

Integrated Science Assessment for Particulate Matter

Includes Errata Sheet created on 2/10/2010

National Center for Environmental Assessment-RTP Division
Office of Research and Development
U.S. Environmental Protection Agency
Research Triangle Park, NC

Disclaimer

This document has been reviewed in accordance with U.S. Environmental Protection Agency policy and approved for publication. Mention of trade names or commercial products does not constitute endorsement or recommendation for use.

**Errata Sheet Created 2/10/2010
for the document titled
Integrated Science Assessment for Particulate Matter, December 2009, Final**

Table or Figure	Page	Erratum
	iv-v	Table of contents for Chapter 2 updated to correct page numbers.
	xv, xxiii	Page numbers for Chapter 2 figures and tables corrected.
	2-9	Replaced reference to “Table 6-14” in the text with “ Table 6-15 ”
	2-10	Replaced reference to “Table 6-14” in the text with “ Table 6-15 ”
	2-11	Replaced reference to “Table 6-14” in the text with “ Table 6-15 ”
	2-12	Replaced the reference to “Figure 7-8” in the text with “ Figure 7-7 ” (cited 3 times)
Figure 2-2	2-15	Mean concentration for Laden et al. (2006, 087605) corrected from 14.8 to 16.4 . Deleted “conducted in locations where the mean annual PM _{2.5} concentrations were <17 µg/m ³ ” in caption.
	2-17	Replaced reference to “Table 6-17” in the text with “ Table 6-18 ”
Figure 6-4	6-72	Figure replaced. Lisabeth et al. (2008, 155939) correctly moved to PM _{2.5} study group.
Figure 6-15	6-148	Updated HERO ID numbers.
Figure 7-6	7-85	PM _{2.5} concentrations for Laden et al. (2006, 087605) corrected from 17.6 to 16.4

Table of Contents

LIST OF TABLES	XV
LIST OF FIGURES	XXIII
PM ISA PROJECT TEAM	XLIII
AUTHORS, CONTRIBUTORS, REVIEWERS	XLVI
CLEAN AIR SCIENTIFIC ADVISORY COMMITTEE FOR PARTICULATE MATTER NAAQS	LII
ACRONYMS AND ABBREVIATIONS	LIV
CHAPTER 1. INTRODUCTION	1-2
1.1. Legislative Requirements	1-4
1.2. History of Reviews of the NAAQS for PM	1-5
1.3. ISA Development	1-9
1.4. Document Organization	1-13
1.5. EPA Framework for Causal Determination	1-14
1.5.1. Scientific Evidence Used in Establishing Causality	1-15
1.5.2. Association and Causation	1-15
1.5.3. Evaluating Evidence for Inferring Causation	1-15
1.5.4. Application of Framework for Causal Determination	1-19
1.5.5. First Step—Determination of Causality	1-20
1.5.6. Second Step—Evaluation of Response	1-22
1.5.6.1. Effects on Human Populations	1-22
1.5.6.2. Effects on Public Welfare	1-24
1.5.7. Concepts in Evaluating Adversity of Health Effects	1-24
1.6. Summary	1-24
Chapter 1 References	1-26
CHAPTER 2. INTEGRATIVE HEALTH AND WELFARE EFFECTS OVERVIEW	2-1
2.1. Concentrations and Sources of Atmospheric PM	2-2
2.1.1. Ambient PM Variability and Correlations	2-2
2.1.1.1. Spatial Variability across the U.S.	2-2
2.1.1.2. Spatial Variability on the Urban and Neighborhood Scales	2-3
2.1.2. Trends and Temporal Variability	2-3
2.1.3. Correlations between Copollutants	2-4
2.1.4. Measurement Techniques	2-4
2.1.5. PM Formation in the Atmosphere and Removal	2-4
2.1.6. Source Contributions to PM	2-5
2.1.7. Policy-Relevant Background	2-6
2.2. Human Exposure	2-6
2.2.1. Spatial Scales of PM Exposure Assessment	2-6
2.2.2. Exposure to PM Components and Copollutants	2-7
2.2.3. Implications for Epidemiologic Studies	2-7

2.3. Health Effects	2-8
2.3.1. Exposure to PM _{2.5}	2-9
2.3.1.1. Effects of Short-Term Exposure to PM _{2.5}	2-9
2.3.1.2. Effects of Long-Term Exposure to PM _{2.5}	2-11
2.3.2. Integration of PM _{2.5} Health Effects	2-13
2.3.3. Exposure to PM _{10-2.5}	2-18
2.3.3.1. Effects of Short-Term Exposure to PM _{10-2.5}	2-18
2.3.4. Integration of PM _{10-2.5} Effects	2-19
2.3.5. Exposure to UFPs	2-21
2.3.5.1. Effects of Short-Term Exposure to UFPs	2-21
2.3.6. Integration of UFP Effects	2-22
2.4. Policy Relevant Considerations	2-23
2.4.1. Potentially Susceptible Populations	2-23
2.4.2. Lag Structure of PM-Morbidity and PM-Mortality Associations	2-24
2.4.2.1. PM-Cardiovascular Morbidity Associations	2-24
2.4.2.2. PM-Respiratory Morbidity Associations	2-24
2.4.2.3. PM-Mortality Associations	2-25
2.4.3. PM Concentration-Response Relationship	2-25
2.4.4. PM Sources and Constituents Linked to Health Effects	2-26
2.5. Welfare Effects	2-27
2.5.1. Summary of Effects on Visibility	2-27
2.5.2. Summary of Effects on Climate	2-28
2.5.3. Summary of Ecological Effects of PM	2-29
2.5.4. Summary of Effects on Materials	2-30
2.6. Summary of Health Effects and Welfare Effects Causal Determinations	2-31
Chapter 2 References	2-34

CHAPTER 3. SOURCE TO HUMAN EXPOSURE **3-1**

3.1. Introduction	3-1
3.2. Overview of Basic Aerosol Properties	3-1
3.3. Sources, Emissions and Deposition of Primary and Secondary PM	3-6
3.3.1. Emissions of Primary PM and Precursors to Secondary PM	3-8
3.3.2. Formation of Secondary PM	3-10
3.3.2.1. Formation of Nitrate and Sulfate	3-10
3.3.2.2. Formation of Secondary Organic Aerosol	3-10
3.3.2.3. Formation of New Particles	3-12
3.3.3. Mobile Source Emissions	3-13
3.3.3.1. Emissions from Gasoline Fueled Engines	3-13
3.3.3.2. Emissions from Diesel Fueled Engines	3-13
3.3.4. Deposition of PM	3-14
3.3.4.1. Deposition Forms	3-16
3.3.4.2. Methods for Estimating Dry Deposition	3-17
3.3.4.3. Factors Affecting Dry Deposition Rates and Totals	3-18
3.4. Monitoring of PM	3-20
3.4.1. Ambient Measurement Techniques	3-20
3.4.1.1. PM Mass	3-20
3.4.1.2. PM Speciation	3-23
3.4.1.3. Multiple-Component Measurements on Individual Particles	3-28
3.4.1.4. UFPs: Mass, Surface Area, and Number	3-29
3.4.1.5. PM Size Distribution	3-29
3.4.1.6. Satellite Measurement	3-29
3.4.2. Ambient Network Design	3-30
3.4.2.1. Monitor Siting Requirements	3-30
3.4.2.2. Spatial and Temporal Coverage	3-31

3.4.2.3.	Network Application for Exposure Assessment with Respect to Susceptible Populations	3-36
3.5.	Ambient PM Concentrations	3-40
3.5.1.	Spatial Distribution	3-41
3.5.1.1.	Variability across the U.S.	3-42
3.5.1.2.	Urban-Scale Variability	3-60
3.5.1.3.	Neighborhood-Scale Variability	3-85
3.5.2.	Temporal Variability	3-91
3.5.2.1.	Regional Trends	3-91
3.5.2.2.	Seasonal Variations	3-96
3.5.2.3.	Hourly Variability	3-97
3.5.3.	Statistical Associations with Copollutants	3-100
3.6.	Mathematical Modeling of PM	3-104
3.6.1.	Estimating Source Contributions to PM Using Receptor Models	3-104
3.6.1.1.	Receptor Models	3-104
3.6.2.	Chemistry Transport Models	3-109
3.6.2.1.	Global Scale	3-111
3.6.2.2.	Regional Scale	3-111
3.6.2.3.	Local or Neighborhood Scale	3-113
3.6.3.	Air Quality Model Evaluation for Air Concentrations	3-113
3.6.3.1.	Ground-based Comparisons of Photochemical Dynamics	3-120
3.6.3.2.	Predicted Chemistry for Nitrates and Related Compounds	3-120
3.6.4.	Evaluating Concentrations and Deposition of PM Components with CTMs	3-126
3.6.4.1.	Global CTM Performance	3-126
3.6.4.2.	Regional CTM Performance	3-127
3.7.	Background PM	3-139
3.7.1.	Contributors to PRB Concentrations of PM	3-139
3.7.1.1.	Estimates of PRB Concentrations in Previous Assessments	3-140
3.7.1.2.	Chemistry Transport Models for Predicting PRB Concentrations	3-142
3.8.	Issues in Exposure Assessment for PM and its Components	3-152
3.8.1.	General Exposure Concepts	3-153
3.8.2.	Personal and Microenvironmental Exposure Monitoring	3-155
3.8.2.1.	New Developments in Personal Exposure Monitoring Instrumentation	3-155
3.8.2.2.	New Developments in Microenvironmental Exposure Monitoring Instrumentation	3-156
3.8.3.	Exposure Modeling	3-157
3.8.3.1.	Time-Weighted Microenvironmental Models	3-157
3.8.3.2.	Stochastic Population Exposure Models	3-158
3.8.3.3.	Dispersion Models	3-160
3.8.3.4.	Land Use Regression and GIS-Based Models	3-160
3.8.4.	Exposure Assessment Studies	3-162
3.8.4.1.	Micro-to-Neighborhood Scale Ambient PM Exposure	3-162
3.8.4.2.	Ambient PM Exposure Estimates from Central Site Monitoring Data	3-165
3.8.4.3.	Infiltration	3-168
3.8.5.	Multicomponent and Multipollutant PM Exposures	3-170
3.8.5.1.	Exposure Issues Related to PM Composition	3-170
3.8.5.2.	Exposure to PM and Copollutants	3-175
3.8.6.	Implications of Exposure Assessment Issues for Interpretation of Epidemiologic Studies	3-176
3.8.6.1.	Measurement Error	3-176
3.8.6.2.	Model-Related Errors	3-177
3.8.6.3.	Spatial Variability	3-179
3.8.6.4.	Temporal Variability	3-181
3.8.6.5.	Use of Surrogates for PM Exposure	3-183
3.8.6.6.	Compositional Differences	3-184
3.8.6.7.	Conclusions	3-184

3.9. Summary and Conclusions	3-185
3.9.1. Concentrations and Sources of Atmospheric PM	3-185
3.9.1.1. PM Source Characteristics	3-185
3.9.1.2. Measurement Techniques	3-185
3.9.1.3. Ambient PM Variability and Correlations	3-186
3.9.1.4. Temporal Variability	3-187
3.9.1.5. Correlations between Copollutants	3-188
3.9.1.6. Source Contributions to PM	3-188
3.9.1.7. Policy-Relevant Background	3-189
3.9.2. Human Exposure	3-189
3.9.2.1. Characterizing Human Exposure	3-189
3.9.2.2. Spatial Scales of PM Exposure Assessment	3-190
3.9.2.3. Multicomponent and Multipollutant PM Exposures	3-191
3.9.2.4. Implications for Epidemiologic Studies	3-191
Chapter 3 References	3-193

CHAPTER 4. DOSIMETRY **4-1**

4.1. Introduction	4-1
4.1.1. Size Characterization of Inhaled Particles	4-2
4.1.2. Structure of the Respiratory Tract	4-3
4.2. Particle Deposition	4-5
4.2.1. Mechanisms of Deposition	4-6
4.2.2. Deposition Patterns	4-7
4.2.2.1. Total Respiratory Tract Deposition	4-8
4.2.2.2. Extrathoracic Region	4-9
4.2.2.3. Tracheobronchial and Alveolar Region	4-10
4.2.2.4. Localized Deposition Sites	4-10
4.2.3. Interspecies Patterns of Deposition	4-11
4.2.4. Biological Factors Modulating Deposition	4-11
4.2.4.1. Physical Activity	4-12
4.2.4.2. Age	4-13
4.2.4.3. Gender	4-14
4.2.4.4. Anatomical Variability	4-14
4.2.4.5. Respiratory Tract Disease	4-15
4.2.4.6. Hygroscopicity of Aerosols	4-16
4.2.5. Summary	4-16
4.3. Clearance of Poorly Soluble Particles	4-17
4.3.1. Clearance Mechanisms and Kinetics	4-17
4.3.1.1. Extrathoracic Region	4-17
4.3.1.2. Tracheobronchial Region	4-18
4.3.1.3. Alveolar Region	4-19
4.3.2. Interspecies Patterns of Clearance and Retention	4-19
4.3.3. Particle Translocation	4-20
4.3.3.1. Alveolar Region	4-21
4.3.3.2. Olfactory Region	4-22
4.3.4. Factors Modulating Clearance	4-23
4.3.4.1. Age	4-23
4.3.4.2. Gender	4-24
4.3.4.3. Respiratory Tract Disease	4-24
4.3.4.4. Particle Overload	4-25
4.3.5. Summary	4-25
4.4. Clearance of Soluble Materials	4-26
4.4.1. Clearance Mechanisms and Kinetics	4-26
4.4.2. Factors Modulating Clearance	4-27
4.4.2.1. Age	4-28

4.4.2.2. Physical Activity	4-28
4.4.2.3. Disease	4-28
4.4.2.4. Concurrent Exposures	4-29
4.4.3. Summary	4-29
Chapter 4 References	4-30

CHAPTER 5. POSSIBLE PATHWAYS/ MODES OF ACTION 5-1

5.1. Pulmonary Effects	5-1
5.1.1. Reactive Oxygen Species	5-1
5.1.2. Activation of Cell Signaling Pathways	5-3
5.1.3. Pulmonary Inflammation	5-4
5.1.4. Respiratory Tract Barrier Function	5-6
5.1.5. Antioxidant Defenses and Adaptive Responses	5-6
5.1.6. Pulmonary Function	5-7
5.1.7. Allergic Disorders	5-8
5.1.8. Impaired Lung Defense Mechanisms	5-8
5.1.9. Resolution of Inflammation/Progression or Exacerbation of Disease	5-8
5.1.9.1. Factors Affecting the Retention of PM	5-9
5.1.9.2. Factors Affecting the Balance of Pro/Anti-Inflammatory Mediators, Oxidants/Anti-Oxidants and Proteases/Anti-Proteases	5-9
5.1.9.3. Pre-Existing Disease	5-10
5.1.10. Pulmonary DNA Damage	5-10
5.1.11. Epigenetic Changes	5-10
5.1.12. Lung Development	5-11
5.2. Systemic Inflammation	5-12
5.2.1. Endothelial Dysfunction and Altered Vasoreactivity	5-13
5.2.2. Activation of Coagulation and Acute Phase Response	5-14
5.2.3. Atherosclerosis	5-15
5.3. Activation of the Autonomic Nervous System by Pulmonary Reflexes	5-16
5.4. Translocation of UFPs or Soluble PM Components	5-17
5.5. Disease of the Cardiovascular and Other Organ Systems	5-18
5.6. Acute and Chronic Responses	5-19
5.7. Results of New Inhalation Studies which Contribute to Modes of Action	5-19
5.8. Gaps in Knowledge	5-22
Chapter 5 References	5-23

CHAPTER 6. INTEGRATED HEALTH EFFECTS OF SHORT-TERM PM EXPOSURE 6-1

6.1. Introduction	6-1
6.2. Cardiovascular and Systemic Effects	6-2
6.2.1. Heart Rate and Heart Rate Variability	6-2
6.2.1.1. Epidemiologic Studies	6-2
6.2.1.2. Controlled Human Exposure Studies	6-8
6.2.1.3. Toxicological Studies	6-10
6.2.2. Arrhythmia	6-13
6.2.2.1. Epidemiologic Studies	6-13
6.2.2.2. Toxicological Studies	6-18
6.2.3. Ischemia	6-20
6.2.3.1. Epidemiologic Studies	6-20
6.2.3.2. Controlled Human Exposure Studies	6-22
6.2.3.3. Toxicological Studies	6-23
6.2.4. Vasomotor Function	6-24

6.2.4.1.	Epidemiologic Studies	6-24
6.2.4.2.	Controlled Human Exposure Studies	6-26
6.2.4.3.	Toxicological Studies	6-29
6.2.5.	Blood Pressure	6-33
6.2.5.1.	Epidemiologic Studies	6-33
6.2.5.2.	Controlled Human Exposure Studies	6-36
6.2.5.3.	Toxicological Studies	6-37
6.2.6.	Cardiac Contractility	6-38
6.2.6.1.	Toxicological Studies	6-38
6.2.7.	Systemic Inflammation	6-39
6.2.7.1.	Epidemiologic Studies	6-40
6.2.7.2.	Controlled Human Exposure Studies	6-44
6.2.7.3.	Toxicological Studies	6-46
6.2.8.	Hemostasis, Thrombosis and Coagulation Factors	6-47
6.2.8.1.	Epidemiologic Studies	6-47
6.2.8.2.	Controlled Human Exposure Studies	6-48
6.2.8.3.	Toxicological Studies	6-50
6.2.9.	Systemic and Cardiovascular Oxidative Stress	6-52
6.2.9.1.	Epidemiologic Studies	6-52
6.2.9.2.	Controlled Human Exposure Studies	6-53
6.2.9.3.	Toxicological Studies	6-54
6.2.10.	Hospital Admissions and Emergency Department Visits	6-56
6.2.10.1.	All Cardiovascular Disease	6-60
6.2.10.2.	Cardiac Diseases	6-64
6.2.10.3.	Ischemic Heart Disease	6-64
6.2.10.4.	Acute Myocardial Infarction	6-67
6.2.10.5.	Congestive Heart Failure	6-68
6.2.10.6.	Cardiac Arrhythmias	6-69
6.2.10.7.	Cerebrovascular Disease	6-70
6.2.10.8.	Peripheral Vascular Disease	6-72
6.2.10.9.	Copollutant Models	6-72
6.2.10.10.	Concentration Response	6-75
6.2.10.11.	Out of Hospital Cardiac Arrest	6-76
6.2.11.	Cardiovascular Mortality	6-77
6.2.12.	Summary and Causal Determinations	6-78
6.2.12.1.	PM _{2.5}	6-78
6.2.12.2.	PM _{10-2.5}	6-81
6.2.12.3.	UFPs	6-83
6.3.	Respiratory Effects	6-84
6.3.1.	Respiratory Symptoms and Medication Use	6-84
6.3.1.1.	Epidemiologic Studies	6-84
6.3.1.2.	Controlled Human Exposure Studies	6-93
6.3.2.	Pulmonary Function	6-94
6.3.2.1.	Epidemiologic Studies	6-95
6.3.2.2.	Controlled Human Exposure Studies	6-98
6.3.2.3.	Toxicological Studies	6-99
6.3.3.	Pulmonary Inflammation	6-101
6.3.3.1.	Epidemiologic Studies	6-101
6.3.3.2.	Controlled Human Exposure Studies	6-104
6.3.3.3.	Toxicological Studies	6-106
6.3.4.	Pulmonary Oxidative Responses	6-110
6.3.4.1.	Controlled Human Exposure Studies	6-111
6.3.4.2.	Toxicological Studies	6-112
6.3.5.	Pulmonary Injury	6-114
6.3.5.1.	Epidemiologic Studies	6-114
6.3.5.2.	Controlled Human Exposure Studies	6-114
6.3.5.3.	Toxicological Studies	6-115
6.3.6.	Allergic Responses	6-122

6.3.6.1. Epidemiologic Studies	6-122
6.3.6.2. Controlled Human Exposure Studies	6-122
6.3.6.3. Toxicological Studies	6-123
6.3.7. Host Defense	6-129
6.3.7.1. Epidemiologic Studies	6-129
6.3.7.2. Toxicological Studies	6-129
6.3.8. Respiratory ED Visits, Hospital Admissions and Physician Visits	6-132
6.3.8.1. All Respiratory Diseases	6-133
6.3.8.2. Asthma	6-137
6.3.8.3. Chronic Obstructive Pulmonary Disease	6-142
6.3.8.4. Pneumonia and Respiratory Infections	6-143
6.3.8.5. Copollutant Models	6-147
6.3.9. Respiratory Mortality	6-149
6.3.10. Summary and Causal Determinations	6-149
6.3.10.1. PM _{2.5}	6-149
6.3.10.2. PM _{10-2.5}	6-152
6.3.10.3. UFPs	6-153
6.4. Central Nervous System Effects	6-154
6.4.1. Epidemiologic Studies	6-154
6.4.2. Controlled Human Exposure Studies	6-155
6.4.3. Toxicological Studies	6-155
6.4.3.1. Urban Air	6-155
6.4.3.2. CAPs	6-156
6.4.3.3. Diesel Exhaust	6-156
6.4.3.4. Summary of Toxicological Study Findings of CNS Effects	6-157
6.4.4. Summary and Causal Determination	6-157
6.5. Mortality	6-158
6.5.1. Summary of Findings from 2004 PM AQCD	6-158
6.5.2. Associations of Mortality and Short-Term Exposure to PM	6-159
6.5.2.1. PM ₁₀	6-160
6.5.2.2. PM _{2.5}	6-174
6.5.2.3. Thoracic Coarse Particles (PM _{10-2.5})	6-184
6.5.2.4. Ultrafine Particles	6-190
6.5.2.5. Chemical Components of PM	6-191
6.5.2.6. Source-Apporioned PM Analyses	6-196
6.5.2.7. Investigation of Concentration-Response Relationship	6-197
6.5.3. Summary and Causal Determinations	6-200
6.5.3.1. PM _{2.5}	6-200
6.5.3.2. PM _{10-2.5}	6-201
6.5.3.3. UFPs	6-202
6.6. Attribution of Ambient PM Health Effects to Specific Constituents or Sources	6-202
6.6.1. Evaluation Approach	6-202
6.6.2. Findings	6-203
6.6.2.1. Epidemiologic Studies	6-203
6.6.2.2. Controlled Human Exposure Studies	6-206
6.6.2.3. Toxicological Studies	6-206
6.6.3. Summary by Health Effects	6-210
6.6.4. Conclusion	6-211
Chapter 6 References	6-213

CHAPTER 7. INTEGRATED HEALTH EFFECTS OF LONG-TERM PM EXPOSURE 7-1

7.1. Introduction	7-1
7.2. Cardiovascular and Systemic Effects	7-1
7.2.1. Atherosclerosis	7-2
7.2.1.1. Epidemiologic Studies	7-2

7.2.1.2.	Toxicological Studies	7-4
7.2.2.	Venous Thromboembolism	7-6
7.2.2.1.	Epidemiologic Studies	7-7
7.2.3.	Metabolic Syndromes	7-7
7.2.3.1.	Epidemiologic Studies	7-7
7.2.3.2.	Toxicological Studies	7-7
7.2.4.	Systemic Inflammation, Immune Function, and Blood Coagulation	7-8
7.2.4.1.	Epidemiologic Studies	7-8
7.2.4.2.	Toxicological Studies	7-8
7.2.5.	Renal and Vascular Function	7-9
7.2.5.1.	Epidemiologic Studies	7-10
7.2.5.2.	Toxicological Studies	7-11
7.2.6.	Autonomic Function	7-12
7.2.6.1.	Toxicological Studies	7-12
7.2.7.	Cardiac changes	7-12
7.2.7.1.	Toxicological studies	7-12
7.2.8.	Left Ventricular Mass and Function	7-13
7.2.9.	Clinical Outcomes in Epidemiologic Studies	7-13
7.2.10.	Cardiovascular Mortality	7-17
7.2.11.	Summary and Causal Determinations	7-18
7.2.11.1.	PM _{2.5}	7-18
7.2.11.2.	PM _{10-2.5}	7-19
7.2.11.3.	UFPs	7-19
7.3.	Respiratory Effects	7-20
7.3.1.	Respiratory Symptoms and Disease Incidence	7-20
7.3.1.1.	Epidemiologic Studies	7-20
7.3.2.	Pulmonary Function	7-26
7.3.2.1.	Epidemiologic Studies	7-26
7.3.2.2.	Toxicological Studies	7-30
7.3.3.	Pulmonary Inflammation	7-32
7.3.3.1.	Epidemiologic Studies	7-32
7.3.3.2.	Toxicological Studies	7-32
7.3.4.	Pulmonary Oxidative Response	7-34
7.3.4.1.	Toxicological Studies	7-34
7.3.5.	Pulmonary Injury	7-35
7.3.5.1.	Toxicological Studies	7-35
7.3.6.	Allergic Responses	7-38
7.3.6.1.	Epidemiologic Studies	7-38
7.3.6.2.	Toxicological Studies	7-39
7.3.7.	Host Defense	7-40
7.3.7.1.	Epidemiologic Studies	7-40
7.3.7.2.	Toxicological Studies	7-40
7.3.8.	Respiratory Mortality	7-41
7.3.9.	Summary and Causal Determinations	7-42
7.3.9.1.	PM _{2.5}	7-42
7.3.9.2.	PM _{10-2.5}	7-43
7.3.9.3.	UFPs	7-44
7.4.	Reproductive, Developmental, Prenatal and Neonatal Outcomes	7-44
7.4.1.	Epidemiologic Studies	7-44
7.4.1.1.	Low Birth Weight	7-45
7.4.1.2.	Preterm Birth	7-48
7.4.1.3.	Growth Restriction	7-51
7.4.1.4.	Birth Defects	7-52
7.4.1.5.	Infant Mortality	7-53
7.4.1.6.	Decrements in Sperm Quality	7-58
7.4.2.	Toxicological Studies	7-58
7.4.2.1.	Female Reproductive Effects	7-59

7.4.2.2.	Male Reproductive Effects	7-60
7.4.2.3.	Multiple Generation Effects	7-62
7.4.2.4.	Receptor Mediated Effects	7-63
7.4.2.5.	Developmental Effects	7-63
7.4.3.	Summary and Causal Determinations	7-67
7.4.3.1.	PM _{2.5}	7-67
7.4.3.2.	PM _{10-2.5}	7-68
7.4.3.3.	UFPs	7-68
7.5.	Cancer, Mutagenicity, and Genotoxicity	7-68
7.5.1.	Epidemiologic Studies	7-69
7.5.1.1.	Lung Cancer Mortality and Incidence	7-70
7.5.1.2.	Other Cancers	7-73
7.5.1.3.	Markers of Exposure or Susceptibility	7-73
7.5.2.	Toxicological Studies	7-75
7.5.2.1.	Mutagenesis and Genotoxicity	7-76
7.5.2.2.	Carcinogenesis	7-79
7.5.2.3.	Summary of Toxicological Studies	7-80
7.5.3.	Epigenetic Studies and Other Heritable DNA mutations	7-80
7.5.4.	Summary and Causal Determinations	7-81
7.5.4.1.	PM _{2.5}	7-81
7.5.4.2.	PM _{10-2.5}	7-82
7.5.4.3.	UFPs	7-82
7.6.	Mortality	7-82
7.6.1.	Recent Studies of Long-Term Exposure to PM and Mortality	7-84
7.6.2.	Composition and Source-Oriented Analyses of PM	7-89
7.6.3.	Within-City Effects of PM Exposure	7-90
7.6.4.	Effects of Different Long-term Exposure Windows	7-92
7.6.5.	Summary and Causal Determinations	7-95
7.6.5.1.	PM _{2.5}	7-95
7.6.5.2.	PM _{10-2.5}	7-97
7.6.5.3.	UFPs	7-97
Chapter 7 References		7-98

CHAPTER 8. POPULATIONS SUSCEPTIBLE TO PM-RELATED HEALTH EFFECTS 8-1

8.1.	Potentially Susceptible Populations	8-3
8.1.1.	Lifestage	8-3
8.1.1.1.	Older Adults	8-3
8.1.1.2.	Children	8-5
8.1.2.	Pregnancy and Developmental Effects	8-5
8.1.3.	Gender	8-6
8.1.4.	Race/Ethnicity	8-7
8.1.5.	Gene-Environment Interaction	8-7
8.1.6.	Pre-Existing Disease	8-9
8.1.6.1.	Cardiovascular Diseases	8-9
8.1.6.2.	Respiratory Illnesses	8-12
8.1.6.3.	Respiratory Contributions to Cardiovascular Effects	8-13
8.1.6.4.	Diabetes and Obesity	8-13
8.1.7.	Socioeconomic Status	8-14
8.1.8.	Summary	8-15
Chapter 8 References		8-17

CHAPTER 9. WELFARE EFFECTS 9-1

9.1.	Introduction	9-1
9.2.	Effects on Visibility	9-1

9.2.1.	Introduction	9-1
9.2.2.	Background	9-2
9.2.2.1.	Non-PM Visibility Effects	9-5
9.2.2.2.	PM Visibility Effects	9-5
9.2.2.3.	Direct Optical Measurements	9-8
9.2.2.4.	Value of Good Visual Air Quality	9-10
9.2.3.	Monitoring and Assessment	9-10
9.2.3.1.	Aerosol Properties	9-11
9.2.3.2.	Spatial Patterns	9-16
9.2.3.3.	Urban and Regional Patterns	9-23
9.2.3.4.	Temporal Trends	9-31
9.2.3.5.	Causes of Haze	9-37
9.2.4.	Urban Visibility Valuation and Preference	9-65
9.2.4.1.	Urban Visibility Preference Studies	9-67
9.2.4.2.	Denver, Colorado Urban Visibility Preference Study	9-68
9.2.4.3.	Phoenix, Arizona Urban Visibility Preference Study	9-69
9.2.4.4.	British Columbia, Canada Urban Visibility Preference Study	9-69
9.2.4.5.	Washington, DC Urban Visibility Preference Studies	9-69
9.2.4.6.	Urban Visibility Valuation Studies	9-71
9.2.5.	Summary of Effects on Visibility	9-72
9.3.	Effects on Climate	9-74
9.3.1.	The Climate Effects of Aerosols	9-74
9.3.2.	Overview of Aerosol Measurement Capabilities	9-82
9.3.2.1.	Satellite Remote Sensing	9-82
9.3.2.2.	Focused Field Campaigns	9-88
9.3.2.3.	Ground-Based In Situ Measurement Networks	9-89
9.3.2.4.	In Situ Aerosol Profiling Programs	9-91
9.3.2.5.	Ground-Based Remote Sensing Measurement Networks	9-95
9.3.2.6.	Synergy of Measurements and Model Simulations	9-96
9.3.3.	Assessments of Aerosol Characterization and Climate Forcing	9-99
9.3.3.1.	The Use of Measured Aerosol Properties to Improve Models	9-100
9.3.3.2.	Intercomparisons of Satellite Measurements and Model Simulation of Aerosol Optical Depth	9-103
9.3.3.3.	Satellite-Based Estimates of Aerosol Direct Radiative Forcing	9-105
9.3.3.4.	Satellite-Based Estimates of Anthropogenic Component of Aerosol Direct Radiative Forcing	9-111
9.3.3.5.	Aerosol-Cloud Interactions and Indirect Forcing	9-112
9.3.3.6.	Remote Sensing of Aerosol-Cloud Interactions and Indirect Forcing	9-113
9.3.3.7.	In Situ Studies of Aerosol-Cloud Interactions	9-116
9.3.4.	Outstanding Issues	9-117
9.3.5.	Concluding Remarks	9-120
9.3.6.	Modeling the Effect of Aerosols on Climate	9-121
9.3.6.1.	Introduction	9-121
9.3.6.2.	Modeling of Atmospheric Aerosols	9-124
9.3.6.3.	Calculating Aerosol Direct Radiative Forcing	9-129
9.3.6.4.	Calculating Aerosol Indirect Forcing	9-137
9.3.6.5.	Aerosol in the Climate Models	9-145
9.3.6.6.	Impacts of Aerosols on Climate Model Simulations	9-153
9.3.6.7.	Outstanding Issues	9-157
9.3.6.8.	Conclusions	9-158
9.3.7.	Fire as a Special Source of PM Welfare Effects	9-159
9.3.8.	Radiative Effects of Volcanic Aerosols	9-160
9.3.8.1.	Explosive Volcanic Activity	9-160
9.3.9.	Other Special Sources and Effects	9-164
9.3.9.1.	Glaciers and Snowpack	9-167
9.3.9.2.	Radiative Forcing by Anthropogenic Surface Albedo Change: BC in Snow and Ice	9-169
9.3.9.3.	Effects on Local and Regional Climate	9-170

9.3.10. Summary of Effects on Climate	9-171
9.4. Ecological Effects of PM	9-172
9.4.1. Introduction	9-172
9.4.1.1. Ecosystem Scale, Function, and Structure	9-173
9.4.1.2. Ecosystem Services	9-174
9.4.2. Deposition of PM	9-174
9.4.2.1. Forms of Deposition	9-175
9.4.2.2. Components of PM Deposition	9-175
9.4.2.3. Magnitude of Dry Deposition	9-179
9.4.3. Direct Effects of PM on Vegetation	9-182
9.4.3.1. Effects of Coarse-mode Particles	9-182
9.4.4. PM and Altered Radiative Flux	9-183
9.4.5. Effects of Trace Metals on Ecosystems	9-183
9.4.5.1. Effects on Soil Chemistry	9-185
9.4.5.2. Effects on Soil Microbes and Plant Uptake via Soil	9-186
9.4.5.3. Plant Response to Metals	9-189
9.4.5.4. Effects on Aquatic Ecosystems	9-192
9.4.5.5. Effects on Animals	9-192
9.4.5.6. Biomagnification across Trophic Levels	9-193
9.4.5.7. Effects near Smelters and Roadsides	9-194
9.4.5.8. Toxicity to Mosses and Lichens	9-196
9.4.6. Organic Compounds	9-196
9.4.7. Summary of Ecological Effects of PM	9-199
9.5. Effects on Materials	9-201
9.5.1. Effects on Paint	9-202
9.5.2. Effects on Metal Surfaces	9-202
9.5.3. Effects on Stone	9-203
9.5.4. Summary of Effects on Materials	9-203
Chapter 9 References	9-204
ANNEX A. ATMOSPHERIC SCIENCE	A-1
Annex A References	A-353
ANNEX B. DOSIMETRY	B-1
Annex B References	B-7
ANNEX C. CONTROLLED HUMAN EXPOSURE STUDIES	C-1
Annex C References	C-14
ANNEX D. TOXICOLOGICAL STUDIES	D-1
Annex D References	D-172
ANNEX E. EPIDEMIOLOGIC STUDIES	E-1
Annex E References	E-524
ANNEX F. SOURCE APPORTIONMENT STUDIES	F-1
Annex F References	F-11

List of Tables

Table 1-1.	Summary of NAAQS promulgated for PM, 1971-2006. _____	1-6
Table 1-2.	Aspects to aid in judging causality. _____	1-20
Table 1-3.	Weight of evidence for causal determination. _____	1-22
Table 2-1.	Summary of causal determinations for short-term exposure to PM _{2.5} . _____	2-9
Table 2-2.	Summary of causal determinations for long-term exposure to PM _{2.5} . _____	2-11
Table 2-3.	Summary of causal determinations for short-term exposure to PM _{10-2.5} . _____	2-18
Table 2-4.	Summary of causal determinations for short-term exposure to UFPs. _____	2-21
Table 2-5.	Summary of causality determination for welfare effects. _____	2-27
Table 2-6.	Summary of PM causal determinations by exposure duration and health outcome. _____	2-32
Table 2-7.	Summary of PM causal determinations for welfare effects _____	2-33
Table 3-1.	Characteristics of ambient fine (ultrafine plus accumulation-mode) and coarse particles. _____	3-4
Table 3-2.	Constituents of atmospheric particles and their major sources. _____	3-7
Table 3-3.	Proximity to PM _{2.5} and PM ₁₀ monitors for total population ^a by city. _____	3-35
Table 3-4.	Proximity to PM _{2.5} and PM ₁₀ monitors for children age 0-4 yr, children age 5-17 yr, and adults age 65 yr and older. ^a _____	3-37
Table 3-5.	Proximity to PM _{2.5} and PM ₁₀ monitors for adults age 65 yr and older ^a by city. _____	3-38
Table 3-6.	Proximity to PM _{2.5} and PM ₁₀ monitors based on the population identified as white, black, Hispanic, or non-Hispanic ^a . _____	3-39
Table 3-7.	Proximity to PM _{2.5} and PM ₁₀ monitors based on the population below or above the poverty line, population over age 25 with less than high school education, population over 25 with high school education, and population over 25 with college education or more ^a . _____	3-40
Table 3-8.	PM _{2.5} distributions derived from AQS data (concentration in µg/m ³). _____	3-44
Table 3-9.	PM _{10-2.5} distributions derived from AQS data (concentration in µg/m ³). _____	3-47
Table 3-10.	PM ₁₀ distributions derived from AQS data (concentration in µg/m ³). _____	3-49
Table 3-11.	Inter-sampler comparison statistics for each pair of 24-h PM _{2.5} monitors reporting to AQS for Boston, MA. _____	3-63
Table 3-12.	Inter-sampler comparison statistics for each pair of 24-h PM _{2.5} monitors reporting to AQS for Pittsburgh, PA. _____	3-67
Table 3-13.	Inter-sampler comparison statistics for each pair of 24-h PM _{2.5} monitors reporting to AQS for Los Angeles, CA. _____	3-69
Table 3-14.	Inter-sampler comparison statistics for each pair of 24-h PM ₁₀ monitors reporting to AQS for Boston, MA. _____	3-75
Table 3-15.	Inter-sampler comparison statistics for each pair of 24-h PM ₁₀ monitors reporting to AQS for Pittsburgh, PA. _____	3-78
Table 3-16.	Inter-sampler comparison statistics for each pair of 24-h PM ₁₀ monitors reporting to AQS for Los Angeles, CA. _____	3-81

Table 3-17.	Example of emissions factors (ng/km) for trace elements under variable speed and steady speed driving conditions for PM emitted by diesel and gasoline engines. _____	3-106
Table 3-18.	Estimates of annual average natural background concentrations of PM _{2.5} and PM ₁₀ (µg/m ³) from Trijonis et al. (1990, 157058). _____	3-140
Table 3-19.	Annual and quarterly mean PM _{2.5} concentrations (µg/m ³) measured at IMPROVE sites in 2004. _____	3-142
Table 3-20.	Annual and quarterly mean PM _{2.5} concentrations (µg/m ³) for the CMAQ “base case” at IMPROVE sites in 2004. _____	3-150
Table 3-21.	Annual and quarterly mean PM _{2.5} concentrations (µg/m ³) for the CMAQ PRB simulations at IMPROVE sites in 2004. _____	3-151
Table 3-22.	Annual and quarterly mean of the CMAQ-predicted base case PM _{2.5} concentrations (µg/m ³) in the U.S. EPA CONUS regions in 2004. _____	3-151
Table 3-23.	Annual and quarterly mean of the CMAQ-predicted PRB PM _{2.5} concentrations (µg/m ³) in the U.S. EPA CONUS regions in 2004. _____	3-152
Table 3-24.	Examples of studies comparing near-road personal exposures with fixed site ambient concentrations. _____	3-164
Table 4-1.	Breathing patterns with activity level in adult human male. _____	4-12
Table 6-1.	Characteristics of epidemiologic studies investigating associations between PM and changes in HRV. _____	6-6
Table 6-2.	Epidemiologic studies of ventricular arrhythmia and ambient PM concentration, in patients with implantable cardioverter defibrillators. _____	6-15
Table 6-3.	PM Concentrations reported in epidemiologic studies ECG changes suggestive of ischemia. _____	6-22
Table 6-4.	PM concentrations reported in epidemiologic studies of vasomotor function. _____	6-26
Table 6-5.	Mean PM concentrations reported in epidemiologic studies of blood pressure. _____	6-35
Table 6-6.	PM concentrations reported in epidemiologic studies of inflammation, hemostasis, thrombosis, coagulation factors and oxidative stress. _____	6-42
Table 6-7.	Description of ICD-9 and ICD-10 codes for diseases of the circulatory system. _____	6-57
Table 6-8.	Characterization of ambient PM concentrations in epidemiologic studies of hospital admission and ED visits for cardiovascular diseases. _____	6-63
Table 6-9.	PM concentrations reported in studies of out-of-hospital cardiac arrest. _____	6-77
Table 6-10.	Characterization of ambient PM concentrations from epidemiologic studies of respiratory morbidity and short-term exposures in asthmatic children and adults. _____	6-87
Table 6-11.	PAMCHAR PM _{10-2.5} inflammation results with ambient PM. _____	6-119
Table 6-12.	Other ambient PM – in vivo PM _{10-2.5} studies – BALF results, 18-24 h post-IT exposure. _____	6-119
Table 6-13.	Description of ICD-9 and ICD-10 codes for diseases of the respiratory system. _____	6-133
Table 6-14.	PM concentrations in epidemiologic studies of respiratory diseases. _____	6-146
Table 6-15.	Overview of U.S. and Canadian multicity PM studies of mortality analyzed in the 2004 PM AQCD and the PM ISA ^b . _____	6-159
Table 6-16.	NMMAPS national and regional percentage increase in all-cause, cardio-respiratory, and other-cause mortality associated with a 10 µg/m ³ increase in PM ₁₀ at lag 1 day for the periods 1987-1994, 1995-2000, and 1987-2000. _____	6-163

Table 6-17.	Effect modification of composition on the estimated percent increase in mortality with a 10 $\mu\text{g}/\text{m}^3$ increase in $\text{PM}_{2.5}$.	6-194
Table 6-18.	Study-specific $\text{PM}_{2.5}$ factor/source categories associated with health effects.	6-207
Table 7-1.	Characterization of ambient PM concentrations from studies of subclinical measures of cardiovascular diseases and long-term exposure.	7-11
Table 7-2.	Characterization of ambient PM concentrations from studies of clinical cardiovascular diseases and long-term exposure.	7-14
Table 7-3.	Characterization of ambient PM concentrations from studies of respiratory symptoms/disease and long-term exposures.	7-22
Table 7-4.	Characterization of ambient PM concentrations from studies of FEV_1 and long-term exposures.	7-27
Table 7-5.	Characterization of ambient PM concentrations from studies of reproductive, developmental, prenatal and neonatal outcomes and long-term exposure.	7-46
Table 7-6.	Characterization of ambient PM concentrations from recent studies of cancer and long-term exposures to PM.	7-70
Table 7-7.	Associations* between ambient PM concentrations from select studies of lung cancer mortality and incidence.	7-72
Table 7-8.	Characterization of ambient PM concentrations from studies of mortality and long-term exposures to PM.	7-83
Table 7-9.	Comparison of results from ACS intra-urban analysis of Los Angeles and New York City using kriging or land use regression to estimate exposure.	7-91
Table 7-10.	Distribution of the effect of a hypothetical reduction of 10 $\mu\text{g}/\text{m}^3$ PM_{10} in 2000 on all-cause mortality 2000-2009 in Switzerland.	7-94
Table 8-1.	Definitions of susceptible and vulnerable in the PM literature.	8-2
Table 8-2.	Susceptibility factors evaluated.	8-3
Table 8-3.	Percent of the U.S. population with respiratory diseases, cardiovascular diseases, and diabetes.	8-11
Table 9-1.	Regional Planning Organization websites with visibility characterization and source attribution assessment information.	9-17
Table 9-2.	Summary of urban visibility preference studies.	9-67
Table 9-3.	Top-of-atmosphere, cloud-free, instantaneous direct aerosol radiative forcing dependence on aerosol and surface properties.	9-81
Table 9-4.	Summary of major satellite measurements currently available for the tropospheric aerosol characterization and radiative forcing research.	9-83
Table 9-5.	List of major intensive field experiments that are relevant to aerosol research in a variety of aerosol regimes around the globe conducted in the past two decades.	9-93
Table 9-6.	Summary of major U.S. surface in situ and remote sensing networks for the tropospheric aerosol characterization and radiative forcing research.	9-94
Table 9-7.	Summary of approaches to estimating the aerosol direct radiative forcing in three categories: (1) satellite retrievals; (2) satellite-model integrations; and (3) model simulations.	9-106
Table 9-8.	Summary of seasonal and annual average clear-sky DRF (W/m^2) at the TOA and the surface (SFC) over global OCEAN derived with different methods and data.	9-109

Table 9-9.	Summary of seasonal and annual average clear-sky DRF (W/m^2) at the TOA and the surface (SFC) over global LAND derived with different methods and data. _____	9-110
Table 9-10.	Estimates of anthropogenic components of aerosol optical depth (T_{ant}) and clear-sky DRF at the TOA from model simulations. _____	9-112
Table 9-11.	Anthropogenic emissions of aerosols and precursors for 2000 and 1750. _____	9-126
Table 9-12.	Summary of statistics of AeroCom Experiment A results from 16 global models. _____	9-127
Table 9-13.	SO_4^{2-} mass loading, MEE and AOD at 550 nm, shortwave radiative forcing at the top of the atmosphere, and normalized forcing with respect to AOD and mass. _____	9-131
Table 9-14.	Particulate organic matter (POM) and BC mass loading, AOD at 550 nm, shortwave radiative forcing at the top of the atmosphere, and normalized forcing with respect to AOD and mass. _____	9-132
Table 9-15.	Differences in present day and pre-industrial outgoing solar radiation (W/m^2) in the different experiments. _____	9-141
Table 9-16.	Forcings used in IPCC AR4 simulations of 20th century climate change. _____	9-145
Table 9-17.	Climate forcings (1880-2003) used to drive GISS climate simulations, along with the surface air temperature changes obtained for several periods. _____	9-154
Table 9-18.	Overview of the different aerosol indirect effects and their sign of the net radiative flux change at the top of the atmosphere (TOA). _____	9-166
Table 9-19.	Overview of the different aerosol indirect effects and their implications for the global mean net shortwave radiation of the surface F_{sfc} (columns 2-4) and for precipitation (columns 5-7). _____	9-166
Table 9-20.	Recent studies highlighting POP occurrence and fate in the major arctic compartments. _____	9-168
Table 9-21.	Factors potentially important in estimating Hg exposure. _____	9-177
Table A-1.	Summary of integrated and continuous samplers included in the field comparison. _____	A-1
Table A-2.	Summary of $PM_{2.5}$ and PM_{10} FRM and FEM samplers. _____	A-5
Table A-3.	Measurement and analytical specifications for filter analysis of mass, elements, ions, and carbon. _____	A-7
Table A-4.	Measurement and analytical specifications for filter analysis of organic species. _____	A-9
Table A-5.	Measurement and analytical specifications for continuous mass and mass surrogate instruments. _____	A-11
Table A-6.	Measurement and analytical specifications for continuous elements. _____	A-14
Table A-7.	Measurement and analytical specifications for continuous NO_3^- . _____	A-15
Table A-8.	Measurement and analytical specifications for continuous SO_4^{2-} . _____	A-17
Table A-9.	Measurement and analytical specifications for ions other than NO_3^- and SO_4^{2-} . _____	A-19
Table A-10.	Measurement and analytical specifications for continuous carbon. _____	A-20
Table A-11.	Summary of mass measurement comparisons. _____	A-23
Table A-12.	Summary of element and liquid water content measurement comparisons. _____	A-31
Table A-13.	Summary of $PM_{2.5}$ NO_3^- measurement comparisons. _____	A-32
Table A-14.	Summary of $PM_{2.5}$ SO_4^{2-} measurement comparisons _____	A-38
Table A-15.	Summary of $PM_{2.5}$ carbon measurement comparisons. _____	A-41

Table A-16.	Summary of particle mass spectrometer measurement comparisons.	A-48
Table A-17.	Summary of key parameters for TD-GC/MS and pyrolysis-GC/MS.	A-52
Table A-18.	Relevant Spatial Scales for PM ₁₀ , PM _{2.5} , and PM _{10-2.5} Measurement	A-54
Table A-19.	Major routine operating air monitoring networks ^a	A-56
Table A-20.	Inter-sampler correlation statistics for each pair of PM _{2.5} monitors reporting to AQS for Atlanta, GA.	A-98
Table A-21.	Inter-sampler correlation statistics for each pair of PM _{2.5} monitors reporting to AQS for Birmingham, AL.	A-102
Table A-22.	Inter-sampler correlation statistics for each pair of PM _{2.5} monitors reporting to AQS for Boston, MA.	A-106
Table A-23.	Inter-sampler correlation statistics for each pair of PM _{2.5} monitors reporting to AQS for Chicago, IL.	A-111
Table A-24.	Inter-sampler correlation statistics for each pair of PM _{2.5} monitors reporting to AQS for Denver, CO.	A-116
Table A-25.	Inter-sampler correlation statistics for each pair of PM _{2.5} monitors reporting to AQS for Detroit, MI.	A-120
Table A-26.	Inter-sampler correlation statistics for each pair of PM _{2.5} monitors reporting to AQS for Houston, TX.	A-123
Table A-27.	Inter-sampler correlation statistics for each pair of PM _{2.5} monitors reporting to AQS for Los Angeles, CA.	A-127
Table A-28.	Inter-sampler correlation statistics for each pair of PM _{2.5} monitors reporting to AQS for New York, NY.	A-131
Table A-29.	Inter-sampler correlation statistics for each pair of PM _{2.5} monitors reporting to AQS for Philadelphia, PA.	A-136
Table A-30.	Inter-sampler correlation statistics for each pair of PM _{2.5} monitors reporting to AQS for Phoenix, AZ.	A-140
Table A-31.	Inter-sampler correlation statistics for each pair of PM _{2.5} monitors reporting to AQS for Pittsburgh, PA.	A-144
Table A-32.	Inter-sampler correlation statistics for each pair of PM _{2.5} monitors reporting to AQS for Riverside, CA.	A-148
Table A-33.	Inter-sampler correlation statistics for each pair of PM _{2.5} monitors reporting to AQS for Seattle, WA.	A-152
Table A-34.	Inter-sampler correlation statistics for each pair of PM _{2.5} monitors reporting to AQS for St. Louis, MO.	A-155
Table A-35.	Inter-sampler correlation statistics for each pair of PM ₁₀ monitors reporting to AQS for Atlanta, GA.	A-159
Table A-36.	Inter-sampler correlation statistics for each pair of PM ₁₀ monitors reporting to AQS for Birmingham, AL.	A-163
Table A-37.	Inter-sampler correlation statistics for each pair of PM ₁₀ monitors reporting to AQS for Boston, MA.	A-166
Table A-38.	Inter-sampler correlation statistics for each pair of PM ₁₀ monitors reporting to AQS for Chicago, IL.	A-170

Table A-39.	Inter-sampler correlation statistics for each pair of PM ₁₀ monitors reporting to AQS for Denver, CO. _____	A-174
Table A-40.	Inter-sampler correlation statistics for each pair of PM ₁₀ monitors reporting to AQS for Detroit, MI. _____	A-178
Table A-41.	Inter-sampler correlation statistics for each pair of PM ₁₀ monitors reporting to AQS for Houston, TX. _____	A-181
Table A-42.	Inter-sampler correlation statistics for each pair of PM ₁₀ monitors reporting to AQS for Los Angeles, CA. _____	A-184
Table A-43.	Inter-sampler correlation statistics for each pair of PM ₁₀ monitors reporting to AQS for New York, NY. _____	A-188
Table A-44.	Inter-sampler correlation statistics for each pair of PM ₁₀ monitors reporting to AQS for Philadelphia, PA. _____	A-191
Table A-45.	Inter-sampler correlation statistics for each pair of PM ₁₀ monitors reporting to AQS for Phoenix, AZ. _____	A-195
Table A-46.	Inter-sampler correlation statistics for each pair of PM ₁₀ monitors reporting to AQS for Pittsburgh, PA. _____	A-200
Table A-47.	Inter-sampler correlation statistics for each pair of PM ₁₀ monitors reporting to AQS for Riverside, CA. _____	A-204
Table A-48.	Inter-sampler correlation statistics for each pair of PM ₁₀ monitors reporting to AQS for Seattle, WA. _____	A-207
Table A-49.	Inter-sampler correlation statistics for each pair of PM ₁₀ monitors reporting to AQS for St. Louis, MO. _____	A-211
Table A-50.	Correlation coefficients of hourly and daily average particle number, surface and volume concentrations in selected particle size ranges. _____	A-212
Table A-51.	Different receptor models used in the Supersite source apportionment studies: chemical mass balance. _____	A-273
Table A-52.	Different receptor models used in the Supersites source apportionment studies: factor analysis. _____	A-274
Table A-53.	Different receptor models used in the Supersites source apportionment studies: tracer-based methods. _____	A-278
Table A-54.	Different receptor models used in the Supersites source apportionment studies: meteorology-based methods. _____	A-280
Table A-55.	Source Profiles: Part I _____	A-286
Table A-56.	PM _{2.5} receptor model results (µg/m ³) _____	A-289
Table A-57.	PM ₁₀ receptor model results (mass percent) _____	A-290
Table A-58.	Exposure Assessment Study Summaries _____	A-291
Table A-59.	Examples of studies showing developments with UFP sampling methods since the 2004 PM AQCD. _____	A-317
Table A-60.	Summary of in-vehicle studies of exposure assessment. _____	A-318
Table A-61.	Summary of personal PM exposure studies with no indoor source during 2002-2008. _____	A-320
Table A-62.	Summary of PM species exposure studies. _____	A-324
Table A-63.	Summary of personal PM exposure source apportionment studies. _____	A-337

Table A-64.	Summary of PM infiltration studies. _____	A-339
Table A-65.	Summary of PM – copollutant exposure studies. _____	A-350
Table B-1.	Ultrafine disposition in humans. _____	B-1
Table B- 2.	Ultrafine disposition in animals. _____	B-2
Table B- 3.	In vitro studies of ultrafine disposition. _____	B-3
Table B-4.	Olfactory particle translocation. _____	B-3
Table B-5.	Studies of respiratory tract mucosal and macrophage clearance as a function of age. _____	B-5
Table C-1.	Cardiovascular effects. _____	C-1
Table C-2.	Respiratory effects. _____	C-9
Table C- 3.	Central nervous system effects. _____	C-13
Table D-1.	Cardiovascular effects. _____	D-1
Table D-2.	Respiratory effects: in vitro studies. _____	D-31
Table D-3.	Respiratory effects: in vivo studies. _____	D-81
Table D-4.	Effects related to immunity and allergy. _____	D-116
Table D-5.	Effects of the central nervous system. _____	D-155
Table D-6.	Reproductive and developmental effects. _____	D-157
Table D-7.	Mutagenic/genotoxic effects in bacterial cultures. _____	D-163
Table D-8.	Mutagenicity and genotoxicity data summary: In vitro and in vivo. _____	D-166
Table E-1	Short-term exposure – cardiovascular morbidity outcomes: PM ₁₀ _____	E-1
Table E-2.	Short-term exposure - cardiovascular morbidity studies: PM _{10-2.5} . _____	E-19
Table E-3.	Short-term exposure - cardiovascular morbidity studies: PM _{2.5} (including PM components/sources). _____	E-21
Table E-4.	Short-term exposure-cardiovascular morbidity studies: Other size fractions. _____	E-79
Table E-5.	Short-term exposure-cardiovascular: ED/HA PM ₁₀ _____	E-85
Table E-6.	Short-term exposure-cardiovascular-ED/HA - PM _{10-2.5} . _____	E-104
Table E-7.	Short-term exposure – cardiovascular: ED/HA PM _{2.5} (including PM components/sources) _____	E-107
Table E-8.	Short-term exposure-cardiovascular-ED/HA-other size fractions. _____	E-130
Table E-9.	Short-term exposure-respiratory morbidity outcomes -PM ₁₀ . _____	E-134
Table E-10.	Short-term exposure - respiratory morbidity outcomes - PM _{10-2.5} . _____	E-169
Table E-11.	Short-term exposure - respiratory morbidity outcomes - PM _{2.5} (including components/sources). _____	E-173
Table E-12.	Short-term exposure-respiratory-ED/HA-PM ₁₀ . _____	E-230
Table E-13.	Short-term exposure-respiratory-ED/HA-PM _{10-2.5} . _____	E-256
Table E-14.	Short-term exposure-respiratory-ED/HA-PM _{2.5} (including PM components/sources). _____	E-262
Table E-15.	Short-term exposure-respiratory-ED/HA-Other Size Fractions. _____	E-284
Table E-16.	Short-term exposure-mortality - PM ₁₀ . _____	E-293
Table E-17.	Short-term exposure-mortality - PM _{10-2.5} . _____	E-343

Table E-18.	Short-term exposure-mortality - PM _{2.5} (including PM components/sources). _____	E-346
Table E-19.	Short-term exposure-mortality - other PM size fractions. _____	E-360
Table E-20.	Long-term exposure - cardiovascular morbidity outcomes - PM ₁₀ . _____	E-363
Table E-21.	Long-term effects-cardiovascular- PM _{2.5} (including PM components/sources). _____	E-372
Table E-22.	Long-term exposure - respiratory morbidity outcomes - PM ₁₀ . _____	E-383
Table E-23.	Long-term exposure - respiratory morbidity outcomes - PM _{10-2.5} . _____	E-407
Table E-24.	Long-term exposure - respiratory morbidity outcomes - PM _{2.5} (including PM components/sources). _____	E-412
Table E-25.	Long-term exposure - respiratory morbidity outcomes - other PM size fractions. _____	E-432
Table E-26.	Long-term exposure - cancer outcomes - PM ₁₀ . _____	E-434
Table E-27.	Long-term exposure - cancer outcomes - PM _{2.5} (including PM components/sources). _____	E-437
Table E-28.	Long-term exposure - cancer outcomes - other PM size fractions. _____	E-440
Table E-29.	Long-term exposure - reproductive outcomes - PM ₁₀ . _____	E-441
Table E-30.	Long-term exposure-mortality - PM ₁₀ . _____	E-491
Table E-31.	Long-term exposure-mortality - PM ₁₀ . _____	E-498
Table E-32.	Long-term exposure-mortality - PM _{10-2.5} . _____	E-499
Table E-33.	Long-term exposure-mortality - PM _{2.5} (including PM components/sources). _____	E-500
Table E-34.	Long-term exposure - central nervous system outcomes - PM. _____	E-521
Table F-1.	Epidemiologic studies of ambient PM sources, factors, or constituents _____	F-1
Table F-2.	Human clinical studies of ambient PM sources, factors, or constituents _____	F-6
Table F-3.	Toxicological studies of ambient PM sources, factors, or constituents _____	F-7

List of Figures

Figure 1-1.	Identification of studies for inclusion in the ISA. _____	1-11
Figure 2-1.	Summary of effect estimates (per 10 $\mu\text{g}/\text{m}^3$) by increasing concentration from U.S. studies examining the association between short-term exposure to $\text{PM}_{2.5}$ and cardiovascular and respiratory effects, and mortality _____	2-14
Figure 2-2.	Summary of effect estimates (per 10 $\mu\text{g}/\text{m}^3$) by increasing concentration from U.S. studies examining the association between long-term exposure to $\text{PM}_{2.5}$ and cardiovascular and respiratory effects, and mortality _____	2-15
Figure 2-3.	Summary of U.S. studies examining the association between short-term exposure to $\text{PM}_{10-2.5}$ and cardiovascular morbidity/mortality and respiratory morbidity/mortality _____	2-20
Figure 3-1.	Particle size distributions by number and volume. _____	3-2
Figure 3-2.	X-ray spectra and scanning electron microscopy images of individual particles. _____	3-5
Figure 3-3.	Detailed source categorization of anthropogenic emissions of primary $\text{PM}_{2.5}$, PM_{10} and gaseous precursor species SO_2 , NO_x , NH_3 and VOCs for 2002 in units of million metric tons (MMT). _____	3-9
Figure 3-4.	Primary emissions and formation of SOA through gas, cloud and condensed phase reactions. _____	3-12
Figure 3-5.	Schematic of the resistance-in-series analogy for atmospheric deposition. _____	3-15
Figure 3-6.	The relationship between particle diameter and V_d for particles. _____	3-19
Figure 3-7.	$\text{PM}_{2.5}$ monitor distribution in comparison with population density, Boston CSA. _____	3-33
Figure 3-8.	PM_{10} monitor distribution in comparison with population density, Boston CSA. _____	3-34
Figure 3-9.	Three-yr avg 24-h $\text{PM}_{2.5}$ concentration by county derived from FRM or FRM-like data, 2005-2007. _____	3-43
Figure 3-10.	Three-yr avg 24-h $\text{PM}_{10-2.5}$ concentration by county derived from co-located low volume FRM PM_{10} and $\text{PM}_{2.5}$ monitors, 2005-2007. _____	3-46
Figure 3-11.	Three-yr avg 24-h PM_{10} concentration by county derived from FRM or FEM monitors, 2005-2007. _____	3-48
Figure 3-12.	Three-yr avg 24-h $\text{PM}_{2.5}$ OC concentrations measured at CSN sites across the U.S., 2005-2007. _____	3-52
Figure 3-13.	Three-yr avg 24-h $\text{PM}_{2.5}$ EC concentrations measured at CSN sites across the U.S., 2005-2007. _____	3-53
Figure 3-14.	Three-yr avg 24-h $\text{PM}_{2.5}$ SO_4^{2-} concentrations measured at CSN sites across the U.S., 2005-2007. _____	3-54
Figure 3-15.	Three-yr avg 24-h $\text{PM}_{2.5}$ NO_3^- concentrations measured at CSN sites across the U.S., 2005-2007. _____	3-55
Figure 3-16.	Three-yr avg 24-h $\text{PM}_{2.5}$ NH_4^+ concentrations measured at CSN sites across the U.S., 2005-2007. _____	3-56
Figure 3-18.	Seasonally-stratified 3-yr avg $\text{PM}_{2.5}$ speciation estimates for 2005-2007 derived using the SANDWICH method. _____	3-58
Figure 3-19.	Locations of $\text{PM}_{2.5}$ monitors and major highways, Boston, MA. _____	3-61

Figure 3-20.	Seasonal distribution of 24-h avg PM _{2.5} concentrations by site for Boston, MA, 2005-2007.	3-62
Figure 3-21.	Locations of PM _{2.5} monitors and major highways, Pittsburgh, PA.	3-65
Figure 3-22.	Seasonal distribution of 24-h avg PM _{2.5} concentrations by site for Pittsburgh, PA, 2005-2007.	3-66
Figure 3-23.	Locations of PM _{2.5} monitors and major highways, Los Angeles, CA.	3-68
Figure 3-24.	Seasonal distribution of 24-h avg PM _{2.5} concentrations by site for Los Angeles, CA, 2005-2007.	3-69
Figure 3-25.	Inter-sampler correlations for 24-h PM _{2.5} as a function of distance between monitors in Boston, MA.	3-71
Figure 3-26.	Inter-sampler correlations for 24-h PM _{2.5} as a function of distance between monitors in Pittsburgh, PA.	3-71
Figure 3-27.	Inter-sampler correlations for 24-h PM _{2.5} as a function of distance between monitors in Los Angeles, CA.	3-72
Figure 3-28.	Seasonal distribution of 24-h avg PM _{10-2.5} concentrations by site	3-73
Figure 3-29.	Locations of PM ₁₀ monitors and major highways, Boston, MA.	3-74
Figure 3-30.	Seasonal distribution of 24-h avg PM ₁₀ concentrations by site for Boston, MA, 2005-2007.	3-75
Figure 3-31.	Locations of PM ₁₀ monitors and major highways, Pittsburgh, PA.	3-76
Figure 3-32.	Seasonal distribution of 24-h avg PM ₁₀ concentrations by site for Pittsburgh, PA, 2005-2007.	3-77
Figure 3-33.	Locations of PM ₁₀ monitors and major highways, Los Angeles, CA.	3-80
Figure 3-34.	Seasonal distribution of 24-h avg PM ₁₀ concentrations by site for Los Angeles, CA, 2005-2007.	3-81
Figure 3-35.	Inter-sampler correlations for 24-h PM ₁₀ as a function of distance between monitors in Boston, MA.	3-82
Figure 3-36.	Inter-sampler correlations for 24-h PM ₁₀ as a function of distance between monitors in Pittsburgh, PA.	3-83
Figure 3-37.	Inter-sampler correlations for 24-h PM ₁₀ as a function of distance between monitors in Los Angeles, CA.	3-83
Figure 3-38.	Bin-wise Spearman correlation coefficients in aerosol particle number concentrations between the lft (urban background) and the Eisenbahn-strasse (city/urban center) sites in Leipzig, Germany.	3-84
Figure 3-39.	Dimensionless concentration as a function of height at windward and leeward locations and street canyon aspect ratios (H/W).	3-86
Figure 3-40.	Inter-sampler correlations for 24-h PM _{2.5} and PM ₁₀ as a function of distance between monitors for samplers located within 4 km (neighborhood scale).	3-87
Figure 3-41.	Particle size distributions measured at various distances from the 710 freeway in Los Angeles, CA (top), and particle number concentration as a function of distance from the 710 freeway (bottom).	3-88
Figure 3-42.	Mass distributions for BaP at a high traffic urban center (HTC), high traffic urban periphery (HTP), low traffic urban center (LTC), low traffic urban periphery (LTP), and low traffic industrial urban periphery (LTIP) in Seville, Spain.	3-90
Figure 3-43.	Mass distributions for 16 PAHs at a high traffic city center in Seville, Spain.	3-91

Figure 3-44.	Ambient 24-h PM _{2.5} concentrations in the U.S., 1999-2007, showing A) ambient concentrations, B) number of trends sites above the 24-h NAAQS and C) trends by U.S. EPA Region.	3-92
Figure 3-45.	Ambient annual PM _{2.5} concentrations in the U.S., 1999-2007, showing A) ambient concentrations, B) number of trends sites above the annual NAAQS and C) trends by U.S. EPA Region.	3-93
Figure 3-46.	Ambient 24-h PM ₁₀ concentrations in the U.S., 1988-2007, showing A) ambient concentrations, B) number of trends sites above the 24-h NAAQS and C) trends by U.S. EPA Region.	3-94
Figure 3-47.	Regional and seasonal trends in annual PM _{2.5} composition from 2002 to 2007 derived using the SANDWICH method.	3-95
Figure 3-48.	UFP size distribution at highway (site A) and background (site B) sites in Los Angeles, CA, during summer and winter seasons, with winter broken into day and evening distributions.	3-97
Figure 3-49.	Diel plot generated from hourly FRM-like PM _{2.5} data (µg/m ³) stratified by weekday (left) and weekend (right) for Pittsburgh, PA, and Seattle, WA, 2005-2007.	3-98
Figure 3-50.	Diel plots generated from hourly FEM PM ₁₀ data (µg/m ³) stratified by weekday (left) and weekend (right) for Chicago, IL, and Phoenix, AZ, 2005-2007.	3-99
Figure 3-51.	Average diel variation in total particle number (ToN) and total particle volume (ToV) on weekdays (left column) and Sundays (right column) from two sites in Denmark: one in a busy street canyon (Jagtv) and one measuring urban background (HCØ).	3-100
Figure 3-52.	Distribution of correlations between 24-h avg PM _{2.5} and co-located 24-h avg PM ₁₀ , PM _{10-2.5} , SO ₂ , NO ₂ and CO and daily max 8-h avg O ₃ for the U.S. stratified by season (2005-2007).	3-101
Figure 3-53.	Distribution of correlations between 24-h avg PM ₁₀ and co-located 24-h avg PM _{2.5} , PM _{10-2.5} , SO ₂ , NO ₂ and CO and daily max 8-h avg O ₃ for the U.S. stratified by season (2005-2007).	3-102
Figure 3-54.	Schematic of organic composition of particulate emissions from gasoline-fueled vehicles.	3-105
Figure 3-55.	Source category contributions to PM _{2.5} at a number of sites in the East derived using PMF.	3-108
Figure 3-56.	Pearson correlation coefficients for source category contributions to PM _{2.5} between the 10 Regional Air Pollution Study/Regional Air Monitoring System (RAPS/RAMS) monitoring sites in St. Louis.	3-109
Figure 3-57.	Pearson correlation coefficients for source contributions to PM _{10-2.5} between the 10 Regional Air Pollution Study/Regional Air Monitoring System (RAPS/RAMS) monitoring sites in St. Louis.	3-109
Figure 3-58.	Eight km southeast U.S. CMAQ-UCD domain zoomed over Tampa Bay, FL.	3-115
Figure 3-59.	Two km southeast U.S. CMAQ-UCD domain zoomed over Tampa Bay, FL.	3-115
Figure 3-60.	Hourly average CMAQ-UCD predictions and measured observations of NO (top), NO ₂ (middle), and total NO _x (bottom) concentrations for May 1-31, 2002.	3-116
Figure 3-61.	CMAQ-UCD predictions and measured observations of ethene concentrations at Sydney, FL for May 1-31, 2002.	3-117
Figure 3-62.	CMAQ-UCD predictions and measured observations of isoprene concentrations at Sydney, FL for May 1-31, 2002.	3-118
Figure 3-63.	CMAQ-UCD predictions and measured observations of PM _{2.5} concentrations at Sidney, FL for May 1-31, 2002.	3-119
Figure 3-64.	CMAQ-UCD predictions of HNO ₃ ⁻ concentrations and corresponding measured observations at Sydney, FL, for May 1-31, 2002.	3-121

Figure 3-65.	CMAQ-UCD predictions of NH ₃ concentrations and corresponding measured observations at Sydney, FL, for May 1-31, 2002. _____	3-122
Figure 3-66.	CMAQ-UCD predictions of pNO ₃ ⁻ concentrations and corresponding measured observations at Sydney, FL, for 1-31 May, 2002. _____	3-123
Figure 3-67.	CMAQ-UCD predictions of the ratio of HNO ₃ to total NO ₃ and corresponding measured observations at Sydney, FL, for May 1-31, 2002. _____	3-124
Figure 3-68.	CMAQ-UCD predicted size and chemical-form fractions of total NO ₃ ⁻ for days in May 2002 with measured observations. _____	3-125
Figure 3-69.	Scatter plot of total nitrate (HNO ₃ plus pNO ₃ ⁻) wet deposition (mg N/m ² /yr) of the model mean versus measurements for the North American Deposition Program (NADP) network. _____	3-127
Figure 3-70.	Scatter plot of total SO ₄ ²⁻ wet deposition (mg S/m ² /yr) of the model mean versus measurements for the National Atmospheric Deposition Program (NADP) network. _____	3-127
Figure 3-71.	CMAQ modeling domains for the OAQPS risk and exposure assessments: 36 km outer parent domain in black; 12 km western U.S. (WUS) domain in red; 12 km eastern U.S. (EUS) domain in blue. _____	3-128
Figure 3-72.	12-km EUS Summer sulfate PM. _____	3-129
Figure 3-73.	12-km EUS Winter nitrate PM. _____	3-130
Figure 3-74.	12-km EUS Winter total nitrate (HNO ₃ + total pNO ₃ ⁻). _____	3-131
Figure 3-75.	12-km EUS annual sulfate wet deposition. _____	3-132
Figure 3-76.	12-km EUS annual nitrate wet deposition. _____	3-133
Figure 3-77.	CMAQ vs. measured air concentrations from east-coast sites in the IMPROVE, CSN (labeled STN), and CASTNet sites in the summer of 2002 for sulfate (left) and ammonium (right). _____	3-134
Figure 3-78.	Comparison of CMAQ-predicted and NADP-measured NH ₄ ⁺ wet deposition _____	3-134
Figure 3-79.	CMAQ-predicted (red symbols and lines) and 12-h measured (blue symbols and lines) NH ₃ and SO ₄ ²⁻ surface concentrations at high and low concentration grid cells in North Carolina in July 2004. _____	3-135
Figure 3-80.	Surface grid cell (layer 1) analysis of the sensitivity of NH _x deposition and transport to the change in NH ₃ V _d in CMAQ. _____	3-136
Figure 3-81.	Total column analysis for NH ₃ (left) and NH _x (right) showing modeled NH ₃ emissions, transformation, and transport throughout the mixed layer and up to the free troposphere. _____	3-136
Figure 3-82.	Range of influence (where 50% of emitted NH ₃ deposits) from the high concentration Sampson County grid cell in the June 2002 CMAQ simulation of V _d sensitivities. _____	3-137
Figure 3-83.	Areal extent of the change in NH _x range of influence as predicted by CMAQ for the Sampson County high concentration grid cell (center of range circles) in June 2002 using the base case and sensitivity case V _d . _____	3-138
Figure 3-84.	IMPROVE monitoring site locations. _____	3-141
Figure 3-85.	12-km EUS Summer SO ₄ ²⁻ PM. _____	3-144
Figure 3-86.	12-km EUS Winter NO ₃ ⁻ PM. _____	3-145
Figure 3-87.	12-km EUS Winter total nitrate (HNO ₃ + total particulate NO ₃ ⁻). _____	3-145
Figure 3-88.	Monthly average of PM _{2.5} concentrations measured at IMPROVE sites in the East and Midwest for 2004. _____	3-146

Figure 3-89.	Monthly average of PM _{2.5} concentrations measured at IMPROVE sites in the West for 2004.	3-147
Figure 3-90.	Distribution of PM _{2.5} concentrations measured at IMPROVE sites in the East and Midwest for 2004.	3-148
Figure 3-91.	Distribution of PM _{2.5} concentrations measured at IMPROVE sites in the West for 2004.	3-149
Figure 3-92.	Model of total personal exposure to PM as a function of ambient and nonambient sources.	3-154
Figure 3-93.	Distribution of time sample population spends in various environments, from the National Human Activity Pattern Survey.	3-159
Figure 3-94.	Total exposure to SO ₄ ²⁻ as a function of measured ambient SO ₄ ²⁻ concentration, from the Vancouver study.	3-166
Figure 3-95.	Estimated ambient exposure to PM _{2.5} as a function of measured ambient PM _{2.5} concentration, from the Vancouver study.	3-166
Figure 3-96.	Total exposure to PM _{2.5} as a function of measured ambient PM _{2.5} concentration, from the Vancouver study.	3-167
Figure 3-97.	F_{inf} as a function of particle size.	3-170
Figure 3-98.	Apportionment of aliphatic carbon, carbonyl, and SO ₄ ²⁻ components of outdoor, indoor, and personal PM _{2.5} samples, for Los Angeles (top), Elizabeth (center), and Houston (bottom).	3-172
Figure 3-99.	Apportionment of infiltrated PM from mechanical generation (top), primary combustion (center), and secondary combustion (bottom).	3-173
Figure 3-100.	Results of the positive matrix factorization model showing differences in the mass of outdoor PM and PM that has infiltrated indoors based on source category.	3-174
Figure 3-101.	Grid resolution of the CMAQ model in Philadelphia compared with distribution of census tracts in which exposure assessment is performed.	3-178
Figure 4-1.	Diagrammatic representation of respiratory tract regions in humans.	4-3
Figure 4-2.	Structure of lower airways with progression from the large airways to the alveolus.	4-4
Figure 4-3.	Comparison of total and regional deposition results from the ICRP and MPPD models for a resting breathing pattern ($V_T = 625$ mL, $f = 12$ min ⁻¹) and corrected for particle inhalability.	4-7
Figure 4-4.	Comparison of total and regional deposition results from the ICRP and MPPD models for a light exercise breathing pattern ($V_T = 1250$ mL, $f = 20$ min ⁻¹) and corrected for particle inhalability.	4-8
Figure 4-5.	Total lung deposition measured in healthy adults (UF, 11 M, 11 F, 31 ± 4 yr; fine and coarse, 11 M, 11 F, 25 ± 4 yr) during controlled breathing on a mouthpiece.	4-9
Figure 4-6.	Total deposition of hygroscopic sodium chloride and hydrophobic aluminosilicate aerosols during oral breathing ($V_T = 1.0$ L; $f = 15$ min ⁻¹).	4-16
Figure 4-7.	Retention of poorly soluble particles (0.5-5 µm) in the alveolar region of the lung over time in various mammalian species.	4-20
Figure 5-1.	PM oxidative potential.	5-2
Figure 5-2.	PM stimulates pulmonary cells to produce ROS/RNS.	5-3
Figure 5-3.	PM activates cell signaling pathways leading to pulmonary inflammation.	5-5
Figure 5-4.	Potential pathways for the effects of PM on the respiratory system.	5-7
Figure 5-5.	Potential pathways for the effects of PM on the cardiovascular system.	5-13

Figure 6-1.	Excess risk estimates per 10 $\mu\text{g}/\text{m}^3$ increase in 24-h avg $\text{PM}_{2.5}$, $\text{PM}_{10-2.5}$, and PM_{10} concentration for CVD ED visits and HAs. _____	6-62
Figure 6-2.	Excess risk estimates per 10 $\mu\text{g}/\text{m}^3$ increase in 24-h avg (unless otherwise noted) $\text{PM}_{2.5}$, $\text{PM}_{10-2.5}$, and PM_{10} concentration for MI and IHD ED visits and HAs. _____	6-66
Figure 6-3.	Excess risk estimates per 10 $\mu\text{g}/\text{m}^3$ increase in 24-h avg $\text{PM}_{2.5}$, $\text{PM}_{10-2.5}$, and PM_{10} concentration for CHF ED visits and HAs. _____	6-69
Figure 6-4.	Excess risk estimates per 10 $\mu\text{g}/\text{m}^3$ increase in 24-h avg $\text{PM}_{2.5}$ and PM_{10} concentration for CBVD ED visits and HAs. _____	6-72
Figure 6-5.	Excess risk estimates per 10 $\mu\text{g}/\text{m}^3$ increase in 24-h avg $\text{PM}_{2.5}$, and $\text{PM}_{10-2.5}$ for cardiovascular disease ED visits or HAs, adjusted for co-pollutants. _____	6-74
Figure 6-6.	Combined random-effect estimate of the concentration-response relationship between MI emergency hospital admissions and PM_{10} , computed by fitting a piecewise linear spline, with slope changes at 20 $\mu\text{g}/\text{m}^3$ and 50 $\mu\text{g}/\text{m}^3$. _____	6-76
Figure 6-7.	Respiratory symptoms and/or medication use among asthmatic children following acute exposure to PM. _____	6-86
Figure 6-8.	Respiratory symptoms and/or medication use among asthmatic adults following acute exposure to particles. _____	6-92
Figure 6-9.	Respiratory symptoms following acute exposure to particles and additional criteria pollutants. _____	6-93
Figure 6-10.	Excess risk estimates per 10 $\mu\text{g}/\text{m}^3$ 24-h avg $\text{PM}_{2.5}$, $\text{PM}_{10-2.5}$, and PM_{10} concentration for ED visits and HAs for respiratory diseases in children. _____	6-134
Figure 6-11.	Excess risks estimates per 10 $\mu\text{g}/\text{m}^3$ increase in 24-h avg $\text{PM}_{2.5}$, $\text{PM}_{10-2.5}$, and PM_{10} for ED visits and HAs for respiratory diseases among adults. _____	6-138
Figure 6-12.	Excess risk estimates per 10 $\mu\text{g}/\text{m}^3$ increase in 24-h avg $\text{PM}_{2.5}$, $\text{PM}_{10-2.5}$, and PM_{10} for asthma ED visits and HAs. _____	6-140
Figure 6-13.	Excess risks estimates per 10 $\mu\text{g}/\text{m}^3$ increase in 24-h avg $\text{PM}_{2.5}$, $\text{PM}_{10-2.5}$, and PM_{10} for COPD ED visits and HAs among older adults (65+ yr, unless other age group is noted). _____	6-143
Figure 6-14.	Excess risks estimates per 10 $\mu\text{g}/\text{m}^3$ increase in 24-h avg $\text{PM}_{2.5}$, $\text{PM}_{10-2.5}$, and PM_{10} for respiratory infection ED visits* and HAs. _____	6-145
Figure 6-15.	Excess risk estimates per 10 $\mu\text{g}/\text{m}^3$ increase in 24-h avg $\text{PM}_{2.5}$, and $\text{PM}_{10-2.5}$ for respiratory disease ED visits or HAs, adjusted for co-pollutants. _____	6-148
Figure 6-16.	National and regional estimates of smooth seasonal effects for PM_{10} at a 1-day lag and their sensitivity to the degrees of freedom assigned to the smooth function of time in the updated NMMAPS data 1987-2000. _____	6-162
Figure 6-17.	Percent increase in the daily number of deaths, for all ages, associated with a 10- $\mu\text{g}/\text{m}^3$ increase in PM_{10} : lag 1 (A) and lags 0 and 1 (B) for all three centers. _____	6-166
Figure 6-18.	Effect modification by city characteristics in 20 U.S. cities. _____	6-168
Figure 6-19.	Percent excess risk in mortality (all-cause [nonaccidental] and cause-specific) per 10 $\mu\text{g}/\text{m}^3$ increase in PM_{10} by individual-level characteristics. _____	6-170
Figure 6-20.	Percent excess risk in mortality (all-cause [nonaccidental] and cause-specific) per 10 $\mu\text{g}/\text{m}^3$ increase in PM_{10} by location of death and by season. _____	6-171
Figure 6-21.	Percent increase in mortality (all-cause [nonaccidental] and cause-specific) per 10 $\mu\text{g}/\text{m}^3$ increase in PM_{10} by contributing causes of death. _____	6-172

Figure 6-22.	Summary of percent increase in all-cause (nonaccidental) mortality from recent multicity studies per 10 $\mu\text{g}/\text{m}^3$ increase in PM_{10} .	6-174
Figure 6-23.	Percent increase in all-cause (nonaccidental) and cause-specific mortality per 10 $\mu\text{g}/\text{m}^3$ increase in the average of 0- and 1-day lagged $\text{PM}_{2.5}$, combined by climatic regions.	6-177
Figure 6-24.	Empirical Bayes-adjusted city-specific percent increase in total (nonaccidental), cardiovascular, and respiratory mortality per 10 $\mu\text{g}/\text{m}^3$ increase in the average of 0- and 1-day lagged $\text{PM}_{2.5}$ by decreasing mean 24-h avg $\text{PM}_{2.5}$ concentrations.	6-178
Figure 6-25.	Summary of percent increase in all-cause (nonaccidental) mortality per 10 $\mu\text{g}/\text{m}^3$ increase in $\text{PM}_{2.5}$ by various effect modifiers.	6-181
Figure 6-26.	Summary of percent increase in all-cause (nonaccidental) and cause-specific mortality per 10 $\mu\text{g}/\text{m}^3$ increase in $\text{PM}_{2.5}$ from recent multicity studies.	6-183
Figure 6-28.	Percent increase in all-cause (nonaccidental) and cause-specific mortality per 10 $\mu\text{g}/\text{m}^3$ increase in the average of 0- and 1-day lagged $\text{PM}_{10-2.5}$, combined by climatic regions.	6-186
Figure 6-29.	Empirical Bayes-adjusted city-specific percent increase in total (nonaccidental), cardiovascular, and respiratory mortality per 10 $\mu\text{g}/\text{m}^3$ increase in the average of 0- and 1-day lagged $\text{PM}_{10-2.5}$ by decreasing 98th percentile of mean 24-h avg $\text{PM}_{10-2.5}$ concentrations.	6-187
Figure 6-30.	Summary of percent increase in total (nonaccidental) and cause-specific mortality per 10 $\mu\text{g}/\text{m}^3$ increase in $\text{PM}_{10-2.5}$ for all U.S.-, Canadian-, and international-based studies.	6-190
Figure 6-31.	Percent increase in PM_{10} risk estimates (point estimates and 95% CIs) associated with a 5th-95th percentile increase in $\text{PM}_{2.5}$ and $\text{PM}_{2.5}$ chemical components.	6-192
Figure 6-32.	Sensitivity of the percent increase in PM_{10} risk estimates (point estimates and 95% CIs) associated with an interquartile increase in Ni.	6-193
Figure 6-33.	Percent excess risk (CI) of total (nonaccidental) mortality per IQR of concentrations.	6-196
Figure 6-34.	Relative risk and CI of cardiovascular mortality associated with estimated $\text{PM}_{2.5}$ source contributions.	6-197
Figure 6-35.	Concentration-response curves (spline model) for all-cause, cardiovascular, respiratory and other cause mortality from the 20 NMMAPS cities.	6-198
Figure 6-36.	Percent increase in the risk of death on days with PM_{10} concentrations in the ranges of 15-24, 25-34, 35-44, and 45 $\mu\text{g}/\text{m}^3$ and greater, compared to a reference of days when concentrations were below 15 $\mu\text{g}/\text{m}^3$.	6-199
Figure 6-37.	Combined concentration-response curves (spline model) for all-cause, cardiovascular, and respiratory mortality from the 22 APHEA cities.	6-200
Figure 7-1.	Risk estimates for the associations of clinical outcomes with long-term exposure to ambient $\text{PM}_{2.5}$ and PM_{10} .	7-15
Figure 7-2.	Adjusted ORs and 95% CIs of symptoms and respiratory diseases associated with a decline of 10 $\mu\text{g}/\text{m}^3$ PM_{10} levels in Swiss Surveillance Program of Childhood Allergy and Respiratory Symptoms.	7-23
Figure 7-3.	Effect of $\text{PM}_{2.5}$ on the association of lung function with asthma.	7-24
Figure 7-4.	Proportion of 18-yr olds with an FEV_1 below 80% of the predicted value plotted against the average levels of pollutants from 1994 through 2000 in the 12 southern California communities of the Children's Health Study.	7-28
Figure 7-5.	Percent increase in postneonatal mortality per 10 $\mu\text{g}/\text{m}^3$ in PM_{10} , comparing risk for total and respiratory mortality.	7-58

Figure 7-6.	Mortality risk estimates associated with long-term exposure to PM _{2.5} from the Harvard Six Cities Study (SCS) and the American Cancer Society Study (ACS).	7-85
Figure 7-7.	Mortality risk estimates, long-term exposure to PM _{2.5} in recent cohort studies.	7-86
Figure 7-8.	Plots of the relative risk of death from cardiovascular disease from the Women's Health Initiative study displaying the between-city and within-city contributions to the overall association between PM _{2.5} and cardiovascular mortality windows of exposure-effects.	7-92
Figure 7-9.	The model-averaged estimated effect of a 10-µg/m ³ increase in PM _{2.5} on all-cause mortality at different lags (in years) between exposure and death.	7-93
Figure 7-10.	Time course of relative risk of death after a sudden decrease in air pollution exposure during the year 2000, assuming a steady state model (solid line) and a dynamic model (bold dashed line).	7-94
Figure 7-11.	Experts' mean effect estimates and uncertainty distributions for the PM _{2.5} mortality concentration-response coefficient for a 1 µg/m ³ change in annual average PM _{2.5} .	7-96
Figure 9-1.	Important factors involved in seeing a scenic vista are outlined.	9-3
Figure 9-2.	Schematic of remote-area (top) and urban (bottom) nighttime sky visibility showing the effects of PM and light pollution.	9-4
Figure 9-3.	Effect of relative humidity on light scattering by mixtures of ammonium nitrate and ammonium sulfate.	9-6
Figure 9-4.	Estimated fractions of total particulate nitrate during each field campaign comprised of ammonium nitrate, reacted sea salt nitrate (shown as NaNO ₃), and reacted soil dust nitrate (shown as Ca(NO ₃) ₂).	9-12
Figure 9-5.	A scatter plot of the original IMPROVE algorithm estimated particle light scattering versus measured particle light scattering.	9-15
Figure 9-6.	Scatter plot of the revised algorithm estimates of light scattering versus measured light scattering.	9-15
Figure 9-7.	IMPROVE network PM species estimated light extinction for 2000 (left) and for 2004 (right).	9-18
Figure 9-8.	Mean estimated light extinction from PM speciation measurements for the first (top left), second (top right), third (bottom left), and fourth (bottom right) calendar quarters of 2004.	9-18
Figure 9-9.	Percent contributions of ammonium nitrate (left column) and ammonium sulfate (right column) to particulate light extinction for each calendar quarter of 2004 (first through fourth quarter arranged from top to bottom).	9-20
Figure 9-10.	Percent contributions of organic mass (left column) and EC (right column) to particulate light extinction for each calendar quarter of 2004 (first through fourth quarter arranged from top to bottom).	9-21
Figure 9-11.	Percent contributions of coarse mass (left column) and fine soil (right column) to particulate light extinction for each calendar quarter of 2004 (first through fourth quarter arranged from top to bottom).	9-22
Figure 9-12.	IMPROVE Mean PM _{2.5} mass concentration determined by summing the major components for the 2000-2004.	9-24
Figure 9-13.	IMPROVE and CSN (STN) mean PM _{2.5} mass concentration determined by summing the major components for 2000-2004.	9-24
Figure 9-14.	IMPROVE mean ammonium nitrate concentrations for 2000-2004.	9-25
Figure 9-15.	IMPROVE and CSN (STN) mean ammonium nitrate concentrations for 2000-2004.	9-25

Figure 9-16.	IMPROVE mean ammonium sulfate concentrations for 2000-2004. _____	9-26
Figure 9-17.	IMPROVE and CSN (STN) mean ammonium sulfate concentrations for 2000-2004. _____	9-26
Figure 9-18.	IMPROVE monitored mean organic mass concentrations for 2000-2004. _____	9-28
Figure 9-19.	IMPROVE and CSN (STN) mean organic mass concentrations for 2000-2004. _____	9-28
Figure 9-20.	IMPROVE mean EC concentrations for 2000-2004. _____	9-29
Figure 9-21.	IMPROVE and CSN (STN) mean EC concentrations for 2000-2004. _____	9-29
Figure 9-22.	IMPROVE mean fine soil concentrations for 2000-2004. _____	9-30
Figure 9-23.	IMPROVE and CSN (STN) fine soil concentrations, 2000-2004. _____	9-30
Figure 9-24.	Regional and local contributions to annual average PM _{2.5} by particulate SO ₄ ²⁻ , nitrate and total carbon (i.e., organic plus EC) for select urban areas based on paired IMPROVE and CSN monitoring sites. _____	9-32
Figure 9-25.	IMPROVE mean coarse mass concentrations for 2000-2004. _____	9-33
Figure 9-26.	Ten-year (1995-2004) haze trends for the mean of the 20% best annual haze conditions. _____	9-34
Figure 9-27.	Ten-year (1995-2004) haze trends for the mean of the 20% worst annual haze conditions. _____	9-35
Figure 9-28.	Ten-year trends in the 80th percentile particulate SO ₄ ²⁻ concentration based on IMPROVE and CASTNet monitoring and net SO ₂ emissions from the National Emissions Trends (NET) data base by region of the U.S. _____	9-36
Figure 9-29.	Map of 10-yr trends (1994-2003) in haze by particulate nitrate contribution to haze for the worst 20% annual haze periods. _____	9-37
Figure 9-30.	Contributions of the Pacific Coast area to the ammonium sulfate (µg/m ³) at 84 remote-area monitoring sites in western U.S. based on trajectory regression for all sample periods from 2000-2002 _____	9-39
Figure 9-31.	Shows the IMPROVE monitoring sites in the WRAP region with at least three years of valid data and identifies the six sites selected to demonstrate the apportionment tools. _____	9-41
Figure 9-32.	Particulate SO ₄ ²⁻ (a) and nitrate (b) source attribution by region using CAMx modeling for six western remote area monitoring sites _____	9-43
Figure 9-33.	Monthly averaged model predicted organic mass concentration apportioned into primary PM and anthropogenic and biogenic secondary PM categories for the Olympic NP (top) and San Geronio W (bottom) monitoring sites. _____	9-44
Figure 9-34.	Monthly averaged model predicted organic mass concentration apportioned into primary PM and anthropogenic and biogenic secondary PM categories for the Yellowstone NP (top) and Grand Canyon (Hopi Point) (bottom) monitoring sites. _____	9-45
Figure 9-35.	Monthly averaged model predicted organic mass concentration apportioned into primary PM and anthropogenic and biogenic secondary PM categories for the Badland NP (top) and Salt Creek W (bottom) monitoring sites. _____	9-46
Figure 9-36.	Comparison of carbon concentrations between Seattle (Puget Sound site) and Mt. Rainer (left) and between Phoenix and Tonto (right) showing the background site concentration (gray) and the urban excess concentration (black) for total, fossil and contemporary carbon during the summer and winter studies. _____	9-47
Figure 9-37.	Average contemporary fraction of PM _{2.5} carbon for the summer (top) and winter (bottom), estimated from IMPROVE monitoring data (June 2004-February 2006) based on EC/TC ratios. _____	9-48

Figure 9-38.	Results of the weighted emissions potential tool applied to primary OC emissions (top) and EC emissions (bottom) for the baseline and projected 2018 emissions inventories for Olympic NP. _____	9-50
Figure 9-39.	Results of the weighted emissions potential tool applied to primary OC emissions (top) and EC emissions (bottom) for the baseline and projected 2018 emissions inventories for San Geronio W. _____	9-51
Figure 9-40.	Results of the weighted emissions potential tool applied to primary OC emissions (top) and EC emissions (bottom) for the baseline and projected 2018 emissions inventories for Yellowstone NP. _____	9-53
Figure 9-41.	Results of the weighted emissions potential tool applied to primary OC emissions (top) and EC emissions (bottom) for the baseline and projected 2018 emissions inventories for Grand Canyon NP. _____	9-54
Figure 9-42.	Results of the weighted emissions potential tool applied to primary OC emissions (top) and EC emissions (bottom) for the baseline and projected 2018 emissions inventories for Badlands NP. _____	9-55
Figure 9-43.	Results of the weighted emissions potential tool applied to primary OC emissions (top) and EC emissions (bottom) for the baseline and projected 2018 emissions inventories for Salt Creek W. _____	9-56
Figure 9-44.	BRAVO study haze contributions for Big Bend NP, TX during a 4-mo period in 1999. _____	9-58
Figure 9-45.	Maps of spatial patterns for average annual particulate nitrate measurements (top), and for ammonia emissions for April 2002 from the WRAP emissions inventory (bottom). _____	9-59
Figure 9-46.	Maps of spatial patterns of annual NO (left) and NO ₂ (right) emissions for 2002 from the WRAP emissions inventory. _____	9-60
Figure 9-47.	Midwest ammonia monitoring network. _____	9-61
Figure 9-48.	Upwind transport probability fields associated with high particulate nitrate concentrations measured at Toronto, Canada; Boundary Water Canoe Area, MN; Shenandoah NP, VA; Lye Brook, VT; and Great Smoky Mountains NP, TN. _____	9-62
Figure 9-49.	Trajectory probability fields for periods with high particulate SO ₄ ²⁻ measured at Underhill, VT and Brigantine, NJ (shown as white stars) associated with oil-burning trace components (left) and with coal-burning trace components (right). _____	9-63
Figure 9-50.	Scatter plots of particulate SO ₄ ²⁻ (left) and particulate SO ₄ ²⁻ and organic mass (right) versus nephelometer measured particle light scattering for Acadia NP, ME. _____	9-64
Figure 9-51.	CMAQ air quality modeling projections of visibility responses on the 20% worst haze days at Great Smoky Mountains NP, NC (top) and Swanquarter W, NC (bottom) to 30% reductions. _____	9-65
Figure 9-52.	Aerosol radiative forcing. _____	9-76
Figure 9-53.	Global average radiative forcing (RF) estimates and uncertainty ranges in 2005, relative to the pre-industrial climate. _____	9-78
Figure 9-54.	Probability distribution functions (PDFs) for anthropogenic aerosol and GHG RFs. _____	9-79
Figure 9-55.	The clear-sky forcing efficiency E _T , defined as the diurnally averaged aerosol direct radiative effect (W/m ²) per unit AOD at 550 nm, calculated at both TOA and the surface, for typical aerosol types over different geographical regions. _____	9-80
Figure 9-56.	A composite of MODIS/Terra observed aerosol optical depth (at 550 nm, green light near the peak of human vision) and fine-mode fraction that shows spatial and seasonal variations of aerosol types. _____	9-87

Figure 9-57.	Oregon fire on September 4, 2003, as observed by MISR: (a) MISR nadir view of the fire plume, with five patch locations numbered and wind-vectors superposed in yellow; (b) MISR aerosol optical depth at 558 nm; and (c) MISR stereo height without wind correction for the same region. _____	9-88
Figure 9-58.	Global maps at 18 km resolution showing monthly average (a) AOD at 865 nm and (b) Ångström exponent of AOD over water surfaces only for June, 1997, derived from radiance measurements by the POLDER. _____	9-89
Figure 9-59.	A dust event that originated in the Sahara desert on 17 August 2007 and was transported to the Gulf of Mexico. _____	9-91
Figure 9-60.	A constellation of five spacecraft that overfly the Equator at about 1:30 p.m., the so-called A-Train, carries sensors having complementary capabilities, offering unprecedented opportunities to study aerosols from space in multiple dimensions. _____	9-92
Figure 9-61.	Geographical coverage of active AERONET sites in 2006. _____	9-95
Figure 9-62.	Comparison of the mean concentration ($\mu\text{g}/\text{m}^3$) and standard deviation of the modeled (STEM) aerosol chemical components with shipboard measurements during INDOEX, ACE-Asia, and ICARTT. _____	9-98
Figure 9-63.	Correlations between one-hour $\text{PM}_{2.5}$ surface measurements in the U.S. and southern Canada reported to AIRNOW and MODIS satellite AOD values for the period between 4 July and 1 September 2009. _____	9-99
Figure 9-64.	Location of aerosol chemical composition measurements with aerosol mass spectrometers. _____	9-101
Figure 9-65.	Scatterplots of the submicrometer POM measured during NEAQS versus A) acetylene and B) iso-propyl nitrate. _____	9-102
Figure 9-66.	Comparison of annual mean aerosol optical depth (AOD). _____	9-104
Figure 9-67.	Percentage contributions of individual aerosol components. _____	9-105
Figure 9-68.	Geographical patterns of seasonally (MAM) averaged aerosol optical depth at 550 nm (left panel) and the diurnally averaged clear-sky aerosol direct radiative (solar spectrum) forcing (W/m^2) at the TOA (right panel) derived from satellite (Terra) retrievals. _____	9-107
Figure 9-69.	Summary of observation- and model-based (denoted as OBS and MOD, respectively) estimates of clear-sky, annual average DRF at the TOA and at the surface. _____	9-108
Figure 9-70.	Scatter plots showing mean cloud drop effective radius (r_e) versus aerosol extinction coefficient (unit: km^{-1}) for various liquid water path (LWP) bands on April 3, 1998 at ARM SGP site. _____	9-115
Figure 9-71.	Sampling the Arctic Haze. Pollution and smoke aerosols can travel long distances, from mid-latitudes to the Arctic, causing "Arctic Haze." _____	9-123
Figure 9-72.	Global annual averaged AOD (upper panel) and aerosol mass loading (lower panel) with their components simulated by 15 models in AeroCom- A (excluding one model which only reported mass). _____	9-130
Figure 9-73.	Aerosol direct radiative forcing in various climate and aerosol models. _____	9-134
Figure 9-74.	Aerosol optical thickness and anthropogenic shortwave all-sky radiative forcing from the AeroCom study. _____	9-135
Figure 9-75.	Radiative forcing from the cloud albedo effect (1st aerosol indirect effect) in the global climate models used from IPCC (2007, 092765), Chapter 2, Figure 2.14, of the IPCC AR4. _____	9-136

Figure 9-76.	Anthropogenic impact on cloud cover, planetary albedo, radiative flux at the surface (while holding sea surface temperatures and sea ice fixed) and surface air temperature change from the direct aerosol forcing (top row), the first indirect effect (second row) and the second indirect effect (third row).	9-139
Figure 9-77.	Global average present-day short wave cloud forcing at TOA (top) and change in whole sky net outgoing shortwave radiation (bottom) between the present-day and pre-industrial simulations for each model in each experiment.	9-140
Figure 9-78.	Direct radiative forcing by anthropogenic aerosols in the GISS model (including sulfates, BC, OC and nitrates).	9-148
Figure 9-79.	Percentage of aerosol optical depth in the GISS, left, based on Liu et al. (2006, 190422), provided by A. Lacis, GISS, and GFDL, right, from Ginoux et al. (2006, 190582).	9-151
Figure 9-80.	Most probable aerosol altitude (in pressure, hPa) from the GISS model in January (top) and July (bottom).	9-153
Figure 9-81.	Time dependence of aerosol optical thickness (left) and climate forcing (right). Note that as specified, the aerosol trends are all "flat" from 1990-2000.	9-155
Figure 9-82.	Change in global mean ocean temperature (left axis) and ocean heat content (right axis) for the top 3000 m due to different forcings in the GFDL model.	9-156
Figure 9-83.	Visible (wavelength 0.55 μm) optical depth estimates of stratospheric SO_4^{2-} aerosols formed in the aftermath of explosive volcanic eruptions that occurred between 1860 and 2000.	9-163
Figure 9-84.	The transfer of POPs between the major abiotic compartments of the Arctic.	9-169
Figure 9-85.	Relationship of plant nutrients and trace metals with vegetation.	9-185
Figure A-1.	PM _{2.5} monitor distribution in comparison with population density, Atlanta, GA.	A-59
Figure A-2.	PM ₁₀ monitor distribution in comparison with population density, Atlanta, GA.	A-60
Figure A-3.	PM _{2.5} monitor distribution in comparison with population density, Birmingham, AL.	A-61
Figure A-4.	PM ₁₀ monitor distribution in comparison with population density, Birmingham, AL.	A-62
Figure A-5.	PM _{2.5} monitor distribution in comparison with population density, Boston, MA.	A-63
Figure A-6.	PM ₁₀ monitor distribution in comparison with population density, Boston, MA.	A-64
Figure A-7.	PM _{2.5} monitor distribution in comparison with population density, Chicago, IL.	A-65
Figure A-8.	PM ₁₀ monitor distribution in comparison with population density, Chicago, IL.	A-66
Figure A-9.	PM _{2.5} monitor distribution in comparison with population density, Denver, CO.	A-67
Figure A-10.	PM ₁₀ monitor distribution in comparison with population density, Denver, CO.	A-68
Figure A-11.	PM _{2.5} monitor distribution in comparison with population density, Detroit, MI.	A-69
Figure A-12.	PM ₁₀ monitor distribution in comparison with population density, Detroit, MI.	A-70
Figure A-13.	PM _{2.5} monitor distribution in comparison with population density, Houston, TX.	A-71
Figure A-14.	PM ₁₀ monitor distribution in comparison with population density, Houston, TX.	A-72
Figure A-15.	PM _{2.5} monitor distribution in comparison with population density, Los Angeles, CA.	A-73
Figure A-16.	PM ₁₀ monitor distribution in comparison with population density, Los Angeles, CA.	A-74
Figure A-17.	PM _{2.5} monitor distribution in comparison with population density, New York, NY.	A-75
Figure A-18.	PM ₁₀ monitor distribution in comparison with population density, New York, NY.	A-76

Figure A-19.	PM _{2.5} monitor distribution in comparison with population density, Philadelphia, PA. _____	A-77
Figure A-20.	PM ₁₀ monitor distribution in comparison with population density, Philadelphia, PA. _____	A-78
Figure A-21.	PM _{2.5} monitor distribution in comparison with population density, Phoenix, AZ. _____	A-79
Figure A-22.	PM ₁₀ monitor distribution in comparison with population density, Phoenix, AZ. _____	A-80
Figure A-23.	PM _{2.5} monitor distribution in comparison with population density, Pittsburgh, PA. _____	A-81
Figure A-24.	PM ₁₀ monitor distribution in comparison with population density, Pittsburgh, PA. _____	A-82
Figure A-25.	PM _{2.5} monitor distribution in comparison with population density, Riverside, CA. _____	A-83
Figure A-26.	PM ₁₀ monitor distribution in comparison with population density, Riverside, CA. _____	A-84
Figure A-27.	PM _{2.5} monitor distribution in comparison with population density, Seattle, WA. _____	A-85
Figure A-28.	PM ₁₀ monitor distribution in comparison with population density, Seattle, WA. _____	A-86
Figure A-29.	PM _{2.5} monitor distribution in comparison with population density, St. Louis, MO. _____	A-87
Figure A-30.	PM ₁₀ monitor distribution in comparison with population density, St. Louis, MO. _____	A-88
Figure A-31.	Three-yr avg of 24-h PM _{2.5} Cu concentrations measured at CSN sites across the U.S., 2005-2007. _____	A-89
Figure A-32.	Three-yr avg of 24-h PM _{2.5} Fe concentrations measured at CSN sites across the U.S., 2005-2007 _____	A-90
Figure A-33.	Three-yr avg of 24-h PM _{2.5} Ni concentrations measured at CSN sites across the U.S., 2005-2007 _____	A-91
Figure A-34.	Three-yr avg of 24-h PM _{2.5} Pb concentrations measured at CSN sites across the U.S., 2005-2007 _____	A-92
Figure A-35.	Three-yr avg of 24-h PM _{2.5} Se concentrations measured at CSN sites across the U.S., 2005-2007 _____	A-93
Figure A-36.	Three-yr avg of 24-h PM _{2.5} V concentrations measured at CSN sites across the U.S., 2005-2007 _____	A-94
Figure A-37.	PM _{2.5} monitor distribution and major highways, Atlanta, GA. _____	A-96
Figure A-38.	Box plots illustrating the seasonal distribution of 24-h avg PM _{2.5} concentrations for Atlanta, GA. _____	A-97
Figure A-39.	PM _{2.5} inter-sampler correlations as a function of distance between monitors for Atlanta, GA. _____	A-99
Figure A-40.	PM _{2.5} monitor distribution and major highways, Birmingham, AL. _____	A-100
Figure A-41.	Box plots illustrating the seasonal distribution of 24-h avg PM _{2.5} concentrations for Birmingham, AL. _____	A-101
Figure A-42.	PM _{2.5} inter-sampler correlations as a function of distance between monitors for Birmingham, AL. _____	A-103
Figure A-43.	PM _{2.5} monitor distribution and major highways, Boston, MA. _____	A-104
Figure A-44.	Box plots illustrating the seasonal distribution of 24-h avg PM _{2.5} concentrations for Boston, MA. _____	A-105
Figure A-45.	PM _{2.5} inter-sampler correlations as a function of distance between monitors for Boston, MA. _____	A-107
Figure A-46.	PM _{2.5} monitor distribution and major highways, Chicago, IL. _____	A-108
Figure A-47.	Box plots illustrating the seasonal distribution of 24-h avg PM _{2.5} concentrations for Chicago, IL. _____	A-110

Figure A-48.	PM _{2.5} inter-sampler correlations as a function of distance between monitors for Chicago, IL.	A-113
Figure A-49.	PM _{2.5} monitor distribution and major highways, Denver, CO.	A-114
Figure A-50.	Box plots illustrating the seasonal distribution of 24-h avg PM _{2.5} concentrations for Denver, CO.	A-115
Figure A-51.	PM _{2.5} inter-sampler correlations as a function of distance between monitors for Denver, CO.	A-117
Figure A-52.	PM _{2.5} monitor distribution and major highways, Detroit, MI.	A-118
Figure A-53.	Box plots illustrating the seasonal distribution of 24-h avg PM _{2.5} concentrations for Detroit, MI.	A-119
Figure A-54.	PM _{2.5} inter-sampler correlations as a function of distance between monitors for Detroit, MI.	A-121
Figure A-55.	PM _{2.5} monitor distribution and major highways, Houston, TX.	A-122
Figure A-56.	Box plots illustrating the seasonal distribution of 24-h avg PM _{2.5} concentrations for Houston, TX.	A-123
Figure A-57.	PM _{2.5} inter-sampler correlations as a function of distance between monitors for Houston, TX.	A-124
Figure A-58.	PM _{2.5} monitor distribution and major highways, Los Angeles, CA.	A-125
Figure A-59.	Box plots illustrating the seasonal distribution of 24-h avg PM _{2.5} concentrations for Los Angeles, CA.	A-126
Figure A-60.	PM _{2.5} inter-sampler correlations as a function of distance between monitors for Los Angeles, CA.	A-127
Figure A-61.	PM _{2.5} monitor distribution and major highways, New York City, NY.	A-128
Figure A-62.	Box plots illustrating the seasonal distribution of 24-h avg PM _{2.5} concentrations for New York, NY.	A-130
Figure A-63.	PM _{2.5} inter-sampler correlations as a function of distance between monitors for New York, NY.	A-133
Figure A-64.	PM _{2.5} monitor distribution and major highways, Philadelphia, PA.	A-134
Figure A-65.	Box plots illustrating the seasonal distribution of 24-h avg PM _{2.5} concentrations for Philadelphia, PA.	A-135
Figure A-66.	PM _{2.5} inter-sampler correlations as a function of distance between monitors for Philadelphia, PA.	A-137
Figure A-67.	PM _{2.5} monitor distribution and major highways, Phoenix, AZ.	A-138
Figure A-68.	Box plots illustrating the seasonal distribution of 24-h avg PM _{2.5} concentrations for Phoenix, AZ.	A-139
Figure A-69.	PM _{2.5} inter-sampler correlations as a function of distance between monitors for Phoenix, AZ.	A-141
Figure A-70.	PM _{2.5} monitor distribution and major highways, Pittsburgh, PA.	A-142
Figure A-71.	Box plots illustrating the seasonal distribution of 24-h avg PM _{2.5} concentrations for Pittsburgh, PA.	A-143
Figure A-72.	PM _{2.5} inter-sampler correlations as a function of distance between monitors for Pittsburgh, PA.	A-145
Figure A-73.	PM _{2.5} monitor distribution and major highways, Riverside, CA.	A-146

Figure A-74.	Box plots illustrating the seasonal distribution of 24-h avg PM _{2.5} concentrations for Riverside, CA.	A-147
Figure A-75.	PM _{2.5} inter-sampler correlations as a function of distance between monitors for Riverside CA.	A-149
Figure A-76.	PM _{2.5} monitor distribution and major highways, Seattle, WA.	A-150
Figure A-77.	Box plots illustrating the seasonal distribution of 24-h avg PM _{2.5} concentrations for Seattle, WA.	A-151
Figure A-78.	PM _{2.5} inter-sampler correlations as a function of distance between monitors for Seattle, WA.	A-152
Figure A-79.	PM _{2.5} monitor distribution and major highways, St. Louis, MO.	A-153
Figure A-80.	Box plots illustrating the seasonal distribution of 24-h avg PM _{2.5} concentrations for St. Louis, MO.	A-154
Figure A-81.	PM _{2.5} inter-sampler correlations as a function of distance between monitors for St. Louis, MO.	A-156
Figure A-82.	PM ₁₀ monitor distribution and major highways, Atlanta, GA.	A-157
Figure A-83.	Box plots illustrating the seasonal distribution of 24-h avg PM ₁₀ concentrations for Atlanta, GA.	A-158
Figure A-84.	PM ₁₀ inter-sampler correlations as a function of distance between monitors for Atlanta, GA.	A-160
Figure A-85.	PM ₁₀ monitor distribution and major highways, Birmingham, AL.	A-161
Figure A-86.	Box plots illustrating the seasonal distribution of 24-h avg PM ₁₀ concentrations for Birmingham, AL.	A-162
Figure A-87.	PM ₁₀ inter-sampler correlations as a function of distance between monitors for Birmingham, AL.	A-164
Figure A-88.	PM ₁₀ monitor distribution and major highways, Boston, MA.	A-165
Figure A-89.	Box plots illustrating the seasonal distribution of 24-h avg PM ₁₀ concentrations for Boston, MA.	A-166
Figure A-90.	PM ₁₀ inter-sampler correlations as a function of distance between monitors for Boston, MA.	A-167
Figure A-91.	PM ₁₀ monitor distribution and major highways, Chicago, IL.	A-168
Figure A-92.	Box plots illustrating the seasonal distribution of 24-h avg PM ₁₀ concentrations for Chicago, IL.	A-169
Figure A-93.	PM ₁₀ inter-sampler correlations as a function of distance between monitors for Chicago, IL.	A-171
Figure A-94.	PM ₁₀ monitor distribution and major highways, Denver, CO.	A-172
Figure A-95.	Box plots illustrating the seasonal distribution of 24-h avg PM ₁₀ concentrations for Denver, CO.	A-173
Figure A-96.	PM ₁₀ inter-sampler correlations as a function of distance between monitors for Denver, CO.	A-175
Figure A-97.	PM ₁₀ monitor distribution and major highways, Detroit, MI.	A-176
Figure A-98.	Box plots illustrating the seasonal distribution of 24-h avg PM ₁₀ concentrations for Detroit, MI.	A-177
Figure A-99.	PM ₁₀ inter-sampler correlations as a function of distance between monitors for Detroit, MI.	A-178
Figure A-100.	PM ₁₀ monitor distribution and major highways, Houston, TX.	A-179

Figure A-101.	Box plots illustrating the seasonal distribution of 24-h avg PM ₁₀ concentrations for Houston, TX. _____	A-180
Figure A-102.	PM ₁₀ inter-sampler correlations as a function of distance between monitors for Houston, TX. _____	A-182
Figure A-103.	PM ₁₀ monitor distribution and major highways, Los Angeles, CA. _____	A-183
Figure A-104.	Box plots illustrating the seasonal distribution of 24-h avg PM ₁₀ concentrations for Los Angeles, CA. _____	A-184
Figure A-105.	PM ₁₀ inter-sampler correlations as a function of distance between monitors for Los Angeles, CA. _____	A-185
Figure A-106.	PM ₁₀ monitor distribution and major highways, New York, NY. _____	A-186
Figure A-107.	Box plots illustrating the seasonal distribution of 24-h avg PM ₁₀ concentrations for New York, NY. _____	A-187
Figure A-108.	PM ₁₀ inter-sampler correlations as a function of distance between monitors for New York, NY. _____	A-188
Figure A-109.	PM ₁₀ monitor distribution and major highways, Philadelphia, PA. _____	A-189
Figure A-110.	Box plots illustrating the seasonal distribution of 24-h avg PM ₁₀ concentrations for Philadelphia, PA. _____	A-190
Figure A-111.	PM ₁₀ inter-sampler correlations as a function of distance between monitors for Philadelphia, PA. _____	A-191
Figure A-112.	PM ₁₀ monitor distribution and major highways, Phoenix, AZ. _____	A-192
Figure A-113.	Box plots illustrating the seasonal distribution of 24-h avg PM ₁₀ concentrations for Phoenix, AZ. _____	A-194
Figure A-114.	PM ₁₀ inter-sampler correlations as a function of distance between monitors for Phoenix, AZ. _____	A-197
Figure A-115.	PM ₁₀ monitor distribution and major highways, Pittsburgh, PA. _____	A-198
Figure A-116.	Box plots illustrating the seasonal distribution of 24-h avg PM ₁₀ concentrations for Pittsburgh, PA. _____	A-199
Figure A-117.	PM ₁₀ inter-sampler correlations as a function of distance between monitors for Pittsburgh, PA. _____	A-201
Figure A-118.	PM ₁₀ monitor distribution and major highways, Riverside, CA. _____	A-202
Figure A-119.	Box plots illustrating the seasonal distribution of 24-h avg PM ₁₀ concentrations for Riverside, CA. _____	A-203
Figure A-120.	PM ₁₀ inter-sampler correlations as a function of distance between monitors for Riverside, CA. _____	A-205
Figure A-121.	PM ₁₀ monitor distribution and major highways, Seattle, WA. _____	A-206
Figure A-122.	Box plots illustrating the seasonal distribution of 24-h avg PM ₁₀ concentrations for Seattle, WA. _____	A-207
Figure A-123.	PM ₁₀ inter-sampler correlations as a function of distance between monitors for Seattle, WA. _____	A-208
Figure A-124.	PM ₁₀ monitor distribution and major highways, St. Louis, MO. _____	A-209
Figure A-125.	Box plots illustrating the seasonal distribution of 24-h avg PM ₁₀ concentrations for St. Louis, MO. _____	A-210
Figure A-126.	PM ₁₀ inter-sampler correlations as a function of distance between monitors for St. Louis, MO. _____	A-212

Figure A-127.	Seasonally averaged PM _{2.5} speciation data for 2005-2007 for a) annual, b) spring, c) summer, d) fall and e) winter derived using the SANDWICH method in Atlanta, GA. _____	A-213
Figure A-128.	Seasonally averaged PM _{2.5} speciation data for 2005-2007 for a) annual, b) spring, c) summer, d) fall and e) winter derived using the SANDWICH method in Birmingham, AL. _____	A-214
Figure A-129.	Seasonally averaged PM _{2.5} speciation data for 2005-2007 for a) annual, b) spring, c) summer, d) fall and e) winter derived using the SANDWICH method in Boston, MA. _____	A-215
Figure A-130.	Seasonally averaged PM _{2.5} speciation data for 2005-2007 for a) annual, b) spring, c) summer, d) fall and e) winter derived using the SANDWICH method in Chicago, IL. _____	A-216
Figure A-131.	Seasonally averaged PM _{2.5} speciation data for 2005-2007 for a) annual, b) spring, c) summer, d) fall and e) winter, derived using the SANDWICH method in Denver, CO. _____	A-217
Figure A-132.	Seasonally averaged PM _{2.5} speciation data for 2005-2007 for a) annual, b) spring, c) summer, d) fall and e) winter derived using the SANDWICH method in Detroit, MI. _____	A-218
Figure A-133.	Seasonally averaged PM _{2.5} speciation data for 2005-2007 for a) annual, b) spring, c) summer, d) fall and e) winter derived using the SANDWICH method in Houston, TX. _____	A-219
Figure A-134.	Seasonally averaged PM _{2.5} speciation data for 2005-2007 for a) annual, b) spring, c) summer, d) fall and e) winter derived using the SANDWICH method in Los Angeles, CA. _____	A-220
Figure A-135.	Seasonally averaged PM _{2.5} speciation data for 2005-2007 for a) annual, b) spring, c) summer, d) fall and e) winter derived using the SANDWICH method in New York, NY. _____	A-221
Figure A-136.	Seasonally averaged PM _{2.5} speciation data for 2005-2007 for a) annual, b) spring, c) summer, d) fall and e) winter derived using the SANDWICH method in Philadelphia, PA. _____	A-222
Figure A-137.	Seasonally averaged PM _{2.5} speciation data for 2005-2007 for a) annual, b) spring, c) summer, d) fall and e) winter derived using the SANDWICH method in Phoenix, AZ. _____	A-223
Figure A-138.	Seasonally averaged PM _{2.5} speciation data for 2005-2007 for a) annual, b) spring, c) summer, d) fall and e) winter derived using the SANDWICH method in Pittsburgh, PA. _____	A-224
Figure A-139.	Seasonally averaged PM _{2.5} speciation data for 2005-2007 for a) annual, b) spring, c) summer, d) fall and e) winter derived using the SANDWICH method in Riverside, CA. _____	A-225
Figure A-140.	Seasonally averaged PM _{2.5} speciation data for 2005-2007 for a) annual, b) spring, c) summer, d) fall and e) winter derived using the SANDWICH method in Seattle, WA. _____	A-226
Figure A-141.	Seasonally averaged PM _{2.5} speciation data for 2005-2007 for a) annual, b) spring, c) summer, d) fall and e) winter derived using the SANDWICH method in St. Louis, MO. _____	A-227
Figure A-142.	Seasonal patterns in PM _{2.5} chemical composition from city-wide monthly average values for Atlanta, GA, 2005-2007. _____	A-228
Figure A-143.	Seasonal patterns in PM _{2.5} chemical composition from city-wide monthly average values for Birmingham, AL, 2005-2007. _____	A-228
Figure A-144.	Seasonal patterns in PM _{2.5} chemical composition from city-wide monthly average values for Boston, MA, 2005-2007. _____	A-229
Figure A-145.	Seasonal patterns in PM _{2.5} chemical composition from city-wide monthly average values for Chicago, IL, 2005-2007. _____	A-229
Figure A-146.	Seasonal patterns in PM _{2.5} chemical composition from city-wide monthly average values for Denver, CO, 2005-2007. _____	A-230
Figure A-147.	Seasonal patterns in PM _{2.5} chemical composition from city-wide monthly average values for Detroit, MI, 2005-2007. _____	A-230

Figure A-148.	Seasonal patterns in PM _{2.5} chemical composition from city-wide monthly average values for Houston, TX, 2005-2007. _____	A-231
Figure A-149.	Seasonal patterns in PM _{2.5} chemical composition from city-wide monthly average values for Los Angeles, CA, 2005-2007. _____	A-231
Figure A-150.	Seasonal patterns in PM _{2.5} chemical composition from city-wide monthly average values for New York, NY, 2005-2007. _____	A-232
Figure A-151.	Seasonal patterns in PM _{2.5} chemical composition from city-wide monthly average values for Philadelphia, PA, 2005-2007. _____	A-232
Figure A-152.	Seasonal patterns in PM _{2.5} chemical composition from city-wide monthly average values for Phoenix, AZ, 2005-2007. _____	A-233
Figure A-153.	Seasonal patterns in PM _{2.5} chemical composition from city-wide monthly average values for Pittsburgh, PA, 2005-2007. _____	A-233
Figure A-154.	Seasonal patterns in PM _{2.5} chemical composition from city-wide monthly average values for Riverside, CA, 2005-2007. _____	A-234
Figure A-155.	Seasonal patterns in PM _{2.5} chemical composition from city-wide monthly average values for Seattle, WA, 2005-2007. _____	A-234
Figure A-156.	Seasonal patterns in PM _{2.5} chemical composition from city-wide monthly average values for St. Louis, MO, 2005-2007. _____	A-235
Figure A-157.	Diel plots generated from all available hourly FRM-like PM _{2.5} data, stratified by weekday (left) and weekend (right), in Atlanta, GA. _____	A-235
Figure A-158.	Diel plots generated from all available hourly FRM-like PM _{2.5} data, stratified by weekday (left) and weekend (right), in Chicago, IL. _____	A-236
Figure A-159.	Diel plots generated from all available hourly FRM-like PM _{2.5} data, stratified by weekday (left) and weekend (right), in Houston, TX. _____	A-236
Figure A-160.	Diel plots generated from all available hourly FRM-like PM _{2.5} data, stratified by weekday (left) and weekend (right), in New York, NY. _____	A-237
Figure A-161.	Diel plots generated from all available hourly FRM-like PM _{2.5} data, stratified by weekday (left) and weekend (right), in Pittsburgh, PA. _____	A-237
Figure A-162.	Diel plots generated from all available hourly FRM-like PM _{2.5} data, stratified by weekday (left) and weekend (right), in Seattle, WA. _____	A-238
Figure A-163.	Diel plots generated from all available hourly FRM-like PM _{2.5} data, stratified by weekday (left) and weekend (right), in St. Louis, MO. _____	A-238
Figure A-164.	Diel plot generated from all available hourly FRM/FEM PM ₁₀ data, stratified by weekday (left) and weekend (right), in Atlanta, GA. _____	A-239
Figure A-165.	Diel plot generated from all available hourly FRM/FEM PM ₁₀ data, stratified by weekday (left) and weekend (right), in Chicago, IL. _____	A-239
Figure A-166.	Diel plot generated from all available hourly FRM/FEM PM ₁₀ data, stratified by weekday (left) and weekend (right), in Denver, CO. _____	A-240
Figure A-167.	Diel plot generated from all available hourly FRM/FEM PM ₁₀ data, stratified by weekday (left) and weekend (right), in Detroit, MI. _____	A-240
Figure A-168.	Diel plot generated from all available hourly FRM/FEM PM ₁₀ data, stratified by weekday (left) and weekend (right), in Los Angeles, CA. _____	A-241

Figure A-169.	Diel plot generated from all available hourly FRM/FEM PM ₁₀ data, stratified by weekday (left) and weekend (right), in Philadelphia, PA. _____	A-241
Figure A-170.	Diel plot generated from all available hourly FRM/FEM PM ₁₀ data, stratified by weekday (left) and weekend (right), in Phoenix, AZ. _____	A-242
Figure A-171.	Diel plot generated from all available hourly FRM/FEM PM ₁₀ data, stratified by weekday (left) and weekend (right), in Pittsburgh, PA. _____	A-242
Figure A-172.	Diel plot generated from all available hourly FRM/FEM PM ₁₀ data, stratified by weekday (left) and weekend (right), in Riverside, CA. _____	A-243
Figure A-173.	Diel plot generated from all available hourly FRM/FEM PM ₁₀ data, stratified by weekday (left) and weekend (right), in Seattle, WA. _____	A-243
Figure A-174.	Diel plot generated from all available hourly FRM/FEM PM ₁₀ data, stratified by weekday (left) and weekend (right), in St. Louis, MO. _____	A-244
Figure A-175.	Correlations between 24-h PM _{2.5} and co-located 24-h avg PM ₁₀ , PM _{10-2.5} , SO ₂ , NO ₂ and CO and daily maximum 8-h avg O ₃ for Atlanta, GA, stratified by season (2005-2007). _____	A-245
Figure A-176.	Correlations between 24-h PM _{2.5} and co-located 24-h avg PM ₁₀ , PM _{10-2.5} , SO ₂ , NO ₂ and CO and daily maximum 8-h avg O ₃ for Birmingham, AL, stratified by season (2005-2007). _____	A-246
Figure A-177.	Correlations between 24-h PM _{2.5} and co-located 24-h avg PM ₁₀ , PM _{10-2.5} , SO ₂ , NO ₂ and CO and daily maximum 8-h avg O ₃ for Boston, MA, stratified by season (2005-2007). _____	A-247
Figure A-178.	Correlations between 24-h PM _{2.5} and co-located 24-h avg PM ₁₀ , PM _{10-2.5} , SO ₂ , NO ₂ and CO and daily maximum 8-h avg O ₃ for Chicago, IL, stratified by season (2005-2007). _____	A-248
Figure A-179.	Correlations between 24-h PM _{2.5} and co-located 24-h avg PM ₁₀ , PM _{10-2.5} , SO ₂ , NO ₂ and CO and daily maximum 8-h avg O ₃ for Denver, CO, stratified by season (2005-2007). _____	A-249
Figure A-180.	Correlations between 24-h PM _{2.5} and co-located 24-h avg PM ₁₀ , PM _{10-2.5} , SO ₂ , NO ₂ and CO and daily maximum 8-h avg O ₃ for Detroit, MI, stratified by season (2005-2007). _____	A-250
Figure A-181.	Correlations between 24-h PM _{2.5} and co-located 24-h avg PM ₁₀ , PM _{10-2.5} , SO ₂ , NO ₂ and CO and daily maximum 8-h avg O ₃ for Houston, TX, stratified by season (2005-2007). _____	A-251
Figure A-182.	Correlations between 24-h PM _{2.5} and co-located 24-h avg PM ₁₀ , PM _{10-2.5} , SO ₂ , NO ₂ and CO and daily maximum 8-h avg O ₃ for Los Angeles, CA, stratified by season (2005-2007). _____	A-252
Figure A-183.	Correlations between 24-h PM _{2.5} and co-located 24-h avg PM ₁₀ , PM _{10-2.5} , SO ₂ , NO ₂ and CO and daily maximum 8-h avg O ₃ for New York, NY, stratified by season (2005-2007). _____	A-253
Figure A-184.	Correlations between 24-h PM _{2.5} and co-located 24-h avg PM ₁₀ , PM _{10-2.5} , SO ₂ , NO ₂ and CO and daily maximum 8-h avg O ₃ for Philadelphia, PA, stratified by season (2005-2007). _____	A-254
Figure A-185.	Correlations between 24-h PM _{2.5} and co-located 24-h avg PM ₁₀ , PM _{10-2.5} , SO ₂ , NO ₂ and CO and daily maximum 8-h avg O ₃ for Phoenix, AZ, stratified by season (2005-2007). _____	A-255
Figure A-186.	Correlations between 24-h PM _{2.5} and co-located 24-h avg PM ₁₀ , PM _{10-2.5} , SO ₂ , NO ₂ and CO and daily maximum 8-h avg O ₃ for Pittsburgh, PA, stratified by season (2005-2007). _____	A-256
Figure A-187.	Correlations between 24-h PM _{2.5} and co-located 24-h avg PM ₁₀ , PM _{10-2.5} , SO ₂ , NO ₂ and CO and daily maximum 8-h avg O ₃ for Riverside, CA, stratified by season (2005-2007). _____	A-257
Figure A-188.	Correlations between 24-h PM _{2.5} and co-located 24-h avg PM ₁₀ , PM _{10-2.5} , SO ₂ , NO ₂ and CO and daily maximum 8-h avg O ₃ for St. Louis, MO, stratified by season (2005-2007). _____	A-258
Figure A-189.	Correlations between 24-h PM ₁₀ and co-located 24-h avg PM _{2.5} , PM _{10-2.5} , SO ₂ , NO ₂ and CO and daily maximum 8-h avg O ₃ for Atlanta, GA, stratified by season (2005-2007). _____	A-259

Figure A-190.	Correlations between 24-h PM ₁₀ and co-located 24-h avg PM _{2.5} , PM _{10-2.5} , SO ₂ , NO ₂ and CO and daily maximum 8-h avg O ₃ for Birmingham, AL, stratified by season (2005-2007). _____	A-260
Figure A-191.	Correlations between 24-h PM ₁₀ and co-located 24-h avg PM _{2.5} , PM _{10-2.5} , SO ₂ , NO ₂ and CO and daily maximum 8-h avg O ₃ for Boston, MA, stratified by season (2005-2007). _____	A-261
Figure A-192.	Correlations between 24-h PM ₁₀ and co-located 24-h avg PM _{2.5} , PM _{10-2.5} , SO ₂ , NO ₂ and CO and daily maximum 8-h avg O ₃ for Chicago, IL, stratified by season (2005-2007). _____	A-262
Figure A-193.	Correlations between 24-h PM ₁₀ and co-located 24-h avg PM _{2.5} , PM _{10-2.5} , SO ₂ , NO ₂ and CO and daily maximum 8-h avg O ₃ for Denver, CO, stratified by season (2005-2007). _____	A-263
Figure A-194.	Correlations between 24-h PM ₁₀ and co-located 24-h avg PM _{2.5} , PM _{10-2.5} , SO ₂ , NO ₂ and CO and daily maximum 8-h avg O ₃ for Detroit, MI, stratified by season (2005-2007). _____	A-264
Figure A-195.	Correlations between 24-h PM ₁₀ and co-located 24-h avg PM _{2.5} , PM _{10-2.5} , SO ₂ , NO ₂ and CO and daily maximum 8-h avg O ₃ for Houston, TX, stratified by season (2005-2007). _____	A-265
Figure A-196.	Correlations between 24-h PM ₁₀ and co-located 24-h avg PM _{2.5} , PM _{10-2.5} , SO ₂ , NO ₂ and CO and daily maximum 8-h avg O ₃ for Los Angeles, CA, stratified by season (2005-2007). _____	A-266
Figure A-197.	Correlations between 24-h PM ₁₀ and co-located 24-h avg PM _{2.5} , PM _{10-2.5} , SO ₂ , NO ₂ and CO and daily maximum 8-h avg O ₃ for New York, NY, stratified by season (2005-2007). _____	A-267
Figure A-198.	Correlations between 24-h PM ₁₀ and co-located 24-h avg PM _{2.5} , PM _{10-2.5} , SO ₂ , NO ₂ and CO and daily maximum 8-h avg O ₃ for Philadelphia, PA, stratified by season (2005-2007). _____	A-268
Figure A-199.	Correlations between 24-h PM ₁₀ and co-located 24-h avg PM _{2.5} , PM _{10-2.5} , SO ₂ , NO ₂ and CO and daily maximum 8-h avg O ₃ for Phoenix, AZ, stratified by season (2005-2007). _____	A-269
Figure A-200.	Correlations between 24-h PM ₁₀ and co-located 24-h avg PM _{2.5} , PM _{10-2.5} , SO ₂ , NO ₂ and CO and daily maximum 8-h avg O ₃ for Pittsburgh, PA, stratified by season (2005-2007). _____	A-270
Figure A-201.	Correlations between 24-h PM ₁₀ and co-located 24-h avg PM _{2.5} , PM _{10-2.5} , SO ₂ , NO ₂ and CO and daily maximum 8-h avg O ₃ for Riverside, CA, stratified by season (2005-2007). _____	A-271
Figure A-202.	Correlations between 24-h PM ₁₀ and co-located 24-h avg PM _{2.5} , PM _{10-2.5} , SO ₂ , NO ₂ and CO and daily maximum 8-h avg O ₃ for St. Louis, MO, stratified by season (2005-2007). _____	A-272

PM ISA Project Team

Executive Direction

Dr. John Vandenberg (Director)—National Center for Environmental Assessment-RTP Division, U.S. Environmental Protection Agency, Research Triangle Park, NC

Ms. Debra Walsh (Deputy Director)—National Center for Environmental Assessment-RTP Division, U.S. Environmental Protection Agency, Research Triangle Park, NC

Dr. Mary Ross (Branch Chief)—National Center for Environmental Assessment, U.S. Environmental Protection Agency, Research Triangle Park, NC

Scientific Staff

Dr. Lindsay Wichers Stanek (PM Team Leader)—National Center for Environmental Assessment, U.S. Environmental Protection Agency, Research Triangle Park, NC

Dr. Jeffrey Arnold—National Center for Environmental Assessment, U.S. Environmental Protection Agency, Research Triangle Park, NC (now at Institute for Water Resources, U.S. Army Corps of Engineers, Washington, D.C.)

Dr. Christal Bowman—National Center for Environmental Assessment, U.S. Environmental Protection Agency, Research Triangle Park, NC

Dr. James S. Brown—National Center for Environmental Assessment, U.S. Environmental Protection Agency, Research Triangle Park, NC

Dr. Barbara Buckley—National Center for Environmental Assessment, U.S. Environmental Protection Agency, Research Triangle Park, NC

Mr. Allen Davis—National Center for Environmental Assessment, U.S. Environmental Protection Agency, Research Triangle Park, NC

Dr. Jean-Jacques Dubois—National Center for Environmental Assessment, U.S. Environmental Protection Agency, Research Triangle Park, NC

Dr. Steven J. Dutton—National Center for Environmental Assessment, U.S. Environmental Protection Agency, Research Triangle Park, NC

Dr. Erin Hines—National Center for Environmental Assessment, U.S. Environmental Protection Agency, Research Triangle Park, NC

Dr. Douglas Johns—National Center for Environmental Assessment, U.S. Environmental Protection Agency, Research Triangle Park, NC

Dr. Ellen Kirrane—National Center for Environmental Assessment, U.S. Environmental Protection Agency, Research Triangle Park, NC

Dr. Dennis Kotchmar—National Center for Environmental Assessment, U.S. Environmental Protection Agency, Research Triangle Park, NC

Dr. Thomas Long—National Center for Environmental Assessment, U.S. Environmental Protection Agency, Research Triangle Park, NC

Dr. Thomas Luben—National Center for Environmental Assessment, U.S. Environmental Protection Agency, Research Triangle Park, NC

Dr. Qingyu Meng—Oak Ridge Institute for Science and Education, Postdoctoral Research Fellow to National Center for Environmental Assessment, U.S. Environmental Protection Agency, Research Triangle Park, NC

Dr. Kristopher Novak—National Center for Environmental Assessment, U.S. Environmental Protection Agency, Research Triangle Park, NC

Dr. Joseph Pinto—National Center for Environmental Assessment, U.S. Environmental Protection Agency, Research Triangle Park, NC

Dr. Jennifer Richmond-Bryant—National Center for Environmental Assessment, U.S. Environmental Protection Agency, Research Triangle Park, NC

Dr. Mary Ross—National Center for Environmental Assessment, U.S. Environmental Protection Agency, Research Triangle Park, NC

Mr. Jason Sacks—National Center for Environmental Assessment, U.S. Environmental Protection Agency, Research Triangle Park, NC

Dr. David Svendsgaard—National Center for Environmental Assessment, U.S. Environmental Protection Agency, Research Triangle Park, NC

Dr. Lisa Vinikoor—National Center for Environmental Assessment, U.S. Environmental Protection Agency, Research Triangle Park, NC

Dr. William Wilson—National Center for Environmental Assessment, U.S. Environmental Protection Agency, Research Triangle Park, NC

Dr. Lori White—National Center for Environmental Assessment, U.S. Environmental Protection Agency, Research Triangle Park, NC (now at National Institute for Environmental Health Sciences, Research Triangle Park, NC)

Technical Support Staff

Mattie Arnold—Senior Environmental Employee Program, National Center for Environmental Assessment, U.S. Environmental Protection Agency, Research Triangle Park, NC

Laeda Baston—Senior Environmental Employee Program, National Center for Environmental Assessment, U.S. Environmental Protection Agency, Research Triangle Park, NC

Kimberly Branch—Student Services Contractor, National Center for Environmental Assessment, U.S. Environmental Protection Agency, Research Triangle Park, NC

Ken Breito—Senior Environmental Employee Program, National Center for Environmental Assessment, U.S. Environmental Protection Agency, Research Triangle Park, NC

Eleanor Jamison—Senior Environmental Employee Program, National Center for Environmental Assessment, U.S. Environmental Protection Agency, Research Triangle Park, NC

Ryan Jones—Oak Ridge Institute for Science and Education, at National Center for Environmental Assessment, U.S. Environmental Protection Agency, Research Triangle Park, NC

Erica Lee—Oak Ridge Institute for Science and Education, at National Center for Environmental Assessment, U.S. Environmental Protection Agency, Research Triangle Park, NC

Barbara Liljequist—Senior Environmental Employee Program, National Center for Environmental Assessment, U.S. Environmental Protection Agency, Research Triangle Park, NC

Ellen Lorang—National Center for Environmental Assessment, U.S. Environmental Protection Agency, Research Triangle Park, NC

Kelsey Matson—Student Services Contractor, National Center for Environmental Assessment, U.S. Environmental Protection Agency, Research Triangle Park, NC

Sandy Pham—Student Services Contractor, National Center for Environmental Assessment, U.S. Environmental Protection Agency, Research Triangle Park, NC

Olivia Phillipott—Senior Environmental Employee Program, National Center for Environmental Assessment, U.S. Environmental Protection Agency, Research Triangle Park, NC

Deborah Wales—National Center for Environmental Assessment, U.S. Environmental Protection Agency, Research Triangle Park, NC

Erica Wilson—Oak Ridge Institute for Science and Education, at National Center for Environmental Assessment, U.S. Environmental Protection Agency, Research Triangle Park, NC

Richard Wilson—National Center for Environmental Assessment, U.S. Environmental Protection Agency, Research Triangle Park, NC

Barbara Wright—Senior Environmental Employee Program, National Center for Environmental Assessment, U.S. Environmental Protection Agency, Research Triangle Park, NC

Authors, Contributors, Reviewers

AUTHORS

Dr. Lindsay Wichers Stanek (PM Team Leader)—National Center for Environmental Assessment, U.S. Environmental Protection Agency, Research Triangle Park, NC

Dr. Jeffrey Arnold—National Center for Environmental Assessment, U.S. Environmental Protection Agency, Research Triangle Park, NC (now at Institute for Water Resources, U.S. Army Corps of Engineers, Washington, D.C)

Dr. Christal Bowman—National Center for Environmental Assessment, U.S. Environmental Protection Agency, Research Triangle Park, NC

Dr. James S. Brown—National Center for Environmental Assessment, U.S. Environmental Protection Agency, Research Triangle Park, NC

Dr. Barbara Buckley—National Center for Environmental Assessment, U.S. Environmental Protection Agency, Research Triangle Park, NC

Mr. Allen Davis—National Center for Environmental Assessment, U.S. Environmental Protection Agency, Research Triangle Park, NC

Dr. Jean-Jacques Dubois—National Center for Environmental Assessment, U.S. Environmental Protection Agency, Research Triangle Park, NC

Dr. Steven J. Dutton—National Center for Environmental Assessment, U.S. Environmental Protection Agency, Research Triangle Park, NC

Dr. Tara Greaver—National Center for Environmental Assessment, U.S. Environmental Protection Agency, Research Triangle Park, NC

Dr. Erin Hines—National Center for Environmental Assessment, U.S. Environmental Protection Agency, Research Triangle Park, NC

Dr. Douglas Johns—National Center for Environmental Assessment, U.S. Environmental Protection Agency, Research Triangle Park, NC

Dr. Ellen Kirrane—National Center for Environmental Assessment, U.S. Environmental Protection Agency, Research Triangle Park, NC

Dr. Dennis Kotchmar—National Center for Environmental Assessment, U.S. Environmental Protection Agency, Research Triangle Park, NC

Dr. Thomas Long—National Center for Environmental Assessment, U.S. Environmental Protection Agency, Research Triangle Park, NC

Dr. Thomas Luben—National Center for Environmental Assessment, U.S. Environmental Protection Agency, Research Triangle Park, NC

Dr. Qingyu Meng—Oak Ridge Institute for Science and Education, Postdoctoral Research Fellow to National Center for Environmental Assessment, U.S. Environmental Protection Agency, Research Triangle Park, NC

Dr. Kristopher Novak—National Center for Environmental Assessment, U.S. Environmental Protection Agency, Research Triangle Park, NC

Dr. Joseph Pinto—National Center for Environmental Assessment, U.S. Environmental Protection Agency, Research Triangle Park, NC

Dr. Jennifer Richmond-Bryant—National Center for Environmental Assessment, U.S. Environmental Protection Agency, Research Triangle Park, NC

Dr. Mary Ross—National Center for Environmental Assessment, U.S. Environmental Protection Agency, Research Triangle Park, NC

Mr. Jason Sacks—National Center for Environmental Assessment, U.S. Environmental Protection Agency, Research Triangle Park, NC

Dr. Timothy J. Sullivan—E&S Environmental Chemistry, Inc., Corvallis, OR

Dr. David Svendsgaard—National Center for Environmental Assessment, U.S. Environmental Protection Agency, Research Triangle Park, NC

Dr. Lisa Vinikoor—National Center for Environmental Assessment, U.S. Environmental Protection Agency, Research Triangle Park, NC

Dr. William Wilson—National Center for Environmental Assessment, U.S. Environmental Protection Agency, Research Triangle Park, NC

Dr. Lori White—National Center for Environmental Assessment, U.S. Environmental Protection Agency, Research Triangle Park, NC (now at National Institute for Environmental Health Sciences, Research Triangle Park, NC)

Dr. Christy Avery—University of North Carolina, Chapel Hill, NC

Dr. Kathleen Belanger—Center for Perinatal, Pediatric and Environmental Epidemiology, Yale University, New Haven, CT

Dr. Michelle Bell—School of Forestry & Environmental Studies, Yale University, New Haven, CT

Dr. William D. Bennett—Center for Environmental Medicine, Asthma and Lung Biology, University of North Carolina, Chapel Hill, NC

Dr. Matthew J. Campen—Lovelace Respiratory Research Institute, Albuquerque, NM

Dr. Leland B. Deck—Stratus Consulting, Inc., Washington, DC

Dr. Janneane F. Gent—Center for Perinatal, Pediatric and Environmental Epidemiology, Yale University, New Haven, CT

Dr. Yuh-Chin Tony Huang—Department of Medicine, Division of Pulmonary Medicine, Duke University Medical Center, Durham, NC

Dr. Kazuhiko Ito—Nelson Institute of Environmental Medicine, NYU School of Medicine, Tuxedo, NY

Mr. Marc Jackson—Integrated Laboratory Systems, Inc., Research Triangle Park, NC

Dr. Michael Kleinman—Department of Community and Environmental Medicine, University of California, Irvine

Dr. Sergey Napelenok—National Exposure Research Laboratory, U.S. Environmental Protection Agency, Research Triangle Park, NC

Dr. Marc Pitchford—National Oceanic and Atmospheric Administration, Las Vegas, NV

Dr. Les Recio—Genetic Toxicology Division, Integrated Laboratory Systems, Inc., Research Triangle Park, NC

Dr. David Quincy Rich—Department of Epidemiology, University of Medicine and Dentistry of New Jersey, Piscataway, NJ

Dr. Timothy Sullivan—E&S Environmental Chemistry, Inc., Corvallis, OR

Dr. George Thurston—Department of Environmental Medicine, NYU, Tuxedo, NY

Dr. Gregory Wellenius—Cardiovascular Epidemiology Research Unit, Beth Israel Deaconess Medical Center, Boston, MA

Dr. Eric Whitsel—Departments of Epidemiology and Medicine, University of North Carolina, Chapel Hill, NC

CONTRIBUTORS

Dr. Philip Bromberg—Department of Medicine, University of North Carolina, Chapel Hill, NC

Mr. Michael Burr—National Center for Environmental Assessment, U.S. Environmental Protection Agency, Research Triangle Park, NC

Mr. Turhan Carroll—Student Services Contractor, National Center for Environmental Assessment, U.S. Environmental Protection Agency, Research Triangle Park, NC

Ms. Rosana Datti—Student Services Contractor, National Center for Environmental Assessment, U.S. Environmental Protection Agency, Research Triangle Park, NC

Mr. Neil Frank—Office of Air Quality Planning and Standards, U.S. Environmental Protection Agency, Research Triangle Park, NC

Mr. Jonathan Krug—Student Services Contractor, National Center for Environmental Assessment, U.S. Environmental Protection Agency, Research Triangle Park, NC

Ms. Katie Lane—Student Services Contractor, National Center for Environmental Assessment, U.S. Environmental Protection Agency, Research Triangle Park, NC

Mr. Phil Lorang—Office of Air Quality Planning and Standards, U.S. Environmental Protection Agency, Research Triangle Park, NC

Ms. Christina Miller—National Center for Environmental Assessment, U.S. Environmental Protection Agency, Research Triangle Park, NC

Ms. Irina Mordukhovich—Oak Ridge Institute for Science and Education, at National Center for Environmental Assessment, U.S. Environmental Protection Agency, Research Triangle Park, NC

Dr. Elizabeth Oesterling Owens—National Center for Environmental Assessment, U.S. Environmental Protection Agency, Research Triangle Park, NC

Dr. Adam Reff—Office of Air Quality Planning and Standards, U.S. Environmental Protection Agency, Research Triangle Park, NC

Ms. Victoria Sandiford—Office of Air Quality Planning and Standards, U.S. Environmental Protection Agency, Research Triangle Park, NC

Dr. Mark Schmidt—Office of Air Quality Planning and Standards, U.S. Environmental Protection Agency, Research Triangle Park, NC

Ms. Angelina Schultz—Student Services Contractor, National Center for Environmental Assessment, U.S. Environmental Protection Agency, Research Triangle Park, NC

Ms. Kirsten Simmons—Student Services Contractor, National Center for Environmental Assessment, U.S. Environmental Protection Agency, Research Triangle Park, NC

Ms. Genee Smith—Oak Ridge Institute for Science and Education, at National Center for Environmental Assessment, U.S. Environmental Protection Agency, Research Triangle Park, NC

Mr. Kurt Susdorf—Student Services Contractor, National Center for Environmental Assessment, U.S. Environmental Protection Agency, Research Triangle Park, NC

Dr. Barbara Turpin—Department of Environmental Sciences, Rutgers University, New Brunswick, NJ

Ms. Lauren Tuttle—Student Services Contractor, National Center for Environmental Assessment, U.S. Environmental Protection Agency, Research Triangle Park, NC

Ms. Rebecca Yang—Student Services Contractor, National Center for Environmental Assessment, U.S. Environmental Protection Agency, Research Triangle Park, NC

PEER REVIEWERS

Dr. Sara Dubowsky Adar, Department of Epidemiology, University of Washington, Seattle, WA

Mr. Chad Bailey, Office of Transportation and Air Quality, Ann Arbor, MI

Mr. Richard Baldauf, Office of Transportation and Air Quality, Ann Arbor, MI

Dr. Prakash Bhawe, National Exposure Research Laboratory, U.S. Environmental Protection Agency, Research Triangle Park, NC

Mr. George Bowker, Office of Atmospheric Programs, U.S. Environmental Protection Agency, Washington, D.C.

Dr. Judith Chow, Division of Atmospheric Sciences, Desert Research Institute, Reno, NV

Dr. Dan Costa, U.S. Environmental Protection Agency, Research Triangle Park, NC

Dr. Ila Cote, National Center for Environmental Assessment, U.S. Environmental Protection Agency, Research Triangle Park, NC

Dr. Robert Devlin, National Health and Environmental Effects Research Laboratory, U.S. Environmental Protection Agency, Research Triangle Park, NC

Dr. David DeMarini, National Health and Environmental Effects Research Laboratory, U.S. Environmental Protection Agency, Research Triangle Park, NC

Dr. Neil Donahue, Department of Chemical Engineering, Carnegie Mellon University, Pittsburgh, PA

Dr. Aimen Farraj, National Health and Environmental Effects Research Laboratory, U.S. Environmental Protection Agency, Research Triangle Park, NC

Dr. Mark Frampton, Department of Environmental Medicine, University of Rochester Medical Center, Rochester, NY

Mr. Neil Frank, Office of Air Quality Planning and Standards, U.S. Environmental Protection Agency, Research Triangle Park, NC

Mr. Tyler Fox, Office of Air Quality Planning and Standards, U.S. Environmental Protection Agency, Research Triangle Park, NC

Dr. Jim Gauderman, Department of Environmental Medicine, Department of Preventive Medicine, University of Southern California, Los Angeles, CA

Dr. Barbara Glenn, National Center for Environmental Research, U.S. Environmental Protection Agency, Washington, D.C.

Dr. Terry Gordon, School of Medicine, New York University, Tuxedo, NY

Mr. Tim Hanley, Office of Air Quality Planning and Standards, U.S. Environmental Protection Agency, Research Triangle Park, NC

Dr. Jack Harkema, Department of Pathobiology and Diagnostic Investigation, Michigan State University, East Lansing, MI

Ms. Beth Hassett-Sipple, Office of Air Quality Planning and Standards, U.S. Environmental Protection Agency, Research Triangle Park, NC

Dr. Amy Herring, Department of Biostatistics, University of North Carolina, Chapel Hill, NC

Dr. Israel Jirak, Department of Meteorology, Embry-Riddle Aeronautical University, Prescott, AZ

Dr. Mike Kleeman, Department of Civil and Environmental Engineering, University of California, Davis, CA

Dr. Petros Koutrakis, Exposure, Epidemiology and Risk Program, Harvard School of Public Health, Boston, MA

Dr. Sagar Krupa, Department of Plant Pathology, University of Minnesota, St. Paul, MN

Mr. John Langstaff, Office of Air Quality Planning and Standards, U.S. Environmental Protection Agency, Research Triangle Park, NC

Dr. Meredith Lassiter, Office of Air Quality Planning and Standards, U.S. Environmental Protection Agency, Research Triangle Park, NC

Mr. Phil Lorang, Office of Air Quality Planning and Standards, U.S. Environmental Protection Agency, Research Triangle Park, NC

Dr. Karen Martin, Office of Air Quality Planning and Standards, U.S. Environmental Protection Agency, Research Triangle Park, NC

Ms. Connie Meacham, National Center for Environmental Assessment, U.S. Environmental Protection Agency, Research Triangle Park, NC

Mr. Tom Pace, Office of Air Quality Planning and Standards, U.S. Environmental Protection Agency, Research Triangle Park, NC

Dr. Jennifer Peel, Department of Environmental and Radiological Health Sciences, College of Veterinary Medicine and Biomedical Sciences, Colorado State University, Fort Collins, CO

Dr. Zackary Pekar, Office of Air Quality Planning and Standards, U.S. Environmental Protection Agency, Research Triangle Park, NC

Mr. Rob Pinder, National Exposure Research Laboratory, U.S. Environmental Protection Agency, Research Triangle Park, NC

Mr. Norm Possiel, Office of Air Quality Planning and Standards, U.S. Environmental Protection Agency, Research Triangle Park, NC

Dr. Sanjay Rajagopalan, Division of Cardiovascular Medicine, Ohio State University, Columbus, OH

Dr. Pradeep Rajan, Office of Air Quality Planning and Standards, U.S. Environmental Protection Agency, Research Triangle Park, NC

Mr. Venkatesh Rao, Office of Air Quality Planning and Standards, U.S. Environmental Protection Agency, Research Triangle Park, NC

Ms. Joann Rice, Office of Air Quality Planning and Standards, U.S. Environmental Protection Agency, Research Triangle Park, NC

Mr. Harvey Richmond, Office of Air Quality Planning and Standards, U.S. Environmental Protection Agency, Research Triangle Park, NC

Ms. Victoria Sandiford, Office of Air Quality Planning and Standards, U.S. Environmental Protection Agency, Research Triangle Park, NC

Dr. Stefanie Sarnat, Department of Environmental and Occupational Health, Emory University, Atlanta, GA

Dr. Frances Silverman, Gage Occupational and Environmental Health, University of Toronto, Toronto, ON

Mr. Steven Silverman, Office of General Council, U.S. Environmental Protection Agency, Washington, D.C.

Dr. Barbara Turpin, Department of Environmental Sciences, Rutgers University, New Brunswick, NJ

Dr. Robert Vanderpool, National Exposure Research Laboratory, U.S. Environmental Protection Agency, Research Triangle Park, NC

Dr. John Vandenberg (Director)—National Center for Environmental Assessment-RTP Division, U.S. Environmental Protection Agency, Research Triangle Park, NC

Dr. Alan Vette, National Exposure Research Laboratory, U.S. Environmental Protection Agency, Research Triangle Park, NC

Ms. Debra Walsh (Deputy Director)—National Center for Environmental Assessment-RTP Division, U.S. Environmental Protection Agency, Research Triangle Park, NC

Mr. Tim Watkins, National Exposure Research Laboratory, U.S. Environmental Protection Agency, Research Triangle Park, NC

Dr. Christopher Weaver, National Center for Environmental Assessment, U.S. Environmental Protection Agency, Research Triangle Park, NC

Mr. Lewis Weinstock, Office of Air Quality Planning and Standards, U.S. Environmental Protection Agency, Research Triangle Park, NC

Ms. Karen Wesson, Office of Air Quality Planning and Standards, U.S. Environmental Protection Agency, Research Triangle Park, NC

Dr. Jason West, Department of Environmental Sciences and Engineering, University of North Carolina, Chapel Hill, NC

Mr. Ronald Williams, National Exposure Research Laboratory, U.S. Environmental Protection Agency, Research Triangle Park, NC

Dr. George Woodall, National Center for Environmental Assessment, U.S. Environmental Protection Agency, Research Triangle Park, NC

Dr. Antonella Zanobetti, Department of Environmental Health, Harvard School of Public Health, Boston, MA

Clean Air Scientific Advisory Committee for Particulate Matter NAAQS

CHAIRPERSON

Dr. Jonathan Samet, Department of Preventive Medicine, Keck School of Medicine, University of Southern California, Los Angeles, CA

MEMBERS

Dr. Lowell Ashbaugh, Crocker Nuclear Lab, University of California, Davis, CA

Dr. Ed Avol, Department of Preventive Medicine, Keck School of Medicine, University of Southern California, Los Angeles, CA

Dr. Joseph Brain*, Department of Environmental Health, Harvard School of Public Health, Harvard University, Boston, MA

Dr. Wayne Cascio, Brody School of Medicine, East Carolina University, Greenville, NC

Dr. Ellis B. Cowling*, Colleges of Natural Resources and Agriculture and Life Sciences, North Carolina State University, Raleigh, NC

Dr. James Crapo*, Department of Medicine, National Jewish Medical and Research Center, Denver, CO

Dr. Douglas Crawford-Brown, Department of Environmental Sciences and Engineering, University of North Carolina at Chapel Hill, Chapel Hill, NC

Dr. H. Christopher Frey*, Department of Civil, Construction and Environmental Engineering, College of Engineering, North Carolina State University, Raleigh, NC

Dr. David Grantz, Botany and Plant Sciences and Air Pollution Research Center, Riverside Campus and Kearney Agricultural Center, University of California, Parlier, CA

Dr. Joseph Helble, Thayer School of Engineering, Dartmouth College, Hanover, NH

Dr. Rogene Henderson**, Lovelace Respiratory Research Institute, Albuquerque, NM

Dr. Philip Hopke, Department of Chemical Engineering, Clarkson University, Potsdam, NY

Dr. Donna Kenski*, Lake Michigan Air Directors Consortium, Rosemont, IL

Dr. Morton Lippmann, Nelson Institute of Environmental Medicine, New York University School of Medicine, Tuxedo, NY

Dr. Helen Suh MacIntosh, Environmental Health, School of Public Health, Harvard University, Boston, MA

Dr. William Malm, National Park Service Air Resources Division, Cooperative Institute for Research in the Atmosphere, Colorado State University, Fort Collins, CO

Mr. Charles Thomas (Tom) Moore, Jr., Western Regional Air Partnership, Western Governors' Association, Fort Collins, CO

Dr. Robert F. Phalen, Center for Occupation & Environment Health, College of Medicine, Department of Community and Environmental Medicine, Air Pollution Health Effects Laboratory, University of California Irvine, Irvine, CA

Dr. Kent Pinkerton, Center for Health and the Environment, University of California, Davis, CA

Mr. Richard L. Poirot, Air Pollution Control Division, Department of Environmental Conservation, Vermont Agency of Natural Resources, Waterbury, VT

Dr. Armistead (Ted) Russell*, Department of Civil and Environmental Engineering, Georgia Institute of Technology, Atlanta, GA

Dr. Frank Speizer, Channing Laboratory, Harvard Medical School, Boston, MA

Dr. Sverre Vedal, Department of Environmental and Occupational Health Sciences, School of Public Health and Community Medicine, University of Washington, Seattle, WA

*Members of the statutory Clean Air Scientific Advisory Committee (CASAC) appointed by the EPA Administrator.

**As immediate past CASAC Chair, Dr. Henderson is invited to participate in CASAC advisory activities for FY 2009.

SCIENCE ADVISORY BOARD STAFF

Dr. Holly Stallworth, Economist and Designated Federal Officer, Clean Air Scientific Advisory Committee, Environmental Economics Advisory Committee, Washington, D.C.

Acronyms and Abbreviations

α	alpha, ambient exposure factor
α -HCH	alpha-hexachlorocyclohexane
Å	Ångström
A	surface albedo
AAC	abdominal aortic calcium
AAS	atomic absorption spectrophotometry
AB	Alcian Blue stain
ABC	Asian Brown Cloud
ABI	ankle-arm or resting blood pressure index
AC	air conditioning
Ace	acenaphthene
ACE-1	angiotensin converting enzyme-1
ACEAsia	(Asian Pacific Regional) Aerosol Characterization Experiment
ACGIH	American Conference of Governmental Industrial Hygienists
ACh	acetylcholine
Acl	acenaphthylene
ACP	accumulation mode particle
ACS	American Cancer Society
Ad4BP	adrenal-4-binding protein
ADEOS-1	Advanced Earth Observing Satellite-1
A-DEP	automobile diesel exhaust particles
ADM	angular distribution model(s), angular dependence model
ADMA	asymmetric dimethylarginine
AD-Net	Asian Dust Network
Ae	AERONET
AeroCom	Aerosol Comparisons between Observations and Models
AERONET	NASA AERosol RObotic NETwork
AF	atrial fibrillation
AGA	appropriate for gestational age
AGE	advanced glycation end product
AHR	airway hyperresponsiveness, airway hyperreactivity
AhR	arylhydrocarbon receptor

AHSMOG	California Seventh Day Adventist study
AI	aerosol index
AIC	Akaike's information criterion
AIM	ambient ion monitor
AIOP	2003 Aerosol Intensive Operating Period
AIRS	Aerometric Information Retrieval System
Al	aluminum
ALI	air liquid interface
AM	alveolar macrophage(s)
AM, AMF	arbuscular mycorrhizal
AMAP	Arctic Monitoring and Assessment Programme
AMDP	annual maximum of daily precipitation
AMI	acute myocardial infarction
AMS	aerosol mass spectrometry
Ang II	angiotensin II
ANOVA	analysis of variance
ANP	atrial natriuretic peptide
ANS	autonomic nervous system
Ant	anthracene
AOD	aerosol optical depth
AP-1	activator protein 1
APC	antigen presenting cell(s)
APCS	Absolute Principal Components Scores
APEX	Air Pollutants Exposure Model
APHEA	Air pollution and Health: a European Approach
APO	apocynin
ApoE	apolipoprotein E
APS	aerodynamic particle sizer, aerosol polarimetry sensor
aPTT	activated partial thromboplastin time
AQCD	Air Quality Criteria Document
AQI	Air Quality Index
AQM	air quality model
AQS	U.S. EPA Air Quality System database
Aqua	NASA satellite
AR4	Fourth Assessment Report (AR4) from the IPCC

ARCTAS	Arctic Research of the Composition of the Troposphere from Aircraft and Satellites
ARD	Air Resources Division
ARDS	adult respiratory distress syndrome
ARI	acute respiratory infection
ARIC	Atherosclerosis Risk in Communities study
ARIES	Aerosol Research and Inhalation Epidemiology Study
ARM	Atmospheric Radiation Measurement program
ARQM	Air Quality Research Branch (Meteorological Service of Canada Toronto)
ARS	Air Resource Specialists
As	arsenic
ASDNN5	mean of the standard deviation in all 5-min segments of a EKG 24 h recording
ASOS	Automated Surface Observing System
ATOFMS	aerosol time-of-flight mass spectrometry
ATP	adenosine triphosphate
A-Train	a group of 5 afternoon overpass satellites (Aura, PARASOL, CALIPSO, CloudSat, Aqua)
ATS	American Thoracic Society
AURA	NASA satellite
avg	average
AVHRR	Advanced Very High Resolution Radiometer
β	beta, beta coefficient, slope
β -HCH	beta-hexachlorocyclohexane(s)
3 β HSD	3 β -hydroxysteroid dehydrogenase
β TGF	β transforming growth factor
b_{ag}	absorption by gases coefficient
b_{ap}	absorption by particles coefficient
b_{ext}	light extinction coefficient
b_{sg}	scattering by gases coefficient
b_{sp}	sum of light scattering by (aerosol) particles coefficient
Ba	barium
BaA	benz[a]anthracene
BAD	bronchial artery diameter
BAL	bronchoalveolar lavage
BALB/c	albino inbred mouse strain

BALF	bronchoalveolar lavage fluid
BALT	bronchus-associated lymphoid tissues
BAM	beta attenuation monitor
BaP	benzo[a]pyrene
BASIC	Brain Attack Surveillance in Corpus Christi
BASE-A	Burning Airborne and Spaceborne Experiment - Amazon and Brazil
BbF	benzo[b]fluoranthene
BC	black carbon
BCC-CMI	Beijing Climate Center – Carbon Mitigation Initiative
BCCR	Bjerknes Centre for Climate Research
BeP	benz[e]pyrene
BghiP, BpPe	benzo[g,h,i]perylene
BGT	beta-gauge technique
BH ₄	tetrahydrobiopterin
bhp	brake horsepower
BkF	benzo[k]fluoranthene
BMI	body mass index
BMP	bone morphogenetic protein
BN/BR	Brown Norway rat strain
BNP	brain natriuretic peptide, B-type natriuretic peptide
BOSS	BYU Organic Sampling System
BP	blood pressure
BPM	blowing PM _{2.5}
BpPe	benzo[ghi]perylene
BPQ	benz(ayrene (BaP)-quinone
Br	bromine
BRAVO	Big Bend Regional Aerosol and Visibility Observational (Study)
BrdU	bromodeoxyuridine
BS	black smoke
BUC	bucillamine (N-[2-mercapto-2-methylpropionyl]-L-cysteine)
BVAIT	B-Vitamin Atherosclerosis Intervention Trial
BYU	Brigham Young University
C	carbon
C ⁴	Center of Clouds, Chemistry and Climate
¹² C	carbon-12

^{13}C	carbon-13
^{14}C	carbon-14
$\text{C}_{60}(\text{OH})_{24}$	water-soluble fullerene
Ca	calcium
CAA	Clean Air Act
CAAA	1977 Clean Air Act Amendments
CAAM	continuous ambient mass monitor
CAC	coronary artery calcification
CaCO_3	calcium carbonate
CAD	coronary artery disease
CALINE	California Line Source Dispersion Model
CALIOP	Cloud and Aerosol Lidar with Orthogonal Polarization
CALIPSO	Cloud-Aerosol Lidar and Infrared Pathfinder Satellite Observations
CAM	Community Atmosphere Model
CAMM	continuous ambient mass monitor
CAMP	Childhood Asthma Management Program
CAMx	comprehensive air quality model with extensions
$\text{Ca}(\text{NO}_3)_2$	calcium nitrate
CAP	concentrated ambient particle
CAPMoN	Canadian Air and Precipitation Monitoring Network
CASAC	Clean Air Scientific Advisory Committee
CaSO_4	calcium sulfate
CASTNet	Clean Air Status and Trends Network
CATS	cumulative air toxics surface
CB	carbon black, chronic bronchitis
CB-Fe	carbon black particles artificially coated with Fe(II) salt.
CB(P)	carbon black (particles)
CBSA	Core-Based Statistical Area
CB-V	carbon black particles artificially coated with a targeted concentration of Vanadium (IV) salt
CBVD	cerebrovascular disease
CC16	Clara cell protein, Clara cell 16 protein
CCCma	Canadian Centre for Climate Modeling and Analysis
CCM3	Community Climate Model
CCN	cloud condensation nuclei
CCPM	continuous coarse particle monitor

CCSM3	Community climate system model, version 3
CCSP	Climate Change Science Program
Cd	cadmium
CDC	Centers for Disease Control and Prevention
CDE	conjugated diene
CDNC	cloud droplet number concentration
CDPHE	Colorado Department of Public Health and Environment
Ce	cerium
CEN	European Committee for Standardization
CenRAP	Central Regional Air Planning Association
CERES	Clouds and the Earth's Radiant Energy System
CERFACS	European Centre for Research and Advanced Training in Scientific Computation
CF	coronary flow, cystic fibrosis
CFA	coal fly ash
CFD	cystic fibrosis disease
CFR	Code of Federal Regulations
CGCM3.1	Coupled global climate model
cGMP	cyclic guanosine monophosphate
CH ₂ Cl ₂	methylene chloride
CH ₂ O	formaldehyde
CH ₄	methane
CHAD	Consolidated Human Activity Database
CHD	chronic heart disease
CHF	congestive heart failure
CHL	crown heel length
CHO	Chinese hamster ovary cells
Chr	chrysene
CHS	Children's Health Study
CI	confidence interval
CIF	carbon-impregnated charcoal filter
CIIT	Chemical Industry Institute of Toxicology
CIMT	carotid intimal-medial thickness
Cl	chlorine
CL	chemiluminescence
CLAMS	Chesapeake Lighthouse and Aircraft Measurements for Satellites

CM	conditioned medium, cell culture medium
CMAQ	Community Multi-scale Air Quality modeling system
CMAR	CSIRO Marine and Atmospheric Research
CMB	chemical mass balance
CMD	count median diameter
CNES	Centre National d'Etudes Spatiales
CNP	carbon nano particle
CNRM	Centre National de Recherches Meteorologiques
CNRM	Center National Weather Research
CNS	central nervous system
Co	cobalt
CO	carbon monoxide
CO ₂	carbon dioxide
COD	coefficient of divergence
COH, CoH	coefficient of haze
CONUS	continental United States
COO ⁻	carboxyl group
COPD	chronic obstructive pulmonary disease
CoPP	cobalt protoporphyrin
COX-2	cyclooxygenase 2 enzyme
CPC	condensation particle counter
CPZ	capsazepine
Cr	chromium
C-R	concentration-response (relationship)
CRP	C-reactive protein
Cs	cesium
¹³⁷ Cs	cesium-137
CS	cigarette smoke
CSA	Combined Statistical Area
CSC	cigarette smoke condensates
CSE	cigarette smoke extract
cSHMT	cytosolic serine hydroxymethyltransferase
CSIRO	Commonwealth Scientific and Industrial Research Organization
CSN	Chemical Speciation Network
CTM	chemistry-transport model, chemical transport model

Cu	copper
CuSO ₄	copper sulfate
Cu/Zn SOD	Cu/Zn superoxide dismutase
CUP	Current Use Pesticide
CV	cardiovascular, coefficient of variation
CVD	cardiovascular disease(s)
CVM	contingent valuation method
CYP	cytochrome P450
CYP 1A1	cytochrome P450 1A1
Δ	delta, change, difference
ΔFEV ₁	change in forced expiratory volume in one second
d ₅₀	50 percent cut point or 50 percent diameter
d _{ae}	aerodynamic diameter of a particle
D	diameter
D _a	Dalton
DAAC	Distributed Active Archive Center
DAASS	Dry Ambient Aerosol Size Spectrometer
DABEX	Dust and Biomass-burning Experiment (in West Africa)
DAR	denuded aortic ring
DAX-1	x-chromosome gene-1
DBA	dibenzo(a,h)thracene
DBP	diastolic blood pressure
DC	dendritic cell
DC	diesel exhaust particles + cigarette smoke condensates
DC8	Douglas aircraft
DCF	direct climate forcing, 2',7'-dichlorofluorescein
DDT	dichlorodiphenyltrichloroethane
DE	diesel exhaust
DEE	diesel exhaust extract
DEP	diesel exhaust particle
DEPAL	diesel exhaust particles aliphatic (extract)
DEPAR	diesel exhaust particles aromatic (extract)
DEPE	diesel exhaust particles extract
DEPM	diesel exhaust particles methanol (extract)
DEPME	diesel exhaust particles methylene chloride extract

DEPPO	diesel exhaust particles polar (extract)
Dex	dexamethasone
<i>d</i> Fld	change fold, unit change in property
DFO	desferrioxamine (Desferral) an iron chelator
DFX	deferasirox (Exjade) an oral iron chelator
DHR	dihydrorhodamine 123
DLCO	carbon monoxide diffusing capacity
DMEM	Dulbecco's modified Eagle's medium (culture medium)
DMSO	dimethyl sulfoxide
DMT1	divalent metal transporter-1 protein
DMTU	dimethylthiourea
DNA	deoxyribonucleic acid
DOE	U.S. Department of Energy
dpc	days post conception
DPC	dodecylphosphocholine
DPCC	1,2-dipalmitoyl-SN-glycero-3-phosphocholine
DPI	diphenyleneiodonium
DPM	diesel particulate matter
DPPC	dipalmitoylphosphatidylcholine
DRE	direct radiative effects
DRF	direct radiative forcing
DRUM	Davis Rotating Uniform size-cut Monitor
DS	diffusion screens
DSP	daily sperm production
DTMA	Dynamic mechanical thermal analysis
DTPA	diethylene triamine pentaacetic acid
DU	dust
<i>dv</i>	deciview(s)
DVT	deep vein thrombosis
EAD	electrical aerosol detector
EANET	Acid Deposition Monitoring Network in East Asia
EARLINET	European Aerosol Research Lidar Network
EarthCARE	Earth Clouds, Aerosols and Radiation Explorer
EAST-AIRE	East Asian Study for Tropospheric Aerosols
EBCT	electron beam computed tomography

EC	elemental carbon
ECE-1	endothelin converting enzyme-1
ECG, EKG	electrocardiogram
ECHAM5	European Centre Hamburg with Hamburg Aerosol Module
ECHO-G	(ECHAM4 + HOPE-G):
ECRHS	European Community Respiratory Health Survey
EC/TC	ratio of elemental carbon to total carbon
ED	emergency room, emergency department
EDGAR	Emissions Database for Global Atmospheric Research
EDTA	ethylenediaminetetraacetic acid
ED-XRF	energy dispersive X-ray fluorescence
EGM	electrogram
EGU	electricity-generating unit
EHC-93	Ottawa dust; urban air particulate matter PM ₁₀ , collected in 1993 in Ottawa, Canada
EKG, ECG	electrocardiogram
ELISA	enzyme-linked immunosorbent assay
EMECAS	Spanish Multi-centric Study on the Relation between Air Pollution and Health
EMEP	European Monitoring and Evaluation Programme
eNO	exhaled nitric oxide
eNOS	endothelial nitric oxide synthase
EOS	Earth Observing System
EPA	U.S. Environmental Protection Agency
ER	estrogen receptor
ERBS	Earth Radiation Budget Satellite
ERK1/2	ERK-1 (MAPK p42) and ERK-2 (MAPK p44)
ESRL	Earth System Research Laboratory
ESTR	expanded simple tandem repeat
E _T	forcing efficiency
ET	extrathoracic region
ET	endothelin
ET _A	endothelin A receptor subtype
ET _B	endothelin B receptor subtype
ETS	environmental tobacco smoke
EU	endotoxin units

F	breathing frequency
f	the ratio of ambient aerosol mass (wet) to dry aerosol mass M .
$f_{\text{sp}}(\text{RH})$	total light scattering coefficient at given relative humidity(RH) values
f_{af}	anthropogenic fraction of fine-mode fraction
f_{f}	fine mode fraction
$f(\text{RH})$	the unitless water growth term that depends on relative humidity
F	fine particles
F344	Fisher 344 strain of rats
F_{a}	adjusted forcings
FA	filtered air
FAC	ferric ammonium citrate
FBI	Federal Bureau of Investigation
FBS	fetal bovine serum
FCS	fetal calf serum
FDMS	Filter Dynamics Measurement System
FDMS-TEOM	Filter Dynamics Measurement System - Tapered Element Oscillating Microbalance
F_e	effective (F_e) forcings
F_{e}	iron
$\text{Fe}_2(\text{SO}_4)_3$	ferric sulfate
FeCl_3	ferric chloride
FEF	forced expiratory flow
FEF_{25-75}	mean forced expiratory flow over the middle half of the forced vital capacity
$\text{FEF}_{50\%}$	mid-expiratory flow
FEM	Federal Equivalent Method
FeNO	fractional exhaled nitric oxide
FERA	Fire and Environmental Research Applications (Team)
FEV_1	forced expiratory volume in one second
FGA	one fibrinogen alpha chain
FGB	one fibrinogen beta chain
FGOALS-g1.0	Flexible Global Ocean-Atmosphere-Land System Model
F_i	instantaneous forcing
FID	flame ionization detection
FIMS	fast integrated mobility scanners
F_{inf}	infiltration factors

FKHR	Proapoptotic Factor FOXO1
Fle	fluorine
Flu	fluoranthene
FMD	flow-mediated dilation
FPG	formamidopyrimidine-DNA glycosylase
f-PM, FPM	fine particulate matter
FR	Federal Register
FRM	Federal Reference Method
FROSTFIRE	The landscape-scale prescribed research burn in the boreal forest of interior Alaska, July 1999; conducted by FERA.
Fs	SST forcing(s), forcing driven by sea surface temperature (SST)
Fsfc	mean net solar flux at the (Earth) surface
FT	free troposphere
FTIR	Fourier transform infrared spectrometry
F/ULP	mix of fine and ultrafine particles, all < 2.5 μm
FVC	forced vital capacity
γ GCS	gamma glutamylcysteine sythetase
Ga	gallium
GAM	generalized additive model
GATOR	Gas, Aerosol, Transport, and Radiation model
GATORG	Gas, Aerosol, Transport, Radiation, and General circulation model
GAW	Global Atmospheric Watch network
GBS	group B streptococcus
GC	gas chromatography
GCM(s)	general circulation model(s), global climate model
GCMOM	General Circulation, Mesoscale and Ocean Model
GC/MS	gas chromatography/mass spectrometry
GCS	gamma glutamylcysteine sythetase
GD	gestational day
GDF	growth differentiation factor (e.g., GDF-9)
GEE	generalized estimating equations, gasoline engine exhaust
GEIA	Global Emissions Inventory Activity
GEM	gaseous elemental mercury
GEOS-Chem	Goddard Earth Observing System-CHEMistry
GFAAS	graphite furnace atomic absorption spectrometry
GFAP	glial fibrillary acidic protein

GFDL	Geophysical Fluid Dynamics Laboratory
GFDL-CM2.x	GFDL Climate Models
GFED	Global Fire Emission Database
GGT	gamma-glutamyltranspeptidase
GHG	greenhouse gas
GIS	Geographic Information System
GISS	Goddard Institute for Space Studies
GISS-AOM	GISS Atmosphere-Ocean Model climate prediction model
GISS-EH	GISS AOM for sea ice model
GISS-ER	GISS AOM for liquid sea model
GLAS	Geoscience Laser Altimeter System
GLM	generalized linear models
GM	geometric mean
GM-CSF	granulocyte macrophage colony-stimulating factor
GMD	Global Monitoring Division
GMS	Greater Mekong Subregion
GOCART	Goddard Chemistry Aerosol Radiation and Transport
GOES	Geostationary Operational Environmental Satellite
GoMACCS	Gulf of Mexico Atmospheric Composition and Climate Study
GPS	Global Positioning System
GSD	geometric standard deviation
GSFC	NASA Goddard Space Flight Center
GSH	glutathione
GSH:GSSG	ratio of reduced glutathione to glutathione disulfide (oxidized glutathione)
GSO, GSNO	S-Nitrosoglutathione
GSSG	glutathione disulfide; oxidized glutathione
GST	glutathione-S-transferase
GSTM1	glutathione S-transferase polymorphism M1
GSTP1	glutathione-S-transferase polymorphism P1
GSTT1	glutathione-S-transferase polymorphism T1
GWP	global warming potential
h	hour
H	atomic hydrogen, hydrogen radical, height, heart rate, high dose, high exposure
H ⁺	hydrogen ion

HR	heart rate
H ₂	molecular hydrogen
H ₂ CO	formaldehyde
H ₂ O	water
H ₂ O ₂	hydrogen peroxide
H ₂ S	hydrogen sulfide
H ₂ SO ₄	sulfuric acid
H9c2	rat embryonic cardiomyocytes cell line
HA	hospital admission
HAEC	Human Aortic Endothelial Cell
HAPC	Harvard ambient particle concentrator
HBE, HBEC	Human Bronchial Epithelial cells
HC	hydrocarbon(s); head circumference
HCB	hexachlorobenzene
HCH	hexachlorocyclohexane(s) (e.g. α -HCH, β -HCH)
HDL	high density lipoprotein
HEAPSS	Health Effects of Air Pollution among Susceptible Subpopulations study
HEI	Health Effects Institute
HEPA	high efficiency particle air (filter)
HERO	Health and Environmental Research Online, NCEA Database System
HF	heart failure, high frequency (HRV parameter), high (dose/exposure) filtered
HFCD	High-Fat Chow Diet
HFE	HFE gene, HFE protein
Hg	mercury
Hg(0)	gaseous elemental mercury
Hg(II)	gaseous divalent (oxidized) mercury
HH	hereditary hemochromatosis
HNRS	Hans Nixdorf Recall Study
HO-1	heme oxygenase-1
hOGG1	8-hydroxyguanine DNA-glycosylase
HOPE-G	Hamburg Atmosphere-Ocean Coupled Circulation Model
hPA	hectopascal
hPAEC	human pulmonary artery endothelial cells
hPBMC	human peripheral blood mononuclear cells

HPLC	high pressure liquid chromatography
HPMF	high particulate matter filtered
hPMVEC	human pulmonary microvascular endothelial cells
HR	heart rate, hazard ratio, high level DE
HRV	heart rate variability
HSD	17 β -hydroxysteroid dehydrogenase
HSP-70	heat shock protein
HSPH	Harvard School of Public Health
HSRL	High Spectral Resolution Lidar
HUVEC	human umbilical vein endothelial cells
h ν	photon
HWS	hardwood smoke
Hz	hertz
IC	ion chromatography
ICAM-1	intercellular adhesion molecule-1
ICARTT	International Consortium for Atmospheric Research on Transport and Transformation
ICAS	Inner-City Asthma Study
ICD	implantable/implanted cardioverter defibrillator
ICD-9	International Classification of Disease 9th revision
ICD-10	International Classification of Disease 10th revision
ICESat	Ice, Cloud and land Elevation Satellite
ICP-AES	inductively coupled plasma-atomic emission spectroscopy
ICP-MS	inductively-coupled plasma-mass spectrometry
ICR	imprinting control region, mouse strain
ICRP	International Commission on Radiological Protection
IDP	indeno[1,2,3-c,d]pyrene
IFN- γ	interferon-gamma
IFS	Integrated Forest Study
Ig	immunoglobulin (e.g., IgE)
IGS	International Genetic Standard
IHD	ischemic heart disease
IIASA	International Institute for Applied Systems Analysis
IL	interleukin
iMDDC	immature monocyte-derived dendritic cells

IMPACT	Interactive Modeling Project for Atmospheric Chemistry and Transport
IMPROVE	Interagency Monitoring of Protected Visual Environment
IN	ice nuclei
INAA	instrumental neutron activation analysis
INCA	Interactions between Chemistry and Aerosol
INDOEX	Indian Ocean Experiment
INGV-SXG	Istituto Nazionale di Geofisica e Vulcanologia coupled to SINTEX-G
INM-CM3.0	Institute of Numerical Mathematics climate model
iNOS	inducible nitric oxide synthase
INTEX	Intercontinental Chemical Transport Experiment
I/O	indoor-outdoor ratio
IOM	Institute of Medicine
i.p.	intraperitoneal
IP	inhalable particle
IPCC	Intergovernmental Panel on Climate Change
IPSL-CM4	Institut Pierre Simon Laplace climate model
IQR	interquartile range
Ir	iridium
IR	incidence rate, infrared radiation
IRE	iron responsive element
IRMS	isotope ratio mass spectrometer
ISA	Integrated Science Assessment
ISO	International Standards Organization
ISO	isoprene, 2-methyl analog of 1,3-butadiene
IT	intratracheal, intratracheally
IUGG	International Union of Geodesy and Geophysics
IUGR	intrauterine growth restriction, intrauterine growth retardation
i.v.	intravenous
JNK	c-jun N-terminal kinase
κB	kappa B
K	potassium
KC	local neutrophil chemoattractant protein
kHz	kilohertz
kJ	kilojoules
KLH	keyhole limpet hemocyanin

km	kilometer
km ⁻¹	inverse kilometer
K _{ow}	octanol-water partition coefficient
L, dL, mL, μL	Liter, deciLiter, milliLiter, microLiter
L	low
La	lanthanum
LAC	light-absorbing carbon
LACE98	Lindenberg Aerosol Characterization Experiment 1998
LBA-SMOCC	Large-Scale Atmosphere-Biosphere Experiment in Amazon
LBW	low birth weight
LC	lethal concentration
LC ₅₀	median lethal concentration
LDH	lactate dehydrogenase
LDL	low-density lipoprotein
LDLR	low-density lipoprotein receptor
LDVP	left developing ventricular pressure
LES	large eddy simulations model
LF	low frequency an HRV parameter
LF/HF	ratio of LF to HF an HRV parameter
LIBS	laser induced breakdown spectroscopy
LIF	leukemia inhibitory factor
LITE	Lidar In-space Technology Experiment
LMD	Laboratoire de Meteorologie Dynamique
LMDz	LMD with Zoom
LMDZ-INCA	LMDZ INTERactive Chemistry and Aerosols model
LMDZ-LOA	LMDZ with Laboratoire d'Optique Atmosphérique model
L-NAME	arginine analog; N(G)-nitro-L- arginine methyl ester
L-NMMA	N(G)-mono-methyl-L-arginine
LnRMSSD	natural log of RMSSD; measure of HRV
lnSDNN	natural log of the standard deviation of NN intervals in an EKG
LOA	Laboratoire d'Optique Atmosphérique
LOESS	locally weighted scatterplot smoothing
LOSU	level of scientific understanding
Lpm	liters per minute (L/min)
LPMF	low particulate matter filtered

LPO	plasma lipid peroxides
LPS	lipopolysaccharide
LRAT	long range atmospheric transport
LROT	long range oceanic transport
LSCE	Laboratoire des Sciences du Climat et de l'Environnement
LSDF	low-sulfur diesel fuel
LTB ₄	leukotriene B ₄
LTE ₄	leukotriene E ₄
LUA NRW	The North Rhine-Westphalia State Environment Agency
LUDEP	LUn g Dose Evaluation Program
LUR	land use regression
LV	left ventricle
LVEDP	left-ventricular end-diastolic pressure,
LVSP	left-ventricular systolic pressure, left ventricular developed pressure
L/W	ratio of lumen to wall
LWC	liquid water content
LWDE	Low Whole Diesel Exhaust
LWP	liquid water path
μg	microgram
μg/m ³	micrograms per cubic meter
μm	micrometer, micron
m, cm, μm, nm	meter(s), centimeter(s), micrometer(s), nanometer(s)
M, mM, μM, nM, pM	Molar, milliMolar, microMolar, nanoMolar, picoMolar
M	dry aerosol mass, medium dose/exposure
ma	moving average
MAM	March-April-May
MAN	Maritime Aerosol Network
MANE-VU	Mid-Atlantic/Northeast Visibility Union
MAP	mitogen-activated protein, mean arterial pressure
MAPK	mitogen-activated protein kinase(s), MAP kinase
MARAMA	Mid Atlantic Regional Air Management Association
MATCH	Model of Atmospheric Transport and Chemistry
max	maximum
MBP	major basic protein
MCAPS	Medicare Air Pollution Study

Mch	methacholine
MCN	mixed carbon nanoparticle
MCP-1	monocyte chemoattractant protein 1
MCV	mean corpuscular volume
MD	mineral dust
MDA	malondialdehyde
MDCT	multidetector computed tomography
ME	Multilinear Engine
MEE	mass extinction efficiency
MEF	maximal expiratory flow
MEF ₅₀	maximum expiratory flow rate at 50% of vital capacity
MeHg	methyl mercury
MENTOR	Modeling Environment for Total Risk Studies
MEP	motorcycle exhaust particulate(s)
MEPE	motorcycle exhaust particulate extract (particle-free)
MESA	Multi-Ethnic Study of Atherosclerosis
MFFSR	multifilter rotating shadowband radiometer
mg/m ³	milligrams per cubic meter
Mg	magnesium
MI	myocardial infarction
MIROC3.x	Model for Interdisciplinary Research on Climate
MILAGRO	Megacity Initiative: Local and Global Research Observations, study of air pollution in Mexico City
min	minute(s), minimum
MINOS	MPI Mediterranean INTensive Oxidant Study
MIP-2	macrophage inflammatory protein-2
MIRAGE	Megacities Impact on Regional and Global Environment program
MIS	mullerian inhibiting substance
MISR	Multi-angle Imaging SpectroRadiometer
Mm	megameter
Mm ⁻¹	inverse megameter
MM	monocyte-derived macrophages
MM5	mesoscale model
MMAD	mass median aerodynamic diameter
MMD	mass median diameter
MMEF	maximal mid-expiratory flow

mmHg	millimeters of mercury
MMP	mitochondria membrane potential
MMP(2,9)	matrix metalloproteinase (2, or 9)
MMT	million metric tons
Mn	manganese
MN	micronuclei
MnSO ₄	manganese sulfate
MnSOD	manganese superoxide dismutase
MnTBAP	manganese tetrakis (4-benzoic acid) porphyrin
mo	month
MOA	mode(s) of action
MODIS	MODerate resolution Imaging Spectroradiometer
MOUDI	Micro-Orifice Uniform Deposit Impactor
MOZART	MOdel for Ozone and Related chemical Tracers
MP	mid polar, myelopeptide
MPC	mean platelet component
MPF	median power frequency
MPG	N-(2-mercaptopropionyl) glycine
MPI	Max Planck Institute for Meteorology
MPLNET	Micro-Pulse Lidar Network
MPO	myeloperoxidase
MPPD	Multiple-Path Particle Dosimetry model
MPV	mean platelet volume
MRI	Meteorological Research Institute
MRI-CGCM	MRI coupled general circulation model
mRNA	messenger RNA
MRPO	Midwest Regional Planning Organization
ms	millisecond
MSA	metropolitan statistical area
MSH	melanocyte stimulating hormone
MSHA	Mount St. Helen ash
MSU	monosodium urate crystals
MT	metric ton
MTHFR	methylenetetrahydrofolate reductase
MTT	methyl thiazol tetrazolium

MV	motor vehicle
MWNT	multiplewall nanotube
<i>M/Z</i>	mass-to-charge ratio
N	nitrogen
N ₂ O	nitrous oxide
Na	sodium
Na ₂ SO ₄	sodium sulfate
NAAQS	National Ambient Air Quality Standards
NAC	N-acetylcysteine, a thiol antioxidant
NaCl	sodium chloride
NADPH	reduced form of nicotinamide adenine dinucleotide phosphate
NAG	N-acetyl-β-D-glucosaminidase
Na,K-ATPase	sodium-potassium adenosine triphosphatase
NAMS	National Ambient Monitoring Stations
NaN ₃	sodium azide
NaNO ₃	sodium nitrate
nano-BAM	low pressure-drop ultrafine particle impactor coupled with a Beta Attenuation Monitor
NAPAP	National Acid Precipitation Assessment Program
NAPCA	National Air Pollution Control Administration
NAS	National Academy of Sciences
NASA	U.S. National Aeronautics and Space Administration
NASDA	National Space Development Agency, Japan
NATA	U.S. EPA's National Air Toxics Assessment
2-NB	2-nitrobenzanthrone
NC	total (particle) number concentration
NCAR	National Center for Atmospheric Research
NCC-MPSP	negatively charged carboxylate-modified polystyrene particle(s)
NCD	Normal Chow Diet
NCEA	National Center for Environmental Assessment
NCHS	National Center for Health Statistics
NCICAS	National Cooperative Inner-City Asthma Study
NCORE	National Core
Nd	drop number concentration
Nd:YAG	neodymium-doped yttrium aluminum garnet laser
NDDN	National Dry Deposition Network

NEAQS	NOAA New England Air Quality Study
NEI	National Emissions Inventory
NESCAUM	Northeast States for Coordinated Air Use Management
NET	National Emissions Trends database
NFκB	nuclear factor kappa-B
NG	neutrophil granulocytes
NH	northern hemisphere
NH ₃	ammonia
NH ₄ ⁺	ammonium ion
NH ₄ NO ₃	ammonium nitrate
(NH ₄) ₂ SO ₄	ammonium sulfate
NHANES	National Health and Nutrition Examination Survey
NHBE(C)	normal human bronchial epithelial cells
NHPAE	normal human pulmonary artery endothelial cells
NHS	Nurses' Health Study
Ni	nickel
NIOSH	National Institute for Occupational Safety and Health
NIST	National Institute of Standards and Technology
NMHC	non-methane volatile hydrocarbon
NMMAPS	U.S. National Morbidity, Mortality, and Air Pollution Study
NO	nitric oxide
NO ₂ , NO ₂ [·]	nitrogen dioxide, nitrogen dioxide radical
NO ₃ ⁻	nitrate
NOAA	National Oceanic and Atmospheric Administration
NOAEL	no observed adverse effect level
NOS	nitric oxide synthase
NOS3	nitric oxide synthase 3
NOx	nitrogen oxides, oxides of nitrogen (NO + NO ₂)
NP	National Park
NPM	non-blowing PM _{2.5}
NPOESS	National Polar-orbiting Operational Environment Satellite System
NPS	National Park Service, U.S. Department of the Interior
NR	not reported
NR5A1	nuclear receptor subfamily 5, group A, member 1
NRC	National Research Council

NRPB	National Radiological Protection Board
NSA	North Slope Alaska
NT	neurotrophin, nitrotyrosine
NWS	National Weather Service
NYHA	New York Heart Association
O	oxygen
O ₂	molecular oxygen
O ₃	ozone
OAQPS	Office of Air Quality Planning and Standards
OC	organic carbon
OCM	organic carbon mass
OE	organic extracts
OGG1	8 oxo-guanine repair enzyme
OH, OH•	hydroxyl group, hydroxyl radical
8-OHdG	8-hydroxydeoxyguanosine
OM	organic matter
OMI	Ozone Monitoring Instrument
OMM	organic molecular marker
OR	odds ratio(s)
OSM	oncostatin M, a cytokine
OSPM	Operational Street Pollution Model
OVA	ovalbumin
oxLDL	oxidation of LDL, marker of oxidative stress
8-oxodG	8-oxo-7-hydrodeoxyguanosine
ox-PAPC	oxidized 1-palmitoyl-2-arachidonoyl-sn-glycero-3-phosphorylcholine
P450	cytochrome P450
P450c17	cytochrome P450 17- α -hydroxylase
P450scc	cytochrome P450 cholesterol side chain cleavage enzyme
P90	90th percentile; Printex 90
p	probability value
P	phosphorus
PA	photoacoustic analyzer, physical activity, plasminogen activator, pulmonary arterial, alveolar pressure
PAF	platelet-activating factor
PAH	polycyclic aromatic hydrocarbon(s)
PAI	plasminogen activator inhibitor, (e.g. PAI-1)

PALMS	NOAA Particle Analysis by Laser Mass Spectrometry instrument
PAMCHAR	Chemical and Biological Characterisation of Ambient Air Coarse, Fine, and Ultrafine Particles for Human Health Risk Assessment in Europe
PAMS	Photochemical Assessment Monitoring Stations network
PAR	photosynthetically active radiation
PAR(s)	Pulmonary Artery Rings
PARASOL	Polarization and Directionality of the Earth's Reflectances, coupled with observations from a Lidar, a CNES satellite
PARP	poly(ADP-ribose) polymerase
PAS	Periodic Acid Schiff stain
Pb	lead
²⁰⁷ Pb	lead-207
PBDE	polybrominated diphenyl ether
PBL	planetary boundary layer
PBMC	peripheral blood mononuclear cell
PBMM	peripheral blood monocyte-derived macrophages
PBP	primary biological particle(s)
PBS	phosphate buffered saline
PC	synthetic carboxylate-modified particles
PCA	principal component analysis
PCA-MPSP	positively-charged amine modified polystyrene particle
PCB	polychlorinated biphenyl(s)
PCDD	polychlorinated dibenzo-p-dioxin
PCIS	Personal Cascade Impactor Sampler
PCM	NCAR Parallel Climate Model
PCPSP	positively charged polystyrene particle
PCR	polymerase chain reaction
PDF	probability distribution functions
pDR	personal DataRam
PE	post exposure, post exercise, phenylephrine
PEACE	Pollution Effects on Asthmatic Children in Europe study
PEC	particulate elemental carbon
PECAM-1	platelet endothelial cell adhesion molecule 1
PEF	peak expiratory flow (L/min)
PEFR	peak expiratory flow rate

PEFT	time to peak flow
PEM	personal exposure monitor
PEM-West	NASA Pacific Exploratory Missions in the western Pacific
Penh	enhanced pause
Per	perylene
PESA	particle elastic scattering analysis
PFDE	particle free diesel exhaust
PGE ₂	prostaglandin E ₂
PGI ₂	prostacyclin
Phe	phenanthrene
PI	post instillation, posterior interval, pulmonary inflammation
PICT	pollution-induced community tolerance
PILS	Particle Into Liquid Sampler
PILS-IC	Particle Into Liquid Sampler-Ion Chromatography
PIXE	Particle Induced X-ray Emission
PKA	protein kinase A
PLS	partial least squares, projection to latent structures
PM	particulate matter
PM _x	particulate matter of a specific size range. X refers to the diameter at which the sampler collects 50% of the particles and rejects 50% of the particles. Collection efficiency increases for particles with smaller diameters and decreases for particles with larger diameters. The variation of collection efficiency with size is given by a collection efficiency curve. The definition of PM _x is frequently abbreviated as “particles with a nominal mean aerodynamic diameter less than or equal to x μm.
PM _{x-y}	particulate matter with a nominal mean diameter greater than x μm and less than y μm where x and y are the numeric mean aerodynamic or mobility diameters (μm).
PM _{0.1}	particulate matter with a nominal mean mobility diameter less than or equal to 0.1 μm (referred to as ultrafine PM)
PM _{2.5}	particulate matter with a nominal mean aerodynamic diameter less than or equal to 2.5 μm (referred to as fine PM)
PM ₁₀	particulate matter with a nominal mean aerodynamic diameter less than or equal to 10 μm
PM _{10-2.5}	particulate matter with a nominal mean aerodynamic diameter greater than 2.5 μm and less than or equal to 10 μm (referred to as thoracic coarse particulate matter or the coarse fraction of PM ₁₀) Concentration may be measured with a dichotomous sampler or calculated as the difference between measured PM ₁₀ and measured PM _{2.5} concentrations.
PMA	phorbol 12-myristate 13-acetate
PMF	particulate matter filtrate, positive matrix factorization

PM-HD	particulate matter at high concentration
PM-LD	particulate matter at low concentration
PMN	polymorphonuclear leukocytes
PN	particle number
PNC	particle number concentration, particle number count
PND, pnd	post-natal day
PNMD	particle number median diameter
PNN	proportion of interval differences of successive normal-beat intervals in EKG
pNN50	proportion of interval differences of successive normal-beat intervals greater than 50 ms in an EKG
PNNL	Pacific Northwest National Laboratory
pNO ₃	particulate nitrate
POA	primary organic aerosol
POC	particulate organic carbon
POLDER	POLarization and Directionality of the Earth's Reflectance
POM	particulate organic matter
POP	persistent organic pollutant
P _p	particle density
PP	pulse pressure
ppb	parts per billion
PPFL	percent predicted lung function
ppm	parts per million
ppt	parts per trillion
PRB	policy-relevant background
PRE	AeroCom Experiment
PRELC	Primary Rat Epithelial Lung Cells
PRIDE	Puerto Rico Dust Experiment
PS	public school
PSAS	The French National Program on Air Pollution Health Effects
PSO	Public Service Company of Oklahoma
pSO ₄	particulate sulfate
PSS	physiologic saline solution
PSU	Pennsylvania State University
PT	prothrombin time
PTT	partial thromboplastin time

PTV	programmable temperature vaporization
PVD	peripheral vascular disease
Pyr	pyrene
Q	cardiac output
Q	coronary flow of the heart
QAI	QA interval
QBQ	backup quartz-fiber filter behind a quartz-fiber filter
QEEG	quantitative electroencephalography
Q_{ext}	the extinction coefficient (a function of particle size distribution and refractive index)
r	correlation coefficient
R^2	coefficient of determination
RAIN	Regional Aerosol Intensive Network
RAMS	real-time total ambient mass sampler
RANTES	regulated upon activation, normal T cell expressed and secreted
RAPS/RAMS	Regional Air Pollution Study / Regional Air Monitoring Study
RAR	rapidly activating receptor(s)
RASMC	rat aortic smooth muscle cells
RAW 264.7	mouse macrophage cell line
RBC	red blood cell
RD	respiratory disease
REALM	Regional East Atmospheric Lidar Mesonet
RF	radiative forcing(s)
r_{eff}	particle effective radius
RFL	Fetal Lung Fibroblasts
RH	relative humidity
RHMVE	rat heart micro-vessel endothelial cell
RHR	Regional Haze Rule
RLF	rat lung fibroblasts
RMC	rat cardiomyocyte(s)
RME	rapeseed oil methyl ester
RMSSD	root mean squared differences of successive normal-beat to normal-beat (NN or RR) time intervals between each QRS complex in the EKG
RMV	respiratory minute volume
RNA	ribonucleic acid

RNS	reactive nitrogen species
RO	residual oil
ROCK	rho associated kinase
ROFA	residual oil fly ash (particles)
ROFA-L	residual oil fly ash leachate
ROI	reactive oxygen intermediates
ROS	reactive oxygen species
RPO	Regional Planning Organizations
RR	risk ratio, relative risk, normal-to-normal (NN or RR) time interval between each QRS complex in the EKG
RS	resuspended soil
RSV	respiratory syncytial virus
RTI	respiratory tract infection
RTM	Radiative Transfer Model
RTP	Research Triangle Park, North Carolina
RV	right ventricular
RVCFB	right ventricular cardio fibroblasts
RVCM	right ventricular cardiomyopathy, rat ventricular cardiomyocytes, reduced volume culture medium
σ	sigma, standard deviation
1σ	one sigma; one standard deviation
σ_g	sigma-g; geometric standard deviation
s	second
S	sulfur
SAB	(EPA) Science Advisory Board
SAFARI	South African Fire-Atmosphere Research Initiative
SAGE	Stratospheric Aerosol and Gas Experiment
SALIA	German study on the Influence of Air Pollution on Lung Function, Inflammation, and Aging
SAM	Stratospheric Aerosol Measurement
SAMUM	Saharan Mineral Dust Experiment
SAP2.3	Synthesis and Assessment Product 2.3
Sb	antimony
SB	strand breaks
SBL	stable boundary layer
SBP	systolic blood pressure

Sc	scandium
SC	summer curbside particles
SCAB	California South Coast Air Basin
SCAR	Smoke/Sulfates, Clouds and Radiation
SCARPOL	Swiss Study on Childhood Allergy and Respiratory Symptoms with Respect to Air Pollution
sCD40L	soluble CD40 ligand
SCE	sister chromatid exchange
SCS	Harvard Six Cities Study
SD	standard deviation; Sprague-Dawley rat
SDANN5	standard deviation of the average of normal to normal (N:N) intervals in all 5-min intervals in a 24-h period
SDNN	standard deviation normal-to-normal (NN or RR) time interval between each QRS complex in the EKG
SDNN24HR	standard deviation of the average of all normal to normal intervals in a 24-h period
Se	selenium
se	standard error
SEARCH	Southeastern Aerosol Research and Characterization
sem	standard error of mean
SEM	scanning electron microscopy
SES	socioeconomic status, sample equilibration system
SF-1	steroidogenic factor -1
SF-UFID	suspension, particle free ultrafine industrial exhaust
SGA	small for gestational age
sGC	soluble guanylate cyclase
SGP	Southern Great Plains
-SH	sulfhydryl group
SH	Mount Saint Helen's ash
SH, SHR	spontaneously hypertensive disease model rat
SHADE	Saharan Dust Experiment
SHEDS	Stochastic Human Exposure and Dose Simulation model
Si	silicon
sICAM-1	soluble intercellular adhesion molecule
SIDS	sudden infant death syndrome
SiO ₂	silicone dioxide
SIPS	State Implementation Plan

SJV	San Joaquin Valley
SLAMS	State and Local Air Monitoring Stations
SME	soybean oil methyl ester
SMOCC	Smoke Aerosols, Clouds, Rainfall and Climate
SMOKE	Spare-Matrix Operator Kernel Emissions system
SMPS	scanning mobility particle sizer
SMPS-APS	scanning mobility particle sizer– aerodynamic particle sizer
SMRA	small mesenteric rat arteries
SNP	single-nucleotide polymorphism, sodium nitroprusside
SNS	sympathetic nervous system
SO ₂	sulfur dioxide
SO ₃	sulfur trioxide
SO ₄ ²⁻	sulfate
SOA	secondary organic aerosol
SOC	semi-volatile organic compound
SOD	superoxide dismutase
SOPHIA	Study of Particulates and Health in Atlanta
SO _x	sulfur oxides, oxides of sulfur
SP	surfactant protein (e.g., SPA, SPD)
SPA	surfactant protein A
SPD	surfactant protein D
SPEW	Speciated Pollutant Emission Wizard
SPG	Southern Great Plains site
SPM	suspended particulate matter
SPRINTARS	Spectral Radiation-Transport Model for Aerosol Species
SRM-154b	NIST standard reference material 154b; (TiO ₂ Titanium dioxide)
SRM1648	NIST standard reference material 1648; (urban particulate matter)
SRM-1649	NIST standard reference material 1649 (Washington, D.C. urban air particulate matter, urban dust)
SRM-1650	NIST standard reference material 1650 (diesel exhaust particulate matter)
SRM-1879	NIST standard reference material 1859; (silicon dioxide, respirable cristobalite [respirable crystalline silica])
SRM-2975	NIST standard reference material 2975 (diesel exhaust particulate matter)
s-ROFA	soluble portion of residual oil fly ash
SS	secondary sulfate, sea salt

SSA	single-scattering albedo
SSR	standardized sex ratio
SST	sea surface temperature
STEM	Sulfur / Sulfate Transport Eulerian Model
STN	EPA Speciation Trend Network
STP	standard temperature and pressure
STZ	Streptozotocin
SUB	summer urban background particles
SURFRAD	NOAA GMD Surface Radiation network
SVA	supraventricular arrhythmia
sVCAM-1	soluble vascular adhesion molecule 1
SVEB	supraventricular ectopic beats
SWNT	singlewalled nanotube
SXRF	Synchrotron X-ray fluorescence
SZA	solar zenith angle
τ	photochemical lifetime
T	body temperature
TAR	IPCC 3rd Assessment Report
TARC	thymus and activation-regulated chemokine
TARFOX	Tropospheric Aerosol Radiative Forcing Observational Experiment
TAT	thrombin-anti-thrombin complexes
TB	tracheobronchial
TBA	thiobarbituric acid
TBAP	tetrakis(4-benzoic acid) porphyrin
TBARS	thiobarbituric acid reactive substances
TBQ	backup quartz-fiber filter behind a Teflon-membrane filter
^{99m}Tc	Technetium-99m
^{99m}Tc -DMTA	^{99m}Tc Dynamic mechanical thermal analysis
^{99m}Tc -DTPA	^{99m}Tc -diethylenetriaminepentaacetic acid
T_{co}	core temperature
TD	thermal desorption, tire debris extracted in methanol
TD-GC/MS	thermal desorption-gas chromatography/mass spectrometry
TEAC	Trolox Equivalent Antioxidant Capacity assay
TEOM	Tapered Element Oscillating Microbalance
TexAQS	Texas Air Quality Field Study

TF	tissue factor
TFPI	tissue factor pathway inhibitor
Tg	teragram
TG	terminal ganglion (neurons)
TGF	transforming growth factor
TGF β	β transforming growth factor
Th	thorium
Th1	T helper cell type 1
Th2	T helper cell type 2
tHcy	total homocysteine
Ti	titanium
TIA	transient ischemic attack
TiFe	iron-loaded fine titanium oxide
TIMP-2	tissue inhibitor of MMP
TiO ₂	titanium dioxide
TK	thymidine kinase
TM	transition metals
TM5	Thematic Mapper, a sensor on Landsat5 satellite
TMTU	tetramethylthiourea
TNF- α	tumor necrosis factor alpha
TOA	top of the atmosphere
TOF-SIMS	time-of-flight - secondary ion mass spectrometry
TOMS	Total Ozone Mapping Spectrometer
TOT/GC	thermal optical transmission analyzer coupled with gas chromatography
TOVS	TIROS-N Operational Vertical Sounder
tPA, t-PA	tissue plasminogen activator
TRACE	Transition Region and Coronal Explorer
TRP	transient receptor potential
TRPV1	transient receptor potential vanilloid-1 receptor
TR-XRF	total reflection X-ray fluorescence
TSA	trichostatin A
TSP	total suspended particulate
TSS	WRAP Technical Support System website
TVOC	total VOC
TWP	Tropical West Pacific island

TXB ₂	thromboxane B-2
U	uranium
UACR	urinary albumin / creatinine ratio
UAE ²	United Arab Emirates Unified Aerosol Experiment
UAP	urban ambient particle
UF	ultrafine, uncertainty factor
UFAA	ultrafine ambient air
UFC	ultrafine carbon
UfCB	ultrafine carbon black
UFDG	ultrafine diesel engine exhaust
UFID	ultrafine industrial exhaust
UFP	ultrafine particle
UFPM	ultrafine particulate matter
UFTiO ₂	ultrafine titanium dioxide
UIO	University of Oslo
U.K.	United Kingdom
UKMO	United Kingdom Meteorological Office
ULAQ	University of IL'Aquila.
ULTRA	Exposure and Risk Assessment for Fine and Ultrafine Particles in Ambient Air
UMI	University of Michigan
UNEP	United Nations Environmental Programme
UP	urban particle
UPM	ultrafine particulate matter
UPSP	unmodified polystyrene particle(s)
URI	upper respiratory infection
URS	upper respiratory symptoms
U.S.	United States of America
U.S.C.	U.S. Code
UV	ultraviolet radiation
V	vanadium
V, mV, μV	volt, millivolt, microvolt
VAQ	visual air quality
VCAM-1	vascular adhesion molecule 1
V _d	deposition velocity
VEAPS	Vitamin E Atherosclerosis Progression Study

VEGF	vascular endothelial growth factor
VEWS	Visibility Information Exchange Web Site
VISTAS	Visibility Improvement State and Tribal Association of the Southeast
VOC	volatile organic compound
VOSO ₄	vanadyl sulfate
VPB	ventricular premature beat
VR	visual range
VR1	vanilloid receptor 1
VSCC	very sharp cut cyclone
VSMC	Vascular Smooth Muscle Cells
V _T	tidal volume
vWF	von Willebrand factor
W	Wilderness
WACAP	Western Airborne Contaminates Assessment Project
WBC	white blood cell(s)
WC	winter curbside particles
WHI	Women's Health Initiative
WHI OS	Women's Health Initiative Observational Study
wk	week(s)
WKY	Wistar-Kyoto rat strain
W/m ² , W m ⁻²	watts per square meter
WMO	World Meteorological Organization
Wnt	wingless gene family
WRAP	Western Regional Air Partnership
WRF	Weather Research and Forecasting model
WS	wood smoke
WSOC	water soluble organic carbon
WUB	winter urban background particles
XAD	polystyrene-divinyl benzene
XPS	X-ray photoelectron spectroscopy
Y	yttrium
yr	year
Z	radar reflectivity (measured in dBZ [decibels of Z, where Z represents the energy reflected back to the radar.])
Zn	zinc
ZnO	zinc oxide

ZnS	zinc sulfide
ZnSO ₄	zinc sulfate
Zr	zirconium

Chapter 1. Introduction

This Integrated Science Assessment (ISA) is a review, synthesis, and evaluation of the most policy-relevant evidence, and communicates critical science judgments relevant to the National Ambient Air Quality Standards (NAAQS) review. As such, the ISA forms the scientific foundation for the review of the primary (health-based) and secondary (welfare-based) NAAQS for particulate matter (PM). The ISA accurately reflects “the latest scientific knowledge useful in indicating the kind and extent of identifiable effects on public health which may be expected from the presence of [a] pollutant in ambient air” (42 U.S.C. 7408). Key information and judgments formerly contained in an Air Quality Criteria Document (AQCD) for PM are incorporated in this assessment. Additional details of the pertinent literature published since the last review, as well as selected older studies of particular interest, are included in a series of annexes. This ISA thus serves to update and revise the evaluation of the scientific evidence available at the time of the previous review of the NAAQS for PM that was concluded in 2006.

The *Integrated Review Plan for the National Ambient Air Quality Standards for Particulate Matter* identifies a series of policy-relevant questions that provide a framework for this assessment of the scientific evidence (U.S. EPA, 2008, [157072](#)). These questions frame the entire review of the NAAQS for PM, and thus are informed by both science and policy considerations. The ISA organizes and presents the scientific evidence such that, when considered along with findings from risk analyses and policy considerations, will help the EPA address these questions during the NAAQS review for PM. In evaluating the health evidence, the focus of this assessment will be on scientific evidence that is most relevant to the following questions that have been taken directly from the Integrated Review Plan:

- Has new information altered the body of scientific support for the occurrence of health effects following short- and/or long-term exposure to levels of fine and thoracic coarse particles found in the ambient air?
- Has new information altered conclusions from previous reviews regarding the plausibility of adverse health effects associated with exposures to PM_{2.5}, PM₁₀, PM_{10-2.5}, or alternative PM indicators that might be considered?
- What evidence is available from recent studies focused on specific size fractions, chemical components, sources, or environments (e.g., urban and non-urban areas) of PM to inform our understanding of the nature of PM exposures that are linked to various health outcomes?
- To what extent is key scientific evidence becoming available to improve our understanding of the health effects associated with various time periods of PM exposures, including not only short-term (daily or multi-day) and chronic (months to years) exposures, but also peak PM exposures (<24 hours)? To what extent is critical research becoming available that could improve our understanding of the relationship between various health endpoints and different lag periods (e.g., <1 day, single day, multi-day distributed lags)?
- What data are available to improve our understanding of spatial and/or temporal heterogeneity of PM exposures considering different size fractions and/or components?
- At what levels of PM exposure do health effects of concern occur? Is there evidence for the occurrence of adverse health effects at levels of PM lower than those observed previously? If so, at what levels and what are the important uncertainties associated with

Note: Hyperlinks to the reference citations throughout this document will take you to the NCEA HERO database (Health and Environmental Research Online) at <http://epa.gov/hero>. HERO is a database of scientific literature used by U.S. EPA in the process of developing science assessments such as the Integrated Science Assessments (ISA) and the Integrated Risk Information System (IRIS).

that evidence? What is the nature of the dose-response relationships of PM for the various health effects evaluated?

- What evidence is available linking particle number concentration with adverse health effects of UF particles?
- Do risk/exposure estimates suggest that exposures of concern for PM-induced health effects will occur with current ambient levels of PM or with levels that just meet the current standards? If so, are these risks/exposures of sufficient magnitude such that the health effects might reasonably be judged to be important from a public health perspective? What are the important uncertainties associated with these risk/exposure estimates?
- To what extent is key evidence becoming available that could inform our understanding of subpopulations that are particularly sensitive or vulnerable to PM exposures? In the last review, sensitive or vulnerable subpopulations that appeared to be at greater risk for PM-related effects included individuals with pre-existing heart and lung diseases, older adults, and children. Has new evidence become available to suggest additional sensitive subpopulations should be given increased focus in this review (e.g., fetuses, neonates, genetically susceptible subpopulations)?
- To what extent is key evidence becoming available to inform our understanding of populations that are particularly vulnerable to PM exposures? Specifically, is there new or emerging evidence to inform our understanding of geographical, spatial, SES, and environmental justice considerations?
- To what extent have important uncertainties identified in the last review been reduced and/or have new uncertainties emerged?
- To what extent is new information available to inform our understanding of non-PM-exposure factors that might influence the associations between PM levels and health effects being considered (e.g., weather-related factors; behavioral factors such as heating/air conditioning use; driving patterns; and time-activity patterns)?

In evaluating evidence on welfare effects of PM, the focus will be on evidence that can help inform these questions from the Integrated Review Plan:

- What new evidence is available on the relationship between PM mass/size fraction and/or specific PM components and visibility impairment and climate-related and other welfare effects?
- To what extent has key scientific evidence now become available to improve our understanding of the nature and magnitude of visibility, climate, and ecosystem responses to PM and the variability associated with those responses (including ecosystem type, climatic conditions, environmental effects and interactions with other environmental factors and pollutants)?
- Do the evidence, the air quality assessment, and the risk/exposure assessment provide support for considering alternative averaging times?
- At what levels of ambient PM do visibility impairment and/or environmental effects of concern occur? Is there evidence for the occurrence of adverse visibility and other welfare-related effects at levels of PM lower than those observed previously? If so, at what levels and what are the important uncertainties associated with the evidence?
- Do the analyses suggest that PM-induced visibility impairment and/or other welfare-effects will occur with current ambient levels of PM or with levels that just meet the current standards? If so, are these effects of sufficient magnitude and/or frequency such

that these effects might reasonably be judged to be important from a public welfare perspective? What are the uncertainties associated with these estimates?

- What new evidence and/or techniques are available to quantify the benefits of improved visibility and/or other welfare-related effects?
- To what extent have important uncertainties identified in the last review been reduced and/or have new uncertainties emerged?

1.1. Legislative Requirements

Two sections of the United States (U.S.) Clean Air Act (CAA, the Act) govern the establishment and revision of the NAAQS. Section 108 of the Act (42 U.S.C. 7408) directs the Administrator to identify and list “air pollutants” that “in his judgment, may reasonably be anticipated to endanger public health and welfare” and whose “presence... in the ambient air results from numerous or diverse mobile or stationary sources” and to issue air quality criteria for those that are listed (42 U.S.C. 7408). Air quality criteria are intended to “accurately reflect the latest scientific knowledge useful in indicating the kind and extent of identifiable effects on public health or welfare which may be expected from the presence of [a] pollutant in ambient air...” 42 U.S.C. 7408(b).

Section 109 of the Act (42 U.S.C. 7409) directs the Administrator to propose and promulgate “primary” and “secondary” NAAQS for pollutants listed under Section 108. 42 U.S.C. 7409(a). Section 109(b)(1) defines a primary standard as one “the attainment and maintenance of which in the judgment of the Administrator, based on such criteria and allowing an adequate margin of safety, are requisite to protect the public health.”¹ 42 U.S.C. 7409(b)(1). A secondary standard, as defined in Section 109(b)(2), must “specify a level of air quality the attainment and maintenance of which, in the judgment of the Administrator, based on such criteria, is required to protect the public welfare from any known or anticipated adverse effects associated with the presence of [the] pollutant in the ambient air.”² 42 U.S.C. 7409(b)(2).

The requirement that primary standards include an adequate margin of safety was intended to address uncertainties associated with inconclusive scientific and technical information available at the time of standard setting. It was also intended to provide a reasonable degree of protection against hazards that research has not yet identified. See *Lead Industries Association v. EPA*, 647 F.2d 1130, 1154 (D.C. Cir. 1980), cert. denied, 449 U.S. 1042 (1980); *American Petroleum Institute v. Costle*, 665 F.2d 1176, 1186 (D.C. Cir. 1981), cert. denied, 455 U.S. 1034 (1982); *American Farm Bureau Federation v. EPA*, 559 F.3d 512, 533 (D.C. Cir. 2009). Both kinds of uncertainties are components of the risk associated with pollution at levels below those at which human health effects can be said to occur with reasonable scientific certainty. Thus, in selecting primary standards that include an adequate margin of safety, the Administrator is seeking not only to prevent pollution levels that have been demonstrated to be harmful, but also to prevent lower pollutant levels that may pose an unacceptable risk of harm, even if the risk is not precisely identified as to nature or degree.

In selecting a margin of safety, the EPA considers such factors as the nature and severity of the health effects involved, the size of the sensitive population(s) at risk, and the kind and degree of the uncertainties that must be addressed. The selection of any particular approach to providing an adequate margin of safety is a policy choice left specifically to the Administrator’s judgment. See *Lead Industries Association v. EPA*, supra, 647 F.2d 1161-62.

In setting standards that are “requisite” to protect public health and welfare, as provided in Section 109(b), the Administrator’s task is to establish standards that are neither more nor less

¹ The legislative history of Section 109 indicates that a primary standard is to be set at “the maximum permissible ambient air level...which will protect the health of any [sensitive] group of the population,” and that for this purpose “reference should be made to a representative sample of persons comprising the sensitive group rather than to a single person in such a group” [S. Rep. No. 91-1196, 91st Cong., 2d Sess. 10 (1970)].

² Welfare effects as defined in Section 302(h) [42 U.S.C. 7602(h)] include, but are not limited to, “effects on soils, water, crops, vegetation, man-made materials, animals, wildlife, weather, visibility and climate, damage to and deterioration of property, and hazards to transportation, as well as effects on economic values and on personal comfort and well-being.”

stringent than necessary. In so doing, EPA may not consider the costs of implementing the standards. See generally *Whitman v. American Trucking Associations*, 531 U.S. 457, 465-472, 475-76 (2001).

Section 109(d)(1) requires that “not later than December 31, 1980, and at 5-yr intervals thereafter, the Administrator shall complete a thorough review of the criteria published under Section 108 and the national ambient air quality standards...and shall make such revisions in such criteria and standards and promulgate such new standards as may be appropriate...” 42 U.S.C. 7409(d)(1). Section 109(d)(2) requires that an independent scientific review...committee “shall complete a review of the criteria and the national primary and secondary ambient air quality standards...and shall recommend to the Administrator any new standards and revisions of existing criteria and standards as may be appropriate...” 42 U.S.C. 7409(d)(2). Since the early 1980s, this independent review function has been performed by the Clean Air Scientific Advisory Committee (CASAC).

1.2. History of Reviews of the NAAQS for PM

PM is the generic term for a broad class of chemically and physically diverse substances that exist as discrete particles (liquid droplets or solids) over a wide range of sizes. Particles originate from a variety of anthropogenic stationary and mobile sources, as well as from natural sources. Particles may be emitted directly or formed in the atmosphere by transformations of gaseous emissions such as sulfur oxides (SO_x), nitrogen oxides (NO_x), and volatile organic compounds (VOC). The chemical and physical properties of PM vary greatly with time, region, meteorology, and source category, thus complicating the assessment of health and welfare effects. Table 1-1 summarizes the NAAQS that have been promulgated for PM to date. These reviews are briefly described below, and further details are provided in the Integrated Review Plan (U.S. EPA, 2008, [157072](#)).

EPA first established NAAQS for PM in 1971 (36 FR 8186, April 30, 1971), based on the original criteria document (NAPCA, 1969, [014684](#)). The reference method specified for determining attainment of the original standards was the high-volume sampler, which collects PM up to a nominal size of 25-45 micrometers (µm) (referred to as total suspended particulates [TSP]). The primary standards (measured by the indicator TSP) were 260 µg/m³, 24-h avg, not to be exceeded more than once per year, and 75 µg/m³, annual geometric mean. The secondary standard was 150 µg/m³, 24-h avg, not to be exceeded more than once per year. In October 1979 (44 FR 56730, October 2, 1979), EPA announced the first periodic review of the air quality criteria and NAAQS for PM, and significant revisions to the original standards were promulgated in 1987 (52 FR 24634, July 1, 1987). In that decision, EPA changed the indicator for particles from TSP to PM₁₀, the latter including particles with a mean aerodynamic diameter¹ ≤ 10 µm, which delineated that subset of inhalable particles small enough to penetrate to the thoracic region (including the tracheobronchial and alveolar regions) of the respiratory tract (referred to as thoracic particles). EPA also revised the level and form of the primary standards by (1) replacing the 24-h TSP standard with a 24-h PM₁₀ standard of 150 µg/m³ with no more than one expected exceedence per year; and (2) replacing the annual TSP standard with a PM₁₀ standard of 50 µg/m³, annual arithmetic mean, averaged over 3 yr.

¹ The more precise term is 50% cut point or 50% diameter (d₅₀). This is the aerodynamic particle diameter for which the efficiency of particle collection is 50%. Larger particles are not excluded altogether, but are collected with substantially decreasing efficiency and smaller particles are collected with increasing (up to 100%) efficiency.

Table 1-1. Summary of NAAQS promulgated for PM, 1971-2006.

Year (Final Rule)	Indicator	Avg Time	Level	Form
1971 (36 FR 8186)	TSP (Total Suspended Particulates)	24 h	260 $\mu\text{g}/\text{m}^3$ (primary) 150 $\mu\text{g}/\text{m}^3$ (secondary)	Not to be exceeded more than once per yr
		Annual	75 $\mu\text{g}/\text{m}^3$ (primary)	Annual geometric mean
1987 (52 FR 24634)	PM ₁₀	24 h	150 $\mu\text{g}/\text{m}^3$	Not to be exceeded more than once per yr on average over a 3-yr period
		Annual	50 $\mu\text{g}/\text{m}^3$	Annual arithmetic mean, averaged over 3 yr
	PM _{2.5}	24 h	65 $\mu\text{g}/\text{m}^3$	98th percentile, averaged over 3 yr
		Annual	15 $\mu\text{g}/\text{m}^3$	Annual arithmetic mean, averaged over 3 yr ¹
1997 (62 FR 38652)	PM ₁₀	24 h	150 $\mu\text{g}/\text{m}^3$	Initially promulgated 99th percentile, averaged over 3 yr; when 1997 standards were vacated in 1999, the form of 1987 standards remained in place (not to be exceeded more than once per yr on average over a 3-yr period)
		Annual	50 $\mu\text{g}/\text{m}^3$	Annual arithmetic mean, averaged over 3 yr
2006 (71 FR 61144)	PM _{2.5}	24 h	35 $\mu\text{g}/\text{m}^3$	98th percentile, averaged over 3 yr
		Annual	15 $\mu\text{g}/\text{m}^3$	Annual arithmetic mean, averaged over 3 yr ²
	PM ₁₀	24 h	150 $\mu\text{g}/\text{m}^3$	Not to be exceeded more than once per yr on average over a 3-yr period

Note: When not specified, primary and secondary standards are identical.

The secondary standard was revised by replacing it with 24-h and annual standards identical in all respects to the primary standards. The revisions also included a new reference method for the measurement of PM₁₀ in the ambient air and rules for determining attainment of the new standards. On judicial review, the revised standards were upheld in all respects. See *Natural Resources Defense Council v. Administrator*, 902 F. 2d 962 (D.C. Cir. 1990), cert. denied, 498 U.S. 1082 (1991).

In April 1994, EPA announced its plans for the second periodic review of the air quality criteria and NAAQS for PM, and promulgated significant revisions to the NAAQS in 1997 (62 FR 38652, July 18, 1997). In that decision, EPA revised the PM NAAQS in several respects. Most significantly, EPA determined that the fine and coarse³ fractions of PM₁₀ should be considered separately. The Administrator's decision to modify the standards was based on evidence that serious health effects were associated with short- and long-term exposure to fine particles in areas that met the existing PM₁₀ standards. EPA accordingly added new standards, using PM_{2.5} as the indicator for fine particles (with PM_{2.5} referring to particles with a nominal mean aerodynamic diameter $\leq 2.5 \mu\text{m}$), and PM₁₀ as the indicator for thoracic coarse particles or coarse-fraction particles (generally including particles with a nominal mean aerodynamic diameter $>2.5 \mu\text{m}$ and $\leq 10 \mu\text{m}$, or PM_{10-2.5}). The EPA established two new PM_{2.5} standards: an annual standard of 15 $\mu\text{g}/\text{m}^3$, based on the 3-yr avg of annual arithmetic mean PM_{2.5} concentrations from single or multiple community-oriented monitors; and a 24-h standard of 65 $\mu\text{g}/\text{m}^3$, based on the 3-yr avg of the 98th percentile of 24-h PM_{2.5} concentrations at each population-oriented monitor within an area. Also, EPA established a new reference method for measuring PM_{2.5} in the ambient air and adopted protocols for determining attainment of the new standards. To continue to address thoracic coarse particles, EPA retained the annual PM₁₀ standard, while revising the form, but not the level, of the

¹ The level of the 1997 annual PM_{2.5} standard was to be compared to measurements made at the community-oriented monitoring site recording the highest level, or, if specific constraints were met, measurements from multiple community-oriented monitoring sites could be averaged ("spatial averaging"). This approach was judged to be consistent with the short-term epidemiologic studies on which the annual PM_{2.5} standard was primarily based, in which air quality data were generally averaged across multiple monitors in an area or were taken from a single monitor that was selected to represent community-wide exposures, not localized "hot spots" (62 FR 38672). These criteria and constraints were intended to ensure that spatial averaging would not result in inequities in the level of protection afforded by the PM_{2.5} standards. Community-oriented monitoring sites were specified to be consistent with the intent that a spatially averaged annual standard provide protection for persons living in smaller communities, as well as those in larger population centers.

² In the revisions to the PM NAAQS finalized in 2006, EPA tightened the constraints on the spatial averaging criteria by further limiting the conditions under which some areas may average measurements from multiple community-oriented monitors to determine compliance (71 FR 61165-61167, October 17, 2006).

³ See definitions of "fine" and "coarse" particles in Section 3.2.

24-h PM₁₀ standard to be based on the 99th percentile of 24-h PM₁₀ concentrations at each monitor in an area. The EPA revised the secondary standards by making them identical in all respects to the primary standards.

Following promulgation of the 1997 PM NAAQS, petitions for review were filed by a large number of parties, addressing a broad range of issues. In May 1999, a three-judge panel of the U.S. Court of Appeals for the District of Columbia Circuit issued an initial decision that upheld EPA's decision to establish fine particle standards, holding that "the growing empirical evidence demonstrating a relationship between fine particle pollution and adverse health effects amply justifies establishment of new fine particle standards." *American Trucking Associations v. EPA* (175 F. 3d 1027, 1055-56 (D.C. Cir. 1999)); rehearing granted in part and denied in part, 195 F. 3d 4 (D.C. Cir. 1999), affirmed in part and reversed in part, *Whitman v. American Trucking Associations* 531 U.S. 457 (2001). The panel also found "ample support" for EPA's decision to regulate coarse particle pollution, but vacated the 1997 PM₁₀ standards, concluding that EPA had not provided a reasonable explanation justifying use of PM₁₀ as an indicator for coarse particles (175 F. 3d at 1054-55). Pursuant to the court's decision, EPA removed the vacated 1997 PM₁₀ standards from the Code of Federal Regulations. The pre-existing 1987 PM₁₀ standards remained in place (65 FR 80776, December 22, 2000). The Court also upheld EPA's determination not to establish more stringent secondary standards for fine particles to address effects on visibility (175 F. 3d at 1027).

More generally, the panel held (over one judge's dissent) that EPA's approach to establishing the level of the standards in 1997, both for the PM and ozone (O₃) NAAQS promulgated on the same day, effected "an unconstitutional delegation of legislative authority" (Id. at 1034-40). Although the panel stated that "the factors EPA uses in determining the degree of public health concern associated with different levels of ozone and PM are reasonable," it remanded the rule to EPA, stating that when EPA considers these factors for potential non-threshold pollutants "what EPA lacks is any determinate criterion for drawing lines" to determine where the standards should be set. Consistent with EPA's long-standing interpretation and D.C. Circuit precedent, the panel also reaffirmed its prior holdings that in setting NAAQS EPA is "not permitted to consider the cost of implementing those standards" (Id. at 1040-41).

On EPA's petition for rehearing, the panel adhered to its position on these points. *American Trucking Associations v. EPA*, 195 F. 3d 4 (D.C. Cir. 1999). The full Court of Appeals denied EPA's suggestion for rehearing en banc, with five judges dissenting (Id. at 13).

Both sides filed cross appeals on these issues to the U.S. Supreme Court, and the Court granted *certiorari*. In February 2001, the Supreme Court issued a unanimous decision upholding EPA's position on both the constitutional and cost issues. *Whitman v. American Trucking Associations*, 531 U.S. 457, 464, 475-76. On the constitutional issue, the Court held that the statutory requirement that NAAQS be "requisite" to protect public health with an adequate margin of safety sufficiently guided EPA's discretion, affirming EPA's approach of setting standards that are neither more nor less stringent than necessary. The Supreme Court remanded the case to the Court of Appeals for resolution of any remaining issues that had not been addressed in that court's earlier rulings (Id. at 475-76). In March 2002, the Court of Appeals rejected all remaining challenges to the standards, holding under the traditional standard of judicial review that PM_{2.5} standards were reasonably supported by the administrative record and were not "arbitrary and capricious" *American Trucking Associations v. EPA*, 283 F. 3d 355, 369-72 (D.C. Cir. 2002).

In October 1997, EPA published its plans for the third periodic review of the air quality criteria and NAAQS for PM (62 FR 55201). After CASAC and public review, EPA finalized the 2004 PM AQCD (U.S. EPA, 2004, [056905](#)) and 2005 Staff Paper (U.S. EPA, 2005, [090209](#)). For the primary fine particle standards, most CASAC PM Panel members favored the option of revising the level of the 24-h PM_{2.5} standard in the range of 35 to 30 µg/m³ with a 98th percentile form, in concert with revising the level of the annual PM_{2.5} standard in the range of 14 to 13 µg/m³ (Henderson, 2005, [188316](#)). Most of the members of the CASAC PM Panel also strongly supported establishing a new, secondary PM_{2.5} standard to protect urban visibility and recommended establishing a sub-daily (4- to 8-h averaging time) PM_{2.5} standard within the range of 20 to 30 µg/m³ with a form within the range of the 92nd to 98th percentile (Henderson, 2005, [188316](#)). For thoracic coarse particles, there was general concurrence among CASAC PM Panel members to revise the PM₁₀ standards by establishing a primary standard specifically targeted to address particles in the size range of 2.5 to 10 µm (PM_{10-2.5}). The CASAC PM Panel was also in general agreement "that coarse particles in urban or industrial areas are likely to be enriched by anthropogenic pollutants that tend to be inherently more toxic than the windblown crustal material which typically dominates coarse particle mass in

arid rural areas.” Based on its review of the Staff Paper, there was general agreement among the CASAC PM Panel members that a 24-h $PM_{10-2.5}$ standard with a level in the range of 50 to 70 $\mu\text{g}/\text{m}^3$, with a 98th percentile form, was reasonably justified and that a $PM_{10-2.5}$ standard with an annual averaging time was not warranted (Henderson, 2005, [156537](#)). On January 17, 2006, EPA proposed to revise the NAAQS for PM (71 FR 2620). For fine particles, EPA proposed to retain $PM_{2.5}$ as the indicator, to retain standards for 24-h and annual exposures, and to revise the form of the annual standard to tighten conditions for demonstrating compliance using spatially averaged monitoring. EPA also proposed to revise the level of the 24-h $PM_{2.5}$ standard to 35 $\mu\text{g}/\text{m}^3$ to provide increased protection against health effects associated with short-term $PM_{2.5}$ exposures, including premature mortality and increased hospital admission and emergency room visits, but proposed to retain the level of the annual $PM_{2.5}$ standard at 15 $\mu\text{g}/\text{m}^3$, continuing protection against health effects associated with long-term exposure including premature mortality and development of chronic respiratory disease. With regard to the primary standards for thoracic coarse particles, EPA proposed to revise the 24-h PM_{10} standard in part by establishing a new indicator for thoracic coarse particles (particles generally between 2.5 and 10 μm in diameter), qualified so as to include any ambient mix of $PM_{10-2.5}$ that was dominated by resuspended dust from high density traffic on paved roads and PM generated by industrial sources and construction sources, and proposed to exclude any ambient mix of $PM_{10-2.5}$ that was dominated by rural windblown dust and soils and $PM_{10-2.5}$ generated by agricultural and mining sources. EPA also proposed a detailed monitoring regime in conjunction with this proposed indicator (71 FR 2710, 2731-42). The EPA proposed to set a 24-h standard (using the proposed indicator) at a level of 70 $\mu\text{g}/\text{m}^3$ to continue to provide a level of protection against health effects associated with short-term exposure (including hospital admissions for cardiopulmonary diseases, increased respiratory symptoms and possibly premature mortality) in those areas where the proposed indicator was found, generally equivalent to the level of protection provided by the existing 24-h PM_{10} standard. Also, EPA proposed to revoke, upon finalization of a primary 24-h standard for thoracic coarse particles, the 24-h PM_{10} standard as well as the annual PM_{10} standard.

EPA proposed to revise the secondary standards by making them identical to the suite of proposed primary standards for fine and coarse particles, providing protection against PM-related public welfare effects including visibility impairment, effects on vegetation and ecosystems, and materials damage and soiling. EPA also solicited comment on adding a new sub-daily $PM_{2.5}$ secondary standard to address visibility impairment in urban areas.

CASAC provided additional advice to EPA in a letter to the Administrator requesting reconsideration of CASAC’s recommendations for both the primary and secondary $PM_{2.5}$ standards, as well as standards for thoracic coarse particles (Henderson, 2006, [156538](#)).

On September 21, 2006, EPA announced its final decisions to revise the primary and secondary NAAQS for PM to provide increased protection of public health and welfare, respectively (71 FR 61144). With regard to the primary and secondary standards for fine particles, EPA revised the level of the 24-h $PM_{2.5}$ standard to 35 $\mu\text{g}/\text{m}^3$, retained the level of the annual $PM_{2.5}$ standard at 15 $\mu\text{g}/\text{m}^3$, and revised the form of the annual $PM_{2.5}$ standard by narrowing the constraints on the optional use of spatial averaging. EPA established the secondary standard for fine particles identical to the primary standards. With regard to the primary and secondary standards for thoracic coarse particles, EPA retained PM_{10} as the indicator for coarse particles, retained the level and form of the 24-h PM_{10} standard (so the standard remains 150 $\mu\text{g}/\text{m}^3$ with a one expected exceedence form) and revoked the annual standard because available evidence generally did not support a link between long-term exposure to current ambient levels of coarse particles and health or welfare effects.

Following promulgation of the revised PM NAAQS in 2006, several parties filed petitions for review with respect to: (1) selecting the level of the annual primary $PM_{2.5}$ standard; (2) setting the secondary $PM_{2.5}$ standards identical to the primary standards; (3) retaining PM_{10} as the indicator for coarse particles and retaining the level and form of the PM_{10} 24-h standard; and (4) revoking the PM_{10} annual standard. On judicial review, the D.C. Circuit remanded the annual standard for fine particles to EPA because EPA failed to adequately explain why the annual $PM_{2.5}$ standard provided the requisite protection from both short- and long-term exposures to fine particles including protection for vulnerable subpopulations. With respect to protection from short-term exposures, in 1997 EPA determined that the annual standard was the generally controlling standard for lowering both short- and long-term $PM_{2.5}$ concentrations and the 24-h standard was set to “provide an adequate margin of safety against infrequent or isolated peak concentrations that could occur in areas that attain the annual standard” (62 FR 38676-77, July 18, 1997). In the 2006 decision, the Administrator considered it appropriate to use a somewhat different evidence-based approach from

that used in 1997 to set the level of the 24-h and annual PM_{2.5} standards. In that decision, the Administrator relied upon evidence from the short-term exposure PM_{2.5} studies as the principal basis for selecting the proposed level of the 24-h standard and relied upon evidence from the long-term exposure PM_{2.5} studies as the principal basis for selecting the level of the annual standard. The court found EPA failed to adequately explain this change in approach in light of CASAC and staff's recommendations to do otherwise. The court also found that EPA had failed to adequately explain why a short-term 24-h standard by itself would provide the protection needed from short-term exposures. *American Farm Bureau Federation v. EPA*, 559 F.3d 512, 520-24 (D.C. Cir. 2009). With respect to protection from long-term exposure, the court found that EPA failed to adequately explain how the current standard provided "an adequate margin of safety for vulnerable subpopulations, such as children, the elderly, or those with conditions that expose them to greater risk from fine particles". Specifically, EPA did not provide a reasonable explanation of why certain studies, including a study of children in Southern California showing lung damage from long-term exposure, did not call for a more stringent annual standard (Id. at 522-23).

The court also remanded the secondary standard for fine particles, based on EPA's failure to adequately explain why setting the secondary NAAQS equivalent to the primary standards provided the required protection for public welfare including protection from visibility impairment. The court found that EPA failed to identify a target level of visibility impairment that would be requisite to protect public welfare. This was contrary to the statute and resulted in a lack of a reasoned basis for the final decision. In addition, EPA's near exclusive reliance on a comparison of numbers of counties that would be in nonattainment under various types of standards was an inadequate basis for making a decision. It did not take into account the relative visibility protection of different standards, as well as the failure of a 24-h standard to address regional differences in humidity and its effect on visibility (Id. at 528-31).

The court upheld EPA's decision to retain the 24-h PM₁₀ standard to provide protection for coarse particle exposures and to revoke the annual PM₁₀ standard. The court found that EPA reasonably included all coarse PM within the standard, both urban and non-urban, to provide nationwide protection for exposure to coarse PM. It rejected arguments that the evidence showed there are no risks from exposure to non-urban coarse PM (Id. at 531-33). The court further found that EPA had a reasonable basis to not set separate standards for urban and non-urban coarse PM, namely the inability to reasonably define what ambient mixes would be included under either "urban" or "non-urban." In addition, the court found that record evidence supported EPA's cautious decision to provide "some protection from exposure to thoracic coarse particles... in all areas." The court also upheld EPA's decision to use PM₁₀ as the indicator for coarse particles and to retain the level of the standard at 150 µg/m³. EPA's final rule acknowledged that evidence of harm from urban-type coarse PM is stronger than for other types, and targeted protection at areas where urban-type coarse PM is most likely present. The targeting is done by using the indicator PM₁₀ for coarse particles. PM₁₀ includes both coarse PM and fine PM. Urban and industrial areas tend to have higher levels of fine PM than rural areas, so that in those areas less coarse PM is allowed – the desired targeting. Conversely, fine PM levels tend to be lower in rural areas, so more coarse particles are allowed in those areas – again the desired targeting. Likewise, the court concluded that the EPA's choice of the level for the PM₁₀ standard was reasonable for many of the same reasons (Id. at 533-36). The court also upheld EPA's decision to revoke the annual PM₁₀ standard (Id. at 537-38).

1.3. ISA Development

EPA initiated the current formal review of the NAAQS for PM on June 28, 2007 with a call for information from the public (72 FR 35462). In addition to the call for information, publications were identified through an ongoing literature search process that includes extensive computer database mining on specific topics. Literature searches were conducted routinely to identify studies published since the last review, focusing on publications from 2002 to May 2009. Search strategies were iteratively modified in an effort to optimize the identification of pertinent publications. Additional papers were identified for inclusion in several ways: review of pre-publication tables of contents for journals in which relevant papers may be published; independent identification of relevant literature by expert authors; and identification by the public and CASAC during the external review process. Generally, only information that had undergone scientific peer review and had been published or

accepted for publication was considered. All relevant epidemiologic, controlled human exposure, animal toxicological, and welfare effects studies published since the last review were considered, including those related to exposure-response relationships, mode(s) of action (MOA), or susceptible populations.

In general, in assessing the scientific quality and relevance of health and environmental effects studies, the following considerations have been taken into account when selecting studies for inclusion in the ISA or its annexes. The selection process for studies included in this ISA is shown in Figure 1-1.

- Are the study populations, subjects, or animal models adequately selected and are they sufficiently well defined to allow for meaningful comparisons between study or exposure groups?
- Are the statistical analyses appropriate, properly performed, and properly interpreted? Are likely covariates adequately controlled or taken into account in the study design and statistical analysis?
- Are the PM aerometric data, exposure, or dose metrics of adequate quality and sufficiently representative of information regarding ambient PM?
- Are the health or welfare effect measurements meaningful and reliable?

In selecting epidemiologic studies, EPA considered whether a given study contained information on associations with short- or long-term PM exposures at or near ambient levels of PM; evaluated health effects of PM size fractions, components or source-related indicators; considered approaches to evaluate issues related to potential confounding by other pollutants; assessed potential effect modifiers; and evaluated important methodological issues (e.g., lag or time period between exposure and effects, model specifications, thresholds, mortality displacement) related to interpretation of the health evidence. Among the epidemiologic studies selected, particular emphasis was placed on those studies most relevant to the review of the NAAQS. Specifically, studies conducted in the U.S. or Canada were discussed in more detail than those from other geographical regions. Particular emphasis was placed on: (1) recent multicity studies that employ standardized analysis methods for evaluating effects of PM and that provide overall estimates for effects based on combined analyses of information pooled across multiple cities; (2) studies that help understand quantitative relationships between exposure concentrations and effects; (3) recent studies (published since the last PM NAAQS review) that provide evidence on effects in susceptible populations; and (4) studies that consider and report PM as a component of a complex mixture of air pollutants.

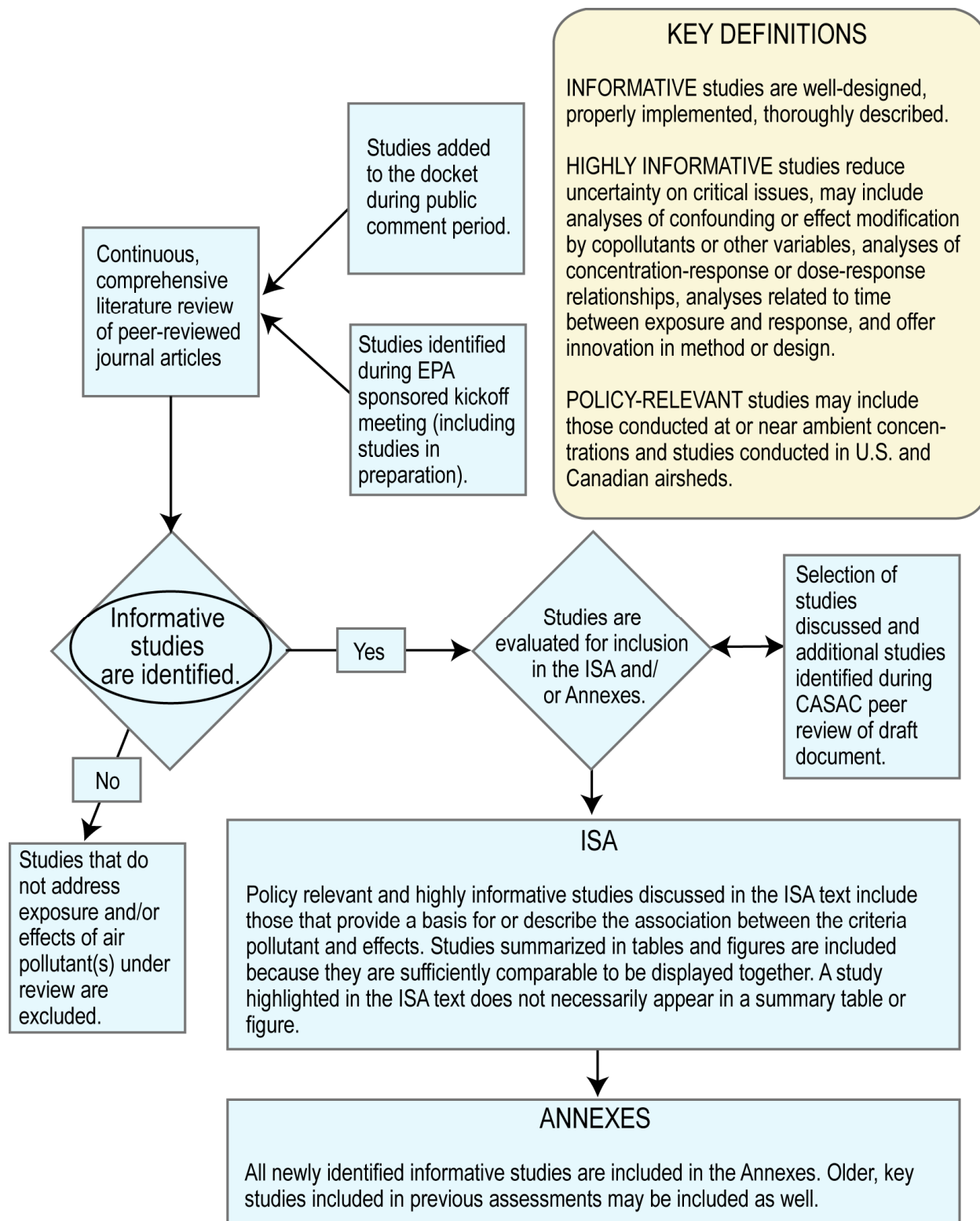


Figure 1-1. Identification of studies for inclusion in the ISA.

Criteria for the selection of research evaluating controlled human exposure or animal toxicological studies included a focus on studies conducted using relevant pollutant exposures. For both types of studies, relevant pollutant exposures are considered to be those generally within one or two orders of magnitude of ambient PM concentrations. Studies in which higher doses were used may also be considered if they provide information relevant to understanding MOAs or mechanisms, as noted below.

Evaluation of controlled human exposure studies focused on those that approximated expected human exposure conditions in terms of concentration and duration. In the selection of controlled human exposure studies, emphasis is placed on studies that: (1) investigate potentially susceptible populations such as people with cardiovascular diseases or asthmatics, particularly studies that compare responses in susceptible individuals with those in age-matched healthy controls; (2) address issues such as concentration-response or time-course of responses; (3) investigate exposure to PM separately and in combination with other pollutants such as O₃; (4) include control exposures to filtered air; and (5) have sufficient statistical power to assess findings.

For selecting toxicological studies for highlighting in the text, emphasis is placed on inhalation studies conducted at concentrations <2 mg/m³ and those studies that approximate expected human dose conditions in terms of concentration, size distributions, and duration, which will depend on the toxicokinetics and biological sensitivity of the particular laboratory animals examined. Studies that elucidated MOAs and/or susceptibility, particularly if the studies were conducted under atmospherically relevant conditions, were emphasized whenever possible. A limited number of toxicological studies were included that employed intratracheal (IT) instillation techniques, mainly for PM_{10-2.5} studies in rodents, that explored new emerging areas of investigation (e.g., vasomotor function), or that evaluated specific potential MOA or mechanisms of response. The sources, transport, and fate of fibers and unique nano-materials (viz., dots, hollow spheres, rods, fibers, tubes) are not reviewed herein because the in vivo disposition of these unique nanomaterials is not necessarily relevant to the behavior of ultrafine (UF) aerosols in the urban environment that are created by combustion sources and photochemical formation of secondary organic aerosols. In considering the potential effects of different components of PM, EPA has focused on studies that have assessed effects for a range of PM sources or components, including those using source apportionment methods or comparing effects for numerous PM components, and not on studies of individual constituents or species. Studies of ubiquitous PM sources as part of a mixture (i.e., diesel exhaust, gasoline exhaust, wood smoke) are included, provided they meet the other remaining selection criteria. Those studies of mixtures that are not a significant source of ambient PM, such as environmental tobacco smoke (ETS), are not included.

These criteria provide benchmarks for evaluating various studies and for focusing on the policy relevant studies in assessing the body of health and welfare effects evidence. Detailed critical analysis of all PM health and welfare effects studies, especially in relation to the above considerations, is beyond the scope of this document. Of most relevance for evaluation of studies is whether they provide useful qualitative or quantitative information on exposure-effect or exposure-response relationships for effects associated with current ambient air concentrations of PM that can inform decisions on whether to retain or revise the standards.

In developing the PM ISA, EPA began by reviewing and summarizing the evidence on (1) atmospheric sciences and exposure; (2) the health effects evidence from in vivo and in vitro animal toxicological, controlled human exposure, and epidemiologic studies; and (3) the welfare effects of PM, including visibility, climate, and ecological effects. In June 2008, EPA held a workshop to obtain review of the scientific content of initial draft materials or sections for the draft ISA and its annexes, that primarily contain summary information. The purpose of the initial peer review workshop was to ensure that the ISA is up to date and focused on the most policy-relevant findings, and to assist EPA with integration of evidence within and across disciplines. Following the peer review workshop, EPA addressed comments from the peer review workshop and completed the initial integration and synthesis of the evidence.

The integration of evidence on health or welfare effects involves collaboration between scientists from various disciplines. As described in the section below, the ISA organization is based on health or welfare effect categories. As an example, an evaluation of health effects evidence would include summaries of findings from epidemiologic, controlled human exposure, and toxicological studies, and integration of the results to draw conclusions based on the causal framework described below. Using the causal framework described in Section 1.5, EPA scientists consider aspects such as strength, consistency, coherence and biological plausibility of the evidence, and develop draft

causality judgments on the nature of the relationships. The draft integrative synthesis sections and conclusions are reviewed by EPA internal experts and, as appropriate, by outside expert authors. In practice, causality determinations often entail an iterative process of review and evaluation of the evidence. The draft ISA is released for review by the CASAC and the public. Comments on the characterization of the science as well as the implementation of the causal framework are carefully considered in revising and completing the ISA.

PM₁₀ health studies are included in this assessment because they provide important evidence regarding the health effects of PM in general. However, the ISA draws no conclusions regarding causality for short- or long-term exposure to PM₁₀, as PM₁₀ is comprised of both fine and thoracic coarse particles. As a result, causality determinations are limited to PM_{2.5}, PM_{10-2.5}, and UF particle (UFP) size fractions. In the cases where it was determined that PM₁₀ is dominated by fine or thoracic coarse PM in specific study locations, these health studies are used in supporting the causality determinations for PM_{2.5} or PM_{10-2.5}. Epidemiologic studies of short-term exposure to PM₁₀ are also relied upon to examine potential effect modifiers, potential confounding by copollutants, and the influence of different modeling approaches on PM-mortality risk estimates, as well as the concentration-response relationship between PM and mortality. Therefore, to the extent possible, the findings of PM₁₀ studies are considered insofar as they provide information relevant to the review of the NAAQS for fine and thoracic coarse particles.

1.4. Document Organization

This ISA is composed of nine chapters. This introductory chapter presents background information, and provides an overview of EPA's framework for making causal judgments. Key findings and conclusions for consideration in the review of the NAAQS for PM from the atmospheric sciences, ambient air data analyses, exposure assessment, dosimetry, health and welfare effects, including judgments on causality for the health and welfare effects of PM exposure, are presented in Chapter 2. More detailed summaries, evaluations and integration of the evidence are included in Chapters 3 through 9.

Chapter 3 highlights key concepts or issues relevant to understanding the atmospheric chemistry, sources, and exposure of and to PM following a "source-to-exposure" paradigm. Chapter 4 summarizes key concepts and recent findings on the dosimetry of PM, and Chapter 5 discusses possible pathways and MOA for the effects of PM. Chapters 6 and 7 evaluate and integrate epidemiologic, controlled human exposure, and animal toxicological information relevant to the review of the primary NAAQS for PM. Health effects related to short-term exposures (hours to days) to PM are the focus of Chapter 6. Chapter 7 evaluates health evidence related to long-term exposures (months to years) to PM. Chapters 6 and 7 are organized by health outcome categories, such as cardiovascular or respiratory effects, and each section includes effects of the various types of PM studied. For each health outcome category, summary sections then integrate the findings to draw conclusions on the evidence for the main size classes of PM (i.e., PM_{2.5}, PM_{10-2.5}, and UFP). Chapter 6 also includes a summary and synthesis of the recent health evidence that uses systematic approaches to assess health effects of sources and constituents of ambient PM; most such studies have evaluated effects of short-term exposure. Chapter 8 evaluates evidence related to populations potentially susceptible to PM-related effects.

Chapter 9 evaluates welfare effects evidence that is relevant to the review of the secondary NAAQS for PM. This chapter includes consideration of effects of PM on visibility impairment, materials damage, effects of PM on climate, and ecological effects of PM that were not addressed in the Integrated Science Assessment for Oxides of Nitrogen and Sulfur—Ecological Criteria (NO_xSO_x ISA) (U.S. EPA, 2008, [157074](#)). The chapter also presents key conclusions and scientific judgments regarding causality for welfare effects of PM. In 2008, EPA completed the NO_xSO_x ISA (U.S. EPA, 2008, [157074](#)), that focused on ecological effects related to the deposition of nitrogen (N)- and sulfur (S)-containing compounds. The 2008 NO_xSO_x ISA included ecological effects from particle-phase compounds (e.g., nitrates and sulfates), primarily effects from acidification and N-nutrient enrichment and eutrophication. In this ISA, the focus is on recent data for direct welfare effects of particle-phase NO_x and SO_x in the ambient air – primarily visibility impairment, damage to materials, and positive and negative climate interactions – not the welfare effects related to deposition of particle-phase NO_x and SO_x.

A series of annexes supplement this ISA. The annexes provide additional details of the pertinent literature published since the last review, as well as selected older studies of particular interest. These annexes contain information on:

- atmospheric chemistry of PM, sampling and analytic methods for measurement of PM, concentrations, emissions, sources and human exposure to PM (Annex A);
- studies on the dosimetry of PM (Annex B);
- controlled human exposure studies of health effects related to exposure to PM (Annex C);
- toxicological studies of health effects related to exposure to PM in laboratory animals and cell cultures (Annex D);
- epidemiologic studies of health effects from short- and long-term exposure to PM (Annex E); and
- studies that evaluate PM-induced health effects attributable to specific constituents or sources (Annex F).

Within Annexes B through F, detailed information about methods and results of health studies is summarized in tabular format, and generally includes information about: concentrations of PM and averaging times; study methods employed; results; and quantitative results for relationships between effects and exposure to PM. As noted in the section above, the most pertinent results of this body of studies are brought into the ISA.

1.5. EPA Framework for Causal Determination

The EPA has developed a consistent and transparent basis to evaluate the causal nature of air pollution-induced health or environmental effects. The framework described below establishes uniform language concerning causality and brings more specificity to the findings. It drew standardized language from across the federal government and wider scientific community, especially from the recent National Academy of Sciences (NAS) Institute of Medicine (IOM) document, *Improving the Presumptive Disability Decision-Making Process for Veterans* (IOM, 2008, [156586](#)), the most recent comprehensive work on evaluating causality.

This introductory section focuses on the evaluation of health effects evidence; while focusing on human health outcomes, the concepts are also generally relevant to causality determination for welfare effects. This section:

- describes the kinds of scientific evidence used in establishing a general causal relationship between exposure and health effects;
- defines cause, in contrast to statistical association;
- discusses the sources of evidence necessary to reach a conclusion about the existence of a causal relationship;
- highlights the issue of multifactorial causation;
- identifies issues and approaches related to uncertainty; and
- provides a framework for classifying and characterizing the weight of evidence in support of a general causal relationship.

Approaches to assessing the separate and combined lines of evidence (e.g., epidemiologic, controlled human exposure, and animal toxicological studies) have been formulated by a number of

regulatory and science agencies, including the IOM of the NAS (IOM, 2008, [156586](#)), International Agency for Research on Cancer (IARC, 2006, [093206](#)), EPA Guidelines for Carcinogen Risk Assessment (U.S. EPA, 2005, [086237](#)), Centers for Disease Control and Prevention (CDC, 2004, [056384](#)), and National Acid Precipitation Assessment Program (NAPAP, 1991, [095894](#)). These formalized approaches offer guidance for assessing causality. The frameworks are similar in nature, although adapted to different purposes, and have proven effective in providing a uniform structure and language for causal determinations. Moreover, these frameworks have supported decision-making under conditions of uncertainty.

1.5.1. Scientific Evidence Used in Establishing Causality

Causality determinations are based on the evaluation and synthesis of evidence from across scientific disciplines; the type of evidence that is most important for such determinations will vary by assessment. The most direct evidence of a causal relationship between pollutant exposures and human health effects comes from controlled human exposure studies. This type of study experimentally evaluates the health effects of administered exposures in human volunteers under highly-controlled laboratory conditions.

In most epidemiologic or observational studies of humans, the investigator does not control exposures or intervene with the study population. Broadly, observational studies can describe associations between exposures and effects. These studies fall into several categories: cross-sectional, prospective cohort, and time-series studies. “Natural experiments” offer the opportunity to investigate changes in health with a change in exposure; these include comparisons of health effects before and after a change in population exposures, such as the closure of a pollution source.

Experimental animal data can help characterize effects of concern, exposure-response relationships, susceptible populations, MOAs and enhance understanding of biological plausibility of observed effects. In the absence of controlled human exposure or epidemiologic data, animal data alone may be sufficient to support a likely causal determination, assuming that similar responses are expected in humans.

1.5.2. Association and Causation

“Cause” is a significant, effectual relationship between an agent and an effect on health or public welfare. “Association” is the statistical dependence among events, characteristics, or other variables. An association is *prima facie* evidence for causation; alone, however, it is insufficient proof of a causal relationship between exposure and disease or health effect. Determining whether an observed association is causal rather than spurious involves consideration of a number of factors, as described below. Much of the newly available health information evaluated in this ISA comes from epidemiologic studies that report a statistical association between ambient exposure and health outcomes.

Many of the health and environmental outcomes reported in these studies have complex etiologies. Diseases such as asthma, coronary artery disease or cancer are typically initiated by a web of multiple agents. Outcomes depend on a variety of factors, such as age, genetic susceptibility, nutritional status, immune competence, and social factors (Gee and Payne-Sturges, 2004, [093070](#); IOM, 2008, [156586](#)). Effects on ecosystems are also multifactorial with a complex web of causation. Further, exposure to a combination of agents could cause synergistic or antagonistic effects. Thus, the observed risk represents the net effect of many actions and counteractions.

1.5.3. Evaluating Evidence for Inferring Causation

Moving from association to causation involves elimination of alternative explanations for the association. In estimating the causal influence of an exposure on health or environmental effects, it is recognized that scientific findings include uncertainty. Uncertainty can be defined as a state of having limited knowledge where it is impossible to exactly describe an existing state or future outcome; the lack of knowledge about the correct value for a specific measure or estimate. Uncertainty characterization and uncertainty assessment are two activities that lead to different degrees of sophistication in describing uncertainty. Uncertainty characterization generally involves a

qualitative discussion of the thought processes that lead to the selection and rejection of specific data, estimates, scenarios, etc. Uncertainty assessment is more quantitative. The process begins with simpler measures (e.g., ranges) and simpler analytical techniques and progresses, to the extent needed to support the decision for which the assessment is conducted, to more complex measures and techniques. Data will not be available for all aspects of an assessment, and those data that are available may be of questionable or unknown quality. In these situations, evaluation of uncertainty can include professional judgment or inferences based on analogy with similar situations. The net result is that the assessments will be based on a number of assumptions with varying degrees of uncertainty. Uncertainties commonly encountered in evaluating health evidence for the criteria air pollutants are outlined below for epidemiologic and experimental studies. Various approaches to characterizing uncertainty include classical statistical methods, sensitivity analysis, or probabilistic uncertainty analysis, in order of increasing complexity and data requirements. The ISA generally evaluates uncertainties qualitatively in assessing the evidence from across studies; in some situations quantitative analysis approaches, such as meta-regression may be used.

It is important to note here that, although the following discussion refers primarily to health effect studies, many parallels exist with welfare effects studies. Controlled exposure studies have been conducted in which plant species have been directly exposed to air pollutants, and the strengths and limitations of that body of studies mirror those of the controlled human exposure studies discussed below. Ecological field or natural gradient studies are similar to epidemiologic studies, for example, in the study of free-living populations and in the challenges faced in distinguishing effects of pollutants within a mixture.

Controlled human exposure studies evaluate the effects of exposures to a variety of pollutants in a highly-controlled laboratory setting. Also referred to as human clinical studies, these experiments allow investigators to expose subjects to fixed concentrations of air pollutants under carefully regulated environmental conditions and activity levels. Controlled human exposures to PM typically involve exposing subjects either at rest or while engaged in intermittent exercise in a whole-body exposure chamber, although mouthpiece and facemask systems can also be used. A variety of different types of particles are used in these studies including ambient outdoor particles, concentrated ambient particles (CAPs), diesel exhaust (DE) from a diesel engine, wood smoke generated in a wood stove, laboratory generated model particles (e.g., elemental carbon [EC] or zinc oxide [ZnO]), or particles collected on a filter, resuspended in saline, and administered either through IT instillation or inhalation. The recovery of particles on filters is variable and some components, such as organics, may be too volatile to be collected. Exposures to artificially generated particles may provide important information on the health effects of PM, but are not truly representative of ambient air pollution particles. The direct exposure of humans to ambient air pollution particles may be complicated by factors that cannot be controlled such as coexposures to other air pollutants (e.g., O₃, SO₂, and NO₂). In concentrating ambient particles, gaseous copollutants are not proportionately concentrated and interactions between PM and the copollutants cannot be investigated unless the latter are re-introduced. These limitations as well as daily variability in concentration and composition can make it difficult to compare the results from controlled human exposure studies employing particles from different sources.

In some instances, controlled human exposure studies can also be used to characterize concentration-response relationships at pollutant concentrations relevant to ambient conditions. Controlled human exposures are typically conducted using a randomized crossover design with subjects exposed both to PM and a clean air control. In this way, subjects serve as their own controls, effectively controlling for many potential confounders. However, controlled human exposure studies are limited by a number of factors including a small sample size and short exposure times. These laboratory studies are often conducted at PM concentrations much higher than those typically observed under ambient conditions, which may result in an overestimate of the acute response to exposure in the general population. Although the repetitive nature of ambient PM exposures may lead to cumulative health effects, this type of exposure is not practical to replicate in a laboratory setting. In addition, while subjects do serve as their own controls, personal exposure to pollutants in the hours and days preceding the controlled exposures may vary significantly between and within individuals. Finally, controlled human exposure studies require investigators to adhere to stringent health criteria for a subject to be included in the study, and therefore the results cannot necessarily be generalized to an entire population. Although some controlled human exposure studies have included health comprised individuals such as asthmatics or individuals with chronic obstructive pulmonary disease (COPD) or coronary artery disease, these individuals must also be relatively healthy and do

not represent the most sensitive individuals in the population. Thus, a lack of observation of effects from controlled human exposure studies does not necessarily mean that a causal relationship does not exist. While controlled human exposure studies provide important information on the biological plausibility of associations observed between air pollutant exposure and health outcomes in epidemiologic studies, observed effects in these studies may underestimate the response in certain subpopulations.

Epidemiologic studies provide important information on the associations between health effects and exposure of human populations to ambient air pollution. In the evaluation of epidemiologic evidence, one important consideration is potential confounding. Confounding is "...a confusion of effects. Specifically, the apparent effect of the exposure of interest is distorted because the effect of an extraneous factor is mistaken for or mixed with the actual exposure effect (which may be null)" (Rothman and Greenland, 1998, [086599](#)). One approach to remove spurious associations from possible confounders is to control for characteristics that may differ between exposed and unexposed persons; this is frequently termed "adjustment." Appropriate statistical adjustment for confounders requires identifying and measuring all reasonably expected confounders. Deciding which variables to control for in a statistical analysis of the association between exposure and disease or health outcome depends on knowledge about possible mechanisms and the distributions of these factors in the population under study. In addition, scientific judgment is needed regarding likely sources and magnitude of confounding, together with consideration of how well the existing constellation of study designs, results, and analyses address this potential threat to inferential validity. One key consideration in this review is evaluation of the potential contribution of PM to health effects when it is a component of a complex air pollutant mixture. Reported PM effect estimates in epidemiologic studies may reflect independent PM effects on respiratory and cardiovascular health. Ambient PM may also be serving as an indicator of complex ambient air pollution mixtures that share the same source as PM (i.e., combustion of S-containing fuels or motor vehicle emissions). Alternatively, copollutants may mediate the effects of PM or PM may influence the toxicity of copollutants.

Another important consideration in the evaluation of epidemiologic evidence is effect modification. "Effect-measure modification differs from confounding in several ways. The main difference is that, whereas confounding is a bias that the investigator hopes to prevent or remove from the effect estimate, effect-measure modification is a property of the effect under study . . . In epidemiologic analysis one tries to eliminate confounding but one tries to detect and estimate effect-measure modification" (Rothman and Greenland, 1998, [086599](#)). Examples of effect modifiers in some of the studies evaluated in this ISA include environmental variables (e.g., temperature or humidity), individual risk factors (e.g., education, cigarette smoking status, age), and community factors (e.g., percent of population > 65 years old). It is often possible to stratify the relationship between health outcome and exposure by one or more of these risk factor variables. Effect modifiers may be encountered (a) within single-city time-series studies; or (b) across cities in a two-stage hierarchical model or meta-analysis.

Several statistical methods are available to detect and control for potential confounders, with none of them being completely satisfactory. Multivariable regression models constitute one tool for estimating the association between exposure and outcome after adjusting for characteristics of participants that might confound the results. The use of multipollutant regression models has been the prevailing approach for controlling potential confounding by copollutants in air pollution health effects studies. Finding the pollutant likely responsible for the health outcome from multipollutant regression models is made difficult by the possibility that one or more air pollutants may be acting as a surrogate for an unmeasured or poorly-measured pollutant or for a particular mixture of pollutants. In addition, more than one pollutant may exert similar health effects, resulting in independently observed associations for multiple pollutants. Further, the correlation between the air pollutant of interest and various copollutants may make it difficult to discern associations between different pollutant exposures and health effects. Thus, results of models that attempt to distinguish gaseous and particle effects must be interpreted with caution. The number and degree of diversity of covariates, as well as their relevance to the potential confounders, remain matters of scientific judgment. Despite these limitations, the use of multipollutant models is still the prevailing approach employed in most air pollution epidemiologic studies, and provides some insight into the potential for confounding or interaction among pollutants.

Adjustment for potential confounders can be influenced by differential exposure measurement error. There are several components that contribute to exposure measurement error in epidemiologic

studies, including the difference between true and measured ambient concentrations, the difference between average personal exposure to ambient pollutants and ambient concentrations at central monitoring sites, and the use of average population exposure rather than individual exposure estimates. Previous AQCDs have examined the role of measurement error in time-series epidemiologic studies using simulated data and mathematical analyses and suggested that “transfer of effects” would only occur under unusual circumstances (i.e., “true” predictors having high positive or negative correlation; substantial measurement error; or extremely negatively correlated measurement errors) (U.S. EPA, 2004, [056905](#)).

Confidence that unmeasured confounders are not producing the findings is increased when multiple studies are conducted in various settings using different subjects or exposures; each of which might eliminate another source of confounding from consideration. Thus, multicity studies which use a consistent method to analyze data from across locations with different levels of covariates can provide insight on potential confounding in associations. Intervention studies, because of their quasi-experimental nature, can be particularly useful in characterizing causation.

In addition to controlled human exposure and epidemiologic studies, the tools of experimental biology have been valuable for developing insights into human physiology and pathology. Animal toxicological studies explore the effects of pollutants on human health, especially through the study of model systems in other species. These studies evaluate the effects of exposures to a variety of pollutants in a highly controlled laboratory setting, and allow exploration of MOAs or mechanisms by which a pollutant may cause effects. Background knowledge of the biological mechanisms by which an exposure might or might not cause disease can prove crucial in establishing, or negating, a causal claim. There are, however, uncertainties associated with quantitative extrapolations between laboratory animals and humans on the pathophysiological effects of any pollutant. Animal species can differ from each other in fundamental aspects of physiology and anatomy (e.g., metabolism, airway branching, hormonal regulation) that may limit extrapolation. The differences between humans and rodents with regard to pollutant absorption and distribution profiles based on breathing pattern, exposure dose, and differences in lung structure and anatomy all have to be taken into consideration.

A relatively new tool available for experimental studies of PM exposure is the particle concentrator. Particle concentrators enable human subjects, animals, or cell culture systems to be exposed to atmospheric PM at concentrations greater than that observed under ambient conditions. As ambient PM is just one component of a complex mixture that interacts with gases and other aerosols, CAPs systems provide a method of exposing subjects to the particle phase. There are several instrument systems used to concentrate ambient PM in controlled human or animal exposure studies (Gordon et al., 1999, [001176](#); Maciejczyk and Chen, 2005, [087456](#); Sioutas et al., 1995, [001629](#); Sioutas et al., 1999, [001633](#)). Gases (such as O₃ and SO₂) are not concentrated nor is PM_{10-2.5} (except for the coarse particle concentrator) and only certain systems are capable of concentrating UFPs. In UF CAPs systems, increased number fraction of organic carbon and PAHs, along with decreased relative percentage of EC particles have been reported in concentrated PM compared to ambient PM (Su et al., 2006, [157021](#)). These data suggest that for UF concentrators, the CAPs do not accurately reflect atmospheric UFP composition.

The ability to extrapolate between species has not generally changed since the 2004 PM AQCD but some considerations related to coarse particles merit attention. The inhalability of particles >2.5 μm in diameter is considerably lower in rats than in humans; however, once inhaled, deposition in the extrathoracic region is near 100% percent for particles >5 μm for most laboratory animal species (rat, mouse, hamster, guinea pig, and dogs). By contrast, penetration of thoracic coarse particles into the lower respiratory tract is greater in humans than rodents due to the moderately less efficient nasal deposition of humans and oronasal breathing (especially during exercise). The extent to which coarse particle deposition in the lower respiratory tract differs between the species is highly dependent on the activity level of the human exposure scenario in contrast with the resting exposure conditions common to rodent exposures. Endotracheal exposures of rodents may be needed to achieve coarse particle tissue doses in the lower respiratory tract of rodents similar to those experienced by humans. For particles <1 μm, including UFPs, deposition is expected to be relatively similar between the species.

There are also differences between species in both the rates of particle clearance from and retention in the lung. The clearance rate of particles from the ciliated airways of rats is considerably greater than humans. There is also evidence of prolonged particle retention in the smaller bronchioles of humans that does not appear to exist or has not been observed in rats. Under most

circumstances, clearance from the alveolar region of rats is also more rapid than observed in humans. Thus, these combined effects contribute to a greater particle burden in the lower respiratory tract of humans relative to rats. An important consideration in studies where rats are chronically exposed to high concentrations of insoluble particles, is the potential for “overload conditions.” Rats, unlike other laboratory animals or humans, may experience a reduction in their alveolar clearance rates and an accumulation of interstitial particle burden and under these conditions, the relevance of tissue burdens and responses to humans is questionable. Considering interspecies differences in both deposition and clearance, greater exposure concentrations are required to achieve coarse particle tissue doses in the lower respiratory tract of rodents similar to those experienced by humans.

1.5.4. Application of Framework for Causal Determination

EPA uses a two-step approach to evaluate the scientific evidence on health or environmental effects of criteria pollutants. The first step determines the weight of evidence in support of causation and characterizes the strength of any resulting causal classification. The second step includes further evaluation of the quantitative evidence regarding the concentration-response relationships and the loads or levels, duration and pattern of exposures at which effects are observed.

To aid judgment, various “aspects”¹ of causality have been discussed by many philosophers and scientists. The most widely cited aspects of causality in epidemiology, and public health, in general, were articulated by Sir Austin Bradford Hill (1965, [071664](#)) and have been widely used (CDC, 2004, [056384](#); IARC, 2006, [093206](#); IOM, 2008, [156586](#); NRC, 2004, [156814](#); U.S. EPA, 2005, [086237](#)). Several adaptations of the Hill aspects have been used in aiding causality judgments in the ecological sciences (Adams, 2003, [156192](#); Collier, 2003, [155736](#); Fox, 1991, [156444](#); Gerritsen et al., 1998, [156465](#)).

These aspects (Hill, 1965, [071664](#)) have been modified (Table 1-2) for use in causal determinations specific to health and welfare effects or pollutant exposures.² Some aspects are more likely than others to be relevant for evaluating evidence on the health or environmental effects of criteria air pollutants. For example, the analogy aspect does not always apply and specificity would not be expected for multi-etiological health outcomes such as asthma or cardiovascular disease, or ecological effects related to acidification. Aspects that usually play a larger role in determination of causality are consistency of results across studies, coherence of effects observed in different study types or disciplines, biological plausibility, exposure-response relationship, and evidence from “natural” experiments.

Although these aspects provide a framework for assessing the evidence, they do not lend themselves to being considered in terms of simple formulas or fixed rules of evidence leading to conclusions about causality (Hill, 1965, [071664](#)). For example, one cannot simply count the number of studies reporting statistically significant results or statistically nonsignificant results and reach credible conclusions about the relative weight of the evidence and the likelihood of causality. In addition, it is important to note that the aspects in Table 1-2 cannot be used as a strict checklist, but rather to determine the weight of the evidence for inferring causality. While these aspects are particularly salient in this assessment, it is also important to recognize that no one aspect is either necessary or sufficient for drawing inferences of causality.

¹ The “aspects” described by Hill (1965, [071664](#)) have become, in the subsequent literature, more commonly described as “criteria.” The original term “aspects” is used here to avoid confusion with ‘criteria’ as it is used, with different meaning, in the Clean Air Act.

² The Hill aspects were developed for interpretation of epidemiologic results. They have been modified here for use with a broader array of data, i.e., epidemiologic, controlled human exposure, and animal toxicological studies, as well as in vitro data, and to be more consistent with EPA’s Guidelines for Carcinogen Risk Assessment.

Table 1-2. Aspects to aid in judging causality.

Aspect	Description
CONSISTENCY OF THE OBSERVED ASSOCIATION	An inference of causality is strengthened when a pattern of elevated risks is observed across several independent studies, conducted in multiple locations by multiple investigators. The reproducibility of findings constitutes one of the strongest arguments for causality. If there are discordant results among investigations, possible reasons such as differences in exposure, confounding factors, and the power of the study are considered.
COHERENCE	An inference of causality from epidemiologic associations may be strengthened by other lines of evidence (e.g., controlled human exposure and animal toxicological studies) that support a cause-and-effect interpretation of the association. Causality is also supported when epidemiologic associations are reported across study designs and across related health outcomes. Evidence on ecological or welfare effects may be drawn from a variety of experimental approaches (e.g., greenhouse, laboratory, and field) and subdisciplines of ecology (e.g., community ecology, biogeochemistry and paleological/ historical reconstructions). The coherence of evidence from various fields greatly adds to the strength of an inference of causality. The absence of other lines of evidence, however, is not a reason to reject causality.
BIOLOGICAL PLAUSIBILITY	An inference of causality tends to be strengthened by consistency with data from experimental studies or other sources demonstrating plausible biological mechanisms. A proposed mechanistic linking between an effect, and exposure to the agent, is an important source of support for causality, especially when data establishing the existence and functioning of those mechanistic links are available. A lack of biological understanding, however, is not a reason to reject causality.
BIOLOGICAL GRADIENT (EXPOSURE-RESPONSE RELATIONSHIP)	A well characterized exposure-response relationship (e.g., increasing effects associated with greater exposure) strongly suggests cause and effect, especially when such relationships are also observed for duration of exposure (e.g., increasing effects observed following longer exposure times). There are, however, many possible reasons that a study may fail to detect an exposure-response relationship. Thus, although the presence of a biological gradient may support causality, the absence of an exposure-response relationship does not exclude a causal relationship.
STRENGTH OF THE OBSERVED ASSOCIATION	The finding of large, precise risks increases confidence that the association is not likely due to chance, bias, or other factors. However, given a truly causal agent, a small magnitude in the effect could follow from a lower level of exposure, a lower potency, or the prevalence of other agents causing similar effects. While large effects support causality, modest effects therefore do not preclude it.
EXPERIMENTAL EVIDENCE	The strongest evidence for causality can be provided when a change in exposure brings about a change in occurrence or frequency of health or welfare effects.
TEMPORAL RELATIONSHIP OF THE OBSERVED ASSOCIATION	Evidence of a temporal sequence between the introduction of an agent and appearance of the effect constitutes another argument in favor of causality.
SPECIFICITY OF THE OBSERVED ASSOCIATION	As originally intended, this refers to increased inference of causality if one cause is associated with a single effect or disease (Hill, 1965, 071664). Based on the current understanding this is now considered one of the weaker guidelines for causality; for example, many agents cause respiratory disease and respiratory disease has multiple causes. At the scale of ecosystems, as in epidemiology, complexity is such that single agents causing single effects, and single effects following single causes, are extremely unlikely. The ability to demonstrate specificity under certain conditions remains, however, a powerful attribute of experimental studies. Thus, although the presence of specificity may support causality, its absence does not exclude it.
ANALOGY	Structure activity relationships and information on the agent's structural analogs can provide insight into whether an association is causal. Similarly, information on mode of action for a chemical, as one of many structural analogs, can inform decisions regarding likely causality.

1.5.5. First Step—Determination of Causality

In the ISA, EPA assesses the results of recent relevant publications, building upon evidence available during the previous NAAQS review, to draw conclusions on the causal relationships between relevant pollutant exposures and health or environmental effects. This ISA uses a five-level

hierarchy that classifies the weight of evidence for causation, not just association¹. In developing this hierarchy, EPA has drawn on the work of previous evaluations, most prominently the IOM's *Improving the Presumptive Disability Decision-Making Process for Veterans* (IOM, 2008, [156586](#)), EPA's Guidelines for Carcinogen Risk Assessment (U.S. EPA, 2005, [086237](#)) and the U.S. Surgeon General's smoking reports (CDC, 2004, [056384](#)). This weight of evidence evaluation is based on various lines of evidence from across the health and environmental effects disciplines. These separate judgments are integrated into a qualitative statement about the overall weight of the evidence and causality. The five descriptors for causal determination are described in Table 1-3.

For PM, this determination of causality step involved a rather complex evaluation of evidence for different PM indices, different types of health or environmental effects, and for short- and long-term exposure periods. There were insufficient data on peak (i.e., <24 h) exposures for any PM size fraction with health effects to make causality determinations for this exposure category. Causality determinations were made for the PM measure (PM_{2.5}, PM_{10-2.5}, and UFPs, to the extent evidence was available for each measure), the overall effect category, and the exposure duration. As noted above, to the extent possible, results of PM₁₀ studies are considered in causality determinations for PM_{2.5} and PM_{10-2.5}. In the evaluation of health effects findings in Chapter 6 (for short-term exposure) and Chapter 7 (for long-term exposure), evidence was evaluated for health outcome categories, such as cardiovascular effects, and then conclusions were drawn based upon the integration of evidence from across disciplines (e.g., epidemiology, controlled human exposure, and toxicology) and also across the suite of related individual health outcomes. Chapters 6 and 7 initially summarize and evaluate findings for individual health outcomes, then integrate the results in summary sections to draw conclusions on causality for each PM indicator. The causality narratives present the weight of evidence that highlights the quality and breadth of the data, including any limitations or uncertainties. In the integrative synthesis and conclusions in Chapter 2, the ISA presents causality determinations and a summary of the underlying basis for those determinations for the PM indicator (e.g., PM_{2.5}), for the exposure time period (e.g., short- and long-term exposure) and for the major health effect categories.

¹ It should be noted that the CDC and IOM frameworks use a four-category hierarchy for the strength of the evidence. A five-level hierarchy is used here to be consistent with the EPA Guidelines for Carcinogen Risk Assessment and to provide a more nuanced set of categories.

Table 1-3. Weight of evidence for causal determination.

Determination	Health Effects	Ecological and Welfare Effects
CAUSAL RELATIONSHIP	Evidence is sufficient to conclude that there is a causal relationship with relevant pollutant exposures. That is, the pollutant has been shown to result in health effects in studies in which chance, bias, and confounding could be ruled out with reasonable confidence. For example: a) controlled human exposure studies that demonstrate consistent effects; or b) observational studies that cannot be explained by plausible alternatives or are supported by other lines of evidence (e.g., animal studies or mode of action information). Evidence includes replicated and consistent high-quality studies by multiple investigators.	Evidence is sufficient to conclude that there is a causal relationship with relevant pollutant exposures. That is, the pollutant has been shown to result in effects in studies in which chance, bias, and confounding could be ruled out with reasonable confidence. Controlled exposure studies (laboratory or small- to medium-scale field studies) provide the strongest evidence for causality, but the scope of inference may be limited. Generally, determination is based on multiple studies conducted by multiple research groups, and evidence that is considered sufficient to infer a causal relationship is usually obtained from the joint consideration of many lines of evidence that reinforce each other.
LIKELY TO BE A CAUSAL RELATIONSHIP	Evidence is sufficient to conclude that a causal relationship is likely to exist with relevant pollutant exposures, but important uncertainties remain. That is, the pollutant has been shown to result in health effects in studies in which chance and bias can be ruled out with reasonable confidence but potential issues remain. For example: a) observational studies show an association, but copollutant exposures are difficult to address and/or other lines of evidence (controlled human exposure, animal, or mode of action information) are limited or inconsistent; or b) animal toxicological evidence from multiple studies from different laboratories that demonstrate effects, but limited or no human data are available. Evidence generally includes replicated and high-quality studies by multiple investigators.	Evidence is sufficient to conclude that there is a likely causal association with relevant pollutant exposures. That is, an association has been observed between the pollutant and the outcome in studies in which chance, bias and confounding are minimized, but uncertainties remain. For example, field studies show a relationship, but suspected interacting factors cannot be controlled, and other lines of evidence are limited or inconsistent. Generally, determination is based on multiple studies in multiple research groups.
SUGGESTIVE OF A CAUSAL RELATIONSHIP	Evidence is suggestive of a causal relationship with relevant pollutant exposures, but is limited because chance, bias and confounding cannot be ruled out. For example, at least one high-quality epidemiologic study shows an association with a given health outcome but the results of other studies are inconsistent.	Evidence is suggestive of a causal relationship with relevant pollutant exposures, but chance, bias and confounding cannot be ruled out. For example, at least one high-quality study shows an effect, but the results of other studies are inconsistent.
INADEQUATE TO INFER A CAUSAL RELATIONSHIP	Evidence is inadequate to determine that a causal relationship exists with relevant pollutant exposures. The available studies are of insufficient quantity, quality, consistency or statistical power to permit a conclusion regarding the presence or absence of an effect.	The available studies are of insufficient quality, consistency or statistical power to permit a conclusion regarding the presence or absence of an effect.
NOT LIKELY TO BE A CAUSAL RELATIONSHIP	Evidence is suggestive of no causal relationship with relevant pollutant exposures. Several adequate studies, covering the full range of levels of exposure that human beings are known to encounter and considering susceptible populations, are mutually consistent in not showing an effect at any level of exposure.	Several adequate studies, examining relationships with relevant exposures, are consistent in failing to show an effect at any level of exposure.

1.5.6. Second Step—Evaluation of Response

Beyond judgments regarding causality are questions relevant to quantifying health or environmental risks based on our understanding of the quantitative relationships between pollutant exposures and health or welfare effects.

1.5.6.1. Effects on Human Populations

Once a determination is made regarding the causal relationship between the pollutant and outcome category, important questions regarding quantitative relationships include:

- What is the concentration-response or dose-response relationship in the human population?
- What exposure conditions (dose or exposure, duration and pattern) are important?
- What subpopulations appear to be differentially affected (i.e., more susceptible to effects)?

To address these questions, in the second step of the EPA framework, the entirety of quantitative evidence is evaluated to best quantify those concentration-response relationships that exist. This requires evaluation of pollutant concentrations and exposure durations at which effects were observed for exposed populations including potentially susceptible populations. This integration of evidence results in identification of a study or set of studies that best approximates the concentration-response relationships between health outcomes and PM indicators for the U.S. population or subpopulations, given the current state of knowledge and the uncertainties that surrounded these estimates.

To accomplish this, evidence from multiple and diverse types of studies is considered. To the extent available, the ISA evaluates results from across epidemiologic studies that use various methods to evaluate the form of relationships between PM and health outcomes, and draws conclusions on the most well-supported shape of these relationships. Controlled human exposure studies can also provide data on the concentration-response relationship. Animal data may inform evaluation of concentration-response relationships, particularly relative to MOAs, and characteristics of susceptible populations. For some health outcomes, the probability and severity of health effects and associated uncertainties can be characterized. Chapter 2 presents the integrated findings informative for evaluation of population risks.

An important consideration in characterizing the public health impacts associated with exposure to a pollutant is whether the concentration-response relationship is linear across the full concentration range encountered, or if nonlinear relationships exist along any part of this range. Of particular interest is the shape of the concentration-response curve at and below the level of the current standards. The shape of the concentration-response curve varies, depending on the type of health outcome, underlying biological mechanisms and dose. At the human population level, however, various sources of variability and uncertainty tend to smooth and “linearize” the concentration-response function (such as the low data density in the lower concentration range, possible influence of measurement error, and individual differences in susceptibility to air pollution health effects). In addition, many chemicals and agents may act by perturbing naturally occurring background processes that lead to disease, which also linearizes population concentration-response relationships (Clewell and Crump, 2005, [156359](#); Crump et al., 1976, [003192](#); Hoel, 1980, [156555](#)). These attributes of population dose-response may explain why the available human data at ambient concentrations for some environmental pollutants (e.g., PM, O₃, lead [Pb], ETS, radiation) do not exhibit evident thresholds for health effects, even though likely mechanisms include nonlinear processes for some key events. These attributes of human population dose-response relationships have been extensively discussed in the broader epidemiologic literature (Rothman and Greenland, 1998, [086599](#)).

Publication bias is a source of uncertainty regarding the magnitude of health risk estimates. It is well understood that studies reporting non-null findings are more likely to be published than reports of null findings, and publication bias can also result in overestimation of effect estimate sizes (Ioannidis, 2008, [188317](#)). For example, effect estimates from single-city epidemiologic studies have been found to be generally larger than those from multicity studies (Anderson et al., 2005, [087916](#)).

Finally, identification of the susceptible population groups contributes to an understanding of the public health impact of pollutant exposures. Epidemiologic studies can help identify susceptible populations by evaluating health responses in the study population. Examples include stratified analyses for subsets of the population under study, or testing for interactions or effect modification by factors such as gender, age group, or health status. Experimental studies using animal models of susceptibility or disease can also inform the extent to which health risks are likely greater in specific population subgroups. Further discussion of these groups is in Chapter 8.

1.5.6.2. Effects on Public Welfare

Key questions for understanding the quantitative relationships between exposure (or concentration or deposition) to a pollutant and risk to the public welfare (e.g., ecosystems, visibility, materials, climate):

- What elements of the ecosystem (e.g., types, regions, taxonomic groups, populations, functions, etc.) appear to be affected, or are more sensitive to effects?
- Under what exposure conditions (amount deposited or concentration, duration and pattern) are effects seen?
- What is the shape of the concentration-response or exposure-response relationship?

Evaluations of causality typically consider the probability of welfare effects changing in response to exposure. A challenge to the quantification of exposure-response relationships for ecological effects is the variability across ecosystems. Ecological responses are evaluated within the range of observations, so a quantitative relationship may be determined for a given ecological system and scale. However, there is great regional and local variability in ecosystems. Thus, exposure-response relationships are often available site by site, rather than at the national or even regional scale. For example, an ecological response to deposition of a given pollutant can differ greatly between ecosystems. Where results from greenhouse or animal ecotoxicological studies are available, they may be used to aid in characterizing exposure-response relationships, particularly relative to mechanisms of action, and characteristics of sensitive biota.

1.5.7. Concepts in Evaluating Adversity of Health Effects

In evaluating the health evidence, a number of factors can be considered in determining the extent to which health effects are “adverse” for health outcomes such as changes in lung function. What constitutes an adverse health effect may vary between populations. Some changes in healthy individuals may not be considered adverse while those of a similar type and magnitude are potentially adverse in more susceptible individuals.

The American Thoracic Society (ATS) published an official statement titled *What Constitutes an Adverse Health Effect of Air Pollution?* (ATS, 2000, [011738](#)). This statement updated the guidance for defining adverse respiratory health effects that had been published 15 years earlier (ATS, 1985, [006522](#)), taking into account new investigative approaches used to identify the effects of air pollution and reflecting concern for impacts of air pollution on specific susceptible groups. In the 2000 update, there was an increased focus on quality of life measures as indicators of adversity and a more specific consideration of population risk. Exposure to air pollution that increases the risk of an adverse effect to the entire population is viewed as adverse, even though it may not increase the risk of any identifiable individual to an unacceptable level; estimated mean population effects do not reflect more severe effects in individuals. For example, a population of asthmatics could have a distribution of lung function such that no identifiable individual has a level associated with significant impairment. Exposure to air pollution could shift the distribution such that no identifiable individual experiences clinically-relevant effects; this shift toward decreased lung function, however, would be considered adverse because individuals within the population would have diminished reserve function and, therefore, would be at increased risk to further environmental insult.

1.6. Summary

This ISA is a review, synthesis, and evaluation of the most policy-relevant science, and communicates critical science judgments relevant to the NAAQS review. It reviews the most policy-relevant evidence from environmental effects studies and includes information on atmospheric chemistry, PM sources and emissions, exposure, and dosimetry. This ISA incorporates clarification and revisions based on advice and comments provided by EPA’s CASAC (Samet, 2009, [190992](#); Samet, 2009, [199522](#)). Annexes to the ISA provide additional details of the literature published since the last review. A framework for making critical judgments concerning causality

appears in this chapter. It relies on a widely accepted set of principles and standardized language to express evaluation of the evidence. This approach can bring rigor and clarity to current and future assessments. This ISA should assist EPA and others, now and in the future, to accurately represent what is presently known—and what remains unknown—concerning the effects of PM on human health and public welfare.

Chapter 1 References

- Adams SM (2003). Establishing causality between environmental stressors and effects on aquatic ecosystems. *Hum Ecol Risk Assess*, 9: 17-35. [156192](#)
- Anderson HR; Atkinson RW; Peacock JL; Sweeting MJ; Marston L (2005). Ambient particulate matter and health effects: Publication bias in studies of short-term associations. *Epidemiology*, 16: 155-163. [087916](#)
- ATS (1985). American Thoracic Society: Guidelines as to what constitutes an adverse respiratory health effect, with special reference to epidemiologic studies of air pollution. *Am Rev Respir Dis*, 131: 666-668. [006522](#)
- ATS (2000). What constitutes an adverse health effect of air pollution? Official statement of the American Thoracic Society. *Am J Respir Crit Care Med*, 161: 665-673. [011738](#)
- CDC (2004). The health consequences of smoking: A report of the Surgeon General. Centers for Disease Control and Prevention, U.S. Department of Health and Human Services. Washington, DC. [056384](#)
- Clewell HJ; Crump KS (2005). Quantitative estimates of risk for noncancer endpoints. *Risk Anal*, 25: 285-289. [156359](#)
- Collier TK (2003). Forensic ecotoxicology: Establishing causality between contaminants and biological effects in field studies. *Hum Ecol Risk Assess*, 9: 259 - 266. [155736](#)
- Crump KS; Hoel DG; Langley CH; Peto R (1976). Fundamental carcinogenic processes and their implications for low dose risk assessment. *Cancer Res*, 36: 2973-2979. [003192](#)
- Fox GA (1991). Practical causal inference for ecoepidemiologists. *J Toxicol Environ Health*, 33: 359-373. [156444](#)
- Gee GC; Payne-Sturges DC (2004). Environmental health disparities: A framework integrating psychosocial and environmental concepts. *Environ Health Perspect*, 112: 1645-1653. [093070](#)
- Gerritsen J; Carlson RE; Dycus DL; Faulkner C; Gibson GR (1998). Lake and reservoir bioassessment and biocriteria: Technical guidance document. US Environmental Protection Agency, Office of Water. Washington, DC. EPA 841-B-98-007. <http://www.epa.gov/owow/monitoring/tech/lakes.html>. [156465](#)
- Gordon T; Gerber H; Fang CP; Chen LC (1999). A centrifugal particle concentrator for use in inhalation toxicology. *Inhal Toxicol*, 11: 71-87. [001176](#)
- Henderson R (2005). Clean Air Scientific Advisory Committee (CASAC) review of the EPA staff recommendations concerning a Potential Thoracic Coarse PM standard in the Review of the National Ambient Air Quality Standards for Particulate Matter: Policy Assessment of Scientific and Technical Information. U.S. Environmental Protection Agency. Washington, DC. [156537](#)
- Henderson R (2005). EPA's Review of the National Ambient Air Quality Standards for Particulate Matter (Second Draft PM Staff Paper, January 2005): A review by the Particulate Matter Review Panel of the EPA Clean Air Scientific Advisory Committee. U.S. Environmental Protection Agency. Washington D.C.. [188316](#)
- Henderson R (2006). Clean Air Scientific Advisory Committee recommendations concerning the proposed National Ambient Air Quality Standards for particulate matter. U.S. Environmental Protection Agency. Washington, DC. [156538](#)
- Hill AB (1965). The environment and disease: Association or causation. *J R Soc Med*, 58: 295-300. [071664](#)
- Hoel DG (1980). Incorporation of background in dose-response models. *Fed Proc*, 39: 73-75. [156555](#)
- IARC (2006). IARC monographs on the evaluation of carcinogenic risks to humans: Preamble. International Agency for Research on Cancer, World Health Organization. Lyon, France . <http://monographs.iarc.fr/ENG/Preamble/CurrentPreamble.pdf> . [093206](#)
- Ioannidis JPA (2008). Why most discovered true associations are inflated. *Epidemiology*, 19: 640-648. [188317](#)

Note: Hyperlinks to the reference citations throughout this document will take you to the NCEA HERO database (Health and Environmental Research Online) at <http://epa.gov/hero>. HERO is a database of scientific literature used by U.S. EPA in the process of developing science assessments such as the Integrated Science Assessments (ISA) and the Integrated Risk Information System (IRIS).

- IOM (2008). Improving the Presumptive Disability Decision-Making Process for Veterans; Committee on Evaluation of the Presumptive Disability Decision-Making Process for Veterans, Board on Military and Veterans Health. Washington, DC: Institute of Medicine of the National Academies, National Academies Press. [156586](#)
- Maciejczyk P; Chen LC (2005). Effects of subchronic exposures to concentrated ambient particles (CAPs) in mice: VIII source-related daily variations in in vitro responses to CAPs. *Inhal Toxicol*, 17: 243-253. [087456](#)
- NAPAP (1991). The experience and legacy of NAPAP report of the Oversight Review Board. National Acid Precipitation Assessment Program. Washington, DC. [095894](#)
- NAPCA (1969). Air quality criteria for particulate matter. National Air Pollution Control Administration. Washington, DC. [014684](#)
- NRC (2004). Research priorities for airborne particulate matter: IV Continuing research progress. National Academies Press. Washington, DC. [156814](#)
- Rothman KJ; Greenland S (1998). Modern epidemiology. Philadelphia, PA: Lippincott-Raven Publishers. [086599](#)
- Samet JM (2009). CASAC Review of integrated science assessment for particulate matter (second external review draft, July 2009). U.S. Environmental Protection Agency. Washington, D.C.. EPA-CASAC-10-001. [199522](#)
- Samet JM (2009). Review of EPA's Integrated Science Assessment for Particulate Matter (First External Review Draft, December 2008). Clean Air Scientific Advisory Committee (CASAC) and members of the CASAC Particulate Matter (PM) Review Panel, Science Advisory Board, U.S. Environmental Protection Agency. Washington, D.C.. EPA-CASAC-09-008. [190992](#)
- Sioutas C; Kim S; Chang M (1999). Development and evaluation of a prototype ultrafine particle concentrator. *J Aerosol Sci*, 30: 1001-1017. [001633](#)
- Sioutas D; Koutrakis P; Ferguson ST; Burton RM (1995). Development and evaluation of a prototype ambient particle concentrator for inhalation exposure studies. *Inhal Toxicol*, 7: 633-644. [001629](#)
- Su Y; Sipin MF; Spencer MT; Qin X; Moffet RC; Shields LG; Prather KA; Venkatachari P; Jeong C-H; Kim E; Hopke PK; Gelein RM; Utell MJ; Oberdörster G; Berntsen J; Devlin RB; Chen LC (2006). Real-time characterization of the composition of individual particles emitted from ultrafine particle concentrators. *Aerosol Sci Technol*, 40: 437-455. [157021](#)
- U.S. EPA (2004). Air quality criteria for particulate matter. U.S. Environmental Protection Agency. Research Triangle Park, NC. EPA/600/P-99/002aF-bF. [056905](#)
- U.S. EPA (2005). Guidelines for carcinogen risk assessment, Final Report. Risk Assessment Forum, U.S. Environmental Protection Agency. Washington, DC. EPA/630/P-03/001F. <http://cfpub.epa.gov/ncea/cfm/recordisplay.cfm?deid=116283>. [086237](#)
- U.S. EPA (2005). Review of the national ambient air quality standards for particulate matter: Policy assessment of scientific and technical information OAQPS staff paper. U.S. Environmental Protection Agency. Washington, DC. EPA/452/R-05-005a. http://www.epa.gov/ttn/naaqs/standards/pm/data/pmstaffpaper_20051221.pdf. [090209](#)
- U.S. EPA (2008). Integrated review plan for the national ambient air quality standards for particulate matter. U.S. Environmental Protection Agency, Office of Research and Development, National Center for Environmental Assessment. Research Triangle Park, NC. [157072](#)
- U.S. EPA (2008). Integrated science assessment for oxides of nitrogen and sulfur: Ecological criteria. U.S. Environmental Protection Agency. Research Triangle Park, NC. EPA/600/R-08/082F. [157074](#)

Chapter 2. Integrative Health and Welfare Effects Overview

The subsequent chapters of this ISA will present the most policy-relevant information related to this review of the NAAQS for PM. This chapter integrates the key findings from the disciplines evaluated in this current assessment of the PM scientific literature, which includes the atmospheric sciences, ambient air data analyses, exposure assessment, dosimetry, health studies (e.g., toxicological, controlled human exposure, and epidemiologic), and welfare effects. The EPA framework for causal determinations described in Chapter 1 has been applied to the body of scientific evidence in order to collectively examine the health or welfare effects attributed to PM exposure in a two-step process.

As described in Chapter 1, EPA assesses the results of recent relevant publications, building upon evidence available during the previous NAAQS reviews, to draw conclusions on the causal relationships between relevant pollutant exposures and health or environmental effects. This ISA uses a five-level hierarchy that classifies the weight of evidence for causation:

- Causal relationship
- Likely to be a causal relationship
- Suggestive of a causal relationship
- Inadequate to infer a causal relationship
- Not likely to be a causal relationship

Beyond judgments regarding causality are questions relevant to quantifying health or environmental risks based on our understanding of the quantitative relationships between pollutant exposures and health or welfare effects. Once a determination is made regarding the causal relationship between the pollutant and outcome category, important questions regarding quantitative relationships include:

- What is the concentration-response or dose-response relationship?
- Under what exposure conditions (amount deposited, dose or concentration, duration and pattern) are effects observed?
- What populations appear to be differentially affected (i.e., more susceptible) to effects?
- What elements of the ecosystem (e.g., types, regions, taxonomic groups, populations, functions, etc.) appear to be affected, or are more sensitive to effects?

To address these questions, in the second step of the EPA framework, the entirety of quantitative evidence is evaluated to identify and characterize potential concentration-response relationships. This requires evaluation of levels of pollutant and exposure durations at which effects were observed for exposed populations including potentially susceptible populations.

This chapter summarizes and integrates the newly available scientific evidence that best informs consideration of the policy-relevant questions that frame this assessment, presented in Chapter 1. Section 2.1 discusses the trends in ambient concentrations and sources of PM and provides a brief summary of ambient air quality. Section 2.2 presents the evidence regarding personal exposure to ambient PM in outdoor and indoor microenvironments, and it discusses the

▪ Note: Hyperlinks to the reference citations throughout this document will take you to the NCEA HERO database (Health and Environmental Research Online) at <http://epa.gov/hero>. HERO is a database of scientific literature used by U.S. EPA in the process of developing science assessments such as the Integrated Science Assessments (ISA) and the Integrated Risk Information System (IRIS).

relationship between ambient PM concentrations and exposure to PM from ambient sources. Section 2.3 integrates the evidence for studies that examine the health effects associated with short- and long-term exposure to PM and discusses important uncertainties identified in the interpretation of the scientific evidence. Section 2.4 provides a discussion of policy-relevant considerations, such as potentially susceptible populations, lag structure, and the PM concentration-response relationship, and PM sources and constituents linked to health effects. Section 2.5 summarizes the evidence for welfare effects related to PM exposure. Finally, Section 2.6 provides all of the causal determinations reached for each of the health outcomes and PM exposure durations evaluated in this ISA.

2.1. Concentrations and Sources of Atmospheric PM

2.1.1. Ambient PM Variability and Correlations

Recently, advances in understanding the spatiotemporal distribution of PM mass and its constituents have been made, particularly with regard to PM_{2.5} and its components as well as ultrafine particles (UFPs). Emphasis in this ISA is placed on the period from 2005-2007, incorporating the most recent validated EPA Air Quality System (AQS) data. The AQS is EPA's repository for ambient monitoring data reported by the national, and state and local air monitoring networks. Measurements of PM_{2.5} and PM₁₀ are reported into AQS, while PM_{10-2.5} concentrations are obtained as the difference between PM₁₀ and PM_{2.5} (after converting PM₁₀ concentrations from STP to local conditions; Section 3.5). Note, however, that a majority of U.S. counties were not represented in AQS because their population fell below the regulatory monitoring threshold. Moreover, monitors reporting to AQS were not uniformly distributed across the U.S. or within counties, and conclusions drawn from AQS data may not apply equally to all parts of a geographic region. Furthermore, biases can exist for some PM constituents (and hence total mass) owing to volatilization losses of nitrates and other semi-volatile compounds, and, conversely, to retention of particle-bound water by hygroscopic species. The degree of spatial variability in PM was likely to be region-specific and strongly influenced by local sources and meteorological and topographic conditions.

2.1.1.1. Spatial Variability across the U.S.

AQS data for daily average concentrations of PM_{2.5} for 2005-2007 showed considerable variability across the U.S. (Section 3.5.1.1). Counties with the highest average concentrations of PM_{2.5} (>18 µg/m³) were reported for several counties in the San Joaquin Valley and inland southern California as well as Jefferson County, AL (containing Birmingham) and Allegheny County, PA (containing Pittsburgh). Relatively few regulatory monitoring sites have the appropriate co-located monitors for computing PM_{10-2.5}, resulting in poor geographic coverage on a national scale (Figure 3-10). Although the general understanding of PM differential settling leads to an expectation of greater spatial heterogeneity in the PM_{10-2.5} fraction, deposition of particles as a function of size depends strongly on local meteorological conditions. Better geographic coverage is available for PM₁₀, where the highest reported annual average concentrations (>50 µg/m³) occurred in southern California, southern Arizona and central New Mexico. The size distribution of PM varied substantially by location, with a generally larger fraction of PM₁₀ mass in the PM_{10-2.5} size range in western cities (e.g., Phoenix and Denver) and a larger fraction of PM₁₀ in the PM_{2.5} size range in eastern U.S. cities (e.g., Pittsburgh and Philadelphia). UFPs are not measured as part of AQS or any other routine regulatory network in the U.S. Therefore, limited information is available regarding regional variability in the spatiotemporal distribution of UFPs.

Spatial variability in PM_{2.5} components obtained from the Chemical Speciation Network (CSN) varied considerably by species from 2005-2007 (Figures 3-12 through 3-18). The highest annual average organic carbon (OC) concentrations were observed in the western and southeastern U.S. OC concentrations in the western U.S. peaked in the fall and winter, while OC concentrations in the Southeast peaked anytime between spring and fall. Elemental carbon (EC) exhibited less seasonality than OC and showed lowest seasonal variability in the eastern half of the U.S. The

highest annual average EC concentrations were present in Los Angeles, Pittsburgh, New York, and El Paso. Concentrations of sulfate (SO_4^{2-}) were higher in the eastern U.S. as a result of higher SO_2 emissions in the East compared with the West. There is also considerable seasonal variability with higher SO_4^{2-} concentrations in the summer months when the oxidation of SO_2 proceeds at a faster rate than during the winter. Nitrate (NO_3^-) concentrations were highest in California and during the winter in the Upper Midwest. In general, NO_3^- was higher in the winter across the country, in part as a result of temperature-driven partitioning and volatilization. Exceptions existed in Los Angeles and Riverside, CA, where high NO_3^- concentrations appeared year-round. There is variation in both $\text{PM}_{2.5}$ mass and composition among cities, some of which might be due to regional differences in meteorology, sources, and topography.

2.1.1.2. Spatial Variability on the Urban and Neighborhood Scales

In general, $\text{PM}_{2.5}$ has a longer atmospheric lifetime than $\text{PM}_{10-2.5}$. As a result, $\text{PM}_{2.5}$ is more homogeneously distributed than $\text{PM}_{10-2.5}$, whose concentrations more closely reflect proximity to local sources (Section 3.5.1.2). Because PM_{10} encompasses $\text{PM}_{10-2.5}$ in addition to $\text{PM}_{2.5}$, it also exhibits more spatial heterogeneity than $\text{PM}_{2.5}$. Urban- and neighborhood-scale variability in PM mass and composition was examined by focusing on 15 metropolitan areas, which were chosen based on their geographic distribution and coverage in recent health effects studies. The urban areas selected were Atlanta, Birmingham, Boston, Chicago, Denver, Detroit, Houston, Los Angeles, New York, Philadelphia, Phoenix, Pittsburgh, Riverside, Seattle and St. Louis. Inter-monitor correlation remained higher over long distances for $\text{PM}_{2.5}$ as compared with PM_{10} in these 15 urban areas. To a large extent, greater variation in $\text{PM}_{2.5}$ and PM_{10} concentrations within cities was observed in areas with lower ratios of $\text{PM}_{2.5}$ to PM_{10} . When the data was limited to only sampler pairs with less than 4 km separation (i.e., on a neighborhood scale), inter-sampler correlations remained higher for $\text{PM}_{2.5}$ than for PM_{10} . The average inter-sampler correlation was 0.93 for $\text{PM}_{2.5}$, while it dropped to 0.70 for PM_{10} (Section 3.5.1.3). Insufficient data were available in the 15 metropolitan areas to perform similar analyses for $\text{PM}_{10-2.5}$ using co-located, low volume FRM monitors.

As previously mentioned, UFPs are not measured as part of AQS or any other routine regulatory network in the U.S. Therefore, information about the spatial variability of UFPs is sparse; however, their number concentrations are expected to be highly spatially and temporally variable. This has been shown on the urban scale in studies in which UFP number concentrations drop off quickly with distance from roads compared to accumulation mode particle numbers.

2.1.2. Trends and Temporal Variability

Overall, $\text{PM}_{2.5}$ concentrations decreased from 1999 (the beginning of nationwide monitoring for $\text{PM}_{2.5}$) to 2007 in all ten EPA Regions, with the 3-yr avg of the 98th percentile of 24-h $\text{PM}_{2.5}$ concentrations dropping 10% over this time period. However from 2002-2007, concentrations of $\text{PM}_{2.5}$ were nearly constant with decreases observed in only some EPA Regions (Section 3.5.2.1). Concentrations of $\text{PM}_{2.5}$ components were only available for 2002-2007 using CSN data and showed little decline over this time period. This trend in $\text{PM}_{2.5}$ components is consistent with trends in $\text{PM}_{2.5}$ mass concentration observed after 2002 (shown in Figures 3-44 through 3-47). Concentrations of PM_{10} also declined from 1988 to 2007 in all ten EPA Regions.

Using hourly PM observations in the 15 metropolitan areas, diel variation showed average hourly peaks that differ by size fraction and region (Section 3.5.2.3). For both $\text{PM}_{2.5}$ and PM_{10} , a morning peak was typically observed starting at approximately 6:00 a.m., corresponding with the start of morning rush hour. There was also an evening concentration peak that was broader than the morning peak and extended into the overnight period, reflecting the concentration increase caused by the usual collapse of the mixing layer after sundown. The magnitude and duration of these peaks varied considerably by metropolitan area investigated.

UFPs were found to exhibit similar two-peaked diel patterns in Los Angeles and the San Joaquin Valley of CA and Rochester, NY as well as in Kawasaki City, Japan, and Copenhagen, Denmark. The morning peak in UFPs likely represents primary source emissions, such as rush-hour traffic, while the afternoon peak likely represents the combination of primary source emissions and nucleation of new particles.

2.1.3. Correlations between Copollutants

Correlations between PM and gaseous copollutants, including SO₂, NO₂, carbon monoxide (CO) and O₃, varied both seasonally and spatially between and within metropolitan areas (Section 3.5.3). On average, PM_{2.5} and PM₁₀ were correlated with each other better than with the gaseous copollutants. Although data are limited for PM_{10-2.5}, the available data suggest a stronger correlation between PM₁₀ and PM_{10-2.5} than between PM_{2.5} and PM_{10-2.5} on a national basis. There was relatively little seasonal variability in the mean correlation between PM in both size fractions and SO₂ and NO₂. CO, however, showed higher correlations with PM_{2.5} and PM₁₀ on average in the winter compared with the other seasons. This seasonality results in part because a larger fraction of PM is primary in origin during the winter. To the extent that this primary component of PM is associated with common combustion sources of NO₂ and CO, then higher correlations with these gaseous copollutants are to be expected. Increased atmospheric stability in colder months also results in higher correlations between primary pollutants (Section 3.5).

The correlation between daily maximum 8-h avg O₃ and 24-h avg PM_{2.5} showed the highest degree of seasonal variability with positive correlations on average in summer (avg = 0.56) and negative correlations on average in the winter (avg = -0.30). During the transition seasons, spring and fall, correlations were mixed but on average were still positive. PM_{2.5} is both primary and secondary in origin, whereas O₃ is only secondary. Photochemical production of O₃ and secondary PM in the planetary boundary layer (PBL) is much slower during the winter than during other seasons. Primary pollutant concentrations (e.g., primary PM_{2.5} components, NO and NO₂) in many urban areas are elevated in winter as the result of heating emissions, cold starts and low mixing heights. O₃ in the PBL during winter is mainly associated with air subsiding from above the boundary layer following the passage of cold fronts, and this subsiding air has much lower PM concentrations than are present in the PBL. Therefore, a negative association between O₃ and PM_{2.5} is frequently observed in the winter. During summer, both O₃ and secondary PM_{2.5} are produced in the PBL and in the lower free troposphere at faster rates compared to winter, and so they tend to be positively correlated.

2.1.4. Measurement Techniques

The federal reference methods (FRMs) for PM_{2.5} and PM₁₀ are based on criteria outlined in the Code of Federal Regulations. They are, however, subject to several limitations that should be kept in mind when using compliance monitoring data for health studies. For example, FRM techniques are subject to the loss of semi-volatile species such as organic compounds and ammonium nitrate (especially in the West). Since FRMs based on gravimetry use 24-h integrated filter samples to collect PM mass, no information is available for variations over shorter averaging times from these instruments. However, methods have been developed to measure real-time PM mass concentrations. Real-time (or continuous and semi-continuous) measurement techniques are also available for PM species, such as particle into liquid sampler (PILS) for multiple ions analysis and aerosol mass spectrometer (AMS) for multiple components analysis (Section 3.4.1). Advances have also been achieved in PM organic speciation. New 24-h FRMs and Federal Equivalent Methods (FEMs) based on gravimetry and continuous FEMs for PM_{10-2.5} are available. FRMs for PM_{10-2.5} rely on calculating the difference between co-located PM₁₀ and PM_{2.5} measurements while a dichotomous sampler is designated as an FEM.

2.1.5. PM Formation in the Atmosphere and Removal

PM in the atmosphere contains both primary (i.e., emitted directly by sources) and secondary components, which can be anthropogenic or natural in origin. Secondary PM components can be produced by the oxidation of precursor gases such as SO₂ and NO_x to acids followed by neutralization with ammonia (NH₃) and the partial oxidation of organic compounds. In addition to being emitted as primary particles, UFPs are produced by the nucleation of H₂SO₄ vapor, H₂O vapor, and perhaps NH₃ and certain organic compounds. Over most of the earth's surface, nucleation is probably the major mechanism forming new UFPs. New UFP formation has been observed in environments ranging from relatively unpolluted marine and continental environments to polluted

urban areas as an ongoing background process and during nucleation events. However, as noted above, a large percentage of UFPs come from combustion-related sources such as motor vehicles.

Developments in the chemistry of formation of secondary organic aerosol (SOA) indicate that oligomers are likely a major component of OC in aerosol samples. Recent observations also suggest that small but significant quantities of SOA are formed from the oxidation of isoprene in addition to the oxidation of terpenes and organic hydrocarbons with six or more carbon atoms. Gasoline engines have been found to emit a mix of nucleation-mode heavy and large polycyclic aromatic hydrocarbons on which unspent fuel and trace metals can condense, while diesel particles are composed of a soot nucleus on which sulfates and hydrocarbons can condense. To the extent that the primary component of organic aerosol is overestimated in emissions from combustion sources, the semi-volatile components are underestimated. This situation results from the lack of capture of evaporated semi-volatile components upon dilution in common emissions tests. As a result, near-traffic sources of precursors to SOA would be underestimated. The oxidation of these precursors results in more oxidized forms of SOA than previously considered, in both near source urban environments and further downwind. Primary organic aerosol can also be further oxidized to forms that have many characteristics in common with oxidized SOA formed from gaseous precursors. Organic peroxides constitute a significant fraction of SOA and represent an important class of reactive oxygen species (ROS) that have high oxidizing potential. More information on sources, emissions and deposition of PM are included in Section 3.3.

Wet and dry deposition are important processes for removing PM and other pollutants from the atmosphere on urban, regional, and global scales. Wet deposition includes incorporation of particles into cloud droplets that fall as rain (rainout) and collisions with falling rain (washout). Other hydrometeors (snow, ice) can also serve the same purpose. Dry deposition involves transfer of particles through gravitational settling and/or by impaction on surfaces by turbulent motions. The effects of deposition of PM on ecosystems and materials are discussed in Section 2.5 and in Chapter 9.

2.1.6. Source Contributions to PM

Results of receptor modeling calculations indicate that $PM_{2.5}$ is produced mainly by combustion of fossil fuel, either by stationary sources or by transportation. A relatively small number of broadly defined source categories, compared to the total number of chemical species that typically are measured in ambient monitoring source receptor studies, account for the majority of the observed PM mass. Some ambiguity is inherent in identifying source categories. For example, quite different mobile sources such as trucks, farm equipment, and locomotives rely on diesel engines and ancillary data is often required to resolve these sources. A compilation of study results shows that secondary SO_4^{2-} (derived mainly from SO_2 emitted by Electricity Generating Units [EGUs]), NO_3^- (from the oxidation of NO_x emitted mainly from transportation sources and EGUs), and primary mobile source categories, constitute most of $PM_{2.5}$ (and PM_{10}) in the East. $PM_{10-2.5}$ is mainly primary in origin, having been emitted as fully formed particles derived from abrasion and crushing processes, soil disturbances, plant and insect fragments, pollens and other microorganisms, desiccation of marine aerosol emitted from bursting bubbles, and hygroscopic fine PM expanding with humidity to coarse mode. Gases such as HNO_3 can also condense directly onto preexisting coarse particles. Suspended primary coarse PM can contain Fe, Si, Al, and base cations from soil, plant and insect fragments, pollen, fungal spores, bacteria, and viruses, as well as fly ash, brake lining particles, debris, and automobile tire fragments. Quoted uncertainties in the source apportionment of constituents in ambient aerosol samples typically range from 10 to 50%. An intercomparison of source apportionment techniques indicated that the same major source categories of $PM_{2.5}$ were consistently identified by several independent groups working with the same data sets. Soil-, sulfate-, residual oil-, and salt-associated mass were most clearly identified by the groups. Other sources with more ambiguous signatures, such as vegetative burning and traffic-related emissions were less consistently identified.

Spatial variability in source contributions across urban areas is an important consideration in assessing the likelihood of exposure error in epidemiologic studies relating health outcomes to sources. Concepts similar to those for using ambient concentrations as surrogates for personal exposures apply here. Some source attribution studies for $PM_{2.5}$ indicate that intra-urban variability increases in the following order: regional sources (e.g., secondary SO_4^{2-} originating from EGUs) < area sources (e.g., on-road mobile sources) < point sources (e.g., metals from stacks of smelters).

Although limited information was available for PM_{10-2.5}, it does indicate a similar ordering, but without a regional component (resulting from the short lifetime of PM_{10-2.5} compared to transport times on the regional scale). More discussion on source contributions to PM is available in Section 3.6.

2.1.7. Policy-Relevant Background

The background concentrations of PM that are useful for risk and policy assessments, which inform decisions about the NAAQS are referred to as policy-relevant background (PRB) concentrations. PRB concentrations have historically been defined by EPA as those concentrations that would occur in the U.S. in the absence of anthropogenic emissions in continental North America defined here as the U.S., Canada, and Mexico. For this document, PRB concentrations include contributions from natural sources everywhere in the world and from anthropogenic sources outside continental North America. Background concentrations so defined facilitated separation of pollution that can be controlled by U.S. regulations or through international agreements with neighboring countries from those that were judged to be generally uncontrollable by the U.S. Over time, consideration of potential broader ranging international agreements may lead to alternative determinations of which PM source contributions should be considered by EPA as part of PRB.

Contributions to PRB concentrations of PM include both primary and secondary natural and anthropogenic components. For this document, PRB concentrations of PM_{2.5} for the continental U.S. were estimated using EPA's Community Multi-scale Air Quality (CMAQ) modeling system, a deterministic, chemical-transport model (CTM), using output from GEOS-Chem a global-scale model for CMAQ boundary conditions. PRB concentrations of PM_{2.5} were estimated to be less than 1 µg/m³ on an annual basis, with maximum daily average values in a range from 3.1 to 20 µg/m³ and having a peak of 63 µg/m³ at the nine national park sites across the U.S. used to evaluate model performance for this analysis. A description of the models and evaluation of their performance is given in Section 3.6 and further details about the calculations of PRB concentrations are given in Section 3.7.

2.2. Human Exposure

This section summarizes the findings from the recent exposure assessment literature. This summary is intended to support the interpretation of the findings from epidemiologic studies and reflects the material presented in Section 3.8. Attention is given to how concentration metrics can be used in exposure assessment and what errors and uncertainties are incurred for different approaches. Understanding of exposure errors is important because exposure error can potentially bias an estimate of a health effect or increase the size of confidence intervals around a health effect estimate.

2.2.1. Spatial Scales of PM Exposure Assessment

Assessing population-level exposure at the urban scale is particularly relevant for time-series epidemiologic studies, which provide information on the relationship between health effects and community-average exposure, rather than an individual's exposure. PM concentrations measured at a central-site ambient monitor are used as surrogates for personal PM exposure. However, the correlation between the PM concentration measured at central-site ambient monitor(s) and the unknown true community average concentration depends on the spatial distribution of PM, the location of the monitoring site(s) chosen to represent the community average, and division of the community by terrain features or local sources into several sub-communities that differ in the temporal pattern of pollution. Concentrations of SO₄²⁻ and some components of SOA measured at central-site monitors are expected to be uniform in urban areas because of the regional nature of their sources. However, this is not true for primary components like EC whose sources are strongly spatially variable in urban areas.

At micro-to-neighborhood scales, heterogeneity of sources and topography contribute to variability in exposure. This is particularly true for PM_{10-2.5} and for UFPs, which have spatially

variable urban sources and loss processes (mainly gravitational settling for $PM_{10-2.5}$ and coagulation for UFPs) that also limit their transport from sources more readily than for $PM_{2.5}$. Personal activity patterns also vary across urban areas and across regions. Some studies, conducted mainly in Europe, have found personal $PM_{2.5}$ and PM_{10} exposures for pedestrians in street canyons to be higher than ambient concentrations measured by urban central site ambient monitors. Likewise, microenvironmental UFP concentrations were observed to be substantially higher in near-road environments, street canyons, and tunnels when compared with urban background concentrations. In-vehicle UFP and $PM_{2.5}$ exposures can also be important. As a result, concentrations measured by ambient monitors likely do not reflect the contributions of UFP or $PM_{2.5}$ exposures to individuals while commuting.

There is significant variability within and across regions of the country with respect to indoor exposures to ambient PM. Infiltrated ambient PM concentrations depend in part on the ventilation properties of the building or vehicle in which the person is exposed. PM infiltration factors depend on particle size, chemical composition, season, and region of the country. Infiltration can best be modeled dynamically rather than being represented by a single value. Season is important to PM infiltration because it affects the ventilation practices (e.g., open windows) used. In addition, ambient temperature and humidity conditions affect the transport, dispersion, and size distribution of PM. Residential air exchange rates have been observed to be higher in the summer for regions with low air conditioning usage. Regional differences in air exchange rates (Southwest < Southeast < Northeast < Northwest) also reflect ventilation practices. Differential infiltration occurs as a function of PM size and composition (the latter of which is described below). PM infiltration is larger for accumulation mode particles than for UFPs and $PM_{10-2.5}$. Differential infiltration by size fraction can affect exposure estimates if not accurately characterized.

2.2.2. Exposure to PM Components and Copollutants

Emission inventories and source apportionment studies suggest that sources of PM exposure vary by region. Comparison of studies performed in the eastern U.S. with studies performed in the western U.S. suggest that the contribution of SO_4^{2-} to exposure is higher for the East (16-46%) compared with the West (~4%) and that motor vehicle emissions and secondary NO_3^- are larger sources of exposure for the West (~9%) as compared with the East (~4%). Results of source apportionment studies of exposure to SO_4^{2-} indicate that SO_4^{2-} exposures are mainly attributable to ambient sources. Source apportionment for OC and EC is difficult because they originate from both indoor and outdoor sources. Exposure to OC of indoor and outdoor origin can be distinguished by the presence of aliphatic C-H groups generated indoors, since outdoor concentrations of aliphatic C-H are low. Studies of personal exposure to ambient trace metal have shown significant variation among cities and over seasons. This is in response to geographic and seasonal variability in sources including incinerator operation, fossil fuel combustion, biomass combustion (wildfires), and the resuspension of crustal materials in the built environment. Differential infiltration is also affected by variations in particle composition and volatility. For example, EC infiltrates more readily than OC. This can lead to outdoor-indoor differentials in PM composition.

Some studies have explored the relationship between PM and copollutant gases and suggested that certain gases can serve as surrogates for describing exposure to other air pollutants. The findings indicate that ambient concentrations of gaseous copollutants can act as surrogates for personal exposure to ambient PM. Several studies have concluded that ambient concentrations of O_3 , NO_2 , and SO_2 are associated with the ambient component of personal exposure to total $PM_{2.5}$. If associations between ambient gases and personal exposure to $PM_{2.5}$ of ambient origin exist, such associations are complex and vary by season and location.

2.2.3. Implications for Epidemiologic Studies

In epidemiologic studies, exposure may be estimated using various approaches, most of which rely on measurements obtained using central site monitors. The magnitude and direction of the biases introduced through error in exposure measurement depend on the extent to which the error is associated with the measured PM concentration. In general, when exposure error is not strongly correlated with the measured PM concentration, bias is toward the null and effect estimates are

underestimated. Moreover, lack of information regarding exposure measurement error can also add uncertainty to the health effects estimate.

One important factor to be considered is the spatial variation in PM concentrations. The degree of urban-scale spatial variability in PM concentrations varies across the country and by size fraction. PM_{2.5} concentrations are relatively well-correlated across monitors in the urban areas examined for this assessment. The limited available evidence indicates that there is greater spatial variability in PM_{10-2.5} concentrations than PM_{2.5} concentrations, resulting in increased exposure error for the larger size fraction. Likewise, studies have shown UFPs to be more spatially variable across urban areas compared to PM_{2.5}. Even if PM_{2.5}, PM_{10-2.5}, or UFP concentrations measured at sites within an urban area are generally highly correlated, significant spatial variation in their concentrations can occur on any given day. In addition, there can be differential exposure errors for PM components (e.g., SO₄²⁻, OC, EC). Current information suggests that UFPs, PM_{10-2.5}, and some PM components are more spatially variable than PM_{2.5}. Spatial variability of these PM indicators adds uncertainty to exposure estimates.

Overall, recent studies generally confirm and build upon the key conclusions of the 2004 PM AQCD: separation of total PM exposures into ambient and nonambient components reduces potential uncertainties in the analysis and interpretation of PM health effects data; and ambient PM concentration can be used as a surrogate for ambient PM exposure in community time-series epidemiologic studies because the change in ambient PM concentration should be reflected in the change in the health risk coefficient. The use of the community average ambient PM_{2.5} concentration as a surrogate for the community average personal exposure to ambient PM_{2.5} is not expected to change the principal conclusions from time-series and most panel epidemiologic studies that use community average health and pollution data. Several recent studies support this by showing how the ambient component of personal exposure to PM_{2.5} could be estimated using various tracer and source apportionment techniques and by showing that the ambient component is highly correlated with ambient concentrations of PM_{2.5}. These studies show that the non-ambient component of personal exposure to PM_{2.5} is largely uncorrelated with ambient PM_{2.5} concentrations. A few panel epidemiologic studies have included personal as well as ambient monitoring data, and generally reported associations with all types of PM measurements. Epidemiologic studies of long-term exposure typically exploit the differences in PM concentration across space, as well as time, to estimate the effect of PM on the health outcome of interest. Long-term exposure estimates are most accurate for pollutants that do not vary substantially within the geographic area studied.

2.3. Health Effects

This section evaluates the evidence from toxicological, controlled human exposure, and epidemiologic studies that examined the health effects associated with short- and long-term exposure to PM (i.e., PM_{2.5}, PM_{10-2.5} and UFPs). The results from the health studies evaluated in combination with the evidence from atmospheric chemistry and exposure assessment studies contribute to the causal determinations made for the health outcomes discussed in this assessment (a description of the causal framework can be found in Section 1.5.4). In the following sections a discussion of the causal determinations will be presented by PM size fraction and exposure duration (i.e., short- or long-term exposure) for the health effects for which sufficient evidence was available to conclude a causal, likely to be causal or suggestive relationship. Although not presented in depth in this chapter, a detailed discussion of the underlying evidence used to formulate each causal determination can be found in Chapters 6 and 7.

2.3.1. Exposure to PM_{2.5}

2.3.1.1. Effects of Short-Term Exposure to PM_{2.5}

Table 2-1. Summary of causal determinations for short-term exposure to PM_{2.5}.

Size Fraction	Outcome	Causality Determination
PM _{2.5}	Cardiovascular Effects	Causal
	Respiratory Effects	Likely to be causal
	Mortality	Causal

Cardiovascular Effects

Epidemiologic studies that examined the effect of PM_{2.5} on cardiovascular emergency department (ED) visits and hospital admissions reported consistent positive associations (predominantly for ischemic heart disease [IHD] and congestive heart failure [CHF]), with the majority of studies reporting increases ranging from 0.5 to 3.4% per 10 µg/m³ increase in PM_{2.5}. These effects were observed in study locations with mean¹ 24-h avg PM_{2.5} concentrations ranging from 7-18 µg/m³ (Section 6.2.10). The largest U.S.-based multicity study evaluated, Medicare Air Pollution Study (MCAPS), provided evidence of regional heterogeneity (e.g., the largest excess risks occurred in the Northeast [1.08%]) and seasonal variation (e.g., the largest excess risks occurred during the winter season [1.49%]) in PM_{2.5} cardiovascular disease (CVD) risk estimates, which is consistent with the null findings of several single-city studies conducted in the western U.S. These associations are supported by multicity epidemiologic studies that observed consistent positive associations between short-term exposure to PM_{2.5} and cardiovascular mortality and also reported regional and seasonal variability in risk estimates. The multicity studies evaluated reported consistent increases in cardiovascular mortality ranging from 0.47 to 0.85% in study locations with mean 24-h avg PM_{2.5} concentrations above 12.8 µg/m³ (Table 6-15).

Controlled human exposure studies have demonstrated PM_{2.5}-induced changes in various measures of cardiovascular function among healthy and health-compromised adults. The most consistent evidence is for altered vasomotor function following exposure to diesel exhaust (DE) or CAPs with O₃ (Section 6.2.4.2). Although these findings provide biological plausibility for the observations from epidemiologic studies, the fresh DE used in the controlled human exposure studies evaluated contains gaseous components (e.g., CO, NO_x), and therefore, the possibility that some of the changes in vasomotor function might be due to gaseous components cannot be ruled out. Furthermore, the prevalence of UFPs in fresh DE limits the ability to conclusively attribute the observed effects to either the UF fraction or PM_{2.5} as a whole. An evaluation of toxicological studies found evidence for altered vessel tone and microvascular reactivity, which provide coherence and biological plausibility for the vasomotor effects that have been observed in both the controlled human exposure and epidemiologic studies (Section 6.2.4.3). However, most of these toxicological studies exposed animals via intratracheal (IT) instillation or using relatively high inhalation concentrations.

In addition to the effects observed on vasomotor function, myocardial ischemia has been observed across disciplines through PM_{2.5} effects on ST-segment depression, with toxicological studies providing biological plausibility by demonstrating reduced blood flow during ischemia (Section 6.2.3). There is also a growing body of evidence from controlled human exposure and toxicological studies demonstrating PM_{2.5}-induced changes on heart rate variability (HRV) and

¹ In this context mean represents the arithmetic mean of 24-h avg PM concentrations.

markers of systemic oxidative stress (Sections 6.2.1 and 6.2.9, respectively). Additional but inconsistent effects of PM_{2.5} on blood pressure (BP), blood coagulation markers, and markers of systemic inflammation have also been reported across disciplines. Toxicological studies have provided biologically plausible mechanisms (e.g., increased right ventricular pressure and diminished cardiac contractility) for the associations observed between PM_{2.5} and CHF in epidemiologic studies.

Together, the collective evidence from epidemiologic, controlled human exposure, and toxicological studies is sufficient to conclude that **a causal relationship exists between short-term exposures to PM_{2.5} and cardiovascular effects.**

Respiratory Effects

The recent epidemiologic studies evaluated report consistent positive associations between short-term exposure to PM_{2.5} and respiratory ED visits and hospital admissions for chronic obstructive pulmonary disease (COPD) and respiratory infections (Section 6.3). Positive associations were also observed for asthma ED visits and hospital admissions for adults and children combined, but effect estimates are imprecise and not consistently positive for children alone. Most studies reported effects in the range of ~1% to 4% increase in respiratory hospital admissions and ED visits and were observed in study locations with mean 24-h avg PM_{2.5} concentrations ranging from 6.1-22 µg/m³. Additionally, multicity epidemiologic studies reported consistent positive associations between short-term exposure to PM_{2.5} and respiratory mortality as well as regional and seasonal variability in risk estimates. The multicity studies evaluated reported consistent, precise increases in respiratory mortality ranging from 1.67 to 2.20% in study locations with mean 24-h avg PM_{2.5} concentrations above 12.8 µg/m³ (Table 6-15). Evidence for PM_{2.5}-related respiratory effects was also observed in panel studies, which indicate associations with respiratory symptoms, pulmonary function, and pulmonary inflammation among asthmatic children. Although not consistently observed, some controlled human exposure studies have reported small decrements in various measures of pulmonary function following controlled exposures to PM_{2.5} (Section 6.3.2.2).

Controlled human exposure studies using adult volunteers have demonstrated increased markers of pulmonary inflammation following exposure to a variety of different particle types; oxidative responses to DE and wood smoke; and exacerbations of allergic responses and allergic sensitization following exposure to DE particles (Section 6.3). Toxicological studies have provided additional support for PM_{2.5}-related respiratory effects through inhalation exposures of animals to CAPs, DE, other traffic-related PM and wood smoke. These studies reported an array of respiratory effects including altered pulmonary function, mild pulmonary inflammation and injury, oxidative responses, airway hyperresponsiveness (AHR) in allergic and non-allergic animals, exacerbations of allergic responses, and increased susceptibility to infections (Section 6.3).

Overall, the evidence for an effect of PM_{2.5} on respiratory outcomes is somewhat restricted by limited coherence between some of the findings from epidemiologic and controlled human exposure studies for the specific health outcomes reported and the sub-populations in which those health outcomes occur. Epidemiologic studies have reported variable results among specific respiratory outcomes, specifically in asthmatics (e.g., increased respiratory symptoms in asthmatic children, but not increased asthma hospital admissions and ED visits) (Section 6.3.8). Additionally, respiratory effects have not been consistently demonstrated following controlled exposures to PM_{2.5} among asthmatics or individuals with COPD. Collectively, the epidemiologic, controlled human exposure, and toxicological studies evaluated demonstrate a wide range of respiratory responses, and although results are not fully consistent and coherent across studies the evidence is sufficient to conclude that **a causal relationship is likely to exist between short-term exposures to PM_{2.5} and respiratory effects.**

Mortality

An evaluation of the epidemiologic literature indicates consistent positive associations between short-term exposure to PM_{2.5} and all-cause, cardiovascular-, and respiratory-related mortality (Section 6.5.2.2.). The evaluation of multicity studies found that consistent and precise risk estimates for all-cause (nonaccidental) mortality that ranged from 0.29 to 1.21% per 10 µg/m³

increase in PM_{2.5} at lags of 1 and 0-1 days. In these study locations, mean 24-h avg PM_{2.5} concentrations were 12.8 µg/m³ and above (Table 6-15). Cardiovascular-related mortality risk estimates were found to be similar to those for all-cause mortality; whereas, the risk estimates for respiratory-related mortality were consistently larger (i.e., 1.01-2.2%) using the same lag periods and averaging indices. The studies evaluated that examined the relationship between short-term exposure to PM_{2.5} and cardiovascular effects (Section 6.2) provide coherence and biological plausibility for PM_{2.5}-induced cardiovascular mortality, which represents the largest component of total (nonaccidental) mortality (~ 35%) (American Heart Association, 2009, [198920](#)). However, as noted in Section 6.3, there is limited coherence between some of the respiratory morbidity findings from epidemiologic and controlled human exposure studies for the specific health outcomes reported and the subpopulations in which those health outcomes occur, complicating the interpretation of the PM_{2.5} respiratory mortality effects observed. Regional and seasonal patterns in PM_{2.5} risk estimates were observed with the greatest effect estimates occurring in the eastern U.S. and during the spring. Of the studies evaluated only Burnett et al. (2004, [086247](#)), a Canadian multicity study, analyzed gaseous pollutants and found mixed results, with possible confounding of PM_{2.5} risk estimates by NO₂. Although the recently evaluated U.S.-based multicity studies did not analyze potential confounding of PM_{2.5} risk estimates by gaseous pollutants, evidence from the limited number of single-city studies evaluated in the 2004 PM AQCD (U.S. EPA, 2004, [056905](#)) suggest that gaseous copollutants do not confound the PM_{2.5}-mortality association. This is further supported by studies that examined the PM₁₀-mortality relationship. An examination of effect modifiers (e.g., demographic and socioeconomic factors), specifically air conditioning use as an indicator for decreased pollutant penetration indoors, has suggested that PM_{2.5} risk estimates increase as the percent of the population with access to air conditioning decreases. Collectively, the epidemiologic literature provides evidence that **a causal relationship exists between short-term exposures to PM_{2.5} and mortality.**

2.3.1.2. Effects of Long-Term Exposure to PM_{2.5}

Table 2-2. Summary of causal determinations for long-term exposure to PM_{2.5}.

Size Fraction	Outcome	Causality Determination
PM _{2.5}	Cardiovascular Effects	Causal
	Respiratory Effects	Likely to be causal
	Mortality	Causal
	Reproductive and Developmental	Suggestive
	Cancer, Mutagenicity, and Genotoxicity	Suggestive

Cardiovascular Effects

The strongest evidence for cardiovascular health effects related to long-term exposure to PM_{2.5} comes from large, multicity U.S.-based studies, which provide consistent evidence of an association between long-term exposure to PM_{2.5} and cardiovascular mortality (Section 7.2.10). These associations are supported by a large U.S.-based epidemiologic study (i.e., Women’s Health Initiative [WHI] study) that reports associations between PM_{2.5} and CVDs among post-menopausal women using a 1-yr avg PM_{2.5} concentration (mean = 13.5 µg/m³) (Section 7.2). However, epidemiologic studies that examined subclinical markers of CVD report inconsistent findings. Epidemiologic studies have also provided some evidence for potential modification of the PM_{2.5}-CVD association when examining individual-level data, specifically smoking status and the use of anti-

hyperlipidemics. Although epidemiologic studies have not consistently detected effects on markers of atherosclerosis due to long-term exposure to PM_{2.5}, toxicological studies have provided strong evidence for accelerated development of atherosclerosis in ApoE^{-/-} mice exposed to CAPs and have shown effects on coagulation, experimentally-induced hypertension, and vascular reactivity (Section 7.2.1.2). Evidence from toxicological studies provides biological plausibility and coherence with studies of short-term exposure and cardiovascular morbidity and mortality, as well as with studies that examined long-term exposure to PM_{2.5} and cardiovascular mortality. Taken together, the evidence from epidemiologic and toxicological studies is sufficient to conclude that **a causal relationship exists between long-term exposures to PM_{2.5} and cardiovascular effects.**

Respiratory Effects

Recent epidemiologic studies conducted in the U.S. and abroad provide evidence of associations between long-term exposure to PM_{2.5} and decrements in lung function growth, increased respiratory symptoms, and asthma development in study locations with mean PM_{2.5} concentrations ranging from 13.8 to 30 µg/m³ during the study periods (Section 7.3.1.1 and Section 7.3.2.1). These results are supported by studies that observed associations between long-term exposure to PM₁₀ and an increase in respiratory symptoms and reductions in lung function growth in areas where PM₁₀ is dominated by PM_{2.5}. However, the evidence to support an association with long-term exposure to PM_{2.5} and respiratory mortality is limited (Figure 7-7). Subchronic and chronic toxicological studies of CAPs, DE, roadway air and woodsmoke provide coherence and biological plausibility for the effects observed in the epidemiologic studies. These toxicological studies have presented some evidence for altered pulmonary function, mild inflammation, oxidative responses, immune suppression, and histopathological changes including mucus cell hyperplasia (Section 7.3). Exacerbated allergic responses have been demonstrated in animals exposed to DE and wood smoke. In addition, pre- and postnatal exposure to ambient levels of urban particles was found to affect lung development in an animal model. This finding is important because impaired lung development is one mechanism by which PM exposure may decrease lung function growth in children. Collectively, the evidence from epidemiologic and toxicological studies is sufficient to conclude that **a causal relationship is likely to exist between long-term exposures to PM_{2.5} and respiratory effects.**

Mortality

The recent epidemiologic literature reports associations between long-term PM_{2.5} exposure and increased risk of mortality. Mean PM_{2.5} concentrations ranged from 13.2 to 29 µg/m³ during the study period in these areas (Section 7.6). When evaluating cause-specific mortality, the strongest evidence can be found when examining associations between PM_{2.5} and cardiovascular mortality, and positive associations were also reported between PM_{2.5} and lung cancer mortality (Figure 7-7). The cardiovascular mortality association has been confirmed further by the extended Harvard Six Cities and American Cancer Society studies, which both report strong associations between long-term exposure to PM_{2.5} and cardiopulmonary and IHD mortality (Figure 7-7). Additional new evidence from a study that used the WHI cohort found a particularly strong association between long-term exposure to PM_{2.5} and CVD mortality in post-menopausal women. Fewer studies have evaluated the respiratory component of cardiopulmonary mortality, and, as a result, the evidence to support an association with long-term exposure to PM_{2.5} and respiratory mortality is limited (Figure 7-7). The evidence for cardiovascular and respiratory morbidity due to short- and long-term exposure to PM_{2.5} provides biological plausibility for cardiovascular- and respiratory-related mortality. Collectively, the evidence is sufficient to conclude that **a causal relationship exists between long-term exposures to PM_{2.5} and mortality.**

Reproductive and Developmental Effects

Evidence is accumulating for PM_{2.5} effects on low birth weight and infant mortality, especially due to respiratory causes during the post-neonatal period. The mean PM_{2.5} concentrations during the study periods ranged from 5.3-27.4 µg/m³ (Section 7.4), with effects becoming more precise and consistently positive in locations with mean PM_{2.5} concentrations of 15 µg/m³ and above (Section 7.4). Exposure to PM_{2.5} was usually associated with greater reductions in birth weight than exposure to PM₁₀. The evidence from a few U.S. studies that investigated PM₁₀ effects on fetal growth, which reported similar decrements in birth weight, provide consistency for the PM_{2.5} associations observed and strengthen the interpretation that particle exposure may be causally related to reductions in birth weight. The epidemiologic literature does not consistently report associations between long-term exposure to PM and preterm birth, growth restriction, birth defects or decreased sperm quality. Toxicological evidence supports an association between PM_{2.5} and PM₁₀ exposure and adverse reproductive and developmental outcomes, but provide little mechanistic information or biological plausibility for an association between long-term PM exposure and adverse birth outcomes (e.g., low birth weight or infant mortality). New evidence from animal toxicological studies on heritable mutations is of great interest, and warrants further investigation. Overall, the epidemiologic and toxicological evidence is **suggestive of a causal relationship between long-term exposures to PM_{2.5} and reproductive and developmental outcomes.**

Cancer, Mutagenicity, and Genotoxicity

Multiple epidemiologic studies have shown a consistent positive association between PM_{2.5} and lung cancer mortality, but studies have generally not reported associations between PM_{2.5} and lung cancer incidence (Section 7.5). Animal toxicological studies have examined the potential relationship between PM and cancer, but have not focused on specific size fractions of PM. Instead they have examined ambient PM, wood smoke, and DEP. A number of studies indicate that ambient urban PM, emissions from wood/biomass burning, emissions from coal combustion, and gasoline and DE are mutagenic, and that PAHs are genotoxic. These findings are consistent with earlier studies that concluded that ambient PM and PM from specific combustion sources are mutagenic and genotoxic and provide biological plausibility for the results observed in the epidemiologic studies. A limited number of epidemiologic and toxicological studies examined epigenetic effects, and demonstrate that PM induces some changes in methylation. However, it has yet to be determined how these alterations in the genome could influence the initiation and promotion of cancer. Additionally, inflammation and immune suppression induced by exposure to PM may confer susceptibility to cancer. Collectively, the evidence from epidemiologic studies, primarily those of lung cancer mortality, along with the toxicological studies that show some evidence of the mutagenic and genotoxic effects of PM is **suggestive of a causal relationship between long-term exposures to PM_{2.5} and cancer.**

2.3.2. Integration of PM_{2.5} Health Effects

In epidemiologic studies, short-term exposure to PM_{2.5} is associated with a broad range of respiratory and cardiovascular effects, as well as mortality. For cardiovascular effects and mortality, the evidence supports the existence of a causal relationship with short-term PM_{2.5} exposure; while the evidence indicates that a causal relationship is likely to exist between short-term PM_{2.5} exposure and respiratory effects. The effect estimates from recent and older U.S. and Canadian-based epidemiologic studies that examined the relationship between short-term exposure to PM_{2.5} and health outcomes with mean 24-h avg PM_{2.5} concentrations <17 µg/m³ are shown in Figure 2-1. A number of different health effects are included in Figure 2-1 to provide an integration of the range of effects by mean concentration, with a focus on cardiovascular and respiratory effects and all-cause (nonaccidental) mortality (i.e., health effects categories with at least a suggestive causal determination). A pattern of consistent positive associations with mortality and morbidity effects can be seen in this figure. Mean PM_{2.5} concentrations ranged from 6.1 to 16.8 µg/m³ in these study locations.

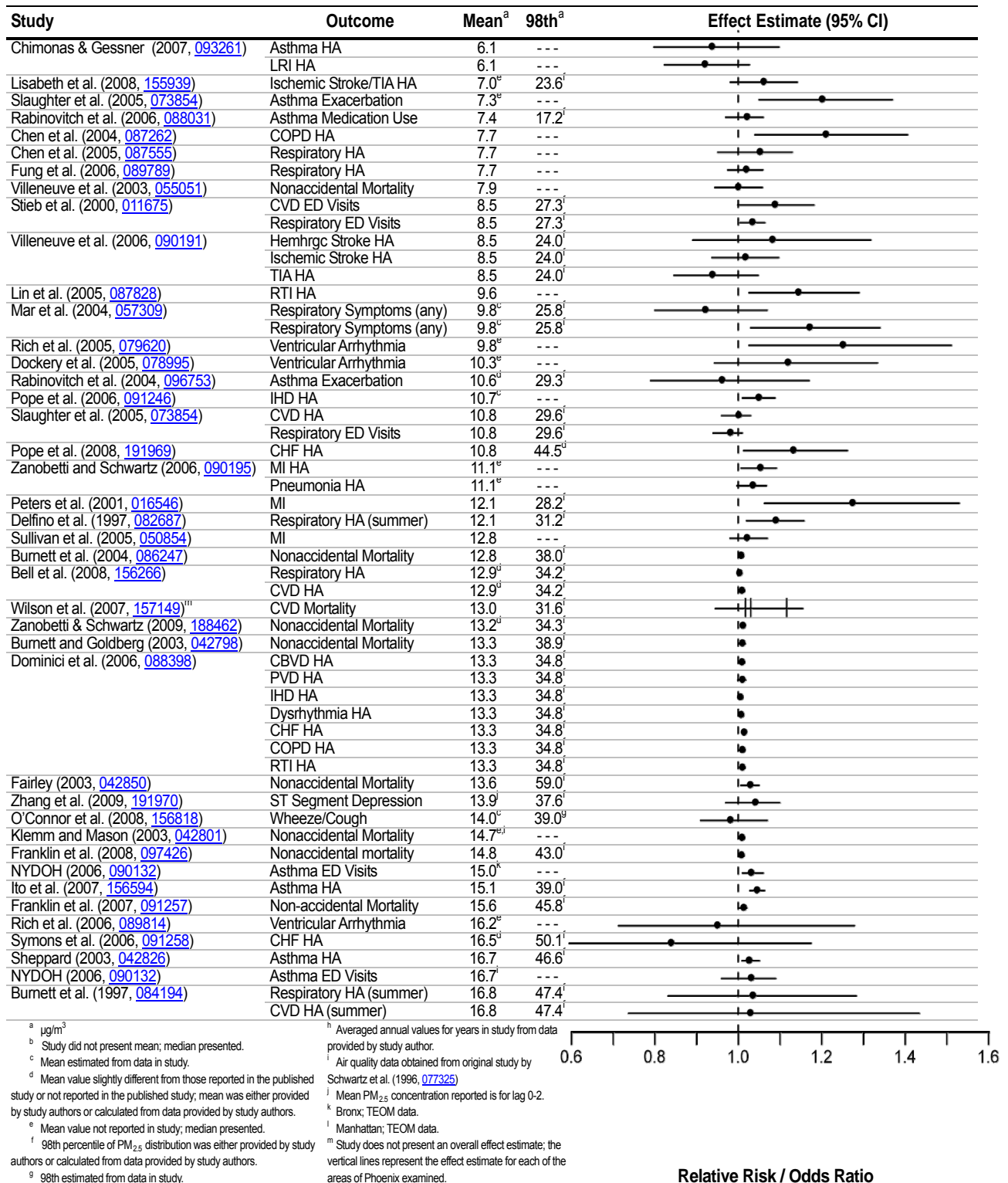


Figure 2-1. Summary of effect estimates (per $10 \mu\text{g}/\text{m}^3$) by increasing concentration from U.S. studies examining the association between short-term exposure to $\text{PM}_{2.5}$ and cardiovascular and respiratory effects, and mortality, conducted in locations where the reported mean 24-h avg $\text{PM}_{2.5}$ concentrations were $<17 \mu\text{g}/\text{m}^3$.

Long-term exposure to PM_{2.5} has been associated with health outcomes similar to those found in the short-term exposure studies, specifically for respiratory and cardiovascular effects and mortality. As found for short-term PM_{2.5} exposure, the evidence indicates that a causal relationship exists between long-term PM_{2.5} exposure and cardiovascular effects and mortality, and that a causal relationship is likely to exist between long-term PM_{2.5} exposure and effects on the respiratory system.

Figure 2-2 highlights the findings of epidemiologic studies where the long-term mean PM_{2.5} concentrations were $\leq 29 \mu\text{g}/\text{m}^3$. A range of health outcomes are displayed (including cardiovascular mortality, all-cause mortality, infant mortality, and bronchitis) ordered by mean concentration. The range of mean PM_{2.5} concentrations in these studies was 10.7-29 $\mu\text{g}/\text{m}^3$ during the study periods. Additional studies not included in this figure that focus on subclinical outcomes, such as changes in lung function or atherosclerotic markers also report effects in areas with similar concentrations (Sections 7.2 and 7.3). Although not highlighted in the summary figure, long-term PM_{2.5} exposure studies also provide evidence for reproductive and developmental effects (i.e., low birth weight) and cancer (i.e., lung cancer mortality) in response to exposure to PM_{2.5}.

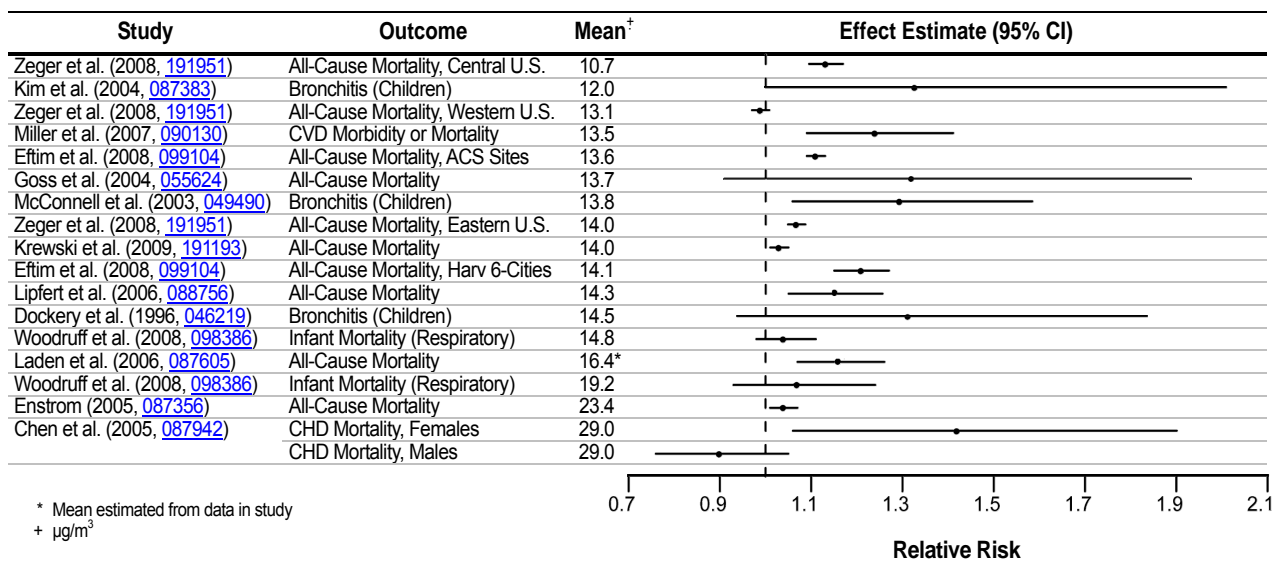


Figure 2-2. Summary of effect estimates (per 10 $\mu\text{g}/\text{m}^3$) by increasing concentration from U.S. studies examining the association between long-term exposure to PM_{2.5} and cardiovascular and respiratory effects, and mortality.

The observations from both the short- and long-term exposure studies are supported by experimental findings of PM_{2.5}-induced subclinical and clinical cardiovascular effects. Epidemiologic studies have shown an increase in ED visits and hospital admissions for IHD upon exposure to PM_{2.5}. These effects are coherent with the changes in vasomotor function and ST-segment depression observed in both toxicological and controlled human exposure studies. It has been postulated that exposure to PM_{2.5} can lead to myocardial ischemia through an effect on the autonomic nervous system or by altering vasomotor function. PM-induced systemic inflammation, oxidative stress and/or endothelial dysfunction may contribute to altered vasomotor function. These effects have been demonstrated in recent animal toxicological studies, along with altered microvascular reactivity, altered vessel tone, and reduced blood flow during ischemia. Toxicological studies demonstrating increased right ventricular pressure and diminished cardiac contractility also provide biological plausibility for the associations observed between PM_{2.5} and CHF in epidemiologic studies.

Thus, the overall evidence from the short-term epidemiologic, controlled human exposure, and toxicological studies evaluated provide coherence and biological plausibility for cardiovascular effects related to myocardial ischemia and CHF. Coherence in the cardiovascular effects observed

can be found in long-term exposure studies, especially for CVDs among post-menopausal women. Additional studies provide limited evidence for subclinical measures of atherosclerosis in epidemiologic studies with stronger evidence from toxicological studies that have demonstrated accelerated development of atherosclerosis in ApoE^{-/-} mice exposed to PM_{2.5} CAPs along with effects on coagulation, experimentally-induced hypertension, and vascular reactivity. Repeated acute responses to PM may lead to cumulative effects that manifest as chronic disease, such as atherosclerosis. Contributing factors to atherosclerosis development include systemic inflammation, endothelial dysfunction, and oxidative stress all of which are associated with PM_{2.5} exposure. However, it has not yet been determined whether PM initiates or promotes atherosclerosis. The evidence from both short- and long-term exposure studies on cardiovascular morbidity provide coherence and biological plausibility for the cardiovascular mortality effects observed when examining both exposure durations. In addition, cardiovascular hospital admission and mortality studies that examined the PM₁₀ concentration-response relationship found evidence of a log-linear no-threshold relationship between PM exposure and cardiovascular-related morbidity (Section 6.2) and mortality (Section 6.5).

Epidemiologic studies have also reported respiratory effects related to short-term exposure to PM_{2.5}, which include increased ED visits and hospital admissions, as well as alterations in lung function and respiratory symptoms in asthmatic children. These respiratory effects were found to be generally robust to the inclusion of gaseous pollutants in copollutant models with the strongest evidence from the higher powered studies (Figure 6-9 and Figure 6-15). Consistent positive associations were also reported between short-term exposure to PM_{2.5} and respiratory mortality in epidemiologic studies. However, uncertainties exist in the PM_{2.5}-respiratory mortality associations reported due to the limited number of studies that examined potential confounders of the PM_{2.5}-respiratory mortality relationship, and the limited information regarding the biological plausibility of the clinical and subclinical respiratory outcomes observed in the epidemiologic and controlled human exposure studies (Section 6.3) resulting in the progression to PM_{2.5}-induced respiratory mortality. Important new findings, which support the PM_{2.5}-induced respiratory effects mentioned above, include associations with post-neonatal (between 1 mo and 1 yr of age) respiratory mortality. Controlled human exposure studies provide some support for the respiratory findings from epidemiologic studies, with demonstrated increases in pulmonary inflammation following short-term exposure. However, there is limited and inconsistent evidence of effects in response to controlled exposures to PM_{2.5} on respiratory symptoms or pulmonary function among healthy adults or adults with respiratory disease. Long-term exposure epidemiologic studies provide additional evidence for PM_{2.5}-induced respiratory morbidity, but little evidence for an association with respiratory mortality. These epidemiologic morbidity studies have found decrements in lung function growth, as well as increased respiratory symptoms, and asthma. Toxicological studies provide coherence and biological plausibility for the respiratory effects observed in response to short and long-term exposures to PM by demonstrating a wide array of biological responses including: altered pulmonary function, mild pulmonary inflammation and injury, oxidative responses, and histopathological changes in animals exposed by inhalation to PM_{2.5} derived from a wide variety of sources. In some cases, prolonged exposures led to adaptive responses. Important evidence was also found in an animal model for altered lung development following pre- and post-natal exposure to urban air, which may provide a mechanism to explain the reduction in lung function growth observed in children in response to long-term exposure to PM.

Additional respiratory-related effects have been tied to allergic responses. Epidemiologic studies have provided evidence for increased hospital admissions for allergic symptoms (e.g., allergic rhinitis) in response to short- and long-term exposure to PM_{2.5}. Panel studies also positively associate long-term exposure to PM_{2.5} and PM₁₀ with indicators of allergic sensitization. Controlled human exposure and toxicological studies provide coherence for the exacerbation of allergic symptoms, by showing that PM_{2.5} can promote allergic responses and intensify existing allergies. Allergic responses require repeated exposures to antigen over time and co-exposure to an adjuvant (possibly DE particles or UF CAPs) can enhance this response. Allergic sensitization often underlies allergic asthma, characterized by inflammation and AHR. In this way, repeated or chronic exposures involving multifactorial responses (immune system activation, oxidative stress, inflammation) can lead to irreversible outcomes. Epidemiologic studies have also reported evidence for increased hospital admissions for respiratory infections in response to both short- and long-term exposures to PM_{2.5}. Toxicological studies suggest that PM impairs innate immunity, which is the first line of

defense against infection, providing coherence for the respiratory infection effects observed in epidemiologic studies.

The difference in effects observed across studies and between cities may be attributed, at least in part, to the differences in PM composition across the U.S. Differences in PM toxicity may result from regionally varying PM composition and size distribution, which in turn reflects differences in sources and PM volatility. A person's exposure to ambient PM will also vary due to regional differences in personal activity patterns, microenvironmental characteristics and the spatial variability of PM concentrations in urban areas. Regional differences in PM_{2.5} composition are outlined briefly in Section 2.1 above and in more detail in Section 3.5. An examination of data from the CSN indicates that East-West gradients exist for a number of PM components. Specifically, SO₄²⁻ concentrations are higher in the East, OC constitutes a larger fraction of PM in the West, and NO₃⁻ concentrations are highest in the valleys of central California and during the winter in the Midwest. However, the available evidence and the limited amount of city-specific speciated PM_{2.5} data does not allow conclusions to be drawn that specifically differentiate effects of PM in different locations.

It remains a challenge to determine relationships between specific constituents, combinations of constituents, or sources of PM_{2.5} and the various health effects observed. Source apportionment studies of PM_{2.5} have attempted to decipher some of these relationships and in the process have identified associations between multiple sources and various respiratory and cardiovascular health effects, as well as mortality. Although different source apportionment methods have been used across these studies, the methods used have been evaluated and found generally to identify the same sources and associations between sources and health effects (Section 6.6). While uncertainty remains, it has been recognized that many sources and components of PM_{2.5} contribute to health effects. Overall, the results displayed in Table 6-18 indicate that many constituents of PM_{2.5} can be linked with multiple health effects, and the evidence is not yet sufficient to allow differentiation of those constituents or sources that are more closely related to specific health outcomes.

Variability in the associations observed across PM_{2.5} epidemiologic studies may be due in part to exposure error related to the use of county-level air quality data. Because western U.S. counties tend to be much larger and more topographically diverse than eastern U.S. counties, the day-to-day variations in concentration at one site, or even for the average of several sites, may not correlate well with the day-to-day variations in all parts of the county. For example, site-to-site correlations as a function of distance between sites (Section 3.5.1.2) fall off rapidly with distance in Los Angeles, but high correlations extend to larger distances in eastern cities such as Boston and Pittsburgh. These differences may be attributed to a number of factors including topography, the built environment, climate, source characteristics, ventilation usage, and personal activity patterns. For instance, regional differences in climate and infrastructure can affect time spent outdoors or indoors, air conditioning usage, and personal activity patterns. Characteristics of housing stock may also cause regional differences in effect estimates because new homes tend to have lower infiltration factors than older homes. Biases and uncertainties in exposure estimates resulting from these aspects can, in turn, cause bias and uncertainty in associated health effects estimates.

The new evidence reviewed in this ISA greatly expands upon the evidence available in the 2004 PM AQCD particularly in providing greater understanding of the underlying mechanisms for PM_{2.5} induced cardiovascular and respiratory effects for both short- and long-term exposures. Recent studies have provided new evidence linking long-term exposure to PM_{2.5} with cardiovascular outcomes that has expanded upon the continuum of effects ranging from the more subtle subclinical measures to cardiopulmonary mortality.

2.3.3. Exposure to PM_{10-2.5}

2.3.3.1. Effects of Short-Term Exposure to PM_{10-2.5}

Table 2-3. Summary of causal determinations for short-term exposure to PM_{10-2.5}.

Size Fraction	Outcome	Causality Determination
PM _{10-2.5}	Cardiovascular Effects	Suggestive
	Respiratory Effects	Suggestive
	Mortality	Suggestive

Cardiovascular Effects

Generally positive associations were reported between short-term exposure to PM_{10-2.5} and hospital admissions or ED visits for cardiovascular causes. These results are supported by a large U.S. multicity study of older adults that reported PM_{10-2.5} associations with CVD hospital admissions, and only a slight reduction in the PM_{10-2.5} risk estimate when included in a copollutant model with PM_{2.5} (Section 6.2.10). The PM_{10-2.5} associations with cardiovascular hospital admissions and ED visits were observed in study locations with mean 24-h avg PM_{10-2.5} concentrations ranging from 7.4 to 13 µg/m³. These results are supported by the associations observed between PM_{10-2.5} and cardiovascular mortality in areas with 24-h avg PM_{10-2.5} concentrations ranging from 6.1-16.4 µg/m³ (Section 6.2.11). The results of the epidemiologic studies were further confirmed by studies that examined dust storm events, which contain high concentrations of crustal material, and found an increase in cardiovascular-related ED visits and hospital admissions. Additional epidemiologic studies have reported PM_{10-2.5} associations with other cardiovascular health effects including supraventricular ectopy and changes in HRV (Section 6.2.1.1). Although limited in number, studies of controlled human exposures provide some evidence to support the alterations in HRV observed in the epidemiologic studies (Section 6.2.1.2). The few toxicological studies that examined the effect of PM_{10-2.5} on cardiovascular health effects used IT instillation due to the technical challenges in exposing rodents via inhalation to PM_{10-2.5}, and, as a result, provide only limited evidence on the biological plausibility of PM_{10-2.5} induced cardiovascular effects. The potential for PM_{10-2.5} to elicit an effect is supported by dosimetry studies, which show that a large proportion of inhaled particles in the 3-6 micron (d_{ae}) range can reach and deposit in the lower respiratory tract, particularly the tracheobronchial (TB) airways (Figures 4-3 and 4-4). Collectively, the evidence from epidemiologic studies, along with the more limited evidence from controlled human exposure and toxicological studies **is suggestive of a causal relationship between short-term exposures to PM_{10-2.5} and cardiovascular effects.**

Respiratory Effects

A number of recent epidemiologic studies conducted in Canada and France found consistent, positive associations between respiratory ED visits and hospital admissions and short-term exposure to PM_{10-2.5} in studies with mean 24-h avg concentrations ranging from 5.6-16.2 µg/m³ (Section 6.3.8). In these studies, the strongest relationships were observed among children, with less consistent evidence for adults and older adults (i.e., ≥ 65). In a large multicity study of older adults, PM_{10-2.5} was positively associated with respiratory hospital admissions in both single and copollutant models with PM_{2.5}. In addition, a U.S.-based multicity study found evidence for an increase in respiratory mortality upon short-term exposure to PM_{10-2.5}, but these associations have not been consistently

observed in single-city studies (Section 6.3.9). A limited number of epidemiologic studies have focused on specific respiratory morbidity outcomes, and found no evidence of an association with lower respiratory symptoms, wheeze, and medication use (Section 6.3.1.1). While controlled human exposure studies have not observed an effect on lung function or respiratory symptoms in healthy or asthmatic adults in response to short-term exposure to PM_{10-2.5}, healthy volunteers have exhibited an increase in markers of pulmonary inflammation. Toxicological studies using inhalation exposures are still lacking, but pulmonary injury has been observed in animals after IT instillation exposure (Section 6.3.5.3). In some cases, PM_{10-2.5} was found to be more potent than PM_{2.5} and effects were not attributable to endotoxin. Both rural and urban PM_{10-2.5} have induced inflammation and injury responses in rats or mice exposed via IT instillation, making it difficult to distinguish the health effects of PM_{10-2.5} from different environments. Overall, epidemiologic studies, along with the limited number of controlled human exposure and toxicological studies that examined PM_{10-2.5} respiratory effects provide evidence that **is suggestive of a causal relationship between short-term exposures to PM_{10-2.5} and respiratory effects.**

Mortality

The majority of studies evaluated in this review provide some evidence for mortality associations with PM_{10-2.5} in areas with mean 24-h avg concentrations ranging from 6.1-16.4 µg/m³. However, uncertainty surrounds the PM_{10-2.5} associations reported in the studies evaluated due to the different methods used to estimate PM_{10-2.5} concentrations across studies (e.g., direct measurement of PM_{10-2.5} using dichotomous samplers, calculating the difference between PM₁₀ and PM_{2.5} concentrations). In addition, only a limited number of PM_{10-2.5} studies have investigated potential confounding by gaseous copollutants or the influence of model specification on PM_{10-2.5} risk estimates.

A new U.S.-based multicity study, which estimated PM_{10-2.5} concentrations by calculating the difference between the county-average PM₁₀ and PM_{2.5}, found associations between PM_{10-2.5} and mortality across the U.S., including evidence for regional variability in PM_{10-2.5} risk estimates (Section 6.5.2.3). Additionally, the U.S.-based multicity study provides preliminary evidence for greater effects occurring during the warmer months (i.e., spring and summer). A multicity Canadian study provides additional evidence for an association between short-term exposure to PM_{10-2.5} and mortality (Section 6.5.2.3). Although consistent positive associations have been observed across both multi- and single-city studies, more data are needed to adequately characterize the chemical and biological components that may modify the potential toxicity of PM_{10-2.5} and compare the different methods used to estimate exposure. Overall, the evidence evaluated **is suggestive of a causal relationship between short-term exposures to PM_{10-2.5} and mortality.**

2.3.4. Integration of PM_{10-2.5} Effects

Epidemiologic, controlled human exposure, and toxicological studies have provided evidence that is suggestive for relationships between short-term exposure to PM_{10-2.5} and cardiovascular effects, respiratory effects, and mortality. Conclusions regarding causation for the various health effects and outcomes were made for PM_{10-2.5} as a whole regardless of origin, since PM_{10-2.5}-related effects have been demonstrated for a number of different environments (e.g., cities reflecting a wide range of environmental conditions). Associations between short-term exposure to PM_{10-2.5} and cardiovascular and respiratory effects, and mortality have been observed in locations with mean PM_{10-2.5} concentrations ranging from 5.6 to 33.2 µg/m³, and maximum PM_{10-2.5} concentrations ranging from 24.6 to 418.0 µg/m³ (Figure 2-3). A number of different health effects are included in Figure 2-3 to provide an integration of the range of effects by mean concentration, with a focus on cardiovascular and respiratory effects, and mortality (i.e., health effects categories with at least a suggestive causal determination). To date, a sufficient amount of evidence does not exist in order to draw conclusions regarding the health effects and outcomes associated with long-term exposure to PM_{10-2.5}.

In epidemiologic studies, associations between short-term exposure to PM_{10-2.5} and cardiovascular outcomes (i.e., IHD hospital admissions, supraventricular ectopy, and changes in HRV) have been found that are similar in magnitude to those observed in PM_{2.5} studies. Controlled human exposure studies have also observed alterations in HRV, providing consistency and coherence

for the effects observed in the epidemiologic studies. To date, only a limited number of toxicological studies have been conducted to examine the effects of PM_{10-2.5} on cardiovascular effects. All of these studies involved IT instillation due to the technical challenges of using PM_{10-2.5} for rodent inhalation studies. As a result, the toxicological studies evaluated provide limited biological plausibility for the PM_{10-2.5} effects observed in the epidemiologic and controlled human exposure studies.

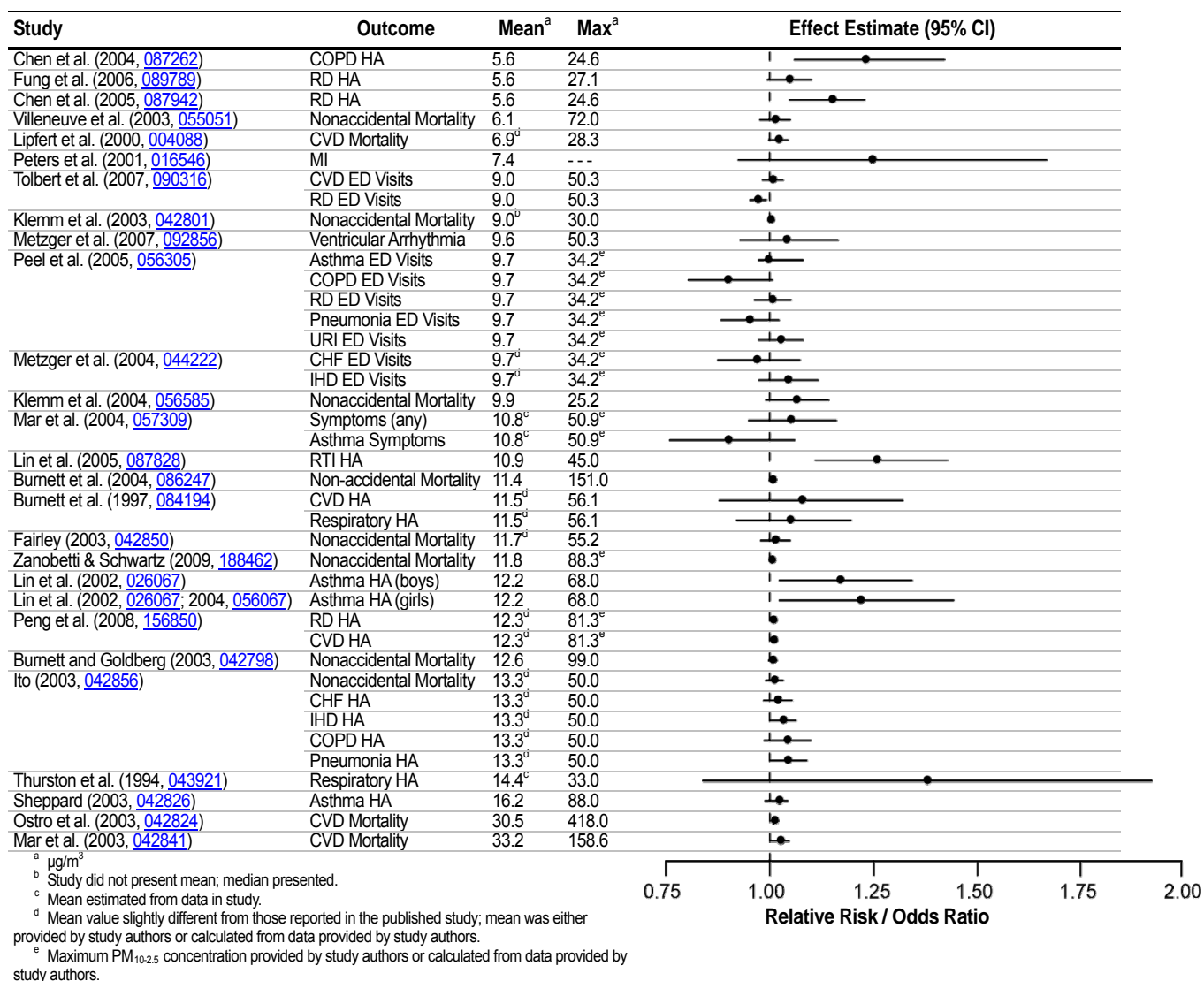


Figure 2-3. Summary of U.S. studies examining the association between short-term exposure to PM_{10-2.5} and cardiovascular morbidity/mortality and respiratory morbidity/mortality. All effect estimates have been standardized to reflect a 10 $\mu\text{g}/\text{m}^3$ increase in mean 24-h avg PM_{10-2.5} concentration and ordered by increasing concentration.

Limited evidence is available from epidemiologic studies for respiratory health effects and outcomes in response to short-term exposure to PM_{10-2.5}. An increase in respiratory hospital admissions and ED visits has been observed, but primarily in studies conducted in Canada and Europe. In addition, associations are not reported for lower respiratory symptoms, wheeze, or medication use. Controlled human exposure studies have not observed an effect on lung function or respiratory symptoms in healthy or asthmatic adults, but healthy volunteers have exhibited pulmonary inflammation. The toxicological studies (all IT instillation) provide evidence of

pulmonary injury and inflammation. In some cases, PM_{10-2.5} was found to be more potent than PM_{2.5} and effects were not solely attributable to endotoxin.

Currently, a national network is not in place to monitor PM_{10-2.5} concentrations. As a result, uncertainties surround the concentration at which the observed associations occur. Ambient concentrations of PM_{10-2.5} are generally determined by the subtraction of PM₁₀ and PM_{2.5} measurements, using various methods. For example, some epidemiologic studies estimate PM_{10-2.5} by taking the difference between collocated PM₁₀ and PM_{2.5} monitors while other studies have taken the difference between county average PM₁₀ and PM_{2.5} concentrations. Moreover, there are potential differences among operational flow rates and temperatures for PM₁₀ and PM_{2.5} monitors used to calculate PM_{10-2.5}. Therefore, there is greater error in ambient exposure to PM_{10-2.5} compared to PM_{2.5}. This would tend to increase uncertainty and make it more difficult to detect effects of PM_{10-2.5} in epidemiologic studies. In addition, the various differences between eastern and western U.S. counties can lead to exposure misclassification, and the potential underestimation of effects in western counties (as discussed for PM_{2.5} in Section 2.3.2).

It is also important to note that the chemical composition of PM_{10-2.5} can vary considerably by location, but city-specific speciated PM_{10-2.5} data are limited. PM_{10-2.5} may contain Fe, Si, Al, and base cations from soil, plant and insect fragments, pollen, fungal spores, bacteria, and viruses, as well as fly ash, brake lining particles, debris, and automobile tire fragments.

The 2004 PM AQCD presented the limited amount of evidence available that examined the potential association between exposure to PM_{10-2.5} and health effects and outcomes. The current evidence, primarily from epidemiologic studies, builds upon the results from the 2004 PM AQCD and indicates that short-term exposure to PM_{10-2.5} is associated with effects on both the cardiovascular and respiratory systems. However, variability in the chemical and biological composition of PM_{10-2.5}, limited evidence regarding effects of the various components of PM_{10-2.5}, and lack of clearly defined biological mechanisms for PM_{10-2.5}-related effects are important sources of uncertainty.

2.3.5. Exposure to UFPs

2.3.5.1. Effects of Short-Term Exposure to UFPs

Table 2-4. Summary of causal determinations for short-term exposure to UFPs.

Size Fraction	Outcome	Causality Determination
UFPs	Cardiovascular Effects	Suggestive
	Respiratory Effects	Suggestive

Cardiovascular Effects

Controlled human exposure studies provide the majority of the evidence for cardiovascular health effects in response to short-term exposure to UFPs. While there are a limited number of studies that have examined the association between UFPs and cardiovascular morbidity, there is a larger body of evidence from studies that exposed subjects to fresh DE, which is typically dominated by UFPs. These studies have consistently demonstrated changes in vasomotor function following exposure to atmospheres containing relatively high concentrations of particles (Section 6.2.4.2). Markers of systemic oxidative stress have also been observed to increase after exposure to various particle types that are predominantly in the UFP size range. In addition, alterations in HRV parameters have been observed in response to controlled human exposure to UF CAPs, with inconsistent evidence for changes in markers of blood coagulation following exposure to UF CAPs

and DE (Sections 6.2.1.2 and 6.2.8.2). A few toxicological studies have also found consistent changes in vasomotor function, which provides coherence with the effects demonstrated in the controlled human exposure studies (Section 6.2.4.3). Additional UFP-induced effects observed in toxicological studies include alterations in HRV, with less consistent effects observed for systemic inflammation and blood coagulation. Only a few epidemiologic studies have examined the effect of UFPs on cardiovascular morbidity and collectively they found inconsistent evidence for an association between UFPs and CVD hospital admissions, but some positive associations for subclinical cardiovascular measures (i.e., arrhythmias and supraventricular beats) (Section 6.2.2.1). These studies were conducted in the U.S. and Europe in areas with mean particle number concentration ranging from ~8,500 to 36,000 particles/cm³. However, UFP number concentrations are highly variable (i.e., concentrations drop off quickly from the road compared to accumulation mode particles), and therefore, more subject to exposure error than accumulation mode particles. In conclusion, the evidence from the studies evaluated **is suggestive of a causal relationship between short-term exposures to UFPs and cardiovascular effects.**

Respiratory Effects

A limited number of epidemiologic studies have examined the potential association between short-term exposure to UFPs and respiratory morbidity. Of the studies evaluated, there is limited, and inconsistent evidence for an association between short-term exposure to UFPs and respiratory symptoms, as well as asthma hospital admissions in locations a median particle number concentration of ~6,200 to a mean of 38,000 particles/cm³ (Section 6.3.10). The spatial and temporal variability of UFPs also affects these associations. Toxicological studies have reported respiratory effects including oxidative, inflammatory, and allergic responses using a number of different UFP types (Section 6.3). Although controlled human exposure studies have not extensively examined the effect of UFPs on respiratory outcomes, a few studies have observed small UFP-induced asymptomatic decreases in pulmonary function. Markers of pulmonary inflammation have been observed to increase in healthy adults following controlled exposures to UFPs, particularly in studies using fresh DE. However, it is important to note that for both controlled human exposure and animal toxicological studies of exposures to fresh DE, the relative contributions of gaseous copollutants to the respiratory effects observed remain unresolved. Thus, the current collective evidence **is suggestive of a causal relationship between short-term exposures to UFPs and respiratory effects.**

2.3.6. Integration of UFP Effects

The controlled human exposure studies evaluated have consistently demonstrated effects on vasomotor function and systemic oxidative stress with additional evidence for alterations in HRV parameters in response to exposure to UF CAPs. The toxicological studies provide coherence for the changes in vasomotor function observed in the controlled human exposure studies. Epidemiologic studies are limited because a national network is not in place to measure UFP in the U.S. UFP concentrations are spatially and temporally variable, which would increase uncertainty and make it difficult to detect associations between health effects and UFPs in epidemiologic studies. In addition, data on the composition of UFPs, the spatial and temporal evolution of UFP size distribution and chemical composition, and potential effects of UFP constituents are sparse.

More limited evidence is available regarding the effect of UFPs on respiratory effects. Controlled human exposure studies have not extensively examined the effect of UFPs on respiratory measurements, but a few studies have observed small decrements in pulmonary function and increases in pulmonary inflammation. Additional effects including oxidative, inflammatory, and pro-allergic outcomes have been demonstrated in toxicological studies. Epidemiologic studies have found limited and inconsistent evidence for associations between UFPs and respiratory effects.

Overall, a limited number of studies have examined the association between exposure to UFPs and morbidity and mortality. Of the studies evaluated, controlled human exposure and toxicological studies provide the most evidence for UFP-induced cardiovascular and respiratory effects; however, many studies focus on exposure to DE. As a result, it is unclear if the effects observed are due to UFP, larger particles (i.e., PM_{2.5}), or the gaseous components of DE. Additionally, UF CAPs systems

are limited as the atmospheric UFP composition is modified when concentrated, which adds uncertainty to the health effects observed in controlled human exposure studies (Section 1.5.3).

2.4. Policy Relevant Considerations

2.4.1. Potentially Susceptible Populations

Upon evaluating the association between short- and long-term exposure to PM and various health outcomes, studies also attempted to identify populations that are more susceptible to PM (i.e., populations that have a greater likelihood of experiencing health effects related to exposure to an air pollutant (e.g., PM) due to a variety of factors including, but not limited to: genetic or developmental factors, race, gender, life stage, lifestyle (e.g., smoking status and nutrition) or preexisting disease; as well as, population-level factors that can increase an individual's exposure to an air pollutant (e.g., PM) such as socioeconomic status [SES], which encompasses reduced access to health care, low educational attainment, residential location, and other factors). These studies did so by conducting stratified analyses; by examining effects in individuals with an underlying health condition; or by developing animal models that mimic the pathophysiologic conditions associated with an adverse health effect. In addition, numerous studies that focus on only one potentially susceptible population provide supporting evidence on whether a population is susceptible to PM exposure. These studies identified a multitude of factors that could potentially contribute to whether an individual is susceptible to PM (Table 8-2). Although studies have primarily used exposures to PM_{2.5} or PM₁₀, the available evidence suggests that the identified factors may also enhance susceptibility to PM_{10-2.5}. The examination of susceptible populations to PM exposure allows for the NAAQS to provide an adequate margin of safety for both the general population and for susceptible populations.

During specific periods of life (i.e., childhood and advanced age), individuals may be more susceptible to environmental exposures, which in turn can render them more susceptible to PM-related health effects. An evaluation of age-related health effects suggests that older adults have heightened responses for cardiovascular morbidity with PM exposure. In addition, epidemiologic and toxicological studies provide evidence that indicates children are at an increased risk of PM-related respiratory effects. It should be noted that the health effects observed in children could be initiated by exposures to PM that occurred during key windows of development, such as in utero. Epidemiologic studies that focus on exposures during development have reported inconsistent findings (Section 7.4), but a recent toxicological study suggests that inflammatory responses in pregnant women due to exposure to PM could result in health effects in the developing fetus.

Epidemiologic studies have also examined whether additional factors, such as gender, race, or ethnicity modify the association between PM and morbidity and mortality outcomes. Although gender and race do not seem to modify PM risk estimates, limited evidence from two studies conducted in California suggest that Hispanic ethnicity may modify the association between PM and mortality.

Recent epidemiologic and toxicological studies provided evidence that individuals with null alleles or polymorphisms in genes that mediate the antioxidant response to oxidative stress (i.e., GSTM1), regulate enzyme activity (i.e., MTHFR and cSHMT), or regulate levels of procoagulants (i.e., fibrinogen) are more susceptible to PM exposure. However, some studies have shown that polymorphisms in genes (e.g., HFE) can have a protective effect against effects of PM exposure. Additionally, preliminary evidence suggests that PM exposure can impart epigenetic effects (i.e., DNA methylation); however, this requires further investigation.

Collectively, the evidence from epidemiologic and toxicological, and to a lesser extent, controlled human exposure studies, indicate increased susceptibility of individuals with underlying CVDs and respiratory illnesses (i.e., asthma) to PM exposure. Controlled human exposure and toxicological studies provide additional evidence for increased PM-related cardiovascular effects in individuals with underlying respiratory health conditions.

Recently studies have begun to examine the influence of preexisting chronic inflammatory conditions, such as diabetes and obesity, on PM-related health effects. These studies have found some evidence for increased associations for cardiovascular outcomes along with pathophysiologic alterations in markers of inflammation, oxidative stress, and acute phase response. However, more

research is needed to thoroughly examine the affect of PM exposure on obese individuals and to identify the biological pathway(s) that could increase the susceptibility of diabetic and obese individuals to PM.

There is also evidence that SES, measured using surrogates such as educational attainment or residential location, modifies the association between PM and morbidity and mortality outcomes. In addition, nutritional status, another surrogate measure of SES, has been shown to have protective effects against PM exposure in individuals that have a higher intake of some vitamins and nutrients.

Overall, the epidemiologic, controlled human exposure, and toxicological studies evaluated in this review provide evidence for increased susceptibility for various populations, including children and older adults, people with pre-existing cardiopulmonary diseases, and people with lower SES.

2.4.2. Lag Structure of PM-Morbidity and PM-Mortality Associations

Epidemiologic studies have evaluated the time-frame in which exposure to PM can impart a health effect. PM exposure-response relationships can potentially be influenced by a multitude of factors, such as the underlying susceptibility of an individual (e.g., age, pre-existing diseases), which could increase or decrease the lag times observed.

An attempt has been made to identify whether certain lag periods are more strongly associated with specific health outcomes. The epidemiologic evidence evaluated in the 2004 PM AQCD supported the use of lags of 0-1 days for cardiovascular effects and longer moving averages or distributed lags for respiratory diseases (U.S. EPA, 2004, [056905](#)). However, currently, little consensus exists as to the most appropriate a priori lag times to use when examining morbidity and mortality outcomes. As a result, many investigators have chosen to examine the lag structure of associations between PM concentration and health outcome instead of focusing on a priori lag times. This approach is informative because if effects are cumulative, higher overall risks may exist than would be observed for any given single-day lag.

2.4.2.1. PM-Cardiovascular Morbidity Associations

Most of the studies evaluated that examined the association between cardiovascular hospital admissions and ED visits report associations with short-term PM exposure at lags 0- to 2-days, with more limited evidence for shorter durations (i.e., hours) between exposure and response for some health effects (e.g., onset of MI) (Section 6.2.10). However, these studies have rarely examined alternative lag structures. Controlled human exposure and toxicological studies provide biological plausibility for the health effects observed in the epidemiologic studies at immediate or concurrent day lags. Although the majority of the evidence supports shorter lag times for cardiovascular health effects, a recent study has provided preliminary evidence suggesting that longer lag times (i.e., 14-day distributed lag model) may be plausible for non-ischemic cardiovascular conditions (Section 6.2.10). Panel studies of short-term exposure to PM and cardiovascular endpoints have also examined the time frame from exposure to health effect using a wide range of lag times. Studies of ECG changes indicating ischemia show effects at lags from several hours to 2 days, while lag times ranging from hours to several week moving averages have been observed in studies of arrhythmias, vasomotor function and blood markers of inflammation, coagulation and oxidative stress (Section 6.2). The longer lags observed in these panel studies may be explained if the effects of PM are cumulative. Although few studies of cumulative effects have been conducted, toxicological studies have demonstrated PM-dependent progression of atherosclerosis. It should be noted that PM exposure could also lead to an acute event (e.g., infarction or stroke) in individuals with atherosclerosis that may have progressed in response to cumulative PM exposure. Therefore, effects have been observed at a range of lag periods from a few hours to several days with no clear evidence for any lag period having stronger associations than another.

2.4.2.2. PM-Respiratory Morbidity Associations

Generally, recent studies of respiratory hospital admissions that evaluate multiple lags, have found effect sizes to be larger when using longer moving averages or distributed lag models. For example, when examining hospital admissions for all respiratory diseases among older adults, the strongest associations were observed when using PM concentrations 2 days prior to the hospital

admission (Section 6.3.8). Longer lag periods were also found to be most strongly associated with asthma hospital admissions and ED visits in children (3-5 days) with some evidence for more immediate effects in older adults (lags of 0 and 1 day), but these observations were not consistent across studies (Section 6.3.8). These variable results could be due to the biological complexity of asthma, which inhibits the identification of a specific lag period. The longer lag times identified in the epidemiologic studies evaluated are biologically plausible considering that PM effects on allergic sensitization and lung immune defenses have been observed in controlled human exposure and toxicological studies. These effects could lead to respiratory illnesses over a longer time course (e.g., within several days respiratory infection may become evident, resulting in respiratory symptoms or a hospital admission). However, inflammatory responses, which contribute to some forms of asthma, may result in symptoms requiring medical care within a shorter time frame (e.g., 0-1 days).

2.4.2.3. PM-Mortality Associations

Epidemiologic studies that focused on the association between short-term PM exposure and mortality (i.e., all-cause, cardiovascular, and respiratory) mostly examined a priori lag structures of either 1 or 0-1 days. Although mortality studies do not often examine alternative lag structures, the selection of the aforementioned a priori lag days has been confirmed in additional studies, with the strongest PM-mortality associations consistently being observed at lag 1 and 0-1-days (Section 6.5). However, of note is recent evidence for larger effect estimates when using a distributed lag model.

Epidemiologic studies that examined the association between long-term exposure to PM and mortality have also attempted to identify the latency period from PM exposure to death (Section 7.6.4). Results of the lag comparisons from several cohort studies indicate that the effects of changes in exposure on mortality are seen within five years, with the strongest evidence for effects observed within the first two years. Additionally, there is evidence, albeit from one study, that the mortality effect had larger cumulative effects spread over the follow-up year and three preceding years.

2.4.3. PM Concentration-Response Relationship

An important consideration in characterizing the PM-morbidity and mortality association is whether the concentration-response relationship is linear across the full concentration range that is encountered or if there are concentration ranges where there are departures from linearity (i.e., nonlinearity). In this ISA studies have been identified that attempt to characterize the shape of the concentration-response curve along with possible PM “thresholds” (i.e., levels which PM concentrations must exceed in order to elicit a health response). The epidemiologic studies evaluated that examined the shape of the concentration-response curve and the potential presence of a threshold have focused on cardiovascular hospital admissions and ED visits and mortality associated with short-term exposure to PM₁₀ and mortality associated with long-term exposure to PM_{2.5}.

A limited number of studies have been identified that examined the shape of the PM-cardiovascular hospital admission and ED visit concentration-response relationship. Of these studies, some conducted an exploratory analysis during model selection to determine if a linear curve most adequately represented the concentration-response relationship; whereas, only one study conducted an extensive analysis to examine the shape of the concentration-response curve at different concentrations (Section 6.2.10.10). Overall, the limited evidence from the studies evaluated supports the use of a no-threshold, log-linear model, which is consistent with the observations made in studies that examined the PM-mortality relationship.

Although multiple studies have previously examined the PM-mortality concentration-response relationship and whether a threshold exists, more complex statistical analyses continue to be developed to analyze this association. Using a variety of methods and models, most of the studies evaluated support the use of a no-threshold, log-linear model; however, one study did observe heterogeneity in the shape of the concentration-response curve across cities (Section 6.5). Overall, the studies evaluated further support the use of a no-threshold log-linear model, but additional issues such as the influence of heterogeneity in estimates between cities, and the effect of seasonal and regional differences in PM on the concentration-response relationship still require further investigation.

In addition to examining the concentration-response relationship between short-term exposure to PM and mortality, Schwartz et al. (2008, [156963](#)) conducted an analysis of the shape of the concentration-response relationship associated with long-term exposure to PM. Using a variety of statistical methods, the concentration-response curve was found to be indistinguishable from linear, and, therefore, little evidence was observed to suggest that a threshold exists in the association between long-term exposure to PM_{2.5} and the risk of death (Section 7.6).

2.4.4. PM Sources and Constituents Linked to Health Effects

Recent epidemiologic, toxicological, and controlled human exposure studies have evaluated the health effects associated with ambient PM constituents and sources, using a variety of quantitative methods applied to a broad set of PM constituents, rather than selecting a few constituents a priori (Section 6.6). There is some evidence for trends and patterns that link particular ambient PM constituents or sources with specific health outcomes, but there is insufficient evidence to determine whether these patterns are consistent or robust.

For cardiovascular effects, multiple outcomes have been linked to a PM_{2.5} crustal/soil/road dust source, including cardiovascular mortality and ST-segment changes. Additional studies have reported associations between other sources (i.e., traffic and wood smoke/vegetative burning) and cardiovascular outcomes (i.e., mortality and ED visits). Studies that only examined the effects of individual PM_{2.5} constituents found evidence for an association between EC and cardiovascular hospital admissions and cardiovascular mortality. Many studies have also observed associations between other sources (i.e., salt, secondary SO₄²⁻/long-range transport, other metals) and cardiovascular effects, but at this time, there does not appear to be a consistent trend or pattern of effects for those factors.

There is less consistent evidence for associations between PM sources and respiratory health effects, which may be partially due to the fact that fewer source apportionment studies have been conducted that examined respiratory-related outcomes (e.g., hospital admissions) and measures (e.g., lung function). However, there is some evidence for associations between respiratory ED visits and decrements in lung function with secondary SO₄²⁻ PM_{2.5}. In addition, crustal/soil/road dust and traffic sources of PM have been found to be associated with increased respiratory symptoms in asthmatic children and decreased PEF in asthmatic adults. Inconsistent results were observed in those PM_{2.5} studies that used individual constituents to examine associations with respiratory morbidity and mortality, although Cu, Pb, OC, and Zn were related to respiratory health effects in two or more studies.

A few studies have identified PM_{2.5} sources associated with total mortality. These studies found an association between mortality and the PM_{2.5} sources: secondary SO₄²⁻/long-range transport, traffic, and salt. In addition, studies have evaluated whether the variation in associations between PM_{2.5} and mortality or PM₁₀ and mortality reflects differences in PM_{2.5} constituents. PM₁₀-mortality effect estimates were greater in areas with a higher proportion of Ni in PM_{2.5}, but the overall PM₁₀-mortality association was diminished when New York City was excluded in sensitivity analyses in two of the studies. V was also found to modify PM₁₀-mortality effect estimates. When examining the effect of species-to-PM_{2.5} mass proportion on PM_{2.5}-mortality effect estimates, Ni, but not V, was also found to modify the association.

Overall, the results indicate that many constituents of PM can be linked with differing health effects and the evidence is not yet sufficient to allow differentiation of those constituents or sources that are more closely related to specific health outcomes. These findings are consistent with the conclusions of the 2004 PM AQCD (U.S. EPA, 2004, [056905](#)) (i.e., that a number of source types, including motor vehicle emissions, coal combustion, oil burning, and vegetative burning, are associated with health effects). Although the crustal factor of fine particles was not associated with mortality in the 2004 PM AQCD (U.S. EPA, 2004, [056905](#)), recent studies have suggested that PM (both PM_{2.5} and PM_{10-2.5}) from crustal, soil or road dust sources or PM tracers linked to these sources are associated with cardiovascular effects. In addition, PM_{2.5} secondary SO₄²⁻ has been associated with both cardiovascular and respiratory effects.

2.5. Welfare Effects

This section presents key conclusions and scientific judgments regarding causality for welfare effects of PM as discussed in Chapter 9. The effects of particulate NO_x and SO_x have recently been evaluated in the ISA for Oxides of Nitrogen and Sulfur – Ecological Criteria (U.S. EPA, 2008, [157074](#)). That ISA focused on the effects from deposition of gas- and particle-phase pollutants related to ambient NO_x and SO_x concentrations that can lead to acidification and nutrient enrichment. Thus, emphasis in Chapter 9 is placed on the effects of airborne PM, including NO_x and SO_x, on visibility and climate, and on the effects of deposition of PM constituents other than NO_x and SO_x, primarily metals and carbonaceous compounds. EPA's framework for causality, described in Chapter 1, was applied and the causal determinations are highlighted.

Table 2-5. Summary of causality determination for welfare effects.

Welfare Effects	Causality Determination
Effects on Visibility	Causal
Effects on Climate	Causal
Ecological Effects	Likely to be causal
Effects on Materials	Causal

2.5.1. Summary of Effects on Visibility

Visibility impairment is caused by light scattering and absorption by suspended particles and gases. There is strong and consistent evidence that PM is the overwhelming source of visibility impairment in both urban and remote areas. EC and some crustal minerals are the only commonly occurring airborne particle components that absorb light. All particles scatter light, and generally light scattering by particles is the largest of the four light extinction components (i.e., absorption and scattering by gases and particles). Although a larger particle scatters more light than a similarly shaped smaller particle of the same composition, the light scattered per unit of mass is greatest for particles with diameters from ~0.3-1.0 μm.

For studies where detailed data on particle composition by size are available, accurate calculations of light extinction can be made. However, routinely available PM speciation data can be used to make reasonable estimates of light extinction using relatively simple algorithms that multiply the concentrations of each of the major PM species by its dry extinction efficiency and by a water growth term that accounts for particle size change as a function of relative humidity for hygroscopic species (e.g., sulfate, nitrate, and sea salt). This permits the visibility impairment associated with each of the major PM components to be separately approximated from PM speciation monitoring data.

Direct optical measurement of light extinction measured by transmissometer, or by combining the PM light scattering measured by integrating nephelometers with the PM light absorption measured by an aethalometer, offer a number of advantages compared to algorithm estimates of light extinction based on PM composition and relative humidity data. The direct measurements are not subject to the uncertainties associated with assumed scattering and absorption efficiencies used in the PM algorithm approach. The direct measurements have higher time resolution (i.e., minutes to hours), which is more commensurate with visibility effects compared with calculated light extinction using routinely available PM speciation data (i.e., 24-h duration).

Particulate sulfate and nitrate have comparable light extinction efficiencies (haze impacts per unit mass concentration) at any relative humidity value. Their light scattering per unit mass concentration increases with increasing relative humidity, and at sufficiently high humidity values (RH>85%) they are the most efficient particulate species contributing to haze. Particulate sulfate is

the dominant source of regional haze in the eastern U.S. (>50% of the particulate light extinction) and an important contributor to haze elsewhere in the country (>20% of particulate light extinction). Particulate nitrate is a minor component of remote-area regional haze in the non-California western and eastern U.S., but an important contributor in much of California and in the upper Midwestern U.S., especially during winter when it is the dominant contributor to particulate light extinction.

EC and OC have the highest dry extinction efficiencies of the major PM species and are responsible for a large fraction of the haze, especially in the northwestern U.S., though absolute concentrations are as high in the eastern U.S. Smoke plume impacts from large wildfires dominate many of the worst haze periods in the western U.S. Carbonaceous PM is generally the largest component of urban excess PM_{2.5} (i.e., the difference between urban and regional background concentration). Western urban areas have more than twice the average concentrations of carbonaceous PM than remote areas sites in the same region. In eastern urban areas PM_{2.5} is dominated by about equal concentrations of carbonaceous and sulfate components, though the usually high relative humidity in the East causes the hydrated sulfate particles to be responsible for about twice as much of the urban haze as that caused by the carbonaceous PM.

PM_{2.5} crustal material (referred to as fine soil) and PM_{10-2.5} are significant contributors to haze for remote areas sites in the arid southwestern U.S. where they contribute a quarter to a third of the haze, with PM_{10-2.5} usually contributing twice that of fine soil. Coarse mass concentrations are as high in the Central Great Plains as in the deserts though there are no corresponding high concentrations of fine soil as in the Southwest. Also the relative contribution to haze by the high coarse mass in the Great Plains is much smaller because of the generally higher haze values caused by the high concentrations of sulfate and nitrate PM in that region.

Visibility has direct significance to people's enjoyment of daily activities and their overall sense of wellbeing. For example, psychological research has demonstrated that people are emotionally affected by poor VAQ such that their overall sense of wellbeing is diminished. Urban visibility has been examined in two types of studies directly relevant to the NAAQS review process: urban visibility preference studies and urban visibility valuation studies. Both types of studies are designed to evaluate individuals' desire for good VAQ where they live, using different metrics. Urban visibility preference studies examine individuals' preferences by investigating the amount of visibility degradation considered unacceptable, while economic studies examine the value an individual places on improving VAQ by eliciting how much the individual would be willing to pay for different amounts of VAQ improvement.

There are three urban visibility preference studies and two additional pilot studies that have been conducted to date that provide useful information on individuals' preferences for good VAQ in the urban setting. The completed studies were conducted in Denver, Colorado, two cities in British Columbia, Canada, and Phoenix, AZ. The additional studies were conducted in Washington, DC. The range of median preference values for an acceptable amount of visibility degradation from the 4 urban areas was approximately 19-33 dv. Measured in terms of visual range (VR), these median acceptable values were between approximately 59 and 20 km.

The economic importance of urban visibility has been examined by a number of studies designed to quantify the benefits (or willingness to pay) associated with potential improvements in urban visibility. Urban visibility valuation research was described in the 2004 PM AQCD (U.S. EPA, 2004, [056905](#)) and the 2005 PM Staff Paper (U.S. EPA, 2005, [090209](#)). Since the mid-1990s, little new information has become available regarding urban visibility valuation (Section 9.2.4).

Collectively, the evidence is sufficient to conclude that **a causal relationship exists between PM and visibility impairment.**

2.5.2. Summary of Effects on Climate

Aerosols affect climate through direct and indirect effects. The direct effect is primarily realized as planet brightening when seen from space because most aerosols scatter most of the visible spectrum light that reaches them. The Intergovernmental Panel on Climate Change (IPCC) Fourth Assessment Report (AR4) (IPCC, 2007, [092765](#)), hereafter IPCC AR4, reported that the radiative forcing from this direct effect was $-0.5 (\pm 0.4) \text{ W/m}^2$ and identified the level of scientific understanding of this effect as 'Medium-low'. The global mean direct radiative forcing effect from individual components of aerosols was estimated for the first time in the IPCC AR4 where they were reported to be (all in W/m^2 units): $-0.4 (\pm 0.2)$ for sulfate, $-0.05 (\pm 0.05)$ for fossil fuel-derived organic

carbon, +0.2 (± 0.15) for fossil fuel-derived black carbon (BC), +0.03 (± 0.12) for biomass burning, -0.1 (± 0.1) for nitrates, and -0.1 (± 0.2) for mineral dust. Global loadings of anthropogenic dust and nitrates remain very troublesome to estimate, making the radiative forcing estimates for these constituents particularly uncertain.

Numerical modeling of aerosol effects on climate has sustained remarkable progress since the time of the 2004 PM AQCD (U.S. EPA, 2004, [056905](#)), PM AQCD, though model solutions still display large heterogeneity in their estimates of the direct radiative forcing effect from anthropogenic aerosols. The clear-sky direct radiative forcing over ocean due to anthropogenic aerosols is estimated from satellite instruments to be on the order of -1.1 (± 0.37) W/m^2 while model estimates are -0.6 W/m^2 . The models' low bias over ocean is carried through for the global average: global average direct radiative forcing from anthropogenic aerosols is estimated from measurements to range from -0.9 to -1.9 W/m^2 , larger than the estimate of -0.8 W/m^2 from the models.

Aerosol indirect effects on climate are primarily realized as an increase in cloud brightness (termed the 'first indirect' or Twomey effect), changes in precipitation, and possible changes in cloud lifetime. The IPCC AR4 reported that the radiative forcing from the Twomey effect was -0.7 (range: -1.1 to $+4$) and identified the level of scientific understanding of this effect as "Low" in part owing to the very large unknowns concerning aerosol size distributions and important interactions with clouds. Other indirect effects from aerosols are not considered to be radiative forcing.

Taken together, direct and indirect effects from aerosols increase Earth's shortwave albedo or reflectance thereby reducing the radiative flux reaching the surface from the Sun. This produces net climate cooling from aerosols. The current scientific consensus reported by IPCC AR4 is that the direct and indirect radiative forcing from anthropogenic aerosols computed at the top of the atmosphere, on a global average, is about -1.3 (range: -2.2 to -0.5) W/m^2 . While the overall global average effect of aerosols at the top of the atmosphere and at the surface is negative, absorption and scattering by aerosols within the atmospheric column warms the atmosphere between the Earth's surface and top of the atmosphere. In part, this is owing to differences in the distribution of aerosol type and size within the vertical atmospheric column since aerosol type and size distributions strongly affect the aerosol scattering and reradiation efficiencies at different altitudes and atmospheric temperatures. And, although the magnitude of the overall negative radiative forcing at the top of the atmosphere appears large in comparison to the analogous IPCC AR4 estimate of positive radiative forcing from anthropogenic GHG of about $+2.9$ (± 0.3) W/m^2 , the horizontal, vertical, and temporal distributions and the physical lifetimes of these two very different radiative forcing agents are not similar; therefore, the effects do not simply off-set one another.

Overall, the evidence is sufficient to conclude that **a causal relationship exists between PM and effects on climate, including both direct effects on radiative forcing and indirect effects that involve cloud feedbacks that influence precipitation formation and cloud lifetimes.**

2.5.3. Summary of Ecological Effects of PM

Ecological effects of PM include direct effects to metabolic processes of plant foliage; contribution to total metal loading resulting in alteration of soil biogeochemistry and microbiology, plant growth and animal growth and reproduction; and contribution to total organics loading resulting in bioaccumulation and biomagnification across trophic levels. These effects were well-characterized in the 2004 PM AQCD (U.S. EPA, 2004, [056905](#)). Thus, the summary below builds upon the conclusions provided in that review.

PM deposition comprises a heterogeneous mixture of particles differing in origin, size, and chemical composition. Exposure to a given concentration of PM may, depending on the mix of deposited particles, lead to a variety of phytotoxic responses and ecosystem effects. Moreover, many of the ecological effects of PM are due to the chemical constituents (e.g., metals, organics, and ions) and their contribution to total loading within an ecosystem.

Investigations of the direct effects of PM deposition on foliage have suggested little or no effects on foliar processes, unless deposition levels were higher than is typically found in the ambient environment. However, consistent and coherent evidence of direct effects of PM has been found in heavily polluted areas adjacent to industrial point sources such as limestone quarries, cement kilns, and metal smelters (Sections 9.4.3 and 9.4.5.7). Where toxic responses have been

documented, they generally have been associated with the acidity, trace metal content, surfactant properties, or salinity of the deposited materials.

An important characteristic of fine particles is their ability to affect the flux of solar radiation passing through the atmosphere, which can be considered in both its direct and diffuse components. Foliar interception by canopy elements occurs for both up- and down-welling radiation. Therefore, the effect of atmospheric PM on atmospheric turbidity influences canopy processes both by radiation attenuation and by changing the efficiency of radiation interception in the canopy through conversion of direct to diffuse radiation. Crop yields can be sensitive to the amount of radiation received, and crop losses have been attributed to increased regional haze in some areas of the world such as China (Section 9.4.4). On the other hand, diffuse radiation is more uniformly distributed throughout the canopy and may increase canopy photosynthetic productivity by distributing radiation to lower leaves. The enrichment in photosynthetically active radiation (PAR) present in diffuse radiation may offset a portion of the effect of an increased atmospheric albedo due to atmospheric particles. Further research is needed to determine the effects of PM alteration of radiative flux on the growth of vegetation in the U.S.

The deposition of PM onto vegetation and soil, depending on its chemical composition, can produce responses within an ecosystem. The ecosystem response to pollutant deposition is a direct function of the level of sensitivity of the ecosystem and its ability to ameliorate resulting change. Many of the most important ecosystem effects of PM deposition occur in the soil. Upon entering the soil environment, PM pollutants can alter ecological processes of energy flow and nutrient cycling, inhibit nutrient uptake, change ecosystem structure, and affect ecosystem biodiversity. The soil environment is one of the most dynamic sites of biological interaction in nature. It is inhabited by microbial communities of bacteria, fungi, and actinomycetes, in addition to plant roots and soil macro-fauna. These organisms are essential participants in the nutrient cycles that make elements available for plant uptake. Changes in the soil environment can be important in determining plant and ultimately ecosystem response to PM inputs.

There is strong and consistent evidence from field and laboratory experiments that metal components of PM alter numerous aspects of ecosystem structure and function. Changes in the soil chemistry, microbial communities and nutrient cycling, can result from the deposition of trace metals. Exposures to trace metals are highly variable, depending on whether deposition is by wet or dry processes. Although metals can cause phytotoxicity at high concentrations, few heavy metals (e.g., Cu, Ni, Zn) have been documented to cause direct phytotoxicity under field conditions. Exposure to coarse particles and elements such as Fe and Mg are more likely to occur via dry deposition, while fine particles, which are more often deposited by wet deposition, are more likely to contain elements such as Ca, Cr, Pb, Ni, and V. Ecosystems immediately downwind of major emissions sources can receive locally heavy deposition inputs. Phytochelatins produced by plants as a response to sublethal concentrations of heavy metals are indicators of metal stress to plants. Increased concentrations of phytochelatins across regions and at greater elevation have been associated with increased amounts of forest injury in the northeastern U.S.

Overall, the ecological evidence is sufficient to conclude that **a causal relationship is likely to exist between deposition of PM and a variety of effects on individual organisms and ecosystems, based on information from the previous review and limited new findings in this review.** However, in many cases, it is difficult to characterize the nature and magnitude of effects and to quantify relationships between ambient concentrations of PM and ecosystem response due to significant data gaps and uncertainties as well as considerable variability that exists in the components of PM and their various ecological effects.

2.5.4. Summary of Effects on Materials

Building materials (metals, stones, cements, and paints) undergo natural weathering processes from exposure to environmental elements (wind, moisture, temperature fluctuations, sunlight, etc.). Metals form a protective film of oxidized metal (e.g., rust) that slows environmentally induced corrosion. However, the natural process of metal corrosion is enhanced by exposure to anthropogenic pollutants. For example, formation of hygroscopic salts increases the duration of surface wetness and enhances corrosion.

A significant detrimental effect of particle pollution is the soiling of painted surfaces and other building materials. Soiling changes the reflectance of opaque materials and reduces the transmission

of light through transparent materials. Soiling is a degradation process that requires remediation by cleaning or washing, and, depending on the soiled surface, repainting. Particulate deposition can result in increased cleaning frequency of the exposed surface and may reduce the usefulness of the soiled material.

Attempts have been made to quantify the pollutant exposure levels at which materials damage and soiling have been perceived. However, to date, insufficient data are available to advance the knowledge regarding perception thresholds with respect to pollutant concentration, particle size, and chemical composition. Nevertheless, the evidence is sufficient to conclude that **a causal relationship exists between PM and effects on materials.**

2.6. Summary of Health Effects and Welfare Effects Causal Determinations

This chapter has provided an overview of the underlying evidence used in making the causal determinations for the health and welfare effects and PM size fractions evaluated. This review builds upon the main conclusions of the last PM AQCD (U.S. EPA, 2004, [056905](#)):

- “A growing body of evidence both from epidemiological and toxicological studies... supports the general conclusion that PM_{2.5} (or one or more PM_{2.5} components), acting alone and/or in combination with gaseous copollutants, are likely causally related to cardiovascular and respiratory mortality and morbidity.” (pg 9-79)
- “A much more limited body of evidence is suggestive of associations between short-term (but not long-term) exposures to ambient coarse-fraction thoracic particles... and various mortality and morbidity effects observed at times in some locations. This suggests that PM_{10-2.5}, or some constituent component(s) of PM_{10-2.5}, may contribute under some circumstances to increased human health risks... with somewhat stronger evidence for... associations with morbidity (especially respiratory) endpoints than for mortality.” (pg 9-79 and 9-80)
- “Impairment of visibility in rural and urban areas is directly related to ambient concentrations of fine particles, as modulated by particle composition, size, and hygroscopic characteristics, and by relative humidity.” (pg 9-99)
- “Available evidence, ranging from satellite to in situ measurements of aerosol effects on incoming solar radiation and cloud properties, is strongly indicative of an important role in climate for aerosols, but this role is still poorly quantified.” (pg 9-111)

The evaluation of the epidemiologic, toxicological, and controlled human exposure studies published since the completion of the 2004 PM AQCD have provided additional evidence for PM-related health effects. Table 2-6 provides an overview of the causal determinations for all PM size fractions and health effects. Causal determinations for PM and welfare effects, including visibility, climate, ecological effects, and materials are included in Table 2-7. Detailed discussions of the scientific evidence and rationale for these causal determinations are provided in the subsequent chapters of this ISA.

Table 2-6. Summary of PM causal determinations by exposure duration and health outcome.

Size Fraction	Exposure	Outcome	Causality Determination
PM _{2.5}	Short-term	Cardiovascular Effects	Causal
		Respiratory Effects	Likely to be causal
		Central Nervous System	Inadequate
		Mortality	Causal
	Long-term	Cardiovascular Effects	Causal
		Respiratory Effects	Likely to be Causal
		Mortality	Causal
		Reproductive and Developmental	Suggestive
		Cancer, Mutagenicity, Genotoxicity	Suggestive
PM _{10-2.5}	Short-term	Cardiovascular Effects	Suggestive
		Respiratory Effects	Suggestive
		Central Nervous System	Inadequate
		Mortality	Suggestive
	Long-term	Cardiovascular Effects	Inadequate
		Respiratory Effects	Inadequate
		Mortality	Inadequate
		Reproductive and Developmental	Inadequate
		Cancer, Mutagenicity, Genotoxicity	Inadequate
UFPs	Short-term	Cardiovascular Effects	Suggestive
		Respiratory Effects	Suggestive
		Central Nervous System	Inadequate
		Mortality	Inadequate
	Long-term	Cardiovascular Effects	Inadequate
		Respiratory Effects	Inadequate
		Mortality	Inadequate
		Reproductive and Developmental	Inadequate
		Cancer, Mutagenicity, Genotoxicity	Inadequate

Table 2-7. Summary of PM causal determinations for welfare effects

Welfare Effects	Causality Determination
Effects on Visibility	Causal
Effects on Climate	Causal
Ecological Effects	Likely to be causal
Effects on Materials	Causal

Chapter 2 References

- American Heart Association (2009). Cardiovascular disease statistics. Retrieved 17-NOV-09, from <http://www.americanheart.org/presenter.jhtml?identifier=4478>. [198920](#)
- ATSDR (2006). A study of ambient air contaminants and asthma in New York City: Part A and B. Agency for Toxic Substances and Disease Registry; Public Health Service; U.S. Department of Health and Human Services. Atlanta, GA. http://permanent.access.gpo.gov/lps88357/ASTHMA_BRONX_FINAL_REPORT.pdf. [090132](#)
- Bell ML; Ebisu K; Peng RD; Walker J; Samet JM; Zeger SL; Dominic F (2008). Seasonal and regional short-term effects of fine particles on hospital admissions in 202 U.S. counties, 1999-2005. *Am J Epidemiol*, 168: 1301-1310. [156266](#)
- Burnett RT; Cakmak S; Brook JR; Krewski D (1997). The role of particulate size and chemistry in the association between summertime ambient air pollution and hospitalization for cardiorespiratory diseases. *Environ Health Perspect*, 105: 614-620. [084194](#)
- Burnett RT; Goldberg MS (2003). Size-fractionated particulate mass and daily mortality in eight Canadian cities. Health Effects Institute. Boston, MA. [042798](#)
- Burnett RT; Stieb D; Brook JR; Cakmak S; Dales R; Raizenne M; Vincent R; Dann T (2004). Associations between short-term changes in nitrogen dioxide and mortality in Canadian cities. *Arch Environ Occup Health*, 59: 228-236. [086247](#)
- Chen LH; Knutsen SF; Shavlik D; Beeson WL; Petersen F; Ghamsary M; Abbey D (2005). The association between fatal coronary heart disease and ambient particulate air pollution: Are females at greater risk? *Environ Health Perspect*, 113: 1723-1729. [087942](#)
- Chen Y; Yang Q; Krewski D; Burnett RT; Shi Y; McGrail KM (2005). The effect of coarse ambient particulate matter on first, second, and overall hospital admissions for respiratory disease among the elderly. *Inhal Toxicol*, 17: 649-655. [087555](#)
- Chen Y; Yang Q; Krewski D; Shi Y; Burnett RT; McGrail K (2004). Influence of relatively low level of particulate air pollution on hospitalization for COPD in elderly people. *Inhal Toxicol*, 16: 21-25. [087262](#)
- Chimonas MA; Gessner BD (2007). Airborne particulate matter from primarily geologic, non-industrial sources at levels below National Ambient Air Quality Standards is associated with outpatient visits for asthma and quick-relief medication prescriptions among children less than 20 years old enrolled in Medicaid in Anchorage, Alaska. *Environ Res*, 103: 397-404. [093261](#)
- Delfino RJ; Murphy-Moulton AM; Burnett RT; Brook JR; Becklake MR (1997). Effects of air pollution on emergency room visits for respiratory illnesses in Montreal, Quebec. *Am J Respir Crit Care Med*, 155: 568-576. [082687](#)
- Dockery DW; Damokosh AI; Neas LM; Raizenne M; Spengler JD; Koutrakis P; Ware JH; Speizer FE (1996). Health effects of acid aerosols on North American children: respiratory symptoms and illness. *Environ Health Perspect*, 104: 500-505. [046219](#)
- Dockery DW; Luttmann-Gibson H; Rich DQ; Link MS; Mittleman MA; Gold DR; Koutrakis P; Schwartz JD; Verrier RL (2005). Association of air pollution with increased incidence of ventricular tachyarrhythmias recorded by implanted cardioverter defibrillators. *Environ Health Perspect*, 113: 670-674. [078995](#)
- Dominici F; Peng RD; Bell ML; Pham L; McDermott A; Zeger SL; Samet JL (2006). Fine particulate air pollution and hospital admission for cardiovascular and respiratory diseases. *JAMA*, 295: 1127-1134. [088398](#)
- Eftim SE; Samet JM; Janes H; McDermott A; Dominici F (2008). Fine particulate matter and mortality: a comparison of the six cities and American Cancer Society cohorts with a medicare cohort. *Epidemiology*, 19: 209-216. [099104](#)
- Enstrom JE (2005). Fine particulate air pollution and total mortality among elderly Californians, 1973-2002. *Inhal Toxicol*, 17: 803-816. [087356](#)

▪ Note: Hyperlinks to the reference citations throughout this document will take you to the NCEA HERO database (Health and Environmental Research Online) at <http://epa.gov/hero>. HERO is a database of scientific literature used by U.S. EPA in the process of developing science assessments such as the Integrated Science Assessments (ISA) and the Integrated Risk Information System (IRIS).

- Fairley D (2003). Mortality and air pollution for Santa Clara County, California, 1989-1996, In: Revised analyses of time-series studies of air pollution and health. Special report. Health Effects Institute. Boston, MA. <http://www.healtheffects.org/Pubs/TimeSeries.pdf> . [042850](#)
- Franklin M; Koutrakis P; Schwartz J (2008). The role of particle composition on the association between PM2.5 and mortality. *Epidemiology*, 19: 680-689. [097426](#)
- Franklin M; Zeka A; Schwartz J (2007). Association between PM2.5 and all-cause and specific-cause mortality in 27 US communities. *J Expo Sci Environ Epidemiol*, 17: 279-287. [091257](#)
- Fung KY; Khan S; Krewski D; Chen Y (2006). Association between air pollution and multiple respiratory hospitalizations among the elderly in Vancouver, Canada. *Inhal Toxicol*, 18: 1005-1011. [089789](#)
- Goss CH; Newsom SA; Schildcrout JS; Sheppard L; Kaufman JD (2004). Effect of ambient air pollution on pulmonary exacerbations and lung function in cystic fibrosis. *Am J Respir Crit Care Med*, 169: 816-821. [055624](#)
- IPCC (2007). *Climate Change 2007: The Physical Science Basis. Contribution of Working Group I to the Fourth Assessment Report (AR4) of the Intergovernmental Panel on Climate Change* . Cambridge, UK and New York, NY: Intergovernmental Panel on Climate Change, Cambridge University Press. [092765](#)
- Ito K (2003). Associations of particulate matter components with daily mortality and morbidity in Detroit, Michigan, In: Revised analyses of time-series studies of air pollution and health. Special report. Health Effects Institute. Boston, MA. R828112. <http://www.healtheffects.org/Pubs/TimeSeries.pdf> . [042856](#)
- Ito K; Thurston GD; Silverman RA (2007). Characterization of PM2.5, gaseous pollutants, and meteorological interactions in the context of time-series health effects models. *J Expo Sci Environ Epidemiol*, 17 Suppl 2: S45-S60. [156594](#)
- Kim JJ; Smorodinsky S; Lipsett M; Singer BC; Hodgson AT; Ostro B (2004). Traffic-related air pollution near busy roads: the East Bay children's Respiratory Health Study. *Am J Respir Crit Care Med*, 170: 520-526. [087383](#)
- Klemm RJ; Lipfert FW; Wyzga RE; Gust C (2004). Daily mortality and air pollution in Atlanta: two years of data from ARIES. *Inhal Toxicol*, 16 Suppl 1: 131-141. [056585](#)
- Klemm RJ; Mason R (2003). Replication of reanalysis of Harvard Six-City mortality study. In HEI Special Report: Revised Analyses of Time-Series Studies of Air Pollution and Health, Part II (pp. 165-172). Boston, MA: Health Effects Institute. [042801](#)
- Krewski D; Jerrett M; Burnett RT; Ma R; Hughes E; Shi Y; Turner MC; Pope AC III; Thurston G; Calle EE; Thun MJ (2009). Extended follow-up and spatial analysis of the American Cancer Society study linking particulate air pollution and mortality. Health Effects Institute. Cambridge, MA. Report Nr. 140. [191193](#)
- Laden F; Schwartz J; Speizer FE; Dockery DW (2006). Reduction in fine particulate air pollution and mortality: extended follow-up of the Harvard Six Cities study. *Am J Respir Crit Care Med*, 173: 667-672. [087605](#)
- Lin M; Chen Y; Burnett RT; Villeneuve PJ; Krewski D (2002). The influence of ambient coarse particulate matter on asthma hospitalization in children: case-crossover and time-series analyses. *Environ Health Perspect*, 110: 575-581. [026067](#)
- Lin M; Stieb DM; Chen Y (2005). Coarse particulate matter and hospitalization for respiratory infections in children younger than 15 years in Toronto: a case-crossover analysis. *Pediatrics*, 116: 235-240. [087828](#)
- Lipfert FW; Baty JD; Miller JP; Wyzga RE (2006). PM2.5 constituents and related air quality variables as predictors of survival in a cohort of U.S. military veterans. *Inhal Toxicol*, 18: 645-657. [088756](#)
- Lipfert FW; Morris SC; Wyzga RE (2000). Daily mortality in the Philadelphia metropolitan area and size-classified particulate matter. *J Air Waste Manag Assoc*, 50: 1501-1513. [004088](#)
- Lisabeth LD; Escobar JD; Dvornich JT; Sanchez BN; Majersik JJ; Brown DL; Smith MA; Morgenstern LB (2008). Ambient air pollution and risk for ischemic stroke and transient ischemic attack. *Ann Neurol*, 64: 53-59. [155939](#)
- Mar TF; Larson TV; Stier RA; Claiborn C; Koenig JQ (2004). An analysis of the association between respiratory symptoms in subjects with asthma and daily air pollution in Spokane, Washington. *Inhal Toxicol*, 16: 809-815. [057309](#)
- Mar TF; Norris GA; Larson TV; Wilson WE; Koenig JQ (2003). Air pollution and cardiovascular mortality in Phoenix, 1995-1997. Health Effects Institute. Cambridge, MA. [042841](#)

- McConnell R; Berhane K; Gilliland F; Molitor J; Thomas D; Lurmann F; Avol E; Gauderman WJ; Peters JM (2003). Prospective study of air pollution and bronchitic symptoms in children with asthma. *Am J Respir Crit Care Med*, 168: 790-797. [049490](#)
- Metzger KB; Klein M; Flanders WD; Peel JL; Mulholland JA; Langberg JJ; Tolbert PE (2007). Ambient air pollution and cardiac arrhythmias in patients with implantable defibrillators. *Epidemiology*, 18: 585-592. [092856](#)
- Metzger KB; Tolbert PE; Klein M; Peel JL; Flanders WD; Todd KH; Mulholland JA; Ryan PB; Frumkin H (2004). Ambient air pollution and cardiovascular emergency department visits. *Epidemiology*, 15: 46-56. [044222](#)
- Miller KA; Siscovick DS; Sheppard L; Shepherd K; Sullivan JH; Anderson GL; Kaufman JD (2007). Long-term exposure to air pollution and incidence of cardiovascular events in women. *N Engl J Med*, 356: 447-458. [090130](#)
- O'Connor GT; Neas L; Vaughn B; Kattan M; Mitchell H; Crain EF; Evans R 3rd; Gruchalla R; Morgan W; Stout J; Adams GK; Lippmann M (2008). Acute respiratory health effects of air pollution on children with asthma in US inner cities. *J Allergy Clin Immunol*, 121: 1133-1139. [156818](#)
- Ostro BD; Broadwin R; Lipsett MJ (2003). Coarse particles and daily mortality in Coachella Valley, California. Health Effects Institute. Boston, MA. [042824](#)
- Peel JL; Tolbert PE; Klein M; Metzger KB; Flanders WD; Knox T; Mulholland JA; Ryan PB; Frumkin H (2005). Ambient air pollution and respiratory emergency department visits. *Epidemiology*, 16: 164-174. [056305](#)
- Peng RD; Chang HH; Bell ML; McDermott A; Zeger SL; Samet JM; Dominici F (2008). Coarse particulate matter air pollution and hospital admissions for cardiovascular and respiratory diseases among Medicare patients. *JAMA*, 299: 2172-2179. [156850](#)
- Peters A; Dockery DW; Muller JE; Mittleman MA (2001). Increased particulate air pollution and the triggering of myocardial infarction. *Circulation*, 103: 2810-2815. [016546](#)
- Pope C; Renlund D; Kfoury A; May H; Horne B (2008). Relation of heart failure hospitalization to exposure to fine particulate air pollution. *Am J Cardiol*, 102: 1230-1234. [191969](#)
- Pope CA III; Muhlestein JB; May HT; Renlund DG; Anderson JL; Horne BD (2006). Ischemic heart disease events triggered by short-term exposure to fine particulate air pollution. *Circulation*, 114: 2443-2448. [091246](#)
- Rabinovitch N; Strand M; Gelfand EW (2006). Particulate levels are associated with early asthma worsening in children with persistent disease. *Am J Respir Crit Care Med*, 173: 1098-1105. [088031](#)
- Rabinovitch N; Zhang LN; Murphy JR; Vedal S; Dutton SJ; Gelfand EW (2004). Effects of wintertime ambient air pollutants on asthma exacerbations in urban minority children with moderate to severe disease. *J Allergy Clin Immunol*, 114: 1131-1137. [096753](#)
- Renwick LC; Brown D; Clouter A; Donaldson K (2004). Increased inflammation and altered macrophage chemotactic responses caused by two ultrafine particle types. *Occup Environ Med*, 61: 442-447. [056067](#)
- Rich DQ; Kim MH; Turner JR; Mittleman MA; Schwartz J; Catalano PJ; Dockery DW (2006). Association of ventricular arrhythmias detected by implantable cardioverter defibrillator and ambient air pollutants in the St Louis, Missouri metropolitan area. *Occup Environ Med*, 63: 591-596. [089814](#)
- Rich DQ; Schwartz J; Mittleman MA; Link M; Luttmann-Gibson H; Catalano PJ; Speizer FE; Dockery DW (2005). Association of short-term ambient air pollution concentrations and ventricular arrhythmias. *Am J Epidemiol*, 161: 1123-1132. [079620](#)
- Schwartz J; Coull B; Laden F; Ryan L (2008). The effect of dose and timing of dose on the association between airborne particles and survival. *Environ Health Perspect*, 116: 64-69. [156963](#)
- Schwartz J; Dockery DW; Neas LM (1996). Is daily mortality associated specifically with fine particles? *J Air Waste Manag Assoc*, 46: 927-939. [077325](#)
- Sheppard L; Levy D; Norris G; Larson TV; Koenig JQ (2003). Effects of ambient air pollution and nonelderly asthma hospital admissions in Seattle, Washington, 1987-1994. *Epidemiology*, 10: 23-30. [042826](#)
- Slaughter JC; Kim E; Sheppard L; Sullivan JH; Larson TV; Claiborn C (2005). Association between particulate matter and emergency room visits, hospital admissions and mortality in Spokane, Washington. *J Expo Sci Environ Epidemiol*, 15: 153-159. [073854](#)

- Stieb DM; Beveridge RC; Brook JR; Smith-Doiron M; Burnett RT; Dales RE; Beaulieu S; Judek S; Mamedov A (2000). Air pollution, aeroallergens and cardiorespiratory emergency department visits in Saint John, Canada. *J Expo Sci Environ Epidemiol*, 10: 461-477. [011675](#)
- Sullivan J; Sheppard L; Schreuder A; Ishikawa N; Siscovick D; Kaufman J (2005). Relation between short-term fine-particulate matter exposure and onset of myocardial infarction. *Epidemiology*, 16: 41-48. [050854](#)
- Symons JM; Wang L; Guallar E; Howell E; Dominici F; Schwab M; Ange BA; Samet J; Ondov J; Harrison D; Geyh A (2006). A case-crossover study of fine particulate matter air pollution and onset of congestive heart failure symptom exacerbation leading to hospitalization. *Am J Epidemiol*, 164: 421-433. [091258](#)
- Thurston GD; Ito K; Hayes CG; Bates DV; Lippmann M (1994). Respiratory hospital admissions and summertime haze air pollution in Toronto, Ontario: consideration of the role of acid aerosols. *Environ Res*, 65: 271-290. [043921](#)
- Tolbert PE; Klein M; Peel JL; Sarnat SE; Sarnat JA (2007). Multipollutant modeling issues in a study of ambient air quality and emergency department visits in Atlanta. *J Expo Sci Environ Epidemiol*, 17: S29-S35. [090316](#)
- U.S. EPA (2004). Air quality criteria for particulate matter. U.S. Environmental Protection Agency. Research Triangle Park, NC. EPA/600/P-99/002aF-bF. [056905](#)
- U.S. EPA (2005). Review of the national ambient air quality standards for particulate matter: Policy assessment of scientific and technical information OAQPS staff paper. U.S. Environmental Protection Agency. Washington, DC. EPA/452/R-05-005a. http://www.epa.gov/ttn/naaqs/standards/pm/data/pmstaffpaper_20051221.pdf. [090209](#)
- U.S. EPA (2008). Integrated science assessment for oxides of nitrogen and sulfur: Ecological criteria. U.S. Environmental Protection Agency. Research Triangle Park, NC. EPA/600/R-08/082F. [157074](#)
- Villeneuve PJ; Burnett RT; Shi Y; Krewski D; Goldberg MS; Hertzman C; Chen Y; Brook J (2003). A time-series study of air pollution, socioeconomic status, and mortality in Vancouver, Canada. *J Expo Sci Environ Epidemiol*, 13: 427-435. [055051](#)
- Villeneuve PJ; Chen L; Stieb D; Rowe BH (2006). Associations between outdoor air pollution and emergency department visits for stroke in Edmonton, Canada. *Eur J Epidemiol*, 21: 689-700. [090191](#)
- Wilson WE; Mar TF; Koenig JQ (2007). Influence of exposure error and effect modification by socioeconomic status on the association of acute cardiovascular mortality with particulate matter in Phoenix. *J Expo Sci Environ Epidemiol*, 17: S11-S19. [157149](#)
- Woodruff TJ; Darrow LA; Parker JD (2008). Air pollution and postneonatal infant mortality in the United States, 1999-2002. *Environ Health Perspect*, 116: 110-115. [098386](#)
- Zanobetti A; Schwartz J (2006). Air pollution and emergency admissions in Boston, MA. *J Epidemiol Community Health*, 60: 890-895. [090195](#)
- Zanobetti A; Schwartz J (2009). The effect of fine and coarse particulate air pollution on mortality: A national analysis. *Environ Health Perspect*, 117: 1-40. [188462](#)
- Zeger S; Dominici F; McDermott A; Samet J (2008). Mortality in the Medicare population and chronic exposure to fine particulate air pollution in urban centers (2000-2005). *Environ Health Perspect*, 116: 1614-1619. [191951](#)
- Zhang Z; Whitsel E; Quibrera P; Smith R; Liao D; Anderson G; Prineas R (2009). Ambient fine particulate matter exposure and myocardial ischemia in the Environmental Epidemiology of Arrhythmogenesis in the Women's Health Initiative (EEAWHI) study. *Environ Health Perspect*, 117: 751-756. [191970](#)

Chapter 3. Source to Human Exposure

3.1. Introduction

This chapter describes basic concepts and new and established findings in atmospheric sciences and human exposure assessment relevant to PM to establish a foundation for the health and ecological effects discussed in subsequent chapters. Information in this chapter builds on previous AQCDs for PM using new data and re-interpretations of extant studies as well. This includes new knowledge of PM chemistry, the latest developments in monitoring methodologies, recent national and local measurements and trends in PM concentrations as a function of size range and composition, advances in receptor and chemistry-transport modeling, revised estimates of policy-relevant background PM, and recent work on exposure assessment.

The chapter and its associated annex material are organized as follows: Section 3.2 presents an overview of basic information related to the size distribution and composition of airborne particles. Section 3.3 provides a brief description of the sources, emissions, and deposition of PM, including discussions of possible mechanisms of secondary PM formation from gaseous precursors and of the atmospheric processes that deposit PM to the earth's surface. Issues related to the measurement of PM and its chemical components and to monitors and networks in the U.S. are covered in Section 3.4; supplementary material on these topics is contained in Annex A, Section A.1. Analyses of data for ambient concentrations of PM and its components are characterized in Section 3.5, and supplementary information can be found in Annex A, Section A.2. Section 3.6 describes methods for determining source contributions to ambient samples by receptor models and presents results from recent receptor modeling studies. In addition, the construction of chemistry-transport models (CTMs) to determine pollutant concentrations is described in Section 3.6. Supplementary information about receptor model methods and results is given in Annex A, Section A.3. Policy relevant background concentrations of PM, i.e., those concentrations defined to result from natural sources everywhere in the world together with anthropogenic sources outside of Canada, the United States, and Mexico, are presented in Section 3.7. Issues related to human exposure assessment including sources of exposure and implications for epidemiologic studies are discussed in Section 3.8. Supplementary information on exposure studies is included in Annex A, Section A.4. Finally, the summary and conclusions from Chapter 3 are presented in Section 3.9.

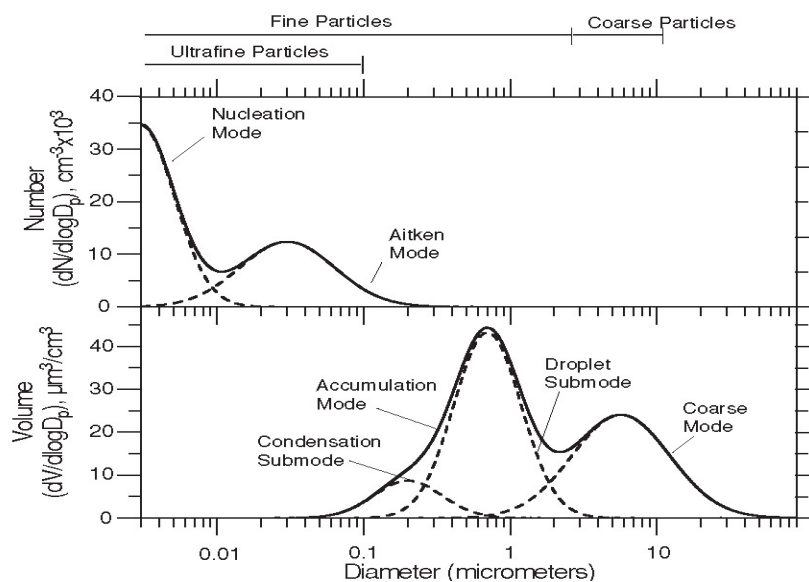
3.2. Overview of Basic Aerosol Properties

Unlike gas-phase pollutants such as SO₂, CO, H₂CO and O₃, which are well-defined chemical entities, atmospheric PM varies in size, shape, and chemical composition. Atmospheric chemical and microphysical processing of direct emissions of PM and its precursors together with mechanical generation of particles tend to produce distinct lognormal modes (Whitby, 1978, [071181](#)) as shown in Figure 3-1. To the extent that information is available, discussions in this and subsequent chapters will focus on particles in specific size ranges (i.e., PM_{2.5}, PM_{10-2.5} and PM₁₀). The subscripts after PM

Note: Hyperlinks to the reference citations throughout this document will take you to the NCEA HERO database (Health and Environmental Research Online) at <http://epa.gov/hero>. HERO is a database of scientific literature used by U.S. EPA in the process of developing science assessments such as the Integrated Science Assessments (ISA) and the Integrated Risk Information System (IRIS).

refer to the aerodynamic diameter¹ (d_{ae}) in micrometers (μm) of 50% cut points of sampling devices. For example, EPA defines PM_{10} as particles collected by a sampler with an upper 50% cut point of $10 \mu\text{m}$ d_{ae} and a specific, fairly sharp, penetration curve, as defined in the Code of Federal Regulations (40 CFR Part 58). $\text{PM}_{2.5}$ is defined in an analogous way. Ultrafine particles (UFPs), defined here as particles with a diameter $\leq 0.1 \mu\text{m}$ (typically based on physical size, thermal diffusivity, or electrical mobility), will also be discussed.

The terms “fine particles” and “coarse particles” have lost the precise meaning as defined in Whitby (1978, [071181](#)), where “fine particles” refers to all particles in the nucleation, Aitken, and accumulation modes; and “coarse particles” characterizes all particles larger than these. UFPs correspond loosely to the nucleation plus Aitken modes (in earlier literature, these modes were not separated and the combination, unresolved by older instruments, was called the Aitken mode). Now, the term “fine particles” is most often associated with the $\text{PM}_{2.5}$ fraction, which includes the nucleation, Aitken and accumulation modes and some particles from the lower-size tail of the coarse particle mode between about 1 and $2.5 \mu\text{m}$ aerodynamic diameter. “Thoracic coarse” is frequently used in reference to $\text{PM}_{10-2.5}$, which does not include the low-end tail of the coarse particle mode. With high relative humidity, larger particles in the accumulation mode could also extend into the 1 to $3 \mu\text{m}$ size range. These relationships can be seen in Figure 3-1, which shows the number distribution for UFPs and the volume distribution (or mass distribution if particle density is constant across the size range) for fine and (thoracic) coarse particles. The figure is arranged this way because particle number is most highly concentrated in the ultrafine (UF) size range but volume (or mass) is most concentrated in the larger size ranges.



Source: Reprinted with Permission of Cambridge University Press from Pandis (2004, [156838](#)).

Figure 3-1. Particle size distributions by number and volume. Dashed lines refer to values in individual modes and solid lines to their sum. Note that ultrafine particles are a subset of fine particles.

¹ Aerodynamic diameter is the diameter of a unit density (1 g/cm^3) sphere that has the same gravitational settling velocity as the particle of interest and is a useful metric for characterizing particles $> 1 \mu\text{m}$. For sub-micron particles, forces other than gravity increase in importance in determining a particle's motion and air can no longer be considered a continuum. Aerodynamic diameter is frequently reported down to $\sim 0.1 \mu\text{m}$ where the assumptions used in its derivation no longer hold. A useful metric for characterizing particles $< 0.5 \mu\text{m}$ is the mobility diameter defined as the diameter of a particle having the same diffusivity or electrical mobility in air as the particle of interest. In the region between ~ 0.5 – $1.0 \mu\text{m}$, aerodynamic and mobility diameters are not necessarily the same. The question of how best to merge these diameters is unresolved and depends on the particle properties of interest.

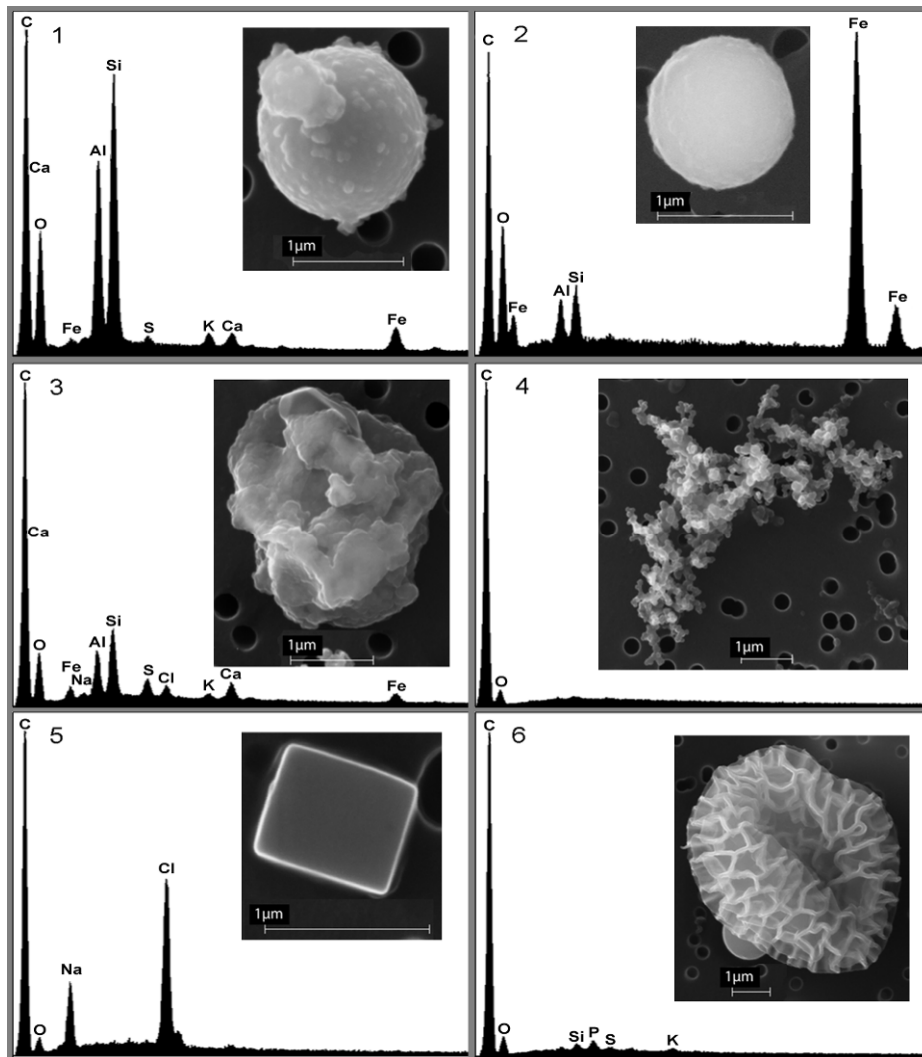
Characterizing particle size is important because different size particles penetrate to different regions of the human respiratory tract. Thoracic particles refer to particles that travel past the larynx to reach the lung airways and the gas-exchange region of the lung, and respirable particles are those that reach the gas-exchange region. The selection of PM_{10} as an indicator of thoracic particles was based in large part on dosimetry (U.S. EPA, 1996, [079380](#)). However, the selection of $PM_{2.5}$ to characterize respirable particles was driven mainly by considerations related to measurement techniques available at the time rather than dosimetry. Currently, cut points other than $2.5\ \mu\text{m}$ are attainable and frequently put into use. For example, the American Conference of Governmental Industrial Hygienists (ACGIH, 2005, [156188](#)), the International Standards Organization, and the European Standardization Committee have adopted a 50% cut point of $4\ \mu\text{m}$ as an indicator of respirable particles. Most commonly, however, $PM_{2.5}$ is used as an indicator of respirable particles, $PM_{10-2.5}$ is used as an indicator of the thoracic component of coarse particles that is sometimes referred to as thoracic coarse (noting that it excludes some coarse particles below $2.5\ \mu\text{m}$ and above $10\ \mu\text{m}$), and PM_{10} is used as an indicator of thoracic particles.

As can be seen from Table 3-1, particles in individual size modes are characterized by rather distinct sources, composition, chemical properties, lifetimes in the atmosphere (τ) and distances over which they can travel. Whereas particles in the smaller size modes are formed mainly by combustion processes and by nucleation and condensation of gases, coarse particles are generated mainly by mechanical activity, such as by the action of wind on either the ground or the sea surface or by construction or by resuspension by traffic. Particles in the UF size range are either emitted directly to the atmosphere or are formed by nucleation of gaseous constituents in the atmosphere. The properties of fibers and engineered nano-objects and nanometer scale products (e.g., dots, hollow spheres, rods, fibers, and tubes) are not reviewed in this chapter because these classes of objects are found mainly in certain occupational settings rather than in ambient air.

Table 3-1. Characteristics of ambient fine (ultrafine plus accumulation-mode) and coarse particles.

	Fine		Coarse
	Ultrafine	Accumulation	
Formation Processes	Combustion, high-temperature processes, and atmospheric reactions		Break-up of large solids/droplets
Formed by	Nucleation of atmospheric gases including H ₂ SO ₄ , NH ₃ and some organic compounds	Condensation of gases Coagulation of smaller particles Reactions of gases in or on particles	Mechanical disruption (crushing, grinding, abrasion of surfaces) Evaporation of sprays Suspension of dusts
	Condensation of gases	Evaporation of fog and cloud droplets in which gases have dissolved and reacted	Reactions of gases in or on particles
Composed of	Sulfate	Sulfate, nitrate, ammonium, and hydrogen ions	Nitrates/chlorides/sulfates from HNO ₃ /HCl/SO ₂ reactions with coarse particles
	EC	EC	Oxides of crustal elements (Si, Al, Ti, Fe)
	Metal compounds	Large variety of organic compounds	CaCO ₃ , CaSO ₄ , NaCl, sea salt
	Organic compounds with very low saturation vapor pressure at ambient temperature	Metals: compounds of Pb, Cd, V, Ni, Cu, Zn, Mn, Fe, etc. Particle-bound water Bacteria, viruses	Bacteria, pollen, mold, fungal spores, plant and animal debris
Solubility	Not well characterized	Largely soluble, hygroscopic, and deliquescent	Largely insoluble and nonhygroscopic
Sources	High temperature combustion Atmospheric reactions of primary, gaseous compounds.	Combustion of fossil and biomass fuels, and high temperature industrial processes, smelters, refineries, steel mills etc.	Resuspension of particles deposited onto roads Tire, brake pad, and road wear debris
		Atmospheric oxidation of NO ₂ , SO ₂ , and organic compounds, including biogenic organic species (e.g., terpenes)	Suspension from disturbed soil (e.g., farming, mining, unpaved roads) Construction and demolition
			Fly ash from uncontrolled combustion of coal, oil, and wood
			Ocean spray
Atmospheric half-life	Minutes to hours	Days to weeks	Minutes to hours
Removal Processes	Grows into accumulation mode	Forms cloud droplets and rains out	Dry deposition by fallout
	Diffuses to raindrops and other surfaces	Dry deposition	Scavenging by falling rain drops
Travel distance	<1 to 10s of km	100s to 1000s of km	<1 to 10s of km (100s to 1,000s of km in dust storms for the small size tail)

Source: Adapted with Permission of the Air & Waste Management Association from Wilson and Suh (1997, [077408](#))



Source: National Exposure Research Laboratory.

Figure 3-2. X-ray spectra and scanning electron microscopy images of individual particles. These include: (1) an aluminum-silicate fly ash sphere emitted from a coal-fired power plant; (2) an iron oxide sphere emitted from a steel manufacturing facility; (3) an aluminum-silicate particle, probably of crustal origin; (4) a carbon soot aggregate from a diesel engine consisting of many sub-micron size carbon particles; (5) a sodium chloride crystal, potentially of marine origin; and (6) a partially collapsed pollen particle. The polycarbonate filter substrate used to collect the particles is visible in the background of each image and contributes to the carbon peak in each spectrum.

Particles appear in a wide variety of shapes such as spheres, ellipsoids, cubes, and irregular or fractal geometries. This is one reason why a standard metric such as aerodynamic diameter is useful for describing the mechanical properties of the particles. The shape of particles is important for determining the optical properties of the particles. The directionality of sunlight scattered by certain shapes of particles, such as plates, also depends strongly on their physical orientation while suspended. The shape of particles also affects the surface area of the particles in contact with the surface it is deposited on, including cell membranes.

Images of six types of individual particles obtained using scanning electron microscope (SEM) and their corresponding x-ray spectra showing their major elemental composition are shown

in Figure 3-2. The images show particles sitting on a thin polycarbonate film with pores and a 1 μm scale bar for size reference. Air is pulled through the filter pores with a vacuum pump and the particles are left behind on the surface. The metal dominated spherical particles (image 2) were formed at high temperatures and were quickly cooled. Particles which are liquid such as sulfate are also spherical. Sodium chloride (NaCl) crystals are cubic (image 5); this particular particle could be marine sea salt due to the proximity to the ocean where the sample was collected. Other particles, such as the carbon chain agglomerates from diesel engines have much more irregular and complex shapes (image 4). Note that these particles were placed under vacuum resulting in volatilization of water and other volatile components and partial collapse of the pollen grain (image 6). Changes in composition and possibly morphology could occur during the sampling, collection and analysis of aerosol samples. For example, particles may be coated with semi-volatile material that evolves off the particles under vacuum and under the electron beam. Similarly, particles in ambient air are generally mixtures or agglomerates of particles coming from multiple sources and have a diverse chemical make-up.

3.3. Sources, Emissions and Deposition of Primary and Secondary PM

PM is composed of both primary (derived directly from emissions) or secondary (derived from atmospheric reactions involving gaseous precursors) components. Table 3-4 summarizes anthropogenic and natural sources for the major primary and secondary aerosol constituents of fine and coarse particles. Anthropogenic sources can be further divided into stationary and mobile sources. Stationary sources include fuel combustion for electrical utilities, residential space heating and cooking; industrial processes; construction and demolition; metal, mineral, and petrochemical processing; wood products processing; mills and elevators used in agriculture; erosion from tilled lands; waste disposal and recycling; and biomass combustion. Biomass combustion encompasses many emission activities including burning of wood for fuel, burning of vegetation to clear land for agriculture and construction, to dispose of agricultural and domestic waste, to control the growth of animal or plant pests, and to manage forest resources (prescribed burning). Wildlands also burn due to lightning strikes and arson. Mobile or transportation-related sources include direct emissions of primary PM and secondary PM precursors from highway vehicles and non-road sources as well as fugitive dust from paved and unpaved roads. Also shown in Table 3-2 are sources for several precursor gases, the oxidation of which can form secondary PM. An overview of estimates of emissions of primary PM and precursors to secondary PM from major sources is given in Section 3.3.1. The transformations from gaseous precursors shown in Table 3-2 to secondary PM are described in Section 3.3.2.

In general, the sources of fine PM are very different from those of coarse PM. Some of the mass in the fine size fraction forms during combustion from material that has volatilized in combustion chambers and then recondensed before emission to the atmosphere. Some ambient $\text{PM}_{2.5}$ forms in the atmosphere from photochemical reactions involving precursor gases. Included in this category is the formation of new UFPs by (1) homogeneous nucleation of precursor gases and (2) the condensation of gases on pre-existing particles. Biological material also exists in the fine fraction including many types of microorganisms, especially viruses and bacteria and fragments of pollens and fungal spores. $\text{PM}_{10-2.5}$ is mainly primary in origin, as it is produced by surface abrasion or by suspension of biological material and fragments of living things (e.g., plant and insect debris). In addition, atmospheric reaction products condense on coarse particles. Because precursor gases undergo mixing during transport from their sources and chemical reactions, and the oxidation of different gases can produce the same reaction products, it is difficult to identify individual sources of secondary PM. Transport and transformation of precursors can occur over distances of hundreds of kilometers. $\text{PM}_{10-2.5}$ has a shorter lifetime in the atmosphere, so its effects tend to be more localized. However, intercontinental transport of dust from African and Asian deserts occurs and some of this material is in the $\text{PM}_{10-2.5}$ size range. Major intercontinental dust events are highly episodic but small contributions can be present at other times (see Section 3.7).

Table 3-2. Constituents of atmospheric particles and their major sources.

Aerosol species	Primary (PM <2.5 µm)		Primary (PM >2.5 µm)		Secondary PM Precursors (PM <2.5 µm)	
	Natural	Anthropogenic	Natural	Anthropogenic	Natural	Anthropogenic
Sulfate (SO ₄ ²⁻)	Sea spray	Fossil fuel combustion	Sea spray	—	Oxidation of reduced sulfur gases emitted by the oceans and wetlands and SO ₂ and H ₂ S emitted by volcanism and forest fires	Oxidation of SO ₂ emitted from fossil fuel combustion
Nitrate (NO ₃ ⁻)	—	Mobile source exhaust	—	—	Oxidation of NO _x produced by soils, forest fires, and lightning	Oxidation of NO _x emitted from fossil fuel combustion and in motor vehicle exhaust
Minerals	Erosion and re-entrainment	Fugitive dust from paved and unpaved roads, agriculture, forestry, construction, and demolition	Erosion and re-entrainment	Fugitive dust, paved and unpaved road dust, agriculture, forestry, construction, and demolition	—	—
Ammonium (NH ₄ ⁺)	—	Mobile source exhaust	—	—	Emissions of NH ₃ from wild animals, and undisturbed soil	Emissions of NH ₃ from motor vehicles, animal husbandry, sewage, and fertilized land
Organic carbon (OC)	Wildfires	Prescribed burning, wood burning, mobile source exhaust, cooking, tire wear and industrial processes	Soil humic matter	Tire and asphalt wear, paved and unpaved road dust	Oxidation of hydrocarbons emitted by vegetation (terpenes, waxes) and wild fires	Oxidation of hydrocarbons emitted by motor vehicles, prescribed burning, wood burning, solvent use and industrial processes
EC	Wildfires	Mobile source exhaust (mainly diesel), wood biomass burning, and cooking	—	Tire and asphalt wear, paved and unpaved road dust	—	—
Metals	Volcanic activity	Fossil fuel combustion, smelting and other metallurgical processes, and brake wear	Erosion, re-entrainment, and organic debris	—	—	—
Bioaerosols	Viruses and bacteria	—	Plant and insect fragments, pollen, fungal spores, and bacterial agglomerates	—	—	—

Dash (—) indicates either very minor source or no known source of component.

Source: U.S. EPA (2004, [056905](#)).

Only major sources for each constituent within each broad category shown at the top of Table 3-2 are listed. Not all sources are equal in magnitude. Chemical characterizations of primary particulate emissions for a wide variety of natural and anthropogenic sources (as shown in Table 3-2) were given in Chapter 5 of the 1996 PM AQCD (U.S. EPA, 1996, [079380](#)). Summary tables of the composition of source emissions presented in the 1996 PM AQCD (U.S. EPA, 1996, [079380](#)) and updates to that information are provided in Appendix 3D to the 2004 PM AQCD (U.S. EPA, 2004, [056905](#)). Source composition profiles are archived by the EPA at <http://www.epa.gov/ttn/chief/software/speciate/>. The profiles of source composition were based in large measure on the results of studies that collected source signatures for use in source apportionment studies.

Natural sources of primary PM include windblown dust from undisturbed land, sea spray, and biological material. The oxidation of a fraction of terpenes emitted by vegetation and reduced sulfur species from anaerobic environments leads to secondary PM formation. Ammonium (NH_4^+) ions, which play a major role in regulating the pH of particles, are derived from emissions of NH_3 gas. Source categories for NH_3 have been divided into emissions from undisturbed soils (natural) and emissions that are related to human activities (e.g., fertilized lands, domestic and farm animal waste). There is ongoing debate about characterizing emissions from wildfires as either natural or anthropogenic. Wildfires have been listed in Table 3-2 as natural in origin, but land management practices and other human actions affect the occurrence and scope of wildfires. For example, fire suppression practices allow the buildup of combustible fuels and increase the susceptibility of forests to more severe and infrequent fires from whatever cause, including lightning strikes. Similarly, prescribed burning is listed as anthropogenic, but can be viewed as a substitute for wildfires that would otherwise occur eventually on the same land.

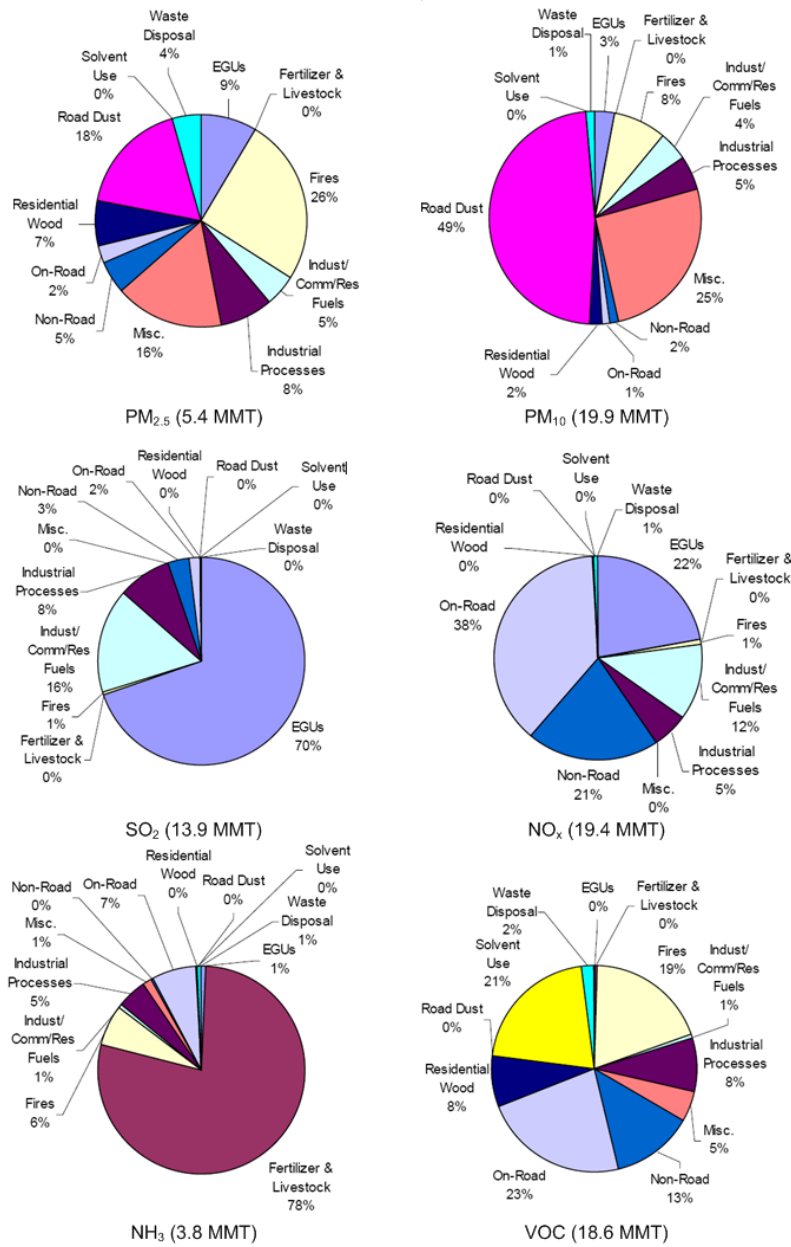
3.3.1. Emissions of Primary PM and Precursors to Secondary PM

U.S. national average emissions of primary $\text{PM}_{2.5}$, PM_{10} and gaseous precursor species (SO_2 , NO_x , NH_3 and VOCs) from different source categories are shown in Figure 3-3. Note that the entries refer mainly to anthropogenic sources, with little information about natural sources. However, for categories such as VOCs, the contribution from biogenic emissions of isoprene and terpenes can be quite large. The entries are continually undergoing revision and are subject to varying degrees of uncertainty. For example, almost all of the sulfur in fuel is released as volatile components (SO_2 or SO_3) during combustion. Hence, sulfur emissions can be calculated on the basis of sulfur content in fuels to a greater accuracy than can be done for other pollutants like nitrogen oxides or primary PM. There have been notable downward revisions to the inventories since 2002 in the emissions of dust from roads. These have resulted in large measure from incorporation of emissions test data with updated methods for measuring dust emissions. Also, the spatial and temporal characterization of wildfire emissions has improved since 2002 by integrating satellite-derived fire detection and state-of-the-art fuels characterization and consumption models (Pouliot et al., 2008, [156883](#)). Emission measurements from high-temperature combustion sources are sensitive to the dilution, temperature, and pre-treatment of dilution air (England et al., 2007, [156420](#); England et al., 2007, [156421](#); Sheya et al., 2008, [156977](#)).

To a large extent, especially with regard to the contribution of road dust to PM, refinements in emission estimates have been guided by the use of receptor modeling. See Section 3.6.1 for a description of receptor modeling techniques and the 2004 PM AQCD (U.S. EPA, 2004, [056905](#)) for the role of receptor models in refining emissions estimates. Note that since the estimates given in Figure 3-3 are U.S. national averages, they may not accurately reflect the contribution of specific local sources determining a person's exposures to PM at any given time and location.

As can be seen from a comparison of the total U.S. emissions (in million metric tons) shown in Figure 3-3, estimates of total emissions of potential precursors to secondary PM formation including SO_2 , NO_x , NH_3 and VOCs are considerably larger than those for primary PM sources. However, translating the emissions of precursors into production rates of secondary PM or using these emissions as a guide to estimate PM composition is highly problematic. A significant fraction of gaseous precursors are lost before they could be converted to PM. Dry deposition and precipitation scavenging of some of these gaseous precursors and their intermediate oxidation products occur before they are transformed in the atmosphere, and most VOCs emitted are oxidized to carbon dioxide (CO_2) rather than to PM. Some of these precursors are also transported outside the United States. Even if gaseous precursors are converted to PM components, the effects of atmospheric transformations must also be considered (discussed in Section 3.3.2 below). As a result of these transformations, ratios of masses of particle phase products to each other will not be the same as those in the emissions inventories for their precursors. For example, SO_2 , NO_x and NH_3 are converted to secondary PM as SO_4^{2-} , NO_3^- and NH_4^+ . The ratios of molecular weights of PM products (SO_4^{2-} , NO_3^- and NH_4^+) to gaseous precursors (SO_2 , NO_x and NH_3) are 1.5, 1.35, and 1.07, respectively. Estimating a conversion factor for carbon in VOCs is less straightforward. The oxidation of VOCs leads to the formation of secondary OC in PM. As the result of atmospheric transformations, nitrogen and oxygen are added to the carbon originally present in VOCs. Turpin and Lim (2001, [017093](#)) recommend adjustment factors ranging from 1.4 to 2.0 to account for the presence of oxygen and nitrogen in organic compounds in OC in the aerosol phase. Because of all

the above issues, the resultant mass and composition of ambient PM is quite different from what might be inferred from examining the emissions inventories alone.



Source: U.S. EPA (2006, [157070](#))

Figure 3-3. Detailed source categorization of anthropogenic emissions of primary PM_{2.5}, PM₁₀ and gaseous precursor species SO₂, NO_x, NH₃ and VOCs for 2002 in units of million metric tons (MMT). EGUs = Electricity Generating Units.

3.3.2. Formation of Secondary PM

Precursors to secondary PM have natural and anthropogenic sources, just as primary PM has natural and anthropogenic sources. A substantial fraction of the fine particle mass, especially during the warmer months of the year, is secondary in nature, formed as the result of atmospheric reactions involving both inorganic and organic gaseous precursors. The major atmospheric chemical transformations leading to the formation of particulate nitrate (pNO_3) and particulate sulfate (pSO_4) are relatively well understood; whereas those involving the formation of secondary organic aerosol (SOA) are less well understood and are subject to much current investigation. A large number of organic precursors are involved and many of the kinetic details still need to be determined. Also, many of the products of the oxidation of hydrocarbons have yet to be identified. However, there has been substantial progress made in understanding the chemistry of SOA formation in the past few years.

3.3.2.1. Formation of Nitrate and Sulfate

The basic mechanism of the gas and aqueous phase oxidation of NO_2 and SO_2 has long been studied and can be found in numerous texts on atmospheric chemistry, e.g., Seinfeld and Pandis (1998, [018352](#)), Finlayson-Pitts and Pitts (2000, [055565](#)), Jacob (1999, [091122](#)), and Jacobson (2002, [090667](#)). The reader is referred to the 2004 PM AQCD (U.S. EPA, 2004, [056905](#)) as well as the 2008 NO_x and SO_x ISAs (U.S. EPA, 2008, [157073](#); U.S. EPA, 2008, [157074](#); U.S. EPA, 2008, [157075](#)) where these processes are described in great detail.

3.3.2.2. Formation of Secondary Organic Aerosol

Some key new findings have altered perceptions of SOA formation since the 2004 PM AQCD (see especially the reviews by Kroll and Seinfeld (2008, [155910](#)) and Rudich et al. (2007, [156059](#))). New measurement techniques for estimating the speciation and water solubility of organic aerosols have noted the dominant contribution of oxygenated species in atmospheric particles. Recent measurements show that the abundance of oxidized SOA exceeds that of more reduced hydrocarbon like organic aerosol in Pittsburgh (Zhang et al., 2005, [157185](#)) and in about 30 other cities across the Northern Hemisphere (Zhang et al., 2007, [101119](#)). Based on aircraft and ship-based sampling of organic aerosols in coastal waters downwind of northeastern U.S. cities, de Gouw et al. (2008, [191757](#)) reported that 40-70% of measured organic mass was water soluble and estimated that approximately 37% of SOA is attributable to aromatic precursors, based on PM yields estimated for NO_x -limited conditions. However, the remaining mass of estimated SOA (63%) was unexplained, possibly due to oxidation of semivolatile precursors not measured by standard gas chromatography. Aerosol yields from the oxidation of aromatic compounds have been reported to be higher when reactions with NO_x are not dominant, suggesting that transport of less reactive compounds (e.g., benzene) out of source regions with high NO_x levels could result in greater overall SOA yields than previously estimated (Ng et al., 2007, [199528](#)). Furthermore, Zhang et al. (2007, [189998](#)) noted that the most common mass spectrum of oxygenated OA measured in ambient air resembles mass spectra measured in irradiated diesel exhaust reported by Robinson et al. (2007, [156053](#)) and Sage et al. (2008, [191758](#)).

Typical dilution sampling of combustion sources employ dilution rate, temperature, pressure, and background aerosol concentrations that can differ substantially from ambient conditions. Lipsky and Robinson (2006, [189891](#)) and Robinson et al. (2007, [156053](#)) showed that under higher dilution conditions, the fraction of diesel engine organic emissions that volatilizes is higher than that measured using common test methods.

Murphy and Pandis (2009, [190095](#)) pointed out the importance of characterizing the volatility distribution of emissions of organic species from combustion sources for more accurately predicting the abundance and oxidation state of SOA in both urban and surrounding regional background environments. They note that in urban areas, volatile emissions can be photochemically oxidized to more non-volatile compounds which then condense, forming oxidized SOA. Braun (2009, [189997](#)) suggested that the weathering of diesel exhaust particles involves the desorption of semi-volatile organic compounds followed by the decomposition and reaction of the amorphous non-volatile carbon. These reactions would result in the formation of a number of functional groups on the

surface of the carbon core including quinones, carbohydroxide and carboxyl groups as well as sulfate. In general, all the above studies underscore the importance of accurately describing the phase distribution of semivolatile organic compounds emitted by combustion sources under atmospheric conditions, and of atmospheric photochemical reactions in modifying the composition of emissions.

Until a few years ago, the oxidation of terpenes and aromatic compounds were considered as sources of SOA, and the oxidation of isoprene was not considered a source of SOA. However, observations of 2-methyl tetrols in ambient samples from a number of different environments suggest that small but not insignificant quantities of SOA are formed from isoprene oxidation (Claeys et al., 2004, [058608](#)). Laboratory studies also indicate the formation of 2-methyl tetrols from isoprene oxidation (Edney et al., 2005, [155760](#); Kleindienst et al., 2006, [156650](#)). Xia and Hopke (2006, [179947](#)) observed the seasonal variations for the two major diastereoisomers produced during the oxidation of isoprene with highest concentrations occurring during summer and lowest concentrations occurring during winter. During summer, the maximum contribution of these two diastereoisomers to OC was 2.8%, however it is not clear if more SOA could have been produced from isoprene oxidation.

Kroll and Seinfeld (2008, [155910](#)) and Rudich et al. (2007, [156059](#)) noted that the composition of SOA evolves from repeated cycles of volatilization and condensation of chemical reaction products in both the particle and gas phases. Rudich et al. (2007, [156059](#)) focused on the oxidation of particle phase species by reaction with gas phase oxidants. Kroll and Seinfeld (2008, [155910](#)) identified three factors that determine the SOA forming potential of organic compounds in the atmosphere:

1. Oxidation reactions of gas-phase organic species. These species include alkanes, alkenes, aromatics, cyclic olefins, isoprene and terpenes. Note that oxidation reactions can either lower volatility by addition of functional groups or increase volatility by cleavage of carbon-carbon bonds;
2. Reactions in the particle, or condensed, phase that can change volatility either by oxidation or formation of high-molecular-weight species. These reactions can lead to the formation of oligomers, thereby decreasing volatility or to the formation of more volatile products; and
3. Ongoing reactions that result from the varied volatility of oxidation products.

Other detailed work has focused on the formation of higher molecular weight particle-phase oligomers (Gao et al., 2004, [156460](#); Kalberer et al., 2004, [156619](#); Tolocka et al., 2004, [087578](#)), the importance of cloud processing in the evolution of SOA (Blando and Turpin, 2000, [155692](#); Gelencser and Varga, 2005, [156463](#)), and the role of acid seeds in oligomer formation (Tolocka et al., 2004, [087578](#)). These results imply that ambient samples could contain mixtures of SOA from different sources at different stages of processing, some with common reaction products making source identification of SOA problematic. Figure 3-4 shows a schematic of processes involved in the formation of SOA.

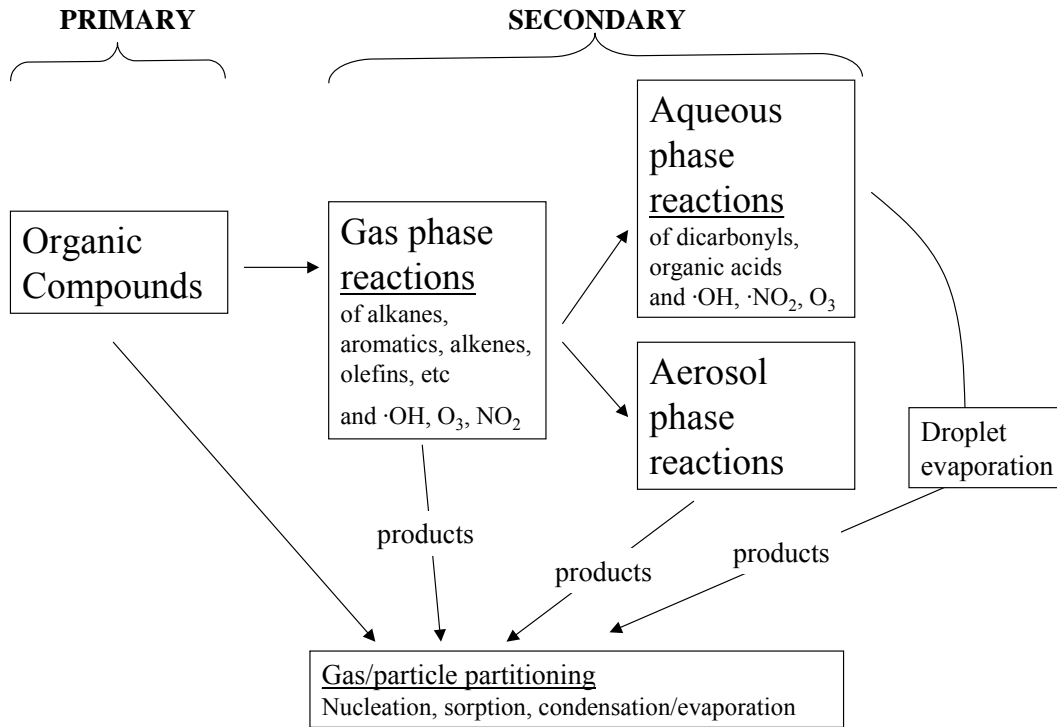


Figure 3-4. Primary emissions and formation of SOA through gas, cloud and condensed phase reactions.

It should be noted that many of the products of terpene oxidation are oxidative in nature, and are not merely nonreactive oxidation products. Organic peroxides represent an important class of reactive oxygen species (ROS) that have high oxidizing potential and could cause oxidative stress in cells on which these species deposit. For example, Docherty (2005, [087613](#)) found evidence for the substantial production of organic hydroperoxides in secondary organic aerosol (SOA) resulting from the reaction of monoterpenes with O_3 . Analysis of the SOA formed in their environmental chamber indicated that the SOA was mainly organic hydroperoxides. In particular, they obtained yields of 47% and 85% of organic peroxides from the oxidation of α - and β -pinene. The hydroperoxides then react with aldehydes in particles to form peroxyhemiacetals, which can either rearrange to form other compounds such as alcohols and acids or revert back to the hydroperoxides. The aldehydes are also produced in large measure during the ozonolysis of the monoterpenes. Monoterpenes also react with OH radicals resulting, however, in the production of more lower molecular weight products than in their reaction with O_3 . Various terpenoid compounds are used in a number of household products and can be oxidized by ozone that has infiltrated from outdoors. The oxidation of terpenoid compounds indoors produces UFPs as described in the 2006 O_3 AQCD (U.S. EPA, 2006, [088089](#)).

3.3.2.3. Formation of New Particles

In addition to being emitted by high temperature combustion sources, new particles can form by nucleation of atmospheric gases. New particle formation has been observed in environments ranging from relatively unpolluted marine and continental environments to polluted urban areas (Kulmala et al., 2004, [089159](#)). These new, nucleation mode particles are formed from molecular clusters. Competition between condensation of gases and clusters onto existing particles and coagulation of clusters determines which process will dominate (McMurry et al., 2005, [191759](#)). Because of this competition, it is expected that particle number concentrations are dominated by primary anthropogenic emissions in highly polluted settings and by nucleation in remote continental sites. However, nucleation still occurs in urban environments and can still be the major source under certain conditions. The composition of UFPs will differ depending on the nature of their sources.

Nucleation is observed in the morning and extending into the afternoon, and occurs at higher rates during summer than during winter, consistent with a photochemical process. New particle formation events have been observed to occur over distances of several hundred kilometers in what have been called regional nucleation events (Shi et al., 2007, [191760](#)).

The major gas phase nucleating species involved are sulfuric acid vapor and water vapor. Kuang et al. (2008, [191196](#)) suggested that the rate of nucleation is second order with respect to H₂SO₄ vapor depending on mechanism. However, other studies (e.g., Kulmala et al., 2007, [097838](#)) have suggested that the nucleation rate is first order with respect to H₂SO₄ vapor. These differences imply that a number of mechanistic details still remain to be determined, including the interactions with other species. However, this disparity is small compared to classical thermodynamic binary nucleation theory involving H₂SO₄ and water vapor, in which the nucleation rate is given by H₂SO₄ vapor to at least the 10th power (Kulmala et al., 1998, [129411](#)). H₂SO₄ vapor is produced by the gas phase oxidation of SO₂ by OH radicals (U.S. EPA, 2008, [157075](#)). Ammonia (Gaydos et al., 2005, [191762](#)) and organic acids and bases (amines) are also involved to some extent (Smith et al., 2008, [199529](#)). The formation of UFPs indoors from the oxidation of terpenoids by O₃ as mentioned above also indicates that nucleation occurs indoors as well (U.S. EPA, 2006, [088089](#)).

3.3.3. Mobile Source Emissions

3.3.3.1. Emissions from Gasoline Fueled Engines

PM emitted from gasoline fueled engines is a mix of OC, EC and small quantities of trace metals and sulfates, with OC constituting anywhere from 26-88% of PM (Cadle et al., 1999, [007636](#); Geller et al., 2006, [139644](#); Schauer et al., 2002, [035332](#)). Most of the compounds in OC have yet to be characterized. High molecular weight and large PAHs have been identified in gasoline fueled vehicle emissions (Phuleria et al., 2006, [156867](#); Riddle et al., 2007, [115272](#)). EPA exhaust emission standards do not control PM from gasoline vehicles as stringently as diesel vehicles. PM emissions from gasoline fueled vehicles decreased greatly as other exhaust emissions (primarily hydrocarbons and carbon monoxide) were controlled by improvements in the catalytic converter and better control of air-to-fuel mixture ratios for the engine intake. When leaded gasoline was used in pre-1975 model year vehicles, gasoline engine PM emissions were relatively large (about 300 mg/mile) and consisted largely of lead salts from combustion of the lead additive. A current gasoline fueled vehicle emits far lower PM, about 1-10 mg/mile. Emissions of gasoline PM increase at colder ambient temperatures and recent rulemaking for air toxics will result in significant reduction of gasoline PM at colder temperatures. Further details about the composition of motor vehicle emissions in the context of source apportionment modeling can be found in Section 3.6.1.

3.3.3.2. Emissions from Diesel Fueled Engines

Matti Maricq (2007, [155973](#)) presents a conceptual model of diesel PM as a mix of nucleation-mode SO₄²⁻ and hydrocarbons from unspent fuel and soot embedded with trace metals on which SO₄²⁻ and hydrocarbons condense. PM emissions from pre-2007 diesels consist largely of EC (about 70% by mass) and OC (high molecular weight compounds derived from both diesel fuel and lubricating oil) which is responsible for about 25% of the PM (Maricq, 2007, [155973](#)). The EC is non-volatile, while the organic material present exhibits temperature-dependent evaporation in similar fashion to a mixture of C₂₄-C₃₂ alkanes (Sakurai et al., 2003, [113924](#)). Sulfates constitute about 5% of the PM. A small fraction of the diesel fuel sulfur (typically about 1-2%) is oxidized to sulfate. Trace elements (such as Zn and halogens, mainly from lubricating oil; and others) are also present. Mass spectra of organic diesel particles from pre-2007 engines appear to be largely similar to engine lube oil with minor contributions from unburned diesel fuel.

Effective with the 2007 model year for on-road diesel heavy-duty highway truck engines, the new EPA PM standard (0.01 g per brake horsepower-hour [g/bhp-h]) reduced PM emission limits by 90% from the prior standard (0.10 g/bhp-h). By comparison, uncontrolled heavy-duty diesels (pre-1988 model years) emitted about 1-2 g/bhp-h of PM. The 2007 standard resulted in the introduction of new emission control technology, mainly the diesel particulate filter (DPF). Other elements of the

new control technology also include water-cooled exhaust gas recirculation (mostly for control of NO_x), a diesel oxidation catalyst (DOC) used in some vehicles and improved fuel injection systems.

Besides the large reduction in diesel PM on a mass basis, the composition of diesel PM changed greatly. EPA regulations required that diesel fuel for on-road vehicles contain no more than 15 ppm sulfur as of January 2007 (Lim et al., 2007, [155931](#)). Prior to that, the limit on diesel fuel sulfur established in 1995 for on-road vehicles was 500 ppm. The HEI-ACES study characterizes emissions from four engines and shows that PM emissions are about 0.001 g/bhp-h or 90% below the level of the current (2007) emission standard (Shimpi et al., 2009, [189888](#)). This study also characterizes the composition of the much lower mass of PM emitted with this new technology. PM samples collected over a composite type test consisted of 53% sulfate, 30% OC, 13% EC and 4% other components, including metals. A substantial fraction of sulfur is converted to sulfate over the diesel particulate filter resulting in the higher fractional content of sulfate emissions. However, due to the much lower mass of PM being emitted (over a 90% reduction compared to earlier diesels) as well as the low sulfur content of the fuel, the total mass of sulfate emitted is somewhat less than that from earlier diesels. This work also shows that UFP number emissions are lower (about 90% lower) and that a number of other emissions are also controlled, including PAHs, nitro-PAHs, carbonyls (such as aldehydes), and metals.

Pre-2007 engines can be retrofitted with exhaust aftertreatment devices, including DPFs, DOCs, and selective catalytic reduction (SCR) systems to reduce emissions (U.S. EPA, 2009, [189885](#)). Hu et al. (2009, [189886](#)) examined emissions of various metals (V, Pt) from various diesel retrofit systems including those using V-SCR and a zeolite-based SCR with a DPF. Pakbin et al. (2009, [189893](#)) shows significant reductions in emissions of various PAHs for diesels with SCR retrofit systems for NO_x control. Biswas et al. (2008, [189969](#)) examined PM size distribution and composition (including semi-volatiles and non-volatiles) from several advanced technology diesels including those with SCR. They showed major reductions in PM number in most driving conditions but did not show a reduction in PM number under cruise conditions. Biswas et al. (2009, [189880](#)) examined four heavy-duty diesel vehicles with various retrofits showing, in general, large reductions in PM but, in some cases, somewhat higher emissions (or smaller decreases than expected) for EC and OC.

In general, under light load conditions such as idle, diesel PM has a higher percentage of OC emissions than at high load conditions. Under lighter loads, organic compounds are not oxidized as effectively as under high loads. Under higher loads, PM contains more EC than under light loads. Also, newer model year diesels through the 2006 model year tend to have a higher fraction of PM that is EC than older models.

Emissions have been measured with the new technology engines under a number of driving cycles besides the Federal Test Procedure. The HEI ACES study examined emissions during a range of test procedures. In general, the low-load test cycle resulted in lower exhaust temperatures and higher emission than did the high-load cycles. Regeneration events also produced short-term increases in particle emissions. However, particle emission measurements on the ACES engines were consistently lower than those on a typical 2004 engine (Shimpi et al., 2009, [189888](#)).

EPA standards will result in non-road diesels also having technology like catalyzed diesel particulate filters starting in 2012. Similar standards have also been promulgated for locomotives powered by diesel engines. Some work has been done with prototype SCR systems for diesel NO_x control such as would be used for the 2010 diesel NO_x standard. This standard will also result in reductions for NO_x similar to those seen for PM in the 2007 standard.

There is no information on emissions from diesel engines with this new technology at temperatures of $\leq 10^{\circ}$ C. In general, the ratio of emissions under cold start conditions at low temperatures to emissions at 24 $^{\circ}$ C is significantly higher for diesel engines with new technology compared to emissions from non-catalyst systems. Note that the engines with the newer technology require time to allow the catalyst to reach normal operating temperatures for full emission reductions. During the period of catalyst heating, particles will be trapped in the DPF, but volatile components can pass through. As a result of this particle-trapping, post-2007 model year engines still emit less than the older engines, even under cold start conditions.

3.3.4. Deposition of PM

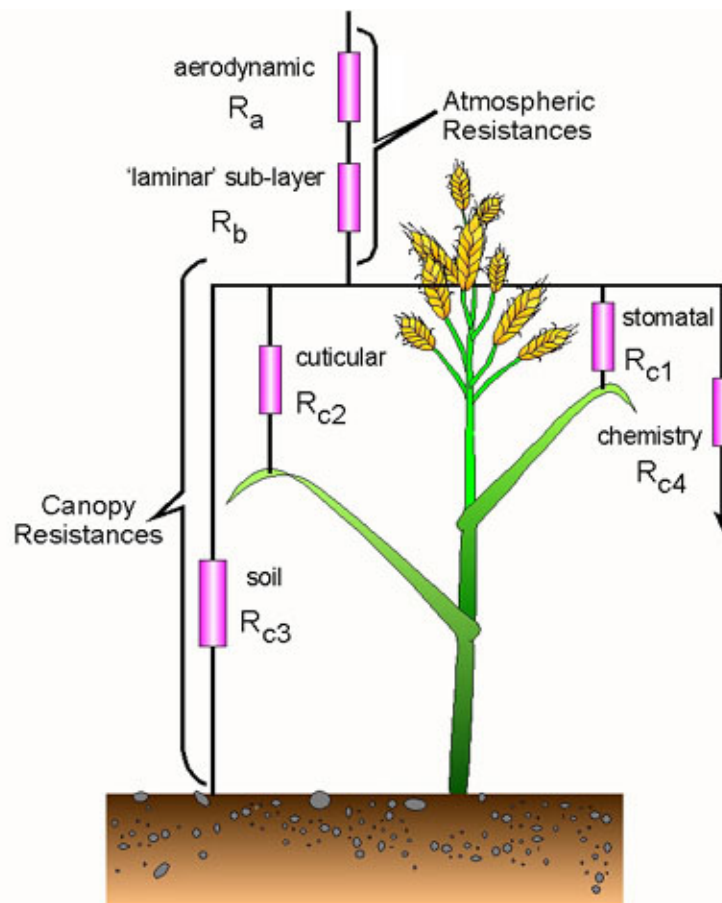
Wet and dry deposition are important processes for removing PM and other pollutants from the atmosphere on urban, regional, and global scales. The conceptual model for dry deposition is to view

the flux deposited on a surface as the product of a concentration (mass or moles of a pollutant/m³) times a deposition velocity (V_d) (m/s). Therefore, deposition has the units of mass per unit time per unit area, or flux. The general approach used to estimate V_d for gases or very small particles is the resistance-in-series method represented by Equation 3-1:

$$V_d = 1 / (R_a + R_b + R_c)$$

Equation 3-1

where R_a , R_b , and R_c represent the resistance due to atmospheric turbulence, transport in the fluid sublayer very near the elements of the surface, such as leaves or soil, and the resistance to uptake of the surface itself, respectively. Typically, these resistances are empirically derived and can vary as a function of wind speed, solar radiation, plant characteristics, precipitation/moisture, and soil/air temperature. These processes are shown schematically in Figure 3-5. This approach works for a range of substances, although it is inappropriate for species with substantial re-emissions from the surface or for species where deposition to the surface depends on concentrations at the surface itself. The approach is also modified somewhat for aerosols where R_b and R_c are replaced with a surface V_d to account for gravitational settling.



Resistance analogy for the deposition of atmospheric pollutants

Source: Courtesy of T. Pierce, USEPA / ORD / NERL / Atmospheric Modeling Division.

Figure 3-5. Schematic of the resistance-in-series analogy for atmospheric deposition.

Wesley and Hicks (2000, [025018](#)) listed several shortcomings of the then-current knowledge of dry deposition. Among those shortcomings were difficulties in representing dry deposition over

varying terrain where horizontal advection plays a significant role in determining the magnitude of R_a and difficulties in adequately determining V_d for extremely stable conditions such as those occurring at night; see the discussion by Mahrt (1998, [048210](#)). Under optimal conditions, when a model is exercised over a relatively small area where dry deposition measurements have been made, models still generally showed uncertainties on the order of $\pm 30\%$ (e.g., Brook et al., 1996, [024023](#); Massman et al., 1994, [043681](#); Padro, 1996, [052446](#); Wesely and Hicks, 2000, [025018](#)). Wesley and Hicks (2000, [025018](#)) concluded that an important result of those comparisons was that the level of sophistication of most dry deposition models was relatively low, and that deposition estimates, therefore, must rely heavily on empirical data. Still larger uncertainties exist when the surface features in the built environment are not well known or when the surface comprises a patchwork of different surface types, as is common in the eastern U.S.

3.3.4.1. Deposition Forms

Wet Deposition

Wet deposition results from the incorporation of atmospheric particles and gases into cloud droplets and their subsequent precipitation as rain or snow, or from the scavenging of particles and gases by raindrops or snowflakes as they fall (Lovett, 1994, [024049](#)). Wet deposition depends on precipitation amount and ambient pollutant concentrations. Vegetation surface properties have little effect on wet deposition, although leaves can retain liquid and solubilized PM.

Landscape characteristics can affect wet deposition via orographic effects and by the closer aerodynamic coupling to the atmosphere of tall forest canopies as compared to the shorter shrub and herbaceous canopies. Following wet deposition, humidity and temperature conditions further affect the extent of drying versus concentrating of solutions on foliar surfaces, which influence the rate of metabolic uptake of surface solutes (Swietlik and Faust, 1984, [046678](#)). The net consequence of these factors on direct physical effects of wet deposited PM on leaves is not known (U.S. EPA, 2004, [056905](#)).

Rainfall introduces new wet deposition and also redistributes throughout the canopy previously dry-deposited particles (Peters and Eiden, 1992, [045277](#)). The concentrations of suspended and dissolved materials are typically highest at the onset of precipitation and decline with duration of individual precipitation events (Hansen et al., 1994, [046634](#)). Sustained rainfall removes much of the accumulation of dry-deposited particles from foliar surfaces, reducing direct foliar effects and combining the associated chemical burden with the wet-deposited material (Lovett, 1994, [024049](#)) for transfer to the soil. Intense rainfall may contribute substantial total particulate inputs to the soil, but it also removes bioavailable or injurious pollutants from foliar surfaces. This washing effect, combined with differential foliar uptake and foliar leaching of different chemical constituents from particles, alters the composition of the rainwater that reaches the soil and the pollutant burden that is taken-up by plants. Once in the soil, these particle constituents may affect biogeochemical cycles of major, minor, and trace elements. Low intensity precipitation events, in contrast, may deposit significantly more particulate pollutants to foliar-surfaces than high intensity precipitation events. Additionally, low-intensity events may enhance foliar uptake through the hydrating of some previously dry-deposited particles (U.S. EPA, 2004, [056905](#)).

Dry Deposition

Dry particulate deposition, especially of heavy metals, base cations, and organic contaminants, is a complex and poorly characterized process. It appears to be controlled primarily by such variables as atmospheric stability, macro- and micro-surface roughness, particle diameter, and surface characteristics (Hosker and Lindberg, 1982, [019118](#)). The range of particle sizes, the diversity of canopy surfaces, and the variety of chemical constituents in airborne particles have made it difficult to predict and to estimate dry particulate deposition (U.S. EPA, 2004, [056905](#)).

Dry deposition of atmospheric particles to plant and soil surfaces affects all exposed surfaces. Larger particles $>5 \mu\text{m}$ diameter are dry-deposited mainly by gravitational sedimentation and inertial impaction. Smaller particles, especially those with diameters between 0.2 and $2.0 \mu\text{m}$, are not readily

dry-deposited and may travel long distances in the atmosphere until their eventual deposition, most often via precipitation. Plant parts of all types, along with exposed soil and water surfaces, receive steady deposits of dry dusts, EC, and heterogeneous secondary particles formed from gaseous precursors (U.S. EPA, 1982, [017610](#)).

Estimates of regional particulate dry deposition infer fluxes from the product of variable and uncertain measured or modeled particulate concentrations in the atmosphere and even more variable and uncertain estimates of V_d parameterized for a variety of specific surfaces (e.g., Brook et al., 1996, [024023](#)). Even for specific sites and well-defined particles, uncertainties are large. Modeling the dry deposition of particles to vegetation is at a relatively early stage of development, and it is not currently possible to identify a best or most generally applicable modeling approach (U.S. EPA, 2004, [056905](#)).

Deposition from Clouds and Fog

The occurrence of cloud and fog deposition tends to be geographically restricted to coastal and high mountain areas. Several factors make it particularly effective for the delivery of dissolved and suspended particles to vegetation. Concentrations of particulate-derived materials are often many-fold higher in cloud or fog water than in precipitation or ambient air due to orographic effects and gas-liquid partitioning. In addition, fog and cloud water deliver particulate chemical species in a bioavailable-hydrated form to foliar surfaces. This enhances deposition by sedimentation and impaction of submicron aerosol particles that exhibit low V_d before fog droplet formation (Fowler et al., 1989, [002515](#)). Deposition to vegetation in fog droplets is proportional to wind speed, droplet size, concentration, and fog density. In some areas, typically along foggy coastlines or at high elevations, this deposition represents a substantial fraction of total deposition to foliar surfaces (Fowler et al., 1991, [046630](#)).

3.3.4.2. Methods for Estimating Dry Deposition

Methods for estimating dry deposition of particles are more restricted than for gaseous species and fall into two major categories: surface analysis methods, which include all types of estimates of contaminant accumulation on surfaces of interest, and atmospheric deposition rate methods, which use measurements of contaminant concentrations in the atmosphere and descriptions of surrounding surface elements to estimate deposition rates (Davidson and Wu, 1990, [036799](#)). Surface extraction or washing methods characterize the accumulation of particles on natural surfaces of interest or on experimental surrogate surfaces. These techniques rely on methods designed specifically to remove only surface-deposited material. Total surface rinsate may be equated to accumulated deposition or to the difference in concentrations in rinsate between exposed and control (sheltered) surfaces and may be used to refine estimates of deposition. Foliar extraction techniques may underestimate deposition to leaves because of uptake and translocation processes that remove pollutants from the leaf surface (Garten and Hanson, 1990, [036803](#); Taylor et al., 1988, [019289](#)). Foliar extraction methods also cannot distinguish gas from particle-phase sources (Bytnerowicz et al., 1987, [036493](#); Dasch, 1987, [036496](#); Kelly, 1988, [037379](#); Lindberg and Lovett, 1985, [036530](#); Van Aalst, 1982, [036481](#)).

The National Dry Deposition Network was established in 1986 to document the magnitude, spatial variability, and trends in dry deposition across the United States. Currently, the network operates as a component of the CASTNet (Clarke et al., 1997, [025022](#)). A significant limitation on current capacity to estimate regional effects of NO_x and SO_x deposition is inadequate knowledge of the mechanisms and factors governing particle dry deposition to diverse surfaces (U.S. EPA, 2004, [056905](#)).

Collection and analysis of stem flow and throughfall can also provide useful estimates of particulate deposition when compared to directly sampled precipitation. The method is most precise for particle deposition when gaseous deposition is a small component of the total dry deposition and when leaching or uptake of compounds of interest out of or into the foliage is not a significant fraction of the deposition because these lead to positive and negative artifacts in the calculated totals.

Foliar washing, whether using precipitation or experimental lavage, is one of the best available methods to determine dry deposition to vegetated ecosystems. Major limitations include the site specificity of the measurements and the restriction to elements that are largely conserved within the

vegetative system. Surrogate surfaces have not been found that can adequately replicate essential features of natural surfaces, and therefore do not produce reliable estimates of particle deposition to the landscape.

Micrometeorological methods employ eddy covariance, eddy accumulation, or flux gradient protocols for quantifying dry deposition. These techniques require measurements of particulate concentrations and of atmospheric transport processes. They are currently well developed for ideal conditions of flat, homogeneous, and extensive landscapes and for chemical species for which accurate and rapid sensors are available. Additional studies are needed to extend these techniques to more complex terrain and more chemical species.

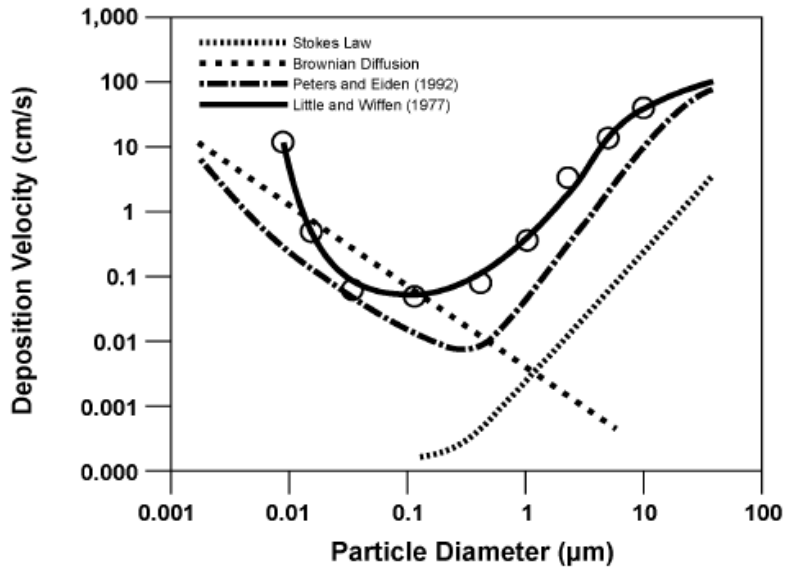
The eddy covariance technique measures vertical fluxes of gases and fine particles from calculations of the mean covariance between the vertical component of wind velocity and pollutant concentration (Wesely et al., 1982, [036564](#)) using sensors acquiring concentration data at 5-20 Hz. For the flux gradient or profile techniques, vertical fluxes are calculated from a concentration difference and an eddy exchange coefficient determined at discrete heights (Erismann et al., 1988, [036510](#); Huebert et al., 1988, [036569](#)). Most measurements of eddy transport of PM have used chemical sensors (rather than mass or particle counting) to focus on specific PM components. These techniques have not been well developed for generalized particles and may be less suitable for coarse particles that are transported efficiently in high frequency eddies (Gallagher et al., 1988, [046631](#)).

3.3.4.3. Factors Affecting Dry Deposition Rates and Totals

In the size range of ~ 0.1 - $1.0 \mu\text{m}$ where V_d is relatively independent of particle diameter as shown in Figure 3-6, particulate deposition is controlled by roughness of the surface and by the stability and turbulence of the atmospheric surface layer. Impaction and interception dominate over diffusion as dry deposition processes, and the V_d is considerably lower than for particles that are either smaller than $\sim 0.1 \mu\text{m}$ or larger than $\sim 1.0 \mu\text{m}$.

Deposition of particles between 1 and $10 \mu\text{m}$ diameter is strongly dependent on particle size as shown in Figure 3-6. Larger particles within this size range are collected more efficiently at typical wind speeds than are smaller particles (Clough, 1975, [070850](#)), suggesting the importance of impaction. Impaction is related to wind speed, the square of the particle diameter, and the inverse of the deposition surface cross-section. As a depositing particle's trajectory deviates from the streamlines of the air in which it is suspended, increasing either wind speed or the ratio of particle size to the deposition surface cross-section increases the probability of collision.

Empirical estimates of V_d for fine particles under wind tunnel and field conditions are often several-fold greater than predicted by theory (Unsworth and Wilshaw, 1989, [046682](#)). A large number of transport phenomena, including streamlining of foliar obstacles, turbulence structure near surfaces, and various phoretic transport mechanisms are not well characterized (U.S. EPA, 2004, [056905](#)). The discrepancy between estimated and predicted values of V_d may reflect model limitations or experimental limitations in the specification of the effective size and number of deposition obstacles. Previous reviews (e.g., U.S. EPA, 1996, [079380](#); U.S. EPA, 2004, [056905](#)) suggest the following generalizations: (1) particles $>10 \mu\text{m}$ exhibit variable V_d between 0.5 and 1.1 cm/s depending on friction velocities, whereas a minimum particle V_d of 0.03 cm/s exists for particles in the size range 0.1 to $1.0 \mu\text{m}$; (2) the V_d of particles is approximately a linear function of friction velocity; and (3) deposition of particles from the atmosphere to a forest canopy is from 2 to 16 times greater than deposition in adjacent open terrain like grasslands or other low vegetation.



Source: U.S. EPA (2004, [056905](#)).

Figure 3-6. The relationship between particle diameter and V_d for particles. Values measured in wind tunnels by Little and Wiffen (1977, [070869](#)) over short grass with wind speed of 2.5 mi/s closely approximate the theoretical distribution determined by Peters and Eiden (1992, [045277](#)) for a tall spruce forest. These distributions reflect the interaction of Brownian diffusivity (descending dashed line), which decreases with particle size and sedimentation velocity (ascending dotted line derived from Stokes Law), which increases with particle size. Intermediate-sized particles (0.1-1.0 μm) are influenced strongly by both particle size and sedimentation velocity, and deposition is relatively independent of size.

Leaf Surface Effects on V_d

The chemical composition of a particle is not usually considered to be a primary determinant of its V_d . Rather, the plant leaf surface has an important influence on the V_d of particles, and therefore on the flux of dry deposition to the terrestrial environment. Relevant leaf surface properties include stickiness, microscale roughness, and cross-sectional area. These properties affect the probability of impaction and particle bounce. The efficiency of deposition to vegetation also varies with leaf shape. Particles impact more frequently on the adaxial (upper) surface than on the abaxial (lower) surface. Most particles accumulate in the midvein, central portion of leaves. The greatest particle loading on dicotyledonous leaves is frequently on the adaxial surface at the base of the blade, just above the petiole junction. Precipitation washing probably plays an important role in this distribution pattern (U.S. EPA, 2004, [056905](#)).

Lead particles have been shown to accumulate to a greater extent on older as compared with younger needles and twigs of white pine, suggesting that wind and rain may be insufficient to fully wash the foliage. Fungal mycelia (derived from windborne spores) were frequently observed in intimate contact with other particles on leaves, which may reflect minimal re-entrainment of the spore due to shelter by the particles, mycelia development near sources of soluble nutrients provided by the particles, or simply co-deposition (Smith and Staskawicz, 1977, [046675](#)).

Leaves with complex shapes tend to collect more particles than do those with shapes that are more regular. For example, conifer needles are more efficient than broad leaves in collecting particles by impaction as a result of the small cross-section of the needles relative to the larger leaf laminae of broadleaves allowing for greater penetration of wind into conifer canopies than broadleaf ones (U.S. EPA, 2004, [056905](#)).

Canopy Surface Effects on V_d

Surface roughness increases particulate deposition, and V_d is usually greater for a forest than for a nonforested area and greater for a field than for a water surface. Different size particles have different transport properties and V_d . The upwind leading edges of forests, hedgerows, and individual plants are primary sites of coarse particle deposition. Impaction at high wind speed and the sedimentation that follows the reduction in wind speed and carrying capacity of the air in these areas lead to preferential deposition of larger particles (U.S. EPA, 2004, [056905](#)).

Air movement is slowed in proximity to vegetated surfaces. Canopies of uneven age or with a diversity of species are typically aerodynamically rougher and receive larger inputs of dry-deposited pollutants than do smooth, low, or monoculture vegetation (Garner et al., 1989, [042085](#); U.S. EPA, 2004, [056905](#)). Canopies on slopes facing the prevailing winds receive larger inputs of pollutants than more sheltered, interior canopy regions.

All foliar surfaces within a forest canopy are not equally exposed to particle deposition. Upper canopy foliage tends to receive maximum exposure to coarse and fine particles, but foliage within the canopy tends to receive primarily fine aerosol exposures. The dry deposition of fine-mode particles and unreactive gases tends to be more evenly distributed throughout the canopy.

Both uptake and release of PM constituents can occur within the canopy. The leaf surface is a region of leaching and uptake. Exchange also occurs with epiphytic organisms and bark and through solubilization of previously dry-deposited PM. Vegetation emits a variety of particles and particulate precursor materials.

3.4. Monitoring of PM

3.4.1. Ambient Measurement Techniques

3.4.1.1. PM Mass

Federal reference methods (FRMs) and federal equivalence methods (FEMs) for PM were discussed in detail in the 2004 PM AQCD (U.S. EPA, 2004, [056905](#)). Issues discussed there include the definition or description of FRMs and FEMs for $PM_{2.5}$ and PM_{10} , and measurement methods for $PM_{10-2.5}$. Also included are detailed descriptions of the WINS impactor, virtual and cascade multistage impactors for $PM_{10-2.5}$ measurement, high-volume and low-volume PM_{10} samplers, and real-time or continuous methods for $PM_{2.5}$ and PM_{10} including:

- Tapered Element Oscillating Microbalance (TEOM) operated at various temperatures;
- Sample Equilibration System (SES)-TEOM;
- Differential TEOM;
- β -Gauge Techniques (BGT);
- Piezoelectric Microbalance;
- Real-Time Total Ambient Mass Sampler (RAMS);
- Continuous Ambient Mass Monitor (CAMM);
- Continuous Coarse Particle Monitor (CCPM);
- Micro-orifice Uniform Deposit Impactor (MOUDI);

- Multichannel diffusion denuder sampling system (BOSS); and
- Light scattering photometric instruments.

In this section, FRMs and FEMs for PM_{2.5}, PM_{10-2.5}, and PM₁₀ will be revisited and evaluated based on the cumulative understanding of these methods with a focus on evaluations performed following the 2004 PM AQCD (U.S. EPA, 2004, [056905](#)), followed by the discussion of new techniques under development or evaluation.

Federal Reference Method and Federal Equivalent Method

FRM and FEM PM samplers are designed to measure the mass concentrations of ambient particulate matter. The FRMs for measuring PM_{2.5}, PM_{10-2.5}, and PM₁₀ are specified in CFR 40 Part 50, Appendices L, O and J, respectively. The FRM for PM_{2.5} is a hybrid-based method that specifies certain aspects of the method (e.g., component dimensions and tolerances, sample handling and analysis) by design specifications and other aspects (e.g., flow control) by performance specifications (U.S. EPA, 2004, [056905](#)). The PM₁₀ FRM is performance-based; particles are inertially separated with a penetration efficiency of 50% at 10 ± 0.5 μm aerodynamic diameter. The required collection efficiency as a function of particle size larger and smaller than 10 μm aerodynamic diameter is explicitly specified by a penetration curve in the CFR. Particles larger than 10 μm in aerodynamic diameter are collected on the filter with diminishing collection efficiency as particle size increases. Likewise, particles smaller than 10 μm in aerodynamic diameter are collected on the filter with increasing collection efficiency as particle size decreases. The FRM for PM_{10-2.5} concentration is computed as the numeric difference between concurrent and co-located PM₁₀ and PM_{2.5} concentrations obtained from low-volume FRM samplers of the same make and model. It should be noted that while the FRM for PM_{2.5} and PM_{10-2.5} reports data under local conditions, the FRM for PM₁₀ reports data corrected to standard temperature (298 K) and pressure (101.3 kPa) (STP).

A very sharp cut cyclone (VSCC) was approved in 2004 as a Class II PM_{2.5} FEM method (Kenny et al., 2004, [155895](#)). The VSCC provides superior performance over long sampling periods under heavy loading and was also incorporated as an optional second-stage separator for the PM_{2.5} FRM (71 FR 61214, October 17, 2006). In 2006, EPA finalized new performance criteria (40 CFR Part 53) for the approval of FEMs as Class II equivalent methods when based on integrated filter sampling and as Class III equivalent methods when based on continuous technologies that can provide at least hourly data reporting. The performance criteria include evaluating additive bias (intercept) and multiplicative bias (slope) as well as correlation with co-located candidate and FRM methods at field studies covering multiple seasons and sampling locations. As a result of these new performance criteria, EPA has recently approved two filter-based PM_{2.5} and two filter-based PM_{10-2.5} Class II FEMs based on the virtual impactor techniques (dichotomous sampler), and five PM_{2.5} and one PM_{10-2.5} Class III continuous FEMs based on BGT or TEOM techniques. The most recent list of FRMs and FEMs can be found in Annex A, Table A-2 and on the following EPA web site: <http://www.epa.gov/ttn/amtic/files/ambient/criteria/reference-equivalent-methods-list.pdf>.

Evaluations of FRMs and FEMs were conducted both in supersite studies and in other research studies (Ayers, 2004, [097440](#); Brown et al., 2006, [097665](#); Butler et al., 2003, [156313](#); Cabada et al., 2004, [148859](#); Chang and Tsai, 2003, [155718](#); Charron et al., 2004, [053849](#); Grover et al., 2005, [090044](#); Hains et al., 2007, [091039](#); Hering et al., 2004, [155837](#); Jaques et al., 2004, [155878](#); Krieger et al., 2007, [129657](#); Lee et al., 2005, [155925](#); Lee et al., 2005, [128139](#); Price et al., 2003, [098082](#); Rees et al., 2004, [097164](#); Russell et al., 2004, [082453](#); Salminen and Karlsson, 2003, [156070](#); Schwab et al., 2004, [098450](#); Schwab et al., 2006, [098449](#); Solomon et al., 2003, [156994](#); Tsai et al., 2006, [098312](#); Vega et al., 2003, [105974](#); Wilson et al., 2006, [091142](#); Yi et al., 2004, [156169](#); Zhu et al., 2007, [098367](#)) (see Annex A, Tables A-3, A-5 and A-11). In general, the co-located FRMs showed very good precision with coefficient of variation (CV) <5%. For different co-located FRMs, the regression slope of one sampler on another is commonly close to unity with R² >0.95. The PM_{2.5} and PM₁₀ concentrations measured by dichotomous samplers were within 10% of the FRM methods, and the differences can be attributed to the sampling artifacts of semi-volatile components; see Section 3.4.1.2 for details. The precision of various TEOMs ranges from 10-30%. The concentration measured by the TEOM operated at 50°C was consistently lower than those measured by the TEOM operated at 30°C. The differences between these monitors were also found to be a function of season

and location. BGTs were highly correlated with FRMs but BGT mass could be higher than the FRM mass (30% higher at the Fresno supersite) (Chow et al., 2008, [156355](#)). Additionally, a number of techniques have been developed to reduce positive and negative sampling artifacts. These are described in the ISA for NO_x and SO_x – Ecological Criteria (U.S. EPA, 2008, [157074](#)).

Several papers (Buser et al., 2007, [156310](#); Buser et al., 2007, [156311](#); Buser et al., 2007, [156312](#)) published since the 2004 PM AQCD (U.S. EPA, 2004, [056905](#)) claim that the EPA FRM samplers for PM₁₀ “oversample certain agricultural and other source emissions.” These claims are based on the erroneous assumption that the “true” PM₁₀ concentration is what would be given by a PM₁₀ sampler that excluded all particles greater than 10 μm aerodynamic diameter and included all particles less than 10 μm aerodynamic diameter. The legal definitions for PM_{2.5} and PM₁₀, as defined in the CFR (40 CFR Part 58), include both a 50% cut-point and a penetration curve. For PM₁₀, the 50% cut-point of 10 ± 0.5 μm aerodynamic diameter means that 50% of particles with aerodynamic diameter of 10 ± 0.5 μm are removed by the inlet and 50% pass through the inlet where they are collected on the filter. The penetration curve specifies, as a function of particle size, the fraction of particles larger than 10 μm that pass through the inlet and the fraction of particles less than 10 μm that are intercepted by the inlet. No effort was made in the development of the FRM to have the PM₁₀ sampler collect all particles less than 10 μm and no particles greater than 10 μm since the sampler was designed to collect a fraction of atmospheric particles similar to the “inhalable” or thoracic fraction, i.e., those particles that would pass through the nose and throat and reach the lungs (Miller et al., 1979, [070577](#); U.S. EPA, 2004, [056905](#)). Thus, the FRM PM₁₀ sampler correctly and intentionally collects particles greater than 10 μm.

For PM_{2.5} and PM₁₀, it has long been known that FRMs are subject to sampling artifacts including particle bounce on heavily-loaded impaction substrates and the loss of semi-volatile components of PM (e.g., NH₄NO₃, and some organics). Although there are no standard reference materials that provide a test of accuracy of the sampling method for airborne PM mass, in comparison with other sampling techniques that can measure both semi-volatile and nonvolatile PM, FRMs reported PM_{2.5} or PM₁₀ mass concentrations biased low by as much as 10-30% (Chow et al., 2008, [156355](#)). The bias of the FRMs depends on the composition of ambient PM and the sampling conditions (e.g., ambient temperature and relative humidity), which vary from day to day and from season to season. Another limitation of the current FRM sampling protocol is that filter samples are typically collected every 3 or 6 days (only ~150 of the 900+ PM_{2.5} FRMs operating in 2007 were scheduled to sample every day). Under this operating condition, the concentration-response relationship in air pollution health studies (especially in time-series studies) cannot be fully evaluated in terms of lag structures and distributed lags between ambient concentration and health outcome (Lippmann, 2009, [190083](#); Solomon and Hopke, 2008, [156997](#)).

Development and Evaluation of New Techniques

Several new innovations have recently emerged to measure both fine and coarse PM fractions in the ambient air. These techniques include the Filter Dynamics Measurement System-TEOM (FDMS-TEOM) (Grover et al., 2006, [138080](#)) for real-time measurement of PM_{2.5} or PM₁₀ and several new methods for measurement of PM_{10-2.5}. In addition, several new techniques exist for measuring UFPs (discussed later in Section 3.4.1.4) and for estimating PM mass concentration indirectly using particle size (discussed later in Section 3.4.1.5).

Real-time Measurement of PM_{2.5} or PM₁₀ using the FDMS-TEOM

The FDMS-TEOM incorporates self-referencing capability to the traditional TEOM by alternating measurement of ambient air and chilled clean air (particles and semivolatile gases are removed by filtration at 4°C after which the clean air is reheated to 30°C) in 6-min intervals. As clean air flows over the sample filter, the semivolatile PM on the sample filter is evaporated. Thus, the instrument provides direct measurements of the nonvolatile particle mass and incorporates an adjustment for the semivolatile NH₄NO₃ and organic material. In a comparison between the TEOM, FDMS-TEOM, and FRM mass, the PM_{2.5} concentration measured by the TEOM operated at 50°C was consistently lower than those measured by the TEOM operated at 30°C. The TEOM operated at 30°C provided concentrations 50% lower than the FDMS-TEOM, and the FDMS-TEOM provided concentrations 10-30% higher than the FRM mass (Chow et al., 2008, [156355](#); Schwab et al., 2006, [098449](#)).

Techniques for Measurement of PM_{10-2.5}

Methods developed to measure PM_{10-2.5} are based on three measurement techniques: (1) virtual impactors using low-volume, high-volume, and real-time techniques; (2) cascade impactors; and (3) passive samplers.

A low-volume dichotomous sampler (operated at 16.7 L/min), based on virtual impaction, was described in the 2004 PM AQCD (U.S. EPA, 2004, [056905](#)). Since then, a high-volume dichotomous sampler was developed to operate at 1,000 L/min (Sardar et al., 2006, [156071](#)). The sampler was evaluated in the field by comparison with a MOUDI sampler, and the measured PM_{10-2.5} mass concentrations were within 10%. The high-volume dichotomous sampler provides sufficient mass collection for comprehensive standard chemical analyses over short sampling intervals. Using the virtual impactor technique in conjunction with a TEOM or BGT as the detector, continuous PM_{10-2.5} measurement techniques were developed (Misra et al., 2001, [018998](#); Misra et al., 2003, [195001](#); Solomon and Sioutas, 2008, [190139](#)). The TEOM method was highly correlated with the PM_{10-2.5} FRM, but mass concentrations measured by the TEOM were 20-30% lower (Solomon and Sioutas, 2008, [190139](#)). The BGT method also agreed well with the PM_{10-2.5} FRM (slopes = 0.88-1.17, and R²>0.95) (Solomon and Sioutas, 2008, [190139](#)).

Case et al. (2008, [155149](#)) evaluated a cascade PM sampler designed to collect PM_{10-2.5} on a foam impactor. Particle bouncing on impactors has long been a concern for PM collection. Porous foam was used to serve as the impactor substrate to reduce particle bounce and to collect relatively large amounts of particles (Demokritou et al., 2004, [186901](#); Demokritou et al., 2004, [190115](#); Huang et al., 2005, [186991](#); Kuo et al., 2005, [186997](#)). The sampler was operated at 5 L/min, and it agreed with a low-volume dichotomous sampler within ±20%. The precision of the sampler was 20% as determined by the CV.

An inexpensive passive sampler for PM_{10-2.5} was also developed (Leith et al., 2007, [098241](#); Ott et al., 2008, [195004](#); Wagner and Leith, 2001, [190153](#); Wagner and Leith, 2001, [190154](#)). The passive sampler collects particles by gravity, diffusion, and convective diffusion onto a glass coverslip, and then an image analysis is conducted on the collected particles to estimate mass flux as a function of aerodynamic diameter. Leith et al. (2007, [098241](#)) conducted a field evaluation of the passive sampler, and the difference between a FRM and the co-located passive sampler was within 1σ of concentrations measured with PM_{10-2.5} FRM samplers. Ott et al. (2008, [119394](#)) reported the precision of the sampler was 11.6% (CV), and the detection limit was 2.3 μg/m³ for a 5-day sample.

3.4.1.2. PM Speciation

The following sections describe recent developments regarding measurement techniques to ascertain quantities of particle-bound water, cations and anions, elemental composition, carbon, and organic species.

Particle-Bound Water

Particle-bound water is an important component of ambient PM (U.S. EPA, 2004, [056905](#)). Recently, a differential method was developed to measure particle-bound water (Santarpia et al., 2004, [156944](#); Stanier et al., 2004, [095955](#)). The dry ambient aerosol size spectrometer (DAASS) can measure particle-bound water in the particle size range from 3 nm-10 μm (Stanier et al., 2004, [095955](#)), by alternatively measuring ambient PM size distribution at low relative humidity (RH) and ambient RH. A comparison of the two size distributions provides information on the water absorption and change in particle size due to RH. Khlystov et al. (2005, [156635](#)) reported that the particle-bound water, measured by DAASS, was underestimated for particles <200 nm and overestimated for particles >200 nm compared with thermodynamic models. The loss of semi-volatile components during measurement may bias the particle-bound water measurement results. Methods and analytical specifications for particle-bound water are listed in Annex A, Table A-12.

Cations and Anions

The measurement of cations and anions including SO_4^{2-} , NO_3^- , NH_4^+ , Cl^- , Na^+ , and K^+ still relies primarily on filter-based collection, water based extraction and ion chromatography (IC) based chemical speciation and quantification. In addition, denuders are frequently used in the sampling system to adjust for sampling artifacts. These methods have been reviewed in the 2004 PM AQCD (U.S. EPA, 2004, [056905](#)). Filter-denuder based integrated sampling methods for SO_4^{2-} , NO_3^- , and NH_4^+ have been detailed in the 2008 SO_x - Health ISA (U.S. EPA, 2008, [157075](#)) and the 2008 NO_x and SO_x - Ecological ISA (U.S. EPA, 2008, [157074](#)).

Recent developments in multiple ion measurements have focused on the coupling of IC and a sample dissolution system, represented by the Particle into Liquid Sampler-Ion Chromatography (PILS-IC) and the Ambient Ion Monitor (AIM) (Orsini et al., 2003, [156008](#); Weber et al., 2001, [024640](#)). When ambient PM passes through the PILS-IC system, water droplets are generated by mixing ambient PM with saturated water vapor and collected by impaction. The resulting liquid stream is then introduced into the IC system for ion speciation and quantification. Hourly concentrations of multiple ions can be obtained with the system, with a CV of 10%. For the AIM system, a parallel plate denuder is used to remove the interfering gases, and then particles enter a super-saturation chamber to form droplets. The collected droplets are then introduced into the IC for analysis. The AIM system can provide hourly concentrations for multiple ions. The particle mass spectrometer is another advance in multiple PM component measurements, but most of these types of measurements are semi-quantitative and will be detailed later in Section 3.4.1.3. Note that measurement and analytical specifications for ions other than SO_4^{2-} and NO_3^- are listed in Annex A, Table A-9.

Sulfate

Methods used for continuous (sampling interval of minutes) measurements of SO_4^{2-} include Aerosol Mass Spectrometry (AMS) (Drewnick et al., 2003, [099160](#); Hogrefe et al., 2004, [099003](#)), PILS-IC (Weber et al., 2001, [024640](#)), flash volatilization techniques (Bae, 2007, [155669](#); Stolzenburg and Hering, 2000, [013289](#)) and the Harvard School of Public Health (HSPH) tube furnace to convert SO_4^{2-} to SO_2 for detection by a SO_2 analyzer (Allen et al., 2001, [156205](#)). These methods are described in detail by Drewnick et al. (2003, [099160](#)), along with an inter-sampler comparison that found overall agreement within 2.9% for all continuous instruments with R^2 of 0.87 or better. When compared with filter samples, Drewnick et al. (2003, [099160](#)) showed differences were less than 25% for the AMS, PILS, flash vaporization, and HSPH continuous SO_4^{2-} monitors. The Thermo 5020 particulate sulfate analyzer (based on the HSPH technique) compared within 80% of 24-h filter-based measurement at a rural site in New York (Schwab et al., 2006, [098449](#)). Annex A, Tables A-8 and A-14, list detailed methods and analytical specifications for sampling SO_4^{2-} .

Nitrate

In addition to the nylon filter-based method and the new developments mentioned for SO_4^{2-} , methods based on flash volatilization-chemiluminescence analysis and catalytic conversion-chemiluminescence analysis have also been developed for continuous NO_3^- measurement (averaging time 30 s-10 min). For the flash volatilization system (Fine et al., 2003, [155775](#); Stolzenburg and Hering, 2000, [013289](#); Stolzenburg et al., 2003, [156102](#)), particles are collected by a humidified impaction process and analyzed in place by flash vaporization and chemiluminescent detection of the evolved NO_x . For the catalytic conversion-chemiluminescence analysis system (Weber et al., 2003, [157129](#)), NO_3^- was measured by conversion of particle NO_3^- into NO , and then detected with the chemiluminescence method. Field and lab comparisons were conducted to compare the different instruments mentioned above. Although the R&P 8400N ambient particulate NO_3^- monitor, which is based on the Stolzenburg flash vaporization technique, could provide 10-min resolution data and showed excellent precision (with a CV <10%) (Harrison et al., 2004, [136787](#); Hogrefe et al., 2004, [099003](#); Long and McClenny, 2006, [098214](#); Rattigan et al., 2006, [115897](#)), it consistently reported NO_3^- concentrations ~30% lower than the denuder-filter systems in both the Baltimore supersite and the multiyear field study in New York (Harrison et al., 2004, [136787](#); Hogrefe et al., 2004, [099003](#); Rattigan et al., 2006, [115897](#)). In the New York measurement campaign, an AMS was also co-located with other instruments to obtain the real-time NO_3^- information. AMS did not always agree well with the denuder-filter system for reasons not

entirely apparent. However, Bae et al. (2007, [156244](#)) reported that some organic compounds can also produce signals at mass-to-charge ratio $m/z = 30$, which is one of the characteristic m/z for NO_3^- . Therefore, the disagreement between the AMS and the filter-based method could be a result of the interference of organic compounds using the AMS. Annex A, Tables A-7 and A-13, list methods and analytical specifications for sampling NO_3^- .

Ammonium

Several continuous and semi-continuous instruments can be used to monitor ambient ammonium concentrations (Al-Horr et al., 2003, [153951](#); Bae, 2007, [155669](#)) including many listed above for SO_4^{2-} and NO_3^- . Bae et al. (2007, [155669](#)) conducted an inter-comparison of three semi-continuous instruments during the New York multiyear air sampling campaign: a PILS-IC, an AMS, and a wet scrubbing-long path absorption photometer. Bae et al. (2007, [155669](#)) reported the inter-sampler coefficients of determination (R^2) between these instruments were above 0.75, and the slopes (with zero intercept) were between 0.71 and 1.04. Annex A, Table A-9 describes measurement of ions other than NO_3^- and SO_4^{2-} , including NH_4^+ .

Elemental Composition

Techniques for measuring the elemental composition of PM samples were reviewed in the 2004 PM AQCD (U.S. EPA, 2004, [056905](#)). These methods include:

- Energy dispersive X-ray fluorescence (ED-XRF);
- Synchrotron X-ray fluorescence (SXRF);
- Particle-induced X-ray emission (PIXE);
- Particle elastic scattering analysis (PESA);
- Total reflection X-ray fluorescence (TR-XRF);
- Instrumental neutron activation analysis (INAA);
- Atomic absorption spectrophotometry (AAS);
- Inductively-coupled plasma-atomic emission spectroscopy (ICP-AES);
- Inductively-coupled plasma-mass spectrometry (ICP-MS); and
- Scanning electron microscopy (SEM).

Recent development in this area focused on the semi-continuous measurement methods, in which elements were analyzed in the lab using the methods mentioned above on time-resolved and/or size resolved samples (Kidwell and Ondov, 2004, [155898](#)). The concentrated slurry/graphite furnace atomic absorption spectrometry (GFAAS) method collects ambient PM as a slurry using impactors, and then the collected PM is analyzed by AAS in the lab. Laser induced breakdown spectroscopy (LIBS) was used to measure seven metals at the Pittsburgh supersite. LIBS concentrates ambient PM using a virtual impactor into a sample cell, and then a Nd:YAG laser-spectrometer is used to identify and quantify different elements. A full listing of measurement techniques and analytical specifications for trace elements is provided in Annex A, Table A-6.

Elemental and Organic Carbon

The large variety of aspects of carbon analyses were reviewed in the 2004 PM AQCD (U.S. EPA, 2004, [056905](#)). Measurement and analytical specifications for carbon measurements are listed in Annex A, Tables A-10 and A-15. Aspects of the measurements include sampling artifacts

associated with the integrated filter-based OC and EC sampling methods, the IMPROVE vs. CSN thermal optical protocols (i.e., different thermal optical methods) and optical techniques to measure light-absorption or BC. One significant change taking place in the CSN is that the method for carbon measurements is being changed from the CSN method to a method designed to be consistent with the IMPROVE carbon analysis protocol. This is a phased process that began in May of 2007 with the conversion of 56 stations. Phase 2 of the carbon sampler conversion occurred in April of 2009 with another 62 stations. The balance of the CSN is scheduled to be converted to IMPROVE-like sampling and IMPROVE analysis in late 2009 (Henderson, 2005, [156537](#)). The CSN network was implemented to support the PM_{2.5} NAAQS and provides data for PM_{2.5} mass, SO₄²⁻, NO₃⁻, NH₄⁺, Na, K, EC, OC, and select trace elements (Al through Pb) at many sites across the U.S. This conversion will increase consistency between these two networks. Also, since the release of the 2004 PM AQCD (U.S. EPA, 2004, [056905](#)), more studies have been conducted to extend the understanding of sampling artifact issues (Chow et al., 2008, [156355](#); Watson et al., 2005, [157125](#)), evaluate different thermal and optical procedures (Chen et al., 2004, [199501](#); Chow et al., 2004, [156347](#); Chow et al., 2005, [155728](#); Chow et al., 2007, [156354](#); Conny et al., 2003, [145948](#); Han et al., 2007, [155823](#); Subramanian et al., 2004, [081203](#); Watson et al., 2005, [157125](#)), develop reference materials (Klouda et al., 2005, [130382](#); Lee, 2007, [155926](#)), create water soluble organic carbon (WSOC) measurement techniques (Andracchio et al., 2002, [155657](#); Yang et al., 2003, [156167](#)), develop semi-continuous/continuous/real-time carbon measurement techniques (Chow et al., 2008, [156355](#); Watson et al., 2005, [157125](#)), and introduce isotope identification into the OC/EC measurement (Huang et al., 2006, [097654](#)).

OC sampling artifact issues were further addressed in various studies (Arhami et al., 2006, [156224](#); Bae et al., 2004, [156243](#); Chow et al., 2005, [155728](#); Fan et al., 2003, [058628](#); Fan et al., 2004, [155770](#); Grover et al., 2008, [156502](#); Lim et al., 2003, [037037](#); Mader et al., 2003, [155955](#); Matsumoto et al., 2003, [124293](#); Muller et al., 2004, [097109](#); Offenbergl et al., 2007, [098101](#); Olson and Norris, 2005, [156005](#); Park et al., 2006, [098104](#); Rice, 2004, [156049](#); Subramanian et al., 2004, [081203](#); ten Brink et al., 2004, [097110](#); ten Brink et al., 2005, [156115](#); Viana et al., 2006, [179987](#)), and were well summarized by Watson et al. (2005, [157125](#)) and Chow et al. (2008, [156355](#)). There are two commonly used methods to correct OC sampling artifacts: the filter with backup filter system (TBQ: placing a backup quartz-fiber filter behind the front Teflon-membrane filter; QBQ: placing a backup quartz-fiber filter behind the front quartz-fiber filter); and the denuder-filter-adsorbent system. Subramanian et al. (2004, [081203](#)) and Chow et al. (2006, [099031](#)) reported that during the Pittsburgh and Fresno supersite studies the positive artifact (organic gases condensed on filters) from TBQ (24-34%, up to 4 µg/m³ OC) was nearly twice that from QBQ (13-17%). With the denuder-filter-adsorbent system, the negative artifact (OC evaporating from the filter) was 5-10%. Watson and Chow (2002, [037873](#)) reported that the XAD-coated denuder could function as efficiently as a parallel plate denuder using carbon-impregnated charcoal filters (CIF) with frequent denuder changes. Huebert and Charlson (2000, [156577](#)) reported that using tandem filter packs may hinder a quantitative analysis of the artifacts.

Different temperature protocols and optical correction methods in thermal-optical analyses were further evaluated by Watson et al. (2005, [157125](#)), Chow et al. (2004, [156347](#); 2005, [155728](#); 2007, [156354](#)), Subramanian et al. (2006, [156107](#)), Conny et al. (2003, [145948](#)), Han et al. (2007, [155823](#)), Chen et al. (2004, [199501](#)) and (Conny et al., 2009, [191999](#)). Solomon et al. (2003, [156994](#)) reported a 20-50% difference for OC and a 20-200% difference for EC using 11 filter samples and 4 different analytical protocols. In an assessment of the different thermal-optical analysis protocols used around the world, Watson et al. (2005, [157125](#)) reported that differences of a factor of 2 to 7 in EC between different methods could be observed, and a factor of 2 was common, while the relative differences in OC between different methods were small. As Watson et al. (2005, [157125](#)) stated, there are 12 major differences among the thermal methods: (1) analysis atmosphere; (2) temperature ramping rates; (3) temperature plateaus; (4) residence time at each plateau; (5) optical pyrolysis monitoring configuration and wavelength; (6) standardization; (7) oxidation and reduction catalysts; (8) sample aliquot and size; (9) evolved carbon detection method; (10) carrier gas flow through or across the sample; (11) location of the temperature monitor relative to the sample; and (12) oven flushing conditions. Chow et al. (2004, [156347](#)) and Chen et al. (2004, [199501](#)) addressed the difference between optical transmission and optical reflectance methods for charring correction, and they reported that the charring OC on the surface of or inside a filter dominated the differences between these two correction methods. The differences between different sampling and measurement methods are also applied to the in-situ/semi-continuous methods, since

most of these methods are also based on thermal-optical analysis of collected filters. Most of these methods agree with integrated filter methods within 30%.

The differences observed between methods for OC and EC come largely from how OC and EC are defined. They are defined on an operational basis, as there are no standard reference materials. Initial efforts have been made to produce OC/EC reference materials at the National Institute of Science and Technology (NIST) (Klouda et al., 2005, [130382](#); Lee, 2007, [155926](#)). Klouda et al. (2005, [130382](#)) described the development of Reference Material 8785: Air Particulate Matter on Filter Media. Each reference filter is uniquely identified by its air PM number and its gravimetrically determined mass of fine Standard Reference Material (SRM) 1649a, and each filter has values assigned for total carbon, EC, and organic carbon mass fractions measured according to both IMPROVE and NIOSH protocols. Lee et al. (2007, [155926](#)) reported a method to create a reference filter with a known amount of OC (as potassium hydrogen phthalate), and EC (as carbon black hydrosol).

Measurement methods for WSOC have been developed recently (Miyazaki et al., 2006, [156767](#); Sullivan and Weber, 2006, [157031](#); Sullivan et al., 2004, [157029](#); Sullivan et al., 2006, [157030](#); Sullivan et al., 2007, [100083](#); Yu et al., 2004, [156172](#)). WSOC can be measured on integrated filter samples, or in-situ measurement can be conducted by coupling with the PILS-IC (Sullivan et al., 2004, [157029](#)). For integrated filter samples, filters are extracted with deionized water and followed by oxidation of total WSOC to CO₂. CO₂ can then be detected by either infrared spectroscopy (IR) (Decesari et al., 2000, [155748](#); Kiss et al., 2002, [156646](#); Yang et al., 2003, [156167](#)), FID (Yang et al., 2003, [156167](#)), or pyrolysis gas chromatography/mass spectrometry (GC/MS) (Gelencsér et al., 2000, [155785](#)). A correlation coefficient of 0.84 was reported by Sullivan et al. (Sullivan et al., 2004, [157029](#)) between in-situ and filter based measurement of WSOC.

Further development and evaluation has been conducted on the measurement of BC with light absorption instruments (Andreae and Gelencsér, 2006, [156215](#); Arnott et al., 2003, [037711](#); Bae et al., 2004, [156243](#); Borak et al., 2003, [156284](#); Cyrus et al., 2003, [049634](#); Kurniawan and Schmidt-Ott, 2006, [098823](#); Park et al., 2006, [098104](#); Saathoff et al., 2003, [156066](#); Sadezky et al., 2005, [097499](#); Slowik et al., 2007, [096177](#); Taha et al., 2007, [096277](#); Virkkula et al., 2007, [157098](#); Wallace, 2000, [000803](#); Weingartner et al., 2003, [156149](#); Williams et al., 2006, [157148](#); Wu et al., 2005, [157155](#)). These instruments include the aethalometer, particle absorption photometer, and photoacoustic analyzer. However, these instruments are subject to interferences by particle scattering, interactions with the filter substrate, particle loading on filters, and other pollutants (e.g., NO₂). Uncertainties of up to 50% were observed in the studies mentioned above by comparing these methods with integrated filter methods and thermal analysis methods.

Huang et al. (2006, [097654](#)) reported the measurement of a stable isotope, ¹³C, in OC and EC with a thermal optical transmission analyzer coupled with gas chromatography-isotope ratio mass spectrometer (TOT-GC-IRMS). The ratio of ¹³C/¹²C in OC and EC can provide useful information on OC/EC source categories and origin. The method was applied to Pacific2001 aerosol samples from the greater Vancouver area in Canada and produced a precision of ~0.03%. Gustafsson et al. (2009, [192000](#)) applied the radiocarbon measurement technique and quantified the source contributions of carbonaceous aerosols to the Indian Ocean “brown cloud,” with particular relevance for understanding and mitigating the climate effects of EC/BC.

Organic Speciation

Organic matter makes up a substantial fraction of PM in all regions of the U.S. (U.S. EPA, 2004, [056905](#)), and 10-40% of the total organic matter is currently quantifiable at the individual compound level (Pöschl, 2005, [156882](#)). Recent advancements in traditional solvent extraction GC/MS and high pressure liquid chromatography (HPLC) as well as application of thermal desorption (TD) techniques are helping to expand the understanding of the composition of organic matter as well as improving detection limits for quantification of organic molecular marker (OMM) compounds (Robinson et al., 2006, [156918](#); Schnelle-Kreis et al., 2005, [112944](#); Sheesley et al., 2007, [112017](#); Shrivastava et al., 2007, [111594](#)). In addition, information about organic functional groups can be obtained with Fourier transform infrared spectrometry (FTIR) (Tsai and Kuo, 2006, [156127](#)).

Recent advancements in GC/MS technology including inert electron ionization sources and improved instrument sensitivity and scan rates for better OMM quantification, have increased its

application in organic aerosol characterization studies (Cass, 1998, [155716](#); Dutton et al., 2009, [194887](#); Fraser et al., 2003, [042231](#); Graham et al., 2003, [156489](#); Hays et al., 2002, [026104](#); Robinson et al., 2006, [156918](#); Schauer et al., 1996, [051162](#); Sheesley et al., 2007, [112017](#); Subramanian et al., 2006, [156107](#); Watson et al., 1998, [012257](#); Zheng et al., 2002, [026100](#); Zheng et al., 2006, [157189](#)). Incorporation of high volume injection using programmable temperature vaporization (PTV) (Engewald et al., 1999, [155765](#)) has further lowered detection limits for trace level OMM compounds. High volume injection has the added benefit of preventing the loss of semivolatile compounds (Swartz et al., 2003, [157035](#)), and has been applied for analysis of PAHs using low volume samplers (down to 5 L/min), allowing for smaller required mass loadings (Bruno et al., 2007, [155706](#); Crimmins and Baker, 2006, [097008](#)). Since last review, HPLC analysis with fluorescence detection has also been used frequently for quantification of semivolatile organic compounds in both the particle and gas phase (Albinet et al., 2007, [154426](#); Barreto et al., 2007, [155676](#); Chow, 2007, [157209](#); Eiguren-Fernandez et al., 2003, [142609](#); Goriaux et al., 2006, [156484](#); Murahashi, 2003, [096539](#); Rynö et al., 2006, [156065](#); Stracquadiano et al., 2005, [156104](#); Temime-Roussel et al., 2004, [098530](#); Temime-Roussel et al., 2004, [098521](#)). Lengthy extraction and analysis times remain a limiting factor for these methods.

TD techniques bypass one of the time consuming steps in traditional solvent extraction analysis for nonpolar organic compounds (n-alkanes, branched alkanes, cyclohexanes, hopanes, steranes, alkenes, phthalates and PAHs). This is achieved by vaporizing and analyzing organic constituents directly from the collection substrate, thereby bypassing the extraction step (Chow, 2007, [157209](#)). Methods exist for both off-line TD analysis of previously collected filter samples and semi-continuous TD analysis. Annex A, Table A-17 is adapted from Chow et al. (2007, [157209](#)) and summarizes recent TD-GC/MS studies. The most common off-line method is TD-GC/MS (Hays and Lavrich, 2007, [155831](#)). Continuous or semi-continuous methods have been developed for direct analysis of individual organic constituents by coupling TD with various forms of mass spectrometry (Smith et al., 2004, [156090](#); Tobias and Ziemann, 1999, [157053](#); Tobias et al., 2000, [156121](#); Voisin et al., 2003, [156141](#); Williams et al., 2006, [156157](#)). A comparison of measurement and analytical specifications for filter analysis using solvent extraction and TD methods for organic speciation are summarized in Annex A, Table A-17.

3.4.1.3. Multiple-Component Measurements on Individual Particles

The 2004 PM AQCD (U.S. EPA, 2004, [056905](#)) discussed the aerosol time-of-flight mass spectrometry (ATOFMS). Recently, the ATOFMS and several other aerosol mass spectrometry methods have been further developed. Both lab and field comparisons have been conducted to evaluate the reliability of these types of instruments.

There are four types of commonly used aerosol mass spectrometry: (1) particle analysis by laser MS (PALMS; National Oceanic and Atmospheric Administration [NOAA]); (2) rapid single particle mass spectrometer (RSMS; University of Delaware); (3) aerosol time-of-flight MS (ATOFMS; TSI, Inc.); and (4) AMS (Aerodyne) (Chow et al., 2008, [156355](#); Nash et al., 2006, [199502](#)). The differences between these instruments primarily come from the particle sizing methods of mass spectrometers, as shown in Annex A, Table A-16. Although the technique varies, the underlying principle is to fragment each particle into ions, using either a high-power laser or a heated surface, and then a mass spectrometer to measure the mass to charge ratio of each ion fragment in a vacuum.

These instruments were evaluated at the Atlanta, Houston, Fresno, Pittsburgh, New York, and Baltimore supersites (Bein et al., 2005, [156265](#); Drewnick et al., 2004, [155755](#); Drewnick et al., 2004, [155754](#); Hogrefe et al., 2004, [099003](#); Jimenez et al., 2003, [156611](#); Lake et al., 2003, [156669](#); Lake et al., 2004, [088411](#); Middlebrook et al., 2003, [042932](#); Phares et al., 2003, [156866](#); Qin and Prather, 2006, [156895](#); Wenzel et al., 2003, [157139](#)). Measurements of the gross composition and abundance of particles by these instruments were generally semi-quantitative, with the exception of AMS. Particles of similar composition (e.g., OC/SO₄²⁻, Na/K/SO₄²⁻, soot/hydrocarbon, and mineral particle types) were characterized by these instruments during the studies mentioned above. NO₃⁻ and SO₄²⁻ concentrations measured with AMS were comparable with other continuous and filter-based methods, as mentioned in Section 3.4.1.2. In addition, concentrations of different particle types can be obtained by the co-location of these aerosol mass spectrometers and other particle sizing instruments, such as particle counters or the Micro-Orifice Uniform Deposit Impactor (MOUDI).

3.4.1.4. UFPs: Mass, Surface Area, and Number

Instruments for measuring UFPs developed during the past decade permit measurement of size distributions of particles down to 3 nm in diameter with mobility particle sizers. Concentrations down to this size range can be obtained by a MOUDI. The recently developed low pressure-drop UFP impactor coupled with a β Attenuation Monitor (nano-BAM) can also provide UFP (<150 nm) mass concentrations (Chakrabarti et al., 2004, [157426](#)). A high correlation coefficient was observed between MOUDIs and nano-BAMs, with a correlation of 0.96. A 50% cut point (d_{50}) of 13-200 nm can be achieved by a high-volume slot-type UFP virtual impactor (Middha and Wexler, 2006, [155982](#)).

Methods are also being developed to measure the surface area of UFPs. Particle surface area is usually measured by attaching labeled (radioactive or electrical labeling) molecules to particles and detecting the radioactive or electrical properties of the attached molecules. Wilson et al. (2007, [098398](#)) suggested that the electrical aerosol detector (EAD, based on diffusion charging) measurement might be a useful indicator of the particle surface area deposited in the lung. This method can be potentially useful for examining the association between health effects and particle surface areas.

Developments involving the condensation particle counter include use of de-ionized water as a condensation medium in lieu of butanol or n-propanol in condensation particle counters (Hering et al., 2005, [155838](#); Hermann et al., 2007, [155840](#); Petäjä et al., 2006, [156021](#)). This development makes the condensation particle counter (CPC) easier to use in field studies because water does not have some of the same chemical properties (with respect to hazard and odor) as butanol or n-propanol. The performance of this CPC was reported to be similar to the conventional butanol based CPC (Hering et al., 2005, [155838](#)). Use of a battery of water and butanol-based CPCs was demonstrated to detect a range of solubilities in nucleation-mode particles (Kulmala et al., 2007, [155911](#)). Additionally, CPCs have been used to measure particles in the smaller end of the UF scale through adjustment of CPC cut-off diameters through tuning the temperature difference between the CPC saturator and condenser (Kulmala et al., 2007, [155911](#)) and improved charge reduction techniques (Winkler et al., 2008, [156160](#)). The latter method was effective in reducing the size of particles detected by a CPC to <2 nm. These studies include assessment of errors related to these developments with the CPC and generally show that counting efficiencies with these devices is upwards of 95% (Hermann et al., 2007, [155840](#)). Additionally, recent advancements have been made in development of fast scanning methods for UFP size distributions, including diffusion screens (DS) (Feldpausch et al., 2006, [155773](#)) and fast integrated mobility scanners (FIMS) (Olfert et al., 2008, [156004](#)).

3.4.1.5. PM Size Distribution

Along with particle density and shape (U.S. EPA, 2004, [056905](#)), the particle size distribution can be used to estimate PM mass concentrations. For particles >0.1 μm , several instruments, including DRUM, MOUDIs, and aerodynamic particle sizer (APS), are available to measure mass-based or count-based particle size distribution. An APS incorporating very sharp cut points between 0.1 and 10 μm is now available (Peters, 2006, [156860](#); Zeng, 2006, [098375](#)). For particles in this range, inertial forces are used to separate particles based on impaction. For particles <0.1 μm , particles can be separated by their electrical mobility, and as a result, electrical mobility diameter is often used to describe UFP size distribution in lieu of aerodynamic diameter. It has been necessary to develop techniques to convert mobility diameters, measured by the scanning mobility particle sizer (SMPS) or the Engine Exhaust Particle Sizer (EEPS), to aerodynamic diameters, measured by the APS, or vice versa, in order to merge the distributions spanning the UF, accumulation, and coarse modes. A variety of techniques for combining SMPS and APS diameters have been reported in the literature (Hand and Kreidenweis, 2002, [155824](#); Khlystov et al., 2004, [155897](#); Morawska et al., 1999, [007609](#); Morawska et al., 2007, [155990](#); Shen et al., 2002, [156086](#); TSI, 2005, [157196](#)). However, each of these techniques incurs some uncertainty of which the user must be aware.

3.4.1.6. Satellite Measurement

Instruments sensing back scattered solar radiation on satellites have made it possible to derive information about tropospheric aerosol properties on the global scale. The satellite borne instruments

vary in their complexity and in the aerosol properties they can measure. Satellite instruments measure radiance (or brightness temperature) that can then be used to provide information on the aerosol column amount, or the aerosol optical depth (AOD). Depending on the wavelengths sampled and the spectral resolution of the instruments, information about the composition of particles of diameter $<2\ \mu\text{m}$ and particles of diameter $>2\ \mu\text{m}$ can be obtained. Data from two main instruments, the moderate resolution imaging spectroradiometer (MODIS) and the multiangle imaging spectroradiometer (MISR) have been used to estimate surface PM in the U.S. MODIS measures the intensity of back scattered sunlight at seven wavelengths through the visible to the near infrared at one viewing direction; and MISR measures the intensity at four wavelengths (from the visible to the near IR) and the same ground pixel at nine viewing angles. The spatial resolution of reported AOD is $17.6 \times 17.6\ \text{km}$ for MISR and either 10×10 or $1 \times 1\ \text{km}$ for MODIS, depending on retrieval algorithm. Since both instruments are located on the same satellite, their times of overpass are the same, about 1330 local time. Due to precession of the satellite's orbit, the satellite does not pass over the same path every day, and instruments cannot sense aerosol properties beneath cloud tops.

The problem of using satellite data to retrieve properties of the atmospheric aerosol is complex because the surface contribution to satellite measured reflectance must be separated from the aerosol signal. Difficulties can arise when attempting to derive aerosol information over land surfaces because of uncertainties in surface reflectivity, similarities between aerosol and surface composition, and high signal-to-noise ratio when viewing AOD over reflective surfaces such as desert and snow. To overcome this difficulty, data from MODIS have been applied over dark land surfaces and ongoing improvements in retrieval algorithms are being developed. Instruments such as the MISR that sense at multiple viewing angles can better cope with the problems over land surfaces because they can use the information on the angular dependence of reflection from the surface and the atmosphere to distinguish between their signals. Not only can total AODs be derived, but fractional AODs that reflect external mixtures characterized by particle shape, effective radius, and single scattering albedo can also be derived. These properties can then be used to infer particle composition. Retrievals over the oceans have had less difficulty because the optical properties of sunlight reflected from the sea surface are much better known, and reflectivities are low over most zenith angles at less than grazing incidence.

Kokhanovsky et al. (2007, [190009](#)) examined the errors associated with MODIS, MISR, and a number of other satellite instruments with respect to associated retrieval algorithms for retrievals over Central Europe. They found a correlation coefficient between MODIS and MISR AOD of 0.62. Both MODIS and MISR AOD tended to underestimate ground-based AOD measurements from AERONET (NASA's AEROSOL ROBOTIC NETWORK) slightly with MODIS generally retrieving higher AODs than MISR. Chu et al. (2003, [190049](#)) found correlations between MODIS and AERONET AODs ranging from 0.82-0.91; and Kahn et al. (2005, [189961](#)) found correlations of 0.7-0.9 between MISR and AERONET AODs.

Further complexity is added when attempting to relate surface $\text{PM}_{2.5}$ to aerosol optical depths. The detailed comparisons of surface measurement and satellite measurements are given in Chapter 9.

3.4.2. Ambient Network Design

3.4.2.1. Monitor Siting Requirements

The EPA Air Quality System database (AQS) contains measurements of air pollutant concentrations in the 50 states, plus the District of Columbia, Puerto Rico, and the Virgin Islands, for the 6 criteria air pollutants as well as a more limited dataset of hazardous air pollutants. In 2007, there were 4,693 PM_{10} monitors and 2,194 $\text{PM}_{2.5}$ monitors reporting values to the AQS. Where SLAMS PM_{10} and $\text{PM}_{2.5}$ monitoring is required, at least one of the sites must be a maximum concentration site for that specific area. The appropriate spatial scales for $\text{PM}_{2.5}$, $\text{PM}_{10-2.5}$, and PM_{10} monitoring differ given the contrasting spatial gradients of coarse PM relative to fine. The relevant scales for each size classification are provided in Annex A, Table A-18.

Criteria for siting ambient monitors for PM at national monitoring networks are summarized below by PM size, and details are given in the CFR 40 Part 58 Appendix D, and SLAMS/NAMS/PAMS Network Review Guidance (U.S. EPA, 1998, [093211](#)). Table A-19 in Annex A provides a summary of the number of sites and operating specifications of these networks. Probing

and monitoring path siting criteria for any specific monitoring site are given in CFR 40 Part 58 Appendix E, including horizontal and vertical placement, spacing from minor source, spacing from obstructions, spacing from trees, and spacing from roadways.

PM_{2.5}

The minimum number of PM_{2.5} monitors required in a metropolitan statistical area is determined by the population and the air quality in the area, as specified in Appendix D of 40 CFR Part 58. The required minimum number of PM_{2.5} monitors ranges from 0 to 3 in any given metropolitan statistical area. Continuous PM_{2.5} monitors must be operated in no fewer than one-half of the minimum required sites in each area. Most PM_{2.5} monitoring in urban areas should be representative of a neighborhood scale (for trends and compliance with standards). Urban or regional scale sites are located to characterize regional transport of PM_{2.5}. In certain instances where population-oriented micro- or middle-scale PM_{2.5} monitoring are determined by the Regional Administrator to represent many such locations throughout a metropolitan area, these smaller scales can be considered to represent community-wide air quality. PM_{2.5} measurements are obtained at local temperature and pressure across the NAMS/SLAMS networks (40 CFR Part 58).

PM_{2.5} chemical speciation monitoring is currently conducted at 197 CSN sites (<http://www.epa.gov/ttn/amtic/specgen.html>). Within the CSN network, 53 locations are recognized as the Speciation Trends Network (STN) operating on a sample schedule of one in every three days, while the rest of the CSN typically operates every sixth day.

PM_{10-2.5}

PM_{10-2.5} monitoring has not been required at SLAMS sites, but will be required at NCore¹ Stations (which is a sub-set of the SLAMS) by January 1, 2011. Middle and neighborhood scale measurements are the most important station classifications for PM_{10-2.5} to assess the variation in coarse particle concentrations that would be expected across populated areas that are in proximity to large emissions sources. PM_{10-2.5} chemical speciation monitoring and analyses will also be required at NCore sites by January 1, 2011. EPA has already approved FRMs and FEMs for PM_{10-2.5} mass; however, methods for PM_{10-2.5} speciation are still being developed (Henderson, 2009, [192001](#)). PM_{10-2.5} measurements are obtained at local temperature and pressure by recalculating the co-located PM₁₀ for local conditions.

PM₁₀

As for PM_{2.5}, the minimum number of PM₁₀ monitors required in a metropolitan statistical area is determined by the population and the air quality in the area, as specified in Appendix D of 40 CFR Part 58. The required minimum number of PM₁₀ monitors ranges from 0 to 8 in any given metropolitan statistical area. Except for some circumstances where microscale (<100 m, for maximum PM₁₀ exposure) monitoring may be appropriate, the most important scales to characterize the emissions of PM₁₀ effectively from both mobile and stationary sources are the middle scale (for short-term public exposure) and neighborhood scale (for trends and compliance with standards). PM₁₀ measurements are obtained at standard temperature and pressure across the NAMS/SLAMS networks (40 CFR Part 58).

3.4.2.2. Spatial and Temporal Coverage

Locations of PM_{2.5} and PM₁₀ Monitors in Selected Metropolitan Areas in the U.S.

Fifteen metropolitan regions were chosen for closer investigation of monitor siting based on their distribution across the nation and relevance to health studies analyzed in subsequent chapters of this ISA. These regions were: Atlanta, Birmingham, Boston, Chicago, Denver, Detroit, Houston, Los Angeles, New York City, Philadelphia, Phoenix, Pittsburgh, Riverside, Seattle, and St. Louis. Core-

¹ For more information on NCore, see the NCore web site at: <http://www.epa.gov/ttn/amtic/ncore/index.html>.

Based Statistical Areas (CBSAs) and Combined Statistical Areas (CSAs), as defined by the U.S. Census Bureau (<http://www.census.gov/>), were used to determine which counties, and hence which monitors, to include for each metropolitan region.¹ Figure 3-7 and Figure 3-8 display PM_{2.5} and PM₁₀ monitor density, respectively, with respect to population density in Boston. Annex A includes similar information for all fifteen metropolitan regions (Figure A-1 through Figure A-30).

¹ A CBSA represents a county-based region surrounding an urban center of at least 10,000 people determined using 2000 census data and replaces the older Metropolitan Statistical Area (MSA) definition from 1990. The CSA represents an aggregate of adjacent CBSAs tied by specific commuting behaviors. The broader CSA definition was used when selecting monitors for the cities listed above with the exception of Los Angeles, Riverside and Phoenix. Los Angeles and Riverside are contained within the same CSA, so the smaller CBSA definition was used to delineate these two cities. Phoenix is not contained within a CSA, so the smaller CBSA definition was used for this city as well.

Boston Combined Statistical Area

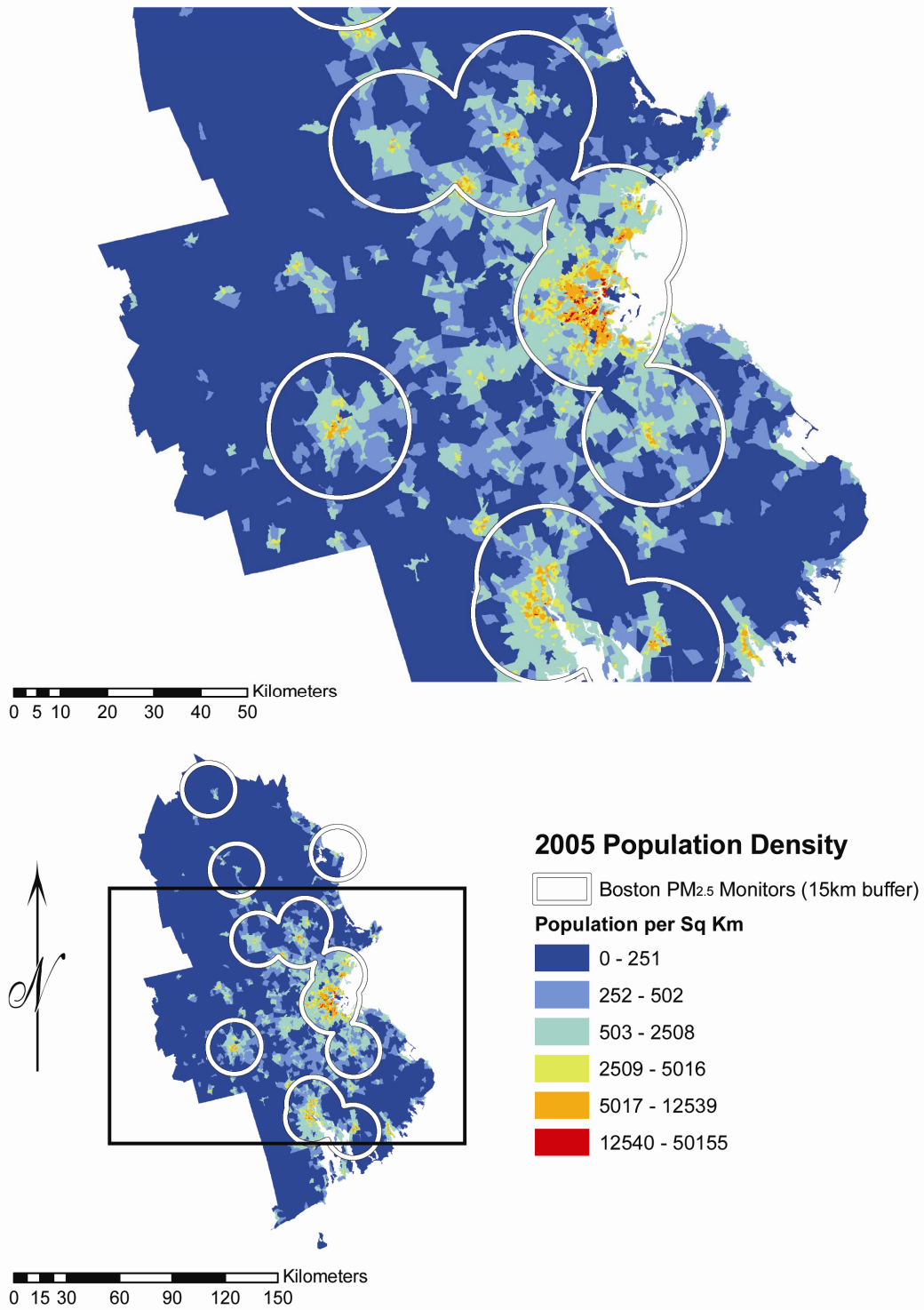


Figure 3-7. PM_{2.5} monitor distribution in comparison with population density, Boston CSA.

Boston Combined Statistical Area

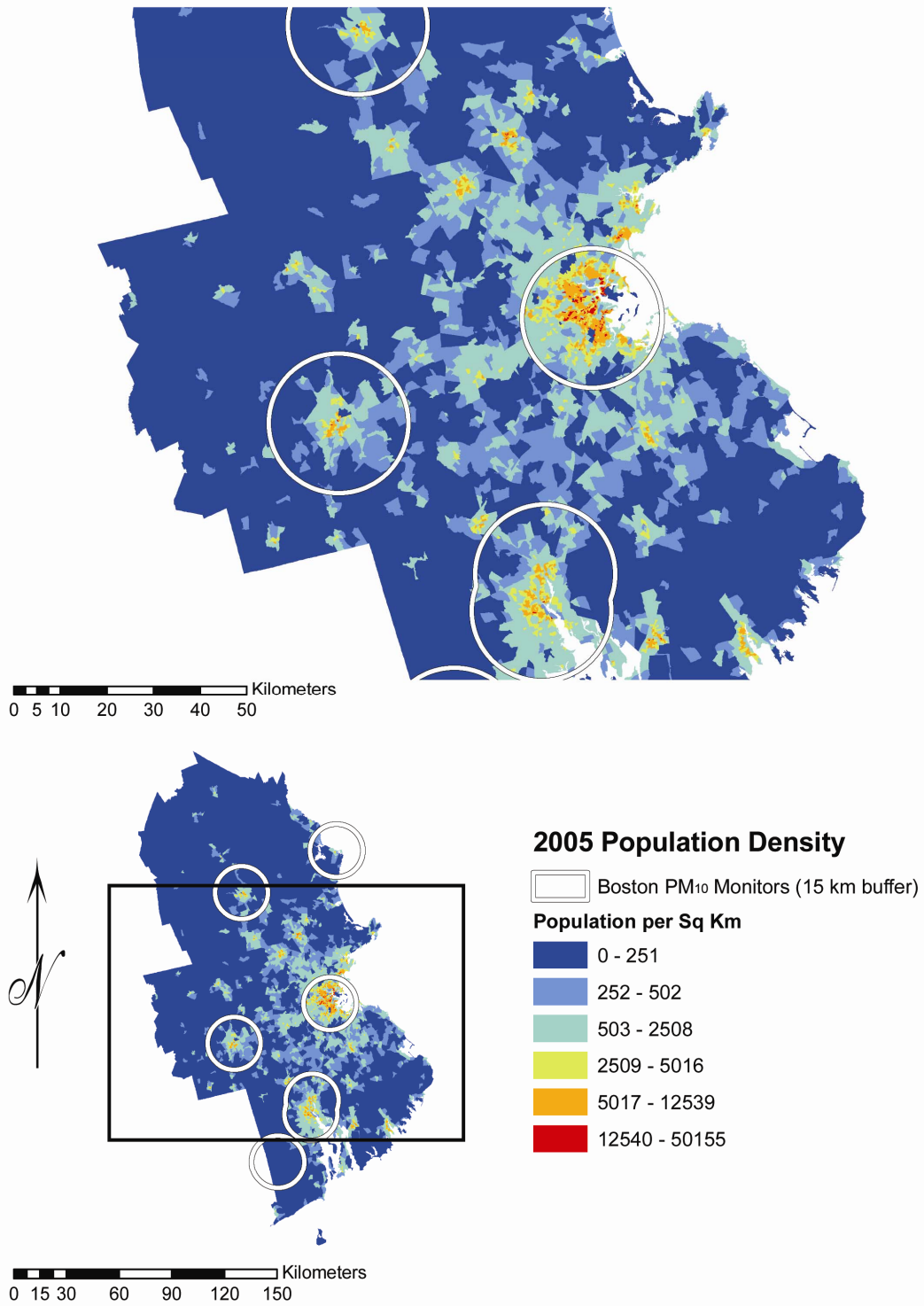


Figure 3-8. PM₁₀ monitor distribution in comparison with population density, Boston CSA.

Table 3-3. Proximity to PM_{2.5} and PM₁₀ monitors for total population^a by city.

Region	Proximity to PM Monitors ^b								
	Total CSA/CBSA	≤ 1 km		≤ 5 km		≤ 10 km		≤ 15 km	
	N	N	%	N	%	N	%	N	%
PROXIMITY TO PM_{2.5} MONITORS									
Atlanta	5,316,742	23,461	0.44	581,461	10.94	1,990,477	37.44	3,179,844	59.81
Birmingham	1,166,100	12,925	1.11	240,383	20.61	666,926	57.19	848,447	72.76
Boston	7,502,707	185,457	2.47	1,877,180	25.02	3,356,019	44.73	4,641,175	61.86
Chicago	9,754,262	177,076	1.82	3,091,573	31.69	6,473,463	66.37	8,185,010	83.91
Denver	2,952,039	40,601	1.38	649,953	22.02	1,548,976	52.47	2,252,657	76.31
Detroit	5,553,465	54,997	0.99	1,174,733	21.15	2,791,555	50.27	3,845,190	69.24
Houston	5,503,320	11,586	0.21	213,708	3.88	905,007	16.44	1,599,079	29.06
Los Angeles	13,061,361	115,477	0.88	2,579,809	19.75	7,544,466	57.76	10,792,727	82.63
New York	22,050,940	717,094	3.25	8,107,764	36.77	13,493,867	61.19	16,571,764	75.15
Philadelphia	6,388,913	117,389	1.84	1,878,373	29.40	3,517,321	55.05	4,393,136	68.76
Phoenix	3,818,147	37,133	0.97	490,072	12.84	1,099,069	28.79	1,739,542	45.56
Pittsburgh	2,515,383	40,574	1.61	587,148	23.34	1,331,230	52.92	1,883,301	74.87
Riverside	3,781,063	43,739	1.16	723,829	19.14	1,855,296	49.07	2,344,394	62.00
Seattle	3,962,434	13,723	0.35	287,373	7.25	931,630	23.51	1,561,792	39.41
St. Louis	2,869,955	37,329	1.30	563,176	19.62	1,338,349	46.63	1,760,985	61.36
PROXIMITY TO PM₁₀ MONITORS									
Atlanta	5,316,742	30,973	0.58	416,440	7.83	1,090,497	20.51	1,837,983	34.57
Birmingham	1,166,100	23,943	2.05	251,310	21.55	473,054	40.57	638,472	54.75
Boston	7,502,707	63,614	0.85	1,090,172	14.53	2,087,770	27.83	2,939,870	39.18
Chicago	9,754,262	55,642	0.57	844,714	8.66	2,374,972	24.35	3,844,297	39.41
Denver	2,952,039	38,449	1.30	521,201	17.66	1,146,286	38.83	1,799,187	60.95
Detroit	5,553,465	14,050	0.25	309,623	5.58	748,971	13.49	1,300,995	23.43
Houston	5,503,320	36,795	0.67	832,767	15.13	2,227,314	40.47	3,141,150	57.08
Los Angeles	13,061,361	52,052	0.40	1,404,389	10.75	4,899,254	37.51	9,075,863	69.49
New York	22,050,940	19,842	0.09	292,105	1.32	592,631	2.69	773,962	3.51
Philadelphia	6,388,913	23,988	0.38	376,966	5.90	1,091,532	17.08	2,238,309	35.03
Phoenix	3,818,147	99,520	2.61	1,255,430	32.88	2,615,738	68.51	3,416,682	89.49
Pittsburgh	2,515,383	65,906	2.62	706,413	28.08	1,291,700	51.35	1,705,451	67.80
Riverside	3,781,063	61,356	1.62	895,615	23.69	2,360,272	62.42	2,922,799	77.30
Seattle	3,962,434	4,851	0.12	220,539	5.57	709,887	17.92	1,211,430	30.57
St. Louis	2,869,955	27,872	0.97	380,411	13.25	891,695	31.07	1,212,543	42.25

^aBased on 2005 population totals.

^bPercentages are given with respect to the total population per city provided.

Table 3-3 shows the population density around PM_{2.5} and PM₁₀ monitors for the total population for each CSA/CBSA individually. Population totals within various distances of PM monitors were calculated assuming equal internal population distribution for individual census blocks. Between-city disparities in population density were large and were dependent primarily on the location and number of PM monitoring sites per CSA/CBSA. For PM_{2.5}, Los Angeles (83%) and Denver (76%) had the largest proportion of the total population within 15 km of a monitor. Houston (29%) had the least population coverage with their PM_{2.5} monitors. For PM₁₀, Phoenix (89%) had the largest proportion of the total population within 15 km of a monitor. Detroit (23%), Boston (39%), Seattle (31%), and Philadelphia (35%) had the smallest proportions of the population within 15 km of a PM₁₀ monitor. Proximity to monitoring stations is considered further in Section 3.5 and Section 3.8 regarding spatial variability within cities. Figure 3-7 shows that the PM_{2.5} network more closely samples near population centers in the Boston CSA compared with the PM₁₀ network shown in Figure 3-8, although both PM_{2.5} and PM₁₀ networks place at least one monitor in the city center.

3.4.2.3. Network Application for Exposure Assessment with Respect to Susceptible Populations

Subject Age

Table 3-4 breaks down the population density around PM_{2.5} and PM₁₀ monitors for sub-populations of children age 0-4 yr, children age 5-17 yr, and elderly adults age 65 yr and over cumulatively for the 15 CSAs/CBSAs examined. Table 3-5 shows the distribution for adults age 65 years and over for each CSA/CBSA individually. This detail of information is not provided for the 0- to 4-yr and 5- to 17-yr age groups because variation in percentage within a certain radius of the monitor was generally fairly low for each city across the child age groups when compared to total population. In the cases of Denver, Detroit, Phoenix, Riverside, and St. Louis for PM_{2.5} and Birmingham, Denver, Riverside, and St. Louis for PM₁₀, the elderly population's distribution around the samplers varied more from the total population compared to other age groups. When all CSAs/CBSAs were considered cumulatively, the percentage of the population within 15 km of a monitor was similar for all age groups for both PM_{2.5} and PM₁₀. Between-city disparities in elderly population density within a sampler radius were larger. For PM_{2.5}, Chicago (87%) and Denver (84%) had the largest proportion of the elderly population within 15 km of a monitor. Houston (31%) had the least population coverage with their PM_{2.5} monitors. For PM₁₀, Phoenix (90%) had the largest proportion of the total population within 15 km of a monitor. New York (4%), Detroit (27%), Seattle (32%), and Philadelphia (39%) had the smallest proportions of the population within 15 km of a PM₁₀ monitor. These differences may reflect overall density of the samplers within a given city, with PM_{2.5} monitors more numerous than PM₁₀ monitors in most of the CSAs/CBSAs, and retirement and settlement trends among elderly adults.

Table 3-4. Proximity to PM_{2.5} and PM₁₀ monitors for children age 0-4 yr, children age 5-17 yr, and adults age 65 yr and older.^a The figures presented here are cumulative for the 15 CSAs/CBSAs examined in Chapter 3.

Age Grouping	Proximity to PM Monitors ^b								
	Total CSA/CBSA	≤ 1 km		≤ 5 km		≤ 10 km		≤ 15 km	
	N	N	%	N	%	N	%	N	%
PROXIMITY TO PM_{2.5} MONITORS									
0-4	6,400,785	109,466	1.71	1,603,000	25.04	3,361,922	52.52	4,462,403	69.72
5-17	17,212,825	275,427	1.60	4,164,132	24.19	8,814,179	51.21	11,813,997	68.63
≥ 65	10,391,023	175,113	1.69	2,570,909	24.74	5,483,776	52.77	7,288,049	70.14
PROXIMITY TO PM₁₀ MONITORS									
0-4	6,400,785	44,384	0.69	695,120	10.86	1,725,419	26.96	2,636,782	41.19
5-17	17,212,825	110,882	0.64	1,756,246	10.20	4,441,239	25.80	6,942,001	40.33
≥ 65	10,391,023	68,367	0.66	1,056,375	10.17	2,631,243	25.32	4,041,802	38.90

^a Based on 2000 population totals.

^b Percentages are given with respect to the total population per city provided.

Race and Hispanic Origin

Table 3-6 shows the percent of the population self-identified as white or black and having a Hispanic or non-Hispanic origin within 1, 5, 10, or 15 km distances from PM_{2.5} and PM₁₀ monitors cumulatively across the fifteen CSAs/CBSAs. For PM_{2.5}, blacks and Hispanics had similar percentages of the population within 15 km of a monitor (86% and 82%, respectively), while a smaller proportion of whites and non-Hispanics were within that same distance (63% and 67%, respectively), across the fifteen CSAs/CBSAs studied. For PM₁₀, Hispanics (54%) represented the subpopulation with the largest percentage of total population within 15 km of a monitor across the fifteen CSAs/CBSAs studied. The percentage of blacks within that same distance was marginally lower (48%), whereas the percentage of whites and non-Hispanics within 15 km of a monitor was approximately two-thirds that of Hispanics (35% and 37%, respectively). Higher percentages of individual ethnic subpopulations within 15 km of a PM_{2.5} monitor most likely represents the fact that more PM_{2.5} monitors are currently deployed compared with PM₁₀ monitors. While no ethnic subpopulation appears to be well represented at the neighborhood scale, greater percentages of the black and Hispanic populations (1% each) are within 1 km of a PM₁₀ monitor than the corresponding white and non-Hispanic populations (0.5% each). Likewise, 2.5% of the black population and 2.8% of the Hispanic population reside within 1 km of a PM_{2.5} monitor compared to 1.4% of the white population and 1.5% of the non-Hispanic population. Furthermore, it is notable that at any scale shown in Table 3-6 for both PM_{2.5} and PM₁₀ monitors, those self-identified as black or Hispanic actually have greater representation by the monitors than those identified as white or non-Hispanic.

Table 3-5. Proximity to PM_{2.5} and PM₁₀ monitors for adults age 65 yr and older^a by city.

Age Grouping	Proximity to PM Monitors ^b									
	Total CSA/CBSA	≤ 1 km		≤ 5 km		≤ 10 km		≤ 15 km		
	N	N	%	N	%	N	%	N	%	
PROXIMITY TO PM_{2.5} MONITORS										
Atlanta	362,201	1,757	0.49	36,772	10.15	136,179	37.60	207,122	57.18	
Birmingham	145,905	1,619	1.11	29,952	20.53	84,223	57.72	106,488	72.98	
Boston	945,790	18,821	1.99	224,628	23.75	438,920	46.41	606,231	64.10	
Chicago	1,018,983	18,539	1.82	348,656	34.22	713,194	69.99	883,112	86.67	
Denver	232,974	3,891	1.67	59,625	25.59	140,523	60.32	196,361	84.28	
Detroit	626,216	5,765	0.92	138,672	22.14	345,808	55.22	469,462	74.97	
Houston	377,586	1,010	0.27	14,911	3.95	66,741	17.68	117,661	31.16	
Los Angeles	1,207,436	9,653	0.80	229,893	19.04	688,844	57.05	984,889	81.57	
New York	2,710,675	78,918	2.91	921,599	34.00	1,619,177	59.73	2,048,842	75.58	
Philadelphia	834,110	13,323	1.60	251,459	30.15	487,003	58.39	605,663	72.61	
Phoenix	388,150	2,738	0.71	39,833	10.26	90,304	23.27	142,084	36.61	
Pittsburgh	449,544	8,933	1.99	111,050	24.70	249,269	55.45	347,711	77.35	
Riverside	342,334	3,024	0.88	50,901	14.87	129,836	37.93	170,933	49.93	
Seattle	390,372	1,721	0.44	29,429	7.54	101,223	25.93	156,562	40.11	
St. Louis	358,747	5,401	1.51	83,528	23.28	192,532	53.67	244,929	68.27	
PROXIMITY TO PM₁₀ MONITORS										
Atlanta	362,201	2,115	0.58	35,448	9.79	93,903	25.93	139,240	38.44	
Birmingham	145,905	3,663	2.51	35,628	24.42	66,839	45.81	86,299	59.15	
Boston	945,790	6,852	0.72	124,911	13.21	262,854	27.79	385,046	40.71	
Chicago	1,018,983	7,619	0.75	107,540	10.55	291,705	28.63	441,771	43.35	
Denver	232,974	3,675	1.58	43,658	18.74	107,548	46.16	168,447	72.30	
Detroit	626,216	1,555	0.25	41,833	6.68	99,680	15.92	167,760	26.79	
Houston	377,586	2,085	0.55	57,413	15.21	166,715	44.15	219,615	58.16	
Los Angeles	1,207,436	4,693	0.39	126,696	10.49	422,725	35.01	810,078	67.09	
New York	2,710,675	2,463	0.09	37,580	1.39	80,222	2.96	104,951	3.87	
Philadelphia	834,110	2,740	0.33	49,413	5.92	154,535	18.53	322,700	38.69	
Phoenix	388,150	8,605	2.22	119,306	30.74	267,456	68.91	348,464	89.78	
Pittsburgh	449,544	13,302	2.96	133,285	29.65	243,723	54.22	314,941	70.06	
Riverside	342,334	4,181	1.22	65,499	19.13	182,615	53.34	236,900	69.20	
Seattle	390,372	503	0.13	22,333	5.72	72,979	18.69	123,054	31.52	
St. Louis	358,747	4,316	1.20	55,833	15.56	117,743	32.82	172,535	48.09	

^aBased on 2000 population totals.

^bPercentages are given with respect to the total population per city provided.

Table 3-6. Proximity to PM_{2.5} and PM₁₀ monitors based on the population identified as white, black, Hispanic, or non-Hispanic^a. The figures presented here are cumulative for the 15 CSAs/CBSAs examined in Chapter 3.

Race or Hispanic Origin	Proximity to PM Monitors ^b								
	Total CSA/CBSA	≤ 1 km		≤ 5 km		≤ 10 km		≤ 15 km	
	N	N	%	N	%	N	%	N	%
PROXIMITY TO PM_{2.5} MONITORS									
White	61,936,855	863,823	1.39	12,257,978	19.79	27,553,900	44.49	39,030,037	63.02
Black	12,668,004	320,447	2.53	4,780,620	37.74	9,241,172	72.95	10,906,346	86.09
Hispanic	15,916,208	445,126	2.80	5,782,482	36.33	10,661,947	66.99	13,094,618	82.27
Non-Hispanic	74,611,962	1,135,999	1.52	16,553,574	22.19	36,318,474	48.68	49,629,054	66.52
PROXIMITY TO PM₁₀ MONITORS									
White	61,936,855	325,771	0.53	5,554,906	8.97	14,041,215	22.67	21,913,907	35.38
Black	12,668,004	134,174	1.06	1,611,263	12.72	3,867,436	30.53	6,020,348	47.52
Hispanic	15,916,208	169,305	1.06	2,496,959	15.69	5,905,322	37.10	8,589,819	53.97
Non-Hispanic	74,611,962	421,917	0.57	6,767,187	9.07	17,261,734	23.14	27,254,421	36.53

^aBased on 2000 population totals

^bPercentages are given with respect to the total population per city provided.

Socioeconomic Status

Table 3-7 shows the percent of the population below and above the poverty level and the percent of the population over age 25 years stratified by education level that reside within 1 km, 5 km, 10 km, and 15 km of a PM_{2.5} and PM₁₀ monitor cumulatively across the 15 CSAs/CBSAs. For PM_{2.5}, 80% of the population below poverty level and 77% of the population with less than high school education are within 15 km of a monitor for the 15 CSAs/CBSAs studied. Populations of those above the poverty line, those with a high school or more education, and those with a college education within 15 km of a monitor were less than the low SES groups (67% for each). For PM₁₀, 47% of the population below the poverty level and 45% of the population with less than a high school education are within 15 km of a monitor, whereas the percentage of those above the poverty line (39%), those with a high school or more education (38%), and those with a college education (35%) were slightly less. Higher percentages of individual SES subpopulations within a given distance of PM_{2.5} monitors relative to PM₁₀ monitors likely reflect the fact that more PM_{2.5} monitors are currently deployed within the 15 CSAs/CBSAs studied compared with PM₁₀ monitors. Lower SES groups are not shown to be well-represented at the neighborhood scale, with 1.2% of the population below the poverty level and 1.0% of the population with less than a high school education residing within 1 km of a PM₁₀ monitor. Likewise, 3.1% of the population below the poverty level and 2.4% of the population with less than high school education reside within 1 km of a PM_{2.5} monitor. However, the populations of low SES groups are more represented at the neighborhood scale than those for higher SES groups. For example, only about 1.5-1.7% of those above the poverty line, those with a high school or more education, or those with a college education are within 1 km of a PM_{2.5} monitor. Moreover, it is notable that at any scale shown in Table 3-7 and for both PM_{2.5} and PM₁₀, those living under the poverty line and those age 25 years and older with less than high school education have greater representation by the monitors than those above the poverty line or those age 25 and older with high school or college education.

Table 3-7. Proximity to PM_{2.5} and PM₁₀ monitors based on the population below or above the poverty line, population over age 25 with less than high school education, population over 25 with high school education, and population over 25 with college education or more^a. The figures presented here are cumulative for the 15 CSAs/CBSAs examined in Chapter 3.

SES	Proximity to PM Monitors ^b								
	Total CSA/CBSA	≤ 1 km		≤ 5 km		≤ 10 km		≤ 15 km	
	N	N	%	N	%	N	%	N	%
PROXIMITY TO PM_{2.5} MONITORS									
Below poverty line	10,645,411	330,970	3.11	3,951,549	37.12	7,107,192	66.76	8,528,731	80.12
Above poverty line	85,551,420	1,297,591	1.52	19,094,985	22.32	41,736,460	48.79	57,070,312	66.71
Less than HS education	11,606,042	276,942	2.39	3,806,208	32.80	7,225,291	62.25	8,930,174	76.94
HS education	30,583,598	444,262	1.45	6,940,261	22.69	15,152,047	49.54	20,489,904	67.00
College education	16,433,811	280,810	1.71	3,451,717	21.00	7,776,218	47.32	11,000,917	66.94
PROXIMITY TO PM₁₀ MONITORS									
Below poverty line	10,645,411	132,979	1.25	1,626,694	15.28	3,504,957	32.92	5,024,714	47.20
Above poverty line	85,551,420	485,874	0.57	8,171,398	9.55	21,096,615	24.66	33,034,279	38.61
Less than HS education	11,606,042	112,901	0.97	1,544,594	13.31	3,537,414	30.48	5,186,441	44.69
HS education	30,583,598	185,439	0.61	2,975,200	9.73	7,580,000	24.78	11,747,653	38.41
College education	16,433,811	59,892	0.36	1,229,885	7.48	3,447,148	20.98	5,722,347	34.82

^aBased on 2000 population totals

^bPercentages are given with respect to the total population per city provided.

3.5. Ambient PM Concentrations

This section describes measurements of ambient PM mass and composition made since the 2004 PM AQCD (U.S. EPA, 2004, [056905](#)) including analyses using AQS data as well as published findings. Emphasis is placed on the period from 2005-2007 which incorporates the most recent validated AQS data available at the time this document was prepared.

When the 2004 PM AQCD (U.S. EPA, 2004, [056905](#)) was written, the full nationwide PM_{2.5} compliance monitoring network had only recently been deployed, providing three years (1999-2001) of completed measurements. Based on observations from these first three years, the 2004 PM AQCD (U.S. EPA, 2004, [056905](#)) found that PM_{2.5} in eastern cities was generally more highly correlated across monitoring sites than in western cities. The higher spatial correlations in the eastern cities resulted from the more regionally dispersed sources of PM_{2.5} in the East. Although PM_{2.5} concentrations at sites within an urban area can be highly correlated, significant differences in concentrations can occur on any given day. The ratio of PM_{2.5} to PM₁₀ was found to be higher in the East than in the West in general, and values for this ratio are consistent with those found in numerous earlier studies presented in the 1996 PM AQCD (U.S. EPA, 1996, [079380](#)). Differences in the composition of PM_{2.5} between eastern and western cities were also found to be consistent with differences found in the 1996 PM AQCD (U.S. EPA, 1996, [079380](#)). Much more limited data were

available for describing the spatial variability of coarse particulate mass measured as PM_{10-2.5}, UFPs, and PM composition. The 2004 PM AQCD (U.S. EPA, 2004, [056905](#)) noted that components produced by area (e.g., traffic) and point sources are more spatially variable than regionally dispersed components (e.g., secondary SO₄²⁻). Spatial variability will affect estimates of community-scale human exposure and caution should be exercised in extrapolating conclusions from one area to another, particularly on a regional scale.

For this PM ISA, the PM_{2.5} monitoring network has been active for 8 or 9 years depending on location. Observations and analyses based on PM_{2.5} measurements reported to AQS are included in this chapter. Furthermore, by selecting locations where PM₁₀ and PM_{2.5} measurements are co-located, information about the spatiotemporal distribution of the PM_{10-2.5} size fraction is investigated. Given the form of the current standard and the relative abundance of PM₁₀ monitors in the AQS network, PM₁₀ mass concentrations are also included in this section with the understanding that PM₁₀ includes mass contributions from the smaller size fractions and therefore overlaps with PM_{2.5}, PM_{10-2.5} and UFP mass concentrations. Although compliance monitoring does not apply for UFPs because there is no ambient standard for them, new observational information is available from detailed studies in several cities. Similarly, advancements have been made in understanding PM composition from the CSN and IMPROVE networks. Descriptions of UFPs and speciated PM are covered throughout this section where information is available.

Unless otherwise specified, the PM_{2.5}, PM_{10-2.5} and PM₁₀ data utilized in this section comes from the AQS. Based on the population and exposure requirements for monitor siting in 40 CFR Part 58 described in Section 3.4.2, monitors reporting to the AQS are not uniformly distributed across the U.S. Monitors are far more abundant in urban areas than rural ones, so actual rural spatiotemporal distributions may differ considerably from those reported here. Furthermore, biases exist for some PM constituents (and hence, total mass) owing to volatilization losses of NO₃⁻ and other semi-volatile compounds and, conversely, retention of particle-bound water with hygroscopic species. The magnitude of these effects is likely to be region-specific.

Spatial distributions of PM across a range of geographic scales are covered in Section 3.5.1. Temporal behavior including trends, seasonality and hourly variability are covered in Section 3.5.2. Finally, statistical associations between different size fractions of PM and copollutants including CO, NO₂, O₃ and SO₂ are covered in Section 3.5.3.

3.5.1. Spatial Distribution

Spatial scales of interest for PM range from global and continental scales (>1000 km) down to micro scale (~5-100 m). Variation in PM concentration depends on the spatial scale and magnitude of PM sources, formation and removal mechanisms, and transport and dispersion of PM. These different sources and processes can cause substantial variation in particle size distribution and chemistry. This section addresses the spatial variability of PM by focusing primarily on AQS data across three different scales: variability across the U.S., urban-scale variability and neighborhood-scale variability. These sections are further subdivided to the extent possible into PM size fractions and composition.

3.5.1.1. Variability across the U.S.

PM_{2.5}

Figure 3-9 shows the 3-yr mean of the 24-h PM_{2.5} concentrations by county across the U.S. for 2005-2007. The data used in generating this map are from FRM or FRM-like¹ data obtained from the AQS database after applying a completeness criterion of 75% per quarter (i.e., 11 out of 15 quarterly measurements for a 1-in-6 day sampling schedule). Counties shown in white did not contain sufficient PM_{2.5} data between 2005-2007 to meet the completeness criterion as a result of either a lack of monitoring sites or a lack of adequate or complete data from existing monitoring sites within the county. Of the 3,225 U.S. counties, 540 (17%) had PM_{2.5} data meeting the completeness criterion in all three years (2005-2007). These 540 counties represent roughly 63% of the U.S. population. The fraction of the population residing within each county-average concentration range is shown on the left-hand margin of Figure 3-9. Given the number of counties with no data, the varying size of counties, and the non-uniform spacing of the monitors and population within each reporting county, this should only be taken as a rough estimate of the relationship between population and average ambient concentrations. As seen in Figure 3-9, Kern County, CA reported the highest 3-yr avg 24-h PM_{2.5} concentration in excess of 20 µg/m³. Average concentrations between 18 and 20 µg/m³ were reported for several counties in the San Joaquin Valley and inland southern California as well as Jefferson County, AL containing Birmingham and Allegheny County, PA containing Pittsburgh.

¹ FRM-like refers to PM_{2.5} concentration data associated with the parameter code “88502 - Acceptable PM_{2.5} AQI and Speciation Mass” in the AQS. These data were collected by continuous instruments which are not approved as FRM or FEM, and consequently EPA does not use these data for regulatory purposes. These data are denoted as “FRM-like” because state and local monitoring agencies have individually decided that the continuous instruments reporting these data have a degree of agreement with FRM/FEM methods that is sufficient in their opinion for the data to be used in public advisories regarding current air quality. In some cases, these data include statistical adjustments by the state/local monitoring agency based on one-time or ongoing correlation analysis with co-located FRM/FEM monitors, intended to improve the “FRM-likeness” of the continuous concentration data (e.g., Bortnick et al., 2002, [156285](#)). State/local monitoring agency decisions about whether to adjust continuous PM_{2.5} data and whether their raw or adjusted continuous PM_{2.5} data should be associated with parameter code 88502 were informed by non-binding EPA guidance issued in 2006 (Technical Note on Reporting PM_{2.5} Continuous Monitoring and Speciation Data to AQS <http://www.epa.gov/ttn/amtic/files/ambient/pm25/datamang/contrept.pdf>).

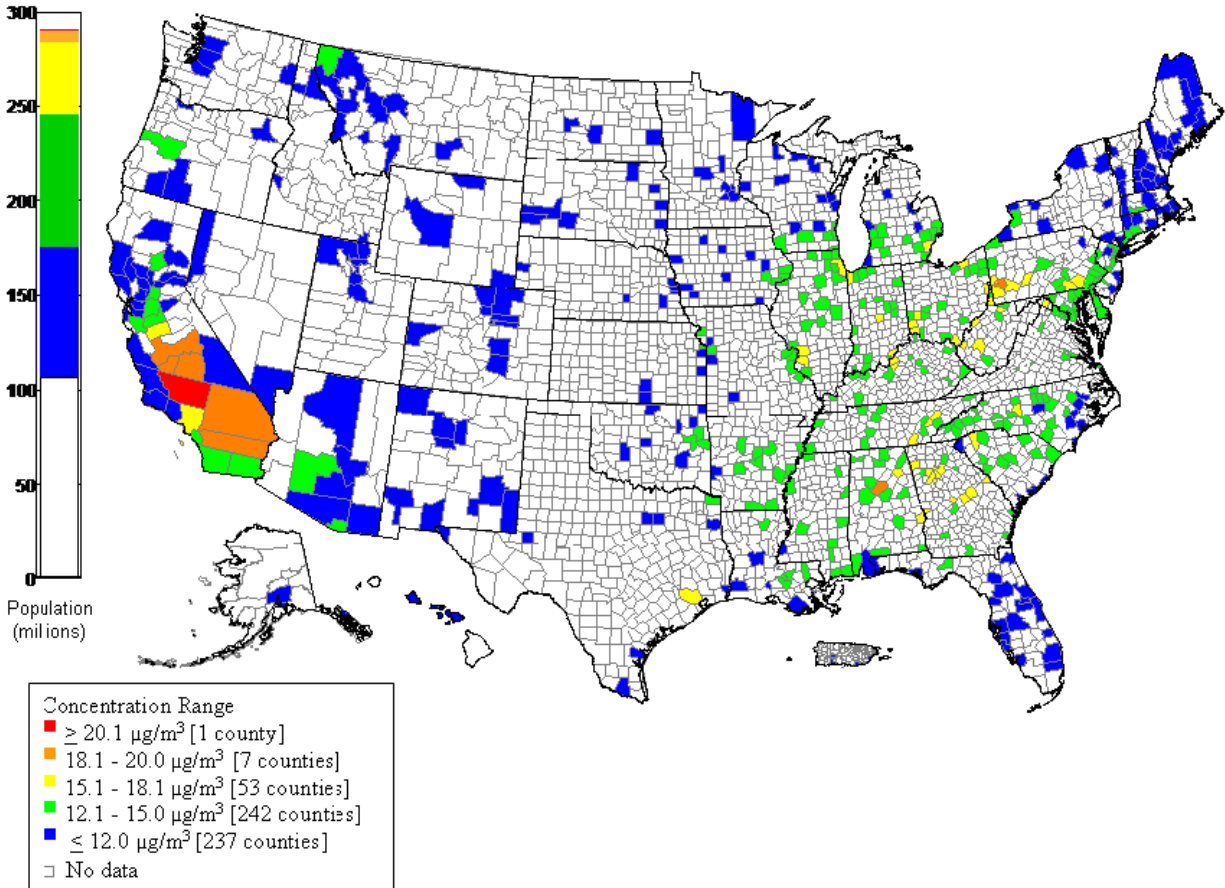


Figure 3-9. Three-yr avg 24-h $\text{PM}_{2.5}$ concentration by county derived from FRM or FRM-like data, 2005-2007. The population bar shows the number of people residing within counties that reported county-wide average concentrations within the specified ranges.

Table 3-8 contains summary statistics for $\text{PM}_{2.5}$ reported to AQS for the period 2005-2007. All 24-h FRM and 1-h FRM-like data reported to AQS and meeting the completeness criterion outlined above are included in the table. The table provides a distributional comparison between annual, 24-h and 1-h averaging times, calendar years (2005, 2006 and 2007) and seasons: winter (December-February), spring (March-May), summer (June-August), and fall (September-November). In addition, 15 CSAs/CBSAs were chosen for their importance in recent PM health studies, as described in Section 3.4, and have been included individually in the table.

The distribution of $\text{PM}_{2.5}$ annual averages (calculated without seasonal weighting and presented in Table 3-8) was generated from 2,382 individual annual means reported by 794 24-h FRM monitors reporting to AQS between 2005 and 2007. The mean of the annual averages was $12 \mu\text{g}/\text{m}^3$, equivalent to the mean of the individual 24-h avg. The maximum annual average $\text{PM}_{2.5}$ concentration calculated from 24-h FRM data over these 3 yr was $23 \mu\text{g}/\text{m}^3$ in Bakersfield, CA (AQS monitor ID: 060290010) during 2007. This site is located in the heavily populated portion of the San Joaquin Valley where air pollution frequently becomes trapped at ground level due to local topography. The distribution of the 24-h and 1-h avg, both generated from the same 1-h FRM-like data, are comparable up to the 90th percentile. The 1-h avg is $3 \mu\text{g}/\text{m}^3$ higher than the 24-h avg at the 95th percentile and $7 \mu\text{g}/\text{m}^3$ higher at the 99th percentile. This deviation between 1-h and 24-h averaging times is a result of short duration spikes in $\text{PM}_{2.5}$ mass lasting long enough to influence the upper percentiles of the 1-h distribution but not necessarily the 24-h avg distribution. Exceptional events were not removed from this data set and are responsible for at least some of the higher

concentrations observed. For example, the maximum 1-h reading of 828 $\mu\text{g}/\text{m}^3$ was reported by a monitor in Boise, ID (AQS monitor ID: 160010011) on July 4, 2007. Nine of the top 12 1-h $\text{PM}_{2.5}$ concentrations reported across the country also occurred on July 4th, implicating fireworks as the common source for these high values.

Table 3-8. $\text{PM}_{2.5}$ distributions derived from AQS data (concentration in $\mu\text{g}/\text{m}^3$).

	n	Mean	Percentiles									Max
			1	5	10	25	50	75	90	95	99	
2005-2007 $\text{PM}_{2.5}$ FOR DIFFERENT AVERAGING PERIODS												
Annual avg ^a (24-h FRM)	2,382	12	5	7	8	10	12	14	16	17	19	23
24-h avg (24-h FRM)	349,028	12	2	4	4	7	10	16	23	28	39	193
24-h avg (1-h FRM-like)	183,057	10	1	2	3	5	8	13	19	24	35	126
1-h avg (1-h FRM-like)	4,403,817	10	0	1	2	4	8	13	21	27	42	828
$\text{PM}_{2.5}$ ANNUAL AND SEASONAL STRATIFICATION USING 24-H AVG FRM DATA												
2005	114,346	13	2	4	5	7	11	17	24	30	42	133
2006	113,197	12	2	4	4	7	10	15	21	26	36	193
2007	121,485	12	2	4	4	7	10	16	22	27	40	145
Winter (December-February)	86,286	12	2	4	5	7	10	15	22	27	44	193
Spring (March-May)	88,489	11	2	3	4	6	9	14	20	24	33	145
Summer (June-August)	86,830	14	2	4	5	8	12	19	26	31	40	133
Fall (September-November)	87,423	12	2	3	4	6	10	15	22	26	39	126
2005-2007 $\text{PM}_{2.5}$ IN INDIVIDUAL CSAS/CBSAS USING 24-H AVG FRM DATA												
Atlanta	4,939	15	4	6	7	10	14	19	25	29	37	145
Birmingham	4,869	16	4	6	7	10	15	21	29	34	47	64
Boston	8,464	10	2	3	4	5	9	13	20	24	32	50
Chicago	10,308	14	3	4	6	8	13	18	25	31	42	65
Denver	4,192	9	2	3	4	6	8	10	14	18	31	61
Detroit	5,223	14	2	3	5	7	12	19	26	31	45	82
Houston	1,342	15	4	6	8	10	14	18	23	26	34	44
Los Angeles	6,600	15	3	5	6	9	13	18	25	32	50	133
New York	15,826	13	2	4	4	6	10	17	24	29	39	58
Philadelphia	7,541	14	3	4	5	8	12	18	25	30	38	63
Phoenix	1,634	10	2	3	4	6	9	12	17	21	32	77
Pittsburgh	5,783	16	3	5	6	9	13	20	29	36	52	101
Riverside	2,751	17	3	5	6	10	14	21	31	40	58	106
Seattle	1,297	9	2	3	3	4	7	10	20	29	43	68
St. Louis	6,887	14	3	5	6	9	13	18	24	29	40	50
All 15 CSAs/CBSAs	87,656	14	2	4	5	7	12	17	25	30	42	145
Not in the 15 CSAs/CBSAs	261,372	12	2	3	4	6	10	15	22	27	38	193

^aStraight annual average without quarterly weighting.

The distribution of the 24-h FRM PM_{2.5} data was similar across the 3 years (2005-2007) investigated. Summer (June-August) had the highest mean and median relative to other seasons, but only by a small margin. For the 99th percentile, winter (December-February) was slightly higher than the other seasons. This is consistent with wintertime stagnation events resulting in short-term elevated PM_{2.5} concentrations. Of the 15 CSAs/CBSAs investigated, the highest mean of 24-h PM_{2.5} concentrations was reported for Riverside (17 µg/m³), Birmingham (16 µg/m³) and Pittsburgh (16 µg/m³); the lowest was reported for Denver (9 µg/m³) and Seattle (9 µg/m³).

PM_{10-2.5}

Since PM_{10-2.5} is not routinely measured and reported to AQS, co-located PM₁₀ and PM_{2.5} measurements from the AQS network were used to investigate the spatial distribution in PM_{10-2.5}. Only low-volume FRM or FRM-like samplers were considered in calculating PM_{10-2.5} to avoid complications with vastly different sampling protocols (e.g., flow rates) between the independent PM₁₀ and PM_{2.5} measurements. The same 11+ days per quarter completeness criterion discussed above was applied to the PM₁₀ and PM_{2.5} measurements. The PM_{2.5} concentrations are reported to AQS at local conditions whereas the PM₁₀ concentrations are reported at standard conditions. Therefore, prior to calculating PM_{10-2.5} by subtraction, the PM₁₀ AQS data were adjusted to local conditions on a daily basis using temperature and pressure measurements from the nearest National Weather Service station. Figure 3-10 shows the 3-yr mean of the 24-h PM_{10-2.5} concentration by county across the U.S. for 2005-2007. There is considerably less coverage for PM_{10-2.5} than for PM_{2.5} or PM₁₀ alone since only a small subset of PM monitors are co-located and low-volume. The 40 counties included in Figure 3-10 incorporate less than 5% of the U.S. population. Of the 3,225 U.S. counties, only 40 (1%) met the completeness and co-location criteria in all 3 yr (2005-2007), and therefore the available measurements do not provide sufficient information to adequately characterize regional-scale coarse PM spatial concentration distributions.

Table 3-9 contains summary statistics for PM_{10-2.5} for the period 2005-2007 similar to those reported in Table 3-8 for PM_{2.5}. Only six of the 15 CSAs/CBSAs had sufficient data for inclusion in Table 3-9. Although fewer monitoring sites within these CSAs/CBSAs were used for PM_{10-2.5} than for PM_{2.5}, Table 3-8 and Table 3-9 provide a rough comparison of the PM present in the fine and thoracic coarse modes for these six cities. The eastern cities including Atlanta, Boston, Chicago and New York all had a higher fraction in the fine mode with the greatest ratio of fine to thoracic coarse in Chicago (14 µg/m³ PM_{2.5}, 5 µg/m³ PM_{10-2.5}, ratio = 2.8). In contrast, Denver (9 µg/m³ PM_{2.5}, 20 µg/m³ PM_{10-2.5}, ratio = 0.45) and Phoenix (10 µg/m³ PM_{2.5}, 22 µg/m³ PM_{10-2.5}, ratio = 0.45) had a higher fraction in the thoracic coarse mode. Given the limited information available from AQS for PM_{10-2.5} and the current NAAQS for PM₁₀, the next section characterizes the more prevalent PM₁₀ data, acknowledging that PM₁₀ incorporates both thoracic coarse and fine particles.

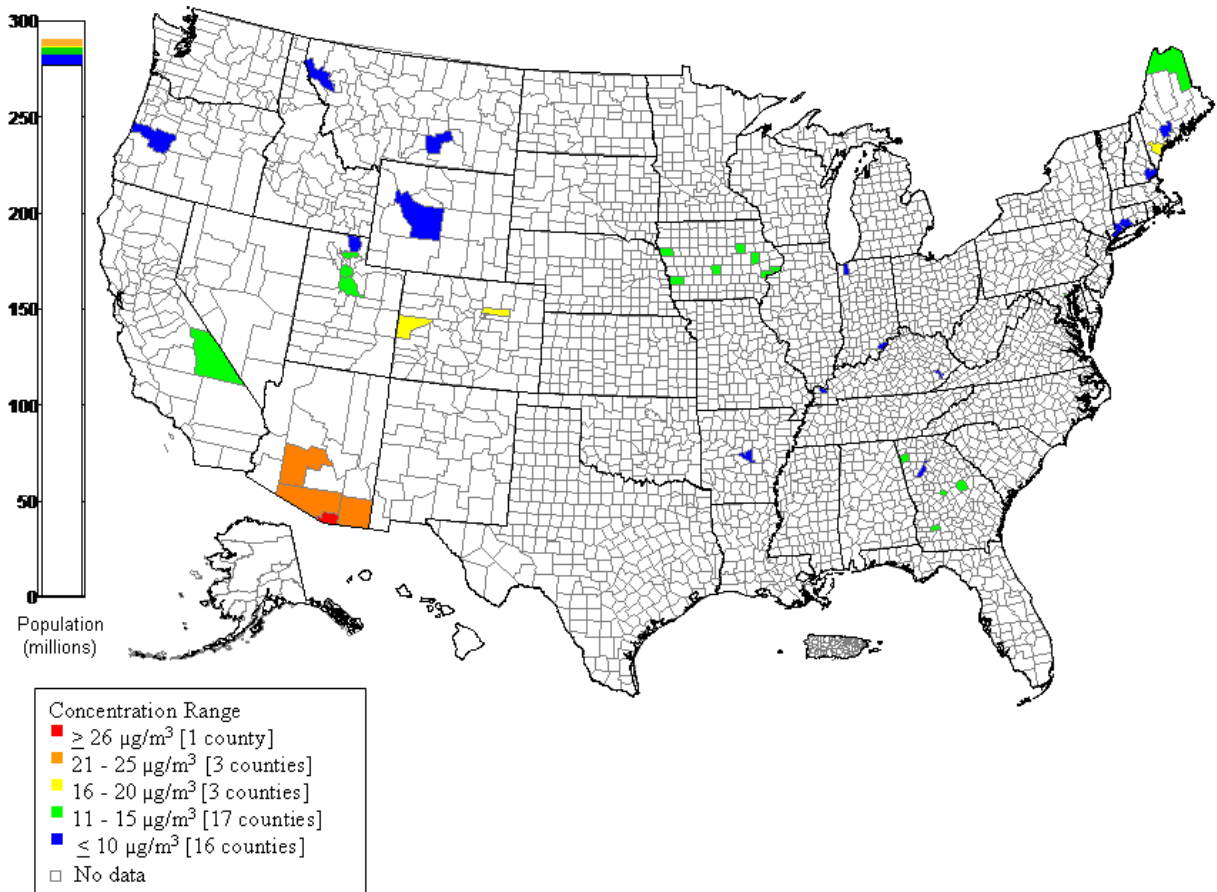


Figure 3-10. Three-yr avg 24-h $\text{PM}_{10-2.5}$ concentration by county derived from co-located low volume FRM PM_{10} and $\text{PM}_{2.5}$ monitors, 2005-2007. The population bar shows the number of people residing within counties that reported county-wide average concentrations within the specified ranges.

Table 3-9. PM_{10-2.5} distributions derived from AQS data (concentration in µg/m³).

	n	Mean	Percentiles									Max
			1	5	10	25	50	75	90	95	99	
2005-2007 PM_{10-2.5} FOR DIFFERENT AVERAGING PERIODS												
Annual avg ^a (low volume FRM)	130	12	3	5	6	9	11	14	19	23	39	43
24-h avg (low volume FRM)	12,027	13	-3	1	2	6	10	17	26	33	54	246
PM_{10-2.5} ANNUAL AND SEASONAL STRATIFICATION USING 24-H AVG LOW VOLUME FRM DATA												
2005	3,990	12	-5	0	2	5	10	16	26	33	52	246
2006	4,037	13	-2	1	2	6	10	17	27	34	56	182
2007	4,000	13	-2	1	3	6	11	18	26	33	56	148
Winter (December-February)	2,942	11	-5	-1	1	4	8	15	27	34	56	246
Spring (March-May)	3,088	13	-2	1	2	5	10	17	26	33	62	151
Summer (June-August)	2,968	14	-2	3	5	8	12	18	25	31	44	93
Fall (September-November)	3,029	14	-2	1	3	6	11	18	28	34	60	148
2005-2007 PM_{10-2.5} IN INDIVIDUAL CSAS/CBSAS USING 24-H AVG LOW VOLUME FRM DATA^b												
Atlanta	167	10	-4	1	2	5	9	13	18	21	30	46
Boston	340	7	-2	1	2	4	6	9	12	16	25	27
Chicago	161	5	-8	-4	-3	1	4	8	14	19	37	37
Denver	353	20	0	4	6	11	19	28	36	42	59	78
New York	338	9	-16	-2	1	5	8	12	17	23	34	56
Phoenix	163	22	-3	8	11	16	20	29	35	46	67	70
All 6 CSAs/CBSAs	1,522	12	-6	0	2	5	10	17	27	34	51	78
Not in the 6 CSAs/CBSAs	10,505	13	-2	1	2	6	10	17	26	33	56	246

^aStraight annual average without quarterly weighting.

^bNo co-located low-volume FRM PM₁₀ and FRM-like PM_{2.5} monitors available for Birmingham, Detroit, Houston, Los Angeles, Philadelphia, Pittsburgh, Riverside, Seattle or St. Louis.

PM₁₀

Figure 3-11 shows the 3-yr mean of the 24-h PM₁₀ concentrations by county across the U.S. for 2005-2007. Both FRM and FEM PM₁₀ data reported to AQS were included and the same 11+ days per quarter completeness criterion described above for PM_{2.5} was applied. The highest 3-yr avg for PM₁₀ (>50 µg/m³) occurred in inland southern California and the populous counties of southern Arizona and central New Mexico. Of the 3,225 U.S. counties, 676 (12%) contained PM₁₀ data meeting the completeness criterion in all three years; these 676 counties incorporate approximately 43% of the U.S. population.

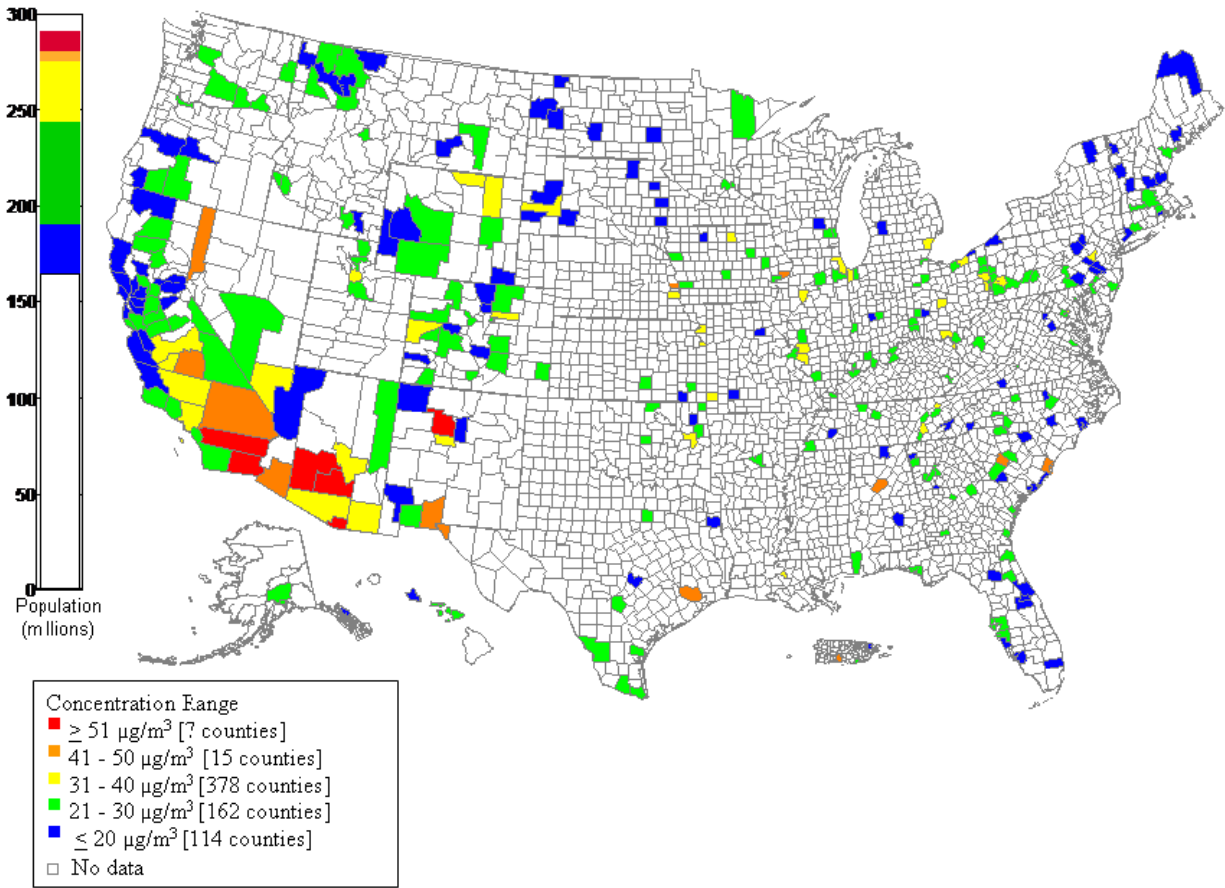


Figure 3-11. Three-yr avg 24-h PM₁₀ concentration by county derived from FRM or FEM monitors, 2005-2007. The population bar shows the number of people residing within counties that reported county-wide average concentrations within the specified ranges.

Table 3-10 contains summary statistics for PM₁₀ reported to AQS for the period 2005-2007. Both 24-h FRM and 1-h FEM data are included in the table. To facilitate a distributional comparison between averaging times, annual, 24-h and 1-h averaging times using the FRM and FEM data have been included separately in Table 3-10. As in the earlier tables, the data is also stratified by year and season and includes the 15 CSAs/CBSAs individually.

Table 3-10. PM₁₀ distributions derived from AQS data (concentration in µg/m³).

	n	Mean	Percentiles									Max
			1	5	10	25	50	75	90	95	99	
2005-2007 PM₁₀ FOR DIFFERENT AVERAGING PERIODS												
Annual avg ^a (24-h FRM and 1-h FEM)	2022	25	10	14	16	19	23	28	35	44	60	85
24-h avg (24-h FRM and 1-h FEM)	326,675	26	3	6	9	14	21	32	46	59	97	8299
24-h avg (24-h FRM)	167,310	25	2	6	9	14	21	31	45	57	91	8299
24-h avg (1-h FEM)	156,931	26	4	7	9	14	21	32	48	62	105	979
1-h avg (1-h FEM)	3,767,533	27	1	4	6	11	19	32	51	69	145	8540
PM₁₀ ANNUAL AND SEASONAL STRATIFICATION USING 24-H AVG FRM AND FEM DATA												
2005	107,524	25	2	6	9	13	21	31	46	58	93	1441
2006	109,505	26	3	6	9	13	21	32	46	59	101	8299
2007	109,646	26	4	7	9	14	21	32	47	60	99	2253
Winter (December-February)	80,959	23	2	5	7	11	17	27	42	57	99	8299
Spring (March-May)	82,772	25	2	6	8	13	20	31	45	58	96	2253
Summer (June-August)	81,351	29	6	10	12	18	25	35	49	60	92	1839
Fall (September-November)	81,593	26	3	7	9	14	21	32	48	62	102	1212
2005-2007 PM₁₀ IN INDIVIDUAL CSAS/CBSAS USING 24-H AVG FRM AND FEM DATA												
Atlanta	1,868	24	6	9	11	16	23	31	39	44	57	108
Birmingham	5,478	34	6	9	12	19	28	43	64	82	120	241
Boston	1,412	17	2	5	7	10	15	22	30	36	50	58
Chicago	6,165	26	6	9	11	16	23	32	45	55	78	214
Denver	4,706	28	5	10	12	18	25	35	47	54	75	118
Detroit	1,407	30	7	10	12	18	26	38	53	64	81	182
Houston	1,397	31	7	10	12	17	23	34	56	80	137	248
Los Angeles	2,020	27	4	8	11	18	25	33	42	51	74	489
New York	514	19	2	6	7	11	17	25	35	40	51	83
Philadelphia	4,207	19	4	7	9	12	17	24	34	40	52	84
Phoenix	12,005	52	7	14	19	29	44	65	91	112	166	2253
Pittsburgh	12,677	24	4	7	9	13	19	31	45	57	83	157
Riverside	4,327	35	4	8	11	19	30	45	64	75	111	1212
Seattle	2,136	19	5	7	9	12	17	23	31	37	52	79
St. Louis	2,464	33	6	10	12	18	28	42	59	74	114	315
All 15 CSAs/CBSAs	62,783	32	5	8	10	16	25	39	60	77	120	2253
Not in the 15 CSAs/CBSAs	263,892	24	2	6	8	13	20	30	43	54	88	8299

^aStraight annual average without quarterly weighting

The maximum annual average PM₁₀ concentration calculated from 24-h FRM data over these three years was 85 µg/m³ in Stanfield, AZ (AQS monitor ID: 040213008) during 2007. Stanfield is a small agricultural town (2007 population = 1074) approximately 64 km south of Phoenix and is in a region heavily influenced by windblown dust. Many of the maximum 24-h and 1-h avg PM₁₀ concentrations in Table 3-10 exceed 1,000 µg/m³, but these represent rare events given the much lower 99th percentiles. Exceptional events were not removed from this data set and are responsible for at least some of the higher concentrations observed.

The distribution of the 24-h FRM and FEM PM₁₀ data was similar across the three years (2005-2007) investigated. Summer (June-August) had the highest mean and median relative to other seasons, consistent with PM_{2.5} observations. Of the 15 CSAs/CBSAs investigated, the highest mean of 24-h PM₁₀ concentrations was reported for Phoenix (52 µg/m³), considerably higher than the means for the other CSAs/CBSAs investigated. The lowest was reported for Boston (17 µg/m³) with New York, Philadelphia and Seattle only slightly higher (19 µg/m³).

On average using the 2005-2007 data for PM_{2.5} in Table 3-8 and PM₁₀ in Table 3-10, the distribution between fine and coarse PM varies substantially by location. A larger fraction of PM mass is present in the thoracic coarse mode in Phoenix and Denver (3-yr mean PM_{2.5}/PM₁₀ ratios of 0.19 and 0.32, respectively). In contrast, a larger fraction is present in the fine mode in Philadelphia (0.74), New York (0.68) and Pittsburgh (0.67). Comparisons of PM_{2.5} to PM₁₀ as reported to AQS should be used with caution, however, since PM_{2.5} concentrations are reported for local conditions while PM₁₀ concentrations are converted to STP before reporting. Nevertheless, these findings are consistent with those in Table 3-9 for PM_{10-2.5} in the subset of 6 cities with available co-located low-volume PM data that have been properly adjusted for temperature and pressure. These findings are also consistent with those reported in the 2004 PM AQCD (U.S. EPA, 2004, [056905](#)) where ratios of PM_{2.5} to PM₁₀ were observed to be highest in the northeast (0.70), southeast (0.70), and industrial Midwest (0.70) and lower in the upper Midwest (0.53), northwest (0.50), southern California (0.47) and southwest (0.38).

UFPs

Little is known about the spatiotemporal distribution or composition of UFPs on a regional scale. New particle formation has been observed in environments ranging from relatively unpolluted marine and continental environments to polluted urban areas as an ongoing background process and during nucleation events (Kulmala et al., 2004, [089159](#)). During nucleation events, which may last for several hours, UFP number concentrations can exceed 10⁴ per cm³ over distances of several hundred kilometers (Kulmala et al., 2004, [089159](#); Qian et al., 2007, [116435](#)). These events occur throughout the year on 5-40% of days, depending on location (Qian et al., 2007, [116435](#)). Cloud condensation nuclei, with diameters between ~10 and ~100 nm have been monitored for several years at a number of nonurban sites in the U.S. (<http://cmdl.noaa.gov/aero/data/>). Average particle number counts at these sites in the U.S. range from several hundred to several thousand per cm³. The particles are formed by nucleation of atmospheric gases with additional contribution from primary emissions in these environments (Pierce and Adams, 2009, [191189](#)).

In an urban setting, a large percentage of UFPs come from combustion-related emissions from mobile sources (Sioutas et al., 2005, [088428](#)). UFP number concentrations drop off quickly with distance from the roadway (Levy et al., 2003, [052661](#); Reponen et al., 2003, [088425](#); Zhu et al., 2005, [157191](#)), and therefore concentrations can be highly heterogeneous in the near-road environment depending on traffic, meteorological and topographic conditions (Baldauf et al., 2008, [190239](#)). Studies characterizing spatial variability in UFPs are currently limited to a handful of close proximity locations and therefore are discussed in Sections 3.5.1.2 and 3.5.1.3 in the context of urban- and neighborhood-scale variability. Further elaboration on the composition of UFPs is included below.

PM Constituents

Only PM_{2.5} is collected routinely at CSN network sites so the majority of this section on PM constituents is devoted to PM_{2.5} composition. PM_{10-2.5} and UFP composition is discussed to the extent possible below. Figure 3-12 through Figure 3-16 contain U.S. concentration maps for OC, EC, SO₄²⁻, NO₃⁻, and NH₄⁺ mass from PM_{2.5} measurements taken as part of the CSN network for the period 2005-2007. Data used in these figures are as reported to AQS: no correction was applied to OC for non-carbon mass and NO₃⁻ represents total particulate nitrate. Figure 3-12 shows regions of

high PM_{2.5} OC mass concentration with annual average concentrations greater than 5 µg/m³ in the western and the southeastern U.S. Concentrations at the western monitors peak in the fall and winter while those in the Southeast peak anywhere from spring through fall. The central and northeastern portions of the U.S. generally contain lower measured OC. Bell et al. (2007, [155683](#)) present a similar map for estimated organic carbon mass (OCM) from 2000-2005 calculated by multiplying the blank corrected OC measurement by 1.4 to account for non-carbon mass. There are a range of estimates in the literature for suggested scaling factors (Turpin and Lim, 2001, [017093](#)), depending predominantly on how highly oxygenated the aerosol is (Pang et al., 2006, [156012](#)). Fresh PM, more common in urban regions, has undergone limited chemical transformation. As the aerosol is transported to rural regions, it becomes more oxygenated. Turpin and Lim (2001, [017093](#)) recommended ratios of 1.6 ± 0.2 for urban and 2.1 ± 0.2 for non-urban aerosols. Estimates range from 1.6 to 2.6 for rural IMPROVE monitors (El-Zanan et al., 2005, [155764](#)). Therefore, applying one correction factor of 1.4 across the entire U.S. will lead to an underestimate of the OCM in rural regions. Therefore, the OC data in Figure 3-12 is presented as measured with a national blank correction, but no adjustment to OCM.

Figure 3-13 contains a similar map for PM_{2.5} EC mass concentration that exhibits smaller seasonal variability than OC, particularly in the eastern half of the U.S. There are isolated monitors spread throughout the country that measure high annual average EC concentrations. These EC 'hot spots' are primarily associated with larger metropolitan areas such as Los Angeles, Pittsburgh, and New York, but El Paso, TX, also reported high annual average EC concentrations (driven by a wintertime average concentration greater than 2 µg/m³). In a similar analysis for EC by Bell et al. (2007, [155683](#)) for 2000-2005 data, there were also high wintertime EC concentrations in eastern Kentucky and western Montana. These particular locations do not stand out in the 2005-2007 data in Figure 3-13.

Figure 3-14 contains a map for PM_{2.5} SO₄²⁻ mass concentration which shows that SO₄²⁻ is more prevalent in the eastern U.S. owing to the strong west-to-east gradient in SO₂ emissions. This gradient is magnified in the summer months when more sunlight is available for photochemical formation of SO₄²⁻. In contrast, PM_{2.5} NO₃⁻ mass concentration in Figure 3-15 is highest in the west, particularly in California. There are also elevated concentrations of NO₃⁻ in the upper Midwest. The seasonal plots show generally higher NO₃⁻ in the wintertime as a result of temperature driven partitioning. Exceptions exist in Los Angeles and Riverside where high NO₃⁻ readings appear year-round. The PM_{2.5} NH₄⁺ mass concentration maps in Figure 3-16 shows spatial patterns related to both SO₄²⁻ and NO₃⁻ resulting from its presence in both (NH₄)₂SO₄ and NH₄NO₃. Figure A-31 through Figure A-36 in Annex A show similar U.S. concentration maps for PM_{2.5} Cu, Fe, Ni, Pb, Se and V mass concentrations as measured by XRF. There is considerably less seasonal variation in the concentration profile for these metals than OC or the ions.

For the 15 metropolitan areas identified earlier, the contribution of the major component classes to total PM_{2.5} mass was derived using the measured sulfate, adjusted NO₃⁻, derived water, inferred carbonaceous mass approach (SANDWICH) (Frank, 2006, [098909](#)). This approach uses the measured FRM PM_{2.5} mass and co-located CSN chemical constituents to perform a mass balance-based estimation of the PM_{2.5} mass fraction attributed to SO₄²⁻, NO₃⁻, EC, OCM, and crustal material. SO₄²⁻ and NO₃⁻ include associated NH₄⁺ mass and estimated particle-bound water. Furthermore, NO₃⁻ is assumed to be fully neutralized as NH₄NO₃ and has been adjusted to represent the amount retained by the FRM monitor. EC is taken as measured, and the crustal component is derived from common oxides contained in the Earth's crust (Pettijohn, 1957, [156862](#)), but can also include significant anthropogenic contributions, such as coal fly ash that are unrelated to soil resuspension. Finally, OCM is estimated using mass balance by subtracting the sum of all other constituents from the FRM PM_{2.5} mass. The SANDWICH method takes into account passive collection of semi-volatile or handling-related mass on the FRM filters in the mass balance calculation. The magnitude of this artifact is assigned a nominal value of 0.5 µg/m³, which is derived from limited analysis of FRM field blanks. Other constituents such as salt and other metallic oxides, however, are not included in these calculations and therefore the OCM fraction estimated by mass balance represents an upper bound on the FRM retained OCM. The calculations and assumptions that go into the SANDWICH method are discussed in detail in Frank (2006, [098909](#)) with further information available on EPA's AirExplorer web site http://www.epa.gov/cgi-bin/htmsQL/mxplorer/query_spe.hspl

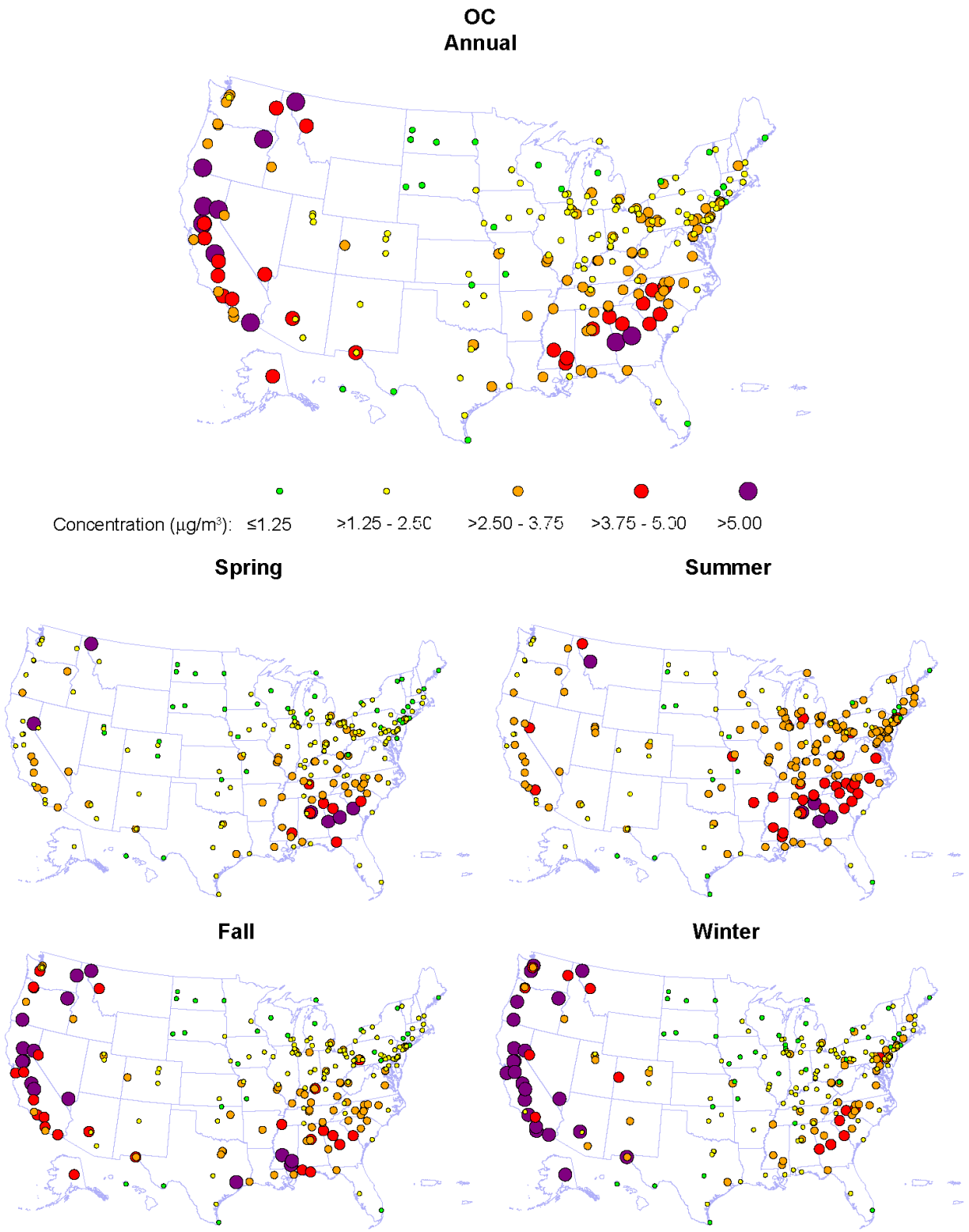


Figure 3-12. Three-yr avg 24-h $\text{PM}_{2.5}$ OC concentrations measured at CSN sites across the U.S., 2005-2007.

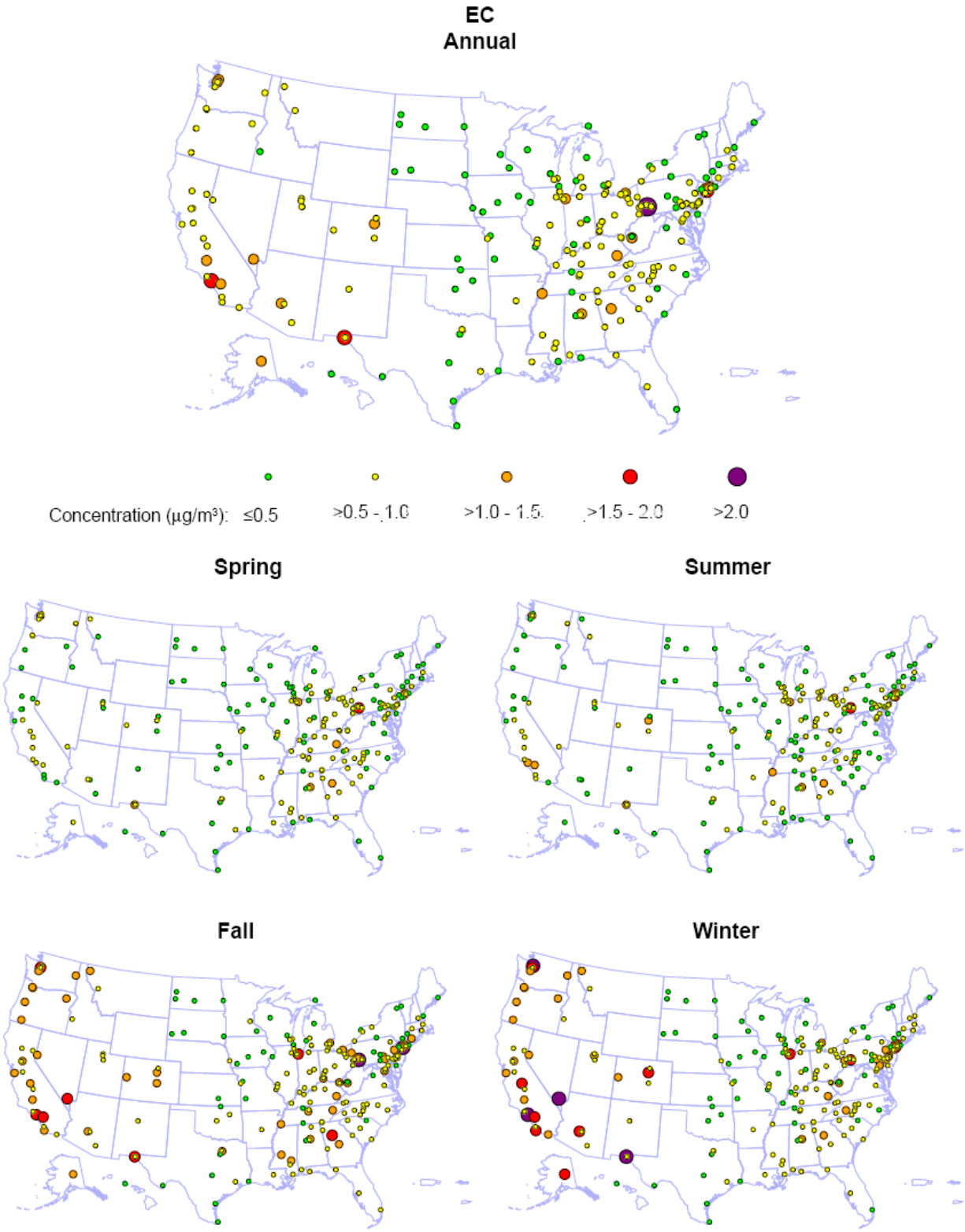


Figure 3-13. Three-yr avg 24-h $\text{PM}_{2.5}$ EC concentrations measured at CSN sites across the U.S., 2005-2007.

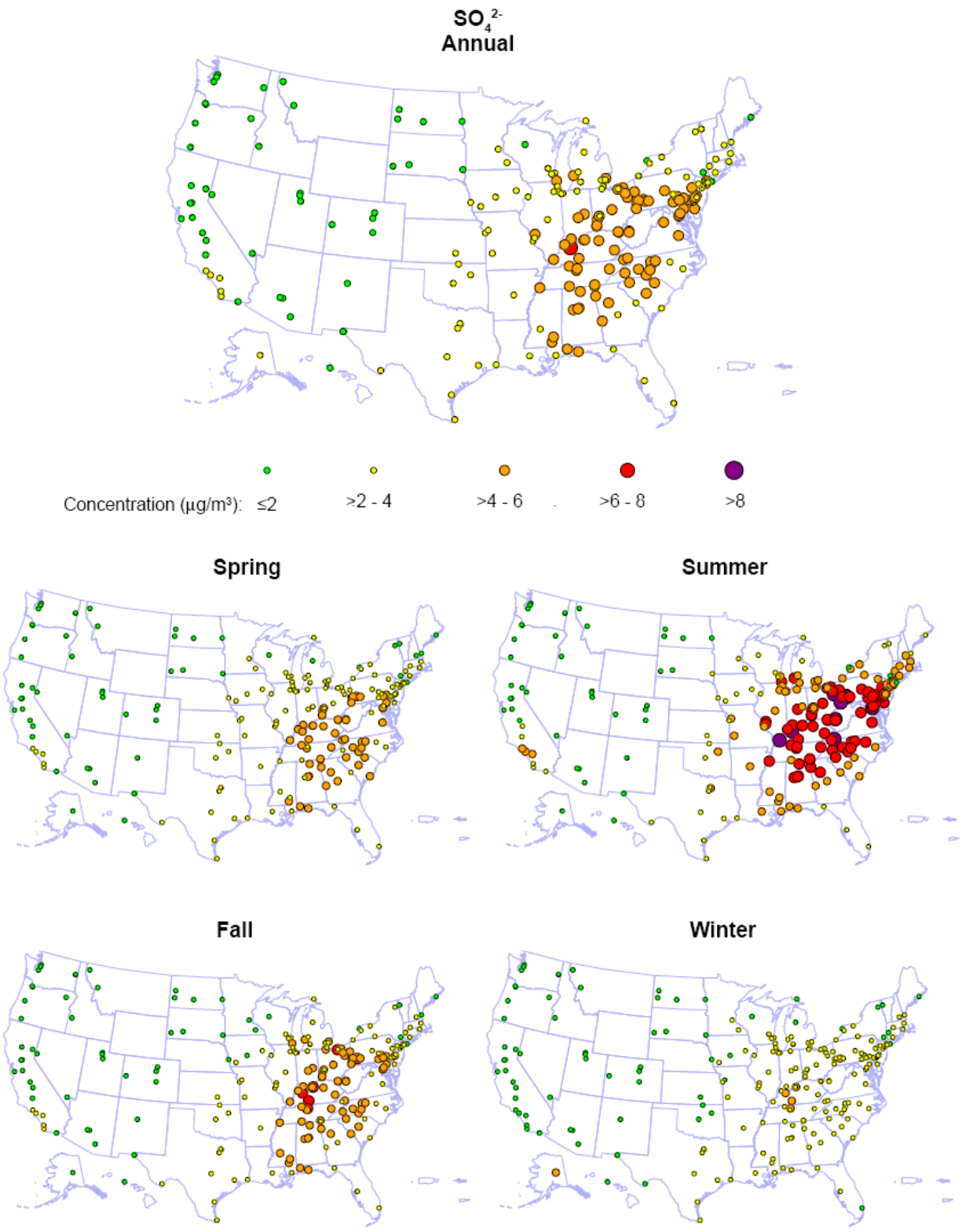


Figure 3-14. Three-yr avg 24-h PM_{2.5} SO₄²⁻ concentrations measured at CSN sites across the U.S., 2005-2007.

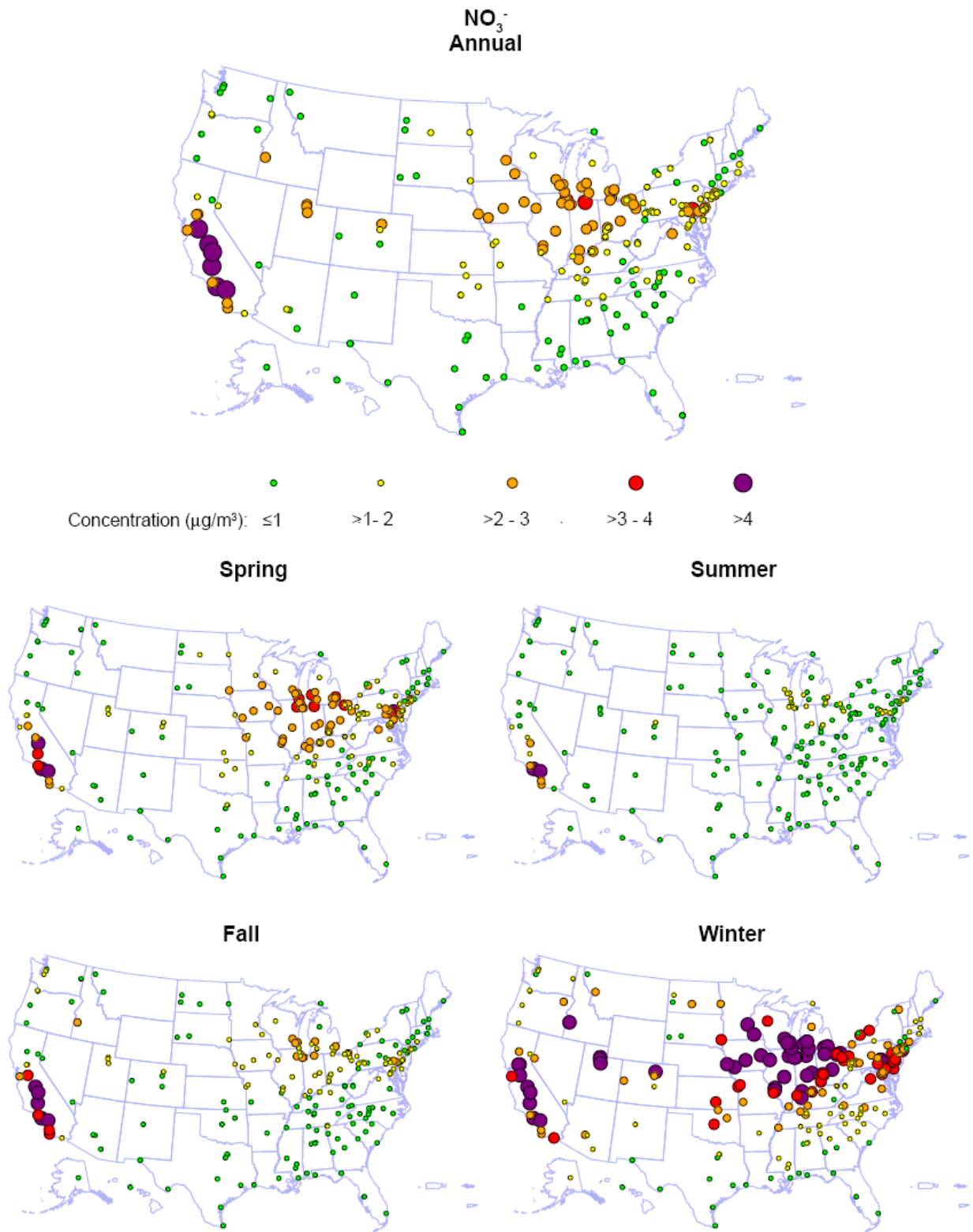


Figure 3-15. Three-yr avg 24-h PM_{2.5} NO₃⁻ concentrations measured at CSN sites across the U.S., 2005-2007.

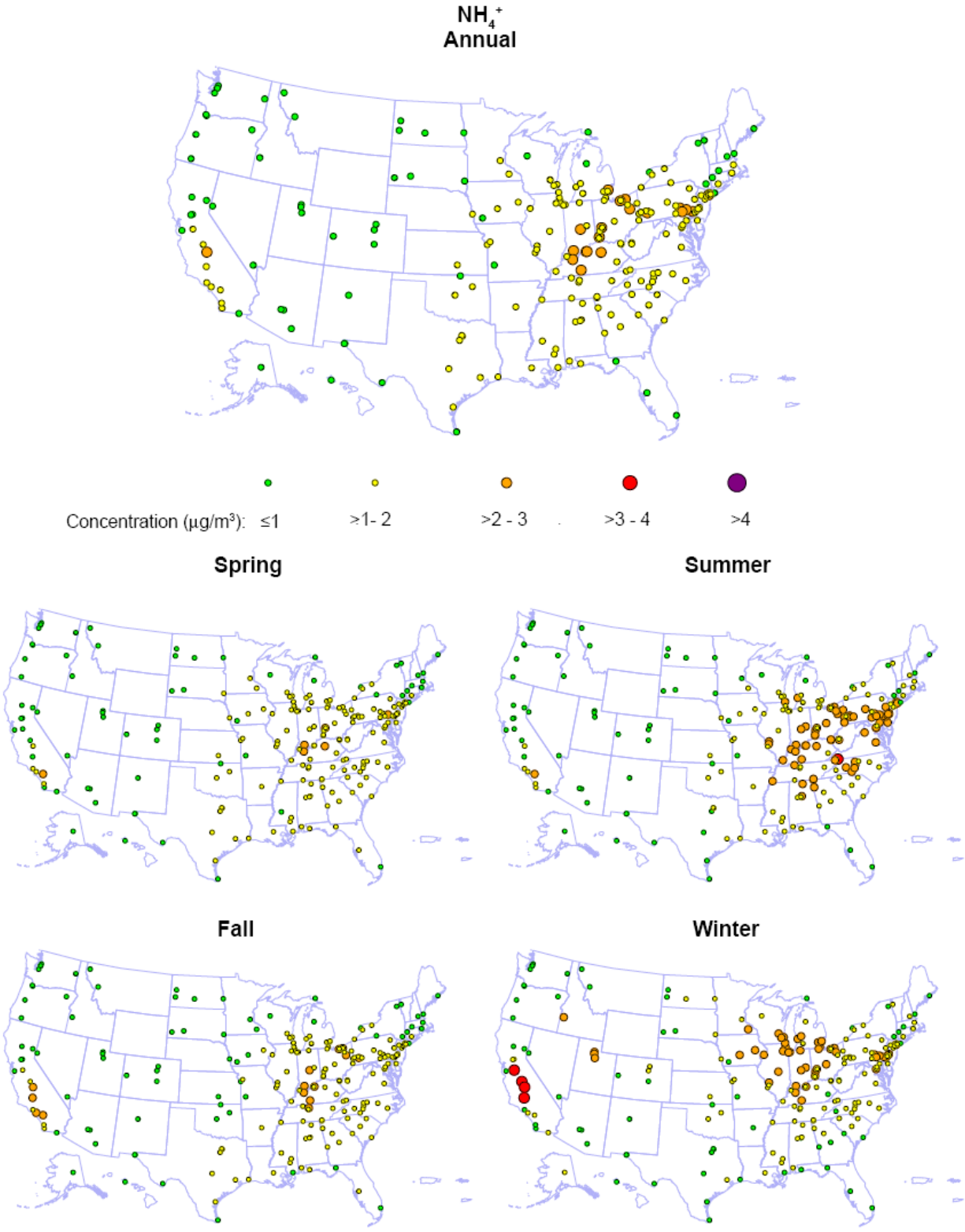


Figure 3-16. Three-yr avg 24-h PM_{2.5} NH₄⁺ concentrations measured at CSN sites across the U.S., 2005-2007.

Figure 3-17 shows the PM_{2.5} compositional breakdown for the 15 CSAs/CBSAs. All available monitoring sites with co-located FRM PM_{2.5} and CSN speciation data reporting in all four seasons for at least one calendar year from 2005-2007 were included. Furthermore, each season was required to contain five reported values for mass and the major PM_{2.5} constituents. This resulted in a varying number of sites (ranging from one to seven, as indicated in the caption to Figure 3-17) used to create the averages shown in the figure. Variability in PM_{2.5} composition within each CSA/CBSA where multiple monitors were available and trends in composition over time are discussed in subsequent sections.

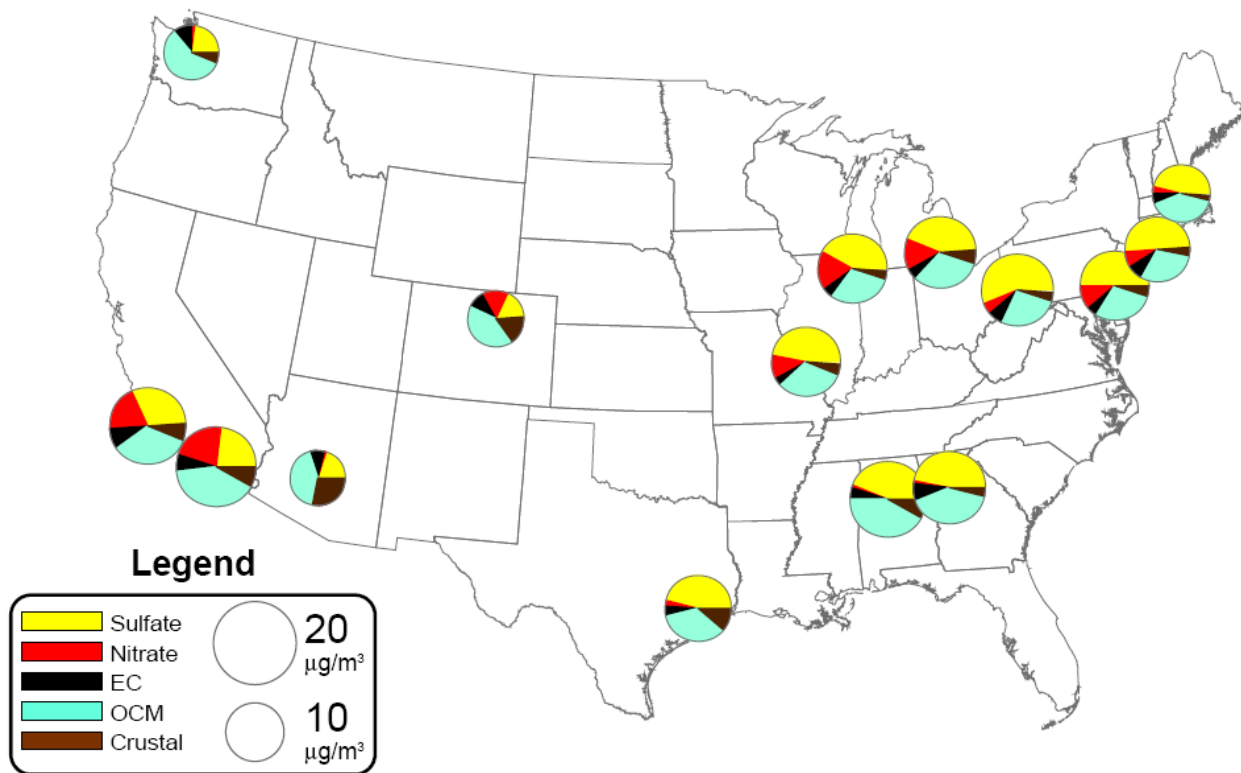


Figure 3-17. Three-yr avg PM_{2.5} speciation estimates for 2005-2007 derived using the SANDWICH method. For the following 15 CSAs/CBSAs (with the number of sites per CSA/CBSA listed in parenthesis): Atlanta, GA (1); Birmingham, AL (3); Boston, MA (4); Chicago, IL (7); Denver, CO (2); Detroit, MI (4); Houston, TX (1); Los Angeles, CA (1); New York City, NY (7); Philadelphia, PA (6); Phoenix, AZ (2); Pittsburgh, PA (4); Riverside, CA (1); Seattle, WA (4); and St. Louis, MO (3). SO₄²⁻ and NO₃⁻ estimates include NH₄⁺ and particle bound water and the circle area is scaled in proportion to FRM PM_{2.5} mass as indicated in the legend.

On an annual average basis, SO₄²⁻ is a dominant PM component in the eastern U.S. cities. For the presented cities, this includes everything east of Houston where the SO₄²⁻ fraction of PM_{2.5} ranges from 42% in Chicago to 56% in Pittsburgh on an annual average basis. OCM is the next largest component in the east ranging from 27% in Pittsburgh to 42% in Birmingham. In the west, OCM is the largest constituent on an annual basis, ranging from 34% in Los Angeles to 58% in Seattle. SO₄²⁻, NO₃⁻ and crustal material are also important in many of the included western cities. In the west, fractional SO₄²⁻ ranges from 18% in Denver to 32% in Los Angeles while fractional NO₃⁻ is relatively large in Riverside (22%), Los Angeles (19%) and Denver (15%) and less important on an annual basis in Phoenix (1%) and Seattle (2%). Crustal material is particularly prevalent in Phoenix (28%). EC makes up a smaller fraction of the PM_{2.5} (4-11%), but it is consistently present in all included cities regardless of region.

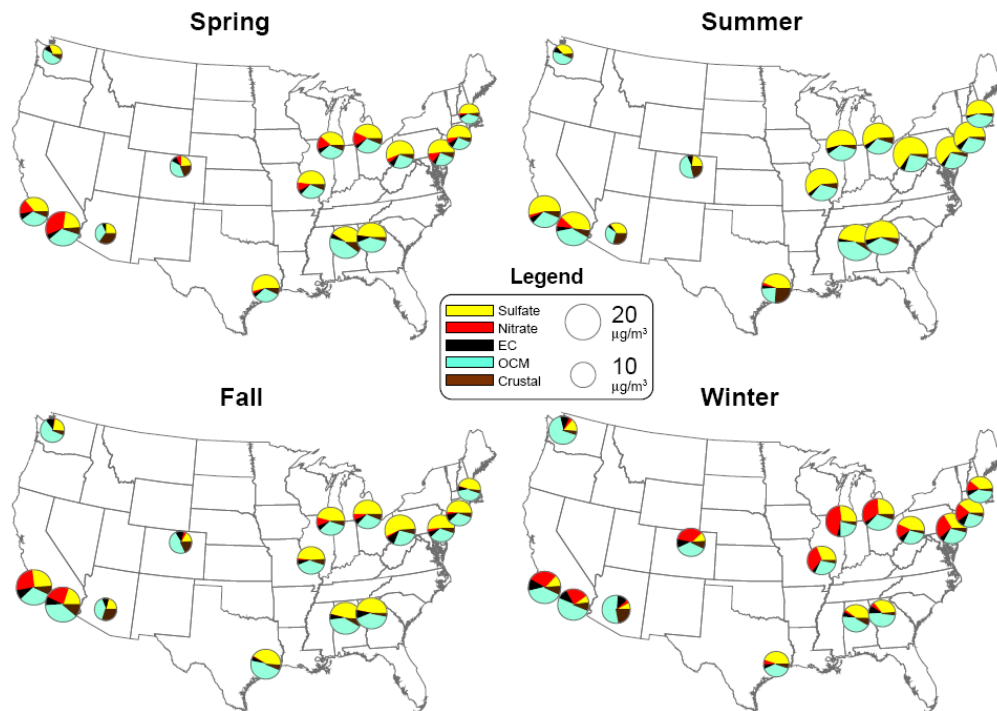


Figure 3-18. Seasonally-stratified 3-yr avg PM_{2.5} speciation estimates for 2005-2007 derived using the SANDWICH method. For the following 15 CSAs/CBSAs: Atlanta, GA; Birmingham, AL; Boston, MA; Chicago, IL; Denver, CO; Detroit, MI; Houston, TX; Los Angeles, CA; New York City, NY; Philadelphia, PA; Phoenix, AZ; Pittsburgh, PA; Riverside, CA; Seattle, WA; and St. Louis, MO. SO₄²⁻ and NO₃⁻ estimates include NH₄⁺ and particle bound water and the circle area is scaled in proportion to FRM PM_{2.5} mass as indicated in the legend.

The seasonal variation in PM_{2.5} composition across the 15 CSAs/CBSAs is shown in Figure 3-18 where the seasons are defined as before. SO₄²⁻ dominates in most metropolitan areas in the summertime, while NO₃⁻ becomes important in the colder wintertime months. Notable exceptions include Denver, Phoenix, Riverside, and Seattle where summertime SO₄²⁻ makes up a smaller fraction of the PM_{2.5} mass compared with other regions. Likewise, NO₃⁻ is less pronounced in the wintertime in Atlanta, Birmingham, Houston, Phoenix, and Seattle compared with other regions. Los Angeles and Riverside exhibit elevated NO₃⁻ from fall through spring. Crustal material is a substantial summertime component in Houston (26%), and is generally low elsewhere in the East in all seasons. In the West, crustal material represents a substantial component year-round in Phoenix and Denver.

The only PM size fraction routinely collected at CSN network sites is PM_{2.5}, resulting in less available information on speciated PM_{10-2.5}. Edgerton et al. (2005, [088686](#); 2009, [180385](#)) published speciated measurements for PM_{2.5} and PM_{10-2.5} obtained using dichotomous samplers from four locations included in the Southeastern Aerosol Research and Characterization (SEARCH) study: Yorkville, GA, Centreville, AL, Birmingham, AL and Atlanta, GA. Samples were collected between 1999 and 2003 on a 1-in-3 day or 1-in-6 day schedule, depending on site. Speciated measurements for both PM_{2.5} and PM_{10-2.5} included SO₄²⁻, NO₃⁻, NH₄⁺, and major metal oxides (MMO). In addition, OC and either black carbon (BC) or EC were reported for PM_{2.5} over the entire study period and for PM_{10-2.5} for a subset of samples extending from April 2003 to April 2004.

For the Atlanta and Birmingham SEARCH sites, the annual average NO₃⁻ mass fraction was approximately equal for PM_{2.5} (5.6% and 5.0%, respectively, for Atlanta and Birmingham) and PM_{10-2.5} (4.9% and 3.3%). Likewise, the OC mass fraction was approximately equal for PM_{2.5} (26% and 26%) and PM_{10-2.5} (24% and 27%). MMO contributed an order of magnitude smaller mass fraction to PM_{2.5} (2.6% and 4.7%) than PM_{10-2.5} (38% and 35%). In contrast, SO₄²⁻ contributed an order of

magnitude greater mass fraction to PM_{2.5} (25.1% and 24.1%) than PM_{10-2.5} (2.8 and 2.1%). BC also contributed a larger mass fraction of PM_{2.5} (8.6% and 10.5%) than EC did for PM_{10-2.5} (2.9% and 2.4%). Based on these findings, MMO are present primarily in the thoracic coarse mode, while SO₄²⁻ and EC/BC are present primarily in the fine mode. NO₃⁻ and OC are present in both modes in approximately equal mass fractions. These results are specific to Atlanta and Birmingham and may not represent other geographic regions.

Information about the composition of ambient UFPs directly emitted by sources is still sparse compared to that for the larger size modes. However, their composition is expected to reflect that of their sources. As noted in Section 3.3 (and references therein), particle number emissions from motor vehicles are dominantly in the UF size range. The composition of gasoline vehicle emissions consists mainly of a mix of OC, EC and small quantities of trace metals and sulfates, with OC constituting anywhere from 26-88% of PM. Diesel PM is generally comprised of an EC and trace metal ash core onto which organic material and nucleation-mode SO₄²⁻ condense. With the introduction of new diesel emissions standards in 2007, total emissions have decreased dramatically, particularly for carbon. In areas where atmospheric nucleation is the dominant source of UFPs, sulfate along with ammonium, and secondary organic compounds are the likely major components of UFPs.

In a study conducted at several urban sites in Southern California, Cass et al. (2000, [020680](#)) found that the composition of UFPs ranged from 32-67% OC, 3.5-17.5% EC, 1-18% SO₄²⁻, 0-19% NO₃⁻, 0-9% NH₄⁺, 1-26% metal oxides, 0-2% Na, and 0-2% Cl. Thus carbon, in various forms, was found to be the major contributor to the mass of UFPs. However, ammonium was found to contribute 33% of the mass of UFPs at one site in Riverside. Fe was the most abundant metal found in the UFPs. Chung et al. (2001, [017105](#)) found that carbon was the major component of the mass of UFPs in a study conducted during January of 1999 in Bakersfield, CA. However, in the study of Chung et al. (2001, [017105](#)), the contribution of carbonaceous species (OC and EC; typically 20-30%) was much lower than that found in the cities in Southern California. They found that Ca was the dominant cation, accounting for about 20% of the mass of UFPs in their samples. Sizable contributions from Si (0-4%) and Al (6-14%) were also found. MOUDIs are used to collect size-segregated filter samples in the UFP compositional analyses described above. Coarse particle bounce is a concern when using MOUDIs and further studies, including scanning electron microscopy, may be needed to quantify the effect of this sampling artifact on UFP compositional analyses.

Herner et al. (2005, [135983](#)) reported a gradual increase in OC mass fraction as particle size decreases from 1 μm (20% OC) to 100 nm (80% OC) in the San Joaquin Valley of California. Sardar et al. (2005, [180086](#)) found OC to be the major component of UFPs at four locations in California, with higher OC mass fraction in the wintertime relative to summertime. EC and SO₄²⁻ were also present in the UFP samples, but at much smaller mass fractions. EC was present year-round, whereas SO₄²⁻ had a summertime increase. More detailed chemical characterization of the OC fraction of ambient UFPs is extremely limited, but recent studies have identified specific organic molecular markers affiliated with motor vehicle emissions including hopanes and PAHs (Fine et al., 2004, [141283](#); Ning et al., 2007, [156809](#); Phuleria et al., 2007, [117816](#)).

As noted in the 2004 PM AQCD (U.S. EPA, 2004, [056905](#)), primary biological aerosol particles (PBAP), which include microorganisms, fragments of living things, and organic compounds of miscellaneous origin in surface deposits on filters, are not distinguishable in analyses of total OC. A clear distinction should be made between PBAP and primary OC that is produced by organisms (e.g., waxes coating the surfaces of organisms) and precursors to secondary OC such as isoprene and terpenes. Indeed, the fields of view of many photomicrographs of PM samples obtained by scanning electron microscopy are often dominated by large numbers of pollen spores, plant and insect fragments, and microorganisms. Bioaerosols such as pollen, fungal spores, and most bacteria are expected to be found mainly in the coarse size fraction (see Figure 3-2 for an illustrative example of a pollen particle). However, allergens from pollens can also be found in respirable particles (Edgerton et al., 2009, [180385](#); Taylor, 2002, [025693](#)). Matthias-Maser et al. (2000, [155972](#)) summarized information about the size distribution of PBAP in and around Mainz, Germany in what is perhaps the most complete study of this sort. Matthias-Maser found that PBAP constituted up to 30% of total particle number and volume in the approximate size range from 0.35-50 μm on an annual basis. Additionally, whereas the contribution of PBAP to the total aerosol volume did not change appreciably with season, the contribution of PBAP to total particle number ranged from about 10% in December and March to about 25% in June and October. Bauer et al. (2008, [189986](#)) measured contributions of fungal spores to OC at an urban and a suburban site in Vienna, Austria in spring and summer. Fungal spores at the suburban site contributed on average 10% to OC in PM₁₀

and 5% at the urban site. At the suburban site, in summer, fungal spores accounted on average for 60% of the OC ($0.56 \mu\text{g}/\text{m}^3$) in $\text{PM}_{10-2.1}$ ($2.6 \mu\text{g}/\text{m}^3$). The contribution to $\text{PM}_{2.1}$ was estimated to be about 10% that in $\text{PM}_{10-2.1}$. Womiloju et al. (2003, [179954](#)) estimated that fungal spores contribute 14-22% of OC in $\text{PM}_{2.5}$ in and around Toronto.

Edgerton et al. (2009, [180385](#)) found that PBAP contributed 60-70% of OC (average $\sim 1.7 \mu\text{g}/\text{m}^3$) in $\text{PM}_{10-2.5}$ at an urban and a rural site in Alabama in fall of 2000 and spring of 2001. The percentage contributions were similar at both sites and higher concentrations were found in spring than in fall. Although results for the U.S. are more limited, they are broadly consistent with the results of the other studies in illustrating the importance of PBAP, at least for fungal spores in OC.

3.5.1.2. Urban-Scale Variability

PM_{2.5}

Data from the 15 CSAs/CBSAs were used to investigate urban-scale variability in PM reported to AQS. $\text{PM}_{2.5}$ has a longer residence time in the atmosphere compared to $\text{PM}_{10-2.5}$ resulting from a slower V_d . As a result, $\text{PM}_{2.5}$ exhibits increased spatial homogeneity with relatively less localized influence from point sources. Maps of $\text{PM}_{2.5}$ monitor locations and box plots of seasonal $\text{PM}_{2.5}$ mass concentration data are provided for Boston (Figure 3-19 and Figure 3-20), Pittsburgh (Figure 3-21 and Figure 3-22), and Los Angeles (Figure 3-23 and Figure 3-24). Figures A-37 through A-80 in Annex A contain similar information for all 15 CSAs/CBSAs under investigation. With very few exceptions, the $\text{PM}_{2.5}$ concentration is quite uniformly distributed across the monitors. Los Angeles has one monitor (Site I) that reported noticeably less $\text{PM}_{2.5}$ in all four seasons than the rest of the monitors in the region. This monitor is located at Lancaster CA, separated from the rest of the Los Angeles region by the San Gabriel Mountains. In general, however, $\text{PM}_{2.5}$ varies approximately the same magnitude between monitors as it does between seasons for the 15 selected cities.

Table 3-11 through Table 3-13 contain pair-wise monitor site comparison statistics for $\text{PM}_{2.5}$ in Boston, Pittsburgh, and Los Angeles, respectively. Tables A-20 through A-34 in Annex A contain the same statistics for $\text{PM}_{2.5}$ measured within all 15 of the CSAs/CBSAs investigated. Comparison statistics shown include the Pearson correlation coefficient (R), the 90th percentile of the absolute difference in concentrations (P90), the coefficient of divergence (COD) and the number of paired observations (n). The COD provides an indication of the variability across the monitoring sites in each CSA/CBSA and is defined as follows:

$$COD_{jk} = \sqrt{\frac{1}{p} \sum_{i=1}^p \left(\frac{X_{ij} - X_{ik}}{X_{ij} + X_{ik}} \right)^2}$$

Equation 3-2

where X_{ij} and X_{ik} represent observed concentrations averaged over some measurement averaging period i (hourly, daily, etc.) at sites j and k , and p is the number of paired observations. A COD of 0 indicates there are no differences between concentrations at paired sites (spatial homogeneity), while a COD approaching 1 indicates extreme spatial heterogeneity.

Temporal correlations between 24-h $\text{PM}_{2.5}$ concentrations in Boston range from 0.61 to 0.97 in Table 3-11. The lowest correlation in this CSA was between Site A located in Fall River, MA, 1 km from the Narragansett Bay and Site L located in Nashua, NH, on the bank of the Merrimack River, 120 km north. The highest correlation was between Sites P and R, located less than a kilometer apart in Providence, RI.

In Pittsburgh, 24-h $\text{PM}_{2.5}$ correlations range from 0.65 to 0.97. The lowest correlation in this CSA was between Sites B and D, located diametrically opposite downtown Pittsburgh and 33 km apart. The highest correlation was for Sites K and D, located 21 km apart and both west of downtown. The prevailing wind in Pittsburgh is from the west, which explains the higher correlation between the two upwind sites.

In Los Angeles, 24-h $\text{PM}_{2.5}$ correlations range from 0.21 to 0.96. The lowest correlation was between Sites I and J located 123 km apart and separated by the San Gabriel Mountains as discussed

earlier. The highest correlation was for sites G and H, located 3.7 km apart and both in Long Beach, CA. Therefore, while distance between monitors plays an important role in how well any two monitors correlate, other factors such as meteorology and topography can be important as well.

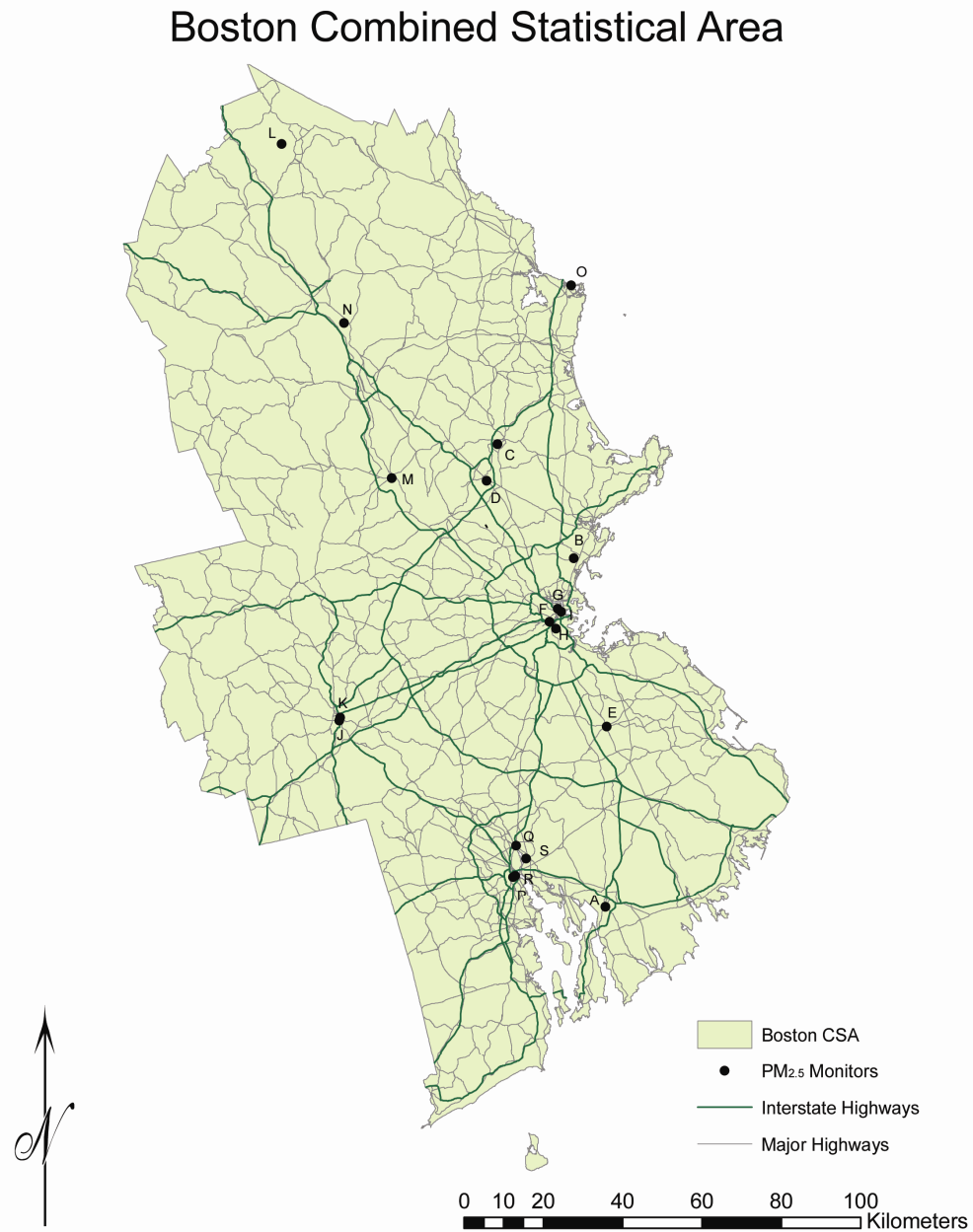


Figure 3-19. Locations of PM_{2.5} monitors and major highways, Boston, MA.

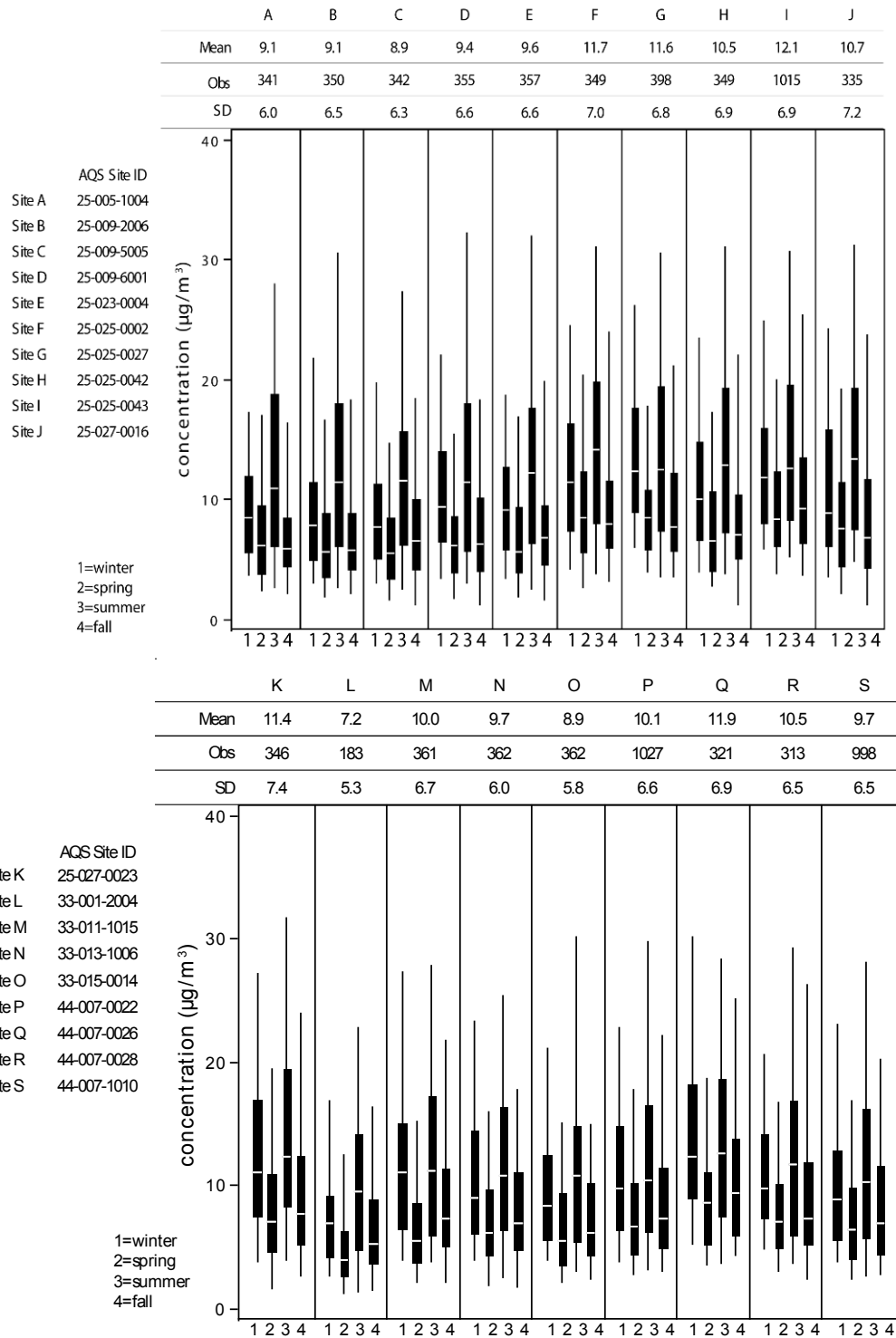


Figure 3-20. Seasonal distribution of 24-h avg PM_{2.5} concentrations by site for Boston, MA, 2005-2007. Box plots show the median and interquartile range with whiskers extending to the 5th and 95th percentiles at each site during (1) winter (December-February), (2) spring (March-May), (3) summer (June-August) and (4) fall (September-November).

Table 3-11. Inter-sampler comparison statistics for each pair of 24-h PM_{2.5} monitors reporting to AQS for Boston, MA.

Site	A	B	C	D	E	F	G	H	I	J
A	1.00 (0.0, 0.00) 341	0.80 (6.6, 0.21) 326	0.77 (6.2, 0.22) 318	0.71 (6.9, 0.23) 323	0.84 (4.8, 0.19) 329	0.79 (8.1, 0.23) 318	0.78 (7.7, 0.24) 319	0.79 (6.8, 0.22) 325	0.79 (7.9, 0.25) 338	0.77 (7.5, 0.24) 310
B		1.00 (0.0, 0.00) 350	0.92 (4.1, 0.17) 328	0.87 (4.1, 0.18) 331	0.87 (4.7, 0.19) 339	0.90 (6.3, 0.21) 326	0.90 (6.2, 0.23) 323	0.90 (4.9, 0.19) 333	0.90 (7.1, 0.26) 343	0.85 (6.5, 0.21) 317
C			1.00 (0.0, 0.00) 342	0.90 (3.5, 0.17) 321	0.85 (5.3, 0.21) 331	0.90 (6.3, 0.23) 316	0.89 (6.3, 0.24) 318	0.90 (5.0, 0.20) 326	0.88 (6.8, 0.26) 336	0.86 (6.2, 0.21) 311
D				1.00 (0.0, 0.00) 355	0.80 (5.6, 0.20) 336	0.88 (5.8, 0.21) 324	0.88 (5.8, 0.22) 329	0.86 (4.6, 0.19) 332	0.86 (7.0, 0.26) 345	0.87 (5.8, 0.19) 313
E					1.00 (0.0, 0.00) 357	0.90 (5.9, 0.19) 330	0.90 (5.8, 0.21) 333	0.89 (5.0, 0.19) 340	0.87 (6.9, 0.24) 350	0.87 (5.4, 0.20) 322
F						1.00 (0.0, 0.00) 349	0.94 (3.8, 0.14) 324	0.94 (3.5, 0.15) 324	0.92 (4.5, 0.17) 339	0.92 (5.4, 0.18) 310
G							1.00 (0.0, 0.00) 398	0.94 (4.0, 0.16) 325	0.94 (4.3, 0.15) 338	0.89 (5.7, 0.20) 308
H								1.00 (0.0, 0.00) 349	0.93 (4.7, 0.19) 342	0.89 (5.0, 0.17) 318
I									1.00 (0.0, 0.00) 1015	0.86 (6.9, 0.23) 330
J										1.00 (0.0, 0.00) 335

Site	K	L	M	N	O	P	Q	R	S
A	0.77 (8.1, 0.23)	0.61 (8.3, 0.29)	0.71 (8.0, 0.23)	0.68 (7.9, 0.23)	0.73 (7.0, 0.22)	0.87 (5.3, 0.18)	0.81 (7.2, 0.23)	0.85 (5.6, 0.20)	0.86 (5.2, 0.18)
	320	173	324	334	331	326	292	285	306
B	0.86 (6.6, 0.21)	0.80 (6.2, 0.23)	0.87 (5.3, 0.19)	0.83 (6.0, 0.21)	0.88 (4.7, 0.18)	0.86 (5.6, 0.19)	0.80 (7.9, 0.26)	0.85 (5.7, 0.21)	0.85 (6.0, 0.19)
	329	175	331	341	336	335	300	288	314
C	0.86 (6.9, 0.21)	0.89 (4.8, 0.23)	0.93 (4.4, 0.17)	0.90 (4.6, 0.19)	0.93 (3.8, 0.18)	0.83 (5.9, 0.21)	0.79 (7.8, 0.26)	0.81 (6.2, 0.23)	0.82 (6.0, 0.21)
	321	173	323	335	328	329	290	281	309
D	0.88 (6.4, 0.19)	0.79 (5.7, 0.25)	0.91 (3.5, 0.16)	0.85 (4.7, 0.19)	0.86 (4.2, 0.18)	0.80 (6.2, 0.20)	0.75 (7.8, 0.25)	0.79 (6.2, 0.21)	0.80 (5.8, 0.20)
	325	174	329	339	334	342	300	287	321
E	0.87 (6.3, 0.20)	0.72 (8.3, 0.27)	0.83 (5.8, 0.17)	0.79 (6.3, 0.20)	0.84 (4.8, 0.18)	0.91 (4.5, 0.17)	0.86 (6.3, 0.22)	0.88 (4.9, 0.18)	0.91 (3.9, 0.17)
	333	179	338	347	343	343	306	295	324
F	0.91 (4.7, 0.17)	0.78 (9.6, 0.33)	0.90 (5.3, 0.18)	0.85 (6.4, 0.20)	0.85 (7.5, 0.22)	0.89 (5.2, 0.16)	0.86 (6.0, 0.16)	0.88 (4.9, 0.16)	0.89 (5.5, 0.17)
	323	168	323	334	330	336	295	281	316
G	0.90 (5.0, 0.19)	0.77 (9.0, 0.33)	0.90 (5.3, 0.19)	0.85 (6.3, 0.20)	0.87 (7.0, 0.22)	0.88 (5.5, 0.17)	0.86 (5.3, 0.17)	0.87 (5.2, 0.17)	0.88 (5.7, 0.19)
	320	172	326	335	329	383	296	282	356
H	0.90 (4.4, 0.17)	0.75 (9.4, 0.30)	0.88 (4.9, 0.18)	0.83 (5.6, 0.21)	0.84 (6.8, 0.21)	0.89 (4.5, 0.16)	0.86 (6.0, 0.19)	0.87 (4.5, 0.16)	0.88 (5.1, 0.17)
	327	175	332	341	336	335	299	289	314
I	0.87 (6.1, 0.20)	0.75 (10.0, 0.36)	0.86 (6.7, 0.22)	0.82 (7.2, 0.23)	0.83 (8.2, 0.25)	0.88 (6.1, 0.20)	0.84 (6.0, 0.16)	0.85 (6.0, 0.18)	0.87 (6.3, 0.21)
	341	181	352	356	357	957	314	306	936
J	0.95 (3.0, 0.14)	0.73 (9.2, 0.28)	0.87 (5.2, 0.18)	0.84 (5.9, 0.20)	0.80 (7.5, 0.22)	0.90 (5.0, 0.17)	0.86 (5.9, 0.20)	0.87 (5.3, 0.17)	0.88 (5.2, 0.18)
	316	167	314	326	323	321	283	272	302
K	1.00 (0.0, 0.00)	0.71 (10.3, 0.31)	0.88 (6.0, 0.16)	0.85 (6.5, 0.19)	0.81 (8.2, 0.22)	0.89 (5.2, 0.16)	0.86 (5.8, 0.18)	0.87 (5.5, 0.16)	0.88 (5.5, 0.18)
	346	170	326	337	332	331	296	286	313
L		1.00 (0.0, 0.00)	0.89 (6.7, 0.24)	0.91 (5.9, 0.23)	0.90 (4.8, 0.21)	0.68 (10.0, 0.29)	0.63 (12.1, 0.35)	0.72 (9.1, 0.30)	0.69 (9.8, 0.29)
		183	176	181	177	181	153	149	164
M			1.00 (0.0, 0.00)	0.94 (3.8, 0.13)	0.90 (4.6, 0.16)	0.83 (5.5, 0.16)	0.81 (7.4, 0.20)	0.82 (5.8, 0.17)	0.84 (5.1, 0.16)
			361	341	336	345	300	288	326
N				1.00 (0.0, 0.00)	0.90 (4.4, 0.17)	0.77 (6.7, 0.19)	0.75 (8.1, 0.22)	0.78 (6.4, 0.20)	0.78 (6.2, 0.19)
				362	346	347	309	297	327
O					1.00 (0.0, 0.00)	0.80 (5.8, 0.19)	0.75 (8.8, 0.25)	0.79 (6.8, 0.21)	0.80 (6.0, 0.19)
					362	348	304	292	330
P						1.00 (0.0, 0.00)	0.95 (3.6, 0.14)	0.97 (2.0, 0.09)	0.97 (2.1, 0.08)
						1027	307	299	943
Q							1.00 (0.0, 0.00)	0.92 (3.1, 0.13)	0.94 (4.0, 0.16)
							321	268	290
R								1.00 (0.0, 0.00)	0.94 (2.7, 0.12)
								313	280
S									1.00 (0.0, 0.00)
									998

LEGEND
Pearson R
(P90, COD)
n

Pittsburgh Combined Statistical Area

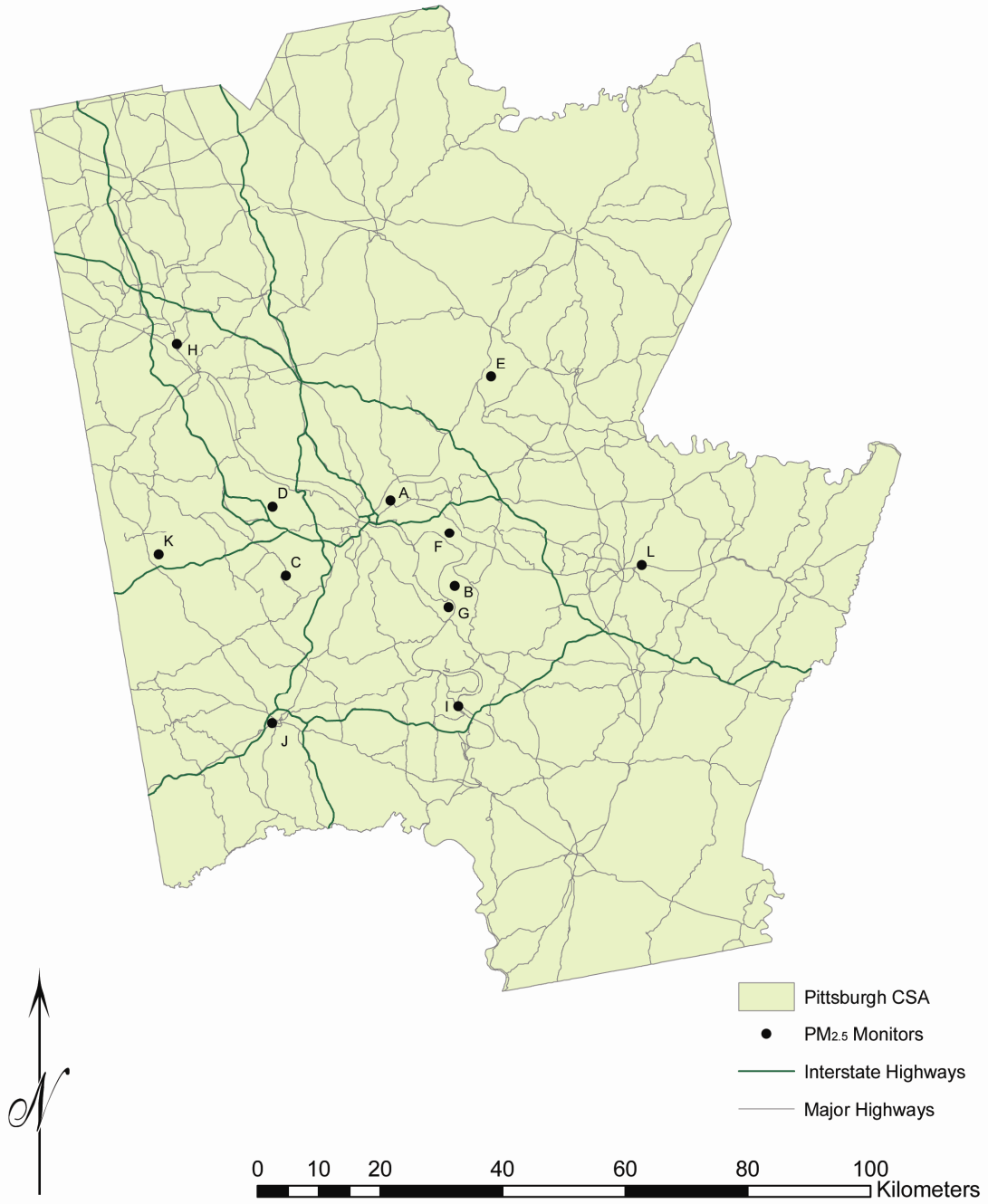


Figure 3-21. Locations of PM_{2.5} monitors and major highways, Pittsburgh, PA.

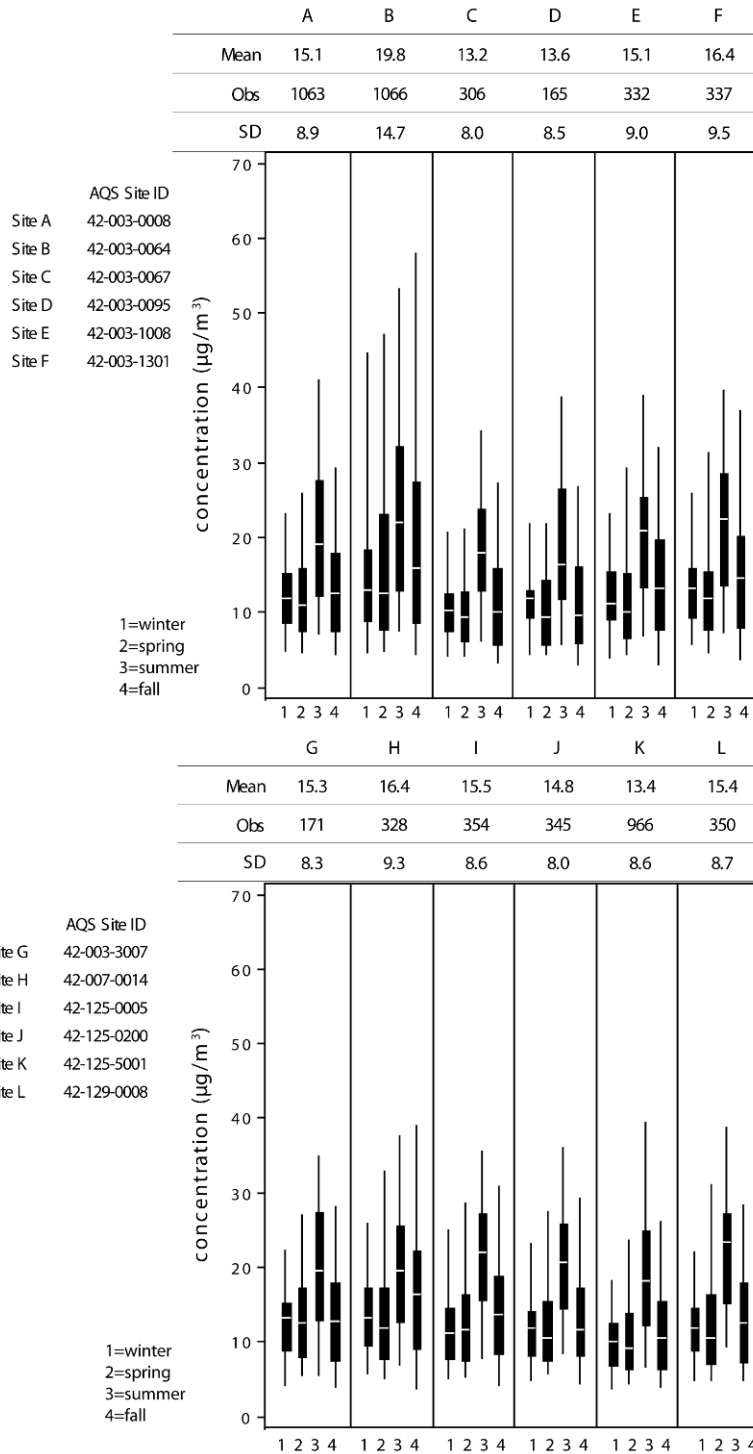


Figure 3-22. Seasonal distribution of 24-h avg PM_{2.5} concentrations by site for Pittsburgh, PA, 2005-2007. Box plots show the median and interquartile range with whiskers extending to the 5th and 95th percentiles at each site during (1) winter (December-February), (2) spring (March-May), (3) summer (June-August) and (4) fall (September-November).

Table 3-12. Inter-sampler comparison statistics for each pair of 24-h PM_{2.5} monitors reporting to AQS for Pittsburgh, PA.

	A	B	C	D	E	F	G	H	I	J	K	L
A	1.00 (0.0, 0.00)	0.79 (15.9, 0.19)	0.95 (5.6, 0.13)	0.92 (4.7, 0.11)	0.93 (4.7, 0.11)	0.95 (4.9, 0.10)	0.95 (3.8, 0.10)	0.85 (6.4, 0.13)	0.90 (6.4, 0.13)	0.93 (5.0, 0.12)	0.91 (6.0, 0.13)	0.88 (5.6, 0.12)
	1063	1035	298	164	323	329	170	319	344	337	934	340
B		1.00 (0.0, 0.00)	0.71 (16.9, 0.24)	0.65 (17.4, 0.25)	0.80 (14.4, 0.19)	0.85 (12.5, 0.14)	0.76 (15.7, 0.20)	0.69 (17.0, 0.19)	0.71 (15.7, 0.21)	0.68 (17.8, 0.23)	0.68 (19.3, 0.25)	0.67 (15.9, 0.21)
		1066	303	165	329	335	171	324	350	341	938	346
C			1.00 (0.0, 0.00)	0.93 (2.8, 0.09)	0.90 (6.6, 0.16)	0.91 (8.7, 0.17)	0.94 (6.0, 0.14)	0.80 (9.4, 0.19)	0.93 (6.7, 0.15)	0.96 (4.6, 0.12)	0.95 (4.5, 0.10)	0.91 (6.5, 0.15)
			306	144	282	282	148	268	290	286	270	286
D				1.00 (0.0, 0.00)	0.84 (6.4, 0.15)	0.87 (8.5, 0.16)	0.91 (5.8, 0.13)	0.79 (9.2, 0.17)	0.89 (5.9, 0.13)	0.91 (4.6, 0.11)	0.97 (3.1, 0.08)	0.85 (6.5, 0.15)
				165	153	161	158	156	158	155	146	157
E					1.00 (0.0, 0.00)	0.90 (6.4, 0.13)	0.90 (6.5, 0.13)	0.84 (6.8, 0.14)	0.85 (8.3, 0.16)	0.86 (7.7, 0.16)	0.88 (7.6, 0.15)	0.83 (7.3, 0.15)
					332	313	157	295	320	315	290	318
F						1.00 (0.0, 0.00)	0.91 (6.7, 0.13)	0.82 (7.4, 0.14)	0.88 (7.1, 0.15)	0.88 (7.9, 0.15)	0.89 (8.8, 0.17)	0.86 (7.0, 0.14)
						337	167	302	327	319	296	322
G							1.00 (0.0, 0.00)	0.78 (7.3, 0.16)	0.94 (4.0, 0.10)	0.93 (5.0, 0.11)	0.90 (6.6, 0.15)	0.91 (5.0, 0.13)
							171	159	163	159	149	161
H								1.00 (0.0, 0.00)	0.80 (8.4, 0.15)	0.78 (8.2, 0.17)	0.82 (9.0, 0.18)	0.70 (9.2, 0.18)
								328	317	309	288	314
I									1.00 (0.0, 0.00)	0.93 (5.0, 0.11)	0.89 (7.2, 0.16)	0.88 (6.0, 0.13)
									354	334	310	339
J										1.00 (0.0, 0.00)	0.93 (5.5, 0.12)	0.88 (5.9, 0.13)
										345	302	331
K											1.00 (0.0, 0.00)	0.86 (6.9, 0.15)
											966	306
L												1.00 (0.0, 0.00)
												350

LEGEND
Pearson R
(P90, COD)
n

Los Angeles Core Based Statistical Area



Figure 3-23. Locations of PM_{2.5} monitors and major highways, Los Angeles, CA.

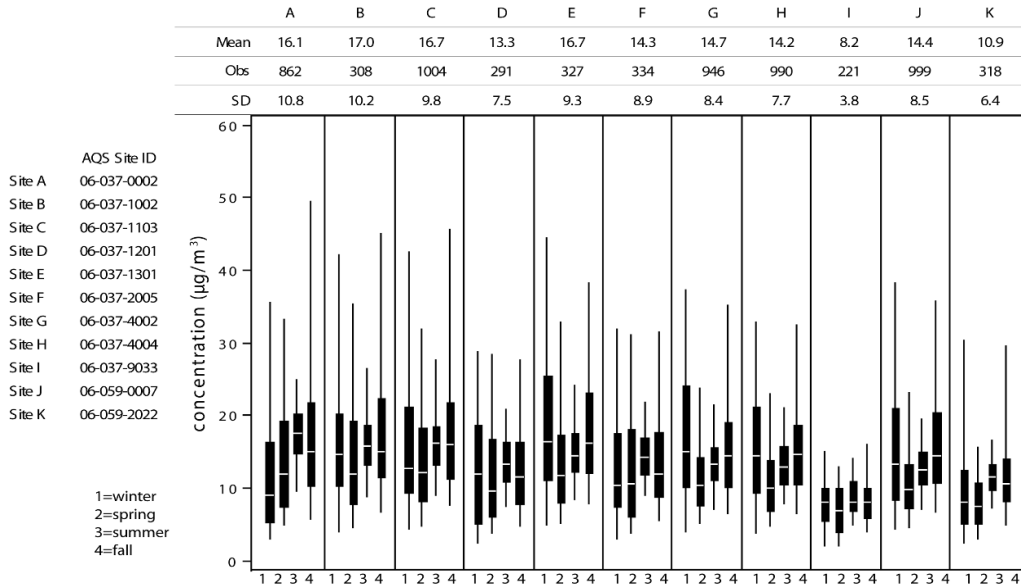


Figure 3-24. Seasonal distribution of 24-h avg PM_{2.5} concentrations by site for Los Angeles, CA, 2005-2007. Box plots show the median and interquartile range with whiskers extending to the 5th and 95th percentiles at each site during (1) winter (December-February), (2) spring (March-May), (3) summer (June-August) and (4) fall (September-November).

Table 3-13. Inter-sampler comparison statistics for each pair of 24-h PM_{2.5} monitors reporting to AQS for Los Angeles, CA.

	A	B	C	D	E	F	G	H	I	J	K
A	1.00 (0.0, 0.00) 862	0.86 (9.0, 0.18) 252	0.87 (7.7, 0.16) 803	0.81 (9.0, 0.19) 238	0.80 (9.7, 0.21) 262	0.88 (5.8, 0.14) 269	0.68 (11.5, 0.22) 761	0.64 (12.4, 0.23) 793	0.30 (18.0, 0.36) 179	0.70 (10.5, 0.21) 804	0.82 (11.4, 0.23) 259
B		1.00 (0.0, 0.00) 308	0.92 (5.5, 0.11) 293	0.87 (9.1, 0.19) 250	0.83 (9.0, 0.15) 278	0.88 (7.6, 0.15) 279	0.77 (9.8, 0.17) 268	0.73 (11.6, 0.18) 282	0.31 (24.1, 0.38) 177	0.74 (11.9, 0.19) 292	0.71 (15.0, 0.27) 277
C			1.00 (0.0, 0.00) 1004	0.80 (9.6, 0.20) 274	0.89 (5.8, 0.11) 315	0.92 (6.4, 0.13) 319	0.84 (9.0, 0.15) 880	0.79 (10.0, 0.17) 913	0.29 (18.6, 0.38) 213	0.82 (9.4, 0.16) 920	0.78 (13.2, 0.25) 305
D				1.00 (0.0, 0.00) 291	0.69 (10.9, 0.23) 263	0.77 (7.4, 0.18) 256	0.63 (11.3, 0.22) 268	0.60 (11.1, 0.22) 164	0.41 (14.8, 0.31) 164	0.64 (9.6, 0.21) 274	0.60 (11.6, 0.23) 261
E					1.00 (0.0, 0.00) 327	0.79 (9.1, 0.19) 301	0.95 (5.9, 0.11) 289	0.92 (7.6, 0.13) 301	0.34 (19.7, 0.39) 192	0.88 (8.2, 0.15) 307	0.76 (13.7, 0.27) 291
F						1.00 (0.0, 0.00) 334	0.70 (10.5, 0.18) 290	0.70 (9.2, 0.19) 302	0.33 (14.8, 0.34) 184	0.69 (9.8, 0.19) 311	0.72 (9.9, 0.21) 293
G							1.00 (0.0, 0.00) 946	0.96 (4.0, 0.09) 859	0.23 (17.0, 0.35) 194	0.92 (5.4, 0.12) 882	0.78 (11.0, 0.21) 277
H								1.00 (0.0, 0.00) 990	0.26 (15.3, 0.34) 208	0.91 (5.9, 0.12) 914	0.77 (9.5, 0.21) 294
I									1.00 (0.0, 0.00) 221	0.21 (18.3, 0.35) 205	0.31 (9.7, 0.28) 180
J										1.00 (0.0, 0.00) 999	0.84 (9.8, 0.19) 298
K											1.00 (0.0, 0.00) 318

To further investigate the relationship between correlation and distance, Figure 3-25 through Figure 3-27 plot inter-sampler correlation as a function of distance between monitors for PM_{2.5} in

Boston, Pittsburgh, and Los Angeles. These three cities were selected to illustrate how this relationship varies across urban areas with different topography and climatology as well as different $PM_{2.5}$ sources, compositions and monitor densities. Plots are provided in Annex A for all 15 CSAs/CBSAs under investigation beginning with Figure A-39. The Boston data exhibit the strongest relationship between inter-sampler correlation and distance, with average inter-sampler correlation remaining higher than 80% when samplers are 95 km apart ($R^2 = 0.55$). This small amount of variability is expected given the consistency between distributions shown in the corresponding box plots (Figure 3-20). The Pittsburgh data show some reductions in inter-sampler correlations at short distances, with the samplers at Sites B and G having only 76% correlation with a distance of less than 4 km. Site B is located in Liberty, PA, a mountainous suburb of Pittsburgh where emissions from steel manufacturing and frequent stable conditions in the planetary boundary layer cause localized events of elevated concentration. In contrast, Site G is in the neighboring town of Clairton, PA, located at a lower elevation on the bank of the opposite side of the Monongahela River from Liberty. On average, inter-sampler correlation remained higher than 80% when samplers were separated by 61 km, but in this case with much greater scatter ($R^2 = 0.22$) than observed in the Boston data. This scatter is driven by the measurements at Site B; Figure 3-22 shows an elevated mean and variability for this site compared with other monitors situated around the Pittsburgh CSA. When data from Site B are removed, the inter-sampler correlation vs. distance plot for Pittsburgh $PM_{2.5}$ resembles the one from Boston (with R^2 increasing to 0.68). The Los Angeles data exhibit a much steeper slope, with average inter-sampler correlation remaining higher than 80% when samplers are 29 km apart ($R^2 = 0.74$). This suggests that other factors, such as mountainous topography separating monitors, the distribution of traffic, re suspension of crustal components, and occurrence of stable boundary layers, may cause more spatial variation in the $PM_{2.5}$ concentration profile within the Los Angeles region when compared with other parts of the country. The Site I monitor, separated from the rest of the Los Angeles region by the San Gabriel Mountains as mentioned above, provides the low correlations grouped in the lower right portion of Figure 3-27. It should also be noted in examining Figure 3-19, Figure 3-21, and Figure 3-23 that some monitors are often located close to major interstate highways while others in the same urban area are not. These differences in proximity of monitors to nearby major roads may also result in lower inter-monitor correlations.

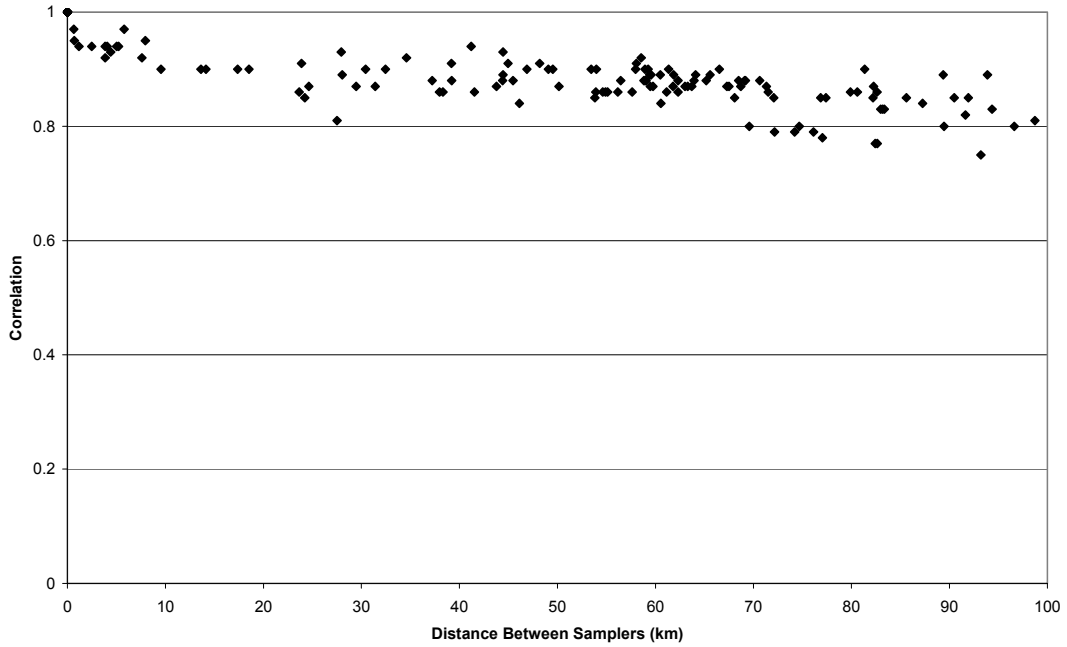


Figure 3-25. Inter-sampler correlations for 24-h PM_{2.5} as a function of distance between monitors in Boston, MA.

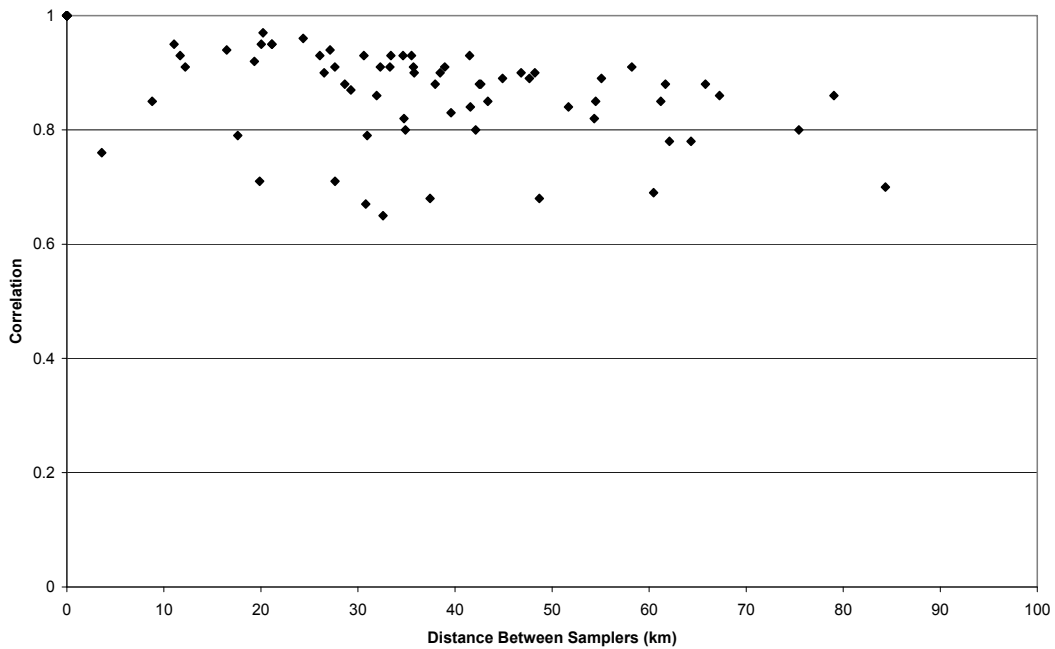


Figure 3-26. Inter-sampler correlations for 24-h PM_{2.5} as a function of distance between monitors in Pittsburgh, PA.

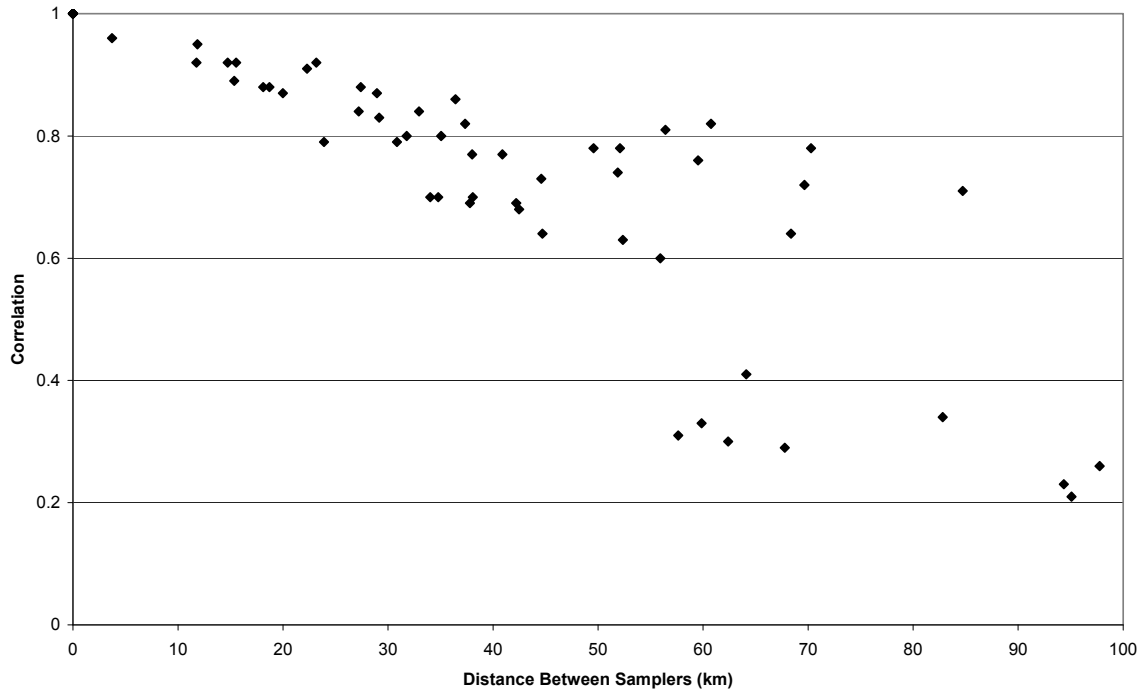


Figure 3-27. Inter-sampler correlations for 24-h $PM_{2.5}$ as a function of distance between monitors in Los Angeles, CA.

PM_{10-2.5}

Given the limited number of co-located low-volume FRM PM_{10} and FRM $PM_{2.5}$ monitors, only a very limited investigation into the intra-urban spatial variability of $PM_{10-2.5}$ was possible using AQS data. Of the 15 cities under investigation, only six (Atlanta, Boston, Chicago, Denver, New York and Phoenix) contained data sufficient for calculating $PM_{10-2.5}$ according to the data completeness and monitor specification requirements discussed earlier. Figure 3-28 contains box plots of $PM_{10-2.5}$ for one or two available sites per CSA/CBSA providing adequate $PM_{10-2.5}$ concentration data. For Boston, the correlation between the two sites for $PM_{10-2.5}$ was 0.45 compared with 0.73 for $PM_{2.5}$ alone and 0.84 for PM_{10} alone (using the same two monitoring sites). For New York, the correlation was slightly higher for the two sites: 0.74 for $PM_{10-2.5}$ compared with 0.93 for $PM_{2.5}$ alone and 0.82 for PM_{10} alone. The COD for $PM_{10-2.5}$ also increases in both cities compared with $PM_{2.5}$ and PM_{10} alone, suggesting less spatial homogeneity for thoracic coarse particles compared with fine particles. Wilson and Suh (1997, [077408](#)) reported $PM_{10-2.5}$ correlations between eight sites in Philadelphia ranging from 0.14 to 0.63 with an average of 0.38. This was considerably less than the corresponding average correlation for $PM_{2.5}$ ($r = 0.90$) and PM_{10} ($r = 0.87$) from the same study. Thornburg et al. (2009, [190999](#)) also reported a high degree of spatial variability in $PM_{10-2.5}$ in Detroit with between-monitor correlations ranging from 0.03 to 0.76. These results suggest that local sources can have a substantial impact on $PM_{10-2.5}$ concentrations, resulting in a higher degree of spatial variability in $PM_{10-2.5}$ relative to $PM_{2.5}$ or PM_{10} .

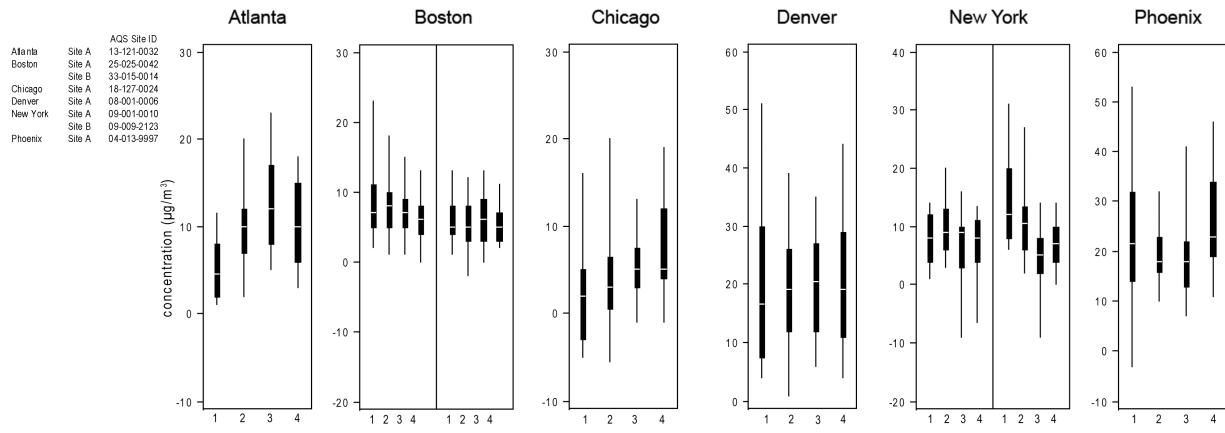


Figure 3-28. Seasonal distribution of 24-h avg $PM_{10-2.5}$ concentrations by site for Atlanta, GA; Boston, MA; Chicago, IL; Denver, CO; New York City, NY; and Phoenix, AZ; 2005-2007. Box plots show the median and interquartile range with whiskers extending to the 5th and 95th percentiles at each site during (1) winter (December-February), (2) spring (March-May), (3) summer (June-August) and (4) fall (September-November). Note the different concentration scales on the y-axes.

PM_{10}

PM_{10} mass concentration has been shown to vary as much as a factor of five over urban-scale distances of 100 km or less, and by a factor of 2 or more on scales as small as 30 km in an analysis of California air quality (Alexis et al., 2001, [079886](#)). This can be attributed to the rapid V_d and resulting short atmospheric lifetime of the coarse-mode particles making up much of PM_{10} mass. As a result, local emission sources often dominate PM_{10} annual average mass at certain monitors. Data from the 15 CSAs/CBSAs were used to investigate urban variability in PM_{10} reported to the AQS database.

Maps of PM_{10} monitor locations and box plots of seasonal PM_{10} mass concentration data are provided for Boston (Figure 3-29 and Figure 3-30), Pittsburgh (Figure 3-31 and Figure 3-32), and Los Angeles (Figure 3-33 and Figure 3-34) similar to the $PM_{2.5}$ maps and box plots shown earlier in Figure 3-19 through Figure 3-24. Annex A, Figures A-82 through A-125 incorporate similar information for all 15 CSAs/CBSAs. Table 3-14 through Table 3-16 contain pair wise, within-city comparison statistics (R, P90, COD and n, as defined above) for PM_{10} measured at the available monitors in Boston (Table 3-14), Pittsburgh (Table 3-15) and Los Angeles (Table 3-16); all 15 CSAs/CBSAs are included in Annex A, Tables A-35 through A-49.

Boston is an example of a city with a wide range in concentrations measured at different sites. Inter-monitor variation in PM_{10} is frequently larger than the seasonal variation measured at any given site. Pairwise correlations between monitors in Boston range from 0.45 to 0.95 in Table 3-14. Pittsburgh is an example of a city with a large number of PM_{10} monitors providing consistent values with a select few reporting higher concentrations (sites D, H, I and K in Figure 3-32). This illustrates the potential influence of localized point or area sources or topography. Correlations between monitors in Pittsburgh range from 0.47 to 0.97 in Table 3-15. Los Angeles shows a high degree of between-season and within-season variability, which is on the order of the between-monitor variation. Correlations between monitors in Los Angeles range from 0.29 to 0.93 in Table 3-16. Once again, the lowest correlations are with the monitor separated from the other monitors by the San Gabriel Mountains (Site E in Figure 3-33).

Boston Combined Statistical Area

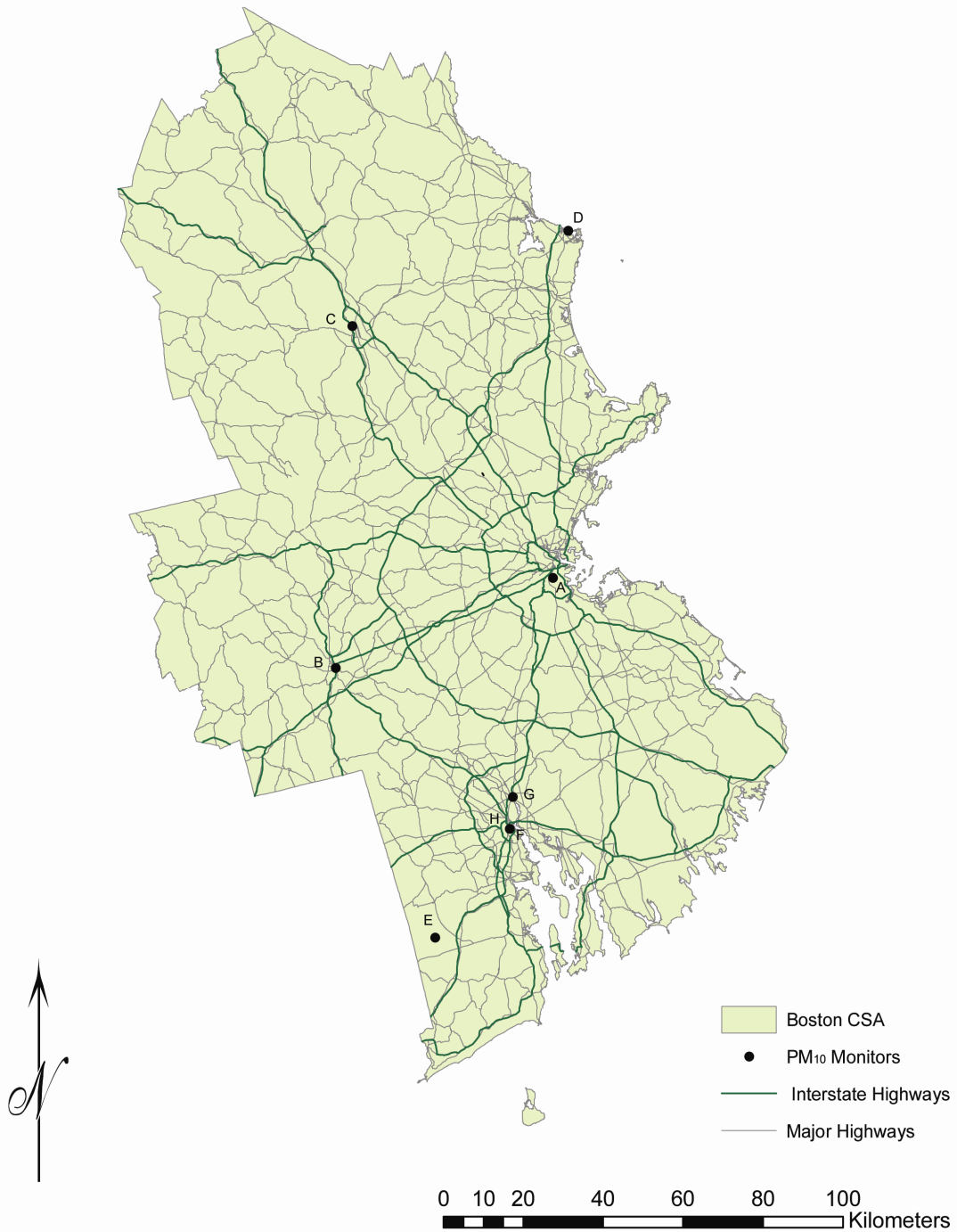


Figure 3-29. Locations of PM₁₀ monitors and major highways, Boston, MA.

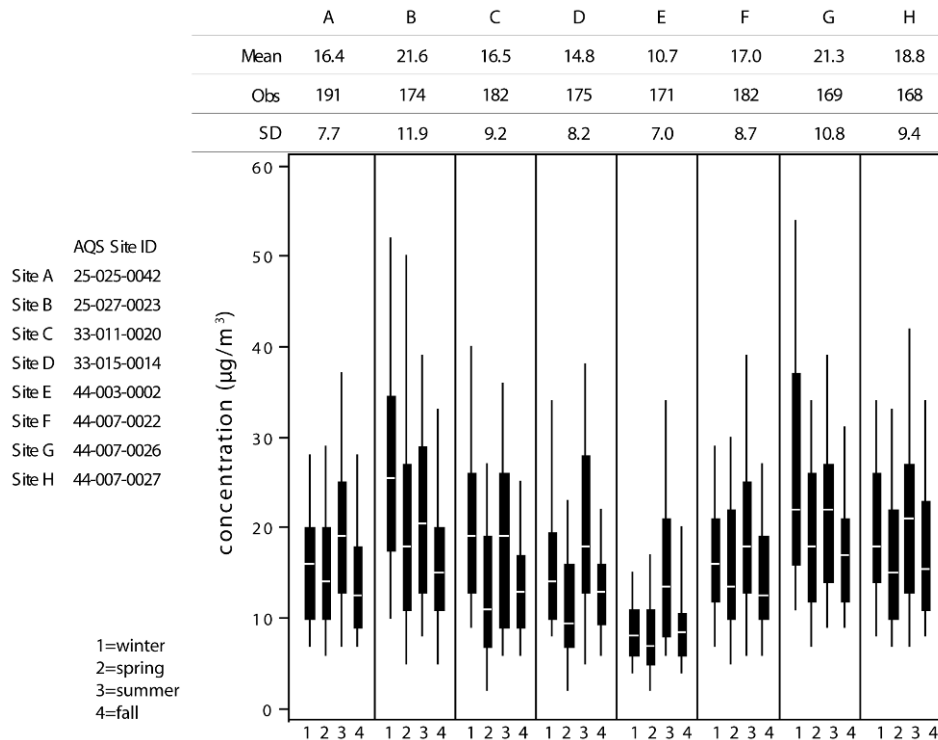


Figure 3-30. Seasonal distribution of 24-h avg PM₁₀ concentrations by site for Boston, MA, 2005-2007. Box plots show the median and interquartile range with whiskers extending to the 5th and 95th percentiles at each site during (1) winter (December-February), (2) spring (March-May), (3) summer (June-August) and (4) fall (September-November).

Table 3-14. Inter-sampler comparison statistics for each pair of 24-h PM₁₀ monitors reporting to AQS for Boston, MA.

Site	A	B	C	D	E	F	G	H
A	1.00 (0.0, 0.00) 191	0.69 (15.0, 0.22) 169	0.69 (12.0, 0.20) 179	0.73 (10.0, 0.22) 173	0.71 (13.0, 0.30) 171	0.84 (8.0, 0.14) 182	0.70 (15.0, 0.20) 169	0.79 (10.0, 0.17) 167
B		1.00 (0.0, 0.00) 174	0.66 (17.0, 0.24) 167	0.56 (19.0, 0.28) 161	0.45 (24.0, 0.39) 158	0.69 (15.0, 0.21) 169	0.77 (12.0, 0.17) 156	0.65 (16.0, 0.20) 154
C			1.00 (0.0, 0.00) 182	0.72 (10.0, 0.22) 170	0.47 (17.0, 0.33) 168	0.62 (12.0, 0.21) 179	0.64 (16.0, 0.26) 166	0.59 (16.0, 0.24) 164
D				1.00 (0.0, 0.00) 175	0.63 (11.0, 0.29) 163	0.68 (10.0, 0.23) 173	0.59 (19.0, 0.30) 161	0.69 (13.0, 0.26) 158
E					1.00 (0.0, 0.00) 171	0.84 (13.0, 0.29) 171	0.58 (22.0, 0.38) 161	0.80 (15.0, 0.33) 157
F						1.00 (0.0, 0.00) 182	0.81 (11.0, 0.16) 169	0.95 (5.0, 0.11) 167
G							1.00 (0.0, 0.00) 169	0.79 (10.0, 0.13) 154
H								1.00 (0.0, 0.00) 168

Pittsburgh Combined Statistical Area

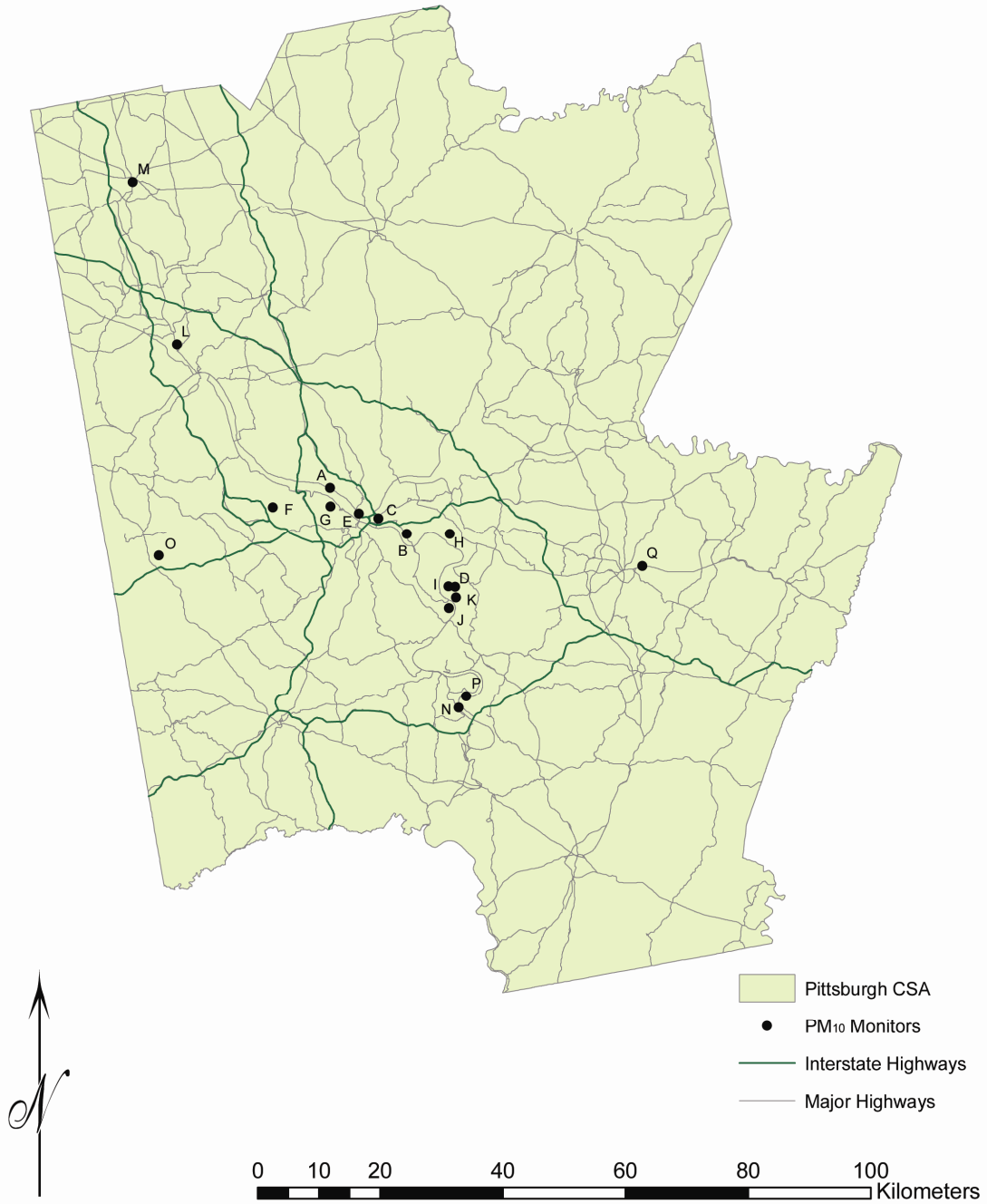


Figure 3-31. Locations of PM₁₀ monitors and major highways, Pittsburgh, PA.

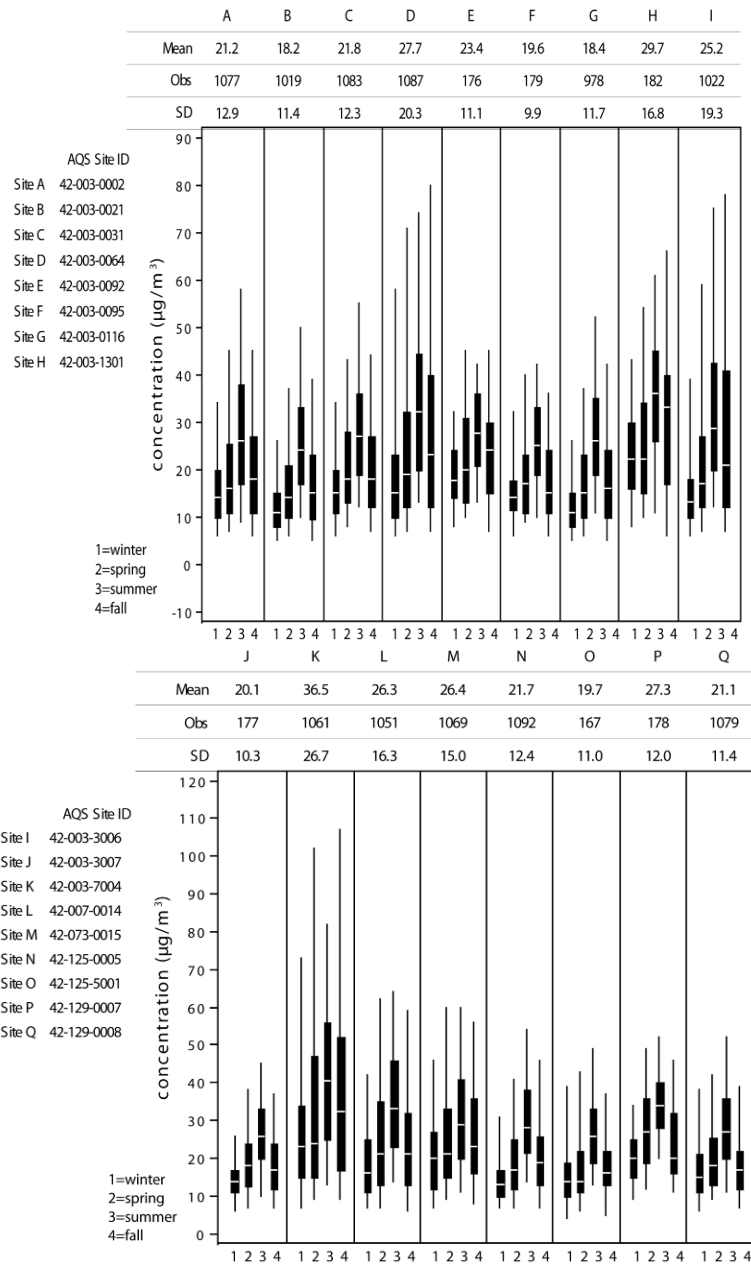


Figure 3-32. Seasonal distribution of 24-h avg PM₁₀ concentrations by site for Pittsburgh, PA, 2005-2007. Box plots show the median and interquartile range with whiskers extending to the 5th and 95th percentiles at each site during (1) winter (December-February), (2) spring (March-May), (3) summer (June-August) and (4) fall (September-November).

Table 3-15. Inter-sampler comparison statistics for each pair of 24-h PM₁₀ monitors reporting to AQS for Pittsburgh, PA.

Site	A	B	C	D	E	F	G	H	I
A	1.00 (0.0, 0.00) 1077	0.93 (9.0, 0.15) 1002	0.93 (8.0, 0.14) 1065	0.80 (23.0, 0.21) 1070	0.92 (8.0, 0.12) 175	0.89 (14.0, 0.18) 178	0.93 (8.0, 0.14) 960	0.79 (16.0, 0.17) 181	0.86 (18.0, 0.18) 1005
B		1.00 (0.0, 0.00) 1019	0.96 (8.0, 0.15) 1007	0.80 (29.0, 0.24) 1012	0.91 (11.0, 0.20) 163	0.92 (6.0, 0.16) 166	0.97 (5.0, 0.10) 911	0.81 (25.0, 0.29) 169	0.89 (22.0, 0.20) 954
C			1.00 (0.0, 0.00) 1083	0.81 (23.0, 0.20) 1075	0.94 (6.0, 0.11) 173	0.93 (7.0, 0.12) 176	0.94 (8.0, 0.13) 966	0.77 (21.0, 0.22) 179	0.87 (19.0, 0.17) 1010
D				1.00 (0.0, 0.00) 1087	0.72 (21.0, 0.20) 176	0.66 (26.0, 0.24) 179	0.76 (27.0, 0.24) 970	0.83 (14.0, 0.18) 182	0.88 (16.0, 0.14) 1014
E					1.00 (0.0, 0.00) 176	0.90 (10.0, 0.14) 173	0.90 (10.0, 0.17) 154	0.78 (20.0, 0.20) 175	0.77 (20.0, 0.19) 166
F						1.00 (0.0, 0.00) 179	0.94 (7.0, 0.12) 157	0.70 (25.0, 0.27) 178	0.74 (25.0, 0.22) 168
G							1.00 (0.0, 0.00) 978	0.70 (22.0, 0.28) 160	0.87 (20.0, 0.19) 910
H								1.00 (0.0, 0.00) 182	0.76 (17.0, 0.20) 171
I									1.00 (0.0, 0.00) 1022

LEGEND
Pearson R
(P90, COD)
n

	J	K	L	M	N	O	P	Q
A	0.84 (14.0, 0.20)	0.76 (40.0, 0.30)	0.88 (15.0, 0.18)	0.85 (16.0, 0.19)	0.86 (11.0, 0.16)	0.77 (16.0, 0.22)	0.78 (15.0, 0.19)	0.86 (11.0, 0.15)
	176	1044	1033	1052	1074	166	177	1061
B	0.93 (7.0, 0.16)	0.76 (43.0, 0.36)	0.88 (19.0, 0.23)	0.81 (20.0, 0.26)	0.91 (10.0, 0.16)	0.76 (12.0, 0.19)	0.83 (18.0, 0.28)	0.88 (10.0, 0.18)
	164	986	982	994	1016	157	165	1003
C	0.90 (8.0, 0.13)	0.75 (39.0, 0.30)	0.88 (14.0, 0.17)	0.83 (15.0, 0.19)	0.89 (9.0, 0.12)	0.78 (12.0, 0.18)	0.88 (13.0, 0.19)	0.90 (9.0, 0.12)
	174	1049	1039	1057	1080	164	175	1067
D	0.73 (24.0, 0.22)	0.84 (24.0, 0.22)	0.80 (20.0, 0.18)	0.78 (20.0, 0.20)	0.76 (25.0, 0.20)	0.57 (28.0, 0.26)	0.64 (20.0, 0.25)	0.74 (26.0, 0.21)
	177	1055	1043	1061	1084	167	178	1071
E	0.86 (10.0, 0.16)	0.65 (36.0, 0.29)	0.83 (16.0, 0.16)	0.80 (14.0, 0.17)	0.84 (12.0, 0.14)	0.77 (14.0, 0.19)	0.84 (13.0, 0.16)	0.85 (11.0, 0.15)
	171	169	169	172	176	161	172	174
F	0.90 (7.0, 0.12)	0.57 (41.0, 0.34)	0.82 (20.0, 0.20)	0.75 (19.0, 0.22)	0.86 (11.0, 0.14)	0.83 (9.0, 0.15)	0.84 (16.0, 0.22)	0.86 (9.0, 0.14)
	174	172	172	175	179	164	175	177
G	0.92 (7.0, 0.13)	0.73 (45.0, 0.35)	0.87 (18.0, 0.21)	0.78 (19.0, 0.24)	0.89 (9.0, 0.15)	0.81 (11.0, 0.17)	0.84 (17.0, 0.26)	0.86 (10.0, 0.16)
	156	955	938	952	975	146	157	967
H	0.74 (23.0, 0.26)	0.68 (26.0, 0.22)	0.77 (15.0, 0.18)	0.78 (17.0, 0.18)	0.74 (21.0, 0.22)	0.60 (27.0, 0.29)	0.65 (19.0, 0.22)	0.76 (21.5, 0.24)
	176	175	175	178	182	167	177	180
I	0.79 (22.0, 0.20)	0.83 (30.0, 0.25)	0.82 (16.0, 0.17)	0.78 (18.0, 0.20)	0.81 (20.0, 0.17)	0.66 (26.0, 0.24)	0.69 (21.0, 0.25)	0.78 (22.0, 0.19)
	166	992	978	998	1019	158	167	1009
J	1.00 (0.0, 0.00)	0.66 (44.5, 0.33)	0.79 (18.0, 0.20)	0.72 (18.0, 0.22)	0.88 (8.0, 0.13)	0.78 (11.0, 0.17)	0.86 (16.0, 0.21)	0.86 (8.0, 0.15)
	177	170	170	173	177	163	173	175
K		1.00 (0.0, 0.00)	0.74 (31.0, 0.26)	0.75 (33.0, 0.24)	0.70 (40.0, 0.30)	0.47 (44.0, 0.36)	0.58 (34.0, 0.30)	0.68 (43.0, 0.30)
		1061	1017	1035	1058	160	171	1048
L		1.00 (0.0, 0.00)	0.87 (13.0, 0.16)	0.87 (13.0, 0.16)	0.85 (16.0, 0.17)	0.70 (22.0, 0.24)	0.74 (17.0, 0.21)	0.80 (18.0, 0.19)
			1051	1025	1048	160	171	1035
M			1.00 (0.0, 0.00)	0.74 (18.0, 0.21)	0.64 (19.0, 0.26)	0.67 (17.0, 0.22)	0.77 (18.0, 0.19)	
			1069	1067	163	174	1053	
N				1.00 (0.0, 0.00)	0.72 (13.0, 0.18)	0.86 (14.0, 0.20)	0.86 (10.0, 0.14)	
				1092	167	178	1076	
O					1.00 (0.0, 0.00)	0.75 (18.0, 0.25)	0.69 (14.0, 0.19)	
					167	163	165	
P						1.00 (0.0, 0.00)	0.84 (15.0, 0.21)	
						178	176	
Q							1.00 (0.0, 0.00)	
							1079	

Los Angeles Core Based Statistical Area

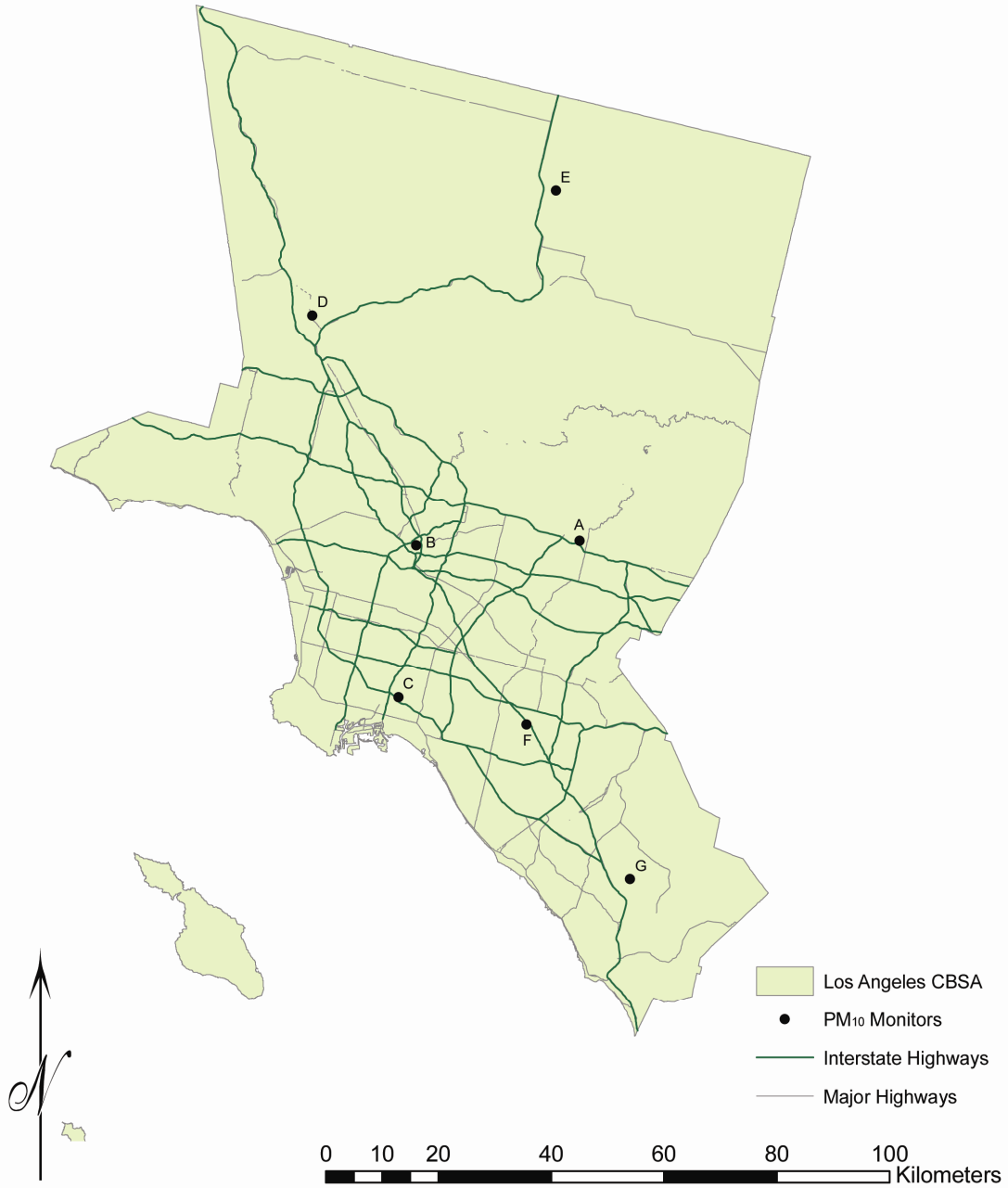


Figure 3-33. Locations of PM₁₀ monitors and major highways, Los Angeles, CA.

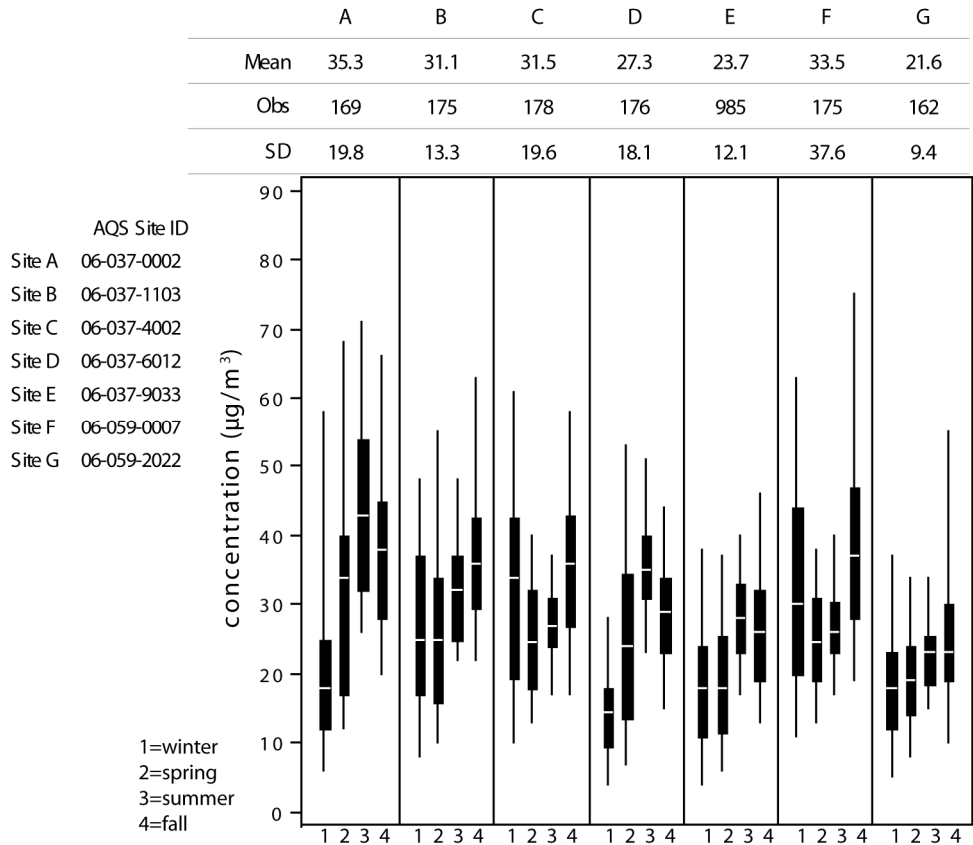


Figure 3-34. Seasonal distribution of 24-h avg PM₁₀ concentrations by site for Los Angeles, CA, 2005-2007. Box plots show the median and interquartile range with whiskers extending to the 5th and 95th percentiles at each site during (1) winter (December-February), (2) spring (March-May), (3) summer (June-August) and (4) fall (September-November).

Table 3-16. Inter-sampler comparison statistics for each pair of 24-h PM₁₀ monitors reporting to AQS for Los Angeles, CA.

Site	A	B	C	D	E	F	G
A	1.00 (0.0, 0.00) 169	0.73 (17.0, 0.17) 153	0.44 (27.0, 0.24) 154	0.73 (24.0, 0.22) 157	0.47 (28.0, 0.26) 169	0.41 (29.0, 0.24) 155	0.65 (30.0, 0.28) 143
B		1.00 (0.0, 0.00) 175	0.61 (14.0, 0.14) 159	0.57 (21.0, 0.24) 159	0.52 (23.0, 0.23) 173	0.42 (15.0, 0.16) 162	0.73 (20.0, 0.23) 149
C			1.00 (0.0, 0.00) 178	0.65 (27.0, 0.28) 158	0.43 (22.0, 0.24) 176	0.93 (11.0, 0.11) 159	0.73 (21.0, 0.22) 148
D				1.00 (0.0, 0.00) 176	0.70 (16.0, 0.20) 175	0.65 (26.0, 0.28) 161	0.57 (19.5, 0.24) 150
E					1.00 (0.0, 0.00) 985	0.29 (26.0, 0.25) 173	0.38 (20.0, 0.24) 159
F						1.00 (0.0, 0.00) 175	0.65 (21.5, 0.22) 150
G							1.00 (0.0, 0.00) 162

Figure 3-35 through Figure 3-37 illustrate the relationship between inter-sampler correlation and distance between sites for PM₁₀ measurements obtained in Boston, Pittsburgh and Los Angeles. Annex A contains similar plots for all 15 CSAs/CBSAs under investigation beginning with Figure A-84. In each plot, substantially more scatter is observed when compared to those for PM_{2.5} (Figure 3-25 through Figure 3-27). This is consistent with the variability observed in the seasonal box plots of concentration shown in Figure 3-30, Figure 3-32, and Figure 3-34. The Boston data exhibit the strongest relationship between inter-sampler correlation and distance, with average inter-sampler correlation remaining higher than 80% when samplers are 44 km apart ($R^2 = 0.61$). The lowest correlations on this plot originate from comparisons between Site B (rural Worcester, MA) and samplers located at Sites E (West Greenwich, RI) and G (Providence, RI). Boston is subject to long range transport of SO₄²⁻, which is a regional pollutant and is a major component of PM_{2.5} and PM₁₀ in the eastern U.S. The Pittsburgh data shows some lower inter-sampler correlations, with one sampler pair having only 66% correlation within a distance of 2 km. On average, inter-sampler correlation remained higher than 80% when samplers were also separated by 44 km, but in this case with much greater scatter ($R^2 = 0.28$) than observed in the Boston data. As seen for the Pittsburgh PM₁₀ box plots in Figure 3-32, sites D, H, I, and K have elevated means and high variability that is driving the observed scatter. These four sites are all located in mountainous suburbs of Pittsburgh (North Braddock, PA, Liberty, PA, Lincoln Boro, PA, and Beaver Falls, PA, respectively), where emissions from steel manufacturing and frequent stable conditions in the planetary boundary layer cause localized events of elevated concentration. When those four sites are removed, scatter decreases greatly ($R^2 = 0.56$). The Los Angeles data exhibit a much steeper slope, with average inter-sampler correlation remaining higher than 80% when samplers are only 30 km apart ($R^2 = 0.56$). The lower inter-sampler correlations in part reflect the fact that some of these monitoring sites are separated from each other by hills or, in the case of one sited at Lancaster, CA (Site I), by the San Gabriel Mountains. The Los Angeles data exhibit greater scatter than the Pittsburgh data. However, the smallest inter-sampler separation distance is 23 km, and there are relatively fewer PM₁₀ samplers. Given the present data, it is not possible to judge how data would correlate on smaller spatial scales.

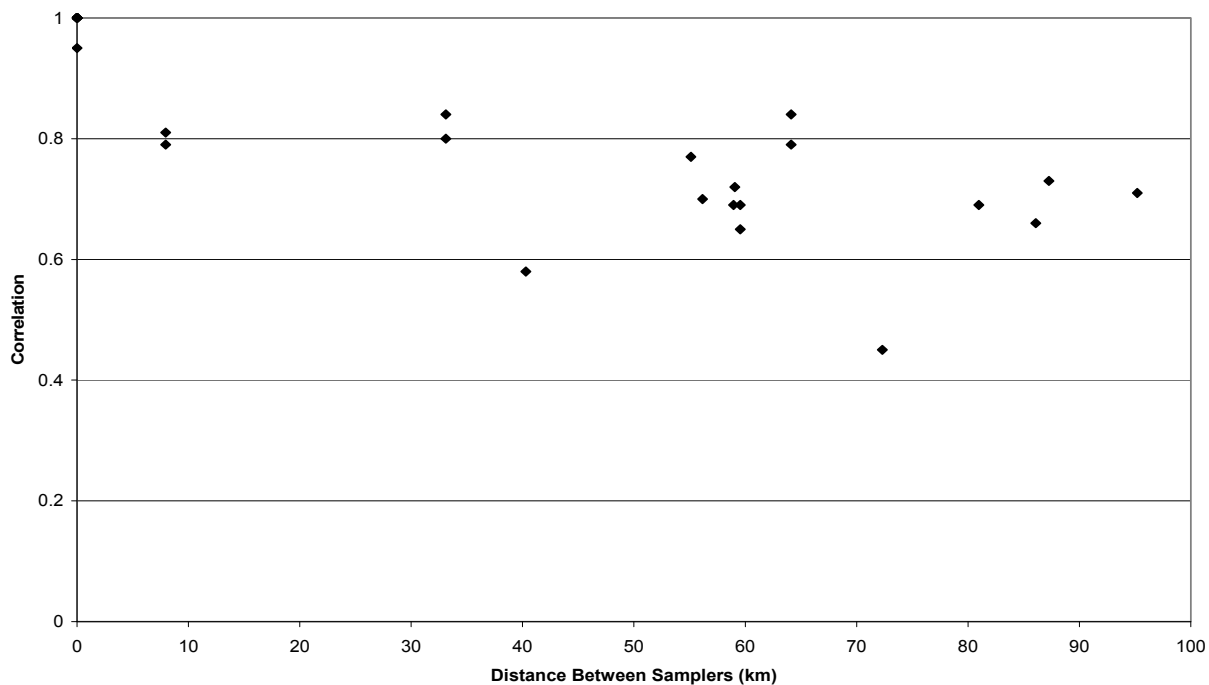


Figure 3-35. Inter-sampler correlations for 24-h PM₁₀ as a function of distance between monitors in Boston, MA.

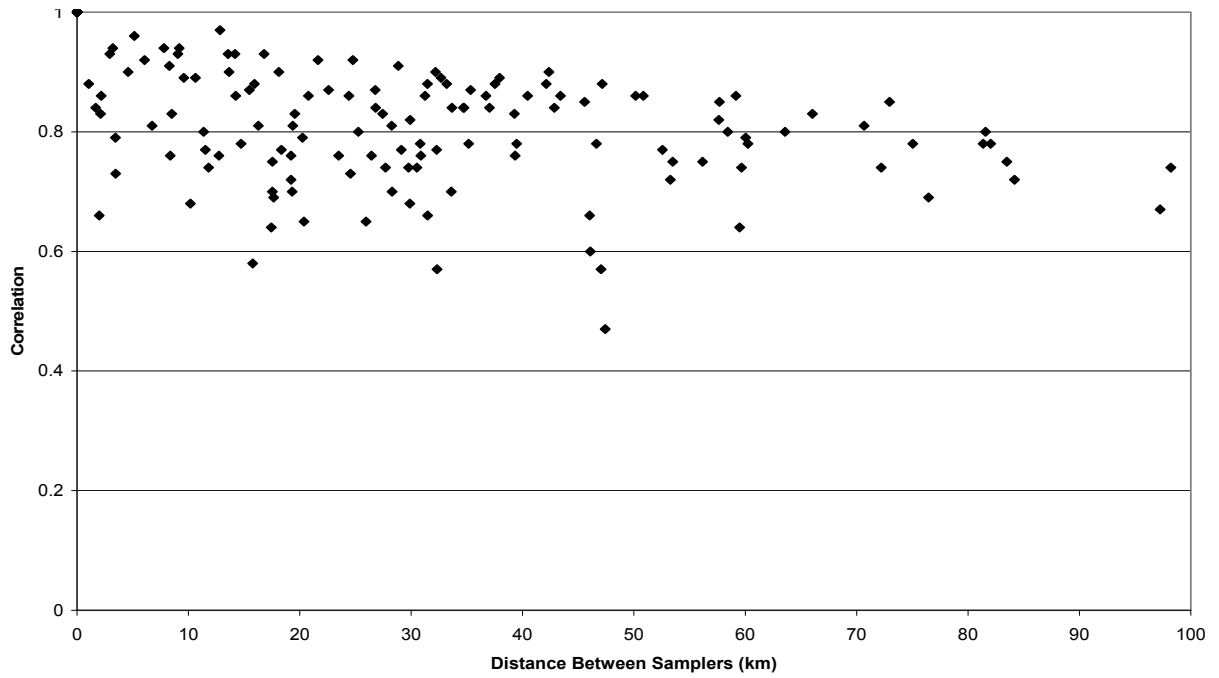


Figure 3-36. Inter-sampler correlations for 24-h PM₁₀ as a function of distance between monitors in Pittsburgh, PA.

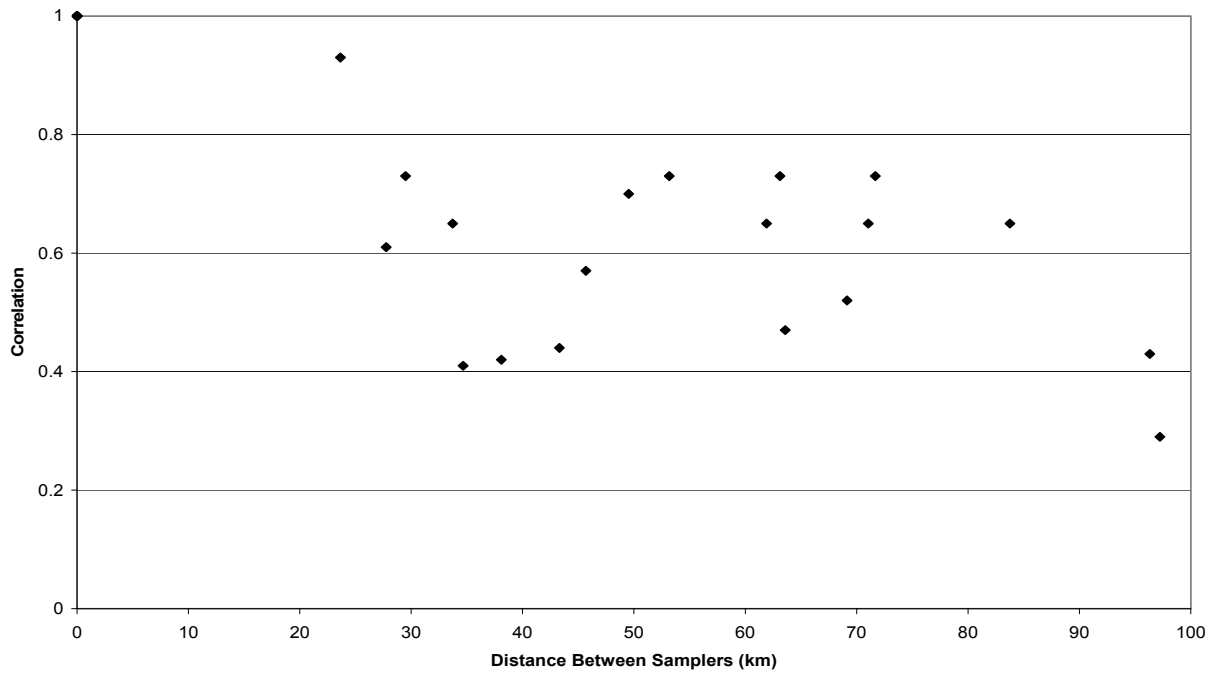
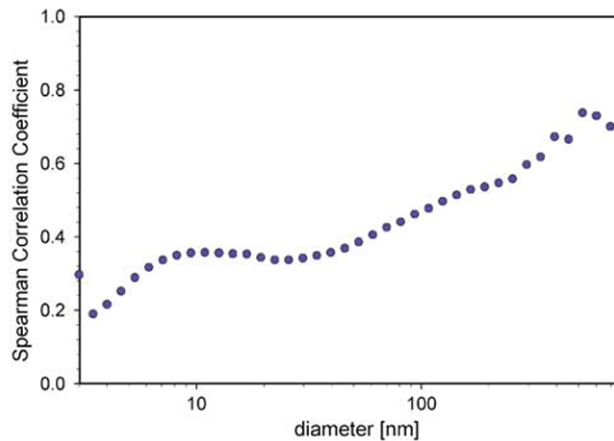


Figure 3-37. Inter-sampler correlations for 24-h PM₁₀ as a function of distance between monitors in Los Angeles, CA.

UFPs

Relatively few studies compare UFP measurements at multiple locations within an urban center. An early study by Buzorius et al. (1999, [081205](#)) suggested spatial homogeneity in total particle number concentrations between multiple locations in Helsinki, Finland. They found correlations in 10-min average at three sites within the city as high as 0.84. The sites, however, were relatively close together (2 km) and all near the same roadway. There was a high degree of correlation between traffic intensity and total aerosol number concentrations, suggesting that traffic was the primary source of the measured particles and the driving force behind the high correlations. Weekend correlations (0.28-0.47) and correlations with a fourth monitor located 22 km outside the city (0.05-0.64) were much lower.

Tuch et al. (2006, [157060](#)) found more spatial heterogeneity in UFP concentrations measured for an entire year at two locations 1.5 km apart in Leipzig, Germany. Figure 3-38 shows the correlation as a function of particle size (mobility diameter) dropping off as the particle size decreases from 0.5 at 100 nm down to 0.2 at 3 nm. Table A-50 in Annex A contains correlation coefficients of hourly and daily average particle number, surface area and volume concentrations as a function of particle diameter adapted from the Tuch et al. (2006, [157060](#)) study. For all days (N = 5481 hourly observations), the correlation between UFPs (10-100 nm) measured at the two sites was 0.31.



Source: Reprinted with Permission of Nature Publishing Group from Tuch et al. (2006, [157060](#))

Figure 3-38. Bin-wise Spearman correlation coefficients in aerosol particle number concentrations between the lft (urban background) and the Eisenbahn-strasse (city/urban center) sites in Leipzig, Germany.

The two sites represented in Figure 3-38 and Table A-44 were relatively close to each other, but one was located in a mixed semi-industrial region while the other was in a street canyon in a residential neighborhood near busy roadways. This suggests a high degree of spatial heterogeneity in UFPs driven primarily by differences in nearby source characteristics. Sioutas et al. (2005, [088428](#)) reviewed studies of the distribution of UFPs and came to the similar conclusion that mobile sources make a large contribution to UFPs and therefore UFP concentrations can exhibit substantial variability in space and time. This is to be expected since UFP concentrations drop off much quicker with distance from roadways than larger particle sizes (Levy et al., 2003, [052661](#); Reponen et al., 2003, [088425](#); Zhu et al., 2005, [157191](#)). Hagler et al. (2009, [191185](#)) showed similar exponential decreases in UFP number concentrations with distance from the road for multiple locations in the U.S. Neighborhood-scale variability and near-roadway concentration gradients for UFPs are discussed further in Section 3.5.1.3.

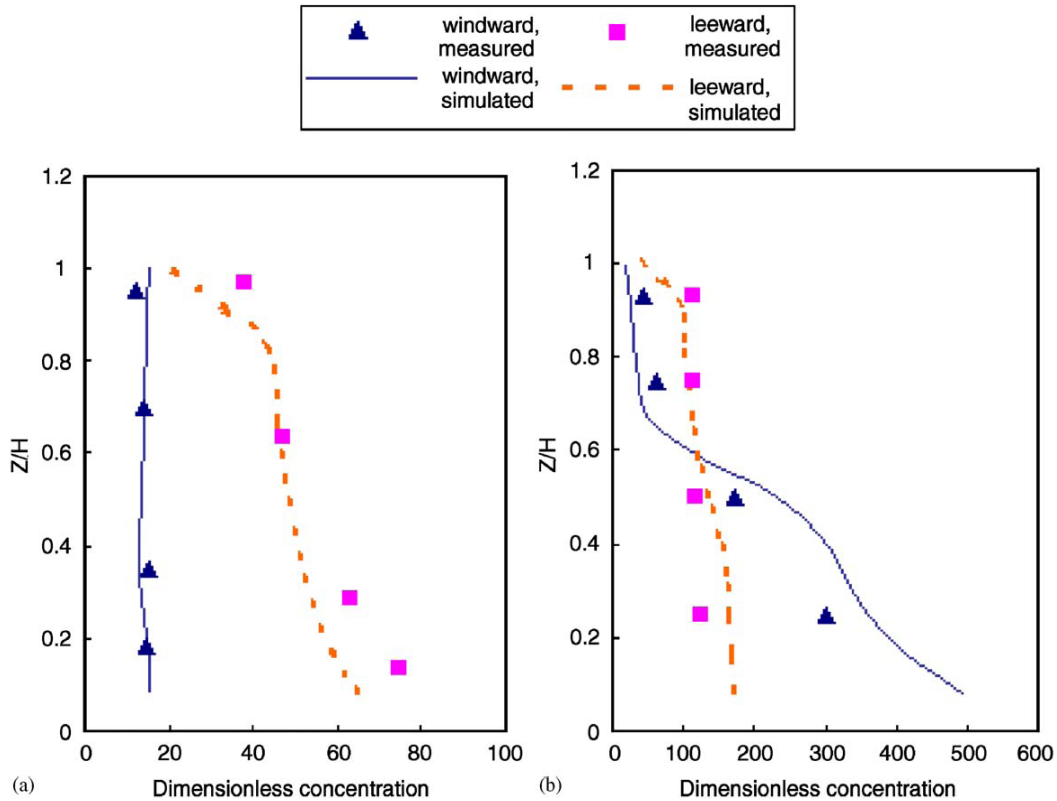
PM Constituents

The pie charts showing PM_{2.5} composition that were generated using the SANDWICH method for the 15 CSAs/CBSAs presented earlier in Figure 3-17 and Figure 3-18 represent the average of all available monitors within each region. Individual pie charts for each monitor are included in Figures A-127 through A-141 in Annex A and provide an indication of the urban-scale spatial variability in PM_{2.5} composition. In the instances where multiple monitors were available, there was a fair degree of spatial homogeneity in PM_{2.5} bulk chemistry within each metropolitan area. Some notable exceptions exist, however. Birmingham and Detroit show variation in the amount of crustal material, both spatially and seasonally. Denver exhibits some spatial variation in NO₃⁻ during the winter, the season with the highest measured PM_{2.5} mass. Several sites in New York and one in Pittsburgh have elevated fractions of EC relative to the other sites within the respective cities, and several sites in New York have been shown to have elevated Ni concentrations in PM_{2.5} samples when compared with surrounding areas (Peltier and Lippmann, 2009, [197455](#); Peltier et al., 2008, [197452](#)). In Phoenix, high winter PM_{2.5} mass is site specific and appears to be associated with high OC; the crustal component also varies and is inversely proportional to total measured mass.

3.5.1.3. Neighborhood-Scale Variability

Neighborhood scale spatial variability in the particle concentration profile is affected by land and building topography, meteorology, particle size distribution, particle composition, and particle volatility. Population density at the neighborhood scale is also an important determinant of the spatial distribution of PM concentration because population density impacts source prevalence, source magnitude, topographical-driven ventilation, and heat island effects (Crist et al., 2008, [156372](#); Makar et al., 2006, [155959](#); Mfula et al., 2005, [123359](#); Rigby and Toumi, 2008, [156050](#)).

A number of computational and wind tunnel modeling street canyon studies have demonstrated the potential variability in pollutant concentrations within a street canyon (Borrego et al., 2006, [155697](#); Chang and Meroney, 2003, [090298](#); Kastner-Klein and Plate, 1999, [001961](#); So et al., 2005, [110746](#); Xiaomin et al., 2006, [156165](#)). Influential parameters include street canyon height to width ratio (H/W), source positioning, wind speed and direction, building shape and upstream configuration of buildings. Figure 3-39 shows pollutant concentrations obtained from wind tunnel and computational fluid dynamics simulations of transport and dispersion in an infinitely long street canyon with a line source centered at the bottom of the canyon (Xiaomin et al., 2006, [156165](#)). When the canyon height was equal to the street width (typical of moderate density suburban or urban fringe residential neighborhoods) and lower background wind speed existed, concentrations on the leeward canyon wall were four times those of the windward wall near ground level. When the canyon height was twice the street width (typical of higher-density urban planning) and background winds were somewhat higher, near ground level concentrations on the windward canyon wall were roughly three times higher than those measured at the leeward wall. Baldauf et al. (2008, [191017](#); 2009, [191766](#)) noted that the presence of noise barriers, vegetation, or changes in topography adjacent to the road can also alter particle dispersion characteristics. Specifically, depressed road segments, where the road bed is below the surrounding terrain, leads to increased air turbulence and pollutant dispersion. These results suggest that micro- and neighborhood-scale variation related to urban topography may have a significant impact on pollutant concentrations at this scale.



Source : Reprinted with Permission of Elsevier Ltd. From Xiaomin et al. (2006, [156165](#)).

Figure 3-39. Dimensionless concentration as a function of height at windward and leeward locations and street canyon aspect ratios (H/W). (a) Dimensionless concentration on the windward and leeward sides of the canyon when H/W = 1 and wind speed = 3 m/s. (b) Dimensionless concentration on the windward and leeward sides of the canyon when H/W = 2 and wind speed = 5 m/s. Computational fluid dynamics modeling was performed, and measurements were obtained in wind tunnel simulations.

PM_{2.5} and PM₁₀

Knowledge of neighborhood-scale variability is important for interpreting data from PM_{2.5} and PM₁₀ community monitors. Figure 3-40 shows data derived from the 15 CSAs/CBSAs for PM_{2.5} and PM₁₀ discussed in Section 3.5.1.2. This figure is limited to the inter-sampler correlations obtained for sampler pairs located within a distance of 4 km (i.e., neighborhood scale). PM_{2.5} data exhibit a flatter slope, with average correlation maintained at 93% within 4 km ($R^2 = 0.22$). There is more scatter and variability among the PM₁₀ data, with an average correlation of 70% within 4 km ($R^2 = 0.03$). The degree of variability in PM₁₀ compared with PM_{2.5} relates to transport and dispersion of the PM_{10-2.5} component of PM₁₀ compared with PM_{2.5}. However, differences in composition, source location, topography, and monitor height—all of which could affect concentrations—could drive the relatively high degree of scatter for both size classes, considering the low computed R^2 values for each of these curves.

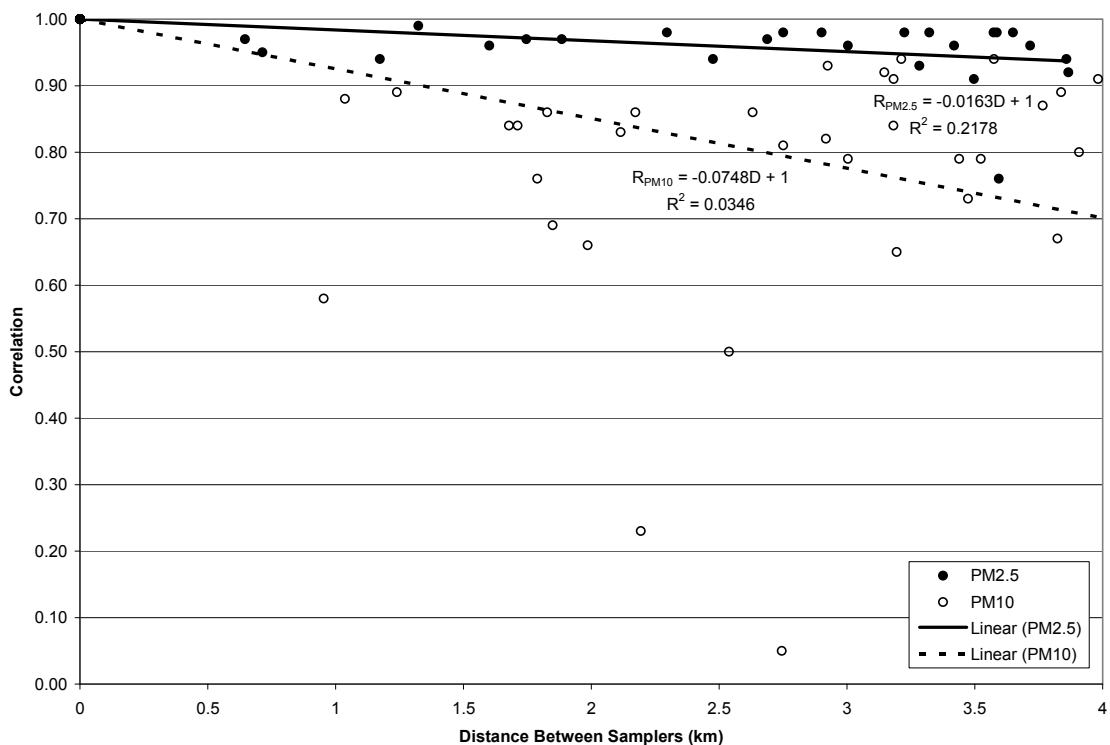


Figure 3-40. Inter-sampler correlations for 24-h PM_{2.5} and PM₁₀ as a function of distance between monitors for samplers located within 4 km (neighborhood scale).

Isakov et al. (2007, [156588](#)) compared PM_{2.5} concentrations from a central monitoring site in Wilmington, DE with PM_{0.3} measurements taken on a mobile platform driven through mostly quite residential streets within a 4 km×4 km grid containing the central monitor. Correlations were generally high (average $r = 0.87$) over all time periods and locations monitored, consistent with the range of correlations for PM_{2.5} shown in Figure 3-40.

PM_{10-2.5}

Neighborhood-scale variability in PM_{10-2.5} was investigated by Chen et al. (2007, [147318](#)) in the Raleigh/Durham area of NC. The average correlation between 26 residential monitors located throughout the region and a centrally located monitor representing a maximum inter-sampler range of 60 km was found to be 0.75 for PM_{10-2.5} compared with 0.92 and 0.94 for PM_{2.5} and PM₁₀, respectively. Based on this study, neighborhood-scale variability is greater for PM_{10-2.5} than for PM_{2.5} or PM₁₀, matching the conclusion drawn above on the broader urban-scale.

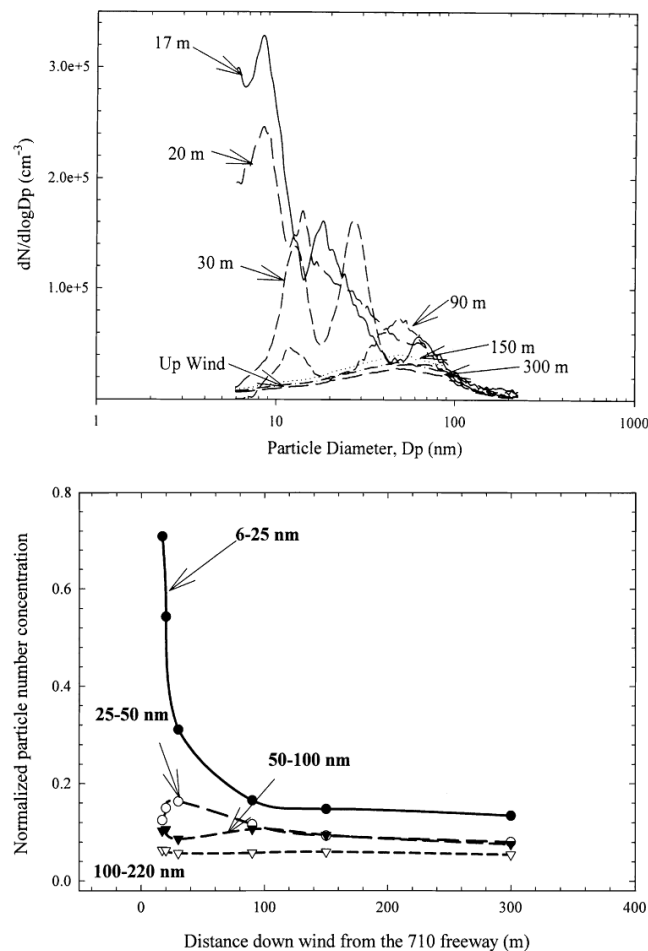
UFPs

Moore et al. (2009, [191004](#)) monitored UFP concentrations throughout the Ports of Los Angeles and Long Beach, through which an interstate highway runs and found that concentrations varied by a factor of 5-7 across sites with substantial differences in the daily concentration time series at each site. Such variability reflects diversity of the sources (some near the Interstate, some near the Port), and the influence of changing meteorology over an urban area. In a mobile platform sampling study, Westerdahl et al. (2005, [086502](#)) and Fruin et al. (2008, [097183](#)) also reported substantial peaks in UFP concentration when sampling at highways in comparison with a background site (the University of Southern California) using the same data set.

Near roadway environments can exhibit high concentration gradients, particularly for UFPs. Ntziachristos et al. (2007, [089164](#)) observed that the near-road particle size distribution was

substantially higher in the UF mobility diameter range and that these results were very sensitive to meteorology (rain) and time of day. Baldauf et al. (2008, [190239](#)) reported elevated UFP number concentrations downwind of a highway in Raleigh, NC, when compared to measurements approximately 100 m upwind of the road. Hagler et al. (2009, [191185](#)) noted a 5-12% decrease in number concentrations per 10 m distance from the road for a number of studies in the U.S. with unobstructed air flow.

After initial emission from a motor vehicle, the evolution of the PM distribution within the plume is a function of (1) the turbulence that dilutes the plume and (2) evaporation or condensation of the volatile portion of the aerosol that results from rapid cooling of the exhaust. Figure 3-41 shows the size distribution measured by Zhu et al. (2002, [041553](#)) at distances of 17-300 m away from the roadway (in this case, Highway 710 in Los Angeles) and at an upwind site. It can be seen that a mode originally measured around 9 nm increases in diameter and decreases in number concentration as distance from the highway increases. Smaller secondary modes appear around 30 m from the roadway with multiple modes at some particle sizes. By 150 m away from the highway, the size distribution flattens with a small mode around 50 nm. It is clear from the bottom figure that the number concentration of larger particles (i.e., 100-220 nm) does not vary as much as UFPs (<100 nm) with increasing distance downwind from the roadway.



Source: Reprinted with Permission of Elsevier Ltd. From Zhu et al. (2002, [041553](#)).

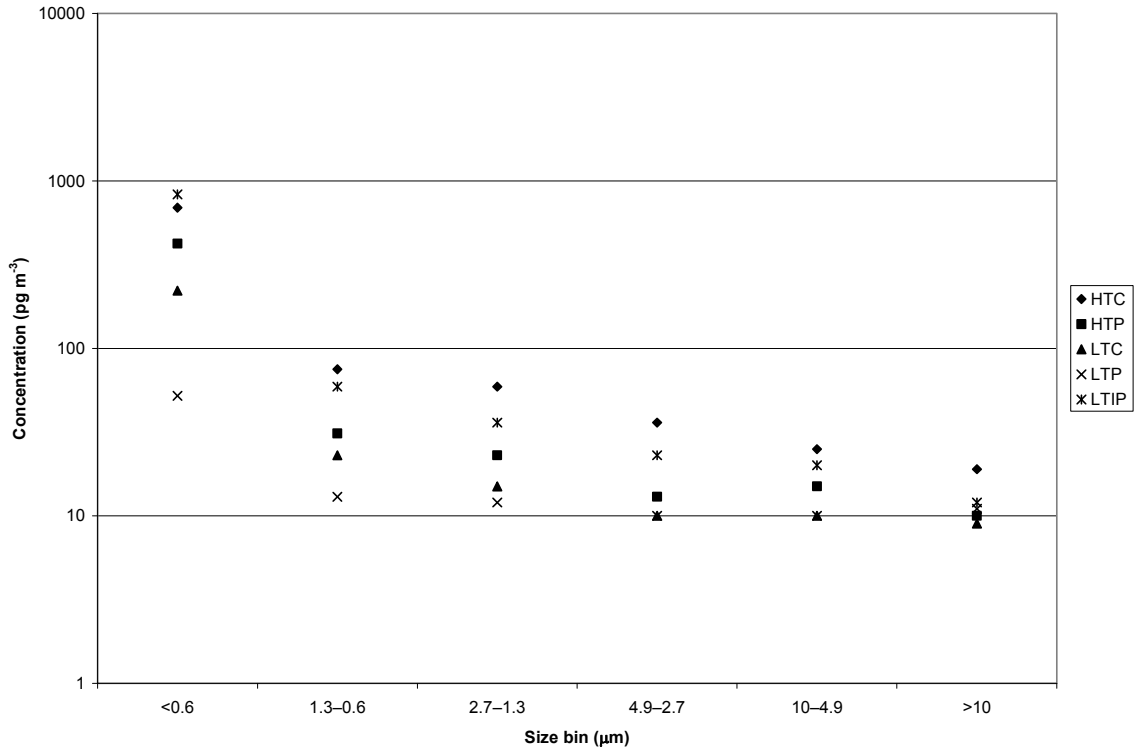
Figure 3-41. Particle size distributions measured at various distances from the 710 freeway in Los Angeles, CA (top), and particle number concentration as a function of distance from the 710 freeway (bottom).

Zhou and Levy (2007, [098633](#)) performed a meta-analysis of traffic-related air pollution literature and found that background pollution and meteorology can have important impacts on the size of the elevated concentration region around the highway. Zhu et al. (2002, [041553](#)) and Zhang et al. (2005, [157185](#)) noted in field measurements of UFPs that small particles can be lost due to evaporation or to coagulation during Brownian diffusion to form bigger particles, resulting in an upward shift in mode diameter with distance from the roadway. Studies of particle sizes on roads (Kittelson et al., 2006, [156649](#); Kittelson et al., 2006, [156648](#)), in tunnels (Venkataraman et al., 1994, [002475](#)), and upwind and downwind of roads (Zhu et al., 2002, [041553](#)) suggest that for well-maintained spark-ignition vehicles, a large fraction of the mass of particles emitted from the vehicles are in the nuclei mode (i.e., smaller than accumulation mode). High-speed highway driving may be associated with a larger fraction of particle mass being emitted in the UF size range, while lower speed operation results in a higher mass fraction in the accumulation mode (Cadle et al., 2001, [017192](#)). In situations in which the dilution rates are lower than in a short tunnel or downwind of a road way, condensation of vapors can give rise to particles in the accumulation mode (Kittelson, 1998, [051098](#)). Diesel engines, in particular, emit black carbon in the lower end of the accumulation mode, with number emissions dominated by semi-volatile material in the nuclei mode (Kittelson, 1998, [051098](#); Kittelson et al., 2006, [156649](#); Kittelson et al., 2006, [156648](#)). Sharp gradients in black carbon mass have been observed along roadways with high diesel traffic (Zhu et al., 2002, [041553](#)). As the traffic pollution moves downwind, the UFPs may grow into the accumulation mode by coagulation or condensation. In addition to Gaussian dispersion and wind eddies caused by the presence of natural and anthropogenic barriers, Sahlodin et al. (2007, [114058](#)) demonstrated that turbulence produced by vehicles can result in modification of the plume emanating from the highway. Hence, on-road turbulence could potentially alter the aerosol size distribution. This added turbulence could cause some evaporation of tiny nucleation particles that have not adsorbed or adsorbed onto soot nuclei, which may affect the rate of coagulation (Jacobson et al., 2005, [191187](#)). The roadway configuration may also affect particle transport and dispersion. Depressed road sections, where the road bed is below the surrounding terrain, leads to increased air turbulence and mixing as air flows up and out of the road depression. This configuration can result in lower particulate concentrations and flatten concentration decay curves away from the road. On the other hand, configurations with the road bed at-grade with surrounding terrain, or elevated above the surrounding terrain with solid fill material resulted in the highest pollutant concentrations and sharpest concentration gradients downwind from the road.

PM Constituents

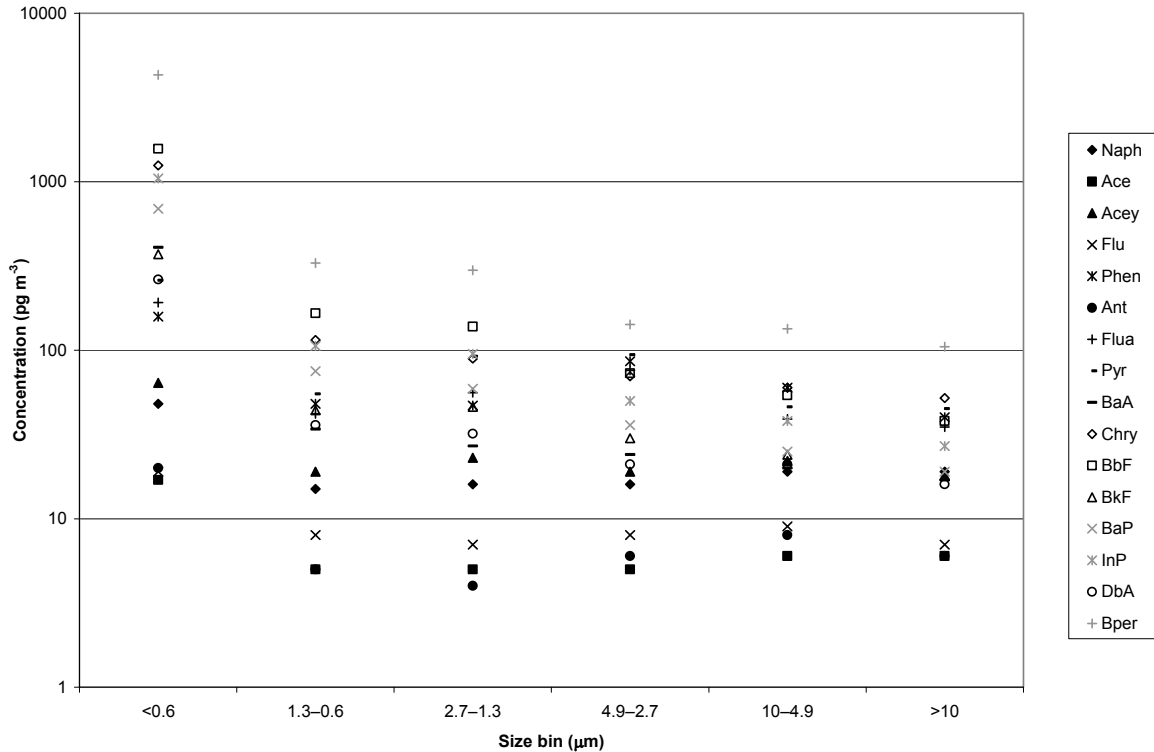
The composition of PM will also vary on the neighborhood-scale in response to local sources and differential dispersion, resulting in variable spatial distribution of individual components. Krudysz et al. (2008, [190064](#)) investigated spatial variation in size-fractionated (<0.25 μm , 0.25-2.5 μm , >2.5 μm) PM composition data at four sites located within 3-6 km of each other in the Long Beach, CA area. Inter-site R^2 values in the 0.25-2.5 μm size range were higher for mass (ranging from 0.56-0.91) than for EC (0.02-0.71) for pair wise site comparisons. Spatial heterogeneity in all size ranges investigated was also found for several elements associated with motor vehicle emissions and resuspended road dust including Cu, Mg, Ba, Ca and Al. Viana et al. (2008, [156135](#)) observed higher concentrations of crustal elements in $\text{PM}_{2.5}$ and PM_{10} samples in rural neighborhoods and higher concentrations of combustion-derived $\text{PM}_{2.5}$ and PM_{10} , such as EC and NO_3^- , in higher density urban areas. Gutiérrez-Dabán et al. (2005, [155818](#)) examined the mass distribution of various PAHs under different traffic and urban density conditions. Figure 3-42 displays the distributions for benz[a]pyrene (BaP) at high and low traffic sites at the urban center, periphery, and industrial areas in Seville, Spain (Gutiérrez-Dabán et al., 2005, [155818](#)). Concentrations were nearly an order of magnitude lower for the low traffic urban periphery location when compared with the high traffic or industrial locations. Particles smaller than ~ 600 nm had roughly an order of magnitude higher concentration than those at larger sizes and tended to have a larger spread in concentrations among sampling sites. Figure 3-43 shows the distributions for sixteen PAHs at a high traffic location at the city center in Seville, Spain (Gutiérrez-Dabán et al., 2005, [155818](#)). PAH species varied in concentration by up to two orders of magnitude for each particle size bin, and the highest concentrations of individual PAHs were generally found for particles smaller than approximately 600 nm. Olson and McDow (2009, [191188](#)) reported decreases by a factor of 1.04-2.37 in select PAH and organic source marker concentrations when comparing measurements 10 m and 275 m from a highway in Raleigh, North Carolina. Phuleria et al. (2006, [156867](#)) sampled

UFPs and PM_{2.5} concentrations and PAH species at the mouth of the Caldecott Tunnel in Orinda, CA and found that the two size classes were highly correlated ($R^2 = 0.97$). Given the size differentials of each size bin presented in the Gutiérrez-Dabán et al. (2005, [155818](#)) study, it is possible that the PM_{2.5} sampled at the tunnel mouth in the latter study represented secondary PM_{2.5} that grew from UFP emissions trapped within the tunnel.



Source: Adapted with Permission of Springer-Verlag from Gutiérrez-Dabán et al. (2005, [155818](#)).

Figure 3-42. Mass distributions for BaP at a high traffic urban center (HTC), high traffic urban periphery (HTP), low traffic urban center (LTC), low traffic urban periphery (LTP), and low traffic industrial urban periphery (LTIP) in Seville, Spain.



Source: Adapted with Permission of Springer-Verlag from Gutiérrez-Dabán et al. (2005, [155818](#)).

Figure 3-43. Mass distributions for 16 PAHs at a high traffic city center in Seville, Spain.

3.5.2. Temporal Variability

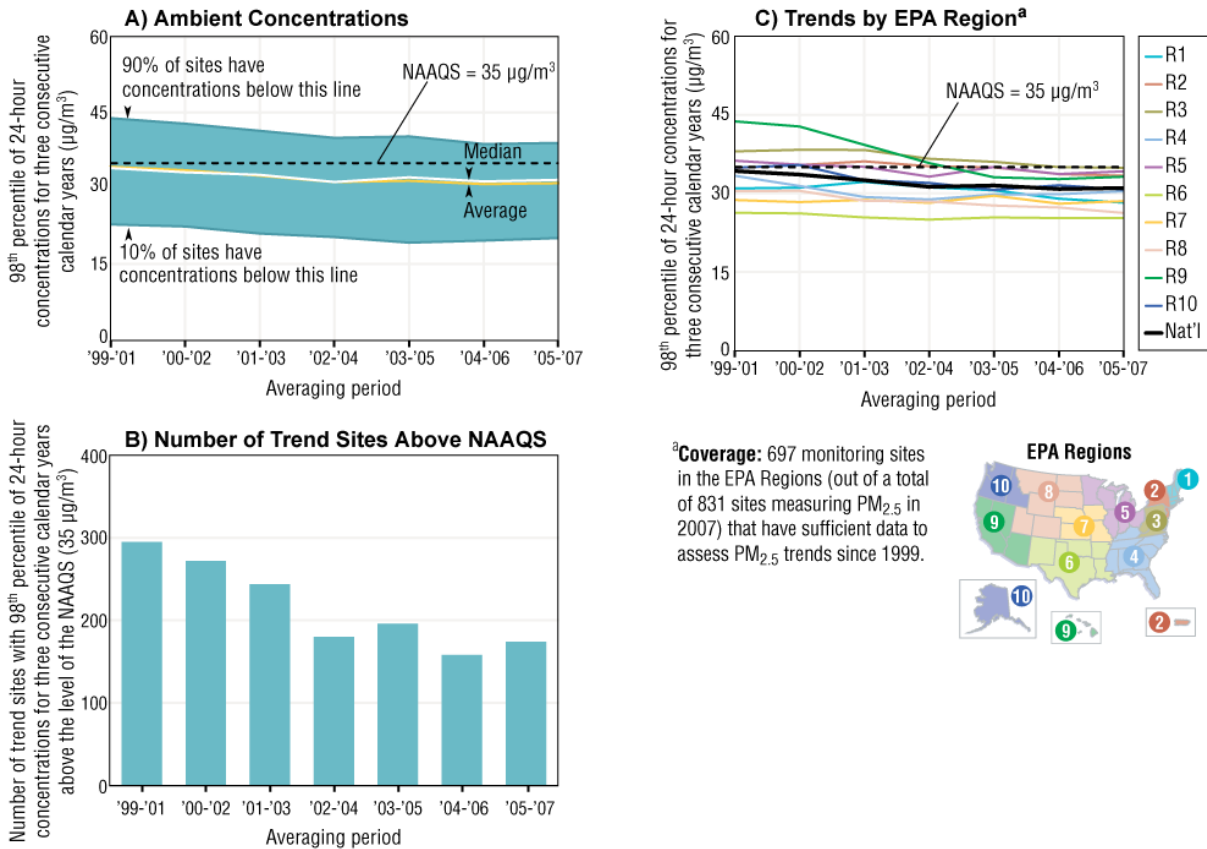
Temporal variability is another important factor in characterizing PM. This section addresses trends as well as seasonal and hourly variability. Trends in $PM_{2.5}$ and PM_{10} are addressed in Section 3.5.2.1 based on AQS data. Seasonality is coupled with spatial variability and has been discussed in the regional context above. Section 3.5.2.2 below briefly investigates the seasonality on a finer time scale, thereby addressing issues relating to the seasonal definitions used earlier. Section 0 addresses hourly patterns, an issue particularly important to understanding the behavior of PM concentrations in reference to sources, human activity patterns and exposure. Hourly patterns are investigated using AQS data on a national basis for $PM_{2.5}$ and PM_{10} . Data for UFPs and PM constituents are presented where available.

3.5.2.1. Regional Trends

This section summarizes available information on trends in PM mass and composition. Mass concentration trends are based on AQS data and incorporate 9 years (1999-2007) of $PM_{2.5}$ data and 20 years (1988-2007) of PM_{10} data. Composition trends are based on six years of available CSN data (2002-2007). Several monitoring sites were excluded from the following trend analyses to provide a consistent basis for comparison over the desired years of monitoring. This included exclusion of sites when there was no corresponding site in later or earlier years. Region-average trends were calculated to facilitate presentation and extrapolation of the results. These region-averages, however, may not necessarily represent the trends that are being observed at any individual monitor or geographical location within the specified region.

PM_{2.5}

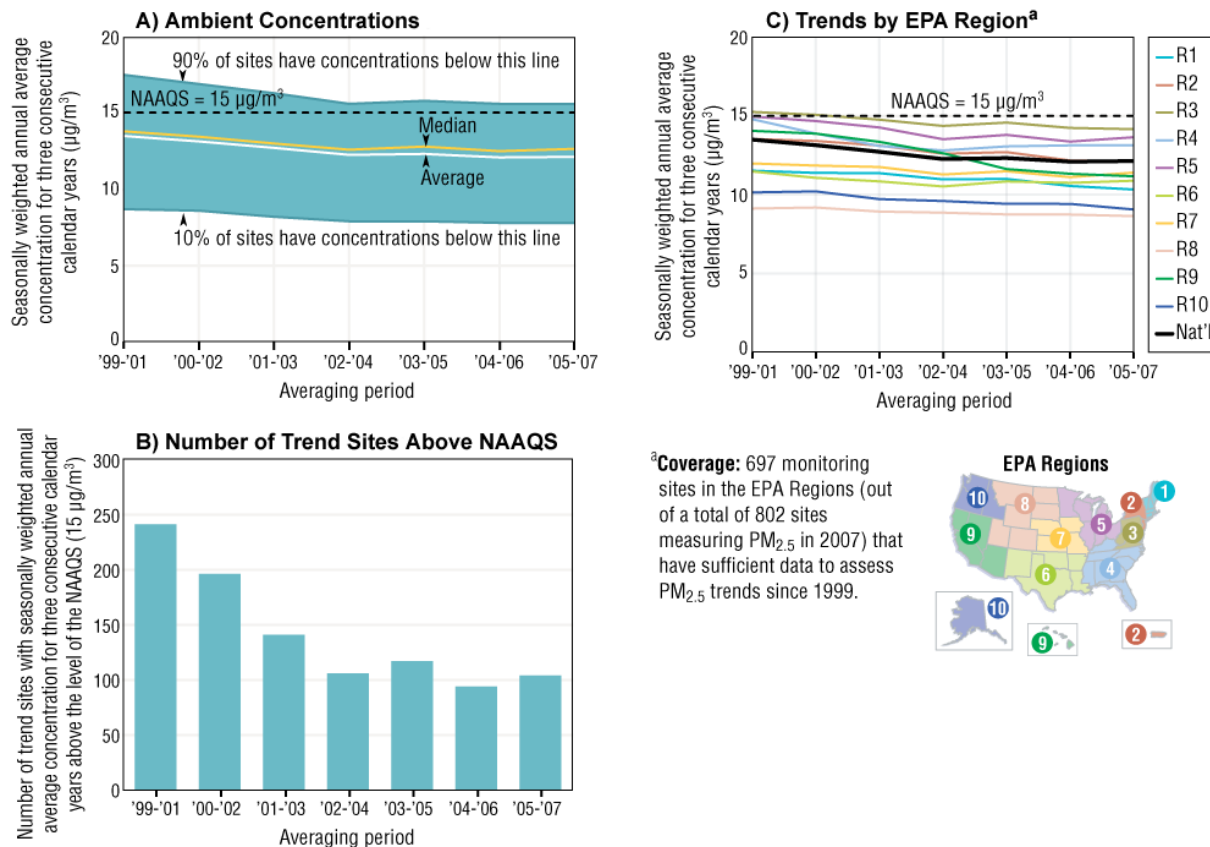
Figure 3-44 shows trends in U.S. ambient 24-h PM_{2.5} concentrations from 1999-2007. In the period 2005-2007, the 3-yr avg of the 98th percentile of 24-h PM_{2.5} concentrations fell 10% relative to the 1999-2001 period (see Figure 3-44A). The number of sites reporting values greater than the 24-h NAAQS was shown to decline 40% in Figure 3-44B. Figure 3-44C illustrates the downward trend in the 98th percentile of 24-h PM_{2.5} concentrations for three consecutive calendar years in all U.S. EPA regions. This trend is most pronounced in Region 9 incorporating Arizona, California and Nevada where this value dropped 25% from the 1999-2001 period to the 2005-2007 period.



Source: U.S. EPA (2008, [157076](#))

Figure 3-44. Ambient 24-h PM_{2.5} concentrations in the U.S., 1999-2007, showing A) ambient concentrations, B) number of trends sites above the 24-h NAAQS and C) trends by U.S. EPA Region.

Figure 3-45 contains similar trend information for the annual PM_{2.5} NAAQS. The seasonally weighted 3-yr avg PM_{2.5} concentrations for the years 2005-2007 were at the lowest since national monitoring began in 1999 (Figure 3-45A). The seasonally weighted 3-yr avg fell 10% between the 1999-2001 averaging period and the 2005-2007 averaging period. The number of sites reporting concentrations above the annual average PM_{2.5} NAAQS fell 56% over these same periods in Figure 3-45B. Figure 3-45C illustrates the annual trends in PM_{2.5} by U.S. EPA region. Declines were the greatest in Region 9 again where annual PM_{2.5} concentrations fell 20% from the 1999-2001 averaging period to the 2005-2007 averaging period.

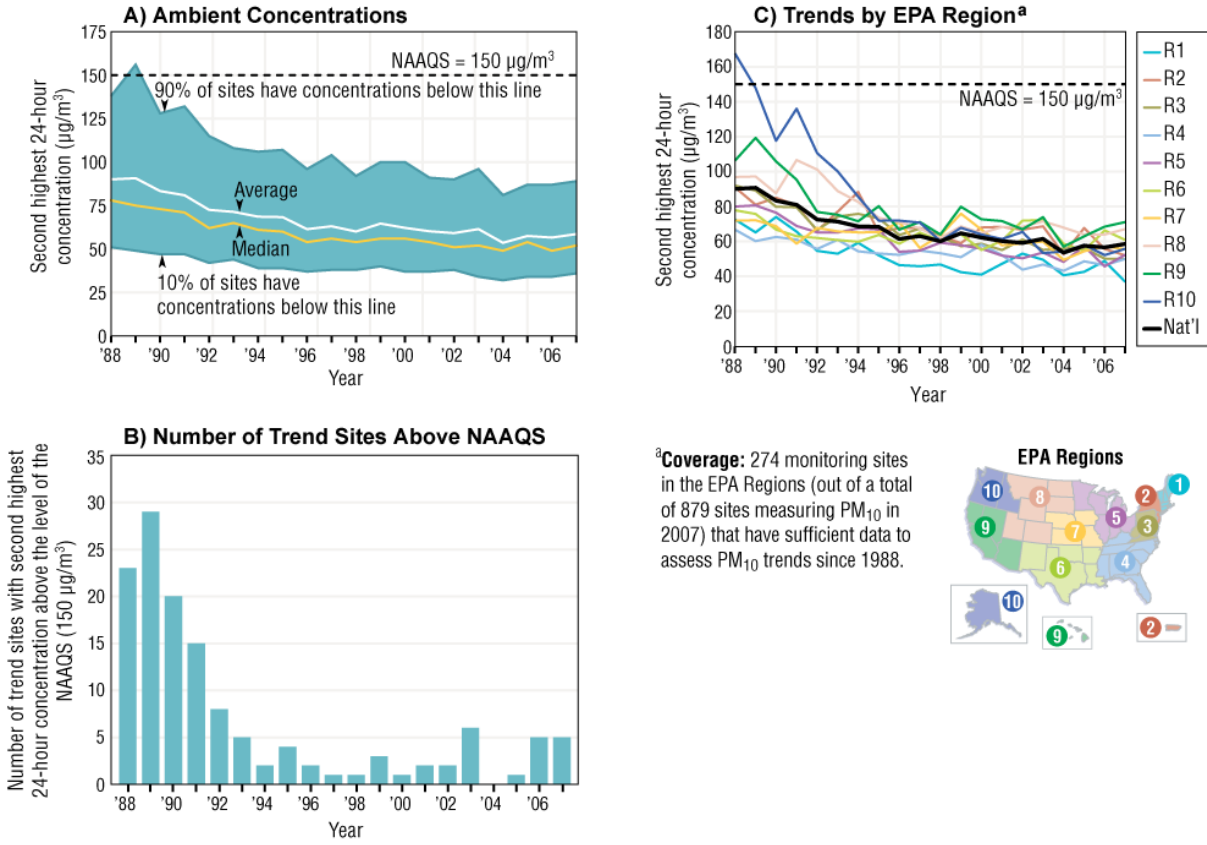


Source: U.S. EPA (2008, [157076](#)).

Figure 3-45. Ambient annual $\text{PM}_{2.5}$ concentrations in the U.S., 1999-2007, showing A) ambient concentrations, B) number of trends sites above the annual NAAQS and C) trends by U.S. EPA Region.

PM₁₀

Figure 3-46 shows trends in U.S. ambient 24-h PM_{10} concentrations from 1988-2007. In 2007, the U.S. national average second highest PM_{10} concentration was 37% lower than in 1988 (Figure 3-46A). Of 281 sites used in this trend analysis, the number reporting concentrations above the 24-h PM_{10} NAAQS ($150 \mu\text{g}/\text{m}^3$) fell from 23 in 1988 to 5 in 2007 with a max of 29 in 1989 (Figure 3-46B). Figure 3-46C shows trends in the second highest 24-h PM_{10} concentrations broken down by U.S. EPA region. All regions exhibit an overall decrease from 1988-2007. Largest decreases occurred in EPA Region 10, which incorporates Washington, Oregon, Idaho and Alaska. Most of the decrease occurred between 1988-1995.



Source: U.S. EPA (2008, [157076](#)).

Figure 3-46. Ambient 24-h PM_{10} concentrations in the U.S., 1988-2007, showing A) ambient concentrations, B) number of trends sites above the 24-h NAAQS and C) trends by U.S. EPA Region.

PM Constituents

The SANDWICH method discussed in Section 3.5.1.1 for estimating $\text{PM}_{2.5}$ composition from FRM mass measurements and CSN bulk composition measurements was used to evaluate trends in $\text{PM}_{2.5}$ constituents. Figure 3-47 includes stacked bar charts of $\text{PM}_{2.5}$ composition from 2002 to 2007 stratified by region and season. The regions used in Figure 3-47 were selected based on common aerosol characteristics including trends, seasonality, size distributions and/or composition as described in chapter 6 of the 1996 PM AQCD (U.S. EPA, 1996, [079380](#)) and differ from the EPA regions used in the preceding figures. Figure 3-47 is based on 42 monitoring locations reporting complete CSN data with 2002 being the first year with sufficient speciation data. The Southwest region incorporating Arizona, New Mexico and parts of Texas and Oklahoma did not contain any complete data and therefore is not represented in this analysis. Two seasons representing different temperature ranges—cool (October-April) and warm (May-September)—were considered in the figure since many $\text{PM}_{2.5}$ components exhibit strong seasonal dependence.

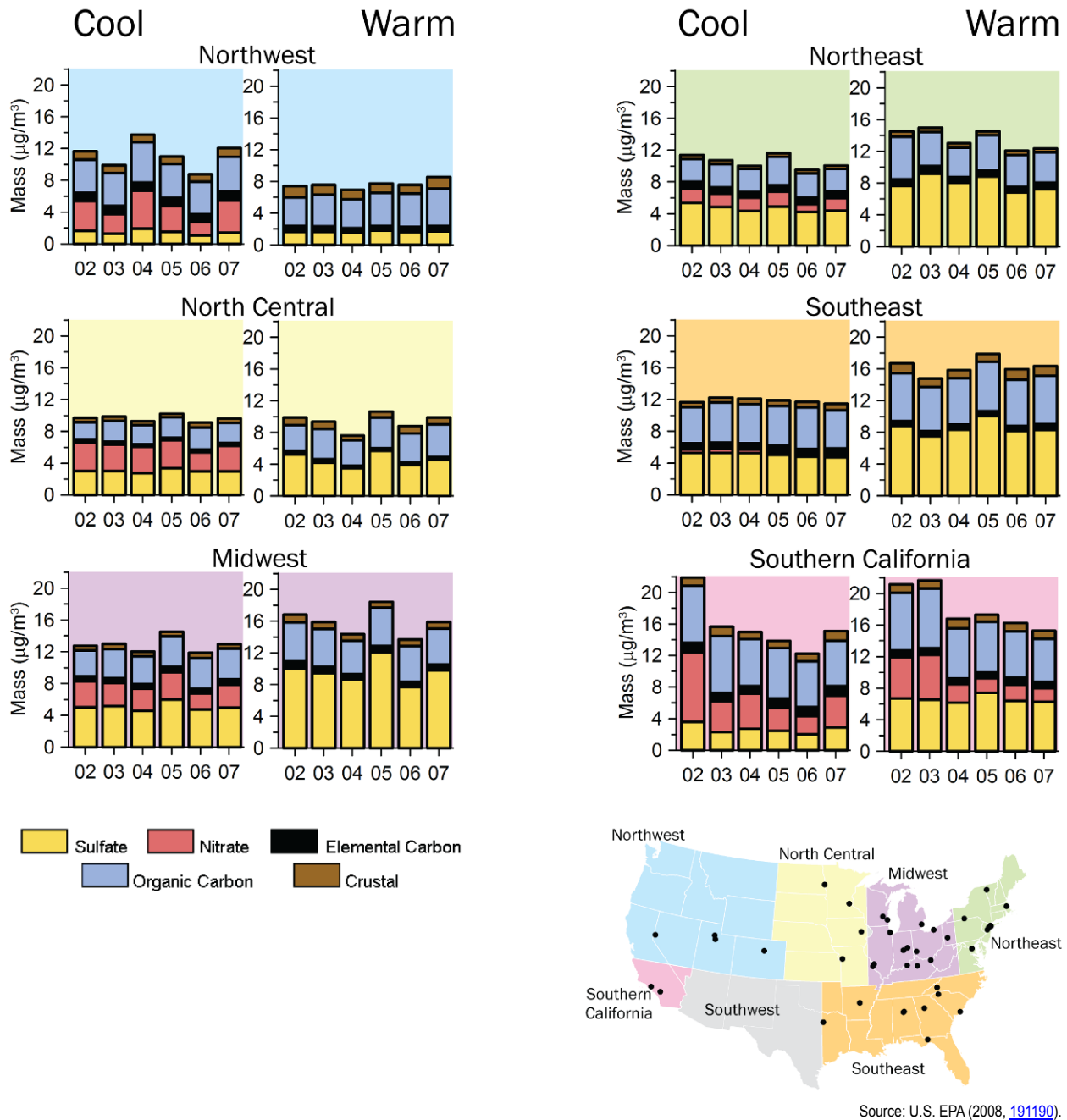


Figure 3-47. Regional and seasonal trends in annual PM_{2.5} composition from 2002 to 2007 derived using the SANDWICH method. Data from the 42 monitoring locations shown on the map were stratified by region and season including cool months (October-April) and warm months (May-September). SO₄²⁻ and NO₃⁻ estimates include NH₄⁺ and particle bound water.

Most of the components showed little discernable trend over the 6-yr period. SO₄²⁻ showed a peak during the warm months of 2005 in the Southeast, Northeast and Midwest, partly due to atypical weather conditions (U.S. EPA, 2008, 191190). However, no trend over the 6-yr time period is present for SO₄²⁻ in any of the regions or seasons. The same is true for EC and crustal material. A slight decline in OC was observed for the Northeast during warm months and in Southern California year-round. The largest decline was for NO₃⁻ in Southern California during both cool and warm

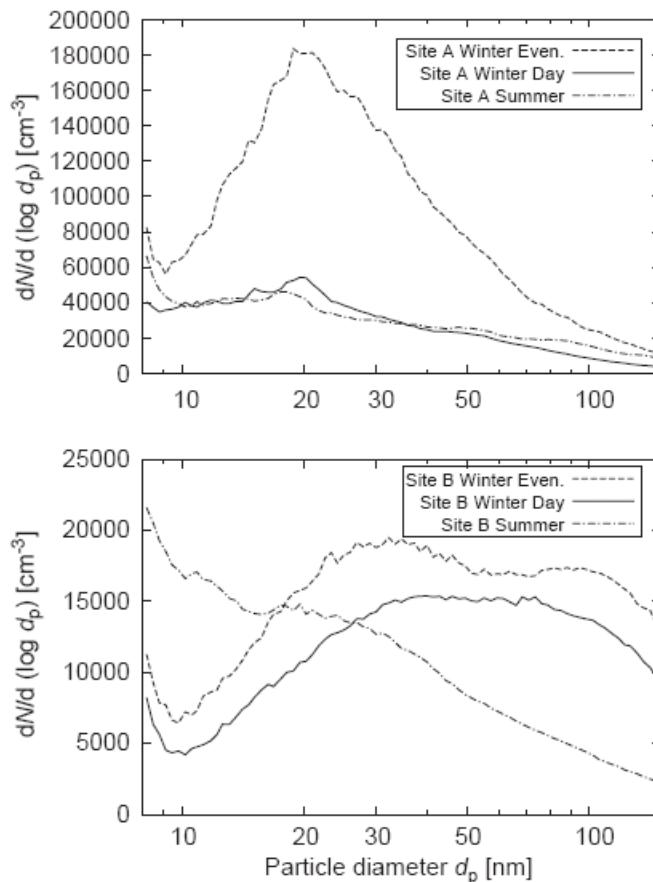
months. A smaller decline in NO_3^- is also observed in the other regions with the exception of the Northwest where no discernible trend is present. This analysis is limited in time and space by the availability of CSN data so a high degree of uncertainty remains regarding $\text{PM}_{2.5}$ compositional trends. However, with the exception of NO_3^- concentrations in Southern California, no major changes in $\text{PM}_{2.5}$ composition are evident based on available CSN data from 2002-2007. This is consistent with Figure 3-44 and Figure 3-45 where the downward trend in $\text{PM}_{2.5}$ mass begins to level off after 2002.

3.5.2.2. Seasonal Variations

Many of the figures and tables presented in the preceding sections have included a seasonal break-down based on the following climatological seasons: winter (December-February), spring (March-May), summer (June-August) and fall (September-November). Figures A-142 through A-156 in Annex A show bar charts of $\text{PM}_{2.5}$ composition by individual month, illustrating intra-annual variability on a finer time scale. The same 15 CSAs/CBSAs are investigated and included in these plots; they are generated from the same data used in the seasonal and annual pie charts based on the SANDWICH method discussed in Section 3.5.1.1 and illustrated in Figure 3-17 and Figure 3-18.

Monthly plots for most of the areas reveal heterogeneity in PM composition within the 3-month long seasonal bins defined earlier. This is especially true in the spring and fall when daily average weather conditions (e.g., temperature) are changing most rapidly, driving fluctuation in $\text{PM}_{2.5}$ composition on relatively short timescales in many cities. For example, the NO_3^- mass in Los Angeles (Figure A-129) and Riverside (Figure A-134) can vary from a small fraction to the most prevalent fraction of $\text{PM}_{2.5}$ mass in a month's time based on the 3-yr aggregate data. Therefore, selecting a different delineation point for the seasons can have an influence on the seasonal composition analysis, specifically for constituents that fluctuate rapidly (e.g., NO_3^-).

Relatively little is known about the seasonal variability in UFPs. Kuhn et al. (2005, [129448](#)) and Zhu et al. (2004, [156184](#)) found that the concentrations in the UF mode in Los Angeles, CA can be much higher during winter, particularly during evenings, because atmospheric dilution is reduced in response to lower mixing heights (Figure 3-48). Jeong et al. (2004, [180350](#)) made similar observations in Rochester, NY, suggesting an inverse relationship between temperature and UFP formation in the 11-470 nm size range. Singh et al. (2006, [190136](#)) reported higher particle number concentrations during winter months, relative to summer and spring, at urban sites in Southern California, and that afternoon particle number concentrations in warm months either occurred during a peak in ozone concentrations or followed shortly thereafter, suggesting a role for photochemistry in addition to meteorological changes in the formation of aerosols. The study also reported increased concentrations of 60-200 nm particles during a labor strike at the Port of Long Beach, suggesting contributions from idling ships. Moore et al. (2009, [191004](#)) also report higher particle number concentrations during cooler months at 14 sites in Long Beach, San Pedro, and Wilmington, CA, a location with diverse industrial and transportation sources. However, they noted substantial heterogeneity in seasonal trends between sites with seasonal numerical size distributions not generalizable across the study area with a maximum monitor separation of under 10 km.



Source: Reprinted with Permission of Elsevier Ltd. from Kuhn et al. (2005, [129448](#)).

Figure 3-48. UFP size distribution at highway (site A) and background (site B) sites in Los Angeles, CA, during summer and winter seasons, with winter broken into day and evening distributions.

Studies reporting higher cold-season particle number concentrations are consistent with vehicle emission studies that found particle emission rates elevated during lower ambient temperatures (Baldauf et al., 2005, [191184](#); Mathis et al., 2005, [155970](#); U.S. EPA, 2008, [191767](#)). Mathis et al. (2005, [155970](#)) found that cold-start conditions produce roughly an order of magnitude greater PM number emissions in gasoline engines and more than two orders of magnitude higher PM number emissions in diesel engines when compared with warm start conditions.

3.5.2.3. Hourly Variability

Hourly $PM_{2.5}$ and PM_{10} measurements are conducted at many sites using beta gauge or TEOM monitors. Many of the hourly measurements for PM_{10} have FRM or FEM status. All available hourly data from FRM, FEM and FRM-like monitors in the 15 CSAs/CBSAs discussed earlier were used to investigate diel variation in PM. Of the 15 CSAs/CBSAs, Atlanta, Chicago, Pittsburgh, Seattle and St. Louis had qualifying hourly $PM_{2.5}$ and PM_{10} data available. Houston and New York had only qualifying $PM_{2.5}$ data. Denver, Detroit, Los Angeles, Philadelphia, Phoenix, and Riverside had only qualifying hourly PM_{10} data. Birmingham and Boston had no qualifying hourly $PM_{2.5}$ or PM_{10} data.

Diel plots for $PM_{2.5}$ stratified by weekdays and weekends for seven of the 15 CSAs/CBSAs with available data between 2005 and 2007 are included in Annex A, Figures A-157 through A-163. In most cities investigated, a morning $PM_{2.5}$ peak is present starting at approximately 6:00 a.m., corresponding with the start of the morning rush hour just before the break-up of overnight stagnation. In Pittsburgh, dispersion behavior during the night results in elevated $PM_{2.5}$.

concentrations throughout the night that blend in with any morning peak. With the exception of Pittsburgh, all seven metropolitan areas show two distinct daily peaks on both the weekdays and weekends. The evening $PM_{2.5}$ concentration peak is broader than the morning peak and extends to overnight hours, reflecting the concentration increase caused by a drop in boundary layer height at night. Figure 3-49 compares the two-peak diel distribution in $PM_{2.5}$ for Seattle with the one-peak distribution in $PM_{2.5}$ for Pittsburgh. Since these figures represent the distribution of hourly observations over a 3-yr period, any fluctuations or changes in the timing of the daily peaks would result in a broadening of the curves shown in the diel plot.

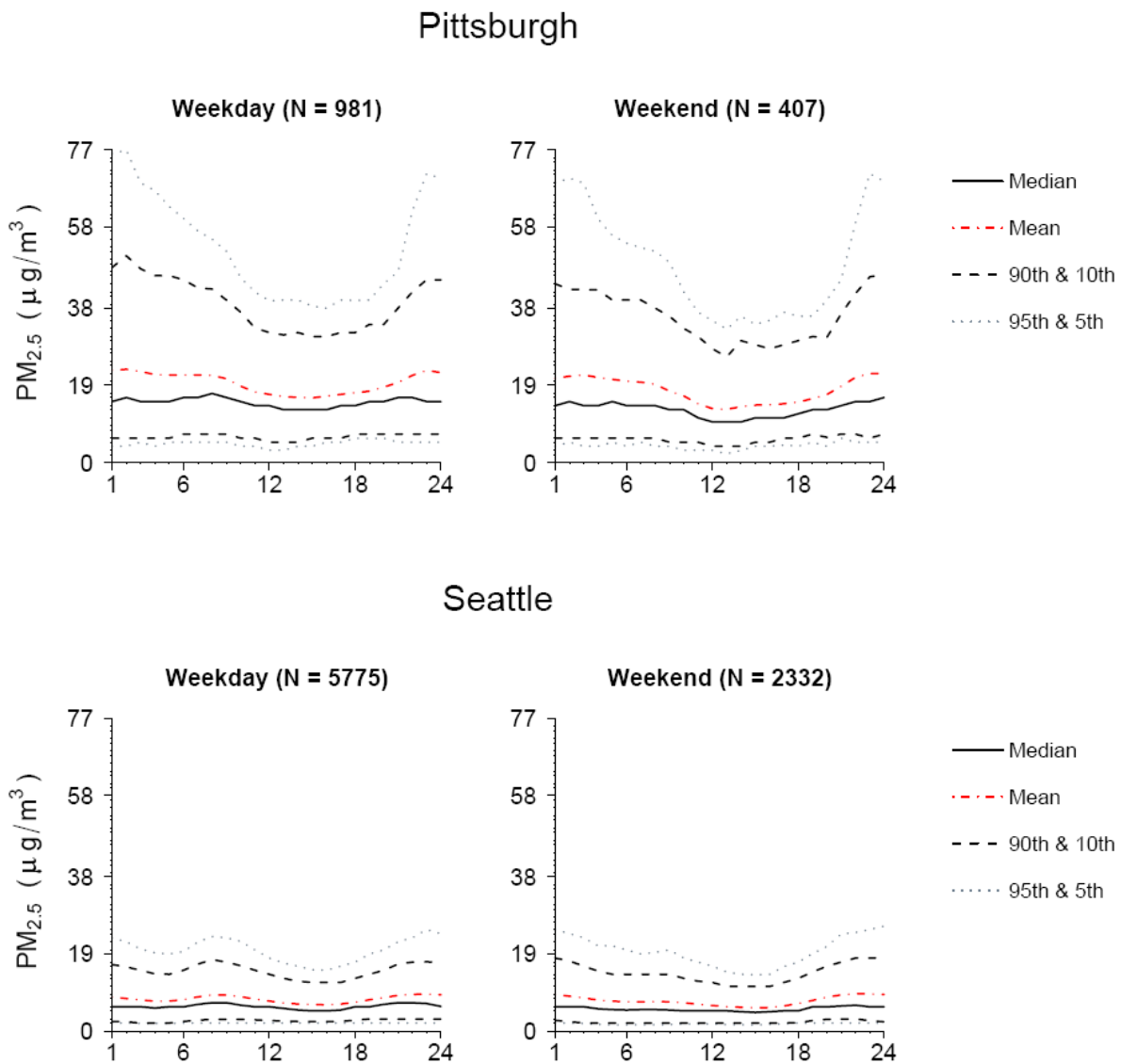


Figure 3-49. Diel plot generated from hourly FRM-like $PM_{2.5}$ data ($\mu\text{g}/\text{m}^3$) stratified by weekday (left) and weekend (right) for Pittsburgh, PA, and Seattle, WA, 2005-2007. Included are the number of monitor days (N) and the median, mean, 5th, 10th, 90th and 95th percentiles for each hour of the day shown on the horizontal axis.

Annex A, Figures A-164 through A-174 show diel patterns for PM₁₀ stratified by weekdays and weekends for eleven of the 15 CSAs/CBSAs with available data between 2005 and 2007. All cities show a gradual morning increase in mean PM₁₀ starting at approximately 6:00 a.m. on weekdays, corresponding with the start of the morning rush hour before the break-up of overnight stagnation. The magnitude and duration of this peak, however, varies considerably by area. Phoenix shows the most pronounced morning PM₁₀ peak concentration, which drops off during the day and reappears in the evening. In contrast, Chicago shows a less pronounced peak with the PM₁₀ concentration remaining elevated throughout the day. Figure 3-50 shows the diel plots of PM₁₀ for Chicago and Phoenix. In both instances, the weekend diel pattern is similar in shape to the weekday pattern with less pronounced peaks. Once again, any fluctuations in the timing of the daily peaks could result in a broadening of the peaks in the 3-yr composite diel figures.

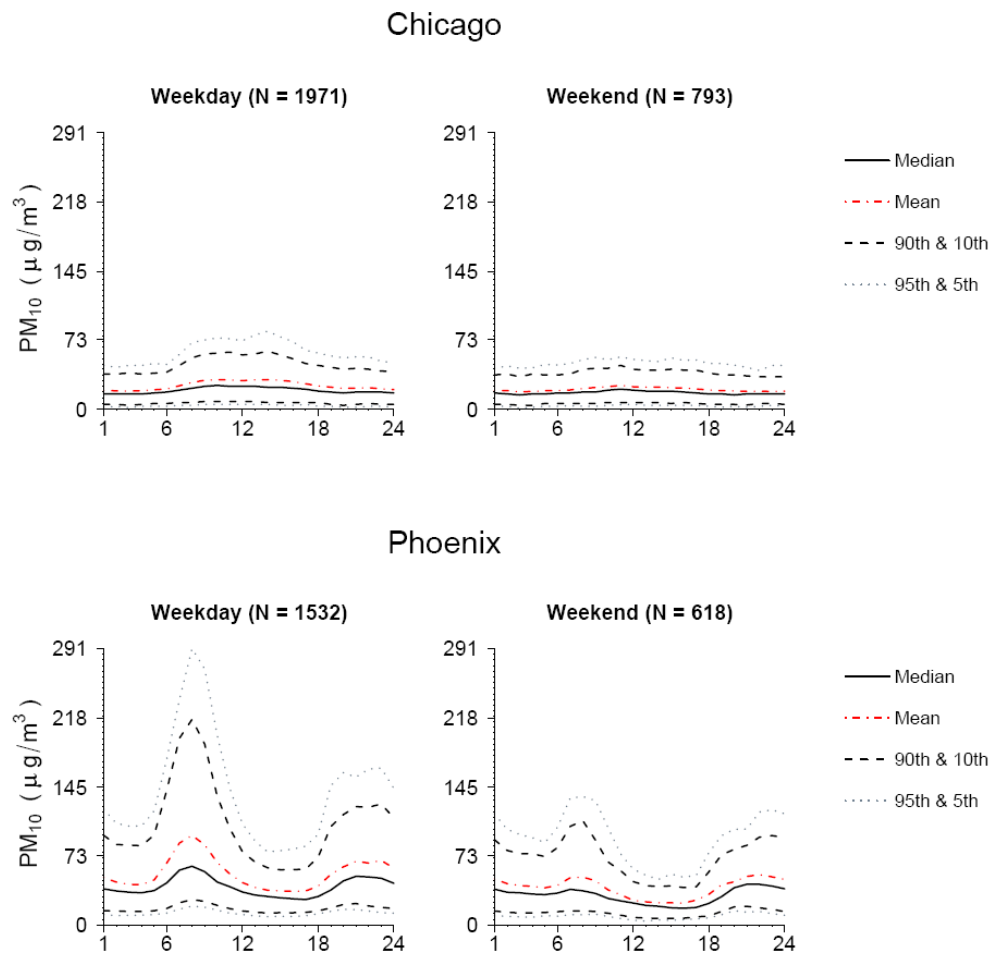
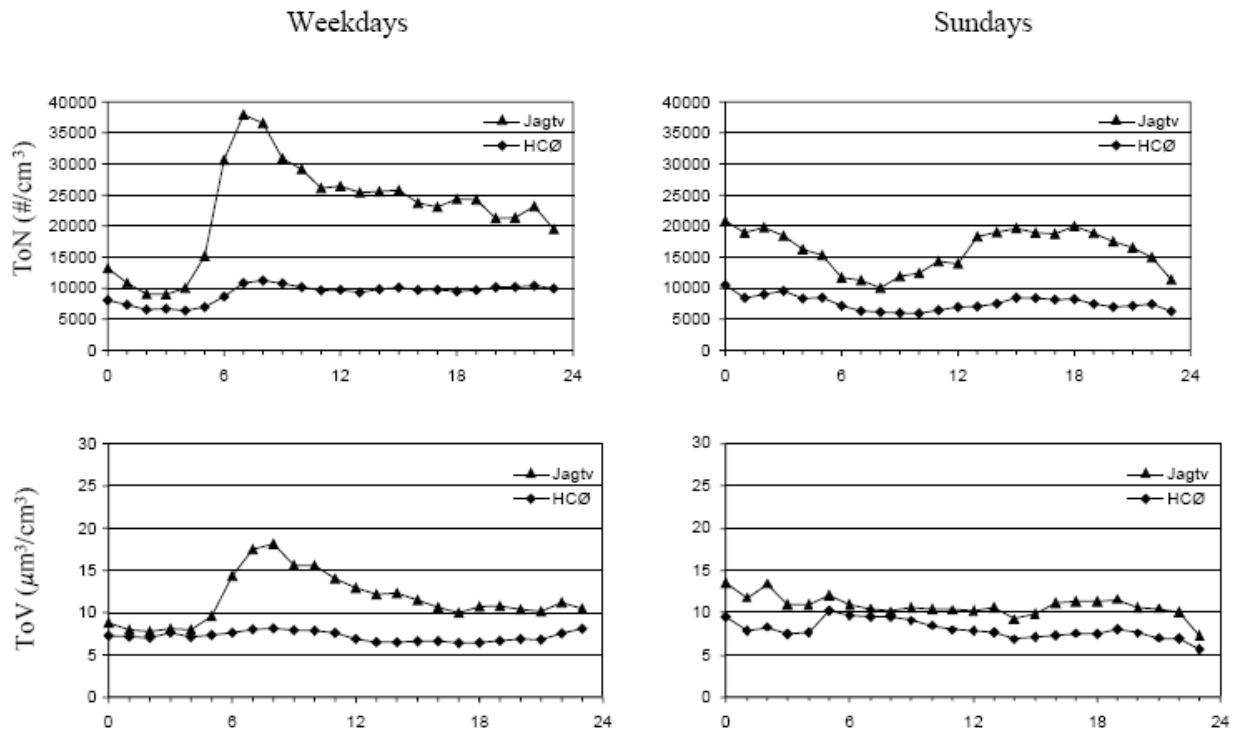


Figure 3-50. Diel plots generated from hourly FEM PM₁₀ data ($\mu\text{g}/\text{m}^3$) stratified by weekday (left) and weekend (right) for Chicago, IL, and Phoenix, AZ, 2005-2007. Included are the number of monitor days (N) and the median, mean, 5th, 10th, 90th and 95th percentiles for each hour of the day shown on the horizontal axis.

UFPs in urban environments have been shown to exhibit a similar two-peaked diel pattern in Los Angeles (Moore et al., 2007, [122445](#); Sardar et al., 2005, [180086](#)) and the San Joaquin Valley (Herner et al., 2005, [135983](#)) in CA, Rochester, NY (Jeong et al., 2004, [180350](#)), Raleigh, NC (Baldauf et al., 2008, [190239](#)) as well as in Kawasaki City, Japan (Hasegawa et al., 2005, [157355](#)) and Copenhagen, Denmark (Ketznel et al., 2003, [131251](#)). Figure 3-51 from the Denmark study

shows a large peak in total particle number (dominated by UFPs) corresponding with the morning rush hour. The morning peak is absent on Sundays, however. Many studies also show a broad afternoon UFP concentration peak, which likely originates from a combination of evening rush-hour traffic, decreased atmospheric dilution and formation of UFPs through nucleation involving products of active photochemistry. Nucleation likely plays an important role since the afternoon peak is present on weekends whereas the morning traffic related peak is absent. This is consistent with observations of particle counts in Atlanta peaking during the mid-afternoon for particles <10 nm (Woo et al., 2001, [011702](#)) resulting from nucleation.



Source: Adapted with Permission of Elsevier Science Ltd. From Ketzel et al. (2003, [131251](#))

Figure 3-51. Average diel variation in total particle number (ToN) and total particle volume (ToV) on weekdays (left column) and Sundays (right column) from two sites in Denmark: one in a busy street canyon (Jagtv) and one measuring urban background (HCØ).

Hourly variability in particle-phase OC and EC were investigated by Bae et al. (2004, [156243](#)) in the urban St. Louis atmosphere. OC diel patterns were similar during weekdays and weekends with a broad morning and evening concentration peak most likely reflecting daily fluctuations in atmospheric mixing height. Weekend EC diel patterns were similar to those for OC, but the weekday patterns showed more abrupt EC concentration peaks in the morning and afternoon, coinciding with rush-hour traffic. The divergent weekday patterns between OC and EC suggests motor vehicles or other EC sources with temporal profiles tracking traffic patterns are primarily responsible for the daily fluctuations in EC concentrations in St. Louis.

3.5.3. Statistical Associations with Copollutants

Associations between different PM size fractions and between PM and other copollutants including SO₂, NO₂, CO and O₃ are investigated in this section. AQS data were obtained from all available co-located monitors across the U.S. after application of a completeness criterion of 11 or

more observations per quarter. Pearson correlation coefficients (r) were calculated using 2005-2007 data. The results are displayed graphically in Figure 3-52 for correlations with $PM_{2.5}$ mass concentration and Figure 3-53 for correlations with PM_{10} mass concentration. The different PM size fractions are compared and contrasted in this section using temporal correlations which should not be confused with average PM mass fraction (e.g., $PM_{2.5}/PM_{10}$) comparisons discussed in Section 3.5.1.1.

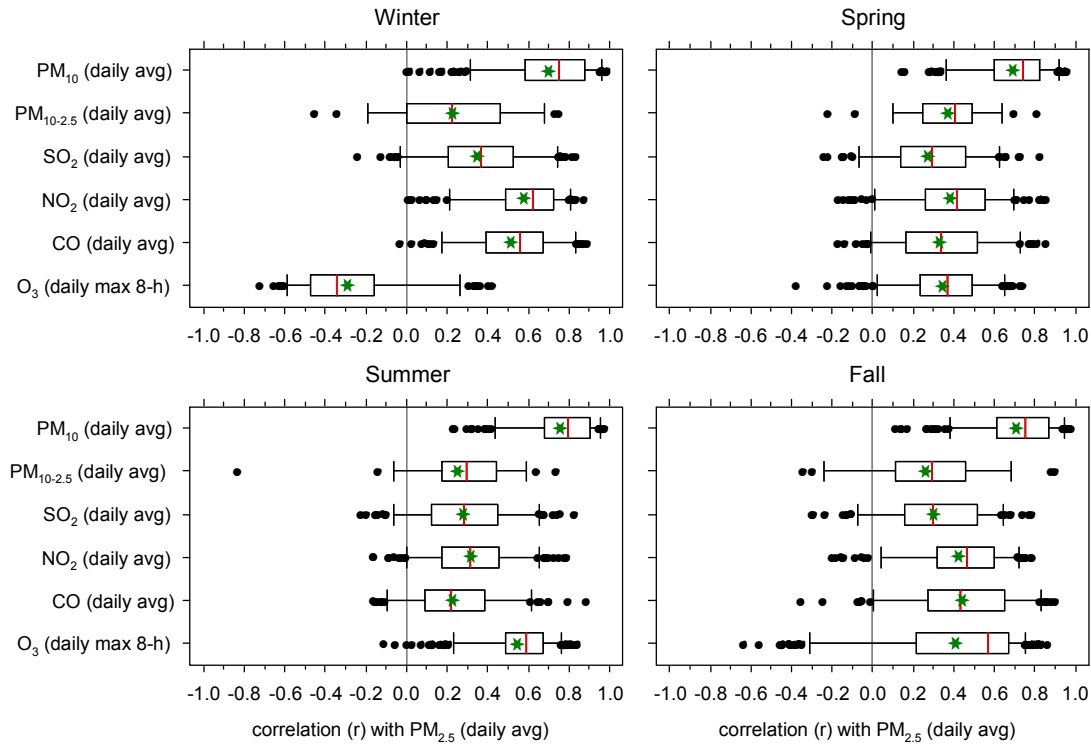


Figure 3-52. Distribution of correlations between 24-h avg $PM_{2.5}$ and co-located 24-h avg PM_{10} , $PM_{10-2.5}$, SO_2 , NO_2 and CO and daily max 8-h avg O_3 for the U.S. stratified by season (2005-2007). Statistics shown include the mean (green star), median (red line), inner quartile range (box), 5th/95th percentiles (whiskers) and outliers (black circles).

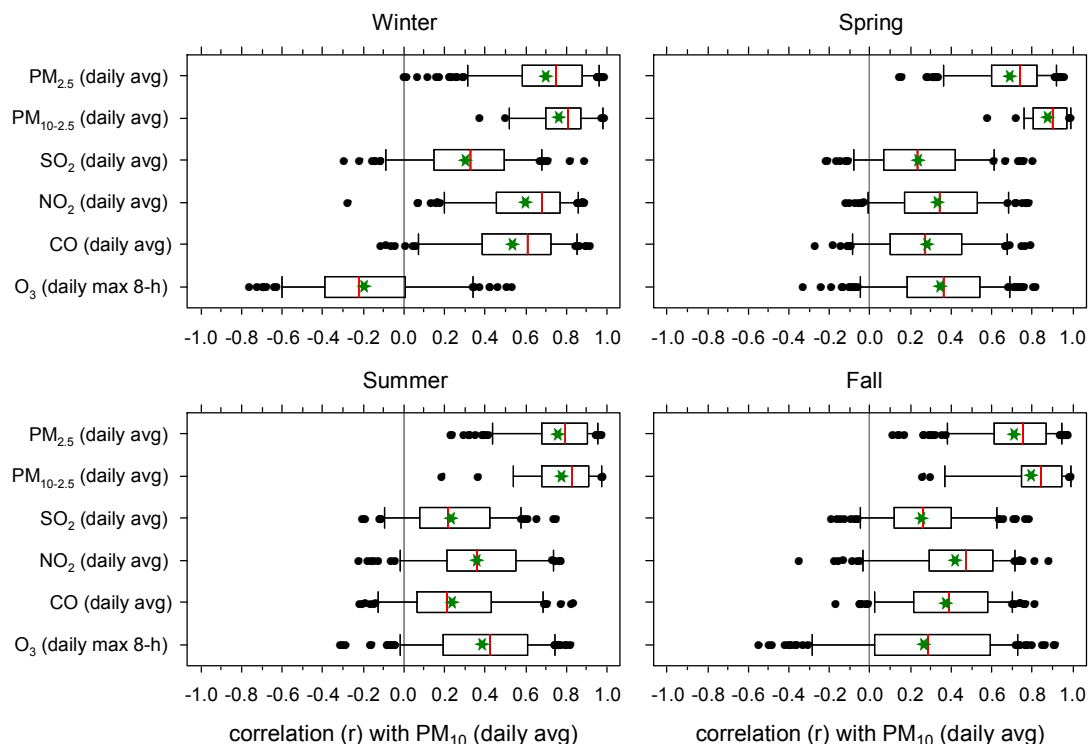


Figure 3-53. Distribution of correlations between 24-h avg PM₁₀ and co-located 24-h avg PM_{2.5}, PM_{10-2.5}, SO₂, NO₂ and CO and daily max 8-h avg O₃ for the U.S. stratified by season (2005-2007). Statistics shown include the mean (green star), median (red line), inner quartile range (box), 5th/95th percentiles (whiskers) and outliers (black circles).

For both PM_{2.5} and PM₁₀ national composite copollutant correlations, there is considerable spread in the observed correlations in all four seasons. On average, PM_{2.5} and PM₁₀ correlate with each other better than with the gaseous copollutants. The correlations between PM_{2.5} and PM₁₀ are all positive but span the range from just above zero to near one. This illustrates the wide variability in correlation between these two PM metrics. Fewer points are available for correlation with PM_{10-2.5} because only data from low-volume FRM/FRM-like samplers were used to calculate PM_{10-2.5}. The available data suggest a stronger correlation between PM₁₀ and PM_{10-2.5} than between PM_{2.5} and PM_{10-2.5} on a national basis.

Correlations among copollutants for individual CSAs/CBSAs are included in Annex A, Figure A-175 through Figure A-188 for PM_{2.5} and Figure A-189 through Figure A-202 for PM₁₀. Each data point in these figures represents a co-located monitor pair. Seattle did not have sufficient co-located data to be included with the other CSAs/CBSAs. As can be seen from the individual CSAs/CBSAs, there can be considerable variation in the correlations even within an individual urban area. For example, correlations between 24-h average PM_{2.5} and PM₁₀ concentrations measured at the five co-located monitor pairs in Boston between 2005 and 2007 ranged from 0.42 to 0.88 during winter and reach as high as 0.98 during the summer (Figure A-177).

Few locations within the 15 CSAs/CBSAs contained adequate data for calculating correlations with PM_{10-2.5} using low-volume PM data: Boston and New York had two locations each, Atlanta, Chicago, Denver and Phoenix had only one location and the remaining CSAs/CBSAs had no locations. Correlations between PM_{2.5} and PM_{10-2.5} varied substantially by CSA/CBSA and season and no general patterns were observed in the limited data set analyzed here. In contrast, correlations between PM₁₀ and PM_{10-2.5} did show some trends by location and season and were greater in all locations than correlations between PM_{2.5} and PM_{10-2.5}. The highest correlations between PM₁₀ and

PM_{10-2.5} were observed in Denver and Phoenix with correlations above 0.88 during all seasons. Atlanta, Boston, Chicago and New York all had lower correlations between PM₁₀ and PM_{10-2.5} ($0.30 \leq r \leq 0.88$), particularly during the fall ($0.30 \leq r \leq 0.56$). The lowest correlations between PM₁₀ and PM_{10-2.5} were observed in New York in the fall and Boston in the summer where they dropped to 0.30 and 0.38, respectively, at one of the two monitor locations in each city. In the four eastern CSAs/CBSAs investigated, correlations between PM₁₀ and PM_{10-2.5} were highest in the spring, in agreement with the national averages shown in Figure 3-53. In Denver and Phoenix, there was less seasonal dependence in the correlation.

A similar analysis of correlations between PM size fractions by region was reported in Table 3-1 of the 2004 PM AQCD (U.S. EPA, 2004, [056905](#)) and Figure 2-20 of the 2005 OAQPS Staff Paper (U.S. EPA, 2005, [090209](#)). In all regions, correlations between PM₁₀ and PM_{10-2.5} were greater than those for PM_{2.5} and PM_{10-2.5}. Correlations between PM₁₀ and PM_{10-2.5} were found to be largest in the southwest and the upper Midwest and smallest in the southeast and the northeast. While these regional analyses used different data inclusion criteria for estimating PM_{10-2.5} than the criteria used in this analysis for the individual CSAs/CBSAs, the results are generally consistent: higher correlations between PM₁₀ and PM_{10-2.5} mass concentrations compared with PM_{2.5} and PM_{10-2.5} mass concentrations in all regions and higher correlations between PM₁₀ and PM_{10-2.5} mass concentrations in the west compared to the east.

The correlation between PM and the gaseous pollutants included in Figure 3-52 and Figure 3-53 also showed a large range in values based on the national composite data. There was little seasonal variability in the mean correlation between PM and SO₂. NO₂ and CO, however, showed higher correlations with PM on average in winter than in the other seasons. This is possibly driven by meteorology with increased frequency of stagnation events in colder months as well as potential concurrent increases in emissions of these compounds from motor vehicles with colder temperatures. The correlation between daily max 8-h avg O₃ and 24-h avg PM showed the highest degree of seasonal variability with positive correlations on average in summer (0.56 for PM_{2.5} and 0.39 for PM₁₀) and negative correlations on average in winter (-0.30 for PM_{2.5} and -0.18 for PM₁₀). During the transition seasons, spring and fall, correlations were mixed but on average were still positive. PM_{2.5} is both primary and secondary in origin, whereas O₃ is only secondary. Photochemical production of O₃ and secondary PM in the planetary boundary layer (PBL) is much slower during the winter than during other seasons. Primary pollutant concentrations (e.g., primary PM_{2.5} components, NO and NO₂) in many urban areas are elevated in winter as the result of heating emissions, cold starts and low mixing heights. O₃ in the PBL during winter is mainly associated with air subsiding from above the boundary layer following the passage of cold fronts, and this subsiding air has much lower PM concentrations than are present in the PBL. Therefore, a negative association between O₃ and PM is frequently observed in the winter. During summer, both O₃ and secondary PM_{2.5} are produced in the PBL and in the lower free troposphere at faster rates compared to winter, and so they tend to be positively correlated. Bell et al. (2007, [093256](#)) also observed wintertime minima in same-day correlations between 24-h avg PM (both PM_{2.5} and PM₁₀) and 24-h avg O₃ using data from 98 U.S. urban communities. The average correlations were positive in winter, unlike those shown in Figure 3-53. Furthermore, the highest national average correlations were in spring and fall in the Bell et al. (2007, [093256](#)) analysis rather than summer as observed in Figure 3-52 and Figure 3-53. This discrepancy could be a result of the different averaging times used for O₃ or the selection of different monitoring networks and/or time periods.

For the PM_{2.5} city-specific correlations shown in Annex A, Figure A-175 through Figure A-188, all selected cities with sufficient data showed negative correlations in the wintertime with daily max 8-h avg O₃ (including Birmingham, Boston, Chicago, Denver, Houston, Los Angeles, Philadelphia, Phoenix, Pittsburgh, Riverside and St. Louis). The remaining four CSAs/CBSAs had insufficient data. In Baltimore, Sarnat et al. (2001, [019401](#)) found a significant (at the $p < 0.05$ level) positive (0.67) and negative (-0.72) correlation between daily PM_{2.5} and O₃ in the summer (June 19-August 23, 1998) and winter (February 2-March 13, 1999), respectively. For PM₁₀, the city-specific correlations with max 8-h avg O₃ shown in Annex A, Figure A-189 through Figure A-202 were more variable. Birmingham, Boston, and St. Louis all showed positive wintertime correlations between PM₁₀ and daily maximum 8-h avg O₃ while Denver, Detroit, Houston, Los Angeles and Phoenix showed negative wintertime correlations. The remaining seven CSAs/CBSAs had insufficient data. These copollutant correlations illustrate the importance of considering seasonality when assessing temporal relationships between air pollutants, particularly PM and O₃.

3.6. Mathematical Modeling of PM

There are two main classes of models used to study atmospheric PM, receptor models and CTMs. Receptor models are statistical models whereas CTMs are numerical models, i.e., they approximate derivatives by finite difference approximations. Finite element models are also numerical models but have not been used as extensively for applications described here, and so are not discussed further. Receptor models are diagnostic in their approach, in that they try to derive source contributions at monitoring locations using either ambient data alone or in combination with data for the chemical composition of sources or in combination with meteorological data. Three-dimensional CTMs are formulated in a prognostic, or predictive manner, that is, they attempt to predict species concentrations by solving a set of coupled, non-linear partial differential equations (continuity equations) for chemical species that include terms based on emissions inventories, atmospheric transport, chemical transformations, and deposition. Monitoring data is used to evaluate the performance of CTMs. Each of these approaches has its own advantages and disadvantages.

3.6.1. Estimating Source Contributions to PM Using Receptor Models

Methods for analyzing the composition of ambient PM samples in terms of contributions from different sources are reviewed in this section. Associations between exposures to ambient PM, as represented by ambient monitors, and health outcomes have been extensively studied. Some health studies, described in Section 6.6, have used source apportionment modeling to evaluate relationships between health outcomes and PM (mainly PM_{2.5}) from different sources. This section is intended to provide background concerning the uses of source apportionment techniques in such studies. Understanding the contribution of different emissions sources to ambient PM has also been used extensively in evaluating air quality data for use in developing control strategies.

3.6.1.1. Receptor Models

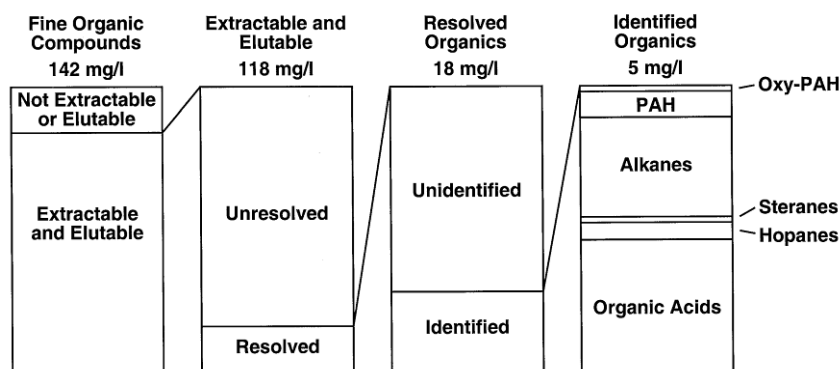
Receptor models have been used mainly as part of the development of air quality management plans. However, there have been several publications relating apportioned source types based on receptor models to human health effects. Discussions in this section will focus mainly on those methods that have been used to relate health outcomes to sources. More complete descriptions of a large number of types of receptor models currently in use are given in Watson et al. (2008, [157128](#)), who summarize the properties of these methods, including the strengths and weaknesses. This compilation of receptor models, broken down into different approaches (i.e., chemical mass balance, factor analysis, tracer-based, meteorology based) is included in Tables A-51 through A-54 in Annex A.

Receptor models such as the chemical mass balance (CMB) model (Watson et al., 1990, [004848](#)) relate source category contributions to ambient PM concentrations based on analyses of the compositional profiles of ambient and source emissions samples. It uses as its basis a mass balance equation that represents all chemical species in an aerosol sample as linear combinations of contributions from a fixed number of independent sources plus an error term representing the portion of the measurement that cannot be fit by the model.

The compositional profiles used in receptor models can be extensive (see for example the SPECIATE data base, <http://www.epa.gov/ttnchie1/software/speciate/index.html>) for a comprehensive collection of results from a large number of studies. As an example, several studies have identified EC and over 100 organic carbon compounds in gasoline PM emissions, including alkanes, PAHs, oxy-PAHs, steranes, hopanes, and organic acids (Maricq, 2007, [155973](#); Schauer et al., 1999, [010582](#); Schauer et al., 2002, [035332](#)). This breakdown in identifiable groups of organic compounds is illustrated in Figure 3-54 and Table 3-17 shows emissions factors for trace elements. Data for the compositional profiles for several other important sources of PM that could be used for CMB modeling are shown in Table A-55 in Annex A.

Source categories are amenable to refinement and to analysis as information on tracers becomes available. For example, PBAP have long been known to be significant constituents of the atmospheric aerosol, but not many studies have evaluated their contributions, largely because of the lack of suitable tracers and the additional equipment needs for sampling and analysis of bioaerosols.

Bauer et al. (2008, [189986](#)) reviewed studies estimating the contribution of fungal spores to PM_{2.5} and PM_{10-2.5} as fungal spores were expected to be major contributors to PBAP. They proposed the use of arabitol and mannitol as unique tracers with an estimated accuracy of ± 50% to apportion the contribution of fungal spores to OC in both PM_{2.5} and PM_{10-2.5}. They estimated 24-h avg contributions of ~ 40% to OC in PM_{10-2.5} during spring and summer in Vienna, with a smaller contribution to PM_{2.5}.



Source: Reprinted with Permission of Elsevier Science Ltd. From Fraser et al. (1999, [010819](#))

Figure 3-54. Schematic of organic composition of particulate emissions from gasoline-fueled vehicles.

One recently-identified concern in the application of CMB-based receptor models with detailed organic marker compounds is the photochemical stability of those species. Robinson et al. (2006, [156918](#)) reported evidence of significant summertime photooxidation of hopanes and long-chain alkenoic acids, low-volatility compounds often used as mobile source and cooking emissions, respectively. Seasonal differences in hopanes/EC ratios differed in a manner consistent with oxidation. Photochemical loss of particle-phase marker species mass complicates the interpretation of model results, as long-range transport and photochemistry may result in the loss of markers for distant sources. Furthermore, photochemical breakdown of organic marker species may cause losses in CMB model performance criteria and possible bias in source contribution estimates. The photooxidation of condensed-phase organic compounds also may affect the polarity and volatility of these compounds.

In other methods, various forms of factor analysis are used that rely on the varying mix of species present in ambient observations of compositional data to derive the source contributions. Standard factor analytic approaches such as Principal Component Analysis (PCA) have been used, but PCA alone can apportion only the variance, not the mass, in an aerosol composition data set. Additional steps in particular the identification of source tracers is required in Absolute Principal Components Scores (APCS) to apportion mass from PCA (Miller et al., 2002, [030661](#); Thurston and Spengler, 1985, [056074](#)). However, it can be difficult to find suitable tracers for some sources because many elements are emitted by more than one source. In Positive Matrix Factorization (PMF) (Paatero and Tapper, 1994, [086998](#)), the ambient compositional data matrix is decomposed into the product of a matrix representing the source contributions and one representing the source profiles. Solutions are obtained by minimizing an object function with respect to these two matrices, and solutions are subject to non-negativity constraints. PMF also allows for the treatment of missing data and data near or below detection limits by weighting elements inversely according to their uncertainties. The PMF approach requires a large number of samples (n typically >50) and are most often applied to time series data, whereas CMB can be applied to a single sample. Both the CMB and the PMF approaches find solutions based on least squares fitting and minimization of an object function. Both methods provide error estimates for the solutions based on estimates of the errors in the input parameters. It should be noted, though, that the error estimates for both methods often contain subjective judgments about the magnitude of the analytical and monitoring errors.

Table 3-17. Example of emissions factors (ng/km) for trace elements under variable speed and steady speed driving conditions for PM emitted by diesel and gasoline engines. Note that emissions are highly variable.

Element	Diesel		Gasoline	
	Transient	Steady State	Transient	Steady State
Al	9108 (5224)	2706	2273 (545)	252
Ca	69,443 (23,640)	16,128	18,247 (3044)	2324
Fe	22,910 (21,448)	2036	10,266 (9928)	138
K	4672 (752)	1191	1935 (558)	117
Mg	3087 (461)	997	5183 (1706)	183
Na	7736 (1751)	1945	2237 (1125)	321
Ba	583 (349)	73	331 (55)	4.8
Be	26 (12)	23	6.7 (1.1)	1.5
Cr	634 (354)	93	138 (6.7)	8.6
Cu	1944 (679)	627	1745 (1803)	16
Li	13 (0.2)	7.9	3.0 (1.4)	0.9
Mn	368 (183)	76	152 (85)	3.4
Ni	2310 (656)	644	107 (0.7)	21
Pb	793 (593)	79	237 (2.3)	11
S	23,750 (5295)	6713	8705 (3375)	349
Ti	2036 (320)	345	118 (9.3)	24
V	28 (9.4)	11	15 (11)	1.8
Zn	21,118 (4422)	5620	4650 (1225)	198

Standard deviations are presented in parenthesis when multiple tests have been averaged.

Source: Adapted with Permission of Elsevier Ltd. from Geller et al. (2006, [139644](#))

The nature of the solutions in terms of source categories is different in the CMB and PMF approaches. In the CMB approach, the composition of the source emissions is assumed to be known based on measurements. These assumptions may or may not reflect the composition of emissions affecting a particular site at any given time or place. However, there may be variations in the composition of individual source categories (e.g., soils, motor vehicle emissions) across a given airshed and even in the composition of the same source with time. Source profiles can also be altered between emission and receptor locations resulting from atmospheric reactions, depending on the source type and species under analysis. The CMB technique was developed for apportioning source categories of primary PM and was not formulated to include sources of secondary PM. CMB might not explain all the mass or produce a valid result unless there is information for the composition of all major sources affecting a given site, and there is confidence that the existing source profiles are specific to those sources. For example, Volckens et al. (2008, [105465](#)) describe PAH emission profiles from hand-held gasoline lawn and garden equipment as found in some CMB source profiles for motor vehicles.

In PMF, the source solutions are more general in that they contain information about the entrainment of emissions from additional sources during transport, the time dependence of the composition of emissions from particular sources, the formation of secondary species and local differences in source compositions. PMF differs from CMB because it derives the mix of factors from measured data. However, the procedure used to find a solution results in some rotational ambiguity (Paatero and Tapper, 1994, [086998](#)). The assignment of sources to PMF factors depends largely on past experience and judgments. Judgments are based to large extent on comparison with data for source profiles and also on the factors that could modify the assignments. These issues are

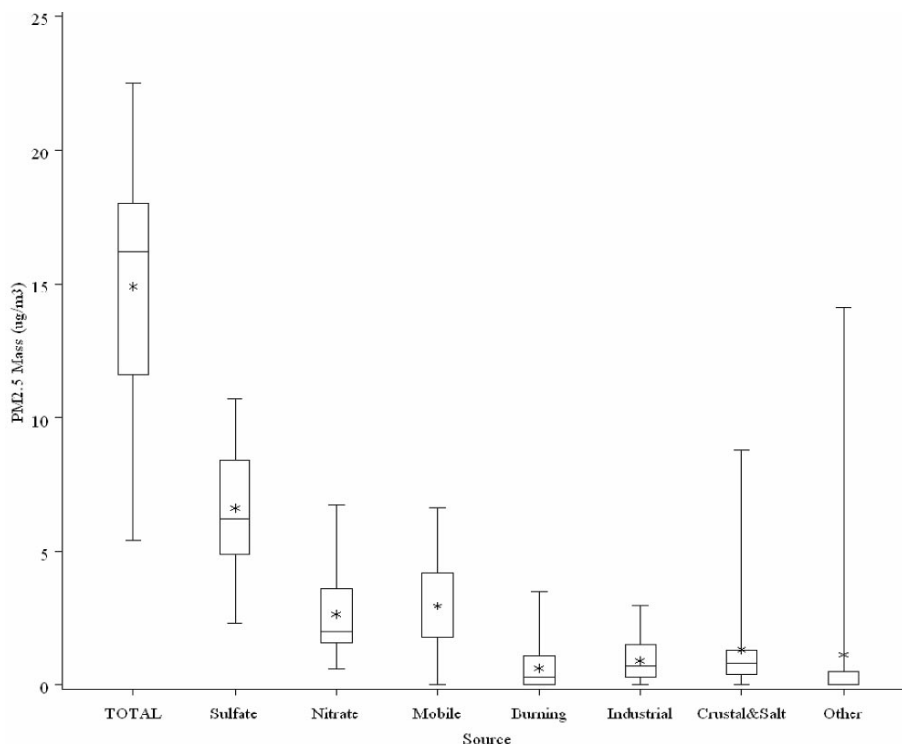
alleviated to some degree by incorporating information about local wind fields and other physical parameters.

The UNMIX model takes a geometric approach that exploits the covariance of the ambient data to determine the number of independent sources, the composition and contributions of the sources, and corresponding uncertainties (Henry, 1997, [020941](#)). UNMIX uses PCA to find edges in m -dimensional space, where m is the number of ambient species. Success of the UNMIX model hinges on the ability to find these “edges” in the ambient data from which the number of source types and the source compositions are extracted. In simplest terms, the approach can be seen to be similar to that for deriving ternary mixing diagrams, except there is extension to higher dimensionality. Measurement errors in the ambient data “fuzz” the edges, making them difficult to find. UNMIX employs an “edge-finding” algorithm to find the best edges in the presence of error. UNMIX does not make explicit use of errors or uncertainties in the ambient concentrations, unlike the methods outlined above. Rather they are implicitly incorporated into the analyses. PMF and UNMIX have also used data for particle size distributions to obtain further information about sources.

Partial least squares (PLS) is another mathematical model related to PCA which has been used in a limited number of PM toxicology studies to establish a relationship between PM constituents and health outcomes (McDonald et al., 2004, [087458](#); Seagrave et al., 2006, [091291](#); Veranth et al., 2006, [087479](#)). Although not really a receptor model and not designed as such, PLS shares some similarities with certain receptor models; and more importantly attempts to link PM components with health outcomes. Unlike PCA and other receptor models discussed in this section, PLS incorporates both predictor variables (e.g., PM component concentrations) and outcome variables (e.g., toxicological responses) into one coupled regression model. Like PCA, PLS groups the observable variables into a reduced number of latent variables, thereby reducing the dimensionality of the model. Typically, PM toxicology studies have been limited to two-component models (two latent variables on the predictor side compared with two on the outcome side), thereby producing a 2×2 loading plot revealing relationships between predictors and outcomes. PLS is particularly useful when there are more predictor variables than observations, which is a situation that other multivariate factor analysis approaches do not handle well. However, since PLS is a variance based approach, it shares the same shortcomings discussed earlier for PCA. PLS has also traditionally been limited to two-component applications even though this is not a strict mathematical limitation.

Results from Receptor Models

Results from receptor modeling calculations indicate that $PM_{2.5}$ is most often produced mainly by fossil fuel combustion. Fugitive dust, found mainly in the $PM_{10-2.5}$ size range, represents the largest source of measured ambient PM_{10} in many locations in the western U.S. Quoted uncertainties in the source apportionment of constituents in ambient aerosol samples typically range from 10 to 50%. It is apparent that a relatively small number of broadly defined source categories, compared to the total number of chemical species that typically are measured in ambient monitoring-source receptor model studies, are needed to account for the majority of the observed mass of PM in these studies. Trying to be more specific about contributions from source categories could result in ambiguity. For example, some stationary sources (e.g., agriculture use engines) and quite different mobile sources (e.g., trucks and locomotives) rely on diesel power and ancillary data is required to resolve contributions from these sources. Compilations of source attribution studies using CMB for PM_{10} have appeared in the 2004 PM AQCD (U.S. EPA, 2004, [056905](#)) and using PMF for $PM_{2.5}$ in Engel-Cox and Weber (2007, [156419](#)). Results of the compilation by Engel-Cox and Weber (2007, [156419](#)) for the eastern U.S. are shown in Figure 3-53. There are only three main source categories in the figure constituting most of the $PM_{2.5}$ mass (i.e., sulfate, nitrate, mobile). Two of these are predominantly secondary and not identified by sources of precursors. Tables A-56 and A-57 in Annex A list results of other receptor modeling studies for $PM_{2.5}$ and PM_{10} , many of which are in the western U.S.

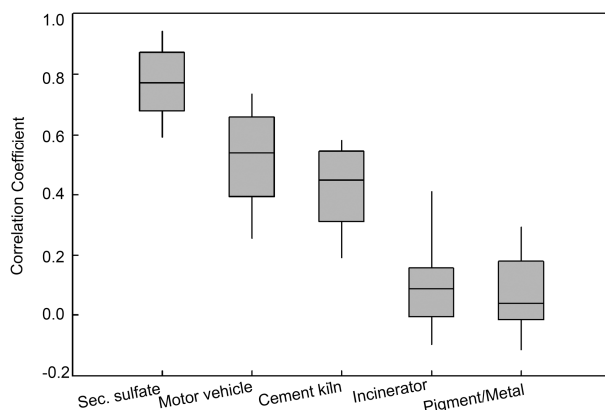


Source: Reprinted with Permission of Air & Waste Management Association from Engel-Cox and Weber (2007, [156419](#)).

Figure 3-55. Source category contributions to PM_{2.5} at a number of sites in the East derived using PMF.

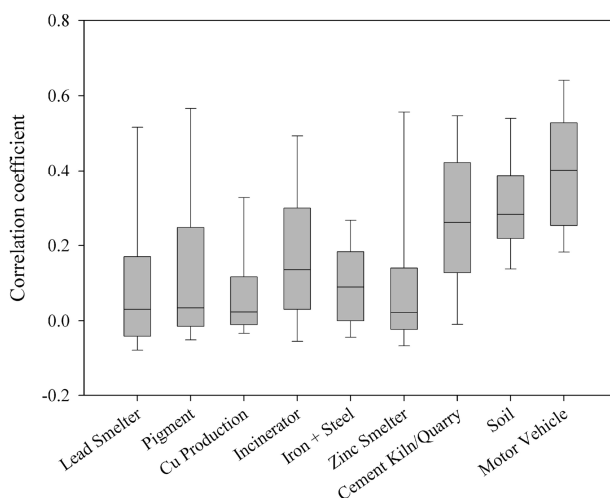
Spatial Variability in Source Contributions to PM Based on Receptor Models

Spatial variability in source contributions across urban areas is an important consideration in assessing the likelihood of exposure measurement error in epidemiologic studies relating health endpoints to sources. Arguments similar to those for using ambient concentrations as surrogates for personal exposures apply here. Studies for PM_{2.5} (Kim et al., 2005, [083181](#); Wongphatarakul et al., 1998, [049281](#)) indicate that intra-urban variability increases in the following order: regional sources (e.g., secondary SO₄²⁻ originating from EGUs) < area sources (e.g., on-road mobile sources) < point sources (e.g., stacks). This point is illustrated in Figure 3-56. The only study available for PM_{10-2.5} (Hwang et al., 2008, [134420](#)) indicates a similar ordering, but without a regional component (resulting from the short lifetime of coarse PM compared to transport times on the regional scale) as shown in Figure 3-57.



Source: Reprinted with Permission of ACS from Kim et al. (2005, [083181](#))

Figure 3-56. Pearson correlation coefficients for source category contributions to PM_{2.5} between the 10 Regional Air Pollution Study/Regional Air Monitoring System (RAPS/RAMS) monitoring sites in St. Louis.



Source: Reprinted with Permission of ACS from Hwang et al. (2008, [194533](#))

Figure 3-57. Pearson correlation coefficients for source contributions to PM_{10-2.5} between the 10 Regional Air Pollution Study/Regional Air Monitoring System (RAPS/RAMS) monitoring sites in St. Louis.

3.6.2. Chemistry Transport Models

CTMs are the prime tools used to compute the interactions among atmospheric pollutants and their transformation products, the production of secondary aerosols, the evolution of particle size distribution, and transport and deposition of pollutants. CTMs are driven by emissions inventories for primary species such as NO_x, SO_x, NH₃, VOCs, and primary PM, and by meteorological fields produced by other numerical prediction models. Values for meteorological state variables such as winds and temperatures are taken from operational analyses, reanalyses, or weather circulation models. In most cases, these are off-line meteorological analyses, meaning that they are not modified

by radiatively active species generated by the air quality model (AQM). Work to integrate meteorology and chemistry was done in the mid-1990s by Lu et al. (1997, [048202](#) and references therein; 1997, [191768](#)) although limits to computing power prevented their wide-spread application. More recently, new, integrated models of meteorology and chemistry are now available as well; see, for example, Binkowski et al. (2007, [090563](#)) and the Weather Research and Forecast model with chemistry (WRF-Chem) (<http://ruc.fsl.noaa.gov/wrf/WG11>).

CTMs have been developed for application over a wide range of spatial scales ranging up from neighborhood to global. CTMs are used to: (1) obtain better understanding of the processes controlling the formation, transport, and destruction of gas- and particle-phase criteria and hazardous air pollutants; (2) understand the relations between concentrations of secondary pollutant products and concentrations of their precursors; (3) understand relations among the concentration patterns of various pollutants that may exert adverse effects; and (4) evaluate how changes in emissions propagate through the atmospheric system to secondary products and deposition.

Emissions of precursor compounds can be divided into anthropogenic and natural source categories. Natural sources can be further divided into biogenic from vegetation, microbes, and animals, and abiotic from biomass burning, lightning, and geogenic sources. However, the distinction between natural sources and anthropogenic sources is often difficult to make in practice, as human activities affect directly or indirectly emissions from what would have been considered natural sources during the preindustrial era. Thus, emissions from plants and animals used in agriculture have been referred to as anthropogenic or biogenic in different applications. Wildfire emissions may be considered natural, except that forest management practices can lead to buildup of fuels on the forest floor, thereby altering the frequency and severity of forest fires.

The initial conditions, or starting concentration fields of all species computed by a model, and the boundary conditions, or concentrations of species along the horizontal and upper boundaries of the model domain throughout the simulation, must be specified at the beginning of the simulation. Both initial and boundary conditions can be estimated from models or data or, more generally, model + data hybrids. Because data for vertical profiles of most species of interest are very sparse, results of model simulations over larger, usually global, domains are often used. As might be expected, the influence of boundary conditions depends on the lifetime of the species under consideration and the time scales for transport from the boundaries to the interior of the model.

Each of the model components described above has associated uncertainties and the relative importance of these uncertainties varies with the modeling application. The largest errors in photochemical modeling are still thought to arise from the meteorological and emissions inputs to the model (Russell and Dennis, 2000, [035563](#)). While the effects of poorly specified boundary conditions propagate through the model's domain, the effects of these errors remain undetermined. Because many meteorological processes occur on spatial scales smaller than the model's vertical or horizontal grid spacing and thus are not calculated explicitly, parameterizations of these processes must be used. These parameterizations introduce additional uncertainty. Because the chemical production and loss terms in the continuity equations for individual species are numerically coupled, the chemical calculations must be performed iteratively until calculated concentrations converge to within some preset criterion. The number of iterations and the convergence criteria chosen also can introduce error.

CTMs in current use mostly have one of two forms. The first, grid-based or Eulerian air quality models subdivide the region to be modeled, the modeling domain, into a three-dimensional array of grid cells. Spatial derivatives in the species continuity equations are cast in finite-difference form over this grid and a system of equations for the concentrations of all the chemical species in the model are solved numerically at each grid point. Time-dependent continuity or mass conservation equations are solved for each species including terms for transport, chemical production and destruction, and emissions and deposition (if relevant), in each grid cell. Chemical processes are simulated with ordinary differential equations, and transport processes are simulated with partial differential equations. Because of a number of factors such as the different time scales inherent in different processes, the coupled, nonlinear nature of the chemical process terms, and computer storage limitations, not all of the terms in the equations are solved simultaneously in three dimensions. Instead, operator splitting, in which terms in the continuity equation involving individual processes are solved sequentially, is used.

In the second common CTM formulation, trajectory or Lagrangian models, a number of hypothetical air parcels are specified as though following wind trajectories. In these models, the

original system of partial differential equations is transformed into a system of ordinary differential equations.

A less common approach is to use a hybrid Lagrangian-Eulerian model, in which certain aspects of atmospheric chemistry and transport are treated with a Lagrangian approach and others are treated in an Eulerian manner (e.g., Stein et al., 2000, [048341](#)).

Each approach has advantages and disadvantages. The Eulerian approach is more general in that it includes processes that mix air parcels and allows integrations to be carried out for long periods during which individual air parcels lose their identity. There are, however, techniques for including the effects of mixing in Lagrangian models such as FLEXPART (Zanis et al., 2003, [053423](#)), ATTILA (Reithmeier and Sausen, 2002, [053447](#)), and CLaMS (McKenna et al., 2002, [053445](#)). Because both the accuracy and the computational intensity of Eulerian models depend strongly on the size of the horizontal and vertical grid spacing, speed and fidelity to actual atmospheric conditions must sometimes be traded-off; that is to say, while finer grid spacing will often capture effects missed at larger grid intervals, models set up in this way require longer to solve. In a similar manner, the accuracy of Lagrangian models depends on the number of air parcels deployed; thus they, too, become computationally intensive when higher-order accuracy is desired. More detailed discussion of CTM applications appears in the 2008 ISA for NO_x and SO_x – Ecological Criteria (U.S. EPA, 2008, [157074](#)).

3.6.2.1. Global Scale

Global-scale CTMs are used to address issues associated with climate change and stratospheric O₃ depletion to characterize long-range air pollution transport, and to provide boundary conditions for the regional-scale models. The CTMs include parameterizations of atmospheric transport; the transfer of solar radiation through the atmosphere; chemical reactions; and removal to the surface by turbulent motions and precipitation for emitted pollutants. The upper boundaries of the CTMs extend anywhere from the tropopause (~8 km at the poles to ~16 km in the tropics) to the mesopause at ~80 km in order to obtain more realistic boundary conditions for problems involving stratospheric dynamics and chemistry.

Global simulations are typically conducted with a horizontal grid spacing of 200 km or more, although some models such as GEOS-Chem have been run at grid spacings of about 100 km (e.g., Wu et al., 2008, [190039](#)) and efforts are being made to achieve even higher spatial resolution. Simulations of the effects of long-range transport at particular locations link multiple horizontal resolutions from the global to the local scale. Finer resolution can only improve scientific understanding to the extent that the governing processes are more accurately described at that scale. Consequently, there is a crucial need for observations at the appropriate scales to evaluate the scientific understanding represented by the models.

3.6.2.2. Regional Scale

Most major regional-scale air-related modeling efforts at EPA use the Community Multi-scale Air Quality modeling system (CMAQ) (Byun and Ching, 1999, [156314](#); Byun and Schere, 2006, [090560](#)). A number of other modeling platforms using Lagrangian and Eulerian frameworks were reviewed in the 2006 O₃ AQCD (U.S. EPA, 2006, [088089](#)) and in Russell and Dennis (2000, [035563](#)). The capabilities of a number of CTMs designed to study local- and regional-scale air pollution problems were summarized by Russell and Dennis (2000, [035563](#)). Evaluations of the performance of CMAQ are given in Arnold et al. (2003, [087579](#)), Eder and Yu (2005, [089229](#)), Appel et al. (2005, [089227](#)), and Fuentes and Raftery (2005, [087580](#)). CMAQ's horizontal domain can extend from a few hundred kilometers on a side to the entire hemisphere. CMAQ is most often driven by the MM5 mesoscale meteorological model (Seaman, 2000, [035562](#)), though it may be driven by other meteorological models including WRF and the Regional Atmospheric Modeling System (RAMS); see <http://atmet.com>. Simulations of pollution episodes over regional domains have been performed with a horizontal resolution as low as 1 km; see the application and general survey results reported in Ching et al. (2006, [090300](#)). However, simulations at such high resolutions require better parameterizations of meteorological processes such as boundary layer fluxes, deep convection and clouds (Seaman, 2000, [035562](#)). Finer spatial resolution is necessary to resolve features such as urban heat island circulation; sea, bay, and land breezes; mountain and valley breezes; and the nocturnal low-level jet, all of which can affect pollutant concentrations.

The most common approach to setting up the horizontal domain is to nest a finer grid within a larger domain of coarser resolution. However, there are other strategies such as the stretched grid and the adaptive grid. In a stretched grid, the grid's resolution continuously varies throughout the domain, thereby eliminating any potential problems with the sudden change from one resolution to another at the boundary. Caution should be exercised in using such a formulation because certain parameterizations like those for convection might be valid on a relatively coarse grid scale but may not be valid on finer scales. Adaptive grids are not fixed at the start of the simulation, but instead adapt to the needs of the simulation as it evolves. They have the advantage that they can resolve processes at relevant spatial scales. However, they can be very slow if the situation to be modeled is complex. Additionally, if adaptive grids are used for separate meteorological, emissions, and photochemical models, there is no reason a priori why the resolution of each grid should match, and the gains realized from increased resolution in one model will be wasted in the transition to another model. The use of finer horizontal resolution in CTMs will necessitate finer-scale inventories of land use and better knowledge of the exact paths of roads, locations of factories, and, in general, better methods for locating sources and estimating their emissions.

The vertical resolution of these CTMs is variable and usually configured to have more layers in the PBL and fewer higher up. Because the height of the boundary layer is of critical importance in simulations of air quality, improved resolution of the boundary layer height would likely improve air quality simulations. Additionally, current CTMs do not adequately resolve fine-scale features such as the nocturnal low-level jet in part because little is known about the nighttime boundary layer.

CTMs require time-dependent, three-dimensional wind fields for the period of simulation. The winds may be generated either by a model using initial fields alone or with four-dimensional data assimilation to improve the model's performance; i.e., model equations can be updated periodically to bring results into agreement with observations. Modeling series durations can range from simulations of several days duration, the typical time scale for individual O₃ episodes, to several months or multiple seasons of the year. The current trend in modeling applications is towards annual simulations. This trend is driven in part by the need to improve understanding of observations of periods of high wintertime PM (Blanchard et al., 2002, [047598](#)) and the need to simulate O₃ episodes occurring in spring, fall, and winter.

Chemical kinetics mechanisms representing the important reactions occurring in the atmosphere are used in CTMs to estimate the rates of chemical formation and destruction of each pollutant simulated as a function of time. Mechanisms that treat the reactions of all individual reactive species explicitly are computationally too demanding to be incorporated into CTMs for regulatory use. Similarly, very extensive "master mechanisms" (Derwent et al., 2001, [047912](#)) that include approximately 10,500 reactions involving 3,603 chemical species (Derwent et al., 2001, [047912](#)) can be combined into mechanisms that group together compounds with similar chemistry. Because of different approaches to the lumping of organic compounds into surrogate groups for computational efficiency, chemical mechanisms can produce different results under similar conditions. The Carbon Bond chemical mechanisms starting with CB-IV (Gery et al., 1989, [043039](#)), the RADM II mechanism (Stockwell et al., 1990, [043095](#)), the SAPRC (e.g., Carter, 1990, [042893](#); Wang et al., 2000, [048357](#); Wang et al., 2000, [048365](#)), and the RACM mechanisms can be used in CMAQ. Jimenez et al. (2003, [156611](#)) provided brief descriptions of the features of the main mechanisms in use and compared concentrations of several key species predicted by seven chemical mechanisms in a box-model simulation over 24 h.

CMAQ and other state-of-the-science CTMs incorporate processes and interactions of aerosol-phase chemistry (Binkowski and Roselle, 2003, [191769](#); Gaydos et al., 2007, [139738](#); Zhang and Wexler, 2008, [191770](#)). There have also been several attempts to study the feedbacks of chemistry on atmospheric dynamics using meteorological models like MM5 and WRF (Grell et al., 2000, [048047](#); Liu et al., 2001, [048201](#); Lu et al., 1997, [048202](#); Park et al., 2001, [044169](#)). This coupling is necessary to accurately simulate feedbacks which may be caused by the heavy aerosol loading found in forest fire plumes (Lu et al., 1997, [048202](#); Park et al., 2001, [044169](#)) or in heavily polluted areas. Photolysis rates in CMAQ can now be calculated interactively with model produced O₃, NO₂, and aerosol fields (Binkowski et al., 2007, [090563](#)).

Spatial and temporal characterizations of anthropogenic and biogenic precursor emissions must be specified as inputs to a CTM. Emissions inventories have been compiled on grids of varying resolution for many hydrocarbons, aldehydes, ketones, CO, NH₃, and NO_x. Emissions inventories for many species require the application of algorithms for calculating the dependence of emissions on physical variables, such as temperature, and to convert the inventories into formatted emission

files which can be used by a CTM. For example, preprocessing of emissions data for CMAQ often is done by the Sparse-Matrix Operator Kernel Emissions (SMOKE) system (<http://smoke-model.org>). For many species, information concerning the temporal variability of emissions is lacking, so long-term annual averages are used in short-term, episodic simulations. Annual emissions estimates are often modified by the emissions model to produce emissions more characteristic of the time of day and season. Significant errors in emissions can occur if inappropriate time dependence is used. Additional complexity arises in model calculations because different chemical mechanisms can include different species, and inventories constructed for use with one mechanism must be adjusted to reflect these differences in another.

3.6.2.3. Local or Neighborhood Scale

The grid spacing in regional CTMs, usually between 1 and 12 km², is usually too coarse to resolve spatial variations on the neighborhood scale. The interface between regional scale models and models of smaller exposure scales is provided by smaller scale dispersion models. Several models could be used to simulate concentration fields near roads, each with its own set of strengths and weaknesses. The California Department of Transportation's most recent line dispersion model is CALINE4; see <http://www.dot.ca.gov/hq/env/air/pages/calinesw.htm>. The CALINE family of models is not supported by the California Department of Transportation for modeling of highway-source PM, however, but only for roadway CO, although PM work with CALINE has been performed for more than ten years; see Wu et al. (2009, 191773) and references therein.

In addition, AERMOD (http://www.epa.gov/scram001/dispersion_prefrec.htm) is a steady-state plume model formulated as a replacement to the ISC3 dispersion model. In the stable boundary layer (SBL), it assumes the concentration distribution to be Gaussian in both the vertical and horizontal dimensions. In the convective boundary layer, the horizontal distribution is also assumed to be Gaussian, but the vertical distribution is described with a bi-Gaussian probability density function (pdf). AERMOD has provisions that can be applied to flat and complex terrain and multiple source types (including, point, area and volume sources) in both urban and rural areas. It incorporates air dispersion based on the structure of turbulence in the PBL and scaling concepts and is meant to treat surface and elevated sources, in both simple and complex terrain in rural and urban areas. The dispersion of emissions from line sources like highways in AERMOD is handled as a source with dimensions set using an area or volume source algorithm in the model; however, actual emissions are usually not in steady state and there are different functional relationships between buoyant plume rise in point and line sources. Moreover, most simple dispersion models including AERMOD are designed without chemical mechanisms and so cannot produce secondary pollutants from their primary emissions.

There are also non-steady state models that incorporate plume rise explicitly from different types of sources. For example, CALPUFF (<http://www.src.com/calpuff/calpuff1.htm>), which is EPA's recommended dispersion model for transport in ranges >50 km, is a non-steady-state puff dispersion model that simulates the effects of time- and space-varying meteorological conditions on pollution transport, transformation, and removal and has provisions for calculating dispersion from surface sources. However, CALPUFF was not designed to treat the dispersion of emissions from roads, and like AERMOD does not include production of secondary pollutants. The distinction between a steady-state and time varying model could be unimportant for long time scales; however, at short time scales, the temporal variability in traffic emissions could result in underestimation of peak concentration and exposures.

3.6.3. Air Quality Model Evaluation for Air Concentrations

Urban and regional air quality is determined by a complex system of coupled chemical and physical processes including emissions of pollutants and pollutant precursors, complex chemical reactions, physical transport and diffusion, and wet and dry deposition. NO_x in these systems has long been known to (1) act nonlinearly in the production of O₃ and other secondary pollutants (Dodge, 1977, 038646); and (2) involve complicated cross-media environmental issues, such as acidic or nutrient deposition to sensitive biota and degradation of visibility.

NO_y species emitted and transformed from emissions control the production and fate of both O₃ and aerosols by sustaining or suppressing OH cycling. Correctly characterizing the interrelated

NO_Y and OH dynamics for O_3 formation and fate in the polluted troposphere depends on new techniques using combinations of several NO_Y species for diagnostically probing the complex atmospheric dynamics in typical urban and regional airsheds.

Evaluation results from a recent EPA exercise of CMAQ in the Tampa Bay, FL, airshed are presented here as an example of the present level of skill of state-of-the-science AQMs for predicting atmospheric concentrations of some of the relevant species for this PM NAAQS assessment. This modeling series exercised CMAQ version 4.4 and with the University of California at Davis (UCD) sectional aerosol module in place of the standard CMAQ modal aerosol module and was driven by meteorology from MM5 v3.6 and with NEI emissions as augmented by continuous emissions monitoring data where available. The UCD size-segregated module was preferred for this application because of the importance of sea salt particles in the bay airshed. Testing of this new engineering extension to CMAQ (termed CMAQ-UCD below) revealed that its performance was very similar to that of CMAQ's standard modal module; hence, model behavior and performance reported here can stand as a general indication of CMAQ's skill.

The CTM was run with 21 vertical layers for the month of May 2002. For this evaluation, CMAQ-UCD was run in a one-way nested series of three domains with 32 km, 8 km, and 2 km horizontal grid spacings from the CONUS (32 km) to central Florida and the eastern Gulf of Mexico (2 km). Depictions of the 8 km and 2 km domains used here zoomed over the central Tampa area are shown in Figure 3-58 and Figure 3-59.



Figure 3-58. Eight km southeast U.S. CMAQ-UCD domain zoomed over Tampa Bay, FL.

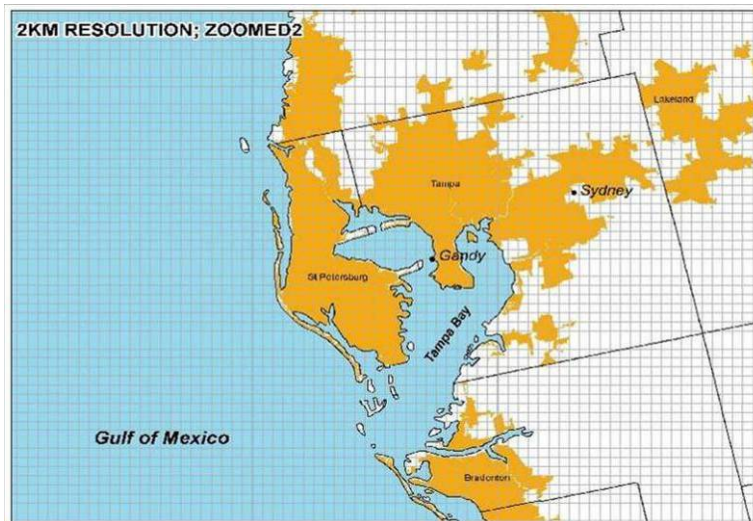


Figure 3-59. Two km southeast U.S. CMAQ-UCD domain zoomed over Tampa Bay, FL.

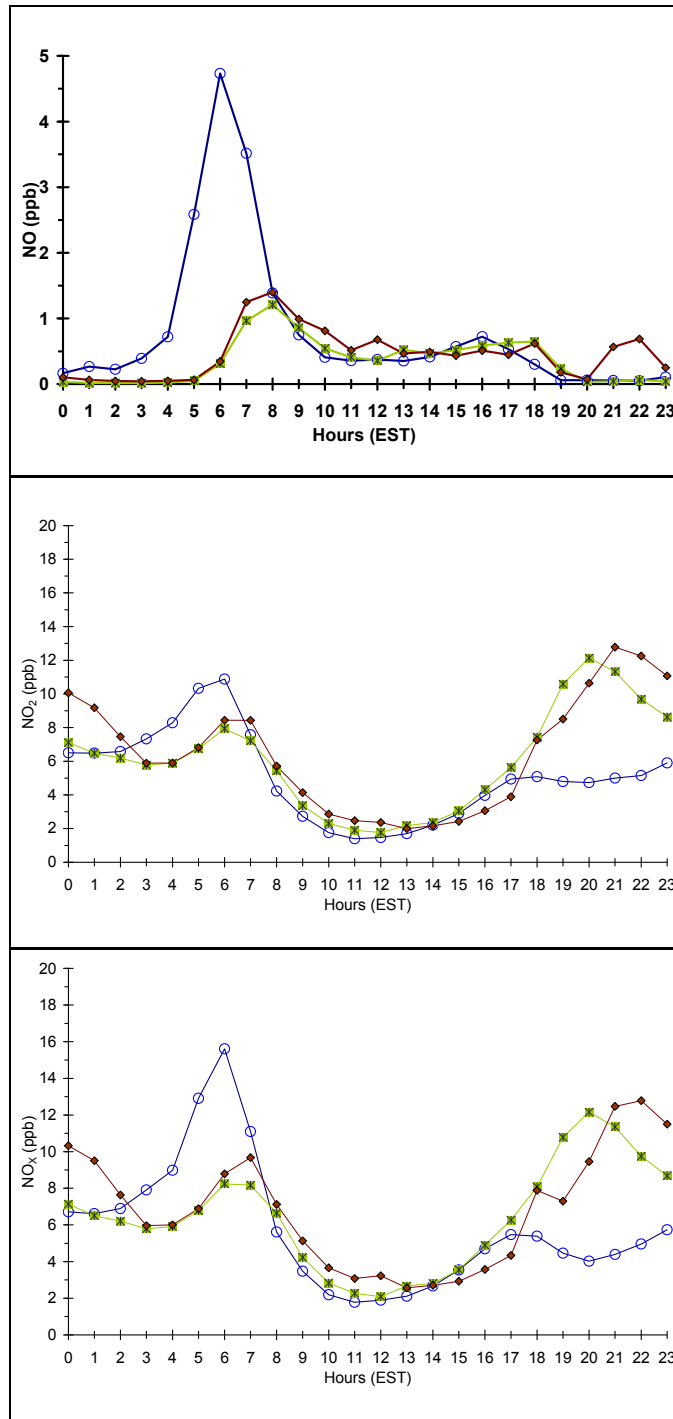


Figure 3-60. Hourly average CMAQ-UCD predictions and measured observations of NO (top), NO₂ (middle), and total NO_x (bottom) concentrations for May 1-31, 2002. Green squares = 8 km solution, red diamonds = 2 km solution, blue circles = observations.

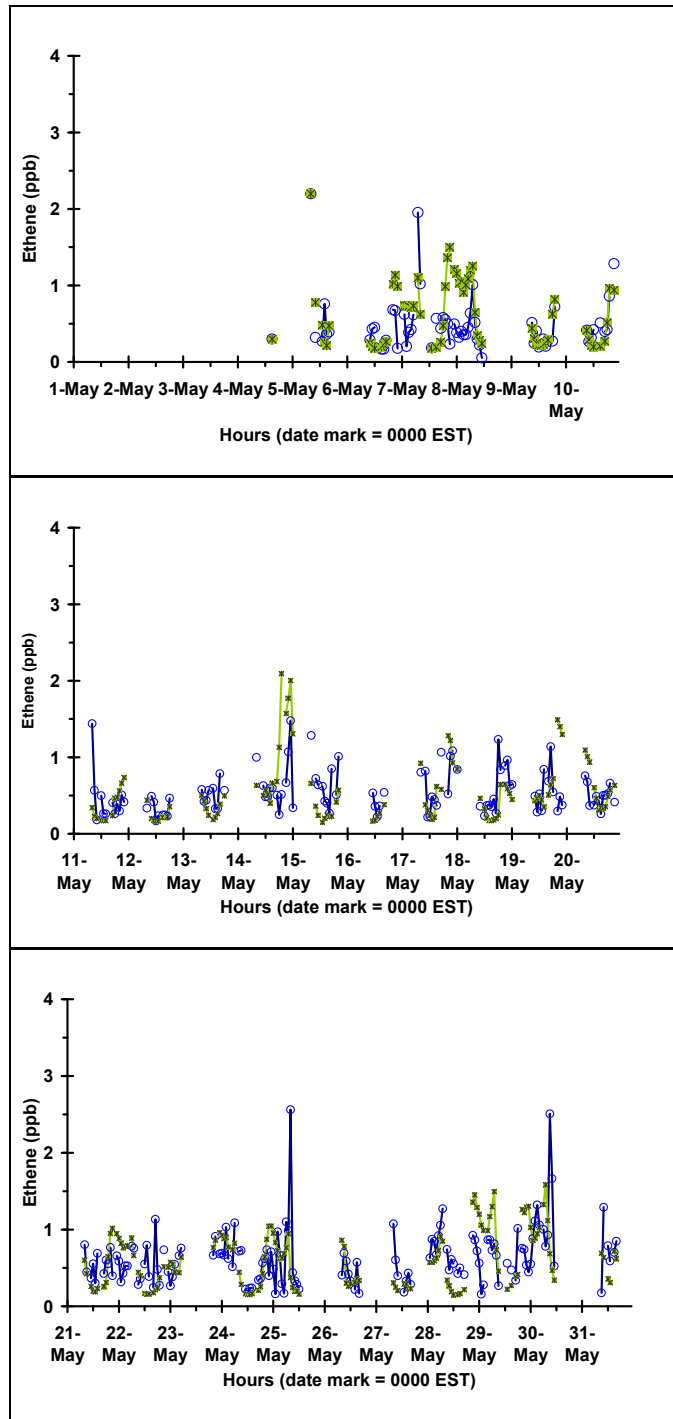


Figure 3-61. CMAQ-UCD predictions and measured observations of ethene concentrations at Sydney, FL for May 1-31, 2002. Green squares = 8 km solution, blue circles = observations.

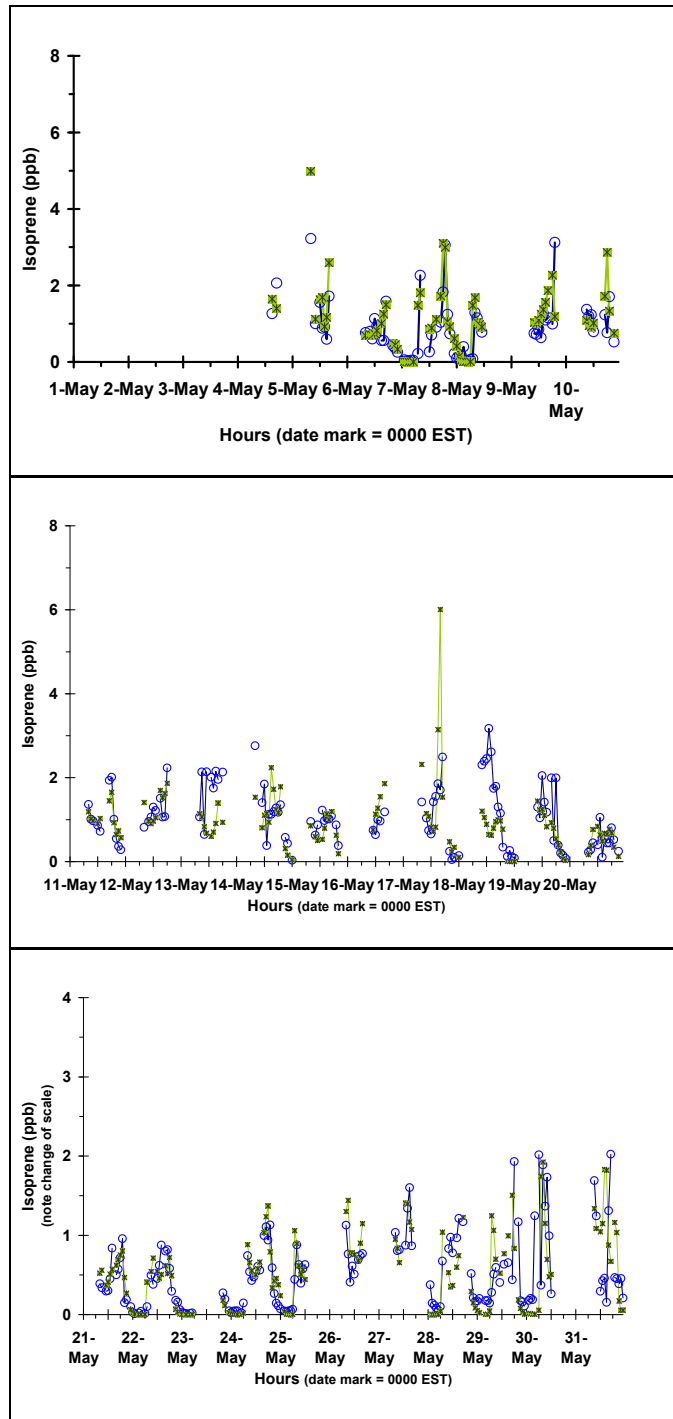


Figure 3-62. CMAQ-UCD predictions and measured observations of isoprene concentrations at Sydney, FL for May 1-31, 2002. Green squares = 8 km solution, blue circles = observations.

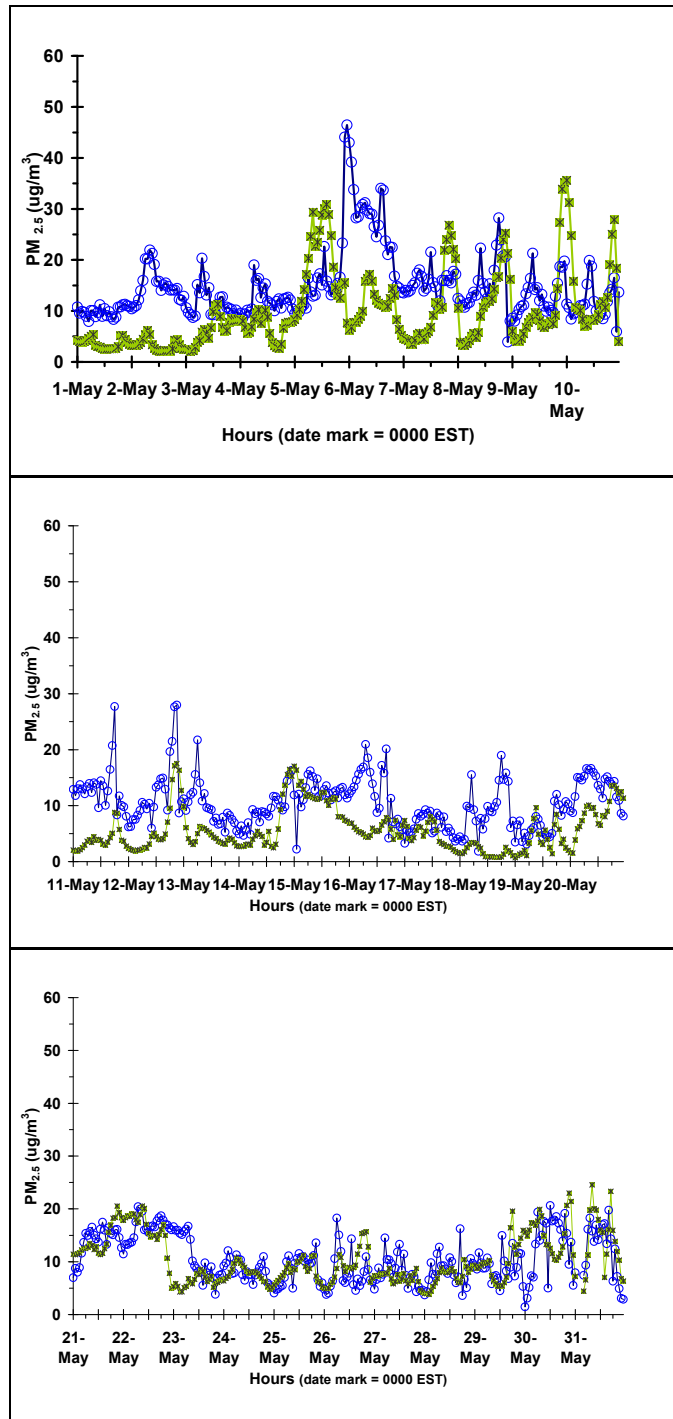


Figure 3-63. CMAQ-UCD predictions and measured observations of $PM_{2.5}$ concentrations at Sidney, FL for May 1-31, 2002. Green squares = 8 km solution, blue circles = observations.

3.6.3.1. Ground-based Comparisons of Photochemical Dynamics

Errors in the NO_x concentrations in the model, most likely from on-road emissions, affected NO_x predictions shown in Figure 3-60, but CMAQ-UCD's general responses were reasonable. The model also replicated anthropogenic and biogenic VOC emissions well; see Figure 3-61 and Figure 3-62, respectively. After initial errors leading to underprediction in the first 21 days, CMAQ-UCD's predictions of hourly $\text{PM}_{2.5}$ concentrations and trends over the whole month also replicated the observed concentrations well (Figure 3-63).

3.6.3.2. Predicted Chemistry for Nitrates and Related Compounds

Particulate NO_3^- (pNO_3^-) plays a crucial and complex role in the health of aquatic and estuarine ecosystems and human drinking water systems. Gas-phase NO_3^- replacement of Cl^- on sea salt particles is often favored thermodynamically and the V_d of the coarse pNO_3^- formed through this replacement is more than an order of magnitude greater than for fine pNO_3^- . Over open bodies of salt water such as the Gulf of Mexico and Tampa Bay, FL, pNO_3^- from this reaction dominates dry deposition and is estimated to be of the same order as pNO_3^- wet deposition.

However, total NO_3^- concentrations are driven, buffered, and altered by a wide range of photochemical gas-phase reactions, heterogeneous reactions, and aerosol dynamics, making them especially difficult to model. Because pNO_3^- is derived mostly from gas-phase HNO_3 and will interact with Na^+ , NH_4^+ , Cl^- , and SO_4^{2-} , all these species and the physical parameters governing their creation, transport, transformation, and fate must be accurately replicated to predict pNO_3^- with high fidelity. This has historically been a difficult problem for numerical process models, owing in large part to the pervasive dearth of reliable ambient measurements of NO_3^- in its various forms. Normalized mean error (NME) for the large-scale Eulerian CTM-predicted pNO_3^- has typically been on the order of a factor of 3 greater than the NME for particulate SO_4^{2-} (pSO_4^{2-}) (Odman et al., 2002, [092474](#); Pun et al., 2003, [047775](#)).

SO_4^{2-} , NH_4^+ , Na^+ , and Cl^- were all predicted to within a factor of 2 and with no significant bias during the photochemical day in the 8 km CMAQ-UCD solution, although a significant bias in Na^+ and Cl^- was evident in the 2 km solution for two near-water sites. This grid-size dependent bias is still being explored. Size segregation maxima were correct to within two size bins every day for which there were observations for both SO_4^{2-} and NH_4^+ (0.2 to 1.0 μm), and Na^+ and Cl^- (2.0-10.0 μm). Cl^- concentrations were greatly overpredicted during dark hours, but were nearer to observed values during the photochemical day. CMAQ-UCD performance for HNO_3 and NH_3 are shown in Figure 3-64 and Figure 3-65, respectively.

Figure 3-66 shows that CMAQ-UCD systematically underpredicted the hourly time series of measured pNO_3^- concentrations at the Sydney supersite, the only location with discrete pNO_3^- data. These time series data establish that CMAQ-UCD's largest errors were on 4 days in the first 2 wk of the month, but that the total peak pNO_3^- concentrations were nearly all underpredicted.

Since pNO_3^- is derived in large part from gas-phase HNO_3 , its underprediction may be due to an underprediction of HNO_3 concentrations or an underrepresentation of the gas- to aerosol-phase change. At Sydney, FL, in fact, both these conditions held. Figure 3-64 depicts the model's bias for HNO_3 underprediction in both the 8 km and 2 km solutions, except for four days of very large peak overpredictions. This pattern of underpredictions was especially evident overnight. On 8 other days the model overpredicted the one hour peak concentration as well, though not so substantially, but the chief effect was still one of an artificial and inappropriate N limitation in the model.

A time series molar equivalent ratio of HNO_3 to total NO_3^- depicts which phase stores the NO_3^- and how that storage ratio changes over time. Figure 3-67 shows that at Sydney, FL, CMAQ-UCD stored too much NO_3^- in the gas phase as HNO_3 (and recall that the daytime HNO_3 concentrations were sometimes overpredicted by the model) and too little in the gas phase overnight, when the model was regularly low against the measurements; compare Figure 3-64 and Figure 3-65. Note again here the similarity of the 8 km and 2 km solutions in this comparison.

Interestingly, the 23-h integrated data did not reveal this important difference in NO_3^- form between the model and measurements as Figure 3-68 shows in the stacked bar percentage plots of fine and coarse pNO_3^- together with gas-phase HNO_3 . Both the 8 km (Figure 3-68, middle panel) and the 2 km (Figure 3-68, bottom panel) solutions predicted distributions between the two general ranges of aerosol size, and between gas and aerosol phases, with good fidelity to the daily observations (Figure 3-68, top panel) at Sydney, FL. This result illustrates that while discrete time

series data are crucial for diagnosing model behavior, on the integrated total daily and longer basis used for computing total annual N loads, CMAQ-UCD predicted approximately the correct distributions for pNO_3^- , even though the total NO_3^- concentration prediction was biased low.

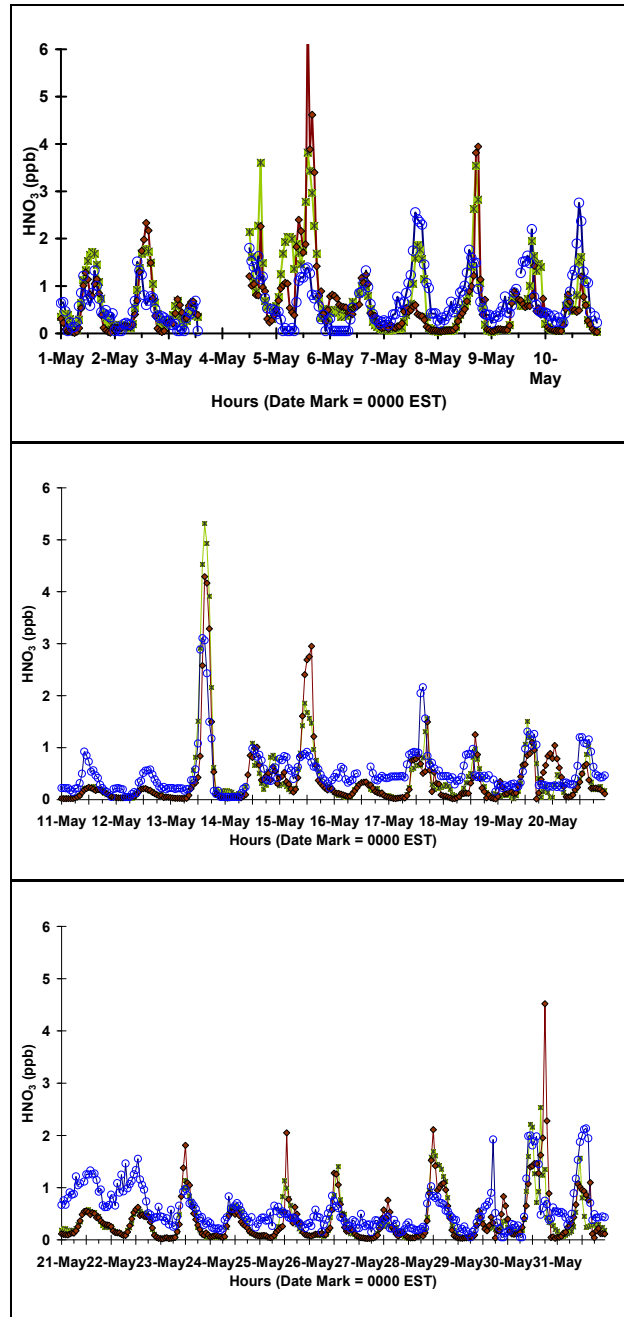


Figure 3-64. CMAQ-UCD predictions of HNO_3^- concentrations and corresponding measured observations at Sydney, FL, for May 1-31, 2002. Green x = 8 km solution, red diamonds = 2 km solution, blue circles = observations.

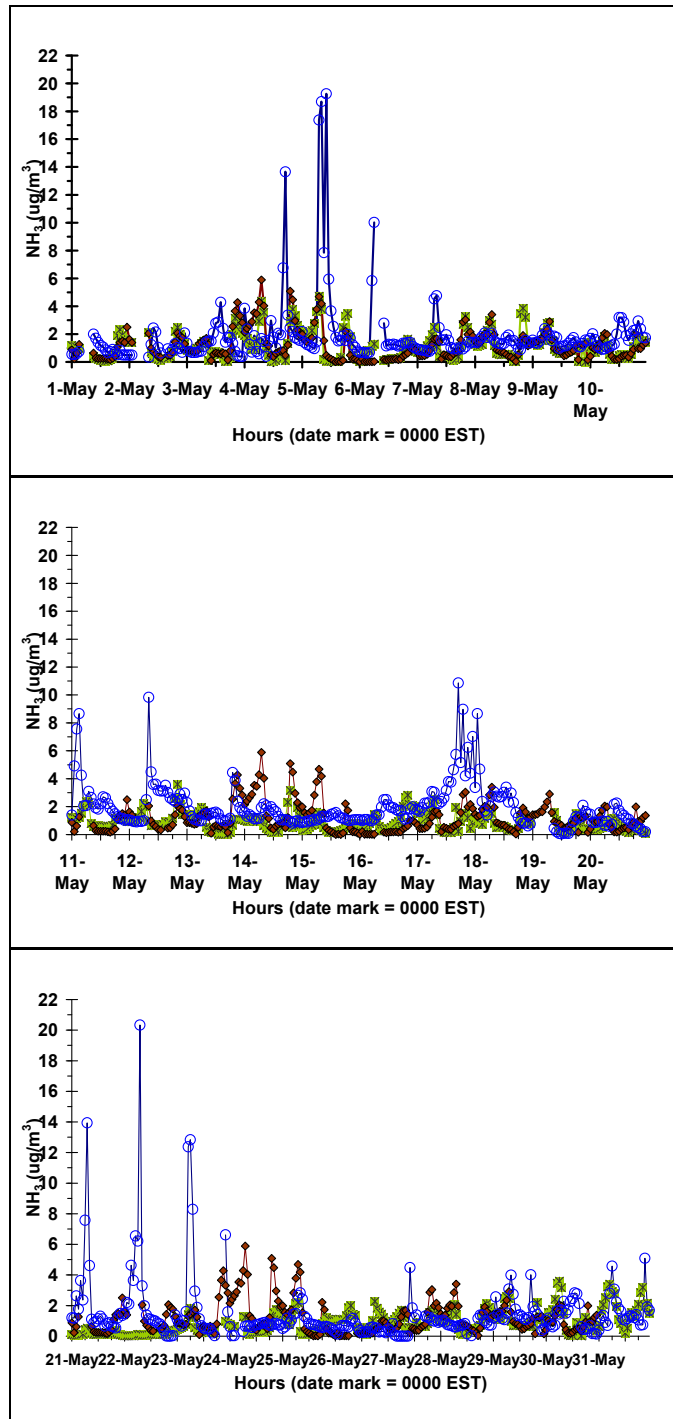


Figure 3-65. CMAQ-UCD predictions of NH₃ concentrations and corresponding measured observations at Sydney, FL, for May 1-31, 2002. Green x = 8 km solution, red diamonds = 2 km solution, blue circles = observations.

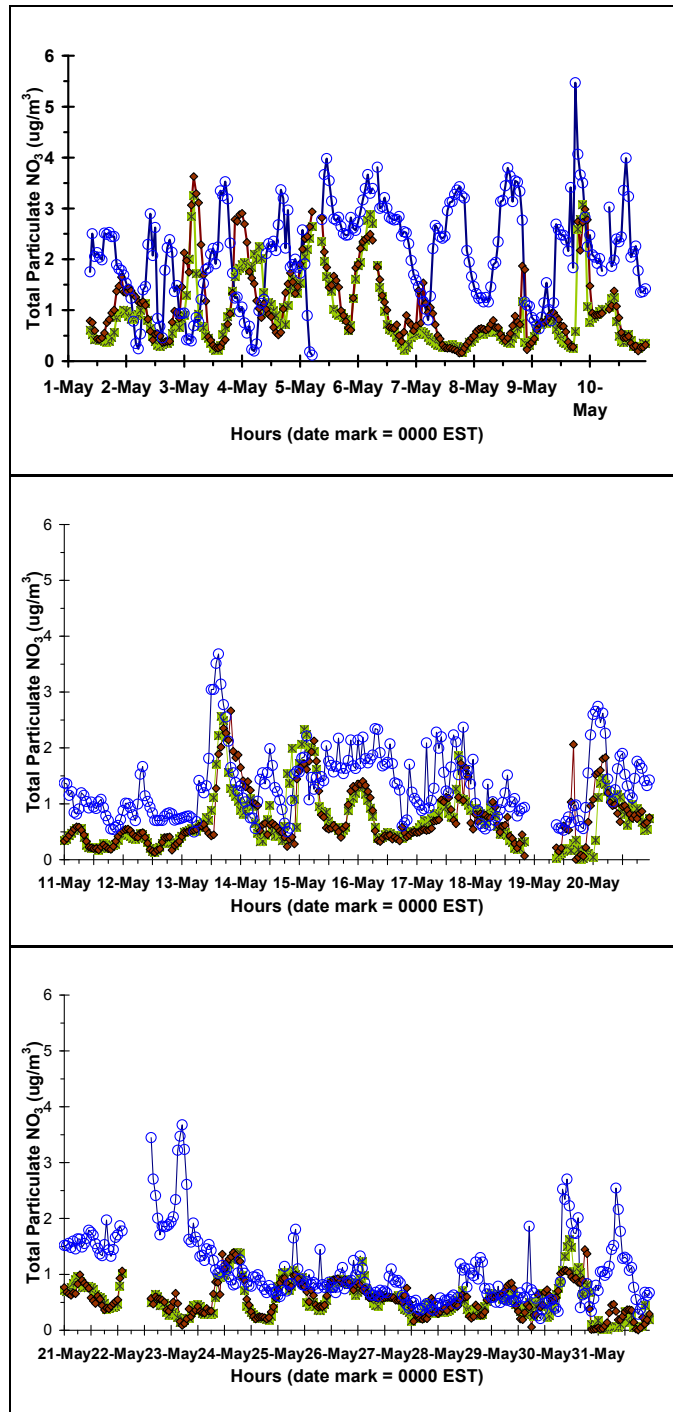


Figure 3-66. CMAQ-UCD predictions of pNO_3^- concentrations and corresponding measured observations at Sydney, FL, for 1-31 May, 2002. Green x = 8 km solution, red diamonds = 2 km solution, blue circles = observations.

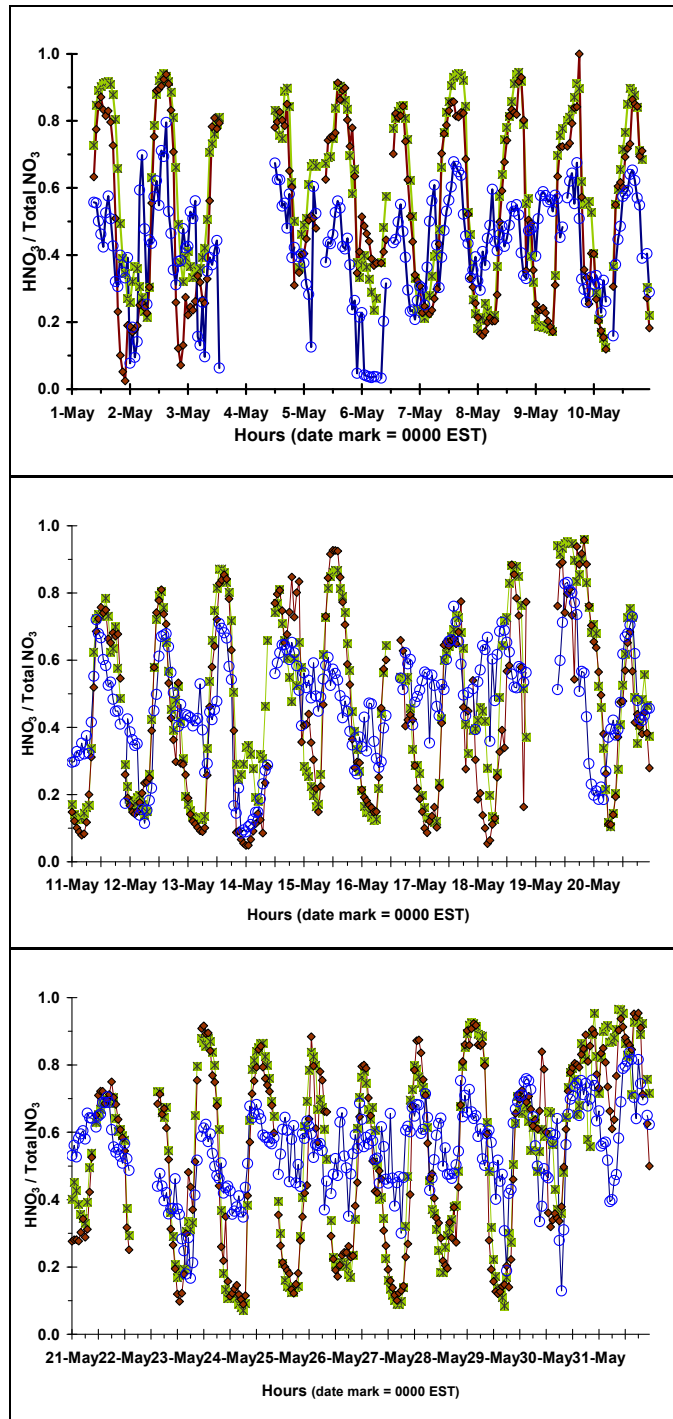


Figure 3-67. CMAQ-UCD predictions of the ratio of HNO₃ to total NO₃ and corresponding measured observations at Sydney, FL, for May 1-31, 2002. Green x = 8 km solution, red diamonds = 2 km solution, blue circles = observations.

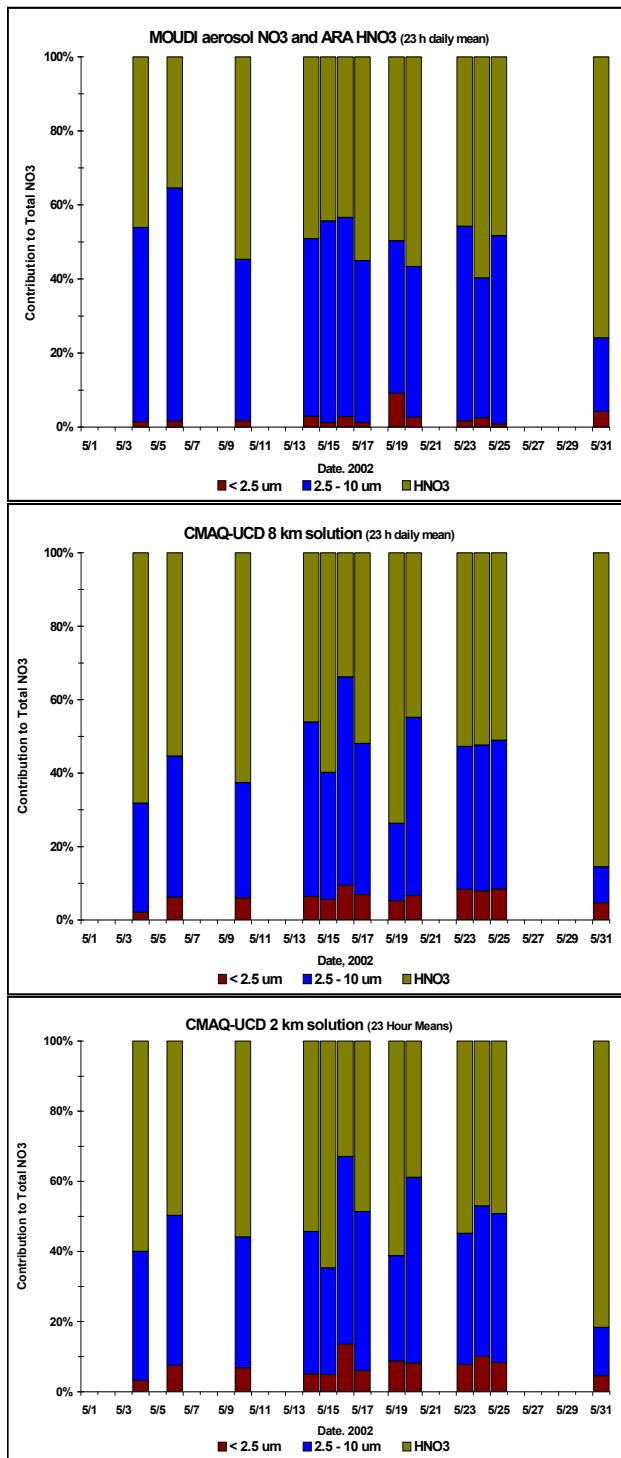


Figure 3-68. CMAQ-UCD predicted size and chemical-form fractions of total NO₃⁻ for days in May 2002 with measured observations. Measured concentrations (top panel); 8 km solution (middle panel); 2 km solution (bottom panel). Red bars = pNO₃⁻ <2.5 μm; blue bars = pNO₃⁻ 2.5-10 μm; green bars = HNO₃.

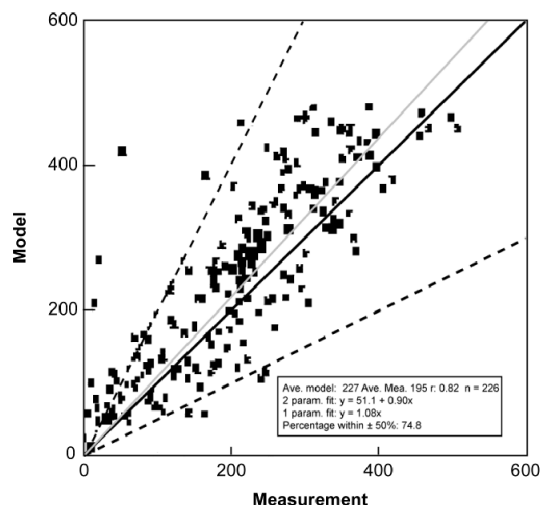
While inorganic aerosol anion totals were dominated by NO_3^- in the coarse fraction and by SO_4^{2-} in the fine fraction, there was sufficient NH_x ($\text{NH}_x = \text{NH}_3 + \text{NH}_4^+$) at Sydney, FL, to form fine aerosol NH_4NO_3 in some circumstances. Figure 3-65 depicts the hourly mass concentration of NH_3 at Sydney, FL, showing again the strong similarity of the 8 km and 2 km solutions. Each solution, however, underpredicted the measured NH_3 concentrations consistently, and especially for the nine very large excursions of 10-20 $\mu\text{g}/\text{m}^3$ during the month.

Overall, CMAQ-UCD was found to be operationally sound in this evaluation of its 8 km and 2 km solutions for the Tampa Bay airshed using the ground-based and aloft data (not shown here) from the May 2002 field intensive. Moreover, results from diagnostic tests of the model's photochemical dynamics were generally in excellent agreement with results from the ambient atmosphere. However, CMAQ-UCD was biased low in this application for total NO_3 and for NO_3 present as gas-phase HNO_3 . In addition, the model was biased low for the HO_x radical reservoir species CH_2O and H_2O_2 (not shown here), though this bias appeared to have been limited to these species. Performance of the new UCD aerosol module was judged to be entirely adequate, allocating aerosols by chemical makeup to the appropriate size fractions. Model performance for fine-mode aerosols was also judged to be fully adequate.

3.6.4. Evaluating Concentrations and Deposition of PM Components with CTMs

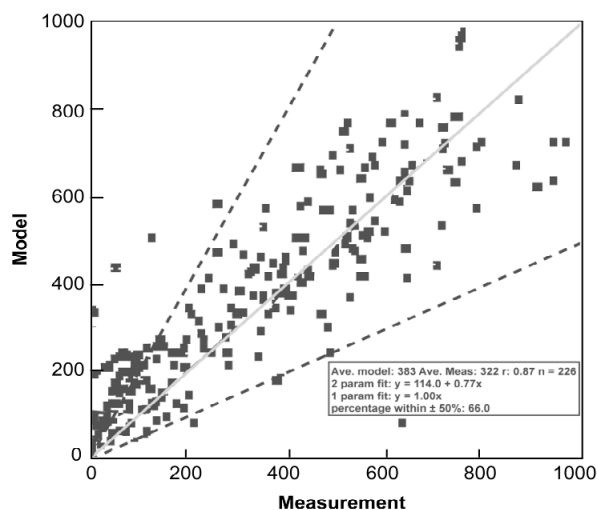
3.6.4.1. Global CTM Performance

The wet and dry deposition processes described in Section 3.3 are of necessity highly parameterized in all CTMs. While all current models implement resistance schemes for dry deposition, the V_d generated from different models can vary highly across terrain types (Stevenson et al., 2006, [089222](#)). The accuracy of wet deposition in global CTMs is tied to spatial and temporal distribution of model precipitation and the treatment of chemical scavenging. Dentener et al. (2006, [088434](#)) compared wet deposition across 23 models with available measurements around the globe. Figure 3-69 and Figure 3-70 extract results of a comparison of the 23-model mean versus observations over the eastern U.S. for pNO_3^- and pSO_4^{2-} deposition, respectively. The mean model results were strongly correlated with the observations ($r > 0.8$), and usually captured the magnitude of wet deposition to within a factor of two over the eastern U.S. Dentener et al. (2006, [088434](#)) concluded that 60-70% of the participating models captured the measurements to within 50% in regions with quality controlled observations.



Source: Adapted with Permission of American Geophysical Union from Dentener et al. (2006, [088434](#)).

Figure 3-69. Scatter plot of total nitrate (HNO_3 plus pNO_3^-) wet deposition ($\text{mg N/m}^2/\text{yr}$) of the model mean versus measurements for the North American Deposition Program (NADP) network. Dashed lines indicate a factor of two. The gray line is a linear regression through zero.



Source: Adapted with Permission of American Geophysical Union from Dentener et al. (2006, [088434](#)).

Figure 3-70. Scatter plot of total SO_4^{2-} wet deposition ($\text{mg S/m}^2/\text{yr}$) of the model mean versus measurements for the National Atmospheric Deposition Program (NADP) network. Dashed lines indicate a factor of two. The gray line is a linear regression through zero.

3.6.4.2. Regional CTM Performance

Regional CTM performance for concentration and deposition of some of the most relevant PM species is illustrated here with examples from CMAQ version 4.6.1 as configured and run for

exposure and risk assessments reported in the *Risk and Exposure Assessment for the Review of the Secondary National Ambient Air Quality Standards for Oxides of Nitrogen and Oxides of Sulfur* (U.S. EPA, 2009, [191774](#)); additional details on the model configuration and application are found there. A map of the 36 km parent domain and two 12 km (east and west) progeny domains appears in Figure 3-71.

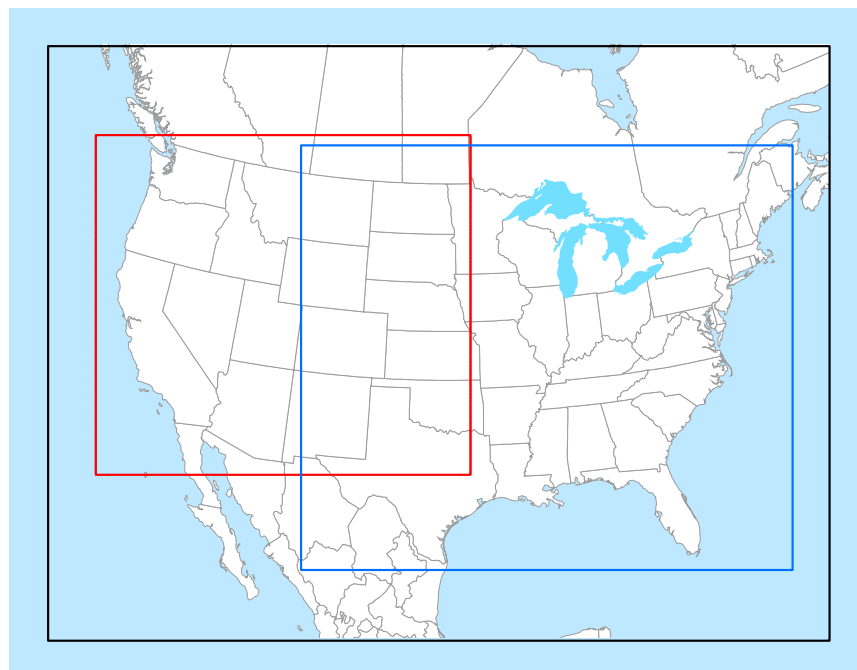


Figure 3-71. CMAQ modeling domains for the OAQPS risk and exposure assessments: 36 km outer parent domain in black; 12 km western U.S. (WUS) domain in red; 12 km eastern U.S. (EUS) domain in blue.

Comparisons from the 2002 annual run of CMAQ for the exposure assessment are shown here against measured concentrations and deposition totals from nodes in three networks: IMPROVE, CSN (labeled STN in the plots) and CASTNet. Comparisons were made as model-observation pairs at all sites having sufficient data for the seasonal or the 2002 annual time period in the two 12 km east and west domains and were evaluated with the following descriptive statistics: correlation, root mean square error, normalized mean bias, and normalized mean error.

Summertime pSO_4^{2-} concentrations are well predicted by CMAQ, to within a factor of 2 at nearly every point, and with $R^2 > 0.8$ across all three networks (Figure 3-72). This result tracks the generally well-predicted SO_4^{2-} concentrations found in earlier CMAQ evaluations: see Eder and Yu (2005, [089229](#)), Mebust et al. (2003, [156749](#)) and Tesche et al. (2006, [157050](#)). Since pSO_4^{2-} concentrations are strongly a function of precipitation, care must be taken to ensure that the meteorological solution driving individual CMAQ chemical applications produces precipitation fields with low bias as discussed by Appel et al. (2008, [155660](#)).

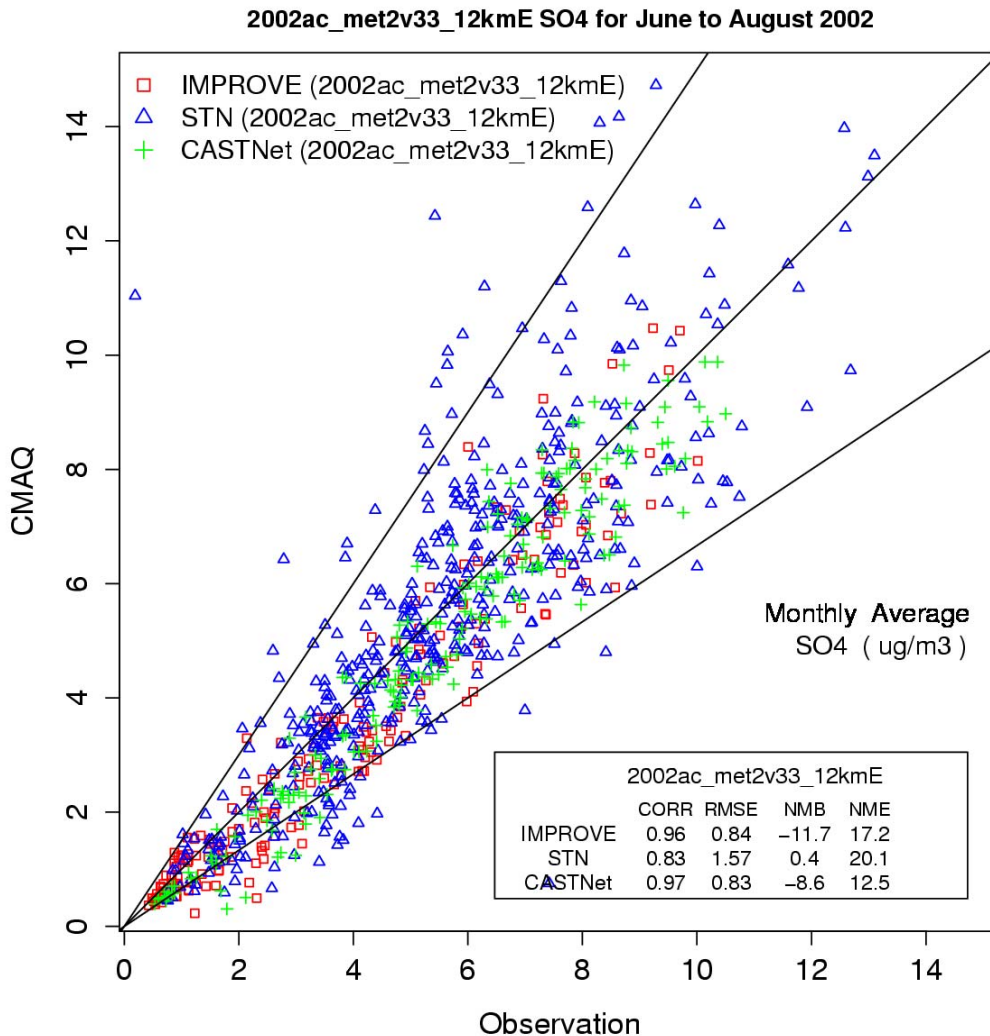


Figure 3-72. 12-km EUS Summer sulfate PM. Each data point represents a paired monthly averaged (June/July/August) observation and CMAQ prediction at a particular IMPROVE, STN, and CASTNet site. Solid lines indicate a factor of two around the 1:1 line shown between them.

Wintertime pNO_3^- (Figure 3-73) and total NO_3 ($\text{HNO}_3 + \text{pNO}_3^-$) (Figure 3-74) concentrations are predicted less well by CMAQ, but NO_3 is a pervasively difficult species to measure and model. Still, at the CASTNet nodes where the total NO_3 concentrations are higher than they are at all but a few of the remote IMPROVE sites, CMAQ predicts concentrations for nearly every node to within a factor of 2 and with an $R^2 > 0.8$. These CMAQ-predicted concentrations, coupled with modeled cloud and precipitation fields produce wet deposition fields for SO_4^{2-} and NO_3^- in the east domain as shown in Figure 3-75 and Figure 3-76, respectively.

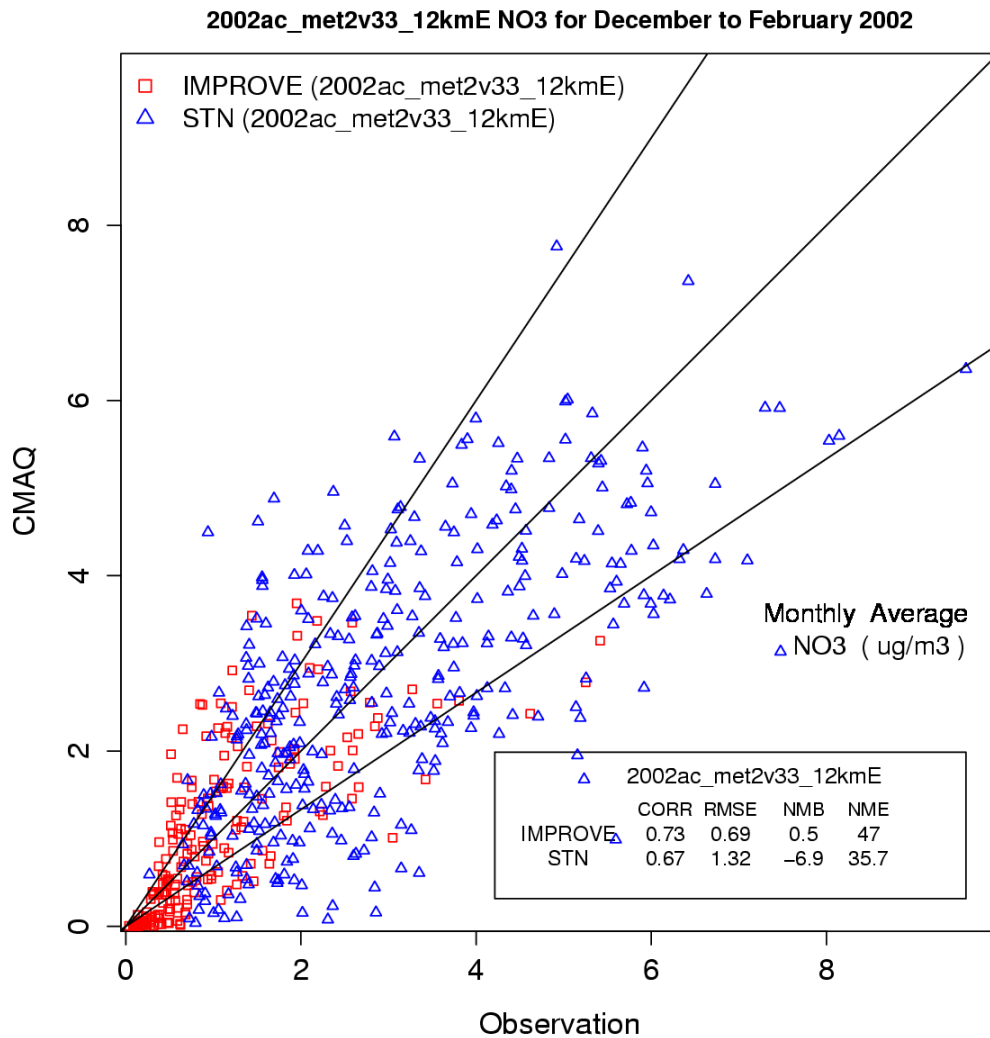


Figure 3-73. 12-km EUS Winter nitrate PM. Each data point represents a paired monthly averaged (December/January/February) observation and CMAQ prediction at a particular IMPROVE and STN site. Solid lines indicate a factor of two around the 1:1 line shown between them.

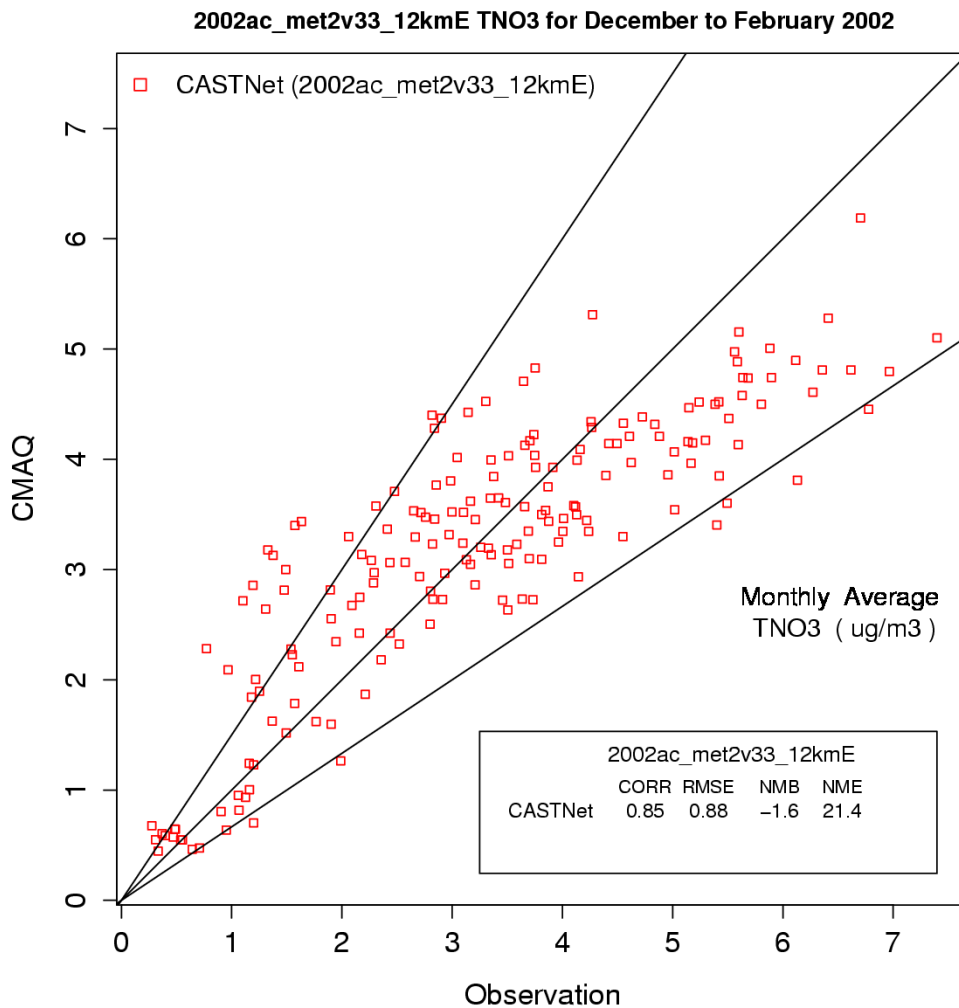


Figure 3-74. 12-km EUS Winter total nitrate ($\text{HNO}_3 + \text{total pNO}_3^-$). Each data point represents a paired monthly averaged (December/January/February) observation and CMAQ prediction at a particular CASTNet site. Solid lines indicate a factor of two around the 1:1 line shown between them.

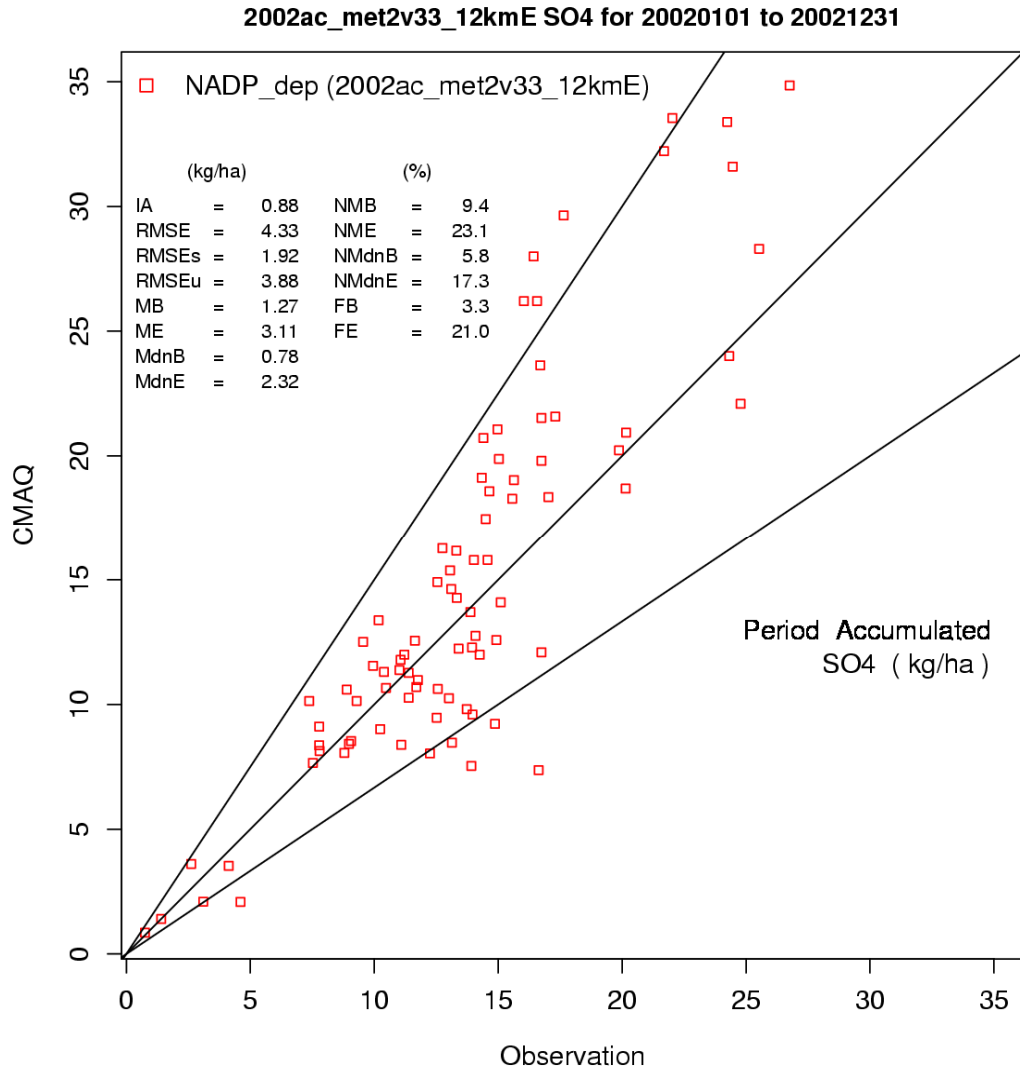


Figure 3-75. 12-km EUS annual sulfate wet deposition. Each data point represents an annual average paired observation and CMAQ prediction at a particular NADP site. Solid lines indicate the factor of 2 around the 1:1 line shown between them.

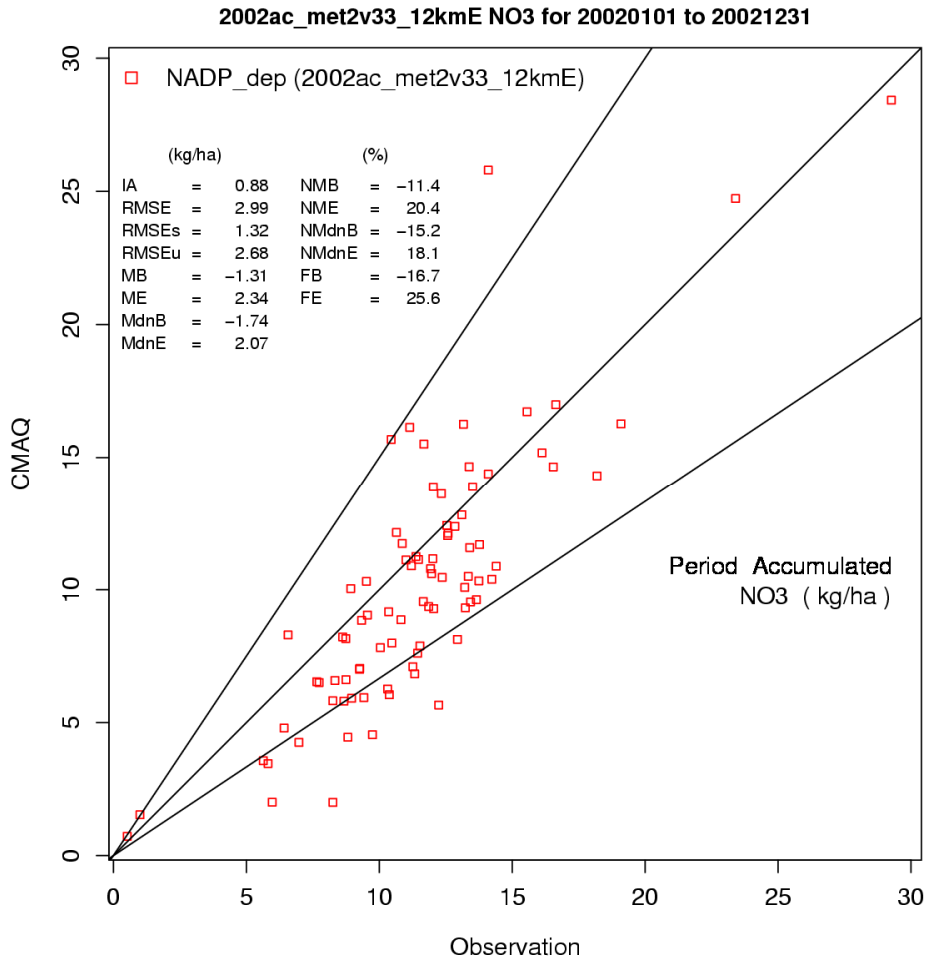


Figure 3-76. 12-km EUS annual nitrate wet deposition. Each data point represents an annual average paired observation and CMAQ prediction at a particular NADP site. Solid lines indicate a factor of two around the 1:1 line shown between them.

Importantly, CMAQ captured the chief spatial patterns and magnitudes of air concentrations and wet deposition relevant to computing concentration and deposition budgets, as shown in Figure 3-77 for concentrations and Figure 3-78 for deposition. More specifically, CMAQ's predictions of NH_3 and SO_4^{2-} for both high and low concentration sites are well within the range of observed measurements (Figure 3-79).

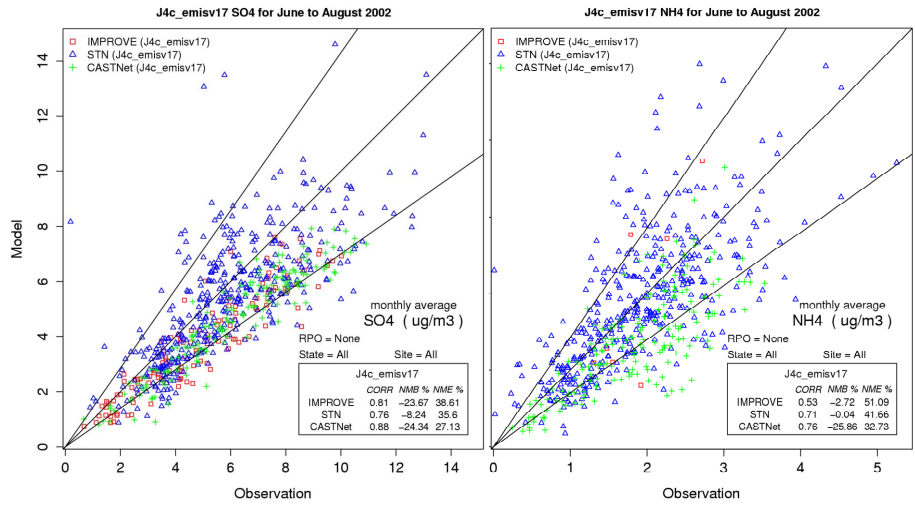


Figure 3-77. CMAQ vs. measured air concentrations from east-coast sites in the IMPROVE, CSN (labeled STN), and CASTNet sites in the summer of 2002 for sulfate (left) and ammonium (right). Solid lines indicate a factor of 2 around the 1:1 line shown between them.

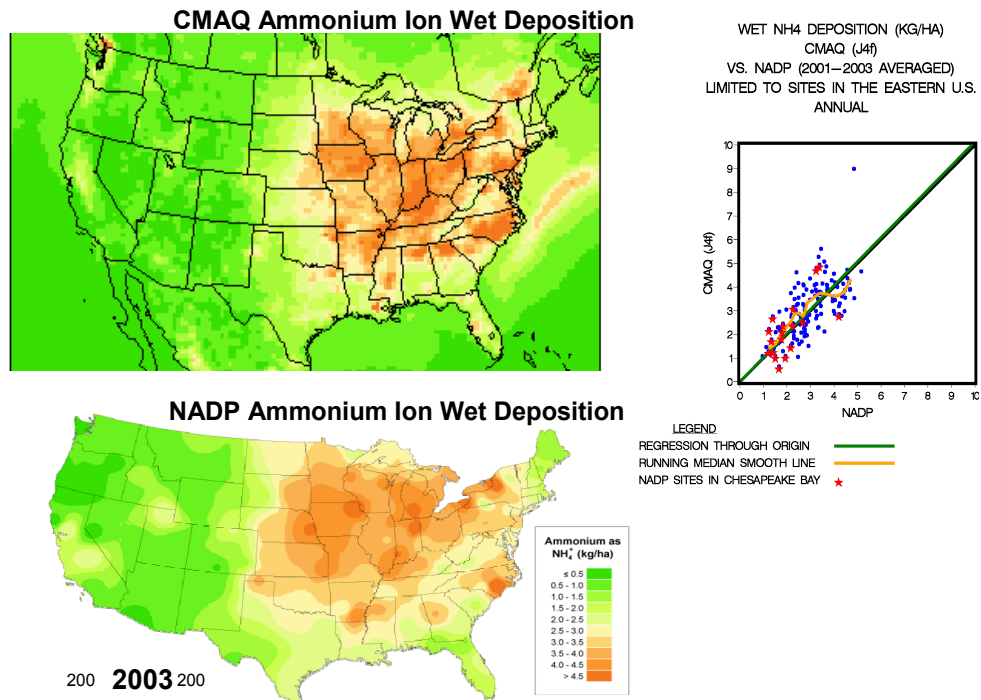


Figure 3-78. Comparison of CMAQ-predicted and NADP-measured NH₄⁺ wet deposition : (top left) CMAQ prediction; (bottom left) NADP-measurements; (right) regression and smoothed median line through CMAQ predictions and NADP measurements with sites in the Chesapeake Bay watershed highlighted.

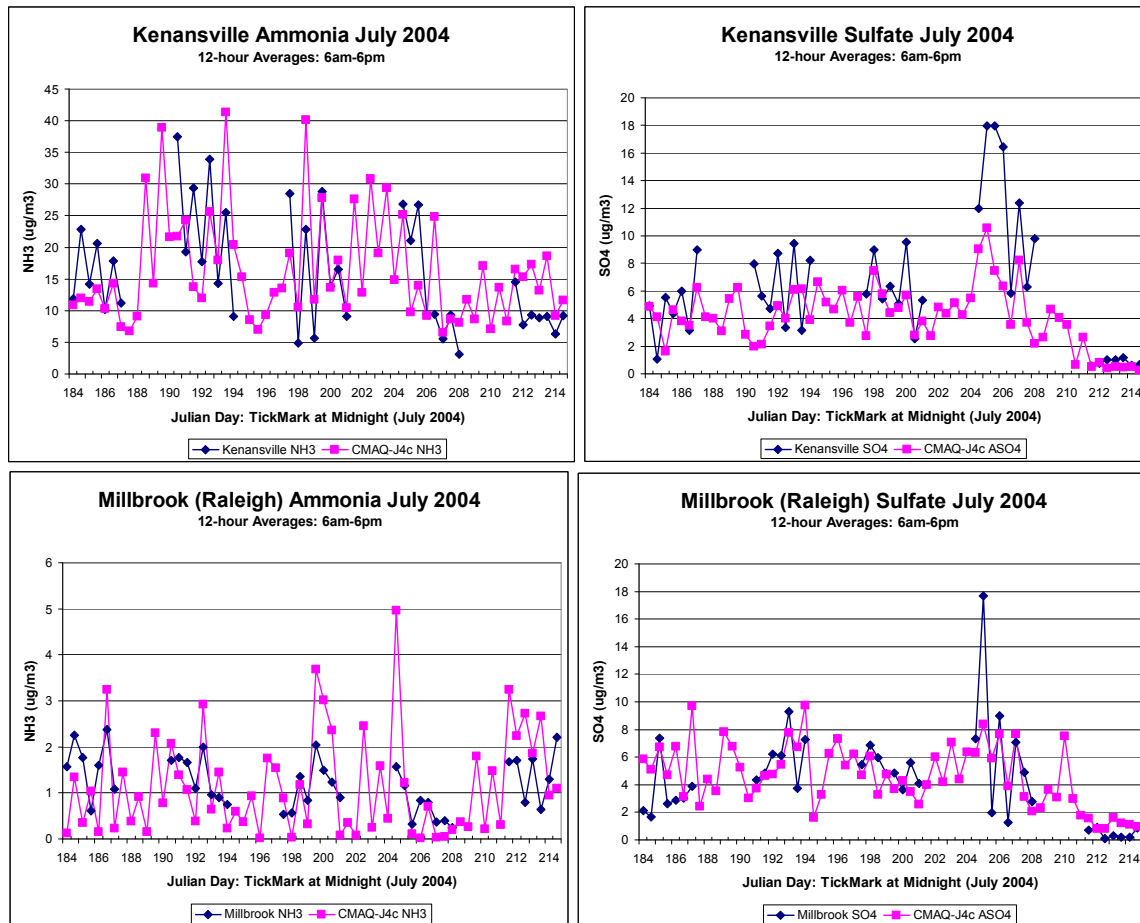


Figure 3-79. CMAQ-predicted (red symbols and lines) and 12-h measured (blue symbols and lines) NH_3 and SO_4^{2-} surface concentrations at high and low concentration grid cells in North Carolina in July 2004. (top left) High concentration NH_3 in Kenansville; (top right) high concentration SO_4^{2-} in Kenansville; (bottom left) low concentration NH_3 in Raleigh; (bottom right) low concentration SO_4^{2-} in Raleigh.

Deposition velocities are difficult to estimate for reasons described in Section 3.3.3. Recent work in EPA's Atmospheric Modeling and Analysis Division with CMAQ showed that the original V_d for NH_3 was very likely too high and should be nearer to the values for SO_2 deposition, or even lower over some land use surface types. A sensitivity study with the model was performed to test the effects of changing V_d for NH_3 on the fraction of NH_3 available for transport away from grid cells with high emissions concentrations. Comparisons were made for the surface grid cells and total column NH_3 concentrations.

In the highest emissions grid cells during June 2002, the surface NH_x budget was dominated by turbulent transport or vertical mixing moving a majority of the surface NH_3 emissions up and away from the surface into the mixed layer. Figure 3-80 depicts the NH_x budget under the base case (Base V_d) and the sensitivity case ($\text{SO}_2 V_d$) for which the $\text{NH}_3 V_d$ was set equal to the $\text{SO}_2 V_d$. Lower $\text{NH}_3 V_d$ decreased NH_x deposition to the surface from 15 to 8%, leaving more NH_x for transport horizontally, 22% up from 20% in the base case, and vertically, 69% up from 64% in the base case. Typically, ~67% of surface emissions were moved aloft where most was advected away from the high emissions grid cell, with a small fraction converted to pNH_4^+ and an even smaller fraction wet-deposited to the surface. The total column analyses for NH_3 and NH_x are shown in Figure 3-81.

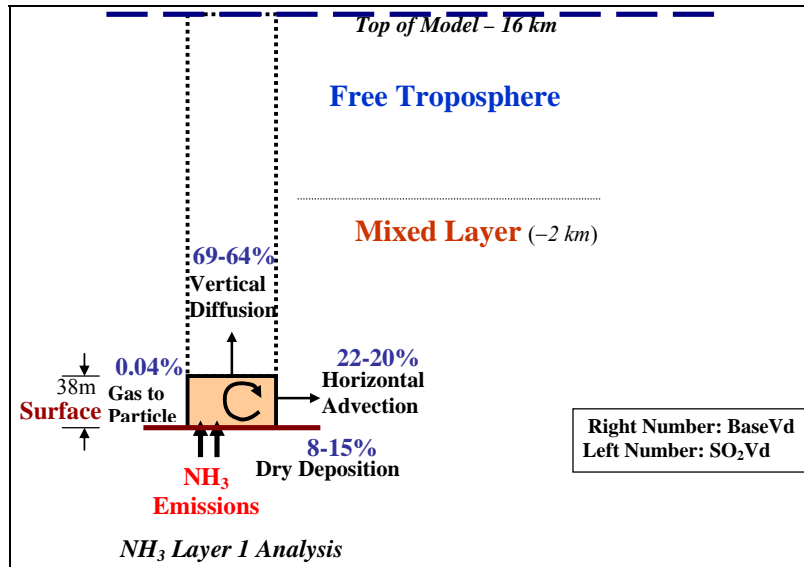


Figure 3-80. Surface grid cell (layer 1) analysis of the sensitivity of NH_x deposition and transport to the change in NH_3 V_d in CMAQ.

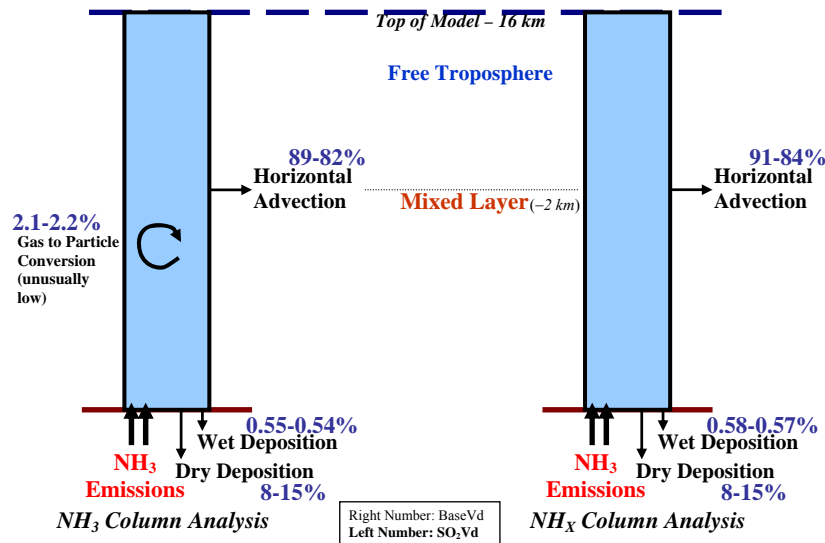


Figure 3-81. Total column analysis for NH_3 (left) and NH_x (right) showing modeled NH_3 emissions, transformation, and transport throughout the mixed layer and up to the free troposphere.

Local total deposition (wet + dry) is a significant but not dominant loss pathway for surface NH_3 emissions. In these simulations, CMAQ deposited ~25% of the NH_3 emissions from the single high concentration grid cell in Sampson County, NC, back into that grid cell. By far, the largest contribution to the local deposition total was dry deposition. Dry-to-wet deposition ratios for the Sampson County high emissions grid cell and surrounding surface grid cells ranged from 2 to 10.

Deposition to grid cells farther away from the high concentration, immediately surrounding grid cells, was significantly affected by the change in NH_3 V_d tested in this case. Figure 3-82 depicts

the range of influence of the high concentration grid cell, where that range is defined to be the distance by which 50% of the emissions attributable to that grid cell have deposited. The range of influence of the high concentration Sampson County grid cell was extended in the V_d sensitivity tested here from ~180 km in the base case to ~400 km in the case using the lower, more realistic V_d for NH_3 . The areal extent of this difference in range of influence is mapped in Figure 3-83.

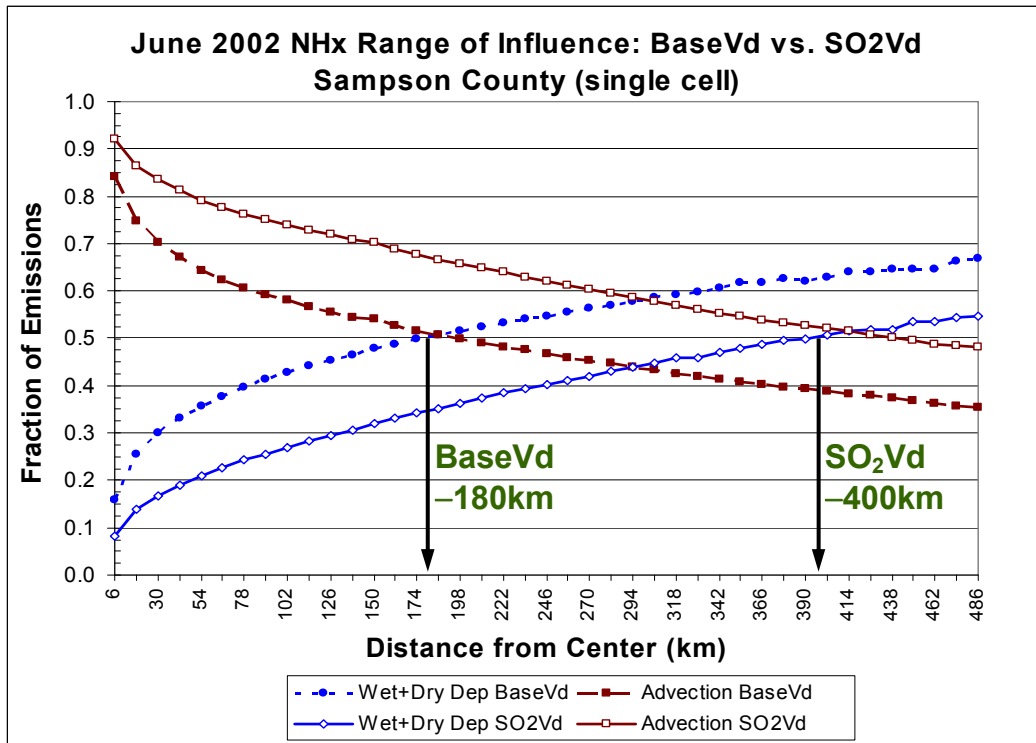


Figure 3-82. Range of influence (where 50% of emitted NH_3 deposits) from the high concentration Sampson County grid cell in the June 2002 CMAQ simulation of V_d sensitivities. Base case and sensitivity case total deposition (blue symbols and lines); base case and sensitivity case advection totals (red symbols and lines).

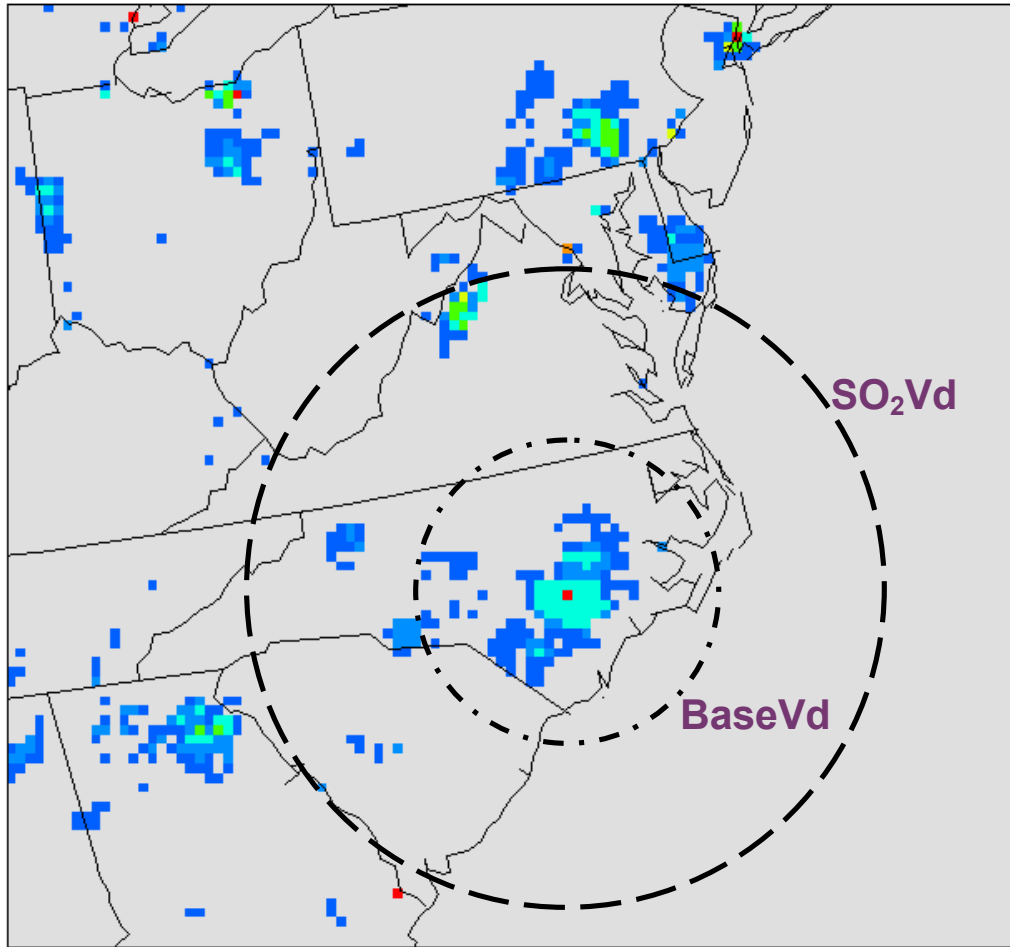


Figure 3-83. Areal extent of the change in NH_x range of influence as predicted by CMAQ for the Sampson County high concentration grid cell (center of range circles) in June 2002 using the base case and sensitivity case V_d .

3.7. Background PM

The background concentrations of PM that are useful for risk and policy assessments informing decisions about the NAAQS are referred to as policy-relevant background (PRB) concentrations. PRB concentrations have historically been defined by EPA as those concentrations that would occur in the U.S. in the absence of anthropogenic emissions in continental North America defined here as the U.S., Canada, and Mexico. For this document, PRB concentrations include contributions from natural sources everywhere in the world and from anthropogenic sources outside continental North America. Background concentrations so defined facilitated separation of pollution that can be controlled by U.S. regulations or through international agreements with neighboring countries from those that were judged to be generally uncontrollable by the U.S. Over time, consideration of potential broader ranging international agreements may lead to alternative determinations of which PM source contributions should be considered by EPA as part of PRB.

3.7.1. Contributors to PRB Concentrations of PM

Contributions to PRB concentrations of PM include both primary and secondary natural and anthropogenic components. Natural sources include wind erosion of natural surfaces (Gillette and Hanson, 1989, [030212](#)); volcanic production of SO_4^{2-} ; PBAP; wildfires producing EC, OC, and inorganic and organic PM precursors; and SOA produced by oxidation of biogenic hydrocarbons such as isoprene and terpenes. However, human intervention can be involved in the formation of SOA, as production of natural SOA depends to a large extent on the presence of anthropogenic NO_x . As described earlier in Section 3.3, prescribed fires are considered part of PRB. In addition to emissions from forest fires in the U.S., emissions from forest fires in other countries can be transported to the U.S. For example, Boreal forest fires in Canada (Mathur, 2008, [156742](#)) and Siberia (Generoso et al., 2007, [155786](#)) and tropical forest fires in the Yucatan Peninsula and Central America (Wang et al., 2006, [157109](#)) have affected PM concentrations in the U.S. PRB PM varies across the contiguous United States (CONUS) by region and season as a function of the complex mechanisms of transport, dispersion, deposition, and reentrainment.

Dust from the Sahara desert and the Sahel in North Africa (Chiapello et al., 2005, [156339](#)) affects mainly the eastern U.S.; dust from the Gobi and Taklimikan deserts in Asia (VanCuren and Cahill, 2002, [157087](#); Yu et al., 2008, [157168](#)) have the largest effects in the western U.S. but also affect air quality in the eastern U.S. Husar et al. (2001, [024947](#)) report that the average PM_{10} concentration at 25 reporting stations throughout the northwestern U.S. reached $65 \mu\text{g}/\text{m}^3$ during an episode in the last week in April 1998, compared to an average of $10\text{-}25 \mu\text{g}/\text{m}^3$ during the rest of April and May. This was accompanied by visual reports of milky-white discoloration of the normally blue sky in non-urban areas along the west coast.

PRB contributions to $\text{PM}_{2.5}$, $\text{PM}_{10-2.5}$, and PM_{10} can also be viewed as coming from two conceptually separate components: a reasonably consistent “baseline” component and an episodic component. The baseline component consists of contributions that are generally well characterized by a reasonably consistent distribution of daily values each year, although there is variability by region and season. The episodic component consists of infrequent, sporadic contributions from natural high-concentration events occurring over shorter periods of time (e.g., hours to several days) both within North America (e.g., volcanic eruptions, large forest fires, dust storms) and outside North America (e.g., transport related to dust storms from deserts in North Africa and China and storms at sea). These episodic natural events, as well as events like the uncontrolled biomass burning in Central America, are essentially uncontrollable and do not necessarily occur in all years.

In-situ measurements provide evidence for the transport of anthropogenic PM from Asia on Mt. Bachelor, OR (Jaffe et al., 2003, [052229](#)). These data show sporadic but well correlated increases in CO , O_3 , total Hg, and aerosol backscatter associated with air coming from Asia. The ITCT-2K2 campaign also found evidence for the oxidation of SO_2 to H_2SO_4 during trans-Pacific transport of Asian emissions. If particulate SO_4^{2-} were to be formed in the polluted boundary layer where it originated, it would likely be deposited prior to transport across the Pacific Ocean (Brock et al., 2004, [156295](#)). Thus, primary species emitted directly and secondary species formed during transport contribute to PRB concentrations. Satellite data have provided images to track clouds of dust and pollution across the oceans and have been used for some quantitative estimation of the flux of material leaving continents. Yu et al. (2008, [157168](#)) used optical thickness data to estimate

column loadings from the MODIS along with satellite assimilated wind fields to estimate the transport of PM from Asia. Three-dimensional, global-scale CTMs have also been used to estimate intercontinental transport of PM pollution (UNCEC, 2007, [157078](#)) and trans-Pacific transport of mineral dust from Asian deserts (Fairlie et al., 2007, [141923](#)) and the Sahara Desert (McKendry et al., 2007, [156748](#)).

Estimates for the contribution of PBAP are highly problematic. Heald and Spracklen (2009, [190014](#)) estimated the contribution of fungal spores to PM_{2.5} based on GEOS-Chem simulations of mannitol, considered to be a unique tracer for fungal spores (Bauer et al., 2008, [189986](#)). They estimated an annual mean contribution of fungal spores to OC ranging from <0.1 µg/m³ in the desert Southwest to ~ 0.5 µg/m³ in the more humid Southeast. It should be noted that these are model derived estimates that still require evaluation against measurements in the U.S. They do, however, provide the only quantitative estimates of PBAP concentrations across the continental U.S.

3.7.1.1. Estimates of PRB Concentrations in Previous Assessments

Estimates of PRB concentrations reported in the 1996 PM AQCD (U.S. EPA, 1996, [079380](#)) and earlier PM AQCDs were based in large measure on estimates by Trijonis et al. (1990, [157058](#)) for the National Acid Precipitation Assessment Program (NAPAP) as shown in Table 3-18. The importance of different sources is likely to be quite different for natural background compared to current conditions in the US, resulting in large changes in relations among different size fractions. For example, PM_{10-2.5} might be expected to dominate under certain conditions in the absence of primary and secondary PM_{2.5} from anthropogenic sources. Different approaches for estimating PRB concentrations in the western and eastern U.S. were taken in the 2004 PM AQCD (U.S. EPA, 2004, [056905](#)). Data obtained at IMPROVE monitoring sites in the western U.S. shown in Figure 3-84 were chosen as estimates of the distribution of daily average PRB concentrations in the West because they were thought to be among the least likely influenced by regional pollution sources especially at the upper end of the concentration distribution. This conclusion was drawn from back trajectory analyses and examination of the trace elemental composition at IMPROVE sites. Because of likely unresolved contamination from pollution sources at other IMPROVE sites, it was recommended to use averaged data from these sites throughout the West. Concentrations distributions from 1988 through 2001 can be found in Appendix 3E of the 2004 PM AQCD (U.S. EPA, 2004, [056905](#)). Median concentrations were ~3 µg/m³. Little interannual variability was observed below the 90th percentile values. However, at the upper end of the concentration distribution substantial interannual variability was observed due mainly to forest fires and dust transport from Asian deserts. It was also recognized that this method would likely overestimate PRB concentrations.

Table 3-18. Estimates of annual average natural background concentrations of PM_{2.5} and PM₁₀ (µg/m³) from Trijonis et al. (1990, [157058](#)). Estimates of PM_{10-2.5} were obtained by subtraction.

	PM _{2.5}	PM ₁₀	PM _{10-2.5}
East	2-5	5-11	≤ 1-9
West	1-4	4-8	≤ 1-7

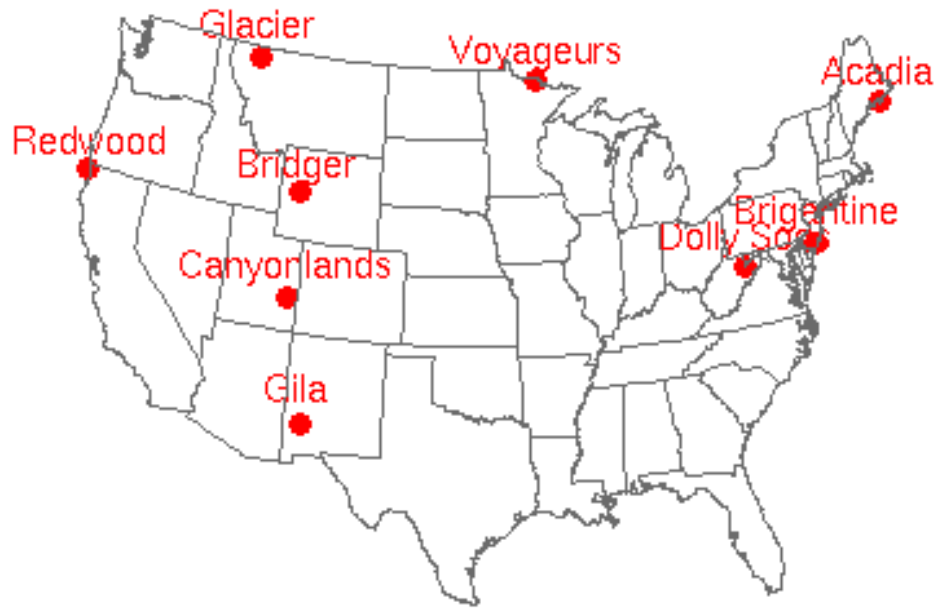


Figure 3-84. IMPROVE monitoring site locations.

Table 3-19 shows annual and quarterly average $PM_{2.5}$ concentrations measured at the IMPROVE sites shown in Figure 3-84 for 2004. Annual average concentrations tend to be slightly higher in the East, particularly in Brigantine and Dolly Sods. When the data are broken down by season, a more complex picture emerges. The highest concentrations in the East and Midwest are found during the 3rd calendar quarter, whereas in the West highest quarterly averages can occur during other quarters. As can also be seen from a comparison with values shown in Table 3-18, $PM_{2.5}$ values measured in the East are much higher than the PRB concentration estimates by Trijonis et al. (1990, [157058](#)) for the NAPAP.

Table 3-19. Annual and quarterly mean PM_{2.5} concentrations (µg/m³) measured at IMPROVE sites in 2004.

	Mean	January-March	April-June	July-September	October-December
EAST					
Acadia	4.5	3.9	4.6	6.0	3.5
Brigantine	9.5	8.1	11.3	11.6	7.3
Dolly Sods	9.5	6.7	9.8	15.5	5.7
MIDWEST					
Voyageurs	3.8	4.1	3.1	4.2	3.6
WEST					
Bridger	2.1	1.2	3.1	2.8	1.3
Canyonlands	2.6	2.2	3.2	2.9	2.1
Gila	2.9	2.0	4.0	3.8	1.8
Glacier	4.8	4.6	4.2	5.3	5.0
Redwood	3.5	2.7	3.6	3.7	3.9

Thus, estimating daily average PRB concentrations in the eastern U.S. using observations is highly problematic because of the widespread mixing of precursors and anthropogenic PM generated in the East. Therefore, results from receptor modeling studies using PMF by Song et al. (2001, [036064](#)) were used in the 2004 PM AQCD (U.S. EPA, 2004, [056905](#)) for the East to separate contributions from likely regional pollution sources from natural and imported pollution. The “background” sources contribute about 7% to annual average PM_{2.5} concentrations at Underhill, VT and about 12% at Brigantine, NJ, i.e., values between 1 and 2 µg/m³. These sites were chosen because they were outside of urban areas making it easier to separate pollution from background components. However, some contribution of regional anthropogenic pollution was still present.

The PM Staff Paper (U.S. EPA, 2006, [157071](#)) adopted a different approach for estimating PRB concentrations. This approach separated out components mainly thought to be emitted by regional pollution sources such as SO₄²⁻, which are obtained directly from observations at many more IMPROVE sites than are shown in Figure 3-84, and to use the remaining PM components in both the East and the West to estimate PRB. Removing regional pollution from data obtained at IMPROVE sites is problematic as it involves assumptions about the relative contributions of regional pollution and background sources. Although sulfate in the East is mainly produced by regional pollution sources, it is not the only component with a regional pollution source. By comparison, sulfate is a very minor component of PM_{2.5} in the West, leading to substantial overestimates in populated states like California. Annual mean estimates in the continental U.S. ranged from 2.5 µg/m³ in the Central West (ID, MT, WY, ND, SD, CO, UT, NZ, AZ) to 5.2 µg/m³ for the Southwest Coast (most of California), the latter value likely reflecting contributions from local, non-sulfate pollution.

In general, the methods outlined in both these documents are of limited utility for two reasons: (1) they lack detailed spatial coverage across the whole U.S., since both methods rely on monitoring data that are limited both spatially and temporally; and (2) PM measurements from even the limited, remote sites used in the previous estimates of PRB can not be completely devoid of contributions from anthropogenic PM. Because of these limitations, numerical modeling can provide superior PM background estimates, as described just below.

3.7.1.2. Chemistry Transport Models for Predicting PRB Concentrations

CTMs can be used to estimate the PRB concentrations of atmospheric components including PM using a “zero-out” approach in which anthropogenic emissions inside continental North America are set to zero while global biogenic emissions and anthropogenic emissions outside continental

North America remain. Numerical modeling can provide more precision in the estimate of PRB PM than measurements since even the most remote measurement sites like some of those in the IMPROVE network (see the discussion in Section 3.7.1.1) will necessarily be affected by non-local non-biogenic pollution, thereby confusing the contributions from these sources. Numerical models are also capable of supplying estimates of PRB concentrations at much higher spatial and temporal resolution than can be obtained by relying on measurements obtained at even the most remote monitoring sites. In this approach, the monitoring data are used to evaluate the CTM's performance.

For this assessment, the global-scale circulation model GEOS-Chem was coupled with the regional scale air quality model CMAQ (Section 3.6.2.2) to simulate one year of air quality data over the CONUS in two series of runs, the first annual series with all anthropogenic and biogenic emissions included and the second annual series with the zero-out approach employed.

The global-scale scale circulation model was set up as follows. GEOS-Chem, version 7, was used, with modifications to include aromatic and biogenic SOA formation; emissions were computed from a variety of sources including the Global Emissions Inventory Activity (GEIA) (Benkovitz et al., 1996, [156267](#)), and Emissions Database for Global Atmospheric Research, version 2 (EDGAR) (Olivier et al., 1996, [156828](#); Olivier et al., 1999, [156829](#)).

Particularized emissions in specific areas used the European Monitoring and Evaluation Program (EMEP) for Europe (Auvray and Bey, 2005, [156237](#)), BRAVO (Kuhns and Knipping, 2005, [156663](#)) for Mexico, and Streets et al. (2006, [157019](#)) for Asia. Emissions from these studies were supplemented with data from Martin et al. (2002, [089380](#)) for additional NO_x emissions from biofuels, lightning, and ship traffic, Bond et al. (2004, [056389](#)) for global primary organic aerosols, and Cooke et al. (1999, [156365](#)) and Park et al. (2003, [156842](#)) for U.S. primary organic aerosols. Biomass burning emissions are not climatological, but were computed with GFEDv2 (Giglio et al., 2006, [156469](#); van der Werf et al., 2006, [157084](#)); monthly values computed using active fire observations from MODIS; global dust fields computed off-line using GOCART (see emissions from DEAD: <http://dust.ess.uci.edu/dead/>) to make annual adjustments to photolysis rates and heterogeneous-phase chemistry.

The regional CTM was set up as follows. CMAQ, version 4.7, (excluding the dynamic coarse mode updates) was used with the SAPRC 99 chemical mechanism and AERO5 aerosol module; emissions were processed through SMOKE (<http://smoke-model.org>), version 2.4, based on the 2004 projections from the NEI with specific CEM, biogenics, and fire updates; MM5, version 3.7.4, was used with the Asymmetric Convective Mixing, version 2.2, PBL scheme; and data nudging was used to analyze fields for winds and temperature.

Model Evaluation

Details from evaluations of the performance of a number of CMAQ applications are given in Arnold et al. (2003, [087579](#)), Eder and Yu (2006, [142721](#)), Appel et al. (2005, [089227](#)), and Fuentes and Raftery (2005, [087580](#)).

In an annual simulation series for 2002 using CMAQ, version 4.6.1, in two 12-km domains for the CONUS (Figure 3-85), predicted concentrations of summertime particulate SO₄, often a major determinant of surface-layer PM concentrations, were well-predicted by CMAQ at a 12-km grid spacing, to within a factor of 2 at nearly every point of comparison and with R² > 0.8 across all three national networks (CASTNet, IMPROVE and CSN); a more detailed description is included in the 2008 NO_xSO_x ISA (U.S. EPA, 2008, [157074](#)). This result for CMAQ, version 4.6.1, for 2002 tracks the generally well-predicted SO₄²⁻ concentrations found in most earlier CMAQ evaluations: see Mebust et al. (2003, [156749](#)), Eder and Yu (2006, [142721](#)), and Tesche et al. (2006, [157050](#)). Since particulate SO₄²⁻ concentrations are strongly a function of precipitation, care must be taken to ensure that the meteorological solution driving individual CMAQ chemical applications produces precipitation fields with low bias as discussed by Appel et al. (2008, [155660](#)).

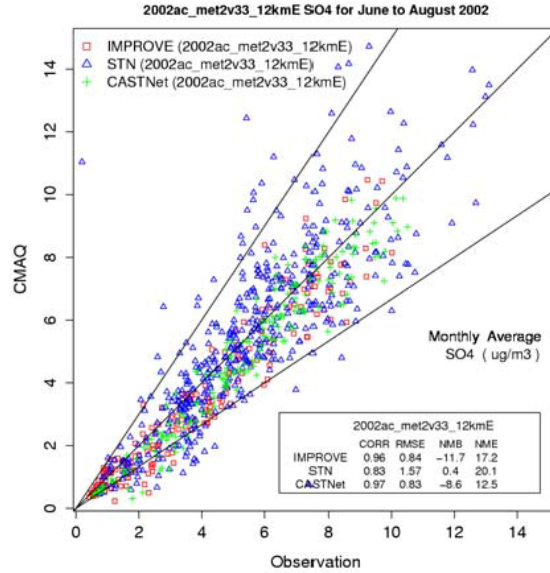


Figure 3-85. 12-km EUS Summer SO_4^{2-} PM. Each data point represents a paired monthly averaged (June/July/August) observation and CMAQ prediction at a particular IMPROVE, STN, and CASTNet site. Solid lines indicate the factor of 2 around the 1:1 line shown between them.

Wintertime particulate NO_3^- (Figure 3-86) and total NO_3 (HNO_3 + particulate NO_3^-) (Figure 3-87) concentrations are predicted as well by CMAQ; however, NO_3^- is a pervasively difficult species to measure and model. Still, at the CASTNet nodes where the total NO_3^- concentrations are higher than they are at all but a few of the remote IMPROVE sites, CMAQ predicts concentrations for nearly every node to within a factor of 2 and with an $R^2 > 0.8$.

A “base case” in which conditions for 2004 including all the anthropogenic and natural sources both within and outside of continental North America was run for comparison with measurements. A PRB simulation was also run by shutting off the anthropogenic sources of primary PM and precursors to secondary PM inside continental North America.

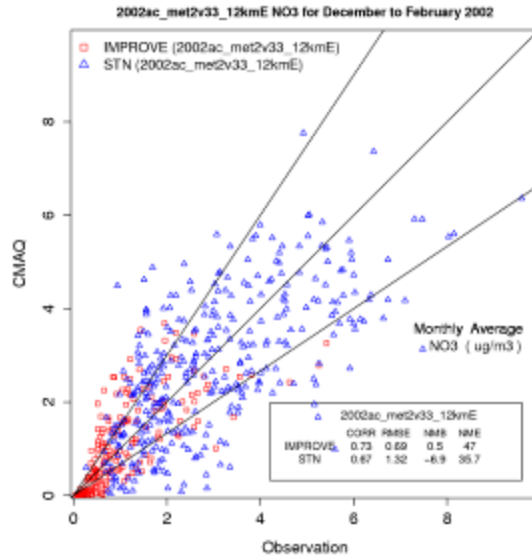


Figure 3-86 12-km EUS Winter NO_3^- PM. Each data point represents a paired monthly averaged (December/January/February) observation and CMAQ prediction at a particular IMPROVE and STN site. Solid lines indicate the factor of 2 around the 1:1 line shown between them.

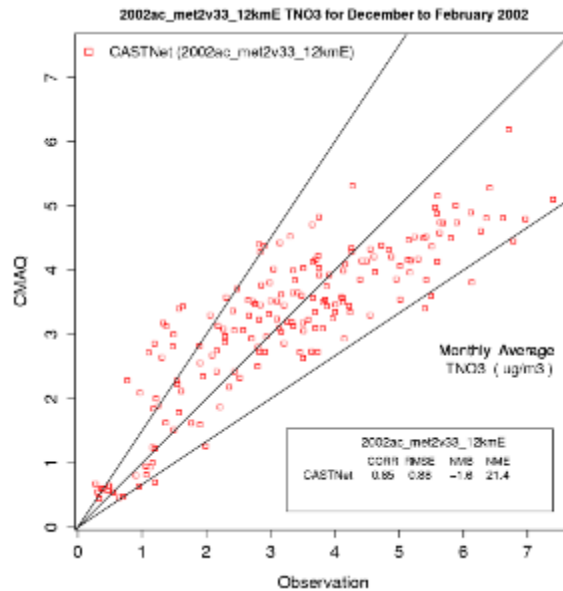


Figure 3-87. 12-km EUS Winter total nitrate ($\text{HNO}_3 + \text{total particulate } \text{NO}_3^-$). Each data point represents a paired monthly averaged (December/January/February) observation and CMAQ prediction at a particular CASTNet site. Solid lines indicate the factor of 2 around the 1:1 line shown between them.

Figure 3-88 and Figure 3-89 show monthly average concentrations, and Figure 3-90 and Figure 3-91 show 24-h avg concentration distributions for 2004 predicted by CMAQ for the base case and for PRB. Measurements are also included for the five western and four eastern/midwestern IMPROVE sites shown in Figure 3-84. Wildfires could have affected the grid cell containing the midwestern Voyageurs site resulting in the high PRB values found for the July average compared to the PRB values for the rest of the year. The “base case” simulations tend to underestimate concentrations throughout most western sites as shown in Figure 3-89 and Figure 3-91. These underestimates are still within the range of a few $\mu\text{g}/\text{m}^3$. However, the base case simulation also greatly over-predicts $\text{PM}_{2.5}$ concentrations at the upper end of the distribution at the Redwoods site (Figure 3-91). This over-prediction results from emissions from wildfires in northern California that are included in the grid cell containing the Redwoods site, but may not have affected the site. However, wildfires indicated by MODIS would have affected other areas either close to these sites or could have affected other locations in between the IMPROVE sites. The simulated monthly average PRB concentrations in the east/midwest range from a minimum of $0.6 \mu\text{g}/\text{m}^3$ at Acadia National Park (NP) in July to $3.7 \mu\text{g}/\text{m}^3$ at Voyageurs NP in July. However, most values are $<1 \mu\text{g}/\text{m}^3$. The monthly average PRB concentrations calculated for the West tend to be lower than for the East and range from $0.2 \mu\text{g}/\text{m}^3$ at Bridger and Glacier NPs in January and February, respectively, to $8.7 \mu\text{g}/\text{m}^3$ at Redwoods NP in November. Excluding values at Redwoods NP which greatly exceed measurements, the highest monthly average concentration was $3.7 \mu\text{g}/\text{m}^3$ at Voyageurs NP in the East/Midwest and $2.4 \mu\text{g}/\text{m}^3$ at Gila NP in the West.

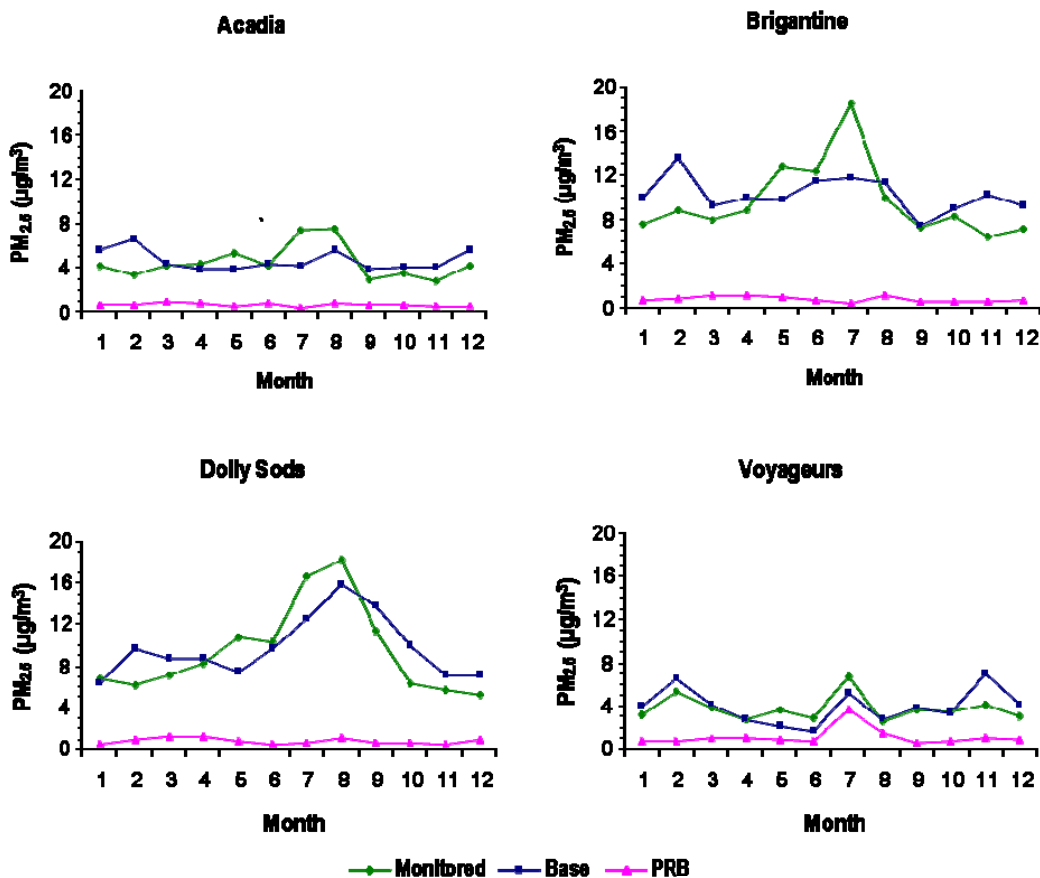


Figure 3-88. Monthly average of $\text{PM}_{2.5}$ concentrations measured at IMPROVE sites in the East and Midwest for 2004. Also shown are distributions of $\text{PM}_{2.5}$ concentrations calculated by CMAQ for the base case and for PRB.

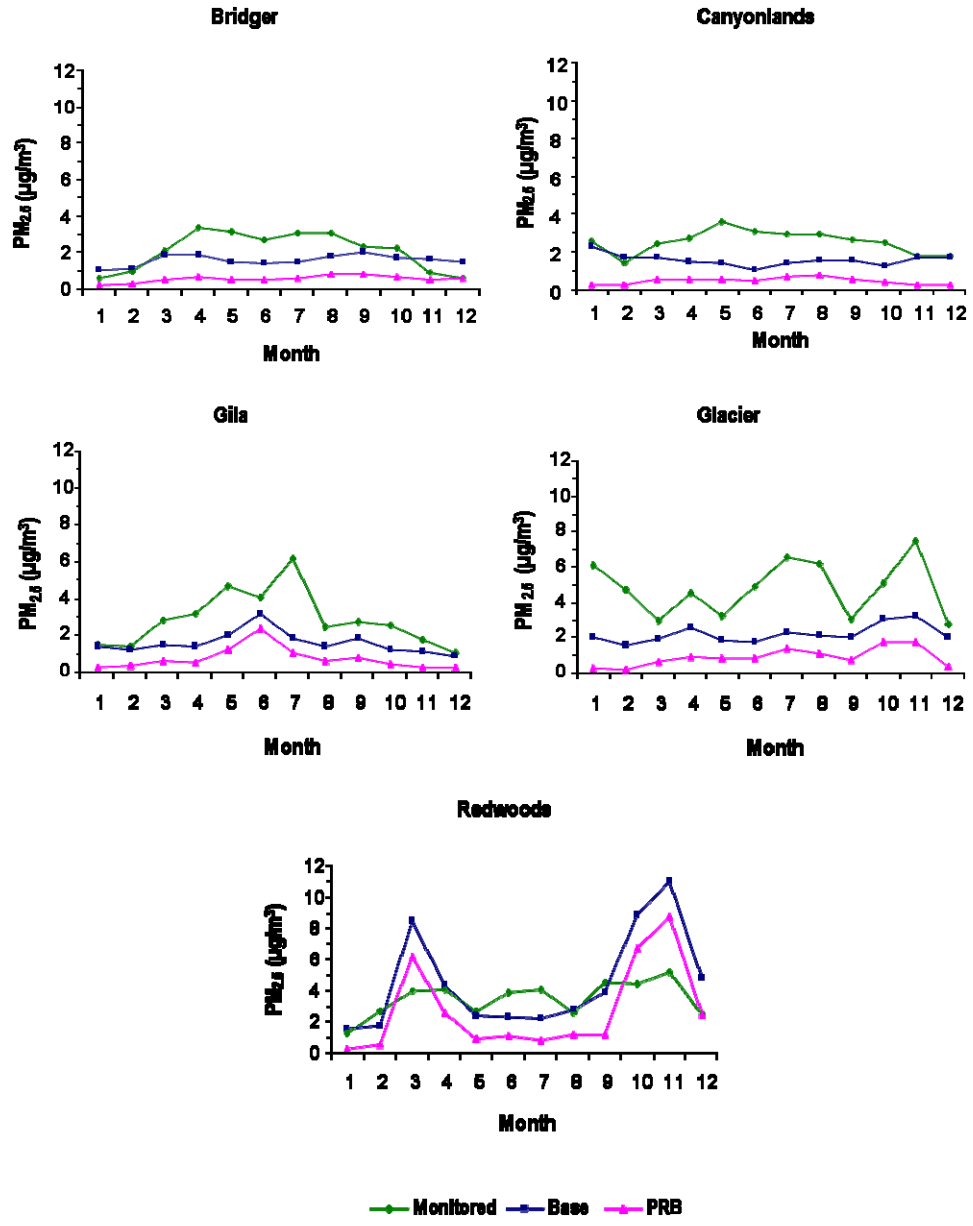


Figure 3-89. Monthly average of PM_{2.5} concentrations measured at IMPROVE sites in the West for 2004. Also shown are distributions of PM_{2.5} concentrations calculated by CMAQ for the base case and for PRB.

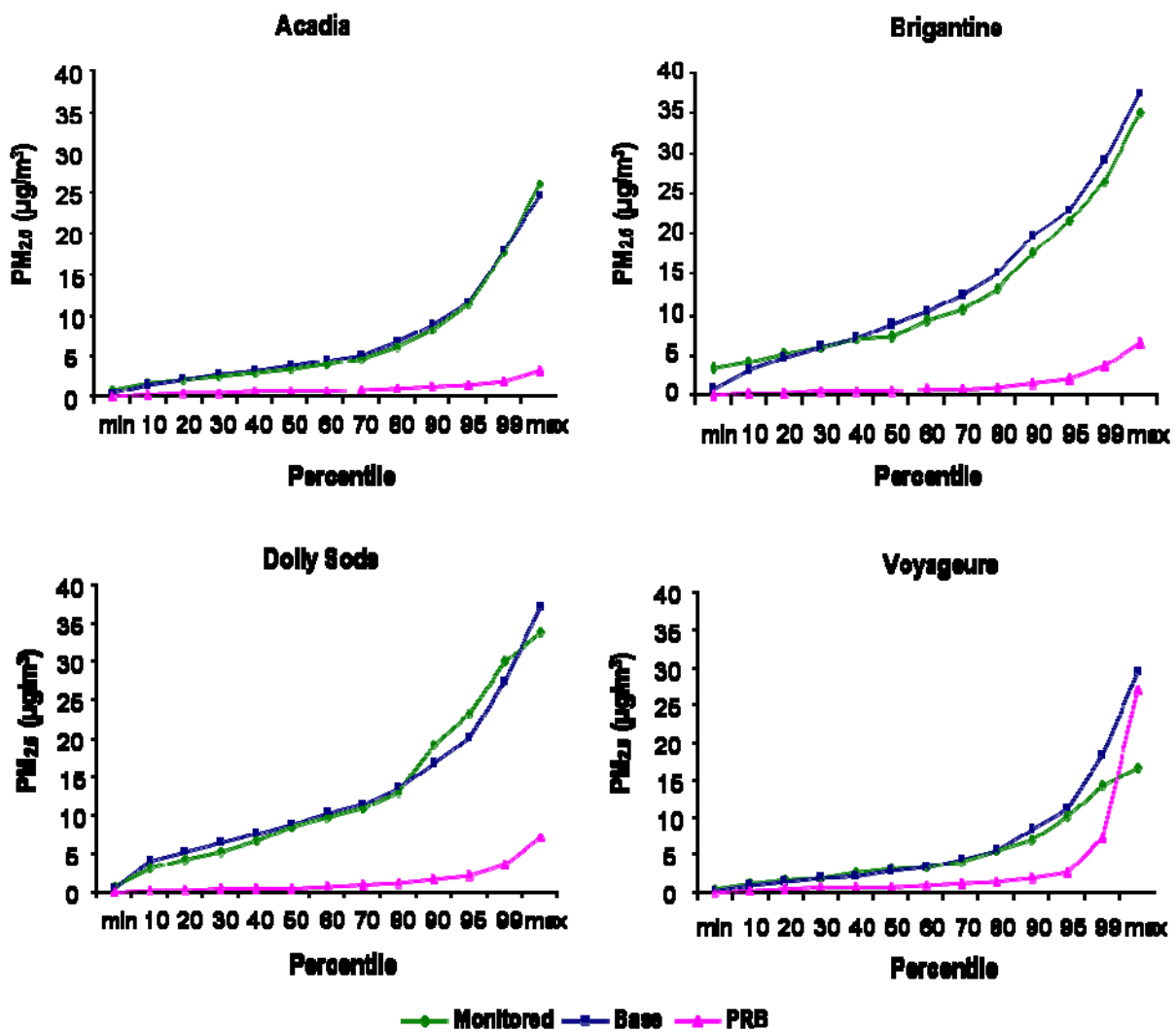


Figure 3-90. Distribution of PM_{2.5} concentrations measured at IMPROVE sites in the East and Midwest for 2004. Also shown are distributions of PM_{2.5} concentrations calculated by CMAQ for the base case and for PRB.

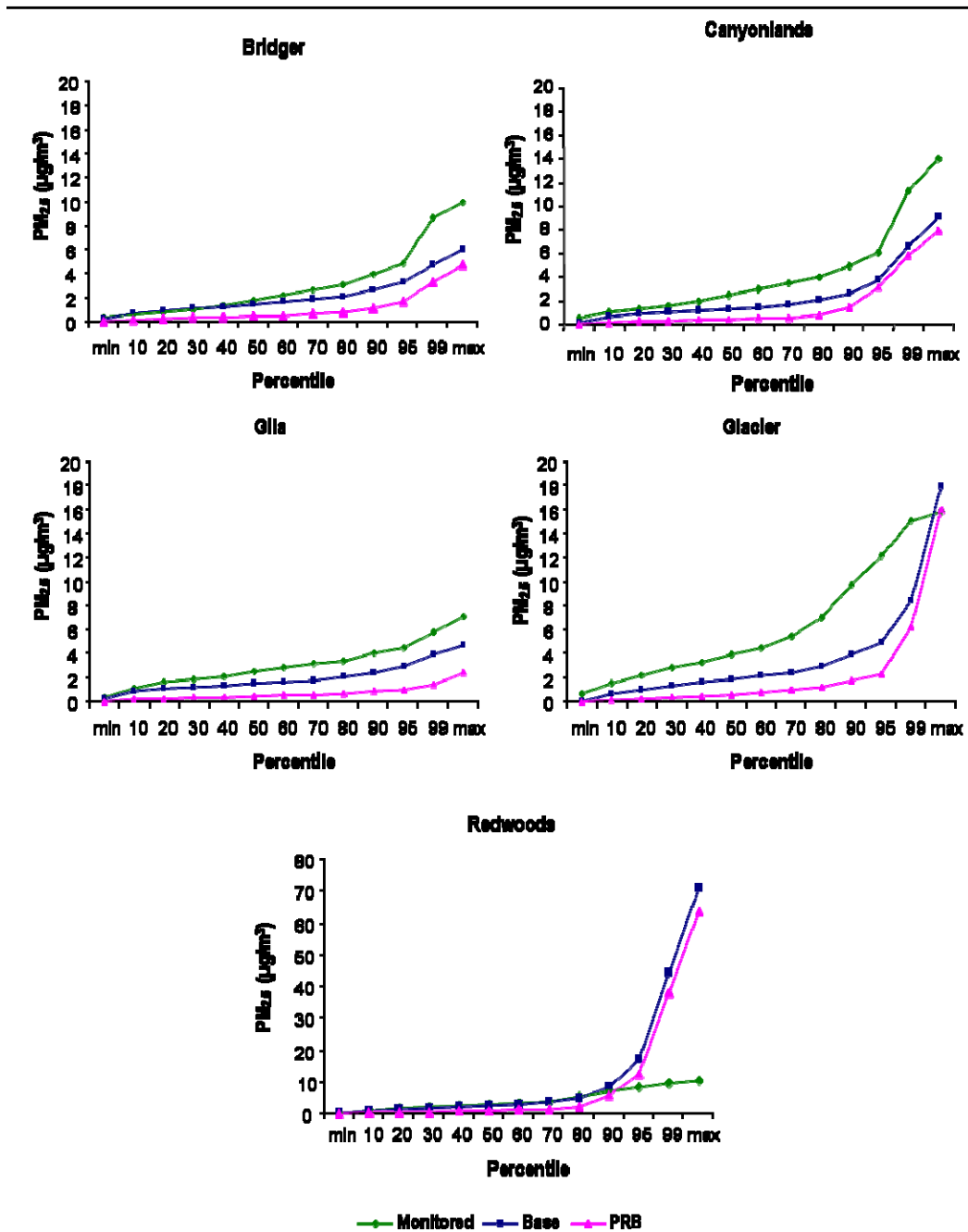


Figure 3-91. Distribution of PM_{2.5} concentrations measured at IMPROVE sites in the West for 2004. Also shown are distributions of PM_{2.5} concentrations calculated by CMAQ for the base case and for PRB. Note the scale change on the y-axis for Redwoods NP.

Table 3-20 gives the annual and quarterly average CMAQ predictions at IMPROVE sites for the “base case” and the ratio of CMAQ predictions to the measured concentrations at those sites in 2004. CMAQ performance for the annual average concentrations and most of the seasonal averages is very good in the East and Midwest, generally falling within 35%. In the West, CMAQ’s prediction of PM_{2.5} mass averages at these remote sites is generally too low in all seasons, often by 50%. Air quality model predictions in the mountainous West are often not as good as those over the flatter

terrain in the East and Midwest because the model's grid spacing (36 km in this case) smoothes over significant variation at the surface that results in differences at such remote sites. However, the model's trend relative to the geospatial difference is correct: the predicted PM_{2.5} concentrations are lower at the western sites than they are at the eastern sites, just as the measurements are. Table 3-21 shows corresponding annual and quarterly mean PRB PM_{2.5} concentrations at IMPROVE sites.

Table 3-20. Annual and quarterly mean PM_{2.5} concentrations (µg/m³) for the CMAQ "base case" at IMPROVE sites in 2004.

	Annual; mod/obs	Jan-March; mod/obs	Apr-Jun; mod/obs	Jul-Sep; mod/obs	Oct-Dec; mod/obs
EAST					
Acadia	4.7; 1.04	5.6; 1.44	4.0; 0.87	4.6; 0.77	4.6; 1.31
Brigantine	10.2; 1.07	10.9; 1.35	10.3; 0.91	10.2; 0.88	9.4; 1.29
Dolly Sods	9.8; 1.03	8.3; 1.24	8.6; 0.88	14.0; 0.90	8.0; 1.40
MIDWEST					
Voyageurs	4.0; 1.05	4.9; 1.19	2.2; 0.71	3.9; 0.93	4.9; 1.36
WEST					
Bridger	1.6; 0.76	1.3; 1.08	1.6; 0.52	1.8; 0.64	1.7; 1.30
Canyonlands	1.6; 0.62	1.9; 0.86	1.4; 0.44	1.5; 0.52	1.6; .76
Gila	1.6; 0.55	1.4; 0.70	2.2; 0.55	1.7; 0.45	1.1; 0.61
Glacier	2.2; 0.45	1.8; 0.39	2.1; 0.50	2.1; 0.40	2.8; 0.56
Redwood	4.6; 1.31	4.0; 1.48	3.0; 0.83	2.9; 0.78	8.4; 2.15

Table 3-22 illustrates CMAQ predictions of seasonal variation in the base case PM_{2.5} concentrations across regions of the CONUS, while Table 3-23 shows CMAQ predictions of the seasonal variation in regional PRB PM_{2.5} concentrations. Highest base case PM_{2.5} concentrations were observed for the Northeast, Southeast, and industrial Midwest, with highest concentrations during the fall and winter (and comparably high concentrations in the summer for the Industrial Midwest). PRB PM_{2.5} concentrations were highest on an annual basis in the Southeast, and peaking during the winter. In the summer, PRB PM_{2.5} is roughly comparable for the Northwest and Southern California and elevated, but slightly lower for the Southwest. These results also likely indicate the influence of sources that are more strongly related to hot and dry conditions such as wildfires and dust suspension.

Table 3-21. Annual and quarterly mean PM_{2.5} concentrations (µg/m³) for the CMAQ PRB simulations at IMPROVE sites in 2004.

	Annual	January-March	April-June	July-September	October-December
EAST					
Acadia	0.70	0.76	0.76	0.65	0.65
Brigantine	0.77	0.86	0.91	0.70	0.63
Dolly Sods	0.79	0.88	0.83	0.75	0.66
MIDWEST					
Voyageurs	1.2	0.83	0.91	2.0	0.93
WEST					
Bridger	0.57	0.33	0.57	0.76	0.61
Canyonlands	0.49	0.38	0.54	0.68	0.35
Gila	0.74	0.42	1.4	0.80	0.32
Glacier	0.91	0.36	0.87	1.1	1.3
Redwood	2.8	2.4	1.5	1.1	6.1

Table 3-22. Annual and quarterly mean of the CMAQ-predicted base case PM_{2.5} concentrations (µg/m³) in the U.S. EPA CONUS regions in 2004.

	Annual	January-March	April-June	July-September	October-December
Northeast	9.76	10.74	8.38	9.55	10.38
Southeast	10.05	12.28	7.72	9.78	10.42
Industrial Midwest	11.38	12.22	9.37	11.89	12.00
Upper Midwest	6.70	8.83	4.95	5.34	7.67
Southwest	3.30	4.08	2.77	3.31	3.03
Northwest	2.72	2.49	2.21	2.71	3.44
Southern California	4.43	4.64	3.93	4.34	4.82

Table 3-23. Annual and quarterly mean of the CMAQ-predicted PRB PM_{2.5} concentrations (µg/m³) in the U.S. EPA CONUS regions in 2004.

	Annual	January-March	April-June	July-September	October-December
Northeast	0.74	0.85	0.78	0.67	0.68
Southeast	1.72	2.43	1.41	1.41	1.64
Industrial Midwest	0.86	0.89	0.89	0.94	0.73
Upper Midwest	0.84	0.79	0.93	0.99	0.66
Southwest	0.62	0.61	0.76	0.70	0.40
Northwest	1.01	0.48	0.81	1.42	1.32
Southern California	0.84	0.54	0.92	1.21	0.67

3.8. Issues in Exposure Assessment for PM and its Components

The purpose of this section is to present the latest exposure assessment studies to characterize the exposure of individuals and populations to PM of ambient origin. Such information will aid the interpretation of epidemiologic studies described in subsequent chapters of this ISA. This section includes descriptions of modeling and monitoring techniques used to capture personal PM exposure, observations reported in the literature at various relevant spatial scales, observations related to PM composition and PM in a mix of copollutants, and the effect of exposure estimates on epidemiologic results. Attention is given to use of community-based monitors at urban spatial scales and use of personal and microenvironmental exposure data to present how each metric can be used in exposure assessment and what errors and uncertainties exist for each approach. Understanding of exposure errors is important because exposure error can potentially bias an estimate of a health effect endpoint, or increase the size of confidence intervals around a health effect estimate. Typically, exposure error biases analyses of health effects towards the null (i.e., no relationship between exposure and health effect).

The information presented in this section builds upon the key findings of the 2004 PM AQCD (U.S. EPA, 2004, [056905](#)). One key finding was that separation of total PM exposures into ambient and nonambient components reduces potential uncertainties in the analysis and interpretation of PM health effects data. At the time of the 2004 PM AQCD (U.S. EPA, 2004, [056905](#)), one study reported that individual daily values of both the total and nonambient personal PM exposure were poorly correlated with the daily ambient PM concentrations, while individual daily values of ambient PM exposure and daily ambient PM concentrations were highly correlated. In pooled studies (different subjects measured on different days), individual, daily values of the total PM exposure were generally shown to be poorly correlated with the daily ambient PM concentrations. In longitudinal studies (each subject measured for multiple days), individual, daily values of the total PM personal exposure and the daily ambient PM concentrations were found to be highly correlated for some, but not all, subjects. Using the PTEAM study data, the 2004 PM AQCD (U.S. EPA, 2004, [056905](#)) also analyzed exposure measurement errors in the context of time-series epidemiology to show that the error introduced by using ambient PM concentrations as a surrogate for ambient PM exposures negatively biases the estimation of health risk coefficients by the ratio of ambient PM exposure to ambient PM concentration. However, it was concluded that the health risk coefficient determined using ambient PM concentrations provides the correct information on the change in health risks that would be produced by a change in ambient concentrations.

Personal exposure to PM can vary considerably depending on PM size and composition, source strength and proximity, season, time of day, region of the country, population density of the environment, personal activity patterns, and ventilation of indoor environments. Table A-58 of Annex A, which summarizes findings from U.S. panel studies of personal exposure to PM with no

indoor sources published between 2002 and 2008 broken down by region of the country, illustrates this variability. For example, Table A-58 presents 24-h personal PM_{2.5} exposures that range from roughly 1-55 µg/m³ with highest exposures in the southwest and northeastern regions of the country and during the summer season. Section 3.8 is designed to present current theory and field results regarding exposure to PM. To illustrate the concept of personal exposure within various microenvironments, a general exposure model is presented in Section 3.8.1. New developments in techniques for measuring personal and indoor PM are presented in Section 3.8.2, followed by exposure modeling techniques in Section 3.8.3. In Section 3.8.4, exposure assessment field studies in the literature are presented. Attention is given to ambient exposure over multiple spatial scales including near-road, in-vehicle, and indoor environments. Section 3.8.5 presents issues related to PM composition and PM in multipollutant mixtures. Finally, implications of exposure assessment issues for epidemiologic studies are presented in Section 3.8.6.

3.8.1. General Exposure Concepts

A theoretical model of personal exposure is presented to highlight what is measurable and what uncertainties exist in this framework. An individual's time-integrated total exposure to airborne PM can be described based on a compartmentalization of the person's activities during a given time period:

$$E_T = \int C_j dt$$

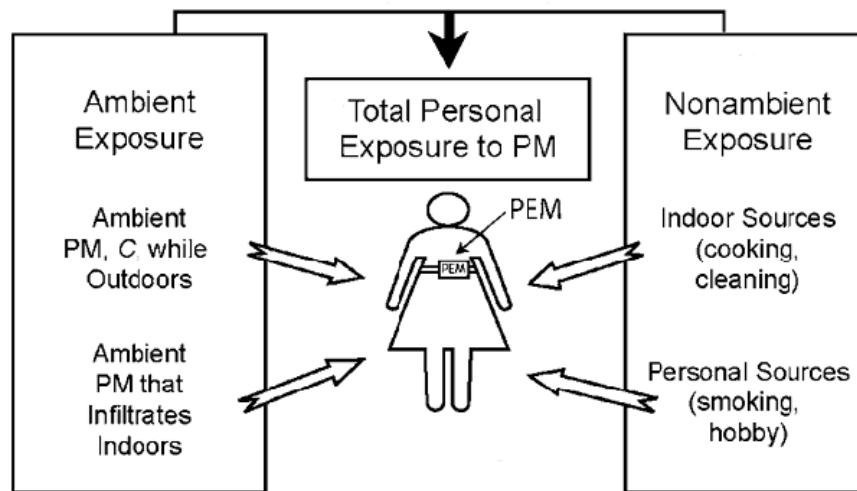
Equation 3-3

where E_T = total exposure over a time period of interest, C_j = airborne PM concentration at microenvironment j , and dt = portion of the time-period spent in microenvironment j . Equation 3-3 can be decomposed into a microenvironmental model that accounts for exposure to PM of ambient (E_a) and nonambient (E_{na}) origin of the form:

$$E_T = E_a + E_{na}$$

Equation 3-4

Figure 3-92 illustrates Equation 3-4. Examples of ambient PM sources include industrial and mobile source emissions, resuspended dust, biomass combustion, and secondary formation. Examples of nonambient sources include smoking, cooking, home heating, cleaning, and indoor air chemistry. PM concentrations generated by ambient and nonambient sources are subject to spatial and temporal variability that can affect estimates of exposure and resulting health effects. Exposure factors affecting interpretation of epidemiology are discussed in detail in Section 3.8.6.



Source: Adapted with permission of Nature Publishing Group from Wilson and Brauer (2006, [088933](#)).

Figure 3-92. Model of total personal exposure to PM as a function of ambient and nonambient sources.

This assessment focuses on the ambient component of exposure because this is more relevant to the NAAQS review. E_a can be decomposed into the fraction of time spent in various outdoor and indoor microenvironments (Wallace et al., 2006, [089190](#); Wilson et al., 2000, [010288](#)):

$$E_a = \sum f_o C_o + \sum f_i F_{inf,i} C_{o,i}$$

Equation 3-5

where f = fraction of the relevant time period (equivalent to dt in Equation 3-2), subscript o = index of outdoor microenvironments, subscript i = index of indoor microenvironments, subscript o,i = index of outdoor microenvironments adjacent to a given indoor microenvironment i , and $F_{inf,i}$ = infiltration factor for indoor microenvironment i . Equation 3-5 is subject to the constraint $\sum f_o + \sum f_i = 1$, and each term on the right hand side of the equation has a summation because it reflects various microenvironmental exposures. Here, “indoors” refers to being inside any aspect of the built environment, e.g., home, office buildings, enclosed vehicles (automobiles, trains, buses), and recreational facilities (movies, restaurants, bars). “Outdoor” exposure can occur in parks or yards, on sidewalks, and on bicycles or motorcycles.

F_{inf} represents the equilibrium fraction of the PM concentration outside the microenvironment that penetrates inside the microenvironment and remains suspended. It is a function of the microenvironmental air exchange characteristics and the particle properties. Assuming steady state conditions, the infiltration factor is a function of the penetration, P , of PM (a fractional quantity representing the portion of outdoor PM that passes through the building envelope), the air exchange rate, a , of the indoor microenvironment, and the rate of PM loss, k , within the indoor microenvironment: $F_{inf} = Pa/(a+k)$. Determination of E_a can be complicated by PM loss through chemical and physical processes in microenvironments, and the composition of PM can be modified during infiltration of outdoor air into microenvironments (Meng et al., 2007, [194618](#); Sarnat et al., 2006, [089166](#)).

In the context of interpreting epidemiologic studies of the effects of ambient pollutants on human health, the association between E_a and concentrations from a central site monitor, C_a , is more relevant than the association between E_T and C_a because nonambient PM is uncorrelated with C_a , as discussed in Section 3.8.4. In ecologic studies of large panels or cohorts, C_a is often used in lieu of outdoor microenvironmental data to represent these exposures based on the availability of data. Thus it is often assumed that $C_o = C_a$ and that the fraction of time spent outdoors can be expressed cumulatively as f_o ; the indoor terms still retain a summation because infiltration differs among

different microenvironments. Under these assumptions, an individual's exposure to ambient PM, first given in Equation 3-5, can be re-expressed as a function of C_a . The following approximation has been employed in the literature to describe ambient exposure based on these assumptions (Wallace et al., 2006, [089190](#); Wilson and Brauer, 2006, [088933](#); Wilson et al., 2000, [010288](#)):

$$E_a = (f_o + \sum f_i F_{\text{inf},i}) C_a$$

Equation 3-6

Particle size, particle composition, meteorology, urban and natural topography, and other factors determine whether or not Equation 3-6 is a reasonable approximation for Equation 3-5. Errors and uncertainties inherent in the use of Equation 3-6 in lieu of Equation 3-5 are described in Section 3.8.6 with respect to implications for epidemiology. If concentration measured at a central site monitor is used to represent ambient concentration, then α , the ratio between personal exposure to ambient PM and the ambient concentration of PM, can be defined as:

$$\alpha = \frac{E_a}{C_a}$$

Equation 3-7

If the assumptions forming the basis for Equation 3-6 are valid, then α is the proportionality factor in Equation 3-6:

$$\alpha = f_o + \sum f_i F_{\text{inf},i}$$

Equation 3-8

α varies between 0 and 1. If a person's exposure occurs in a single microenvironment, the ambient component of a microenvironmental PM concentration can be represented as the product of the ambient concentration and F_{inf} . Wallace et al. (2006, [089190](#)) note that time-activity data and corresponding estimates of F_{inf} for each microenvironmental exposure are needed to compute an individual's α with accuracy. If significant local sources and sinks are not captured by central site monitors, then the ambient component of outdoor air must be estimated using dispersion models, land use regression (LUR) models, receptor models, fine scale CTMs or some combination of these techniques. Modeling methods are described in Section 3.8.3.

3.8.2. Personal and Microenvironmental Exposure Monitoring

The purpose of this section is to present new discoveries related to measuring microenvironmental PM concentrations or personal exposure to PM. A review of over 100 personal and microenvironmental PM exposure studies published since 2002 (see Table A-58 of Annex A) reveals that the majority of the monitoring techniques in use were previously reviewed in the 2004 PM AQCD (U.S. EPA, 2004, [056905](#)) for PM. Detailed descriptions of these methodologies are provided in that document and therefore will not be repeated in this document. The following sections will include only findings from 2002 or later regarding monitoring and modeling methodologies in common use and significant advancements in understanding the capabilities and limitations of these methods for assessment of PM exposure.

3.8.2.1. New Developments in Personal Exposure Monitoring Instrumentation

Current personal exposure sampling methodology consists largely of integrated filter sampling using a cyclone or personal exposure monitor (PEM) to achieve a cut point at a desired particle size. This method of sampling facilitates speciation work because the filters can be archived for chemical and gravimetric analysis. Additionally, light scattering aerosol detection instruments, such as the personal DataRam (pDR) and SidePak personal aerosol monitor have seen some use in personal PM_{2.5}, PM₁₀, and PM₁ monitoring (e.g., Lewne et al., 2006, [090556](#); Wallace et al., 2006, [088211](#)). Several researchers have noted that relative humidity causes overestimation of the particle mass in

light-scattering personal exposure monitors (e.g., Lowenthal et al., 1995, [045134](#); Ramachandran et al., 2003, [195017](#)); a correction factor has been applied to concentrations to address this issue. In the DEARS, Williams et al. (2008, [191201](#)) attempted to reduce humidity of the sample stream by placing a drying column upstream of the pDR's detector. Although this addressed the humidity issue, the drying column occasionally released particles and therefore caused artificial concentration peaks. For this reason, Williams et al. (2008, [191201](#)) determined that the humidity correction approach is preferable.

One area of further development is in personal sampling of the thoracic and respirable particle size distribution. Variations of the cascade impactor have been developed for personal sampling and tested for use in field studies (Case et al., 2008, [155149](#); Lee et al., 2006, [098249](#); Singh et al., 2003, [156088](#)). The model developed and tested by Lee et al. (2006, [098249](#)) operates with a 1- μm cut point and therefore can characterize respirable particles well. The Case et al. (2008, [155149](#)) two-stage cascade impactor separated $\text{PM}_{10-2.5}$ from $\text{PM}_{2.5}$ for personal monitoring and sampled within $\pm 20\%$ of a reference method. Hsiao et al. (2009, [191001](#)) developed a mini-cyclone with a 1 μm or 0.3 μm cut point for sampling accumulation mode and UFPs. The Personal Cascade Impactor Sampler (PCIS) has the capability to sample down to a cut point of 250 nm (Singh et al., 2003, [156088](#)). For $\text{PM}_{2.5}$, the difference between the PCIS and the MOUDI cascade impactor was 11%, while the difference between the PCIS and the SMPS-APS was only 2%. Differences between the PCIS and the MOUDI for $\text{PM}_{2.5}$ species compared with the MOUDI was generally higher: 11% for SO_4^{2-} , 22% for NO_3^- , 19% for EC, and 94% for OC. Mass was overestimated by 3%, 16%, and 31% for $\text{PM}_{1-0.5}$, $\text{PM}_{0.5-0.25}$, and $\text{PM}_{0.25}$, respectively, when compared with the SMPS-APS. Similarly, Case et al. (2008, [155149](#)) found a mass difference ranging from -11 to +10% for $\text{PM}_{10-2.5}$ with the Personal Respirable Particulate Sampler (PRPS), and Lee et al. (2006, [098249](#)) found a mass difference of -6 to 0% for $\text{PM}_{2.5}$ and -6 to -1% for PM_{10} when comparing results from this device with those from the PEM. Leith et al. (2007, [098241](#)) redesigned the Wagner-Leith passive sampler for measuring $\text{PM}_{10-2.5}$. In this work, the difference between a $\text{PM}_{10-2.5}$ FRM and the co-located passive sampler was within 1 standard deviation of concentrations measured by the FRM samplers.

A number of personal PM monitors are under development as part of the National Institutes of Health Genes, Environment, and Health Initiative (<http://www.gei.nih.gov/exposurebiology/program/sensor.asp>). Funded projects for miniature personal monitors include a platform that records real-time BC and PM concentrations and archives PM for further analysis, a badge containing a sensor array that detects several compounds found in diesel PM, a micro-nephelometer recording PM and endotoxin exposure, a complementary metal-oxide-semiconductor (CMOS) fitting in the nose to measure allergen PM, and a micro-thermofluidic nanoparticle sensor. The mini-cyclone cited above was designed to operate upwind of the micro-thermofluidic sensor (Hsiao et al., 2009, [191001](#)). LeVine et al. (2009, [192091](#)) and Schwartz et al. (2008, [192094](#)) described use of the CMOS technology for real-time DNA detection. Mulchandani et al. (2001, [191003](#)) reviewed amperometric biosensors used for organophosphate pesticide detection that are the basis of the diesel detection badge; several additional articles have been published by this group that describe applications of amperometric sensors.

3.8.2.2. New Developments in Microenvironmental Exposure Monitoring Instrumentation

The majority of developments since the 2004 PM AQCD (U.S. EPA, 2004, [056905](#)) regarding microenvironmental PM characterization have involved real-time instrumentation in the UFP size range. Because these methods are also used for ambient sampling, they are described in Section 3.4 and in Annex Table A-59.

New developments in microenvironmental sampling for exposure assessment have also included construction, testing, and implementation of mobile environmental sampling laboratories for PM mass, particle count, and composition, as well as other criteria pollutants (CO , SO_2 , NO_2 , O_3). These mobile laboratories typically contain a suite of real-time equipment with short sampling intervals (e.g., 1-10 min), such as an SMPS with CPC, APS, laser photometers, and aethalometers for aerosols; monitors for the gaseous criteria pollutants; a weather station for meteorological variables; and a Global Positioning System (GPS) for position. Videotape or journal observations are sometimes logged simultaneously to track local on-road sources of pollution. One key application of mobile laboratory technology is assessment of the outdoor microscale environments and in-vehicle microenvironments on roadways for determining exposure during on-road transportation (Pirjola et

al., 2004, [117564](#); Sabin et al., 2005, [087728](#); Weijers et al., 2004, [104186](#); Westerdahl et al., 2005, [086502](#)). For instance, Sabin et al. (2005, [087728](#)) used videotape records to determine whether BC detected on a school bus was the result of local outdoor sources from other vehicles or “self-pollution” from the school bus’s own engine exhaust. Westerdahl et al. (2005, [086502](#)) used the GPS time series to determine that minima in the UFP time series corresponded to passage through residential areas of Long Beach and Pasadena, in contrast to the pollution spikes observed along highways. Studies have also shown that detection of PM from vehicle exhaust could be improved through use of combined measurement results to improve statistical analysis (Ntziachristos and Samaras, 2006, [116722](#)).

3.8.3. Exposure Modeling

This section describes a variety of techniques used to model PM exposure. Many of these methods are used in combination to link ambient PM levels in the atmosphere or source characteristics to human exposure among individuals or sample populations. Recent developments in exposure modeling are described in this subsection, and errors and uncertainties of these approaches are described in Section 3.8.6.2.

3.8.3.1. Time-Weighted Microenvironmental Models

An individual’s exposure is dictated by his or her activity patterns, as modeled by f_o and f_i in Equation 3-5. A number of panel studies have tracked subject exposures using questionnaires, time-activity diaries, or global positioning systems(e.g., Cohen et al., 2009, [190639](#); Elgethun et al., 2003, [190640](#); Johnson et al., 2000, [001660](#); Olson and Burke, 2006, [189951](#); Wallace et al., 2006, [089190](#)). In many cases, the time-activity tracking is performed in conjunction with personal exposure and/or indoor and outdoor PM concentration monitoring to estimate overall PM exposure. Wu (2005, [086397](#)) described a microenvironmental model of total personal exposure:

$$E_T = f_{oh}C_o + f_{oa}C_a + f_iC_i$$

Equation 3-9

where f_{oh} = fraction of time spent outdoors at home, f_{oa} = fraction of time spent outdoors away from home, C_o = PM concentration outside the home, and C_i = indoor PM concentration. In Equation 3-9, E_T can be calculated based on time-activity diary data and time-resolved PM concentration measurements. E_T can be expressed as a time-resolved value or cumulatively over a time period of interest using this formulation. In this model, ambient and nonambient exposure cannot be separated because it incorporates indoor concentrations that are a function of both ambient and nonambient sources. Additionally, Equation 3-9 distinguishes ambient concentration measured at a monitor from that measured immediately outside the home. Liu et al. (2003, [073841](#)) found that this model predicted elderly exposures adequately but was a poor predictor of PM_{2.5} exposure for asthmatic children. Wu et al. (2005, [086397](#)) point out that this may be due to lack of availability of the children’s time-activity data in school where children spend a substantial portion of their day. In a study of school children’s exposure patterns, DeCastro et al. (2007, [190996](#)) computed odds ratios of a panel subject’s location within a given microenvironment using multivariate logistic models of the indoor school, indoor home, and outdoor microenvironments. They found that (1) the city of residence was a significant predictor of being indoors at school; (2) having an afterschool job was a significant predictor of being indoors at home; and (3) age and having an afterschool job were significant predictors of being outdoors. The results of the DeCastro et al. (2007, [190996](#)) study were designed to predict f_i and f_o in exposure modeling.

A second approach proposed by Wu et al. (2005, [086397](#)) is similar in formulation to Equation 3-5 because it computes ambient PM exposure by considering the amount of outdoor PM infiltrated indoors. This version also incorporates C_o and C_a :

$$E_a = f_{oh}C_o + f_{oa}C_a + f_iF_{inf}C_o$$

Equation 3-10

Equation 3-10 differs from Equation 3-5 because it accounts for concentrations immediately outside the building rather than considering all outdoor exposures to be a function of that measured at a community monitor. Factors influencing the contribution of E_a to E_T may include sample population characteristics, location of a site for microenvironmental monitoring, seasonal trends in PM concentration, and regional differences affecting ambient concentration and infiltration.

Regression based approaches can also be incorporated into time-weighted microenvironmental modeling. Chang et al. (2003, [053789](#)) used data from the Scripted Activity Study and the Older Adults Study, both conducted in Baltimore in 1998 and 1999, to compute total personal exposure based on time-weighted microenvironmental exposures for each panel subject:

$$E_T = ME_i\beta_i \sum_k f_k C_k + ME_o\beta_o \sum_k f_k C_k$$

Equation 3-11

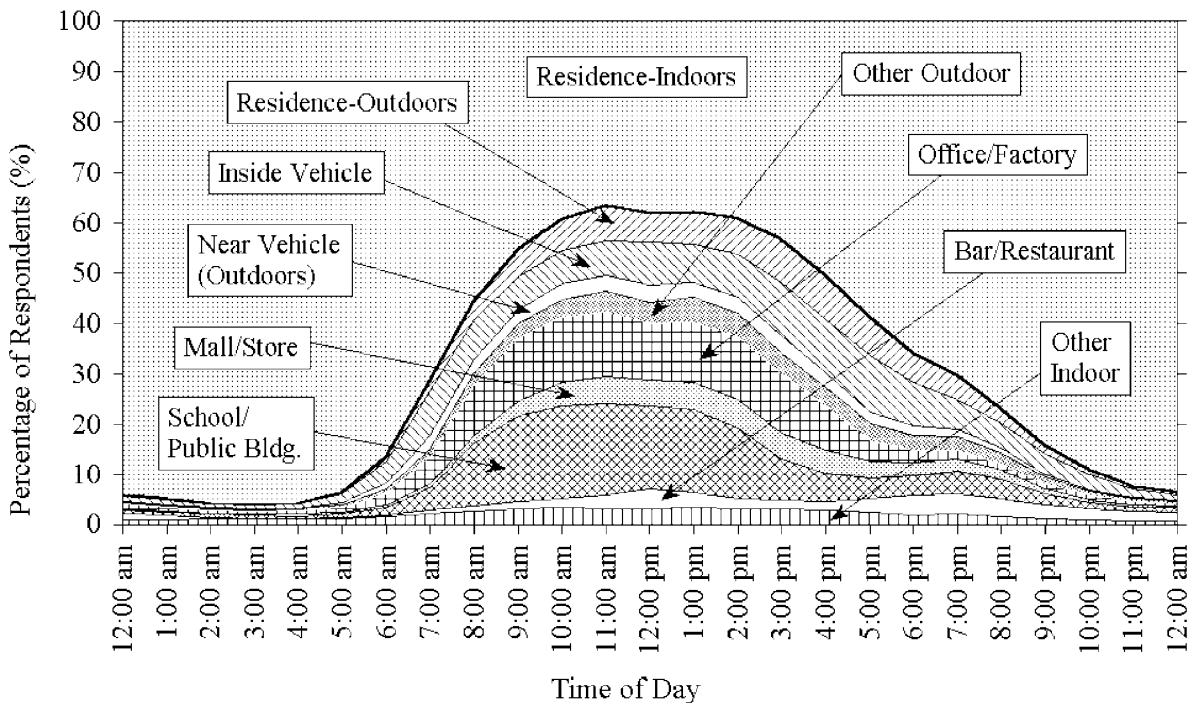
where ME = microenvironment (indoor or outdoor), β = regression coefficient reflecting the accuracy of the exposure estimate for a given microenvironment, f_k = fraction of time performing an activity k , and C_k = personal exposure while performing activity k . In this work, Chang et al. (2003, [053789](#)) tested the models with hourly personal exposure data, hourly ambient concentration data, and daily ambient concentration data. The study found that time-activity data improved estimates of 24-h $PM_{2.5}$ exposure in comparison with using 24-h ambient $PM_{2.5}$ data, but the use of hourly ambient data was comparable to personal microenvironmental data in estimating exposure. When using ambient concentration data, β reflected infiltration for the indoor microenvironmental estimates for a sample population. Using a similar activity-based exposure modeling approach for a panel study in Seattle from 1999-2002, Allen et al. (2004, [190089](#)) found that subjects' PM exposures were best represented by modeling ambient and nonambient exposures separately because ambient PM personal exposure was well correlated with PM concentration at central site monitors, while nonambient PM exposure was not.

3.8.3.2. Stochastic Population Exposure Models

Population-based methods, such as the Air Pollution Exposure (APEX), Stochastic Human Exposure and Dose Simulation (SHEDS), and EXPOLIS (exposure in polis, or cities) models, involve stochastic treatment of the model input factors (http://www.epa.gov/ttn/fera/human_apex.html; (Burke et al., 2001, [014050](#); Kruiize et al., 2003, [156661](#)). These are described in detail in Annex 3.7 of the 2008 NO_x ISA (U.S. EPA, 2008, [157073](#)). Stochastic models utilize distributions of pollutant-related and individual-level variables, such as ambient and local PM concentration source contributions and breathing rate, respectively, to compute the distribution of individual exposures across the modeled population. Using distributions of input parameters in the model framework rather than point estimates allows the models to explicitly incorporate uncertainty and variability into exposure estimates (Zidek et al., 2007, [190076](#)). These models estimate time-weighted exposure for modeled individuals by summing exposure in each microenvironment visited during the exposure period. The models also have the capability to estimate received dose through a dosimetry model. The initial set of input data for population exposure models is ambient air quality data, which may come from a monitoring network or model estimates. Estimates of concentrations in a set of microenvironments are generated either by mass balance methods or microenvironmental factors. Microenvironments modeled include residential indoor microenvironments; other indoor microenvironments, such as schools, offices, and public buildings; vehicles; and outdoor microenvironments. The sequence of microenvironments and exertion levels during the exposure period is determined from characteristics of each modeled individual. The APEX model does this by generating a profile for each simulated individual by sampling from distributions of demographic variables such as age, gender, and employment; physiological variables, such as height and weight; and situational variables, such as living in a house with a gas stove or air conditioning. Activity patterns from a database such as Consolidated Human Activity Database (CHAD) are assigned to the simulated individual using age, gender, and

biometric characteristics. Breathing rates are calculated for each activity based on exertion level, and the corresponding received dose is then computed. For APEX, the PM dosimetry algorithm is based on the International Commission on Radiological Protection's Human Respiratory Tract Model for Radiological Protection (ICRP, 1995, [006988](#)), and calculates the rate of mass deposition of PM in the respiratory system (U.S. EPA, 2008, [191775](#)). Summaries of individual- and population-level metrics are produced, such as maximum exposure or dose, number of individuals exceeding a specified exposure/dose threshold, and number of person-days at or above certain exposure levels. The models also consider the non-ambient contribution to total exposure. Nonambient source terms are added to the infiltration of ambient pollutants to calculate the total concentration in the microenvironment. Output from model runs with and without nonambient sources can be compared to estimate the ambient contribution to total exposure and dose.

Recent larger-scale human activity databases, such as those developed for CHAD or the National Human Activity Pattern Survey (NHAPS), have been designed to characterize exposure patterns among much larger population subsets than can be examined during individual panel studies (Klepeis et al., 2001, [002437](#); McCurdy et al., 2000, [000782](#)). CHAD consists of a consolidation of human activity data obtained during several panel studies in which diary or retrospective activity data were obtained, while NHAPS acquired sample population time-activity data through surveys about human activity (Klepeis et al., 2001, [002437](#)). The complex human activity patterns across the population (all ages) for NHAPS are illustrated in Figure 3-93 (Klepeis et al., 2001, [002437](#)). This figure is presented to illustrate the diversity of daily activities among the entire population as well as the proportion of time spent in each microenvironment. Different patterns would be anticipated when breaking down activity patterns for subgroups, such as children or the elderly. With data for average PM concentrations in each microenvironment, population exposures can be estimated from this break-down of time-activity data.



Source: Reprinted with Permission of Nature Publishing Group from Klepeis et al. (2001, [002437](#)).

Figure 3-93. Distribution of time sample population spends in various environments, from the National Human Activity Pattern Survey.

Stochastic and deterministic methods are often combined, as described below. Recently, SHEDS has been linked with the Modeling Environment for Total Risk Studies (MENTOR) model to expand population exposure assessment to individual risk assessment (Georgopoulos et al., 2005, [080269](#)). In this formulation, CMAQ was used to predict initial concentrations at a coarse scale, and then a spatiotemporal random field method (Vyas and Christakos, 1997, [156142](#)) was applied to interpolate the concentration to census tract scale in which exposure estimates are made. CHAD can also be incorporated into MENTOR so that estimates of exposure are related to dose and metabolic distributions to estimate risk of specific health impacts.

3.8.3.3. Dispersion Models

Dispersion models have been used both for direct estimation of exposure and as inputs for stochastic modeling systems, as described above. Location-based exposures have been predicted using models such as CALINE, AERMOD, CALPUFF, (all described in Section 3.6.2.3) or the Operational Street Pollution Model (OSPM) for estimation of street-level PM pollution coupled with infiltration models to represent indoor exposure to ambient levels (Gilliam et al., 2005, [056749](#); Mensink et al., 2008, [155980](#); Wilson and Zawar-Reza, 2006, [088292](#)). For instance, CALPUFF was used to model transport and dispersion in lower Manhattan following the September 11, 2001 World Trade Center collapse to determine average location-based exposures (Gilliam et al., 2005, [056750](#)). Wilson and Zawar-Reza (2006, [088292](#)) used The Air Pollution Model (TAPM), which integrated an emissions model with a mesoscale meteorological driver, to assess PM₁₀ dispersion and potential for exposure in Christchurch, New Zealand. Gulliver and Briggs (2005, [191079](#)) used the Atmospheric Dispersion Modeling System (ADMS) to model dispersion of “line-source” traffic emissions in an urban environment. In a method similar to that employed by Georgopoulos et al. (Georgopoulos et al., 2005, [080269](#)) with SHEDS, Wu et al. (2005, [058570](#)) used CALINE to predict street-level concentrations of pollutants and input the results of that dispersion model into an individual exposure model that accounts for infiltration of specific building characteristics. Wu et al. (2005, [058570](#)) employed CHAD to estimate the time-basis of exposures from the CALINE predictions. With an individualized exposure approach, the model is deterministic. However, population exposures can be estimated by performing repeated simulations using various housing characteristics and then computing a posterior probability distribution function for exposure. Isakov et al. (2009, [191192](#)) developed a methodology to link a CTM (used to compute regional scale spatiotemporally-varying concentration in an urban area) with stochastic population exposure models to predict annual and seasonal variation in urban population exposure within urban microenvironments.

3.8.3.4. Land Use Regression and GIS-Based Models

LUR models have also been developed to describe pollution levels as a function of source characteristics (Briggs et al., 1997, [025950](#); Gilliland et al., 2005, [098820](#); Ryan and LeMasters, 2007, [156063](#)). LUR is a regression derived from monitored concentration values as a function of data from a combination of factors (e.g., land use designation, traffic counts, home heating usage, point source strength, and population density). The regression is then computed for multiple locations based on the independent variables at locations without monitors. At the census tract level, a LUR is a multivariate description of pollution as a function of traffic, land use, and topographic variables (Briggs et al., 1997, [025950](#)). Originally, LUR was used for NO₂ dispersion, but it was adapted for PM_{2.5} exposure estimation by Brauer et al. (2003, [155702](#)) for Stockholm, Sweden, Munich, Germany, and throughout The Netherlands. This study found a measure of traffic density to be the most significant variable predicting PM_{2.5} exposure. Ryan et al. (2008, [156064](#)) reported on a LUR model for childhood exposure to traffic-derived EC for the Cincinnati Allergy and Air Pollution Study and also found traffic to be the most important determinant of diesel exhaust particle exposure. In this case, wind direction was also factored into the model as a determinant of EC mixing. Like deterministic dispersion models, LUR can be performed over wide areas to develop a posterior probability distribution function of exposure at the urban scale. However, Hoek et al. (2008, [195851](#)) warn of several limitations of LUR, including distinguishing real associations between pollutants and covariates from those of correlated copollutants, limitations in spatial resolution from monitor data, applicability of the LUR model under changing temporal conditions, and introduction of confounding factors when LUR is used in epidemiologic studies.

A GIS platform is typically used to organize the independent variable data and map the results. The GIS software creates numerous lattice points for the regression of concentration as a function of the covariates. For instance, Krewski et al. (2009, [191193](#)) computed PM_{2.5} concentrations for the New York City and Los Angeles metropolitan areas. For the Los Angeles analysis, the LUR was applied at 18,000 points in the simulation domain, and an inverse distance weighting kriging method was applied to interpolate the predicted concentration. In New York City, the LUR was applied at 49 monitors for a 3-yr model and 36 monitors for a model of winter 2000; kriging was employed only for the purpose of visualizing the concentration between monitors. The models explained 69% and 66% of the variation in PM_{2.5} in Los Angeles and New York City, respectively.

GIS-based spatial smoothing models can be used to estimate PM concentration levels where monitors are not located. Yanosky et al. (2008, [099467](#)) described an approach to estimate concentrations using a combination of reported AQS data and GIS-based and meteorological covariates. Temporally stationary covariates included distance to nearest road for different PM size fractions, urban land use, population density, point source emissions within 1 and 10 km buffers, and elevation above sea level. Time-varying covariates included area source emissions, precipitation, and wind speed. In this analysis, the GIS-based covariates were temporally stationary, while the meteorological and PM monitored concentration inputs were time-varying. This approach was applied to estimate PM_{2.5}, PM_{10-2.5}, and PM₁₀ exposures for the Nurse's Health Study and provided estimates of concentration at approximately 70,000 nodes with PM_{2.5} and/or PM₁₀ data input from more than 900 AQS sites with good validation of the PM_{2.5} and PM₁₀ models (Paciorek et al., 2009, [190090](#); Yanosky et al., 2008, [099467](#); Yanosky et al., 2009, [190114](#)).

GIS-based methods can also be applied to integrate exposures over different microenvironments. For example, Gulliver and Briggs (2005, [191079](#)) described development of the Space-Time Exposure Modeling System (STEMS) to model PM₁₀ concentration. STEMS is a multipronged model that links traffic emissions estimates, dispersion, background PM estimates, and time-activity data within a GIS framework to create exposure estimates. Traffic emissions estimates and meteorological parameters are input into the ADMS dispersion model, which along with background PM measurements, are used to create hourly point estimates of PM concentration. Based on the time-activity data, the concentration estimates were then used to calculate exposures to traffic-related PM₁₀ along a commuting path while an individual is in transit. PM₁₀ was used by Gulliver and Briggs (2005, [191079](#)) because ADMS had not yet been validated for smaller PM size fractions. In an analysis of the sensitivity of included variables, Gulliver and Briggs (2005, [191079](#)) showed the model to be most sensitive to fluctuations in local meteorology followed by sudden vehicle speed reductions of 10 km/h. The STEMS model was primarily designed to model exposures during transit, but the authors state that this technique can be applied to modeling other microenvironmental exposures.

Source proximity is sometimes used as a covariate in GIS-based regression models. For instance, Baxter et al. (2007, [092725](#)) predicted indoor exposure to PM_{2.5}, EC, and NO_x based on distance to roadways, indoor source characteristics, window opening, and ambient concentrations in the Boston metropolitan area. In this effort, Baxter et al. examined a variety of factors estimated using GIS including roadway density, roadway length, average daily traffic, and population density to determine which variables were significant predictors. They found that point estimates of PM_{2.5} were largely influenced by regional ambient PM_{2.5} while EC estimates were more influenced by local mobile sources. However, Baxter et al. (2008, [191194](#)) found no association between distance to a bridge toll booth station and indoor EC concentration in Detroit homes when studying the impact of diesel emissions from traffic on the Ambassador Bridge as part of the Detroit Exposure and Aerosol Research Study (DEARS). Being located downwind of the booth, however, was a significant predictor of indoor EC concentration. Corburn (2007, [155738](#)) tested two distinct modeling approaches, the cumulative air toxics surface (CATS) and the U.S. EPA's National Air Toxics Assessment (NATA) to determine how these approaches can yield estimates of human exposure to diesel exhaust and 33 air toxics for environmental impact assessment. The CATS approach included an exposure term incorporating source density and distance to source, and the sources include traffic as well as bus depots and transfer stations, airports, and industrial point sources. Corburn's results demonstrated that robust land use data can provide an approximation for urban exposures, although he cautioned that such estimates should not supersede environmental monitoring. In using these approaches, Huang and Batterman (2000, [156572](#)) warn that geographic divisions must be sufficiently small to avoid inter-zone variability in source and exposure characteristics. Moreover, the HEI Report on Traffic Related Health Effects (2009, [191009](#))

discourages use of source proximity as a surrogate for traffic exposure in epidemiologic studies because it is not specific to particular pollutants and can be subject to confounding factors such as SES.

3.8.4. Exposure Assessment Studies

Table A-61 in Annex A lists exposure assessment studies performed in the U.S. by region of the country with personal, microenvironmental, and ambient mass concentrations presented (note that chemical speciation data, where available, are discussed below). The majority of urban-scale studies focus on $PM_{2.5}$ because $PM_{2.5}$ concentrations are more homogeneously distributed. Studies of microscale to neighborhood scale dispersion more commonly include data on UF and thoracic coarse PM in addition to $PM_{2.5}$ because they travel over shorter distances from the site of generation, as described in Section 3.5. Some of these studies present the outdoor concentration measured outside the test building, while others use ambient concentration obtained from a community site monitor. As would be expected, there is considerable variability within and across regions of the country with respect to indoor exposures and ambient concentrations. Furthermore, some regions are represented by only one or two studies, while other regions have many studies. Most studies have been conducted in only one or two metropolitan areas. Thus, the results presented may not be broadly representative.

Results of these studies highlight the uncertainties surrounding various estimates of the ambient contribution to personal exposure. This variation can be attributed to a number of factors, including PM size distribution, scope and magnitude of microenvironmental sources, proximity to microenvironmental sources, ambient concentrations of PM, percentages of time spent in various microenvironments, the age and condition of indoor microenvironments, natural and urban topography, and outdoor meteorology. Errors in exposure estimation are linked to the spatial scale of concentration measurements because pollutant transport and dispersion varies over different spatial scales as a function of the many factors mentioned in the previous sentence. Findings related to identifying the ambient components of personal exposure and modes of PM infiltration indoors are discussed in the subsequent subsections with respect to multiple spatial scales.

3.8.4.1. Micro-to-Neighborhood Scale Ambient PM Exposure

Near-Road Exposures

Sections 3.3 and 3.5 describe the physical and chemical composition of traffic emissions as well as characterization of the plume away from roads. Table 3-24 contains data from recent studies comparing outdoor personal exposure to fixed site monitors. Only studies where samples were obtained outdoors and compared with a community-based ambient monitoring site were included because indoor microenvironments have penetration losses that affect the comparability of the results. Note that some of these studies included enclosed transportation microenvironments (e.g., cars, buses, subways), but all studies examined personal exposure in the outdoor microscale environment. Also note that studies must be reviewed cautiously because most used different instrumentation for personal, microenvironmental, and ambient measurements, and measurement artifacts related to each instrument may differ. The Violante et al. (2006, [156140](#)) study showed that outdoor personal exposure to PM_{10} was significantly higher than fixed community-based ambient PM_{10} measurements in downtown Bologna, Italy. Likewise, the Kaur et al. (2005, [088175](#)), Kaur et al. (2005, [086504](#)), and Adams et al. (2001, [019350](#)) studies showed $PM_{2.5}$ measurements to be significantly higher than fixed community-based ambient $PM_{2.5}$ monitoring site measurements in central London, U.K. Kinney et al. (2000, [001774](#)) performed personal exposure monitoring on study volunteers on streets in Manhattan and showed that $PM_{2.5}$ concentrations were not significantly different from ambient $PM_{2.5}$ measurements; this is more consistent with the urban-scale homogeneity in concentration of $PM_{2.5}$.

Morwaska et al. (2008, [191006](#)) stated that UFP number concentrations in the near-road environment were roughly 18 times higher than in a non-urban background environment, while measured concentrations in street canyons and tunnels were 27 and 64 times higher, respectively

than background. This suggests that trapping of sources in a semi-enclosed environment can lead to higher UFP exposures. Additionally, fresh emission of short-lived UFPs would explain substantially higher concentrations near the site of emission. By sampling UFP number concentrations at multiple sites in Los Angeles, Moore et al. (2009, [191004](#)) demonstrated five- to seven-fold differences between concentrations measured directly next to a freeway and an oceanside site during morning rush hour with substantial variability among sites throughout the day. When comparing sampling campaign data for clear weather and rainy days next to the I-710 freeway in Los Angeles, Ntziachristos et al. (2007, [089164](#)) found that particle number concentration obtained with a CPC was 2.4 times higher in clear weather than when raining; particle surface area was 3.7 times larger in clear weather; and, black carbon concentration was 1.7 times higher in clear weather. However, SMPS data reported for rainy day particle number concentrations were almost 29 times higher in this study. Likewise, Zhou and Levy (2007, [098633](#)) noted in a meta-analysis of near-road studies that the concentrations are generally elevated within 300-400 m of a roadway for EC and UFPs. Kinney et al. (2000, [001774](#)) showed EC to increase linearly with increasing traffic counts and large spatial variations in two sites that had concentrations significantly higher than ambient measurements. These observations suggest caution should be taken regarding the representativeness of community averaged monitoring data for assessing exposures.

Particle chemistry is also an important consideration, because exposure may differ among PM components. Farmer et al. (2003, [089017](#)) found that exposure to particle-bound PAHs, including benzo[a]pyrene, can be 2-3 times higher among those routinely exposed to outdoor traffic emissions (e.g., police, bus drivers) compared with control subjects. Particle-bound PAH exposure can also vary with vehicle operation. For example, Kinsey et al. (2007, [190073](#)) estimated from continuous idling and restart school bus operating conditions (without retrofitting) that over a 10-min period of waiting at a bus stop, continuous idling resulted in exposure to 33% more particle-bound PAH than in the case where the bus was restarted 2 min into the simulation and idled for 8 min. Continuous idling produced approximately 34 times more particle-bound PAH than in another scenario where the bus was off for 10 min then restarted.

Table 3-24. Examples of studies comparing near-road personal exposures with fixed site ambient concentrations.

Reference and Site	Ambient monitors	Personal monitors	Microenvironment, other variables	Ambient v. Personal Association	Primary Findings																					
Violante et al. (2006, 156140) Bologna, Italy	Fixed PM ₁₀ and benzene monitoring station (method not specified).	Active pump with PM ₁₀ PEM, passive sample for benzene desorbed and analyzed by GC-MS.	Localized traffic density (vehicles/h); Meteorology (wind speed, wind direction, visibility, relative humidity).	Personal: 185.10 ± 38.52 µg/m ³ Fixed: 43.56 ± 24.10 µg/m ³ (p<0.0001)	Fixed PM ₁₀ correlated with multivariate model of traffic and meteorology, but not personal PM ₁₀ ; relationship between benzene and PM ₁₀ not explored.																					
Kaur et al. (2005, 086504) London, U.K.	Fixed TEOM for PM _{2.5} and fixed CO monitor at ambient and curbside sites.	High flow personal samplers for PM _{2.5} , P-Trak monitors for UFP, Langan T15 and T15v for CO.	Exposures stratified by mode of transport (walk, cycle, bus, car, taxi).	Average PM _{2.5} sampled by TEOM was 3 times lower than average personal PM _{2.5} sample, and 8 times lower than maximum personal PM _{2.5} sample.	PM _{2.5} exposures during walking significantly lower than during car and taxi rides, UFP exposures during walking significantly lower than bus and car rides, cycling exposures to PM _{2.5} and UFP not significantly different from those on bus, car, or taxi.																					
Kaur et al. (2005, 088175) London, U.K.	Fixed TEOM for PM _{2.5} and fixed CO monitor at ambient and curbside sites.	High flow personal samplers for PM _{2.5} analyzed post-sample for reflectance for EC, P-Trak monitors for UFP, Langan T15 and T15v for CO.	Volunteers walking at set times and directions along Marylebone Rd in London.	Fixed vs. personal PM _{2.5} : slope = 0.29, R = 0.6; personal PM _{2.5} measurements were >2 times background levels and more than 15 µg/m ³ greater than curbside measurements.	Pedestrian exposures were significantly higher than fixed site curbside or ambient measurements. Results indicate that exposure declined up to 10% from curbside to building edge within a street canyon.																					
Adams et al. (2001, 019350) London, U.K.	Fixed TEOM for PM _{2.5} and fixed CO monitor at ambient and curbside sites.	High flow personal samplers for PM _{2.5} .	Exposures stratified by mode of transport (cycle, bus, car, subway).	Median values: (µg/m ³) <table border="1" style="display: inline-table; vertical-align: middle;"> <tr><td></td><td>Summer</td><td>Winter</td></tr> <tr><td>Cycle</td><td>34.5</td><td>23.5</td></tr> <tr><td>Bus</td><td>39.0</td><td>38.9</td></tr> <tr><td>Car</td><td>37.7</td><td>33.7</td></tr> <tr><td>Subway</td><td>247.2</td><td>157.3</td></tr> <tr><td>Fixed</td><td>15</td><td>13</td></tr> <tr><td>Curb</td><td>24</td><td>37</td></tr> </table>		Summer	Winter	Cycle	34.5	23.5	Bus	39.0	38.9	Car	37.7	33.7	Subway	247.2	157.3	Fixed	15	13	Curb	24	37	Exposures were 2.3-16.5 times higher than ambient and 1.4-10.3 times higher than curbside during summer. During winter, only subway exposures were appreciably higher (4.3 times) than curbside.
	Summer	Winter																								
Cycle	34.5	23.5																								
Bus	39.0	38.9																								
Car	37.7	33.7																								
Subway	247.2	157.3																								
Fixed	15	13																								
Curb	24	37																								
Kinney et al. (2000, 001774) New York City, NY (Harlem)	Ambient site filter in greased impactor with pump for PM _{2.5} ; absorbance testing on filter for EC.	Three high traffic sites filter in greased impactor with pump; absorbance testing on filter for EC.	Localized traffic density (vehicles/h).	Mean values: (µg/m ³) <table border="1" style="display: inline-table; vertical-align: middle;"> <tr><td></td><td>PM_{2.5}</td><td>EC</td></tr> <tr><td>Site 1</td><td>45.7 (10.1)</td><td>6.2 (1.9)</td></tr> <tr><td>Site 2</td><td>47.1 (16.4)</td><td>3.7 (0.6)</td></tr> <tr><td>Site 3</td><td>36.6 (10.8)</td><td>2.3 (0.9)</td></tr> <tr><td>Ambient</td><td>38.7 (10.9)</td><td>1.5 (0.5)</td></tr> </table>		PM _{2.5}	EC	Site 1	45.7 (10.1)	6.2 (1.9)	Site 2	47.1 (16.4)	3.7 (0.6)	Site 3	36.6 (10.8)	2.3 (0.9)	Ambient	38.7 (10.9)	1.5 (0.5)	PM _{2.5} at high traffic sites was not significantly higher than ambient; EC was significantly higher than ambient at 2 sites. EC increased linearly with traffic counts.						
	PM _{2.5}	EC																								
Site 1	45.7 (10.1)	6.2 (1.9)																								
Site 2	47.1 (16.4)	3.7 (0.6)																								
Site 3	36.6 (10.8)	2.3 (0.9)																								
Ambient	38.7 (10.9)	1.5 (0.5)																								

In-Vehicle and In-Transit Exposures

In-vehicle pollution has been identified in various studies as a source of exposure to PM_{2.5}, PM₁₀, and UFPs (Briggs et al., 2008, [156294](#); Diapouli et al., 2007, [156397](#); Fruin et al., 2008, [097183](#); Gómez-Perales et al., 2004, [054418](#); Gómez-Perales et al., 2007, [138816](#); Gulliver and Briggs, 2004, [053238](#); Gulliver and Briggs, 2007, [155814](#); Rossner et al., 2008, [156927](#); Sabin et al., 2005, [087728](#)). Results from recent studies are provided in Table A-60 of Annex A. In many of these studies, in-vehicle exposures are shown to be comparable to or less than that of walkers on the same route. Typically, in-vehicle exposures were also higher than community-based ambient monitor concentrations for TSP and PM₁₀ (Diapouli et al., 2008, [190119](#)). Curbside measurements of UFPs and PM_{2.5} obtained at a fixed site in the Kaur et al. (2005, [088175](#); 2005, [086504](#)) studies were generally lower than exposures during transit, including during walking and cycling. In contrast, the Adams et al. (2001, [019350](#)) study demonstrated that fixed site PM_{2.5} concentrations were higher than curbside during the summer and lower than curbside during the winter. As particle size decreased to the fine and UF range, less difference between in-vehicle and ambient concentrations was observed for PM mass or count, with the exception of the Diapouli et al. (2008, [190119](#)) study where in-bus UFP concentrations were several times higher than indoor or outdoor residential and school concentrations.

Fruin et al. (2008, [097183](#)) and Westerdahl et al. (2005, [086502](#)) observed that in-vehicle UFP concentrations increased for freeways in comparison with arterial roads. They estimated that 36% of exposure to UFPs occurred during a total daily commuting time of 1.5 h (6% of the day) in Los Angeles; 22% of total exposure occurred during 0.5 h spent on freeways. Gong et al. (2009, [190124](#)) demonstrated that UFP deposition rate increased with decreasing particle size (down to ~30 nm) and increasing surface area inside the vehicle, where deposited PM on the seats and dashboard can be resuspended and then inhaled or ingested. UFP deposition rate also rose slightly with increased number of passengers. Zhu et al. (2007, [179919](#)) found that in-vehicle UFP counts were 85% lower than outdoors when the fan was operating in recirculation mode. They estimated that a 1-h commute (4% of the day) accounts for 10-50% of daily exposure to UFPs generated by traffic. Based on the American Time Use Survey estimation of an average of 70.2 min spent in vehicles per person each day (U.S. Bureau of Labor Statistics <http://www.bls.gov/tus/>), cumulative in-vehicle exposure can become important.

In a study of PM_{2.5} exposure on school buses, Adar et al. (2008, [191200](#)) found that PM_{2.5} on school buses was 2 times higher than on-road levels and 4 times higher than central site measurements. Sabin et al. (2005, [087728](#)) demonstrated for school buses that emission control technologies had a significant impact on in-bus concentrations of black carbon mass, and Hammond et al. (2007, [190135](#)) demonstrated significant reductions of particle number concentration measured for 0.02-1 μm particles when comparing buses using clean diesel or retrofits compared with non-retrofitted buses. Although not tested here for other vehicle types with respect to PM, these findings suggest that a portion of in-vehicle concentrations are due to self-pollution, defined by Behrentz et al. (2004, [155682](#)) as the fraction of a vehicle's own exhaust entering the vehicle microenvironment. Behrentz et al. (2004, [155682](#)) tested self-pollution with school buses using SF₆ tracer gas and demonstrated that 0.3% of in-vehicle air comes from self-pollution, and that this number was roughly 10 times greater than in-vehicle concentrations related to self-pollution on newer buses. The Behrentz et al. (2004, [155682](#)) study also measured EC and particle-bound PAH and found that 25% of the variability in EC concentration was related to self-pollution. Adar et al. (2008, [191200](#)) estimated that 35.5% of PM_{2.5} mass on school buses was from self-pollution. These findings are important for exposure estimation when partitioning local and ambient sources of pollution during transport in vehicles.

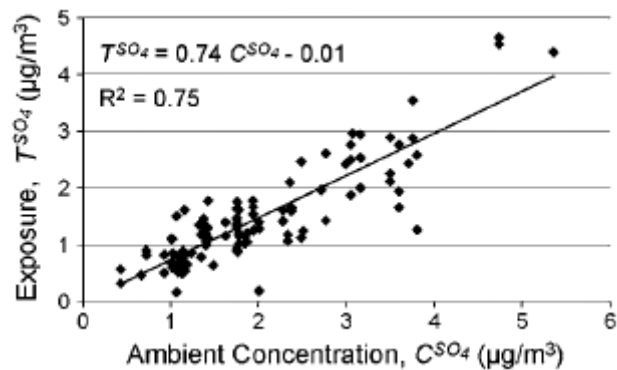
3.8.4.2. Ambient PM Exposure Estimates from Central Site Monitoring Data

The following paragraphs describe studies that estimate personal exposure to ambient PM from central site monitoring data. As shown in Figure 3-93, the large majority of an individual's time is spent indoors. Although calculation of infiltration and indoor personal exposure is an important part of this assessment, such exposures are described with respect to central site monitors. Assessing population-level exposure at the urban scale is particularly relevant for epidemiologic studies, which typically provide information on the relationship between health effects and community-averaged, rather than individual, exposure.

Indoor or other nonambient sources could significantly affect assessment of a person's total exposure to many pollutants. For this reason, many studies use PM components to estimate infiltration of ambient PM to indoor environments. Wilson et al. (2000, [010288](#)) first proposed that SO₄²⁻ could be used as a tracer of the ambient PM_{2.5} infiltration rate. Sarnat et al. (2002, [037056](#)) also noted that it is reasonable to assume that the size distribution of ambient SO₄²⁻ particles is sufficiently similar to the size distribution of ambient PM_{2.5}, and therefore that the ambient SO₄²⁻ to personal SO₄²⁻ ratio is an acceptable surrogate for the ratio of the ambient PM_{2.5} exposure to the ambient PM_{2.5} concentration. Sulfate has been used this way in several studies, including Ebel et al. (2005, [056907](#)), Wallace and Williams (2005, [057485](#); 2006, [089190](#)) and Wilson and Brauer (2006, [088933](#)). For this method to be successful, indoor or other nonambient sources of the tracer must be small compared to ambient sources over the period of sampling. Wilson and Brauer (2006, [088933](#)) noted that environmental tobacco smoke and tap water used in showers or humidifiers are indoor sources of SO₄²⁻. Other concerns in using SO₄²⁻ as a tracer for PM_{2.5} arise because SO₄²⁻ tends to be concentrated in the accumulation mode and thus it might not capture any coarse PM found in the upper end of the PM_{2.5} distribution, which can include larger particles in the tail end of the coarse mode (Wallace and Williams, 2005, [057485](#)). Strand et al. (2007, [157018](#)) suggested that Fe be used as an additional tracer to correct for the infiltration of larger PM_{2.5} particles. Their study took place in Denver, where indoor sources of Fe were small. However, there could be more substantial

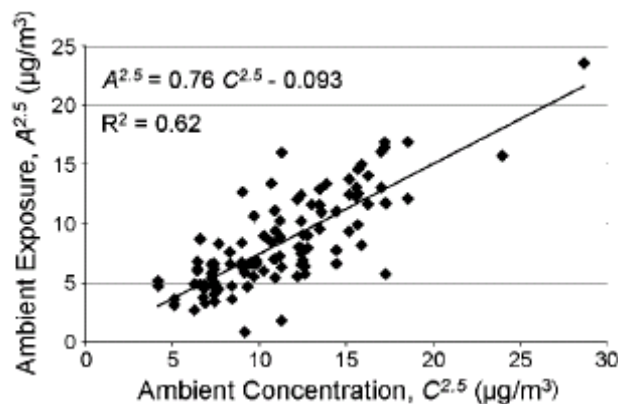
contributions from tracking iron in soil indoors in other locations. The spatial variability of Fe is also larger than that of PM_{2.5} across urban areas. Volatilization of nitrate or organic compounds after infiltration of PM_{2.5} indoors could lead to bias in exposure estimates (Sarnat et al., 2006, [089166](#)). This could be a large problem in areas in which PM contains a large semi-volatile component.

Figure 3-94 shows total exposure to SO₄²⁻ as a function of measured ambient SO₄²⁻ concentration. Figure 3-95 shows estimated ambient exposure to PM_{2.5} as a function of measured ambient PM_{2.5} concentration, where ambient personal exposure is calculated from the ambient exposure factor for SO₄²⁻. Close agreement between these figures can be observed. Figure 3-96 shows total exposure to PM_{2.5} as a function of measured ambient PM_{2.5} concentration. However, the total exposure to PM_{2.5} shows virtually no association with ambient PM_{2.5} because it contains nonambient contributions to PM_{2.5}.



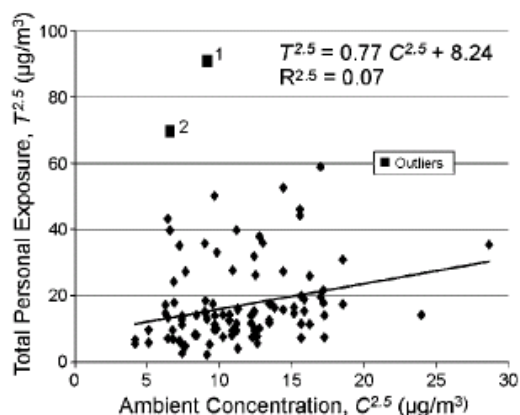
Source: Reprinted with Permission of Nature Publishing Group from Wilson and Brauer (2006, [088933](#))

Figure 3-94. Total exposure to SO₄²⁻ as a function of measured ambient SO₄²⁻ concentration, from the Vancouver study. Vancouver British Columbia, April-September 1998, with 16 non-smoking subjects aged 54-86 yr.



Source: Reprinted with Permission of Nature Publishing Group from Wilson and Brauer (2006, [088933](#))

Figure 3-95. Estimated ambient exposure to PM_{2.5} as a function of measured ambient PM_{2.5} concentration, from the Vancouver study (Vancouver, British Columbia, April-September 1998, with 16 non-smoking subjects aged 54-86 yr).



Source: Reprinted with Permission of Nature Publishing Group from Wilson and Brauer (2006, [088933](#))

Figure 3-96. Total exposure to $\text{PM}_{2.5}$ as a function of measured ambient $\text{PM}_{2.5}$ concentration, from the Vancouver study. Vancouver, British Columbia, April-September 1998, with 16 non-smoking subjects aged 54-86 yr.

The estimated ambient exposure to $\text{PM}_{2.5}$ is well correlated with measured ambient $\text{PM}_{2.5}$ concentration with zero intercept, implying that nonambient sources were minor. This technique works well in areas where SO_4^{2-} is a regional pollutant, because its spatial variability is small (Kim et al., 2005, [083181](#); U.S. EPA, 2004, [056905](#)). Wilson and Brauer (2006, [088933](#)) reported that the pooled Pearson correlation coefficient was 0.79 for personal ambient exposures (estimated by the tracer element method) vs. ambient concentrations of $\text{PM}_{2.5}$, and it was 0.001 for personal nonambient $\text{PM}_{2.5}$ exposure vs. ambient concentrations. Strand et al. (2006, [089203](#)) conducted an exposure study in Denver (2002-2004) for 6-12 year-old school children. Up to 10 personal exposure samples were collected on each day, and ambient concentrations were measured simultaneously at a fixed site located at the school. The daily average personal SO_4^{2-} exposure was strongly associated with ambient SO_4^{2-} concentration ($r = 0.96$, $120 > N > 100$). Koutrakis et al. (2005, [095800](#)) reported the median Spearman correlation coefficients between personal SO_4^{2-} exposure and ambient SO_4^{2-} concentration were above 0.60 during both winter and summer in Boston and Baltimore (15 subjects with 12 consecutive measurements during each season in both Boston and Baltimore). For another Baltimore cohort (15 senior subjects with up to 23 consecutive measurements for each person), Hopke et al. (2003, [095544](#)) reported that the median Pearson correlation coefficient between personal exposure to the SO_4^{2-} factor and the ambient SO_4^{2-} factor was 0.93 (ranging from 0.56 to 0.98 for different subjects), while the median Pearson correlation coefficients were 0.25 for the crustal factor (ranging from -0.46 to 0.66) and 0.22 for a factor whose origin was not identified (ranging from -0.19 to 0.88). The inferences drawn from using the SO_4^{2-} component of $\text{PM}_{2.5}$ as an indicator for personal exposure to ambient $\text{PM}_{2.5}$ may apply in areas where SO_4^{2-} is a minor component of $\text{PM}_{2.5}$ or in the absence of significant nonambient sources of SO_4^{2-} (Sarnat et al., 2001, [019401](#)).

Source apportionment techniques could also be used, in principle, to derive ambient personal $\text{PM}_{2.5}$ exposures. They would be especially useful in areas where the application of a tracer method might be problematic. Hopke et al. (2003, [095544](#)) noted that four outdoor factors (NH_4NO_3^- and $(\text{NH}_4)_2\text{SO}_4$, secondary SO_4^{2-} , OC, motor vehicle exhaust) would constitute an estimate of the personal ambient $\text{PM}_{2.5}$ concentration. However, the data used in this portion of the analysis were obtained only with fixed monitors and did not include measurements made by PEMS. They also used the Multilinear Engine to derive factors that were required to contribute jointly to central indoor and outdoor, individual apartment, and PEM samples of a panel of residents. Hopke et al. (2003, [095544](#)) used PMF to derive source contributions to community, outdoor, and indoor PM exposures at a retirement facility in Towson, MD. Hopke et al. (2003, [095544](#)) found three sources: SO_4^{2-} , unknown (perhaps combustion related, according to the authors), and soil, jointly contributing 46%, 13%, and 4% of $\text{PM}_{2.5}$ to the PEM samples, respectively. Further source resolution was not possible because there was a lack of data for a number of components in the PEM samples. The largest and most clearly identified contribution to personal exposure was from the SO_4^{2-} factor. This study also

determined that a few minor indoor and personal activity sources contributed <10% of the ambient SO_4^{2-} source to personal exposures.

Wilson and Brauer (2006, [088933](#)) presented an adaptation of the SO_4^{2-} method for estimating exposure to $\text{PM}_{10-2.5}$. α is computed based on the SO_4^{2-} method as the ratio of exposure to ambient SO_4^{2-} (as measured by a personal monitor) to ambient SO_4^{2-} concentration. Then, knowing an individual subjects' time diary and the penetration and loss properties of SO_4^{2-} , the air exchange rate for an individual location can be calculated from Equation 3-5 and Equation 3-7. Finally, the penetration and loss rates of $\text{PM}_{10-2.5}$ from the PTEAM database (Ozkaynak et al., 1996, [073986](#)) can be input into the individual exposure model along with the individual activity pattern and residential air exchange rate to compute the ambient $\text{PM}_{10-2.5}$ exposure factor and the ambient $\text{PM}_{10-2.5}$ exposure if $\text{PM}_{10-2.5}$ concentration is measured; in the Wilson and Brauer (2006, [088933](#)) paper, $\text{PM}_{10-2.5}$ was estimated from ambient PM_{10} and $\text{PM}_{2.5}$ concentrations. Given that $\text{PM}_{10-2.5}$ deposits more readily and therefore disperses over a shorter distance than $\text{PM}_{2.5}$, it is possible that use of ambient $\text{PM}_{10-2.5}$ concentration may incur more error than in using this method for $\text{PM}_{2.5}$. Ebel et al. (2005, [056907](#)) observed in a Vancouver, Canada panel study that the correlation between ambient $\text{PM}_{10-2.5}$ exposure and ambient PM_{10} exposure ($r = 0.72$) was lower than the correlation between ambient $\text{PM}_{2.5}$ exposure and ambient PM_{10} exposure ($r = 0.92$). This is attributed to both a smaller F_{inf} for $\text{PM}_{10-2.5}$ and $\text{PM}_{2.5}$ comprising a greater fraction of the PM_{10} for the Vancouver study. In this study, $\text{PM}_{10-2.5}$ mass concentration was calculated from the difference between ambient PM_{10} and $\text{PM}_{2.5}$ mass concentration.

Wilson and Brauer (2006, [088933](#)) state that their methodology for computing the ambient exposure factor based on the $\text{PM}_{2.5}$ SO_4^{2-} method can be applied to PM in the 0.1-0.5 μm size range. Little SO_4^{2-} mass is found below 0.1 μm , so the SO_4^{2-} tracer method would not be applicable for UFPs. Given the short atmospheric lifetime of UFPs resulting from particle growth and evaporation processes, primary UFPs are most prevalent at microscale rather than at an urban spatial scale (Sioutas et al., 2005, [088428](#)). Moore et al. (2009, [191004](#)) found substantial spatial, hourly, and daily variability in UFP concentration in a saturation study of Los Angeles. Moore et al. (2009, [191004](#)) and Harrison and Jones (2005, [191005](#)) also found that UFPs and $\text{PM}_{2.5}$ measurements were poorly correlated at the monitoring sites.

3.8.4.3. Infiltration

F_{inf} varies substantially given a vast array of conditions, and it can best be modeled dynamically based on a distribution of air exchange and deposition or other UF, accumulation mode, fine, and coarse PM loss rates rather than a single value (Bennett and Koutrakis, 2006, [089184](#); Wallace et al., 2006, [089190](#)). Given that air exchange rates within a building vary as a function of ambient temperature and pressure, F_{inf} is subject to seasonal and regional changes (Meng et al., 2005, [058595](#); Sarnat et al., 2006, [089166](#); Wallace and Williams, 2005, [057485](#)). These factors make F_{inf} a more accurate descriptor of infiltration than a simple I/O ratio because the I/O ratio also includes contributions from indoor sources in addition to PM that infiltrates from outdoors. Wallace et al. (2006, [089190](#)) identified several significant factors affecting F_{inf} , including window opening, age of an indoor microenvironment, number of occupants, location on a dirt road, dryer usage, and air conditioning usage. This term becomes even more complex when one considers transformation of the size distribution and chemical composition of the PM through chemical reactions on the particle surface, agglomeration, growth, and evaporation given that F_{inf} depends on particle size (Keller and Siegmann, 2001, [025881](#)). F_{inf} for PM is influenced by physical mechanisms, such as Brownian diffusion, thermophoresis, and impaction, all of which are functions of particle size (Bennett and Koutrakis, 2006, [089184](#); Tung et al., 1999, [049003](#)). These differential effects are summarized below. Recent studies on infiltration are summarized in Table A-64 of Annex A. F_{inf} and I/O are listed where available, although it is recognized that I/O is not as meaningful a descriptor but provides an approximation of F_{inf} .

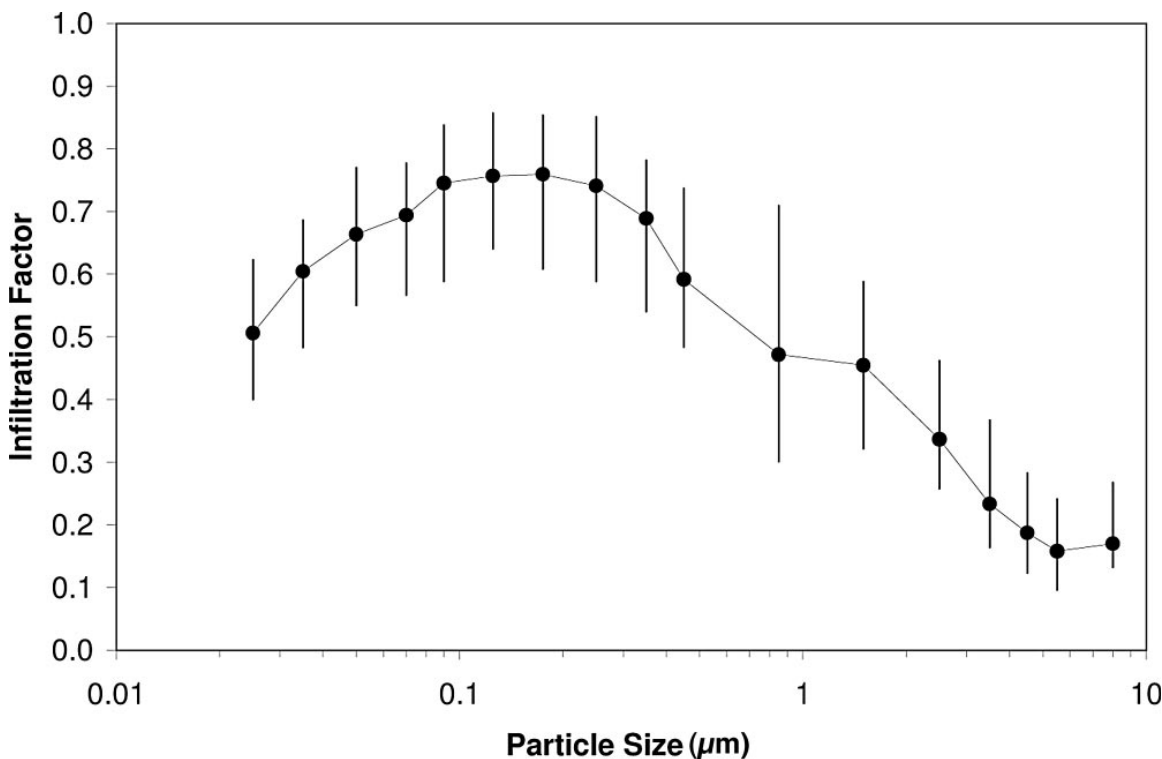
A number of studies have examined the impact of season on PM infiltration. Season is important because it affects the ventilation practices used (e.g., open windows, air conditioning or heating use) and ambient temperature and humidity conditions influence the transport, dispersion, and size distribution of the PM. Pandian et al. (1998, [090552](#)) found that nationwide residential air exchange rates vary by season as: summer > spring > winter > fall with summer air exchange roughly 1.5-2 times greater than average air exchange rate for the entire year because the rates are driven by home air conditioning and heating usage. Allen (2003, [053578](#)) provided information on

the range and distribution of F_{inf} for $\text{PM}_{2.5}$ at 44 residences in Seattle. The mean F_{inf} was calculated using light scattering measurements in a recursive mass balance method with no species data. For all sampling days, F_{inf} (\pm SD) was 0.65 ± 0.21 . Differences in infiltration were observed for the heating season (0.53 ± 0.16), when windows would be expected to be closed, and for the non-heating season (0.79 ± 0.18). Residences with open windows had a mean F_{inf} of 0.69 vs. 0.58 for residences with closed windows. The authors combined the light scattering results with indoor and outdoor sulfur measurements to estimate that $79 \pm 17\%$ of indoor $\text{PM}_{2.5}$ was generated outdoors. This study provides important data on the distribution of residential F_{inf} values and illustrates the magnitude of the effect of season and window position on infiltration rates. Barn et al. (2008, [156252](#)) and Baxter et al. (2007, [092725](#)) also noted that window opening was an important variable. Barn et al. (2008, [156252](#)) found F_{inf} of 0.61 ± 0.27 for 13 homes during summer and 0.27 ± 0.18 for 19 homes during winter in Canada for $\text{PM}_{2.5}$ from forest fires and wood smoke.

Likewise, location could impact residential ventilation practices and infiltration. Using the SO_4^{2-} method for estimating $\text{PM}_{2.5}$ infiltration, Cohen et al. (2009, [190639](#)) noted differences in median infiltration among eight areas (including three comprising the Los Angeles region and two comprising the New York City region). Indoor-outdoor SO_4^{2-} ratio was noted to be highest in New York City (median: 0.85) and Los Angeles (median: 0.84) and lowest in St. Paul (median: 0.54). Pandian et al. (1998, [090552](#)) observed that residential air exchange rates vary by region as: southwest > southeast > northeast > northwest, which reflects regional use of air conditioning. Sarnat et al. (2006, [089166](#)) noted differences in $\text{PM}_{2.5}$ infiltration between coastal and inland residences, although these differences were not statistically significant.

Differential Infiltration Related to PM Size

Differential infiltration as a function of particle size has been observed to occur. Infiltration factors for particle diameters ranging from 20 nm to 10 μm were measured using continuous SMPS-APS monitoring in Boston by Long et al. (2001, [011526](#)) during summer and fall for nighttime periods, when personal activity patterns would be less likely to generate indoor PM. The maximum infiltration factor was reported for particles between 80 and 500 nm to range from 0.8 to 1.0. Summer values were uniformly higher than fall values, consistent with higher observed air exchange rates. The infiltration factor decreased with size above 500 nm, reaching 0.1-0.2 for 6-10 μm particles. Particles smaller than 80 nm also were reported to have lower infiltration factors. This demonstrates the size dependence of PM infiltration, which has been further studied by recent investigators. Sarnat et al. (2006, [089166](#)) examined infiltration as a function of particle size and found that I/O varies by particle diameter, as measured by a SMPS-APS system. Figure 3-97 presents I/O values for size fractions ranging from 0.02 to 10 μm . The maximum infiltration was observed around the accumulation mode (0.1-0.5 μm), with I/O = 0.7-0.8. Reduced infiltration was observed for coarse-mode PM (0.1-0.2 for $D_p = 5\text{-}10 \mu\text{m}$) and, to a lesser extent, UFPs (0.5-0.7 for $D_p = 0.02\text{-}0.1 \mu\text{m}$). This is consistent with increased removal mechanisms for those size fractions. Deposition is caused by settling for coarse-mode particles. Deposition of UFP can occur by diffusion leading to agglomeration into larger particles and subsequent settling, as well as losses to walls.



Source: Reprinted with Permission of Air & Waste Management Association from Samat et al. (2006, [089166](#)).

Figure 3-97. F_{inf} as a function of particle size.

3.8.5. Multicomponent and Multipollutant PM Exposures

3.8.5.1. Exposure Issues Related to PM Composition

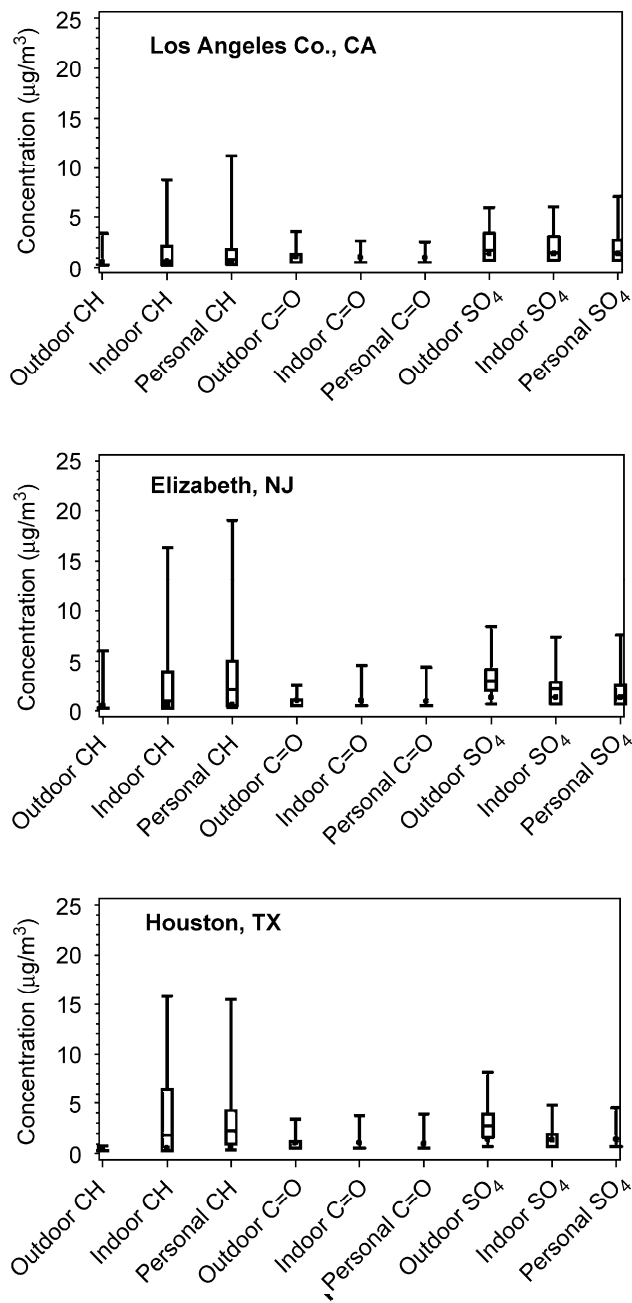
Annex A presents exposure studies that include chemical speciation data in Table A-62. Some of these studies focused on SO_4^{2-} , NO_3^- , or carbonaceous aerosols (EC, OC, particle-bound PAHs), while others measured concentrations of trace elements from crustal (Ca, Fe, Mn, K, Al, S, Cl in salt), mobile (Al, Ca, Fe, K, Mg, Na, Ba, Cr, Cu, Mn, Ni, Pb, S, Ti, V, and Zn), or industrial (particle-bound Hg, Cl, V, Zn, Ti, Cu, Pb) sources. A number of source apportionment studies have been performed over the last five years to determine the contribution of outdoor sources to indoor and personal PM constituents.

Source apportionment studies by Kim et al. (2005, [083181](#)), Hopke et al. (2003, [095544](#)) and Zhao et al. (2006, [156181](#)) have shown that secondary SO_4^{2-} provides the largest ambient contribution to personal and indoor exposures. These studies took place in Baltimore, MD and Raleigh/Chapel Hill, NC. In a source apportionment study in Seattle, vegetative burning was the most significant source of outdoor origin (Larson et al., 2004, [098145](#)). Zhao et al. (2007, [156182](#)) performed a source apportionment study of personal exposure to $\text{PM}_{2.5}$ among residents in Denver and also observed lower contributions from secondary SO_4^{2-} in comparison with motor vehicle emissions and secondary NO_3^- . This suggests that personal exposure to SO_4^{2-} in parts of the West is lower than in the Mid-Atlantic. These observations are consistent with the composition distribution shown in Figure 3-17 and Figure 3-18. Viana et al. (2008, [156135](#)) selected 4 sites of varying population density to represent exposures of pregnant subjects in an early childhood epidemiologic study. Viana et al. (2008, [156135](#)) analyzed $\text{PM}_{2.5}$ and PM_{10} samples for several species along urban-to-rural gradients centered in Valencia, Spain and found gradients for both size fractions in anthropogenically-generated SO_4^{2-} , OC, EC, NO_3^- , Fe, and NH_4^+ , but not in mineral species.

Combined, these findings suggest urban- and regional-scale variation in species composition can influence exposure estimates. Personal PM exposure studies including source apportionment analysis along with chemical speciation are presented in Annex A, Table A-63.

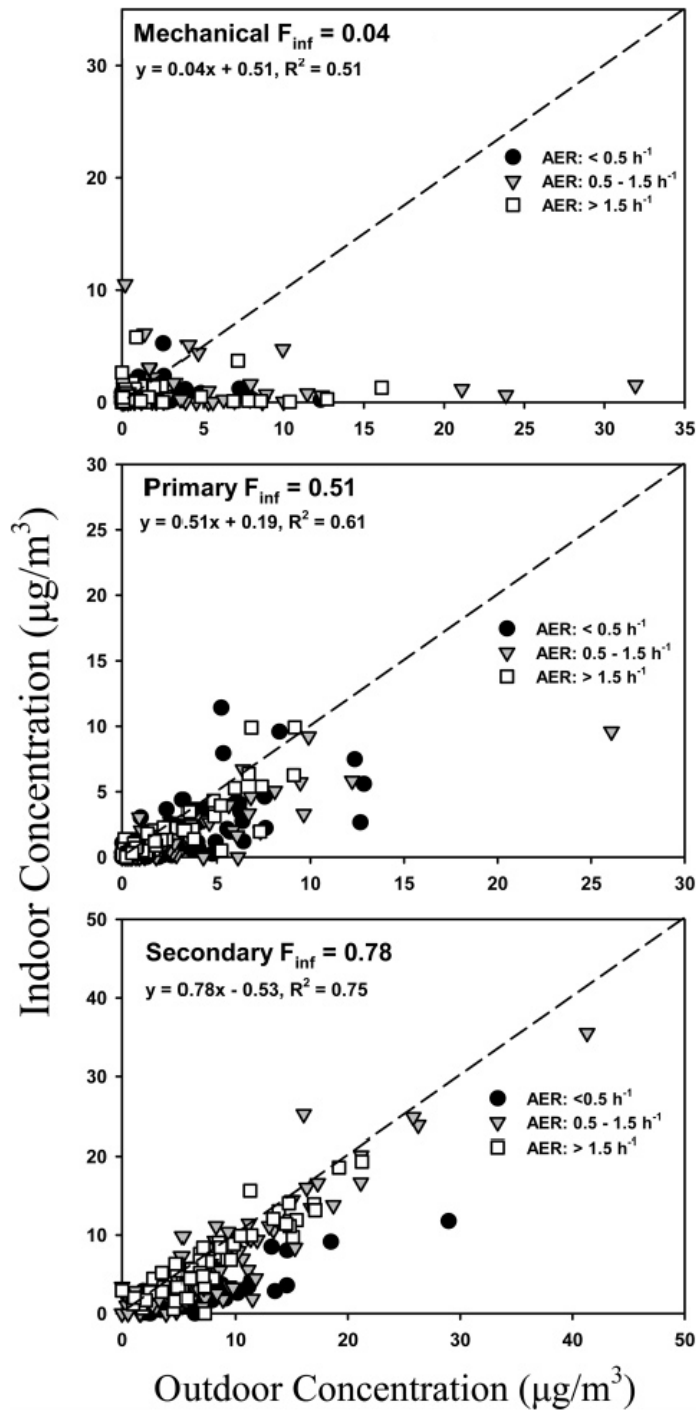
Source apportionment for carbonaceous aerosols is complicated by the fact that they can be derived from indoor and outdoor combustion sources. Carbonaceous aerosols are difficult to trace to specific indoor and outdoor sources because combustion is widespread. Sørensen et al. (2005, [089428](#)), Ho et al. (2004, [056804](#)), Larson et al. (2004, [098145](#)), and Jansen et al. (2005, [082236](#)) all found that personal and microenvironmental exposure to total carbon or BC was lower than that measured outdoors, while Sarnat et al. (2006, [089166](#)) showed significant associations between personal and ambient measurements of EC for measurements taken during the fall for low and high ventilation conditions (slope = 0.66-0.73) and during the summer for high ventilation conditions (slope = 0.41). Wu et al. (2006, [179950](#)), Delfino et al. (2006, [090745](#)), Olson and Norris (2005, [156005](#)) and Turpin et al. (2007, [157062](#)) all demonstrated much higher levels of OC compared with EC in personal samples, possibly due to indoor sources of OC from cooking and home heating. Reff et al. (2007, [156045](#)) and Meng et al. (2007, [194618](#)) both reported findings from the Relationships between Indoor, Outdoor, and Personal Air (RIOPA) study in Los Angeles, Houston, and Elizabeth, NJ. Results from Reff et al. (2007, [156045](#)) reveal significantly higher detection of aliphatic C-H functional groups indoors and in personal samples compared with outdoors (Figure 3-98). This information may help to distinguish carbonaceous compounds of indoor and outdoor origin in future source apportionment studies of PM exposure. Little regional variation in the aliphatic, carbonyl, or SO_4^{2-} groups tested were reported in this study. In Meng et al. (2007, [194618](#)), indoor exposures were shown to decrease for secondary formation aerosols including SO_4^{2-} but not NO_3^- (not tested) when compared with outdoor concentrations. In this study, indoor exposures to mechanically generated aerosols decreased in comparison with outdoors (Figure 3-99).

Trace metal studies have shown variable results regarding personal exposure to ambient constituents. For instance, Molnár et al. (2006, [156773](#)) found that personal exposure was higher than outdoor and ambient concentrations for mostly crustal Cl, K, Ca, Ti, Fe, and Cu. However, Adgate et al. (2007, [156196](#)) found that personal exposures were higher than ambient for Fe, Mg, K, Zn, Cu, Pb, and Mn but lower than ambient for Al, Na, and Ti. Larson et al. (2004, [098145](#)) found that personal exposure to Ca and Cl were higher than concentrations measured at ambient (central site) and residential outdoor monitors, lower for Fe, K, Mn, and As and the same for Al, Br, Cr, and Cu. Source apportionment for trace metals can vary significantly among cities and over seasons. For instance, in a Baltimore source apportionment study, exposure to Mn could be attributed nearly equally to the Quebec wildfires, roadway wear, and soil, while Pb exposure was largely found to be due to a local incinerator (Ogulei et al., 2006, [119973](#)). In this case, the Quebec wildfires were a transient episodic source, while roadway wear and incineration were continuous. However, in Larson et al. (2004, [098145](#)), Mn and Pb exposures in Seattle were largely attributable to mobile source and stationary source emissions. For this reason, source composition behavior cannot be generalized for characterizing exposures and resulting health effects across multiple locations or times.



Source: Reprinted with Permission of Elsevier Ltd. from Reff et al. (2007, [156045](#))

Figure 3-98. Apportionment of aliphatic carbon, carbonyl, and SO₄²⁻ components of outdoor, indoor, and personal PM_{2.5} samples, for Los Angeles (top), Elizabeth (center), and Houston (bottom).

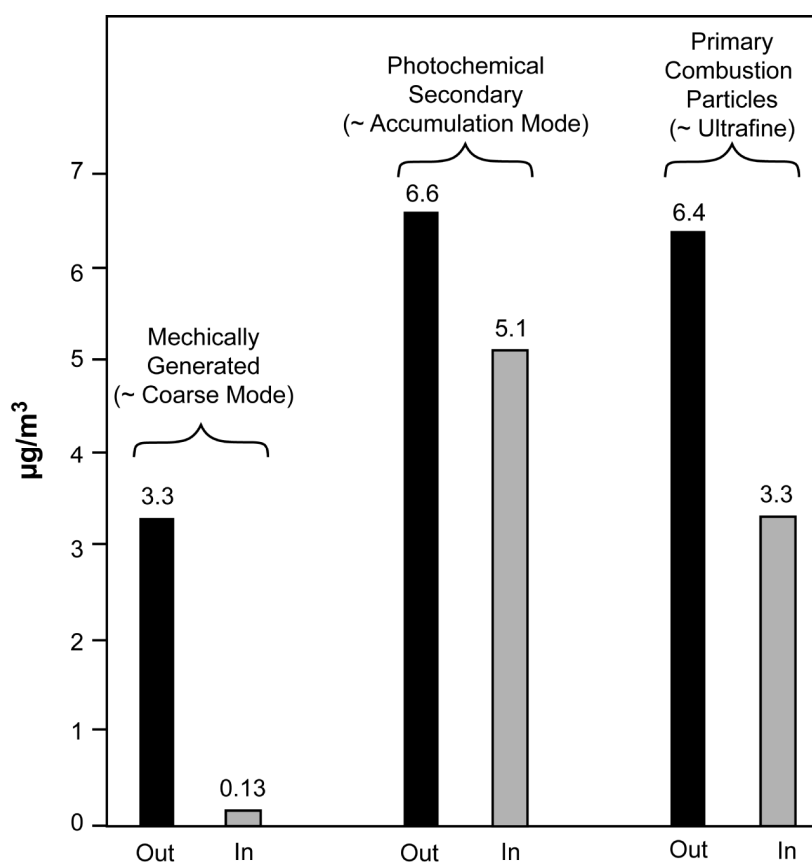


Source: Reprinted with Permission of ACS from Meng et al. (2007, [194618](#)).

Figure 3-99. Apportionment of infiltrated PM from mechanical generation (top), primary combustion (center), and secondary combustion (bottom).

Differential Infiltration Related to PM Composition

A number of chemical factors influence the tendency for differential infiltration in PM. Lunden et al. (2003, [156718](#)) studied infiltration of BC and OC aerosols and found that F_{inf} can vary substantially as a function of gas transport properties with differing air exchange rates. This study and Sarnat et al. (2006, [089166](#)) also showed that BC aerosol infiltration is considerably higher than infiltration of OC, and that carbonaceous aerosol infiltration differed substantially from NO_3^- and SO_4^{2-} aerosols under the same building air exchange conditions. These disparities are likely related to differences in the particle size distribution of PM components, as described in Section 3.8.4.3. As shown in Figure 3-100, the composition of indoor PM that has infiltrated from outdoors is different from that of outdoor PM (Meng et al., 2007, [194618](#)). In this case, the particles containing photochemical products (primarily accumulation mode) have a higher infiltration rate than the larger (primarily coarse mode) mechanically generated particles or the smaller primary combustion particles (likely to consist mostly of UFPs in the nucleation or Aitken nuclei mode).



Source: Reprinted with Permission of ACS from Meng et al. (2007, [194618](#)).

Figure 3-100. Results of the positive matrix factorization model showing differences in the mass of outdoor PM and PM that has infiltrated indoors based on source category.

PM species enriched in the accumulation mode, such as SO_4^{2-} , will infiltrate more efficiently than components with larger size distributions, such as iron (Strand et al., 2007, [157018](#)). Lunden et al. (2008, [155949](#)) also compared I/O ratios for $\text{PM}_{2.5}$, total carbon, OC, and BC in an unoccupied house and found the lowest ratio for $\text{PM}_{2.5}$ (0.41 ± 0.2), the highest for BC (0.61 ± 0.2), and intermediate values for total carbon (0.50 ± 0.2) and OC (0.47 ± 0.2). The authors attributed the

lower PM_{2.5} I/O ratio to indoor loss of NH₄NO₃ aerosol. The authors note that their BC I/O of 0.6 is somewhat lower than BC ratios measured in occupied spaces (Polidori et al., 2007, [156877](#)). Conversely, indoor sources in occupied residences contribute to observed OC I/O ratios greater than 1 in other studies (Polidori et al., 2006, [156876](#); Sawant et al., 2004, [056798](#)). Analytical results for PM_{2.5} components from the Baxter et al. (2007, [092726](#)) study found F_{inf} of 0.95 ± 0.07 for S and 0.60 ± 0.04 for V, the two components identified as having no indoor sources and which had I/O ratios significantly less than 1 (Baxter et al., 2007, [092726](#)). It is possible that association of V with larger particles of lower penetration efficiency could contribute to a lower infiltration rate. Meng et al. (2005, [058595](#)) also noted that the lack of indoor sources of S and V result in much lower variability in penetration and loss rates.

Volatilization of PM during infiltration can cause differences between the composition of indoor and outdoor PM. NO₃⁻, a prevalent PM component year-round in the western U.S. and during winter throughout the mid-western and northeastern states, has a decreased F_{inf} due to volatilization of NO₃⁻ indoors. Sarnat et al. (2006, [089166](#)) calculated F_{inf} values for NO₃⁻, PM_{2.5}, and BC, and found the values to increase in that order. NO₃⁻ was low (median = 0.18, IQR = 0.12-0.33), while BC was high (median = 0.84, IQR = 0.70-0.96); the intermediate value of PM_{2.5} (median = 0.48, IQR = 0.39-0.57) reflected its composition as a mixture of those two components (among others). Indoor volatilization of NO₃⁻ enriches indoor ambient PM in other components, creating differences in toxicity between indoor and outdoor ambient PM. The high infiltration of non-volatile BC creates additional sorption sites for organics, including indoor-generated compounds. Meng et al. (2007, [194618](#)) found that secondary formation accounts for 55% of indoor PM of outdoor origin, while primary combustion accounts for 43%, and mechanical generation accounts for 2%. Meng et al. (2007, [194618](#)) noted that secondary formation processes often result in more accumulation mode particles, so that diffusion losses are not as great as for primary combustion particles that are composed primarily of nucleation and condensation size modes (Figure 3-100). Likewise, Polidori et al. (2007, [156877](#)) suggest that similarities in the EC and OC size distributions and infiltration factors reflect low vapor pressure secondary organic aerosols in the OC component. Sioutas et al. (2005, [088428](#)) suggest that volatilization of UFPs while crossing the building envelope may impede infiltration in this size range. Variations in the presence of outdoor PM indoors, and resulting changes in removal behavior once indoors, relate to the species composition of PM.

3.8.5.2. Exposure to PM and Copollutants

Analysis of personal exposure to multipollutant mixtures is an area of growing research. Several multipollutant studies involving UF, fine, and coarse PM are presented in Table A-65. Sarnat et al. (2001, [019401](#)) found significant associations between personal exposure to PM_{2.5} and ambient concentrations of O₃, NO₂, CO (significant only for winter), and SO₂ in a panel study conducted in Baltimore. Personal exposures to PM_{2.5} and personal exposures to the gases were not correlated in this study. This result may have arisen in part because personal exposures to the gases were often beneath detection limits of the personal monitoring devices. Schwartz et al. (2007, [090220](#)) also used data from the Baltimore panel study to simulate distributions of personal exposures and ambient concentrations of PM_{2.5}, PM₁₀, SO₄²⁻, NO₂, and O₃. They found that personal exposure to ambient PM_{2.5} was significantly associated with ambient concentrations of PM_{2.5}, NO₂, and O₃ (O₃ in an inverse relationship). They also reported that personal exposure to SO₄²⁻ was significantly positively associated with ambient PM_{2.5} and O₃ concentrations.

There is evidence that associations between ambient gases and personal exposure to PM_{2.5} of ambient origin exist but are complex and vary by season and region. Seasonality of the associations could be a result of seasonal variability in photochemistry, source generation, and building ventilation. Sarnat et al. (2005, [087531](#)) observed associations between personal exposure to total PM_{2.5} and ambient concentrations of O₃, NO₂, and SO₂ measured at community-based monitors for groups of healthy senior citizens and school children in Boston during the summer. In this study, significant associations between personal exposure to ambient PM_{2.5} and personal O₃ exposures were observed in summer and between personal PM_{2.5} and personal NO₂ in winter and summer, unlike the Baltimore study in which only summertime personal PM_{2.5} and personal NO₂ were associated (Sarnat et al., 2001, [019401](#)). In their study of personal exposure to ambient air pollutants in Steubenville, OH, Sarnat et al. (2006, [090489](#)) found low but significant associations for ambient O₃ with personal PM_{2.5}, SO₄²⁻, and EC in the summer. Low but significant associations between ambient SO₂ and personal PM_{2.5}, and between ambient NO₂ and personal EC, were also observed. In the fall,

ambient O₃ had a weak but significant association with personal EC, and SO₂ had a weak but significant association with personal SO₄²⁻. Ambient NO₂ was also significantly associated with personal PM_{2.5}, SO₄²⁻, and EC with somewhat higher coefficient of determination ($R^2 = 0.25-0.49$) in the fall.

3.8.6. Implications of Exposure Assessment Issues for Interpretation of Epidemiologic Studies

Environmental epidemiologic study designs vary by many factors, including study sample size, measurement time interval, study duration, monitor type, and spatial distribution of the study sample. A panel epidemiology study consists of a relatively small sample (typically tens) of study participants followed over a period of days to months. Time-activity diary studies are examples of panel studies (e.g., Cohen et al., 2009, [190639](#); Elgethun et al., 2003, [190640](#); Johnson et al., 2000, [001660](#); Olson and Burke, 2006, [189951](#)), and a microenvironmental model might be applied to represent exposure in this case. Community time-series studies may involve millions of people whose exposure and health status is estimated over the course of a few years using a short monitoring interval (hours to days). Because so many people are involved, community-averaged concentration is typically used as a surrogate for exposure in community time-series studies. Exposures and health effects are spatially aggregated over the time intervals of interest because they are designed to examine health effects and their potential causes at the community level (e.g., Dominici et al., 2000, [005828](#); Peng et al., 2005, [087463](#)). A longitudinal cohort epidemiology study typically involves hundreds or thousands of subjects followed over several years or decades. Concentrations are generally aggregated over time and by community to estimate exposures (e.g., Dockery et al., 1993, [044457](#); Krewski et al., 2000, [012281](#)). The importance of exposure misclassification varies with study design based on the spatial and temporal aspects of the design. Other factors that could influence exposure estimates in PM epidemiologic studies include source characteristics, particle size distribution, and particle composition. Potential issues that could influence estimates of PM exposure include measurement, modeling, spatial variability, temporal variability, use of surrogates for PM exposure, and compositional differences. These are described in detail in the following sections.

3.8.6.1. Measurement Error

Measurement Error at Community-Based Ambient Monitors and Exposure Assessment

Community-based ambient monitors are employed for time-series and longitudinal studies, although they can be used for panel studies as well. Section 3.4 discusses potential errors in measuring ambient PM in detail. Because there will likely be some random component to instrumental measurement error, the correlation of the measured PM mass with the true PM mass is expected to be <1. Sheppard et al. (2005, [079176](#)) indicate that instrument error in the hourly or daily average concentrations has “the effect of attenuating the estimate of α .” Zeger et al. (2000, [001949](#)) suggest that in order for this error to cause substantial bias in later estimation of a health outcome, the measurement error must be strongly correlated with the measured concentrations. Positive and negative artifacts resulting from sampling volatile PM may therefore lead to lack of association with health endpoints in time-series and longitudinal studies. In multicity longitudinal studies, where PM composition and associated artifacts may vary across cities, the cumulative influence of such artifacts on exposure estimates is more difficult to predict.

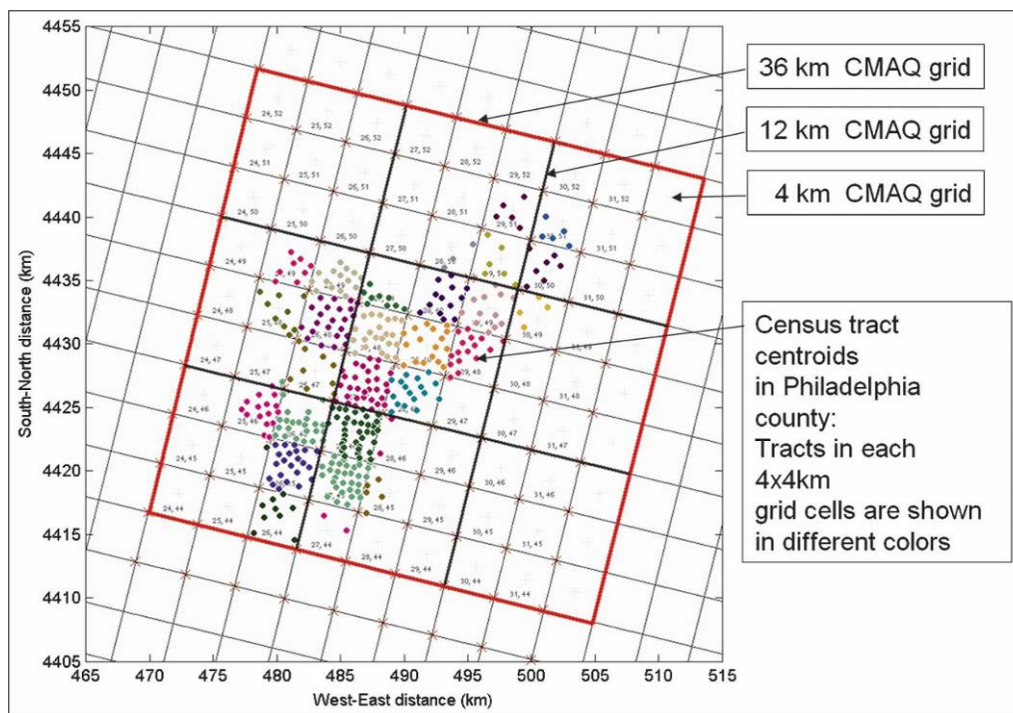
Measurement Error for Personal Exposure Monitors

PEMs are primarily used in panel exposure studies to measure total exposure to PM (e.g., Cohen et al., 2009, [190639](#); Elgethun et al., 2003, [190640](#); Johnson et al., 2000, [001660](#); Olson and Burke, 2006, [189951](#)). PEMs are specialized monitors that, because people must carry them, have to

be small, light, quiet, and battery operated or passive. As a result, they may have lower face velocities across the filter and lower pressure drops than ambient-based filter measurements of PM, which typically sample at much higher flow rates, and consequently at much higher face velocities. Light scattering measurements are biased when relative humidity is high and are sensitive to size distribution (Lowenthal et al., 1995, [045134](#); Sioutas et al., 2000, [025223](#)). Positive artifacts resulting from adsorption of vapor-phase organic compounds and negative artifacts from evaporation of semi-volatile PM also create challenges for interpreting personal exposure monitoring data (e.g., Pang et al., 2002, [030353](#)). Olson and Norris (2005, [156005](#)) attributed more OC particle mass collection to face velocity differences when using PEMS compared with FRMs. Data quality of PEMS is described in much greater detail in the 2004 PM AQCD (U.S. EPA, 2004, [056905](#)). The artifacts listed here could result in either negative or positive sampling bias.

3.8.6.2. Model-Related Errors

When models are used in lieu of or to supplement measurements of ambient PM exposure or community-based ambient PM concentration, it is important to identify errors and uncertainties that could affect estimates of PM-related health effects. Model-related errors are determined by four factors: representativeness of the mathematical model, accuracy of model inputs, scale of model resolution, and model sensitivity. If verification errors related to these four factors are minimized, then the model can be evaluated against physical data to determine how well the model truly captures a real situation (Roache, 1998, [156915](#)). Detail of the model design and inputs can have significant impact on validation, as observed in Meng et al. (2005, [058595](#)) and Hering (2007, [155839](#)). Meng et al. (2005, [058595](#)) demonstrated how use of an increasingly more detailed mathematical model decreases the variability of the results with respect to modeled indoor PM_{2.5} concentration of outdoor origin and to modeled infiltration factor. Hering (2007, [155839](#)) compared infiltration model results for PM-based EC, NO₃⁻, and SO₄²⁻. Model inputs were from a central site monitor only, central site monitor with air exchange data, and detailed inputs related to initial outdoor (outside test building) and indoor concentrations. Use of more detailed inputs resulted in significant reductions in error for indoor EC concentration, smaller improvements for indoor SO₄²⁻, and negligible improvement in model results for indoor NO₃⁻. This illustrates the impact of differential infiltration discussed in Sections 3.8.4 and 3.8.5.



Source: Reprinted with Permission of ACS from Isakov et al. (2007, [195880](#)).

Figure 3-101. Grid resolution of the CMAQ model in Philadelphia compared with distribution of census tracts in which exposure assessment is performed.

For any spatial interpolation models, grid resolution is another source of error. Isakov et al. (2007, [195880](#)) linked CMAQ with the Hazardous Air Pollutant Exposure Model for exposure assessment in Philadelphia. Their simulation was implemented on a 4 km nested grid within 12 km and 36 km grids to bring the scale of their model from national to urban. However, the census tracts in which Isakov et al. (2007, [195880](#)) sought to describe exposure were distributed on a much finer scale (Figure 3-101). They supplemented the CMAQ model with an Industrial Source Complex Short Term (ISCST) dispersion model to resolve the subgrid scale behavior. If concentrations were averaged across the cell in lieu of a more detailed subgrid representation, Isakov et al. (2007, [195880](#)) found that exposures were overestimated by a factor of 2. Appel et al. (2008, [155660](#)) noted that their 36 km simulations provided a closer estimate of SO_4^{2-} aerosol concentration than did their 12 km nested simulation, which overestimated concentrations. Hogrefe et al. (2007, [156561](#)) also noted overestimation of the CMAQ model at the 12 km scale, where multiple point interpolation was used to obtain subgrid estimates. Model convergence theory would suggest that the 36 km simulation is not actually more accurate but coincidentally closer to the observed concentrations (Roache, 1998, [156915](#)). It is possible that if secondary pollutants are more regionally dispersed, lower spatial resolution would be required to attain a converged solution of the spatial concentration field. However, higher spatial resolution in the simulation should produce very similar results if the solution is convergent.

Use of geospatial statistical methods for grid interpolation, as performed in the SHEDS/MENTOR simulation by Georgopoulos et al. (2005, [080269](#)), provides another methodology for grid interpolation. Similar to Isakov et al. (2007, [195880](#)), Georgopoulos et al. (2005, [080269](#)) linked CMAQ with an exposure model for estimation of neighborhood-scale exposures using a 4 km resolution grid nested within 12 km and 36 km grids. The authors found that CMAQ underestimated $\text{PM}_{2.5}$ concentration at many times during the simulation. Kim et al. (2009, [188446](#)) compared results from an exposure model using six different levels of spatial resolution. The model predicted $\text{PM}_{2.5}$ at monitor locations as a function of the mean concentration and spatial and random errors. The 6 levels of spatial resolution were simulated through assignment of the spatial and random error terms and by defining the distance over which spatial errors are correlated.

Between monitors, Kim et al. (2009, [188446](#)) compared results from assigning nearest monitor values and from kriging. They found that model prediction error and bias in health effects estimates decreased with increased spatial resolution of the error terms, as well as with kriging over a nearest monitor scheme.

For GIS-based models designed to improve spatial resolution of exposure estimates, Yanosky et al. (2008, [099467](#)) described three sources from which they derived an estimate of total model uncertainty: transient model components, stationary model components, and residual spatial and temporal components of variance. When analyzing relative contributions to uncertainty, they found that unexplained local spatial variability was the largest contributor. With model inputs from PM₁₀ monitors for this study, poor model performance and high uncertainty were observed where monitors were sparsely located. High uncertainties were also calculated in a few select urban areas (New York City, Detroit, Cleveland, and Pittsburgh) where concentrations tend to be higher, although the latter may have been related to the Taylor series approximation used for the residual uncertainty term. Spatial and temporal uncertainties were also reduced when temporal resolution was increased in the model implementation.

In his review of various exposure assessment modeling techniques, Jerrett et al. (2005, [092864](#)) reviewed source proximity and LUR for application to exposure assessment. The literature contains mixed evidence of the association between health effects and source proximity (e.g., Langholz et al., 2002, [191771](#); Maheswaran and Elliott, 2003, [125271](#); Venn et al., 2000, [007895](#); Venn et al., 2001, [023644](#)). Jerrett et al. (2005, [092864](#)) contend that source proximity modeling is limited because other confounding covariates, such as SES, may be related to source proximity. Additionally, subjects' time-activity patterns may vary from locations modeled through source proximity. Wind direction and topography may bring PM plumes away from a site located even in very close proximity to the source, so that high concentrations would be found at distances far downwind of a source. Jerrett et al. (2005, [092864](#)) state that LUR is an adaptable framework allowing adaptation to localized conditions, but they caution that LUR is limited to fairly homogeneous spatial regions. They point to Briggs' (2000, [191772](#)) simulation of Amsterdam as an example of LUR surfaces produced with little spatial variability.

LUR and kriging were both used in the ACS data reanalysis by Krewski et al. (2009, [191193](#)) to study mortality as a function of spatial variability in PM_{2.5} in New York and Los Angeles, as described in Section 3.8.3.4. The LUR solution produced some observed overpredictions near freeways. Kriged results were compared with LUR for both cities. For New York City, kriging produced slightly attenuated mortality risk estimates, while for Los Angeles, kriging did not exhibit as much spatial variability as LUR. The latter may be due to the fact that the monitoring network in Los Angeles was not situated to capture spatial variability in PM_{2.5} concentration occurring near areas of high traffic. Despite similarities in the LUR performance, health effects predictions were quite different for New York City and Los Angeles, with increased hazard ratios of 1.56 and 1.39, respectively using the same LUR covariates. Krewski et al. (2009, [191193](#)) noted that in New York City, the healthiest (and wealthiest) segment of the population lived in the most polluted areas, while in Los Angeles, there was a strong association between pollution and mortality. This finding implies that, because geographic regions may differ by multiple factors, such as building and power plant fuel use, roadway design, traffic patterns, and building design, significant variables in an LUR analysis may also differ by region.

3.8.6.3. Spatial Variability

For PM, spatial and temporal distribution as a function of particle size and composition also plays a large role in the selection of an exposure model. For instance, use of Equation 3-6 might be employed for a study of ambient PM_{2.5} exposure because spatial variability in PM_{2.5} concentration can be low over urban to regional scales in comparison with more spatially variable PM_{10-2.5} and UFPs, as described in Section 3.8.4. Spatial issues leading to exposure misclassification are discussed below.

In panel studies, exposure error will be introduced if the ambient PM concentration measured at the central site monitor is used as an exposure surrogate and differs from the actual ambient PM concentration outside a subject's residence and/or worksite. Filleul et al. (2006, [089862](#)) computed exposure based on varying contributions of community-based ambient monitors (deemed background) and proximal monitors (to represent a receptor) in Le Havre, France for black smoke measurements. They found that using a weighted mean with increasing weight for proximal monitors

resulted in non-significant but increased mean exposure estimates. Moore et al.'s (2009, [191004](#)) finding of high variability in UFPs across Los Angeles also suggests that exposure error would occur from using one or a few UFP monitors. In an example using AQS data, PM₁₀ monitors in the Chicago CSA are south of the most populated areas within Chicago (Figure A-8 in Annex A), where intersampler correlations for urban scale PM₁₀ data for several monitor pairs are below 0.4 (Table A-23 in Annex A). In another example from AQS data, PM_{2.5} and PM₁₀ monitor locations in the Riverside CBSA are shown to correspond more closely with higher population density areas (Figures A-25 and A-26 in Annex A), where urban scale intersampler correlations for both PM_{2.5} and PM₁₀ are below 0.4 for several monitor pairs. For most cities, intersampler correlation is much higher for PM_{2.5} than for PM₁₀. This is in accord with the findings of Sarnat et al. (2009, [180084](#)) where, in an Atlanta time-series study of the effect of spatial variation in concentration on epidemiologic associations, spatially homogeneous PM_{2.5} and O₃ were found to be consistently associated with emergency room visits using any monitor within the study area, while associations were less consistent across monitors for spatially heterogeneous CO and NO₂ among the entire population studied. Considering results reported in the literature along with inter-sampler correlations (reported in Annex A, Section A.2 for PM_{2.5} and PM₁₀, and their corresponding monitor locations shown in Annex A, Section A.1), the magnitude of spatial exposure error likely depends on particle size as well as monitor location, source location, and characteristics such as urban and natural topography and meteorological trends.

Spatial variability among various studies further suggests that use of a single or small number of ambient monitors introduces uncertainty in exposure assessment panel studies. Violante et al. (2006, [156140](#)) studied personal exposures to traffic of parking police in Bologna, Italy to determine how personal exposure to outdoor PM₁₀ and benzene compares with that measured at a community-based monitor. This study found that personal exposures to PM₁₀ were significantly higher than at the community-based monitor, although the authors were not able to demonstrate significant effects of meteorology or traffic on those exposures. Nerriere et al. (2007, [156801](#)) observed spatial heterogeneity of personal exposures to metals in PM_{2.5} and PM₁₀, with higher levels found near high-traffic and industrial areas. In a Bayesian hierarchical model analysis of personal exposure and ambient PM_{2.5} data from the pilot Baltimore Epidemiology-Exposure Panel Study of 16 subjects, McBride et al. (2007, [124058](#)) showed that community monitors overestimated personal exposures for the panel subjects, and that these results were not sensitive to model selection.

For community time-series epidemiology, the community-average concentration, not the concentration at each fixed monitoring site, is the concentration variable of concern (Zeger et al., 2000, [001949](#)). Because variation in trends is of interest, bias in the central site monitor data will not affect health effects estimates unless the central site monitor is not correlated with the community-average concentration. The latter condition will cause the health effect estimate to be biased towards the null (Sheppard et al., 2005, [079176](#)). The correlation between the concentration at a central community ambient monitor and the community-average concentration depends on homogeneity of the spatial distribution and representativeness of the central-site monitor location. Kim et al. (2005, [083181](#)) noted that spatial variability among PM species can add uncertainty to exposure estimates in community time-series epidemiology studies exploring source contributions to health effects. The monitoring site is selected to represent the community average of the PM characteristic (mass and/or species) of interest. If the selected site is far from PM sources, then the average measurement may be lower than actual ambient PM concentrations. Likewise, if the site is selected to measure a "hot spot" or pollution from a nearby source, exposure estimates across the community could be skewed upwards.

Intra-urban spatial heterogeneity could affect health effects estimates derived from community time-series studies if a community is divided by urban or natural topographic features or by source locations into several sub-communities that differ in the temporal pattern of pollution. Intra-urban spatial heterogeneity is discussed in detail in Section 3.5. Community exposure may not be well-represented when monitors cover large areas with several sub-communities having different sources and topographies. This point is illustrated for Los Angeles in Figure 3-27 and Figure 3-37 where intersampler correlation decreases with respect to distance more so than for other cities shown. Using zip code classified mortality data in a study of SES and acute cardiovascular mortality in Phoenix, high risk ratios were computed when a small area near the monitoring site was studied (Mar et al., 2003, [042841](#); Wilson et al., 2007, [157149](#)), while use of larger-area county-wide data produced non-significant associations (Moolgavkar, 2000, [010305](#); Smith et al., 2000, [010335](#)). At least part of the heterogeneity found between cities in multicity studies may be due to the use of a large

geographic area that is composed of several sub-communities that differ in the spatiotemporal distribution of air pollutants. Note that when zip codes cover large areas (e.g., in western mountain states) or when counties cover small areas (e.g., in the northeast), then assumptions change regarding use of zip code- or county-level data for epidemiologic studies. For all metropolitan areas investigated in this assessment, the PM₁₀ data have significantly more scatter than PM_{2.5}. This suggests that the uncertainty of the community average concentration would increase in the coarse PM range. Metrics have been developed and used to compare the spatial variability of air pollutants (Wongphatarakul et al., 1998, [049281](#)). These metrics are useful in assessing the potential for exposure error in the epidemiologic studies, especially when different monitors are used on different days to construct city-wide averages.

Epidemiologic studies of long-term exposure rely on differences among communities in long-term average ambient concentrations. If exposure errors are different in the different communities, the differences in long-term ambient concentrations among communities may not represent the differences in long-term average exposures (Dockery et al., 1993, [044457](#)). Thus, in a regression of health effects against average concentration as an indicator for average exposure, there could be a different magnitude and direction of error in the exposure indicator for each spatial area. This could bias the slope up or down. The following epidemiologic studies, described in detail in Section 7.6, are cited here to illustrate the effect of spatial exposure error on health effects estimates. The Harvard Six-City Study dealt with this issue by design, where the members of the cohort in each city were located in a relatively small area near the monitor (Dockery et al., 1993, [044457](#)). In the ACS study, the spatial area was the Metropolitan Statistical Area (MSA) (Krewski et al., 2000, [012281](#)); other studies have used counties as the spatial area (Enstrom, 2005, [087356](#); Lipfert et al., 2000, [004087](#)). In a comparison of several of the larger long-term cohort studies, those using county level spatial areas (Enstrom, 2005, [087356](#); Lipfert et al., 2000, [004087](#)) sometimes did not find significant associations, whereas those using MSAs (Pope et al., 1995, [045159](#); Pope et al., 2002, [024689](#)) or cities (Dockery et al., 1993, [044457](#)) did find significant associations. Jerrett et al. (2005, [087600](#)) used smaller zip code areas within Los Angeles County and found effects that were both significant and largest in magnitude compared to those reported for other long-term cohort studies. Krewski et al. (2009, [191193](#)) suggested that significant associations between cardiovascular health effects estimates and PM_{2.5} observed in Los Angeles but not in New York City were related to spatial homogeneity of PM_{2.5} concentration in New York City. The Nurses' Health Study examined associations of mortality with PM₁₀ and found higher and more significant associations when using estimated concentrations at subjects' individual residences (Puett et al., 2008, [156891](#)) in lieu of county-level concentrations (Fuentes et al., 2006, [097647](#)). These considerations suggest that studies that include large U.S. counties as spatial areas and find no significant associations of health effects with pollution cannot be considered definitive, because the likelihood of exposure error increases in this situation. Reducing the exposure error by using concentrations based on residence address or small zip code areas is associated with larger relative risk than those obtained with county-wide averages of concentrations.

3.8.6.4. Temporal Variability

Temporal Correlation

Concentration time series analyzed for community time-series epidemiologic studies can include those averaged over several monitors, a single monitor used as an estimate of the true community average exposure, or a monitor used to represent nearby exposures. Within a city, lack of correlation of relevant time series at various sites results in smoothing the exposure surrogate concentration function over time and resulting loss of peak structure from the data series. Burnett and Goldberg (2003, [042798](#)) found that community time-series epidemiology results reflect actual population dynamics only when five conditions are met: environmental covariates are fixed spatially but vary temporally; the probability of the health effect estimate is small at any given time; each member of the population has the same probability of the health effect estimate at any given time after adjusting for risk factors; each member of the population is equally affected by environmental covariates; and, if risk factors are averaged across members of the population, they will exhibit smooth temporal variation. For this study, mortality was examined, but the temporal considerations

are generalizable to other health outcomes. Dominici et al. (2000, [005828](#)) note that ensuring correlation between ambient and community-average exposure time series is made difficult by limitations in availability and duration of detailed ambient concentration and exposure time series data and, as a result, is often a source of uncertainty. Sheppard et al. (2005, [079176](#)) also add that the health effect estimate can be biased by time-dependent error in α in a time-series study if the spatial variation in PM concentration is not significant. The direction of bias is related to seasonal correlation between α and C_{α} .

Seasonality

Community time-series studies can be designed to investigate seasonal effects by incorporating seasonal interaction terms for the exposure surrogate and/or meteorology (e.g., Dominici et al., 2000, [005828](#)). Studies from Section 6.5 are briefly mentioned here to illustrate how seasonal exposures can influence health effect estimates. Bell et al. (2008, [156266](#)) and Peng et al. (2005, [087463](#)) observed higher health effect estimates and stronger seasonal dependence in the northeast than in the rest of the country for PM_{2.5} and PM₁₀, respectively. Peng et al. (2005, [087463](#)) stated that these results generated three hypotheses. First, the PM composition and resulting toxicity might vary with season. Bell et al. (2008, [156266](#)) showed seasonal differences between respiratory and cardiovascular effect estimates that the authors hypothesized related to seasonal differences in dominance of a given PM species. Second, Peng et al. (2005, [087463](#)) suggested that less seasonality in regions other than the northeast may reflect regional tendencies for spending more or less time outdoors. Exposure estimates for time spent outdoors may be less subject to exposure error because uncertainties related to infiltration are not a factor during that time. At the same time, air conditioning usage, which is more common in the summer and in warm climates (Pandian et al., 1998, [090552](#)), has been associated with decreased association between PM_{2.5} and cardiovascular morbidity (Bell et al., 2009, [191007](#)). Third, infectious diseases are more prevalent during winter and so may influence health outcomes. However, it would be expected that regions other than the northeast would be affected by influenza in winter. Uncertainty in sources of seasonal bias may also indicate other unknown factors.

Data Frequency

Most panel and many time-series studies examine the associations of health outcomes only with exposure (or exposure surrogates) on the day of exposure (lag 0). Zanobetti et al. (2000, [004133](#)) and Lokken et al. (2009, [186774](#)) suggest that health effects may not occur until subsequent days or be distributed over several days. When PM measurements are obtained every three or six days, it is difficult to refine the study lag structure down to the day-level. In studies of the effects of short-term PM_{2.5} exposure on cardiovascular and respiratory hospitalization in >200 urban U.S. counties, Bell et al. (2008, [156266](#)) and Dominici et al. (2006, [088398](#)) worked with a combination of air quality measurements obtained daily, those obtained every 3 days, and daily hospitalization data. Time lags of 0, 1, and 2 days were applied, such that PM_{2.5} data obtained only on day 0 would be applied as lag 0 for the corresponding day's hospitalization record, as lag 1 for the next day's hospitalization, and as lag 2 for the following day. No lag 0 data would be available for day 1, and no lag 0 or 1 data would be available for day 2 in this example. This analysis could be performed with sufficient statistical power despite the reduction in days of PM data because a large number of counties were analyzed. Single city studies using data obtained every three or six days could employ the same approach but would lose statistical power compared with daily data because fewer data points would exist for each lag. Likewise, Dominici et al. (2006, [088398](#)) only applied distributed lag analysis to the daily hospitalization data where daily PM_{2.5} concentration data were also available.

3.8.6.5. Use of Surrogates for PM Exposure

Surrogates for Infiltration Tracers

In panel studies, a tracer can be used for PM that infiltrates indoors, such as sulfate as a surrogate for PM_{2.5}, as described in Section 3.8.4. For this method to be successful, indoor or other nonambient sources of the tracer must be small compared to ambient sources over the period of sampling. Wallace and Williams (2005, [057485](#)) observed that, because SO₄²⁻ particles are typically smaller than other PM contributing to measurable PM_{2.5} mass, F_{inf} may be biased by using this term to describe PM_{2.5} infiltration. Other concerns in using SO₄²⁻ as a tracer for PM_{2.5} arise because SO₄²⁻ tends to be concentrated in smaller particles and thus it might be a better tracer for fine mode particles than for the coarse fraction at the upper tail of the PM_{2.5} particle size distribution. Volatilization of ammonium nitrate or organic compounds after infiltration of PM_{2.5} indoors results in these components being poor surrogates for ambient PM in exposure estimates (Lunden et al., 2003, [081201](#)).

Use of Ambient PM Concentration in Lieu of Ambient PM Exposure

Ambient PM concentration is often used as a surrogate for exposure to ambient PM in epidemiologic studies. The ambient concentration may be based on measurements made just outside the primary microenvironment, at the nearest community monitor, at a single community monitor, or as the average of several community monitors. Based on the information presented in Section 3.8.4 related to urban-scale PM distribution, there is less exposure error for accumulation mode PM because it has a more homogeneous spatial distribution and higher infiltration indoors, compared with coarse or UFPs. If appropriate measurements are made, it is also possible to estimate the ambient and nonambient components of total personal exposure and use four exposure surrogates in panel epidemiologic studies: C_a , E_T , E_a , and E_{na} (Ebelt et al., 2005, [056907](#); Koenig et al., 2005, [087384](#); Strand et al., 2006, [089203](#); Wilson and Brauer, 2006, [088933](#)). Results from Wilson and Brauer (2006, [088933](#)) showed that exposure error is introduced by 1) using C_a instead of E_a and 2) assuming E_a and E_{na} have the same effects on health outcomes. There was essentially no association of the effect with E_T or E_{na} . Wilson and Brauer (2006, [088933](#)) noted that exposure to nonambient PM will not affect the relationship between C_a and E_a , but “the difference between ambient concentration and ambient exposure will bias the relative risk derived from epidemiologic studies.” Strand et al. (2006, [089203](#)) also noted that inclusion of nonambient PM_{2.5} would not be expected to change health effect estimates because ambient and nonambient PM_{2.5} calculations were not correlated.

Zeger et al. (2000, [001949](#)) pointed out that for community time-series epidemiology, it is the correlation of the daily community-average personal exposure to the ambient concentration with daily community-average concentration that is important, not the correlation of each individual's daily exposure with the daily community-average concentration. Thus, the low correlation of individual daily exposure with the daily community-average concentration, as frequently found in pooled panel exposure studies, is not relevant to error in community time-series epidemiologic analysis. Sheppard et al. (2005, [079176](#)) also notes that an insufficient number of total personal exposure samples used in a time-series design would introduce large classical measurement errors related to high variability in E_{na} . Sheppard et al. (2005, [079176](#)) further maintain that these errors can be minimized by using the average concentration measured at community-based ambient monitors. However, overestimation of the community-average exposure by substituting C_a for E_a leads to underestimation of the effect estimate per unit mass of ambient PM. City-to-city variations in the indoor air exchange rate, related to differences in climate or housing stock, will cause city-to-city differences in the health effect endpoint estimate obtained from the study using C_a even if the endpoint remained the same using the community-average exposure.

Relationship between PM and Copollutants

Uncertainties in the composition of multipollutant mixtures of gases and PM to which the population is exposed can introduce uncertainties in health effects estimates. When copollutant associations exist, as described in Section 3.8.5, the potential for one pollutant to act as a surrogate for another pollutant or mix of pollutants introduces uncertainty into epidemiologic models (Sarnat et al., 2001, [019401](#)). For example, O₃ may be an indicator of photochemical oxidation products including organic PM. SO₂ may be an indicator of Ni emissions from smelters, V from oil fired power plants, or As, Se or Hg from coal-fired power plants. In another example, the HEI Report on traffic-related health effects (2009, [191009](#)) lists CO, NO₂, PM_{2.5} and PM₁₀ mass, UFP count, EC, benzene, and traffic metrics (e.g., count, fuel consumption) all as potential surrogates for traffic or for the mix of all PM and gaseous pollutants in traffic because all of these pollutants are found in mobile source emissions. Furthermore, in a multipollutant model, transfer of association can occur by an increase in the slope of a confounding copollutant and a concurrent decrease in the slope of the truly causal covariate. This can occur when copollutants are highly correlated with larger error for the true copollutant, smaller error for the confounder, and correlation between the copollutant measurement errors (U.S. EPA, 2004, [056905](#); Zeger et al., 2000, [001949](#); Zidek et al., 1996, [051879](#)). For these reasons, this is an important area of uncertainty for interpretation of the multipollutant models discussed in Chapter 6.

3.8.6.6. Compositional Differences

Differences between the composition of ambient PM and the ambient PM that has infiltrated indoors may affect exposure estimates. Numerous differential infiltration studies related to indoor-outdoor changes in size distribution and chemical composition are cited in Sections 3.8.4 and 3.8.5, respectively. If differential infiltration results in differences in PM size distribution and chemical composition between indoor-ambient PM and outdoor-ambient PM, then use of outdoor-ambient PM could bias health effects estimates related to particular species. Baxter et al. (2007, [092726](#)) showed that V tends to have lower F_{inf} , perhaps because metals exist more in the coarse range, while S has F_{inf} close to unity. Epidemiologic studies cited in Section 6.6 indicate that significant associations between health effects estimates and PM trace metal exposures exist and may be modified by season. Trace metal penetration efficiency estimates are thus relevant to those findings. Section 6.6 also discusses significant associations between health effects endpoints and exposure to EC and OC in PM. After initial emission, traffic-related PM is generally in the accumulation mode with volatile components; accumulation mode PM tends to have the highest infiltration factors, but volatile components may be lost during infiltration (Sarnat et al., 2006, [089166](#)). If outdoor residential or central-site measurements are used for an exposure surrogate, differences in indoor and outdoor PM composition related to infiltration could introduce uncertainty into effects estimates.

Ebelt et al. (2005, [056907](#)) illustrated that exposure error occurs when the PM on one or more days is not representative of the normal community PM. Section 6.3.2.1 discusses this COPD panel study of the association between respiratory and cardiovascular measures (i.e., lung function, blood pressure, heart rate, HRV, and ectopic beats) and PM_{2.5}, PM_{10-2.5}, and PM₁₀. In their analysis, one day of dust from the Gobi Desert caused an increase in the concentration of fine and coarse PM. When this day was deleted from the analysis, the associations of health effects estimates with PM₁₀ and especially with PM_{10-2.5} became larger and more significant. Similar peaks in PM₁₀ concentration have been observed on the Iberian Peninsula as a result of high transport events carrying dust from the Sahara Desert that could affect epidemiologic associations on given days (Artinano et al., 2001, [190099](#)).

3.8.6.7. Conclusions

This section presents considerations for exposure assessment and the exposure misclassification issues that can potentially affect health effects estimates. These issues can be categorized into six areas: measurement, modeling, spatial variability, temporal variability, use of surrogates for PM exposure, and compositional differences. Potential influences of each of these sources on health effects estimates derived from panel, time-series, and longitudinal epidemiologic studies are described above. Additionally, error sources often interact with each other and are driven

by particle size distribution. For example, fresh diesel-generated PM is characterized by UFPs that dynamically grow and change in chemical composition over short time and spatial scales, and lack of spatial and temporal resolution in measurements or models can result in misclassifying this exposure (Moore et al., 2009, [191004](#)). For this reason, conclusions regarding UFP exposure cannot be drawn from PM_{2.5} concentration data, in part because PM_{2.5} concentration is more spatially homogeneous across a city. In most circumstances, exposure error tends to bias a health effect estimate downward (Sheppard et al., 2005, [079176](#); Zeger et al., 2000, [001949](#)). Insufficient spatial or temporal resolution to capture true variability and correlation of PM with copollutants are examples of sources of uncertainty that could widen confidence intervals and so potentially reduce the significance of health effects estimates.

3.9. Summary and Conclusions

3.9.1. Concentrations and Sources of Atmospheric PM

This section summarizes sources and concentrations of atmospheric PM. The following summaries cover source characteristics from Section 3.3, measurement techniques from Section 3.4, spacial and temporal variability and copollutant correlations from Section 3.5, source contributions from Section 3.6 and policy relevant background concentrations from Section 3.7.

3.9.1.1. PM Source Characteristics

PM in the atmosphere contains both primary (i.e., emitted directly by sources) and secondary components, which can be anthropogenic or natural in origin. Secondary components are produced by the oxidation of precursor gases such as SO₂ and NO_x and reactions of acidic products with NH₃ and organic compounds. Developments in the chemistry of formation of SOA indicate that oligomers are likely a major component of OC in aerosol samples. Recent observations suggest that small, but still significant quantities of SOA are formed from isoprene oxidation. Gasoline engines have been found to emit a mix of OC, EC, and nucleation-mode heavy and large polycyclic aromatic hydrocarbons on which unspent fuel and trace metals condense, while diesel particles are composed of a soot nucleus on which SO₄²⁻ and hydrocarbons condense. Data from standard emissions tests in which there is insufficient dilution of fresh exhaust from combustion sources tend to overestimate the primary component of organic aerosol at the expense of the semi-volatile components. These semi-volatile components are precursors to secondary organic aerosol formation and their oxidation results in more oxidized forms of SOA than previously considered, both in near source urban environments and further downwind.

3.9.1.2. Measurement Techniques

The federal reference methods for PM_{2.5} and PM₁₀ are based on criteria outlined in the CFR. They are, however, subject to several limitations that should be kept in mind when using compliance monitoring data for health outcome studies. FRM methods are subject to the loss of semi-volatile species such as organic compounds and ammonium nitrate (especially in the West). Since FRM gravimetric methods involve 24-h integrated filter samples, no information is available for variations over shorter averaging times. However, methods have been developed to measure real-time PM_{2.5} or PM₁₀ mass concentrations (e.g., FDMS-TEOM). New FRMs and FEMs are available for PM_{10-2.5} and various methods (dichotomous samplers, cascade impactors, and passive sampling techniques) are under evaluation to improve PM_{10-2.5} measurements. Techniques are available to characterize UFP mass, surface area, and number concentrations. Continuous and semi-continuous measurement techniques are also available for PM species, such as PILS for multiple ion analysis and AMS for multiple component analysis. Advances have also been achieved in PM organic speciation (e.g., TD-GC/MS).

3.9.1.3. Ambient PM Variability and Correlations

Advances in understanding the spatiotemporal distribution of PM mass and constituents have recently been made, particularly with regard to PM_{2.5} mass and chemical composition and UFP concentrations. Emphasis in this ISA was on the period 2005-2007 so that the most recent validated EPA Air Quality System (AQS) data were used. Note, however, that a majority of U.S. counties were not represented by AQS data since their population fell below the regulatory monitoring threshold for PM. Moreover, monitors reporting to AQS were not uniformly distributed across the U.S. or within counties, and conclusions drawn from AQS data may not apply equally to all parts of a geographic region. Furthermore, biases can exist for some PM constituents (and hence total mass) owing to volatilization losses of nitrates and other semi-volatile compounds, and, conversely, to retention of particle-bound water by hygroscopic species. The degree of spatial variability in PM is likely to be region-specific and strongly influenced by region-specific sources and meteorological and topographic conditions.

Spatial Variability across the U.S.

County-scale, 24-h avg concentration data for PM_{2.5} between 2005-2007 showed considerable variability across the U.S.. The highest reported 3-yr avg concentrations were for six counties within the San Joaquin Valley and inland southern California, as well as Jefferson County, AL (containing Birmingham) and Allegheny County, PA (containing Pittsburgh). The lowest reported annual average PM_{2.5} concentrations were contained within 237 counties distributed throughout many western and northern states as well as Florida and the Carolinas. Of the 15 individual CSAs/CBSAs selected for detailed investigation based on their geographic distribution and importance in recent health effect studies, the highest mean 24-h PM_{2.5} concentrations were reported for Riverside (17 µg/m³), Birmingham (16 µg/m³) and Pittsburgh (16 µg/m³); the lowest were reported for Denver (9 µg/m³) and Seattle (9 µg/m³).

Since PM_{10-2.5} is not routinely measured and reported to AQS, co-located low-volume PM₁₀ and PM_{2.5} measurements from the AQS network were used to investigate the spatial distribution in PM_{10-2.5}. Current data coverage (see Figure 3-10) and measurement errors limit the ability to draw any meaningful conclusions regarding the large-scale spatial distribution of PM_{10-2.5} in urban areas. Only 6 of the 15 CSAs/CBSAs chosen for closer investigation had sufficient data for calculating PM_{10-2.5}. In general, in the eastern metropolitan areas including Atlanta, Boston, Chicago and New York, most of the mass of PM₁₀ was in the PM_{2.5} size fraction, with the highest ratio of PM_{2.5} to PM_{10-2.5} in Chicago (14 µg/m³ PM_{2.5}, 5 µg/m³ PM_{10-2.5}, ratio = 2.8). In contrast, Denver (9 µg/m³ PM_{2.5}, 20 µg/m³ PM_{10-2.5}, ratio = 0.45) and Phoenix (10 µg/m³ PM_{2.5}, 22 µg/m³ PM_{10-2.5}, ratio = 0.45) contained most of PM₁₀ in the thoracic coarse mode.

Given the limited information available from AQS for PM_{10-2.5} and the current National Ambient Air Quality Standard for PM₁₀, analyses were performed on the more prevalent PM₁₀ data acknowledging that PM₁₀ incorporates both thoracic coarse and fine particles. The highest reported 3-yr avg PM₁₀ concentrations (>51 µg/m³) occurred in two counties in southern California and five counties in southern Arizona and central New Mexico. The lowest reported annual average PM₁₀ concentrations (≤ 20 µg/m³) were within 114 counties distributed fairly uniformly across the U.S. Of the 15 CSAs/CBSAs investigated, the highest mean 24-h PM₁₀ concentrations was reported for Phoenix (52 µg/m³), considerably higher than the means for the other CSAs/CBSAs investigated. The lowest was reported for Boston (17 µg/m³) with New York, Philadelphia and Seattle only slightly higher (19 µg/m³).

Spatial variability in PM_{2.5} components obtained from the CSN varied considerably by species. The highest annual average OC concentrations (>5 µg/m³) were observed in the western and southeastern U.S. Concentrations in the West peaked in the fall and winter, while concentrations in the Southeast peaked anytime between spring and fall. Of the 15 CSAs/CBSAs investigated, OC was the dominant PM_{2.5} component on an annual basis in the western cities, ranging from 34% of PM_{2.5} mass in Los Angeles to 58% in Seattle. EC exhibited less seasonal variability than OC and was particularly stable in the eastern half of the U.S. Annual average EC concentrations greater than 1.5 µg/m³ were present in Los Angeles, Pittsburgh, New York and El Paso. Concentrations of SO₄²⁻ were higher in the eastern U.S. resulting from higher SO₂ emissions in the East compared with the West. There is also considerable seasonal variability with higher SO₄²⁻ concentrations in the summer months when the oxidation of SO₂ proceeds at a faster rate than during the winter. Of the 15

CSAs/CBSAs selected, sulfate was the dominant PM_{2.5} component on an annual basis in the eastern cities, ranging from 42% of PM_{2.5} mass in Chicago to 56% in Pittsburgh. NO₃⁻ concentrations were highest in California, with annual averages >4 μg/m³ at many monitoring locations. There were also elevated concentrations of NO₃⁻ in the Midwest (>2 μg/m³), with wintertime concentrations exceeding 4 μg/m³. In general, NO₃⁻ was higher in the winter across the country, resulting from a number of factors including: (1) lower temperatures which favor partitioning into particles; (2) higher relative humidity, mainly in dry areas; (3) lower sulfate, allowing higher uptake of NO₃⁻; and (4) residential wood burning in specific areas of the U.S., especially in the Northwest. Exceptions existed in Los Angeles and Riverside, where high NO₃⁻ readings appeared year-round. Crustal material constituted a substantial fraction of PM_{2.5} year-round in Phoenix (28%) and Denver (16%), and during the summer in Houston (26%).

Clearly there are variations in both PM_{2.5} mass and composition by city resulting from numerous controlling variables (e.g., meteorology, the nature of sources, proximity to sources, topography). These variables are frequently poorly characterized on a broad scale, making it difficult to draw general conclusions regarding PM_{2.5} mass and composition across all cities within a given geographic region.

Spatial Variability on the Urban and Neighborhood Scales

In general, PM_{2.5} has a longer atmospheric lifetime than PM_{10-2.5} because larger particles have a higher gravitational settling velocity. For PM_{2.5}, most metropolitan areas exhibited high correlations (generally >0.75) between monitoring sites out to a distance of 100 km. Notable exceptions were Denver, Los Angeles and Riverside where correlations dropped below 0.75 somewhere between 20 and 50 km. Insufficient data were available in the 15 metropolitan areas to perform similar analyses for PM_{10-2.5} using co-located, low volume FRM monitors. More abundant PM₁₀ data, however, showed larger declines in inter-monitor correlations as a function of distance relative to PM_{2.5}. Atlanta, Boston, Denver, Los Angeles, New York City, Philadelphia, Phoenix, Pittsburgh and Riverside all showed an average correlation of 0.75 at 40 km or greater monitor separation while Birmingham, Chicago, Detroit, Houston and St. Louis had correlations that dropped off much more quickly with distance (average correlation of 0.75 at 6 km or less monitor separation). Furthermore, correlations between PM₁₀ concentrations exhibited substantially more scatter relative to PM_{2.5}. Shorter atmospheric lifetimes for PM₁₀ can result in local emission sources dominating PM₁₀ annual average mass concentrations at particular monitors. Although the general understanding of PM differential settling leads to an expectation of greater spatial heterogeneity in the PM_{10-2.5} fraction relative to the PM_{2.5} fraction in urban areas, deposition of particles as a function of size depends strongly on local meteorological conditions, in particular on the degree of turbulence in the mixing layer. Therefore, the findings from these 15 CSAs/CBSAs may not apply to all locations or at all times.

Population density and associated building density are also important determinants of the spatial distribution of PM concentrations. Inter-sampler correlations as a function of distance between monitors obtained for sampler pairs located less than 4 km apart (i.e., on a neighborhood scale) showed a shallower slope for PM_{2.5} than for PM₁₀. The average correlation was 0.93 for PM_{2.5}, but it dropped to 0.70 for PM₁₀.

Few studies have performed direct comparisons of UFP measurements at multiple locations within an urban area. A decrease in the number of UFPs was demonstrated with shifts from a dominant mode at around 10 nm within 20 m of a freeway to a flattened dominant mode at around 50 nm at a distance of roughly 100-150 m. At the same time, accumulation mode particle number concentration remained relatively constant to within ~300 m from the freeway. These findings suggest a high degree of spatial heterogeneity in UFPs compared with accumulation mode particles on the urban scale.

3.9.1.4. Temporal Variability

A steady decrease in PM_{2.5} concentrations from 1999 (the beginning of nationwide monitoring for PM_{2.5}) to 2007 was observed in all 10 EPA Regions, with the 3-yr avg of the 98th percentile of 24-h PM_{2.5} concentrations dropping 10% over this time period. Similar trends in PM₁₀ concentrations show a steady decline from 1988 to 2007 in all 10 EPA Regions.

Using hourly PM observations in the 15 metropolitan areas, diel variation showed peaks that differ by PM size fraction and region. For PM_{2.5}, a morning peak was observed starting at approximately 6:00 a.m., corresponding with the start of morning rush hour. There was also an evening PM_{2.5} concentration peak that was broader than the morning peak and extended into the overnight period, likely reflecting a combination of evening rush hour and the concentration increase caused by the usual collapse of the mixed layer after sundown. PM_{2.5} concentrations in Pittsburgh remained elevated throughout the night, obscuring the morning peak. For PM₁₀, all areas showed a morning and afternoon peak in mean concentrations. The magnitude and duration of this peak varied considerably by metropolitan area.

Studies indicate that UFPs in urban environments exhibit similar two-peaked diel patterns in Los Angeles and the San Joaquin Valley as well as in Kawasaki City, Japan and Copenhagen, Denmark. The afternoon peak in UFPs likely represents the combination of primary source emissions such as evening rush-hour traffic and photochemical formation of secondary organic aerosol and sulfate. Comparison between weekdays and Sundays as well as an urban street canyon site and an urban background site in this figure suggest traffic is a major source of UFPs within a street canyon during the morning rush hour. Any fluctuations or changes in the timing of the individual daily peaks during the 3-yr period would result in a broadening of the distribution shown in the diel plots.

3.9.1.5. Correlations between Copollutants

Correlations between PM size fractions and between PM and gaseous copollutants including SO₂, NO₂, CO and O₃ varied both seasonally and spatially between and within metropolitan areas. On average, PM₁₀ and PM_{2.5} were correlated with each other better than with the gaseous copollutants. Correlations between PM₁₀ and PM_{10-2.5} were greater in all locations than correlations between PM_{2.5} and PM_{10-2.5}. Correlations between PM₁₀ and PM_{10-2.5} were particularly high in Denver and Phoenix ($r > 0.88$ in all seasons). There was relatively little seasonal variability in the mean correlation between PM in both size fractions and SO₂ and NO₂. CO, however, showed higher correlations with PM₁₀ and PM_{2.5} on average in the winter compared with the other seasons. This seasonality results in part because a larger fraction of PM is primary in origin during the winter. To the extent that this primary component of PM is associated with common sources of NO₂ and CO, then higher correlations with these gaseous copollutants are to be expected. Increased atmospheric stability in colder months would also reinforce these associations. The correlation between daily maximum 8-h avg O₃ and PM showed the highest degree of seasonal variability with positive correlations on average in the spring, summer and fall, and negative correlations on average in the winter. This situation arises as the result of seasonal differences in PM primary emissions and photochemical production of secondary PM_{2.5} and O₃.

3.9.1.6. Source Contributions to PM

Results of receptor modeling calculations indicate that PM_{2.5} is produced mainly by combustion of fossil fuel, either by stationary sources or by transportation. It is apparent that a relatively small number of source categories, compared to the total number of chemical species that typically are measured in ambient monitoring source receptor model studies, are needed to account for the majority of the observed mass of PM in these studies. Trying to be more specific about contributions from source categories could result in ambiguity. For example, quite different mobile sources (e.g., trucks and locomotives) rely on diesel power and ancillary data is required to resolve contributions from these sources. A compilation of study results shows that secondary sulfate (mainly from EGUs), nitrate (from the oxidation of NO_x emitted mainly from transportation and EGUs), and primary mobile source categories constitute most of PM_{2.5} (and PM₁₀) in the East. Fugitive dust, found mainly in the PM_{10-2.5} size range, represents the largest source of ambient PM₁₀ in many locations in the western U.S. Quoted uncertainties in the source apportionment of constituents in ambient aerosol samples typically range from 10 to 50%. A comparison of source apportionment techniques indicated that the same major source categories of PM_{2.5} were consistently identified by several independent groups working with the same data sets. Soil-, sulfate-, residual oil-, and salt-associated mass were most clearly identified by the groups. Other sources with more ambiguous signatures, such as vegetative burning and traffic-related emissions were less consistently identified.

Spatial variability in source contributions across urban areas is an important consideration in assessing the likelihood of exposure error in epidemiologic studies relating health endpoints to sources. Concepts similar to those for using ambient concentrations as surrogates for personal exposures apply here. Studies for PM_{2.5} indicate that intra-urban variability increases in the following order: regional (e.g., secondary SO₄²⁻ from EGUs) < area (e.g., on-road mobile sources) < point (e.g., stacks) sources. Only one study was available for PM_{10-2.5}, indicating a similar ordering, but without a regional component (resulting from the short lifetime of PM_{10-2.5} compared to transport times on the regional scale).

3.9.1.7. Policy-Relevant Background

The background concentrations of PM that are useful for risk and policy assessments informing decisions about the NAAQS are referred to as policy-relevant background (PRB) concentrations. PRB concentrations have historically been defined by EPA as those concentrations that would occur in the U.S. in the absence of anthropogenic emissions in continental North America defined here as the U.S., Canada, and Mexico. For this document, PRB concentrations include contributions from natural sources everywhere in the world and from anthropogenic sources outside continental North America. Background concentrations so defined facilitated separation of pollution that can be controlled by U.S. regulations or through international agreements with neighboring countries from those that were judged to be generally uncontrollable by the U.S. Over time consideration of potential broader ranging international agreements may lead to alternative determinations of which PM source contributions should be considered by EPA as part of PRB. Contributions to PRB concentrations of PM include both primary and secondary natural and anthropogenic components. For this document, PRB concentrations for the continental U.S. were estimated using EPA's CMAQ modeling system, a deterministic CTM and with GEOS-Chem, a global-scale model for CMAQ boundary conditions. PRB concentrations of PM_{2.5} were estimated to be less than 1 µg/m³ on an annual basis, with maximum daily average values in a range from 3.1 to 20 µg/m³ and having a peak of 63 µg/m³ at the nine national park sites across the U.S. used to evaluate model performance for this analysis. For further information on methods used in modeling of PRB concentrations see Section 3.6, and for further information on the results of calculation of PRB concentrations see Section 3.7.

3.9.2. Human Exposure

This section summarizes the findings from the recent exposure assessment literature, which include the assessment of exposure to ambient PM, infiltration of ambient PM to indoor environments, and source apportionment of PM exposure. This summary is intended to support the interpretation of the findings from epidemiologic studies. For more detailed explication see Section 3.8.

3.9.2.1. Characterizing Human Exposure

A number of techniques have been applied in the literature to model human exposure to PM. Several studies have used time-weighted microenvironmental models to define total or ambient PM exposure. Time-activity diaries or global positioning systems have been employed to capture the time-basis for those models. Stochastic population exposure models, such as APEX and SHEDS, are applied for PM exposure risk assessment among the population. Concentrations from chemistry transport models have also been used to provide input to the stochastic exposure models at particular locations. LUR models have been applied for individual exposures at the intra-urban scale to examine exposure to pollution surrogates, such as traffic counts, land use, or topographic variables. Source proximity and kriging have also been applied. GIS-based models have been used to model exposure over large regions (e.g., for the Nurse's Health Study) using spatial smoothing models of AQS data and incorporating GIS-based and meteorological covariates. GIS approaches have also been used for intra-urban scale exposure studies. These methods all have their own uses and caveats. LUR is an adaptable framework allowing adaptation to localized conditions but might best be applied in relatively spatially homogeneous areas. In a comparison of LUR with kriging, kriging produced slightly attenuated mortality risk estimates for New York City, while for Los Angeles,

kriging did not exhibit as much spatial variability as LUR. Source proximity modeling is relatively simple to apply but is limited because other confounding covariates, such as socioeconomic status, may be related to source proximity. Additionally, source proximity models do not incorporate time-activity data.

New advancements in personal and microenvironmental monitoring techniques have been reported. Personal monitoring developments include new models of cascade impactors and cyclones to sample in the UF size range and miniature monitors for species detection. Additionally, new work on microenvironmental modeling using mobile platforms and GPS technology has been reported. The reader is referred to the 2004 PM AQCD (U.S. EPA, 2004, [056905](#)) for descriptions of most real-time and filter-based personal and microenvironmental PM monitors currently available.

3.9.2.2. Spatial Scales of PM Exposure Assessment

Assessing population-level exposure at the urban scale is particularly relevant for time-series epidemiologic studies, which provide information on the relationship between health effects and community-average exposure, rather than variations in individual exposure. The correlation between the PM concentration measured at a central-site community ambient monitor and the true community average concentration depends on the spatial distribution of the PM, location of the monitoring site chosen to represent the community average, and division of the community by terrain features or source locations into several sub-communities that differ in the temporal pattern of pollution. Concentrations of SO_4^{2-} and some components of SOA measured at central-site monitors are expected to be uniform in urban areas given the regional nature of their sources. However, this is not true for primary components like EC whose sources are strongly spatially variable in urban areas. Given that roughly 90% of an individual's day is spent indoors, assessment of exposure to infiltrated ambient SO_4^{2-} , whose formation and dispersion also occurs over urban-to-regional scales and whose size distribution is in the accumulation mode, is commonly used to assess ambient $\text{PM}_{2.5}$ exposure. This technique has also been applied to assess $\text{PM}_{10-2.5}$ exposure but likely with more error than for $\text{PM}_{2.5}$ because $\text{PM}_{10-2.5}$ is more highly spatially variable than $\text{PM}_{2.5}$. Source apportionment techniques have also been applied to assess urban-scale $\text{PM}_{2.5}$ exposures using community-based ambient monitoring, outdoor, and indoor samples.

At micro-to-neighborhood scales, heterogeneity of sources and topography may cause more variability in exposure. This is particularly true for $\text{PM}_{10-2.5}$ and for UFPs, both of which are more highly spatially variable than $\text{PM}_{2.5}$. Particle chemistry and source behavior also contribute to spatial heterogeneity of PM concentration. Some studies, conducted mainly in Europe, have found personal $\text{PM}_{2.5}$ and PM_{10} exposures for pedestrians in street canyons to be higher than ambient concentrations measured by urban background ambient monitors. Likewise, microenvironmental UFP concentrations were observed to be substantially higher in near-road environments, street canyons, and tunnels when compared with other environments in urban areas. In-vehicle UFP exposures can also be important. As a result, ambient monitors located at background, central urban, road side, or near-residential sites might not reflect peak exposures to individuals who commute.

PM infiltration factors, F_{inf} , depend on particle size, chemical composition, season, and region of the country. Infiltration can best be modeled dynamically based on a distribution of air exchange and deposition PM loss rates rather than being represented by a single value. There is significant variability within and across regions of the country with respect to indoor exposures to ambient PM. Infiltrated ambient PM concentrations depend in part on the ventilation properties of the building or vehicle in which the person is exposed. Season is important to PM infiltration because it affects the ventilation practices used, and ambient temperature and humidity conditions affect the transport, dispersion, and size distribution of PM. Residential air exchange rates have been observed to be higher in summer for regions with low air conditioning usage, and regional differences in air exchange rates (Southwest < Southeast < Northeast < Northwest) also reflect ventilation practices. Differential infiltration occurs as a function of PM size and composition. PM infiltration is largest for accumulation mode particles, and decreases for UFPs lost to diffusion and for coarse PM lost through inertial impaction mechanisms. Differential infiltration by size fraction can affect exposure estimates if not properly characterized.

3.9.2.3. Multicomponent and Multipollutant PM Exposures

Emission inventories and source apportionment studies suggest that sources of PM exposure vary by region. Comparison of studies performed in the eastern U.S. with studies performed in the western U.S. suggest that the contribution of SO_4^{2-} to personal exposure is higher for the East (16-46%) compared with the West (~4%) and that motor vehicle emissions and secondary NO_3^- are larger sources of personal exposure for the West (~9%) as compared with the East (~4%). Results of source apportionment studies of personal exposure to SO_4^{2-} indicate that personal SO_4^{2-} exposures are mainly attributable to ambient sources. Source apportionment for OC and EC is difficult because they originate from both indoor and outdoor sources. Exposure to OC of indoor and outdoor origin can be distinguished by the presence of aliphatic C-H groups generated indoors, since outdoor concentrations of aliphatic C-H are low. Trace metal studies have shown variable results regarding personal exposure to ambient constituents with significant variation among cities and over seasons that can be related to incinerator operation, fossil fuel combustion, biomass combustion (wildfires), and presence of crustal materials in the built environment, among other sources. Differential infiltration is also affected by variations in particle composition and volatility. For example EC infiltrates more readily than OC. This can lead to outdoor-indoor differentials in PM toxicity.

A number of studies have examined whether gaseous copollutants could act as surrogates for exposure to ambient PM. Several studies have concluded that ambient concentrations of O_3 , NO_2 , and SO_2 are associated with the ambient component of personal exposure to total $\text{PM}_{2.5}$ as opposed to the ambient component of personal exposures to the gases. However, in some studies this result may have arisen in part because personal exposure to the gases was often beneath the detection limits of the personal monitoring devices. Thus, the evidence that ambient gases can be considered surrogates of $\text{PM}_{2.5}$ exposure is mixed. It is likely that associations between ambient gases and personal exposure to $\text{PM}_{2.5}$ of ambient origin exist, but they are complex and vary by season and location.

3.9.2.4. Implications for Epidemiologic Studies

The importance of exposure error varies with study design based on the spatial and temporal aspects of the design. For PM epidemiology studies, source characteristics, particle size distribution, and particle composition are also important factors in interpreting exposure error for an epidemiology study. Potential sources of error that could influence estimates of PM exposure include measurements, use of surrogates for PM exposure, modeling, spatial variability, temporal variability, and compositional differences.

PM exposure estimates are subject to monitoring and modeling errors. Ambient and personal exposure monitoring errors can bias health effects estimates if the error is strongly correlated with the measurements of concentration. This can be an issue for sampling semi-volatile organic compounds in PM, especially where PM exposures in cities with different PM composition are compared. Ambient monitor height also affects estimates of exposure because PM concentration varies as a function of height. Within a street canyon, changes in wind direction and speed cause significant variability over a small distance. Wind tunnel studies have shown street canyon effects exist for suburban settings as well as for heavily urbanized settings. Additionally, model-based exposure estimates are subject to errors related to the spatial resolution of the modeling technique and the measurement-based inputs used.

Variations in PM and its components could lead to errors in using ambient PM measures as surrogates for PM exposure. $\text{PM}_{2.5}$ concentrations are relatively well-correlated across monitors in the urban areas examined. Correlation coefficients tend to be lower, and concentration differences tend to be higher between PM_{10} monitoring sites than between $\text{PM}_{2.5}$ monitoring sites. Likewise, studies have shown UFPs to be more spatially variable across urban areas. Even if $\text{PM}_{2.5}$, $\text{PM}_{10-2.5}$, and UFP concentrations measured at sites within an urban area are highly correlated, significant differences in their concentrations can occur on any given day. The degree of urban-scale spatial variability in PM concentrations varies across the country and with size fraction. Current information suggests that UFPs, $\text{PM}_{10-2.5}$, and many PM components are more spatially variable than $\text{PM}_{2.5}$. These factors should be considered in using data obtained from monitoring networks to estimate community-scale human exposure to ambient PM, and caution should be exercised in extrapolating conclusions obtained from one urban area to another.

Community time-series epidemiologic studies use the average community PM concentration as a surrogate for the average personal exposure to ambient PM. The resulting health effect risk estimate, based on the average community ambient concentration, differs from the risk that would be estimated if the average community ambient exposure were used in the epidemiologic study. However, the risk estimate based on the ambient concentration gives the change in health effects resulting from a change in ambient PM concentration and is, therefore, an appropriate measure for risk assessment and risk management. Variations in ambient concentrations across a community, variations in individual ambient exposures around the community average, and seasonal or daily variation in the ambient exposure estimate may increase standard errors of PM health effects estimates, making it more difficult to detect a true underlying association between the correct exposure metric and the health outcome studied. Likewise, sampling time interval and lag time selection both determine whether an epidemiologic model captures the phenomena of interest with sufficient resolution. The use of the community average ambient PM_{2.5} concentration as a surrogate for the community average personal exposure to ambient PM_{2.5} is not expected to change the principal conclusions from PM_{2.5} epidemiologic studies that use community average health and pollution data. Several recent studies support this by showing how the ambient component of personal exposure to PM_{2.5} could be estimated using various tracer and source apportionment techniques and that it is highly correlated with ambient concentrations of PM_{2.5}. These studies also show that the non-ambient component of personal exposure to PM_{2.5} is basically uncorrelated with ambient PM_{2.5} concentrations. For long-term studies that use differences in long-term community average ambient PM concentrations as an exposure metric, the effect of possible community-to-community differences in the average ambient exposure factor or in the average non-ambient exposure are less understood. For panel epidemiologic studies, the most appropriate exposure metric may depend on the health outcome measured. However, sufficient information should be obtained to enable determining the association of the health outcome with ambient concentration, ambient exposure, non-ambient exposure, and total personal exposure.

Exposure error may occur if a measured PM component acts as a surrogate for another PM constituent. Differences between composition of outdoor and indoor ambient PM may also cause error in exposure assessment related either to differential losses of UF or coarse PM from diffusion, evaporation of semi-volatile PM, or impaction. The resulting differences in PM size distribution and chemical composition between indoor-ambient PM and outdoor-ambient PM are expected to cause differences in toxicity that could affect health outcomes. Lack of information regarding these relationships adds uncertainty to the health effects estimate.

Chapter 3 References

- ACGIH (2005). TLVs and BEIs: Based on the documentation of the threshold limit values for chemical substances and physical agents and biological exposure indices. American Conference of Governmental Industrial Hygienists. Cincinnati, Ohio. [156188](#)
- Adams HS; Nieuwenhuijsen MJ; Colvile RN; McMullen MAS; Khandelwal P (2001). Fine particle (PM_{2.5}) personal exposure levels in transport microenvironments, London, UK. *Sci Total Environ*, 279: 29-44. [019350](#)
- Adar SD; Davey M; Sullivan JR; Compher M; Szpiro A; Liu L-J (2008). Predicting airborne particle levels aboard Washington State school buses. *Atmos Environ*, 42: 7590-7599. [191200](#)
- Adgate JL; Mongin SJ; Pratt GC; Zhang J; Field MP; Ramachandran G; Sexton K (2007). Relationships between personal, indoor, and outdoor exposures to trace elements in PM_{2.5}. *Sci Total Environ*, 386: 21-32. [156196](#)
- Al-Horr R; Samanta G; Dasgupta PK (2003). A Continuous Analyzer for Soluble Anionic Constituents and Ammonium in Atmospheric Particulate Matter. *Environ Sci Technol*, 37: 5711-5720. [153951](#)
- Albinet A; Leoz-Garziandia E; Budzinski H; Villenave E (2007). Sampling precautions for the measurement of nitrated polycyclic aromatic hydrocarbons in ambient air. *Atmos Environ*, 41: 4988-4994. [154426](#)
- Alexis A; Garcia A; Nystrom M; Rosenkranz K (2001). The 2001 California almanac of emissions and air quality. Retrieved 10-AUG-05, from <http://www.arb.ca.gov/aqd/almanac/almanac01/almanac01.htm>. [079886](#)
- Allen GA; Harrison D; Koutrakis P (2001). A New Method for Continuous Measurement of Sulfate in the Ambient Atmosphere. Presented at American Association for Aerosol Research, 20th Annual Conference. [156205](#)
- Allen R; Larson T; Sheppard L; Wallace L; Liu L-JS (2003). Use of real-time light scattering data to estimate the contribution of infiltrated and indoor-generated particles to indoor air. *Environ Sci Technol*, 37: 3484-3492. [053578](#)
- Allen R; Wallace L; Larson T; Sheppard L; Liu LJ (2004). Estimated hourly personal exposures to ambient and nonambient particulate matter among sensitive populations in Seattle, Washington. *J Air Waste Manag Assoc*, 54: 1197-1211. [190089](#)
- Andracchio A; Cavicchi C; Tonelli D; Zappoli S (2002). A new approach for the fractionation of water-soluble organic carbon in atmospheric aerosols and cloud drops. *Atmos Environ*, 36: 5097-5107. [155657](#)
- Andreae MO; Gelencsér A (2006). Black carbon or brown carbon? The nature of light-absorbing carbonaceous aerosols. *Atmos Chem Phys*, 6: 3131-3148. [156215](#)
- Appel K; Bhave PV; Gilliland AB; Sarwar G; Roselle SJ (2008). Evaluation of the community multiscale air quality (CMAQ) model version 4.5: Sensitivities impacting model performance; Part II: particulate matter. *Atmos Environ*, 42: 6057-6066. [155660](#)
- Appel KW; Gilliland A; Eder B (2005). An operational evaluation of the 2005 release of models-3 CMAQ version 4.5. National Oceanic and Atmospheric Administration—Air Resources. Washington DC. [089227](#)
- Arhami M; Kuhn T; Fine PM; Delfino RJ; Sioutas C (2006). Effects of Sampling Artifacts and Operating Parameters on the Performance of a Semicontinuous Particulate Elemental Carbon/Organic Carbon Monitor. *Environ Sci Technol*, 40: 945-954. [156224](#)
- Arnold JR; Dennis RL; Tonnesen GS (2003). Diagnostic evaluation of numerical air quality models with specialized ambient observations: testing the Community Multiscale Air Quality modeling system (CMAQ) at selected SOS 95 ground sites. *Atmos Environ*, 37: 1185-1198. [087579](#)
- Arnott WP; Moosmüller H; Sheridan PJ; Ogren JA; Raspet R; Slaton WV; Hand JL; Kreidenweis SM; Collett JL Jr (2003). Photoacoustic and filter-based ambient aerosol light absorption measurements: Instrument comparisons and the role of relative humidity. *J Geophys Res*, 108: AAC 15-1. [037711](#)

Note: Hyperlinks to the reference citations throughout this document will take you to the NCEA HERO database (Health and Environmental Research Online) at <http://epa.gov/hero>. HERO is a database of scientific literature used by U.S. EPA in the process of developing science assessments such as the Integrated Science Assessments (ISA) and the Integrated Risk Information System (IRIS).

- Artinano B; Querol X; Salvador P; Rodriguez S; Alonso DG; Alastuey A (2001). Assessment of airborne particulate levels in Spain in relation to the new EU-directive. *Atmos Environ*, 35: S43-S53. [190099](#)
- Auvray M; Bey I (2005). Long-range transport to Europe: Seasonal variations and implications for the European ozone budget. *J Geophys Res*, 110: D11303.1-D11303.22. [156237](#)
- Ayers GP (2004). Potential for simultaneous measurement of PM10, PM25 and PM1 for air quality monitoring purposes using a single TEOM. *Atmos Environ*, 38: 3453-3458. [097440](#)
- Bae MS (2007). Intercomparison of Real Time Ammonium Measurements at Urban and Rural Locations in New York. *Aerosol Sci Technol*, 41: 329-341. [155669](#)
- Bae MS; Schauer JJ; Deminter JT; Turner JR (2004). Hourly and daily patterns of particle-phase organic and elemental carbon concentrations in the urban atmosphere. *J Air Waste Manag Assoc*, 54: 823-833. [156243](#)
- Bae MS; Schwab JJ; Zhang Q; Hogrefe O; Demerjian KL; Weimer S; Rhoads K; Orsini D; Venkatachari P; Hopke PK (2007). Interference of organic signals in highly time resolved nitrate measurements by low mass resolution aerosol mass spectrometry. *J Geophys Res*, 112: D22305-D22305 (1-16). [156244](#)
- Baldauf R; Thoma E; Hays M; Shores R; Kinsey J; Gullett B; Kimbrough S; Isakov V; Long T; Snow R; Khlystov A; Weinstein J; Chen FL; Seila R; Olson D; Gilmour I; Cho SH; Watkins N; Rowley P; Bang J (2008). Traffic and meteorological impacts on near-road air quality: Summary of methods and trends from the Raleigh near-road study. *J Air Waste Manag Assoc*, 58: 865-878. [190239](#)
- Baldauf R; Thoma E; Khlystov A; Isakov V; Bowker G; Long T; Snow R (2008). Impacts of noise barriers on near-road air quality. *Atmos Environ*, 42: 7502-7507. [191017](#)
- Baldauf R; Watkins N; Heist D; Bailey C; Rowley P; Shores R (2009). Near-road air quality monitoring: Factors affecting network design and interpretation of data. *Air Qual. Atmos. Health*, 2: 1-9. [191766](#)
- Baldauf RW; Gabele P; Crews W; Snow R; Cook JR (2005). Criteria and air-toxic emissions from in-use automobiles in the national low-emission vehicle program. *J Air Waste Manag Assoc*, 55: 1263-1268. [191184](#)
- Barn P; Larson T; Noullett M; Kennedy S; Copes R; Brauer M (2008). Infiltration of forest fire and residential wood smoke: an evaluation of air cleaner effectiveness. *J Expo Sci Environ Epidemiol*, 18: 503-511. [156252](#)
- Barreto RP; Albuquerque FC; Netto ADP (2007). Optimization of an improved analytical method for the determination of 1-nitropyrene in milligram diesel soot samples by high-performance liquid chromatography–mass spectrometry. *J Chromatogr A*, 1163: 219-227. [155676](#)
- Bauer H; Schueller E; Weinke G; Berger A; Hitzemberger R; Marr I; Puxbaum H (2008). Significant contributions of fungal spores to the organic carbon and to the aerosol mass balance of the urban atmospheric aerosol. *Atmos Environ*, 42: 5542-5549. [189986](#)
- Baxter LK; Barzyk TM; Vette VF; Croghan C; Williams RW (2008). Contributions of diesel truck emissions to indoor elemental carbon concentrations in homes in proximity to Ambassador Bridge. *Atmos Environ*, 42: 9080-9086. [191194](#)
- Baxter LK; Clougherty JE; Laden F; Levy JI (2007). Predictors of concentrations of nitrogen dioxide, fine particulate matter, and particle constituents inside of lower socioeconomic status urban homes. *J Expo Sci Environ Epidemiol*, 17: 433-444. [092726](#)
- Baxter LK; Clougherty JE; Paciorek CJ; Wright RJ; Levy JI (2007). Predicting residential indoor concentrations of nitrogen dioxide, fine particulate matter, and elemental carbon using questionnaire and geographic information system based data. *Atmos Environ*, 41: 6561-6571. [092725](#)
- Behrentz E; Fitz DR; Pankratz DV; Sabin LD; Colome SD; Fruin SA; Winer AM (2004). Measuring self-pollution in school buses using a tracer gas technique. *Atmos Environ*, 38: 3735-3746. [155682](#)
- Bein KJ; Zhao Y; Wexler AS; Johnston MV (2005). Speciation of size-resolved individual ultrafine particles in Pittsburgh, Pennsylvania. *J Geophys Res*, 110: D07S05. [156265](#)
- Bell ML; Dominici F; Ebisu K; Zeger SL; Samet JM (2007). Spatial and Temporal Variation in PM2.5 Chemical Composition in the United States for Health Effects Studies. *Environ Health Perspect*, 115: 989-995. [155683](#)
- Bell ML; Ebisu K; Peng RD; Dominici F (2009). Adverse health effects of particulate air pollution: modification by air conditioning. *Epidemiology*, 20: 682-686. [191007](#)

- Bell ML; Ebisu K; Peng RD; Walker J; Samet JM; Zeger SL; Dominic F (2008). Seasonal and regional short-term effects of fine particles on hospital admissions in 202 U.S. counties, 1999-2005. *Am J Epidemiol*, 168: 1301-1310. [156266](#)
- Bell ML; Kim JY; Dominici F (2007). Potential confounding of particulate matter on the short-term association between ozone and mortality in multisite time-series studies. *Environ Health Perspect*, 115: 1591-1595. [093256](#)
- Benkovitz CM; Scholtz MT; Pacyna J; Tarrason L; Dignon J; Voldner EC; Spiro PA; Logan JA; Graedel TE (1996). Global gridded inventories of anthropogenic emissions of sulfur and nitrogen: North Atlantic Regional Experiment(NARE). *J Geophys Res*, 101: 29239-29253. [156267](#)
- Bennett DH; Koutrakis P (2006). Determining the infiltration of outdoor particles in the indoor environment using a dynamic model. *J Aerosol Sci*, 37: 766-785. [089184](#)
- Binkowski F; Roselle S (2003). Models-3 Community Multiscale Air Quality(CMAQ) model aerosol component 1. Model description. *J Geophys Res*, 108: 4183. [191769](#)
- Binkowski FS; Arunachalam S; Adelman Z; Pinto JP (2007). Examining photolysis rates with a prototype online photolysis module in CMAQ. *J Appl Meteor Climatol*, 46: 1252-1256. [090563](#)
- Biswas S; Hu S; Verma V; Herner J; Robertson W; Ayala A; Sioutas C (2008). Physical properties of particulate matter (PM) from late model heavy-duty diesel vehicles operating with advanced PM and NOx emission control technologies. *Atmos Environ*, 42: 5622-5634. [189969](#)
- Biswas S; Verma V; Schauer JJ; Sioutas C (2009). Chemical speciation of PM emissions from heavy-duty diesel vehicles equipped with diesel particulate filter (DPF) and. *Atmos Environ*, 43: 1917-1925. [189880](#)
- Blanchard P; Brook JR; Brazil P (2002). Chemical characterization of the organic fraction of atmospheric aerosol at two sites in Ontario, Canada. *J Geophys Res*, 107: ICC10.1-ICC10.8 . [047598](#)
- Blando JD; Turpin BJ (2000). Secondary organic aerosol formation in cloud and fog droplets: a literature evaluation of plausibility. *Atmos Environ*, 34: 1623-1632. [155692](#)
- Bond TC; Streets DG; Yarber KF; Nelson SM; Woo J-H; Klimont Z (2004). A technology-based global inventory of black and organic carbon emissions from combustion. *J Geophys Res*, 109: D14203. [056389](#)
- Borak J; Sirianni G; Cohen HJ; Chemerynski S; Wheeler R (2003). Comparison of NIOSH 5040 Method versus Aethalometer™ to Monitor Diesel Particulate in School Buses and at Work Sites. *AIHA J*, 64: 260-268. [156284](#)
- Borrego C; Tchepel O; Costa AM; Martins H; Ferreira J; Miranda AI (2006). Traffic-related particulate air pollution exposure in urban areas. *Atmos Environ*, 40: 7205-7214. [155697](#)
- Bortnick SM; Coutant BW; Eberly SI (2002). Using continuous PM2.5 monitoring data to report an air quality index. *J Air Waste Manag Assoc*, 52: 104-112. [156285](#)
- Brauer M; Hoek G; van Vliet P; Meliefste K; Fischer P; Gehring U; Heinrich J; Cyrus J; Bellander T; Lewne M; Brunekreef B (2003). Estimating long-term average particulate air pollution concentrations: application of traffic indicators and geographic information systems. *Epidemiology*, 14: 228-239. [155702](#)
- Braun A (2009). Two-process model for the atmospheric weathering, oxidation and ageing of diesel soot. *Geophys Res Lett*, 36: L07810. [189997](#)
- Briggs D (2000). Exposure assessment. In *Spatial Epidemiology: Methods and Applications* (pp. 335-359). Oxford: Oxford University Press. [191772](#)
- Briggs DJ; Collins S; Elliott P; Fischer P; Kingham S; Lebreton E; Pyl K; Van Reeuwijk H; Smallbone K; Van Der Veen A (1997). Mapping urban air pollution using GIS: a regression-based approach. *Int J Geogr Inform Sci*, 11: 699-718. [025950](#)
- Briggs DJ; de Hoogh K; Morris C; Gulliver J (2008). Effects of travel mode on exposures to particulate air pollution. *Environ Int*, 34: 12-22. [156294](#)
- Brock CA; Hudson PK; Lovejoy ER; Sullivan A; Nowak JB; Huey LG; Cooper OR; Cziczo DJ; de Gouw J; Fehsenfeld FC (2004). Particle characteristics following cloud-modified transport from Asia to North America. *J Geophys Res*, 109: D23S26. [156295](#)
- Brook JR; Sirois A; Clarke JF (1996). Comparison of dry deposition velocities for SO₂, HNO₃, and SO₄(²⁻) estimated with two inferential models. *Water Air Soil Pollut*, 87: 205-218. [024023](#)

- Brown AS; Yardley RE; Quincey PG; Butterfield DM (2006). Studies of the effect of humidity and other factors on some different filter materials used for gravimetric measurements of ambient particulate matter. *Atmos Environ*, 40: 4670-4678. [097665](#)
- Bruno P; Caselli M; de Gennaro G; Tutino M (2007). Determination of polycyclic aromatic hydrocarbons (PAHs) in particulate matter collected with low volume samplers. *Talanta*, 72: 1357-1361. [155706](#)
- Burke JM; Zufall MJ; Ozkaynak H (2001). A population exposure model for particulate matter: case study results for PM_{2.5} in Philadelphia, PA. *J Expo Sci Environ Epidemiol*, 11: 470-489. [014050](#)
- Burnett RT; Goldberg MS (2003). Size-fractionated particulate mass and daily mortality in eight Canadian cities. Health Effects Institute. Boston, MA. [042798](#)
- Buser MD; Parnell Jr CB; Shaw BW; Lacey RE (2007). Particulate matter sampler errors due to the interaction of particle size and sampler performance characteristics: Ambient PM₁₀ samplers. *Trans ASAE*, 50: 229-240. [156311](#)
- Buser MD; Parnell Jr CB; Shaw BW; Lacey RE (2007). Particulate matter sampler errors due to the interaction of particle size and sampler performance characteristics: Ambient PM_{2.5} samplers. *Trans ASAE*, 50: 241-254. [156310](#)
- Buser MD; Parnell Jr CB; Shaw BW; Lacey RE (2007). Particulate matter sampler errors due to the interaction of particle size and sampler performance characteristics: Background and Theory. *Trans ASAE*, 50: 221-228. [156312](#)
- Butler AJ; Andrew MS; Russell AG (2003). Daily sampling Of PM_{2.5} in Atlanta: Results of the first year of the Assessment of Spatial Aerosol Composition. *J Geophys Res*, 108: 8415. [156313](#)
- Buzorius G; Hameri K; Pekkanen J; Kulmala M (1999). Spatial variation of aerosol number concentration in Helsinki city. *Atmos Environ*, 33: 553-565. [081205](#)
- Bytnerowicz A; Miller PR; Olszyk DM (1987). Dry deposition of nitrate, ammonium and sulfate to a *Ceanothus crassifolius* canopy and surrogate surfaces. *Atmos Environ*, 21: 1749-1757. [036493](#)
- Byun D; Schere KL (2006). Review of the governing equations, computational algorithms, and other components of the models-3 community multiscale air quality (CMAQ) modeling system. *Appl. Mech. Rev.*, 59: 51-77. [090560](#)
- Byun DW; Ching JKS (eds) (1999). Science algorithms of the EPA models-3 community multiscale air quality (CMAQ) modeling system. U.S. Environmental Protection Agency, Office of Research and Development. Washington, DC. EPA/600-R-99-030. <http://www.epa.gov/asmdnerl/CMAQ/CMAQscienceDoc.html>. [156314](#)
- Cabada JC; Rees S; Takahama S; Khlystov A; Pandis SN; Davidson CI; Robinson AL (2004). Mass size distributions and size resolved chemical composition of fine particulate matter at the Pittsburgh supersite. *Atmos Environ*, 38: 3127-3141. [148859](#)
- Cadle SH; Mulawa P; Groblicki P; Laroo C; Ragazzi RA; Nelson K; Gallagher G; Zielinska B (2001). In-use light-duty gasoline vehicle particulate matter emissions on the FTP, REPO5, and UC cycles [final report]. [017192](#)
- Cadle SH; Mulawa PA; Hunsanger EC; Nelson K; Ragazzi RA; Barrett R; Gallagher GL; Lawson DR; Knapp KT; Snow R (1999). Composition of light-duty motor vehicle exhaust particulate matter in the Denver, Colorado area. *Environ Sci Technol*, 33: 2328-2339. [007636](#)
- Carter WPL (1990). A detailed mechanism for the gas-phase atmospheric reactions of organic compounds. *Atmos Environ*, 24: 481-518. [042893](#)
- Case MW; Williams R; Yeatts K; Chen F-L; Scott J; Svendsen E; Devlin RB (2008). Evaluation of a direct personal coarse particulate matter monitor. *Atmos Environ*, 42(19): 4446-4452. [155149](#)
- Cass GR (1998). Organic molecular tracers for particulate air pollution sources. *Trends Analyt Chem*, 17: 356-366. [155716](#)
- Cass GR; Hughes LA; Bhave P; Kleeman MJ; Allen JO; Salmon LG (2000). The chemical composition of atmospheric ultrafine particles. *Proc Biol Sci*, 358: 2581-2592. [020680](#)
- Chakrabarti B; Singh M; Sioutas C (2004). Development of a Near-Continuous Monitor for Measurement of the Sub-150 nm PM Mass Concentration. *Aerosol Sci Technol*, 38: 239-252. [157426](#)
- Chang C-H; Meroney RN (2003). Concentration and flow distributions in urban street canyons: wind tunnel and computational data. *J Wind Eng Ind Aerod*, 91: 1141-1154. [090298](#)
- Chang CT; Tsai CJ (2003). A model for the relative humidity effect on the readings of the PM₁₀ beta-gauge monitor. *J Aerosol Sci*, 34: 1685-1697. [155718](#)

- Chang L-T; Koutrakis P; Catalano PJ; Suh HH (2003). Assessing the importance of different exposure metrics and time-activity data to predict 24-h personal PM_{2.5} exposures. *J Toxicol Environ Health A Curr Iss*, 66: 1825-1846. [053789](#)
- Charron A; Harrison RM; Moorcroft S; Booker J (2004). Quantitative interpretation of divergence between PM₁₀ and PM_{2.5} mass measurement by TEOM and gravimetric (Partisol) instruments. *Atmos Environ*, 38: 415-423. [053849](#)
- Chen FL; Williams R; Svendsen E; Yeatts K; Creason J; Scott J; Terrell D; Case M (2007). Coarse particulate matter concentrations from residential outdoor sites associated with the North Carolina Asthma and Children's Environment Studies (NC-ACES). *Atmos Environ*, 41: 1200-1208. [147318](#)
- Chen LWA; Chow JC; Watson JG; Moosmuller H; Arnott WP (2004). Modeling reflectance and transmittance of quartz-fiber filter samples containing elemental carbon particles: Implications for thermal/optical analysis. *J Aerosol Sci*, 35: 765-780. [199501](#)
- Chiapello I; Moulin C; Prospero JM (2005). Understanding the long-term variability of African dust transport across the Atlantic as recorded in both Barbados surface concentrations and large-scale Total Ozone Mapping Spectrometer (TOMS) optical thickness. *J Geophys Res*, 110: D18S10. [156339](#)
- Ching J; Herwehe J; Swall J (2006). On joint deterministic grid modeling and sub-grid variability conceptual framework for model evaluation. *Atmos Environ*, 40: 4935-4945. [090300](#)
- Chow JC (2007). The application of thermal methods for determining chemical composition of carbonaceous aerosols: A review. *J Environ Sci Health A Tox Hazard Subst Environ Eng*, 42: 1521-1541. [157209](#)
- Chow JC; Doraiswamy P; Watson JG; Chen LW; Ho SS; Sodeman DA (2008). Advances in integrated and continuous measurements for particle mass and chemical composition. *J Air Waste Manag Assoc*, 58: 141-163. [156355](#)
- Chow JC; Watson JG; Chen LW; Chang MC; Robinson NF; Trimble D; Kohl S (2007). The IMPROVE_A temperature protocol for thermal/optical carbon analysis: maintaining consistency with a long-term database. *J Air Waste Manag Assoc*, 57: 1014-1023. [156354](#)
- Chow JC; Watson JG; Chen LWA; Arnott WP; Moosmuller H; Fung K (2004). Equivalence of elemental carbon by thermal/optical reflectance and transmittance with different temperature protocols. *Environ Sci Technol*, 38: 4414-4422. [156347](#)
- Chow JC; Watson JG; Louie PKK; Chen LWA; Sin D (2005). Comparison of PM_{2.5} carbon measurement methods in Hong Kong, China. *Environ Pollut*, 137: 334-344. [155728](#)
- Chow JC; Watson JG; Park K; Lowenthal DH; Robinson NF; Magliano KA (2006). Comparison of particle light scattering and fine particulate matter mass in central California. *J Air Waste Manag Assoc*, 56: 398-410. [099031](#)
- Chu D; Kaufman Y; Zibordi G; Chern J; Mao J; Li C; Holben B (2003). Global monitoring of air pollution over land from the Earth Observing System-Terra Moderate Resolution Imaging Spectroradiometer (MODIS). *J Geophys Res*, 108: 4661. [190049](#)
- Chung A; Herner JD; Kleeman MJ (2001). Detection of alkaline ultrafine atmospheric particles at Bakersfield, California. *Environ Sci Technol*, 35: 2184-2190. [017105](#)
- Claeys M; Graham B; Vas G; Wang W; Vermeylen R; Pashynska V; Cafmeyer J; Guyon P; Andreae MO; Artaxo P; Maenhaut W (2004). Formation of secondary organic aerosols through photooxidation of isoprene. *Sci New York*, 303: 1173-1176. [058608](#)
- Clarke JF; Edgerton ES; Martin BE (1997). Dry deposition calculations for the clean air status and trends network. *Atmos Environ*, 31: 3667-3678. [025022](#)
- Clough WS (1975). The deposition of particles on moss and grass surfaces. *Atmos Environ*, 9: 1113-1119. [070850](#)
- Cohen M; Adar S; Allen R; Avol E; Curl C; Gould T; Hardie D; Ho A; Kinney P; Larson T (2009). Approach to estimating participant pollutant exposures in the multi-ethnic study of atherosclerosis and air pollution (MESA Air). *Environ Sci Technol*, 43: 4687-4693. [190639](#)
- Conny JM; Klinedinst DB; Wight SA; Paulsen JL (2003). Optimizing thermal-optical methods for measuring atmospheric elemental (black) carbon: A response surface study. *Aerosol Sci Technol*, 37: 703-723. [145948](#)
- Conny JM; Norris GA; Gould TR (2009). Factorial-based response-surface modeling with confidence intervals for optimizing thermal-optical transmission analysis of atmospheric black carbon. *Anal Chim Acta*, 635: 144-156. [191999](#)

- Cooke WF; Lioussé C; Cachier H; Feichter J (1999). Construction of a 1 ° x 1 ° fossil fuel emission data set for carbonaceous aerosol and implementation and radiative impact in the ECHAM 4 model. *J Geophys Res*, 104: 22137-22162. [156365](#)
- Corburn J (2007). Urban land use, air toxics and public health: Assessing hazardous exposures at the neighborhood scale. *Environ Impact Assess Rev*, 27: 145-160. [155738](#)
- Crimmins BS; Baker JE (2006). Improved GC/MS methods for measuring hourly PAH and nitro-PAH concentrations in urban particulate matter. *Atmos Environ*, 40: 6764-6779. [097008](#)
- Crist KC; Liu B; Kim M; Deshpande SR; John K (2008). Characterization of fine particulate matter in Ohio: Indoor, outdoor, and personal exposures. *Environ Res*, 106: 62-71. [156372](#)
- Cyrus J; Heinrich J; Hoek G; Meliefste K; Lewne M; Gehring U; Bellander T; Fischer P; Van Vliet P; Brauer M; Wichmann HE; Brunekreef B (2003). Comparison between different traffic-related particle indicators: elemental carbon (EC), PM25 mass, and absorbance. *J Expo Sci Environ Epidemiol*, 13: 134-143. [049634](#)
- Dasch JM (1987). Measurement of dry deposition to surfaces in deciduous and pine canopies. *Environ Pollut*, 44: 261-277. [036496](#)
- Davidson CI; Wu Y-L (1990). Dry deposition of particles and vapors. In Lindberg, S. E.; Page, A. L.; Norton, S. A. (Ed.), *Acidic precipitation: v. 3, sources, deposition, and canopy interactions* New York, NY: Springer-Verlag. [036799](#)
- deCastro BR; Sax AN; Chillrud SN; Kinney PL; Spengler JD (2007). Modeling time-location patterns of inner-city high school students in New York and Los Angeles using a longitudinal approach with generalized estimating equations. *J Expo Sci Environ Epidemiol*, 17: 233-247. [190996](#)
- Decesari S; Facchini MC; Fuzzi S; Tagliavini E (2000). Characterization of water-soluble organic compounds in atmospheric aerosol: A new approach. *J Geophys Res*, 105: 1481-1489. [155748](#)
- Delfino RJ; Staimer N; Gillen D; Tjoa T; Sioutas C; Fung K; George SC; Kleinman MT (2006). Personal and ambient air pollution is associated with increased exhaled nitric oxide in children with asthma. *Environ Health Perspect*, 114: 1736-1743. [090745](#)
- Demokritou P; Lee S; Koutrakis P (2004). Development and evaluation of a high loading PM2.5 speciation sampler. *Aerosol Sci Technol*, 38: 111-119. [186901](#)
- Demokritou P; Lee SJ; Ferguson ST; Koutrakis P (2004). A compact multistage (cascade) impactor for the characterization of atmospheric aerosols. *J Aerosol Sci*, 35: 281-299. [190115](#)
- Dentener F; Stevenson D; Ellingsen K; Van Noije T; Schultz M; Amann M; Atherton C; Bell N; Bergmann D; Bey I; Bouwman L; Butler T; Cofala J; Collins B; Drevet J; Doherty R; Eickhout B; Eskes H; Fiore A; Gauss M; Hauglustaine D; Horowitz L; Isaksen ISA; Josse B; Lawrence M; Krol M; Lamarque JF; Montanaro V; Muller JF; Peuch VH; Pitari G; Pyle J; Rast S; Rodriguez J; Sanderson M; Savage NH; Shindell D; Strahan S; Szopa S; Sudo K; Van Dingenen R; Wild O; Zeng G (2006). The global atmospheric environment for the next generation. *Environ Sci Technol*, 40: 3586-3594. [088434](#)
- Derwent RG; Collins WJ; Johnson CE; Stevenson DS (2001). Transient behaviour of tropospheric ozone precursors in a global 3-D CTM and their indirect greenhouse effects. *Clim Change*, 49: 463-487. [047912](#)
- Diapouli E; Chaloulakou A; Spyrellis N (2007). Levels of ultrafine particles in different microenvironments--implications to children exposure. *Sci Total Environ*, 388: 128-136. [156397](#)
- Diapouli E; Grivas G; Chaloulakou A; Spyrellis N (2008). PM10 and ultrafine particles counts in-vehicle and on-road in the Athens area. *Water Air Soil Pollut*, 8: 89-97. [190119](#)
- Docherty KS; Wu W; Lim YB; Ziemann PJ (2005). Contributions of organic peroxides to secondary aerosol formed from reactions of monoterpenes with O₃. *Environ Sci Technol*, 39: 4049-4059. [087613](#)
- Dockery DW; Pope CA III; Xu X; Spengler JD; Ware JH; Fay ME; Ferris BG Jr; Speizer FE (1993). An association between air pollution and mortality in six US cities. *N Engl J Med*, 329: 1753-1759. [044457](#)
- Dodge MC (1977). Combined use of modeling techniques and smog chamber data to derive ozone-precursor relationships. Presented at International Conference on Photochemical Oxidant Pollution and Its Control, 09/12/1976-09/17/1976, Research Triangle Park, NC. [038646](#)

- Dominici F; Peng RD; Bell ML; Pham L; McDermott A; Zeger SL; Samet JL (2006). Fine particulate air pollution and hospital admission for cardiovascular and respiratory diseases. *JAMA*, 295: 1127-1134. [088398](#)
- Dominici F; Zeger SL; Samet JM (2000). A measurement error model for time-series studies of air pollution and mortality. *Biostatistics*, 1: 157-175. [005828](#)
- Drewnick F; Jayne JT; Canagaratna M; Worsnop DR; Demerjian KL (2004). Measurement of Ambient Aerosol Composition During the PMTACS-NY 2001 Using an Aerosol Mass Spectrometer. Part II: Chemically Speciated Mass Distributions. *Aerosol Sci Technol*, 38: 104-117. [155755](#)
- Drewnick F; Schwab J; Jayne J; Canagaratna M; Worsnop D; Demerjian K (2004). Measurement of Ambient Aerosol Composition During the PMTACS-NY 2001 Using an Aerosol Mass Spectrometer. Part I: Mass Concentrations. *Aerosol Sci Technol*, 38: 92-103. [155754](#)
- Drewnick F; Schwab JJ; Hogrefe O; Peters S; Husain L; Diamond D; Weber R; Demerjian KL (2003). Intercomparison and evaluation of four semi-continuous PM_{2.5} sulfate instruments. *Atmos Environ*, 37: 3335-3350. [099160](#)
- Dutton SJ; Williams DE; Garcia JK; Vedal S; Hannigan MP (2009). PM_{2.5} characterization for time series studies: organic molecular marker speciation methods and observations from daily measurements in Denver. *Atmos Environ*, 43: 2018-2030. [194887](#)
- Ebelt ST; Wilson WE; Brauer M (2005). Exposure to ambient and nonambient components of particulate matter: a comparison of health effects. *Epidemiology*, 16: 396-405. [056907](#)
- Eder B; Kang D; Mathur R; Yu S; Schere K (2006). An operational evaluation of the Eta-CMAQ air quality forecast model. *Atmos Environ*, 40: 4894-4905. [142721](#)
- Eder B; Yu S (2005). A performance evaluation of the 2004 release of Models-3 CMAQ. *Atmos Environ*, 40: 4811-4824. [089229](#)
- Egerton ES; Casucelo GS; Saylor RD; Lersch TL; Hartsell BE; Jansen JJ; Hansen DA (2009). Measurements of OC and EC in coarse particulate matter in the southeastern United States. *J Air Waste Manag Assoc*, 59: 78-90. [180385](#)
- Egerton ES; Hartsell BE; Saylor RD; Jansen JJ; Hansen DA; Hidy GM (2005). The Southeastern Aerosol Research and Characterization Study: Part II Filter-based measurements of fine and coarse particulate matter mass and composition. *J Air Waste Manag Assoc*, 55: 1527-1542. [088686](#)
- Edney EO; Lewandowski M; Offenberg JH; Wang W; Claeys M; Kleindienst TE; Jaoui M (2005). Formation of 2-methyl tetrols and 2-methylglyceric acid in secondary organic aerosol from laboratory irradiated isoprene/NOX/SO₂/air mixtures and their detection in ambient PM_{2.5} samples collected in the eastern United States. *Atmos Environ*, 39: 5281-5289. [155760](#)
- Eiguren-Fernandez A; Miguel AH; Jaques PA; Sioutas C (2003). Evaluation of a denuder-MOUDI-PUF sampling system to measure the size distribution of semi-volatile polycyclic aromatic hydrocarbons in the atmosphere. *Aerosol Sci Technol*, 37: 201-209. [142609](#)
- El-Zanan HS; Lowenthal DH; Zielinska B; Chow JC; Kumar N (2005). Determination of the organic aerosol mass to organic carbon ratio in IMPROVE samples. *Chemosphere*, 60: 485-496. [155764](#)
- Elgethun K; Fenske R; Yost M; Palcisko G (2003). Time-location analysis for exposure assessment studies of children using a novel global positioning system instrument. *Environ Health Perspect*, 111: 115-122. [190640](#)
- Engel-Cox JA; Weber SA (2007). Compilation and assessment of recent positive matrix factorization and UNMIX receptor model studies on fine particulate matter source apportionment for the eastern United States. *J Air Waste Manag Assoc*, 57: 1307-1316. [156419](#)
- Engewald W; Teske J; Efer J (1999). Programmed temperature vaporisers-based large volume injection in capillary gas chromatography. *J Chromatogr A*, 842: 143-161. [155765](#)
- England GC; Watson JG; Chow JC; Zielinska B; Chang M (2007). Dilution-Based Emissions Sampling from Stationary Sources: Part 2- Gas-Fired Combustors Compared with Other Fuel-Fired Systems. *J Air Waste Manag Assoc*, 57: 79-93. [156421](#)
- England GC; Watson JG; Chow JC; Zielinska B; Oliver Chang MC; Loos KR; Hidy GM (2007). Dilution-based emissions sampling from stationary sources: Part 1-Compact sampler methodology and performance. *J Air Waste Manag Assoc*, 57: 65-78. [156420](#)

- Enstrom JE (2005). Fine particulate air pollution and total mortality among elderly Californians, 1973-2002. *Inhal Toxicol*, 17: 803-816. [087356](#)
- Erisman J-W; Vermetten AWM; Asman WAH; Waijers-Ijpelaar A; Slanina J (1988). Vertical distribution of gases and aerosols: the behaviour of ammonia and related components in the lower atmosphere. *Atmos Environ*, 22: 1153-1160. [036510](#)
- Fairlie TD; Jacob DJ; Park RJ (2007). The impact of transpacific transport of mineral dust in the United States. *Atmos Environ*, 41: 1251-1266. [141923](#)
- Fan X; Brook JR; Mabury SA (2003). Sampling atmospheric carbonaceous aerosols using an integrated organic gas and particle sampler. *Environ Sci Technol*, 37: 3145-3151. [058628](#)
- Fan X; Lee PKH; Brook JR; Mabury SA (2004). Improved Measurement of Seasonal and Diurnal Differences in the Carbonaceous Components of Urban Particulate Matter Using a Denuder-Based Air Sampler. *Aerosol Sci Technol*, 38: 63-69. [155770](#)
- Farmer PB; Singh R; Kaur B; Sram RJ; Binkova B; Kalina I; Popov TA; Garte S; Taioli E; Gabelova A; Cebulska-Wasilewska A (2003). Molecular epidemiology studies of carcinogenic environmental pollutants: effects of polycyclic aromatic hydrocarbons (PAHs) in environmental pollution on exogenous and oxidative DNA damage. *Mutat Res*, 544: 397-402. [089017](#)
- Feldpausch P; Fiebig M; Fritzsche L; Petzold A (2006). Measurement of ultrafine aerosol size distributions by a combination of diffusion screen separators and condensation particle counters. *J Aerosol Sci*, 37: 577-597. [155773](#)
- Filleul L; Zeghnoun A; Cassadou S; Declercq C; Eilstein D; Le Tertre A; Medina S; Pascal L; Prouvost H; Saviuc P; Quenel P (2006). Influence of set-up conditions of exposure indicators on the estimate of short-term associations between urban pollution and mortality. *Sci Total Environ*, 355: 90-97. [089862](#)
- Fine PM; Chakrabarti B; Krudysz M; Schauer JJ; Sioutas C (2004). Diurnal Variations of Individual Organic Compound Constituents of Ultrafine and Accumulation Mode Particulate Matter in the Los Angeles Basin. *Environ Sci Technol*, 38: 1296-1304. [141283](#)
- Fine PM; Jaques PA; Hering SV; Sioutas C (2003). Performance Evaluation and Use of a Continuous Monitor for Measuring Size-Fractionated PM 2.5 Nitrate. *Aerosol Sci Technol*, 37: 342 - 354. [155775](#)
- Finlayson-Pitts BJ; Pitts JN Jr (2000). *Chemistry of the upper and lower atmosphere: theory, experiments and applications*. San Diego, CA: Academic Press. [055565](#)
- Fowler D; Cape JN; Unsworth MH (1989). Deposition of atmospheric pollutants on forests. *Proc Biol Sci*, 324: 247-265. [002515](#)
- Fowler D; Duyzer JH; Baldocchi DD (1991). Inputs of trace gases, particles and cloud droplets to terrestrial surfaces. *Proc Roy Soc Edinb B Biol*, 97: 35-59. [046630](#)
- Frank NH (2006). Retained nitrate, hydrated sulfates, and carbonaceous mass in federal reference method fine particulate matter for six eastern U.S. cities. *J Air Waste Manag Assoc*, 56: 500-11. [098909](#)
- Fraser MP; Cass GR; Simoneit BRT (1999). Particulate organic compounds emitted from motor vehicle exhaust and in the urban atmosphere. *Atmos Environ*, 33: 2715-2724. [010819](#)
- Fraser MP; Yue ZW; Buzcu B (2003). Source apportionment of fine particulate matter in Houston, TX, using organic molecular markers. *Atmos Environ*, 37: 2117-2123. [042231](#)
- Fruin S; Westerdahl D; Sax T; Sioutas C; Fine PM (2008). Measurements and predictors of on-road ultrafine particle concentrations and associated pollutants in Los Angeles. *Atmos Environ*, 42: 207-219. [097183](#)
- Fuentes M; Raftery AE (2005). Model evaluation and spatial interpolation by Bayesian combination of observations with outputs from numerical models. *Biometrics*, 61: 36-45. [087580](#)
- Fuentes M; Song HR; Ghosh SK; Holland DM; Davis JM (2006). Spatial association between speciated fine particles and mortality. *Biometrics*, 62: 855-863. [097647](#)
- Gallagher MW; Choularton TW; Morse AP; Fowler D (1988). Measurements of the size dependence of cloud droplet deposition at a hill site. *Q J Roy Meteorol Soc*, 114: 1291-1303. [046631](#)

- Gao S; Ng NL; Keywood M; Varutbangkul V; Bahreini R; Nenes A; He J; Yoo KY; Beauchamp JL; Hodyss RP; Flagan RC; Seinfeld JH (2004). Particle phase acidity and oligomer formation in secondary organic aerosol. *Environ Sci Technol*, 38: 6582-6589. [156460](#)
- Garner JHB; Pagano T; Cowling EB (1989). An evaluation of the role of ozone, acid deposition, and other airborne pollutants in the forests of eastern North America. Southeastern Forest Experiment Station, Asheville, NC. [042085](#)
- Garten CT Jr; Hanson PJ (1990). Foliar retention of 15N-nitrate and 15N-ammonium by red maple (*Acer rubrum*) and white oak (*Quercus alba*) leaves from simulated rain. *Environ Exp Bot*, 30: 333-342. [036803](#)
- Gaydos TM; Pinder R; Koo B; Fahey KM; Yarwood G; Pandis SN (2007). Development and application of a three-dimensional aerosol chemical transport model, PMCAMx. *Atmos Environ*, 41: 2594-2611. [139738](#)
- Gaydos TM; Stanier CO; Pandis SN (2005). Modeling of in situ ultrafine atmospheric particle formation in the eastern United States. *J Geophys Res*, 110: D07S12. [191762](#)
- Gelencsér A; Mészáros T; Blazsó M; Kiss G; Krivácsy Z; Molnár A; Mészáros E (2000). Structural Characterisation of Organic Matter in Fine Tropospheric Aerosol by Pyrolysis-Gas Chromatography-Mass Spectrometry. *J Atmos Chem*, 37: 173-183. [155785](#)
- Gelencser A; Varga Z (2005). Evaluation of the atmospheric significance of multiphase reactions in atmospheric secondary organic aerosol formation. *Atmos Chem Phys*, 5: 2823-2831. [156463](#)
- Geller MD; Ntziachristos L; Mamakos A; Samaras Z; Schmitz DA; Froines JR; Sioutas C (2006). Physicochemical and redox characteristics of particulate matter (PM) emitted from gasoline and diesel passenger cars. *Atmos Environ*, 40: 6988-7004. [139644](#)
- Generoso S; Bey I; Attié J-L; Bréon F-M (2007). A satellite- and model-based assessment of the 2003 Russian fires: impact on the arctic region. *J Geophys Res*, 112: 5302. [155786](#)
- Georgopoulos PG; Wang S-W; Vyas VM; Sun Q; Burke J; Vedantham R; McCurdy T; Ozkaynak H (2005). A source-to-dose assessment of population exposures to fine PM and ozone in Philadelphia, PA, during a summer 1999 episode. *J Expo Sci Environ Epidemiol*, 15: 439-457. [080269](#)
- Gery MW; Whitten GZ; Killus JP; Dodge MC (1989). A photochemical kinetics mechanism for urban and regional scale computer modeling. *J Geophys Res*, 94: 12,925-12,956. [043039](#)
- Giglio L; van der Werf GR; Randerson JT; Collatz GJ; Kasibhatla P (2006). Global estimation of burned area using MODIS active fire observations. *Atmos Chem Phys*, 6: 957-974. [156469](#)
- Gillette DA; Hanson KJ (1989). Spatial and temporal variability of dust production caused by wind erosion in the United States. *J Geophys Res*, 94: 2197-2206. [030212](#)
- Gilliam RC; Childs PP; Huber AH; Raman S (2005). Metropolitan-scale transport and dispersion from the New York World Trade Center following September 11, 2001 Part I: an evaluation of the CALMET meteorological model. *Pure Appl Geophys*, 162: 1981-2003. [056749](#)
- Gilliam RC; Huber AH; Raman S (2005). Metropolitan-scale transport and dispersion from the New York World Trade Center following September 11, 2001 Part II: an application of the CALPUFF plume model. *Pure Appl Geophys*, 162: 2005-2028. [056750](#)
- Gilliland F; Avol E; Kinney P; Jerrett M; Dvonch T; Lurmann F; Buckley T; Breyse P; Keeler G; de Villiers T; McConnell R (2005). Air pollution exposure assessment for epidemiologic studies of pregnant women and children: lessons learned from the Centers for Children's Environmental Health and Disease Prevention Research. *Environ Health Perspect*, 113: 1447-54. [098820](#)
- Gómez-Perales JE; Colville RN; Fernández-Bremauntz AA; Gutiérrez-Avedoy V; Páramo-Figueroa VH; Blanco-Jiménez S; Bueno-López E; Bernabé-Cabanillas R; Mandujano F; Hidalgo-Navarro M; Nieuwenhuijsen MJ (2007). Bus, minibus, metro inter-comparison of commuters' exposure to air pollution in Mexico City. *Atmos Environ*, 41: 890-901. [138816](#)
- Gómez-Perales JE; Colville RN; Nieuwenhuijsen MJ; Fernández-Bremauntz A; Gutiérrez-Avedoy VJ; Páramo-Figueroa VH; Blanco-Jiménez S; Bueno-López E; Mandujano F; Bernabé-Cabanillas R (2004). Commuters' exposure to PM_{2.5}, CO, and benzene in public transport in the metropolitan area of Mexico City. *Atmos Environ*, 38: 1219-1229. [054418](#)

- Gong L; Xu B; Zhu Y (2009). Ultrafine particles deposition inside passenger vehicles . *Aerosol Sci Technol*, 43: 544-553. [190124](#)
- Goriaux M; Jourdain B; Temime B; Besombes JL; Marchand N; Albinet A; Leoz-Garziandia E; Wortham H (2006). Field comparison of particulate PAH measurements using a low-flow denuder device and conventional sampling systems. *Environ Sci Technol*, 40: 6398-6404. [156484](#)
- Gouw Jd; Brock C; Atlas E; Bates T; Fehsenfeld F; Goldan P; Holloway J; Kuster W; Lerner B; Matthew B; Middlebrook A; Onasch T; Peltier R; Quinn P; Senff C; Stohl A; Sullivan A; Trainer M; Warneke C; Weber R; Williams E (2008). Sources of particulate matter in the northeastern United States in summer: 1. Direct emissions and secondary formation of organic matter in urban plumes. *J Geophys Res*, 113: D08301. [191757](#)
- Graham B; Guyon P; Taylor PE; Artaxo P; Maenhaut W; Glovsky MM; Flagan RC; Andreae MO (2003). Organic compounds present in the natural Amazonian aerosol: Characterization by gas chromatography-mass spectrometry. *J Geophys Res*, 108: 4766. [156489](#)
- Grell GA; Emeis S; Stockwell WR; Schoenemeyer T; Forkel R; Michalakes J; Knoche R; Seidl W (2000). Application of a multiscale, coupled MM5/chemistry model to the complex terrain of the VOTALP valley campaign. *Atmos Environ*, 34: 1435-1453. [048047](#)
- Grover BD; Eatough NL; Eatough DJ; Chow JC; Watson JG; Ambs JL; Meyer MB; Hopke PK; Al-Horr R; Later DW; Wilson WE (2006). Measurement of Both Nonvolatile and Semi-Volatile Fractions of Fine Particulate Matter in Fresno, CA. *Aerosol Sci Technol*, 40: 811-826. [138080](#)
- Grover BD; Kleinman M; Eatough NL; Eatough DJ; Cary RA; Hopke PK; Wilson WE (2008). Measurement of fine particulate matter nonvolatile and semi-volatile organic material with the Sunset Laboratory Carbon Aerosol Monitor. *J Air Waste Manag Assoc*, 58: 72-77. [156502](#)
- Grover BD; Kleinman M; Eatough NL; Eatough DJ; Hopke PK; Long RW; Wilson WE; Meyer MB; Ambs JL (2005). Measurement of total PM_{2.5} mass (nonvolatile plus semivolatile) with the Filter Dynamic Measurement System tapered element oscillating microbalance monitor. *J Geophys Res*, 110: D07S03. [090044](#)
- Gulliver J; Briggs DJ (2004). Personal exposure to particulate air pollution in transport microenvironments. *Atmos Environ*, 38: 1-8. [053238](#)
- Gulliver J; Briggs DJ (2005). Time-space modeling of journey-time exposure to traffic-related air pollution using GIS. *Environ Res*, 97: 10-25. [191079](#)
- Gulliver J; Briggs DJ (2007). Journey-time exposure to particulate air pollution. *Atmos Environ*, 41: 7195-7207. [155814](#)
- Gustafsson O; Kruså M; Zencak Z; Sheesley RJ; Granat L; Engström E; Praveen PS; Rao PS; Leck C; Rodhe H (2009). Brown clouds over South Asia: biomass or fossil fuel combustion? *Science*, 323: 495-498. [192000](#)
- Gutiérrez-Dabán A; Fernández-Espinosa AJ; Ternero-Rodríguez M; Fernández-Álvarez F (2005). Particle-size distribution of polycyclic aromatic hydrocarbons in urban air in southern Spain. *Anal Bioanal Chem*, 381: 721-736. [155818](#)
- Hagler GSW; Baldauf RW; Thoma ED; Long TR; Snow RF; Kinsey JS; Oudejans L; Gullett BK (2009). Ultrafine particles near a major roadway in Raleigh, North Carolina: Downwind attenuation and correlation with traffic-related pollutants. *Atmos Environ*, 43: 1229-1234. [191185](#)
- Hains JC; Chen L-WA; Taubman BF; Doddridge BG; Dickerson RR (2007). A side-by-side comparison of filter-based PM_{2.5} measurements at a suburban site: a closure study. *Atmos Environ*, 41: 6167-6184. [091039](#)
- Hammond DM; Lalor MM; Jones SL (2007). In-vehicle measurement of particle number concentrations on school buses equipped with diesel retrofits . *Water Air Soil Pollut*, 179: 217-225. [190135](#)
- Han Y; Cao J; Chow JC; Watson JG; An Z; Jin Z; Fung K; Liu S (2007). Evaluation of the thermal/optical reflectance method for discrimination between char-and soot-EC. *Chemosphere*, 69: 569-574. [155823](#)
- Hand JL; Kreidenweis SM (2002). A New Method for Retrieving Particle Refractive Index and Effective Density from Aerosol Size Distribution Data. *Aerosol Sci Technol*, 36: 1012-1026. [155824](#)
- Hansen K; Draaijers GPJ; Ivens WPMF; Gundersen P; van Leeuwen NFM (1994). Concentration variations in rain and canopy throughfall collected sequentially during individual rain events. *Atmos Environ*, 28: 3195-3205. [046634](#)
- Harrison D; Shik Park S; Ondov J; Buckley T; Roul Kim S; Jayanty RKM (2004). Highly time resolved fine particle nitrate measurements at the Baltimore Supersite. *Atmos Environ*, 38: 5321-5332. [136787](#)

- Harrison RM; Jones AM (2005). Multisite study of particle number concentrations in urban air. *Environ Sci Technol*, 39: 6063-6070. [191005](#)
- Hasegawa S; Hirabayashi M; Kobayashi S; Moriguchi Y; Kondo Y; Tanabe K; Wakamatsu (2005). Size Distribution and Characterization of Ultrafine Particles in Roadside Atmosphere. *J Environ Sci Health A Tox Hazard Subst Environ Eng*, 39: 2671-2690. [157355](#)
- Hays MD; Geron CD; Linna KJ; Smith ND; Schauer JJ (2002). Speciation of gas-phase and fine particle emissions from burning of foliar fuels. *Environ Sci Technol*, 36: 2281-2295. [026104](#)
- Hays MD; Lavrich RJ (2007). Developments in direct thermal extraction gas chromatography-mass spectrometry of fine aerosols. *Trends Analyt Chem*, 26: 88-102. [155831](#)
- Heald C; Spracklen D (2009). Atmospheric budget of primary biological aerosol particles from fungal sources. *Geophys Res Lett*, 36: L09806. [190014](#)
- HEI (2009). Traffic-related air pollution: A critical review of the literature on emissions, exposure, and health effects. Health Effects Institute. Boston. Special Report 17. [191009](#)
- Henderson R (2005). Clean Air Scientific Advisory Committee (CASAC) review of the EPA staff recommendations concerning a Potential Thoracic Coarse PM standard in the Review of the National Ambient Air Quality Standards for Particulate Matter: Policy Assessment of Scientific and Technical Information. U.S. Environmental Protection Agency. Washington, DC. [156537](#)
- Henderson R (2009). Clean Air Scientific Advisory Committee (CASAC) letter to the Administrator: Consultation on monitoring issues related to the NAAQS for particulate matter. U.S. Environmental Protection Agency. Washington, DC. EPA-CASAC-09-006. [192001](#)
- Henry RC (1997). History and fundamentals of multivariate air quality receptor models. *Chemometr Intell Lab Syst*, 37: 37-42. [020941](#)
- Hering S; Fine PM; Sioutas C; Jaques PA; Ambs JL; Hogrefe O; Demerjian KL (2004). Field assessment of the dynamics of particulate nitrate vaporization using differential TEOM® and automated nitrate monitors. *Atmos Environ*, 38: 5183-5192. [155837](#)
- Hering SV (2007). Using Regional Data and Building Leakage to Assess Indoor Concentrations of Particles of Outdoor Origin. *Aerosol Sci Technol*, 41: 639-654. [155839](#)
- Hering SV; Stolzenburg MR; Quant FR; Oberreit DR; Keady PB (2005). A Laminar-Flow, Water-Based Condensation Particle Counter (WCPC). *Aerosol Sci Technol*, 39: 659-672. [155838](#)
- Hermann M; Wehner B; Bischof O; Han HS; Krinke T; Liu W; Zerrath A; Wiedensohler A (2007). Particle counting efficiencies of new TSI condensation particle counters. *J Aerosol Sci*, 38: 674-682. [155840](#)
- Herner JD; Aw J; Gao O; Chang DP; Kleeman MJ (2005). Size and composition distribution of airborne particulate matter in Northern California: I - Particulate mass, carbon, and water-soluble ions. *J Air Waste Manag Assoc*, 55: 30-51. [135983](#)
- Ho KF; Cao JJ; Harrison RM; Lee SC (2004). Indoor/outdoor relationships of organic carbon (OC) and elemental carbon (EC) in PM_{2.5} in roadside environment of Hong Kong. *Atmos Environ*, 38: 6327-6335. [056804](#)
- Hoek G; Beelen R; de Hoogh K; Vienneau D; Gulliver J; Fischer P; Briggs D (2008). A review of land-use regression models to assess spatial variation of outdoor air pollution. *Atmos Environ*, 42: 7561-7578. [195851](#)
- Hogrefe C; Hao W; Civerolo K; Ku JY; Sistla G; Gaza RS; Sedefian L; Schere K; Gilliland A; Mathur R (2007). Daily Simulation of Ozone and Fine Particulates over New York State: Findings and Challenges. *J Appl Meteor Climatol*, 46: 961-979. [156561](#)
- Hogrefe O; Schwab JJ; Drewnick F; Lala GG; Peters S; Demerjian KL; Rhoads K; Felton HD; Rattigan OV; Husain L; Dutkiewicz VA (2004). Semicontinuous PM_{2.5} sulfate and nitrate measurements at an urban and a rural location in New York: PMTACS-NY summer 2001 and 2002 campaigns. *J Air Waste Manag Assoc*, 54: 1040-1060. [099003](#)
- Hopke PK; Ramadan Z; Paatero P; Norris GA; Landis MS; Williams RW; Lewis CW (2003). Receptor modeling of ambient and personal exposure samples: 1998 Baltimore Particulate Matter Epidemiology-Exposure Study. *Atmos Environ*, 37: 3289-3302. [095544](#)

- Hosker RP Jr; Lindberg SE (1982). Review: atmospheric deposition and plant assimilation of gases and particles. *Atmos Environ*, 16: 889-910. [019118](#)
- Hsiao T-C; Chen D-R; Son SY (2009). Development of mini-cyclones as the size-selective inlet of miniature particle detectors. *J Aerosol Sci*, 40: 481-491. [191001](#)
- Hu S; Herner JD; Shafer M; Robertson W; Schauer JJ; Dwyer H; Collins J; Huai T; Ayala A (2009). Metals emitted from heavy-duty diesel vehicles equipped with advanced PM and NO_x emission controls. *Atmos Environ*, 43: 2950-2959. [189886](#)
- Huang C; Chang C; Chang S; Tsai C; Shih T; Tang D (2005). Use of porous foam as the substrate of an impactor for respirable aerosol sampling. *J Aerosol Sci*, 36: 1373-1386. [186991](#)
- Huang L; Brook JR; Zhang W; Li SM; Graham L; Ernst D; Chivulescu A; Lu G (2006). Stable isotope measurements of carbon fractions (OC/EC) in airborne particulate: A new dimension for source characterization and apportionment. *Atmos Environ*, 40: 2690-2705. [097654](#)
- Huang YL; Batterman S (2000). Selection and evaluation of air pollution exposure indicators based on geographic areas. *Sci Total Environ*, 253: 127-144. [156572](#)
- Huebert BJ; Charlson RJ (2000). Uncertainties in data on organic aerosols. *Tellus B Chem Phys Meteorol*, 52: 1249-1255. [156577](#)
- Huebert BJ; Luke WT; Delany AC; Brost RA (1988). Measurements of concentrations and dry surface fluxes of atmospheric nitrates in the presence of ammonia. *J Geophys Res*, 93: 7127-7136. [036569](#)
- Husar RB; Tratt DM; Schichtel BA; Falke SR; Li F; Jaffe D; Gasso S; Gill T; Laulainen NS; Lu F; Reheis MC; Chun Y; Westphal D; Holben BN; Gueymard C; McKendry I; Kuring N; Feldman GC; McClain C; Frouin RJ; Merrill J; DuBois D; Vignola F; Murayama T; Nickovic S; Wilson WE; Sassen K; Sugimoto N; Malm WC (2001). Asian dust events of April 1998. *J Geophys Res*, 106: 18,317-18,330. [024947](#)
- Hwang IJ; Hopke PK; Pinto JP (2008). Source apportionment and spatial distributions of coarse particles during the regional air pollution study. *Environ Sci Technol*, 42: 3524-3530. [194533](#)
- Hwang K-W; Lee J-H; Jeong D-Y; Lee C-H; Bhatnagar A; Park J-M; Kim S-H (2008). Observation of difference in the size distribution of carbon and major inorganic compounds of atmospheric aerosols after the long-range transport between the selected days of winter and summer. *Atmos Environ*, 42: 1057-1063. [134420](#)
- ICRP (1995). Human respiratory tract model for radiological protection: a report of a task group of the International Commission on Radiological Protection. *Ann ICRP*, 24: 1-482. [006988](#)
- Isakov V; Irwin JS; Ching J (2007). Using CMAQ for exposure modeling and characterizing the subgrid variability for exposure estimates. *J Appl Meteor Climatol*, 46: 1354-1371. [195880](#)
- Isakov V; Touma JS; Burke J; Lobdell DT; Palma T; Rosenbaum A; Ozkaynak H (2009). Combining regional- and local-scale air quality models with exposure models for use in environmental health studies. *J Air Waste Manag Assoc*, 59: 461-472. [191192](#)
- Isakov V; Touma JS; Khlystov A (2007). A method of assessing air toxics concentrations in urban areas using mobile platform measurements. *J Air Waste Manag Assoc*, 57: 1286-1295. [156588](#)
- Jacob DJ (1999). Introduction to atmospheric chemistry. New Jersey: Princeton University Press. [091122](#)
- Jacobson MZ (2002). Atmospheric pollution: history, science, and regulation. New York: Cambridge University Press. [090667](#)
- Jacobson MZ; Kittelson DB; Watts WF (2005). Enhanced coagulation due to evaporation and its effect on nanoparticle evolution. *Environ Sci Technol*, 39: 9486-9492. [191187](#)
- Jaffe D; Price H; Parrish D; Goldstein A; Harris J (2003). Increasing background ozone during spring on the west coast of North America. *Geophys Res Lett*, 30: 1613. [052229](#)
- Jansen KL; Larson TV; Koenig JQ; Mar TF; Fields C; Stewart J; Lippmann M (2005). Associations between health effects and particulate matter and black carbon in subjects with respiratory disease. *Environ Health Perspect*, 113: 1741-1746. [082236](#)
- Jaques PA; Ambs JL; Grant WL; Sioutas C (2004). Field evaluation of the differential TEOM monitor for continuous PM_{2.5} mass concentrations. *Aerosol Sci Technol*, 38: 49-59. [155878](#)

- Jeong CH; Hopke PK; Chalupa D; Utell M (2004). Characteristics of nucleation and growth events of ultrafine particles measured in Rochester, NY. *Environ Sci Technol*, 38: 1933-1940. [180350](#)
- Jerrett M; Arain A; Kanaroglou P; Beckerman B; Potoglou D; Sahuvaroglu T; Morrison J; Giovis C (2005). A review and evaluation of intraurban air pollution exposure models. *J Expo Sci Environ Epidemiol*, 15: 185-204. [092864](#)
- Jerrett M; Burnett RT; Ma R; Pope CA III; Krewski D; Newbold KB; Thurston G; Shi Y; Finkelstein N; Calle EE; Thun MJ (2005). Spatial analysis of air pollution and mortality in Los Angeles. *Epidemiology*, 16: 727-736. [087600](#)
- Jimenez JL; Jayne JT; Shi Q; Kolb CE; Worsnop DR; Yourshaw I; Seinfeld JH; Flagan RC; Zhang X; Smith KA (2003). Ambient aerosol sampling using the Aerodyne Aerosol Mass Spectrometer. *J Geophys Res*, 108: 8425. [156611](#)
- Johnson T; Long T; Ollison W (2000). Prediction of hourly microenvironmental concentrations of fine particles based on measurements obtained from the Baltimore scripted activity study. *J Expo Sci Environ Epidemiol*, 10: 403-411. [001660](#)
- Kahn R; Gaitley B; Martonchik J; Diner D; Crean K; Holben B (2005). Multiangle Imaging Spectroradiometer (MISR) global aerosol optical depth validation based on 2 years of coincident Aerosol Robotic Network (AERONET) observations. *J Geophys Res*, 110: D10S04. [189961](#)
- Kalberer M; Paulsen D; Sax M; Steinbacher M; Dommen J; Prevot ASH; Fisseha R; Weingartner E; Frankevich V; Zenobi R (2004). Identification of Polymers as Major Components of Atmospheric Organic Aerosols. *Science*, 303: 1659-1662. [156619](#)
- Kastner-Klein P; Plate EJ (1999). Wind-tunnel study of concentration fields in street canyons. *Atmos Environ*, 33: 3973-3979. [001961](#)
- Kaur S; Nieuwenhuijsen M; Colvile R (2005). Personal exposure of street canyon intersection users to PM_{2.5}, ultrafine particle counts and carbon monoxide in central London, UK. *Atmos Environ*, 39: 3629-3641. [086504](#)
- Kaur S; Nieuwenhuijsen MJ; Colvile RN (2005). Pedestrian exposure to air pollution along a major road in Central London, UK. *Atmos Environ*, 39: 7307-7320. [088175](#)
- Keller A; Siegmann HC (2001). The role of condensation and coagulation in aerosol monitoring. *J Expo Sci Environ Epidemiol*, 11: 441-448. [025881](#)
- Kelly JM (1988). Annual elemental input/output estimates for two forested watersheds in eastern Tennessee. *J Environ Qual*, 17: 463-468. [037379](#)
- Kenny LC; Merrifield T; Mark D; Gussman R; Thorpe A (2004). The Development and Designation Testing of a New USEPA-Approved Fine Particle Inlet: A Study of the USEPA Designation Process. *Aerosol Sci Technol*, 38: 15-22. [155895](#)
- Ketzel M; Wahlin P; Berkowicz R; Palmgren F (2003). Particle and trace gas emission factors under urban driving conditions in Copenhagen based on street and roof-level observations. *Atmos Environ*, 37: 2735-2749. [131251](#)
- Khlystov A; Stanier C; Pandis SN (2004). An Algorithm for Combining Electrical Mobility and Aerodynamic Size Distributions Data when Measuring Ambient Aerosol. *Aerosol Sci Technol*, 38: 229-238. [155897](#)
- Khlystov A; Stanier CO; Takahama S; Pandis SN (2005). Water content of ambient aerosol during the Pittsburgh Air Quality Study. *J Geophys Res*, 110: D07S10. [156635](#)
- Kidwell CB; Ondov JM (2004). Elemental Analysis of Sub-Hourly Ambient Aerosol Collections. *Aerosol Sci Technol*, 38: 205-218. [155898](#)
- Kim E; Hopke PK; Pinto JP; Wilson WE (2005). Spatial variability of fine particle mass, components, and source contributions during the regional air pollution study in St Louis. *Environ Sci Technol*, 39: 4172-4179. [083181](#)
- Kim SY; Sheppard L; Kim H (2009). Health effects of long-term air pollution: influence of exposure prediction methods. *Epidemiology*, 20: 442-50. [188446](#)
- Kinney PL; Aggarwal M; Northridge ME; Janssen NAH; Shepard P (2000). Airborne concentrations of PM_{2.5} and diesel exhaust particles on Harlem sidewalks: a community-based pilot study. *Environ Health Perspect*, 108: 213-218. [001774](#)
- Kinsey JS; Williams DC; Dong Y; Logan R (2007). Characterization of fine particle and gaseous emissions during school bus idling. *Environ Sci Technol*, 41: 4972-4979. [190073](#)

- Kiss G; Varga B; Galambos I; Ganszky I (2002). Characterization of water-soluble organic matter isolated from atmospheric fine aerosol. *J Geophys Res*, 107: 8339. [156646](#)
- Kittelson DB (1998). Engines and nanoparticles: a review. *J Aerosol Sci*, 29: 575-588. [051098](#)
- Kittelson DB; Schauer JJ; Lawson DR; Watts WF; Johnson JP (2006). On-road and laboratory evaluation of combustion aerosols-Part 2: Summary of spark ignition engine results. *J Aerosol Sci*, 37: 931-949. [156648](#)
- Kittelson DB; Watts WF; Johnson JP (2006). On-road and laboratory evaluation of combustion aerosols—Part 1: Summary of diesel engine results. *J Aerosol Sci*, 37: 913-930. [156649](#)
- Kleindienst TE; Edney EO; Lewandowski M; Offenberg JH; Jaoui M (2006). Secondary Organic Carbon and Aerosol Yields from the Irradiations of Isoprene and-Pinene in the Presence of NO_x and SO₂. *Environ Sci Technol*, 40: 3807-3812. [156650](#)
- Klepeis NE; Nelson WC; OttWR; Robinson JPTsang AM; Switzer P; Behar JV; Hern SC; Engelmann WH (2001). The National Human Activity Pattern Survey (NHAPS): a resource for assessing exposure to environmental pollutants. *J Expo Sci Environ Epidemiol*, 11: 231-252. [002437](#)
- Klouda GA; Filliben JJ; Parish HJ; Chow JC; Watson JG; Cary RA (2005). Reference material 8785: Air particulate matter on filter media. *Aerosol Sci Technol*, 39: 173-183. [130382](#)
- Koenig JQ; Mar TF; Allen RW; Jansen K; Lumley T; Sullivan JH; Trenga CA; Larson T; Liu LJ (2005). Pulmonary effects of indoor- and outdoor-generated particles in children with asthma. *Environ Health Perspect*, 113: 499-503. [087384](#)
- Kokhanovsky A; Breon F; Cacciari A; Carboni E; Diner D; Di Nicolantonio W; Grainger R; Grey W; Höller R; Lee K (2007). Aerosol remote sensing over land: a comparison of satellite retrievals using different algorithms and instruments. *Atmos Res*, 85: 372-394. [190009](#)
- Koutrakis P; Suh HH; Sarnat JA; Brown KW; Coull BA; Schwartz J (2005). Characterization of particulate and gas exposures of sensitive subpopulations living in Baltimore and Boston. Health Effects Institute. Boston, MA. 131. <http://pubs.healtheffects.org/view.php?id=91>. [095800](#)
- Krewski D; Burnett RT; Goldberg MS; Hoover K; Siemiatycki J; Jerrett M; Abrahamowicz M; White WH (2000). Reanalysis of the Harvard Six Cities study and the American Cancer Society study of particulate air pollution and mortality. Health Effects Institute. Cambridge, MA. <http://pubs.healtheffects.org/view.php?id=6>. [012281](#)
- Krewski D; Jerrett M; Burnett RT; Ma R; Hughes E; Shi Y; Turner MC; Pope AC III; Thurston G; Calle EE; Thun MJ (2009). Extended follow-up and spatial analysis of the American Cancer Society study linking particulate air pollution and mortality. Health Effects Institute. Cambridge, MA. Report Nr. 140. [191193](#)
- Krieger UK; Rupp S; Hausammann E; Peter T (2007). Simultaneous measurements of PM₁₀ and PM₁ using a single TEOM. *Aerosol Sci Technol*, 41: 975-980. [129657](#)
- Kroll JH; Seinfeld JH (2008). Chemistry of secondary organic aerosol: Formation and evolution of low-volatility organics in the atmosphere. *Atmos Environ*, 42: 3593-3624. [155910](#)
- Krudysz MA; Froines JR; Fine PM; Sioutas C (2008). Intra-community spatial variation of size-fractionated PM mass, OC, EC, and trace elements in the Long Beach, CA area. *Atmos Environ*, 42: 5374-5389. [190064](#)
- Kruize H; Hanninen O; Breugelmans O; Lebet E; Jantunen M (2003). Description and demonstration of the EXPOLIS simulation model: two examples of modeling population exposure to particulate matter. *J Expo Sci Environ Epidemiol*, 13: 87-99. [156661](#)
- Kuang C; McMurry PH; McCormick AV; Eisele FL (2008). Dependence of nucleation rates on sulfuric acid vapor concentration in diverse atmospheric locations. *J Geophys Res*, 113: D10209. [191196](#)
- Kuhn T; Biswas S; Sioutas C (2005). Diurnal and seasonal characteristics of particle volatility and chemical composition in the vicinity of a light-duty vehicle freeway. *Atmos Environ*, 39: 7154-7166. [129448](#)
- Kuhns H; Knipping EM (2005). Development of a United States-Mexico emissions inventory for the Big Bend Regional Aerosol and Visibility Observational (BRAVO) Study. *J Air Waste Manag Assoc*, 55: 677-692. [156663](#)
- Kulmala M; Laaksonen A; Pirjola L (1998). Parameterizations for sulfuric acid/water nucleation rates. *J Geophys Res*, 103: 8301-8307. [129411](#)

- Kulmala M; Mordas G; Petäjä T; Grönholm T; Aalto PP; Vehkamäki H; Hienola AI; Herrmann E; Sipilä M; Riipinen I (2007). The condensation particle counter battery (CPCB): A new tool to investigate the activation properties of nanoparticles. *J Aerosol Sci*, 38: 289-304. [155911](#)
- Kulmala M; Riipinen I; Sipilä M; Manninen HE; Petaja T; Junninen H; Maso MD; Mordas G; Mirme A; Vana M; Hirsikko A; Laakso L; Harrison RM; Hanson I; Leung C; Lehtinen KE; Kerminen VM (2007). Toward direct measurement of atmospheric nucleation. *Science*, 318: 89-92. [097838](#)
- Kulmala M; Vehkamäki H; Petaja T; Dal Maso M; Lauri A; Kerminen V-M; Birmili W; McMurry PH (2004). Formation and growth rates of ultrafine atmospheric particles: a review of observations. *J Aerosol Sci*, 35: 143-176. [089159](#)
- Kuo Y; Huang S; Shih T; Chen C; Weng Y; Lin W (2005). Development of a size-selective inlet-simulating ICRP lung deposition fraction. *Aerosol Sci Technol*, 39: 437-443. [186997](#)
- Kurniawan A; Schmidt-Ott A (2006). Monitoring the soot emissions of passing cars. *Environ Sci Technol*, 40: 1911-5. [098823](#)
- Lake DA; Tolocka MP; Johnston MV; Wexler AS (2003). Mass Spectrometry of Individual Particles between 50 and 750 nm in Diameter at the Baltimore Supersite. *Environ Sci Technol*, 37: 3268-3274. [156669](#)
- Lake DA; Tolocka MP; Johnston MV; Wexler AS (2004). The character of single particle sulfate in Baltimore. *Atmos Environ*, 38: 5311-5320. [088411](#)
- Langholz B; Ebi K; Thomas D; Peters J; London S (2002). Traffic density and the risk of childhood leukemia in a Los Angeles case-control study. *Ann Epidemiol*, 12: 482-487. [191771](#)
- Larson T; Gould T; Simpson C; Liu LJ; Claiborn C; Lewtas J (2004). Source apportionment of indoor, outdoor, and personal PM_{2.5} in Seattle, Washington, using positive matrix factorization. *J Air Waste Manag Assoc*, 54: 1175-87. [098145](#)
- Lee HM (2007). Fabrication of Reference Filter for Measurements of EC (Elemental Carbon) and OC (Organic Carbon) in Aerosol Particles. *Aerosol Sci Technol*, 41: 284-294. [155926](#)
- Lee JH; Hopke PK; Holsen TM; Lee DW; AJaques P; Sioutas C; Ambs JL (2005). Performance evaluation of continuous PM_{2.5} mass concentration monitors. *J Aerosol Sci*, 36: 95-109. [155925](#)
- Lee JH; Hopke PK; Holsen TM; Polissar AV; Lee DW; Edgerton ES; Ondov JM; Allen G (2005). Measurements of fine particle mass concentrations using continuous and integrated monitors in Eastern US Cities. *Aerosol Sci Technol*, 39: 261-275. [128139](#)
- Lee SJ; Demokritou P; Koutrakis P; Delgado-Saborit JM (2006). Development and evaluation of personal respirable particulate sampler (PRPS). *Atmos Environ*, 40: 212-224. [098249](#)
- Leith D; Sommerlatt D; Boundy MG (2007). Passive sampler for PM_{10-2.5} aerosol. *J Air Waste Manag Assoc*, 57: 332-6. [098241](#)
- Levine PM; Gong P; Levicky R; Shepard KL (2009). Real-time, multiplexed electrochemical DNA detection using an active complementary metal-oxide-semiconductor biosensor array with integrated sensor electronics. *Biosens Bioelectron*, 24: 1995-2001. [192091](#)
- Levy JI; Bennett DH; Melly SJ; Spengler JD (2003). Influence of traffic patterns on particulate matter and polycyclic aromatic hydrocarbon concentrations in Roxbury, Massachusetts. *J Expo Sci Environ Epidemiol*, 13: 364-371. [052661](#)
- Lewne M; Nise G; Lind ML; Gustavsson P (2006). Exposure to particles and nitrogen dioxide among taxi, bus and lorry drivers. *Int Arch Occup Environ Health*, 79: 220-226. [090556](#)
- Lim H-J; Turpin BJ; Edgerton E; Hering SV; Allen G; Maring H; Solomon P (2003). Semi-continuous aerosol carbon measurements: Comparison of Atlanta supersite measurements. *J Geophys Res*, 108: 8419. [037037](#)
- Lim MCH; Ayoko GA; Morawska L; Ristovski ZD; Jayaratne ER (2007). The effects of fuel characteristics and engine operating conditions on the elemental composition of emissions from heavy duty diesel buses. *Fuel*, 86: 1831-1839. [155931](#)
- Lindberg SE; Lovett GM (1985). Field measurements of particle dry deposition rates to foliage and inert surfaces in a forest canopy. *Environ Sci Technol*, 19: 238-244. [036530](#)

- Lipfert FW; Perry HM Jr; Miller JP; Baty JD; Wyzga RE; Carmody SE (2000). The Washington University-EPRI veterans' cohort mortality study: preliminary results. *Inhal Toxicol*, 4: 41-73. [004087](#)
- Lippmann M (2009). Semi-continuous speciation analyses for ambient air particulate matter: an urgent need for health effects studies. *J Expo Sci Environ Epidemiol*, 19: 235-247. [190083](#)
- Lipsky E; Robinson A (2006). Effects of dilution on fine particle mass and partitioning of semivolatile organics in diesel exhaust and wood smoke. *Environ Sci Technol*, 40: 155-162. [189891](#)
- Little P; Wiffen RD (1977). Emission and deposition of petrol engine exhaust Pb--I deposition of exhaust Pb to plant and soil surfaces. *Atmos Environ*, 11: 437-447. [070869](#)
- Liu L-J; Box M; Kalman D; Kaufman J; Koenig J; Larson T; Lumley T; Sheppard L; Wallace L (2003). Exposure assessment of particulate matter for susceptible populations in Seattle. *Environ Health Perspect*, 11: 909-918. [073841](#)
- Liu XH; Hegg DA; Stoelinga MT (2001). Numerical simulation of new particle formation over the northwest Atlantic using the MM5 mesoscale model coupled with sulfur chemistry. *J Geophys Res*, 106: 9697-9715. [048201](#)
- Lokken PR; Wellenius GA; Coull BA; Burger MR; Schlaug G; Suh HH; Mittleman MA (2009). Air Pollution and Risk of Stroke: Underestimation of Effect Due to Misclassification of Time of Event Onset. *Epidemiology*, 20: 137-142. [186774](#)
- Long CM; Suh HH; Catalano PJ; Koutrakis P (2001). Using time- and size-resolved particulate data to quantify indoor penetration and deposition behavior. *Environ Sci Technol*, 35: 2089-2099. [011526](#)
- Long RW; McClenny WA (2006). Laboratory and field evaluation of instrumentation for the semicontinuous determination of particulate nitrate (and other water-soluble particulate components). *J Air Waste Manag Assoc*, 56: 294-305. [098214](#)
- Lovett GM (1994). Atmospheric deposition of nutrients and pollutants in North America: an ecological perspective. *Ecol Appl*, 4: 629-650. [024049](#)
- Lowenthal DH; Rogers CF; Saxena P; Watson JG; Chow JC (1995). Sensitivity of estimated light extinction coefficients to model assumptions and measurement errors. *Atmos Environ*, 29: 751-766. [045134](#)
- Lu R; Turco RP; Jacobson MZ (1997). An integrated air pollution modeling system for urban and regional scales: 1. Structure and performance. *J Geophys Res*, 102: 6063-6079. [048202](#)
- Lu R; Turco RP; Jacobson MZ (1997). An integrated air pollution modeling system for urban and regional scales: 2. Simulations for SCAQS 1987. *J Geophys Res*, 102: 6081-6098. [191768](#)
- Lunden MM; Kirchstetter TW; Thatcher TL; Hering SV; Brown NJ (2008). Factors affecting the indoor concentrations of carbonaceous aerosols of outdoor origin. *Atmos Environ*, 42: 5660-5671. [155949](#)
- Lunden MM; Revzan KL; Fischer ML; Thatcher TL; Littlejohn D; Hering SV; Brown NJ (2003). The transformation of outdoor ammonium nitrate aerosols in the indoor environment. *Atmos Environ*, 37: 5633-5644. [081201](#)
- Lunden MM; Thatcher TL; Hering SV; Brown NJ (2003). The use of time- and chemically resolved particulate data to characterize the infiltration of outdoor PM_{2.5} into a residence in the San Joaquin Valley. *Environ Sci Pol*, 37: 4724-4732. [156718](#)
- Mader BT; Schauer JJ; Seinfeld JH; Flagan RC; Yu JZ; Yang H; Lim HJ; Turpin BJ; Deminter JT; Heidemann G (2003). Sampling methods used for the collection of particle-phase organic and elemental carbon during ACE-Asia. *Atmos Environ*, 37: 1435-1449. [155955](#)
- Maheswaran R; Elliott P (2003). Stroke mortality associated with living near main roads in England and Wales: a geographical study. *Stroke*, 34: 2776-2780. [125271](#)
- Mahrt L (1998). Stratified atmospheric boundary layers and breakdown of models. *Theor Comput Fluid Dynam*, 11: 263-279. [048210](#)
- Makar PA; Gravel S; Chirkov V; Strawbridge KB; Froude F; Arnold J; Brook J (2006). Heat flux, urban properties, and regional weather. *Atmos Environ*, 40: 2750-2766. [155959](#)
- Mar TF; Norris GA; Larson TV; Wilson WE; Koenig JQ (2003). Air pollution and cardiovascular mortality in Phoenix, 1995-1997. Health Effects Institute. Cambridge, MA. [042841](#)

- Maricq MM (2007). Chemical characterization of particulate emissions from diesel engines: A review. *J Aerosol Sci*, 38: 1079-1118. [155973](#)
- Martin RV; Chance K; Jacob DJ; Kurosu TP; Spurr RJD; Bucsele E; Gleason JF; Palmer PI; Bey I; Fiore AM; Li Q; Yantosca RM; Koelemeijer RBA (2002). An improved retrieval of tropospheric nitrogen dioxide from GOME. *J Geophys Res*, 107: 1-21. [089380](#)
- Massman WJ; Pederson J; Delany A; Grantz D; Denhartog G; Neumann HH; Oncley SP; Pearson R; Shaw RH (1994). An evaluation of the regional acid deposition model surface module for ozone uptake at 3 sites in the San-Joaquin valley of California. *J Geophys Res*, 99: 8281-8294. [043681](#)
- Mathis U; Mohr M; Forss AM (2005). Comprehensive particle characterization of modern gasoline and diesel passenger cars at low ambient temperatures. *Atmos Environ*, 39: 107-117. [155970](#)
- Mathur R (2008). Estimating the impact of the 2004 Alaskan forest fires on episodic particulate matter pollution over the eastern United States through assimilation of satellite-derived aerosol optical depths in a regional air quality model. *J Geophys Res*, 113: D17302. [156742](#)
- Matsumoto K; Hayano T; Uematsu M (2003). Positive artifact in the measurement of particulate carbonaceous substances using an ambient carbon particulate monitor. *Atmos Environ*, 37: 4713-4717. [124293](#)
- Matthias-Maser S; Bogs B; Jaenicke R (2000). The size distribution of primary biological aerosol particles in cloud water on the mountain Kleiner Feldberg/Taunus (FRG). *Atmos Res*, 54: 1-13. [155972](#)
- McBride SJ; Williams RW; Creason J (2007). Bayesian hierarchical modeling of personal exposure to particulate matter. *Atmos Environ*, 41: 6143-6155. [124058](#)
- McCurdy T; Glen G; Smith L; Lakkadi Y (2000). The National Exposure Research Laboratory's consolidated human activity database. *J Expo Sci Environ Epidemiol*, 10: 566-578. [000782](#)
- McDonald JD; Eide I; Seagrave J; Zielinska B; Whitney K; Lawson DR; Mauderly JL (2004). Relationship between composition and toxicity of motor vehicle emission samples. *Environ Health Perspect*, 112: 1527-1538. [087458](#)
- McKendry IG; Strawbridge KB; O'Neill NT; Macdonald AM; Liu PSK; Leitch WR; Anlauf KG; Jaegle L; Fairlie TD; Westphal DL (2007). Trans-Pacific transport of Saharan dust to western North America: A case study. *J Geophys Res*, 112: D01103. [156748](#)
- McKenna DS; Konopka P; Grooss J-U; Gunther G; Muller R; Spang R; Offermann D; Orsolini Y (2002). A new chemical Lagrangian model of the stratosphere (CLaMS) 1. formulation of advection and mixing. *J Geophys Res*, 107: 4309. [053445](#)
- McMurry PH; Fink M; Sakurai H; Stolzenburg MR; Mauldin RL III; Smith J; Eisele F; Moore K; Sjostedt S; Tanner D; Huey LG; Nowak JB; Edgerton E; Voisin D (2005). A criterion for new particle formation in the sulfur-rich Atlanta atmosphere. *J Geophys Res*, 110: 1-10. [191759](#)
- Mebust MR; Eder BK; Binkowski FS; Roselle SJ (2003). Models-3 community multiscale air quality (CMAQ) model aerosol component 2. Model evaluation. *J Geophys Res*, 108: 4184. [156749](#)
- Meng QY; Turpin BJ; Korn L; Weisel CP; Morandi M; Colome S; Zhang J; Stock T; Spektor D; Winer A; Zhang L; Lee JH; Giovanetti R; Cui W; Kwon J; Alimokhtari S; Shendell D; Jones J; Farrar C; Maberti S (2005). Influence of ambient (outdoor) sources on residential indoor and personal PM_{2.5} concentrations: analyses of RIOPA data. *J Expo Sci Environ Epidemiol*, 15: 17-28. [058595](#)
- Meng QY; Turpin BJ; Lee JH; Polidori A; Weisel CP; Morandi M; Colome S; Zhang JF; Stock T; Winer A (2007). How does infiltration behavior modify the composition of ambient PM_{2.5} in indoor spaces? An analysis of RIOPA data. *Environ Sci Tech*, 41: 7315-7321. [194618](#)
- Mensink C; De Ridder K; Deutsch F; Lefebvre F; Van de Vel K (2008). Examples of scale interactions in local, urban, and regional air quality modelling. *Atmos Res*, 89: 351-357. [155980](#)
- Mfula AM; Kukadia V; Griffiths RF; Hall DJ (2005). Wind tunnel modelling of urban building exposure to outdoor pollution. *Atmos Environ*, 39: 2737-2745. [123359](#)
- Middha P; Wexler A (2006). Design of a Slot Nanoparticle Virtual Impactor. *Aerosol Sci Technol*, 40: 737-743. [155982](#)

- Middlebrook AM; Murphy DM; Lee S-H; Thomson DS; Prather KA; Wenzel RJ; Liu D-Y; Phares DJ; Rhoads KP; Wexler AS; Johnston MV; Jimenez JL; Jayne JT; Worsnop DR; Yourshaw I; Seinfeld JH; Flagan RC (2003). A comparison of particle mass spectrometers during the 1999 Atlanta Supersites project. *J Geophys Res*, 108: 8424. [042932](#)
- Miller FJ; Gardner DE; Graham JA; Lee RE Jr; Wilson WE; Bachmann JD (1979). Size considerations for establishing a standard for inhalable particles. *J Air Waste Manag Assoc*, 29: 610-615. [070577](#)
- Miller SL; Anderson MJ; Daly EP; Milford JB (2002). Source apportionment of exposures to volatile organic compounds I Evaluation of receptor models using simulated exposure data. *Atmos Environ*, 36: 3629-3641. [030661](#)
- Misra C; Geller MD; Shah P; Sioutas C; Solomon PA (2001). Development and evaluation of a continuous coarse (PM10-PM25) particle monitor. *J Air Waste Manag Assoc*, 51: 1309-1317. [018998](#)
- Misra C; Geller MD; Sioutas C; Solomon PA (2003). Development and evaluation of a PH10 impactor-inlet for a continuous coarse particle monitor. *Aerosol Sci Technol*, 37: 271-281. [195001](#)
- Miyazaki Y; Kondo Y; Takegawa N; Komazaki Y; Fukuda M; Kawamura K; Mochida M; Okuzawa K; Weber RJ (2006). Time-resolved measurements of water-soluble organic carbon in Tokyo. *J Geophys Res*, 111: D23206. [156767](#)
- Molnár P; Johannesson S; Boman J; Barregard L; Sallsten G (2006). Personal exposures and indoor, residential outdoor, and urban background levels of fine particle trace elements in the general population. *J Environ Monit*, 8: 543-551. [156773](#)
- Moolgavkar SH (2000). Air pollution and hospital admissions for diseases of the circulatory system in three US metropolitan areas. *J Air Waste Manag Assoc*, 50: 1199-1206. [010305](#)
- Moore K; Krudysz M; Pakbin P; Hudda N; Sioutas C (2009). Intra-community variability in total particle number concentrations in the San Pedro Harbor Area (Los Angeles, California). *Aerosol Sci Technol*, 43: 587-603. [191004](#)
- Moore KF; Ning Z; Ntziachristos L; Schauer JJ; Sioutas C (2007). Daily variation in the properties of urban ultrafine aerosol-Part I: Physical characterization and volatility. *Atmos Environ*, 41: 8633-8646. [122445](#)
- Morawska L; Keogh DU; Thomas SB; Mengersen K (2007). Modality in ambient particle size distributions and its potential as a basis for developing air quality regulation. *Atmos Environ*, 42: 1617-1628. [155990](#)
- Morawska L; Ristovski Z; Jayaratne ER; Keogh DU; Ling X (2008). Ambient nano and ultrafine particles from motor vehicle emissions: Characteristics, ambient processing and implications on human exposure. *Atmos Environ*, 42: 8113-8138. [191006](#)
- Morawska L; Thomas S; Jamriska M; Johnson G (1999). The modality of particle size distributions of environmental aerosols. *Atmos Environ*, 33: 4401-4411. [007609](#)
- Mulchandani A; Chen W; Mulchandani P; Rogers KR (2001). Biosensors for direct determination of organophosphate pesticides. *Biosens Bioelectron*, 16: 225-230. [191003](#)
- Muller K; Spindler G; Maenhaut W; Hitzemberger R; Wieprecht W; Baltensperger U; ten Brink H (2004). INTERCOMP2000, a campaign to assess the comparability of methods in use in Europe for measuring aerosol composition. *Atmos Environ*, 38: 6459-6466. [097109](#)
- Murahashi T (2003). Determination of mutagenic 3-nitrobenzanthrone in diesel exhaust particulate matter by three-dimensional high-performance liquid chromatography. *Analyst*, 128: 42-5. [096539](#)
- Murphy BN; Pandis SN (2009). Simulating the formation of semivolatile primary and secondary organic aerosol in a regional chemical transport model. *Environ Sci Technol*, 43: 4722-4728. [190095](#)
- Nash DG; Tomas Baer T; Johnston MV (2006). Aerosol mass spectrometry: an introductory review. *Int J Mass Spectrom*, 258: 2-12. [199502](#)
- Nerriere E; Guegan H; Bordigoni B; Hautemaniere A; Momas I; Ladner J; Target A; Lameloise P; Delmas V; Personnaz MB; Koutrakis P; Zmirou-Navier D (2007). Spatial heterogeneity of personal exposure to airborne metals in French urban areas. *Sci Total Environ*, 373: 49-56. [156801](#)
- Ng NL; Kroll JH; Chan AWH; Chhabra PS; Flagan RC; Seinfeld JH (2007). Secondary organic aerosol formation from m-xylene, toluene, and benzene. *Atmos Chem Phys Discuss*, 7: 4085-4126. [199528](#)
- Ning Z; Geller MD; Moore KF; Sheesley R; Schauer JJ; Sioutas C (2007). Daily Variation in Chemical Characteristics of Urban Ultrafine Aerosols and Inference of Their Sources. *Environ Sci Technol*, 41: 6000-6006. [156809](#)

- Ntziachristos L; Ning Z; Geller MD; Sioutas C (2007). Particle concentration and characteristics near a major freeway with heavy-duty diesel traffic. *Environ Sci Technol*, 41: 2223-2230. [089164](#)
- Ntziachristos L; Samaras Z (2006). Combination of aerosol instrument data into reduced variables to study the consistency of vehicle exhaust particle measurements. *Atmos Environ*, 40: 6032-6042. [116722](#)
- Odman MT; Boylan JW; Wilkinson JG; Russell AG; Mueller SF; Imhoff RE; Doty KG; Norris WB; McNider RT (2002). SAMI air quality modeling: final report. [092474](#)
- Offenberg JH; Lewandowski M; Edney EO; Kleindienst TE; Jaoui M (2007). Investigation of a systematic offset in the measurement of organic carbon with a semicontinuous analyzer. *J Air Waste Manag Assoc*, 57: 596-9. [098101](#)
- Ogulei D; Hopke PK; Zhou L; Patrick Pancras J; Nair N; Ondov JM (2006). Source apportionment of Baltimore aerosol from combined size distribution and chemical composition data. *Atmos Environ*, 40: 396-410. [119973](#)
- Olfert JS; Kulkarni P; Wang J (2008). Measuring aerosol size distributions with the fast integrated mobility spectrometer. *J Aerosol Sci*, 39: 940-956. [156004](#)
- Olivier JGJ; Bouwman AF; Berdowski JJM; Veldt C; Bloos JPJ; Visschedijk AJH; van der Maas CWM; Zandveld PYJ (1999). Sectoral emission inventories of greenhouse gases for 1990 on a per country basis as well as on 1°× 1°. *Environ Sci Pol*, 2: 241-263. [156829](#)
- Olivier JGJ; Bouwman AF; Berdowski JJM; Veldt C; Bloos JPJ; Visschedijk AJH; Zandveld PYJ; Haverlag JL (1996). Description of EDGAR Version 2.0: A set of global emission inventories of greenhouse gases and ozone-depleting substances for all anthropogenic and most natural sources on a per country basis and on 1 degree x 1 degree grid. [156828](#)
- Olson DA; Burke JM (2006). Distributions of PM_{2.5} source strengths for cooking from the Research Triangle Park particulate matter panel study. *Environ Sci Technol*, 40: 163-169. [189951](#)
- Olson DA; Mcdow SR (2009). Near roadway concentrations of organic source markers. *Atmos Environ*, 43: 2862-2867. [191188](#)
- Olson DA; Norris GA (2005). Sampling artifacts in measurement of elemental and organic carbon: Low-volume sampling in indoor and outdoor environments. *Atmos Environ*, 39: 5437-5445. [156005](#)
- Orsini DA; Ma Y; Sullivan A; Sierau B; Baumann K; Weber RJ (2003). Refinements to the particle-into-liquid sampler (PILS) for ground and airborne measurements of water soluble aerosol composition. *Atmos Environ*, 37: 1243-1259. [156008](#)
- Ott DK; Cyrs W; Peters TM (2008). Passive measurement of coarse particulate matter, PM_{10-2.5}. *J Aerosol Sci*, 39: 156-167. [195004](#)
- Ott DK; Kumar N; Peters TM (2008). Passive sampling to capture spatial variability in PM₁₀₋₂₅. *Atmos Environ*, 42: 746-756. [119394](#)
- Ozkaynak H; Xue J; Zhou H; Raizenne M (1996). Associations between daily mortality and motor vehicle pollution in Toronto, Canada. U.S. Environmental Protection Agency, Office of Reserch and Development, National Exposure Research Laboratory. Research Triangle Park, NC. EPA/600/R-95/098. [073986](#)
- Paatero P; Tapper U (1994). Positive matrix factorization: a non-negative factor model with optimal utilization of error estimates of data values. *Environmetrics*, 5: 111-126. [086998](#)
- Paciorek CJ; Yanosky JD; Puett RC; Laden F; Suh HH (2009). Practical large-scale spatio-temporal modeling of particulate matter concentrations. *Ann Appl Stat*, 3: 370-397. [190090](#)
- Padro J (1996). Summary of ozone dry deposition velocity measurements and model estimates over vineyard, cotton, grass and deciduous forest in summer. *Atmos Environ*, 30: 2363-2369. [052446](#)
- Pakbin P; Ning Z; Schauer J; Sioutas C (2009). Characterization of Particle Bound Organic Carbon from Diesel Vehicles Equipped with Advanced Emission Control Technologies. *Environ Sci Technol*, 43: 4679-4686. [189893](#)
- Pandian MD; Behar JV; Ott WR; Wallace LA; Wilson AL; Colome S D (1998). Correcting errors in the nationwide data base of residential air exchange rates. *J Expo Sci Environ Epidemiol*, 8: 577-586. [090552](#)
- Pandis SN (2004). Atmospheric aerosol processes. In McMurry PH; Shepard, M; Vickery JS (Ed.), *Particulate Matter Science for Policy Makers: A NARSTO Assessment* Cambridge, UK: Cambridge University Press. [156838](#)

- Pang Y; Eatough NL; Modey WK; Eatough DJ (2002). Evaluation of the RAMS continuous monitor for determination of PM_{2.5} mass including semi-volatile material in Philadelphia, PA. *J Air Waste Manag Assoc*, 52: 563-572. [030353](#)
- Pang Y; Turpin BJ; Gundel LA (2006). On the Importance of Organic Oxygen for Understanding Organic Aerosol Particles. *Aerosol Sci Technol*, 40: 128-133. [156012](#)
- Park J; Mitchell MJ; McHale PJ; Christopher SF; Myers TP (2003). Interactive effects of changing climate and atmospheric deposition on N and S biogeochemistry in a forested watershed of the Adirondack Mountains, New York State. *Global Change Biol*, 9: 1602-1619. [156842](#)
- Park K; Chow JC; Watson JG; Trimble DL; Doraiswamy P; Arnott WP; Stroud KR; Bowers K; Bode R; Petzold A; Hansen AD (2006). Comparison of continuous and filter-based carbon measurements at the Fresno supersite. *J Air Waste Manag Assoc*, 56: 474-91. [098104](#)
- Park RJ; Stenchikov GL; Pickering; Dickerson RR; Allen DJ; Kondragunta S (2001). Regional air pollution and its radiative forcing: studies with a single column chemical and radiation transport model. *J Geophys Res*, 106: 28,751-28,770. [044169](#)
- Peltier RE; Hsu S-I; Lall R; Lippmann M (2008). Residual oil combustion: A major source of airborne nickel in New York City. *J Expo Sci Environ Epidemiol*, 19: 603-612. [197452](#)
- Peltier RE; Lippmann M (2009). Residual oil combustion: 2. Distributions of airborne nickel and vanadium within New York City. *J Expo Sci Environ Epidemiol*, TBD: 1-9. [197455](#)
- Peng RD; Dominici F; Pastor-Barriuso R; Zeger SL; Samet JM (2005). Seasonal analyses of air pollution and mortality in 100 US cities. *Am J Epidemiol*, 161: 585-594. [087463](#)
- Petäjä T; Mordas G; Manninen H; Aalto PP; Hmeri K; Kulmala M (2006). Detection efficiency of a water-based TSI condensation particle counter 3785. *Aerosol Sci Technol*, 40: 1090-1097. [156021](#)
- Peters K; Eiden R (1992). Modelling the dry deposition velocity of aerosol particles to a spruce forest. *Atmos Environ*, 26: 2555-2564. [045277](#)
- Peters TM (2006). Use of the Aerodynamic Particle Sizer to Measure Ambient PM_{10-2.5}: The Coarse Fraction of PM₁₀. *J Air Waste Manag Assoc*, 56: 411-416. [156860](#)
- Pettijohn FJ (1957). *Sedimentary rocks*. New York: Harper & Brothers. [156862](#)
- Phares DJ; Rhoads KP; Johnston MV; Wexler AS (2003). Size-resolved ultrafine particle composition analysis 2. Houston. *J Geophys Res*, 108: 8420. [156866](#)
- Phuleria HC; Geller MD; Fine PM; Sioutas C (2006). Size-Resolved emissions of organic tracers from light-and heavy-duty vehicles measured in a California roadway tunnel. *Environ Sci Technol*, 40: 4109-4118. [156867](#)
- Phuleria HC; Sheesley RJ; Schauer JJ; Fine PM; Sioutas C (2007). Roadside measurements of size-segregated particulate organic compounds near gasoline and diesel-dominated freeways in Los Angeles, CA. *Atmos Environ*, 41: 4653-4671. [117816](#)
- Pierce JR; Adams PJ (2009). Uncertainty in global CCN concentrations from uncertain aerosol nucleation and primary emission rates. *Atmos Chem Phys*, 9: 1339-1356. [191189](#)
- Pirjola L; Parviainen H; Hussein T; Valli A; Haameri K; Aalto P; Virtanen A; Keskinen J; Pakkanen TA; Maekelae T; Hillamo RE (2004). 'Sniffer': a novel tool for chasing vehicles and measuring traffic pollutants. *Atmos Environ*, 38: 3625-3635. [117564](#)
- Polidori A; Arhami M; Sioutas C; Delfino RJ; Allen R (2007). Indoor/outdoor relationships, trends, and carbonaceous content of fine particulate matter in retirement homes of the Los Angeles Basin. *J Air Waste Manag Assoc*, 57: 366-379. [156877](#)
- Polidori A; Turpin B; Meng QY; Lee JH; Weisel C; Morandi M; Colome S; Stock T; Winer A; Zhang J; Kwon J; Alimokhtari S; Shendell D; Jones J; Farrar C; Maberti S (2006). Fine organic particulate matter dominates indoor-generated PM_{2.5} in RLOPA homes. *J Expo Sci Environ Epidemiol*, 16: 321-331. [156876](#)
- Pope CA III; Burnett RT; Thun MJ; Calle EE; Krewski D; Ito K; Thurston GD (2002). Lung cancer, cardiopulmonary mortality, and long-term exposure to fine particulate air pollution. *JAMA*, 287: 1132-1141. [024689](#)

- Pope CA III; Thun MJ; Namboodiri MM; Dockery DW; Evans JS; Speizer FE; Heath CW Jr (1995). Particulate air pollution as a predictor of mortality in a prospective study of US adults. *Am J Respir Crit Care Med*, 151: 669-674. [045159](#)
- Pöschl U (2005). Atmospheric aerosols: composition, transformation, climate and health effects. *Angew Chem Weinheim Bergstr Ger*, 44: 7520-7540. [156882](#)
- Pouliot G; Pace TG; Roy B; Pierce T; Mobley D (2008). Development of a biomass burning emissions inventory by combining satellite and ground-based information. *J of Applied Remote Sensing*, 2: 021501-021517. [156883](#)
- Price M; Bulpitt S; Meyer MB (2003). A comparison of PM10 monitors at a Kerbside site in the northeast of England. *Atmos Environ*, 37: 4425-4434. [098082](#)
- Puett RC; Schwartz J; Hart JE; Yanosky JD; Speizer FE; Suh H; Paciorek CJ; Neas LM; Laden F (2008). Chronic particulate exposure, mortality, and coronary heart disease in the nurses' health study. *Am J Epidemiol*, 168: 1161-1168. [156891](#)
- Pun BK; Seigneur C; White W (2003). Day-of-week behavior of atmospheric ozone in three US cities. *J Air Waste Manag Assoc*, 53: 789-801. [047775](#)
- Qian S; Sakurai H; McMurry PH (2007). Characteristics of regional nucleation events in urban East St Louis. *Atmos Environ*, 41: 4119-4127. [116435](#)
- Qin X; Prather KA (2006). Impact of biomass emissions on particle chemistry during the California Regional Particulate Air Quality Study. *Int J Mass Spectrom*, 258: 142-150. [156895](#)
- Ramachandran G; Adgate JL; Pratt GC; Sexton K (2003). Characterizing indoor and outdoor 15 minute average PM2.5 concentrations in urban neighborhoods. *Aerosol Sci Technol*, 37: 33-45. [195017](#)
- Rattigan OV; Hogrefe O; Felton HD; Schwab JJ; Roychowdhury UK; Husain L; Dutkiewicz VA; Demerjian KL (2006). Multi-year urban and rural semi-continuous PM2.5 sulfate and nitrate measurements in New York state: Evaluation and comparison with filter based measurements. *Atmos Environ*, 40: 192-205. [115897](#)
- Rees SL; Robinson AL; Khlystov A; Stanier CO; Pandis SNSN (2004). Mass balance closure and the Federal Reference Method for PM2.5 in Pittsburgh, Pennsylvania. *Atmos Environ*, 38: 3305-3318. [097164](#)
- Reff A; Weisel CP; Zhang J; Morandi M; Stock T; Colome S; Winer A; Turpin BJ; Offenberg JH (2007). A functional group characterization of organic PM2.5 exposure: Results from the RIOPA study. *Atmos Environ*, 41: 4585-4598. [156045](#)
- Reithmeier C; Sausen R (2002). ATTLA: atmospheric tracer transport in a Lagrangian model. *Tellus Dyn Meteorol Oceanogr*, 54B: 278-299. [053447](#)
- Reponen T; Grinshpun SA; Trakumas S; Martuzevicius D; Wang Z-M; LeMasters G; Lockey JE; Biswas P (2003). Concentration gradient patterns of aerosol particles near interstate highways in the Greater Cincinnati airshed. *J Environ Monit*, 5: 557-562. [088425](#)
- Rice J (2004). Comparison of Integrated Filter and Automated Carbon Aerosol Measurements at Research Triangle Park, North Carolina. *Aerosol Sci Technol*, 38: 23-36. [156049](#)
- Riddle SG; Jakober CA; Robert MA; Cahill TM; Charles MJ; Kleeman MJ (2007). Large PAHs detected in fine particulate matter emitted from light-duty gasoline vehicles. *Atmos Environ*, 41: 8658-8668. [115272](#)
- Rigby M; Toumi R (2008). London air pollution climatology: Indirect evidence for urban boundary layer height and wind speed enhancement. *Atmos Environ*, 42: 4932-4947. [156050](#)
- Roache PJ (1998). Verification and validation in computational science and engineering. Socorro New Mexico: Hermosa Publishing. [156915](#)
- Robinson AL; Donahue NM; Rogge WF (2006). Photochemical oxidation and changes in molecular composition of organic aerosol in the regional context. *J Geophys Res*, 111: D03302. [156918](#)
- Robinson AL; Donahue NM; Shrivastava MK; Weitkamp EA; Sage AM; Grieshop AP; Lane TE; Pierce JR; Pandis SN (2007). Rethinking organic aerosols: Semivolatile emissions and photochemical aging. *Science*, 315: 1259-1262. [156053](#)

- Rossner P; Svecova V; Milcova A; Lnenickova Z; Solansky N; Sram RJ (2008). Seasonal variability of oxidative stress markers in city bus drivers - Part I. Oxidative damage to DNA. *Mutat Res Fund Mol Mech Mutagen*, 642: 14-20. [156927](#)
- Rudich Y; Donahue NM; Mentel TF (2007). Aging of Organic Aerosol: Bridging the Gap Between Laboratory and Field Studies. *Annu Rev Phys Chem*, 58: 321. [156059](#)
- Russell A; Dennis R (2000). NARSTO critical review of photochemical models and modeling. *Atmos Environ*, 34: 2283-2324. [035563](#)
- Russell M; Allen DT; Collins DR; Fraser MP (2004). Daily, seasonal and spatial trends in PM_{2.5} mass and composition in southeast Texas. *Aerosol Sci Technol*, 1: 14-26. [082453](#)
- Ryan PH; LeMasters GK (2007). A review of land-use regression models for characterizing intraurban air pollution exposure. *Inhal Toxicol*, 19: 127. [156063](#)
- Ryan PH; LeMasters GK; Levin L; Burkle J; Biswas P; Hu S; Grinshpun S; Reponen T (2008). A land-use regression model for estimating microenvironmental diesel exposure given multiple addresses from birth through childhood. *Sci Total Environ*, 404: 139-147. [156064](#)
- Rynö M; Rantanen L; Papaioannou E; Konstandopoulos AG; Koskentalo T; Savela K (2006). Comparison of pressurized fluid extraction, Soxhlet extraction and sonication for the determination of polycyclic aromatic hydrocarbons in urban air and diesel exhaust particulate matter. *J Environ Monit*, 8: 488-493. [156065](#)
- Saathoff H; Naumann KH; Schnaiter M; Schöck W; Weingartner E; Baltensperger U; Krämer L; Bozoki Z; Pöschl U; Niessner R (2003). Carbon mass determinations during the AIDA soot aerosol campaign 1999. *J Aerosol Sci*, 34: 1399-1420. [156066](#)
- Sabin LD; Kozawa K; Behrentz E; Winer AM; Fitz DR; Pankratz DV; Colome SD; Fruin SA (2005). Analysis of real-time variables affecting children's exposure to diesel-related pollutants during school bus commutes in Los Angeles. *Atmos Environ*, 39: 5243-5254. [087728](#)
- Sadezky A; Muckenhuber H; Grothe H; Niessner R; Pöschl U (2005). Raman microspectroscopy of soot and related carbonaceous materials: Spectral analysis and structural information. *Carbon N Y*, 43: 1731-1742. [097499](#)
- Sage AM; Weitkamp EA; Robinson AL; Donahue NM (2008). Evolving mass spectra of the oxidized component of organic aerosol: results from aerosol mass spectrometer analyses of aged diesel emissions. *Atmos Chem Phys*, 8: 1139-1152. [191758](#)
- Sahlodin AM; Sotudeh-Gharebagh R; Zhu Y (2007). Modeling of dispersion near roadways based on the vehicle-induced turbulence concept. *Atmos Environ*, 41: 92-102. [114058](#)
- Sakurai H; Tobias HJ; Park K; Zarling D; Docherty KS; Kittelson DB; McMurry PH; Ziemann PJ (2003). On-line measurements of diesel nanoparticle composition and volatility. *Atmos Environ*, 37: 1199-1210. [113924](#)
- Salminen K; Karlsson V (2003). Comparability of low-volume PM₁₀ sampler with β -attenuation monitor in background air. *Atmos Environ*, 37: 3707-3712. [156070](#)
- Santarpia JL; Li RJ; Collins DR (2004). Direct measurement of the hydration state of ambient aerosol populations. *J Geophys Res*, 109: D18209. [156944](#)
- Sardar SB; Fine PM; Mayo PR; Sioutas C (2005). Size-fractionated measurements of ambient ultrafine particle chemical composition in Los Angeles using the NanoMOUDI. *Environ Sci Technol*, 39: 932-944. [180086](#)
- Sardar SB; Solomon PA; Geller MD; Sioutas C (2006). Development and evaluation of a high-volume dichotomous sampler for chemical speciation of coarse and fine particles. *J Aerosol Sci*, 37: 1455-1466. [156071](#)
- Sarnat JA; Brown KW; Schwartz J; Coull BA; Koutrakis P (2005). Ambient gas concentrations and personal particulate matter exposures: implications for studying the health effects of particles. *Epidemiology*, 16: 385-395. [087531](#)
- Sarnat JA; Long CM; Koutrakis P; Coull BA; Schwartz J; Suh HH (2002). Using sulfur as a tracer of outdoor fine particulate matter. *Environ Sci Technol*, 36: 5305-5314. [037056](#)
- Sarnat JA; Schwartz J; Catalano PJ; Suh HH (2001). Gaseous pollutants in particulate matter epidemiology: Confounders or surrogates? *Environ Health Perspect*, 109: 1053-1061. [019401](#)
- Sarnat SE; Coull BA; Ruiz PA; Koutrakis P; Suh HH (2006). The influences of ambient particle composition and size on particle infiltration in Los Angeles, CA residences. *J Air Waste Manag Assoc*, 56: 186-196. [089166](#)

- Sarnat SE; Klein M; Sarnat JA; Flanders WD; Waller LA; Mulholland JA; Russell AG; Tolbert PE (2009). An examination of exposure measurement error from air pollutant spatial variability in time-series studies. *J Expo Sci Environ Epidemiol*, In Press: 1-12. [180084](#)
- Sarnat SE; Suh HH; Coull BA; Schwartz J; Stone PH; Gold DR (2006). Ambient particulate air pollution and cardiac arrhythmia in a panel of older adults in Steubenville, Ohio. *Occup Environ Med*, 63: 700-706. [090489](#)
- Sawant AA; Na K; Zhu X; Cocker K; Butt S; Song C; Cocker DR III (2004). Characterization of PM_{2.5} and selected gas-phase compounds at multiple indoor and outdoor sites in Mira Loma, California. *Atmos Environ*, 38: 6269-6278. [056798](#)
- Schauer JJ; Kleeman MJ; Cass GR; Simoneit BRT (1999). Measurement of emissions from air pollution sources 2 C₁ through C₃₀ organic compounds from medium duty diesel trucks. *Environ Sci Technol*, 33: 1578-1587. [010582](#)
- Schauer JJ; Kleeman MJ; Cass GR; Simoneit BRT (2002). Measurement of emissions from air pollution sources 5 C₁ - C₃₂ organic compounds from gasoline-powered motor vehicles. *Environ Sci Technol*, 36: 1169-1180. [035332](#)
- Schauer JJ; Rogge WF; Hildemann LM; Mazurek MA; Cass GR (1996). Source apportionment of airborne particulate matter using organic compounds as tracers. *Atmos Environ*, 30: 3837-3855. [051162](#)
- Schnelle-Kreis J; Sklorz M; Peters A; Cyrys J; Zimmermann R (2005). Analysis of particle-associated semi-volatile aromatic and aliphatic hydrocarbons in urban particulate matter on a daily basis. *Atmos Environ*, 39: 7702-7714. [112944](#)
- Schwab JJ; Felton HD; Rattigan OV; Demerjian KL (2006). New York State urban and rural measurements of continuous PM_{2.5} mass by FDMS, TEOM, and BAM: Evaluations and Comparisons with the FRM. *J Air Waste Manag Assoc*, 56: 372-83. [098449](#)
- Schwab JJ; Hogrefe O; Demerjian KL; Ambs JL (2004). Laboratory characterization of modified tapered element oscillating microbalance samplers. *J Air Waste Manag Assoc*, 54: 1254-63. [098450](#)
- Schwartz DE; Gong P; Shepard KL (2008). Time-resolved Förster-resonance-energy-transfer DNA assay on an active CMOS microarray. *Biosens Bioelectron*, 24: 383-390. [192094](#)
- Schwartz J; Sarnat JA; Coull BA; Wilson WE (2007). Effects of exposure measurement error on particle matter epidemiology: a simulation using data from a panel study in Baltimore, MD. *J Expo Sci Environ Epidemiol*, 17: S2-S10. [090220](#)
- Seagrave JC; McDonald JD; Bedrick E; Edgerton ES; Gigliotti AP; Jansen JJ; Ke L; Naeher LP; Seilkop SK; Zheng M; Mauderley JL (2006). Lung toxicity of ambient particulate matter from southeastern US sites with different contributing sources: relationships between composition and effects. *Environ Health Perspect*, 114: 1387-93. [091291](#)
- Seaman NL (2000). Meteorological modeling for air quality assessments. *Atmos Environ*, 34: 2231-2259. [035562](#)
- Seinfeld JH; Pandis SN (1998). Atmospheric chemistry and physics: from air pollution to climate change. New York: John Wiley & Sons. [018352](#)
- Sheesley RJ; Schauer JJ; Meiritz M; Deminter JT; Bae M-S; Turner JR (2007). Daily Variation in Particle-Phase Source Tracers in an Urban Atmosphere. *Aerosol Sci Technol*, 41: 981-993. [112017](#)
- Shen S; Jaques PA; Zhu Y; Geller MD; Sioutas C (2002). Evaluation of the SMPS-APS system as a continuous monitor for measuring PM_{2.5}, PM₁₀ and coarse (PM_{2.5-10}) concentrations. *Atmos Environ*, 36: 3939-3950. [156086](#)
- Sheppard L; Slaughter JC; Schildcrout J; Liu L-JS; Lumley T (2005). Exposure and measurement contributions to estimates of acute air pollution effects. *J Expo Sci Environ Epidemiol*, 15: 366-376. [079176](#)
- Sheya SA; Glowacki C; Chang MC; Chow JC; Watson JG (2008). Hot filter/impinger and dilution sampling for fine particulate matter characterization from ferrous metal casting processes. *J Air Waste Manag Assoc*, 58: 553-561. [156977](#)
- Shi Q; Sakurai H; McMurry PH (2007). Climatology of Regional Nucleation Events in Urban East St. Louis. *Atmos Environ*, 41: 4119-4127. [191760](#)
- Shimpi S; Khalek I; Bougher T; Tennant C (2009). Number count measurements of particulate trap-equipped diesel truck exhaust from engines that meet 2007 US on-highway emission regulations. Presented at A&WMA's 102nd Annual Conference and Exhibition, June 16-19, 2009, Pittsburgh, PA. [189888](#)

- Shrivastava MK; Subramanian R; Rogge WF; Robinson AL (2007). Sources of organic aerosol: Positive matrix factorization of molecular marker data and comparison of results from different source apportionment models. *Atmos Environ*, 41: 9353-9369. [111594](#)
- Singh M; Misra C; Sioutas C (2003). Field evaluation of a personal cascade impactor sampler (PCIS). *Atmos Environ*, 37: 4781-4793. [156088](#)
- Singh M; Phuleria HC; Bowers K; Sioutas C (2006). Seasonal and spatial trends in particle number concentrations and size distributions at the children's health study sites in Southern California. *J Expo Sci Environ Epidemiol*, 16: 3-18. [190136](#)
- Sioutas C; Delfino RJ; Singh M (2005). Exposure assessment for atmospheric ultrafine particles (UFPs) and implications in epidemiologic research. *Environ Health Perspect*, 113: 947-955. [088428](#)
- Sioutas C; Kim S; Chang M; Terrell LL; Gong H Jr (2000). Field evaluation of a modified DataRAM MIE scattering monitor for real-time PM_{2.5} mass concentration measurements. *Atmos Environ*, 34: 4829-4838. [025223](#)
- Slowik JG; Cross ES; Han J-H; Davidovits P; Onasch TB; Jayne JT; Williams LR; Canagaratna MR; Worsnop DR; Chakrabarty RK; Moosm; uuml; Iler H; Arnott WP; Schwarz JP; Gao R-S; Fahey DW; Kok GL; Petzold A (2007). An Inter-Comparison of Instruments Measuring Black Carbon Content of Soot Particles. *Aerosol Sci Technol*, 41: 295 - 314. [096177](#)
- Smith JN; Dunn MJ; VanReken TM; Iida K; Stolzenburg MR; McMurry PH; Huey LG (2008). Chemical composition of atmospheric nanoparticles formed from nucleation in Tecamac, Mexico: evidence for an important role for organic species in nanoparticle growth. *Geophys Res Lett*, 35: L04808. [199529](#)
- Smith JN; Moore KF; McMurry PH; Eisele FL (2004). Atmospheric Measurements of Sub-20 nm Diameter Particle Chemical Composition by Thermal Desorption Chemical Ionization Mass Spectrometry. *Aerosol Sci Technol*, 38: 100-110. [156090](#)
- Smith RL; Spitzner D; Kim Y; Fuentes M (2000). Threshold dependence of mortality effects for fine and coarse particles in Phoenix, Arizona. *J Air Waste Manag Assoc*, 50: 1367-1379. [010335](#)
- Smith WH; Staskawicz BJ (1977). Removal of atmospheric particles by leaves and twigs of urban trees: some preliminary observations and assessment of research needs. *J Environ Manage*, 1: 317-330. [046675](#)
- So ESP; Chan ATY; Wong AYT (2005). Large-eddy simulations of wind flow and pollutant dispersion in a street canyon. *Atmos Environ*, 39: 3573-3582. [110746](#)
- Solomon P; Baumann K; Edgerton E; Tanner R; Eatough D; Modey W; Marin H; Savoie D; Natarajan S; Meyer MB (2003). Comparison of integrated samplers for mass and composition during the 1999 Atlanta supersites project. *J Geophys Res*, 108: 8423. [156994](#)
- Solomon PA; Hopke PK (2008). A Special Issue of JA&WMA Supporting Key Scientific and Policy-and Health-Relevant Findings from EPA's Particulate Matter Supersites Program and Related Studies: An Integration and Synthesis of Results. *J Air Waste Manag Assoc*, 58: 137. [156997](#)
- Solomon PA; Sioutas C (2008). Continuous and semicontinuous monitoring techniques for particulate matter mass and chemical components: a synthesis of findings from EPA's Particulate Matter Supersites Program and related studies. *J Air Waste Manag Assoc*, 58: 164-195. [190139](#)
- Song CH; Carmichael GR (2001). A three-dimensional modeling investigation of the evolution processes of dust and sea-salt particles in east Asia. *J Geophys Res*, 106: 18,131-18,154. [036064](#)
- Stanier CO; Khlystov AY; Chan WR; Mandiro M; Pandis SN (2004). A Method for the In Situ Measurement of Fine Aerosol Water Content of Ambient Aerosols: The Dry-Ambient Aerosol Size Spectrometer (DAASS). *Aerosol Sci Technol*, 38: 215 - 228. [095955](#)
- Stein AF; Lamb D; Draxler RR (2000). Incorporation of detailed chemistry into a three-dimensional Lagrangian-Eulerian hybrid model: application to regional tropospheric ozone. *Atmos Environ*, 34: 4361-4372. [048341](#)
- Stevenson D; Dentener FJ; Schultz MG; Ellingsen K; Van Noije TPC; Wild O; Zeng G; Amann M; Atherton CS; Bell N; Bergmann DJ; Bey I; Butler T; Cofala J; Collins WJ; Derwent RG; Doherty RM; Drevet J; Eskes HJ; Fiore AM; Gauss M; Hauglustaine DA; Horowitz LW; Isaksen ISA; Krol MC; Lamarque J-F; Lawrence MG; Montanaro V; Muller J-F; Pitari G; Prather MJ; Pyle JA; Rast S; Rodriguez JM; Sanderson MG (2006). Multimodel ensemble simulations of present-day and near-future tropospheric ozone. *J Geophys Res*, 111: D08301. [089222](#)

- Stockwell WR; Middleton P; Chang JS; Tang X (1990). The second generation Regional Acid Deposition Model chemical mechanism for regional air quality modeling. *J Geophys Res*, 95: 16,343-16,367. [043095](#)
- Stolzenburg MR; Dutcher DD; Kirby BW; Hering SV (2003). Automated Measurement of the Size and Concentration of Airborne Particulate Nitrate. *Aerosol Sci Technol*, 37: 537-546. [156102](#)
- Stolzenburg MR; Hering SV (2000). Method for the automated measurement of fine particle nitrate in the atmosphere. *Environ Sci Technol*, 34: 907-914. [013289](#)
- Stracquadanio M; Bergamini D; Massaroli E; Trombini C (2005). Field evaluation of a passive sampler of polycyclic aromatic hydrocarbons (PAHs) in an urban atmosphere (Bologna, Italy). *J Environ Monit*, 7: 910-915. [156104](#)
- Strand M; Hopke PK; Zhao W; Vedal S; Gelfand E; Rabinovitch N (2007). A study of health effect estimates using competing methods to model personal exposures to ambient PM_{2.5}. *J Expo Sci Environ Epidemiol*, 17: 549-558. [157018](#)
- Strand M; Vedal S; Rodes C; Dutton SJ; Gelfand EW; Rabinovitch N (2006). Estimating effects of ambient PM_{2.5} exposure on health using PM_{2.5} component measurements and regression calibration. *J Expo Sci Environ Epidemiol*, 16: 30-38. [089203](#)
- Streets DG; Zhang Q; Wang L; He K; Hao J; Wu Y; Tang Y; Carmichael GR (2006). Revisiting China's CO emissions after the Transport and Chemical Evolution over the Pacific (TRACE-P) mission: Synthesis of inventories, atmospheric modeling, and observations. *J Geophys Res*, 111: D14306. [157019](#)
- Subramanian R; Khlystov A; Robinson A (2006). Effect of Peak Inert-Mode Temperature on Elemental Carbon Measured Using Thermal-Optical Analysis. *Aerosol Sci Technol*, 40: 763-780. [156107](#)
- Subramanian R; Khlystov AY; Cabada JC; Robinson AL (2004). Positive and negative artifacts in particulate organic carbon measurements with denuded and undenuded sampler configurations. *Aerosol Sci Technol*, 1: 27-48. [081203](#)
- Sullivan AP; Peltier RE; Brock CA; de Gouw JA; Holloway JS; Warneke C; Wollny AG; Weber RJ (2006). Airborne measurements of carbonaceous aerosol soluble in water over northeastern United States: Method development and an investigation into water-soluble organic carbon sources. *J Geophys Res*, 111: 1-14. [157030](#)
- Sullivan AP; Weber RJ (2006). Chemical characterization of the ambient organic aerosol soluble in water: 1. Isolation of hydrophobic and hydrophilic fractions with a XAD-8 resin. *J Geophys Res*, 111: D05314. [157031](#)
- Sullivan AP; Weber RJ; Clements AL; Turner JR; Bae MS; Schauer JJ (2004). A method for on-line measurement of water-soluble organic carbon in ambient aerosol particles: Results from an urban site. *Geophys Res Lett*, 31: L13105. [157029](#)
- Sullivan JH; Hubbard R; Liu SL; Shepherd K; Trenga CA; Koenig JQ; Chandler WL; Kaufman JD (2007). A community study of the effect of particulate matter on blood measures of inflammation and thrombosis in an elderly population. *Environ Health Perspect*, 6: 3. [100083](#)
- Swartz E; Stockburger L; Gundel LA (2003). Recovery of semivolatile organic compounds during sample preparation: Implications for characterization of airborne particulate matter. *Environ Sci Technol*, 37: 597-605. [157035](#)
- Swietlik D; Faust M (1984). Foliar nutrition of fruit crops. *Hortic Rev (Am Soc Hortic Sci)*, 6: 287-355. [046678](#)
- Sørensen M; Loft S; Andersen HV; Raaschou-Nielsen O; Skovgaard LT; Knudsen LE; Nielsen IV; Hertel O (2005). Personal exposure to PM_{2.5}, black smoke and NO₂ in Copenhagen: relationship to bedroom and outdoor concentrations covering seasonal variation. *J Expo Sci Environ Epidemiol*, 15: 413-422. [089428](#)
- Taha G; Box GP; Cohen DD; Stelcer E (2007). Black Carbon Measurement using Laser Integrating Plate Method. *Aerosol Sci Technol*, 41: 266 - 276. [096277](#)
- Taylor DA (2002). Dust in the wind. *Environ Health Perspect*, 110: A80-A87. [025693](#)
- Taylor GE Jr; Hanson PJ; Baldocchi DD (1988). Pollutant deposition to individual leaves and plant canopies: sites of regulation and relationship to injury. In Heck, W. W.; Taylor, O. C.; Tingey, D. T. (Ed.), *Assessment of crop loss from air pollutants* (pp. 227-257). New York, NY: Elsevier Applied Science. [019289](#)
- Temime-Roussel B; Monod A; Massiani C; Wortham H (2004). Evaluation of an annular denuder for atmospheric PAH partitioning studies--2: evaluation of mass and number particle losses. *Atmos Environ*, 38: 1925-1932. [098530](#)

- Temime-Roussel B; Monod A; Massiani C; Wortham H (2004). Evaluation of an annular denuder tubes for atmospheric PAH partitioning studies--1: evaluation of the trapping efficiency of gaseous PAHS. *Atmos Environ*, 38: 1913-1924. [098521](#)
- ten Brink H; Hoek G; Khlystov A (2005). An approach to monitor the fraction of elemental carbon in the ultrafine aerosol. *Atmos Environ*, 39: 6255-6259. [156115](#)
- ten Brink H; Maenhaut W; Hitzenberger R; Gnauk T; Spindler G; Even A; Chi X; Bauer H; Puxbaum H; Putaud J-P; Tursic J; Berner A (2004). INTERCOMP2000: the comparability of methods in use in Europe for measuring the carbon content of aerosol. *Atmos Environ*, 38: 6507-6519. [097110](#)
- Tesche TW; Morris R; Tonnesen G; McNally D; Boylan J; Brewer P (2006). CMAQ/CAMx annual 2002 performance evaluation over the eastern US. *Atmos Environ*, 40: 4906-4919. [157050](#)
- Thornburg J; Rodesa CE; Lawless PA; Williams R (2009). Spatial and Temporal Variability of Outdoor Coarse Particulate Matter Mass Concentrations Measured with a New Coarse Particle Sampler During the Detroit Exposure and Aerosol Research Study . *Atmos Environ*, 43: 4251-4258. [190999](#)
- Thurston GD; Spengler JD (1985). A quantitative assessment of source contributions to inhalable particulate matter pollution in metropolitan Boston. *Atmos Environ*, 19: 9-25. [056074](#)
- Tobias HJ; Kooiman PM; Docherty KS; Ziemann PJ (2000). Real-Time Chemical Analysis of Organic Aerosols Using a Thermal Desorption Particle Beam Mass Spectrometer. *Aerosol Sci Technol*, 33: 170-190. [156121](#)
- Tobias HJ; Ziemann PJ (1999). Compound Identification in Organic Aerosols Using Temperature-Programmed Thermal Desorption Particle Beam Mass Spectrometry. *Anal Chem*, 71: 3428-3435. [157053](#)
- Tolocka M; Jang PM; Ginter JM; Cox FJ; Kamens RM; Johnston MV (2004). Formation of oligomers in secondary organic aerosol. *Environ Sci Technol*, 38: 1428-1434. [087578](#)
- Trijonis JC; Malm WC; Pitchford M; White WH; Charlson R (1990). Acidic deposition: State of science and technology. Report 24. Visibility: Existing and historical conditions-causes and effects. Final report. [157058](#)
- Tsai CJ; Chang CT; Huang CH (2006). Direct field observation of the relative humidity effect on the beta-gauge readings. *J Air Waste Manag Assoc*, 56: 834-40. [098312](#)
- Tsai YI; Kuo SC (2006). Development of diffuse reflectance infrared Fourier transform spectroscopy for the rapid characterization of aerosols. *Atmos Environ*, 40: 1781-1793. [156127](#)
- TSI (2005). Data Merge Software Module for merging and fitting of SMPA and APS Data Files, P/N 1930074, User's Guide, Model 390069, Revision A. St. Paul, MN. A. St Paul, MN: TSI, Incorporated [157196](#)
- Tuch TM; Herbarth O; Franck U; Peters A; Wehner B; Wiedensohler A; Heintzenberg J (2006). Weak correlation of ultrafine aerosol particle concentrations < 800 nm between two sites within one city. *J Expo Sci Environ Epidemiol*, 16: 486-491. [157060](#)
- Tung TCW; Chao CYH; Burnett J (1999). A methodology to investigate the particulate penetration coefficient through building shell. *Atmos Environ*, 33: 881-893. [049003](#)
- Turpin BJ; Lim H-J (2001). Species contributions to PM25 mass concentrations: revisiting common assumptions for estimating organic mass. *Aerosol Sci Technol*, 35: 602-610. [017093](#)
- Turpin BJ; Weisel CP; Morandi M; Colome S; Stock T; Eisenreich S; Buckley B (2007). Relationships of Indoor, Outdoor, and Personal Air (RIOPA): Part II. Analyses of concentrations of particulate matter species. [157062](#)
- U.S. EPA (1982). Air quality criteria for particulate matter and sulfur oxides, Vol 1, 2, 3. U.S. Environmental Protection Agency, Environmental Criteria and Assessment Office. Washington, D.C.. EPA 600/8-82-029a; EPA 600/8-82-029b; EPA 600/8-82-029c. <http://nepis.epa.gov/Exe/ZyPURL.cgi?Dockey=3000188Z.txt>; <http://nepis.epa.gov/Exe/ZyPURL.cgi?Dockey=300018EV.txt>; <http://nepis.epa.gov/Exe/ZyPURL.cgi?Dockey=300053KV.txt>. [017610](#)
- U.S. EPA (1996). Air quality criteria for particulate matter. U.S. Environmental Protection Agency. Research Triangle Park, NC. EPA/600/P-95/001aF-cF. [079380](#)
- U.S. EPA (1998). SLAMS/NAMS/PAMS network review guidance. [093211](#)
- U.S. EPA (2004). Air quality criteria for particulate matter. U.S. Environmental Protection Agency. Research Triangle Park, NC. EPA/600/P-99/002aF-bF. [056905](#)

- U.S. EPA (2005). Review of the national ambient air quality standards for particulate matter: Policy assessment of scientific and technical information OAQPS staff paper. U.S. Environmental Protection Agency. Washington, DC. EPA/452/R-05-005a. http://www.epa.gov/ttn/naaqs/standards/pm/data/pmstaffpaper_20051221.pdf . [090209](#)
- U.S. EPA (2006). 2002 National Emissions Inventory Data and Documentation. Retrieved 02-DEC-09, from <http://www.epa.gov/ttnchie1/net/2002inventory.html>. [157070](#)
- U.S. EPA (2006). Air quality criteria for ozone and related photochemical oxidants. EPA. DC. [088089](#)
- U.S. EPA (2006). Provisional Assessment of Recent Studies on Health Effects of Particulate Matter Exposure. U.S. Environmental Protection Agency. Research Triangle Park, NC. [157071](#)
- U.S. EPA (2008). Analysis of particulate matter emissions from light-duty gasoline vehicles in Kansas City. U.S. Environmental Protection Agency. Washington, D.C.. EPA420-R-08-010. [191767](#)
- U.S. EPA (2008). Integrated Science Assessment for Oxides of Nitrogen - Health Criteria. U.S. Environmental Protection Agency. Research Triangle Park, NC. EPA/600/R-08/071. [157073](#)
- U.S. EPA (2008). Integrated science assessment for oxides of nitrogen and sulfur: Ecological criteria. U.S. Environmental Protection Agency. Research Triangle Park, NC. EPA/600/R-08/082F. [157074](#)
- U.S. EPA (2008). Integrated Science Assessment for Sulfur Oxides - Health Criteria. U.S. Environmental Protection Agency. Research Triangle Park, NC. EPA/600/R-08/047F. <http://cfpub.epa.gov/ncea/cfm/recordisplay.cfm?deid=198843>. [157075](#)
- U.S. EPA (2008). National Air Quality Status and Trends Through 2007. U.S. Environmental Protection Agency. Research Triangle Park. EPA-454/R-08-006 . [191190](#)
- U.S. EPA (2008). Total Risk Integrated Methodology (TRIM) Air Pollutants Exposure Model Documentation (TRIM.Expo/APEX, Version 4.3). Volume 1: User's Guide. U.S. Environmental Protection Agency, Office of Air Quality Planning and Standards. Research Triangle Park, NC. EPA-452/B-08-001b. [191775](#)
- U.S. EPA (2008). U.S. EPA's 2008 Report on the Environment (Final Report). U.S. Environmental Protection Agency. DC. [157076](#)
- U.S. EPA (2009). Risk and Exposure Assessment for Review of the Secondary National Ambient Air Quality Standards for Oxides of Nitrogen and Oxides of Sulfur Second Draft. U.S. Environmental Protection Agency. Washington, D.C.. EPA-452/P-09-004a. http://www.epa.gov/ttnnaaqs/standards/no2so2sec/cr_rea.html. [191774](#)
- U.S. EPA (2009). Verified Retrofit Technologies. Retrieved 02-DEC-09, from <http://www.epa.gov/otaq/retrofit/index.htm>. [189885](#)
- UNCEC (2007). Hemispheric Transport of Air Pollution 2007. New York: United Nations Publications. [157078](#)
- Unsworth MH; Wilshaw JC (1989). Wet, occult and dry deposition of pollutants on forests. *Agr Forest Meteorol*, 47: 221-238. [046682](#)
- VanCuren RA; Cahill TA (2002). Asian aerosols in North America: Frequency and concentration of fine dust. *J Geophys Res*, 107: 4804. [157087](#)
- Van Aalst RM (1982). Dry deposition of NO_x. In Schneider, T.; Grant, L. (Ed.), *Air pollution by nitrogen oxides* Amsterdam, The Netherlands: Elsevier Scientific Publishing Company. [036481](#)
- van der Werf GR; Randerson JT; Giglio L; Collatz GJ; Kasibhatla PS; Arellano Jr AF (2006). Interannual variability in global biomass burning emissions from 1997 to 2004. *Atmos Chem Phys*, 6: 3423–3441. [157084](#)
- Vega E; Reyes E; Wellens A; Sanchez G; Chow JC; Watson JG (2003). Comparison of continuous and filter based mass measurements in Mexico City. *Atmos Environ*, 37: 2783-2793. [105974](#)
- Venkataraman C; Lyons JM; Friedlander SK (1994). Size distributions of polycyclic aromatic hydrocarbons and elemental carbon 1 Sampling, measurement methods, and source characterization. *Environ Sci Technol*, 28: 555-562. [002475](#)
- Venn A; Lewis S; Cooper M; Hubbard R; Hill I; Boddy R; Bell M; Britton J (2000). Local road traffic activity and the prevalence, severity and persistence of wheeze in school children: combined cross sectional and longitudinal study. *Occup Environ Med*, 57: 152-158. [007895](#)
- Venn AJ; Lewis SA; Cooper M; Hubbard R; Britton J (2001). Living near a main road and the risk of wheezing illness in children. *Am J Respir Crit Care Med*, 164: 2177-2180. [023644](#)

- Veranth JM; Moss TA; Chow JC; Labban R; Nichols WK; Walton JC; Walton JG; Yost GS (2006). Correlation of in vitro cytokine responses with the chemical composition of soil-derived particulate matter. *Environ Health Perspect*, 114: 341-349. [087479](#)
- Viana M; Chi X; Maenhaut W; Cafmeyer J; Querol X; Alastuey A; Mikuska P; Vecera Z (2006). Influence of Sampling Artefacts on Measured PM, OC, and EC Levels in Carbonaceous Aerosols in an Urban Area. *Aerosol Sci Technol*, 40: 107-117. [179987](#)
- Viana M; Querol X; Alastuey A; Ballester F; Llop S; Esplugues A; Fernandez-Patier R; Garca dos Santos S; Herce MD (2008). Characterising exposure to PM aerosols for an epidemiological study. *Atmos Environ*, 42: 1552-1568. [156135](#)
- Violante FS; Barbieri A; Curti S; Sanguinetti G; Grazioli F; Mattioli S (2006). Urban atmospheric pollution: Personal exposure versus fixed monitoring station measurements. *Chemosphere*, 64: 1722-1729. [156140](#)
- Virkkula A; Makela T; Hillamo R; Yli-Tuomi T; Hirsikko A; Hameri K; Koponen IK (2007). A simple procedure for correcting loading effects of aethalometer data. *J Air Waste Manag Assoc*, 57: 1214-1222. [157098](#)
- Voisin D; Smith JN; Sakurai H; McMurry PH; Eisele FL (2003). Thermal Desorption Chemical Ionization Mass Spectrometer for Ultrafine Particle Chemical Composition. *Aerosol Sci Technol*, 37: 471-475. [156141](#)
- Volckens J; Olson DA; Hays MD (2008). Carbonaceous species emitted from handheld two-stroke engines. *Atmos Environ*, 42: 1239-1248. [105465](#)
- Vyas VM; Christakos G (1997). Spatiotemporal analysis and mapping of sulfate deposition data over Eastern USA. *Atmos Environ*, 31: 3623-3633. [156142](#)
- Wagner J; Leith D (2001). Passive aerosol sampler. Part I: Principle of operation. *Aerosol Sci Technol*, 34: 186-192. [190153](#)
- Wagner J; Leith D (2001). Passive aerosol sampler. Part II: Wind tunnel experiments. *Aerosol Sci Technol*, 34: 193-201. [190154](#)
- Wallace L (2000). Real-time monitoring of particles, PAH, and CO in an occupied townhouse. *J Occup Environ Hyg*, 15: 39-47. [000803](#)
- Wallace L; Williams R (2005). Use of personal-indoor-outdoor sulfur concentrations to estimate the infiltration factor and outdoor exposure factor for individual homes and persons. *Environ Sci Technol*, 39: 1707-1714. [057485](#)
- Wallace L; Williams R; Rea A; Croghan C (2006). Continuous weeklong measurements of personal exposures and indoor concentrations of fine particles for 37 health-impaired North Carolina residents for up to four seasons. *Atmos Environ*, 40: 399-414. [088211](#)
- Wallace L; Williams R; Suggs J; Jones P (2006). Estimating contributions of outdoor fine particles to indoor concentrations and personal exposures: effects of household characteristics and personal activities. U.S. Environmental Protection Agency; National Exposure Research Laboratory. Research Triangle Park, NC. EPA/600/R-06/023. [089190](#)
- Wang J; Christopher SA; Nair US; Reid JS; Prins EM; Szykman J; Hand JL (2006). Mesoscale modeling of Central American smoke transport to the United States: 1. "Top-down" assessment of emission strength and diurnal variation impacts. *J Geophys Res*, 111: D05S17. [157109](#)
- Wang LH; Milford JB; Carter WPL (2000). Reactivity estimates for aromatic compounds Part 2 uncertainty in incremental reactivities. *Atmos Environ*, 34: 4349-4360. [048365](#)
- Wang LH; Milford JB; Carter WPL (2000). Reactivity estimates for aromatic compounds Part I: uncertainty in chamber-derived parameters. *Atmos Environ*, 34: 4337-4348. [048357](#)
- Watson JG; Chen LW; Chow JC; Doraiswamy P; Lowenthal DH (2008). Source apportionment: findings from the U.S. Supersites Program. *J Air Waste Manag Assoc*, 58: 265-288. [157128](#)
- Watson JG; Chow JC (2002). Comparison and evaluation of in situ and filter carbon measurements at the Fresno Supersite. *J Geophys Res*, 107: 8341. [037873](#)
- Watson JG; Chow JC; Chen LWA (2005). Summary of organic and elemental carbon/black carbon analysis methods and intercomparisons. *Aerosol Air Qual Res*, 5: 69-102. [157125](#)
- Watson JG; Fujita EM; Chow JC; Zielinska B; Richards LW; Neff W; Dietrich D (1998). Northern front range air quality study Final report. [012257](#)

- Watson JG; Robinson NF; Chow JC; Henry RC; Kim BM; Pace TG; Meyer EL; Nguyen Q (1990). The USEPA/DRI chemical mass balance receptor model, CMB 70. *Environ Software*, 5: 38-49. [004848](#)
- Weber RJ; Orsini D; Daun Y; Lee Y-N; Kotz PJ; Brechtel F (2001). A particle-into-liquid collector for rapid measurement of aerosol bulk chemical composition. *Aerosol Sci Technol*, 35: 718-727. [024640](#)
- Weber RJ; Orsini D; Duan Y; Baumann K; Kiang CS; Chameides W; Lee YN; Brechtel F; Klotz P; Jongejan P (2003). Intercomparison of near real time monitors of PM_{2.5} nitrate and sulfate at the US Environmental Protection Agency Atlanta Supersite. *J Geophys Res*, 108: 8421. [157129](#)
- Weijers EP; Khlystov AY; Kos GPA; Erisman JW (2004). Variability of particulate matter concentrations along roads and motorways determined by a moving measurement unit. *Atmos Environ*, 38: 2993-3002. [104186](#)
- Weingartner E; Saathoff H; Schnaiter M; Streit N; Bitnar B; Baltensperger U (2003). Absorption of light by soot particles: determination of the absorption coefficient by means of aethalometers. *J Aerosol Sci*, 34: 1445-1463. [156149](#)
- Wenzel RJ; Liu DY; Edgerton ES; Prather KA (2003). Aerosol time-of-flight mass spectrometry during the Atlanta Supersite Experiment: 2. Scaling procedures. *J Geophys Res*, 108: 8426. [157139](#)
- Wesely ML; Eastman JA; Stedman DH; Yalvac ED (1982). An eddy-correlation measurement of NO₂ flux to vegetation and comparison to O₃ flux. *Atmos Environ*, 16: 815-820. [036564](#)
- Wesely ML; Hicks BB (2000). A review of the current status of knowledge on dry deposition. *Atmos Environ*, 34: 2261-2282. [025018](#)
- Westerdahl D; Fruin S; Sax T; Fine PM; Sioutas C (2005). Mobile platform measurements of ultrafine particles and associated pollutant concentrations on freeways and residential streets in Los Angeles. *Atmos Environ*, 39: 3597-3610. [086502](#)
- Whitby KT (1978). The physical characteristics of sulfur aerosols. *Atmos Environ*, 12: 135-159. [071181](#)
- Williams B; Goldstein A; Kreisberg N; Hering S (2006). An In-Situ Instrument for Speciated Organic Composition of Atmospheric Aerosols: Thermal Desorption Aerosol GC/MS-FID (TAG). *Aerosol Sci Technol*, 40: 627-638. [156157](#)
- Williams R; Rea A; Vette A; Croghan C; Whitaker D; Stevens C; McDow S; Fortmann R; Sheldon L; Wilson H; Thornburg J; Phillips M; Lawless P; Rodes C; Daughtrey H (2008). The design and field implementation of the Detroit exposure and aerosol research study. *J Expo Sci Environ Epidemiol*, 19: 643-659. [191201](#)
- Williams TC; Shaddix CR; Jensen KA; Suo-Anttila JM (2006). Measurements of the Dimensionless Extinction Coefficient of Soot Within Laminar Diffusion Flames. *Combust Flame*, 50: 1616-1630. [157148](#)
- Wilson JG; Zawar-Reza P (2006). Intraurban-scale dispersion modelling of particulate matter concentrations: applications for exposure estimates in cohort studies. *Atmos Environ*, 40: 1053-1063. [088292](#)
- Wilson WE; Brauer M (2006). Estimation of ambient and non-ambient components of particulate matter exposure from a personal monitoring panel study. *J Expo Sci Environ Epidemiol*, 16: 264-274. [088933](#)
- Wilson WE; Grover BD; Long RW; Eatough NL; Eatough DJ (2006). The measurement of fine particulate semivolatile material in urban aerosols. *J Air Waste Manag Assoc*, 56: 384-387. [091142](#)
- Wilson WE; Mage DT; Grant LD (2000). Estimating separately personal exposure to ambient and nonambient particulate matter for epidemiology and risk assessment: why and how. *J Air Waste Manag Assoc*, 50: 1167-1183. [010288](#)
- Wilson WE; Mar TF; Koenig JQ (2007). Influence of exposure error and effect modification by socioeconomic status on the association of acute cardiovascular mortality with particulate matter in Phoenix. *J Expo Sci Environ Epidemiol*, 17: S11-S19. [157149](#)
- Wilson WE; Stanek J; Han HS; Johnson T; Sakurai H; Pui DY; Turner J; Chen DR; Duthie S (2007). Use of the electrical aerosol detector as an indicator of the surface area of fine particles deposited in the lung. *J Air Waste Manag Assoc*, 57: 211-20. [098398](#)
- Wilson WE; Suh HH (1997). Fine particles and coarse particles: concentration relationships relevant to epidemiologic studies. *J Air Waste Manag Assoc*, 47: 1238-1249. [077408](#)
- Winkler PM; Steiner G; Vrtala A; Vehkamäki H; Noppel M; Lehtinen KEJ; Reischl GP; Wagner PE; Kulmala M (2008). Heterogeneous Nucleation Experiments Bridging the Scale from Molecular Ion Clusters to Nanoparticles. *Science*, 319: 1374-1377. [156160](#)

- Womilaju TO; Miller JD; Mayer PM; Brook JR (2003). Methods to determine the biological composition of particulate matter collected from outdoor air. *Atmos Environ*, 37: 4335-4344. [179954](#)
- Wongphatarakul V; Friedlander SK; Pinto JP (1998). A comparative study of PM_{2.5} ambient aerosol chemical databases. *Environ Sci Technol*, 32: 3926-3934. [049281](#)
- Woo K-S; Chen D-R; Pui DYH; McMurry PH (2001). Measurement of Atlanta aerosol size distributions: observations of ultrafine particle events. *Aerosol Sci Technol*, 34: 75-87. [011702](#)
- Wu C-F; Delfino RJ; Floro JN; Quintana; (2005). Exposure assessment and modeling of particulate matter for asthmatic children using personal nephelometers. *Atmos Environ*, 39: 3457-3469. [086397](#)
- Wu CF; Delfino RJ; Floro JN; Samimi BS; Quintana PJ; Kleinman MT; Liu LJ (2005). Evaluation and quality control of personal nephelometers in indoor, outdoor and personal environments. *J Expo Sci Environ Epidemiol*, 15: 99-110. [157155](#)
- Wu CF; Jimenez J; Claiborn C; Gould T; Simpson CD; Larson T; Liu LJS (2006). Agricultural burning smoke in Eastern Washington: Part II. Exposure assessment. *Atmos Environ*, 40: 5379-5392. [179950](#)
- Wu J; Houston D; Lurmann F; Ong P; Winer A (2009). Exposure of PM_{2.5} and EC from diesel and gasoline vehicles in communities near the Ports of Los Angeles and Long Beach, California. *Atmos Environ*, 43: 1962-1971. [191773](#)
- Wu J; Lurmann F; Winer A; Lu R; Turco R; (2005). Development of an individual exposure model for application to the Southern California children's health study. *Atmos Environ*, 39: 259-273. [058570](#)
- Wu S; Mickley L; Jacob D; Rind D; Streets D (2008). Effects of 2000-2050 changes in climate and emissions on global tropospheric ozone and the policy-relevant background surface ozone in the United States. *J Geophys Res*, 113: D18312. [190039](#)
- Xia X; Hopke PK (2006). Seasonal Variation of 2-Methyltetrols in Ambient Air Samples. *Environ Sci Technol*, 40: 6934-6937. [179947](#)
- Xiaomin X; Zhen H; Jiasong W (2006). The impact of urban street layout on local atmospheric environment. *Build Environ*, 41: 1352-1363. [156165](#)
- Yang H; Li Q; Yu JZ (2003). Comparison of two methods for the determination of water-soluble organic carbon in atmospheric particles. *Atmos Environ*, 37: 865-870. [156167](#)
- Yanosky JD; Paciorek CJ; Schwartz J; Laden F; Puett R; Suh HH (2008). Spatio-temporal modeling of chronic PM₁₀ exposure for the Nurses' Health Study. *Atmos Environ*, 42(18): 4047-4062. [099467](#)
- Yanosky JD; Paciorek CJ; Suh HH (2009). Predicting chronic fine and coarse particulate exposures using spatiotemporal models for the northeastern and midwestern United States. *Environ Health Perspect*, 117: 522-529. [190114](#)
- Yi SM; Ambs JL; Patashnick H; Rupprecht G; Hopke PK (2004). Particle Collection Characteristics of a Prototype Electrostatic Precipitator (ESP) for a Differential TEOM System. *Aerosol Sci Technol*, 38: 46-51. [156169](#)
- Yu H; Remer LA; Chin M; Bian H; Kleidman RG; Diehl T (2008). A satellite-based assessment of transpacific transport of pollution aerosol. *J Geophys Res*, 113: 1-15. [157168](#)
- Yu JZ; Yang H; Zhang H; Lau AKH (2004). Size distributions of water-soluble organic carbon in ambient aerosols and its size-resolved thermal characteristics. *Atmos Environ*, 38: 1061-1071. [156172](#)
- Zanis P; Trickl T; Stohl A; Wernli H; Cooper O; Zerefos C; Gaeggeler H; Schnabel C; Tobler L; Kubik PW; Priller A; Scheel HE; Kanter HJ; Cristofanelli P; Forster C; James P; Gerasopoulos E; Delcloo A; Papayannis A; Claude H (2003). Forecast, observation and modelling of a deep stratospheric intrusion event over Europe. *Atmos Chem Phys*, 3: 763-777. [053423](#)
- Zanobetti A; Wand MP; Schwartz J; Ryan LM (2000). Generalized additive distributed lag models: quantifying mortality displacement. *Biostatistics*, 1: 279-292. [004133](#)
- Zeger SL; Thomas D; Dominici F; Samet JM; Schwartz J; Dockery D; Cohen A (2000). Exposure measurement error in time-series studies of air pollution: concepts and consequences. *Environ Health Perspect*, 108: 419-426. [001949](#)
- Zeng Y (2006). A comprehensive particulate matter monitoring system and dosimetry-based ambient particulate matter standards. *J Air Waste Manag Assoc*, 56: 518-29. [098375](#)

- Zhang K; Wexler A (2008). Modeling urban and regional aerosols—Development of the UCD Aerosol Module and implementation in CMAQ model. *Atmos Environ*, 42: 3166-3178 . [191770](#)
- Zhang Q; Jimenez JL; Canagaratna MR; Allan JD; Coe HL Ulbrich I; Alfarra MR; Takami A; Middlebrook AM; Sun YL; Dzepina K; Dunlea E; Docherty K; DeCarlo PF; Salcedo D; Onasch T; Jayne JR; Miyoshi T; Shimo A; Hatakeyama S; Takegawa N; Kondo Y; Schneider J; Drewnick F; Borrmann S; Weimer S; Demerjian K; Williams P; Bower K; Bahreini R; Cottrell L; Griffin RJ; Rautiainen J; Sun JR; Zhang YM; Worsnop DR (2007). Ubiquity and dominance of oxygenated species in organic aerosols in anthropogenically-influenced Northern Hemisphere midlatitudes. *Geophys Res Lett*, 34: L13801. [189998](#)
- Zhang Q; Jimenez JL; Canagaratna MR; Jayne JT; Worsnop DR (2005). Time- and size-resolved chemical composition of submicron particles in Pittsburgh: Implications for aerosol sources and processes. *J Geophys Res*, 110: 1-19. [157185](#)
- Zhang X; Zhuang G; Guo J; Yin K; Zhang P (2007). Characterization of aerosol over the Northern South China Sea during two cruises in 2003. *Atmos Environ*, 41: 7821-7836. [101119](#)
- Zhao W; Hopke PK; Norris G; Williams R; Paatero P (2006). Source apportionment and analysis on ambient and personal exposure samples with a combined receptor model and an adaptive blank estimation strategy. *Atmos Environ*, 40: 3788-3801. [156181](#)
- Zhao W; Rabinovitch N; Hopke PK; Gelfand EW (2007). Use of an expanded receptor model for personal exposure analysis in schoolchildren with asthma. *Atmos Environ*, 41: 4084-4096. [156182](#)
- Zheng M; Cass GR; Schauer JJ; Edgerton ES (2002). Source apportionment of PM_{2.5} in the southeastern United States using solvent-extractable organic compounds as tracers. *Environ Sci Technol*, 36: 2361-2371. [026100](#)
- Zheng M; Ke L; Edgerton ES; Schauer JJ; Dong M; Russell AG (2006). Spatial distribution of carbonaceous aerosol in the southeastern United States using molecular markers and carbon isotope data. *J Geophys Res*, 111: D10S06. [157189](#)
- Zhou Y; Levy JI (2007). Factors influencing the spatial extent of mobile source air pollution impacts: a meta-analysis. *BMC Public Health*, 7: 89. [098633](#)
- Zhu K; Zhang J; Liou PJ (2007). Evaluation and comparison of continuous fine particulate matter monitors for measurement of ambient aerosols. *J Air Waste Manag Assoc*, 57: 1499-506. [098367](#)
- Zhu Y; Eiguren-Fernandez A; Hinds WC; Miguel AH (2007). In-Cabin Commuter Exposure to Ultrafine Particles on Los Angeles Freeways. *Environ Sci Technol*, 41: 2138-2145. [179919](#)
- Zhu Y; Hinds WC; Kim S; Shen S; Sioutas C (2002). Study of ultrafine particles near a major highway with heavy-duty diesel traffic. *Atmos Environ*, 36: 4323-4335. [041553](#)
- Zhu Y; Hinds WC; Shen S; Sioutas C (2004). Seasonal trends of concentration and size distribution of ultrafine particles near major highways in Los Angeles. *Aerosol Sci Technol*, 38: 5-13. [156184](#)
- Zhu Y; Kuhn T; Mayo P; Hinds WC (2005). Comparison of Daytime and Nighttime Concentration Profiles and Size Distributions of Ultrafine Particles near a Major Highway. *Environ Sci Technol*, 39: 2531-2536. [157191](#)
- Zidek JV; Shaddick G; Meloche J; Chatfield C; White R (2007). A framework for predicting personal exposures to environmental hazards. *Environ Ecol Stat*, 14: 411-431. [190076](#)
- Zidek JV; Wong H; Le ND; Burnett R (1996). Causality, measurement error and multicollinearity in epidemiology. *Environmetrics*, 7: 441-451. [051879](#)

Chapter 4. Dosimetry

4.1. Introduction

Particle dosimetry refers to the characterization of deposition, translocation, clearance, and retention of particles and their constituents within the respiratory tract and extrapulmonary tissues. This chapter summarizes basic concepts presented in dosimetry chapters of the 1996 and 2004 PM AQCDs (U.S. EPA, 1996, [079380](#); U.S. EPA, 2004, [056905](#)), and updates the state of the science based upon new literature appearing since publication of these PM AQCDs. Although the basic understanding of the mechanisms governing deposition and clearance of inhaled particles has not changed, there is significant additional information on the role of certain biological determinants such as gender, age and lung disease on deposition and clearance. Additionally, new studies have further characterized the retention and translocation of ultrafine particles (UFPs; also commonly referred to as nanoparticles) following deposition in the respiratory tract.

The dose from inhaled particles deposited and retained in the respiratory tract is governed by a number of factors. These include exposure concentration and duration, activity and ventilatory parameters, and particle properties (e.g., particle size, hygroscopicity, and solubility in airway fluids and cellular components). The basic characteristics of particles as they relate to deposition and retention, as well as anatomical and physiological factors influencing particle deposition and retention, were discussed in depth in Chapter 10 of 1996 PM AQCD and updated in Chapter 6 of the 2004 PM AQCD. Species differences between humans and rats in particle exposures, deposition patterns, and pulmonary retention were also reviewed in Brown et al. (2005, [089308](#)). The current review of PM dosimetry focuses mainly on issues that may affect the susceptibility of an individual to adverse effects as well as issues that affect our ability to extrapolate findings between studies (e.g., in vitro to in vivo) and between species. Other than a brief overview in this introductory section, the disposition (i.e., deposition, absorption, distribution, metabolism, and elimination) of fibers and unique nano-objects (viz., dots, hollow spheres, rods, fibers, tubes) is not reviewed herein. Substantial exposures to fibers and unique nano-objects generally occur in the occupational settings rather than the ambient environment.

The deposition by interception of micro-sized fibers was briefly discussed in the 1996 and 2004 PM AQCD, but fiber retention in the respiratory tract was not addressed. Airborne fibers (length/diameter ratio ≥ 3), can exceed 150 μm in length and appear to be relatively stable in air. This is because their aerodynamic size is determined predominantly by their diameter, not their length. Fibers longer than 10 μm can deposit by interception and when aligned with the direction of airflow may penetrate deep into the respiratory tract. Once deposited, macrophage mediated clearance is the primary mechanism of removing micro-sized particles from the pulmonary region. The length of fibers can, however, affect their phagocytosis and clearance. For example, fibers of $>17 \mu\text{m}$ in length are too long to be fully engulfed by rat alveolar macrophages and can protrude from macrophages (i.e., macrophage frustration) (Zeidler-Erdely et al., 2006, [190967](#)). Further discussion of the fiber disposition in the respiratory tract is beyond the scope of this chapter.

The term “ultrafine particle” has traditionally been used by the aerosol research and occupational and environmental health communities to describe airborne particles or other laboratory generated aerosols used in toxicological studies that are $<100 \text{ nm}$ in size (based on physical size, diffusivity, or electrical mobility). Generally consistent with the definition of an UFP, the International Organization for Standardization (ISO) recently defined a nanoparticle as an object with all 3 external dimensions in the nanoscale, i.e., from approximately 1 and 100 nm (ISO, 2008, [190066](#)). The ISO also defined a nano-object as a material with one or more external dimensions in

Note: Hyperlinks to the reference citations throughout this document will take you to the NCEA HERO database (Health and Environmental Research Online) at <http://epa.gov/hero>. HERO is a [database of scientific literature](#) used by U.S. EPA in the process of developing science assessments such as the [Integrated Science Assessments \(ISA\)](#) and the [Integrated Risk Information System \(IRIS\)](#).

the nanoscale. The terms, nanoparticle and UFP, have been used rather synonymously in the recent literature. However, the terms nanoparticle and nano-object are more commonly associated with engineered materials that are created for consumer products and industrial applications. With the current interest in nanotechnologies, many nano-objects have been created by manipulating materials at the atomic or molecular scale for the purpose of forming new materials, structures, and devices that exploit the unique physical and chemical properties associated with their nanoscale. Toxicological studies are becoming available that evaluate in vivo translocation and health effects unique of nano-objects (viz., dots, hollow spheres, rods, tubes). The in vivo disposition of these unique nano-objects is not, however, necessarily relevant to the behavior of UF aerosols in the urban environment that are created by combustion sources and photochemical formation of secondary organic aerosols. Therefore, the disposition of unique nano-objects (viz., dots, hollow spheres, rods, fibers, tubes) is not considered in this chapter.

4.1.1. Size Characterization of Inhaled Particles

Particle size is a major determinant of the fraction of inhaled particles depositing in and cleared from various regions of the respiratory tract. The distribution of particle sizes in an aerosol is typically described by the lognormal distribution (i.e., the situation in which the logarithms of particle diameter are distributed normally). The geometric mean is the median of the distribution, and the variability around the median is the geometric standard deviation (GSD or σ_g) and is given by:

$$GSD = \sigma_g = \frac{d_{84\%}}{d_{50\%}} = \frac{d_{50\%}}{d_{16\%}}$$

Equation 4-1

where: $d_{16\%}$, $d_{50\%}$, $d_{84\%}$ are the particle diameters associated with the 16th, 50th (i.e., the median), and the 84th percentiles from the cumulative frequency distribution of particle sizes. By definition, GSD must be greater than one. The particle size associated with any percentile of the distribution, d_i , is given by:

$$d_i = d_{50\%} \sigma_g^{z(P)}$$

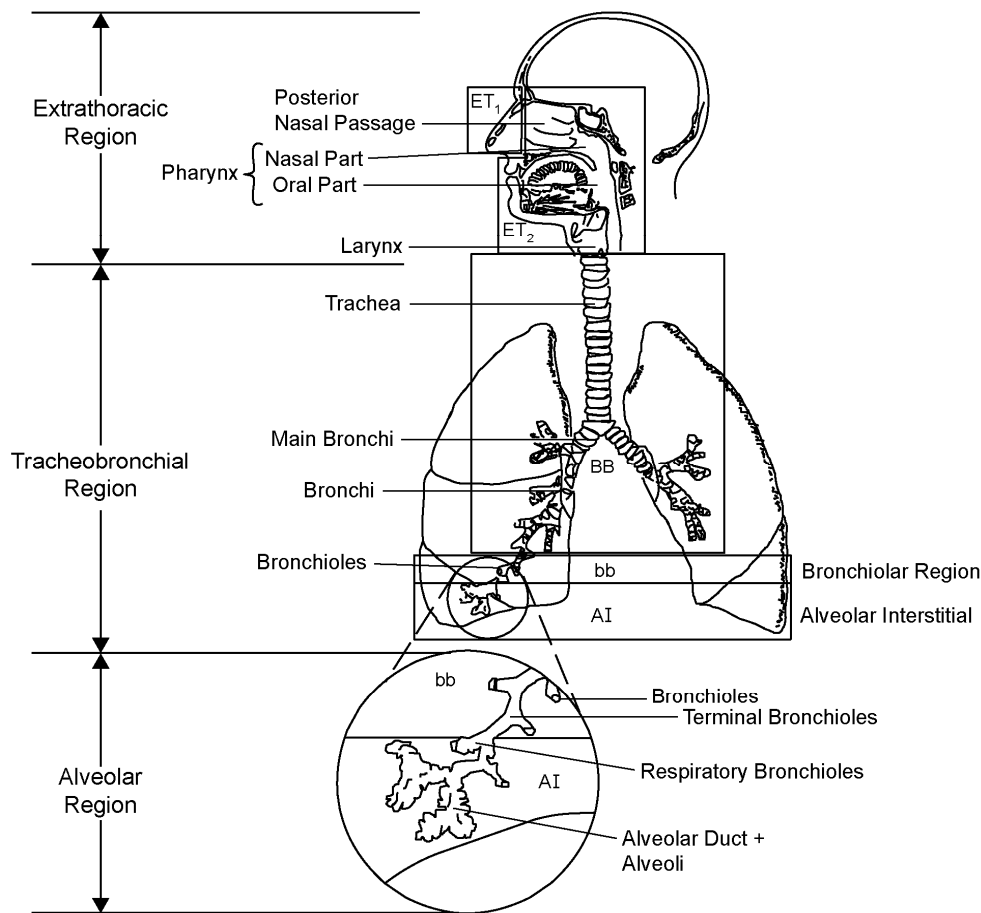
Equation 4-2

where: $z(P)$ is the normal standard deviate for a given probability. In most cases, the aerosols to which people are naturally exposed are polydisperse. By contrast, most experimental studies of particle deposition and clearance in the lung use monodisperse particles (GSD <1.15). Ambient aerosols may also be composed of multiple size modes, each mode should be described by its specific median diameter and GSD.

Aerosol size distributions may be measured and described in various ways. When a distribution is described by counting particles, the median is called the count median diameter (CMD). On the other hand, the median of a distribution based on particle mass in an aerosol is the mass median diameter (MMD). Impaction and sedimentation of particles in the respiratory tract depend on a particle's aerodynamic diameter (d_{ae}), which is the size of a sphere of unit density that has the same terminal settling velocity as the particle of interest. The size distribution is frequently described in terms of d_{ae} as the mass median aerodynamic diameter (MMAD), which is the median of the distribution of mass with respect to aerodynamic equivalent diameter. Alternative descriptions should be used for particles with actual physical sizes below $\approx 0.5 \mu\text{m}$ because, for these sized particles, aerodynamic properties become less important and diffusion becomes ever more important. For these smaller particles, their physical diameter or CMD are typically used since diffusivity is not a function of particle density. For small irregular shaped particles and aggregates, the diameter of a spherical particle that has the same diffusion coefficient in air as the particle in question is appropriate.

4.1.2. Structure of the Respiratory Tract

The basic structure of the human respiratory tract is illustrated in Figure 4-1. In the literature, the terms extrathoracic (ET) region and upper airways are used synonymously. The term lower airways is used to refer to the intrathoracic airways, i.e., the combination of the tracheobronchial (TB) region which is the conducting airways and the alveolar region which is the functional part or parenchyma of the lung. A recent review of interspecies similarities and differences in the structure and function of the respiratory tract is provided by Phalen et al. (2008, [156865](#)). Although the structure varies, the illustrated anatomic regions are common to all mammalian species with the exception of the respiratory bronchioles. Respiratory bronchioles, the transition region between ciliated and fully alveolated airways, are found in humans, dogs, ferrets, cats, and monkeys. Respiratory bronchioles are absent in rats and mice and abbreviated in hamsters, guinea pigs, oxen, sheep, and pigs. The branching structure of the ciliated bronchi and bronchioles also differs between species from being a rather symmetric and dichotomous branching network of airways in humans to a more monopodial branching network in other mammals.

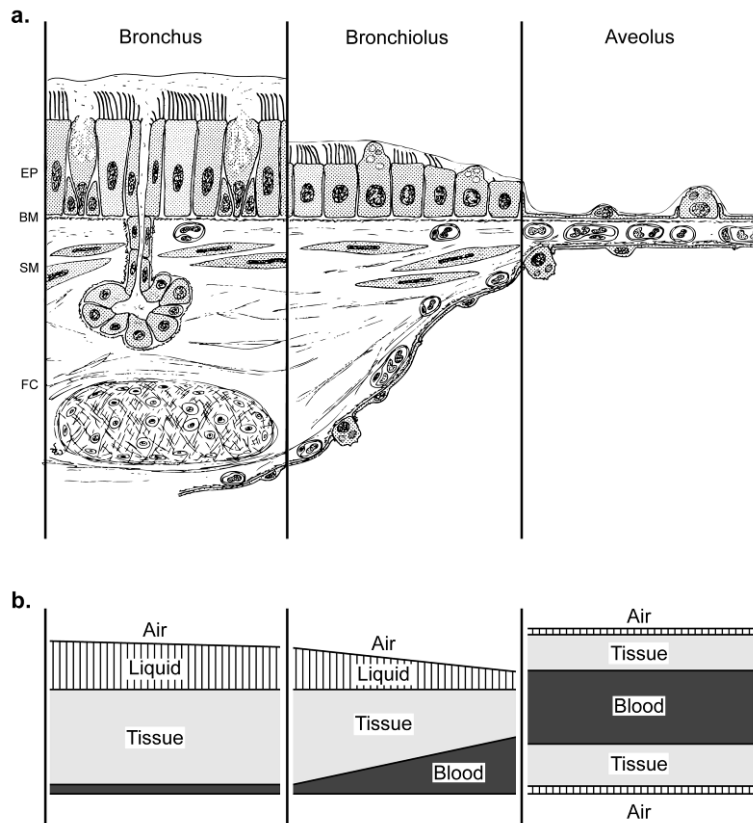


Source: Based on ICRP (1995, [006988](#)).

Figure 4-1. Diagrammatic representation of respiratory tract regions in humans. Structures are anterior nasal passages, ET₁; oral airway and posterior nasal passages, ET₂; bronchial airways, BB; bronchioles, bb; and alveolar interstitial, AI.

Another species difference relevant to particle dosimetry is the route of breathing. For instance, rodents are obligate nose breathers, whereas most humans are oronasal breathers who breathe through the nose when at rest and increasingly through the mouth with increasing activity

level. There is inter-individual variability in the route by which people breathe. Most people, 87% (26 of 30) in the Niinimaa et al. (1981, [071758](#)) study, breathed through their nose until an activity level was reached where they switched to oronasal breathing. Thirteen percent (4 of 30) of the subjects, however, were oronasal breathers even at rest. These two subject groups are commonly referred to in the literature (e.g. ICRP, 1995, [006988](#)) as “normal augmenters” and “mouth breathers,” respectively. In contrast to healthy subjects, Chadha et al. (1987, [037365](#)) found that the majority (11 of 12) of patients with asthma or allergic rhinitis breathe oronasally even at rest.



Source: Panel (a) reprinted with permission from McGraw Hill (Fishman and Elias, 1980, [156436](#))

Figure 4-2. Structure of lower airways with progression from the large airways to the alveolus. Panel (a) illustrates basic airway anatomy. Structures are epithelial cells, EP; basement membrane, BM; smooth muscle cells, SM; and fibrocartilaginous coat, FC. Panel (b) illustrates the relative amounts of liquid, tissue, and blood with distal progression.

The site of particle deposition within the respiratory tract has implications related to lung retention and surface dose of particles as well as potential systemic distribution of particles or their constituents. Figure 4-2 illustrates the progressive change in airway anatomy with distal progression into the lower respiratory tract. In the bronchi there is a thick liquid lining and mucociliary clearance rapidly moves deposited particles toward the mouth. In general, in the bronchi, only highly soluble materials moving from the air into the liquid layer will have systemic access via the blood. With distal progression, the protective liquid lining diminishes and clearance rates slow. Soluble compounds and some poorly soluble UFPs may cross the air-liquid interface to enter the tissues and the blood especially in the alveolar region.

4.2. Particle Deposition

Inhaled particles may be either exhaled or deposited in the ET, TB, or alveolar region. A particle becomes deposited when it moves from the airway lumen to the wall of an airway. The deposition of particles in the respiratory tract depends primarily on inhaled particle size, route of breathing (nasal or oronasal), tidal volume (V_T), breathing frequency (f), and respiratory tract morphology. The distinction between air passing through the nose versus the mouth is important since the nasal passages more effectively remove inhaled particles than the oral passage. Respiratory tract morphology, which affects particle transport and deposition, varies between species, the size of an animal or human, and health status.

The fraction of inhaled aerosol becoming deposited in the human respiratory tract has been measured experimentally. Studies, using light scattering or particle counting techniques to quantify the amount of aerosol in inspired and expired breaths, have characterized total particle deposition for varied breathing conditions and particle sizes. The vast majority of in vivo data on the regional particle deposition has been obtained by scintigraphic methods where external monitors are used to measure gamma emissions from radiolabeled particles. These scintigraphic data have shown highly variable regional deposition with sites of highly localized deposition or “hot spots” in the obstructed lung relative to the healthy lung. Even in the healthy lung, “hot spots” occur in the region of airway bifurcations. Mathematical models aid in predicting the mixed effects of particle size, breathing conditions, and lung volume on total and regional deposition. Experimentally, however, there is considerable inter-individual variability in total and regional deposition even when inhaled particle size and breathing conditions are strictly controlled. Section 4.2.4 on Biological Factors Modulating Deposition provides more detailed information on factors affecting deposition among individuals.

In order to potentially become deposited in the respiratory tract, particles must first be inhaled. The inspirable particulate mass fraction of an aerosol is that fraction of the ambient airborne particles that can enter the uppermost respiratory tract compartment, i.e., the head (Soderholm, 1985, [156992](#)). The American Conference of Governmental Industrial Hygienists (ACGIH) and the International Commission on Radiological Protection (ICRP) have established inhalability criteria for humans (ACGIH, 2005, [156188](#); ICRP, 1995, [006988](#)). These criteria are indifferent to route of breathing and assume random orientation with respect to wind direction. They are based on experimental inhalability data for $d_{ae} \leq 100 \mu\text{m}$ at wind speeds of between 1 and 8 m/s. For the ACGIH criterion, inhalability is 97% for an $d_{ae} = 1 \mu\text{m}$, 87% for an $d_{ae} = 5 \mu\text{m}$, 77% for an $d_{ae} = 10 \mu\text{m}$, and plateaus at 50% for d_{ae} above $\sim 40 \mu\text{m}$. The ICRP criterion, which also plateaus at 50% for very large d_{ae} , does not become of real importance until an $d_{ae} = 5 \mu\text{m}$ where inhalability is 97%. Dai et al. (2006, [156377](#)) reported slightly lower nasal particle inhalability in humans during moderate exercise than rest (e.g., 89.2 versus 98.1% for $13 \mu\text{m}$ particles, respectively). Nasal particle inhalability is similar between an adult and 7-year-old child (Hsu and Swift, 1999, [155855](#)). Inhalability into the mouth from calm air in humans also becomes important for $d_{ae} > 10 \mu\text{m}$ (Anthony and Flynn, 2006, [155659](#); Brown, 2005, [156299](#)). Unlike the inhalability from high wind speeds which plateaus at 50% for d_{ae} greater than $\sim 40 \mu\text{m}$, particle inhalability from calm air continues to decrease toward zero with increasing d_{ae} .

Inhalability data in laboratory animals, such as rats, are only available for breathing from relatively calm air (velocity $\leq 0.3 \text{ m/s}$). For nasal breathing, inhalability becomes an important consideration for d_{ae} of above $1 \mu\text{m}$ in rodents and $10 \mu\text{m}$ in humans (Ménache et al., 1995, [006533](#)). The inhalability of particles having d_{ae} of 2.5, 5, and $10 \mu\text{m}$ is 80, 65, and 44% in rats, respectively, whereas it only decreases to 96% for an d_{ae} of $10 \mu\text{m}$ in humans during nasal breathing (Ménache et

al., 1995, [006533](#)). Asgharian et al. (2003, [153068](#)) suggested that an even more rapid decrease in inhalability with increasing d_{ae} may occur in rats. Inhalability is a particularly important consideration for rodent exposures. Section 4.2.3 provides additional discussion of interspecies patterns of particle deposition.

4.2.1. Mechanisms of Deposition

Particle deposition in the lung is predominantly governed by diffusion, impaction, and sedimentation. Most discussion herein focuses on these three dominant mechanisms of deposition. Simple interception, which is an important mechanism of fiber deposition, is not discussed in this chapter. Electrostatic and thermophoretic forces as mechanisms of deposition have not been thoroughly evaluated and receive limited discussion. Some generalizations with regard to deposition by these mechanisms follows, but should not be viewed as absolute rules. Both experimental studies and mathematical models have demonstrated that breathing patterns can dramatically alter regional and total deposition for all sized particles. The combined processes of aerodynamic and diffusive (or thermodynamic) deposition are important for particles in the range of 0.1 μm to 1 μm . Aerodynamic processes predominate above and thermodynamic processes predominate below this range.

Diffusive deposition, by the process of Brownian diffusion, is the primary mechanism of deposition for particles having physical diameters of less than 0.1 μm . For particles having physical diameters of roughly between 0.05 and 0.1 μm , diffusive deposition occurs mainly in the small distal bronchioles and the pulmonary region of the lung. However, with further decreases in particle diameter below $\sim 0.05 \mu\text{m}$, increases in particle diffusivity shift more deposition proximally to the bronchi and ET regions.

Governed by inertial or aerodynamic properties, impaction and sedimentation increase with d_{ae} . When a particle has sufficient inertia, it is unable to follow changes in flow direction and strikes a surface thus depositing by the process of impaction. Impaction occurs predominantly at bifurcations in the proximal airways, where linear velocities and secondary eddies are at their highest. Sedimentation, caused by the gravitational settling of a particle, is most important in the distal airways and pulmonary region of the lung. In these regions, residence time is the greatest and the distances that a particle must travel to reach the wall of an airway are minimal.

The electrical charge on some particles may result in an enhanced deposition over what would be expected based on size alone. With an estimated charge of 10-50 negative ions per 0.5 μm particle, Scheuch et al. (1990, [006948](#)) found deposition in humans ($V_T = 500 \text{ mL}$, $f = 15 \text{ min}^{-1}$) to increase from 13.4% (no charge) to 17.8% (charged). This increase in deposition is thought to result from image charges induced on the surface of the airway by charged particles. Yu (1985, [006963](#)) estimated a charge threshold level above which deposition fractions would be increased of about 12, 30, and 54% for 0.3, 0.6, and 1.0 μm diameter particles, respectively. Electrostatic deposition is generally considered negligible for particles below 0.01 μm because so few of these particles carry a charge at Boltzmann equilibrium. This mechanism is also thought to be a minor contributor to overall particle deposition, but it may be important in some laboratory studies due to specific aerosol generation techniques such as nebulization. Laboratory methods such as passage of aerosols through a Kr-85 charge neutralizer prior to inhalation are commonly used to mitigate this effect.

The National Radiological Protection Board (NRPB) recently evaluated the potential for corona discharges from high voltage power lines to charge particles and enhance particulate doses (NRPB, 2004, [156815](#)). They concluded that electrostatic effects would be the most important for particles in the size range from about 0.1-1 μm , where deposition may theoretically increase by a factor of three to ten. However, given that only a small fraction of ambient particles would pass through the corona to become charged, the small range of relevant particle sizes (0.1-1 μm), and the subsequent required transport of charged particles to expose individuals; the NRPB concluded that effects, if any, of electric fields on particle deposition in the human respiratory tract would likely be minimal.

Thermophoretic forces on particles occur due to temperature differences between respired air and respiratory tract surfaces. Temperature gradients of around 20°C are thought to produce sufficient thermophoretic force to oppose diffusive and electrostatic deposition during inspiration and to perhaps augment deposition by these mechanisms during expiration (Jeffers, 2005, [156608](#)). Thermophoresis is only relevant in the extrathoracic and large bronchi airways and reduces to zero as the temperature gradient decreases deeper in the lung. Theoretical analysis of thermophoresis has been done for smooth walled tubes and is important over distances that are several orders of

magnitude smaller than the diameter of the trachea. The alteration of the flow patterns by airway surface features such as cartilaginous rings may affect particle transport and deposition over far greater distances than thermophoretic force.

4.2.2. Deposition Patterns

Knowledge of sites where particles of different sizes deposit in the respiratory tract and the amount of deposition therein is necessary for understanding and interpreting the health effects associated with exposure to particles. Particles deposited in the various respiratory tract regions are subjected to large differences in clearance mechanisms and pathways and, consequently, retention times. Deposition patterns in the human respiratory tract were described in considerable detail in dosimetry chapters of prior PM AQCD (U.S. EPA, 1996, [079380](#); U.S. EPA, 2004, [056905](#)); as such, they are only briefly described here.

Predicted total and regional deposition for an adult male during rest and light exercise are illustrated in Figure 4-3 and Figure 4-4, respectively. Note that a large proportion of inhaled coarse particles in the 3-6 μm (d_{ae}) range can reach and deposit in the lower respiratory tract, particularly the TB airways. Although these figures were provided in Chapter 6 of the 2004 PM AQCD, they are reproduced here to illustrate changes in deposition as a function of particle size and breathing conditions. The predictions were based on two publicly available particle deposition models, the ICRP (1995, [006988](#)) and the Multi-Path Particle Dosimetry model (MPPD; Version 1.0, ©2002). The ICRP (1995, [006988](#)) model was implemented by Lung Dose Evaluation Program (LUDEP; Version 2.07, June 2000). The MPPD¹ model was developed by the CIIT Centers for Health Research with support from the Dutch National Institute of Public Health and the Environment.

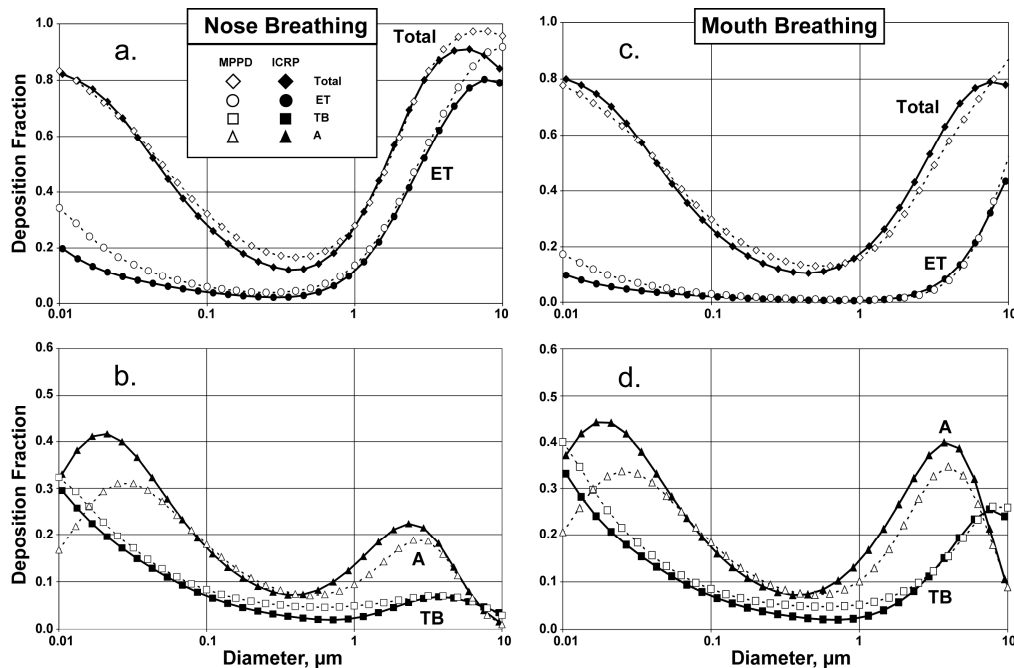


Figure 4-3. Comparison of total and regional deposition results from the ICRP and MPPD models for a resting breathing pattern ($V_T = 625 \text{ mL}$, $f = 12 \text{ min}^{-1}$) and corrected for particle inhalability. Regions are extrathoracic, ET; tracheobronchial, TB; and alveolar, A. Panels a-b are for nose breathing; panels c-d are for mouth breathing.

¹ For more information about this model, the reader is referred to: http://www.ara.com/products/mppd_capabilities.htm.

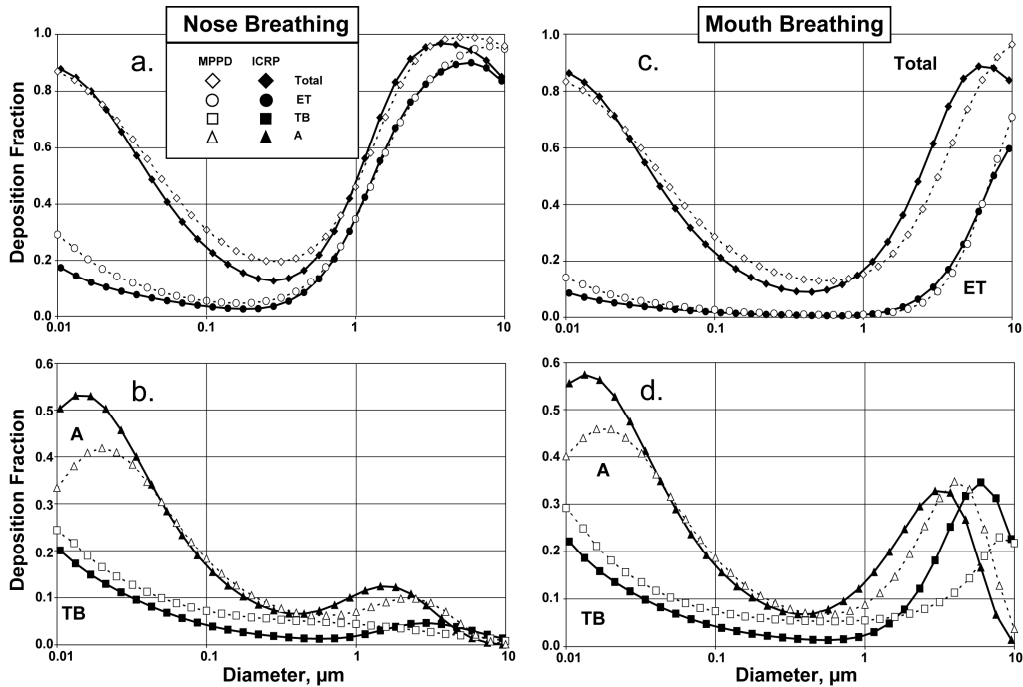
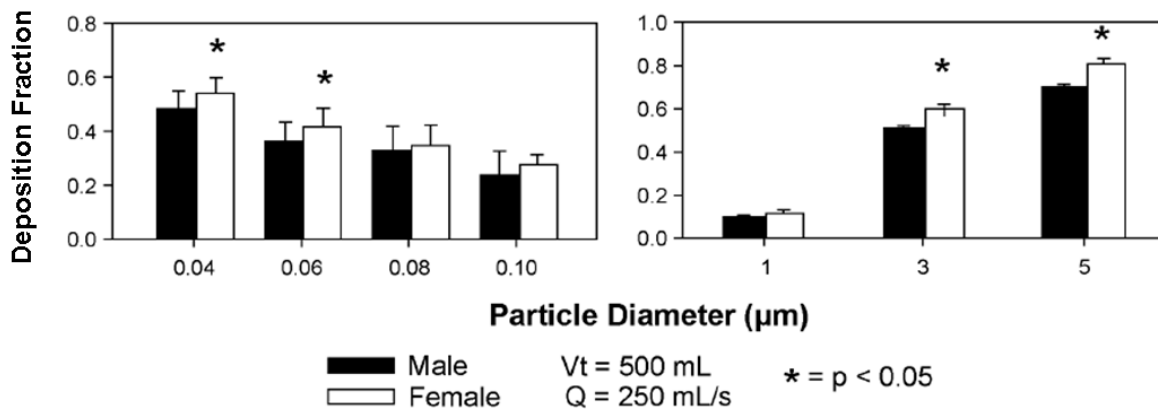


Figure 4-4. Comparison of total and regional deposition results from the ICRP and MPPD models for a light exercise breathing pattern ($V_T = 1250 \text{ mL}$, $f = 20 \text{ min}^{-1}$) and corrected for particle inhalability. Regions are extrathoracic, ET; tracheobronchial, TB; and alveolar, A. Panels a-b are for nose breathing; panels c-d are for mouth breathing.

4.2.2.1. Total Respiratory Tract Deposition

The efficiency of deposition in the respiratory tract may generally be described as a “U-shaped” curve on a plot of deposition efficiency versus the log of particle diameter. Total deposition shows a minimum for particle diameters in the range of 0.1 to 1.0 μm , where particles are small enough to have minimal sedimentation or impaction and sufficiently large so as to have minimal diffusive deposition. Total deposition does not decrease to zero for any sized particle, in part, because of mixing between particle laden tidal air and residual lung air. The particles mixed into residual air remain in the lung following a breath and are removed on subsequent breaths or gradually deposited. Total deposition approaches 100% for particles of roughly 0.01 μm (physical diameter) due to diffusive deposition and for particles of around 10 μm (d_{ac}) due to the efficiency of sedimentation and impaction.

Total human lung deposition, as a function of particle size, is depicted in Figure 4-5. These experimental data were obtained by using monodisperse spherical test particles in healthy adults during controlled breathing on a mouthpiece. Despite the control of inhaled particle size and breathing conditions, this figure illustrates variability in deposition efficiencies due to inter-individual differences in lung size and anatomical variability in airway dimensions and branching patterns.



Source: Data from Kim and Hu (1998, [086066](#)) and Kim and Jaques (2000, [012811](#)).

Figure 4-5. Total lung deposition measured in healthy adults (UF, 11 M, 11 F, 31 ± 4 yr; fine and coarse, 11 M, 11 F, 25 ± 4 yr) during controlled breathing on a mouthpiece. Deposition calculated from aerosol bolus measurements between 50 and 500 mL into a breath with 50 mL increments. Illustrated data are means and standard errors. Asterisk indicates significantly greater total deposition in females versus males.

4.2.2.2. Extrathoracic Region

The first line of defense for protecting the lower respiratory tract from inhaled particles is the nose and mouth. Particle deposition in the ET region, especially the nasal passages, reduces the amount available for deposition in the TB and alveolar regions. Recent data have become available, but are largely derived from computational fluid dynamics (CFD) modeling and experimental measurements in casts. As most of these studies do not substantially improve our understanding of deposition in the ET region they are not reviewed here.

For particles >1 μm d_{ae}, deposition efficiency in the oral and nasal passages has been generally described as a function of an impaction parameter (Stokes number) with the addition of a flow regime parameter (Reynolds number) for the oral passages (Finlay and Martin, 2008, [155776](#); Grgic et al., 2004, [155810](#); Kelly et al., 2005, [155894](#); Schroeter et al., 2006, [156076](#)). For an adult male, the CFD simulations of Schroeter et al. (2006, [156076](#)) predicted nasal deposition of 10 μm d_{ae} particles was 90%, and 100% for a V_E of 7.5 L/min (rest) and 15 L/min (light activity), respectively. Thus, relatively few large coarse particles will pass through the nasal passages into the lungs. Since the nasal passages are more efficient at removing inhaled particles than the oral passage, an individual's mode of breathing (i.e., oral versus nasal) influences the quantity of particles penetrating to the lung.

In limited studies, it has been shown that children tend to have more oral breathing both at rest and during exercise and also displayed more variability than adults (Becquemin et al., 1999, [155679](#); Bennett et al., 2008, [156269](#); James et al., 1997, [042422](#)). In contrast to adults, there is little data on the uptake of particles for oral or nasal breathing in children. Theoretical calculations by Xu and Yu (1986, [072697](#)) predict enhanced deposition of particles (>2 μm) in the head region for children when compared to adults. Studies of fine particle deposition in physical models of the nose, scaled to adult versus children sizes, predict that deposition efficiency in the nose is a function of pressure drop across the nose (Phalen et al., 1989, [156023](#)). Consequently, these model analyses suggest that, when properly scaled physiological flows are used in the calculation of nasal deposition, children, who have higher nasal resistance than adults, should have higher nasal deposition compared to adults. Surprisingly, the few studies reporting measures of nasal deposition in children, found lower nasal deposition efficiencies for fine particles (1-3 μm d_{ae}) as compared to adults, despite their higher nasal resistances (Becquemin et al., 1991, [009187](#); Bennett et al., 2008, [156269](#)). These findings of lesser nasal versus oral breathing and less efficient nasal deposition suggest that children's lower respiratory tract (i.e., the TB and alveolar regions) may receive a higher dose of

ambient PM compared to adults. Normalized to lung surface area, the dose rate to the lower airways of children versus adults is increased further because children breathe at higher minute ventilations relative to their lung volumes (see Section 4.2.4.2 on age as a factor modulating deposition).

4.2.2.3. Tracheobronchial and Alveolar Region

Inhaled particles passing the ET region enter and may become deposited in the lungs. For any given particle size, the pattern of particle deposition influences clearance by partitioning deposited material among lung regions. Deposition in the tracheobronchial airways and alveolar region cannot be directly measured *in vivo*. Much of the available deposition data for the TB and alveolar regions have been obtained from experiments with radioactively labeled, poorly soluble particles (U.S. EPA, 1996, [079380](#)) or by use of aerosol bolus techniques (U.S. EPA, 2004, [056905](#)). In general, the ability of these experimental data to define specific sites of particle deposition is limited to anatomically large regions of the respiratory tract such as the head, larynx, bronchi, bronchioles, and alveolar region. Mathematical modeling can provide more refined predictions of deposition sites. Comparisons of the modeling results obtained with two publicly available models were provided in Figure 4-3 and Figure 4-4. Highly localized sites of deposition within the bronchi are described in Section 4.2.2.4. Both experimental and modeling techniques are based on many assumptions that may be relatively good for the healthy lung but not for the diseased lung. For discussion of these issues, the reader is referred to Sections 4.2.4.4 and 4.2.4.5.

4.2.2.4. Localized Deposition Sites

From a toxicological perspective, it is important to realize that not all epithelial cells in an airway will receive the same dose of deposited particles. Localized deposition in the vicinity of airway bifurcations has been analyzed using experimental and mathematical modeling techniques. In the 1996 PM AQCD, experimental data were available illustrating the peak deposition of coarse particles (3, 5, and 7 μm d_{ae}) in daughter airways during inspiration and the parent airway during expiration, but always near the carinal ridge (Kim and Iglesias, 1989, [078539](#); Kim et al., 1989, [078538](#)). In the 2004 PM AQCD, mathematical models predicted distinct “hot spots” of deposition in the vicinity of the carinal ridge for both coarse (10 μm) and UF (0.01 μm) particles (Heistracher and Hofmann, 1997, [047514](#); Hofmann et al., 1996, [047515](#)). In a model of lung generations 4-5 during inspiration, hot spots occurred at the carinal ridge for 10 μm d_{ae} particles due to inertial impaction and for 0.01 μm particles due to secondary flow patterns formed at the bifurcation. During expiration, preferential sites of deposition for both particle sizes occurred 1) approaching the juncture of daughter airways on the walls forming and across the lumen from the carinal ridge; and 2) the top and bottom (visualizing the Y-shaped geometry laying horizontal) of the parent airway downstream of the bifurcation.

Recent studies further support these findings (Balashazy et al., 2003, [155671](#); Farkas and Balásházy, 2008, [157358](#); Farkas et al., 2006, [155771](#); Isaacs et al., 2006, [155861](#)). Most of these studies quantified localized deposition in terms of an enhancement factor. Typically, the enhancement factor is the ratio of the deposition in a pre-specified surface area (e.g., 100 \times 100 μm which corresponds to $\sim 10 \times 10$ epithelial cells) to the average deposition density for the whole airway geometry. These enhancement factors are very sensitive to the size of the surface considered (Balashazy et al., 1999, [043201](#)). The studies by Farkas et al. (2006, [155771](#)) and Farkas and Balásházy (2008, [157358](#)) investigated the phenomena of localized deposition down to 0.001 μm particles. The deposition of 0.001 μm was rather uniform, however, the deposition pattern became increasingly less uniform with increasing particle size. These studies indicate that, for particles greater than ~ 0.01 μm , some cells located near the carinal ridge of bronchial bifurcations may receive hundreds to thousands times the average dose (particles per unit surface area) of the parent and daughter airways. Furthermore, the inertial impaction of particles ≥ 1 μm d_{ae} at the carinal ridge of large bronchi will increase with increasing inspiratory flows. In a comparison of constricted versus healthy airways, Farkas et al. (2006, [155771](#)) also reported that the overall deposition efficiency of 10 μm d_{ae} particles at bifurcations downstream of a constriction may be increased by 18 times. Given these considerations, Phalen and Oldham (2006, [156024](#)) noted that substantial doses of particles (≥ 1 μm d_{ae}) may be justified for *in vitro* studies using tracheobronchial epithelial cell cultures.

4.2.3. Interspecies Patterns of Deposition

The primary purpose of this document is to assess the health effects of particles in humans. As such, human dosimetry studies have been stressed in this chapter. Such studies avoid the uncertainties associated with the extrapolation of dosimetric data from laboratory animals to humans. However, animal models have been and continue to be used in evaluating PM health effects because of ethical considerations regarding the types of studies that can be performed with human subjects. Thus, there is a considerable need to understand dosimetry in animals and dosimetric differences between animals and humans. Limited new data are becoming available. Similar deposition efficiencies have been reported in nasal casts of human and rhesus monkey for 1-10 μm d_{ae} for inspiratory flows mimicking resting breathing patterns (Kelly et al., 2005, [155894](#)). Oldham and Robinson (2007, [156003](#)) recently provided morphological data and predicted particle deposition in an asthma mouse model.

Interspecies similarities and differences in deposition were described in detail in the last two PM AQCDs (U.S. EPA, 1996, [079380](#); U.S. EPA, 2004, [056905](#)). It was concluded that the general pattern of total particle deposition efficiency was similar between laboratory animals and humans: deposition increases on both sides of a minimum that occurs for particles of 0.2-1 μm . There are, however, marked interspecies differences in uptake into the respiratory tract and regional deposition. For instance, the nasal inhalability of 10 μm d_{ae} particles is predicted to be 96% in humans, whereas it is only 44% in rats (Ménache et al., 1995, [006533](#)). In most laboratory animal species (rat, mouse, hamster, guinea pig, and dogs), deposition in the ET region is near 100% for particles >5 μm d_{ae} (Raabe et al., 1988, [001439](#)), indicating greater efficiency than that seen in humans. Detailed presentation of dosimetric difference between rats and humans are available elsewhere (Brown et al., 2005, [089308](#); Jarabek et al., 2005, [056756](#)).

Brown et al. (2005, [089308](#)) conducted a thorough evaluation of extrapolations between rats and humans in relation to PM exposures. One of many factors they considered was the choice of a dose metric appropriate for comparison between species. For example, deposited mass may be an appropriate PM indicator for health effects associated with soluble PM constituents. For health effects associated with insoluble PM, the particle number, surface area, or mass may be appropriate indicators. Given interspecies differences in deposition patterns and clearance rates, the question of retained versus deposited dose was also discussed. It was concluded that for acute effects, the incremental dose may be the appropriate type of dose metric. For chronic effects, long-term burden may be more appropriate. For various dose metrics, estimates of particle concentration and exposure duration required for a rat to receive the same dose as received by a human were obtained with consideration of activity levels, mode of breathing, and particle size distributions. It was noted that high PM exposures over the period of months can lead to particle overload in rats (see Section 4.3.4.4). Exposure regimes were derived as a function of particle size and exposure duration that should avoid overwhelming macrophage mediated clearance achieving particle overload in rats (see Table 12 in Brown et al., 2005, [089308](#)). The dosimetric calculations indicated that to achieve nominally similar acute doses per surface area in rats, relative to humans undergoing moderate to high exertion, PM exposure concentrations for rats would need to be somewhat higher than for humans. Since particle clearance from the lungs of rats is faster than humans, much higher exposure concentrations are required for the rat to simulate retained burdens of humans. Illustrating the complexity of such analyses, in some cases, rats were found to require lower exposures than humans to have comparable doses (generally when considering a scenario of humans at rest).

4.2.4. Biological Factors Modulating Deposition

Evaluation of factors affecting particle deposition is important to help understand potentially susceptible subpopulations. Differences in biological response following pollutant exposure may be caused by dosimetry differences as well as by differences in innate sensitivity. The effects of different biological factors on deposition were discussed in the 2004 PM AQCD (U.S. EPA, 2004, [056905](#)) and are summarized briefly here.

4.2.4.1. Physical Activity

The activity level of an individual is well recognized to affect their minute ventilation and route of breathing. Changes in minute ventilation during exercise are accomplished by increasing both V_T and f (Table 4-1). Humans are oronasal breathers tending to breathe through the nose when at rest and increasingly through the mouth with increasing activity level. There is considerable inter-individual variability in both the route by which people breathe and the way breathing pattern changes occur.

Table 4-1. Breathing patterns with activity level in adult human male.

Activity	Awake Rest ^a	Slow Walk ^a	Light Exertion ^a	Moderate Exertion ^a	Heavy Exertion ^b
Breaths/min	12	16	19	28	26
Tidal volume, mL	625	813	1000	1429	1923
Minute ventilation, L/min	7.5	13	19	40	50

Sources: ^aWinter-Sorkina and Cassee (2002, [043670](#)); ^bICRP (1995, [006988](#))

Individuals typically breathe through their nose while at rest, switching to oronasal breathing as ventilation increases (Bennett et al., 2003, [191977](#); Niinimaa et al., 1981, [071758](#)). The role of the nose in filtering particles is diminished as airflow is diverted from the nose to the mouth during exercise, bringing more particles to the lower respiratory tract. A recent study in adults (Bennett et al., 2003, [191977](#)) found that nasal ventilation during exercise varied as a function of both race and gender. African-Americans possessed a greater nasal contribution to breathing during exercise than Caucasians. At similar exercise efforts (i.e., normalized to a % maximum work capacity) the females also had a greater nasal contribution to breathing during exercise than males.

In addition, when individuals increase their ventilation with activity the total number of particles inhaled per unit time (i.e., exposure rate) increases, but the fractional deposition of particles in each breath also changes with breathing pattern. Figure 4-3 and Figure 4-4 illustrate predicted deposition fractions in the respiratory tract during rest versus light exercise, respectively. During exercise, both V_T and f increase. Fractional deposition for all particles increases with increased V_T . Increasing the f , however, decreases the fractional deposition of fine and UFPs due to decreased time for gravitational and diffusive deposition. For particles larger than a d_{ac} of roughly 3 μm , increasing f can increase the deposition fraction due to increased impaction in the extrathoracic and TB airways. Thus, it should be expected that the change in deposition fraction with activity will vary among individuals depending on the relative influences of these two variables (i.e., V_T and f) in a given subject and the particle size to which they are exposed. Experimentally, the lung deposition fractions of fine particles during moderate exercise and mouth breathing are unchanged between rest and exercise (Bennett et al., 1985, [190034](#); Morgan et al., 1984, [190035](#)). Kim (2000, [013112](#)) evaluated differences in deposition of 1, 3, and 5 μm (MMAD) particles under varying breathing patterns (simulating breathing conditions of sleep, resting, and mild exercise). Total lung deposition increased with increasing V_T at a given flow rate and with increasing flow rate at a given breathing period. These experimental studies suggest that the total deposited dose rate (i.e., deposition per unit time) of particles will generally increase in direct proportion to the increase in minute ventilation associated with exercise.

The changes in ventilation, i.e., breathing pattern and flow rate, may also alter the regional deposition of particles. Coarse particle deposition increases in the TB and ET regions during exercise due to the increased flow rates and associated impaction. A rapid-shallow breathing pattern during exercise may result in more bronchial airway versus alveolar deposition, while a slow-deep pattern will shift deposition to deeper lung regions (Valberg et al., 1982, [190019](#)). Bennett et al. (1985, [190034](#)) showed for 2.6 μm particles that moderate exercise shifted deposition from the lung periphery towards ET and larger, bronchial airways. Similarly, Morgan et al. (1984, [190035](#)) showed that even for fine particles (0.7 μm) TB deposition was enhanced with exercise. This shift in deposition toward the bronchial airways results in a much greater dose per unit surface area of tissue in those regions. Morgan et al. (1984, [190035](#)) also found that the apical-to-basal distribution of fine

particles increased with exercise, i.e., a shift towards increased deposition in the lung apices. This shift may be less likely for larger particles, however, whose deposition in large airway bifurcations may preclude their transport to these more apical regions (Bennett et al., 1985, [190034](#)).

4.2.4.2. Age

Airway structure and respiratory conditions vary with age, and these variations may alter the amount and site of particle deposition in the respiratory tract. It was concluded in the 2004 PM AQCD (U.S. EPA, 2004, [056905](#)) that significant differences between adults and children had been predicted by mathematical models and observed in experimental studies. Studies generally indicated that ET and TB deposition was greater in children and that children received greater doses of particles per lung surface area than adults. Deposition studies in the elderly are still quite limited.

A few studies have attempted to measure oronasal breathing in children as compared to adults (Becquemin et al., 1999, [155679](#); Bennett et al., 2008, [156269](#); James et al., 1997, [042422](#)). This is important since particles deposit with greater efficiency in the nose relative to the mouth, thereby affecting exposure of the lower respiratory tract. James et al. (1997, [042422](#)) found that children (age 7-16 yr, n = 10) displayed more variability than adults with respect to their oronasal pattern of breathing with exercise. However, it was not possible to predict the pattern of the partitioning of ventilation during exercise based on age, gender, or nasal airway resistance. Further, in a limited number of children (age 8-16 yr, n = 10), Becquemin et al. (1999, [155679](#)) found that the children tended to display more oral breathing both at rest and during exercise than the adults. The highest oral fractions were also found in the youngest children. None of these studies, however, was able to show a relationship between nasal resistance and the relative contribution of nasal breathing in children. Bennett et al. (2008, [156269](#)) made preliminary measurements of the relative contributions of oral versus nasal breathing at rest and during incrementally graded submaximal exercise on the cycle ergometer for children (age 6-10 yr, n = 12) and adults (age 18-27 yr, n = 11). There was a trend for children to have a lesser nasal contribution to breathing at rest and during exercise, but the differences from adults were not statistically significant.

Breathing patterns are well recognized to change with increasing age, i.e., V_T increase and respiratory rates decrease (Tabachnik et al., 1981, [157036](#); Tobin et al., 1983, [156122](#)). Bennett and Zeman (1998, [076182](#)) measured the deposition fraction of inhaled, fine particles ($2 \mu\text{m } d_{ae}$) in children (age 7-14 yr, n=16) and adults (age 19-35 yr, n=12) as they breathed the aerosol with their natural, resting breathing pattern. Among the children, variation in deposition fractions, measured by photometry at the mouth, was highly dependent on intersubject variation in V_T . On the other hand, they found no difference in deposition fractions between children versus adults for these fine particles. This finding and the modeling predictions (Hofmann et al., 1989, [006922](#)) are explained in part by the smaller V_T and faster breathing rate of children relative to adults for natural breathing conditions. Bennett et al. (2008, [156269](#)) also recently reported measures of fine particle (1 and $2 \mu\text{m } d_{ae}$) deposition at ventilation rates typical of light exercise in children (age 6-10 yr, n=12) and adults (age 18-27 yr, n=11) and showed that, like with resting breathing, deposition fractions were predicted by breathing pattern and did not differ or tended to be less in children compared to adults. On the other hand, because children breathe at higher minute ventilations relative to their lung volumes, the rate of deposition of fine particles normalized to lung surface area may be greater in children versus adults (Bennett and Zeman, 1998, [076182](#)).

Bennett and Zeman (2004, [155686](#)) expanded their measures of fine particle deposition during resting breathing to a larger group of healthy children (6-13 yr; 20 boys, 16 girls) and found again that the variation in total deposition was best predicted by V_T ($r = 0.79$, $p < 0.001$). But both V_T and resting minute ventilation increased with both height and body mass index (BMI) of the children. Interestingly, these data suggest that for a given height and age, children with higher BMI have larger minute ventilations and V_T at rest than those with lower BMI. These differences in breathing patterns as a function of BMI translated into increased deposition of fine particles in the heaviest children. The rate of deposition (i.e., particles depositing per unit time) in the overweight children was 2.8 times that of the leanest children ($p < 0.02$). Among all children, the rate of deposition was significantly correlated with BMI ($r = 0.46$, $p < 0.004$). Some of the increase in deposition fractions of heavier children may be due to their elevated V_T , which was well correlated with BMI ($r = 0.72$, $p < 0.001$).

In 62 healthy adults with normal lung function aged 18-80 yr, Bennett et al. (1996, [083284](#)) showed there was no effect of age on the whole lung deposition fractions of $2\text{-}\mu\text{m}$ particles under

natural breathing conditions. Across all subjects, the deposition fractions were found to be independent of age, depending on breathing period ($r = 0.58$, $p < 0.001$) and airway resistance ($r = 0.46$, $p < 0.001$). In the same adults breathing with a fixed pattern (360 mL V_T , 3.4 sec breathing period), there was a mild decrease in deposition with increasing age, which could be attributed to increased peripheral airspace dimensions in the elderly.

4.2.4.3. Gender

Males and females differ in body size, conductive airway size, and ventilatory parameters; therefore, gender differences in deposition might be expected. In some of the controlled studies, however, the men and women were constrained to breathe at the same V_T and f . Since women are generally smaller than men, the increased minute ventilation of women compared to their normal ventilation could affect deposition patterns. This may help explain why gender related effects on deposition have been observed in some studies.

Kim and Hu (1998, [086066](#)) assessed the regional deposition patterns of 1-, 3-, and 5- μm MMAD particles in healthy adult males and females using controlled breathing. The total fractional deposition in the lungs was similar for both genders with the 1- μm particle size, but was greater in women for the 3- and 5- μm particles. Deposition also appeared to be more localized in the lungs of females compared to those of males. Kim and Jaques (2000, [012811](#)) measured deposition in healthy adults using sizes in the UF mode (0.04-0.1 μm). Total fractional lung deposition was greater in females than in males for 0.04- and 0.06- μm particles. The region of peak fractional deposition was shifted closer to the mouth and peak height was slightly greater for women than for men for all exposure conditions. The total lung deposition data from these studies are illustrated in Figure 4-5. These differences were generally attributed to the smaller size of the upper airways, particularly of the laryngeal structure, in females.

In another study (Bennett et al., 1996, [083284](#)), the total respiratory tract deposition of 2- μm particles was examined in adult males and females aged 18-80 yr who breathed with a normal resting pattern. There was a tendency for greater deposition fractions in females compared to males. However, since males had greater minute ventilation, the deposition rate (i.e., deposition per unit time) was greater in males than in females. More recently, Bennett and Zeman (2004, [155686](#)) found no difference in the deposition of 2- μm particles in boys versus girls aged 6-13 yr ($n = 36$).

4.2.4.4. Anatomical Variability

Anatomical variability, even in the absence of respiratory disease, can affect deposition throughout the respiratory tract. The ET region is the first exposed to inhaled particles and, therefore, deposition within this region would reduce the amount of particles available for deposition in the lungs. Variations in relative deposition within the ET region will, therefore, propagate through the rest of the respiratory tract, creating differences in calculated doses among individuals.

The influence of variations in nasal airway geometry on particle deposition has been investigated. Cheng et al. (1996, [047520](#)) examined nasal airway deposition in healthy adults using particles ranging in size from 0.004 to 0.15 μm and at 2 constant inspiratory flow rates, 167 and 333 mL/s. Inter-individual variability in deposition was correlated with the wide variation of nasal dimensions; in that, greater surface area, smaller cross-sectional area, and increasing complexity of airway shape were all associated with enhanced deposition. Bennett and Zeman (2005, [155687](#)) have also shown that nasal anatomy influences the efficiency of particle uptake in the noses of adults. For light exercise breathing conditions in adults, their study demonstrated that nasal deposition efficiencies for both 1- and 2- μm monodisperse particles were significantly less in African Americans versus Caucasians. The lesser nasal efficiencies in African-Americans were associated with both lower nasal resistance and less elliptical nostrils compared to Caucasians.

Within the lungs, the branching structure of the airways may also differ between individuals. Zhao et al. (2009, [157187](#)) recently examined the bronchial anatomy of the left lung in patients (132 M, 84 W; mean age 47 yr) that underwent conventional thoracic computed tomography scans for various reasons. At the level of the segmental bronchus in the upper and lower lobes, a bifurcation occurred in the majority of patients. A trifurcation, however, was observed in 23% of the upper and 18% of the lower lobes. Other more unusual findings were also reported such as four bronchi arising from the left upper lobe bronchus. As described in Section 4.2.2.4, deposition can be highly localized near the carinal ridge of bifurcations. The effect of a bifurcation versus other

branching patterns on airflow patterns and particle deposition has not been described in the literature. Martonen et al. (1994, [000847](#)) showed that a wide blunt carinal ridge shape dramatically affected the flow stream lines relative to a narrower and more rounded ridge shape. Specifically, there were high flow velocities across the entire area of the blunt carinal ridge versus a smoother division of the airstream in the case of the narrow rounded ridge shape. The implication may be that localized particle deposition on the carinal ridge would increase with ridge width. A similar situation might be expected for a trifurcation versus a bifurcation. These differences in branching patterns provide a clear example of anatomical variability among individuals that might affect both air flow patterns and sites of particle deposition.

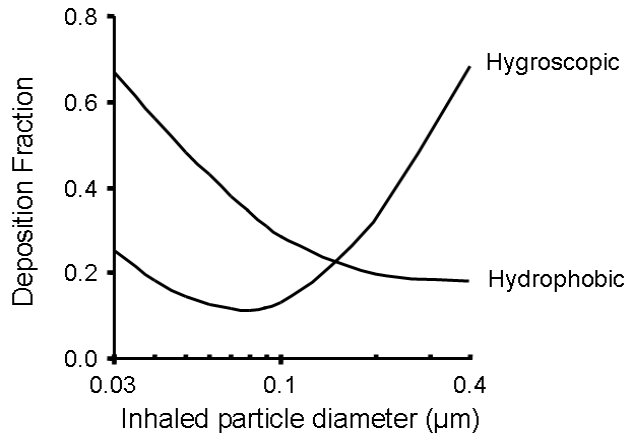
4.2.4.5. Respiratory Tract Disease

The presence of respiratory tract disease can affect airway structure and ventilatory parameters, thus altering deposition compared to that occurring in healthy individuals. The effect of airway diseases on deposition has been studied extensively, as described in the 1996 and 2004 PM AQCD (U.S. EPA, 1996, [079380](#); U.S. EPA, 2004, [056905](#)). Studies described therein showed that people with chronic obstructive pulmonary disease (COPD) had very heterogeneous deposition patterns and differences in regional deposition compared to healthy individuals. People with obstructive pulmonary diseases tended to have greater deposition in the TB region than did healthy people. Furthermore, there tended to be an inverse relationship between bronchoconstriction and the extent of deposition in the alveolar region, whereas total respiratory tract deposition generally increased with increasing degrees of airway obstruction.

The vast majority of deposition studies in individuals with respiratory disease have been performed during controlled breathing, i.e., all subjects breathed with the same V_T and f . However, although resting V_T is similar or elevated in people with COPD compared to healthy individuals, the former tend to breathe at a faster rate, resulting in higher than normal tidal peak flow and resting minute ventilation. Thus, given that breathing patterns differ between healthy and obstructed individuals, particle deposition data for controlled breathing may not be appropriate for estimating respiratory doses from ambient PM exposures.

Bennett et al. (1997, [078839](#)) measured the fractional deposition of insoluble 2- μm particles in moderate-to-severe COPD patients ($n = 13$; mean age 62 yr) and healthy older adults ($n = 11$; mean age 67 yr) during natural resting breathing. COPD patients had about a 50% greater deposition fraction and a 50% increase in resting minute ventilation relative to the healthy adults. As a result, the patients had an average deposition rate of about 2.5 times that of healthy adults. Similar to previously reviewed studies (U.S. EPA, 1996, [079380](#); U.S. EPA, 2004, [056905](#)), these investigators observed an increase in deposition with an increase in airway resistance, suggesting that deposition increased with the severity of airway disease.

Brown et al. (2002, [043216](#)) measured the deposition of an UF aerosol ($\text{CMD} = 0.033 \mu\text{m}$) during natural resting breathing in 10 patients with moderate-to-severe COPD (mean age 61 yr) and 9 healthy adults (mean age 53 yr). The COPD group consisted of 7 patients with chronic bronchitis and 3 patients with emphysema. The total deposition fraction in the bronchitic patients (0.67) was significantly ($p < 0.02$) greater than in either the patients with emphysema (0.48) or the healthy subjects (0.54). Minute ventilation increased with disease severity (healthy, 5.8 L/min; chronic bronchitic, 6.9 L/min; emphysema, 11 L/min). Relative to the healthy subjects, the average dose rate was significantly ($p < 0.05$) increased by 1.5 times in the COPD patients, whereas the average deposition fraction only tended to be increased by 1.1 times. These data further demonstrate the need to consider dose rates (which depend on minute ventilation) rather than just deposition fractions when evaluating the effect of respiratory disease on particle deposition and dose.



Source: Data from Tu and Knutson (1984, [072870](#)).

Figure 4-6. Total deposition of hygroscopic sodium chloride and hydrophobic aluminosilicate aerosols during oral breathing ($V_T = 1.0$ L; $f = 15$ min⁻¹).

4.2.4.6. Hygroscopicity of Aerosols

Experimental and modeling studies of hygroscopic aerosol growth and deposition in the lung were extensively discussed in Section 10.4.3.1 of the 1996 PM AQCD (U.S. EPA, 1996, [079380](#)). Hygroscopic ambient aerosols include sulfates, nitrates, some organics, and aerosols laden with sodium or potassium. The high relative humidity in the lungs contributes to rapid growth of hygroscopic particles and dramatically alters the deposition characteristics of ambient hygroscopic aerosols relative to nonhygroscopic aerosols. Nonhygroscopic particles in the range of 0.3 µm have minimal intrinsic mobility and low total deposition in the lungs. However, a 0.3 µm salt particle (dry) will grow in vivo to nearly 2 µm and deposit to a far greater extent (Anselm et al., 1990, [156217](#)). The hygroscopic growth of particles in the respiratory tract decreases diffusive deposition and increases aerodynamic deposition as illustrated in Figure 4-6.

4.2.5. Summary

Particle deposition in the respiratory tract occurs predominantly by diffusion, impaction, and sedimentation. Deposition is minimal for particle diameters in the range of 0.1 to 1.0 µm, where particles are small enough to have minimal sedimentation or impaction and sufficiently large so as to have minimal diffusive deposition. In humans, total respiratory tract deposition approaches 100% for particles of roughly 0.01 µm (physical diameter) due to diffusive deposition and for particles of around 10 µm d_{ae} due to the efficiency of sedimentation and impaction.

The first line of defense for protecting the lower respiratory tract from inhaled particles is the nose and mouth. Nasal deposition approaches 100% in the average human for 10 µm d_{ae} particles. Experimental studies show lower nasal particle deposition in children than adults. Relative to adults, children also tend to breathe more through their mouth which is less efficient for removing inhaled particles than the nose. These findings suggest that the lower respiratory tract of children may receive a higher dose of ambient PM compared to adults. Since children breathe at higher minute ventilations relative to their lung volumes, the rate of particle deposition normalized to lung surface area may be further increased relative to adults.

People with COPD generally have greater total deposition and more heterogeneous deposition patterns compared to healthy individuals. The observed increase in deposition correlates with increases in airway resistance, suggesting that deposition increases with the severity of airway disease. COPD patients also have an increased resting minute ventilation relative to the healthy adults. This demonstrates the need to consider dose rates (which depend on minute ventilation)

rather than just deposition fractions when evaluating the effect of respiratory disease on particle deposition and dose.

Modeling studies indicate that, for particles greater than $\sim 0.01 \mu\text{m}$, some cells located near the carinal ridge of bronchial bifurcations may receive hundreds to thousands times the average dose (particles per unit surface area) of the parent and daughter airways. The inertial impaction of particles $\geq 1 \mu\text{m } d_{ae}$ at the carinal ridge of large bronchi increases with increasing inspiratory flows. Airway constriction can further augment the overall deposition efficiency of coarse particles at downstream bifurcations. These findings suggest that substantial doses of particles ($\geq 1 \mu\text{m } d_{ae}$) may be justified for in vitro studies using tracheobronchial epithelial cell cultures.

Our ability to extrapolate between species has not generally changed since the 2004 PM AQCD (U.S. EPA, 2004, [056905](#)). However, some considerations related to coarse particles warrant comment. The inhalability of particles having d_{ae} of 2.5, 5, and 10 μm is 80, 65, and 44% in rats, respectively, whereas it remains near 100% for a d_{ae} of 10 μm in humans. In most laboratory animal species (rat, mouse, hamster, guinea pig, and dogs), deposition in the extrathoracic region is near 100% for particles greater than 5 $\mu\text{m } d_{ae}$. By contrast, in humans nasal deposition approaches 100% for 10 $\mu\text{m } d_{ae}$. Oronasal breathing versus obligate nasal breathing further contributes to greater penetration of coarse particles into the lower respiratory tract of humans than rodents.

4.3. Clearance of Poorly Soluble Particles

This section discusses the clearance and translocation of poorly soluble particles that have deposited in the respiratory tract. The term “clearance” is used here to refer to the processes by which deposited particles are removed by mucociliary action or phagocytosis from the respiratory tract. “Translocation” is used here mainly to refer to the movement of free particles across cell membranes and to extrapulmonary sites. In the literature, translocation may also refer to the extra- and intracellular dissolution of particles and the subsequent transfer of dissociated material to the blood through extra- and intracellular fluids and across the various cell membranes and lung tissues. The clearance and distribution of soluble particles and soluble constituents of particles are discussed in Section 4.4.

A basic overview of biological mechanisms and clearance pathways from various regions of the respiratory tract are presented in the following sections. Then regional kinetics of particle clearance are addressed. Subsequently, an update on interspecies patterns and rates of particle clearance is provided. The translocation of UFPs is also discussed. Finally, information on biological factors that may modulate clearance is presented.

4.3.1. Clearance Mechanisms and Kinetics

For any given particle size, the deposition pattern of poorly soluble particles influences clearance by partitioning deposited material between lung regions. Tracheobronchial clearance of poorly soluble particles in humans, with some exceptions, is thought (in general) to be complete within 24-48 h through the action of the mucociliary escalator. Clearance of poorly soluble particles from the alveolar region is a much slower process which may continue from months to years.

4.3.1.1. Extrathoracic Region

Particles deposited in either the nasal or oral passages are cleared by several mechanisms. Particles depositing in the mouth may generally be assumed to be swallowed or removed by expectoration. Particles deposited in the posterior portions of the nasal passages are moved via mucociliary transport towards the nasopharynx and swallowed. Mucus flow in the most anterior portion of the nasal passages is forward, toward the vestibular region where removal occurs by sneezing, wiping, or nose blowing.

4.3.1.2. Tracheobronchial Region

Mucociliary clearance in the TB region has generally been considered to be a rapid process that is relatively complete by 24-48 h post-inhalation in humans. Mucociliary clearance is frequently modeled as a series of “escalators” moving material proximally from one generation to the next. As such, the removal rate of particles from an airway generation increases with increasing tracheal mucus velocity. Assuming continuity in the amount of mucus between airway generations, mucus velocities decrease and transit times within an airway generation increase with distal progression. Although clearance from the TB region is generally rapid, experimental evidence discussed in the 1996 and 2004 PM AQCD (U.S. EPA, 1996, [079380](#); U.S. EPA, 2004, [056905](#)) showed that a fraction of material deposited in the TB region is retained much longer.

The slow-cleared TB fraction (i.e., the fraction of particles deposited in the TB region that are subject to slow clearance) was thought to increase with decreasing particle size. For instance, Roth et al. (1993, [156928](#)) showed approximately 93% retention of UFPs (30 nm median diameter) thought to be deposited in the TB region at 24 h post-inhalation. The slow phase clearance of these UFPs continued with an estimated half-time ($t_{1/2}$) of around 40 days. Using a technique to target inhaled particles (monodisperse 4.2 μm MMAD) to the conducting airways, Möller et al. (2004, [155987](#)) observed that $49 \pm 9\%$ of particles cleared rapidly ($t_{1/2}$ of 3.0 ± 1.6 h), whereas the remaining fraction cleared considerably slower ($t_{1/2}$ of 109 ± 78 days). The ICRP (1995, [006988](#)) human respiratory tract model assumes particles ≤ 2.5 μm (physical diameter) to have a slow-cleared TB fraction of 50%. The slow-cleared fraction assumed by the ICRP (1995, [006988](#)) decreases with increasing particle size to $<1\%$ for 9 μm particles. Considering the UF data of Roth et al. (1993, [156928](#)) in addition to data considered by the ICRP (1995, [006988](#)), Bailey et al. (1995, [190057](#)) estimated a slow-cleared TB fraction of 75% for UFPs. At that time, they (Bailey et al. 1995) also estimated the slow-cleared fraction to decrease with increasing particle size to 0% for particles ≥ 6 μm . Recent experimental evidence from the same group (Smith et al., 2008, [190037](#)) showed no difference in TB clearance among humans for particles with geometric sizes of 1.2 versus 5 μm , but the same d_{ae} (5 μm) so as to deposit similarly in the TB airways. For at least micron-sized particles, these recent findings do not support the particle size dependence of a slow-cleared TB fraction. As discussed further below, much of the apparent slow-cleared TB fraction may be accounted for by differences in deposition patterns, i.e., greater deposition in the alveolar region than expected.

A portion of the slow cleared fraction from the TB region appears to be associated with small bronchioles. For large particles ($d_{ae} = 6.2$ μm) inhaled at a very slow rate to theoretically deposit mainly in small ciliated airways, 50% had cleared by 24 h post-inhalation. Of the remaining particles, 20% cleared with a $t_{1/2}$ of 2.0 days and 80% with a $t_{1/2}$ of 50 days (Falk et al., 1997, [086080](#)). Using the same techniques, Svartengren et al. (2005, [157034](#)) also reported the existence of long-term clearance in humans from the small airways. It should be noted that the clearance rates for the slow-cleared TB fraction still exceeds the clearance rate of the alveolar region in humans. Kreyling et al. (1999, [039175](#)) targeted inhaled particle ($d_{ae} = 2.2$ and 2.5 μm) deposition to the TB airways of adult beagle dogs and subsequently quantified particle retention using scintigraphic and morphometric analyses. Despite the use of shallow aerosol bolus inhalation to a volumetric lung depth of less than the anatomic dead space, 2.5-25% of inhaled particles deposited in alveoli. At 24 and 96 h post-inhalation, more than 50% of the retained particles were in alveoli. However, 40% of particles present at 24 and 96 h were localized to small TB airways of between 0.3 and 1 mm in diameter. Collectively, these studies suggest that although mucociliary clearance is fast and effective in healthy large airways, it is less effective and sites of longer retention exist in the smaller TB airways.

The underlying sites and mechanisms of long-term TB retention in the smaller airways remain largely unknown. Several factors may contribute to the existence or experimental artifact of slow clearance from the smaller TB airways. Even when inhaled to very shallow lung volumes, some particles reach the alveolar region (Kreyling et al., 1999, [039175](#)). Therefore, experiments utilizing bolus techniques to target inhaled particle deposition to the TB airways may have had some deposition in the alveolar region. This may occur due to variability in path length and the number of generations to the alveoli (Asgharian et al., 2001, [017025](#)) and/or differences in regional ventilation (Brown and Bennett, 2004, [190032](#)). Nonetheless, the experimentally measured clearance rates measured for the slow cleared TB fraction are faster than that of the alveolar region in both humans and canines. Thus, although experimental artifacts likely occur, they do not discount the existence of a slow cleared TB fraction. To some extent, it is possible that the slow cleared TB fraction may be due to bronchioles that do not have a continuous ciliated epithelium as in the larger bronchi. Neither

path length, ventilation distribution, nor a discontinuous ciliated epithelium explains an apparently slow cleared TB fraction with decreasing particle size below 0.1 μm . As discussed in Section 4.3.3 on Particle Translocation, UFPs cross cell membranes by mechanisms different from larger ($\sim 1 \mu\text{m}$) particles. Based on that body of literature, particles smaller than a micron may enter epithelial cells resulting in their prolonged retention, particularly in the bronchioles where the residence time is longer and distances necessary to reach the epithelium are shorter compared to that in the bronchi.

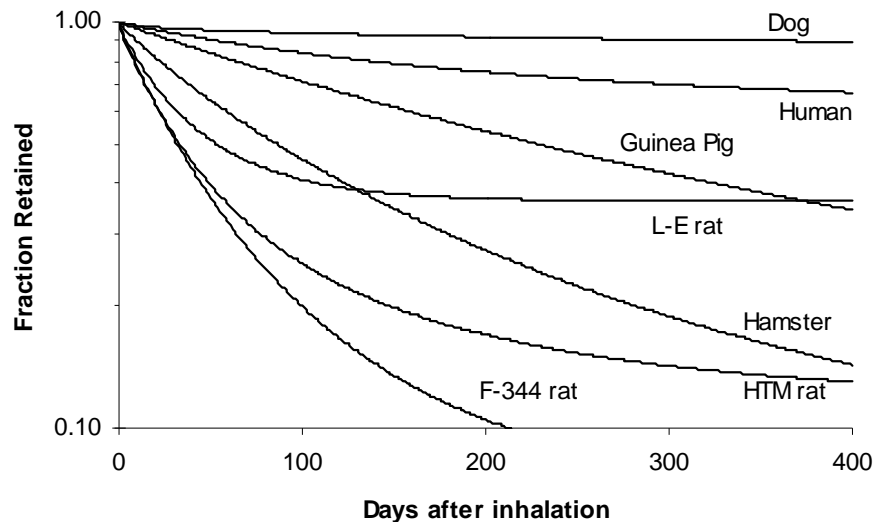
4.3.1.3. Alveolar Region

The primary alveolar clearance mechanism is macrophage phagocytosis and migration to terminal bronchioles where the cells are cleared by the mucociliary escalator. Alveolar macrophages originate from bone marrow, circulate briefly as monocytes in the blood, and then become pulmonary interstitial macrophages before migrating to the luminal surfaces. Under normal conditions, a small fraction of ingested particles may also be cleared through the lymphatic system. This may occur by transepithelial migration of alveolar macrophage following particle ingestion or free particle translocation with subsequent uptake by interstitial macrophages. Snipes et al. (1997, [156092](#)) have also demonstrated the importance of neutrophil phagocytosis in clearance of particles from the alveolar region. Rates of alveolar clearance of poorly soluble particles vary between species and are briefly discussed in Section 4.3.2. The translocation of particles from their site of deposition is discussed in Section 4.3.3.

The efficiency of macrophage phagocytosis is thought to be greatest for particles between 1.5 and 3 μm (Oberdörster, 1988, [006857](#)). The decreased efficiency of alveolar macrophage for engulfing UFPs increases the time available for these particles to be taken up by epithelial cells and moved into the interstitium (Ferin et al., 1992, [044401](#)). Consistent with this supposition (i.e., translocation increases with time), an increase in titanium dioxide (TiO_2) particle transport to lymph nodes has been reported following inhalation of a cytotoxin to macrophages (Greenspan et al., 1988, [045031](#)). Interestingly, the long-term clearance kinetics of the poorly soluble UF (15-20 nm CMD) iridium (Ir) particles were found to be similar to the kinetics reported in the literature for micrometer-sized particles (Semmler et al., 2004, [055641](#); Semmler-Behnke et al., 2007, [156080](#)). Semmler-Behnke et al. (2007, [156080](#)) concluded that UF Ir particles are less phagocytized by alveolar macrophage than larger particles, but are effectively removed from the airway surface into the interstitium. Particles are then engulfed by interstitial macrophages which then migrate to the airway lumen and are removed by mucociliary clearance to the larynx. The major role of macrophage-mediated clearance was supported by lavage of relatively few free particles versus predominantly phagocytized particles at time-points of up to 6 mo. It is also possible that some free particles as well as particle-laden macrophages were carried from interstitial sites via the lymph flow to bronchial and bronchiolar sites, including bronchial-associated lymphatic tissue, where they were excreted again into the airway lumen.

4.3.2. Interspecies Patterns of Clearance and Retention

There are differences between species in both the rates of particle clearance from the lung and manner in which particles are retained in the lung. For instance, based on models of mucociliary clearance from un-diseased airways, >95% of particles deposited in the tracheobronchial airways of rats are predicted to be cleared by 5 h post deposition, whereas it takes nearly 40 h for comparable clearance in humans (Hofmann and Asgharian, 2003, [055579](#)). As noted in Section 4.3.1.2, however, there is considerable evidence that a sizeable fraction of particles deposited at the bronchiolar level of the ciliated airways in humans (as well as canines) are cleared at a far slower rate. The slow cleared TB fraction appears to increase with decreasing particle size.



Source: Data from Kreyling and Scheuch (2000, [056281](#)).

Figure 4-7. Retention of poorly soluble particles (0.5-5 μm) in the alveolar region of the lung over time in various mammalian species.

Figure 4-7 illustrates rates of alveolar clearance for 0.5-5 μm particles in various mammalian species. The alveolar clearance rate of particles smaller than 0.1 μm and larger than 5 μm is slower than that of particles in the 0.5-5 μm range. From interspecies comparisons of alveolar clearance, the path length from alveoli to ciliated terminal bronchioles may affect the particle transport rate (Kreyling and Scheuch, 2000, [056281](#)). The average path length from alveoli to ciliated terminal bronchioli is longer in humans, monkeys, and dogs, than in sheep, rats, hamsters, and mice. Transport time and hence retention times may increase with path length. This hypothesis fits with all species in this comparison, except guinea pigs, which have a short path length yet particle retention that is nearly as long as in humans, monkeys, and dogs. However, sheep have a short path length and particle transport as fast as rodents. In general, alveolar clearance rates appear to increase with increasing path length from the alveoli to ciliated airways.

There are also distinct differences in the sites of particle retention between species. Large mammals retain particles in interstitial tissues under normal conditions, whereas rats retain particles in alveolar macrophages (Snipes, 1996, [076041](#)). In rats with chronic high doses there is a shift in the pattern of dust accumulation and response from that observed at lower doses in the lungs (Snipes, 1996, [076041](#); Vincent and Donaldson, 1990, [002462](#)). Rats chronically exposed to high concentrations of insoluble particles experience a reduction in their alveolar clearance rates and an accumulation of interstitial particle burden (Bermudez et al., 2002, [055578](#); Bermudez et al., 2004, [056707](#); Ferin et al., 1992, [044401](#); Oberdörster et al., 1994, [046203](#); Oberdörster et al., 1994, [056285](#); Warheit et al., 1997, [086055](#)). The influence of exposure concentration on the pattern of particle retention in rats (exposed to diesel soot) and humans (exposed to coal dust) was examined by Nikula et al. (2001, [016641](#)). In rats, the diesel particles were found to be primarily in the lumens of the alveolar duct and alveoli; whereas in humans, retained dust was found primarily in the interstitial tissue within the respiratory acini.

4.3.3. Particle Translocation

Mucociliary and macrophage mediated clearance of poorly soluble particles from the respiratory tract was discussed in Section 4.3.1. There is evidence that particles may cross cell membranes and move from their site of deposition by other mechanisms. The following subsections discuss the movement of particles from the luminal surfaces of the alveolar region and from the olfactory mucosa. The clearance and distribution of soluble particles and soluble constituents of particles are discussed in Section 4.4.

4.3.3.1. Alveolar Region

Numerous studies have examined the translocation of UFPs from their site of deposition in the lung. Traditionally viewed as a relatively inert particle type, UF TiO₂ has received the most study. At the time the 2004 PM AQCD was released, there were conflicting results regarding the rate and magnitude of UF carbon translocation from the human lung. Since that time, it has become well-established that the transport of UF carbon particles from the human lung is far slower than that of soluble materials. However, it has also been shown in animal studies (primarily of rats) that UFPs cross cell membranes by mechanisms different from larger (~1 μm) particles and that a small fraction of these particles enter capillaries and may distribute systemically. Described in brief below, details of selected new studies investigating the disposition of poorly soluble particles are provided in Annex B.

There has been some contention regarding ability of UF carbon particles to rapidly diffuse from the lungs into the systemic circulation. Based on their study of 5 healthy volunteers, Nemmar et al. (2002, [024914](#)) suggested that UF carbon particles (<100 nm) pass rapidly into the systemic circulation. However, Brown et al. (2002, [043216](#)) found that the majority of UF carbon particles (CMD, 33 ± 2 nm) were still in the lungs of healthy human adult volunteers (n = 9; aged 40-67 yr) and COPD patients (n = 10; 45-70 yr) at 24 h post-inhalation. Brown et al. (2002, [043216](#)) and Burch (2002, [056754](#)) contended that the findings reported by Nemmar et al. (2002, [024914](#)) were consistent with soluble pertechnetate clearance, but not insoluble UF carbon particles. Highly soluble in normal saline, pertechnetate clears rapidly from the lung with a half-time of ~10 min and accumulates most notably in the bladder, stomach, thyroid, and salivary glands. Three recent studies have confirmed that the majority (>95%) of UF carbon particles deposited in the lungs of human volunteers are retained at 24 h post-inhalation (Mills et al., 2006, [088770](#); Wiebert et al., 2006, [157146](#); Wiebert et al., 2006, [156154](#)). Wiebert et al. (2006, [157146](#)) modified their aerosol generation system to reduce leaching of the ^{99m}Tc radiolabel from carbon particles. Except for a small amount of radiotracer leaching from particles (1.0 ± 0.6% of initially deposited activity in urine by 24 h), these investigators found negligible radiolabel and associated particle clearance from the lungs by 70 h. The available data show that there is not a rapid or significant amount of UF carbon particle migration into circulation (Brown et al., 2002, [043216](#); Burch, 2002, [056754](#); Mills et al., 2006, [088770](#); Möller et al., 2008, [156771](#); Wiebert et al., 2006, [157146](#); Wiebert et al., 2006, [156154](#)).

Although human studies show that the vast majority of UF carbon particles are retained in the lungs until at least 24 h post-inhalation, both in vitro and in vivo studies support the rapid (≤ 1 h) translocation of free UF TiO₂ particles across pulmonary cell membranes (Churg et al., 1998, [085815](#); Ferin et al., 1992, [044401](#); Geiser et al., 2005, [087362](#)). Peculiar to TiO₂ aerosols, there is evidence that particle aggregates may disassociate once deposited in the lungs. This disassociation makes inhaled aggregate size the determinant of deposition amount and site, but primary particle size the determinant of subsequent clearance (Bermudez et al., 2002, [055578](#); Ferin et al., 1992, [044401](#); Takenaka et al., 1986, [046210](#)). Following disaggregation, the UF TiO₂ particles are cleared more slowly and cause a greater inflammatory response (neutrophil influx) than fine TiO₂ particles (Bermudez et al., 2002, [055578](#); Ferin et al., 1992, [044401](#); Oberdörster et al., 1994, [046203](#); Oberdörster et al., 1994, [056285](#); Oberdörster et al., 2000, [039014](#)). The differences in inflammatory effects and possibly lymph burdens between fine and UF TiO₂ in many studies appear related to lung burden in terms of particle surface area and not particle mass or number (Oberdörster, 1996, [039852](#); Oberdörster et al., 1992, [045110](#); Oberdörster et al., 2000, [039014](#); Tran et al., 2000, [013071](#)). More recently, others have noted that particle surface area is not an appropriate metric across all particle types (Warheit et al., 2006, [088436](#)). Surface characteristics such as roughness can also affect protein binding and potentially clearance kinetics, with smoother TiO₂ surfaces being more hydrophobic (Sousa et al., 2004, [089866](#)).

Geiser et al. (2005, [087362](#)) conducted a detailed examination of the disposition of inhaled UF TiO₂ in 20 healthy adult rats. They found that distributions of particles among lung tissue compartments appeared to follow the volume fraction of the tissues and did not significantly differ between 1 and 24 h post-inhalation. Averaging 1- and 24-h data, 79.3 ± 7.6% of particles were on the luminal side of the airway surfaces, 4.6 ± 2.6% were in epithelial or endothelial cells, 4.8 ± 4.5% were in connective tissues, and 11.3 ± 3.9% were within capillaries. Particles within cells were not membrane bound. It is not clear why the fraction of particles identified in compartments such as the capillaries did not differ between 1 and 24 h post-inhalation. These findings were consistent with the smaller study of 5 rats by Kapp et al. (2004, [156624](#)) who reported identifying TiO₂ aggregates in a

type II pneumocyte; a capillary close to the endothelial cells; and within the surface-lining layer close to the alveolar epithelium immediately following a 1-h exposure. These studies effectively demonstrate that some inhaled UF TiO₂ particles, once deposited on the pulmonary surfaces, can rapidly (≤ 1 h) translocate beyond the epithelium and potentially into the vasculature.

Extrapulmonary translocation has also been described for poorly soluble UF gold and Ir particles. In male Wistar-Kyoto rats exposed to UF gold particles (5-8 nm), Takenaka et al. (2006, [156110](#)) reported a low but significant fraction (0.03 to 0.06% of lung concentration) of gold in the blood from 1 to 7 days post-inhalation. Semmler et al. (2004, [055641](#)) also found small but detectable amounts of poorly soluble Ir particle (15 and 20 nm CMD) translocation from the lungs of male Wistar-Kyoto rats to secondary target organs like the liver, spleen, brain, and kidneys. Each of these organs contained about 0.2% of deposited Ir. The peak levels in these organs were found 7 days post-inhalation. The translocated particles were largely cleared from extrapulmonary organs by 20 days and Ir levels were near background at 60 days post-inhalation. Particles may have been distributed systemically via the gastrointestinal tract. Immediately after the 6-h inhalation exposure, $18 \pm 5\%$ of the deposited Ir particles had already cleared into the gastrointestinal tract. After 3 wk, $31 \pm 5\%$ of the deposited particles were retained in the lung. By 2 and 6 mo post-inhalation, lung retention was 17 ± 3 and $7 \pm 1\%$, respectively. The particles appeared to be cleared predominantly from the peripheral lung via the mucociliary escalator into the GI tract and were found in feces.

A few recent studies have characterized differences in the behavior of fine and UF particles in vitro. Geiser et al. (2005, [087362](#)) found that both UF and fine (0.025 μm gold, 0.078 μm TiO₂, and 0.2 μm TiO₂) particles cross cellular membranes by non-endocytic (i.e., involving vesicle formation) mechanisms such as adhesive interactions and diffusion, whereas the phagocytosis of larger 1 μm TiO₂ particles is ligand-receptor mediated. Edetsberger et al. (2005, [155759](#)) found that UFPs (0.020 μm polystyrene) translocated into cells by first measurement (~ 1 min after particle application). Intracellular agglomerates of 88-117 nm were seen by 15-20 min and of 253-675 nm by 50-60 min after particle application. These intracellular aggregates were thought to result from particle incorporation into endosomes or similar structures since Genistein or Cytochalasin treatment generally blocked aggregate formation. Interestingly, particles did not translocate into dead cells, rather they attached to the outside of the cell membrane. Amine- or carboxyl-modified surfaces (46 nm polystyrene) did not affect translocation across cultures of human bronchial epithelial cells with about 6% regardless of the surface characteristics (Geys et al., 2006, [155789](#)).

4.3.3.2. Olfactory Region

Numerous studies have demonstrated the translocation of soluble and poorly soluble particles from the olfactory mucosa via the axons to the olfactory bulb of the brain. The vast majority of these studies were conducted in rodents. However, DeLorenzo (1970, [156391](#)) observed the rapid (within 30-60 min) movement of 50 nm silver-coated colloidal gold particles instilled on the olfactory mucosa into the olfactory bulb of squirrel monkeys. The specifics of this and other key studies that have investigated the translocation of particles to the olfactory bulb are provided in Annex B.

Two recent studies reported the movement of UFPs deposited in the olfactory region of the nose along the olfactory nerve and into the olfactory bulb of the brain in rats. Oberdörster et al. (2004, [055639](#)) exposed rats to UF carbon particles (36 nm CMD, 1.7 σ_g) containing ¹³C in a whole-body chamber for 6 h. The distribution of ¹³C was followed for 7 days postexposure. There was a significant increase in ¹³C in the olfactory bulb on Day 1 with persistent and continued increase through Day 7. Elder et al. (2006, [089253](#)) exposed rats to manganese (Mn) oxide (~ 30 nm equivalent sphere with 3-8 nm primary particles) via whole-body inhalation exposure for 12 days (6 h/day, 5 days/wk) with both nares open or Mn oxide for 2 days (6 h/day) with right nostril blocked. After the 12 days exposure via both nostrils, Mn in the olfactory bulb increased 3.5-fold. After the 2-day exposure with the right nostril blocked, Mn was found mainly in the left olfactory bulb (2.4-fold increase). These studies suggest the neuronal uptake and translocation of UFPs without particle dissolution and in the absence of mucosal injury.

Elder et al. (2006, [089253](#)) also addressed the issue of whether solubilization of particles was requisite for translocation along the olfactory nerve and into the brain. Similar amounts of soluble manganese chloride (MnCl₂) and poorly soluble Mn oxide were instilled onto the left naris of anesthetized rats. At 24 h post-instillation, similar amounts of Mn were found in the left olfactory bulb of rats instilled with MnCl₂ ($8.2 \pm 3.6\%$ of instilled) and Mn oxide ($8.2 \pm 0.7\%$ of instilled). If solubilization were required for translocation, then a lower amount of Mn oxide than MnCl₂ should

have reached the olfactory bulb. Following 14 consecutive days of aerosol exposure, Dorman et al. (2001, [055433](#)) demonstrated that more soluble Mn sulfate reaches the olfactory bulb and striatum of rat brains than the poorly soluble form of Mn tetroxide. Nonetheless, the Mn levels were statistically increased in both the olfactory bulb and striatum following exposure to Mn tetroxide relative to filtered air. In a subsequent 13-wk exposure study, Dorman et al. (2004, [155752](#)) also demonstrated that more soluble manganese sulfate (MnSO₄) reached the olfactory bulb than was observed for the less soluble Mn form (hureaulite). Both the soluble and less soluble forms of Mn resulted in statistically increased levels of Mn in the olfactory bulb relative to air exposed controls. The soluble MnSO₄ was also observed to reach the striatum and cerebellum. In addition, Yu et al. (2003, [156171](#)) demonstrated increased Mn levels in the brains of rats exposed to welding-fumes for 60 days, however, the role of transport via the blood is less clear in this study.

The translocation of zinc (Zn) and TiO₂ to the olfactory bulb has also been reported in the literature. Persson et al. (2003, [051846](#)) observed the translocation of Zn to the olfactory bulbs following instillation in both rats and freshwater pike. Wang et al. (2007, [156146](#)) reported the translocation of both fine (155 nm) and UF (21 and 71 nm) TiO₂ particles in mice. Interestingly, a qualitative analysis of the data showed that more of the fine TiO₂ than UF TiO₂ reached the olfactory bulb. Wang et al. (2007, [156146](#)) suggested that a strong hydrophilic character and propensity for aggregation reduced the translocation of the UF TiO₂.

The importance of particle translocation to the brain is not yet understood. Translocation via the axon to the olfactory bulb has been observed for numerous compounds of varying composition, particle size, and solubility. Although the rate of translocation is rapid, perhaps less than an hour, the magnitude of transport remains poorly characterized. With regard to the magnitude of transport, Elder et al. (2006, [089253](#)) found that as much as 8% of both soluble and insoluble forms of Mn were translocated to the olfactory bulb in rats following intranasal instillation. It is also still unclear to what extent translocation to the olfactory bulb and other brain regions may vary between species. The olfactory mucosa covers approximately 50% of the nasal epithelium in rodents versus only about 5% in primates (Aschner et al., 2005, [155663](#)). Additionally, a greater portion of inhaled air passes through the olfactory region of rats relative to primates (Kimbell, 2006, [155902](#)). These differences may predispose rats, more so than humans, to deposition of particles in the olfactory region with subsequent particle translocation to the olfactory bulb.

4.3.4. Factors Modulating Clearance

4.3.4.1. Age

It was previously concluded that there appeared to be no clear evidence for any age-related differences in clearance from the lung or total respiratory tract, either from child to adult, or young adult to elderly (U.S. EPA, 1996, [079380](#); U.S. EPA, 2004, [056905](#)). Studies showed either no change or some slowing in mucus clearance with age after maturity. Although some differences in alveolar macrophage function were reported between mature and senescent mice, no age-related decline in macrophage function had been observed in humans. A comprehensive review of the recent and older literature supports a decrease in mucociliary clearance with increasing age beyond adulthood in humans and animals. Limited animal data also suggest macrophage-mediated alveolar clearance may also decrease with age.

Studies addressing the effects of age on respiratory tract clearance are provided in Annex B. Ho et al. (2001, [156549](#)) demonstrated that nasal mucociliary clearance rates were about 40% lower in old (age >40-90 yr) versus young (age 11-40 yr) men and women. Tracheal mucus velocities in elderly (or aged) humans and beagle dogs are about 50% that of young adults (Goodman et al., 1978, [071130](#); Whaley et al., 1987, [156153](#)). Several human studies have demonstrated decreasing rates of mucociliary particle clearance from the large and small bronchial airways with increasing age (Puchelle et al., 1979, [006863](#); Svartengren et al., 2005, [157034](#); Vastag et al., 1985, [157088](#)). Linear fits to the data show that rapid clearance (within 1 h) from large bronchi and prolonged clearance (between 1-21 days) from the small bronchioles in an 80-year-old is only about 50% of that in a 20-year-old (Svartengren et al., 2005, [157034](#); Vastag et al., 1985, [157088](#)). One study reported that alveolar particle clearance rates decreased by nearly 40% in old versus young rats (Muhle et al., 1990, [006853](#)). Another study has reported that older rats have an increased susceptibility to

pulmonary infection due to altered alveolar macrophage function and slowed bacterial clearance (Antonini et al., 2001, [156219](#)). Although data are somewhat limited, they consistently show a depression of clearance throughout the respiratory tract with increasing age from young adulthood in humans and laboratory animals.

4.3.4.2. Gender

Gender was not found to affect clearance rates in prior reviews (U.S. EPA, 1996, [079380](#); U.S. EPA, 2004, [056905](#)). Studies not included in those reviews also show that human males and females have similar nasal mucus clearance rates (Ho et al., 2001, [156549](#)), tracheal mucus velocities (Yeates et al., 1981, [095391](#)), and large bronchial airway clearance rates (Vastag et al., 1985, [157088](#)).

4.3.4.3. Respiratory Tract Disease

At the time of the last two reviews (U.S. EPA, 1996, [079380](#); U.S. EPA, 2004, [056905](#)), it was well recognized that obstructive airways disease may influence both the site of initial deposition and the rate of mucociliary clearance from the airways. When deposition patterns are matched, mucociliary clearance rates are reduced in patients with COPD relative to healthy controls. The effects of acute bacterial/viral infections and cough on mucociliary clearance were briefly summarized in Section 10.4.2.5 (EPA, 1996, [079380](#)) and Section 6.3.4.4 (EPA, 2004, [056905](#)) of past reviews. While cough is generally a reaction to some inhaled stimulus, in some cases, especially respiratory disease, it can also serve to clear the upper bronchial airways of deposited substances by dislodging mucus from the airway surface. One of the difficulties in assessing effects on infection on mucociliary clearance is that spontaneous coughing increases during acute infections. Cough has been shown to supplement mucociliary clearance of secretions, especially in patients with obstructive lung disease and primary ciliary dyskinesia.

Using a bolus technique to target specific lung regions, Möller et al. (2008, [156771](#)) examined particle clearance from the ciliated airways and alveolar region of healthy subjects, smokers, and patients with COPD. Airway retention after 1.5 hours was significantly lower in healthy subjects ($89 \pm 6\%$) than smokers ($97 \pm 3\%$) or COPD patients ($96 \pm 6\%$). At 24 and 48 h, retention remained significantly higher in COPD patients ($86 \pm 6\%$ and $82 \pm 6\%$, respectively) than healthy subjects ($75 \pm 10\%$ and $70 \pm 9\%$, respectively). However, these findings are confounded by the more central pattern of deposition in the healthy subjects than in the smokers and COPD patients. Alveolar retention of particles was similar between the groups at 48 h post-inhalation.

The effect of asthma on lung clearance of particles may depend on disease status. Lay et al. (2009, [190060](#)) found significantly ($p < 0.01$) more rapid particle ($0.22 \mu\text{m}$) mucociliary clearance over a 2-h period post-inhalation in mild asthmatics than in healthy volunteers. Although the pattern of deposition tended to be more central in the asthmatics, there was not a statistically significant difference from healthy controls. In vivo uptake by airway macrophages in mild asthmatics was also enhanced relative to healthy volunteers ($p < 0.01$). In an ex vivo study, airway macrophages from individuals with more severe asthma had impaired phagocytic capacity relative to less severely affected asthmatics and healthy volunteers (Alexis et al., 2001, [190013](#)). Lay et al. (2009, [190060](#)) concluded that enhanced uptake and processing of particulate antigens could contribute to the pathogenesis and progression of allergic airways disease in asthmatics and may contribute to an increased risk of exacerbations with particulate exposure.

Chen et al. (2006, [147267](#)) investigated the effect of endotoxin on the disposition of particles. Healthy rats and those pretreated with endotoxin (12 h before particle instillation) were instilled with UF (56.4 nm) or fine (202 nm) particles. In healthy rats, there were no marked differences in lung retention or systemic distribution between the UF and fine particles. In healthy animals, UFPs were primarily retained in lungs ($72 \pm 10\%$ at 0.5-2 h; $65 \pm 1\%$ at 1 day; $62 \pm 5\%$ at 5 days). Particles were also detected in the blood ($2 \pm 1\%$ at 0.5-2 h; $0.1 \pm 0.1\%$ at 5 days) and liver ($3 \pm 2\%$ at 0.5-2 h; $1 \pm 0.1\%$ at 5 days) of the healthy animals. At 1 day post-instillation, about 13% of the particles were excreted in the urine or feces of the healthy animals. In rats pretreated with endotoxin, by 2 h post-instillation, the UFPs accessed the blood (5 versus 2%) and liver (11 versus 4%) to a significantly greater extent than fine particles. The endotoxin-treated rats also had significantly greater amounts of UFPs in the blood (5% versus 2%) and liver (11% versus 3%) relative to the

healthy control rats. This study demonstrates that acute pulmonary inflammation caused by endotoxin increases the migration of UFPs into systemic circulation.

Adamson and Preditis (1995, [189982](#)) investigated the possibility that particle deposition into an already injured lung might affect particle retention and enhance the toxicity of “inert” particles. Bleomycin was instilled into mice to induce epithelial necrosis and subsequent pulmonary fibrosis. Instilled 3 days following bleomycin treatment, while epithelial permeability was compromised, carbon black particles in treated mice were translocated to the interstitium and showed increased pulmonary retention relative to untreated mice. When instilled 4 wk post-bleomycin treatment, after epithelial integrity was restored, carbon black particle retention was similar between treated and untreated mice with minimal translocation to the interstitium. The instillation of carbon particles did not appear to increase lung injury in the bleomycin treated mice at either time point. This study shows that integrity of the epithelium affects particle retention and translocation into interstitial tissues.

4.3.4.4. Particle Overload

Unlike other laboratory animals, rats appear susceptible to “particle overload” effects due to impaired macrophage-mediated alveolar clearance. Numerous reviews have discussed this phenomenon and the difficulties it poses for the extrapolation of chronic effects in rats to humans (International, 2000, [002892](#); Miller, 2000, [011822](#); Morrow, 1994, [006850](#); Oberdorster, 1995, [046596](#); Oberdorster, 2002, [021111](#)). Large mammals have slow pulmonary particle clearance and retain particles in interstitial tissues under normal conditions, whereas rats have rapid pulmonary clearance and retain particles in alveolar macrophages (Snipes, 1996, [076041](#)). With chronic high doses of PM there is a shift in the pattern of dust accumulation and response from that observed at lower doses in rat lungs (Snipes, 1996, [076041](#); Vincent and Donaldson, 1990, [002462](#)). Rats chronically exposed to high concentrations of insoluble particles experience a reduction in their alveolar clearance rates and an accumulation of interstitial particle burden (Bermudez et al., 2002, [055578](#); Bermudez et al., 2004, [056707](#); Ferin et al., 1992, [044401](#); Oberdörster et al., 1994, [046203](#); Oberdörster et al., 1994, [056285](#); Warheit et al., 1997, [086055](#)). With continued exposure, some rats eventually develop pulmonary fibrosis and both benign and malignant tumors (Lee et al., 1985, [067628](#); Lee et al., 1986, [067629](#); Warheit et al., 1997, [086055](#)). Oberdörster (1996, [039852](#); 2002, [021111](#)) proposed that high-dose effects observed in rats may be associated with two thresholds. The first threshold is the pulmonary dose that results in a reduction in macrophage-mediated clearance. The second threshold, occurring at a higher dose than the first, is the dose at which antioxidant defenses are overwhelmed and pulmonary tumors develop. Intrapulmonary tumors following TiO₂ exposures are exclusive to rats and are not found in mice or hamsters (Mauderly, 1997, [084631](#)). Moreover, Lee et al. (1985, [067628](#)) noted that the squamous cell carcinomas observed with prolonged high concentration TiO₂ exposures developed from the alveolar lining cells adjacent to the alveolar ducts, whereas squamous cell carcinomas in humans which are generally linked with cigarette smoking are thought to arise from basal cells of the bronchial epithelium. Quoting Lee et al. (1986, [067629](#)), “Since the lung tumors were a unique type of experimentally induced tumor under exaggerated exposure conditions and have not usually been seen in man or animals, their relevance to man is questionable.”

4.3.5. Summary

For any given particle size, the pattern of poorly soluble particle deposition influences clearance by partitioning deposited material between regions of the respiratory tract. Particles depositing in the mouth may generally be assumed to be swallowed or removed by expectoration. Particles deposited in the posterior portions of the nasal passages or the TB airways are moved via mucociliary transport towards the nasopharynx and swallowed. Although clearance from the TB region is generally rapid, there appears to be fraction of material deposited in the TB region of humans that is retained much longer. The underlying sites and mechanisms of long-term TB retention are not known. The primary alveolar clearance mechanism is macrophage phagocytosis and migration to terminal bronchioles where the cells are cleared by the mucociliary escalator. Clearance from both the TB and alveolar region is more rapid in rodents than humans. Mucociliary and macrophage-mediated clearance decreases with age beyond adulthood.

Human data show that there is not a rapid or significant amount of UF carbon particle migration into circulation. However, both in vitro and in vivo animal studies support the rapid (≤ 1 h) translocation of free UF TiO_2 particles across pulmonary cell membranes. Extrapulmonary translocation has also been described in rats for poorly soluble UF gold and Ir particles. A low, but statistically significant, fraction (0.03-0.06% of lung concentration) of UF gold particles has been observed in the blood of rats from 1 to 7 days post-inhalation. The translocation in detectable amounts ($<1\%$ of deposited material) of poorly soluble Ir particles (15 and 20 nm CMD) from the lungs of rats to secondary target organs like the liver, spleen, brain, and kidneys has also been reported. However, the systemic distribution of particles may have occurred via normal clearance from the lungs to the gastrointestinal tract.

Although the importance of particle translocation to the brain is not yet understood, translocation from the olfactory mucosa via the axon to the olfactory bulb has been reported in primates, rodents, and freshwater pike for numerous compounds of varying composition, particle size, and solubility. The rate of translocation is rapid, perhaps less than an hour. In rats, as much as 8% of material may become translocated to the olfactory bulb following intranasal instillation. It is unclear to what extent translocation to the olfactory bulb and other brain regions may vary between species. Interspecies differences may predispose rats, more so than humans, to the deposition of particles in the olfactory region with subsequent translocation to the olfactory bulb.

4.4. Clearance of Soluble Materials

Soluble particles and soluble constituents of particles may be absorbed through the epithelium and distributed systemically or retained in the lung. The rate of dissolution depends on a number of factors, including particle surface area and chemical structure. Some dissolved materials bind to proteins or other components in the airway surface liquid layer. In the ciliated airways, solutes are cleared by mucociliary transport and diffuse into underlying tissues and the blood. In the alveolar regions, the thin barrier between the air and blood allows for rapid transport of solutes into the blood. The movement of soluble materials depends on the site of deposition in the lung, the rate of material dissolution from particles, and the molecular weight of the solute. The rate of soluble material clearance from the lungs depends on epithelial permeability which may be affected by age, respiratory disease, and concurrent exposures. While enhanced clearance of insoluble particles acts to reduce dose to airway tissue, increased transport of soluble matter into the blood stream may enhance effects on extra-pulmonary organs.

4.4.1. Clearance Mechanisms and Kinetics

The rate of absorption across the epithelium for materials that dissolve in the airway or alveolar lining fluid is fairly rapid (minutes to hours) and is a function of their molecular size and their water or lipid solubility (Enna and Schanker, 1972, [155767](#); Huchon et al., 1987, [024923](#); Oberdörster, 1988, [006857](#); Schanker et al., 1986, [005100](#)). Huchon et al. (1987, [024923](#)) studied the clearance of a variety of aerosolized solutes from the lungs of dogs. Solute clearance was inversely related to molecular weight. Negligible clearance of the largest molecular weight solute (transferrin mol wt $\sim 76,000$ daltons) in their study was found over a 30-min observation period. At the other extreme, free pertechnetate (mol wt ~ 163 daltons) had a clearance rate of 6% per min. Clearance of hydrophilic solutes is diffusion limited by pore sizes associated with intercellular tight junctions (estimated at 0.6-1.5 nm). Absorption of lipophilic compounds that pass easily through cell membranes is perfusion limited and thus generally occurs very rapidly. However, if lipophilic materials are adsorbed onto insoluble particles their retention in the lung may be prolonged (Creasia et al., 1976, [059713](#)). In addition to diffusion through intercellular junctions, transcellular transport of large solutes by pinocytosis into epithelial cells has also been observed (Chinard, 1980, [156341](#)).

A portion of poorly soluble particles may become dissolved with subsequent solute clearance. More rapid dissolution of poorly soluble nano- or UF particles relative to micro-sized particles occurs due to an increasing surface-to-volume ratio with decreasing particle size. Kreyling et al. (2002, [037332](#)) examined the dissolution of poorly soluble UF Ir particle agglomerates (15-80 nm CMD) composed of 5 nm primary particles. After 7 days, $<1\%$ of the particles were dissolved in buffered saline, whereas 6% dissolved in 1 N hydrochloric acid after 1 day. Thus, the high surface-

to-volume ratio of UFPs should not be misconstrued to imply rapid dissolution of poorly soluble particles following deposition in the respiratory tract. However, poorly soluble particles that become phagocytosed may slowly dissolve in the acidic (pH of 4.3-5.3) environment of the phagolysosome to be released in their solubilized form from the cell and potentially move across the epithelium into the bloodstream. The dissolution rate is inversely related to particle size and directly related to specific surface area (Kreyling and Scheuch, 2000, [056281](#)) and facilitated by the acidic environment of the macrophage (Kreyling, 1992, [067243](#)).

There is considerable evidence that soluble particles depositing in the bronchial airways are cleared by dual mechanisms (Bennett and Ilowite, 1989, [000835](#); Lay et al., 2003, [155920](#); Matsui et al., 1998, [040405](#); Sakagami et al., 2002, [156936](#); Wagner and Foster, 2001, [156143](#)). The relative contribution of their removal by transepithelial absorption versus mucociliary clearance is likely a function of both the molecular size and water or lipid solubility of the material (Enna and Schanker, 1972, [155767](#); Huchon et al., 1987, [024923](#); Oberdörster, 1988, [006857](#); Sakagami et al., 2002, [156936](#)). Furthermore, the rate of mucociliary transport for soluble particles may be less than that of insoluble particles (Lay et al., 2003, [155920](#)). Consequently, non-permeating hydrophilic solutes may remain in contact with the airway epithelium for a longer period than insoluble particles. This may be due to diffusion of a greater portion of the solute into the periciliary sol layer which may be transported less efficiently than the mucus layer during mucociliary clearance. Bronchial blood flow has also been shown to modulate airway retention of soluble particles (Wagner and Foster, 2001, [156143](#)), i.e., decreasing blood flow increases airway retention of soluble particles.

As an example of how transport of soluble components of PM may clear the lung by transepithelial absorption, Wallenborn et al. (2007, [156144](#)) measured elemental content of lungs, plasma, heart, and liver of healthy male WKY rats (12-15 wk old) 4 or 24 h following a single intratracheal (IT) instillation of saline or 8.33 mg/kg of oil combustion PM containing a variety of transition metals with differing water and acid solubility. Metals with high water solubility and relatively high concentration in oil combustion PM were increased in extrapulmonary organs. Elements with low water or acid solubility, like silicon and aluminum, were not detected in extrapulmonary tissues despite decreased levels in the lung suggesting they cleared the lung primarily by mucociliary clearance. Thus, PM-associated metals deposited in the lung may be released into systemic circulation at different rates depending on their water/acid solubility.

The amount and type of water soluble or leachable metals associated with PM varies with location and by source. Furthermore some metals such as Zn, Cu, and Fe are essential to body function while others such as vanadium and nickel are nonessential metals. Consequently the body and the lung have different ways of dealing with excesses in inhaled soluble metals associated with PM. Bioavailability, and potentially the toxicity, of leachable metals may be altered by protein binding within the lung and blood as well as the affinities of these binding sites. For example Zn is tightly regulated by a variety of metal binding proteins, including metallothionein and a family of Zn specific transporters. In the plasma, Zn binds to many proteins, including α 2-macroglobulin and albumin. Zn is an example of a common abundant water soluble metal in ambient air that may contribute to increased respiratory and cardiovascular disease risk associated with PM exposure. Wallenborn et al. (2009, [191172](#)) recently showed that soluble Zn sulfate (in the form of ^{70}Zn , a rare isotope of Zn) introduced into the lungs by instillation not only reaches, but accumulates in extrapulmonary organs, including the heart and liver, following pulmonary exposure. However, the retention of greater than 50% of ^{70}Zn in the lung at 4 h post-instillation suggested that the transepithelial absorption of soluble Zn was indeed slowed by binding to proteins in the lungs. While it could not be ascertained if ^{70}Zn measured in the heart was replacing endogenous Zn pools, any accumulation in cardiac Zn levels could lead to mitochondrial dysfunction and ion channel disruption, possibly explaining adverse cardiac effects from inhalation of Zn-rich PM. Effects of Zn instillation on epithelial integrity were not evaluated.

4.4.2. Factors Modulating Clearance

A number of studies have evaluated the epithelial permeability by measuring the clearance of $^{99\text{m}}\text{Tc}$ -diethylenetriaminepentaacetic acid ($^{99\text{m}}\text{Tc}$ -DTPA), a small hydrophilic solute (492 daltons, 0.57 nm). These studies are the basis for much of the discussion in this section.

4.4.2.1. Age

In humans, the clearance of water-soluble particles (^{99m}Tc -DTPA) from the alveolar epithelium generally slows with increasing age (Braga et al., 1996, [156289](#); Pigorini et al., 1988, [156027](#)). However, Tankersley et al. (2003, [096363](#)) recently showed enhanced permeability of soluble particles (^{99m}Tc -DTPA) in terminally senescent mice just before death, suggesting that a disintegration of the epithelial barrier may be a feature of lung homeostatic loss during this period of terminal senescence.

4.4.2.2. Physical Activity

The transepithelial transport rates of soluble particles, ^{99m}Tc -DTPA, have also been found to increase during exercise (Hanel et al., 2003, [155826](#); Lorino et al., 1989, [155946](#); Meignan et al., 1986, [156752](#)). This enhancement was linked to increases in V_T associated with exercise (Lorino et al., 1989, [155946](#)). Regionally, this effect was dominated by increased apical lung clearance and attributed to an increase in apical blood flow (Meignan et al., 1986, [156752](#)). The increased permeability with exercise appears to resolve to baseline after a short period post exercise, i.e., within a couple hours (Hanel et al., 2003, [155826](#)).

4.4.2.3. Disease

Because the integrity of the epithelial surface lining of the lungs may be damaged from lung disease, particles (either insoluble or soluble) may gain greater access to the interstitium, lymph, and blood stream. Damage to the epithelial barrier is most likely to acutely affect transepithelial transport rates of soluble particles. From bronchial biopsies, Laitinen et al. (1985, [037521](#)) found various degrees of epithelial damage, from loosening of tight junctions to complete denudation of the airway epithelium, in asthmatics. Consistent with these findings, Ilowite et al. (1989, [156584](#)) found that asthmatics had increased permeability of the bronchial mucosa to the hydrophilic solute ^{99m}Tc -DTPA. On the other hand, a more recent study in a sheep model showed that the presence of bronchial edema could slow the uptake of soluble DTPA into the blood and enhanced retention in the airways, likely within the expanded interstitial barrier (Foster and Wagner, 2001, [155778](#)). Both a leaky epithelial barrier and expanded interstitial barrier associated with asthma may result in enhanced exposure of submucosal immune and smooth muscle cells to xenobiotic substances.

Alveolar epithelial permeability was also shown to be affected by the presence of lung inflammation. The most common finding has been a clear increase in alveolar permeability induced by cigarette smoking (Jones et al., 1980, [155883](#)). This effect appears to be dependent on the recent cigarette smoke exposure as indexed by carboxyhaemoglobin (Jones et al., 1983, [155884](#)) and is rapidly reversible within a week of smoking cessation (Mason et al., 1983, [013169](#)). In fact, Huchon et al. (1984, [156576](#)) demonstrated that COPD patients who have stopped smoking have normal clearance of ^{99m}Tc -DTPA.

In general, increased alveolar permeability to ^{99m}Tc -DTPA has been found to be associated with any lung syndrome characterized by pulmonary edema. While the trans-alveolar transport of a small solute like DTPA is very sensitive to even mild acute lung injury (such as that associated with even mild cigarette smoking), increased transport rates of larger molecules (>100K daltons) across the alveolar epithelium require more severe damage like that seen in adult respiratory distress syndrome (ARDS) (Braude et al., 1986, [155701](#); Peterson et al., 1989, [024922](#)). Interstitial lung disease and pulmonary fibrosis are also characterized by increased alveolar permeability (Antoniou et al., 2006, [156220](#); Bodolay et al., 2005, [156280](#); Watanabe et al., 2007, [157115](#)). Interestingly, these recent studies have also shown that the increased permeability in these patients could be corrected with immunosuppressive/steroid treatments (Bodolay et al., 2005, [156280](#); Watanabe et al., 2007, [157115](#)). Furthermore, studies of DTPA clearance in bleomycin injured dogs, a model of pulmonary fibrosis, suggest that the enhanced permeability is associated with the initial acute phase of the lung damage, with clearance rates returning to normal as chronic fibrosis developed over time (Suga et al., 2003, [157024](#)).

Finally, as evidence of lung complications associated with non-insulin dependent diabetes (type 2), Lin et al. (2002, [155932](#)) found impairment of alveolar integrity as shown by increased transport rates of both hydrophilic and lipophilic solutes from the lungs in these patients. By contrast, a number of other studies have found epithelial permeability reduced, i.e., slower transport

rates, in diabetes (Caner et al., 1994, [156320](#); Mousa et al., 2000, [156786](#); Ozsahin et al., 2006, [156833](#)) that may be related to disease duration and metabolic control (Ozsahin et al., 2006, [156833](#)). These findings are consistent with thickening of alveolar basement membrane detected in autopsies of diabetes patients (Weynand et al., 1999, [157140](#)).

4.4.2.4. Concurrent Exposures

The integrity of the alveolar epithelium may be disrupted by co-pollutants such that soluble components of inhaled particles can more easily enter the interstitium and blood stream. Like active cigarette smoking discussed previously, Beadsmoore et al. (2007, [156259](#)) showed clearance half-times in healthy passive smokers to be shorter compared with healthy non-smokers but still longer than in healthy smokers. These findings show a progressive increase in epithelial permeability with exposure to cigarette smoke. Similarly, acute exposure of humans to 0.4 ppm ozone for 2 h with intermittent exercise has been shown to alter epithelial integrity and increase clearance of soluble hydrophilic particles from the alveolar surfaces of the lung (Kehrl et al., 1987, [040824](#)). This effect persists to at least 24 h post-exposure even following lower exposure levels (0.24 ppm average for 130 min) of ozone (Foster and Stetkiewicz, 1996, [079920](#)). Similarly, 0.8 ppm O₃ exposure for 2 h in rats caused increased permeability to macromolecules at all levels of the respiratory tract (Bhalla et al., 1986, [040407](#)) that persisted in the alveolar region beyond 24 h post-exposure. Cohen et al. (1997, [009213](#)) may have best illustrated the competing effects of mucociliary and transepithelial transport by showing that coexposure to ozone affected the retention of inhaled chromium in rats differently depending on its solubility. In its soluble potassium chromate form, ozone decreased the retention of chromium, but when chromium was inhaled as insoluble barium chromate, its retention in the lung was increased by ozone coexposure. Similarly, a study that showed decreased clearance of insoluble cesium oxide particles following influenza infection also showed a virus-induced enhancement of clearance for a soluble cesium chloride (Lundgren et al., 1978, [155950](#)). Chang et al. (2005, [097776](#)) also recently showed that UF carbon black acts through a reactive oxygen species (ROS) dependent pathway to increase epithelial permeability in mice.

Chronic exposure to other particulate or gaseous pollutants does not always led to increased epithelial permeability. Studying subjects with a variety of occupational exposures, Kaya et al. (2006, [156632](#)) showed that nonsmoking welders actually have decreased epithelial permeability relative to nonsmoking control subjects, and occupational exposure of painters to isocyanates has no effect on bronchoalveolar epithelial permeability (Kaya et al., 2003, [156631](#)).

4.4.3. Summary

The healthy airway and alveolar epithelium is generally impermeable to very large insoluble macromolecules and particles. Water and acid soluble particles may more rapidly move through the epithelium as they dissolve on the airway surface or within the phagolysosomes of macrophages. The presence of airway inflammation in a variety of airway diseases (e.g., asthma, fibrosis, ARDS, pulmonary edema, inflammation from smoking) alters epithelial integrity to allow more rapid movement of these solutes into the bloodstream. While diabetics are another group recently shown to have increased susceptibility to particulate air pollution (Zanobetti and Schwartz, 2002, [034821](#)), it is unclear whether transport of soluble particles across the epithelium is affected in these patients. In general, it appears that coexposure to irritant pollutants results in a disruption of epithelial integrity and macrophage function which, on the one hand, retards mucociliary and alveolar clearance, but also allows for a more rapid movement of soluble constituents across the epithelial surface into the interstitium and blood stream. Alterations in epithelial permeability by disease, pollutant exposure, or infection may partially explain increased susceptibility to PM associated with these co-conditions.

Chapter 4 References

- ACGIH (2005). TLVs and BEIs: Based on the documentation of the threshold limit values for chemical substances and physical agents and biological exposure indices. American Conference of Governmental Industrial Hygienists. Cincinnati, Ohio. [156188](#)
- Adamson I; Prieditis H (1995). Response of mouse lung to carbon deposition during injury and repair. *Environ Health Perspect*, 103: 72-76. [189982](#)
- Alexis N; Soukup J; Nierkens S; Becker S (2001). Association between airway hyperreactivity and bronchial macrophage dysfunction in individuals with mild asthma. *Am J Physiol Lung Cell Mol Physiol*, 280: L369-L375. [190013](#)
- Anselm A; Heibel T; Gebhart J; Ferron GA (1990). In vivo studies of growth factors of sodium chloride particles in the human respiratory tract. *J Aerosol Sci*, 21: S427-430. [156217](#)
- Anthony TR; Flynn MR (2006). Computational fluid dynamics investigation of particle inhalability. *J Aerosol Sci*, 37: 750-765. [155659](#)
- Antonini JM; Roberts JR; Clarke RW; Yang HM; Barger MW; Ma JYC; Weissman DN (2001). Effect of age on respiratory defense mechanisms: pulmonary bacterial clearance in Fischer 344 rats after intratracheal instillation of *Listeria monocytogenes*. *Chest*, 120: 240-249. [156219](#)
- Antoniou KM; Malagari K; Tzanakis N; Perisinakis K; Symvoulakis EK; Karkavitsas N; Siafakas NM; Bouros D (2006). Clearance of technetium-99m-DTPA and HRCT findings in the evaluation of patients with Idiopathic Pulmonary Fibrosis. *BMC Pulm Med*, 6: 4. [156220](#)
- Aschner M; Erikson KM; Dorman DC (2005). Manganese Dosimetry: Species Differences and Implications for Neurotoxicity. *Crit Rev Toxicol*, 35: 1-32. [155663](#)
- Asgharain B; Kelly JT; Tewksbury EW (2003). Respiratory deposition and inhalability of monodisperse aerosols in Long-Evans rats. *Toxicol Sci*, 71: 104-111. [153068](#)
- Asgharian B; Hofmann W; Miller FJ (2001). Mucociliary clearance of insoluble particles from the tracheobronchial airways of the human lung. *J Aerosol Sci*, 32: 817-832. [017025](#)
- Bailey M; Dorrian M; Birchall A (1995). Implications of airway retention for radiation doses from inhaled radionuclides. *J Aerosol Med*, 8: 373-390. [190057](#)
- Balashazy I; Hofmann W; Heistracher T (1999). Computation of local enhancement factors for the quantification of particle deposition patterns in airway bifurcations. *J Aerosol Sci*, 30: 185-203. [043201](#)
- Balashazy I; Hofmann W; Heistracher T (2003). Local particle deposition patterns may play a key role in the development of lung cancer. *J Appl Physiol*, 94: 1719-1725. [155671](#)
- Beadsmoore C; Cheow HK; Szczepura K; Ruparella P; Peters AM (2007). Healthy passive cigarette smokers have increased pulmonary alveolar permeability. *Nucl Med Comm*, 28: 75-77. [156259](#)
- Becquemin MH; Swift DL; Bouchikhi A; Roy M; Teillac A (1991). Particle deposition and resistance in the noses of adults and children. *Eur Respir J*, 4: 694-702. [009187](#)
- Becquemin MM; Bertholon JF; Bouchikhi A; Malarbet JL; Roy M (1999). Oronasal Ventilation Partitioning in Adults and Children: Effect on Aerosol Deposition in Airways. *Radiat Prot Dosimetry*, 81: 221-228. [155679](#)
- Bennett W; Messina M; Smaldone G (1985). Effect of exercise on deposition and subsequent retention of inhaled particles. *J Appl Physiol*, 59: 1046-1054. [190034](#)
- Bennett W; Zeman K; Jarabek A (2003). Nasal contribution to breathing with exercise: effect of race and gender. *J Appl Physiol*, 95: 497-503. [191977](#)
- Bennett WD; Ilowite JS (1989). Dual pathway clearance of 99mTc-DTPA from the bronchial mucosa. *Am Rev Respir Dis*, 139: 1132-1138. [000835](#)

Note: Hyperlinks to the reference citations throughout this document will take you to the NCEA HERO database (Health and Environmental Research Online) at <http://epa.gov/hero>. HERO is a database of scientific literature used by U.S. EPA in the process of developing science assessments such as the Integrated Science Assessments (ISA) and the Integrated Risk Information System (IRIS).

- Bennett WD; Zeman KL (1998). Deposition of fine particles in children spontaneously breathing at rest. *Inhal Toxicol*, 10: 831-842. [076182](#)
- Bennett WD; Zeman KL (2004). Effect of body size on breathing pattern and fine-particle deposition in children. *J Appl Physiol*, 97: 821-826. [155686](#)
- Bennett WD; Zeman KL (2005). Effect of Race on Fine Particle Deposition for Oral and Nasal Breathing. *Inhal Toxicol*, 17: 641-648. [155687](#)
- Bennett WD; Zeman KL; Jarabek AM (2008). Nasal contribution to breathing and fine particle deposition in children versus adults. *J Toxicol Environ Health A Curr Iss*, 71: 227-237. [156269](#)
- Bennett WD; Zeman KL; Kim C (1996). Variability of fine particle deposition in healthy adults: effect of age and gender. *Am J Respir Crit Care Med*, 153: 1641-1647. [083284](#)
- Bennett WD; Zeman KL; Kim C; Mascarella J (1997). Enhanced deposition of fine particles in COPD patients spontaneously breathing at rest. *Inhal Toxicol*, 9: 1-14. [078839](#)
- Bermudez E; Mangum JB; Asgharian B; Wong BA; Reverdy EE; Janszen DB; Hext PM; Warheit DB; Everitt JI (2002). Long-term pulmonary responses of three laboratory rodent species to subchronic inhalation of pigmentary titanium dioxide particles. *Toxicol Sci*, 70: 86-97. [055578](#)
- Bermudez E; Mangum JB; Wong BA; Asgharian B; Hext PM; Warheit DB; Everitt JI (2004). Pulmonary responses of mice, rats, and hamsters to subchronic inhalation of ultrafine titanium dioxide particles. *Toxicol Sci*, 77: 347-357. [056707](#)
- Bhalla DK; Mannix RC; Kleinman MT; Crocker TT (1986). Relative permeability of nasal, tracheal, and bronchoalveolar mucosa to macromolecules in rats exposed to ozone. *J Toxicol Environ Health*, 17: 269-283. [040407](#)
- Bodolay E; Szekanez Z; Devenyi K; Galuska L; Csipo I; Vegh J; Garai I; Szegedi G (2005). Evaluation of interstitial lung disease in mixed connective tissue disease (MCTD). *Rheumatology*, 44: 656-661. [156280](#)
- Braga F; Mango JC; Souza JF; Ferrioli E; De Andrade J; Iazigi N (1996). Age-related reduction in 99Tcm-DTPA alveolar-capillary clearance in normal humans. *Nucl Med Comm*, 17: 971-974. [156289](#)
- Braude S; Nolop KB; Hughes JMB; Barnes PJ; Royston D (1986). Comparison of lung vascular and epithelial permeability indices in the adult respiratory distress syndrome. *Am Rev Respir Dis*, 133: 1002-1005. [155701](#)
- Brown J; Bennett W (2004). Deposition of coarse particles in cystic fibrosis: model predictions versus experimental results. *J Aerosol Med*, 17: 239-248. [190032](#)
- Brown JS (2005). Particle inhalability at low wind speeds. *Inhal Toxicol*, 17: 831-837. [156299](#)
- Brown JS; Wilson WE; Grant LD (2005). Dosimetric comparisons of particle deposition and retention in rats and humans. *Inhal Toxicol*, 17: 355-385. [089308](#)
- Brown JS; Zeman KL; Bennett WD (2002). Ultrafine particle deposition and clearance in the healthy and obstructed lung. *Am J Respir Crit Care Med*, 166: 1240-1247. [043216](#)
- Burch WM (2002). Comment on "Passage of inhaled particles into the blood circulation in humans". *Circulation*, 106: e141-e142. [056754](#)
- Caner B; Ugur O; Bayraktar M; Ulutuncel N; Menten T; Telatar F; Bekdik C (1994). Impaired lung epithelial permeability in diabetics detected by technetium-99m-DTPA aerosol scintigraphy. *J Nucl Med*, 35: 204-206. [156320](#)
- Chadha TS; Birch S; Sackner MA (1987). Oronasal distribution of ventilation during exercise in normal subjects and patients with asthma and rhinitis. *Chest*, 92: 1037-1041. [037365](#)
- Chang C-C; Chiu H-F; Wu Y-S; Li Y-C; Tsai M-L; Shen C-K; Yang C-Y (2005). The induction of vascular endothelial growth factor by ultrafine carbon black contributes to the increase of alveolar-capillary permeability. *Environ Health Perspect*, 113: 454-460. [097776](#)
- Chen J; Tan M; Nemmar A; Song W; Dong M; Zhang G; Li Y (2006). Quantification of extrapulmonary translocation of intratracheal-instilled particles in vivo in rats: effect of lipopolysaccharide. *Toxicology*, 222: 195-201. [147267](#)
- Cheng K-H; Cheng Y-S; Yeh H-C; Guilmette RA; Simpson SQ; Yang Y-H; Swift DL (1996). In vivo measurements of nasal airway dimensions and ultrafine aerosol deposition in the human nasal and oral airways. *J Aerosol Sci*, 27: 785-801. [047520](#)

- Chinard FP (1980). The alveolar-capillary barrier: some data and speculations. *Microvasc Res*, 19: 1-17. [156341](#)
- Churg A; Stevens B; Wright JL (1998). Comparison of the uptake of fine and ultrafine TiO₂ in a tracheal explant system. *Am J Physiol*, 274: L81-L86. [085815](#)
- Cohen MD; Zelikoff JT; Chen L-C; Schlesinger RB (1997). Pulmonary retention and distribution of inhaled chromium: effects of particle solubility and coexposure to ozone. *Inhal Toxicol*, 9: 843-865. [009213](#)
- Creasia DA; Poggenburg JK Jr; Nettesheim P (1976). Elution of benzo[a]pyrene from carbon particles in the respiratory tract of mice. *J Toxicol Environ Health*, 1: 967-975. [059713](#)
- Dai YT; Juang YJ; Wu Y; Breyse PN; Hsu DJ (2006). In vivo measurements of inhalability of ultralarge aerosol particles in calm air by humans. *J Aerosol Sci*, 37: 967-973. [156377](#)
- DeLorenzo AJD (1970). The olfactory neuron and the blood-brain barrier. In *Taste and Smell in Vertebrates* (pp. 151-175). London: Churchill Livingstone. [156391](#)
- Dorman DC; McManus BE; Parkinson CU; Manuel CA; McElveen AM; Everitt JI (2004). Nasal Toxicity of Manganese Sulfate and Manganese Phosphate in Young Male Rats Following Subchronic (13-Week) Inhalation Exposure. *Inhal Toxicol*, 16: 481-488. [155752](#)
- Dorman DC; Struve MF; James RA; Marshall MW; Parkinson CU; Wong BA (2001). Influence of particle solubility on the delivery of inhaled manganese to the rat brain: manganese sulfate and manganese tetroxide pharmacokinetics following repeated (14-day) exposure. *Toxicol Appl Pharmacol*, 170: 79-87. [055433](#)
- Edetsberger M; Gaubitzer E; Valic E; Waigmann E; Köhler G (2005). Detection of nanometer-sized particles in living cells using modern fluorescence fluctuation methods. *Biochem Biophys Res Commun*, 332: 109-116. [155759](#)
- Elder A; Gelein R; Silva V; Feikert T; Opanashuk L; Carter J; Potter R; Maynard A; Ito Y; Finkelstein J; Oberdorster G (2006). Translocation of inhaled ultrafine manganese oxide particles to the central nervous system. *Environ Health Perspect*, 114: 1172-1178. [089253](#)
- Enna SJ; Schanker LS (1972). Absorption of drugs from the rat lung. *Am J Physiol*, 223: 1227-1231. [155767](#)
- Falk R; Philipson K; Svartengren M; Jarvis N; Bailey M; Camner P (1997). Clearance of particles from small ciliated airways. *Exp Lung Res*, 23: 495-515. [086080](#)
- Farkas A; Balásházy I (2008). Quantification of particle deposition in asymmetrical tracheobronchial model geometry. *Comput Biol Med*, 38: 508-18. [157358](#)
- Farkas A; Balashazy I; SzQcs K (2006). Characterization of Regional and Local Deposition of Inhaled Aerosol Drugs in the Respiratory System by Computational Fluid and Particle Dynamics Methods. *J Aerosol Med*, 19: 329-343. [155771](#)
- Ferin J; Oberdorster G; Penney DP (1992). Pulmonary retention of ultrafine and fine particles in rats. *Am J Respir Cell Mol Biol*, 6: 535-542. [044401](#)
- Finlay WH; Martin AR (2008). Recent advances in predictive understanding of respiratory tract deposition. *J Aerosol Med Pulm Drug Deliv*, 21: 189-206. [155776](#)
- Fishman AP; Elias JA (1980). *Fishman's Pulmonary diseases and disorders*. New York: McGraw-Hill. [156436](#)
- Foster WM; Stetkiewicz PT (1996). Regional clearance of solute from the respiratory epithelia: 18--20 h postexposure to ozone. *J Appl Physiol*, 81: 1143-1149. [079920](#)
- Foster WM; Wagner EM (2001). Bronchial edema alters 99mTc-DTPA clearance from the airway surface in sheep. *J Appl Physiol*, 91: 2567-2573. [155778](#)
- Geiser M; Rothen-Rutishauser B; Kapp N; Schurch S; Kreyling W; Schulz H; Semmler M; Im Hof V; Heyder J; Gehr P (2005). Ultrafine particles cross cellular membranes by nonphagocytic mechanisms in lungs and in cultured cells. *Environ Health Perspect*, 113: 1555-1560. [087362](#)
- Geys J; Coenegrachts L; Vercammen J; Engelborghs Y; Nemmar A; Nemery B; Hoet PHM (2006). In vitro study of the pulmonary translocation of nanoparticles A preliminary study. *Toxicol Lett*, 160: 218-226. [155789](#)
- Goodman RM; Yergin BM; Landa JF; Golinviaux MH; Sackner MA (1978). Relationship of smoking history and pulmonary function tests to tracheal mucous velocity in nonsmokers, young smokers, ex-smokers, and patients with chronic bronchitis. *Am Rev Respir Dis*, 117: 205-214. [071130](#)

- Greenspan BJ; Morrow PE; Ferin J (1988). Effects of aerosol exposures to cadmium chloride on the clearance of titanium dioxide from the lungs of rats. *Exp Lung Res*, 14: 491-499. [045031](#)
- Grgic B; Finlay WH; Burnell PKP; Heenan AF (2004). In vitro intersubject and intrasubject deposition measurements in realistic mouth–throat geometries. *J Aerosol Sci*, 35: 1025-1040. [155810](#)
- Hanel B; Law I; Mortensen J (2003). Maximal rowing has an acute effect on the blood-gas barrier in elite athletes. *J Appl Physiol*, 95: 1076-1082. [155826](#)
- Heistracher T; Hofmann W (1997). Flow and deposition patterns in successive airway bifurcations. Presented at In: Cherry, N.; Ogden, T., eds. *Inhaled Particles VIII: proceedings of an international symposium on inhaled particles organised by the British Occupational Hygiene Society; August 1996; Cambridge, UK. Ann. Occup. Hyg.* 41(suppl.): 537-542. [047514](#)
- Ho JC; Chan KN; Hu WH; Lam WK; Zheng L; Tipoe GL; Sun J; Leung R; Tsang KW (2001). The effect of aging on nasal mucociliary clearance, beat frequency, and ultrastructure of respiratory cilia. *Am J Respir Crit Care Med*, 163: 983-988. [156549](#)
- Hofmann W; Asgharian B (2003). The effect of lung structure on mucociliary clearance and particle retention in human and rat lungs. *Toxicol Sci*, 73: 448-456. [055579](#)
- Hofmann W; Balashazy I; Heistracher T; Koblinger L (1996). The significance of particle deposition patterns in bronchial airway bifurcations for extrapolation modeling. *Aerosol Sci Technol*, 25: 305-327. [047515](#)
- Hofmann W; Martonen TB; Graham RC (1989). Predicted deposition of nonhygroscopic aerosols in the human lung as a function of subject age. *J Aerosol Med*, 2: 49-68. [006922](#)
- Hsu DJ; Swift DL (1999). The measurements of human inhalability of ultralarge aerosols in calm air using mannikins. *J Aerosol Sci*, 30: 1331-1343. [155855](#)
- Huchon GJ; Montgomery AB; Lipavsky A; Hoefel JM; Murray JF (1987). Respiratory clearance of aerosolized radioactive solutes of varying molecular weight. *J Nucl Med*, 28: 894-902. [024923](#)
- Huchon GJ; Russell JA; Barritault LG; Lipavsky A; Murray JF (1984). Chronic air-flow limitation does not increase respiratory epithelial permeability assessed by aerosolized solute, but smoking does. *Am Rev Respir Dis*, 130: 457-460. [156576](#)
- ICRP (1995). Human respiratory tract model for radiological protection: a report of a task group of the International Commission on Radiological Protection. *Ann ICRP*, 24: 1-482. [006988](#)
- Ilowite JS; Bennett WD; Sheetz MS; Groth ML; Nierman DM (1989). Permeability of the bronchial mucosa to ^{99m}Tc-DTPA in asthma. *Am Rev Respir Dis*, 139: 1139-1143. [156584](#)
- International Life Sciences Institute (2000). The relevance of the rat lung response to particle overload for human risk assessment: A workshop consensus report. *Inhal Toxicol*, 12: 1-17. [002892](#)
- Isaacs KK; Schlesinger RB; Martonen TB (2006). Three-dimensional computational fluid dynamics simulations of particle deposition in the tracheobronchial tree. *J Aerosol Med*, 19: 344-352. [155861](#)
- ISO (2008). Nanotechnologies -- Terminology and definitions for nano-objects -- Nanoparticle, nanofibre and nanoplate. International Organization for Standardization. Geneva. [190066](#)
- James DS; Stidley CA; Lambert WE; Chick TW; Mermier CM; Samet JM (1997). Oronasal distribution of ventilation at different ages. *Arch Environ Occup Health*, 52: 118-123. [042422](#)
- Jarabek AM; Asgharian B; Miller FJ (2005). Dosimetric adjustments for interspecies extrapolation of inhaled poorly soluble particles (PSP). *Inhal Toxicol*, 17: 317-334. [056756](#)
- Jeffers DE (2005). Relative magnitudes of the effects of electrostatic image and thermophoretic forces on particles in the respiratory tract. *Radiat Prot Dosimetry*, 113: 189-194. [156608](#)
- Jones JG; Minty BD; Lawler P; Hulands G; Crawley JC; Veall N (1980). Increased alveolar epithelial permeability in cigarette smokers. *Lancet*, 1: 66-68. [155883](#)
- Jones JG; Minty BD; Royston D; Royston JP (1983). Carboxyhaemoglobin and pulmonary epithelial permeability in man. *Thorax*, 38: 129-133. [155884](#)

- Kapp N; Kreyling W; Schulz H; Im Hof V; Gehr P; Semmler M; Geiser M (2004). Electron energy loss spectroscopy for analysis of inhaled ultrafine particles in rat lungs. *Microsc Res Tech*, 63: 298-305. [156624](#)
- Kaya E; Fidan F; Unlu M; Sezer M; Tetik L; Acar M (2006). Evaluation of alveolar clearance by Tc-99m DTPA radioaerosol inhalation scintigraphy in welders. *Ann Nucl Med*, 20: 503-510. [156632](#)
- Kaya M; Salan A; Tabakoglu E; Aydogdu N; Berkarda S (2003). The bronchoalveolar epithelial permeability in house painters as determined by Tc-99m DTPA aerosol scintigraphy. *Ann Nucl Med*, 17: 305-308. [156631](#)
- Kehrl HR; Vincent LM; Kowalsky RJ; Horstman DH; O'Neil JJ; McCartney WH; Bromberg PA (1987). Ozone exposure increases respiratory epithelial permeability in humans. *Am J Respir Crit Care Med*, 135: 1124-1128. [040824](#)
- Kelly JT; Asgharian B; Wong BA (2005). Inertial Particle Deposition in a Monkey Nasal Mold Compared with that in Human Nasal Replicas. *Inhal Toxicol*, 17: 823-830. [155894](#)
- Kim CS (2000). Methods of calculating lung delivery and deposition of aerosol particles. *Respir Care*, 45: 695-711. [013112](#)
- Kim CS; Hu SC (1998). Regional deposition of inhaled particles in human lungs: comparison between men and women. *J Appl Physiol*, 84: 1834-1844. [086066](#)
- Kim CS; Iglesias AJ (1989). Deposition of inhaled particles in bifurcating airway models: I inspiratory deposition. *J Aerosol Med*, 2: 1-14. [078539](#)
- Kim CS; Iglesias AJ; Garcia L (1989). Deposition of inhaled particles in bifurcating airway models: II expiratory deposition. *J Aerosol Med*, 2: 15-27. [078538](#)
- Kim CS; Jaques PA (2000). Respiratory dose of inhaled ultrafine particles in healthy adults. *Philos Transact A Math Phys Eng Sci*, 358: 2693-2705. [012811](#)
- Kimbell JS (2006). Nasal Dosimetry of Inhaled Gases and Particles: Where Do Inhaled Agents Go in the Nose? *Toxicol Pathol*, 34: 270-273. [155902](#)
- Kreyling WG (1992). Intracellular particle dissolution in alveolar macrophages. *Environ Health Perspect*, 97: 121-126. [067243](#)
- Kreyling WG; Blanchard JD; Godleski JJ; Haeussermann S; Heyder J; Hutzler P; Schulz H; Sweeney TD; Takenaka S; Ziesenis A (1999). Anatomic localization of 24- and 96-h particle retention in canine airways. *J Appl Physiol*, 87: 269-284. [039175](#)
- Kreyling WG; Scheuch G (2000). Clearance of particles deposited in the lungs. In Gehr, P.; Heyder, J. (Ed.), *Particle-lung interactions* (pp. x). New York, NY: Marcel Dekker, Inc. [056281](#)
- Kreyling WG; Semmler M; Erbe F; Mayer P; Takenaka S; Schulz H; Oberdorster G; Ziesenis A (2002). Translocation of ultrafine insoluble iridium particles from lung epithelium to extrapulmonary organs is size dependent but very low. *J Toxicol Environ Health A Curr Iss*, 65: 1513-1530. [037332](#)
- Laitinen LA; Heino M; Laitinen A; Kava T; Haahtela T (1985). Damage of the airway epithelium and bronchial reactivity in patients with asthma. *Am Rev Respir Dis*, 131: 599-606. [037521](#)
- Lay J; Alexis N; Zeman K; Peden D; Bennett W (2009). In vivo uptake of inhaled particles by airway phagocytes is enhanced in patients with mild asthma compared with normal volunteers. *Thorax*, 64: 313-320. [190060](#)
- Lay JC; Stang MR; Fisher PE; Yankaskas JR; Bennett WD (2003). Airway Retention of Materials of Different Solubility following Local Intrabronchial Deposition in Dogs. *J Aerosol Med*, 16: 153-166. [155920](#)
- Lee KP; Henry NW III; Trochimowicz HJ; Reinhardt CF (1986). Pulmonary response to impaired lung clearance in rats following excessive TiO₂ dust deposition. *Environ Res*, 41: 144-167. [067629](#)
- Lee KP; Trochimowicz HJ; Reinhardt CF (1985). Transmigration of titanium dioxide (TiO₂) particles in rats after inhalation exposure. *Exp Mol Pathol*, 42: 331-343. [067628](#)
- Lin CC; Chang CT; Li TC; Kao A (2002). Objective Evidence of Impairment of Alveolar Integrity in Patients with Non-Insulin-Dependent Diabetes Mellitus Using Radionuclide Inhalation Lung Scan. *Lung*, 180: 181-186. [155932](#)
- Lorino AM; Meignan M; Bouissou P; Atlan G (1989). Effects of sustained exercise on pulmonary clearance of aerosolized 99mTc-DTPA. *J Appl Physiol*, 67: 2055-2059. [155946](#)
- Lundgren DL; Hahn FF; Crain CR; Sanchez A (1978). Effect of influenza virus infection on the pulmonary retention of inhaled 144Ce and subsequent survival of mice. *Health Phys*, 34: 557-567. [155950](#)

- Martonen TB; Yang Y; Xue ZQ (1994). Effects of carinal ridge shapes on lung airstreams. *Aerosol Sci Technol*, 21: 119-136. [000847](#)
- Mason GR; Uszler JM; Effros RM; Reid E (1983). Rapidly reversible alterations of pulmonary epithelial permeability induced by smoking. *Chest*, 83: 6-11. [013169](#)
- Matsui H; Randell SH; Peretti SW; Davis CW; Boucher RC (1998). Coordinated clearance of periciliary liquid and mucus from airway surfaces. *J Clin Invest*, 102: 1125-1131. [040405](#)
- Mauderly JL (1997). Relevance of particle-induced rat lung tumors for assessing lung carcinogenic hazard and human lung cancer risk. *Environ Health Perspect*, 105 (Suppl 5): 1337-1346. [084631](#)
- Meignan M; Rosso J; Leveau J; Katz A; Cinotti L; Madelaine G; Galle P (1986). Exercise increases the lung clearance of inhaled technetium-99m DTPA. *J Nucl Med*, 27: 274-280. [156752](#)
- Ménache MG; Miller FJ; Raabe OG (1995). Particle inhalability curves for humans and small laboratory animals. *Ann Occup Hyg*, 39: 317-328. [006533](#)
- Miller FJ (2000). Dosimetry of particles in laboratory animals and humans in relationship to issues surrounding lung overload and human health risk assessment: a critical review. *Inhal Toxicol*, 12: 19-57. [011822](#)
- Mills NL; Amin N; Robinson SD; Anand A; Davies J; Patel D; de la Fuente JM; Cassee FR; Boon NA; Macnee W; Millar AM; Donaldson K; Newby DE (2006). Do inhaled carbon nanoparticles translocate directly into the circulation in humans? *Am J Respir Crit Care Med*, 173: 426-431. [088770](#)
- Möller W; Felten K; Sommerer K; Scheuch G; Meyer G; Meyer P; Haussinger K; Kreyling WG (2008). Deposition, retention, and translocation of ultrafine particles from the central airways and lung periphery. *Am J Respir Crit Care Med*, 177: 426-432. [156771](#)
- Möller W; Haussinger K; Winkler-Heil R; Stahlhofen W; Meyer T; Hofmann W; Heyder J (2004). Mucociliary and long-term particle clearance in the airways of healthy nonsmoker subjects. *J Appl Physiol*, 97: 2200-2206. [155987](#)
- Morgan W; Ahmad D; Chamberlain M; Clague H; Pearson M; Vinitski S (1984). The effect of exercise on the deposition of an inhaled aerosol. *Respir Physiol*, 56: 327-338. [190035](#)
- Morrow PE (1994). Mechanisms and significance of "particle overload". In Mohr U (Ed.), *Toxic and Carcinogenic Effects of Solid Particles in the Respiratory Tract* (pp. 17-25). Washington, DC: ILSI Press. [006850](#)
- Mousa K; Onadoko BO; Mustafa HT; Mohamed M; Nabilla A; Omar A; Al-Bunni A; Elgazzar A (2000). Technetium 99mTc-DTPA clearance in the evaluation of pulmonary involvement in patients with diabetes mellitus. *Respir Med*, 94: 1053-1056. [156786](#)
- Muhle H; Creutzenberg O; Bellmann B; Heinrich U; Mermelstein R (1990). Dust overloading of lungs: investigations of various materials, species differences, and irreversibility of effects. *J Aerosol Med*, 1: S111-S128. [006853](#)
- Nemmar A; Hoet PHM; Vanquickenborne B; Dinsdale D; Thomeer M; Hoylaerts MF; Vanbilloen H; Mortelmans L; Nemery B (2002). Passage of inhaled particles into the blood circulation in humans. *Circulation*, 105: 411-414. [024914](#)
- Niinimaa V; Cole P; Mintz S; Shephard RJ (1981). Oronasal distribution of respiratory airflow. *Respir Physiol Neurobiol*, 43: 69-75. [071758](#)
- Nikula KJ; Vallyathan V; Green FHY; Hahn FF (2001). Influence of exposure concentration or dose on the distribution of particulate material in rat and human lungs. *Environ Health Perspect*, 109: 311-318. [016641](#)
- NRPB (2004). Particle deposition in the vicinity of power lines and possible effects on health: Report of an independent advisory group on non-ionising radiation and its ad hoc group on corona ions. National Radiological Protection Board. Oxfordshire, England. [156815](#)
- Oberdörster G (1988). Lung clearance of inhaled insoluble and soluble particles. *J Aerosol Med*, 1: 289-330. [006857](#)
- Oberdörster G (1995). Lung particle overload: implications for occupational exposures to particles. *Regul Toxicol Pharmacol*, 27: 123-135. [046596](#)
- Oberdörster G (1996). Significance of particle parameters in the evaluation of exposure-dose-response relationships of inhaled particles. *Inhal Toxicol*, 8 Supplement: 73-89. [039852](#)
- Oberdörster G (2002). Toxicokinetics and effects of fibrous and nonfibrous particles. *Inhal Toxicol*, 14: 29-56. [021111](#)

- Oberdörster G; Ferin J; Gelein R; Soderholm SC; Finkelstein J (1992). Role of the alveolar macrophage in lung injury: studies with ultrafine particles. *Environ Health Perspect*, 97: 193-199. [045110](#)
- Oberdörster G; Ferin J; Lehnert BE (1994). Correlation between particle size, in vivo particle persistence, and lung injury. *Environ Health Perspect*, 102 : 173-179. [046203](#)
- Oberdörster G; Ferin J; Soderholm S; Gelein R; Cox C; Baggs R; Morrow PE (1994). Increased pulmonary toxicity of inhaled ultrafine particles: due to lung overload alone? *Ann Occup Hyg*, 38: 295-302. [056285](#)
- Oberdörster G; Finkelstein JN; Johnston C; Gelein R; Cox C; Baggs R; Elder ACP (2000). Acute pulmonary effects of ultrafine particles in rats and mice. Health Effects Institute. Boston. Report Number 96. [039014](#)
- Oberdörster G; Sharp Z; Atudorei V; Elder A; Gelein R; Kreyling W; Cox C (2004). Translocation of inhaled ultrafine particles to the brain. *Inhal Toxicol*, 16: 437-445. [055639](#)
- Oldham MJ; Robinson RJ (2007). Predicted tracheobronchial and pulmonary deposition in a murine asthma model. *Anat Rec*, 290: 1309-1314. [156003](#)
- Ozsahin K; Tugrul A; Mert S; Yüksel M; Tugrul G (2006). Evaluation of pulmonary alveolo-capillary permeability in Type 2 diabetes mellitus Using technetium 99mTc-DTPA aerosol scintigraphy and carbon monoxide diffusion capacity. *J Diabetes Complications*, 20: 205-209. [156833](#)
- Persson E; Henriksson J; Tallkvist J; Rouleau C; Tjalve H (2003). Transport and subcellular distribution of intranasally administered zinc in the olfactory system of rats and pikes. *Toxicology*, 191: 97-108. [051846](#)
- Peterson BT; Dickerson KD; James HL; Miller EJ; McLarty JW; Holiday DB (1989). Comparison of three tracers for detecting lung epithelial injury in anesthetized sheep. *J Appl Physiol*, 66: 2374-2383. [024922](#)
- Phalen RF; Oldham MJ (2006). Aerosol dosimetry considerations. *Clin Occup Environ Med*, 5: 773-784. [156024](#)
- Phalen RF; Oldham MJ; Mautz WJ (1989). Aerosol Deposition in the Nose As a Function of Body Size. *Health Phys*, 57: 299-305. [156023](#)
- Phalen RF; Oldham MJ; Wolff RK (2008). The relevance of animal models for aerosol studies. *J Aerosol Med Pulm Drug Deliv*, 21: 113-124. [156865](#)
- Pigorini F; Maini CL; Pau F; Giosue S (1988). The influence of age on the pulmonary clearance of 99Tcm-DTPA radioaerosol. *Nucl Med Comm*, 9: 965-971. [156027](#)
- Puchelle E; Zahm J-M; Bertrand A (1979). Influence of age on bronchial mucociliary transport. *Scand J Respir Dis*, 60: 307-313. [006863](#)
- Raabe OG; Al-Bayati MA; Teague SV; Rasolt A (1988). Regional deposition of inhaled monodisperse, coarse, and fine aerosol particles in small laboratory animals. In *Inhaled particles VI: Proceedings of an international symposium and workshop on lung dosimetry* (pp. 53-63). Cambridge, U.K.: Pergamon Press. [001439](#)
- Roth C; Scheuch G; Stahlhofen W (1993). Clearance of the human lungs for ultrafine particles. *J Aerosol Sci*, 24: S95-S96. [156928](#)
- Sakagami M; Byron PR; Venitz J; Rypacek F (2002). Solute disposition in the rat lung in vivo and in vitro: determining regional absorption kinetics in the presence of mucociliary escalator. *J Pharmacol Sci*, 91: 594-604. [156936](#)
- Schanker LS; Mitchell EW; Brown RA Jr (1986). Species comparison of drug absorption from the lung after aerosol inhalation or intratracheal injection. *Drug Metab Dispos*, 14: 79-88. [005100](#)
- Scheuch G; Gebhart J; Roth C (1990). Uptake of electrical charges in the human respiratory tract during exposure to air loaded with negative ions. *J Aerosol Sci*, 21: S439-S442. [006948](#)
- Schroeter JD; Kimbell JS; Asgharian B (2006). Analysis of particle deposition in the turbinate and olfactory regions using a human nasal computational fluid dynamics model. *J Aerosol Med Pulm Drug Deliv*, 19: 301-313. [156076](#)
- Semmler M; Seitz J; Erbe F; Mayer P; Heyder J; Oberdörster G; Kreyling WG (2004). Long-term clearance kinetics of inhaled ultrafine insoluble iridium particles from the rat lung, including transient translocation into secondary organs. *Inhal Toxicol*, 16: 453-459. [055641](#)
- Semmler-Behnke M; Takenaka S; Fertsch S; Wenk A; Seitz J; Mayer P; Oberdörster G; Kreyling WG (2007). Efficient elimination of inhaled nanoparticles from the alveolar region: evidence for interstitial uptake and subsequent reentrainment onto airways epithelium. *Environ Health Perspect*, 115: 728-733. [156080](#)

- Smith JR; Bailey MR; Etherington G; Shutt AL; Youngman MJ (2008). Effect of particle size on slow particle clearance from the bronchial tree. *Exp Lung Res*, 34: 287-312. [190037](#)
- Snipes MB (1996). Current information on lung overload in nonrodent mammals: contrast with rats. *Inhal Toxicol*, 8: 91-109. [076041](#)
- Snipes MB; Harkema JR; Hotchkiss JA; Bice DE (1997). Neutrophil Involvement in the Retention and Clearance of Dust Intratracheally Instilled into the LUNGS of F344/N Rats. *Exp Lung Res*, 23: 65-84. [156092](#)
- Soderholm SC (1985). Size-selective sampling criteria for inspirable mass fraction. In *Particle size-selective sampling in the workplace : report of the ACGIH Technical Committee on Air Sampling Procedures* (pp. 27-32). Cincinnati, Ohio: American Conference of Governmental Industrial Hygienists. [156992](#)
- Sousa SR; Moradas-Ferreira P; Saramago B; Viseu ML; Barbosa MA (2004). Human serum albumin adsorption on TiO₂ from single protein solutions and from plasma. *Langmuir*, 20: 9745-9754. [089866](#)
- Suga K; Yuan Y; Ogasawara N; Tsukuda T; Matsunaga N (2003). Altered Clearance of Gadolinium Diethylenetriaminepentaacetic Acid Aerosol from Bleomycin-injured Dog Lungs: Initial Observations. *Am J Respir Crit Care Med*, 167: 1704-1710. [157024](#)
- Svartengren M; Falk R; Philipson K (2005). Long-term clearance from small airways decreases with age. *Eur Respir J*, 26: 609-615. [157034](#)
- Tabachnik E; Muller N; Toye B; Levison H (1981). Measurement of ventilation in children using the respiratory inductive plethysmograph. *J Pediatr*, 99: 895-899. [157036](#)
- Takenaka S; Dornhofer-Takenaka H; Muhle H (1986). Alveolar distribution of fly ash and of titanium dioxide after long-term inhalation by Wistar rats. *J Aerosol Sci*, 17: 361-364. [046210](#)
- Takenaka S; Karg E; Kreyling W; Lentner B; Möller W; Behnke-Semmler M; Jennen L; Walch A; Michalke B; Schramel P (2006). Distribution Pattern of Inhaled Ultrafine Gold Particles in the Rat Lung. *Inhal Toxicol*, 18: 733-740. [156110](#)
- Tankersley CG; Shank JA; Flanders SE; Soutiere SE; Rabold R; Mitzner W; Wagner EM (2003). Changes in lung permeability and lung mechanics accompany homeostatic instability in senescent mice. *J Appl Physiol*, 95: 1681-1687. [096363](#)
- Tobin MJ; Chadha TS; Jenouri G; Birch SJ; Gazeroglu HB; Sackner MA (1983). Breathing patterns. 1. Normal subjects. *Chest*, 84: 202-205. [156122](#)
- Tran CL; Buchanan D; Cullen RT; Searl A; Jones AD; Donaldson K (2000). Inhalation of poorly soluble particles II Influence of particle surface area on inflammation and clearance. *Inhal Toxicol*, 12: 1113-1126. [013071](#)
- Tu KW; Knutson EO (1984). Total deposition of ultrafine hydrophobic and hygroscopic aerosols in the human respiratory system. *Aerosol Sci Technol*, 3: 453-465. [072870](#)
- U.S. EPA (1996). Air quality criteria for particulate matter. U.S. Environmental Protection Agency. Research Triangle Park, NC. EPA/600/P-95/001aF-cF. [079380](#)
- U.S. EPA (2004). Air quality criteria for particulate matter. U.S. Environmental Protection Agency. Research Triangle Park, NC. EPA/600/P-99/002aF-bF. [056905](#)
- Valberg P; Brain J; Sneddon S; LeMott S (1982). Breathing patterns influence aerosol deposition sites in excised dog lungs. *J Appl Physiol*, 53: 824-837. [190019](#)
- Vastag E; Matthys H; Kohler D; Gronbeck L; Daikeler G (1985). Mucociliary clearance and airways obstruction in smokers, ex-smokers and normal subjects who never smoked. *Eur J Respir Dis*, 139: 93-100. [157088](#)
- Vincent JH; Donaldson K (1990). A dosimetric approach for relating the biological response of the lung to the accumulation of inhaled mineral dust. *Br J Ind Med*, 47: 302-307. [002462](#)
- Wagner EM; Foster WM (2001). Interdependence of bronchial circulation and clearance of ^{99m}Tc-DTPA from the airway surface. *J Appl Physiol*, 90: 1275-1281. [156143](#)
- Wallenborn JG; Kovalcik KD; McGee JK; Landis MS; Kodavanti UP (2009). Systemic translocation of (70)zinc: kinetics following intratracheal instillation in rats. *Toxicol Appl Pharmacol*, 234: 25-32. [191172](#)
- Wallenborn JG; McKee JK; Schladweiler MC; Ledbetter AD; Kodavanti UP (2007). Systemic translocation of particulate matter-associated metals following a single intratracheal instillation in rats. *J Toxicol Sci*, 98: 231-239. [156144](#)

- Wang JX; Chen CY; Yu HW; Sun J; Li B; Li YF; Gao YX; He W; Huang YY; Chai ZF (2007). Distribution of TiO₂ particles in the olfactory bulb of mice after nasal inhalation using microbeam SRXRF mapping techniques. *Journal of Radioanal Chem*, 272: 527-531. [156146](#)
- Warheit DB; Hansen JF; Yuen IS; Kelly DP; Snajdr SI; Hartsky MA (1997). Inhalation of high concentrations of low toxicity dusts in rats results in impaired pulmonary clearance mechanisms and persistent inflammation. *Toxicol Appl Pharmacol*, 145: 10-22. [086055](#)
- Warheit DB; Webb TR; Sayes CM; Colvin VL; Reed KL (2006). Pulmonary instillation studies with nanoscale TiO₂ rods and dots in rats: Toxicity is not dependent upon particle size and surface area. *Toxicol Sci*, 91: 227-236. [088436](#)
- Watanabe N; Tanada S; Sasaki Y (2007). Pulmonary clearance of aerosolized ^{99m}Tc-DTPA in sarcoidosis I patients. *Q J Nucl Med Mol Imaging*, 51: 82-90. [157115](#)
- Weynand B; Jonckheere A; Frans A; Rahier J; Saint-Luc CU (1999). Diabetes mellitus Induces a Thickening of the Pulmonary Basal Lamina. *Respiration*, 66: 14-19. [157140](#)
- Whaley SL; Muggenburg BA; Seiler FA; Wolff RK (1987). Effect of aging on tracheal mucociliary clearance in beagle dogs. *J Appl Physiol*, 62: 1331-1334. [156153](#)
- Wiebert P; Sanchez-Crespo A; Falk R; Philipson K; Lundin A; Larsson S; Möller W; Kreyling W; Svartengren M (2006). No Significant Translocation of Inhaled 35-nm Carbon Particles to the Circulation in Humans. *Inhal Toxicol*, 18: 741-747. [156154](#)
- Wiebert P; Sanchez-Crespo A; Seitz J; Falk R; Philipson K; Kreyling WG; Moller W; Sommerer K; Larsson S; Svartengren M (2006). Negligible clearance of ultrafine particles retained in healthy and affected human lungs. *Eur Respir J*, 28: 286-290. [157146](#)
- Winter-Sorkina Rde; Cassee FR (2002). From concentration to dose: factors influencing airborne particulate matter deposition in humans and rats. National Institute for Public Health and the Environment. Bilthoven, Netherlands. 650010031/2002. www.rivm.nl/bibliotheek/rapporten/650010031.html. [043670](#)
- Xu GB; Yu CP (1986). Effects of age on deposition of inhaled aerosols in the human lung. *Aerosol Sci Technol*, 5: 349-357. [072697](#)
- Yeates DB; Gerrity TR; Garrard CS (1981). Particle deposition and clearance in the bronchial tree. *Ann Biomed Eng*, 9: 577-592. [095391](#)
- Yu CP (1985). Theories of electrostatic lung deposition of inhaled aerosols. *Ann Occup Hyg*, 29: 219-227. [006963](#)
- Yu IJ; Park JD; Park ES; Song KS; Han KT; Han JH; Chung YH; Choi BS; Chung KH; Cho MH (2003). Manganese distribution in brains of Sprague-Dawley rats after 60 days of stainless steel welding-fume exposure. *Neurotoxicology*, 24: 777-785. [156171](#)
- Zanobetti A; Schwartz J (2002). Cardiovascular damage by airborne particles: are diabetics more susceptible? *Epidemiology*, 13: 588-592. [034821](#)
- Zeidler-Erdely PC; Calhoun WJ; Ameredes BT; Clark MP; Deye GJ; Baron P; Jones W; Blake T; Castranova V (2006). In vitro cytotoxicity of Manville Code 100 glass fibers: Effect of fiber length on human alveolar macrophages. *Part Fibre Toxicol*, 28: 3:5. [190967](#)
- Zhao X; Ju Y; Liu C; Li J; Huang M; Sun J; Wang T (2009). Bronchial anatomy of left lung: a study of multi-detector row CT. *Surg Rad Anat*, 31: 85-91. [157187](#)

Chapter 5. Possible Pathways/ Modes of Action

The mechanisms underlying pulmonary effects of inhaled PM have been well-studied in the laboratory and there is general agreement regarding the key roles played by cellular injury and inflammation. These pathways are initiated following the deposition of inhaled particles on respiratory tract surfaces. Since most of these studies were conducted at concentrations of PM much higher than ambient levels, there is some question regarding the relevance of these responses and mechanisms to ambient exposures.

Interestingly, inhaled PM may also affect the cardiovascular, hematopoietic and other systems. Mechanisms underlying these extra-pulmonary effects are incompletely understood. However, pulmonary inflammation can lead to systemic inflammation and pulmonary reflexes can activate the autonomic nervous system (ANS). These latter responses may mediate cardiovascular and other systemic effects, as will be discussed below. In addition, it has been proposed that PM or soluble components of PM reach the circulation by translocating across the epithelial and endothelial barriers of the respiratory tract. In this way, PM or its components may interact directly with cells in the vasculature and blood and be transported to the heart and other organs. At this time, evidence clearly supports the translocation of small solutes following inhalation exposures and the translocation of soluble components of PM following some high dose exposures involving intratracheal (IT) instillation. However, there is insufficient evidence to support translocation of appreciable amounts of intact particles following inhalation exposures at lower concentrations (Section 4.3.3.1). Future studies will be required to resolve these issues.

The following sections discuss biological pathways which comprise proposed modes of action for the pulmonary and extra-pulmonary effects of inhaled PM. Overall themes are emphasized and supportive evidence from new in vitro and in vivo animal studies is cited. The characterization of evidence here is for PM in general, since most of the potential pathways or modes of action do not appear to be specific to a particular size class of PM. However, characteristics of ultrafine particles (UFPs) may allow for unique modes of action or effects disproportionate to their mass, as will be described below. Recent studies suggest an enhanced potential of this size class of PM to cause adverse effects; however evidence supporting this hypothesis is limited. Finally, a compilation of results from new inhalation studies which are relevant to ambient PM exposures and which confirm and extend these proposed mechanisms is found at the end of this chapter. Detailed descriptions of these key new studies are found in Chapters 6 and 7.

5.1. Pulmonary Effects

5.1.1. Reactive Oxygen Species

A great deal of research interest has focused on the role of reactive oxygen species (ROS) in the initiation of pulmonary injury and inflammation following exposure to PM. Numerous studies have demonstrated PM oxidative potential in in vitro and in vivo assay systems (Ayres et al., 2008, [155666](#); Cho et al., 2005, [087937](#); Shi et al., 2003, [088248](#); Tao et al., 2003, [156111](#)). Both redox active surface components, such as metals and organic species, and the surface characteristics of crystal structures have been shown to contribute to oxidative potential (Jiang et al., 2008, [156609](#); Tao et al., 2003, [156111](#); Warheit et al., 2007, [090482](#)). In this way, PM may be a direct source of ROS in the respiratory tract (Figure 5-1).

Note: Hyperlinks to the reference citations throughout this document will take you to the NCEA HERO database (Health and Environmental Research Online) at <http://epa.gov/hero>. HERO is a database of scientific literature used by U.S. EPA in the process of developing science assessments such as the Integrated Science Assessments (ISA) and the Integrated Risk Information System (IRIS).

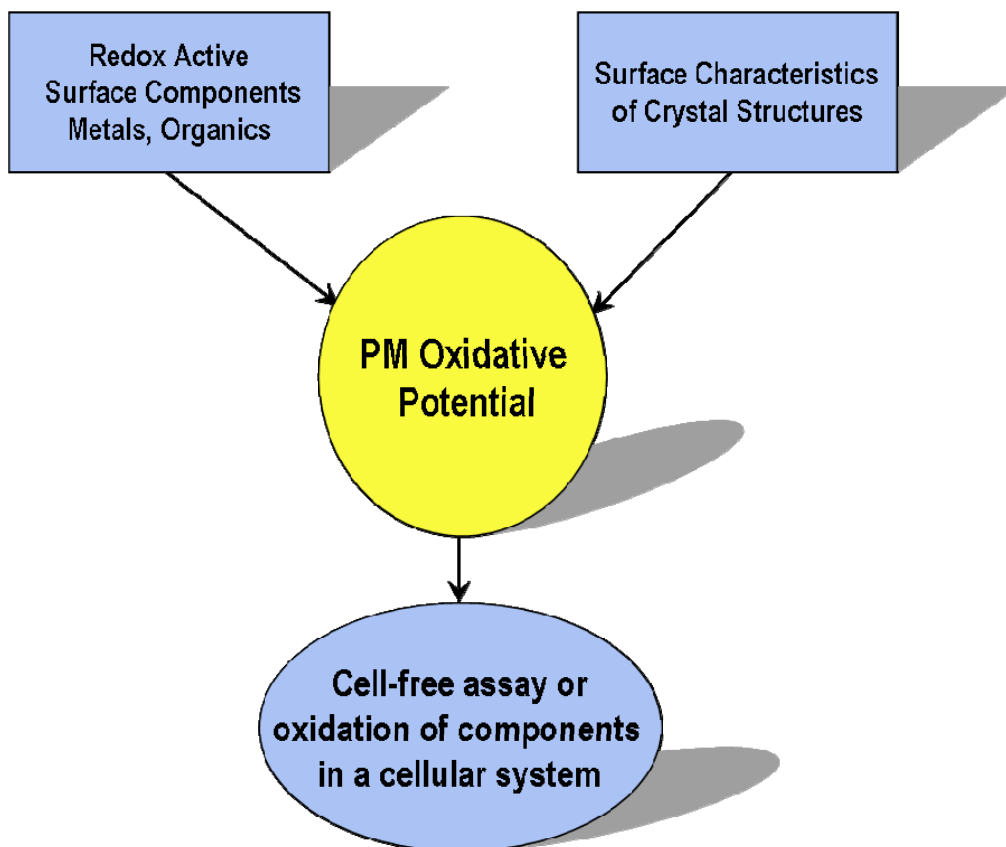


Figure 5-1. PM oxidative potential.

PM may also act as an indirect source of ROS in the respiratory tract by stimulating cells to produce ROS (Ayres et al., 2008, [155666](#); Tao et al., 2003, [156111](#)) (Figure 5-2). This may explain the observation that the oxidative potential of isolated PM does not always correlate with cellular or tissue oxidative stress induced by PM exposure. Exposure to PM increases intracellular production of ROS by a variety of mechanisms. For example, PM interaction with cell surfaces results in stimulation of NADPH oxidase in macrophages (i.e., the respiratory burst) (Dostert et al., 2008, [155753](#)) and in epithelial cells (Amara et al., 2007, [156212](#); Becher et al., 2007, [097125](#); Tamaoki et al., 2004, [157040](#)). Absorption of PM soluble components (e.g., PAH, transition metals) by respiratory tract cells can occur (Penn et al., 2005, [088257](#)) and be followed by microsomal transformation of PAHs to quinones or by redox cycling of transition metals with production of intracellular ROS (Molinelli et al., 2002, [035347](#); Xia et al., 2004, [087486](#)). Disruption of intracellular iron homeostasis with the subsequent generation of ROS has also been demonstrated following PM exposure (Ghio and Cohen, 2005, [088272](#)). In some cases, mitochondria serve as the source of ROS in response to PM (Huang et al., 2003, [156573](#); Risom and Loft, 2005, [089070](#); Soberanes et al., 2006, [156991](#); Soberanes et al., 2009, [190483](#)). Furthermore, PM interaction with cells can lead to the induction of nitric oxide synthase (Becher et al., 2007, [097125](#); Lindbom et al., 2007, [155934](#); Xiao et al., 2005, [156164](#); Zhao et al., 2006, [100996](#)) and the production of nitric oxide and other reactive nitrogen species (RNS).

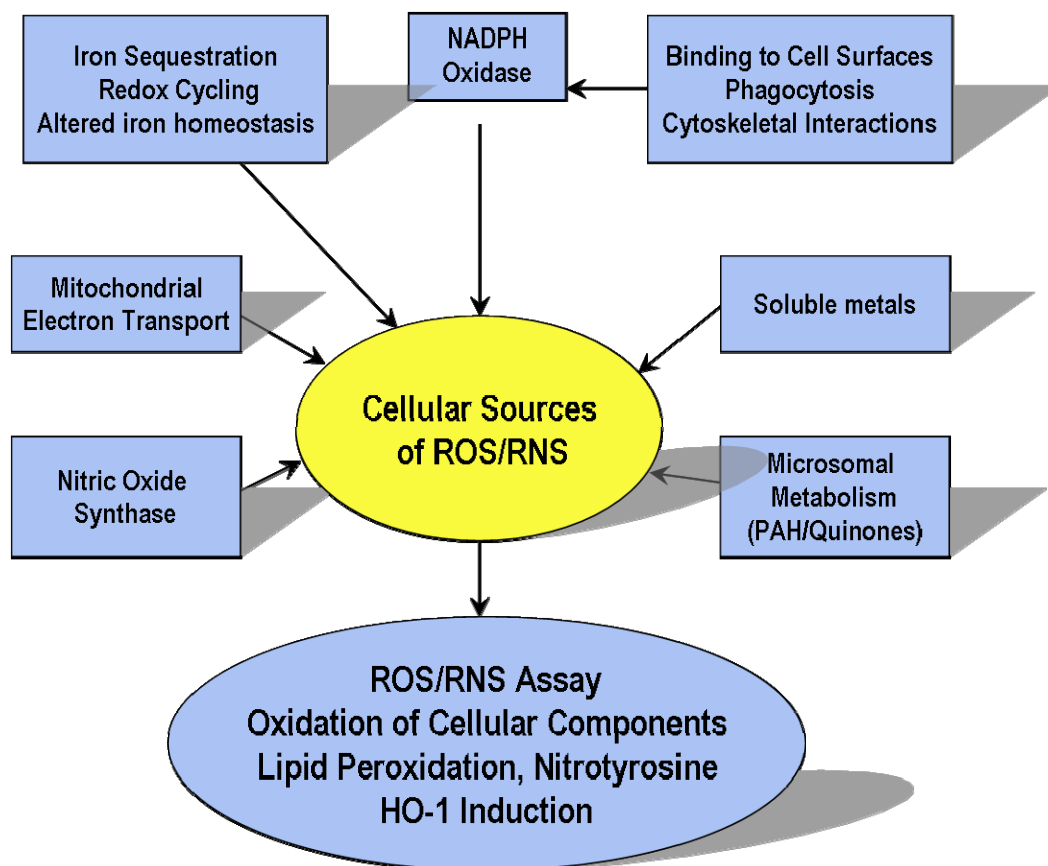


Figure 5-2 PM stimulates pulmonary cells to produce ROS/RNS.

Although all size fractions of PM may contribute to oxidative and nitrosative stress, UFPs may contribute disproportionately to their mass due to their large surface/volume ratio. The relative enrichment of redox active surface components, such as metals and organics, per unit mass may translate to a relatively greater oxidative potential of UFPs compared with larger particles with similar surface components. In addition, the greater surface per unit volume could potentially deliver relatively more adsorbed soluble components to cells. These components may undergo intracellular redox cycling following cellular uptake. Furthermore, per unit mass, UFPs may have more opportunity to interact with cell surfaces due to their greater surface area and their greater particle number compared with larger PM. These interactions with cell surfaces can lead to ROS generation, as described above. Recent studies have also demonstrated that UFPs have the capacity to cross cellular membranes by non-endocytotic mechanisms involving adhesive interactions and diffusion (Geiser et al., 2005, [087362](#)), as described in Chapter 4. This may allow UFPs to interact with or penetrate intracellular organelles.

In general, high levels of intracellular ROS/RNS can lead to irreversible protein modifications, loss of cellular membrane integrity, DNA damage and cellular toxicity. Lower levels of ROS/RNS may cause reversible protein modifications that trigger intracellular signaling pathways and/or adaptive responses. Thus PM-dependent generation of ROS may be responsible for a continuum of responses from cell signaling to cellular injury.

5.1.2. Activation of Cell Signaling Pathways

Activation of cell signaling pathways by ROS/RNS has received increasing attention by numerous investigators over the years. An early example was provided by Kaul and Forman (1996, [155892](#)) who demonstrated that respiratory burst-derived H_2O_2 activates the transcription factor

nuclear factor kappa-light-chain-enhancer of activated B cells (NF- κ B). Numerous studies since then have demonstrated that PM, which serves as both a direct and indirect source of ROS/RNS, activates cell signaling pathways by this mechanism.

PM also has the potential to activate cell signaling by mechanisms that are independent of ROS/RNS. For example, PM delivers water-soluble components, such as endotoxin and zinc (Zn), to cell surfaces. Endotoxin binds to toll-like receptors on alveolar macrophages and other cells, resulting in the upregulation of cytokines (Becker et al., 2002, [052419](#)). Zn, a transition metal which does not redox cycle, inhibits protein tyrosine phosphatases in airway epithelial cells resulting in a cascade of cell signaling events (Tal et al., 2006, [108588](#)). Similarly, PM-mediated delivery of lipid soluble components such as PAH results in binding and activation of the arylhydrocarbon receptor (AhR). AhR is a transcription factor responsible for the upregulation of CYP1A1, a cytochrome oxidase involved in PAH biotransformation to metabolites capable of forming DNA adducts or eliciting oxidative stress responses (Rouse et al., 2008, [156930](#)). In addition, interaction of PM with cell surfaces may activate cell signaling by perturbation of the cytoskeleton, adherence, internalization, or receptor-mediated pathways.

Recent studies involving PM exposures have focused on intracellular pathways involving protein kinases, such as mitogen-activated protein kinase (MAPK) (Bayram et al., 2006, [088439](#); Lee et al., 2005, [156682](#); Roberts et al., 2003, [156051](#); Soberanes et al., 2009, [190483](#)); AKT (Ahsan et al., 2005, [156200](#)); src (Cao et al., 2007, [156322](#)) and epidermal growth factor receptor (Blanchet et al., 2004, [087982](#); Cao et al., 2007, [156322](#); Tamaoki et al., 2004, [157040](#)), as well as ras (Tamaoki et al., 2004, [157040](#)), toll-like receptors (Becker et al., 2002, [052419](#); Becker et al., 2005, [088590](#)), protein tyrosine phosphatases (Tal et al., 2006, [108588](#)), phospholipases A₂ (Lee et al., 2003, [156678](#)), calcium (Agopyan et al., 2003, [155649](#); Brown et al., 2004, [155705](#); Brown et al., 2004, [088663](#); Geng et al., 2005, [096689](#); 2006, [097026](#); Sakamoto et al., 2007, [096282](#)), caspases (Soberanes et al., 2006, [156991](#); Zhang et al., 2007, [156179](#)), poly (ADP-ribose) polymerase family member 1 (PARP-1) (Zhang et al., 2007, [156179](#)) and histone acetylation (Gilmour et al., 2003, [096959](#)). The transcription factors regulated by these pathways, including NF- κ B (Bayram et al., 2006, [088439](#); Lee et al., 2005, [156682](#); Takizawa et al., 2003, [157039](#)), activator protein 1 (AP-1) (Donaldson et al., 2003, [156408](#)), signal transducers and activators of transcription protein (STAT) (Cao et al., 2007, [156322](#)), antioxidant response element (ARE) (Li and Nel, 2006, [156694](#)), and AhR (Rouse et al., 2008, [156930](#)) have also been studied following PM exposures. Activation of these intracellular pathways and transcription factors leads to the upregulation of genes responsible for inflammatory, immune and acute phase responses as well as genes responsible for antioxidant defense and xenobiotic metabolism.

5.1.3. Pulmonary Inflammation

Following PM exposure, transcription factor activation in macrophages and epithelial cells stimulates the synthesis and release of soluble mediators involved in inflammatory and immune responses including cytokines, chemokines, proteases and eicosanoids (Figure 5-3). These substances play a role in recruiting inflammatory cells such as neutrophils, monocytes, mast cells and eosinophils to the lung. Interactions between macrophages and epithelial cells enhance these responses (Tao and Kobzik, 2002, [157044](#)).

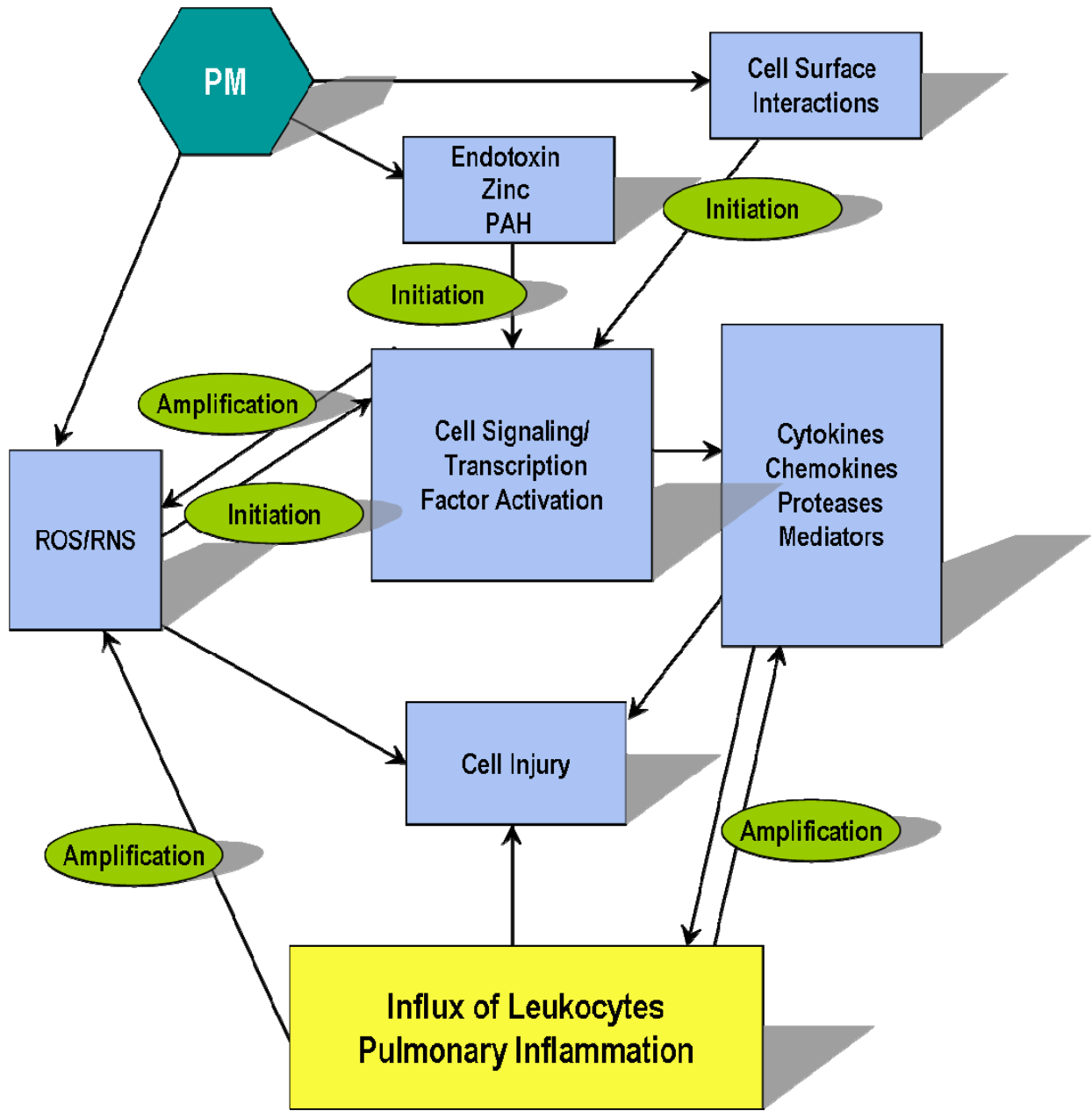


Figure 5-3. PM activates cell signaling pathways leading to pulmonary inflammation.

Inflammatory cells can serve as a source of extracellular ROS which, along with soluble mediators derived from the inflammatory cells, amplify the inflammatory response. Unchecked inflammation may cause cellular and tissue injury through the generation of excess amounts of ROS and soluble mediators. In some cases the oxidative potential of PM is well-correlated with the degree of inflammation (Dick et al., 2003, [036605](#)), suggesting that the inflammation is a direct consequence of PM-generated ROS. However, in other cases the oxidative potential of PM is not well-correlated with the degree of inflammation (Beck-Speier et al., 2005, [156262](#)), suggesting that the inflammation is a consequence of the ROS-independent mechanisms by which PM activates intracellular signaling pathways. Particle surface area has been identified as a key determinant of the extent of inflammation in the case of low-toxicity, low-solubility particles (Donaldson et al., 2008,

[190217](#)). Moreover, UFPs may cause inflammation disproportionately to their mass compared with PM of larger sizes given their large surface/volume ratio compared with other PM fractions.

PM exposure often results in neutrophilic inflammation in laboratory studies (Tao et al., 2003, [156111](#)). Neutrophilic inflammation is also associated with acute lung injury in humans as well as chronic lung diseases such as COPD and certain forms of asthma (Barnes, 2007, [191139](#); Cowburn et al., 2008, [191142](#)). Circulating neutrophils respond to chemotactic factors in the lung such as leukotriene B₄ and IL-8 (Barnes, 2007, [191139](#)). They migrate into the lung parenchyma across the pulmonary capillary network and into the airways from the bronchial circulation (Cowburn et al., 2008, [191142](#)). As a consequence of priming by inflammatory mediators or contact with extracellular matrix components, neutrophils become hyperresponsive to activating signals and insensitive to chemotactic signals (Cowburn et al., 2008, [191142](#)). Activation results in neutrophil degranulation, respiratory burst responses and soluble mediator release (Cowburn et al., 2008, [191142](#)). Neutrophils eventually undergo apoptosis and are phagocytized by inflammatory macrophages (Cowburn et al., 2008, [191142](#)). This is accompanied by the release of anti-inflammatory mediators such as IL-10 and transforming growth factor- β (TGF- β) (Cowburn et al., 2008, [191142](#)). These steps are key to the resolution of inflammation and prevent unregulated release of toxic neutrophil products such as neutrophil elastase (Cowburn et al., 2008, [191142](#)). Thus, circumstances leading to the decreased ingestion of apoptotic neutrophils by macrophages may lead to tissue injury. Impairment of macrophage function may serve as an important mechanism by which PM contributes to disease.

5.1.4. Respiratory Tract Barrier Function

Epithelial injury can lead to an increase in permeability of the airway epithelial and alveolar-capillary barriers (Braude et al., 1986, [155701](#)). Enhanced transport of soluble and possibly of insoluble PM components into the circulation may occur under these conditions. Increased epithelial permeability is also associated with enhanced immune responses to proteins, including allergens, on the epithelial surface, presumably due to the greater availability of antigens to underlying immune cells (Wan et al., 1999, [191903](#)). Furthermore, endothelial injury can compromise the integrity of the alveolar-capillary barrier resulting in transvascular fluid and solute flux (Braude et al., 1986, [155701](#)). Soluble mediators derived from inflammatory and lung cells (Chang et al., 2005, [097776](#)) and peptides released by some nerve cells (Widdicombe and Lee, 2001, [019049](#)) can increase the permeability of the alveolar-capillary barrier and result in alveolar edema. Compromised barrier function in the airways may lead to airway edema. Edema occurring secondarily to nerve cell stimulation is one component of the process termed neurogenic inflammation.

Given the small size of UFPs, modest changes in epithelial permeability may particularly affect the disposition of this fraction. Enhanced translocation to interstitial compartments or to the circulation may be important sequelae. A recent study described in Section 4.3.4.3 demonstrated greater translocation of UFPs compared with PM_{2.5} into the circulation of rodents treated with endotoxin to induce acute lung injury prior to IT instillation of PM (Chen et al., 2006, [147267](#)). Furthermore, epithelial injury in another model resulted in greater translocation of UFPs into the interstitial compartment (Adamson and Prieditis, 1995, [189982](#)).

5.1.5. Antioxidant Defenses and Adaptive Responses

Antioxidant defenses and adaptive responses are important modulators of oxidative stress and other cellular stresses resulting from PM exposure. Antioxidants are present in the epithelial lining fluid in all regions of the respiratory tract. In addition, they are present in cells of the lung parenchyma and inflammatory cells found in airways and alveoli. Some antioxidants act directly against oxidant species (e.g., glutathione, ascorbate, superoxide dismutase) while others act indirectly (e.g., gamma-glutamylcysteine synthetase [γ GCS], glutathione reductase). Furthermore, some antioxidants (e.g., Phase 2 enzymes heme oxygenase-1[HO-1], NADPH quinone oxidoreductase 1 [NQO1], glutathione-S-transferase [GST]) are inducible via activation of the nuclear factor (erythroid-derived 2)-related factor 2 (Nrf2)-ARE pathway, which occurs as an adaptive response to stress (Cho et al., 2006, [156345](#); Li and Nel, 2006, [156694](#)). Antioxidants play

an important role in reducing the oxidative potential of those PM species that directly generate ROS. They also inhibit responses due to generation of intracellular ROS.

Recently a three-tier response to oxidative stress was proposed (Li and Nel, 2006, [156694](#)). In this scheme, mild oxidative stress enhances antioxidant defenses by upregulating Phase 2 and other antioxidant enzymes (Tier 1). Further increase in oxidative stress induces inflammation (Tier 2) and cell death (Tier 3). Experimental evidence is supportive of this scheme. Numerous studies have demonstrated that enhancement of lung and cellular antioxidant defenses inhibits inflammation, cytotoxicity and other responses following exposure to PM (Ahsan et al., 2005, [156200](#); Bachoual et al., 2007, [155667](#); Bayram et al., 2006, [088439](#); Chang et al., 2005, [097776](#); Imrich et al., 2007, [155859](#); Koike and Kobayashi, 2005, [088303](#); Koike et al., 2004, [058555](#); Li et al., 2007, [155929](#); Ramage and Guy, 2004, [055640](#); Rhoden et al., 2004, [087969](#); Steerenberg et al., 2004, [087981](#); Takizawa et al., 2003, [157039](#); Tao et al., 2003, [156111](#); Upadhyay et al., 2003, [097370](#); Wan and Diaz-Sanchez, 2006, [097399](#); Wan and Diaz-Sanchez, 2007, [156145](#); Yin et al., 2004, [087983](#)).

Cellular and tissue exposure to xenobiotics carried by PM can lead to induction of Phase 1 and Phase 2 detoxifying enzymes following the activation of cell signaling pathways and transcription factors AhR and ARE, respectively (Rengasamy et al., 2003, [156907](#); Rouse et al., 2008, [156930](#); Zhao et al., 2006, [100996](#)).

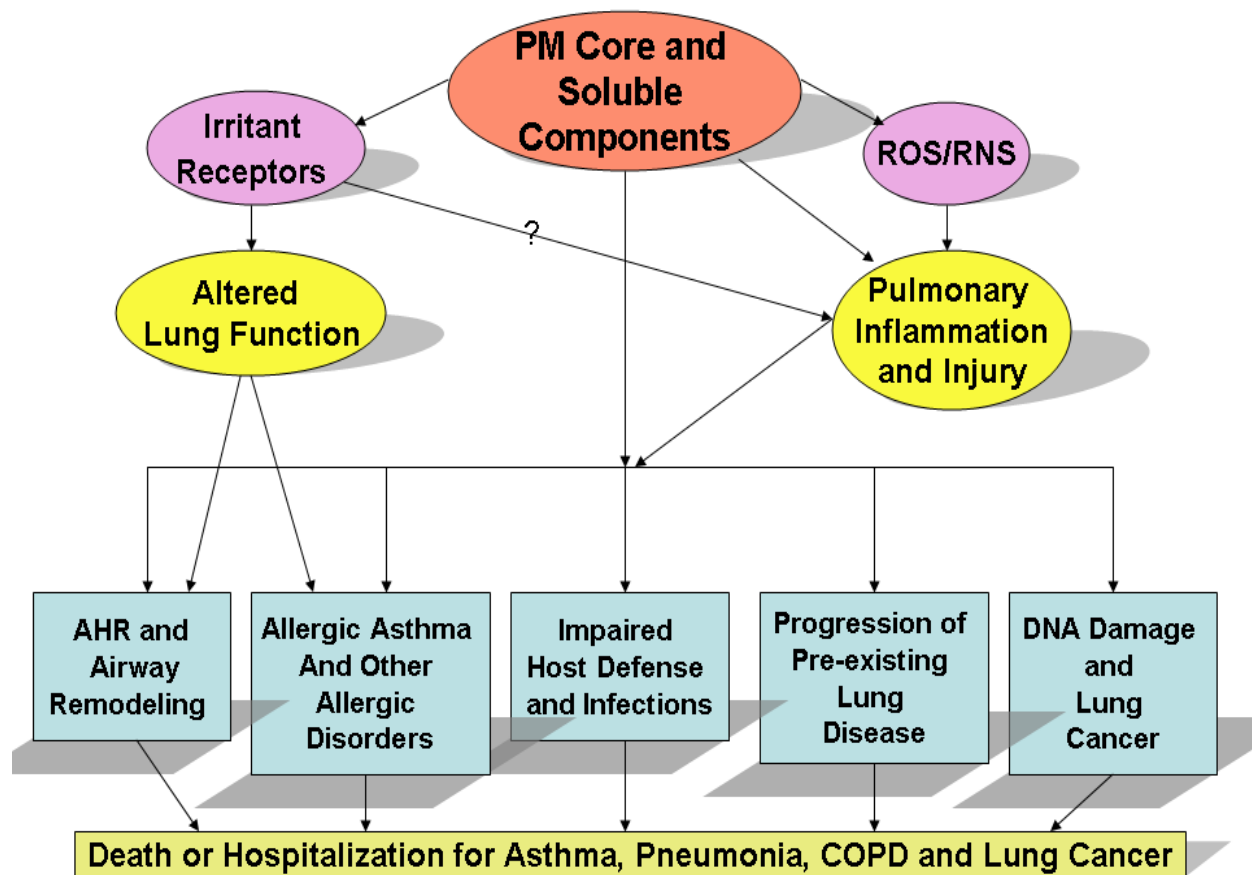


Figure 5-4. Potential pathways for the effects of PM on the respiratory system.

5.1.6. Pulmonary Function

PM exposure may alter pulmonary function by a variety of different mechanisms (Figure 5-4). In the short-term, airway hyperresponsiveness (AHR) may ensue due to the influence of inflammatory mediators. In the long-term, morphological changes may occur, in some cases leading to mucus hypersecretion and airway remodeling. Activation of irritant receptors and stimulation of the ANS in the respiratory tract is another mechanism by which PM exposure may alter pulmonary function (Section 5.4).

5.1.7. Allergic Disorders

PM exposure sometimes leads to the development of allergic immune responses (Figure 5-4). These responses are predominately mediated by T helper 2 cells (Th2). Th1 responses, characterized by IFN- γ and classical macrophage activation, are inflammatory; in excess they can lead to tissue damage. Alternatively, Th2 responses are associated with allergy and asthma and are characterized by IL-4, IL-5, IL-13, influx of eosinophils, B-lymphocyte production of IgE, and alternative macrophage activation. PM exposure can also lead to the exacerbation of airway allergic responses, such as antigen-specific IgE production and AHR.

Due to soluble mediators and immune cell trafficking, pulmonary exposure may result in systemic immune alterations. Not only do macrophages ingest PM, but they are also antigen presenting cells whose level of activation dictates costimulation and thus subsequent T cell responses. These cells are highly mobile and can transport PM to other sites such as lymph nodes. Dendritic cells (DC) also play a key role as antigen presenting cells and in modulating T and B cell activity. A cell culture model of the human epithelial airway wall was used to demonstrate that DC extended processes between epithelial cells through the tight junctions, collected particles in the luminal space and transported them across the epithelium (Blank et al., 2007, [096521](#)). DC also transmigrated through the epithelium to take up particles on the epithelial surface (Blank et al., 2007, [096521](#)). Furthermore, DC interacted with particle-loaded macrophages on top of the epithelium and with other DC within or beneath the epithelium to transfer particles (Blank et al., 2007, [096521](#)). In vitro studies also demonstrated that the adjuvant activity of diesel exhaust particles (DEPs) involved stimulation of immature monocyte-derived dendritic cells (iMDDC) to undergo maturation in response to an altered airway epithelial cell-derived microenvironment (Bleck et al., 2006, [096560](#)). Additionally, DEP directly influenced the profile of cytokines secreted by DC and caused a predisposition toward Th2-mediated or allergic responses (Chan et al., 2006, [097468](#)). Thus PM can negatively affect both innate immunity through effects on macrophage pathogen handling (Section 5.1.8) as well as adaptive immunity by altering macrophage or DC antigen presenting activity and subsequent T cell responses.

Moreover, recent studies have demonstrated that ambient PM can act as an adjuvant for allergic sensitization with UFPs having a greater effect than fine particles (de Haar et al., 2006, [144746](#); Li et al., 2009, [190457](#)). This has been attributed to higher oxidative potential of the UFPs compared with the same mass of particles of larger size (Li et al., 2009, [190457](#)), although the larger surface area and particle number per unit mass as well as the propensity of UFPs for trans-epithelial movement may also contribute to this effect.

5.1.8. Impaired Lung Defense Mechanisms

PM exposure may impair lung defense mechanisms and result in frequent or persistent infections (Figure 5-4). Potential targets include mucociliary transport, surfactant function and pathogen clearance. Pathogen clearance is dependent on the integrity of macrophages and their migration, phagocytosis and respiratory burst functions. PM-mediated cytotoxicity of macrophages with the concomitant release of lysosomal contents may affect pathogen clearance and cause damage to nearby cells and tissues. IT instillation and cell culture experiments have demonstrated PM-dependent impairment of lung defense mechanisms (Jaspers et al., 2005, [088115](#); Kaan and Hegele, 2003, [095753](#); Long et al., 2005, [087454](#); Moller et al., 2005, [156770](#); Monn et al., 2003, [052418](#); Roberts et al., 2007, [097623](#); Yin et al., 2004, [087983](#)).

5.1.9. Resolution of Inflammation/Progression or Exacerbation of Disease

Resolution of pulmonary inflammation and injury has been demonstrated in many experimental models using higher than ambient concentrations of PM. Factors contributing to this complex process are likely to include the uptake and clearance of PM by macrophages; the retention of PM in parenchymal cells and tissues; the balance of pro/anti-inflammatory soluble mediators, oxidants/antioxidants and proteases/anti-proteases; and the presence of pre-existing disease. These factors may also influence the resolution of pulmonary responses to ambient PM exposures (Figure 5-4). The long-term consequences of prolonged inflammation are not likely to be beneficial and may lead to remodeling of the respiratory tract and to the progression or exacerbation of disease.

5.1.9.1. Factors Affecting the Retention of PM

Clearance of poorly soluble particles from ET, TB and alveolar regions is extensively discussed in Section 4.3. While clearance from ET and TB regions generally occurs over hours to days, clearance from the alveolar compartment is much slower, occurring over months to years depending on the species. Phagocytosis by alveolar macrophages and transport by the mucociliary escalator is the primary mechanism of clearance from the alveolar compartment although neutrophil phagocytosis also plays a role (Snipes et al., 1997, [156092](#)). Pre-existing disease can alter the extent and localization of PM deposition as discussed in Section 4.2.4.5. In addition, mechanisms of clearance may be altered in cases of pre-existing disease as discussed in Section 4.3.4.3. While mild asthma was associated with enhanced mucociliary clearance, acute lung injury was associated with enhanced particle translocation to the circulation and the interstitial compartment. Whether retained particles are localized in alveolar macrophages or parenchymal tissue also differs according to species (Snipes, 1996, [076041](#)).

UFPs may have a special propensity for retention given the decreased efficiency of alveolar macrophages for phagocytosis of this size particle (Oberdörster, 1988, [006857](#)) and the demonstration that UFPs can readily cross cellular membranes (Geiser et al., 2005, [087362](#)). Some studies suggest that UFPs are taken up by epithelial cells and move to the interstitium where they are cleared by other pathways (Semmler-Behnke et al., 2007, [156080](#)); however clearance mechanisms are not entirely understood.

Enhanced deposition of particles in “hot spots” may influence retention. For example, deposition in the centriacinar or proximal alveolar region, where clearance is slow, may result in accumulated particle dose in this region and the potential for prolonged inflammation at the site leading to the development of pulmonary fibrosis or emphysema (Donaldson et al., 2008, [190217](#)). A recent study suggests an important role for retained particles in the progression of disease. Complexation of endogenous iron by retained particles resulted in retained particles growing larger over time. The authors suggested that redox cycling of complexed iron may be responsible for disease progression (Ghio and Cohen, 2005, [088272](#); Ghio et al., 2004, [155790](#)).

5.1.9.2. Factors Affecting the Balance of Pro/Anti-Inflammatory Mediators, Oxidants/Anti-Oxidants and Proteases/Anti-Proteases

Inflammation can be enhanced by pro-inflammatory mediators or dampened by anti-inflammatory mediators. Production of anti-inflammatory mediators normally occurs at several steps of the inflammation pathway, such as the release of IL-10 and TGF- β during phagocytosis of apoptotic neutrophils by macrophages (Cowburn et al., 2008, [191142](#)). Dysregulation of the inflammatory process may prevent the resolution of inflammation. PM exposure may result in the production of pro-inflammatory mediators as well as decrease the production of anti-inflammatory mediators by impairing macrophage function.

An unfavorable balance of oxidants to antioxidants in the lung is associated with inflammatory lung diseases including asthma and COPD (Rahman et al., 2006, [191165](#)). PM is likely to contribute to an unfavorable balance through its oxidative potential and capacity to promote cellular production of ROS. Exacerbations of asthma and COPD resulting from bacterial and viral infections are also associated with increased oxidative stress (Barnes, 2007, [191139](#)). Conversely, antioxidants may reduce neutrophilic inflammation associated with oxidative stress (Barnes, 2007, [191139](#)).

Protease/anti-protease balance has long been tied to the pathogenesis of emphysema and other forms of COPD (Owen, 2008, [191162](#)). Key steps include the release of proteinases by inflammatory cells which degrade the extracellular matrix components of alveolar walls. Destruction of alveolar walls and airspace enlargement ensues. Endogenous anti-protease defenses in the lung modulate this response but may be insufficient to prevent it during prolonged inflammation. Proteases also play a role in pathologies which lead to small airway fibrosis (Owen, 2008, [191162](#)). Oxidative stress has been linked to both activation of proteases and inactivation of anti-proteases (Owen, 2008, [191162](#)). PM may contribute to an unfavorable protease/anti-protease balance through the generation of ROS.

Although there are numerous inflammatory cell-derived proteases and lung anti-proteases, many recent studies have focused on matrix metalloproteinases (MMPs). MMPs are a family of Zn-containing enzymes normally found in an inactive pro-enzyme form. Activation involves proteolytic cleavage or oxidation of the “cysteine switch” (Pardo and Selman, 2005, [191163](#)). Inhibitors include tissue inhibitors of metalloproteinases (TIMPs) (Pardo and Selman, 2005, [191163](#)). In particular, MMP-1 is well-studied and found to play an important role in physiological processes such as development and wound repair as well as in diseases such as pulmonary emphysema, fibrosis, asthma and bronchial carcinoma (Li et al., 2009, [190424](#); Pardo and Selman, 2005, [191163](#)). In addition to its activity in degrading collagenase, MMP-1 also acts on non-matrix substrates and cell surface molecules suggesting that it may influence cell signaling (Pardo and Selman, 2005, [191163](#)). MMP-2 and MMP-9 are thought to be involved in the pathogenesis of disease through their gelatinase activity. Interestingly, recent in vitro studies have demonstrated upregulation of MMP-1 by hydrogen peroxide, cigarette smoke and DEPs (Amara et al., 2007, [156212](#); Li et al., 2009, [190424](#); Mercer et al., 2004, [191180](#)), and up-regulation of MMP-12 following instillation of PM collected from the Paris subway (Bachoual et al., 2007, [155667](#)). These considerations suggest that particulate air pollution may act via MMP to mediate progression or exacerbation of lung disease.

5.1.9.3. Pre-Existing Disease

In addition to its effects on deposition, retention and clearance of PM described above, pre-existing disease may also alter the balance of the aforementioned factors. For example, acute exacerbations of COPD are characterized by a rapid influx of neutrophils into the airways (Owen, 2008, [191162](#)). However, clearance of apoptotic neutrophils by macrophages is impaired in COPD leading to greater release of neutrophil-derived inflammatory mediators, oxidants and proteases (Owen, 2008, [191162](#)). Thus, exacerbation of disease may occur as a result of unchecked inflammation.

5.1.10. Pulmonary DNA Damage

Pulmonary DNA damage can occur primarily or secondarily to PM exposure. Primary effects include oxidative DNA injury or DNA adduct formation due directly to PM while secondary effects occur due to PM-mediated inflammation (De Kok et al., 2005, [088656](#); Gabelová et al., 2007, [156457](#); Gallagher et al., 2003, [140171](#); Schins and Knaapen, 2007, [156074](#)). These responses may lead to chromosomal aberrations or DNA strand breaks. PM effects on cell cycle arrest, proliferation, apoptosis, and DNA repair mechanisms may also influence the genotoxic, mutagenic or carcinogenic potential of DNA damage as reviewed by Schins et al. (2007, [156074](#)).

5.1.11. Epigenetic Changes

Epigenetic mechanisms regulate the transcription of genes without altering the nucleotide sequence of DNA. These mechanisms generally involve DNA methylation and histone modifications, leading to alterations which may have long-term consequences or are heritable (Jones and Baylin, 2007, [191153](#); Keverne and Curley, 2008, [191154](#)). DNA methylation and histone modifications, which include methylation, acetylation, phosphorylation, ubiquitylation and sumoylation, are known to be linked (Hitchler and Domann, 2007, [191151](#); Jones and Baylin, 2007, [191153](#)). Numerous studies have identified epigenetic processes in the control of cancer (Foley et al., 2009, [191144](#); Gopalakrishnan et al., 2008, [191147](#); Jones and Baylin, 2007, [191153](#); Valinluck et al., 2004, [191170](#)), embryonic development (Foley et al., 2009, [191144](#); Gopalakrishnan et al., 2008,

[191147](#); Keverne and Curley, 2008, [191154](#)) and inflammation and other immune system functions (Adcock et al., 2007, [191178](#)).

Epigenetic modifications resulting in decreased expression of tumor suppressor genes and increased expression of transforming genes have been observed in human tumors (Valinluck et al., 2004, [191170](#)). In general, transcription repression is associated with DNA methylation in promoter regions of genes. Cytosine methylation in CpG dinucleotides has emerged as an important, heritable epigenetic modification which can result in chromatin remodeling and decreased gene expression (Valinluck et al., 2004, [191170](#)). Global changes in DNA methylation are also seen in cancer and hypomethylation is associated with genomic instability (Gopalakrishnan et al., 2008, [191147](#)).

Embryonic development is characterized by several phases of epigenetic modifications. DNA methylation is very dynamic following fertilization, with demethylation and re-methylation of egg and sperm genomes occurring immediately (Foley et al., 2009, [191144](#)). Imprinted genes, however, retain the methylation profile of the parent of origin (Foley et al., 2009, [191144](#)). Epigenetic changes accumulated through a life course may be passed from parent to offspring in the germline (i.e., germline transmission of epimutation) if they survive the epigenetic remodeling that occurs during gametogenesis and early embryogenesis (Foley et al., 2009, [191144](#)). Early development is characterized by the process of cell differentiation, which produces different cell types and involves the selective activation of some sets of genes and the silencing of others in a temporal pattern (Foley et al., 2009, [191144](#); Gopalakrishnan et al., 2008, [191147](#)). DNA methylation is postulated to provide a basis for cell differentiation (Gopalakrishnan et al., 2008, [191147](#)).

In the lung, histone acetylation and methylation have been linked to inflammatory gene expression, T cell differentiation, and the regulation of macrophage function following pathogen challenge (Adcock et al., 2007, [191178](#)). Furthermore, altered patterns of methylation and acetylation have been reported in inflammatory diseases (Adcock et al., 2007, [191178](#)). Reduced expression and activity of histone deacetylase have been demonstrated in lung and inflammatory cells in COPD and asthma (Adcock et al., 2007, [191178](#); Barnes, 2007, [191139](#)). Consequently, histone deacetylase has been identified as a potential therapeutic target for epigenetic therapy (Adcock et al., 2007, [191178](#); Jones and Baylin, 2007, [191153](#)).

Epigenetic mechanisms have been identified as potential targets for gene-environment interactions and recent studies have demonstrated that diet, cigarette smoking, endocrine disruptors, heavy metals and bacterial infection can alter the epigenetic profile in animals and humans (Foley et al., 2009, [191144](#)). A role for PM in promoting epigenetic changes has been proposed and new studies, discussed in later chapters, provide some evidence for this pathway (Baccarelli et al., 2009, [192155](#); Liu et al., 2008, [156709](#); Reed et al., 2008, [156903](#); Tarantini et al., 2009, [192010](#); Tarantini et al., 2009, [192153](#); Yauk et al., 2008, [157164](#)).

Early life exposures may be especially important in this regard since periods of rapid cell division and epigenetic remodeling are likely to occur at this time (Foley et al., 2009, [191144](#); Keverne and Curley, 2008, [191154](#); Wright and Baccarelli, 2007, [191173](#)). This may provide a basis for fetal origins of adult disease.

It has been suggested that DNA methylation is regulated by oxygen gradients and redox status (Hitchler and Domann, 2007, [191151](#)). While this is of particular importance during development where oxygen gradients and redox status are linked to cellular differentiation, these processes are also important for cell signaling during all stages of life. A common metabolic precursor for both methylation reactions and glutathione availability (involved in redox status) is methionine (Hitchler and Domann, 2007, [191151](#)). Methionine availability regulates the cell's ability to generate S-adenosyl methionine which is directly involved in DNA and histone methylation and the cell's ability to generate homocysteine/cysteine which is involved in glutathione biosynthesis (Hitchler and Domann, 2007, [191151](#)). Furthermore, the folate cycle is a key determinant of methionine bioavailability (Hitchler and Domann, 2007, [191151](#)). In this way, cellular intermediary metabolism is linked to epigenetic processes, with oxidative stress necessitating a metabolic shift resulting in decreased DNA methylation and increased glutathione production.

5.1.12. Lung Development

Lung development is a multi-step process which begins in embryogenesis and continues to adult life (Pinkerton and Joad, 2006, [091237](#)). This allows for a long period of potential vulnerability to environmental and other stressors. Furthermore, enzymatic systems responsible for detoxification of xenobiotic compounds are not fully developed until the postnatal period (Pinkerton and Joad,

2006, [091237](#)). Disruption of cell signaling during development could affect cellular differentiation, branching morphogenesis and overall lung growth, possibly leading to life-long consequences. Although very little is known about the effects of maternal exposure to PM on the fetus or the effects of exposure during childhood, recent animal studies demonstrate respiratory and immune system effects of perinatal exposure to sidestream cigarette smoke (Pinkerton and Joad, 2006, [091237](#); Wang and Pinkerton, 2007, [179975](#)).

5.2. Systemic Inflammation

Pulmonary inflammation resulting from PM exposure may trigger systemic inflammation through the action of cytokines and other soluble mediators which leave the lung and enter the circulation (Figure 5-5). Epithelial permeability may exert an important influence on this process (Section 5.1.4). Cytokines released by alveolar macrophages can stimulate bone marrow production of leukocytes resulting in an increased number of total and immature leukocytes in the circulation (Van and Hogg, 2002, [088111](#); Van Eeden et al., 2001, [019018](#)). They also can activate neutrophils and promote their sequestration in microvascular beds (Van Eeden et al., 2001, [019018](#)). The time course of these responses varies according to the acute or chronic nature of the PM exposure (van Eeden et al., 2005, [157086](#)).

Systemic inflammation is seen under conditions of mild pulmonary inflammation – and sometimes under conditions of no measurable pulmonary inflammation – following PM exposure. The time-dependent nature of pulmonary and systemic inflammatory responses may in part explain these findings since biomarkers of inflammation are frequently measured only at one time point. Furthermore, chronic exposures may lead to adaptive responses. In general, systemic inflammation is associated with changes in circulating white blood cells, the acute phase response, pro-coagulation effects, endothelial dysfunction and the development of atherosclerosis (Figure 5-5). Adverse effects on the cardiovascular and cerebrovascular systems such as thrombosis, plaque rupture, MI and stroke may result. Systemic inflammation may affect other organ systems such as the liver or the CNS.

One recent study demonstrated that alveolar macrophage-derived IL-6 mediated pro-coagulation effects in mice exposed by IT instillation to PM₁₀ (Mutlu et al., 2007, [121441](#)). This study provides a clear link between lung cytokines and systemic responses in one model system. Whether this mechanism or others account for the majority of extra-pulmonary effects following inhalation of PM at concentrations relevant to ambient exposures is not yet known.

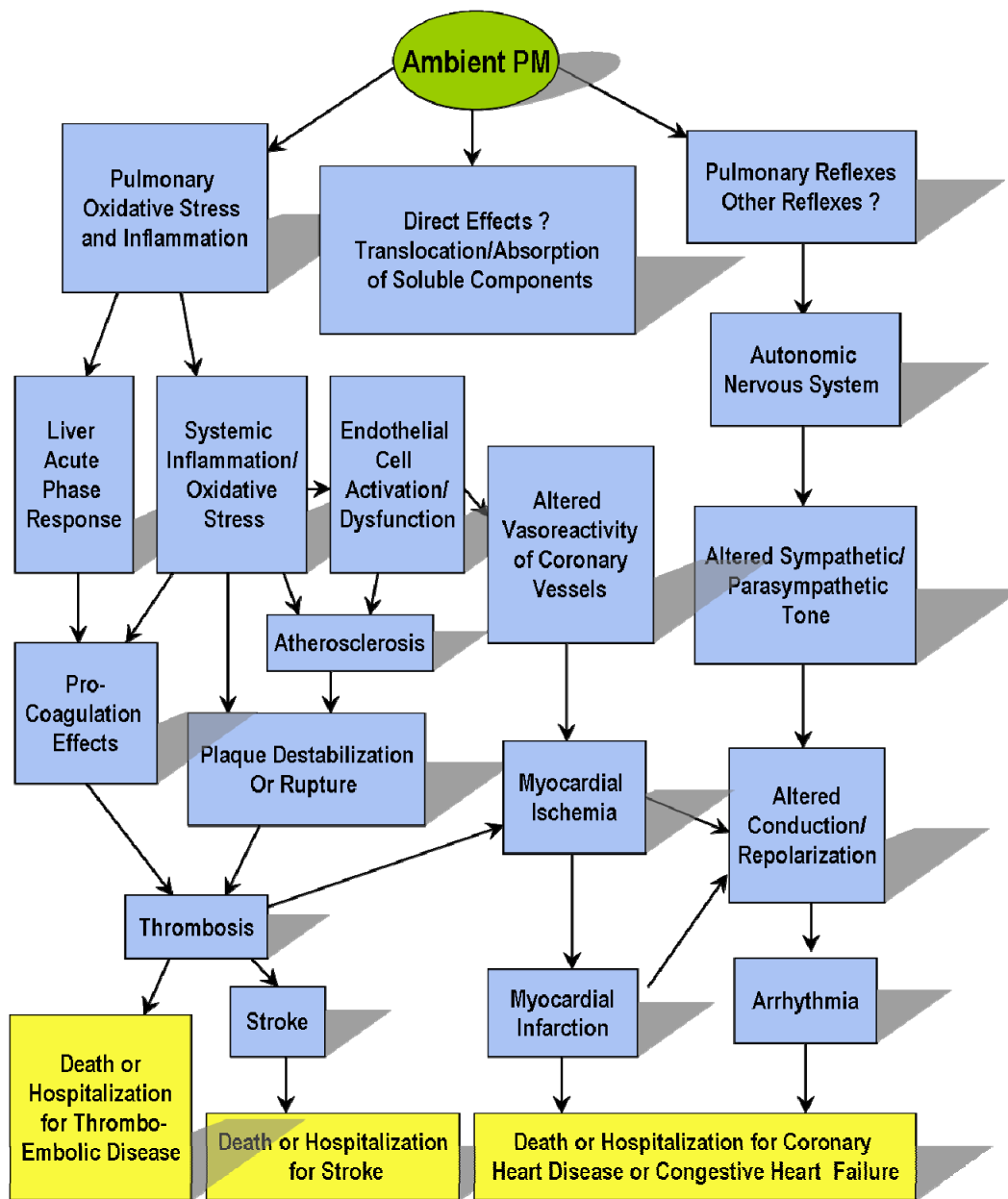


Figure 5-5. Potential pathways for the effects of PM on the cardiovascular system.

5.2.1. Endothelial Dysfunction and Altered Vasoreactivity

The luminal surface of blood vessels is lined by endothelial cells which, in addition to providing a barrier function, are key regulators of vascular homeostasis. Endothelial cells synthesize and release vasodilators such as nitric oxide (NO) and prostacyclin and vasoconstrictors such as endothelin (ET), which act on neighboring smooth muscle cells. ET also stimulates endothelial NO synthesis through a feedback mechanism. Inhalation of high concentrations of PM has been reported to increase ET levels in the circulation (Thomson et al., 2005, [087554](#)). ET has also been proposed to play a role in hypoxia-induced MI (Caligiuri et al., 1999, [157365](#)). However, the role of ET in mediating cardiovascular effects following ambient PM exposures is unclear (Section 6.2.4.3).

Endothelial dysfunction can lead to or follow endothelial activation under conditions of systemic inflammation and/or vascular oxidative stress. Both systemic inflammation and vascular oxidative stress have been associated with PM exposure (Nurkiewicz et al., 2006, [088611](#); Van Eeden et al., 2001, [019018](#)). Cytokines activate endothelial cells and upregulate endothelial cell adhesion molecules. They also promote the sequestration of neutrophils in microvascular beds. Neutrophil sequestration is sometimes associated with the deposition of myeloperoxidase (MPO) on endothelial cell surfaces (Nurkiewicz et al., 2006, [088611](#)). ROS-derived from neutrophils, MPO, other adhered inflammatory cells and/or other sources can perturb the balance of vasodilator and vasoconstrictor species produced by endothelial cells. Oxidative stress can result in decreased synthesis of NO due to limitation of the redox-sensitive essential cofactor tetrahydrobiopterin and in decreased bioavailability of NO due to reaction with superoxide. Prostacyclin synthesis is also decreased by oxidative stress. Importantly, these processes can affect vasoreactivity such that blood vessels may be unable to respond to vasoconstrictor stimuli with compensatory vasodilation.

Loss of NO and prostacyclin synthesis due to PM-dependent vascular oxidative stress may have other consequences since both exert negative influences on platelet and neutrophil activation. While endothelial surfaces normally are anti-thrombotic, endothelial dysfunction can contribute to thrombus formation. Furthermore, inflammation and oxidative stress associated with endothelial dysfunction can contribute to the development or progression of atherosclerosis (van Eeden et al., 2005, [157086](#)).

5.2.2. Activation of Coagulation and Acute Phase Response

The primary function of the coagulation cascade is to stop the loss of blood after vascular injury by forming a fibrin clot. However in some cases, activation of coagulation can promote intravascular thrombosis (Karoly et al., 2007, [155890](#)). It has been proposed that air pollution-associated PM can activate clotting pathways and enhance the likelihood of an obstructive cardiac ischemic event (e.g., MI) or cerebral event (e.g., stroke) (Seaton et al., 1995, [045721](#)).

Coagulation is regulated by intrinsic and extrinsic pathways. The intrinsic pathway occurs following activation of Factor XII and does not require the addition of an exogenous agent (Mackman, 2005, [156722](#)). On the other hand, the extrinsic pathway is an inducible signaling cascade that can be activated by tissue factor (TF) produced in response to inflammation or endothelial injury (Karoly et al., 2007, [155890](#)).

In general, platelets, red blood cells (RBCs) and endothelial cells are effector cells for inducing a pro-coagulant state in the vasculature. Circulating factors may enhance coagulation or promote activation of platelets. Cytokines formed during tissue damage and inflammation lead to TF induction. TF is the initiating stimulus for coagulation following vascular injury or plaque erosion. Complexes of TF:Factor VIIa form on endothelial cell surfaces and play a key role in thrombin generation by initiating the extrinsic blood coagulation pathway (Gilmour et al., 2005, [087410](#)). Thrombin generates fibrin from fibrinogen and amplifies the intrinsic pathway (Karoly et al., 2007, [155890](#)). TF and thrombin also have pro-inflammatory actions independent of coagulation functions (Chu, 2005, [155730](#)); thus activation of coagulation may lead to or potentiate inflammation. Endothelial cell-derived von Willebrand factor also contributes to coagulation.

The fibrinolytic system opposes these processes by facilitating the removal of a clot. The fibrinolytic pathway is regulated by the ratio of tissue plasminogen activator (tPA) and plasminogen activator inhibitor (PAI). Furthermore, the endothelial cell surface has anti-thrombotic properties due to the expression of tissue factor pathway inhibitor (TFPI) and thrombomodulin (Mackman, 2005, [156722](#)).

Inhibition of the fibrinolytic pathway, along with increased plasma viscosity and increased concentrations of plasma fibrinogen and Factor VII, contributes to a pro-thrombotic state (Gilmour et al., 2005, [087410](#)). In acute lung injury, vascular cells have enhanced pro-coagulant activity and impaired fibrinolytic activity (Gilmour et al., 2005, [087410](#)). In arterial atherosclerosis, TF expression is increased within plaques. As a result, spontaneous plaque rupture may trigger intravascular clotting (Karoly et al., 2007, [155890](#)).

Acute phase responses also play a role in hemostasis by exerting pro-coagulant effects. Cytokines such as IL-6 stimulate the liver to produce acute phase proteins including C-reactive protein (CRP), fibrinogen and antiproteases (van Eeden et al., 2005, [157086](#)). To date, there is limited evidence supporting a role for ambient PM in stimulating acute phase responses (Ruckerl et al., 2007, [156931](#) and reviewed therein) (also Section 6.2.7 and 6.2.8 in this ISA).

5.2.3. Atherosclerosis

Atherosclerosis is a chronic progressive disease which contributes greatly to cardiovascular morbidity (Libby, 2002, [192009](#)). Mainly a disease of the large arteries, it is characterized by the accumulation of lipid and fibrous tissue in atheromas, or swellings of the vessel wall (Libby, 2002, [192009](#)). Although a strong link is known to exist between hypercholesterolemia and atherogenesis, there is growing appreciation of the key role played by inflammation in the initiation and progression of atherosclerosis (Libby, 2002, [192009](#)). Furthermore, inflammation has the potential to promote thrombosis which can complicate this disorder and lead to MI and stroke (Libby, 2002, [192009](#)). As discussed above, PM exposure is associated with systemic inflammation, potentially contributing to the development of atherosclerosis.

Atheroma formation in experimental animals fed a high fat diet begins with the accumulation of modified lipoprotein particles in the arterial intima, as reviewed by Libby (2002, [192009](#)). The modification of lipoprotein particles often involves oxidation. As discussed above, PM exposure is associated with oxidative stress, suggesting a potential role for PM in the modification of lipoprotein particles. Endothelial dysfunction may also be key to these early events (Halvorsen et al., 2008, [191149](#)). Recent studies, which are discussed in later chapters, demonstrate PM-dependent endothelial dysfunction (Nurkiewicz et al., 2009, [191961](#)). As described by Libby (2002, [192009](#)), oxidative stress leads to lipid modification and uptake by endothelial cells and initiates an inflammatory response by activating NF- κ B. As a result, cell adhesion molecules such as vascular cell adhesion molecule-1 (VCAM-1) are upregulated and expressed in endothelial cells. Pro-inflammatory cytokines associated with systemic inflammation may also contribute to adhesion molecule upregulation. Subsequently, monocytes and T cell lymphocytes adhere to the activated endothelium, then migrate into the tunica intima directed by chemokines such as monocyte chemoattractant protein-1 (MCP-1) and IL-8. Monocytes undergo transformation to tissue macrophages and later to foam cells. As a part of this transformation, monocyte/macrophages express scavenger receptors and bind to and internalize the modified lipoprotein particles. These cells secrete growth factors and cytokines, produce ROS, replicate within the lesion and contribute to further lesion progression. Macrophage colony-stimulating factor (M-CSF) and granulocyte-macrophage colony-stimulating factor (GM-CSF) are thought to be involved in these latter steps which eventually lead to the formation of a fatty streak. T cell lymphocytes also become activated in the atheroma and secrete pro- or anti-inflammatory cytokines. Degranulation of mast cells found in the atheroma may also contribute to the lesion.

Atheroma progression involves the proliferation of smooth muscle cells, which is stimulated by macrophage-derived growth factors (Libby, 2002, [192009](#)). This results in smooth muscle accumulation in the lesion, the elaboration of extracellular matrix material and the formation of a more bulky lesion which can occlude the arterial lumen. Matrix proteins contribute to the evolution of the lesion from a fatty streak to a fibrous plaque. Mechanisms which trigger plaque disruption, including endothelial erosions and plaque rupture, can result in thrombosis as well as in further expansion of the lesion. Resident T cells, mast cells and circulating platelets may also play a role in destabilizing plaques (Halvorsen et al., 2008, [191149](#)). It is thought that most atheromatous lesions progress in a discontinuous manner due to cycles of disruption, expansion and repair.

A major factor regulating plaque disruption is the thickness of the fibrous cap, with more stable plaques characterized by a thick fibrous cap (Libby, 2002, [192009](#)). Collagen in the fibrous cap can be degraded by proteases, especially MMPs. Inflammation in the intima reduces collagen production by smooth muscle cells and promotes the expression and activation of MMPs. ROS may mediate MMP upregulation (Lund et al., 2009, [180257](#)). Both macrophages and smooth muscle cells produce MMPs in the lesion areas (Halvorsen et al., 2008, [191149](#)); fully differentiated macrophages selectively upregulate certain MMPs with more destructive potential (Newby, 2008, [191161](#)). Rupture of the fibrous cap allows pro-thrombotic factors within the plaque (e.g., TF) to come into contact with coagulation factors in the blood possibly resulting in the formation of an occlusive blood clot. However in some cases, blood fibrinolytic mechanisms minimize clot formation and repair processes ensue. The result is a more fibrous plaque and/or an expanded lesion. The proposed role of PM in activating coagulation pathways, which was discussed above, may influence the outcome of plaque disruption.

In this manner oxidative stress, inflammation and pro-coagulant activity in the blood are involved in the initiation and progression of atheromatous lesions as well as plaque disruption and occlusive blood clot formation. PM exposure may contribute to these pathways and in fact, studies

described in later chapters demonstrate PM-dependent effects on atherosclerosis progression (Araujo et al., 2008, [156222](#); Chen and Nadziejko, 2005, [087219](#); Sun et al., 2005, [087952](#); Ying et al., 2009, [190111](#)).

5.3. Activation of the Autonomic Nervous System by Pulmonary Reflexes

Chemosensitive receptors, including rapidly adapting receptors (RARs) and sensory C-fiber receptors, are found at all levels of the respiratory tract and are sensitive to irritant particles as well as to irritant gases (Alarie, 1973, [070967](#); Coleridge and Coleridge, 1994, [156362](#); Widdicombe, 2006, [155519](#)). Activation of trigeminal afferents in the nose causes CNS reflexes resulting in decreases in respiratory rate through a lengthened expiratory phase, closure of the glottis, closure of the nares with increased nasal airflow resistance and effects on the cardiovascular system such as bradycardia, peripheral vasoconstriction and a rise in systolic arterial blood pressure (Alarie, 1973, [070967](#)). Sneezing, rhinorrhea and vasodilation with subsequent nasal vascular congestion are also nasal reflex responses involving the trigeminal nerve (Sarin et al., 2006, [191166](#)). Activation of vagal afferents in the tracheobronchial and alveolar regions of the respiratory tract causes CNS reflexes resulting in bronchoconstriction, mucus secretion, mucosal vasodilation, cough, apnea followed by rapid shallow breathing and effects on the cardiovascular system such as bradycardia and hypotension or hypertension (Coleridge and Coleridge, 1994, [156362](#); Widdicombe, 2003, [157145](#); 2006, [155519](#); Widdicombe and Lee, 2001, [019049](#)). Some evidence suggests that cardiovascular responses may be mediated primarily by the C-fiber receptors (Coleridge and Coleridge, 1994, [156362](#)) and that irritants in the lower respiratory tract cause more pronounced cardiovascular responses than irritants in the upper respiratory tract (Widdicombe and Lee, 2001, [019049](#)).

Early experiments demonstrated that sectioning of the trigeminal nerve abrogated irritant effects on respiratory rate, heart rate and systolic arterial blood pressure (Alarie, 1973, [070967](#)). These nasal reflexes were attributed to the ophthalmic branch of the trigeminal nerve since they were identical to reflex responses following diving or immersion of the face in water (Alarie, 1973, [070967](#)). Early experiments also demonstrated that non-nasal reflexes were mediated by cholinergic parasympathetic pathways involving the vagus nerve and inhibited by atropine (Grunstein et al., 1977, [071445](#); Nadel et al., 1965, [014846](#)). More recent experiments have shown that noncholinergic mechanisms may also be involved. For example, stimulation of C-fiber receptors can activate local axon reflexes. These local axon pathways are responsible for secretion of neuropeptides and the development of neurogenic inflammation (Widdicombe and Lee, 2001, [019049](#)). It has been proposed that, in some cases, neurogenic pulmonary responses can switch from their normally protective function to one that perpetuates pulmonary inflammation (Wong et al., 2003, [097707](#)). Differences in respiratory tract innervation between rodents and humans suggest that C-fiber mediated neurogenic inflammation may be more important in rodents than in humans (Groneberg et al., 2004, [138134](#); Widdicombe, 2003, [157145](#); Widdicombe and Lee, 2001, [019049](#)) However, the role of neurogenic inflammation in mediating pulmonary responses in humans is an active area of investigation.

VR1 receptors represent a subset of neuropeptide and acid-sensitive irritant receptors which belong to the transient receptor potential (TRP) family. They are located on the sensory C-fibers which lie underneath and between lung epithelial cells and on immune and non-immune airway cells. Some investigators have focused on the role played by these receptors in mediating inflammation following exposure to PM (Veronesi and Oortgiesen, 2001, [015977](#)). Exposure of bronchial epithelial cells and neurons to PM in vitro has been shown to result in an immediate increase in intracellular calcium followed by the release of neuropeptides and inflammatory cytokines (Veronesi et al., 1999, [048764](#); Veronesi et al., 2000, [017062](#)). In one study, this response was found to be due to an intrinsic property of the particle core and was not metal-dependent (Oortgiesen et al., 2000, [013998](#)), while in another study electrostatic charge was found to activate VR1 receptors (Veronesi et al., 2003, [094384](#)). PM-mediated activation of VR1 receptors which results in increases in intracellular calcium and apoptosis in epithelial cells has also been demonstrated (Agopyan et al., 2003, [155649](#)). New studies, discussed in later chapters, provide evidence for the involvement of TRPV1 irritant receptor involvement in PM-dependent responses (Ghelfi et al., 2008, [156468](#); Rhoden et al., 2005, [087878](#)).

Recently it has been proposed that pulmonary reflex responses may be modulated by CNS plasticity (Bonham et al., 2006, [191140](#); Sekizawa et al., 2008, [191167](#)). Plasticity is a property of neurons or synapses which allows change in response to previous events. In the case of the respiratory tract, visceral afferent inputs to the CNS are integrated primarily in the nucleus tractus solitarius (NTS) region of the brain (Bonham et al., 2006, [191140](#)). Inputs from local networks, higher brain regions and circulating mediators contribute to the reflex output (Bonham et al., 2006, [191140](#)). This integration allows for plasticity in that repeated or prolonged exposure to a particular stimuli may lead to altered reflex responses to the same or subsequent stimuli. An exaggerated reflex response was recently observed in guinea pigs exposed to ETS for an extended period of time (Sekizawa et al., 2008, [191167](#)). It is not known whether CNS plasticity influences responses following acute and chronic exposure to ambient PM, but it is a mechanism that may possibly explain hyperresponsiveness and/or adaptation of reflex-related responses.

At this time, it is not clear how activation of the ANS by pulmonary reflexes contributes to the kinds of altered conduction and/or repolarization properties of the heart which may be linked to arrhythmias (Figure 5-5). Pulmonary reflexes, as they are currently understood, initially lead to increases in parasympathetic tone. However, decreased heart rate variability appears to be reflective of decreased parasympathetic tone and/or increased sympathetic tone. A PM-dependent sympathetic stress response mediated by cytokines has been postulated (Godleski et al., 2000, [000738](#)), but there is little new information to support this mechanism. Thus, activation of the autonomic nervous system by mechanisms other than pulmonary reflexes seems likely in response to PM. Very little is known about putative alternative mechanisms leading to sympathoexcitatory responses although one study demonstrated a role for the olfactory bulb-NTS pathway in regulating cardiovascular functions following smoke exposure (Moffitt et al., 2002, [191160](#)). In addition, sympathoexcitatory responses occur during myocardial ischemia, mediated by the release of adenosine or the production of ROS by the myocardium (Longhurst et al., 2001, [191158](#)). Hence, PM-dependent effects leading to myocardial ischemia may stimulate sympathoexcitatory responses. Furthermore, the effects of pre-existing alterations in the ANS due to disease processes (e.g., increased sympathetic tone observed in cardiac diseases) on PM responses are not understood. Possibly, integration of neural signals resulting from pulmonary and cardiac reflexes at the level of the NTS may have an influence on ANS responses to PM. Further investigation will be required to clarify these mechanisms.

5.4. Translocation of UFPs or Soluble PM Components

UFPs can translocate across cell membranes by non-endocytotic mechanisms involving adhesive interactions and diffusion (Geiser et al., 2005, [087362](#)), as described in Section 4.3.3.1. In this study, there was no measurable loss of PM from the lung over 24 h despite the rapid translocation of inhaled UFPs into alveolar epithelial cells and capillary endothelial cells. In another study, UFPs were localized in macrophage mitochondria as demonstrated by electron microscopy (Li et al., 2003, [042082](#)). Other studies found extrapulmonary translocation of poorly soluble UFPs, but the process was slow and resulted in only a small amount leaving the lung. It is possible that in these studies PM gained access to the circulation after initial transport to the lymph nodes or the gastrointestinal system. Hence, there is limited evidence to date that UFPs or other PM size fractions access the circulation by traversing the epithelial barrier of the respiratory tract.

However, soluble components from all size fractions of PM have the potential to translocate across the airway epithelium into the bronchial circulation or across the alveolar epithelium into the systemic circulation as depicted in Figure 5-5. Absorption across nasal epithelium may also occur (Illum, 2006, [191205](#)). Factors affecting this process include the rate of dissolution of the solute from the particle and the molecular weight of the solute (Section 4.4). More rapid dissolution of soluble components may occur in the case of UFPs due to the higher surface/volume ratios compared with larger particles.

Several interesting studies investigated the translocation of water-soluble metals from the lung. Gilmour et al. (2006, [156472](#)) demonstrated the rapid appearance of Zn in the plasma of rats following IT instillation of zinc sulfate (ZnSO₄). Similarly, Wallenborn et al. (2007, [156144](#)) demonstrated the rapid appearance of water-soluble metals in the blood, heart and liver following IT instillation of oil combustion PM in rats. Using a more sensitive technique, these same investigators demonstrated the accumulation of ⁷⁰Zn, a rare isotope of Zn, in blood, heart and liver following IT

instillation of ZnSO₄ (Wallenborn et al., 2009, [191172](#)). In three other studies, soluble Zn and Cu were associated with cardiac effects following IT instillation of rats with different forms of Zn- and Cu-containing PM (Gilmour et al., 2006, [088489](#); Gottipolu et al., 2008, [191148](#); Kodavanti et al., 2008, [155907](#)). These results suggest the possibility that PM-derived soluble Zn and Cu translocated across the alveolar-capillary barrier into the circulation and exerted effects on the heart. However, in the two studies in which barrier function was measured it was found to be compromised (Gilmour et al., 2006, [088489](#); Gottipolu et al., 2008, [191148](#)) suggesting an acute lung injury response to IT instillation of high concentrations of metal. Acute lung injury is not likely to occur in healthy individuals exposed to PM at concentrations relevant to ambient levels. Cardiac effects were also observed following subchronic inhalation exposure to low concentrations of aerosolized ZnSO₄ (Wallenborn et al., 2008, [191171](#)). Since it was not possible to measure extra-pulmonary Zn in this study, it remains unclear whether cardiac effects were a direct effect of translocated Zn or an indirect effect of exposure to Zn-containing PM. Nonetheless, translocation of soluble components derived from inhaled PM remains a viable hypothesis to explain some extra-pulmonary effects.

Epithelial permeability is a key determinant of translocation and is discussed in detail in Section 4.4.2. In brief, a number of studies have measured clearance of ^{99m}Tc-DTPA as an index of alveolar epithelial membrane integrity and permeability of alveolar-capillary barrier (Braude et al., 1986, [155701](#)). Endothelial integrity also contributes to the alveolar-capillary barrier and is measured by transvascular protein flux but is not discussed here (Braude et al., 1986, [155701](#)). In laboratory animals, increased alveolar permeability was shown in terminally senescent mice (Tankersley et al., 2003, [096363](#)). In human volunteers, epithelial permeability was transiently increased following 3 h of moderate exercise but not following 24-h exposure to particle-rich urban air (Brauner et al., 2009, [190244](#)). A previous study found that the exercise-induced increase in epithelial permeability was transient and suggested that it was due to increased ventilation and elevated vascular pressure which altered the properties of tight junctions (Hanel et al., 2003, [155826](#)). Smokers (Jones et al., 1983, [155884](#)) and individuals with acute respiratory distress syndrome (Braude et al., 1986, [155701](#)) or interstitial lung disease (Rinderknecht et al., 1980, [191965](#)) also exhibited increased alveolar epithelial permeability. The changes in smokers were reversible upon cessation of smoking. Increased airway epithelial permeability was found in asthmatics when ^{99m}Tc-DTPA clearance was used to measure the permeability of the bronchial mucosa (Ilowite et al., 1989, [156584](#)). These studies demonstrate that epithelial permeability is increased following moderate exercise and in lung syndromes associated with inflammation and suggest that compromised epithelial barrier functions in the lung may contribute to PM-mediated effects.

Interaction of circulating PM or soluble PM components with vascular endothelial cells, platelets, and other leukocytes is a potential mechanism underlying the cardiovascular and systemic effects of inhaled PM. A role for PM-derived ROS and/or cellular-derived ROS has been proposed. Furthermore, soluble metals that do not redox-cycle may activate cell signaling pathways without the generation of ROS. In this way, PM may promote adverse cardiovascular effects such as endothelial dysfunction, atherosclerosis and thrombosis. Circulating PM or soluble PM components also have the potential to impact other organ systems. However, convincing evidence that this occurs to an appreciable extent in healthy individuals following inhalation of PM at concentrations relevant to ambient exposures is lacking.

5.5. Disease of the Cardiovascular and Other Organ Systems

As discussed above, deposition of PM in the lung may lead not only to pulmonary disease but also to diseases of other systems (Figure 5-5). In the cardiovascular system, myocardial ischemia and MI may occur as a result of the above proposed effects of PM on atherosclerosis, plaque instability, thrombosis, plaque rupture and/or altered vasoreactivity of coronary vessels. Myocardial ischemia and MI may alter the conduction and depolarization properties of the heart and lead to arrhythmic events. In addition, thrombosis may lead to stroke and/or thromboembolic disease. Many of these processes may be interlinked and responses to ambient PM exposures may involve multiple mechanisms simultaneously with some variability depending on PM composition. Furthermore, it is not clear at this time whether PM initiates cardiovascular disease or whether it perturbs existing disease.

In addition, recent studies which are discussed in later chapters have demonstrated PM-dependent effects on the CNS (Campbell et al., 2005, [087217](#); Kleinman et al., 2008, [190074](#); Sirivelu et al., 2006, [111151](#); Veronesi et al., 2005, [087481](#); Win-Shwe et al., 2008, [190146](#)). At this time, it is not known whether this is a direct or indirect consequence of PM exposure. Translocation of soluble and poorly soluble particles from the olfactory mucosa via the axons to the olfactory bulb of the brain has been proposed as a possible mechanism by which PM or its components may directly access the CNS. Evidence for this pathway is discussed in Section 4.3.3.2. Alternative mechanisms proposed for PM-mediated CNS effects involve systemic inflammation and autonomic responses. These are new and intriguing possibilities which warrant further investigation.

PM-dependent effects on the reproductive system, reproductive outcomes and perinatal development have also been identified and are discussed in a later chapter. Mechanisms involved in these responses have not been determined. However, it seems possible that systemic inflammation and/or oxidative stress may play a role. Developmental windows of susceptibility may also be an important consideration. Furthermore, it has been hypothesized that oxygen gradients and redox status are key to cell differentiation and epigenetic processes occurring during development (Section 5.1.11) (Hitchler and Domann, 2007, [191151](#)).

5.6. Acute and Chronic Responses

In general, repeated acute responses may lead to cumulative effects which manifest as chronic disease. Several examples relevant to the modes of action discussed in this chapter are that of allergic responses, atherosclerosis and lung development. Allergic responses require repeated exposures to antigen over time. Co-exposure to an adjuvant, possibly DEP or ultrafine concentrated ambient particles (CAPs), can enhance this response. Furthermore, the presence of oxidative stress, as may occur in response to PM, can contribute to allergic responses. Allergic sensitization often underlies allergic asthma, characterized by inflammation and AHR. In this way, repeated or chronic exposures involving multifactorial responses (immune system activation, oxidative stress, inflammation) can lead to irreversible outcomes. Similarly, the development of atherosclerosis involves inflammation and remodeling of the blood vessel wall. Factors contributing to this process include systemic inflammation, endothelial dysfunction, oxidative stress and high levels of circulating lipids. PM exposure is associated with three out of four of these processes. The role of PM in initiating, promoting or complicating this disease or its outcomes has yet to be determined. Critical windows of susceptibility during development also provide an opportunity for repeated exposures to injurious agents to lead to irreversible changes in organ structure and function. The extended period of postnatal lung development in humans and other species heightens this vulnerability. PM may serve as such an injurious agent as has been demonstrated previously for hyperoxia (Randell et al., 1990, [191956](#)).

Furthermore, adverse outcomes may be precipitated by acute events superimposed on chronic disease states. In the case of allergic asthma, acute PM exposure may provoke asthmatic responses through oxidative stress and inflammatory pathways. Additionally, PM can act as a carrier of aeroallergens and other biological materials which can potentially trigger asthma attacks. Similarly, PM exposure may provoke inflammatory or thrombotic responses leading to rupture of an atherosclerotic plaque which subsequently results in acute MI. In this way, the outcome of an acute exposure to PM may be drastically worsened by the underlying chronic disease.

5.7. Results of New Inhalation Studies which Contribute to Modes of Action

Prior to this review, much of the evidence for the proposed modes of action was obtained from animal studies involving IT instillation or inhalation of high concentrations of PM and from cell culture experiments. In many cases, the types of PM used were of questionable relevance to ambient exposures (i.e., high concentrations of ROFA, metals and ambient PM collected on filters). Since then, many inhalation studies have been conducted using CAPs, combustion-derived PM, urban air

and carbon black, generally using concentrations of PM lower than 1 mg/m³. Much of this research has been conducted in animal models of disease. These key new studies, described in detail in Chapters 6 and 7, add to the understanding of modes of action which are relevant to ambient PM exposure. A compilation of pertinent results is found below.

- Altered lung function including changes in respiratory frequency and AHR following short-term exposures to CAPs and combustion-derived PM (Section 6.3.2.3)
- Mild pulmonary inflammation in response to short-term exposures to CAPs, urban air, combustion-derived PM and carbon black (Section 6.3.3.3)
- Mild pulmonary injury in response to short-term exposure to CAPs and combustion-derived PM (Section 6.3.5.3)
- Inhibition of cell proliferation in the proximal alveolar region of neonatal animals following short-term exposure to iron-soot (Section 6.3.5.3)
- Pulmonary oxidative stress in response to short-term exposure to CAPs, urban air, combustion-derived PM, carbon black and iron-soot; pulmonary nitrosative stress in response to titanium dioxide (TiO₂) (Section 6.3.4.2)
- Antioxidant intervention which ameliorates PM effects on oxidative stress, allergic responses, and AHR (Sections 6.3.4.2)
- Allergic sensitization and exacerbation of allergic responses in response to CAPs and combustion-derived PM (Section 6.3.6.3)
- Altered methylation of promoter regions of IFN- γ and IL-4 genes suggestive of pro-allergic Th2 gene activation following short-term exposure to combustion-derived PM in an allergy model (Section 6.3.6.3)
- Increased susceptibility to respiratory infection following exposure to combustion-derived PM (Section 6.3.7.2)
- Effects on nasal epithelial mucosubstances, airway morphology and airway mucosubstances following chronic exposure to urban air-derived PM and woodsmoke (Section 7.3.5.1)
- Worsening of papain-induced emphysema following chronic exposure to urban air-derived PM (Section 7.3.5.1)
- Effects on lung development following chronic exposure to urban air-derived PM (Sections 7.3.2.2 and 7.3.5.1)
- Prolonged exposure to CAPs and combustion-derived PM leading sometimes to mild pulmonary inflammation, oxidative stress and injury and sometimes to loss of inflammatory, oxidative stress and AHR responses which were observed after short-term exposures (Sections 7.3.2.2, 7.3.3.2, 7.3.4.1, 7.3.5.1 and 7.3.6.2)
- Hypermethylation of lung DNA following chronic exposure to combustion-derived PM (Section 7.3.5.1)
- A role for TRPV1 irritant receptors in activating local axon and CNS reflexes following short-term exposure to CAPs and combustion-derived PM (Section 6.2.9.3)

- A role for TRPV1 irritant receptors in mediating lung and heart oxidative stress through increased parasympathetic and sympathetic activity in response to CAPs (Sections 6.2.9.3 and 6.3.4.2)
- Altered heart rate variability in response to CAPs, combustion-derived PM and carbon black (Section 6.2.1.3)
- Arrhythmic events in response to CAPs and combustion-derived PM (Section 6.2.2.2)
- Altered cardiac contractility following short-term exposure to CAPs and carbon black (Section 6.2.6.1)
- Enhanced myocardial ischemia following short-term exposure to CAPs (Section 6.2.3.3)
- Endothelial dysfunction and altered vascular reactivity following short-term exposure to CAPs, combustion-derived PM and TiO₂ (Section 6.2.4.3)
- Increases in blood pressure following short-term exposure to CAPs and carbon black (Section 6.2.5.3)
- Changes in blood leukocyte counts following short-term exposure to CAPs and carbon black (Section 6.2.7.3)
- Increased levels of blood coagulation factors following short-term exposure to CAPs and on-road highway aerosols (Section 6.2.8.3)
- Systemic and cardiovascular oxidative stress in response to short-term exposure to CAPs, road dust and combustion-derived PM (Section 6.2.9.3)
- Progression of atherosclerosis, induction of TF in aortic plaques, vascular oxidative stress and altered vasomotor function following long-term exposure to CAPs in a susceptible animal model (Section 7.2.1.2)
- Vascular remodeling following chronic exposure to urban air-derived PM (Section 7.2.1.2).
- Enhanced angiotensin II-induced hypertension accompanied by vascular oxidative stress and altered vasoreactivity in response to chronic exposure to CAPs (Section 7.2.5.2)
- Exaggerated insulin resistance, visceral adiposity and systemic inflammation in response to chronic exposure to CAPs and a high-fat diet (Section 7.2.3.1)
- CNS responses following short- and long-term exposures to CAPs and combustion-derived PM (Section 6.4.3)
- Effects on the reproductive system, reproductive outcomes and developmental outcomes following chronic exposure to urban-air derived PM (Section 7.4.2)
- DNA adducts in nose, lung and liver following chronic exposure to urban air (Section 7.5.2.1)
- Germ line mutations, DNA strand breaks and global hypermethylation in sperm following chronic exposure to urban air-derived PM (Section 7.5.3)

5.8. Gaps in Knowledge

The new studies highlighted in Section 5.7 confirm and extend findings from older studies. However, this increasing body of evidence does not provide a complete picture of the biological pathways involved in mediating PM effects. For example, a lack of information regarding the time-dependence of many responses makes it difficult to understand the underlying biological mechanisms. Existing gaps in knowledge include:

- The spatial distribution of retained particles in the lung and its impact
- The deposition, uptake and clearance of UFPs in the lung
- Effects of ambient PM exposures on epithelial barrier function in the lung
- Time dependence of responses
- The putative modulation of neural reflexes by pre-existing disease or other factors
- The putative role of neural reflexes besides those involving pulmonary irritant receptors
- The putative role of ET in altering vasomotor tone following PM exposure
- The putative translocation of PM or soluble components across the epithelial barrier of the lung into the circulation
- The putative translocation of PM from olfactory epithelium to the olfactory bulb and other brain regions

Additional studies will be required to clarify the biological mechanisms underlying the health effects of PM.

Chapter 5 References

- Adamson I; Prieditis H (1995). Response of mouse lung to carbon deposition during injury and repair. *Environ Health Perspect*, 103: 72-76. [189982](#)
- Adcock IM; Tsaprouni L; Bhavsar P; Ito K (2007). Epigenetic regulation of airway inflammation. *Curr Opin Immunol*, 19: 694-700. [191178](#)
- Agopyan N; Bhatti T; Yu S; Simon SA (2003). Vanilloid receptor activation by 2- and 10- μ m particles induces responses leading to apoptosis in human airway epithelial cells. *Toxicol Appl Pharmacol*, 192: 21-35. [155649](#)
- Ahsan MK; Nakamura H; Tanito M; Yamada K; Utsumi H; Yodoi J (2005). Thioredoxin-1 suppresses lung injury and apoptosis induced by diesel exhaust particles (DEP) by scavenging reactive oxygen species and by inhibiting DEP-induced downregulation of Akt. *Free Radic Biol Med*, 39: 1549-1559. [156200](#)
- Alarie Y (1973). Sensory irritation by airborne chemicals. *Crit Rev Toxicol*, 2: 299-363. [070967](#)
- Amara N; Bachoual R; Desmard M; Golda S; Guichard C; Lanone S; Aubier M; Ogier-Denis E; Boczkowski J (2007). Diesel exhaust particles induce matrix metalloproteinase-1 in human lung epithelial cells via a NADPH oxidase/NOX4 redox-dependent mechanism. *Am J Physiol Lung Cell Mol Physiol*, 293: L170-L181. [156212](#)
- Araujo JA; Barajas B; Kleinman M; Wang X; Bennett BJ; Gong KW; Navab M; Harkema J; Sioutas C; Lusa AJ; Nel AE (2008). Ambient particulate pollutants in the ultrafine range promote early atherosclerosis and systemic oxidative stress. *Circ Res*, 102: 589-596. [156222](#)
- Ayres JG; Borm P; Cassee FR; Castranova V; Donaldson K; Ghio A; Harrison RM; Hider R; Kelly F; Kooter IM; Marano F; Maynard RL; Mudway I; Nel A; Sioutas C; Smith S; Baeza-Squiban A; Cho A; Duggan S; Froines J (2008). Evaluating the Toxicity of Airborne Particulate Matter and Nanoparticles by Measuring Oxidative Stress Potential - A Workshop Report and Consensus Statement. *Inhal Toxicol*, 20: 75 - 99. [155666](#)
- Baccarelli A; Wright RO; Bollati V; Tarantini L; Litonjua AA; Suh HH; Zanobetti A; Sparrow D; Vokonas PS; Schwartz J (2009). Rapid DNA Methylation Changes after Exposure to Traffic Particles. *Am J Respir Crit Care Med*, 179: 572-578. [192155](#)
- Bachoual R; Boczkowski J; Goven D; Amara N; Tabet L; On D; Lecon-Malas V; Aubier M; Lanone S (2007). Biological effects of particles from the Paris subway system. *Chem Res Toxicol*, 20: 1426-1433. [155667](#)
- Barnes PJ (2007). New molecular targets for the treatment of neutrophilic diseases. *J Clin Immunol*, 119: 1055-62. [191139](#)
- Bayram H; Ito K; Issa R; Ito M; Sukkar M; Chung KF (2006). Regulation of human lung epithelial cell numbers by diesel exhaust particles. *Eur Respir J*, 27: 705-713. [088439](#)
- Becher R; Bucht A; Ovrevik J; Hongslo JK; Dahlman HJ; Samuelsen JT; Schwarze PE (2007). Involvement of NADPH oxidase and iNOS in rodent pulmonary cytokine responses to urban air and mineral particles. *Inhal Toxicol*, 19: 645-655. [097125](#)
- Beck-Speier I; Dayal N; Karg E; Maier KL; Schumann G; Schulz H; Semmler M; Takenaka S; Stettmaier K; Bors W; Ghio A; Samet JM; Heyder J (2005). Oxidative stress and lipid mediators induced in alveolar macrophages by ultrafine particles. *Free Radic Biol Med*, 38: 1080-1092. [156262](#)
- Becker S; Fenton MJ; Soukup JM (2002). Involvement of microbial components and toll-like receptors 2 and 4 in cytokine responses to air pollution particles. *Am J Respir Cell Mol Biol*, 27: 611-618. [052419](#)
- Becker S; Mundandhara S; Devlin RB; Madden M (2005). Regulation of cytokine production in human alveolar macrophages and airway epithelial cells in response to ambient air pollution particles: further mechanistic studies. *Toxicol Appl Pharmacol*, 207: 269-275. [088590](#)
- Blanchet S; Ramgolam K; Baulig A; Marano F; Baeza-Squiban A (2004). Fine particulate matter induces amphiregulin secretion by bronchial epithelial cells. *Am J Respir Cell Mol Biol*, 30: 421-427. [087982](#)

Note: Hyperlinks to the reference citations throughout this document will take you to the NCEA HERO database (Health and Environmental Research Online) at <http://epa.gov/hero>. HERO is a database of scientific literature used by U.S. EPA in the process of developing science assessments such as the Integrated Science Assessments (ISA) and the Integrated Risk Information System (IRIS).

- Blank F; Rothen-Rutishauser B; Gehr P (2007). Dendritic cells and macrophages form a transepithelial network against foreign particulate antigens. *Am J Respir Cell Mol Biol*, 36: 669-77. [096521](#)
- Bleck B; Tse Doris B; Jaspers I; de Lafaille Maria AC; Reibman J (2006). Diesel exhaust particle-exposed human bronchial epithelial cells induce dendritic cell maturation. *J Immunol*, 176: 7431-7437. [096560](#)
- Bonham AC; Chen CY; Sekizawa S; Joad JP (2006). Plasticity in the nucleus tractus solitarius and its influence on lung and airway reflexes. *J Appl Physiol*, 101: 322-7. [191140](#)
- Braude S; Nolop KB; Hughes JMB; Barnes PJ; Royston D (1986). Comparison of lung vascular and epithelial permeability indices in the adult respiratory distress syndrome. *Am Rev Respir Dis*, 133: 1002-1005. [155701](#)
- Brauner EV; Mortensen J; Moller P; Bernard A; Vinzents P; Wahlin P; Glasius M; Loft S (2009). Effects of ambient air particulate exposure on blood-gas barrier permeability and lung function. *Inhal Toxicol*, 21: 38-47. [190244](#)
- Brown DM; Donaldson K; Borm PJ; Schins RP; Dehnhardt M; Gilmour P; Jimenez LA; Stone V (2004). Calcium and ROS-mediated activation of transcription factors and TNF-alpha cytokine gene expression in macrophages exposed to ultrafine particles. *Am J Physiol*, 286: L344-L353. [155705](#)
- Brown DM; Donaldson K; Stone V (2004). Effects of PM10 in human peripheral blood monocytes and J774 macrophages. *Respir Res*, 5: 29. [088663](#)
- Caligiuri G; Levy B; Pernow J; Thoren P; Hansson GK (1999). Myocardial infarction mediated by endothelin receptor signaling in hypercholesterolemic mice. *PNAS*, 96: 6920-4. [157365](#)
- Campbell A; Oldham M; Becaria A; Bondy SC; Meacher D; Sioutas C; Misra C; Mendez LB; Kleinman M (2005). Particulate matter in polluted air may increase biomarkers of inflammation in mouse brain. *Neurotoxicology*, 26: 133-140. [087217](#)
- Cao D; Tal TL; Graves LM; Gilmour I; Linak W; Reed W; Bromberg PA; Samet JM (2007). Diesel exhaust particulate-induced activation of Stat3 requires activities of EGFR and Src in airway epithelial cells. *Am J Physiol Lung Cell Mol Physiol*, 292: L422-L429. [156322](#)
- Chan RC-F; Wang M; Li N; Yanagawa Y; Onoe K; Lee JJ; Nel AE (2006). Pro-oxidative diesel exhaust particle chemicals inhibit LPS-induced dendritic cell responses involved in T-helper differentiation. *J Allergy Clin Immunol*, 118: 455-465. [097468](#)
- Chang C-C; Chiu H-F; Wu Y-S; Li Y-C; Tsai M-L; Shen C-K; Yang C-Y (2005). The induction of vascular endothelial growth factor by ultrafine carbon black contributes to the increase of alveolar-capillary permeability. *Environ Health Perspect*, 113: 454-460. [097776](#)
- Chen J; Tan M; Nemmar A; Song W; Dong M; Zhang G; Li Y (2006). Quantification of extrapulmonary translocation of intratracheal-instilled particles in vivo in rats: effect of lipopolysaccharide. *Toxicology*, 222: 195-201. [147267](#)
- Chen LC; Nadziejko C (2005). Effects of subchronic exposures to concentrated ambient particles (CAPs) in mice V CAPs exacerbate aortic plaque development in hyperlipidemic mice. *Inhal Toxicol*, 17: 217-224. [087219](#)
- Cho AK; Sioutas C; Miguel AH; Kumagai Y; Schmitz DA; Singh M; Eiguren-Fernandez A; Froines JR (2005). Redox activity of airborne particulate matter at different sites in the Los Angeles Basin. *Environ Res*, 99: 40-47. [087937](#)
- Cho H-Y; Reddy SP; Kleeberger SR (2006). Nrf2 defends the lung from oxidative stress. *Antioxid Redox Signal*, 8: 76-87. [156345](#)
- Chu AJ (2005). Tissue factor mediates inflammation. *Arch Biochem Biophys*, 440: 123-132. [155730](#)
- Coleridge HM; Coleridge JCG (1994). Pulmonary Reflexes: Neural Mechanisms of Pulmonary Defense. *Annu Rev Physiol*, 56: 69-91. [156362](#)
- Cowburn AS; Condliffe AM; Farahi N; Summers C; Chilvers ER (2008). Advances in neutrophil biology: clinical implications. *Chest*, 134: 606-12. [191142](#)
- de Haar C; Hassing I; Bol M; Bleumink R; Pieters R (2006). Ultrafine but not fine particulate matter causes airway inflammation and allergic airway sensitization to co-administered antigen in mice. *Clin Exp Allergy*, 36: 1469-1479. [144746](#)
- De Kok TM; Hogervorst JG; Briede JJ; Van Herwijnen MH; Maas LM; Moonen EJ; Driee HA; Kleinjans JC (2005). Genotoxicity and physicochemical characteristics of traffic-related ambient particulate matter. *Environ Mol Mutagen*, 46: 71-80. [088656](#)

- Dick CAJ; Brown DM; Donaldson K; Stone V (2003). The role of free radicals in the toxic and inflammatory effects of four different ultrafine particle types. *Inhal Toxicol*, 15: 39-52. [036605](#)
- Donaldson K; Borm PJA; Oberdorster G; Pinkerton KE; Stone V; Tran CL (2008). Concordance between in vitro and in vivo dosimetry in the proinflammatory effects of low-toxicity, low-solubility particles: the key role of the proximal alveolar region. *Inhal Toxicol*, 20: 53-62. [190217](#)
- Donaldson K; Stone V; Borm PJA; Jimenez LA; Gilmour PS; Schins RPF; Knaapen AM; Rahman I; Faux SP; Brown DM; MacNee W (2003). Oxidative stress and calcium signaling in the adverse effects of environmental particles (PM10). *Free Radic Biol Med*, 34: 1369-1382. [156408](#)
- Dostert C; Petrilli V; Van Bruggen R; Steele C; Mossman BT; Tschopp J (2008). Innate Immune Activation Through Nalp3 Inflammasome Sensing of Asbestos and Silica. *Science*, 320: 674-677. [155753](#)
- Foley DL; Craig JM; Morley R; Olsson CA; Dwyer T; Smith K; Saffery R (2009). Prospects for epigenetic epidemiology. *Am J Epidemiol*, 169: 389-400. [191144](#)
- Gabelová A; Valovicova Z; Labaj J; Bacova G; Binkova B; Farmer Peter B (2007). Assessment of oxidative DNA damage formation by organic complex mixtures from airborne particles PM(10). *Mutat Res*, 620: 135-144. [156457](#)
- Gallagher J; Sams R; Inmon J; Gelein R; Elder A; Oberdorster G; Prahald AK (2003). Formation of 8-oxo-7,8-dihydro-2'-deoxyguanosine in rat lung DNA following subchronic inhalation of carbon black. *Toxicol Appl Pharmacol*, 190: 224-231. [140171](#)
- Geiser M; Rothen-Rutishauser B; Kapp N; Schurch S; Kreyling W; Schulz H; Semmler M; Im Hof V; Heyder J; Gehr P (2005). Ultrafine particles cross cellular membranes by nonphagocytic mechanisms in lungs and in cultured cells. *Environ Health Perspect*, 113: 1555-1560. [087362](#)
- Geng H; Meng Z; Zhang Q (2005). Effects of blowing sand fine particles on plasma membrane permeability and fluidity, and intracellular calcium levels of rat alveolar macrophages. *Toxicol Lett*, 157: 129-137. [096689](#)
- Geng H; Meng Z; Zhang Q (2006). In vitro responses of rat alveolar macrophages to particle suspensions and water-soluble components of dust storm PM(2.5). *Toxicol In Vitro*, 20: 575-584. [097026](#)
- Ghelfi E; Rhoden CR; Wellenius GA; Lawrence J; Gonzalez-Flecha B (2008). Cardiac oxidative stress and electrophysiological changes in rats exposed to concentrated air particles are mediated by TRP-dependent pulmonary reflexes. *Toxicol Sci*, 102: 328-336. [156468](#)
- Ghio AJ; Churg A; Roggli VL (2004). Ferruginous bodies: Implications in the mechanism of fiber and particle toxicity. *Toxicol Pathol*, 32: 643-649. [155790](#)
- Ghio AJ; Cohen MD (2005). Disruption of iron homeostasis as a mechanism of biologic effect by ambient air pollution particles. *Inhal Toxicol*, 17: 709-716. [088272](#)
- Gilmour PS; Morrison ER; Vickers MA; Ford I; Ludlam CA; Greaves M; Donaldson K; MacNee W (2005). The procoagulant potential of environmental particles (PM10). *Occup Environ Med*, 62: 164-171. [087410](#)
- Gilmour PS; Nyska A; Schladweiler MC; McGee JK; Wallenborn JG; Richards JH; Kodavanti UP (2006). Cardiovascular and blood coagulative effects of pulmonary zinc exposure. *Toxicol Appl Pharmacol*, 211: 41-52. [088489](#)
- Gilmour PS; Rahman I; Donaldson K; MacNee W (2003). Histone acetylation regulates epithelial IL-8 release mediated by oxidative stress from environmental particles. *Am J Physiol Lung Cell Mol Physiol*, 284: L533-L540. [096959](#)
- Gilmour PS; Schladweiler MC; Nyska A; McGee JK; Thomas R; Jaskot RH; Schmid J; Kodavanti UP (2006). Systemic imbalance of essential metals and cardiac gene expression in rats following acute pulmonary zinc exposure. *J Toxicol Environ Health A Curr Iss*, 69: 2011-2032. [156472](#)
- Godleski JJ; Verrier RL; Koutrakis P; Catalano P; Coull B; Reinisch U; Lovett EG; Lawrence J; Murthy GG; Wolfson JM; Clarke RW; Nearing BD; Killingsworth C (2000). Mechanisms of morbidity and mortality from exposure to ambient air particles. *Res Rep Health Eff Inst*, 91: 5-88; discussion 89-103. [000738](#)
- Gopalakrishnan S; Van Emburgh BO; Robertson KD (2008). DNA methylation in development and human disease. *Mutat Res*, 647: 30-38. [191147](#)
- Gottipolu RR; Landa ER; Schladweiler MC; McGee JK; Ledbetter AD; Richards JH; Wallenborn GJ; Kodavanti UP (2008). Cardiopulmonary responses of intratracheally instilled tire particles and constituent metal components. *Inhal Toxicol*, 20: 473-84. [191148](#)

- Groneberg DA; Quarcoo D; Frossard N; Fischer A (2004). Neurogenic mechanisms in bronchial inflammatory diseases. *Allergy*, 59: 1139-52. [138134](#)
- Grunstein MM; Hazucha M; Sorli J; Milic-Emili J (1977). Effect of SO₂ on control of breathing in anesthetized cats. *J Appl Physiol*, 43: 844-851. [071445](#)
- Halvorsen B; Otterdal K; Dahl TB; Skjelland M; Gullestad L; Oie E; Aukrust P (2008). Atherosclerotic plaque stability-- what determines the fate of a plaque? *Prog Cardiovasc Dis*, 51: 183-94. [191149](#)
- Hanel B; Law I; Mortensen J (2003). Maximal rowing has an acute effect on the blood-gas barrier in elite athletes. *J Appl Physiol*, 95: 1076-1082. [155826](#)
- Hitchler MJ; Domann FE (2007). An epigenetic perspective on the free radical theory of development. *Free Radic Biol Med*, 43: 1023-1036. [191151](#)
- Huang Y-CT; Soukup J; Harder S; Becker S (2003). Mitochondrial oxidant production by a pollutant dust and NO-mediated apoptosis in human alveolar macrophage. *Am J Physiol Lung Cell Mol Physiol*, 284: C24-C32. [156573](#)
- Illum L (2006). Nasal clearance in health and disease. *J Aerosol Med*, 19: 92-99. [191205](#)
- Ilowite JS; Bennett WD; Sheetz MS; Groth ML; Nierman DM (1989). Permeability of the bronchial mucosa to 99mTc-DTPA in asthma. *Am Rev Respir Dis*, 139: 1139-1143. [156584](#)
- Imrich A; Ning Y; Lawrence J; Coull B; Gitin E; Knutson M; Kobzik L (2007). Alveolar macrophage cytokine response to air pollution particles: oxidant mechanisms. *Toxicol Appl Pharmacol*, 218: 256-264. [155859](#)
- Jaspers I; Ciencewicz JM; Zhang W; Brighton LE; Carson JL; Beck MA; Madden MC (2005). Diesel exhaust enhances influenza virus infections in respiratory epithelial cells. *Toxicol Sci*, 85: 990-1002. [088115](#)
- Jiang J; Oberdrster G; Elder A; Gelein R; Mercer P; Biswas P (2008). Does nanoparticle activity depend upon size and crystal phase? *Nanotoxicology*, 2: 33-42. [156609](#)
- Jones JG; Minty BD; Royston D; Royston JP (1983). Carboxyhaemoglobin and pulmonary epithelial permeability in man. *Thorax*, 38: 129-133. [155884](#)
- Jones PA; Baylin SB (2007). The epigenomics of cancer. *Cell*, 128: 683-92. [191153](#)
- Kaan PM; Hegele RG (2003). Interaction between respiratory syncytial virus and particulate matter in guinea pig alveolar macrophages. *Am J Respir Cell Mol Biol*, 28: 697-704. [095753](#)
- Karoly ED; Li Z; Dailey LA; Hyseni X; Huang YCT (2007). Up-regulation of Tissue Factor in Human Pulmonary Artery Endothelial Cells after Ultrafine Particle Exposure. *Environ Health Perspect*, 115: 535-540. [155890](#)
- Kaul N; Forman HJ (1996). Activation of NF- κ B by the respiratory burst of macrophages. *Free Radic Biol Med*, 21: 401-405. [155892](#)
- Keverne EB; Curley JP (2008). Epigenetics, brain evolution and behaviour. *Front Neuroendocrinol*, 29: 398-412. [191154](#)
- Kleinman MT; Araujo JA; Nel A; Sioutas C; Campbell A; Cong PQ; Li H; Bondy SC (2008). Inhaled ultrafine particulate matter affects CNS inflammatory processes and may act via MAP kinase signaling pathways. *Toxicol Lett*, 178: 127-130. [190074](#)
- Kodavanti UP; Schladweiler MC; Gilmour PS; Wallenborn JG; Mandavilli BS; Ledbetter AD; Christiani DC; Runge MS; Karoly ED; Costa DL; Peddada S; Jaskot R; Richards JH; Thomas R; Madamanchi NR; Nyska A (2008). The role of particulate matter-associated zinc in cardiac injury in rats. *Environ Health Perspect*, 116: 13-20. [155907](#)
- Koike E; Hirano S; Furuyama A; Kobayashi T (2004). cDNA microarray analysis of rat alveolar epithelial cells following exposure to organic extract of diesel exhaust particles. *Toxicol Appl Pharmacol*, 201: 178-185. [058555](#)
- Koike E; Kobayashi T (2005). Organic extract of diesel exhaust particles stimulates expression of Ia and costimulatory molecules associated with antigen presentation in rat peripheral blood monocytes but not in alveolar macrophages. *Toxicol Appl Pharmacol*, 209: 277-285. [088303](#)
- Lee CC; Cheng YW; Kang JJ (2005). Motorcycle exhaust particles induce IL-8 production through NF- κ B activation in human airway epithelial cells. *J Toxicol Environ Health A Curr Iss*, 68: 1537-1555. [156682](#)
- Lee SS; Woo CH; Chang JD; Kim JH (2003). Roles of Rac and cytosolic phospholipase A2 in the intracellular signalling in response to titanium particles. *Cell Signal*, 15: 339-345. [156678](#)

- Li J; Ghio AJ; Cho SH; Brinckerhoff CE; Simon SA; Liedtke W (2009). Diesel exhaust particles activate the matrix-metalloproteinase-1 gene in human bronchial epithelia in a beta-arrestin-dependent manner via activation of RAS. *Environ Health Perspect*, 117: 400-409. [190424](#)
- Li N; Nel AE (2006). Role of the Nrf2-mediated signaling pathway as a negative regulator of inflammation: Implications for the impact of particulate pollutants on asthma. *Antioxid Redox Signal*, 8: 88-98. [156694](#)
- Li N; Sioutas C; Cho A; Schmitz D; Misra C; Sempf J; Wang M; Oberley T; Froines J; Nel A (2003). Ultrafine particulate pollutants induce oxidative stress and mitochondrial damage. *Environ Health Perspect*, 111: 455-460. [042082](#)
- Li N; Wang M; Bramble LA; Schmitz DA; Schauer JJ; Sioutas C; Harkema JR; Nel AE (2009). The adjuvant effect of ambient particulate matter is closely reflected by the particulate oxidant potential. *Environ Health Perspect*, 117: 1116-1123. [190457](#)
- Li Y-J; Kawada T; Matsumoto A; Azuma A; Kudoh S; Takizawa H; Sugawara I (2007). Airway inflammatory responses to oxidative stress induced by low-dose diesel exhaust particle exposure differ between mouse strains. *Exp Lung Res*, 33: 227-244. [155929](#)
- Libby P (2002). Inflammation in atherosclerosis. *Nature*, 420: 868-874. [192009](#)
- Lindbom J; Gustafsson M; Blomqvist G; Dahl A; Gudmundsson A; Swietlicki E; Ljungman AG (2007). Wear particles generated from studded tires and pavement induces inflammatory reactions in mouse macrophage cells. *Chem Res Toxicol*, 20: 937-946. [155934](#)
- Liu J; Ballaney M; Al-Alem U; Quan C; Jin X; Perera F; Chen LC; Miller RL (2008). Combined Inhaled Diesel Exhaust Particles and Allergen Exposure Alter Methylation of T Helper Genes and IgE Production In Vivo. *Toxicol Sci*, 102: 76-81. [156709](#)
- Long JF; Waldman WJ; Kristovich R; Williams M; Knight D; Dutta PK (2005). Comparison of ultrastructural cytotoxic effects of carbon and carbon/iron particulates on human monocyte-derived macrophages. *Environ Health Perspect*, 113: 170-174. [087454](#)
- Longhurst JC; Tjen-a-looi SC; Fu LW (2001). Cardiac sympathetic afferent activation provoked by myocardial ischemia and reperfusion. Mechanisms and reflexes. *Ann N Y Acad Sci*, 940: 74-95. [191158](#)
- Lund AK; Lucero J; Lucas S; Madden MC; McDonald JD; Seagrave JC; Knuckles TL; Campen MJ (2009). Vehicular emissions induce vascular MMP-9 expression and activity associated with endothelin-1 mediated pathways. *Arterioscler Thromb Vasc Biol*, 29: 511-517. [180257](#)
- Mackman N (2005). Tissue-Specific Hemostasis in Mice. *Arterioscler Thromb Vasc Biol*, 25: 2273-2281. [156722](#)
- Mercer BA; Kolesnikova N; Sonett J; D'Armiento J (2004). Extracellular regulated kinase/mitogen activated protein kinase is up-regulated in pulmonary emphysema and mediates matrix metalloproteinase-1 induction by cigarette smoke. *J Biol Chem*, 279: 17690-17696. [191180](#)
- Moffitt JA; Grippo AJ; Holmes PV; Johnson AK (2002). Olfactory bulbectomy attenuates cardiovascular sympathoexcitatory reflexes in rats. *Am J Physiol Heart Circ Physiol*, 283: H2575-H2583. [191160](#)
- Molinelli AR; Madden MC; McGee JK; Stonehuerner JG; Ghio AJ (2002). Effect of metal removal on the toxicity of airborne particulate matter from the Utah Valley. *Inhal Toxicol*, 14: 1069-1086. [035347](#)
- Moller W; Brown DM; Kreyling WG; Stone V (2005). Ultrafine particles cause cytoskeletal dysfunctions in macrophages: role of intracellular calcium. *Part Fibre Toxicol*, 2: 7. [156770](#)
- Monn C; Naef R; Koller T (2003). Reactions of macrophages exposed to particles <10 "micron"m. *Environ Res*, 91: 35-44. [052418](#)
- Mutlu GM; Green D; Bellmeyer A; Baker CM; Burgess Z; Rajamannan N; Christman JW; Foiles N; Kamp DW; Ghio AJ; Chandel NS; Dean DA; Sznajder JI; Budinger GR (2007). Ambient particulate matter accelerates coagulation via an IL-6-dependent pathway. *J Clin Invest*, 117: 2952-2961. [121441](#)
- Nadel JA; Salem H; Tamplin B; Tokiwa Y (1965). Mechanism of bronchoconstriction during inhalation of sulfur dioxide. *J Appl Physiol*, 20: 164-167. [014846](#)
- Newby AC (2008). Metalloproteinase expression in monocytes and macrophages and its relationship to atherosclerotic plaque instability. *Arterioscler Thromb Vasc Biol*, 28: 2108-2114. [191161](#)

- Nurkiewicz TR; Porter DW; Barger M; Millecchia L; Rao KMK; Marvar PJ; Hubbs AF; Castranova V; Boegehold MA (2006). Systemic microvascular dysfunction and inflammation after pulmonary particulate matter exposure. *Environ Health Perspect*, 114: 412-419. [088611](#)
- Nurkiewicz TR; Porter DW; Hubbs AF; Stone S; Chen BT; Frazer DG; Boegehold MA; Castranova V (2009). Pulmonary nanoparticle exposure disrupts systemic microvascular nitric oxide signaling. *Toxicol Sci*, 110: 191-203. [191961](#)
- Oberdörster G (1988). Lung clearance of inhaled insoluble and soluble particles. *J Aerosol Med*, 1: 289-330. [006857](#)
- Oortgiesen M; Veronesi B; Eichenbaum G; Kiser PF; Simon SA (2000). Residual oil fly ash and charged polymers activate epithelial cells and nociceptive sensory neurons. *Am J Physiol*, 278: L683-L695. [013998](#)
- Owen CA (2008). Roles for proteinases in the pathogenesis of chronic obstructive pulmonary disease. *Int J of COPD*, 3: 253-268. [191162](#)
- Pardo A; Selman M (2005). MMP-1: the elder of the family. *Int J Biochem Cell Biol*, 37: 283-8. [191163](#)
- Penn A; Murphy G; Barker S; Henk W; Penn L (2005). Combustion-derived ultrafine particles transport organic toxicants to target respiratory cells. *Environ Health Perspect*, 113: 956-963. [088257](#)
- Pinkerton KE; Joad JP (2006). Influence of air pollution on respiratory health during perinatal development. *Clin Exp Pharmacol Physiol*, 33: 269-272. [091237](#)
- Rahman I; Biswas SK; Kode A (2006). Oxidant and antioxidant balance in the airways and airway diseases. *Eur J Pharmacol*, 533: 222-39. [191165](#)
- Ramage L; Guy K (2004). Expression of C-reactive protein and heat-shock protein-70 in the lung epithelial cell line A549, in response to PM10 exposure. *Inhal Toxicol*, 16: 447-452. [055640](#)
- Randell SH; Mercer RR; Young SL (1990). Neonatal hyperoxia alters the pulmonary alveolar and capillary structure of 40-day-old rats. *Am J Pathol*, 136: 1259-1266. [191956](#)
- Reed MD; Barrett EG; Campen MJ; Divine KK; Gigliotti AP; McDonald JD; Seagrave JC; Mauderly JL; Seilkop SK; Swenberg JA (2008). Health effects of subchronic inhalation exposure to gasoline engine exhaust. *Inhal Toxicol*, 20: 1125-1143. [156903](#)
- Rengasamy A; Barger MW; Kane E; Ma JKH; Castranova V; Ma JYC (2003). Diesel exhaust particle-induced alterations of pulmonary phase I and phase II enzymes of rats. *J Toxicol Environ Health A Curr Iss*, 66: 153-167. [156907](#)
- Rhoden CR; Lawrence J; Godleski JJ; Gonzalez-Flecha B (2004). N-acetylcysteine prevents lung inflammation after short-term inhalation exposure to concentrated ambient particles. *Toxicol Sci*, 79: 296-303. [087969](#)
- Rhoden CR; Wellenius GA; Ghelfi E; Lawrence J; Gonzalez-Flecha B (2005). PM-induced cardiac oxidative stress and dysfunction are mediated by autonomic stimulation. *Biochim Biophys Acta*, 1725: 305-313. [087878](#)
- Rinderknecht J; Shapiro L; Krauthammer M; Taplin G; Wasserman K; Uszler JM; Effros RM (1980). Accelerated clearance of small solutes from the lungs in interstitial lung disease. *Am Rev Respir Dis*, 121: 105-117. [191965](#)
- Risom L Moller P; Loft S (2005). Oxidative stress-induced DNA damage by particulate air pollution. *Mutat Res*, 592: 119-137. [089070](#)
- Roberts ES; Richards JH; Jaskot R; Dreher KL (2003). Oxidative stress mediates air pollution particle-induced acute lung injury and molecular pathology. *Inhal Toxicol*, 15: 1327-1346. [156051](#)
- Roberts JR; Young S-H; Castranova V; Antonini JM (2007). Soluble metals in residual oil fly ash alter innate and adaptive pulmonary immune responses to bacterial infection in rats. *Toxicol Appl Pharmacol*, 221: 306-319. [097623](#)
- Rouse RL; Murphy G; Boudreaux MJ; Paulsen DB; Penn AL (2008). Soot nanoparticles promote biotransformation, oxidative stress, and inflammation in murine lungs. *Am J Respir Cell Mol Biol*, 39: 198-207. [156930](#)
- Ruckerl R; Greven S; Ljungman P; Aalto P; Antoniadis C; Bellander T; Berglind N; Chrysohoou C; Forastiere F; Jacquemin B; von Klot S; Koenig W; Kuchenhoff H; Lanki T; Pekkanen J; Perucci CA; Schneider A; Sunyer J; Peters A (2007). Air pollution and inflammation (interleukin-6, C-reactive protein, fibrinogen) in myocardial infarction survivors. *Environ Health Perspect*, 115: 1072-1080. [156931](#)
- Sakamoto N; Hayashi S; Gosselink J; Ishii H; Ishimatsu Y; Mukae H; Hogg JC; van Eeden SF (2007). Calcium dependent and independent cytokine synthesis by air pollution particle-exposed human bronchial epithelial cells. *Toxicol Appl Pharmacol*, 225: 134-141. [096282](#)

- Sarin S; Undem B; Sanico A; Togias A (2006). The role of the nervous system in rhinitis. *J Allergy Clin Immunol*, 118: 999-1016. [191166](#)
- Schins RPF; Knaapen AM (2007). Genotoxicity of poorly soluble particles. *Inhal Toxicol*, 19 Suppl 1: 189-198. [156074](#)
- Seaton A; MacNee W; Donaldson K; Godden D (1995). Particulate air pollution and acute health effects. *Lancet*, 345: 176-178. [045721](#)
- Sekizawa S; Chen CY; Bechtold AG; Tabor JM; Bric JM; Pinkerton KE; Joad JP; Bonham AC (2008). Extended secondhand tobacco smoke exposure induces plasticity in nucleus tractus solitarius second-order lung afferent neurons in young guinea pigs. *Eur J Neurosci*, 28: 771-81. [191167](#)
- Semmler-Behnke M; Takenaka S; Fertsch S; Wenk A; Seitz J; Mayer P; Oberdörster G; Kreyling WG (2007). Efficient elimination of inhaled nanoparticles from the alveolar region: evidence for interstitial uptake and subsequent reentrainment onto airways epithelium. *Environ Health Perspect*, 115: 728-733. [156080](#)
- Shi T; Knaapen AM; Begerow J; Birmili W; Borm PJA; Schins RPF (2003). Temporal variation of hydroxyl radical generation and 8-hydroxy-2'-deoxyguanosine formation by coarse and fine particulate matter. *Occup Environ Med*, 60: 315-321. [088248](#)
- Sirivelu MP; MohanKumar SMJ; Wagner JG; Harkema JR; MohanKumar PS (2006). Activation of the stress axis and neurochemical alterations in specific brain areas by concentrated ambient particle exposure with concomitant allergic airway disease. *Environ Health Perspect*, 114: 870-874. [111151](#)
- Snipes MB (1996). Current information on lung overload in nonrodent mammals: contrast with rats. *Inhal Toxicol*, 8: 91-109. [076041](#)
- Snipes MB; Harkema JR; Hotchkiss JA; Bice DE (1997). Neutrophil Involvement in the Retention and Clearance of Dust Intratracheally Instilled into the LUNGS of F344/N Rats. *Exp Lung Res*, 23: 65-84. [156092](#)
- Soberanes S; Panduri V; Mutlu GM; Ghio A; Bundinger GRS; Kamp DW (2006). p53 mediates particulate matter-induced alveolar epithelial cell mitochondria-regulated apoptosis. *Am J Respir Crit Care Med*, 174: 1229-1238. [156991](#)
- Soberanes S; Urich D; Baker CM; Burgess Z; Chiarella SE; Bell EL; Ghio AJ; De Vizcaya-Ruiz A; Liu J; Ridge KM; Kamp DW; Chandel NS; Schumacker PT; Mutlu GM; Budinger GRS (2009). Mitochondrial complex III-generated oxidants activate ASK1 and JNK to induce alveolar epithelial cell death following exposure to particulate matter air pollution. *J Biol Chem*, 284: 2176-2186. [190483](#)
- Steenberg PA; Withagen CET; van Dalen WJ; Dormans JAMA; van Loveren H (2004). Adjuvant Activity of Ambient Particulate Matter in Macrophage Activity-Suppressed, N-Acetylcysteine-Treated, iNOS- and IL-4-Deficient Mice. *Inhal Toxicol*, 16: 835-843. [087981](#)
- Sun Q; Wang A; Jin X; Natanzon A; Duquaine D; Brook RD; Aguinaldo JG; Fayad ZA; Fuster V; Lippmann M; Chen LC; Rajagopalan S (2005). Long-term air pollution exposure and acceleration of atherosclerosis and vascular inflammation in an animal model. *JAMA*, 294: 3003-3010. [087952](#)
- Takizawa H; Abe S; Okazaki H; Kohyama T; Sugawara I; Saito Y; Ohtoshi T; Kawasaki S; Desaki M; Nakahara K; Yamamoto K; Matsushima K; Tanaka M; Sagai M; Kudoh S (2003). Diesel exhaust particles upregulate eotaxin gene expression in human bronchial epithelial cells via nuclear factor-kappa B-dependent pathway. *Am J Physiol Lung Cell Mol Physiol*, 284: L1055-L1062. [157039](#)
- Tal TL; Graves LM; Silbajoris R; Bromberg PA; Wu W; Samet JM (2006). Inhibition of protein tyrosine phosphatase activity mediates epidermal growth factor receptor signaling in human airway epithelial cells exposed to Zn²⁺. *Toxicol Appl Pharmacol*, 214: 16-23. [108588](#)
- Tamaoki J; Isono K; Takeyama K; Tagaya E; Nakata J; Nagai A (2004). Ultrafine carbon black particles stimulate proliferation of human airway epithelium via EGF receptor-mediated signaling pathway. *Am J Physiol Lung Cell Mol Physiol*, 287: L1127-L1133. [157040](#)
- Tankersley CG; Shank JA; Flanders SE; Soutiere SE; Rabold R; Mitzner W; Wagner EM (2003). Changes in lung permeability and lung mechanics accompany homeostatic instability in senescent mice. *J Appl Physiol*, 95: 1681-1687. [096363](#)
- Tao F; Gonzalez-Flecha B; Kobzik L (2003). Reactive oxygen species in pulmonary inflammation by ambient particulates. *Free Radic Biol Med*, 35: 327-340. [156111](#)

- Tao F; Kobzik L (2002). Lung macrophage-epithelial cell interactions amplify particle-mediated cytokine release. *Am J Respir Cell Mol Biol*, 26: 499-505. [157044](#)
- Tarantini L; Bonzini M; Apostoli P; Pegoraro V; Bollati V; Marinelli B; Cantone L; Rizzo G; Hou L; Schwartz J; Bertazzi PA; Baccarelli A (2009). Effects of particulate matter on genomic DNA methylation content and iNOS promoter methylation. *Environ Health Perspect*, 117: 217-222. [192010](#)
- Tarantini L; Bonzini M; Apostoli P; Pegoraro V; Bollati V; Marinelli B; Cantone L; Rizzo G; Hou L; Schwartz J; Bertazzi PA; Baccarelli A (2009). Errata to Effects of particulate matter on genomic DNA methylation content and iNOS promoter methylation. *Environ Health Perspect*, 117: A143. [192153](#)
- Thomson E; Kumarathasan P; Goegan P; Aubin RA; Vincent R (2005). Differential regulation of the lung endothelin system by urban particulate matter and ozone. *Toxicol Sci*, 88: 103-113. [087554](#)
- Upadhyay D; Panduri V; Ghio A; Kamp DW (2003). Particulate matter induces alveolar epithelial cell DNA damage and apoptosis: role of free radicals and the mitochondria. *Am J Respir Cell Mol Biol*, 29: 180-187. [097370](#)
- Valinluck V; Tsai HH; Rogstad DK; Burdzy A; Bird A; Sowers LC (2004). Oxidative damage to methyl-CpG sequences inhibits the binding of the methyl-CpG binding domain (MBD) of methyl-CpG binding protein 2 (MeCP2). *Nucleic Acids Res*, 32: 4100-8. [191170](#)
- Van Eeden SF; Hogg JC (2002). Systemic inflammatory response induced by particulate matter air pollution: the importance of bone-marrow stimulation. *J Toxicol Environ Health A Curr Iss*, 65: 65:1597-1613. [088111](#)
- Van Eeden SF; Tan WC; Suwa T; Mukae H; Terashima T; Fujii T; Qui D; Vincent R; Hogg JC (2001). Cytokines involved in the systemic inflammatory response induced by exposure to particulate matter air pollutants (PM10). *Am J Respir Crit Care Med*, 164: 826-830. [019018](#)
- van Eeden SF; Yeung A; Quinlan K; Hogg JC (2005). Systemic response to ambient particulate matter: relevance to chronic obstructive pulmonary disease. *Proc Am Thorac Soc*, 2: 61-67. [157086](#)
- Veronesi B; Makwana O; Pooler M; Chen LC (2005). Effects of subchronic exposures to concentrated ambient particles: VII. Degeneration of dopaminergic neurons in Apo E^{-/-} mice. *Inhal Toxicol*, 17: 235-241. [087481](#)
- Veronesi B; Oortgiesen M (2001). Neurogenic inflammation and particulate matter (PM) air pollutants. *Neurotoxicology*, 22: 795-810. [015977](#)
- Veronesi B; Oortgiesen M; Carter JD; Devlin RB (1999). Particulate matter initiates inflammatory cytokine release by activation of capsaicin and acid receptors in a human bronchial epithelial cell line. *Toxicol Appl Pharmacol*, 154: 106-115. [048764](#)
- Veronesi B; Oortgiesen M; Roy J; Carter JD; Simon SA; Gavett SH (2000). Vanilloid (capsaicin) receptors influence inflammatory sensitivity in response to particulate matter. *Toxicol Appl Pharmacol*, 169: 66-76. [017062](#)
- Veronesi B; Wei G; Zeng JQ; Oortgiesen M (2003). Electrostatic charge activates inflammatory vanilloid (VR1) receptors. *Neurotoxicology*, 24: 463-473. [094384](#)
- Wallenborn JG; Evansky P; Shannahan JH; Vallanat B; Ledbetter AD; Schladweiler MC; Richards JH; Gottipolu RR; Nyska A; Kodavanti UP (2008). Subchronic inhalation of zinc sulfate induces cardiac changes in healthy rats. *Toxicol Appl Pharmacol*, 232: 69-77. [191171](#)
- Wallenborn JG; Kovalcik KD; McGee JK; Landis MS; Kodavanti UP (2009). Systemic translocation of (70)zinc: kinetics following intratracheal instillation in rats. *Toxicol Appl Pharmacol*, 234: 25-32. [191172](#)
- Wallenborn JG; McKee JK; Schladweiler MC; Ledbetter AD; Kodavanti UP (2007). Systemic translocation of particulate matter-associated metals following a single intratracheal instillation in rats. *J Toxicol Sci*, 98: 231-239. [156144](#)
- Wan H; Winton HL; Soeller C; Tovey ER; Gruenert DC; Thompson PJ; Stewart GA; Taylor GW; Garrod DR; Cannell MB; Robinson C (1999). Der p 1 facilitates transepithelial allergen delivery by disruption of tight junctions. *J Clin Invest*, 104: 123-133. [191903](#)
- Wan J; Diaz-Sanchez D (2006). Phase II enzymes induction blocks the enhanced IgE production in B cells by diesel exhaust particles. *J Immunol*, 177: 3477-3483. [097399](#)
- Wan J; Diaz-Sanchez D (2007). Antioxidant enzyme induction: a new protective approach against the adverse effects of diesel exhaust particles. *Inhal Toxicol*, 19 Suppl 1: 177-182. [156145](#)

- Wang L; Pinkerton KE (2007). Air pollutant effects on fetal and early postnatal development. *Birth Defects Res C Embryo Today*, 81: 144-154. [179975](#)
- Warheit DB; Webb TR; Colvin VL; Reed KL; Sayes CM (2007). Pulmonary bioassay studies with nanoscale and fine-quartz particles in rats: toxicity is not dependent upon particle size but on surface characteristics. *Toxicol Sci*, 95: 270-280. [090482](#)
- Widdicombe J (2006). Reflexes from the lungs and airways: historical perspective. *J Appl Physiol*, 101: 628-634. [155519](#)
- Widdicombe J; Lee L-Y (2001). Airway reflexes, autonomic function, and cardiovascular responses. *Environ Health Perspect*, 4: 579-584. [019049](#)
- Widdicombe JG (2003). Overview of neural pathways in allergy and asthma. *Pulm Pharmacol Ther*, 16: 23-30. [157145](#)
- Win-Shwe TT; Yamamoto S; Fujitani Y; Hirano S; Fujimaki H (2008). Spatial learning and memory function-related gene expression in the hippocampus of mouse exposed to nanoparticle-rich diesel exhaust. *Neurotoxicology*, 29: 940-947. [190146](#)
- Wong SS; Sun NN; Keith I; Kweon C-B; Foster DE; Schauer James J; Witten ML (2003). Tachykinin substance P signaling involved in diesel exhaust-induced bronchopulmonary neurogenic inflammation in rats. *Arch Toxicol*, 77: 638-650. [097707](#)
- Wright RO; Baccarelli A (2007). Metals and neurotoxicology. *J Nutr*, 137: 2809-2813. [191173](#)
- Xia T; Korge P; Weiss JN; Li N; Venkatesen MI; Sioutas C; Nel A (2004). Quinones and aromatic chemical compounds in particulate matter induce mitochondrial dysfunction: implications for ultrafine particle toxicity. *Environ Health Perspect*, 112: 1347-1358. [087486](#)
- Xiao GG; Nel AE; Loo JA (2005). Nitrotyrosine-modified proteins and oxidative stress induced by diesel exhaust particles. *Electrophoresis*, 26: 280-292. [156164](#)
- Yauk C; Polyzos A; Rowan-Carroll A; Somers CM; Godschalk RW; Van Schooten FJ; Berndt ML; Pogribny IP; Koturbash I; Williams A; Douglas GR; Kovalchuk O (2008). Germ-line mutations, DNA damage, and global hypermethylation in mice exposed to particulate air pollution in an urban/industrial location. *PNAS*, 105: 605-610. [157164](#)
- Yin XJ; Ma JYC; Antonini JM; Castranova V; Ma JKH (2004). Roles of reactive oxygen species and heme oxygenase-1 in modulation of alveolar macrophage-mediated pulmonary immune responses to listeria monocytogenes by diesel exhaust particles. *Toxicol Sci*, 82: 143-153. [087983](#)
- Ying Z; Kampfrath T; Thurston G; Farrar B; Lippmann M; Wang A; Sun Q; Chen LC; Rajagopalan S (2009). Ambient particulates alter vascular function through induction of reactive oxygen and nitrogen species. *Toxicol Sci*, 111: 80-88. [190111](#)
- Zhang J; Ghio AJ; Chang W; Kamdar O; Rosen GD; Upadhyay D (2007). Bim mediates mitochondria-regulated particulate matter-induced apoptosis in alveolar epithelial cells. *FEBS Lett*, 581: 4148-4152. [156179](#)
- Zhao H; Barger MW; Ma JKH; Castranova V; Ma JYC (2006). Cooperation of the inducible nitric oxide synthase and cytochrome P450 1A1 in mediating lung inflammation and mutagenicity induced by diesel exhaust particles. *Environ Health Perspect*, 114: 1253-1258. [100996](#)

Chapter 6. Integrated Health Effects of Short-Term PM Exposure

6.1. Introduction

This chapter reviews, summarizes, and integrates the evidence of relationships between short-term exposures to PM and a variety of health-related outcomes and endpoints. Cardiovascular and respiratory health effects of short-term exposure to various size fractions and sources of PM have been examined in numerous epidemiologic, controlled human exposure and toxicological studies. In addition, there is a large body of literature evaluating the relationship between mortality and short-term exposure to PM. The association between PM exposure and central nervous system function has also been assessed, although far fewer studies are available. The research approaches used to evaluate health effects of PM exposure are described in Section 1.5 along with advantages and limitations of the various study types. Chapter 5 provides an overview of the potential pathophysiological pathways and modes of action underlying the PM-induced health effects observed in animal and human studies. Evidence from the scientific literature of specific cardiovascular and systemic effects, respiratory effects, and central nervous system (CNS) effects associated with exposure to PM are presented in Sections 6.2, 6.3, and 6.4, respectively. Evidence of associations between short-term exposure to PM and mortality are described in Section 6.5. The chapter concludes with an evaluation of PM-induced health effects attributable to specific constituents or sources (Section 6.6). More detailed descriptions of each study evaluated for this assessment are presented in Annexes C, D, E, and F.

Findings for cardiovascular and respiratory effects are presented by specific endpoint or measure of effect, leading from more subtle health outcome measures (e.g., heart rate variability [HRV]) to the more severe, such as hospitalization and mortality for cardiovascular disease. Conclusions from the 2004 PM AQCD (U.S. EPA, 2004, [056905](#)) are briefly summarized at the beginning of each section, and the evaluation of evidence from recent studies builds upon what was available during the previous review. For each health outcome, results are summarized for studies from the specific scientific discipline, i.e., epidemiologic, controlled human exposure, and toxicological studies. The sections conclude with summaries of the evidence on the various health outcomes and integration of the findings that leads to conclusions regarding causality based upon the framework described in Chapter 1. Determination of causality is made for the overall health effect category, such as cardiovascular effects, with coherence, consistency and biological plausibility being based upon the evidence from across disciplines and also across the suite of related health outcomes ranging from the more subtle health outcomes to cause-specific mortality. In the summary sections for cardiovascular and respiratory effects and all-cause mortality, the evidence is summarized and independent conclusions drawn for relationships with PM_{2.5}, PM_{10-2.5}, and ultrafine particles (UFPs) (Sections 6.2.12, 6.3.10, and 6.5.3, respectively). Evidence of central nervous system effects is also divided by scientific discipline; however, the lack of data does not allow for informative summaries of effect by PM metric in discussing CNS effects (Section 6.4.4).

▪ Note: Hyperlinks to the reference citations throughout this document will take you to the NCEA HERO database (Health and Environmental Research Online) at <http://epa.gov/hero>. HERO is a database of scientific literature used by U.S. EPA in the process of developing science assessments such as the Integrated Science Assessments (ISA) and the Integrated Risk Information System (IRIS).

6.2. Cardiovascular and Systemic Effects

6.2.1. Heart Rate and Heart Rate Variability

Heart rate (HR), HRV, and BP are all regulated, in part, by the sympathetic and parasympathetic nervous systems. Changes in one or more may increase the risk of cardiovascular events (e.g., arrhythmias, MI, etc.). Decreases in HRV have been associated with cardiovascular mortality/morbidity in older adults and those with significant heart disease (TFESC, 1996, [003061](#)). In addition, decreased HRV may precede some clinically important arrhythmias, such as atrial fibrillation, as well as sudden cardiac death, in high risk populations (Chen and Tan, 2007, [197461](#); Sandercock and Brodie, 2006, [197465](#); Thong and Raitt, 2007, [197462](#)).

HRV is measured using electrocardiograms (ECG) and can be analyzed in the time domain (e.g., standard deviation of all NN intervals [SDNN], square root of the mean squared successive NN interval differences [rMSSD]), and/or the frequency domain measured by power spectral analysis (e.g., high frequency [HF], low frequency [LF], ratio of LF to HF [LF/HF]). SDNN generally reflects the overall modulation of HR by the autonomic nervous system (ANS), whereas rMSSD and frequency variations in HR generally reflect parasympathetic activity. Thus, rMSSD is generally well correlated with HF, which also reflects the parasympathetic modulation of HR. LF is predominately determined by both sympathetic and parasympathetic tone and increased LF/HF indicates sympathoexcitation, which correlates with decreased overall HRV (SDNN, rMSSD). Thus LF/HF is thought to estimate the ratio of sympathetic influences on HR to parasympathetic influences.

While HRV is commonly described as being a reflection of vagal and adrenergic input to the heart, there is clearly a more complex phenomenon reflected in HRV parameters. Rowan et al. (2007, [191911](#)) provide a review of HRV and its use and interpretation with respect to air pollution studies. To summarize, HRV indices are excellent measures of extrapulmonary effects from inhaled pollutants, but the characterization of the acute, reversible responses to air pollution as being either parasympathetic or sympathetic in origin, much less predictive of some adverse outcomes such as ventricular arrhythmia, is relatively unsupported by the clinical literature. This is consistent with the 2004 PM AQCD (U.S. EPA, 2004, [056905](#)) which stated that there is inherent variability in the minute-to-minute spectral measurements, but long-term HRV measures demonstrate excellent day-to-day reproducibility.

The 2004 PM AQCD (U.S. EPA, 2004, [056905](#)) presented limited evidence of PM-induced changes in HRV. However, findings from epidemiologic, controlled human exposure and toxicological studies demonstrated both decreases and increases in HRV following PM exposure. Recent epidemiologic studies have demonstrated a more consistent decrease in HRV (SDNN and rMSSD), which is supported by several controlled human exposure studies published since 2003. In these studies, decreases in HRV were observed among healthy adults following short-term exposures to PM_{2.5} and PM_{10-2.5} CAPs. It is interesting to note that these effects were not observed in adults with asthma or COPD. The effect of PM on HRV observed in animal toxicological studies continues to vary greatly, which may be due in part to strain differences in baseline HRV.

6.2.1.1. Epidemiologic Studies

The 2004 PM AQCD (U.S. EPA, 2004, [056905](#)) reviewed several studies of PM exposure and HR or HRV and described mixed findings across studies. Several additional studies have investigated the association between acute changes in multiple HRV parameters and ambient air pollutant concentrations in the U.S., Canada, Europe, Mexico, and Asia. Features and results of these studies are presented in Table 6-1, and are summarized below.

In a multicity study, Liao and colleagues (2004, [056590](#)) used data from the fourth cohort evaluation of the Atherosclerosis Risk in Communities (ARIC) Study (1996-1998). The 6,784 subjects were 45-64 yr of age and lived in Washington County, MD, Forsyth County, NC, or the suburbs of Minneapolis, MN. Linear regression models were used to examine the change in HRV associated with PM₁₀, O₃, SO₂, CO, and NO₂ concentrations in the 1-3 days prior to ECG measurement. Among all subjects, each 11.5 µg/m³ increase in mean daily PM₁₀ concentration 1 day before the ECG measurement was associated with a 0.06 ms² decrease in log-transformed HF (95%

CI: -0.10 to -0.02) and a 1.03 ms decrease in SDNN (95% CI: -1.64 to -0.42). A smaller non-significant decrease was also observed for log transformed LF. This reduction in cardiac autonomic control was larger among hypertensive subjects, suggesting that this group may be susceptible to the effects of PM.

In a study of randomly selected participants in the Women's Health Initiative (WHI), a multicity U.S. study, Whitsel et al. (2009, [191980](#)) found decreases in rMSSD and SDNN in association with PM₁₀ concentration. The associations were stronger among participants with diabetes. For example, in subjects with impaired fasting glucose, the reduction in rMSSD was 8.3% (-13.9, -2.4) among those with high levels of insulin and 0.6% (-2.1, 1.6) among those with low levels of insulin. Similar results were observed comparing high and low levels of insulin resistance.

Timonen et al. (2006, [088747](#)) conducted a multicity panel study of elderly subjects with stable coronary heart disease who lived in 3 European cities (Amsterdam, the Netherlands; Erfurt, Germany; or Helsinki, Finland). They collected ECGs biweekly for six months in each subject. This analysis, done as part of the ULTRA Study, examined changes in HRV (resting, paced breathing, supine, and 5-min beat-to-beat NN intervals) associated with changes in fixed monitor particulate concentrations (PM_{2.5}, PM_{10-2.5}) with an emphasis on counts of UFPs (0.01-0.1 μm particles) and accumulation mode particles (ACP; 0.1-1.0 μm particles). Mixed models were first fit to estimate the change in HRV associated with PM (UFP, ACP, PM_{2.5}, and PM_{10-2.5}) concentrations on the same and previous 4 days in each city. In pooled analyses, the most consistent results identified were for LF/HF (Table 6-1). Estimates for PM_{2.5}, however, differed across cities. PM_{2.5} was associated with decreased HF power and increased LF/HF in Helsinki, increased HF power and decreased LF/HF in Erfurt, and not associated with any HRV metric in Amsterdam. In a subsequent analysis, de Hartog et al. (2009, [191904](#)) investigated whether exposure misclassification, effect modification by medication use, or particle composition differences across the three cities could explain the result observed. These authors found that PM_{2.5} apportioned from traffic, long-range transported PM_{2.5} and outdoor PM_{2.5} were associated with reduced HRV most strongly among those not taking beta-blockers (Table 6-1). Indoor and personal PM_{2.5} were not associated with decreased HRV in this study. Therefore, the authors concluded that effect modification by medication use and particle composition differences across the three cities may, in part, explain the heterogeneous PM_{2.5} findings in the previous analysis.

The association between HRV and short-term increases in PM_{2.5}, PM_{10-2.5}, PM₁₀, other size fractions and components was also examined in single-city studies conducted in the U.S. or Canada (Table 6-1). Among U.S. and Canadian cities, increases in PM_{2.5} were generally associated with decreased SDNN and/or decreased HF power but not in all studies. However, studies also reported increased SDNN associated with PM_{2.5} concentrations (Riediker et al., 2004, [056992](#); Wheeler et al., 2006, [088453](#)). In addition, Yeatts et al. (2007, [091266](#)) reported increased rMSSD and HF power with increased PM_{2.5} concentrations as well as SDANN5 (standard deviation of the average of normal to normal intervals in all 5-min intervals in a 24-h period), and SDNN24HR (standard deviation of the average of all normal to normal intervals in a 24-h period).

Other size fractions (e.g. coarse PM and UFPs) were also associated with decreases in HRV metrics in several single-city studies conducted in the U.S. or Canada. Lipsett et al. (2006, [088753](#)) reported significantly decreased SDNN associated with increases in 2- and 6-h mean PM₁₀ and PM_{10-2.5} concentrations. Yeatts et al. (2007, [091266](#)) reported decreased rMSSD, SDNN24HR, SDANN5, ASDNN5 (mean of the standard deviation in all 5-min segments of a 24-h recording), proportion of NN intervals <50 m apart (pNN50) (7 min and 24 h), and HF power associated with increased PM_{10-2.5} concentration. Of those studies examining HRV associations with particle counts (Adar et al., 2007, [001458](#); Park et al., 2005, [057331](#)), only Adar et al. (2007, [001458](#)) found clear evidence of such effects (e.g., decreased SDNN, LF, HF). Decreased HRV was also associated with increases in ambient mean SO₄²⁻ concentration (Luttmann-Gibson et al., 2006, [089794](#)), ambient mean BC concentration (Park et al., 2005, [057331](#); Schwartz et al., 2005, [074317](#)), and traffic generated particles/pollution (Adar et al., 2007, [001458](#); Riediker et al., 2004, [056992](#)) in these single-city studies.

Studies in Asia, Europe, and Mexico have also reported decreases in one or several HRV metrics (Table 6-1) associated with increases in PM_{2.5} concentration or other size fractions. However, a study conducted in Scotland reported no PM-HRV associations (Barclay et al., 2009, [179935](#)). Riojas-Rodriguez et al. (2006, [156913](#)) reported significantly decreased LF and HF power associated with each 1 ppm increase in CO concentration, but only small non-significant decreases associated with PM_{2.5}.

Summary of Epidemiologic Studies of Heart Rate and HRV

HRV studies investigated lagged pollutant concentrations from 2 h-5 days before ECG measurement, reporting effects associated with mean pollutant concentrations lagged as short as 1-2 h, and more consistently with lags of 24-48 h. Taken together, these international and U.S./Canadian studies show decreases in HRV associated with PM_{2.5} in most studies that use SDNN, rMSSD or HF power. The effects of PM_{10-2.5}, UFPs, and components were evaluated in fewer studies but associations with decreased HRV (e.g., both time and frequency measures) were observed. PM₁₀ studies also found evidence for PM-induced alterations in HRV, however, it is difficult to determine which size fraction of PM₁₀ (e.g., PM_{10-2.5}, PM_{2.5} or UFPs) imparts the effects observed. As a result, PM₁₀ studies provide supportive evidence for the overall effect of PM on HRV, but not for a specific size fraction. The proportion of studies reporting decreases in HRV may be inflated by publication bias (i.e., studies showing little or no effects are not submitted for publication).

HRV Studies Investigating Specific Mechanisms

Panel studies investigating PM-HRV associations have also been useful in investigating potential mechanistic pathways by which PM may elicit a cardiovascular response. A series of analyses using data from the Normative Aging Study, a cohort of older men living in the Boston metropolitan area, has also provided mechanistic insights into the PM-HRV association (Baccarelli et al., 2008, [191959](#); Chahine et al., 2007, [156327](#); Park et al., 2005, [057331](#); Park et al., 2006, [091245](#); Park et al., 2008, [156845](#); Schwartz et al., 2005, [086296](#)).

Park et al. (2005, [057331](#)) studied the association between short-term increases in ambient air pollution and changes in HRV using males enrolled in the Normative Aging Study. Using linear regression models, the association between HRV metrics and PM_{2.5}, O₃, NO₂, SO₂, CO, BC, and particle number count (PNC) moving averages (ma) in the previous 4, 24, and 48 h were examined. The modifying effects of hypertension, diabetes, ischemic heart disease (IHD), and use of hypertensive medications were also estimated. Of the pollutants examined, only PM_{2.5} and O₃ were associated with reductions in HRV, and each pollutant's effect appeared independent of the other. Each 8 µg/m³ increase in mean PM_{2.5} concentration in the previous 48 h was associated with a 20.8% decrease in HF power (95% CI: -34.2 to -4.6), with larger effects among subjects with hypertension, IHD, and diabetes. The authors state that since BC concentrations were also associated with adverse changes in HRV, this suggests that traffic pollution may be partially responsible for the HRV changes.

Schwartz et al. (2005, [086296](#)) examined the hypothesis that adverse changes in HRV due to PM_{2.5} are mediated by an oxidative stress response among participants in the Normative Aging Study. They examined whether the change in HF power associated with each 10 µg/m³ increase in 48-h mean PM_{2.5} was modified by the presence or absence of the allele for glutathione S-transferase M1 (GSTM1), use of statins, obesity, high neutrophil counts, higher blood pressure (BP), and/or older age. In subjects without the GSTM1 allele and its protection against oxidative stress, each 10 µg/m³ increase in 48-h mean PM_{2.5} concentration was associated with a 34% decrease in HF power (95% CI: -52 to -9). There was no association among those with at least one copy of the allele. Obesity and high neutrophil counts also worsened the effect of PM on HRV regardless of allele.

Park et al. (2006, [091245](#)) investigated whether transition metals may be responsible for cardiorespiratory effects that are observed in association with PM_{2.5}. Again using the Normative Aging Study cohort, they investigated whether subjects with two hemochromatosis (HFE) polymorphisms associated with increased iron uptake had a smaller decrease in HF power associated with PM than those subjects without either variant. Each 10 µg/m³ increase in 48-h mean PM_{2.5} was associated with a 31.7% decrease in HF (95% CI: -48.1 to -10.3) among subjects without either polymorphism, but not among those with the 2 protective HFE alleles.

Chahine et al. (2007, [156327](#)) reported a 10.5% reduction in SDNN (95% CI: -18.2 to -2.2) associated with each 10 µg/m³ increase in the mean 48-h PM_{2.5} concentration among Normative Aging Study participants without the GSTM1 allele, but only a 2.0% SDNN decrease (95% CI: -11.3, 8.3) in those with the allele. This supports the PM-HF power findings of Schwartz et al. (2005, [086296](#)). Further, subjects with the long repeat polymorphism in the HO-1 promoter had a greater decline in SDNN associated with each 10 µg/m³ increase in the mean 48-h PM_{2.5}

concentration (-8.5% [95% CI: -14.8 to -1.8]) than those with the short repeat polymorphism in HO-1 (7.4 % increase [95% CI: -8.7 to 26.2]). Again, this suggests that PM-HRV changes are mediated, in part, by oxidative stress.

Baccarelli et al. (2008, [191959](#)) investigated whether the PM_{2.5}-HRV association was modified by dietary intakes of methyl nutrients (folate, vitamins B6 and B12, and methionine) and related gene polymorphisms thought to either confer increased or decreased risk of CVD among men enrolled in the Normative Aging Study. Each 10 µg/m³ increase in PM_{2.5} in the previous 48 h was associated with -8.8% (95% CI: -16.7 to -0.2) and -11.8% (95% CI: -20.8 to -1.8) decreases in SDNN, among those with CC/TT genotypes of the C677T methylenetetrahydrofolate reductase (MTHFR) polymorphism, and the CC genotype of the C1420T cytoplasmic serine hydroxymethyltransferase (cSHMT) polymorphism, respectively. There were no changes among those with CC MTHFR and CC/TT cSHMT. Further, there were similar HRV reductions in those subjects with lower intakes of B6, B12, and/or methionine, but no decreases in those with high intakes. Thus these genetic and nutritional variations in the methionine cycle may modify the PM-HRV association.

Finally, among those Normative Aging Study subjects with high chronic lead exposure as measured using X-ray fluorescence of the tibia, each 7 µg/m³ increase in mean PM_{2.5} concentration in the previous 48 h was associated with a 22% decrease in HF power (95% CI: -37.4 to -1.7) (Park et al., 2008, [093027](#)). Decreases in HF HRV were also associated with each 2.5 µg/m³ increase in mean SO₄²⁻ concentration in the previous 48 h (22% decrease [95% CI: -40.4 to 1.6]). The authors suggest that these findings are consistent with an oxidative stress response. Although this series of studies suggest a role of oxidative stress and perhaps methyl nutrients and related polymorphisms in these short-term associations of PM_{2.5} with HRV, replication by other investigators in other cities and in other populations will aid interpretations of these findings.

Using data from a randomized controlled trial in Mexico City, Romieu et al. (2005, [086297](#)) investigated whether omega-3 fatty acids in fish oil supplements would mitigate the adverse effects of acute PM exposure on HRV. Residents of a Mexico City nursing home were randomized to either 2 g/day of fish oil or 2 g/day of soy oil. They used random-effects regression models to estimate the change in HRV associated with mean PM_{2.5} concentration in the pre-supplementation and supplementation phases. In the group receiving the fish oil supplement, each 8 µg/m³ increase in 24-h mean total PM_{2.5} exposure (weighted average of indoor and outdoor PM_{2.5} based on time activity diaries) was associated with a 54% reduction (95% CI: -72 to -24) in log transformed HF power in the pre-supplementation phase. However, in the supplementation phase of the trial, each 8 µg/m³ increase in 24-h mean total PM_{2.5} concentration was associated with only a 7% reduction in log transformed HF power (95% CI: -20 to 7). Decreases in other HRV parameters associated with PM_{2.5} were also muted in the supplementation phase. In the group receiving the soy oil supplement, the reduction in HF power was also smaller in magnitude during the supplementation phase. However, among those receiving the soy oil supplement, the differences between the pre-supplementation PM_{2.5}-HF change and the supplementation PM_{2.5}-HF change were smaller compared to those receiving the fish oil, and were not statistically significant. Romieu et al. (2008, [156922](#)) also report that omega-3 polyunsaturated fatty acids appear to modulate the adverse effect of PM_{2.5} based on measured biomarkers of oxidative response (Section 6.2.9.1).

Summary of HRV Studies Investigating Specific Mechanisms

In summary, several analyses of data from the Normative Aging Study have provided evidence that effect of PM_{2.5} on HRV is modulated by genetic polymorphisms related to oxidative stress (Chahine et al., 2007, [156327](#); Park et al., 2006, [091245](#); Schwartz et al., 2005, [086296](#)) or dietary methyl nutrients or related genetic polymorphisms (Baccarelli et al., 2008, [191959](#)). In addition, preexisting conditions such as diabetes, IHD, and hypertension (Park et al., 2005, [057331](#); Whitsel et al., 2009, [191980](#)), beta-blocker use (Folino et al., 2009, [191902](#); Park et al., 2005, [057331](#)), chronic lead exposure (Park et al., 2008, [093027](#)) and omega-3 fatty acid (Romieu et al., 2005, [086297](#)) are reported to modulate the effect of PM_{2.5} on HRV.

Table 6-1. Characteristics of epidemiologic studies investigating associations between PM and changes in HRV.

	PM Type, Exposure Lag	Study Subjects	Ambient Concentration ($\mu\text{g}/\text{m}^3$)*	Recording Length	SDNN	LF	HF, rMSSD	LF/HF
MULTICITY STUDIES								
Liao et al. (2004, 056590)	PM ₁₀ , 24-h, lag 1-day	N=6784 (mean age = 62 yrs), ARIC study: MD, NC, MN	24.3	5-min	↓	↓	↓	
Whitsel et al. (2009, 191980)	PM ₁₀ , 24-h, 3-d avg within 5 days preceding exam	N=4295 randomly selected participants in the WHI Trial	28 visit 1 27 visit 2 27 visit 3	10 second	↓		↓	
	UFP, lags 0-2 days		Amsterdam: 17,300 particles/cm ³ Erfurt: 21,100 particles/cm ³ Helsinki: 17,000 particles/cm ³		↓		↑	↓
Timonen et al. (2006, 088747)	AC, lags 0-2 days	Stable IHD patients (65+ yr) Amsterdam, Netherlands (N=37) Erfurt, Germany (N=47) Helsinki, Finland (N=47)	Amsterdam: 2100 particles/cm ³ Erfurt: 1800 particles/cm ³ Helsinki: 1400 particles/cm ³	5-min (Pooled estimates during paced breathing presented to the right)	↓		↑	↓
	PM _{2.5} , lags 0-2 days		Amsterdam: 20.0 Erfurt: 23.1 Helsinki: 12.7		↓		↑	↓
	PM _{10-2.5} , 2-day lag		Amsterdam: 15.3 Erfurt: 3.7 Helsinki: 6.7		→		→	↓
De Hartog et al. (2009, 191904)	24 h PM _{2.5} outdoor, PM _{2.5} traffic, long-range transported PM _{2.5}	Stable IHD patients (65+) Amsterdam, Netherlands (N=37) Erfurt, Germany (N=47) Helsinki, Finland (N=47) (Effects strongest among those NOT taking beta-blockers)	Median Outdoor: Amsterdam: 16.7 Erfurt: 16.3 Helsinki: 10.6	5 min	↓		↓	
U.S. AND CANADIAN STUDIES								
Park et al. (2005, 057331)	PM _{2.5} , 48-h avg	N=497 men (mean age = 73 yr), Normative Aging Study	24-h: 11.4 98th: 30.58		↓	↓	↓	↑
	PNC, 48-h avg	Boston, MA	24-h: 28,942 (13,527) particles/cm ³	4-min	→	↓	↓	↓
	BC, 48-h avg		24-h: 0.92		↓	↓	↓	↑
Riediker et al. (2004, 056992)	In-vehicle PM _{2.5} (mass) 9-h avg	N=9 healthy state police	9-h in-vehicle: 23	10-min	↑	→	↑	↓
	BC, 24-h		24-h Median: 1.0		↓		↓	↑
Schwartz et al. (2005, 074317)	PM _{2.5} , 24-h	N=28 older adults (61-89 yr), 12 wk follow-up, Boston, MA	24-h Median: 10	23-min	↓		↓	↑
	Secondary PM (estimated), 1-h		1-h Median: -1.7		↓		↓	↑
Yeatts et al. (2007, 091266)	PM _{10-2.5} , 24-h	N=12 adult asthmatics, Chapel Hill, NC	24-h: 5.3	5-min	↓	↓	↓	
	PM _{2.5} , 24-h		24-h: 12.5		↑	↓	↑	

	PM Type, Exposure Lag	Study Subjects	Ambient Concentration ($\mu\text{g}/\text{m}^3$)*	Recording Length	SDNN	LF	HF, rMSSD	LF/HF
Wheeler et al. (2006, 088453)	PM _{2.5} , 4-h avg	N=18 COPD, Atlanta, GA	4-h: 17.8	20-min	↑	↑	↑	↑
	PM _{2.5} , 4-h avg	N=12 MI, Atlanta, GA			↓	↑	↓	↓
	EC, 4-h avg	N=18 COPD, Atlanta, GA	4-h: 2.3		↑			
	EC, 4-h avg	N=12 MI, Atlanta, GA			↓			
Dales 2004 (2004, 099036)	PM _{2.5} , 24-h avg (personal)	N=36 IHD patients, Toronto, Canada	24-h personal: 19.9	Not described	→	→	→	→
Luttmann-Gibson et al. (2006, 089794)	PM _{2.5} , lag 1-day	N=32 (65+ yr) Steubenville, OH	24-h: 19.7	~30-min	↓	↓	↓	
	Sulfate, lag 1-day		24-h: 6.9		↓	↓	↓	
	Nonsulfate PM, lag 1-day		24-h: 10.0		↓	↓	↓	
	EC, lag 1-day		24-h: 1.1		↑	↓	→	
Adar et al. (2007, 001458)	PM _{2.5} , 24-h avg	N=44 (60+ yr), diesel bus riders St. Louis, MO	24-h: 10.17	5-min	↓	↓	↓	↑
	BC, 24-h avg		98th: 22.43		↓	↓	↓	↑
	PNC fine		330 ng/m ³		↓	↓	↓	↑
	PNC course		42 particles/cm ³		↑	↑	↑	↓
Pope et al. (2004, 055238)	PM _{2.5} (FRM), 24-h, lag 1-day	N=88 (65+ yr; 250 p-days), Utah Valley	23.7	24-h	↓		↓	
Sullivan et al. (2005, 109418)	PM _{2.5} , 1, 2, 24-h avg	N=21 (65+ yr) with CVD, Seattle WA	Median: 10.7	20-min	→		→	
		N=13 (65+ yr) w/out CVD, Seattle WA			→		→	
Lipsett et al. (2006, 088753)	PM ₁₀	N=19 IHD (65+ yr), 12 wk fu, Coachella Valley, CA	31.0 and 46.1	5-min	↓	↓	↓	
	PM _{10-2.5}		None given	Frequency domain; 2-h, 24-h Time domain	↓	↓	→	
	PM _{2.5}		14 and 23.2		↓	↓	↑	
Ebelt et al. (2005, 056907)	PM ₁₀ , 24 h	N=16 COPD, Vancouver, Canada	17	24-h	↓		↓	
	PM _{10-2.5}		5.6		↑		→	
	PM _{2.5} , 24-h		11.4		↓		↓	
	PM _{2.5} Sulfate, 24-h outdoor		98th: 23		↓		↓	
	PM _{2.5} Sulfate, 24-h outdoor		2.0		↓		→	
Baccarelli et al. (2008, 191959)	PM _{2.5} , 48 h	N=549 Normative Aging Study and residents of Boston metropolitan area	Geometric mean (95% confidence interval) 10.5 (10.0, 10.9)	7 min	↓			
Fan et al. (2008, 191979)	PM _{2.5} personal, 1 h	N=11 crossing guards in New Jersey	Only change in 1-h PM _{2.5} reported Morning shift: 35.2 Afternoon shift: 24.1	24 h	↓			
INTERNATIONAL STUDIES								
Chan et al. (2004, 087398)	NC _{0.02-1} , 1-4 h	N=9 adults (19-29 yr) with lung function impairment, Taipei, Taiwan	23,407 (19,836) particles/cm ³	5 min	↓	↓	↓	↓
		N=10 adults (42-79 yr) with lung function impairment, Taipei, Taiwan	25,529 (20,783) particles/cm ³		↓	↓	↓	↓
Chuang et al. (2005, 087989)	PM _{1.0-0.3} , 1-4 h	N=16, Patients with IHD/hypertension, Taipei, Taiwan	37.2	5-min	↓	↓	↓	↑
	PM _{2.5-1.0} , 1-4 h		12.6	↓	↓	↓	↑	
	PM _{10-2.5} , 1-4 h		14.0	↓	↓	↓	↑	

	PM Type, Exposure Lag	Study Subjects	Ambient Concentration ($\mu\text{g}/\text{m}^3$)*	Recording Length	SDNN	LF	HF, rMSSD	LF/HF
	PM _{1.0-0.3} , 1-4 h		26.8		↓	↓	↓	→
	PM _{2.5-1.0} , 1-4 h	N=10 IHD, Taipei, Taiwan	10.9		↓	↓	↓	↓
	PM _{10-2.5} , 1-4 h		16.4		↓	↓	↓	↑
Holguin et al. (2003, 057326)	PM _{2.5} , 24-h	N=21 without hypertension (60-96 yr), Mexico City N=13 with hypertension (60-88 yr), Mexico City	37.2	5-min			↓	↑
				6-min			↓	↑
Romieu et al. (2005, 086297)	PM _{2.5} , 24-h (outdoor and indoor)	N=50 nursing home residents 65+ yr, Mexico City	Outdoor: 19.4 Indoor: 18.3	(Indoor PM _{2.5} , pre-supplement phase presented)	↓	↓	↓	
Riojas-Rodriguez et al. (2006, 156913)	Personal PM _{2.5}	N=30 IHD patients, Mexico City	Geometric mean: 46.8	5-min		↓	↓	
Barclay et al. (2009, 179935)	PM ₁₀ , daily PNC, daily Estimated PM _{2.5} and PNC	N=132, stable coronary heart failure Aberdeen, Scotland	Range of daily means: 7.4 to 68	24 h		→		
Cárdenas et al. (2008, 191900)	PM _{2.5} -outdoor PM _{2.5} -indoor	N=52 (31 women, 21 men; 20-40 yr), southeast of Mexico City	Median PM _{2.5} outdoor: 28.3 $\mu\text{g}/\text{m}^3$ Median PM _{2.5} indoor: 10.8	15 min		↓	↓	↓
Folino et al. (2009, 191902)	PM ₁₀ , 24 h PM _{2.5} , 24 h PM _{0.25} , 24 h	N=39 (36 male, 3 female; mean age = 60 yr) Padua, Italy	PM ₁₀ Summer: 46.4 Winter: 73.0 Spring: 38.3 PM _{2.5} Summer: 33.9 Winter: 62.1 Spring: 30.8 PM _{0.25} Summer: 17.6 Winter: 30.5 Spring: 18.8	24 h		↓		
Min et al. (2008, 191901)	PM ₁₀ , 12 h	N=1349 (596 males; mean age = 44 yr), Korea	1-h avg: 33.2	5 min	↓	↓	↓	

Notes: Increases (↑), decreases (↓) and no effects (→) in HRV associated with PM concentration are indicated. Statistical significance was not necessary to categorize an effect as an increase or decrease. For time domain measures moving average lags up to 24-h were explored. For frequency domain measures lags of 2-h, 4-h and 24-h were explored.
** All concentrations are means measured in $\mu\text{g}/\text{m}^3$, unless otherwise noted.

6.2.1.2. Controlled Human Exposure Studies

The 2004 PM AQCD (U.S. EPA, 2004, [056905](#)) cited one study in which HRV indicators of parasympathetic activity increased relative to filtered air control following a 2-h exposure with intermittent exercise to PM_{2.5} CAPs (avg concentration 174 $\mu\text{g}/\text{m}^3$) in both healthy and asthmatic volunteers (Gong et al., 2003, [042106](#)). This effect was observed immediately following exposure and at 1 day post-exposure, but not at 4 h post-exposure. Although not statistically significant, HRV (total power) increased following exposure to filtered air and decreased following exposure to CAPs. More recent controlled human exposure studies are described below.

CAPs

Two new studies have evaluated the effect of PM_{2.5} CAPs (2-h exposures to concentrations of 20-200 $\mu\text{g}/\text{m}^3$) on HRV in elderly subjects (Devlin et al., 2003, [087348](#); Gong et al., 2004, [087964](#)). In both studies, subjects experienced significant decreases in HRV following exposure to CAPs relative to filtered air exposures. Interestingly, Gong et al. (2004, [087964](#)) found that decreases in HRV were more pronounced in healthy older adults than in those with COPD. In another study,

healthy and asthmatic adults were exposed to PM_{10-2.5} CAPs (avg concentration 157 µg/m³) for 2 h with intermittent exercise (Gong et al., 2004, [055628](#)). HRV was not affected immediately following the exposure, but decreased in both groups at 4 and 22 h after the end of the exposure, with greater responses observed in non-asthmatics. In a recent study among healthy adults exposed for 2 h with intermittent exercise to PM_{10-2.5} CAPs (avg concentration 89 µg/m³, MMAD 3.59 µm, Chapel Hill, NC), Graff et al. (2009, [191981](#)) observed a significant decrease in overall HRV (SDNN) at 20 h post-exposure, although no other measures of HRV were affected. Using a similar study design, the same laboratory also evaluated the effect of ultrafine CAPs (avg concentration 49.8 µg/m³, <0.16 µm in diameter) on various HRV parameters (Samet et al., 2009, [191913](#)) Relative to filtered air, both HF and LF power increased 18 h following exposure to UF CAPs (36-42% increase per 10⁵ particles/cm³). Exposure to UF CAPs, expressed as mass concentration, was not associated with changes in HF power, and time domain parameters of HRV did not differ between CAPs and filtered air in the 24 h following exposure. Gong et al. (2008, [156483](#)) also recently evaluated changes in HRV following controlled human exposures to UF CAPs and reported a small and transient decrease in LF power (p < 0.05) among healthy (n = 17) and asthmatic (n = 14) adults 4 h after the completion of a 2-h exposure with intermittent exercise in Los Angeles (avg concentration 100 µg/m³, avg PNC 145,000/cm³). No other measure of HRV was shown to be significantly affected by exposure to UF CAPs. In one of the largest studies of controlled human exposures to CAPs conducted to date, Fakhri et al. (2009, [191914](#)) evaluated changes in HRV among 50 adult volunteers during 2-h exposures to PM_{2.5} CAPs (127 µg/m³) and O₃ (114 ppb), alone and in combination. Neither exposure to CAPs nor O₃ resulted in any significant changes in HRV relative to filtered air. However, trends were observed suggesting a negative concentration-response relationship between CAPs concentration and SDNN, rMSSD, HF power and LF power when subjects were concomitantly exposed to O₃.

Diesel Exhaust

In a double-blind, crossover, controlled-exposure study, Peretz et al. (2008, [156855](#)) exposed three healthy adult volunteers and 13 adults with metabolic syndrome while at rest to filtered air and two levels of diluted DE (PM_{2.5} concentrations of 100 and 200 µg/m³) in 2-h sessions. HRV parameters were assessed prior to exposure, as well as at 1, 3, 6 and 22 h following the start of exposure, and included both time domain (SDNN and rMSSD) and frequency domain parameters (HF power, LF power, and the LF/HF ratio). In an analysis including all 16 subjects, the authors observed an increase in HF power and a decrease in LF/HF 3 h after the start of exposure to 200 µg/m³ relative to filtered air. Although these changes were statistically significant (p < 0.05) the effects were not consistent among the study subjects. No other significant effect of DE on HRV was observed at either concentration or time point. The authors attributed the lack of consistent effects to the small and non-homogeneous population and the timing of measurement. There was no difference in either baseline or diesel-induced changes in HRV parameters between normal individuals and patients with metabolic syndrome, although the number of normal individuals was quite small. It is unclear if patients with metabolic syndrome were taking any medications.

Model Particles

Several additional recent controlled human exposure studies have evaluated the effect of laboratory generated particles on HRV in healthy and health-compromised individuals. In a random order crossover controlled human exposure study, Routledge et al. (2006, [088674](#)) examined the effects of UF elemental carbon (EC) particles (50 µg/m³) alone and in combination with 200 ppb SO₂ on HRV among 20 healthy older adults (age 56-75 yr), as well as 20 older adults with coronary artery disease (age 52-74 yr). Five minute recordings of HRV data were obtained prior to and immediately following the 1-h exposure, as well as 3 h post-exposure. In healthy subjects, exposure to EC particles resulted in small increases in RR-interval, SDNN, rMSSD, and LF power immediately following exposure compared to filtered air control. At 3 h post-exposure, there were no significant differences in HRV measures between EC particle and filtered air exposures. Conversely, SO₂-induced decreases in HRV were observed at 3 h, but not immediately following exposure. Concomitant exposure to EC particles and SO₂ followed a pattern similar to that observed with SO₂

alone, but did not reach statistical significance. Subjects with coronary artery disease did not experience any significant changes in HRV following exposure to either pollutant. The authors postulated that this lack of effect may be due to differences in medication between the two groups, as 70% of subjects with stable angina reported using β blockers, which are known to increase cardiac vagal control. The lack of any significant effects on HRV following exposure to EC particles is an important finding, as it provides evidence to suggest that the health effects observed following exposure to PM may be due to particle constituents other than carbon, or to reactive species found on the surface of the particle. These findings are in agreement with those of Zareba et al. (2009, [190101](#)) who reported small and variable changes in HRV among a group of healthy adults following exposure to UF EC. While exposure both at rest and during exercise to $10 \mu\text{g}/\text{m}^3$ UF EC resulted in an increase in time domain parameters (rMSSD and SNDD), no such effect was observed following exposure to a higher concentration of UF EC ($25 \mu\text{g}/\text{m}^3$) in the same subjects. A recent pilot study reported no effect of exposure to EC and ammonium nitrate particles ($250\text{-}300 \mu\text{g}/\text{m}^3$) on HRV parameters in five adults with allergic asthma (Power et al., 2008, [191982](#)). However, when the exposure occurred concomitantly with O_3 (0.2 ppm), subjects were observed to experience significant changes in both time and frequency HRV parameters. These observations should be considered very preliminary as the study was limited by a small sample size ($n = 5$) and did not evaluate the effect of exposure to O_3 without particles. However, these findings are in agreement with the previously described study of CAPs and O_3 conducted by Fakhri et al. (2009, [191914](#)). In addition to the studies of laboratory generated carbon described above, Beckett et al. (2005, [156261](#)) used ZnO as a model particle and exposed twelve resting, healthy adults for 2 h to filtered air and $500 \mu\text{g}/\text{m}^3$ in the ultrafine ($40.4 \pm 2.7 \text{ nm}$) and fine ($291.2 \pm 20.2 \text{ nm}$) modes. Neither ultrafine nor fine ZnO produced a significant change in any time or frequency domain parameter of HRV.

Summary of Controlled Human Exposure Study Findings for Heart Rate Variability

The results of several new controlled human exposure studies provide limited evidence to suggest that acute exposure to near ambient levels of PM may be associated with small changes in HRV. Changes in HRV parameters, however, are variable with some showing increased parasympathetic activity relative to sympathetic activity and others showing the opposite. Although a direct comparison between younger and older adults has not been made, PM exposure appears to result in a decrease in HRV more consistently in healthy older adults (Devlin et al., 2003, [087348](#); Gong et al., 2004, [087964](#)).

6.2.1.3. Toxicological Studies

Toxicological studies that examined HR and HRV are presented in the 2004 PM AQCD (U.S. EPA, 2004, [056905](#)) and overall demonstrated differing responses, which were collectively characterized as providing limited evidence for PM-related cardiovascular effects. The studies described that reported HR or HRV effects following PM exposure were conducted with a variety of particle types (CAPs, diesel, ROFA, metals), exposure methods (inhalation and IT instillation), and doses ($100\text{-}3,000 \mu\text{g}/\text{m}^3$ for inhalation; up to $8.3 \text{ mg}/\text{kg}$ for IT instillation).

CAPs

Two groups of SH rats exposed to CAPs in Tuxedo, NY for 4 h (single-day mean $\text{PM}_{2.5}$ concentrations 80 and $66 \mu\text{g}/\text{m}^3$; February 2001 and May 2001, respectively) demonstrated decreased HR when exposure groups were combined that returned to baseline values when exposure ceased (Nadziejko et al., 2002, [087460](#)). Fine or UF H_2SO_4 exposure (mean concentration 225 and $468 \mu\text{g}/\text{m}^3$) did not induce any HR effects. Another study demonstrated a trend toward increased HR in WKY rats following a 1- or 4-day $\text{PM}_{2.5}$ CAPs exposure in Yokohama City, Japan (4.5 h/day; May 2004, November 2004, and September 2005), but the correlation between change in HR and cumulative PM mass collected was not significant (Ito et al., 2008, [096823](#)). Increased HR was observed in SH rats exposed to $\text{PM}_{2.5}$ CAPs for two 5-h periods during the spring (mean mass concentration $202 \mu\text{g}/\text{m}^3$) in a suburb of Taipei, Taiwan (Chang et al., 2004, [055637](#)). The response

was less prominent in the summer (mean mass concentration $141 \mu\text{g}/\text{m}^3$), despite the number concentrations being similar for the two seasons (2.30×10^5 and 2.78×10^5 particles/ cm^3 , respectively).

For HRV, decreased SDNN was observed in SH rats exposed to $\text{PM}_{2.5}$ CAPs (mean mass concentration $202 \mu\text{g}/\text{m}^3$; mean number concentration 2.30×10^5 particles/ cm^3) for two 5-h periods separated by 24 h (Chang et al., 2005, [088662](#)). Each of the four animals served as their own control and the estimated mean PM effects for the SDNN decreases during exposure were 85-60% of baseline. CAPs effects on rMSSD were less remarkable. In a study of Tuxedo, NY $\text{PM}_{2.5}$ CAPs, no acute changes in rMSSD or SDNN were observed in either ApoE^{-/-} or C57 mice when the 48-h time period postexposure was evaluated (6 h/day \times 5 day/wk; mean mass concentration over 5-mo period $110 \mu\text{g}/\text{m}^3$) (Chen and Hwang, 2005, [087218](#)).

Diesel Exhaust

Anselme et al. (2007, [097084](#)) used a MI model of congestive heart failure (CHF) where the left anterior descending coronary artery of WKY rats was occluded to induce ischemia. After 3 mo of recovery, rats were exposed to diesel emissions for 3 h (PM concentration $500 \mu\text{g}/\text{m}^3$; mass mobility diameter 85 nm; NO_2 1.1 ppm; CO 4.3 ppm) and decreases in rMSSD were observed during the first 2 h of the exposure, which returned to baseline values for the last hour of exposure. Healthy rats also demonstrated decreased rMSSD when measured over the entire exposure period.

Model Particles

In WKY rats exposed to UF carbon particles (mass concentration $180 \mu\text{g}/\text{m}^3$; mean number concentration 1.6×10^7 particles/ cm^3) for 24 h, HR increased and SDNN decreased during particle inhalation (Harder et al., 2005, [087371](#)). These measures returned to baseline values during the recovery period. This study provides evidence that ultrafine carbon exerts its effects through changes in ANS mediation, as the HR and HRV responses occurred quickly after exposure started and pulmonary inflammation was only observed at the 24-h time point (and not at 4 h). SH rats exposed to ultrafine carbon particles under the same conditions (mass concentration $172 \mu\text{g}/\text{m}^3$; mean number concentration 9.0×10^6 particles/ cm^3) demonstrated similar responses, albeit not until recovery days 2 and 3 (Upadhyay et al., 2008, [159345](#)).

A model of premature senescence has been developed by Tankersley et al. (2003, [053919](#)), using aged AKR mice whose body weight abruptly declines ~ 5 wk prior to death and is accompanied by deficiencies in other vital physiological function including HR and temperature regulation. When exposed to carbon black ([CB]; mean concentration $160 \mu\text{g}/\text{m}^3$; 3 h/day \times 3 day), terminal senescent mice responded with robust cardiovascular effects, including bradycardia and increased rMSSD and SDNN (Tankersley et al., 2004, [094378](#)). SDNN and LF/HF were also increased in healthy senescent mice exposed to CB. These studies indicate that HR regulatory mechanisms are altered in susceptible mice exposed to PM (sympathetic and parasympathetic changes in healthy senescent mice and increased parasympathetic influence in terminally senescent mice), which may translate into lowered homeostatic competence in these animals. Results from the near-terminal group should be interpreted with caution, as only three mice were in this group.

Subsequent research with a similar exposure protocol (mean CB concentration $159 \mu\text{g}/\text{m}^3$) used C57BL/6J and C3H/HeJ mice to determine whether an acute PM challenge can modify HR regulation in two mice strains with differing baseline HR (Tankersley et al., 2007, [097910](#)). There were no CB-specific effects on HR or HRV in C3H/HeJ compared to C57BL/6J mice (average HR ~ 80 bpm lower than C3H/HeJ at baseline). Administration of a sympathetic antagonist (propranolol) to C57BL/6J mice prior to CB exposure resulted in elevated HR and decreased rMSSD compared to air during the last 2 h of exposure, indicating withdrawal of parasympathetic tone. There may be differences in regional particle deposition based on strain-specific breathing patterns that may affect HR and HRV responses. However, this study revealed that inherent autonomic tone, which is genetically varied between these mouse strains, may affect cardiovascular responses following PM exposure. In extrapolating these results to humans, individual variation in genetic factors likely plays some role in PM-induced adjustments in HR control via the ANS.

A recent study in mice (C3H/HeJ, C57BL/6J, and C3H/HeOuJ) examined the effects of a 2-h O_3 (mean concentration 0.584 ppm) pretreatment followed by a 3-h exposure to CB (mean

concentration 536 $\mu\text{g}/\text{m}^3$) on HR and HRV measures (Hamade et al., 2008, [156515](#)) HR decreased to the greatest extent during O₃ pre-exposure for all strains that were then exposed to CB. The percent change in SDNN and rMSSD were increased in C3H mice during O₃ pre-exposure and CB exposure compared to the filtered air group; however, these HRV parameters gradually decreased over the duration of the experiment and appeared to be O₃ dependent. Together, these findings indicate that increases in parasympathetic tone and/or decreases in sympathetic input may explain the observed bradycardia. In a subset of all mice pre-exposed to O₃, rMSSD remained significantly elevated during the CB exposure compared to filtered air. The results from this study confirm what was observed in Tankersley et al. (2007, [097910](#)) in that genetic determinants affect HR regulation in mice with exposure to air pollutants.

Summary of Toxicological Study Findings for Heart Rate and Heart Rate Variability

Both increases and decreases in HR have been observed in rats or mice following PM exposure. Fine or UF H₂SO₄ did not result in HR changes in SH rats. Similarly, decreased SDNN was reported for UF CAPs exposure and lowered rMSSD was observed with diesel exposure. In near-terminal senescent mice, HRV responses were robust following CB exposure and represented increased parasympathetic influence. Strain differences in baseline HR and HRV likely contribute to PM responses. HRV changes with preexposure to O₃ and CB appeared to be O₃ dependent, although rMSSD remained elevated during PM exposure.

Source Apportionment and PM Components

An additional analysis of CAPs data (Chen and Hwang, 2005, [087218](#); Hwang et al., 2005, [087957](#)) was conducted to link short-term HR and HRV effects to major PM source categories using source apportionment methodology (Lippmann et al., 2005, [087453](#)).

The source categories were: (1) regional secondary SO₄²⁻ comprised of high S, Si, and OC (mean 63.41 $\mu\text{g}/\text{m}^3$); (2) resuspended soil characterized by high concentrations of Ca, Fe, Al, and Si (mean concentration 5.88 $\mu\text{g}/\text{m}^3$); (3) fly ash emissions from power plants burning residual oil in the eastern U.S. and containing high levels of V, Ni, and Se (mean concentration 1.53 $\mu\text{g}/\text{m}^3$); and (4) motor vehicle traffic and other unknown sources (34.92 $\mu\text{g}/\text{m}^3$) (Lippmann et al., 2005, [087453](#)). Exposures occurred from 9:00 a.m. to 3:00 p.m., 5 days/wk for 5 mo. PM_{2.5} mass was associated with a daily interquartile change of -4.1 beat/min HR during exposure in ApoE^{-/-} mice¹ and a similar magnitude of effect was observed with resuspended soil (-4.5 beat/min). Resuspended soil was also associated with a HR increase in the afternoon post-exposure (2.6 beat/min); the secondary SO₄²⁻ factor was linked to lowered HR in the same period (-2.5 beat/min). A 6.2% increase in rMSSD collected in the afternoon post-exposure was associated with the residual oil factor, compared to a 5.6% and 2.4% decrease in rMSSD at night for secondary SO₄²⁻ and PM_{2.5} mass, respectively. Resuspended soil was associated with a 4.3% increase in rMSSD the night following CAPs exposure. The residual oil and secondary SO₄²⁻ categories showed similar statistically significant parameter estimates for SDNN as rMSSD.

Recent studies of ECG alterations in mice have indicated a role for PM-associated Ni in driving the cardiovascular effects. Lippman et al. (2006, [091165](#)) presented a posthoc analysis of daily variations in PM_{2.5} CAPs (mean concentration: 85.6 $\mu\text{g}/\text{m}^3$; 7/21/ 2004–1/12/2005; Tuxedo, NY) and changes in cardiac dynamics in ApoE^{-/-} mice. On the 14 days that the exposed mice had

¹ Atherosclerosis and related pathways have been studied primarily in the Apolipoprotein E (ApoE) knockout mouse. Developed by Nobuyo Maeda's group in 1992 (Piedrahita et al., 1992, [156868](#); Zhang et al., 1992, [157180](#)), the ApoE^{-/-} mouse and related models have become the workhorse of atherosclerosis research over the past 15 years. The ApoE molecule is involved in the clearance of fats and cholesterol. When ApoE (or the LDL receptor) is deleted from the genome, mice develop severely elevated lipid and cholesterol profiles; ApoE^{-/-} mice on a high-fat ("Western") diet exhibit cholesterol levels exceeding 1000 mg/dL (normal is ~150 mg/dL) (Huber et al., 1999, [156575](#); Moore et al., 2005, [156780](#)). As a result, the lipid uptake into the vasculature is increased and the atherosclerotic process is dramatically hastened. Furthermore, the LDLs in ApoE^{-/-} mice are highly susceptible to oxidation (Hayek et al., 1994, [156527](#)), which may be a crucial event in the air pollution-mediated vascular changes. However it should be noted that this model is primarily one of peripheral vascular disease rather than coronary artery disease.

unusually elevated HR, Ni, Cr, and Fe comprised 12.4% of the PM mass, compared to only 1.5% on the other 89 days. Back trajectory analyses indicated high-altitude winds from the northwest that did not traverse population centers and industrial areas except the Sudbury Ni smelter in Ontario, Canada. On the 14 days that high HR was observed, the HR elevation lasted for two days, but only the current day CAPs concentration was statistically significant. SDNN decreases were statistically significant for all three lags (0, 1, 2 days). The GAM regression analysis showed that only Ni produced a statistically significant effect for HR and SDNN.

6.2.2. Arrhythmia

Epidemiologic and toxicological studies presented in the 2004 PM AQCD (U.S. EPA, 2004, [056905](#)) provided some evidence of arrhythmia following exposure to PM. However, a positive association between PM and ventricular arrhythmias among patients with implantable cardioverter defibrillators was only observed in one study conducted in Boston, MA, while toxicological studies reported arrhythmogenesis in rodents following exposure to ROFA, DE, or metals. Recent epidemiologic studies have confirmed the findings of PM-induced ventricular arrhythmias in Boston, MA, and have also reported increases in ectopic beats in studies conducted in the Midwest and Pacific Northwest regions of the U.S. In addition, two studies from Germany have demonstrated positive associations between traffic and combustion particles and changes in repolarization parameters among patients with IHD. Findings of recent toxicological studies are mixed, with both demonstrated decreases and increases in frequency of arrhythmia following exposure to CAPs.

6.2.2.1. Epidemiologic Studies

Studies of Arrhythmias Using Implantable Cardioverter Defibrillators

One study reviewed in the 2004 PM AQCD assessed the effect of short-term fluctuations in PM_{2.5} on ventricular arrhythmias and several recent studies examining this relationship have been conducted. Ventricular ectopy and arrhythmia include ventricular premature beats (VPBs), ventricular tachycardia (VT), and ventricular fibrillation (VF). VPBs are spontaneous beats originating from either the right or left ventricles. VT refers to three or more VPBs in succession at a rate of 100 beats per minute or greater, while VF is characterized by rapid and disorganized ventricular electrical activation incapable of generating an organized mechanical contraction or cardiac output. AF is the most common type of arrhythmia. In this condition, ectopic electrical impulses arising in the atria or pulmonary veins, i.e., outside their normal anatomic origin (the sinoatrial node), can result in atrioventricular dilatation, dysfunction, and/or thromboembolism. Despite being common, clinical and subclinical forms of AF are associated with reduced functional status and quality of life. Moreover, the arrhythmia accounts for a large proportion of ischemic stroke (Laupacis et al., 1994, [190901](#); Prystowsky et al., 1996, [156031](#)) and is a strong risk factor for CHF (Roy et al., 2009, [190902](#)), contributing to both cardiovascular disease (CVD) and all-cause mortality (Kannel et al., 1983, [156623](#)).

Ventricular arrhythmia is commonly associated with myocardial infarction, heart failure, cardiomyopathy, and other forms of structural (e.g., valvular) heart disease. Pathophysiologic mechanisms underlying this established cause of sudden cardiac death include activators and facilitators of arrhythmia, such as electrolyte abnormalities, modulation of the ANS, membrane channels, gap junctions, oxidant stress, myocardial stretch and ischemia.

Previously, Peters et al. (2000, [011347](#)) conducted a pilot study in Boston, MA to examine the association between short-term changes in ambient air pollutant concentrations and increased risk of ventricular arrhythmias, among a cohort of patients with implantable cardioverter defibrillators (ICD). ICDs continuously monitor cardiac rhythm and upon detection of an abnormal rhythm (i.e., rapid HR), they can be programmed to deliver pacing and/or shock therapy to restore normal sinus rhythm. Those abnormal rhythms that are most severe or rapid are assumed to be due to VT or VF (i.e., life-threatening arrhythmias), and are thus treated with electric shock. These ICD devices also store information on each abnormal rhythm detected, including the date, time, and therapy given. Thus, using the date and time of those arrhythmias resulting in electric shock, Peters et al. (2000,

[011347](#)) reported an increased risk of ICD shock associated with mean NO₂ concentration in the previous two days. Among subjects with frequent events (10 or more during 3 yr of follow-up) an increased risk of ICD shock was also associated with interquartile range increases in CO, NO₂, PM_{2.5}, and BC in the previous 2 days. Several studies were conducted to confirm these findings. The study characteristics, as well as the reported effect estimates and 95% CI associated with each PM metric, are shown in Table 6-2.

Dockery et al. (2005, [078995](#); 2005, [090743](#)) conducted a follow-up study of ICD patients living in eastern Massachusetts and followed subjects for a longer period of time (up to 7 yr). They were the first to review the ECG, classify each ICD-detected arrhythmia (e.g., ventricular arrhythmia, VF, atrial tachycardia, sinus tachycardia, etc.), and include only ventricular arrhythmias (VF or VT; excluding supraventricular arrhythmias). In single-pollutant models using generalized estimating equations, increased risks of confirmed ventricular arrhythmias were associated with IQR increases in every pollutant (PM_{2.5}, BC, SO₄²⁻, NO₂, SO₂, O₃, and PNC). Among those with a prior ventricular arrhythmia in the past three days, interquartile range increases in 2-calendar-day mean PM_{2.5}, NO₂, SO₂, CO, O₃, SO₄²⁻, and BC concentrations were all associated with significant and markedly higher risks of ventricular arrhythmia than among those without a prior arrhythmia. The pollutants associated with increased risk of ventricular arrhythmia implicate traffic pollution.

Rich et al. (2005, [079620](#)) conducted a case-crossover analysis of these same data to investigate moving average pollutant concentrations lagged <48 h. They reported an increased risk of ventricular arrhythmia associated with mean PM_{2.5} and O₃ concentrations in the 24 h before the arrhythmia. Each pollutant effect appeared independent in two pollutant models. In single-pollutant models, NO₂ and SO₂ were associated with increased risk, but when included in two pollutant models with PM_{2.5}, only PM_{2.5} remained associated with increased risk. They did not, however, find evidence of a more acute arrhythmic response to pollution (i.e., larger risk estimates associated with moving averages <24 h before arrhythmia detection). In an ancillary case-crossover analysis of data from the Boston ICD study, Rich et al. (2006, [088427](#)) identified 91 confirmed episodes of paroxysmal AF among 29 subjects. In single pollutant models, they reported a significantly increased risk of AF associated with mean O₃ and PM_{2.5} concentrations in the hour before the arrhythmia and BC concentration in the 24 h before the arrhythmia.

Rich et al. (2006, [089814](#)) conducted another case-crossover study in the St. Louis, MO metropolitan area. Using the same methods as in Boston, they reported increased risk of ventricular arrhythmia associated with mean SO₂ concentration in the 24 h before the arrhythmia, but not PM_{2.5} (in single-pollutant models). Again, they found no evidence of an arrhythmic response with moving average pollutant concentrations <24 h before the arrhythmia.

In Vancouver, Canada, Vedal et al. (2004, [055630](#)) did not find increased risk of ICD shocks associated with increases in any pollutant concentration (PM₁₀, O₃, SO₂, NO₂, and CO). Secondary analyses among those subjects with two or more discharges per year, and analyses stratified by season were also null for PM₁₀, although an association with SO₂ (lag 2 days) was observed. A case crossover analysis of these same data examining additional particle pollutant concentrations available for a shorter time frame (e.g., PM_{2.5}, SO₄²⁻, EC, and OC) also found no increased risk of ICD shock associated with any pollutant (Rich et al., 2004, [055631](#)).

The largest ICD study to date examined the risk of ventricular arrhythmias associated with increases in the daily concentration of numerous PM and gaseous pollutants in Atlanta, GA (Metzger et al., 2007, [092856](#)) (see Table 6-2 for specific pollutants evaluated). Similar to Vedal et al. (2004, [055630](#)), they did not find significant or consistently increased risk of a ventricular arrhythmia associated with any IQR increase in mean daily PM or gaseous pollutant concentration at any lag examined.

Ljungman et al. (2008, [180266](#)) conducted a similar study, using case-crossover methods, on ICD patients in Gothenburg and Stockholm, Sweden. They investigated the triggering of confirmed ventricular arrhythmias by ambient PM₁₀ and NO₂ concentrations, and reported increased relative odds of ventricular arrhythmia associated with each 10 µg/m³ increase in the 2-h ma PM₁₀ concentration (OR = 1.22 [95% CI: 1.00-1.51]), with a smaller non-significant risk associated with each 10.3 µg/m³ increase in the 24-h ma PM₁₀ concentration (OR = 1.23 [95% CI: 0.87-1.73]). The NO₂ and PM_{2.5} effect estimates were much smaller and not statistically significant. Effect estimates were larger for events occurring near the air pollution monitors in Gothenburg (compared to Stockholm).

Albert et al. (2007, [156201](#)), although not investigating associations with ambient pollution, conducted a case-crossover study of the association between ventricular arrhythmia and traffic

exposure in the hours before the arrhythmia. They reported an increased risk of ventricular arrhythmia associated with traffic exposure or driving in the previous hour. They hypothesized that this increased risk was due to either a stress response from being in a car in heavy traffic, or from traffic-generated air pollution, or a combination of both.

Table 6-2. Epidemiologic studies of ventricular arrhythmia and ambient PM concentration, in patients with implantable cardioverter defibrillators.

Reference	Outcome and Sample Size	Study Design and Analytic Method	Copollutants	PM Metric	Ambient Concentration	Lag and its Increment Units	OR	95% Confidence Interval
Dockery et al. (2005, 078995 ; 2005, 090743) Eastern MA	N=670 days with ≥ 1 confirmed ventricular arrhythmias among n=84 subjects	Generalized estimating equations Lags Evaluated: 2 calendar day means	NO ₂ , CO, SO ₂ , O ₃	PM _{2.5}	Daily Median: 10.3 µg/m ³	2 day 6.9 µg/m ³	1.08	0.96, 1.22
				BC	Daily Median: 0.98 µg/m ³	2 day 0.74 µg/m ³	1.11	0.95, 1.28
				Sulfate	Daily Median: 2.55 µg/m ³	2 day 2.04 µg/m ³	1.05	0.92, 1.20
				PNC	Daily Median: 29,300 particles/cm ³	2 day 19,120 particles/cm ³	1.14	0.87, 1.50
Rich et al. (2005, 079620) Eastern MA	N=798 confirmed ventricular arrhythmias among n=84 subjects	Time-stratified case--crossover study. Conditional logistic regression. Lags evaluated: 3, 6, 24, 48-h ma	NO ₂ , CO, SO ₂ , O ₃	PM _{2.5}	Daily Median: 9.8 µg/m ³	24-h ma 7.8 µg/m ³	1.19	1.02, 1.38
				BC	Daily Median: 0.94 µg/m ³	24-h ma 0.83 µg/m ³	0.93	0.74, 1.18
Rich et al. (2006, 089814) St. Louis metro area	N=139 confirmed ventricular arrhythmias among n=56 subjects	Time-stratified case-crossover study. Conditional logistic regression. Lags Evaluated: 6, 12, 24, 48-h ma	NO ₂ , CO, SO ₂ , O ₃	PM _{2.5}	Daily Median: 16.2 µg/m ³	24-h ma 9.7 µg/m ³	0.95	0.72, 1.27
				EC	Daily Median: 0.6 µg/m ³	24-h ma 0.5 µg/m ³	1.18	0.93, 1.50
				Organic Carbon	Daily Median: 4.0 µg/m ³	24-h ma 2.3 µg/m ³	1.08	0.81, 1.43
Vedal et al. (2004, 055630) Vancouver, BC, Canada	N=257 days with ≥ 1 ICD shock among n=50 subjects	Generalized estimating equations Lags Evaluated: 0, 1, 2, 3 daily ma	NO ₂ , CO, SO ₂ , O ₃	PM ₁₀	Daily Median: 11.6 µg/m ³	Lag Day 0 5.6 µg/m ³	1.00*	0.82, 1.19*
Ljungman et al. (2008, 180266) Gothenburg and Stockholm, Sweden	N=114 ventricular arrhythmias among 73 subjects. 211 total subjects were followed.	Conditional logistic regression Lags evaluated: 2 h, 24 h	NO ₂	PM ₁₀	Median Gothenburg 2 h: 18.95 µg/m ³ 24 h: 19.92 µg/m ³	2-h ma: 14.16 µg/m ³	2 h: 1.31	1.00, 1.72
					Stockholm 2 h: 14.62 µg/m ³ 24 h: 15.23 µg/m ³	24-h ma: 11:49 µg/m ³	24 h: 1.24	
				PM _{2.5}	Median Stockholm µg/m ³	2-h ma: 6.69 µg/m ³	2 h: 1.23	0.84, 1.80
					2 h: 9.17 24 h: 9.49 µg/m ³	24-h ma: 5.27 µg/m ³	24 h: 1.28	
Rich et al. (2004, 055631) Vancouver, BC, Canada	N=77 to 98 days with ≥ 1 ICD shock among n=34 subjects	Ambi-directional case-crossover study. Conditional logistic regression Lags Evaluated: 0, 1, 2, and 3 day ma	NO ₂ , CO, SO ₂ , O ₃	PM _{2.5}	Daily Mean: 8.2 µg/m ³	Lag Day 0 5.2 µg/m ³	1.0†	0.9, 1.1†
				PM ₁₀	Daily Mean: 13.3 µg/m ³	Lag Day 0 7.4 µg/m ³	0.9†	0.5, 1.5†
				EC	Daily Mean: 0.8 µg/m ³	Lag Day 0 0.4 µg/m ³	1.1†	0.9, 1.3†
				Organic Carbon	Daily Mean: 4.5 µg/m ³	Lag Day 0 2.2 µg/m ³	1.1†	0.9, 1.3†
				Sulfate	Daily Mean: 1.3 µg/m ³	Lag Day 0 0.9 µg/m ³	0.9†	0.7, 1.2†

Reference	Outcome and Sample Size	Study Design and Analytic Method	Copollutants	PM Metric	Ambient Concentration	Lag and its Increment Units	OR	95% Confidence Interval
Metzger et al. (2007, 092856) Atlanta, GA	N=6287 confirmed ventricular arrhythmias among n=518 subjects	Generalized estimating equations Lags Evaluated: 0, 1, and 2 day ma	NO ₂ , CO, SO ₂ , O ₃	PM _{2.5}	Daily Median: 16.2 µg/m ³	24-h ma 10 µg/m ³	1.00	0.95, 1.0
				PM ₁₀	Daily Median: 26.4 µg/m ³	24-h ma 10 µg/m ³	1.00	0.97, 1.03
				PM _{10-2.5}	Daily Median: 8.7 µg/m ³	24-h ma 5 µg/m ³	1.03	1.00, 1.07
				PM _{2.5} EC	Daily Median: 1.4 µg/m ³	24-h ma 1 µg/m ³	1.01	0.98, 105
				PM _{2.5} OC	Daily Median: 3.9 µg/m ³	24-h ma 2 µg/m ³	1.01	0.98, 1.03
				PM _{2.5} SO ₄ ²⁻	Daily Median: 4.1 µg/m ³	24-h ma 5 µg/m ³	0.99	0.93, 1.06
				PM _{2.5} water soluble elements	Daily Median: 0.022 µg/m ³	24-h ma 0.03 µg/m ³	0.95	0.90, 1.00

Estimated from Figure 3 Vedal et al. (2004, [055630](#)).† Estimated from Figure 3 Rich et al. (2004, [055631](#))

Summary of Epidemiologic Studies of Arrhythmias using ICDs

Since 2004, only two studies (in Boston and Sweden), reported adverse associations of PM_{2.5}, other size fractions and components with ICD-detected ventricular arrhythmias (Dockery et al., 2005, [078995](#); Dockery et al., 2005, [090743](#); Ljungman et al., 2008, [180266](#); Rich et al., 2005, [079620](#)). Studies of ICD-detected ventricular arrhythmias conducted elsewhere did not report associations (Dusek et al., 2006, [155756](#); Metzger et al., 2007, [092856](#); Rich et al., 2004, [055631](#); Vedal et al., 2004, [055630](#)) nor was an association observed in a study of PM₁₀ and ICD shock in Vancouver, Canada (Vedal et al., 2004, [055630](#)). A range in exposure lags was evaluated in the Boston study (3 h-3 days) (Dockery et al., 2005, [078995](#); Dockery et al., 2005, [090743](#); Rich et al., 2005, [079620](#)) and Sweden study (2 h and 24 h) (Ljungman et al., 2008, [180266](#)). Reasons for the inconsistent findings may include differing degrees of exposure misclassification within each study or city due to differences in PM composition and pollutant mixes (e.g., less transition metals and sulfates in the Pacific Northwest than the Northeast U.S.), and differences in the size of study areas (Boston: within 40 km of PM_{2.5} monitoring site; Vancouver: Lower Mainland of British Columbia 90 km east of Vancouver). In addition, Rich et al. (2005, [079620](#)) reported that use of the mean pollutant concentration from the specific 24 h before the arrhythmia rather than just the day of the arrhythmia, resulted in less exposure misclassification and less bias towards the null, possibly explaining the lack of association when using just the day of ICD discharge and daily PM concentrations.

Ectopy Studies Using ECG Measurements

A few panel studies have used ECG recordings to evaluate associations between ectopic beats (ventricular or supraventricular) and mean PM concentrations in the previous hours and/or days (Berger et al., 2006, [098702](#); Ebelt et al., 2005, [056907](#); Liao et al., 2009, [199519](#); Sarnat et al., 2006, [090489](#)).

Ectopic beats are defined as heart beats that originate at a location in the heart outside of the sinus node. They are the most common disturbance in heart rhythm. Ectopic beats are usually benign, and may present with or without symptoms, such as palpitations or dizziness. Such beats can arise in the atria, AV node, conduction system or ventricles. When the origin is in the atria the beat is called an atrial or supraventricular ectopic beat. When such a beat occurs earlier than expected it is referred to as a premature supraventricular or atrial premature beat. Likewise, when the origin is in

the ventricle the beat is defined as a ventricular ectopic beat, or when early a premature ventricular beat. When three or more occur ectopic beats occur in succession, this is called a non-sustained run of either supraventricular (atrial) or ventricular origin. When the rate of the run is greater than 100 beats per minute it is defined as a tachycardia. Sustained VT are the arrhythmias investigated in the ICD studies described above.

Using data from the WHI done in 59 U.S. exam sites in 24 cities, Liao et al. (2009, [199519](#)) estimated mean PM_{2.5} and PM₁₀ concentrations at the addresses of 57,422 study subjects undergoing ECG monitoring. They then estimated the risks of ventricular and supraventricular ectopy during that 10-s ECG recording associated with increases in mean PM₁₀ and PM_{2.5} concentrations on the same day and previous 2 days, as well as over the previous 30 days. Mean PM_{2.5} and PM₁₀ concentrations during the study period were 13.8 and 27.5 µg/m³, respectively. Using a 2-stage random effects model, they reported that among smoking subjects, each 10 µg/m³ increase in PM_{2.5} concentration on lag day 1 was associated with a significantly increased risk of ventricular ectopy (OR = 2.0 [95% CI: 1.32-3.3]). Similarly, each 10 µg/m³ increase in lag 1 PM₁₀ concentration was associated with an increased risk of ventricular ectopy (OR = 1.32 [95% CI: 1.07-1.65]). The lag day 2 PM_{2.5} risk estimate was similar in size, but not statistically significant. There were no associations between PM₁₀, PM_{2.5} and supraventricular ectopy among smokers or non-smokers, and no association with any PM metric and ventricular ectopy among non-smokers.

Sarnat et al. (2006, [090489](#)) conducted a panel study among 32 nonsmoking older adults residing in Steubenville, OH. In this study, the median daily PM_{2.5}, SO₄²⁻, and EC concentrations were 17.7, 5.7, and 1.0 µg/m³, respectively. They used logistic regression models to examine lagged effects of 1- to 10-day moving average concentrations of PM_{2.5}, SO₄²⁻, EC, O₃, NO₂, and SO₂. Supraventricular ectopy and ventricular ectopy were measured using Holter monitors during a 30-minute protocol of alternating rest in the supine position, standing, walking and paced breathing. In single-pollutant models, each 10.0 µg/m³ increase in 5-day mean PM_{2.5} concentration was associated with increased risk of supraventricular ectopy (OR = 1.42 [95% CI: 0.99-2.04]), but not ventricular ectopy (OR = 1.02 [95% CI: 0.63-1.65]). Similarly, increased risk of supraventricular ectopy, but not ventricular ectopy, was associated with each interquartile range increase in 5-day mean SO₄²⁻ and O₃ concentration.

Ebelt et al. (2005, [056907](#)) conducted a repeated measures panel study of 16 patients with COPD in Vancouver, British Columbia. Their goal was to evaluate the relative impact of ambient and non-ambient exposures to PM_{2.5}, PM₁₀, and PM_{10-2.5} on several health measures. Subjects wore an ambulatory ECG monitor for 24 h to record heart rhythm data and ascertain supraventricular ectopic beats. The mean PM_{2.5} concentration during this study was 11.4 µg/m³. Using mixed models with random subject effects to investigate only same-day PM concentrations, an increase in supraventricular ectopic beats was associated with same day ambient exposures to each PM size fraction.

Berger and colleagues (2006, [098702](#)) conducted a panel study of 57 men with coronary heart disease living in Erfurt, Germany. Using 24-h ECG measurements made once every 4 wk, they studied associations between runs of supraventricular and ventricular tachycardia and lagged concentrations of PM_{2.5}, UFP (0.01-0.1 µm), ACP (0.1-1.0 µm), SO₂, NO₂, CO, and NO. Using GAMs, as well as Poisson and linear regression models, they reported increases in supraventricular tachycardia and the number of runs of ventricular tachycardia associated with 5-day mean PM_{2.5}, UFP counts, and ACP counts. They found these associations at all lags evaluated (during ECG recording, 0-23 h before, 24-47 h before, 48-71 h before, 72-95 h before, and 5-day mean), but the largest effect estimates were generally associated with the 24- to 47-h mean and the 5-day mean.

Summary of Ectopy Studies Using ECG Measurements

Four studies of ectopic beats and runs of supraventricular and ventricular tachycardia, captured using ECG measurements, all report at least one positive association. Further, they report findings in regions other than Boston and Sweden (i.e., Midwest U.S., Pacific Northwest, 24 U.S. cities, and Erfurt, Germany). A range of lags and/or moving averages were investigated (0-30 days) with the strongest effects observed for either the 5-day mean, same day, or 1-day lagged PM concentrations. Taken together, these ICD studies and ectopy studies provide evidence of an arrhythmic response to PM, although further study is needed to understand the variable ICD study findings.

ECG Abnormalities Associated with the Modulation of Repolarization

No reported investigations of the relationship of PM concentration and ECG abnormalities indicating arrhythmia were conducted prior to 2002 and thus were not included in the 2004 PM AQCD (U.S. EPA, 2004, [056905](#)). Abnormalities in the myocardial substrate, myocardial vulnerability, and resulting repolarization abnormalities are believed to be key factors contributing to the development of arrhythmogenic conditions such as those discussed above. These abnormalities include ECG measures of repolarization such as QT duration (time for depolarization and repolarization of the ventricles), T-wave complexity (a measure of repolarization morphology), and T-wave amplitude (height of the T-wave). Abnormalities in repolarization may also identify subjects potentially at risk of more serious events such as sudden cardiac death (Atiga et al., 1998, [156231](#); Berger et al., 1997, [155688](#); Chevalier et al., 2003, [156338](#); Okin et al., 2000, [156002](#); Zabel et al., 1998, [156176](#)). Recent studies of changes in these measures following acute increases in air pollution are described below.

Two studies conducted in Erfurt, Germany, (Henneberger et al., 2005, [087960](#); Yue et al., 2007, [097968](#)) examined the association between measures of repolarization (QT duration, T-wave complexity, T-wave amplitude, T-wave amplitude variability) and particulate air pollution. Henneberger et al. (2005, [087960](#)) conducted a panel study of 56 males with IHD. Each subject was measured every 2 wk for 6 mo. During the study, the median daily PM_{2.5}, EC, and OC concentrations were 14.9, 1.8, and 1.4 µg/m³, respectively. The median count of UFP was 11,444 particles/cm³, while the median count of ACP (0.1-1.0 µm) was 1,238 particles/cm³. They examined the change in these ECG parameters associated with the mean pollutant (UFP, ACP, PM_{2.5}, OC, and EC) concentrations 0-5, 6-11, 12-17, 18-23, and 0-23 h before, and 2-5 days before the ECG measurement. Significant decreases in T-wave amplitude were associated with PM_{2.5} mass, UFP, and ACP. Each 16.4 µg/m³ increase in the mean PM_{2.5} concentration in the previous 5 h was associated with a 6.46 µV decrease in T-wave amplitude (95% CI: -10.88 to -2.04). Each 0.7 µg/m³ increase in the mean OC concentration in the previous 5 h was associated with a 4.15 ms increase in QT interval (95% CI: 0.22-8.09). There was a similar sized effect for 24-h mean OC concentration. Significant increases in the variability of T-wave complexity were also associated with acute increases in EC and OC concentration.

Yue et al. (2007, [097968](#)) then used positive matrix factorization to identify 5 sources of ambient PM (airborne soil, local traffic-related UFP, combustion-generated aerosols, diesel traffic-related particles, and secondary aerosols). Using similar statistical models, they examined the association between these same repolarization changes and incremental increases in the mean concentration of each particle source in the 24 h before the ECG measurement. They also examined associations with CRP and vWF concentrations in the blood. Both UFP from local traffic and diesel particles from traffic had the strongest associations with repolarization parameters.

Summary of Epidemiologic Studies of ECG Abnormalities Associated with the Modulation of Repolarization

These two analyses demonstrate associations between PM pollution and repolarization changes, at lags of 5 h to 2 days. Moreover, the findings from the Yue et al. (2007, [097968](#)) study demonstrate a potential role of traffic particles/pollution.

6.2.2.2. Toxicological Studies

The ECG of animal research models frequently exhibit different characteristics than that of humans. Mice and rats are notable in this regard, as they do not have an isoelectric ST-segment typical of larger species, likely owing to their rapid heart rates (~600 and ~350 bpm, respectively) and repolarizing currents. However, the ultimate function of the pumping heart is conserved and reflected by the ECG in a remarkably consistent manner across species. Thus, atrial depolarization causes an electrical inflection represented by the P-wave, ventricular depolarization elicits the QRS complex, and the T-wave represents repolarization of the ventricles.

The earliest indication that there may be cardiovascular system effects of PM came from ECG studies in susceptible animal models (rats with pulmonary hypertension and dogs with coronary occlusion), which were summarized in the 2004 PM AQCD (U.S. EPA, 2004, [056905](#)). However, a study of dogs exposed to ROFA did not demonstrate ECG changes, perhaps due to differences in disease state, as these were the oldest dogs in the colony with signs of preexisting, naturally occurring heart disease (Muggenburg et al., 2000, [010279](#)). Much of the research conducted since the release of the last PM AQCD has been focused on exploring susceptibility or varying exposure methodologies, with little new evidence into the mechanisms for ECG changes of inhaled PM.

CAPs

Wellenius et al. (2004, [087874](#)) used a susceptible model that was previously shown to produce significant results with exposures to ROFA (Wellenius et al., 2002, [025405](#)) to examine ECG-related PM_{2.5} effects. Using an anesthetized model of post-infarction myocardium sensitivity, Wellenius and colleagues tested the effects of Boston, MA CAPs on the induction of spontaneous arrhythmias in SD rats (1 h; mean mass concentration 523.11 µg/m³; range of mass concentration 60.3-2202 µg/m³). Decreased (67.1%) VPB frequency was observed during the post-exposure period in rats with a high number of pre-exposure VPB. No interaction was observed with coexposure to CO (35 ppm). CAPs number concentration or the mass concentration of any single element did not predict VPB frequency. In a follow-up publication, a decreased number of supraventricular ectopic beats (SVEB) was reported with CAPs (mean mass concentration 645.7 µg/m³) (Wellenius et al., 2006, [156152](#)). Furthermore, an increase in CAPs number concentration of 1,000 particles/cm³ was associated with a 3.3% decrease in SVEB frequency. The findings of decreased ventricular arrhythmia differ from those observed following ROFA exposure in the same animal model in that an increased frequency of premature ventricular complexes was observed with ROFA, albeit the ROFA exposure concentration was >3,000 µg/m³ (Wellenius et al., 2002, [025405](#)). It is difficult to directly compare the results of these studies due to differences in exposure concentrations and particle type, but collectively they may suggest an important role for the soluble components of PM, including transition metals, as only ROFA induced increases in ventricular arrhythmia occurrence.

In older rats (Fisher 344; ~18 months) exposed to PM_{2.5} CAPs in Tuxedo, NY (4 h; mean concentration 180 µg/m³; August 2000), the frequency of delayed beats was greater than in rats exposed to air (Nadziejko et al., 2004, [055632](#)). The majority of these beats were characterized as pauses (a delay of 2.5 times the adjacent interbeat intervals) rather than premature beats. When the same animals were exposed to generated UF carbon particles (single-day concentrations 500 and 1280 µg/m³) or SO₂ (1.2 ppm), no significant differences were observed in arrhythmia frequency between air controls and exposed animals. The authors also report using the same protocol for young WKY rats (concentration 215 µg/m³) and very few arrhythmias were observed, thus precluding statistical analysis. The results of this study indicate (1) involvement of the sino-atrial node, as the observed arrhythmias were mostly of a delayed nature; and (2) particle size and PM_{2.5} constituents may play a role in these effects.

Diesel and Gasoline Exhaust

Anselme and colleagues (2007, [097084](#)) exposed rats with and without induced CHF to DE for 3 h (PM concentration 500 µg/m³; mass mobility diameter 85 nm; NO₂ 1.1 ppm; CO 4.3 ppm). While no dramatic change was noted in HR, prominent increases in the incidence of VPB were observed in CHF rats, which lasted at least 4-5 h after exposure ceased. The duration of VPB attributable to diesel exposure in CHF rats lasted much longer than the rMSSD change (>5 h post-exposure), indicating that the HRV response was not driving the increased arrhythmia incidence. It is interesting to contrast the work of Anselme with the studies by Wellenius et al. (2002, [025405](#); 2004, [087874](#); 2006, [156152](#)), as the arrhythmia incidence in the acute infarction model was greatest with ROFA, while the CHF model demonstrated sensitivity to DE exposure. However, several differences in the research designs preclude strong comparisons.

Using ApoE^{-/-} mice on a high-fat diet as a model of pre-existing coronary insufficiency (Caligiuri et al., 1999, [157365](#)), Campen and colleagues studied the impact of inhaled diesel and gasoline exhaust and road dust (6 h/day×3 day) on ECG morphology (Campen et al., 2005, [083977](#);

2006, [096879](#)). Moreover, a high efficiency particle filter was used to compare the whole exhaust with an atmosphere containing only the gaseous components. For gasoline exhaust, the PM-containing atmosphere (PM mean concentration 61 $\mu\text{g}/\text{m}^3$; PNMD 15 nm; NO_x mean concentration 18.8 ppm; CO mean concentration 80 ppm) induced T-wave morphological alterations, while the PM-filtered atmosphere did not (Campen et al., 2006, [096879](#)). Resuspended road dust ($\text{PM}_{2.5}$), at up to 3500 $\mu\text{g}/\text{m}^3$ had no impact on ECG. For DE (PM mean concentration 512, 770, or 3,634 $\mu\text{g}/\text{m}^3$; MMD 100 nm, CMD 80 nm; NO_x mean concentration 19, 105, 102 ppm for low whole exhaust, high PM filtered, and high whole exhaust, respectively), dramatic bradycardia, decreased T-wave area, and arrhythmia (atrioventricular-node block and VPB) were only observed in mice exposed to high filtered and high whole exhaust (Campen et al., 2005, [083977](#)). These effects remained after filtration of PM, suggesting that the gaseous components of the whole DE drove the cardiovascular findings. The diesel- and gasoline-induced ECG changes contrast, in that the gasoline exhaust required particles to induce T-wave changes, whereas the DE did not require PM to cause an effect on ECG. However, the differing responses could be attributable to higher PM concentrations in the whole DE.

Summary of Toxicological Study Findings for ECG Abnormalities

The above toxicological studies demonstrate mixed results for arrhythmias, which may be somewhat attributable to the different disease models used. Wellenius et al. (2004, [087874](#); 2006, [156152](#)) showed decreased frequency of VPB and SVEB following $\text{PM}_{2.5}$ CAPs exposure in rats with induced MI (>12 h prior to exposure). One study reported increased frequency of premature beats in older rats exposed to CAPs, which were not observed with UF carbon particles (Nadziejko et al., 2004, [055632](#)). Rats with a MI model of CHF (3-mo recovery) had increased incidence of VPB with DE exposure (Anselme et al., 2007, [097084](#)). As for ECG morphology changes, T-wave alterations were reported for gasoline exhaust that were absent when the PM was filtered (Campen et al., 2006, [096879](#)). However, for DE, increased atrioventricular-node block, VPB, and decreased T-wave area were observed with whole exhaust and remained after filtration of PM, indicating that the gases were responsible for the effects (Campen et al., 2005, [083977](#)).

6.2.3. Ischemia

Although no evidence from epidemiologic or controlled human exposure studies of PM-induced myocardial ischemia was included in the 2004 PM AQCD (U.S. EPA, 2004, [056905](#)), one toxicological study was cited that observed ST-segment changes in dogs following a 3-day exposure to CAPs. In epidemiologic studies published since the 2004 PM AQCD (U.S. EPA, 2004, [056905](#)), associations have been demonstrated between PM and ST-segment depression, and one new controlled human exposure study reported significant increases in exercise-induced ST-segment depression among men with prior MI following a controlled exposure to DE. Results from recent toxicological studies confirm the findings presented in the 2004 PM AQCD (U.S. EPA, 2004, [056905](#)) and provide coherence and biological plausibility for the effects observed in epidemiologic and controlled human exposure studies.

6.2.3.1. Epidemiologic Studies

ECG Changes Suggestive of Increased Ischemia

The ST-segment duration is typically in the range of 0.08-0.12 s (80-120 ms). The direction of the ST change is influenced by the extent of the acute myocardial injury. If the ischemia or infarction is transmural, i.e., penetrates the entire thickness of the ventricular wall, it usually causes ST-segment elevation, while ischemia confined primarily to the ventricular endocardium often causes ST-segment depression. Clinical ischemia is typically defined to include a downsloping ST segment depression of ≥ 0.1 mV (ECG voltages are calibrated such that 1 mV equals 10 mm in the vertical direction). The studies described below evaluate a range of ECG changes suggestive of increased

ischemia including subclinical ST segment depressions (e.g. less than 0.1 mV or 1 mm) in relation to ambient PM concentration.

In a large study of the WHI Trial, Zhang et al. (2009, [191970](#)) examined the change and risk of subclinical ST-segment abnormalities, T-wave abnormalities, and T-wave amplitude associated with ambient PM_{2.5} concentrations on the same and previous 6 days. Using logistic regression, each 10 µg/m³ increase in the mean PM_{2.5}, on lag days 0-2, was associated with a 4% (95% CI: -3 to 10) increase in the relative odds of a ST-segment abnormality, and a 5% (95% CI: 0-9) increase in the relative odds of a T-wave abnormality.

Gold et al. (2005, [087558](#)) studied 24 elderly residents of Boston, MA (aged 61-88 yr) residing at or near an apartment complex that was ~ 0.5 km from an air pollution monitoring station. A protocol of continuous Holter monitoring including 5 min of rest, 5 min of standing, 5 min of outdoor exercise, 5 min of rest, and then 20 cycles of paced breathing was done up to 12 times for each subject (n = 269 ECG measurements for analysis). From these ECG measurements, they identified occurrences of ST-segment depression and examined whether mean BC, CO, and PM_{2.5} concentrations in the previous 5 and 12 h were associated with ST-segment depression. The median 5-h and 12-h mean BC concentrations were 1.28 and 1.14 µg/m³, respectively (PM_{2.5} concentrations are in Table 6-3). The mean BC concentrations in the 5 and 12 h before testing predicted ST-segment depression in most portions of the protocol. However, these effects were strongest in the post-exercise periods. For example, during the post-exercise rest period, each 10th-90th percentile increase (1.59 µg/m³) in the mean 5-h BC concentration was associated with a -0.11 mm ST-segment depression (95% CI: -0.18 to -0.05). In two pollutant models, CO did not appear to confound this association. PM_{2.5} was not associated with ST-segment depression in this study. These findings suggest traffic-generated particulate pollution may be associated with ST-segment depression.

Previously, Pekkanen et al. (2002, [035050](#)) conducted a panel study of 45 subjects with stable coronary heart disease living in Helsinki, Finland. Each subject had biweekly sub-maximal exercise testing for 6 mo (n = 342 exercise tests with 72 exercise-induced ST-segment depressions). The median daily count of ACP (ACP: 0.1-1.0 µm) was 1,200 particles/cm³ (PM_{2.5} concentrations are found in Table 6-3). They examined the risk of ST-segment depression associated with mean pollutant concentrations (UFP, ACP, PM₁, PM_{2.5}, PM_{10-2.5}, NO₂, CO) in the previous 24 h, and the 3 previous lagged 24-h periods. Each 7.9 µg/m³ increase in mean PM_{2.5} concentration, lagged 2 days, was associated with significantly increased risk of ST-segment depression >0.1 mV (OR: 2.84 [95% CI: 1.42-5.66]). Each 760 particles/cm³ increase in the count of ACP, lagged 2 days, was also associated with significantly increased risk of ST-segment depression >0.1 mV (OR: 3.29 [95% CI: 1.57-6.92]). Similarly sized increased risks of ST-segment depression were also found for other particulate pollutants, including PM_{10-2.5}, PM₁, and UFP counts.

This same research group, then conducted a principal components analysis to identify five PM_{2.5} sources (crustal, long range transport, oil combustion, salt, and local traffic) (Lanki et al., 2006, [088412](#)). Using similar statistical models, each 1 µg/m³ increase in “local traffic” particle concentration, lagged 2 days, was associated with increased risk of ST-segment depression (OR: 1.53 [95% CI: 1.19-1.97]). Similarly, each 1 µg/m³ increase in “long-range transport” particle concentration was also associated with increased risk of ST-segment depression (OR: 1.11 [95% CI: 1.02-1.20]). No significant associations for other sources were reported for any lag time.

In Boston, Chuang et al. (2008, [155731](#)) studied 48 patients with a prior percutaneous intervention following MI, acute coronary syndrome (ACS) without MI, or stable coronary artery disease without ACS. Each patient had a 24-h ECG measurement up to four times during study follow-up. Using logistic regression, they estimated the risk of ST-segment depression of ≥0.1 mm, during 30-min segments, associated with increases in the mean PM_{2.5}, BC, CO, NO₂, O₃, and SO₂ concentration in the previous 24 h. Each 6.93 µg/m³ increase in mean PM_{2.5} concentration was associated with a significantly increased risk of ST-segment depression (OR = 1.50 [95% CI: 1.19-1.89]). Using linear additive models to estimate the change in ST level associated with the same PM_{2.5} change, they observed a significant -0.031 mm change (95% CI: -0.042 to -0.019). In single pollutant models, risk estimates were of similar magnitude and statistically significant for BC, NO₂, and SO₂. In two pollutant models, however, PM_{2.5} risk estimates were reduced to 1.0 in all models with BC, NO₂, and SO₂. In contrast, the risk estimates for BC, NO₂, and SO₂ remained elevated and statistically significant when modeled with PM_{2.5}.

In a panel study of 14 Helsinki resident, non-smoking, elderly subjects with coronary artery disease, Lanki et al. (2008, [191984](#)) used logistic regression to report that each 10 µg/m³ increase in personal PM_{2.5} concentration in the previous hour was associated with a significantly increased risk

of ST-segment depression (OR = 3.26 [95% CI: 1.07-9.98]). In addition, each 10 $\mu\text{g}/\text{m}^3$ increase in outdoor mean $\text{PM}_{2.5}$ concentration in the previous 4 h was also associated with an increased risk (OR = 2.47 [95% CI: 1.05-5.85]). Last, the risk estimates for all time lags examined (1, 4, 8, 12, and 22 or 24 h) for all PM size fractions were increased, but none other than those described above were statistically significant.

Summary of Epidemiologic Study Findings for Ischemia

These studies demonstrate associations between $\text{PM}_{2.5}$ pollution and ST-segment depression at lags of 1 h-2 days. Moreover, these findings demonstrate a potential role for traffic (Chuang et al., 2008, [155731](#); Gold et al., 2005, [087558](#)) and long-range transported $\text{PM}_{2.5}$ (Lanki et al., 2006, [089788](#)). Mean and upper percentile concentrations reported in these studies are found in Table 6-3.

Table 6-3. PM Concentrations reported in epidemiologic studies ECG changes suggestive of ischemia.

Author	Location	Mean Concentration ($\mu\text{g}/\text{m}^3$)	Upper Percentile Concentrations ($\mu\text{g}/\text{m}^3$)
<i>PM_{2.5}</i>			
Zhang et al. (2009, 191970)	Multicity, US:WHI Clinical Trial	NR	NR
Pekkanen et al. (2002, 035050)	Helsinki, Finland	24-h avg: 10.6 (median)	75th: 16.0 Max: 39.8
Gold et al. (2005, 087558)	Boston, MA	5-h avg: 9.5 (median)	5-h avg 90th: 25.6 Max: 41.0
		12-h avg: 9.8 (median)	12-h avg 90th: 25.9 Max: 35.6
Chuang et al. (2008, 155731)	Boston, MA	12-h avg: 9.91 (median)	12-h avg 75th: 13.18
		24-h avg: 9.20 (median)	24-h avg max: 40.38
		Personal	Personal
Lanki et al. (2008, 191984)	Helsinki, Finland	1-h avg: 11.5 (median)	1-h avg 75th: 17.2; Max: 746.3
		4-h avg: 10.1 (median)	4-h avg 75th: 15.7; Max: 189.6
		22-h avg: 9.3 (median)	22-h avg 75th: 13.2; Max: 52.9
		Outdoor	Outdoor
		24-h avg: 12.5	24-h avg 75th: 17.7; Max: 30.5
<i>PM_{10-2.5}</i>			
Pekkanen et al. (2002, 035050)	Helsinki, Finland	24-h avg: 4.8 (median)	75th: 8.5 Max: 37.0

6.2.3.2. Controlled Human Exposure Studies

Diesel Exhaust

Among a group of 20 men with prior MI, Mills et al. (2007, [091206](#)) found that DE (300 $\mu\text{g}/\text{m}^3$ particle concentration, median particle diameter 54 nm) significantly increased exercise-induced ischemic burden during exposure, calculated as the product of exercise duration and change in ST-segment amplitude. The mechanism by which DE induced the exacerbation of ischemic burden remains unclear, and appears to be unrelated to impaired vasodilation. However, the

authors suggest that this discrepancy may be due to the timing of the vascular assessment, as measures of blood-flow were taken 5 h after the observed increase in ischemic burden. Although it is reasonable to assume that the observed increase in ST-segment depression during exercise represents an increased magnitude of ischemia, it is important to note that there are other potential explanations for the ST change. For example, it is possible that the ST-segment depression could be secondary to heterogeneity of electrophysiological responses of particle exposure on the myocardium that is enhanced by the metabolic and ionic conditions associated with ischemia or increased HR. It is also important to note that the effects observed in this study cannot be conclusively attributed to the particles per se, as subjects were also exposed relatively high levels of NO (3.45 ppm), NO₂ (1.01 ppm), CO (2.9 ppm), and total hydrocarbons (2.8 ppm).

6.2.3.3. Toxicological Studies

CAPs

A study that examined ECG changes in dogs (female; retired mongrel breeder dogs) following PM_{2.5} CAPs exposure in Boston, MA (mean mass concentration 345 µg/m³; 9/2000-3/2001) and left anterior descending coronary artery occlusion as an indicator of myocardial ischemia reported changes in ST-segment (Wellenius et al., 2003, [055691](#)). The experimental protocol was a 6-h exposure to CAPs via tracheostomy, followed by a preconditioning occlusion (5 min), rest interval (20 min), and the experimental occlusion (5 min). Increased ST-segment elevation was observed following PM_{2.5} during the experimental occlusion period compared to filtered air. Furthermore, peak ST-segment elevation attributable to CAPs was reported with the experimental occlusion, which remained elevated 24 h post-exposure. Ventricular arrhythmias were rarely observed during occlusion and when observed, were unrelated to CAPs exposure. The results from this study support those previously observed (Godleski et al., 2000, [000738](#)) and provides greater support that enhanced myocardial ischemia occurs relatively quickly (within hours) following PM exposure.

The Wellenius et al. (2003, [055691](#)) study also attempted to link ST-segment changes with four CAPs elements (Si, Ni, S, and BC) as tracers of PM_{2.5} sources in Boston. In the multivariate regression analyses, peak ST-segment elevation and integrated ST-segment change were significantly associated with only the mass concentration of Si (Si mean concentration 8.17 µg/m³; Si concentration 2.31-13.93 µg/m³). In the univariate regression analyses, Pb also demonstrated a significant association for both ST-segment measures, although the p-value was greater than that observed with Si.

A recent study in dogs (female mixed-breed canines) evaluated myocardial blood flow during myocardial ischemia following 5-h PM_{2.5} Boston CAPs exposures (daily mean mass concentration 94.1-1556.8 µg/m³; particle number concentration 3-69.3×10³ particles/cm³; BC concentration 1.3-32.0 µg/m³) (Bartoli et al., 2009, [179904](#)). Similar methods were used for the coronary occlusion and exposure method as Wellenius et al. (2003, [055691](#)). Immediately following exposure, microspheres were injected (15 µm diameter) into the left atrium after 3 min of ischemia during the second occlusion. Post-mortem analysis of cardiac tissue and blood samples allowed for quantification of microspheres. CAPs-exposed dogs had decreased total myocardial blood flow and increased coronary vascular resistance during occlusion that was greatest in tissue within or near the ischemic zone. The rate-pressure product (product of HR and SBP) during occlusion was unchanged in animals exposed to CAPs, indicating that cardiac metabolic demand was not altered. The multilevel linear mixed models demonstrated that myocardial blood flow and coronary vascular resistance during occlusion were inversely and significantly associated with CAPs mass concentration, particle number concentration, and BC concentration, with the strongest effects observed with particle number concentration. The results of this study provide evidence that exacerbation of myocardial ischemia following PM exposure is due to reduced myocardial blood flow, perhaps via dysfunctional collateral vessels.

Intratracheal Instillation

Cozzi et al. (2006, [091380](#)) exposed ICR mice to UF PM (100 µg IT instillation), followed by ischemia/reperfusion injury to the left anterior coronary artery 24 h later. The area-at-risk (the region of tissue perfused by the left anterior descending coronary artery) and the infarct size were measured 2 h following reperfusion, and while the area-at-risk was not affected by PM exposure, the infarct size was nearly doubled in mice who received UF PM. Increases in infarct size were associated with increased myocardial neutrophil density in the infarct zone and lipid peroxidation in the myocardium.

Summary of Toxicological Study Findings for Ischemia

The studies described above provide evidence that PM can induce greater myocardial responses following ischemic events, as demonstrated by, enhanced ischemia, decreased myocardial blood flow and increased coronary vascular resistance, and increased infarct size.

6.2.4. Vasomotor Function

The most noteworthy new cardiovascular-related revelation in the past six years with regards to PM exposure is that the systemic vasculature may be a target organ. The vasculature of all tissues is lined with endothelial cells that will naturally encounter any systemically absorbed toxin. The endothelium (1) maintains barrier integrity to ensure fluid compartmentalization; (2) communicates dilatory and constrictive stimuli to vascular smooth muscle cells; and (3) recruits inflammatory cells to injured regions. Smooth muscle cells lie within the layer of endothelium and are crucial to the regulation of blood flow and pressure. In states of injury and disease, both cell types can exhibit dysfunction and even pathological responses.

Endothelial dysfunction is a factor in many diseases and may contribute to the origin and/or exacerbation of perfusion-limited diseases, such as MI or IHD, as well as hypertension. Endothelial dysfunction is also a characteristic feature of early and advanced atherosclerosis. A primary outcome of endothelial dysfunction is impaired vasodilatation, frequently due to uncoupling of NOS. It is this uncoupling that appears central to impaired vasodilation and thus endothelial dysfunction.

One controlled human exposure study cited in the 2004 PM AQCD (U.S. EPA, 2004, [056905](#)) reported a decrease in bronchial artery diameter (BAD) among healthy adults following exposure to CAPs in combination with O₃. Conclusions based on this finding were limited due to the concomitant exposure to O₃ as well as a lack of published results from epidemiologic and toxicological studies. Recent controlled human exposure studies have provided support to the findings described in the 2004 PM AQCD (U.S. EPA, 2004, [056905](#)), with changes in vasomotor function observed following controlled exposures to DE and EC particles. In addition, epidemiologic studies have observed associations between PM and decreases in BAD and flow mediated dilatation (FMD) in healthy adults and diabetics. These findings are further supported by a large body of new toxicological evidence of impaired vasodilation following exposure to PM.

6.2.4.1. Epidemiologic Studies

O'Neill et al. (2005, [088423](#)) examined the association between 2 measures of vascular reactivity, non-endothelium dependent nitroglycerin mediated reactivity and endothelium-dependent flow-mediated reactivity, and ambient mean particulate pollutant concentration (PM_{2.5}, SO₄²⁻, BC, PNC) on the same and previous few days. They studied a panel of 270 subjects with diabetes or at risk for diabetes, who lived in the greater Boston metropolitan area. Using linear regression models, the change in vascular reactivity associated with moving average pollutant concentrations across the same and previous 5 days was estimated. Interquartile range (values not reported) increases in mean PM_{2.5} concentration, BC concentration, and PNC over the previous 6 days were associated with decreased vascular reactivity among diabetics, but not among subjects at risk for diabetes. For SO₄²⁻, the mean concentration on lag day 0, lag day 1, and the 3-day, 4-day, and 5-day ma all were associated with similarly sized reductions in both metrics of vascular reactivity. Among diabetics, each interquartile range increase in the mean SO₄²⁻ concentration over the previous 6 days was

associated with a 5.4% decrease in nitroglycerin-mediated reactivity (95% CI: -10.5 to -0.1) and flow-mediated reactivity (-10.7% [95% CI: -17.3 to -3.5]). Also among diabetics, each interquartile range increase in the mean PM_{2.5} concentration over the previous 6 days was associated with a 7.6% decrease in nitroglycerin-mediated reactivity (95% CI: -12.8 to -2.1) and a non-significant 7.6% decrease in flow-mediated reactivity (95% CI: -14.9 to 0.4). Each interquartile range increase in the mean BC concentration over the previous 6 days was associated with a 12.6% decrease in flow mediated reactivity (95% CI: -21.7 to -2.4), but not nitroglycerin-mediated reactivity. PNC was associated with non-significant decreases in both measures. Effect estimates were larger for type 2 diabetics than type 1 diabetics.

Dales et al. (2007, [155743](#)) conducted a panel study of 39 healthy volunteers who sat at 1 of 2 bus stops in Ottawa, Canada for 2 h. FMD of the brachial artery was measured immediately after the bus stop exposure, but not before. They examined the association between FMD and 2-h mean PM_{2.5}, PM₁, NO₂, and traffic density at the bus stop (vehicles/h). The authors report that each 30 µg/m³ increase in 2-h mean PM_{2.5} concentration was associated with a significant 0.48% reduction in FMD. This represented a 5% relative change in the maximum ability to dilate.

This same research group conducted a panel study of 25 type 1 or 2 diabetic subjects living in Windsor, Ontario (aged 18-65 yr) (Liu et al., 2007, [156705](#)). For each subject, personal PM₁₀ concentrations were measured for 24 h before measurements of BAD, FMD, and other biomarkers. Each 10 µg/m³ increase in personal 24-h mean PM₁₀ concentration was associated with a 0.20% increase in end-diastolic FMD (95% CI: 0.04-0.36) and a 0.38% increase in end-systolic FMD (95% CI: 0.03-0.73), but decreases in end-diastolic basal diameter (-2.52 µm [95% CI: -8.93 to 3.89]) and end-systolic basal diameter (-9.02 µm [95% CI: -16.04 to -2.00]).

Rundell et al. (2007, [156060](#)) examined the change in FMD associated with high and low PM₁ (0.02-1.0 µm) pollution in a panel of 16 young intercollegiate athletes (mean age = 20.5±2.4 yr) in Scranton, PA, who were non-smokers, non-asthmatics, and free of cardiovascular disease (Rundell et al., 2007, [156060](#)). Each subject had FMD of the brachial artery measured 10-20 min before and 20-30 min after each of two 30-min exercise tests (85-90% of maximal HR). The exercise tests were done outside either on an inner campus location free of automobile and truck traffic (low PM₁; mean = 5,309±1,942 particles/cm³) or on a soccer field adjacent to a major highway (high PM₁; mean = 143,501±58,565 particles/cm³). The order of the exercise test locations was chosen randomly. Using paired t-tests for analysis, they reported FMD was impaired after high PM₁ exposure (pre-exercise: 6.8±3.58%; post-exercise: 0.30±2.74%), but not low PM₁ exposure (pre-exercise: 6.6±4.04%; post-exercise: 4.89±4.42%). Further, they found basal brachial artery vasoconstriction (4%; pre-exercise BAD: 4.66±0.61 mm; post-exercise BAD: 4.47±0.63 mm) after the 'high PM₁' exposure, but not the 'low PM₁' exposure (-0.3% pre-exercise BAD: 4.66±0.63 mm; post-exercise BAD: 4.68±0.61 mm).

In a prospective panel study of 22 type 2 diabetics (aged 61 ± 8 yr), Schneider et al. (2008, [191985](#)) examined the change in FMD, BAD, small artery elasticity index, larger artery elasticity index, and systemic vascular resistance associated with ambient PM_{2.5} as measured in Chapel Hill, NC (November 2004-December 2005). Using additive mixed models with a random subject effect, each 10 µg/m³ increase in PM_{2.5} in the previous 24 h was associated with a decrease in FMD (-17.3% [95% CI: -34.6 to 0.0]). Similarly, each 10 µg/m³ increases in PM_{2.5} was associated with a decrease in small artery elasticity index lagged 1 day (-15.1% [95% CI: -29.3 to -0.9]), and lagged 3 days (-25.4% [95% CI: -45.4 to -5.3]). Significant decreases in larger artery elasticity index and increases in systemic vascular resistance lagged 2 and 4 days were also reported. Further, effects were greatest among those with high BMI, high glycosylated hemoglobin A1c, low adiponectin, or the null GSTM1 polymorphism. However, high myeloperoxidase (MPO) levels were associated with greater PM_{2.5} effects on these measures.

In a similar study done in Paris, France, Briet (2007, [093049](#)) similarly reported that each increase in PM_{2.5} was associated with a -0.32% decrease in FMD (95% CI: -1.10 to 0.46). Significant FMD reductions were associated with increased SO₂, NO₂, and CO concentrations. Each 1 standard deviation increase (units not given) in PM_{2.5} in the previous 2 wk was associated with a 15.68% (95% CI: 7.11-23.30) increase in small artery reactive hyperemia. Each 1 standard deviation increase (units not given) in PM₁₀ in the previous 2 wk was associated with a 15.91% (95% CI: 7.74-24.0) increase in small artery reactive hyperemia.

Summary of Epidemiologic Study Findings for Vasomotor Function

Vasomotor function has been evaluated using several metrics in the studies described above, including FMD, small artery elasticity index, larger artery index, systemic vascular resistance, BAD, end diastolic basal diameter, and nitroglycerin-mediated reactivity. The most common measures evaluated were BAD, a measure of the relatively static, anatomic/physiological baseline vasomotor function, and FMD, the dynamic measure of post- minus pre-occlusion BAD. Each study demonstrated an acute association between these measures of vascular function and ambient PM_{2.5} concentrations (Briet et al., 2007, [093049](#); Dales et al., 2007, [155743](#); Liu et al., 2007, [156705](#); O'Neill et al., 2005, [088423](#); Rundell et al., 2007, [156060](#); Schneider et al., 2008, [191985](#)). An association with PM₁₀ was observed in a study conducted in Windsor Ontario (Liu et al., 2007, [156705](#)). Three studies evaluated effects on diabetics (Liu et al., 2007, [156705](#); O'Neill et al., 2005, [088423](#); Schneider et al., 2008, [191985](#)), and three evaluated PM-related changes in vasomotor function on young healthy subjects (Briet et al., 2007, [093049](#); Dales et al., 2007, [155743](#); Rundell et al., 2007, [156060](#)). Only two studies investigated multiple lags (lag days 0 to 6) (O'Neill et al., 2005, [088423](#); Schneider et al., 2008, [191985](#)), with one reporting the strongest association with the 6-day mean PM concentration (O'Neill et al., 2005, [088423](#)), and the other with lag day 0. In other studies, responses were observed in as short as 30 min after the exposure (Rundell et al., 2007, [156060](#)). The Rundell et al. (2007, [156060](#)) findings are consistent with other studies showing an adverse response to ambient particulate pollution emitted from vehicular traffic (Adar et al., 2007, [098635](#); Adar et al., 2007, [001458](#); Riediker et al., 2004, [056992](#); Riediker et al., 2004, [091261](#)). Mean and upper percentile concentrations reported in these studies are found in Table 6-4.

Table 6-4. PM concentrations reported in epidemiologic studies of vasomotor function.

Author	Location	Mean Concentration ($\mu\text{g}/\text{m}^3$)	Upper Percentile Concentrations ($\mu\text{g}/\text{m}^3$)
PM_{2.5}			
Briet (2007, 093049)	Paris, France	NR	NR
Dales (2007, 155743)	Ottawa, Canada (bus stops)	Bus stop 1: 40 Bus stop 2: 10	NR
O'Neill (2005, 088423)	Boston, MA	11.5	Range: 1.1 - 20.0
Schneider (2008, 191985)	Chapel Hill, NC	13.6	NR
PM₁₀			
Briet (2007, 093049)	Paris, France	NR	NR
Liu (2007, 156705)	Windsor, Ontario	24h (personal): 25.5	5th to 95th: 9.8 – 133

6.2.4.2. Controlled Human Exposure Studies

Some evidence of a PM-induced increase in brachial artery vasoconstriction is presented in the 2004 PM AQCD (U.S. EPA, 2004, [056905](#)). Brook et al. (2002, [024987](#)) exposed 24 healthy adults to PM_{2.5} CAPs (150 $\mu\text{g}/\text{m}^3$) along with 120 ppb O₃ for a period of 2 h. A significant decrease in BAD was observed immediately following exposure compared with filtered air control. No significant changes were observed in either endothelial-dependent or endothelial-independent vasomotor function, as determined by FMD and nitroglycerin-mediated dilatation, respectively. As described below, many more recent studies have evaluated the effects of various types of particles on vasomotor function following controlled exposures among healthy and health-compromised individuals.

CAPs

A subsequent analysis of the CAPs constituents from the Brook et al. (2002, [024987](#)) study revealed a significant negative association between the post-exposure change in BAD and both the OC and EC concentrations of CAPs (Urch et al., 2004, [055629](#)). However, the observed vasomotor effects cannot conclusively be attributed to PM_{2.5}, as subjects were exposed concurrently to PM_{2.5} and O₃. Mills et al. (2008, [156766](#)) evaluated the effect of fine and UF CAPs on vasomotor function in a group of 12 males with stable coronary heart disease (average age 59 yr), as well as in 12 healthy males (average age 54 yr). Relative to filtered air exposure, exposure to PM (average concentration 190 µg/m³) did not significantly affect vascular function in either group. The authors attributed the lack of response in endothelial function to the composition of the CAPs used in the study, which were low in combustion-derived particles and consisted largely of sea salt.

Urban Traffic Particles

The effect of exposure to urban traffic particles on vasomotor function has recently been evaluated among a group of adult volunteers (Bräuner et al., 2008, [191966](#)). In this study, healthy young adults (average age 27 yr) exposed for 24 h to urban traffic particles (average PM_{2.5} concentration 10.5 µg/m³) were not observed to experience any change in microvascular function after 6 or 24 h of exposure relative to filtered air.

Diesel Exhaust

Mills et al. (2005, [095757](#)) exposed 30 healthy men (20-38 yr) to both diluted DE (300 µg/m³) and filtered air control for 1 h with intermittent exercise. Half of the subjects underwent vascular assessments at 6-8 h following exposure to DE or filtered air, while in the other 15 subjects, vascular assessments were performed at 2-4 h post-exposure. DE attenuated forearm blood flow increase induced by bradykinin, acetylcholine (ACh), and sodium nitroprusside (SNP) infusion measured 2 and 6 h after exposure. The authors postulated that the effect of DE on vasomotor function may be the result of reduced NO bioavailability in the vasculature stemming from oxidative stress induced by the nanoparticulate fraction of DE. A DE-induced decrease in the release of tPA was also observed at 6 h post-exposure, which may provide additional mechanistic evidence supporting the observed association between air pollution and MI. As presented in Tornqvist et al. (2007, [091279](#)), changes in vascular function were also evaluated 24 h following exposure in 15 of the 30 subjects. Compared with filtered air, exposure to DE significantly reduced endothelium-dependent (ACh) vasodilation at 24 h post exposure. Bradykinin-induced vasodilation was marginally attenuated by DE, while no effects of diesel on endothelium-independent vasodilation (SNP) were observed. Although the release of tPA was not affected by DE 24 h following exposure, the authors suggest that the persistent association between diesel exposure and vasomotor function observed in this study provides supporting mechanistic evidence of increases in cardiovascular events occurring 24 h after a peak in PM concentration.

To further investigate the effects of DE on vasomotor function, Mills et al. (2007, [091206](#)) exposed 20 men (avg age 60 yr) with previous MI on two separate occasions to dilute DE (300 µg/m³; mean particle size 54 nm) or filtered air for 1 h with intermittent exercise. Contrary to previous findings in younger, healthy adults (Mills et al., 2005, [095757](#)), DE was found not to affect vasomotor function in peripheral resistance vessels at 6 h post-exposure as measured by endothelium-dependent (ACh) and endothelium-independent (SNP) vasodilation (forearm blood flow). However, vascular assessments were not performed at 2 h post-exposure in this study. The same laboratory evaluated the effect of exposure to DE with slightly higher particle concentrations (330 µg/m³, particle number 1.26×10⁶/cm³) on arterial stiffness among healthy adults (Lundbäck et al., 2009, [191967](#)). Using radial artery pulse wave analysis, significant increases in augmentation pressure and augmentation index, as well as a significant reduction in the time to wave reflection were observed 10 and 20 min following exposure to DE relative to filtered air. This finding of a DE-induced reduction in arterial compliance provides additional evidence to suggest that exposure to particles may adversely affect vasomotor function.

Peretz et al. (2008, [156854](#)) exposed both healthy adults (n = 10) and adults with metabolic syndrome (n = 17) for 2 h to filtered air and two concentrations of diluted DE (PM_{2.5} concentrations of 100 and 200 µg/m³). Compared with filtered air, DE at 200 µg/m³ elicited a statistically significant decrease in BAD (0.11 mm [95% CI: 0.02-0.18 mm]) immediately following exposure. A smaller DE-induced decrease in BAD (0.05 mm) was observed following exposure to 100 µg/m³. Although this latter decrease was not statistically significant, the average decrease was approximately 50% of the decrease at the higher particle concentration, which provides suggestive evidence of a linear concentration response in this range of concentrations. Exposure to DE was not shown to significantly affect endothelium-dependent FMD. Plasma levels of endothelin-1 (ET-1) were observed to increase relative to filtered air exposure approximately 1 h after exposure to 200 µg/m³ DE (p = 0.01). Samples collected following the 100 µg/m³ exposure session were not assayed for ET-1. The results of this study provide evidence of an acute endothelial response and arterial vasoconstriction resulting from short-term exposure to DE. DE-induced changes in vasoconstriction and ET-1 release were more pronounced in the healthy subjects than in the subjects with metabolic syndrome. The authors postulated that subjects with metabolic syndrome may have stiffer vessels that are not as responsive to vasoconstrictor stimuli. In a study utilizing a similar exposure protocol, Lund et al. (2009, [180257](#)) observed a significant increase in ET-1 in healthy adults following a 2-h exposure to DE with a particle concentration of 100 µg/m³.

In the previously described studies by Mills et al. (2005, [095757](#); 2007, [091206](#)), Peretz et al. (2008, [156854](#)), Tornqvist et al. (2007, [091279](#)) and Lund et al. (2009, [180257](#)), subjects were exposed to DE, which, in addition to PM, includes DE gases such as NO_x, CO, and hydrocarbons. Therefore, it is possible that the observed effects may be due in part to exposure to non-particle components of DE. While the majority of these DE exposures have contained relatively high levels of gaseous emissions including NO₂ concentrations >2 ppm, the concentrations of these gases were much lower in the Peretz et al. (2008, [156854](#)) study (NO₂ concentrations ≈ 20 ppb) which used a newer diesel engine (2002 Cummins B-series) operating under load at 75% of rated capacity. In this study, an apparent linear concentration response relationship was observed between increasing DE exposure and decreases in BAD at particle concentrations between 100 and 200 µg/m³.

Gasoline Emissions

Rundell and Caviston (2008, [191986](#)) exposed 15 college athletes to particles generated using a 2.5 hp gasoline engine, as well as a clean air control during 6-min periods of maximal exercise on a cycle ergometer. Subjects were exposed twice under each condition, with the two clean air exposures occurring first, separated by 3 days. The 2 exposures to gasoline emissions were also separated by 3 days, with the first exposure occurring 7 days after the second clean air exposure. During exposures to gasoline emissions, average PNC of PM <1.0 µm were reported as 336,730 and 396,200 particles/cm³ during the first and second exposures, respectively, with an average CO concentration of 6.3 ppm. There were no differences observed in total work done (kJ) over the 6-min exercise periods between the two clean air exposures or between the clean air exposures and the first exposure to gasoline exhaust. However, the second gasoline exhaust exposure was demonstrated to significantly decrease work accumulated over the 6-min exercise period compared with either of the other exposure conditions. The results of this study provide limited evidence to suggest that a very short term exposure to gasoline emissions may affect exercise performance in healthy adults. The authors speculated that the observed effect of exposure on work accumulated during maximal exercise could be due to vasoconstriction and decrease in blood flow in the skeletal muscle microcirculation. However, the effect of exposure on vasoreactivity was not explicitly assessed.

Model Particles

The results of a recent study by Shah et al. (2008, [156970](#)) provides evidence that exposure to UF EC particles (50 µg/m³) without coexposure to organics, metals, or gaseous copollutants may alter vasomotor function in healthy adults. In this study, venous occlusion plethysmography was used to measure reactive hyperemia of the forearm prior to exposure, immediately following exposure, and 3.5 h, 21 h, and 45 h following a 2-h exposure with intermittent exercise. Peak

forearm blood flow was observed to increase after exposure to filtered air, but not following exposure to UF EC at 3.5 h post-exposure ($p = 0.03$).

Summary of Controlled Human Exposure Study Findings for Vasomotor Function

Taken together, the two studies by Mills et al. (2005, [095757](#); 2007, [091206](#)) along with the studies by Peretz et al. (2008, [156854](#)), Lund et al. (2009, [180257](#)) and Tornqvist et al. (2007, [091279](#)) suggest that, in healthy subjects, DE exposure inhibits endothelium-dependent and endothelium-independent vasodilation acutely (within 2-6 h), and that the suppression of endothelium-dependent vasodilation may remain up to 24 h following exposure. In patients with coronary artery disease, vasodilator function does not appear to be affected 6-8 h following exposure; however, vascular assessments were not performed at earlier time points. In addition, the use of medications in these patients may have blunted the response to PM. The findings of Shah et al. (2008, [156970](#)) suggest that UFP carbon core may be sufficient to produce small changes in systemic vascular function, but the mechanisms remain obscure. The authors demonstrated a decrease in nitrate levels following exposure to UF EC; however, venous nitrite level, which more closely reflects NO production, was unchanged. Exposure to urban traffic particles was not demonstrated to alter vasomotor function among healthy adults.

6.2.4.3. Toxicological Studies

Vascular dysfunction is a function of altered production of vasoconstrictors and vasodilators. In the 2004 PM AQCD (U.S. EPA, 2004, [056905](#)), studies examining ET as an activator of vasoconstriction were limited to those conducted by Bouthiller et al. (1998, [087110](#)) and Vincent et al. (2001, [021184](#)), in which increased plasma ET levels were observed in rats exposed to high concentrations (40 or 5 mg/m^3) of resuspended Ottawa (EHC-93) or diesel PM, respectively. The authors postulated that PM altered vasoconstriction via elevated ET. No studies were cited in the 2004 PM AQCD (U.S. EPA, 2004, [056905](#)) that looked at direct measures of vasoreactivity.

As this area is newly emerging, some studies are included below that utilize IT exposure or high concentrations; the studies that exposed vessels directly to particles *ex vivo* are included in Annex D only, as their relevance is questionable. There is clearly a need for more toxicological research examining the relationship between vascular measurements and PM exposures using ambient particles at lower concentrations. Furthermore, no new studies have advanced the knowledge in regards to ET as a biomarker of PM-induced vasoconstriction since the last PM review.

CAPs

SD rats were exposed to $\text{PM}_{2.5}$ CAPs (5 h/day \times 3 days; daily mean mass concentration 73.5-733 $\mu\text{g}/\text{m}^3$; Boston, MA; 3/1997-6/1998) then the pulmonary arterial vasculature was evaluated (Batalha et al., 2002, [088109](#)). Some animals were repeatedly exposed to SO_2 (5 h/day \times 5 days/wk \times 6 wk) to induce chronic bronchitis. Morphometric measurements indicated that the pulmonary artery lumen-to-wall (L/W) ratio (an indicator of arterial narrowing) was decreased for the both CAPs groups compared to the normal/air group. Furthermore, decreased L/W ratio in CAPs-exposed animals (regardless of pre-treatment) was significantly associated with particle mass and composition when the mean concentrations from the second and third exposure days were used in a univariate linear regression. These results indicate a change in vascular tone following acute exposure to PM. Univariate analyses were conducted that regressed log L/W on differential exposure concentrations of tracer elements determined using principal components analysis (Batalha et al., 2002, [088109](#)). For CAPs exposure (regardless of pretreatment), CAPs mass, Si, Pb, SO_4^{2-} , EC, and OC were all negatively correlated with L/W ratio. Si and SO_4^{2-} were negatively correlated with L/W ratio in normal rats and Si and OC were negatively correlated with L/W ratio in bronchitic rats. When a multivariate analysis was conducted using normal and bronchitic animals, only the association with Si remained significant. V was not associated with L/W ratio in any analysis.

Diesel Exhaust

The venous circulation plays a prominent role in heart failure exacerbation (Gehlbach and Geppert, 2004, [155784](#)). In heart failure, patients are often volume overloaded and are subsequently placed on diuretics to alleviate symptoms of pulmonary congestion and chest pain. Knuckles et al. (2008, [191987](#)) hypothesized that if veins constrict in a manner similar to arteries, then patients with severe CHF may have temporary shunting of fluid to the pulmonary circulation, which may elicit signs and symptoms of CHF. Using mesenteric vessels from mice (C57BL/6) exposed to DE (350 $\mu\text{g}/\text{m}^3 \times 4$ h; MMD 100 nm, CMD 80 nm), the authors reported a significant enhancement of ET-1-induced vasoconstriction in veins with much weaker responses in arteries. In an ex vivo experiment, venous constriction was blocked by the arginine analog, L-NAME, which eliminates the feedback NOS activation via endothelial ET_B receptors; this is indicative of impaired or uncoupled eNOS. The authors hypothesized that volatile organic compounds might be responsible these effects, but no significant effects were observed for acetaldehyde, formaldehyde, acetone, hexadecane, or pristane.

Model Particles

A study by Nurkiewicz et al. (2008, [156816](#)) compared the arteriole dilation responses in the spinotrapezius muscle with inhalation exposure to fine or UF TiO₂ (1 μm and 21 nm, respectively; mean mass concentration 3-16 and 1.5-12 mg/m^3 , respectively) for durations of 4-12 h in SD rats. Both size fractions of TiO₂ induced impaired dilation with a NO-dependent Ca²⁺ ionophore in a dose-dependent manner. When fine and UF TiO₂ were compared at similar mass doses, the systemic microvascular dysfunction was greater with the UFPs. Furthermore, three exposures of differing durations and concentrations that produced equal calculated pulmonary deposition of UF TiO₂ (30 μg) demonstrated similar dilation responses, indicating that impairment is dependent upon the time \times concentration product. No effects on dilation were observed with a dose of 4 μg UF TiO₂ (1.5 mg/m^3 for 4 h) or 8 μg fine TiO₂ (3 mg/m^3 for 4 h).

In a follow-up study, Nurkiewicz et al. (2009, [191961](#)) examined the effect of pulmonary fine and UF TiO₂ exposure on endogenous microvasculature NO production in SD rats. The exposure concentrations and durations were selected to produce ~50% impairment of microvascular reactivity (67 and 10 μg for fine¹ and UF² TiO₂, respectively). Similar to the study above (Nurkiewicz et al., 2008, [156816](#)), impaired endothelium-dependent arteriolar dilation was observed 24 h post-exposure with infusion of a Ca²⁺ ionophore. Earlier studies that used residual oil fly ash (ROFA) or TiO₂ via IT instillation reported similar findings, regardless of particle type (Nurkiewicz et al., 2004, [087968](#); Nurkiewicz et al., 2006, [088611](#)). There was no difference in arteriolar dilation between sham and TiO₂ exposed groups with direct administration of the NO donor SNP to the exterior arteriolar wall and this response was consistent with that observed following ROFA administered intratracheally (Nurkiewicz et al., 2004, [087968](#)). The lack of response to SNP indicates that vascular smooth muscle sensitivity to NO is not altered after particle exposure. The amount of ROS in the microvascular wall was increased following exposure to either TiO₂ size. Local ROS may consume endothelial-derived NO and generate peroxynitrite radicals, as microvascular nitrotyrosine (NT) formation (the end product of peroxynitrite reactions) was demonstrated after TiO₂ exposure. NO production was compromised in a dose-dependent manner following particle exposure (8-90 μg for fine and 4-38 μg for UF TiO₂), and was partially restored with agents for radical scavenging or enzyme inhibition for NADPH oxidase and MPO.

Intratracheal Instillation

Nurkiewicz et al. (2004, [087968](#); 2006, [088611](#)) have shown impairment of endothelium-dependent dilation in the systemic microvasculature of SD rats following ROFA or TiO₂ exposure (0.1 or 0.25 mg/rat). NO-independent arteriolar dilation was also impaired by ROFA,

¹ Produced by a 300-min exposure to 16 mg/m^3 of fine TiO₂

² Produced by a 240-min exposure to 6 mg/m^3 of ultrafine TiO₂

but arteriole adrenergic sensitivity to phenylephrine (PHE) was not affected by 0.25 mg ROFA, indicating that contractile activity was unchanged. In addition, increased venular leukocyte rolling and adhesion in the spinotrapezius muscle was also observed following ROFA exposure (Nurkiewicz et al., 2004, [087968](#)).

Further characterization of the leukocyte adherence and “rolling” effects for both ROFA and TiO₂ were indicative of an activated endothelium (Nurkiewicz et al., 2006, [088611](#)). Vascular deposition of MPO was observed in the spinotrapezius muscle 24 h post-exposure and the authors suggested that the adherent leukocytes may have deposited the MPO to be taken up by endothelial cells (Nurkiewicz et al., 2006, [088611](#)). However, this is in contrast to another study (Cozzi et al., 2006, [091380](#)) that did not find changes in blood neutrophil MPO release in ICR mice exposed to UF PM (100 µg from Chapel Hill, NC; assessed 24 h post-exposure), although this finding may be a reflection of differing protocols. Increased oxidative stress in the arteriolar wall was also reported with exposure to 0.25 mg ROFA. TiO₂ and ROFA induced varying degrees of pulmonary inflammation in these animals, but elicited very similar vascular effects, indicating that the vascular responses may be due to PM presence in the lung rather than its physiochemical properties or intrinsic pulmonary toxicity.

PM₁₀

Tamagawa et al. (2008, [191988](#)) reported reduced ACh-stimulated relaxation in carotid arteries from rabbits (New Zealand White) exposed to PM₁₀ (EHC-93) via intrapharyngeal instillation for 5 days or 4 wk (total doses 8 and 16 mg/kg, respectively). Endothelium-dependent NO-mediated vasorelaxation correlated with increased serum IL-6 levels in the acute study and during wk 1 and 2 of the 4-wk exposure, which may indicate a role for systemic inflammation in the response. Maximal SNP-induced dilation was not affected by PM exposure, indicating that the dilatory response was not acting via endothelium-independent NO-mediated mechanisms. This finding is consistent with that by Nurkiewicz et al. (2004, [087968](#)) and suggests that the arteriolar smooth muscle is not involved in the PM-impaired dilatation response.

Vasoreactivity of aortic rings was measured in SH rats following exposure to 10 mg/kg PM₁₀ (EHC-93), with an increase in ACh-induced vasorelaxation observed (Bagate et al., 2004, [087945](#)). This endothelium-dependent response was greatest at 4 h and was still present at 24 h. Similarly, vasorelaxation induced by SNP 4-h post-PM exposure was enhanced. The vasorelaxation response was attenuated after denudation of the aortic rings, suggesting that the effect was endothelium dependent. The findings of enhanced dilation with PM exposure contrast with those reported by Nurkiewicz et al. (2004, [087968](#); 2006, [088611](#)), Tamagawa et al. (2008, [191988](#)), and Cozzi et al. (2006, [091380](#)) and may be attributable to differences in PM type, animal species, or disease models. The authors attribute their findings to the SH rat as a well-documented model of sympathetic hyperactivity (increased affinity of aortic smooth muscle α-adrenergic receptors) that demonstrates upregulation of NO formation and/or release (Safar et al., 2001, [156068](#)). No change in vasoconstriction was observed with PM with PHE or potassium chloride.

Consistent with the impaired vasodilatory responses observed in the microvasculature and aortic rings following PM exposure, Courtois et al. (2008, [156369](#)) demonstrated less relaxation to ACh in intrapulmonary arteries of Wistar rats exposed to a high dose (5 mg) of ambient PM (SRM1648). This response was only observed 12 h after PM exposure and not at shorter (6 h) or longer (24 or 72 h) time points. Fine TiO₂ did not alter ACh-induced relaxation.

Ultrafine PM

Cozzi et al. (2006, [091380](#)) used ICR mice to examine the effects of UF PM exposure (100 µg collected from Chapel Hill, NC) on vascular reactivity following PM exposure and ischemia/reperfusion injury. Aortic rings were evaluated for their contractile and dilatory responses 24 h post-exposure and following the ischemia/reperfusion protocol. Maximum ACh-induced relaxation was impaired in UF PM-exposed vessels, as well as a rightward shift in sensitivity to ACh. There was no difference in constriction to PHE between aortic rings from control and PM-exposed mice. The reduced ACh-induced relaxation may be important for reperfusion of critical vascular beds following occlusion, potentially leading to a greater area of infarction (as in this study). A new study in dogs supports the results observed in the above study and provides evidence of reduced myocardial blood flow following PM exposure (Bartoli et al., 2009, [179904](#)), and is discussed in more detail in Section 6.2.3.3.

Summary of Toxicological Study Findings for Vasoreactivity

The toxicological findings with respect to vascular reactivity are generally in agreement and demonstrate impaired dilation following PM exposure that is likely endothelium dependent. These effects have been demonstrated in varying vessels (right spinotrapezius muscle, carotid arteries, and aortic rings) and in response to different PM types (ROFA, TiO₂, EHC-93, UF ambient PM). The work by Nurkiewicz et al. (2004, [087968](#); 2006, [088611](#); 2008, [156816](#); 2009, [191961](#)) supports a role for increased ROS and RNS production in the microvascular wall that leads to altered NO bioavailability and dysfunction following particle exposure. Only one study showed enhanced dilation with PM exposure, but the authors attributed the conflicting results to the SH rat. No constriction changes in response to PHE were observed following PM exposure. The responses observed in the pulmonary circulation after PM exposure include pulmonary vasoconstriction, decreased L/W ratio, and impaired vasodilation in intrapulmonary arteries. These results are consistent and indicate altered vascular tone. Enhancement of vasoconstriction in mesenteric veins following DE is the first study of its kind to report on venous circulatory effects.

Endothelin

In addition to studies that look at vascular reactivity, three recent studies have examined plasma ET levels following exposure to vehicle emissions and a few studies examined the mRNA expression of ET-1 and ET receptors in the hearts of rodents following PM exposure.

CAPs

The upregulation of mRNA expressions of ET-1 and the ET_A receptor in WKY rats exposed to CAPs (1 or 4 days; 4.5 h/day; mean mass concentration range 1,000-1,900 µg/m³; Yokohama City, Japan) was correlated with increasing PM cumulative mass collected on chamber filters (Ito et al., 2008, [096823](#)). Furthermore, relative cardiac mRNA expressions of ET-1 and ET_A receptor were significantly correlated with CYP1B1 and HO-1 expression, indicating a possible relationship between ET-1 metabolism and oxidative stress.

Another plasma mediator of vasomotor tone is asymmetric dimethylarginine (ADMA), which is an endogenous inhibitor of NOS that is associated with impaired vascular function and increased cardiovascular events. Dvonch et al. (2004, [055741](#)) assessed levels of ADMA in Brown Norway rats 24 h following a 3-day PM_{2.5} CAPs exposure in southwest Detroit (8 h/day; July 2002). CAPs (mean mass concentration 354 µg/m³) resulted in increased plasma ADMA compared to air controls, although the levels reported were well below the 2 µM range associated with increased CVD risk in humans in chronic studies. Therefore, the preliminary results identified a new potential biomarker of vascular tone that had not previously been used in air pollution toxicological studies.

Traffic-Related Particles

A study of old rats (21 mo; F344) exposed to on-road highway aerosols (number concentration range 0.95-3.13×10⁵ particles/cm³; Interstate 90 between Rochester and Buffalo, NY) for 6 h demonstrated decreased plasma ET-2 (18 h post-exposure) and unchanged levels of ET-1 and ET-3 (Elder et al., 2004, [087354](#)).

Gasoline Exhaust

In contrast to the study above, circulating levels of ET-1 (measured 18 h post-exposure) were elevated in animals exposed to gasoline exhaust and filtration of particles did not reduce this effect (study details in Section 6.2.2.2) (Campen et al., 2006, [096879](#)). The results of Campen et al. (2006, [096879](#)) are consistent with those observed by Bouthillier et al. (1998, [087110](#)) following a very high exposure to EHC-93, but it is difficult to attribute the effects to PM alone, as Campen et al. (2006, [096879](#)) showed that the gaseous components of the gasoline mixture were required for the ET-1 increase.

Aorta ET-1 mRNA expression was increased with a 7-day gasoline exhaust exposure (60 µg/m³) in ApoE^{-/-} mice, but was not changed following a single-day exposure (Lund et al., 2009, [180257](#)). The expression and activity of MMP-2 and -9 and oxidative stress in aortas of exposed

mice were also elevated. The ET-1 and MMP-9 mRNA expressions were attenuated with the addition of an ET_A receptor antagonist (but not a radical scavenger), indicating that ET-1 may mediate the expression of MMP-9 through the ET_A receptor.

Model Particles

Another study examined the effects of UF carbon particles (mass concentration 172 µg/m³; mean number concentration 9.0×10⁶ particles/cm³) and there was no difference in ET-1, ET_A or ET_B receptor mRNA expression between air- and particle-exposed SH rats 1 or 3 days post-exposure (Upadhyay et al., 2008, [159345](#)). In lung homogenates, ET-1, ET_A and ET_B receptor mRNA expressions were elevated 3 days after exposure to UF carbon particles (Upadhyay et al., 2008, [159345](#)).

Summary of Toxicological Study Findings for Endothelin

The ET responses were mixed, with one study demonstrating ET-1 increases after exposure to gasoline emissions that were particle independent and another reported decreased ET-2, but no change in ET-1 or ET-3 with on-road highway exposure. Elevated levels of ET-1 and ET_A receptor mRNA expression were noted in hearts of rats exposed to CAPs, but not in rats exposed to UF carbon particles. However, ET-1, ET_A and ET_B receptor mRNA expressions were increased in lung homogenates of rats following UF carbon exposure. The ET_A receptor was found to be involved in the ET-1 and MMP-9 responses in the aortas of mice exposed to gasoline exhaust. A relatively novel marker, ADMA, was used to evaluate vasomotor tone in rats and was found to be elevated following exposure to CAPs, although the results are preliminary and have not been confirmed.

6.2.5. Blood Pressure

One of the potential outcomes of air pollution-mediated alterations in vascular tone is its impact on variable BP or hypertension. BP is tightly regulated by autonomic (central and local), cardiac, renal, and regional vascular homeostatic mechanisms with changes in arterial tone being countered by changes in cardiac contractility, HR, or fluid volume. The evidence of PM-induced changes in BP presented in the 2004 PM AQCD (U.S. EPA, 2004, [056905](#)) is limited and inconsistent. Recent epidemiologic, controlled human exposure, and toxicological studies have similarly reported conflicting results regarding the effect of PM on BP. However, the majority of these studies have evaluated changes in BP at some point following exposure to PM. Significant increases in DBP have been observed in controlled human exposure studies that evaluated BP during exposure (concomitant exposure to CAPs and O₃). In addition, evidence from toxicological studies suggests that the effect of PM on BP may be modified by health status, as PM-induced increases in BP have been more consistently observed in SH rats.

6.2.5.1. Epidemiologic Studies

Increased BP was associated with PM concentration in two of three studies reviewed in the 2004 PM AQCD (U.S. EPA, 2004, [056905](#)). Increases in left ventricular BP (systolic and diastolic) are well established risk factors for cardiovascular mortality/morbidity (Welin et al., 1993, [156151](#)). Changes in HR and BP both reflect changes in autonomic tone, and have been examined following short-term increases in PM pollution in several recent studies.

Ibald-Mulli et al. (2004, [087415](#)) examined associations between BP and ambient PM_{2.5} concentrations, UFP counts, and ACP counts in a multicity panel study (Amsterdam, the Netherlands; Helsinki, Finland; Erfurt, Germany) of 131 adults with coronary heart disease. Although based on the same ULTRA Study (Timonen et al., 2006, [088747](#)) with study methods as described previously in Section 6.2.1.1, the study period was different. They investigated changes in BP (SBP and DBP) associated with mean PM_{2.5}, UFP, and ACP concentration/counts (lag days 0, 1, and 2, as well as the 5-day mean) in each city and then generated a pooled estimate across the cities. The median PM_{2.5} concentration for each city is provided in Table 6-5. Pooled analyses across all 3 cities showed small, but statistically significant decreases in SBP and DBP associated with various single day lagged concentrations/counts of each particulate pollutant. Each 10 µg/m³ increase in the

mean PM_{2.5} concentration over the previous 5 days was associated with a 0.36 mmHg decrease in SBP (95% CI: -0.99 to 0.27) and a 0.39 mmHg decrease in DBP (95% CI: -0.75 to -0.03). Each 10,000 particles/cm³ increase in UFP was associated with a 0.72 mmHg decrease in SBP (95% CI: -1.92 to 0.49), and a 0.70 mmHg decrease in DBP (95% CI: -1.38 to -0.02). Each 1,000 particles/cm³ increase in 5-day avg ACP was associated with a 1.11 mmHg decrease in SBP (95% CI: -2.12 to -0.09) and a 0.95 mmHg decrease in DBP (95% CI: -1.53 to -0.37). The authors concluded that these findings do not support previous findings of an increase in BP associated with increases in particulate pollutant concentrations.

Single-city studies examining the association between BP and particulate air pollution have been done in several U.S. and Canadian cities. Dales et al. (2007, [155743](#)) conducted a panel study of 39 healthy volunteers who sat outside at two different bus stops for 2-h in Ottawa, Canada. The median PM_{2.5} concentrations measured at the bus stops during each 2-h exposure session were 40 and 10 µg/m³. Post-exposure SBP and DBP were not associated with the mean PM_{2.5} concentration measured at the bus stops during the 2-h exposure session. The change in BP from pre- to post-exposure was not evaluated, as health measurements were only made after the 2-h exposure sessions.

Jansen et al. (2005, [082236](#)) studied changes in BP among 16 older subjects (aged 60-86 yr) with asthma or COPD in Seattle, Washington, associated with indoor, outdoor, and personal PM₁₀, PM_{2.5}, and BC concentrations on 12 consecutive days. The study authors reported that no associations were observed between BP and daily mean PM₁₀, PM_{2.5}, or BC concentrations.

Zanobetti et al. (2004, [087489](#)) examined the association between BP (SBP, DBP, and mean arterial BP) and mean PM_{2.5} concentrations in the previous 24, 48, 72, 96, and 120 h in 62 elderly, cardiac rehabilitation patients in Boston, MA (Zanobetti et al., 2004, [087489](#)). Each 10.4 µg/m³ increase in mean PM_{2.5} concentration in the previous 120 h was associated with significant increases in resting DBP (2.82 mmHg [95% CI: 1.26-4.41]), SBP (2.68 mmHg [95% CI: 0.04-5.38]), and mean arterial BP (2.76 mmHg [95% CI: 1.07-4.48]).

Mar et al. (2005, [087566](#)) studied this same PM_{2.5}-BP association in 88 subjects aged >57 yr in Seattle, WA. Among healthy subjects taking medications (bronchodilators, inhaled corticosteroids, anti-hypertensives, β-blockers, calcium channel blockers, and/or cardiac glycosides), each 10 µg/m³ increase in mean outdoor PM_{2.5} concentration on the same day as the BP measurement was made was associated with small increases in SBP and DBP. However, among all subjects, each 10 µg/m³ increase in same day mean PM_{2.5} concentration was associated with non-significant decreases in SBP (-0.81 mmHg [95% CI: -2.34 to 0.73]) and DBP (-0.46 mmHg [95% CI: -1.49 to 0.57]).

As described earlier, Ebelt et al. (2005, [056907](#)) conducted a repeated measures panel study of 16 patients with COPD in the summer of 1998 in Vancouver, British Columbia to evaluate the relative impact of ambient and non-ambient exposures to PM_{2.5}, PM₁₀, and PM_{10-2.5} on multiple health outcomes including ectopy and BP. Using the same analytic methods, pollutant concentrations, and lags, they reported decreased SBP associated with same day ambient exposures to each PM size fraction.

Two similar studies were done in Incheon, South Korea (Choi et al., 2007, [093196](#)) and Taipei, Taiwan (Chuang et al., 2005, [156356](#)). Choi et al. (2007, [093196](#)) reported significantly increased SBP and DBP associated with the mean PM₁₀ concentration over the same and previous 2 days in the warm season only (July to September). Chuang et al. (2005, [156356](#)) reported significant increases in SBP and DBP associated with the mean UFP count (0.01-0.1 µm particles) 1-3 h before the BP measurement.

Summary of Epidemiologic Studies of Blood Pressure

These studies (Choi et al., 2007, [093196](#); Chuang et al., 2005, [156356](#); Dales et al., 2007, [155743](#); Ibalid-Mulli et al., 2004, [087415](#); Mar et al., 2005, [087566](#); Zanobetti et al., 2004, [087489](#)) are not entirely consistent with regard to their BP-PM associations. Most have reported increases in SBP and DBP associated with increases in either PM_{2.5}, PM₁₀, or UFP (Choi et al., 2007, [093196](#); Chuang et al., 2005, [156356](#); Mar et al., 2005, [087566](#); Zanobetti et al., 2004, [087489](#)). However, two studies reported small decreases in BP associated with multiple particulate pollutants (Ibalid-Mulli et al., 2004, [087415](#); Mar et al., 2005, [087566](#)), Dales et al. (2007, [155743](#)) reported no change in BP associated with a 2-h exposure to bus stop PM_{2.5} and Jansen et al. (2005, [082236](#)) reported null findings among older adults in Seattle, WA. Exposure lags ranging from 1-3 h (Chuang et al., 2005,

[156356](#)), to the same day (Ebelt et al., 2005, [056907](#); Mar et al., 2005, [087566](#)), to the mean across the previous 5 days (Zanobetti et al., 2004, [087489](#)) were reported as having the strongest associations with BP. Mean and upper percentile concentrations for PM from these studies are presented in Table 6-5.

Table 6-5. Mean PM concentrations reported in epidemiologic studies of blood pressure.

Author	Location	Mean Concentration ($\mu\text{g}/\text{m}^3$)	Upper Percentile Concentrations ($\mu\text{g}/\text{m}^3$)
<i>PM_{2.5}</i>			
Dales (2007, 155743)	Ottawa, Canada (bus stops)	Bus stop 1: 40 Bus stop 2: 10	NR
Ebelt (2005, 056907)	Vancouver, Canada	Ambient (measured): 11.4 Personal (estimated): 7.9 Personal (measured): 18.5	Ambient (measured) range: 4.2-28.7 Personal (estimated) range: 0.9-21.3 Personal (measured) range: 2.2-90.9
	Amsterdam, Netherlands	20	50th: 16.9 75th: 23.9 Max: 82.2
Ibald-Mulli (2004, 087415)	Erfurt, Germany	23.1	50th: 16.3 75th: 27.4 Max: 118.1
	Helsinki, Finland	12.7	50th: 10.6 75th: 16 Max: 39.8
Jansen (2005, 082236)	Seattle, WA	10.47	NR
Mar (2005, 087566)	Seattle, WA	Healthy: Personal- 9.3 Indoor- 7.4 Outdoor- 9 CVD: Personal- 10.8 Indoor- 9.5 Outdoor- 12.6 COPD: Personal- 10.5 Indoor- 8.5 Outdoor- 9.2	NR
Zanobetti (2004, 087489)	Boston, MA	Median: 8.8	90th: 17.6
<i>PM_{10-2.5}</i>			
Ebelt (2005, 056907)	Vancouver, Canada	Ambient (calculated): 5.6 Personal (estimated): 2.4	Ambient (calculated) range: -1.2 to 11.9 Personal (estimated) range: -0.4 to 7.2
<i>PM₁₀</i>			
Choi (2007, 093196)	Incheon, South Korea	July-Sept: 42.1 Oct.-Dec: 53.5	July-Sept.: 75%: 52.2 Max: 136.7 Oct.-Dec.: 75%: 64.5 Max: 209.6

Author	Location	Mean Concentration ($\mu\text{g}/\text{m}^3$)	Upper Percentile Concentrations ($\mu\text{g}/\text{m}^3$)
Chuang (2005, 156356)	Taipei, Taiwan	54.1	Range: 10.3-139.8
Ebelt (2005, 056907)	Vancouver, Canada	Ambient (calculated): 17 Personal (estimated): 10.3	Ambient (calculated) range: 7-36 Personal (estimated) range: 1.5-23.8
Jansen (2005, 082236)	Seattle, WA	13.47	NR
Mar (2005, 087566)	Seattle, Washington	Healthy: 14.5 CVD: 18 COPD: 14.3	NR

Right Ventricular Pressure

Several recent studies, summarized in the section on hospital admissions and emergency department (ED) visits for CVD causes, have reported increased risk of hospital admissions for CHF associated with increased PM concentration on the same day (Wellenius et al., 2005, [087483](#); 2006, [088748](#)). As a possible mechanism for these reported associations, Rich et al. (2008, [156910](#)) hypothesized that these hospital admissions for decompensation of heart failure would be preceded by more subtle increases in pulmonary arterial (PA) and right ventricular (RV) diastolic pressures. They used passively monitored PA and RV pressures on 5,807 person-days, among 11 subjects implanted with the Chronicle Implantable Hemodynamic Monitor [Medtronic, Inc. Medtronic, MN]). Using a two-stage modeling process, they examined the change in daily mean right heart pressures associated with mean $\text{PM}_{2.5}$ concentration on the same and previous 6 days. Each $11.62 \mu\text{g}/\text{m}^3$ increase in same day mean $\text{PM}_{2.5}$ concentration was associated with small, but statistically significant increases in estimated PA diastolic pressure (0.19 mmHg [95% CI: 0.05-0.33]) and RV diastolic pressure (0.23 mmHg [95% CI: 0.11-0.34]). These effects were not attenuated when controlling for all lags simultaneously. Thus, PM induced right heart pressure increases may mark another potential pathway between PM exposure and incidence of cardiovascular events, but further studies on this same hypothesis are needed for confirmation.

Wellenius et al. (2007, [092830](#)) conducted a panel study of 28 subjects living in the greater Boston metropolitan area, each with chronic stable heart failure and impaired systolic function. They hypothesized that circulating levels of B-type natriuretic peptide (BNP), measured in whole blood at 0, 6, and 12 wk, were associated with acute changes in ambient air pollution, as a possible mechanistic explanation for the observed association between hospital admissions for CHF and ambient PM concentration (Wellenius et al., 2005, [087483](#); 2006, [088748](#)). During the study, the mean $\text{PM}_{2.5}$ concentration was $10.9 \mu\text{g}/\text{m}^3$, while the mean BC concentration was $0.73 \mu\text{g}/\text{m}^3$. Using linear mixed models, they reported no association between any pollutant ($\text{PM}_{2.5}$, CO, SO_2 , NO_2 , O_3 , and BC) and BNP at any lag (e.g., each $10 \mu\text{g}/\text{m}^3$ increase in mean daily $\text{PM}_{2.5}$ concentration [0.8% increase in BNP (95% CI: -16.4 to 21.5)]) (Wellenius et al., 2007, [092830](#)). However, BNP the active peptide has a very short half-life and might not be the best biomarker for such a study. Thus the absence of a correlation between PM and BNP may not suggest that PM does not have an impact on RV or LV function in individuals with impaired cardiac mechanics.

6.2.5.2. Controlled Human Exposure Studies

Only one controlled human exposure study cited in the 2004 PM AQCD (U.S. EPA, 2004, [056905](#)) reported any PM-induced changes in BP. Gong et al. (2003, [042106](#)) found that exposure to $\text{PM}_{2.5}$ ($174 \mu\text{g}/\text{m}^3$) decreased SBP in asthmatics, but increased SBP in healthy subjects. Among healthy adults, BP was not affected following 2-h exposures to $200 \mu\text{g}/\text{m}^3$ diesel PM (Nightingale et al., 2000, [011659](#)), $150 \mu\text{g}/\text{m}^3$ $\text{PM}_{2.5}$ CAPs with 120 ppb O_3 (Brook et al., 2002, [024987](#)), or $10 \mu\text{g}/\text{m}^3$ UF carbon particles (Frampton, 2001, [019051](#)). The effect of PM on BP has been further investigated in several recent controlled human exposure studies, which are described below.

CAPs

One recent study demonstrated a significant increase (9.3%) in DBP among healthy adults immediately prior to the end of a 2-h exposure to 150 $\mu\text{g}/\text{m}^3$ PM_{2.5} CAPs in combination with 120 ppb O₃ (Urch et al., 2005, [081080](#)). The authors also found that the magnitude of change in BP was significantly associated with PM_{2.5} carbon content, but not total PM_{2.5} mass. It was postulated that the disparity between these findings and those of a similar study by the same group (Brook et al., 2002, [024987](#)) could be due to differences in experimental methods. The Brook et al. (2002, [024987](#)) study measured post-exposure BP approximately 10 min following exposure, while the study by Urch et al. (2005, [081080](#)) measured BP during exposure. In a follow up study that evaluated changes in BP during a 2-h exposure to PM_{2.5} CAPs, Fakhri et al. (2009, [191914](#)) reported a significant increase in DBP with exposure to CAPs with, but not without, coexposure to O₃.

Diesel Exhaust

Several recent studies have assessed BP changes following a 1-h exposure to DE with a particle concentration of 300 $\mu\text{g}/\text{m}^3$. Mills et al. (2005, [095757](#)) evaluated changes in BP 2 h following exposure to DE and found a 6 mmHg increase in DBP of marginal statistical significance ($p = 0.08$) compared to filtered air control. In this same group of subjects, Tornqvist et al. (2007, [091279](#)) did not observe any such changes in BP 24 h following DE exposure. At lower particle concentrations in diluted DE (100-200 $\mu\text{g}/\text{m}^3$ PM_{2.5}), Peretz et al. (2008, [156854](#)) did not observe any changes in systolic or DBP in either healthy adults or adults with metabolic syndrome immediately following a 2-h exposure. Further, although Lundback et al. (2009, [191967](#)) reported an increase in arterial stiffness following exposure to DE with a particle concentration of 330 $\mu\text{g}/\text{m}^3$ among healthy young adults, no changes in systolic or diastolic BP were observed during or following exposure relative to filtered air.

Model Particles

Routledge et al. (2006, [088674](#)) did not observe any changes in BP among healthy older adults and older adults with stable angina following a 1-h exposure to UF EC (50 $\mu\text{g}/\text{m}^3$), with or without coexposure to 200 ppb SO₂. Similarly, neither Shah et al. (2008, [156970](#)), nor Beckett et al. (2005, [156261](#)) reported any changes in BP among healthy adults following exposure to UF EC (50 $\mu\text{g}/\text{m}^3$) or ZnO (500 $\mu\text{g}/\text{m}^3$ fine and ultrafine), respectively.

Summary of Controlled Human Exposure Study Findings for BP

The findings of these new studies do not provide convincing evidence of an association between PM exposure and an increase in BP; however, they do suggest that there is a need for additional investigations of PM-induced changes in BP at various time points following exposure.

6.2.5.3. Toxicological Studies

In healthy animal models, little evidence exists for significant BP changes following inhalation exposure to environmentally-relevant concentrations of PM. Only one animal toxicological study is mentioned in the 2004 PM AQCD (U.S. EPA, 2004, [056905](#)) that examined BP with PM exposure and no effect was observed (Vincent et al., 2001, [021184](#)).

CAPs

In a recent study of dogs, exposure to PM_{2.5} CAPs from Boston (mean mass concentration 358.1 $\mu\text{g}/\text{m}^3$; mass concentration 94.1-1557 $\mu\text{g}/\text{m}^3$) for 5 h resulted in increased SBP (2.7 mmHg), DBP (4.1 mmHg), mean arterial pressure (3.7 mmHg), and lowered pulse pressure (1.7 mmHg) when measured upstream of the femoral artery (Bartoli et al., 2009, [156256](#)). Administration of an

α -adrenergic antagonist (prazosin) prior to CAPs attenuated the BP responses. These findings indicate that CAPs exposure may have activated α -adrenergic receptors and increased peripheral vascular resistance. Baroreflex sensitivity was measured immediately before and after exposure during a transient elevation of arterial pressure that was induced by PHE; increased baroreflex sensitivity was observed in subgroup of dogs exposed to CAPs, which is consistent with an upregulation of vagal reflexes.

Chang et al. (2004, [055637](#)) noted slight increases in SH rat BP (5-10 mmHg) when exposed to PM_{2.5} CAPs (mean mass concentration 202 $\mu\text{g}/\text{m}^3$) during spring months. However, during summer months, when the CAPs exposure level was less (140 $\mu\text{g}/\text{m}^3$), this effect was not observed. It was unclear, therefore, whether the effects were seasonal or dose-related. In a preliminary study of SH rats exposed to CAPs during a dust storm event, mean BP was elevated the third and fourth hour of a 6-h exposure, although interpretation of this finding is difficult due to few animals in the exposure group (n = 2) (Chang et al., 2007, [155719](#)). In another study, the increased change in mean BP measured using the tail cuff method following CAPs exposure weakly correlated with PM mass accumulated on chamber filters over the entire exposure duration (Section 6.2.4.3 for details) (Ito et al., 2008, [096823](#)). Furthermore, ET_A receptor mRNA expression in cardiac tissue was positively correlated with the change in mean BP.

Model Particles

In WKY rats, 24-h exposure to UF carbon particles (mass concentration 180 $\mu\text{g}/\text{m}^3$; mean number concentration 1.6×10^7 particles/cm³) did not alter mean BP during exposure or the recovery periods (Harder et al., 2005, [087371](#)). SH rats exposed to UF carbon particles for 24 h (mass concentration 172 $\mu\text{g}/\text{m}^3$; mean number concentration 9.0×10^6 particles/cm³) resulted in elevated mean BP (by 6 mmHg) on the first and second days of recovery following exposure that was attributable to increases in both SBP and DBP (Upadhyay et al., 2008, [159345](#)). Increased plasma renin concentrations were observed in CB-exposed rats on the first and second days of recovery, although renin activity and angiotensin (Ang) I and II concentrations were not affected by particle exposure.

Summary of Toxicological Study Findings for Blood Pressure

Limited toxicological evidence provides support for elevated BP in dogs or compromised rats with CAPs, UF CAPs, CAPs during a dust storm event, or UF carbon particle exposure. However, most of the CAPs studies were conducted outside of the U.S.

6.2.6. Cardiac Contractility

The 2004 PM AQCD (U.S. EPA, 2004, [056905](#)) did not include any toxicological studies that evaluated cardiac contractility either directly or indirectly following exposure to PM. Two recent animal toxicological studies have demonstrated reductions in cardiac fractional shortening, diminished ejection shortening, or changes in the QA interval following PM exposure. The results of these studies provide some evidence of PM-induced changes in cardiac contractility in animal models.

6.2.6.1. Toxicological Studies

The strength of the contracting heart is reflected by its contractility. In heart failure, contractility wanes significantly and the heart cannot compensate during periods of increased physical activity. Measuring true contractility in a whole animal is difficult, requiring extensive surgical instrumentation and monitoring.

CAPs

Using radiotelemetry to indirectly measure cardiac contractility through the QA interval, SH rats were repeatedly and alternately exposed to UF CAPs in Taiwan on separate days in spring or summer (details provided in Section 6.2.5.3) (Chang et al., 2004, [055637](#)). The QA interval was calculated as the time duration between the Q wave in the ECG and point A (upstroke in aortic pressure) in the pressure trace and is not as reliable as other measures, such as echocardiography. During the spring exposure, QA interval decreased by 1.6 ms (as demonstrated by fixed effects in linear mixed-effects modeling), which indicates an increase in cardiac contractility. There were no changes in QA interval observed for the summer months, which may be attributable to lower UF PM concentrations (mean mass concentration 140 $\mu\text{g}/\text{m}^3$) or differing PM compositions.

Model Particles

A recent study using old (18-28-mo) mice (C57BL/6, C3H/HeJ, and B6C3F1) demonstrated significant reductions in cardiac fractional shortening (due to increased left ventricular end-diastolic and end-systolic diameters) following a 4-day (3 h/day) exposure to CB (PM_{2.5} mean concentration 401 $\mu\text{g}/\text{m}^3$; PM₁₀ mean concentration 553 $\mu\text{g}/\text{m}^3$) using echocardiography (Tankersley et al., 2008, [157043](#)). Hemodynamic measurements of diminished ejection fraction and maximum change in pressure over time further supported lowered myocardial contractility. Furthermore, increased right ventricular pressure associated with elevated right atrial and pulmonary vascular pressures and resistance, was indicative of pulmonary vasoconstriction in CB-exposed mice. Heart tissue and isolated cardiomyocytes from exposed animals demonstrated enhanced ROS that was partially attributable to NOS3-uncoupling and elevated MMP-2 and MMP-9 levels, which may implicate myocardial remodeling. The combined results from this study suggest that cellular mechanisms involving NOS-uncoupled ROS generation likely mediate PM-induced cardiac effects. Furthermore, mRNA expression for atrial and brain natriuretic peptides was increased in hearts from exposed mice compared to control, which is consistent with pulmonary congestion. There were no reported strain-related differences in any response.

Intratracheal Instillation

Similar to the responses observed by Tankersley et al. (2008, [157043](#)), decreases in fractional shortening and increases in left ventricular end diastolic diameter measured by echocardiography were also reported for SD rats at 24 h post-IT exposure to DE particles (250 μg) (Yan et al., 2008, [098625](#)). A subset of rats received isoproterenol to induce myocardial injury prior to IT instillation of DE particles and these animals demonstrated lowered fractional shortening at baseline, which was decreased to an even greater extent with DE particle exposure; left ventricular end diastolic diameter was not affected by DE particles in these rats.

Summary of Toxicological Study Findings for Cardiac Contractility

The studies above provide some evidence that cardiac contractility may be altered immediately following PM exposure in animal models. Results from the Tankersley (2008, [157043](#)) and Yan (2008, [098625](#)) studies provide the strongest support for PM-induced contractility changes with inhalation exposure, as echocardiography and hemodynamic measurements are well-established for examining cardiac function.

6.2.7. Systemic Inflammation

The evidence presented in the 2004 PM AQCD (U.S. EPA, 2004, [056905](#)) of increases in markers of systemic inflammation associated with PM was limited and not sufficient to formulate a definitive conclusion. Recent controlled human exposure and toxicological studies continue to provide mixed results for an effect of PM on markers of systemic inflammation including cytokine

levels, C-reactive protein (CRP), and white blood cell (WBC) count. While results from recent epidemiologic studies have also been inconsistent across studies, there is some evidence to suggest that PM levels may have a greater effect on inflammatory markers among populations with preexisting diseases.

6.2.7.1. Epidemiologic Studies

Several studies reviewed in the 2004 PM AQCD (U.S. EPA, 2004, [056905](#)) investigated the association of short-term fluctuations in PM concentration with markers of inflammation. These studies were found to offer limited support for mechanistic explanations of the associations between PM concentration and heart disease outcomes. Recent studies, published since 2002, are reviewed below. CRP was measured in multiple studies, allowing the consistency of findings across epidemiologic studies to be evaluated. Several other markers were examined in only a few studies, in relation to a wide range PM size fractions and components. These markers included IL-6, TNF- α , vascular cell adhesion molecule-1 (VCAM-1), intercellular adhesion molecule-1 (ICAM-1), soluble CD40 ligand (sCD40L), WBCs, and soluble adhesion molecules (sP-selectin and e-selectin).

Diez-Roux et al. (2006, [156400](#)) examined whether CRP increased in response to changes in the mean ambient PM_{2.5} concentrations in the prior day, prior 2 days, prior week, prior 30 days, and prior 60 days among participants in the Multi-Ethnic Study of Atherosclerosis (MESA) cohort. Subjects (n = 5,634) lived in either Baltimore City or County, MD, Chicago, IL, Forsyth County, NC, Los Angeles County, CA, Northern Manhattan and the Bronx, NY, or St. Paul, MN. The authors report finding no evidence of a short-term effect of PM_{2.5} on CRP in their population-based sample. Of the five exposure measures examined, only the 30-day and 60-day mean exposures showed positive associations with PM_{2.5} (3% [95% CI: -2 to 10] and 4% [95% CI: -3 to 11] per 10 $\mu\text{g}/\text{m}^3$, respectively).

Ruckerl et al. (2007, [156931](#)) conducted a multicity longitudinal study to examine whether changes in markers of inflammation were associated with short-term increases in particulate concentrations (PM₁₀, PM_{2.5}, PNC) and gaseous pollutant (NO₂, SO₂, CO, O₃). Study subjects were MI survivors (n= 1,003) living in either Athens, Greece; Augsburg, Germany; Barcelona, Spain; Helsinki, Finland; Rome, Italy; or Stockholm, Sweden. Repeated measurements of IL-6 and CRP were made during the study. Fibrinogen was also measured in this study and results are discussed in Section 6.2.8.1. The mean city-specific pollutant concentrations during the study are shown below in Table 6-6. In pooled analyses, each interquartile range (not provided) increase in PNC in the 12-17 h before the health measurement was associated with a 2.7% increase in the geometric mean IL-6 levels (95% CI: 1.0-4.6). None of the pollutants, at any lag, were associated with CRP levels in these subjects. There did not appear to be effect modification of these results by smoking, diabetes, or heart failure. Ljungman et al. (2009, [191983](#)) studied the modification of the IL-6 association with several PM size fractions (PM₁₀, PM_{2.5}, PNC) by three IL-6 SNPs, one fibrinogen α chain (FGA) single-nucleotide polymorphism (SNP) and one fibrinogen β chain (FGB) SNP. The associations of PM_{2.5} and PM₁₀ with plasma level of IL-6 were stronger among those with the homozygous minor allele genotype of FGB rs1800790 and among those homozygous for the major allele genotype of IL-6 rs2069832. Gene-environment interactions were most pronounced for CO. Modification the PNC-IL-6 association by genotype was not apparent in these data, nor was modification of the PM-IL-6 associations by FBA.

Single-city studies of systemic inflammation have also been conducted in the U.S. and Canada. Delfino et al. (2008, [156390](#)) measured CRP, IL-6, TNF- α , sP-selectin, sVCAM-1 and sICAM-1 in blood during a period of 12 wk. Associations of these markers with average PM concentration (PM_{0.25}, PM_{0.25-2.5}, PM_{10-2.5}, PNC, EC, OC, BC, primary OC, secondary OC) 24 h to 9 days prior to the blood draw were examined. Subjects included residents of two downtown Los Angeles nursing homes who were >65 yr old with a history of coronary artery disease. Both 24-h avg and multiday average concentrations of PM_{0.25}, EC, primary OC, BC, PNC and gaseous pollutants were associated with CRP, IL-6 and sP-selectin.

Pope et al. (2004, [055238](#)) conducted a panel study of 88 non-smoking, elderly subjects residing in the Salt Lake City, Ogden, and Provo metropolitan area of Utah. Each 100 $\mu\text{g}/\text{m}^3$ increase in same day mean PM_{2.5} concentration was associated with a 0.81 mg/dL increase in CRP (95% CI: 0.48-1.14), but not WBCs. However, when excluding 1 influential subject, each 100 $\mu\text{g}/\text{m}^3$ increase in same day mean PM_{2.5} concentration was associated with only a 0.19 mg/dL increase in

CRP (95% CI: -0.01 to 0.39). Several markers of coagulation were examined in this study and are discussed in Section 6.2.8.1.

Zeka et al. (2006, [157177](#)) studied 710 elderly members of the VA Normative Aging Study to examine changes in CRP, sediment rate and WBCs with acute changes in PM concentrations in the previous 48 h, 1 wk, and 4 wk. Results for fibrinogen are discussed in Section 6.2.8.1. They did not find consistent or significant associations with any pollutant and CRP or WBC count. Sediment rate was significantly increased with PNC, BC and PM_{2.5} concentration averaged over the previous 4 wk period. Modification of these PM effects by obesity, GSTM1 genotype and statin use was suggested in this study.

O'Neill et al. (2007, [091362](#)) conducted a cross-sectional study of 92 Boston residents with type 2 diabetes, to examine the association between plasma levels of ICAM-1, VCAM-1 and PM concentrations. Results for markers of coagulation measured in this study are discussed in Section 6.2.8.1. PM_{2.5}, BC, and SO₄²⁻ concentrations were measured 0.5 km from the patient exam site. For all moving averages examined (1-6 days), increases in mean PM_{2.5} and BC concentration were associated with increased ICAM-1 and VCAM-1 concentrations. Each 7.6 µg/m³ increase in the mean PM_{2.5} concentration over the previous 6 days was associated with a 11.76 ng/mL increase in VCAM-1 (95% CI: 3.48-20.70), and each 0.6 µg/m³ increase in the mean BC concentration over the previous 6 days was associated with a 27.51 ng/mL increase in VCAM-1 (95% CI: 11.96-45.21). There were no consistent associations between mean SO₄²⁻ concentration and any marker at any lag.

Sullivan et al. (2007, [100083](#)) conducted a panel study of 47 subjects (aged >55 yr) either with COPD (n = 23) or without COPD (n = 24) in Seattle, WA. They examined the association between levels of CRP and mean daily PM_{2.5} concentration. Most values for IL-6 and TNF-α were below the limit of detection, so these cytokines were not included in the analyses. Results for fibrinogen and D-dimer are discussed in Section 6.2.8.1. They did not find any associations between 24-h mean PM_{2.5} concentrations and levels of CRP in individuals with or without COPD.

In the study by Liu et al. (2006, [192002](#); 2007, [156705](#)), conducted in Toronto, Ontario, neither CRP (0.11 µg/mL [95% CI: -0.03 to 0.25]) nor TNF-α (0.03 pg/mL [95% CI: -0.07 to 0.13]) was associated with personal exposure to PM₁₀ (24-h averaging time).

Similarly, there was no association with IL-6. However, significant positive associations with markers of oxidative stress, FMD and BP were found and are discussed in Sections 6.2.9.1, 6.2.4.1, and 6.2.5.1, respectively.

In the St. Louis Bus Study, each 5.4 µg/m³ increase in the mean PM_{2.5} concentration over the previous week was associated with 5.5% increase in WBCs (95% CI: 0.10-11) (Dubowsky et al., 2006, [088750](#)). Each 6.1 µg/m³ increase in the mean PM_{2.5} concentration over the previous 5 days was associated with a 14% increase in CRP among all subjects (95% CI: -5.4 to 37), but an 81% increase in CRP (95% CI: 21-172) among subjects with diabetes, obesity, and/or hypertension. Associations between PM_{2.5} and IL-6 were only observed among those with diabetes, obesity, and/or hypertension. In another study of in-vehicle PM_{2.5}, each 10 µg/m³ increase during a work-shift was associated with decreased lymphocytes, increased mean corpuscular volume, neutrophils, and CRP over the next 10-14 h among 9 healthy North Carolina state troopers (Riediker et al., 2004, [056992](#)). Associations of roadside and ambient PM_{2.5} with systemic inflammatory markers were weaker and non-significant in this population.

International studies of the effect of air pollution on markers of inflammation have been conducted with mixed results. Two studies conducted among 57 male patients with coronary heart disease in Erfurt, Germany, found associations of UFP, ACP and PM₁₀ with CRP (Ruckerl et al., 2006, [088754](#)) and UFP and ACP with sCD40L, a marker for platelet activation (Ruckerl et al., 2007, [156931](#)). In a large cross-sectional study of healthy subjects in Tel Aviv, Steinvil et al. (2008, [188893](#)) examined biological markers of inflammation (CRP and WBCs) collected as part of routine health examinations for 3,659 individuals. Associations with air pollutants (including PM₁₀) measured at local monitoring sites for the day of the examination and up to 7 days prior were examined. No significant associations were found between pollutant levels and indications of enhanced inflammation. By contrast, PM₁₀, PM_{2.5}, SO₄²⁻ and nitrate (3-day avg concentrations) were associated with increases in hs-CRP in healthy students in Taiwan (Chuang et al., 2007, [091063](#)). PM₁₀, PM_{2.5} and PM_{0.25} were not associated with CRP in a study of MI patients in Italy, although associations with autonomic dysregulation and more severe arrhythmias were observed (Folino et al., 2009, [191902](#)). Kelishadi et al. (2009, [191960](#)) reports that CRP, as well as markers of insulin resistance and oxidative stress (discussed in Section 6.2.9.1), were associated with PM₁₀ in a cross-

sectional study of a population-based sample of children 10-18 yr old in Iran (mean PM₁₀ concentration 122.08 µg/m³).

Summary of Epidemiologic Study Findings for Systemic Inflammation

The most commonly measured marker of inflammation in the studies reviewed was CRP. CRP was not consistently associated with short-term PM concentrations (PM_{2.5}, PM₁₀, SO₄²⁻, EC, OC, PNC). A multicity study of MI survivors in Europe (Ruckerl et al., 2007, [156931](#)) failed to provide evidence of an effect of PM (e.g., PM₁₀, PM_{2.5}, PNC) on CRP and no effect was observed by Diez-Roux et al. (2006, [156400](#)) in a population-based study when concentrations were averaged over periods less than 30 days. Several other markers of inflammation have been examined in relation to several PM size fractions and components, but the number of studies examining the same marker/PM metric combination is too few to allow results to be compared across epidemiologic studies. Mean and upper percentile concentrations for those epidemiologic studies that evaluated systemic inflammation are included in Table 6-6.

Table 6-6. PM concentrations reported in epidemiologic studies of inflammation, hemostasis, thrombosis, coagulation factors and oxidative stress.

Author	Location	Mean Concentration (µg/m ³)	Upper Percentile Concentrations (µg/m ³)
PM_{2.5}			
Chuang (2007, 091063)	Taipei, Taiwan	1-day avg: 31.8	1-day avg (range): 16.2-50.1
		2-day avg: 36.4	2-day avg (range): 15-53.4
		3-day avg: 36.5	3-day avg (range): 12.7-59.5
Diez-Roux (2006, 156400)	Chicago, IL	Prior day (median): 14.3	Prior day (75th): 20.9
	Baltimore, MD	Prior 2 days (median): 14.4	Prior 2 days (75th): 20.35
	Forsyth County, NC	Prior 7 days (median): 15.24	Prior 7 days (75th): 19.7
	Los Angeles, CA	Prior 30 days (median): 15.69	Prior 30 days (75th): 19.22
	New York City, NY	Prior 60 days (median): 15.9	Prior 60 days (75th): 19.08
	St. Paul, MN		
Dubowsky (2006, 088750)	St. Louis (bus stops)	16	75th: 22 100th: 28
Folino (2009, 191902)	Padua, Italy	Summer: 33.9	
		Winter: 62.1	NR
		Spring: 30.8	
O'Neill (2007, 091362)	Boston, MA	11.4	Range: 0.07-33.7
Park (2008, 156845)	Boston, MA	12	Range: 2-62
Peters (2009, 191992)	Helsinki, Finland	Helsinki: 8.2	Helsinki (range): 1-28
	Stockholm, Sweden	Stockholm: 8.8	Stockholm (range): 0-27
	Augsburg, Germany	Augsburg: 17.4	Augsburg (range): 6-39
	Rome, Italy	Rome: 24.5	Rome (range): 4-95
	Barcelona, Spain	Barcelona: 24.2	Barcelona (range): 3-95
		Total: 16.4	Total (range): 0-95

Author	Location	Mean Concentration ($\mu\text{g}/\text{m}^3$)	Upper Percentile Concentrations ($\mu\text{g}/\text{m}^3$)
Pope (2004, 055238)	Salt Lake City, Ogden, Provo Utah	FRM-Filled: 23.7 Not filled: 25.8 TEOM: 18.9 RAMS/PC-BOSS: 26.5	FRM-Filled (range): 1.7-74 Not filled (range): 1.7-74 TEOM (range): 2.2-61.5 RAMS/PC-BOSS (range): 5.6-72.4
Riediker (2004, 056992)	North Carolina State Troopers	Light Scatter: 24.1 Mass: 23 Ambient: 32.3 Roadside: 32.1	Light Scatter (range): 4.5-54.4 Mass (range): 7.1-38.7 Ambient (range): 9.9-68.9 Roadside (range): 8.9-62.2
Ruckerl (2007, 156931)	Helsinki, Finland	8.2 (19.4)	NR
	Stockholm, Sweden	8.8 (19.1)	NR
	Augsburg, Germany	17.4 (29.3)	NR
	Rome, Italy	24.5 (54.1)	NR
	Barcelona, Spain	24.2 (64.7)	NR
	Athens, Greece	23 (46)	NR
Sørensen (2003, 157000)	Copenhagen, Denmark	Personal (median): 16.1 Urban background (median): 9.2	Personal (Q25-Q75): 10-24.5 Urban background (Q25-Q75): 5.3-14.8
Sullivan (2007, 100083)	Seattle, WA	Outdoor (median): 7.7 Indoor (median): 7.7	Outdoor: 75th- 11.5 90th- 19.9 Max- 33.9
			Indoor: 75th- 12.1 90th- 16 Max- 81.4
			75th: 14.57 90th: 21.48
<i>PM_{10-2.5}</i>			
Delfino (2008, 156390)	Los Angeles, CA	Outdoor: 10.04 (4.07) Indoor: 4.12 (4.76)	Outdoor (range): 1.76-22.38 Indoor (range): 0.12-37.63
Peters (2009, 191992)	Helsinki, Finland	Helsinki: 8.9	Helsinki (range): 1-38
	Stockholm, Sweden	Stockholm: 9	Stockholm (range): 0-40
	Augsburg, Germany	Augsburg: 15.8	Augsburg (range): -1 to 35
	Rome, Italy	Rome: 16.8	Rome (range): -33 to 65
	Barcelona, Spain	Barcelona: 16.5	Barcelona (range): 1-102
	Total: 13.3	Total (range): -33 to 102	
<i>PM₁₀</i>			
Baccarelli (2007, 090733)	Lombardia Region, Italy	Sep-Nov (median): 51.2	Sep-Nov (max): 148.9
		Dec-Feb (median): 68.5	Dec-Feb (max): 238.3
		Mar-May (median): 64.1	Mar-May (max): 158.5
		Jun-Aug (median): 44.3	Jun-Aug (max): 94.7
Baccarelli (2007, 091310)	Lombardia Region, Italy	Median: 34.1	Maximum: 390
Chuang (2007, 091063)	Taipei, Taiwan	1-day avg: 49.2	1-day avg (range): 29.5-83.4
		2-day avg: 55.3	2-day avg (range): 25.5-85.1
		3-day avg: 54.9	3-day avg (range): 22.2-87.2

Author	Location	Mean Concentration ($\mu\text{g}/\text{m}^3$)	Upper Percentile Concentrations ($\mu\text{g}/\text{m}^3$)
Folino (2009, 191902)	Padua, Italy	Summer: 46.4 Winter: 73 Spring: 38.3	NR
Kelishadi (2009, 191960)	Isfahan, Iran	122.08	75th: 153 100th: 191
Liao (2005, 088677)	Washington County, MD Forsyth County, NC Minneapolis, MN (suburbs)	29.9	Q4: 47.3
Liu (2007, 156705)	Windsor, Ontario, Canada	Personal (median): 0-24 h before clinical visit: 25.5 0-6 h before clinical visit: 15.3 7-12 h before clinical visit: 17 13-18 h before clinical visit: 28.5 19-24 h before clinical visit: 30.5	Personal (5th to 95th): 0-24 h before clinical visit: 9.8-133 0-6 h before clinical visit: 5.3-83.2 7-12 h before clinical visit: 7.1-186.3 13-18 h before clinical visit: 11.4-167 19-24 h before clinical visit: 10.1-148.2
Peters (2009, 191992)	Helsinki, Finland Stockholm, Sweden Augsburg, Germany Rome, Italy Barcelona, Spain	Helsinki: 17.1 Stockholm: 17.8 Augsburg: 33.1 Rome: 42.1 Barcelona: 40.7 Total: 30.3	Helsinki (range): 4-53 Stockholm (range): 0-57 Augsburg (range): 7-71 Rome (range): 15-91 Barcelona (range): 6-194 Total (range): 0-194
Ruckerl (2007, 156931)	Helsinki, Finland Stockholm, Sweden Augsburg, Germany Rome, Italy Barcelona, Spain Athens, Greece	17.1 17.8 33.1 42.1 40.7 38.5	NR NR NR NR NR NR
Steinvil (2008, 188893)	Tel Aviv, Israel	64.5	75th: 60.7

6.2.7.2. Controlled Human Exposure Studies

Several controlled human exposure studies were included in the 2004 PM AQCD (U.S. EPA, 2004, [056905](#)) which evaluated markers of systemic inflammation following exposure to PM. Salvi et al. (1999, [058637](#)) exposed 15 healthy volunteers (21-28 yr) for 1 h to DE (300 $\mu\text{g}/\text{m}^3$ particle concentration) and observed a significant increase in neutrophils in peripheral blood 6 h post-exposure compared with filtered air control. However, Ghio et al. (2003, [087363](#)) reported no changes in plasma cytokine levels (e.g., IL-6 and TNF- α), WBC count, or CRP 0 or 24 h following a 2-h exposure to PM_{2.5} CAPs (120 $\mu\text{g}/\text{m}^3$). Gong et al. (2003, [042106](#)) did not observe any effect of PM_{2.5} CAPs (174 $\mu\text{g}/\text{m}^3$) on serum amyloid A, while Frampton (2001, [019051](#)) reported no change in leukocyte activation following exposure to a low concentration (10 $\mu\text{g}/\text{m}^3$) of UF carbon. The results of studies published since the completion of the 2004 PM AQCD (U.S. EPA, 2004, [056905](#)) are discussed below.

CAPs

Several controlled human exposure studies have reported no change in plasma CRP levels 0-24 h after exposure to UF (avg concentration 50-100 $\mu\text{g}/\text{m}^3$), $\text{PM}_{2.5}$ (avg concentration 190 $\mu\text{g}/\text{m}^3$), or $\text{PM}_{10-2.5}$ (avg concentration 89 $\mu\text{g}/\text{m}^3$) CAPs (Gong et al., 2008, [156483](#); Graff et al., 2009, [191981](#); Mills et al., 2008, [156766](#); Samet et al., 2009, [191913](#)). In a study of exposures to $\text{PM}_{2.5}$ CAPs (200 $\mu\text{g}/\text{m}^3$), Gong et al. (2004, [087964](#)) observed increased peripheral basophils 4 h following a 2-h exposure in a group of healthy older adults, which provides limited evidence of a CAPs-induced systemic inflammatory response.

Urban Traffic Particles

In a recent investigation of controlled exposures (24 h) to urban traffic particles, Bräuner et al. (2008, [191966](#)) observed no effect of PM concentration (avg $\text{PM}_{2.5}$ concentration 10.5 $\mu\text{g}/\text{m}^3$) on markers of inflammation including CRP, IL-6 and TNF- α in peripheral venous blood.

Diesel Exhaust

Recent controlled human exposure studies have observed no effect of DE on plasma CRP concentrations or peripheral blood cell counts (Blomberg et al., 2005, [191991](#); Carlsten et al., 2007, [155714](#); Mills et al., 2005, [095757](#); Mills et al., 2007, [091206](#); Tornqvist et al., 2007, [091279](#)). Mills et al. (2005, [095757](#)) found no effect of DE (300 $\mu\text{g}/\text{m}^3$) on serum IL-6 or TNF- α among healthy adult volunteers 6 h after exposure. However, as reported by Tornqvist et al. (2007, [091279](#)), a significant increase in these cytokines was observed 24 h after exposure. Although the physiological significance of this finding is unclear, this study does provide evidence of a mild systemic inflammatory response induced by exposure to DE. In an effort to better understand the inflammatory response of exposure to PM, Peretz et al. (2007, [156853](#)) conducted a pilot study in which gene expression in peripheral blood mononuclear cells (PBMCs) of healthy human volunteers was evaluated following a 2-h controlled exposure to DE (200 $\mu\text{g}/\text{m}^3$ $\text{PM}_{2.5}$). Adequate RNA samples for microarray analysis from both pre- and 4 h post-exposure to filtered air and DE were available in 4 of the 11 subjects enrolled. The authors found differential expression of 10 genes involved in the inflammatory response when comparing DE exposure (8 upregulated, 2 downregulated) to filtered air. Two participants had paired samples from 20 h post-exposure which were adequate for analysis. At this time point, DE was associated with 4 differentially expressed genes (1 upregulated, 3 downregulated). However, this study is limited by a small sample size with limited statistical power.

Wood Smoke

Barregard et al. (2006, [091381](#)) recently reported an increase in serum amyloid A at 0, 3, and 20 h following a 4-h exposure to wood smoke ($\text{PM}_{2.5}$ concentrations of 240-280 $\mu\text{g}/\text{m}^3$) among a group of 13 healthy adults (20-56 yr).

Model Particles

Frampton et al. (2006, [088665](#)) evaluated the effect of varying concentrations (10-50 $\mu\text{g}/\text{m}^3$) of UF EC on blood leukocyte expression of adhesion molecules in healthy and asthmatic adults. Healthy subjects ($n = 40$) were exposed for 2 h to filtered air and UF EC under three separate protocols: 10 $\mu\text{g}/\text{m}^3$ at rest ($n = 12$), 10 and 25 $\mu\text{g}/\text{m}^3$ with intermittent exercise ($n = 12$), and 50 $\mu\text{g}/\text{m}^3$ with intermittent exercise ($n = 16$). Asthmatics ($n = 16$) were exposed at a single concentration (10 $\mu\text{g}/\text{m}^3$) for 2 h with intermittent exercise. Leukocyte expression of surface markers were quantified using flow cytometry on peripheral venous blood samples collected prior to and immediately following exposure, as well as at 3.5 and 21 h post-exposure. Among healthy resting adults, UF EC exposure at a concentration of 10 $\mu\text{g}/\text{m}^3$ had no effect on blood leukocytes. The expression of adhesion molecules CD54 and CD18 on monocytes, and CD18 on PMNs was shown

to decrease with UF EC exposure in healthy exercising adults. In exercising asthmatics, expression of CD11b on monocytes and eosinophils, as well as CD54 on PMNs were reduced following exposure to UF EC. In both asthmatics and healthy adults, a UF EC-induced decrease in eosinophils and basophils was observed 0-21 h following exposure. Although the clinical significance of these findings is unclear, the authors concluded that their findings of UF EC-induced changes in leukocyte distribution and expression were consistent with increased retention of leukocytes in the pulmonary vasculature, which may be due to an increase in pulmonary vasoconstriction. Other studies have reported no changes in plasma cytokine levels, peripheral blood counts, or CRP following exposure to ZnO or UF EC (Beckett et al., 2005, [156261](#); Routledge et al., 2006, [088674](#)).

Summary of Controlled Human Exposure Study Findings for Systemic Inflammation

New studies involving controlled exposures to various particle types have provided limited and inconsistent evidence of a PM-induced increase in markers of systemic inflammation.

6.2.7.3. Toxicological Studies

There has been limited evidence that enhanced hematopoiesis may occur in animals exposed to PM. Two studies in the 2004 PM AQCD (U.S. EPA, 2004, [056905](#)) provided support for this effect, with one study measured stimulated release of PMNs from bone marrow and another examined peripheral blood PMN and blood cell counts; however, one study did not find associations between CAPs and peripheral blood counts. Thus, it was concluded that consistent evidence of PM-induced hematopoiesis remained to be demonstrated. However, in a study of humans exposed to biomass burning during the 1997 Southeast Asian smoke-haze episodes, PM₁₀ demonstrated the best relationship with blood PMN band cell counts expressed as a percentage of total PMN at lag 0 and 1, indicating a relatively quick response (Tan et al., 2000, [002304](#)).

CAPs

A 2-day CAPs study employing SH rats did not report increased WBCs 18-20 h post-exposure (Kodavanti et al., 2005, [087946](#)). A study utilizing fine and/or UF CAPs demonstrated decreased WBCs in SH rats 18 h after a 2-day (6 h/day) exposure (Kooter et al., 2006, [097547](#)). The decrease was largely attributable to lowered neutrophils in the fine CAPs-exposed rats and reduced lymphocytes in the fine+UF CAPs-exposed animals.

Model Particles

In a study of fine and UF CB particles (WKY rats; 7 h; mean mass concentration 1,400 and 1,660 $\mu\text{g}/\text{m}^3$ for fine and UF CB, respectively; mean number concentration 3.8×10^3 and 5.2×10^4 particles/ cm^3 , respectively), only UF CB induced elevated blood leukocytes at 0 and 48 h post-exposure compared to the control rats and no effect was observed at 16 h (Gilmour et al., 2004, [054175](#)). In another study of SH rats exposed to UF carbon particles for 24 h (mass concentration 172 $\mu\text{g}/\text{m}^3$; mean number concentration 9.0×10^6 particles/ cm^3), the percent neutrophils and lymphocytes were increased on the first recovery day, but not the third day (Upadhyay et al., 2008, [159345](#)); CRP was unchanged. In another study, blood neutrophils were decreased in SH rats exposed to UF CB for 6 h and no effects were observed in old F344 rats (Elder et al., 2004, [055642](#)). Plasma IL-6 levels were unchanged (Elder et al., 2004, [055642](#)).

Coal Fly Ash

Smith et al. (2006, [110864](#)) examined the hematology parameters in SD rats following a 3-day inhalation exposure (4 h/day) to coal fly ash (mean mass concentration 1,400 $\mu\text{g}/\text{m}^3$) and reported increased blood neutrophils and reduced blood lymphocytes at 36 h but not 18 h post-exposure.

Intratracheal Instillation

Elevated systemic IL-6 and TNF- α levels were observed following PM₁₀ instillation in mice (details provided in Section 6.2.8.3) (Mutlu et al., 2007, [121441](#)). IL-6 was decreased with PM exposure in macrophage-depleted mice, indicating that some of the IL-6 release originated from macrophages. For mice (male C57Bl/6J) exposed to PM_{10-2.5} derived from coal fly ash (200 μg), increased plasma IL-6 levels were only observed in animals that also received 100 μg of LPS (Finnerty et al., 2007, [156434](#)) and this response was not observed with LPS alone, indicating a role for PM_{10-2.5}.

Summary of Toxicological Study Findings for Systemic Inflammation

Overall, these studies provide evidence of time-dependent responses of systemic inflammation induced by PM exposure. Alterations in WBCs have been reported generally as elevations immediately (0 h) or <36 h post-exposure and no change or reductions are noted from 18-24 h.

6.2.8. Hemostasis, Thrombosis and Coagulation Factors

The 2004 PM AQCD (U.S. EPA, 2004, [056905](#)) presented limited and inconsistent evidence from epidemiologic, controlled human exposure, and toxicological studies of PM-induced changes in blood coagulation markers. The body of scientific literature investigating hemostatic effects of PM has grown significantly since the publication of the 2004 PM AQCD (U.S. EPA, 2004, [056905](#)), with a limited number of epidemiologic studies demonstrating consistent increases in von Willebrand factor (vWf) associated with PM and less consistent associations with fibrinogen. Recent controlled human exposure and toxicological studies have also observed changes in blood coagulation markers (e.g., fibrinogen, vWf, factor VII, t-PA) following exposure to PM. However, the findings of these studies are somewhat inconsistent, which may be due in part to differences in the post-exposure timing of the assessment.

6.2.8.1. Epidemiologic Studies

Several studies investigating the association of short-term fluctuations in PM concentration with markers of coagulation (e.g., blood viscosity and fibrinogen) were included in the 2004 PM AQCD (U.S. EPA, 2004, [056905](#)). These preliminary studies offered limited support for mechanistic explanations of the associations of PM concentration with heart disease outcomes. New studies, published since 2002, are reviewed in this section. Only vWF and fibrinogen were measured in enough comparable studies to allow the consistency of findings to be evaluated across epidemiologic studies. Other markers of coagulation studied included D-dimer, prothrombin time, Factor VII/VIII and tPA.

Liao et al. (2005, [088677](#)) used a cross-sectional study to examine the association between short-term increases in air pollutant concentrations (mean PM₁₀, NO₂, CO, SO₂, and O₃ over the previous 3 days) and several plasma hemostatic markers (fibrinogen, factor VIII-C, vWF, albumin). Study subjects were middle aged participants in the ARIC (Atherosclerosis Risk in Communities) study (n = 10,208), and were residents of Washington County, MD, Forsyth County, NC, selected suburbs of Minneapolis, MN, or Jackson, MS. Each 12.8 $\mu\text{g}/\text{m}^3$ increase in the mean PM₁₀ concentration 1 day before the health measurements were made was associated with a 3.93% increase in vWF (95% CI: 0.40-7.46) among diabetics, but not among non-diabetics (-0.54% [95% CI: -1.68 to 0.60]). Each 12.8 $\mu\text{g}/\text{m}^3$ increase in the mean PM₁₀ concentration 1 day before the health measurements were made was also associated with a 0.006 g/dL decrease in serum albumin (95% CI: -0.012 to 0.000) among those with cardiovascular disease (CVD), but not among those without CVD (0.029 g/dL increase [95% CI: -0.004 to 0.062]). The mean CO concentration on the previous day was also associated with a significant decrease in serum albumin. The authors reported significant curvilinear associations between PM₁₀ and factor VIII-C, which may indicate a threshold effect. Similar curvilinear associations were observed between O₃ with fibrinogen, and vWF, and SO₂ with factor VIII-C, WBC, and serum albumin (Liao et al., 2005, [088677](#)). No significant associations with fibrinogen and PM₁₀ or gaseous pollutants were observed.

In the European multicity study described in Section 6.2.7.1, Ruckerl et al. (2007, [156931](#)) found that each 13.5 $\mu\text{g}/\text{m}^3$ increase in the mean PM_{10} concentration over the previous 5 days was associated with a 0.6% increase in the arithmetic mean fibrinogen level (95% CI: 0.1-1.1). Further these investigators found that promoter polymorphisms within FGA and FGB modified the association of 5-day avg PM_{10} concentration with plasma fibrinogen levels (Peters et al., 2009, [191992](#)). This association was 8-fold higher among those homozygous for the minor allele genotype of FGB rs1800790 compared with those homozygous for the major allele.

Several smaller studies have been conducted in the U.S. and Canada. Delfino et al. (2008, [156390](#)) measured fibrinogen and D-dimer in blood of subjects who resided at two downtown Los Angeles nursing homes. As described in Section 6.2.7.1, measurements were made over a period of 12 wk and subjects were >65 yr old with a history of coronary artery disease. These markers were not associated with the broad array PM metrics studied (e.g., $\text{PM}_{0.25}$, $\text{PM}_{0.25-2.5}$, $\text{PM}_{10-2.5}$, EC, OC, primary OC, BC). In the study of 92 Boston residents with type 2 diabetes described previously, O'Neill et al. (2007, [091362](#)) found that increases in mean $\text{PM}_{2.5}$ and BC concentration were associated with vWF concentrations for all moving averages examined (1-6 days). Reidiker et al. (2004, [056992](#)) reported that in-vehicle $\text{PM}_{2.5}$ was associated with increased vWF over the next 10-14 h among nine police troopers. Sullivan et al. (2007, [100083](#)) did not observe associations with fibrinogen, or D-dimer in individuals with or without COPD. Red blood cells (RBCs), platelets, nor blood viscosity were associated with $\text{PM}_{2.5}$ concentration in a panel study of 88 non-smoking elderly subjects residing in the Salt Lake City, Ogden and Provo metropolitan area of Utah (Pope et al., 2004, [055238](#)). Although Zeka et al. (2006, [157177](#)) did not observe an association with CRP in the analysis of the Normative Aging Study population in Boston (Section 6.3.7.1), increased fibrinogen level was associated with increases in the number of particles/ cm^3 over the previous 48 h and 1 wk, and an incremental increase in BC concentration over the previous 4 wk. There were no consistent findings for lagged $\text{PM}_{2.5}$ or sulfates (Zeka et al., 2006, [157177](#)).

Several studies of coagulation markers were conducted outside the U.S. and Canada. In a study of healthy individuals in Taiwan, associations were observed for $\text{PM}_{2.5}$, PM_{10} , nitrate, and SO_4^{2-} concentrations with fibrinogen and plasminogen activator fibrinogen inhibitor-1 (PAI-1) (Chuang et al., 2007, [091063](#)). In a large cross-sectional study of healthy subjects in Tel-Aviv, Steinvil et al. (2008, [188893](#)) examined fibrinogen collected as part of routine health examinations for 3,659 individuals. No significant associations were found between pollutant levels (lagged 1-7 days) and fibrinogen. Finally, Baccarelli and colleagues reported associations between PM_{10} and prothrombin time among normal subjects (Baccarelli et al., 2007, [090733](#)).

Summary of Epidemiologic Study Findings for Hemostasis, Thrombosis and Coagulation

The most commonly measured markers of coagulation in the studies reviewed were fibrinogen and vWF. Associations of PM_{10} (Liao et al., 2005, [088677](#)) and $\text{PM}_{2.5}$ (O'Neill et al., 2007, [091362](#); Riediker et al., 2004, [056992](#)) with increased vWF were observed across the limited number of studies examining this association among both diabetics and healthy state troopers (Liao et al., 2005, [088677](#); Riediker et al., 2004, [056992](#)). Results for fibrinogen were not consistent across epidemiologic studies. Positive associations with fibrinogen were reported in older adults residing in Boston (Zeka et al., 2006, [157177](#)) and in the multicity European study of MI survivors. Liao et al. (2005, [088677](#)) in a population based multicity study and Sullivan et al. (2007, [100083](#)) did not observe associations of PM_{10} or $\text{PM}_{2.5}$ with fibrinogen. Several other markers have been examined (e.g., D-dimer, prothrombin time), but not in adequate numbers of studies to allow comparisons across epidemiologic studies. Mean and upper percentile concentrations of the studies discussed in this section are listed in Table 6-6.

6.2.8.2. Controlled Human Exposure Studies

In two separate studies conducted by Ghio and colleagues, controlled exposures (2 h) to fine CAPs (Chapel Hill, NC) at concentrations between 15 and 350 $\mu\text{g}/\text{m}^3$ were shown to increase blood fibrinogen 18-24 h following exposure among healthy adults (Ghio et al., 2000, [012140](#); Ghio et al., 2003, [087363](#)). Increases in blood fibrinogen or factor VII would suggest an increase in blood coagulability, which could result in an increased risk of coronary thrombosis. However, a similar

study conducted in Los Angeles observed a PM_{2.5} CAPs-induced decrease in factor VII blood levels in healthy subjects and found no association between PM_{2.5} CAPs and blood fibrinogen among healthy and asthmatic volunteers (Gong et al., 2003, [042106](#)). Since the publication of the 2004 PM AQCD (U.S. EPA, 2004, [056905](#)), several new controlled human exposure studies have evaluated the effects of PM on blood coagulation markers.

CAPs

Two studies of controlled human exposures to Los Angeles CAPs among older adults with COPD (PM_{2.5} CAPs) and adults with and without asthma (UF CAPs) reported no significant association between exposure and blood coagulation markers at 0, 4, or 22 h post-exposure (Gong et al., 2004, [087964](#); 2008, [156483](#)). Graff et al. (2009, [191981](#)) observed a decrease in the concentration of D-dimer of marginal statistical significance in healthy adults (11.3% decrease per 10 µg/m³, p = 0.07) following exposure to PM_{10-2.5} CAPs (89 µg/m³). At 20 h post-exposure, levels of tPA in plasma were shown to decrease by 32.9% from baseline per 10 µg/m³ increase in CAPs concentration. No other markers of hemostasis or thrombosis were affected by exposure to PM_{10-2.5} CAPs. However, in a similar study from the same laboratory, Samet et al. (2009, [191913](#)) reported a statistically significant increase in D-dimer immediately following, as well as 18 h, after a 2-h exposure to UF CAPs (49.8 µg/m³; 120,662 particles/cm³) in a group of healthy adults (18-35 yr). Plasma concentrations of PAI-1 were also reported to increase 18 h after exposure to UF CAPs, although this increase was not statistically significant (p = 0.1). No changes in fibrinogen, tPA, vWF, plasminogen, or factor VII were observed. The finding of an increase in D-dimer following exposure to UF CAPs provides potentially important information in elucidating the relationship between elevated concentrations of PM and cardiovascular morbidity and mortality observed in epidemiologic studies. Whereas many coagulation markers provide evidence of an increased potential to form clots (e.g., an increase in fibrinogen or a decrease in tPA), D-dimer is a degradation product of a clot that has formed.

Urban Traffic Particles

In a study of controlled 24-h exposures to urban traffic particles (avg PM_{2.5} concentration 10.5 µg/m³) among 29 healthy adults, Bräuner et al. (2008, [191966](#)) did not observe any particle-induced change in plasma fibrinogen, factor VII, or platelet count after 6 or 24 h of exposure. Similarly, Larsson et al. (2007, [091375](#)) observed no change in PAI-1 or fibrinogen in peripheral blood of healthy adult volunteers 14 h after a 2-h exposure to road tunnel traffic with a PM_{2.5} concentration of 46-81 µg/m³.

Diesel Exhaust

Mills and colleagues have recently demonstrated a significant effect of DE (particle concentration 300 µg/m³) on fibrinolytic function both in healthy men (n = 30) and in men with coronary heart disease (n = 20) (Mills et al., 2005, [095757](#); 2007, [091206](#)). In both groups of volunteers, bradykinin-induced release of tPA was observed to decrease 6 h following exposure to DE compared to filtered air exposure. The same laboratory did not observe an attenuation of tPA release 24 h after a 1-h exposure to DE (300 µg/m³) in a group of health adults (Tornqvist et al., 2007, [091279](#)), or observe any change in markers of hemostasis or thrombosis 6 or 24 h following DE exposure at the same particle concentration among a group of older adults with COPD (Blomberg et al., 2005, [191991](#)). Carlsten et al. (2007, [155714](#)) conducted a similar study involving exposure of healthy adults to DE with a PM_{2.5} concentration of 200 µg/m³. Although the authors observed an increase in D-dimer, vWF, and platelet count 6 h following exposure to DE, these increases did not reach statistical significance. In a subsequent study with a similar study design, the same laboratory found no effect of a 2-h exposure to DE (100 and 200 µg/m³ PM_{2.5}) on prothrombotic markers in a group (n = 16) of adults with metabolic syndrome (Carlsten et al., 2008, [156323](#)). The authors postulated that the lack of significant findings could be due to a relatively small sample size. In addition, Carlsten et al. (2007, [155714](#); 2008, [156323](#)) exposed subjects at rest

while Mills et al. (2005, [095757](#)) exposed subjects to a higher concentration ($300 \mu\text{g}/\text{m}^3$) with intermittent exercise. A more recent study of DE which exposed healthy adults to a slightly higher particle concentration ($330 \mu\text{g}/\text{m}^3$) evaluated the effect of DE on thrombus formation using an ex vivo perfusion chamber (Lucking et al., 2008, [191993](#)). Thrombus formation, as well as in vivo platelet activation, was observed to significantly increase 2 h following exposure to DE relative to filtered air, thus providing some evidence of a potential physiological mechanism which may explain in part the associations between PM and cardiovascular events observed in epidemiologic studies.

Wood Smoke

Barregard et al. (2006, [091381](#)) recently evaluated the effect of wood smoke on markers of coagulation, inflammation, and lipid peroxidation. Subjects ($n = 13$) were healthy males and females (20-56 yr) and were exposed for 4 h to $\text{PM}_{2.5}$ concentrations of 240-280 $\mu\text{g}/\text{m}^3$. The authors reported an increase in the ratio of factor VIII/vWF, which is an indicator of an increased risk of venous thromboembolism, at 0, 3, and 20 h following exposure to wood smoke.

Model Particles

Routledge et al. (2006, [088674](#)) did not observe any changes in fibrinogen or D-dimer following a 1-h exposure to UF carbon among a group of resting healthy older adults and older adults with stable angina. Similarly, Beckett et al. (2005, [156261](#)) found no changes in hemostatic markers (e.g., factor VII, fibrinogen, and vWF) following exposure to UF and fine ZnO ($500 \mu\text{g}/\text{m}^3$).

Summary of Controlled Human Exposure Study Findings for Hemostasis, Thrombosis and Coagulation

Taken together, these new studies have provided some additional evidence that short-term exposure to PM at near ambient levels may have small, yet statistically significant effects on hemostatic markers in healthy subjects or patients with coronary artery disease.

6.2.8.3. Toxicological Studies

In general, the limited toxicological studies reviewed in the 2004 PM AQCD (U.S. EPA, 2004, [056905](#)) reported positive and negative findings for plasma fibrinogen levels or other factors involved in the coagulation cascade. Rats exposed to New York City CAPs did not have any exposure-related effects on any measured coagulation markers (Nadziejko et al., 2002, [050587](#)), whereas rats exposed to a high concentration of ROFA demonstrated increased plasma fibrinogen (Kodavanti et al., 2002, [025236](#)).

CAPs

A $\text{PM}_{2.5}$ CAPs exposure conducted for 2 days (4 h/day; mean mass concentration 144-2,758 $\mu\text{g}/\text{m}^3$; 8-10/2001; RTP, NC) in SH rats induced plasma fibrinogen increases (measured 18-20 h post-exposure) in 5 of 7 separate studies (Kodavanti et al., 2005, [087946](#)). Fibrinogen was not different from the air control group on the two days with the highest CAPs concentrations (1,129 and 2,758 $\mu\text{g}/\text{m}^3$), indicating that the response was likely not attributable to mass alone.

In SH rats exposed to $\text{PM}_{2.5}$ CAPs for 6 h in one of three locations in the Netherlands (mean mass concentration range 270-2,400; 335-3,720; and 655-3,660 $\mu\text{g}/\text{m}^3$), plasma fibrinogen was increased 48 h post-exposure when all CAP-exposed animals were combined in the analysis (Cassee et al., 2005, [087962](#)). In WKY rats pre-exposed to O_3 (8 h; 1,600 $\mu\text{g}/\text{m}^3$) and CAPs for 6 h, increases in RBCs, hemoglobin, and hematocrit were observed 2 days after CAPs exposure. For SH rats exposed to CAPs only, decreased mean corpuscular hemoglobin concentration were reported.

A similar study conducted by the same group (Kooter et al., 2006, [097547](#)) reported no changes in plasma fibrinogen measured 18 h after a 2-day exposure (6 h/day) to PM_{2.5} or PM_{2.5}+UF CAPs (mean mass concentration range 399.0-1,067.5 and 269.0-555.8 µg/m³, respectively; 1/2003-4/2004). However, elevated vWF was observed in SH rats exposed to the highest concentration of PM_{2.5} CAPs. Decreases in mean corpuscular volume (MCV), and elevations in mean platelet volume (MPV) and mean platelet component (MPC) were reported in SH rats 18 h following a 2-day exposure to PM_{2.5}+UF CAPs in a freeway tunnel.

Traffic-Related Particles

Plasma fibrinogen levels were elevated 18 h following a single 6-h exposure to on-road highway aerosols when groups of rats pretreated with saline or influenza virus were combined (i.e., there was a significant effect of particles) (Elder et al., 2004, [087354](#)).

Model Particles

The coagulation effects of inhaled UF CB at a concentration of 150 µg/m³ (number count not provided) for 6 h were evaluated 24 h post-exposure in two aged rat models (11-14 mo SH and 23 mo F344), some of which received LPS via intraperitoneal injection prior to particle exposure (Elder et al., 2004, [055642](#)). LPS has been shown to induce the expression of molecules involved in coagulation, inflammation, oxidative stress, and the acute-phase response. In those animals only exposed to CB, SH rats demonstrated increased thrombin-anti-thrombin complexes (TAT) and decreased fibrinogen. For F344 rats, TAT complexes and fibrinogen were elevated only in those that received LPS and CB. Whole-blood viscosity was not altered in either rat strain with particle exposure.

In another study of SH rats exposed to UF carbon particles for 24 h (mass concentration 172 µg/m³; mean number concentration 9.0×10^6 particles/cm³), the number of RBCs and platelets and hematocrit percent, were unchanged 1 and 3 days following exposure (Upadhyay et al., 2008, [159345](#)). Fibrinogen levels were similar in both air and UF carbon-exposed groups. However, mRNA expression of PAI-1 and TF in lung homogenates (but not in heart) was increased on recovery day 3 after exposure. A study of similar design that employed SH rats did not report any effect on plasma fibrinogen 4 or 24 h following UF carbon exposure (mass concentration 180 µg/m³; mean number concentration 1.6×10^7 particles/cm³) (Harder et al., 2005, [087371](#)). Similarly, clotting factor VIIa and thrombomodulin, PAI-1, and tPA mRNA expression were not affected by UF carbon exposure at 24 h post-exposure.

Coal Fly Ash

One study that employed coal fly ash (mean mass concentration 1,400 µg/m³; 4 h/day×3 days) demonstrated increases in hematocrit and MCV in SD rats at 36 h but not 16 h post-exposure (Smith et al., 2006, [110864](#)).

Intratracheal Instillation

Mutlu et al. (2007, [121441](#)) used a PM₁₀ sample collected from Dusseldorf, Germany, in mice (C57BL/6) with and without the gene coding for IL-6. The authors report using a moderate IT instillation dose (10 µg/mouse; roughly equivalent to 400-500 µg/kg); the PM sample had previously been characterized as having significant Fe, Ni, and V content (Upadhyay et al., 2003, [097370](#)). In C57BL/6 mice, the Dusseldorf PM shortened bleeding (32%), prothrombin (13%), and activated partial thromboplastin (16%) times and increased platelet count, fibrinogen, and Factors II, VIII, and X activities 24 h following exposure. The authors further demonstrated accelerated coagulation by a reduction in the left carotid artery occlusion time (experimentally-derived by direct application of FeCl₃). Additional experiments demonstrated that IL-6^{-/-} or macrophage-depleted mice showed dramatically attenuated effects of PM₁₀ on hemostatic indices, thrombin generation, and occlusion

time. In IL-6^{-/-} mice, there was no change in total cell counts or differentials in BALF compared to the wild-type mice, despite the lack of IL-6. In contrast, the model of macrophage depletion had reduced levels of macrophages and IL-6 in BALF, following PM exposure. These studies suggest that instillation of Dusseldorf PM₁₀ activates clotting through an alveolar macrophage-dependent release of IL-6; however, other factors may also be involved in the prothrombotic response (i.e., activation of neutrophils, other inflammatory cells, or alterations in the levels of other cytokines).

In a study employing PM_{10-2.5} collected from six European locations with contrasting traffic profiles, fibrinogen increases were observed in SH rats exposed to 10 mg/kg via IT instillation at 24 h post-exposure and similar responses were observed with PM_{2.5} (Gerlofs-Nijland et al., 2007, [097840](#)). PM_{10-2.5} and PM_{2.5} samples from Prague or Barcelona administered intratracheally to SH rats (7 mg/kg) resulted in elevated plasma fibrinogen levels 24 h post-exposure compared to rats instilled with water (Gerlofs-Nijland et al., 2009, [190353](#)). No changes were observed in vWF for whole particle suspensions, but Barcelona PM_{10-2.5} organic extract induced greater levels of vWF than Barcelona PM_{10-2.5}.

Summary of Toxicological Study Findings for Hemostasis, Thrombosis and Coagulation

Increases in coagulation and thrombotic markers were observed in some studies of rats or mice exposed to PM. Plasma TAT complexes were increased in CB-exposed SH rats and shortened bleeding, prothrombin, and activated partial thromboplastin times were observed in mice exposed via IT instillation to PM₁₀. Furthermore, the latter study also reported increased levels of Factors II, VIII, and X activities in mice. Another study demonstrated increased vWF in response to PM_{2.5} CAPs. As for plasma fibrinogen, these studies provide some evidence that increased levels are observed 18-48 h post-exposure to PM, although one study reported no change and another reported a decrease in this biomarker. Alterations in platelet measurements have also been observed with PM exposure, including increased platelet number, mean platelet volume, and mean platelet component. The toxicological results of RBC-related measurements are limited and inconsistent following PM exposure, which may be attributable to different exposure protocols, time of analysis, or rat strain.

6.2.9. Systemic and Cardiovascular Oxidative Stress

Very little information on systemic oxidative stress associated with PM was available for inclusion in the 2004 PM AQCD (U.S. EPA, 2004, [056905](#)). However, recent epidemiologic studies have provided consistent evidence of PM-induced increases in markers of systemic oxidative stress including plasma thiobarbituric acid reactive substances (TBARS), CuZn-superoxide dismutase (SOD), 8-oxo-7-hydrodeoxyguanosine (8-oxodG), and total homocysteine. This is supported by a limited number of controlled human exposure studies that observed PM-induced increases in free-radical mediated lipid peroxidation, as well as upregulation of the DNA repair gene hOGG1. In addition, recent toxicological studies have demonstrated an increase in cardiovascular oxidative stress following PM exposure in rats.

6.2.9.1. Epidemiologic Studies

No studies of markers of oxidative stress were reviewed in the 2004 PM AQCD (U.S. EPA, 2004, [056905](#)). Since 2002, numerous studies have examined whether short-term increases in mean PM concentrations are associated with changes in systemic markers of oxidative stress.

In an analysis of the randomized trial of omega-3 fatty acid supplementation in Mexico City nursing home residents described previously (Section 6.2.1.1), Romieu et al. (2008, [156922](#)) investigated the effect of this intervention on markers of systemic oxidative stress (Cu/Zn SOD activity, LPO in plasma and GSH in plasma). A significant decrease of Cu/Zn SOD was associated with a 10 µg/m³ increase of PM_{2.5} in both groups (Fish oil: β = -0.17 [SE = 0.05], p = 0.002; Soy oil: β = -0.06 [SE = 0.02], p < 0.001). A decrease in GSH was associated with a 10 µg/m³ increase in PM_{2.5} in the fish oil group (β = -0.09 [SE = 0.04], p = 0.017).

Two studies evaluated plasma homocysteine levels in relation to PM. Baccarelli et al. (2007, [091310](#)) investigated fasting and post-methionine load total homocysteine (tHcy) among 1,213 normal subjects in Lombardia, Italy. Plasma homocysteine is a risk factor for CVD and a marker for oxidative stress. Among smokers, average PM₁₀ level during the 24 h preceding the measurement was associated with 6.3% (95% CI: 1.3-11.6) and 4.9% (95% CI: 0.5-9.6) increases in fasting and post-methionine load tHcy, respectively. No associations were observed among non-smokers. Park et al. (2008, [156845](#)) investigated the association of BC, OC, SO₄²⁻ and PM_{2.5} with tHcy among 960 male participants of the Normative Aging Study. Effect modification by folate and vitamins B6 and B12 was also examined. BC and OC were associated with increases in tHcy and associations were more pronounced in those with lower plasma folate and vitamin B12.

In smaller studies with 25-50 healthy or diseased participants, several markers of oxidative stress have been associated with PM size fractions or components. These associations include TBARS with 24-h PM₁₀ (Liu et al., 2006, [192002](#)); Cu/Zn-SOD with several PM metrics (e.g., UF, PM_{10-2.5}, EC, OC, BC and PNC) (Delfino et al., 2008, [156390](#)); PM_{2.5}, BC, V and Cr with plasma proteins (Sørensen et al., 2003, [157000](#)); DNA damage assessed by 8-oxodG in lymphocytes (Sørensen et al., 2003, [157000](#)), and 8-OHdG with sulfates (Chuang et al., 2007, [091063](#)). In addition, a cross-sectional study of children (10-18 yr) in Iran showed an association of PM₁₀ with oxidized LDL (oxLDL), malondialdehyde (MDA) and conjugated diene (CDE) (Kelishadi et al., 2009, [191960](#)).

Summary of Epidemiologic Study Findings for Systemic and Cardiovascular Oxidative Stress

Oxidative stress responses measured by one or more markers (plasma tHcy, CuZn-SOD, TBARS, 8-oxodG, oxLDL and MDA) have been consistently observed (Baccarelli et al., 2007, [091310](#); Chuang et al., 2007, [091063](#); Delfino et al., 2008, [156390](#); Kelishadi et al., 2009, [191960](#); Liu et al., 2007, [156705](#); Romieu et al., 2008, [156922](#); Sørensen et al., 2003, [157000](#)). In addition, a series of analyses examining the modification the PM-HRV association by genetic polymorphisms related to oxidative stress has provided insight into the possible mechanisms of CVD observed in association with PM concentrations (Section 6.2.1.1). Mean and upper percentile concentrations of the epidemiologic studies of systemic oxidative stress are included in Table 6-6.

6.2.9.2. Controlled Human Exposure Studies

Urban Traffic Particles

Bräuner et al. (2007, [091152](#)) recently investigated the effect of urban traffic particles on oxidative stress-induced damage to DNA. Healthy adults (20-40 yr) were exposed to low concentrations of urban traffic particles as well as filtered air for periods of 24 h, with and without two 90-min periods of exercise. Exposures took place in an exposure chamber above a busy road with high traffic density in Copenhagen. Non-filtered air was pumped into the chamber from above the street, with avg PM_{2.5} and PM_{10-2.5} mass concentrations of 9.7 µg/m³ and 12.6 µg/m³, respectively. The UF/PM_{2.5} (6-700 nm) particle number concentration was continuously monitored throughout the exposure (avg PNC 10,067 particles/cm³). The PM_{2.5} fraction was rich in sulfur, V, Cr, Fe, and Cu. PBMCs were isolated from blood samples collected at 6 and 24 h. DNA damage, as measured by strand breaks (SB) and formamidopyrimidine-DNA glycosylase (FPG) sites, was evaluated using the Comet assay. The activity and mRNA levels of the DNA repair enzyme 7,8-dihydro-8-oxoguanine-DNA glycosylase (OGG1) were also measured. The authors observed increased levels of DNA strand breaks and FPG sites following 6 and 24 h of exposure to PM. Using a mixed-effects regression model, the particle concentration at the 57 nm mode was found to be the major contributor of these measures of DNA damage. The results of this study suggest that short-term (6-24 h) exposure to ambient levels of UFPs cause systemic oxidative stress resulting in damage to DNA.

Diesel Exhaust

Tornqvist et al. (2007, [091279](#)) reported an increase in plasma antioxidant capacity in a group of healthy volunteers 24 h after a 1-h exposure to DE with a particle concentration of 300 $\mu\text{g}/\text{m}^3$. The investigators suggested that systemic oxidative stress occurring following exposure may have caused this up-regulation in antioxidant defense. Peretz et al. (2007, [156853](#)) observed some significant differences in expression of genes involved in oxidative stress pathways between exposure to DE (200 $\mu\text{g}/\text{m}^3$ $\text{PM}_{2.5}$) and filtered air. However, the conclusions of this investigation are limited by a small number of subjects (n = 4).

Wood Smoke

In a controlled human exposure study of controlled exposure to wood smoke, Barregard et al. (2006, [091381](#)) found an increase in urinary excretion of free 8-iso-prostaglandin 2α among healthy adults (n = 9) approximately 20 h following a 4-h exposure to $\text{PM}_{2.5}$ (mass concentration of 240-280 $\mu\text{g}/\text{m}^3$). This finding provides evidence of a PM-induced increase in free-radical mediated lipid peroxidation. From the same study, Danielsen et al. (2008, [156382](#)) reported an increase in the mRNA levels of the DNA repair gene hOGG1 in peripheral mononuclear cells 20 h after exposure to wood smoke relative to filtered air.

Summary of Controlled Human Exposure Study Findings for Systemic and Cardiovascular Oxidative Stress

Based on the results of these studies, it appears that exposure to PM at or near ambient levels may increase systemic oxidative stress in human subjects.

6.2.9.3. Toxicological Studies

Very little information was available for inclusion in the 2004 PM AQCD (U.S. EPA, 2004, [056905](#)) on oxidative stress in the cardiovascular system. A few new studies have evaluated ROS in blood or the heart following PM exposure. Some studies have used chemiluminescence (CL), which is measured using the decay of excited states of molecular oxygen, and may also be prone to artifact.

CAPs

Gurgueira et al. (2002, [036535](#)) measured oxidative stress in SD rats immediately following a 5-h CAPs exposure ($\text{PM}_{2.5}$ mean mass concentration 99.6-957.5 $\mu\text{g}/\text{m}^3$; Boston, MA; 7/2000-2/2001) and reported increased in situ CL in hearts of CAPs-exposed animals. CL evaluated after 1- and 3-h CAPs exposure did not demonstrate changes from the filtered air group, although a 5-h exposure resulted in increased CL in hearts. When animals were allowed to recover for 24 h, oxidative stress returned to control values. To compare potential particle-induced differences in CL, rats were exposed to ROFA (1.7 mg/m^3 for 30 min) or CB (170 $\mu\text{g}/\text{m}^3$ for 5 h) and only the ROFA-treated animals exhibited increased CL in cardiac tissue. Additionally, levels of antioxidant enzymes in the heart (Cu/Zn-SOD and MnSOD) were increased in CAPs-exposed rats. Individual PM component concentrations were linked to CL levels in rat heart tissue using separate univariate linear regression models, with total PM mass, Al, Si, Ti, and Fe having p-values ≤ 0.007 (Gurgueira et al., 2002, [036535](#)). The highest R^2 value in the regression analyses was for Al (0.67) and its concentration ranged from 0.000 to 8.938 $\mu\text{g}/\text{m}^3$.

Recently, Rhoden et al. (2005, [087878](#)) tested the role of the ANS in driving CAPs-induced cardiac oxidative stress in heart tissues of SD rats. At $\text{PM}_{2.5}$ mass concentrations of 700 $\mu\text{g}/\text{m}^3$ (Boston, MA), pretreatment with an antioxidant, a β_1 -receptor antagonist, or a muscarinic receptor antagonist attenuated the CL and TBARS effects observed in the heart following a 5-h $\text{PM}_{2.5}$ exposure. The wet/dry ratio (edema) of cardiac tissue also returned to control values in animals treated with the antioxidant prior to CAPs. These combined results indicate involvement of both the

sympathetic and parasympathetic pathways in the cardiac oxidative stress response observed following PM exposure.

More recently, a type of irritant receptor, the transient receptor potential vanilloid receptor 1 (TRPV1), was identified as central to the inhaled CAPS-mediated induction of cardiac tissue CL and TBARS in SD rats (Ghelfi et al., 2008, [156468](#)). In these studies (PM_{2.5} mean mass concentration 218 µg/m³; Boston, MA), capsazapine (a TRPV1 inhibitor) abrogated cardiac CL, TBARS, edema, and QT-interval shortening when measured at the end of the 5-h exposure. These studies provide some evidence that the ANS may be involved in producing cardiac oxidative stress following exposure to CAPs. Furthermore, this response could be acting, at least in part, via TRPV receptors.

In WKY rats exposed to PM_{2.5} CAPs in Japan, relative mRNA expression of HO-1 was increased in cardiac tissue and was also significantly correlated with the cumulative mass of PM collected on chamber filters throughout the exposure (Ito et al., 2008, [096823](#)).

Road Dust

A composite of PM_{2.5} road dust samples obtained from New York City, Los Angeles, and Atlanta induced cardiac ROS as measured by CL in the low exposure group (306 µg/m³) and TBARS in the high exposure group (954 µg/m³); thus, the CL and TBARS methods provided different results for the various source types (Seagrave et al., 2008, [191990](#)).

Gasoline and Diesel Exhaust

Gasoline exhaust exposure also resulted in increased ROS (measured by TBARS) in aortas of ApoE^{-/-} mice, as discussed in Section 6.2.4.3 (Lund et al., 2009, [180257](#)). Similarly, a 6-h exposure to gasoline exhaust (PM mass concentration 60 µg/m³, CMD 15-20 nm; MMD 150 nm; CO concentration 104 ppm, NO concentration 16.7 ppm, NO₂ concentration 1.1 ppm, SO₂ concentration 1.0 ppm) in SD rats demonstrated increased CL in the heart, but no change in TBARS and the CL response was not duplicated when the particles were filtered (Seagrave et al., 2008, [191990](#)). Increased lipid peroxides in the serum of male SH rats exposed to gasoline exhaust (PM mass concentration 59.1 µg/m³; NO concentration 18.4 ppm; NO₂ concentration 0.9 ppm; CO concentration 107.3 ppm; SO₂ concentration 0.62 ppm) was observed following a 1-wk exposure to gasoline exhaust and this effect was attenuated with particle filtration (Reed et al., 2008, [156903](#)). An IT instillation study of diesel particles in mice demonstrated increased myocardial MPO activity 12 and 24 h post-exposure to the residual particle component that remained after extraction with dichloromethane (Yokota et al., 2008, [190109](#)).

Model Particles

Other studies previously presented also demonstrated ROS (via CL) and NT expression (via ELISA) in the left ventricle with CB exposure (Tankersley et al., 2008, [157043](#)) and oxidative stress in the systemic microvasculature following TiO₂ inhalation (Nurkiewicz et al., 2009, [191961](#)) or ROFA IT instillation exposure (Nurkiewicz et al., 2006, [088611](#)). Decreased HO-1 mRNA expression in hearts of SH rats exposed to UF carbon particles was observed 3 days following exposure (Upadhyay et al., 2008, [159345](#)) and there was a trend toward increased HO-1 mRNA expression 1 day post-exposure.

Summary of Toxicological Study Findings for Systemic and Cardiovascular Oxidative Stress

When considered together, the above studies provide evidence that PM exposure results in oxidative stress as measured in cardiac tissue by CL, TBARS, HO-1 mRNA expression, and NT expression. However, the PM concentration/dose and method of ROS measurement could also affect the response. Cardiac oxidative stress may have resulted from PM stimulation of the ANS, although these studies have only been conducted in one laboratory. Multiple studies from two different

laboratories provide support for vascular oxidative stress as demonstrated in aortas following gasoline exhaust exposure and in the microvasculature after TiO₂ inhalation or ROFA IT exposure.

6.2.10. Hospital Admissions and Emergency Department Visits

The 1996 PM AQCD (U.S. EPA, 1996, [079380](#)) considered just two time-series studies regarding the association between daily variations in PM levels and the risk of CVD morbidity as measured by the number of daily hospitalizations with primary discharge diagnoses related to CVD (Burnett et al., 1995, [077226](#); Schwartz and Morris, 1995, [046186](#)). In contrast, the 2004 PM AQCD (U.S. EPA, 2004, [056905](#)) reviewed more than 25 publications relating PM and risk of CVD hospitalizations. Results from a handful of larger multicity studies were emphasized, with the greatest emphasis placed on findings from the U.S. National Morbidity, Mortality, and Air Pollution Study (NMMAPS) (Samet et al., 2000, [010269](#)) and a subsequent reanalysis (Zanobetti and Schwartz, 2003, [157174](#)). The NMMAPS study evaluated the effect of daily changes in ambient PM levels on total CVD hospitalizations among elderly Medicare beneficiaries in 14 U.S. cities and found a ~1% excess risk per 10 µg/m³ increase in PM₁₀. The 2004 PM AQCD concluded that these results, along with those of the other single- and multicity studies reviewed “generally appear to confirm likely excess risk of CVD-related hospital admissions for U.S. cities in the range of [0.6-1.7% per 10 µg/m³] PM₁₀, especially among the elderly” (U.S. EPA, 2004, [056905](#)). The 2004 PM AQCD (U.S. EPA, 2004, [056905](#)) also concluded that there was some evidence from single-city studies suggesting an excess risk specifically for hospitalizations related to IHD and heart failure. Furthermore, the 2004 PM AQCD (U.S. EPA, 2004, [056905](#)) found that “insufficient data exist from the time-series CVD admissions studies [...] to provide clear guidance as to which ambient PM components, defined on the basis of size or composition, determine ambient PM CVD effect potency” (U.S. EPA, 2004, [056905](#)). The key studies reviewed in the 2004 PM AQCD (U.S. EPA, 2004, [056905](#)) on this topic included those by Burnett and colleagues (1997, [084194](#); 1999, [017269](#)), Lippman and colleagues (2000, [011938](#)), Ito (2003, [042856](#)), and Peters et al. (2001, [016546](#)).

Recent large studies conducted in the U.S., Europe, and Australia and New Zealand have confirmed these findings for PM₁₀, and have also observed consistent associations between PM_{2.5} and cardiovascular hospitalizations. However, findings from single-city studies have demonstrated regional heterogeneity in effect estimates. It is apparent from these recent studies that the observed increases in cardiovascular hospitalizations are largely due to admissions for IHD and CHF rather than CBVDs (such as stroke). The new literature on hospitalizations and ED visits for cardiovascular causes published since 2002 is reviewed in the following sections. First, the specific CVD outcomes captured using ICD codes from hospital admissions databases are discussed. Second, the methods used in the large and multicity studies are described. For each outcome considered, evidence from large/multicity studies is emphasized and results from U.S. and Canadian single-city studies are also discussed. Although the single-city studies may lack statistical power needed to evaluate interactions and detect some of the subtle effects of air pollution, they inform the interpretation of the heterogeneous effect estimates that have been observed across North America.

Cardiovascular Disease ICD Codes

When the 2004 PM AQCD (U.S. EPA, 2004, [056905](#)) was written, few studies had evaluated the link between ambient PM and specific CVD outcomes such as CHF, IHD or ischemic stroke. In contrast, the majority of recent studies have focused on specific CVD outcomes. This trend is justified by the fact that the short-term exposure effects of PM may be very different for different cardiovascular outcomes. For example, given the current putative biological pathways involved in the acute response to PM exposure, there is no *a priori* reason why short-term fluctuations in PM levels would have similar effects on the risk of acute MI, chronic atherosclerosis of the coronary arteries, and hemorrhagic stroke.

Almost all of the published time-series studies of cardiovascular hospitalizations and ED visits identified cases based on administrative discharge diagnosis codes as defined by the International Classification of Disease 9th revision (ICD-9) or 10th revision (ICD-10) (NCHS, 2007, [157194](#)). A complicating factor in interpreting the results of these studies is the lack of consistency in both defining specific health outcomes and in the nomenclature used.

Table 6-7. Description of ICD-9 and ICD-10 codes for diseases of the circulatory system.

Description	ICD-9 Codes	ICD-10 Codes
All Cardiovascular Disease	390-459	I00-I99
IHD	410-414	I20-I25
Acute MI	410	I21
Diseases Of Pulmonary Circulation	415-417	I26-I28
CHF	428	I50
Arrhythmia	427	I47, I48, I49
CBVD	430-438	I60-I69
Ischemic Stroke And Transient Ischemic Attack (TIA)	430-432	I63
Hemorrhagic Stroke	433-435	I60-I62
Peripheral Vascular Disease (PVD)	440-448	I70-I79

Table 6-7 shows major groups of diagnostic codes used in air pollution studies for diseases of the circulatory system. The codes ICD-9: 390-459 are frequently used to identify all CVD morbidity. Note that this definition of CVD includes diseases of the heart and coronary circulation, CBVD, and peripheral vascular disease. In contrast, the term cardiac disease specifically excludes diseases not involving the heart or coronary circulation. While this distinction is conceptually straightforward, the implementation of the definition of cardiac disease in terms of ICD-9 or ICD-10 codes varies among authors. Even greater heterogeneity can be found among studies in the implementation of definitions related to CBVD.

Design and Methods of Large and Multicity Hospital Admission and ED Visit Studies

Recently, multiple research groups in the U.S., Europe, and Australia have created large datasets to evaluate specific CVD and respiratory endpoints using more detailed and relevant measures of PM concentration. In the U.S., the MCAPS analyses of Dominici et al. (2006, [088398](#)), Bell et al. (2008, [156266](#)) and Peng et al. (2008, [156850](#)) are large, comprehensive and informative studies based on Medicare hospitalization data. Likewise, the Atlanta-based SOPHIA study (Metzger et al., 2004, [044222](#); Peel et al., 2005, [056305](#); Tolbert et al., 2007, [090316](#)) is the largest and most comprehensive study of U.S. cardiovascular and respiratory ED visits. In Europe, the APHEA initiative (Le Tertre et al., 2002, [023746](#); Le Tertre et al., 2003, [042820](#)) the more recent HEAPSS study (Von Klot et al., 2005, [088070](#)), and the French PSAS program (Host et al., 2008, [155852](#); Larrieu et al., 2007, [093031](#)) are similarly noteworthy for their large sample size, geographic diversity, and consideration of specific CVD and/or respiratory endpoints. These studies contain adequate data to examine interactions by season and region; the effects of different size fractions, components and sources of PM; or the effect of PM on susceptible populations. The following section provides a detailed review of the study design and methods used by each of the large studies. A discussion of the results of each study can be found later in Section 6.2.10.

MCAPS: Medicare Air Pollution Study

Dominici et al. (2006, [088398](#)) created a database of daily time-series of hospital admission rates (1999-2002) for a range of cardiovascular and respiratory outcomes among Medicare beneficiaries aged ≥ 65 yr, ambient PM_{2.5} levels, and meteorological variables for 204 U.S. urban counties. The specific CVD outcomes considered were: CBVD (ICD-9: 430-438), peripheral vascular disease (440-448), IHD (410-414, 429), heart rhythm disturbances (426, 427), and CHF

(428). Injuries (800-849) were evaluated as a control outcome. Gaseous and other particulate pollutant size fractions were not considered.

Data on PM_{2.5} were obtained from the AQS database of the U.S. EPA. Within each county, associations between cause-specific hospitalization rates and same-day PM_{2.5} levels were evaluated using Poisson regression models controlling for long-term temporal trends and meteorologic conditions with natural cubic splines. County-specific results were subsequently averaged using Bayesian hierarchical models. In addition to evaluating single-day lags, 3-day distributed lag models (lags 0, 1, and 2 days) were also considered in a subset of 90 U.S. counties with daily PM_{2.5} data available during the study time period.

Subsequently, Peng et al. (2008, [156850](#)) and Bell et al. (2008, [156266](#)) extended the database of daily time-series of hospital admissions, PM_{2.5}, and other covariates for 202 U.S. counties through 2005. Importantly, Peng et al. (2008, [156850](#)) added data on PM_{10-2.5} to this database for 108 U.S. counties with one or more co-located PM_{2.5} and PM₁₀ monitors. Analyses with PM_{10-2.5} were carried out using similar methods to those of Dominici et al. (2006, [088398](#)). Peng et al. (2008, [156850](#)) evaluated the robustness of PM_{2.5} associations to adjustment for PM_{10-2.5} (Peng et al., 2008, [156850](#)). Gaseous pollutants were not considered in these analyses.

SOPHIA: Study of Particulates and Health in Atlanta

SOPHIA investigators (Metzger et al., 2004, [044222](#); Peel et al., 2005, [056305](#); Tolbert et al., 2000, [010320](#)) compiled data on 4,407,535 ED visits between 1993 and 2000 to 31 hospitals in the Atlanta metropolitan statistical area (20 counties). Specific cardiovascular outcomes considered were: IHD (ICD-9: 410-414), acute MI (410), cardiac dysrhythmias (427), cardiac arrest (427.5), CHF (428), peripheral vascular and CBVD (433-437, 440, 443-444, 451-453), atherosclerosis (440), and stroke (436). Finger wounds (883.0) were evaluated as a control outcome.

The air quality data included measurements of criteria pollutants (PM and gaseous pollutants) for the entire study period, as well as detailed measurements of mass concentrations for PM_{2.5} and PM_{10-2.5} and several physical and chemical characteristics of PM_{2.5} for the final 25 mo of the study using data from the ARIES monitoring station. Rates of ED visits for specific causes were assessed in relation to the 3-day moving average (lags 0-2 days) of daily measures of air pollutants using Poisson generalized linear models (GLMs) controlling for long-term temporal trends and meteorologic conditions with cubic splines. Tolbert et al. (2007, [090316](#)) published interim results of this study in relation to both cardiovascular and respiratory disease visits, Metzger et al. (2004, [044222](#)) published the main results for CVD visits, and Peel et al. (2005, [056305](#)) published the main results for respiratory conditions. An analysis of co-morbid conditions that may make individuals more susceptible to PM-related cardiovascular risk was carried out by Peel et al. (2007, [090442](#)). Tolbert et al. (2007, [090316](#)) extended the available data through 2002 and compared results from single and multipollutant models, while Sarnat et al. (2008, [097972](#)) evaluated the risk of ED visits for cardiovascular and respiratory diseases in relation to specific sources of ambient PM using the extended dataset.

APHEA and APHEA-2: Air Pollution and Health: a European Approach

APHEA-2 investigators compiled daily data on cardiovascular (Le Tertre et al., 2002, [023746](#); 2003, [042820](#)) and respiratory (Atkinson et al., 2001, [021959](#); 2003, [042797](#)) disease hospital admissions in the following 8 European locations: Barcelona, Birmingham, London, Milan, the Netherlands (considered a “city” for this study, due to its small size and dense population), Paris, Rome, and Stockholm. (The publications on respiratory diseases were reviewed in the 2004 PM AQCD). The specific CVD outcomes considered in each city were: cardiac diseases (ICD-9: 390-429), IHD (410-413) and CBVDs (430-438). Routine registers in all cities provided daily data on hospitalizations. Only emergency hospitalizations were considered, except in Milan, Paris, and Rome where only general admissions data were available.

Ambient PM₁₀ levels were available in all cities except Paris (PM₁₃ used), and Milan and Rome (TSP used). Data on gaseous pollutants (NO₂, SO₂, CO, and O₃) were also available in most cities. Five of the eight cities provided data on black smoke (BS). The length of the available time-series varied by city but generally spanned from the early to mid-1990s.

Within each city, associations between cause-specific hospitalization rates and same-day PM_{2.5} levels were evaluated using Poisson GAMs controlling for long-term temporal trends and meteorologic conditions. City-specific results were subsequently averaged using standard

meta-analytic methods. The original analyses (Atkinson et al., 2001, [021959](#); Le Tertre et al., 2002, [023746](#)) were carried out using general additive models (GAM) and LOESS smoothers. Following reports of problems associated with using the default convergence criteria in the standard S-plus GAM procedure (Dominici et al., 2002, [030458](#)), study authors reanalyzed the data on cardiac admissions using GAMs and stricter convergence criteria, and GLMs with natural splines and penalized splines (Atkinson et al., 2003, [042797](#); Le Tertre et al., 2003, [042820](#)). The authors found that the results of the original analyses were insensitive to the choice of convergence criteria and that the use of GLMs with penalized splines yielded very similar results.

HEAPSS: Health Effects of Air Pollution among Susceptible Subpopulations

HEAPSS investigators collected data on patients hospitalized for a first MI in five European cities between 1992 and 2000. Patients were identified from MI registers in Augsburg and Barcelona, and from hospital discharge registers in Helsinki, Rome and Stockholm. Data on daily levels of PM₁₀, were measured at central monitoring sites in each city. Particle number concentration was measured for a year in each city and then modeled retrospectively for the whole study period. Associations of outcomes with gaseous criteria pollutants were also evaluated.

Von Klot et al. (2005, [088070](#)) identified 22,006 survivors of a first MI in the five participating European cities and collected data on subsequent first cardiac re-hospitalizations between 1992 and 2001. Readmissions of interest were those with primary diagnoses of acute MI, angina pectoris, or cardiac disease (which additionally includes dysrhythmias and CHF). Within each city, associations between cause-specific hospitalization rates and same-day levels of PM₁₀ were evaluated using Poisson GAMs controlling for long-term temporal trends and meteorologic conditions using penalized splines. City-specific results were combined using standard meta-analytic methods. Subsequently, Lanki et al. (2006, [089788](#)) used HEAPSS data from 26,854 patients to evaluate the association between daily PM₁₀ and particle number concentrations and the risk of hospitalization for first MI.

PSAS: The French National Program on Air Pollution Health Effects

Larrieu et al. (2007, [093031](#)) evaluated the association between PM₁₀ and the risk of hospitalization in eight French cities between 1998 and 2003. The cities examined were: Bordeaux, Le Havre, Lille, Lyon, Marseille, Paris, Rouen and Toulouse. The specific CVD outcomes considered in each city included: total CVD (ICD-10: I00-I99), cardiac disease (I00-I52), IHD (I20-I25) and stroke (I60-I64, G45-G46). The available data did not differentiate between emergency and non-emergency hospitalizations. Daily mean PM₁₀ and NO₂ levels as well as 8-h max O₃ levels were obtained from a network of monitors in each city.

Within each city, associations between cause-specific hospitalization rates and 2-day ma (lag 0-1 days) levels of PM₁₀ were evaluated using Poisson GAMs controlling for long-term temporal trends and meteorologic conditions using penalized splines. City-specific results were combined using standard meta-analytic methods. Host et al. (2008, [155852](#)) used a subset of these data (6 cities, 2000-2003) to compare the effects of PM_{2.5} and PM_{10-2.5} on the risk of cardiovascular and respiratory admissions. CVD outcomes assessed in this analysis were all CVD (ICD-10 I00-I99), cardiac disease (I00-I52) and IHD (I20-I25). PM_{2.5} levels were obtained from the same network of background monitors described above. PM_{10-2.5} was calculated by subtracting PM_{2.5} levels from PM₁₀ levels. Gaseous pollutants and hospital admissions for stroke were not considered in this analysis.

Multicity Studies in Australia and New Zealand

Barnett et al. (2006, [089770](#)) collected data on daily CVD emergency hospital admissions among older adults and pollution data between 1998 and 2001 in five Australian cities (Brisbane, Canberra, Melbourne, Perth, Sydney) and two cities in New Zealand (Auckland, Christchurch). In 2001, these cities covered 53% of the Australian population and 44% of the New Zealand population. The specific outcomes considered in each city were: all circulatory diseases (ICD-9 390-429, ICD-10 I00-I99 with exclusions); CHF (ICD-9 428, ICD-10 I50); arrhythmia (ICD-9 427 ICD-10 I46-49); cardiac disease (ICD-9 390-429, ICD-10 I00-I52, I97.0, I97.1, I98.1); IHD (ICD-9 410-413, ICD-10 I20-24, I25.2); acute MI (ICD-9 410, ICD-10 I21-22); and stroke (ICD-9 430-438, ICD-10 I60-66, I67, I68, I69, G45-46 with exclusions).

Air pollutants considered were 24-h avg PM₁₀, 24-h avg PM_{2.5}, BSP and gaseous pollutants. Within each city, associations between cause-specific hospitalization rates and 2-day ma (lags 0-1 days) of PM₁₀ were evaluated using the time-stratified case-crossover approach which controls for long-term and seasonal time trends by design rather than analytically. City-specific results were combined using random effects meta-analytic methods.

EMECAS: Spanish Multicentric Study on the Relation between Air Pollution and Health

Ballester et al. (2006, [088746](#)) collected data on daily cardiovascular emergency hospital admission and air pollution data between approximately 1995 and 1999 in 14 cities in Spain. The specific outcomes considered in each city were: total CVD (ICD-9: 390-459) and heart diseases (410-414, 427, 428). Air pollutants considered were PM₁₀, TSP, BS, SO₂, NO₂ (24-h avg), CO and O₃ (8-h max).

Within each city, associations between cause-specific hospitalization rates and daily levels of each pollutant metric were evaluated using Poisson GAMs with strict convergence criteria. In all models, pollutants were entered as linear continuous variables and included control for confounding by meteorological variables, influenza rates, long-term time trends, and unusual events. The authors considered both distributed lag models (lags 0-3 days) and the 2-day ma of pollution (lags 0-1 days). City-specific results were combined using standard meta-analytic methods.

6.2.10.1. All Cardiovascular Disease

The 2004 PM AQCD (U.S. EPA, 2004, [056905](#)) incorporated the results of a large number of time-series studies in the U.S. and elsewhere relating ambient PM levels and risk of hospitalization for CVD. The 2004 PM AQCD (U.S. EPA, 2004, [056905](#)) noted that the strongest evidence for this association came from the NMMAPS study (Samet et al., 2000, [010269](#)) and the subsequent reanalysis by Zanobetti and Schwartz (2003, [157174](#)).

Since then, the U.S. MCAPS study evaluated the association between PM_{2.5} and risk of CVD hospitalization in 202 U.S. counties between 1999 and 2005 and found a 0.8% (95% posterior interval (PI): 0.6-1.0) increase in risk per 10 µg/m³ increase in PM_{2.5} on the same day (Bell et al., 2008, [156266](#); Peng et al., 2008, [156850](#)). In 108 U.S. counties with co-located PM₁₀ and PM_{10-2.5} monitors, Peng et al. found a 0.4% (95% PI, 0.1- 0.7, lag 0) increase in risk per 10 µg/m³ PM_{10-2.5} and no associations at lags of 1 and 2 days (Peng et al., 2008, [156850](#)). In a two-pollutant model adjusted for PM_{2.5}, the association between PM_{10-2.5} and CVD hospitalization lost precision (0.3% [95% PI: -0.1 to 0.6, lag 0]). Bell et al. (2008, [156266](#)) found evidence of substantial and statistically significant variability in the effects of PM_{2.5} on cardiovascular hospitalizations by season and region, with the highest national average estimates occurring in the winter and the highest regional estimates in the northeastern U.S. (1.08% [95% PI: 0.79-1.37, lag 0, per 10 µg/m³ increase in PM_{2.5}]). Estimates for the nation (1.49% [95% PI: 1.09-1.89, lag 0]) and northeast (2.01% [95% PI: 1.39-2.63, lag 0]) were highest in the winter.

Bell et al. (2009, [191997](#)) and Peng et al. (2009, [191998](#)) used data from the MCAPS study and the EPA's Speciation Trends Network (STN) to identify the components of PM_{2.5} that are most strongly associated with hospitalizations for CVD. Peng et al. (2009, [191998](#)) focused on the components that make up the majority of PM_{2.5} mass (SO₄²⁻, NO₃⁻, Si, EC, OC, Na⁺ and NH₄⁺) and found that in multipollutant models, only EC and OC were significantly associated with risk of hospitalization for CVD. Bell et al. (2009, [191997](#)) used data from 20 PM_{2.5} components and found that EC, Ni, and V were most positively and significantly associated with the risk of cardiovascular hospitalizations. These results suggest that the observed associations between PM_{2.5} and CVD hospitalizations may be primarily due to particles from oil combustion and traffic.

Additional evidence is provided by several large multicity studies conducted outside of the U.S. The European APHEA2 study (Le Tertre et al., 2002, [023746](#)) looked at admissions for CVD among those aged ≥65 and found a 0.7% (95% CI: 0.4-1.0, lag 0-1 day avg) increase in risk per 10 µg/m³ PM₁₀. The Spanish EMECAS study (Ballester et al., 2006, [088746](#)) looked at admissions for CVD and found a 0.9% (95% CI: 0.4-1.5, lag 0-1 day avg) increase in risk per 10 µg/m³ PM₁₀. The French PSAS program looked at CVD hospitalizations among the elderly and found a 1.9% (95% CI: 0.9-3.0, lag 0-1 day avg) increase in risk with a 10 µg/m³ increase in PM_{2.5} and a 1.1% (95% CI: 0.5-1.7) increase in risk with PM₁₀ (Host et al., 2008, [155852](#); Larrieu et al., 2007, [093031](#)). Non-significant increases in CVD hospital admissions association with PM_{10-2.5} were

reported (1.0% [95% CI: -1.0 to 3.0]) (Host et al., 2008, [155852](#)). In multiple cities across New Zealand and Australia, Barnett et al. (2006, [089770](#)) found a 1.3% (95% CI: 0.6-2.0, lag 0-1 day avg) increase in risk per 10 $\mu\text{g}/\text{m}^3$ increase in $\text{PM}_{2.5}$.

The Atlanta-based SOPHIA study found a 3.3% (95% CI: 1.0-5.6, lag 0-2 day avg) and a 0.9% (95% CI: -0.2 to 1.9, lag 0-2 day avg) increase in risk with a 10 $\mu\text{g}/\text{m}^3$ increase in $\text{PM}_{2.5}$ and PM_{10} , respectively (Metzger et al., 2004, [044222](#)). In a more recent analysis from this study with an additional four years of data, ED visits for CVD were not significantly associated with PM_{10} or $\text{PM}_{2.5}$, but were significantly associated with total carbon (1.6% [95% CI: 0.5-2.6, per IQR increase]), EC (1.5% [95% CI: 0.5-2.5, per IQR increase]) and OC (1.5% [95% CI: 0.5-2.6, per IQR increase]) components of $\text{PM}_{2.5}$ (2007, [090316](#)). A weak non-significant association $\text{PM}_{10-2.5}$ was observed in these data (Tolbert et al., 2007, [090316](#)). More recently, Sarnat et al. (2008, [097972](#)) used multiple source-apportionment methods to evaluate the association between all CVD ED visits and specific $\text{PM}_{2.5}$ sources and found consistent positive associations with sources related to motor vehicles and biomass combustion. These results were insensitive to the source-apportionment technique used. It is noteworthy that other traffic-related gaseous pollutants were associated with CVD ED visits in the SOPHIA study (Metzger et al., 2004, [044222](#)).

Using meta-regression techniques and the reported association between PM_{10} and CVD hospitalizations from the 14 cities included in the NMMAPS analysis, Janssen et al. (2002, [016743](#)) examined whether the between-city variability in relative risk estimates were related to the local contribution of a number of PM sources. The authors found that in multivariate analyses PM_{10} coefficients increased significantly with increasing percentage of PM_{10} emissions from highway vehicles/diesels and oil combustion.

A small number of additional single-city studies have been published showing positive associations between hospital admissions and ambient PM in Copenhagen, Denmark (Andersen et al., 2007, [093201](#)), weak nonsignificant associations in Spokane, WA (Schreuder et al., 2006, [097959](#); Slaughter et al., 2005, [073854](#)), and no associations in two small counties in Idaho (Ulirsch et al., 2007, [091332](#)). Schreuder et al. (2006, [097959](#)) performed a source apportionment analysis using seven years of daily speciation data from the same residential monitor in Spokane, WA used by Slaughter et al. (2005, [073854](#)). These authors related daily levels of four sources (wood smoke, an As-rich source, motor vehicle emissions, and airborne soil) to the excess risk of cardiovascular ED visits. During the heating season, the only notable association for CVD-related ED visits was with wood smoke, while in the non-heating season the only notable association was with airborne soil. While neither of these associations reached statistical significance, the study likely lacked the statistical power to find effects of the expected magnitude. In fact, it is doubtful that studies conducted outside of large metropolitan areas have sufficient statistical power to detect associations of the expected magnitude. Delfino et al. (2009, [191994](#)) evaluated the effects of the 2003 California wildfires and observed a slightly larger excess risk of total CVD admissions during the wildfire period compared to the period prior to the wildfire, although excess risk estimates were generally weak and non-significant.

Studies in several cities in Australia have investigated the association of CVD admissions with PM concentration and sources. A study from Sydney, Australia found a 1.8% (95% CI: 0.4-3.2) and 0.3% (95% CI: -0.8 to 1.4) excess risk per 10 $\mu\text{g}/\text{m}^3$ increase in the 2-day ma (lags 0-1 days) in $\text{PM}_{2.5}$ and PM_{10} , respectively (Jalaludin et al., 2006, [189416](#)). Johnston et al. (2007, [155882](#)) and Hanigan et al. (2008, [156518](#)) studied the association between PM_{10} and cardiovascular and respiratory hospitalizations in Darwin, Australia, where the predominant source of PM is from biomass combustion. The authors found little or no evidence of an association between PM_{10} and CVD hospital admissions in the general population.

Crustal material has also been investigated in an effort to explain associations of PM concentration with CVD admissions. Studies of a dust storm in the Gobi desert that transported PM across the Pacific Ocean reaching the western U.S. in the spring of 1998 have been conducted. An analysis of the health impacts of this event on the population of British Columbia's (Canada) Lower Fraser Valley found no excess risk of cardiac or respiratory hospital admissions despite hourly PM_{10} levels $>100 \mu\text{g}/\text{m}^3$ (Bennett et al., 2006, [088061](#)). On the other hand, a number of studies in Asia and eastern Europe have reported associations between CVD hospital admissions and dust storm events. Middleton et al. (2008, [156760](#)) found that dust storms in Cyprus were associated with a 4.7% (95% CI: 0.7-9.0) and 10.4% (95% CI: -4.7 to 27.9) increase in risk of hospitalization for all causes and CVD, respectively. Chan et al. (2008, [093297](#)) studied the effects of Asian dust storms on cardiovascular hospital admissions in Taipei, Taiwan and also found significant adverse effects

during 39 Asian dust events with high PM₁₀ levels (daily PM₁₀ >90 µg/m³). Bell et al. (2008, [091268](#)) analyzed these data independently and concluded that Asian dust storms were positively associated with risk of hospitalization for IHD.

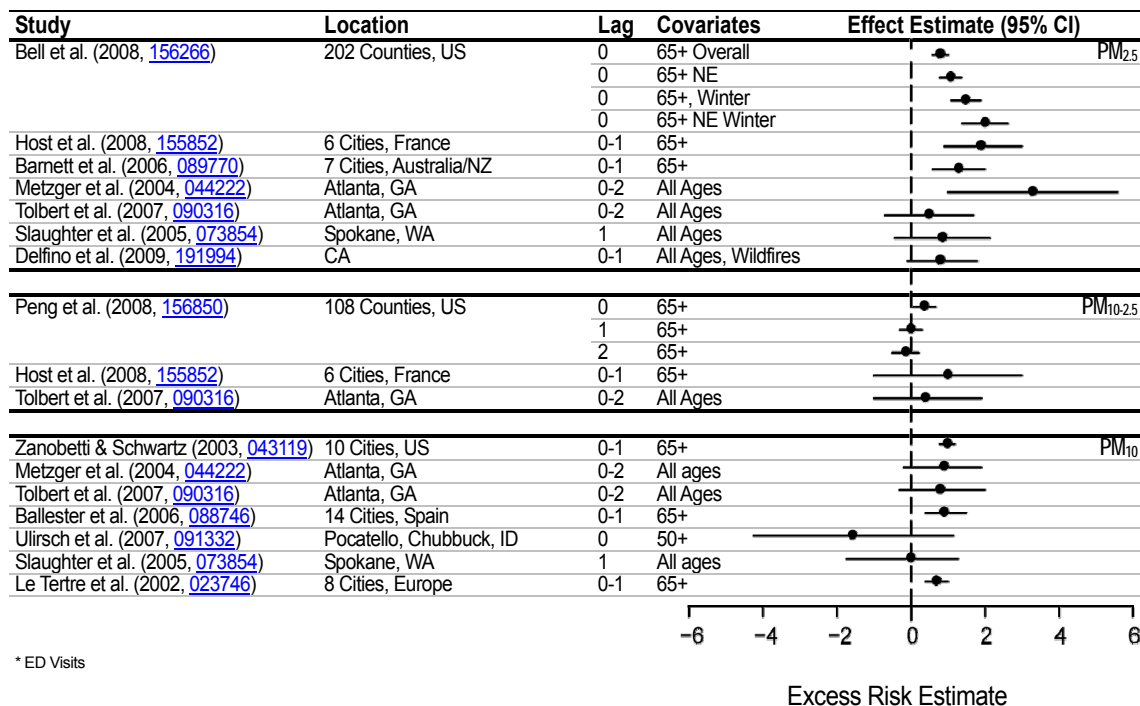


Figure 6-1. Excess risk estimates per 10 µg/m³ increase in 24-h avg PM_{2.5}, PM_{10-2.5}, and PM₁₀ concentration for CVD ED visits and HAs. Studies represented in the figure include all multicity studies, as well as single-city studies conducted in the U.S. or Canada.

The effect estimates from multicity studies and single-city studies conducted in the U.S. and Canada are included in Figure 6-1. Information on PM concentrations during the relevant study period is presented in Table 6-8. In summary, large studies from the U.S., Europe, and Australia/New Zealand published since the 2004 PM AQCD (U.S. EPA, 2004, [056905](#)) provide support for an association between short-term increases in ambient levels of PM_{2.5} and PM₁₀ and increased risk of hospitalization for total CVD. The evidence for an association of CVD hospitalization with PM_{10-2.5} is relatively limited. Peng et al. (2008, [156850](#)) reported that their PM_{10-2.5} estimate was not robust to adjustment for PM_{2.5} and estimates from the other studies are imprecise. The average excess risk among the U.S. elderly is likely in the range of 0.5-1.0% per 10 µg/m³ increase in PM_{2.5}, although substantial variability by region of the country and season has been demonstrated. An excess risk of ED visits for CVD of a similar magnitude appears likely. The excess risk of CVD hospitalization may be somewhat greater in Europe and Australia/New Zealand than in the U.S. Sources including wood burning, oil burning, traffic and crustal material have been associated with increases in cardiovascular hospitalization or ED visits, but the best evidence suggests that in the U.S., oil combustion, wood burning, and traffic are likely the sources of PM_{2.5} most strongly associated with cardiovascular hospitalizations or ED visits.

Table 6-8. Characterization of ambient PM concentrations in epidemiologic studies of hospital admission and ED visits for cardiovascular diseases.

Pollutant	Study	Location	Mean Concentration ($\mu\text{g}/\text{m}^3$)	Upper Percentile Concentration ($\mu\text{g}/\text{m}^3$)
<i>PM_{2.5}</i>				
	Barnett et al. (2006, 089770)	7 cities in Australia	8.1-11.0	NR
	Bell et al. (2008, 156266)	202 counties in the U.S.	12.92	34.16
	Burnett et al. (1999, 017269)	Toronto Canada	18	95th: 34.0, Max: 90
	Dominici et al. (2006, 088398)	204 counties in the U.S.	13.4	NR
	Delfino et al. (2009, 191994)	6 counties CA	18.4-32.7	45.3-76.1 (wildfire period)
	Host et al. (2008, 155852)	6 cities in France	13.8-18.8	95th: 25-33
	Ito et al. (2003, 042856); Lippman (2000, 011938)	Detroit, MI	18	98th: 55.2
	Lisabeth et al. (2008, 155939)		7	75th: 10
	Metzger et al. (2004, 044222)	Atlanta, GA	17.8	90th: 32.3 98th: 39.8
	Pope et al. (2006, 091246)	Wasatch Front, Utah	10.1-11.3	Max: 82-144
	Slaughter et al. (2005, 073854)	Spokane, WA	NR	90th: 20.2
	Sullivan et al. (2005, 050854)	King County, WA	12.8	90th 27.3, Max: 147
	Symons et al. (2006, 091258)	Baltimore, MD	16	Max: 69.2
	Tolbert et al. (2007, 090316)	Atlanta, GA	17.1	98th: 38.7
	Villeneuve et al. (2006, 090191)	Edmonton, Canada	8.5	75th: 11
	Zanobetti and Schwartz (2005, 088069)	Boston, MA	11.1 (median)	95th: 26.31 98th: 55.2
<i>PM_{10-2.5}</i>				
	Burnett et al. (1999, 017269)	Toronto, Canada	12.2	Max: 68
	Host et al. (2008, 155852)	6 cities in France	7-11	95th: 12.5-21.0
	Ito et al. (2003, 042856); Lippman (2000, 011938)	Detroit, MI	13	Max: 50
	Le Tertre et al. (2002, 023746)	8 cities in Europe	NR	NR
	Metzger et al. (2004, 044222)	Atlanta, GA	9.1	90th: 16.2
	Peng et al. (2008, 156850)	204 cities in the U.S.	9.8 (Median)	75th: 15.0
	Peters et al. (2001, 016546)	Boston, MA	7.4	95th: 15.2
	Slaughter et al. (2005, 073854)	Spokane, WA	NR	NR
	Tolbert et al. (2007, 090316)	Atlanta, GA	9	Max: 50.3
<i>PM₁₀</i>				
	Ballester et al. (2006, 088746)	14 cities in Spain	32.8-43.2	90th: 50.3-62.6
	Barnett et al. (2006, 089770)	7 cities in Australia and New Zealand	16.5-20.6	NR
	Burnett et al. (1999.017269)	Toronto, Canada	30.2	95th: 56.0
	Ito et al. (2003, 042856); Lippman (2000, 011938)	Detroit, MI	31	NR
	Jalaludin et al. (2006, 189416)	Sydney, Australia	16.8	75th: 19.9 Max: 103.9
	Larrieu et al. (2007, 093031)	8 cities in France	21.0-28.9	NR
	Le Tertre et al. (2002, 023746)	8 cities in Europe	Range: 15.5-55.7	Range 75th: 19.9-66

Pollutant	Study	Location	Mean Concentration ($\mu\text{g}/\text{m}^3$)	Upper Percentile Concentration ($\mu\text{g}/\text{m}^3$)
	Linn et al. (2000, 002839)	Los Angeles, California	45	78 (summer) -132 (fall)
	Metzger et al. (2004, 044222)	Atlanta, GA	26.3	90th: 44.7
	Morris et al. (1998, 024924)	Chicago, Illinois	41	75th: 51 Max: 117
	Peters et al. (2001, 016546)	Boston, MA	19.4	95th: 37.0
	Schwartz et al. (1995, 046186)	Detroit, MI	48	90th: 82
	Slaughter et al. (2005, 073854)	Spokane, WA	NR	90th: 41.9
	Tolbert et al. (2007, 090316)	Atlanta, GA	26.6	Max: 98.4
	Ulirsch et al. (2007, 091332)*	2 cities in southeast Idaho	24.2/23.2	90th: 40.7/37.4
	Wellenius et al. (2005, 087483)	Pittsburgh, PA	31.1	95th: 70.5
	Wellenius et al. (2005, 088685)	9 cities in the U.S.	28.4 (median)	90th: 57.9
	Wellenius et al. (2006, 088748)	7 cities in the U.S.	28.3 (median)	90th: 57
	Zanobetti and Schwartz (2005, 088069)	Boston, MA	28.4 (median)	90th: 53.6

*Results presented separately for 2 separate time series

6.2.10.2. Cardiac Diseases

Cardiac disease represents a subset of CVD which specifically excludes hospitalizations for CBVD, peripheral vascular disease, and other circulatory diseases not involving the heart or coronary circulation. Only a small number of studies published since the 2004 PM AQCD (U.S. EPA, 2004, [056905](#)) have evaluated the association between ambient PM and hospitalizations for cardiac diseases, as most investigators have focused instead on more narrowly defined outcomes.

The French PSAS program found a 2.4% (95% CI: 1.2-3.7, lag 0-1) and 1.5% (95% CI: 0.5-2.2, lag 0-1) excess risk among the elderly per 10 $\mu\text{g}/\text{m}^3$ increase in $\text{PM}_{2.5}$ and PM_{10} , respectively (Host et al., 2007, [155851](#); Larrieu et al., 2007, [093031](#)). Host et al. (2008, [155852](#)) also found a positive less precise association with $\text{PM}_{10-2.5}$, (excess relative risk per 10 $\mu\text{g}/\text{m}^3$: 1.6% [95% CI: -0.8 to 4.1]). The European HEAPSS study looked at cardiac readmissions among survivors of a first MI and found a 2.1% (95% CI: 0.4-3.9, lag 0) excess risk per 10 $\mu\text{g}/\text{m}^3$ increase in PM_{10} (Von Klot et al., 2005, [088070](#)). A 1.9% (95% CI: 1.0-2.7, lag 0-1) excess risk per 10 $\mu\text{g}/\text{m}^3$ increase in $\text{PM}_{2.5}$ was observed in several cities in Australia and New Zealand (Barnett et al., 2006, [089770](#)). Single-city studies of hospital admissions from Kaohsiung and Taipei, Taiwan, and an ED visit study from Sydney, Australia also reported statistically significant positive associations (Chang et al., 2005, [080086](#); Jalaludin et al., 2006, [189416](#); Yang et al., 2004, [094376](#)). On the other hand, Slaughter et al. (2005, [073854](#)) found no association between either $\text{PM}_{2.5}$ or PM_{10} and risk of cardiac hospitalization in Spokane, Washington.

In summary, although relatively few studies have focused on all cardiac diseases, large studies from Europe and Australia/New Zealand published since the 2004 PM AQCD (U.S. EPA, 2004, [056905](#)) report positive associations between short-term increases in ambient levels of $\text{PM}_{2.5}$, $\text{PM}_{10-2.5}$, and PM_{10} and increased risk of hospitalization for cardiac disease. The results from small single-city studies are less consistent. The excess risk for cardiac hospitalizations may be somewhat larger than for total CVD hospitalizations.

6.2.10.3. Ischemic Heart Disease

IHD represents a subset of all cardiac disease hospitalizations and typically includes acute MI (ICD 9: 410), other acute and subacute forms of IHD (411), old MI (412), angina pectoris (413), and other forms of chronic IHD (414). Some authors term this category coronary heart disease. Published studies evaluating IHD as a single outcome are considered first, followed by consideration of studies looking at acute MI, a specific form of IHD.

In one of the first studies to evaluate IHD, Schwartz and Morris (1995, [046186](#)) reported a 0.6% (95% CI: 0.2-1.0) excess risk of hospitalization for IHD per 10 $\mu\text{g}/\text{m}^3$ increase in mean PM_{10}

levels over the previous two days among elderly Medicare beneficiaries living in Detroit between 1986 and 1989. As reviewed in the 2004 PM AQCD (U.S. EPA, 2004, [056905](#)), similar associations were subsequently observed in many single-city studies including: London, England (Atkinson et al., 1999, [007882](#)), Toronto, Canada (Burnett et al., 1999, [017269](#)), and Seoul, Korea (Lee et al., 2003, [095552](#)). Studies in Hong Kong (Wong et al., 1999, [009172](#); Wong et al., 2002, [023232](#)), Birmingham, England (Anderson et al., 2001, [017033](#)), and London, England (Wong et al., 2002, [023232](#)) yielded positive point estimates of a similar magnitude, but did not reach statistical significance.

The positive associations between short-term changes in PM and IHD hospitalizations observed in the early single-city studies have been confirmed in several large multicity studies. The U.S. MCAPS study (Dominici et al., 2006, [088398](#)) found a 0.4% (95% CI: 0.0-0.8) excess risk of hospitalization for IHD per 10 $\mu\text{g}/\text{m}^3$ increase in $\text{PM}_{2.5}$ two days earlier. The European APHEA-2 study (Le Tertre et al., 2002, [023746](#)) considered PM_{10} and found a 0.8% (95% CI: 0.3-1.2, lag 0-1) excess risk among those aged ≥ 65 yr. Among the elderly in 5 cities in Australia and New Zealand (Barnett et al., 2006, [089770](#)) there was a 4.3% (95% CI: 1.9-6.4, lag 0-1) excess risk per 10 $\mu\text{g}/\text{m}^3$ increase in $\text{PM}_{2.5}$. Among the elderly in several French cities there was a 4.5% (95% CI: 2.3-6.8, lag 0-1), 6.4% (95% CI: 1.6-11.4, lag 0-1) and 2.9% (95% CI: 1.5-4.3, lag 0-1) excess risk per 10 $\mu\text{g}/\text{m}^3$ increase in $\text{PM}_{2.5}$, $\text{PM}_{10-2.5}$ (Host et al., 2008, [155852](#)), and PM_{10} , respectively (Larrieu et al., 2007, [093031](#)).

With regard to ED visits, the Atlanta-based SOPHIA study (Metzger et al., 2004, [044222](#)) found positive associations with $\text{PM}_{2.5}$ and PM_{10} (ranging from 1.1 to 2.3%), but the effect estimates did not reach statistical significance. Similarly, associations of EC and OC with IHD were increased but not significant. In 6 cities across Canada, Szyszkowicz (2009, [191996](#)) observed a 2.4% (95% CI: 1.2-3.6) and 1.4% (95% CI: 0.7-2.0) excess risk of ED visits for angina per 10 $\mu\text{g}/\text{m}^3$ increase in same-day $\text{PM}_{2.5}$ and PM_{10} , respectively. Although excess risks were generally weak and non-significant, Delfino et al. (2009, [191994](#)) observed a slightly larger excess risk of IHD during wildfires compared to the pre-wildfire period. In Sydney, Australia, Jalaludin et al. (2006, [189416](#)) found a 2.6% (95% CI: 0.1-5.2) and 0.8% (95% CI: -1.2 to 2.8) excess risk of ED visits for IHD per 10 $\mu\text{g}/\text{m}^3$ increase in 2-day ma of $\text{PM}_{2.5}$ and PM_{10} , respectively. A recent study in Helsinki, Finland, found no evidence of an association of IHD hospital admissions with UFP, ACP, $\text{PM}_{2.5}$, $\text{PM}_{10-2.5}$, or source-specific $\text{PM}_{2.5}$ (Halonen et al., 2009, [180379](#)).

To explore this link further, Pope et al. (2006, [091246](#)) used data from an ongoing registry of patients undergoing coronary angiography at a single referral center in Salt Lake City, UT, between 1994-2004. The authors found a 4.8% (95% CI: 1.0-8.8, lag 0) excess risk of acute MI or unstable angina per 10 $\mu\text{g}/\text{m}^3$ increase in $\text{PM}_{2.5}$ among 4,818 patients. These results were robust to changes in the definition of the outcome. The results of this study are particularly noteworthy given the high specificity of the outcome definition.

In summary, large studies from the U.S., Europe, and Australia/New Zealand published since the 2004 PM AQCD (U.S. EPA, 2004, [056905](#)) provide support for an association between short-term increases in ambient levels of PM_{10} and $\text{PM}_{2.5}$ and increased risk of hospitalization or ED visits for ischemic heart diseases. Although estimates are less precise for $\text{PM}_{10-2.5}$, most results from single pollutant models provide evidence of a positive association between $\text{PM}_{10-2.5}$ and IHD. Moreover, Host et al. (2008, [155852](#)) found that the effect estimates for the association of $\text{PM}_{2.5}$ and $\text{PM}_{10-2.5}$ with IHD were very similar when scaled to the IQR of each metric. Estimates of the excess risk vary considerably between studies, but as was the case for total CVD hospitalizations, the excess risk appears to somewhat greater in Europe and Australia/New Zealand. Results from multicity studies and U.S. and Canadian single-city studies are presented in Figure 6-2.

Study	Location	Lag	Age	Effect Estimate (95% CI)
ISCHEMIC HEART DISEASE				
Ito (2003, 042856)	Detroit, MI	1	65+	[Red X]
Pope et al. (2006, 091246)	Utah Valley, UT	0	All	
Host et al. (2007, 155851)	6 Cities, France	0-1	All	
Metzger et al. (2004, 044222)*	Atlanta, GA	0-3	All	
Barnett et al. (2006, 089770)	Australia/NZ	0-1	15-64	
Dominici et al. (2006, 088398)	204 Counties, US	0	65+	
		1	65+	
		2	65+	
		0-2 DL	65+	
Barnett et al. (2006, 089770)	Australia/NZ	0-1	65+	
Host et al. (2007, 155851)	6 Cities, France	0-1	65+	
Burnett et al. (1999, 017269)	Toronto, Can	0,1	All	
Delfino et al. (2009, 191994)	6 Counties, CA (Wildfires)	0,1	All	
<hr/>				
Ito (2003, 042856)	Detroit, MI	1	65+	PM _{2.5}
Metzger et al. (2004, 044222)*	Atlanta, GA	0-3	All	
Host et al. (2007, 155851)	6 Cities, France	0-1	All	
Burnett et al. (1999, 017269)	Toronto, Can	0	All	
<hr/>				
Ito (2003, 042856)	Detroit, MI	1	65+	PM ₁₀
Le Tertre et al. (2002, 023746)	8 Cities, Europe	0-1	<65	
Metzger et al. (2004, 044222)*	Atlanta, GA	0-2	All	
Larrieu et al. (2007, 093031)	8 Cities, France	0-1	All	
Burnett et al. (1999, 017269)	Toronto, Can	0-1	All	
Le Tertre et al. (2002, 023746)	8 Cities, Europe	0-1	65+	
Jalaludin et al. (2006, 189416)*	Sydney, Australia	0-1	65+	
Larrieu et al. (2007, 093031)	8 Cities, France	0-1	65+	
<hr/>				
MYOCARDIAL INFARCTION				
Peters et al. (2001, 016546)	Boston, MA	2 h	61.6 Mean	PM _{2.5}
		24 h	61.6 Mean	
		1 h	21-98	
		2 h	21-98	
		4 h	21-98	
Sullivan et al. (2005, 050854)	King County, WA	24 h	21-98	
		0	65+	
Zanobetti & Schwartz (2006, 090195)	Boston, MA	0	65+	
<hr/>				
Peters et al. (2001, 016546)	Boston, MA	2 h	61.6 Mean	PM _{10-2.5}
		24 h	61.6 Mean	
<hr/>				
Linn et al. (2000, 002839)	Los Angeles, CA	0	>30	PM ₁₀
Peters et al. (2001, 016546)	Boston, MA	2 h	61.6 Mean	
		24 h	61.6 Mean	
Zanobetti & Schwartz (2005, 088069)	21 Cities, US	0	65+	

* ED Visits
DL Distributed Lag

Excess Risk (%)

Figure 6-2. Excess risk estimates per 10 µg/m³ increase in 24-h avg (unless otherwise noted) PM_{2.5}, PM_{10-2.5}, and PM₁₀ concentration for MI and IHD ED visits and HAs. Studies represented in the figure include all multi-city studies as well as single-city studies conducted in U.S. or Canada.

6.2.10.4. Acute Myocardial Infarction

Because even IHD refers to a heterogeneous collection of diseases and syndromes, several authors have evaluated the association between short-term fluctuations in ambient PM and acute MI, a specific form of IHD.

In 2001, Peters et al. (2001, [016546](#)) published their study evaluating the effects of PM on the risk of MI among 772 Boston-area participants in the Determinants of MI Onset Study. The authors found that a 10 $\mu\text{g}/\text{m}^3$ increase in the 2-h or 24-h avg levels of $\text{PM}_{2.5}$ was associated with a 17% (95% CI: 4-32) and 27% (95% CI: 6-53) excess risk of MI, respectively. An imprecise, non-significant association between $\text{PM}_{10-2.5}$ and onset of MI was observed in Boston. In contrast, a study among 5793 patients in King County, WA that used similar methods, found no association with $\text{PM}_{2.5}$ with lag times of 1, 2, 4, or 24 h (Sullivan et al., 2005, [050854](#)). Among 852 hospitalized patients in Augsburg, Germany, Peters et al. (2005, [087759](#)) also found no association between $\text{PM}_{2.5}$ and MI risk within this time frame, although they did find a positive and statistically significant association with time spent in traffic (Peters et al., 2004, [087464](#)).

These three studies are particularly important because in each one: (1) cases were prospectively identified based on clinical criteria rather than retrospectively based on discharge diagnoses; and (2) time of MI symptom onset was used for exposure assessment rather than date of hospital admission. Whether the discrepant results among these studies are due to regional differences in population characteristics and/or air pollution sources remains unclear. The King County study suggests that differences in statistical approaches are unlikely to account for the discrepant results (Sullivan et al., 2005, [050854](#)). Analyses from the U.S. MCAPS study suggest that substantial heterogeneity of effects are to be expected across regions of the country (Bell et al., 2008, [156266](#)).

Several studies have assessed the association between acute exposure to ambient PM and MI using administrative databases. In the U.S., MI was not one of the specific endpoints evaluated in the MCAPS study (Dominici et al., 2006, [088398](#)) or in the Atlanta-based SOPHIA study of ED visits (Metzger et al., 2004, [044222](#)). However, Zanobetti and Schwartz (2005, [088069](#)) found a 0.7% (95% CI: 0.3-1.0) excess risk of MI per 10 $\mu\text{g}/\text{m}^3$ increase in same-day PM_{10} among elderly Medicare beneficiaries in 21 cities. Subsequently, the same authors found that among elderly Medicare beneficiaries living in the Boston metropolitan region, a 10 $\mu\text{g}/\text{m}^3$ increase in $\text{PM}_{2.5}$ was associated with a 4.9% (95% CI: 1.1-8.2) excess risk on the same day (Zanobetti and Schwartz, 2006, [090195](#)).

This body of evidence may implicate traffic-related pollution generally as a risk factor for MI. In the study described above, Peters et al. (2001, [016546](#)) found positive associations between risk of hospitalization for MI and potential markers of traffic-related pollution measured at a central monitor including BC, CO and NO_2 . However, none of these associations were statistically significant in models adjusting for season, meteorological variables, and day of week. Zanobetti and Schwartz (2006, [090195](#)) examined the association between traffic-related pollution and risk of hospitalization for MI among Medicare beneficiaries in the Boston area and found that MI risk was positively and significantly associated with measures of $\text{PM}_{2.5}$, BC, NO_2 , and CO, but not with levels of non-traffic-related $\text{PM}_{2.5}$. Peters et al. (2004, [087464](#)) interviewed 691 subjects with MI who survived at least 24-h after the event and found a strong positive association between self-reported exposure to traffic and the onset of MI within 1 h (OR: 2.9 [95% CI: 2.2-3.8]). The association was somewhat stronger among subjects traveling by bicycle or public transportation in the hour prior to the event. Of note, however, this study did not directly measure traffic-related pollution.

Similar studies with administrative databases have been conducted in Europe, Australia, and New Zealand. Barnett et al. (2006, [089770](#)) observed that in five cities in Australia and New Zealand, a 10 $\mu\text{g}/\text{m}^3$ increase in $\text{PM}_{2.5}$ was associated with a 7.3% (95% CI: 3.5-11.4, lag 0-1 day) excess risk. In Rome, D'Ippoliti et al. (2003, [074311](#)) carried out a case-crossover study and found a statistically significant positive association between TSP and the risk of hospitalization for MI. In contrast, the HEAPSS study found no evidence of an association between PM_{10} and risk of hospitalization for a first MI in five European cities (Lanki et al., 2006, [089788](#)), although there is some indication that among survivors of a first MI, risk of re-hospitalization for MI may be related to transient elevations in PM_{10} (Von Klot et al., 2005, [088070](#)).

In summary, large studies from the U.S., Europe, and Australia/New Zealand published since the 2004 PM AQCD (U.S. EPA, 2004, [056905](#)) provide support for an association between short-term increases in ambient levels of $\text{PM}_{2.5}$ and PM_{10} and increased risk of hospitalization for MI. Some of the heterogeneity of results is likely explained by regional differences in pollution sources,

components, and measurement error. One study of the effect of 2- and 24-h avg $PM_{10-2.5}$ concentration on admissions for MI produced effect estimates that were positive, but imprecise (Peters et al., 2001, [016546](#)). These results need to be interpreted together with those studies evaluating hospitalization for IHD since MIs make up the majority of hospitalizations for IHD. U.S. studies of MI are included in Figure 6-2.

6.2.10.5. Congestive Heart Failure

Perhaps the first suggestion of an association between ambient PM and hospitalization for CHF was provided by the study of Schwartz and Morris (1995, [046186](#)). These authors reported that among elderly Medicare beneficiaries living in Detroit between 1986-1989, a $10 \mu\text{g}/\text{m}^3$ increase in mean PM_{10} levels over the previous two days was associated with a 1.0% (95% CI: 0.4-1.6) increase in risk of hospitalization for CHF. As reviewed in the 2004 PM AQCD (U.S. EPA, 2004, [056905](#)), using similar approaches, statistically significant positive associations with $PM_{2.5}$ or PM_{10} were subsequently reported in single-city studies looking at hospitalizations for CHF in Toronto (Burnett et al., 1999, [017269](#)), Hong Kong (Wong et al., 1999, [009172](#)), and Detroit (Ito, 2003, [042856](#)), but not Los Angeles (Linn et al., 2000, [002839](#)) or Denver (Koken et al., 2003, [049466](#)). Burnett et al. (1999, [017269](#)) reports a significantly increased risk of CHF hospitalization with $PM_{10-2.5}$ while Metzger et al. (2004, [044222](#)) and Ito et al. found (2003, [042856](#)) less precise associations.

Subsequent multicity studies support the presence of a positive association between PM concentration and CHF hospitalization. In the U.S., the MCAPS study found a 1.3% (95%: 0.8-1.8) excess risk per $10 \mu\text{g}/\text{m}^3$ increase in same-day $PM_{2.5}$ (Dominici et al., 2006, [088398](#)). In addition, Wellenius et al. (2006, [088748](#)) reported a 0.7% (95% CI: 0.4-1.1) excess risk of hospitalization for CHF per $10 \mu\text{g}/\text{m}^3$ increase in same-day PM_{10} among elderly Medicare beneficiaries in seven cities. In Australia and New Zealand, Barnett et al. (2006, [089770](#)) found a 9.8% (95% CI: 4.8-14.8, lag 0-1 day) and 4.6% (95% CI: 2.8-6.3, lag 0-1 days) excess risk of hospitalization for CHF associated with a $10 \mu\text{g}/\text{m}^3$ increase in $PM_{2.5}$ and PM_{10} , respectively. Results from more recent single-city studies in Pittsburgh (Wellenius et al., 2005, [087483](#)), Utah's Wasatch Front (Pope et al., 2008, [191969](#)), Kaohsiung, Taiwan (Lee et al., 2007, [196613](#)) and Taipei, Taiwan (Yang, 2008, [157160](#)) have also reported positive associations between PM and CHF hospital admissions. In addition, Yang et al. (2009, [190341](#)) found that hospitalizations for CHF were elevated during or immediately following 54 Asian dust storm events (while single day lags 0-3 were evaluated, maximum excess risk occurred at lag 1: 11.4% [95% CI: -0.7 to 25.0]). Delfino et al. (2009, [191994](#)) observed a slightly larger excess risk of total CHF during wildfires occurring in California compared to the period before the wildfires.

While most studies suggest an association at very short lags (0-1 days), the study by Pope et al. (2008, [191969](#)) failed to find such short term associations and instead suggested that $PM_{2.5}$ levels averaged over the past 2-3 wk may be more important. Pope et al. (2008, [191969](#)) observed a 13.1% (95% CI: 1.3-26.2) increase in CHF hospitalization per $10 \mu\text{g}/\text{m}^3$ increase in $PM_{2.5}$ (imputed values used in analysis). Whether findings at longer lags in this population represent true cumulative effects of PM or are due to misclassification of symptom onset times remains to be determined.

Findings from the Atlanta-based SOPHIA study (Metzger et al., 2004, [044222](#)) also support the presence of a positive association between PM and CHF ED visits. Specifically, the SOPHIA study found a 5.5% (95% CI: 0.6-10.5, lag 0-2 days) excess risk of ED visits for CHF per $10 \mu\text{g}/\text{m}^3$ increase in the 3-day ma of $PM_{2.5}$. Positive associations were also observed for CHF and EC and OC components of $PM_{2.5}$. No associations were observed with PM_{10} and a weak, imprecise increase was observed in association with $PM_{10-2.5}$.

Only one published study has attempted to evaluate the effects of ambient particles on CHF symptom exacerbation using data which was not derived from administrative databases. Symons et al. (2006, [091258](#)) interviewed 135 patients with prevalent CHF hospitalized for symptom exacerbation in Baltimore, MD. The authors found a 7.4% (95% CI: -7.5 to 24.2) excess risk of hospitalization per $10 \mu\text{g}/\text{m}^3$ increase in $PM_{2.5}$ two days prior to symptom onset. This finding did not reach statistical significance and may be attributable to the lack of statistical power needed to find an effect of the expected magnitude.

In summary, large studies from the U.S., Europe, and Australia/New Zealand published since the 2004 PM AQCD (U.S. EPA, 2004, [056905](#)) provide support for an association between short-term increases in ambient levels of $PM_{2.5}$ and PM_{10} and increased risk of hospitalization and ED visits for CHF. Although the number of studies is fewer (and only Metzger et al., 2004, [044222](#)

is new since the 2005 AQCD), elevated risks of hospitalization or ED visits for CHF in association with PM_{10-2.5} have been observed. The excess risks associated with CHF hospitalizations and ED visits are consistently greater than those observed for other CVD endpoints. The results of multicity studies and U.S. and Canadian single-city studies are summarized in Figure 6-3.

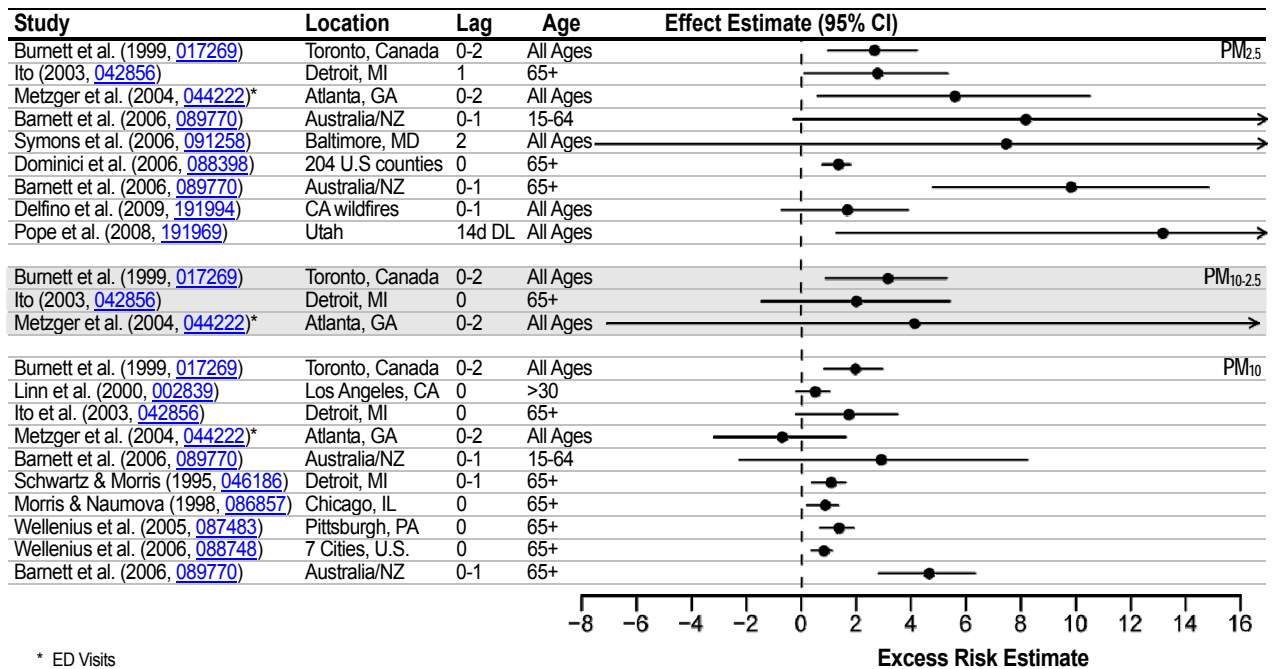


Figure 6-3. Excess risk estimates per 10 µg/m³ increase in 24-h avg PM_{2.5}, PM_{10-2.5}, and PM₁₀ concentration for CHF ED visits and HAs. Studies represented in the figure include all multicity studies as well as single-city studies conducted in the U.S. and Canada.

6.2.10.6. Cardiac Arrhythmias

A number of studies based on administrative databases have sought to evaluate the association between short-term fluctuations in ambient PM levels and the risk of hospitalization for cardiac arrhythmias (also known as dysrhythmias). Typically in these studies a primary discharge diagnosis of ICD-9 427 has been used to identify hospitalized patients. However, ICD-9 427 includes a heterogeneous group of arrhythmias including paroxysmal ventricular or supraventricular tachycardia, atrial fibrillation and flutter, ventricular fibrillation and flutter, cardiac arrest, premature beats, and sinoarterial node dysfunction. One study in the Netherlands found that the positive predictive value of ICD-9 codes related to ventricular arrhythmias and sudden cardiac death was 82% (De Bruin et al., 2005, [155746](#)). The positive predictive value of other codes related to cardiac arrhythmias is unknown, but likely to be lower.

The results from early studies of arrhythmia-related hospitalizations have been inconsistent, with positive findings in Toronto (Burnett et al., 1999, [017269](#)) and null findings in Detroit (Schwartz and Morris, 1995, [046186](#)), Los Angeles (Linn et al., 2000, [002839](#)), and Denver (Koken et al., 2003, [049466](#)). The U.S. MCAPS study found a statistically significant 0.6% (95% CI: 0.0-1.2) excess risk of hospitalization for the combined outcome of cardiac arrhythmias and conduction disorders (ICD-9: 426, 427) per 10 µg/m³ increase in same-day PM_{2.5} (Dominici et al., 2006, [088398](#)). A multicity study in Australia and New Zealand found no evidence of an association between arrhythmia hospitalizations and either PM_{2.5} or PM₁₀ (Barnett et al., 2006, [089770](#)). A study in Helsinki, Finland, found no evidence of an association between either PM_{2.5} or PM_{10-2.5} and risk of hospitalization for arrhythmias (Halonen et al., 2009, [180379](#)), although there was an association with smaller particles (0.03-0.1 µm).

With regard to ED visits, the Atlanta-based SOPHIA study found no evidence of an association between any measure of ambient PM and the rate of ED visits for cardiac arrhythmias (Metzger et al., 2004, [044222](#)). However, in São Paulo, Brazil, Santos et al. (2008, [192004](#)) found a 3.0% (95% CI: 0.5-5.4) excess risk of ED visits for arrhythmias per 10 $\mu\text{g}/\text{m}^3$ increase in PM_{10} on the same day.

In summary, the current evidence does not support the presence of a consistent association between short-term increases in ambient levels of $\text{PM}_{2.5}$, $\text{PM}_{10-2.5}$, or PM_{10} and increased risk of hospitalization for cardiac arrhythmias. However, it should be noted that studies of hospital admissions or ED visits are ill-suited to the study of cardiac arrhythmias since most arrhythmias do not lead to hospitalization. Studies in patients with implanted defibrillators, human panel studies with ambulatory ECG recordings, and animal toxicological studies provide a more appropriate setting for evaluating this endpoint. Results of these studies are described in Section 6.2.2.

6.2.10.7. Cerebrovascular Disease

Time-series studies evaluating the hypothesis that short-term increases in ambient $\text{PM}_{2.5}$ or PM_{10} levels are associated with increased risk of hospitalization for CBVD have been inconsistent, with few studies reporting positive associations (Chan et al., 2006, [090193](#); Dominici et al., 2006, [088398](#); Metzger et al., 2004, [044222](#); Wordley et al., 1997, [082745](#)), and several studies reporting null or negative associations (Anderson et al., 2001, [017033](#); Barnett et al., 2006, [089770](#); Burnett et al., 1999, [017269](#); Halonen et al., 2009, [180379](#); Jalaludin et al., 2006, [189416](#); Larrieu et al., 2007, [093031](#); Le Tertre et al., 2002, [023746](#); Peel et al., 2007, [090442](#); Villeneuve et al., 2006, [090191](#); Wong et al., 1999, [009172](#)).

The U.S. MCAPS study found a 0.8% (95% CI: 0.3-1.4) excess risk of hospitalization for CBVD per 10 $\mu\text{g}/\text{m}^3$ increase in same-day $\text{PM}_{2.5}$ (Dominici et al., 2006, [088398](#)). The association showed regional variability with the strongest associations observed in the eastern U.S. The Atlanta-based SOPHIA study found a 5.0% (95% CI: 0.8-9.3, lag 0-2 days) excess risk of ED visits for cerebrovascular and peripheral vascular disease combined (excluding hemorrhagic strokes) per 10 $\mu\text{g}/\text{m}^3$ increase in $\text{PM}_{2.5}$ and a 2.0% (95% CI: -0.1 to 4.3, lag 0-2 days) excess risk for PM_{10} (Metzger et al., 2004, [044222](#)). Delfino et al. (2009, [191994](#)) observed a weak association between excess risk of CBVD admissions before and during a wildfire occurring in California and slightly higher risks after the wildfire period.

Large multicity studies conducted outside of North America have failed to observe an association between PM and CBVD hospitalizations. The APHEA study found no excess risk (0.0% [95% CI: -0.3 to 0.3]) of hospitalization for CBVD per 10 $\mu\text{g}/\text{m}^3$ increase in the 2-day ma of PM_{10} in 8 European cities (Le Tertre et al., 2002, [023746](#)). Investigators from the French PSAS program reported a 0.8% (95% CI: -0.9 to 2.5, lag 0-1 days) excess risk per 10 $\mu\text{g}/\text{m}^3$ increase in PM_{10} among patients aged ≥ 65 yr and a 0.2% (95% CI: -1.6 to 1.9, lag 0-1 days) excess risk among all patients (Larrieu et al., 2007, [093031](#)). Although neither estimate was statistically significant, the estimated excess risk among the elderly is very similar to that observed in the U.S. MCAPS study. Barnett et al. (2006, [089770](#)) examined this hypothesis in New Zealand and Australia and reported no association.

All of the above studies have identified cases of CBVD based on ICD-9 or ICD-10 codes (most commonly ICD-9 430-438). However, the range of ICD codes commonly used in these studies includes ischemic strokes, hemorrhagic strokes, transient ischemic attacks (TIAs) and several poorly defined forms of acute neurological events (e.g., seizures from a vascular cause) (Table 6-7). It is plausible that ambient PM has different effects on each of these disparate outcomes.

Ischemic Strokes and Transient Ischemic Attacks

An increasing number of studies have specifically evaluated the association between PM_{10} and $\text{PM}_{2.5}$ and the risk of ischemic stroke (Chan et al., 2006, [090193](#); Henrotin et al., 2007, [093270](#); Linn et al., 2000, [002839](#); Lisabeth et al., 2008, [155939](#); Low et al., 2006, [090441](#); Szyszkowicz, 2008, [192128](#); Tsai et al., 2003, [080133](#); Villeneuve et al., 2006, [090191](#); Wellenius et al., 2005, [087483](#)). Linn et al. (2000, [002839](#)) found a 1.3% (95% CI: 1.0-1.6 per 10 $\mu\text{g}/\text{m}^3$, PM_{10} lag 0) excess risk of hospitalization for ischemic stroke in the Los Angeles metropolitan area. Wellenius et al. (2005, [087483](#)) reported a statistically significant 0.4% (95% CI: 0.0-0.9) excess risk per 10 $\mu\text{g}/\text{m}^3$ increase

in same-day PM₁₀ among elderly Medicare beneficiaries in nine U.S. cities. Low et al. (2006, [090441](#)) reported an absolute increase of 0.08 (95% CI: 0.002-0.16) ischemic stroke hospitalizations per 10 µg/m³ increase in PM₁₀ in New York City. In Kaohsiung, Taiwan, Tsai et al. (2003, [080133](#)) found a 5.9% (95% CI: 4.3-7.4, lag 0-2 days) excess risk of hospitalization for ischemic stroke per 10 µg/m³ increase in PM₁₀ after excluding days with mean daily temperature <20°C. Meanwhile, in Taipei, Taiwan, Chan et al. (2006, [090193](#)) found a 3.0% (95% CI: -0.8 to 6.6, lag 3) and 1.6% (95% CI: -0.8 to 3.9, lag 3) excess risk per 10 µg/m³ increase in PM_{2.5} and PM₁₀, respectively. Villeneuve et al. (2006, [090191](#)) and Szyszkowicz et al. (2008, [192128](#)) found no association between either PM_{2.5} or PM₁₀ and ED visits for acute ischemic stroke in Edmonton, Canada.

Two recent studies are particularly noteworthy given the high specificity of the outcome definition. Henrotin et al. (2007, [093270](#)) used data on 1432 confirmed cases of ischemic stroke from the French Dijon Stroke Register and found 0.9% (95% CI: -7.0 to 9.4) excess risk of ischemic stroke per 10 µg/m³ increase in PM₁₀ on the same day and a 1.1% (95% CI: -0.2 to 9.4) excess risk on the previous day (lag 1 day). Lisabeth et al. (2008, [155939](#)) used data on 2,350 confirmed cases of ischemic stroke and 1,158 cases of TIA from the Brain Attack Surveillance in Corpus Christi Project (BASIC), a population-based stroke surveillance project designed to capture all strokes in Nueces County, Texas. The authors found a 6.0% (95% CI: -0.8 to 13.2) and 6.0% (95% CI: -1.8 to 14.4) excess risk of ischemic stroke/TIA per 10 µg/m³ increase in PM_{2.5} on the previous day and the same day, respectively.

Only the study by Villeneuve et al. (2006, [090191](#)) specifically evaluated the association between ambient PM and the risk of TIAs. This study failed to find any evidence of an association with either PM_{2.5} or PM₁₀.

A limitation of all of these studies is that they have assessed exposure based on the date of hospital admission or ED presentation rather than the date and time of stroke symptom onset. It has been shown that this can bias health effect estimates towards the null by up to 60% (Lokken et al., 2009, [186774](#)). Therefore, if there is a causal link between PM and the risk of stroke, it is likely that the existing studies underestimate the true effects. Moreover, most of these studies have evaluated only very short-term effects (lags of 0-2 days) and none have considered lags longer than 5 days. It is possible that the lag structure of the association between PM and stroke differs from that of other CVDs and it might even differ by stroke type.

Hemorrhagic Strokes

Most of the studies in the preceding section also evaluated the association between ambient PM and the risk of hemorrhagic stroke (Chan et al., 2006, [090193](#); Henrotin et al., 2007, [093270](#); Tsai et al., 2003, [080133](#); Villeneuve et al., 2006, [090191](#); Wellenius et al., 2005, [087483](#)). In Kaohsiung, Taiwan, Tsai et al. (2003, [080133](#)) noted a 6.7% (95% CI: 4.2-9.4, lag 0-2 days) excess risk of hospitalization for hemorrhagic stroke per 10 µg/m³ increase in PM₁₀, after excluding days where the mean temperature was <20°C. However, in the U.S., Wellenius et al. (2005, [088685](#)) failed to find any association between ambient PM₁₀ levels and risk of hemorrhagic stroke among Medicare beneficiaries in nine U.S. cities. Similarly, Villeneuve et al. (2006, [090191](#)) found no evidence of an association between ED visits for hemorrhagic stroke and either PM_{2.5} or PM₁₀ levels in Edmonton, Canada. Henrotin et al. (2007, [093270](#)) found no evidence of an association between risk of hospitalization and PM₁₀ levels in Dijon, France, and Chan et al. (2006, [090193](#)) found no evidence of an association between risk of hospitalization and either PM_{2.5} or PM₁₀ levels in Taipei, Taiwan.

In summary, large studies from the U.S., Europe, and Australia/New Zealand published since the 2004 PM AQCD (U.S. EPA, 2004, [056905](#)) provide inconsistent support for an association between short-term increases in ambient levels of PM_{2.5} and PM₁₀ and risk of hospitalization and ED visits for CBVD (Figure 6-4). Studies of PM_{10-2.5} and CBVD or stroke have not been conducted. The heterogeneity in results is likely partly attributed to: (1) differences in the sensitivity and specificity of the various outcome definitions used in the studies; (2) lag structures between PM exposure and stroke onset which may vary by stroke type and patient characteristics; and (3) exposure misclassification due to the use of hospital admission date rather than stroke onset time, which may vary by region, population characteristics, and stroke type. Effect estimates from multicity studies and single-city U.S. and Canadian studies are included in Figure 6-4.

6.2.10.8. Peripheral Vascular Disease

In the U.S., the large MCAPS study Dominici et al. (2006, 088398) evaluated the association between mean daily PM_{2.5} levels and the risk of hospitalization among elderly Medicare beneficiaries in 204 urban counties and found that a 10 µg/m³ increase in PM_{2.5} was not significantly associated with risk of hospitalization for peripheral vascular disease 0-2 days later. An earlier study in Toronto (Burnett et al., 1999, 017269) found a negative association with PM_{2.5} (point estimate and confidence intervals not reported), a positive statistically significant association with PM_{10-2.5} (2.2% [95% CI: 0.1-4.3]), and a positive non-significant association with PM₁₀ (0.5% [95% CI: -0.5 to 1.6]). The Atlanta-based SOPHIA study (Metzger et al., 2004, 044222) of ED visits grouped visits for PVD with those for CBVD, making interpretation of these results challenging.

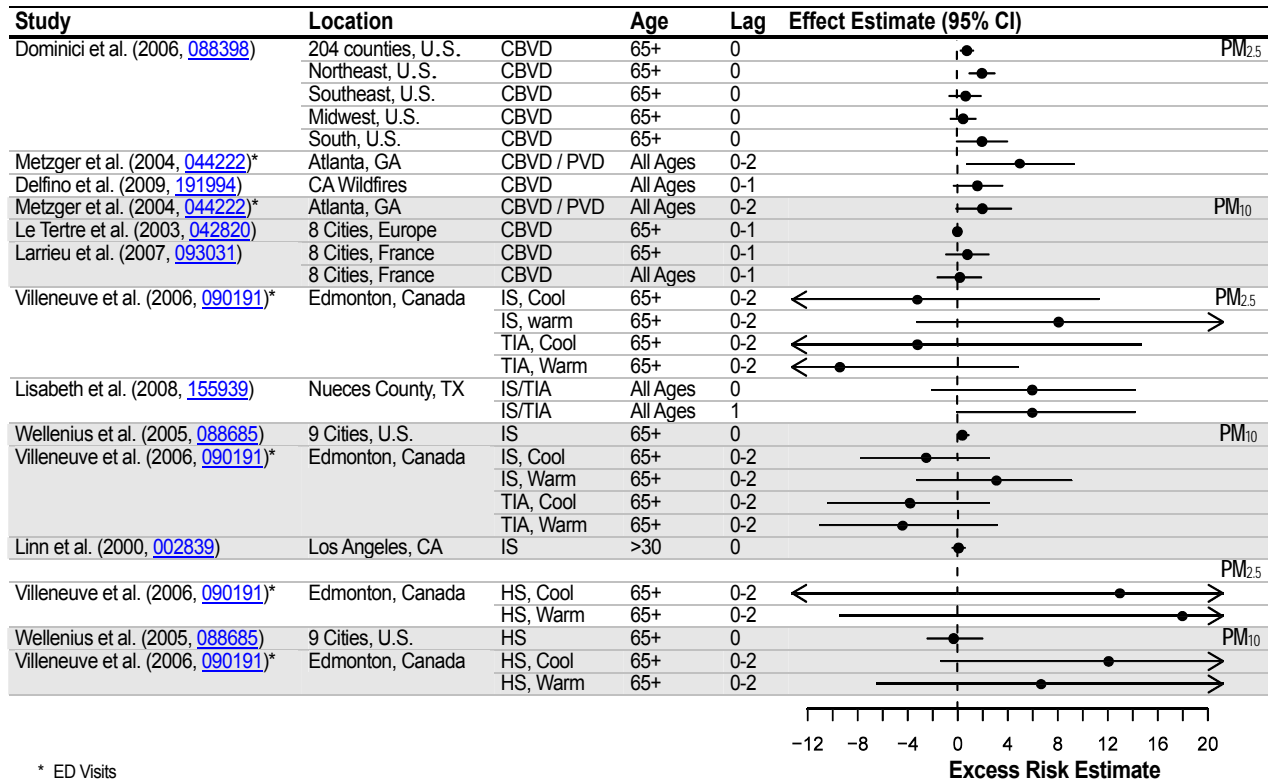


Figure 6-4. Excess risk estimates per 10 µg/m³ increase in 24-h avg PM_{2.5} and PM₁₀ concentration for CBVD ED visits and HAs. Studies represented in the figure include all multicity studies as well as single-city studies conducted in the U.S. and Canada.

In summary, there is insufficient published data to determine whether or not there may be an association between short-term increases in ambient levels of PM_{2.5}, PM_{10-2.5}, or PM₁₀ and increased risk of hospitalization and ED visits for PVD.

6.2.10.9. Copollutant Models

Relatively few studies have evaluated the effects of PM_{2.5} and PM_{10-2.5} on the risk of hospital admissions and ED visits in the context of two-pollutant models. Generally, results for health effects of both size fractions are similar even after controlling for SO₂ or O₃ levels (Figure 6-5). However, controlling for NO₂ or CO has yielded mixed results. Among the large multicity studies, the Atlanta-based SOPHIA study found that the association between PM_{2.5} (total carbon) and risk of cardiovascular ED visits was somewhat attenuated in two-pollutant models additionally controlling for either CO or NO₂ (Tolbert et al., 2007, 090316). Barnett et al. (2006, 089770) found that the

associations they observed between PM_{2.5} and cardiac hospitalizations in Australia and New Zealand were attenuated after control for 24-h NO₂, but not after control for CO.

Only a few studies have attempted to evaluate the effects of one PM size fraction while controlling for another PM size fraction. The large U.S. MCAPS study evaluating the effects of PM_{10-2.5} on cardiovascular hospital admissions lost precision after controlling for PM_{2.5}, but did not consider gaseous pollutants (Peng et al., 2008, [156850](#)). Andersen et al. (2008, [189651](#)) found that associations between both PM₁₀ and PM_{2.5} and cardiovascular hospitalizations in Copenhagen were not attenuated by control for particle number concentration.

A number of studies have also evaluated PM₁₀ effects in the context of two-pollutant models with inconsistent results. The multicity Spanish EMECAS study (Ballester et al., 2006, [088746](#)) found that the statistically significant positive associations observed between PM₁₀ and cardiac hospitalizations were robust to control for other pollutants in two-pollutant models. Jalaludin et al. (2006, [189416](#)) found that the effects of PM₁₀ as well as PM_{2.5} on cardiovascular ED visits in Sydney Australia were attenuated by additional control for either NO₂ or CO. Wellenius et al. (2005, [087483](#)) found that the PM₁₀-related risk of hospitalization for CHF in Allegheny County, PA, was attenuated in two-pollutant models controlling for either CO or NO₂. In contrast, Chang et al. (2005, [080086](#)) examined CVD hospitalizations in Taipei and found attenuation of PM₁₀ effects by control for NO₂ or CO, but only during warm days. In Kaohsiung, Taiwan, Tsai et al. (2003, [080133](#)) found that the association between PM₁₀ and ischemic stroke hospitalizations was not materially attenuated in two-pollutant models controlling for either NO₂ or CO.

The inconsistent findings after controlling for gaseous pollutants or other size fractions are likely due to differences in the correlation structure among pollutants, as well as differing degrees of exposure measurement error.

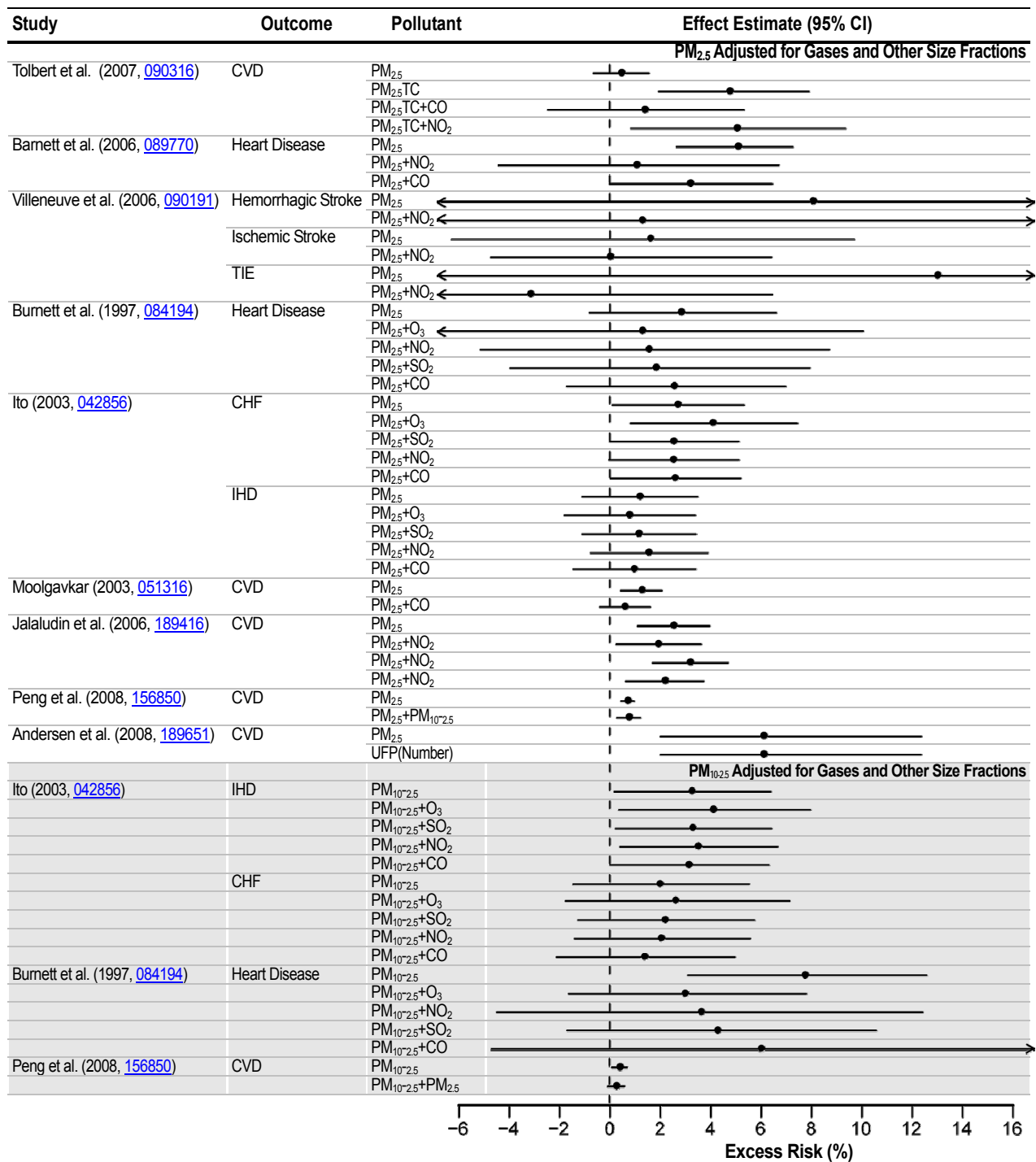


Figure 6-5. Excess risk estimates per 10 µg/m³ increase in 24-h avg PM_{2.5}, and PM_{10-2.5} for cardiovascular disease ED visits or HAs, adjusted for co-pollutants.

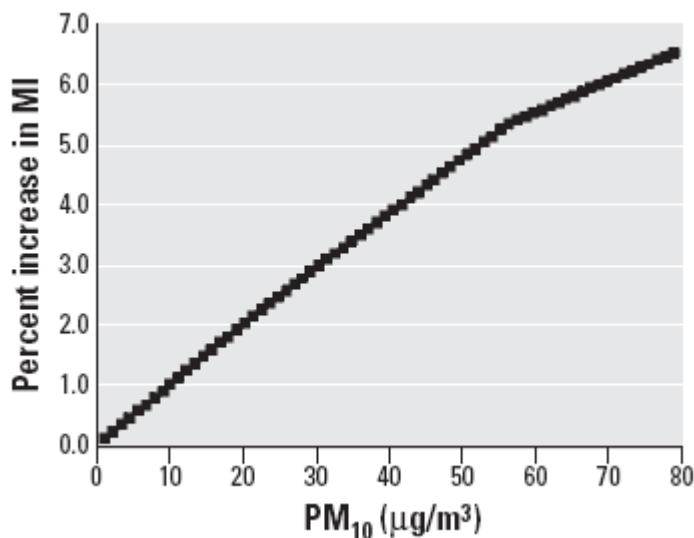
6.2.10.10. Concentration Response

The concentration-response relationship has been extensively analyzed primarily through studies that examined the relationship between PM and mortality. These studies, which have focused on short- and long-term exposures to PM have consistently found no evidence for deviations from linearity or a safe threshold (Daniels et al., 2004, [087343](#); Samoli et al., 2005, [087436](#); Schwartz, 2004, [078998](#); Schwartz et al., 2008, [156963](#)) (Sections 6.5.2.7 and 7.1.4). Although on a more limited basis, studies that have examined PM effects on cardiovascular hospital admissions and ED visits have also analyzed the PM concentration-response relationship, and contributed to the overall body of evidence which suggests a log-linear, no-threshold PM concentration-response relationship.

The evaluation of cardiovascular hospital admission and ED visit studies in 2004 PM AQCD (U.S. EPA, 2004, [056905](#)) found no evidence for a threshold in the dose-response relationship between short-term exposure to PM₁₀ and IHD hospital admissions (Schwartz and Morris, 1995, [046186](#)). An evaluation of recent single- and multicity studies of hospital admission and ED visits for CVD further supports this finding.

Ballester et al. (2006, [088746](#)) examined the linearity of the relationship between air pollutants (including PM₁₀) and cardiovascular hospital admissions in 14 Spanish cities within the EMECAM project. In this exploratory analysis, the authors examined the models used when pollutants were added in either a linear or non-linear way (i.e., with a spline smoothing function) to the model. Although the study does not present the results for each of the pollutants evaluated individually, overall Ballester et al. (2006, [088746](#)) found that the shape of the pollutant-cardiovascular hospital admission relationship was most compatible with a linear curve. Wellenius et al. (2005, [087483](#)) conducted a similar analysis when examining the relationship between PM₁₀ and CHF hospital admissions among Medicare beneficiaries. The authors examined the assumption of linearity using fractional polynomials and linear splines. The results of both approaches contributed to Wellenius et al. (2005, [087483](#)) concluding that the assumption of linearity between the log relative risk of cardiovascular hospital admissions and PM concentration was reasonable.

Unlike the aforementioned studies that examined the linearity in the concentration-response curve as part of the model selection process (i.e., to determine the most appropriate model to use to examine the relationship between PM and cardiovascular hospital admissions and ED visits), Zanobetti and Schwartz (2005, [088069](#)) conducted an extensive analysis of the shape of the concentration-response curve and the potential presence of a threshold when examining the association between PM₁₀ and MI hospital admissions among older adults in 21 U.S. cities. The authors examined the concentration-response curve by fitting a piecewise linear spline with slope changes at 20 and 50 $\mu\text{g}/\text{m}^3$. This approach resulted in an almost linear concentration-response relationship between PM₁₀ and MI hospital admissions with a steeper slope occurring below 50 $\mu\text{g}/\text{m}^3$ (Figure 6-6). Additionally, Zanobetti and Schwartz (2005, [088069](#)) found no evidence for a threshold.



Source: Zanobetti and Schwartz (2005, [088069](#)).

Figure 6-6. Combined random-effect estimate of the concentration-response relationship between MI emergency hospital admissions and PM₁₀, computed by fitting a piecewise linear spline, with slope changes at 20 µg/m³ and 50 µg/m³.

Overall, the limited evidence from the studies that examined the concentration-response relationship between PM and cardiovascular hospital admissions and ED visits supports a no-threshold, log-linear model, which is consistent with the observations made in studies that examined the PM-mortality relationship (Section 6.5.2.7).

6.2.10.11. Out of Hospital Cardiac Arrest

One study of out of hospital cardiac death conducted in Seattle, WA (Checkoway et al., 2000, [015527](#)), which reported no association with PM was included in the 2004 PM AQCD (U.S. EPA, 2004, [056905](#)). In the U.S., the survival rate of sudden cardiac arrest is less than 5%. In addition, as discussed in Section 6.5, Zeka et al. (2006, [088749](#)) found that the estimated mortality risk due to short-term exposure to PM₁₀ was much higher for out-of-hospital cardiovascular deaths than for in-hospital cardiovascular deaths. The analysis of studies that examine the association between PM and cardiac arrest could provide evidence for an important link between the morbidity and mortality effects attributed to PM.

Sullivan et al. (2003, [043156](#)) examined the association between the incidence of primary cardiac arrest and daily measures of PM_{2.5} (measured by nephelometry) using a case-crossover analysis of 1,206 Washington State out-of-hospital cardiac arrests (1985-1994) among persons with (n = 774) and without (n = 432) clinically recognized heart disease. The authors examined PM associations at 0- through 2-day lags using the time-stratified referent sampling scheme (i.e., the same day of the week and month of the same year). The estimated relative risk for a 13.8-µg/m³ increase in 1-day lag PM_{2.5} (nephelometry: IQR = 0.54 10⁻¹ km⁻¹ bsp) was 0.94 (95% CI: 0.88-1.02), or 0.96 (95% CI: 0.91-1.0) per 10 µg/m³ increase. Similar estimates were reported for 0- or 2-day lags. The presence or absence of clinically recognized heart disease did not alter the result. This finding is consistent with the previous study of cardiac arrest in Seattle (Levy et al., 2001, [017171](#)) that reported no PM association. It is also consistent with the Sullivan et al. (2005, [050854](#)) analysis of PM and onset of MI, and the Sullivan et al. (2007, [100083](#)) analysis of PM and blood markers of inflammation in the elderly population, both of which were conducted in Seattle. Note also that the analysis of the NMMAPS data for the years 1987-1994 also found no PM₁₀ association for all-cause mortality in Seattle. Overall, the results of studies conducted in Seattle consistently found no association between PM and cardiovascular outcomes or all-cause mortality.

Rosenthal et al. (2008, [156925](#)) examined associations between PM_{2.5} and out-of-hospital cardiac arrests in Indianapolis, Indiana for the years 2002-2006 using a case-crossover design with time-stratified referent sampling. Using all the cases (n = 1,374), they found no associations between PM_{2.5} and cardiac arrest in any of the 0- through 3-day lags or multiday averages thereof (e.g., for 0-day lag, OR = 1.02 [CI: 0.94-1.11] per 10 µg/m³ increase in PM_{2.5}). However, for cardiac arrests witnessed by bystanders (n = 511), they found a significant association with PM_{2.5} exposure (by TEOM, corrected with FRM measurements) during the hour of the arrest (OR = 1.12 [CI: 1.01-1.25] per 10 µg/m³ increase in PM_{2.5}), and even larger risk estimates for older adults (age 60-75) or those that presented with asystole. There have been very few PM studies that used hourly PM measurements, and further studies are needed to confirm associations at such time scales.

In Rome, Forastiere et al. (2005, [086323](#)) examined associations between air pollution (PNC, PM₁₀, CO, NO₂, and O₃) and out-of-hospital coronary deaths (n = 5,144) for the study period of 1998-2000. A case-crossover design with the time-stratified referent sampling was used to examine the pollution indices at lag 0- through 3 days and the average of 0-1 lags. They found associations between deaths and PNC (lag 0 and 0-1), PM₁₀ (lag 0, 1, and 0-1), and CO (lag 0 and 0-1) but not with NO₂ or O₃. The risk estimate for 0-day lag PM₁₀ was 1.59% (CI: 0.03-3.18) per 10 µg/m³ increase. The older adults (65-74 and ≥75 age groups) showed higher risk estimates than the younger (35-64) age group. Because PNC is considered to be associated with UFPs, and CO was also associated with out-of-hospital cardiac arrests, combustion sources were implicated.

In summary, only a few studies have examined out-of-hospital cardiac arrest or deaths. The two studies from Seattle, WA consistently found no association (also consistent with other cardiac effects and mortality studies conducted in that locale); a study in Indianapolis, IN found an association with hourly PM_{2.5} but not daily PM_{2.5}; and a study in Rome found an association with PM₁₀, but also with PNC and CO. Because multicity mortality studies examining this association found heterogeneity in PM risk estimates across regions, future studies of out-of-hospital cardiac arrest will need to consider location and the air pollution mixture during their design. Mean and upper percentile concentrations are found in Table 6-9.

Table 6-9. PM concentrations reported in studies of out-of-hospital cardiac arrest.

Author	Location	Mean Concentration (µg/m ³)	Upper Percentile Concentrations (µg/m ³)
PM_{2.5}			
Sullivan et al. (2003, 043156)	Washington State	Nephelometry: 0.71 x 10 ⁻¹ km ⁻¹ bsp	Maximum: 5.99 x 10 ⁻¹ km ⁻¹ bsp
Rosenthal et al. (2008, 156925)	Indianapolis, Indiana	NR	NR
PM₁₀			
Sullivan et al. (2003, 043156)	Washington State	28.05	89.83
Zeka et al. (2006, 088749)		Range in Means: 15.9 (Honolulu) - 37.5 (Cleveland)	NR
Forastiere et al. (2005, 086323)	Rome, Italy	52.1	75th: 65.7

6.2.11. Cardiovascular Mortality

An evaluation of studies that examined the association between short-term exposure to PM_{2.5} and PM_{10-2.5} and mortality provides additional evidence for PM-related cardiovascular health effects. Although the primary analysis in the majority of mortality studies evaluated consists of an examination of the relationship between PM_{2.5} or PM_{10-2.5} and all-cause (nonaccidental) mortality, some studies have examined associations with cause-specific mortality including cardiovascular-related mortality.

Multicity mortality studies that examined the PM_{2.5}-cardiovascular mortality relationship on a national scale (Franklin et al. (2007, [091257](#)) – 27 U.S. cities; Franklin et al. (2008, [097426](#)) – 25 U.S. cities; and Zanobetti and Schwartz (2009, [188462](#)) – 112 U.S. cities) have found consistent positive associations between short-term exposure to PM_{2.5} and cardiovascular mortality ranging from 0.47 to 0.85% per 10 µg/m³ at lag 0-1 (Section 6.5). The associations observed on a national scale are consistent with those presented by Ostro et al. (2006, [087991](#)) in a study that examined the PM_{2.5}-mortality relationship in nine California counties (0.6% [95% CI: 0-1.1] per 10 µg/m³). Of the multicity studies evaluated, one examined single day lags and found evidence for slightly larger effects at lag 1 compared to the average of lag days 0 and 1 for cardiovascular mortality (94% [95% CI: -0.14 to 2.02] per 10 µg/m³) (Franklin et al., 2007, [091257](#)). Although the overall effect estimates reported in the multicity studies evaluated are consistently positive, it should be noted that a large degree of variability exists between cities when examining city-specific effect estimates potentially due to differences between cities and regional differences in PM_{2.5} composition (Figure 6-24). Only a limited number of studies that examined the PM_{2.5}-mortality relationship have conducted analyses of potential confounders, such as gaseous copollutants, and none examined the effect of copollutants on PM_{2.5} cardiovascular mortality risk estimates. Although the recently evaluated multicity studies did not extensively examine whether PM_{2.5} mortality risk estimates are confounded by gaseous copollutants, evidence from the limited number of single-city studies evaluated in the 2004 PM AQCD (U.S. EPA, 2004, [056905](#)) suggests that gaseous copollutants do not confound the PM_{2.5}-cardiovascular mortality association. This is further supported by studies that examined the PM₁₀-mortality relationship in both the 2004 PM AQCD (U.S. EPA, 2004, [056905](#)) and this review. The evidence from epidemiologic, controlled human exposure, and toxicological studies that examined the association between short-term exposure to PM_{2.5} and cardiovascular morbidity provide coherence and biological plausibility for the cardiovascular mortality effects observed. Overall, the cardiovascular mortality PM_{2.5} effects were similar to those reported for all-cause (nonaccidental) mortality (Section 6.5), and are consistent with the effect estimates observed in the single- and multicity studies evaluated in the 2004 PM AQCD (U.S. EPA, 2004, [056905](#)).

Zanobetti and Schwartz (2009, [188462](#)) also examined PM_{10-2.5} mortality associations in 47 U.S. cities and found evidence for cardiovascular mortality effects (0.32% [95% CI: 0.00-0.64] per 10 µg/m at lag 0-1) similar to those reported for all-cause (nonaccidental) mortality (0.46% [95% CI: 0.21-0.67] per 10 µg/m). In addition, Zanobetti and Schwartz (2009, [188462](#)) reported seasonal (i.e., larger in spring and summer) and regional differences in PM_{10-2.5} cardiovascular mortality risk estimates. A few single-city studies evaluated also reported associations, albeit somewhat larger than the multicity study, between PM_{10-2.5} and cardiovascular mortality in Phoenix, AZ (Wilson et al., 2007, [157149](#)) (3.4-6.6% at lag 1) and Vancouver, Canada (Villeneuve et al., 2003, [055051](#)) (5.4% at lag 0). The difference in the PM_{10-2.5} risk estimates observed between the multi- and single-city studies could be due to a variety of factors including differences between cities and compositional differences in PM_{10-2.5} across regions (Figure 6-29). Only a small number of studies have examined potential confounding by gaseous copollutants or the influence of model specification on PM_{10-2.5} mortality risk estimates, but the effects are relatively consistent with those studies evaluated in the 2004 PM AQCD (U.S. EPA, 2004, [056905](#)).

6.2.12. Summary and Causal Determinations

6.2.12.1. PM_{2.5}

Several studies cited in the 2004 AQCD reported positive associations between short-term PM_{2.5} concentrations and hospital admissions or ED visits for CVD, although few were statistically significant. In addition, U.S. and Canadian-based studies (both multi- and single-city) that examined the PM_{2.5}-mortality relationship reported associations for cardiovascular mortality consistent with those observed for all-cause (nonaccidental) mortality and relatively stronger than those for respiratory mortality. Significant associations were also observed between MI and short-term PM_{2.5} concentrations (averaged over 2 or 24 h), as well as decreased HRV in association with PM_{2.5}. Several controlled human exposure and animal toxicological studies demonstrated HRV effects from exposure to PM_{2.5} CAPs, as well as changes in blood coagulation markers. However, the effects in these studies were variable. Arrhythmogenesis was reported for toxicological studies and generally

these results were observed in animal models of disease (SH rat, MI, pulmonary hypertension) exposed to combustion-derived PM_{2.5} (i.e., ROFA, DE, metals). One study demonstrated significant vasoconstriction in healthy adults following controlled exposures to CAPs, although this response could not be conclusively attributed to the particles as subjects were concomitantly exposed to relatively high levels of O₃. The results reported for systemic inflammation in toxicological studies were mixed.

A large body of evidence from studies of the effect of PM_{2.5} on hospital admissions and ED visits for CVD has been published since the 2004 PM AQCD. Associations with PM_{2.5} are consistently positive with the majority of studies reporting increases in hospital admissions or ED visits ranging from 0.5 to 3.4% per 10 µg/m³ increase in PM_{2.5} (Section 6.2.10). The largest U.S.-based multicity study, MCAPs, reported excess risks in the range of approximately 0.7% with the largest excess risks in the Northeast (1.08%) and in the winter (1.49%), providing evidence of regional and seasonal heterogeneity (Bell et al., 2008, [156266](#); Dominici et al., 2006, [088398](#)). Weak or null findings for PM_{2.5} have been observed in two single-city studies both conducted in Washington state (Slaughter et al., 2005, [073854](#); Sullivan et al., 2007, [100083](#)) and may be explained by this heterogeneity. Weak associations were also reported in Atlanta for PM_{2.5} and CVD ED visits, with PM_{2.5} traffic components being more strongly associated with CVD ED visits than other components (Tolbert et al., 2007, [090316](#)). Multicity studies conducted outside the U.S. and Canada have shown positive associations with PM_{2.5}. Studies of specific CVD outcomes indicate that IHD and CHF may be driving the observed associations (Sections 6.2.10.3 and 6.2.10.5, respectively). Although estimates from studies of cerebrovascular diseases are less precise and consistent, ischemic diseases appear to be more strongly associated with PM_{2.5} compared to hemorrhagic stroke (Section 6.2.10.7). The available evidence suggests that these effects occur at very short lags (0-1 days), although effects at longer lags have rarely been evaluated. Overall, the results of these studies provide support for associations between short-term PM_{2.5} exposure and increased risk of cardiovascular hospital admissions in areas with mean concentrations ranging from 7 to 18 µg/m³.

Epidemiologic studies that examined the association between PM_{2.5} and mortality provide additional evidence for PM_{2.5}-related cardiovascular effects (Section 6.2.11). The multicity studies evaluated found consistent, precise positive associations between short-term exposure to PM_{2.5} and cardiovascular mortality ranging from 0.47 to 0.85% at mean 24-h avg PM_{2.5} concentrations above 13 µg/m³. These associations were reported at short lags (0-1 days), which is consistent with the associations observed in the hospital admission and ED visit studies discussed above. Although only a limited number of studies examined potential confounders of the PM_{2.5}-cardiovascular mortality relationship, the studies evaluated in both this review and the 2004 PM AQCD (U.S. EPA, 2004, [056905](#)) support an association between short-term exposure to PM_{2.5} and cardiovascular mortality.

Recent studies that apportion ambient PM_{2.5} into sources and components suggest that cardiovascular hospital admissions associated with PM_{2.5} may be attributable to traffic-related pollution and, in some cases, biomass burning (Section 6.2.10). Further supporting evidence is provided by studies that have used PM₁₀ collection filters (median diameter generally <2.5 µm) to identify combustion- or traffic-related sources associated with cardiovascular hospital admissions. Metals have also been implicated in these effects (Bell et al., 2009, [191997](#)). A limited number of older publications have reported that particle acidity of PM_{2.5} is not more strongly associated with CVD hospitalizations or ED visits than other PM metrics.

Changes in various measures of cardiovascular function have been demonstrated by multiple independent laboratories following controlled human exposures to different types of PM_{2.5}. The most consistent effect is changes in vasomotor function, which has been demonstrated following exposure to CAPs and DE. The majority of the new evidence of particle-induced changes in vasomotor function comes from studies of exposures to DE (Section 6.2.4.2). None of these studies have evaluated the effects of DE with and without a particle trap. Therefore, the changes in vasomotor function cannot be conclusively attributed to the particles in DE as subjects are also concomitantly exposed to relatively high levels of NO₂, NO, CO, and hydrocarbons. However, it is important to note that a study by Peretz et al. (2008, [156854](#)) used a newer diesel engine with lower gaseous emissions and reported significant DE-induced decreases in BAD. In addition, increasing the particle exposure concentration from 100 to 200 µg/m³, without proportional increases in NO, NO₂, or CO, resulted in an approximate 100% increase in response. An additional consideration is that, while fresh DE used in these studies contains relatively high concentrations of PM_{2.5}, the MMAD is typically ≤ 100 nm, which makes it difficult to determine whether the observed effects are due to

PM_{2.5} or, more specifically, due to the UF fraction. Further evidence of a particle effect on vasomotor function is provided by significant changes in BAD demonstrated in healthy adults following controlled exposure to CAPs with O₃ (Brook et al., 2002, [024987](#)). These findings are consistent with epidemiologic studies of various measures of vasomotor function (e.g., FMD and BAD were the most common), which have demonstrated an association with short-term PM_{2.5} concentration in healthy and diabetic populations (Section 6.2.4.1). A limited number of epidemiologic studies examined multiple lags and the strongest associations were with either the 6-day mean concentration (O'Neill et al., 2005, [088423](#)) or the concurrent day (Schneider et al., 2008, [191985](#)).

The toxicological findings with respect to vascular reactivity are generally in agreement and demonstrate impaired dilation following PM_{2.5} exposure that is likely endothelium dependent (Section 6.2.4.3). These effects have been demonstrated in varying vessels and in response to different PM_{2.5} types, albeit using IT instillation exposure in most studies. Further support is provided by IT instillation studies of ambient PM₁₀ that also demonstrate impaired vasodilation and a PM_{2.5} CAPs study that reported decreased L/W ratio of the pulmonary artery. An inhalation study of Boston PM_{2.5} CAPs reported increases in coronary vascular resistance during ischemia, which indicated a possible role for PM-induced coronary vasoconstriction. The mechanism behind impaired dilation following PM exposure may include increased ROS and RNS production in the microvascular wall that leads to altered NO bioavailability and endothelial dysfunction. Despite the limited number of inhalation studies conducted with concentrations near ambient levels, the toxicological studies collectively provide coherence and biological plausibility for the myocardial ischemia observed in controlled human exposure and epidemiologic studies.

Consistent with the observed effects on vasomotor function, one recent controlled human exposure study reported an increase in exercise-induced ST-segment depression (a potential indicator of ischemia) during exposure to DE in a group of subjects with prior MI (Mills et al., 2007, [091206](#)). In addition, toxicological studies from Boston that employed CAPs provide further evidence for PM_{2.5} effects on ischemia, with changes in ST-segment and decreases in total myocardial blood flow reported (Section 6.2.3.3). These findings from toxicological and controlled human exposure studies provide coherence and biological plausibility for the associations observed in epidemiologic studies, particularly those of increases in hospital admissions and ED visits for IHD. Several epidemiology studies have reported associations between short-term PM_{2.5} concentration (including traffic sources or components such as BC) and ST-segment depression or abnormality (Section 6.2.3.1).

Toxicological studies provide biological plausibility for the PM_{2.5} associations with CHF hospital admissions by demonstrating increased right ventricular pressure and diminished cardiac contractility in rodents exposed to CB and DE (Section 6.2.6.1). Similarly, increased coronary vascular resistance was observed following PM_{2.5} CAPs exposure in dogs with experimentally-induced ischemia. Further, a recent epidemiology study reported small but statistically significant decreases in passively monitored diastolic pressure and right ventricular diastolic pressure (Rich et al., 2008, [156910](#)).

In addition to the effects of PM on vasomotor response, there is a growing body of evidence that demonstrates changes in markers of systemic oxidative stress following controlled human exposures to DE, wood smoke, and urban traffic particles. However, these effects may be driven in part by the UF fraction of PM_{2.5}. Toxicological studies provide evidence of increased cardiovascular ROS following PM_{2.5} exposure to CAPs, road dust, CB, and TiO₂, as well as increased systemic ROS in rats exposed to gasoline exhaust (Section 6.2.9.3). Epidemiologic studies of markers of oxidative stress (e.g., tHcy, CuZn-SOD, TBARS, 8-oxodG, oxLDL and MDA) are consistent with these toxicological findings (Section 6.2.9.1).

A few epidemiologic studies of ventricular arrhythmias recorded on ICDs that were conducted in Boston and Sweden (Table 6-2) found associations with short-term PM_{2.5} concentration (also BC and sulfate). While Canadian and U.S. studies conducted outside of Boston did not find positive associations between PM_{2.5} and ICD recorded ventricular arrhythmias, several such studies observed associations with ectopic beats and runs of supraventricular or ventricular tachycardias (Section 6.2.2.1). Toxicological studies also provide limited evidence of arrhythmia, mainly in susceptible animal models (i.e., older rats, rats with CHF) (Section 6.2.2.2).

Most epidemiologic studies of HRV have reported decreases in SDNN, LF, HF, and rMSSD (Section 6.2.1.1). While there are also a significant number of controlled human exposure studies reporting PM-induced changes in HRV, these changes are often variable and difficult to interpret (Section 6.2.1.2). Similarly, HRV increases and decreases have been observed in animal toxicological studies that employed CAPs or CB (Section 6.2.1.3). In a study in mice, resuspended

soil, secondary sulfate, residual oil, and motor vehicle/other sources, as well as Ni were implicated in HRV effects (Lippmann et al., 2006, [091165](#)). Further, cardiac oxidative stress has been implicated as a consequence of ANS stimulation in response to CAPs. Modification of the PM-HRV association by genetic polymorphisms related to oxidative stress has been observed in a series of analyses of the population enrolled in the Normative Aging Study. Changes in HRV measures (whether increased or decreased) are likely to be more useful as indicators of PM exposure rather than predictive of some adverse outcome. Furthermore, the HRV result may be reflecting a fundamental response of an individual that is determined in part by a number of factors including age and pre-existing conditions.

Although not consistently observed across studies, some investigators have reported PM_{2.5}-induced changes in BP, blood coagulation markers, and markers of systemic inflammation in controlled human exposure studies (Sections 6.2.5.2, 6.2.8.2, and 6.2.9.2, respectively). Findings from epidemiologic studies, which are largely cross-sectional and measure a wide array markers of inflammation and coagulation, are not consistent; however, a limited number of recent studies of gene-environment interactions offer insight into potential individual susceptibility to these effects (Ljungman et al., 2009, [191983](#); Peters et al., 2009, [191992](#)). Similarly, toxicological studies demonstrate mixed results for systemic inflammatory markers and generally indicate relatively little change at 16-20 h post-exposure (Section 6.2.7.3). Increases in BP have been observed in toxicological studies (Section 6.2.5.3), with the strongest evidence coming from dogs exposed to PM_{2.5} CAPs. For blood coagulation parameters, the most commonly reported change in animal toxicological studies is elevated plasma fibrinogen levels following PM_{2.5} exposure, but this response is not consistently observed (Section 6.2.8.3).

In summary, associations of hospital admissions or ED visits with PM_{2.5} for CVD (predominantly IHD and CHF) are consistently positive with the majority of studies reporting increases ranging from 0.5 to 3.4% per 10 µg/m³ increase in PM_{2.5}. Seasonal and regional variation observed in the large multicity study of Medicare recipients is consistent with null findings reported in several single city studies conducted in the Western U.S. The results from the hospital admission and ED visit studies are supported by the associations observed between PM_{2.5} and cardiovascular mortality, which also provide additional evidence for regional and seasonal variability in PM_{2.5} risk estimates. Changes in various measures of cardiovascular function that may explain these epidemiologic findings have been demonstrated by multiple independent laboratories following controlled human exposures to different types of PM_{2.5}. The most consistent PM_{2.5} effect is for vasomotor function, which has been demonstrated following exposure to CAPs and DE. Toxicological studies finding reduced myocardial blood flow during ischemia and altered vascular reactivity provide coherence and biological plausibility for the myocardial ischemia that has been observed in both controlled human exposure and epidemiologic studies. Further, PM_{2.5} effects on ST-segment depression have been observed across disciplines. In addition to ischemia, PM_{2.5} may act through several other pathways. Plausible biological mechanisms (e.g., increased right ventricular pressure and diminished cardiac contractility) for the associations of PM_{2.5} with CHF have also been proposed based on toxicological findings. There is a growing body of evidence from controlled human exposure, toxicological and epidemiologic studies demonstrating changes in markers of systemic oxidative stress with PM_{2.5} exposure. Inconsistent effects of PM on BP, blood coagulation markers and markers of systemic inflammation have been reported across the disciplines. Together, the collective **evidence is sufficient to conclude that a causal relationship exists between short-term PM_{2.5} exposures and cardiovascular effects.**

6.2.12.2. PM_{10-2.5}

There was little evidence in the 2004 AQCD regarding PM_{10-2.5} cardiovascular health effects. Two single-city epidemiologic studies found positive associations of PM_{10-2.5} with cardiovascular hospital admissions in Toronto (Burnett et al., 1999, [017269](#)) and Detroit, MI (Ito, 2003, [042856](#); Lippmann, 2000, [024579](#)) and the effect estimates were of the same general magnitude as for PM₁₀ and PM_{2.5}. Both studies reported positive associations and estimates appeared robust to adjustment for gaseous copollutants in two-pollutant models. An imprecise, non-significant association between PM_{10-2.5} and onset of MI was observed in Boston (Peters et al., 2001, [016546](#)). No controlled human exposure or toxicological studies of PM_{10-2.5} were presented in the 2004 AQCD.

Several recent epidemiologic studies of the effect of ambient PM_{10-2.5} concentration on hospital admissions or ED visits for CVD were conducted (Section 6.2.10). In a study of Medicare patients in

108 U.S. counties, Peng et al. (2008, [156850](#)) reported a significant association between PM_{10-2.5} and CVD hospitalizations in their single pollutant model. In a study of six French cities, Host et al. (2008, [155852](#)) reported a significant increase in IHD hospital admissions in association with PM_{10-2.5}. In contrast, associations of cardiovascular outcomes with PM_{10-2.5} were weak for CHF and null for IHD in the Atlanta-based SOPHIA study (Metzger et al., 2004, [044222](#)). Results from single-city studies are generally positive, but effect sizes are heterogeneous and estimates are imprecise (Section 6.2.10). Crustal material from a dust storm in the Gobi desert that was largely coarse PM (generally indicated using PM₁₀) was associated with hospitalizations for CVD, including IHD and CHF in most studies (Section 6.2.10). Mean PM_{10-2.5} concentrations in the hospital admission and ED visit studies ranged from 7.4-13 µg/m³. A few epidemiologic studies that examined the association between short-term exposure to PM_{10-2.5} and cardiovascular mortality (Section 6.2.11) provide supporting evidence for the hospital admission and ED visit studies at similar 24-h avg PM_{10-2.5} concentrations (i.e., 6.1-16.4 µg/m³). A multicity study reported risk estimates for cardiovascular mortality of similar magnitude to those for all-cause (nonaccidental) mortality (Zanobetti and Schwartz, 2009, [188462](#)). However, the single-city studies evaluated (Villeneuve et al., 2003, [055051](#); Wilson et al., 2007, [157149](#)) reported substantially larger effect estimates, but this could be due to differences between cities and compositional differences in PM_{10-2.5} across regions. Of note is the lack of analyses within the studies evaluated that examined potential confounders of the PM_{10-2.5}-cardiovascular mortality relationship.

The U.S. study of Medicare patients (Peng et al., 2008, [156850](#)) and the multicity study that examined the association between PM_{10-2.5} and mortality (Zanobetti and Schwartz, 2009, [188462](#)) were the only studies to adjust PM_{10-2.5} for PM_{2.5}. Peng, et al. (2008, [156850](#)) found that the PM_{10-2.5} association with CVD hospitalizations remained, but diminished slightly after adjustment for PM_{2.5}. These results are consistent with those reported by Zanobetti and Schwartz (2009, [188462](#)), which found PM_{10-2.5}-cardiovascular mortality risk estimates remained relatively robust to the inclusion of PM_{2.5} in the model. Because of the greater spatial heterogeneity of PM_{10-2.5}, exposure measurement error is more likely to bias health effect estimates towards the null for epidemiologic studies of PM_{10-2.5} versus PM₁₀ or PM_{2.5}, making it more difficult to detect an effect of the coarse size fraction. In addition, models that include both PM_{10-2.5} and PM_{2.5} may suffer from instability due to collinearity. Further, the lag structure of PM_{10-2.5} effects on risk of cardiovascular hospital admissions and ED visits, as well as mortality, has not been examined in detail.

Several epidemiologic studies of cardiovascular endpoints including HRV, BP, ventricular arrhythmia, and ECG changes indicating ectopy or ischemia were conducted since publication of the 2004 PM AQCD. Supraventricular ectopy and ST-segment depression were associated with PM_{10-2.5} (Section 6.2.3.1), and the only study to examine the effect of PM_{10-2.5} on BP reported a decrease in SBP (Ebelt et al., 2005, [056907](#)) (Section 6.2.5.1). HRV findings were mixed across the epidemiologic studies (Section 6.2.1.1). A limited number of studies have evaluated the effect of controlled exposures to PM_{10-2.5} CAPs on cardiovascular endpoints in human subjects. These studies have provided some evidence of decreases in HRV (SDNN) and tPA concentration among healthy adults approximately 20 hours following exposure (Section 6.2.1.2). However, it is important to note that no other measures of HRV (e.g., LF, HF, or LF/HF), nor other hemostatic or thrombotic markers (e.g., fibrinogen) were significantly affected by particle exposure in these studies.

There are very few toxicological studies that examined the effect of exposure to PM_{10-2.5} on cardiovascular endpoints or biomarkers in animals. The few studies that evaluated cardiovascular responses were comparative studies of various size fractions, and only blood or plasma parameters were measured (Sections 6.2.7.3 and 6.2.8.3). These studies used IT instillation methodologies, as there are challenges to exposing rodents via inhalation to PM_{10-2.5}, due to near 100% deposition in the ET region for particles >5 µm (Raabe et al., 1988, [001439](#)) and only 44% nasal inhalability of a 10 µm particle in the rat (Ménache et al., 1995, [006533](#)). These studies also employed relatively high doses of PM_{10-2.5}. Despite these shortcomings, increased plasma fibrinogen was observed and the response was similar to that observed with PM_{2.5}. At this time, evidence of biological plausibility for cardiovascular morbidity effects following PM_{10-2.5} exposure is sparse, due to the small number of studies, few endpoints examined, and the limitations related to the interpretation of IT instillation exposures.

In summary, several epidemiologic studies report associations with cardiovascular endpoints including IHD hospitalizations, supraventricular ectopy, and changes in HRV. Further, dust storm events resulting in high concentrations of crustal material are linked to increases in cardiovascular disease hospital admissions or ED visits for cardiovascular diseases. A large proportion of inhaled

coarse particles in the 3-6 μm (d_{ae}) range can reach and deposit in the lower respiratory tract, particularly the TB airways (Figures 4-3 and 4-4). The few toxicological and controlled human exposure studies examining the effects of $\text{PM}_{10-2.5}$ provide limited evidence of cardiovascular effects and biological plausibility to support the epidemiologic findings. Therefore the available evidence is **suggestive of a causal relationship between $\text{PM}_{10-2.5}$ exposures and cardiovascular effects.**

6.2.12.3. UFPs

There was very little evidence available in the 2004 PM AQCD (U.S. EPA, 2004, [056905](#)) on the cardiovascular effects of UFPs. Findings from one study presented in the 2004 PM AQCD (U.S. EPA, 2004, [056905](#)) of controlled exposures to UF EC suggested no particle-related effects on various cardiovascular endpoints including blood coagulation, HRV, and systemic inflammation. No epidemiologic studies of short-term UFP concentration and cardiovascular endpoints were included in the 2004 AQCD and there were no relevant toxicological studies reviewed in the 2004 PM AQCD (U.S. EPA, 2004, [056905](#)) that exposed animals to UFPs. A small number of new epidemiologic studies, as well as several controlled human exposure and toxicological studies have been conducted in recent years, but substantial uncertainties remain as to the cardiovascular effects of UFPs. For a given mass, the enormous number and large surface area of UFPs highlight the importance of considering the size of the particle in assessing response. For example, UFPs with a diameter of 20 nm, when inhaled at the same mass concentration, have a number concentration that is approximately six orders of magnitude higher than for a 2.5- μm diameter particle. Particle surface area is also greatly increased with UFPs. Many studies suggest that the surface of particles or substances released from the surface (e.g., transition metals, organics) interact with biological substrates, and that surface-associated free radicals or free radical-generating systems may be responsible for toxicity, resulting in greater toxicity of UFPs per particle surface area than larger particles. Additionally, smaller particles may have greater potential to cross cell membranes and epithelial barriers.

Controlled human exposure studies are increasingly being utilized to evaluate the effect of UFPs on cardiovascular function. While the number of studies of exposure to UFPs is still limited, there is a relatively large body of evidence from exposure to fresh DE, which is typically dominated by UFPs. As described under the summary for $\text{PM}_{2.5}$, studies of controlled exposures to DE (100-300 $\mu\text{g}/\text{m}^3$) have consistently demonstrated effects on vasomotor function among adult volunteers (Section 6.2.4.2). In addition, exposure to UF EC (50 $\mu\text{g}/\text{m}^3$, 10.8×10^6 particles/ cm^3) was recently shown to attenuate FMD (Shah et al., 2008, [156970](#)). Changes in vasomotor function have been observed in animal toxicological studies of UFPs, although very few studies have been conducted (Section 6.2.4.3). Inhaled UF TiO_2 impaired arteriolar dilation when compared to fine TiO_2 at similar mass doses (Nurkiewicz et al., 2008, [156816](#)). This response may have been due to ROS in the microvascular wall, which may have led to consumption of endothelial-derived NO and generation of peroxynitrite radicals. Support for an UFP effect on altered vascular reactivity is also provided by studies of DE and IT instillation exposure to ambient PM. The response to DE did not appear to be due to VOCs. One epidemiologic study showed that PNC was associated with a nonsignificant decrease in flow- and nitroglycerine-mediated reactivity as measures of vasomotor function in diabetics living in Boston (O'Neill et al., 2005, [088423](#)).

New studies have reported increases in markers of systemic oxidative stress in humans following controlled exposures to different types of PM consisting of relatively high concentrations of UFPs from sources including wood smoke, urban traffic particles, and DE (Section 6.2.9.2). Increased cardiac oxidative stress has been observed in mice and rats following gasoline exhaust exposure and it appeared the effect was particle-dependent (Section 6.2.9.3).

The associations between UFPs and HRV measures in epidemiologic studies include increases and decreases (Section 6.2.1.1), providing some evidence for an effect. Exposure to UF CAPs has been observed to alter parameters of HRV in controlled human exposure studies, although this effect has been variable between studies (Section 6.2.1.2). Alterations in HR, HRV, and BP were reported in rats exposed to <200 $\mu\text{g}/\text{m}^3$ UF CB (< 1.6×10^7 particles/ cm^3) (Sections 6.2.1.3 and 6.2.5.3). The effects of UFPs on BP have been mixed in epidemiologic studies (Section 6.2.5.1).

There is some evidence of changes in markers of blood coagulation in humans following controlled exposure to UF CAPs, as well as wood smoke and DE; however, these effects have not

been consistently observed across studies (Section 6.2.8.2). Toxicological studies demonstrate mixed results for systemic inflammation and blood coagulation as well (Sections 6.2.7.3 and 6.2.8.3).

Few time-series studies of CVD hospital admissions have evaluated UFPs. The SOPHIA study found no association between any outcome studied (all CVD, dysrhythmia, CHF, IHD, peripheral vascular and cerebrovascular disease) and 24-h mean levels of UFP (Metzger et al. 2004). The median UF particle count in Atlanta during the study period was 25,900 particles/cm³. UFP were not associated with CVD hospitalizations in the elderly in Copenhagen, Denmark, but were associated with cardiac readmission or fatal MI in the European HEAPSS study (Section 6.2.10). In the Copenhagen study, the mean count of particles with a 100 nm mean diameter was 0.68×10⁴ particles/cm³, whereas the PNC range was approximately 1.2-7.6×10⁴ particles/cm³ in HEAPSS study. Spatial variation in UFP concentration, which diminishes within a short distance from the roadway, may introduce exposure measurement error, making it more difficult to observe an association if one exists.

A limited number of epidemiologic studies have evaluated subclinical cardiovascular measures and a number of these were conducted in Boston. UFPs have been linked to ICD-recorded arrhythmias in Boston and supraventricular ectopic beats in Erfurt, Germany (Section 6.2.2.1). One study reported no UFP association with ectopy (Barclay et al., 2009, [179935](#)). ST-segment depression in subjects with stable coronary heart disease was associated with UFPs in Helsinki (Section 6.2.3.1). The limited number of studies that examine this size fraction makes it difficult to draw conclusions about these cardiovascular measures.

In summary, there is a relatively large body of evidence from controlled human exposure studies of fresh DE, which is typically dominated by UFPs, demonstrating effects of UFP on the cardiovascular system. In addition, cardiovascular effects have been demonstrated by a limited number of laboratories in response to UF CB, urban traffic particles and CAPs. Responses include altered vasomotor function, increased systemic oxidative stress and altered HRV parameters. Studies using UF CAPs, as well as wood smoke and DE, provide some evidence of changes in markers of blood coagulation, but findings are not consistent. Toxicological studies conducted with UF TiO₂, CB, and DE demonstrate changes in vasomotor function as well as in HRV. Effects on systemic inflammation and blood coagulation are less consistent. PM-dependent cardiac oxidative stress was noted following exposure to gasoline exhaust. The few epidemiologic studies of UFPs conducted do not provide strong support for an association of UFPs with effects on the cardiovascular system. Based on the above findings, the evidence is **suggestive of a causal relationship between ultrafine PM exposure and cardiovascular effects.**

6.3. Respiratory Effects

6.3.1. Respiratory Symptoms and Medication Use

The 2004 PM AQCD (U.S. EPA, 2004, [056905](#)) presented evidence from epidemiologic studies of increases in respiratory symptoms associated with PM, although this was not supported by the findings of a limited number of controlled human exposure studies. Recent epidemiologic studies have provided evidence of an increase in respiratory symptoms and medication use associated with PM among asthmatic children, with less evidence of an effect in asthmatic adults. The lack of an observed effect of PM exposure on respiratory symptoms in controlled human exposure studies does not necessarily contradict these findings, as very few studies of controlled exposures to PM have been conducted among groups of asthmatic or healthy children.

6.3.1.1. Epidemiologic Studies

The 2004 PM AQCD (U.S. EPA, 2004, [056905](#)) concluded that the effects of PM₁₀ on respiratory symptoms in asthmatics tended to be positive, although they were somewhat less consistent than PM₁₀ effects on lung function. Most studies showed increases in cough, phlegm, difficulty breathing, and bronchodilator use, although these increases were generally not statistically significant for PM₁₀. The results from one study of respiratory symptoms and PM_{10-2.5} (Schwartz and

Neas, 2000, [007625](#)) found a statistically significant association with cough with PM_{10-2.5}. The results of two studies examining respiratory symptoms and PM_{2.5} revealed slightly larger effects for PM_{2.5} than for PM₁₀.

Asthmatic Children

Two large, longitudinal studies in urban areas of the U.S. investigated the effects of ambient PM on respiratory symptoms and/or asthma medication use with similar analytic techniques (i.e., multistaged modeling and generalized estimating equations [GEE]): the Childhood Asthma Management Program (CAMP) (Schildcrout et al., 2006, [089812](#)) and the National Cooperative Inner-City Asthma Study (NCICAS) (Mortimer et al., 2002, [030281](#)). A number of smaller panel studies conducted in the U.S. evaluated the effects of ambient PM concentrations on respiratory symptoms and medication use among asthmatic children (Delfino et al., 2002, [093740](#); 2003, [090941](#); 2003, [050460](#); Gent et al., 2003, [052885](#); 2009, [180399](#); 2006, [088031](#); Slaughter et al., 2003, [086294](#)).

In the CAMP study, the association between ambient air pollution and asthma exacerbations in children (n = 990) from eight North American cities was investigated (Schildcrout et al., 2006, [089812](#)). In contrast to several past studies (Delfino et al., 1996, [080788](#); 1998, [051406](#)), no associations were observed between PM₁₀ and asthma exacerbations or medication use. PM₁₀ concentrations were measured on less than 50% of study days in all cities except Seattle and Albuquerque. While PM₁₀ effects were not observed for the entire panel of children, they were observed in recent reports on the children participating at the Seattle center (Slaughter et al., 2003, [086294](#); Yu et al., 2000, [013254](#)). In a smaller panel study of asthmatic children (n = 133) enrolled in the CAMP study, daily particle concentrations averaged over three central sites in Seattle was used as the exposure metric (Slaughter et al., 2003, [086294](#)). Children were followed for 2 months, on average. Daily health outcomes included both a 3-category measure of asthma severity based on symptom duration and frequency, and inhaled albuterol use. In single-pollutant models, an increased risk of asthma severity was associated with a 10 µg/m³ increase in lag 1 PM_{2.5} (OR 1.20 [95% CI: 1.05-1.37]) and with a 10 µg/m³ increase in lag 0 PM₁₀ (OR 1.12 [95% CI: 1.05-1.22]). In copollutant models with CO, the associations remained (OR for PM_{2.5} 1.16 [95% CI: 1.03-1.30]; OR for PM₁₀ 1.11 [95% CI: 1.03-1.19]). Associations between inhaler use and PM were positive in single-pollutant models (RR lag 1 PM_{2.5} 1.08 [95% CI: 1.01-1.15]; RR lag 0 PM₁₀ 1.05 [95% CI: 1.00-1.09]), but attenuated and no longer statistically significant in copollutant models.

The eight cities included in the NCICAS (Mortimer et al., 2002, [030281](#)) were all in the East or Midwest: New York City (Bronx, E. Harlem), Baltimore, Washington DC, Cleveland, Detroit, St. Louis, and Chicago. In this study, 864 asthmatic children, aged 4-9 yr, were followed daily for four 2-wk periods over the course of nine months. Morning and evening asthma symptoms (analyzed as none vs. any) and peak flow were recorded. For the three urban areas with air quality data, each 10 µg/m³ increase in the mean of the previous 2 days (lag 1-2) PM₁₀, increased the risk for morning asthma symptoms (OR 1.12 [95% CI: 1.00-1.26]). This effect was robust to the inclusion of O₃ (OR 1.12 [95% CI: 0.98-1.27]). In a related study, O'Connor et al. (2008, [156818](#)) examined the relationship between short-term fluctuations in outdoor air pollutant concentrations and changes in pulmonary function and respiratory symptoms among children with asthma in seven U.S. inner-city communities. PM_{2.5} concentration was not statistically associated with respiratory symptoms in this study.

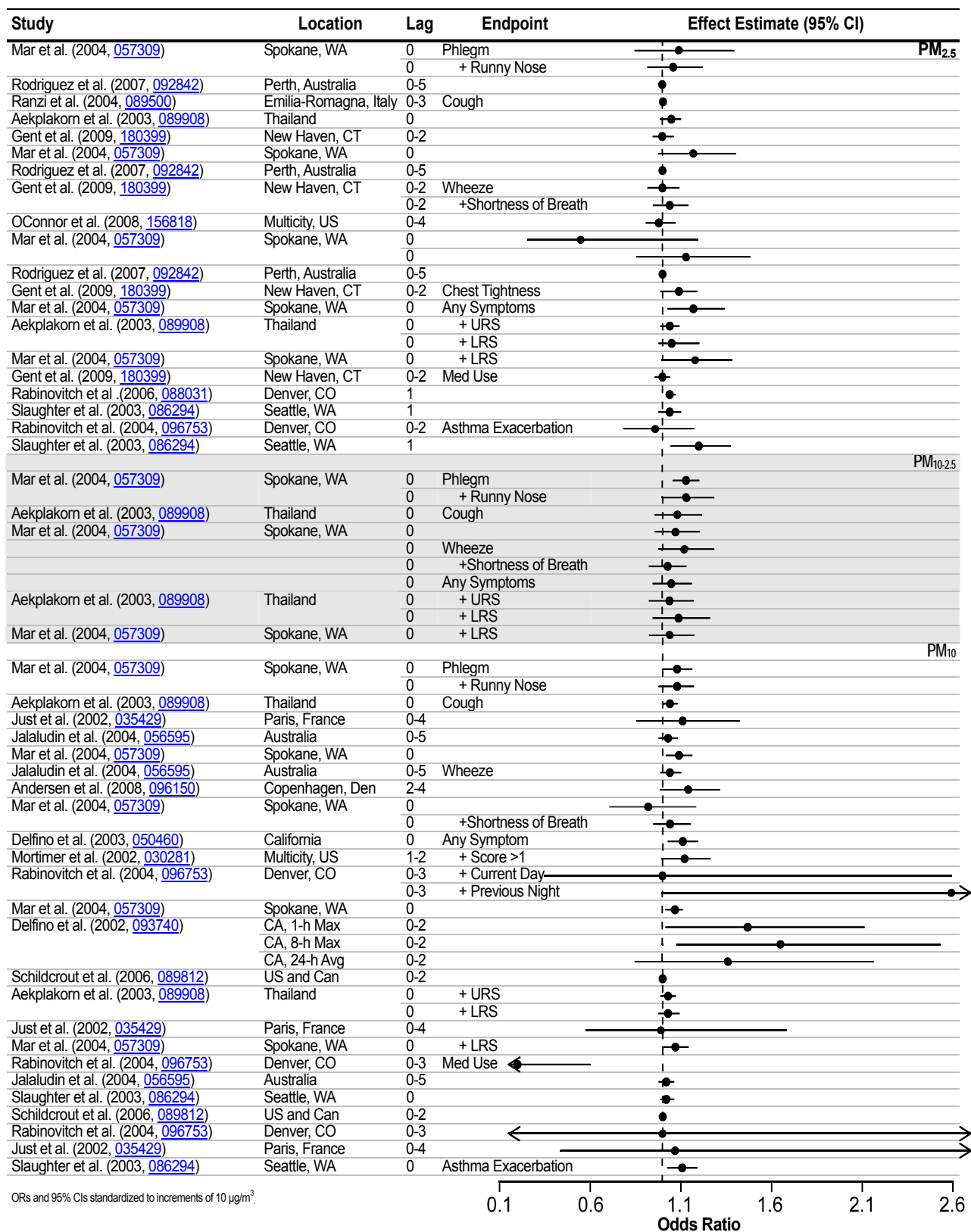


Figure 6-7. Respiratory symptoms and/or medication use among asthmatic children following acute exposure to PM.

Table 6-10. Characterization of ambient PM concentrations from epidemiologic studies of respiratory morbidity and short-term exposures in asthmatic children and adults. All concentrations are for the 24-h avg unless otherwise noted.

Study	Location	Mean Concentration ($\mu\text{g}/\text{m}^3$)	Upper Percentile Concentrations ($\mu\text{g}/\text{m}^3$)
<i>PM_{2.5}</i>			
Adamkiewicz et al. (2004, 087925)	Steubenville, OH	20.43	75th: 23 98th: 51.79 Max: 51.79
Adar et al. (2007, 001458)	St. Louis, MO	10.13	98th: 22.43 Max: 23.24
Aekplakorn et al. (2003, 089908)	North Thailand		Max: 24.8-26.3
Allen et al. (2008, 156208)	Seattle, WA	11.2	Max: 40.38
Barraza-Villarreal et al. (2008, 156254)	Mexico City	8-h max: 28.9	Max: 102.8
Bourotte et al. (2007, 150040)	Sao Paulo, Brazil	11.9	Max: 26.6
de Hartog et al. (2003, 001061)	Multicity, Europe	12.8-23.4	Max: 39.8-118.1
Delfino et al. (2006, 090745)	Southern CA	3.9-6.9	Max: 8.8-11.6
DeMeo et al. (2004, 087346)	Boston, MA	10.8	NR
Ebelt et al. (2005, 056907)	Vancouver, Canada	11.4	98th: 23 Max: 28.7
Ferdinands et al. (2008, 156433)	Atlanta, GA	27.2	Max: 34.7
Fischer et al. (2007, 156435)	The Netherlands	56	75th: 187
Gent et al. (2003, 052885)	CT & MA	13.1	60th: 12.1 80th: 19.0
Gent et al. (2009, 180399)	New Haven, CT	17.0	NR
Girardot et al. (2006, 088271)	Smoky Mountains	13.9	Max: 38.4
Hogervorst et al. (2006, 156559)	The Netherlands	19.0	NR
Hong et al. (2007, 091347)	Incheon City, Korea	20.27	Max: 36.28
Jansen et al. (2005, 082236)	Seattle, WA	14.0	Max: 44
Johnston et al. (2006, 091386)	Darwin, Australia	11.1	Max: 36.5
Koenig et al. (2003, 156653)	Seattle, WA	13.3	Max: 40.4
Lagorio et al. (2006, 089800)	Rome, Italy	27.2	Max: 100
Lee et al. (2007, 093042)	Seoul, South Korea	51.15	75th: 87.54 Max: 92.71
Lewis et al. (2004, 097498)	Detroit, MI	15.7-17.5	Max: 56.1
Liu et al. (2009, 192003)	Windsor, Ontario	7.1	95th: 19.0 98th: 19.0.
Mar et al. (2004, 057309)	Spokane, WA	8.1-11.0	NR
Mar et al. (2005, 088759)	Seattle, WA	5-26	NR
McCreanor et al. (2007, 092841)	London, England	1-h avg: 11.9-28.3	1-h max: 55.9-76.1
Moshhammer et al. (2006, 090771)	Linz, Austria	8-h avg: 15.70	Max 24-h avg: 76.39
Murata et al. (2007, 189159)	Tokyo, Japan	39.0	Max 1-h avg: 120
O'Connor et al. (2008, 156818)	Multicity, U.S.	14	Max: 35

Study	Location	Mean Concentration ($\mu\text{g}/\text{m}^3$)	Upper Percentile Concentrations ($\mu\text{g}/\text{m}^3$)
Peled et al. (2005, 156015)	Multicity, Israel	23.9-29.2	NR
Penttinen et al. (2006, 087988)	Helsinki, Finland	8.37	75th: 11.15 Max: 33.53
Rabinovitch et al. (2004, 096753)	Denver, CO	10.8	98th: 29.3 Max: 53.5
Rabinovitch et al. (2006, 088031)	Denver, CO	10.8	98th: 23.4
Ranzi et al. (2004, 089500)	Emilia-Romagna, Italy	Urban: 53.07 Rural: 29.11	NR
Rodriguez et al. (2007, 092842)	Perth, Australia	1-h avg: 20.8 24-h avg: 8.5	Max 1-h avg: 93.4 Max 24-h avg: 39.4
Slaughter et al. (2003, 086294)	Seattle, WA	7.3 ^a	75th: 11.3
Strand et al. (2006, 089203)	Denver, CO	12.7	Max: 32.3
Timonen et al. (2004, 087915)	Multicity, Europe	12.7-23.1	Max: 39.8-118.1
Trenga et al. (2006, 155209)	Seattle, WA	8.6-9.6 ^a	75th: 13.1-14.8 Max: 40.4-41.5
von Klot et al. (2002, 034706)	Erfurt, Germany	30.3 ^b	75th: 41.3 ^b Max: 133.8 ^b
Ward et al. (2002, 025839)	Birmingham and Sandwell, U.K.	12.3-12.7	Max: 28-37
<i>PM_{10-2.5}</i>			
Aekplakorn et al. (2003, 089908)	North Thailand	NR	NR
Bourotte et al. (2007, 150040)	Sao Paulo, Brazil	21.7	Max: 62.0
Ebelt et al. (2005, 056907)	Vancouver, Canada	5.6	Max: 11.9
Lagorio et al. (2006, 089800)	Rome, Italy	15.6	Max: 39.6
Mar et al. (2004, 057309)	Spokane, WA	8.7-13.5	NR
von Klot et al. (2002, 034706)	Erfurt, Germany	10.3	75th: 14.6 Max: 64.3
<i>PM₁₀</i>			
Aekplakorn et al. (2003, 089908)	North Thailand	31.9-37.5	Max: 113.3-153.3
Andersen et al. (2008, 096150)	Copenhagen, Denmark	25.1	75th: 30.2
Boezen et al. (2005, 087396)	The Netherlands	26.6-44.1	Max: 89.9-242.2
de Hartog et al. (2003, 001061)	Multicity, Europe	19.6-36.5	Max: 67.4-112.0
Delfino et al. (2002, 093740)	Alpine, CA	20	90th: 32 Max: 42
Delfino et al. (2003, 050460)	Los Angeles, CA	59.9	90th: 86/0/Max: 126
Delfino et al. (2004, 056897)	Alpine, CA	29.7	90th: 40.9 Max: 50.7
Delfino et al. (2006, 090745)	Southern CA	35.7-70.8	Max: 105.5-154.1
Desqueyroux et al. (2002, 026052)	Paris, France	23-28	Max: 63-84
Ebelt et al. (2005, 056907)	Vancouver, Canada	17	Max: 36
Hong et al. (2007, 091347)	Incheon City, Korea	35.3	Max: 124.87
Jalaludin et al. (2004, 056595)	Sydney, Australia	22.8	75th: 122.8
Jansen et al. (2005, 082236)	Seattle, WA	18.0	Max: 51

Study	Location	Mean Concentration ($\mu\text{g}/\text{m}^3$)	Upper Percentile Concentrations ($\mu\text{g}/\text{m}^3$)
Johnston et al. (2006, 091386)	Darwin, Australia	20	Max: 43.3
Just et al. (2002, 035429)	Paris, France	23.5	Max: 44.0
Lagorio et al. (2006, 089800)	Rome, Italy	42.8	Max: 123
Laurent et al. (2008, 156672)	Strasbourg, France	20.8	Max: 106.3
Lee et al. (2007, 093042)	Seoul, South Korea	71.40	75th: 87.54 Max: 148.34
Mar et al. (2004, 057309)	Spokane, WA	16.8-24.5	NR
Mortimer et al. (2002, 030281)	Multicity, U.S.	53	NR
Moshhammer et al. (2006, 090771)	Linz, Austria	8-h avg: 24.85	Max 24-h: 76.39
Odajima et al. (2008, 192005)	Fukuoka, Japan	3-h avg: 32.6-41.5	Max 3-h avg: 126.0-191.3
Peacock et al. (2003, 042026)	Southern England	21.2	Max: 87.9
Peled et al. (2005, 156015)	Multicity, Israel	31.0-67.1	NR
Preutthipan et al. (2004, 055598)	Bangkok, Thailand	111.0	Max: 201
Rabinovitch et al. (2004, 096753)	Denver, CO	28.1	Max: 102.0
Ségala et al. (2004, 090449)	Paris, France	24.2	Max: 97.4
Schildcrout et al. (2006, 089812)	Multicity, U.S.	17.7-32.4 ^a	75th: 26.2-42.7 90th: 32.5-53.9
Slaughter et al. (2003, 086294)	Seattle, WA	21.0 ^a	75th: 29.3
Steinvil et al. (2008, 188893)	Tel Aviv, Israel	64.5	75th: 60.7
von Klot et al. (2002, 034706)	Erfurt, Germany	45.4	75th: 59.7 Max: 172.4

^aMedian

^bIncludes UFP, for complete information on number concentration from this study, please see corresponding table in Annex E.

Mar et al. (2004, [057309](#)) studied asthmatic children (n = 9) in Spokane, WA. Increases in 0-, 1- or 2-day lags of each of the PM size classes studied were associated with cough. When all lower respiratory tract symptoms (wheeze, cough, shortness of breath, sputum production) were grouped together, positive associations were reported for each 10 $\mu\text{g}/\text{m}^3$ increase in same-day PM₁₀ (OR 1.07 [95% CI: 1.00-1.14]), or lag 0 or lag 1 PM_{2.5} (OR 1.18 [95% CI: 1.00-1.38]; OR 1.21 [95% CI: 1.00-1.46], respectively), and 10 $\mu\text{g}/\text{m}^3$ increase in lag 0 and lag 1 PM_{1.0} (OR 1.21 [95% CI: 1.01-1.44]; OR 1.25 [95% CI: 1.01-1.55], respectively). No associations were reported for PM_{10-2.5} and grouped lower respiratory tract symptoms (Mar et al., 2004, [057309](#)).

Gent et al. (2003, [052885](#)) reported on daily symptom and medication use during one summer for 271 asthmatic children living in southern New England. In single-pollutant models for users of maintenance medication (n = 130), PM_{2.5} $\geq 19 \mu\text{g}/\text{m}^3$ lagged by 1 day was associated with a 10-25% increase in risk of symptoms compared to PM_{2.5} $< 6.9 \mu\text{g}/\text{m}^3$: OR for persistent cough 1.12 (95% CI: 1.02-1.24); OR for chest tightness 1.21 (95% CI: 1.00-1.46); OR for shortness of breath 1.26 (95% CI: 1.02-1.54). Effects were attenuated in models including O₃ (OR for persistent cough 1.00 [95% CI: 0.88-1.15]; OR for chest tightness 0.91 [95% CI: 0.71-1.17]; OR for shortness of breath 1.20 [95% CI: 0.94-1.52]). No statistical associations between ambient particle exposure and respiratory health were found for asthmatic children not on maintenance medication.

Annual PM_{2.5} levels at monitoring sites in New Haven, CT exceed the annual standard of 15 $\mu\text{g}/\text{m}^3$. Gent et al. (2009, [180399](#)) conducted a study here to examine the associations between daily exposure to PM_{2.5} components and sources identified through source apportionment, and daily symptoms and medication use in asthmatic children. Asthmatic children (n = 149) aged 4-12 yr were enrolled in the study between 2000 and 2003. Factor analysis was used to identify six sources of PM_{2.5} (motor vehicle, road dust, sulfur, biomass burning, oil, and sea salt). Total PM_{2.5} was not associated with any symptoms or medication use; however trace elements originating from motor vehicle, road dust, biomass burning and oil sources were associated with symptoms and/or

medication use. For example, an increased risk of wheeze, shortness of breath, chest tightness or short-acting inhaler use was associated with increasing EC mass concentration. Risks remain in models that include all six PM_{2.5} sources as well as NO₂, which may be considered a marker for traffic. NO₂ was found to be an independent risk factor for increased wheeze.

Two panel studies were conducted over the course of three winters at a school in Denver (Rabinovitch et al., 2004, [096753](#); 2006, [088031](#)). In the first report, approximately 86 different children contributed data on asthma symptoms and medication use over three consecutive winters (Rabinovitch et al., 2004, [096753](#)). The exposure metric was the 3-day average concentration of PM_{2.5} measured at a site located next to the school for the first two winters and from a central site located 4.8 km (3 miles) away for the third. A strong correlation was observed during the first two winters between PM_{2.5} values measured locally and at a downtown monitoring station (Pearson product-moment correlation = 0.93) and between PM₁₀ values measured locally and at a downtown monitoring station (correlation = 0.84). Therefore, in year 3, all ambient data were collected from nearby community monitoring stations. No statistical associations were found between asthma symptoms or medication use and PM. Rabinovitch et al. (2006, [088031](#)) enrolled a panel of 73 children and evaluated associations with morning maximum PM_{2.5} measured at the central site. PM measurements were available hourly from two co-located monitors, an FRM and a TEOM monitor. Each 10 µg/m³ increase in morning maximum 1-h PM_{2.5} concentration was associated with an increased likelihood of rescue medication use (OR for FRM 1.02 [95% CI: 1.01-1.03]; OR for TEOM 1.03 [95% CI: 1.00-1.6]). Interestingly, the association between inhaler use and particle exposure was not evident when the 24-h avg PM_{2.5} was used in the model.

Two smaller panel studies enrolling asthmatic children conducted by Delfino et al. (2002, [093740](#); 2003, [050460](#)) in southern California examined the health effects of different averaging times for PM₁₀ (1-h, 8-h, 24-h) (Delfino et al., 2002, [093740](#)), and 24-h avg of two PM₁₀ components (EC and OC) (Delfino et al., 2003, [050460](#)). In the first study, 22 children living in a “lower” pollution area were followed daily for two months in spring. In contrast with Gent et al. (2003, [052885](#)), positive statistical associations with asthma symptoms (measured on a 6-point severity scale) were found only for the children not taking anti-inflammatory medication. For these 12 children, in single-pollutant models each 10 µg/m³ increase in lag 0 1-h max PM₁₀ nearly doubled the risk of clinically meaningful symptoms (i.e., an asthma symptom score ≥3) (OR 1.14 [95% CI: 1.04-1.24]) and each 10 µg/m³ increase in 3-day avg 24-h PM₁₀ increased the risk by 1.25 (95% CI: 1.06-1.48). No statistical associations were found between exposure to ambient particles and symptoms in the ten children who were taking anti-inflammatory medication. No multipollutant models were reported. The second study enrolled 22 asthmatic children living in an area of higher pollution. For children living in this community, each 10 µg/m³ increase in lag 0, 24-h PM₁₀ was associated with an increased risk of asthma symptom score >1: OR 1.10, (95% CI: 1.03-1.19) (Delfino et al., 2003, [050460](#)). The correlation among PM₁₀, EC and OC was substantial: 0.80 between PM₁₀ and either EC or OC, and 0.94 between EC and OC. Associations between EC or OC and asthma symptoms were very similar to those for PM₁₀: each 3 µg/m³ increase in lag 0, 24-h EC or 5 µg/m³ increase in lag 0, 24-h OC was associated with an increased risk of asthma symptoms (OR 1.85 [95% CI: 1.11-3.08] or OR 1.88 [95% CI: 1.12-3.17], respectively) (Delfino et al., 2003, [050460](#)).

The association between incident wheezing symptoms and air pollution was assessed in the Copenhagen Prospective Study of Asthma in Children among a birth cohort of 205 children in Copenhagen, Denmark. In addition to PM₁₀ and other gaseous air pollutants, the study examined UFP concentrations collected from a central background monitoring station. This is the only study identified that examined the association between UFPs and respiratory symptoms in children. There were strong adverse effects for PM₁₀ and UFPs, as well as for NO₂, NO_x, and CO for wheezing symptoms in infants which attenuated after the age of 1 yr (lag 2-4 PM₁₀ OR 1.21 (95% CI 0.99-1.48); lag 2-4 UFP OR 1.92 (95% CI: 0.98-3.76)). These associations remained in copollutant models including NO₂, NO_x and CO.

Studies from Australia (Rodriguez et al., 2007, [092842](#)), Europe (Andersen et al., 2008, [096150](#); Laurent et al., 2008, [156672](#); Laurent et al., 2009, [192129](#); Ranzi et al., 2004, [089500](#)), and Asia (Aekplakorn et al., 2003, [089908](#)) provide additional evidence of an association between ambient PM and respiratory symptoms and/or medication use among asthmatic children. Two studies (Jalaludin et al., 2004, [056595](#); Just et al., 2002, [035429](#)) found no association between ambient PM levels and these health endpoints.

Asthmatic Adults

Since the 2004 PM AQCD (U.S. EPA, 2004, [056905](#)), one U.S. and several European studies have investigated the effects of ambient PM levels on respiratory symptoms and medication use among asthmatic adults. The respiratory symptom and medication use results from these studies are summarized by particle size and displayed in Table 6-10 and Figure 6-8. Relatively few studies examined these effects in healthy adults, and they did not identify a relationship between ambient PM levels and respiratory symptoms or medication use. These studies of healthy adults are summarized in Annex E, but will not be described in detail in this section.

Mar et al. (2004, [057309](#)) studied asthmatic adults ($n = 16$) in Spokane, WA over a 3-yr time period. No associations were found between PM and respiratory symptoms among the adults.

Several panel studies conducted in Europe have examined effects of daily exposures to air pollution on adults with asthma, including studies in the Pollution Effects on Asthmatic Children in Europe (PEACE) study (Boezen et al., 2005, [087396](#)), Exposure and Risk Assessment for Fine and UFPs in Ambient Air (ULTRA) study (De Hartog et al., 2003, [001061](#)), in Germany (Von et al., 2002, [034706](#)), and in Paris (Desqueyroux et al., 2002, [026052](#); 2004, [090449](#)). Boezen et al. (2005, [087396](#)) enrolled 327 elderly adults in the Netherlands to examine the role of airway hyperresponsiveness (AHR) and IgE levels in susceptibility to air pollution. For subjects with both AHR (defined as $\geq 20\%$ FEV₁ decline at ≤ 2 mg cumulative methacholine [Mch]) and high total IgE (>20 kU/L), each $10 \mu\text{g}/\text{m}^3$ increase in lag 2 PM₁₀ concentration was associated with an increased risk of upper respiratory symptoms (URS) among males (OR 1.06 [95% CI: 1.02-1.10]), and at lag 0 with increased cough among females (OR 1.04 [95% CI: 1.00-1.08]). Each $10 \mu\text{g}/\text{m}^3$ increase in BS at lag 0, lag 1, and the 5-day mean was associated with URS and cough among males. The strongest association in both cases was for the 5-day mean (OR for URS 1.43 [95% CI: 1.20-1.69]; OR for cough 1.16 [95% CI: 1.05-1.29]). The authors suggest that the sex differences observed may be explained by differential daily exposure to traffic exhaust experienced by men compared to women (Boezen et al., 2005, [087396](#)).

As part of the multicenter ULTRA study, de Hartog et al. (2003, [001061](#)) enrolled 131 older adults with coronary artery disease in three cities (Amsterdam, Erfurt [Germany], and Helsinki). Pooling data from all 3 cities, associations were observed between PM_{2.5} and shortness of breath and phlegm: each $10 \mu\text{g}/\text{m}^3$ increase in the 5-day avg PM_{2.5} was associated with an increased risk of symptoms (OR for shortness of breath 1.12 [95% CI: 1.02-1.24]; OR for phlegm 1.16 [95% CI: 1.03-1.32]). Unlike fine particles, UFPs were not consistently associated with symptoms.

In a study that took place in Erfurt, Germany, von Klot et al. (2002, [034706](#)) examined daily, winter time exposure to ambient PM_{10-2.5}, PM_{2.5-0.01} and PM_{0.1-0.01} and respiratory health effects in 53 adult asthmatics. The authors examined associations between wheeze, use of inhaled, short-acting β_2 -agonists or inhaled corticosteroids and exposure to particles in single and multipollutant models. Particle exposure metrics examined included same-day, 5-day and 14-day average concentrations. No effects were observed for wheeze and exposure to PM_{10-2.5} for any averaging time. The strongest association between wheeze and exposure to UFPs was for a 14-day avg: each 7,700 increase in the NC_{0.01-0.1} increased the risk of wheeze by 27% (OR 1.27 [95% CI: 1.13-1.43]). The effect was attenuated in copollutant models that also included PM_{2.5-0.01} (OR 1.12 [95% CI: 1.01-1.24]), NO₂ (OR 1.12 [95% CI: 0.99-1.26]), CO (OR 1.05 [95% CI: 0.92-1.19]) or SO₂ (OR 1.14 [95% CI: 1.04-1.26]). The correlations between UFPs and two gaseous pollutants, NO₂ and CO, were high: 0.66 for each.

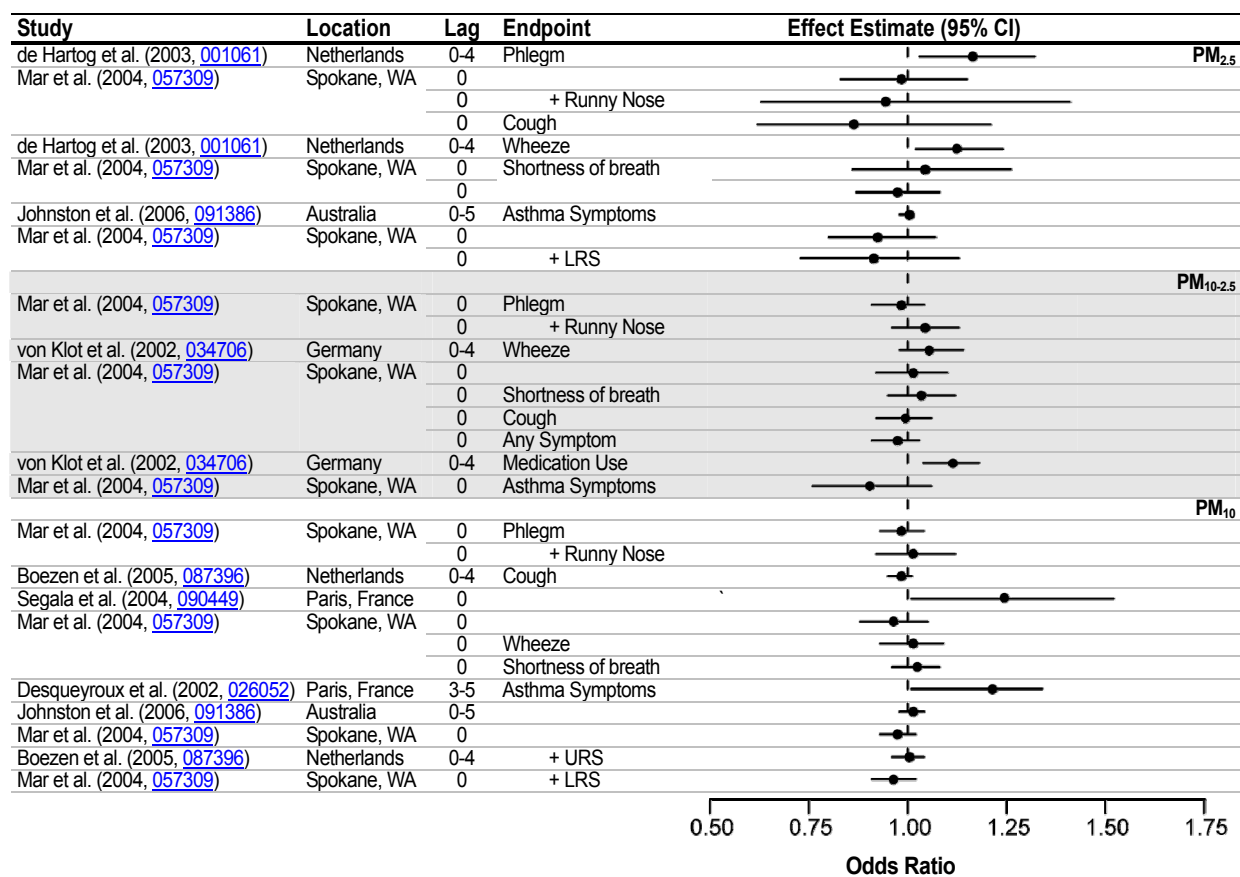


Figure 6-8. Respiratory symptoms and/or medication use among asthmatic adults following acute exposure to particles. Summary of studies using 24-h avg of PM₁₀, PM_{2.5}, PM_{10-2.5}. ORs and 95% CIs were standardized to increments of 10 µg/m³.

In the same study, no association was found between exposure to PM_{10-2.5}, PM_{2.5}, or UFPs and use of short-acting inhalers, though there was an association with maintenance medication. Increased likelihood of maintenance medication was significantly associated with PM of all sizes and all averaging times (same-day, 5- and 14-day avg) and gaseous copollutants in single or copollutant models. The strongest effects were seen for 14-day avg of PM_{10-2.5} (for each 10 µg/m³ increase OR 1.43 [95% CI: 1.28-1.60]), PM_{2.5-0.01} (for each 20 µg/m³ increase OR 1.54 [95% CI: 1.43-1.66]), NC_{0.01-0.1} (for each 7,700 increase OR 1.45 [95% CI: 1.29-1.63]). For PM_{2.5-0.01}, effects were unchanged in copollutant models, including a model with UFPs. The authors conclude that this is evidence for independent effects of PM_{2.5} and UFPs (Von et al., 2002, [034706](#)).

In Paris, Segala et al. (2004, [090449](#)) recruited 78 adults from an otolaryngology clinic and followed them for three months. Both PM₁₀ and BS (which were highly correlated [r = .88]) were associated with cough: OR 1.24 (95% CI: 1.01-1.52) for a 10 µg/m³ increase in mean 0-4 day PM₁₀ and OR 1.18 (95% CI: 1.02-1.39) for a 10 µg/m³ increase in BS.

Also in Paris, 60 severe asthmatics were followed for 13 months and the relationship between daily air quality (including 24-h PM₁₀ as measured at the site nearest to the subject's home) and asthma attack (defined as the need to increase rescue medication use and one or more positive signs on clinical exam of wheezing, expiratory brake, thoracic distention, hypertension with tachycardia, polypnea) were examined with GEE models (Desqueyroux et al., 2002, [026052](#)). Each 10 µg/m³ increase in PM₁₀ increased the risk of asthma attack, but only after lags of 3-5 days. The strongest effect was seen for the mean lag of days 3-5 (OR 1.21 [95% CI: 1.04-1.40]). Effect sizes were larger among patients not on regular oral steroid therapy: for PM₁₀ lag 3-5 (OR 1.41 [95% CI: 1.15-1.73]). This effect persisted in copollutant models for winter time levels of PM₁₀ and SO₂ (OR 1.51 [95%

CI: 1.20-1.90]) or NO₂ (OR 1.43 [95% CI: 1.16-1.76]), but not in summer time models with O₃ (OR 1.09 [95% CI: 0.71-1.67]).

Copollutant Models

A limited number of respiratory symptoms studies reported results of copollutant models. Generally, the associations between respiratory symptoms and PM were robust to the inclusion of copollutants (Figure 6-9), though Desqueyroux et al. (2002, [026052](#)) indicate the effects of PM may be potentiated by NO₂ and SO₂ during the winter months. Gent et al. (2003, [052885](#)) also reported the results of copollutant models, though the categorical exposure groups used in the analysis did not allow these results to be included in Figure 6-9. As reported above, the investigators found that effects were attenuated in models including O₃.

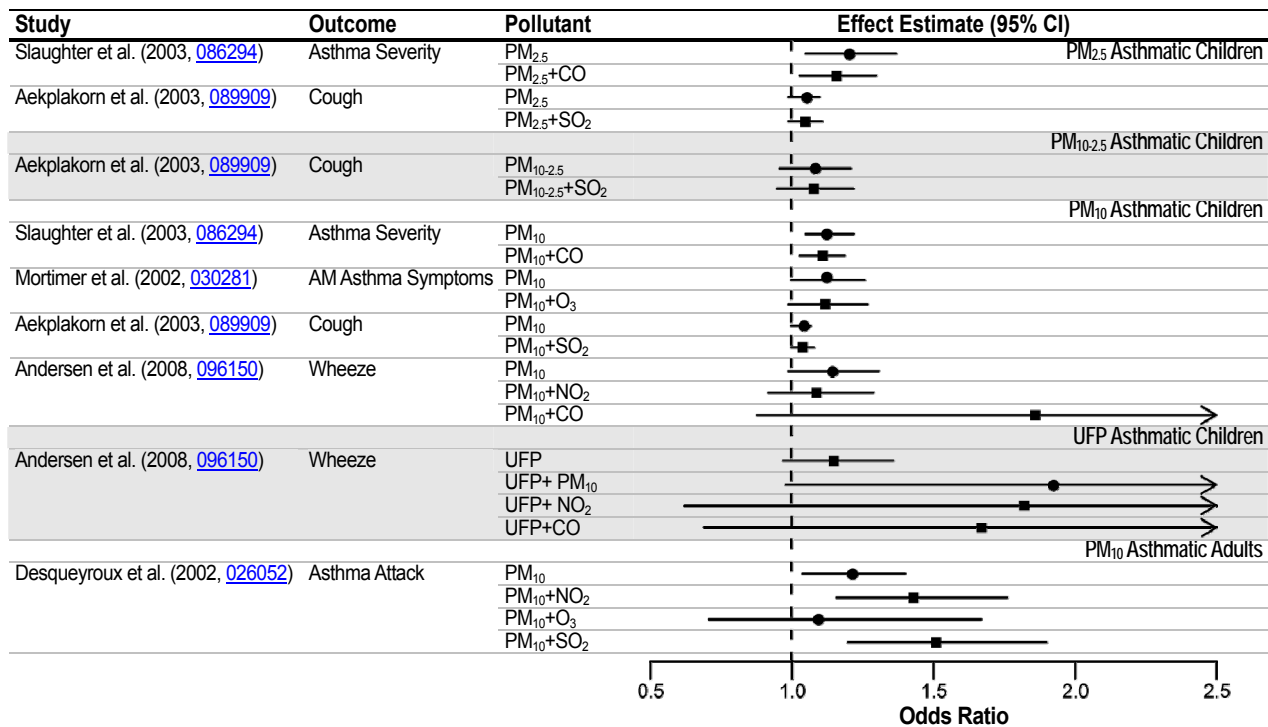


Figure 6-9. Respiratory symptoms following acute exposure to particles and additional criteria pollutants. Circles represent single pollutant effect estimates and squares represent copollutant effect estimates.

6.3.1.2. Controlled Human Exposure Studies

CAPs

Neither new controlled human exposure studies nor studies cited in the 2004 PM AQCD (U.S. EPA, 2004, [056905](#)) have found significant effects of CAPs on respiratory symptoms among healthy or asthmatic adults, or among older adults with COPD (Gong et al., 2000, [155799](#); 2003, [042106](#); 2004, [087964](#); 2004, [055628](#); 2005, [087921](#); 2008, [156483](#); Petrovic et al., 2000, [004638](#)).

Urban Traffic Particles

One new study reported an increase in respiratory symptoms (upper and lower airways) among healthy volunteers (19-59 yr) during a 2-h exposure to road tunnel traffic (PM_{2.5} concentration 46-81 µg/m³) (Larsson et al., 2007, [091375](#)). However, information on specific respiratory symptoms (e.g., throat irritation, wheeze or chest tightness) was not provided. In addition, this study only evaluated respiratory symptoms pre- versus post-exposure, and did not compare response with a filtered air control exposure.

Diesel Exhaust

Respiratory symptoms including mild nose and throat irritation have been reported following controlled exposure to DE; however, other symptoms such as cough, wheeze and chest tightness have not been observed (Mudway et al., 2004, [180208](#)).

Model Particles

Pietropaoli et al. (2004, [156025](#)) found no association between exposure to UF carbon particles and respiratory symptoms in healthy adults at concentrations between 10 and 50 µg/m³, or asthmatics at a concentration of 10 µg/m³. Beckett et al. (2005, [156261](#)) exposed healthy subjects to UF and fine ZnO (500 µg/m³) and observed no difference in respiratory symptoms compared to filtered air control 24 h following exposure. In a study evaluating respiratory effects of exposure to ammonium bisulfate or aerosolized H₂SO₄ (200 and 2,000 µg/m³) among healthy and asthmatic adults, Tunnicliffe et al. (2003, [088744](#)) observed no change in respiratory symptoms with either particle type or concentration relative to filtered air. This finding is in agreement with many similar older studies which have generally reported no increase in respiratory symptoms following exposure to acid aerosols at concentrations <1,000 µg/m³ (U.S. EPA, 1996, [079380](#); 2004, [056905](#)).

Summary of Controlled Human Exposure Study Findings for Respiratory Symptoms

These new studies confirm previous reports that have found no association between PM exposure and respiratory symptoms.

6.3.2. Pulmonary Function

Epidemiologic studies cited in the 2004 PM AQCD (U.S. EPA, 2004, [056905](#)) observed small decrements in pulmonary function associated with both PM_{2.5} and PM₁₀ (U.S. EPA, 2004, [056905](#)). The majority of controlled human exposure studies reported no effect of PM on pulmonary function, while the results from toxicological studies were mixed, with some evidence of changes in tidal volume and respiratory rate following exposure to CAPs. Epidemiologic studies published since the 2004 PM AQCD (U.S. EPA, 2004, [056905](#)) have reported an association between PM_{2.5} concentration and decrements in forced expiratory volume in one second (FEV₁), particularly among asthmatic children. These findings are coherent with recent toxicological evidence of AHR following CAPs exposure. Results from recent controlled human exposure studies have been inconsistent, with some studies demonstrating small decreases in arterial oxygen saturation, FEV₁ or maximal mid-expiratory flow following exposure to CAPs or EC. It is interesting to note that these effects appear to be more pronounced among healthy adults than adults with asthma or COPD. A number of recent animal toxicological studies demonstrated alterations in respiratory frequency following short-term exposure to CAPs.

6.3.2.1. Epidemiologic Studies

The 2004 PM AQCD (U.S. EPA, 2004, [056905](#)) concluded that both PM_{2.5} and PM₁₀ appeared to affect lung function in asthmatics. A limited number of studies evaluated UFPs and found them to be associated with a decrease in peak expiratory flow (PEF). Few analyses were able to clearly distinguish the effects of PM_{2.5} and PM₁₀ from other pollutants. Results for PM₁₀ PEF analyses in non-asthmatic studies were inconsistent, with fewer studies reporting strong associations.

Asthmatic Children

Several recent panel studies have been conducted in the U.S. examining the association of exposure to ambient PM and lung function in asthmatic children (Allen et al., 2008, [156208](#) in Seattle; Lewis et al., 2003, [088413](#) in Southern California; 2004, [097498](#); Lewis et al., 2005, [081079](#) in Detroit; O'Connor et al., 2008, [156818](#); Rabinovitch et al., 2004, [096753](#) in Denver). Mean concentration data from these studies are summarized in Table 6-10. In the Inner-City Asthma Study (ICAS), FEV₁ and PEF tidal were statistically related to the 5-day avg of PM_{2.5} but not to the 1-day avg concentration (O'Connor et al., 2008, [156818](#)). The risk of experiencing a percent-predicted FEV₁ more than 10% below personal best was related to the 5-day avg concentration of PM_{2.5} (1.14 [95% CI: 1.01-1.29]). The risk of experiencing a percent-predicted PEF rate more than 10% below personal best was related to PM_{2.5} (1.18 [95% CI: 1.03-1.35]). This effect remained robust in copollutant models with O₃ and NO₂ for the FEV₁ effect, but not the PEF rate effect.

The Denver study (Rabinovitch et al., 2004, [096753](#)), described in Section 6.3.1.1, also examined daily FEV₁ and PEF in 86 asthmatic children over the course of three winters (some subjects participated in more than one winter). Lung function measurements were performed under supervision daily at the elementary school where all subjects attended, and without supervision every evening and on nonschool days. As described above, the authors chose to use a 3-day moving average of 24-h PM_{2.5} or PM₁₀ as the exposure metric. No statistical associations were observed between morning or afternoon FEV₁ or PEF and particle exposure. The same group of researchers (Strand et al., 2006, [089203](#)) used regression calibration to estimate personal exposures to ambient PM_{2.5} and found that a 10 µg/m³ increase in PM_{2.5} was associated with a 2.2% (95% CI: 0.0-4.3) decrease in FEV₁ at a 1-day lag as compared with the estimate of a 1.0% decrease in FEV₁ using ambient PM_{2.5} concentrations from fixed monitors. These results underscore the effects of exposure error on epidemiologic study results; the effect estimate using an estimate of personal exposure to ambient PM_{2.5} was twice that for central site PM_{2.5}.

From winter 2001 to the spring of 2002, the same number (n = 86) of primary school-age asthmatic children participated in six 2-wk seasonal assessments of lung function in Detroit (Lewis et al., 2005, [081079](#)). Using a protocol similar to that used in Rabinovitch et al. (2004, [096753](#)), morning lung function measurements (FEV₁, PEF) were self-administered at school under supervision by research staff. Evening and weekend measurements were recorded by subjects at home, without supervision from research staff. Community-level exposure was assessed using monitors placed on a school roof top of both of the communities. Most of the subjects (82 of 86) lived within 5 km of their respective community monitors. In single-pollutant models using GEE and only among children reporting the use of maintenance medication (corticosteroids), each 10 µg/m³ increase in lag 2 PM₁₀ was associated with a decrease in the lowest daily percent predicted FEV₁ (a reduction of 1.15%, [95% CI: -2.1 to -0.25]). Among children reporting presence of URI on the day of lung function measurement, increases in the average of lag 3-5 of either PM_{2.5} or PM₁₀ resulted in a decrease in the lowest daily FEV₁ (for a 10 µg/m³ increase in PM_{2.5} the reduction was 2.24% [95% CI: -4.4 to -0.25]; and for a 10 µg/m³ increase in PM₁₀ the reduction was 2.4% [95% CI: -4.5 to -0.3]). In copollutant models that included one particle pollutant and O₃, and among children using maintenance medication, lag 3-5 PM_{2.5} continued to be associated with lowest daily FEV₁ as well as diurnal FEV₁ variability: each 10 µg/m³ increase was associated with a 2.23% decrease in FEV₁ (95% CI: -3.92 to -0.57) and a 2.22% increase in FEV₁ variability (95% CI: 1.0 to 3.50). Increases in lag 1 or lag 2 of PM₁₀ were associated with FEV₁ and FEV₁ diurnal variability in copollutant models. The strongest association was with lag 2 for diurnal variability (for each 10 µg/m³ increase variability increased by 7.0% [95% CI: 4.2-9.6]). It is unclear what role the lack of supervision during the evening and weekend measures may have had on these diurnal results.

Two panel studies in southern California examined the association of PM exposure on lung function in asthmatic children (Delfino et al., 2003, [050460](#); 2004, [056897](#)). In Delfino et al. (2003,

[050460](#)), described above, no association between exposure to particles and PEF was found for 22 Hispanic, asthmatic children living in an area of relatively high pollution. In Delfino et al. (2004, [056897](#)) 19 asthmatic children, aged 9-17 yr, were followed for 2 weeks and daily, self-administered FEV₁ measurements were taken. Particle exposures studied included central-site PM₁₀ in addition to personal PM (in the range of 0.1-10 μm range, with the highest response in the fine PM range), and home stationary measurements of both PM_{2.5} and PM₁₀. The authors report inverse associations between percent expected FEV₁ and PM indicators. The strongest association for exposure to personal PM was for a 5-day moving average of 12-h daytime PM: for each 10 μg/m³ increase, FEV₁ decreased by 7.1% (95% CI: -9.9 to -2.9). Effects for all stationary sites (inside and outside of residence, central site) for PM_{2.5} were on the order of 1-2% reductions in FEV₁, with the strongest associations for the 5-day moving average (presented in figures only). Likewise for PM₁₀ measured at stationary sites, the strongest effects were for the 5-day moving average and ranged from approximately 3.8% reduction associated with indoor monitors to about 1.5% for both the outdoor and central site monitors (presented in figures only). A helpful comparison among all 24-h measures is given for 10 μg/m³ increases in personal PM and PM_{2.5} associated with decreases in percent predicted FEV₁: an increase of 10 μg/m³ personal PM is associated with a decrease in FEV₁ of 3.0% (95% CI: -5.6 to -0.5); 10 μg/m³ increase in indoor PM with 2.4% decrease (95% CI: -4.2 to -0.6); 10 μg/m³ increase in outdoor PM with 1.5% decrease (95% CI: -3.4 to 0.1); 10 μg/m³ increase in central site PM with 0.9% decrease (95% CI: -2.6 to 0.5).

Trenga et al. (2006, [155209](#)) reported associations among personal, residential, and central site PM_{2.5} and lung function in 17 asthmatic children in Seattle. The only statistical association with decline in FEV₁ was with indoor measurements of PM_{2.5}: each 10 μg/m³ increase in lag 1 indoor PM_{2.5} was associated with a decline in FEV₁ of 64.8 mL (95% CI: -111.3 to 18.3) (a 3.4% decline from the mean of 1.9 L). Indoor PM_{2.5} (lag 1) was also associated with declines in PEF (by 9.2 L/min [95% CI: -17.5 to -0.9], a 3.6% decline from the 254 L/min avg) and in maximal mid-expiratory flow (MMEF) for the six subjects not taking anti-inflammatory medication (by 12.6 L/min [95% CI: -20.7 to -4.6], a 13.7% decline from the 92 L/min avg). Personal PM_{2.5} (lag 1) was only statistically associated with PEF for the six subjects not on anti-inflammatory medication: each 10 μg/m³ increase resulted in a 10.5 L/min ([95% CI: -18.7 to -2.3], a 4.5% decline from the 233 L/min avg) reduction in PEF. Anti-inflammatory medication use attenuated associations with PM_{2.5}.

Also in Seattle, Allen et al. (2008, [156208](#)) evaluated the effect of different PM_{2.5} exposure metrics in relation to lung function among children in wood smoke-impacted areas. The authors found that the ambient-generated component of PM_{2.5} exposure was associated with decrements in lung function only among children not using inhaled corticosteroids, whereas no association was reported with the nonambient exposure component. All of the ambient concentrations were associated with decrements in both PEF and maximal expiratory flow (MEF). There were no associations between any exposure metrics and forced vital capacity (FVC). The authors suggest that lung function may be especially sensitive to the combustion-generated component of ambient PM_{2.5}, whereas airway inflammation may be more closely related to some other source.

In a longitudinal study, Liu et al. (2009, [192003](#)) examined the association between acute increases in ambient air pollutants and pulmonary function among children (ages 9-14 yr) with asthma. FEV₁ and FEF_{25-75%} exhibited a consistent trend of negative associations with PM_{2.5} across lag days 0, 1, 0-1, and 0-2, with the strongest effects for FEF_{25-75%} on lag day 0 (-1.12% [95% CI: -2.06 to -0.18]) and lag days 0-1 (-1.18% [95% CI: -2.24 to -0.12]). Copollutant models including O₃, SO₂ or NO₂ did not result in marked changes in the PM_{2.5} risk estimates for FEV₁ or FEF_{25-75%}.

Moshhammer and Neuberger (2003, [041956](#)) used a novel technique for assessing exposure to PM in a study they conducted in Austria. They employed a diffusion charging particle sensor (model LQ 1-DC, Matter Engineering AG, Wohlen, Switzerland) and a photoelectric aerosol sensor (model PAS 2000 CE, EcoChem Analytics, League City, TX) to relate the spirometry scores of Upper Austrian children, aged 7-10 yr, to particle surface area and particle-bound PAH concentration, respectively. Details on these methods for measuring surface area and PAH can be found in Shi et al. (2001, [078292](#)) and Burtscher (2005, [155710](#)), respectively. By measuring the surface area distribution, it was possible to understand potential for contact area with respiratory tract cells. The authors found that acute decrements of pulmonary function (FVC, FEV₁, MEF₅₀) were related to the active surface of particles after adjustment for PM₁₀. For short-term lung impairments, this indicates that active particle surface is a better index of exposure than PM mass.

A number of additional panel studies conducted outside of the U.S. and Canada also examined lung function using more traditional exposure metrics. Several European and Asian studies reported

associations with PM measurements and decrements in pulmonary function (FEV₁, FVC, FEF, MEF, PEF rate) (Hogervorst et al., 2006, [156559](#); Hong et al., 2007, [091347](#); Moshhammer et al., 2006, [090771](#); Odajima et al., 2008, [192005](#); Peacock et al., 2003, [042026](#); Peled et al., 2005, [156015](#)). Others found little evidence for a relationship between PM and daily changes in PEF after correction for the confounding effects of weather, trends in the data, and autocorrelation (Fischer et al., 2002, [025731](#); Holguin et al., 2007, [099000](#); Just et al., 2002, [035429](#); Preutthipan et al., 2004, [055598](#); Ranzi et al., 2004, [089500](#); Ward, 2003, [157111](#)).

Adults

Trenga et al. (2006, [155209](#)) examined personal, residential, and central site monitoring of particles and the relationship with lung function in Seattle. In models controlling for gaseous copollutants (CO, NO₂), adults, regardless of COPD status, experienced a decline in FEV₁ associated only with measurements of PM_{2.5} at the central site: each 10 µg/m³ increase in lag 0 PM_{2.5} was associated with a 35.3 mL (95% CI: -70 to -1.0) decrease in FEV₁. This represents a 2.2% decline in mean FEV₁ (mean 1.6 L during the study). Results for personal, indoor and outdoor measures of PM_{2.5} were inconsistent. No statistical associations were reported with outdoor PM_{10-2.5}.

Girardot et al. (2006, [088271](#)) assessed the effects of PM_{2.5} on the pulmonary function of adult day hikers in the Great Smoky Mountains National Park. Hikers performed spirometry both before their hike and when they returned from their hike. The authors reported no statistically significant responses in pulmonary function with an average of five hours of outdoor exercise at ambient PM_{2.5} levels that were below the current NAAQS. Specifically, post-hike percentage changes in FVC, FEV₁, FEV₁/FVC, FEF₂₅₋₇₅, and PEF were not associated with PM_{2.5} exposure.

Ebelt et al. (2005, [056907](#)) developed an approach to separately estimate exposures to PM of ambient and non-ambient origin based on a mass balance model. These exposures were linked with respiratory and cardiovascular health endpoints for 16 patients with COPD in Vancouver, Canada (mean age 74 yr). Effect estimates for estimated ambient exposure were generally equal to or larger than those for the respective ambient concentration levels for post-FEV and ΔFEV₁, and were statistically significant for all ΔFEV₁ comparisons (estimated from figure).

Several studies outside of the U.S. and Canada examined the relationship between PM concentrations and lung function and all reported a decrease in lung function in adults (FEV₁, FVC, PEF) associated with PM exposure (Boezen et al., 2005, [087396](#); Bourotte et al., 2007, [150040](#); Lagorio et al., 2006, [089800](#); Lee et al., 2007, [093042](#); McCreanor et al., 2007, [092841](#); Penttinen et al., 2006, [087988](#)).

Measures of Oxygen Saturation

Oxygen saturation measures the percentage of hemoglobin binding sites in the bloodstream occupied by oxygen. DeMeo et al. (2004, [087346](#)) estimated the change in oxygen saturation and mean PM_{2.5} concentration in the previous 24 h in a panel of elderly subjects. They used the same panel of elderly Boston residents (n = 28) and study protocol and analytic methods (12 wk of repeated oxygen saturation measurements) as Gold et al. (2005, [087558](#)) and Schwartz et al. (2005, [074317](#)) in studies of ST-segment depression and HRV, respectively. At each clinic visit, subjects had 5 min each of rest, standing, post-exercise rest, and 20 cycles of paced breathing. The median PM_{2.5} concentration during the study period was 10.0 µg/m³ (Schwartz et al., 2005, [074317](#)). Each 10 µg/m³ increase in the mean PM_{2.5} concentration in the previous 6 h was associated with a 0.15% decrease in oxygen saturation (95% CI: -0.22 to 0.0) during the baseline rest period. Each 10 µg/m³ increase in mean 6-h PM_{2.5} concentration was also associated with a decline in oxygen saturation during the post-exercise period (-0.15% [95% CI: -0.22 to 0.0]), and post-exercise paced breathing period (-0.07% [95% CI: -0.22 to 0.0]), but not during the exercise period. The authors suggest that these oxygen saturation reductions may result from pulmonary vascular and inflammatory changes.

In a similar study, Goldberg et al. (2008, [180380](#)) examined the association between oxygen saturation, pulse rate, and ambient PM_{2.5}, NO₂, and SO₂ concentrations in a panel of 31 subjects in Montreal, with NYHA Class II or III heart failure who were aged 50-85 yr. Although each 10 µg/m³ increase in PM_{2.5} on lag day 0 was associated with a -0.119 (95% CI = -0.196 to -0.042) change in oxygen saturation in unadjusted models, once adjusted for temperature and barometric pressure, the estimated change was smaller and no longer significant (-0.077 [95% CI = -0.160 to 0.007]). Only

SO₂ was significantly associated with reduced oxygen saturation in copollutant models. None of the pollutants examined, including PM_{2.5}, were associated with a change in pulse rate.

6.3.2.2. Controlled Human Exposure Studies

As with respiratory symptoms, there is little evidence from controlled human exposure studies of PM-induced changes in pulmonary function. One study cited in the 2004 PM AQCD (U.S. EPA, 2004, [056905](#)) noted a significant decrement in thoracic gas volume in healthy adults following a 2-h exposure to PM_{2.5} CAPs (92 µg/m³); however, no significant changes were observed in spirometric measurements, diffusing capacity (DLCO), total lung capacity, or airways resistance (Petrovic et al., 2000, [004638](#)). Other studies found no significant changes in pulmonary function in healthy adults following exposure to inhaled iron oxide particles (Lay et al., 2001, [020613](#)) or UF EC (Frampton, 2001, [019051](#)), or in healthy and asthmatic adults following exposure to CAPs (Ghio et al., 2000, [012140](#); Gong et al., 2000, [155799](#); 2003, [087365](#)). Rudell et al. (1996, [056577](#)) reported a significant increase in specific airways resistance following exposure to DE, an effect that was not attenuated by reducing the particle number by 46% (2.6×10^6 particles/cm³ compared with 1.4×10^6 particles/cm³) using a particle trap. The particle trap did not affect the concentrations of other measured diesel emissions including NO₂, NO, CO, or total hydrocarbons. As described below, more recent controlled human exposure studies provide limited and inconsistent evidence of changes in lung function following exposure to particles from various sources.

CAPs

Among a group of healthy and asthmatic adults exposed to UFPs (Los Angeles, mean concentration 100 µg/m³), Gong et al. (2008, [156483](#)) observed small, yet statistically significant decrements in arterial oxygen saturation immediately following exposure, 4 h post-exposure, and 22 h post-exposure (0.5% mean decrease relative to filtered air across all time points, $p < 0.05$). A statistically significant decrease in FEV₁ was also observed, but only at 22 h post-exposure (2% decrease relative to filtered air, $p < 0.05$). The responses demonstrated in this study were not affected by health status. No such effects were observed in a similar study conducted in Chapel Hill, NC which exposed healthy adults to a lower concentration of UF CAPs (49.8 µg/m³) (Samet et al., 2009, [191913](#)). In addition, two studies evaluating effects of exposure to PM_{10-2.5} CAPs (average concentration 89-157 µg/m³) on lung function observed no changes in spirometric measurements, DLCO or arterial oxygen saturation 0-22 h post-exposure in asthmatic or healthy adults (Gong et al., 2004, [055628](#); Graff et al., 2009, [191981](#)). While Gong et al. (2004, [087964](#)) did not observe a significant association between exposure to PM_{2.5} CAPs and spirometry in older subjects (60-80 yr), the investigators did report a decrease in oxygen saturation immediately following CAPs exposure. This effect was observed more consistently in healthy older adults than in older adults with COPD. These findings were confirmed by a subsequent study conducted by the same laboratory (Gong et al., 2005, [087921](#)). The authors also observed a small decrease in MMEF following a 2-h exposure to PM_{2.5} CAPs (200 µg/m³) which was more pronounced in healthy subjects.

Urban Traffic Particles

Neither short-term exposure to relatively high levels of urban traffic particles nor longer exposures to lower concentrations of urban particles have been observed to alter pulmonary function in controlled exposures among healthy adults. Larsson et al. (2007, [091375](#)) exposed 16 adults for 2 h to PM_{2.5} concentrations of 46-81 µg/m³ in a room adjacent to a busy road tunnel, with concomitant exposure to NO₂ (0.12 ppm), NO (0.71 ppm), and CO (5 ppm). Although respiratory effects in this study were not compared to filtered air control, no difference in lung function was observed 14 h after exposure to traffic particles relative to lung function measured on a day following typical activities that did not include transit through a road tunnel. In a study of 24-h exposures to urban traffic particles (PM_{2.5} 9.7 µg/m³), no change in lung function was reported at 2.5 h after the start of exposure relative to filtered air (Brauner et al., 2009, [190244](#)).

Diesel Exhaust

Mudway et al. (2004, [180208](#)) exposed 25 healthy adults to DE with an average particle concentration of $100 \mu\text{g}/\text{m}^3$ and observed mild bronchoconstriction (airways resistance) immediately following exposure relative to filtered air. No changes were observed in FEV₁ or FVC following DE exposure in these subjects, or in a group of 15 asthmatics exposed using the same protocol (Mudway et al., 2004, [180208](#); Stenfors et al., 2004, [157009](#)).

Model Particles

Pietropaoli et al. (2004, [156025](#)) observed a reduction in MMEF and DLCO in healthy adults 21 h after a 2-h exposure to UF carbon particles ($50 \mu\text{g}/\text{m}^3$). This reduction in DLCO may reflect a PM-induced vasoconstrictive effect on the pulmonary vasculature. Tunnicliffe et al. (2003, [088744](#)) did not observe any significant change in lung function following exposure to ammonium bisulfate or aerosolized H₂SO₄ (200 and 2,000 $\mu\text{g}/\text{m}^3$) in healthy or asthmatic adults, which is consistent with findings of the majority of studies of controlled exposures to acid aerosols presented in the last two PM AQCDs (U.S. EPA, 1996, [079380](#); 2004, [056905](#)).

Summary of Controlled Human Exposure Study Findings for Pulmonary Function

Taken together, the majority of controlled human exposure studies do not provide evidence of PM-induced changes in pulmonary function; however, some investigators have observed slight decreases in DLCO, MMEF, FEV₁, oxygen saturation, or increases in airways resistance following exposure to CAPs, DE, or UF EC.

6.3.2.3. Toxicological Studies

The 2004 PM AQCD (U.S. EPA, 2004, [056905](#)) included three animal toxicological studies which measured pulmonary function following multiday short-term inhalation exposure to CAPs. A decreased respiratory rate was noted in the one study involving dogs. Increased tidal volume was observed in one study involving rats while no changes were observed in the other rat study. AHR was found in four studies of mice, healthy rats or SH rats exposed to ROFA by IT instillation or inhalation. Studies conducted since the last review are discussed below.

CAPs

SH rats exposed to Tuxedo, NY CAPs via nose-only inhalation for 4 h (mean concentration $73 \mu\text{g}/\text{m}^3$; single-day concentrations 80 and $66 \mu\text{g}/\text{m}^3$; 2/2001 and 5/2001, respectively) had a statistically significant decreased respiratory rate compared with air-exposed controls (Nadziejko et al., 2002, [087460](#)). This measure was obtained from BP fluctuations using radiotelemetry. The decrease in respiratory rate of 25-30 breaths/min was an immediate response to CAPs, beginning shortly after the exposure began and ceasing with the end of exposure. It was accompanied by a decrease in HR (Section 6.2.1.3). Rats were also exposed to fine (MMAD 160 nm; $49\text{-}299 \mu\text{g}/\text{m}^3$) and UF H₂SO₄ (MMAD 50-75 nm; $140\text{-}750 \mu\text{g}/\text{m}^3$) (Nadziejko et al., 2002, [087460](#)) because H₂SO₄ aerosols have the potential to activate irritant receptors. Irritant receptors, found at all levels of the respiratory tract, include rapidly-adapting receptors and sensory C-fiber receptors (Alarie, 1973, [070967](#); Bernardi et al., 2001, [019040](#); Coleridge and Coleridge, 1994, [156362](#); Widdicombe, 2003, [157145](#); Widdicombe, 2006, [155519](#)). Activation of trigeminal afferents in the nose causes CNS reflexes resulting in decreases in respiratory rate through a lengthened expiratory phase, closure of the glottis, closure of the nares with increased nasal airflow resistance and effects on the cardiovascular system such as bradycardia, peripheral vasoconstriction and a rise in systolic arterial blood pressure. Sneezing, rhinorrhea and vasodilation with subsequent nasal vascular congestion are also nasal reflex responses involving the trigeminal nerve (Sarin et al., 2006, [191166](#)). Activation of vagal afferents in the tracheobronchial and alveolar regions of the respiratory tract causes CNS reflexes resulting in bronchoconstriction, mucus secretion, mucosal vasodilation, cough, and apnea

followed by rapid shallow breathing. Besides effects on the respiratory system, effects on the cardiovascular system can also occur including bradycardia and hypotension or hypertension. Fine H₂SO₄ induced an overall decrease in respiratory rate, with UF H₂SO₄ resulting in elevated respiratory rate compared to control (Nadziejko et al., 2002, [087460](#)). The authors suggested that both CAPs and fine H₂SO₄ aerosols activated sensory irritant receptors in the upper airways, resulting in a decreased respiratory rate. The response to UF H₂SO₄ aerosols differed from the other responses and was thought to be due to deposition of UFPs deeper into the lung with the subsequent activation of pulmonary irritant receptors which trigger an increase in respiratory rate. Since irritant receptors in nasal, tracheobronchial and alveolar regions act via trigeminal- and vagal-mediated pathways, this study indicates a role for neural reflexes in respiratory responses to CAPs.

Kodavanti et al. (2005, [087946](#)) measured respiratory frequency 1 day after a 2-day exposure of SH and WKY rats to CAPs from RTP, NC (mean mass concentration range 144-2,758 µg/m³; <2.5 µm in size; 8/27-10/24/2001) for 4 h/day. Increases in inspiratory and expiratory times were seen in SH, but not WKY rats, exposed to CAPs compared with filtered air controls.

Effects of CAPs on pulmonary function were also investigated in a rat model of pulmonary hypertension using SD rats pre-treated with monocrotaline (Lei et al., 2004, [087999](#)). In this study, rats were exposed to CAPs from an urban high traffic area in Taiwan (mean mass concentration 371 µg/m³) for 6 h/day on three consecutive days and pulmonary function was evaluated 5 h post-exposure using whole-body plethysmography. A statistically significant decrease in respiratory frequency and an increase in tidal volume were observed following CAPs exposure, along with an increase in airway responsiveness (measured as Penh) following Mch challenge.

In many animal studies changes in ventilatory patterns are assessed using whole body plethysmography, for which measurements are reported as enhanced pause (Penh). Some investigators report increased Penh as an indicator of AHR, but these are inconsistently correlated and many investigators consider Penh solely an indicator of altered ventilatory timing in the absence of other measurements to confirm AHR. Therefore use of the terms AHR or airway responsiveness has been limited to instances in which the terminology has been similarly applied by the study investigators.

Diesel Exhaust

Li et al. (2007, [155929](#)) exposed BALB/c and C57BL/6 mice to clean air or to low dose DE (containing 100 µg/m³ particles) for 7 h/day and 5 days/wk for 1, 4 and 8 wk. Average gas concentrations were reported to be 3.5 ppm CO, 2.2 ppm NO₂, and <0.01 ppm SO₂. AHR was evaluated by whole-body plethysmography at day 0 and after 1, 4 and 8 wk of exposure. Exposure to DE for 1 wk resulted in an increased sensitivity of airways to Mch, measured as Penh, in C57BL/6 but not BALB/c, mice. Other short-term responses of this study are discussed in Sections 6.3.3.3 and 6.3.4.2.

McQueen et al. (2007, [096266](#)) investigated the role of vagally-mediated pathways in respiratory responses to PM. Respiratory minute volume (RMV) was increased in anesthetized Wistar rats 6 h after treatment with 500 µg DE particles (SRM2975) by IT instillation. This response was blocked by severing the vagus nerve or pretreatment with atropine. The absence of a respiratory response with vagotomy or atropine indicated that the increase in RMV following DE particle exposure involved a neural reflex acting via vagal afferents. No statistically significant changes in mean BP, HR or HRV were observed in response to DE particles in this study. Vagally-mediated inflammatory responses to DEP were also observed in this study and are discussed in Section 6.3.3.3.

Model Particles

In a study by Last et al. (2004, [097334](#)), BALB/c mice were exposed to 250 µg/m³ laboratory-generated iron-soot (size range 80-110 nm; about 200 µg/m³ as soot) for 4 h/day and 3 days/wk for 2 wk. Pulmonary function was measured by whole-body plethysmography after challenge with Mch. No AHR, as measured by Penh, was observed following 2-wk exposure to iron-soot. Other findings of this study are reported in Sections 6.3.3.3 and 6.3.5.3.

Summary of Toxicological Study Findings for Pulmonary Function

Several recent studies demonstrated alterations in respiratory frequency and in airway responsiveness following short-term exposure to CAPs and DE. Two studies provide evidence for the involvement of irritant receptors and vagally-mediated neural reflexes in mediating changes in respiratory functions.

6.3.3. Pulmonary Inflammation

The discussion of the effects of PM on pulmonary inflammation in the 2004 PM AQCD (U.S. EPA, 2004, [056905](#)) was limited by a relative lack of information from controlled human exposure and toxicological studies. Although no epidemiologic studies of pulmonary inflammation were described in the 2004 PM AQCD (U.S. EPA, 2004, [056905](#)), several recent studies have observed a positive association between PM concentration and exhaled NO (eNO). New controlled human exposure and toxicological studies have also generally observed an increase in markers of inflammation in the pulmonary compartment following exposure to PM.

6.3.3.1. Epidemiologic Studies

No epidemiologic studies of pulmonary inflammation were described in the 2004 PM AQCD (U.S. EPA, 2004, [056905](#)).

Exhaled Nitric Oxide – Asthmatic Children

Exhaled NO, a biomarker for airway inflammation, was the outcome studied in panels of asthmatic children in southern California (Wu et al., 2006, [157156](#)) and Seattle (Allen et al., 2008, [156208](#); Koenig et al., 2003, [156653](#); 2005, [087384](#); Mar et al., 2005, [088759](#)). Mean concentration data from these studies are summarized in Table 6-10. Delfino et al. (2006, [157156](#)) followed 45 asthmatic children for ten days with offline fractional eNO and examined the associations with exposures to personal PM_{2.5} and 24-h PM_{2.5}, EC and OC as well as ambient PM_{2.5}, EC and OC. The strongest associations were between eNO and 2-day avg pollutant concentrations: for a 10 µg/m³ increase in personal PM_{2.5}, eNO increased by 0.46 ppb (95% CI: 0.04-0.79); for 0.6 µg/m³ personal EC, eNO increased by 0.7 ppb (95% CI: 0.3-1.1). An association with exposure to ambient PM_{2.5} was only statistically significant in 19 subjects taking inhaled corticosteroids: for each 10 µg/m³ increase in PM_{2.5}, eNO increased by 0.77 ppb (95% CI: 0.07-1.47).

In a panel of 19 asthmatic children in Seattle, effects were observed only among the ten non-users of inhaled corticosteroids. For each 10 µg/m³ increase in personal, outdoor, indoor, or central site PM_{2.5}, eNO increased from 3.82 ppb (associated with central site, 95% CI: 1.22-6.43) to 4.48 ppb (with personal PM_{2.5}, 95% CI: 1.02-7.93) (Koenig et al., 2003, [156653](#)). Further analysis examining the association between eNO and outdoor and indoor-generated particles suggested that eNO was associated more strongly with ambient particles, but only for non-users of medication: each 10 µg/m³ increase in estimated ambient PM_{2.5} results in an increase in eNO of 4.98 ppb (95% CI: 0.28-9.69) (Koenig et al., 2005, [087384](#)).

Also in Seattle, WA, Mar et al. (2005, [088759](#)) examined the association between eNO and ambient PM_{2.5} concentration among children (aged 6-13 yr) recruited from an asthma/allergy clinic. Fractional exhaled nitric oxide (FeNO) was associated with hourly averages of PM_{2.5} up to 10-12 h after exposure. Each 10 µg/m³ increase in 1-h mean PM_{2.5} concentration was associated with a 6.99 ppb increase in eNO (95% CI: 3.43-10.55) among children not taking inhaled corticosteroids, but associated with only a 0.77 ppb decrease in eNO (95% CI: -4.58 to 3.04) among those taking inhaled corticosteroids.

Allen et al. (2008, [156208](#)), in a reanalysis of data from Koenig et al. (2005, [087384](#)), evaluated the effect of different PM_{2.5} exposure metrics in relation to airway inflammation among children in wood smoke-impacted areas of Seattle. The authors found that for the nine non-users of inhaled corticosteroids, the ambient-generated component of PM_{2.5} exposure was associated with respiratory responses, both airway inflammation and decrements in lung function, whereas the non-ambient PM_{2.5} exposure component was not. They did note, however, different relationships for

airway inflammation and decrements in lung function, with the former significantly associated with total personal PM_{2.5}, personal light-absorbing carbon (LAC), and ambient generated personal PM_{2.5} and the latter related to ambient PM_{2.5} and its combustion markers. The different results between FeNO and lung function were not unexpected; epidemiologic data show that airway inflammation indicated by FeNO does not correlate strongly with either respiratory symptoms or lung function (Smith and Taylor, 2005, [192176](#)). The authors conclude that lung function decrements may be associated with the combustion-generated component of ambient PM_{2.5}, whereas airway inflammation may be related to some other component of the ambient PM_{2.5} mixture.

In a longitudinal study, Liu et al. (2009, [192003](#)) examined the association between acute increases in ambient air pollutants and FeNO among children (ages 9-14 yr) with asthma. FeNO had a trend of positive associations with PM_{2.5}, with the strongest association on lag day 0 (3.12% [95% CI: -2.12 to 8.82]). Copollutant models including O₃, SO₂ or NO₂ did not result in marked changes in the PM_{2.5} risk estimates for FeNO.

A few studies outside of the U.S. examined eNO in relation to PM exposure among children. Fischer et al. (2002, [025731](#)) and Murata et al. (2007, [189159](#)) found a statistical association between increases in PM and increases in the percent of eNO. Holguin et al. (2007, [099000](#)) found no association between exposure to PM and eNO. However, they did see statistical associations between increases in eNO for the 95 asthmatic subjects and measures of road density of roads 50- and 75-m from the home.

Exhaled Nitric Oxide – Adults

Three recent panel studies examined the effects of particle exposure on eNO measured in older adults (Adamkiewicz et al., 2004, [087925](#) in Steubenville, OH; Adar et al., 2007, [001458](#); Jansen et al., 2005, [082236](#) in Seattle). Mean concentration data from these studies are characterized in Table 6-10. Breath samples were collected weekly for 12 weeks from a group of 29 elderly adults in Steubenville, OH (Adamkiewicz et al., 2004, [087925](#)). In single-pollutant models, each 10 µg/m³ increase in 24-h ambient PM_{2.5} increased eNO by 0.82 ppb (95% CI: 0.19-1.45), a change of 15% compared to mean eNO (9.9 ppb). Effects were essentially unchanged in copollutant models that included ambient and/or indoor NO. The effect estimates for the seven COPD subjects were higher than for normal subjects (2.20 vs. 0.45 ppb, p = 0.03) (Adamkiewicz et al., 2004, [087925](#)).

In the Seattle panel of older adults (aged 60-86 yr), seven subjects were asthmatic and nine had a diagnosis of COPD (five with asthma and four without) (Jansen et al., 2005, [082236](#)). Exhaled NO was measured daily for 12 days, along with personal, indoor, outdoor and central site PM₁₀, PM_{2.5} and BC. The strongest associations between 24-h avg PM and eNO were found for the asthmatic subjects: 10 µg/m³ increases in outdoor levels (measured outside the subjects' homes) of PM_{2.5} or PM₁₀ were associated with increases in eNO of 4.23 ppb (95% CI: 1.33-7.13), an increase of 22% above the group mean of 19.2 ppb, and 5.87 ppb (95% CI: 2.87-8.88), an increase of 31%, respectively. BC measured indoors, outdoors or personally was also associated with increases in eNO (of 3.97, 2.32, and 1.20 ppb, respectively) (Jansen et al., 2005, [082236](#)).

Adar et al. (2007, [001458](#)) conducted a panel study of 44 non-smoking senior citizens residing in St. Louis, MO. As part of the study, subjects were taken on group trips to a theater performance, Omni movie, outdoor band concert, and a Mississippi River boat cruise. Subjects were driven to and from each event aboard a diesel bus. Before and after each bus trip, eNO was measured on each subject. Two carts containing continuous air pollution monitors were used to measure group-level micro-environmental exposures to PM_{2.5}, BC, and size-specific particle counts (0.3-2.5 µm and 2.5-10 µm) on the day of each trip. Each 10 µg/m³ increase in 24-h mean PM_{2.5} concentration was associated with a 36% increase in eNO pre-trip (95% CI: 5-71). Each 10 µg/m³ increase in micro-environmental PM_{2.5} concentration (i.e., during the bus ride) was associated with a 27% increase in eNO post-trip (95% CI: 17-38).

These studies all demonstrated an association between increased levels of eNO and increases in PM in the previous 4-24 h. Further, three studies demonstrated effects in elderly populations (Adamkiewicz et al., 2004, [087925](#); Adar et al., 2007, [001458](#); Jansen et al., 2005, [082236](#)) while four others reported a similar acute increase in eNO among children (Delfino et al., 2006, [090745](#); Koenig et al., 2003, [156653](#); 2005, [087384](#); 2005, [088999](#)).

Outside of the U.S., one study examined eNO in a panel of 60 adult asthmatic subjects in London. McCreanor et al. (2007, [092841](#)) reported that 1 µg/m³ increase in personal exposure to EC

was associated with increases of approximately 1.75-2.25% in eNO (results were presented graphically only) for up to 22 h post-exposure.

Other Biomarkers of Pulmonary Inflammation and Oxidative Stress

Other biomarkers of respiratory distress that have been examined in recent panel studies include urinary leukotriene E₄ (LTE₄) in asthmatic children (Rabinovitch et al., 2006, [088031](#)); two oxidative stress markers: TBARS and 8-isoprostane in asthmatic children (Liu et al., 2009, [192003](#)) and breath acidification in adolescent athletes (Ferdinands et al., 2008, [156433](#)). Mean concentration data from these studies are characterized in Table 6-10.

In Rabinovitch et al. (2006, [088031](#)), LTE₄, an asthma-related biological mediator, was used to study the response to short-term particle exposure. In the second winter of their 2-yr study of asthmatic children (described above in Section 6.3.1.1), urine samples were collected at approximately the same time of day from 57 subjects for eight consecutive days. Controlling for days with URI symptoms, each 10 µg/m³ increase in morning maximum PM_{2.5} (measured by TEOM), was associated with an increase in LTE₄ levels by 5.1% (95% CI: 1.6-8.7). No statistically significant effects were observed on the same day or up to 3 days later based on 24-h averaged concentrations from the TEOM monitor or from the FRM central site monitor.

In a longitudinal study conducted in Windsor, Ontario, Liu et al. (2009, [192003](#)) examined the association between acute increases in ambient air pollutants and TBARS and 8-isoprostane among children (ages 9-14 yr) with asthma. TBARS, but not 8-isoprostane, was positively associated with PM_{2.5} (percent change in TBARS 40.6% [95% CI: 11.8-81.3], lag 0-2 days). The association with TBARS persisted for at least three days. Adverse changes in pulmonary function (Section 6.3.2.1) were consistent with those of TBARS in response to PM_{2.5} with a similar lag structure, suggesting a coherent outcome for small airway function and oxidative stress.

The effects of vigorous outdoor exercise during peak smog season in Atlanta, GA on breath pH, a biomarker of airway inflammation, in adolescent athletes (n = 16, mean age = 14.9 yr) were examined by Ferdinands et al. (2008, [156433](#)). Median pre-exercise breath pH was 7.58 (range 4.39-8.09) and median post-exercise breath pH was 7.68 (range 3.78-8.17). The authors observed no significant association between ambient PM and post-exercise breath pH. However both pre- and post-exercise breath pH were strikingly low in these athletes when compared to 14 relatively sedentary healthy adults and to published values of breath pH in healthy subjects. The authors speculate that repetitive vigorous exercise may induce airway acidification.

Effect of Measurement Location on Studies of Pulmonary Function and Inflammation

A number of studies examining exposure to PM_{2.5} and pulmonary function and inflammation have compared the results of exposure assessment based on concentrations recorded from personal, indoor, outdoor, and/or ambient monitors (Allen et al., 2008, [156208](#); Delfino et al., 2004, [056897](#); Delfino et al., 2006, [090745](#); Koenig et al., 2005, [087384](#); Trenga et al., 2006, [155209](#)). Two investigations evaluated PM_{2.5} concentrations from indoor, outdoor, personal and central site monitors and the relationship with FEV₁. Delfino et al. (2004, [056897](#)) reported that personal exposure estimates showed a stronger association with FEV₁ than any of the stationary exposures, and that indoor exposure estimates were associated with a stronger effect than either outdoor or central site exposure estimates. However, Trenga et al. (2006, [155209](#)) reported the largest declines in FEV₁ associated with central site exposure estimates, though the most consistent association with declines in FEV₁ came from the exposure estimates measured by indoor monitors. Delfino et al. (2006, [090745](#)) used personal and ambient exposure estimates in a study of FeNO among asthmatic children and found that the personal exposure estimates were more robust than the ambient exposure estimates. Two studies conducted in Seattle, WA partitioned personal exposure to PM_{2.5} into its ambient-generated and indoor-generated components. Koenig et al. (2005, [087384](#)) reported that ambient-generated PM_{2.5} was consistently associated with an increase in FeNO, while the indoor-generated component of PM_{2.5} was less strongly associated with FeNO. This could reflect the difference in composition of indoor-generated PM_{2.5} as compared to ambient-generated PM_{2.5}. Similarly, Allen et al. (2008, [156208](#)) found that FeNO was associated with the ambient-generated

component of personal PM_{2.5} exposure, but not with ambient PM_{2.5} concentrations measured by central site monitors. Overall, these studies provide a unique perspective on how measurement location influences the findings of epidemiologic studies. This small group of studies indicates that effects are associated with all types of PM measurement, suggesting health effects of both ambient-generated and indoor-generated particles. It is likely that variability in season, meteorology, topography, geography, behavior and exposure patterns contribute to the observed differences.

6.3.3.2. Controlled Human Exposure Studies

Studies of controlled human exposures presented in the 2004 PM AQCD (U.S. EPA, 2004, [056905](#)) provided evidence of pulmonary inflammation induced by exposure to PM. Lay et al. (1998, [007683](#)) found that instillation of iron oxide particles (2.6 µm) produced an increase in alveolar macrophages and neutrophils in bronchoalveolar lavage fluid (BALF) collected 24 h post-instillation. Ghio and Devlin (2001, [017122](#)) evaluated the inflammatory response following bronchial instillation of particles extracted from filters collected in the Utah Valley both prior to and after the closure of an area steel mill. Subjects who underwent pulmonary instillation of particles (500 µg) collected while the steel mill was operating (n = 16) had significantly higher levels of neutrophils 24 h post-instillation compared with either saline instillation or with subjects (n = 8) who were instilled with the same mass of PM collected during the mill's closure. This finding indicates that metals may be an important PM component for this health outcome. In an inhalation study of exposure to PM_{2.5} CAPs (23-311 µg/m³) from Chapel Hill, NC, Ghio et al. (2000, [012140](#)) observed an increase in airway and alveolar neutrophils 18 h after the 2-h exposure. A similar finding was reported by Rudell et al. (1999, [001964](#)) following exposure to DE among healthy adults. In this study, reducing the particle number from 2.6×10⁶ particles/cm³ to 1.3×10⁶ particles/cm³ while maintaining the concentration of gaseous diesel emissions was not observed to attenuate the response. One study of controlled exposures to UF EC among healthy adults did not report particle-related effects on eNO (Frampton, 2001, [019051](#)). As summarized below, several recent studies of controlled exposures have provided some additional evidence of pulmonary inflammation associated with PM.

CAPS

A series of exposures to UF, PM_{2.5}, and PM_{10-2.5} CAPs from Los Angeles with average particle concentrations between 100 and 200 µg/m³ have not been shown to have a significant effect on markers of airway inflammation in healthy or health-compromised adults (Gong et al., 2004, [087964](#); 2004, [055628](#); 2005, [087921](#); 2008, [156483](#)). However, two recent studies conducted in Chapel Hill, NC reported significant increases in percent PMNs and concentration of IL-8 in BALF among healthy adults 18-20 h following controlled exposures to PM_{10-2.5} (89 µg/m³) and UF (49.8 µg/m³) CAPs, respectively (Graff et al., 2009, [191981](#); Samet et al., 2009, [191913](#)). As discussed above, the same laboratory previously reported a mild inflammatory response in the lower respiratory tract following exposure to PM_{2.5} CAPs (Ghio et al., 2000, [012140](#)). In a follow-up analysis, Huang et al. (2003, [087377](#)) found the increase in BALF neutrophils demonstrated by Ghio et al. (2000, [012140](#)) to be positively associated with the Fe, Se, and SO₄²⁻ content of the particles.

Alexis et al. (2006, [154323](#)) recently evaluated the effect of PM_{10-2.5} on markers of airway inflammation, specifically focusing on the impact of biological components of PM_{10-2.5}. Healthy men and women (n = 9) between the ages of 18 and 35 inhaled nebulized saline (0.9%) as well as aerosolized PM_{10-2.5} collected from ambient air. Subjects were exposed to PM_{10-2.5} on two separate occasions, once using PM_{10-2.5} that had been heated to inactivate biological material and once using non-heated PM_{10-2.5}. Approximately 0.65 mg PM_{10-2.5} was deposited in the respiratory tract of subjects during the exposures. Markers of inflammation and immune function were analyzed in induced sputum collected 2-3 h after inhalation of saline or PM_{10-2.5}. Both heated and non-heated PM_{10-2.5} were observed to increase the neutrophil response compared with saline. Exposure to non-heated PM_{10-2.5} was found to increase levels of monocytes, eotaxin, macrophage TNF-α mRNA, and was also associated with an upregulation of macrophage cell surface markers. No such effects were observed following exposure to biologically inactive PM_{10-2.5}. These results suggest that while PM_{10-2.5}-induction of neutrophil response is not dependent on biological components, heat sensitive

components of PM_{10-2.5} (e.g., endotoxin) may be responsible for PM-induced alveolar macrophage activation.

Traffic Particles

Larsson et al. (2007, [091375](#)) exposed 16 healthy adults to air pollution in a road tunnel for 2 h during the afternoon rush hour in Stockholm, Sweden. The median PM_{2.5} and PM₁₀ concentrations during the road tunnel exposures were 64 µg/m³ and 176 µg/m³, respectively. Bronchial biopsies were obtained and bronchoscopy and BAL were performed 14 h after the exposure. The results were compared with a control exposure which consisted of exposure to urban air during normal activity. The authors reported significant BALF increases in percentage of lymphocytes, total cell number, and alveolar macrophages following exposure to road tunnel exposure versus control. These results provide evidence of a significant association between exposure to road tunnel air pollution and airway inflammation. However, unlike other controlled exposure studies, the control exposure was not a true clean air control, but only a lower exposure group with no characterization of personal exposure. In addition, it is not possible to separate out the contributions of each air pollutant, including PM, on the observed inflammatory response.

Diesel Exhaust

In a recent study evaluating the effect of DE exposure on markers of airway inflammation, Behndig et al. (2006, [088286](#)) exposed healthy adults (n = 15) for 2 h with intermittent exercise to filtered air or DE with a reported PM₁₀ concentration of 100 µg/m³. Eighteen hours after exposure to DE, the authors found significant increases in neutrophil and mast cell numbers in bronchial tissue, as well as significant increases in neutrophil numbers and IL-8 in BALF compared with filtered air control. Similarly, Stenfors et al. (2004, [157009](#)) observed an increase in pulmonary inflammation (e.g., airways neutrophilia and an increase in IL-8 in BALF) among healthy adults 6 h following exposure to DE (PM₁₀ average concentration 108 µg/m³). It is interesting to note, however, that no such inflammatory effects were observed in a group of mild asthmatic subjects in the same study. The DE-induced neutrophil response in the airways of healthy subjects observed in these two studies (Behndig et al., 2006, [088286](#); Stenfors et al., 2004, [157009](#)) is qualitatively consistent with the findings of Ghio et al. (2000, [012140](#)) who exposed healthy subjects to Chapel Hill PM_{2.5} CAPs. In a group of healthy volunteers, Bosson et al. (2007, [156286](#)) demonstrated that exposure to O₃ (2 h at 0.2 ppm) may enhance the airway inflammatory response of DE relative to clean air (1-h exposure to 300 µg/m³). Exposure to O₃ was conducted 5 h after exposure to DE, and resulted in an increase in the percentage of neutrophils in induced sputum collected 18 h after exposure to O₃. In a subsequent study using a similar protocol at the same concentrations, prior exposure to DE was shown to increase the inflammatory effects of O₃ exposure, demonstrated as an increase in neutrophil and macrophage numbers in bronchial wash (Bosson et al., 2008, [196659](#)).

Wood Smoke

Barregard et al. (2008, [155675](#)) examined the effect of a short-term exposure (4 h) to wood smoke (240-280 µg/m³) on markers of pulmonary inflammation in a group of healthy adults. Exposure to wood smoke increased alveolar NO compared to filtered air (2.0 ppb versus 1.3 ppb) 3 h after exposure. Although these results provide some evidence of a PM-induced increase in pulmonary inflammation, the physiological significance of the relatively small increase in alveolar NO is unclear.

Model Particles

Pietropaoli et al. (2004, [156025](#)) observed a lack of airway inflammatory response 21 h after exposure to UF EC particles (10-50 µg/m³) among healthy and asthmatic adults. The same laboratory reported no effect of exposure to UF or fine ZnO (500 µg/m³) on total or differential sputum cell

counts 24 h after exposure in a group of healthy adults (Beckett et al., 2005, [156261](#)). Tunnicliffe et al. (2003, [088744](#)) measured levels of eNO as a marker of airway inflammation following 1-h controlled exposures to ammonium bisulfate or aerosolized H₂SO₄ (200 and 2,000 µg/m³) in a group of healthy and asthmatic adults. While exposure to ammonium bisulfate increased the concentration of eNO immediately following exposure in asthmatics, no such effect was observed in healthy adults, or in either healthy or asthmatic adults following exposure to aerosolized H₂SO₄.

Instillation

Schaumann et al. (2004, [087966](#)) investigated the inflammatory response of human subjects instilled with PM_{2.5} (100 µg) collected from two different cities in Germany, Hettstedt and Zerbst. Although endobronchial instillation of PM from both cities were shown to induce airway inflammation, instillation of PM from the more industrial area (Hettstedt) resulted in greater influxes of BALF monocytes compared to PM collected from Zerbst. The authors postulated that the difference in response between PM from the two cities may be due to the higher concentration of transition metals observed in the samples collected from Hettstedt. Another study reported no change in inflammatory markers in nasal lavage fluid 4 and 96 h following intranasal instillation of DEP (300 µg/nostril) in asthmatics and healthy adults (Kongerud et al., 2006, [156656](#)). Pre-exposure of DEP to O₃ was not shown to have any effect on the response. Although not a cross-over design, these findings suggest that exposure to DEP without the gaseous component of DE may have little effect on inflammatory responses in human subjects.

Summary of Controlled Human Exposure Study Findings for Pulmonary Inflammation

These new studies strengthen the evidence of PM-induced pulmonary inflammation; however, the response appears to vary significantly depending on the source and composition of the particles.

6.3.3.3. Toxicological Studies

The 2004 PM AQCD (U.S. EPA, 2004, [056905](#)) discussed numerous studies investigating pulmonary inflammation in response to CAPs, ROFA, DEPs, metals and acid aerosols. A wide variety of responses was reported depending on the type of PM and route of administration. In general, IT instillation exposure to fly ash and metal PM resulted in notable pulmonary inflammation. In contrast, inhalation of sulfates and acid aerosols had minimal, if any, effect on pulmonary inflammation. More recent animal toxicological studies using CAPs, DE and other relevant PM types are summarized below.

CAPs

The 2004 PM AQCD (U.S. EPA, 2004, [056905](#)) found that exposure to PM_{2.5} CAPs at concentrations of 100-1,000 µg/m³ for 1-6 h/day and 1-3 days generally resulted in minimal to mild inflammation in rats and dogs. Somewhat enhanced inflammation was observed in a model of chronic bronchitis. Since the last review, numerous studies have investigated inflammatory responses to PM_{2.5} and UF CAPs in both healthy and compromised animal models.

In one study of healthy animals, SD rats were exposed to CAPs for 4 h/day on 3 consecutive days in Fresno, CA, in fall 2000 and winter 2001 (PM_{2.5} mean mass concentration 190-847 µg/m³) (Smith et al., 2003, [042107](#)). The particle concentrator used in these studies was capable of enhancing the concentration of UF as well as fine particles. Immediately after exposure on the third day, BALF was collected and analyzed for total cells and neutrophils. Statistically significant increases were observed in numbers of neutrophils during the first week of the fall exposure period and in numbers of total cells, neutrophils and macrophages during the first week of the winter exposure period. CAPs concentrations were >800 µg/m³ during both of those weeks.

Two studies were conducted using CAPs in Boston. In a study by Godleski et al. (2002, [156478](#)), healthy SD rats were exposed for 5 h/day for 3 consecutive days to CAPs ranging in

concentration from 73.5-733.0 $\mu\text{g}/\text{m}^3$. BALF and lung tissue were collected for analysis 1 day later. Neutrophilic inflammation was indicated by a statistically significant increase in percent neutrophils in BALF. Microarray analysis of RNA from lung tissue and BALF cells demonstrated increased gene expression of pro-inflammatory mediators, markers of vascular activation and enzymes involved in organic chemical detoxification. This study overlapped in part with previously described studies by Saldiva et al. (2002, [025988](#)) and Batalha et al. (2002, [088109](#)) (Section 6.2.4.3). In another study (Rhoden et al., 2004, [087969](#)), healthy SD rats were exposed for 5 h to CAPs (mean mass concentration 1228 $\mu\text{g}/\text{m}^3$; June 20-August 16, 2002). A statistically significant increase in BALF neutrophils was observed 24 h following CAPs exposure. Histological analysis confirmed the influx of inflammatory cells (Section 6.3.5.3). Inflammation was accompanied by injury which is discussed in Section 6.3.5.3.

Kodavanti et al. (2005, [087946](#)) reported two sets of studies involving $\text{PM}_{2.5}$ CAPs exposure during fall months in RTP, NC. In the first study, SH rats were exposed to filtered air or CAPs (mean mass concentration range 1,138-1,765 $\mu\text{g}/\text{m}^3$; $<2.5 \mu\text{m}$) for 4 h and analyzed 1-3 h later. No increase in BALF inflammatory cells or other measured parameter was observed. In the second study, SH and WKY rats were exposed to filtered air or CAPs (mean mass concentration range 144-2,758 $\mu\text{g}/\text{m}^3$; $<2.5 \mu\text{m}$) for 4 h/day on 2 consecutive days and analyzed 1 day afterward. Differences in baseline parameters were noted for the two rat strains since SH rats had greater numbers of BALF neutrophils than WKY rats. Following the 2-day CAPs exposure, increased BALF neutrophils were observed in the WKY rats but not in the SH rats compared with filtered air controls. Inflammation was not accompanied by increases in BALF markers of injury (Section 6.3.5.3).

Two CAPs studies involving SH rats were conducted in the Netherlands. In the first, SH rats were exposed by nose-only inhalation to CAPs (ranging in concentration from 270-3,660 $\mu\text{g}/\text{m}^3$ and in size from 0.15-2.5 μm) from three different sites in the Netherlands (suburban, industrial and near-freeway) for 6 h (Cassee et al., 2005, [087962](#)). Increased numbers of neutrophils were observed in BALF 2 days post-exposure compared to air controls. When CAPs exposure was used as a binary term, the relationship between CAPs concentration and number of PMN in BALF was statistically significant. In contrast, Kooter et al. (2006, [097547](#)) reported no changes in markers of pulmonary inflammation measured 18 h after a 2-day exposure (6 h/day) of SH rats to $\text{PM}_{2.5}$ or $\text{PM}_{2.5}+\text{UFP}$ CAPs from sites in the Netherlands (mean mass concentration range 399-3613 and 269-556 $\mu\text{g}/\text{m}^3$, respectively; $\text{PM}_{2.5}$ CAPs site in Bilthoven and $\text{PM}_{2.5}+\text{UF}$ CAPs site in freeway tunnel in Hendrik-Ido-Ambacht).

Pulmonary inflammation was investigated in two studies using a rat model of pulmonary hypertension (i.e., SD rats pre-treated with monocrotaline). In the first study, rats were exposed to $\text{PM}_{2.5}$ CAPs from an urban high traffic area in Taiwan (mean mass concentration of 371 $\mu\text{g}/\text{m}^3$) (Lei et al., 2004, [087999](#)) for 6 h/day on 3 consecutive days and BALF was collected 2 days later. A statistically significant increase in total cells and neutrophils was observed in BALF. Levels of TNF- α and IL-6 in the BALF were not altered by CAPs exposure. In the second study, rats were exposed to $\text{PM}_{2.5}$ CAPs (mean mass concentration 315.6 and 684.5 $\mu\text{g}/\text{m}^3$ for 6 and 4.5 h, respectively; Chung-Li area, Taiwan) during a dust storm event occurring March 18-19, 2002 (Lei et al., 2004, [087884](#)). Only one animal served as control during the 6-h exposure (from 2100-300 on the first exposure day) so results from that one animal were combined with that of three control animals from the 4.5-h exposure (from 300-730) on the second exposure day. A statistically significant increase in total cells and neutrophils in BALF occurred in both CAPs-exposed groups. In addition, increases in BALF IL-6 and markers of injury (Section 6.3.5.3) were observed as a function of CAPs exposure.

In summary, pulmonary inflammation was noted in all three studies involving multiday exposure of healthy rats to CAPs from different locations. No pulmonary inflammation was seen in one study of SH rats exposed to CAPs for 4 h and analyzed 1-3 h later. In studies involving multiday exposure of SH rats, one demonstrated pulmonary inflammation while two did not. In the rat monocrotaline model of pulmonary hypertension, both single-day and multiday exposures to CAPs resulted in mild pulmonary inflammation.

On-Road Exposures

In a study by Elder et al. (2004, [087354](#)) old rats (21 mo) were exposed to on-road highway aerosols (particle concentration range $0.95\text{-}3.13 \times 10^5$ particles/ cm^3 ; mass concentration estimated to be 37-106 $\mu\text{g}/\text{m}^3$; Interstate 90 between Rochester and Buffalo, NY) for 6 h on one or three

consecutive days. No increase in BALF inflammatory cells was observed 18 h post-exposure in any of the treatment groups.

Urban Air

To evaluate inflammatory responses to ambient particles from vehicles, Wistar rats were exposed to ambient urban air from a high traffic site (concentration range 22-225 $\mu\text{g}/\text{m}^3$ PM_{10} ; Porto Alegre, Brazil) or to the same air which was filtered to remove the PM (Pereira et al., 2007, [156019](#)). Concentrations of gases were not reported. Compared with controls exposed to filtered urban air, a significant increase in total number of BALF cells was observed 24 h following the 20 h continuous exposure, but not following the 6 h of exposure to unfiltered urban air.

Diesel Exhaust

The 2004 PM AQCD (U.S. EPA, 2004, [056905](#)) summarized findings of the 2002 EPA Diesel Document regarding the health effects of DE. Short-term inhalation exposure to low levels of DE results in the accumulation of diesel PM in lung tissue, pulmonary inflammation and alveolar macrophage aggregation and accumulation near the terminal bronchioles. More recent studies are summarized below.

Pulmonary inflammatory responses were investigated in C57BL/6 mice exposed to DE 7 h/day for 6 consecutive days (Harrod et al., 2003, [097046](#)). Compared with controls, inflammatory cell counts in BALF were increased in mice exposed to the higher concentration of DE (1,000 $\mu\text{g}/\text{m}^3$ PM) but not in mice exposed to the lower concentration of DE (30 $\mu\text{g}/\text{m}^3$ PM). Concentrations of gases present in the higher dose DE were reported to be 43 ppm NO_x , 20 ppm CO and 364 ppb SO_2 .

In a second study evaluating DE effects on BALF inflammatory cells, no increases in numbers of neutrophils, lymphocytes or eosinophils were observed in BALB/c mice exposed by inhalation to 500 or 2,000 $\mu\text{g}/\text{m}^3$ DE particles for 4 h/day on 5 consecutive days (Stevens et al., 2008, [157010](#)). Concentrations of gases reported in this study were 4.2 ppm CO, 9.2 ppm NO, 1.1 ppm NO_2 , and 0.2 ppm SO_2 for the higher concentration of DE. Transcriptional microarray analysis demonstrated upregulation of chemokine and inflammatory cytokine genes, as well as genes involved in growth and differentiation pathways, in response to the higher concentration of DE. No gene expression results were reported for the lower concentration of DE. Sensitization and challenge with ovalbumin (OVA) significantly altered these findings (Section 6.3.6.2). These results demonstrate that changes in gene expression can occur in the absence of measurable pulmonary inflammation or injury markers (Section 6.3.5.3).

Li et al. (2007, [155929](#)) exposed mice to clean air or to low dose DE (100 $\mu\text{g}/\text{m}^3$ PM) for 7 h/day and 5 days/wk for 1, 4 and 8 wk as described in Section 6.3.2.3. Analysis of BALF and histology of lung tissues was carried out at day 0 and after 1, 4 and 8 wk of exposure. Total numbers of cells and macrophages in BALF were significantly increased in C57BL/6 mice, but not in BALB/c mice, after 1-wk exposure to DE compared with 0 day controls. Neutrophils and lymphocytes were increased after 1-wk exposure to DE in both strains compared with 0 day controls. Differences in BALF cytokines were also noted between the two strains after 1-wk exposure to DE. No changes were observed by histological analysis. Pulmonary function and oxidative responses were also evaluated (Sections 6.3.2.3 and 6.3.4.2). Long-term exposure responses are discussed in Sections 7.3.2.2, 7.3.3.2 and 7.3.4.1.

Healthy F344 rats and A/J mice were exposed to DE containing 30, 100, 300 and 1,000 $\mu\text{g}/\text{m}^3$ PM by whole body inhalation for 6 h/day, 7 days/wk for either 1 wk or 6 months in a study by Reed et al. (2004, [055625](#)). Concentrations of gases were reported to be from 2.0-45.3 ppm NO, 0.2-4.0 ppm NO_2 , 1.5-29.8 ppm CO and 8-365 ppb for SO_2 in these exposures. One week of exposure resulted in no measurable effects on pulmonary inflammation. Long-term exposure responses are discussed in Section 7.3.3.2.

In a study by Wong et al. (2003, [097707](#)), also reported by Witten et al. (2005, [087485](#)), F344/NH rats were exposed nose-only to filtered room air or to DE at concentrations of 35.3 $\mu\text{g}/\text{m}^3$ and 669.3 $\mu\text{g}/\text{m}^3$ PM (particle size range 7.2-294.3 nm) for 4 h/day and 5 days/wk for 3 wk. Gases associated with the high dose exposure were reported to be 3.59 ppm NO, 3.69 ppm NO_x , 0.1 ppm NO_2 , 2.95 ppm CO, 518.96 ppm CO_2 and 0.031 ppm total hydrocarbon. The focus of this study was

on the possible role of neurogenic inflammation in mediating responses to DE. Neurogenic inflammation is characterized by both the influx of inflammatory cells and plasma extravasation into the lungs following the release of neuropeptides from bronchopulmonary C-fibers. Pulmonary inflammation was evaluated by histological analysis of lung tissue at the end of the 3-wk exposure period. Following high, but not low, concentration exposure to DE, a large number of alveolar macrophages was found in the lungs. Small black particles, presumably DE particles, were found in the cytoplasm of these alveolar macrophages. Perivascular cuffing consisting of mononuclear cells was also observed in high dose-exposed animals. Influx of neutrophils or eosinophils was not seen, although mast cell number was increased in high-dose exposed animals. Pulmonary plasma extravasation was measured by the ^{99m}Tc-Technecium-albumin technique and found to be dose-dependently increased in the bronchi and lung parenchyma. Alveolar edema was also observed by histology in high concentration-exposed animals. A significant decrease in substance P content in lung tissue was reported in DE-exposed rats. These responses initially suggested that DE resulted in stimulation of C-fibers and activation of a local axon reflex resulting in the repeated release of the stored neuropeptide substance P. Subsequent experiments were conducted using capsaicin pretreatment, which inhibits neurogenic inflammation by activating C-fibers and causing the depletion of neuropeptide stores. Pretreatment with capsaicin was found to reduce the influx of inflammatory cells, but not plasma extravasation, in response to DE. Hence, DE is unlikely to act through bronchopulmonary C-fibers to cause neurogenic edema in this model, although there may be a different role for bronchopulmonary C-fibers in mediating the inflammatory cell influx.

Stimulation of bronchopulmonary C-fibers can result in activation of both local and CNS reflexes through vagal parasympathetic pathways. McQueen et al. (2007, [096266](#)) investigated the role of vagally-mediated pathways in acute inflammatory responses to DE particles. A statistically significant increase in BALF neutrophils was observed 6 h after IT instillation treatment of anesthetized Wistar rats with 500 µg DE particles (SRM2975). This response was blocked by severing the vagus nerve or pretreatment with atropine (McQueen et al., 2007, [096266](#)). Similarly, atropine treatment blocked the increase in BALF neutrophils seen 6 h after DE particle exposure in conscious Wistar rats. These results provide evidence for the involvement of a pulmonary vagal reflex in the inflammatory response to DE particles.

In summary, several studies demonstrate that short-term inhalation exposure to DE (100-1,000 µg/m³ PM) causes pulmonary inflammation in rodents. No attempt was made in these studies to determine whether the responses were due to PM components or to gaseous components. However, PM from DE was found to be capable of inducing an inflammatory response, as demonstrated by the one IT instillation study described above. Evidence was presented suggesting that DEP may act through bronchopulmonary C-fibers to stimulate pulmonary inflammation.

Gasoline Emissions and Road Dust

Healthy male Swiss mice were exposed to gasoline exhaust (635 µg/m³ PM and associated gases) or filtered air for 15 min/day for 7, 14, and 21 days (Sureshkumar et al., 2005, [088306](#)). BALF was collected for analysis 1 h after the last exposure. Histological analysis was also carried out at 7, 14, and 21 days. The number of leukocytes in BALF was increased after exposure to gasoline exhaust, but this increase did not achieve statistical significance. However, levels of the pro-inflammatory cytokines TNF-α and IL-6 were significantly increased in BALF following 14 and 21 days of exposure. Furthermore, inflammatory cell infiltrate in the peribronchiolar and alveolar regions were observed by histology. Evidence of lung injury was also found (Section 6.3.5.3). In this study, BALF analysis of inflammatory cells was a less sensitive indicator of pulmonary inflammation than BALF analysis of cytokines and histological analysis of lung tissue. Results of this study cannot entirely be attributed to the presence of PM in the gasoline exhaust since 0.11 mg/m³ SO_x, 0.49 mg/m³ of NO_x and 18.7 ppm of CO were also present during exposure.

Using ApoE^{-/-} mice on a high-fat diet, Campen et al. (2006, [096879](#)) studied the impact of inhaled gasoline emissions and road dust (6 h/day×3 day) on pulmonary inflammation. For gasoline emissions, the PM-containing atmosphere (PM mean concentration 61 µg/m³; NO_x mean concentration 18.8 ppm; CO mean concentration 80 ppm) failed to increase numbers of inflammatory cells in BALF collected 18 h after the last exposure. However, a statistically significant increase in total cells and macrophages was observed in response to resuspended road dust (PM_{2.5}) at 3,500 µg/m³, but not at 500 µg/m³.

Model Particles

In a study by Elder et al. (2004, [055642](#)), pulmonary inflammation was investigated in two compromised, aged animal models (11-14 mo old SH and 23 mo old F344) exposed by inhalation to UF CB (count median diameter = 36 nm) at a relevant concentration ($150 \mu\text{g}/\text{m}^3$). No changes in BALF cells were seen 24 h post-exposure in either model.

An increase in BALF neutrophils was observed at 24 h, but not at 4 h, in WKY rats exposed to UF carbon particles (median particle size 38 nm; mass concentration $180 \mu\text{g}/\text{m}^3$; mean number concentration 1.6×10^7 particles/ cm^3) for up to 24 h (Harder et al., 2005, [087371](#)). Changes in HR and HRV demonstrated in this study (Section 6.2.1.3) occurred much more rapidly than the inflammatory response.

No evidence of pulmonary inflammation was found by analysis of BALF or histology one or three days following 24-h exposure of SH rats to UF carbon particles under similar conditions (median particle size 31 nm; mass concentration $172 \mu\text{g}/\text{m}^3$; mean number concentration 9.0×10^6 particles/ cm^3) (Upadhyay et al., 2008, [159345](#)). However increased expression of HO-1, ET-1, ET_A and ET_B, tPA and plasminogen activator-1 was found in lung tissue three days following exposure.

In a study by Gilmour et al. (2004, [054175](#)), adult Wistar rats were exposed for 7 h to fine and UF CB particles (mean mass concentration $1,400$ and $1,660 \mu\text{g}/\text{m}^3$ for fine and UF CB, respectively; mean number concentration 3.8×10^3 and 5.2×10^4 particles/ cm^3 , respectively; count median aerodynamic diameter 114 nm and 268 nm, respectively). Both treatments resulted in increased BALF neutrophils 16 h post-exposure, with the UFPs having the greater response. UFPs also increased total BALF leukocytes and macrophage inflammatory protein-2 (MIP-2) mRNA in BALF cells. Although these exposures may not be relevant to ambient exposures, this study demonstrated the greater propensity of UF CB particles to cause a pro-inflammatory response compared with fine CB particles.

In a study by Last et al. (2004, [097334](#)), mice were exposed to $250 \mu\text{g}/\text{m}^3$ laboratory-generated iron-soot over a 2-wk period as described in Section 6.3.2.3. BALF was collected 1-h after the last exposure and analyzed for total cells. No increase in total cell number was observed following iron-soot exposure. Other findings of this study are described in Sections 6.3.2.3 and 6.3.5.3.

Pinkerton et al. (2008, [190471](#)) exposed young adult male SD rats to filtered air, iron, soot or iron-soot for 6 h/day for 3 days. The iron particles were mainly less than 100 nm aerodynamic diameter, while the soot particles were initially 20-40 nm in diameter but formed clusters of 100-200 nm in diameter. The size-distribution of iron-soot particles was bimodal over 10-250 nm and averaged 70-80 nm in diameter. Rats were exposed to 45 , 57 and $90 \mu\text{g}/\text{m}^3$ iron or to $250 \mu\text{g}/\text{m}^3$ soot alone or in combination with $45 \mu\text{g}/\text{m}^3$ iron. Increased levels of the pro-inflammatory cytokine IL-1 β were observed in lung tissue of rats exposed for 6 h/day for 3 days to $90 \mu\text{g}/\text{m}^3$, but not $57 \mu\text{g}/\text{m}^3$, iron. No change in BALF inflammatory cells was observed after exposure to $57 \mu\text{g}/\text{m}^3$ or $90 \mu\text{g}/\text{m}^3$ iron. Exposures to $250 \mu\text{g}/\text{m}^3$ soot in combination with $45 \mu\text{g}/\text{m}^3$ iron also resulted in increased levels of lung IL-1 β and activation of the transcription factor NF- κ B. Levels of lung IL-1 β were increased in neonatal rats exposed to $250 \mu\text{g}/\text{m}^3$ soot in combination with 100, but not 30, $\mu\text{g}/\text{m}^3$ iron. Other endpoints of this study are described in Section 6.3.4.2.

Summary of Toxicological Study Findings for Pulmonary Inflammation

New studies involving short-term exposures to CAPs and urban air strengthen the evidence of PM-induced pulmonary inflammation. In addition, several studies demonstrated pulmonary inflammation in response to diesel and gasoline exhaust; however it is not known whether PM or gaseous components of the exhaust were responsible for these effects. Mixed results were obtained in studies using model particles such as CB and iron-soot.

6.3.4. Pulmonary Oxidative Responses

The results of a small number of controlled human exposure and toxicological studies presented in the 2004 PM AQCD (U.S. EPA, 2004, [056905](#)) provided some initial evidence of an association between exposure to PM and pulmonary oxidative stress. Recent controlled human

exposure studies have provided support for previous findings of an increase in markers of pulmonary oxidative stress following exposure to DE, and one new study has observed a similar effect following controlled exposure to wood smoke. New findings from toxicological studies provide further evidence that oxidative species are involved in PM-mediated effects. No epidemiologic studies have evaluated the association between PM concentration and pulmonary oxidative response.

6.3.4.1. Controlled Human Exposure Studies

Two studies cited in the 2004 PM AQCD (U.S. EPA, 2004, [056905](#)) observed effects on markers of airway oxidative response in healthy adults following controlled exposures to fresh DE or resuspended DE particles (Blomberg et al., 1998, [051246](#); Nightingale et al., 2000, [011659](#)). Several recent studies are described below which have further evaluated the oxidative response following exposure to particles in human volunteers.

Diesel Exhaust

Pourazar et al. (2005, [088305](#)) exposed 15 adults (11 males and four females) for 1 h to air or DE (PM₁₀ concentration 300 µg/m³) in a controlled cross-over study. Bronchoscopy with airway biopsy was performed 6 h after exposure. The expression of NF-κB, AP-1 (c-jun and c-fos), p38, and JNK in bronchial epithelium was quantified using immunohistochemical staining. DE was observed to significantly increase nuclear translocation of NF-κB, AP-1, phosphorylated p38, and phosphorylated JNK; however, the findings of this study require confirmation with more quantitative methods such as Western blot analysis. The observed activation of redox-sensitive transcription factors by DE may result in the induction of pro-inflammatory cytokines. There is some evidence to suggest that this bronchial response to DE is mediated through the epidermal growth factor receptor signaling pathway (Pourazar et al., 2008, [156884](#)). Behndig et al. (2006, [088286](#)) evaluated the upregulation of endogenous antioxidant defenses following exposure to DE (100 µg/m³ PM₁₀) in a group of 15 healthy adults. Increases in urate and reduced GSH were observed in alveolar lavage, but not bronchial wash, 18 h after exposure. In a study utilizing the same exposure protocol, Mudway et al. (2004, [180208](#)) observed an increase in GSH and ascorbate in nasal lavage fluid 6 h following exposure to DE in a group of 25 healthy adults.

Wood Smoke

Barregard et al. (2008, [155675](#)) observed a significant increase in malondialdehyde levels in breath condensate of healthy volunteers (n = 13) immediately following and 20 h after a 4-h exposure to wood smoke (240-280 µg/m³ PM).

Endobronchial Instillation

Schaumann et al. (2004, [087966](#)) demonstrated an increased oxidant radical generation of BALF cells following endobronchial instillation of urban particles compared with instillation of particles collected in a rural area. The authors suggested that this difference was likely due to the greater concentration of transition metals found in the urban particles.

Summary of Controlled Human Exposure Study Findings for Pulmonary Oxidative Responses

Taken together, these studies suggest that short-term exposure to PM at near ambient levels may produce mild oxidative stress in the lung. Limited data suggest that proximal and distal lung regions may be subject to different degrees of oxidative stress during exposures to different pollutant particles.

6.3.4.2. Toxicological Studies

The 2004 PM AQCD (U.S. EPA, 2004, [056905](#)) reported one study which provided evidence that ROS were involved in PM-mediated responses. This particular study used pre-treatment with the antioxidant DMTU to block the neutrophilic response to ROFA. More recently, several studies evaluated the effects of PM exposure on pulmonary oxidative stress. Oxidative stress can be directly determined by measuring ROS or oxidation products of lipids and proteins. An indirect assay involves measurement of the enzyme HO-1 or of the antioxidant enzymes SOD or catalase, all of which can be induced by oxidative stress. Antioxidant interventions which inhibit or prevent responses are a further indirect measure of oxidative stress playing a role in the pathway of interest.

CAPs

Gurgueira et al. (2002, [036535](#)) measured oxidative stress as in situ CL. Immediately following a 5-h PM_{2.5} CAPs exposure (mean mass concentration range 99.6-957.5 µg/m³; Boston, MA) increased CL was observed in lungs of CAPs-exposed rats. CL evaluated after CAPs exposure durations of 3 h was also increased but did not achieve statistical significance compared to the filtered air group. When animals were allowed to recover for 24 h following the 5-h CAPs exposure, CL levels returned to control values. Interestingly, a decrease in lung CL was observed in rats breathing filtered air for three days compared with rats breathing room air for the same duration. To compare potential particle-induced differences in in situ CL, rats were exposed to ROFA (1.7 mg/m³ for 30 min) or CB (170 µg/m³ for 5 h). Only the ROFA-treated animals exhibited increased CL in lung tissue. Additionally, levels of antioxidant enzymes in the lung (MnSOD and catalase) were increased in CAPs-exposed rats. A CAPs-associated increase in CL was also seen in the heart (Section 6.2.9.3), but not the liver.

In a similar study, Rhoden et al. (2004, [087969](#)) exposed SD rats for 5 h to PM_{2.5} CAPs from Boston (mean mass concentration 1,228 µg/m³) or to filtered air. Significant increases in TBARS and protein carbonyl content (a measure of protein oxidation) were observed 24 h post-exposure to CAPs. Pretreatment with the thiol antioxidant NAC (50 mg/kg i.p.) 1-h prior to exposure prevented not only the lipid and protein oxidation observed in response to CAPs, but also the increase in BALF neutrophils and pulmonary edema in this model (Sections 6.3.3.3 and 6.3.5.3). Results of this study demonstrate the key role played by oxidative stress in these CAPs-mediated effects.

A later study by Rhoden et al. (2008, [190475](#)) investigated the role of superoxide in mediating pulmonary inflammation following exposure to ambient air particles. In this study, adult SD rats were exposed by IT instillation to 1 mg of SRM1649. Two hours prior to exposure, half of the rats were pretreated with the membrane-permeable SOD mimetic MnTBAP (10 mg/kg, i.p.). MnTBAP abrogated the inflammatory response, measured by increased BALF inflammatory cells, and the increase in lung superoxide, measured by CL, observed 4 h following exposure to urban air particles.

Kooter et al. (2006, [097547](#)) reported an increase in HO-1 in BALF and lung tissue measured 18 h after a 2-day exposure (6 h/day) of SH rats to PM_{2.5} or PM_{2.5}+UF CAPs (mean mass concentration range 399-3613 and 269-556 µg/m³, respectively; PM_{2.5} CAPs site in Bilthoven and PM_{2.5}+UF site in freeway tunnel in Hendrik-Ido-Ambacht, the Netherlands). This occurred in the absence of any measurable pulmonary inflammation (Section 6.3.3.3).

Urban Air

To evaluate oxidative stress responses to ambient particles from vehicles, Wistar rats were exposed to ambient urban air from a high traffic site (concentration range 22-225 µg/m³ PM₁₀; Porto Alegre, Brazil) or to the same air which was filtered to remove the PM (Pereira et al., 2007, [156019](#)). Several exposure regimens were carried out: 6- and 20-h continuous exposures or to intermittent exposures of 5 h/day for four consecutive days. A significant increase in lipid peroxidation (measured as malondialdehyde) was seen in lung tissue immediately following the 20-h continuous exposure, but not following the 6-h exposure or the intermittent exposures. Inflammation-related endpoints are described in Section 6.3.3.3.

Diesel Exhaust

Li et al. (2007, [155929](#)) exposed mice to clean air or to low dose DE (100 $\mu\text{g}/\text{m}^3$ PM) for 7 h/day and 5 days/wk for 1, 4 and 8 wk as described in Section 6.3.2.3. HO-1 mRNA and protein were increased in lung tissues of both mouse strains after 1 wk of DE exposure. In addition, AHR and changes in BALF cells and cytokines were observed (Sections 6.3.2.3 and 6.3.3.3). Pretreatment with the thiol antioxidant NAC (320 mg/kg, i.p.) on days 1-5 of DE exposure greatly attenuated the AHR and inflammatory response seen after 1 wk of DE exposure. Long-term responses are discussed in Sections 7.3.2.2, 7.3.3.2 and 7.3.4.1.

A study by Whitekus et al. (2002, [157142](#)) investigated the adjuvant effects of DE particles in an allergic animal model and is discussed in detail below (Section 6.3.6.3). Intervention with the thiol antioxidants mucillamine and NAC inhibited the increases in allergen-specific IgE and IgG₁ as well as the increases in protein carbonyl and lipid hydroperoxides in the lung following DE particle exposure.

Gasoline Exhaust

Pulmonary oxidative stress was evaluated by measurement of CL and TBARS following exposure of SD rats to gasoline engine exhaust (Seagrave et al., 2008, [191990](#)). Animals were exposed for 6 h in a nose-only inhalation exposure system. PM mass concentration was reported to be 60 $\mu\text{g}/\text{m}^3$; count median diameter 20 nm; mass median diameter 150 nm; while the concentrations of gaseous copollutants were 104 ppm CO, 16.7 ppm NO, 1.1 ppm NO₂ and 1.0 ppm SO₂. A statistically significant increase in lung CL was observed without a concomitant increase in lung TBARS. Discordant results were also observed for road dust exposures in the heart (Section 6.2.9.3). The discrepancy between oxidative stress indicators suggests that the responses may follow different time courses. Furthermore, no CL was seen when the gasoline exhaust was filtered to remove the particulate fraction.

Model Particles

Increased expression of HO-1 was observed in lung tissue three days following 24-h exposure of SH rats to UF carbon particles (median particle size 31 nm; mass concentration 172 $\mu\text{g}/\text{m}^3$; mean number concentration 9.0×10^6 particles/cm³) despite no evidence of pulmonary inflammation (Section 6.3.3.3) (Upadhyay et al., 2008, [159345](#))

In a study conducted by Pinkerton et al. (2008, [190471](#)), young adult male SD rats were exposed to filtered air, soot, iron or iron-soot for 6 h/day for three days as described in Section 6.3.3.3. A statistically significant decrease in total antioxidant power and a statistically significant increase in glutathione-S-transferase activity were observed in lung tissue from rats exposed to 90 $\mu\text{g}/\text{m}^3$ iron. This high concentration iron exposure also resulted in increased levels of ferritin protein in lung tissue, indicating the presence of free iron which has the potential to redox cycle and cause oxidative stress. Lung tissue total antioxidant power was decreased and glutathione redox ratio was increased by the combined exposure to 250 $\mu\text{g}/\text{m}^3$ soot and 45 $\mu\text{g}/\text{m}^3$ iron. The iron-soot exposure also increased oxidized glutathione in BALF and lung tissue. These results demonstrate that co-exposure to soot enhanced iron-mediated oxidative stress. Furthermore, co-exposure to soot and iron resulted in increased expression of cytochrome P450 isozymes CYP1A1 and CYP2E1 in lung tissue, an effect not observed in response to either agent alone. Inflammation-related endpoints observed in this study are described in Section 6.3.3.3.

In a parallel study, Pinkerton et al. (2008, [190471](#)) exposed neonatal male SD rats to iron-soot or filtered air 6 h/day for three days during the second and fourth week of life. Both 30 $\mu\text{g}/\text{m}^3$ and 100 $\mu\text{g}/\text{m}^3$ iron in combination with 250 $\mu\text{g}/\text{m}^3$ soot resulted in increased BALF oxidized glutathione, glutathione redox ratio and glutathione-S-transferase activity and decreased total antioxidant power. The higher concentration exposure resulted in increased ferritin expression in lung tissue. Effects on cellular proliferation in specific regions of the lung were also noted as described in Section 6.3.5.3.

Nurkiewicz et al. (2009, [191961](#)) exposed SD rats to fine (count median diameter 710 nm) and UF (count median diameter 100 nm) TiO₂ particles via aerosol inhalation at concentrations of 1.5-16

mg/m³ for 240-720 min. These exposures were chosen in order to produce deposition of 4-90 µg/rat, which was demonstrated in a previous study to result in different degrees of impaired microvascular function (Nurkiewicz et al., 2008, [156816](#)). Histological analysis of lung tissue did not find any significant inflammation, although particle accumulation in alveolar macrophages and a frequent association of alveolar macrophage with the alveolar wall was observed 24 h following exposure (Nurkiewicz et al., 2008, [156816](#)). Although the main focus of the more recent study was on effects of TiO₂ on NO production and microvascular reactivity in the spinotrapezius muscle (Section 6.2.4.3), the presence of nitrotyrosine was determined in both lung tissue and spinotrapezius muscle as a measure of peroxynitrite formation. Peroxynitrite formation occurs mainly as a result of the rapid reaction of NO with superoxide and suggests an increase in local superoxide production. The area of lung tissue containing nitrotyrosine immunoreactivity increased three-fold 24 h following exposure to 10 µg UF TiO₂. Nitrotyrosine immunoreactivity was localized in inflammatory cells found in the alveolar region of the lung.

Summary of Toxicological Study Findings for Pulmonary Oxidative Responses

New studies involving short-term exposure to CAPs, urban air, diesel and gasoline exhaust, and model particles such as CB, iron-soot and TiO₂ consistently demonstrate pulmonary oxidative responses. Furthermore, antioxidant treatment ameliorated effects observed in response to CAPs, DE and DE particles.

6.3.5. Pulmonary Injury

The 2004 PM AQCD (U.S. EPA, 2004, [056905](#)) presented evidence from several toxicological studies of small PM-induced increases in markers of pulmonary injury including thickening of alveolar walls and increases in BALF protein. These findings are consistent with the results of recent toxicological and controlled human exposure studies demonstrating mild pulmonary injury accompanying inflammatory responses to CAPs and wood smoke. One recent epidemiologic study has also observed a positive association between PM and urinary concentrations of lung Clara cell protein.

6.3.5.1. Epidemiologic Studies

One epidemiologic study examined biomarkers of pulmonary injury. The mean concentration data from this study are characterized in Table 6-10. Timonen et al. (2004, [087915](#)) enrolled subjects with coronary heart disease in Amsterdam (n = 37), Erfurt, Germany (n = 47) and Helsinki (n = 47) to study daily variation in PM and urinary concentrations of lung Clara cell protein (CC16). No associations were seen between the PNC of the smallest particles (NC_{0.01-0.1}) and CC16. Significant associations with NC_{0.1-1} and PM_{2.5} (which were strongly correlated with each other [r = 0.8]) were seen only for Helsinki subjects: same day, lag 3 and 5-day mean NC_{0.1-1} increases of 1000 particles/cm³ were associated with increases in ln (CC16/creatinine) of 15.5% (95% CI: 0.001-30.9), 17.4% (95% CI: 3.4-31.4), and 43.2% (95% CI: 17.4-69.0), respectively. Similar associations were seen for 10 µg/m³ increases in PM_{2.5}: lag 0 and 5-day mean PM_{2.5} were associated with increases in ln (CC16/creatinine) of 23.3% (95% CI: 6.3-40.3) and 38.8% (95% CI: 15.8-61.8), respectively.

6.3.5.2. Controlled Human Exposure Studies

No studies of controlled human exposures presented in the 2004 PM AQCD (U.S. EPA, 2004, [056905](#)) specifically examined the effect of PM on pulmonary injury. However, several recent studies have evaluated changes in markers of injury and increased alveolar permeability following exposures to various types of particles.

Urban Traffic Particles

Bräuner et al. (2009, [190244](#)) evaluated the effect of exposure to urban traffic particles (24-h exposure, $PM_{2.5}$ $9.7 \mu\text{g}/\text{m}^3$) on the integrity of the alveolar epithelial membrane in a group of 29 healthy adults, with and without exercise. Following 2.5 h of exposure, alveolar epithelial permeability was assessed by measuring the pulmonary clearance of $^{99\text{m}}\text{Tc}$ -DTPA, which was administered as an aerosol during 3 min of tidal breathing. While pulmonary clearance of $^{99\text{m}}\text{Tc}$ -DTPA was observed to increase following exercise, there was no significant difference in clearance between exposure to urban traffic particles and filtered air. In addition, PM exposure was not observed to affect the level of CC16 in plasma or urine at 6 or 24 h after the start of exposure.

Diesel Exhaust

Relative to filtered air, exposure for 1 h to DE ($300 \mu\text{g}/\text{m}^3$ PM) was not observed to affect the plasma CC16 concentration at 6 or 24 h post exposure in a group of 15 former smokers with COPD (Blomberg et al., 2005, [191991](#)).

Wood Smoke

In a study examining the respiratory effects of wood smoke, Barregard et al. (2008, [155675](#)) exposed two groups of healthy adults in separate 4-h sessions to wood smoke with median particle concentrations of 243 and $279 \mu\text{g}/\text{m}^3$. At 20 h post-exposure, the mean serum CC16 concentration was significantly higher after exposure to wood smoke when compared with filtered air. However, when the analysis was stratified by exposure session, a statistically significant effect of wood smoke on serum CC16 was observed in the subjects in session 1 but not those in session 2. It is interesting to note that while the mean particle concentration was only slightly higher in session 1, the mean particle number in session 1 was almost 90% higher than the particle number in session 2, with geometric mean particle diameters of 42 and 112 nm, respectively.

Summary of Controlled Human Exposure Study Findings for Pulmonary Injury

The findings from these studies provide limited evidence to suggest that exposures to particles may increase markers of pulmonary injury in healthy adults.

6.3.5.3. Toxicological Studies

The 2004 PM AQCD (U.S. EPA, 2004, [056905](#)) reported mild increases in BALF protein, a marker of pulmonary injury, in several studies involving inhalation exposure to CAPs. In addition, histological analysis demonstrated that the bronchoalveolar junction was the site of the greatest inflammation following CAPs exposure. Low level exposure to DE was associated with Type 2 cell proliferation and thickening of alveolar walls near alveolar macrophages according to the 2002 EPA Diesel Document (U.S. EPA, 2002, [042866](#)). In addition, IT instillation of fly ash and metal-containing PM generally caused pulmonary injury as measured by increases in BALF protein, LDH and albumin. Proliferation of bronchiolar epithelium was also noted. More recent studies of BALF markers of pulmonary injury and histological analysis of lung tissue are summarized below.

BALF Markers of Pulmonary Injury and Increased Permeability

CAPs

Kodavanti et al. (2005, [087946](#)) exposed SH and WKY rats to filtered air or $PM_{2.5}$ CAPs from RTP, NC as described in Section 6.3.3.3. Differences in baseline parameters were noted for the two rat strains since SH rats had greater levels of protein and lower levels of LDH, NAG, ascorbate and

uric acid in the BALF compared with WKY rats. One day after the 2-day CAPs exposure, increased levels of GGT were observed in BALF (a marker of epithelial injury) of SH rats, but not WKY rats, compared with filtered air controls. Injury was not accompanied by inflammation (Section 6.3.3.3).

In a study by Cassee et al. (2005, [087962](#)), SH rats were exposed for 6 h by nose-only inhalation to CAPs from three different sites in the Netherlands as described in Section 6.3.3.3. The pulmonary injury marker CC16 was increased in BALF two days following CAPs exposure. Inflammation was also observed (Section 6.3.3.3).

Gurgueira et al. (2002, [036535](#)) exposed SD rats to Boston, MA CAPs as described in Section 6.3.4.2 and reported a small but statistically significant increase in lung wet/dry ratios after 3 and 5 h of exposure, indicating the presence of mild edema. This response was accompanied by increased oxidative stress as measured by in situ CL (Section 6.3.4.2). In a similar study, Rhoden et al. (2004, [087969](#)) reported an increase in lung wet/dry ratio in rats 24 h following a 5-h exposure to Boston CAPs which was diminished by pre-treatment of the antioxidant NAC (Section 6.3.4.2).

Pulmonary injury was investigated in two studies using a rat model of pulmonary hypertension (SD rats pre-treated with monocrotaline) which is described in greater detail in Section 6.3.3.3 (Lei et al., 2004, [087999](#)). Significant increases in BALF LDH and protein were observed in response to CAPs. Pulmonary inflammation was observed in both of these studies (Section 6.3.3.3).

Diesel Exhaust

In a study evaluating the effects of DE, no changes were observed in BALF protein and LDH in mice exposed by inhalation to concentrations of 50 and 2000 $\mu\text{g}/\text{m}^3$ DE particles for 4 h/day on 5 consecutive days as described in Section 6.3.3.3 (Stevens et al., 2008, [157010](#)). Changes in gene expression were observed in the higher exposure group. This study demonstrates that changes in gene expression can occur in the absence of measurable markers of injury or pulmonary inflammation.

In a study by Wong et al. (2003, [097707](#)), also reported by Witten et al. (2005, [087485](#)), rats were exposed nose-only to filtered room air or to DE over a 3-wk period. This study, focusing on neurogenic inflammation, is described in greater detail in Section 6.3.3.3. Pulmonary plasma extravasation was measured by the $^{99\text{m}}$ Technecium-albumin technique and found to be dose-dependently increased in the bronchi and lung. Pretreatment with capsaicin, which inhibits neurogenic inflammation by activating C-fibers and causing the depletion of neuropeptide stores, did not reduce plasma extravasation following DE exposure. Hence, DE is unlikely to act through bronchopulmonary C-fibers to cause neurogenic edema in this model. Inflammatory responses measured in this study are discussed in Section 6.3.3.3.

Gasoline Exhaust

Healthy male Swiss mice were exposed to gasoline exhaust (635 $\mu\text{g}/\text{m}^3$ PM and associated gases) or filtered air for 15 min/day for 7, 14, and 21 days as described in Section 6.3.3.3 (Sureshkumar et al., 2005, [088306](#)). BALF was collected for analysis 1-h after the last exposure. Statistically significant increases in BALF markers of lung injury, alkaline phosphatase, gamma-glutamyl transferase and LDH, were observed at all time points studied. Alveolar edema was noted following 14 and 21 days of exposure. Other findings of this study, including inflammation and histopathological changes, are discussed in Section 6.3.3.3 and below.

Histopathology

CAPs

Histopathological changes were demonstrated in rats exposed for 5 h to Boston CAPs as described in Section 6.3.3.3 (Rhoden et al., 2004, [087969](#)). Slight bronchiolar inflammation and thickened vessels at the bronchiole were observed 24 h post-exposure, consistent with the influx of polymorphonuclear leukocytes observed in BALF (Section 6.3.3.3).

Diesel Exhaust

In a study by Wong et al. (2003, [097707](#)), also reported by Witten et al. (2005, [087485](#)), rats were exposed nose-only to filtered room air or to DE over a 3-wk period. This study, focusing on neurogenic inflammation, is described in greater detail in Section 6.3.3.3. Pulmonary inflammation was evaluated by histological analysis of lung tissue. Following high, but not low, concentration-exposure to DE, a large number of alveolar macrophages was found in the lungs. Small black particles, presumably DE particles, were found in the cytoplasm of these alveolar macrophages. Perivascular cuffing consisting of mononuclear cells was also observed in the high exposure animals. Influx of neutrophils or eosinophils was not seen although mast cell number was increased. Other indices of injury demonstrated in this study are described above.

Gasoline Exhaust

Another study, which is described in greater detail in Section 6.3.3.3, demonstrated histopathological responses to gasoline exhaust in mice exposed to gasoline exhaust or filtered air for 15 min/day for 7, 14, and 21 days (Sureshkumar et al., 2005, [088306](#)). Histological observations showed inflammatory cell infiltrate in the peribronchiolar and alveolar region, alveolar edema and thickened alveolar septa at 14 and 21 days post-exposure. Levels of pro-inflammatory cytokines and marker enzymes of lung damage were also increased in BALF. The numbers of inflammatory cells in BALF was increased but not significantly, demonstrating that BALF analysis of inflammatory cells was a less sensitive indicator of pulmonary inflammation in this study than histological analysis. Other indices of injury found in this study are described above.

Model Particles

In a study investigating the effects of iron-soot, mice were exposed to 250 $\mu\text{g}/\text{m}^3$ laboratory-generated iron-soot as described in Sections 6.3.2.3 and 6.3.3.3 (Last et al., 2004, [097334](#)). Analysis of airway collagen content was conducted by histology and by biochemical analysis of microdissected airways. No increases in airway collagen content were found by either method in mice exposed to iron-soot for two weeks. Furthermore, no goblet cells were observed in airways of air or iron-soot exposed animals. Other findings of this study are described in Sections 6.3.2.3 and 6.3.3.3.

One study demonstrating histopathological responses to PM in neonatal rats was reported by Pinkerton et al. (2004, [087465](#)). Rat pups (10 days old) were exposed to soot and iron particles (mean mass concentration of 243 $\mu\text{g}/\text{m}^3$; iron concentration 96 $\mu\text{g}/\text{m}^3$; size range 10-50 nm) for 6 h/day on 3 consecutive days. Cell proliferation in different lung regions was evaluated following bromodeoxyuridine injection 2 h prior to necropsy. The rate of cell proliferation in the proximal alveolar region (immediately beyond the terminal bronchioles) was significantly reduced in iron-soot exposed animals compared to controls. This was a region-specific response since the rate of cell proliferation was not altered in the terminal bronchioles or the general lung parenchyma. However alveolar septation, the process by which alveoli are formed during development, and alveolar growth were not altered by iron-soot exposure. Decreased cell viability and increased LDH was also noted in BALF of neonatal rats (Pinkerton et al., 2008, [190471](#)). The authors suggest the possibility of greater susceptibility to air pollution during the critical postnatal lung development period which occurs in animals and humans and that neonatal exposure to PM may contribute to impaired lung growth seen in children.

Summary of Toxicological Study Findings for Pulmonary Injury

New studies involving short-term exposure to CAPs and diesel and gasoline exhaust demonstrate mild pulmonary injury, including enhanced BALF markers of injury, pulmonary edema and histopathology. In general, injury responses were accompanied by inflammatory responses. In addition, altered cellular proliferation in the proximal alveolar region was observed in neonatal rats exposed to iron-soot, suggesting the possibility of greater susceptibility to PM during postnatal lung development.

Relative Toxicity of PM Size Fractions

Ambient PM Studies

A recently undertaken multinational project entitled “Chemical and biological characterization of ambient thoracic coarse (PM_{10-2.5}), fine (PM_{2.5-0.2}), and UFPs (PM_{0.2}) for human health risk assessment in Europe” (PAMCHAR) takes a systematic approach to expanding the present knowledge about the physiochemical and toxicological effects of these three PM size fractions. Six European cities were selected that represented contrasting ambient PM profiles: Helsinki, Duisburg, Prague, Amsterdam, Barcelona, and Athens. For PM collected at all sites, PM_{10-2.5} induced the greatest pulmonary effects in C57BL/6J mice IT instilled with 1, 3, or 10 mg/kg of particles (Happo et al., 2007, [096630](#)). Dose-response relationships in BALF parameters measured 24 h post-IT instillation exposure, including cell number and protein, were observed for all sites following PM_{10-2.5}, and neutrophils were the predominant cell type present in the BALF (Happo et al., 2007, [096630](#)). Prague PM_{10-2.5} exposure resulted in decreased macrophages in BALF at 12 h, and Amsterdam, Barcelona, and Athens PM_{10-2.5} induced lymphoplasmacytic cells in BALF (Happo et al., 2007, [096630](#)). No inflammatory responses were observed for UFPs measured 12-h after exposure. Protein was elevated for PM_{10-2.5} for all locations with the 10 mg/kg dose; Athens UFPs induced protein release only at the two lowest doses 12 h post-exposure. For TNF- α and IL-6, the greatest response was observed with PM_{10-2.5} 4 h following exposure (Happo et al., 2007, [096630](#)). Exposure to UFPs from Duisburg resulted in elevated TNF- α for the 1 and 3 mg/kg doses. Only the Helsinki sample appeared to induce the same level of IL-6 release for PM_{10-2.5} and PM_{0.2} at 10 mg/kg, albeit the collection times differed. In vitro TNF- α and IL-6 responses did not always reflect in vivo effects (Table 6-11), as the Duisburg PM_{10-2.5} sample was the most potent in vivo compared to the other sites and elicited much lower cytokine release compared to other cities (except Helsinki) in vitro (Happo et al., 2007, [096630](#); Jalava et al., 2006, [155872](#); Jalava et al., 2008, [098968](#)). Helsinki PM was collected in the spring and generally had the lowest in vivo and in vitro activity for PM_{10-2.5} compared to the other cities (Happo et al., 2007, [096630](#); Jalava et al., 2006, [155872](#); Jalava et al., 2008, [098968](#)). Spring-time samples were collected because episodes of resuspended road dust occur frequently during this season (Pennanen et al., 2007, [155357](#)). There was a high correlation between EC content in PM_{2.5} and PM_{10-2.5}, indicating that traffic impacted both size fractions (Sillanpaa et al., 2005, [156980](#)). Duisburg PM collected in fall had the greatest amounts of Mn and Zn compared to PM samples from other locations (Pennanen et al., 2007, [155357](#)). Metals industries in Duisburg are likely contributors to the observed PM metals concentrations. For the Prague winter PM samples, the As content was higher than at any other location (Pennanen et al., 2007, [155357](#)). Prague also had the highest PAH levels in all three size fractions, possibly attributable to stable atmosphere conditions and incomplete combustion of coal and biomass in residential heating (Pennanen et al., 2007, [155357](#)). High levels of ammonium and nitrate in PM samples from Amsterdam suggest traffic as a large source of air pollution (Pennanen et al., 2007, [155357](#)). Approximately one-third of PM_{10-2.5} mass from Amsterdam was comprised of sea salt (Sillanpaa et al., 2005, [156980](#)), double that of any other city. In Barcelona and Athens, high calcium or Ca²⁺ contents in spring and summer PM_{2.5} and PM_{10-2.5} are indicative of resuspended soil-derived particles (Pennanen et al., 2007, [155357](#)).

Table 6-11. PAMCHAR PM_{10-2.5} inflammation results with ambient PM.

City and Season	In Vivo ^a (mg/kg)					In Vitro ^b (µg/mL)			
	BALF protein	BALF TNF-α	BALF IL-6	BALF KC	BALF PMN	BALF AM	TNF-α	IL-6	MIP-2
Helsinki spring	+10	+10	+10	[+3 10]	+10	--	+150,300	+150,300	+150,300
Duisburg fall	+10	+10	+10	+10	+10	--	+150,300	+150,300	+300
Prague winter	+10	[+3 10]	+10	[+3 10]	+10	+10	+150,300	+150,300	+150,300
Amsterdam winter	+10	+10	+10	+10	+10	--	+150	+150,300	+150,300
Barcelona spring	+10	+10	[+3 10]	+10	+10	--	+150,300	+150,300	+150,300
Athens summer	+10	[+3 10]	[+3 10]	[+3 10]	+10	--	+150,300	+150,300	+150,300

^aSource: Happo et al. (2007, [096630](#)); 2 cell lines used for in vitro study were RAW264.7
^bSource: Jalava et al. (2006, [155872](#)); + indicates increased response and numbers that follow indicate at which dose the response was observed

Schins et al. (2004, [054173](#)) employed PM from two cities in Germany, Duisburg and Borken, in another study. In contrast to the PAMCHAR study where animals were administered PM suspended in pathogen-free water (Happo et al., 2007, [096630](#)), animals received PM via IT instillation suspended in saline at a dose of 320 µg (Schins et al., 2004, [054173](#)). In female Wistar rats, neutrophils in BALF were significantly elevated for PM_{10-2.5} from Duisburg and Borken (Table 6-12), albeit the percent of neutrophils with the PM_{10-2.5} from Borken was nearly double that of Duisburg. The responses with PM_{2.5} were much smaller. When these PM_{10-2.5} particles were introduced into whole blood to determine overall inflammatory capacity, IL-8 and TNF-α were released in greater quantities than in response to PM_{2.5}. Furthermore, PM_{10-2.5} from Borken induced higher cytokine responses than Duisburg PM_{10-2.5}.

An in vivo study involving SH rats was conducted using PM_{10-2.5} and PM_{2.5} from six different European locations with varying traffic densities (3 or 10 mg/kg IT instillation; UFPs were not collected) (Gerlofs-Nijland et al., 2007, [097840](#)). It was reported that PM_{10-2.5} generally induced greater responses than PM_{2.5}. IT instillation of PM_{10-2.5} from a location with high traffic influence in Munich, Germany, demonstrated the greatest response in terms of LDH activity, protein, total cells, neutrophils, and lymphocytes in BALF 24 h post-exposure. PM_{10-2.5} collected from a low traffic site in Munich induced the greatest cytokine response for TNF-α and MIP-2. Some correlations were observed between PM_{10-2.5} components (Ba and Cu) and BALF parameters, but were largely driven by one location (Gerlofs-Nijland et al., 2007, [097840](#)).

Table 6-12. Other ambient PM – in vivo PM_{10-2.5} studies – BALF results, 18-24 h post-IT exposure.

Location	Endotoxin (~ Values)	Dose (mg/kg)	Cell Differentials	Cytokines	Injury Biomarkers	Reference
Germany, Borken; rural Feb-May 2000	6.6 EU/mg	0.58-0.91	↑* % PMN	↑ TNF-α		Schins et al. (2004, 054173)
Germany, Duisburg; heavy industry Feb-May 2000	5.0 EU/mg	0.58-0.91	↑ % PMN	↑ MIP-2		Schins et al. (2004, 054173)
USA, Seattle, WA Feb-March 2004	6.0 EU/mg	1.25, 5.0				Gilmour, et al. (2007, 096433)
USA, Salt Lake City, UT Apr-May 2004	6.3 EU/mg	1.25, 5.0			↑ protein	Gilmour, et al. (2007, 096433)
USA, South Bronx, NY Dec 2003-Jan 2004	2.8 EU/mg	1.25, 5.0	↑ PMN	↑ MIP-2		Gilmour, et al. (2007, 096433)
USA, Sterling Forest, NY Dec 2003-Jan 2004	2.9 EU/mg	1.25, 5.0				Gilmour, et al. (2007, 096433)

Location	Endotoxin (~ Values)	Dose (mg/kg)	Cell Differentials	Cytokines	Injury Biomarkers	Reference
USA, RTP, NC Oct-Nov 1996	0.96 EU/mg	0.5, 2.5, 5.0	↑↑ PMN	↑ IL-6		Dick (2003, 088776)
Germany, Munich Ost Bahnhof; high traffic A Aug 2002	2.9 EU/mg	3, 10	↑↑* total cells ↑↑ AM ↑↑* PMN ↑↑* Lymph	↑↑ MIP-2 ↑↑ TNF-α	↑↑* LDH ↑* protein	Gerlofs-Nijland, et al. (2007, 097840)
Netherlands, Hendrik-Ido-Ambacht; high traffic Sept 2002	6.5 EU/mg	3, 10	↑↑ total cells ↑↑* AM ↑↑ PMN ↑↑ Lymph	↑ MIP-2 ↑↑ TNF-α	↑↑ LDH ↑ protein	Gerlofs-Nijland, et al. (2007, 097840)
Italy, Rome; high traffic Apr 2002	1.5 EU/mg	3, 10	↑ total cells ↑↑ AM ↑↑ PMN ↑↑ Lymph	↑↑ MIP-2 ↑↑ TNF-α	↑↑ LDH	Gerlofs-Nijland, et al. (2007, 097840)
Netherlands, Dordrecht; moderate traffic Apr 2002	0.6 EU/mg	3, 10	↑↑ total cells ↑ AM ↑↑ PMN ↑ Lymph		↑↑ LDH ↑ protein	Gerlofs-Nijland, et al. (2007, 097840)
Germany, Munich Grosshadern Hospital; low traffic Jun-Jul 2002	2.9 EU/mg	3, 10	↑ total cells ↑↑ AM ↑↑ PMN ↑↑ Lymph	↑↑* MIP-2 ↑↑* TNF-α	↑↑* LDH ↑ protein	Gerlofs-Nijland, et al. (2007, 097840)
Sweden, Lycksele; low traffic Feb-March 2002	0.9 EU/mg	3, 10	↑↑ total cells ↑ AM ↑↑ PMN ↑ Lymph		↑↑ LDH ↑ protein	Gerlofs-Nijland, et al. (2007, 097840)

For Gerlofs-Nijland study, composition data were averaged across seasons. † significant only at highest dose.

†† Significant at lowest and highest dose.

* Greatest potency for that endpoint and study. Gilmour et al. (2007, [096433](#)) exposure was via aspiration.

A more recent study by these investigators (Gerlofs-Nijland et al., 2009, [190353](#)) compared responses to PM from three different European cities based on size fraction and content of metals and PAH. SH rats were IT instilled with 7 mg/kg PM, and markers of toxicity and inflammation were measured in BALF 24 h later. Blood markers of coagulation were also measured and are described in Section 6.2.8.3. In the first part of the study, both PM_{2.5} and PM_{10-2.5} from Duisburg were found to have dramatic effects on inflammatory cell influx and activation as well as on the injury markers LDH, protein and albumin in the BALF. The antioxidant species uric acid was increased in BALF from rats exposed to both size fractions and was interpreted as an adaptive response to oxidative stress. Statistical analysis demonstrated that PM_{10-2.5} was more potent in eliciting these responses than PM_{2.5}. In the second part of the study, responses to metal-rich PM from Duisburg and metal-poor PM from Prague were determined. A statistically significant greater enhancement of BALF markers of inflammation and injury was observed for the Duisburg PM compared with the Prague PM. Furthermore, responses to PAH-rich PM_{10-2.5} from Prague and PAH-poor PM_{10-2.5} from Barcelona were determined. PM_{10-2.5} from Prague was found to have statistically significant greater effects compared with PM_{10-2.5} from Barcelona. However, organic extracts of these PM_{10-2.5} fractions had very little capacity to produce inflammation or toxicity in this model. These findings suggest an important role for specific components associated with PM_{10-2.5} in mediating the pro-inflammatory effects.

In another study investigating specific components of PM_{10-2.5}, BALB/c mice were IT instilled with 25 and 50 µg PM_{10-2.5} from a rural area of the San Joaquin Valley, California (Wegesser and Last, 2008, [190506](#)). Inflammatory cell influx into BALF began at 6 h and peaked at 24 h following IT instillation with 50 µg PM, with the increase in neutrophils preceding the increase in macrophages. Pro-inflammatory effects were found to be mainly due to insoluble components of PM. Furthermore, heat-treatment, which was capable of inactivating endotoxin, had no effect on inflammation. Numbers of neutrophils in the BALF were found to correlate with the content of MIP-2, a known neutrophil chemoattractant released from macrophages and epithelial cells. Taken together, these results demonstrate that the pro-inflammatory effect of this PM_{10-2.5} was associated with insoluble components and not with endotoxin.

In an in vivo study that employed ambient PM collected in fall 1996 from RTP, NC, neutrophilic influx was observed in BALF of female CD1 mice 18 h post-IT instillation (10, 50 or 100 µg) of coarse PM (3.5-20 µm), although a dose-response relationship was not evident (Dick et al., 2003, [088776](#)). Mice were also exposed to fine (1.7-3.5 µm) and fine/ultrafine (<1.7 µm) PM fractions. Only the two highest doses of PM for the smaller size fractions induced elevated neutrophils. Significant responses in albumin and TNF-α were only observed for the fine PM (1.7-3.5 µm) exposure group. Total protein, LDH and NAG responses were unchanged from control levels for all PM size fractions. Levels of IL-6 were elevated in mice exposed to 100 µg for coarse, fine, and fine/ultrafine (<1.7 µm) PM. When dimethylthiourea (DMTU) was administered intravenously prior to exposure, the neutrophil response was attenuated in all groups to levels below control.

Another study compared PM_{10-2.5}, PM_{2.5}, and UFPs collected in Seattle, WA, Salt Lake City, UT, South Bronx, NY, and Sterling Forest, NY (Gilmour et al., 2007, [096433](#)). In female BALB/c mice, the 100 µg dose of PM_{10-2.5} (approximately 5 mg/kg) from Salt Lake City induced a significant increase in protein in BALF, and the level released was almost as high as that observed after LPS exposure. PM_{10-2.5} from the South Bronx resulted in dose-related increases in neutrophil number and MIP-2 levels in BALF. In contrast, no effects were observed with PM_{10-2.5} from Sterling Forest. The greatest amount of LPS was observed in the Salt Lake City and Seattle PM_{10-2.5} samples. There was a less discernable pattern of response with fine and UFPs.

Coal Fly Ash

Coal fly ash of differing size fractions and composition was administered to female CD1 mice via oropharyngeal aspiration (25 or 100 µg) to assess lung inflammation and injury 18 h following exposure (Gilmour et al., 2004, [057420](#)). Montana (low-sulfur subbituminous; 0.83% sulfur, 11.72% ash content) or western Kentucky (high-sulfur bituminous; 3.11% sulfur, 8.07% ash content) coal was combusted using a laboratory-scale down-fired furnace. Interestingly, no significant effects on BALF neutrophils, TNF-α, MIP-2, albumin, total protein, LDH activity, or NAG activity were observed 18 h post-exposure to PM_{10-2.5} from either coal fly ash. However, the UF fraction (PM_{0.2}) of combusted Montana coal induced greater numbers of neutrophils than PM_{10-2.5} or PM_{2.5} at both doses. TNF-α was only elevated in animals exposed to 100 µg of the Montana UFPs; MIP-2 was also increased at both doses. The PM_{2.5} western Kentucky coal fly ash caused increased BALF neutrophils, MIP-2, albumin, and protein (Gilmour et al., 2004, [057420](#)).

In a similar study employing Montana subbituminous coal fly ash particles >2.5 µm, C57BL/6J mice were IT instilled with PM alone or PM+LPS and BALF was obtained 18 h post-exposure (Finnerty et al., 2007, [156434](#)). TNF-α and IL-6 in lung homogenates were only elevated in the animals exposed to PM+100 µg LPS, although it appeared that there was a greater-than additive effect. Total cells and cell differentials were not measured.

Summary of Toxicological Study Findings for Relative Toxicity of PM Size Fractions

Biomarkers of injury and inflammation were measured in in vivo and in vitro studies comparing the toxicity of different size fractions of ambient PM from various locations. Responses were measured in BALF from rodents following IT instillation or aspiration of PM. In general, the PM_{10-2.5} size fraction was more potent than PM_{2.5} or UFPs and endotoxin levels did not appear responsible. In one study, rural PM_{10-2.5} from Germany induced a greater inflammatory and cytokine response than PM_{10-2.5} from an industrial location. In contrast, PM_{10-2.5} from Sterling Forest, NY did not lead to any change in BALF inflammation or injury markers. A study that employed coal fly ash

indicated that the UF fraction was the most inflammogenic. All of these studies were conducted using high doses of PM (0.58-10 mg/kg) and it is unclear if similar effects would be observed at lower doses.

6.3.6. Allergic Responses

A large number of toxicological and controlled human exposure studies cited in the 2004 PM AQCD (U.S. EPA, 2004, [056905](#)) reported an exacerbation of existing allergic airway disease following exposure to laboratory-generated and ambient particles. In addition, numerous studies have demonstrated that PM can alter the immune response to challenge with specific antigens and suggest that PM may act as an adjuvant to promote allergic sensitization. Recent toxicological studies have provided evidence of enhanced allergic responses and allergic sensitization following exposure to CAPs and DE that is consistent with the findings presented in the 2004 PM AQCD. PM can enhance allergic responses by facilitating delivery of allergenic material and promoting subsequent immune reactivity. The initiation or exacerbation of allergic responses has important implications for allergic asthma, the most common form of asthma. Additionally, PM has been shown to alter ventilatory measures in non-allergic animal models, suggesting a possible role in other forms of asthma.

6.3.6.1. Epidemiologic Studies

Allergy contributes to a number of respiratory morbidity outcomes, including asthma. However, relatively few epidemiologic studies of PM have specifically examined indicators of allergy. The 2004 PM AQCD (U.S. EPA, 2004, [056905](#)) presented one study (Hajat et al., 2001, [016693](#)) showing an association between doctor visits for allergic rhinitis and PM₁₀ among children in London. This association was strongest at a lag of 3 or 4 days. Similar results were obtained in a new study by Tecer et al. (2008, [180030](#)), which found significant associations between PM_{2.5}, PM_{10-2.5}, and PM₁₀ with hospital admissions for allergic rhinitis in Turkish children, particularly at lag day 4. While exacerbation of allergic symptoms may occur relatively rapidly, repeated or longer exposures may be required for allergic sensitization to develop; a number of studies associating long-term exposure to PM with specific indicators of allergic sensitization are described in Chapter 7.

6.3.6.2. Controlled Human Exposure Studies

Exacerbation of Allergic Responses

Diesel Exhaust and Diesel Exhaust Particles

Exposure to DE particles was shown to increase the allergic response among atopic individuals in several controlled human exposure studies cited in the 2004 PM AQCD (U.S. EPA, 2004, [056905](#)). Nordenhall et al. (2001, [025185](#)) found that exposure to DE significantly decreased the concentration of Mch required to induce a 20% decrease in FEV₁ in a group of atopic asthmatics 24 h post-exposure. In addition, Diaz-Sanchez et al. (1997, [051247](#)) demonstrated an increase in allergen-specific IgE following exposure via intranasal spray to ragweed plus DE particles (0.3 mg) relative to ragweed allergen alone. Decreases in IFN- γ and IL-2, as well as increases in IL-4, IL-5, IL-6, IL-10, and IL-13 were also observed when ragweed allergen was administered with DE particles. It should be noted that the DE particles used in this study were collected during a cold start of a light-duty Isuzu diesel engine, and thus contained relatively high levels of incomplete combustion materials and semi-volatiles organics (e.g., PAHs). One new study using the same source of DE particles (Bastain et al., 2003, [098690](#)) also observed an increase in IL-4 and allergen specific IgE, as well as a decrease in IFN- γ following intranasal administration of ragweed allergen with DE particles (0.3 mg) in atopic adults. The protocol was repeated in this study for all subjects, and the enhancement of allergic response by coexposure to DE particles was observed to be highly reproducible within individuals. In addition, Gilliland et al. (2004, [156471](#)) demonstrated that GST

polymorphisms may alter the adjuvant effects of DE particles on allergic response, with individuals with GSTM1 null or GSTP1 I105 wild type genotypes showing the largest effects.

Allergic Sensitization

Diesel Exhaust Particles

One controlled human exposure study has demonstrated that de novo sensitization to a neoantigen can be induced by exposure to DE particles. In this study, Diaz-Sanchez et al. (1999, [011346](#)) dosed 25 atopic adults intranasally with 1 mg keyhole limpet hemocyanin (KLH), followed by two biweekly challenges with 100 µg KLH. In 15 of the 25 subjects, cold-start DE particles (0.3 mg) were administered intranasally 24 h prior to each KLH exposure, while in the other ten subjects, no DE particles were administered. No KLH-specific IgE was observed in the nasal lavage fluid of any of the subjects exposed to KLH without exposure to DE particles. However, KLH-specific IgE was present in the nasal lavage fluid of 9 out of 15 subjects 28-32 days after the initial KLH immunization when exposures were preceded by administration of DE particles.

CAPs

Increased levels of eotaxin, a marker of allergic activation, were observed in healthy adult volunteers after inhalation of nebulized ambient Chapel Hill PM_{10-2.5} (Alexis et al., 2006, [154323](#)). This particular effect was found to be due to endotoxin, based on its elimination by heat-inactivation; study details are provided in Section 6.3.3.2.

6.3.6.3. Toxicological Studies

Exacerbation of Allergic Responses

Increased use of actual ambient air particle mixes in toxicological studies since the 2004 CD has greatly expanded evidence relevant to assessing these and other immunotoxic effects. A number of studies have also included ambient-level concentrations, although many still include relatively high doses of questionable relevance compared to the doses inhaled by humans. Recent dosimetric models reveal that a small fraction of epithelial cells located at the carinal ridges of airway bifurcations can receive massive doses that may be even a few hundred times higher than the average dose for the whole airway (Chapter 4). These areas, coincidentally, are locations of bronchus associated lymphoid tissues (BALT) which are sites at which interaction of T and B lymphocytes with antigen presenting cells (APC) occurs. Hence the deposited particles are in near-ideal proximity to immunologically active tissues. Doses used for assessing PM immunotoxicity should be viewed with this perspective. In many animal studies, changes in ventilatory patterns are assessed using whole body plethysmography, for which measurements are reported as enhanced pause (Penh). Some investigators report increased Penh as an indicator of AHR, but these are inconsistently correlated and many investigators consider Penh solely an indicator of altered ventilatory timing in the absence of other measurements to confirm AHR. Therefore use of the terms AHR or airway responsiveness has been limited to instances in which the terminology has been similarly applied by the study investigators.

CAPs

Existing allergic sensitization confers susceptibility to the effects of PM in rodent models. For example, studies in allergic rats (Harkema et al., 2004, [056842](#); Morishita et al., 2004, [087979](#)) suggest that allergic sensitization enhances the retention of PM in the airways. Recovery of anthropogenic trace elements (La, V, Mn, S) from lung tissue was greater for Detroit PM_{2.5} CAPs exposed OVA sensitized/challenged BN rats than for air exposed or non-allergic CAPs exposed controls (24 h post-exposure for 4 or 5 consecutive 10-h days during July or September; time weighted avg mass concentration of 676 ± 288 or 313 ± 119 µg/m³, respectively) (Harkema et al.,

2004, [056842](#)). Interestingly, despite lower avg mass concentration, increases in these elements were observed in September, when the avg number concentration of UFPs was nearly double that of July ($10,879 \pm 5,126$ vs. $5,753 \pm 2,566$ particles/cm³). September CAPs was associated with eosinophil influx and BALF protein content, as well as significantly increased airway mucosubstances, and the authors speculated that the high concentration of UFPs facilitated particle penetration into the alveolar region of the lungs. IT instillation of fractionated insoluble PM_{2.5} collected from this period resulted in a mild pulmonary neutrophilic inflammation in healthy BN rats, but no differential effects were obtained after IT instillation of total, soluble, or insoluble PM_{2.5} in allergic rats.

Research has also been conducted to determine the effect of proximity to the roadway on exacerbation of existing allergic disease. OVA-allergic BALB/c mice were exposed to PM_{2.5} or UF (≤ 0.15 μm) CAPs, (avg total concentration $400 \mu\text{g}/\text{m}^3$) for five 4-h days a week over 2 wk at 50 or 150 m downwind of a heavily trafficked road (Kleinman et al., 2005, [087880](#)). Markers of allergy (serum OVA-specific IgE and IgG1, lung IL-5 and eosinophils) were significantly higher in mice exposed to CAPs (PM_{2.5} or UF) than in air-exposed mice after OVA challenge. IL-5, IgG1, and eosinophils were higher in mice closer to the roadway (50 m) than in mice 150 m downwind. The authors suggest that the enhanced responses closer to the roadway may reflect a greater proportion of UFPs in this vicinity, given that the concentrations of sub-25-nm particles decrease rapidly with distance from the roadway and the PM_{2.5} CAPs closer to the roadway contained a greater number of particles for a similar mass, a portion of which were UF. Animal-to-animal variability among the biomarkers tested made it necessary to combine values from two exposures spanning two years for statistical power (determined prior to the start of the experiment). A subsequent publication (Kleinman et al., 2007, [097082](#)) included a third exposure regimen as well as compositional analysis. PM_{2.5} CAPs mass concentration was intentionally adjusted to an avg concentration of approximately $400 \mu\text{g}/\text{m}^3$, ranging from 163 to $500 \mu\text{g}/\text{m}^3$, with an estimated particle number of 2.1×10^5 particles/cm³ at 50 m and 1.6×10^5 particles/cm³ at 150 m. UFPs ranged from 146 to $430 \mu\text{g}/\text{m}^3$, with particle counts of $4.9 \pm 1.4 \times 10^5$ particles/cm³ at 50 m, and $4.4 \pm 2.1 \times 10^5$ particles/cm³ at 150 m. Analysis of results from the three exposures indicated that OVA-sensitized mice exposed 50 m downwind of the roadway exhibited increased levels of IL-5 and IgG₁ compared to mice exposed 150 m downwind or exposed to air. No markers of allergy-related responses were observed in the 150 m exposure groups, and very little difference was seen between PM_{2.5} and UF CAPs responses, perhaps because PM_{2.5} contained 20-32% UF components. The strongest associations between component concentrations and biological markers of allergy (IL-5 and IgG₁) were with EC and OC. These studies demonstrate that CAPs can enhance allergic responses, and that proximity to a source may be an important factor.

In a BN rat model for allergic asthma (Heidenfelder et al., 2009, [190026](#)), thirteen 8-h days of exposure to Grand Rapids, MI PM_{2.5} CAPs alone did not result in differential gene expression or indicators of asthmatic pathology in the lung, but the combination of CAPs and OVA resulted in differential expression of genes predominantly related to inflammation and airway remodeling, along with significant increases in IgE, mucin, and total protein in BALF. Consistent with these changes in gene expression and BALF markers, OVA with CAPs also induced a more severe allergic bronchopneumonia (distribution and severity of bronchiolitis and alveolitis) and increased mucus cell metaplasia/hyperplasia and mucosubstances, indicating exacerbation of allergic or asthmatic disease. CAPs was collected in July and characterized as having an average mass of 493 ± 391 , OC 244 ± 144 , EC 10 ± 4 , SO₄²⁻ 79 ± 131 (13 day avg was only about 10% of the CAPs, but a spike occurred during the first week), nitrate 39 ± 67 , ammonium 39 ± 59 , and urban dust (estimated from Fe, Al, Ca, and Si) 18 ± 6 (mean \pm SD in $\mu\text{g}/\text{m}^3$).

Diesel Exhaust Particles

Resuspended DE particles influences airway responses in mice with existing allergic sensitization. A single 5-h nose-only exposure to $870 \mu\text{g}/\text{m}^3$ aerosolized filter-collected DE particles (PM_{2.5}) increased Mch-induced increases in ventilatory timing (Penh) in OVA sensitized/challenged C57BL/6J mice (Farraj et al., 2006, [088469](#)). Intranasal pretreatment with an antibody against the pan neurotrophin receptor p75 attenuated the DE particle-induced increase in airflow obstruction, indicating a role for neurotrophins. Neurotrophins are expressed by various structural, nerve and immune cells within the respiratory tract and are linked to the etiology of asthma in both humans and animal models. DE particles alone in unsensitized mice caused a significant increase in lung macrophages; this response was also inhibited by anti-p75, which may suggest mediation of macrophage influx by neurotrophin or alternatively may reflect anti-p75 dependent depletion of

macrophages due to expression of the p75 receptor. Aside from increased macrophages, the single exposure to DE particles had little effect on other markers of airway inflammation. In a similar subsequent study, these authors demonstrate neurotrophin-mediated DE particle-induced airflow obstruction in OVA sensitized and challenged BALB/c mice (Farraj et al., 2006, [141730](#)), in this case using a higher 2000 $\mu\text{g}/\text{m}^3$ single 5-h exposure to aerosolized filter-collected $\text{PM}_{2.5}$. Differences between whole body plethysmography and tracheal ventilation measurements indicated that airflow obstruction may have originated in the nasal passages. Again, very few indices of inflammation were increased; however, similar neurotrophin-dependent increases in lung macrophages were observed after DE particle exposure alone, and BALF IL-4 protein levels were increased 5-fold in sensitized, challenged, DE particle-exposed mice. This neurotrophin-dependent IL-4 response was not evident in the first study, and may be related to the higher dose used in the second study or the characteristic allergic/Th2 bias of the BALB/c strain. Airflow obstruction in the absence of airway inflammation in OVA-sensitized animals seen in both studies by Farraj et al. (2006, [088469](#); 2006, [141730](#)) may reflect DE particle-induced acute enhancement of neurogenic as opposed to immunologic inflammation.

Diesel Exhaust

Exposure to relatively low doses of DE has been shown to exacerbate asthmatic responses in OVA sensitized/challenged BALB/c mice (Matsumoto et al., 2006, [098017](#)). Mice were intranasally challenged one day prior to chamber exposure to DE (100 $\mu\text{g}/\text{m}^3$ PM; CO, 3.5 ppm; NO_2 , 2.2 ppm; SO_2 <0.01 ppm) for 1 day or 1, 4, or 8 wk (7h/day, 5 days/wk, endpoints 12-h post-DE exposure). Results from the 8 wk study are described in Section 7.3.6.2. It should be noted that control mice were left in a clean room as opposed to undergoing chamber exposure to filtered air. Significant AHR upon Mch challenge was observed after 1 and 4 wk of exposure, and airway sensitivity (provocative concentration of Mch causing a 200% increase in Penh) was significantly increased after 1 wk of exposure but not 4 wk. DE had no effect on total cells in BALF, but transiently increased expression of IL-4, IL-5, and IL-13 after 1 day of exposure, MDC after 1 wk, and RANTES after 2 and 3 wk. Eotaxin, TARC, and MCP-1 were elevated without statistical significance after short-term (1 day or wk) exposure. Statistical power may have been lacking due to few animals in the exposure group ($n=3$). Protein levels of IL-4 and RANTES were significantly elevated after one day of DE exposure. DE had no effect on OVA challenge-induced peribronchial inflammatory or mucin positive cells. Therefore DE-induced AHR was observed in the absence of neutrophilic inflammation, similar to the responses described for aerosolized or nebulized DE particles by Farraj et al. (2006, [088469](#); 2006, [141730](#)) and Hao et al. (2003, [096565](#)).

Gasoline Exhaust

Acute exposure to fresh gasoline engine exhaust PM does not appear to exacerbate allergic responses (Day et al., 2008, [190204](#)). BALB/c mice were exposed to whole exhaust diluted 1:10 (H), 1:15 (M), or 1:90 (L), filtered exhaust at the 1:10 (HF), or clean air for 6 h/day over three days. Analytes for the high (H) and high filtered (HF) concentrations were: PM mass ($\mu\text{g}/\text{m}^3$) 59.1 \pm 28.3 (H) and 2.3 \pm 2.6 (HF); PM number (particles/ cm^3) 5.0 \times 10⁵ and 1.1 \times 10⁴; CO (mg/m^3) 102.8 \pm 33.0 and 99.5 \pm 1.6; NO (mg/m^3) 18.4 \pm 2.8 and 17.2 \pm 1.9; NO_2 (mg/m^3) 1.4 \pm 0.3 and 1.7 \pm 0.2; SO_2 ($\mu\text{g}/\text{m}^3$) 1366.8 \pm 56.0 and 1051.1 \pm 43.0; NH_3 ($\mu\text{g}/\text{m}^3$) 1957.7 \pm 8.1 and 1241.5 \pm 6.1; NMHC (mg/m^3) 15.9 and 25.9. Particles represented only 0.04% of the total exposure mass and particle size in the H exposure ranged from 5.5 to 150 nm with the majority between 5-20 nm (MMD 150 nm) (McDonald et al., 2008, [191978](#)). Although particles were filtered out, it should be noted that NMHC (non-methane volatile organics) increased by 62%. Mice were exposed with or without prior sensitization to OVA, after one aerosol challenge and with or without secondary challenge. Acute gasoline engine exhaust exposure had variable effects on inflammatory and allergic markers depending on the exposure protocol, but there were no statistically significant differences between the H and HF exposure results, suggesting that the PM fraction of gasoline engine exhaust does not appear to contribute significantly to observed health effects.

Hardwood Smoke

One study indicated that hardwood smoke exposure only minimally exacerbated indices of allergic airway inflammation in an OVA-sensitized BALB/c mouse model and did not alter Th1/Th2

cytokine levels (Barrett et al., 2006, [155677](#)). Trend analysis indicated increasing BALF eosinophils with increasing dose of hardwood smoke, becoming significantly elevated at 300 $\mu\text{g}/\text{m}^3$ (CO, 1.6 \pm 0.3 ppm; total vapor hydrocarbon, 0.6 \pm 0.2 ppm; NO_x, below limit of quantitation, PM MMAD 0.35 \pm 2.0 μm), and increasing, but not significantly, OVA-specific IgE levels with hardwood smoke up to 1,000 $\mu\text{g}/\text{m}^3$.

Model Particles

Exposures to an aerosol of soot and iron oxide generated from ethylene (0.235 mg/m³ PM_{2.5}) were conducted to test whether the sequence of exposure to OVA aerosol challenge and PM affected the observed response of OVA sensitized BALB/c mice (Last et al., 2004, [097334](#)). Though called PM_{2.5}, the authors characterized the PM material as UF, 80-110 nm, with the iron oxide crystals often spatially segregated from the soot (200 $\mu\text{g}/\text{m}^3$ soot, remainder iron oxide, CO <0.8 ppm, NO_x <0.4 ppm, PAH below detection). Mice were exposed to PM via chamber inhalation for 2 wk (4h/day, 3 days/wk) before or after 4 wk of OVA inhalation, or simultaneously to PM and OVA for 6 wk. Among endpoints (BALF cells, Penh, airway collagen, and goblet cells) only goblet cell counts were significantly increased with PM exposure in any combination with OVA. There was a trend toward increased Penh responses with exposure to PM alone or with OVA, particularly when PM exposure immediately preceded Mch challenge (after or during OVA challenge). Results from this study are difficult to interpret due to the varied elapsed times between cessation of PM or OVA treatment and endpoint determination. The mild responses to PM may be related to the intraperitoneal sensitization protocol used, reputed to generate a highly allergic mouse in which any additive effects of PM may be obscured by maximal responses to antigen challenge (Deurloo et al., 2001, [156396](#); Hao et al., 2003, [096565](#)).

Residual Oil Fly Ash

Arantes-Costa and colleagues (2008, [187137](#)) estimated that 60 μg of ROFA would be inhaled by a mouse during one day of exposure to Sao Paulo air. This dose, given intranasally every other day for 4 days, increased AHR in both nonsensitized and OVA sensitized/challenged BALB/c mice upon Mch challenge 2 days after the last exposure. ROFA had no significant impact on eosinophil or macrophage numbers in the lung, nor did it increase the chronic lung inflammation or thickening induced by OVA. In many studies, particular effects such as airway obstruction are only evident when allergic sensitization precedes exposure, but this study and a few others demonstrate allergen-independent AHR after exposure to PM including CAPs (Lei et al., 2004, [087999](#)) and DE or DE particles (Hao et al., 2003, [096565](#); Li et al., 2007, [155929](#)).

Allergy in Pregnancy or Early Life

Pregnancy or in utero exposure may confer susceptibility to PM-induced asthmatic responses. Exposure of pregnant BALB/c mice to aerosolized ROFA leachate by inhalation or to DE particles intranasally increased asthma susceptibility in their offspring (Fedulov et al., 2008, [097482](#); Hamada et al., 2007, [091235](#)). The offspring from dams exposed for 30 min to 50 mg/mL ROFA 1, 3, or 5 days prior to delivery responded to OVA immunization and aerosol challenge with AHR and increased antigen-specific IgE and IgG1 antibodies. AHR was also observed in the offspring of dams intranasally instilled with 50 μg of DE particles or TiO₂, or 250 μg CB, indicating that the same effect could be demonstrated using relatively “inert” particles. Pregnant mice were particularly sensitive to exposure to DE particles or TiO₂ particles, and genetic analysis indicated differential expression of 80 genes in response to TiO₂ on the pregnant background. Thus pregnancy may enhance responses to PM, and exposure to even relatively inert particles may result in offspring predisposed to asthma.

Allergic Sensitization

A large number of in vivo animal studies and in vitro studies have demonstrated that particles can alter the immune response to challenge with specific antigens and suggest that PM acts as an adjuvant to promote allergic sensitization. This phenomenon was introduced in the 2002 Diesel

Document, and has been noted in multiple animal and human studies by the 2004 PM AQCD (U.S. EPA, 2004, [056905](#)). Adjuvants enhance the immune response to antigens through various means, including chemoattraction, cytokines, or enhanced antigen presentation and costimulation, and may act on a number of cell types. Importantly, adjuvants may be major contributors to the development of inappropriate immune responses. These immune responses, mediated by T helper cells, fall along a continuum from T helper type 1 (Th1) to T helper type 2 (Th2). Th1 responses, characterized by IFN- γ , are inflammatory and in excess can lead to tissue damage. Alternatively, Th2 responses are characterized by IL-4, IL-5, IL-13, eosinophils, and IgE, and are associated with allergy and asthma. Autoimmune diseases may be driven by Th1, Th2, or mixed responses, but allergic diseases are predominantly Th2 mediated, and many of the immunologic effects observed for PM fall into the Th2 category.

It has been suggested that the capacity of particles to enhance allergic sensitization is associated more strongly with particle number and surface area than particle mass, and several studies comparing size fractions of the same material show greater adjuvant activity for an equivalent mass dose of smaller particles (de Haar et al., 2006, [144746](#); Inoue et al., 2005, [088625](#); Nygaard et al., 2004, [058558](#)). This is particularly true of inert or homogeneous materials, such as carbon, polystyrene, and TiO₂, which vary little in composition with size fraction. Studies using CAPs have also observed that adjuvancy and allergic exacerbation are more strongly associated with the UF fraction, possibly due to greater oxidative potential (Kleinman et al., 2005, [087880](#); Kleinman et al., 2007, [097082](#); Li et al., 2009, [190457](#)). In some studies of ambient PM, however, PM_{10-2.5} or PM₁₀ have demonstrated equal or greater adjuvancy compared to PM_{2.5} (Nygaard et al., 2004, [058558](#); Steerenberg et al., 2004, [096024](#); Steerenberg et al., 2005, [088649](#)). More inhalation studies to compare size fractions are needed in order to elucidate the role of particle size in mediating adjuvancy, but this may prove difficult given the influence of composition, e.g., combustion related materials (Steerenberg et al., 2006, [088249](#)) and metal content (Gavett et al., 2003, [053153](#)), which differs among various size fractions and sources.

CAPs

As little as 0.1 μg of UF Los Angeles CAPs administered intranasally with OVA was able to significantly boost allergic antibody responses in BALB/c mice (Li et al., 2009, [190457](#)). A comparison of UFPs (aerodynamic diameter $<0.15 \mu\text{m}$) with a mix of sub-2.5 μm particles (PM_{2.5}/UFP) collected 200 m from a major freeway delivered intranasally five times over the course of nine days showed that UFP but not PM_{2.5}/UFP were associated with significant adjuvant effects. 0.5 μg of UFP with OVA (but not alone) led to an increase in BALF eosinophils, allergic cytokines, inflammatory mediators, and serum OVA-specific IgE/IgG1, as well as allergic tissue inflammation in the upper and lower airways. Adjuvant effects of UFP were observed with two independently collected samples (1/2007 and 9/2006) and could not be replicated by administering the same amount of endotoxin measured in the particles, indicating that the effects were not unique to the sampling period nor mediated by contaminating endotoxin. UFP had a greater OC and PAH content than PM_{2.5}/UFP, and induced greater oxidative stress in vitro. Partial blocking of the adjuvant effects by antioxidant administration implicates redox potential as a key factor in mediating these effects. The authors suggest that the lack of adjuvancy for UF carbon particles (being mostly EC) is due to a lack of redox cycling compounds, but this was not tested. In contrast, UF (30-50 nm) CB particles have demonstrated intranasal adjuvant activity in other studies (de Haar et al., 2005, [097872](#)) when administered with OVA over three consecutive days. A 200- μg dose increased serum OVA-specific IgE, local lymph node dendritic cells and OVA-specific Th2 lymphocytes in the lung draining lymph nodes and lung, as well as post-challenge airway eosinophilia. Doses as low as 20 μg were able to activate adoptively transferred OVA-specific T cells.

Diesel Exhaust Particles

Resuspended DE particles have been shown to enhance OVA-specific IgG1 and IgE in BALB/c mice exposed via inhalation to doses as low as 200 and 600 $\mu\text{g}/\text{m}^3$, respectively (Whitekus et al., 2002, [157142](#)). Mice were exposed to DE particles (200, 600 and 2,000 $\mu\text{g}/\text{m}^3$) for 1 h daily for 10 days prior to aerosol OVA challenge. Compared with responses to OVA alone, antibody levels were increased by all OVA+DE particle exposures. Statistical significance was reached for IgG1 at all DE particle exposure levels, whereas OVA specific IgE was significantly increased at the 600 and 2,000 $\mu\text{g}/\text{m}^3$ doses and total IgE was significantly elevated at 2,000 $\mu\text{g}/\text{m}^3$. Although strong adjuvant

effects were observed, no general markers of inflammation such as eosinophils, IL-5, GM-CSF, mucin, morphological changes, or eosinophilic major basic protein (MBP) deposition in the airways were observed in exposed mice. In vitro experiments using the RAW 264.7 macrophage-like cell line indicated a DE particle-induced lipid peroxidation and protein oxidation, which could be inhibited by a variety of antioxidants. Also observed was a decrease in the GSH:GSSG ratio and an increase in HO-1 expression, both of which were inhibited only by the thiol antioxidants NAC and BUC. These same thiol antioxidants were able to completely block DE particle-related increases in IgE and IgG1, as well as lipid peroxides and oxidized proteins recovered from BALF at the 2,000 $\mu\text{g}/\text{m}^3$ dose. Thus solid correlations between in vivo and in vitro antioxidant activities were found, and the reversal of adjuvant effects by antioxidants in vivo clearly indicates a link between oxidative stress and DE particle adjuvancy. However, the intranasal adjuvant activity of Ottawa, Canada, dust (EHC-93) in the same strain of mice was not inhibited by NAC pretreatment (Steerenberg et al., 2004, [087981](#)), suggesting that disparate pathways may be utilized by different materials to exert immune stimulation.

Diesel Exhaust

DE inhalation during allergen exposure has been shown to augment IgE production and alter methylation of T helper genes in BALB/c mice (Liu et al., 2008, [156709](#)). Animals were exposed to DE (1280 $\mu\text{g}/\text{m}^3$ PM) over a 3-wk period, 5 h per day, concurrent with periodic intranasal sensitization to the common fungus *Aspergillus fumigatus*. Gas concentrations were not reported. Total IgE and BALF eosinophils were elevated with *A. fumigatus* sensitization and further increased by concomitant DE exposure. Greater methylation of the IFN- γ promoter was observed following DE and *A. fumigatus* exposure (but not DE alone) compared to *A. fumigatus* alone, indicating that combined DE and allergen exposure might induce methylation and thus suppress expression of Th1 genes. Furthermore, hypomethylation of the IL-4 promoter was detected after exposure to *A. fumigatus* and DE compared with exposure to *A. fumigatus* or DE alone, suggesting pro-allergic Th2 gene activation upon combined exposure to allergen and DE. The changes in methylation status of these genes were associated with alterations in IgE levels in individual animals, indicating that modifications at the genetic level could result in predicted downstream effects. This study shows for the first time that DE exposure can exert pro-allergic in vivo effects on the mouse immune system at the epigenetic level.

A toxicogenomic approach to investigate early response mechanisms of DE adjuvancy was taken by Stevens et al. (2008, [157010](#)). BALB/c mice were chamber exposed to filtered air, 500 or 2,000 $\mu\text{g}/\text{m}^3$ PM in DE for 4 h/day over 5 consecutive days and intranasally exposed to OVA on each of the first 3 days. In the low (500 $\mu\text{g}/\text{m}^3$) vs. high (2,000 $\mu\text{g}/\text{m}^3$) DE exposures, CO, NO, NO₂, and SO₂ were <0.1 versus 4.3, <2.5 vs. 9.2, <0.25 vs. 1.1 and <0.06 vs. 0.2 ppm; particle number median diameters were 80 and 86 nm, and volume median diameters were 184 and 195 nm, respectively. Lung tissues were assessed for alterations in global gene expression (n = 4) 4 h after the last DE exposure on day 4. Mice were intranasally challenged with OVA or saline on day 18 and then with OVA on day 28. Post-challenge results demonstrated mild adjuvancy with antigen and DE exposure as evidenced by significant increases in eosinophils, neutrophils, lymphocytes, and IL-6 in the BALF. Antibody responses were not significantly affected by DE exposure, although a slight increase in IgE after high concentration exposure was observed. DE alone only increased neutrophils, indicating the need for combined exposure to DE and antigen in the development of allergic outcomes. Comparison of low DE/OVA vs. air/OVA resulted in no significant changes in gene sets associated with this treatment. Comparison of the high DE/OVA versus air/OVA, however, showed significant changes in 23 gene sets, including neutrophil homing and other chemokines, inflammatory cytokines, numerous interleukins and TNF subtypes, and growth/differentiation pathways.

Summary of Toxicological Study Findings for Allergic Responses

Studies conducted since the last review confirm and extend the 2004 PM AQCD's (U.S. EPA, 2004, [056905](#)) finding that PM can modulate immune reactivity in both humans and animals to promote allergic sensitization and exacerbate allergic responses. Numerous forms of PM, including inert materials, have been shown to function as adjuvants, and although toxicological studies of relatively homogeneous materials demonstrate greater adjuvancy for smaller particles, some analyses

of ambient PM do not. Recent toxicological studies comparing size fractions of well-characterized ambient PM for adjuvant activity in a direct, controlled fashion via inhalation exposure suggest a role for oxidative potential, but thus far the relative contributions of size and composition are not entirely clear. Although epidemiologic studies examining specific allergic outcomes and short-term exposure PM are relatively rare, the available studies, conducted primarily in Europe, positively associate various PM size fractions with allergic rhinitis. Similar findings from a number of long term studies are described in Chapter 7.

6.3.7. Host Defense

The normal and very important role of respiratory immune defense is the detection and/or destruction of pathogens that enter the lung via inhalation and removal of damaged, transformed (cancerous), or infected cells. Innate immune defenses of the respiratory tract include mucociliary clearance, release of toxic antimicrobial proteins into airway surface liquid, and activation of alveolar macrophages. The innate immune system is the earliest responder to irritation or infection, initiating the normal inflammatory response including the majority of detrimental inflammatory processes discussed. Activated macrophages and epithelial cells release cytokines and chemokines that can bring into play the adaptive immune system, which in turn can produce long-lasting pathogen-specific immune responses critical for resolving and preventing infections.

6.3.7.1. Epidemiologic Studies

Collectively, results from multicity studies of hospital admissions and ED visits for respiratory infection as well as single-city studies conducted in the U.S. and Canada (summarized in Figure 6-14) show a positive association between PM and respiratory infections. Lag structure was not investigated in most studies and effects have been observed in association with current day concentration (Zanobetti and Schwartz, 2006, [090195](#)) as well as with concentrations modeled using a 14-day distributed lag function (Peel et al., 2005, [056305](#)). Of studies examining multiple lag times, associations with increasing lag times were observed (Dominici et al., 2006, [088398](#); Peel et al., 2005, [056305](#); Peng et al., 2008, [156850](#)). Although no significant positive associations were reported, Slaughter et al. (2005, [073854](#)) observed a trend of increasing association with increasing lag for acute respiratory infection ED visits with PM₁, PM_{2.5}, PM₁₀ and PM_{10-2.5}. This delay in the onset of disease may reflect the time necessary for an infection to become established and symptomatic. The majority of toxicological evidence, described below and in the 2004 PM AQCD (U.S. EPA, 2004, [056905](#)), suggests that PM impairs innate immunity, the first line of defense in preventing infection.

6.3.7.2. Toxicological Studies

Several toxicological studies were cited in the 2004 PM AQCD (U.S. EPA, 2004, [056905](#)) that demonstrated increased susceptibility to infectious agents following exposure to PM. A limited number of new studies have evaluated the effect of PM on host defense in rodents. Two recent studies have observed an increase in susceptibility to influenza infection and respiratory syncytial virus in mice. However, one new study found that wood smoke had no effect on bacterial clearance in rodents.

Bacterial Infection

Several studies included in the 2004 PM AQCD (U.S. EPA, 2004, [056905](#)) demonstrated increased susceptibility to infectious agents following exposure to various forms of PM. CAPs exposed aged rats demonstrated increased *S. pneumoniae* burdens when a 24-h exposure (65 µg/m³) followed infection (Zelikoff et al., 2003, [039009](#)). In another study, IT instillation exposure to ROFA was found to affect bacterial clearance (Antonini et al., 2002, [035342](#)). Examinations of mechanisms related to PM interference with host defenses have demonstrated impaired mucociliary clearance and modified macrophage phagocytosis and chemotaxis. Prolonged exposure to inhaled particles at sufficiently high concentrations can lead to diminished clearance of PM from the alveolar region of

the lung, resulting in the accumulation of retained particles and an accompanying chronic alveolar inflammation. Diminished clearance of PM may also increase susceptibility to pulmonary infection by impeding clearance of pathogens. Impaired phagocytosis by alveolar macrophages may contribute to a decrease in the lung's capacity to deal with increased particle loads (as occurs during high-pollution episodes) or infections and affect the local and systemic responses through the release of biologically active compounds (cytokines, ROS, NO, isoprostanes).

Diesel Exhaust

Since the last review, several additional studies have reported impairment of pathogen clearance following exposure to various sources of PM. All levels of DE (30, 100, 300 or 1,000 $\mu\text{g}/\text{m}^3$) decreased lung bacterial clearance in C57BL/6 mice exposed for 1 wk (7 days/wk, 6 h/day) prior to infection with *Pseudomonas aeruginosa* (Harrod et al., 2005, [088144](#)). This effect appeared concentration dependent up to 100 $\mu\text{g}/\text{m}^3$ and was not enhanced at higher concentrations. Lung inflammation was not induced by DE in the absence of infection, but infection-induced inflammation was exacerbated by DE at all concentrations without apparent concentration dependency. Measures of histopathology in infected animals were increased by DE exposure in a concentration-dependent manner, peaking at 100 $\mu\text{g}/\text{m}^3$ and leveling off or decreasing with higher concentrations. Particle deposition was readily apparent in the lungs after exposure to the lowest concentration of 30 $\mu\text{g}/\text{m}^3$. A loss of ciliated cells was observed at 30 $\mu\text{g}/\text{m}^3$ and 100 $\mu\text{g}/\text{m}^3$ in large airways and in small airways at the higher concentration. Alterations in Clara cell morphology and function were observed at both concentrations as well. Concentrations of gases were reported to be 2.0-45.3 ppm NO, 0.2-4.0 ppm NO₂, 1.5-29.8 ppm CO and 8-365 ppb for SO₂ (McDonald et al., 2004, [055644](#)). PM mass median diameter was ~100-150 nm at all exposure levels (>90% below 1 μm in aerodynamic diameter), with lower exposure concentrations having a slightly smaller size distribution (Reed et al., 2004, [055625](#)).

Gasoline Exhaust

In a study by Reed et al. (2008, [156903](#)), short or long-term exposure to fresh gasoline exhaust (6h/day, 7day/wk for 1 wk or 6 mo) did not affect clearance of *P. aeruginosa* from the lungs of C57BL/6 mice. Atmospheric characterizations are described above for the Day et al. (2008, [190204](#)) and McDonald et al. (2008, [191978](#)) studies in Section 6.3.6.3.

Hardwood Smoke

Similar to gasoline exhaust, hardwood smoke does not appear to have significant impact on pathogen clearance. C57BL/6 mice were exposed to 30-1,000 $\mu\text{g}/\text{m}^3$ hardwood smoke by whole-body inhalation for 1 wk and 6 months (Reed et al., 2006, [156043](#)). Long-term responses are discussed in Sections 7.3.3.2 and 7.3.7.2. Concentrations of gases ranged from 229.0-14,887.6 mg/m³ for CO, 54.9-139.3 $\mu\text{g}/\text{m}^3$ for ammonia, and 177.6-3,455.0 $\mu\text{g}/\text{m}^3$ for nonmethane volatile organic carbon in these exposures. Bacterial clearance of instilled *P. aeruginosa* was unaffected by hardwood smoke.

Intratracheal Instillation

Studies demonstrate that ROFA impairs host defenses and that soluble metals are important contributors. Antonini et al. (2004, [097199](#)) compared sources of ROFA in SD rats. Precipitator ROFA induced an inflammatory response and diminished pulmonary clearance of *L. monocytogenes* while air heater ROFA had no effect on lung bacterial clearance at the same IT dose of 1 mg/100g body weight. Precipitator ROFA generated a metal-dependent hydroxyl radical suggesting that differences in metal composition were a determinant of the immunotoxicity of ROFA. Subsequent studies using soluble extracts of ROFA with or without a chelating agent confirmed that soluble metals were responsible for weakening defenses against bacterial infection and impairing both innate and adaptive lung immune responses (Roberts et al., 2004, [196994](#); Roberts et al., 2007, [097623](#)) ROFA has also been shown to result in ciliated cell loss in BALB/c mice after intranasal administration of 60 μg every other day for 4 days (Arantes-Costa et al., 2008, [187137](#)).

Viral Infection

Diesel Exhaust

Viral respiratory infections in early life are associated with increased incidence of childhood asthma and other pulmonary diseases. DE exposure can enhance the progression of influenza infection. BALB/c mice that were chamber exposed to DE 4 h/day for 5 days and subsequently IT instilled with influenza A/Bangkok/1/79 virus had increased susceptibility to influenza infection (Cienciewicki et al., 2007, [096557](#)). Exposures to two concentrations of DE were conducted: 500 $\mu\text{g}/\text{m}^3$ (0.9 ppm CO, <0.25 ppm NO₂, <2.5 ppm NO, and 0.06 ppm SO₂) and 2,000 $\mu\text{g}/\text{m}^3$ (5.4 ppm CO, 1.13 ppm NO₂, 10.8 ppm NO, and 0.32 ppm SO₂). Responses were greater for animals exposed to 500 $\mu\text{g}/\text{m}^3$ DE than to 2,000 $\mu\text{g}/\text{m}^3$, and were associated with a significant increase in IL-6 protein and mRNA expression and IFN- β expression. The authors present the possibility that damage to the epithelium at the higher exposure prevented viral infection and replication. After exposure to 500 $\mu\text{g}/\text{m}^3$ DE alone or prior to infection, decreased expression of surfactant proteins (SP) A and D was observed. These proteins are part of the IFN-independent defense against influenza.

Similarly, Harrod et al. (2003, [097046](#)) demonstrated decreased SP-A expression in the lungs following DE exposure and linked it to increased susceptibility to respiratory syncytial virus (RSV), the most common cause of respiratory infection in young children. C57BL/6 mice, a relatively RSV-resistant strain, were exposed via inhalation to DE at a concentration of 30 or 1,000 $\mu\text{g}/\text{m}^3$ PM 6h/day for 7 consecutive days prior to intratracheal viral inoculation. Gaseous copollutants ranged from 2.0-43.3 ppm for NO_x (~ 90% NO), 0.94-29.0 ppm CO, and 8.3-364.9 ppb SO₂. Exposure to 30 $\mu\text{g}/\text{m}^3$ DE did not induce a statistically significant increase in BALF cell numbers compared to air-treated, infected animals. However, distinct consolidated inflammatory infiltrates were observed in the peribronchial regions of RSV-infected animals exposed to this concentration, along with alterations in Clara cell morphology, decreased CCSP production by these cells, and occasional regional myofibril layer thickening. These changes were more pronounced in RSV-infected animals exposed to 1000 $\mu\text{g}/\text{m}^3$, and the higher concentration also resulted in significant increases in inflammatory cells, predominantly macrophages, in both uninfected and infected mice compared to air-exposed controls. Both doses elicited significant levels of TNF- α and IFN- γ in the lungs of infected animals, but decreased levels of SP-A. Consistent with this study's finding of decreased SP-A and increased viral gene and inflammatory cytokine expression after DE exposure, SP-A^{-/-} mice demonstrate decreased clearance of RSV concordant with increased lung inflammation (Levine et al., 1999, [156687](#)). Thus, DE may enhance susceptibility to respiratory viral infections by reducing the expression and production of SP (Cienciewicki et al., 2007, [096557](#); Harrod et al., 2003, [097046](#)), although the contribution of gaseous copollutants, in some instances concentrated 1,000 times, should be considered for both studies. SP are also essential for clearance of other pathogens, including group B *Streptococcus* (GBS), *Haemophilus influenzae*, and *P. aeruginosa* (LeVine and Whitsett, 2001, [155928](#)).

A reduction in host defense molecules and an increase in viral entry sites was observed by Gowdy et al. (2008, [097226](#)) after BALB/c mice were exposed to HEPA filtered room air or DE at 0.5 or 2.0 mg/m³ for 4hr/day for one or five consecutive days [O₂ (%) 21.0 \pm 0.10 or 20.7 \pm 0.09, CO (ppm) 1.7 \pm 0.15 or 5.4 \pm 0.07, NO_x (ppm) 2.0 \pm 0.36 or 7.4 \pm 0.61, SO₂ (ppm) 0.0 \pm 0.0 or 0.4 \pm 0.3, number median (nm) 96.2 \pm 2 or 97 \pm 2, volume median (nm) 238 \pm 2 or 249 \pm 2, OC/EC (wt ratio) 0.4 \pm 0.04 or 0.4 \pm 0.07 for the 0.5 or 2.0 mg/m³ exposures, respectively]. One of the more notable features of this study was the observation that effects of extended exposure to the lower concentration (0.5 mg/m³ for 5 days) tended to persist beyond 18 h post-exposure. Exposure to DE significantly increased BALF neutrophils in the higher exposure group, and this response persisted beyond 18 h only after the five day exposure. An increase in ICAM-1 expression (a viral entry site) was observed in both exposure groups, and was persistent in the lower concentration group after a 5-day exposure. Persistently elevated expression of pro-inflammatory cytokines IL-6 and TNF- α and pro-allergic cytokine IL-13 was observed after five days of low concentration exposure. Non-statistically significant effects of either concentration or exposure regimen included increased IFN- γ and MIP-2. Host defense molecules CCSP, SP-A and SP-D were decreased after either exposure regimen, persisting beyond 18 h in the low concentration group.

Taken together, these data suggest that exposure to DE can weaken host defenses, in some cases persistently. A role for PM in these responses is supported by studies demonstrating changes in host defense molecules and viral entry sites in vitro consistent with those observed in vivo. In lung epithelial cells, DE particles increased the mRNA expression of ICAM-1, LDL and platelet-activating factor (PAF) receptors, which can act as receptors for viruses or bacteria (Ito et al., 2006, [096648](#)). DE particles may therefore enhance the susceptibility to infection by the upregulation of bacterial and viral invasion sites in the lungs. Expression of the β -defensin-2 gene, which is one antimicrobial mechanism of host defense in the airway, was significantly inhibited by V and not Ni or Fe in airway epithelial cells incubated with aqueous leachate of ROFA (Klein-Patel et al., 2006, [097092](#)).

Immunosuppressive Effects of PM

Diesel Exhaust

DE may affect systemic immunity. Decreased thymus weight was observed in female F344 rats exposed to 300 $\mu\text{g}/\text{m}^3$ DE for 1 wk by Reed et al. (2004, [055625](#)). Concentrations of gases for this PM concentration were reported to be approximately 16.1 ppm for NO, 0.8 ppm for NO₂, 9.8 ppm for CO, and 115 ppb for SO₂. Long-term responses are discussed in Section 7.3.8.

Summary of Toxicological Study Findings for Host Defense

Toxicological studies demonstrate that short-term inhalation exposures to CAPs and DE, but not gasoline exhaust or wood smoke, can increase susceptibility to infection by bacterial and viral pathogens. While gaseous copollutants may be contributing factors, a role for particles is demonstrated by studies utilizing IT instillation exposure and in vitro studies of PM where biomarkers parallel those observed in vivo. Although ethical considerations limit controlled exposure studies in humans, epidemiologic evidence reflects an association between most PM size fractions and hospital admissions for respiratory infections. Importantly, toxicological studies demonstrate impaired host defense against the etiological agents of influenza, pneumonia (*S. pneumoniae*), and bronchiolitis (RSV), which are commonly reported respiratory morbidities associated with PM.

6.3.8. Respiratory ED Visits, Hospital Admissions and Physician Visits

The epidemiologic evidence presented in the 2004 PM AQCD (U.S. EPA, 2004, [056905](#)) linking short-term increases in PM concentration with respiratory hospitalizations and ED visits was consistent across studies. Recent investigations provide further support for this relationship, with larger effect estimates observed among children and older adults. However, effect estimates are clearly heterogeneous, with evidence of both regional and seasonal differences at play.

Excess risk estimates for hospitalizations or ED visits for all respiratory diseases combined, reported in studies reviewed in the 2004 PM AQCD (U.S. EPA, 2004, [056905](#)) fell within the range of approximately 1-4% per 10 $\mu\text{g}/\text{m}^3$ increase in PM₁₀. On average, excess risks for asthma were higher than excess risks for COPD and pneumonia. Associations with PM_{2.5} (including PM₁) and PM_{10-2.5} were also reported in the limited body of evidence reviewed in the 2004 AQCD. Excess risk estimates fell within the range of approximately 2.0-6.0% per 10 $\mu\text{g}/\text{m}^3$ increases in PM_{2.5} or PM_{10-2.5} for all respiratory diseases combined as well as COPD admissions. Larger estimates were reported for asthma admissions. Many of the associations of respiratory admissions and ED visits with short-term PM_{2.5} concentration were statistically significant. The associations with PM_{10-2.5} were less precise with fewer reaching statistical significance (U.S. EPA, 2004, [056905](#)). Finally, several studies reviewed in the 2004 AQCD reported associations of PM with outpatient physician visits, suggesting that the population impacted by short-term increases in PM is not restricted to those admitted to the hospital or seeking medical attention through an ED.

Table 6-13. Description of ICD-9 and ICD-10 codes for diseases of the respiratory system.

Description	ICD 9 Codes	ICD 10 Codes
Diseases of the Respiratory System	460-519	J00-J99
Asthma	493	J45
COPD and allied conditions	490-496 (asthma, chronic bronchitis, emphysema, bronchiectasis, extrinsic allergic alveolitis)	
Chronic lower respiratory diseases		J40-J47 (bronchitis, emphysema, other COPD, asthma, status asthmaticus, bronchiectasis)
Acute Respiratory Infections	460-466 (common cold, sinusitis, pharyngitis, tonsillitis, laryngitis & tracheitis, bronchitis & bronchiolitis)	
Acute Upper Respiratory Infections		J00-J06 (common cold, sinusitis, pharyngitis, tonsillitis, laryngitis & tracheitis, croup & epiglottitis)
Acute bronchitis and bronchiolitis	466	J20-J22
Allergic Rhinitis	477	J30.1
Pneumonia	480-486	J13-J18
Wheezing	786.09	

Hospital admissions or ED visits for respiratory diseases and ambient concentrations of PM have been the subject of more than 90 peer-reviewed research publications since 2002 (Annex E). Included among these new publications are several large single-city and multicity studies. These new studies complement those reviewed in the 2004 AQCD by examining the effect of several PM size fractions and components on increasingly specific disease endpoints, as well as evaluating the presence of effect modification by factors such as season and region.

Specific design and methodological considerations of the large and multicity studies included in this review were discussed previously (Section 6.2.10). Like the CVD endpoints discussed, the respiratory endpoints examined in these studies were heterogeneous and approaches to selecting cases for inclusion in the studies were varied. ICD codes commonly used in hospital admission and ED visits studies for diseases of the respiratory system are found in Table 6-13.

6.3.8.1. All Respiratory Diseases

Findings from new studies of PM and respiratory hospitalization and ED visits among children are summarized in Figure 6-10. Results from new studies of adults are summarized in Figure 6-11. Information on the PM concentrations during the relevant study periods is found in Table 6-14.

Children

Barnett et al. (2005, [087394](#)) used a case-crossover design to study respiratory hospital admissions (ICD-9 460-519) of children (age groups 0, 1-4, and 5-14 yr) in seven cities in Australia and New Zealand from 1998 to 2001. All respiratory diseases (ICD10 J00-J99) except Mendelson's Syndrome, post-procedural disorders, asphyxia and certain other symptoms (ICD10 codes J95.4-J95.9, R09.1, R09.8) were included in the study. In addition, scheduled admissions and transfers from other hospitals were excluded. Using an a priori lag (0- to 1-day avg), increases in respiratory hospital admissions of 2.0% (95% CI: -0.13 to 4.3) among infants <1 yr old, 2.3% (95% CI: 1.9-7.3) among children 1-4 yr old and 2.5% (95% CI: 0.1-5.1) among children 5-14 yr old per 10 $\mu\text{g}/\text{m}^3$ increase in 24-h avg PM_{10} were observed. Increases of 6.4% (95% CI: 2.7-10.3) among infants <1 yr and 4.5% (95% CI: 1.9-7.3) among children 1-4 yr per 10 $\mu\text{g}/\text{m}^3$ increase in $\text{PM}_{2.5}$ were observed.

Ostro et al. (2009, [191971](#)) studied the effect of $\text{PM}_{2.5}$ and components on respiratory disease (ICD9 460-519) hospitalizations among children <19 yr from 2000 to 2003 in six counties in California. The nine components examined (EC, OC, nitrates, sulfates, Cu, Fe, K, Si and Zn), were chosen because they made up relatively large proportion of $\text{PM}_{2.5}$, had a signal to noise ratio >2, or

the majority of their values were greater than the level of detection. Single day lags of 0-3 days were evaluated. The largest risks were observed at lag 3 days for PM_{2.5} (2.8% [95%CI: 1.2-4.3] per 10 µg/m³), EC (5.4% [95% CI: 0.8-10.3] per IQR) and Fe (4.7% [95% CI: 2.2-7.2] per IQR increase). Although not as great, positive associations were also observed for OC, SO₄²⁻, nitrate, Cu and Zn.

In a study of PM_{2.5} from wildfires in California during 2003, Delfino et al. (2009, 191994) evaluated conducted stratified analyses comparing PM_{2.5} associations pre-, post- and during the wildfires. Four age groups (0-4, 5-19, 20-64 and ≥65 yr) were considered in these analyses. Authors found increased respiratory disease admissions in the periods before (2.6% [95%CI: -5.4 to 11.3]) and during (2.7% [95%CI: -1.6 to 7.6]) the wildfires among children 5-19 yr old, but not after the wildfire period. Among younger children (0-4 yr), hospital admissions were increased during fire periods (4.5% [95% CI: 1-8.2]), but not before or after the wildfire period. Estimated zip code level PM_{2.5} concentrations were 90 µg/m³ and 75 µg/m³ during heavy and light smoke conditions, respectively, compared to 20 µg/m³ during non-fire periods.

In the study of six cities in France described previously (PSAS), investigators report a change of 0.4% (95%CI: -1.2 to 2) per 10 µg/m³ increases in PM_{2.5} for all respiratory diseases combined (ICD-10: J00-J99) among children from 0-14 yr old (Host et al., 2008, 155852). The same study reported a larger increase associated with PM_{10-2.5} of 6.2% (95% CI: 0.4-12.3, 0-1 day avg) per 10 µg/m³ increase among children. A relatively large effect for PM_{10-2.5} (31% [95% CI: -4.7 to 80]) was also observed in a single-city study of children <3 yr in Vancouver (Yang et al., 2004, 087488). The non-significant PM_{2.5} effect estimates were not presented in the publication. Luginaah et al. (2005, 057327) did not observe significant increases in respiratory hospitalizations with increasing PM₁₀ concentrations among male or female children in Ontario Canada, while Ulirsch et al. (2007, 091332) reported increased admissions for respiratory hospitalizations, ED and urgent care visits combined among children <17 yr in association with PM₁₀.

As shown in Figure 6-10, studies of respiratory hospitalizations or ED visits reported increased risks to children in association with all size fractions. However, increased risk among boys was not observed in Ontario (Luginaah et al., 2005, 057327). Estimates are imprecise and it is not clear if associations with PM_{2.5}, PM_{10-2.5}, or both are driving associations observed with PM₁₀.

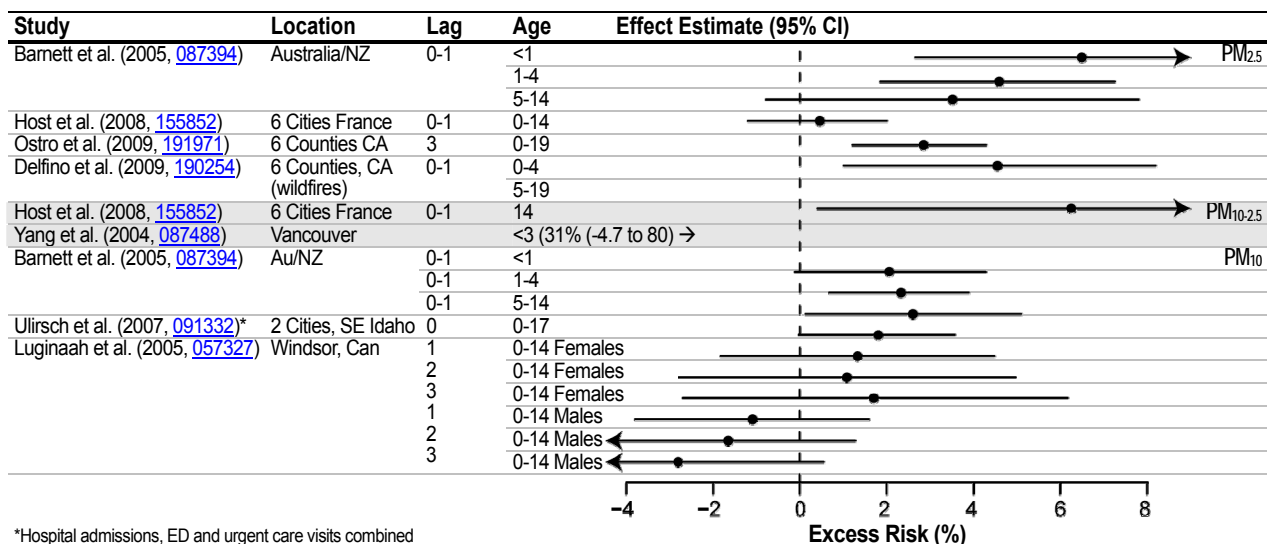


Figure 6-10. Excess risk estimates per 10 µg/m³ 24-h avg PM_{2.5}, PM_{10-2.5}, and PM₁₀ concentration for ED visits and HAs for respiratory diseases in children. Studies represented in the figure include all multicity studies as well as single-city studies conducted in the U.S. or Canada.

Adults and All Ages Combined

In the study of four million ED visits from 31 hospitals in Atlanta described previously, SOPHIA investigators reported an excess risk of 1.3% (95% CI: 0.4-2.1, lag 0-2) per 10 $\mu\text{g}/\text{m}^3$ increase in 24-h avg PM_{10} for ED visits for respiratory causes combined (ICD-9: 460-466, 477, 480-486, 491-493, 496, 786.09) among all ages during January 1993-August 2000 (Peel et al., 2005, [056305](#)). $\text{PM}_{2.5}$, $\text{PM}_{10-2.5}$, UF number count and $\text{PM}_{2.5}$ components (SO_4^{2-} , acidity, EC, OC, and an index of water-soluble transition metals) were available for inclusion in analyses beginning August 1, 1998. Excess risks of 1.6% (95% CI: -0.003 to 3.5) per 10 $\mu\text{g}/\text{m}^3$ increase in 24-h avg $\text{PM}_{2.5}$ and 0.6% (95% CI: -3.6 to 5.1) per 10 $\mu\text{g}/\text{m}^3$ increase in $\text{PM}_{10-2.5}$ were reported. Weaker, less precise associations with components were reported and no increase with UF PNC was observed.

Analyses with four additional years of data were conducted and more recently reported by SOPHIA investigators (Tolbert et al., 2007, [090316](#)). Single-pollutant results are included in Figure 6-11. The effect of PM_{10} remained with the additional years of data, while the effect of $\text{PM}_{2.5}$ was diminished and a decrease in ED visits with $\text{PM}_{10-2.5}$ was observed. The association of PM_{10} with respiratory disease ED visits was robust to adjustment for O_3 , CO and NO_2 . In another recent analysis using SOPHIA data from 1998 through 2002 to compare source apportionment methods, Sarnat et al. (2008, [097972](#)) reported that $\text{PM}_{2.5}$ from mobile sources, $\text{PM}_{2.5}$ from biomass burning and SO_4^{2-} -rich secondary $\text{PM}_{2.5}$ were associated with respiratory ED visits and associations were robust to the choice of the method. Excess risks were statistically significant, ranging from approximately 2-4%, depending on the method.

In a French multicity study, larger increases were observed in association with 24-h avg $\text{PM}_{10-2.5}$ concentration compared to $\text{PM}_{2.5}$ concentration among adults as well as children. Among adults 15-64 yr, investigators reported increases in respiratory hospitalizations of 0.8% (95%CI: -0.7 to 2.3) and 2.6% (95%CI: -0.5 to 5.8) per 10 $\mu\text{g}/\text{m}^3$ for $\text{PM}_{2.5}$ and $\text{PM}_{10-2.5}$, respectively (lag 0-1 days) (Host et al., 2008, [155852](#)).

In a study of respiratory hospital admission and ED visits (ICD-9 Codes 460-519) among all ages conducted in Spokane, Washington, no associations were observed with any size fraction of PM considered (e.g., PM_1 , $\text{PM}_{2.5}$, $\text{PM}_{10-2.5}$, PM_{10}) (Slaughter et al., 2005, [073854](#)). Furthermore, several of the same investigators conducted a source apportionment analysis using daily $\text{PM}_{2.5}$ filter samples from the same residential monitor in Spokane (Schreuder et al., 2006, [097959](#)). In this investigation, $\text{PM}_{2.5}$ from vegetative burning in the previous day (lag 1) was associated with respiratory hospital admissions (2.3% [95% CI: 0.9-3.8] per interquartile range increase in the source marker). In a study of $\text{PM}_{2.5}$ from wildfires in California during 2003, associations with respiratory hospitalizations were generally stronger relative to associations in the periods before and after the fires (Delfino et al., 2009, [191994](#)). Among adults 20-64 yr, an increase of 2.4% (95% CI: 0.5-4.4 per 10 $\mu\text{g}/\text{m}^3$) was reported during the wildfire period compared to 0.9% (95%CI: -0.1 to 1.8 per 10 $\mu\text{g}/\text{m}^3$) for all periods combined (pre-, post- and during wildfires).

Luginaah et al. (2005, [057327](#)) examined respiratory hospital admissions in relation to PM_{10} concentration across strata for age and gender and compared time series to case-crossover approaches. The results for all ages combined, which were relatively precise, stratified by gender and all lags are presented in Figure 6-11; the largest estimates for PM_{10} were for adult males (15-64 yr old). Fung et al. (2005, [093262](#)) did not report evidence of an association between respiratory admissions and 24-h PM_{10} concentration among adults <65 yr, in a study in Ontario, Canada, while Ulirsch et al. (2007, [091332](#)) reported a significant positive association among all ages and adults (18-64 yr) in two Southeast Idaho cities for hospitalizations, ED and urgent care visits combined. This estimate was robust to adjustment for gaseous pollutants.

Older Adults

Among older adults, MCAPS investigators observed largely null findings for $\text{PM}_{2.5}$ and respiratory hospitalizations (ICD-9: 490-492, 464-466, 480-487) for the U.S. as a whole, but reported heterogeneity in effect estimates across the country that were explained by regional and seasonal factors (Bell et al., 2008, [156266](#)). The nationwide excess risk of respiratory admissions with $\text{PM}_{2.5}$ was 0.22% (95% PI: -0.12 to 0.56, lag 0) (Bell et al., 2008, [156266](#)). The largest increase was observed during the winter in the Northeast (1.76% [95% PI: 0.60-2.93], lag 0). Significant increases in respiratory admissions were also observed at lag 2. In an analysis of $\text{PM}_{10-2.5}$, MCAPS

investigators observed small imprecise increases in respiratory admissions with 24-h $PM_{10-2.5}$ concentration (0.33% [95% PI: -0.21 to 0.86, per $10 \mu\text{g}/\text{m}^3$, lag 0]) (Peng et al., 2008, [156850](#)), which decreased after adjustment for $PM_{2.5}$ (0.26% [95% PI: -0.32 to 0.84 per $10 \mu\text{g}/\text{m}^3$ lag 0]). Associations with $PM_{2.5}$ increased (0.7% [95% PI: 0-1.5, lag 0]) or persisted (0.6% [95% PI: -0.2 to 1.25, lag 2]), after adjustment for $PM_{10-2.5}$.

Two recent MCAPS analyses evaluate the effect of $PM_{2.5}$ components on respiratory hospital admissions. Bell et al. (2009, [191997](#)) analyzed a subset of MCAPS data restricted to 106 counties with data available for both long-term average concentrations of $PM_{2.5}$ components (Bell et al., 2007, [155683](#)) and $PM_{2.5}$ total mass (1999-2005). The components evaluated included 20 chemicals with demonstrated toxicity or that contribute a large proportion of $PM_{2.5}$ mass (Al, NH_4^+ , As, Ca, Cl, Cu, EC, OCM, Fe, Pb, Mg, Ni, NO_3^- , K, Si, Na^+ , Ti, V, Zn). Increases in effect estimates of 511% (95% PI: 80.7-941) for EC, 223% (95% PI: 36.9-410) for Ni and 392% (95% CI: 46.3-738) for V per IQR increases in county-specific component fraction were observed. Associations were somewhat reduced and non-significant in two-pollutant models. When Queens or New York County were excluded, the association of V with hospital admissions lost significance. Associations were also diminished when alternative lag structures were considered.

Peng et al. (2009, [191998](#)) linked data on hospital admissions for respiratory causes among older adults from 2000-2006 to daily air levels from the STN in 119 counties in which both sets of data were available. Chemical constituents evaluated were SO_4^{2-} , nitrate, Si, EC, OCM, sodium and ammonium ions. Single-day lags of 0-2 days were considered. These investigators found a 0.82% increase (95% PI: 0.22-1.44) per IQR increase in same day OCM. After adjustment for the other components, a 1.01% (95% PI: 0.04-1.98, lag 0) increase in respiratory admissions per IQR increase OCM was observed.

French PSAS investigators reported a non-significant increase in hospitalizations for respiratory diseases (ICD-10 J00-J99) with 24-h avg $PM_{10-2.5}$ among older adults. $PM_{2.5}$ estimates were also not significant (Host et al., 2008, [155852](#)). Adjusted estimates from two-pollutant models were not presented. Positive associations of first hospitalization, overall hospitalizations and readmission for respiratory diseases and $PM_{10-2.5}$ were also reported among older adults in Vancouver (Chen et al., 2005, [087555](#)). $PM_{10-2.5}$ was associated with an increase of 15% (95% CI: 4.8-22.8) in overall admissions per $10 \mu\text{g}/\text{m}^3$. Increases associated with $PM_{10-2.5}$ were larger for readmissions compared to overall admissions. The association for $PM_{2.5}$ with overall admissions was 5.1% (95% CI: -4.9 to 13) and the association with readmissions was not larger. In this study, effect estimates for $PM_{10-2.5}$ and PM_{10} lost precision, but were robust to adjustment for gaseous pollutants, while the estimate for $PM_{2.5}$ was null after adjustment for gaseous pollutants. In Vancouver, Fung et al. (2006, [089789](#)) report increased admissions of 1.8% (95% CI: -2.5 to 5.8) per $10 \mu\text{g}/\text{m}^3$ increase in $PM_{2.5}$ and 3.8% (95% CI: 0-7.6) per $10 \mu\text{g}/\text{m}^3$ increase in $PM_{10-2.5}$ (lag 0-1 day avg) among adults ≥ 65 yr.

In a multicity Australian study, Simpson et al. (2005, [087438](#)) examined the association between $PM_{2.5}$ measured by nephelometry and respiratory hospital admissions (ICD-9 460-519) among older adults (≥ 65 yr) and reported significant associations (1.055 [95% CI: 1.008-1.1045], lag 0-1 day avg) from a meta-analysis combining effect estimates from all cities. Results from three statistical models were considered, including standard GAM, which produced similar results.

Delfino et al. (2009, [191994](#)) reported that $PM_{2.5}$ from wildfire in California was associated with respiratory hospital admissions among older adults (3% 95% CI: 1.1-4.9 per $10 \mu\text{g}/\text{m}^3$). In two analyses of data collected in Copenhagen, Denmark between 1999 and 2004, several size fractions including UF and accumulation mode (Andersen et al., 2008, [189651](#)) and PM_{10} sources (Andersen et al., 2007, [093201](#)) were investigated in relation to respiratory hospitalizations (J41-42, J43, J44-46) among adults >65 yr of age. Of the size fractions examined (NC total, NC median diameter of 12 nm [NC_{a12}], NC_{a23} , NC_{a57} , NC_{a100} , NC_{a212} , PM_{10} , $PM_{2.5}$) NC_{a212} , typically aged secondary long-range transported, NC_{a57} and PM_{10} were significantly associated with respiratory hospitalizations (Andersen et al., 2008, [189651](#)). PM_{10} sources including biomass combustion, secondary inorganic compounds, oil combustion, and crustal were associated with respiratory hospitalizations (excess risks ranged from 3.5% to 5.4% per interquartile range, respectively) (Andersen et al., 2007, [093201](#)). PM_{10} associations were diminished somewhat in two-pollutant models (Andersen et al., 2007, [093201](#); 2008, [189651](#)); the authors note that it was difficult to separate the effects of PM_{10} and NC_{a212} , which were highly correlated in these data. $PM_{2.5}$ was not associated with respiratory hospitalizations in these data.

Results from other single-city studies offer somewhat consistent evidence for the effect of PM_{10} on respiratory admissions among older age groups. Ulirsch et al. (2007, [091332](#)) found

increases in hospitalizations, ED and urgent care visits combined among this age group in two cities of Southeast Idaho. Two studies in Vancouver report increased admissions for respiratory causes with the largest effects observed for a 3-day ma (0-2 days) (Chen et al., 2005, [087555](#); Fung et al., 2006, [089789](#)). Fung et al. (2005, [093262](#)) observed non-significant increases in admissions with PM₁₀ among older adults in Ontario, Canada, while another study conducted in Ontario (Luginaah et al., 2005, [057327](#)) did not provide compelling evidence for an effect that was robust to method selection, although some increases among males were observed. Finally, a study of hospital admissions for cardiopulmonary conditions combined among older adults (≥ 65 yr) in Allegheny County, PA found a positive association with PM₁₀ at lag 0 (Arena et al., 2006, [088631](#)).

Effect estimates for adults (and combined age groups) as well as older adults are found in Figure 6-11. Effects observed in single-city studies are generally imprecise but most studies report positive associations. Regional and seasonal variation was observed with the largest effect estimate reported by Bell et al. (2008, [156266](#)) in the Northeast during the winter. Although the number of studies examining components or sources was limited, EC, OC, Ni, V, and PM_{2.5} from mobile sources were associated with increased respiratory admissions. Several additional studies conducted outside the U.S. and Canada reported positive associations of respiratory hospitalizations with PM₁₀ for different age groups and lags (Bedeschi et al., 2007, [090712](#); Chen et al., 2005, [087555](#); Chen et al., 2006, [087947](#); Hanigan et al., 2008, [156518](#); Lai and Cheng, 2008, [180301](#); Larrieu et al., 2009, [180294](#); Middleton et al., 2008, [156760](#); Oftedal et al., 2003, [055623](#)), PM_{2.5} (Hinwood et al., 2006, [088976](#); Neuberger et al., 2004, [093249](#); Vigotti et al., 2007, [090711](#)), BS (Bartzokas et al., 2004, [093252](#); Tecer et al., 2008, [180030](#)) and with PM_{10-2.5} (Tecer et al., 2008, [180030](#)). Other studies reported no associations with PM₁₀ (Vegni and Ros, 2004, [087448](#)) or TSP (Llorca et al., 2005, [087825](#)).

6.3.8.2. Asthma

Results from multicity studies of hospital admissions and ED visits for asthma as well as single-city studies conducted in the U.S. and Canada are summarized in Figure 6-12. Studies reviewed in the 2004 AQCD are included for continuity. Concentrations of PM for the relevant study period are found in Table 6-14.

Children

SOPHIA investigators (Peel et al., 2005, [056305](#)) reported that, of the PM mass indicators examined, the largest effect estimate observed using the a priori lag (0- to 2-day avg) was the association of PM₁₀ with pediatric (2-18 yr) asthma ED visits (1.6% [95% CI: -0.2 to 3.4]). ED visits for both asthma (ICD-9: 493) and wheezing (ICD-9: 786.09) were included in their study. New York State DOH (2006, [090132](#)) conducted a study comparing effect estimates for ED visits for asthma and 24-h PM_{2.5} and 1-h PM_{2.5} across two communities in New York City (the Bronx and Manhattan). No associations with 24-h PM_{2.5} were reported for either borough for age categories 0-4 or 5-18 yr. Non-significant increases with 1-h maximum PM_{2.5} were reported for the Bronx. Asthma hospital admissions (ICD-10 J45, J46, J44.8) in children <14 yr were examined in the Australia/New Zealand multicity study (Barnett et al., 2005, [087394](#)). In this study, associations for asthma hospital admissions with PM_{2.5} and PM₁₀ were increased but imprecise.

Lin et al. (2002, [026067](#)) used both time series and case-crossover approaches to investigate the influence of PM on asthma hospitalization in children, 6-12 yr old, in Toronto from 1981 to 1993. These authors report relatively small differences in results obtained through bi-directional case crossover and time series approaches, but indicate that unidirectional case-crossover methods may overestimate the relative risks. Single- to 7-day avg lags were investigated and estimates appeared to increase and then level off at the longer lags (0- to 2-day and 0- to 5-day lags are shown in Figure 6-12). Effect estimates for PM_{2.5} are not easily distinguished from the null, but PM_{10-2.5} is significantly associated with asthma admissions among boys and among girls. These associations were imprecise, but robust to adjustment for gaseous pollutants, among all children combined.

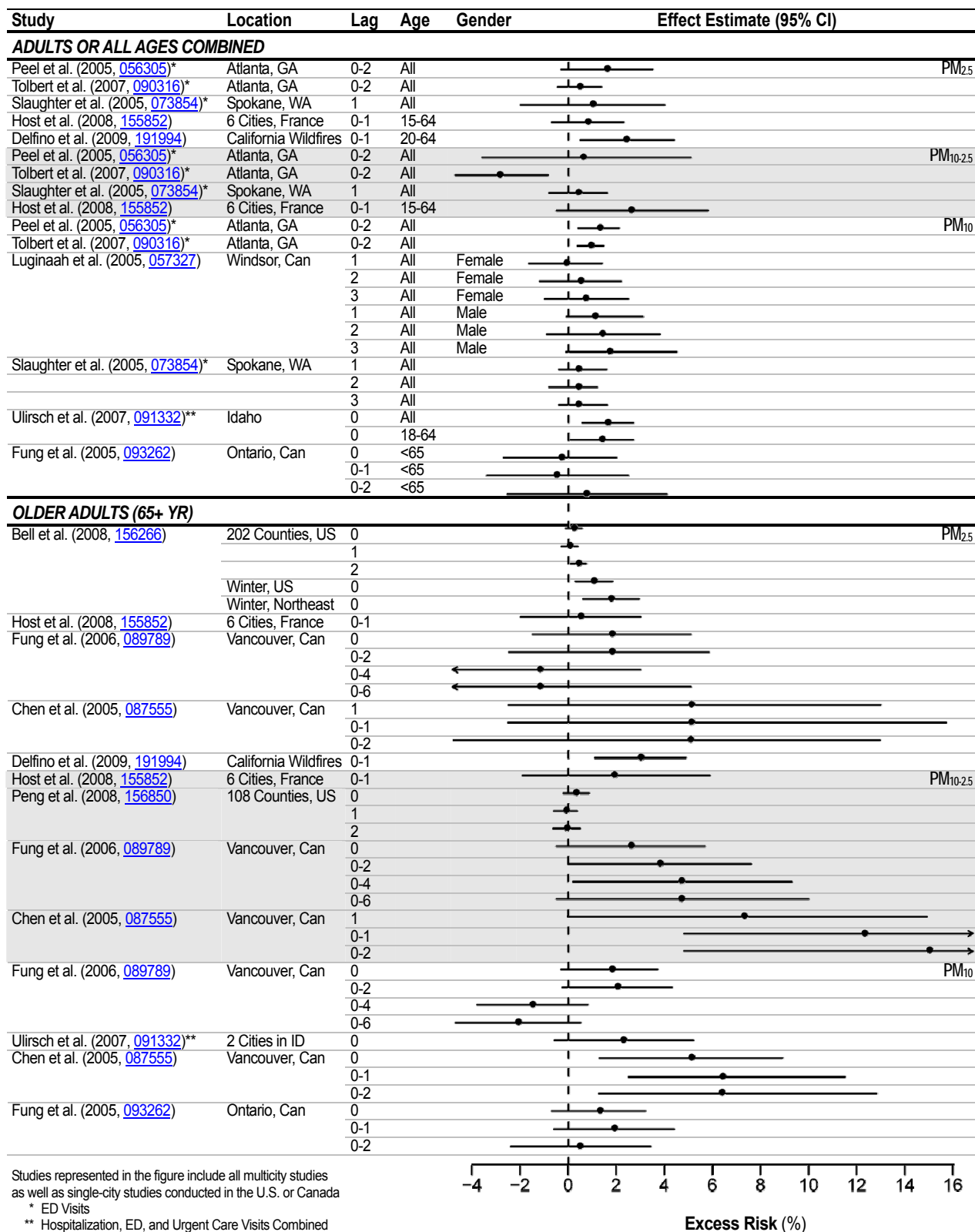


Figure 6-11. Excess risks estimates per 10 µg/m³ increase in 24-h avg PM_{2.5}, PM_{10-2.5}, and PM₁₀ for ED visits and HAs for respiratory diseases among adults.

Although Ostro et al. (2009, [191971](#)) presented estimates for all respiratory diseases combined, these authors note that PM_{2.5} and its components were associated with asthma hospitalizations among the children in six counties of Los Angeles studied. Delfino et al. (2009, [191994](#)) examined the association of PM_{2.5} before, during, and after wildfires in California with asthma hospitalizations among age and gender subgroups. Associations were observed for children 0-4 yr among children during the wildfire period (8.3% [95% CI: 2.1-14.9] per 10 µg/m³), but not before or after the wildfire period. For older children, 5-19 yr, non-significant increases in asthma hospitalizations were found before the wildfire period, but not during or after the fires.

Hirshon et al. (2008, [180375](#)) studied hospital admissions and ED visits by children 0-17 yr old in Baltimore, MD from June 2002-November 2002, in relation to Zn as a component in PM_{2.5}. Single day lags from 0-2 days were tested with the highest estimates observed for the previous day. A 23% (95% CI: 7-41) increase in admissions was observed comparing medium (8.63-20.76 ng/m³) concentrations on the previous day to low concentrations (<8.63 ng/m³) on the previous day. Previous day high concentration (>20.76 ng/m³) was associated with an increase in admissions of 16% (95% CI: -3 to 39) compared to previous day low concentration. Zinc associations were robust to adjustment for EC, CO, NO₂, Ni, and Cr. However, evidence of effect modification by EC and NO₂ at lags 1 and 2 was observed.

Mohr et al. (2008, [180215](#)) used measurements of EC, O₃, SO₂, and total NO_x from the EPA supersite in St. Louis for June 2001-May 2003, to examine the association of EC, temperature and season with asthma ED visits among children 2-17 yr old. The association of EC with asthma ED visits varied by age, season and weekday versus weekend. The largest associations were observed for 2-5 yr olds during the fall weekends (3% [95% CI: 1-5] per 0.1 µg/m³) and 11-17 yr olds during winter weekdays (3% [95% CI: 0-5] per 0.1 µg/m³) and summer weekends (9% [95% CI: 2-17] per 0.1 µg/m³). Investigators also report that temperature modified the effect of EC after adjusting for gaseous copollutants, such that the association of ED visits with EC increased with increasing temperature during the summer and increased with decreasing temperature during the winter. Authors attribute the temperature modification to time-activity patterns among this age group.

Sinclair and Tolsma (2004, [088696](#)) investigated respiratory ambulatory care visits using ARIES data in Atlanta, GA (also used by SOPHIA investigators) and health insurance records. These authors evaluated three 3-day ma lags (0-2, 2-5 and 6-8 days) and reported relative risks, with no confidence intervals, for significant results only (not included in Figure 6-12). For childhood asthma outpatient visits, OHC, PM_{10-2.5}, PM₁₀, EC and OC were significantly associated with ambulatory care visits at lags 0-2 or 2-5 days.

A study in Anchorage used medical records to examine effects of particle exposure on pediatric asthma outpatient visits, inpatient visits and prescriptions for short-acting inhalers (Chimonas and Gessner, 2007, [093261](#)). Authors examined Medicaid claims for asthma-related and lower respiratory infection visits among children less than 20 yr of age for 5 yr (approximately 25,000 children were enrolled in Medicaid each year between 1999 and 2003). Citing work done in the mid-1980's, the authors describe their city's particles as arising primarily from natural, geologic sources (PM₁₀), and to a lesser extent from local automotive emissions (PM_{2.5}) (Pritchett and Cooper, 1985, [156886](#)). Using GEE in a time-series analysis of daily and weekly effects of particle exposure on health outcomes, the authors found that each 10 µg/m³ increase in 24-h avg PM₁₀ was associated with a 0.6% increase (95% CI: 0.1-1.3) in outpatient visits for asthma. The same increase in weekly PM₁₀ concentration resulted in a 2.1% increase (95% CI: 0.4-3.8) in asthma visits, after adjustment for gaseous pollutants. No meaningful associations were observed for PM_{2.5}.

In Copenhagen, Denmark, Anderson et al. (2007, [093201](#)) found an association between PM₁₀ attributed to vehicle emissions and asthma hospitalizations among children 5-18 yr (5.4% 95% CI: 0.57-22.9 per 10 µg/m³, 0- to 5-day avg). In an analysis of size distribution and number concentration, accumulation mode particles were most strongly associated with asthma admissions (8% [95% CI: 0-17] per 495 particles/cm³, lag 0-5). (Andersen et al., 2008, [189651](#)). In Helsinki, Halonen et al. (2008, [189507](#)) examined the association of various size fractions of PM (e.g., Aitken, accumulation mode, PM_{2.5}, PM_{10-2.5}) with ED visits for asthma among children <15 yr. These authors evaluated lags 0-5 and noted a different lag structure depending on age with children experiencing greater effects at lags 3-5 days compared to adults at lag 0. Aitken, accumulation mode particles and traffic-related PM were significantly and most strongly associated with asthma visits among children, while no association with PM_{10-2.5} was observed in this age group.

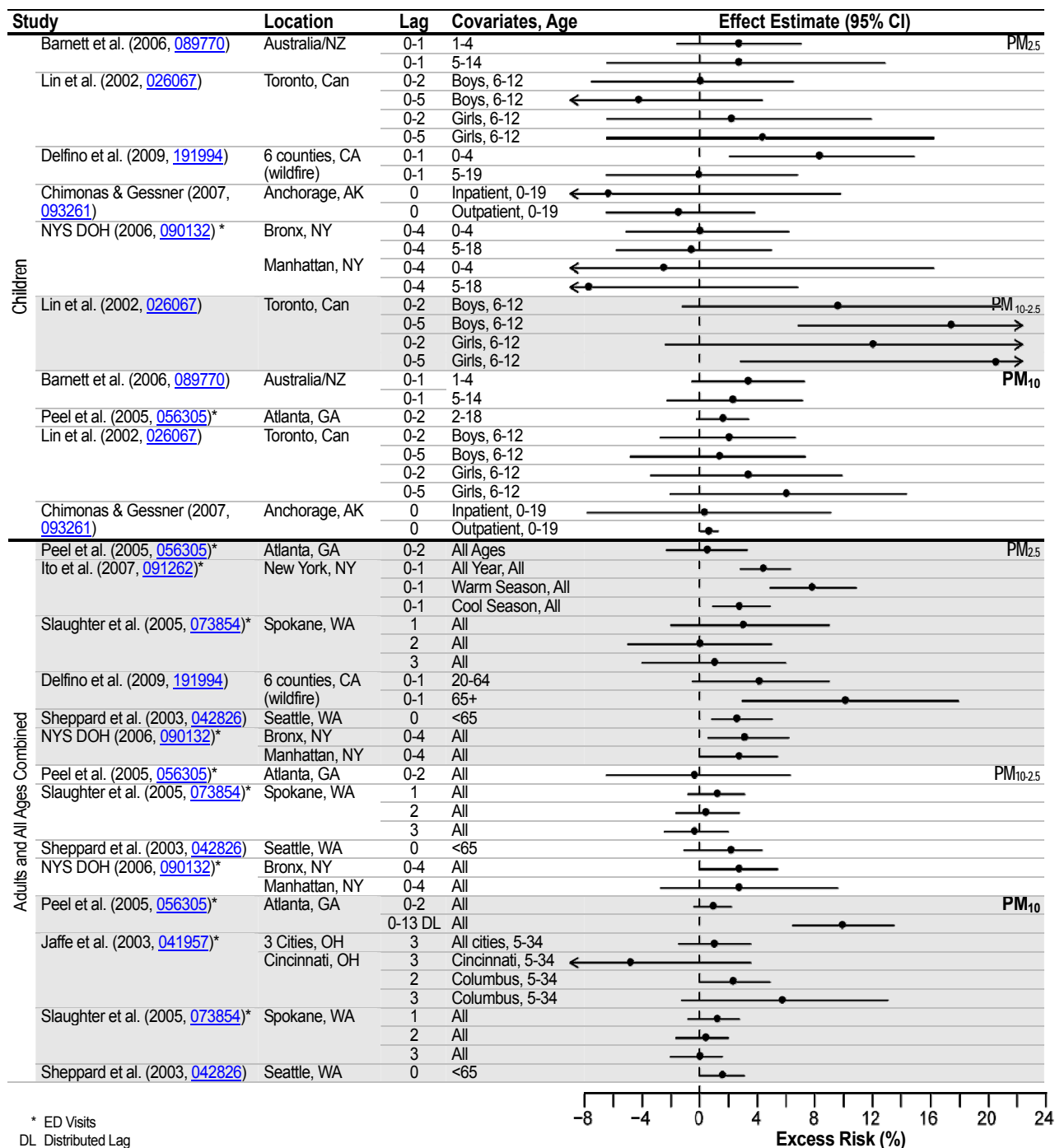


Figure 6-12. Excess risk estimates per 10 µg/m³ increase in 24-h avg PM_{2.5}, PM_{10-2.5}, and PM₁₀ for asthma ED visits and HAs. Studies represented in the figure include all multicounty studies as well as single-city studies conducted in the U.S. or Canada.

Adults and All Ages Combined

Results from the Atlanta SOPHIA study based on the a priori models examining a 3-day moving average (lag 0-2 days) revealed no statistically significant associations with asthma (ICD-9 493, 786.09)

among all ages for any of the PM metrics studied (e.g., PM_{2.5}, PM_{10-2.5}, PM₁₀, UF PNC, PM components) (Peel et al., 2005, [056305](#)). However, the 14-day unconstrained distributed lag model produced an excess risk of 9.9% (95% CI: 6.5-13.5 per 10 µg/m³ PM₁₀). The authors note that associations of PM_{2.5} and OC with asthma tended to be stronger during the warmer months. Sinclair and Tolsma (2004, [088696](#)) report a significant association between adult outpatient visits for asthma and UFPs, but not other PM size fractions (not included in Figure 6-12 because only significant results were presented).

Jaffe et al. (2003, [041957](#)) examined the effects of ambient pollutants (PM₁₀, O₃, NO₂ and SO₂) during the summer months (June through August) on the daily number of ED visits for asthma among Medicaid recipients aged 5-34 yr from 1991 to 1996 in Cincinnati, Columbus, and Cleveland. Lags 1 to 3 were tested and only statistically significant lags were presented. For all cities combined, the overall effect estimate for 24-h avg PM₁₀ was 1.0% (95% CI: -1.44 to 3.54 per 10 µg/m³ increase). The effect estimate for Cleveland was the only significantly elevated estimate (2.3% [95% CI: 0.0-4.9] per 10 µg/m³ increase) when the cities were examined independently. The authors reported results from analyses indicating a possible concentration response for O₃, but no consistent effects for PM₁₀.

In New York City, Ito et al. (2007, [156594](#)) examined numbers of ED visits for asthma among all ages (ICD-9 493) in relation to pollution levels from 1999 to 2002; several weather models were evaluated. Although the association with NO₂ was the strongest, PM_{2.5} was significantly associated with asthma ED visits in each weather model (strongest during the warm months) and remained significant after adjustment for O₃, NO₂, CO and SO₂. Slaughter et al. (2005, [073854](#)) reported no associations with ED visits or hospitalizations for asthma, among all ages, in Spokane, Washington for the PM size fractions studied (PM₁, PM_{2.5}, PM₁₀, PM_{10-2.5}). An association with CO, which the authors attribute to combustion related pollution in general, was observed. The effect of 24-h avg and 1-h max PM_{2.5}, PM_{10-2.5}, EC and OC on ED visits for asthma among all ages combined, comparing two communities in New York City was investigated (ATSDR, 2006, [090132](#)). In the Bronx, an increase in visits of 3.1% (95% CI: 0.6-6.2 per 10 µg/m³) was observed in relation to 24-h avg PM_{2.5}. For PM_{10-2.5}, an increase of 2.7% (95% CI: 0.0-5.4) was observed in the Bronx. Smaller, less precise estimates were observed for Manhattan. Increased asthma visits were observed with OC, EC and total metals. In the Bronx, the association of 1-h max PM_{2.5} with ED visits was larger than the association with 24-h PM_{2.5} when standardized to the mean concentration for both communities and was generally robust to adjustment for copollutants.

Delfino et al. (2009, [191994](#)) examined the association of PM_{2.5} before, during and after wildfires in California with asthma hospitalizations among age and gender subgroups. The increase among older adults >65 yr of 10% (95% CI: 3-17.8 per 10 µg/m³) was larger than the increase among adults 20-64 yr of 4.1% (95% CI: -0.5 to 9 per 10 µg/m³). For older adults, the association was stronger during the wildfire period compared to the pre-wildfire period and did not diminish during the post-wildfire period.

Effect estimates from studies of hospital admissions and ED visits for asthma are summarized in Figure 6-12. Associations with PM_{2.5} concentration among children are imprecise and not consistently positive across different age groups and lags. Findings from two studies of PM_{10-2.5} (Sinclair and Tolsma, 2004, [088696](#)), as well as PM₁₀ studies both show positive associations, although estimates lack precision. Among adults and adults and children combined, associations of asthma hospital admissions and ED visits with PM_{2.5} concentration were observed in most studies. Positive, non-significant associations of PM_{10-2.5} concentration with asthma admissions and ED visits were observed in some studies of adults. Again, PM₁₀ estimates are more consistently positive and precise compared to other size fractions. Associations were observed with several PM_{2.5} components (e.g., EC, OC and Zn) and sources (e.g., traffic, wildfires). Many factors (e.g., the underlying distribution of individual sensitivity and severity, medication use and other personal behaviors) can influence the lag time observed in observational studies (Forastiere et al., 2008, [186937](#)). Excess risk estimates for asthma were generally sensitive to choice of lag and increase with longer or cumulative lags times. Most additional single-city studies conducted in Europe, South America and Asia, have investigated the associations of asthma hospitalizations, ED visits or doctor visits and most have reported evidence of an association with TSP (Arbex et al., 2007, [091637](#); Migliaretti and Cavallo, 2004, [087425](#); 2005, [088689](#)), PM₁₀ (Bell et al., 2008, [156266](#); Bell et al., 2008, [091268](#); Chardon et al., 2007, [091308](#); Chen et al., 2006, [087947](#); Erbas et al., 2005, [073849](#); Galan et al., 2003, [087408](#); Jalaludin et al., 2004, [056595](#); Kim et al., 2007, [092837](#); Ko et al., 2007, [091639](#); Kuo et al., 2002, [036310](#); Lee et al., 2002, [034826](#); Lee et al., 2006, [090176](#)) and PM_{2.5} (Chardon et al., 2007, [091308](#);

Ko et al., 2007, [091639](#); Ko et al., 2007, [092844](#)) while a few have not shown an association with PM₁₀ (Larrieu et al., 2009, [180294](#); Masjedi et al., 2003, [052100](#); Tsai et al., 2006, [089768](#); Yang and Chen, 2007, [092847](#); Yang et al., 2007, [092848](#)).

6.3.8.3. Chronic Obstructive Pulmonary Disease

Results from multicity studies of hospital admissions and ED visits for COPD as well as single-city studies conducted in the U.S. and Canada are summarized in Figure 6-13. Studies reviewed in the AQCD are included in the figure for continuity. Concentrations of PM for the relevant study period are found in Table 6-14.

In a study of Medicare recipients in 204 U.S. counties, Dominici et al. (2006, [088398](#)) reported an overall increase of about 1% in COPD hospitalizations (ICD-9 490-492) associated with 24-h avg PM_{2.5}, with the largest effects at lags 0 and 1. In this study effect estimates were heterogeneous across the U.S. with a significant increase of about 4% observed in the Southeast at lag 0. In another study using Medicare data in 36 U.S. cities (1986-1999) short-term exposure to PM₁₀ was associated with an increase in COPD hospital admissions (ICD-9 490-496, excluding 493) of 1.47% (95% CI: 0.93-2.01, lag 1) during the warm season (Medina-Ramon et al., 2006, [087721](#)). A smaller effect was observed during the cold season.

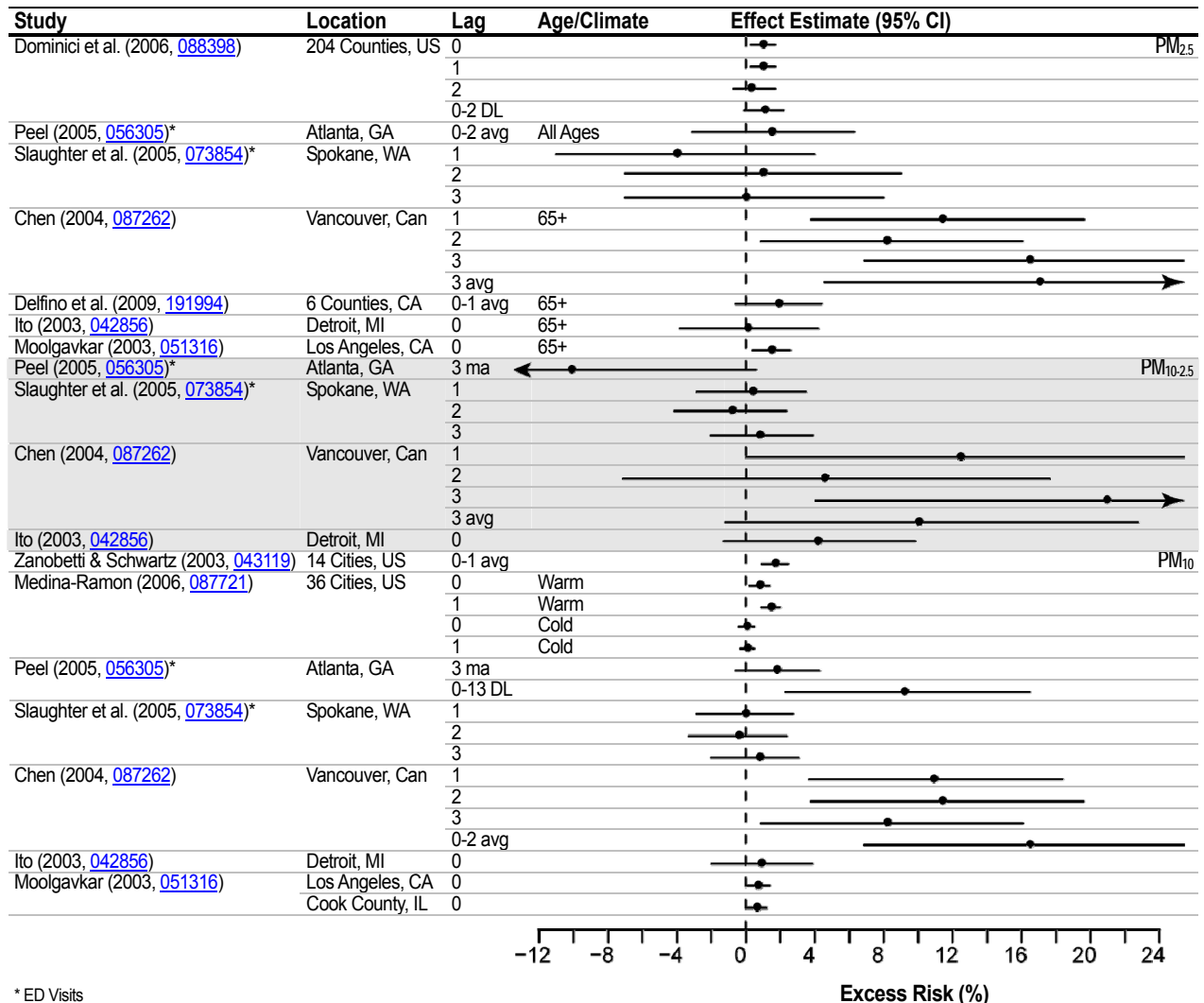
In Atlanta, SOPHIA investigators reported a comparably sized effect estimate for COPD (ICD-9 491, 492, 496) and 24-h avg PM_{2.5} (1.5% [95% CI: -3.1 to 6.3], 0- to 2-day avg)]. The association of PM₁₀ with COPD reported by Peel et al. (2005, [056305](#)) was 1.8% (95% CI: -0.6 to 4.3). No associations were observed for PM_{10-2.5}, UF or PM_{2.5} components. Slaughter et al. (2005, [073854](#)) reported no associations between any size fraction of PM in Spokane, Washington (PM_{2.5}, PM_{10-2.5}, PM₁₀) and COPD (ICD-9 491, 492, 494, 496). In contrast, Chen et al. (2004, [087262](#)) reported increases in COPD admissions (ICD-9 490-492, 494, 496) for PM_{2.5} (17.1% [95% CI: 4.6-31.0], 0- to 2-day avg), PM_{10-2.5} (10.0% [95% CI: -1.2 to 22.8, 0- to 2-day avg]), and PM₁₀ (16.5% [95% CI: 6.88-27.02], 0- to 2-day avg)]. However, the estimates for PM metrics were diminished after adjustment for NO₂.

Delfino et al. (2009, [191994](#)) examined the association of PM_{2.5} from the wildfires of 2003 in California with COPD hospitalizations among age and gender subgroups. Among older adults (≥65 years), associations were similar across pre-, post- and wildfire periods with none reaching significance. The increase for all periods combined in this age group was 1.9% (95% CI: -0.6 to 4.4, per 10 μg/m³). Michaud et al. (2004, [188530](#)) reported an association for asthma and COPD ED visits combined with PM₁ (lag 1) in Hilo, Hawaii in a study designed to investigate the effect of volcanic fog.

Halonen et al. (2008, [189507](#)) conducted a study of ED visits for COPD and asthma combined (J41, J44-J46) among adults 15-64 yr and older adults >65 yr. These authors examined the effects of Aitken mode particles, accumulation mode particles, PM_{2.5} and PM_{10-2.5} as well as several sources of PM_{2.5} (traffic, long range transported particles, road dust and coal/oil combustion). Concentrations, lagged from 0-5 days, were examined and the largest effects among older adults were observed in association with concurrent day PM_{2.5}, PM_{10-2.5}, accumulation mode particles, NO₂, and CO concentrations. The PM_{2.5} association was diminished with adjustment for UFPs, NO₂ and CO. A similar diminishment was observed when PM_{10-2.5} was adjusted for PM_{2.5}, NO₂ and CO. However, traffic related particles and long range transported particles (e.g., accumulation mode particles such as carbon compounds, sulfates and nitrates from central Europe and Russia) were associated with COPD and asthma among older adults. This same research group conducted additional analyses of hospital admissions using the same PM metrics focusing on older adults (≥65 yr) (Halonen et al., 2009, [180379](#)). The PM_{2.5} results and lag structure were similar to the earlier ED visit study. The strongest effect was for accumulation mode particles with COPD/asthma admissions. Traffic related PM_{2.5} was associated with COPD/asthma admissions at lag 1 while no effect was observed with concurrent day concentration. Long range transported particles and road dust were also associated with admissions for asthma and COPD.

With the exception of one study conducted in Spokane Washington (Slaughter et al., 2005, [073854](#)), associations have been consistently observed for PM_{2.5} and PM₁₀ with COPD in multicity and single-city studies conducted in the U.S. and Canada. Associations with PM_{10-2.5} are fewer and less consistent. A study that examined seven single-day lags in association with pooled COPD and asthma ED visits in Finland reported that PM_{2.5}, PM_{10-2.5}, traffic sources as well as gaseous pollutants

had a more immediate effect in older adults (lags 0 and 1) compared to children experiencing asthma (3- to 5-day lags) (Halonen et al., 2008, [189507](#)). Larger estimates at shorter lags were not observed consistently across other studies. Most single-city studies conducted outside of the U.S. or Canada focused on PM₁₀ (Chiu et al., 2008, [191989](#); Hapcioglu et al., 2006, [093263](#); Ko et al., 2007, [091639](#); Ko et al., 2007, [092844](#); Martins et al., 2002, [035059](#); Masjedi et al., 2003, [052100](#); Sauerzapf et al., 2009, [180082](#); Yang and Chen, 2007, [092847](#)).



* ED Visits

Figure 6-13. Excess risks estimates per 10 µg/m³ increase in 24-h avg PM_{2.5}, PM_{10-2.5}, and PM₁₀ for COPD ED visits and HAs among older adults (65+ yr, unless other age group is noted). Studies represented in the figure include all multicounty studies as well as single-city studies conducted in the U.S. or Canada.

6.3.8.4. Pneumonia and Respiratory Infections

Results from multicounty studies of hospital admissions and ED visits for respiratory infection as well as single-city studies conducted in the U.S. and Canada are summarized in Figure 6-14. The figure includes studies of respiratory infection reviewed in the 2004 AQCD. Concentrations of PM for the relevant study period are found in Table 6-14.

Children

In the study of seven cities in Australia and New Zealand, associations of PM_{2.5} with pneumonia and acute bronchitis (ICD-10 J12-J17, J18.0, J18.1, J18.8, J18.9, J20, J21) were observed among infants <1 yr old (4.54% [95% CI: 0.00-9.20]) and children 1-4 yr old (6.44% [95% CI: 0.26-12.85]) (Barnett et al., 2005, [087394](#)). Although quantitative results were only presented for all respiratory diseases combined, Ostro et al. (2009, [191971](#)) examined several specific respiratory diseases including acute bronchitis and pneumonia. They reported that PM_{2.5} and its components were more strongly associated with these endpoints compared to other respiratory diseases. Delfino et al. (2009, [191994](#)) reports imprecise increases in admissions among children during wildfire periods for acute bronchitis and bronchiolitis, as well as pneumonia.

Inpatient and outpatient visits for lower respiratory tract infections among children in Anchorage, Alaska, were not associated with PM_{2.5} or PM₁₀ (Chimonas and Gessner, 2007, [093261](#)). Lin et al. (2005, [087828](#)) observed associations of respiratory infections (ICD-9 464, 466, 480-487) with PM_{10-2.5} and PM₁₀ that persisted after adjustment for gaseous pollutants among subjects <15 yr old living in Toronto. Analyses were stratified by gender and both single and multiple day lags were examined (4- and 6-day avg were presented). The largest significant effect estimates were for PM_{10-2.5}. The size of the PM_{2.5} estimate varied by gender and was sensitive to the choice of lag. PM_{2.5} results were not generally robust to adjustment for gases.

All Ages and Older Adults

SOPHIA investigators examined ED visits for upper respiratory tract infections (URI) (ICD-9 460-466, 477) and pneumonia (ICD-9 480-486) among all ages. An excess risk of 1.4% (95% CI: 0.4-2.5 per 10 µg/m³, lag 0- to 2-day avg) for PM₁₀ was associated with URI visits. With the exception of a small increase in risk for OC of 2.8% (95% CI: 0.4-5.3 per 2 µg/m³, 0- to 2-day avg) with pneumonia visits, Peel et al. (2005, [056305](#)) reported no association with other PM size fractions or components evaluated. However, Sinclair and Tolsma (2004, [088696](#)), who also used ARIES data in their analysis, reported significant associations with outpatient visits for LRI. These associations were generally observed for 3- to 5-day ma lags, in association with PM_{10-2.5}, PM₁₀, EC, OC, and PM_{2.5} water soluble metals (not pictured in figure because only significant lags were reported). No associations with pneumonia for any size fractions were observed among all ages in a study conducted in Spokane, Washington (effect estimates were not reported) (Slaughter et al., 2005, [073854](#)).

French PSAS investigators examined the effect of PM_{2.5} and PM_{10-2.5} on hospital admissions for respiratory infection (ICD-10: J10-22) among all ages. Increases of 2.5% (95% CI: 0.1-4.8) and 4.4% (95%CI: 0.9-8.0) per 10 µg/m³ were observed in association with PM_{2.5} and PM_{10-2.5}, respectively (Host et al., 2008, [155852](#)). In a multicity study of older adults (≥65 yr) Medina-Ramon et al. (2006, [087721](#)) examined hospital admissions for pneumonia (ICD-9 480-487) in 36 U.S. cities in relation to 24-h avg PM₁₀ concentration. An increase in pneumonia admissions of 0.84% (95% CI: 0.50-1.19 per 10 µg/m³, lag 0) was reported by these investigators during the warm season. Cold season associations were weaker (0.30% [95% CI: 0.07-0.53] per 10 µg/m³, lag 0) as were lag 1 associations. Dominici et al. (2006, [088398](#)) investigated hospital admissions for all respiratory infections including pneumonia (ICD-9 464-466, 480-487) among older adults in 204 urban U.S. counties in relation to PM_{2.5} and reported a significant increased risk only at lag 2. Heterogeneity in effect estimates was observed across the U.S. with the largest associations reported for the South and Southeast.

In Boston, excess risks of pneumonia hospitalization in association with PM_{2.5}, BC, and CO were observed among older adults (Zanobetti and Schwartz, 2006, [090195](#)). A measure of non-traffic PM, e.g., the residuals from the regression of PM_{2.5} on BC, was not associated with pneumonia hospitalization in these data. In a California study (Delfino et al., 2009, [190254](#)), effect estimates were of similar magnitude for pneumonia admissions associated with PM_{2.5} from wildfires among all ages combined and older adults (2.8% [95% CI: 0.7-5.0] per 10 µg/m³, all ages combined). The PM_{2.5} association with acute bronchitis and bronchiolitis admissions during the wildfire period for all age groups showed an approximately 10% increase (9.6% 95% CI: 1.8-17.9, per 10 µg/m³). The increase was not larger during the wildfire period compared to the pre-fire period for either outcome.

In a study of four cities in Australia, statistically significant associations of pneumonia and acute bronchitis with particles measured by nephelometry (but not PM_{2.5} mass) and NO₂ were observed among older adults (Simpson et al., 2005, [087438](#)). Halonen et al. (2009, [180379](#)) examined pneumonia among older adults (ICD10 J12-J15) in their most recent analysis. Associations of PM_{2.5} (5.0% [95% CI: 1.0-9.3] per 10 µg/m³, lag 5-day mean), as well as accumulation mode particles, with pneumonia admissions were observed.

Although the body of literature is small, several studies of children reported associations of PM_{2.5}, PM_{10-2.5} and PM₁₀ with respiratory infections but the outcomes studied are heterogeneous and effect estimates are imprecise. Studies of adults show a similar pattern of increased risk for each of these size fractions. Several other single-city studies conducted outside the U.S. and Canada reported associations for PM₁₀ (Cheng et al., 2007, [093034](#); Hwang and Chan, 2002, [023222](#); Nascimento et al., 2006, [093247](#)) and PM_{2.5} (Hinwood et al., 2006, [088976](#)) with hospitalization or ED visits for respiratory infections.

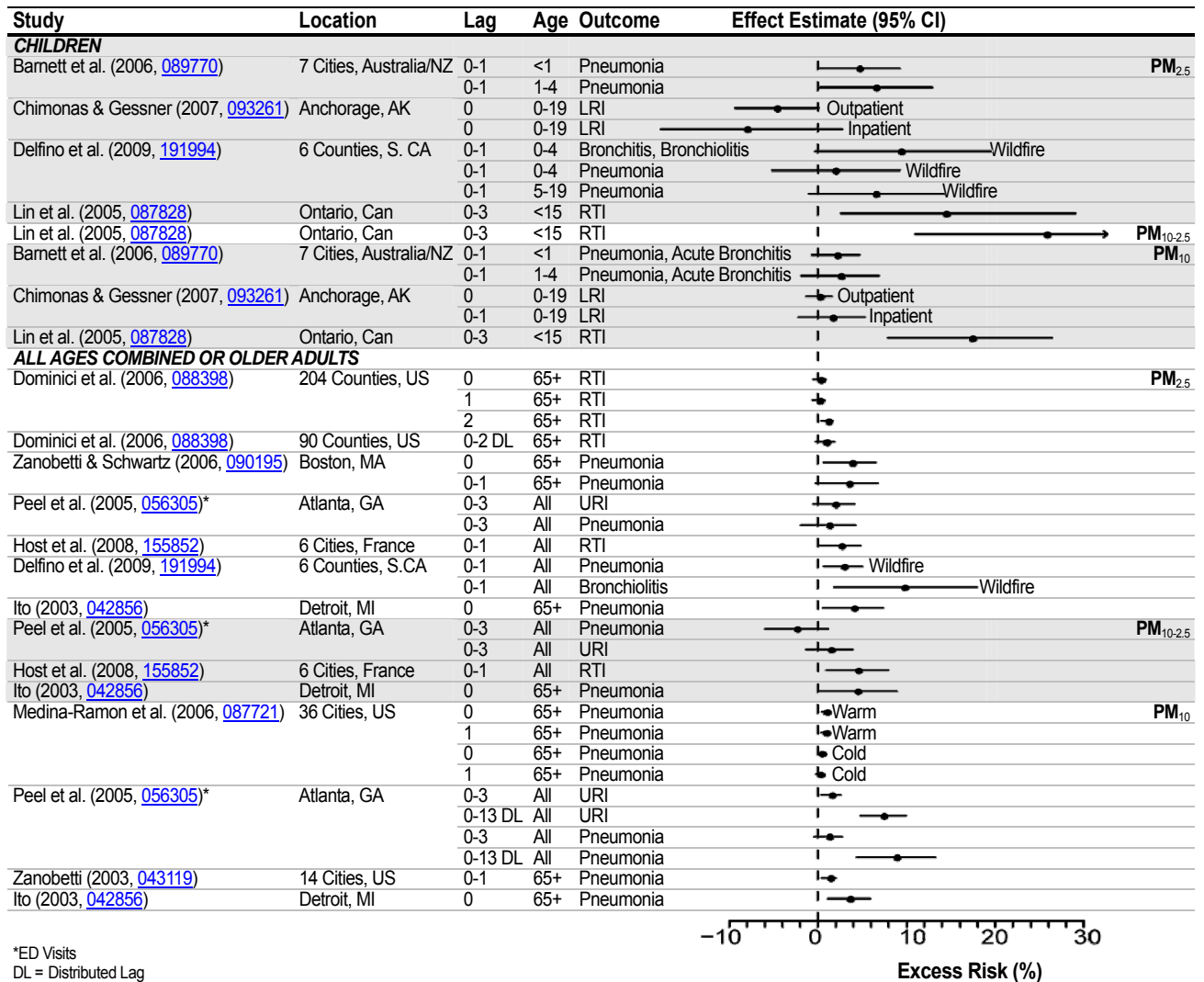


Figure 6-14. Excess risks estimates per 10 µg/m³ increase in 24-h avg PM_{2.5}, PM_{10-2.5}, and PM₁₀ for respiratory infection ED visits* and HAs. Studies represented in the figure include all multicity studies as well as single-city studies conducted in the U.S.

Table 6-14. PM concentrations in epidemiologic studies of respiratory diseases.

Study	Location	Mean Concentration ($\mu\text{g}/\text{m}^3$)	Upper Percentile concentrations ($\mu\text{g}/\text{m}^3$)
<i>PM_{2.5}</i>			
Andersen et al. (2007, 093201)	Copenhagen, Denmark	10	99th: 28
Barnett et al. (2005, 087394)	7 Cities Australia, NZ	8.1-11	Max: 29.3-122.8
Bell et al. (2008, 156266)	202 U.S. counties	12.92	98th: 34.16
Chardon et al. (2007, 091308)	Paris, France	14.7	75th: 18.2
Chen et al. (2004, 087262 ; 2005, 087555)	Vancouver, Canada	7.7	Max: 32
Chimonas and Gessner (2007, 093261)	Anchorage, AK	6.1	Max: 69.8
Delfino et al. (2009, 191994)	6 counties, CA	18.4-32.7	45.3-76.1 (mean during wildfire period)
Dominici et al. (2006, 088398)	204 U.S. counties	13.4	75th: 15.2
Fung et al. (2006, 089789)	Vancouver, Canada	7.72	Max: 32
Halonen et al. (2008, 189507)	Helsinki, Finland	NR; Median = 9.5	Max: 69.5
Host et al. (2008, 155852)	6 Cities France	13.8-18.8	95th: 25.0-33.0
Ito et al. (2007, 091262)	New York, NY	All yr: 15.1	All yr: 95th: 32
Lin et al. (2002, 026067)	Toronto Canada	17.99	Max: 89.59
Lin et al. (2005, 087828)	Ontario, Canada	9.59	Max: 73
Moolgavkar (2003, 051316)	Los Angeles, CA	22 (median)	Max: 86
New York State DOH (2006, 090132)	Bronx/Manhattan	15.0/16.7	NR
Peel et al. (2005, 056305)	Atlanta, GA	19.2	90th: 32.3; 98th: 39.8
Sinclair and Tolsma (2004, 088696)	Atlanta, GA	17.62	NR
Sheppard et al. (2003, 042826)	Seattle, WA	16.7	98th: 46.6
Slaughter et al. (2005, 073854)	Spokane, WA	NR	Max: 20.2 (using 90% of concentrations)
Tolbert et al. (2007, 090316)	Atlanta, GA	17.1	90th: 28.8; 98th: 38.7
Yang et al. (2004, 087488)	Vancouver, Canada	7.7	Max: 32.0
Zanobetti and Schwartz (2006, 090195)	112 U.S. cities	11.1 (Median)	95th: 26.31
<i>PM_{10-2.5}</i>			
Chen et al. (2004, 087262 ; 2005, 087555)	Vancouver, Canada	5.6	Max: 24.6
Fung et al. (2006, 089789)	Vancouver, Canada	5.6	Max: 27.07
Halonen et al. (2008, 189507)	Helsinki, Finland	NR; Median: 9.9	Max: 101.4
Host et al. (2008, 155852)	6 Cities France	7.0-11.0	95th: 12.5-21.0
Lin et al. (2002, 026067)	Toronto, Canada	12.17	Max: 68.00
Lin et al. (2005, 087828)	Ontario, Canada	10.86	Max: 45
New York State DOH	Bronx/Manhattan	7.69/7.10	NR
Peel et al. (2005, 056305)	Atlanta, GA	9.7	90th: 16.2
Peng et al. (2008, 156850)	108 U.S. counties	NR; Median: 9.8	75th: 15.0
Sinclair and Tolsma (2004, 088696)	Atlanta, GA	9.67	NR
Sheppard et al. (2003, 042826)	Seattle, WA	16.2	Max: 88
Slaughter et al. (2005, 073854)	Spokane, WA	NR	NR
Tolbert et al. (2007, 090316)	Atlanta, GA	9	90th: 15.1; Max: 50.3
Yang et al. (2004, 087488)	Vancouver, Canada	7.7	Max: 24.6
<i>PM₁₀</i>			
Andersen et al. (2007, 093201)	Copenhagen, Denmark	25/24	75th: 30 / 99th: 72
Barnett et al. (2005, 087394)	7 Cities, Australia, NZ	16.5-20.6	Max: 50.2-156.3
Chardon et al. (2007, 091308)	Paris, France	23	Max: 97.3
Chen et al. (2004, 087262 ; 2005, 087555)	Vancouver, Canada	13.3	Max: 52.2
Chimonas and Gessner (2007, 093261)	Anchorage, AK	27.6	Max: 421
Fung et al. (2005, 093262)	Ontario, Canada	38	Max: 248
Fung et al. (2006, 089789)	Vancouver, Canada	13.3	Max: 52.17
Gordian and Choudhury (2003, 054842)	Anchorage, AK	36.11	Max: 210.0
Jaffe et al. (2003, 041957)	Cincinnati, OH	43	Max: 90

Study	Location	Mean Concentration ($\mu\text{g}/\text{m}^3$)	Upper Percentile concentrations ($\mu\text{g}/\text{m}^3$)
Jalaludin et al. (2004, 056595)	Sydney, Australia	22.8	Max: 44.9
Lin et al. (2002, 026067)	Toronto, Canada	30.16	Max: 116.20
Lin et al. (2005, 087828)	Ontario, Canada	20.41	Max: 73
Luginaah et al. (2005, 057327)	Ontario, Canada	50.6	Max: 349
Medina-Ramon et al. (2006, 087721)	36 U.S. Cities	15.9-44.0	NR
Moolgavkar (2003, 051316)	Los Angeles, CA	22 (median)	Max: 86
Moolgavkar (2003, 051316)	Cook County, IL	35 (median)	Max: 365
Peel et al. (2005, 056305)	Atlanta, GA	27.9	Max: 44.7
Sinclair and Tolsma (2004, 088696)	Atlanta, GA	29.03	NR
Slaughter et al. (2005, 073854)	Spokane, WA	NR	Max: 41.9 (using 90% of concentrations)
Tolbert et al. (2007, 090316)	Atlanta, GA	26.6	90th: 42.8
Ulirsch et al. (2007, 091332)	Idaho	23.2	Max: 183.0
Yang et al. (2004, 087488)	Vancouver, Canada	13.3	Max: 52.2
Zanobetti (2003, 043119); Samet et al. (2000, 010269)	14 U.S. Cities	24.4-45.3	Max 94.8-605.8

UFP

Andersen et al. (2008, 189651)	Copenhagen, Denmark	Mean particles/cm ³ : 6847	99th: 19,895 particles/cm ³
Halonen et al. (2008, 189507)		NR: Median particles/cm ³ : 8,203	Max: 50,990 particles/cm ³

6.3.8.5. Copollutant Models

Some studies have investigated potential confounding by copollutants through the application of multipollutant models (Figure 6-15). Several Canadian studies of respiratory hospital admissions reported larger effects for PM_{10-2.5} compared to PM_{2.5} that were robust to adjustment for gaseous pollutants (Chen et al., 2005, [087555](#); Lin et al., 2002, [026067](#); Yang et al., 2004, [087488](#)). The COPD associations between PM_{2.5} and PM_{10-2.5} reported by Chen et al. (2004, [087262](#)) remained positive but were diminished slightly after adjustment for NO₂. The associations reported by Ito et al. (2003, [042856](#)) of PM_{2.5} and PM_{10-2.5} with pneumonia hospital admissions remained after adjustment for gases, while the association of PM_{10-2.5} with COPD admissions was not robust to adjustment for O₃. Associations reported by Burnett et al. (1997, [084194](#)), Moolgavkar et al. (2003, [042864](#)) and Delfino et al. (1998, [093624](#)) were not consistently robust to adjustment for gaseous copollutants. In the MCAPS study, the effect of PM_{2.5} was robust to adjustment for PM_{10-2.5}, while the PM_{10-2.5} effect on respiratory admissions was diminished after adjustment for PM_{2.5} (Peng et al., 2008, [156850](#)). Effect estimates for PM₁₀ were robust to adjustment for gases in several recent studies (Andersen et al., 2007, [093201](#); Tolbert et al., 2007, [090316](#); Ulirsch et al., 2007, [091332](#)).

Multiple pollutant analyses for other size fractions and components have been conducted in some additional studies. PM₁₀ associations with respiratory disease did not change in models also containing total PNC, nor did the association of ACP diminish after adjustment for UFP concentration (Andersen et al., 2008, [189651](#)). Peng et al. (2009, [191998](#)) reports an OCM effect that was robust to adjustment for other components while the associations with Ni, V, and EC were somewhat diminished in models containing multiple components.

Inconsistency across these study findings is likely due to differences in the correlation structure among pollutants as well as differing degrees of exposure measurement error.

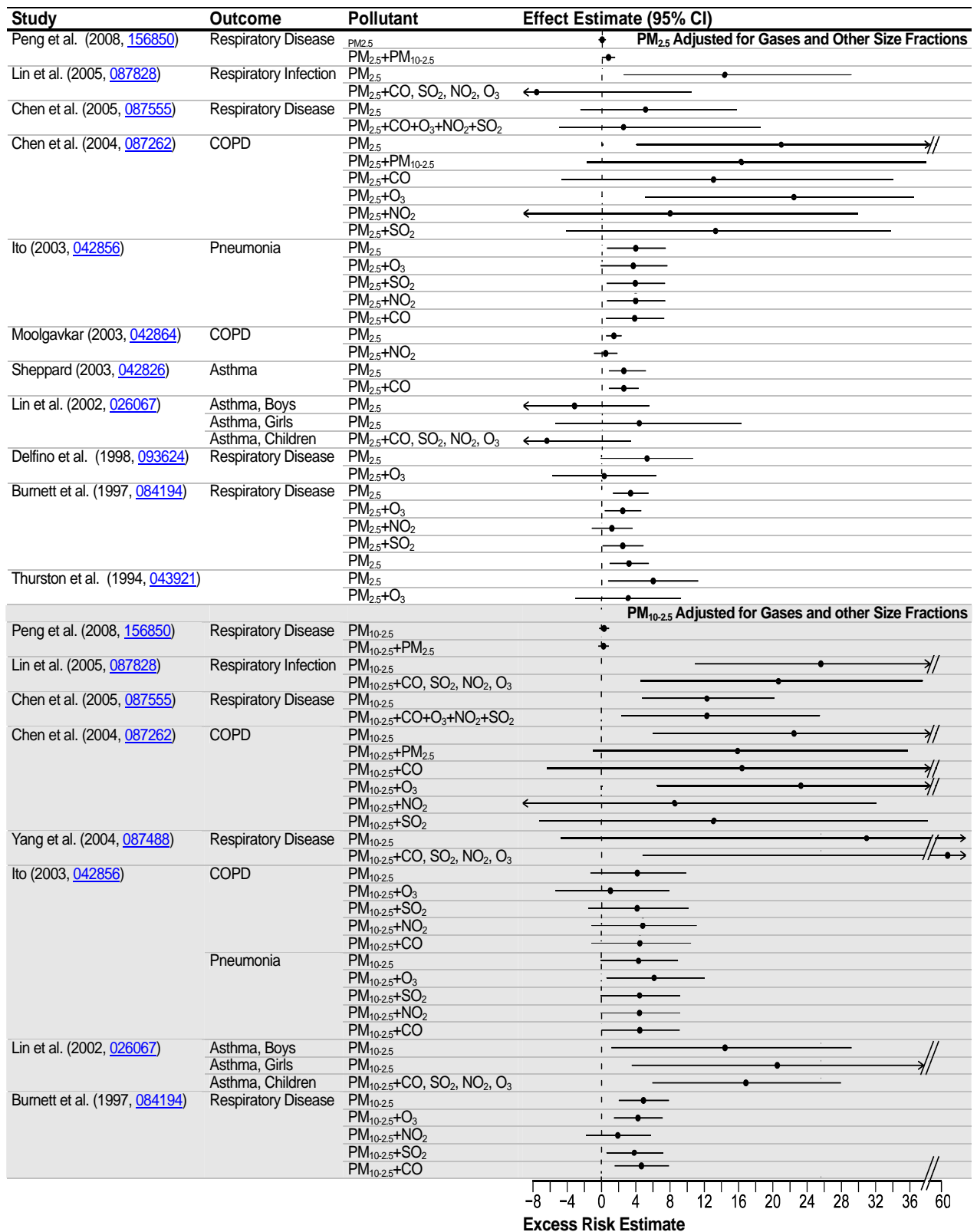


Figure 6-15. Excess risk estimates per 10 µg/m³ increase in 24-h avg PM_{2.5}, and PM_{10-2.5} for respiratory disease ED visits or HAs, adjusted for co-pollutants.

6.3.9. Respiratory Mortality

An evaluation of studies that examined the association between short-term exposure to PM_{2.5} and PM_{10-2.5} and mortality provides additional evidence for PM-related respiratory health effects. Although the primary analysis in the majority of mortality studies evaluated consists of an examination of the relationship between PM_{2.5} or PM_{10-2.5} and all-cause (nonaccidental) mortality, some studies have examined associations with cause-specific mortality including respiratory-related mortality.

Multicity mortality studies that examine the PM-respiratory mortality relationship on a national scale – Franklin et al. (2007, [091257](#)): 27 U.S. cities and Zanobetti and Schwartz (2009, [188462](#)): 112 U.S. cities – have found consistent positive associations between short-term exposure to PM_{2.5} and respiratory mortality of approximately 1.68% per 10 µg/m³ at lag 0-1 (Section 6.5). The associations observed on a national scale are consistent with those presented by Ostro et al. (2006, [087991](#)) in a study that examined the PM_{2.5}-mortality relationship in nine California counties (2.2% [95% CI: 0.6-3.9] per 10 µg/m³). An evaluation of studies that examined additional lag structures of associations found smaller respiratory mortality effect estimates when using the average of lag days 1 and 2 (1.01% [95% CI: -0.03 to 2.05] per 10 µg/m³) (Franklin et al., 2008, [097426](#)), and associations consistent with those observed at lag 0-1 when examining single-day lags, specifically lag 1 (1.78% [95% CI: 0.2-3.36]). Although the overall effect estimates reported in the multicity studies evaluated are consistently positive, it should be noted that a large degree of variability exists between cities when examining city-specific effect estimates potentially due to differences between cities and regional differences in PM_{2.5} composition (Figure 6-25). Only a limited number of studies that examined the PM_{2.5}-mortality relationship have conducted analyses of potential confounders, such as gaseous copollutants, and none examined the effect of copollutants on PM_{2.5} respiratory mortality risk estimates. Although the recently evaluated multicity studies did not extensively examine whether PM_{2.5} mortality risk estimates are confounded by gaseous pollutants, evidence from the limited number of single-city studies evaluated in the 2004 PM AQCD (U.S. EPA, 2004, [056905](#)) suggest that gaseous copollutants do not confound the PM_{2.5}-respiratory mortality association. This is further supported by studies that examined the PM₁₀-mortality relationship in both the 2004 PM AQCD (U.S. EPA, 2004, [056905](#)) and this review. Overall, the respiratory PM_{2.5} effects observed in the new studies evaluated were larger, but less precise than those reported for all-cause (nonaccidental) mortality (Section 6.5), and are consistent with the effect estimates observed in the single- and multicity studies evaluated in the 2004 PM AQCD (U.S. EPA, 2004, [056905](#)).

Zanobetti and Schwartz (2009, [188462](#)) also examined PM_{10-2.5} mortality associations in 47 U.S. cities and found evidence for respiratory mortality effects (1.16% [95% CI: 0.43-1.89] per 10 µg/m³ at lag 0-1), which are somewhat larger than those reported for all-cause (nonaccidental) mortality (0.46% [95% CI: 0.21-0.671] per 10 µg/m³). In addition, Zanobetti and Schwartz (2009, [188462](#)) reported seasonal (i.e., larger in spring) and regional differences in PM_{10-2.5} respiratory mortality risk estimates. However, single-city studies conducted in Atlanta, GA (Klemm et al., 2004, [056585](#)) and Vancouver, Canada ((Villeneuve et al., 2003, [055051](#)) reported no associations between short-term exposure to PM_{10-2.5} and respiratory mortality. The difference in the results observed between the multi- and single-city studies could be due to a variety of factors including differences between cities and compositional differences in PM_{10-2.5} across regions (Figure 6-30). Only a small number of studies have examined potential confounding by gaseous copollutants or the influence of model specification on PM_{10-2.5} mortality risk estimates, but the effects are relatively consistent with those studies evaluated in the 2004 PM AQCD (U.S. EPA, 2004, [056905](#)).

6.3.10. Summary and Causal Determinations

6.3.10.1. PM_{2.5}

Several studies of the effect of PM_{2.5} on hospital admissions for respiratory diseases reviewed in the 2004 AQCD (U.S. EPA, 2004, [056905](#)) reported positive associations for several diseases. The 2004 AQCD (U.S. EPA, 2004, [056905](#)) presented limited epidemiologic evidence of PM_{2.5} being associated with respiratory symptoms (including cough, phlegm, difficulty breathing, and bronchodilator use); observations for PM_{2.5} were positive, with slightly larger effects for PM_{2.5} than

for PM₁₀. In addition, mortality studies reported relatively higher PM_{2.5} risk estimates for respiratory-related mortality compared to all-cause (nonaccidental) mortality. Controlled human exposure studies did not provide support for effects of CAPs on respiratory symptoms. Small decrements in peak flow for both PM_{2.5} and PM₁₀ in asthmatics and nonasthmatics were reported in epidemiologic studies included in the 2004 PM AQCD (U.S. EPA, 2004, [056905](#)), whereas controlled human exposure and animal toxicological studies reported few or no effects on pulmonary function with inhalation of CAPs. In addition, the 2004 PM AQCD (U.S. EPA, 2004, [056905](#)) presented a number of controlled human exposure and toxicological studies that reported mild pulmonary inflammation following exposure to PM_{2.5} CAPs and DE or DE particles, as well as ROFA or other metal-containing PM in animals. The 2004 PM AQCD (U.S. EPA, 2004, [056905](#)) described controlled human exposure studies showing increases in allergic responses among previously sensitized atopic subjects after short-term exposure to DE particles. These observations were supported by many toxicological studies that added to existing evidence demonstrating that various types of PM could promote allergic disease and exacerbate allergic asthma in animal models. Toxicological studies also indicated that PM_{2.5} increased susceptibility to respiratory infection.

Overall, in recent studies PM_{2.5} effects on respiratory hospitalizations and ED visits have been consistently observed. Most effect estimates were in the range of ~1-4% and were observed in areas with mean 24-h PM_{2.5} concentrations between 6.1 and 22 µg/m³. Further, recent studies have focused on increasingly specific disease endpoints such as asthma, COPD, and respiratory infection. The strongest recent evidence of an association comes from large multicity studies of COPD, respiratory tract infection, and all respiratory diseases among Medicare recipients (≥65 yr) (Bell et al., 2008, [156266](#); Dominici et al., 2006, [088398](#)). Studies of children have also found evidence of an effect of PM_{2.5} on hospitalization for all respiratory diseases, including asthma and respiratory infection. However, many of these effect estimates are imprecise, their magnitude and statistical significance are sensitive to choice of lag, and some null associations were observed. Although the association of PM_{2.5} with pediatric asthma was not examined specifically, it is noteworthy that one of the strongest associations observed in the Atlanta-based SOPHIA study was between PM₁₀ and pediatric asthma visits; PM_{2.5} makes up a large proportion of PM₁₀ in Atlanta (Peel et al., 2005, [056305](#)). Positive associations between PM_{2.5} (or PM₁₀) and hospital admissions for respiratory infection (Figure 6-14) are supported by animal toxicological studies which add to previous findings of increased susceptibility to infection following exposure to PM_{2.5}. These include studies demonstrating reduced clearance of bacteria (*Pseudomonas*, *Listeria*) or enhanced pathogenesis of viruses (influenza, RSV) after exposure to DE or ROFA.

Epidemiologic studies that examined the association between PM_{2.5} and mortality provide additional evidence for PM_{2.5}-related respiratory effects (Section 6.3.9). The multicity studies evaluated found consistent, precise positive associations between short-term exposure to PM_{2.5} and respiratory mortality ranging from 1.67 to 2.20% increases at mean 24-h PM_{2.5} avg concentrations above 13 µg/m³. Although only a limited number of studies examined potential confounders of the PM_{2.5}-respiratory mortality relationship, the studies evaluated in both this review and the 2004 PM AQCD (U.S. EPA, 2004, [056905](#)) support an association between short-term exposure to PM_{2.5} and respiratory mortality.

Epidemiologic studies of asthmatic children have observed increases in respiratory symptoms and asthma medication use associated with higher PM_{2.5} or PM₁₀ concentrations. Associations with respiratory symptoms and medication use are less consistent among asthmatic adults, and there is no evidence to suggest an association between respiratory symptoms with PM_{2.5} among healthy individuals. In addition, respiratory symptoms have not been reported following controlled exposures to PM_{2.5} among healthy or health-compromised adults (Section 6.3.1.2).

Although more recent epidemiologic studies of pulmonary function and PM_{2.5} have yielded somewhat inconsistent results, the majority of studies have found an association between PM_{2.5} concentration and FEV₁, PEF, and/or MMEF. In asthmatic children, a 10 µg/m³ increase in PM_{2.5} is associated with a decrease in FEV₁ ranging from 1-3.4% (Section 6.3.2.1). A limited number of controlled human exposure studies have reported small decreases in arterial oxygen saturation and MMEF following exposure to PM_{2.5} CAPs with more pronounced effects observed in healthy adults than in asthmatics or older adults with COPD (Section 6.3.2.2). In toxicological studies, changes in pulmonary function have been observed in healthy and compromised rodents after inhalation exposures to CAPs from a variety of locations or DE. A role for the PM fraction of DE is supported by altered pulmonary function in healthy rats after IT instillation of DE particles (Section 6.3.2.3).

Several lines of evidence suggest that PM_{2.5} promotes and exacerbates allergic disease, which often underlies asthma (Section 6.3.6). Although epidemiologic studies examining specific allergic outcomes and short-term exposure to PM are relatively rare, the available studies, conducted primarily in Europe, positively associate PM_{2.5} and PM₁₀ with allergic rhinitis or hay fever and skin prick reactivity to allergens. Short-term exposure to DE particles in controlled human exposure studies has been shown to increase the allergic response among previously sensitized atopic subjects, as well as induce de novo sensitization to an antigen. Toxicological studies continue to provide evidence that PM_{2.5}, in the form of CAPs, resuspended DE particles, or DE, but not wood smoke, spurs and intensifies allergic responses in rodents. Proposed mechanisms for these effects include mediation by neurotrophins and oxidative stress, and one study demonstrated that effects were mediated at the epigenetic level (Liu et al., 2008, [156709](#)).

A large body of evidence, primarily from toxicological studies, indicates that various forms of PM induce oxidative stress, pulmonary injury, and inflammation. Notably, CAPs from a variety of locations induce inflammatory responses in rodent models, although this generally requires multiday exposures. The toxicology findings are consistent with several recent epidemiologic studies of PM_{2.5} and the inflammatory marker eNO, which reported statistically significant, positive effect estimates with some inconsistency in the lag times and use of medication. In asthmatic children, a 10 µg/m³ increase in PM_{2.5} is associated with an increase in eNO ranging from 0.46 to 6.99 ppb. Several new controlled human exposure studies report traffic or DE-induced increases in markers of inflammation (e.g., neutrophils and IL-8) in BALF from healthy adults. Recent studies have provided additional evidence in support of a pulmonary oxidative response to DE in humans, including induction of redox-sensitive transcription factors and increased urate and GSH concentrations in nasal lavage. In addition, exposure to wood smoke has recently been demonstrated to increase the levels of eNO and malondialdehyde in breath condensate of healthy adults (Barregard et al., 2008, [155675](#)). Preliminary findings indicate little to no pulmonary injury in humans following controlled exposures to PM_{2.5} urban traffic particles or DE, in contrast to a number of toxicological studies demonstrating injury with CAPs or DE (Sections 6.3.5.2 and 6.3.5.3, respectively).

Recent studies have reported associations of hospital admissions, ED or urgent care visits for several respiratory diseases with PM_{2.5} components and sources including Ni, V, OC and EC, wood smoke and traffic emissions, in studies of both children and adults. Delfino et al. (2003, [090941](#); 2006, [090745](#)) found positive associations between EC and OC components of PM and asthma symptoms and between EC and eNO. Particle composition and/or source also appears to heavily influence the increase in markers of pulmonary inflammation demonstrated in studies of controlled human exposures to PM_{2.5}. For example, whereas exposures to PM_{2.5} CAPs from Chapel Hill, NC have been shown to increase BALF neutrophils in healthy adults, no such effects have been observed in similar studies conducted in Los Angeles. In addition, differential inflammatory responses have been observed following bronchial instillation of particles collected at different times or from different areas (Section 6.3.3.2). One new study found that the increased airway neutrophils previously observed by Ghio et al. (2000, [012140](#)) in human volunteers after Chapel Hill CAPs exposure could be largely attributed to the content of sulfate, Fe, and Se in the soluble fraction (Huang et al., 2003, [087377](#)).

In summary, new evidence of ED visits and hospital admissions builds upon the positive and statistically significant evidence presented in the 2004 PM AQCD to support a consistent association with ambient concentrations of PM_{2.5}. Most effect estimates with respiratory hospitalizations and ED visits were in the range of ~1-4% and were observed in areas with mean 24-h PM_{2.5} concentrations between 6.1 and 22 µg/m³. The evidence for PM_{2.5}-induced respiratory effects is strengthened by similar hospital admissions and ED visit associations for PM₁₀, along with the consistent positive associations observed between PM_{2.5} and respiratory mortality in multicity studies. Panel studies also indicate associations with PM_{2.5} and respiratory symptoms, pulmonary function, and pulmonary inflammation among asthmatic children. Further support for these observations is provided by recent controlled human exposure studies in adults demonstrating increased markers of pulmonary inflammation following DE and other traffic-related exposures, oxidative responses to DE and wood smoke, and exacerbations of allergic responses and allergic sensitization following exposure to DE particles. Although not consistent across studies, some controlled human exposure studies have reported small decrements in various measures of pulmonary function following exposures to PM_{2.5}. Numerous toxicological studies demonstrating a wide range of responses provide biological plausibility for the associations between PM_{2.5} and respiratory morbidity observed in epidemiologic studies. Altered pulmonary function, mild pulmonary inflammation and injury, oxidative responses,

AHR in allergic and non-allergic animals, exacerbations of allergic responses and increased susceptibility to infections were observed in a large number of studies involving exposure to CAPs, DE, other traffic-related PM, and wood smoke. The evidence for an effect of PM_{2.5} on respiratory outcomes is somewhat restricted by limited coherence between some of the findings from epidemiologic and controlled human exposure studies for the specific health outcomes reported and the sub-populations in which those health outcomes occur. For instance, although there is evidence for respiratory symptoms among asthmatic children in epidemiologic panel studies, the studies of hospital admissions and ED visits provide more evidence for effects from COPD and respiratory infections than for asthma. Additionally, controlled human exposure studies report greater effects in healthy adults when compared to asthmatics or those suffering from COPD. Finally, there is limited information which could explain the relationship between the clinical and subclinical respiratory outcomes observed and the magnitude of the PM_{2.5}-respiratory mortality associations reported. Therefore, the evidence is sufficient to conclude that a **causal relationship is likely to exist between short-term PM_{2.5} exposures and respiratory effects.**

6.3.10.2. PM_{10-2.5}

The 2004 PM AQCD (U.S. EPA, 2004, [056905](#)) presented the results from several epidemiologic studies of respiratory symptoms and PM_{10-2.5}, which provided limited evidence for cough and effects on morning PEF. Toxicology data for PM_{10-2.5} were extremely limited, and there were no controlled human exposure studies presented in the 2004 PM AQCD (U.S. EPA, 2004, [056905](#)) that evaluated the effect of PM_{10-2.5} on respiratory symptoms, pulmonary function, or inflammation. Epidemiologic studies of the effect of PM_{10-2.5} on hospitalizations or ED visits for respiratory diseases (i.e., pneumonia, COPD and respiratory diseases combined) reviewed in the 2004 AQCD (U.S. EPA, 2004, [056905](#)) reported positive associations. Additionally, the few mortality studies that examined cause-specific mortality suggested somewhat larger risk estimates for respiratory mortality compared to all-cause (nonaccidental) mortality.

Several new studies report associations between PM_{10-2.5} and respiratory hospitalizations with the most consistent evidence among children (Figure 6-10 through Figure 6-14), however, effect estimates are imprecise. Although a number of studies provide evidence of respiratory effects in older adults, a recent analysis of MCAPS data reports that weak associations of PM_{10-2.5} with respiratory hospitalizations are further diminished after adjustment for PM_{2.5}. It is not clear that PM_{10-2.5} estimates across all populations and regions are confounded by PM_{2.5}. An examination of PM_{10-2.5} mortality associations on a national scale found a strong association between PM_{10-2.5} and respiratory mortality, but this association varied when examining city-specific risk estimates (Zanobetti and Schwartz, 2009, [188462](#)). The regional variability in PM_{10-2.5} mortality risk estimates is further confirmed by the negative associations reported in the single-city studies evaluated. However, there is greater spatial heterogeneity in PM_{10-2.5} compared to PM_{2.5} and consequently greater potential for exposure measurement error in epidemiologic studies relying on central site monitors. This exposure measurement error may bias effect estimates toward the null and could explain some of the regional variability in the observed associations between PM_{10-2.5} and respiratory morbidity and mortality.

Mar et al. (2004, [057309](#)) provide evidence for an association with increased respiratory symptoms in asthmatic children, but not asthmatic adults. Consistent with this, controlled human exposures to PM_{10-2.5} have not been observed to affect lung function or respiratory symptoms in healthy or asthmatic adults. However, increases in markers of pulmonary inflammation have been demonstrated in healthy volunteers. In these studies, an increase in neutrophils in BALF or induced sputum was observed, with additional evidence of alveolar macrophage activation associated with biological components of PM_{10-2.5} (i.e., endotoxin). Toxicological studies using inhalation exposures are still lacking, but pulmonary injury and inflammation have been observed in animals after IT instillation exposure and both rural and urban PM_{10-2.5} have induced these responses. In some cases, PM_{10-2.5} from urban air was more potent than PM_{2.5} (Section 6.3.3.3). PM_{10-2.5} respiratory effects may be due to components other than endotoxin (Wegesser and Last, 2008, [190506](#)).

Overall, the most compelling new evidence comes from a number of recent epidemiology studies conducted in Canada and France showing significant associations between respiratory ED visits or hospitalization and short-term exposure to PM_{10-2.5}. Effects have been observed in areas where the mean 24-h avg PM_{10-2.5} concentrations ranged from 7.4 to 13.0 µg/m³. The strongest relationships were observed among children, whereas studies of adults and older adults show less

consistent evidence of an association. While controlled human exposure studies have not observed an effect on lung function or respiratory symptoms in healthy or asthmatic adults in response to exposure to PM_{10-2.5}, healthy volunteers have exhibited increases in markers of pulmonary inflammation. Toxicological studies using inhalation exposures are still lacking, but pulmonary injury has been observed in animals after IT instillation exposure to both rural and urban PM_{10-2.5}, which may not be entirely attributed to endotoxin. Overall, epidemiologic studies, along with the limited number of controlled human exposure and toxicological studies that examined PM_{10-2.5} and respiratory outcomes, provide evidence that is **suggestive of a causal relationship between short-term PM_{10-2.5} exposures and respiratory effects.**

6.3.10.3. UFPs

The 2004 PM AQCD (U.S. EPA, 2004, [056905](#)) included a few epidemiologic and controlled human exposure studies that examined the effect of UFPs on respiratory morbidity. Collectively these studies provided limited evidence of an association between UFPs and respiratory symptoms, medication use, inflammation, and decreased pulmonary function. Evidence from toxicological studies presented in the 2004 AQCD, although limited, suggested that exposure via inhalation to high concentrations of UF TiO₂ may increase pulmonary inflammation in healthy rodents. Since the publication of the 2004 AQCD there has been an increased focus among the scientific community on gaining a better understanding of the potential health effects associated with exposure to UFPs (U.S. EPA, 2004, [056905](#)). A number of recent controlled human exposure and toxicological studies have evaluated respiratory responses following exposures to UF CAPs, model particles, and fresh diesel or gasoline exhaust. While DE contains both PM_{2.5} and UFPs, the MMAD is typically ≤ 100 nm, and therefore the results of these studies may be used to support findings from studies utilizing other sources of UFP.

UFPs were associated with incident wheezing symptoms among infants (<1 yr) in a study conducted in Copenhagen, Denmark, where the mean UFP number concentration was 8,092 particles/cm³, though this association did not persist for children between ages 1-3 yr (Andersen et al., 2008, [096150](#)). Recent epidemiologic studies conducted in Copenhagen, Denmark and Helsinki, Finland, reported associations between UFPs and hospital admissions or ED visits for respiratory diseases, including childhood asthma and pneumonia in adults (Andersen et al., 2008, [189651](#); Halonen et al., 2008, [189507](#)). The median UFP number concentrations in Copenhagen and Helsinki were 6,243 particles/cm³ and 8,203 particles/cm³, respectively. Associations between UFP and ED visits for respiratory diseases were not observed in the Atlanta-based SOPHIA study, where the mean UFP number concentration was 38,000 particles/cm³.

A single recent epidemiologic study has examined associations between UFP and pulmonary function, and observed that asthmatic adults exhibited decreased lung function after exposure to diesel traffic pollution in London (McCreanor et al., 2007, [092841](#)). Two new controlled human exposure studies have reported small decreases in pulmonary function among healthy adults approximately following exposure to Los Angeles UF CAPs or UF EC (Gong et al., 2008, [156483](#); Pietropaoli et al., 2004, [156025](#)). Exposures to lower concentrations of UF CAPs from Chapel Hill, NC did not result in any changes in pulmonary function (Samet et al., 2009, [191913](#)). However, while Gong et al. (2008, [156483](#)) did not observe any effect of exposure to UF CAPs on markers of pulmonary inflammation, Samet et al. (2009, [191913](#)) reported an UF CAPs-induced increase in IL-8 in BALF at 18 hours post-exposure. A limited number of controlled human exposure studies have also demonstrated increases in the pulmonary inflammatory response following exposure to UF and PM_{2.5} from DE, which may be enhanced by exposure to O₃ (Section 6.3.3.2).

Altered pulmonary function and inflammation have also been observed in toxicological studies of DE and UF model particles (Sections 6.3.2.3 and 6.3.3.3). In one rat model, pulmonary inflammation was observed after exposure to UF CB at concentrations as low as 180 µg/m³ (Harder et al., 2005, [087371](#)). However, inflammatory responses vary considerably depending on the animal model, dose, test material, and exposure duration. In cases where pulmonary inflammation was not observed, oxidative stress was often evident (Section 6.3.4.2). Oxidative stress is a major mechanism by which PM may exert effects (Chapter 5), and some toxicological studies suggest that UFPs are more potent than PM_{2.5}, possibly due to a higher proportion of pro-oxidative OC and PAH content and greater surface area with which to deliver these components.

The relationship between exposure to UFP and pulmonary injury has not been widely examined. No association with pulmonary injury biomarkers was found for UFP in a European

multicity epidemiologic study (Timonen et al., 2004, [087915](#)). In controlled human exposure studies, UFP from wood smoke resulted in significantly increased markers of injury in healthy adults, but this effect was not evident in COPD sufferers exposed to DE (Section 6.3.5.2). Exposure of neonatal rats to UF iron-soot particles resulted in a significantly reduced rate of cell proliferation in the proximal alveolar region, which suggests that postnatal lung development may be susceptible to air pollution, consistent with impaired lung function growth observed in children (Pinkerton et al., 2004, [087465](#)). In contrast, no histopathological responses were evident in adult mice exposed to UF iron-soot particles (Last et al., 2004, [097334](#)). Some toxicological studies have reported pulmonary injury after inhalation of DE or gasoline exhaust (Section 6.3.5.3). In studies that evaluated ambient PM size fractions from a variety of European and U.S. cities for relative toxicity in rodents following IT instillation exposure, UFPs were generally less injurious than the larger size fractions. However, the UF fraction of Montana coal fly ash induced greater injury and inflammation than the PM_{10-2.5} fraction (Gilmour et al., 2004, [057420](#)).

In rodent studies, UF CAPs appeared to be more potent than PM_{2.5} CAPs in inducing and exacerbating allergic responses (Section 6.3.6.3). In addition to CAPs, UF CB or iron-soot particles, but not particles from fresh gasoline exhaust, have been shown to induce or exacerbate allergic responses in mice. Bacterial clearance appears unaffected by hardwood smoke or gasoline engine exhaust. However, host defenses are impaired by DE, which has been shown to reduce bacterial clearance, impair defenses against viral infection, and reduce thymus weight, indicating systemic immunosuppression.

Several toxicological studies demonstrated oxidative, inflammatory, and allergic responses following exposure to a number of different UFP types, including model particles (i.e., CB, iron-soot particles), CAPs, and DE. Although the respiratory effects of controlled exposures to UFPs have not been extensively examined in humans, two controlled human exposure studies have observed small UFP-induced decreases in pulmonary function; however, no increases in respiratory symptoms have been reported. In a limited number of studies, markers of pulmonary inflammation were increased following controlled human exposures to UFP, which has been most consistently observed in studies using fresh DE. In both controlled human exposure and animal toxicological studies using fresh DE, the relative contributions of gaseous copollutants to the observed effects remain unresolved. However, similar effects are reported using resuspended DE particles, and although not UFPs, these particles can be assumed to have similar composition. A limited number of epidemiologic studies have provided some evidence of an association between short-term exposure to UFPs and respiratory symptoms, as well as asthma hospitalizations. However, the interpretation of these findings is difficult due to the spatial variability of UFPs. Thus, the current collective evidence is **suggestive of a causal relationship between short-term UFP exposure and respiratory effects.**

6.4. Central Nervous System Effects

While evidence of an effect of PM on the CNS was not presented in the 2004 PM AQCD (U.S. EPA, 2004, [056905](#)), a limited number of recent epidemiologic, controlled human exposure and toxicological studies provide some evidence that exposure to PM may be associated with changes in neurological function. The majority of studies included in this section are of short-term exposure, however, there are also a few studies of long-term exposure. As CNS effects of PM are a newly emerging area, and since there are so few studies, all studies that evaluate CNS responses are included in this section.

6.4.1. Epidemiologic Studies

Chen and Schwartz (2009, [179945](#)) used extant data on CNS function from the Third National Health and Nutrition Examination Survey (NHANES III) to characterize the association between cognitive function in adults (ages 20-59 yr) and exposure to ambient air pollution. Three computerized neurobehavioral tests were used: a simple reaction time test (SRTT), a basic measure of visuomotor speed; a symbol digit substitution test (SDST) on coding ability; and a serial digit learning test (SDLT) on attention and short-term memory. The authors used annual PM₁₀ concentrations to approximate the long-term exposure to ambient air pollution prior to the

NHANES-III examination. Increased PM₁₀ levels were associated with reduced performance in all three neurobehavioral tests, and were particularly strong for SDST and SDLT scores in models adjusted for age and sex. However, after additional adjustment for race/ethnicity or SES, the magnitudes of these associations were greatly diminished and largely null. It is possible that the observed associations disappeared after adjustment for race/ethnicity and SES due to the potential confounding by residential segregation of ethnic minorities and poorer people in areas with high levels of ambient PM₁₀ concentrations.

Two additional epidemiologic studies evaluated the effect of ambient PM on the CNS (Calderón-Garcidueñas et al., 2008, [156317](#); Suglia et al., 2008, [157027](#)). These studies examined long-term exposure to non-specific PM indicators and are detailed in Annex E.

6.4.2. Controlled Human Exposure Studies

In a recent controlled human exposure study, Cruţ et al. (2008, [156374](#)) exposed 10 healthy males (18-39 yr) to filtered air and dilute DE (300 µg/m³ PM) for 1 h using a randomized crossover study design. Changes in brain activity were measured during and following exposure using quantitative electroencephalography (QEEG). Exposure to DE was observed to significantly increase the median power frequency (MPF) in the frontal cortex during exposure, as well as in the hour following the completion of the exposure. While this study does provide some evidence of an acute cortical stress response to DE, it is important to note that the QEEG findings are very nonspecific, and could have been caused by factors other than diesel PM such as DE gases (e.g., CO, NO and NO₂) or the odor of the DE.

6.4.3. Toxicological Studies

Evidence is mounting that the CNS may be a critical target of PM and that adverse health effects may result from PM exposure. Whether these health effects are a direct or indirect effect of PM has not yet been established. One hypothesis suggests that UFPs which deposit onto nasal olfactory epithelium enter the CNS by axonal olfactory transport to the olfactory bulb and lead to a cascade of effects involving inflammatory cytokines and ROS. An increased potential for neurodegenerative processes may ensue. Evidence for translocation of UFPs to the olfactory bulb via olfactory neurons is discussed in Chapter 4, but its relevance to CNS health effects is unknown. Another hypothesis suggests that brain inflammation occurs secondarily to PM-mediated systemic inflammation. Finally, it has been suggested that PM-stimulation of the ANS via respiratory tract receptors results in inflammatory or other effects in the CNS. This is an emerging field with many unknowns.

6.4.3.1. Urban Air

Calderon-Garciduenas et al. (2003, [156316](#)) conducted a long-term observational study in mongrel dogs from Mexico City and Tlaxcala. DNA damage and inflammation in the brain and respiratory tract were evaluated in dogs living in Mexico City (exposed group) and dogs living in Tlaxcala (control group). These cities are similar in altitude but differ in air pollutant levels. Measurements of air pollutant levels were presented only for Mexico City, the more polluted city. Statistically significant greater levels of apurinic/aprimidinic sites (an indicator of DNA damage) were observed in the olfactory bulbs and hippocampus of Mexico City dogs compared with controls. These differences were not seen in other brain regions examined or in nasal respiratory epithelium. In addition, Mexico City dogs demonstrated greater histopathological changes in the respiratory and olfactory epithelium of the nasal cavity compared with controls. Immunohistochemical staining of brain tissue from the Mexico City dogs demonstrated greater immunoreactivity for NF-κB, iNOS, cyclooxygenase-2, glial fibrillary acidic protein (GFAP), ApoE, amyloid precursor product and β-amyloid compared with controls. These results are indicative of inflammation and stress protein responses. This study has several limitations given that the dogs were of mixed breeds and of variable ages and that there was no standardization of exposures or diets. However results suggest a possible relationship between air pollution and brain inflammation.

6.4.3.2. CAPs

Several new inhalation studies have provided evidence of CNS effects due to ambient PM exposures. In one study, Campbell et al. (2005, [087217](#)) exposed OVA-sensitized BALB/c mice to filtered air or near-highway Los Angeles CAPs (a 20-fold concentration of PM_{2.5}+UFPs or UFPs only; mean exposure concentration UFPs 282.5 µg/m³ and PM_{2.5} 441.7 µg/m³) for 4 h/day and 5 days/wk over a 2-wk period. The animals were subsequently challenged with OVA to elicit an allergic response in the lungs; brain tissue was obtained one day later. Exposure to CAPs, but not filtered air, resulted in activation of the immune-related transcription factor NF-κB and upregulation of the cytokines TNF-α, and IL-1α in the brain, demonstrating pro-inflammatory responses that could contribute to neurodegenerative disease. While this study demonstrates CAPs effects in an allergic animal model, it is not known whether these responses also occur in non-allergic animals.

In a second study, control or OVA-sensitized and challenged Brown Norway rats were exposed for 8 h to filtered air or PM_{2.5} CAPs (500 µg/m³) in Grand Rapids, MI (Sirivelu et al., 2006, [111151](#)). Brain tissue was obtained 1 day later. CAPs exposure resulted in brain region-specific modulation of neurotransmitters. In animals which were not pretreated with OVA, statistically significant increases in norepinephrine were observed in the paraventricular nucleus and olfactory bulb of CAPs-exposed rats compared with filtered air controls. In animals which were pretreated with OVA, a statistically significant increase in dopamine was observed in the medial preoptic area in CAPs-exposed rats compared with controls. Furthermore, exposure to CAPs resulted in a statistically significant increase in serum corticosterone. These data suggest that the hypothalamo-pituitary-adrenal axis (i.e., stress axis) may be activated by PM exposure, causing aggravation of allergic airway disease. The authors discuss the possible role of the olfactory bulb in mediating neuroendocrine control of autonomic activities involved in respiratory and cardiovascular functions; however these relationships require clarification.

Pro-inflammatory responses were examined in a subchronic CAPs study involving normal (C57BL/6J) and ApoE^{-/-} mice (Kleinman et al., 2008, [190074](#)). Mice were exposed to filtered air or to two concentrations of UF CAPs from a near-highway area of central Los Angeles (average of 30.4 and 114.2 µg/m³) for 5 h/day and 3 days/wk over a 6-wk period. Brain tissue was harvested one day after the last exposure and cortical samples prepared. CAPs exposure resulted in activation of transcription factors, with a dose-dependent increase observed for AP-1 and an increase in NF-κB observed at the higher concentration. Increased levels of GFAP (representing activation of astrocytes) and phosphorylated JNK (representing MAP kinase activation) were observed at the lower but not higher concentration of CAPs. No changes were observed in levels of or activation of the other MAP kinases p38 and ERK or of IκB. These findings provide evidence that inhalation of CAPs can lead to activation of cell signaling pathways involved in upregulation of pro-inflammatory cytokine genes in the cortical region of the mouse brain.

In another study utilizing normal (C57BL/6) and ApoE^{-/-} mice, brain histopathology was examined following a 4-month chronic exposure to PM_{2.5} CAPs from Tuxedo, NY (March, April or May through September 2003) (Veronesi et al., 2005, [087481](#)). The average PM_{2.5} exposure concentration was 110 µg/m³. CAPs exposure resulted in a statistically significant decrease in dopaminergic neurons, measured by tyrosine hydroxylase immunoreactivity, in the substantia nigra of ApoE^{-/-} mice but not in control mice. This population of neurons is targeted in neurodegenerative diseases such as Parkinson's. Furthermore, a statistically significant increase in GFAP immunoreactivity, a marker for astrocytes, was observed in the nucleus compacta of CAPs-exposed ApoE^{-/-} mice compared to air-exposed ApoE^{-/-} mice. These results suggest that the ApoE^{-/-} mice, a genetic model involving increased oxidative stress, are susceptible to PM-induced neurodegeneration. Evidence for brain oxidative stress has also been found in normal animals following IT instillation of high concentrations of PM_{2.5} from Taiyuan, China (Liu and Meng, 2005, [088650](#)) and of gasoline exhaust (Che et al., 2007, [096460](#)) and following chronic exposure to ROFA by intranasal instillation (Zanchi et al., 2008, [157173](#)).

6.4.3.3. Diesel Exhaust

A recent study tested the effects of DE inhalation on spatial learning and memory function-related gene expression in the hippocampus (Win-Shwe et al., 2008, [190146](#)). Male BALB/c mice were exposed to DE (148.86 µg/m³ PM) for 5 h/day and 5 day/wk over a 4-wk period. Particle size was 26.21±1.50 nm and PNC was 1.92×10⁶ ± 6.18×10⁴ particles/m³. Concentrations of gases were

3.27 ppm CO, 0.01 ppm SO₂, 0.53 ppm NO₂, 0.98 ppm NO and 0.07 ppm CO₂. Half of the animals were injected i.p. once per week with lipoteichoic acid (LTA), a bacterial cell wall component used to induce systemic inflammation. The ability of the mice to perform spatial learning tasks was examined the day after the final exposure to DE and on two subsequent days. Impaired acquisition of spatial learning was observed in DE-exposed mice on the first day and on all three days in DE-exposed mice that had also been treated with LTA. LTA by itself had no effect. Since the NMDA (a type of neurotransmitter) receptors in the hippocampus play an important role in spatial learning ability, mice were sacrificed and total RNA from hippocampus was extracted and analyzed for expression of NMDA receptor subunits. DE exposure resulted in a statistically significant increase in the expression of one subunit while the combined exposure to DE and LTA resulted in statistically significant increases in the expression of three subunits compared with controls. The expression of pro-inflammatory cytokines was also examined in the hippocampus. DE exposure resulted in a statistically significant increase in TNF- α mRNA, while LTA exposure resulted in a statistically significant increase IL-1 β mRNA compared with controls. Neither exposure altered the expression of HO-1. These results demonstrated that subchronic exposure to UF-rich DE resulted in impaired spatial learning and altered expression of hippocampal genes involved in memory function and inflammation. These responses were modulated by systemic inflammation.

6.4.3.4. Summary of Toxicological Study Findings of CNS Effects

In summary, PM may produce adverse effects in the CNS by direct or indirect mechanisms which are at present incompletely understood. Two recent short-term PM_{2.5} CAPs inhalation studies demonstrated pro-inflammatory responses in the brain and brain region-specific modulation of neurotransmitters and suggest the involvement of neuroimmunological pathways. One recent chronic PM_{2.5} CAPs inhalation study demonstrated loss of dopaminergic neurons in the substantia nigra and suggested that oxidative stress contributes to neurodegeneration. Veronesi et al. (2005, [087481](#)) have noted that the brain is very vulnerable to the oxidative stress induced by PM due to the brain's high energy demands, low levels of endogenous free radical scavengers, and high content of lipids and proteins. PM-mediated upregulation of inflammatory cytokines and mediators may also contribute to neurodegeneration. In fact, a recent subchronic study involving UF CAPs demonstrated the activation of cell signaling pathways associated with upregulation of pro-inflammatory cytokines in brain cortical regions. Furthermore, a subchronic study involving UF-rich DE demonstrated impaired spatial learning and altered expression of pro-inflammatory and neurotransmitter receptor genes in the hippocampus. Further investigations are required to delineate mechanisms involved in these responses.

6.4.4. Summary and Causal Determination

Recent animal toxicological studies involving acute or chronic CAPs exposure have demonstrated pro-inflammatory responses in the brain, brain region-specific modulation of neurotransmitters and loss of dopaminergic neurons in the substantia nigra (Campbell et al., 2005, [087217](#); Kleinman et al., 2008, [190074](#); Sirivelu et al., 2006, [111151](#); Veronesi et al., 2005, [087481](#)). However, the mechanisms underlying these effects need to be delineated. A single controlled human exposure study provides some evidence of an acute cortical stress response to DE, though these findings are nonspecific and could have been caused by DE gases rather than DE particles (Cruts et al., 2008, [156374](#)). Similar consideration is warranted for the single animal toxicological study involving DE which demonstrated impaired spatial learning and altered expression of pro-inflammatory and neurotransmitter genes in the hippocampus following subchronic exposure (Win-Shwe et al., 2008, [190146](#)). The single epidemiology study that examined CNS outcomes did not find associations between long-term exposure to PM₁₀ and cognitive function in adults after adjustment for race/ethnicity or SES (Chen and Schwartz, 2009, [179945](#)). Though the effect of ambient air pollution on CNS outcomes has recently begun to draw more attention, the evidence for a PM-induced CNS effect is limited. While most available studies have evaluated the effects of fine particle exposures, there is insufficient evidence to draw conclusions regarding effects of specific PM size fractions. Overall, the **evidence is inadequate to determine if a causal relationship exists between short-term exposures to PM_{2.5}, PM_{10-2.5}, or UFPs and CNS effects.**

6.5. Mortality

The relationship between short-term exposure to PM and mortality has been extensively addressed in previous PM assessments (U.S. EPA, 1982, [017610](#); 1996, [079380](#); 2004, [056905](#)). A positive association between PM concentration and mortality was consistently demonstrated across studies cited in the 2004 PM AQCD (U.S. EPA, 2004, [056905](#)); these results are summarized below in Section 6.5.1. Numerous studies have been published since the previous review, including a number of multicity analyses and many single-city studies. The current body of evidence examines the association between short-term exposure to PM of various size fractions (i.e., PM₁₀, PM_{10-2.5}, PM_{2.5}, and UFPs) and mortality through the use of time-series and/or case-crossover studies. Both study designs aim to disentangle the PM-mortality effect through either complex modeling (i.e., time-series) or matching strategies (i.e., case-crossover). Overall, the results of the more recent studies build upon the conclusions from the previous review, showing consistent positive associations between mortality and short-term exposure to PM_{2.5} and PM_{10-2.5}.

Section 6.5.2 reviews and summarizes the results of recent studies that examined mortality associations with the four PM size classes listed above. Each section integrates the results of recent studies with those available in previous PM reviews. This assessment first focuses on multicity studies that examined mortality associations with PM₁₀ because this is an important body of literature that provides information on potential effect modifiers, potential confounding by copollutants, evaluation of concentration-response relationships, and the influence of different modeling approaches on the PM-mortality relationship (Section 6.5.2.1). The PM₁₀ studies have provided the most data among the PM indices thus far; therefore this evaluation begins with the consideration of those findings as they relate to the general association between PM and mortality. It is difficult to interpret the extent to which these studies inform an evaluation of the effects of PM_{2.5} or PM_{10-2.5}, since data are combined from multiple cities with different PM composition. Interpretations of the PM size fraction that contributes the most to the PM₁₀ effects observed are provided when appropriate in the following review. The multicity studies that examine the association between PM₁₀ and mortality also offer new evidence on regional and seasonal differences in effect estimates, building upon observations made in the 2004 PM AQCD (U.S. EPA, 2004, [056905](#)).

Recent study findings on associations with PM_{2.5}, PM_{10-2.5}, and UFPs are evaluated in Sections 6.5.2.2, 6.5.2.3, and 6.5.2.4, respectively. For PM_{2.5}, the focus of the assessment remains on multicity study findings; however, for PM_{10-2.5} and UFPs, some additional emphasis is placed on single-city studies, due to the relative sparseness of peer-reviewed literature on these size fractions. Some studies have also evaluated relationships between mortality and specific components and sources of PM, and the results are summarized in Sections 6.5.2.4 and 6.5.2.5. Finally, Section 6.5.2.6 assesses evidence on the concentration-response relationship between short-term PM exposure and mortality.

6.5.1. Summary of Findings from 2004 PM AQCD

The 2004 PM AQCD (U.S. EPA, 2004, [056905](#)) found strong evidence that PM₁₀ and PM_{2.5}, or one or more PM_{2.5} components, acting alone and/or in combination with gaseous copollutants, are associated with total (nonaccidental) mortality and various cause-specific mortality outcomes. For PM₁₀, several multicity studies in the U.S., Canada, and Europe provided strong support for this conclusion, reporting associations with total mortality highlighted by effect estimates ranging from ~0.2 to 0.7% (per 10 µg/m³ increase in PM₁₀) (U.S. EPA, 2004, [056905](#)). Numerous studies also reported PM₁₀ associations with cause-specific mortality, specifically cardiovascular- and respiratory-related mortality. For PM_{2.5}, the strength of the evidence varied across categories of cause-specific mortality, with relatively stronger evidence for associations with cardiovascular compared to respiratory mortality. The resulting effect estimates reported from the U.S.- and Canadian-based studies (both multi- and single-city) analyzed for these two categories ranged from 1.2 to 2.7% for cardiovascular-related mortality and 0.8 to 2.7% for respiratory-related mortality, per 10 µg/m³ increase in PM_{2.5} (U.S. EPA, 2004, [056905](#)). In regards to PM_{10-2.5}, the PM AQCD found a limited body of evidence that was suggestive of associations between short-term exposure to ambient PM_{10-2.5} and various mortality outcomes (e.g., 0.08-2.4% increase in total [nonaccidental] mortality per 10 µg/m³ increase in PM_{10-2.5}). The positive effect estimates obtained from studies that analyzed the association between PM_{10-2.5} and mortality resulted in the conclusion that PM_{10-2.5}, or some

constituent component(s) (including those on the surface) of PM_{10-2.5}, may contribute, in certain circumstances, to increased human health risks.

Some additional studies examined the association between specific PM_{2.5} chemical components and mortality. These studies observed associations for SO₄²⁻, NO₃⁻, and CoH₂, but not crustal particles. The strength of the association for each component varied from city to city (U.S. EPA, 2004, [056905](#)). Source-oriented analyses were also conducted to identify specific source-types associated with mortality. These studies implicate PM_{2.5} from anthropogenic origin, such as motor vehicle emissions, coal combustion, oil burning, and vegetative burning, as being important in contributing to increased mortality (U.S. EPA, 2004, [056905](#)).

6.5.2. Associations of Mortality and Short-Term Exposure to PM

The recent literature examines the association between short-term exposure to various PM size fractions (i.e., PM₁₀, PM_{10-2.5}, PM_{2.5}, UFPs, or species [e.g., OC, EC, transition metals, etc.]) and mortality. This ISA, similar to previous AQCDs, focuses more heavily on multicity studies, and especially those conducted in the U.S. and Canada (Table 6-15). By using this approach it is possible to: (1) obtain a more representative sample of or insight into the PM-mortality relationship observed across the U.S.; (2) analyze the association between mortality and short-term exposure to PM at or near ambient conditions observed in the U.S.; (3) examine the potential heterogeneity in effect estimates between cities and regions; and (4) analyze the confounders and/or effect modifiers that may explain the PM-mortality relationship in the U.S. Although this section focuses on mortality outcomes in response to short-term exposure to PM, it does not evaluate studies that examine the association between PM and infant mortality. These studies are evaluated in Section 7.5., although it is possible that short- and long-term in utero exposures may contribute to infant mortality. In addition, the exposure windows of interest for this unique health outcome can be difficult to characterize and may span both short- and long-term exposure periods.

Table 6-15. Overview of U.S. and Canadian multicity PM studies of mortality analyzed in the 2004 PM AQCD and the PM ISA^b.

Study	Location	Mean Concentration (µg/m ³)	98th; 99th Percentiles (µg/m ³)	Upper Percentile: Concentrations (µg/m ³)
PM₁₀				
Dominici et al. (2003, 156407) ^a	90 U.S. cities	15.3-53.2	---	NR
Burnett and Goldberg (2003, 042798) ^a	8 Canadian cities	25.9	---	95th: 54; Maximum: 121
Peng et al. (2005, 087463)	100 U.S. cities	13-49	---	50th: 27.1; 75th: 32.0 Maximum: 48.7
Dominici et al. (2007, 097361) ^f	100 U.S. cities	13-49	---	50th: 27.1; 75th: 32.0 Maximum: 48.7
Welty and Zeger (2005, 087484) ^f	100 U.S. cities	13-49	---	50th: 27.1; 75th: 32.0 Maximum: 48.7
Bell et al. (2009, 191007)	84 U.S. urban communities	NR	---	NR
Burnett et al. (2004, 086247)	12 Canadian cities	NR	---	NR
Samoli et al. (2008, 188455)	12 Canadian cities 90 U.S. cities ^e 22 European cities	NR	---	NR
Schwartz (2004, 078998)	14 U.S. cities	23-36 ^d	---	75th: 31-57
Schwartz (2004, 053506)	14 U.S. cities	23-36 ^d	---	75th: 31-57
Zeka et al. (2005, 088068)	20 U.S. cities	15-37.5	---	NR
Zeka et al. (2006, 088749)	20 U.S. cities	15.9-37.5	---	NR

Study	Location	Mean Concentration ($\mu\text{g}/\text{m}^3$)	98th; 99th Percentiles ($\mu\text{g}/\text{m}^3$)	Upper Percentile: Concentrations ($\mu\text{g}/\text{m}^3$)
<i>PM_{2.5}</i>				
Burnett and Goldberg (2003, 042798) ^a	8 Canadian cities	13.3	38.9; 45.4	95th: 32; Maximum: 86
Dominici et al. (2007, 097361)	96 U.S. cities	NR	---	NR
Zanobetti and Schwartz (2009, 188462)	112 U.S. cities	13.2	34.3; 38.6	Maximum: 57.4
Franklin et al. (2007, 091257)	27 U.S. cities	15.6	45.8; 54.7	Maximum: 239
Franklin et al. (2008, 097426) ^g	25 U.S. cities	14.8	43.0; 50.9	Maximum: 239.2
Ostro et al. (2006, 087991)	9 California counties	19.9	68.2; 82.0	95th: 61.3; Maximum: 160.0
Ostro et al. (2007, 091354)	6 California counties	18.4	61.2; 70.1	Maximum: 116.1
Burnett et al. (2004, 086247)	12 Canadian cities	12.8	38.0; 45.0	Maximum: 86.0
<i>PM_{10-2.5}</i>				
Burnett and Goldberg (2003, 042798) ^a	8 Canadian cities	12.6	---	95th: 30; Maximum: 99
Zanobetti and Schwartz (2009, 188462)	47 U.S. cities	11.8	40.2; 47.2	Maximum: 88.3
Burnett et al. (2004, 086247)	12 Canadian cities	11.4	---	Maximum: 151
Villeneuve et al. (2003, 055051)	Vancouver, Canada	6.1	---	90th: 13.0; Maximum: 72.0
Klemm et al. (2004, 056585)	Atlanta, Georgia	9.7	20.7	50th: 9.34; 75th: 11.94 Maximum: 25.17
Slaughter et al. (2005, 073854)	Spokane, Washington	NR	---	NR
Wilson et al. (2007, 157149)	Phoenix, Arizona	NR	---	NR
Kettunen et al. (2007, 091242)	Helsinki, Finland	Cold season: 6.7 ^d Warm season: 8.4 ^d	---	Cold season: 50th: 6.7 75th: 12.5; Maximum: 101.4 Warm season: 50th: 8.4 75th: 11.8; Maximum: 42.0
Perez et al. (2008, 156020)	Barcelona, Spain	Saharan Dust Days: 16.4 Non-Saharan Dust Days: 14.9	---	Saharan Dust Days 50th: 14.8; 75th: 21.8 Maximum: 36.7 Non-Saharan Dust Days 50th: 12.6; 75th: 18.9 Maximum: 93.1

^a Multicity studies examined in the 2004 PM AQCD (U.S. EPA, 2004, [056905](#))

^b Because only two multicity study was identified that examined PM_{10-2.5}, single-city and international studies that examined PM_{10-2.5} were analyzed in this ISA and are included in this table.

^c The majority of multicity studies examined in the PM ISA provide the mean PM concentration of each individual city, not an overall PM concentration across all cities. As a result, the range of PM concentrations for a particular study are presented, which represents the lowest and highest mean PM concentrations reported across cities, if an overall mean is not provided within the study.

^d Median PM concentration.

^e The study included 90 U.S. cities in the 1-day lag analysis, but only 15 U.S. cities in the analysis of the average of lag days 0-1.

^f The concentrations reported for these studies were estimated from Peng et al. (2005, [087463](#)) because they used the same number of cities and years of data from NMMAPS.

^g This study did not present an overall mean 24-h avg PM_{2.5} concentration across all cities for each season. The range of mean 24-h avg concentrations reported in this table for each season represents the lowest mean 24-h avg PM_{2.5} concentration and the highest 24-h avg PM_{2.5} concentration reported across all cities included in the study.

6.5.2.1. PM₁₀

The majority of studies that examined the association between short-term exposure to PM and mortality focused on effects attributed to PM₁₀. Although these studies do not characterize the compositional differences in PM₁₀ across the cities examined in each of the studies evaluated, they can provide an underlying basis for the overall pattern of associations observed when examining the relationship between PM_{10-2.5} and PM_{2.5} and mortality. The studies evaluated in this review analyzed the PM₁₀-mortality relationship through either a time-series or case-crossover design.¹

¹ Schwartz (1981, [078988](#)) used a case-crossover study design, but also conducted a time-series analysis to validate the results obtained using the case-crossover approach.

Time-Series Analyses

Mortality associations with short-term exposure to PM₁₀ in the U.S. have been examined in several updated time-series analyses of the NMMAPS. In the previous NMMAPS analysis (Dominici et al., 2003, [156407](#); Samet et al., 2000, [005809](#); Samet et al., 2000, [010269](#)) of the 1987-1994 data, which was reviewed in the 2004 PM AQCD (U.S. EPA, 2004, [056905](#)), the strongest association was found for nonaccidental mortality for 1-day lag, with a combined estimate across 90 cities of 0.21% (95% PI: 0.09-0.33) per 10 µg/m³ increase in PM₁₀. The association was found to be robust to the inclusion of other gaseous copollutants in the regression models, but the investigators found heterogeneity across regions, with the strongest associations in northeastern cities. In the new updated analyses, the investigators examined additional issues surrounding the association between PM and mortality including: seasonal effect modification; change in risk estimates over time; sensitivity of results to alternative weather models; and effect modification by air conditioning use. The NMMAPS data has also been used to examine the PM concentration-response relationship using PM₁₀ data from 20 cities (Section 6.5.2.7). A few multicounty studies conducted in Canada and Europe provide additional information, which further clarifies and supports the association between PM and mortality presented in the NMMAPS analyses.

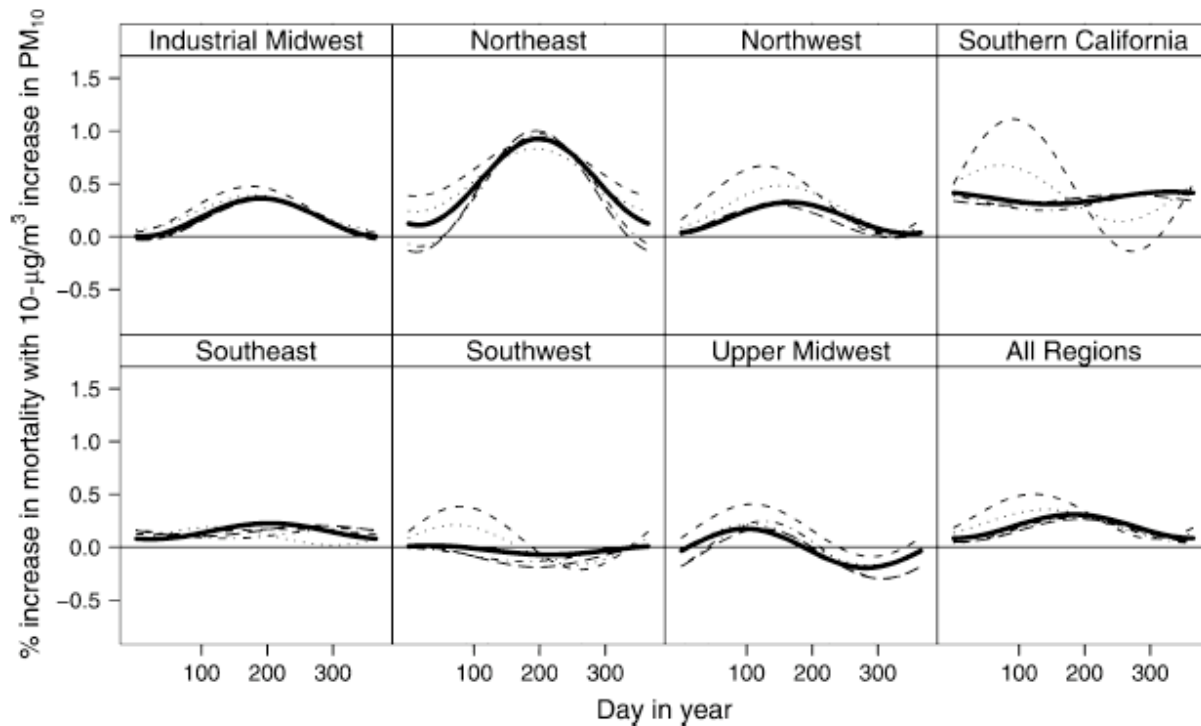
Seasonal Analyses of PM₁₀-Mortality Associations

Using the updated NMMAPS data, which consisted of 100 U.S. cities for the period 1987-2000, Peng et al. (2005, [087463](#)) examined the effect of season on PM₁₀-mortality associations. In their first stage regression model, for each city, the PM₁₀ effect was modeled to have a sinusoidal shape that completes a cycle in a year, but was constrained to be periodic across years using sine/cosine terms. The authors also considered a model that consisted of PM₁₀-season interactions using season indicators. Both of these models also included covariates that were used in their earlier NMMAPS analyses. In the second stage model, the seasonal patterns of PM₁₀ mortality coefficients were estimated for seven geographic regions and on average for the entire U.S. Peng et al. (2005, [087463](#)) found for 1-day lag, at the national level, season specific increases in nonaccidental mortality per 10 µg/m³ increase in PM₁₀ of: 0.15% (95% PI: -0.08 to 0.39), 0.14% (95% PI: -0.14 to 0.42), 0.36% (95% PI: 0.11-0.61), and 0.14% (95% PI: -0.06 to 0.34) for winter, spring, summer, and fall, respectively. The corresponding all-season estimate was 0.19% (95% PI: 0.10-0.28). After the inclusion of SO₂, O₃, or NO₂ in the model with PM₁₀ in a subset of cities (i.e., 45 cities) for which data existed, PM₁₀ risk estimates remained fairly robust. An analysis by geographic region found a strong seasonal pattern in the Northeast. Figure 6-16 presents the estimated seasonal pattern of PM₁₀ risk estimates by region from Peng et al. (2005, [087463](#)), which includes a sensitivity analysis aimed to determine the appropriate number of degrees of freedom for temporal adjustment. It is clear from Figure 6-16 that the Northeast has the strongest association with PM₁₀ and mortality, which peaks in the summer and is robust to the extent of temporal adjustment. The industrial Midwest also shows the summer peak, but with smaller risk estimates. Other regions have either no seasonal pattern (Southeast) or a suggestion of a spring peak that appears to be sensitive to the extent of temporal adjustment. On a nationwide basis, the PM₁₀ risk estimates appear to peak between spring and summer. Overall, this study identified an effect modifier that may be useful in identifying the specific chemical component(s) of PM that are related to specific regions and times of the year.

Change in PM₁₀-Mortality Associations over Time

Dominici et al. (2007, [097361](#)) conducted an analysis of the extended NMMAPS data set (i.e., 1987-2000) to examine if short-term PM₁₀-mortality risk estimates changed during the course of the study period. The investigators estimated the average PM₁₀ mortality risk coefficient for 1-day lag, using essentially the same model specification as in their 2003 analysis, separately for three time periods (i.e., 1987-1994, 1995-2000, and 1987-2000) the “eastern U.S.” (62 counties), the “western U.S.” (38 counties), and all 100 U.S. counties. To produce national and regional estimates, two-stage hierarchical models were used as in the previous NMMAPS studies. As shown in Table 6-16, the authors found a continuation of the PM₁₀-mortality association in the nationwide data for the entire study period. A comparison of the relative risk estimates for 1987-1994 vs. 1995-2000 suggests weak evidence (not a statistically significant difference) that short-term effects declined. Most of the decline in the national estimate appears to be attributable to the eastern U.S. counties. However, the decline in the risk estimate for all-cause mortality in the eastern U.S. appears to be

disproportionately influenced by the reduction in the risk estimate for the “other” mortality category (i.e., all-cause minus cardio-respiratory category, which may be 40-50% of all-cause deaths in U.S. cities). Likewise, the apparent increase in the risk estimate for all-cause mortality in the western U.S. appears to be affected by the increase in the risk estimate for the “other” mortality category. Because the study does not clearly identify the specific cause(s) in the “other” mortality category that are affected by PM, interpreting the reduction in risk estimates for all-cause mortality requires caution. In contrast, the apparent reductions (~23%) in PM₁₀ risk estimates for cardio-respiratory deaths were more comparable between the two regions.



Source: Reprinted with Permission of Oxford University Press from Peng et al. (2005, [087463](#))

Figure 6-16. National and regional estimates of smooth seasonal effects for PM₁₀ at a 1-day lag and their sensitivity to the degrees of freedom assigned to the smooth function of time in the updated NMMAPS data 1987-2000. Note: The degrees of freedom chosen were 3 df (short-dashed line), 5 df (dotted line), 7 df (solid line), 9 df (dotted-and-dashed line), and 11 df (long-dashed line) per year of data.

In addition, the investigators estimated time-varying PM₁₀ mortality risk as a linear function of calendar time for the period 1987-2000, producing the percentage rate change in the PM₁₀ risk estimate with a change in time of 1 yr. The estimated rate of decline in slope for all-cause mortality and the combination of cardiovascular and respiratory mortality were -0.012 (95% PI: -0.037 to 0.014) and -0.016 (95% PI: -0.058 to 0.027), respectively. The authors also estimated a PM_{2.5} mortality risk for the period 1999-2000 (discussed in Section 6.5.2.2.).

Table 6-16. NMMAPS national and regional percentage increase in all-cause, cardio-respiratory, and other-cause mortality associated with a 10 $\mu\text{g}/\text{m}^3$ increase in PM_{10} at lag 1 day for the periods 1987-1994, 1995-2000, and 1987-2000.

	1987-1994	95% PI	1996-2000	95% PI	1987-2000	95% PI
ALL CAUSE						
East	0.29	0.12, 0.46	0.13	-0.19, 0.44	0.25	0.11, 0.39
West	0.12	-0.07, 0.30	0.18	-0.07, 0.44	0.12	-0.02, 0.26
National	0.21	0.10, 0.32	0.18	0.00, 0.35	0.19	0.10, 0.28
CARDIORESPIRATORY						
East	0.39	0.16, 0.63	0.30	-0.13, 0.73	0.34	0.15, 0.54
West	0.17	-0.07, 0.40	0.13	-0.23, 0.50	0.14	-0.05, 0.33
National	0.28	0.14, 0.43	0.21	-0.03, 0.44	0.24	0.13, 0.36
OTHER						
East	0.21	-0.03, 0.44	0.00	-0.49, 0.50	0.15	-0.09, 0.39
West	0.09	-0.21, 0.38	0.23	-0.15, 0.62	0.11	-0.10, 0.33
National	0.15	-0.02, 0.32	0.17	-0.07, 0.41	0.15	0.00, 0.29

Source: Reprinted with Permission of HEI from Dominici et al. (2007, [097361](#))

The objective of the Dominici et al. (2007, [097361](#)) study described above was motivated by accountability research, the idea of measuring the impact of policy interventions. However, unlike the intervention studies conducted in Hong Kong (Hedley et al., 2002, [040284](#)) and Dublin, Ireland (Clancy et al., 2002, [035270](#)) that were reviewed in the 2004 PM AQCD (U.S. EPA, 2004, [056905](#)), this study was not designed to estimate a reduction in mortality in response to a sudden change in air pollution. In fact, the figure of observed trend in PM_{10} levels presented in the Dominici et al. (2007, [097361](#)) study indicates that the decline in PM_{10} levels during the study period was very gradual, with much of the decline appearing in the first few years (median values of $\sim 33 \mu\text{g}/\text{m}^3$ in 1987 to $\sim 25 \mu\text{g}/\text{m}^3$ in 1992, then down to $\sim 23 \mu\text{g}/\text{m}^3$ in 2000). A flaw in the use of the time-series study design for this type of analysis is that it adjusts for long-term trends, and, therefore, does not estimate the change in mortality in response to the gradual change in PM_{10} . The apparent change, though weak, in the PM_{10} risk estimates may also reflect a potential change in the composition of PM_{10} (i.e., $\text{PM}_{10-2.5}$ or $\text{PM}_{2.5}$). The study listed a number of PM_{10} -related air pollution control programs that were implemented between 1987 and 2000. Some of these programs, such as the Acid Rain Control Program, did result in major reductions in emissions, and, therefore, could have contributed to the results observed, but the analytic approach used in the study does not allow for a systematic analysis of the effect of air pollution policies on the risk of mortality.

Sensitivity of PM-Mortality Associations to Alternative Weather Models

To examine the sensitivity of PM_{10} -mortality risk estimates to alternative weather models that consider longer lags, Welty and Zeger (2005, [087484](#)) analyzed the updated NMMAPS 100 U.S. cities data. All of the previous NMMAPS analyses only considered temperature and dew point up to 3-day lags. In this analysis, the authors considered various forms of a constrained distributed lag model: (1) containing a step function of temperature with steps at lag 0, 2, 7 and extended to 14 days; (2) similar to (1) but with time-varying coefficients to change over season and study period; and, (3) containing a smooth function to account for non-linearity in the temperature-mortality relationship. With the combination of degrees of freedom for temporal trends and the number of distributed lags, more than 20 models were applied to each of the 3 lag days (0, 1, and 2) of PM_{10} . These city-specific risk estimates were then combined across the 100 cities in the second stage Bayesian model. The combined PM_{10} risk estimates were generally consistent within the lag. In particular, the risk estimates for nonaccidental mortality for lag 1 day ranged between 0.15% and

0.25% per 10 $\mu\text{g}/\text{m}^3$ increase in PM_{10} , and were always statistically significant regardless of the model used. In addition, the range of these point estimates across the models was found to be much narrower than the regression posterior intervals. Thus, the PM_{10} risk estimates at lag 1 day were robust to alternative temperature models that considered temperature effects lasting up to a 2-week period.

In summary, the above three analyses of the updated NMMAPS data provided useful information on PM -mortality risks, resulting in the following conclusions: (1) estimated PM_{10} mortality risk is particularly high in the northeast and in the summer; (2) there remains an overall PM_{10} -mortality association in the 1987-2000 time period as well as the 1995-2000 time period; (3) there is a weak indication that PM_{10} -mortality risk estimates are declining; and (4) PM_{10} -mortality risk estimates were not sensitive to alternative temperature models.

Effect Modification of PM_{10} -Mortality Associations by Air Conditioning Use

It has been hypothesized that air conditioning (AC) use reduces an individual's exposure to PM and subsequently modifies the PM -mortality association. Bell et al. (2009, [191007](#)) investigated the role of AC use on the relationship between PM_{10} and all-cause mortality using the NMMAPS PM_{10} risk estimates from 84 U.S. urban communities from 1987-2000.¹ Bayesian hierarchical modeling was used to examine if AC prevalence (i.e., fraction of households with central or any AC) explained city-to-city variation in PM_{10} risk estimates. The authors calculated yearly, summer-only, and winter-only effect estimates stratified by housing stock that had either central AC or any AC, which includes window units. Risk estimates for lag 1 (previous day) were used in the analysis because this lag showed the strongest association with mortality in the original NMMAPS analyses. Community-specific AC prevalence was calculated from national survey U.S. Census American Housing Survey (AHS) data, which is available every two years. The investigators computed percent change in PM_{10} effect estimates per an additional 20% of the population acquiring AC.

The AC variables were not strongly correlated with socio-economic variables (poverty rate, unemployment, and education) from the U.S. Census (correlation ranged from -0.27 to 0.29). Bell et al. (2009, [191007](#)) found that communities with higher AC prevalence had lower PM_{10} mortality risk estimates for all-cause mortality (-30.4% [95% PI: -80.4 to 19.6] per an additional 20% of the population acquiring any AC; -39.0% [95% PI: -81.4 to 3.3] for central AC), but results were not statistically significant. When restricting the analysis to the summer months and focusing on the 45 cities with summer-peaking PM_{10} concentrations, the authors reported positive, non-significant risk estimates (29.9% [95% PI: -84.0 to 144] per an additional 20% of the population acquiring any AC; -2.0% [95% PI: -60.3 to 64.3] for central AC). A similar analysis was conducted for winter months using data from six cities with winter peaking PM_{10} concentrations, but the confidence bands were too wide (due to the small sample size) for meaningful interpretation.

Although the estimated reductions in PM_{10} all-cause mortality risks from AC use reported in the Bell et al. (2009, [191007](#)) study were not statistically significant, their large magnitude suggests that AC use may reduce an individual's exposure to PM . Given the expected additional increase in AC use in the future, and the results from recent multicity studies, which have reported stronger PM -mortality associations during the warm season, AC use may play a larger role in determining an individual's exposure to PM . Studies that have examined the effect of AC use on the $\text{PM}_{2.5}$ -mortality association have reported similar results. For example, Franklin et al. (2007, [091257](#)) (discussed in detail in Section 6.5.2.2) found that AC use non-significantly modified $\text{PM}_{2.5}$ mortality risk estimates, but the result was suggestive of higher $\text{PM}_{2.5}$ effects in cities with lower AC use, especially in cities with summer-peaking $\text{PM}_{2.5}$ concentrations. Overall, further investigation is needed to fully understand the relationship between AC use and mortality attributed to short-term exposure to PM .

PM_{10} -Mortality Associations in Canada and Europe

Burnett et al. (2004, [086247](#)) examined the association between mortality and various air pollutants in 12 Canadian cities, and reported that the most consistent association was found for NO_2 . For this analysis, PM was measured every 6th day for the majority of the study period, and the PM_{10} concentrations used in the study represent the sum of the $\text{PM}_{2.5}$ and $\text{PM}_{10-2.5}$, which were directly measured by dichotomous samplers. The authors found that the simultaneous inclusion of

¹ This study also examined risk estimates for cardiovascular and respiratory hospital admissions in older adults (≥ 65).

NO₂ and PM₁₀ in a model, on those days with PM data, greatly reduced the PM₁₀ association with nonaccidental mortality, from 0.47% (95% CI: 0.04-0.89) to 0.07% (95% CI: -0.44 to 0.58) per 10 µg/m³ increase. The previous Canadian multicity analysis (Burnett and Goldberg, 2003, [042798](#)), a re-analysis of Burnett et al. (2000, [010273](#)) reviewed in the 2004 PM AQCD (U.S. EPA, 2004, [056905](#)), did not consider gaseous pollutants. Thus, PM₁₀ risk estimates in the Canadian data appear to be more sensitive to NO₂ than those estimates reported in U.S. studies.

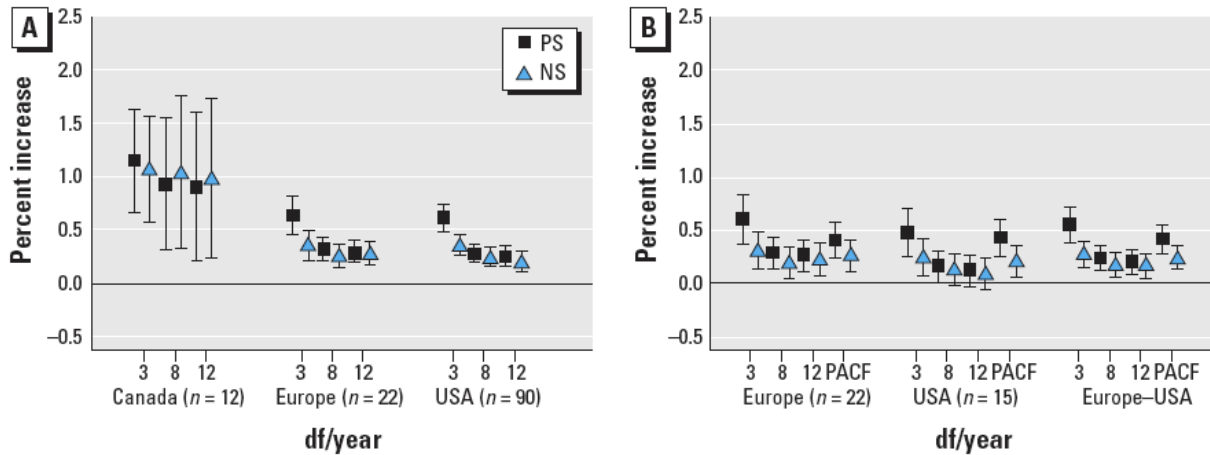
The association between PM₁₀ and mortality in Europe was also reviewed in the 2004 PM AQCD (U.S. EPA, 2004, [056905](#)) through Katsouyanni et al. (2003, [042807](#)), which presented results from the APHEA-2 study, a multicity study that examined PM₁₀ effects on total mortality in 29 European cities. Analitis et al. (2006, [088177](#)) published a brief report on effect estimates for cardiovascular and respiratory deaths also based on the 29 European cities, within the APHEA2 study. They reported for the average of 0- and 1-day lags, PM₁₀ risk estimates per 10 µg/m³ of 0.76% (95% CI: 0.47-1.05) for cardiovascular deaths and 0.71% (95% CI: 0.22-1.20) for respiratory deaths in random effects models.

Comparison of PM-Mortality Associations in Europe, Canada, and the U.S.

The APHENA study (Samoli et al., 2008, [188455](#)) was a collaborative effort by the APHEA, NMMAPS, and the Canadian multicity study investigators to evaluate the coherence of PM₁₀ mortality risk estimates across locations and possible effect modifiers of the PM-mortality relationship using a common protocol. To adjust for temporal trends, Samoli et al. (2008, [188455](#)) used 3, 8, and 12 degrees of freedom (df) with natural splines and penalized splines, as well as the minimization of the sum of the absolute values of the partial auto-correlation function (PACF). The investigators also included a smooth function of temperature on the same day of death and the day before death. The study reported risk estimates for a 1-day lag (from all three data sets), the average of lag day 0 and 1 (all but for the Canadian data because PM data was collected every 6th day), and an unconstrained distributed lag model using lags of 0, 1, and 2 days (all but for the Canadian data). The second-stage regression included: (a) the average pollution level and mix in each city; (b) air pollution exposure characterization (e.g., number of monitors, density of monitors); (c) the health status of the population (e.g., cardio-respiratory deaths as a percentage of total mortality, crude mortality rate, etc.); and (d) climatic conditions (e.g., mean and variance of temperature). In addition, unemployment rate was examined for 14 European cities and all U.S. cities. Effect modification patterns were examined only for cities with complete time-series data and using the average of lags 0 and 1 day, resulting in the exclusion of the Canadian data.

Generally, the risk estimates from Europe and the U.S. were similar, but those from Canada were substantially higher.¹ For example, the percent excess risks per 10 µg/m³ increase in PM₁₀ for all ages using 8 df/yr and penalized splines were 0.84% (95% CI: 0.30-1.40), 0.33% (95% CI: 0.22-0.44), and 0.29% (95% CI: 0.18-0.40) for the Canadian, European, and U.S. data, respectively. Note that the risk estimate for the 90 U.S. cities is slightly larger than that reported in the original NMMAPS study (0.21%, using natural splines, and more temperature variables). In the all ages model, the average of lag days 0 and 1, and the distributed lag model with lags 0, 1, and 2 did not result in larger risk estimates compared to those for a 1 day lag. In copollutant models, PM₁₀ risk estimates did not change when controlling for O₃. Figure 6-17 shows the risk estimates from the three data sets for alternative extent of temporal smoothing and smoothing methods. The Canadian data appear less sensitive to the extent of temporal smoothing or smoothing methods (Panel A of Figure 6-17). When stratifying by age the risk estimates for the older age group (≥ 75 yr) were consistently larger than those for the younger age group (<75 yr) (e.g., 0.47% vs. 0.12% for the U.S. data) for all the three data sets. Although the study did not quantitatively present the results from the effect modification analyses, some evidence of effect modification across the study regions was observed. The investigators reported that, in the European data, higher levels of NO₂ and a larger NO₂/PM₁₀ ratio were associated with greater PM₁₀ risk estimates, and that while this pattern was also present in the U.S. data, it was less pronounced. Additionally, in the U.S. data, smaller PM₁₀ risk estimates were observed among older adults in cities with higher O₃ levels. Effect modification by temperature was also observed, but only in the European data.

¹ The risk estimate reported for the 12 Canadian cities examined in the APHENA study is higher than that reported by Burnett et al. (2004, [086247](#)). This is because the APHENA study did not use the 12 cities data from Burnett et al. (2004, [086247](#)), but instead used a composite of the data from three previous studies conducted by the same group by the same group (Burnett and Goldberg, 2003, [042798](#); 1998, [029505](#); Burnett et al., 2000, [010273](#)).



Source: Samoli et al. (2008, [188455](#))

Figure 6-17. Percent increase in the daily number of deaths, for all ages, associated with a 10-µg/m³ increase in PM₁₀: lag 1 (A) and lags 0 and 1 (B) for all three centers. PACF indicates df based on minimization of PACF.

In this study, the underlying basis for the larger PM₁₀ risk estimates (by twofold) in the Canadian data compared to the European and U.S. data could not be identified, even when consistent statistical methods were applied across each of the data sets. Because the effect modification of PM₁₀ risk estimates were not examined in the Canadian data, the potential influence of air pollution type or mixture could not be ruled out as a potential source of heterogeneity across the three data sets. It should be noted that both the original U.S. and European studies reported regional heterogeneity in PM risk estimates, and the U.S. data also demonstrated seasonal heterogeneity. In both of these cases the specific characteristics associated with the regions that contributed to the heterogeneity observed were not identified. Thus, further investigation is needed to identify factors that influence the heterogeneity in PM risk estimates observed between different countries and across regions.

Case-Crossover Analyses

Since the 2004 PM AQCD (U.S. EPA, 2004, [056905](#)) investigators have used the case-crossover study design more frequently as an alternative to time-series analyses to examine the association between short-term exposure to PM and mortality. This study design allows for the control of seasonal variation, time trends, and slow time varying confounders without the use of complex models. However, similar to any study design, biases can be introduced into the study depending on the control (i.e., referent) period selected (Janes et al., 2005, [087535](#)). The multicity case-crossover analyses discussed below match cases (i.e., days in which a death occurred) to controls (i.e., days in which a death did not occur), to control for (1) seasonal patterns and gaseous pollutants; or (2) temperature. In addition, the studies attempted to examine the heterogeneity of effect estimates through the analysis of individual-level and city-specific effect modification.

Controlling for Temperature

Schwartz (2004, [078998](#)) investigated the PM₁₀-mortality association in 14 U.S. cities for the years 1986-1993 (some cities started in later years because of PM₁₀ data availability) using a case-crossover study design. Note that in this analysis, four more cities (Boulder, CO; Cincinnati, OH; Columbus, OH; and Provo-Orem, UT) were added to the cities Schwartz (2003, [042800](#)) previously analyzed using a time-series study design. These cities were chosen for this analysis because they collected daily PM₁₀ data, unlike most U.S. cities, which only monitor PM₁₀ every six days. Lag 1-day PM₁₀ risk estimates were computed using several methods. Model 1 (i.e., the main model) and Model 2 were constructed from a case-crossover analysis with bidirectional control days

(7-15 days before and after the case). Model 1 obtained city-specific estimates in the first stage analysis, followed by a second stage random-effects model to obtain a combined estimate. Model 2 is the same as Model 1, but consisted of a single stage model, which included data from all 14 cities. Models 3 and 4 were also constructed from a case-crossover analysis, but used time-stratified control days (i.e., matched on season and temperature within the same degree in Celsius). Model 3 obtained single-city estimates in the first stage analysis, followed by a second stage random-effects model to obtain combined estimates. Model 4 used the same approach as Model 3, but consisted of a single stage model including data from all 14 cities. The final model, Model 5 consisted of a two-stage Poisson time-series model, which produced city-specific estimates in the first stage, and combined estimates across cities in the second stage. In the main model the estimated excess risk for nonaccidental mortality was 0.36% (95% CI: 0.22-0.50) per 10 $\mu\text{g}/\text{m}^3$ increase in PM_{10} . The other models yielded a similar magnitude of effect estimates, ranging from 0.32% (Model 2) to 0.53% (Model 4). Thus, the methods used to select control days and adjust for weather in the case-crossover design did not result in major differences in effect estimates, and in addition, were comparable to the estimates obtained from the time-series analysis, 0.40% (Model 5).

Controlling for Gaseous Pollutants

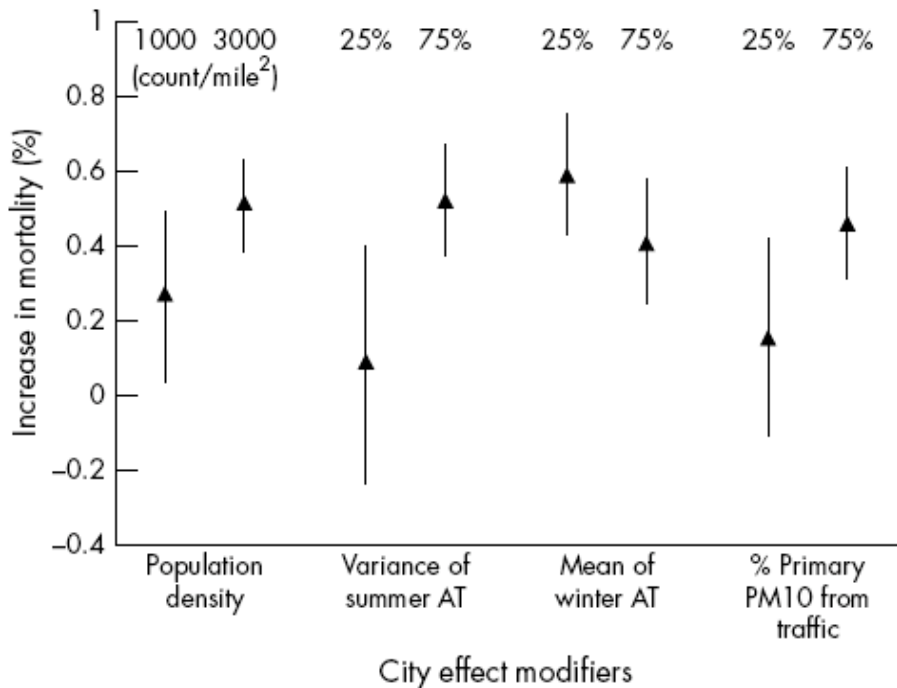
In a subsequent analysis, Schwartz (2004, [053506](#)) analyzed the same 14 cities data described above, using a case-crossover design, to investigate the potential confounding effects of gaseous pollutants. For each case day, control days were selected from all other days of the same month of the same year. In addition, control days were selected if they had gaseous pollutant concentrations within: 1 ppb, 1 ppb, 2 ppb, or 0.03 ppm for SO_2 , NO_2 , 1-h max O_3 , and CO, respectively, of the case day. Unlike the study described above (Schwartz, 2004, [078998](#)) in this analysis, the excess risk was estimated for the average of 0- and 1-day lag PM_{10} (rather than 1-day lag). In addition, apparent temperature (a composite index of temperature and humidity) was used rather than temperature and humidity individually. The case-crossover analysis was conducted in each city, and a combined estimate was computed in a second-stage random effects model. The number of cities analyzed varied across pollutants depending on the availability of monitors. The study reported PM_{10} risk estimates for nonaccidental mortality of 0.81% (95% CI: 0.47-1.15), 0.78% (95% CI: 0.42-1.15), 0.45% (95% CI: 0.12-0.78), and 0.53% (95% CI: 0.04-1.02) per 10 $\mu\text{g}/\text{m}^3$ increase, for the analysis matched by SO_2 (10 cities), NO_2 (8 cities), O_3 (13 cities), and CO (13 cities), respectively.

Schwartz (2004, [053506](#)) only presented PM_{10} risk estimates matched by gaseous pollutants, therefore, it is unclear in this analysis how matching by gaseous pollutants affected (i.e., reduced or increased) unmatched PM_{10} risk estimates. The estimates reported were computed using the average of 0- and 1-day lagged PM_{10} and, therefore, cannot be directly compared to the 1-day lag PM_{10} risk estimates obtained in the Schwartz (2004, [078998](#)) 14-city study described above. The estimates reported in the case-crossover analysis that controlled for gaseous pollutants (Schwartz, 2004, [053506](#)) are generally larger than those obtained in the analysis that controlled for temperature (Schwartz, 2004, [078998](#)), which was expected since the Schwartz (2004, [053506](#)) analysis used 2-day avg PM_{10} . However, the estimates reported in Schwartz (2004, [053506](#)) are comparable to the average of 0- and 1-day lagged PM_{10} risk estimate for nonaccidental mortality (0.55% [95% CI: 0.39-0.70]) per 10 $\mu\text{g}/\text{m}^3$ increase from the 10-city study (Schwartz, 2003, [042800](#)), which was reviewed in the 2004 PM AQCD (U.S. EPA, 2004, [056905](#)). Overall, Schwartz (2004, [053506](#)) provided an alternative method to assess the influence of gaseous copollutants. The results suggest that PM_{10} is significantly associated with all-cause mortality after controlling for each of the gaseous copollutants.

City-Level Effect Modification

Zeka et al. (2005, [088068](#)) expanded the 14 cities analyses conducted by Schwartz (2004, [078998](#); 2004, [053506](#)) to 20 cities, added more years of data (1989-2000), and investigated PM_{10} effects on total and cause-specific mortality using a case-crossover design. Individual 0-, 1-, and 2-day lags as well as an unconstrained distributed lag model with 0, 1, and 2 lag days were examined. For each case day, control days were defined as every third day in the same month of the same year, to eliminate serial correlation. The authors also investigated potential effect modifiers in the second stage regression using city-specific variables including percent using AC, population density, standardized mortality rates, the proportion of elderly in each city, daily minimum apparent

temperature in summer, daily maximum apparent temperature in winter, and the estimated percentage of primary PM₁₀ from traffic sources.



Source: Reprinted with Permission of BMJ Group from Zeka et al. (2005, [088068](#))

Figure 6-18. Effect modification by city characteristics in 20 U.S. cities. Note: The two estimates and their CI for each of the modifying factors represent the percentage increase in mortality for a 10 µg/m³ increase in PM₁₀, for the 25th percentile, and 75th percentile of the modifier distribution across the 20 cities.

The investigators found that, for all-cause (nonaccidental) mortality, lag 1 day showed the largest risk estimate (0.35% [95% CI: 0.21-0.49] per 10 µg/m³) among the individual lags. Respiratory mortality exhibited associations at lag 0, 1, and 2 days (0.34%, 0.52%, and 0.51%, respectively), whereas cardiovascular mortality was most strongly associated with PM₁₀ at lag day 2 (0.37%). The sum of the distributed lag risk estimates (e.g., 0.45% [95% CI: 0.25-0.65] for all-cause mortality) was generally larger than those for single-day lag estimates. The excess risk estimates for single-day lags for specific respiratory and cardiovascular causes had generally wider confidence intervals due to their smaller daily mortality counts, but some of the categories showed markedly larger estimates when included in the combined distributed lag model (e.g., pneumonia 1.24% [95% CI: 0.46-2.02]). As shown in Figure 6-18, Zeka et al. (2005, [088068](#)) also found evidence indicative of several PM₁₀ effect modifiers including higher population density and the estimated percentage of primary PM₁₀ from traffic. When 25th versus 75th percentiles of these city-specific variables were evaluated, the estimated percent increase in mortality attributed to PM₁₀ appears to contrast substantially (e.g., 0.09% vs. 0.52% for variance of summer time apparent temperature).

The effect modifiers investigated by Zeka et al. (2005, [088068](#)) consisted of city-specific variables. Some of these variables are ecological in nature, and therefore, interpreting the meaning of “effect modification” requires some caution. As the investigators pointed out, the population density and the estimated percentage of primary PM₁₀ from traffic were correlated in this data set ($r = 0.65$)¹. These variables may also be a surrogate for another or composite aspects of “urban” characteristics.

¹ The correlation coefficient was calculated based on the numbers provided in Table 1 of Zeka et al. (2005, [088068](#)).

Thus, the apparent effect modification by traffic-related PM₁₀ needs further investigation. Interestingly, the percent of homes with central AC was not a significant effect modifier of PM₁₀ risk estimates, which questions the impact of reduced building ventilation rates on PM exposure. Overall, this study presented PM₁₀ risk estimates that are consistent with those found in other analyses, but also provided new information on the risk estimated for broad and specific respiratory and cardiovascular mortality designations, along with possible effect modifying city-specific characteristics.

Individual-level Effect Modification

In an additional analysis, Zeka et al. (2006, [088749](#)) examined individual-level, instead of city-specific, effect modification of PM₁₀-mortality associations in the 20 U.S. cities described above using the same case-crossover design. City-specific estimates were obtained in the first stage model, followed by a second stage model which estimated the overall effects across all cities. Figure 6-19 shows PM₁₀ excess risks by four of the individual characteristics examined in the study (i.e., gender, race, age group, and education). It should be noted that the lag and averaging of days for the associations reported varied across the outcomes: all-cause and heart disease deaths used the average of lag 1 and 2 days; respiratory deaths used the average of lag 0 through 2 days; MI deaths used lag 0 day; and stroke deaths used lag 1 day. PM₁₀ risk estimates do not appear to differ by gender or by race. However, significant differences were found for the youngest vs. oldest age groups for all-cause and heart disease mortality. For all-cause mortality, the level of education appeared to be inversely related to the PM₁₀ risk estimates (i.e., greater risk for lower education level), but this observation was not statistically significant. The study also examined effect modification by location of death (“out-of-hospital” versus “in-hospital”) and season (Figure 6-20). The “out-of-hospital” deaths showed larger PM₁₀ risk estimates than were found for “in-hospital deaths” with a significant difference per 10 µg/m³ for all-cause (0.71% versus 0.22%) and heart disease (0.93% versus 0.15%) deaths. Stroke deaths also showed a significant difference (0.87% vs. 0.06%, not shown in Figure 6-20).

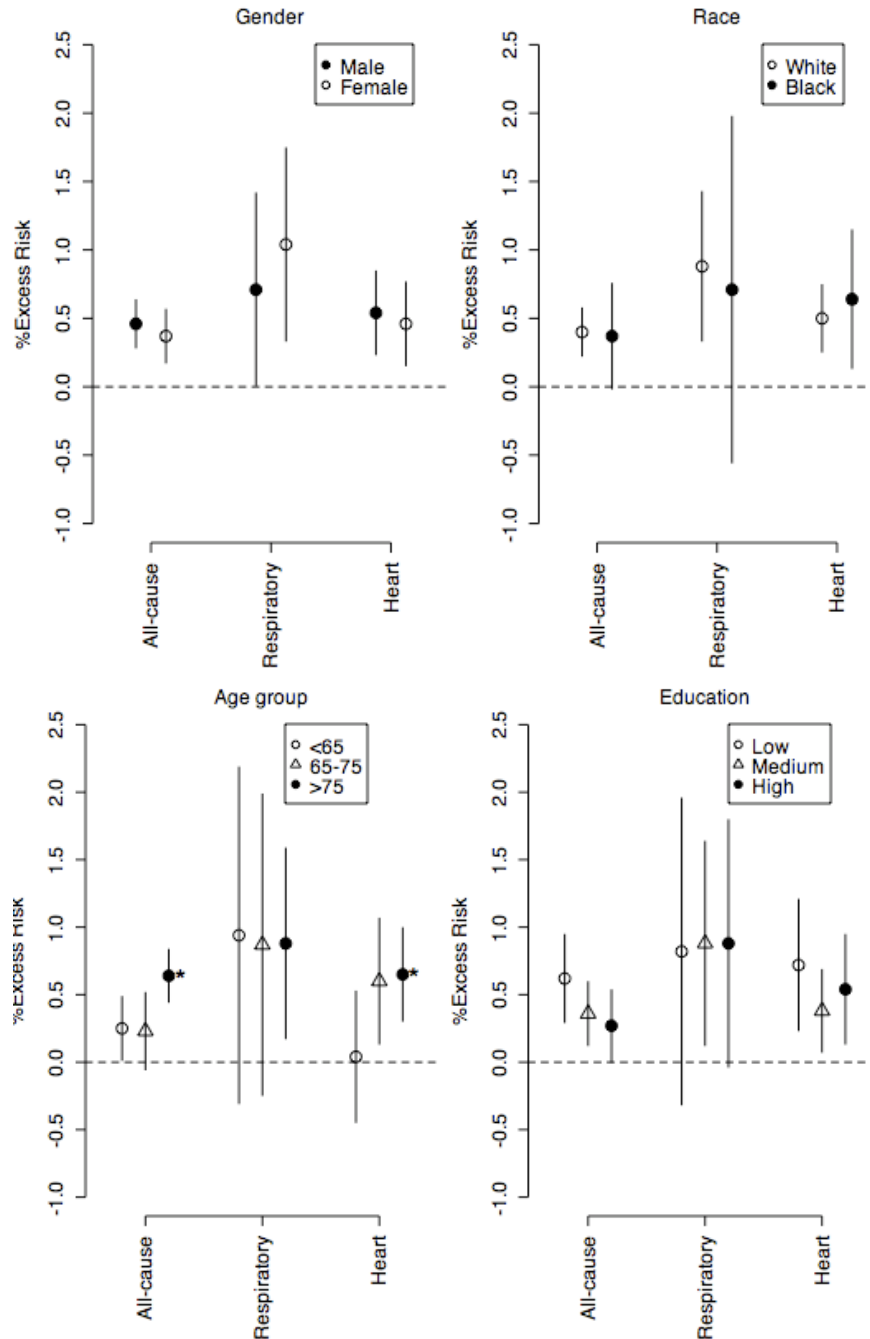


Figure 6-19. Percent excess risk in mortality (all-cause [nonaccidental] and cause-specific) per $10 \mu\text{g}/\text{m}^3$ increase in PM_{10} by individual-level characteristics. The risk estimates and 95% confidence intervals were plotted using numerical results from tables in Zeka et al. (2006, [088749](#)). The estimates with * next to them are significantly higher than the lowest estimate in the group.

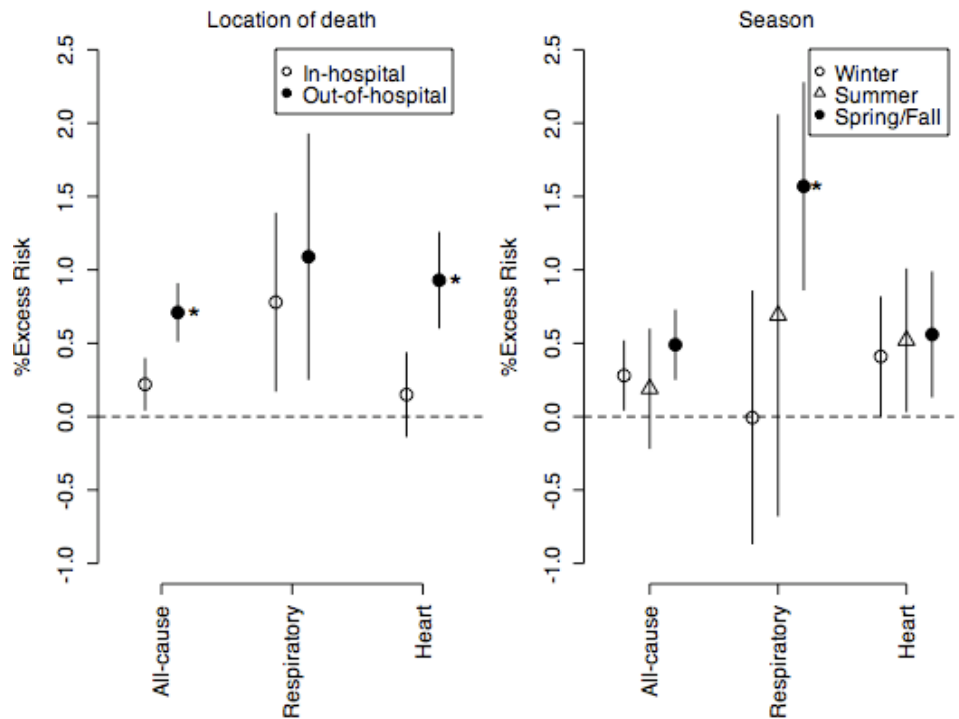
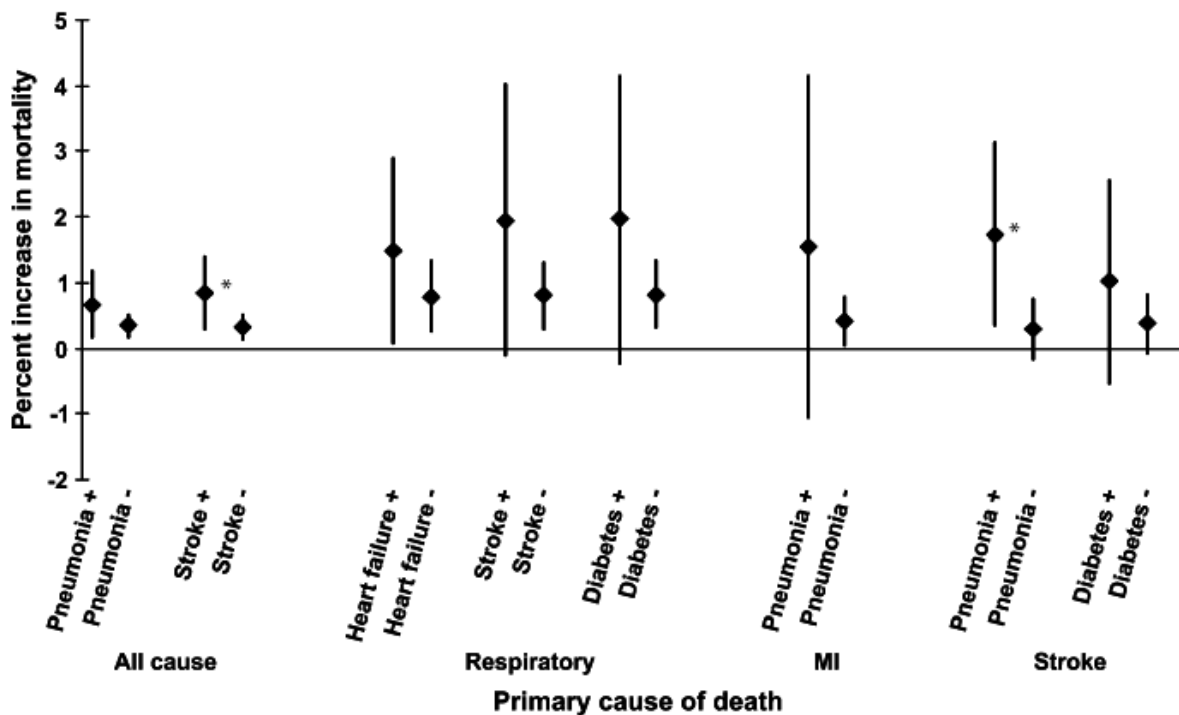


Figure 6-20. Percent excess risk in mortality (all-cause [nonaccidental] and cause-specific) per $10 \mu\text{g}/\text{m}^3$ increase in PM_{10} by location of death and by season. The risk estimates and 95% confidence intervals were plotted using numerical results from tables in Zeka et al. (2006, [088749](#)). The estimates with * next to them are significantly higher than the lowest estimate in the group.

Overall, Zeka et al. (2006, [088749](#)) showed a consistent pattern of effect modification by contributing causes of death (i.e., pneumonia, stroke, heart failure, and diabetes) on PM_{10} risk estimates for primary causes of death (Figure 6-21; not all results for contributing cause are shown). However, because the contributing causes of death counts were relatively small, as reflected by the wide confidence intervals in Figure 6-21, most of the differences observed did not achieve statistical significance.



Source: Adapted with Permission of Oxford University Press from Zeka et al. (2006, [088749](#))

Figure 6-21. Percent increase in mortality (all-cause [nonaccidental] and cause-specific) per 10 $\mu\text{g}/\text{m}^3$ increase in PM_{10} by contributing causes of death. The estimates with * (added to the original figure) indicates a significant difference.

In addition, when examining the other effect modifiers, the results that show no difference in PM_{10} risk estimates between gender or race for all-cause and cardiovascular deaths are important, given the relatively narrow confidence bands of these estimates. The effect modification by the location of death has been reported previously in smaller studies, but the large contrast found for all-cause and cardiovascular mortality in this large multicity analysis is noteworthy. The elevated PM_{10} risks reported by Zeka et al. (2006, [088749](#)) for all-cause, heart disease (and stroke) “out-of-hospital” deaths are also consistent with the hypothesis of acute PM_{10} effects on “sudden deaths” brought on by systemic inflammation or dysregulation of the ANS. The finding regarding the seasonal effect modification, though significant only for respiratory deaths, is somewhat in contrast with the Peng et al. (2005, [087463](#)) analysis of the extended NMMAPS data, which observed the greatest effects during the summer season. The apparent inconsistency may be due to the difference in geographic coverage (i.e., 20 versus 100 cities) or methodology (i.e., case-crossover with referent days in the same month of the same year vs. time-series analysis with adjustment for temporal trend in the regression model).

Summary of PM_{10} Risk Estimates

Overall, the recent studies continue to show an association between short-term exposure to PM and mortality. Although these studies do not examine mortality effects attributed to PM size fractions that compose PM_{10} , the regional, seasonal, and effect modification analyses conducted contribute to the evidence for the $\text{PM}_{2.5}$ and $\text{PM}_{10-2.5}$ associations presented in Sections 6.5.2.2 and 6.5.2.3, respectively. Of the PM_{10} studies evaluated, depending on the lag/averaging time and the number of cities included, the estimates for all-cause (nonaccidental) mortality for all ages ranged from 0.12% (Dominici et al., 2007, [097361](#)) to 0.84% (Samoli et al., 2008, [188455](#)) per 10 $\mu\text{g}/\text{m}^3$ increase in PM_{10} , regardless of the study design used (i.e., time-series vs. case crossover). Although this range of PM mortality risk estimates is smaller than those reported for $\text{PM}_{10-2.5}$ and $\text{PM}_{2.5}$ they do support the

association between PM and mortality. The majority of studies examined present estimates for either a lag of 1 day or a 2-day avg (lag 0-1), both of which have been found to be strongly associated with the risk of death (Schwartz, 2004, [078998](#); 2004, [053506](#)). The use of a distributed lag model (using lag 0, 1, and 2 days) was found to result in slightly larger (by ~30%) estimates compared to those for single-day lags in the 20 cities study (Zeka et al., 2005, [088068](#)), but when using the 15 cities data from NMMAPS analyzed in the APHENA study (Samoli et al., 2008, [188455](#)), the 1-day lag combined risk estimate was larger than the distributed lag (lag, 0, 1, and 2 days) estimate. Overall, an examination of the PM₁₀ risk estimates stratified by cause-specific mortality and age, for all U.S.- and Canadian-based studies, further supports the findings of the multicity studies discussed in the 2004 PM AQCD (U.S. EPA, 2004, [056905](#)) (i.e., consistent positive associations between short-term exposure to PM₁₀ and mortality) and this ISA, however, it must be noted that a large degree of variability exists between cities when examining city-specific risk estimates.

The variability in PM₁₀ mortality risk estimates reported within and between multicity studies may be due to the difference in the cities analyzed and the potential regional differences in PM composition. The NMMAPS studies have found that geographic regions and seasons are the two most important factors that determine the variability in risk estimates, with estimates being larger in the eastern U.S. and during the summer. These findings were fairly consistent across studies, but Zeka et al. (2006, [088749](#)) observed the strongest association during the transition period (spring and fall); however, this may be due to the difference in geographic coverage or the difference in the model specification used compared to Peng et al. (2005, [087463](#)).

Finally, examination of potential confounders showed that the size of PM₁₀ risk estimates are fairly robust to the inclusion of gaseous copollutants in models (Peng et al., 2005, [087463](#)) or by matching days with similar gaseous pollutant concentrations (Schwartz, 2004, [053506](#)). These findings further confirmed that PM₁₀ risk estimates are not, at least in a straightforward manner, confounded by gaseous copollutants.

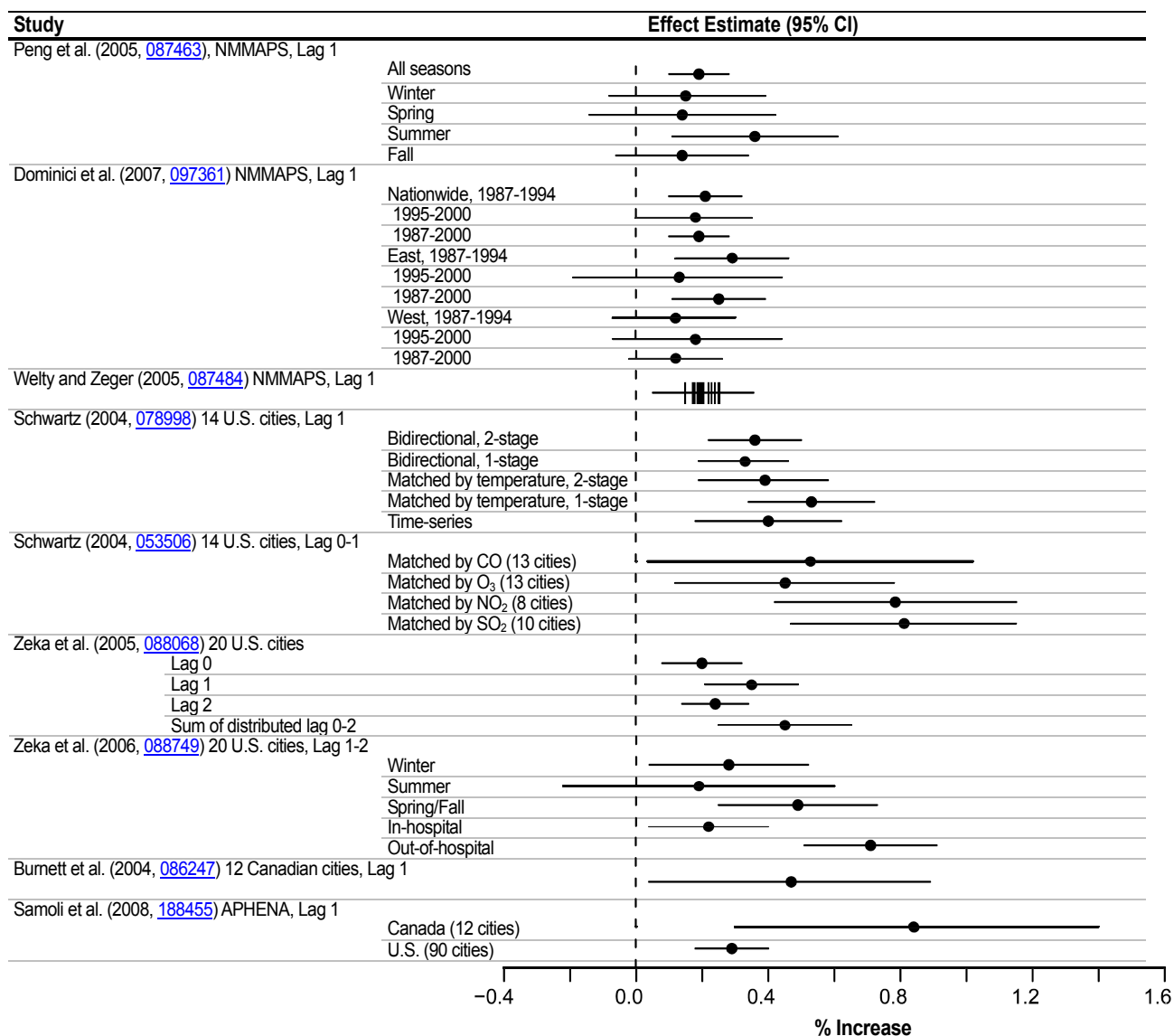


Figure 6-22. Summary of percent increase in all-cause (nonaccidental) mortality from recent multicity studies per 10 $\mu\text{g}/\text{m}^3$ increase in PM_{10} . The number after the study location indicates lag/average used for PM_{10} (e.g., “01” indicates the average of lag 0 and 1 days). For Welty and Zeger (2005, 087484), the vertical lines represent point estimates for 23 different weather models, and the horizontal band spans the 95% posterior intervals of these point estimates.

6.5.2.2. $\text{PM}_{2.5}$

A nationwide monitoring system for $\text{PM}_{2.5}$ was not established until 1999. This in conjunction with the unavailability of nationwide mortality data from the National Center of Health Statistics (NCHS) starting in 2001¹, has contributed to the relatively small literature base that has examined

¹ In 2008 the EPA facilitated the availability of the mortality data for EPA-funded researchers, which should eventually increase the literature base of studies that examine the association between short-term exposure to $\text{PM}_{2.5}$ and mortality.

the association between short-term exposure to PM_{2.5} and mortality. To date, the studies that have been conducted examined national (i.e., in multiple cities across the country) or regional (i.e., in one location of the country) PM_{2.5} associations with mortality.

PM_{2.5} – Mortality Associations on a National Scale

The NMMAPS study conducted by Dominici et al. (2007, [097361](#)) (described in Section 6.5.2.1), also conducted a national analysis of PM_{2.5}-mortality associations using the same methodology and data for 1999-2000. The PM_{2.5} risk estimates at lag 1 day were 0.29% (95%PI: 0.01-0.57) and 0.38% (95%PI: -0.07 to 0.82) per 10 µg/m³ increase for all-cause and cardio-respiratory mortality, respectively. The authors also conducted a sensitivity analysis of the risk estimates based on the extent of adjustment for temporal trends in the model, changing the degrees of freedom (df) of temporal adjustment from 1 to 20/yr (the main result used 7 df/yr). In comparison to the PM₁₀ results, the PM_{2.5} risk estimates appeared more sensitive to the extent of temporal adjustment between 5 and 10 df/yr, but this may be in part due to the much smaller sample size used for the PM_{2.5} analysis (i.e., mortality counts from 1999-2000) compared to the PM₁₀ analysis (i.e., mortality counts from 1987-2000).

Franklin et al. (2007, [091257](#)) analyzed 27 cities across the U.S. that had PM_{2.5} monitoring and daily mortality data for at least two years of a 6-yr period, 1997-2002. The mortality data up to year 2000 were obtained from the NCHS, while the 2001-2002 data were obtained from six states (CA, MI, MN, PA, TX, and WA), resulting in 12 out of the 27 cities having data up to 2002. The start year for each city included in the study was set at 1999, except for Milwaukee, WI (1997) and Boston, MA (1998), which is due to PM_{2.5} data availability in these two cities. In the case-crossover analysis in each city, control days for each death were chosen to be every 3rd-day within the same month and year that death occurred in order to reduce autocorrelation. The first stage regression examined the interaction of effects with age and gender, while the second stage random effects model combined city-specific PM_{2.5} risk estimates and examined possible effect modifiers using city-specific characteristics (e.g., prevalence of central AC and geographic region). For all of the mortality categories, the estimates for lag 1 day showed the largest estimates. The combined estimates at lag 1 day were: 1.2% (95%CI: 0.29-2.1), 0.94% (95%CI: -0.14 to 2.0), 1.8% (95%CI: 0.20-3.4), and 1.0% (95%CI: 0.02-2.0) for all-cause, cardiovascular, respiratory, and stroke deaths, respectively, per 10 µg/m³. When examining the city-specific risk estimates most of the cities with negative estimates were also those with a high prevalence of central AC (Dallas, 89%; Houston, 84%; Las Vegas, 93%; Birmingham, 77%). It is unclear why these cities exhibit negative (and significant) risk estimates rather than null effects.

In the analysis of effect modifiers, Franklin et al. (2007, [091257](#)) found that individuals ≥ 75 yr showed significantly higher PM_{2.5} risk estimates than those individuals < 75 yr. The estimated effects were also found to vary by geographic location with larger estimates in the East than in the West, which are consistent with the regional pattern found in the NMMAPS PM₁₀ risk estimates. In addition, a higher prevalence of central AC was associated with decreased PM_{2.5} risk estimates when comparing the lower (25th percentile) versus the higher (75th percentile) AC use rates, especially in the cities where PM_{2.5} concentrations peak in the summer. Finally, the risk estimates were not found to be different between communities with PM_{2.5} concentrations ≤ 15 vs. >15 µg/m³. The risk estimates for each effect modifier are presented in Figure 6-25. Note the wide confidence intervals associated with each of the risk estimates, specifically for Franklin et al. (2007, [091257](#)) and Ostro et al. (2006, [087991](#)), which suggests low statistical power for testing the differences between effect modifiers.

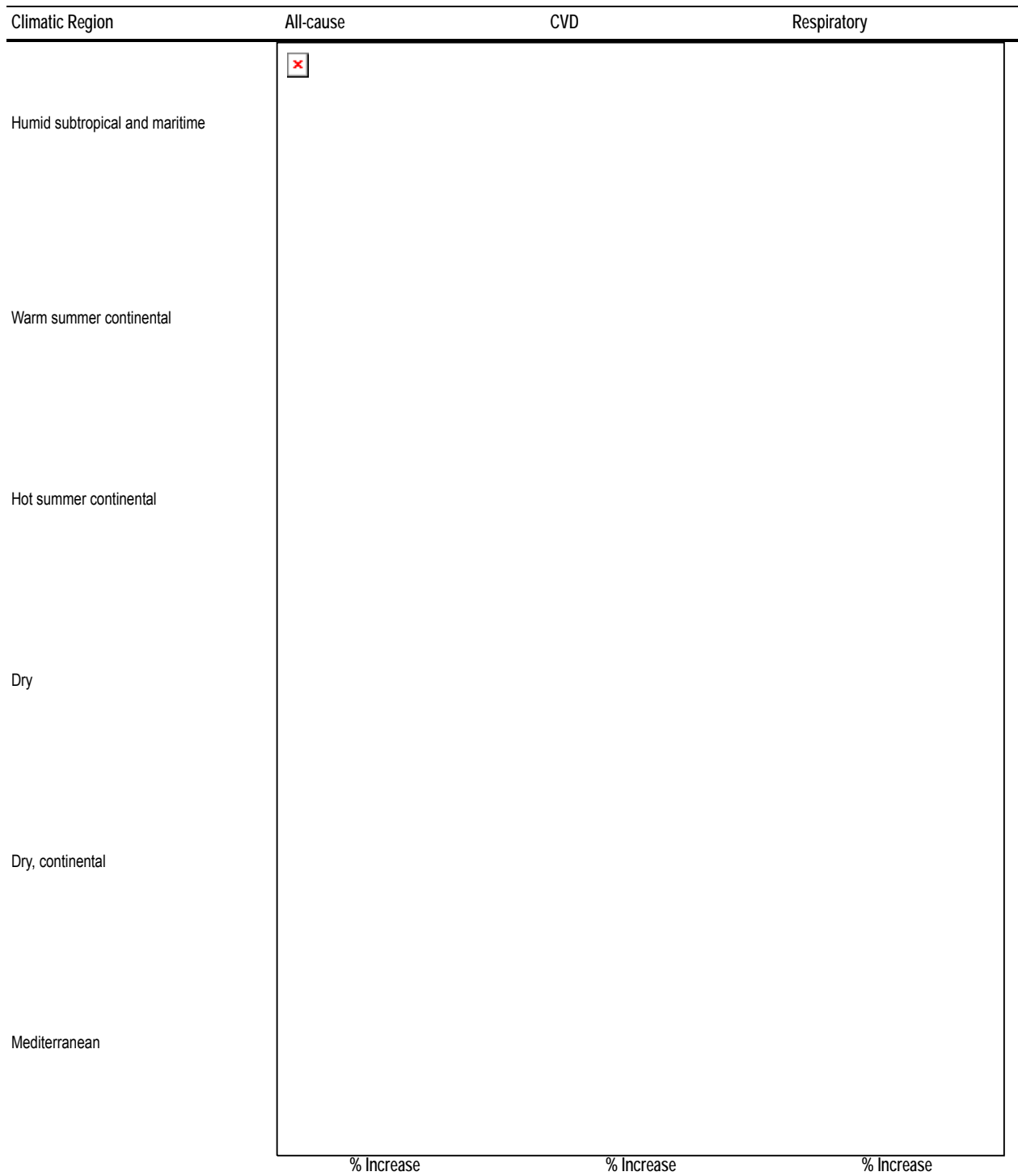
Franklin et al. (2008, [097426](#)) analyzed 25 cities that had PM_{2.5} monitoring and daily mortality data between the years 2000-2005 (with the study period varying from city to city). The choice of the 25 communities was based on the availability of PM_{2.5} mass concentrations and daily mortality records for at least four years, along with PM_{2.5} speciation data for at least 2 years between 2000 and 2005. Similar to Franklin et al. (2007, [091257](#)), all-cause, cardiovascular, respiratory, and stroke deaths were examined; however, of the 25 cities included in the study, only 15 overlap with the 27 cities analyzed in Franklin et al. (2007, [091257](#)). The authors obtained mortality data from the NCHS and various state health departments (CA, MA, MI, MN, MO, OH, PA, TX, and WA). Although the main objective of the study was to examine the role of PM_{2.5} chemical species in the second stage analysis (Section 6.5.2.5), the first stage analysis conducted a time-series regression of

mortality on PM_{2.5}. In addition, the first stage regression performed a seasonal analysis in order to take advantage of seasonal variation in PM_{2.5} chemical species across cities and to possibly explain the city-to-city variation in PM_{2.5} mortality risk estimates. From this analysis a strong seasonal pattern was observed with the greatest effects occurring in the spring and summer seasons (Figure 6-25).

Overall, the risk estimates for all-cause, cardiovascular, and respiratory deaths reported by Franklin et al. (2008, [097426](#)) are comparable to those presented in the 27 cities study (2007, [091257](#)), as shown in Figure 6-26. When comparing the 2007 and 2008 studies conducted by Franklin et al. (2007, [091257](#); 2008, [097426](#)), although only 15 cities overlap between the two studies and each study was designed differently (i.e., time-series vs. case-crossover), the magnitude of the PM_{2.5} risk estimates reported were similar for the same averaging time, and both studies reported a regional pattern (East > West) similar to that found in the NMMAPS studies previously discussed.

Zanobetti and Schwartz (2009, [188462](#)) conducted a multicity time-series study to examine associations between PM_{2.5} and mortality in 112 U.S. cities. The cities included in this analysis encompass the majority of cities included in the Franklin et al. (2007, [091257](#); 2008, [097426](#)) analyses. In this analysis a city represents a single county; however, 14 of the cities represent a composite of multiple counties. In addition to examining PM_{2.5}, the investigators also analyzed PM_{10-2.5}; these results are discussed in Section 6.5.2.3. Zanobetti and Schwartz (2009, [188462](#)) analyzed PM_{2.5} associations with all-cause, cardiovascular disease (CVD), MI, stroke, and respiratory mortality for the years 1999-2005. To be included in the analysis, each of the cities selected had to have at least 265 days of PM_{2.5} data per year and at least 300 days of mortality data per year. The authors conducted a city- and season-specific Poisson regression to estimate excess risk for PM_{2.5} lagged 0- and 1-days, adjusting for smooth functions (natural cubic splines) of days (1.5 df per season), the same-day and previous day temperature (3 df each), and day-of-week. The city specific estimates were then combined using a random effects model. Based on the assumption that climate affects PM exposures (e.g., ventilation and particle characteristics), the investigators combined city-specific estimates into six regions based on the Köppen climate classification scheme (e.g., “Mediterranean climates” for CA, OR, WA, etc.).

The overall combined excess risk estimates were: 0.98 % (95% CI: 0.75, 1.22) for all-cause; 0.85 % (95% CI: 0.46-1.24) for CVD, 1.18 % (95% CI: 0.48-1.89) for MI; 1.78 % (95% CI: 0.96-2.62) for stroke, and 1.68 % (95% CI: 1.04-2.33) for respiratory mortality for a 10 µg/m³ increase in PM_{2.5} at lag 0-1. When the risk estimates were combined by season, the spring estimates were the largest for all-cause and for all of the cause-specific mortality outcomes examined. For example, the risk estimate for all-cause mortality for the spring was 2.57% (95% CI: 1.96-3.19) with the estimates for the other seasons ranging from 0.25% to 0.95%. When examining cities that had both PM_{2.5} and PM_{10-2.5} data (i.e., 47 cities), the addition of PM_{10-2.5} in the model did not alter the PM_{2.5} estimates substantially, only decreasing slightly from 0.94% in a single pollutant model to 0.77% in a copollutant model with PM_{10-2.5}. When the risk estimates were combined by climatic regions, the estimated PM_{2.5} risk for all-cause mortality were similar (all above 1% per 10 µg/m³ increase) for all the regions except for the “Mediterranean” region (0.5%) which includes cities in CA, OR and WA, though the estimates in that region were significantly heterogeneous (Figure 6-24).



Source: Data from Zanobetti and Schwartz (2009, [188462](#)).

Figure 6-23. Percent increase in all-cause (nonaccidental) and cause-specific mortality per $10 \mu\text{g}/\text{m}^3$ increase in the average of 0- and 1-day lagged $\text{PM}_{2.5}$, combined by climatic regions.

The PM_{2.5} risk estimate for all-cause mortality reported by Zanobetti and Schwartz (2009, [188462](#)) for 112 cities (0.98% per 10 µg/m³ increase in the average of 0- and 1-day lags) is generally consistent with that reported by Franklin et al. (2007, [091257](#)) for 27 cities (0.82% [0.02-1.63]) and Franklin et al. (2008, [097426](#)) for 25 cities (0.74% [95% CI: 0.41-1.07]) using the same 0- and 1-day avg exposure time. The seasonal pattern (i.e., higher risk estimates in the spring) found in this study is also consistent with the result from Franklin et al. (2008, [097426](#)). Figure 6-23 highlights the risk estimates for all-cause, CVD, and respiratory mortality combined by region. The regional division based on climatic types used in this study makes it difficult to directly compare the regional pattern of results from previous studies. However, an examination of empirical Bayes-adjusted effect estimates for each of the cities included in the analysis further confirms the heterogeneity observed between some cities and regions of the country (Figure 6-24). It is noteworthy that, unlike NMMAPS, which focused on PM₁₀ and indicated larger risk estimates in the northeast, Zanobetti and Schwartz (2009, [188462](#)) found that the all-cause mortality risk estimates were fairly uniform across the climatic regions, except for the “Mediterranean” region.

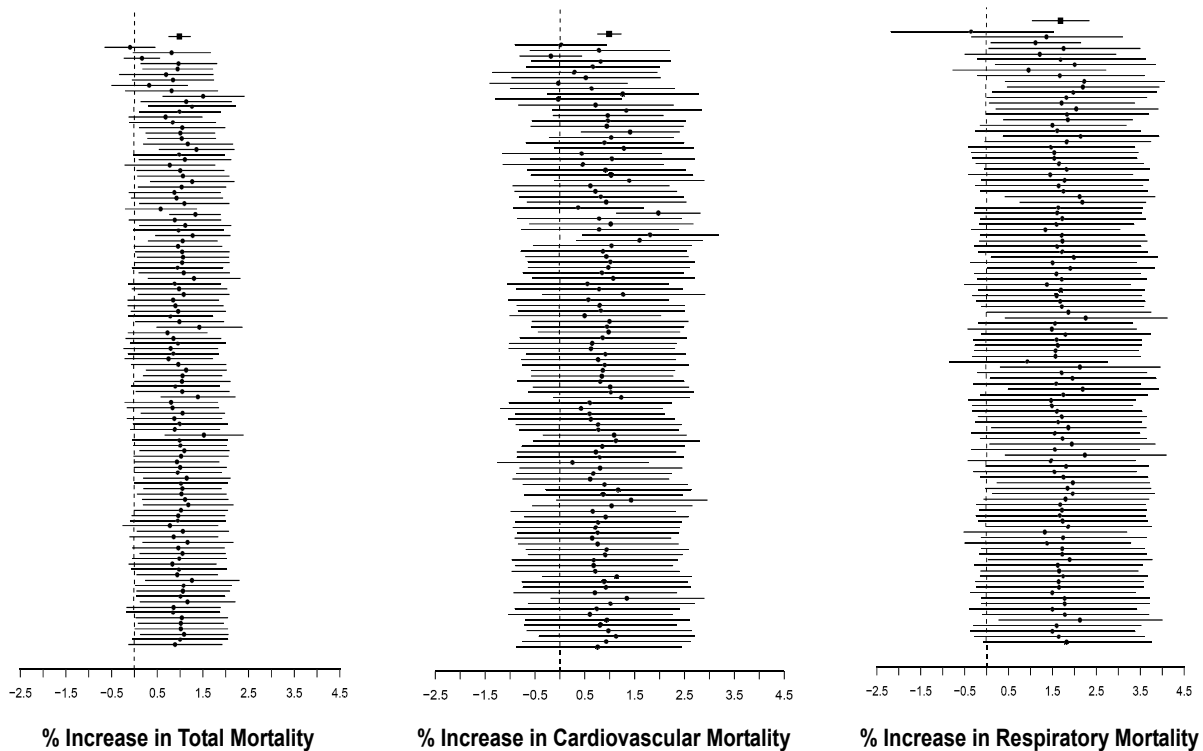


Figure 6-24. Empirical Bayes-adjusted city-specific percent increase in total (nonaccidental), cardiovascular, and respiratory mortality per 10 µg/m³ increase in the average of 0- and 1-day lagged PM_{2.5} by decreasing mean 24-h avg PM_{2.5} concentrations. Based on estimates calculated from Zanobetti and Schwartz (2009, [188462](#)) using the approach specified in Le Tertre et al. (2005, [087560](#)).

Key to Figure 6-24

City	Mean	98 th	City	Mean	98 th	City	Mean	98 th	City	Mean	98 th
Rubidoux, CA	24.7	68.0	Taylors, SC	15.0	32.2	Waukesha, WI	13.4	35.3	Phoenix, AZ	11.4	30.7
Bakersfield, CA	21.7	80.3	Toledo, OH	14.9	36.6	Baton Rouge, LA	13.4	30.1	Tacoma, WA	11.4	38.1
Los Angeles, CA	19.7	51.1	Anaheim, CA	14.9	44.1	Memphis, TN	13.3	32.4	Port Arthur, TX	11.1	25.7
Fresno, CA	18.7	64.9	New York, NY	14.7	38.1	Erie, PA	12.9	36.1	Cedar Rapids, IA	11.0	31.0
Atlanta, GA	17.6	38.2	Washington, PA	14.7	37.0	Dallas, TX	12.8	28.7	Dodge, WI	10.9	32.9
Steubenville, OH	17.1	41.4	Winston, NC	14.7	34.1	Houston, TX	12.8	27.5	Oklahoma, OK	10.8	26.1
Cincinnati, OH	17.1	39.9	Elizabeth, NJ	14.6	38.2	Chesapeake, VA	12.8	29.8	Des Moines, IA	10.5	27.9
Birmingham, AL	16.5	38.8	Philadelphia, PA	14.6	36.6	Wilkes-Barre, PA	12.8	32.5	Jacksonville, FL	10.5	25.3
Middletown, OH	16.5	38.4	St. Louis, MO	14.5	33.7	Norfolk, VA	12.7	29.6	Omaha, NE	10.5	28.0
Indianapolis, IN	16.4	38.2	Allentown, PA	14.4	38.9	Sacramento, CA	12.6	45.0	Denver, CO	10.5	26.4
Cleveland, OH	16.3	40.5	Richmond, VA	14.3	33.0	Springfield, MA	12.5	35.1	Pinellas, FL	10.4	23.1
Dayton, OH	16.3	38.3	Spartanburg, SC	14.2	31.4	New Orleans, LA	12.5	29.0	Austin, TX	10.4	24.5
Columbus, OH	16.2	38.3	Durham, NC	14.2	32.9	Ft. Worth, TX	12.4	27.7	Orlando, FL	10.3	24.3
Detroit, MI	16.2	41.0	Little Rock, AR	14.2	31.8	Pensacola, FL	12.3	31.2	Klamath, OR	10.2	40.7
Akron, OH	16.0	39.0	Easton, PA	14.2	39.7	Davenport, IA	12.3	32.1	Seattle, WA	10.1	27.9
Louisville, KY	15.9	38.0	Raleigh, NC	14.1	31.8	Avondale, LA	12.3	28.6	Medford, OR	10.0	37.3
Chicago, IL	15.8	39.1	Greensboro, NC	14.1	31.0	Boston, MA	12.3	30.2	Bath, NY	9.6	29.3
Pittsburgh, PA	15.7	43.1	Mercer, PA	14.1	36.4	Holland, MI	12.1	35.0	Provo, UT	9.5	38.5
Harrisburg, PA	15.6	40.2	Annandale, VA	14.0	34.6	Charleston, SC	12.1	27.9	Miami, FL	9.4	20.5
Baltimore, MD	15.6	38.8	Nashville, TN	13.9	31.0	Tampa, FL	12.1	25.8	El Paso, TX	9.0	24.4
Youngstown, OH	15.6	38.1	Dumbarton, VA	13.8	31.9	Tulsa, OK	12.1	32.3	Spokane, WA	8.9	30.6
Knoxville, TN	15.5	32.9	Columbia, SC	13.7	30.7	Kansas, MO	12.0	28.6	San Antonio, TX	8.9	21.9
Gary, IN	15.5	37.5	Milwaukee, WI	13.7	36.3	Scranton, PA	11.9	33.0	Portland, OR	8.9	25.4
Charlotte, NC	15.3	32.7	New Haven, CT	13.6	36.8	Hartford, CT	11.8	33.5	Davie, FL	8.4	19.1
Warren, OH	15.2	37.4	Grand Rapids, MI	13.6	36.4	Minneapolis, MN	11.6	31.6	Eugene, OR	8.1	29.9
Washington, DC	15.2	37.2	El Cajon, CA	13.5	34.9	Worcester, MA	11.5	30.2	Palm Beach, FL	7.8	18.4
Wilmington, DE	15.1	37.6	Gettysburg, PA	13.4	36.5	Salt Lake, UT	11.5	52.4	Bend, OR	7.7	23.5
Carlisle, PA	15.1	40.0	State College, PA	13.4	38.5	Providence, RI	11.5	30.5	Albuquerque, NM	6.6	17.9

Note: The top effect estimate in the figures represents the overall effect estimate for that mortality outcome across all cities. The remaining effect estimates are ordered by the highest (i.e., Rubidoux, CA) to lowest (i.e., Albuquerque, NM) mean 24-h PM_{2.5} concentrations across the cities examined. In the key the cities are reported in this order, which represents the policy relevant concentrations for the annual standard, but the policy relevant PM_{2.5} concentrations for the daily standard (i.e., 98th percentile of the 24-h average) are also listed for each city (from Zanobetti and Schwartz (2009, [188462](#))).

PM_{2.5}-Mortality Associations on a Regional Scale: California

Ostro et al. (2006, [087991](#)) examined associations between PM_{2.5} and daily mortality in nine heavily populated California counties (Contra Costa, Fresno, Kern, Los Angeles, Orange, Riverside, Sacramento, San Diego, and Santa Clara) using data from 1999 through 2002. The authors used a two-stage model to examine all-cause, respiratory, cardiovascular, ischemic heart disease, and diabetes mortality individually and by potential effect modifier (i.e., age, gender, race, ethnicity, and education level). The a priori exposure periods examined included the average of 0- and 1-day lags (lag 0-1) and the 2-day lag (lag 2). The authors selected these non-overlapping lags (i.e., rather than selecting lag 1 as the single-day lag) because previous studies have reported stronger associations at lags of 1 or 2 days or with cumulative exposure over three days. It is unclear why the investigators chose these non-overlapping lags (i.e., single-day lag of 2 instead of 1) even though they state they based the selection of their lag days on results presented in previous studies, which found the strongest association for PM lagged 1 or 2 days. Using the average of 0- and 1-day lags Ostro et al.

(2006, [087991](#)) reported combined estimates of: 0.6% (95% CI: 0.2-1.0), 0.6% (95% CI: 0.0-1.1), 0.3% (95% CI: -0.5 to 1.0), 2.2% (95% CI: 0.6-3.9), and 2.4% (95% CI: 0.6-4.2) for all-cause, cardiovascular, ischemic heart disease, respiratory, and diabetes deaths, respectively, per 10 $\mu\text{g}/\text{m}^3$. The authors also conducted a sensitivity analysis of risk estimates based on the extent of temporal adjustment, which showed monotonic reductions for all of the death categories examined when 4, 8, and 12 degrees of freedom per year were used.

Five of the nine counties examined in the Ostro et al. (2006, [087991](#)) analysis contain cities that are among the 27 cities examined in the Franklin et al. (2007, [091257](#)) analysis for the same period, 1999-2002. While the lags used were different between these two studies, both presented $\text{PM}_{2.5}$ risk estimates in individual cities or counties (graphically in the Franklin et al. study (2007, [091257](#)); in a table in the Ostro et al. study (2006, [087991](#))), which allowed for a cursory evaluation of consistency between the two analyses. In Franklin et al. (2007, [091257](#)), $\text{PM}_{2.5}$ risk estimates at lag 1 day for the cities Los Angeles and Riverside were slightly negative, whereas Fresno, Sacramento, and San Diego showed positive values above 1% per 10 $\mu\text{g}/\text{m}^3$ increase in $\text{PM}_{2.5}$. The 2-day lag result presented in Ostro et al. (2006, [087991](#)) is qualitatively consistent, with Los Angeles and Riverside, both of which show slightly negative estimates, while the other 3 locations all show positive, but somewhat smaller estimates, than those reported by Franklin et al. (2007, [091257](#)). The estimates for the average of 0- and 1-day lags for these five counties in Ostro et al. (2006, [087991](#)), which contain cities examined in Franklin et al. (2007, [091257](#)), were all positive. Thus, these two $\text{PM}_{2.5}$ studies showed some consistencies in risk estimates even though they used different lag periods and a different definition for the study areas of interest (i.e., counties vs. cities). The risk estimates for Franklin et al. (2007, [091257](#)) and Ostro et al. (2006, [087991](#)), stratified by various effect modifiers (e.g., gender, race, etc.), are summarized in Figure 6-25. Of note is the contrast in the results presented for the effect modification analysis for “in-hospital” versus “out-of-hospital” deaths for Ostro et al. (2006, [087991](#)), which differs from the results presented in the PM_{10} study conducted by Zeka et al. (2006, [088749](#)). Ostro et al. (2006, [087991](#)) observed comparable risk estimates for “in-hospital” vs. “out-of-hospital” deaths, whereas Zeka et al. (2006, [088749](#)) observed a large difference between the two in the 20 cities study discussed earlier. This difference in effects observed between the two studies is more than likely due to the compositional differences in PM_{10} in the cities examined in Zeka et al. (2006, [088749](#)) (i.e., PM_{10} more or less dominated by $\text{PM}_{2.5}$ and the subsequent composition of $\text{PM}_{2.5}$).

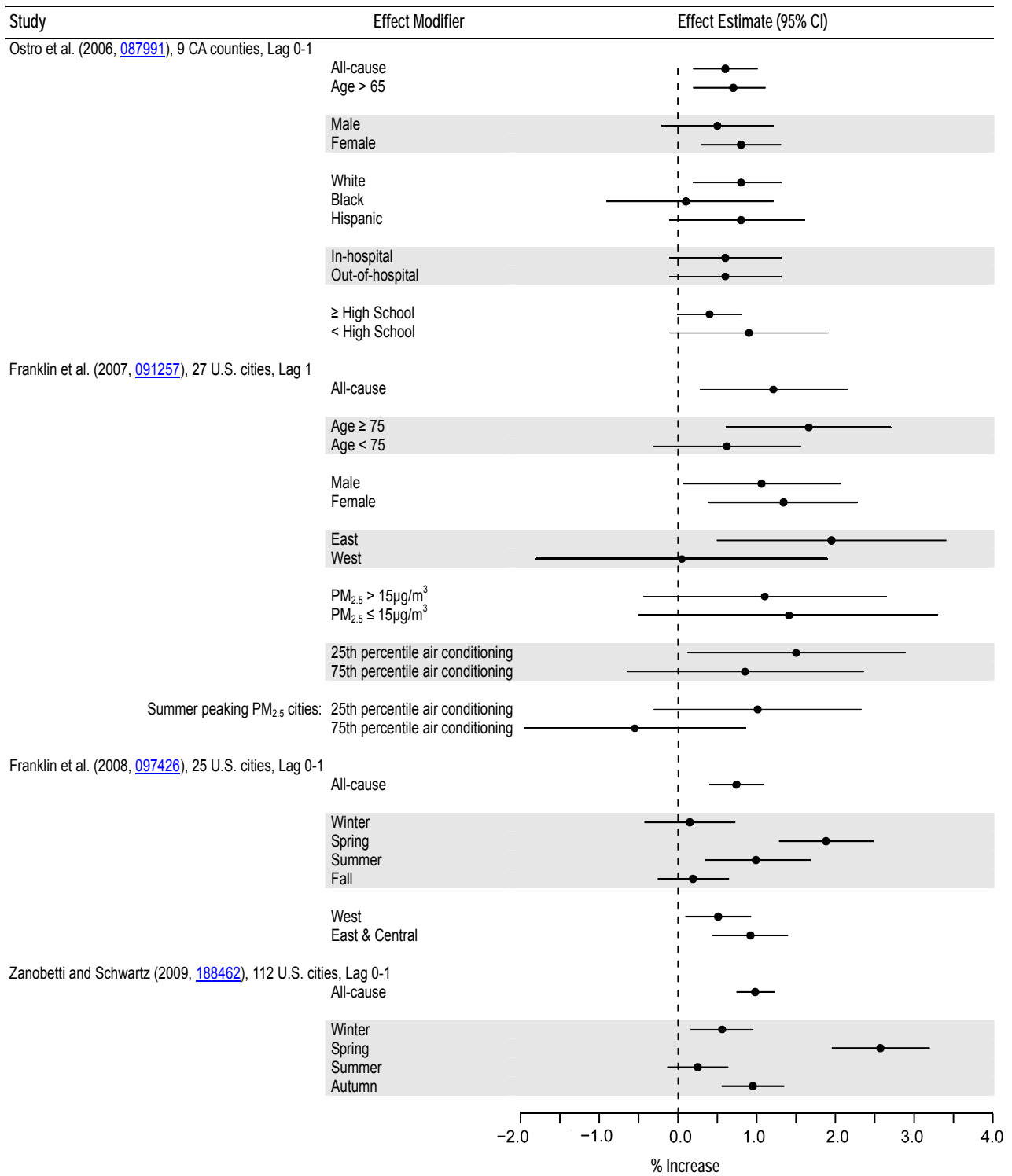


Figure 6-25. Summary of percent increase in all-cause (nonaccidental) mortality per 10 µg/m³ increase in PM_{2.5} by various effect modifiers.

PM_{2.5}-Mortality Associations in Canada

An analysis of multiple pollutants, including PM_{2.5}, in 12 Canadian cities found the most consistent associations for NO₂ (Burnett et al., 2004, [086247](#)). In this analysis, PM_{2.5} was only measured every 6th day in much of the study period, and the simultaneous inclusion of NO₂ and PM_{2.5} in a model on the days when PM_{2.5} data were available eliminated the PM_{2.5} association (from 0.60% to -0.10% per 10 µg/m³ increase in PM_{2.5}). However, the investigators noted that during the later study period of 1998-2000 when daily TEOM PM_{2.5} data were available for 11 of the 12 cities, a simultaneous inclusion of NO₂ and PM_{2.5} resulted in considerable reduction of the NO₂ risk estimate, while the PM_{2.5} risk estimate was only slightly reduced from 1.1% to 0.98% (95% CI: -0.16 to 2.14). Thus, the relative importance of NO₂ and PM_{2.5} on mortality effect estimates has not been resolved when using the Canadian data sets.

Summary of PM_{2.5} Risk Estimates

The risk estimates for all-cause mortality for all ages ranged from 0.29% Dominici et al. (2007, [097361](#)) to 1.21% Franklin et al. (2007, [091257](#)) per 10 µg/m³ increase in PM_{2.5} (Figure 6-26). An examination of cause-specific risk estimates found that PM_{2.5} risk estimates for cardiovascular deaths are similar to those for all-cause deaths (0.30-1.03%), while the effect estimates for respiratory deaths were consistently larger (1.01-2.2%), albeit with larger confidence intervals, than those for all-cause or cardiovascular deaths using the same lag/averaging indices. Figure 6-27 summarizes the PM_{2.5} risk estimates for all U.S.- and Canadian-based studies by cause-specific mortality.

An examination of lag structure observed results similar to those reported for PM₁₀ with most studies reporting either single day lags or two-day avg lags with the strongest effects observed on lag 1 or lag 0-1. In addition, seasonal patterns of PM_{2.5} risk estimates were found to be similar to those reported for PM₁₀, with the warmer season showing the strongest association. An evaluation of regional associations found that in most cases the eastern U.S. had the highest PM_{2.5} mortality risk estimates, but this was dependent on the geographic designations made in the study. When grouping cities by climatic regions, similar PM_{2.5} mortality risk estimates were observed across the country except in the Mediterranean region, which included CA, OR, and WA.

Of the studies evaluated, only Burnett et al. (2004, [086247](#)), a Canadian multicity study, analyzed gaseous pollutants and found mixed results, with possible confounding of PM_{2.5} risk estimates by NO₂. Although the recently evaluated U.S.-based multicity studies did not analyze potential confounding of PM_{2.5} risk estimates by gaseous pollutants, evidence from single-city studies evaluated in the 2004 PM AQCD (U.S. EPA, 2004, [056905](#)) suggest that gaseous copollutants do not confound the PM_{2.5}-mortality association, which is further supported by studies that examined the PM₁₀-mortality relationship.

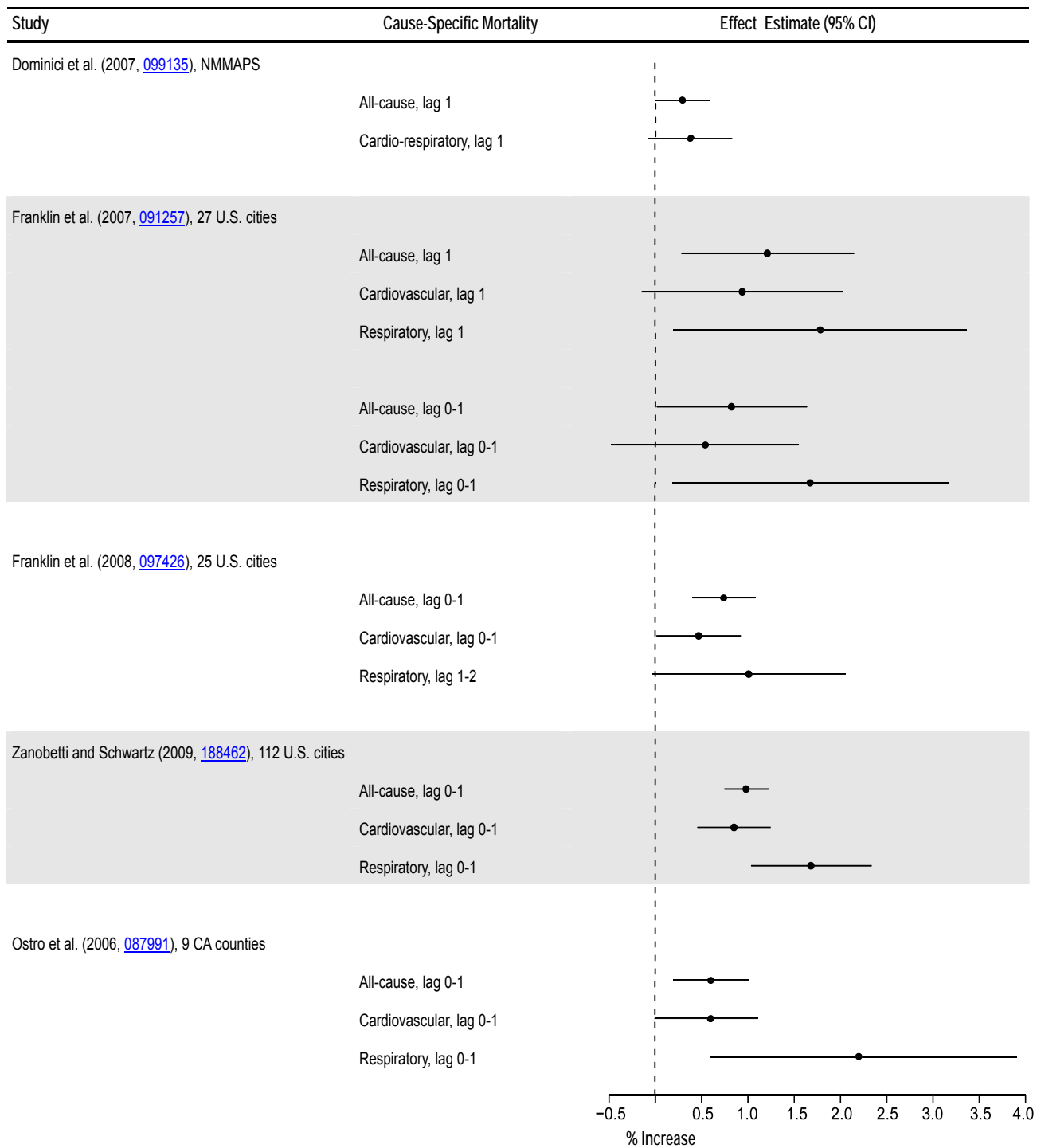


Figure 6-26. Summary of percent increase in all-cause (nonaccidental) and cause-specific mortality per 10 $\mu\text{g}/\text{m}^3$ increase in $\text{PM}_{2.5}$ from recent multicity studies.

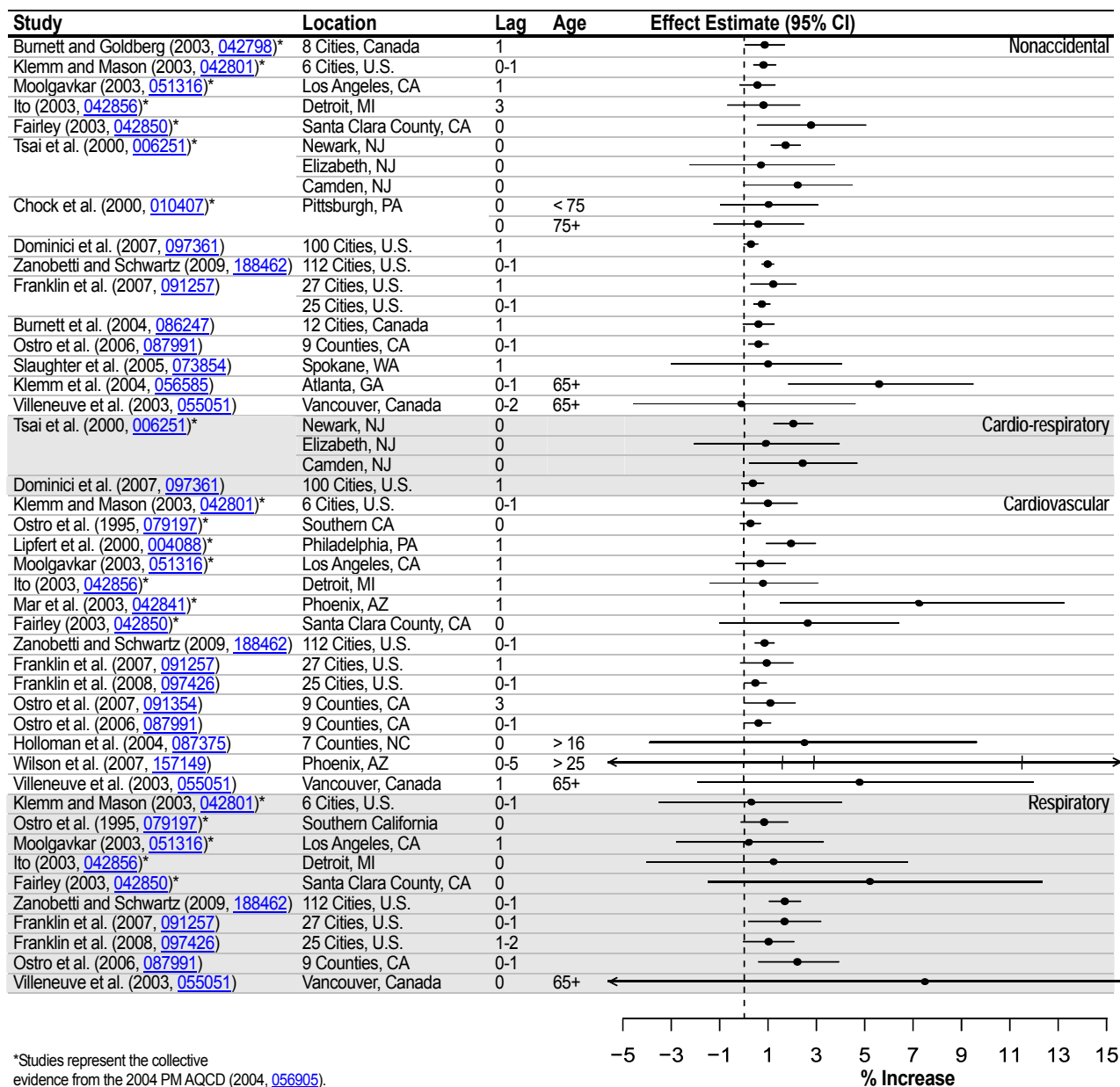


Figure 6-27. Summary of percent increase in all-cause (nonaccidental) and cause-specific mortality per 10 µg/m³ increase in PM_{2.5} for all U.S.- and Canadian-based studies. The three vertical lines for the Wilson et al. (2007, [157149](#)) estimate represent the central, middle, and outer Phoenix estimates.

6.5.2.3. Thoracic Coarse Particles (PM_{10-2.5})

In the 2004 PM AQCD (U.S. EPA, 2004, [056905](#)), a limited number of studies, mostly single-city analyses, were evaluated that examined thoracic coarse (PM_{10-2.5}) PM for its association with mortality. Of these studies a small number examined both PM_{2.5} and PM_{10-2.5} effects, and found some evidence for PM_{10-2.5} effects of the same magnitude as PM_{2.5}. However, multiple limitations in these studies were identified including measurement and exposure issues for PM_{10-2.5} and the correlation between PM_{2.5} and PM_{10-2.5}. These limitations increased the uncertainty surrounding the concentrations at which PM_{10-2.5}-mortality associations are observed.

A thorough analysis of PM_{10-2.5} mortality associations requires information on the speciation of PM_{10-2.5}. This is because, while a large percent of the composition of coarse particles may consist of crustal materials by mass, depending on available sources, the surface chemical characteristics of PM_{10-2.5} may also vary from city to city. Thus, without information on the chemical speciation of PM_{10-2.5}, the apparent variability in observed associations between PM_{10-2.5} and mortality across cities is difficult to characterize. Although this type of information is not available in the current literature, the relative importance of the associations observed between PM_{10-2.5} and mortality in the following studies is of interest.

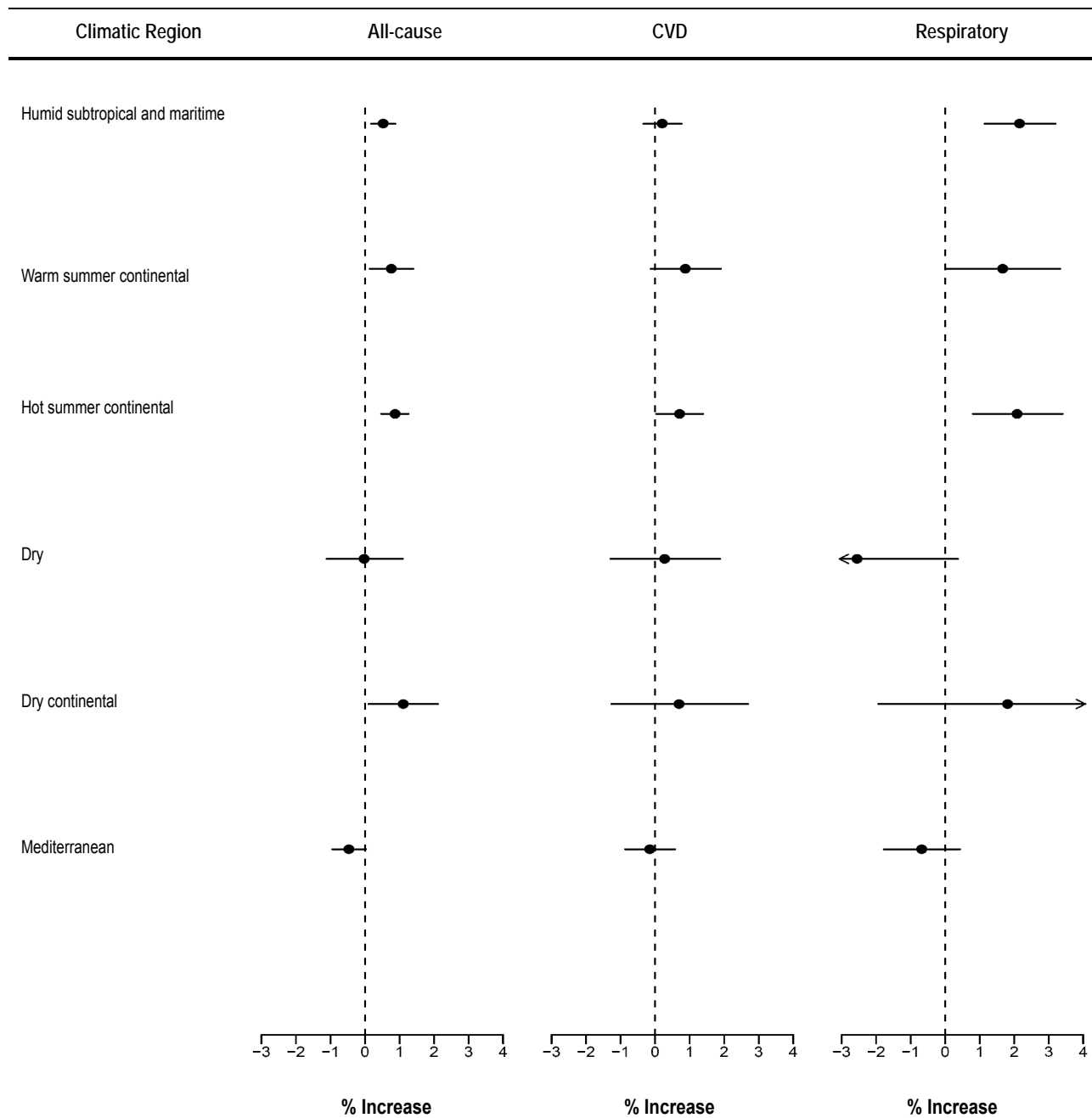
PM_{10-2.5} Concentrations Estimated Using the Difference Method

The Zanobetti and Schwartz (2009, [188462](#)) multicity analysis, described for PM_{2.5} section (Section 6.5.2.2), also examined the association between computed PM_{10-2.5} and all-causes, cardiovascular disease (CVD), MI, stroke, and respiratory mortality for the years 1999-2005. Of the 112 cities included in the PM_{2.5} analysis only 47 cities had both PM_{2.5} and PM₁₀ data available. PM_{10-2.5} was estimated in these cities by differencing the countywide averages of PM₁₀ and PM_{2.5}. In addition to examining the association between PM_{10-2.5} and mortality for the average of lags 0 and 1 day, the investigators also considered a distributed lag of 0-3 days. The risk estimates for PM_{10-2.5} were presented for both a single pollutant model and a copollutant model with PM_{2.5}, and were also combined by season and climatic regions as was done in the PM_{2.5} analysis.

The study found a significant association between the computed PM_{10-2.5} and all-cause, CVD, stroke, and respiratory mortality. The combined estimate for the 47 cities using the average of 0- and 1-day lag PM_{10-2.5} for all-cause mortality was 0.46% (95% CI: 0.21-0.71) per 10 µg/m³ increase. The estimate obtained using the distributed lag model was smaller (0.31% [95% CI: 0.00-0.63]). The seasonal analysis showed larger risk estimates in the spring for all-cause (1.01%) and respiratory mortality (2.56%) (i.e., the same pattern observed in the PM_{2.5} analysis); however, for CVD mortality, the estimates for spring (0.95%) and summer (1.00%) were comparable. When the risk estimates were combined by climatic region (Figure 6-28), for all-cause mortality, the “dry, continental” region (which included Salt Lake City, Provo, and Denver, all of which had relatively high estimated PM_{10-2.5} concentrations) showed the largest risk estimate (1.11% [95% CI: 0.11-2.11]), but the “dry” region (which included Phoenix and Albuquerque, the two cities with high PM_{10-2.5} concentrations) and the “Mediterranean” region (which included cities in CA, OR, and WA) did not show positive associations. The other three regions (i.e., “hot summer, continental,” “warm summer, continental,” and “humid, subtropical and maritime”), which included cities that correspond to the mid-west, southeast, and northeast geographic regions as defined in previous NMMAPS analyses, all showed significantly positive associations. Similar regional patterns of associations were found for CVD and respiratory mortality, which are further confirmed when examining the empirical Bayes-adjusted city-specific estimates in Figure 6-29. The regional pattern of associations for MI and stroke are less clear, because of the wider confidence intervals due to the smaller number of deaths in these specific categories. The lack of a PM_{10-2.5}-mortality association in the “dry” region reported in this study is in contrast to the results from three studies that analyzed Phoenix data and found associations, as reviewed in the 2004 PM AQCD (U.S. EPA, 2004, [056905](#)), and Wilson et al. (2007, [157149](#)) (discussed below).

Although the results from this analysis are informative because it is the first multicity U.S.-based study that examined the association between short-term exposure to PM_{10-2.5} and mortality on a large scale, some limitations do exist. Specifically, it is not clear how the computed PM_{10-2.5} measurements used by Zanobetti and Schwartz (2009, [188462](#)) compare with the PM_{10-2.5} concentrations obtained by directly measuring PM_{10-2.5} using a dichotomous sampler, or the PM_{10-2.5} concentrations computed using the difference of PM₁₀ and PM_{2.5} measured at co-located samplers.

Additional studies evaluated the association between short-term exposure to PM_{10-2.5} and mortality using PM_{10-2.5} concentrations estimated by subtracting PM₁₀ from PM_{2.5} concentrations at co-located monitors. Although PM_{10-2.5} concentrations estimated using this approach are not ideal, the results from these studies are informative in evaluating the PM_{10-2.5} mortality association.



Source: Data from Zanobetti and Schwartz (2009, [188462](#)).

Figure 6-28. Percent increase in all-cause (nonaccidental) and cause-specific mortality per $10 \mu\text{g}/\text{m}^3$ increase in the average of 0- and 1-day lagged $\text{PM}_{10-2.5}$, combined by climatic regions.

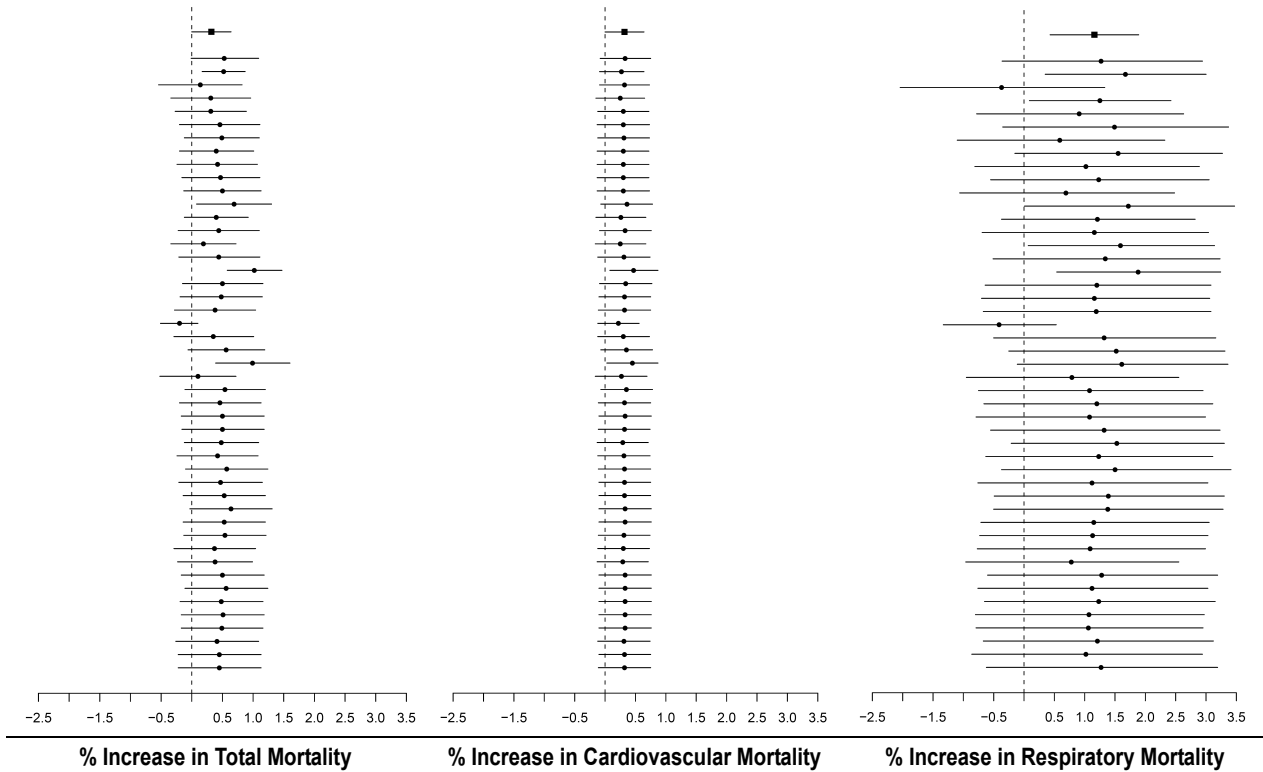


Figure 6-29. Empirical Bayes-adjusted city-specific percent increase in total (nonaccidental), cardiovascular, and respiratory mortality per $10 \mu\text{g}/\text{m}^3$ increase in the average of 0- and 1-day lagged $\text{PM}_{10-2.5}$ by decreasing 98th percentile of mean 24-h avg $\text{PM}_{10-2.5}$ concentrations. Based on estimates calculated from Zanobetti and Schwartz (2009, [188462](#)) using the approach specified in Le Tertre et al. (2005, [087560](#)).

Key for Figure 6-29

City	98th	Mean	City	98th	Mean	City	98th	Mean	City	98th	Mean
El Paso, TX	105.1	25.4	Cleveland, OH	51.2	15.2	Sacramento, CA	31.5	10.2	Louisville, KY	23.3	8.3
St. Louis, MO	81.9	15.2	Davenport, IA	49.9	15.3	Tampa, FL	29.1	12.9	Wilkes-Barre, PA	22.2	6.2
Phoenix, AZ	80.1	33.3	Birmingham, AL	49.6	14.2	Toledo, OH	28.8	7.6	New York, NY	22.0	6.4
Detroit, MI	77.5	17.3	Provo, UT	49.3	18.2	Washington, PA	27.8	6.5	Wilmington, DE	21.8	7.0
Gary, IN	71.3	6.9	Chicago, IL	46.1	12.4	Allentown, PA	27.8	4.5	Raleigh, NC	20.9	6.9
Omaha, NE	65.6	24.7	Easton, PA	43.9	12.0	Atlanta, GA	27.4	8.6	Scranton, PA	19.2	6.1
Albuquerque, NM	64.3	22.9	Steubenville, OH	43.5	12.1	Davie, FL	25.5	9.4	Harrisburg, PA	18.6	5.4
New Haven, CT	58.4	11.9	Columbia, SC	42.9	8.4	Taylors, SC	25.4	8.0	Akron, OH	17.7	5.3
Bakersfield, CA	55.9	16.1	Los Angeles, CA	42.5	13.5	Memphis, TN	24.3	9.3	Charleston, SC	17.6	6.6
Des Moines, IA	55.0	16.2	Spokane, WA	41.8	13.8	Seattle, WA	23.7	9.0	Winston, NC	16.5	7.4
Denver, CO	53.8	18.1	Columbus, OH	40.0	11.2	Baltimore, MD	23.5	8.9	Erie, PA	14.9	3.1
Salt Lake, UT	52.6	19.2	Pittsburgh, PA	32.0	9.4	Cincinnati, OH	23.3	7.8			

Note: The top effect estimate in the figures represents the overall effect estimate for that mortality outcome across all cities. The remaining effect estimates are ordered by the highest (i.e., El Paso, TX) to lowest (i.e., Erie, PA) 98th percentile of the mean 24-h $PM_{10-2.5}$ concentrations across the cities examined, which is the policy relevant concentration for the daily standard [from Zanobetti and Schwartz (2009, 188462)].

Slaughter et al. (2005, [073854](#)) examined the association of various PM size fractions (PM_1 , $PM_{2.5}$, PM_{10} , $PM_{10-2.5}$) and CO with ED visits, HAs, and mortality in Spokane, WA for the period 1995-2001. Although the authors did not report mortality risk estimates for $PM_{10-2.5}$, they did not find an association between any PM size fraction (or CO) and mortality or cardiac HAs at lags of 0-3 days.

Wilson et al. (2007, [157149](#)) examined the association between size-fractionated PM ($PM_{2.5}$ and $PM_{10-2.5}$) and cardiovascular mortality in Phoenix for the study period 1995-1997, using mortality data aggregated for three geographic regions: “Central Phoenix,” “Middle Ring,” and “Outer Phoenix,” which were constructed as a composite of zip codes of residence in order to compare population size among the three areas. The authors reported apparently different patterns of associations between $PM_{2.5}$ and $PM_{10-2.5}$ in terms of the size of the risk estimate across the three areas and temporal patterns of associations. In the “Middle Ring” where $PM_{10-2.5}$ showed the strongest association, the estimated risk per $10 \mu\text{g}/\text{m}^3$ increase for a 1 day lag was 3.4% (95% CI: 1.0-5.8). The estimated risk for $PM_{2.5}$ found for “Central Phoenix” was 6.6% (95% CI: 1.1-12.5) for lag 1. The authors speculated that the apparent difference in estimated risks across the areas might be due to the lower SES in “Central Phoenix” or the lower exposure error, but the relatively wide confidence bands of these estimates make it difficult to establish such relationships (Section 8.1.7 for a detailed discussion on SES and susceptibility to PM exposure).

Kettunen et al. (2007, [091242](#)) analyzed UFPs, $PM_{2.5}$, PM_{10} , $PM_{10-2.5}$, and gaseous pollutants for their associations with stroke mortality in Helsinki during the study period of 1998-2004. The authors did not observe an association between air pollution and mortality for the whole year or cold season, but they did find associations for $PM_{2.5}$ (13.3% [95% CI: 2.3-25.5] per $10 \mu\text{g}/\text{m}^3$), PM_{10} , and CO during the warm season, most strongly at lag 1 day. An association was also observed for $PM_{10-2.5}$ during the warm season (7.8% [95% CI: -7.4 to 25.5] per $10 \mu\text{g}/\text{m}^3$ at lag 1 day); however, it was weaker than $PM_{2.5}$.

The Perez et al. (2008, [156020](#)) analysis tested the hypothesis that outbreaks of Saharan dust exacerbate the effects of $PM_{2.5}$ and $PM_{10-2.5}$ on daily mortality. Changes of effects between Saharan and non-Saharan dust days were assessed using a time-stratified case-crossover design involving 24,850 deaths between March 2003 and December 2004 in Barcelona, Spain. Saharan dust days were identified from back-trajectory and satellite images. Chemical speciation, but not an analysis for microbes or fungi, was conducted approximately once a week during the study period. On Saharan dust days, mean concentrations were 1.2 times higher for $PM_{2.5}$ ($29.9 \mu\text{g}/\text{m}^3$) and 1.1 times higher for $PM_{10-2.5}$ ($16.4 \mu\text{g}/\text{m}^3$) than on non-Saharan dust days. During Saharan dust days (90 days out of 602), the $PM_{10-2.5}$ risk estimate was 8.4% (95% CI: 1.5-15.8) per $10 \mu\text{g}/\text{m}^3$ increase at lag 1 day, compared with 1.4% (95% CI: -0.8 to 3.4) during non-Saharan dust days. In contrast, there was not an additional increased risk of daily mortality for $PM_{2.5}$ during Saharan dust days (5.0%

[95% CI: 0.5-9.7]) compared with non-Saharan dust days (3.5% [95% CI: 1.6-5.5]). However, differences in chemical composition (i.e., PM_{2.5} was primarily composed of nonmineral carbon and secondary aerosols; whereas PM_{10-2.5} was dominated by crustal elements) did not explain these observations. Note also when examining all days combined, both size fractions were associated with mortality, but the PM_{2.5} association was found to be stronger.

PM_{10-2.5} Concentrations Directly Measured

In Burnett et al. (2004, [086247](#)), which analyzed the association of multiple pollutants with mortality in 12 Canadian cities, described previously; the authors also examined PM_{10-2.5}. In this study the authors collected PM_{10-2.5} using dichotomous samplers with an every-6th-day schedule. When both NO₂ and PM_{10-2.5} were included in the regression model, the PM_{10-2.5} effect estimate was reduced from 0.65% (95% CI: -0.10 to 1.4) to 0.31% (95% CI: -0.49 to 1.1) per 10 µg/m³ increase in 1-day lag PM_{10-2.5}. These risk estimates are similar to those reported for PM_{2.5}, which were also reduced upon the inclusion of NO₂ in the two-pollutant model, but to a greater extent, from 0.60% (95% CI: -0.03 to 1.2) to -0.1% (95% CI: -0.86 to 0.67).

Villeneuve et al. (2003, [055051](#)) analyzed the association between PM_{2.5}, PM_{10-2.5}, TSP, PM₁₀, SO₄²⁻, and gaseous copollutants in Vancouver, Canada, using a cohort of approximately 550,000 whose vital status was ascertained between 1986 and 1999. In this study PM_{2.5} and PM_{10-2.5} were directly measured using dichotomous samplers. The authors examined the association of each air pollutant with all-cause, cardiovascular, and respiratory mortality, but only observed significant results for cardiovascular mortality at lag 0 for both PM_{10-2.5} and PM_{2.5}. They found that PM_{10-2.5} (5.4% [95% CI: 1.1-9.8] per 10 µg/m³), was more strongly associated with cardiovascular mortality than PM_{2.5} (4.8% [95% CI: -1.9 to 12.0] per 10 µg/m³).

Klemm et al. (2004, [056585](#)) analyzed various components of PM and gaseous pollutants for their associations with mortality in Fulton and DeKalb Counties, Georgia for the 2-yr period, 1998-2000. PM_{10-2.5} concentrations were obtained from the ARIES database, which directly measured PM_{10-2.5} using dichotomous samplers. In this analysis the authors adjusted for temporal trend using quarterly, monthly, and biweekly knots, and reported estimates for all-cause, circulatory, respiratory, cancer, and other causes mortality for each scenario. Overall, PM_{2.5} was, more strongly associated with mortality than PM_{10-2.5}. For example, using the average of 0- and 1-day lags, the risk estimates for PM_{2.5} and PM_{10-2.5} in the monthly knots model for all-cause mortality, ages ≥ 65 yr were 5.6% (95% CI: 1.9-9.5) and 6.4% (95% CI: -0.5 to 14.1) per 10 µg/m³ increase, respectively.¹

Summary of PM_{10-2.5} Risk Estimates

The results from newly available studies that examined the association between short-term exposure to PM_{10-2.5} primarily consisted of single-city studies. Collectively these studies found consistent, positive associations, with the precision of each association varying by study location. The evidence from those single-city studies conducted in the U.S. and Canada in combination with the multicity studies evaluated (i.e., in the U.S. and Canada), provide evidence for PM_{10-2.5} effects. However, the various methods used to estimate exposure to PM_{10-2.5} (e.g., direct measurement of PM_{10-2.5} using dichotomous samplers, calculating the difference between PM₁₀ and PM_{2.5} concentrations) in the studies evaluated add uncertainty to the associations observed. Specifically, a new U.S. multicity study (Zanobetti and Schwartz, 2009, [188462](#)) estimated PM_{10-2.5} by calculating the difference between the county-average PM₁₀ and PM_{2.5} concentrations. Although there are limitations in the method used by Zanobetti and Schwartz (2009, [188462](#)) associations between PM_{10-2.5} and mortality were observed throughout multiple regions of the country. However, some of the findings of this new multicity study (e.g., no associations in “dry” region where PM_{10-2.5} levels are high) are not consistent with the findings of the PM_{10-2.5} studies evaluated in the 2004 PM AQCD (U.S. EPA, 2004, [056905](#)), and suggest that the coarse fraction is associated with mortality in areas of the U.S. where PM_{10-2.5} levels are not high. Limitations also exist in the PM_{10-2.5} associations reported due to the small number of PM_{10-2.5} studies that have investigated confounding by gaseous

¹ The monthly knot model was selected for comparison because, overall, PM_{2.5} showed the strongest association with all-cause mortality among the 15 air pollution indices examined when using this model.

copollutants or the influence of model specification on PM_{10-2.5} risk estimates. Additionally, more data is needed to characterize the chemical and biological components that may modify the potential toxicity of PM_{10-2.5}. Figure 6-30 summarizes the PM_{10-2.5} risk estimates for all U.S.-, Canadian-, and international-based studies by cause-specific mortality.

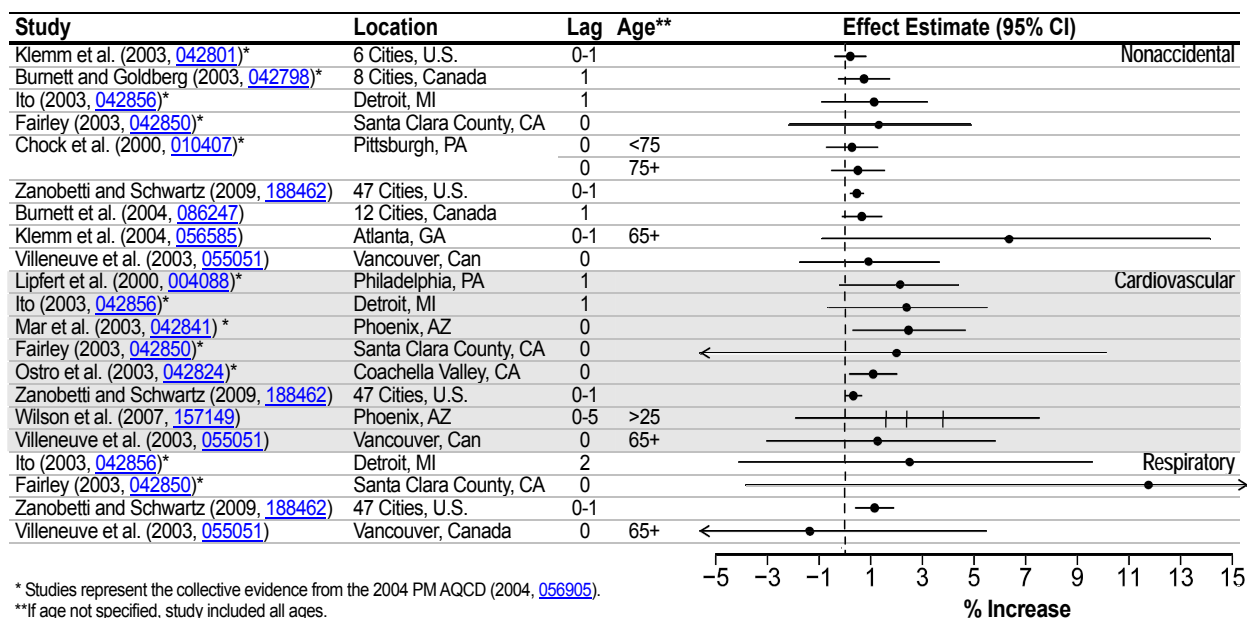


Figure 6-30. Summary of percent increase in total (nonaccidental) and cause-specific mortality per 10 µg/m³ increase in PM_{10-2.5} for all U.S., Canadian, and international-based studies. The three vertical lines for the Wilson et al. (2007, [157149](#)) estimate represent the central, middle, and outer Phoenix estimates.

6.5.2.4. Ultrafine Particles

The 2004 PM AQCD (U.S. EPA, 2004, [056905](#)) reviewed Wichmann et al.'s (reanalyzed by Stölzel et al., 2003, [042842](#); 2000, [013912](#)) study of fine and ultrafine particles (UFPs) (diameter: 0.01-0.1 µm) in Erfurt, Germany, for the study period 1995-1998. Stölzel et al. (2007, [091374](#)) extended the study period to include the years 1995-2001 and updated the analysis. Number concentrations (NC) for four size ranges of UFPs (0.01-0.1, 0.01-0.03, 0.03-0.05, and 0.05-0.1 µm) as well as mass concentration (MC) for three size ranges (0.01-2.5, 0.1-0.5, and 10 µm) were analyzed. The authors found associations with UFP NC and all-cause as well as cardio-respiratory mortality, each for a 4 day lag. The risk estimates associated with a 9,748/cm³ increase in UFP NC was 2.9% (95% CI: 0.3-5.5) for all-cause mortality and 3.1% (95% CI: 0.3-6.0) for cardio-respiratory mortality. The UFP-mortality association, and the lag structure of association, is consistent with the results from their earlier analysis, but the PM_{2.5} association found in the previous study was not observed in the updated analysis. Both UFP and PM_{2.5} concentrations were higher during the cold season in this locale.

Breitner et al. (2009, [188439](#)) analyzed UFP data from Erfurt, Germany, over a 10.5-yr period (October 1991-March 2002) after the German unification, when air quality improved. In this analysis associations between all-cause mortality and UFPs and PM_{2.5} were analyzed from September 1995 to March 2002, while PM₁₀, NO₂ and CO was analyzed for the whole study duration. The exposure time window / averages used in this study were different from those used by Stölzel (2003, [042842](#)) and Stölzel et al. (2007, [091374](#)). Breitner et al. (2009, [188439](#)) investigated the cumulative effect of air pollution on mortality at lags 0-5 and 0-14, using (a) a semiparametric Poisson regression model; and (b) a third degree polynomial distributed lag (PDL) model. The authors estimated the mortality risk for the entire study period as well as specific time periods to examine the effect of declining air pollution levels on the air pollution-mortality association. Of the air pollutants examined, UFPs were

found to be most consistently associated with mortality. NO₂ and CO were also found to be significantly associated with mortality using the 15-day PDL and 15-day avg models, respectively. PM_{2.5} and PM₁₀ also showed positive, but much weaker associations with mortality. In this data set, UFPs were only moderately correlated with PM_{2.5} (r = 0.48) and PM₁₀ (r = 0.57). Of the pollutants examined, NO₂ showed the strongest (but overall a moderate) correlation with UFPs (r = 0.62). When the risk estimates were compared between the two latter time periods of the study (September 1995-February 1998; and March 1998-March 2002), the estimates obtained using the 6-day avg for these pollutants generally declined. For example, the all-cause mortality risk estimates associated with a 8,439/cm³ increase in UFP NC was 5.5% (95% CI: 1.1-10.5) for the earlier period and -1.1% (95% CI: -6.8 to 4.9) for the later period. However, such patterns were less clear when using 15-day avg pollutant concentrations. In summary, UFPs appear to be the pollutant most consistently associated with mortality in Erfurt, Germany, but combined with the results for NO₂ and CO, these associations may implicate the role of local combustion sources on the mortality association observed.

Kettunen et al.'s (2007, [091242](#)) study in Helsinki also examined the relationship between UFPs and stroke mortality. As described earlier, PM_{2.5}, PM₁₀, and CO was associated with stroke mortality only during the warm season. The association with UFPs was borderline non-significant (8.5% [95% CI: -1.2 to 19.1] per 4,979/cm³ increase in UFPs at lag 1 day), but its lag structure of association and the magnitude of the effect estimate per interquartile-range are similar to those for PM_{2.5}. Note that the UFP NC levels in Helsinki (median equals 8,986/cm³ during the cold season and 7,587/cm³ during the warm season) are lower than those in Erfurt (mean = 13,549/cm³), but clearly higher in the cold season.

Summary of UFP Risk Estimates

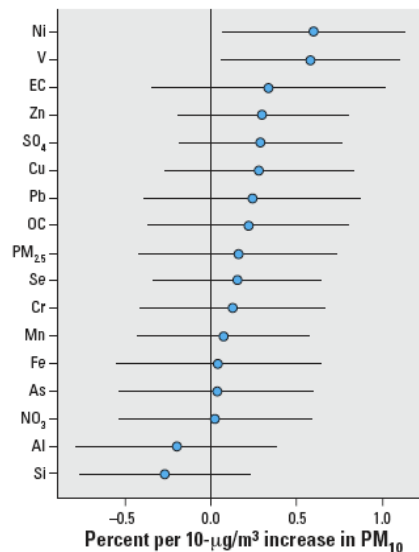
Only a few new studies, all of them conducted in Europe, examined and reported associations between UFPs and mortality. In Erfurt, UFPs showed the strongest associations with mortality among all of the PM indices, but its lag structure of association is either unique with the strongest association at lag 4 days in Stölzel et al. (2007, [091374](#)), not consistent with the lag structure of associations found in other mortality studies, or the time-windows examined are longer (0-5 and 0-14 days) ((Breitner et al., 2009, [188439](#)), making it difficult to compare whether the associations observed are consistent with those reported in other studies. In Helsinki, the association between UFPs and stroke mortality was weaker than that for PM_{2.5}, but its lag structure of association was similar to that for PM_{2.5} (strongest at lag 1 day). However, Kettunen et al. (2007, [091242](#)) only examined lags 0-3 days. Overall, the results of these studies should be viewed with caution because UFPs were consistently found to be correlated with gaseous pollutants derived from local combustion sources, and one or more of the gaseous pollutants were also found to be associated with mortality. Clearly, more research is needed to further investigate the role of UFPs on PM-mortality associations.

6.5.2.5. Chemical Components of PM

A few recent studies have examined the association between mortality and components of PM_{2.5}. This endeavor has been undertaken by some investigators through the use of the newly available PM_{2.5} chemical speciation network data. The PM_{2.5} chemical speciation network consists of more than 250 monitors that have been collecting over 40 chemical species since 2000; however, most sites started collecting data in 2001. One caveat to the new network is that because the sampling frequencies of the monitors are either every third day or every sixth day, there have not been, generally, a sufficient number of days to examine associations with mortality in single cities. To circumvent this issue, some investigators (Bell et al., 2009, [191997](#); Dominici et al., 2007, [099135](#); Franklin et al., 2008, [097426](#); Lippmann et al., 2006, [091165](#)) have used the PM_{2.5} chemical species data in a second stage regression to explain the heterogeneity in PM₁₀ or PM_{2.5} mortality risk estimates across cities. However, it should be noted these studies assume that the relative contributions of PM_{2.5} have remained the same over time. There have also been some studies that directly analyzed speciated PM_{2.5} data (e.g., Klemm et al., 2004, [056585](#); Ostro et al., 2007, [091354](#)).

Explaining the Heterogeneity of PM₁₀ Risk Estimates Using PM_{2.5} Chemical Speciation Data

Lippmann et al. (2006, [091165](#)), in addition to their primary analysis¹, investigated the consistency of the associations between specific elements and health outcomes by examining the heterogeneity of published 1-day lagged NMMAPS PM₁₀ mortality risk estimates for 1987-1994 across cities as a function of the average PM_{2.5} chemical components across cities. They matched PM_{2.5} chemical species in 60 out of 90 cities. Lippmann et al. (2006, [091165](#)) noted that the concentrations of the 16 chemical species examined averaged over the years 2000-2003 were highly skewed across cities. They therefore regressed PM₁₀ risk estimates on each of the PM_{2.5} components, raw and log-transformed, with weights based on the standard error of the PM₁₀ risk estimates. The log-transformed values yielded better predictive power, and the authors subsequently presented the results with log-transformed values. As shown in Figure 6-31, the 16 PM_{2.5} species showed varying extent of predictive power in explaining the PM₁₀ risk estimates across 60 cities, with Ni and V being the best predictors.



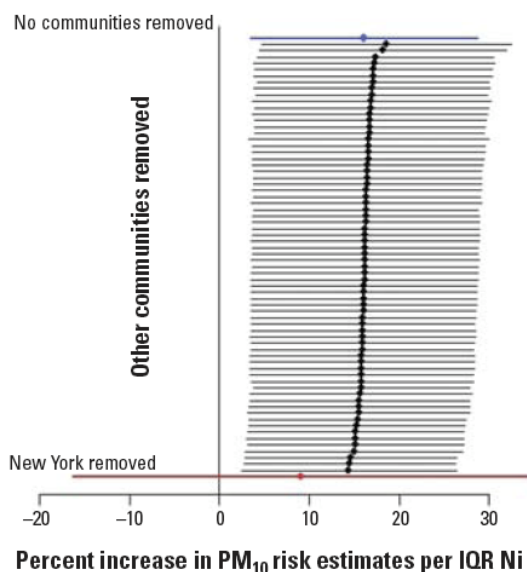
Source: Lippmann et al. (2006, [091165](#))

Figure 6-31. Percent increase in PM₁₀ risk estimates (point estimates and 95% CIs) associated with a 5th-95th percentile increase in PM_{2.5} and PM_{2.5} chemical components. The PM_{2.5} chemical components were log-transformed in the regression. The PM₁₀ risk estimates were for 60 NMMAP cities for 1987-1994.

Dominici et al. (2007, [099135](#)) examined the influence of Ni and V on the updated NMMAPS PM₁₀ mortality risk estimates for 1987-2000, using 72 counties in which Ni and V data were collected. A Bayesian hierarchical model was used to estimate the role of Ni and V on the heterogeneity of PM₁₀ risk estimates. While they found both Ni and V to be significant predictors of variation in PM₁₀ mortality risk estimates across cities, they also noted that this result was sensitive to the inclusion of the New York City data. Lippmann et al. (2006, [091165](#)) and Dominici et al. (2007, [099135](#)) both reported that the Ni levels in New York City are particularly high (~10 times the national average). Figure 6-32 shows the result of the sensitivity analysis for Ni. Note that the Ni in this result was not log-transformed, as clearly reflected in the change in the width of confidence bands when the New York data were removed (i.e., a skewed distribution produces narrow bands).

¹ The main focus of the study was to examine the role of PM_{2.5} chemical components in a mouse model of atherosclerosis (ApoE^{-/-}) exposed to concentrated fine PM (CAPs) in Tuxedo, NY.

Dominici et al. (2007, [099135](#)) further noted that they reached “the same conclusion” when log-transformed data were used in the analysis, but the results were not presented.



Source: Reprinted with Permission of Oxford University Press from Dominici et al. (2007, [099135](#))

Figure 6-32. Sensitivity of the percent increase in PM₁₀ risk estimates (point estimates and 95% CIs) associated with an interquartile increase in Ni. The Ni concentration was not log-transformed in this regression model. The PM₁₀ risk estimates were for 72 NMMAP cities for 1987-2000. The top estimate is achieved by including data for all the 69 communities. The other estimates are calculated by excluding one of the 69 communities at a time.

Bell et al. (2009, [191997](#)) presented a supplemental analysis similar to both Lippmann et al. (2006, [091165](#)) and Dominici et al. (2007, [099135](#)) in their examination of whether the variation in PM_{2.5} risks for cardiovascular and respiratory hospital admissions is due to differences in PM_{2.5} chemical composition. The authors used the 100 U.S. cities included in the Peng et al. (2005, [087463](#)) analysis and PM₁₀ data for the years 1987-2000 along with PM_{2.5} chemical component data for 2000-2005. Using a Bayesian hierarchical model, Bell et al. (2009, [191997](#)) found that PM₁₀ relative risks for total mortality were greater in counties and during seasons with higher PM_{2.5} Ni concentrations. However, in a sensitivity analysis when selectively removing cities from the overall estimate, the significant association between the PM₁₀ mortality risk estimate and the PM_{2.5} Ni fraction was diminished upon removing New York city from the analysis, which is consistent with the results presented by Dominici et al. (2007, [099135](#)).

Explaining the Heterogeneity of PM_{2.5} Risk Estimates Using PM_{2.5} Chemical Speciation Data

The first stage of the Franklin et al. (2008, [097426](#)) 25 cities study, described previously, focused on a time-series regression of mortality on PM_{2.5} by season. In the second stage random effects meta regression, the PM_{2.5} mortality risk estimates (25 cities×4 seasons = 100 estimates) were regressed on the ratio of mean seasonal PM_{2.5} species to the total PM_{2.5} mass. The authors included those species that had at least 25% of the reported concentrations above the minimum detection limit, which resulted in 18 species being included in the analysis. Their rationale for using species proportions as effect modifiers, according to the investigators, was that “in the first stage of the analysis the mortality risk was estimated per unit of the total PM_{2.5} mass, which encompassed all

measured species, and therefore it would not be meaningful to use the species concentrations directly as the effect modifier” (Franklin et al., 2008, [097426](#)). In the second stage regression model, Franklin et al. (2008, [097426](#)) also included a quadratic function of seasonally averaged temperature to capture the inverted U-shape relationship between PM_{2.5} penetration and temperature. They found that the fitted relationship between PM_{2.5} risk estimates across cities and seasonally averaged temperature substantiates the use of temperature as a surrogate for ventilation (Franklin et al., 2008, [097426](#)). Table 6-17 shows the resulting effect modification by PM_{2.5} species. Al, As, Ni, Si, and SO₄²⁻ were found to be significant effect modifiers of PM_{2.5} risk estimates, and simultaneously including Al, Ni, and SO₄²⁻ together, or Al, Ni, and As together further increased explanatory power. Of all the species examined, Al and Ni explained the most residual heterogeneity. Franklin et al. (2008, [097426](#)) also examined the effect of demographic variables on PM_{2.5} risk estimates and found that only median household income was significantly associated with mortality.

Table 6-17. Effect modification of composition on the estimated percent increase in mortality with a 10 µg/m³ increase in PM_{2.5}.

Cause	Species	p-value for effect modification by species to PM _{2.5} mass proportion	% increase in nonaccidental mortality per 10 µg/m ³ increase in PM _{2.5} for an interquartile increase in species to PM _{2.5} mass proportion*	Heterogeneity explained (%) [†]
Nonaccidental Univariate	Al	<0.001	0.58	45
	As	0.02	0.55	35
	Br	0.11	0.38	5
	Cr	0.12	0.33	16
	EC	0.79	0.06	0
	Fe	0.43	0.12	3
	K	0.10	0.41	28
	Mn	0.42	0.14	10
	Na+	0.22	0.20	14
	Ni	0.01	0.37	41
	NO ₃	0.07	-0.49	28
	NH ₄ ⁺	0.84	0.04	3
	OC	0.59	-0.02	4
	Pb	0.31	0.17	11
	Si	0.03	0.41	25
SO ₄ ²⁻	0.01	0.51	33	
V	0.28	0.30	3	
Zn	0.19	0.23	15	
Nonaccidental Multivariate (1)	Al	<0.001	0.79	100
	Ni	0.01	0.34	
	SO ₄ ²⁻	<0.001	0.75	
Nonaccidental Multivariate (2)	Al	<0.001	0.61	100
	Ni	0.01	0.35	
	As	<0.001	0.58	

*Adjusted for temperature

[†]Includes heterogeneity explained by temperature

Source: Reprinted with Permission of Lippincott Williams & Wilkins from Franklin et al. (2008, [097426](#))

Although Lippmann et al. (2006, [091165](#)) used NMMAPS PM₁₀ risk estimates and Franklin et al. (2008, [097426](#)) used PM_{2.5} risk estimates to examine effect modification due to various PM

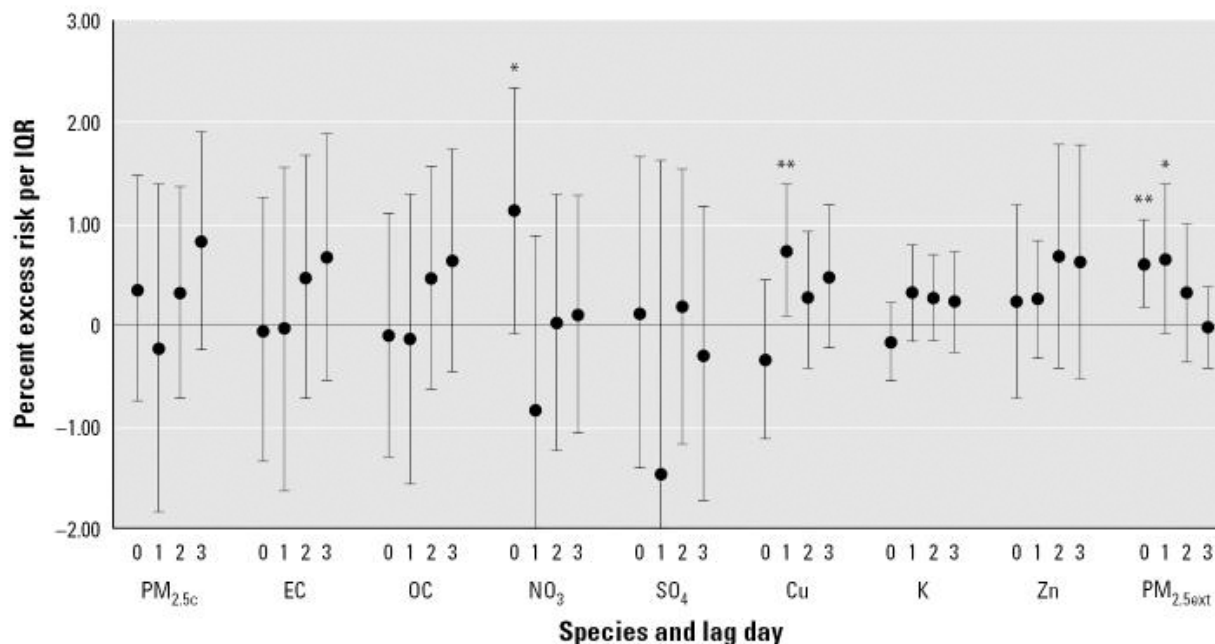
species, 14 out of the 18 species analyzed in these two studies overlap (Figure 6-31 and Table 6-17). Both studies found that Ni explained the heterogeneity in PM risk estimates. Note that New York City was not included in the 25 cities examined in Franklin et al. (2008, [097426](#)) and, thus, could not influence the result. Sulfate positively, but not significantly, explained the PM₁₀ risk estimates in the Lippmann et al. (2006, [091165](#)) analysis. However, SO₄²⁻ was a significant predictor of PM_{2.5} risk estimates in the Franklin et al. (2008, [097426](#)) analysis. Al and Si were negative (i.e., less than the average PM₁₀ risk estimates across cities), though not significant predictors in the Lippmann et al. (2006, [091165](#)) analysis. Unlike the Franklin et al. (2008, [097426](#)) analysis, arsenic (As) showed no association with mortality in the Lippmann et al. (2006, [091165](#)) analysis. The source of these differences may be due to the difference in geographic coverage, PM size (PM_{2.5} may represent more secondary aerosols than PM₁₀), or the difference in the analytical methods used in each study. Specifically, the analytical approach used by Franklin et al. (2008, [097426](#)) does have an advantage of delineating seasonal variations in PM components and the associated potential seasonal mortality effects.

In light of the results presented in speciation studies it must be noted that second stage analyses that use PM chemical species as effect modifiers have some limitations. Unlike analyses that directly examine the associations between chemical species and mortality, if an effect modification is observed it may be confounded if the variations of the mean levels of the chemical species examined are correlated with other demographic factors that vary across cities. Thus, more concrete conclusions could be formulated if direct associations are found between mortality and PM chemical components in time-series analyses.

Association between PM_{2.5} Chemical Components and Mortality

Ostro et al. (2007, [091354](#)) examined associations between PM_{2.5} chemical components and mortality in six California counties (Fresno, Kern, Riverside, Sacramento, San Diego, and Santa Clara), which had at least 180 days of speciation data for the years 2000-2003. The study examined all-cause, cardiovascular, and respiratory mortality for individual lags of 19 specific PM_{2.5} chemical components. The second stage random-effects model combined risk estimates at each lag across cities. The number of available days for chemical species data ranged from 243 (San Diego County) to 395 (Sacramento County). The authors found an association between mortality, especially cardiovascular mortality, and several chemical components. For example, cardiovascular mortality was associated with EC, OC, nitrate, Fe, K, and Ti at various lags.

Even though this was a multicounty study, the relatively small number of available days and the every-third-day (or every-sixth-day) sampling frequency for PM_{2.5} chemical species made it difficult to interpret the results of the lag structure of associations observed for the chemical species. To evaluate the impact of non-daily sampling frequency, Ostro et al. (2007, [091354](#)) examined both the PM_{2.5} series that coincides with the speciation sampling days (for the initial six counties [i.e., PM_{2.5c}]) and PM_{2.5} data that was available on all days for an extended set of counties (the initial six counties plus Contra Costa, Los Angeles, and Orange Counties [i.e., PM_{2.5ext}]). Figure 6-33 shows the association between all-cause mortality and selected PM_{2.5} chemical species as well as for PM_{2.5c} and PM_{2.5ext}. Note the wide confidence bands for the risk estimates for each PM_{2.5} chemical species and PM_{2.5c}, apparently reflecting the low statistical power of the data. The lag structure of associations is more clearly defined for PM_{2.5ext}, and appears to be different from that for PM_{2.5}.



Source: Ostro et al. (2007, [091354](#))

Figure 6-33. Percent excess risk (CI) of total (nonaccidental) mortality per IQR of concentrations. Note: $PM_{2.5}$ has the same sampling days as chemical species. $PM_{2.5}$ has all available $PM_{2.5ext}$ data for nine counties. * $p < 0.10$; ** $p < 0.05$

Ostro et al. (2008, [097971](#)) used the speciation data from the six counties analyzed in their 2007 analysis, described above, in an additional analysis to examine effect modification of cardiovascular mortality effects, which showed the strongest association in the 2007 analysis, attributed to $PM_{2.5}$ and 13 chemical components by socio-economic and demographic factors. The results of the analysis were combined using random effects meta-analysis. The investigators tested statistical differences in risk estimates between strata using a t-test, and reported that, for many of the $PM_{2.5}$ chemical species; there were significantly higher effect estimates among those with lower educational attainment and Hispanics. While these patterns were apparent in their results table, interpretation of the results is not straightforward because the table only presented the most significant (and positive) lags, and they were often different between the strata (e.g., the most frequent significant lag for the Hispanic group was 1 day, while it was 2 or 3 days for the White group). As the investigators pointed out, the every-third-day sampling frequency of the speciation data also complicates the interpretation of the results for different lags.

Overall, the two studies by Ostro et al. (2007, [091354](#)) were the first attempt to directly analyze associations between the newly available chemical speciation data and mortality. While suggestive associations between several chemical species and mortality were reported, a longer length of observations is needed to more clearly determine the associations.

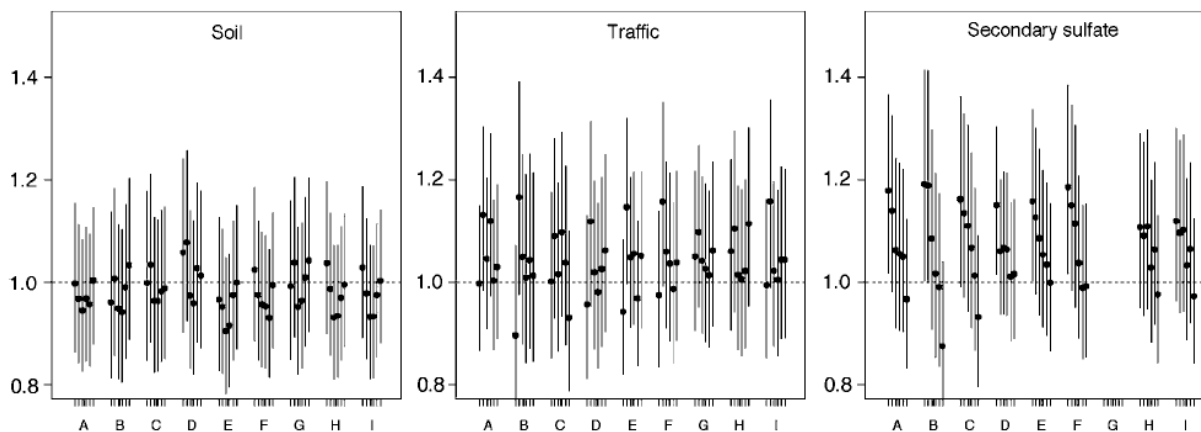
6.5.2.6. Source-Apportioned PM Analyses

Chemically speciated PM data allow for the source apportionment of PM. The idea of using source-apportioned PM for health effects analyses is appealing because, if such source-apportionment could be reliably conducted, it would allow for an evaluation of $PM_{2.5}$ mass concentrations by source types. However, the uncertainties associated with source-apportionment methods have not been well characterized.

To address this issue, in 2003, several groups of EPA-funded researchers organized a workshop and independently conducted source apportionment on two sets of data: Phoenix, AZ, and Washington, DC, compared the results (Hopke et al., 2006, [088390](#)), and then conducted time-series

mortality regression analyses using each group's source-apportioned data (Ito et al., 2006, [088391](#); Mar et al., 2006, [086143](#); Thurston et al., 2005, [097949](#)). The various research groups generally identified the same major source types, each with similar elemental compositions. Inter-group correlation analyses indicated that soil-, SO_4^{2-} -, residual oil-, and salt-associated mass concentrations were most unambiguously identified by various methods, whereas vegetative burning and traffic were less consistent. Aggregate source-specific mortality relative risk (RR) estimate confidence intervals overlapped each other, but the SO_4^{2-} -related $\text{PM}_{2.5}$ component was most consistently significant across analyses in these cities.

The results from the source-apportionment workshop quantitatively characterized the uncertainties associated with the factor analysis-based methods, but they also raised new issues. The mortality analyses conducted in Phoenix, AZ, and Washington, DC, both found that different source-types showed varying lag structure of associations with mortality. For example, Figure 6-34 shows cardiovascular mortality risk estimates for three of the $\text{PM}_{2.5}$ sources from the Phoenix, AZ, analysis (Mar et al., 2006, [086143](#)). The strongest associations for "traffic" $\text{PM}_{2.5}$ was found for lag 1-day, while for "secondary SO_4^{2-} " $\text{PM}_{2.5}$, it was lag 0, with a monotonic decline towards longer lags. These results are consistent with those in the 2004 PM AQCD (U.S. EPA, 2004, [056905](#)), in which associations were reported with combustion-related $\text{PM}_{2.5}$, but not crustal source $\text{PM}_{2.5}$. It is conceivable that PM from different source types produces different lagged effects, but it is also likely that different PM species have varying lagged correlations with the covariates in the health effects regression models (e.g., temperature, day-of-week) resulting in apparent differences in lagged associations with mortality. Thus, interpretation of these source-apportioned PM health effect estimates remains challenging.



Source: Reprinted with Permission of Nature Publishing Group from Mar et al. (2006, [086143](#))

Figure 6-34. Relative risk and CI of cardiovascular mortality associated with estimated $\text{PM}_{2.5}$ source contributions. Y-axis: relative risk per 5th-to-95th percentile increment of estimated $\text{PM}_{2.5}$ source contribution. X-axis: the alphabet denotes investigator/method; lagged $\text{PM}_{2.5}$ source contribution for lag 0 through 5 days, left to right, are shown for each investigator/method.

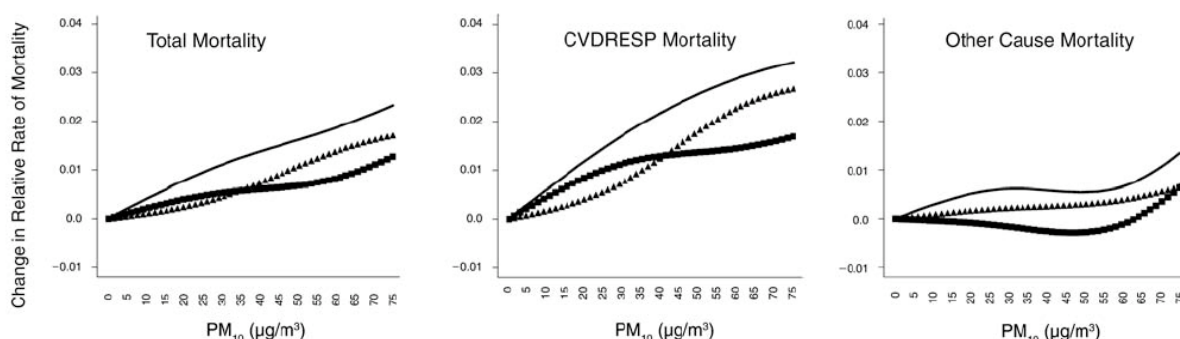
6.5.2.7. Investigation of Concentration-Response Relationship

The results from large multicity studies reviewed in the 2004 PM AQCD (U.S. EPA, 2004, [056905](#)) suggested that strong evidence did not exist for a clear threshold for PM mortality effects. However, as discussed in the 2004 PM AQCD (U.S. EPA, 2004, [056905](#)), there are several challenges in determining and interpreting the shape of PM-mortality concentration-response functions and the presence of a threshold, including: (1) limited range of available concentration levels (i.e., sparse data at the low and high end); (2) heterogeneity of susceptible populations; and (3)

the influence of measurement error. Regardless of these limitations, studies have continued to investigate the PM-mortality concentration-response relationship.

Daniels et al. (2004, [087343](#)) evaluated three concentration-response models: (1) log-linear models (i.e., the most commonly used approach, from which the majority of risk estimates are derived); (2) spline models that allow data to fit possibly non-linear relationship; and (3) threshold models, using PM₁₀ data in 20 cities from the 1987-1994 NMMAPS data. They reported that the spline model, combined across the cities, showed a linear relation without indicating a threshold for the relative risks of death for all-causes and for cardiovascular-respiratory causes in relation to PM₁₀, but “the other cause” deaths (i.e., all cause minus cardiovascular-respiratory) showed an apparent threshold at around 50 µg/m³ PM₁₀, as shown in Figure 6-35. For all-cause and cardio-respiratory deaths, based on the Akaike’s Information Criterion (AIC), a log-linear model without threshold was preferred to the threshold model and to the spline model.

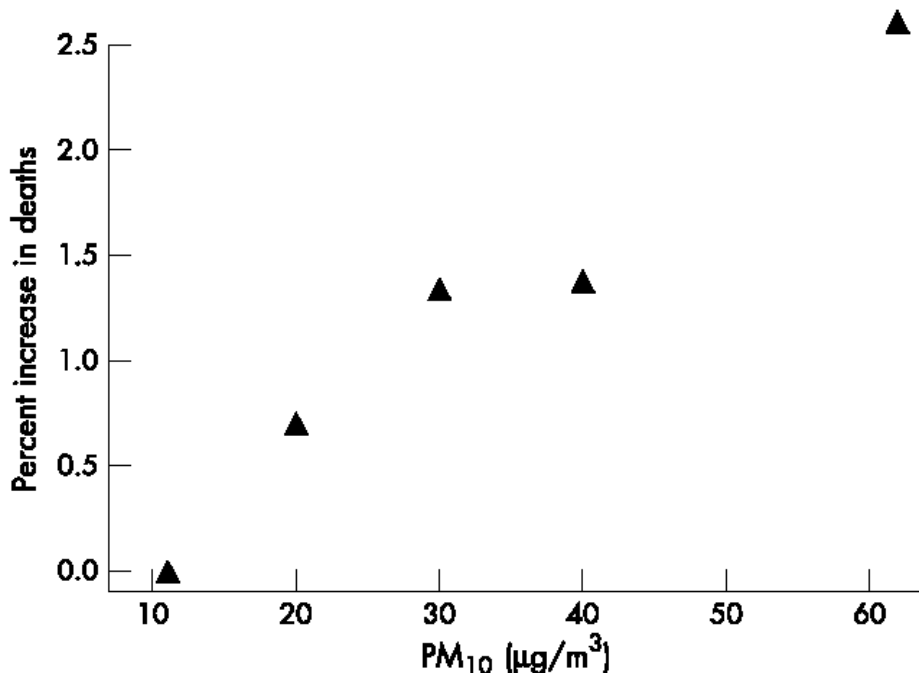
The HEI review committee commented that interpretation of these results required caution, because (1) the measurement error could obscure any threshold; (2) the city-specific concentration-response curves exhibited a variety of shapes; and (3) the use of AIC to choose among the models might not be appropriate due to the fact it was not designed to assess scientific theories of etiology. Note, however, that there has been no etiologically credible reason suggested thus far to choose one model over others for aggregate outcomes. Thus, at least statistically, the result of Daniels et al. (2004, [087343](#)) suggests that the log-linear model is appropriate in describing the relationship between PM₁₀ and mortality.



Source: Reprinted with Permission of HEI from Daniels et al. (2004, [087343](#))

Figure 6-35. Concentration-response curves (spline model) for all-cause, cardiovascular, respiratory and other cause mortality from the 20 NMMAPS cities. Estimates are posterior means under Bayesian random effects model. Solid line is mean lag, triangles are lag 0 (current day), and squares are lag 1 (previous day).

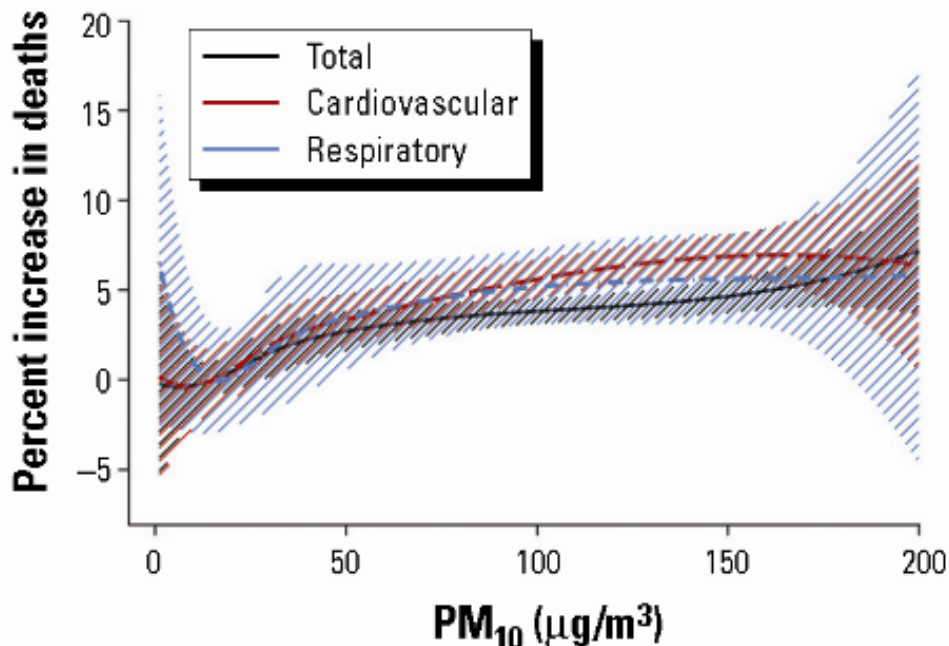
The Schwartz (2004, [078998](#)) analysis of PM₁₀ and mortality in 14 U.S. cities, described in Section 6.5.2.1, also examined the shape of the concentration-response relationship by including indicator variables for days when concentrations were between 15 and 25 µg/m³, between 25 and 34 µg/m³, between 35 and 44 µg/m³, and 45 µg/m³ and above. In the model, days with concentrations below 15 µg/m³ served as the reference level. This model was fit using the single stage method, combining strata across all cities in the case-crossover design. Figure 6-36 shows the resulting relationship, which does not provide sufficient evidence to suggest that a threshold exists. The authors did not examine city-to-city variation in the concentration-response relationship in this study.



Source: Reprinted with Permission of BMJ Group from Schwartz (2004, [078998](#))

Figure 6-36. Percent increase in the risk of death on days with PM₁₀ concentrations in the ranges of 15-24, 25-34, 35-44, and 45 µg/m³ and greater, compared to a reference of days when concentrations were below 15 µg/m³. Risk is plotted against the mean PM₁₀ concentration within each category.

Samoli et al. (2005, [087436](#)) investigated the concentration-response relationship between PM₁₀ and mortality in 22 European cities (and BS in 15 of the cities) participating in the APHEA project. In nine of the 22 cities, PM₁₀ levels were estimated using a regression model relating co-located PM₁₀ to BS or TSP. They used regression spline models with two knots (30 and 50 µg/m³) and then combined the individual city estimates of the splines across cities. The investigators concluded that the association between PM and mortality in these cities could be adequately estimated using the log-linear model. However, in an ancillary analysis of the concentration-response curves for the largest cities in each of the three distinct geographic areas (western, southern, and eastern European cities): London, England; Athens, Greece; and Cracow, Poland, Samoli et al. (2005, [087436](#)) observed a difference in the shape of the concentration-response curve across cities. Thus, while the combined curves (Figure 6-37) appear to support no-threshold relationships between PM₁₀ and mortality, the heterogeneity of the shapes across cities makes it difficult to interpret the biological relevance of the shape of the combined curves.



Source: Samoli et al. (2005, [087436](#))

Figure 6-37. Combined concentration-response curves (spline model) for all-cause, cardiovascular, and respiratory mortality from the 22 APHEA cities.

The results from the three multicity studies discussed above support no-threshold log-linear models, but issues such as the possible influence of exposure error and heterogeneity of shapes across cities remain to be resolved. Also, given the pattern of seasonal and regional differences in PM risk estimates depicted in recent multicity study results (e.g., Peng et al., 2005, [087463](#)), the very concept of a concentration-response relationship estimated across cities and for all-year data may not be very informative.

6.5.3. Summary and Causal Determinations

6.5.3.1. PM_{2.5}

The 2004 PM AQCD (U.S. EPA, 2004, [056905](#)) found that the strength of evidence from U.S.- and Canadian-based studies (both multi- and single-city) for PM_{2.5} mortality associations varied across outcomes, with relatively stronger evidence for associations with cardiovascular compared to respiratory causes. The resulting effect estimates reported for these two endpoints ranged from 1.2 to 2.7% for cardiovascular-related mortality and 0.8 to 2.7% for respiratory-related mortality, per 10 µg/m³ increase in PM_{2.5} (U.S. EPA, 2004, [056905](#)).

In the current review, PM_{2.5} risk estimates were found to be consistently positive, and slightly larger than those reported for PM₁₀ for all-cause, and respiratory- and cardiovascular-related mortality. The risk estimates for all-cause (nonaccidental) mortality ranged from 0.29% (Dominici et al., 2007, [097361](#)) to 1.21% (Franklin et al., 2007, [091257](#)) per 10 µg/m³ increase in PM_{2.5}. These associations were consistently observed at lag 1 and lag 0-1, which have been confirmed through extensive analyses in PM₁₀-mortality studies. Cardiovascular-related mortality risk estimates were found to be similar to those for all-cause mortality; whereas, the risk estimates for respiratory-related mortality were consistently larger: 1.01% (Franklin et al., 2007, [091257](#)) to 2.2% (Ostro et al., 2006, [087991](#)) using the same lag (i.e., lag 1 and lag 0-1) and averaging indices. The studies evaluated that examined the relationship between short-term exposure to PM_{2.5} and cardiovascular effects (section

6.2) provide coherence and biological plausibility for PM_{2.5}-induced cardiovascular mortality, which represents the largest component of total (nonaccidental) mortality (~ 35%) (American Heart Association, 2009, [198920](#)). However, as noted in section 6.3, there is limited coherence between some of the respiratory morbidity findings from epidemiologic and controlled human exposure studies for the specific health outcomes reported and the subpopulations in which those health outcomes occur, complicating the interpretation of the PM_{2.5} respiratory mortality effects observed.

Regional and seasonal patterns in PM_{2.5} risk estimates were observed with results similar to those presented for PM₁₀ (Dominici et al., 2007, [097361](#); Peng et al., 2005, [087463](#); Zeka et al., 2006, [088749](#)), with the greatest effects occurring in the eastern U.S. (Franklin et al., 2007, [091257](#); Franklin et al., 2008, [097426](#)) and during the spring (Franklin et al., 2007, [091257](#); Zanobetti and Schwartz, 2009, [188462](#)). Of the studies evaluated only Burnett et al. (2004, [086247](#)), a Canadian multicity study, analyzed gaseous pollutants and found mixed results, with possible confounding of PM_{2.5} risk estimates by NO₂. Although the recently evaluated U.S.-based multicity studies did not analyze potential confounding of PM_{2.5} risk estimates by gaseous pollutants, evidence from single-city studies evaluated in the 2004 PM AQCD (U.S. EPA, 2004, [056905](#)) suggest that gaseous copollutants do not confound the PM_{2.5}-mortality association, which is further supported by studies that examined the PM₁₀-mortality relationship. An examination of effect modifiers (e.g., demographic and socioeconomic factors), specifically AC use which is sometimes used as a surrogate for decreased pollutant penetration indoors, has suggested that PM_{2.5} risk estimates increase as the percent of the population with access to AC decreases (Franklin et al., 2007, [091257](#); 2008, [097426](#)). Collectively, the epidemiologic evidence is sufficient to conclude that **a causal relationship exists between short-term exposure to PM_{2.5} and mortality.**

6.5.3.2. PM_{10-2.5}

The 2004 PM AQCD (U.S. EPA, 2004, [056905](#)) found a limited body of evidence that was suggestive of associations between short-term exposure to ambient PM_{10-2.5} and various mortality outcomes (e.g., 0.08 to 2.4% increase in total [nonaccidental] mortality per 10 µg/m³ increase in PM_{10-2.5}). As a result, the AQCD concluded that PM_{10-2.5}, or some constituent component(s) (including those on the surface) of PM_{10-2.5}, may contribute, in certain circumstances, to increased human health risks.

The majority of studies evaluated in this review that examined the relationship between PM_{10-2.5} and mortality reported consistent positive associations in areas with mean 24-h avg concentrations ranging from 6.1-16.4 µg/m³. However, uncertainty surrounds the PM_{10-2.5} associations reported due to the different methods used to estimate PM_{10-2.5} concentrations across studies (e.g., direct measurement of PM_{10-2.5} using dichotomous samplers, calculating the difference between PM₁₀ and PM_{2.5} concentrations).

A new study of 47 U.S. cities (Zanobetti and Schwartz, 2009, [188462](#)), which estimated PM_{10-2.5} by calculating the difference between the county-average PM₁₀ and PM_{2.5}, found associations between PM_{10-2.5} and mortality across the U.S., including regions where PM_{10-2.5} levels are not high. In addition, one well conducted multicity Canadian study (Burnett et al., 2004, [086247](#)) provided evidence for an association between short-term exposure to PM_{10-2.5} and mortality. However, unlike PM_{2.5} very few of the PM_{10-2.5} studies have investigated confounding by gaseous copollutants or the influence of model specification on PM_{10-2.5} risk estimates. Zanobetti and Schwartz (2009, [188462](#)) did provide preliminary evidence for greater effects occurring during the warmer months (i.e., spring and summer), which is consistent with the results from PM₁₀-mortality studies (Peng et al., 2005, [087463](#); Zeka et al., 2006, [088749](#)). Overall, although more data is needed to: adequately characterize the chemical and biological components that may modify the potential toxicity of PM_{10-2.5} and compare the different methods used to estimate exposure, consistent positive associations between short-term exposure to PM_{10-2.5} and mortality were observed in the U.S. and Canadian-based multicity studies evaluated, as well as the single-city studies conducted in these locations. Therefore, the epidemiologic evidence **is suggestive of a causal relationship between short-term exposure to PM_{10-2.5} and mortality.**

6.5.3.3. UFPs

Limited evidence was available during the review of the 2004 PM AQCD (U.S. EPA, 2004, [056905](#)) regarding the potential association between UFPs and mortality. The lone study evaluated was conducted in Germany and provided some evidence for an association, but this association was reduced upon the inclusion of gaseous pollutants in a two-pollutant model.

Only a few new studies, all of them from Europe, were identified during this review, which examined the association between short-term exposure to UFPs and mortality. Inconsistencies were observed in the lag structure of association reported by each study in terms of both the lag day with the greatest association and the number of lag days considered in the study. Overall the studies consistently found that UFPs were correlated with gaseous pollutants derived from local combustion sources and that one or more of the gaseous pollutants were also associated with mortality. The limited number of studies available and the discrepancy in results between studies further confirms the need for additional data to examine the UFP-mortality relationship. In conclusion, the epidemiologic evidence **is inadequate to infer a causal association between short-term exposure to UFPs and mortality.**

6.6. Attribution of Ambient PM Health Effects to Specific Constituents or Sources

From a mechanistic perspective, it is highly plausible that the chemical composition of PM would be a better predictor of health effects than particle size. The observed geographical gradients in a number of PM_{2.5} constituents (e.g., EC, OC, nitrate, and SO₄²⁻) and regional heterogeneity in PM-related health effects reported in epidemiologic studies are consistent with this hypothesis. Recent studies in epidemiology, controlled human exposure, and toxicology have begun using information on ambient PM composition, and apportionment of constituents into sources, in an attempt to identify those with links to health outcomes and endpoints.

This section focuses on short-term exposure studies that (1) assessed health effects for ambient PM sources or components; and (2) used quantitative methods to relate those sources and components to health effects. Epidemiologic, controlled human exposure, and toxicological studies that took into consideration a large set of PM constituents (typically minerals, metals, EC, OC, and ions such as SO₄²⁻) and aimed to segregate which constituents or groups of constituents may be responsible for the PM-related health effects observed are included. Most of these studies were reviewed earlier in this chapter and evaluated the relationship between specific chemical constituents derived from ambient PM and health effects. However, there were many studies presented earlier, as well as others only included in the Annexes, which only selected one or a small number of PM constituents *a priori*. Several controlled human exposure and toxicological studies likewise used a single compound found in PM rather than ambient PM. Additionally, studies that presented ambient PM composition and health data without systematically and explicitly investigating relationships are not included in this section. The few epidemiologic studies of long-term exposure that examined potential relationships between composition and sources of PM with mortality are discussed in Section 7.6.2.

Prior to the 2004 PM AQCD (U.S. EPA, 2004, [056905](#)), only a handful of epidemiologic studies had attempted to relate specific constituents or sources of ambient PM to health outcomes without selecting constituents *a priori*. In this review, approximately 40 new epidemiologic, controlled human exposure, and toxicological studies explore the health effects attributed to chemical constituents and sources of ambient PM. The following summary (Section 6.6.3) provides a synthesis of the findings, including discussions on the coherence and consistency of the results.

6.6.1. Evaluation Approach

Relating a large number of ambient PM constituents with a large number of health outcomes presents difficulties that are related to both the nature of PM and methods of quantitative analysis. First, the number of constituents that comprise PM is not only large, but the correlations between them can be high. Reducing the correlation between constituents has been accomplished in most of

the recent studies through various forms of factor analysis, which limits the correlations between constituents by grouping the most highly correlated ambient PM constituents into less correlated groups or factors. Some studies identify the resulting groups or factors with named sources of ambient PM, but many do not draw explicit links between factors and actual sources. The methods used in estimating source contributions to ambient PM are reviewed in Section 3.6.1.

Most studies reviewed herein, regardless of discipline, were based on data for between 7 and 20 ambient PM constituents, with EC, OC, SO₄, and NO₃ most commonly measured. Most studies first reduced the number of ambient PM constituents by grouping them with various factorization or source apportionment techniques and the majority labeled the constituent groupings according to their presumed source. A separate analysis was then used to examine the relationship between the grouped PM constituents and various health effects. A few performed these two steps simultaneously using Partial Least Squares (PLS) procedures or Structural Equation Modeling (SEM). A small number of controlled human exposure and toxicological studies did not apply any kind of grouping to the ambient PM speciation data.

There are some differences in the type of PM constituent data used in epidemiologic, controlled human exposure and toxicological studies. In epidemiologic studies, ambient PM speciation data is obtained from atmospheric monitors; for controlled human exposure and toxicological studies, the technique used in the experimental exposure determines the type of PM data. Thus, all epidemiologic studies relied on monitor data, while all of the controlled human exposure and the majority of the toxicological studies used CAPs (and analyzed the concentrations of constituents therein). The remaining toxicological studies used ambient PM samples collected on filters at various U.S. sites. Further details on the studies included can be found in Appendix F.

Some important limitations in interpreting these studies together is that few, if any of the results are easily comparable, due to: (1) differences in the sets of ambient PM constituents that make up each of the factors; (2) the subjectivity involved in labeling factors as sources; (3) the numerous potential health effects examined in these studies, including definitive outcomes (e.g., HAs) as well as physiological alterations (e.g., increased inflammatory response); and (4) the various statistical methods and analytical approaches used in the studies. There are no well-established, objective methods for conducting the various forms of factor analysis and source apportionment, leaving much of the model operation and factor assignment open to judgment by the individual investigator. For example, the Al/Si factor identified in one study may differ from the Al/Ca/Fe/Si factor from another study, and the “Resuspended Soil” factor from a third study. After factorization or apportionment of the ambient PM data, the methods used for analyzing the potential association between ambient PM constituents or sources and health effects also varied. Except for the studies that used PLS or SEM, controlled human exposure and toxicological studies all used univariate mixed model regression for every identified PM factor or source. A number of toxicological studies followed the univariate step with multivariate regression for all factors. Epidemiologic studies generally related short-term exposure to sources with health outcomes through various forms of Poisson regression.

6.6.2. Findings

The results that follow are organized by discipline, with epidemiologic studies followed by controlled human exposure and toxicological studies. This section ends with a summary table, Table 6-18. Table 6-18 is broken out by PM_{2.5} sources, and includes those epidemiologic, controlled human exposure, and in vivo toxicological studies that either grouped ambient PM_{2.5} constituents or used tracers for each source. The table does not include all factors or sources examined in the studies listed: those factors or sources for which no association with effects was found not included.

6.6.2.1. Epidemiologic Studies

Results from the 2004 PM AQCD

Three epidemiologic studies that examined the association between PM constituents or sources and specific health effects were evaluated in the 2004 PM AQCD (U.S. EPA, 2004, [056905](#)). Of

these studies, one study associated daily mortality with a mobile sources PM factor in Knoxville, TN and St. Louis, MO and coal in Boston, MA, while the crustal factor was not found to be significant for any of the six cities studied (Laden et al., 2000, [012102](#); Schwartz, 2003, [042811](#)). Another study demonstrated an association between a regional SO_4^{2-} factor and total mortality at lag 0 in Phoenix and factors for regional SO_4^{2-} , motor vehicles, and vegetative burning with cardiovascular mortality at lags of 0, 1, and 3, respectively (Mar et al., 2000, [001760](#); 2003, [042841](#)). Negative associations were observed between total mortality and regional SO_4^{2-} at lag 3, along with local SO_2 and soil factors (Mar et al., 2000, [001760](#); 2003, [042841](#)). Finally, Tsai et al. (2000, [006251](#)) identified significant associations between PM_{15} -derived industrial sources and total daily deaths in Newark and Camden, NJ; SO_4^{2-} was also linked to cardiopulmonary deaths in both locations. Total mortality and cardiopulmonary deaths were also significantly associated with PM from oil burning in Camden (2000, [006251](#)).

Comparative Analyses of Source Apportionment Methods

Hopke et al. (2006, [088390](#)) conducted a comparative analysis of source apportionment techniques used by investigators at multiple institutions, and subsequently used in epidemiologic analyses (Ito et al., 2006, [088391](#); Mar et al., 2006, [086143](#)). An overarching conclusion of this set of analyses, reported in Thurston et al. (2005, [097949](#)), is that variation in the source apportionment methods was not a major source of uncertainty in the epidemiologic effect estimates. In the primary analyses, mortality was associated with secondary SO_4^{2-} in both Phoenix and Washington D.C., although lag times differed (0 and 3, respectively). The SO_4^{2-} effect was stronger for total mortality in Washington D.C. and for cardiovascular mortality in Phoenix (Ito et al., 2006, [088391](#); Mar et al., 2006, [086143](#)). In addition, Ito et al. (2006, [088391](#)) found some evidence for associations with primary coal and traffic with total mortality in Washington D.C. (Ito et al., 2006, [088391](#)) while copper smelter, traffic, and sea salt were associated with cardiovascular mortality in Phoenix at various lag times (Mar et al., 2006, [086143](#)). In contrast to Phoenix, sea salt and traffic were not associated with mortality in Washington D.C. (Ito et al., 2006, [088391](#)), but in both locations no associations were observed between biomass/wood combustion and mortality (Ito et al., 2006, [088391](#); Mar et al., 2006, [086143](#)). In an additional study that compared three source apportionment methods in Atlanta—PMF, modified CMB, and a single-species tracer approach—found that the epidemiologic results were robust to the choice of analytic method (Sarnat et al., 2008, [097972](#)). There were consistent associations between ED visits for cardiovascular diseases with $\text{PM}_{2.5}$ from mobile sources (gasoline and diesel) and biomass combustion (primarily prescribed forest burning and residential wood combustion), whereas $\text{PM}_{2.5}$ from secondary SO_4^{2-} was associated with respiratory disease ED visits (Sarnat et al., 2008, [097972](#)). Sarnat et al. (2008, [097972](#)) also found that the primary power plant $\text{PM}_{2.5}$ source identified by the CMB approach was negatively associated with respiratory ED visits while no association was found for $\text{PM}_{2.5}$ from soil and secondary nitrates/ammonium nitrate. In these studies, effect estimates based on the different source apportionment methods were generally in close agreement.

Source Apportionment Studies

A study that examined associations with mortality in Santiago, Chile, identified a motor vehicle source of $\text{PM}_{2.5}$ as having the greatest association with total and cardiac mortality at lag 1 (Cakmak et al., 2009, [191995](#)). There was effect modification by age, with the total mortality relative risks associated with $\text{PM}_{2.5}$ from motor vehicles being greatest for those >85 yr. Soil and combustion sources were also associated with cardiac mortality. Risk estimates for respiratory mortality were the greatest for the motor vehicle source, with combustion and soil source factors also demonstrating positive associations for lag 1 (Cakmak et al., 2009, [191995](#)).

An epidemiologic study that evaluated respiratory ED visits was conducted in Spokane, WA and used tracers as indicators of ambient $\text{PM}_{2.5}$ sources (Schreuder et al., 2006, [097959](#)). In this study, only $\text{PM}_{2.5}$ from vegetative burning (total carbon) was associated with increased respiratory ED visits for lag 1, while $\text{PM}_{2.5}$ indicators for motor vehicles (Zn) and soil (Si) were not associated with cardiac hospital or respiratory ED visits. Andersen et al. (2007, [093201](#)) conducted a source apportionment analysis to identify the sources of ambient PM_{10} associated with cardiovascular and

respiratory hospital admissions in older adults and children (ages 5-18) in Copenhagen, including two-pollutant models with various sources of PM₁₀. Andersen et al. (2007, [093201](#)) found that secondary and crustal sources of PM₁₀ were associated with cardiovascular hospital admissions; biomass sources were associated with respiratory hospital admissions; and vehicle sources were associated with asthma hospital admissions.

Several panel epidemiologic studies have examined the association between PM sources and physiological alterations in cardiovascular function. Lanki et al. (2006, [089788](#)) reported positive associations between PM_{2.5} from local traffic (measured as absorbance, which is correlated with EC content) and long-range transported PM_{2.5} with ST-segment depression in elderly adults in a study conducted in Helsinki, Finland. Positive associations with ST-segment depression were also reported with PM_{2.5} from crustal and salt sources, but these associations were not statistically significant. In an additional study, Yue et al. (2007, [097968](#)) found that adult males with coronary artery disease in Erfurt, Germany, demonstrated changes in repolarization parameters associated with traffic-related PM_{2.5}, with increased vWF linked to traffic and combustion-generated particles, although the source apportionment was based solely on particle size distribution. In addition, elevated CRP levels were associated with all sources of PM_{2.5} (soil, local traffic, secondary aerosols from local fuel combustion, diesel, and secondary aerosols from multiple sources) (Yue et al., 2007, [097968](#)). Reidiker et al. (2004, [056992](#)), in a study of young male highway patrol officers, found that the most significant effects (HRV, supraventricular ectopic beats, hematological markers, vWF) were associated with a speed-change factor for PM_{2.5} (2004, [056992](#)). In addition, the authors observed an association between crustal factor and cardiovascular effects, but no health-related associations with steel wear or gasoline PM_{2.5} source factors.

Two recent studies have examined the associations between ambient PM_{2.5} sources and respiratory symptoms and lung function. Positive associations with PM_{2.5} motor vehicle and road dust sources were reported for respiratory symptoms and inhaler use in asthmatic children in New Haven, CT, and negative associations with wheeze or inhaler use for biomass burning at lag 0-2 (Gent et al., 2009, [180399](#)). These positive effects for motor vehicle and road dust sources were robust to the inclusion of a gaseous copollutant (NO₂, CO, SO₂, or O₃) in the regression model. Penttinen et al. (2006, [087988](#)) in a study consisting of asthmatic adults living in Helsinki, Finland, found that decrements in PEF were associated with ambient PM_{2.5} soil, long-range transport, and local combustion sources at lags from 0-5 days. In addition, negative associations with asthma symptoms and medication use were reported for PM_{2.5} from sea salt and long-range transport sources (Penttinen et al., 2006, [087988](#)).

PM Constituent Studies

Some studies considered large sets of ambient PM constituents and attempted to identify which were associated with various health effects, but without grouping them into factors, or identifying sources. The majority of these studies focused on health effects associated with short-term exposure to PM_{2.5}. Peng et al. (2009, [191998](#)) examined the association between PM_{2.5} constituents (i.e., EC, OC, SO₄²⁻, NO₃⁻, Si, Na, NH₄⁺) and cardiovascular and respiratory hospital admissions in 119 U.S. cities. When including each constituent in a multipollutant model, they found that EC and OC were robust to the inclusion of the other constituents at lag 0 for cardiovascular and respiratory hospital admissions, respectively. Although this study did not include analyses to identify sources of the constituents examined, EC and OC are often attributed to motor vehicle emissions, particularly diesel engines, and wood burning (Peng et al., 2009, [191998](#)). Ostro et al. (2007, [091354](#); 2008, [097971](#)) conducted two studies in six California counties to examine the association between ambient PM constituents and mortality. In the 2007 analysis, Ostro et al. (2006, [087991](#)) found associations between Cu and all-cause mortality; EC, K, and Zn and CVD mortality; and Cu and Ti and respiratory mortality at lags ranging from 0 to 3 days. Associations during the summer were only observed between K for both CVD and respiratory mortality; and Al, Cl, Cu, Pb, Ti, and Zn and respiratory mortality. Overall, the most consistent associations were observed during the cool season. In a subsequent analysis, Ostro et al. (2008, [097971](#)) examined the association between ambient PM constituents and cardiovascular mortality in potentially susceptible subpopulations. The authors found positive associations between EC, OC, NO₃⁻, SO₄²⁻, K, Cu, Fe, and Zn and cardiovascular mortality. These associations were higher in individuals with lower educational

attainment and of Hispanic ethnicity. In addition, similar to the 2007 analysis, associations were observed at lags ranging from 0 to 3 days.

Evaluation of Effect Modification by PM Constituents

Several studies have conducted secondary analyses to examine whether the variation in associations between PM_{2.5} and morbidity and mortality or PM₁₀ and mortality reflects differences in PM_{2.5} constituents. An assumption in these types of analyses, especially when examining the effects on PM₁₀ mortality risk estimates, is that the relative contributions of PM_{2.5} have remained the same over time; these studies used PM₁₀ data for years prior to 2000, while PM_{2.5} speciation data has only been routinely collected since about 2000. Bell et al. (2009, [191997](#)) found statistically significant associations between the county average concentrations of V, Ni, and EC (106 counties) and effect estimates for both cardiovascular and respiratory hospital admissions with short-term exposure to PM_{2.5}. In this analysis the ambient PM_{2.5} constituents that comprised the majority of PM_{2.5} total mass in the study locations were NH₄⁺, EC, OC, NO₃⁻, and SO₄²⁻. Bell et al. (2009, [191997](#)) also conducted a similar analysis for PM₁₀-mortality risk estimates and found that only Ni increased the risk estimate. However, in a sensitivity analysis, when selectively dropping out the communities examined one at a time, removing New York City diminished the Ni association. Both Lippmann et al. (2006, [091165](#)) and Dominici et al. (2007, [099135](#)) conducted similar analyses, albeit using a smaller subset of cities and/or different years of PM₁₀ data. In both studies, Ni and V were found to modify the PM₁₀-mortality risk estimates. Similar to Bell et al. (2009, [191997](#)), Dominici et al. (2007, [099135](#)) also found that excluding New York City as part of a sensitivity analysis resulted in a diminished association with Ni and V. In an additional study, Franklin et al. (2008, [097426](#)) examined the potential modification of the PM_{2.5}-mortality relationship by PM constituents in 25 U.S. cities. In a second-stage analysis using the species-to-PM_{2.5} mass proportion of multiple constituents, the authors found that Al, As, Ni, Si, and SO₄²⁻ significantly modified the association between PM_{2.5} and nonaccidental mortality.

6.6.2.2. Controlled Human Exposure Studies

A few controlled human exposure studies employed PCA, although not all linked groupings of PM constituents to the measured physiological parameters. Huang et al. (2003, [087377](#)) demonstrated associations between increased fibrinogen and Cu/Zn/V and increased BALF neutrophils and Fe/Se/SO₄ in young, healthy adults exposed to RTP, NC CAPs; however, only water-soluble constituents were analyzed. In the other study that examined physiological cardiovascular effects, Fe and EC were associated with changes in ST-segment, while SO₄²⁻ was associated with decreased SBP in asthmatic and healthy human volunteers exposed to Los Angeles CAPs ([2003, 087377](#)). In Gong et al. (2003, [087365](#)) the majority of the PM was in the thoracic coarse fraction. In the other study that used Los Angeles CAPs, the only observed association was between SO₄²⁻ content and decreased lung function (FEV₁ and FVC) in elderly volunteers with and without COPD (Gong et al., 2005, [087921](#)). Two additional controlled human exposure studies that did not perform grouping and employed Toronto CAPs plus O₃ demonstrated increased DBP and increased brachial artery vasoconstriction associated with carbon content (Urch et al., 2004, [055629](#); 2005, [081080](#)).

6.6.2.3. Toxicological Studies

The only toxicological in vivo study that characterized PM sources corresponding to identified sources was conducted in Tuxedo, NY, over a 5-mo period. This study reported that all sources (regional SO₄²⁻, resuspended soil, residual oil, traffic and other unknown sources) were linked to HR or HRV changes in mice at one time or another during or after daily exposure (Lippmann et al., 2005, [087453](#)). In a simultaneous in vitro study using CAPs from the same location, NF-κB in BEAS-2B cells were correlated with the oil combustion factor (r = 0.289 and 0.302 for V and Ni, respectively) (Maciejczyk and Chen, 2005, [087456](#)). The other in vitro toxicological study (Duvall et al., 2008, [097969](#)) that named sources employed samples from 5 U.S. cities and found a good fit for the regression model with increased IL-8 release in primary human airway epithelium cells and coal combustion (R² = 0.79), secondary nitrate (R² = 0.63), and mobile sources (R² = 0.39). In addition, soil (R² = 0.48), residual oil combustion (R² = 0.38), and wood combustion (R² = 0.33) were

associated with COX-2 effects; whereas, secondary SO_4^{2-} ($R^2 = 0.51$) was correlated with HO-1. Wood combustion and soil were negatively associated with HO-1.

Several toxicological studies employed Boston CAPs and identified at least four groupings of ambient $\text{PM}_{2.5}$ constituents (V/Ni, S, Al/Si, and Br/Pb), but they named sources only partially and tentatively (Batalha et al., 2002, [088109](#); Clarke et al., 2000, [011806](#); Godleski et al., 2002, [156478](#); Nikolov et al., 2008, [156808](#); Saldiva et al., 2002, [025988](#); Wellenius et al., 2003, [055691](#)). When examining cardiovascular effects these studies reported that Si was associated with changes in the ST-segment of dogs (Wellenius et al., 2003, [055691](#)) and decreased L/W ratio in rat pulmonary arteries (Batalha et al., 2002, [088109](#)) in multivariate analyses. In addition, blood hematological results were associated with V/Ni, Al/Si, Na/Cl, and S in dogs (Clarke et al., 2000, [011806](#)). An examination of respiratory effects in the latter study found that V/Ni and Br/Pb were associated with increased inflammation in BALF for only the third day of exposure (Clarke et al., 2000, [011806](#)). Decreased respiratory rate and increased airway irritation (Penh) in dogs were associated with road dust (Al) and motor vehicles (OC), respectively (Nikolov et al., 2008, [156808](#)). Individual $\text{PM}_{2.5}$ constituents associated with elevated neutrophils in BALF were Br, EC, OC, Pb, and SO_4^{2-} (Godleski et al., 2002, [156478](#)), which is consistent with the findings (Br, EC, OC, Pb, V, and Cl) of Saldiva et al. (2002, [025988](#)).

The two toxicological studies that used PLS methodologies identified $\text{PM}_{2.5}$ constituents linked to respiratory parameters. Seagrave et al. (2006, [091291](#)) demonstrated associations between cytotoxic responses and a gasoline plus nitrates source factor (OC, Pb, hopanes/steranes, nitrate, and As) along with inflammatory responses and a gasoline plus diesel source factor (including major metal oxides) in rats exposed via IT instillation. In the other study, Veranth et al. (2006, [087479](#)) collected loose surface soil from 28 sites in the Western U.S. and exposed BEAS-2B cells to $\text{PM}_{2.5}$. OC_1 , OC_3 , OC_2 , EC_2 , Br, EC_1 , and Ni correlated with IL-8 release, decreased IL-6 release, and decreased viability at low and high doses (10 and 80 $\mu\text{g}/\text{cm}^2$, respectively).

Table 6-18. Study-specific $\text{PM}_{2.5}$ factor/source categories associated with health effects.

Source Category	Location	Health Effects	Time	Type of Study ¹	Species	Reference
CRUSTAL/SOIL/ROAD DUST						
Al, Si, Fe	Phoenix, AZ	negative association with total mortality	Lag 2	E	Human	Mar et al. (2000, 001760)
Not provided	Washington, D.C.	↑CV mortality	Lag 4	E	Human	Ito et al. (2006, 088391)
Al, Ca, Fe, Si	Santiago, Chile	↑CV mortality ↑respiratory mortality	Lag 1	E	Human	Cakmak et al. (2009, 191995)
Al, Si, Ca, K, Fe	Helsinki, Finland	ST-segment depression	Lag 3	E	Human	Lanki et al. (2006, 089788)
Al, Si, Ca, K, Fe	Los Angeles, CA	↓ST-segment voltage	2 days post-exposure	H	Human	Gong et al. (2003, 042106)
Al, Si	Boston, MA	ST-segment change	Following exposure	T	Dog	Wellenius et al. (2003, 055691)
Al, Si, Ca	Boston, MA	↓ lumen/wall ratio	24 h post-exposure	T	Rat	Batalha et al. (2002, 088109)
Al, Si, Ti, Fe	Wake County, NC	↑ uric acid ↑ mean cycle length	Lag 15 h	E	Human	Riediker et al. (2004, 056992)
Al, Si, Ca, Fe	Tuxedo, NY	↓ HR ↑ HR ↑ SDNN, ↑ RMSSD	During exposure Afternoon post-exposure Night post-exposure	T	Mouse	Lippmann et al. (2005, 087453)
Al, Si	Boston, MA	↑ blood PMN % ↓ blood lymphocytes % ↑ WBC	Following exposure	T	Dog	Clarke et al. (2000, 011806)
Si, Fe, Al, Ca, Ba, Ti	New Haven, CT	↑ respiratory symptoms and inhaler use	Lag 0-2	E	Human	Gent et al. (2009, 180399)

Source Category	Location	Health Effects	Time	Type of Study ¹	Species	Reference
Si, Al, Ca, Fe, Mn	Helsinki, Finland	↓ mean PEF	Lag 3	E	Human	Penttinen et al. (2006, 087988)
Al	Boston, MA	↓ airway irritation (penh)	During exposure	T	Dog	Nikolov et al. (2008, 156808)
SALT						
Not provided	Phoenix, AZ	↑CV mortality ↑total mortality negative association with total mortality	Lag 5 Lag 0	E	Human	Mar et al. (2006, 086143)
Na, Cl	Helsinki, Finland	ST-segment depression	Lag 3	E	Human	Lanki et al. (2006, 089788)
Na, Cl	Boston, MA	↑ blood lymphocyte %	Following exposure	T	Dog	Clarke et al.(2000, 011806)
Na, Cl	Helsinki, Finland	Negatively associated with bronchodilator use and corticosteroid use	Lag 0-5 avg	E	Human	Penttinen et al. (2006, 087988)
Na, Cl	Boston, MA	↑ lung PMN density	24 h post-exposure	T	Rat	Saldiva et al. (2002, 025988)
SECONDARY SO₄²⁻ / LONG-RANGE TRANSPORT						
S	Phoenix, AZ	↑ total mortality negative association with total mortality	Lag 0 Lag 5	E	Human	Mar et al. (2000, 001760)
Not provided	Washington, D.C.	↑ total mortality	Lag 3	E	Human	Ito et al. (2006, 088391)
Not provided	Phoenix, AZ	↑CV mortality	Lag 0	E	Human	Mar et al. (2006, 086143)
S, K, Zn, Pb	Helsinki, Finland	ST-segment depression	Lag 2	E	Human	Lanki et al. (2006, 089788)
SO ₄ ²⁻	Los Angeles, CA	↓ SBP	4 h post-exposure	H	Human	Gong et al. (2003, 042106)
S, Si, OC	Tuxedo, NY	↓ HR ↓ SDNN, ↓ RMSSD	Afternoon post-exposure Night post-exposure	T	Mouse	Lippmann et al. (2005, 087453)
S	Boston, MA	↓ RBC ↑ hemoglobin	Following exposure	T	Dog	Clarke et al. (2000, 011806)
SO ₄ ²⁻ , NH ₄ ⁺ , OC	Atlanta, GA	↑ respiratory ED visits	Lag 0	E	Human	Sarnat et al. (2008, 097972)
S, K, Zn, PM mass	Helsinki, Finland	↓ mean PEF. Negative association with asthma symptom prevalence	Lag 1 Lag 3	E	Human	Penttinen et al. (2006, 087988)
SO ₄ ²⁻ (+NO ₂)	Los Angeles, CA	↓ FEV ₁ ↓ FVC	Following exposure	H	Human	Gong et al. (2005, 087921)
TRAFFIC						
Pb, Br, Cu	Harvard Six Cities	↑ total mortality	Lag 0-1	E	Human	Laden et al. (2000, 012102)
Not provided	Phoenix, AZ	↑CV mortality	Lag 1	E	Human	Mar et al. (2006, 086143)
Mn, Fe, Zn, Pb, OC, EC, CO, NO ₂	Phoenix, AZ	↑ CV mortality	Lag 1	E	Human	Mar et al. (2000, 001760)
CO, NO ₂ , EC, OC	Santiago, Chile	↑CV mortality ↑ respiratory mortality	Lag 1	E	Human	Cakmak et al. (2009, 191995)
Gasoline (OC, NO ₃ ⁻ , NH ₄ ⁺)	Atlanta, GA	↑ CVD ED visits	Lag 0	E	Human	Sarnat et al. (2008, 097972)
Diesel (EC, OC, NO ₃ ⁻)	Atlanta, GA	↑ CVD ED visits	Lag 0	E	Human	Sarnat et al. (2008, 097972)
NO _x , EC, ultrafine count	Helsinki, Finland	ST-segment depression	Lag 2	E	Human	Lanki et al. (2006, 089788)

Source Category	Location	Health Effects	Time	Type of Study ¹	Species	Reference
Speed-change factor (Cu, S, aldehydes)	Wake County, NC	↑ blood urea nitrogen ↑ mean red cell volume ↑ blood PMN % ↓ blood lymphocytes % ↑ von Willebrand factor (vWF) ↓ protein C ↑ mean cycle length ↑ SDNN ↑ PNN50 ↑ supraventricular ectopic beats	Lag 15 h	E	Human	Riediker et al. (2004, 056992)
Motor vehicle/other (Br, Pb, Se, Zn, NO ₃ -)	Tuxedo, NY	↓ RMSSD	Afternoon post-exposure	T	Mouse	Lippmann et al. (2005, 087453)
EC, Zn, Pb, Cu, Se	New Haven, CT	↑ respiratory symptoms	Lag 0-2	E	Human	Gent et al. (2009, 180399)
Local combustion (NO _x , ultrafine PM, Cu, Zn, Mn, Fe)	Helsinki, Finland	↓ mean PEF	Lag 0-5 avg	E	Human	Penttinen et al. (2006, 087988)
Gasoline+secondary nitrate*	Birmingham, AL; Atlanta, GA; Pensacola, FL; Centreville, AL	cytotoxic responses (potency)	24 h post-exposure	T	Rat	Seagrave et al. (2006, 091291)
Gasoline+diesel*	Birmingham, AL; Atlanta, GA; Pensacola, FL; Centreville, AL	inflammatory responses (potency)	24 h post-exposure	T	Rat	Seagrave et al. (2006, 091291)
OIL COMBUSTION						
V, Ni	Boston, MA	↑ blood PMN % ↓ blood lymphocytes % ↑ BALF AM %	Following exposure Following exposure 24 h post-exposure	T	Dog	Clarke et al. (2000, 011806)
V, Ni, Se	Tuxedo, NY	↓ SDNN ↓ RMSSD	Afternoon post-exposure	T	Mouse	Lippmann et al. (2005, 087453)
Ni	Boston, MA	↓ respiratory rate	During exposure	T	Dog	Nikolov et al. (2008, 156808)
V, Ni	Boston, MA	↑ lung PMN density	24 h post-exposure	T	Rat	Saldiva et al. (2002, 025988)
COAL COMBUSTION						
Se, SO ₄ ²⁻	Harvard Six Cities	↑ total mortality	Lag 0-1	E	Human	Laden et al. (2000, 012102)
Not provided	Washington, D.C.	↑ total mortality	Lag 3	E	Human	Ito et al. (2006, 088391)
OTHER METALS						
Cu smelter (not provided)	Phoenix, AZ	↑ CV mortality ↑ total mortality	Lag 0	E	Human	Mar et al. (2006, 086143)
Incinerator	Washington, D.C.	Negative association with total and CV mortality	Lag 0	E	Human	Ito et al. (2006, 088391)
Metal processing (SO ₄ ²⁻ , Fe, NH ₄ ⁺ , EC, OC)	Atlanta, GA	↑ CVD ED visits	Lag 0	E	Human	Sarnat et al. (2008, 097972)

Source Category	Location	Health Effects	Time	Type of Study ¹	Species	Reference
Combustion (Cr, Cu, Fe, Mn, Zn)	Santiago, Chile	↑CV mortality ↑respiratory mortality	Lag 1	E	Human	Cakmak et al. (2009, 191995)
WOODSMOKE / VEGETATIVE BURNING						
OC, K	Phoenix, AZ	↑ CV mortality	Lag 3	E	Human	Mar et al. (2000, 001760)
OC, EC, K, NH ₄ ⁺	Atlanta, GA	↑ CVD ED visits	Lag 0	E	Human	Sarnat et al. (2008, 097972)
Total C	Spokane, WA	↑ respiratory ED visits	Lag 1	E	Human	Schreuder et al. (2006, 097959)
UNNAMED FACTORS						
Zn-Cu-V	Chapel Hill, NC	↑ blood fibrinogen	18 h post-exposure	H	Human	Huang et al. (2003, 087377)
Fe-Se-SO ₄ ²⁻	Chapel Hill, NC	↑ BALF PMN	18 h post-exposure	H	Human	Huang et al. (2003, 087377)
Br, Cl, Pb	Santiago, Chile	↑CV mortality ↑respiratory mortality	Lag 1	E	Human	Cakmak et al. (2009, 191995)
Br, Pb	Boston, MA	↑ BALF PMN %	24 h post-exposure	T	Dog	Clarke et al. (2000, 011806)
Br, Pb	Boston, MA	↑ lung PMN density	24 h post-exposure	T	Rat	Saldiva et al. (2002, 025988)

*Constituents not provided.

¹ E = Epidemiologic study; H = Controlled human exposure study; T = Toxicological study

An *in vitro* toxicological study that employed Chapel Hill PM₁₀ used PCA but did not name specific PM sources (Becker et al., 2005, [088590](#)). In this study, the release of IL-6 from human alveolar macrophages and IL-8 from normal human bronchial epithelial cells was associated with a PM₁₀ factor comprised of Cr, Al, Si, Ti, Fe, and Cu. No statistically significant effects were observed for a second PM₁₀ factor (Zn, As, V, Ni, Pb, and Se).

Those toxicological studies that did not apply groupings to the ambient PM_{2.5} speciation data demonstrated a variety of results. Two Boston CAPs studies demonstrated lung oxidative stress correlated with a number of individual PM_{2.5} constituents including, Mn, Zn, Fe, Cu, and Ca (Gurgueira et al., 2002, [036535](#)) and Al, Si, Fe, K, Pb, and Cu (Rhoden et al., 2004, [087969](#)) in rats using univariate regression.

The remaining toxicological study that did not use ambient PM constituent groupings reported a correlation between Zn and plasma fibrinogen in SH rats when constituents were normalized per unit mass of CAPs (Kodavanti et al., 2002, [035344](#)).

6.6.3. Summary by Health Effects

Recent epidemiologic, toxicological, and controlled human exposure studies have evaluated the health effects associated with ambient PM constituents and sources, using a variety of quantitative methods applied to a broad set of PM constituents, rather than selecting a few constituents a priori. As shown in Table 6-18, numerous ambient PM_{2.5} source categories have been associated with health effects, including factors for PM from crustal and soil, traffic, secondary SO₄²⁻, power plants, and oil combustion sources. There is some evidence for trends and patterns that link particular ambient PM constituents or sources with specific health outcomes, but there is insufficient evidence to determine whether these patterns are consistent or robust.

For cardiovascular effects, multiple outcomes have been linked to a PM crustal/soil/road dust source, including cardiovascular mortality in Washington D.C. (Ito et al., 2006, [088391](#)) and Santiago, Chile, (Cakmak et al., 2009, [191995](#)) and ST-segment changes in Helsinki (Lanki et al., 2006, [089788](#)), Los Angeles (Gong et al., 2003, [042106](#)), and Boston (Wellenius et al., 2003, [055691](#)). Interestingly, the ST-segment changes have been observed in an epidemiologic panel study, a controlled human exposure study, and a toxicological study, although the majority of the CAPs in the controlled human exposure study was PM_{10-2.5}. Further support for a crustal/soil/road dust source associated with cardiovascular health effects comes from a PM₁₀ source apportionment study in Copenhagen that reported increased cardiovascular hospital admissions (Andersen et al., 2007, [093201](#)).

PM_{2.5} traffic and wood smoke/vegetative burning sources have also been linked to cardiovascular effects. Cardiovascular mortality in Phoenix (Mar et al., 2000, [001760](#); 2006, [086143](#)) and Santiago, Chile, (Cakmak et al., 2009, [191995](#)) was associated with traffic at lag 1. Gasoline and diesel sources were associated with ED visits in Atlanta for cardiovascular disease at lag 0 (Sarnat et al., 2008, [097972](#)). Cardiovascular mortality in Phoenix (Mar et al., 2000, [001760](#)) and ED visits in Atlanta (Sarnat et al., 2008, [097972](#)) were associated with wood smoke/vegetative burning.

Studies that only examined the effects of individual PM_{2.5} constituents linked EC to cardiovascular hospital admissions in a multicity analysis (Peng et al., 2009, [191998](#)) and cardiovascular mortality in California (Ostro et al., 2007, [091354](#); 2008, [097971](#)).

These studies suggest that cardiovascular effects may be associated with PM_{2.5} from motor vehicle emissions, wood or biomass burning, and PM (both PM_{2.5} and PM_{10-2.5}) from crustal or road dust sources. In addition, there are many studies that observed associations between other sources (i.e., salt, secondary SO₄²⁻/long-range transport, other metals) and cardiovascular effects, but at this time, there does not appear to be a consistent trend or pattern of effects for those factors.

There is less consistency in observed associations between PM sources and respiratory health effects, which may be partially due to the fact that fewer studies have been conducted that evaluated respiratory-related outcomes and measures. However, there is some evidence for associations with secondary SO₄²⁻ PM_{2.5}. Sarnat et al. (2008, [097972](#)) found an increase in respiratory ED visits in Atlanta that was associated with a PM_{2.5} secondary SO₄²⁻ factor. Decrements in lung function in Helsinki (Lanki et al., 2006, [089788](#)) and Los Angeles (Gong et al., 2005, [087921](#)) in asthmatic and healthy adults, respectively, were also linked to this factor. Health effects relating to the crustal/soil/road dust and traffic sources of PM included increased respiratory symptoms in asthmatic children (Gent et al., 2009, [180399](#)) and decreased PEF in asthmatic adults (Penttinen et al., 2006, [087988](#)). Inconsistent results were also observed in those PM_{2.5} studies that use individual constituents to examine associations with respiratory morbidity and mortality, although Cu, Pb, OC, and Zn were related to respiratory health effects in two or more studies.

A few studies have identified PM_{2.5} sources associated with total mortality. These studies found an association between mortality and a PM_{2.5} coal combustion factor (Laden et al., 2000, [012102](#)), while others linked mortality to a secondary SO₄²⁻/long-range transport PM_{2.5} source (Ito et al., 2006, [088391](#); Mar et al., 2006, [086143](#)).

Recent studies have evaluated whether the variation in associations between PM_{2.5} and morbidity and mortality or PM₁₀ and mortality reflects differences in PM_{2.5} constituents (Bell et al., 2009, [191997](#); Dominici et al., 2007, [099135](#); Lippmann et al., 2006, [091165](#)). In three studies (Bell et al., 2009, [191997](#); Dominici et al., 2007, [099135](#); Lippmann et al., 2006, [091165](#)) PM₁₀-mortality effect estimates were greater in areas with a higher proportion of Ni in PM_{2.5}, but the overall PM₁₀-mortality association was diminished when New York City was excluded in a sensitivity analysis in two of the studies. V was also found to modify PM₁₀-mortality effect estimates as well as those for PM_{2.5} with respiratory and cardiovascular hospital admissions (Bell et al., 2009, [191997](#)). When examining the effect of species-to-PM_{2.5} mass proportion on PM_{2.5}-mortality effect estimates Ni was found to modify the association along with Al, As, Si, and SO₄²⁻, but not V (Franklin et al., 2008, [097426](#)).

6.6.4. Conclusion

Recent studies show that source apportionment methods have the potential to add useful insights into which sources and/or PM constituents may contribute to different health effects. Of particular interest are several epidemiologic studies that compared source apportionment methods and the associated results. One set of studies compared epidemiologic associations with PM_{2.5} source factors using several methods - PCA, PMF, and UNMIX - independently analyzed by separate research groups (Hopke et al., 2006, [088390](#); Ito et al., 2006, [088391](#); Mar et al., 2006, [086143](#); Thurston et al., 2005, [097949](#)). Schreuder et al. (2006, [097959](#)) compared UPM and two versions of UNMIX to derive tracers and Sarnat et al. (2008, [097972](#)) compared PMF, modified CMB, and a single-species tracer approach. In all analyses, epidemiologic results based on the different methods were generally in close agreement. The variation in risk estimates for daily mortality between source categories was significantly larger than the variation between research groups (Ito et al., 2006, [088391](#); Mar et al., 2006, [086143](#); Thurston et al., 2005, [097949](#)). Additionally, the variation in risk estimates based on the source apportionment model used had a much smaller effect than the

variation caused by the different source constituents. Further, the most strongly associated source types were consistent across all groups. This supports the general validity of such approaches, though greater integration of results would be possible if the methods employed for grouping PM constituents were more consistent across studies and disciplines. Further research would aid understanding of the contribution of different factors, sources, or source tracers of PM to health effects by increasing the number of locations where similar health endpoints or outcomes are examined.

Overall, the results displayed in Table 6-18 indicate that many constituents of PM can be linked with differing health effects and the evidence is not yet sufficient to allow differentiation of those constituents or sources that are more closely related to specific health outcomes. These findings are consistent with the conclusions of the 2004 PM AQCD (U.S. EPA, 2004, [056905](#)), that a number of source types, including motor vehicle emissions, coal combustion, oil burning, and vegetative burning, are associated with health effects. Although the crustal factor of fine particles was not associated with mortality in the 2004 PM AQCD (U.S. EPA, 2004, [056905](#)), recent studies have suggested that PM (both PM_{2.5} and PM_{10-2.5}) from crustal, soil or road dust sources or PM tracers linked to these sources are associated with cardiovascular effects. In addition, secondary SO₄²⁻ PM_{2.5} has been associated with both cardiovascular and respiratory effects.

Chapter 6 References

- Adamkiewicz G; Ebelt S; Syring M; Slater J; Speizer FE; Schwartz J; Suh H; Gold DR (2004). Association between air pollution exposure and exhaled nitric oxide in an elderly population. *Thorax*, 59: 204-209. [087925](#)
- Adar SD; Adamkiewicz G; Gold DR; Schwartz J; Coull BA; Suh H (2007). Ambient and microenvironmental particles and exhaled nitric oxide before and after a group bus trip. *Environ Health Perspect*, 115: 507-512. [098635](#)
- Adar SD; Gold DR; Coull BA; Schwartz J; Stone PH; Suh H (2007). Focused exposures to airborne traffic particles and heart rate variability in the elderly. *Epidemiology*, 18: 95-103. [001458](#)
- Aekplakorn W; Loomis D; Vichit-Vadakan N; Shy C; Plungchuchon S (2003). Acute effects of SO₂ and particles from a power plant on respiratory symptoms of children, Thailand. *Southeast Asian J Trop Med Public Health*, 34: 906-914. [089908](#)
- Alarie Y (1973). Sensory irritation by airborne chemicals. *Crit Rev Toxicol*, 2: 299-363. [070967](#)
- Albert CM; Rosenthal L; Calkins H; Steinberg JS; Ruskin JN; Wang P; Muller JE; Mittleman MA (2007). Driving and Implantable Cardioverter-Defibrillator Shocks for Ventricular Arrhythmias: Results From the TOVA Study. *J Am Coll Cardiol*, 50: 2233-2240. [156201](#)
- Alexis NE; Lay JC; Zeman K; Bennett WE; Peden DB; Soukup JM; Devlin RB; Becker S (2006). Biological material on inhaled coarse fraction particulate matter activates airway phagocytes in vivo in healthy volunteers. *J Allergy Clin Immunol*, 117: 1396-1403. [154323](#)
- Allen RW; Mar T; Koenig J; Liu LJ; Gould T; Simpson C; Larson T (2008). Changes in lung function and airway inflammation among asthmatic children residing in a woodsmoke-impacted urban area. *Inhal Toxicol*, 20: 423-433. [156208](#)
- American Heart Association (2009). Cardiovascular disease statistics. Retrieved 17-NOV-09, from <http://www.americanheart.org/presenter.jhtml?identifier=4478>. [198920](#)
- Analitis A; Katsouyanni K; Dimakopoulou K; Samoli E; Nikoloulopoulos AK; Petasakis Y; Touloumi G; Schwartz J; Anderson HR; Cambra K; Forastiere F; Zmirou D; Vonk JM; Clancy L; Kriz B; Bobvos J; Pekkanen J (2006). Short-term effects of ambient particles on cardiovascular and respiratory mortality. *Epidemiology*, 17: 230-233. [088177](#)
- Andersen ZJ; Loft S; Ketzel M; Stage M; Scheike T; Mette MN; Bisgaard H (2008). Ambient Air Pollution Triggers Wheezing Symptoms in Infants. *Thorax*, 63: 710-716. [096150](#)
- Andersen ZJ; Wahlin P; Raaschou-Nielsen O; Ketzel M; Scheike T; Loft S (2008). Size distribution and total number concentration of ultrafine and accumulation mode particles and hospital admissions in children and the elderly in Copenhagen, Denmark. *Occup Environ Med*, 65: 458-66. [189651](#)
- Andersen ZJ; Wahlin P; Raaschou-Nielsen O; Scheike T; Loft S (2007). Ambient particle source apportionment and daily hospital admissions among children and elderly in Copenhagen. *J Expo Sci Environ Epidemiol*, 17: 625-636. [093201](#)
- Anderson HR; Bremner SA; Atkinson RW; Harrison RM; Walters S (2001). Particulate matter and daily mortality and hospital admissions in the west midlands conurbation of the United Kingdom: associations with fine and coarse particles, black smoke and sulphate. *Occup Environ Med*, 58: 504-510. [017033](#)
- Anselme F; Lorient S; Henry J-P; Dionnet F; Napoleoni J-G; Thnillez C; Morin J-P (2007). Inhalation of diluted diesel engine emission impacts heart rate variability and arrhythmia occurrence in a rat model of chronic ischemic heart failure. *Arch Toxicol*, 81: 299-307. [097084](#)
- Antonini JM; Roberts JR; Jernigan MR; Yang H-M; Ma JYC; Clarke RW (2002). Residual oil fly ash increases the susceptibility to infection and severely damages the lungs after pulmonary challenge with a bacterial pathogen. *Toxicol Sci*, 70: 110-119. [035342](#)

■Note: Hyperlinks to the reference citations throughout this document will take you to the NCEA HERO database (Health and Environmental Research Online) at <http://epa.gov/hero>. HERO is a database of scientific literature used by U.S. EPA in the process of developing science assessments such as the Integrated Science Assessments (ISA) and the Integrated Risk Information System (IRIS).

- Antonini JM; Taylor MD; Leonard SS; Lawryk NJ; Shi X; Clarke RW; Roberts JR (2004). Metal composition and solubility determine lung toxicity induced by residual oil fly ash collected from different sites within a power plant. *Mol Cell Biochem*, 255: 257-265. [097199](#)
- Arantes-Costa F; Lopes F; Toledo A; Magliarelli-Filho P; Moriya H; Carvalho-Oliveira R; Mauad T; Saldiva P; Martins M (2008). Effects of residual oil fly ash (ROFA) in mice with chronic allergic pulmonary inflammation. *Toxicol Pathol*, 36: 680-686. [187137](#)
- Arbex MA; Martins LC; De Oliveira RC; Pereira LA; Arbex FF; Cancado JE; Saldiva PH; Braga AL (2007). Air pollution from biomass burning and asthma hospital admissions in a sugar cane plantation area in Brazil. *J Epidemiol Community Health*, 61: 395-400. [091637](#)
- Arena VC; Mazumdar S; Zborowski JV; Talbott EO; He S; Chuang YH; Schwerha JJ (2006). A retrospective investigation of PM10 in ambient air and cardiopulmonary hospital admissions in Allegheny County, Pennsylvania: 1995-2000. *J Occup Environ Med*, 48: 38-47. [088631](#)
- Atiga WL; Calkins H; Lawrence JH; Tomaselli GF; Smith JM; Berger RD (1998). Beat-to-beat repolarization lability identifies patients at risk for sudden cardiac death. *J Cardiovasc Electrophysiol*, 9: 899-908. [156231](#)
- Atkinson RW; Anderson HR; Sunyer J; Ayres J; Baccini M; Vonk JM; Boumghar A; Forastiere F; Forsberg B; Touloumi G; Schwartz J; Katsouyanni K (2001). Acute effects of particulate air pollution on respiratory admissions: results from APHEA 2 project. *Am J Respir Crit Care Med*, 164: 1860-1866. [021959](#)
- Atkinson RW; Anderson HR; Sunyer J; Ayres J; Baccini M; Vonk JM; Boumghar A; Forastiere F; Forsberg B; Touloumi G; Schwartz J; Katsouyanni K (2003). Acute effects of particulate air pollution on respiratory admissions. Health Effects Institute. Cambridge, MA. [042797](#)
- Atkinson RW; Bremner SA; Anderson HR; Strachan DP; Bland JM; Ponce de Leon A (1999). Short-term associations between emergency hospital admissions for respiratory and cardiovascular disease and outdoor air pollution in London. *Arch Environ Occup Health*, 54: 398-411. [007882](#)
- ATSDR (2006). A study of ambient air contaminants and asthma in New York City: Part A and B. Agency for Toxic Substances and Disease Registry; Public Health Service; U.S. Department of Health and Human Services. Atlanta, GA. http://permanent.access.gpo.gov/lps88357/ASTHMA_BRONX_FINAL_REPORT.pdf. [090132](#)
- Baccarelli A; Cassano P; Litonjua A; Park S; Suh H; Sparrow D; Vokonas P; Schwartz J (2008). Cardiac autonomic dysfunction: effects from particulate air pollution and protection by dietary methyl nutrients and metabolic polymorphisms. *Circulation*, 117: 1802. [191959](#)
- Baccarelli A; Zanobetti A; Martinelli I; Grillo P; Hou L; Giacomini S; Bonzini M; Lanzani G; Mannucci PM; Bertazzi PA; Schwartz J (2007). Effects of exposure to air pollution on blood coagulation. *J Thromb Haemost*, 5: 252-260. [090733](#)
- Baccarelli A; Zanobetti A; Martinelli I; Grillo P; Hou L; Lanzani G; Mannucci PM; Bertazzi PA; Schwartz J (2007). Air pollution, smoking, and plasma homocysteine. *Environ Health Perspect*, 115: 176-181. [091310](#)
- Bagate K; Meiring JJ; Gerlofs-Nijland ME; Vincent R; Cassee FR; Borm PJA (2004). Vascular effects of ambient particulate matter instillation in spontaneous hypertensive rats. *Toxicol Appl Pharmacol*, 197: 29-39. [087945](#)
- Ballester F; Rodriguez P; Iniguez C; Saez M; Daponte A; Galan I; Taracido M; Arribas F; Bellido J; Cirarda FB; Canada A; Guillen JJ; Guillen-Grima F; Lopez E; Perez-Hoyos S; Lertxundi A; Toro S (2006). Air pollution and cardiovascular admissions association in Spain: results within the EMECAS project. *J Epidemiol Community Health*, 60: 328-336. [088746](#)
- Barclay JL; Miller BG; Dick S; Dennekamp M; Ford I; Hillis GS; Ayres JG; Seaton A (2009). A panel study of air pollution in subjects with heart failure: negative results in treated patients. *Occup Environ Med*, 66: 325-334. [179935](#)
- Barnett AG; Williams GM; Schwartz J; Best TL; Neller AH; Petroschevsky AL; Simpson RW (2006). The effects of air pollution on hospitalizations for cardiovascular disease in elderly people in Australian and New Zealand cities. *Environ Health Perspect*, 114: 1018-1023. [089770](#)
- Barnett AG; Williams GM; Schwartz J; Neller AH; Best TL; Petroschevsky AL; Simpson RW (2005). Air pollution and child respiratory health: a case-crossover study in Australia and New Zealand. *Am J Respir Crit Care Med*, 171: 1272-1278. [087394](#)

- Barraza-Villarreal A; Sunyer J; Hernandez-Cadena L; Escamilla-Nunez MC; Sienra-Monge JJ; Ramirez-Aguilar M; Cortez-Lugo M; Holguin F; Diaz-Sanchez D; Olin AC; Romieu I (2008). Air pollution, airway inflammation, and lung function in a cohort study of Mexico City schoolchildren. *Environ Health Perspect*, 116: 832-838. [156254](#)
- Barregard L; Sallsten G; Andersson L; Almstrand AC; Gustafson P; Andersson M; Olin AC (2008). Experimental exposure to wood smoke: effects on airway inflammation and oxidative stress. *Occup Environ Med*, 65: 319-324. [155675](#)
- Barregard L; Sallsten G; Gustafson P; Andersson L; Johansson L; Basu S; Stigendal L (2006). Experimental exposure to wood-smoke particles in health humans: effects on markers of inflammation, coagulation, and lipid peroxidation. *Inhal Toxicol*, 18: 845-853. [091381](#)
- Barrett EG; Henson RD; Seilkop SK; McDonald JD; Reed MD (2006). Effects of hardwood smoke exposure on allergic airway inflammation in mice. *Inhal Toxicol*, 18: 33-43. [155677](#)
- Bartoli CR; Wellenius GA; Coull BA; Akiyama I; Diaz EA; Lawrence J; Okabe K; Verrier RL; Godleski JJ (2009). Concentrated ambient particles alter myocardial blood flow during acute ischemia in conscious canines. *Environ Health Perspect*, 117: 333-337. [179904](#)
- Bartoli CR; Wellenius GA; Diaz EA; Lawrence J; Coull BA; Akiyama I; Lee LM; Okabe K; Verrier RL; Godleski JJ (2009). Mechanisms of Inhaled Fine Particulate Air Pollution-Induced Arterial Blood Pressure Changes. *Environ Health Perspect*, 117: 361-366. [156256](#)
- Bartzokas A; Kassomenos P; Petrakis M; Celessides C (2004). The effect of meteorological and pollution parameters on the frequency of hospital admissions for cardiovascular and respiratory problems in Athens. *Indoor Built Environ*, 13: 271-275. [093252](#)
- Bastain TM; Gilliland FD; Li Y-F; Saxon A; Diaz-Sanchez D (2003). Intraindividual reproducibility of nasal allergic responses to diesel exhaust particles indicates a susceptible phenotype. *Clin Immunol*, 109: 130-136. [098690](#)
- Batalha JR; Saldiva P H; Clarke RW; Coull BA; Stearns RC; Lawrence J; Murthy GG; Koutrakis P; Godleski JJ (2002). Concentrated ambient air particles induce vasoconstriction of small pulmonary arteries in rats. *Environ Health Perspect*, 110: 1191-1197. [088109](#)
- Becker S; Mundandhara S; Devlin RB; Madden M (2005). Regulation of cytokine production in human alveolar macrophages and airway epithelial cells in response to ambient air pollution particles: further mechanistic studies. *Toxicol Appl Pharmacol*, 207: 269-275. [088590](#)
- Beckett WS; Chalupa DF; Pauly-Brown A; Speers DM; Stewart JC; Frampton MW; Utell MJ; Huang LS; Cox C; Zareba W; Oberdorster G (2005). Comparing inhaled ultrafine versus fine zinc oxide particles in healthy adults - A human inhalation study. *Am J Respir Crit Care Med*, 171: 1129-1135. [156261](#)
- Bedeschi E; Campari C; Candela S; Collini G; Caranci N; Frasca G; Galassi C; Francesca G; Vigotti MA (2007). Urban air pollution and respiratory emergency visits at pediatric unit, Reggio Emilia, Italy. *J Toxicol Environ Health A Curr Iss*, 70: 261-265. [090712](#)
- Behndig AF; Mudway IS; Brown JL; Stenfors N Helleday R Duggan ST; Wilson SJ; Boman C Cassee FR; Frew AJ; Kelly FJ; Sandstrom T Blomberg A (2006). Airway antioxidant and inflammatory responses to diesel exhaust exposure in healthy humans. *Eur Respir J*, 27: 359-365. [088286](#)
- Bell M; Ebisu K; Peng R; Samet J; Dominici F (2009). Hospital Admissions and Chemical Composition of Fine Particle Air Pollution. *Am J Respir Crit Care Med*, 179: 1115-1120. [191997](#)
- Bell ML; Dominici F; Ebisu K; Zeger SL; Samet JM (2007). Spatial and Temporal Variation in PM_{2.5} Chemical Composition in the United States for Health Effects Studies. *Environ Health Perspect*, 115: 989-995. [155683](#)
- Bell ML; Ebisu K; Peng RD; Dominici F (2009). Adverse health effects of particulate air pollution: modification by air conditioning. *Epidemiology*, 20: 682-686. [191007](#)
- Bell ML; Ebisu K; Peng RD; Walker J; Samet JM; Zeger SL; Dominic F (2008). Seasonal and regional short-term effects of fine particles on hospital admissions in 202 U.S. counties, 1999-2005. *Am J Epidemiol*, 168: 1301-1310. [156266](#)
- Bell ML; Levy JK; Lin Z (2008). The effect of sandstorms and air pollution on cause-specific hospital admissions in Taipei, Taiwan. *Occup Environ Med*, 65: 104-111. [091268](#)
- Bennett CM; McKendry IG; Kelly S; Denike K; Koch T (2006). Impact of the 1998 Gobi dust event on hospital admissions in the Lower Fraser Valley, British Columbia. *Sci Total Environ*, 366: 918-925. [088061](#)

- Berger A; Zareba W; Schneider A; Ruckerl R; Ibal-Mulli A; Cyrys J; Wichmann HE; Peters A (2006). Runs of ventricular and supraventricular tachycardia triggered by air pollution in patients with coronary heart disease. *J Occup Environ Med*, 48: 1149-58. [098702](#)
- Berger RD; Kasper EK; Baughman KL; Marban E; Calkins H; Tomaselli GF (1997). Beat-to-beat QT interval variability: novel evidence for repolarization lability in ischemic and nonischemic dilated cardiomyopathy. *Circulation*, 96: 1557-1565. [155688](#)
- Bernardi L; Passino C; Wilmerding V; Dallam GM; Parker DL; Robergs RA; Appenzeller O (2001). Breathing patterns and cardiovascular autonomic modulation during hypoxia induced by simulated altitude. *J Hypertens*, 19: 947-958. [019040](#)
- Blomberg A; Sainsbury C; Rudell B; Frew AJ; Holgate ST; Sandstrom T; Kelly FJ (1998). Nasal cavity lining fluid ascorbic acid concentration increases in healthy human volunteers following short term exposure to diesel exhaust. *Free Radic Res*, 28: 59-67. [051246](#)
- Blomberg A; Tornqvist H; Desmyter L; Deneys V; Hermans C (2005). Exposure to diesel exhaust nanoparticles does not induce blood hypercoagulability in an at-risk population. *J Thromb Haemost*, 3: 2103-2105. [191991](#)
- Boezen HM; Vonk JM; Van Der Zee SC; Gerritsen J; Hoek G; Brunekreef B; Schouten JP; Postma DS (2005). Susceptibility to air pollution in elderly males and females. *Eur Respir J*, 25: 1018-1024. [087396](#)
- Bosson J; Barath S; Pourazar J; Behndig AF; Sandstrom T; Blomberg A; Adelroth E (2008). Diesel exhaust exposure enhances the ozone-induced airway inflammation in healthy humans. *Eur Respir J*, 31: 1234-40. [196659](#)
- Bosson J; Pourazar J; Forsberg B; Adelroth E; Sandstrom T; Blomberg A (2007). Ozone enhances the airway inflammation initiated by diesel exhaust. *Respir Med*, 101: 1140-1146. [156286](#)
- Bourotte C; Curi-Amarante A-P; Forti M-C; APereira LA; Braga AL; Lotufo PA (2007). Association between ionic composition of fine and coarse aerosol soluble fraction and peak expiratory flow of asthmatic patients in Sao Paulo city (Brazil). *Atmos Environ*, 41: 2036-2048. [150040](#)
- Bouthillier L; Vincent R; Goegan P; Adamson IYR; Bjarnason S; Stewart M; Guenette J; Potvin M; Kumarathasan P (1998). Acute effects of inhaled urban particles and ozone: lung morphology, macrophage activity, and plasma endothelin-1. *Am J Pathol*, 153: 1873-1884. [087110](#)
- Brauner EV; Forchhammer L; Moller P; Simonsen J; Glasius M; Wahlin P; Raaschou-Nielsen O; Loft S (2007). Exposure to ultrafine particles from ambient air and oxidative stress-induced DNA damage. *Environ Health Perspect*, 115: 1177-82. [091152](#)
- Brauner EV; Mortensen J; Moller P; Bernard A; Vinzents P; Wahlin P; Glasius M; Loft S (2009). Effects of ambient air particulate exposure on blood-gas barrier permeability and lung function. *Inhal Toxicol*, 21: 38-47. [190244](#)
- Bräuner EV; Møller P; Barregard L; Dragsted LO; Glasius M; Wåhlin P; Vinzents P; Raaschou-Nielsen O; Loft S (2008). Exposure to ambient concentrations of particulate air pollution does not influence vascular function or inflammatory pathways in young healthy individuals. *Part Fibre Toxicol*, 5: 13. [191966](#)
- Breitner S; Stölzel M; Cyrys J; Pitz M; Wölke G; Kreyling W; Küchenhoff H; Heinrich J; Wichmann H; Peters A (2009). Short-Term Mortality Rates during a Decade of Improved Air Quality in Erfurt, Germany. *Environ Health Perspect*, 117: 448-454. [188439](#)
- Briet M; Collin C; Laurent S; Tan A; Azizi M; Agharazii M; Jeunemaitre X; Alhenc-Gelas F; Boutouyrie P (2007). Endothelial function and chronic exposure to air pollution in normal male subjects. *Hypertension*, 50: 970-976. [093049](#)
- Brook RD; Brook JR; Urch B; Vincent R; Rajagopalan S; Silverman F (2002). Inhalation of fine particulate air pollution and ozone causes acute arterial vasoconstriction in healthy adults. *Circulation*, 105: 1534-1536. [024987](#)
- Brown TP; Rushton L; Muggleston MA; Meehan DF (2003). Health effects of a sulphur dioxide air pollution episode. *J Publ Health Med*, 25: 369-371. [089909](#)
- Burnett RT; Brook J; Dann T; Delocla C; Philips O; Cakmak S; Vincent R; Goldberg MS; Krewski D (2000). Association between particulate- and gas-phase components of urban air pollution and daily mortality in eight Canadian cities. *Inhal Toxicol*, 12: 15-39. [010273](#)
- Burnett RT; Cakmak S; Brook JR (1998). The effect of the urban ambient air pollution mix on daily mortality rates in 11 Canadian cities. *Can J Public Health*, 89: 152-156. [029505](#)

- Burnett RT; Cakmak S; Brook JR; Krewski D (1997). The role of particulate size and chemistry in the association between summertime ambient air pollution and hospitalization for cardiorespiratory diseases. *Environ Health Perspect*, 105: 614-620. [084194](#)
- Burnett RT; Dales R; Krewski D; Vincent R; Dann T; Brook JR (1995). Associations between ambient particulate sulfate and admissions to Ontario hospitals for cardiac and respiratory diseases. *Am J Epidemiol*, 142: 15-22. [077226](#)
- Burnett RT; Goldberg MS (2003). Size-fractionated particulate mass and daily mortality in eight Canadian cities. Health Effects Institute. Boston, MA. [042798](#)
- Burnett RT; Smith-Doiron M; Stieb D; Cakmak S; Brook JR (1999). Effects of particulate and gaseous air pollution on cardiorespiratory hospitalizations. *Arch Environ Occup Health*, 54: 130-139. [017269](#)
- Burnett RT; Stieb D; Brook JR; Cakmak S; Dales R; Raizenne M; Vincent R; Dann T (2004). Associations between short-term changes in nitrogen dioxide and mortality in Canadian cities. *Arch Environ Occup Health*, 59: 228-236. [086247](#)
- Burtscher H (2005). Physical characterization of particulate emissions from diesel engines: a review. *J Aerosol Sci*, 36: 896-932. [155710](#)
- Cakmak S; Dales RE; Vida CB (2009). Components of particulate air pollution and mortality in Chile. *Int J Occup Environ Health*, 15: 152-158. [191995](#)
- Calderón-Garcidueñas L; Maronpot RR; Torres-Jardon R; Henriquez-Roldan C; Schoonhoven R; Acuna-Ayala H; Villarreal-Calderon A; Nakamura J; Fernando R; Reed W; Azzarelli B; Swenberg JA (2003). DNA damage in nasal and brain tissues of canines exposed to air pollutants is associated with evidence of chronic brain inflammation and neurodegeneration. *Toxicol Pathol*, 31: 524-538. [156316](#)
- Calderón-Garcidueñas L; Mora-Tiscareno A; Ontiveros E; Gomez-Garza G; Barragan-Mejia G; Broadway J; Chapman S; Valencia-Salazar G; Jewells V; Maronpot RR; Henriquez-Roldan C; Perez-Guille B; Torres-Jardon R; Herrit L; Brooks D; Osnaya-Brizuela N; Monroy M (2008). Air pollution, cognitive deficits and brain abnormalities: A pilot study with children and dogs. *Brain Cognit*, 68: 117-127. [156317](#)
- Caligiuri G; Levy B; Pernow J; Thoren P; Hansson GK (1999). Myocardial infarction mediated by endothelin receptor signaling in hypercholesterolemic mice. *PNAS*, 96: 6920-4. [157365](#)
- Campbell A; Oldham M; Becaria A; Bondy SC; Meacher D; Sioutas C; Misra C; Mendez LB; Kleinman M (2005). Particulate matter in polluted air may increase biomarkers of inflammation in mouse brain. *Neurotoxicology*, 26: 133-140. [087217](#)
- Campen MJ; Babu NS; Helms GA; Pett S; Wernly J; Mehran R; McDonald JD (2005). Nonparticulate components of diesel exhaust promote constriction in coronary arteries from ApoE^{-/-} mice. *Toxicol Sci*, 88: 95-102. [083977](#)
- Campen MJ; McDonald JD; Reed MD; Seagrave J (2006). Fresh gasoline emissions, not paved road dust, alter cardiac repolarization in ApoE^{-/-} mice. *Cardiovasc Toxicol*, 6: 199-210. [096879](#)
- Cárdenas M; Vallejo M; Romano-Riquer P; Ruiz-Velasco S; Ferreira-Vidal AD; Hermosillo AG (2008). Personal exposure to PM_{2.5} air pollution and heart rate variability in subjects with positive or negative head-up tilt test. *Environ Res*, 108: 1-6. [191900](#)
- Carlsten C; Kaufman JD; Trenga CA; Allen J; Peretz A; Sullivan JH (2008). Thrombotic markers in metabolic syndrome subjects exposed to diesel exhaust. *Inhal Toxicol*, 20: 917-921. [156323](#)
- Carlsten C; Kaufman Joel D; Peretz A; Trenga Carol A; Sheppard L; Sullivan Jeffrey H (2007). Coagulation markers in healthy human subjects exposed to diesel exhaust. *Thromb Res Suppl*, 120: 849-855. [155714](#)
- Cassee FR; Boere AJF; Fokkens PHB; Leseman DLAC; Sioutas C; Kooter IM; Dormans JAMA (2005). Inhalation of concentrated particulate matter produces pulmonary inflammation and systemic biological effects in compromised rats. *J Toxicol Environ Health A Curr Iss*, 68: 773-796. [087962](#)
- Chahine T; Baccarelli A; Litonjua A; Wright RO; Suh H; Gold DR; Sparrow D; Vokonas P; Schwartz J (2007). Particulate air pollution, oxidative stress genes, and heart rate variability in an elderly cohort. *Environ Health Perspect*, 115: 1617-1622. [156327](#)
- Chan C-C; Chuang K-J; Chien L-C; Chen W-J; Chang W-T (2006). Urban air pollution and emergency admissions for cerebrovascular diseases in Taipei, Taiwan. *Eur Heart J*, 27: 1238-1244. [090193](#)

- Chan CC; Chuang KJ; Chen WJ; Chang WT; Lee CT; Peng CM (2008). Increasing cardiopulmonary emergency visits by long-range transported Asian dust storms in Taiwan. *Environ Res*, 106: 393-400. [093297](#)
- Chan CC; Chuang KJ; Shiao GM; Lin LY (2004). Personal exposure to submicrometer particles and heart rate variability in human subjects. *Environ Health Perspect*, 112: 1063-1067. [087398](#)
- Chang C-C; Hwang J-S; Chan C-C; Wang P-Y; Cheng T-J (2007). Effects of concentrated ambient particles on heart rate, blood pressure, and cardiac contractility in spontaneously hypertensive rats during a dust storm event. *Inhal Toxicol*, 19: 973-978. [155719](#)
- Chang C-C; Hwang J-S; Chan C-C; Wang P-Y; Hu T-H; Cheng T-J (2004). Effects of concentrated ambient particles on heart rate, blood pressure, and cardiac contractility in spontaneously hypertensive rats. *Inhal Toxicol*, 16: 421-429. [055637](#)
- Chang C-C; Tsai S-S; Ho S-C; Yang C-Y (2005). Air pollution and hospital admissions for cardiovascular disease in Taipei, Taiwan. *Environ Res*, 98: 114-119. [080086](#)
- Chang CC; Hwang JS; Chan CC; Wang PY; Hu TH; Cheng TJ (2005). Effects of concentrated ambient particles on heart rate variability in spontaneously hypertensive rats. *J Occup Health*, 47: 471-480. [088662](#)
- Chardon B; Lefranc A; Granados D; Gremy I (2007). Air pollution and doctors' house calls for respiratory diseases in the greater Paris area (2000-3). *Occup Environ Med*, 64: 320-324. [091308](#)
- Che W; Zhang Z; Zhang H; Wu M; Liang Y; Liu F; Shu Y; Li N (2007). Compositions and oxidative damage of condensate, particulate and semivolatile organic compounds from gasoline exhausts. *Environ Toxicol Pharmacol*, 24: 11-18. [096460](#)
- Checkoway H; Levy D; Sheppard L; Kaufman J; Koenig J; Siscovick D (2000). A case-crossover analysis of fine particulate matter air pollution and out-of-hospital sudden cardiac arrest. Health Effects Institute. Cambridge, MA. [015527](#)
- Chen C-H; Xirasagar S; Lin H-C (2006). Seasonality in adult asthma admissions, air pollutant levels, and climate: a population-based study. *J Asthma*, 43: 287-292. [087947](#)
- Chen J-C; Schwartz J (2009). Neurobehavioral effects of ambient air pollution on cognitive performance in US adults. *Neurotoxicology*, 30: 231-239. [179945](#)
- Chen LC; Hwang JS (2005). Effects of subchronic exposures to concentrated ambient particles (CAPs) in mice IV Characterization of acute and chronic effects of ambient air fine particulate matter exposures on heart-rate variability. *Inhal Toxicol*, 17: 209-216. [087218](#)
- Chen PS; Tan AY (2007). Autonomic nerve activity and atrial fibrillation. *Heart Rhythm*, 4: S61-S64. [197461](#)
- Chen Y; Yang Q; Krewski D; Burnett RT; Shi Y; McGrail KM (2005). The effect of coarse ambient particulate matter on first, second, and overall hospital admissions for respiratory disease among the elderly. *Inhal Toxicol*, 17: 649-655. [087555](#)
- Chen Y; Yang Q; Krewski D; Shi Y; Burnett RT; McGrail K (2004). Influence of relatively low level of particulate air pollution on hospitalization for COPD in elderly people. *Inhal Toxicol*, 16: 21-25. [087262](#)
- Cheng M-F; Tsai S-S; Wu T-N; Chen P-S; Yang C-Y (2007). Air pollution and hospital admissions for pneumonia in a tropical city: Kaohsiung, Taiwan. *J Toxicol Environ Health A Curr Iss*, 70: 2021-2026. [093034](#)
- Chevalier P; Burri H; Adeleine P; Kirkorian G; Lopez M; Leizorovicz A; Andre-Fouet X; Chapon P; Rubel P; Touboul P (2003). QT dynamicity and sudden death after myocardial infarction: results of a long-term follow-up study. *J Cardiovasc Electrophysiol*, 14: 227-233. [156338](#)
- Chimonas MA; Gessner BD (2007). Airborne particulate matter from primarily geologic, non-industrial sources at levels below National Ambient Air Quality Standards is associated with outpatient visits for asthma and quick-relief medication prescriptions among children less than 20 years old enrolled in Medicaid in Anchorage, Alaska. *Environ Res*, 103: 397-404. [093261](#)
- Chiu H; Tiao M; Ho S; Kuo H; Wu T; Yang C (2008). Effects of Asian Dust Storm events on hospital admissions for chronic obstructive pulmonary disease in Taipei, Taiwan. *Inhal Toxicol*, 20: 777-781. [191989](#)
- Chock DP; Winkler SL; Chen C (2000). A study of the association between daily mortality and ambient air pollutant concentrations in Pittsburgh, Pennsylvania. *J Air Waste Manag Assoc*, 50: 1481-1500. [010407](#)

- Choi JH; Xu QS; Park SY; Kim JH; Hwang SS; Lee KH; Lee HJ; Hong YC (2007). Seasonal variation of effect of air pollution on blood pressure. *J Epidemiol Community Health*, 61: 314-318. [093196](#)
- Chuang K-J; Chan C-C; Chen N-T; Su T-C; Lin L-Y (2005). Effects of particle size fractions on reducing heart rate variability in cardiac and hypertensive patients. *Environ Health Perspect*, 113: 1693-1697. [087989](#)
- Chuang K-J; Chan C-C; Su T-C; Lee C-T; Tang C-S (2007). The effect of urban air pollution on inflammation, oxidative stress, coagulation, and autonomic dysfunction in young adults. *Am J Respir Crit Care Med*, 176: 370-376. [091063](#)
- Chuang KJ; Chan CC; Shiao GM; Su TC (2005). Associations between submicrometer particles exposures and blood pressure and heart rate in patients with lung function impairments. *J Occup Environ Med*, 47: 1093-1098. [156356](#)
- Chuang KJ; Coull BA; Zanobetti A; Suh H; Schwartz J; Stone PH; Litonjua A; Speizer FE; Gold DR (2008). Particulate Air Pollution as a Risk Factor for ST-Segment Depression in Patients With Coronary Artery Disease. *Circulation*, 118: 1314-1320. [155731](#)
- Ciencewicki J; Gowdy K; Krantz QT; Linak WP; Brighton L; Gilmour MI; Jaspers I (2007). Diesel exhaust enhanced susceptibility to influenza infection is associated with decreased surfactant protein expression. *Inhal Toxicol*, 19: 1121-1133. [096557](#)
- Clancy L; Goodman P; Sinclair H; Dockery DW (2002). Effect of air pollution control on death rates in Dublin, Ireland: an intervention study. *Lancet*, 360: 1210-1214. [035270](#)
- Clarke RW; Catalano P; Coull B; Koutrakis P; Krishna Murthy GG; Rice T; Godleski JJ (2000). Age-related responses in rats to concentrated urban air particles (CAPs). Presented at In: Phalen, R. F., ed. *Inhalation toxicology: proceedings of the third colloquium on particulate air pollution and human health (first special issue)*; June, 1999; Durham, NC. *Inhalation Toxicol*. 12(suppl. 1): 73-84. [011806](#)
- Coleridge HM; Coleridge JCG (1994). Pulmonary Reflexes: Neural Mechanisms of Pulmonary Defense. *Annu Rev Physiol*, 56: 69-91. [156362](#)
- Courtois A; Andujar P; Ladeiro Y; Baudrimont I; Delannoy E; Leblais V; Begueret H; Galland MAB; Brochard P; Marano F (2008). Impairment of NO-Dependent Relaxation in Intralobar Pulmonary Arteries: Comparison of Urban Particulate Matter and Manufactured Nanoparticles. *Environ Health Perspect*, 116: 1294-1299. [156369](#)
- Cozzi E; Hazarika S; Stallings HW; Cascio WE; Devlin RB; Lust RM; Wingard CJ; Van Scott MR (2006). Ultrafine particulate matter exposure augments ischemia-reperfusion injury in mice. *Am J Physiol*, 291: H894-H903. [091380](#)
- Cruts B; van Etten L; Tornqvist H; Blomberg A; Sandstrom T; Mills NL; Borm PJ (2008). Exposure to diesel exhaust induces changes in EEG in human volunteers. *Part Fibre Toxicol*, 5: 4. [156374](#)
- D'Ippoliti D; Forastiere F; Ancona C; Agabiti N; Fusco D; Michelozzi P; Perucci CA (2003). Air pollution and myocardial infarction in Rome: a case-crossover analysis. *Epidemiology*, 14: 528-535. [074311](#)
- Dales R (2004). Ambient carbon monoxide may influence heart rate variability in subjects with coronary artery disease. *J Occup Environ Med*, 46: 1217-1221. [099036](#)
- Dales R; Liu L; Szyszkowicz M; Dalipaj M; Willey J; Kulka R; Ruddy TD (2007). Particulate air pollution and vascular reactivity: the bus stop study. *Int Arch Occup Environ Health*, 81: 159-164. [155743](#)
- Daniels MJ; Dominici F; Zeger SL; Samet JM (2004). The national morbidity, mortality, and air pollution study Part III: PM10 concentration-response curves and thresholds for the 20 largest US cities. Health Effects Institute. Cambridge, MA. [087343](#)
- Danielsen PH; Brauner EV; Barregard L; Sallsten G; Wallin M; Olinski R; Rozalski R; Moller P; Loft S (2008). Oxidatively damaged DNA and its repair after experimental exposure to wood smoke in healthy humans. *Mutat Res Fund Mol Mech Mutagen*, 642: 37-42. [156382](#)
- Day KC; Reed MD; McDonald JD; Keilkop SK; Barrett EG (2008). Effects of gasoline engine emissions on preexisting allergic airway responses in mice. *Inhal Toxicol*, 20: 1145-1155. [190204](#)
- Delfino R; Brummel S; Wu J; Stern H; Ostro B; Lipsett M; Winer A; Street D; Zhang L; Tjoa T (2009). The relationship of respiratory and cardiovascular hospital admissions to the southern California wildfires of 2003. *Occup Environ Med*, 66: 189. [191994](#)

- Delfino RJ; Chang J; Wu J; Ren C; Tjoa T; Nickerson B; Cooper D; Gillen DL (2009). Repeated hospital encounters for asthma in children and exposure to traffic-related air pollution near the home. *Ann Allergy Asthma Immunol*, 102: 138-44. [190254](#)
- Delfino RJ; Coate BD; Zeiger RS; Seltzer JM; Street DH; Koutrakis P (1996). Daily asthma severity in relation to personal ozone exposure and outdoor fungal spores. *Am J Respir Crit Care Med*, 154: 633-641. [080788](#)
- Delfino RJ; Gone H; Linn WS; Pellizzari ED; Hu Y (2003). Asthma symptoms in Hispanic children and daily ambient exposures to toxic and criteria air pollutants. *Environ Health Perspect*, 111: 647-656. [050460](#)
- Delfino RJ; Gong H; Linn WS; Hu Y; Pellizzari ED (2003). Respiratory symptoms and peak expiratory flow in children with asthma in relation to volatile organic compounds in exhaled breath and ambient air. *J Expo Sci Environ Epidemiol*, 13: 348-363. [090941](#)
- Delfino RJ; Murphy-Moulton AM; Becklake MR (1998). Emergency room visits for respiratory illnesses among the elderly in Montreal: association with low level ozone exposure. *Environ Res*, 76: 67-77. [093624](#)
- Delfino RJ; Quintana PJE; Floro J; Gastanaga VM; Samimi BS; Kleinman MT; Liu L-JS; Bufalino C; Wu C-F; McLaren CE (2004). Association of FEV1 in asthmatic children with personal and microenvironmental exposure to airborne particulate matter. *Environ Health Perspect*, 112: 932-941. [056897](#)
- Delfino RJ; Staimer N; Gillen D; Tjoa T; Sioutas C; Fung K; George SC; Kleinman MT (2006). Personal and ambient air pollution is associated with increased exhaled nitric oxide in children with asthma. *Environ Health Perspect*, 114: 1736-1743. [090745](#)
- Delfino RJ; Staimer N; Tjoa T; Polidori A; Arhami M; Gillen DL; Kleinman MT; Vaziri ND; Longhurst J; Zaldivar F; Sioutas C (2008). Circulating biomarkers of inflammation, antioxidant activity, and platelet activation are associated with primary combustion aerosols in subjects with coronary artery disease. *Environ Health Perspect*, 116: 898-906. [156390](#)
- Delfino RJ; Zeiger RS; Seltzer JM; Street DH (1998). Symptoms in pediatric asthmatics and air pollution: differences in effects by symptom severity, anti-inflammatory medication use and particulate averaging time. *Environ Health Perspect*, 106: 751-761. [051406](#)
- Delfino RJ; Zeiger RS; Seltzer JM; Street DH; McLaren CE (2002). Association of asthma symptoms with peak particulate air pollution and effect modification by anti-inflammatory medication use. *Environ Health Perspect*, 110: A607-A617. [093740](#)
- DeMeo DL; Zanobetti A; Litonjua AA; Coull BA; Schwartz J; Gold DR (2004). Ambient air pollution and oxygen saturation. *Am J Respir Crit Care Med*, 170: 383-387. [087346](#)
- Desqueyroux H; Pujet J-C; Prosper M; Squinazi F; Momas I (2002). Short-term effects of low-level air pollution on respiratory health of adults suffering from moderate to severe asthma. *Environ Res*, 89: 29-37. [026052](#)
- Deurloo DT; van Esch BC; Hofstra CL; Nijkamp FP; van Oosterhout AJ (2001). CTLA4-IgG reverses asthma manifestations in a mild but not in a more "severe" ongoing murine model. *Am J Respir Cell Mol Biol*, 25: 751-760. [156396](#)
- Devlin RB; Ghio AJ; Kehrl H; Sanders G; Cascio W (2003). Elderly humans exposed to concentrated air pollution particles have decreased heart rate variability. *Eur Respir J*, 40: 76S-80S. [087348](#)
- De Bruin ML; van Hemel NM; Leufkens HG; Hoes AW (2005). Hospital discharge diagnoses of ventricular arrhythmias and cardiac arrest were useful for epidemiologic research. *J Clin Epidemiol*, 58: 1325-1329. [155746](#)
- de Haar C; Hassing I; Bol M; Bleumink R; Pieters R (2005). Ultrafine carbon black particles cause early airway inflammation and have adjuvant activity in a mouse allergic airway disease model. *Toxicol Sci*, 87: 409-418. [097872](#)
- de Haar C; Hassing I; Bol M; Bleumink R; Pieters R (2006). Ultrafine but not fine particulate matter causes airway inflammation and allergic airway sensitization to co-administered antigen in mice. *Clin Exp Allergy*, 36: 1469-1479. [144746](#)
- De Hartog JJ; Hoek G; Peters A; Timonen KL; Ibalid-Mulli A; Brunekreef B; Heinrich J; Tiittanen P; Van Wijnen JH; Kreyling W; Kulmala M; Pekkanen J (2003). Effects of fine and ultrafine particles on cardiorespiratory symptoms in elderly subjects with coronary heart disease: the ULTRA study. *Am J Epidemiol*, 157: 613-623. [001061](#)

- de Hartog JJ; Lanki T; Timonen KL; Hoek G; Janssen NA; Ibaldo-Mulli A; Peters A; Heinrich J; Tarkiainen TH; van Grieken R; van Wijnen JH; Brunekreef B; Pekkanen J (2009). Associations between PM_{2.5} and heart rate variability are modified by particle composition and beta-blocker use in patients with coronary heart disease. *Environ Health Perspect*, 117: 105-111. [191904](#)
- Diaz-Sanchez D; Garcia MP; Wang M; Jyrala M; Saxon A (1999). Nasal challenge with diesel exhaust particles can induce sensitization to a neoallergen in the human mucosa. *J Allergy Clin Immunol*, 104: 1183-1188. [011346](#)
- Diaz-Sanchez D; Tsien A; Fleming J; Saxon A (1997). Combined diesel exhaust particulate and ragweed allergen challenge markedly enhances human in vivo nasal ragweed-specific IgE and skews cytokine production to a T helper cell 2-type pattern. *J Immunol*, 158: 2406-2413. [051247](#)
- Dick CA; Singh P; Daniels M; Evansky P; Becker S; Gilmour MI (2003). Murine pulmonary inflammatory responses following installation of size-fractionated ambient particulate matter. *J Toxicol Environ Health A Curr Iss*, 66: 2193-2207. [088776](#)
- Diez Roux AV; Auchincloss AH; Astor B; Barr RG; Cushman M; Dvornch T; Jacobs DR Jr; Kaufman J; Lin X; Samson Px (2006). Recent exposure to particulate matter and C-reactive protein concentration in the multi-ethnic study of atherosclerosis x. *Am J Epidemiol*, 164: 437-448. [156400](#)
- Dockery DW; Luttmann-Gibson H; Rich DQ; Link MS; Mittleman MA; Gold DR; Koutrakis P; Schwartz JD; Verrier RL (2005). Association of air pollution with increased incidence of ventricular tachyarrhythmias recorded by implanted cardioverter defibrillators. *Environ Health Perspect*, 113: 670-674. [078995](#)
- Dockery DW; Luttmann-Gibson H; Rich DQ; Link MS; Schwartz JD; Gold DR; Koutrakis P; Verrier RL; Mittleman MA (2005). Particulate air pollution and nonfatal cardiac events Part II Association of air pollution with confirmed arrhythmias recorded by implanted defibrillators. Health Effects Institute. Cambridge, MA. [090743](#)
- Dominici F; McDermott A; Daniels M; Zeger SL; Samet J (2003). Revised Analyses of Time-Series Studies of Air Pollution and Health: Mortality Among Residents of 90 Cities. Health Effects Institute. Boston, MA. [156407](#)
- Dominici F; McDermott A; Zeger SL; Samet JM (2002). On the use of generalized additive models in time-series studies of air pollution and health. *Am J Epidemiol*, 156: 193-203. [030458](#)
- Dominici F; Peng RD; Bell ML; Pham L; McDermott A; Zeger SL; Samet JL (2006). Fine particulate air pollution and hospital admission for cardiovascular and respiratory diseases. *JAMA*, 295: 1127-1134. [088398](#)
- Dominici F; Peng RD; Ebisu K; Zeger SL; Samet JM; Bell ML (2007). Does the effect of PM₁₀ on mortality depend on PM nickel and vanadium content? A reanalysis of the NMMAPS data. *Environ Health Perspect*, 115: 1701-1703. [099135](#)
- Dominici F; Peng RD; Zeger SL; White RH; Samet JM (2007). Particulate air pollution and mortality in the United States: did the risks change from 1987 to 2000? *Am J Epidemiol*, 166: 880-888. [097361](#)
- Dubowsky SD; Suh H; Schwartz J; Coull BA; Gold DR (2006). Diabetes, obesity, and hypertension may enhance associations between air pollution and markers of systemic inflammation. *Environ Health Perspect*, 114: 992-998. [088750](#)
- Dusek R; Frank GP; Hildebrandt L; Curtius J; Schneider J; Walter S; Chand D; Drewnick F; Hings S; Jung D; Borrmann S; Andreae MO (2006). Size matters more than chemistry for cloud-nucleating ability of aerosol particles. *Science*, 312: 1375-1378. [155756](#)
- Duvall RM; Norris GA; Dailey LA; Burke JM; McGee JK; Gilmour MI; Gordon T; Devlin RB (2008). Source apportionment of particulate matter in the US and associations with lung inflammatory markers. *Inhal Toxicol*, 20: 671-683. [097969](#)
- Dvornch JT; Brook RD; Keeler GJ; Rajagopalan S; D'Alecy LG; Marsik FJ; Morishita M; Yip FY; Brook JR; Timm EJ; Wagner JG; Harkema JR (2004). Effects of concentrated fine ambient particles on rat plasma levels of asymmetric dimethylarginine. *Inhal Toxicol*, 16: 473-480. [055741](#)
- Ebelt ST; Wilson WE; Brauer M (2005). Exposure to ambient and nonambient components of particulate matter: a comparison of health effects. *Epidemiology*, 16: 396-405. [056907](#)
- Elder A; Gelein R; Finkelstein J; Phipps R; Frampton M; Utell M; Kittelson DB; Watts WF; Hopke P; Jeong CH; Kim E; Liu W; Zhao W; Zhuo L; Vincent R; Kumarathasan P; Oberdorster G (2004). On-road exposure to highway aerosols. 2. Exposures of aged, compromised rats. *Inhal Toxicol*, 16 Suppl 1: 41-53. [087354](#)

- Elder ACP; Gelein R; Azadniv M; Frampton M; Finkelstein J; Oberdorster G (2004). Systemic effects of inhaled ultrafine particles in two compromised, aged rat strains. *Inhal Toxicol*, 16: 461-471. [055642](#)
- Erbas B; Kelly A-M; Physick B; Code C; Edwards M (2005). Air pollution and childhood asthma emergency hospital admissions: estimating intra-city regional variations. *Int J Environ Health Res*, 15: 11-20. [073849](#)
- Fairley D (2003). Mortality and air pollution for Santa Clara County, California, 1989-1996, In: Revised analyses of time-series studies of air pollution and health. Special report. Health Effects Institute. Boston, MA. <http://www.healtheffects.org/Pubs/TimeSeries.pdf>. [042850](#)
- Fakhri AA; Ilic LM; Wellenius GA; Urch B; Silverman F; Gold DR; Mittleman MA (2009). Autonomic effects of controlled fine particulate exposure in young healthy adults: Effect modification by ozone. *Environ Health Perspect*, 117: 1287-1292. [191914](#)
- Fan Z; Meng Q; Weisel C; Laumbach R; Ohman-Strickland P; Shalat S; Hernandez M; Black K (2008). Acute exposure to elevated PM (2.5) generated by traffic and cardiopulmonary health effects in healthy older adults. *J Expo Sci Environ Epidemiol*, 19: 525-533. [191979](#)
- Farraj AK; Haykal-Coates N; Ledbetter AD; Evansky PA; Gavett SH (2006). Inhibition of pan neurotrophin receptor p75 attenuates diesel particulate-induced enhancement of allergic airway responses in C57/B16J mice. *Inhal Toxicol*, 18: 483-491. [088469](#)
- Farraj AK; Haykal-Coates N; Ledbetter AD; Evansky PA; Gavett SH (2006). Neurotrophin mediation of allergic airways responses to inhaled diesel particles in mice. *Toxicol Sci*, 94: 183-192. [141730](#)
- Fedulov AV; Leme A; Yang Z; Dahl M; Lim R; Mariani TJ; Kobzik L (2008). Pulmonary exposure to particles during pregnancy causes increased neonatal asthma susceptibility. *Am J Respir Cell Mol Biol*, 38: 57-67. [097482](#)
- Ferdinands JM; Crawford CA; Greenwald R; Van Sickle D; Hunter E; Teague WG (2008). Breath acidification in adolescent runners exposed to atmospheric pollution: a prospective, repeated measures observational study. *Environ Health Global Access Sci Source*, 7: 10. [156433](#)
- Finnerty K; Choi J-E; Lau A; Davis-Gorman G; Diven C; Seaver N; Linak William P; Witten M; McDonagh Paul F (2007). Instillation of coarse ash particulate matter and lipopolysaccharide produces a systemic inflammatory response in mice. *J Toxicol Environ Health A Curr Iss*, 70: 1957-1966. [156434](#)
- Fischer PH; Steerenberg PA; Snelder JD; Van Loveren H; Van Amsterdam JGC (2002). Association between exhaled nitric oxide, ambient air pollution and respiratory health in school children. *Int Arch Occup Environ Health*, 75: 348-353. [025731](#)
- Fischer SL; Koshland CP (2007). Daily and peak 1 h indoor air pollution and driving factors in a rural Chinese village. *Environ Sci Technol*, 41: 3121-3126. [156435](#)
- Folino AF; Scapellato ML; Canova C; Maestrelli P; Bertorelli G; Simonato L; Iliceto S; Lotti M (2009). Individual exposure to particulate matter and the short-term arrhythmic and autonomic profiles in patients with myocardial infarction. *Eur Heart J*, 30: 1614-1620. [191902](#)
- Forastiere F; Stafoggia M; Berti G; Bisanti L; Cernigliaro A; Chiusolo M; Mallone S; Miglio R; Pandolfi P; Rognoni M; Serinelli M; Tessari R; Vigotti M; Perucci C (2008). Particulate Matter and Daily Mortality: A Case-Crossover Analysis of Individual Effect Modifiers. *Epidemiology*, 19: 571-580. [186937](#)
- Forastiere F; Stafoggia M; Picciotto S; Bellander T; D'Ippoliti D; Lanki T; Von Klot S; Nyberg F; Paatero P; Peters A; Pekkanen J; Sunyer J; Perucci CA (2005). A case-crossover analysis of out-of-hospital coronary deaths and air pollution in Rome, Italy. *Am J Respir Crit Care Med*, 172: 1549-1555. [086323](#)
- Frampton MW (2001). Systemic and cardiovascular effects of airway injury and inflammation: ultrafine particle exposure in humans. *Environ Health Perspect*, 109: 529-532. [019051](#)
- Frampton MW; Stewart JC; Oberdorster G; Morrow PE; Chalupa D; Pietropaoli AP; Frasier LM; Speers DM; Cox C; Huang LS; Utell MJ (2006). Inhalation of ultrafine particles alters blood leukocyte expression of adhesion molecules in humans. *Environ Health Perspect*, 114: 51-58. [088665](#)
- Franklin M; Koutrakis P; Schwartz J (2008). The role of particle composition on the association between PM2.5 and mortality. *Epidemiology*, 19: 680-689. [097426](#)
- Franklin M; Zeka A; Schwartz J (2007). Association between PM2.5 and all-cause and specific-cause mortality in 27 US communities. *J Expo Sci Environ Epidemiol*, 17: 279-287. [091257](#)

- Fung KY; Khan S; Krewski D; Chen Y (2006). Association between air pollution and multiple respiratory hospitalizations among the elderly in Vancouver, Canada. *Inhal Toxicol*, 18: 1005-1011. [089789](#)
- Fung KY; Luginaah IKMG; Webster G (2005). Air pollution and daily hospitalization rates for cardiovascular and respiratory diseases in London, Ontario. *Int J Environ Stud*, 62: 677-685. [093262](#)
- Galan I; Tobias A; Banegas JR; Aranguiz E (2003). Short-term effects of air pollution on daily asthma emergency room admissions. *Eur Respir J*, 22: 802-808. [087408](#)
- Gavett SH; Haykal-Coates N; Copeland L B; Heinrich J; Gilmour MI (2003). Metal composition of ambient PM_{2.5} influences severity of allergic airways disease in mice. *Environ Health Perspect*, 111: 1471-1477. [053153](#)
- Gehlbach BK; Geppert E (2004). The pulmonary manifestations of left heart failure. *Chest*, 125: 669-682. [155784](#)
- Gent JF; Koutrakis P; Belanger K; Triche E; Holford TR; Bracken MB; Leaderer BP (2009). Symptoms and medication use in children with asthma and traffic-related sources of fine particle pollution. *Environ Health Perspect*, 117: 1168-1174. [180399](#)
- Gent JF; Triche EW; Holford TR; Belanger K; Bracken MB; Beckett WS; Leaderer BP (2003). Association of low-level ozone and fine particles with respiratory symptoms in children with asthma. *JAMA*, 290: 1859-1867. [052885](#)
- Gerlofs-Nijland ME; Rummelhard M; Boere AJF; Leseman DLAC; Duffin R; Schins RPF; Borm PJA; Sillanpaa M; Salonen RO; Cassee FR (2009). Particle induced toxicity in relation to transition metal and polycyclic aromatic hydrocarbon contents. *Environ Sci Technol*, 43: 4729-4736. [190353](#)
- Gerlofs-Nijland ME; Dormans JA; Bloemen HJ; Leseman DL; John A; Boere F; Kelly FJ; Mudway IS; Jimenez AA; Donaldson K; Guastadisegni C; Janssen NA; Brunekreef B; Sandstrom T; van Bree L; Cassee FR (2007). Toxicity of coarse and fine particulate matter from sites with contrasting traffic profiles. *Inhal Toxicol*, 19: 1055-1069. [097840](#)
- Ghelfi E; Rhoden CR; Wellenius GA; Lawrence J; Gonzalez-Flecha B (2008). Cardiac oxidative stress and electrophysiological changes in rats exposed to concentrated air particles are mediated by TRP-dependent pulmonary reflexes. *Toxicol Sci*, 102: 328-336. [156468](#)
- Ghio AJ; Devlin RB (2001). Inflammatory lung injury after bronchial instillation of air pollution particles. *Am J Respir Crit Care Med*, 164: 704-708. [017122](#)
- Ghio AJ; Hall A; Bassett MA; Cascio WE; Devlin RB (2003). Exposure to concentrated ambient air particles alters hematologic indices in humans. *Inhal Toxicol*, 15: 1465-1478. [087363](#)
- Ghio AJ; Kim C; Devlin RB (2000). Concentrated ambient air particles induce mild pulmonary inflammation in healthy human volunteers. *Am J Respir Crit Care Med*, 162: 981-988. [012140](#)
- Gilliland FD; Li YF; Saxon A; Diaz-Sanchez D (2004). Effect of glutathione-S-transferase M1 and P1 genotypes on xenobiotic enhancement of allergic responses: randomised, placebo-controlled crossover study. *Lancet*, 363: 119-125. [156471](#)
- Gilmour MI; McGee J; Duvall Rachelle M; Dailey L; Daniels M; Boykin E; Cho S-H; Doerfler D; Gordon T; Devlin Robert B (2007). Comparative toxicity of size-fractionated airborne particulate matter obtained from different cities in the United States. *Inhal Toxicol*, 19 Suppl 1: 7-16. [096433](#)
- Gilmour MI; O'Connor S; Dick CAJ; Miller CA; Linak WP (2004). Differential pulmonary inflammation and in vitro cytotoxicity of size-fractionated fly ash particles from pulverized coal combustion. *J Air Waste Manag Assoc*, 54: 286-295. [057420](#)
- Gilmour PS; Ziesenis A; Morrison ER; Vickers MA; Drost EM; Ford I; Karg E; Mossa C; Schroepel A; Ferron GA; Heyder J; Greaves M; MacNee W; Donaldson K (2004). Pulmonary and systemic effects of short-term inhalation exposure to ultrafine carbon black particles. *Toxicol Appl Pharmacol*, 195: 35-44. [054175](#)
- Girardot SP; Ryan PB; Smith SM; Davis WT; Hamilton CB; Obenour RA; Renfro JR; Tromatore KA; Reed GD (2006). Ozone and PM₂₅ exposure and acute pulmonary health effects: a study of hikers in the Great Smoky Mountains National Park. *Environ Health Perspect*, 113: 612-617. [088271](#)
- Godleski JJ; Clarke RW; Coull BA; Saldiva PHN; Jiang NF; Lawrence J; Koutrakis P (2002). Composition of inhaled urban air particles determines acute pulmonary responses. *Ann Occup Hyg*, 46: 419-424. [156478](#)

- Godleski JJ; Verrier RL; Koutrakis P; Catalano P; Coull B; Reinisch U; Lovett EG; Lawrence J; Murthy GG; Wolfson JM; Clarke RW; Nearing BD; Killingsworth C (2000). Mechanisms of morbidity and mortality from exposure to ambient air particles. *Res Rep Health Eff Inst*, 91: 5-88; discussion 89-103. [000738](#)
- Gold DR; Litonjua AA; Zanobetti A; Coull BA; Schwartz J; MacCallum G; Verrier RL; Nearing BD; Canner MJ; Suh H; Stone PH (2005). Air pollution and ST-segment depression in elderly subjects. *Environ Health Perspect*, 113: 883-887. [087558](#)
- Goldberg MS; Giannetti N; Burnett RT; Mayo NE; Valois MF; Brophy JM (2008). A panel study in congestive heart failure to estimate the short-term effects from personal factors and environmental conditions on oxygen saturation and pulse rate. *Occup Environ Med*, 65: 659-666. [180380](#)
- Gong H Jr; Sioutas C; Linn WS (2003). Controlled exposures of healthy and asthmatic volunteers to concentrated ambient particles in metropolitan Los Angeles. Health Effects Institute. Boston, MA. [087365](#)
- Gong H; Sioutas C; Linn WS; Clark KW; Terrell SL; Terrell LL; Anderson KR; Kim S; Chang MC (2000). Controlled human exposures to concentrated ambient fine particles in metropolitan Los Angeles: Methodology and preliminary health-effect findings. *Inhal Toxicol*, 12: 107-119. [155799](#)
- Gong H Jr; Linn WS; Clark KW; Anderson KR; Geller MD; Sioutas C (2005). Respiratory responses to exposures with fine particulates and nitrogen dioxide in the elderly with and without COPD. *Inhal Toxicol*, 17: 123-132. [087921](#)
- Gong H Jr; Linn WS; Clark KW; Anderson KR; Sioutas C; Alexis NE; Cascio WE; Devlin RB (2008). Exposures of healthy and asthmatic volunteers to concentrated ambient ultrafine particles in Los Angeles. *Inhal Toxicol*, 20: 533-545. [156483](#)
- Gong H Jr; Linn WS; Sioutas C; Terrell SL; Clark KW; Anderson KR; Terrell LL (2003). Controlled exposures of healthy and asthmatic volunteers to concentrated ambient fine particles in Los Angeles. *Inhal Toxicol*, 15: 305-325. [042106](#)
- Gong H Jr; Linn WS; Terrell SL; Anderson KR; Clark KW; Sioutas C; Cascio WE; Alexis N; Devlin RB (2004). Exposures of elderly volunteers with and without chronic obstructive pulmonary disease (COPD) to concentrated ambient fine particulate pollution. *Inhal Toxicol*, 16: 731-744. [087964](#)
- Gong H Jr; Linn WS; Terrell SL; Clark KW; Geller MD; Anderson KR; Cascio WE; Sioutas C (2004). Altered heart-rate variability in asthmatic and healthy volunteers exposed to concentrated ambient coarse particles. *Inhal Toxicol*, 16: 335-343. [055628](#)
- Gordian ME; Choudhury AH (2003). PM10 and asthma medication in schoolchildren. *Arch Environ Occup Health*, 58: 42-47. [054842](#)
- Gowdy K; Krantz QT; Daniels M; Linak WP; Jaspers I; Gilmour MI (2008). Modulation of pulmonary inflammatory responses and antimicrobial defenses in mice exposed to diesel exhaust. *Toxicol Appl Pharmacol*, 229: 310-319. [097226](#)
- Graff D; Cascio W; Rappold A; Zhou H; Huang Y; Devlin R (2009). Exposure to concentrated coarse air pollution particles causes mild cardiopulmonary effects in healthy young adults. *Environ Health Perspect*, 117: 1089-1094. [191981](#)
- Gurgueira SA; Lawrence J; Coull B; Murthy GGK; Gonzalez-Flecha B (2002). Rapid increases in the steady-state concentration of reactive oxygen species in the lungs and heart after particulate air pollution inhalation. *Environ Health Perspect*, 110: 749-755. [036535](#)
- Hajat S; Haines A; Atkinson RW; Bremner SA; Anderson HR; Emberlin J (2001). Association between air pollution and daily consultations with general practitioners for allergic rhinitis in London, United Kingdom. *Am J Epidemiol*, 153: 704-714. [016693](#)
- Halonen JI; Lanki T; Yli-Tuomi T; Kulmala M; Tiittanen P; Pekkanen J (2008). Urban air pollution, and asthma and COPD hospital emergency room visits. *Thorax*, 63: 635-641. [189507](#)
- Halonen JI; Lanki T; Yli-Tuomi T; Tiittanen P; Kulmala M; Pekkanen (2009). Particulate air pollution and acute cardiorespiratory hospital admissions and mortality among the elderly. *Epidemiology*, 20: 143-153. [180379](#)
- Hamada K; Suzaki Y; Leme A; Ito T; Miyamoto K; Kobzik L; Kimura H (2007). Exposure of pregnant mice to an air pollutant aerosol increases asthma susceptibility in offspring. *J Toxicol Environ Health A Curr Iss*, 70: 688-695. [091235](#)
- Hamade AK; Rabold R; Tankersley CG (2008). Adverse cardiovascular effects with acute particulate matter and ozone exposures: interstrain variation in mice. *Environ Health Perspect*, 116: 1033-1039. [156515](#)

- Hanigan IC; Johnston FH; Morgan GG (2008). Vegetation fire smoke, indigenous status and cardio respiratory hospital admissions in Darwin, Australia, 1996-2005: a time-series study. *Environ Health*, 7: 42. [156518](#)
- Hao M; Comier S; Wang M; Lee James J; Nel A (2003). Diesel exhaust particles exert acute effects on airway inflammation and function in murine allergen provocation models. *J Allergy Clin Immunol*, 112: 905-914. [096565](#)
- Hapcioglu B; Issever H; Kocyigit E; Disci R; Vatansever S; Ozdilli K (2006). The effect of air pollution and meteorological parameters on chronic obstructive pulmonary disease at an Istanbul hospital. *Indoor Built Environ*, 15: 147-153. [093263](#)
- Happo MS; Salonen RO; Halinen AI; Jalava PI; Pennanen AS; Kosma VM; Sillanpaa M; Hillamo R; Brunekreef B; Katsouyanni K; Sunyer J; Hirvonen MR (2007). Dose and time dependency of inflammatory responses in the mouse lung to urban air coarse, fine, and ultrafine particles from six European cities. *Inhal Toxicol*, 19: 227-246. [096630](#)
- Harder V; Gilmour P; Lentner B; Karg E; Takenaka S; Ziesenis A; Stampfl A; Kodavanti U; Heyder J; Schulz H (2005). Cardiovascular responses in unrestrained WKY rats to inhaled ultrafine carbon particles. *Inhal Toxicol*, 17: 29-42. [087371](#)
- Harkema JR; Keeler G; Wagner J; Morishita M; Timm E; Hotchkiss J; Marsik F; Dvonch T; Kaminski N; Barr E (2004). Effects of concentrated ambient particles on normal and hypersecretory airways in rats. Health Effects Institute. Boston, MA. [056842](#)
- Harrod KS; Jaramillo RJ; Berger JA; Gigliotti AP; Seilkop SK; Reed MD (2005). Inhaled diesel engine emissions reduce bacterial clearance and exacerbate lung disease to *Pseudomonas aeruginosa* infection in vivo. *Toxicol Sci*, 83: 155-165. [088144](#)
- Harrod KS; Jaramillo RJ; Rosenberger CL; Wang S-Z; Berger JA; McDonald JD; Reed MD (2003). Increased susceptibility to RSV infection by exposure to inhaled diesel engine emissions. *Am J Respir Cell Mol Biol*, 28: 451-463. [097046](#)
- Hayek T; Oiknine J; Brook JG; Aviram M (1994). Increased plasma and lipoprotein lipid peroxidation in apo E-deficient mice. *Biochem Biophys Res Commun*, 201: 1567-1574. [156527](#)
- Hedley AJ; Wong C-M; Thach TQ; Ma S; Lam T-H; Anderson HR (2002). Cardiorespiratory and all-cause mortality after restrictions on sulphur content of fuel in Hong Kong: an intervention study. *Lancet*, 360: 1646-1652. [040284](#)
- Heidenfelder BL; Reif DM; Harkema JR; Cohen Hubal EA; Hudgens EE; Bramble LA; Wagner JG; Morishita M; Keeler GJ; Edwards SW; Gallagher JE (2009). Comparative microarray analysis and pulmonary changes in brown Norway rats exposed to ovalbumin and concentrated air particulates. *Toxicol Sci*, 108: 207-221. [190026](#)
- Henneberger A; Zareba W; Ibaldo-Mulli A; Ruckerl R; Cyrys J; Couderc J-P; Mykies B; Woelke G; Wichmann H-E; Peters A (2005). Repolarization changes induced by air pollution in ischemic heart disease patients. *Environ Health Perspect*, 113: 440-446. [087960](#)
- Henrotin JB; Besancenot JP; Bejot Y; Giroud M (2007). Short-term effects of ozone air pollution on ischaemic stroke occurrence: A case-crossover analysis from a 10-year population-based study in Dijon, France. *Occup Environ Med*, 64: 439-445. [093270](#)
- Hinwood AL; De Klerk N; Rodriguez C; Jacoby P; Runnion T; Rye P; Landau L; Murray F; Feldwick M; Spickett J (2006). The relationship between changes in daily air pollution and hospitalizations in Perth, Australia 1992-1998: A case-crossover study. *Int J Environ Health Res*, 16: 27-46. [088976](#)
- Hirshon JM; Shardell M; Alles S; Powell JL; Squibb K; Ondov J; Blaisdell CJ (2008). Elevated ambient air zinc increases pediatric asthma morbidity. *Environ Health Perspect*, 116: 826-831. [180375](#)
- Hogervorst JG; de Kok TM; Briede JJ; Wesseling G; Kleinjans JC; van Schayck CP (2006). Relationship between radical generation by urban ambient particulate matter and pulmonary function of school children. *J Toxicol Environ Health A Curr Iss*, 69: 245-262. [156559](#)
- Holguin F; Flores S; Ross Z; Cortez M; Molina M; Molina L; Rincon C; Jerrett M; Berhane K; Granados A; Romieu I (2007). Traffic-related exposures, airway function, inflammation, and respiratory symptoms in children. *Am J Respir Crit Care Med*, 176: 1236-1242. [099000](#)
- Holguin F; Tellez-Rojo MM; Hernandez M; Cortez M; Chow JC; Watson JG; Mannino D; Romieu I (2003). Air pollution and heart rate variability among the elderly in Mexico City. *Epidemiology*, 14: 521-527. [057326](#)

- Holloman CH; Bortnick SM; Morara M; Strauss WJ; Calder CA (2004). A Bayesian hierarchical approach for relating PM_{2.5} exposure to cardiovascular mortality in North Carolina. *Environ Health Perspect*, 112: 1282-1288. [087375](#)
- Hong Y-C; Hwang S-S; Kim JH; Lee K-H; Lee H-J; Lee K-H; Yu S-D; Kim D-S (2007). Metals in particulate pollutants affect peak expiratory flow of schoolchildren. *Environ Health Perspect*, 115: 430-434. [091347](#)
- Hopke PK; Ito K; Mar T; Christensen WF; Eatough DJ; Henry RC; Kim E; Laden F; Lall R; Larson TV; Liu H; Neas L; Pinto J; Stolzel M; Suh H; Paatero P; Thurston GD (2006). PM source apportionment and health effects: 1 Intercomparison of source apportionment results. *J Expo Sci Environ Epidemiol*, 16: 275-286. [088390](#)
- Host S; Larrieu S; Pascal L; Blanchard M; Declercq C; Fabre P; Jusot JF; Chardon B; Le Tertre A; Wagner V; Prouvost H; Lefranc A (2007). Short-term Associations between Fine and Coarse Particles and Cardiorespiratory Hospitalizations in Six French Cities. *Occup Environ Med*, 18: S107-S108. [155851](#)
- Host S; Larrieu S; Pascal L; Blanchard M; Declercq C; Fabre P; Jusot JF; Chardon B; Le Tertre A; Wagner V; Prouvost H; Lefranc A (2008). Short-term associations between fine and coarse particles and hospital admissions for cardiorespiratory diseases in six French cities. *Occup Environ Med*, 65: 544-551. [155852](#)
- Huang Y-CT; Ghio AJ; Stonehuerner J; McGee J; Carter JD; Grambow SC; Devlin RB (2003). The role of soluble components in ambient fine particles-induced changes in human lungs and blood. *Inhal Toxicol*, 15: 327-342. [087377](#)
- Huber SA; Sakkinen P; Conze D; Hardin N; Tracy R (1999). Interleukin-6 exacerbates early atherosclerosis in mice. *Arterioscler Thromb Vasc Biol*, 19: 2364-2367. [156575](#)
- Hwang J-S; Chan C-C (2002). Effects of air pollution on daily clinic visits for lower respiratory tract illness. *Am J Epidemiol*, 155: 1-10. [023222](#)
- Hwang J-S; Nadziejko C; Chen LC (2005). Effects of subchronic exposures to concentrated ambient particles (CAPs) in mice: III Acute and chronic effects of CAPs on heart rate, heart-rate fluctuation, and body temperature. *Inhal Toxicol*, 17: 199-207. [087957](#)
- Ibald-Mulli A; Timonen KL; Peters A; Heinrich J; Wolke G; Lanki T; Buzorius G; Kreyling WG; De Hartog J; Hoek G; Ten Brink HM; Pekkanen J (2004). Effects of particulate air pollution on blood pressure and heart rate in subjects with cardiovascular disease: a multicenter approach. *Environ Health Perspect*, 112: 369-377. [087415](#)
- Inoue K; Takano H; Yanagisawa R; Sakurai M; Ichinose T; Sadakane K; Yoshikawa T (2005). Effects of nano particles on antigen-related airway inflammation in mice. *Respir Res*, 6: 106. [088625](#)
- Ito K (2003). Associations of particulate matter components with daily mortality and morbidity in Detroit, Michigan, In: Revised analyses of time-series studies of air pollution and health. Special report. Health Effects Institute. Boston, MA. R828112. <http://www.healtheffects.org/Pubs/TimeSeries.pdf>. [042856](#)
- Ito K; Christensen WF; Eatough DJ; Henry RC; Kim E; Laden F; Lall R; Larson TV; Neas L; Hopke PK; Thurston GD (2006). PM source apportionment and health effects: 2 An investigation of intermethod variability in associations between source-apportioned fine particle mass and daily mortality in Washington, DC. *J Expo Sci Environ Epidemiol*, 16: 300-310. [088391](#)
- Ito K; Thurston GD; Silverman RA (2007). Characterization of PM_{2.5}, gaseous pollutants, and meteorological interactions in the context of time-series health effects models. *J Expo Sci Environ Epidemiol*, 17 Suppl 2: S45-S60. [156594](#)
- Ito K; Thurston GD; Silverman RA; (2007). Association between coarse particles and asthma emergency department (ED) visits in New York City. Presented at American Thoracic Society international conference 2007, San Francisco, CA. [091262](#)
- Ito T; Okumura H; Tsukue N; Kobayashi T; Honda K; Sekizawa K (2006). Effect of diesel exhaust particles on mRNA expression of viral and bacterial receptors in rat lung epithelial L2 cells. *Toxicol Lett*, 165: 66-70. [096648](#)
- Ito T; Suzuki T; Tamura K; Nezu T; Honda K; Kobayashi T (2008). Examination of mRNA expression in rat hearts and lungs for analysis of effects of exposure to concentrated ambient particles on cardiovascular function. *Toxicol Sci*, 243: 271-283. [096823](#)
- Jaffe DH; Singer ME; Rimm AA (2003). Air pollution and emergency department visits for asthma among Ohio Medicaid recipients, 1991-1996. *Environ Res*, 91: 21-28. [041957](#)

- Jalaludin B; Morgan G; Lincoln D; Sheppard V; Simpson R; Corbett S (2006). Associations between ambient air pollution and daily emergency department attendances for cardiovascular disease in the elderly (65+ years), Sydney, Australia. *J Expo Sci Environ Epidemiol*, 16: 225-237. [189416](#)
- Jalaludin BB; O'Toole BI; Leeder SR (2004). Acute effects of urban ambient air pollution on respiratory symptoms, asthma medication use, and doctor visits for asthma in a cohort of Australian children. *Environ Res*, 95: 32-42. [056595](#)
- Jalava PI; Salonen RO; Halinen AI; Penttinen P; Pennanen AS; Sillanpaa M; Sandell E; Hillamo R; Hirvonen M-R (2006). In vitro inflammatory and cytotoxic effects of size-segregated particulate samples collected during long-range transport of wildfire smoke to Helsinki. *Toxicol Appl Pharmacol*, 215: 341-353. [155872](#)
- Jalava PI; Salonen RO; Pennanen AS; Happonen MS; Penttinen P; Halinen AI; Sillanpaa M; Hillamo R; Hirvonen MR (2008). Effects of solubility of urban air fine and coarse particles on cytotoxic and inflammatory responses in RAW 264.7 macrophage cell line. *Toxicol Appl Pharmacol*, 229: 146-60. [098968](#)
- Janes H; Sheppard L; Lumley T (2005). Case-crossover analyses of air pollution exposure data: referent selection strategies and their implications for bias. *Epidemiology*, 16: 717-726. [087535](#)
- Jansen KL; Larson TV; Koenig JQ; Mar TF; Fields C; Stewart J; Lippmann M (2005). Associations between health effects and particulate matter and black carbon in subjects with respiratory disease. *Environ Health Perspect*, 113: 1741-1746. [082236](#)
- Janssen NAH; Schwartz J; Zanobetti A; Suh HH (2002). Air conditioning and source-specific particles as modifiers of the effect of PM10 on hospital admissions for heart and lung disease. *Environ Health Perspect*, 110: 43-49. [016743](#)
- Johnston FH; Bailie RS; Pilotto LS; Hanigan IC (2007). Ambient biomass smoke and cardio-respiratory hospital admissions in Darwin, Australia. *BMC Public Health*, 7: 240. [155882](#)
- Johnston FH; Webby RJ; Pilotto LS; Bailie RS; Parry DL; Halpin SJ (2006). Vegetation fires, particulate air pollution and asthma: a panel study in the Australian monsoon tropics. *Int J Environ Health Res*, 16: 391-404. [091386](#)
- Just J; Segala C; Sahraoui F; Priol G; Grimfeld A; Neukirch F (2002). Short-term health effects of particulate and photochemical air pollution in asthmatic children. *Eur Respir J*, 20: 899-906. [035429](#)
- Kannel WB; Abbott RD; Savage DD; McNamara PM (1983). Coronary heart disease and atrial fibrillation: the Framingham Study. *Am Heart J*, 106: 389-396. [156623](#)
- Katsouyanni K; Touloumi G; Samoli E; Petasakis Y; Analitis A; Le Tertre A; Rossi G; Zmirou D; Ballester F; Boumghar A; Anderson HR; Wojtyniak B; Paldy A; Braunstein R; Pekkanen J; Schindler C; Schwartz J (2003). Sensitivity analysis of various models of short-term effects of ambient particles on total mortality in 29 cities in APHEA2. [042807](#)
- Kelishadi R; Mirghaffari N; Poursafa P; Gidding S (2009). Lifestyle and environmental factors associated with inflammation, oxidative stress and insulin resistance in children. *Atherosclerosis*, 203: 311-319. [191960](#)
- Kettunen J; Lanki T; Tiittanen P; Aalto PP; Koskentalo T; Kulmala M; Salomaa V; Pekkanen J (2007). Associations of fine and ultrafine particulate air pollution with stroke mortality in an area of low air pollution levels. *Stroke*, 38: 918-922. [091242](#)
- Kim SY; O'Neill MS; Lee JT; Cho Y; Kim J; Kim H (2007). Air pollution, socioeconomic position, and emergency hospital visits for asthma in Seoul, Korea. *Int Arch Occup Environ Health*, 80: 701-710. [092837](#)
- Klein-Patel ME; Diamond G; Boniotto M; Saad S; Ryan LK (2006). Inhibition of beta-defensin gene expression in airway epithelial cells by low doses of residual oil fly ash is mediated by vanadium. *Toxicol Sci*, 92: 115-125. [097092](#)
- Kleinman M; Sioutas C; Stram D; Froines J; Cho A; Chakrabarti B; Hamade A; Meacher D; Oldham M (2005). Inhalation of concentrated ambient particulate matter near a heavily trafficked road stimulates antigen-induced airway responses in mice. *J Air Waste Manag Assoc*, 55: 1277-1288. [087880](#)
- Kleinman MT; Araujo JA; Nel A; Sioutas C; Campbell A; Cong PQ; Li H; Bondy SC (2008). Inhaled ultrafine particulate matter affects CNS inflammatory processes and may act via MAP kinase signaling pathways. *Toxicol Lett*, 178: 127-130. [190074](#)
- Kleinman MT; Sioutas C; Froines JR; Fanning E; Hamade A; Mendez L; Meacher D; Oldham M (2007). Inhalation of concentrated ambient particulate matter near a heavily trafficked road stimulates antigen-induced airway responses in mice. *Inhal Toxicol*, 19 Suppl 1: 117-126. [097082](#)

- Klemm RJ; Lipfert FW; Wyzga RE; Gust C (2004). Daily mortality and air pollution in Atlanta: two years of data from ARIES. *Inhal Toxicol*, 16 Suppl 1: 131-141. [056585](#)
- Klemm RJ; Mason R (2003). Replication of reanalysis of Harvard Six-City mortality study. In HEI Special Report: Revised Analyses of Time-Series Studies of Air Pollution and Health, Part II (pp. 165-172). Boston, MA: Health Effects Institute. [042801](#)
- Knuckles TL; Lund AK; Lucas SN; Campen MJ (2008). Diesel exhaust exposure enhances venoconstriction via uncoupling of eNOS. *Toxicol Appl Pharmacol*, 230: 346-351. [191987](#)
- Ko FWS; Tam W; Wong TW; Chan DPS (2007). Temporal relationship between air pollutants and hospital admissions for chronic obstructive pulmonary disease in Hong Kong. *Thorax*, 62: 780-785. [091639](#)
- Ko FWS; Tam W; Wong TW; Lai CKW; (2007). Effects of air pollution on asthma hospitalization rates in different age groups in Hong Kong. *Clin Exp Allergy*, 37: 1312-1319. [092844](#)
- Kodavanti UP; Schladweiler MC; Ledbetter AD; Hauser R; Christiani DC; McGee J; Richards JR; Costa DL (2002). Temporal association between pulmonary and systemic effects of particulate matter in healthy and cardiovascular compromised rats. *J Toxicol Environ Health A Curr Iss*, 65: 1545-1569. [025236](#)
- Kodavanti UP; Schladweiler MC; Ledbetter AD; McGee JK; Walsh L; Gilmour PS; Highfill JW; Davies D; Pinkerton KE; Richards JH; Crissman K; Andrews D; Costa DL (2005). Consistent pulmonary and systemic responses from inhalation of fine concentrated ambient particles: roles of rat strains used and physicochemical properties. *Environ Health Perspect*, 113: 1561-1568. [087946](#)
- Kodavanti UP; Schladweiler MCJ; Ledbetter AD; Hauser R; Christiani DC; Samet JM; McGee J; Richards JH; Costa DL (2002). Pulmonary and systemic effects of zinc-containing emission particles in three rat strains: multiple exposure scenarios. *Toxicol Sci*, 70: 73-85. [035344](#)
- Koenig J; Allen R; Larson T; Liu S (2005). Response to "Indoor- and Outdoor-Generated Particles and Children with asthma" [letter]. *Environ Health Perspect*, 113: A581. [088999](#)
- Koenig JQ; Jansen K; Mar TF; Lumley T; Kaufman J; Trenga CA; Sullivan J; Liu LJ; Shapiro GG; Larson TV (2003). Measurement of offline exhaled nitric oxide in a study of community exposure to air pollution. *Environ Health Perspect*, 111: 1625-1629. [156653](#)
- Koenig JQ; Mar TF; Allen RW; Jansen K; Lumley T; Sullivan JH; Trenga CA; Larson T; Liu LJ (2005). Pulmonary effects of indoor- and outdoor-generated particles in children with asthma. *Environ Health Perspect*, 113: 499-503. [087384](#)
- Koken PJM; Piver WT; Ye F; Elixhauser A; Olsen LM; Portier CJ (2003). Temperature, air pollution, and hospitalization for cardiovascular diseases among elderly people in Denver. *Environ Health Perspect*, 111: 1312-1317. [049466](#)
- Kongerud J; Madden MC; Hazucha M; Peden D (2006). Nasal responses in asthmatic and nonasthmatic subjects following exposure to diesel exhaust particles. *Inhal Toxicol*, 18: 589-594. [156656](#)
- Kooter IM; Boere AJ; Fokkens PH; Leseman DL; Dormans JA; Cassee FR (2006). Response of spontaneously hypertensive rats to inhalation of fine and ultrafine particles from traffic: experimental controlled study. *Part Fibre Toxicol*, 15: 3-7. [097547](#)
- Kuo HW; Lai JS; Lee MC; Tai RC; Lee MC (2002). Respiratory effects of air pollutants among asthmatics in central Taiwan. *Arch Environ Occup Health*, 57: 194-200. [036310](#)
- Laden F; Neas LM; Dockery DW; Schwartz J (2000). Association of fine particulate matter from different sources with daily mortality in six US cities. *Environ Health Perspect*, 108: 941-947. [012102](#)
- Lagorio S; Forastiere F; Pistelli R; Iavarone I; Michelozzi P; Fano V; Marconi A; Ziemacki G; Ostro BD (2006). Air pollution and lung function among susceptible adult subjects: a panel study. *Environ Health*, 5: 11. [089800](#)
- Lai LW; Cheng WL (2008). The impact of air quality on respiratory admissions during Asian dust storm periods. *Int J Environ Health Res*, 18: 429-450. [180301](#)
- Lanki T; De Hartog JJ; Heinrich J; Hoek G; Janssen NAH; Peters A; Stolzel M; Timonen KL; Vallius M; Vanninen E; Pekkanen J (2006). Can we identify sources of fine particles responsible for exercise-induced ischemia on days with elevated air pollution? The ULTRA study. *Environ Health Perspect*, 114: 655-660. [088412](#)
- Lanki T; Hoek G; Timonen K; Peters A; Tiittanen P; Vanninen E; Pekkanen J (2008). Hourly variation in fine particle exposure is associated with transiently increased risk of ST segment depression. *Br Med J*, 65: 782-786. [191984](#)

- Lanki T; Pekkanen J; Aalto P; Elosua R; Berglind N; D'Ippoliti D; Kulmala M; Nyberg F; Peters A; Picciotto S; Salomaa V; Sunyer J; Tiittanen P; Von Klot S; Forastiere F; for the HEAPSS Study Group (2006). Associations of traffic-related air pollutants with hospitalisation for first acute myocardial infarction: the HEAPSS study. *Occup Environ Med*, 63: 844-851. [089788](#)
- Larrieu S; Jusot J-F; Blanchard M; Prouvost H; Declercq C; Fabre P; Pascal L; Le Tertre A; Wagner V; Riviere S; Chardon B; Borelli D; Cassadou S; Eilstein D; Lefranc A (2007). Short term effects of air pollution on hospitalizations for cardiovascular diseases in eight French cities: The PSAS program. *Sci Total Environ*, 387: 105-112. [093031](#)
- Larrieu S; Lefranc A; Gault G; Chatignoux E; Couvy F; Jouves B; Filleul L (2009). Are the Short-term Effects of Air Pollution Restricted to Cardiorespiratory Diseases? *Am J Epidemiol*, 169: 1-8. [180294](#)
- Larsson B-M; Sehistedt M; Grunewald J; Skold CM; Lundin A; Blomberg A; Sandstrom T; Eklund A; Svartengren M (2007). Road tunnel air pollution induces bronchoalveolar inflammation in healthy subjects. *Eur Respir J*, 29: 699-705. [091375](#)
- Last JA; Ward R; Temple L; Pinkerton KE; Kenyon NJ (2004). Ovalbumin-induced airway inflammation and fibrosis in mice also exposed to ultrafine particles. *Inhal Toxicol*, 16: 93-102. [097334](#)
- Laupacis A; Boysen G; Connolly S (1994). Risk factors for stroke and efficacy of antithrombotic therapy in atrial fibrillation: Analysis of pooled data from five randomized controlled trials. *Arch Intern Med*, 154: 1449-1457. [190901](#)
- Laurent O; Pedrono G; Filleul L; Segala C; Lefranc A; Schillinger C; Riviere E; Bard D (2009). Influence of socioeconomic deprivation on the relation between air pollution and beta-agonist sales for asthma. *Chest*, 135: 717-723. [192129](#)
- Laurent O; Pedrono G; Segala C; Filleul L; Havard S; Deguen S; Schillinger C; Riviere E; Bard D (2008). Air pollution, asthma attacks, and socioeconomic deprivation: a small-area case-crossover study. *Am J Epidemiol*, 168: 58-65. [156672](#)
- Lay JC; Bennett WD; Kim CS; Devlin RB; Bromberg PA (1998). Retention and intracellular distribution of instilled iron oxide particles in human alveolar macrophages. *Am J Respir Cell Mol Biol*, 18: 687-695. [007683](#)
- Lay JC; Zeman KL; Ghio AJ; Bennett WD (2001). Effects of inhaled iron oxide particles on alveolar epithelial permeability in normal subjects. *Inhal Toxicol*, 13: 1065-1078. [020613](#)
- Le Tertre A; Schwartz J; Touloumi G (2005). Empirical Bayes and adjusted estimates approach to estimating the relation of mortality to exposure of PM10. *Risk Anal*, 25: 711-718. [087560](#)
- Lee IM; Tsai SS; Ho CK; Chiu HF; Yang CY (2007). Air pollution and hospital admissions for congestive heart failure in a tropical city: Kaohsiung, Taiwan. *Inhal Toxicol*, 19: 899-904. [196613](#)
- Lee J-T; Kim H; Song H; Hong Y-C; Cho Y-S; Shin S-Y; Hyun Y-J; Kim Y-S (2002). Air pollution and asthma among children in Seoul, Korea. *Epidemiology*, 13: 481-484. [034826](#)
- Lee J-T; Son J-Y; Cho Y-S (2007). A comparison of mortality related to urban air particles between periods with Asian dust days and without Asian dust days in Seoul, Korea, 2000-2004. *Environ Res*, 105: 409-13. [093042](#)
- Lee JT; Kim H; Cho YS; Hong YC; Ha EH; Park H (2003). Air pollution and hospital admissions for ischemic heart diseases among individuals 64+ years of age residing in Seoul, Korea. *Arch Environ Health*, 58: 617-623. [095552](#)
- Lee SL; Wong WHS; Lau YL (2006). Association between air pollution and asthma admission among children in Hong Kong. *Clin Exp Allergy*, 36: 1138-1146. [090176](#)
- Lei Y-C; Chan C-C; Wang P-Y; Lee C-T; Cheng T-J (2004). Effects of Asian dust event particles on inflammation markers in peripheral blood and bronchoalveolar lavage in pulmonary hypertensive rats. *Environ Res*, 95: 71-76. [087884](#)
- Lei YC; Chen MC; Chan CC; Wang PY; Lee CT; Cheng TJ (2004). Effects of concentrated ambient particles on airway responsiveness and pulmonary inflammation in pulmonary hypertensive rats. *Inhal Toxicol*, 16: 785-792. [087999](#)
- Levine AM; Gwozdz J; Stark J; Bruno M; Whitsett J; Korfhagen T (1999). Surfactant protein-A enhances respiratory syncytial virus clearance in vivo. *J Clin Invest*, 103: 1015-1021. [156687](#)
- LeVine AM; Whitsett JA (2001). Pulmonary collectins and innate host defense of the lung. *Microb Infect*, 3: 161-166. [155928](#)

- Levy D; Sheppard L; Checkoway H; Kaufman J; Lumley T; Koenig J; Siscovick D (2001). A case-crossover analysis of particulate matter air pollution and out-of-hospital primary cardiac arrest. *Epidemiology*, 12: 193-199. [017171](#)
- Lewis CW; Klouda GA; Ellenson WD (2004). Radiocarbon measurement of the biogenic contribution to summertime PM-2.5 ambient aerosol in Nashville, TN. *Atmos Environ*, 38: 6053-6061. [097498](#)
- Lewis CW; Norris GA; Conner TL; Henry RC (2003). Source apportionment of Phoenix PM2.5 aerosol with the Unmix Receptor model. *J Air Waste Manag Assoc*, 53: 325-338. [088413](#)
- Lewis TC; Robins TG; Dvonch JT; Keeler GJ; Yip FY; Mentz GB; Lin X; Parker EA; Israel BA; Gonzalez L; Hill Y (2005). Air pollution-associated changes in lung function among asthmatic children in Detroit. *Environ Health Perspect*, 113: 1068-1075. [081079](#)
- Le Tertre A; Medina S; Samoli E; Forsberg B; Michelozzi P; Boumghar A; Vonk JM; Bellini A; Atkinson R; Ayres JG; Sunyer J; Schwartz J; Katsouyanni K (2002). Short term effects of particulate air pollution on cardiovascular diseases in eight European cities. *J Epidemiol Community Health*, 56: 773-779. [023746](#)
- Le Tertre A; Medina S; Samoli E; Forsberg B; Michelozzi P; Boumghar A; Vonk JM; Bellini A; Atkinson R; Ayres JG; Sunyer J; Schwartz J; Katsouyanni K (2003). Short-term effects of particulate air pollution on cardiovascular diseases in eight European cities. In *HEI Special Report: Revised Analyses of Time-Series Studies of Air Pollution and Health, Part II* (pp. 173-176). Boston: HEI. [042820](#)
- Li N; Wang M; Bramble LA; Schmitz DA; Schauer JJ; Sioutas C; Harkema JR; Nel AE (2009). The adjuvant effect of ambient particulate matter is closely reflected by the particulate oxidant potential. *Environ Health Perspect*, 117: 1116-1123. [190457](#)
- Li Y-J; Kawada T; Matsumoto A; Azuma A; Kudoh S; Takizawa H; Sugawara I (2007). Airway inflammatory responses to oxidative stress induced by low-dose diesel exhaust particle exposure differ between mouse strains. *Exp Lung Res*, 33: 227-244. [155929](#)
- Liao D; Duan Y; Whitsel EA; Zheng Z-J; Heiss G; Chinchilli VM; Lin H-M (2004). Association of higher levels of ambient criteria pollutants with impaired cardiac autonomic control: a population-based study. *Am J Epidemiol*, 159: 768-777. [056590](#)
- Liao D; Heiss G; Chinchilli VM; Duan Y; Folsom AR; Lin HM; Salomaa V (2005). Association of criteria pollutants with plasma hemostatic/inflammatory markers: a population-based study. *J Expo Sci Environ Epidemiol*, 15: 319-328. [088677](#)
- Liao D; Whitsel EA; Duan Y; Lin HM; Quibrera PM; Smith R; Peuquet DJ; Prineas RJ; Zhang ZM; Anderson G (2009). Ambient particulate air pollution and ectopy—the environmental epidemiology of arrhythmogenesis in Women's Health Initiative Study, 1999-2004. *J Toxicol Environ Health A Curr Iss*, 72: 30-38. [199519](#)
- Lin M; Chen Y; Burnett RT; Villeneuve PJ; Krewski D (2002). The influence of ambient coarse particulate matter on asthma hospitalization in children: case-crossover and time-series analyses. *Environ Health Perspect*, 110: 575-581. [026067](#)
- Lin M; Stieb DM; Chen Y (2005). Coarse particulate matter and hospitalization for respiratory infections in children younger than 15 years in Toronto: a case-crossover analysis. *Pediatrics*, 116: 235-240. [087828](#)
- Linn WS; Szlachet Y; Gong H Jr; Kinney PL; Berhane KT (2000). Air pollution and daily hospital admissions in metropolitan Los Angeles. *Environ Health Perspect*, 108: 427-434. [002839](#)
- Lipfert FW; Morris SC; Wyzga RE (2000). Daily mortality in the Philadelphia metropolitan area and size-classified particulate matter. *J Air Waste Manag Assoc*, 50: 1501-1513. [004088](#)
- Lippmann M (2000). *Environmental toxicants: human exposures and their health effects*. New York: John Wiley and Sons. [024579](#)
- Lippmann M; Hwang J; Maciejczyk P; Chen L (2005). PM source apportionment for short-term cardiac function changes in ApoE^{-/-} mice. *Environ Health Perspect*, 113: 1575-1579. [087453](#)
- Lippmann M; Ito K; Hwang JS; Maciejczyk P; Chen LC (2006). Cardiovascular effects of nickel in ambient air. *Environ Health Perspect*, 114: 1662-1669. [091165](#)
- Lippmann M; Ito K; Nadas A; Burnett RT (2000). Association of particulate matter components with daily mortality and morbidity in urban populations. Health Effects Institute. Cambridge, MA. [011938](#)

- Lipsett MJ; Tsai FC; Roger L; Woo M; Ostro BD (2006). Coarse particles and heart rate variability among older adults with coronary artery disease in the Coachella Valley, California. *Environ Health Perspect*, 114: 1215-1220. [088753](#)
- Lisabeth LD; Escobar JD; Dvonch JT; Sanchez BN; Majersik JJ; Brown DL; Smith MA; Morgenstern LB (2008). Ambient air pollution and risk for ischemic stroke and transient ischemic attack. *Ann Neurol*, 64: 53-59. [155939](#)
- Liu J; Ballaney M; Al-Alem U; Quan C; Jin X; Perera F; Chen LC; Miller RL (2008). Combined Inhaled Diesel Exhaust Particles and Allergen Exposure Alter Methylation of T Helper Genes and IgE Production In Vivo. *Toxicol Sci*, 102: 76-81. [156709](#)
- Liu L; Poon R; Chen L; Frescura AM; Montuschi P; Ciabattini G; Wheeler A; Dales R (2009). Acute effects of air pollution on pulmonary function, airway inflammation, and oxidative stress in asthmatic children. *Environ Health Perspect*, 117: 668-674. [192003](#)
- Liu L; Ruddy TD; Dalipaj M; Szyszkowicz M; You H; Poon R; Wheeler A; Dales R (2007). Influence of personal exposure to particulate air pollution on cardiovascular physiology and biomarkers of inflammation and oxidative stress in subjects with diabetes. *J Occup Environ Med*, 49: 258-265. [156705](#)
- Liu SX; Hou FF; Guo ZJ; Nagai R; Zhang WR; Liu ZQ; Zhou ZM; Zhou M; Xie D; Wang GB; Zhang X (2006). Advanced oxidation protein products accelerate atherosclerosis through promoting oxidative stress and inflammation. *Arterioscler Thromb Vasc Biol*, 26: 1156-1162. [192002](#)
- Liu X; Meng Z (2005). Effects of airborne fine particulate matter on antioxidant capacity and lipid peroxidation in multiple organs of rats. *Inhal Toxicol*, 17: 467-473. [088650](#)
- Ljungman P; Bellander T; Schneider A; Breitner S; Forastiere F; Hampel R; Illig T; Jacquemin B; Katsouyanni K; von Klot S (2009). Modification of the interleukin-6 response to air pollution by interleukin-6 and fibrinogen polymorphisms. *Environ Health Perspect*, 117: 1373-1379. [191983](#)
- Ljungman PLS; Berglund N; Holmgren C; Gadler F; Edvardsson N; Pershagen G; Rosenqvist M; Sjögren B; Bellander T (2008). Rapid effects of air pollution on ventricular arrhythmias. *Eur Heart J*, 29: 2894-2901. [180266](#)
- Llorca J; Salas A; Prieto-Salceda D; Chinchon-Bengoechea V; Delgado-Rodriguez M (2005). Nitrogen dioxide increases cardiorespiratory admissions in Torrelavega (Spain). *J Environ Health*, 68: 30-35. [087825](#)
- Lokken PR; Wellenius GA; Coull BA; Burger MR; Schlaug G; Suh HH; Mittleman MA (2009). Air Pollution and Risk of Stroke: Underestimation of Effect Due to Misclassification of Time of Event Onset. *Epidemiology*, 20: 137-142. [186774](#)
- Low RB; Bielory L; Qureshi AI; Dunn V; Stuhlmiller DF; Dickey DA (2006). The relation of stroke admissions to recent weather, airborne allergens, air pollution, seasons, upper respiratory infections, and asthma incidence, September 11, 2001, and day of the week. *Stroke*, 37: 951-957. [090441](#)
- Lucking A; Lundback M; Mills N; Faratian D; Barath S; Pourazar J; Cassee F; Donaldson K; Boon N; Badimon J; Sandstorm T; Blomberg A; Newby D (2008). Diesel exhaust inhalation increases thrombus formation in man. *Eur Heart J*, 29: 3043-3051. [191993](#)
- Luginaah IN; Fung KY; Gorey KM; Webster G; Wills C (2005). Association of ambient air pollution with respiratory hospitalization in a government designated "area of concern": the case of Windsor, Ontario. *Environ Health Perspect*, 113: 290-296. [057327](#)
- Lund AK; Lucero J; Lucas S; Madden MC; McDonald JD; Seagrave JC; Knuckles TL; Campen MJ (2009). Vehicular emissions induce vascular MMP-9 expression and activity associated with endothelin-1 mediated pathways. *Arterioscler Thromb Vasc Biol*, 29: 511-517. [180257](#)
- Lundbäck M; Mills NL; Lucking A; Barath S; Donaldson K; Newby DE; Sandström T; Blomberg A (2009). Experimental exposure to diesel exhaust increases arterial stiffness in man. *Part Fibre Toxicol*, 6: 7. [191967](#)
- Luttmann-Gibson H; Suh HH; Coull BA; Dockery DW; Sarnet SE; Schwartz J; Stone PH; Gold DR (2006). Short-term effects of air pollution on heart rate variability in senior adults in Steubenville, Ohio. *J Occup Environ Med*, 48: 780-788. [089794](#)
- Maciejczyk P; Chen LC (2005). Effects of subchronic exposures to concentrated ambient particles (CAPs) in mice: VIII source-related daily variations in in vitro responses to CAPs. *Inhal Toxicol*, 17: 243-253. [087456](#)

- Mar TF; Ito K; Koenig JQ; Larson TV; Eatough DJ; Henry RC; Kim E; Laden F; Lall R; Neas L; Stolzel M; Paatero P; Hopke PK; Thurston GD (2006). PM source apportionment and health effects: 3 Investigation of inter-method variations in associations between estimated source contributions of PM_{2.5} and daily mortality in Phoenix, AZ. *J Expo Sci Environ Epidemiol*, 16: 311-320. [086143](#)
- Mar TF; Jansen K; Shepherd K; Lumley T; Larson TV; Koenig JQ (2005). Exhaled nitric oxide in children with asthma and short-term PM_{2.5} exposure in Seattle. *Environ Health Perspect*, 113: 1791-1794. [088759](#)
- Mar TF; Koenig JQ; Jansen K; Sullivan J; Kaufman J; Trenga CA; Siahpush SH; Liu L-JS; Neas L (2005). Fine particulate air pollution and cardiorespiratory effects in the elderly. *Epidemiology*, 16: 681-687. [087566](#)
- Mar TF; Larson TV; Stier RA; Claiborn C; Koenig JQ (2004). An analysis of the association between respiratory symptoms in subjects with asthma and daily air pollution in Spokane, Washington. *Inhal Toxicol*, 16: 809-815. [057309](#)
- Mar TF; Norris GA; Koenig JQ; Larson TV (2000). Associations between air pollution and mortality in Phoenix, 1995-1997. *Environ Health Perspect*, 108: 347-353. [001760](#)
- Mar TF; Norris GA; Larson TV; Wilson WE; Koenig JQ (2003). Air pollution and cardiovascular mortality in Phoenix, 1995-1997. Health Effects Institute. Cambridge, MA. [042841](#)
- Martins LC; Latorre MRDO; Saldiva PHN; Braga ALF (2002). Air pollution and emergency room visits due to chronic lower respiratory diseases in the elderly: An ecological time-series study in Sao Paulo, Brazil. *J Occup Environ Med*, 44: 622-627. [035059](#)
- Masjedi MR; Jamaati HR; Dokouhaki P; Ahmadzadeh Z; Taheri SA; Bigdeli M; Izadi S; Rostamian A; Aagin K; Ghavam SM (2003). The effects of air pollution on acute respiratory conditions. *Respirology*, 8: 213-230. [052100](#)
- Matsumoto A; Hiramatsu K; Li Y; Azuma A; Kudoh S; Takizawa H; Sugawara I (2006). Repeated exposure to low-dose diesel exhaust after allergen challenge exaggerates asthmatic responses in mice. *Clin Immunol*, 121: 227-235. [098017](#)
- McCreanor J; Cullinan P; Nieuwenhuijsen MJ; Stewart-Evans J; Malliarou E; Jarup L; Harrington R; Svartengren M; Han I-K; Ohman-Strickland P; Chung KF; Zhang J (2007). Respiratory effects of exposure to diesel traffic in persons with asthma. *N Engl J Med*, 357: 2348-2358. [092841](#)
- McDonald J; Barr E; White R; Kracko D; Chow J; Zielinska B; Grosjean E (2008). Generation and characterization of gasoline engine exhaust inhalation exposure atmospheres. *Inhal Toxicol*, 20: 1157-1168. [191978](#)
- McDonald JD; Barr EB; White RK; Chow JC; Schauer JJ; Zielinska B; Grosjean E (2004). Generation and characterization of four dilutions of diesel engine exhaust for a subchronic inhalation study. *Environ Sci Technol*, 38: 2513-2522. [055644](#)
- McQueen DS; Donaldson K; Bond SM; McNeilly JD; Newman S; Barton NJ; Duffin R (2007). Bilateral vagotomy or atropine pre-treatment reduces experimental diesel-soot induced lung inflammation. *Toxicol Appl Pharmacol*, 219: 62-71. [096266](#)
- Medina-Ramon M; Zanobetti A; Schwartz J (2006). The effect of ozone and PM₁₀ on hospital admissions for pneumonia and chronic obstructive pulmonary disease: a national multicity study. *Am J Epidemiol*, 163: 579-588. [087721](#)
- Ménache MG; Miller FJ; Raabe OG (1995). Particle inhalability curves for humans and small laboratory animals. *Ann Occup Hyg*, 39: 317-328. [006533](#)
- Metzger KB; Klein M; Flanders WD; Peel JL; Mulholland JA; Langberg JJ; Tolbert PE (2007). Ambient air pollution and cardiac arrhythmias in patients with implantable defibrillators. *Epidemiology*, 18: 585-592. [092856](#)
- Metzger KB; Tolbert PE; Klein M; Peel JL; Flanders WD; Todd KH; Mulholland JA; Ryan PB; Frumkin H (2004). Ambient air pollution and cardiovascular emergency department visits. *Epidemiology*, 15: 46-56. [044222](#)
- Michaud JP; Grove JS; Krupitsky DCEH (2004). Emergency department visits and "vog"-related air quality in Hilo, Hawai'i. *Environ Res*, 95: 11-9. [188530](#)
- Middleton N; Yiallourous P; Kleanthous S; Kolokotroni O; Schwartz J; Dockery DW; Demokritou P; Koutrakis P (2008). A 10-year time-series analysis of respiratory and cardiovascular morbidity in Nicosia, Cyprus: the effect of short-term changes in air pollution and dust storms. *Environ Health*, 7: 39. [156760](#)
- Migliaretti G; Cadum E; Migliore E; Cavallo F (2005). Traffic air pollution and hospital admission for asthma: a case-control approach in a Turin (Italy) population. *Int Arch Occup Environ Health*, 78: 164-169. [088689](#)

- Migliaretti G; Cavallo F (2004). Urban air pollution and asthma in children. *Pediatr Pulmonol*, 38: 198-203. [087425](#)
- Mills NL; Robinson SD; Fokkens PH; Leseman DL; Miller MR; Anderson D; Freney EJ; Heal MR; Donovan RJ; Blomberg A; Sandstrom T; MacNee W; Boon NA; Donaldson K; Newby DE; Cassee FR (2008). Exposure to concentrated ambient particles does not affect vascular function in patients with coronary heart disease. *Environ Health Perspect*, 116: 709-715. [156766](#)
- Mills NL; Törnqvist H; Gonzalez MC; Vink E; Robinson SD; Soderberg S; Boon NA; Donaldson K; Sandstrom T; Blomberg A; Newby DE (2007). Ischemic and thrombotic effects of dilute diesel-exhaust inhalation in men with coronary heart disease. *N Engl J Med*, 357: 1075-1082. [091206](#)
- Mills NL; Törnqvist H; Robinson SD; Gonzalez M; Darnley K; MacNee W; Boon NA; Donaldson K; Blomberg A; Sandstrom T; Newby DE (2005). Diesel exhaust inhalation causes vascular dysfunction and impaired endogenous fibrinolysis. *Circulation*, 112: 3930-3936. [095757](#)
- Min KB; Min JY; Cho SI; Paek D (2008). The relationship between air pollutants and heart-rate variability among community residents in Korea. *Inhal Toxicol*, 4: 435-444. [191901](#)
- Mohr LB; Luo S; Mathias E; Tobing R; Homan S; Sterling D (2008). Influence of season and temperature on the relationship of elemental carbon air pollution to pediatric asthma emergency room visits. *J Asthma*, 45: 936-943. [180215](#)
- Moolgavkar SH (2003). Air pollution and daily deaths and hospital admissions in Los Angeles and Cook counties. Health Effects Institute. Boston, MA. [042864](#)
- Moolgavkar SH (2003). Air pollution and daily mortality in two US counties: season-specific analyses and exposure-response relationships. *Inhal Toxicol*, 15: 877-907. [051316](#)
- Moore KJ; Kunjathoor VV; Koehn SL; Manning JJ; Tseng AA; Silver JM; McKee M; Freeman MW (2005). Loss of receptor-mediated lipid uptake via scavenger receptor A or CD36 pathways does not ameliorate atherosclerosis in hyperlipidemic mice. *J Clin Invest*, 115: 2192-2201. [156780](#)
- Morishita M; Keeler G; Wagner J; Marsik F; Timm E; Dvonch J; Harkema J (2004). Pulmonary retention of particulate matter is associated with airway inflammation in allergic rats exposed to air pollution in urban Detroit. *Inhal Toxicol*, 16: 663-674. [087979](#)
- Morris RD; Naumova EN (1998). Carbon monoxide and hospital admissions for congestive heart failure: evidence of an increased effect at low temperatures. *Environ Health Perspect*, 106: 649-653. [086857](#)
- Morrison D; Skwarski D; Millar AM; Adams W; MacNee W (1998). A comparison of three methods of measuring 99mTc-DTPA lung clearance and their repeatability. *Eur Respir J*, 11: 1141-1146. [024924](#)
- Mortimer KM; Neas LM; Dockery DW; Redline S; Tager IB (2002). The effect of air pollution on inner-city children with asthma. *Eur Respir J*, 19: 699-705. [030281](#)
- Moshhammer H; Hutter H-P; Hauck H; Neuberger M (2006). Low levels of air pollution induce changes of lung function in a panel of schoolchildren. *Eur Respir J*, 27: 1138-1143. [090771](#)
- Moshhammer H; Neuberger M (2003). The active surface of suspended particles as a predictor of lung function and pulmonary symptoms in Austrian school children. *Atmos Environ*, 37: 1737-1744. [041956](#)
- Mudway IS; Stenfors N; Duggan ST; Roxborough H; Zielinski H; Marklund SL; Blomberg A; Frew AJ; Sandstrom T; Kelly FJ (2004). An in vitro and in vivo investigation of the effects of diesel exhaust on human airway lining fluid antioxidants. *Arch Biochem Biophys*, 423: 200-212. [180208](#)
- Muggenburg BA; Barr EB; Cheng YS; Seagrave JC; Tilley LP; Mauderly JL (2000). Effect of inhaled residual oil fly ash on the electrocardiogram of dogs. Presented at In: Grant, L. D., ed. PM2000: particulate matter and health. *Inhalation Toxicol*. 12(suppl. 4): 189-208. [010279](#)
- Murata A; Kida K; Hasunuma H; Kanegae H; Ishimaru Y; Motegi T; Yamada K; Yoshioka H; Yamamoto K; Kudoh S (2007). Environmental influence on the measurement of exhaled nitric oxide concentration in school children: special reference to methodology. *J Nippon Med Sch*, 74: 30-6. [189159](#)
- Mutlu GM; Green D; Bellmeyer A; Baker CM; Burgess Z; Rajamannan N; Christman JW; Foiles N; Kamp DW; Ghio AJ; Chandel NS; Dean DA; Sznajder JI; Budinger GR (2007). Ambient particulate matter accelerates coagulation via an IL-6-dependent pathway. *J Clin Invest*, 117: 2952-2961. [121441](#)

- Nadziejko C; Fang K; Chen LC; Cohen B; Karpatkin M; Nadas A (2002). Effect of concentrated ambient particulate matter on blood coagulation parameters in rats. [050587](#)
- Nadziejko C; Fang K; Nadziejko E; Narciso SP; Zhong M; Chen LC (2002). Immediate effects of particulate air pollutants on heart rate and respiratory rate in hypertensive rats. *Cardiovasc Toxicol*, 2: 245-252. [087460](#)
- Nadziejko C; Fang K; Narciso S; Zhong M; Su WC; Gordon T; Nadas A; Chen LC (2004). Effect of particulate and gaseous pollutants on spontaneous arrhythmias in aged rats. *Inhal Toxicol*, 16: 373-380. [055632](#)
- Nascimento LF; Pereira LA; Braga AL; Modolo MC; Carvalho JA Jr (2006). Effects of air pollution on children's health in a city in southeastern Brazil. *Rev Saude Publica*, 40: 77-82. [093247](#)
- NCHS (2007). Classification of Diseases, Functioning, and Disability...Monitoring the Nation's Health. Retrieved 10-DEC-09, from <http://www.cdc.gov/nchs/icd9.htm>. [157194](#)
- Neuberger M; Schimek MG; Horak F Jr; Moshhammer H; Kundi M; Frischer T; Gomiscek B; Puxbaum H; Hauck H; AUPHEP-Team (2004). Acute effects of particulate matter on respiratory diseases, symptoms and functions: epidemiological results of the Austrian Projects on Health Effects of Particulate Matter (AUPHEP). *Atmos Environ*, 38: 3971-3981. [093249](#)
- Nightingale JA; Maggs R; Cullinan P; Donnelly LE; Rogers DF; Kinnersley R; Chung KF; Barnes PJ; Ashmore M; Newman-Taylor A (2000). Airway inflammation after controlled exposure to diesel exhaust particulates. *Am J Respir Crit Care Med*, 162: 161-166. [011659](#)
- Nikolov MC; Coull BA; Catalano PJ; Diaz E; Godleski JJ (2008). Statistical methods to evaluate health effects associated with major sources of air pollution: a case-study of breathing patterns during exposure to concentrated Boston air particles. *J Roy Stat Soc C Appl Stat*, 57: 357-378. [156808](#)
- Nordenhall C; Pourazar J; Ledin M-C; Levin J-O; Sandstrom T; Adelroth E (2001). Diesel exhaust enhances airway responsiveness in asthmatic subjects. *Eur Respir J*, 17: 909-915. [025185](#)
- Nurkiewicz TR; Porter DW; Barger M; Castranova V; Boegehold MA (2004). Particulate matter exposure impairs systemic microvascular endothelium-dependent dilation. *Environ Health Perspect*, 112: 1299-1306. [087968](#)
- Nurkiewicz TR; Porter DW; Barger M; Millecchia L; Rao KMK; Marvar PJ; Hubbs AF; Castranova V; Boegehold MA (2006). Systemic microvascular dysfunction and inflammation after pulmonary particulate matter exposure. *Environ Health Perspect*, 114: 412-419. [088611](#)
- Nurkiewicz TR; Porter DW; Hubbs AF; Cumpston JL; Chen BT; Frazer DG; Castranova V (2008). Nanoparticle inhalation augments particle-dependent systemic microvascular dysfunction. *Part Fibre Toxicol*, 5: 1. [156816](#)
- Nurkiewicz TR; Porter DW; Hubbs AF; Stone S; Chen BT; Frazer DG; Boegehold MA; Castranova V (2009). Pulmonary nanoparticle exposure disrupts systemic microvascular nitric oxide signaling. *Toxicol Sci*, 110: 191-203. [191961](#)
- Nygaard UC; Samuelsen M; Aase A; Lovik M (2004). The capacity of particles to increase allergic sensitization is predicted by particle number and surface area, not by particle mass. *Toxicol Sci*, 82: 515-524. [058558](#)
- O'Connor GT; Neas L; Vaughn B; Kattan M; Mitchell H; Crain EF; Evans R 3rd; Gruchalla R; Morgan W; Stout J; Adams GK; Lippmann M (2008). Acute respiratory health effects of air pollution on children with asthma in US inner cities. *J Allergy Clin Immunol*, 121: 1133-1139. [156818](#)
- O'Neill MS; Veves A; Sarnat JA; Zanobetti A; Gold DR; Economides PA; Horton ES; Schwartz J (2007). Air pollution and inflammation in type 2 diabetes: a mechanism for susceptibility. *Occup Environ Med*, 64: 373-379. [091362](#)
- O'Neill MS; Veves A; Zanobetti A; Sarnat JA; Gold DR; Economides PA; Horton ES; Schwartz J (2005). Diabetes enhances vulnerability to particulate air pollution-associated impairment in vascular reactivity and endothelial function. *Circulation*, 111: 2913-2920. [088423](#)
- Odajima H; Yamazaki S; Nitta H (2008). Decline in peak expiratory flow according to hourly short-term concentration of particulate matter in asthmatic children. *Inhal Toxicol*, 20: 1263-1272. [192005](#)
- Oftedal B; Nafstad P; Magnus P; Bjorkly S; Skrondal A (2003). Traffic related air pollution and acute hospital admission for respiratory diseases in Drammen, Norway 1995-2000. *Eur J Epidemiol*, 18: 671-675. [055623](#)
- Okin PM; Devereux RB; Howard BV; Fabsitz RR; Lee ET; Welty TK (2000). Assessment of QT interval and QT dispersion for prediction of all-cause and cardiovascular mortality in American Indians: The Strong Heart Study. *Circulation*, 101: 61-66. [156002](#)

- Ostro B (1995). Fine particulate air pollution and mortality in two Southern California counties. *Environ Res*, 70: 98-104. [079197](#)
- Ostro B; Broadwin R; Green S; Feng W-Y; Lipsett M (2006). Fine particulate air pollution and mortality in nine California counties: results from CALFINE. *Environ Health Perspect*, 114: 29-33. [087991](#)
- Ostro B; Feng W-Y; Broadwin R; Green S; Lipsett M (2007). The effects of components of fine particulate air pollution on mortality in California: results from CALFINE. *Environ Health Perspect*, 115: 13-19. [091354](#)
- Ostro B; Roth L; Malig B; Marty M (2009). The effects of fine particle components on respiratory hospital admissions in children. *Environ Health Perspect*, 117: 475-480. [191971](#)
- Ostro BD; Broadwin R; Lipsett MJ (2003). Coarse particles and daily mortality in Coachella Valley, California. Health Effects Institute. Boston, MA. [042824](#)
- Ostro BD; Feng WY; Broadwin R; Malig BJ; Green RS; Lipsett MJ (2008). The impact of components of fine particulate matter on cardiovascular mortality in susceptible subpopulations. *Occup Environ Med*, 65: 750-756. [097971](#)
- Park SK; O'Neill MS; Vokonas PS; Sparrow D; Schwartz J (2005). Effects of air pollution on heart rate variability: The VA normative aging study. *Environ Health Perspect*, 113: 304-309. [057331](#)
- Park SK; O'Neill MS; Vokonas PS; Sparrow D; Spiro A 3rd; Tucker KL; Suh H; Hu H; Schwartz J (2008). Traffic-related particles are associated with elevated homocysteine: the VA normative aging study. *Am J Respir Crit Care Med*, 178: 283-289. [156845](#)
- Park SK; O'Neill MS; Vokonas PS; Sparrow D; Wright RO; Coull B; Nie H; Hu H; Schwartz J (2008). Air pollution and heart rate variability: effect modification by chronic lead exposure. *Epidemiology*, 19: 111-120. [093027](#)
- Park SK; O'Neill MS; Wright RO; Hu H; Vokonas PS; Sparrow D; Suh H; Schwartz J (2006). HFE genotype, particulate air pollution, and heart rate variability; a gene-environmental interaction. *Circulation*, 114: 2798-2805. [091245](#)
- Peacock JL; Symonds P; Jackson P; Bremner SA; Scarlett JF; Strachan DP; Anderson HR (2003). Acute effects of winter air pollution on respiratory function in schoolchildren in southern England. *Occup Environ Med*, 60: 82-89. [042026](#)
- Peel JL; Metzger KB; Klein M; Flanders WD; Mulholland JA; Tolbert PE (2007). Ambient air pollution and cardiovascular emergency department visits in potentially sensitive groups. *Am J Epidemiol*, 165: 625-633. [090442](#)
- Peel JL; Tolbert PE; Klein M; Metzger KB; Flanders WD; Knox T; Mulholland JA; Ryan PB; Frumkin H (2005). Ambient air pollution and respiratory emergency department visits. *Epidemiology*, 16: 164-174. [056305](#)
- Pekkanen J; Peters A; Hoek G; Tiittanen P; Brunekreef B; de Hartog J; Heinrich J; Ibaldo-Mulli A; Kreyling WG; Lanki T; Timonen KL; Vanninen E (2002). Particulate air pollution and risk of ST-segment depression during repeated submaximal exercise tests among subjects with coronary heart disease: the exposure and risk assessment for fine and ultrafine particles in ambient air (ULTRA) study. *Circulation*, 106: 933-938. [035050](#)
- Peled R; Friger M; Bolotin A; Bibi H; Epstein L; Pilpel D; Scharf S (2005). Fine particles and meteorological conditions are associated with lung function in children with asthma living near two power plants. *Public Health*, 119: 418-425. [156015](#)
- Peng R; Bell M; Geyh A; McDermott A; Zeger S; Samet J; Dominici F (2009). Emergency admissions for cardiovascular and respiratory diseases and the chemical composition of fine particle air pollution. *Environ Health Perspect*, 117: 957-963. [191998](#)
- Peng RD; Chang HH; Bell ML; McDermott A; Zeger SL; Samet JM; Dominici F (2008). Coarse particulate matter air pollution and hospital admissions for cardiovascular and respiratory diseases among Medicare patients. *JAMA*, 299: 2172-2179. [156850](#)
- Peng RD; Dominici F; Pastor-Barriuso R; Zeger SL; Samet JM (2005). Seasonal analyses of air pollution and mortality in 100 US cities. *Am J Epidemiol*, 161: 585-594. [087463](#)
- Pennanen AS; Sillanpaa M; Hillamo R; Quass U; John AC; Branis M; Hunova I; Meliefste K; Janssen NA; Koskentalo T; Castano-Vinyals G; Bouso L; Chalbot MC; Kavouras IG; Salonen RO (2007). Performance of a high-volume cascade impactor in six European urban environments: mass measurement and chemical characterization of size-segregated particulate samples. *Sci Total Environ*, 374: 297-310. [155357](#)
- Penttinen P; Vallius M; Tiittanen P; Ruuskanen J; Pekkanen J (2006). Source-specific fine particles in urban air and respiratory function among adult asthmatics. *Inhal Toxicol*, 18: 191-198. [087988](#)

- Pereira CEL; Heck TG; Saldiva PHN; Rhoden CR (2007). Ambient particulate air pollution from vehicles promotes lipid peroxidation and inflammatory responses in rat lung. *Braz J Med Biol Res*, 40: 1353-1359. [156019](#)
- Peretz A; Kaufman JD; Trenga CA; Allen J; Carlsten C; Aulet MR; Adar SD; Sullivan JH (2008). Effects of diesel exhaust inhalation on heart rate variability in human volunteers. *Environ Res*, 107: 178-184. [156855](#)
- Peretz A; Peck EC; Bammler TK; Beyer RP; Sullivan JH; Trenga CA; Srinouanprachnah S; Farin FM; Kaufman JD (2007). Diesel exhaust inhalation and assessment of peripheral blood mononuclear cell gene transcription effects: an exploratory study of healthy human volunteers. *Inhal Toxicol*, 19: 1107-1119. [156853](#)
- Peretz A; Sullivan JH; Leotta DF; Trenga CA; Sands FN; Allen J; Carlsten C; Wilkinson CW; Gill EA; Kaufman JD (2008). Diesel exhaust inhalation elicits acute vasoconstriction in vivo. *Environ Health Perspect*, 116: 937-942. [156854](#)
- Perez L; Tobias A; Querol X; Kunzli N; Pey J; Alastuey A; Viana M; Valero N; Gonzalez-Cabre M; Sunyer J (2008). Coarse particles from Saharan dust and daily mortality. *Epidemiology*, 19: 800-807. [156020](#)
- Peters A (2005). Particulate matter and heart disease: evidence from epidemiological studies. *Toxicol Appl Pharmacol*, 207: S477-S482. [087759](#)
- Peters A; Dockery DW; Muller JE; Mittleman MA (2001). Increased particulate air pollution and the triggering of myocardial infarction. *Circulation*, 103: 2810-2815. [016546](#)
- Peters A; Greven S; Heid I; Baldari F; Breitner S; Bellander T; Chrysohoou C; Illig T; Jacquemin B; Koenig W (2009). Fibrinogen genes modify the fibrinogen response to ambient particulate matter. *Am J Respir Crit Care Med*, 179: 484-491. [191992](#)
- Peters A; Liu E; Verrier RL; Schwartz J; Gold DR; Mittleman M; Baliff J; Oh JA; Allen G; Monahan K; Dockery DW (2000). Air pollution and incidence of cardiac arrhythmia. *Epidemiology*, 11: 11-17. [011347](#)
- Peters A; Von Klot S; Heier M; Trentinaglia I; Hormann A; Wichmann HE; Lowel H (2004). Exposure to traffic and the onset of myocardial infarction. *N Engl J Med*, 351: 1721-1730. [087464](#)
- Petrovic S; Urch B; Brook J; Datema J; Purdham J; Liu L; Lukic Z; Zimmerman B; Tofler G; Downar E; Corey P; Tarlo S; Broder I; Dales R; Silverman F (2000). Cardiorespiratory effects of concentrated ambient PM_{2.5}: A pilot study using controlled human exposures. *Inhal Toxicol*, 1: 173-188. [004638](#)
- Piedrahita JA; Zhang SH; Hagaman JR; Oliver PM; Maeda N (1992). Generation of mice carrying a mutant apolipoprotein E gene inactivated by gene targeting in embryonic stem cells. Presented at Proceedings of the National Academy of Science, 5/15/1992. [156868](#)
- Pietropaoli AP; Frampton MW; Hyde RW; Morrow PE; Oberdorster G; Cox C; Speers DM; Frasier LM; Chalupa DC; Huang LS; Utell MJ (2004). Pulmonary function, diffusing capacity, and inflammation in healthy and asthmatic subjects exposed to ultrafine particles. *Inhal Toxicol*, 16: 59-72. [156025](#)
- Pinkerton KE; Zhou Y; Teague SV; Peake JL; Walther RC; Kennedy IM; Leppert VJ; Aust AE (2004). Reduced lung cell proliferation following short-term exposure to ultrafine soot and iron particles in neonatal rats: key to impaired lung growth? *Inhal Toxicol*, 1: 73-81. [087465](#)
- Pinkerton KE; Zhou Y; Zhong C; Smith KR; Teague SV; Kennedy IM; Ménache MG (2008). Mechanisms of particulate matter toxicity in neonatal and young adult rat lungs. Health Effects Institute. Boston, MA. 135. [190471](#)
- Pope C; Renlund D; Kfoury A; May H; Horne B (2008). Relation of heart failure hospitalization to exposure to fine particulate air pollution. *Am J Cardiol*, 102: 1230-1234. [191969](#)
- Pope CA; Hansen ML; Long RW; Nielsen KR; Eatough NL; Wilson WE; Eatough DJ (2004). Ambient particulate air pollution, heart rate variability, and blood markers of inflammation in a panel of elderly subjects. *Environ Health Perspect*, 112: 339-345. [055238](#)
- Pope CA III; Muhlestein JB; May HT; Renlund DG; Anderson JL; Horne BD (2006). Ischemic heart disease events triggered by short-term exposure to fine particulate air pollution. *Circulation*, 114: 2443-2448. [091246](#)
- Pourazar J; Blomberg A; Kelly FJ; Davies DE; Wilson SJ; Holgate ST; Sandstrom T (2008). Diesel exhaust increases EGFR and phosphorylated C-terminal Tyr 1173 in the bronchial epithelium. *Part Fibre Toxicol*, 5: 8. [156884](#)

- Pourazar J; Mudway IS; Samet JM; Helleday R; Blomberg A; Wilson SJ; Frew AJ; Kelly FJ; Sandstrom T (2005). Diesel exhaust activates redox-sensitive transcription factors and kinases in human airways. *Am J Physiol*, 289: L724-L730. [088305](#)
- Power K; Balmes J; Solomon C (2008). Controlled exposure to combined particles and ozone decreases heart rate variability. *J Occup Environ Med*, 50: 1253-1260. [191982](#)
- Preuthipan A; Udomsubpayakul U; Chaisupamongkollarp T; Pentamwa P (2004). Effect of PM10 pollution in Bangkok on children with and without asthma. *Pediatr Pulmonol*, 37: 187-192. [055598](#)
- Pritchett LC; Cooper JA (1985). Aerosol Characterization Study of Anchorage, Alaska: Chemical Analysis and Source Apportionment. [156886](#)
- Prystowsky EN; Benson DW Jr; Fuster V; Hart RG; Kay GN; Myerburg RJ; Naccarelli GV; Wyse DG (1996). Management of patients with atrial fibrillation. A Statement for Healthcare Professionals. From the Subcommittee on Electrocardiography and Electrophysiology, American Heart Association. *Circulation*, 93: 1262-1277. [156031](#)
- Raabe OG; Al-Bayati MA; Teague SV; Rasolt A (1988). Regional deposition of inhaled monodisperse, coarse, and fine aerosol particles in small laboratory animals. In *Inhaled particles VI: Proceedings of an international symposium and workshop on lung dosimetry* (pp. 53-63). Cambridge, U.K.: Pergamon Press. [001439](#)
- Rabinovitch N; Strand M; Gelfand EW (2006). Particulate levels are associated with early asthma worsening in children with persistent disease. *Am J Respir Crit Care Med*, 173: 1098-1105. [088031](#)
- Rabinovitch N; Zhang LN; Murphy JR; Vedal S; Dutton SJ; Gelfand EW (2004). Effects of wintertime ambient air pollutants on asthma exacerbations in urban minority children with moderate to severe disease. *J Allergy Clin Immunol*, 114: 1131-1137. [096753](#)
- Ranzi A; Gambini M; Spattini A; Galassi C; Sesti D; Bedeschi M; Messori A; Baroni A; Cavagni G; Lauriola P (2004). Air pollution and respiratory status in asthmatic children: Hints for a locally based preventive strategy AIRE study. *Eur J Epidemiol*, 19: 567-576. [089500](#)
- Reed MD; Barrett EG; Campen MJ; Divine KK; Gigliotti AP; McDonald JD; Seagrave JC; Mauderly JL; Seilkop SK; Swenberg JA (2008). Health effects of subchronic inhalation exposure to gasoline engine exhaust. *Inhal Toxicol*, 20: 1125-1143. [156903](#)
- Reed MD; Campen MJ; Gigliotti AP; Harrod KS; McDonald JD; Seagrave JC; Mauderly JL; Seilkop SK (2006). Health effects of subchronic exposure to environmental levels of hardwood smoke. *Inhal Toxicol*, 18: 523-539. [156043](#)
- Reed MD; Gigliotti AP; McDonald JD; Seagrave JC; Seilkop SK; Mauderly JL (2004). Health effects of subchronic exposure to environmental levels of diesel exhaust. *Inhal Toxicol*, 16: 177-193. [055625](#)
- Rhoden CR; Ghelfi E; González-Flecha B (2008). Pulmonary inflammation by ambient air particles is mediated by superoxide anion. *Inhal Toxicol*, 20: 11-15. [190475](#)
- Rhoden CR; Lawrence J; Godleski JJ; Gonzalez-Flecha B (2004). N-acetylcysteine prevents lung inflammation after short-term inhalation exposure to concentrated ambient particles. *Toxicol Sci*, 79: 296-303. [087969](#)
- Rhoden CR; Wellenius GA; Ghelfi E; Lawrence J; Gonzalez-Flecha B (2005). PM-induced cardiac oxidative stress and dysfunction are mediated by autonomic stimulation. *Biochim Biophys Acta*, 1725: 305-313. [087878](#)
- Rich DQ; Freudenberger RS; Ohman-Strickland P; Cho Y; Kipen HM (2008). Right heart pressure increases after acute increases in ambient particulate concentration. *Environ Health Perspect*, 116: 1167-1171. [156910](#)
- Rich DQ; Kim MH; Turner JR; Mittleman MA; Schwartz J; Catalano PJ; Dockery DW (2006). Association of ventricular arrhythmias detected by implantable cardioverter defibrillator and ambient air pollutants in the St Louis, Missouri metropolitan area. *Occup Environ Med*, 63: 591-596. [089814](#)
- Rich DQ; Mittleman MA; Link MS; Schwartz J; Luttmann-Gibson H; Catalano PJ; Speizer FE; Gold DR; Dockery DW (2006). Increased risk of paroxysmal atrial fibrillation episodes associated with acute increases in ambient air pollution. *Environ Health Perspect*, 114: 120-123. [088427](#)
- Rich DQ; Schwartz J; Mittleman MA; Link M; Luttmann-Gibson H; Catalano PJ; Speizer FE; Dockery DW (2005). Association of short-term ambient air pollution concentrations and ventricular arrhythmias. *Am J Epidemiol*, 161: 1123-1132. [079620](#)

- Rich KE; Petkau J; Vedal S; Brauer M (2004). A case-crossover analysis of particulate air pollution and cardiac arrhythmia in patients with implantable cardioverter defibrillators. *Inhal Toxicol*, 16: 363-372. [055631](#)
- Riediker M; Cascio WE; Griggs TR; Herbst MC; Bromberg PA; Neas L; Williams RW; Devlin RB (2004). Particulate matter exposure in cars is associated with cardiovascular effects in healthy young men. *Am J Respir Crit Care Med*, 169: 934-940. [056992](#)
- Riediker M; Devlin RB; Griggs TR; Herbst MC; Bromberg PA; Williams RW; Cascio WE (2004). Cardiovascular effects in patrol officers are associated with fine particulate matter from brake wear and engine emissions. *Part Fibre Toxicol*, 1: 2. [091261](#)
- Riojas-Rodriguez H; Escamilla-Cejudo JA; Gonzalez-Hermosillo JA; Tellez-Rojo MM; Vallejo M; Santos-Burgoa C; Rojas-Bracho L (2006). Personal PM_{2.5} and CO exposures and heart rate variability in subjects with known ischemic heart disease in Mexico City. *J Expo Sci Environ Epidemiol*, 16: 131-137. [156913](#)
- Roberts JR; Taylor MD; Castranova V; Clarke RW; Antonini JM (2004). Soluble metals associated with residual oil fly ash increase morbidity and lung injury after bacterial infection in rats. *J Toxicol Environ Health A Curr Iss*, 67: 251-263. [196994](#)
- Roberts JR; Young S-H; Castranova V; Antonini JM (2007). Soluble metals in residual oil fly ash alter innate and adaptive pulmonary immune responses to bacterial infection in rats. *Toxicol Appl Pharmacol*, 221: 306-319. [097623](#)
- Rodriguez C; Tonkin R; Heyworth J; Kusel M; De Klerk N; Sly PD; Franklin P; Runnion T; Blockley A; Landau L; Hinwood AL (2007). The relationship between outdoor air quality and respiratory symptoms in young children. *Int J Environ Health Res*, 17: 351-360. [092842](#)
- Romieu I; Garcia-Esteban R; Sunyer J; Rios C; Alcaraz-Zubeldia M; Velasco SR; Holguin F (2008). The effect of supplementation with omega-3 polyunsaturated fatty acids on markers of oxidative stress in elderly exposed to PM_{2.5}. *Environ Health Perspect*, 116: 1237-1242. [156922](#)
- Romieu I; Tellez-Rojo MM; Lazo M; Manzano-Patino Cortez-Lugo M; Julien P; Belanger MC; Hernandez-Avila MHolguin F (2005). Omega-3 fatty acid prevents heart rate variability reductions associated with particulate matter. *Am J Respir Crit Care Med*, 172: 1534-1540. [086297](#)
- Rosenthal FS; Carney JP; Olinger ML (2008). Out-of-hospital cardiac arrest and airborne fine particulate matter: a case-crossover analysis of emergency medical services data in Indianapolis, Indiana. *Environ Health Perspect*, 116: 631-636. [156925](#)
- Routledge HC; Manney S; Harrison RM; Ayres JG; Townend JN (2006). Effect of inhaled sulphur dioxide and carbon particles on heart rate variability and markers of inflammation and coagulation in human subjects. *Heart*, 92: 220-227. [088674](#)
- Rowan 3rd WH; Campen MJ; Wichers LB; Watkinson WP (2007). Heart rate variability in rodents: uses and caveats in toxicological studies. *Cardiovasc Toxicol*, 7: 28-51. [191911](#)
- Roy D; Talajic M; Dubuc M; Thibault B; Guerra P; Macle L; Khairy P (2009). Atrial fibrillation and congestive heart failure. *Curr Opin Cardiol*, 24: 29. [190902](#)
- Ruckerl R; Greven S; Ljungman P; Aalto P; Antoniadis C; Bellander T; Berglund N; Chrysohoou C; Forastiere F; Jacquemin B; von Klot S; Koenig W; Kuchenhoff H; Lanki T; Pekkanen J; Perucci CA; Schneider A; Sunyer J; Peters A (2007). Air pollution and inflammation (interleukin-6, C-reactive protein, fibrinogen) in myocardial infarction survivors. *Environ Health Perspect*, 115: 1072-1080. [156931](#)
- Ruckerl R; Ibaldo-Mulli A; Koenig W; Schneider A; Woelke G; Cyrys J; Heinrich J; Marder V; Frampton M; Wichmann HE; Peters A (2006). Air pollution and markers of inflammation and coagulation in patients with coronary heart disease. *Environ Health Perspect*, 114: 432-441. [088754](#)
- Rudell B; Blomberg A; Helleday R; Ledin M-C; Lundback B; Stjernberg N; Horstedt P; Sandstrom T (1999). Bronchoalveolar inflammation after exposure to diesel exhaust: Comparison between unfiltered and particle trap filtered exhaust. *Occup Environ Med*, 56: 527-534. [001964](#)
- Rudell B; Ledin M-C; Hammarstrom U; Stjernberg N; Lundback B; Sandstrom T (1996). Effects on symptoms and lung function in humans experimentally exposed to diesel exhaust. *Occup Environ Med*, 53: 658-662. [056577](#)
- Rundell KW; Caviston R (2008). Ultrafine and fine particulate matter inhalation decreases exercise performance in healthy subjects. *J Strength Cond Res*, 22: 2-5. [191986](#)

- Rundell KW; Hoffman JR; Caviston R; Bulbulian R; Hollenbach AM (2007). Inhalation of ultrafine and fine particulate matter disrupts systemic vascular function. *Inhal Toxicol*, 19: 133-140. [156060](#)
- Safar M; Chamiot-Clerc P; Dagher G; Renaud JF (2001). Pulse pressure, endothelium function, and arterial stiffness in spontaneously hypertensive rats. *Hypertension*, 38: 1416-1421. [156068](#)
- Saldiva PHN; Clarke RW; Coull BA; Stearns RC; Lawrence J; Krishna-Murthy GG; Diaz E; Koutrakis P; Suh H; Tsuda A; Godleski JJ (2002). Lung inflammation induced by concentrated ambient air particles is related to particle composition. *Am J Respir Crit Care Med*, 165: 1610-1617. [025988](#)
- Salvi S; Blomberg A; Rudell B; Kelly F; Sandstrom T; Holgate ST; Frew A (1999). Acute inflammatory responses in the airways and peripheral blood after short-term exposure to diesel exhaust in healthy human volunteers. *Am J Respir Crit Care Med*, 159: 702-709. [058637](#)
- Samet JM; Dominici F; Zeger SL; Schwartz J; Dockery DW (2000). National morbidity, mortality, and air pollution study. Part I: Methods and methodologic issues. Health Effects Institute. Cambridge, MA. [005809](#)
- Samet JM; Rappold A; Graff D; Cascio WE; Berntsen JH; Huang YC; Herbst M; Bassett M; Montilla T; Hazucha MJ; Bromberg PA; Devlin RB (2009). Concentrated ambient ultrafine particle exposure induces cardiac changes in young healthy volunteers. *Am J Respir Crit Care Med*, 179: 1034-1042. [191913](#)
- Samet JM; Zeger SL; Dominici F; Curriero F; Coursac I; Dockery DW; Schwartz J; Zanobetti A (2000). The national morbidity, mortality, and air pollution study Part II: morbidity, mortality, and air pollution in the United States. Health Effects Institute. Cambridge, MA. [010269](#)
- Samoli E; Analitis A; Touloumi G; Schwartz J; Anderson HR; Sunyer J; Bisanti L; Zmirou D; Vonk JM; Pekkanen J; Goodman P; Paldy A; Schindler C; Katsouyanni K (2005). Estimating the exposure-response relationships between particulate matter and mortality within the APHEA multicity project. *Environ Health Perspect*, 113: 88-95. [087436](#)
- Samoli E; Peng R; Ramsay T; Pipikou M; Touloumi G; Dominici F; Burnett R; Cohen A; Krewski D; Samet J (2008). Acute effects of ambient particulate matter on mortality in Europe and North America: results from the APHENA study. *Environ Health Perspect*, 116: 1480-1486. [188455](#)
- Sandercock GRH; Brodie DA (2006). The role of heart rate variability in prognosis for different modes of death in chronic heart failure. *Pacing Clin Electrophysiol*, 29: 892-904. [197465](#)
- Santos U; Terra-Filho M; Lin C; Pereira L; Vieira T; Saldiva P; Braga A (2008). Cardiac arrhythmia emergency room visits and environmental air pollution in Sao Paulo, Brazil. *J Epidemiol Community Health*, 62: 267-272. [192004](#)
- Sarin S; Undem B; Sanico A; Togias A (2006). The role of the nervous system in rhinitis. *J Allergy Clin Immunol*, 118: 999-1016. [191166](#)
- Sarnat JA; Marmur A; Klein M; Kim E; Russell AG; Sarnat SE; Mulholland JA; Hopke PK; Tolbert PE (2008). Fine particle sources and cardiorespiratory morbidity: An application of chemical mass balance and factor analytical source-apportionment methods. *Environ Health Perspect*, 116: 459-466. [097972](#)
- Sarnat SE; Suh HH; Coull BA; Schwartz J; Stone PH; Gold DR (2006). Ambient particulate air pollution and cardiac arrhythmia in a panel of older adults in Steubenville, Ohio. *Occup Environ Med*, 63: 700-706. [090489](#)
- Sauerzapf V; Jones AP; Cross J (2009). Environmental factors and hospitalisation for chronic obstructive pulmonary disease in a rural county of England. *J Epidemiol Community Health*, 63: 324-328. [180082](#)
- Schaumann F; Borm PJA; Herbrich A; Knoch J; Pitz M; Schins RPF; Luettig B; Hohlfeld JM; Heinrich J; Krug N (2004). Metal-rich ambient particles (particulate matter 2.5) cause airway inflammation in healthy subjects. *Am J Respir Crit Care Med*, 170: 898-903. [087966](#)
- Schilderout JS; Sheppard L; Lumley T; Slaughter JC; Koenig JQ; Shapiro GG (2006). Ambient air pollution and asthma exacerbations in children: An eight-city analysis. *Am J Epidemiol*, 164: 505-517. [089812](#)
- Schins RPF; Lightbody JH; Borm PJA; Shi T; Donaldson K; Stone V (2004). Inflammatory effects of coarse and fine particulate matter in relation to chemical and biological constituents. *Toxicol Appl Pharmacol*, 195: 1-11. [054173](#)
- Schneider A; Neas L; Herbst M; Case M; Williams R; Cascio W; Hinderliter A; Holguin F; Buse J; Dungan K (2008). Endothelial dysfunction: associations with exposure to ambient fine particles in diabetic individuals. *Environ Health Perspect*, 116: 1666-1674. [191985](#)

- Schreuder AB; Larson TV; Sheppard L; Claiborn CS (2006). Ambient woodsmoke and associated respiratory emergency department visits in Spokane, Washington. *Int J Occup Environ Health*, 12: 147-153. [097959](#)
- Schwartz J (2003). Airborne particles and daily deaths in 10 US cities. [042800](#)
- Schwartz J (2003). Daily deaths associated with air pollution in six US cities and short-term mortality displacement in Boston. [042811](#)
- Schwartz J (2004). Is the association of airborne particles with daily deaths confounded by gaseous air pollutants? An approach to control by matching. *Environ Health Perspect*, 112: 557-561. [053506](#)
- Schwartz J (2004). The effects of particulate air pollution on daily deaths: a multi-city case crossover analysis. *Occup Environ Med*, 61: 956-961. [078998](#)
- Schwartz J; Coull B; Laden F; Ryan L (2008). The effect of dose and timing of dose on the association between airborne particles and survival. *Environ Health Perspect*, 116: 64-69. [156963](#)
- Schwartz J; Litonjua A; Suh H; Verrier M; Zanobetti A; Syring M; Nearing B; Verrier R; Stone P; MacCallum G; Speizer FE; Gold DR (2005). Traffic related pollution and heart rate variability in a panel of elderly subjects. *Thorax*, 60: 455-461. [074317](#)
- Schwartz J; Morris R (1995). Air pollution and hospital admissions for cardiovascular disease in Detroit, Michigan. *Am J Epidemiol*, 142: 23-35. [046186](#)
- Schwartz J; Neas LM (2000). Fine particles are more strongly associated than coarse particles with acute respiratory health effects in schoolchildren. *Epidemiology*, 11: 6-10. [007625](#)
- Schwartz J; Park SK; O'Neill MS; Vokonas PS; Sparrow D; Weiss S; Kelsey K (2005). Glutathione-S-transferase M1, obesity, statins, and autonomic effects of particles: gene-by-drug-by-environment interaction. *Am J Respir Crit Care Med*, 172: 1529-1533. [086296](#)
- Seagrave J; Campen M; McDonald J; Mauderly J; Rohr A (2008). Oxidative stress, inflammation, and pulmonary function assessment in rats exposed to laboratory-generated pollutant mixtures. *J Toxicol Environ Health A Curr Iss*, 71: 1352-1362. [191990](#)
- Seagrave JC; McDonald JD; Bedrick E; Edgerton ES; Gigliotti AP; Jansen JJ; Ke L; Naeher LP; Seilkop SK; Zheng M; Mauderly JL (2006). Lung toxicity of ambient particulate matter from southeastern US sites with different contributing sources: relationships between composition and effects. *Environ Health Perspect*, 114: 1387-93. [091291](#)
- Segala C; Poizeau D; Neukirch F; Aubier M; Samson J; Gehanno P (2004). Air pollution, passive smoking, and respiratory symptoms in adults. *Arch Environ Occup Health*, 59: 669-676. [090449](#)
- Shah AP; Pietropaoli AP; Frasier LM; Speers DM; Chalupa DC; Delehanty JM; Huang LS; Utell MJ; Frampton MW (2008). Effect of inhaled carbon ultrafine particles on reactive hyperemia in healthy human subjects. *Environ Health Perspect*, 116: 375-380. [156970](#)
- Sheppard L; Levy D; Norris G; Larson TV; Koenig JQ (2003). Effects of ambient air pollution and nonelderly asthma hospital admissions in Seattle, Washington, 1987-1994. *Epidemiology*, 10: 23-30. [042826](#)
- Shi JP; Harrison RM; Evans D (2001). Comparison of ambient particle surface area measurement by epiphaniometer and SMPS/APS. *Atmos Environ*, 35: 6193-6200. [078292](#)
- Sillanpaa M; Frey A; Hillamo R; Pennanen AS; Salonen RO (2005). Organic, elemental and inorganic carbon in particulate matter of six urban environments in Europe. *Atmos Chem Phys*, 5: 2869-2879. [156980](#)
- Simpson R; Williams G; Petroeschevsky A; Best T; Morgan G; Denison L; Hinwood A; Neville G (2005). The short-term effects of air pollution on hospital admissions in four Australian cities. *Aust N Z J Public Health*, 29: 213-221. [087438](#)
- Sinclair AH; Tolsma D (2004). Associations and lags between air pollution and acute respiratory visits in an ambulatory care setting: 25-month results from the aerosol research and inhalation epidemiological study. *J Air Waste Manag Assoc*, 54: 1212-1218. [088696](#)
- Sirivelu MP; MohanKumar SMJ; Wagner JG; Harkema JR; MohanKumar PS (2006). Activation of the stress axis and neurochemical alterations in specific brain areas by concentrated ambient particle exposure with concomitant allergic airway disease. *Environ Health Perspect*, 114: 870-874. [111151](#)

- Slaughter JC; Kim E; Sheppard L; Sullivan JH; Larson TV; Claiborn C (2005). Association between particulate matter and emergency room visits, hospital admissions and mortality in Spokane, Washington. *J Expo Sci Environ Epidemiol*, 15: 153-159. [073854](#)
- Slaughter JC; Lumley T; Sheppard L; Koenig JQ; Shapiro GG (2003). Effects of ambient air pollution on symptom severity and medication use in children with asthma. *Ann Allergy Asthma Immunol*, 91: 346-353. [086294](#)
- Smith AD; Taylor DR (2005). Is exhaled nitric oxide measurement a useful clinical test in asthma? *Curr Opin Allergy Clin Immunol*, 5: 49-56. [192176](#)
- Smith KR; Kim S; Recendez JJ; Teague SV; Menache MG; Grubbs DE; Sioutas C; Pinkerton KE (2003). Airborne particles of the California Central Valley alter the lungs of healthy adult rats. *Environ Health Perspect*, 111: 902-908. [042107](#)
- Smith KR; Veranth JM; Kodavanti UP; Aust AE; Pinkerton KE (2006). Acute pulmonary and systemic effects of inhaled coal fly ash in rats: comparison to ambient environmental particles. *Toxicol Sci*, 93: 390-399. [110864](#)
- Steenenberg PA; Van Amelsvoort L; Lovik M; Hetland RB; Alberg T; Halatek T; Bloemen HJT; Rydzynski K; Swaen G; Schwarze P; Dybing E; Cassee FR (2006). Relation between sources of particulate air pollution and biological effect parameters in samples from four European cities: an exploratory study. *Inhal Toxicol*, 18: 333-346. [088249](#)
- Steenenberg PA; Withagen CE; van Dalen WJ; Dormans JA; Heisterkamp SH; van Loveren H; Cassee FR (2005). Dose dependency of adjuvant activity of particulate matter from five European sites in three seasons in an ovalbumin-mouse model. *Inhal Toxicol*, 17: 133-145. [088649](#)
- Steenenberg PA; Withagen CET; van Dalen WJ; Dormans JAMA; Cassee FR; Heisterkamp SH; van Loveren H (2004). Adjuvant activity of ambient particulate matter of different sites, sizes, and seasons in a respiratory allergy mouse model. *Toxicol Appl Pharmacol*, 200: 186-200. [096024](#)
- Steenenberg PA; Withagen CET; van Dalen WJ; Dormans JAMA; van Loveren H (2004). Adjuvant Activity of Ambient Particulate Matter in Macrophage Activity-Suppressed, N-Acetylcysteine-Treated, iNOS- and IL-4-Deficient Mice. *Inhal Toxicol*, 16: 835-843. [087981](#)
- Steinvil A; Kordova-Biezuner L; Shapira I; Berliner S; Rogowski O (2008). Short-term exposure to air pollution and inflammation-sensitive biomarkers. *Environ Res*, 106: 51-61. [188893](#)
- Stenfors N; Nordenhall C; Salvi SS; Mudway I; Soderberg M; Blomberg A; Helleday R; Levin JO; Holgate ST; Kelly FJ; Frew AJ; Sandstrom T (2004). Different airway inflammatory responses in asthmatic and healthy humans exposed to diesel. *Eur Respir J*, 23: 82-86. [157009](#)
- Stevens T; Krantz QT; Linak WP; Hester S; Gilmour MI (2008). Increased transcription of immune and metabolic pathways in naive and allergic mice exposed to diesel exhaust. *Toxicol Sci*, 102: 359-370. [157010](#)
- Stölzel M; Breitner S; Cyrus J; Pitz M; Wolke G; Kreyling W; Heinrich J; Wichmann H-E; Peters A (2007). Daily mortality and particulate matter in different size classes in Erfurt, Germany. *J Expo Sci Environ Epidemiol*, 17: 458-467. [091374](#)
- Stolzel M; Peters A; Wichmann H-E (2003). Daily mortality and fine and ultrafine particles in Erfurt, Germany. [042842](#)
- Strand M; Vedal S; Rodes C; Dutton SJ; Gelfand EW; Rabinovitch N (2006). Estimating effects of ambient PM2.5 exposure on health using PM2.5 component measurements and regression calibration. *J Expo Sci Environ Epidemiol*, 16: 30-38. [089203](#)
- Suglia SF; Gryparis A; Wright RO; Schwartz J; Wright RJ (2008). Association of black carbon with cognition among children in a prospective birth cohort study. *Am J Epidemiol*, 167: 280-286. [157027](#)
- Sullivan J; Ishikawa N; Sheppard L; Siscovick D; Checkoway H; Kaufman J (2003). Exposure to ambient fine particulate matter and primary cardiac arrest among persons with and without clinically recognized heart disease. *Am J Epidemiol*, 157: 501-509. [043156](#)
- Sullivan J; Sheppard L; Schreuder A; Ishikawa N; Siscovick D; Kaufman J (2005). Relation between short-term fine-particulate matter exposure and onset of myocardial infarction. *Epidemiology*, 16: 41-48. [050854](#)
- Sullivan JH; Hubbard R; Liu SL; Shepherd K; Trenga CA; Koenig JQ; Chandler WL; Kaufman JD (2007). A community study of the effect of particulate matter on blood measures of inflammation and thrombosis in an elderly population. *Environ Health Perspect*, 6: 3. [100083](#)

- Sullivan JH; Schreuder AB; Trenga CA; Liu SL; Larson TV; Koenig JQ; Kaufman JD (2005). Association between short term exposure to fine particulate matter and heart rate variability in older subjects with and without heart disease. *Thorax*, 60: 462-466. [109418](#)
- Sureshkumar V; Paul B; Uthirappan M; Pandey R; Sahu AP; Lal K; Prasad AK; Srivastava S; Saxena A; Mathur N; Gupta YK (2005). Proinflammatory and anti-inflammatory cytokine balance in gasoline exhaust induced pulmonary injury in mice. *Inhal Toxicol*, 17: 161-168. [088306](#)
- Symons JM; Wang L; Guallar E; Howell E; Dominici F; Schwab M; Ange BA; Samet J; Ondov J; Harrison D; Geyh A (2006). A case-crossover study of fine particulate matter air pollution and onset of congestive heart failure symptom exacerbation leading to hospitalization. *Am J Epidemiol*, 164: 421-433. [091258](#)
- Szyszkowicz M (2008). Ambient air pollution and daily emergency department visits for ischemic stroke in Edmonton, Canada. *Int J Occup Med Environ Health*, 21: 295-300. [192128](#)
- Szyszkowicz M (2009). Air pollution and ED visits for chest pain. *Am J Emerg Med*, 27: 165-168. [191996](#)
- Sørensen M; Daneshvar B; Hansen M; Dragsted LO; Hertel O; Knudsen L; Loft S (2003). Personal PM2.5 exposure and markers of oxidative stress in blood. *Environ Health Perspect*, 111: 161-166. [157000](#)
- Tamagawa E; Bai N; Morimoto K; Gray C; Mui T; Yatera K; Zhang X; Xing L; Li Y; Laher I (2008). Particulate matter exposure induces persistent lung inflammation and endothelial dysfunction. *Am J Physiol Lung Cell Mol Physiol*, 295: L79-L85. [191988](#)
- Tan WC; Qiu D; Liam BL; Ng TP; Lee SH; Van Eeden SF; D'Yachkova Y; Hogg JC (2000). The human bone marrow response to acute air pollution caused by forest fires. *Am J Respir Crit Care Med*, 161: 1213-1217. [002304](#)
- Tankersley CG; Bierman A; Rabold R (2007). Variation in heart rate regulation and the effects of particle exposure in inbred mice. *Inhal Toxicol*, 19: 621-629. [097910](#)
- Tankersley CG; Campen M; Bierman A; Flanders SE; Broman KW; Rabold R (2004). Particle effects on heart-rate regulation in senescent mice. *Inhal Toxicol*, 16: 381-390. [094378](#)
- Tankersley CG; Champion HC; Takimoto E; Gabrielson K; Bedja D; Misra V; El-Haddad H; Rabold R; Mitzner W (2008). Exposure to inhaled particulate matter impairs cardiac function in senescent mice. *Am J Physiol Regul Integr Comp Physiol*, 295: R252-R263. [157043](#)
- Tankersley CG; Irizarry R; Flanders SE; Rabold R; Frank R (2003). Unstable heart rate and temperature regulation predict mortality in AKR/J mice. *Am J Physiol*, 284: R742-R750. [053919](#)
- Tecer LH; Alagha O; Karaca F; Tuncel G; Eldes N (2008). Particulate Matter (PM2.5, PM10-2.5, and PM10) and Children's Hospital Admissions for Asthma and Respiratory Diseases: A Bidirectional Case-Crossover Study. *J Toxicol Environ Health A Curr Iss*, 71: 512-520. [180030](#)
- TFESC (1996). Heart rate variability: Standards of measurement, physiological interpretation, and clinical use. Task Force of the European Society of Cardiology. North American Society of Pacing and Electrophysiology. *Eur Heart J*, 17: 354-381. [003061](#)
- Thackara JW (1981). An acute inhalation toxicity study of AC-7987-001 in rats with attachments and cover letter dated 1/24/92. [078988](#)
- Thong T; Raitt MH (2007). Predicting imminent episodes of ventricular tachyarrhythmias using heart rate. *Pacing Clin Electrophysiol*, 30: 874-884. [197462](#)
- Thurston G; Ito K; Mar T; Christensen WF; Eatough DJ; Henry RC; Kim E; Laden F; Lall R; Larson TV; Liu H; Neas L; Pinto J; Stolzel M; Suh H; Hopke PK (2005). Results and implications of the workshop on the source apportionment of PM health effects. *Epidemiology*, 16: S134-S135. [097949](#)
- Thurston GD; Ito K; Hayes CG; Bates DV; Lippmann M (1994). Respiratory hospital admissions and summertime haze air pollution in Toronto, Ontario: consideration of the role of acid aerosols. *Environ Res*, 65: 271-290. [043921](#)
- Timonen KL; Hoek G; Heinrich J; Bernard A; Brunekreef B; De Hartog J; Hameri K; Ibaldo-Mulli A; Mirme A; Peters A; Tiittanen P; Kreyling WG; Pekkanen J (2004). Daily variation in fine and ultrafine particulate air pollution and urinary concentrations of lung Clara cell protein CC16. *Occup Environ Med*, 61: 908-914. [087915](#)

- Timonen KL; Vanninen E; De Hartog J; Ibaldo-Mulli A; Brunekreef B; Gold DR; Henrich J; Hoek G; Lanki T; Peters A; Tarkiainen T; Tiittanen P; Kreyling W; Pekkanen J (2006). Effects of ultrafine and fine particulate and gaseous air pollution on cardiac autonomic control in subjects with coronary artery disease: The ULTRA study. *J Expo Sci Environ Epidemiol*, 16: 332-341. [088747](#)
- Tolbert PE; Klein M; Metzger KB; Peel J; Flanders WD; Todd K; Mulholland JA; Ryan PB; Frumkin H (2000). Interim results of the study of particulates and health in Atlanta (SOPHIA). *J Expo Sci Environ Epidemiol*, 10: 446-460. [010320](#)
- Tolbert PE; Klein M; Peel JL; Sarnat SE; Sarnat JA (2007). Multipollutant modeling issues in a study of ambient air quality and emergency department visits in Atlanta. *J Expo Sci Environ Epidemiol*, 17: S29-S35. [090316](#)
- Tornqvist H; Mills NL; Gonzalez M; Miller MR; Robinson SD; Megson IL; MacNee W; Donaldson K; Soderberg S; Newby DE; Sandstrom T; Blomberg A (2007). Persistent endothelial dysfunction in humans after diesel exhaust inhalation. *Am J Respir Crit Care Med*, 176: 395-400. [091279](#)
- Trenga CA; Sullivan JH; Schildcrout JS; Shepherd KP; Shapiro GG; Liu LJ; Kaufman JD; Koenig JQ (2006). Effect of particulate air pollution on lung function in adult and pediatric subjects in a Seattle panel study. *Chest*, 129: 1614-1622. [155209](#)
- Tsai FC; Apte MG; Daisey JM (2000). An exploratory analysis of the relationship between mortality and the chemical composition of airborne particulate matter. *Inhal Toxicol*, 12: 121-135. [006251](#)
- Tsai S-S; Cheng M-H; Chiu H-F; Wu T-N; Yang C-Y (2006). Air pollution and hospital admissions for asthma in a tropical city: Kaohsiung, Taiwan. *Inhal Toxicol*, 18: 549-554. [089768](#)
- Tsai S-S; Goggins WB; Chiu H-F; Yang C-Y (2003). Evidence for an association between air pollution and daily stroke admissions in Kaohsiung, Taiwan. *Stroke*, 34: 2612-2616. [080133](#)
- Tunnicliffe WS; Harrison RM; Kelly FJ; Dunster C; Ayres JG (2003). The effect of sulphurous air pollutant exposures on symptoms, lung function, exhaled nitric oxide, and nasal epithelial lining fluid antioxidant concentrations in normal and asthmatic adults. *Occup Environ Med*, 60: 1-7. [088744](#)
- U.S. EPA (1982). Air quality criteria for particulate matter and sulfur oxides, Vol 1, 2, 3. U.S. Environmental Protection Agency, Environmental Criteria and Assessment Office. Washington, D.C.. EPA 600/8-82-029a; EPA 600/8-82-029b; EPA 600/8-82-029c. <http://nepis.epa.gov/Exe/ZyPURL.cgi?Dockey=3000188Z.txt>; <http://nepis.epa.gov/Exe/ZyPURL.cgi?Dockey=300018EV.txt>; <http://nepis.epa.gov/Exe/ZyPURL.cgi?Dockey=300053KV.txt>. [017610](#)
- U.S. EPA (1996). Air quality criteria for particulate matter. U.S. Environmental Protection Agency. Research Triangle Park, NC. EPA/600/P-95/001aF-cF. [079380](#)
- U.S. EPA (2002). Health assessment document for diesel engine exhaust. U.S. Environmental Protection Agency. Washington, DC. [042866](#)
- U.S. EPA (2004). Air quality criteria for particulate matter. U.S. Environmental Protection Agency. Research Triangle Park, NC. EPA/600/P-99/002aF-bF. [056905](#)
- Ulirsch GV; Ball LM; Kaye W; Shy CM; Lee CV; Crawford-Brown D; Symons M; Holloway T (2007). Effect of particulate matter air pollution on hospital admissions and medical visits for lung and heart disease in two southeast Idaho cities. *J Expo Sci Environ Epidemiol*, 17: 478-487. [091332](#)
- Upadhyay D; Panduri V; Ghio A; Kamp DW (2003). Particulate matter induces alveolar epithelial cell DNA damage and apoptosis: role of free radicals and the mitochondria. *Am J Respir Cell Mol Biol*, 29: 180-187. [097370](#)
- Upadhyay S; Stoeger T; Harder V; Thomas RF; Schladweiler MC; Semmler-Behnke M; Takenaka S; Karg E; Reitmeir P; Bader M; Stampfl A; Kodovanti U; Schulz H (2008). Exposure to ultrafine carbon particles at levels below detectable pulmonary inflammation affects cardiovascular performance in spontaneously hypertensive rats. *Part Fibre Toxicol*, 5: 19. [159345](#)
- Urch B; Brook JR; Wasserstein D; Brook RD; Rajagopalan S; Corey P; Silverman F (2004). Relative contributions of PM_{2.5} chemical constituents to acute arterial vasoconstriction in humans. *Inhal Toxicol*, 16: 345-352. [055629](#)
- Urch B; Silverman F; Corey P; Brook JR; Lukic KZ; Rajagopalan S; Brook RD (2005). Acute blood pressure responses in healthy adults during controlled air pollution exposures. *Environ Health Perspect*, 113: 1052-1055. [081080](#)

- Vedal S; Rich K; Brauer M; White R; Petkau J (2004). Air pollution and cardiac arrhythmias in patients with implantable cardiovascular defibrillators. *Inhal Toxicol*, 16: 353-362. [055630](#)
- Vegni FE; Ros O (2004). Hospital accident and emergency burden is unaffected by today's air pollution levels. *Eur J Emerg Med*, 11: 86-88. [087448](#)
- Veranth JM; Moss TA; Chow JC; Labban R; Nichols WK; Walton JC; Walton JG; Yost GS (2006). Correlation of in vitro cytokine responses with the chemical composition of soil-derived particulate matter. *Environ Health Perspect*, 114: 341-349. [087479](#)
- Veronesi B; Makwana O; Pooler M; Chen LC (2005). Effects of subchronic exposures to concentrated ambient particles: VII. Degeneration of dopaminergic neurons in Apo E^{-/-} mice. *Inhal Toxicol*, 17: 235-241. [087481](#)
- Vigotti MA; Chiaverini F; Biagiola P; Rossi G (2007). Urban air pollution and emergency visits for respiratory complaints in Pisa, Italy. *J Toxicol Environ Health A Curr Iss*, 70: 266-269. [090711](#)
- Villeneuve PJ; Burnett RT; Shi Y; Krewski D; Goldberg MS; Hertzman C; Chen Y; Brook J (2003). A time-series study of air pollution, socioeconomic status, and mortality in Vancouver, Canada. *J Expo Sci Environ Epidemiol*, 13: 427-435. [055051](#)
- Villeneuve PJ; Chen L; Stieb D; Rowe BH (2006). Associations between outdoor air pollution and emergency department visits for stroke in Edmonton, Canada. *Eur J Epidemiol*, 21: 689-700. [090191](#)
- Vincent R; Kumarathasan P; Goegan P; Bjarnason SG; Guenette J; Berube D; Adamson IY; Desjardins S; Burnett RT; Miller FJ; Battistini B (2001). Inhalation toxicology of urban ambient particulate matter: acute cardiovascular effect in rats. [021184](#)
- Von Klot S; Wolke G; Tuch T; Heinrich J; Dockery DW; Schwartz J; Kreyling WG; Wichmann HE; Peters A (2002). Increased asthma medication use in association with ambient fine and ultrafine particles. *Eur Respir J*, 20: 691-702. [034706](#)
- Von Klot S; Peters A; Aalto P; Bellander T; Berglind N; D'Ippoliti D; Elosua R; Hormann A; Kulmala M; Lanki T; Lowel H; Pekkanen J; Picciotto S; Sunyer J; Forastiere F; Health Effects of Particles on Susceptible Subpopulations (HEAPSS) Study Group (2005). Ambient air pollution is associated with increased risk of hospital cardiac readmissions of myocardial infarction survivors in five European cities. *Circulation*, 112: 3073-3079. [088070](#)
- Ward DJ; Roberts KT; Jones N; Harrison RM; Ayres JG; Hussain S; Walters S (2002). Effects of daily variation in outdoor particulates and ambient acid species in normal and asthmatic children. *Thorax*, 57: 489-502. [025839](#)
- Ward PA (2003). Acute lung injury: how the lung inflammatory response works. *Eur Respir J*, 44: 22s-23s. [157111](#)
- Wegesser TC; Last JA (2008). Lung response to coarse PM: bioassay in mice. *Toxicol Appl Pharmacol*, 230: 159-166. [190506](#)
- Welin L; Eriksson H; Larsson B; Svärdsudd K; Wilhelmsen L; Tibblin G (1993). Risk Factors for Coronary Heart Disease during 25 Years of Follow-Up. *Cardiology*, 82: 223-228. [156151](#)
- Wellenius GA; Batalha JRF; Diaz EA; Lawrence J; Coull BA; Katz T; Verrier RL; Godleski JJ (2004). Cardiac effects of carbon monoxide and ambient particles in a rat model of myocardial infarction. *Toxicol Sci*, 80: 367-376. [087874](#)
- Wellenius GA; Bateson TF; Mittleman MA; Schwartz J (2005). Particulate air pollution and the rate of hospitalization for congestive heart failure among medicare beneficiaries in Pittsburgh, Pennsylvania. *Am J Epidemiol*, 161: 1030-1036. [087483](#)
- Wellenius GA; Coull BA; Batalha JRF; Diaz EA; Lawrence J; Godleski JJ (2006). Effects of ambient particles and carbon monoxide on supraventricular arrhythmias in a rat model of myocardial infarction. *Inhal Toxicol*, 18: 1077-1082. [156152](#)
- Wellenius GA; Coull BA; Godleski JJ; Koutrakis P; Okabe K; Savage ST (2003). Inhalation of concentrated ambient air particles exacerbates myocardial ischemia in conscious dogs. *Environ Health Perspect*, 111: 402-408. [055691](#)
- Wellenius GA; Saldiva PHN; Batalha JRF; Murthy GGK; Coull BA; Verrier RL; Godleski JJ (2002). Electrocardiographic changes during exposure to residual oil fly ash (ROFA) particles in a rat model of myocardial infarction. *Toxicol Sci*, 66: 327-335. [025405](#)
- Wellenius GA; Schwartz J; Mittleman MA (2005). Air pollution and hospital admissions for ischemic and hemorrhagic stroke among medicare beneficiaries. *Stroke*, 36: 2549-2553. [088685](#)

- Wellenius GA; Schwartz J; Mittleman MA (2006). Particulate air pollution and hospital admissions for congestive heart failure in seven United States cities. *Am J Cardiol*, 97: 404-408. [088748](#)
- Wellenius GA; Yeh GY; Coull BA; Suh HH; Phillips RS; Mittleman MA (2007). Effects of ambient air pollution on functional status in patients with chronic congestive heart failure: a repeated-measures study. *Environ Health*, 6: 1-7. [092830](#)
- Welty LJ; Zeger SL (2005). Are the acute effects of particulate matter on mortality in the National Morbidity, Mortality, and Air Pollution study the result of inadequate control for weather and season? A sensitivity analysis using flexible distributed lag models. *Am J Epidemiol*, 162: 80-88. [087484](#)
- Wheeler A; Zanobetti A; Gold DR; Schwartz J; Stone P; Suh HH (2006). The relationship between ambient air pollution and heart rate variability differs for individuals with heart and pulmonary disease. *Environ Health Perspect*, 114: 560-566. [088453](#)
- Whitekus MJ; Li N; Zhang M; Wang M; Horwitz MA; Nelson SK; Horwitz LD; Brechun N; Diaz-Sanchez D; Nel AE (2002). Thiol antioxidants inhibit the adjuvant effects of aerosolized diesel exhaust particles in a murine model for ovalbumin sensitization. *J Immigr Minor Health*, 168: 2560-2567. [157142](#)
- Whitsel E; Quibrera P; Christ S; Liao D; Prineas R; Anderson G; Heiss G (2009). Heart rate variability, ambient particulate matter air pollution, and glucose homeostasis: the environmental epidemiology of arrhythmogenesis in the Women's Health Initiative. *Am J Epidemiol*, 169: 693-703. [191980](#)
- Wichmann H-E; Spix C; Tuch T; Wolke G; Peters A; Heinrich J; Kreyling WG; Heyder J (2000). Daily mortality and fine and ultrafine particles in Erfurt, Germany Part I: role of particle number and particle mass. Health Effects Institute. Boston, MA. [013912](#)
- Widdicombe J (2006). Reflexes from the lungs and airways: historical perspective. *J Appl Physiol*, 101: 628-634. [155519](#)
- Widdicombe JG (2003). Overview of neural pathways in allergy and asthma. *Pulm Pharmacol Ther*, 16: 23-30. [157145](#)
- Wilson WE; Mar TF; Koenig JQ (2007). Influence of exposure error and effect modification by socioeconomic status on the association of acute cardiovascular mortality with particulate matter in Phoenix. *J Expo Sci Environ Epidemiol*, 17: S11-S19. [157149](#)
- Win-Shwe TT; Yamamoto S; Fujitani Y; Hirano S; Fujimaki H (2008). Spatial learning and memory function-related gene expression in the hippocampus of mouse exposed to nanoparticle-rich diesel exhaust. *Neurotoxicology*, 29: 940-947. [190146](#)
- Witten ML; Wong SS ; Sun NN; Keith I; Kweon C; Foster DE; Schauer JJ; Sherrill DL (2005). Neurogenic responses in rat lungs after nose-only exposure to diesel exhaust. Health Effects Institute. Boston, MA. [087485](#)
- Wong C-M; Atkinson RW; Anderson HR; Hedley AJ; Ma S; Chau PY-K; Lam T-H (2002). A tale of two cities: effects of air pollution on hospital admissions in Hong Kong and London compared. *Environ Health Perspect*, 110: 67-77. [023232](#)
- Wong SS; Sun NN; Keith I; Kweon C-B; Foster DE; Schauer James J; Witten ML (2003). Tachykinin substance P signaling involved in diesel exhaust-induced bronchopulmonary neurogenic inflammation in rats. *Arch Toxicol*, 77: 638-650. [097707](#)
- Wong TW; Lau TS; Yu TS; Neller A; Wong SL; Tam W; Pang SW (1999). Air pollution and hospital admissions for respiratory and cardiovascular diseases in Hong Kong. *Occup Environ Med*, 56: 679-683. [009172](#)
- Wordley J; Walters S; Ayres JG (1997). Short term variations in hospital admissions and mortality and particulate air pollution. *Occup Environ Med*, 54: 108-116. [082745](#)
- Wu J; M Winer A; J Delfino R (2006). Exposure assessment of particulate matter air pollution before, during, and after the 2003 Southern California wildfires. *Atmos Environ*, 40: 3333-3348. [157156](#)
- Yan YH; Huang CH; Chen WJ; Wu MF; Cheng TJ (2008). Effects of diesel exhaust particles on left ventricular function in isoproterenol-induced myocardial injury and healthy rats. *Inhal Toxicol*, 20: 199-203. [098625](#)
- Yang C-Y; Chen Y-S; Yang C-H; Ho S-C (2004). Relationship between ambient air pollution and hospital admissions for cardiovascular diseases in Kaohsiung, Taiwan. *J Toxicol Environ Health A Curr Iss*, 67: 483-493. [094376](#)
- Yang CY (2008). Air pollution and hospital admissions for congestive heart failure in a subtropical city: Taipei, Taiwan. *J Toxicol Environ Health A Curr Iss*, 71: 1085-1090. [157160](#)

- Yang CY; Chen CC; Chen CY; Kuo HW (2007). Air pollution and hospital admissions for asthma in a subtropical city: Taipei, Taiwan. *J Toxicol Environ Health A Curr Iss*, 70: 111-117. [092848](#)
- Yang CY; Chen CJ (2007). Air pollution and hospital admissions for chronic obstructive pulmonary disease in a subtropical city: Taipei, Taiwan. *J Toxicol Environ Health A Curr Iss*, 70: 1214-1219. [092847](#)
- Yang CY; Cheng MH; Chen CC (2009). Effects of Asian Dust Storm Events on Hospital Admissions for Congestive Heart Failure in Taipei, Taiwan. *J Toxicol Environ Health A Curr Iss*, 72: 324-328. [190341](#)
- Yang Q; Chen Y; Krewski D; Shi Y; Burnett RT; McGrail KM (2004). Association between particulate air pollution and first hospital admission for childhood respiratory illness in Vancouver, Canada. *Arch Environ Occup Health*, 59: 14-21. [087488](#)
- Yeatts K; Svendsen E; Creason J; Alexis N; Herbst M; Scott J; Kupper L; Williams R; Neas L; Cascio W; Devlin RB; Peden DB (2007). Coarse particulate matter (PM25-10) affects heart rate variability, blood lipids, and circulating eosinophils in adults with asthma. *Environ Health Perspect*, 115: 709-714. [091266](#)
- Yokota S; Seki T; Naito Y; Tachibana S; Hirabayashi N; Nakasaka T; Ohara N; Kobayashi H (2008). Tracheal instillation of diesel exhaust particles component causes blood and pulmonary neutrophilia and enhances myocardial oxidative stress in mice. *J Toxicol Sci*, 33: 609-620. [190109](#)
- Yu O; Sheppard L; Lumley T; Koenig JQ; S (2000). Effects of ambient air pollution on symptoms of asthma in Seattle-area children enrolled in the CAMP study. *Environ Health Perspect*, 108: 1209-1214. [013254](#)
- Yue W; Schneider A; Stolzel M; Ruckerl R; Cyrus J; Pan X; Zareba W; Koenig W; Wichmann HE; Peters A (2007). Ambient source-specific particles are associated with prolonged repolarization and increased levels of inflammation in male coronary artery disease patients. *Mutat Res Fund Mol Mech Mutagen*, 621: 50-60. [097968](#)
- Zabel M; Klingenhoben T; Franz MR; Hohnloser SH (1998). Assessment of QT Dispersion for Prediction of Mortality or Arrhythmic Events After Myocardial Infarction : Results of a Prospective, Long-term Follow-up Study. *Circulation*, 97: 2543-2550. [156176](#)
- Zanchi AC; Venturini CD; Saiki M; Nascimento Saldiva PH; Tannhauser Barros HM; Rhoden CR (2008). Chronic nasal instillation of residual-oil fly ash (ROFA) induces brain lipid peroxidation and behavioral changes in rats. *Inhal Toxicol*, 20: 795-800. [157173](#)
- Zanobetti A; Canner MJ; Stone PH; Schwartz J; Sher D; Eagan-Bengston E; Gates KA; Hartley LH; Suh H; Gold DR (2004). Ambient pollution and blood pressure in cardiac rehabilitation patients. *Circulation*, 110: 2184-2189. [087489](#)
- Zanobetti A; Schwartz J (2003). Airborne particles and hospital admissions for heart and lung disease. [043119](#)
- Zanobetti A; Schwartz J (2003). Airborne particles and hospital admissions for heart and lung disease. In: Revised analyses of time-series studies of air pollution and health. Special Report. [157174](#)
- Zanobetti A; Schwartz J (2005). The effect of particulate air pollution on emergency admissions for myocardial infarction: A multicity case-crossover analysis. *Environ Health Perspect*, 113: 978-982. [088069](#)
- Zanobetti A; Schwartz J (2006). Air pollution and emergency admissions in Boston, MA. *J Epidemiol Community Health*, 60: 890-895. [090195](#)
- Zanobetti A; Schwartz J (2009). The effect of fine and coarse particulate air pollution on mortality: A national analysis. *Environ Health Perspect*, 117: 1-40. [188462](#)
- Zareba W; Couderc JP; Oberdörster G; Chalupa D; Cox C; Huang LS; Peters A; Utell MJ; Frampton MW (2009). ECG parameters and exposure to carbon ultrafine particles in young healthy subjects. *Inhal Toxicol*, 21: 223-233. [190101](#)
- Zeka A; Sullivan JR; Vokonas PS; Sparrow D; Schwartz J (2006). Inflammatory markers and particulate air pollution: characterizing the pathway to disease. *Int J Epidemiol*, 35: 1347-1354. [157177](#)
- Zeka A; Zanobetti A; Schwartz J (2005). Short term effects of particulate matter on cause specific mortality: effects of lags and modification by city characteristics. *Occup Environ Med*, 62: 718-725. [088068](#)
- Zeka A; Zanobetti A; Schwartz J (2006). Individual-level modifiers of the effects of particulate matter on daily mortality. *Am J Epidemiol*, 163: 849-859. [088749](#)
- Zelikoff JT; Chen LC; Cohen MD; Fang K; Gordon T; Li Y; Nadziejko C; Schlesinger RB (2003). Effects of inhaled ambient particulate matter on pulmonary antimicrobial immune defense. *Inhal Toxicol*, 15: 131-150. [039009](#)

Zhang SH; Reddick RL; Piedrahita JA; Maeda N (1992). Spontaneous hypercholesterolemia and arterial lesions in mice lacking apolipoprotein E. *Science*, 258: 468-471. [157180](#)

Zhang Z; Whitsel E; Quibrera P; Smith R; Liao D; Anderson G; Prineas R (2009). Ambient fine particulate matter exposure and myocardial ischemia in the Environmental Epidemiology of Arrhythmogenesis in the Women's Health Initiative (EEAWHI) study. *Environ Health Perspect*, 117: 751-756. [191970](#)

Chapter 7. Integrated Health Effects of Long-Term PM Exposure

7.1. Introduction

This chapter reviews, summarizes, and integrates the evidence on relationships between health effects and long-term exposures to various size fractions and sources of PM. Cardiopulmonary health effects of long-term exposure to PM have been examined in an extensive body of epidemiologic and toxicological studies. Both epidemiologic and toxicological studies provide a basis for examining reproductive and developmental and cancer health outcomes with regard to long-term exposure to PM. In addition, there is a large body of epidemiologic literature evaluating the relationship between mortality and long-term exposure to PM.

Conclusions from the 2004 PM AQCD are summarized briefly at the beginning of each section, and the evaluation of evidence from recent studies builds upon what was available during the previous review. For each health outcome (e.g., respiratory infections, lung function), results are summarized for studies from the specific scientific discipline, i.e., epidemiologic and toxicological studies. The major sections (i.e., cardiovascular, respiratory, reproductive/developmental, cancer) conclude with summaries of the evidence for the various health outcomes within that category and integration of the findings that lead to conclusions regarding causality based upon the framework described in Chapter 1. Determination of causality is made for the overall health effect category, such as cardiovascular effects, with coherence and plausibility being based upon the evidence from across disciplines and also across the suite of related health outcomes including cause-specific mortality. Section 7.6 provides detailed discussions on the epidemiologic literature for long-term exposure to PM and mortality. In each summary section (7.2.11, 7.3.9, 7.4.3, 7.5.4, and 7.6.5), the evidence is briefly reviewed and independent conclusions drawn for relationships with PM_{2.5}, PM_{10-2.5}, and UF particles (UFPs).

7.2. Cardiovascular and Systemic Effects

Studies examining associations between long-term exposure to ambient PM (over months to years) and CVD morbidity had not been conducted and thus were not included in the 1996 or 2004 PM Air Quality Criteria Documents (U.S. EPA, 1996, [079380](#); U.S. EPA, 2004, [056905](#)). A number of studies were included in the 2004 PM AQCD that evaluated the effect of long-term PM_{2.5} exposure on cardiovascular mortality and found consistent associations. No toxicological studies examined chronic atherosclerotic effects of PM exposure in animal models. However, a subchronic study that evaluated atherosclerosis progression in hyperlipidemic rabbits was discussed and this study provided the foundation for the subsequent work that has been conducted in this area (Suwa et al., 2002, [028588](#)). No previous toxicological studies evaluated effects of subchronic or chronic PM exposure on diabetes measures, or HR or HRV changes, nor were there animal toxicological studies included in the 2004 PM AQCD that evaluated systemic inflammatory or blood coagulation markers following subchronic or chronic PM exposure.

Several new epidemiologic studies have examined the long-term PM-CVD association among U.S. and European populations. The studies investigate the association of both PM_{2.5} and PM₁₀ exposures with a variety of clinical and subclinical CVD outcomes. Epidemiologic and toxicological studies have provided evidence of the adverse effects of long-term exposure to PM_{2.5} on

Note: Hyperlinks to the reference citations throughout this document will take you to the NCEA HERO database (Health and Environmental Research Online) at <http://epa.gov/hero>. HERO is a database of scientific literature used by U.S. EPA in the process of developing science assessments such as the Integrated Science Assessments (ISA) and the Integrated Risk Information System (IRIS).

cardiovascular outcomes, including atherosclerosis, clinical and subclinical markers of cardiovascular morbidity, and cardiovascular mortality. The evidence of these effects from long-term exposure to PM_{10-2.5} is weaker.

7.2.1. Atherosclerosis

Atherosclerosis is a progressive disease that contributes to several adverse outcomes, including acute coronary syndromes such as myocardial infarction, sudden cardiac death, stroke and vascular aneurysms. It is multifaceted, beginning with an early injury or inflammation that promotes the extravasation of inflammatory cells. Under conditions of oxidative or nitrosative stress and high lipid or cholesterol concentrations, the vessel wall undergoes a chronic remodeling that is characterized by the presence of foam cells, migrated and differentiated smooth muscle cells, and ultimately a fibrous cap. The advanced lesion that develops from this process can occlude perfusion to distal tissue, causing ischemia, and erode, degrade, or even rupture, revealing coagulant initiators (tissue factor) that promote thrombosis, stenosis, and infarction or stroke. Several detailed reviews of atherosclerosis pathology have been published elsewhere (Ross, 1999, [156926](#); Stocker and Keaney, 2004, [157013](#)).

7.2.1.1. Epidemiologic Studies

Measures of Atherosclerosis

Although no study has examined the association between long-term PM exposure and longitudinal change in subclinical markers of atherosclerosis, several cross sectional studies have been conducted. Markers of atherosclerosis used in these studies include coronary artery calcium (CAC), carotid intima-media thickness (CIMT), ankle-brachial index (ABI), and abdominal aortic calcium (AAC). These measures are described briefly below.

CAC represents the accumulation of calcium in coronary artery macrophages and represents an advanced stage of atherosclerosis. As such CAC is a measure of atherosclerosis assessed by non-contrast, cardiac-gated electron beam computed tomography (EBCT) or multidetector computed tomography (MDCT) of the coronary arteries in the heart (Greenland and Kizilbash, 2005, [156496](#); Hoffmann et al., 2005, [156556](#); Mollet et al., 2005, [155988](#)). The prevalence of CAC is strongly related to age. Few people have detectable CAC in their second decade of life but the prevalence of CAC rises to approximately 100% by age 80 (Ardehali et al., 2007, [155662](#)). Previous studies suggest that while the absence of CAC does not rule out atherosclerosis, it does imply a very low likelihood of significant arterial obstruction (Achenbach and Daniel, 2001, [156189](#); Arad et al., 1996, [155661](#); Shaw et al., 2003, [156083](#); Shemesh et al., 1996, [156085](#)). Conversely, the presence of CAC confirms the existence of atherosclerotic plaque and the amount of calcification varies directly with the likelihood of obstructive disease (Ardehali et al., 2007, [155662](#)). CAC is a quantified using the Agatston method (Agatston et al., 1990, [156197](#)). Its repeatability depends on the laboratory and the method of calculation (O'Rourke et al., 2000, [192159](#)). Agatston scores are frequently used to classify individuals into one of five groups (zero; mild; moderate; severe; extensive) or according to age- and sex-specific percentiles of the CAC distribution (Erbel et al., 2007, [155768](#)).

CIMT is a measure of atherosclerosis assessed by high-resolution, B-mode ultrasonography of the carotid arteries in the neck, the walls of which have inner (intimal), middle (medial) and outer (adventitial) layers (Craven et al., 1990, [155740](#); O'Leary et al., 1999, [156826](#); Wendelhag et al., 1993, [157136](#)). CIMT estimates the distance in mm or μm between the innermost (blood-intima) and outermost (media-adventitia) interfaces, often by averaging over three arterial segments in the common carotid, carotid bulb, and internal carotid artery (Amato et al., 2007, [155656](#)). CIMT has been associated with atherosclerosis risk factors (Heiss et al., 1991, [156535](#); O'Leary et al., 1992, [156825](#); Salonen and Salonen, 1991, [156938](#)), prevalent coronary heart disease (Chambless et al., 1997, [156329](#); Geroulakos et al., 1994, [155788](#)), and incident coronary and cerebral events (O'Leary et al., 1999, [156826](#); van der Meer et al., 2004, [156129](#)). Several studies have indicated that CIMT measurements are accurate (Girerd et al., 1994, [156474](#); Pignoli et al., 1986, [156026](#); Wendelhag et

al., 1991, [157135](#)) and reproducible (Montauban et al., 1999, [156777](#); Smilde et al., 1997, [156988](#); Willekes et al., 1999, [157147](#)), especially for the common carotid artery (Montauban et al., 1999, [156777](#)).

ABI, which is also known as the ankle-arm or resting (blood) pressure index, is a measure of lower extremity arterial occlusive disease commonly caused by advanced atherosclerosis (Weitz et al., 1996, [156150](#)). It is assessed by continuous wave Doppler and manual or automated oscillometric sphygmomanometry, the latter having been shown to have higher repeatability and validity (Weitz et al., 1996, [156150](#)). ABI is defined as the unitless ratio of ankle to brachial systolic blood pressures measured in mmHg. As ankle pressure is normally equal to or slightly higher than arm pressure (resulting in an ABI ≥ 1.0), epidemiologic studies typically define the normal ABI range as 0.90 to 1.50 (Resnick et al., 2004, [156048](#)). Low ABI has been associated with all-cause and CVD mortality (Newman et al., 1993, [156805](#); Vogt et al., 1993, [157100](#)), as well as myocardial infarction and stroke (Karthikeyan and Lip, 2007, [156626](#)).

AAC is a measure of atherosclerosis assessed by non-contrast, EBCT or MDCT of the abdominal aorta. It is scored much like CAC (Agatston et al., 1990, [156197](#)), but the age-specific prevalence and extent of AAC is greater, particularly among women and at ages >50 yr. Although AAC has not been studied as extensively as CAC, it is associated with carotid and coronary atherosclerosis as well as cardiovascular morbidity and mortality (Allison et al., 2004, [156210](#); Allison et al., 2006, [155653](#); Hollander et al., 2003, [156562](#); Khoury et al., 1997, [156636](#); Oei et al., 2002, [156820](#); Walsh et al., 2002, [157103](#); Wilson et al., 2001, [156159](#); Wittman et al., 1986, [156161](#)) and measurements are sufficiently reproducible to allow serial investigations over time (Budoff et al., 2005, [192105](#)).

Study Findings

Diez Roux et al. (2008, [156401](#)) conducted cross-sectional analyses of the association of three of these subclinical markers of atherosclerosis (CAC, CIMT and ABI), collected from 2000 to 2003 during baseline examinations of participants enrolled in the Multi-Ethnic Study of Atherosclerosis (MESA), with long-term exposure to PM_{2.5} and PM₁₀. The study population included 5,172 ethnically diverse people (53% female) residing in Baltimore, MD; Chicago, IL; Forsyth County, NC; Los Angeles, CA; New York, NY; and St. Paul, MN ranging in age from 45 to 84 yr old. Authors used spatio-temporal modeling of pollutant concentrations, weather and demographic data to impute 20-yr avg exposures to PM_{2.5} and PM₁₀. They reported small increases in CIMT of 1% (95% CI: 0-1.4) and 0.5% (95% CI: 0-1), which correspond to absolute changes of 8 (95% CI: 0-12) and 7 (95% CI: 0-14) μm , per 10 $\mu\text{g}/\text{m}^3$ increase in 20-yr avg PM₁₀ and PM_{2.5} concentration, respectively. Evidence of age-, gender-, lipid- and smoking-related susceptibility was lacking. They also reported weak, non-significant increases in the relative prevalence of CAC of 1% (95% CI: -2 to 4) and 0.5% (95% CI: -2 to 3) per 10 $\mu\text{g}/\text{m}^3$ increase in PM₁₀ and PM_{2.5}, respectively. Among the subset of 2,586 participants with EBCT-identified calcification, similarly weak associations were observed. There was little evidence of modification of the CAC associations by demographic, socioeconomic or clinical characteristics. Finally, the authors report no differences in mean ABI with PM₁₀ or PM_{2.5} concentrations. The null findings for ABI exhibited little heterogeneity among participant subgroups and were similarly null when ABI was modeled as a dichotomous outcome using a cutpoint of 0.9 units.

MESA investigators also examined the chronic PM_{2.5}-AAC association in a residentially stable subset of 1,147 participants (mean age = 66 yr; 50% female) randomly selected from all MESA centers, except Baltimore, MD for enrollment in its Aortic Calcium Ancillary Study (Allen et al., 2009, [156209](#)). The authors used kriging and inverse residence-to-monitor distance-weighted averaging of EPA AQS data to estimate 2-yr mean exposures to PM_{2.5}. In cross-sectional analyses, the authors found a 6% (95% CI: -4 to 16) excess risk of a non-zero Agatston score and an 8% (95% CI: -30 to 46) increase in AAC, i.e., approximately 50 (95% CI: -251 to 385) Agatston units, per 10 $\mu\text{g}/\text{m}^3$ increase in PM_{2.5} concentration. These associations were stronger among users than non-users of lipid lowering drugs.

Kunzli et al. (2005, [087387](#)) used baseline data collected between 1998-2003 from two randomized placebo-controlled clinical trials, the Vitamin E Atherosclerosis Progression Study (VEAPS) and the B-Vitamin Atherosclerosis Intervention Trial (BVAIT), for their ancillary cross-sectional analyses of the effect of long-term PM_{2.5} exposure on CIMT. The study population included 798 residents of the greater Los Angeles, CA area who were more than 40 yr old at baseline and 44% were female. The authors used universal kriging of PM_{2.5} data from 23 state and local monitors

operating in 2000 to estimate 1-yr avg exposure to PM_{2.5} at each participant's geocoded U.S. Postal Service ZIP code. They found a 4.2% (95% CI: -0.2 to 8.9) or approximately 32 (95% CI: -2 to 68) μm increase in CIMT per 10 $\mu\text{g}/\text{m}^3$ increase in PM_{2.5} concentration. In contrast to findings from the relatively large, ethnically diverse, yet geographically overlapping MESA ancillary study described above, PM-related increases in CIMT were two- to three-fold larger among older and female participants taking lipid lowering drugs in this study. PM-related increases in CIMT were also higher in never smokers when compared with current or former smokers.

Hoffmann et al. (2007, [091163](#)) conducted a cross-sectional analysis of data collected at baseline (2000-2003) for 4,494 residents of Essen, Mülheim and Bochum, Germany enrolled in the Heinz Nixdorf Recall Study from 2000 to 2003. The age of participants ranged from 45-74 yr and 51% were female. In this cross-sectional study the authors used dispersion and chemistry transport modeling of emissions, climate and topography data to estimate 1-yr avg exposure to PM_{2.5} in 2002 (the midpoint of the baseline exam.) They reported an imprecise 43% (95% CI: -15 to 115) or 102 (95% CI: -77 to 273) Agatston unit increase in CAC per 10 $\mu\text{g}/\text{m}^3$ increase in PM_{2.5}. Differences in strength of association between subgroups defined by demographic and clinical characteristics were small. The authors reported a more consistent association of CAC with traffic exposure (distance from a major roadway) than with PM_{2.5} in this study.

In a subsequent analysis of these data, Hoffmann et al. (2009, [190376](#)) examined the PM-ABI association in this population. In this cross-sectional study, no changes in ABI were observed in association with PM_{2.5} concentration nor was evidence of effect modification by demographic and clinical characteristics apparent. As in the previous study (Hoffmann et al., 2007, [091163](#)), residing near a major roadway was a stronger predictor of atherosclerotic changes. Absolute changes in ABI of -0.024 (95% CI: -0.047 to -0.001) were associated with living within 50 m of a major roadway compared to living more than 200 m away.

Each of the studies described above relied on cross-sectional analyses examining differences in long-term average PM_{2.5} concentrations across space (as well as time to the extent baseline examinations were conducted over time). Such associations may reflect the effect of compositional differences in PM_{2.5} as well as the effect of higher PM_{2.5} concentrations. Most associations of PM_{2.5} with CAC (Diez et al., 2008, [156401](#); Hoffmann et al., 2007, [091163](#)), CIMT (Diez et al., 2008, [156401](#); Kunzli et al., 2005, [087387](#)), ABI (Diez et al., 2008, [156401](#); Hoffmann et al., 2009, [190376](#)) and AAC (Allen et al., 2009, [156209](#)) reviewed in this section were weak and/or imprecise. However, several factors including exposure measurement error, variation in baseline measures atherosclerosis, as well as limited power may contribute to the insensitivity of these cross-sectional studies to detect small differences in CAC, CIMT, ABI and AAC. The study by Hoffmann et al. (2007, [091163](#)), which reported large, imprecise and non-significant increases in CAC in association with PM_{2.5}, is not distinguished from the other studies reviewed by a superior study design or larger sample size. The several fold difference in the magnitude of CIMT associations reported by Kunzli et al. (2005, [087387](#)) and Diez Roux et al. (2008, [156401](#)) may be related to differences between the study populations. The ambient PM concentrations from these studies are characterized in Table 7-1.

7.2.1.2. Toxicological Studies

In the only study of this kind described in the 2004 PM AQCD, Suwa et al. (2002, [028588](#)) demonstrated more advanced atherosclerotic lesions based on phenotype and volume fraction in the left main and right coronary arteries of rabbits exposed to PM₁₀ (5 mg/kg, 2 times/wk×4 wk). Although this study was conducted using IT exposure methodology at a relatively high dose, it provided the first experimental evidence that PM exposure may result in progression of atherosclerosis. Recent toxicological studies conducted using inhalation exposures have replicated these findings at relevant concentrations and are discussed below.

CAPs

New studies have demonstrated increased atherosclerotic plaque area in aortas of ApoE^{-/-} mice exposed to PM_{2.5} CAPs for 4-6 mo (6 h/day×5 days/wk). Average CAPs concentrations ranged from 85 to 138 $\mu\text{g}/\text{m}^3$ and all of the studies were conducted in Tuxedo or Manhattan, NY. Chen and Nadziejko (2005, [087219](#)) reported that the percentage of aortic intimal surface covered by atherosclerotic lesions in ApoE^{-/-} mice was increased. In male ApoE^{-/-}/LDLR^{-/-} mice, both lesion area

and cellularity in the aortic root were enhanced by Tuxedo, NY CAPs exposure, although there was no change in lipid content. Genetic profiles within plaques recovered from ApoE^{-/-} mice included many of the molecular pathways known to contribute to atherosclerosis, including inflammation (Floyd et al., 2009, [190350](#)). Sun (2005, [087952](#)) similarly demonstrated an enhancement of atherosclerosis in ApoE^{-/-} mice exposed Tuxedo, NY CAPs. Plaque area in the aortic arch and abdominal aorta was significantly increased in the PM-exposed, high fat-chow group compared to air-exposed, high fat-chow group. Macrophage infiltration in the abdominal aorta was also observed in the groups exposed to CAPs. A study conducted in Manhattan for 4 mo (May- September 2007) showed that PM_{2.5} CAPs exposure increased atherosclerotic plaque area and led to higher levels of macrophage infiltration, collagen deposition, and lipid composition in thoracic aortas of ApoE^{-/-} mice (Ying et al., 2009, [190111](#)), which is consistent with the previous two studies described that were conducted in Tuxedo, NY.

Alteration of vasomotor function has been observed in aortic rings of ApoE^{-/-} mice on a high fat diet with long-term exposure to CAPs (Sun et al., 2005, [087952](#); Ying et al., 2009, [190111](#)). Sun (2005, [087952](#)) reported that. PM_{2.5}-exposed animals exhibited increased vasoconstrictor responsiveness to serotonin and PE. Increased ROS and elevated iNOS protein expression in aortic sections of CAPs-exposed mice may have resulted alterations in the NO pathway and generation of peroxynitrite that could have affected vascular reactivity. In contrast, Ying, et al. (2009, [190111](#)) demonstrated decreased maximum constriction induced by PE following Manhattan CAPs exposure. Pretreatment with the soluble guanylate cyclase (sGC) inhibitor ODQ attenuated the response, indicating that CAPs exposure resulted in abnormal NO/sGC signaling. Expression of iNOS mRNA and protein was increased in aortas of CAPs-exposed mice, further supporting a role for NO production. In conjunction with increased NO, aortic superoxide production was demonstrated that appeared to be partially driven by increased NADPH oxidase activity. The difference in vasoconstrictor responses between these two studies may be attributable to varying durations (6 versus 4 mo, respectively) or CAPs compositions.

Sun (2005, [087952](#)) and Ying et al. (2009, [190111](#)) reported similar relaxation responses to ACh for air- and CAPs-exposed mice. However, Manhattan CAPs-exposed mice had a markedly decreased response to A23187, indicating that NO release occurred via Ca²⁺-dependent mechanisms (Ying et al., 2009, [190111](#)). Abnormal eNOS function is likely responsible for the decreased relaxation response, as activation of eNOS (but not iNOS) is Ca²⁺-dependent.

A recent study (Sun et al., 2008, [157033](#)) that was part of the research described above (Sun et al., 2005, [087952](#)) investigated tissue factor (TF) expression in aortas, which is a major regulator of hemostasis and thrombosis following vascular injury or plaque erosion. In PM_{2.5}-exposed ApoE^{-/-} mice on a high-fat diet, TF was significantly elevated in the plaques of aortic sections compared to air-exposed mice on the high-fat diet. TF expression was generally detected in (1) the extracellular matrix surrounding macrophages and foam cell-rich areas; and (2) around smooth muscle cells.

One new study of CAPs PM_{2.5} or UFPs derived from traffic was conducted. Araujo et al. (2008, [156222](#)) compared the relative impact of UF (0.01-0.18 μm) and fine (0.01-2.5 μm) PM inhalation on aortic lesion development in ApoE^{-/-} mice following a 40-day exposure (5 h/day×3 days/wk for 75 total h). Animals were on a normal chow diet and exposed to CAPs in a mobile inhalation laboratory parked 300 m from a freeway in downtown Los Angeles. Exposure concentrations were ~440 μg/m³ for PM_{2.5} and ~110 μg/m³ for UFPs, and the number concentrations were roughly equivalent (4.56×10⁵ and 5.59×10⁵ particles/cm³ for PM_{2.5} and UFPs, respectively). Significant increases in plaque size (estimated by lesions at the aortic root) were reported for mice exposed to UFPs only. The lesions were largely comprised of macrophages with intracellular lipid accumulation. Increased total cholesterol measured at the end of the exposure protocol was observed only in the PM_{2.5} group. HDL isolated from the UF PM-exposed mice demonstrated decreased anti-inflammatory protective capacity against LDL-induced monocyte chemotactic activity in an in vitro assay. The livers from the UFP-exposed mice demonstrated significant increases in lipid peroxidation and several stress-related gene products (catalase, glutathione S-transferase Y_a, NADPH-quinone oxidoreductase1, superoxide dismutase 2). Thus, UFPs in these exposures had a substantially greater impact on the systemic response than did PM_{2.5}.

Ambient Air

A study employing young BALB/c mice examined the effects of a 4-month exposure (24 h/day×7 days/wk) to ambient air on arterial histopathology (Lemos et al., 2006, [088594](#)). Outdoor exposure chambers were located in downtown Sao Paulo, Brazil next to streets of high traffic density. In the control chamber, PM₁₀ and NO₂ were filtered with 50% and 75% efficiency, respectively. The average pollutant concentrations were 2.06 ppm for CO (8-h mean), 104.75 µg/m³ for NO₂ (24-h mean), 11.07 µg/m³ for SO₂ (24-h mean), and 35.52 µg/m³ for PM₁₀ (24-h mean) at a monitoring site within 100 m of the inhalation chambers. The pulmonary and coronary arteries demonstrated significant decreases in L/W ratio for animals exposed to the entire ambient mixture compared to controls, indicating thicker walls in these vessels. There was no difference reported for the L/W ratio in renal arteries. Morphologic examination suggested that the increases in L/W ratio were due to muscular hypertrophy rather than fibrosis. The results of this study indicate vascular remodeling of the pulmonary and coronary arteries, as opposed to changes in tone.

To examine the role of systemic inflammation and recruitment of monocytes into plaque tissue as a possible pathway for accelerated atherosclerosis, Yatera et al. (2008, [157162](#)) exposed female Watanabe heritable hyperlipidemic rabbits (42 week old) to Ottawa PM₁₀ (EHC-93) via IT instillation (5 mg/rabbit; approximately 1.56 mg/kg) twice a week for 4 wk. Transfusion of whole blood harvested from exposed and non-exposed animals to donor rabbits supplied labeled monocytes for assessment of monocyte recruitment from the blood to the aortic wall. The fraction of aortic surface and volume of aortic wall taken up by atherosclerotic plaque was increased and the number of labeled monocytes in the atherosclerotic plaques was elevated in rabbits exposed to PM₁₀. In addition, labeled monocytes were attached onto the endothelium overlying atherosclerotic plaques and the number that migrated into the smooth muscle underneath plaques in aortic vessel walls was greater with PM₁₀ exposure compared to control. These responses were not observed in normal vessel walls. ICAM-1 and VCAM-1 expression was elevated in atherosclerotic lesions, likely indicating enhanced monocyte adhesion to endothelium and migration into plaques. Monocytes in plaque tissue stained with immunogold demonstrated foam cell characteristics, which were more numerous in the rabbits exposed to PM₁₀.

Gasoline Exhaust

Lund and colleagues (2007, [125741](#)) used whole emissions from gasoline exhaust to investigate changes in the transcriptional regulation of several gene products with known roles in both the chronic promotion and acute degradation/destabilization of atheromatous plaques. These 50-day exposures (6 h/day×7 days/wk) employed ApoE^{-/-} mice on high-fat chow and the concentrations of the high exposure group were 61 µg/m³ for PM, 19 ppm for NO_x, 80 ppm for CO, and 12.0 ppm for total hydrocarbons. The average particle number median diameter was approximately 15 nm (McDonald et al., 2007, [156746](#)). Dilutions of gasoline engine emissions induced a concentration-dependent increase in transcription of matrix metalloproteinase (MMP) isoform 9, ET-1, and HO-1 in aortas; MMP-3 and -9 mRNA levels were only increased in animals in the highest exposure group. Strong increases in oxidative stress markers (nitrotyrosine and TBARS) in the aortas were also observed. However, using a high-efficiency particle trap, they established that most of the effects were caused by the gaseous portion of the emissions and not the particles. This study did not directly address lesion area.

7.2.2. Venous Thromboembolism

One epidemiologic study examined the relationship between long term PM₁₀ concentration, venous thromboembolism, and laboratory measures of hemostasis (prothrombin and activated partial thromboplastin times [PT; PTT]). PT and PTT measure the extrinsic and intrinsic blood coagulation pathways, the former activated in response to blood vessel injury, the latter, key to subsequent amplification of the coagulation cascade and propagation of thrombus (Mackman et al., 2007, [156723](#)). Decreases in PT and PTT are consistent with a hypercoagulable, prothrombotic state.

7.2.2.1. Epidemiologic Studies

Baccarelli et al. (2008, [157984](#)) studied 2,081 residents (56% female) of the Lombardy region of Italy whose ages ranged from 18 to 84 yr old. In this case-control study of 871 patients with ultrasonographically or venographically diagnosed lower extremity deep vein thrombosis (DVT) and 1,210 of their healthy friends or relatives (1995-2005), the authors used arithmetic averaging of PM₁₀ data available at 53 monitors in nine geographic areas to estimate 1-yr avg residence-specific exposures. They found -0.06 (95% CI: -0.11 to 0) and -0.12 (95% CI: -0.23 to 0) decreases in standardized correlation coefficients for PT as well as 0.01 (95% CI: -0.03 to 0.04) and -0.09 (95% CI: -0.19 to 0.01) decreases in standardized correlation coefficients for PTT among cases and controls, respectively, per 10 µg/m³ increase in PM₁₀. Patients with DVT who were taking heparin or coumarin anticoagulants were not asked to stop taking them before measurement of PT and aPTT. Of additional note, PT was neither adjusted for differences in reagents used to determine it nor conventionally reported as the International Normalized Ratio (INR). The ambient PM concentrations from this study are characterized in Table 7-1.

7.2.3. Metabolic Syndromes

7.2.3.1. Epidemiologic Studies

Chen and Schwartz (2008, [190106](#)) studied 2,978 residentially stable participants in 33 U.S. communities (age range = 20-89 yr; 49% female) who were examined during phase 1 of the National Health and Nutrition Examination Survey III (1989-1991). In this cross-sectional study, the authors used inverse-distance weighted averaging of U.S. EPA AQS monitored data from participant and adjacent counties of residence to estimate 1-yr avg exposures to PM₁₀. They found that after adjustment, residents of communities with lower PM₁₀ concentrations had fewer white blood cells than residents of communities with higher PM₁₀ concentrations. This difference increased with increasing number of metabolic abnormalities (insulin resistance; hypertension; hypertriglyceridemia; low high-density lipoprotein cholesterol; abdominal obesity) reported by the participant. This observed difference across individuals with different degrees of metabolic abnormalities supports the concept that the presence of a metabolic syndrome may impart greater susceptibility to PM-associated long-term CVD effects.

7.2.3.2. Toxicological Studies

Diabetics as a potentially susceptible subpopulation have only recently been evaluated. A toxicological study of a diet-induced obesity mouse model (C57BL/6 fed high-fat chow for 10 wk) examined the effects of a 128-day PM_{2.5} CAPs exposure (mean mass concentration 72.7 µg/m³; Tuxedo, NY) on insulin resistance, adipose inflammation, and visceral adiposity (Sun et al., 2009, [190487](#)). Elevated fasting glucose and insulin levels were observed in CAPs-exposed mice compared to air-exposed during the glucose tolerance test. Aortic rings of mice exposed to CAPs demonstrated decreased peak relaxation to ACh or insulin, which was associated with reduced NO bioavailability. Additionally, insulin signaling was impaired in aortic tissue via lowered endothelial Akt phosphorylation. Increases in adipokines and systemic inflammatory markers (i.e., TNF-α, IL-6, E-selectin, ICAM-1, PAI-1, resistin, leptin) were reported for CAPs-exposed mice. CAPs resulted in increased visceral and mesenteric fat mass, as well as greater adipose tissue macrophages in epididymal fat pads and larger adipocyte size compared to mice in the filtered air group. The results of this study demonstrate that PM_{2.5} exposure can exaggerate insulin resistance, visceral adiposity, and inflammation in mice fed high-fat chow.

7.2.4. Systemic Inflammation, Immune Function, and Blood Coagulation

7.2.4.1. Epidemiologic Studies

As discussed in Section 7.2.3.1, Chen and Schwartz (2008, [190106](#)) conducted a cross-sectional study in 33 U.S. communities and used inverse-distance weighted averaging of U.S. EPA AQS monitored data from participant and adjacent counties of residence to estimate 1-yr avg exposures to PM₁₀ (median concentration within quartiles = 23.1, 31.2, 38.8 and 53.7 µg/m³). They found that after adjustment, residents of communities in quartile 1 had 138 (95% CI: 2-273) fewer white blood cells (×10⁶/L) than residents of communities in quartiles 2-4. This difference increased with increasing number of metabolic abnormalities.

Forbes et al. (2009, [190351](#)) studied approximately 25,000 adults (age ≥ 16 yr; 53% female) who were representatively sampled from 720 English postcode sectors and participated in the Health Survey for England (1994, 1998 and 2003). In this fixed-effects meta-analysis of year-specific cross-sectional findings, the authors used dispersion modeling of emissions and weather data to estimate 2-yr avg exposures to PM₁₀ at participant postcode sector centroids (median in 1994, 1998 and 2003 = 19.5, 17.9 and 16.2 µg/m³, respectively). They found little evidence of a PM₁₀-inflammatory marker association, i.e., only a -0.08% (95% CI: -0.25 to 0.10) decrease in fibrinogen concentration and a 0.14% (95% CI: -1.00 to 1.30) increase in CRP concentration per 1 µg/m³ increase in PM₁₀.

Calderon-Garciduenas et al. (2007, [091252](#)) compared residentially stable, non-smoking healthy children (age range: 6-13 yr) living and attending school between 2003-2004 in Mexico City (historically high PM; altitude 2,250 m) and Polotitlán (historically low PM; altitude 2,380 m). In this ecologic study, residents of Mexico City (n = 59; 93% female) had fewer white blood cells and neutrophils (×10⁹/L) than residents of Polotitlán (n = 22; 69% female): unadjusted mean 6.2 (95% CI: 5.7-6.6) versus 6.9 (95% CI: 6.3-7.5) and 2.9 (95% CI: 2.3-3.5) versus 3.8 (95% CI: 3.2-4.4), respectively.

Calderon-Garciduenas et al. (2009, [192107](#)) subsequently compared 37 unadjusted mean measures of immune function and inflammation among an expanded number of these participants. They found that under a two-sided type I error rate (α) = 0.05, 16 (43%) of the measures were significantly different in residents of southwest Mexico City (n = 66; 48% female) than those in Polotitlán (n = 93; 57% female). However, only 8 measures were significantly different after Bon Ferroni-correction (α = 0.05 / 37 = 0.001) and even fewer would be after adjustment for reported correlation between the measures of immune function and inflammation, e.g., CRP and lipopolysaccharide binding protein (Pearson's r = 0.71).

Two cross-sectional analyses of PM₁₀ concentration and markers of immune function or inflammation have been conducted with significant changes observed in the NHANES population (stronger effects among those with metabolic disorders) (Chen and Schwartz, 2008, [190106](#)) but not in a relative large survey of adults, which was conducted in England (Forbes et al., 2009, [190351](#)). Ecological analyses comparing children in high versus low pollution regions in Mexico show differences in unadjusted blood markers that may be related to PM concentration or other unmeasured risk factors that differs across the communities studied (Calderon-Garciduenas et al., 2007, [091252](#); Calderón-Garcidueñas et al., 2009, [192107](#)).

7.2.4.2. Toxicological Studies

In addition to the PM_{2.5} study mentioned previously that showed increased TF expression (an important initiator of thrombosis) in aortas of ApoE^{-/-} mice following subchronic CAPs exposure (Sun et al., 2008, [157033](#)), three recent studies examined hematology and clotting parameters in rats and mice exposed to DE, gasoline exhaust, or hardwood smoke for 1 week or 6 mo (Reed et al., 2004, [055625](#); Reed et al., 2006, [156043](#); Reed et al., 2008, [156903](#)). In all studies, male and female F344 rats were exposed to the mixtures by whole-body inhalation for 6 h/day, 7 day/wk. Respiratory effects for these studies are presented in Section 7.3.3.

Diesel Exhaust

The target PM concentrations in the DE study was 30, 100, 300, and 1,000 $\mu\text{g}/\text{m}^3$ and the MMAD was 0.10-0.15 μm (Reed et al., 2004, [055625](#)). Male and female rats exposed to DE at the highest concentration (NO concentration 45.3 ppm; NO₂ concentration 4.0 ppm; CO concentration 29.8 ppm; SO₂ concentration 365 ppb) for 6 mo demonstrated decreased serum Factor VII, but no change in plasma fibrinogen or thrombin anti-thrombin complex (TAT) (Reed et al., 2004, [055625](#)). White blood cells were decreased only in female rats in the highest exposure group. Another DE study of shorter duration (4 wk, 4 h/day, 5day/wk; PM mass concentration 507 or 2201 $\mu\text{g}/\text{m}^3$, CO 1.3 and 4.8 ppm, NO <2.5 and 5.9 ppm, NO₂ <0.25 and 1.2 ppm, SO₂ 0.2 and 0.3 ppm for low and high PM exposures, respectively) did not demonstrate changes in hematologic parameters or those related to coagulation (i.e., PT, PPT, plasma fibrinogen, D-dimer) or inflammation (i.e., CRP) in SH or WKY rats (Gottipolu et al., 2009, [190360](#)). Together, these findings do not support a DE-related stimulation of blood coagulation following 1 or 6 mo of exposure.

Hardwood Smoke

The target PM concentrations in the hardwood smoke study was 30, 100, 300, and 1,000 $\mu\text{g}/\text{m}^3$ and the MMAD was 0.25-0.36 μm (Reed et al., 2006, [156043](#)). In male rats exposed to hardwood smoke, the mid-low group (PM concentration 113 $\mu\text{g}/\text{m}^3$; NO, NO₂, SO₂ concentrations 0 ppm; CO concentration 1,832.3 ppm) had the greatest responses in hematology parameters, including increased hematocrit, hemoglobin, lymphocytes, and decreased segmented neutrophils (Reed et al., 2006, [156043](#)). Platelets were elevated in male and female rats after 1 week of exposure, but this response returned to control values following the 6-month exposure. No changes were observed for any coagulation markers at 6 mo.

Gasoline Exhaust

PM mass in the gasoline exhaust study ranged from 6.6 to 59.1 $\mu\text{g}/\text{m}^3$, with the corresponding number concentration between 2.6×10^4 and 5.0×10^5 particles/cm³; the dilutions for the gasoline exhaust were 1:10, 1:15 or 1:90 and filtered PM at the 1:10 dilution (Reed et al., 2008, [156903](#)). Similar to the responses observed with hardwood smoke, male and female rats in the mid- and high-gasoline exhaust exposure groups (NO concentrations 11.9 and 18.4 ppm; NO₂ concentrations 0.5 and 0.9 ppm; CO concentration 73.2 and 107.3 ppm; SO₂ concentration 0.38 and 0.62 ppm, respectively) demonstrated elevated hematocrit and hemoglobin; RBC count was also elevated in these groups (Reed et al., 2008, [156903](#)). The only response that appeared somewhat dependent on the presence of particles was increased RBC in female rats at 6 mo, although the authors attributed the observed increases to the high concentration of CO.

Collectively, these studies do not indicate robust systemic inflammation or coagulation responses in F344 rats following 6-month exposures to diesel, hardwood smoke, or gasoline exhaust. The limited effects that were observed could possibly be due to the varying gas concentrations in the exposure mixtures.

7.2.5. Renal and Vascular Function

Two recent epidemiologic studies have tested associations between PM exposure and indicators of renal and vascular function (urinary albumin to creatinine ratio [UACR] and blood pressure). UACR is a measure of urinary albumin excretion (National Kidney Foundation, 2008, [156796](#)). When calculated as the ratio of albumin to creatinine concentrations in untimed (“spot”) urine samples, UACR approximates 24-h urinary albumin excretion and can be used to identify albuminuria, a marker of generalized vascular endothelial damage (Xu et al., 2008, [157157](#)). Values ≥ 30 mg/g (3.5 mg/mmol) and ≥ 300 mg/g (34 mg/mmol) usually define micro- and macroalbuminuria, both of which are associated with increases in CVD incidence and mortality (Bigazzi et al., 1998, [156272](#); Deckert et al., 1996, [156389](#); Dinneen and Gerstein, 1997, [156403](#); Gerstein et al., 2001, [156466](#); Mogensen, 1984, [156769](#)). Several researchers have called the

dichotomization of albuminuria into question, observing that there is no threshold below which risk of cardiovascular and end-stage kidney disease disappears (Forman and Brenner, 2006, [156439](#); Knight and Curhan, 2003, [179900](#); Ruggenti and Remuzzi, 2006, [156933](#)).

Systolic, diastolic, pulse, and mean arterial blood pressures (SBP; DBP; PP; MAP) in mmHg have also been used as measures of cardiovascular disease. Franklin et al. (1997, [156446](#)) suggested that SBP and PP were the only two measures predictive of carotid stenosis in a multivariable analysis considering all 4 measures, whereas Khattar et al. (2001, [155896](#)) suggested that their prognostic significance in hypertensive populations may differ by age, with SBP and PP being most predictive among those ≥ 60 yr and DBP among those <60 yr old (Khattar et al., 2001, [155896](#)).

7.2.5.1. Epidemiologic Studies

O'Neill et al. (2007, [156006](#)) examined the association of UACR with PM_{2.5} and PM₁₀ among members of the MESA population described previously (Diez et al., 2008, [156401](#)). For this study of UACR, which included cross-sectional and longitudinal analyses, the study population was restricted to a subset of 3,901 participants (mean age = 63 yr; 52% female) with complete covariate, outcome and exposure data at their first through third exams (2000-2004). In cross-sectional analyses, the authors found that after adjustment for demographic and clinical characteristics, 10 $\mu\text{g}/\text{m}^3$ increases in 20-yr imputed exposures to PM_{2.5} and PM₁₀ were associated with negligible 0.002 (95% CI: -0.048 to 0.052) and -0.002 (95% CI: -0.038 to 0.035) mean differences in baseline log UACR, respectively. Similarly, small statistically non-significant decreases in the prevalence of microalbuminuria (defined in this setting as ≥ 25 mg/g) provided little evidence of an effect on renal function. These largely null cross-sectional findings mirrored those based on the study's shorter-term (30- and 60-day) PM_{2.5} and PM₁₀ exposures. Moreover, longitudinal analyses revealed only a weak association between 3-yr change in log UACR and 20-yr PM₁₀ exposure. Evidence of effect modification by demographic and geographic characteristics was not apparent in either the cross-sectional or longitudinal analyses.

Auchincloss et al. (2008, [156234](#)) focused on automated, oscillometric, sphygmomanometric measures of blood pressures in mmHg (SBP; DBP; PP; MAP). Like O'Neill (2007, [156006](#)), Diez et al. (2008, [156401](#)) and Allen et al. (2007, [156006](#)), Auchincloss et al. (2008, [156234](#)) based their examination on the previously described MESA population. The authors included 5,112 study participants (age range = 45-84 yr; 52% female) who were free of clinically manifested CVD at their baseline exam in one of six primarily urban U.S. locations (2000-2002). In this cross-sectional study, they used arithmetic averaging of EPA AQS PM_{2.5} data available at the monitor nearest to each participant's geocoded U.S. Postal Service ZIP code centroid to estimate 30- and 60-day avg exposures to PM_{2.5}. They found small nonsignificant increases of 1.5 (95% CI: -0.2 to 3.2), 0.2 (95% CI: -0.7 to 1.0), 1.3 (95% CI: 0.1 to 2.6), and 0.6 (95% CI: -0.4 to 1.7) mmHg increases in SBP, DBP, PP and MAP, respectively, per 10 $\mu\text{g}/\text{m}^3$ increase in 30-day avg PM_{2.5} exposure. Associations were slightly weaker for 60-day avg PM_{2.5} exposure and among participants without hypertension, during cooler weather, in the presence of low NO₂, residing >300 m from a highway, or surrounded by lower road density.

Finally, the Calderon-Garciduenas et al. (2007, [091252](#)) ecologic study introduced in Section 7.2.3.1 also found that children residing in Mexico City had higher mean pulmonary artery pressure as assessed by Doppler echocardiography and fasting plasma endothelin-1 (ET-1) than residents in Polotitlán: unadjusted mean 17.5 (95% CI: 15.7-19.4) versus 14.6 (95% CI: 13.8-15.4) mmHg and 2.23 (95% CI: 1.93-2.53) versus 1.23 (95% CI: 1.11-1.35) pg/mL, respectively. Within Mexico City, ET-1 was higher in residents of the Northeast (historically higher PM_{2.5}) than those of the Southwest (historically lower PM_{2.5}).

The MESA analyses of UACR (O'Neill et al., 2007, [156006](#)) and the ecologic study of children living in a highly polluted area of Mexico (Calderon-Garciduenas et al., 2007, [091252](#)) provide little evidence that long-term exposure to PM_{2.5} had an effect on renal and vascular function, respectively. Auchincloss et al. (2008, [156234](#)) reports small nonsignificant associations of blood pressure with 30- and 60-day avg PM_{2.5} concentrations. PM concentrations from the analyses are characterized in Table 7-1.

Table 7-1. Characterization of ambient PM concentrations from studies of subclinical measures of cardiovascular diseases and long-term exposure.

Study	Location	Mean Concentration ($\mu\text{g}/\text{m}^3$)	Upper Percentile Concentrations ($\mu\text{g}/\text{m}^3$)
<i>PM₁₀</i>			
Diez Roux et al. (2008, 156401)	MESA: 6 Cities U.S.	20 yr imputed mean: 34	NR
O'Neill et al. (2007, 156006)	MESA: 6 Cities U.S.	Long-Term Exposure: 1982-2002: 34.7 1982-1987: 40.5 1988-1992: 38 1993-1997: 30.6 1998-2002: 29.7 Previous Month: 27.5	NR
Baccarelli et al. (2008, 157984)	Lombardy Region Italy	NR	NR
Rosenlund et al. (2006, 089796)	Stockholm, Sweden	30-y avg PM ₁₀ (traffic) Cases: 2.6 Controls: 2.4	5th-95th %: 0.5-6 0.6-5.9
Chen and Swartz (2008, 190106)	US Population (NHANES)	Annual avg: 36.8	NR
Forbes et al. (2009, 190351)	British Population	1994: 19.5 (median) 1998: 17.9 (median) 2003: 16.2 (median)	1994, Min-Max: 12.5-36.1 1998, Min-Max: 12.6-27.0 2003, Min-Max: 11.0-22.7
<i>PM_{2.5}</i>			
Hoffmann et al. (2007, 091163)	HNRS, 3 Cities Germany	Annual avg: 22.8	NR
Allen et al. (2009, 156209)	MESA: 5 Cities	Annual avg: 15.8	Min-Max: 10.6-24.7
Kunzli et al. (2005, 087387)	VEAPS BVAIT	Annual avg: 20.3	Min-Max: 5.2-26.9
Auchincloss et al. (2008, 156234)	MESA: 6 Cities	Prior 30 days: 16.8 Prior 60 days: 16.7	NR
O'Neill (2007, 156006)	MESA: 6 Cities U.S.	Previous Month: 16.5	NR
Diez Roux et al. (2008, 156401)	MESA: 6 Cities U.S.	20-y imputed mean: 21.7	NR
Hoffmann et al. (2009, 190376)	HNRS: 3 Cities Germany	Annual avg: 22.8	Min-max: 19.8-26.8
Calderon-Garciduenas et al. (2009, 192107)	Southwest Mexico (high pollution) Potitlan (low pollution)	Annual avg: 25 Annual avg: <15	NR NR
Calderon-Garciduenas et al. (2007, 091252)	Southwest Mexico (high pollution) Potitlan (low pollution)	NR NR	NR NR

MESA: Multi-Ethnic Study of Atherosclerosis
HNRS: Heinz Nixdorf Recall Study
VEAPS: Vitamin E Atherosclerosis Progression Study
BVAIT: B-Vitamin Atherosclerosis Intervention Trial

7.2.5.2. Toxicological Studies

In a PM_{2.5} CAPs study of 10 wk (6 h/day×5 days/wk) in Tuxedo, NY (mean mass concentration 79.1 $\mu\text{g}/\text{m}^3$), there was no difference in mean arterial pressure (MAP) in SD rats between groups (Sun et al., 2008, [157032](#)). When angiotensin II (Ang II) was infused during the last week of exposure to induce systemic hypertension, the MAP slope was consistently greater in the CAPs-exposed rats compared to the filtered air group. Furthermore, thoracic aortic rings were more responsive to phenylephrine-induced constriction and less responsive to ACh-induced relaxation in the PM+Ang II vessels. In contrast to the latter findings, the relaxation response was exaggerated in the PM+Ang II aortic segments with a Rho-kinase (ROCK) inhibitor. Superoxide production in aortic rings increased in the PM+Ang II group compared to the filtered air group and the addition of

NAD(P)H oxidase inhibitor (apocynin) or a NOS inhibitor (L-NAME) attenuated the superoxide generation. The levels of tetrahydrobiopterin (BH₄) were decreased in mesenteric vasculature and the heart by 46% and 41% in the PM+Ang II group compared to controls, respectively; furthermore, levels of BH₄ in the liver were similarly reduced, which is consistent with a systemic effect of CAPs. Together, these findings indicate that CAPs potentiate Ang II-induced hypertension and alter vascular reactivity, perhaps through activated NADPH oxidase and eNOS uncoupling that result in oxidative stress generation and triggering of the Rho/ROCK signaling pathway.

7.2.6. Autonomic Function

7.2.6.1. Toxicological Studies

Hwang et al. (2005, [087957](#)) and Chen and Hwang (2005, [087218](#)) used radiotelemetry to examine the chronic changes in HR and HRV resulting from the same CAPs exposures described previously (Chen and Nadziejko, 2005, [087219](#)). The overall average CAPs exposure concentration was 133 µg/m³ and results indicate differing responses to CAPs between ApoE^{-/-} mice and their genetic background strain, C57BL/6J mice (Hwang et al., 2005, [087957](#)). Using the time period of 1:30-4:30 a.m., C57BL/6J mice showed a HR increase only over the last month of exposure. In contrast, ApoE^{-/-} mice had chronic decreases of 33.8 beat/min for HR. Changes in HRV (SDNN and rMSSD) were somewhat more complicated, with biphasic responses in ApoE^{-/-} mice over the 5-month period (initial increase over first 6 wk, decrease over next 12 wk, and slight upward turn for remainder of the study)(Chen and Hwang, 2005, [087218](#)). Increasing linear trends were observed in C57BL/6J mice for SDNN and rMSSD. The average CAPs concentration for the HRV study was 110 µg/m³. However, only three C57BL/6J mice in the exposure group were included in the analysis compared to ten ApoE^{-/-} animals, thus making it difficult to interpret the C57BL/6J mice responses (Chen and Hwang, 2005, [087218](#); Hwang et al., 2005, [087957](#)).

7.2.7. Cardiac changes

7.2.7.1. Toxicological studies

Two recent toxicological studies have evaluated the effects of PM on cardiac effects including pathology and gene expression. Cardiac mitochondrial function has also been evaluated following PM exposure in rats.

Diesel Exhaust

A recent study of DE exposure (PM mass concentration 507 or 2,201 µg/m³, CO 1.3 or 4.8 ppm, NO <2.5 or 5.9 ppm, NO₂ <0.25 or 1.2 ppm, SO₂ 0.2 or 0.3 ppm for low and high PM exposures, respectively; geometric median number diameter 85 nm) indicated a hypertensive-like cardiac gene expression in WKY rats that mimicked baseline patterns in air-exposed SH rats (Gottipolu et al., 2009, [190360](#)). Exposure to the high concentration of DE for 4 wk (4 h/day, 5 day/wk) led to downregulation of genes involved in stress, antioxidant compensatory response, growth and extracellular matrix regulation, membrane transport of molecules, mitochondrial function, thrombosis regulation, and immune function. No genes were affected by DE in SH rats. A dose-dependent inhibition of mitochondrial aconitase activity in both rat strains was observed, indicating a DE effect on oxidative stress. It should be noted that while DE-related cardiovascular effects were found in WKY rats only, pulmonary inflammation and injury were observed in both strains (Sections 7.3.3.2 and 7.3.5.1).

Model Particles

Wallenborn et al. (2008, [191171](#)) examined the subchronic (5 h/day, 3 day/wk, 16 wk) pulmonary, cardiac, and systemic effects of nose-only exposure to particulate ZnSO₄ (9, 35, or 120 µg/m³) in WKY rats. Particle size was reported to be 31-44 nm measured as number median diameter. Although changes in pulmonary inflammation or injury and cardiac pathology were not observed, effects on cardiac mitochondrial protein and enzyme levels were noted (i.e., increased ferritin levels, decrease in succinate dehydrogenase activity), possibly indicating a small degree of mitochondrial dysfunction. Glutathione peroxidase, an antioxidant enzyme, was also decreased in the cardiac cytosol. Gene expression analysis identified alterations in cardiac genes involved in cell signaling events, ion channels regulation, and coagulation in animals exposed to the highest ZnSO₄ concentration only. This study demonstrates a possible direct effect of ZnSO₄ on extrapulmonary systems, as suggested by the lack of pulmonary effects (Section 7.3.3.2).

7.2.8. Left Ventricular Mass and Function

Van Hee et al. (2009, [192110](#)) studied 3,827 participants (age range = 45-84 yr; 53% female) who underwent magnetic resonance imaging (MRI) of the heart at the baseline examination of the MESA cohort (2000-2002). This cross-sectional study focused on two MRI-based outcome measures: left ventricular mass index (LVMI, g/m²) and ejection fraction (EF, %), the former estimated using the DuBois formula for body surface area, the latter as the ratio of stroke volume to end diastolic volume. The study also estimated annual mean exposures to PM_{2.5} at participants' geocoded residential addresses in 2000 using ordinary kriging of U.S. EPA AQS concentration data. In fully adjusted models, it found 3.8 (95% CI: -6.1 to 13.7) g/m² and -3.0% (-8.0 to 2.0) differences in LVMI and EF per 10 µg/m³ increment in PM_{2.5}. The findings were small and imprecise, albeit suggestive of a slight, PM-associated increase in the mass and decrease in the function of the left ventricle. The effect of living within 50 m of a major roadway on LVMI was greater than the effect of PM_{2.5} (i.e., 1.4 g/m² [95% CI: 0.3-2.5] per 10 µg/m³).

7.2.9. Clinical Outcomes in Epidemiologic Studies

Several epidemiologic studies of U.S. and European populations have examined associations between long-term PM exposures and clinical CVD events (Baccarelli et al., 2008, [157984](#); Hoffmann et al., 2006, [091162](#); Hoffmann et al., 2009, [190376](#); Maheswaran et al., 2005, [088683](#); Maheswaran et al., 2005, [090769](#); Miller et al., 2007, [090130](#); Rosenlund et al., 2006, [089796](#); Solomon et al., 2003, [156994](#); Zanobetti and Schwartz, 2007, [091247](#)). Results from these studies are summarized in Figure 7-1. The ambient PM concentrations from these studies are characterized in Table 7-2.

Coronary Heart Disease

Epidemiologic studies examining the association of coronary heart disease (CHD) with long-term PM exposure are discussed below (Hoffmann et al., 2006, [091162](#); Maheswaran et al., 2005, [090769](#); Miller et al., 2007, [090130](#); Puett et al., 2008, [156891](#); Rosenlund et al., 2006, [089796](#); Rosenlund et al., 2009, [190309](#); Zanobetti and Schwartz, 2007, [091247](#)). Cases of CHD were variably defined in these studies to include history of angina pectoris, MI, coronary artery revascularization (bypass graft; angioplasty; stent; atherectomy), and congestive heart failure (CHF). Results pertaining to death from CHD are described in Section 7.6.

Miller et al. (2007, [090130](#)) studied incident, validated MI, revascularization, and CHD death, both separately and collectively, among 58,610 post-menopausal female residents of 36 U.S. metropolitan areas (age range = 50-79 yr) enrolled in the Women's Health Initiative Observational Study (WHI OS, 1994-1998). In this prospective cohort study of participants free of CVD at baseline (median duration of follow-up = 6 yr), the authors used arithmetic averaging of year 2000 EPA AQS PM_{2.5} data available at the monitor nearest to each participant's geocoded U.S. Postal Service five-digit ZIP code centroid to estimate 1-yr avg exposures. They found 6% (95% CI: -15 to 34), 20% (95% CI: 0-43) and 21% (95% CI: 4-42) increases in the overall risk of MI, revascularization, and

their combination with CHD death per 10 $\mu\text{g}/\text{m}^3$ increase in $\text{PM}_{2.5}$, respectively. Hazards were higher within than between cities and in the obese. For the combined CVD outcome (MI, revascularization, stroke, CHD death, cerebrovascular disease), authors reported a 24% (95% CI: 9-41) increase in risk that was higher among participants at higher than lower quintiles of body mass index, waist-to-hip ratio, and waist circumference. The $\text{PM}_{2.5}$ -CVD association was stronger among non-diabetic than diabetic participants.

Table 7-2. Characterization of ambient PM concentrations from studies of clinical cardiovascular diseases and long-term exposure.

Study	Location	Mean Annual Concentration ($\mu\text{g}/\text{m}^3$)	Upper Percentile Concentrations ($\mu\text{g}/\text{m}^3$)
<i>PM₁₀</i>			
Puett et al. (2008, 156891)	13 U.S. States	21.6	
Zanobetti and Schwartz (2007, 091247)	21 U.S. Cities	28.8	Overall range NR
		30 y avg PM_{10} (traffic)	5th-95th Percentile
Rosenlund et al. (2006, 089796)	Stockholm, Sweden	Cases: 2.6 Controls: 2.4	0.5-6.0 0.6-5.9
		5-yr avg PM_{10} from traffic:	
Rosenlund et al. (2009, 190309)	Stockholm, Sweden	Cases: 2.4 (median) Controls: 2.2 (median)	
Maheswaran et al. (2005, 090769)	Sheffield, U.K.	Range of means in each quintile: 16-23.3	NR
Baccarelli et al. (2008, 157984)	Lombardia Region, Italy	NR	NR
<i>PM_{2.5}</i>			
Miller et al. (2007, 090130)	WHI: 36 Metropolitan areas	Citywide avg (yr 2000): 13.5	Min-max: 4-19.3
Hoffmann et al. (2006, 091162)	HNRS: 2 Cities Germany	23.3	NR
Hoffman et al. (2009, 190376)	HRNS: 2 Cities German	22.8	NR

WHI: Womens Health Initiative
HNRS: Hans Nixdorf Recall Study

Puett et al. (2008, [156891](#)) studied incident, validated CHD, CHD death, and non-fatal MI among 66,250 female residents (mean age = 62 yr) of metropolitan statistical areas in thirteen northeastern U.S. states who were enrolled in the Nurses' Health Study (NHS, 1992-2002). In this prospective cohort study of women without a history of non-fatal MI at baseline (maximum duration of follow-up = 4 yr), the authors used two-stage, spatially smoothed, land use regression to estimate residence-specific, 1-yr ma PM_{10} exposures from U.S. EPA AQS and emissions, IMPROVE, and Harvard University monitor data. They found a 10% (95% CI: -6 to 29) increase in risk of first CHD event per 10 μm^3 increase in 1-yr avg PM_{10} exposure, while the association with MI was close to the null value. The association with fatal CHD event of 30% (95% CI: 0-71) was stronger. Furthermore, associations with CHD death were higher in the obese and in the never smokers.

Rosenlund et al. (2006, [089796](#)) studied 2,938 residents of Stockholm County, Sweden (age range = 45-70 yr; 34% female). In this case-control study of 1,085 patients with their first, validated non-fatal MI and an age-, gender-, and catchment-stratified random sample of 1,853 controls without MI (1992-1994), the authors used street canyon-adjusted dispersion modeling of emissions data to estimate 30-yr avg exposure to PM_{10} (median = 2.4 $\mu\text{g}/\text{m}^3$). They found that the OR for prevalent MI per 10 $\mu\text{g}/\text{m}^3$ increase in PM_{10} was 0.85 (95% CI: 0.50-1.42). The OR for fatal MI was elevated, but not statistically significant.

In a more recent study, Rosenlund et al. (2009, [190309](#)) evaluated 554,340 residents (age range = 15-79 yr; 49% female) of Stockholm County, Sweden (1984-1996). In this population-based, case-control study of 43,275 cases of incident, validated MI, the authors used dispersion modeling of traffic emissions and land use data to estimate 5-yr avg exposure to PM_{10} . They found that after

adjustment for demographic, temporal, and socioeconomic characteristics, the OR for MI per 5 $\mu\text{g}/\text{m}^3$ increase in PM_{10} was 1.04 (95% CI: 1.00-1.09). ORs were higher after restriction to fatal cases, in- or out-of-hospital deaths, and participants who did not move between population censuses. Authors state that control for confounding was superior in their previous study (Rosenlund et al., 2006, [089796](#)) although the size of the population was larger in this recent study (Rosenlund et al., 2009, [190309](#)).

Zanobetti and Schwartz (2007, [091247](#)) studied ICD-coded recurrent MI (ICD 9 410) and post-infarction CHF (ICD 9 428) among 196,131 Medicare recipients (age ≥ 65 yr; 50% female) discharged alive following MI hospitalization in 21 cities from 12 U.S. states (1985-1999). In this ecologic, open cohort study of re-hospitalization among MI survivors (mean duration of follow-up = 3.6 and 3.7 yr for MI and CHF, respectively), the authors used arithmetic averaging of EPA AQS PM_{10} data available in the county of hospitalization to estimate 1-yr avg exposures. They found 17% (95% CI: 5-31) and 11% (95% CI: 3-21) increases in the risk of recurrent MI and post-infarction CHF, respectively, per 10 $\mu\text{g}/\text{m}^3$ increase in PM_{10} exposure. Hazards were somewhat higher among persons aged >75 yr.

Hoffmann et al. (2006, [091162](#)) studied self-reported CHD (MI or revascularization) among 3,399 residents of Essen and Mülheim, Germany (age range = 45-75 yr; 51% female) at the baseline exam of the Heinz Nixdorf Recall Study (2000-2003) introduced previously. In this cross-sectional ancillary study, the authors used dispersion modeling of emissions, climate and topography data to estimate 1-yr avg exposure to $\text{PM}_{2.5}$ (mean = 23.3 $\mu\text{g}/\text{m}^3$). They found little evidence of an association between $\text{PM}_{2.5}$ and CHD in these data. After adjustment for geographic, demographic and clinical characteristics, the OR for prevalent CHD per 10 $\mu\text{g}/\text{m}^3$ increase in exposure was 0.55 (95% CI: 0.14-2.11).

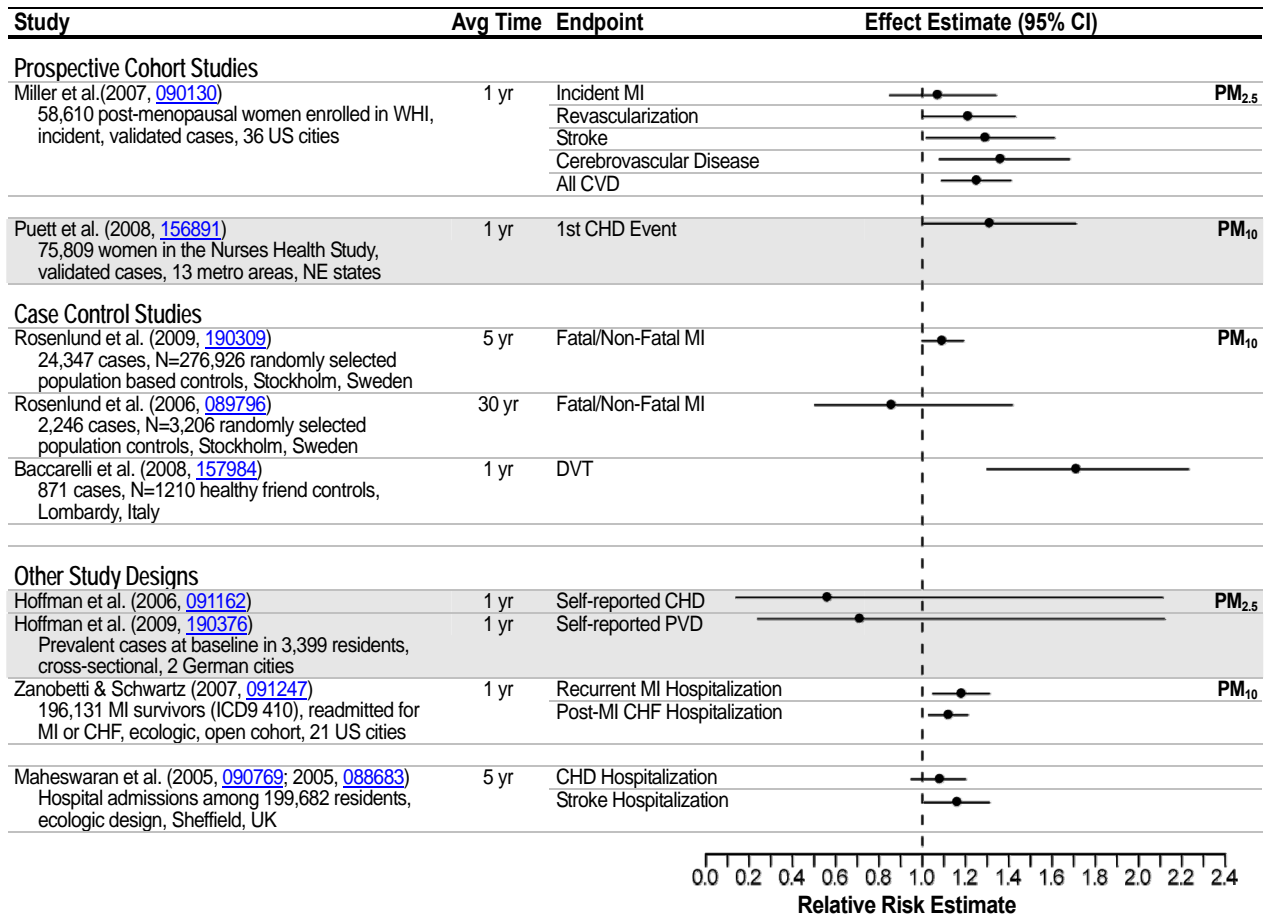


Figure 7-1. Risk estimates for the associations of clinical outcomes with long-term exposure to ambient $\text{PM}_{2.5}$ and PM_{10} .

In the study of 1,030 census enumeration districts in Sheffield, U.K. described previously, Maheswaran et al. (2005, [090769](#)) studied 11,407 ICD-10-coded emergency hospitalizations for CHD (ICD10 I20-25) among 199,682 residents (age \geq 45 yr; 45% female). In this ecologic study, the authors used dispersion modeling of emissions and climate data to estimate 5-yr avg exposure to PM₁₀. They found that after adjusting for smoking prevalence, controlling for socioeconomic factors, and smoothing, the age- and gender-standardized rate ratios for CHD admission were 1.01 (95% CI: 0.92-1.11), 1.04 (95% CI: 0.93-1.15), 0.97 (95% CI: 0.87-1.08), and 1.07 (95% CI: 0.95-1.20) across PM₁₀ quintiles. The linear trend was somewhat stronger for CHD mortality (Section 7.3).

The study of post-menopausal women enrolled in the WHI OS by Miller et al. (2007, [090130](#)) was the only U.S. study to examine the effect of PM_{2.5} rather than PM₁₀. This study, which provides strong evidence of an association, was distinguished by its prospective cohort design, validation of incident cases and large population. Puett et al. (2008, [156891](#)), the other U.S. study with comparable design features, provides evidence of an association of incident CHD with long-term PM₁₀ exposure. Findings from Swedish case control studies of incident validated cases of MI were not consistent. A cross-sectional study of self-reported CHD did not provide evidence of an association with PM_{2.5}, while findings from two ecologic studies of PM₁₀ indicated positive associations of CHD hospitalizations with PM₁₀ (Maheswaran et al., 2005, [088683](#); Zanobetti and Schwartz, 2007, [091247](#)).

Stroke

Miller et al. (2007, [090130](#)) found 28% (95% CI: 2-61) and 35% (95% CI: 8-68) increases in the overall risk of validated stroke and cerebrovascular disease, respectively, per 10 $\mu\text{g}/\text{m}^3$ increase in 1-yr avg PM_{2.5} exposure. Risks were higher within than between cities. In the study of 1030 Census of enumeration districts in Sheffield, U.K. described previously, Maheswaran et al. (2005, [088683](#)) studied 5,122 ICD-10-coded emergency hospital admissions for stroke (I60-69) among 199,682 residents (age \geq 45 yr; 45% female) of 1,030 census enumeration districts in Sheffield, U.K. (1994-1999). In this ecologic study, the authors used dispersion modeling of emissions and climate data to estimate 5-yr avg exposure to PM₁₀. They found that the age- and gender-standardized rate ratios for stroke admission were 1.05 (95% CI: 0.94-1.17), 1.07 (95% CI: 0.95-1.20), 1.06 (95% CI: 0.94-1.20), and 1.15 (95% CI: 1.01-1.31) across PM₁₀ quintiles. Linear trend was somewhat stronger for stroke mortality (Section 7.6).

These studies examining the long-term PM-stroke relationship provide evidence of association. Maheswaran et al. (2005, [088683](#)) examined emergency room hospital admissions in Sheffield, U.K. using an ecologic design while results reported by Miller et al. (2007, [090130](#)) are based on the prospective cohort study of the WHI OS population (both introduced previously).

Peripheral Arterial Disease

The German Heinz Nixdorf Recall cross-sectional study described in Section 7.2.1.1 (Hoffmann et al., 2009, [190376](#)) also evaluated the association between 1-yr avg exposure to PM_{2.5} and peripheral arterial disease (self-reported history of a surgical or procedural intervention or an ABI $<$ 0.9 in one or both legs). The authors found no evidence of an increase in risk. The OR for peripheral arterial disease was 0.87 (95% CI: 0.57-1.34) per 3.9 $\mu\text{g}/\text{m}^3$ increase in PM_{2.5}. However, evidence of an association with traffic exposure was present in these data. ORs of 1.77 (95% CI: 1.01-3.10), 1.02 (95% CI: 0.58-1.80), and 1.07 (95% CI: 0.68-1.68) for residing \leq 50, 50-100, and 100-200 m of a major road (reference category: $>$ 200 m), respectively were observed. ORs were higher among participants with CAC scores \leq 75th percentile, women, and smokers.

Deep Vein Thrombosis

The Italian case-control study (introduced in Section 7.2.1.2) also examined the chronic PM₁₀-DVT association (Baccarelli et al., 2008, [157984](#)). The authors found a 70% (95% CI: 30-223) increase in the odds of DVT per 10 $\mu\text{g}/\text{m}^3$ increase in 1-yr avg PM₁₀ exposure. This finding was consistent with the decreases in PT and PTT also observed among controls in this context as well as

the 47% (95% CI: 11-96) increase in the odds of DVT per inter-decile range (242 m) increase in the residence-to-major-roadway distance observed among a subset of cases and controls (Baccarelli et al., 2009, [188183](#)). The PM₁₀-DVT and distance-DVT associations were both weaker among women and among users of oral contraceptives or hormone therapy.

7.2.10. Cardiovascular Mortality

New epidemiologic evidence reports a consistent association between long-term exposure to PM_{2.5} and increased risk of cardiovascular mortality. There is little evidence for the long-term effects of PM_{10-2.5} on cardiovascular mortality. This section focuses on cardiovascular mortality outcomes in response to long-term exposure to PM. The studies that investigate long-term exposure and mortality due to any specific or all (nonaccidental) causes are evaluated in Section 7.6. A summary of the mean PM concentrations reported for the studies characterized in this section is presented in Table 7-8, and the effect estimates are presented in Figure 7-7 and Figure 7-8.

A number of large, U.S. cohort studies have found consistent associations between long-term exposure to PM_{2.5} and cardiovascular mortality. The American Cancer Society (ACS) (Pope et al. (2004, [055880](#)) reported positive associations with deaths from specific cardiovascular diseases, particularly ischemic heart disease, and a group of cardiac conditions including dysrhythmia, heart failure and cardiac arrest (RR for cardiovascular mortality = 1.12 [95% CI: 1.08-1.15] per 10 µg/m³ PM_{2.5}). In an additional reanalysis that extended the follow-up period for the ACS cohort to 18 yr (1982-2000) (Krewski et al., 2009, [191193](#)), investigators found effect estimates that were similar, though generally higher, than those reported in previous ACS analyses.

A follow-up to the Harvard Six Cities study (Laden et al., 2006, [087605](#)) used updated air pollution and mortality data and found positive associations between long-term exposure to PM_{2.5} and mortality. Of special note is a statistically significant reduction in mortality risk reported with reduced long-term fine particle concentrations. This reduced mortality risk was observed for deaths due to cardiovascular and respiratory causes, but not for lung cancer deaths.

The WHI cohort study (Miller et al., 2007, [090130](#)) (described previously) found that each 10 µg/m³ increase of PM_{2.5} was associated with a 76% increase in the risk of death from cardiovascular disease (hazard ratio, 1.76 [95% CI: 1.25-2.47]). The WHI study not only confirms the ACS and Six City Study associations with cardiovascular mortality in yet another well characterized cohort with detailed individual-level information, it also has been able to consider the individual medical records of the thousands of WHI subjects over the period of the study. This has allowed the researchers to examine not only mortality, but also related morbidity in the form of heart problems (cardiovascular events) experienced by the subjects during the study. These morbidity co-associations with PM_{2.5} in the same population lend even greater support to the biological plausibility of the air pollution-mortality associations found in this study.

In an analysis for the Seventh-Day Adventist cohort in California (AHSMOG), a positive association with coronary heart disease mortality was reported among females (92 deaths; RR = 1.42 [95% CI: 1.06-1.90] per 10 µg/m³ PM_{2.5}), but not among males (53 deaths; RR = 0.90 [95% CI: 0.76-1.05] per 10 µg/m³ PM_{2.5}) (Chen et al., 2005, [087942](#)). Associations were strongest in the subset of postmenopausal women (80 deaths; RR = 1.49 [95% CI: 1.17-1.89] per 10 µg/m³ PM_{2.5}). The authors speculated that females may be more sensitive to air pollution-related effects, based on differences between males and females in dosimetry and exposure. As was found with PM_{2.5}, a positive association with coronary heart disease mortality was reported for PM_{10-2.5} and PM₁₀ among females (RR = 1.38 [95% CI: 0.97-1.95] per 10 µg/m³ PM_{10-2.5}; RR = 1.22 [95% CI: 1.01-1.47] per 10 µg/m³ PM₁₀), but not for males (RR = 0.92 [95% CI: 0.66-1.29] per 10 µg/m³ PM_{10-2.5}; RR = 0.94 [95% CI: 0.82-1.08] per 10 µg/m³ PM₁₀); associations were strongest in the subset of postmenopausal women (80 deaths) (Chen et al., 2005, [087942](#)).

Two additional studies explored the effects of PM₁₀ on cardiovascular mortality. The Nurses' Health Study (Puett et al., 2008, [156891](#)) is an ongoing prospective cohort study examining the relation of chronic PM₁₀ exposures with all-cause mortality and incident and fatal coronary heart disease consisting of 66,250 female nurses in MSAs in the northeastern region of the U.S. The association with fatal CHD occurred with the greatest magnitude when compared with other specified causes of death (hazard ratio 1.42 [95% CI: 1.11-1.81]). The North Rhine-Westphalia State Environment Agency (LUA NRW) initiated a cohort of approximately 4,800 women, and assessed whether long-term exposure to air pollution originating from motorized traffic and industrial sources was associated with total and cause-specific mortality (Gehring et al., 2006, [089797](#)). They found

that cardiopulmonary mortality was associated with PM₁₀ (RR = 1.52 [95% CI: 1.09-2.15] per 10 µg/m³ PM₁₀).

In summary, the 2004 PM AQCD concluded that there was strong evidence that long-term exposure to PM_{2.5} was associated with increased cardiopulmonary mortality. Recent studies investigating cardiovascular mortality provide some of the strongest evidence for a cardiovascular effect of PM. A number of large cohort studies have been conducted throughout the U.S. and reported consistent increases in cardiovascular mortality related to PM_{2.5} concentrations. The results of two of these studies have been replicated in independent reanalyses. These effects are coherent with short-term epidemiologic studies of CVD morbidity and mortality and with long-term epidemiologic studies of CVD morbidity. In addition, biological plausibility and coherence are provided by toxicological studies demonstrating short-term cardiovascular effects as well as PM_{2.5}-related plaque progression in chronically exposed mice.

7.2.11. Summary and Causal Determinations

7.2.11.1. PM_{2.5}

Epidemiologic studies examining associations between long-term exposure to ambient PM (over months to years) and CVD morbidity had not been conducted and thus were not included in the 1996 or 2004 PM AQCDs (U.S. EPA, 1996, [079380](#); U.S. EPA, 2006, [157071](#)). A number of studies were included in the 2004 AQCD that evaluated the effect of long-term PM_{2.5} exposure on cardiovascular mortality and found strong and consistent associations. No toxicological studies had evaluated the effects of subchronic or chronic PM exposure on CVD effects in the 2004 PM AQCD. Recently, epidemiologic and toxicological studies have provided evidence of the adverse effects of long-term exposure to PM_{2.5} on cardiovascular outcomes and endpoints, including atherosclerosis and clinical and subclinical markers of cardiovascular morbidity.

The strongest evidence for a CVD health effect related to long-term PM_{2.5} exposure comes from epidemiologic studies of cardiovascular mortality. A number of large, multicity U.S. studies (the ACS, Six Cities Study, WHI, and AHSMOG) provide consistent evidence of an effect between long-term exposure to PM_{2.5} and cardiovascular mortality (Section 7.2.10). These studies were conducted in urban areas across the U.S. where mean concentrations ranged from 10.2-29.0 µg/m³ (Table 7-8). An epidemiologic study investigating the relationship between PM_{2.5} and clinical CVD morbidity among post-menopausal women (Miller et al., 2007, [090130](#)) provides evidence of an effect that is coherent with the cardiovascular mortality studies. This large, prospective cohort study of incident, validated cases found large increases in the adjusted risk of MI, revascularization, and stroke using a 1-yr avg PM_{2.5} concentration (mean = 13.5 µg/m³). A cross-sectional analyses of self-reported prevalence of CHD and peripheral arterial disease found no such increase in the odds of CVD morbidity (Hoffmann et al., 2006, [091162](#)); the inconsistency of these findings with Miller et al. (2007, [090130](#)) may be explained by differences in study design or location.

The effect of long-term PM_{2.5} exposure on pre-clinical measures of atherosclerosis (CIMT, CAC, AAC or ABI) has been studied in several populations using a cross-sectional study design. The magnitude of the PM_{2.5} effects and their consistency across different measures of atherosclerosis in these studies varies widely, and they may be limited in their ability to discern small changes in these measures. Kunzli et al. (2005, [087387](#)) observed a non-significant 4.2% increase in CIMT associated with long-term PM_{2.5} exposure among participants of a clinical trial in greater Los Angeles, which was several fold higher than the 0.5% increase observed by Diez-Roux et al. (2008, [156401](#)) in their analyses of MESA baseline data. The associations in MESA of CAC and ABI with long-term PM_{2.5} exposure were largely null (Diez et al., 2008, [156401](#)), while an increase in AAC with long-term PM_{2.5} exposure was reported (Chang et al., 2008, [180393](#)). By contrast, a 43% increase in CAC was associated with long-term PM_{2.5} exposure in a German study, but no similar association with ABI was observed (Hoffmann et al., 2009, [190376](#)). Although the number of studies examining these relationships is limited, effect modification by use of lipid lowering drugs and smoking status was reported in more than one study of long-term PM_{2.5} and PM₁₀ exposure.

Evidence of enhanced atherosclerosis development was demonstrated in new toxicological studies that report increased plaque and lesion areas, lipid deposition, and TF in aortas of ApoE^{-/-} mice exposed to CAPs (Section 7.2.1.2). In addition, alterations in vasoreactivity were observed,

suggesting an impaired NO pathway. Additional toxicological studies of PM₁₀ are consistent with these results. Further support is provided by a study that reported decreased L/W ratio in the pulmonary and coronary arteries of mice exposed to ambient air. However, PM_{2.5} CAPs derived from traffic in Los Angeles did not affect plaque size (Araujo et al., 2008, [156222](#)). Collectively, these toxicological studies provide biological plausibility for the associations reported in epidemiologic studies.

There is limited evidence for the effects of PM_{2.5} on renal or vascular function. Cross-sectional and longitudinal epidemiologic analyses of PM_{2.5} and UACR revealed no evidence of an effect (O'Neill et al., 2007, [156006](#)), while small non-statistically significant increases in BP with 30- and 60-day avg PM_{2.5} concentrations were reported (Auchincloss et al., 2008, [156234](#)). A toxicological study did not show changes in MAP with CAPs, but indicated a CAPs-related potentiation of experimentally-induced hypertension (Sun et al., 2008, [157032](#)). In addition, CAPs has induced changes in insulin resistance, visceral adiposity, and inflammation in a diet-induced obesity mouse model (Sun et al., 2009, [190487](#)), indicating that diabetics may be a potentially susceptible population to PM exposure.

In summary, a number of large U.S. cohort studies report associations of long-term PM_{2.5} concentration with cardiovascular mortality. These studies provide the strongest evidence for an effect of long-term PM_{2.5} exposure on CVD effects. Additional evidence comes from a methodologically rigorous epidemiology study that demonstrates coherent associations between long-term PM_{2.5} exposure and CVD morbidity among post-menopausal women. Toxicological studies demonstrate that this effect is biologically plausible and the effect is coherent with studies of short-term PM_{2.5} exposure and CVD morbidity and mortality, and with long-term exposure to PM_{2.5} and CVD mortality. Associations between PM_{2.5} and subclinical measures of atherosclerosis are inconsistent, but cross-sectional studies may be limited in their ability to discern small changes in these measures. In addition, potential modification of the PM_{2.5}-CVD association by smoking status and the use of lipid lowering drugs has been demonstrated in epidemiologic studies that used individual-level data. Toxicological studies provide evidence for accelerated development of atherosclerosis in ApoE^{-/-} mice exposed to CAPs and show effects on coagulation factors, experimentally-induced hypertension, and vascular reactivity. Available studies of clinical cardiovascular disease outcomes report inconsistent results. Based on the above findings, the epidemiologic and toxicological evidence is **sufficient to infer a causal relationship between long-term PM_{2.5} exposures and cardiovascular effects.**

7.2.11.2. PM_{10-2.5}

One epidemiologic study evaluated the relationship between long-term exposure to PM_{10-2.5} and cardiovascular mortality and found a positive association with coronary heart disease mortality among females, but not for males; associations were strongest in the subset of post-menopausal women (Chen et al., 2005, [087942](#)). No toxicological studies of long-term exposure to ambient PM_{10-2.5} and cardiovascular effects have been conducted to date. Evidence is **inadequate to infer the presence or absence of a causal relationship.**

7.2.11.3. UFPs

A few toxicological studies of long-term exposure to UFPs have been conducted. Increased plaque size was reported in mice exposed to UF CAPs derived from traffic (Araujo et al., 2008, [156222](#)). Studies of diesel and gasoline exhaust reported relatively few changes in hematologic or coagulation parameters (Section 7.2.4.2) and one DE study demonstrated altered cardiac gene expression in normotensive rats that reflected the development of hypertension (Gottipolu et al., 2009, [190360](#)). Whole and filtered gasoline exhaust induced increases in gene products involved in atheromatous plaque formation and/or degradation, but these effects were largely due to the gaseous emissions (Lund et al., 2007, [125741](#)). Evidence from these studies alone is **inadequate to infer the presence or absence of a causal relationship.**

7.3. Respiratory Effects

Several cohort studies reviewed in the 2004 PM AQCD provided evidence for relationships between long-term PM exposure and effects on the respiratory system, though it did not rule out the possibility that the observed respiratory effects may have been confounded by other pollutants. In 12 southern California communities in the Children's Health Study (CHS), Gauderman et al. (2000, [012531](#); 2002, [026013](#)) found that decreases in lung function growth among schoolchildren were associated with long-term exposure to PM. Declines in pulmonary function were reported with all three major PM size classes – PM₁₀, PM_{10-2.5} and PM_{2.5} – though the three PM measures were highly correlated. In another analysis of data from the CHS cohort, McConnell et al. (1999, [007028](#)), reported an increased risk of bronchitis symptoms in children living in communities with higher PM₁₀ and PM_{2.5} concentrations. These results were found to be consistent with results of cross-sectional analyses of the 24-city study by Dockery et al. (1996, [046219](#)) and Raizenne et al. (1996, [077268](#)), that were assessed in the 1996 PM AQCD. These studies reported associations between increased bronchitis rates and decreased peak flow with fine particle sulfate and fine particle acidity. However, the high correlation of PM₁₀, acid vapor and NO₂ precluded clear attribution of the bronchitis effects reported by McConnell et al. (1999, [007028](#)) to PM alone. In a prospective cohort study among a subset of children in the CHS (n = 110) who moved to other locations during the study period, Avol et al. (2001, [020552](#)) reported that those subjects who moved to areas of lower PM₁₀ showed increased growth in lung function compared with subjects who moved to communities with higher PM₁₀ concentrations. Finally, the 2004 PM AQCD concluded that there was strong epidemiologic evidence for associations between long-term exposures to PM_{2.5} and cardiopulmonary mortality, though the respiratory effects were not separated from the cardiovascular effects in this conclusion.

The 2004 PM AQCD (U.S. EPA, 2004, [056905](#)) concluded that the evidence for an association between long-term exposure to PM and respiratory effects may be confounded by other pollutants. Gauderman et al. (2002, [026013](#)) reported declines for FEV₁ and McConnell et al. (1999, [007028](#)) reported increased ORs for bronchitic symptoms in asthmatics for PM₁₀ and PM_{2.5}. Recent epidemiologic literature includes results from several prospective cohort studies, which found consistent, positive associations between long-term exposure to PM and respiratory morbidity. Associations were reported with PM_{2.5} and PM₁₀, and the studies showing associations only with PM₁₀ were conducted in locations where the PM consisted predominantly of fine particles, providing support for associations with long-term exposure to fine particles. These results are summarized below; further details of these studies are summarized in Annex E.

Very few subchronic and chronic toxicological studies investigating respiratory effects were available in the 2004 PM AQCD. However, the 2002 EPA Health Assessment Document for DE reported that chronic exposure to DE was associated with histopathology including alveolar histiocytosis, aggregation of alveolar macrophages, tissue inflammation, increased polymorphonuclear leukocytes, hyperplasia of bronchiolar and Type 2 epithelial cells, thickened alveolar septa, edema, fibrosis, emphysema and lesions of the trachea and bronchi. Since then a number of animal toxicological studies have been conducted involving inhalation exposure to CAPs, urban air, DE, gasoline exhaust, and wood smoke. These subchronic and chronic studies provide evidence of altered pulmonary function, inflammation, histopathological changes and oxidative and allergic responses following PM_{2.5} exposures. These results are summarized below; further details of these studies are summarized in Annex D.

7.3.1. Respiratory Symptoms and Disease Incidence

7.3.1.1. Epidemiologic Studies

New longitudinal cohort studies provide the best evidence to evaluate the relationship between long-term exposure to ambient PM and increased incidence of respiratory symptoms or disease. A summary of the mean PM concentrations reported for the long-term exposure studies characterized in this section is presented in Table 7-3.

Bayer-Oglesby et al. (2005, [086245](#)) examined the decline of ambient pollution levels and improved respiratory health demonstrated by a reduction in respiratory symptoms and diseases in school children (n = 9,591) in Switzerland. Reduced air pollution exposure resulted in improved respiratory health of children. Further, the average reduction of symptom prevalence was more pronounced in areas with stronger reduction of air pollution levels. The average decline of PM₁₀ between 1993 and 2000 across the nine study regions was 9.8 µg/m³ (29%). Declining levels of PM₁₀ were associated with declining prevalence of chronic cough, bronchitis, common cold, nocturnal dry cough, and conjunctivitis symptoms, but no significant associations were reported for wheezing, sneezing, asthma, and hay fever, as shown in Figure 7-2. In Figure 7-2, Panel (B) illustrates that on an aggregate level across regions, the mean change in adjusted prevalence of chronic cough is associated with the mean change in PM₁₀ levels (r = 0.78; p = 0.02). Similar associations were seen for nocturnal dry cough and conjunctivitis symptoms and PM₁₀ levels. Rösli et al. (2000, [010296](#); 2001, [108738](#); 2005, [156923](#)) have demonstrated that PM₁₀ levels are homogeneously distributed within regions of Basel, Switzerland and are not substantially affected by local traffic, justifying the single-monitor approach for assignment of PM₁₀ exposures. Based on parallel measurements of PM_{2.5} and PM₁₀ at seven sites in Switzerland, PM_{2.5} and PM₁₀ at all sites are generally highly correlated (r² ranging from 0.85 to 0.98) (Gehrig and Buchmann, 2003, [139678](#)), indicating that PM₁₀ consists predominantly of fine particles in these locations.

Schindler et al. (2009, [191950](#)) reported that sustained reduction in ambient PM₁₀ concentrations can lead to decreases in respiratory symptoms among Swiss adults in the SAPALDIA study. They compared baseline data in 1991 to a follow-up interview in 2002 after a substantial decline in PM₁₀ concentrations served as a natural experiment. Each subject was assigned model-based estimates of PM₁₀ concentrations averaged over the 12 mo preceding each health assessment with mean decline in PM₁₀ levels of 6.2 µg/m³ (SD = 3.9 µg/m³). When the authors tested the joint hypothesis of no association between the PM₁₀ difference and symptom incidence or persistence, positive results were obtained for regular cough, chronic cough or phlegm and wheezing but not regular phlegm or wheezing without a cold.

Pierse et al. (2006, [088757](#)) studied the association between primary PM₁₀ (particles directly emitted from local sources/traffic) and the prevalence and incidence of respiratory symptoms in a randomly sampled cohort of 4,400 children (aged 1-5 yr) in Leicestershire, England surveyed in 1998 and again in 2001. Annual exposure to primary PM₁₀ was calculated for the home address using the Airviro statistical dispersion model. After adjusting for confounders, mean annual exposure to locally generated PM₁₀ was associated with an increased prevalence of cough without a cold in both the 1998 (OR 1.21 [95% CI: 1.07-1.38], n = 2,164) and 2001 surveys (OR 1.56 [95% CI: 1.32-1.84], n = 1,756).

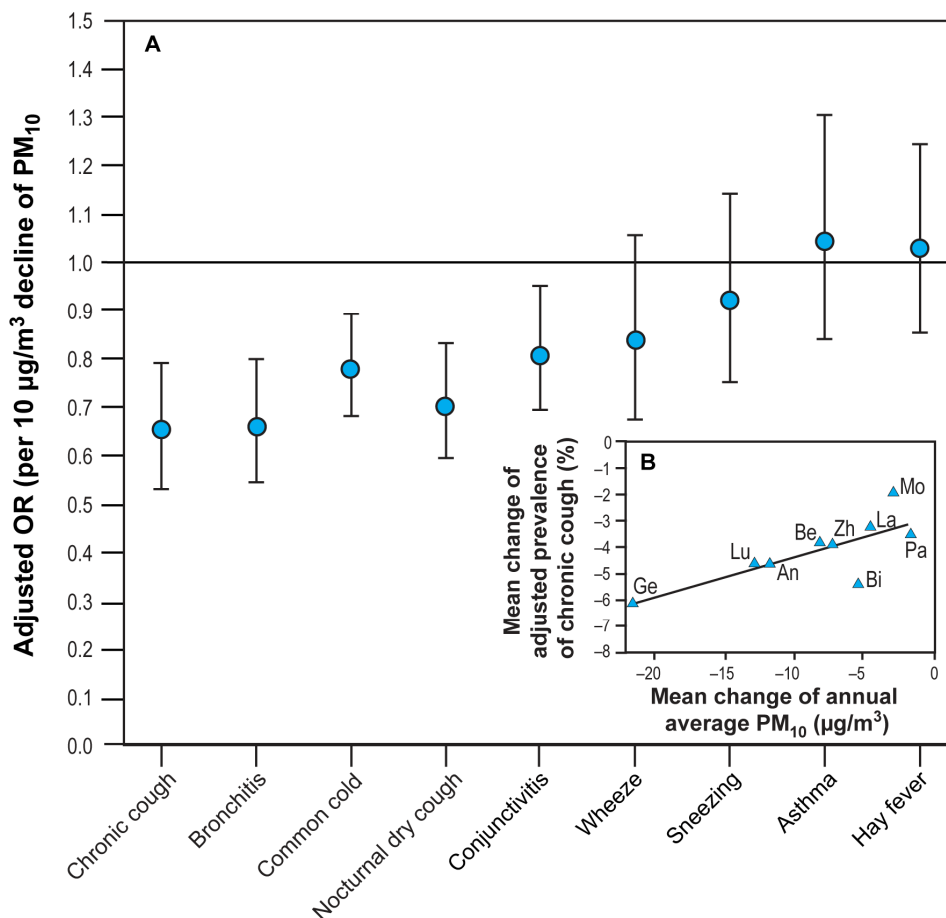
Nordling et al. (2008, [097998](#)) examined the relationship between estimated PM exposure levels and respiratory health effects in a Swedish birth cohort of preschool children (n = 4,089). The spatial distributions of PM from traffic in the study area were estimated with emission databases and statistical dispersion modeling. Children were examined at 2 mo and 1, 2, and 4 yr of age. Using GIS methods, the average contribution of traffic-generated PM₁₀ above regional background to the children's residential outdoor air pollution levels was determined. To evaluate the exposure assessment, the authors compared the estimated levels of traffic-generated PM₁₀ with PM_{2.5} measurements from 42 locations (Hoek et al., 2002, [042364](#)) and reported modeled traffic-generated PM₁₀ correlated reasonably well with measured PM_{2.5} (r = 0.61). Persistent wheezing (cumulative incidence up to age 4 yr) was associated with exposure to traffic-generated PM₁₀ (OR 2.28 [95% CI: 0.84-6.24] per 10 µg/m³ increase) while transient and late onset wheezing was not associated. This study demonstrates that respiratory effects may be present in preschool children.

Table 7-3. Characterization of ambient PM concentrations from studies of respiratory symptoms/disease and long-term exposures.

Study	Location	Mean Annual Concentration ($\mu\text{g}/\text{m}^3$)	Upper Percentile Concentrations ($\mu\text{g}/\text{m}^3$)
<i>PM_{2.5}</i>			
Annesi-Maesano et al. (2007, 093180)	6 French Cities	Range of means across sites: 8.7-23.0 Avg of means across sites: 15.5	
Brauer et al. (2007, 090691)	The Netherlands	16.9	75th: 18.1 90th: 19.0 Max: 25.2
Goss et al. (2004, 055624)	U.S.	13.7	75th: 15.9
Islam et al. (2007, 090697)	12 CHS/CA communities		Max: 29.5
Janssen et al. (2003, 133555)	The Netherlands	20.5	75th: 22.1 Max: 24.4
Kim et al. (2004, 087383)	San Francisco, CA	Range of means across sites: 11-15 Avg of means across sites: 12	
McConnell et al. (2003, 049490)	12 CHS/CA communities	13.8	Max: 28.5
Morgenstern et al. (2008, 156782)	Munich, Germany	11.1	
<i>PM₁₀</i>			
Bayer-Oglesby et al. (2005, 086245)	Nine study regions in Switzerland		Max: 46
Kunzli et al. (2009, 191949)	Switzerland	21.5	
Nordling et al. (2008, 097998)	Sweden	4*	
Schindler et al. (2009, 191950)	Switzerland	**	
McConnell et al. (2003, 049490)	12 CHS/CA communities	30.8	Max: 63.5
Pierse et al. (2006, 088757)	Leicestershire, U.K.	1.33	75th: 1.84

*Source specific; PM₁₀ from traffic

**Only reported change in PM concentration



Source: Bayer-Oglesby et al. (2005, [086245](#))

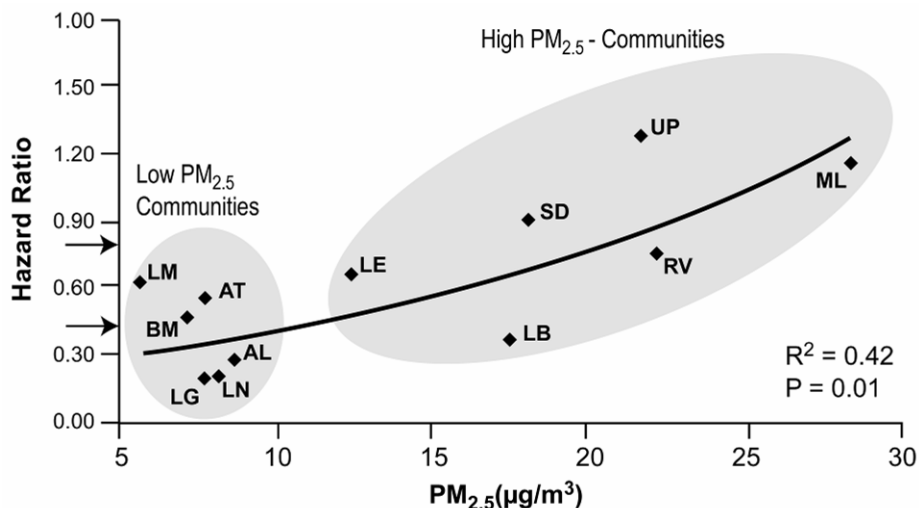
Figure 7-2. Adjusted ORs and 95% CIs of symptoms and respiratory diseases associated with a decline of 10 µg/m³ PM₁₀ levels in Swiss Surveillance Program of Childhood Allergy and Respiratory Symptoms¹. Inset: Mean change in adjusted prevalence (1998-2001 to 1992-1993) versus mean change in regional annual averages of PM₁₀ (1997-2000 to 1993) for chronic cough, across nine SCARPOL regions (An: Anières. Be: Bern. Bi: Biel. Ge: Geneva. La: Langnau. Lu: Lugano. Mo: Montana. Pa: Payerne. Zh: Zürich).

McConnell et al. (2003, [049490](#)) conducted a prospective study examining the association between air pollution and bronchitic symptoms in 475 school children with asthma in 12 Southern California communities as part of the CHS from 1996 to 1999. They investigated both the differences between- communities with 4-yr avg and within-communities yearly variation in PM (i.e., PM₁₀, PM_{2.5}, PM_{10-2.5}, EC, and OC). Based on a 10 µg/m³ change in PM_{2.5}, within-communities effects were larger (OR 1.90 [95% CI: 1.10-2.70]) than those for between-communities (OR 1.30 [95% CI: 1.10-1.50]). The OR for the 10 µg/m³ range in 4-yr avg PM_{2.5} concentrations across the 12 communities was 1.29 (95% CI: 1.06-1.58). Similar results were reported for PM₁₀ and PM_{10-2.5} but the effect estimates were smaller in magnitude and generally not statistically significant. Within-community associations were not confounded by any time-fixed personal covariates. In two-

¹ Adjusted for age, sex, nationality, parental education, number of siblings; farming status, low birth weight, breastfeeding, child who smokes, family history of asthma, bronchitis, and/or atopy, mother who smokes, indoor humidity, mode of heating and cooking, carpeting, pets allowed in bedroom, removal of carpet and/or pets for health reasons, person who completed questionnaire, month when questionnaire was completed, number of days with the maximum temperature <0°C, and belief of mother that there is an association between environmental exposures and children's respiratory health

pollutant models, the within-community effect estimates for PM_{2.5} and OC were significant in the presence of several other pollutants. While the within-community single-pollutant effect of PM_{2.5} ($\beta = 0.085/\mu\text{g}/\text{m}^3$) was only modestly attenuated after adjusting for some pollutants, it was markedly reduced after adjusting for NO₂ or OC. The between-community effect estimates generally were not significant in the presence of other pollutants in copollutant models.

In the CHS, Islam et al. (2007, [090697](#)) examined the hypothesis that ambient air pollution attenuates the reduced risk for childhood asthma that is associated with higher lung function (n = 2,057). At each age a distribution of pulmonary functions exists. Haland et al. (2006, [156511](#)) found evidence that children with high lung function have a reduced risk for asthma. Islam et al. (2007, [090697](#)) used the CHS data to study how the association of asthma incidence with lung function is modified by long-term PM exposure. The incidence rate (IR) of newly diagnosed asthma increased from 9.5/1,000 person-years for children with percent-predicted FEF₂₅₋₇₅ values $\geq 120\%$ to 20.4/1,000 person-years for children with FEF₂₅₋₇₅ value $\leq 100\%$. Over the 10th-90th percentile range for FEF₂₅₋₇₅ (57.1%), the hazard ratio of new onset asthma was 0.50 (95% CI: 0.35-0.71). The IR of asthma for FEF₂₅₋₇₅ $\geq 120\%$ in the “high” PM_{2.5} (13.7-29.5 $\mu\text{g}/\text{m}^3$) communities was 15.9/1,000 person-years compared to 6.4/1,000 person-years in “low” PM_{2.5} (5.7-8.5 $\mu\text{g}/\text{m}^3$) communities. Loss of protection by high lung function against new onset asthma in the “high” PM_{2.5} communities was observed for all the lung function measures. Figure 7-3 shows the effect of PM_{2.5} on the association of lung function with asthma. Of all the pollutants examined (NO₂, PM₁₀, PM_{2.5}, acid vapor, O₃, EC, and OC), PM_{2.5} appeared to have the strongest modifying effect on the association between lung function with asthma as it had the highest R² value (0.42). Over the 10th-90th percentile range of FEF₂₅₋₇₅, the hazard ratio of new onset asthma was 0.34 (95% CI: 0.21-0.56) in a community with low PM_{2.5} ($<13.7 \mu\text{g}/\text{m}^3$) and 0.76 (95% CI: 0.45-1.26) in a community with high PM_{2.5} ($\geq 13.7 \mu\text{g}/\text{m}^3$). The data do not indicate that PM exposure increased rates of incident asthma among children with poor lung function at study entry because rates among those with poor lung function were similar in both low and high pollution communities.



Source: Reprinted with Permission of BMJ Publishing Group Ltd & British Thoracic Society from Islam et al. (2007, [090697](#))

Figure 7-3. Effect of PM_{2.5} on the association of lung function with asthma. Community-specific hazard ratio of newly diagnosed asthma over 10-90th percentile range (57.1%) of FEF_{25-75%} by level of ambient PM_{2.5} ($\mu\text{g}/\text{m}^3$). The 12 CHS communities are shown.

In a prospective birth cohort study (n = 4,000) in The Netherlands, Brauer et al. (2007, [090691](#)) assessed the development of asthma, allergic symptoms, and respiratory infection during the first 4 yr of life in relation to long-term PM_{2.5} concentration at the home address with a validated model using GIS. PM_{2.5} was associated with doctor-diagnosed asthma (OR = 1.32 [95% CI:

1.04-1.69]) for a cumulative lifetime indicator. These findings extend observations made at 2 yr of age in the same cohort (Brauer et al., 2002, [035192](#)) providing greater confidence in the association. No associations were observed for bronchitis.

Kunzli et al. (2009, [191949](#)) used the SAPALDIA cohort study discussed previously in this section to evaluate the relationship between the 11-yr change (1991-2002) in traffic-related PM₁₀ and asthma incidence-adult onset asthma. In a cohort of 2,725 never-smokers without asthma at baseline (age: 18-60 yr in 1991), subjects reporting doctor-diagnosed asthma at follow-up were considered incident cases. Modeled traffic-related PM₁₀ levels were used. Cox proportional hazard models for time to asthma onset were used with adjustments for cofounders. The study findings suggest that PM contributes to asthma development and that reductions in PM decrease asthma risk. A strong feature of SAPALDIA is the ability to assign space, time, and source-specific pollution to each subject. Further, Kunzli et al. (2008, [129258](#)) discusses the impact of attributable health risk models for exposures that are assumed to cause both chronic disease and its exacerbations. The added impact of causing disease increases the risk compared to only exacerbations.

A matched case-control study of infant bronchiolitis (ICD 9 code 466.1) hospitalization and two measures of long-term exposure – the month prior to hospitalization (subchronic) and the lifetime average (chronic) – to PM_{2.5} and gaseous air pollutants in the South Coast Air Basin of southern California was conducted by Karr et al. (2007, [090719](#)) among 18,595 infants born between 1995-2000. For each case, 10 controls matched on date were randomly selected from birth records. Exposure was based on PM_{2.5} measurements collected every third day. The mean distance between the subjects' residential ZIP code and the assigned monitor was generally 4-6 mi with a maximum distance of 30 mi. For 10 µg/m³ increases in both sub-chronic and chronic PM_{2.5} exposure, an adjusted OR of 1.09 (95% CI: 1.04-1.14) was observed. In multipollutant model analyses, the association with PM_{2.5} was robust to the inclusion of gaseous pollutants. Also, in a cohort of children in Germany, Morgenstern et al. (2008, [156782](#)) modeled PM_{2.5} data at birth addresses found statistically significant effects for asthmatic bronchitis, hay fever, and allergic sensitization to pollen.

Goss et al. (2004, [055624](#)) conducted a national study examining the relationship between air pollutants and health effects in a cohort of cystic fibrosis (CF) patients (n = 11,484) over the age of 6 yr (mean age = 18.4, SD = 10) enrolled in the Cystic Fibrosis Foundation National Patient Registry in 1999 and 2000. Exposure was assessed by linking air pollution values from the closest population monitor from the Air Quality System (AQS) with the centroid of the patient's home ZIP code that was within 30 mi. The mean distance from the patient's ZIP code to monitors for PM_{2.5} and PM₁₀ was 10.8 mi (SD 7.8) and 11.5 mi (SD 7.9), respectively. PM_{2.5} and PM₁₀ 24-h avg were collected every 1 to 12 days. CF diagnosis involves genetic screening panels and a common severe mutation used is the loss of phenylalanine at the 508th position. Genotyping was available in 74% of the population and of those genotyped, 66% carried one or more delta F508 deletions. After adjusting for cofounders, a 10 µg/m³ increase in PM_{2.5} or PM₁₀ was associated with a 21% (95% CI: 7-33) or 8% (95% CI: 2-15) increase in the odds of two or more exacerbations, respectively. The exacerbations were defined as a CF-related pulmonary condition requiring admission to the hospital or use of home intravenous antibiotics. The estimate for the associations between pulmonary exacerbations and PM_{2.5} and PM₁₀ were attenuated when the models were adjusted for lung function. Brown et al. (2001, [012307](#)) found that particle deposition was increased in CF and that particle distribution in the lungs was enhanced in poorly ventilated tracheobronchial regions in CF patients. Such focal deposition may partially explain the association of PM and CF exacerbation.

Annesi-Maesano (2007, [093180](#)) relate individual data on asthma and allergy from 5,338 school children (10.4 ± 0.7 yr) attending 108 randomly chosen schools in 6 French cities to the concentration of PM_{2.5} monitored in school yards. Atopic asthma was related to PM_{2.5} (OR 1.43 [95% CI: 1.07-1.91]) when high PM_{2.5} concentrations (20.7 µg/m³) were compared to low PM_{2.5} concentrations (8.7 µg/m³). The report is consistent with the results in an earlier paper (Penard-Morand et al., 2005, [087951](#)) in the same sample of children that related the findings to PM₁₀.

Kim et al. (2004, [087383](#)) conducted a school-based cross-sectional study in the San Francisco metropolitan area in 2001 comprised of 10 neighborhoods to examine the relationship between traffic-related pollutants and current bronchitic symptoms and asthma obtained by parental questionnaire (n = 1,109). They related traffic-related pollutants (PM) and bronchitic and asthma symptoms in the past 12 mo. No multipollutant models were evaluated because of the high interpollutant correlations. PM_{2.5} levels ranged across the school sites from 11 to 15 µg/m³.

Schikowski et al. (2005, [088637](#)) examined the relationship between both long-term air pollution exposure and living close to busy roads and COPD in the Rhine-Ruhr Basin of Germany

from 1985 to 1994 using consecutive cross-sectional studies. Seven monitoring stations that were <8 km to a woman's home address provided TSP data that PM₁₀ was estimated from using a conversion factor (obtained from parallel measurement of TSP and PM₁₀ conducted at 7 sites in the Ruhr area). Distance to a major road was determined using GIS. The results of the study suggest that long-term exposure to air pollution from PM₁₀ and living near a major road might increase the risk of developing COPD and can have a detrimental effect on lung function. All ORs for 5-yr exposures were stronger than those for 1-yr exposures.

In summary, the 2004 PM AQCD evaluated the available studies which primarily related effects to bronchitic symptoms in school-age children. New studies are using several different methods to include individual estimates of exposure to ambient PM that may reduce the impact of exposure error. The strength and consistency of the outcomes is enhanced by results being reported by several different researchers in different countries using different designs. Most recent studies have focused on children, but a few studies have also reported associations in adults.

The CHS (McConnell et al., 2003, [049490](#)) provides evidence in a prospective longitudinal cohort study that relates PM_{2.5} and bronchitic symptoms and reports larger associations for within-community effects that are less subject to confounding than between-community effects. Several new studies report similar findings with long-term exposure to PM₁₀ in areas where fine particles are the predominant fraction of PM₁₀. In England, in a cohort of 4,400 children (aged 1-5 yr), an association is seen with an increased prevalence of cough without a cold. Further evidence includes a reduction of respiratory symptoms corresponding to decreasing PM levels in "natural experiments" in both a cohort of Swiss school children (Bayer-Oglesby et al., 2005, [086245](#)) and adults (Schindler et al., 2009, [191950](#)).

In a separate analysis of the CHS, Islam et al. (2007, [090697](#)) showed that PM_{2.5} had the strongest modifying effect on the association between lung function with asthma such that loss of protection by high lung function against new onset asthma in high PM_{2.5} communities was observed for all the lung function measures from 10 to 18 yr of age. This relates new onset asthma to long-term PM exposure. In the Netherlands, Brauer et al. (2007, [090691](#)) augments the literature with data examining the first 4 yr of life in a birth cohort showing an association with doctor-diagnosed asthma. Further, in an adult cohort in the SALPALDIA study, Kunzli et al. (2009, [191949](#)) relate PM to asthma incidence.

7.3.2. Pulmonary Function

Several cohort studies reviewed in the 2004 PM AQCD provided evidence for relationships between long-term PM exposure and effects on the respiratory system. In 12 southern California communities in the Children's Health Study (CHS), Gauderman et al. (2000, [012531](#); 2002, [026013](#)) found that decreases in lung function growth among school children were associated with long-term exposure to PM. Declines in pulmonary function were reported with all three major PM size classes – PM₁₀, PM_{10-2.5} and PM_{2.5} – though the three PM measures were highly correlated. These results were found to be consistent with results of cross-sectional analyses of Raizenne et al. (1996, [077268](#)), that was assessed in the 1996 PM AQCD. That study reported associations between decreased peak flow with fine particle sulfate and fine particle acidity. Finally, in a prospective cohort study among a subset of children in the CHS (n = 110) who moved to other locations during the study period, Avol et al. (2001, [020552](#)) reported that those subjects who moved to areas of lower PM₁₀ showed increased growth in lung function compared with subjects who moved to communities with higher PM₁₀ concentrations who showed decrease growth in lung function.

7.3.2.1. Epidemiologic Studies

New longitudinal cohort studies have evaluated the relationship between long-term exposure to PM and changes in measures of pulmonary function (FVC, FEV₁, and measures of expiratory flow). Cross-sectional studies also offer supportive information (Annex E) and may provide insights derived from within community analysis. Lung function increases continue through early adulthood with growth and development, then declines with aging (Stanojevic et al., 2008, [157007](#); Thurlbeck, 1982, [093260](#); Zeman and Bennett, 2006, [157178](#)). A summary of the mean PM concentrations reported for the long-term exposure studies characterized in this section is presented in Table 7-4.

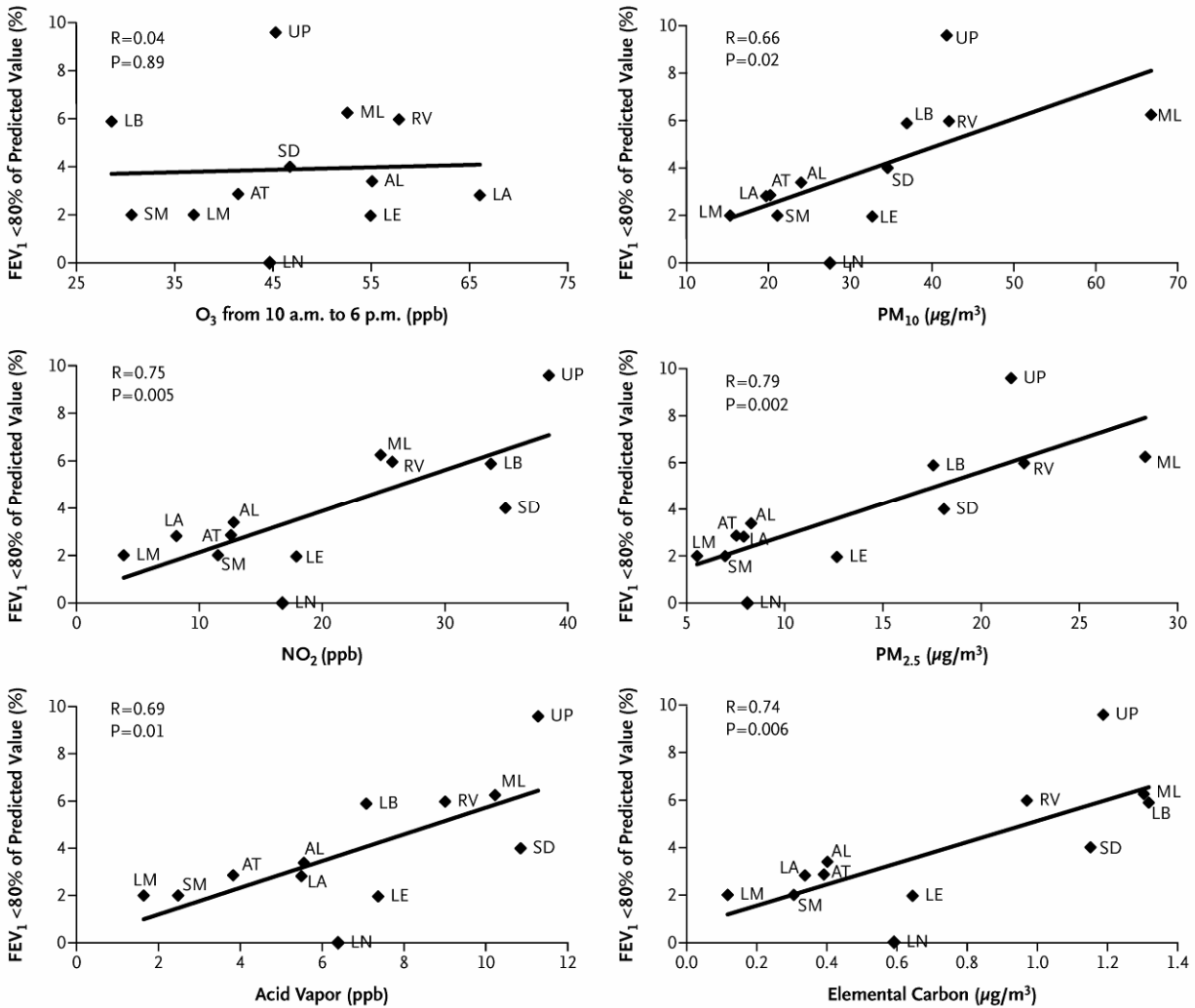
Table 7-4. Characterization of ambient PM concentrations from studies of FEV₁ and long-term exposures.

Study	Location	Mean Annual Concentration (µg/m ³)	Upper Percentile Concentrations (µg/m ³)
PM_{2.5}			
Gauderman et al. (2002, 026013)	12 CHS/CA communities	5-30	
Gauderman et al. (2004, 056569)	12 CHS/CA communities	6-27	
Goss et al. (2004, 055624)	U.S.	13.7	75th: 15.9
Gotschi et al. (2008, 180364)	21 European cities	Range of means across sites: 3.7-44.7 Avg of mean across sites: 16.8	
PM₁₀			
Downs et al. (2007, 092853)	8 cities in Switzerland	Range of means across sites: 9-46 Avg of mean across sites: 21.6	
Gauderman et al. (2002, 026013)	12 CHS/CA communities	Range of means across sites: 13-78 Avg of mean across sites: NR	
Gauderman et al. (2004, 056569)	12 CHS/CA communities	Range of means across sites: 18-68 Avg of mean across sites: NR	
Nordling et al. (2008, 097998)	Sweden	Modeled exposure	
Avol et al. (2001, 020552)	Southern CA/CHS	Range of means across sites: 15.0-66.2	
Rojas-Martinez et al. (2007, 091064)	Mexico City, Mexico	75.6	75th: 92.2 90th: 112.7

The CHS prospectively examined the relationship between air pollutants and lung function (FVC, FEV₁, MMEF) in a cohort (n = 1,759) of children between the ages of 10 and 18 yr, a period of rapid lung development (Gauderman et al., 2004, [056569](#)). Air pollution monitoring stations provided data in each of the 12 study communities from 1994-2000. The results for O₃, PM₁₀, NO₂, PM_{2.5}, acid vapor, and EC are depicted in Figure 7-4. In general, copollutant models for any pair of pollutants did not provide a substantially better fit to the data than the corresponding single-pollutant models due to the strong correlation between most pollutants. The pollution-related deficits in the average growth in lung function over the 8-yr period resulted in clinically important deficits in attained lung function at the age of 18.

Downs et al. (2007, [092853](#)) prospectively examined 9,651 randomly selected adults (18-60 yr of age) in eight cities in Switzerland (see also Ackermann-Liebrich et al., 1997, [077537](#)) to ascertain the relationship between reduced exposure to PM₁₀ and age-related decline in lung function (FVC, FEV₁, and FEF₂₅₋₅₀). An evaluated statistical dispersion model (Liu et al., 2007, [093093](#)) provided spatially resolved concentrations of PM₁₀ that enabled assignment to residential addresses for the participant examinations in 1991 and 2002 that yielded a median decline of 5.3 µg/m³ (IQR 4.1-7.5). Decreasing PM₁₀ concentrations attenuated the decline in lung function. Effects were greater in tests reflecting small airway function. No other pollutant relationships were evaluated, though a related study indicated that levels of NO₂ also declined over the same period (Ackermann-Liebrich et al., 2005, [087826](#)). Generalized cross-validation essentially chose a linear fit for the concentration-response curve for age-related decline in lung function.

These data show that improvement in air quality may slow the annual rate of decline in lung function in adulthood indicating positive consequences for public health. Further evidence on improvement in respiratory health with reduction in air pollution levels is provided from studies conducted in East Germany related to dramatic emissions reductions after the reunification in 1990 (Fryer and Collins, 2003, [156454](#); Heinrich et al., 2002, [034825](#); Sugiri et al., 2006, [088760](#)). This type of “natural experiment” provides additional support for epidemiologic findings that relatively low levels of airborne particles have respiratory effects.



Source: Adapted from Gauderman et al. (2004, [056569](#))
 Copyright © 2004 Massachusetts Medical Society. All rights reserved.

Figure 7-4. Proportion of 18-yr olds with an FEV₁ below 80% of the predicted value plotted against the average levels of pollutants from 1994 through 2000 in the 12 southern California communities of the Children’s Health Study. AL = Alpine; AT = Atascadero; LA = Lake Arrowhead; LB = Long Beach; LE = Lake Elsinore; LM = Lompoc; LN = Lancaster; ML = Mira Loma; RV = Riverside; SD = San Dimas; SM = Santa Maria; UP = Upland.

In a prospective cohort study consisting of school-age children (n = 3,170) who were 8 yr of age at the beginning of the study, had not been diagnosed with asthma, and were located in Mexico City, Rojas-Martinez et al. (2007, [091064](#)) evaluated the association between long-term exposure to PM₁₀, O₃ and NO₂ and lung function growth every 6 mo from April 1996 through May 1999. Exposure data were provided by 10 air quality monitor stations located within 2 km of each child’s school. The multipollutant model effect of PM₁₀ over the age of 8-10 yr of life in this cohort on FVC, FEV₁, and FEF₂₅₋₇₅ showed an association. Single pollutant models showed an association between ambient pollutants (O₃, PM₁₀ and NO₂) and deficits in lung function growth. The association between PM₁₀ and FEF₂₅₋₇₅ was not statistically significant. While the estimates from copollutant models were not substantially different than single pollutant models, independent effects for pollutants could not be estimated accurately because the traffic-related pollutants were correlated.

Although no PM_{2.5} data were presented in this study, in a separate study Chow et al. (2002) report that during the winter of 1997 approximately 50% of PM₁₀ was in the PM_{2.5} fraction in Mexico City.

Gotschi et al. (2008, [156485](#)) examined the relationship between air pollution and lung function in adults in the European Community Respiratory Health Survey (ECRHS). FEV₁ and FVC were assessed at baseline and after 9 yr of follow-up from 21 European centers (followed-up sample n = 5,610). No statistically significant associations were found between city-specific annual mean PM_{2.5} and average lung function levels which is in contrast to the results seen by Ackermann-Lieblich (1997, [077537](#)) (SAPALDIA) and Schikowski et al. (2005, [088637](#)) (SALIA) which compared across far more homogenous populations than for the population assessed in the ECRHS. Misclassification and confounding may partially explain the discrepancy in findings.

In a birth cohort (n = 2,170) in Oslo, Norway, Oftedal et al. (2008, [093202](#)) examined effects of exposure to PM_{2.5} and PM₁₀ on lung function (FVC, FEV₁, FEF_{50%}). Spirometry was performed in 2,307 children aged 9-10 yr in 2001-2002. Residential air pollution levels over the time period 1992-2002 were calculated using EPISODE dispersion models to provide three time scales of exposure: (1) first year of life; (2) lifetime exposure; and (3) just before the lung function test. Only single pollutant models were evaluated because air pollutants were highly correlated (r = 0.83-0.95). PM exposure was associated with changes in adjusted peak respiratory flow, especially in girls. No effect was found for forced volumes. Adjusting for contextual socioeconomic factors diminished associations. Results for PM₁₀ were similar to those for PM_{2.5}.

In an exploratory study, Mortimer et al. (2008, [187280](#)) examined the association of prenatal and lifetime exposure to air pollutants using geocoded monthly average PM₁₀ levels with pulmonary function in a San Joaquin Valley, California cohort of 232 children (ages 6-11 yr) with asthma. First and second trimester PM₁₀ exposures (based on monthly average concentrations) had a negative effect on pulmonary function and may relate to prenatal exposures affecting the lungs as they begin to develop at 6-wk gestation.

Dales et al. (2008, [156378](#)) in a cross-sectional prevalence study examined the relationship of pulmonary function and PM measures, other pollutants, and indicators of motor vehicle emissions in Windsor, Ontario, in a cohort of 2,402 school children. PM_{2.5} and PM₁₀ concentrations were estimated for each child's residence at the postal code level. Each 10 µg/m³ increase in PM_{2.5} was associated with a 7.0% decrease in FVC expressed in a percentage of predicted.

In Leicester, England, investigators examined the carbon content of airway macrophages in induced sputum in 64 of 114 healthy 8-15 year-old children (Grigg et al., 2008, [156499](#); Kulkarni et al., 2006, [089257](#)). The carbon content of airway macrophages (Finch et al., 2002, [054603](#); Strom et al., 1990, [157020](#)) was used as a marker of individual exposure to PM₁₀. Near each child's home, exposure to PM₁₀ was estimated using a statistical dispersion model (Pierse et al., 2006, [088757](#)). The authors reported a dose-dependent inverse association between the carbon content of airway macrophages and lung function in children and found no evidence that reduced lung function itself causes an increase in carbon content. Consistent results were obtained for both FVC and FEF₂₅₋₇₅. Caution should be used when interpreting these results as the accuracy of the estimates on individual PM₁₀ exposures were not validated; there is potential for confounding by ethnic origin; and there is concern that the magnitude of the changes in pulmonary function associated with increased particle area appear large (Boushey et al., 2008, [192162](#)).

Nordling et al. (2008, [097998](#)) discussed above in the respiratory symptoms section, also reported that lower PEF at age 4 was associated with exposure to traffic-related PM₁₀ (-8.93 L/min [95% CI: -17.78 to -0.088]). Goss et al. (2004, [055624](#)), discussed in Section 7.3.1.1, found strong inverse relationships between FEV₁ and PM_{2.5} concentrations in both cross-sectional and longitudinal analyses.

In summary, recent studies have greatly expanded the evidence available for the 2004 PM AQCD. The earlier CHS studies followed young children for 2-4 yr. New analyses have been conducted that include longer follow-up periods of this cohort through 18 yr of age (considered early adulthood for lung development (Stanojevic et al., 2008, [157007](#)) and provide evidence that effects from exposure to PM_{2.5} persist into early adulthood. Longitudinal studies follow effects over time and are considered to provide the best evidence as opposed to studies across communities as in cross-sectional studies. The longitudinal cohort studies in the 2004 PM AQCD provided data for children in one location in one study and new longitudinal studies have been conducted in other locations.

Gauderman et al. (2004, [056569](#)) reported that PM_{2.5} exposure was associated with clinically and statistically significant deficits in FEV₁ attained at the age of 18 yr. Clinical significance was

defined as a FEV₁ below 80% of the predicted value, a criterion commonly used in clinical settings to identify persons at increased risk for adverse respiratory conditions. This clinical aspect is an important enhancement over the earlier results reported in the 2004 PM AQCD. Further, the association reported in this study that evaluated the 8-yr time period into early adulthood not only provided evidence for the persistence of the effect, but in addition the strength and robustness of the outcomes were more positive, larger, and more certain than previous CHS studies of shorter follow-up.

Supporting this result are new longitudinal cohort studies conducted by other researchers in other locations with different methods. Though these studies report results for PM₁₀, available data discussed above indicate that the majority of PM₁₀ is composed of PM_{2.5} in these areas. New studies provide positive results from Mexico City, Sweden, and a national cystic fibrosis cohort in the U.S. One study reported null results in a European cohort described as having potential misclassification and confounding concerns as well as lacking a homogenous population potentially rendering the outcome as non-informative. A natural experiment in Switzerland, where PM levels had decreased, reported that improvement in air quality may slow the annual rate of decline in lung function in adulthood, indicating positive consequences for public health. These natural experiments are considered especially supportive.

The relationship between long-term PM exposure and decreased lung function is thus seen during lung growth and lung development in school-age children into adulthood. At adult ages studies continue to show a relationship between decreased lung function and long-term PM exposure. Some newer studies attempting to study the relationship of long-term PM exposure from birth through preschool are reporting a relationship. Thus, the impact of long-term PM exposure is seen over the time period of lung function growth and development and the decline of lung function with aging.

Overall, effect estimates from these studies are negative (i.e., indicating decreasing lung function) and the pattern of effects are similar between the studies for FVC and FEV₁. Thus, the data are consistent and coherent across several designs, locations, and researchers. With cautions noted, the results relating carbon content of airway macrophages to decreased measures of pulmonary function add plausibility to the epidemiologic findings. Some new studies are using individual estimates of exposure to ambient PM to reduce the impact of exposure error (Downs et al., 2007, [092853](#); Jerrett et al., 2005, [087381](#)).

As was found in the 2004 PM AQCD, the studies report associations with PM_{2.5} and PM₁₀, while most did not evaluate PM_{10-2.5}. Associations have been reported with fine particle components, particularly EC and OC. Source apportionment methods generally have not been used in these long-term exposure studies. However, numerous studies have evaluated exposures to PM related to traffic or motor vehicle sources. For example, Meng et al. (2007, [093275](#)) investigated the associations between traffic and outdoor pollution levels and poorly controlled asthma among adults who were respondents to the California Health Interview Survey and found associations for traffic density and PM₁₀, but not PM_{2.5}.

7.3.2.2. Toxicological Studies

Urban Air

One new study evaluated the effects of chronic exposure to ambient levels of urban particles on lung development in the mouse (Mauad et al., 2008, [156743](#)). Both functional and anatomical indices of lung development were measured. Male and female BALB/c mice were continuously exposed to ambient or filtered Sao Paulo air for 8 mo. Concentrations in the “polluted chamber” versus “clean chamber” were 16.8 versus 2.9 µg/m³ PM_{2.5}. Thus PM levels were reduced by filtration but not entirely eliminated. Ambient concentrations of CO, NO₂ and SO₂ were 1.7 ppm, 89.4 µg/m³ and 8.1 µg/m³, respectively. Concentrations of gaseous pollutants were assumed to be similar to ambient levels in both chambers. After 4 mo, the animals were mated and the offspring were divided into 4 groups to provide for a prenatal exposure group, a postnatal exposure group, a pre and postnatal exposure group and a control group. Animals were sacrificed at 15 and 90 days of age for histological analysis of lungs. Pulmonary pressure-volume measurements were also conducted in the 90-day-old offspring. Statistically significant reductions in inspiratory and

expiratory volumes were found in the group receiving both prenatal and postnatal exposure, but not in the groups receiving only prenatal exposure or only postnatal exposure, compared with controls. These changes in pulmonary function correlated with anatomical changes which are discussed in Section 7.3.5.1.

Diesel Exhaust

Li et al. (2007, [155929](#)) exposed BALB/c and C56BL/6 mice to clean air or to low-dose DE (at a PM concentration of $100 \mu\text{g}/\text{m}^3$) for 7 h/day and 5 days/week for 1, 4 and 8 wk. Average gas concentrations were reported to be 3.5 ppm CO, 2.2 ppm NO₂, and less than 0.01 ppm SO₂. Airway hyperresponsiveness (AHR) was evaluated by whole-body plethysmography at Day 0 and after 1, 4 and 8 wk of exposure. Short-term exposure responses are discussed in Section 6.3.2.3, 6.3.3.3 and 6.3.4.2. The increased sensitivity of airways to methacholine (measured as Penh) seen in C57BL/6 but not BALB/c mice at 1 week was also seen at 4 wk but not at 8 wk. This study suggests that adaptation occurs during prolonged DE exposure. Influx of inflammatory cells, markers of oxidative stress and effects of antioxidant intervention were also evaluated (Sections 7.3.3.2 and 7.3.4.1). Although no attempt was made in this study to determine the effects of gaseous components of DE on the measured responses, concentrations of gases were very low suggesting that PM may have been responsible for the observed effects.

In many animal studies changes in ventilatory patterns are assessed using whole-body plethysmography, for which measurements are reported as enhanced pause (Penh). Some investigators report increased Penh as an indicator of AHR, but these are inconsistently correlated and many investigators consider Penh solely an indicator of altered ventilatory timing in the absence of other measurements to confirm AHR. Therefore use of the terms AHR or airway responsiveness has been limited to instances in which the terminology has been similarly applied by the study investigators.

Gottipolu et al. (2009, [190360](#)) exposed WKY and SH rats to filtered air or DE (particulate concentration 500 and 2,000 $\mu\text{g}/\text{m}^3$) for 4 h/day and 5 days/wk over a 4-wk period. Concentrations of gases were 1.3 and 4.8 ppm CO, NO <2.5 and 5.9 ppm NO, <0.25 and 1.2 ppm NO₂, 0.2 and 0.3 ppm SO₂ for low and high PM exposures, respectively. Particle size, measured as geometric median number and volume diameters, was 85 and 220 nm, respectively. No DE-related effects were found for breathing parameters measured by whole-body plethysmography. Other pulmonary effects are described in Sections 7.3.3.2 and 7.3.5.1.

Woodsmoke

One study evaluated the effects of subchronic woodsmoke exposure on pulmonary function in Brown Norway rats. Rats were exposed 3 h/day and 5 days/week for 4 and 12 wk to air or to concentrated wood smoke from the pinyon pine which is native to the U.S. Southwest (Tesfaigzi et al., 2002, [025575](#)). PM concentrations in the woodsmoke were 1,000 and 10,000 $\mu\text{g}/\text{m}^3$. The particles in this woodsmoke had a bimodal size distribution with the smaller size fraction (74%) characterized by a MMAD of 0.405 μm and the larger size fraction (26%) characterized by a MMAD of 6.7-11.7 μm . Many of these larger particles would not be inhalable by the rat since 8 μm MMAD particles are about 50% inhalable (Ménache et al., 1995, [006533](#)). Concentrations of gases were reported to be 15-106.4 ppm CO, 2.2-18.9 ppm NO, 2.4-19.7 ppm NO_x and 3.5-13.8 ppm total hydrocarbon in these exposures. Respiratory function measured by whole-body plethysmography demonstrated a statistically significant increase in total pulmonary resistance in rats exposed to 1000 $\mu\text{g}/\text{m}^3$ woodsmoke. Additional effects were found at 10,000 $\mu\text{g}/\text{m}^3$. Inflammatory and histopathological responses were also evaluated (Sections 7.3.3.2 and 7.3.5.1).

7.3.3. Pulmonary Inflammation

7.3.3.1. Epidemiologic Studies

One epidemiologic study examined the relationship of airway inflammation (eNO) and PM measures, other pollutants, and indicators of motor vehicle emissions in Windsor, Ontario (Dales et al., 2008, [156378](#)). This cohort of 2,402 school children estimated PM_{2.5} and PM_{10-2.5} for each child's residence at the postal code level with an evaluated statistical model (Wheeler et al., 2006, [103905](#)). Each 10 µg/m³ increase in 1-yr PM_{2.5} was associated with a 39% increase in eNO (p = 0.058). Associations between eNO and PM_{10-2.5} were positive but not statistically significant.

7.3.3.2. Toxicological Studies

CAPs Studies

A set of subchronic studies involved exposure of normal (C57BL1/6) mice, ApoE^{-/-} and the double-knockout ApoE^{-/-}/LDLR^{-/-} mice to Tuxedo, NY CAPs for 5-6 month (March, April or May through September 2003 (Lippmann et al., 2005, [087452](#)). The average PM_{2.5} exposure concentration was 110 µg/m³. Animals were fed a normal chow diet during the CAPs exposure period. No pulmonary inflammation was observed in response to CAPs exposure as measured by BALF cell counts and histology. The lack of a persistent pulmonary response may have been due to adaptation of the lung following repeated exposures. In fact, a parallel study examined CAPs-related gene expression in the double-knockout animals and found upregulation of numerous genes in lung tissue (Gunnison and Chen, 2005, [087956](#)). An in vitro study conducted simultaneously found daily variations in CAPs-mediated NF-κB activation in cultured human bronchial epithelial cells, suggesting that transcription factor-mediated gene upregulation could occur in response to CAPs (Maciejczyk and Chen, 2005, [087456](#)). It should be noted that significant cardiovascular effects were observed in these subchronic studies which are discussed in Section 7.2.1.2.

Araujo et al. (2008, [156222](#)) compared the relative impact of UF (0.01-0.18 µm) versus fine (0.01-2.5 µm) PM inhalation in ApoE^{-/-} mice following a 40 day exposure (5 h/day×3 days/wk for 75 total hours). Animals were fed a normal chow diet and exposed to PM from November 3 -December 12, 2005 in a mobile inhalation laboratory that was parked 300 m from the 110 Freeway in downtown Los Angeles. Particles were concentrated to ~440 µg/m³ for PM_{2.5} exposures and ~110 µg/m³ for the UF exposures, representing a roughly 15-fold increase in concentration from ambient levels; the number concentration of PM in the fine and UF chambers were roughly equivalent (4.56×10⁵ and 5.59×10⁵ particles/cm³, respectively). Over 50% of the UFPs were comprised of OC compared to only 25% for PM_{2.5}. No major increase in BALF inflammatory cells was found in response to PM. However UFP exposure resulted in significant cardiovascular and systemic effects (Section 7.2.1.2).

Diesel Exhaust

Gottipolu et al. (2009, [190360](#)) exposed WKY and SH rats to filtered air or DE for 4 wk as described in Section 7.3.2.2. Previous studies from this laboratory have shown enhanced effects of PM in SH compared with WKY rats. Although the main focus of this recent study was on DE-induced mitochondrial oxidative stress and hypertensive gene expression in the heart (Section 7.2.7.1), some pulmonary effects were also found. Subchronic exposure to DE resulted in a dose-dependent increase in BALF neutrophils in both rat strains although levels of measured cytokines were not altered. Histological analysis of lung tissue from rats exposed to the higher concentration of DE demonstrated accumulation of particle-laden macrophages as well as focal alveolar hyperplasia and inflammation. Effect on indices of injury are discussed in Section 7.3.5.1.

Ishihara and Kagawa (2003, [096404](#)) exposed Wistar rats to filtered air and DE containing 200, 1,000 and 3,000 µg/m³ PM for 16 h/day and 6 days/wk for 6, 12, 18 or 24 mo. The mass median particle diameter was reported to be between 0.3 and 0.5 µm. Concentrations of gases ranged from

2.93-35.67 ppm NO_x, 0.23-4.57 ppm SO₂, 1.8-21.9 ppm CO in the DE exposures. Statistically significant increases in total numbers of inflammatory cells and neutrophils in BALF were observed beginning at 6-12 mo of exposure to DE containing 1,000 and 3,000 µg/m³ PM. When rats were exposed to DE containing 1,000 µg/m³ PM, which was filtered to remove PM, the inflammatory cell response was significantly diminished. These results implicate the PM fraction of DE as a key determinant of the inflammation. The PM fraction was also found to mediate the increase in protein levels, the decrease in PGE₂ levels and alterations in mucus and surfactant components observed in BALF (Section 7.3.5.1).

Li et al. (2007, [155929](#)) exposed BALB/c and C56BL/6 mice to low dose DE as described in Section 7.3.2.2. for 1, 4 and 8 wk. Increases in numbers of BALF macrophages and total inflammatory cells were observed in BALB/c mice at 8 wk but not 4 wk of DE exposure. Persistent increases in numbers of BALF neutrophils and lymphocytes were observed in both strains at 4 and 8 wk of DE exposure. Corresponding increases in BALF cytokines differed between the two strains. These results should be interpreted with caution since comparisons were made with Day 0 controls rather than age-matched controls. No histopathological changes in the lungs were seen at any time point after DE exposure. This study demonstrated differences in pulmonary responses to low dose DE between two mouse strains. AHR, pulmonary inflammation, markers of oxidative stress and effects of antioxidant intervention were also evaluated (Sections 7.3.2.2 and 7.3.4.1). Although no attempt was made in this study to determine the effects of gaseous components of DE on the measured responses, concentrations of gases were very low suggesting that PM may have been responsible for the observed effects.

In a study by Hiramatsu et al. (2003, [155846](#)), BALB/c and C57BL/6 mice were exposed to DE (PM concentrations 100 and 3,000 µg/m³) for 1 or 3 mo. Concentrations of gases were reported to be 3.5-9.5 ppm CO, 2.2-14.8 ppm NO_x, and less than 0.01 ppm SO₂. Modest increases in BALF neutrophils and lymphocytes were observed in response to DE in both mouse strains at 1 and 3 mo. Histological analysis demonstrated diesel exposure particle-laden alveolar macrophages in alveoli and peribronchial tissues at both time points. Bronchus-associated lymphoid tissue developed after 3-month exposure to the higher concentration of DE in both mouse strains. Mac-1 positive cells (a marker of phagocytic activation of alveolar macrophages) were also increased in BALF of BALB/c mice exposed to the higher concentration of DE for 1 and 3 mo. Increased expression of several cytokines and decreased expression of iNOS mRNA was observed in DE-exposed mice at 1 and 3 mo. NF-κB activation was also noted following 1-month exposure to the lower concentration of DE. No attempt was made in this study to determine the responses to gaseous components of the DE.

In a study by Reed et al. (2004, [055625](#)), healthy Fisher 344 rats and A/J mice were exposed to DE (PM concentration = 30, 100, 300 and 1,000 µg/m³) by whole body inhalation for 6 h/day, 7 days/wk for either 1 week or 6 mo. Concentrations of gases were reported to be 2.0-45.3 ppm NO, 0.2-4.0 ppm NO₂, 1.5-29.8 ppm CO and 8-365 ppb SO₂. Short-term responses are discussed in Section 6.3.3.3 and 6.3.7.2, and sub-chronic systemic effects are presented in Section 7.2.4.1. Six months of exposure resulted in no measurable effects on pulmonary inflammation. However numerous black particles were observed within alveolar macrophages after 6 mo of exposure.

Seagrave et al. (2005, [088000](#)) evaluated pulmonary responses in male and female CDF (F-344)/CrIBR rats exposed 6 h/day for 6 mo to filtered air or DE at concentrations ranging from 30-1000 µg/m³ PM. Concentrations of gases were reported for the highest exposure as 45.3 ppm NO, 4.0 ppm NO₂, 29.8 ppm CO and 2.2 ppm total vapor hydrocarbon. No changes in BALF cells were noted. A small decrease in TNF-α was seen in BALF of female rats exposed to the highest concentration of DE for 6 mo. Pulmonary injury also was evaluated (Section 7.3.5.1). Thus changes in BALF markers were modest and gender-specific.

Woodsmoke

Seagrave et al. (2005, [088000](#)) also evaluated pulmonary responses in male and female CDF (F344)/CrIBR rats exposed 6 h/day for 6 mo to filtered air or hardwood smoke concentrations ranging from 30-1,000 µg/m³ PM. Concentrations of gases were reported for the highest exposure as 3.0 ppm CO and 3.1 ppm total vapor hydrocarbon. A small increase in BALF neutrophils was observed in male rats exposed to the lowest concentration of hardwood smoke. Female rats exhibited a decrease in BALF macrophage inflammatory protein-2 (MIP-2) at the highest concentration of hardwood smoke. Pulmonary injury also was evaluated (Section 7.3.5.1). In general, responses to

hardwood smoke were more remarkable than responses to DE seen in a parallel study. However these gender-specific responses were modest and difficult to interpret.

In a study by Reed et al. (2006, [156043](#)), Fisher 344 rats, SHR rats, A/J mice and C57BL/6 mice were exposed to clean air or hardwood smoke (PM concentrations 30, 100, 300 and 1,000 $\mu\text{g}/\text{m}^3$) by whole body inhalation for 6 h/day, 7 days/wk for either 1 week or 6 mo. Concentrations of gases ranged from 229.0-14887.6 mg/m^3 for CO, 54.9-139.3 $\mu\text{g}/\text{m}^3$ for ammonia, and 177.6- 3455.0 $\mu\text{g}/\text{m}^3$ nonmethane VOC in these exposures. Short-term responses are discussed in Section 6.3.7.2 and sub-chronic effects are presented in Section 7.2.4.1. Histological analysis of lung tissue showed minimal increases in alveolar macrophages. The effects of hardwood smoke on bacterial clearance are discussed below (Section 7.3.7.2).

Another study evaluated the effects of subchronic woodsmoke exposure in Brown Norway rats and is described in detail in Section 7.3.2.2 (Tesfaigzi et al., 2002, [025575](#)). Numbers of alveolar macrophages in BALF were significantly increased in rats exposed to 1,000 $\mu\text{g}/\text{m}^3$ woodsmoke for 12 wk, but no changes were seen in numbers of other inflammatory cells. A large percent of BALF macrophages contained carbonaceous material. Histological analysis of lung tissue showed minimal to mild inflammation in the epiglottis of the larynx in rats exposed to both concentrations of woodsmoke.

Ramos et al. (2009, [190116](#)) examined the effects of subchronic woodsmoke exposure on the development of emphysema in guinea pigs. Inflammation is thought to be involved in the pathogenesis of this form of COPD. Statistically significant increases in total numbers of BALF cells were observed in guinea pigs exposed to smoke for 1-7 mo, with numbers of macrophages increased at 1-4 mo and numbers of neutrophils increased at 4-7 mo. At 4 mo, alveolar mononuclear phagocytic and lymphocytic peribronchiolar inflammation were observed by histological analysis of lung tissue. This study is discussed in depth in Section 7.2.5.1.

Model Particles

Wallenborn et al. (2008, [191171](#)) examined the pulmonary, cardiac and systemic effects of subchronic exposure to particulate ZnSO_4 . WKY rats were exposed nose-only to 10, 30, or 100 $\mu\text{g}/\text{m}^3$ UFP of ZnSO_4 for 5 h/day and 3 day/wk over a 16-wk period. Particle size was reported to be 31-44 nm measured as number median diameter. No changes in pulmonary inflammation or injury were observed although cardiac effects were noted (Section 7.2.7.1). This study possibly demonstrates a direct effect of ZnSO_4 on extrapulmonary systems, as suggested by the lack of pulmonary effects.

7.3.4. Pulmonary Oxidative Response

7.3.4.1. Toxicological Studies

Urban Air

One new study evaluated the effects of subchronic exposure to ambient levels of urban particles on the development of emphysema in papain-treated mice (Lopes et al., 2009, [190430](#)). Since oxidative stress is thought to contribute to the development of emphysema, 8-isoprostane levels were measured in lung tissue from the four groups of mice used in this study. A statistically significant increase in 8-isoprostane, a marker of oxidative stress, was observed in lungs from mice treated with papain and exposed to ambient air compared with the other groups of mice. This study is described in greater depth in Section 7.3.5.1.

Diesel Exhaust

Li et al. (2007, [155929](#)) exposed mice to low dose DE for 1, 4 and 8 wk as described in Section 7.3.2.2. Markers of oxidative stress and effects of antioxidant intervention were evaluated in this model. While HO-1 mRNA and protein were increased in lung tissues of both mouse strains after 1 week of DE exposure (Section 6.3.4.2), at 8 wk of DE exposure, HO-1 protein levels remained high in C57BL/6 mice but returned to control values in BALB/c mice. This study demonstrates differences in pulmonary responses to low dose DE between two mouse strains. Furthermore, this study suggests that adaptation occurs in BALB/c mice during prolonged DE exposure since the increase in HO-1 protein seen in both strains at 1 week of exposure was only seen in C57BL/6 mice at 8 wk. AHR (Section 7.3.2.2) and pulmonary inflammation (Section 7.3.3.2) were also evaluated. Although no attempt was made in this study to determine the effects of gaseous components of DE on the measured responses, concentrations of gases were very low. This suggests that PM may have been responsible for the observed effects.

7.3.5. Pulmonary Injury

7.3.5.1. Toxicological Studies

Urban Air

One new study evaluated the effects of chronic exposure to ambient levels of urban particles on lung development in the mouse (Mauad et al., 2008, [156743](#)). Both functional and anatomical indices of lung development were measured in mice exposed prenatally and/or postnatally as described in Section 7.3.2.2. Animals were sacrificed at 15 and 90 days of age for histological analysis of lungs. Histological analysis demonstrated the presence of mild foci of macrophages containing black dots of carbon pigment in the prenatal and postnatal exposure group at 90 days. In addition, the alveolar spaces of 15-day old mice in the prenatal and postnatal exposure group were enlarged compared with controls. Morphometric analysis demonstrated statistically significant decreases in surface to volume ratio at 15 and 90 days in the prenatal and postnatal exposure group compared with controls. Since alveolarization is normally complete by 15 days of age, these results suggest incomplete alveolarization in the 15-day-old group and an enlargement of air spaces in the 90-day-old group. These anatomical changes correlated with decrements in pulmonary function which are discussed in Section 7.3.2.2.

Prolonged exposure to low levels of ambient air pollution beginning in early life has been linked to secretory changes in the nasal cavity of mice, specifically increased production of acidic mucosubstances (Pires-Neto et al., 2006, [096734](#)). Six-day-old Swiss mice were continuously chamber exposed to ambient or filtered São Paulo air for 5 mo. Concentrations in the “polluted chamber” versus “clean chamber” were (in $\mu\text{g}/\text{m}^3$) 59.52 versus 37.08 for NO_2 , 12.52 versus 0 for BC, and 46.49 versus 18.62 for $\text{PM}_{2.5}$. Thus, pollutant levels were reduced by filtration but not entirely eliminated. Compared to filtered air, exposure to ambient air resulted in increased total mucus and acidic mucus in the epithelium lining the nasal septum, but no statistically significant differences in other parameters (amount of neutral mucus, volume proportions of neutral mucus, total mucus, or nonsecretory epithelium, epithelial thickness, or ratio between neutral and acidic mucus). The physicochemical properties of mucus glycoproteins are critical to the protective function of the airway mucus layer. Acidified mucus is more viscous, and is associated with a decrease in mucociliary transport. Thus acidic mucosubstances may represent impaired defense mechanisms in the respiratory tract.

One new study evaluated the effects of subchronic exposure to ambient levels of urban particles on the development of emphysema in papain-treated mice (Lopes et al., 2009, [190430](#)). Emphysema is a form of COPD caused by the destruction of extracellular matrix in the alveolar region of the lung which results in airspace enlargement, airflow limitation and a reduction of the gas-exchange area of the lung. Inflammation, oxidative stress, protease imbalance and apoptosis are thought to contribute to the development of emphysema. In this study, male BALB/c mice were

continuously exposed to ambient or filtered Sao Paulo air for 2 mo. Concentrations of PM_{2.5} in the “polluted chamber” versus “clean chamber” were 33.86 ± 2.09 versus 2.68 ± 0.38 $\mu\text{g}/\text{m}^3$. Thus filtration reduced PM levels considerably. Ambient concentrations of CO and SO₂ were 1.7 ppm and 16.2 $\mu\text{g}/\text{m}^3$ respectively. No significant difference was observed in the concentrations of NO₂ in the “polluted chamber” versus “clean chamber” (60-80 $\mu\text{g}/\text{m}^3$). Half of the mice were pre-treated with papain by intranasal instillation in order to induce emphysema. Morphometric analysis of lung tissue demonstrated a statistically significant increase in mean linear intercept, a measure of airspace enlargement, in papain-treated mice compared with saline-treated controls exposed to filtered air. While exposure to ambient air failed to increase mean linear intercept values in saline-treated mice, mean linear intercept values were significantly increased in papain-treated mice exposed to ambient air compared with papain-treated mice exposed to filtered air. A similar pattern of responses was observed for the volume proportion of collagen and elastin fibers in alveolar tissue, which are markers of alveolar wall remodeling. Lung immunohistochemical analysis demonstrated an effect of papain, but not ambient air, on macrophage cell density and matrix metalloproteinase 12-positive cell density. No differences in caspase-3 positive cells, a marker of apoptosis, were observed between the four groups of mice. Oxidative stress was evaluated in this model as described in Section 7.3.4.1. Taken together, results of this study demonstrate that urban levels of PM, mainly from traffic sources, worsen protease-induced emphysema in an animal model.

Pulmonary vascular remodeling, measured by a decrease in the lumen to wall ratio, was observed in mice exposed to ambient São Paulo air for 4 mo (Lemos et al., 2006, [088594](#)). This study is described in greater detail in Section 7.2.1.2.

Kato and Kagawa (2003, [089563](#)) exposed Wistar rats to roadside air contaminated mainly with automobile emissions (55.7-65.2 ppb NO₂ and 63-65 $\mu\text{g}/\text{m}^3$ suspended PM [SPM]) and examined the effects on respiratory tissue after 24, 48, or 60 wk of exposure. The surface of the lungs was light gray in color after all durations of exposure, and BC particle deposits accumulated with prolonged exposure. These characteristics were not evident in filtered air-exposed control animals, although filtered air contained low levels of air pollutants (≤ 6.2 ppb NO₂ and 15 $\mu\text{g}/\text{m}^3$ SPM). The most common change observed using transmission electron microscopy was the presence of particle laden (anthracotic) alveolar macrophages, or anthracosis, in a wide range of pulmonary tissues, including the submucosa, tracheal- and bronchiole-associated lymph nodes, alveolar wall and space, pleura, and perivascular connective tissue. These changes were evident after 24 wk and increased with duration of exposure. Other changes included increases in the number of mucus granules in goblet cells, mast cell infiltration (but no degranulation) after 24 wk, increased lysosomes in ciliated cells, some altered morphology of Clara cells, and hypertrophy of the alveolar walls after 48 wk. No goblet cell proliferation was observed, but slight, variable acidification of mucus granules appeared after 24 and 48 wk and disappeared after 60 wk. Anthracotic macrophages were seen in contact with plasma cells and lymphocytes in the lymphoid tissue, suggesting immune cell interaction in the immediate vicinity of particles. Even after 60 wk, no lymph node anthracosis was observed in the filtered air group.

In a post-mortem study of lung tissues from 20 female lifelong residents of Mexico City, a high PM locale, histology demonstrated significantly greater amounts of fibrous tissue and muscle in the airway walls compared to subjects from Vancouver (Churg et al., 2003, [087899](#)), a city with relatively low PM levels. Electron microscopy showed carbonaceous aggregates of UFPs, which the authors conclude penetrate into and are retained in the walls of small airways. The study shows an association between retained particles and airway remodeling in the form of excess muscle and fibrotic walls. The subjects were deemed suitable for examination based on never-smoker status, no use of biomass fuels for cooking, no known occupational particle/dust exposure, death by cause other than respiratory disease, and extended residence in each locale (lifelong for Mexico City and >20 yr for Vancouver). However, subjects from the two locales were not matched with respect to ethnicity, sex (20 females from Mexico City versus 13 females and 7 males from Vancouver), or mean age at death (66 ± 9 versus 76 ± 11), and other possibly influential factors such as exercise or diet were not considered.

Diesel Exhaust

Gottipolu et al. (2009, [190360](#)) exposed WKY and SH rats to filtered air or DE as described in Section 7.3.2.2. Previous studies from this laboratory have shown enhanced effects of PM in SH

compared with WKY rats. Although the main focus of this recent study was on DE-induced mitochondrial oxidative stress and hypertensive gene expression in the heart (Section 7.2.7.1), some pulmonary effects were found. Inflammatory effects are described in Section 7.3.3.2. GGT activity in BALF was increased in both strains in response to the higher concentration of DE. No DE-related changes were observed in BALF protein or albumin. Histological analysis of lung tissue from rats exposed to the higher concentration of DE demonstrated accumulation of particle-laden macrophages as well as focal alveolar hyperplasia and inflammation. No effects on indices of pulmonary function were observed (Section 7.3.2.2.)

Ishihara and Kagawa (2003, [096404](#)) exposed rats to DE for up to 24 mo as described in Section 7.3.3.2. A statistically significant increase in BALF protein was observed at 12 mo of exposure to DE containing 1,000 $\mu\text{g}/\text{m}^3$ PM. This response was attenuated when the DE was filtered to remove PM. Pulmonary inflammation was noted and is described in Section 7.3.3.2.

Seagrave et al. (2005, [088000](#)) evaluated pulmonary responses in rats exposed to DE for up to 6 mo as described in Section 7.3.3.2. A small increase in LDH was seen in BALF of female rats exposed to the highest concentration of DE for 6 mo. Pulmonary inflammation was also evaluated (Section 7.3.3.2). The changes in BALF markers in this study were modest and gender-specific.

Gasoline Exhaust

Reed et al. (2008, [156903](#)) examined a variety of health effects following subchronic inhalation exposure to gasoline engine exhaust. Male and female CDF (F344)/CrIBR rats, SHR rats and male C57BL/6 mice were exposed for 6 h/day and 7 days/wk for a period of 3 days-6 mo. The dilutions for the gasoline exhaust were 1:10, 1:15 and 1:90; filtered PM was at the 1:10 dilution. PM mass ranged from 6.6 to 59.1 $\mu\text{g}/\text{m}^3$, with the corresponding number concentration between 2.6×10^4 and 5.0×10^5 particles/ cm^3 . Concentrations of gases ranged from 12.8-107.3 ppm CO, 2.0-17.9 ppm NO, 0.1-0.9 ppm NO₂, 0.09-0.62 ppm SO₂ and 0.38-3.37 ppm NH₃. Other effects are described in Sections 7.2.4.1 and 7.3.6.1. No pulmonary inflammation or histopathological changes were noted in the F344 rats and A/J mice, except for a time-dependent increase in the number of macrophages containing PM. However statistically significant increases of 47% and 29% in BALF LDH were observed in female and male F344 rats, respectively, after 6 mo of exposure to the highest concentration of engine exhaust. This response was absent when gasoline exhaust was filtered, implicating PM as a key determinant of this response. In addition, exposure to the highest concentration of gasoline exhaust resulted in statistically significant decreases in hydrogen peroxide and superoxide production in unstimulated and stimulated BALF macrophages. Hypermethylation of lung DNA was observed in male F344 rats following 6 mo of exposure to gasoline exhaust containing 30 $\mu\text{g}/\text{m}^3$ PM. This response was PM-dependent since it was absent in mice exposed to filtered gasoline exhaust. The significance of this epigenetic change in terms of respiratory health effects is not known. However, altered patterns of DNA methylation can affect gene expression and are sometimes associated with altered immune responses and/or the development of cancer.

Woodsmoke

Seagrave et al. (2005, [088000](#)) also evaluated pulmonary responses in rats exposed to hardwood smoke for 6 mo as described in Section 7.3.3.2. Increases in BALF LDH and protein were seen in male but not female rats. Female rats exhibited a decrease in BALF glutathione at the highest concentration of hardwood smoke. Decreases in BALF alkaline phosphatase were found in both males and females exposed to 1,000 $\mu\text{g}/\text{m}^3$ hardwood smoke. Male rats exposed to 100 and 300 $\mu\text{g}/\text{m}^3$ hardwood smoke exhibited a decrease in BALF β -glucuronidase activity. Pulmonary inflammation was also evaluated (Section 7.3.3.2). These changes in BALF markers in this study were modest and gender-specific.

Another study evaluated the effects of subchronic woodsmoke exposure in Brown Norway rats as described in Section 7.3.2.2. (Tesfaigzi et al., 2002, [025575](#)). Exposure to 1,000 $\mu\text{g}/\text{m}^3$ woodsmoke for 12 wk resulted in a statistically significant increase in Alcian Blue- (AB) and Periodic Acid Schiff- (PAS) positive airway epithelial cells compared to controls, indicating an increase in mucous secretory cells containing neutral and acid mucus, respectively. More significant histopathological responses were found following exposure to 10,000 $\mu\text{g}/\text{m}^3$ of DE. Pulmonary

function and inflammation were evaluated also but are not discussed here due to the extremely high exposure level (Sections 7.3.2.2. and 7.3.3.2).

Ramos et al. (2009, [190116](#)) examined the effects of subchronic woodsmoke exposure on the development of emphysema in guinea pigs. In particular, the involvement of macrophages and macrophage-derived MMP in woodsmoke-related responses was investigated. Guinea pigs were exposed to ambient air or to whole smoke from pine wood for 3 h/day and 5 days/wk over a 7-month period. PM₁₀ and PM_{2.5} concentrations in the exposure chambers were reported to be 502 ± 34 and 363 ± 23 µg/m³, respectively, while the concentration of CO was less than 80 ppm. COHb levels were reported to be 6% in controls and 15-20% in smoke-exposed guinea pigs. Statistically significant decreases in body weight were observed in guinea pigs exposed to smoke for 4 or more months compared with controls. Statistically significant increases in total numbers of BALF cells were observed in guinea pigs exposed to smoke for 1-7 mo, with numbers of macrophages increased at 1-4 month and numbers of neutrophils increased at 4-7 mo. At 4 mo, alveolar mononuclear phagocytic and lymphocytic peribronchiolar inflammation, as well as bronchiolar epithelial and smooth muscle hyperplasia, were observed by histological analysis of lung tissue. Emphysematous lesions, smooth muscle hyperplasia and pulmonary arterial hypertension were noted at 7 mo. Morphometric analysis of lung tissue demonstrated statistically significant increases in mean linear intercept values, a measure of airspace enlargement, in guinea pigs at 6 and 7 mo of exposure. Statistically significant increases in elastolytic activity was observed in BALF macrophages and lung tissue homogenates at 1-7 mo of exposure. Lung collagenolytic activity was also increased at 4-7 mo of exposure and corresponded in time with the presence of active forms of MMP-2 and MMP-9 in lung tissue homogenates and BALF. Furthermore, MMP-1 and MMP-9 immunoreactivity was detected in macrophages, epithelial and interstitial cells in smoke-exposed animals at 7 mo. Increased levels of MMP-2 and MMP-9 mRNA were also found in smoke-exposed guinea pigs after 3-7 mo. Apoptosis was found in BALF macrophages (TUNEL assay) from guinea pigs exposed to smoke for 3-7 mo and in alveolar epithelial cells (caspase-3 immunoreactivity) after 7 mo. Taken together, these results provide evidence that subchronic exposure to woodsmoke leads to the development of emphysematous lesions accompanied by the accumulation of alveolar macrophages, increased levels and activation of MMPs, connective tissue remodeling and apoptosis. However, the high levels of CO and COHb reported in this study make it difficult to conclude that woodsmoke PM alone is responsible for these dramatic effects.

7.3.6. Allergic Responses

7.3.6.1. Epidemiologic Studies

A number of epidemiologic studies have found associations between PM and allergic (or atopic) indicators. Allergy is a major driver of asthma, which has been associated with PM in studies discussed in previous sections. In a study by Annesi-Maesano (2007, [093180](#)) (described in Section 7.3.1.1) atopic asthma was related to PM_{2.5} (OR 1.43 [95% CI: 1.07-1.91]) and positive skin prick test to common allergens was also increased with higher PM levels. This report is consistent with the results from an earlier study (Penard-Morand et al., 2005, [087951](#)) in the same sample of children that associated allergic rhinitis and atopic dermatitis with PM₁₀. Also, Morgenstern et al. (2008, [156782](#)) found statistically significant effects for asthmatic bronchitis, hay fever, and allergic sensitization to pollen in a cohort of children in Germany examining modeled PM_{2.5} data at birth addresses. Distance to a main road had a dose-response relationship with sensitization to outdoor allergens. Nordling et al. (2008, [097998](#)) (discussed above in Section 7.3.2.1) reported a positive association of PM₁₀ exposure during the first year of life with allergenic sensitization (IgE antibodies) to inhaled allergens, especially pollen. In a study by Brauer et al. (2007, [090691](#)) (discussed above in Section 7.3.1.1) an interquartile range increase in PM_{2.5} was associated with an increased risk of sensitization to food allergens (OR 1.75 [95% CI 1.23-2.47]). A significant association was found for sensitization to any allergen, but none was found for sensitization to specific indoor or outdoor aeroallergens or atopic dermatitis (eczema). In a study by Janssen et al. (2003, [133555](#)), PM_{2.5} was associated with allergic indicators such as hay fever (ever), skin prick test reactivity to outdoor allergens, current itchy rash, and conjunctivitis in Dutch children. These same outcomes were also associated with proximity of the school to truck traffic but not car traffic,

suggesting a role for diesel-related pollution. Consistent with the aforementioned Dutch study by Brauer et al. (2007, [090691](#)), PM_{2.5} was not associated with eczema.

Mortimer et al. (2008, [187280](#)) examined the association between prenatal and early-life exposures to air pollutants with allergic sensitization in a cohort of 170 children with asthma, ages 6-11 yr, living in central California. Sensitization to at least one allergen was associated with higher levels of PM₁₀ and CO during the entire pregnancy and 2nd trimester and higher PM₁₀ during the first 2 yr of life. Sensitization to at least one indoor allergen was associated with higher exposures to PM₁₀ and CO in during the entire pregnancy and during the 2nd trimester. However, no significant associations remained for PM₁₀ after adjustment for copollutants, effect modifiers, or potential cofounders in addition to year of birth. The authors advise that the large number of comparisons may be of concern and this study should be viewed as an exploratory, hypothesis-generating undertaking. In examining the National Health Interview Survey for the years 1997-2006, Bhattacharyya et al. (2009, [180154](#)) found relationships between air quality and the prevalence of hay fever and sinusitis. However, the air quality data were not clearly defined and as such caution is required in interpretation of these results. In contrast, Bayer-Oglesby et al. (2005, [086245](#)) found no significant association between declining levels of PM₁₀ and hay fever in Switzerland. In a study by Oftedal et al. (2007, [191948](#)) conducted in Oslo, Norway, early-life exposure to PM₁₀ or PM_{2.5} was generally not associated with sensitization to allergens in 9- to 10-yr-old children; lifetime exposures to PM₁₀ and PM_{2.5} were associated with dust mite allergy, but the association was diminished by adjustment for socioeconomic factors. In Norway, wood burning in the wintertime is thought to account for about half of the PM_{2.5} levels. Although associations between PM and reactivity to specific allergens have been reported in long-term studies, there is a consistent lack of correlation between PM and total IgE levels, indicating a selective enhancement of allergic responses.

7.3.6.2. Toxicological Studies

Diesel Exhaust

Exposure to relatively low doses of DE has been shown to exacerbate asthmatic responses in ovalbumin (OVA) sensitized and challenged BALB/c mice (Matsumoto et al., 2006, [098017](#)). Mice were intraperitoneally sensitized and intranasally challenged 1 day prior to inhalation exposure to DE (PM concentration 100 µg/m³; CO, 3.5 ppm; NO₂, 2.2 ppm; SO₂ <0.01 ppm) for 1 day or 1, 4, or 8 wk (7/h/day, 5 days/wk, endpoints 12 h post DE exposure). Results from the 1- and 4-wk exposures are described in Section 6.3.6.3. It should be noted that control mice were left in a clean room as opposed to undergoing chamber exposure to filtered air. The significant increases in AHR and airway sensitivity observed following shorter exposure periods did not persist at 8 wk. BALF cytokines were altered by DE exposure with only RANTES significantly elevated after 8 wk. DE had no effect on OVA challenge-induced peribronchial inflammatory or mucin positive cells. These results suggest that adaptive processes may have occurred during prolonged exposure to DE.

Gasoline Exhaust

In a study by Reed et al. (2008, [156903](#)), BALB/c mice were exposed to whole gasoline exhaust diluted 1:10 (H), 1:15 (M), or 1:90 (L), filtered exhaust at the 1:10 (HF), or clean air for 6 h/day (atmospheric characterization described in Section 6.3.6.3). GEE exposure from conception through 4 wk of age induced slight but non-significant increases in OVA-specific IgG1 in offspring but had no significant effect on airway reactivity, BALF cytokine or cell concentrations, although there were non-significant increases in lung neutrophils and eosinophils. Significant increases in total serum IgE were observed, but this effect persisted after filtration of particles and was thus attributed to gas phase components.

Woodsmoke

In a study by Tesfaigzi et al. (2005, [156116](#)), Brown Norway rats were sensitized and challenged with OVA. Rats were exposed for 70 days to filtered air or to 1,000 $\mu\text{g}/\text{m}^3$ hardwood smoke. Particles were characterized by a MMAD of 0.36 μm . Concentrations of gases were reported to be 13.0 ppm CO and 3.1 ppm total vapor hydrocarbon with negligible NO_x . Respiratory function was measured in anesthetized animals by whole-body plethysmography and demonstrated a significant increase in functional residual capacity as well as a significant increase in dynamic lung compliance in hardwood smoke-exposed animals compared to controls. No change in total pulmonary resistance or airway responsiveness to methacholine was observed. BALF inflammatory cells were not increased, although histological analysis demonstrated focal inflammation including granulomatous lesion and eosinophilic infiltrations in hardwood smoke-exposed rats. Alterations of several cytokines in BALF and plasma were noted. Changes in airway epithelial mucus cells and intraepithelial stored mucosubstances were modest and did not achieve statistical significance. Results of this study demonstrate that subchronic exposure to hardwood smoke had minimal effects on pulmonary responses in a rat model of allergen sensitization and challenge.

7.3.7. Host Defense

7.3.7.1. Epidemiologic Studies

Epidemiologic studies of respiratory infections indicate an association with PM. This is more evident when considering short-term exposures (Chapter 6), but studies of long-term exposures have observed associations with general respiratory symptoms often caused by infection, such as bronchitis. In a birth cohort study of approximately 4,000 Dutch children, Brauer et al. (2007, [090691](#)) (described in Section 7.3.1.1) found significant positive associations for $\text{PM}_{2.5}$ with ear/nose/throat infections and doctor-diagnosed flu/serious cold in the first 4 yr of life. These results are consistent with an earlier study by Brauer et al. (2006, [090757](#)), which found that an increase of 10 $\mu\text{g}/\text{m}^3$ $\text{PM}_{2.5}$ was associated with increased risk for ear infections in the Netherlands [OR 1.50 (95% CI, 1.00-2.22)]. A Swiss study by Bayer-Oglesby et al. (2005, [086245](#)), discussed in Section 7.3.1.1 above, demonstrated that declining levels of PM_{10} were associated with declining prevalence of common cold and conjunctivitis. Because traffic-related pollutants such as UFPs are high near major roadways and then decay exponentially over a short distance, Williams, et al. (2009, [191945](#)) assessed exposure according to residential proximity to major roads in a Seattle area study of postmenopausal women. Proximity to major roads was associated with a 21% decrease in natural killer cell function, which is an important defense against viral infection and tumors. This finding was limited to women who reported exercising near traffic; other markers of inflammation and lymphocyte proliferation did not consistently differ according to proximity to major roads. In the Puget Sound region of Washington, Karr et al. (2009, [191946](#)) reported that there may be a modest increased risk of bronchiolitis related to $\text{PM}_{2.5}$ exposure for infants born just before the peak respiratory syncytial virus (RSV) season. Risk estimates were stronger when restricted to cases specifically attributed to RSV and for infants residing closer to highways. Emerging evidence suggests that respiratory infections, particularly infection by viruses such as RSV, can cause asthma or trigger asthma attacks.

7.3.7.2. Toxicological Studies

Diesel Exhaust

DE may affect systemic immunity. The proliferative response of A/J mouse spleen cells following stimulation with T cell mitogens was suppressed by 6 mo of daily exposure to DE at concentrations at or above 300 $\mu\text{g}/\text{m}^3$ PM (Burchiel et al., 2004, [055557](#)). B cell proliferation was increased at 300 $\mu\text{g}/\text{m}^3$ but unaffected at higher concentrations (up to 1,000 $\mu\text{g}/\text{m}^3$). Concentrations of gases and were reported in the parallel study by Reed et al. (2004, [055625](#)), described in

Section 7.3.3.2. The Reed study reported a decrease in spleen weight in male mice (27% reduction in the 300 $\mu\text{g}/\text{m}^3$ exposure group). The immunosuppressive effects of DE were not due to PAHs or benzo(a)pyrene (BaP)-quinones (BPQs) since there were little, if any, of these compounds present in the chamber atmosphere. It should be noted that sentinel animals were negative for mouse parvovirus at the start of the study, but seroconverted by the end of the study, indicating possible infection. Parvovirus can interfere with the modulation of lymphocyte mitogenic responses (Baker, 1998, [156245](#)). A 6-month exposure (6h/day, 7d/wk) to 30, 100, 300 or 1,000 $\mu\text{g}/\text{m}^3$ of PM in DE did not significantly affect bacterial clearance in C57BL/6 mice infected with *Pseudomonas aeruginosa*, although all levels reduced bacterial clearance when the exposure only lasted a week (Harrod et al., 2005, [088144](#)). Characterization of the exposure atmosphere was given by Reed et al. (2004, [055625](#)) (Section 7.3.3.2.).

Gasoline Exhaust

In a study by Reed et al. (2008, [156903](#)) (described in Section 6.3.7.2) long-term exposure to fresh gasoline exhaust (6h/day, 7d/wk for 6 mo) did not affect clearance of *P. aeruginosa* from the lungs of C57BL/6 mice.

Hardwood Smoke

One study demonstrated immunosuppressive effects of hardwood smoke (Burchiel et al., 2005, [088090](#)). Exposure to hardwood smoke increased proliferation of T cells from A/J mice exposed daily to 100 $\mu\text{g}/\text{m}^3$ PM for 6 mo, but produced a concentration-dependent suppression of proliferation at PM concentrations $>300 \mu\text{g}/\text{m}^3$. No effects on B cell proliferation were observed. Concentrations of NO and NO₂ were not detectable or <40 ppb for all exposure levels. CO was reported to be 2, 4, and 13 ppm for the 100, 300 and 1,000 $\mu\text{g}/\text{m}^3$ PM concentrations, respectively. Exposure atmospheres contained significant levels of naphthalene and methylated naphthalenes, fluorene, phenanthrene, and anthracene, as well as low concentrations of several metals (K, Ca, and Fe) (Burchiel et al., 2005, [088090](#)). It should be noted that serologic analysis of study sentinel animals indicated infection with parvovirus, which can interfere with the modulation of lymphocyte mitogenic responses (Baker, 1998, [156245](#)). In another study by Reed et al. (2006, [156043](#)) C57BL/6 mice were exposed to 30-1,000 $\mu\text{g}/\text{m}^3$ hardwood smoke by whole-body inhalation for 6 mo prior to instillation of *P. aeruginosa*. Exposure characterizations are described in Section 7.3.3.2. Although there was a trend toward increased clearance with increasing exposure concentrations, there was no statistically significant effect of hardwood smoke exposure on bacterial clearance.

7.3.8. Respiratory Mortality

Two large U.S. cohort studies examined the effect of long-term exposure to PM_{2.5} on respiratory mortality with mixed results. In the ACS study, Pope et al. (2004, [055880](#)) reported positive associations with deaths from specific cardiovascular diseases, but no PM_{2.5} associations were found with respiratory mortality. A follow-up to the Harvard Six Cities study (Laden et al., 2006, [087605](#)) used updated air pollution and mortality data and found positive associations between long-term exposure to PM_{2.5} and mortality. Of special note is a statistically significant reduction in mortality risk reported with reduced long-term fine particle concentrations observed for deaths due to cardiovascular and respiratory causes, but not for lung cancer deaths. There is some evidence for an association between PM_{2.5} and respiratory mortality among post-neonatal infants (ages 1 month-1 year) (Section 7.4.1). In summary, when deaths due to respiratory causes are separated from all-cause (nonaccidental) and cardiopulmonary deaths, there is limited and inconsistent evidence for an effect of PM_{2.5} on respiratory mortality, with one large cohort study finding a reduction in deaths due to respiratory causes associated with reduced PM_{2.5} concentrations, and another large cohort study finding no PM_{2.5} associations with respiratory mortality.

7.3.9. Summary and Causal Determinations

7.3.9.1. PM_{2.5}

The epidemiologic studies reviewed in the 2004 PM AQCD suggested relationships between long-term PM₁₀ and PM_{2.5} (or PM_{2.1}) exposures and increased incidence of respiratory symptoms and disease. One of these studies indicated associations with bronchitis in the 24-city cohort (Dockery et al., 1996, [046219](#)). They also suggested relationships between long-term exposure to PM_{2.5} and pulmonary function decrements in the CHS (Gauderman et al., 2000, [012531](#); Gauderman et al., 2002, [026013](#)). These findings added to the database of the earlier 22-city study of PM_{2.1} (Raizenne et al., 1996, [077268](#)) that found an association between exposure to ambient particle strong acidity and impairment of lung function in children. No long-term exposure toxicological studies were reported in the 2004 PM AQCD.

Recent studies have greatly expanded the evidence available since the 2004 PM AQCD. New analyses have been conducted that include longer follow-up periods of the CHS cohort through 18 yr of age and provide evidence that effects from exposure to PM_{2.5} persist into early adulthood. Gauderman et al. (2004, [056569](#)) reported that PM_{2.5} exposure was associated with clinically and statistically significant deficits in FEV₁ attained at the age of 18 yr. In addition, the strength and robustness of the outcomes were larger in magnitude, and more precise than previous CHS studies with shorter follow-up periods. Supporting this result are new longitudinal cohort studies conducted by other researchers in other locations with different methods. These studies report results for PM₁₀ that is dominated by PM_{2.5}. New studies provide positive associations from Mexico City, Sweden, and a national cystic fibrosis cohort in the U.S. A natural experiment in Switzerland, where PM levels had decreased, reported that improvement in air quality may slow the annual rate of decline in lung function in adulthood, indicating positive consequences for public health. Thus, the data are consistent and coherent across several study designs, locations and researchers. As was found in the 2004 PM AQCD, the studies report associations with PM_{2.5} and PM₁₀, while most did not evaluate PM_{10-2.5}. Associations have been reported with fine particle components, particularly EC and OC. Source apportionment methods generally have not been used in these long-term exposure studies.

Coherence and biological plausibility for the observed associations with lung function decrements is provided by toxicological studies (Section 7.3.2.2). A recent study demonstrated that pre- and postnatal exposure to ambient levels of urban particles affected mouse lung development, as measured by anatomical and functional indices (Mauad et al., 2008, [156743](#)). Another study suggested that the developing lung may be susceptible to PM since acute exposure to UF iron-soot decreased cell proliferation in the proximal alveolar region of neonatal rats (Pinkerton et al., 2004, [087465](#)) (Section 6.3.5.3). Impaired lung development is a viable mechanism by which PM may reduce lung function growth in children. Other animal toxicological studies have demonstrated alterations in pulmonary function following exposure to DE and wood smoke (Section 7.3.2.2).

An expanded body of epidemiologic evidence for the effect of PM_{2.5} on respiratory symptoms and asthma incidence now includes prospective cohort studies conducted by different researchers in different locations, both within and outside the U.S. with different methods. The CHS provides evidence in a prospective longitudinal cohort study that relates PM_{2.5} and bronchitic symptoms and reports larger associations for within-community effects that are less subject to confounding than between-community effects (McConnell et al., 2003, [049490](#)). Several new studies report similar findings with long-term exposure to PM₁₀ in areas where fine particles predominate. In England, an association was seen with an increased prevalence of cough without a cold. Further evidence includes a reduction of respiratory symptoms corresponding to decreasing PM levels in natural experiments in cohorts of Swiss school children (Bayer-Oglesby et al., 2005, [086245](#)) and adults (Schindler et al., 2009, [191950](#)).

New studies examined the relationship between long-term PM_{2.5} exposure and asthma incidence. PM_{2.5} had the strongest modifying effect on the association between lung function with asthma in an analysis of the CHS (Islam et al., 2007, [090697](#)). The loss of protection by high lung function against new onset asthma in high PM_{2.5} communities was observed for all the lung function measures. In the Netherlands, an association with doctor-diagnosed asthma was found in a birth cohort examining the first 4 yr of life (Brauer et al., 2007, [090691](#)). Further, findings from an adult cohort suggest that traffic-related PM₁₀ contributes to asthma development and that reductions in PM decrease asthma risk (Kunzli et al., 2009, [191949](#)).

A large proportion of asthma is driven by allergy, and the majority of recent epidemiologic studies examining allergic (or atopic) indicators found positive associations with PM_{2.5} or PM₁₀ (Section 7.3.6.1). Limited evidence for PM-mediated allergic responses is provided by toxicological studies of DE and woodsmoke, while effects of gasoline exhaust were attributed to gaseous components (Section 7.3.6.2).

Long-term PM_{2.5} exposure is associated with pulmonary inflammation and oxidative responses. An epidemiologic study found a relationship between PM_{2.5} and increased inflammatory marker eNO among school children (Dales et al., 2008, [156378](#)). Toxicological studies of pulmonary inflammation have demonstrated mixed results, with subchronic DE exposures generating increases and CAPs and wood smoke inducing little or no response (Section 7.3.3.2). The pulmonary inflammation observed with DE was attributable to the particle fraction. Toxicological studies also reported evidence of oxidative responses (Section 7.3.4.1). Adaptation to prolonged DE was observed for some oxidative responses in addition to some allergic and pulmonary function responses (Section 7.3.2.2 and 7.3.6.2).

Additional support for the relationship between long-term PM_{2.5} exposures and respiratory outcomes is provided by pulmonary injury responses observed in toxicological studies (Section 7.3.5.1). Markers of pulmonary injury were increased in rats exposed to DE and gasoline exhaust; and these changes were attributable to PM. Further, lung DNA methylation was observed in the gasoline exhaust study. Histopathological changes have also been reported following exposure to heavily-trafficked urban air and woodsmoke. Findings include nasal and airway mucous cell hyperplasia accompanied by alterations in mucus production which can lead to a loss of mucus-mediated protective functions; exacerbation of protease-induced emphysema; and mast cell infiltration and hypertrophy of alveolar walls. These results provide biological plausibility for adverse respiratory outcomes following long-term PM exposure.

Limited information is available on host defense responses (Section 7.3.7) and respiratory mortality (Section 7.3.8) resulting from PM_{2.5} exposure. Several recent epidemiologic studies suggest a relationship between long-term exposure to PM_{2.5} or PM₁₀ and infection in children and infants (Section 7.3.7.1). A few toxicological studies suggest that DE exposure affects systemic immunity, and although impaired bacterial clearance is associated with short-term exposures to DE, neither DE or gasoline exhaust seems to have this effect after longer exposures (Section 7.3.7.2).

In summary, the strongest evidence for a relationship between long-term exposure to PM_{2.5} and respiratory morbidity is provided by epidemiologic studies demonstrating associations with decrements in lung function growth in children and with respiratory symptoms and disease incidence in adults. Mean PM_{2.5} concentrations in these study locations ranged from 13.8 to 30 µg/m³ during the study periods. These studies provide evidence for associations in areas where PM is predominantly fine particles. A major challenge to interpreting the results of these studies is that the PM size fractions and concentrations of other air pollutants are often correlated; however, the consistency of findings across different locations supports an independent effect of PM_{2.5}. Recent toxicological studies provide support for the associations with PM_{2.5} and decreases in lung function growth in children. Pre- and postnatal exposure to ambient levels of urban particles was found to affect mouse lung development, which provides biological plausibility for the epidemiologic findings. Recent subchronic and chronic toxicological studies also demonstrate altered pulmonary function, mild inflammation, oxidative responses, histopathological changes including mucus cell hyperplasia and enhanced allergic responses in response to CAPs, DE, urban air and woodsmoke and provide further coherence and biological plausibility. Exacerbation of emphysematous lesions was noted in one study involving exposure to urban air in a heavily-trafficked area. **Collectively, the evidence is sufficient to conclude that the relationship between long-term PM_{2.5} exposure and respiratory effects is likely to be causal.**

7.3.9.2. PM_{10-2.5}

The 2004 PM AQCD did not report long-term exposure studies for PM_{10-2.5}. The only recent study to evaluate long-term exposure to PM_{10-2.5} found positive, but not statistically significant associations with eNO (Dales et al., 2008, [156378](#)). The evidence is **inadequate to determine if a causal relationship exists between long-term PM_{10-2.5} exposures and respiratory effects.**

7.3.9.3. UFPs

The 2004 PM AQCD did not report long-term exposure studies for UFPs. The current evidence for long-term UFP effects is limited to toxicological studies. Generally, subchronic exposure to DE induced pulmonary inflammation, which was in contrast to UF CAPs exposure (Section 7.3.3.2) It appeared that the PM fraction was responsible for the inflammatory response with DE exposure. Long-term exposure to DE also resulted in oxidative and allergic responses, although lung injury was not remarkable (Sections 7.3.4.1 and 7.3.6.2). The evidence is **inadequate to determine if a causal relationship exists between long-term UFP exposures and respiratory effects.**

7.4. Reproductive, Developmental, Prenatal and Neonatal Outcomes

7.4.1. Epidemiologic Studies

This section evaluates and summarizes the scientific evidence on PM and developmental and pregnancy outcomes and infant mortality. Infants and fetal development processes may be particularly vulnerable to PM exposure, and although the physical mechanisms are not fully understood, several hypotheses have been proposed involving direct effects on fetal health, altered placenta function, or indirect effects on the mother's health (Bracken et al., 2003, [156288](#); Clifton et al., 2001, [156360](#); Maisonet et al., 2004, [156725](#); Schatz et al., 1990, [156073](#); Sram et al., 2005, [087442](#)). Study of these outcomes can be difficult given the need for detailed data and potential residential movement of mothers during pregnancy. Two recent articles have reviewed methodological issues relating to the study of outdoor air pollution and adverse birth outcomes (Ritz and Wilhelm, 2008, [156914](#); Slama et al., 2008, [156985](#)). Some of the key challenges to interpretation of these study results include the difficulty in assessing exposure as most studies use existing monitoring networks to estimate individual exposure to ambient PM; the inability to control for potential confounders such as other risk factors that affect birth outcomes (e.g., smoking); evaluating the exposure window (e.g., trimester) of importance; and limited evidence on the physiological mechanism of these effects (Ritz and Wilhelm, 2008, [156914](#); Slama et al., 2008, [156985](#)). Another uncertainty is whether PM effects differ by the child's sex. A review of preterm birth and low birth weight studies found limited indication that effects may differ by gender, however sample size was limited (Ghosh et al., 2007, [091233](#)).

Previous summaries of the association between PM concentrations and pregnancy outcomes and infant mortality were presented in previous PM AQCDs. The 1996 PM AQCD concluded that although few studies had been conducted on the link between PM and infant mortality, the research "suggested an association," particularly for post-neonates (U.S. EPA, 1996, [079380](#)). In the 2004 PM AQCD, additional evidence was available on PM's effect on fetal and early postnatal development and mortality (U.S. EPA, 2004, [056905](#)) and although some studies indicated a relationship between PM and pregnancy outcomes, others did not. Studies identifying associations found that exposure to PM₁₀ early during pregnancy (first month of pregnancy) or late in the pregnancy (6 wk prior to birth) were linked with higher risk of preterm birth, including models adjusted for other pollutants, and that PM_{2.5} during the first month of pregnancy was associated with intrauterine growth restriction. However, other work did not identify relationships between PM₁₀ exposure and low birth weight. The state of the science at that time, as indicated in the 2004 PM AQCD, was that the research provided mixed results based on studies from multiple countries, and that additional research was required to better understand the impact of PM on pregnancy outcomes and infant mortality. Considering evidence from recent studies discussed below, along with previous AQCD conclusions, epidemiologic studies consistently report associations between PM₁₀ and PM_{2.5} exposure and low birth weight and infant mortality, especially during the post-neonatal period. Animal toxicological evidence supports these associations with PM_{2.5}, but provides little mechanistic information or biological plausibility. Information on the ambient concentrations of PM₁₀ and PM_{2.5} in these study locations can be found in Table 7-5.

7.4.1.1. Low Birth Weight

A large number of studies have investigated exposure to ambient PM and low birth weight at term, including a U.S. national study, as well as two studies in the northeast U.S., and four in California. Parker and Woodruff (2008, [156846](#)) linked U.S. birth records for singletons delivered at 40-wk gestation in 2001-2003 during the months of March, June, September and December to quarterly estimates of PM exposure by county of residence and month of birth. They found an association between PM_{10-2.5} and birthweight (-13 g [95% CI: -18.3 to -7.6]) per 10 µg/m³ increase), but no such association for PM_{2.5}.

Maisonet et al. (2001, [016624](#)) analyzed 89,557 births (1994-96) in six northeastern cities (Boston and Springfield MA; Hartford CT; Philadelphia and Pittsburgh PA; and Washington DC). Each city had three PM₁₀ monitors measuring every sixth day. Results from multiple monitors were averaged in each city. Exposure was determined for each trimester of pregnancy and categorized by quartiles (<25, 25-30, 31-35, 36-43 µg/m³) and 95th percentile (>43µg/m³). There was no increased risk for low birth weight at term associated with PM₁₀ exposure during any trimester of pregnancy. When birth weight was considered as a continuous outcome, exposure to PM₁₀ was not associated with a reduction in mean birth weight.

In contrast, Bell et al. (2007, [093256](#)) reported positive associations for both PM_{2.5} and PM₁₀ with birth weight in a study of births (n = 358,504) in Connecticut and Massachusetts (1999-2002). Birth data indicated county, not street address or ZIP code, so women were assigned exposure based on county residence at delivery. The difference in birth weight per 10 µg/m³ associated with PM_{2.5} was -66.8 (95% CI: -77.7 to -55.9) g. For PM₁₀ it was -11.1 (95% CI: -15.0 to -7.2) g. The increased risk for low birth weight was OR = 1.054 (95% CI: 1.022-1.087) for PM_{2.5} and OR = 1.027 (95% CI: 0.991-1.064) for PM₁₀, based on average exposure during pregnancy. Reductions in birth weight were also associated with third trimester exposure to PM₁₀ and second and third trimester exposure to PM_{2.5}. Comparing this study to Maisonet et al. (2001, [016624](#)), a larger sample size was able to detect a small increase in risk. In addition, birth weight was reduced more by exposure to PM_{2.5} than by exposure to PM₁₀. Measured PM_{2.5} concentrations were not available in the earlier study.

The Children's Health Study is a population based cohort of children living in 12 southern California communities, selected on the basis of differing levels of air pollution (Salam et al., 2005, [087885](#)), as previously discussed in Section 7.3. The children in grades 4, 7 and 10 were recruited through schools. A subset of this cohort (n = 6,259) were born in California from 1975-1987. Of these, birth certificates were located for 4,842, including 3,901 infants born at term and 72 cases of low birth weight at term. Using the mother's ZIP code at the time of birth, exposure was determined by inverse distance weighting of up to three PM₁₀ monitors within 50 km of the ZIP code centroid. If there was a PM₁₀ monitor within 5 km of the ZIP code centroid (40% of data), exposure from that monitor was used. Exposure was calculated for the entire pregnancy, and for each trimester of pregnancy. A 10 µg/m³ increase in PM₁₀ during the third trimester reduced mean birth weight -10.9 g (95% CI: -21.1 to -0.6) in single pollutant models, but became non-significant in copollutant models controlling for the effects of O₃. Increased risks of low birth weight (<2,500 g) were not statistically significant (OR = 1.3 [95% CI: 0.9-1.9]). A strength of this study was the cohort data available included information on SES and smoking during pregnancy. A limitation is the assignment of exposure based on monitoring stations up to 50 km distant; this may have introduced substantial exposure misclassification obscuring some associations.

Table 7-5. Characterization of ambient PM concentrations from studies of reproductive, developmental, prenatal and neonatal outcomes and long-term exposure.

Study	Location	Mean Annual Concentration ($\mu\text{g}/\text{m}^3$)	Upper Percentile Concentrations ($\mu\text{g}/\text{m}^3$)
<i>PM_{2.5}</i>			
Basu et al. (2004, 087896)	CA	Range of means across sites: 14.5-18.2 Avg of means across sites: 16.2	Max: 26.3-34.1
Bell et al. (2007, 091059)	CT & MA	22.3	
Brauer et al. (2008, 156292)	Vancouver, Canada	5.3	Max: 37.0
Huynh et al. (2006, 091240)	CA	Range of means across trimesters: 17.5-18.8 Avg of means across trimesters: 18.2	
Jalaludin et al. (2007, 156601)	Sydney, Australia	9.0	
Liu (2007, 090429)	Multicity, Canada	12.2	75th: 15
Loomis et al. (1999, 087288)	Mexico City	27.4	Max: 85
Mannes et al. (2005, 087895)	Sydney, Australia	9.4	75th: 11.2; Max: 82.1
Parker et al. (2005, 087462)	CA	15.4	
Ritz et al. (2007, 096146)	Los Angeles, CA	20.0	
Wilhelm and Ritz (2005, 088668)	Los Angeles, CA	21.0	Max: 38.9-48.5
Woodruff et al. (2006, 088758)	CA	19.2 ^a	75th: 22.7
Woodruff et al. (2008, 098386)	U.S.	Range of means across effects: 14.5-14.9 ^a Avg of means across effects: 14.8 ^a	75th: 18.5-18.7
<i>PM_{10-2.5}</i>			
Parker et al. (2008, 156013)	U.S.	13.2	75th: 17.5
<i>PM₁₀</i>			
Bell et al. (2007, 093256)	CT & MA	22.3	
Brauer et al. (2008, 156292)	Vancouver, Canada	12.7	Max: 35.4
Chen et al. (2002, 024945)	Washoe County, NV	31.53	75th: 39.35; Max: 157.32
Gilboa et al. (2005, 087892)	TX	23.8 ^a	75th: 29
Ha et al. (2003, 042552)	Seoul, South Korea	69.2	75th: 87.7; Max: 245.4
Hansen et al. (2006, 089818)	Brisbane, Australia	19.6	Max: 171.7
Hansen et al. (2007, 090703)	Brisbane, Australia	19.6	75th: 22.7; Max: 171.7
Jalaludin et al. (2007, 156601)	Sydney, Australia	16.3	
Kim et al. (2007, 156642)	Seoul, Korea	Range of means across time: 88.7-89.7 Avg of means across time: 89.2	
Lee et al. (2003, 043202)	Seoul, Korea	71.1	75th: 89.3; Max: 236.9
Leem et al. (2006, 089828)	Incheon, Korea	53.8 ^a	75th: 64.6; Max: 106.39
Lipfert et al. (2000, 004103)	U.S.	33.1	Max: 59
Maisonet et al. (2001, 016624)	NE U.S.	31.0 ^a	75th: 36.1; Max: 46.5
Mannes et al. (2005, 087895)	Sydney, Australia	16.8	75th: 19.9; Max: 104.0
Pereira et al. (1998, 007264)	Sao Paulo, Brazil	65.04	Max: 192.8
Ritz et al. (2000, 012068)	CA	49.3	Max: 178.8
Ritz et al. (2006, 089819)	CA	46.3	Max: 83.5

Study	Location	Mean Annual Concentration ($\mu\text{g}/\text{m}^3$)	Upper Percentile Concentrations ($\mu\text{g}/\text{m}^3$)
Rogers and Dunlop (2006, 091232)	GA	3.75	75th: 15.07
Romieu et al. (2004, 093074)	Ciudad Juarez, Mexico	33.0-45.9	
Sagiv et al. (2005, 087468)	PA	Range of means across time: 25.3-27.1 Avg of means across time: 26.2	Max: 68.9-156.3
Salam et al. (2005, 087885)	CA	Range of means across trimesters: 45.4-46.6 Avg of means across trimesters: 45.8	
Suh et al. (2008, 192077)	Seoul, Korea	Range of means across trimesters: 54.6-61.1 Avg of means across trimesters: 58.27	75th: 62.8-67.8 Max: 85.1-107.36
Tsai et al. (2006, 090709)	Kaohsiung, Taiwan	81.5	75th: 111.5; Max: 232.0
Wilhelm and Ritz (2005, 088668)	Los Angeles, CA	38.1	Max: 74.6-103.7
Woodruff et al. (2008, 098386)	U.S.	Range of means across effects: 28.6-29.8 ^a Avg of means across effects: 29.1 ^a	75th: 33.8-36.5
Yang et al. (2006, 090760)	Taipei, Taiwan	53.2	75th: 64.9; Max: 234.9

^aMedian concentration

Parker et al. (2005, [087462](#)) examined births in California within 5 miles of a monitoring station ($n = 18,247$). Only infants born at 40 wk gestation were included. Thus all infants were the same gestational age, and had been exposed in the same year. Exposure to $\text{PM}_{2.5}$ in quartiles (<11.9 , 11.9 - 13.9 , 14.0 - 18.4 , >18.4) was associated with decrements in birth weight. Infants exposed to $>13.9 \mu\text{g}/\text{m}^3$ experienced reductions in birth weight (third quartile -13.7 g (95% CI: -34.2 to 6.9), fourth quartile -36.1 g (95% CI: -55.8 to -16.5). These are larger reductions than have been seen in some other studies. However, this study reduced misclassification by including only women living within 5 miles of a monitoring station, and only included births at 40 wk gestation. Reducing misclassification should lead to a stronger association, if the association is causal.

The effects of spatial variation in exposure were also investigated by Wilhelm and Ritz (2005, [088668](#)). Their study included all women living in ZIP codes where 60% of the ZIP code was within two miles of a monitoring station in the Southern California Basin, and women with known addresses in Los Angeles County within 4 miles of a monitoring station. Exposure to average PM_{10} in the third trimester was analyzed for increased risk of low birth weight at term (≥ 37 -wk gestation). Analysis at the ZIP code level did not detect increased risk (per $10 \mu\text{g}/\text{m}^3 \text{ PM}_{10}$, OR = 1.03 [95% CI: 0.97-1.09]). However the analysis based on geocoded addresses indicated that increasing exposure to PM_{10} was associated with increased risk of low birth weight for women living within 1 mile of the station where PM_{10} was measured. For these women ($n = 247$ cases, 10,981 non-cases), each $10 \mu\text{g}/\text{m}^3$ increase in PM_{10} was associated with a 22% increase in risk of term low birth weight (OR = 1.22 [95% CI: 1.05-1.41]). In the categorical analysis, exposure to $\text{PM}_{10} >44.4 \mu\text{g}/\text{m}^3$ was associated with a 48% increase in risk (OR = 1.48 [95% CI: 1.00-2.19]). Increased risk of low birth weight also was associated with exposure to CO in single pollutant models. However, when multipollutant models were considered, the effects of CO were attenuated but the effects of PM_{10} increased. Controlling for CO, NO_2 , and O_3 , each $10 \mu\text{g}/\text{m}^3$ increase in exposure to PM_{10} increased risk of low birth weight 36% (OR = 1.36 [95% CI: 1.12-1.65]).

Spatial variation in $\text{PM}_{2.5}$ exposure was investigated by Basu et al. (2004, [087896](#)). They included only mothers who lived within 5 miles of a $\text{PM}_{2.5}$ monitor and within a California county with at least 1 monitor. To minimize potential confounding, they included only white ($n = 8,597$) or Hispanic ($n = 8,114$) women, who were married, between 20 and 30 yr of age, completed at least high school and were having their first child. Consistently, $\text{PM}_{2.5}$ exposure measured by the county monitor was more strongly associated with reductions in birth weight than exposure measured by the neighborhood monitor. The results were replicated in both the white and the Hispanic samples. Reductions in birth weight ranged from 15.2 to 43.5 g per $10 \mu\text{g}/\text{m}^3$ increase in $\text{PM}_{2.5}$.

In the remaining U.S. study, Chen et al. (2002, [024945](#)) analyzed 33,859 birth certificates of residents of Washoe County in northern Nevada (1991-1999). There were four sites monitoring PM_{10} during the study period, it appears (not stated) that exposure was averaged over the county. A

10 $\mu\text{g}/\text{m}^3$ increase in exposure to PM_{10} during the third trimester of pregnancy was associated with an 11 g reduction in birth weight (95% CI: -2.3 to -19.8). Effects on risk of low birth weight were not statistically significant. For exposure in the third trimester of 19.77 to 44.74 $\mu\text{g}/\text{m}^3$ compared to <19.74 $\mu\text{g}/\text{m}^3$ the odds ratio for low birth weight was 1.05 (95% CI: 0.81-1.36). Comparing exposure >44.74 to the same reference category, the odds ratio was 1.10 (95% CI: 0.71-1.71). Misclassification of exposure may have occurred when exposure was averaged over a large geographic area (16,968 km^2).

Recent international studies investigating effects of particles on low birth weight include one in Munich (Slama et al., 2007, [093216](#)), two in Canada (Brauer et al., 2008, [156292](#); Dugandzic et al., 2006, [088681](#)), two in Australia (Hansen et al., 2007, [090703](#); Mannes et al., 2005, [087895](#)), two in Taiwan (Lin et al., 2004, [089827](#); Yang et al., 2003, [087886](#)) one in Korea (Ha et al., 2003, [042552](#)) and two in Sao Paulo, Brazil (Gouveia et al., 2004, [055613](#); Medeiros and Gouveia, 2005, [089824](#)). The majority of these studies found that PM concentrations were associated with low birth weight, though two studies (Hansen et al., 2007, [090703](#); Lin et al., 2004, [089827](#)) found no associations. The effect estimates were similar in magnitude to those reported in the U.S. studies.

Considerations in Interpreting Results of Low Birth Weight Studies

Studies included subjects at distances from monitoring stations varying from as close as 1 mile or 2 km, to as far as 50 km or the size of the county. Studies that only included subjects living within a short distance (1 mile, 2 km) of the monitoring station (thus likely reducing exposure measurement error) were more likely to find that PM exposure was associated with increased risk of low birth weight. However, Basu et al. (2004, [087896](#)) reported a stronger association between $\text{PM}_{2.5}$ exposure and birth weight when exposure was estimated based on the county monitor, rather than the monitor within 5 miles of the residence. They suggest that county level exposure may be more representative of where women spend their time, including not only home, but also other time spent away from home. Other pollutants also appeared to influence the risk associated with particle exposure. In one study, exposure to PM_{10} in a single pollutant model reduced birth weight by 11 g, but became non-significant in copollutant models with O_3 (Salam et al., 2005, [087885](#)). In another study the risk associated with PM_{10} exposure increased from 22% to 36% when other pollutants were included in the model (Wilhelm and Ritz, 2005, [088668](#)). All but one study in the U.S. found some association between particle exposure and reduced birth weight (Maisonet et al., 2001, [016624](#)). The results of international studies were inconsistent. This might be related to the chemical composition of particles in the U.S., or to differences in the pollutant mixture. Studies with null results must be interpreted with caution when the comparison groups have significant exposure. This was certainly the situation in studies in Taiwan and Korea (Lee et al., 2003, [043202](#); Lin et al., 2004, [089827](#); Yang et al., 2003, [087886](#)). Differences in geographical locations, study samples and linkage decisions may contribute to the diverse findings in the literature on the association between PM and birthweight, even within the U.S. (Parker and Woodruff, 2008, [156846](#)).

7.4.1.2. Preterm Birth

A potential association of exposure to airborne particles and preterm birth has been investigated in numerous epidemiologic studies, including some conducted in the U.S. and others in foreign countries. Three U.S. studies have been carried out by the same group of investigators in California.

A natural experiment occurred when an open-hearth steel mill in Utah Valley was closed from August 1986 through September 1987. Parker et al. (2008, [156013](#)) compared birth outcomes for Utah mothers within and outside of the Utah Valley, before, during, and after the mill closure. They report that mothers who were pregnant around the time of the closure of the mill were less likely to deliver prematurely than mothers who were pregnant before or after. The strongest effect estimates were observed for exposure during the second trimester (14% decrease in risk of preterm birth during mill closure). Preterm birth outside of the Utah Valley did not change during the time of the mill closure.

In 2000, Ritz et al. (2000, [012068](#)) published the first study investigating the association of preterm birth with PM in the U.S. The study population was women living in the southern California Basin. There were eight monitoring stations measuring PM_{10} every 6th day during the study period.

Birth certificates (1989-1993) were analyzed for women living in ZIP codes within 2 miles of a monitoring station. Women with multiple gestations, chronic disease prior to pregnancy and women who delivered by cesarean section were excluded resulting in a study population of 48,904 women. The risk of preterm birth increased by 4% (RR = 1.04 [95% CI: 1.02-1.6]) per 10 $\mu\text{g}/\text{m}^3$ increase in PM_{10} averaged in the 6 wk before birth. Exposure to PM_{10} in the first month of pregnancy resulted in a 3% increase in risk (RR = 1.03 [95% CI: 1.01-1.05]). These results were robust in multipollutant models.

Wilhelm and Ritz (2005, [088668](#)) reinvestigated this association among women in the same area in 2005, when air pollution had declined from a mean level near 50 $\mu\text{g}/\text{m}^3$ to a mean level near 40 $\mu\text{g}/\text{m}^3$. Birth certificate data from 1994-2000 was analyzed for women living in ZIP codes within 2 miles of a monitoring station, or with addresses within 5 miles of a monitoring station. No significant effects of exposure to PM_{10} were reported. Exposure to $\text{PM}_{2.5}$ 6 wk before birth resulted in an increase in preterm birth (RR = 1.19 [95% CI: 1.02-1.40]) for the highest quartile of exposure ($\text{PM}_{2.5} > 24.3 \mu\text{g}/\text{m}^3$). Using a continuous measure of $\text{PM}_{2.5}$, there was a 10% increase in risk for each 10 $\mu\text{g}/\text{m}^3$ increase in $\text{PM}_{2.5}$ (RR = 1.10 [95% CI: 1.00-1.21]).

There have been two major criticisms of air pollution studies using birth certificate data. First, that birth certificates only indicate the address at birth and the exposure of women who moved during pregnancy may be misclassified; second, that information about some important confounders may not be available (e.g., smoking). To obtain more precise information about these variables, Ritz et al. (2007, [096146](#)) conducted a case-control study nested within a cohort of birth certificates (Jan 2003-Dec 2003) in Los Angeles County. Births to women residing in ZIP codes (n = 24) close to monitoring stations or major population centers or roadways (n = 87) were eligible (n = 58,316 births). All cases of low birth weight or preterm birth and an equal number of randomly sampled controls in the 24 ZIP codes close to monitors were selected. In the other 87 ZIP codes, 30% of cases and an equal number of controls were randomly sampled. Of 6,374 women selected for the case control study, 2,543 (40%) were interviewed. The association of preterm birth with exposure to $\text{PM}_{2.5}$ differed between women responding to the survey and women who did not respond. Among responders, exposure to each 10 $\mu\text{g}/\text{m}^3$ increase in $\text{PM}_{2.5}$ concentration in the first trimester increased risk to preterm birth by 23% (RR = 1.23 [95% CI: 1.02-1.48]). There was no increase in risk among non-responders (RR = 0.95 [95% CI: 0.82-1.10]), or in the entire birth cohort (RR = 1.00 [95% CI: 0.94-1.07]).

An additional case control study of preterm birth and $\text{PM}_{2.5}$ exposure (Huynh et al., 2006, [091240](#)) used California birth certificate data. Singleton preterm infants (24-36-wk gestation) born in California (1999-2000) whose mothers lived within 5 miles of a $\text{PM}_{2.5}$ monitor were eligible. Each of these 10,673 preterm infants were matched to three term (39- to 44-wk gestation) controls (having a last menstrual period within 2 wk of the case infant), resulting in a study population of 42,692. Controlling for maternal race/ethnicity, education, marital status, parity and CO exposure, exposure to $\text{PM}_{2.5} > 17.7 \mu\text{g}/\text{m}^3$ increased the risk of preterm birth by 14% (OR = 1.14 [95% CI: 1.07-1.23]). Averaging $\text{PM}_{2.5}$ exposure over the first month of pregnancy, the last 2 wk before birth, or the entire pregnancy did not substantially change the risk estimate.

Two additional studies of preterm birth and exposure to particulate air pollution have been conducted in the U.S. Each has used a unique methodology. Sagiv et al. (2005, [087468](#)) used time series to analyze births in four Pennsylvania counties between January 1997 and December 2001. In this analysis, exposure to PM_{10} is compared to the rate of preterm births each day. Both acute exposure (on the day of birth) and longer term exposure (average exposure for the preceding 6 wk) were considered in the analysis. An advantage of this analysis is that days, rather than individuals are compared, so confounding by individual risk factors is minimized. For exposure averaged over the 6 wk prior to birth, there was an increase in risk (RR = 1.07 [95% CI: 0.98-1.18]), which persisted for acute exposure with a 2-day lag (RR = 1.10 [95% CI: 1.00-1.21]) and 5-day lag (RR = 1.07 [95% CI: 0.98-1.18]).

Rogers and Dunlop (2006, [091232](#)) examined exposure to particles and risk of delivery of an infant weighing less than 1,500 g (all of which were preterm) from 24 counties in Georgia. The study included 69 preterm, small for gestational age (SGA) infants, 59 preterm appropriate for gestational age (AGA) infants and 197 term AGA controls. Exposure was estimated using an environmental transport model that considered PM_{10} emissions from 32 geographically located industrial point sources, meteorological factors, and geographic location of the birth home. Exposure was categorized by quartiles. Comparing women who delivered a preterm AGA infant to those who

delivered a term AGA infant, exposure to $PM_{10} > 15.07 \mu\text{g}/\text{m}^3$ tripled the risk (OR = 3.68 [95% CI: 1.44-9.44]).

Brauer et al. (2008, [156292](#)) evaluated the impacts of $PM_{2.5}$ on preterm birth using spatiotemporal exposure metrics in Vancouver, Canada. The authors found similar results when they used a land-use regression model or inverse distance weighting as the exposure metric. For preterm births <37 wk, they reported an OR of 1.06 (95% CI: 1.01-1.11), and for preterm births <35 wk the OR increased to 1.12 (95% CI: 1.02-1.24). There were no consistent trends for early or late gestational period to be more strongly associated with preterm births.

Suh et al. (2008, [192077](#)) conducted a study to determine if the effects of exposure to PM_{10} during pregnancy on preterm delivery are modified by maternal polymorphisms in metabolic genes. They analyzed the effects of the gene-environment interaction between the GSTM1, GSTT1, CYP1a1-T6235C and -1462V polymorphisms and exposure to PM_{10} during pregnancy on preterm birth in a case-control study in Seoul, Korea. PM_{10} concentration \geq 75th percentile alone was significant in the third trimester of pregnancy (OR = 2.33 [95% CI: 1.33-4.80]), but not in the first or second trimester. The risk of preterm delivery conferred by the GSTM1 null genotype was increased, and the highest risk was found during the third trimester of pregnancy (OR = 2.58 [95% CI: 1.34-4.97]). There were no statistical associations with the GSTT1 or CYP1A1 genotypes. When the gene-environment interaction was analyzed, the risk for preterm birth was substantially higher for women who carried the GSTM1 null genotype and were exposed to high levels of PM_{10} (\geq 75th percentile) than for those who carried the GSTM1 positive genotype but were only exposed to low levels of PM_{10} (<75th percentile) during the third trimester of pregnancy (OR = 6.22, 95% CI: 2.14-18.08).

In Incheon, Korea, Leem et al. (2006, [089828](#)) estimated PM_{10} exposure spatially as well as temporally. Exposure was based on 26 monitors and kriging was used to determine exposure for 120 dong (administrative districts, mean area 7.82 km^2 , median area 1.42 km^3). The sample included 52,113 births, from 2001-2002. PM_{10} was very weakly correlated with other pollutants. Exposure was compared in quartiles for the first and third trimester of pregnancy. In the first trimester, relative risks for the second, third and fourth quartiles were RR = 1.14 (95% CI: 0.97-1.34), RR = 1.07 (95% CI: 0.94-1.37), and RR = 1.24 (95% CI: 1.09-1.41), respectively. Exposure to PM_{10} in quartile one (reference group) was $26.9\text{-}45.9 \mu\text{g}/\text{m}^3$; fourth quartile exposure equaled $64.6\text{-}106.4 \mu\text{g}/\text{m}^3$. The p-value for trend was 0.02. Exposure in the third trimester was not related to preterm birth, however no information was provided to determine how exposure in the third trimester was adjusted for women who delivered preterm.

Two studies investigating risks of preterm birth related to particle exposure have been reported from Australia. In Brisbane, Hansen et al. (2006, [089818](#)) studied 28,200 births (2000-2003) in an area of low PM_{10} concentrations. Exposure to an interquartile range increase in PM_{10} exposure in the first trimester resulted in a 15% increased risk of preterm birth (OR = 1.15 [95% CI: 1.06-1.25]). This result was strongly influenced by the effect of PM_{10} exposure in the first month of pregnancy (OR = 1.19 [95% CI: 1.13-1.26]). PM_{10} was correlated with O_3 ($r = 0.77$) in this study and O_3 also increased risk in the first trimester. No effects were associated with exposure to PM_{10} in the third trimester.

In Sydney, associations between exposure to particles and preterm birth varied by season. Jalaludin et al. (2007, [156601](#)) obtained information on all births in metropolitan Sydney (1998-2000). Exposure to $PM_{2.5}$ in the 3 mo preceding birth was associated with an increased risk of preterm birth (OR = 1.11 [95% CI: 1.04-1.19]). Additional effects were dependent on season of conception. Both PM_{10} (OR = 1.3 [95% CI: 1.2-1.5]) and $PM_{2.5}$ (OR = 1.4 [95% CI: 1.3-1.6]) were associated with increased risk for conceptions in the winter. Conceptions in summer were associated with reductions in risk (PM_{10} OR = 0.91 [95% CI: 0.88-0.93]) ($PM_{2.5}$ OR = 0.87 [95% CI: 0.84-0.92]). Due to both positive and negative findings, the authors recommend caution in interpreting their results.

Considerations in Analyzing Environmental Exposures and Preterm Birth

A major issue in studying environmental exposures and preterm birth is selecting the relevant exposure period, since the biological mechanisms leading to preterm birth and the critical periods of vulnerability are poorly understood (Bobak, 2000, [011448](#)). Exposures proximate to the birth may be most relevant if exposure causes an acute effect. However, exposure occurring in early gestation

might affect placentation, with results observable later in pregnancy, or cumulative exposure during pregnancy may be the most important determinant. The studies reviewed have dealt with this issue in different ways. Many have considered several exposure metrics based on different periods of exposure.

Often the time periods used are the first month (or first trimester) of pregnancy and the last month (or 6 wk) prior to delivery. Using a time interval prior to delivery introduces an additional problem since cases and controls are not in the same stage of development when they are compared. For example, a preterm infant delivered at 36 wk is a 32-week fetus 4 wk prior to birth, while an infant born at term (40 wk) is a 36-week fetus 4 wk prior to birth. Only one study (Huynh et al., 2006, [091240](#)) adjusted for this in the design.

Many of these studies compare exposure in quartiles, using the lowest quartile as the reference (or control) group. No studies use a truly unexposed control group. If exposure in the lowest quartile confers risk, then it may be difficult to demonstrate additional risk associated with a higher quartile. Thus negative studies must be interpreted with caution.

Preterm birth occurs both naturally (*idiopathic preterm*), and as a result of medical intervention (*iatrogenic preterm*). Ritz et al. (2000, [012068](#); 2007, [096146](#)) excluded all births by Cesarean section, to limit their studies to idiopathic preterm. No other studies attempted to distinguish the type of preterm birth, although PM exposure maybe associated with only one type. This is a source of potential effect misclassification.

7.4.1.3. Growth Restriction

Low birth weight has often been used as an outcome measure because it is easily available and accurately recorded on birth certificates. However, low birth weight may result from either short gestation, or inadequate growth in utero. Most of the studies investigating air pollution exposure and low birth weight, limited their analysis to term infants to focus on inadequate growth. A number of studies were identified that specifically addressed growth restriction in utero by identifying infants who failed to meet specific growth standards. Usually these infants had birth weights less than the 10th percentile for gestational age, using an external standard. Many of these studies have been previously discussed, since they also examined other reproductive outcomes (low birth weight or preterm delivery).

Three studies in the U.S. examined intrauterine growth. A recent study (Rich et al., 2009, [180122](#)) investigated very small for gestational age (defined as a fetal growth ratio <0.75), small for gestational age (defined as ≥ 75 and <85) and “reference” births (≥ 85) to women residing in New Jersey and mean air pollutant concentrations during the first, second and third trimesters. They reported an increased risk of SGA associated with first and third trimester PM_{2.5} concentrations (1.116 [95% CI: 1.012, 1.232], and 1.106 [1.008-1.212], per 10 $\mu\text{g}/\text{m}^3$ PM_{2.5}, respectively). Parker et al. (2005, [087462](#)) reported a positive association between exposure to PM_{2.5}. Since this study only included singleton live births at 40-wk gestation, birth weights less than 2,872 g for girls and 2,986 g for boys were designated SGA, based on births in California. Infants exposed to the highest quartile PM_{2.5} ($>18.4 \mu\text{g}/\text{m}^3$) compared to the lowest quartile PM_{2.5} ($<11.9 \mu\text{g}/\text{m}^3$) were 23% more likely to be small for gestational age (OR = 1.23 [95% CI: 1.03-1.50]). Very similar results were found for exposure in each of the three trimesters respectively (OR = 1.26 [95% CI: 1.04-1.51], OR = 1.24 [95% CI: 1.04-1.49], OR = 1.21 [95% CI: 1.02-1.43]). These results controlled for exposure to CO, which did not increase risk for SGA.

In contrast, Salam et al. (2005, [087885](#)) found no association between exposure to PM₁₀ and intrauterine growth retardation (IUGR) in the California Children’s Health Study. IUGR was defined as less than the 15th percentile of predicted birth weight based on gestational age and sex in term infants. Apparently no external standard was used since 15% of infants in the study were designated as IUGR. An IQR increase in PM₁₀ exposure was not significantly associated with IUGR for the whole pregnancy (OR = 1.1 [95% CI: 0.9-1.3]) or for any specific trimester. Differences between this study and the study by Parker et al. (2005, [087462](#)) include measurement of PM₁₀ versus PM_{2.5}, a less stringent definition of IUGR, and exposures determined by monitors located much farther away from the subjects’ residences (up to 50 km versus within 5 mi). All of these factors could lead to misclassification.

Two studies investigating particle exposure and SGA were conducted in Australia, with differing results (Hansen et al., 2007, [090703](#); Mannes et al., 2005, [087895](#)). Mannes et al. (2005, [087895](#)) defined SGA as birth weight less than two standard deviations below the national mean

birth weight for gestational age. In this study there was a statistically significant effect of exposure to both PM₁₀ (OR = 1.10 [95% CI: 1.00-1.48], per 10 µg/m³ increase) and PM_{2.5} (OR = 1.34 [95% CI: 1.10-1.63], per 10 µg/m³ increase) for exposure during the second trimester. When analysis was restricted to births within 5 km of the monitoring station, the association for PM₁₀ became slightly stronger (OR = 1.22 [95% CI: 1.10-1.34]). Exposure during other trimesters of pregnancy was not associated with IUGR.

In Brisbane, Hansen et al. (2007, [090703](#)) examined head circumference (HC), crown heel length (CHL) and risk of SGA, defined as less than the tenth percentile of weight for gestational age and gender based on an Australian national standard. There was no consistent relationship between PM₁₀ exposure and SGA, HC or CHL in any trimester of pregnancy. PM₁₀ exposure was determined by averaging values from the five monitoring stations. Due to the sample size and limited number of monitoring stations, it was not possible to analyze the data for women living within 5 km of a monitoring station, as was done in Sydney.

In Canada, Liu et al. (2007, [090429](#)) investigated the effect of PM_{2.5} exposure on fetal growth in three cities, Calgary, Edmonton and Montreal. IUGR was defined as birth weight below the tenth percentile, by sex and gestational week (37-42) for all singleton live births in Canada between 1986 and 2000. Models were adjusted for maternal age, parity, infant sex, season of birth, city of residence, and year of birth. A 10 µg/m³ increase in PM_{2.5} was associated with an increased risk for IUGR (OR = 1.07 [95% CI: 1.03-1.10]) in the first trimester, and similar risks were associated with exposure in the second or third trimesters. The effect of PM_{2.5} was reduced in multipollutant models including CO and NO₂.

Brauer et al. (2008, [156292](#)) observed consistent increased risks of SGA for PM_{2.5}, PM₁₀, NO₂, NO and CO in Vancouver, Canada (20% increase in risk in PM_{2.5} and PM₁₀ per 10 µg/m³ increase). The effects were similar for exposure estimates based on nearest monitor, inverse distance weighting, and land-use regression modeling. ORs for early or late pregnancy exposure windows were remarkably similar to those for the full duration of pregnancy.

7.4.1.4. Birth Defects

Four recent studies examined PM and birth defects. The Seoul, Korea study discussed above also considered congenital anomalies, defined as a defect in the child's body structure (Kim et al., 2007, [156642](#)). PM₁₀ levels were associated with higher risk of birth defects for the second trimester, with a 16% (95% CI: 0-34) increase in risk per 10 µg/m³ in PM₁₀.

Two U.S. studies examined air pollution and risk of birth defects. Data were collected from the California Birth Defects Monitoring Program for four counties in Southern California (Los Angeles, Riverside, San Bernardino, and Orange) for the period 1987-1993, although each county included a subset of this period (Ritz et al., 2002, [023227](#)). Cases (i.e., infants with birth defects) were identified as live birth infants and fetal deaths from 20-wk gestation to 1 yr post-birth, with isolated, multiple, syndrome, or chromosomal cardiac or orofacial cleft defects. Cases were restricted to those with registry data for gestational age and residence ZIP code, and those with residences <10 miles from an air pollution monitor. Six types of categories were included: aortic defects; atrium and atrium septum defects; endocrinal and mitral valve defects; pulmonary artery and valve defects; conotruncal defects; and ventricular septal defects not part of the conotruncal category. PM₁₀ measurements were available every 6 days. While results indicated increased risk of birth defects for higher levels of CO or O₃, the authors determined that results for PM₁₀ were inconclusive, finding no consistent trend of effect after adjustment for CO and O₃.

The other U.S. study examined birth defects through a case-control design in seven Texas counties for the period 1997-2000 (Gilboa et al., 2005, [087892](#)). Births were excluded for parents <18 yr and several non-air pollution risk factors known to be associated with birth defects (e.g., maternal diabetes, holoprosencephaly in addition to oral cleft). Comparison of the highest (≥ 29.0 µg/m³) and lowest (<19.521 µg/m³) quartiles of PM₁₀ for exposure defined as the third to eighth week of pregnancy generated an OR of 2.27 (95% CI: 1.43-3.60) for risk of isolated atrial septal defects and 1.26 (95% CI: 1.03-1.55) for individual atrial septal defects. Including other pollutants (CO, NO₂, O₃, SO₂) in the model did not greatly alter results; numerical results for copollutant analysis were not provided. Strong evidence was not observed for a relationship between PM₁₀ and the other birth defect categories. Review articles have concluded that the scientific literature is not sufficient to conclude a relationship between air pollution and birth defects (Sram et al., 2005, [087442](#)).

A recent study of oral clefts conducted in Taiwan found no association between this birth defect and concentrations of PM₁₀ during the first or second gestational month (Hwang and Jaakkola, 2008, [193794](#)). This population-based case-control study included 653 cases and a random sample of 6,530 controls born in Taiwan between 2001 and 2003.

7.4.1.5. Infant Mortality

Many studies have identified strong associations between exposure to particles and increased risk of mortality in adults or the general population, including for short- and long-term exposure (Sections 6.5 and 7.6). Less evidence is available for the potential impact on infant mortality, although studies have been conducted in several countries. The results of these infant mortality studies are presented here with the other reproductive and developmental outcomes because it is likely that in vitro exposures contribute to this outcome. Both long-term and short-term exposure studies of infant mortality are included in this section. Results on PM and infant mortality includes a range of findings, with some studies finding associations and many statistically non-significant or null effects. Yet, more consistency is observed when results are divided into the type of health outcome based on the age of infant and cause of death.

An important question regarding the association between PM and infant mortality is the critical window of exposure during development for which infants are susceptible. Several age intervals have been explored: neonatal (<1 mo); infants (<1 yr); and postneonatal (1 mo-1 yr). Within these various age categories, multiple causes of deaths have been investigated, particularly total deaths and respiratory-related deaths. The studies reflect a variety of study designs, particle size ranges, exposure periods, regions, and adjustment for confounders.

Stillbirth

Only one study of stillbirths and PM was identified. A prospective cohort of pregnant women in Seoul, Korea from 2001 to 2004 was examined with respect to exposure to PM₁₀ (Kim et al., 2007, [156642](#)). Gestational age was estimated by the last menstrual period or by ultrasound. Whereas many of the previously discussed studies of PM and pregnancy outcomes were based on national registries, this study examined medical records and gathered individual information through interviews on socioeconomic condition, medical history, pregnancy complications, smoking, second-hand smoke exposure, and alcohol use. Mother's exposure to PM₁₀ was based on residence for each month of pregnancy, each trimester defined as a three month period, and the 6 wk prior to death. Exposure was assigned by the nearest monitor. A 10 µg/m³ increase in PM₁₀ in the third trimester was associated with an 8% (95% CI: 2-14) increase in risk of stillbirth.

In São Paulo, Brazil, Poisson regression of stillbirth counts for the period 1991-1992 found that a 10 µg/m³ increase in PM₁₀ was associated with a 0.8% increase in stillbirth rates (Pereira et al., 1998, [007264](#)). When other pollutants (NO₂, SO₂, CO, O₃) were included simultaneously in the model, the association did not remain. Stillbirths were defined as fetal loss at >28 wk of pregnancy age, weight >1,000 g, or length of fetus >35 cm.

Neonatal Mortality and Neonatal Respiratory Mortality, <1 Month

Studies on PM and neonatal mortality (<1 month) included a time-series analysis of PM₁₀ for 4 yr of data (1998-2000) for São Paulo, Brazil (Lin et al., 2004, [095787](#)). The analysis used daily counts of deaths from government registries and adjusted for temporal trend, day of the week, weather, and holidays. Findings indicated that a 10 µg/m³ increase in PM₁₀ was associated with a 1.71% (95% CI: 0.31-3.32) increase in risk of neonatal death.

A case-crossover study of 11 yr (1989-2000) in Southern California did not find an association between PM₁₀ and neonatal deaths (Ritz et al., 2006, [089819](#)). Quantitative results were not provided. The authors considered adjustment for season, county, parity, gender, prenatal care, and maternal age, education, and race/ethnicity.

These results add to previous work on PM and neonatal death, including studies identifying higher risk of neonatal mortality with higher TSP in the Czech Republic in an ecological analysis (Bobak and Leon, 1992, [044415](#)) and case-crossover study (Bobak and Leon, 1999, [007678](#)), and a

Poisson model study in Kagoshima City, Japan (Shinkura et al., 1999, [090050](#)). An ecological study evaluated U.S. PM₁₀ data for the year 1990 using long-term pollution levels in 180 U.S. counties (Lipfert et al., 2000, [004103](#)). Analysis considered birth weight, sex, month of birth, location by state and county, prenatal care, and mother's race, age, educational level, marital status, and smoking status. County-level variables were included for socioeconomic status, altitude, and climate. Results indicate a 13.1% increase in neonatal mortality (95% CI: 4.4-22.6) per 10 µg/m³ PM₁₀ for non-low birth weight infants. Statistically significant associations were also observed considering all infants or low birth weight infants. However, higher levels of SO₂ were associated with lower risk of infant mortality. When sulfate and an estimate of non-sulfate particles were included in the regression simultaneously, associations were observed with non-sulfate particles and an inverse relationship with sulfate particles. Respiratory neonatal mortality was not associated with higher TSP in the Czech Republic case-control study (Bobak and Leon, 1999, [007678](#)).

Infant Mortality and Infant Respiratory Mortality, <1Year

A literature search did not reveal new studies on PM and infant mortality (<1 year) since the previous PM AQCD. Previously conducted studies include a case-control study that reported associations between infant mortality and TSP levels over the period between birth and death for infants in the Czech Republic (Bobak and Leon, 1999, [007678](#)). An ecological study evaluated U.S. PM₁₀ data for the year 1990 using long-term pollution levels in 180 U.S. counties (Lipfert et al., 2000, [004103](#)). The authors found a 9.64% (95% CI: 4.60-14.9) increase in risk of infant mortality for non-low birth weight infants per 10 µg/m³ increase in PM₁₀, a 13.4% (95% CI: -10.3 to 43.5) increase in non-low birth weight respiratory-disease related deaths (ICD 9 460-519) and a 19.5% (95% CI: 0.07-42.8) increase in all non-low birth weight respiratory-related infant deaths (ICD 9 460-519, 769, 770).

Postneonatal Mortality and Postneonatal Respiratory Mortality, 1 Month–1 Year

Several studies have been conducted on PM and postneonatal mortality since the previous PM AQCD, including three from the U.S., one from Mexico, and three from Asia. Two case-control studies examined the risk of PM to postneonatal death in California. Research focused on Southern California for the period 1989-2000 linked birth and death certificates and considered PM₁₀ 2 mo prior to death with adjustment for prenatal care, gender, parity, county, season, and mother's age, race/ethnicity, and education (Ritz et al., 2006, [089819](#)). As previously noted, this study did not find an association between PM₁₀ and neonatal mortality (<1 month), however an association was observed for post-neonatal mortality, with a 10 µg/m³ increase in PM₁₀ associated with a 4% (95% CI: 1-6) increase in risk. The exposure period of 2 wk before death was also considered, producing effect estimates of 5% (95% CI: 1-10) for the same PM₁₀ increment. Even larger effect estimates were observed for those who died at ages 4-12 mo. When CO, NO₂, and O₃ were simultaneously included with PM₁₀ in the model, the central estimate reduced to 2% for the 2-wk exposure period and 4% for the 2-mo exposure period, and both estimates lost statistical significance. The other case-control study of California considered PM_{2.5} from 1999 to 2000 for infants born to mothers within five miles of a PM_{2.5} monitoring station (Woodruff et al., 2006, [088758](#)). Infants who died during the postneonatal period were matched to infants with date of birth within 2 wk and birth weight category. Exposure was estimated from the time of birth to death. Models considered parity and maternal race, education, age, and marital status. A 10 µg/m³ increase in PM_{2.5} was associated with a 7% (95% CI: -7 to 24) increase in postneonatal death

County-level PM₁₀ and PM_{2.5} for the first 2 mo of life for births in urban U.S. counties (≥ 250,000 residents) from 1999 to 2002 were evaluated in relation to postneonatal mortality with GEE models (Woodruff et al., 2008, [098386](#)). Births were restricted to singleton births with gestational age ≤ 44 wk, same county of residence at birth and death, and non-missing data on birth order, birth weight, and maternal race, education, and marital status. Higher levels of either PM metric were associated with higher risk of postneonatal mortality, with 4% (95% CI: -1 to 10) increase in mortality risk per 10 µg/m³ in PM₁₀ and 4% (95% CI: -2 to 11) increase in mortality risk for the same increment of PM_{2.5}. This work builds on a previous study of 86 U.S. urban areas from

1989 to 1991, finding a 4% (95% CI: 2-7) increase in postneonatal mortality per 10 $\mu\text{g}/\text{m}^3$ county-level PM_{10} over the first 2 mo of life (Woodruff et al., 1997, [084271](#)).

In Ciudad Juarez, Mexico, a case-crossover approach was applied to data from 1997 to 2001 based on death certificates and the cumulative PM_{10} for the day of death and previous two days (Romieu et al., 2004, [093074](#)). A case-crossover study of Kaohsiung, Taiwan from 1994 to 2000 compared the average of PM_{10} on the day of death and two previous days to PM_{10} in control periods a week before and week after death (Tsai et al., 2006, [090709](#)). A similar approach was also applied to 1994-2000 data from Taipei, Taiwan, also using case-crossover methods for the lag 0-2 PM_{10} with referent periods the week before and after death (Yang et al., 2006, [090760](#)). In these case-crossover studies, season was addressed through matching in the study design. A 10 $\mu\text{g}/\text{m}^3$ increase in PM_{10} was associated with a 2.0% (95% CI: -2.8 to 7.0) increase in the Mexico study, a 0.59 (95% CI: -15.0 to 18.8) increase in postneonatal death in the Kaohsiung study, and a 1.02% (95% CI: -13.2 to 17.6) increase in the Taipei study. A study in Seoul, South Korea from 1995 to 1999 used time-series approaches adjusted for temporal trend and weather, based on national death registries excluding accidental deaths (Ha et al., 2003, [042552](#)). A 10 $\mu\text{g}/\text{m}^3$ increase in PM_{10} was associated with a 3.14% (95% CI: 2.16-4.14) increase in risk of death for postneonates.

A subset of the studies examining postneonatal mortality also considered the subset of postneonatal deaths from respiratory causes. These include the time-series study in South Korea, finding a 17.8% (95% CI: 14.4-21.2) increase in respiratory-mortality per 10 $\mu\text{g}/\text{m}^3$ increase in PM_{10} (Ha et al., 2003, [042552](#)) and the case-crossover study in Mexico, for which the same increment in PM_{10} was associated with a 1.5% (95% CI: -14.1 to 13.0) decrease in risk (Romieu et al., 2004, [093074](#)). Both California case-control studies identified associations, with a 5% (95% CI: 1-10) increase in risk in Southern California (Ritz et al., 2006, [089819](#)) and 57.4% (95% CI: 7.0-132) increase in California per 10 $\mu\text{g}/\text{m}^3$ PM_{10} (Woodruff et al., 2006, [088758](#)). The U.S. study found this increment in PM_{10} to be linked with a 16% (95% CI: 6.0-28.0) increase in respiratory postneonatal mortality, although effect estimates for $\text{PM}_{2.5}$ were not statistically significant (Woodruff et al., 2008, [098386](#)). Earlier studies on respiratory-related postneonatal mortality include the study of 86 U.S. urban areas, finding statistically significant effects (Woodruff et al., 1997, [084271](#)).

Sudden Infant Death Syndrome

Three studies examining the relationship between PM and sudden infant death syndrome (SIDS) have been published from 2002 onward. These studies examined infant mortality and were thereby discussed in this section previously. A case-control study over a 12-year period (1989 to 2000) matched 10 controls to deaths (cases) in Southern California (Ritz et al., 2006, [089819](#)). A 10 $\mu\text{g}/\text{m}^3$ increase in PM_{10} the 2 mo prior to death was associated with a 3% (95% CI: -1 to 8) increase in SIDS. Adjusted for other pollutants (CO, NO_2 , and O_3), the effect estimate reduced to 1% (95% CI: -5 to 7).

A case-control study, also based in California, found an OR of 1.008 (95% CI: 1.006-1.012) per 10 $\mu\text{g}/\text{m}^3$ increase in $\text{PM}_{2.5}$, considering a SIDS definition of ICD 10 R95 (Woodruff et al., 2006, [088758](#)). Due to changes in SIDS diagnosis, another SIDS definition was explored for ICD 10 R99 in addition to ICD 10 R95. Under this SIDS definition, the effect estimate changed to 1.03 (95% CI: 0.79-1.35). The authors also examined whether the relationship between $\text{PM}_{2.5}$ and SIDS differed by season, finding no significant difference. PM_{10} and $\text{PM}_{10-2.5}$ were not associated with risk of SIDS; numerical results were not provided for these PM metrics. The third recent study of PM and SIDS examined U.S. urban counties from 1999 to 2002 (Woodruff et al., 2008, [098386](#)). Statistically non-significant relationships were observed between SIDS and PM_{10} or $\text{PM}_{2.5}$ in the first 2 mo of life.

These studies add to earlier work, such as a U.S. study that found higher risk of SIDS with higher annual $\text{PM}_{2.5}$ levels, including in a separate analysis of normal birth weight infants (Lipfert et al., 2000, [004103](#)), and a U.S. study identifying a 12% (95% CI: 7-17) increase in SIDS risk per 10 $\mu\text{g}/\text{m}^3$ in PM_{10} for the first 2 mo of life for normal weight births (Woodruff et al., 1997, [084271](#)). A study based on Taiwan found higher SIDS risk with lower visibility (Knöbel et al., 1995, [155905](#)), whereas a 12-city Canadian time-series study identified no significant associations (Dales et al., 2004, [087342](#)).

Deaths by SIDS were identified by different methods in the studies, partly due to transition from ICD 9 to ICD 10 codes, but also due to different choices within the research design. Two studies examined multiple approaches (ICD 10 R95, ICD 10 R95 and R99) (Woodruff et al., 2006,

[088758](#); Woodruff et al., 2008, [098386](#)), and other studies investigated ICD 9 798.0 and ICD 10 R95 (Ritz and Wilhelm, 2008, [156914](#)), ICD 9 798.0 (Woodruff et al., 1997, [084271](#)), ICD 9 798.0 and 799.0 (Knöbel et al., 1995, [155905](#)), as well as a sudden unexplained death of infant <1 year for which an autopsy did not identify a specific cause of death (Dales et al., 2004, [087342](#)). These variations in the definition of health outcomes add to differences in populations and study designs.

Although some findings indicate a potential effect of PM on risk of SIDS, with the strongest evidence perhaps from the case-control study in California (Woodruff et al., 2006, [088758](#)), others do not find an effect or observe an uncertain association. For the relationship between PM and SIDS, a 2004 review article concluded consistent evidence exists compared to evidence for other infant mortality effects (Glinianaia et al., 2004, [087898](#)), whereas other reviews found weaker or insufficient evidence (Heinrich and Slama, 2007, [156534](#)). Another review concluded that the scientific literature on air pollution and SIDS suggests an effect, but that further research is needed to draw a conclusion (Tong and Colditz, 2004, [087883](#)).

Considerations for Comparisons across Studies

Comparison of results across studies can be challenging due to several issues, including differences in methodologies, populations and study areas, pollution levels, and the exposure timeframes used. Given the large variation in study designs, the methods to address potential confounders vary. For example, weather and season were addressed in the case-control studies by matching, in the time-series study through non-linear functions of temperature and temporal trend, and in the ecological study through county-level variables. All studies included consideration of seasonality and weather. Researchers used different definitions of respiratory-related deaths, including ICD 9 460-519 (Bobak and Leon, 1999, [007678](#); Lipfert et al., 2000, [004103](#)); ICD 9 460-519, 769-770 (Lipfert et al., 2000, [004103](#)); ICD 9 460-519, 769, 770.4, 770.7, 770.8, 770.9, and ICD 10 J00-J98, P22.0, P22.9, P27.1, P27.9, P28.0, P28.4, P28.5, and P28.9 (Ritz et al., 2006, [089819](#)); and ICD 9 460-519 and ICD 10 J00-J99 for any cause on death certificate (Romieu et al., 2004, [093074](#)); ICD 10 J00-99 and P27.1 excluding J69.0 (Woodruff et al., 2006, [088758](#); Woodruff et al., 2008, [098386](#)); and ICD 9 460-519 (Woodruff et al., 1997, [084271](#)).

Socioeconomic conditions were included at the individual level, typically maternal education, in many studies (e.g., Bobak and Leon, 1999, [007678](#); Ritz and Wilhelm, 2008, [156914](#); Ritz et al., 2006, [089819](#); Woodruff et al., 1997, [084271](#); Woodruff et al., 2006, [088758](#)) and at the community-level in others (e.g., Bobak and Leon, 1992, [044415](#); Penna and Duchade, 1991, [073325](#)) or for both individual and community-level data (e.g., Lipfert et al., 2000, [004103](#)). The time-series approach is unlikely to be confounded by socioeconomic and other variables that do not exhibit day-to-day variation. Similarly, case-crossover methods use each case as his/her own control, thereby negating the need for individual-level confounders such as socioeconomic status (e.g., Romieu et al., 2004, [093074](#); Tsai et al., 2006, [090709](#); Yang et al., 2006, [090760](#)). All studies published after 2001 incorporated individual-level socioeconomic data or were of case-crossover or time-series design. One study specifically examined whether socioeconomic status modified the PM and mortality relationship, dividing subjects into three socioeconomic strata based on the ZIP code of residence at death (Romieu et al., 2004, [093074](#)). This work, based in Mexico, found that at lower socioeconomic levels the association between PM₁₀ and postneonatal mortality increased. Although the overall association showed higher risk of death with higher PM₁₀ with statistical uncertainty, for the lowest socio-economic group, a 10 µg/m³ increment in cumulative PM₁₀ over the 2 days before death was associated with a 60% (95% CI: 3-149) increase in postneonatal death. A trend of higher effect for lower socio-economic condition is observed in all 3 lag structures.

Studies differ in terms of the time frame of pregnancy that was used to estimate exposure. Exposure to PM for infant mortality (<1 yr) was estimated as the levels between birth and death (Bobak and Leon, 1999, [007678](#)), annual community levels (Lipfert et al., 2000, [004103](#); Penna and Duchade, 1991, [073325](#)) and the 3-5 days prior to death (Loomis et al., 1999, [087288](#)). For neonatal deaths, exposure timeframes considered were the time between birth and death (Bobak and Leon, 1992, [044415](#); Bobak and Leon, 1999, [007678](#)), annual levels (Bobak and Leon, 1999, [007678](#); Lipfert et al., 2000, [004103](#)), monthly levels (Shinkura et al., 1999, [090050](#)), the same day concentrations (Lin et al., 2004, [095787](#)), and the 2 mo or 2 wk prior to death (Ritz et al., 2006, [089819](#)). Postneonatal mortality was associated with PM concentrations based on annual levels (Bobak and Leon, 1992, [044415](#); Lipfert et al., 2000, [004103](#)), between birth and death (Bobak and

Leon, 1999, [007678](#); Woodruff et al., 2006, [088758](#)), 2 mo before death (Ritz et al., 2006, [089819](#)), the first 2 mo of life (Woodruff et al., 1997, [084271](#); Woodruff et al., 2006, [088758](#)), the day of death (Ha et al., 2003, [042552](#)), and the average of the same day as death and previous 2 days (Romieu et al., 2004, [093074](#); Tsai et al., 2006, [090709](#); Yang et al., 2006, [090760](#)). Thus, no consistent window of exposure was identified across the studies.

PM₁₀ concentrations were highest in South Korea (69.2 µg/m³) (Ha et al., 2003, [042552](#)) and Taiwan (81.45 µg/m³) (Tsai et al., 2006, [090709](#)), and lowest in the U.S. (29.1 µg/m³) (Woodruff et al., 2008, [098386](#)) and Japan (21.6 µg/m³) (Shinkura et al., 1999, [090050](#)). All studies used community-level exposure information based on ambient monitors, as opposed to exposure measured at the individual level (e.g., subject's home) or personal monitoring.

Given similar sources for multiple pollutants (e.g., traffic), disentangling the health responses of copollutants is a challenge in the study of ambient air pollution. Several studies examined multiple pollutants, most by estimating the effect of different pollutants through several univariate models. Some studies noted the difficulty of separating PM effects from those of other pollutants, but noted stronger evidence for particles than other pollutants (Bobak and Leon, 1999, [007678](#)). A few studies applied copollutant models by including multiple pollutants simultaneously in the same model. Effect estimates for the relationship between PM₁₀ and neonatal deaths in São Paulo were reduced to a null effect when SO₂ was incorporated (Lin et al., 2004, [095787](#)). Associations between PM₁₀ and postneonatal mortality or respiratory postneonatal mortality remained but lost statistical significance in a multiple pollutant model with CO, NO₂, and O₃ (Ritz et al., 2006, [089819](#)).

Several review articles in recent years have examined whether exposure to PM affects risk of infant mortality, generally concluding that more consistent evidence has been observed for postneonatal mortality, particularly from respiratory causes (Bobak and Leon, 1999, [007678](#); Heinrich and Slama, 2007, [156534](#); Lacasaña et al., 2005, [155914](#); Sram et al., 2005, [087442](#)). In one review authors identified 14 studies on infant mortality and air pollution and determined that studies on PM and infant mortality do not provide consistent results, although more evidence was present for an association for some subsets of infant mortality such as postneonatal respiratory-related mortality (Bobak and Leon, 1999, [007678](#)). The relationship between PM and postneonatal respiratory mortality was concluded to be causal in one review (Sram et al., 2005, [087442](#)), and strong and consistent in another (Heinrich and Slama, 2007, [156534](#)). Meta-analysis using inverse-variance weighting of PM₁₀ studies found that a 10 µg/m³ increase in acute PM₁₀ exposure was associated with 3.3% (95% CI: 2.4-4.3) increase in risk of postneonatal mortality, whereas the same increment of chronic PM₁₀ exposure was linked with a 4.8% (95% CI: 2.2-7.2) increase in postneonatal mortality and a 21.6% (95% CI: 10.2-34.2) increase for respiratory postneonatal mortality (Lacasaña et al., 2005, [155914](#)).

Studies that examined multiple outcomes and ages of death allow a direct comparison based on the same study population and methodologies, thereby negating the concern that inconsistent results are due to underlying variation in population, approaches, etc. In this review, one study, based in Southern California identified no association for neonatal effects (numerical results not provided) but statistically significant results for postneonatal mortality (Ritz et al., 2006, [089819](#)). Figure 7-5 compares risk for the postneonatal period for respiratory and total mortality. In six of the seven studies, higher effect estimates were observed for respiratory-related mortality. Results from the neonatal period found higher effects for total mortality compared to respiratory mortality (Bobak and Leon, 1999, [007678](#)) and the reverse for a study examining infant mortality (Lipfert et al., 2000, [004103](#)). Thus, there exists evidence for a stronger effect at the postneonatal period and for respiratory-related mortality, although this trend is not consistent across all studies.

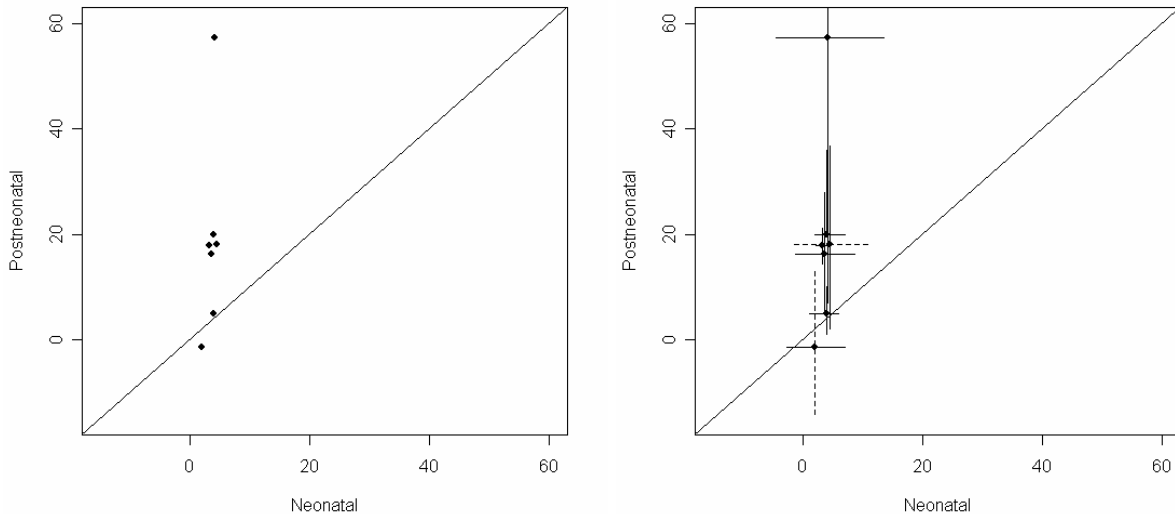


Figure 7-5. Percent increase in postneonatal mortality per 10 $\mu\text{g}/\text{m}^3$ in PM_{10} , comparing risk for total and respiratory mortality. Panel a (left) provides central estimates; panel b (right) also adds the 95% intervals. The points reflect central estimates and the lines the 95% intervals. Solid lines represent statistically significant effect estimates; dashed lines represent non-statistically significant estimates.¹

7.4.1.6. Decrements in Sperm Quality

Limited research conducted in the Czech Republic on the effect of ambient air pollution on sperm production has found associations between elevated air pollution and decrements in proportionately fewer motile sperm, proportionately fewer sperm with normal morphology or normal head shape, proportionately more sperm with abnormal chromatin (Selevan et al., 2000, [012578](#)), and an increase in the percentage of sperm with DNA fragmentation (Rubes et al., 2005, [078091](#)). These results were not specific to PM, but for exposure to a high-, medium- or low-polluted air mixture. Similarly, in Salt Lake City, Utah, $\text{PM}_{2.5}$ was associated with decreased sperm motility and morphology (Hammoud et al., 2009, [192156](#)). Research in Los Angeles, California examined 5,134 semen samples from 48 donors in relation to ambient air pollution measured 0-9, 10-14, 70-90 days before semen collection over a 2-yr period (1996-1998). Ambient O_3 during all exposure periods had a significant negative correlation with average sperm concentration, and no other pollutant measures were significantly associated with sperm quality parameters, or presented quantitatively (Sokol et al., 2006, [098539](#)).

7.4.2. Toxicological Studies

This section summarizes recent evidence on reproductive health effects reported with exposure to ambient PM; no evidence was presented in this area in the 2004 PM AQCD. Studies from different toxicological rodent models allow for investigation of specific mechanisms and modes of

¹ Studies included are Bobak and Leon (1999, [007678](#)), Ha et al. (2003, [042552](#)), Ritz et al. (2006, [089819](#)), Romieu et al. (2004, [093074](#)), Romieu et al. (2008, [156922](#)), Woodruff et al. (1997, [084271](#)), Woodruff et al. (2006, [088758](#)). Findings from Bobak and Leon (1999, [007678](#)) were based on TSP and were converted to PM_{10} estimates assuming $\text{PM}_{10}/\text{TSP} = 0.8$ as per summary data in the original article (Bobak and Leon, 1999, [007678](#)). Findings from Woodruff et al. (1997, [084271](#)) for respiratory-related mortality were based on non-low birth weight infants. Results for Woodruff et al. (2006, [088758](#)) were based on $\text{PM}_{2.5}$ and were converted to PM_{10} assuming $\text{PM}_{2.5}/\text{PM}_{10} = 0.6$.

action for reproductive changes. Emphasis is placed here on results from different windows of development, i.e., exposure in utero, neonatally or as an adult can affect reproductive outcomes as an adult. In addition, studies evaluating whether fertility is affected in female and/or male animals by a similar exposure, and how exposures are transmitted to the fertility of the F₁ offspring, are summarized. Hormonal changes which can lead to decreased sperm count or changes in the estrous cycle are also of interest. Studies of pregnancy losses and placental sufficiency are also reported. Most recently, the role of environmental chemicals in shifting sex ratios (also seen in epidemiologic studies) and in affecting heritable DNA changes have become outcomes of interest.

7.4.2.1. Female Reproductive Effects

Urban Air

Windows of exposure are important in determining reproductive success as an adult. Exposure as a neonate may have a drastically different impact than does a similar adult exposure. To test this, female BALB/C mice were exposed to ambient air in Sao Paulo as neonates or as adults and then were bred to non-exposed males (Mohallem et al., 2005, [088657](#)). Ambient concentrations of the pollutants CO, NO₂, PM₁₀, and SO₂ were 2.2 ± 1.0 ppm, 107.8 ± 42.3 $\mu\text{g}/\text{m}^3$, 35.5 ± 12.8 $\mu\text{g}/\text{m}^3$, and 11.2 ± 5.3 $\mu\text{g}/\text{m}^3$, respectively. They reported decreased fertility in animals exposed as newborns, but not in adult-exposed female BALB/c mice. There were a significantly higher number of liveborn pups from dams housed in filtered chambers (PM and gaseous components removed) versus animals exposed to ambient air as newborns. There was also a higher incidence of implantation failures in dams reared as newborns in polluted chambers. Sex ratio, number of pregnancies per group, resorptions, fetal deaths, and fetal placental weights did not differ significantly by exposure group. Thus, in these studies, exposure to ambient air pollution affected future reproductive success of females if they were exposed as neonates and not if exposed as adults.

Diesel Exhaust

Significant work has been done in male rodent models to determine the effect of PM exposure on reproductive outcomes, with fewer studies conducted using female rodents. Tsukue et al. (2004, [096643](#)) exposed pregnant C57-BL mice to DE (0.1 mg/m^3) or to clean air (controls) for 8 h/day from GD2-13. The concentration of the gaseous materials including NO, NO_x, NO₂, CO and SO₂ are 2.2 ± 0.34 ppm, 2.5 ± 0.34 ppm, 0.0 ppm, 9.8 ± 0.69 ppm, and <0.1 ppm (not detectable), respectively. At GD14 female fetuses were collected for analysis of mRNA for two genes involved in sexual differentiation (Ad4BP-1/SF-1 and MIS), and found no significant changes. Work by Yoshida et al. (2006, [097015](#)) showed changes in these two transcripts in male ICR fetuses exposed to similar concentrations of DE, albeit with different daily durations of exposure. Further work by Yoshida et al. (2006, [097015](#)) showed that of three mouse strains tested, ICR male fetuses were the most sensitive to DE-dependent changes in these two genes. Nonetheless, strain sensitivity to DE particles may also differ by sex. Thus, it appears that female mice exposed in utero to DE show a lack of response at the mRNA level of MIS or Ad4BP-1/SF-1, important genes in male sexual differentiation that showed DE-dependent changes in male pups from dams exposed in utero. Female fetuses have shown a decrease in BMP-15, which is related to oocyte development (Tsukue et al., 2004, [096643](#)).

A sensitive measure of androgenic activity in male rodents is anogenital distance (AGD), i.e., decreased AGD is seen with exposure to anti-androgenic environmental chemicals, the phthalates (Foster et al., 1980, [094701](#); Foster et al., 2001, [156442](#)). To assess the role of DE exposure on reproductive success and anti-androgenic effects on offspring, Tsukue et al. (2002, [030593](#)) exposed 6 week-old female C57-BL mice to 4 mo of DE (0.3 , 1.0 , or 3.0 mg/m^3 ; PM MMAD of 0.4 μm) or filtered air. DE-exposed estrous females had significantly decreased uterine weight (1.0 mg/m^3). Some of the DE-exposed females were bred to unexposed males and DE-exposure led to increased, albeit not significantly increased, rates of pregnancy loss in mated females (up to 25%). Offspring were weighed after birth and decreases in body weight were observed at 6 and 8 wk (males and females, 1.0 and 3.0 mg/m^3) and 9 wk (females, 1.0 and 3.0 mg/m^3). Anogenital distance was decreased in 70-day old DE-exposed male offspring (0.3 mg/m^3). In female offspring at 70 days of

age, lower organ weights (adrenals, liver, and thymus) were observed (1.0 mg/m^3) compared to controls; thymus weight of the 0.3 mg/m^3 females was also lower at 70 days. Crown to rump length in females from dams exposed to DE (1.0 and 3.0 mg/m^3) was less than the control group. In conclusion, adult exposure to DE led to maternal-dependent reproductive changes that affected outcomes in offspring that manifested as decreased pup body weight, anti-androgenic effects like decreased AGD and decreased organ weight (which may have been confounded by changes in body weight because weights were not reported as relative organ weights).

7.4.2.2. Male Reproductive Effects

Diesel Exhaust

Studies were performed to determine PM-dependent strain sensitivity of the male reproductive tract using male steroidogenic enzymes as the model pathway. Three strains of pregnant mice (ICR, C57Bl/6J or ddY mice) were continuously exposed to DE at 0.1 mg/m^3 via inhalation or clean air over gestational days 2-13 (Yoshida et al., 2006, [156170](#)). At GD14, dams were euthanized and fetuses were collected. Male fetuses were collected from each dam for mRNA analysis of genes related to male gonad development including Mullerian inhibiting substance (MIS; crucial for sexual differentiation including Mullerian duct regression in males), steroid transgenic factor (Ad4BP/SF-1, an enzyme in the testosterone synthesis pathway), cytochrome P450 cholesterol side chain cleavage enzyme (P450scc), and other steroidogenic enzymes [17β -hydroxysteroid dehydrogenase (HSD), cytochrome P450 17α -hydroxylase (P450c17), and 3β -hydroxysteroid dehydrogenase (3β HSD)]. There were significant decreases in MIS (ICR and C57BL/6 mice) and Ad4BP/SF-1 (ICR mice) compared to the control groups. The ddY strain demonstrated no changes in Ad4BP/SF-1 or MIS, which may be due to marked changes in 3β -hD expression compared to non-DE exposed controls. From these studies, it appears that mouse strains with in utero exposure to DE show differential sensitivity in gonadal differentiation genes (mRNA) expression in male offspring; ICR are the most sensitive, followed by C57BL/6, with ddY mice being the least sensitive.

Yoshida et al. (2006, [097015](#)) also monitored changes in the male reproductive tract after in utero exposure to DE. Timed-pregnant ICR dams were exposed during gestation (2 days post-coitus [dpc]-16 dpc) to continuous DE (0.3 , 1.0 or 3.0 mg/m^3) or clean air. The reproductive tracts of male offspring were monitored at 4 wk postnatally. These pups received possible continued exposure through lactation as dams were exposed to DE during gestation and nursed pups. Exposure to 0.3 mg/m^3 of DE had no effect on male reproductive organ weight or serum testosterone. The intermediate concentration of 1.0 mg/m^3 induced increases in serum testosterone. Exposure to the higher concentration (1.0 and 3.0 mg/m^3) of DE led to significant increases in reproductive gland weight (testis, prostate, and coagulating gland). The organ weights are presented as absolute numbers and not adjusted for body weight, which is sometimes problematic for complete representation of hormonal changes, as body weight may confound absolute organ weight changes. Transcripts relating to male sexual differentiation (MIS and AD4BP/SF-1, 1.0 and 3.0 mg/m^3) were also significantly decreased. Sexual differentiation is a tightly regulated process and these changes in transcription may lead to changes that can affect genitalia development.

The effects of DE exposure on male spermatogenesis have also been demonstrated. Exposure of pregnant ICR mice to DE (2-16 dpc continuous inhalation exposure to 1.0 mg/m^3 or filtered clean air) led to impaired spermatogenesis in offspring (Ono et al., 2007, [156007](#)). Male offspring were followed at PND 8, 16, 21 (3 wk), 35 (5 wk) and 84 (12 wk). After 16 dpc, but before termination of the study, all of the animals were transferred to a regular animal care facility and received clean air exposure until the termination of the study. No cross fostering was performed in this experiment, so pups that were born to DE-exposed dams were also nursed on these dams and may have received lactational exposure to DE. The gaseous components of the diluted DE included NO, NO₂, SO₂, and CO₂ at concentrations of 11.75 ± 1.18 , 4.62 ± 0.36 , 0.21 ± 0.01 , and 4922 ± 244 ppm, respectively. Body weight was significantly depressed at PNDs 8 and 35. Accessory gland relative weight was significantly increased at PND8 and PND16 only. Serum testosterone was significantly decreased at 3 wk and was significantly increased at 12 wk. At 5 and 12 wk, daily sperm production (DSP) was significantly decreased. FSH receptor and StAR mRNA levels were significantly increased at 5 and 12 wk, respectively. Relative testis weight and relative epididymal weight were unchanged at all

time points. Histological changes showed sertoli cells with partial vacuolization and a significant increase in testicular multinucleated giant cells in the seminiferous tubules of DE-exposed animals compared to control. This study indicates that in utero exposure to DE had effects on spermatogenesis in offspring at the histological, hormonal and functional levels.

In utero exposure to DE and its effect on adult body weight, sex ratio, and male reproductive gland weight was measured by Yoshida et al. (2006, [097015](#)). Pregnant ICR mice were exposed by inhalation to DE (0.3, 1.0 or 3.0 mg/m³) or clean air from 2 dpc to 16 dpc. Pups were allowed to nurse in clean air on exposed dams until weaning and at PND28, male pups were sacrificed. At this time, serum testosterone and pup reproductive gland weight was determined. Significant increases in relative reproductive organ weights were reported at 1.0 and 3.0 mg/m³ for the seminal vesicle, testis, epididymis, coagulating gland, prostate and liver. Male pup serum testosterone was significantly increased at 1.0 mg/m³. Mean testosterone positively correlated with testis weight, DSP, aromatase and steroidogenic enzyme message levels (P450cc, c17 lyase, and P450 aromatase). Sex ratio did not differ in DE-exposed animals versus control. Male pup body weight of DE-exposed animals was significantly increased at PND28 (1.0 and 3.0 mg/m³). These studies show that in utero DE-exposure led to increased serum testosterone and increased reproductive gland weight in male offspring early in life.

The effects of DE on murine adult male reproductive function were studied by exposing ICR male mice (6 wk of age) to DE (clean air control, 0.3, 1.0 or 3.0 mg/m³) for 12 h/day for 6 mo with another group receiving a 1-mo recovery of clean air post-exposure (Yoshida and Takeda, 2004, [097760](#)). After 6 mo of DE exposure, there was a concentration-dependent increase in degeneration of seminiferous tubules and a decrease in DSP/g of testis tissue. After 6 mo exposure to DE particles plus 1 mo of recovery in clean air, significant decreases remained in DSP at the two highest concentrations. The effect of ingestion of deposited PM on the fur with grooming cannot be ruled out as a possible exposure pathway in this experiment.

To expand on PM-dependent changes in spermatogenesis, an eloquent DE-exposure model was designed to determine if PM or the gaseous phase of DE was responsible for changes in sperm production in rodents (Watanabe, 2005, [087985](#)). Pregnant dams (F344/DuCrj rats) exposed to DE (6 h/day exposure to 0.17 or 1.71 mg/m³; <90% of PM less than 0.5 μm; NO₂ concentrations 0.10 and 0.79 ppm, respectively) or filtered air (removing PM only, low concentration filtered air and high concentration filtered air) from GD7 to parturition produced adult male offspring with a decreased number of sertoli cells and decreased DSP (PND 96) when compared to control mice exposed to clean air. The concentrations of NO₂ for the low and high filtered exposure groups were 0.1 and 0.8 ppm, respectively. Because both PM-filtered and DE-exposure groups showed the same outcomes, the effects are likely due to gaseous components of DE.

Motorcycle Exhaust

Adult male (8-wk old) Wistar rats were exposed to motorcycle exhaust (ME) for 1 h in the morning and 1 h in the afternoon (5 day/wk) at 1:50 dilution for 4 wk (group A), 1:10 dilution for 2 wk (group B) or 4 wk (group C), or to clean air (Huang et al., 2008, [156574](#)). After 4 wk of exposure, both exposed groups had significantly decreased body weight compared to the control group. All three ME exposure groups showed a decreased number of spermatids in the testis. Both 1:10 exposure groups also demonstrated decreased caudal epididymal sperm counts. Group C had significant decreased testicular weight, decreased mRNA expression for the cytochrome P450 substrate 7-ethoxycoumarin O-de-ethylase, and increased IL-6, IL-1β, and COX-2 mRNA levels. Decreased protein levels of the antioxidant, superoxide dismutase, and increased IL-6 protein were reported for group C when compared to control. In addition, serum testosterone was significantly decreased in group C. Co-treatment with the antioxidant vitamin E resulted in partial attenuation of serum testosterone levels and caudal epididymal sperm counts, and returned IL-6, IL-1β, and COX-2 ME exposure-dependent message levels to baseline. The glutathione antioxidant system and lipid peroxidation were unchanged. In conclusion, male animals exposed to ME showed significant decrements in body weight, spermatid number, and serum testosterone with an increase in inflammatory cytokines. Vitamin E co-treatment with ME-exposure led to an attenuation of inflammation and a partial rescue of testosterone levels and sperm numbers.

Summary of Toxicological Study Findings for Male Reproductive Effects

In summary, laboratory animals exposed to DE in utero or as adults manifest with abnormal effects on the male reproductive system. In utero exposure to DE induced increased reproductive gland weight and increased serum testosterone in early life (PND28), which may lead to early puberty (albeit not measured in this study). With similar in utero DE exposures, later life outcomes include decreased DSP, aberrant sperm morphology, and hormonal changes (testosterone and FSHr decrements). Chronic exposure of adult mice to DE also induced decreased DSP and seminiferous tubule degeneration. DE-dependent effects on male reproductive function have been reported in multiple animal models, with only one model separating exposure based on particulate versus gaseous components. DE and filtered air (gaseous phase only) exposure in utero induced sertoli cell and DSP decrements in both groups, indicating that the gaseous phase of DE was causative. Adult male rats exposed to ME manifested with decreased spermatid number, serum testosterone, and an increase in inflammatory cytokines. Significant effects on the male reproductive system have been demonstrated after exposure to ambient PM sources (DE or ME). Nonetheless, these models often include a complex mixture of gaseous component and PM exposure, which makes interpreting the contribution from PM alone difficult.

7.4.2.3. Multiple Generation Effects

Urban Air

Veras et al. (2009, [190496](#)) investigated pregnancy and female reproductive outcomes in BALB/c female mice exposed to ambient air or PM-filtered ambient air at one of two different time periods (before conception and during pregnancy) near an area of high traffic density in Sao Paulo, Brazil. Exposures were 27.5 and 6.5 $\mu\text{g}/\text{m}^3$ $\text{PM}_{2.5}$ for ambient and PM-filtered air chambers, respectively, with 101 $\mu\text{g}/\text{m}^3$ NO_2 , 1.81 $\mu\text{g}/\text{m}^3$ CO , and 7.66 ppm SO_2 in both chambers. Two groups of 2nd generation (G2) nulliparous female mice were continuously exposed from birth. Estrous cyclicity and ovarian follicle classification were followed at PND60 (reproductive maturation) in one group. A further group was subdivided into four groups by exposures during pregnancy following reproductive capability and pregnancy outcomes of the G2 mice. Animals exposed to ambient air versus PM-filtered air had an extended time in estrous and thus, a reduction in the number of cycles during the study period. The number of antral follicles was significantly decreased in the ambient air versus the PM-filtered air animals. Other follicular quantification (number of small, growing or preovulatory follicles) showed no differences between the two chambers. There was an increase in the time necessary for mating, a decrease in the fertility index, and an increase in the pregnancy index in the ambient air group versus the PM-filtered group. Specifically, in the ambient air groups, there was a significant increase in rate of the post-implantation loss in G1 and G2 groups. However, there was no statistically significant change in number of pups in the litter. Fetal weight was decreased in all treatment groups (ambient air groups G1 and G2, and PM-filtered G2) when compared to the PM-filtered G1 group or animals raised entirely in filtered air, showing that fetal weight was affected by both pre-gestational and gestational PM exposure.

PM exposure prior to conception is associated with increased time in estrous, which in other animal models can be related to ovarian hormone dysfunction and ovulatory problems. These estrous alterations can contribute to fecundity issues. There was no significant difference in number of preovulatory follicles in the above model, but there was a statistically significant decrease in the number of antral follicles (Veras et al., 2009, [190496](#)). Antral follicles are the last stage in follicle development prior to ovulation, and a decrease in antral follicle number can be related to premature reproductive senescence, premature ovarian failure, or early menopause, which were not followed in this study.

In this study (Veras et al., 2009, [190496](#)), the males that were used to generate the G1 and G2 groups were also exposed to ambient air or PM-filtered ambient air, and thus the reproductive contribution of these males to the overall fertility and mating changes in the females cannot be totally eliminated as a possible confounder to the observed effects. Thus, these effects are hard to differentiate as male- or female-dependent and likely indicate a general loss of reproductive fitness. Interestingly, both pre- and gestational exposure to ambient air induced a significant loss in post-

implantation of fetuses and this may be related to placental insufficiency as has been described in other work by this lab (Veras et al., 2008, [190493](#)).

7.4.2.4. Receptor Mediated Effects

Arylhydrocarbon Receptor (AhR)

Diesel Exhaust Particles

The AhR is often activated by chemicals classified as endocrine disrupting compounds (EDCs), exogenous chemicals that behave as hormonally active agents, disrupting the physiological function of endogenous hormones. DE particles are known to activate the AhR. A recent study by Izawa et al. (2007, [190387](#)) showed that certain polyphenols (quercetin from the onion) and food extracts (Ginkgo biloba extract) are able to attenuate DE particle-dependent AhR activation when measured with the Ah-Immunoassay, thus possibly attenuating the EDC activity of DE particles.

7.4.2.5. Developmental Effects

Sex Ratio

Urban Air

A correlation between PM₁₀ exposure and a decrease in standardized sex ratios (SSRs) has been reported in humans exposed to air pollution (Lichtenfels et al., 2007, [097041](#); Wilson et al., 2000, [010288](#)), with fewer numbers of male births reported. To understand this shift, two groups (control and exposed) of male Swiss mice were housed concurrently in Sao Paulo and received either ambient air exposure or filtered air (chemical and particulate filtering) from PND10 for 4 mo (Lichtenfels et al., 2007, [097041](#)). Filtration efficiency for PM_{2.5}, CB, and NO₂ inside the chamber was found to be 55%, 100%, and 35%, respectively. After this exposure, non-exposed females were placed in either chamber to mate. After mating, the males were sacrificed and testes collected; males exposed to ambient air showed decreased testicular and epididymal sperm counts, decreased total number of germ cells, and decreased elongated spermatids, but no significant change in litter size. Females were housed in the chambers and sacrificed on GD19 when the number of pups born alive and the sex ratio were obtained. There was a significant decrease in the SSR for pups born after living in the ambient air-exposed chamber compared to the filtered chamber. In this study, a shift in SSR has been shown for both humans and rodents exposed to air pollution, but other studies with DE exposure (Yoshida et al., 2006, [156170](#)) or ambient air in Sao Paulo (Mohallem et al., 2005, [088657](#)) showed no changes in rodent sex ratio. Possible exposure to PM and other components of ambient air via ingestion during grooming cannot be ruled out in this rodent model.

Immunological Effects: Placenta

Diesel Exhaust

Placental insufficiency can lead to the loss of a pregnancy or to adverse fetal outcomes. DE-exposure has been shown to induce inflammation in various models. Fujimoto et al. (2005, [096556](#)) assessed cytokine/immunological changes of DE-dependent inhalation exposure on the placenta during pregnancy. Pregnant Slc:CR mice were exposed to DE (0.3, 1.0, or 3.0 mg/m³; PM MMAD of 0.4 μm) or clean air from 2 to 13 dpc and dams, placenta, and pups were collected at 14 dpc. There was a significant increase in the number of absorbed placentas in DE-exposed animals (0.3

and 3.0 mg/m³) with a significant decrease in the number of absorbed placentas in DE-exposed animals at the middle concentration (1.0 mg/m³). Absorbed placentas from DE exposed mice had undetectable levels of CYP1A1 and twofold increases in TNF- α ; CYP1A1 placental mRNA from healthy placentas of DE-exposed mice was unchanged versus control. IL-2, IL-5, IL-12 α , IL-12 β and GM-CSF mRNA significantly increased in placentas of DE-exposed animals (0.3 and 3.0 mg/m³). Fujimoto et al. (2005, [096556](#)) reported DE-induced significant increases in multiple inflammatory markers in the placenta with significant increases in the number of absorbed placentas.

Immunological Effects: Asthma

Model Particles

In utero exposure may confer susceptibility to PM-induced asthmatic responses in offspring. Exposure of pregnant BALB/c mice to aerosolized ROFA leachate by inhalation or to DE particles intranasally increases asthma susceptibility to their offspring (Fedulov et al., 2008, [097482](#); Hamada et al., 2007, [091235](#)). The offspring from dams exposed for 30 min to 50 mg/mL ROFA 1, 3, or 5 days prior to delivery responded to OVA immunization and aerosol challenge with airway hyperreactivity and increased antigen-specific IgE and IgG1 antibodies (Hamada et al., 2007, [091235](#)). Airway hyperreactivity was also observed in the offspring of dams intranasally instilled with 50 μ g of DE particles or TiO₂, or 250 μ g CB, indicating that the same effect could be demonstrated using relatively “inert” particles (Fedulov et al., 2008, [097482](#)). Pregnant mice were particularly sensitive to exposure to DE or TiO₂ particles, and genetic analysis indicated differential expression of 80 genes in response to TiO₂ in pregnant dams. Thus pregnancy and in utero exposure may enhance responses to PM, and exposure to even relatively inert particles may result in offspring predisposed to asthma.

Placental Morphology

Urban Air

Exposure to ambient air pollution during pregnancy is associated with reduced fetal weight in both human and animal models. The effect of particulate urban air pollution on the functional morphology of the mouse placenta was explored by exposing second generation mice in one of four groups to urban Sao Paulo air (PM was 67% PM_{2.5}, mainly of vehicular origin) or filtered air (Veras et al., 2008, [190493](#)). Experimental design was: group F-F comprised of mice that were raised in filtered air chambers and completed pregnancy in filtered air chambers; group F-nF raised in filtered air and pregnant in ambient air; group nF-nF raised and completed pregnancy in non-filtered air chambers; and group nF-F mice raised in ambient air and received filtered air during pregnancy. Mean PM_{2.5} concentrations in the F and nF chambers were 6.5 and 27.5 μ g/m³, respectively. Exposure was from PND20-PND60. After this exposure, the animals were mated and then maintained in their respective chambers during pregnancy. Pregnancy was terminated at GD8 (near term) with placentas and fetuses collected for analysis.

Exposure to ambient PM pre-gestationally or gestationally led to significantly smaller fetal weight (total litter weight). Pregestational exposure to ambient air induced significant increases in fetal capillary surface area and total mass-specific conductance, but this may be explained by reduced maternal/dam blood space and diameters. Gestational exposure to non-filtered air was associated with reduced volume, diameter (caliber) and surface area of maternal blood space with compensatory greater fetal capillary surface and oxygen diffusion conduction rates. Intravascular barrier thickness, a quantitative relationship between trophoblast volume and the combined surfaces of maternal blood spaces and fetal capillaries, was not reduced with ambient air exposure. This study provides evidence that fetal/placental circulatory adaptation to maternal blood deficits after ambient PM exposure may not be sufficient to overcome PM-dependent birth weight deficits in mice exposed to ambient air, with the magnitude of this effect greater in the gestationally-exposed groups.

Placental Weights and Birth Outcomes

Urban Air

Pregnant female Swiss mice were exposed to ambient air (Sao Paulo) or filtered air over various portions of gestation to determine if there was an association between fetal or placental weight or birth outcomes with exposure to air pollution (Rocha et al., 2008, [096685](#)). The reported ambient concentrations of PM₁₀ ($42 \pm 17 \mu\text{g}/\text{m}^3$), NO₂ ($97 \pm 39 \mu\text{g}/\text{m}^3$), and SO₂ ($9 \pm 4 \mu\text{g}/\text{m}^3$) were measured 100 m away from the rodent exposure chambers. By using six time windows of exposure that covered 1-3 wk of gestation (the entire gestation period in a mouse), a significant decrease in near-term fetal weight (GD19) was induced by ambient air-exposure during the first week of gestation. Decreased placental weight could be induced by ambient air exposure during any of the 3 wk of gestation. This study points to possible windows of exposure that may be important in evaluating epidemiologic study results.

Neurodevelopmental Effects

Diesel Exhaust

The diagnosis of autism is on the rise in the Western world with its etiology mostly unknown. Autism-associated cell loss is brain region-specific and hypothesized to be developmental in origin. Sugamata et al. (2006, [097166](#)) exposed pregnant ICR mice to DE ($0.3 \text{ mg}/\text{m}^3$) continuously from 2 dpc to 16 dpc. Pups with in utero exposure to DE were nursed in clean air chambers, but may have received gastro-intestinal exposure via lactational transfer of various components of DE. At 11 wk of age, cerebellar brain tissue was collected. Earlier work has shown that DE particles ($<0.1 \mu\text{m}$) have been detected in the brains (cerebral cortex and hippocampus) of newborn pups who were born to dams exposed to DE during pregnancy (Sugamata et al., 2006, [097166](#)). Histological analysis of DE-exposed pup cerebella revealed significant increases in caspase-3 (c-3) positive cells compared to control and significant decreases in cerebella Purkinje cell numbers in DE-exposed animals versus control. The ratio of cells positive for apoptosis (c-3 positive) showed a nearly significant sex difference with males displaying increased apoptosis versus females ($p = 0.09$). In humans with autism, the cerebellum has a decreased number of Purkinje cells, which is thought to be fetal and developmental in origin; further, these authors speculate that humans may be more sensitive to DE-dependent neuronal brain changes, as the human placenta is two-layers thick compared to the mouse placenta that is four layers thick.

Behavioral Effects

Diesel Exhaust Particles

Body weight decrements at birth have recently been associated through the Barker hypothesis with adverse adult outcomes. Thus, many publications have begun to focus on decreased birth weight for gestational age and associated adult changes. Hougaard et al. (2008, [156570](#)) exposed 40 timed-pregnant C57BL/6 dams to DE particles reference materials (SRM 2975) via inhalation over GD7-GD19 of pregnancy. They found significantly decreased pup weight at weaning, albeit not at birth. PM-dependent liver changes were monitored by following various inflammatory and genotoxicity-related mRNA transcripts and there were no significant differences in pups at PND2. The comet assay from PND2 pup livers showed no significant differences in DNA damage between DE particle-exposed and control animals. The prohormone, thyroxine, was unchanged in control and DE particle-exposed dams and offspring at weaning. At 2 mo, female DE particle-exposed pups required less time than controls to locate the platform in its new location during the first trial of the spatial reversal learning task in the Morris water maze. Thus, DE particle exposure during in utero development led to behavioral changes without body weight at weaning or changes in inflammatory markers or thyroid hormone levels.

Diesel Exhaust

The effect of in utero DE exposure on CNS motor function was evaluated in male pups (ICR mice) after dams received DE exposure (8h/d×5d/wk) from GD2-GD17 (Yokota et al., 2009, [190518](#)). The exposure atmosphere contained concentrations of 1.0 mg/m³ for particle mass, 2.67 ppm CO, 0.23 ppm NO₂, and <0.01 ppm SO₂. Spontaneous motor activity was significantly decreased in pups (PND35), as was the dopamine metabolite homovanillic acid measured in the striatum and nucleus accumbens, indicating decreased dopamine (DA) turnover. However, DA levels were unchanged in the same areas of the brain. The authors conclude that these data demonstrate that maternal exposure to DE induced hypolocomotion, similar to earlier studies with adult and neonatal DE particle exposure (Peters et al., 2000, [001756](#)), with decreased extracellular DA release.

Lactation

Diesel Exhaust

Tozuka et al. (2004, [090864](#)) monitored the transfer of PAHs to fetuses and breast milk of F344 rats exposed to DE (6h/day) for 2 wk from GD7-GD 20 (minus 4 days for the weekend when no exposure occurred) with PM₁₀ concentration of 1.73 mg/m³. At PND 14, breast milk was collected. Fifteen PAHs were monitored in the DE exposure chamber and seven were quantified in dam blood with levels of phenanthrene (Phe), anthracene (Ant) and benz[a]anthracene (BaA) in the DE group being significantly higher than the control group. In breast milk, Ant, fluoranthene (Flu), pyrene (Pyr), and chrysene (Chr) showed significant increases in the DE group compared to the control group. BaA tended to be about fourfold higher than the control group in breast milk, but the increase was not significant. PAHs in dam livers of DE versus control were not significantly different. The results of this study demonstrate that PAHs derived from DE are transferred across the placenta from the DE-exposed dam to the fetus. Lactational transfer through the breast milk is also likely as PAHs were detected in dam breast milk, but this should be confirmed in future studies that cross foster control and exposed dams and pups. The lipophilicity of the PAH based on its structure likely affected its uptake in the dam, as PAHs with 3 or 4 rings were found in maternal blood and PAHs with 5 or 6 rings were not detected.

Heritable DNA Changes and Epigenetic Changes

Ambient Air

To address the role of ambient air exposure on heritable changes, Somers et al. (2004, [078098](#)) exposed mice to ambient air in at a rural Canadian site or at an urban site near a steel mill. They showed that offspring of mice exposed to ambient air in urban regions inherited paternal-origin expanded simple tandem repeat (ESTR) mutations 1.9-2.1 times more frequently than offspring of mice exposed to HEPA filtered air or those exposed to rural ambient air. Mouse expanded simple tandem repeat (ESTR) DNA is composed of short base pair repeats which are unstable in the germline and tend to mutate by insertion or deletion of repeat units. In vivo and in situ studies have shown that murine ESTR loci are susceptible to ionizing radiation, and other environmental mutagen-dependent germline mutations, and are thus good markers of exposure to environmental contaminants.

Expanding upon the above work and to determine if PM or the gaseous phase of the urban air was responsible for heritable mutations, Yauk et al. (2008, [157164](#)) exposed mature male C57Bl×CBA F1 hybrid mice to either HEPA-filtered air or to ambient air in Hamilton, Ontario, Canada for 3 or 10 wk, or 10 wk plus 6 wk of clean air exposure (16 wk). Sperm DNA was monitored for expanded simple tandem repeat (ESTR) mutations. In addition, male-germ line (spermatogonial stem cell) DNA methylation was monitored post-exposure. This area in Hamilton is near two steel mills and a major highway. Air quality data provided by the Ontario Ministry of the Environment showed the highest concentrations of TSP and metals at week 4 (93.8 ± 17 and 3.6 ± 0.7 µg/m³, respectively) and PAH at week 3 (8.3 ± 1.7 ng/m³). Mutation frequency at ESTR

Ms6-hm locus in sperm DNA from mice exposed 3 or 10 wk did not show elevated ESTR mutation frequencies, but there was a significant increase in ESTR mutation frequency at 16 wk in ambient air-exposed males versus HEPA filter-exposed animals, pointing to a PM-dependent mechanism of action. When compared to HEPA filter air-exposed males, ambient air-exposed males manifested with hypermethylation of germ-line DNA at 10 and 16 wk. These PM-dependent epigenetic modifications (hypermethylation) were not seen in the haploid stage (3 wk) of spermatogenesis, but were nonetheless seen in early stages of spermatogenesis (10 wk) and remained significantly elevated in mature sperm even after removal of the mouse from the environmental exposure (16 wk). Thus, these studies indicate that the ambient PM phase and not the gaseous phase is responsible for the increased frequency of heritable DNA mutations and epigenetic modifications.

7.4.3. Summary and Causal Determinations

7.4.3.1. PM_{2.5}

The 1996 PM AQCD concluded that while few studies had been conducted on the link between PM and infant mortality, the research “suggested an association,” particularly for post-neonates (U.S. EPA, 1996, [079380](#)). In the 2004 PM AQCD, additional evidence was available on PM’s effect on fetal and early postnatal development and mortality and while some studies indicated a relationship between PM and pregnancy outcomes, others did not (U.S. EPA, 2004, [056905](#)). Studies identifying associations found that exposure to PM₁₀ early during pregnancy (first month of pregnancy) or late in the pregnancy (6 wk prior to birth) were linked with higher risk of preterm birth, including models adjusted for other pollutants, and that PM_{2.5} during the first month of pregnancy was associated with IUGR. However, other work did not identify relationships between PM₁₀ exposure and low birth weight. The state of the science at that time, as indicated in the 2004 PM AQCD, was that the research provided mixed results based on studies from multiple countries.

Building on the evidence characterized in the previous AQCDs, recent epidemiologic studies conducted in the U.S. and Europe were able to examine the effects of PM_{2.5}, and all found an increased risk of low birth weight (Section 7.4.1). Exposure to PM_{2.5} was usually associated with greater reductions in birth weight than exposure to PM₁₀. All of the studies that examined the relationship between PM_{2.5} and preterm birth report positive associations, and most were statistically significant. The studies evaluating the association between PM_{2.5} and growth restriction all found positive associations, with the strongest evidence coming when exposure was assessed during the first or second trimester (Section 7.4.1). For infant mortality (<1 yr), several studies examined PM_{2.5} and found positive associations (Section 7.4.1).

Animal toxicological studies reported effects including decreased uterine weight, limited evidence of male reproductive effects, and conflicting reports of reproductive outcomes in male offspring, particularly in studies of DE (Section 7.4.2). Toxicological studies also reported effects for several development outcomes, including immunological effects (placental and related to asthma), neurodevelopmental and behavioral effects (Section 7.4.2).

In summary evidence is accumulating from epidemiologic studies for effects on low birth weight and infant mortality, especially due to respiratory causes during the post-neonatal period. The mean PM_{2.5} concentrations during the study periods ranged from 5.3-27.4 µg/m³. Exposure to PM_{2.5} was usually associated with greater reductions in birth weight than exposure to PM₁₀. Several U.S. studies of PM₁₀ investigating fetal growth reported 11-g decrements in birth weight associated with PM₁₀ exposure. Most of these studies were conducted in California, where PM_{2.5} and PM_{10-2.5} contribute almost equally to the PM₁₀ mass concentration. So while these results can not be attributed to one size fraction or the other, the consistency of the results strengthens the interpretation that particle exposure may be causally related to reductions in birth weight. Similarly, animal evidence supported an association between PM_{2.5} and PM₁₀ exposure and adverse reproductive and developmental outcomes, but provided little mechanistic information or biological plausibility for an association between long-term PM exposure and adverse birth outcomes, including low birth weight, or infant mortality. Epidemiologic studies do not consistently report associations between PM exposure and preterm birth, growth restriction, birth defects or decreased sperm quality. New evidence from animal toxicological studies on heritable mutations is of great interest, and warrants further investigation. Overall, the epidemiologic and toxicological evidence is **suggestive of a**

causal relationship between long-term exposures to PM_{2.5} and reproductive and developmental outcomes.

7.4.3.2. PM_{10-2.5}

Evidence is **inadequate to determine if a causal relationship exists between long-term exposure to PM_{10-2.5} and developmental and reproductive outcomes** because studies have not been conducted in sufficient quantity or quality to draw any conclusion. A single study found an association between PM_{10-2.5} and birthweight (-13 g [95% CI: -18.3 to -7.6] per 10 µg/m³ increase), but no such association for PM_{2.5} (Parker et al., 2008, [156013](#)).

7.4.3.3. UFPs

The 2004 PM AQCD did not report long-term exposure studies for UFPs. No epidemiologic or animal toxicology studies have been conducted to evaluate the effects of long-term UFP exposure and reproductive and developmental effects. Ambient air exposures, which likely include UFPs, are reported in this ISA but there is no delineation of the separate contribution from UFPs. The evidence is **inadequate to determine if a causal relationship exists between long-term UFP exposures and reproductive and developmental effects.**

7.5. Cancer, Mutagenicity, and Genotoxicity

Evidence from epidemiologic and animal toxicological studies has been accumulating for more than three decades regarding the mutagenicity and carcinogenicity of PM in the ambient air. DE has been identified as one source of PM in ambient air, and has been extensively studied for its carcinogenic potential. In 1989, the International Agency for Research on Cancer (IARC) found that there was sufficient evidence that extracts of DE particles were carcinogenic in experimental animals and that there was limited evidence for the carcinogenic effect of DE in humans (IARC, 1989, [002958](#)). This conclusion was based on studies in which organic extracts of DE particles were used to evaluate the effects of concentrates of the organic compounds associated with carbonaceous soot particles. These extracts were applied to the skin or administered by IT instillation or intrapulmonary implantation to mice, rats, or Syrian hamsters and an excess of tumors on the skin, lung or at the site of injection were observed.

In 2002, the U.S. EPA reviewed over 30 epidemiologic studies that investigated the potential carcinogenicity of DE. These studies, on average, found that long-term occupational exposures to DE were associated with a 40% increase in the relative risk of lung cancer (U.S. EPA, 2002, [042866](#)). In the same report the U.S. EPA concluded that extensive studies with salmonella had unequivocally demonstrated mutagenic activity in both particulate and gaseous fractions of DE. They further concluded that DE may present a lung cancer hazard to humans (U.S. EPA, 2002, [042866](#)). The particulate phase appeared to have the greatest contribution to the carcinogenic effect. Both the particle core and the associated organic compounds demonstrated carcinogenic properties, although a role for the gas-phase components of DE could not be ruled out. Almost the entire diesel particle mass is ≤ 10 µm in diameter (PM₁₀), with approximately 94% of the mass of these particles <2.5 µm in diameter (PM_{2.5}), including a subgroup with a large number of UFPs (U.S. EPA, 2002, [042866](#)). U.S. EPA considered the weight of evidence for potential human carcinogenicity for DE to be strong, even though inferences were involved in the overall assessment, and concluded that DE is “likely to be carcinogenic to humans by inhalation” and that this hazard applies to environmental exposures (U.S. EPA, 2002, [042866](#)).

Two recent reviews of the mutagenicity (Claxton et al., 2004, [089008](#)) and carcinogenicity (Claxton and Woodall, 2007, [180391](#)) of ambient air have characterized the animal toxicological literature on ambient air pollution and cancer. The majority of these toxicological studies have been conducted using IT instillation or dermal routes of exposure. Generally, the toxicological evidence reviewed in this ISA has been limited to inhalation studies conducted with lower concentrations of

PM (<2 mg/m³), relevant to current ambient concentrations and the current regulatory standard (Section 1.3). Because this ISA focuses on toxicological studies which use the inhalation route of exposure, it is possible that important evidence for the role of PM in mutagenicity, tumorigenicity, and/or carcinogenicity may be missed. In order to accurately characterize the relationship between PM and cancer and be consistent with the EPA Guidelines for Carcinogen Risk Assessment (U.S. EPA, 2005, [086237](#)), these reviews (that include studies that employ IT instillation and dermal routes of exposure) are summarized briefly.

Claxton et al. (2004, [089008](#)) reviewed the mutagenicity of air in the Salmonella (Ames) assay, and showed that hundreds of compounds identified in ambient air from varying chemical classes are mutagenic and that the commonly monitored PAHs could not account for the majority of mutagenicity associated with most airborne particles. They concluded that the smallest particles have the highest toxicity per particulate mass, with the PM_{2.5} size fraction having greater mutagenic and cytotoxic potential than the PM₁₀ size fraction, which had a higher mutagenic potential than the TSP size fraction. One study reviewed by Claxton et al. (2004, [089008](#)) found that the cytotoxic potential of PM_{2.5} was higher in wintertime samples than in summertime samples. A series of studies on source apportionment for ambient particle mutagenic activity reviewed by Claxton et al. (2004, [089008](#)) indicate that mobile sources (cars and diesel trucks) account for most of the mutagenic activity.

Claxton and Woodall (2007, [180391](#)) reviewed many studies that examined the rodent carcinogenicity of extracts of ambient PM samples; the PM was of various size classes, often from TSP samples. Among a variety of mouse and rat strains, application methods, and samples employed, the authors found no pattern that would suggest the routine use of a particular strain or protocol would be more informative than another. The primary conclusion that comes from the analysis of rodent carcinogenicity studies is that the most polluted urban air samples tested to date are carcinogenic; the contribution of PM and different size classes of PM to the carcinogenic effects of ambient air has not been delineated. The differences in response by the various strains of inbred mice indicate that the genetic background of an individual can influence tumorigenic response. Studies examining different components of ambient PM (e.g., PAHs) confirm that ambient air contains multiple carcinogens, and that the carcinogenic potential of particles from different airsheds can be quite different. Therefore, one would expect the incidence of cancers related to ambient air exposure in different metropolitan areas to differ.

Numerous epidemiologic and animal toxicological studies of ambient PM and their contributing sources have been conducted to assess the relative mutagenic or genotoxic potential. Studies previously reviewed in the 2004 PM AQCD (U.S. EPA, 2004, [056905](#)) provide evidence that ambient PM as well as PM from specific combustion sources (e.g., fossil fuels) is mutagenic in vivo and in vitro. Building on these results, data from recent epidemiologic and animal toxicological studies that evaluated the carcinogenic, mutagenic and/or genotoxic effects of PM, PM-constituents, and combustion emission source particles are reviewed in this section.

7.5.1. Epidemiologic Studies

The 2004 PM AQCD reported on original and follow-up analyses for three prospective cohort studies that examined the relationship between PM and lung cancer incidence and mortality. Based on these findings, as well as on the results from case-control and ecologic studies, the 2004 PM AQCD concluded that long-term PM exposure may increase the risk of lung cancer incidence and mortality. The largest of the three prospective cohort studies included in the 2004 PM AQCD was the ACS study (Pope et al., 2002, [024689](#)). This study was the follow-up to the original ACS study (Pope et al., 1995, [045159](#)), and included a longer follow-up period and reported a statistically significant association between PM_{2.5} exposure and lung cancer mortality.

A 14- to 16-yr prospective study conducted using the Six Cities Study cohort reported a slightly elevated risk of lung cancer mortality for individuals living in the most polluted city (mean PM₁₀: 46.5 µg/m³; mean PM_{2.5} 29.6 µg/m³) as compared to the least polluted city (mean PM₁₀: 18.2 µg/m³; mean PM_{2.5} 11.0 µg/m³) but the association was not statistically significant (Dockery et al., 1993, [044457](#)).

Re-analysis of the AHSMOG cohort, a study of non-smoking whites living in California, concluded that elevated long-term exposure to PM₁₀ was associated with lung cancer incidence among both men and women (Beeson et al., 1998, [048890](#)). The original study had reported an excess of incident lung cancers only among women (Abbey et al., 1991, [042668](#)). Further reanalysis

of this cohort revealed an association between PM₁₀ and lung cancer mortality among men but no association among women (Abbey et al., 1999, [047559](#)). In addition, McDonnell et al. (2000, [010319](#)) reported increases in lung cancer mortality with long-term exposure to PM_{2.5} in the AHSMOG cohort; no association was seen for PM_{10-2.5}.

7.5.1.1. Lung Cancer Mortality and Incidence

The following sections will examine extensions of the above mentioned cohort studies and new studies published since the 2004 PM AQCD. The section includes discussion of both lung cancer incidence and mortality, as well as markers of exposure/susceptibility. A summary of the mean PM concentrations reported for the new studies is presented in Table 7-6. In addition, a summary of the associations for lung cancer mortality and incidence are presented in Table 7-7 and Figure 7-7 (Section 7.6) Further discussion of all-cause and cause-specific mortality is presented in Section 7.6.

Table 7-6. Characterization of ambient PM concentrations from recent studies of cancer and long-term exposures to PM.

Study	Location	Pollutant	Mean Annual Concentration (µg/m ³)	Upper Percentile Concentrations (µg/m ³)
Brunekreef et al. (2009, 191947)	The Netherlands	PM _{2.5}	28.3	Max: 36.8
Bonner et al. (2005, 088993)	Western NY State	TSP	44	
Jerret et al. (2005, 087600)	Los Angeles, California	PM _{2.5}		Max:27.1
Laden et al. (2006, 087605)	6 U.S. cities	PM _{2.5}	Range of means across sites: 10.2-29.0 Avg of means across sites: 16.4	
Naess et al. (2007, 090736)	Oslo, Norway	PM _{2.5}	15	Max: 22
		PM ₁₀	19	Max: 30
Palli et al. (2008, 156837)	Florence, Italy	PM ₁₀	NR	
Pedersen et al. (2006, 156848)	Czech Republic	PM _{2.5}		Max: 46-120
		PM ₁₀		Max: 120-238.6
Sorensen et al. (2005, 083053)	Copenhagen, Denmark	PM _{2.5}	Range of means across sites: 12.6-20.7 Avg of means across sites: 16.7	75th: 24.3-27.7
Sram et al. (2007, 188457)	Czech Republic	PM ₁₀		Max: 55
		PM _{2.5}		Max: 38
Sram et al. (2007, 192084)	Czech Republic	PM ₁₀	Range of means across sites: 36.4-55.6 Avg of means across sites: 46.0	
		PM _{2.5}	Range of means across sites: 24.8-44.4 Avg of means across sites: 34.6	
Vineis et al. (2006, 192089)	Multi-city, Europe	PM ₁₀	Range of means across sites: 19.9-73.4 Avg of means across sites: 35.4	
Vinzents et al. (2005, 087482)	Copenhagen, Denmark	PM ₁₀	Range of means across sites: 16.9-23.5 Avg of means across sites: 20.2	

A subset of the ACS cohort study from 1982 to 2000 that included only residents of Los Angeles, California was used to examine the association between PM_{2.5} and lung cancer mortality while adjusting for both individual and neighborhood covariates (Jerrett et al., 2005, [087600](#)). There was a positive association between PM_{2.5} and lung cancer mortality when adjusting for 44 individual covariates (RR 1.44 [95% CI: 0.98-2.11] per 10 µg/m³ increase in PM_{2.5}). However, including all potential individual and neighborhood covariates associated with mortality reduced the association

(RR 1.20 [95% CI: 0.79-1.82] per 10 $\mu\text{g}/\text{m}^3$ increase in $\text{PM}_{2.5}$). A recent re-analysis of the full ACS cohort also demonstrated a positive association between $\text{PM}_{2.5}$ and lung cancer mortality (RR 1.11 [95% CI: 1.04-1.18]) (Krewski et al., 2009, [191193](#)). The authors observed modification of this risk by educational attainment, with those completing a high school degree or less having greater risk. In addition to utilizing the ACS cohort for a nationwide analysis, this same study conducted two regional assessments, one in the New York City area and the other in the Los Angeles area. No association was detected between $\text{PM}_{2.5}$ and lung cancer mortality in the analysis of the region included in the New York City analysis. A positive association was observed in the Los Angeles-area analysis using an unadjusted model, but this association did not persist after control for individual, ecologic, and copollutant covariates.

The Six Cities Study was extended to include data from 1990-1998, a period including 1,368 deaths and 54,735 person-years (Laden et al., 2006, [087605](#)). An elevated risk ratio for lung cancer mortality was reported when the entire follow-up period (1974-1998) was included in the analysis (RR 1.27 [95% CI 0.96-1.69] per 10 $\mu\text{g}/\text{m}^3$ increase in average annual $\text{PM}_{2.5}$). However, estimated decreases in $\text{PM}_{2.5}$ were not associated with reduced lung cancer mortality (RR 1.06 (95% CI: 0.43-2.62] for every 10 $\mu\text{g}/\text{m}^3$ reduction in $\text{PM}_{2.5}$).

Naess et al. (2007, [090736](#)) studied individuals aged 51-90 yr living in Oslo, Norway in 1992. Death certificate data were obtained for 1992-1998 and information on PM was collected from 1992-1995. Women had a larger association of lung cancer mortality with $\text{PM}_{2.5}$ compared to men. Similar results were reported for PM_{10} .

Most recently, Brunekreef et al. (2009, [191947](#)) used the Netherlands cohort study (NLCS) on diet and cancer to conduct a re-analysis of the research performed by Beelen et al. (2008, [156263](#)) examining the association between PM and both lung cancer mortality and incidence. After 10 yr of follow-up, there was no association between $\text{PM}_{2.5}$ and lung cancer mortality for either the analysis of the full cohort (n = 105,296) (RR 1.06 [95% CI: 0.82-1.38] per 10 $\mu\text{g}/\text{m}^3$ increase in $\text{PM}_{2.5}$) or the case-cohort (n = 4,075) (RR 0.87 [95% CI: 0.52-1.47]). There was also no association with black smoke or traffic density variables, although living near a major roadway was associated with an elevated relative risk for lung cancer in the full cohort analysis (RR 1.20 [95% CI: 0.98-1.47]). The association was not present in the case-cohort analysis (RR 1.07 [95% CI: 0.70-1.64]).

In addition to lung cancer mortality, Brunekreef et al. (2009, [191947](#)) also examined the association with lung cancer incidence using 11.3 yr of follow-up data. In both the full cohort and the case-cohort analyses no association was reported between $\text{PM}_{2.5}$ and lung cancer incidence (full cohort: RR 0.81 [95% CI: 0.63-1.04]; case-cohort: RR 0.67 [95% CI: 0.41-1.10] per 10 $\mu\text{g}/\text{m}^3$ increase in $\text{PM}_{2.5}$). The same was true for analyses of BS and traffic density variables.

The association between PM and incident lung cancers was examined in the European Prospective Investigation into Cancer and Nutrition study (EPIC) (Vineis et al., 2006, [192089](#)). Within this cohort, a nested case-control study, the GenAir study, included cases of incident cancer and controls matched on age, gender, smoking status, country of recruitment, and time between recruitment and diagnosis. Only non-smokers and former smokers who had quit smoking at least 10 yr prior were included. The study included 113 cases and 312 controls. No association was seen between PM_{10} and lung cancer (OR 0.91 [95% CI: 0.70-1.18] per 10 $\mu\text{g}/\text{m}^3$). The OR was elevated when cotinine, a marker for cigarette exposure, was included in the model but the authors state that this is probably due to small study size (OR 2.85 [95% CI: 0.97-8.33] comparing $\geq 11 \mu\text{g}/\text{m}^3$ to $<11 \mu\text{g}/\text{m}^3$). Control for other potential confounders, such as BMI, education level, and intake of fruit and vegetables, did not have a large impact on the estimate.

Table 7-7. Associations* between ambient PM concentrations from select studies of lung cancer mortality and incidence.

Study	Cohort	Location	Years	Analysis subgroup	Effect Estimate (95% CI)
MORTALITY - PM_{2.5}					
Dockery et al. (1993, 044457) [†]	Six-Cities	Six cities across the U.S.	1974-1991		1.18 (0.89-1.57)
Krewski et al. (2000, 012281) [†]	Six-Cities-Re-analysis	Six cities across the U.S.	1974-1991		1.16 (0.86-1.23)
Laden et al. (2006, 087605)	Six-Cities	Six cities across the U.S.	1974-1998		1.27 (0.96-1.69)
Beelen et al. (2008, 156263)	NLCS	Netherlands	1987-1996	Full Cohort	1.06 (0.82-1.38)
Beelen et al. (2008, 156263)	NLCS	Netherlands	1987-1996	Case Cohort	0.87 (0.52-1.47)
Brunekreef et al. (2009, 191947)	NLCS-Re-analysis	Netherlands	1987-1996	Full Cohort	1.06 (0.82-1.38)
Brunekreef et al. (2009, 191947)	NLCS-Re-analysis	Netherlands	1987-1996	Case Cohort	0.87 (0.52-1.47)
Pope et al. (1995, 045159) [†]	ACS	U.S.	1982-1989		1.01 (0.91-1.12)
Pope et al. (2002, 024689) [†]	ACS	U.S.	1982-2000		1.13 (1.04-1.22)
Jerret et al. (2005, 087600)	ACS-LA	Los Angeles	1982-2000	Intra-metro Los Angeles	1.44 (0.98-2.11)
Krewski et al. (2009, 191193)	ACS-Re-analysis	U.S.	1982-2000		1.11 (1.04-1.18)
Krewski et al. (2009, 191193)	ACS-Re-analysis	New York City	1982-2000	Intra-metro New York City	0.90 (0.29-2.78)
Krewski et al. (2009, 191193)	ACS-Re-analysis	Los Angeles	1982-2000	Intra-metro Los Angeles	1.31 (0.90-1.92)
McDonnell et al. (2000, 010319) [†]	AHSMOG	California	1973-1977	Men	1.39 (0.79-2.46)
Naess et al. (2007, 090736)		Oslo, Norway	1992-1998	Men, 51-70 yrs	1.18 (0.93-1.52)
Naess et al. (2007, 090736)		Oslo, Norway	1992-1998	Men, 71-90 yrs	1.18 (0.93-1.52)
Naess et al. (2007, 090736)		Oslo, Norway	1992-1998	Women, 51-70 yrs	1.83 (1.36-2.47)
Naess et al. (2007, 090736)		Oslo, Norway	1992-1998	Women, 71-90 yrs	1.45 (1.05-2.02)
MORTALITY - PM₁₀					
McDonnell et al. (2000, 010319) [†]	AHSMOG	California	1973-1977	Men	1.23 (0.84-1.80)
Naess et al. (2007, 090736) [†]		Oslo, Norway	1992-1998	Men, 51-70 yrs	1.12 (0.95-1.33)
Naess et al. (2007, 090736)		Oslo, Norway	1992-1998	Men, 71-90 yrs	1.14 (0.97-1.36)
Naess et al. (2007, 090736) [†]		Oslo, Norway	1992-1998	Women, 51-70 yrs	1.50 (1.23-1.84)
Naess et al. (2007, 090736) [†]		Oslo, Norway	1992-1998	Women, 71-90 yrs	1.29 (1.03-1.60)
INCIDENCE - PM_{2.5}					
Beelen et al. (2008, 155681)	NLCS	Netherlands	1987-1996	Full Cohort	0.81 (0.63-1.04)
Beelen et al. (2008, 155681)	NLCS	Netherlands	1987-1996	Case Cohort	0.65 (0.41-1.04)
Brunekreef et al. (2009, 191947)	NLCS-Re-analysis	Netherlands	1987-1996	Full Cohort	0.81 (0.63-1.04)
Brunekreef et al. (2009, 191947)	NLCS-Re-analysis	Netherlands	1987-1996	Case Cohort	0.67 (0.41-1.10)
INCIDENCE - PM₁₀					
Beeson et al. (1998, 048890)	AHSMOG	California	1977-1992	Men	1.99 (1.32-3.00)
Vineis et al. (2006, 192089)	GenAir	Europe	1993-1999	Case-Control	0.91 (0.70-1.18)

*per 10 µg/m³ increase

†Results from the paper were standardized to 10 µg/m³ [For McDonnell et al. (2000, [010319](#)) the non-standardized results were reported based on IQR increments (24.3 µg/m³ for PM_{2.5} and 29.5 µg/m³ for PM₁₀). For Naess et al. (2007, [090736](#)) the original hazard ratios were calculated based on quartiles of PM exposure. The results were converted to 10 µg/m³ using the mean range of the four quartiles (3.95 µg/m³ for PM_{2.5} and 5.88 µg/m³ for PM₁₀)].

‡Study was included in the 2004 PM AQCD

7.5.1.2. Other Cancers

Bonner et al. (2005, [088993](#)) conducted a population-based, case-control study of the association between ambient exposure to PAHs in early life and breast cancer incidence among women living in Erie and Niagara counties in the state of New York. Cases (n = 1,166 of which 841 were post-menopausal) were women with primary breast cancer, and controls (n = 2,105 of which 1,495 were post-menopausal) were frequency matched to the cases by age, race, and county of residence. TSP was used as a proxy for PAH exposure. Annual average TSP concentrations (1959-1997) were obtained from the New York State Department of Environmental Conservation for Erie and Niagara Counties. Among postmenopausal women, exposure to high concentrations of TSP (>140 $\mu\text{g}/\text{m}^3$) at birth was associated with an OR of 2.42 for breast cancer (95% CI: 0.97-6.09) relative to low concentrations of TSP (<84 $\mu\text{g}/\text{m}^3$). ORs were elevated for pollution exposures at age of menarche (OR: 1.45 [95% CI: 0.74-2.87]) and age at first birth (OR: 1.33 [95% CI: 0.87-2.06]) among postmenopausal women. Among premenopausal women, exposure to high concentrations of TSP at birth was associated with an OR for breast cancer incidence of 1.79 (95% CI: 0.62-5.10) relative to low exposure levels, exposure at age of menarche was associated with an OR of 0.66 (95% CI: 0.38-1.16), and exposure at age of first birth was associated with an OR of 0.52 (95% CI: 0.22-1.20).

7.5.1.3. Markers of Exposure or Susceptibility

Several studies looked at markers of exposure or susceptibility as the outcome associated with short-term exposure. These studies are included here because they may be relevant to the mechanism that leads to cancer associated with long-term exposures. For example, inflammation can contribute to carcinogenesis by inducing genomic instability, which can then lead to altered gene expression, enhanced proliferation, and resistance to apoptotic signals. Reactive oxygen and nitrogen species, provided by PM components or inflammation pathways, can cause molecular damage leading to cellular transformation. Elevated inflammatory cytokines, chemokines, and prostaglandins promote tumor growth and angiogenesis, which in turn promotes metastasis and malignant invasion. In particular, IL-6, IL-8, IL-1 β , COX-2, and TNF- α have been implicated in these processes (Kundu and Surh, 2008, [198840](#)). Several lines of evidence support the involvement of COX-2 in the pathogenesis of lung cancer (Lee et al., 2008, [198811](#)). Both short- and long-term exposure studies demonstrate relationships between various forms of PM and increased production of these inflammatory mediators, both in the lungs and circulation. Additionally, limited evidence suggests that exposure to PM (Chen and Schwartz, 2008, [190106](#)), or traffic (Williams et al., 2009, [191945](#)), or residence in a polluted airshed (Calderon-Garciduenas et al., 2007, [091252](#); Calderón-Garciduenas et al., 2009, [192107](#)) are associated with decreases in the number or function of natural killer cells or other white blood cells, indicating suppression of anti-tumor defenses.

A study performed in the Czech Republic compared 53 male policemen working at least 8 hours per day outdoors in urban air with age- and sex-matched controls who spent at least 90% of their day indoors (n = 52) (Sram et al., 2007, [188457](#)). During the sampling period, two monitors from downtown and suburban areas detected levels of air pollutants in the following ranges: PM₁₀ 32-55 $\mu\text{g}/\text{m}^3$, PM_{2.5} 27-38 $\mu\text{g}/\text{m}^3$, c-PAHs 18-22 ng/m^3 , and B[a]P 2.5-3.1 ng/m^3 using a VAPS monitor (measurements taken with a HiVol monitor, which has a lower flow rate, had a mean for PM₁₀ of 62.6 $\mu\text{g}/\text{m}^3$). c-PAHs detected on personal monitors during sampling days had a mean of 12.04 ng/m^3 among the policemen and 6.17 ng/m^3 among the controls. No difference in percent of chromosomal aberrations was observed between the policemen and control group using conventional cytogenetic analysis. However, using fluorescent in situ hybridization (FISH), a difference in chromosomal aberrations between the policemen and control group was reported. For example, the percentage of aberrant cells, as well as the genomic frequency of translocations per 100 cells, was about 1.4-fold greater in the policemen. This was largely driven by a difference in chromosomal aberrations between nonsmoking policemen and nonsmoking controls. A similar study that included only the policemen (n = 60), reported that the mean exposure to c-PAHs and B[a]P for 40-50 days before sampling was associated with chromosomal aberrations when analyzed with FISH (Sram et al., 2007, [192084](#)). However, when included in a model with other covariates, the association with these variables was null. No association was present with use of conventional cytogenetic analysis.

Palli et al. (2008, [156837](#)) investigated the correlation between ambient PM₁₀ concentrations and individual levels of DNA bulky adducts. Study participants were 214 healthy adults aged

35-64 yr at enrollment who resided in the city of Florence, Italy. This study was conducted between 1993 and 1998. PM₁₀ exposure levels were based on daily environmental measures provided by two types of urban monitoring stations (high-traffic and low-traffic). The researchers assessed correlation between DNA bulky adducts measured in blood samples and PM₁₀ concentrations prior to blood sample collection. Time windows of PM₁₀ exposure evaluated in this study were 0-5 days, 0-10 days, 0-15 days, 0-30 days, 0-60 days, and 0-90 days prior to blood sample collection. Overall, average PM₁₀ concentrations decreased during the study period, with some fluctuations. Quantitative values were not reported, but PM₁₀ appeared to range between approximately 30 and 100 µg/m³ for high-traffic stations, and between approximately 20 and 50 µg/m³ for low-traffic stations. This study found that levels of DNA bulky adducts among non-smoking workers with occupational traffic exposure were positively correlated with cumulative PM₁₀ levels from high-traffic stations during approximately 2 wk preceding blood sample collection (0-5 days: $r = 0.55$, $p = 0.03$; 0-10 days: $r = 0.58$, $p = 0.02$; 0-15 days: $r = 0.56$, $p = 0.02$). DNA bulky adducts were not associated with PM₁₀ levels among Florence residents with no occupational exposure to vehicle emissions or among smokers. DNA bulky adducts were not associated with PM₁₀ levels assessed by low-traffic urban monitoring stations.

The association between personal exposure to water-soluble transition metals in PM_{2.5} and oxidative stress-induced DNA damage was investigated among 49 students from Central Copenhagen, Denmark (Sorensen et al., 2005, [083053](#)). Researchers assessed PM_{2.5} exposure by personal sampling over two weekday periods twice in one year (November 1999 and August 2000), and determined the concentration of water-soluble transition metals (V, Cr, Fe, Ni, Cu and Pt) in these samples. In addition, lymphocyte and 24-h urine samples were analyzed for DNA damage by measuring 7-hydro-8-oxo-2'-deoxyguanosine (8-oxodG). Mean concentrations and corresponding IQR of these metals differed between months of sample collection. This study found that 8-oxodG concentration in lymphocytes was significantly associated with V and Cr concentrations, with a 1.9% increase in 8-oxodG per 1 µg/L increase in V concentration and a 2.2% increase in 8-oxodG per 1 µg/L increase in Cr concentration; these associations were independent of the PM_{2.5} mass concentration. The other transition metals were not significantly associated with the 8-oxodG concentration in lymphocytes, and none of the six measured transition metals was associated with the 8-oxodG concentration in urine.

Vinzents et al. (2005, [087482](#)) investigated the association between UFP and PM₁₀ concentrations with levels of purine oxidation and strand breaks in DNA using a crossover design in Copenhagen, Denmark. Study participants were 15 healthy nonsmoking individuals with a mean age of 25 yr. UFP exposure was evaluated using number concentration obtained in the breathing zone by portable instruments in six 18-h weekday periods from March to June 2003. Ambient concentrations for PM₁₀ and UFP were also measured on all exposure days at curbside street stations and at one urban background station. Oxidative DNA damage was assessed by evaluating strand breaks and oxidized purines in mononuclear cells isolated from venous blood the morning after exposure measurement. Mean number concentration of UFPs (street station) was 30.4×10^3 UFPs/mL (standard deviation [SD]: 1.38), mean mass concentration of PM₁₀ at a background monitoring station was $16.9 \mu\text{g}/\text{m}^3$ (SD: 1.53), and mean mass concentration of PM₁₀ at a street station was $23.5 \mu\text{g}/\text{m}^3$ (SD: 1.48). Mean personal exposure to UFPs was 32.4×10^3 UFPs/mL (SD: 1.49) while bicycling (5 occasions), 19.6×10^3 UFPs/mL (SD: 1.78) during other outdoor activities (6 occasions), and 13.4×10^3 UFPs/mL (SD: 1.96) while indoors (6 occasions). The regression coefficients of the mixed-effects models looking at level of purine oxidation were estimated as 1.50×10^{-3} (95% CI: 0.59×10^{-3} to 2.42×10^{-3} ; $p = 0.002$) for cumulative outdoor exposure and 1.07×10^{-3} (95% CI: 0.37×10^{-3} to 1.77×10^{-3} ; $p = 0.003$) for cumulative indoor exposure. Neither cumulative outdoor nor cumulative indoor exposures to UFPs were associated with strand breaks. Neither ambient air concentrations of PM₁₀ nor number concentrations of UFPs at monitoring stations were significant predictors of DNA damage.

Additionally, a number of studies employed ecologic study designs, comparing the prevalence of biomarkers in populations from more polluted locations to those in less polluted locations. In a pilot study conducted in the Czech Republic (Pedersen et al., 2006, [156848](#)), children age 5-11 yr provided 5 mL blood samples and the frequency of micronuclei (MN) in peripheral blood lymphocytes was analyzed as a measure of cytogenetic effects. Significantly higher frequencies of MN were found in younger children living in Teplice (PM_{2.5} concentration = $120 \mu\text{g}/\text{m}^3$) than in Prachatice (PM_{2.5} concentration = $46 \mu\text{g}/\text{m}^3$). The levels of c-PAHs were also much higher in Teplice (nearly $30 \text{ ng}/\text{m}^3$ in Teplice and about $15 \text{ ng}/\text{m}^3$ in Prachatice). The difference in MN frequencies

observed in the children from the two locations may be attributable to differences in exposure to air pollution, but could also be due to differences in diet or other environmental exposures. This finding is noteworthy considering MN formation in peripheral blood lymphocytes is thought to be biologically relevant for carcinogenesis.

Avogbe et al. (2005, [087811](#)) showed a correlation between the level of oxidative DNA damage in individuals and exposure to ambient UFPs. Formamidopyrimidine DNA glycosylase sensitive sites and the presence of DNA strand breaks were assessed in blood and urine samples obtained from healthy, non-smoking male volunteers that lived and worked in different areas of Cotonou, Benin. Exposure to benzene was assessed by urinary excretion of S-phenylmercapturic acid. There was a high degree of correlation between exposure to benzene and UFPs and the presence of DNA strand breaks and formamidopyrimidine DNA glycosylase sensitive sites (rural subjects < suburban subjects < residents living near high traffic roads < taxi drivers). Genotyping studies showed that the magnitude of the effects of benzene and UFPs may be modified by polymorphisms in GSTP1 and NQO1 genes.

Tovalin et al. (2006, [091322](#)) evaluated the association between exposure to air pollutants and the level of DNA damage using the single cell gel electrophoresis (comet) assay. Mononuclear lymphocytes from outdoor and indoor workers from two areas in Mexico, Mexico City (large city) and Puebla (medium size city), were evaluated. The outcomes showed that the outdoor workers in Mexico City exhibited greater DNA damage than indoor workers in the same region. Similar levels of DNA damage were observed between indoor and outdoor workers in Puebla. The level of observed DNA damage was correlated with exposure to O₃ and PM_{2.5}.

In summary, several recent studies have reported an association between lung cancer mortality and long-term PM_{2.5} exposure. Although many of the estimates include the null in the confidence interval, overall the results have shown a positive relationship. The two recent studies that looked at lung cancer incidence did not report an association with PM_{2.5} (Brunekreef et al., 2009, [191947](#)) or PM₁₀ (Vineis et al., 2006, [192089](#)). Studies of exposure/susceptibility markers have reported inconsistent outcomes, with some markers being associated with PM and others not.

7.5.2. Toxicological Studies

Over the past 30 yr numerous mutagenicity and genotoxicity studies of ambient PM and their contributing sources have been conducted to assess the relative mutagenic or genotoxic potential. Studies previously reviewed in the 2004 PM AQCD (U.S. EPA, 2004, [056905](#)) provide compelling evidence that ambient PM and PM from specific combustion sources (e.g., fossil fuels) are mutagenic in vivo and in vitro. Research cited in the 2004 AQCD demonstrated mutagenic activity of ambient PM from urban centers in California, Germany and the Netherlands. These studies suggested that ubiquitous emission sources, particularly motor vehicle emissions, rather than isolated point sources were largely responsible for the mutagenic effects. In addition, the mutagenicity was dependent upon the chemical composition of the PM with unsubstituted polyaromatic compounds and semi-polar compounds being highly mutagenic. Mutagenicity was also dependent on size, with the fine fraction of urban PM having greater effects than the coarse fraction. Genotoxic activity was demonstrated for ambient PM from two high traffic areas (one upwind and one downwind) and a rural site. In addition, the 2004 AQCD reported that exhausts from gasoline and diesel engines were mutagenic and that DE was more potent. More mutagenicity was observed for exhaust from cold starts than starts at room temperature. Both gaseous and particulate fractions of DE were found to be mutagenic. Sequential fractionation of extracts from gasoline and DE implicated the polar fractions, especially nitrated polynuclear aromatic compounds, as contributing greatly to mutagenicity. Among some of the other mutagenically active compounds found in the gas phase of DE are ethylene, benzene, 1,3-butadiene, acrolein and several PAHs, all of which are also present in gasoline exhaust. Also cited in the 2004 AQCD were studies demonstrating mutagenic effects of emissions from wood/biomass burning, which were primarily attributable to the organic fraction and not the condensate. It was noted that wood smoke induced both frameshift mutations and base pair substitution but not DNA adducts. Further, emissions from coal combustion in China were found to be mutagenic, with both polar and aromatic fractions contributing to effects. Little data were available on the mutagenicity of coal fly ash emissions from U.S. conventional combustion plants. In conclusion, these studies provide evidence that ambient PM and combustion-derived PM are mutagenic/genotoxic. The 2004 AQCD noted that there is not a simple relationship between

mutagenic potential and carcinogenic potential in animals or humans. No studies evaluating carcinogenic effects of PM were reported in the 2004 AQCD.

Building on results of earlier studies in the 2004 PM AQCD, data from newly published studies that evaluated the mutagenic, genotoxic and carcinogenic effects of PM, PM-constituents, and combustion emission source particles are reviewed. Pertinent studies are described briefly in the following paragraphs. A summary table is provided in Annex D, Tables D7 and D8).

7.5.2.1. Mutagenesis and Genotoxicity

In Vitro Studies

In general, studies have focused on PM and PM extracts for mutagenicity testing using bacteria and mammalian cell lines. PM and/or PM extracts from ambient air samples, wood smoke, and coal, diesel, or gasoline combustion have all been reported to induce mutation in *S. typhimurium* and in cultured human cells (Abou et al., 2007, [098819](#); Gabelová et al., 2007, [156457](#); Gabelová et al., 2007, [156458](#); Hannigan et al., 1997, [083598](#); Hornberg et al., 1998, [095741](#)). In addition, effects associated with PM and PM-associated constituents include induction of MN formation, DNA adduct formation, SCE, DNA strand breaks, frameshifts and inhibition of gap-junction intercellular communication (Alink et al., 1998, [087159](#); Arlt et al., 2007, [097257](#); Avogbe et al., 2005, [087811](#); Gabelová et al., 2007, [156457](#); Gabelová et al., 2007, [156458](#); Healey et al., 2006, [156532](#); Hornberg et al., 1996, [087164](#); Hornberg et al., 1998, [095741](#); Sevastyanova et al., 2007, [156969](#)).

Constituents adsorbed onto individual particles play a large role in the genotoxic potential of PM. Poma et al. (2006, [096903](#)) showed that fine CB particles were consistently less genotoxic than similar concentrations of PM_{2.5} extracts, suggesting that the adsorbed components play a role in the genotoxic potential of PM. Total PAH and carcinogenic PAH content were correlated with the genotoxic effects of PM (De Kok et al., 2005, [088656](#); Sevastyanova et al., 2007, [156969](#)). Comparison of different extracts (water-soluble versus organic) by Gutierrez-Castillo et al. (2006, [089030](#)) indicated that water-soluble extracts were more genotoxic than the corresponding organic extracts. Sharma et al. (2007, [156975](#)) reported that mutagenic activity of extracted PM samples collected in and around a waste incineration plant was attributed to the moderately polar and polar fractions. The polar and crude fractions were mutagenic without metabolic activation, suggesting a direct mutagenic effect. No mutagenic activity was observed from any of the nonpolar samples evaluated. Arlt and colleagues (2007, [097257](#)) have shown that the PM constituents 2-nitrobenzanthrone (2-NB) and 3-nitrobenzanthrone were genotoxic in a variety of bacterial and mammalian cell systems.

Conflicting data have been reported on the role of metabolic enzymes in the genotoxicity of PM and their adsorbed constituents. Arlt et al. (2007, [097257](#)) reported that the PM constituent 2-NB was genotoxic in bacterial and mammalian cells. However, metabolic activation with the human N-acetyltransferase 2 or sulfotransferase (SULT1A1) enzyme was needed for the effect to be observed in human cells. Erdinger et al. (2005, [156423](#)) demonstrated that mutagenic activity was not affected when metabolism was induced. de Kok et al. (2005, [088656](#)) evaluated the relationship between the physical, chemical, and genotoxic effects of ambient PM. TSP, PM₁₀, and PM_{2.5} were sampled at different locations and the extracts were assessed for mutagenicity and induction of DNA adducts in cells. Overall, induction of rat liver S9 metabolism generally reduced the mutagenic potential via the Ames assay of the particle fractions and DNA reactivity (induction of DNA adducts) was generally higher after metabolic activation. Binková et al. (2003, [156274](#)) found that the addition of S9 increased PM₁₀-dependent DNA adduct formation.

Ambient Air

A limited number of studies evaluated the impact of the season on the genotoxic effects of ambient PM. A few studies have indicated that greater genotoxic effects were associated with samples collected during the winter months compared to those collected in the summer (Abou et al., 2007, [098819](#); Gabelová et al., 2007, [156457](#); Gabelová et al., 2007, [156458](#)). In contrast, Hannigan et al. (1997, [083598](#)) indicated that no seasonal variation was observed. Studies have also shown that greater genotoxic effects were associated with smaller particle size extracts (e.g., PM_{2.5}>PM₁₀) and

from samples collected in urban areas or closer to higher trafficked areas (Abou et al., 2007, [098819](#); Hornberg et al., 1998, [095741](#)).

de Kok et al. (2005, [088656](#)) found the direct mutagenicity (Ames assay) and the direct DNA reactivity (DNA adduct formation) of the PM_{2.5} size fraction was significantly higher than that of the larger size fractions (TSP, PM₁₀) at most locations.

DNA damage was assessed by the Comet assay in A549 cells exposed to PM collected from a high traffic area in Copenhagen, Denmark (TSP approximately 30 µg/m³) and compared to the results from exposure of A549 cells to standard reference materials (SRM1650 or SRM2975) at the same concentrations (2.5-250 µg/ml) (Danielsen et al., 2008, [192092](#)). All three particles induced strand breaks and oxidized purines in a dose-dependent manner and there were no obvious differences in potency. In contrast, only the ambient PM formed 8-oxodG when incubated with calf thymus DNA, which may be due to the concentration of transition metals.

Diesel and Gasoline Exhaust

Automobile DE particles (A-DE particles) was tested in *S. typhimurium* strains TA98, TA100, and its derivatives (e.g., TA98NR and YG1021) and found to be more mutagenic than forklift DE particles (f-DE particles, derivative SRM2975), based on PM mass. A-DE particles had 227 times more PAH-type mutagenic activity and 8-45 times more nitroarene-type mutagenic activity (DeMarini et al., 2004, [066329](#)). Using a diesel engine without an oxidation catalytic converter (OCC), the diesel engine exhaust particle extract produced the highest number of revertant colonies in strains TA98 and TA100 with and without S9 at several tested loads when compared to extracts from low-sulfur diesel fuel (LSDF), rapeseed oil methyl ester (RME), and soybean oil methyl ester (SME). When an OCC was installed in the exhaust pipe of the engine, all extracts reduced the number of revertant colonies in both strains with and without S9 at partial loads but increased the number of revertant colonies without S9 at rated power. At idling, DE particles extracts increased the number of revertant colonies with and without S9 (Bunger et al., 2006, [156303](#)). In a separate study, engine emissions (particle extracts and condensates) from rapeseed (canola) oil were found to produce greater mutagenic effects in *S. typhimurium* strains TA98 and TA100 than DE particles (Bunger et al., 2007, [156304](#)). Additionally, DE extract (DEE) from diesel fuel containing various percentages of ethanol was also observed to induce mutational response in two Salmonella strains. Base diesel fuel DEE and DEE from fuel with 20% ethanol caused more significant DNA damage in rat fibrocytes L-929 cells than extracts containing 5, 10, or 15% ethanol (Song et al., 2007, [155306](#)).

DE and gasoline engine exhaust particles, as well as their semi-volatile organic compound (SVOC) extracts, induced mutations in the two *S. typhimurium* strains YG1024 and YG1029 in the absence and presence of S9; the PM extracts were more mutagenic than the SVOC extracts. Additionally, all extracts except the DE extract induced DNA damage and MN formation in Chinese hamster lung V79 cells (Liu et al., 2005, [097019](#)). Another study demonstrated that gasoline engine exhaust significantly increased colony formation in TA98 with and without S9 (Zhang et al., 2007, [157186](#)).

Jacobsen et al. (2008, [156597](#)) used the FE1-MutaTM Mouse lung epithelial cell line to investigate putative mechanisms of DE particle-induced mutagenicity. Mutation ion frequencies and ROS were determined after cells were incubated with 37.5 or 75 µg/ml DE particles (SRM1650) for 72-h (n = 8). The mutation frequency at the 75 µg/ml dose was significantly increased (1.55-fold; p<0.001) in contrast to cells treated with 37.5 µg/ml DE particles. DE particles-induced ROS generation 1.6- to 1.9-fold in the epithelial cell cultures after 3 h of exposure compared with the 3- to 10-fold increase in ROS production previously reported for CB. The authors concluded that the mutagenic activity of DE particles is likely attributable to activity from the organic fraction that both contains reactive species and can generate ROS.

In human A549 and CHO-K1 cells, the organic fraction of DE particles significantly increased the amount of Comet and MN formation, respectively, in the presence and absence of SKF-525A (a CYP450 inhibitor) and S9, respectively (Oh and Chung, 2006, [088296](#)). The organic base and neutral fractions of DE particles also significantly induced DNA damage but only without SKF-525A, and all fractions but the moderately polar fraction (phthalates and PAH oxyderivatives) induced MN formation with and without S9 (Bao et al., 2007, [097258](#)). Gasoline engine exhaust significantly induced DNA damage as measured in the Comet assay and increased the frequency of MN in human A549 cells (Zhang et al., 2007, [157186](#)). In human-hamster hybrid (A_L) cells, DE particles (SRM 2975) dose-dependently increased the mutation yield at the CD59 locus; this was

significantly reduced by simultaneous treatment with phagocytosis inhibitors (Bao et al., 2007, [097258](#)).

Wood Smoke

The mutagenicity of wood smoke and cigarette smoke (CS) extracts was assayed in *S. typhimurium* strains TA98 and TA100 (Ames assay) using the pre-incubation assay with exogenous metabolic activation (rat liver S-9). Extracts of both samples (62.5 or 125 µg total PM equivalent/ml) were equally mutagenic to strain TA98 but the wood smoke extract was less mutagenic than the CS extracts in strain TA100 (Iba et al., 2006, [156582](#)).

In Vivo studies

Ambient Air

The contribution of ambient urban roadside air exposure (4, 12, 24, 48 or 60 wk) to DNA damage was examined in the lungs, nasal mucosa, and livers of adult male Wistar rats in Kawasaki, Japan (Sato et al., 2003, [096615](#)). Messenger RNA levels of CYP450 enzymes that catalyze the transformation of PAHs to reactive metabolites were also evaluated. Concentrations of gases were reported to be 12-182 ppb NO and 0-9 ppb NO₂ in the filtered air chamber and 33-280 ppb NO and 42-81 ppb NO₂ in the experimental group chamber. Suspended PM concentrations were 11-19 µg/m³ in the filtered air chamber and 42-100 µg/m³ (average 63 µg/m³) in the experimental group chamber. Body weight significantly decreased in exposed animals at 24, 48 and 60 wk. A 4-wk exposure to urban roadside air resulted in significant increases in multiple DNA adducts (lung, nasal, and liver DNA adducts). With longer exposures, there were significant increases in lung (48 wk), nasal (60 wk), and liver DNA adducts (60 wk). Changes were seen in CYP1A2 mRNA at 4 wk with a 2.3-fold increase in exposed animals compared to the control group with no change observed at 60 wk; CYP1A1 mRNA was unchanged. These results indicate that exposure to ambient air in this roadside area could induce DNA adduct formation, which may be important for carcinogenicity. Earlier studies (Ichinose et al., 1997, [053264](#)) have shown that 8-oxodG, a DNA adduct, is elevated along with tumor formation in a dose-dependent manner in mice administered DE particles. The finding of adducts in the liver indicated that deposition of PM and its associated PAHs in the lung can have indirect effects on extrapulmonary organs. It should be noted that PM deposition on the fur and ingestion during grooming cannot be ruled out as a possible exposure route.

Another animal toxicological study employed “non-carcinogenic” particles obtained from pooled non-cancerous lung tissue collected during surgical lung resection from three non-smoking male patients diagnosed with lung adenocarcinomas (Tokiwa et al., 2005, [191952](#)). Particles were partially purified to remove organic compounds. Morphologically the particles were similar to DE or ambient air PM and the organic extracts from the particles were directly mutagenic in *S. typhimurium* tester strains TA98, YG1021 and YG1024. BALB/c and ICR mice were intratracheally instilled with particles at doses of 0.25, 0.5, 1.0, or 2.0 mg/mouse. After 24 h, 8-oxodG was measured in lung DNA and found to be increased in ICR mice in a dose-dependent manner, reaching a maximum of ~2.75 8-oxodG/10⁵ dG at the 2.0 mg dose. The response was statistically significant at doses of 0.5, 1.0, and 2.0 mg. The increased 8-oxodG levels observed in vivo was reported to be likely due to hydroxyl radicals presumed to be involved in phagocytosis of non-mutagenic particles by inflammatory cells that could induce hydroxylation of guanine residue on DNA.

Diesel Exhaust

An in vivo study employed *gtp* delta transgenic mice carrying the lambda EG10 on each Chromosome 17 from a C57BL/6J background to investigate the effects of DE particles on mutation frequency (Hashimoto et al., 2007, [097261](#)). Mice were exposed via inhalation to DE particles or via IT instillation to DE particles or DE particle extract and lambda EG10 phages were rescued; *E. coli* YG6020 was infected with the phage and screened for 6-thioguanine resistance. The mutagenic potency (mutation frequency per mg) caused by DE particle extract was twice that of DE particles, suggesting that the mutagenicity of DE particles is attributed primarily to compounds in the extract,

since ≈50% of the weight of DE particles was provided by the extract. There was no difference in mutation frequency between the 1 and 3 mg/m³ DE particle groups after 12 wk of exposure.

Wood Smoke

One recent study measured the effect of freshly generated hardwood smoke on CYP1A1 activity based on ethoxyresorufin O-deethylase in pulmonary microsomes recovered from male Sprague-Dawley rats exposed to hardwood smoke by nose-only inhalation exposure (Iba et al., 2006, [156582](#)). CYP1A1 activity in rat lung explants treated with extracts of the total PM (TPM) from hardwood smoke samples and from freshly generated cigarette smoke (CS) was also evaluated. Unlike CS, hardwood smoke did not induce pulmonary CYP1A1 activity or mRNA (assessed by northern blot analysis) nor did extracts of hardwood smoke TPM induce CYP1A1 protein (assessed by western blot analysis) in cultured rat lung explants. The results suggest that unique constituents that are activated by CYP1A1 may be present in CS but not hardwood smoke.

7.5.2.2. Carcinogenesis

Studies published prior to the 2004 AQCD that evaluated the carcinogenicity of ambient air were reviewed by Claxton and Woodall (2007, [180391](#)). Five studies involved chronic inhalation exposures in rodents. No statistically significant increase in tumorigenesis was observed following chronic exposure to urban air pollution in Los Angeles (Gardner, 1966, [015129](#); Gardner et al., 1969, [015130](#); Wayne and Chambers, 1968, [038537](#)). However in a study conducted in Brazil, urban air pollution was found to enhance the formation of urethane-induced lung tumors in mice (Cury et al., 2000, [192100](#); Reymao et al., 1997, [084653](#)).

Two recent studies evaluated the carcinogenic potential of chronic inhalation exposures to DE (Reed et al., 2004, [055625](#)) and hardwood smoke (Reed et al., 2006, [156043](#)). Two indicators of carcinogenic potential, formation of MN and tumorigenesis were measured in strain A/J mice, which is a mouse model that spontaneously develops lung tumors. Exposure to DE or hardwood smoke at concentrations of 1,000 µg/m³ and below did not cause increased formation of MN or an increased rate of lung tumors in this cancer-prone rodent model. These studies are described below.

Diesel Exhaust

A/J mice were exposed to 30, 100, 300 and 1000 µg/m³ DE for 6 h/day and 7 days/wk for 6 mo (Reed et al., 2004, [055625](#)). The concentration of gases in this including NO_x, NO₂, CO, SO₂, NH₃, methane, non-methane VOC, and FID total hydrocarbon ranged from control to high dose group values of 0 to 50.4 ± 0.6 ppm, 0.2 ± 0.2 to 6.9 ± 3.3 ppm, 0.3 ± 0.1 to 30.9 ± 4.5 ppm, not detectable to 955.2 ± 58.4 ppb, 176.5 ± 8.8 to 9.1 ± 0.2 µg/m³, 1406.5 ± 253.2 to 2642.1 ± 455.9 µg/m³, 134.0 ± 52.1 to 1578.6 ± 256.2 µg/m³, 0.1 ± 0.1 to 2.2 ± 0.2 ppm, respectively. Particle sizes in the four exposure groups ranged from 0.10-0.15 µm MMAD with geometric standard deviations of 1.4-1.8. Following the 6-mo exposure and a 6-mo recovery period, mice were collected and MN formation in blood and tumor multiplicity and tumor incidence were measured in lungs. No increases in formation of MN or numbers of lung adenomas were observed in DE-exposed mice compared with controls.

Wood Smoke

A/J mice were exposed to 30, 100, 300 and 1,000 µg/m³ hardwood smoke or to 30, 100, 300 and 1,000 µg/m³ DE for 6 h/day and 7 days/wk for 6 mo (Reed et al., 2006, [156043](#)). Gaseous components of the hardwood smoke included CO, NH₃, and non-methane VOC with concentrations from control levels to high dose hardwood smoke exposure ranging from 229 ± 31 to 14887.6 ± 832.3 ppm, 139.3 ± 2.3 to 54.9 ± 1.2 µg/m³ and 177.6 ± 10.4 to 3455.0 ± 557.2 µg/m³, respectively. Concentrations of NO_x, NO₂ and SO₂ were reported to be null. Particle sizes in the four exposure groups ranged from 0.25-0.36 µm MMAD with geometric standard deviations of 2.0-3.3. Following the 6-mo exposure and a 6-mo recovery period, mice were collected and MN formation in blood and tumor multiplicity and tumor incidence were measured in lungs. No increases in formation of MN or

numbers of lung adenomas were observed in hardwood smoke-exposed mice compared with controls. However, hardwood smoke from this study was mutagenic in the Ames reverse mutation assay.

7.5.2.3. Summary of Toxicological Studies

In summary, numerous new *in vitro* studies confirm and extend findings reported in the 2004 AQCD that ambient PM from urban sites and combustion-derived PM are mutagenic and genotoxic. A small number of new studies were conducted *in vivo*. One of these studies demonstrated increased mutagenic potency in mice exposed to DE particles and DE particle extract. Another study found increased formation of 8-oxodG, a DNA adduct, following IT instillation of PM in mice. A chronic inhalation study of rats exposed to urban roadside air reported increased formation of DNA adducts in nose, lung, and liver and induction of CYP1A2. Inhalation exposure of rats to hardwood smoke failed to induce CYP1A1 in another study. Finally, two chronic inhalation studies found no evidence of carcinogenic potential for DE and hardwood smoke in a cancer-prone mouse model. Collectively, these results provide some evidence, mainly from *in vitro* studies, to support the biological plausibility of ambient PM-lung cancer relationships observed in epidemiology studies.

7.5.3. Epigenetic Studies and Other Heritable DNA mutations

Two epidemiologic epigenetic studies examined the effect of PM on DNA methylation. Both studies examined methylation of Alu and long interspersed nuclear element-1 (LINE-1) sequences, which are located in repetitive elements. In previous studies, methylation of these sequences has been linked to global genomic DNA methylation content (Weisenberger et al., 2005, [192101](#); Yang et al., 2004, [192102](#)).

The first study included men age 55 and older who were part of the Normative Aging Study in the Boston area (Baccarelli et al., 2009, [192155](#)). A stationary monitoring site located 1 km from the examination site was used to estimate ambient PM_{2.5} exposure for the duration of the study (1999-2007). During the study period, the median level of PM_{2.5}, averaged over 7-day periods, was 9.8 µg/m³ (interquartile range 8.0-12.0 µg/m³). There was no association between PM_{2.5} and Alu methylation. LINE-1 methylation was associated with PM_{2.5} measured over the 7 days before the examinations.

The second study included 63 healthy men aged 27-55 yr working at an electric furnace steel plant (Tarantini et al., 2009, [192010](#)). Blood samples were taken twice, once in the morning after 2 days of not working and once in the morning after 3 full days of work. PM₁₀ was measured in 11 work areas and individuals completed daily logs about the amount of time spent in each area. On average, individuals had an estimated exposure of 233.4 µg/m³ PM₁₀ (range 73.4-1220.2 µg/m³). Short-term exposure did not alter the methylation of Alu and LINE-1. To examine effects of long-term exposure, both blood samples were considered independent of time, and Alu and LINE-1 were examined with respect to overall estimated PM₁₀ exposure using mixed effects models. There was a negative association between increasing levels of PM₁₀ exposure and Alu and LINE-1 methylation, indicating that PM₁₀ causes epigenetic changes to occur with long-term exposure. This study also looked at levels of iNOS gene, which is a gene suppressed by DNA methylation. iNOS expression was not associated with long term exposure to PM₁₀ but was affected by methylation in the short term.

Animal toxicology studies evaluating the effect of PM exposure on changes in the epigenome and other non-epigenetic heritable DNA changes have only recently been conducted. After earlier work showed increased germline mutation rates in herring gulls nesting near steel mills on Lake Ontario (Yauk and Quinn, 1996, [089093](#)) further work was conducted to address air-dependent contribution to germline mutations by housing male and female Swiss Webster mice in the same area and comparing mutation rates in those animals with mutation rates of animals housed in a rural setting with less air pollution (Somers et al., 2002, [078100](#)). To determine if PM or the gaseous phase of the urban air was responsible for heritable mutations, Yauk et al. (2008, [157164](#)) exposed mature male C57Bl×CBA F1 hybrid mice to either HEPA-filtered air or to ambient air in Hamilton, Ontario, Canada for 3 or 10 wk, or 10 wk plus 6 wk of clean air exposure (16 wk) (also discussed in Section 7.4.2.5). Sperm DNA was monitored for ESTR mutations, testicular sample bulky DNA adducts, and DNA single or double strand breaks. In addition, male-germ line (spermatogonial stem

cell) DNA methylation was monitored post-exposure. This area in Hamilton is near two steel mills and a major highway. Air composition showed mean concentrations for TSP of $93.8 \pm 17 \mu\text{g}/\text{m}^3$, PAH of $8.3 \pm 1.7 \text{ ng}/\text{m}^3$, and metal of $3.6 \pm 0.7 \mu\text{g}/\text{m}^3$. Mutation frequency at ESTR Ms6-hm locus in sperm DNA from mice exposed 3 or 10 wk did not show elevated ESTR mutation frequencies, but there was a significant increase in ESTR mutation frequency at 16 wk compared to HEPA-filter control animals, pointing to a PM-dependent mechanism of action. No detectable DNA adducts were observed in testes samples at any of the time points monitored. To verify inhalation exposure to particles, DNA adducts were reported in the lungs of mice exposed for 3 wk to ambient air; no other time points showed detectable DNA adduct formation. Hypermethylation of germ-line DNA was also observed in mice exposed to ambient air for 10 and 16 wk. These PM-dependent epigenetic modifications (hypermethylation) were not seen in the haploid stage (3 wk) of spermatogenesis, but were nonetheless seen in early stages of spermatogenesis (10 wk) and remained significantly elevated in mature sperm even after removal of the mouse from the environmental exposure (16 wk). Thus, these studies indicate that the ambient PM phase and not the gaseous phase is responsible for the increased frequency of heritable DNA mutations and epigenetic modifications.

Based on the limited evidence from these epigenetics studies, long-term exposure to PM_{10} may result in epigenetic changes. $\text{PM}_{2.5}$ also potentially affects some DNA methylation content. As epigenetic research progresses, future studies examining the relationship between PM and DNA methylation will be important in more thoroughly characterizing these associations.

The effect of ambient PM on heritable DNA mutations and the epigenome has been well characterized in a Canadian steel mill area. Mice exposed to ambient PM plus gases developed paternally-derived heritable DNA mutations and epigenetic changes in sperm DNA that were not observed in mice exposed to ambient air that was HEPA-filtered. This is the first animal toxicology study showing heritable effects of PM exposure on DNA mutation and the epigenome. Because the epigenetics field is so new, further work in this emerging area will expand on these PM-dependent methylation changes to determine if the results can be recapitulated at other urban sites.

7.5.4. Summary and Causal Determinations

7.5.4.1. $\text{PM}_{2.5}$

The 2004 PM AQCD reported on original and follow-up analyses for three prospective cohort studies that reported positive relationships between $\text{PM}_{2.5}$ and lung cancer mortality. Several recent, well-conducted epidemiologic studies have extended the evidence for a positive association between $\text{PM}_{2.5}$ and lung cancer mortality (Section 7.5.1.1). Generally, studies have not reported associations between long-term exposure to $\text{PM}_{2.5}$ or PM_{10} and lung cancer incidence (Section 7.5.1.1). Animal toxicological studies did not focus on specific size fractions of PM, but rather examined ambient PM, wood smoke, and DE particles (Section 7.5.2). A number of recent studies indicate that ambient urban PM, emissions from wood/biomass burning, emissions from coal combustion, and gasoline and DE are mutagenic and that PAHs are genotoxic (Section 7.5.2). These findings are consistent with earlier studies that concluded that ambient PM and PM from specific combustion sources are mutagenic and genotoxic and provide biological plausibility for the results observed in the epidemiologic studies. A limited number of epidemiologic and toxicological studies on the epigenome demonstrate that PM induces changes in methylation (Section 7.5.3), a new area of research that will likely be expanded in the future. However, it has yet to be determined how these alterations in the genome could influence the initiation and promotion of cancer. Overall, the evidence is **suggestive of a causal relationship between relevant $\text{PM}_{2.5}$ exposures and cancer, with the strongest evidence from the epidemiologic studies of lung cancer mortality.** This evidence is limited by the non-specific measure of PM size fraction in some of the epidemiologic studies and most of the animal toxicological studies, and the inconsistency in evidence with recent epidemiologic studies for an effect on cancer incidence. There is no epidemiologic evidence for cancer related to long-term exposure to PM in organs or systems other than the lung.

7.5.4.2. PM_{10-2.5}

The 2004 PM AQCD did not report long-term exposure studies for PM_{10-2.5}. No epidemiologic studies have been conducted to evaluate the effects of long-term PM_{10-2.5} exposure and cancer. The evidence is **inadequate to assess the association between PM_{10-2.5} and UFP exposures and cancer.**

7.5.4.3. UFPs

The 2004 PM AQCD did not report long-term exposure studies for UFPs. No epidemiologic studies have been conducted to evaluate the effects of long-term UFP and cancer. The evidence is **inadequate to determine if a causal relationship exists between long-term UFP exposures and cancer.**

7.6. Mortality

In the 1996 PM AQCD, results were presented for three prospective cohort studies of adult populations: the Six Cities Study (Dockery et al., 1993, [044457](#)); the ACS Study (Pope et al., 1995, [045159](#)); and the AHSMOG Study (Abbey et al., 1995, [000669](#)). The 1996 AQCD concluded that the chronic exposure studies, taken together, suggested associations between increases in mortality and long-term exposure to PM_{2.5}, though there was no evidence to support an association with PM_{10-2.5} (U.S. EPA, 1996, [079380](#)).

Discussions of mortality and long-term exposure to PM in the 2004 PM AQCD emphasized the results of four U.S. prospective cohort studies, but the greatest weight was placed on the findings of the ACS and the Harvard Six Cities studies, which had each undergone extensive independent reanalysis, and which were based on cohorts that were broadly representative of the U.S. population. The 2004 PM AQCD concluded that the results from the Seventh-Day Adventist (AHSMOG) cohort provided some suggestive (but less conclusive) evidence for associations, while results from the Veterans Cohort provided inconsistent evidence for associations between long-term exposures to PM_{2.5} and mortality. Collectively, the 2004 PM AQCD found that these studies provided strong evidence that long-term exposure to PM_{2.5} was associated with increased risk of human mortality. Effect estimates for all-cause mortality ranged from 6 to 13% increased risk per 10 µg/m³ PM_{2.5}, while effect estimates for cardiopulmonary mortality ranged from 6 to 19% per 10 µg/m³ PM_{2.5}. For lung cancer mortality, the effect estimate was a 13% increase per 10 µg/m³ PM_{2.5}, based upon the results of the extended analysis from the ACS cohort (Pope et al., 2002, [024689](#)). With regard to PM_{10-2.5}, the 2004 PM AQCD reported that no association was observed between mortality and long-term exposure to PM_{10-2.5} in the ACS study (Pope et al., 2002, [024689](#)), while a positive but statistically non-significant association was reported in males in the AHSMOG cohort (McDonnell et al., 2000, [010319](#)). Thus, the 2004 PM AQCD concluded that there was insufficient evidence for associations between long-term exposure to PM_{10-2.5} and mortality. Overall, the 2004 PM AQCD concluded that there was strong epidemiologic evidence for associations between long-term exposures to PM_{2.5} and excess all-cause and cardiopulmonary mortality.

At the time of the 2004 PM AQCD, only a limited number of the chronic-exposure cohort studies had considered direct measurements of constituents of PM, other than sulfates. With regard to source-oriented evaluations of mortality associations with long-term exposure, the 2004 PM AQCD noted only the study by Hoek et al. (2002, [042364](#)), in which the authors concluded that long-term exposure to traffic-related air pollution may shorten life expectancy. However, Hoek et al. (2002, [042364](#)) also noted that living near a major road might include other factors that contribute to mortality associations. There was not sufficient evidence at the time of the 2004 PM AQCD to draw conclusions on effects associated with specific components or sources of PM.

New epidemiologic evidence reports a consistent association between long-term exposure to PM_{2.5} and increased risk of mortality. There is little evidence for the long-term effects of PM_{10-2.5} on mortality. Although this section focuses on mortality outcomes in response to long-term exposure to PM, it does not evaluate studies that examine the association between PM and infant mortality.

These studies are evaluated in Section 7.5 because it is possible that in utero exposures contribute to infant mortality. A summary of the mean PM concentrations reported for the studies characterized in this section is presented in Table 7-8.

Table 7-8. Characterization of ambient PM concentrations from studies of mortality and long-term exposures to PM.

Study	Location	Mean Concentration ($\mu\text{g}/\text{m}^3$)	Upper Percentile Concentrations ($\mu\text{g}/\text{m}^3$)
<i>PM_{2.5}</i>			
Brunekreef et al. (2009, 191947)	The Netherlands	28	95th: 32 99th: 33 Max: 37
Chen et al. (2005, 087942)	Multicity, CA	29.0	
Eftim et al. (2008, 099104)	U.S.	13.6-14.1	Max: 19.1-25.1
Enstrom (2005, 087356)	CA	23.4	Max: 36.1
Goss et al. (2004, 055624)	U.S.	13.7	75th: 15.9
Janes et al. (2007, 090927)	U.S.	14.0	
Jerrett et al. (2005, 087600)	Los Angeles, CA		Max: 27.1
			75 th : 16.00
Krewski et al. (2009, 191193)	U.S.	14.02	90th: 26.75 95th: 27.89 Max: 30.01
Laden et al. (2006, 087605)	Multicity, U.S.	10.2-29.0	
Lipfert et al. (2006, 088218)	U.S.	14.3	
Miller et al. (2007, 090130)	U.S.	13.5	75th: 18.3 Max: 28.3
Pope et al. (2004, 055880)	U.S.	17.1	
Schwartz et al. (2008, 156963)	Multicity, U.S.	17.5	Max: 40
Zeger et al. (2007, 157176)	U.S.		17.0
Zeger et al. (2008, 191951)	U.S.	13.2	75th: 14.9
<i>PM_{10-2.5}</i>			
Chen et al. (2005, 087942)	Multicity, CA	25.4	
Lipfert et al. (2006, 088218)	U.S.	16.0	
<i>PM₁₀</i>			
Chen et al. (2005, 087942)	Multicity, CA	52.6	
Gehring et al. (2006, 089797)	North Rhine, Germany	43.7-48.0	Max: 52.5-56.1
Goss et al. (2004, 055624)	U.S.	24.8	75th: 28.9
Puett et al. (2008, 156891)	NE U.S.	21.6	
Zanobetti et al. (2008, 156177)	U.S.	29.4	

7.6.1. Recent Studies of Long-Term Exposure to PM and Mortality

Studies since the last PM AQCD include results of new analyses and insights for the ACS and Harvard Six Cities studies, further analyses from the AHSMOG and Veterans study cohorts, as well as analyses of a Cystic Fibrosis cohort and subsets of the ACS from Los Angeles and New York City. In the original analyses of the Six Cities and ACS cohort studies, no associations were found between long-term exposure to PM_{10-2.5} and mortality, and the extended and follow-up analyses did not evaluate associations with PM_{10-2.5}. The historical and more recent results for PM_{2.5} of both the ACS and the Harvard Six Cities studies are compiled in Figure 7-6. Moreover, since the last PM AQCD, there is a major new cohort that investigates the effects of PM_{2.5} on cardiovascular mortality in the literature: the WHI study (Miller et al., 2007, [090130](#)). Most recently, an ecologic cohort study of the nation's Medicare population has been completed (Eftim et al., 2008, [099104](#)). These new findings further strengthen the evidence linking long-term exposure to PM_{2.5} and mortality, while providing indications that the magnitude of the PM_{2.5}-mortality association is larger than previously estimated (Figure 7-7). Two recent reports from the AHSMOG and Veterans study cohorts have provided some limited evidence for associations between long-term exposure to PM_{10-2.5} and mortality. The original analyses of the AHSMOG cohort study found positive associations between long-term concentrations of PM₁₀ and 15-yr mortality due to natural causes and lung cancer (Abbey et al., 1999, [047559](#)). McDonnell et al. (2000, [010319](#)) reanalyzed these data and concluded that previously observed association of long-term ambient PM₁₀ concentrations with mortality for males were best explained by a relationship of mortality with the fine fraction of PM₁₀ rather than the thoracic coarse fraction of PM₁₀. Recent reports from the AHSMOG study cohort, as well as the Nurses' Health Study and a cohort of women in Germany have provided some evidence for associations between long-term exposure to PM₁₀ and mortality among women.

Harvard Six Cities: A follow-up study has used updated air pollution and mortality data; an additional 1,368 deaths occurred during the follow-up period (1990-1998) versus 1,364 deaths in the original study period (1974-1989) (Laden et al., 2006, [087605](#)). Statistically significant associations are reported between long-term exposure to PM_{2.5} and mortality for data for the two periods (RR = 1.16 [95% CI: 1.07-1.26] per 10 µg/m³ PM_{2.5}). Of special note is a statistically significant reduction in mortality risk reported with reduced long-term PM_{2.5} concentrations (RR = 0.73 [95% CI: 0.57-0.95] per 10 µg/m³ PM_{2.5}). This is equivalent to an RR of 1.27 for reduced mortality risks with reduced long-term PM_{2.5} concentrations. This reduced mortality risk was observed for deaths due to cardiovascular and respiratory causes, but not for lung cancer deaths. The PM_{2.5} concentrations for recent years were estimated from visibility data, which introduces some uncertainty in the interpretation of the results from this study. Coupled with the results of the original analysis (Dockery et al., 1993, [044457](#)), this study strongly suggests that a reduction in PM_{2.5} pollution yields positive health benefits.

ACS Extended Analyses/Reanalysis II: Two new analyses further evaluated the associations of long-term PM_{2.5} exposures with risk of mortality in 50 U.S. cities reported by Pope and colleagues (2002, [024689](#)), adding new details about deaths from specific cardiovascular and respiratory causes (Krewski, 2009, [190075](#); Pope et al., 2004, [055880](#)). Pope et al. (2004, [055880](#)) reported positive associations with deaths from specific cardiovascular diseases, particularly ischemic heart disease (IHD), and a group of cardiac conditions including dysrhythmia, heart failure and cardiac arrest (RR for cardiovascular mortality = 1.12, 95% CI 1.08-1.15 per 10 µg/m³ PM_{2.5}), but no PM associations were found with respiratory mortality.

In an additional reanalysis that extended the follow-up period for the ACS cohort to 18 yr (1982-2000) (Krewski et al., 2009, [191193](#)), investigators found effect estimates that were similar, though generally higher, than those reported in previous ACS analyses. This reanalysis also included data for seven ecologic (neighborhood-level) contextual (i.e., not individual-level) covariates, each of which represents local factors known or suspected to influence mortality, such as poverty level, educational attainment, and unemployment. The effect estimate for all cause mortality, based on PM_{2.5} concentrations measured in 1999-2000 was 1.03 (95% CI: 1.01-1.05). The corresponding effect estimates for deaths due to IHD and lung cancer were 1.15 (95% CI: 1.04-1.18) and 1.11 (95% CI: 1.04-1.18), respectively. In earlier analyses of this cohort, investigators found that increasing education levels appeared to reduce the effect of PM_{2.5} exposure on mortality. Results from this reanalysis show a similar pattern, although with somewhat less certainty, for all causes of death except IHD, for which the pattern was reversed. Overall, although the addition of random effects modeling and contextual covariates to the ACS model made most effect estimates higher (but

some lower), they were not statistically different from the earlier ACS effect estimates. Thus, these new analyses, with their more extensive consideration of potentially confounding factors, confirm the published ACS PM_{2.5}-mortality results to be robust.

California Cancer Prevention Study: In a cohort of elderly people in 11 California counties (mean age 73 yr in 1983), an association was reported for long-term PM_{2.5} exposure with all-cause deaths from 1973-1982 (RR = 1.04 [95% CI: 1.01-1.07] per 10 µg/m³ PM_{2.5}) (Enstrom, 2005, 087356). However, no significant associations were reported with deaths in later time periods when PM_{2.5} levels had decreased in the most polluted counties (1983-2002) (RR = 1.00 [95% CI: 0.98-1.02] per 10 µg/m³ PM_{2.5}). The PM_{2.5} data were obtained from the EPA's Inhalation Particle Network (collected 1979-1983), and the locations represented a subset of data used in the 50-city ACS study (Pope et al., 1995, 045159). However, the use of average values for California counties as exposure surrogates likely leads to significant exposure error, as many California counties are large and quite topographically variable.

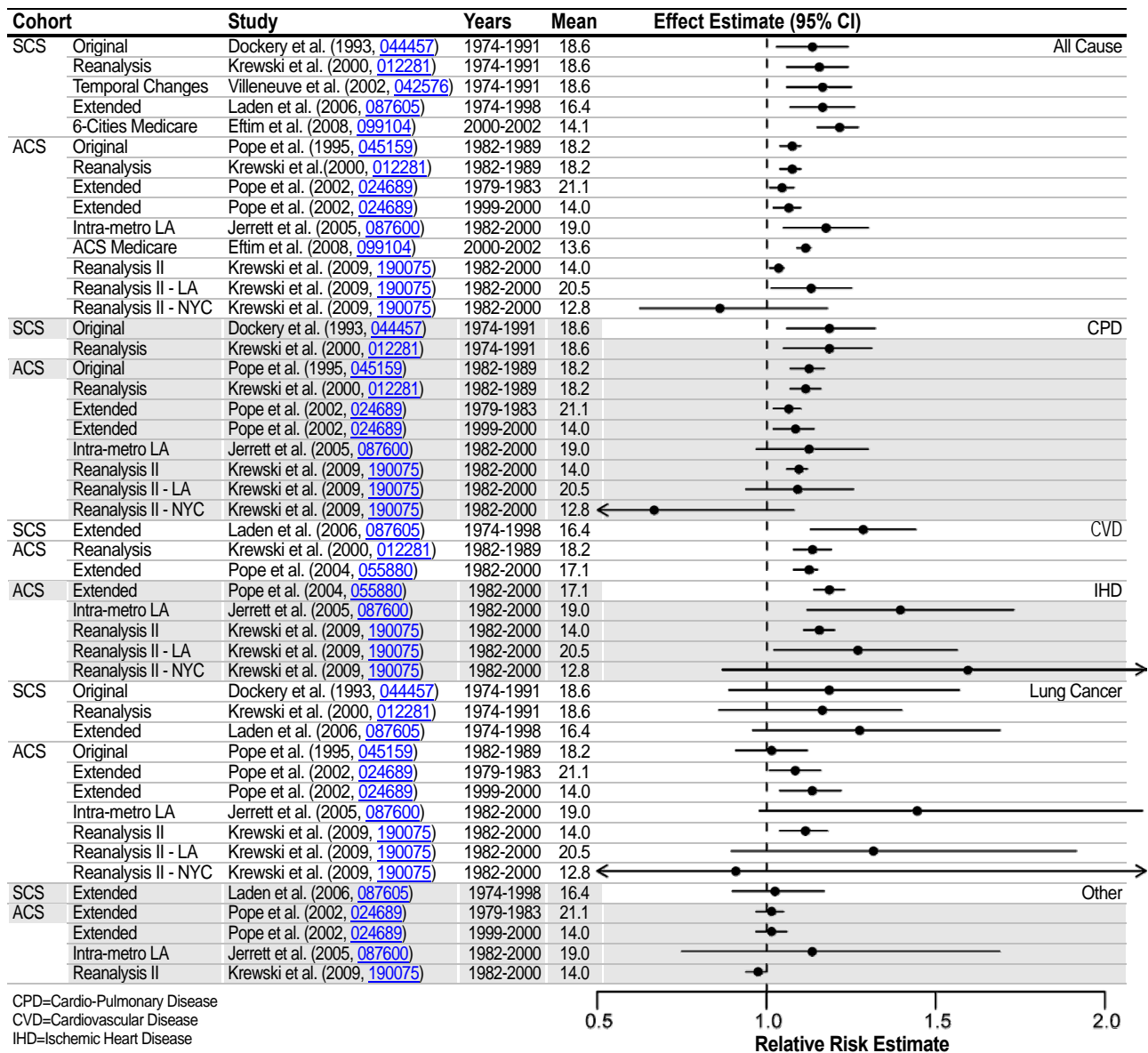


Figure 7-6. Mortality risk estimates associated with long-term exposure to PM_{2.5} from the Harvard Six Cities Study (SCS) and the American Cancer Society Study (ACS).

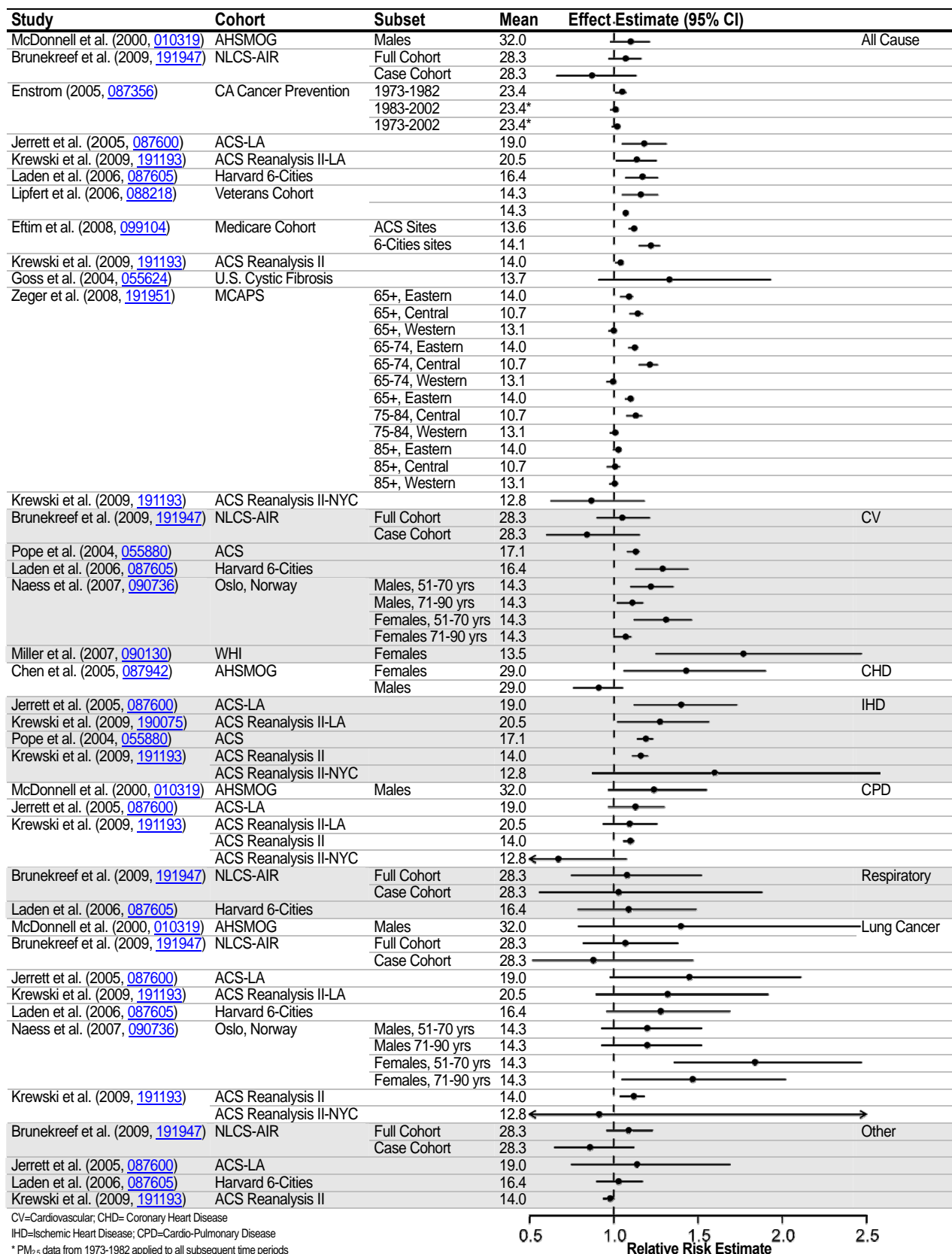


Figure 7-7. Mortality risk estimates, long-term exposure to PM_{2.5} in recent cohort studies.

AHSMOG: In this analysis for the Seventh-Day Adventist cohort in California, a positive, statistically significant, association with coronary heart disease mortality was reported among females (92 deaths; RR = 1.42 [95% CI: 1.06-1.90] per 10 $\mu\text{g}/\text{m}^3$ $\text{PM}_{2.5}$), but not among males (53 deaths; RR = 0.90 [95% CI: 0.76-1.05] per 10 $\mu\text{g}/\text{m}^3$ $\text{PM}_{2.5}$) (Chen et al., 2005, [087942](#)). Associations were strongest in the subset of postmenopausal women (80 deaths; RR = 1.49 [95% CI: 1.17-1.89] per 10 $\mu\text{g}/\text{m}^3$ $\text{PM}_{2.5}$). The authors speculated that females may be more sensitive to air pollution-related effects, based on differences between males and females in dosimetry and exposure. As was found with $\text{PM}_{2.5}$, a positive association with coronary heart disease mortality was reported for $\text{PM}_{10-2.5}$ and PM_{10} among females (RR = 1.38 [95% CI: 0.97-1.95] per 10 $\mu\text{g}/\text{m}^3$ $\text{PM}_{10-2.5}$; RR = 1.22 [95% CI: 1.01-1.47] per 10 $\mu\text{g}/\text{m}^3$ PM_{10}), but not for males (RR = 0.92 [95% CI: 0.66-1.29] per 10 $\mu\text{g}/\text{m}^3$ $\text{PM}_{10-2.5}$; RR = 0.94 [95% CI: 0.82-1.08] per 10 $\mu\text{g}/\text{m}^3$ PM_{10}); associations were strongest in the subset of postmenopausal women (80 deaths) (Chen et al., 2005, [087942](#)).

U.S. Cystic Fibrosis cohort: A positive, but not statistically significant, association was reported for $\text{PM}_{2.5}$ in this study (RR = 1.32 [95% CI: 0.91-1.93] per 10 $\mu\text{g}/\text{m}^3$ $\text{PM}_{2.5}$) that primarily focused on evidence of exacerbation of respiratory symptoms (Goss et al., 2004, [055624](#)). No clear association was reported for PM_{10} . However, only 200 deaths had occurred in the cohort of over 11,000 people (average age in cohort was 18.4 yr), so the power of this study to detect associations was relatively low.

Women's Health Initiative (WHI) Study: This nationwide cohort study considered 65,893 post-menopausal women with no history of cardiovascular disease who lived in 36 U.S. metropolitan areas from 1994 to 1998 (Miller et al., 2007, [090130](#)). The study had a median subject follow-up time of 6 years. Miller and colleagues assessed each woman's exposure to air pollutants using the monitor located nearest to their residence. Hazard ratios were estimated for the first cardiovascular event, adjusting for age, race or ethnic group, smoking status, educational level, household income, body-mass index, and presence or absence of diabetes, hypertension, or hypercholesterolemia. Overall, this study concludes that "long-term exposure to fine particulate air pollution is associated with the incidence of cardiovascular disease and death among postmenopausal women." In terms of effect size, the study found that each increase of 10 $\mu\text{g}/\text{m}^3$ of $\text{PM}_{2.5}$ was associated with a 24% increase in the risk of a cardiovascular event (hazard ratio, 1.24 [95% CI: 1.09-1.41]) and a 76% increase in the risk of death from cardiovascular disease (hazard ratio, 1.76 [95% CI: 1.25-2.47]). While this study found results confirmatory to the ACS and Six Cities Study, it reports much larger relative risk estimates per $\mu\text{g}/\text{m}^3$ $\text{PM}_{2.5}$. In addition, since the study included only women without pre-existing cardiovascular disease, it could potentially be a healthier cohort population than that considered by the ACS and Six Cities Study. Indeed, the WHI Study reported only 216 cardiovascular deaths in 349,643 women-yr of follow-up, or a rate of 0.075% deaths per year (Miller et al., 2007, [090130](#)), while the ACS Study reported that 10% of subjects died of cardiovascular disease over a 16-yr follow-up period, yielding a rate of 0.625% per year, or approximately 8 times the cardiovascular mortality rate of the WHI population (Pope et al., 2004, [055880](#)). Thus, $\text{PM}_{2.5}$ impacts may yield higher relative risk estimates in the WHI population because the $\text{PM}_{2.5}$ risk is being compared to a much lower prevailing risk of cardiovascular death in this select study population.

The WHI study not only confirms the ACS and Six City Study associations with mortality in yet another well characterized cohort with detailed individual-level information, it also has been able to consider the individual medical records of the thousands of WHI subjects over the period of the study. This has allowed the researchers to examine not only mortality, but also related morbidity in the form of heart problems (cardiovascular events) experienced by the subjects during the study. As reported in this paper, this examination confirmed that there is an increased risk of cardiovascular morbidity, as well (Section 7.2.9). These morbidity co-associations with $\text{PM}_{2.5}$ in the same population lend even greater support to the biological plausibility of the air pollution-mortality associations found in this study.

Medicare Cohort Studies: Using Medicare data, Eftim and co-authors (2008, [099104](#)) assessed the association of $\text{PM}_{2.5}$ with mortality for the same locations included in the ACS and Six City Study. For these locations, they estimated the chronic effects of $\text{PM}_{2.5}$ on mortality for the period 2000-2002 using mortality data for cohorts of Medicare participants and average $\text{PM}_{2.5}$ levels from monitors in the same counties included in the two studies. Using aggregate counts of mortality by county for three age groups, they estimated mortality risk associated with air pollution adjusting for age and sex and area-level covariates (education, income level, poverty, and employment), and controlled for potential confounding by cigarette smoking by including standardized mortality ratios

for lung cancer and COPD. This study is, therefore, an ecological analysis, similar to past published cross-sectional analyses, in that area-level covariates (education, income level, poverty, and employment) are employed as controlling variables, since individual level information is not available from the Medicare database (other than age and sex), which includes virtually all Americans aged 65 or greater. Exposures are also ecological in nature, as central site data are used as indices of exposure. These results indicated that a 10 $\mu\text{g}/\text{m}^3$ increase in the yearly average $\text{PM}_{2.5}$ concentration is associated with 10.9% (95% CI: 9.0-12.8) and with 20.8% (95% CI: 14.8-27.1) increases in all-cause mortality for the ACS and Six Cities Study counties, respectively. The estimates are somewhat higher than those reported by the original investigators, and there may be several possible explanations for this apparent increase, especially that this is an older population than the ACS cohort. Perhaps the most likely explanation is that the lack of personal confounder information (e.g., past personal smoking information) led to an insufficient control for the effects of these other variables' effects on mortality, inflating the pollution effect estimates somewhat, similar to what has been found in the ACS analyses when only ecological-level control variables were included. The ability of the Eftim et al. (2008, [099104](#)) study results to qualitatively replicate the original individual-level cohort study (e.g., ACS and Six Cities Study) results suggests that past ecological cross-sectional mortality study results may also provide useful insights into the nature of the association, especially when used for consideration of time trends, or for comparisons of the relative (rather than absolute) sizes of risks between different pollutants or PM components in health effects associations.

Janes et al. (2007, [090927](#)) used the same nationwide Medicare mortality data to examine the association between monthly averages of $\text{PM}_{2.5}$ over the preceding 12 mo and monthly mortality rates in 113 U.S. counties from 2000 to 2002. They decomposed the association between $\text{PM}_{2.5}$ and mortality into two components: (1) the association between "national trends" in $\text{PM}_{2.5}$ and mortality; and (2) the association between "local trends," defined as county-specific deviations from national trends. This second component is posited to provide evidence as to whether counties having steeper declines in $\text{PM}_{2.5}$ also have steeper declines in mortality relative to the national trend. They report that the exposure effect estimates are different at these two spatiotemporal scales, raising concerns about confounding bias in these analyses. The authors assert that the association between trends in $\text{PM}_{2.5}$ and mortality at the national scale is more likely to be confounded than is the association between trends in $\text{PM}_{2.5}$ and mortality at the local scale and, if the association at the national scale is set aside, that there is little evidence of an association between 12-month exposure to $\text{PM}_{2.5}$ and mortality in this analysis. However, in response, Pope and Burnett (2007, [090928](#)) point out that such use of long-term time trends as the primary source of exposure variability has been avoided in most other air pollution epidemiology studies because of such concerns about potential confounding of such time-trend associations.

By linking monitoring data to the U.S. Medicare system by county of residence, Zeger et al. (2007, [157176](#)) analyzed Medicare mortality records, comprising over 20 million enrollees in the 250 largest counties during 2000-2002. The authors estimated log-linear regression models having age-specific county level mortality rates as the outcome and, as the main predictor, the average $\text{PM}_{2.5}$ pollution level in each county during 2000. Area-level covariates were used to adjust for socio-economic status and smoking. The authors reported results under several degrees of adjustment for spatial confounding and with stratification into eastern, central and western U.S. counties. A 10 $\mu\text{g}/\text{m}^3$ increase in $\text{PM}_{2.5}$ was associated with a 7.6% increase in mortality (95% CI: 4.4-10.8). When adjusted for spatial confounding, the estimated log-relative risks dropped by 50%. Zeger et al. (2007, [157176](#)) found a stronger association in the eastern counties than nationally, with no evidence of an association in western counties.

In a subsequent report, Zeger et al. (2008, [191951](#)) created a new retrospective cohort, the Medicare Cohort Air Pollution Study (MCAPS), consisting of 13.2 million persons residing in 4,568 ZIP codes in urban areas having geographic centroids within 6 miles of a $\text{PM}_{2.5}$ monitor. Using this cohort, they investigated the relationship between 6-yr avg exposure to $\text{PM}_{2.5}$ and mortality risk over the period 2000-2005. When divided by region, the associations between long-term exposure to $\text{PM}_{2.5}$ and mortality for the eastern and central ZIP codes were qualitatively similar to those reported in the ACS and Six Cities Study, with 11.4% (95% CI: 8.8-14.1) and 20.4% (95% CI: 15.0-25.8) increases per 10 $\mu\text{g}/\text{m}^3$ increase in $\text{PM}_{2.5}$ in the eastern and central regions, respectively. The MCAPS results included evidence of differing $\text{PM}_{2.5}$ relative risks by age and geographic location, where risk declines with increasing age category until there is no evidence of an association among persons

≥ 85 yr of age, and there is no evidence of a positive association for the 640 urban ZIP codes in the western region of the U.S.

Using hospital discharge data, Zanobetti et al. (2008, [156177](#)) constructed a cohort of persons discharged with COPD using Medicare data between 1985 and 1999. Positive associations in the survival analyses were reported for single year and multiple-year lag exposures, with a hazard ratio for total mortality of 1.22 (95% CI: 1.17-1.27) per 10 $\mu\text{g}/\text{m}^3$ increase in PM_{10} over the previous 4 years.

Veterans Cohort: A recent reanalysis of the Veterans cohort data focused on exposure to traffic-related air pollution (traffic density based on traffic flow rate data and road segment length) reported a stronger relationship between mortality with long-term exposure to traffic than with $\text{PM}_{2.5}$ mass (Lipfert et al., 2006, [088218](#)). A significant association was reported between total mortality and $\text{PM}_{2.5}$ in single-pollutant models (RR = 1.12 [95% CI: 1.04-1.20] per 10 $\mu\text{g}/\text{m}^3$ $\text{PM}_{2.5}$). This risk estimate is larger than results reported in a previous study of this cohort. In multipollutant models including traffic density, the association with $\text{PM}_{2.5}$ was reduced and lost statistical significance. Traffic emissions contribute to $\text{PM}_{2.5}$ so it would be expected that the two would be highly correlated, and, thus, these multipollutant model results should be interpreted with caution. In a companion study, Lipfert et al. (2006, [088218](#)) used data from EPA's fine particle speciation network, and reported findings for $\text{PM}_{2.5}$ which were similar to those reported by Lipfert et al. (2006, [088218](#)). In this study (Lipfert et al., 2006, [088218](#)), a significant association was reported between long-term exposure to $\text{PM}_{10-2.5}$ and total mortality in a single-pollutant model (RR = 1.07, 95% CI: 1.01-1.12 per 10 $\mu\text{g}/\text{m}^3$ $\text{PM}_{10-2.5}$). However, the association became negative and not statistically significant in a model that included traffic density. As it would be expected that traffic would contribute to the $\text{PM}_{10-2.5}$ concentrations, it is difficult to interpret the results of these multipollutant analyses.

Nurses' Health Study Cohort: The Nurses' Health Study (Puett et al., 2008, [156891](#)) is an ongoing prospective cohort study examining the relation of chronic PM_{10} exposures with all-cause mortality and incident and fatal CHD consisting of 66,250 female nurses in MSAs in the northeastern region of the U.S. All cause mortality was statistically significantly associated with average PM_{10} exposures in the time period 3-48 mo preceding death. The association was strongest with average PM_{10} exposure in the 24 mo prior to death (hazard ratio 1.16 [95% CI: 1.05-1.28]) and weakest with exposure in the month prior to death (hazard ratio 1.04 [95% CI: 0.98-1.11]). The association with fatal CHD occurred with the greatest magnitude with mean exposure in the 24 mo prior to death (hazard ratio 1.42 [95% CI: 1.11-1.81]).

Netherlands Cohort Study (NLCS): The Netherlands Cohort Study (Brunekreef et al., 2009, [191947](#)) estimates the effects of traffic-related air pollution on cause specific mortality in a cohort of approximately 120,000 subjects aged 55-69 yr at enrollment. For a 10 $\mu\text{g}/\text{m}^3$ increase in $\text{PM}_{2.5}$ concentration, the relative risk for natural-cause mortality in the full cohort was 1.06 (95% CI: 0.97-1.16), similar in magnitude to the results reported by the ACS. In a case-cohort analysis adjusted for additional potential confounders, there were no associations between air pollution and mortality.

German Cohort: The North Rhine-Westphalia State Environment Agency (LUA NRW) initiated a cohort of approximately 4,800 women, and assessed whether long-term exposure to air pollution originating from motorized traffic and industrial sources was associated with total and cause-specific mortality (Gehring et al., 2006, [089797](#)). They found that cardiopulmonary mortality was associated with PM_{10} (RR = 1.52 [95% CI: 1.09-2.15] per 10 $\mu\text{g}/\text{m}^3$ PM_{10}).

7.6.2. Composition and Source-Oriented Analyses of PM

As discussed in the 2004 PM AQCD, only a very limited number of the chronic exposure cohort studies have included direct measurements of chemical-specific PM constituents other than sulfates, or assessments of source-oriented effects, in their analyses. One exception is the Veterans Cohort Study, which looked at associations with some constituents, and traffic.

Veterans Cohort: Using data from EPA's fine particle speciation network, Lipfert et al. (2006, [088756](#)) reported a positive association for mortality with sulfates. Using 2002 data from the fine particle speciation network, positive associations were found between mortality and long-term exposures to nitrates, EC, Ni and V, as well as traffic density and peak O_3 concentrations. In

multipollutant models, associations with traffic density remained significant, as did nitrates, Ni and V in some models.

Netherlands Cohort Study: Beelen et al. (2008, [156263](#)) studied the association between long-term exposure to traffic-related air pollution and mortality in a Dutch cohort. They used data from an ongoing cohort study on diet and cancer with 120,852 subjects who were followed from 1987 to 1996. Exposure to BS, NO₂, SO₂, and PM_{2.5}, as well as various exposure variables related to traffic, were estimated at the home address. Traffic intensity on the nearest road was independently associated with mortality. Relative risks (CI) for a 10 µg/m³ increase in BS concentrations (difference between 5th and 95th percentile) were 1.05 (95% CI: 1.00-1.11) for natural cause, 1.04 (95% CI: 0.95-1.13) for cardiovascular, 1.22 (95% CI: 0.99-1.50) for respiratory, 1.03 (95% CI: 0.88-1.20) for lung cancer, and 1.04 (95% CI: 0.97-1.12) for mortality other than cardiovascular, respiratory, or lung cancer. Results were similar for NO₂ and PM_{2.5}, but no associations were found for SO₂. Traffic-related air pollution and several traffic exposure variables were associated with mortality in the full cohort, although the relative risks were generally small. Associations between natural-cause and respiratory mortality were statistically significant for NO₂ and BS. These results add to the evidence that long-term exposure to traffic-related particulate air pollution is associated with increased mortality.

Given the general dearth of published source-oriented studies of the mortality impacts of long-term PM exposure components, and given that the recent Medicare Cohort study now indicates that such ecological cross-sectional studies can be useful for evaluating time trends and/or comparisons across pollution components, it may well be that examining past cross-sectional studies comparing source-oriented components of PM may be informative. In particular, Ozkaynak and Thurston (1987, [072960](#)), utilized the chemical speciation conducted in the Inhalable Particle (IP) Network to conduct a chemical constituent and source-oriented evaluation on long-term PM exposure and mortality in the U.S. They analyzed the 1980 U.S. vital statistics and available ambient air pollution data bases for sulfates and fine, inhalable, and TSP mass. Using multiple regression analyses, they conducted a cross-sectional analysis of the association between various particle measures and total mortality. Results from the various analyses indicated the importance of considering particle size, composition, and source information in modeling of particle pollution health effects. Of the independent mortality predictors considered, particle exposure measures most related to the respirable fraction of the aerosols, such as fine particles and sulfates, were most consistently and significantly associated with the reported SMSA-specific total annual mortality rates. On the other hand, particle mass measures that included PM_{10-2.5} (e.g., total suspended particles and inhalable particles) were often found to be non-significant predictors of total mortality. Furthermore, based on the application of PM_{2.5} source apportionment, particles from industrial sources and from coal combustion were indicated to be more significant contributors to human mortality than fine soil-derived particles.

7.6.3. Within-City Effects of PM Exposure

Much of the exposure gradient in the national-scale cohort studies was due to city-to-city differences in regional air pollution, raising the possibility that some or all of the original PM-survival associations may have been driven instead by city-to-city differences in some unknown (non-pollution) confounder variable. This has been evaluated by three recent studies.

ACS, Los Angeles: To investigate this issue, two new analyses using ACS data focused on neighborhood-to-neighborhood differences in urban air pollutants, using data from 23 PM_{2.5} monitoring stations in the Los Angeles area, and applying interpolation methods (Jerrett et al., 2005, [087600](#)) or land use regression methods (Krewski et al., 2009, [191193](#)) to assign exposure levels to study individuals. This resulted in both improved exposure assessment and an increased focus on local sources of PM_{2.5}. Significant associations between PM_{2.5} and mortality from all causes and cardiopulmonary diseases were reported with the magnitude of the relative risks being greater than those reported in previous assessments. In general, the associations for PM_{2.5} and mortality using these two methods for exposure assessment were similar, though the use of land use regression resulted in somewhat smaller hazard ratios and tighter CIs (see Table 7-9). This indicates that city-to-city confounding was not the cause of the associations found in the earlier ACS Cohort studies. This provides evidence that reducing exposure error can result in stronger associations between PM_{2.5} and mortality than generally observed in broader studies having less exposure detail.

Table 7-9. Comparison of results from ACS intra-urban analysis of Los Angeles and New York City using kriging or land use regression to estimate exposure.

Cause of Death	Los Angeles:	Los Angeles:	New York City:
	Hazard Ratio ¹ and 95% Confidence Interval Using Kriging ² (Jerrett et al., 2005, 087600)	Hazard Ratio ¹ and 95% Confidence Interval Using Land Use Regression ³ (Krewski et al., 2009, 191193)	Hazard Ratio ¹ and 95% Confidence Interval Using Land Use Regression ⁴ (Krewski et al., 2009, 191193)
All Cause	1.11 (0.99-1.25)	1.13 (1.01-1.25)	0.86 (0.63-1.18)
IHD	1.25 (0.99-1.59)	1.26 (1.02-1.56)	1.56 (0.87-2.88)
CPD	1.07 (0.91-1.26)	1.09 (0.94-1.26)	0.66 (0.41-1.08)
Lung Cancer	1.20 (0.79-1.82)	1.31 (0.90-1.92)	0.90 (0.29-2.78)

¹Hazard ratios presented per 10 µg/m³ increase in PM_{2.5}

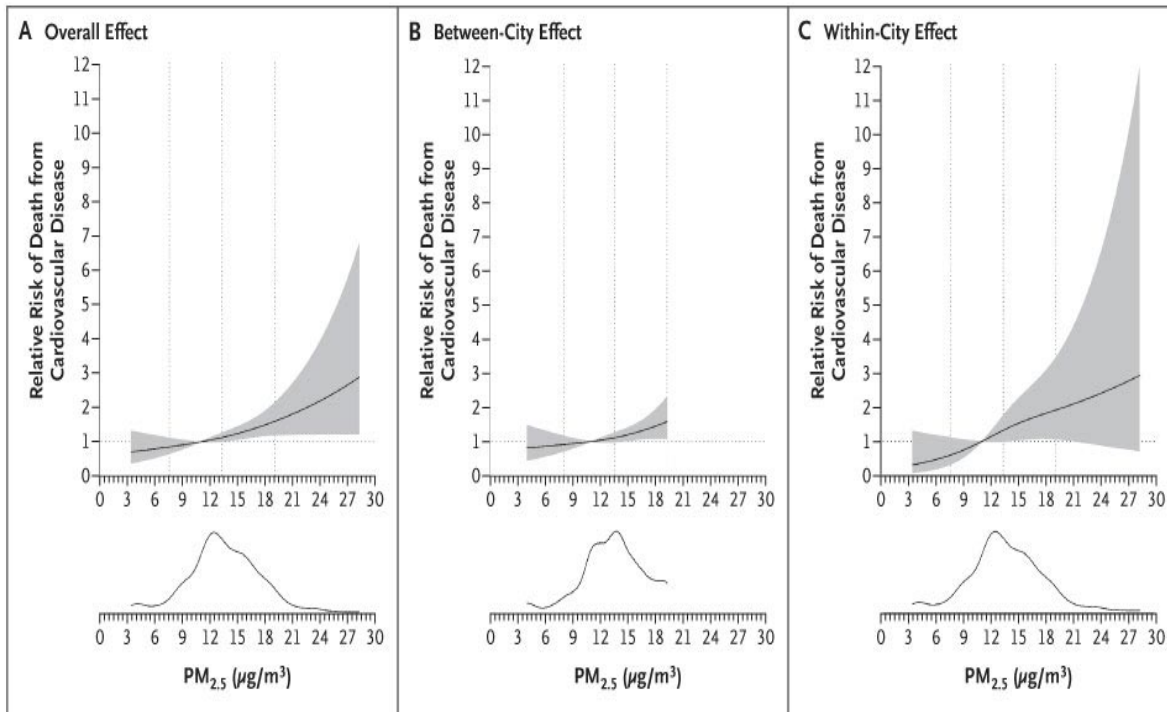
²Model included parsimonious contextual covariates

³Model included parsimonious individual level (23) and ecologic (4) covariates

⁴Model included all 44 individual level and 7 ecologic covariates.

ACS, New York: Krewski et al. (2009, [191193](#)) applied the same techniques used in the land use regression analysis of Los Angeles to an investigation conducted in New York City. Annual average concentrations were calculated for each of 62 monitors from 3 yr of daily monitoring data for 1999-2001. Those data were combined with land-use data collected from traffic counting systems, roadway network maps, satellite photos of the study area, and local government planning and tax-assessment maps to assign estimated exposures to the ACS participants. The investigators did not observe elevated effect estimates for all cause, CPD or lung cancer deaths, but IHD did show a positive association with PM_{2.5} concentration. The difference between the 90th and 10th percentiles of the 3-yr avg PM_{2.5} concentration was 1.5 µg/m³ and the difference between the minimum and maximum values of the 3-yr avg PM_{2.5} concentration was 7.8 µg/m³. This narrow range in PM_{2.5} exposure contrasts across the New York City metropolitan area and may well account for the inconclusive results in this city-specific analysis. Relatively uniform exposures would reduce the power of the statistical models to detect patterns of mortality relative to exposure and estimate the association with precision.

WHI Study: This study also investigated the within- versus between-city effects in its cities. As shown in Figure 7-8, similar effects for both the within and between-city analyses demonstrate that this association is not due to some other (non-pollution) confounder differing between the various cities, strengthening confidence in the overall pollution-effect estimates.

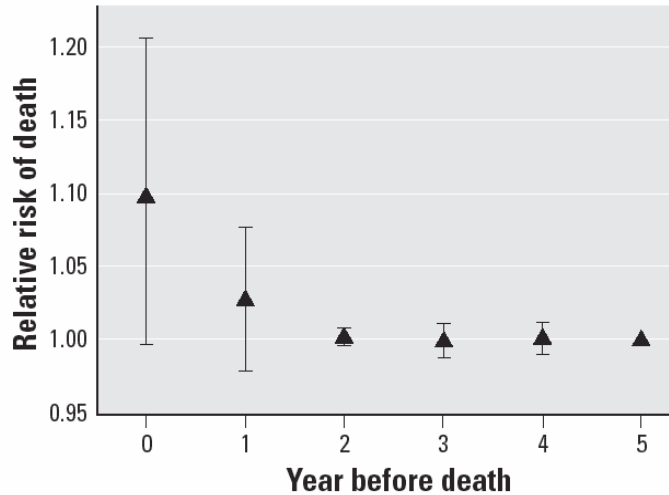


Source: Miller et al. (2007, [090130](#))
 Copyright © 2007 Massachusetts Medical Society. All rights reserved.

Figure 7-8. Plots of the relative risk of death from cardiovascular disease from the Women’s Health Initiative study displaying the between-city and within-city contributions to the overall association between PM_{2.5} and cardiovascular mortality windows of exposure-effects.

7.6.4. Effects of Different Long-term Exposure Windows

The delay between changes in exposure and changes in health has important policy implications. Schwartz et al. (2008, [156963](#)) investigated this issue using an extended follow-up of the Harvard Six Cities Study. Cox proportional hazards models were fit to control for smoking, body mass index, and other covariates. Penalized splines were fit in a flexible functional form to the concentration response to examine its shape, and the degrees of freedom for the curve were selected based on Akaike’s information criterion (AIC). The researchers also used model averaging as an alternative approach, where multiple models are fit explicitly and averaged, weighted by their probability of being correct given the data. The lag relationship by model was averaged across a range of unconstrained distributed lag models (i.e., same year, 1 yr prior, 2 yr prior, etc.). Results of the lag comparison are shown in Figure 7-9 indicating that the effects of changes in exposure on mortality are seen within 2 yr. The authors also noted that the concentration-response curve was linear, clearly continuing below the level of the current U.S. air quality standard of 15 $\mu\text{g}/\text{m}^3$.

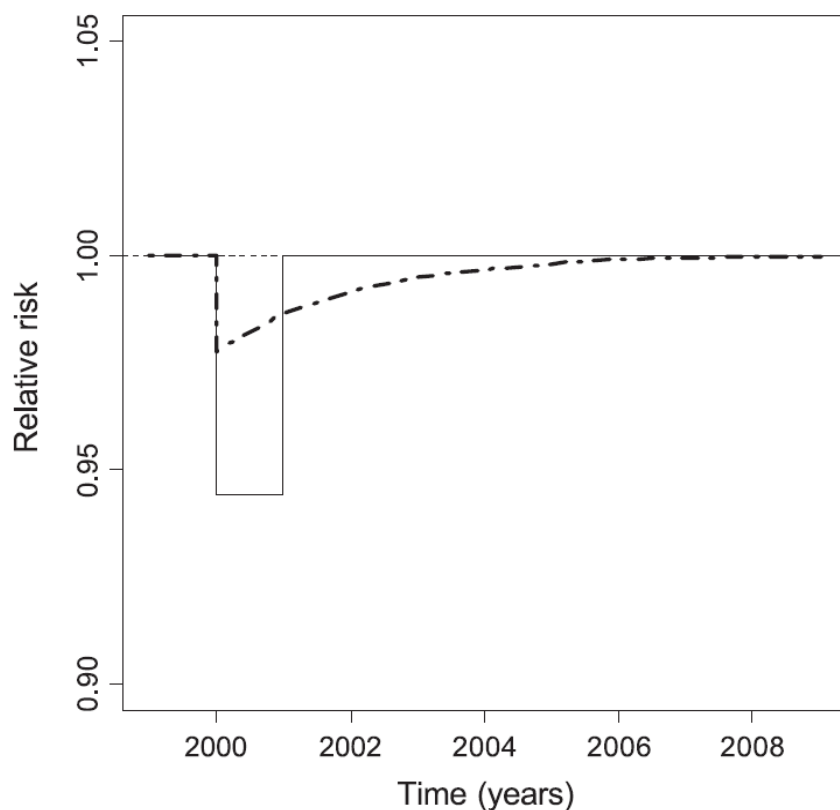


Source: Schwartz et al. (2008, [156963](#))

Figure 7-9. The model-averaged estimated effect of a 10- $\mu\text{g}/\text{m}^3$ increase in $\text{PM}_{2.5}$ on all-cause mortality at different lags (in years) between exposure and death. Each lag is estimated independently of the others. Also shown are the pointwise 95% CIs for each lag, based on jackknife estimates.

Similarly, the effect of long-term exposure to PM_{10} on the risk of death in a large multicity study of elderly subjects discharged alive following an admission for COPD found the effect was not limited to the exposure in each year of follow-up, and had larger cumulative effects spread over the follow-up year and three preceding years (Zanobetti et al., 2008, [156177](#)).

Röösli et al. (2005, [156923](#)) took an alternative approach to determining the window over which the mortality effects of long-term pollution exposures occurred. They fit the model shown in Figure 7-10 using $k = 0.5$ based on the Utah Steel Strike (Pope, 1989, [044461](#)) and the Ireland coal ban study (Clancy et al., 2002, [035270](#)). They found that roughly 75% of health benefits are observed in the first 5 years, as shown in Table 7-10. These results are consistent with the findings of Schwartz et al. (2008, [156963](#)). Puett et al. (2008, [156891](#)) also compared different long-term exposure lags, with exposure periods ranging from 1 month to 48 mo prior to death. They found statistically significant associations with average PM_{10} exposures in the time period 3-48 mo prior to death, with the strongest associations in the 24 mo prior to death and the weakest with exposure in the 1 mo prior to death.



Source: Reprinted with Permission from Oxford University Press & the International Epidemiological Society from Rösli et al. (2005, [156923](#))

Figure 7-10. Time course of relative risk of death after a sudden decrease in air pollution exposure during the year 2000, assuming a steady state model (solid line) and a dynamic model (bold dashed line). The thin dashed line refers to the reference scenario.

Table 7-10. Distribution of the effect of a hypothetical reduction of $10 \mu\text{g}/\text{m}^3$ PM_{10} in 2000 on all-cause mortality 2000-2009 in Switzerland.

Year	1999	2000	2001	2002	2003	2004	2005	2006	2007	2008	2009
Proportion of total effect (%)	-	39.3	23.9	14.5	8.8	5.3	3.2	2.0	1.2	0.7	0.4
Relative risk (per $10 \mu\text{g}/\text{m}^3$ reduction in PM_{10})	1.0	0.9775	0.9863	0.9917	0.9950	0.9969	0.9981	0.9989	0.9993	0.9996	0.9997

Relative risk and proportion of total effect in each year are shown, assuming a time constant k of 0.5

Source: Rösli et al. (2005, [156923](#))

In the reanalysis of the ACS cohort, the investigators calculated time windows of exposure as average concentrations during successive 5-yr periods preceding the date of death (Krewski et al., 2009, [191193](#)). The investigators considered the time window with the best-fitting model (judged by the AIC statistic) to be the period during which pollution had the strongest influence on mortality. Overall, the differences between the time periods were small and demonstrated no definitive patterns. High correlations between exposure levels in the three periods may have reduced the ability of this analysis to detect any differences in the relative importance of the time windows. The investigators did not analyze any time periods smaller than 5 yr, so the results are not directly comparable to those reported by Schwartz et al. (2008, [156963](#)), Rösli et al. (2005, [156923](#)), and Puett et al. (2008, [156891](#)).

Generally, these results indicate a developing coherence of the air pollution mortality literature, suggesting that the health benefits from reducing air pollution do not require a long latency period and would be expected within a few years of intervention.

7.6.5. Summary and Causal Determinations

7.6.5.1. PM_{2.5}

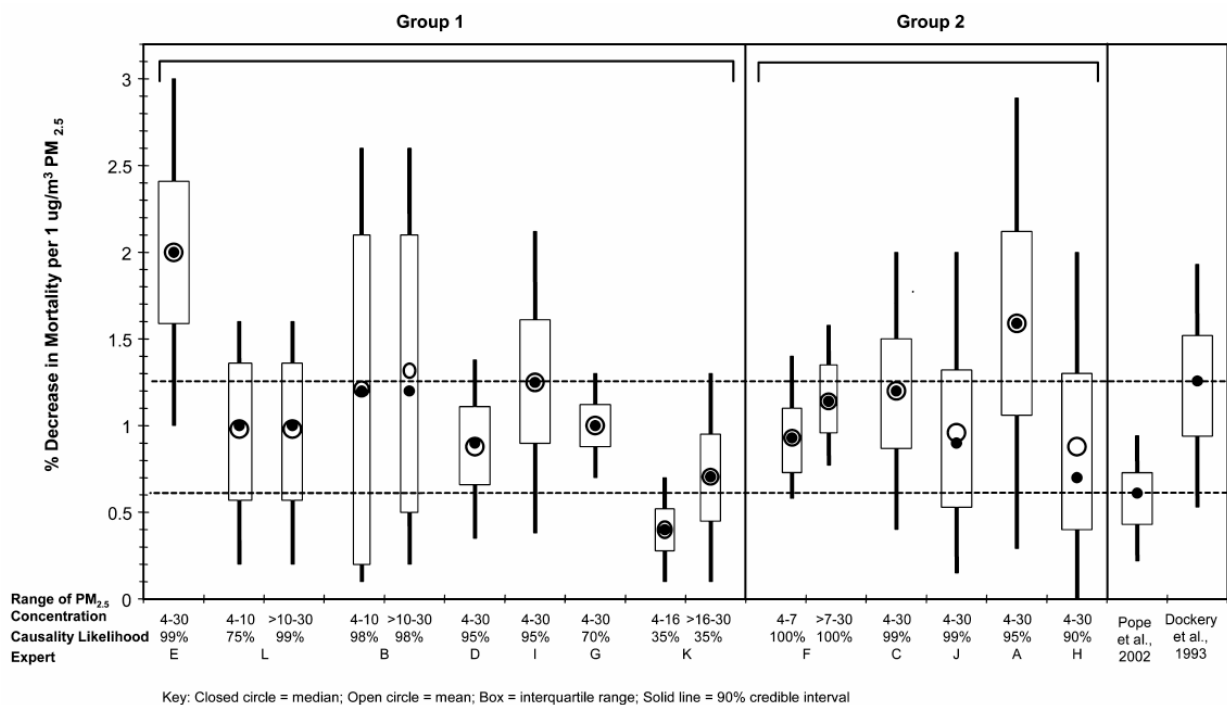
In the 1996 PM AQCD (U.S. EPA, 1996, [079380](#)), results were presented for three prospective cohort studies of adult populations: the Six Cities Study (Dockery et al., 1993, [044457](#)); the ACS Study (Pope et al., 1995, [045159](#)); and the AHSMOG Study (Abbey et al., 1995, [000669](#)). The 1996 AQCD concluded that the chronic exposure studies, taken together, suggested associations between increases in mortality and long-term exposure to PM_{2.5}, though there was no evidence to support an association with PM_{10-2.5} (U.S. EPA, 1996, [079380](#)). Discussions of mortality and long-term exposure to PM in the 2004 PM AQCD emphasized the results of four U.S. prospective cohort studies, but the greatest weight was placed on the findings of the ACS and the Harvard Six Cities studies, which had undergone extensive independent reanalysis, and which were based on cohorts that were broadly representative of the U.S. population. Collectively, the 2004 PM AQCD found that these studies provided strong evidence that long-term exposure to PM_{2.5} was associated with increased risk of human mortality.

The recent evidence is largely consistent with past studies, further supporting the evidence of associations between long-term PM_{2.5} exposure and increased risk of human mortality (Section 7.6) in areas with mean concentrations from 13.2 to 29 µg/m³ (Figure 7-7). New evidence from the Six Cities cohort study shows a relatively large risk estimate for reduced mortality risk with decreases in PM_{2.5} (Laden et al., 2006, [087605](#)). The results of new analyses from the Six Cities cohort and the ACS study in Los Angeles suggest that previous and current studies may have underestimated the magnitude of the association (Jerrett et al., 2005, [087600](#)). With regard to mortality by cause-of-death, recent ACS analyses indicate that cardiovascular mortality primarily accounts for the total mortality association with PM_{2.5} among adults, and not respiratory mortality. The recent WHI cohort study shows even higher cardiovascular risks per µg/m³ than found in the ACS study, but this is likely due to the fact that the study included only post-menopausal women without pre-existing cardiovascular disease (Miller et al., 2007, [090130](#)). There is additional evidence for an association between PM_{2.5} exposure and lung cancer mortality (Section 7.5.1.1). The WHI study also considered within versus between city mortality, as well as morbidity co-associations with PM_{2.5} in the same population. The first showed that the results are not due to between city confounding, and the morbidity analyses show the coherence of the mortality association across health endpoints, supporting the biological plausibility of the air pollution-mortality associations found in these studies.

Results from a new study examining the relationship between life expectancy and PM_{2.5} and the findings from a multiyear expert judgment study that comprehensively characterizes the size and uncertainty in estimates of mortality reductions associated with decreases in PM_{2.5} in the U.S draw conclusions that are consistent with an association between long-term exposure to PM_{2.5} and mortality (Pope et al., 2009, [190107](#); Roman et al., 2008, [156921](#)). Pope et al. (2009, [190107](#)) report that a decrease of 10 µg/m³ in the concentration of PM_{2.5} is associated with an estimated increase in mean (± SE) life expectancy of 0.61 ± 0.20 year. For the approximate period of 1980-2000, the average increase in life expectancy was 2.72 yr among the 211 counties in the analysis. The authors note that reduced air pollution was only one factor contributing to increased life expectancies, with its effects overlapping with those of other factors.

Roman et al. (2008, [156921](#)) applied state-of-the-art expert judgment elicitation techniques to develop probabilistic uncertainty distributions that reflect the broader array of uncertainties in the concentration-response relationship. This study followed best standard practices for expert elicitations based on the body of literature accumulated over the past two decades. The resulting PM_{2.5} effect estimate distributions, elicited from 12 of the world's leading experts on this issue, are shown in Figure 7-11. They indicate both larger central estimates of mortality reductions for decreases in long-term PM_{2.5} exposure in the U.S. (averaging almost 1% per µg/m³ PM_{2.5}) than reported (for example) by the ACS Study (i.e., 0.6% per µg/m³ PM_{2.5} in Pope et al. (2002, [024689](#)),

and a wider distribution of uncertainty by each expert than provided by any one of the PM_{2.5} epidemiologic studies. However, a composite uncertainty range of the overall mean effect estimate (i.e., based upon all 12 experts' estimates, but not provided in Figure 7-11) would be much narrower, and closer to that derived from the ACS study than indicated for any one expert shown in Figure 7-11.



Source: Reprinted with Permission of ACS from Roman et al. (2008, [156921](#))

Figure 7-11. Experts' mean effect estimates and uncertainty distributions for the PM_{2.5} mortality concentration-response coefficient for a 1 µg/m³ change in annual average PM_{2.5}.

Overall, recent evidence supports the strong evidence reported in the 2004 PM AQCD (U.S. EPA, 2004, [056905](#)) that long-term exposure to PM_{2.5} is associated with an increased risk of human mortality. When looking at the cause of death, the strongest evidence comes from mortality due to cardiovascular disease, with additional evidence supporting an association between PM_{2.5} and lung cancer mortality (Figure 7-7). Fewer studies evaluate the respiratory component of cardiopulmonary mortality, and the evidence to support an association with long-term exposure to PM_{2.5} and respiratory mortality is weak (Figure 7-7). Together these findings are consistent and coherent with the evidence from epidemiologic, controlled human exposure, and animal toxicological studies for the effects of short- and long-term exposure to PM on cardiovascular effects presented in Sections 6.2 and 7.2, respectively. Evidence of short- and long-term exposure to PM_{2.5} and respiratory effects (Sections 6.3 and 7.3, respectively) and infant mortality (Section 7.4) are coherent with the weak respiratory mortality effects. Additionally, the evidence for short- and long-term cardiovascular and respiratory morbidity provides biological plausibility for mortality due to cardiovascular or respiratory disease. The most recent evidence for the association between long-term exposure to PM_{2.5} and mortality is particularly strong for women. Collectively, the evidence is **sufficient to conclude that the relationship between long-term PM_{2.5} exposures and mortality is causal.**

7.6.5.2. PM_{10-2.5}

In the 2004 PM AQCD, results from the ACS and Six Cities study analyses indicated that PM_{10-2.5} was not associated with mortality. Evidence is still limited to adequately characterize the association between PM_{10-2.5} and PM sources and/or components. The new findings from AHSMOG and Veterans cohort studies provide limited evidence of associations between long-term exposure to PM_{10-2.5} and mortality in areas with mean concentrations from 16 to 25 µg/m³. The evidence **for PM_{10-2.5} is inadequate to determine if a causal relationship exists between long-term exposures and mortality.**

7.6.5.3. UFPs

The 2004 PM AQCD did not report long-term exposure studies for UFPs. No epidemiologic studies have been conducted to evaluate the effects of long-term UFP exposure and mortality. The evidence is **inadequate to determine if a causal relationship exists between long-term UFP exposures and mortality.**

Chapter 7 References

- Abbey DE; Lebowitz MD; Mills PK; Petersen FF; Beeson WL; Burchette RJ (1995). Long-term ambient concentrations of particulates and oxidants and development of chronic disease in a cohort of nonsmoking California residents. Presented at In: Phalen, R. F.; Bates, D. V., eds. Proceedings of the colloquium on particulate air pollution and human mortality and morbidity; January 1994; Irvine, CA. [000669](#)
- Abbey DE; Mills PK; Petersen FF; Beeson WL (1991). Long-term ambient concentrations of total suspended particulates and oxidants as related to incidence of chronic disease in California Seventh-Day Adventists. *Environ Health Perspect*, 94: 43-50. [042668](#)
- Abbey DE; Nishino N; McDonnell WF; Burchette RJ; Knutsen SF; Beeson WL; Yang JX (1999). Long-term inhalable particles and other air pollutants related to mortality in nonsmokers. *Am J Respir Crit Care Med*, 159: 373-382. [047559](#)
- Abou Chakra OR; Joyeux M; Nerriere E; Strub MP; Zmirou-Navier D (2007). Genotoxicity of organic extracts of urban airborne particulate matter: an assessment within a personal exposure study. *Chemosphere*, 66: 1375-81. [098819](#)
- Achenbach S; Daniel WG (2001). Noninvasive coronary angiography--an acceptable alternative? *N Engl J Med*, 345: 1909-1910. [156189](#)
- Ackermann-Lieblich U; Kuna-Dibbert B; Probst-Hensch NM; Schindler C; Dietrich DF; Stutz EZ; Bayer-Oglesby L; Baum F; Brandli O; Brutsche M; Downs SH; Keidel D; Gerbase MW; Imboden M; Keller R; Knopfli B; Kunzli Nellweger J-P; Leuenberger P; SALPADIA Team (2005). Follow-up of the Swiss Cohort study on air pollution and lung diseases in adults (SAPALDIA 2) 1991-2003: methods and characterization of participants. *Int J Public Health*, 50: 245-263. [087826](#)
- Ackermann-Lieblich U; Leuenberger P; Schwartz J; Schindler C; Monn C; Bolognini B; Bongard JP; Brandli O; Domenighetti G; Elsasser S; Grize L; Karrer W; Keller R; Keller-Wossidlo H; Kunzli N; Martin BW; Medici TC; Pliger B; Wuthrich B; Zellweger JP; Zemp E (1997). Lung function and long term exposure to air pollutants in Switzerland. *Am J Respir Crit Care Med*, 155: 122-129. [077537](#)
- Agatston AS; Janowitz WR; Hildner FJ; Zusmer NR; Viamonte M Jr; Detrano R (1990). Quantification of coronary artery calcium using ultrafast computed tomography. *J Am Coll Cardiol*, 15: 827-832. [156197](#)
- Alink GM; Sjogren M; Bos RP; Doekes G; Kromhout H; Scheepers PTJ (1998). Effect of airborne particles from selected indoor and outdoor environments on gap-junctional intercellular communication. *Toxicol Lett*, 96/97: 209-213. [087159](#)
- Allen RW; Criqui MH; Diez Roux AV; Allison M; Shea S; Detrano R; Sheppard L; Wong N; Hinckley Stukovsky K; Kaufman JD (2009). Fine particulate air pollution, proximity to traffic, and aortic atherosclerosis: The multi-ethnic study of atherosclerosis. *Epidemiology*, 20: 254-264. [156209](#)
- Allison MA; Cheung P; Criqui MH; Langer RD; Wright CM (2006). Mitral and aortic annular calcification are highly associated with systemic calcified atherosclerosis. *Circulation*, 113: 861-866. [155653](#)
- Allison MA; Criqui MH; Wright CM (2004). Patterns and risk factors for systemic calcified atherosclerosis. *Arterioscler Thromb Vasc Biol*, 24: 331-336. [156210](#)
- Amato M; Montorsi P; Ravani A; Oldani E; Galli S; Ravagnani PM; Tremoli E; Baldassarre D (2007). Carotid intima-media thickness by B-mode ultrasound as surrogate of coronary atherosclerosis: correlation with quantitative coronary angiography and coronary intravascular ultrasound findings. *Eur Heart J*, 28: 2094-2101. [155656](#)
- Annesi-Maesano I; Moreau D; Caillaud D; Lavaud F; Le Moullec Y; Taytard A; Pauli G; Charpin D (2007). Residential proximity fine particles related to allergic sensitisation and asthma in primary school children. *Respir Med*, 101: 1721-1729. [093180](#)

Note: Hyperlinks to the reference citations throughout this document will take you to the NCEA HERO database (Health and Environmental Research Online) at <http://epa.gov/hero>. HERO is a database of scientific literature used by U.S. EPA in the process of developing science assessments such as the Integrated Science Assessments (ISA) and the Integrated Risk Information System (IRIS).

- Arad Y; Spadaro LA; Goodman K; Lledo-Perez A; Sherman S; Lerner G; Guerci AD (1996). Predictive value of electron beam computed tomography of the coronary arteries. 19-month follow-up of 1173 asymptomatic subjects. *Circulation*, 93: 1951-1953. [155661](#)
- Araujo JA; Barajas B; Kleinman M; Wang X; Bennett BJ; Gong KW; Navab M; Harkema J; Sioutas C; Lusk AJ; Nel AE (2008). Ambient particulate pollutants in the ultrafine range promote early atherosclerosis and systemic oxidative stress. *Circ Res*, 102: 589-596. [156222](#)
- Ardehali R; Nasir K; Kolandaivelu A; Budoff MJ; Blumenthal RS (2007). Screening patients for subclinical atherosclerosis with non-contrast cardiac CT. *Atherosclerosis*, 192: 235-242. [155662](#)
- Arlt VM; Glatt H; Gamboa da Costa G; Reynisson J; Takamura-Enya T; Phillips DH (2007). Mutagenicity and DNA adduct formation by the urban air pollutant 2-nitrobenzanthrone. *Toxicol Sci*, 98: 445-57. [097257](#)
- Auchincloss AH; Roux AV; Dvonch JT; Brown PL; Barr RG; Daviglus ML; Goff DC; Kaufman JD; O'Neill MS (2008). Associations between Recent Exposure to Ambient Fine Particulate Matter and Blood Pressure in the Multi-Ethnic Study of Atherosclerosis (MESA). *Environ Health Perspect*, 116: 486-491. [156234](#)
- Avogbe PH; Ayi-Fanou L; Autrup H; Loft S; Fayomi B; Sanni A; Vinzents P; Moller P (2005). Ultrafine particulate matter and high-level benzene urban air pollution in relation to oxidative DNA damage. *Carcinogenesis*, 26: 613-620. [087811](#)
- Avol EL; Gauderman WJ; Tan SM; London SJ; Peters JM (2001). Respiratory effects of relocating to areas of differing air pollution levels. *Am J Respir Crit Care Med*, 164: 2067-2072. [020552](#)
- Baccarelli A; Martinelli I; Pegoraro V; Melly S; Grillo P; Zanobetti A; Hou L; Bertazzi PA; Mannucci PM; Schwartz J (2009). Living near Major Traffic Roads and Risk of Deep Vein Thrombosis. *Circulation*, 119: 3118-3124. [188183](#)
- Baccarelli A; Martinelli I; Zanobetti A; Grillo P; Hou LF; Bertazzi PA; Mannucci PM; Schwartz J (2008). Exposure to Particulate Air Pollution and Risk of Deep Vein Thrombosis. *Arch Intern Med*, 168: 920-927. [157984](#)
- Baccarelli A; Wright RO; Bollati V; Tarantini L; Litonjua AA; Suh HH; Zanobetti A; Sparrow D; Vokonas PS; Schwartz J (2009). Rapid DNA Methylation Changes after Exposure to Traffic Particles. *Am J Respir Crit Care Med*, 179: 572-578. [192155](#)
- Baker DG (1998). Natural pathogens of laboratory mice, rats, and rabbits and their effects on research. *Clin Microbiol Rev*, 11: 231-266. [156245](#)
- Bao L; Chen S; Wu L; Hei Tom K; Wu Y; Yu Z; Xu A (2007). Mutagenicity of diesel exhaust particles mediated by cell-particle interaction in mammalian cells. *Toxicol Sci*, 229: 91-100. [097258](#)
- Basu R; Woodruff TJ; Parker JD; Saulnier L; Schoendorf KC (2004). Comparing exposure metrics in the relationship between PM25 and birth weight in California. *J Expo Sci Environ Epidemiol*, 14: 391-396. [087896](#)
- Bayer-Oglesby L; Grize L; Gassner M; Takken-Sahli K; Sennhauser FH; Neu U; Schindler C; Braun-Fahrlander C (2005). Decline of ambient air pollution levels and improved respiratory health in Swiss children. *Environ Health Perspect*, 113: 1632-1637. [086245](#)
- Beelen R; Hoek G; van den Brandt PA; Goldbohm RA; Fischer P; Schouten LJ; Armstrong B; Brunekreef B (2008). Long-term exposure to traffic-related air pollution and lung cancer risk. *Epidemiology*, 19: 702-710. [155681](#)
- Beelen R; Hoek G; van den Brandt PA; Goldbohm RA; Fischer P; Schouten LJ; Jerrett M; Hughes E; Armstrong B; Brunekreef B (2008). Long-term effects of traffic-related air pollution on mortality in a Dutch cohort (NLCS-AIR study). *Environ Health Perspect*, 116: 196-202. [156263](#)
- Beeson WL; Abbey DE; Knutsen SF (1998). Long-term concentrations of ambient air pollutants and incident lung cancer in California adults: results from the AHSMOG study. *Environ Health Perspect*, 106: 813-823. [048890](#)
- Bell ML; Ebisu K; Belanger K (2007). Ambient air pollution and low birth weight in Connecticut and Massachusetts. *Environ Health Perspect*, 115: 1118-24. [091059](#)
- Bell ML; Kim JY; Dominici F (2007). Potential confounding of particulate matter on the short-term association between ozone and mortality in multisite time-series studies. *Environ Health Perspect*, 115: 1591-1595. [093256](#)
- Bhattacharyya N (2009). Air quality influences the prevalence of hay fever and sinusitis. *Laryngoscope*, 119: 429-433. [180154](#)

- Bigazzi R; Bianchi S; Baldari D; Campese VM (1998). Microalbuminuria predicts cardiovascular events and renal insufficiency in patients with essential hypertension. *J Hypertens*, 16: 1325-1333. [156272](#)
- Binková B; Cerná M; Pastorková A; Jeli'nek R; Beneš I; Novák J; Šrám RJ (2003). Biological activities of organic compounds adsorbed onto ambient air particles: comparison between the cities of Teplice and Prague during the summer and winter seasons 2000–2001. *Mutat Res Fund Mol Mech Mutagen*, 525: 43-59. [156274](#)
- Bobak M (2000). Outdoor air pollution, low birth weight, and prematurity. *Environ Health Perspect*, 108: 173-176. [011448](#)
- Bobak M; Leon DA (1992). Air pollution and infant mortality in the Czech Republic, 1986-1988. *Lancet*, 339: 1010-1014. [044415](#)
- Bobak M; Leon DA (1999). The effect of air pollution on infant mortality appears specific for respiratory causes in the postneonatal period. *Epidemiology*, 10: 666-670. [007678](#)
- Bonner MR; Han D; Nie J; Rogerson P; Vena JE; Muti P; Trevisan M; Edge SB; Freudenheim JL (2005). Breast cancer risk and exposure in early life to polycyclic aromatic hydrocarbons using total suspended particulates as a proxy measure. *Cancer Epidemiol Biomarkers Prev*, 14: 53-60. [088993](#)
- Boushey HA; Armstrong B; Brauer M; Brunekreef B; Buckpitt A; Hoidal JR; London S; Reid N; Rom WN; Russell A (2008). Critique, Health Review Committee. In Grigg J; Kulkarni N; Pierse N; Rushton L; O'Callaghan C; Rutman A (Ed.), Research report 134: Black-pigmented material in airway macrophages from healthy children: Association with lung function and modeled PM10 (pp. 25-33). Boston, MA: Health Effects Institute. [192162](#)
- Bracken MB; Triche EW; Belanger K; Saftlas A; Beckett WS; Leaderer BP (2003). Asthma symptoms, severity, and drug therapy: a prospective study of effects on 2205 pregnancies. *Obstet Gynecol*, 102: 739-753. [156288](#)
- Brauer M; Gehring U; Brunekreef B; De Jongste J; Gerritsen J; Rovers M; Wichmann H-E; Wijga A; Heinrich J (2006). Traffic-related air pollution and otitis media. *Environ Health Perspect*, 114: 1414-1418. [090757](#)
- Brauer M; Hoek G; Smit HA; De Jongste JC; Gerritsen J; Postma DS; Kerkhof M; Brunekreef B (2007). Air pollution and development of asthma, allergy and infections in a birth cohort. *Eur Respir J*, 29: 879-888. [090691](#)
- Brauer M; Hoek G; Van Vliet P; Meliefste K; Fischer PH; Wijga A; Koopman LP; Neijens HJ; Gerritsen J; Kerkhof M; Heinrich J; Bellander T; Brunekreef B (2002). Air pollution from traffic and the development of respiratory infections and asthmatic and allergic symptoms in children. *Am J Respir Crit Care Med*, 166: 1092-1098. [035192](#)
- Brauer M; Lencar C; Tamburic L; Koehoorn M; Demers P; Karr C (2008). A cohort study of traffic-related air pollution impacts on birth outcomes. *Environ Health Perspect*, 116: 680-686. [156292](#)
- Brown JS; Zeman KL; Bennett WD (2001). Regional deposition of coarse particles and ventilation distribution in healthy subjects and patients with cystic fibrosis. *J Aerosol Med Pulm Drug Deliv*, 14: 443-454. [012307](#)
- Brunekreef B; Beelen R; Hoek G; Schouten L; Bausch-Goldbohm S; Fischer P; Armstrong B; Hughes E; Jerrett M; van den Brandt P (2009). Effects of long-term exposure to traffic-related air pollution on respiratory and cardiovascular mortality in the Netherlands: The NLCS-AIR Study. Health Effects Institute. Boston, MA. 139. [191947](#)
- Budoff MJ; Takasu J; Katz R; Mao S; Shavelle DM; O'Brien KD; Blumenthal RS; Carr JJ; Kronmal R (2005). Reproducibility of CT measurements of aortic valve calcification, mitral annulus calcification, and aortic wall calcification in the multi-ethnic study of atherosclerosis. *Acad Radiol*, 13: 166-172. [192105](#)
- Bunger J; Krahl J; Weigel A; Schroder O; Bruning T; Muller M; Hallier E; Westphal G (2006). Influence of fuel properties, nitrogen oxides, and exhaust treatment by an oxidation catalytic converter on the mutagenicity of diesel engine emissions. *Arch Toxicol*, 80: 540-546. [156303](#)
- Bunger J; Schappler-Scheele B; Hilgers R; Hallier E (2007). A 5-year follow-up study on respiratory disorders and lung function in workers exposed to organic dust from composting plants. *Int Arch Occup Environ Health*, 80: 306-312. [156304](#)
- Burchiel SW; Lauer FT; Dunaway SL; Zawadzki J; McDonald JD; Reed MD (2005). Hardwood smoke alters murine splenic T cell responses to mitogens following a 6-month whole body inhalation exposure. *Toxicol Appl Pharmacol*, 202: 229-236. [088090](#)
- Burchiel SW; Lauer FT; McDonald JD; Reed MD (2004). Systemic immunotoxicity in AJ mice following 6-month whole body inhalation exposure to diesel exhaust. *Toxicol Appl Pharmacol*, 196: 337-345. [055557](#)

- Calderón-Garcidueñas L; Macías-Parra M; Hoffmann HJ; Valencia-Salazar G; Henríquez-Roldán C; Osnaya N; Monte OC; Barragán-Mejía G; Villarreal-Calderon R; Romero L; Granada-Macías M; Torres-Jardón R; Medina-Cortina H; Maronpot RR (2009). Immunotoxicity and environment: immunodysregulation and systemic inflammation in children. *Toxicol Pathol*, 37: 161-169. [192107](#)
- Calderon-Garciduenas L; Vincent R; Mora-Tiscareno A; Franco-Lira M; Henriquez-Roldan C; Barragan-Mejia G; Garrido-Garcia L; Camacho-Reyes L; Valencia-Salazar G; Paredes R; Romero L; Osnaya H; Villarreal-Calderon R; Torres-Jardon (2007). Elevated plasma endothelin-1 and pulmonary arterial pressure in children exposed to air pollution. *Environ Health Perspect*, 115: 1248-1253. [091252](#)
- Chambless LE; Heiss G; Folsom AR; Rosamond W; Szklo M; Sharrett AR; Clegg LX (1997). Association of coronary heart disease incidence with carotid arterial wall thickness and major risk factors: the Atherosclerosis Risk in Communities (ARIC) Study, 1987-1993. *Am J Epidemiol*, 146: 483-494. [156329](#)
- Chang J; Delfino RJ; Gillen D; Tjoa T; Nickerson B; Cooper D (2008). Repeated respiratory hospital encounters among children with asthma and residential proximity to traffic. *J Occup Environ Med*, 66: 90-98. [180393](#)
- Chen JC; Schwartz J (2008). Metabolic syndrome and inflammatory responses to long-term particulate air pollutants. *Environ Health Perspect*, 116: 612-617. [190106](#)
- Chen L; Yang W; Jennison BL; Goodrich A; Omaye ST (2002). Air pollution and birth weight in northern Nevada, 1991-1999. *Inhal Toxicol*, 14: 141-157. [024945](#)
- Chen LC; Hwang JS (2005). Effects of subchronic exposures to concentrated ambient particles (CAPs) in mice IV Characterization of acute and chronic effects of ambient air fine particulate matter exposures on heart-rate variability. *Inhal Toxicol*, 17: 209-216. [087218](#)
- Chen LC; Nadziejko C (2005). Effects of subchronic exposures to concentrated ambient particles (CAPs) in mice V CAPs exacerbate aortic plaque development in hyperlipidemic mice. *Inhal Toxicol*, 17: 217-224. [087219](#)
- Chen LH; Knutsen SF; Shavlik D; Beeson WL; Petersen F; Ghamsary M; Abbey D (2005). The association between fatal coronary heart disease and ambient particulate air pollution: Are females at greater risk? *Environ Health Perspect*, 113: 1723-1729. [087942](#)
- Churg A; Brauer M; del Carmen Avila-Casado M; Fortoul TI; Wright JL (2003). Chronic exposure to high levels of particulate air pollution and small airway remodeling. *Environ Health Perspect*, 111: 714-718. [087899](#)
- Clancy L; Goodman P; Sinclair H; Dockery DW (2002). Effect of air pollution control on death rates in Dublin, Ireland: an intervention study. *Lancet*, 360: 1210-1214. [035270](#)
- Claxton LD; Matthews PP; Warren SH (2004). The genotoxicity of ambient outdoor air, a review: Salmonella mutagenicity. *DNA Repair (Amst)*, 567: 347-399. [089008](#)
- Claxton LD; Woodall GM (2007). A review of the mutagenicity and rodent carcinogenicity of ambient air. *Mutat Res Rev Mutat Res*, 636: 36-94. [180391](#)
- Clifton VL; Giles WB; Smith R; Bisits AT; Hempenstall PA; Kessell CG; Gibson PG (2001). Alterations of placental vascular function in asthmatic pregnancies. *Am J Respir Crit Care Med*, 164: 546-554. [156360](#)
- Craven TE; Ryu JE; Espeland MA; Kahl FR; McKinney WM; Toole JF; McMahan MR; Thompson CJ; Heiss G; Crouse JR 3rd (1990). Evaluation of the associations between carotid artery atherosclerosis and coronary artery stenosis. A case-control study. *Circulation*, 82: 1230-1242. [155740](#)
- Cury PM; Lichtenfels AJ; Reymão MS; Conceição GM; Capelozzi VL; Saldiva PH (2000). Urban levels of air pollution modifies the progression of urethane-induced lung tumours in mice. *Pathol Res Pract*, 196: 627-633. [192100](#)
- Dales R; Burnett RT; Smith-Doiron M; Stieb DM; Brook JR (2004). Air pollution and sudden infant death syndrome. *Pediatrics*, 113: 628-631. [087342](#)
- Dales R; Wheeler A; Mahmud M; Frescura AM; Smith-Doiron M; Nethery E; Liu L (2008). The Influence of Living Near Roadways on Spirometry and Exhaled Nitric Oxide in Elementary Schoolchildren. *Environ Health Perspect*, 116: 1423-1427. [156378](#)
- Danielsen PH; Loft S; Møller P (2008). DNA damage and cytotoxicity in type II lung epithelial (A549) cell cultures after exposure to diesel exhaust and urban street particles. *Part Fibre Toxicol*, 5: 6. [192092](#)

- Deckert T; Yokoyama H; Mathiesen E; Ronn B; Jensen T; Feldt-Rasmussen B; Borch-Johnsen K; Jensen JS (1996). Cohort study of predictive value of urinary albumin excretion for atherosclerotic vascular disease in patients with insulin dependent diabetes. *Br Med J*, 312: 871-874. [156389](#)
- DeMarini DM; Brooks LR; Warren SH; Kobayashi T; Gilmour MI; Singh P (2004). Bioassay-directed fractionation and Salmonella mutagenicity of automobile and forklift diesel exhaust particles. *Environ Health Perspect*, 112: 814-819. [066329](#)
- De Kok TM; Hogervorst JG; Briede JJ; Van Herwijnen MH; Maas LM; Moonen EJ; Driee HA; Kleinjans JC (2005). Genotoxicity and physicochemical characteristics of traffic-related ambient particulate matter. *Environ Mol Mutagen*, 46: 71-80. [088656](#)
- Diez Roux AV; Auchincloss AH; Franklin TG; Raghunathan T; Barr RG; Kaufman J; Astor B; Keeler J (2008). Long-term exposure to ambient particulate matter and prevalence of subclinical atherosclerosis in the Multi-Ethnic Study of Atherosclerosis. *Am J Epidemiol*, 167: 667-675. [156401](#)
- Dinneen SF; Gerstein HC (1997). The association of microalbuminuria and mortality in non-insulin-dependent diabetes mellitus. A systematic overview of the literature. *Arch Intern Med*, 157: 1413-1418. [156403](#)
- Dockery DW; Damokosh AI; Neas LM; Raizenne M; Spengler JD; Koutrakis P; Ware JH; Speizer FE (1996). Health effects of acid aerosols on North American children: respiratory symptoms and illness. *Environ Health Perspect*, 104: 500-505. [046219](#)
- Dockery DW; Pope CA III; Xu X; Spengler JD; Ware JH; Fay ME; Ferris BG Jr; Speizer FE (1993). An association between air pollution and mortality in six US cities. *N Engl J Med*, 329: 1753-1759. [044457](#)
- Downs SH; Schindler C; Liu L-JS; Keidel D; Bayer-Oglesby L; Brutsche MH; Gerbase MW; Keller R; Kunzli N; Leuenberger P; Probst-Hensch NM; Tschopp J-M; Zellweger J-P; Rochat T; Schwartz J; Ackermann-Liebrich U; (2007). Reduced exposure to PM10 and attenuated age-related decline in lung function. *J Expo Sci Environ Epidemiol*, 15: 185-204. [092853](#)
- Dugandzic R; Dodds L; Stieb D; Smith-Doiron M (2006). The association between low level exposures to ambient air pollution and term low birth weight: A retrospective cohort study. *Environ Health*, 5: 3. [088681](#)
- Eftim SE; Samet JM; Janes H; McDermott A; Dominici F (2008). Fine particulate matter and mortality: a comparison of the six cities and American Cancer Society cohorts with a medicare cohort. *Epidemiology*, 19: 209-216. [099104](#)
- Enstrom JE (2005). Fine particulate air pollution and total mortality among elderly Californians, 1973-2002. *Inhal Toxicol*, 17: 803-816. [087356](#)
- Erbel R; Mohlenkamp S; Kerkhoff G; Budde T; Schmermund A (2007). Non-invasive screening for coronary artery disease: calcium scoring. *Heart*, 93: 1620-1629. [155768](#)
- Erdinger L; Durr M; Hopker KA (2005). Correlations between mutagenic activity of organic extracts of airborne particulate matter, NOx and sulphur dioxide in southern Germany: results of a two-year study. *Environ Sci Pollut Res Int*, 12: 10-20. [156423](#)
- Fedulov AV; Leme A; Yang Z; Dahl M; Lim R; Mariani TJ; Kobzik L (2008). Pulmonary exposure to particles during pregnancy causes increased neonatal asthma susceptibility. *Am J Respir Cell Mol Biol*, 38: 57-67. [097482](#)
- Finch GL; Hobbs CH; Blair LF; Barr EB; Hahn FF; Jaramillo RJ; Kubatko JE; March TH; White RK; Krone JR; Menache MG; Nikula KJ; Mauderly JL; Van Gerpen J; Merceica MD; Zielinska B; Stankowski L; Burling K; Howell S; Mauderly JL (2002). Effects of subchronic inhalation exposure of rats to emissions from a diesel engine burning soybean oil-derived biodiesel fuel. *Inhal Toxicol*, 14: 1017-1048. [054603](#)
- Floyd HS; Chen LC; Vallanat B; Dreher K (2009). Fine ambient air particulate matter exposure induces molecular alterations associated with vascular disease progression within plaques of atherosclerotic susceptible mice. *Inhal Toxicol*, 21: 394-403. [190350](#)
- Forbes LJ; Patel MD; Rudnicka AR; Cook DG; Bush T; Stedman JR; Whincup PH; Strachan DP; Anderson RH (2009). Chronic exposure to outdoor air pollution and markers of systemic inflammation. *Epidemiology*, 20: 245-253. [190351](#)
- Forman JP; Brenner BM (2006). 'Hypertension' and 'microalbuminuria': the bell tolls for thee. *Kidney Int*, 69: 22-28. [156439](#)

- Foster PMD; Mylchreest E; Gaido KW; Sar M (2001). Effects of phthalate esters on the developing reproductive tract of male rats. *Hum Reprod Update*, 7: 231-235. [156442](#)
- Foster PMD; Thomas LV; Cook MW; Gangolli SD (1980). Study of the testicular effects and changes in zinc excretion produced by some n-alkyl phthalates in the rat. *Toxicol Appl Pharmacol*, 54: 392-398. [094701](#)
- Franklin SS; Sutton-Tyrrell K; Belle SH; Weber MA; Kuller LH (1997). The importance of pulsatile components of hypertension in predicting carotid stenosis in older adults. *J Hypertens*, 15: 1143-1150. [156446](#)
- Fryer ME; Collins CD (2003). Model intercomparison for the uptake of organic chemicals by plants. *Environ Sci Technol*, 37: 1617-1624. [156454](#)
- Fujimoto A; Tsukue N; Watanabe M; Sugawara I; Yanagisawa R; Takano H; Yoshida S; Takeda K (2005). Diesel exhaust affects immunological action in the placentas of mice. *Environ Toxicol*, 20: 431-440. [096556](#)
- Gabelová A; Valovicova Z; Bacova G; Labaj J; Binkova B; Topinka J; Sevastyanova O; Sram RJ; Kalina I; Habalova V; Popov TA; Panev T; Farmer PB (2007). Sensitivity of different endpoints for in vitro measurement of genotoxicity of extractable organic matter associated with ambient airborne particles (PM10). *Mutat Res Fund Mol Mech Mutagen*, 620: 103-113. [156458](#)
- Gabelová A; Valovicova Z; Labaj J; Bacova G; Binkova B; Farmer Peter B (2007). Assessment of oxidative DNA damage formation by organic complex mixtures from airborne particles PM(10). *Mutat Res*, 620: 135-144. [156457](#)
- Gardner MB (1966). Biological effects of urban air pollution III Lung tumors in mice. *Arch Environ Occup Health*, 12: 305-313. [015129](#)
- Gardner MB; Loosli CG; Hanes B; Blackmore W; Teebken D (1969). Histopathologic findings in rats exposed to ambient and filtered air. *Arch Environ Occup Health*, 19: 637-647. [015130](#)
- Gauderman WJ; Avol E; Gilliland F; Vora H; Thomas D; Berhane K; McConnell R; Kuenzli N; Lurmann F; Rappaport E; Margolis H; Bates D; Peters J (2004). The effect of air pollution on lung development from 10 to 18 years of age. *N Engl J Med*, 351: 1057-1067. [056569](#)
- Gauderman WJ; Gilliland GF; Vora H; Avol E; Stram D; McConnell R; Thomas D; Lurmann F; Margolis HG; Rappaport EB; Berhane K; Peters JM (2002). Association between air pollution and lung function growth in southern California children: results from a second cohort. *Am J Respir Crit Care Med*, 166: 76-84. [026013](#)
- Gauderman WJ; McConnell R; Gilliland F; London S; Thomas D; Avol E; Vora H; Berhane K; Rappaport EB; Lurmann F; Margolis HG; Peters J (2000). Association between air pollution and lung function growth in southern California children. *Am J Respir Crit Care Med*, 162: 1383-1390. [012531](#)
- Gehrig R; Buchmann B (2003). Characterising seasonal variations and spatial distribution of ambient PM10 and PM25 concentrations based on long-term Swiss monitoring data. *Atmos Environ*, 37: 2571-2580. [139678](#)
- Gehring U; Heinrich J; Kramer U; Grote V; Hochadel M; Sugiri D; Kraft M; Rauchfuss K; Eberwein HG; Wichmann H-E (2006). Long-term exposure to ambient air pollution and cardiopulmonary mortality in women. *Epidemiology*, 17: 545-551. [089797](#)
- Geroulakos G; O'Gorman DJ; Kalodiki E; Sheridan DJ; Nicolaides AN (1994). The carotid intima-media thickness as a marker of the presence of severe symptomatic coronary artery disease. *Eur Heart J*, 15: 781-785. [155788](#)
- Gerstein HC; Mann JF; Yi Q; Zinman B; Dinneen SF; Hoogwerf B; Halle JP; Young J; Rashkow A; Joyce C; Nawaz S; Yusuf S (2001). Albuminuria and risk of cardiovascular events, death, and heart failure in diabetic and nondiabetic individuals. *JAMA*, 286: 421-426. [156466](#)
- Ghosh R; Rankin J; Pless-Mulloli T; Glinianaia S (2007). Does the effect of air pollution on pregnancy outcomes differ by gender? A systematic review. *Environ Res*, 105: 400-408. [091233](#)
- Gilboa SM; Mendola P; Olshan AF; Langlois PH; Savitz DA; Loomis D; Herring AH; Fixler DE (2005). Relation between ambient air quality and selected birth defects, seven county study, Texas, 1997-2000. *Am J Epidemiol*, 162: 238-252. [087892](#)
- Girerd X; Mourad JJ; Acar C; Heudes D; Chiche S; Bruneval P; Mignot JP; Billaud E; Safar M; Laurent S (1994). Noninvasive measurement of medium-sized artery intima-media thickness in humans: in vitro validation. *J Vasc Res*, 31: 114-120. [156474](#)

- Glinianaia FV; Rankin J; Bell R; Pless-Mulloli T; Howel D (2004). Does particulate air pollution contribute to infant death? A systematic review. *Environ Health Perspect*, 112: 1365-1371. [087898](#)
- Goss CH; Newsom SA; Schildcrout JS; Sheppard L; Kaufman JD (2004). Effect of ambient air pollution on pulmonary exacerbations and lung function in cystic fibrosis. *Am J Respir Crit Care Med*, 169: 816-821. [055624](#)
- Gotschi T; Heinrich J; Sunyer J; Kunzli N (2008). Long-term effects of ambient air pollution on lung function: A review. *Epidemiology*, 19: 690-701. [156485](#)
- Gotschi T; Sunyer J; Chinn S; de Marco R; Forsberg B; Gauderman JW; Garcia-Esteban R; Heinrich J; Jacquemin B; Jarvis D; Ponzio M; Villani S; Kunzli N (2008). Air pollution and lung function in the European Community Respiratory Health Survey. *Int J Epidemiol*, 37: 1349-1358. [180364](#)
- Gottipolu RR; Wallenborn JG; Karoly ED; Schladweiler MC; Ledbetter AD; Krantz T; Linak WP; Nyska A; Johnson JA; Thomas R; Richards JE; Jaskot RH; Kodavanti UP (2009). One-month diesel exhaust inhalation produces hypertensive gene expression pattern in healthy rats. *Environ Health Perspect*, 117: 38-46. [190360](#)
- Gouveia N; Bremner SA; Novaes HMD (2004). Association between ambient air pollution and birth weight in Sao Paulo, Brazil. *J Epidemiol Community Health*, 58: 11-17. [055613](#)
- Greenland P; Kizilbash MA (2005). Coronary computed tomography in coronary risk assessment. *J Cardpulm Rehabil*, 25: 3-10. [156496](#)
- Grigg J; Kulkarni N; Pierse N; Rushton L; O'Callaghan C; Rutman A (2008). Black-pigmented material in airway macrophages from healthy children: association with lung function and modeled PM10. Heath Effects Institute. Boston, MA. Research Report 134. [156499](#)
- Gunnison A; Chen LC (2005). Effects of subchronic exposures to concentrated ambient particles (CAPs) in mice VI Gene expression in heart and lung tissue. *Inhal Toxicol*, 17: 225-233. [087956](#)
- Gutierrez-Castillo ME; Roubicek DA; Cebrian-Garcia ME; De Vizcaya-Ruiz A; Sordo-Cedeno M; Ostrosky-Wegman P (2006). Effect of chemical composition on the induction of DNA damage by urban airborne particulate matter. *Environ Mol Mutagen*, 47: 199-211. [089030](#)
- Ha E-H; Lee J-T; Kim H; Hong Y-C; Lee (2003). Infant susceptibility of mortality to air pollution in Seoul, South Korea. *Pediatrics*, 111: 284-290. [042552](#)
- Haland G; Carlsen KC; Sandvik L; Devulapalli CS; Munthe-Kaas MC; Pettersen M; Carlsen KH (2006). Reduced lung function at birth and the risk of asthma at 10 years of age. *N Engl J Med*, 355: 1682-1689. [156511](#)
- Hamada K; Suzaki Y; Leme A; Ito T; Miyamoto K; Kobzik L; Kimura H (2007). Exposure of pregnant mice to an air pollutant aerosol increases asthma susceptibility in offspring. *J Toxicol Environ Health A Curr Iss*, 70: 688-695. [091235](#)
- Hammoud A; Carrell DT; Gibson M; Sanderson M; Parker-Jones K; Matthew Peterson C (2009). Decreased sperm motility is associated with air pollution in Salt Lake City. *Fertil Steril*, TBD: TBD. [192156](#)
- Hannigan MP; Cass GR; Penman BW; Crespi CL; Lafleur AL; Busby WF Jr; Thilly WG (1997). Human cell mutagens in Los Angeles air. *Environ Sci Technol*, 31: 438-447. [083598](#)
- Hansen C; Neller A; Williams G; Simpson R (2006). Maternal exposure to low levels of ambient air pollution and preterm birth in Brisbane, Australia. *BJOG*, 113: 935-941. [089818](#)
- Hansen C; Neller A; Williams G; Simpson R (2007). Low levels of ambient air pollution during pregnancy and fetal growth among term neonates in Brisbane, Australia. *Environ Res*, 103: 383-389. [090703](#)
- Harrod KS; Jaramillo RJ; Berger JA; Gigliotti AP; Seilkop SK; Reed MD (2005). Inhaled diesel engine emissions reduce bacterial clearance and exacerbate lung disease to *Pseudomonas aeruginosa* infection in vivo. *Toxicol Sci*, 83: 155-165. [088144](#)
- Hashimoto AH; Amanuma K; Hiyoshi K; Sugawara Y; Goto S; Yanagisawa R; Takano H; Masumura K-I; Nohmi T; Aoki Y (2007). Mutations in the lungs of gpt delta transgenic mice following inhalation of diesel exhaust. *Environ Mol Mutagen*, 48: 682-693. [097261](#)
- Healey K; Smith EC; Wild CP; Routledge MN (2006). The mutagenicity of urban particulate matter in an enzyme free system is associated with the generation of reactive oxygen species. *Mutat Res Fund Mol Mech Mutagen*, 602: 1-6. [156532](#)

- Heinrich J; Hoelscher B; Frye C; Meyer I; Pitz M; Cyrys J; Wjst M; Neas L; Wichmann H-E (2002). Improved air quality in reunified Germany and decreases in respiratory symptoms. *Epidemiology*, 13: 394-401. [034825](#)
- Heinrich J; Slama R (2007). Fine particles, a major threat to children. *Int J Hyg Environ Health*, 210: 617-622. [156534](#)
- Heiss G; Sharrett AR; Barnes R; Chambless LE; Szklo M; Alzola C (1991). Carotid atherosclerosis measured by B-mode ultrasound in populations: associations with cardiovascular risk factors in the ARIC study. *Am J Epidemiol*, 134: 250-256. [156535](#)
- Hiramatsu K; Azuma A; Kudoh S; Desaki M; Takizawa H; Sugawara I (2003). Inhalation of diesel exhaust for three months affects major cytokine expression and induces bronchus-associated lymphoid tissue formation in murine lungs. *Exp Lung Res*, 29: 607-622. [155846](#)
- Hoek G; Brunekreef B; Goldbohm S; Fischer P; Van den Brandt PA (2002). Association between mortality and indicators of traffic-related air pollution in the Netherlands: A cohort study. *Lancet*, 360: 1203-1209. [042364](#)
- Hoffmann B; Moebus S; Kroger K; Stang A; Mohlenkamp S; Dragano N; Schmermund A; Memmesheimer M; Erbel R; Jockel K-H (2009). Residential exposure to urban pollution, ankle-brachial index, and peripheral arterial disease. *Epidemiology*, 20: 280-288. [190376](#)
- Hoffmann B; Moebus S; Mohlenkamp S; Stang A; Lehmann N; Dragano N; Schmermund A; Memmesheimer M; Mann K; Erbel R; Jockel K-H; Heinz Nixdorf Recall Study Investigative Group (2007). Residential exposure to traffic is associated with coronary atherosclerosis. *Circulation*, 116: 489-496. [091163](#)
- Hoffmann B; Moebus S; Stang A; Beck E-M; Dragano N; Mohlenkamp S; Schmermund A; Memmesheimer M; Mann K; Erbel R; Jockel K-H; Heinz Nixdorf RECALL Study Investigative Group (2006). Residence close to high traffic and prevalence of coronary heart disease. *Eur Heart J*, 27: 2696-2702. [091162](#)
- Hoffmann MH; Shi H; Schmitz BL; Schmid FT; Lieberknecht M; Schulze R; Ludwig B; Kroschel U; Jahnke N; Haerer W; Brambs HJ; Aschoff AJ (2005). Noninvasive coronary angiography with multislice computed tomography. *JAMA*, 293: 2471-2478. [156556](#)
- Hollander M; Hak AE; Koudstaal PJ; Bots ML; Grobbee DE; Hofman A; Witteman JC; Breteler MM (2003). Comparison between measures of atherosclerosis and risk of stroke: the Rotterdam Study. *Stroke*, 34: 2367-2372. [156562](#)
- Hornberg C; Maciuleviciute L; Seemayer NH (1996). Sister chromatid exchanges in rodent tracheal epithelium exposed in vitro to environmental pollutants. *Toxicol Lett*, 88: 45-53. [087164](#)
- Hornberg C; Maciuleviciute L; Seemayer NH; Kainka E (1998). Induction of sister chromatid exchanges (SCE) in human tracheal epithelial cells by the fractions PM-10 and PM-25 of airborne particulates. *Toxicol Lett*, 96/97: 215-220. [095741](#)
- Hougaard KS; Jensen KA; Nordly P; Taxvig C; Vogel U; Saber AT; Wallin H (2008). Effects of prenatal exposure to diesel exhaust particles on postnatal development, behavior, genotoxicity and inflammation in mice. *Part Fibre Toxicol*, 5: 3. [156570](#)
- Huang JY; Liao JW; Liu YC; Lu SY; Chou CP; Chan WH; Chen SU; Ueng TH (2008). Motorcycle exhaust induces reproductive toxicity and testicular interleukin-6 in male rats. *Toxicol Sci*, 103: 137-148. [156574](#)
- Huynh M; Woodruff TJ; Parker JD; Schoendorf KC (2006). Relationships between air pollution and preterm birth in California. *Paediatr Perinat Epidemiol*, 20: 454-461. [091240](#)
- Hwang BF; Jaakkola JJ (2008). Ozone and other air pollutants and the risk of oral clefts. *Environ Health Perspect*, 116: 1411-1415. [193794](#)
- Hwang J-S; Nadziejko C; Chen LC (2005). Effects of subchronic exposures to concentrated ambient particles (CAPs) in mice: III Acute and chronic effects of CAPs on heart rate, heart-rate fluctuation, and body temperature. *Inhal Toxicol*, 17: 199-207. [087957](#)
- IARC (1989). Diesel and gasoline engine exhausts. Lyon, France: International Agency for Research on Cancer. [002958](#)
- Iba MM; Fung J; Chung L; Zhao J; Winnik B; Buckley BT; Chen LC; Zelikoff JT; Kou YR (2006). Differential inducibility of rat pulmonary CYP1A1 by cigarette smoke and wood smoke. *Mutat Res Fund Mol Mech Mutagen*, 606: 1-11. [156582](#)
- Ichinose T; Yajima Y; Nagashima M; Takenoshita S; Nagamachi Y; Sagai M (1997). Lung carcinogenesis and formation of 8-hydroxy-deoxyguanosine in mice by diesel exhaust particles. *Carcinogenesis*, 18: 185-192. [053264](#)

- Ishihara Y; Kagawa J (2003). Chronic diesel exhaust exposures of rats demonstrate concentration and time-dependent effects on pulmonary inflammation. *Inhal Toxicol*, 15: 473-492. [096404](#)
- Islam T; Gauderman WJ; Berhane K; McConnell R; Avol E; Peters JM; Gilliland FD (2007). The relationship between air pollution, lung function and asthma in adolescents. *Thorax*, 62: 957-963. [090697](#)
- Izawa H; Watanabe G; Taya K; Sagai M (2007). Inhibitory effects of foods and polyphenols on activation of aryl hydrocarbon receptor induced by diesel exhaust particles. *Environ Sci J Integr Environ Res*, 14: 149-156. [190387](#)
- Jacobsen NR; Mrller P; Cohn CA; Loft S; Vogel U; Wallin H (2008). Diesel exhaust particles are mutagenic in FE1-Muta™ Mouse lung epithelial cells. *Mutat Res Fund Mol Mech Mutagen*, 641: 54-57. [156597](#)
- Jalaludin B; Mannes T; Morgan G; Lincoln D; Sheppard V; Corbett S (2007). Impact of ambient air pollution on gestational age is modified by season in Sydney, Australia. *Environ Health*, 6: 16. [156601](#)
- Janes H; Dominici F; Zeger SL (2007). Trends in air pollution and mortality: an approach to the assessment of unmeasured confounding. *Epidemiology*, 18: 416-423. [090927](#)
- Janssen NAH; Brunekreef B; van Vliet P; Aarts F; Maliefste K; Harssema H; Fischer P (2003). The relationship between air pollution from heavy traffic and allergic sensitization, bronchial hyperresponsiveness, and respiratory symptoms in Dutch schoolchildren. *Epidemiology*, 111: 1512-1518. [133555](#)
- Jerrett M; Burnett RT; Ma R; Pope CA III; Krewski D; Newbold KB; Thurston G; Shi Y; Finkelstein N; Calle EE; Thun MJ (2005). Spatial analysis of air pollution and mortality in Los Angeles. *Epidemiology*, 16: 727-736. [087600](#)
- Jerrett M; Buzzelli M; Burnett RT; DeLuca PF (2005). Particulate air pollution, social confounders, and mortality in small areas of an industrial city. *Soc Sci Med*, 60: 2845-2863. [087381](#)
- Karr C; Lumley T; Schreuder A; Davis R; Larson T; Ritz B; Kaufman J (2007). Effects of subchronic and chronic exposure to ambient air pollutants on infant bronchiolitis. *Am J Epidemiol*, 165: 553-560. [090719](#)
- Karr C; Rudra C; Miller K; Gould T; Larson T; Sathyanarayana S; Koenig J (2009). Infant exposure to fine particulate matter and traffic and risk of hospitalization for RSV bronchiolitis in a region with lower ambient air pollution. *Environ Res*, 109: 321-327. [191946](#)
- Karthikeyan VJ; Lip GYH (2007). Peripheral artery disease and hypertension: the relation between ankle-brachial index and mortality. *J Hum Hypertens*, 21: 762-765. [156626](#)
- Kato A; Kagawa J (2003). Morphological effects in rat lungs exposed to urban roadside air. *Inhal Toxicol*, 15: 799-818. [089563](#)
- Khattar RS; Swales JD; Dore C; Senior R; Lahiri A (2001). Effect of aging on the prognostic significance of ambulatory systolic, diastolic, and pulse pressure in essential hypertension. *Circulation*, 104: 783-789. [155896](#)
- Khoury Z; Schwartz R; Gottlieb S; Chenzbraun A; Stern S; Keren A (1997). Relation of coronary artery disease to atherosclerotic disease in the aorta, carotid, and femoral arteries evaluated by ultrasound. *Am J Cardiol*, 80: 1429-1433. [156636](#)
- Kim JJ; Smorodinsky S; Lipsett M; Singer BC; Hodgson AT; Ostro B (2004). Traffic-related air pollution near busy roads: the East Bay children's Respiratory Health Study. *Am J Respir Crit Care Med*, 170: 520-526. [087383](#)
- Kim OJ; Ha EH; Kim BM; Park HS; Jung WJ; Lee BE; Suh YJ; Kim YJ; Lee JT; Kim H; Hong YC (2007). PM10 and pregnancy outcomes: a hospital-based cohort study of pregnant women in Seoul. *J Occup Environ Med*, 49: 1394-1402. [156642](#)
- Knight EL; Curhan GC (2003). Albuminuria: moving beyond traditional microalbuminuria cut-points. *Current Opinion Nephrol Hypertens*, 12: 283-284. [179900](#)
- Knöbel HH; Chen CJ; Liang KY (1995). Sudden infant death syndrome in relation to weather and optometrically measured air pollution in Taiwan. *Pediatrics*, 96: 1106-1110. [155905](#)
- Krewski D (2009). Evaluating the effects of ambient air pollution on life expectancy. *N Engl J Med*, 360: 413-415. [190075](#)
- Krewski D; Burnett RT; Goldberg MS; Hoover K; Siemiatycki J; Jerrett M; Abrahamowicz M; White WH (2000). Reanalysis of the Harvard Six Cities study and the American Cancer Society study of particulate air pollution and mortality. Health Effects Institute. Cambridge, MA. <http://pubs.healtheffects.org/view.php?id=6>. [012281](#)

- Krewski D; Jerrett M; Burnett RT; Ma R; Hughes E; Shi Y; Turner MC; Pope AC III; Thurston G; Calle EE; Thun MJ (2009). Extended follow-up and spatial analysis of the American Cancer Society study linking particulate air pollution and mortality. Health Effects Institute. Cambridge, MA. Report Nr. 140. [191193](#)
- Kulkarni N; Pierse N; Rushton L; Grigg J (2006). Carbon in airway macrophages and lung function in children. *N Engl J Med*, 355: 21-30. [089257](#)
- Kundu JK; Surh YJ (2008). Inflammation: Gearing the journey to cancer. *Mutat Res*, 659: 15-30. [198840](#)
- Kunzli N; Bridevaux P-O; Liu S; Garcia-Esteban R; Schindler C; Gerbase M; Sunyer J; Keidel D; Rochat T (2009). Traffic-related air pollution correlates with adult-onset asthma among never-smokers. *Thorax*, 64: 664-670. [191949](#)
- Kunzli N; Jerrett M; Mack WJ; Beckerman B; LaBree L; Gilliland F; Thomas D; Peters J; Hodis HN (2005). Ambient air pollution and atherosclerosis in Los Angeles. *Environ Health Perspect*, 113: 201-206. [087387](#)
- Kunzli N; Perez L; Lurmann F; Hricko A; Penfold B; McConnell R (2008). An Attributable Risk Model for Exposures Assumed to Cause Both Chronic Disease and its Exacerbations. *Epidemiology*, 19: 179-185. [129258](#)
- Lacasaña M; Esplugues A; Ballester F (2005). Exposure to ambient air pollution and prenatal and early childhood health effects. *Eur J Epidemiol*, 20: 183-199. [155914](#)
- Laden F; Schwartz J; Speizer FE; Dockery DW (2006). Reduction in fine particulate air pollution and mortality: extended follow-up of the Harvard Six Cities study. *Am J Respir Crit Care Med*, 173: 667-672. [087605](#)
- Lee BE; Ha EH; Park HS; Kim YJ; Hong YC; Kim H; Lee JT (2003). Exposure to air pollution during different gestational phases contributes to risks of low birth weight. *Hum Reprod*, 18: 638-643. [043202](#)
- Lee JS; Kim KI; Baek SH (2008). Nuclear receptors and coregulators in inflammation and cancer. *Cancer Lett*, 267: 189-196. [198811](#)
- Leem J-H; Kaplan BM; Shim YK; Pohl HR; Gotway CA; Bullard SM; Rogers JF; Smith MM; Tylenda CA (2006). Exposures to air pollutants during pregnancy and preterm delivery. *Environ Health Perspect*, 114: 905-910. [089828](#)
- Lemos M; Mohallen S; Macchione M; Dolhnikoff M; Assunção J; Godleski J; Saldiva P (2006). Chronic exposure to urban air pollution induces structural alterations in murine pulmonary and coronary arteries. *Inhal Toxicol*, 18: 247-253. [088594](#)
- Li Y-J; Kawada T; Matsumoto A; Azuma A; Kudoh S; Takizawa H; Sugawara I (2007). Airway inflammatory responses to oxidative stress induced by low-dose diesel exhaust particle exposure differ between mouse strains. *Exp Lung Res*, 33: 227-244. [155929](#)
- Lichtenfels AJFC; Gomes JB; Pieri PC; Miraglia SGEK; Hallak J; Saldiva PHN (2007). Increased levels of air pollution and a decrease in the human and mouse male-to-female ration in Sao Paulo, Brazil. *Fertil Steril*, 87: 230-232. [097041](#)
- Lin C-M; Li C-Y; Mao I-F (2004). Increased risks of term low-birth-weight infants in a petrochemical industrial city with high air pollution levels. *Arch Environ Occup Health*, 59: 663-668. [089827](#)
- Lin CA; Pereira LAA; Nishioka DC; Conceicao GMS; Graga ALF; Saldiva PHN (2004). Air pollution and neonatal deaths in Sao Paulo, Brazil. *Braz J Med Biol Res*, 37: 765-770. [095787](#)
- Lipfert FW; Baty JD; Miller JP; Wyzga RE (2006). PM2.5 constituents and related air quality variables as predictors of survival in a cohort of U.S. military veterans. *Inhal Toxicol*, 18: 645-657. [088756](#)
- Lipfert FW; Wyzga RE; Baty JD; Miller JP (2006). Traffic density as a surrogate measure of environmental exposures in studies of air pollution health effects: long-term mortality in a cohort of US veterans. *Atmos Environ*, 40: 154-169. [088218](#)
- Lipfert FW; Zhang J; Wyzga RE (2000). Infant mortality and air pollution: a comprehensive analysis of US data for 1990. *J Air Waste Manag Assoc*, 50: 1350-1366. [004103](#)
- Lippmann M; Gordon T; Chen LC (2005). Effects of subchronic exposures to concentrated ambient particles in mice. IX. Integral assessment and human health implications of subchronic exposures of mice to CAPs. *Inhal Toxicol*, 17: 255-261. [087452](#)
- Liu L-JS; Curjuric I; Keidel D; Heldstab J; Kunzli N; Bayer-Oglesby L; Ackermann-Liebrich U; Schindler C; SAPALDIA team (2007). Characterization of source-specific air pollution exposure for a large population-based Swiss cohort (SAPALDIA). *Environ Health Perspect*, 115: 1638-1645. [093093](#)

- Liu S; Krewski D; Shi Y; Chen Y; Burnett R (2007). Association between maternal exposure to ambient air pollutants during pregnancy and fetal growth restriction. *J Expo Sci Environ Epidemiol*, 17: 426-432. [090429](#)
- Liu Y-Q; Keane M; Ensell M; Miller W; Kashon M; Ong T-m; Mauderly J; Lawson D; Gautam M; Zielinska B; Whitney K; Eberhardt J; Wallace W (2005). In vitro genotoxicity of exhaust emissions of diesel and gasoline engine vehicles operated on a unified driving cycle. *J Environ Monit*, 7: 60-66. [097019](#)
- Loomis D; Castillejos M; Gold DR; McDonnell W; Borja-Aburto VH (1999). Air pollution and infant mortality in Mexico City. *Epidemiology*, 10: 118-123. [087288](#)
- Lopes FD; Pinto TS; Arantes-Costa FM; Moriya HT; Biselli PJ; Ferraz LF; Lichtenfels AJ; Saldiva PH; Mauad T; Martins MA (2009). Exposure to ambient levels of particles emitted by traffic worsens emphysema in mice. *Environ Res*, 109: 544-551. [190430](#)
- Lund AK; Knuckles TL; Obot Akata C; Shohet R; McDonald JD; Gigliotti A; Seagrave JC; Campen MJ (2007). Gasoline exhaust emissions induce vascular remodeling pathways involved in atherosclerosis. *Toxicol Sci*, 95: 485-94. [125741](#)
- Maciejczyk P; Chen LC (2005). Effects of subchronic exposures to concentrated ambient particles (CAPs) in mice: VIII source-related daily variations in in vitro responses to CAPs. *Inhal Toxicol*, 17: 243-253. [087456](#)
- Mackman N; Tilley RE; Key NS (2007). Role of the extrinsic pathway of blood coagulation in hemostasis and thrombosis. *Arterioscler Thromb Vasc Biol*, 27: 1687-1693. [156723](#)
- Maheswaran R; Haining RP; Brindley P; Law J; Pearson T; Fryers PR; Wise S; Campbell MJ (2005). Outdoor air pollution and stroke in Sheffield, United Kingdom: A small-area level geographical study. *Stroke*, 36: 239-243. [088683](#)
- Maheswaran R; Haining RP; Brindley P; Law J; Pearson T; Fryers PR; Wise S; Campbell MJ (2005). Outdoor air pollution, mortality, and hospital admissions from coronary heart disease in Sheffield, UK: A small-area level ecological study. *Eur Heart J*, 26: 2543-2549. [090769](#)
- Maisonet M; Bush TJ; Correa A; Jaakkola JJK (2001). Relation between ambient air pollution and low birth weight in the northeastern United States. *Environ Health Perspect*, 109: 351-356. [016624](#)
- Maisonet M; Correa A; Misra D; Jaakkola JJ (2004). A review of the literature on the effects of ambient air pollution on fetal growth. *Environ Res*, 95: 106-115. [156725](#)
- Mannes T; Jalaludin B; Morgan G; Lincoln D; Sheppard V; Corbett S (2005). Impact of ambient air pollution on birth weight in Sydney, Australia. *Occup Environ Med*, 62: 524-530. [087895](#)
- Matsumoto A; Hiramatsu K; Li Y; Azuma A; Kudoh S; Takizawa H; Sugawara I (2006). Repeated exposure to low-dose diesel exhaust after allergen challenge exaggerates asthmatic responses in mice. *Clin Immunol*, 121: 227-235. [098017](#)
- Mauad T; Rivero DH; de Oliveira RC; Lichtenfels AJ; Guimaraes ET; de Andre PA; Kasahara DI; Bueno HM; Saldiva PH (2008). Chronic exposure to ambient levels of urban particles affects mouse lung development. *Am J Respir Crit Care Med*, 178: 721-728. [156743](#)
- McConnell R; Berhane K; Gilliland F; London SJ; Vora H; Avol E; Gauderman WJ; Margolis HG; Lurmann F; Thomas DC; Peters JM (1999). Air pollution and bronchitic symptoms in southern California children with asthma. *Environ Health Perspect*, 107: 757-760. [007028](#)
- McConnell R; Berhane K; Gilliland F; Molitor J; Thomas D; Lurmann F; Avol E; Gauderman WJ; Peters JM (2003). Prospective study of air pollution and bronchitic symptoms in children with asthma. *Am J Respir Crit Care Med*, 168: 790-797. [049490](#)
- McDonald JD; Reed MD; Campen MJ; Barrett EG; Seagrave J; Mauderly JL (2007). Health effects of inhaled gasoline engine emissions. *Inhal Toxicol*, 19 Suppl 1: 107-116. [156746](#)
- McDonnell WF; Nishino-Ishikawa N; Petersen FF; Chen LH; Abbey DE (2000). Relationships of mortality with the fine and coarse fractions of long-term ambient PM10 concentrations in nonsmokers. *J Expo Sci Environ Epidemiol*, 10: 427-436. [010319](#)
- Medeiros A; Gouveia N (2005). Relacao entre baixo peso ao nascer e a poluicao do ar no Municipio de Sao Paulo [Relationship between low birthweight and air pollution in the city of Sao Paulo, Brazil]. *Rev Saude Publica*, 39: 965-972. [089824](#)

- Ménache MG; Miller FJ; Raabe OG (1995). Particle inhalability curves for humans and small laboratory animals. *Ann Occup Hyg*, 39: 317-328. [006533](#)
- Meng YY; Wilhelm M; Rull RP; English P; Ritz B (2007). Traffic and outdoor air pollution levels near residences and poorly controlled asthma in adults. *Ann Allergy Asthma Immunol*, 98: 455-463. [093275](#)
- Miller KA; Siscovick DS; Sheppard L; Shepherd K; Sullivan JH; Anderson GL; Kaufman JD (2007). Long-term exposure to air pollution and incidence of cardiovascular events in women. *N Engl J Med*, 356: 447-458. [090130](#)
- Mogensen CE (1984). Microalbuminuria predicts clinical proteinuria and early mortality in maturity-onset diabetes. *N Engl J Med*, 310: 356-360. [156769](#)
- Mohallem SV; de Araujo Lobo DJ; Pesquero CR; Assuncao JV; de Andre PA; Saldiva PH; Dolhnikoff M (2005). Decreased fertility in mice exposed to environmental air pollution in the city of Sao Paulo. *Environ Res*, 98: 196-202. [088657](#)
- Mollet NR; Cademartiri F; de Feyter PJ (2005). Non-invasive multislice CT coronary imaging. *Heart*, 91: 401-407. [155988](#)
- Montauban van Swijndregt AD; De Lange EE; De Groot E; Ackerstaff RG (1999). An in vivo evaluation of the reproducibility of intima-media thickness measurements of the carotid artery segments using B-mode ultrasound. *Ultrasound Med Biol*, 25: 323-330. [156777](#)
- Morgenstern V; Zutavern A; Cyrys J; Brockow I; Koletzko S; Kramer U; Behrendt H; Herbarth O; von Berg A; Bauer CP; Wichmann HE; Heinrich J (2008). Atopic diseases, allergic sensitization, and exposure to traffic-related air pollution in children. *Am J Respir Crit Care Med*, 177: 1331-1337. [156782](#)
- Mortimer K; Neugebauer R; Lurmann F; Alcorn S; Balmes J; Tager I (2008). Early-Lifetime exposure to air pollution and allergic sensitization in children with asthma. *J Asthma*, 45: 874-881. [187280](#)
- Naess O; Nafstad P; Aamodt G; Claussen B; Rosland P (2007). Relation between concentration of air pollution and cause-specific mortality: four-year exposures to nitrogen dioxide and particulate matter pollutants in 470 neighborhoods in Oslo, Norway. *Am J Epidemiol*, 165: 435-443. [090736](#)
- National Kidney Foundation (2008). Chronic Kidney Disease: Evaluation, Classification, and Stratification. The National Kidney Foundation . Kidney Disease Outcomes Quality Initiative. [156796](#)
- Newman AB; Sutton-Tyrrell K; Vogt MT; Kuller LH (1993). Morbidity and mortality in hypertensive adults with a low ankle/arm blood pressure index. *JAMA*, 270: 487-489. [156805](#)
- Nordling E; Berglind N; Melen E; Emenius G; Hallberg J; Nyberg F; Pershagen G; Svartengren M; Wickman M; Bellander T (2008). Traffic-related air pollution and childhood respiratory symptoms, function and allergies. *Epidemiology*, 19: 401-8. [097998](#)
- O'Leary DH; Polak JF; Kronmal RA; Kittner SJ; Bond MG; Wolfson SK Jr; Bommer W; Price TR; Gardin JM; Savage PJ (1992). Distribution and correlates of sonographically detected carotid artery disease in the Cardiovascular Health Study. The CHS Collaborative Research Group. *Stroke*, 23: 1752-1760. [156825](#)
- O'Leary DH; Polak JF; Kronmal RA; Manolio TA; Burke GL; Wolfson SK Jr (1999). Carotid-artery intima and media thickness as a risk factor for myocardial infarction and stroke in older adults. Cardiovascular Health Study Collaborative Research Group. *N Engl J Med*, 340: 14-22. [156826](#)
- O'Neill MS; Diez-Roux AV; Auchincloss AH; Franklin TG; Jacobs Jnr DR; Astor BC; Dvonch JT; Kaufman J (2007). Airborne particulate matter exposure and urinary albumin excretion: The Multi-Ethnic Study of Atherosclerosis. *Occup Environ Med*, 65: 534-540. [156006](#)
- O'Rourke RA; Brundage BH; Froelicher VF; Greenland P; Grundy SM; Hachamovitch R; Pohost GM; Shaw LJ; Weintraub WS; Winters WL; Forrester JS; Douglas PS; Faxon DP; Fisher JD; Gregoratos G; Hochman JS; Hutter AM; Kaul S; Wolk MJ (2000). American College of Cardiology/American Heart Association Expert Consensus document on electron-beam computed tomography for the diagnosis and prognosis of coronary artery disease. *Circulation*, 102: 126-140. [192159](#)
- Oei HH; Vliementhart R; Hak AE; Iglesias del Sol A; Hofman A; Oudkerk M; Witteman JC (2002). The association between coronary calcification assessed by electron beam computed tomography and measures of extracoronary atherosclerosis: the Rotterdam Coronary Calcification Study. *J Am Coll Cardiol*, 39: 1745-1751. [156820](#)
- Oftedal B; Brunekreef B; Nystad W; Madsen C; Walker S-E; Nafstad P (2008). Residential outdoor air pollution and lung function in schoolchildren. *Epidemiology*, 19: 129-137. [093202](#)

- Oftedal B; Brunekreef B; Nystad W; Nafstad P (2007). Residential outdoor air pollution and allergen sensitization in schoolchildren in Oslo, Norway. *Clin Exp Allergy*, 37: 1632. [191948](#)
- Oh S-M; Chung K-H (2006). Identification of mammalian cell genotoxins in respirable diesel exhaust particles by bioassay-directed chemical analysis. *Toxicol Lett*, 161: 226-235. [088296](#)
- Ono N; Oshio S; Niwata Y; Yoshida S; Tsukue N; Sugawara I; Takano H; Takeda K (2007). Prenatal exposure to diesel exhaust impairs mouse spermatogenesis. *Inhal Toxicol*, 19: 275-281. [156007](#)
- Ozkaynak H; Thurston GD (1987). Associations between 1980 US mortality rates and alternative measures of airborne particle concentration. *Risk Anal*, 7: 449-461. [072960](#)
- Palli D; Saieva C; Munnia A; Peluso M; Grechi D; Zanna I; Caini S; Decarli A; Sera F; Masala G (2008). DNA adducts and PM10 exposure in traffic-exposed workers and urban residents from the EPIC-Florence City study. *Sci Total Environ*, 403: 105-112. [156837](#)
- Parker JD; Mendola P; Woodruff TJ (2008). Preterm birth after the Utah Valley Steel Mill closure: a natural experiment. *Epidemiology*, 19: 820-823. [156013](#)
- Parker JD; Woodruff TJ (2008). Influences of study design and location on the relationship between particulate matter air pollution and birthweight. *Paediatr Perinat Epidemiol*, 22: 214-227. [156846](#)
- Parker JD; Woodruff TJ; Basu R; Schoendorf KC (2005). Air pollution and birth weight among term infants in California. *Pediatrics*, 115: 121-128. [087462](#)
- Pedersen M; Vinzents P; Petersen JH; Kleinjans JC; Plas G; Kirsch-Volders M; Dostal M; Rossner P; Beskid O; Sram RJ; Merlo DF; Knudsen LE (2006). Cytogenetic effects in children and mothers exposed to air pollution assessed by the frequency of micronuclei and fluorescence in situ hybridization (FISH): a family pilot study in the Czech Republic. *Mutat Res Fund Mol Mech Mutagen*, 608: 112-120. [156848](#)
- Penard-Morand C; Charpin D; Raherison C; Kopferschmitt C; Caillaud D; Lavaud F; Annesi-Maesano I (2005). Long-term exposure to background air pollution related to respiratory and allergic health in schoolchildren. *Clin Exp Allergy*, 35: 1279-1287. [087951](#)
- Penna MLF; Duchiae MP (1991). Air pollution and infant mortality from pneumonia in the Rio de Janeiro metropolitan area. *Bull Pan Am Health Organ*, 25: 47-54. [073325](#)
- Pereira LAA; Loomis D; Conceicao GMS; Braga ALF; Arcas RM; Kishi HS; Singer JM; Bohm GM; Saldiva PHN (1998). Association between air pollution and intrauterine mortality in Sao Paulo, Brazil. *Environ Health Perspect*, 106: 325-329. [007264](#)
- Peters A; Skorkovsky J; Kotesovec F; Brynda J; Spix C; Wichmann HE; Heinrich J (2000). Associations between mortality and air pollution in central Europe. *Environ Health Perspect*, 108: 283-287. [001756](#)
- Pierse N; Rushton L; Harris RS; Kuehni CE; Silverman M; Grigg J (2006). Locally-generated particulate pollution and respiratory symptoms in young children. *Thorax*, 61: 216-220. [088757](#)
- Pignoli P; Tremoli E; Poli A; Oreste P; Paoletti R (1986). Intimal plus medial thickness of the arterial wall: a direct measurement with ultrasound imaging. *Circulation*, 74: 1399-1406. [156026](#)
- Pinkerton KE; Zhou Y; Teague SV; Peake JL; Walther RC; Kennedy IM; Leppert VJ; Aust AE (2004). Reduced lung cell proliferation following short-term exposure to ultrafine soot and iron particles in neonatal rats: key to impaired lung growth? *Inhal Toxicol*, 1: 73-81. [087465](#)
- Pires-Neto RC; Lichtenfels AJ; Soares SR; Macchione M; Saldiva PHN; Dolhnikoff M (2006). Effects of Sao Paulo air pollution on the upper airways of mice. *Environ Res*, 101: 356-361. [096734](#)
- Poma A; Limongi T; Pisani C; Granato V; Picozzi P (2006). Genotoxicity induced by fine urban air particulate matter in the macrophages cell line RAW 264.7. *Toxicol In Vitro*, 20: 1023-1029. [096903](#)
- Pope CA III (1989). Respiratory disease associated with community air pollution and a steel mill, Utah Valley. *Am J Public Health*, 79: 623-628. [044461](#)
- Pope CA III; Burnett RT (2007). Confounding in air pollution epidemiology: the broader context. *Epidemiology*, 18: 424-426. [090928](#)
- Pope CA III; Burnett RT; Thun MJ; Calle EE; Krewski D; Ito K; Thurston GD (2002). Lung cancer, cardiopulmonary mortality, and long-term exposure to fine particulate air pollution. *JAMA*, 287: 1132-1141. [024689](#)

- Pope CA III; Thun MJ; Namboodiri MM; Dockery DW; Evans JS; Speizer FE; Heath CW Jr (1995). Particulate air pollution as a predictor of mortality in a prospective study of US adults. *Am J Respir Crit Care Med*, 151: 669-674. [045159](#)
- Pope III CA; Burnett RT; Thurston GD; Thun MJ; Calle EE; Krewski D; Godleski JJ (2004). Cardiovascular mortality and long-term exposure to particulate air pollution: epidemiological evidence of general pathophysiological pathways of disease. *Circulation*, 109: 71-77. [055880](#)
- Pope III CA; Ezzati M; Dockery DW (2009). Fine-particulate air pollution and life expectancy in the United States. *N Engl J Med*, 360: 376-386. [190107](#)
- Puett RC; Schwartz J; Hart JE; Yanosky JD; Speizer FE; Suh H; Paciorek CJ; Neas LM; Laden F (2008). Chronic particulate exposure, mortality, and coronary heart disease in the nurses' health study. *Am J Epidemiol*, 168: 1161-1168. [156891](#)
- Raizenne M; Neas LM; Damokosh AI; Dockery DW; Spengler JD; Koutrakis P; Ware JH; Speizer FE (1996). Health effects of acid aerosols on North American children: pulmonary function. *Environ Health Perspect*, 104: 506-514. [077268](#)
- Ramos C; Cisneros J; Gonzalez-Avila G; Becerril C; Ruiz V; Montaña M (2009). Increase of matrix metalloproteinases in woodsmoke-induced lung emphysema in guinea pigs. *Inhal Toxicol*, 21: 119-132. [190116](#)
- Reed MD; Barrett EG; Campen MJ; Divine KK; Gigliotti AP; McDonald JD; Seagrave JC; Mauderly JL; Seilkop SK; Swenberg JA (2008). Health effects of subchronic inhalation exposure to gasoline engine exhaust. *Inhal Toxicol*, 20: 1125-1143. [156903](#)
- Reed MD; Campen MJ; Gigliotti AP; Harrod KS; McDonald JD; Seagrave JC; Mauderly JL; Seilkop SK (2006). Health effects of subchronic exposure to environmental levels of hardwood smoke. *Inhal Toxicol*, 18: 523-539. [156043](#)
- Reed MD; Gigliotti AP; McDonald JD; Seagrave JC; Seilkop SK; Mauderly JL (2004). Health effects of subchronic exposure to environmental levels of diesel exhaust. *Inhal Toxicol*, 16: 177-193. [055625](#)
- Resnick HE; Lindsay RS; McDermott MM; Devereux RB; Jones KL; Fabsitz RR; Howard BV (2004). Relationship of high and low ankle brachial index to all-cause and cardiovascular disease mortality: the Strong Heart Study. *Circulation*, 109: 733-739. [156048](#)
- Reymao MSF; Cury PM; Lichtenfels AJFC; Lemos M; Battlehner CN; Conceicao GMS; Capelozzi VL; Montes GS; Junior MF; Martins MA; Bohm GM; Saldiva PHN (1997). Urban air pollution enhances the formation of urethane-induced lung tumors in mice. *Environ Res*, 74: 150-158. [084653](#)
- Rich DQ; Demissie K; Lu SE; Kamat L; Wartenberg D; Rhoads GG (2009). Ambient air pollutant concentrations during pregnancy and the risk of fetal growth restriction. *J Epidemiol Community Health*, 63: 488-496. [180122](#)
- Ritz B; Wilhelm M (2008). Ambient air pollution and adverse birth outcomes: methodologic issues in an emerging field. *Basic Appl Ecol*, 102: 182-190. [156914](#)
- Ritz B; Wilhelm M; Hoggatt KJ; Ghosh JK (2007). Ambient air pollution and preterm birth in the environment and pregnancy outcomes study at the University of California, Los Angeles. *Am J Epidemiol*, 166: 1045-1052. [096146](#)
- Ritz B; Wilhelm M; Zhao Y (2006). Air pollution and infant death in southern California, 1989-2000. *Pediatrics*, 118: 493-502. [089819](#)
- Ritz B; Yu F; Chapa G; Fruin S (2000). Effect of air pollution on preterm birth among children born in Southern California between 1989 and 1993. *Epidemiology*, 11: 502-511. [012068](#)
- Ritz B; Yu F; Fruin S; Chapa G; Shaw GM; Harris JA (2002). Ambient air pollution and risk of birth defects in Southern California. *Am J Epidemiol*, 155: 17-25. [023227](#)
- Rocha ESIR; Lichtenfels AJ; Amador Pereira LA; Saldiva PH (2008). Effects of ambient levels of air pollution generated by traffic on birth and placental weights in mice. *Fertil Steril*, 90: 1921-1924. [096685](#)
- Rogers JF; Dunlop AL (2006). Air pollution and very low birth weight infants: a target population? *Pediatrics*, 118: 156-164. [091232](#)
- Rojas-Martinez R; Perez-Padilla R; Olaiz-Fernandez G; Mendoza-Alvarado L; Moreno-Macias H; Fortoul T; McDonnell W; Loomis D; Romieu I (2007). Lung function growth in children with long-term exposure to air pollutants in Mexico City. *Am J Respir Crit Care Med*, 176: 377-384. [091064](#)

- Roman HA; Walker KD; Walsh TL; Conner L; Richmond HM; Hubbell BJ; Kinney PL (2008). Expert judgment assessment of the mortality impact of changes in ambient fine particulate matter in the U.S. *Environ Sci Technol*, 42: 2268-2274. [156921](#)
- Romieu I; Garcia-Esteban R; Sunyer J; Rios C; Alcaraz-Zubeldia M; Velasco SR; Holguin F (2008). The effect of supplementation with omega-3 polyunsaturated fatty acids on markers of oxidative stress in elderly exposed to PM(2.5). *Environ Health Perspect*, 116: 1237-1242. [156922](#)
- Romieu I; Ramirez-Aguilar M; Moreno-Macias H; Barraza-Villarreal A; Miller P; Hernandez-Cadena L; Carbajal-Arroyo LA; Hernandez-Avila M (2004). Infant mortality and air pollution: modifying effect by social class. *J Occup Environ Hyg*, 46: 1210-1216. [093074](#)
- Röösli M; Braun-Fahrlander C; Kunzli N; Oglesby L; Theis G; Camenzind M; Mathys P; Staehelin J (2000). Spatial variability of different fractions of particulate matter within an urban environment and between urban and rural sites. *J Air Waste Manag Assoc*, 50: 1115-1124. [010296](#)
- Röösli M; Kunzli N; Braun-Fahrlander C; Egger M (2005). Years of life lost attributable to air pollution in Switzerland: dynamic exposure-response model. *Int J Epidemiol*, 34: 1029-1035. [156923](#)
- Röösli M; Theis G; Kunzli N; Staehelin J; Mathys P; Oglesby L; Camenzind M; Braun-Fahrlander C (2001). Temporal and spatial variation of the chemical composition of PM10 at urban and rural sites in the Basel area, Switzerland. *Atmos Environ*, 35: 3701-3713. [108738](#)
- Rosenlund M; Bellander T; Nordquist T; Alfredsson L (2009). Traffic-generated air pollution and myocardial infarction. *Epidemiology*, 20: 265-71. [190309](#)
- Rosenlund M; Berglund N; Pershagen G; Hallqvist J; Jonson T; Bellander T (2006). Long-term exposure to urban air pollution and myocardial infarction. *Epidemiology*, 17: 383-390. [089796](#)
- Ross R (1999). Atherosclerosis--an inflammatory disease. *N Engl J Med*, 340: 115-126. [156926](#)
- Rubes J; Selevan SG; Evenson DP; Zudova D; Vozdova M; Zudova Z; Robbins WA; Perreault SD (2005). Episodic air pollution is associated with increased DNA fragmentation in human sperm without other changes in semen quality. *Hum Reprod*, 20: 2776-2783. [078091](#)
- Ruggenenti P; Remuzzi G (2006). Time to abandon microalbuminuria? *Kidney Int*, 70: 1214-1222. [156933](#)
- Sagiv SK; Mendola P; Loomis D; Herring AH; Neas LM; Savitz DA; Poole C (2005). A time-series analysis of air pollution and preterm birth in Pennsylvania, 1997-2001. *Environ Health Perspect*, 113: 602-606. [087468](#)
- Salam MT; Millstein J; Li Y-F; Lurmann FW; Margolis HG; Gilliland FD (2005). Birth outcomes and prenatal exposure to ozone, carbon monoxide, and particulate matter: results from the Children's Health Study. *Environ Health Perspect*, 113: 1638-1644. [087885](#)
- Salonen JT; Salonen R (1991). Ultrasonographically assessed carotid morphology and the risk of coronary heart disease. *Arterioscler Thromb Vasc Biol*, 11: 1245-1249. [156938](#)
- Sato H; Suzuki Kazuo T; Sone H; Yamano Y; Kagawa J; Aoki Y (2003). DNA-adduct formation in lungs, nasal mucosa, and livers of rats exposed to urban roadside air in Kawasaki City, Japan. *Environ Res*, 93: 36-44. [096615](#)
- Schatz M; Zeiger RS; Hoffman CP (1990). Intrauterine growth is related to gestational pulmonary function in pregnant asthmatic women. Kaiser-Permanente Asthma and Pregnancy Study Group. *Chest*, 98: 389-392. [156073](#)
- Schikowski T; Sugiri D; Ranft U; Gehring U; Heinrich J; Wichmann HE; Kramer U (2005). Long-term air pollution exposure and living close to busy roads are associated with COPD in women. *Respir Res*, 22: 152-161. [088637](#)
- Schindler C; Keidel D; Gerbase MW; Zemp E; Bettschart R; Brandli O; Brutsche MH; Burdet L; Karrer W; Knopfli B; Pons M; Rapp R; Bayer-Oglesby L; Kunzli N; Schwartz J; Liu L-JS; Ackermann-Liebrich U; Rochat T; the SAPALDIA Team (2009). Improvements in PM10 exposure and reduced rates of respiratory symptoms in a cohort of swiss adults (SAPALDIA). *Am J Respir Crit Care Med*, 179: 579-587. [191950](#)
- Schwartz J; Coull B; Laden F; Ryan L (2008). The effect of dose and timing of dose on the association between airborne particles and survival. *Environ Health Perspect*, 116: 64-69. [156963](#)
- Seagrave J; McDonald JD; Reed MD; Seilkop SK; Mauderly JL (2005). Responses to subchronic inhalation of low concentrations of diesel exhaust and hardwood smoke measured in rat bronchoalveolar lavage fluid. *Inhal Toxicol*, 17: 657-670. [088000](#)

- Selevan SG; Borkovec L; Slott VL; Zudova Z; Rubes J; Evenson DP; Perreault SD (2000). Semen quality and reproductive health of young Czech men exposed to seasonal air pollution. *Environ Health Perspect*, 108: 887-894. [012578](#)
- Sevastyanova O; Binkova B; Topinka J; Sram RJ; Kalina I; Popov T; Novakova Z; Farmer PB (2007). In vitro genotoxicity of PAH mixtures and organic extract from urban air particles part II: human cell lines. *Mutat Res Fund Mol Mech Mutagen*, 620: 123-134. [156969](#)
- Sharma AK; Jensen KA; Rank J; White PA; Lundstedt S; Gagne R; Jacobsen NR; Kristiansen J; Vogel U; Wallin H (2007). Genotoxicity, inflammation and physico-chemical properties of fine particle samples from an incineration energy plant and urban air. *Mutat Res Fund Mol Mech Mutagen*, 633: 95-111. [156975](#)
- Shaw LJ; Raggi P; Schisterman E; Berman DS; Callister TQ (2003). Prognostic value of cardiac risk factors and coronary artery calcium screening for all-cause mortality. *Radiology*, 228: 826-833. [156083](#)
- Shemesh J; Tenenbaum A; Fisman EZ; Apter S; Rath S; Rozenman J; Itzhak Y; Motro M (1996). Absence of coronary calcification on double-helical CT scans: predictor of angiographically normal coronary arteries in elderly women? *Radiology*, 199: 665-668. [156085](#)
- Shinkura R; Fujiyama C; Akiba S (1999). Relationship between ambient sulfur dioxide levels and neonatal mortality near the Mt Sakurajima volcano in Japan. *J Epidemiol*, 9: 344-349. [090050](#)
- Slama R; Darrow L; Parker J; Woodruff TJ; Strickland M; Nieuwenhuijsen M; Glinianaia S; Hoggatt KJ; Kannan S; Hurley F; Kalinka J; Sram R; Brauer M; Wilhelm M; Heinrich J; Ritz B (2008). Meeting report: atmospheric pollution and human reproduction. *Environ Health Perspect*, 116: 791-798. [156985](#)
- Slama R; Morgenstern V; Cyrus J; Zutavern A; Herbarth O; Wichmann HE; Heinrich J; LISA Study Group (2007). Traffic-related atmospheric pollutants levels during pregnancy and offspring's term birth weight: a study relying on a land-use regression exposure model. *Environ Health Perspect*, 115: 1283-1292. [093216](#)
- Smilde TJ; Wollersheim H; Van Langen H; Stalenhoef AF (1997). Reproducibility of ultrasonographic measurements of different carotid and femoral artery segments in healthy subjects and in patients with increased intima-media thickness. *Clin Sci (Lond)*, 93: 317-324. [156988](#)
- Sokol RZ; Kraft P; Fowler IM; Mamet R; Kim E; Berhane KT (2006). Exposure to environmental ozone alters semen quality. *Environ Health Perspect*, 114: 360-5. [098539](#)
- Solomon P; Baumann K; Edgerton E; Tanner R; Eatough D; Modey W; Marin H; Savoie D; Natarajan S; Meyer MB (2003). Comparison of integrated samplers for mass and composition during the 1999 Atlanta supersites project. *J Geophys Res*, 108: 8423. [156994](#)
- Somers CM; McCarry BE; Malek F; Quinn JS (2004). Reduction of particulate air pollution lowers the risk of heritable mutations in mice. *Science*, 304: 1008-1010. [078098](#)
- Somers CM; Yauk CL; White PA; Parfett CLJ; Quinn JS (2002). Air pollution induces heritable DNA mutations. *PNAS*, 99: 15904-15907. [078100](#)
- Song CL; Zhou YC; Huang RJ; Wang YQ; Huang QF; Lu G; Liu KM (2007). Influence of ethanol-diesel blended fuels on diesel exhaust emissions and mutagenic and genotoxic activities of particulate extracts. *J Hazard Mater*, 149: 355-363. [155306](#)
- Sorensen M; Schins RPF; Hertel O; Loft S (2005). Transition metals in personal samples of PM_{2.5} and oxidative stress in human volunteers. *Cancer Epidemiol Biomarkers Prev*, 14: 1340-1343. [083053](#)
- Sram R; Beskid O; Binkova B; Chvatalova I; Lnenickova Z; Milcova A; Solansky I; Tulupova E; Bavorova H; Ocadlikova D (2007). Chromosomal aberrations in environmentally exposed population in relation to metabolic and DNA repair genes polymorphisms. *Mutat Res Fund Mol Mech Mutagen*, 620: 22-33. [188457](#)
- Sram RJ; Beskid O; Rössnerova A; Rössner P; Lnenickova Z; Milcova A; Solansky I; Binkova B (2007). Environmental exposure to carcinogenic polycyclic aromatic hydrocarbons--the interpretation of cytogenetic analysis by FISH. *Toxicol Lett*, 172: 12-20. [192084](#)
- Sram RJ; Binkova B; Dejmeek J; Bobak M (2005). Ambient air pollution and pregnancy outcomes: a review of the literature. *Environ Health Perspect*, 113: 375-382. [087442](#)
- Stanojevic S; Wade A; Stocks J; Hankinson J; Coates AL; Pan H; Rosenthal M; Corey M; Lebecque P; Cole TJ (2008). Reference ranges for spirometry across all ages: a new approach. *Am J Respir Crit Care Med*, 177: 253-260. [157007](#)

- Stocker R; Keaney Jr JF (2004). Role of oxidative modifications in atherosclerosis. *Physiol Rev*, 84: 1381-1478. [157013](#)
- Strom KA; Garg BD; Johnson JT; D'Arcy JB; Smiler KL (1990). Inhaled particle retention in rats receiving low exposures of diesel exhaust. *J Toxicol Environ Health*, 29: 377-398. [157020](#)
- Sugamata M; Ihara T; Takano H; Oshio S; Takeda K (2006). Maternal diesel exhaust exposure damages newborn murine brains. *Eisei Kagaku*, 52: 82-84. [097166](#)
- Sugiri D; Ranft U; Schikowski T; Kramer U (2006). The influence of large-scale airborne particle decline and traffic-related exposure on children's lung function. *Environ Health Perspect*, 114: 282-288. [088760](#)
- Suh YJ; Ha EH; Park H; Kim YJ; Kim H; Hong YC (2008). GSTM1 polymorphism along with PM10 exposure contributes to the risk of preterm delivery. *Mutat Res*, 656: 62-67. [192077](#)
- Sun Q; Wang A; Jin X; Natanzon A; Duquaine D; Brook RD; Aguinardo JG; Fayad ZA; Fuster V; Lippmann M; Chen LC; Rajagopalan S (2005). Long-term air pollution exposure and acceleration of atherosclerosis and vascular inflammation in an animal model. *JAMA*, 294: 3003-3010. [087952](#)
- Sun Q; Yue P; Deiluiis JA; Lumeng CN; Kampfrath T; Mikolaj MB; Cai Y; Ostrowski MC; Lu B; Parthasarathy S; Brook RD; Moffatt-Bruce SD; Chen LC; Rajagopalan S (2009). Ambient air pollution exaggerates adipose inflammation and insulin resistance in a mouse model of diet-induced obesity. *Circulation*, 119: 538-546. [190487](#)
- Sun Q; Yue P; Kirk RI; Wang A; Moatti D; Jin X; Lu B; Schechter AD; Lippmann M; Gordon T; Chen LC; Rajagopalan S (2008). Ambient air particulate matter exposure and tissue factor expression in atherosclerosis. *Inhal Toxicol*, 20: 127-137. [157033](#)
- Sun Q; Yue P; Ying Z; Cardounel AJ; Brook RD; Devlin R; Hwang JS; Zweier JL; Chen LC; Rajagopalan S (2008). Air Pollution Exposure Potentiates Hypertension Through Reactive Oxygen Species-Mediated Activation of Rho/ROCK. *Arterioscler Thromb Vasc Biol*, 28: 1760-1766. [157032](#)
- Suwa T; Hogg JC; Quinlan KB; Ohgami A; Vincent R; Van Eeden SF (2002). Particulate air pollution induces progression of atherosclerosis. *J Am Coll Cardiol*, 39: 935-942. [028588](#)
- Tarantini L; Bonzini M; Apostoli P; Pegoraro V; Bollati V; Marinelli B; Cantone L; Rizzo G; Hou L; Schwartz J; Bertazzi PA; Baccarelli A (2009). Effects of particulate matter on genomic DNA methylation content and iNOS promoter methylation. *Environ Health Perspect*, 117: 217-222. [192010](#)
- Tesfaigzi Y; McDonald JD; Reed MD; Singh SP; De Sanctis GT; Eynott PR; Hahn FF; Campen MJ; Mauderly JL (2005). Low-level subchronic exposure to wood smoke exacerbates inflammatory responses in allergic rats. *Toxicol Sci*, 88: 505-513. [156116](#)
- Tesfaigzi Y; Singh SP; Foster JE; Kubatko J; Barr EB; Fine PM; McDonald JD; Hahn FF; Mauderly JL (2002). Health effects of subchronic exposure to low levels of wood smoke in rats. *Toxicol Sci*, 65: 115-125. [025575](#)
- Thurlbeck WM (1982). Postnatal human lung growth. *Thorax*, 37: 564-571. [093260](#)
- Tokiwa H; Sera N; Nakanishi Y (2005). Involvement of alveolar macrophages in the formation of 8-oxodeoxyguanosine associated with exogenous particles in human lungs. *Inhal Toxicol*, 17: 577-585. [191952](#)
- Tong S; Colditz P (2004). Air pollution and sudden infant death syndrome: a literature review. *Paediatr Perinat Epidemiol*, 18: 327-335. [087883](#)
- Tovalin H; Valverde M; Morandi MT; Blanco S; Whitehead L; Rojas E (2006). DNA damage in outdoor workers occupationally exposed to environmental air pollutants. *Occup Environ Med*, 63: 230-236. [091322](#)
- Tozuka Y; Watanabe N; Ohsawa M; Toriba A; Kizu R; Hayakawa K (2004). Transfer of polycyclic aromatic hydrocarbons to fetuses and breast milk of rats exposed to diesel exhaust. *Eisei Kagaku*, 50: 497-502. [090864](#)
- Tsai S-S; Chen C-C; Hsieh H-J; Chang C-C; Yang C-Y (2006). Air pollution and postneonatal mortality in a tropical city: Kaohsiung, Taiwan. *Inhal Toxicol*, 18: 185-189. [090709](#)
- Tsukue N; Tsubone H; Suzuki AK (2002). Diesel exhaust affects the abnormal delivery in pregnant mice and the growth of their young. *Inhal Toxicol*, 14: 635-651. [030593](#)
- Tsukue N; Yoshida S; Sugawara I; Taked K (2004). Effect of diesel exhaust on development of fetal reproductive function in ICR female mice. *Eisei Kagaku*, 50: 174-80. [096643](#)

- U.S. EPA (1996). Air quality criteria for particulate matter. U.S. Environmental Protection Agency. Research Triangle Park, NC. EPA/600/P-95/001aF-cF. [079380](#)
- U.S. EPA (2002). Health assessment document for diesel engine exhaust. U.S. Environmental Protection Agency. Washington, DC. [042866](#)
- U.S. EPA (2004). Air quality criteria for particulate matter. U.S. Environmental Protection Agency. Research Triangle Park, NC. EPA/600/P-99/002aF-bF. [056905](#)
- U.S. EPA (2005). Guidelines for carcinogen risk assessment, Final Report. Risk Assessment Forum, U.S. Environmental Protection Agency. Washington, DC. EPA/630/P-03/001F. <http://cfpub.epa.gov/ncea/cfm/recordisplay.cfm?deid=116283>. [086237](#)
- U.S. EPA (2006). Provisional Assessment of Recent Studies on Health Effects of Particulate Matter Exposure. U.S. Environmental Protection Agency. Research Triangle Park, NC. [157071](#)
- van der Meer IM; Bots ML; Hofman A; del Sol AI; van der Kuip DA; Witteman JC (2004). Predictive value of noninvasive measures of atherosclerosis for incident myocardial infarction: the Rotterdam Study. *Circulation*, 109: 1089-1094. [156129](#)
- Van Hee VC; Adar SD; Szpiro AA; Barr RG; Bluemke DA; Diez Roux AV; Gill EA; Sheppard L; Kaufman JD (2009). Exposure to traffic and left ventricular mass and function: the Multi-Ethnic Study of Atherosclerosis. *Am J Respir Crit Care Med*, 179: 827-834. [192110](#)
- Veras MM; Damaceno-Rodrigues NR; Caldini EG; Maciel Ribeiro AA; Mayhew TM; Saldiva PH; Dolhnikoff M (2008). Particulate urban air pollution affects the functional morphology of mouse placenta. *Biol Reprod*, 79: 578-584. [190493](#)
- Veras MM; Damaceno-Rodrigues NR; Guimarães Silva RM; Scoriza JN; Saldiva PH; Caldini EG; Dolhnikoff M (2009). Chronic exposure to fine particulate matter emitted by traffic affects reproductive and fetal outcomes in mice. *Environ Res*, 109: 536-543. [190496](#)
- Villeneuve PJ; Goldberg MS; Krewski D; Burnett RT; Chen Y (2002). Fine particulate air pollution and all-cause mortality within the Harvard six-cities study: variations in risk by period of exposure. *Ann Epidemiol*, 12: 568-576. [042576](#)
- Vineis P; Hoek G; Krzyzanowski M; Vigna-Taglianti F; Veglia F; Airoidi L; Autrup H; Dunning A; Garte S; Hainaut P; Malaveille C; Matullo G; Overvad K; Raaschou-Nielsen O; Clavel-Chapelon F; Linseisen J; Boeing H; Trichopoulos A; Palli D; Peluso M; Krogh V; Tumino R; Panico S; Bueno-De-Mesquita HB; Peeters PH; Lund EE; Gonzalez CA; Martinez C; Dorronsoro M; Barricarte A; Cirera L; Quiros JR; Berglund G; Forsberg B; Day NE; Key TJ; Saracci R; Kaaks R; Riboli E (2006). Air pollution and risk of lung cancer in a prospective study in Europe. *Int J Cancer*, 119: 169-174. [192089](#)
- Vinzents PS; Moller P; Sorensen M; Knudsen LE; Herte LQ; Jensen FP; Schibye B; Loft S (2005). Personal exposure to ultrafine particles and oxidative DNA damage. *Environ Health Perspect*, 113: 1485-1490. [087482](#)
- Vogt MT; Cauley JA; Newman AB; Kuller LH; Hulley SB (1993). Decreased ankle/arm blood pressure index and mortality in elderly women. *JAMA*, 270: 465-469. [157100](#)
- Wallenborn JG; Evansky P; Shannahan JH; Vallanat B; Ledbetter AD; Schladweiler MC; Richards JH; Gottipolu RR; Nyska A; Kodavanti UP (2008). Subchronic inhalation of zinc sulfate induces cardiac changes in healthy rats. *Toxicol Appl Pharmacol*, 232: 69-77. [191171](#)
- Walsh CR; Cupples LA; Levy D; Kiel DP; Hannan M; Wilson PW; O'Donnell CJ (2002). Abdominal aortic calcific deposits are associated with increased risk for congestive heart failure: the Framingham Heart Study. *Am Heart J*, 144: 733-739. [157103](#)
- Watanabe N (2005). Decreased number of sperms and Sertoli cells in mature rats exposed to diesel exhaust as fetuses. *Toxicol Lett*, 155: 51-58. [087985](#)
- Wayne LG; Chambers LA (1968). Biological effects of urban air pollution: V a study of effects of Los Angeles atmosphere on laboratory rodents. *Arch Environ Occup Health*, 16: 871-885. [038537](#)
- Weisenberger DJ; Campan M; Long TI; Kim M; Woods C; Fiala E; Ehrlich M; Laird PW (2005). Analysis of repetitive element DNA methylation by MethyLight. *Nucleic Acids Res*, 33: 6823-36. [192101](#)

- Weitz JI; Byrne J; Clagett GP; Farkouh ME; Porter JM; Sackett DL; Strandness DE Jr; Taylor LM (1996). Diagnosis and treatment of chronic arterial insufficiency of the lower extremities: a critical review. *Circulation*, 94: 3026-3049. [156150](#)
- Wendelhag I; Gustavsson T; Suurkula M; Berglund G; Wikstrand J (1991). Ultrasound measurement of wall thickness in the carotid artery: fundamental principles and description of a computerized analysing system. *Clinical Physiol*, 11: 565-577. [157135](#)
- Wendelhag I; Wiklund O; Wikstrand J (1993). Atherosclerotic changes in the femoral and carotid arteries in familial hypercholesterolemia. Ultrasonographic assessment of intima-media thickness and plaque occurrence. *Arterioscler Thromb Vasc Biol*, 13: 1404-1411. [157136](#)
- Wheeler AJ; Villeneuve P; Smith-Doiron M; Mahmud M; Dales R; Brook JR (2006). Children's exposure to ambient air pollution: the application of different exposure assessment methodologies. *Epidemiology*, 17: S33-S34. [103905](#)
- Wilhelm M; Ritz B (2005). Local variations in CO and particulate air pollution and adverse birth outcomes in Los Angeles County, California, USA. *Environ Health Perspect*, 113: 1212-1221. [088668](#)
- Willekes C; Brands PJ; Willigers JM; Hoeks AP; Reneman RS (1999). Assessment of local differences in intima-media thickness in the human common carotid artery. *J Vasc Res*, 36: 222-228. [157147](#)
- Williams L; Ulrich C; Larson T; Wener M; Wood B; Campbell P; Potter J; McTiernan A; De Roos A (2009). Proximity to Traffic, Inflammation, and Immune Function among Women in the Seattle, Washington, Area. *Environ Health Perspect*, 117: 373. [191945](#)
- Wilson PW; Kauppila LI; O'Donnell CJ; Kiel DP; Hannan M; Polak JM; Cupples LA (2001). Abdominal aortic calcific deposits are an important predictor of vascular morbidity and mortality. *Circulation*, 103: 1529-1534. [156159](#)
- Wilson WE; Mage DT; Grant LD (2000). Estimating separately personal exposure to ambient and nonambient particulate matter for epidemiology and risk assessment: why and how. *J Air Waste Manag Assoc*, 50: 1167-1183. [010288](#)
- Witteman JC; Kok FJ; van Saase JL; Valkenburg HA (1986). Aortic calcification as a predictor of cardiovascular mortality. *Lancet*, 2: 1120-1122. [156161](#)
- Woodruff TJ; Darrow LA; Parker JD (2008). Air pollution and postneonatal infant mortality in the United States, 1999-2002. *Environ Health Perspect*, 116: 110-115. [098386](#)
- Woodruff TJ; Grillo J; Schoendorf KC (1997). The relationship between selected causes of postneonatal infant mortality and particulate air pollution in the United States. *Environ Health Perspect*, 105: 608-612. [084271](#)
- Woodruff TJ; Parker JD; Schoendorf KC (2006). Fine particulate matter (PM_{2.5}) air pollution and selected causes of postneonatal infant mortality in California. *Environ Health Perspect*, 114: 785-790. [088758](#)
- Xu J; Lee ET; Devereux RB; Umans JG; Bella JN; Shara NM; Yeh J; Fabsitz RR; Howard BV (2008). A longitudinal study of risk factors for incident albuminuria in diabetic American Indians: the Strong Heart Study. *Am J Kidney Dis*, 51: 415-424. [157157](#)
- Yang AS; Estécio MR; Doshi K; Kondo Y; Tajara EH; Issa JP (2004). A simple method for estimating global DNA methylation using bisulfite PCR of repetitive DNA elements. *Nucleic Acids Res*, 32: e38. [192102](#)
- Yang C-Y; Hsieh H-J; Tsai S-S; Wu T-N; Chiu H-F (2006). Correlation between air pollution and postneonatal mortality in a subtropical city: Taipei, Taiwan. *J Toxicol Environ Health A Curr Iss*, 69: 2033-2040. [090760](#)
- Yang C-Y; Tseng Y-T; Chang C-C (2003). Effects of air pollution on birthweight among children born between 1995 and 1997 in Kaohsiung, Taiwan. *J Toxicol Environ Health A Curr Iss*, 66: 807-816. [087886](#)
- Yatera K; Hsieh J; Hogg James C; Tranfield E; Suzuki H; Shih C-H; Behzad Ali R; Vincent R; van Eeden Stephan F (2008). Particulate matter air pollution exposure promotes recruitment of monocytes into atherosclerotic plaques. *Am J Physiol Heart Circ Physiol*, 294: H944-H953. [157162](#)
- Yauk C; Polyzos A; Rowan-Carroll A; Somers CM; Godschalk RW; Van Schooten FJ; Berndt ML; Pogribny IP; Koturbash I; Williams A; Douglas GR; Kovalchuk O (2008). Germ-line mutations, DNA damage, and global hypermethylation in mice exposed to particulate air pollution in an urban/industrial location. *PNAS*, 105: 605-610. [157164](#)
- Yauk CL; Quinn JS (1996). Multilocus DNA fingerprinting reveals high rate of heritable genetic mutation in herring gulls nesting in an industrialized urban site. *PNAS*, 93: 12137-12141. [089093](#)

- Ying Z; Kampfrath T; Thurston G; Farrar B; Lippmann M; Wang A; Sun Q; Chen LC; Rajagopalan S (2009). Ambient particulates alter vascular function through induction of reactive oxygen and nitrogen species. *Toxicol Sci*, 111: 80-88. [190111](#)
- Yokota S; Mizuo K; Moriya N; Oshio S; Sugawara I; Takeda K (2009). Effect of prenatal exposure to diesel exhaust on dopaminergic system in mice. *Neurosci Lett*, 449: 38-41. [190518](#)
- Yoshida S; Ono N; Tsukue N; Oshio S; Umeda T; Takano H; Takeda K (2006). In utero exposure to diesel exhaust increased accessory reproductive gland weight and serum testosterone concentration in male mice. *Environ Sci J Integr Environ Res*, 13: 139-147. [097015](#)
- Yoshida S; Takeda K (2004). The effects of diesel exhaust on murine male reproductive function. *Eisei Kagaku*, 50: 210-214. [097760](#)
- Yoshida S; Yoshida M; Sugawara I; Takeda K (2006). Mice strain differences in effects of fetal exposure to diesel exhaust gas on male gonadal differentiation. *Environ Sci J Integr Environ Res*, 13: 117-123. [156170](#)
- Zanobetti A; Bind MAC; Schwartz J (2008). Particulate air pollution and survival in a COPD cohort. *Environ Health Perspect*, 7: 48. [156177](#)
- Zanobetti A; Schwartz J (2007). Particulate air pollution, progression, and survival after myocardial infarction. *Environ Health Perspect*, 115: 769-775. [091247](#)
- Zeger S; Dominici F; McDermott A; Samet J (2008). Mortality in the Medicare population and chronic exposure to fine particulate air pollution in urban centers (2000-2005). *Environ Health Perspect*, 116: 1614-1619. [191951](#)
- Zeger S; McDermott A; Dominici F; Samet J (2007). Mortality in the medicare population and chronic exposure to fine particulate air pollution. Johns Hopkins University. Baltimore. <http://www.bepress.com/jhubiostat/paper133>. [157176](#)
- Zeman KL; Bennett WD (2006). Growth of the small airways and alveoli from childhood to the adult lung measured by aerosol-derived airway morphometry. *J Appl Physiol*, 100: 965-971. [157178](#)
- Zhang Z; Che W; Liang Y; Wu M; Li N; Shu Y; Liu F; Wu D (2007). Comparison of cytotoxicity and genotoxicity induced by the extracts of methanol and gasoline engine exhausts. *Toxicol In Vitro*, 21: 1058-1065. [157186](#)

Chapter 8. Populations Susceptible to PM-related Health Effects

Interindividual variation in human responses to air pollutants indicates that some populations are at increased risk for the detrimental effects of ambient exposure to an air pollutant (e.g., PM) (Kleeberger and Ohtsuka, 2005, [130489](#)). The NAAQS are intended to provide an adequate margin of safety for both general populations and sensitive subgroups, or those individuals potentially at increased risk for health effects in response to ambient air pollution (see Section 1.1). To facilitate the identification of populations at the greatest risk for PM-related health effects, studies have evaluated factors that contribute to the susceptibility and/or vulnerability of an individual to PM. The definition for both of these terms has been found to vary across studies, but in most instances susceptibility refers to biological or intrinsic factors (e.g., lifestage, gender) while vulnerability refers to non-biological or extrinsic factors (e.g., socioeconomic status [SES]) (see Table 8-1). Additionally, in some cases, the terms “at-risk” and sensitive populations have been used to encompass these concepts more generally. However, in many cases a factor identified that increases an individual's risk for morbidity or mortality effects from exposure to an air pollutant (e.g., PM) can not be easily categorized as a susceptibility or vulnerability factor. For example, a population that is characterized as having low SES, traditionally defined as a vulnerability factor, may have less access to healthcare resulting in the manifestation of disease (i.e., a susceptibility factor), but they may also reside in a location that results in exposure to higher concentrations of an air pollutant, increasing their vulnerability. Therefore, the terms susceptibility and vulnerability are intertwined and at times can not be distinguished from one another.

As a result of the inconsistencies in the definition of susceptibility and vulnerability presented in the literature as well as the inability to clearly delineate whether an identified factor increases an individual's susceptibility or vulnerability to an air pollutant, in this ISA, the term ‘susceptible population’ will be used as a blanket term and defined as the following:

Populations that have a greater likelihood of experiencing health effects related to exposure to an air pollutant (e.g., PM) due to a variety of factors including, but not limited to: genetic or developmental factors, race, gender, lifestage, lifestyle (e.g., smoking status and nutrition) or preexisting disease; as well as, population-level factors that can increase an individual's exposure to an air pollutant (e.g., PM) such as socioeconomic status [SES], which encompasses reduced access to health care, low educational attainment, residential location, and other factors.

Note: Hyperlinks to the reference citations throughout this document will take you to the NCEA HERO database (Health and Environmental Research Online) at <http://epa.gov/hero>. HERO is a database of scientific literature used by U.S. EPA in the process of developing science assessments such as the Integrated Science Assessments (ISA) and the Integrated Risk Information System (IRIS).

Table 8-1. Definitions of susceptible and vulnerable in the PM literature.

Definition	Reference
Susceptible: predisposed to develop a noninfectious disease	Merriam-Webster (2009, 192146)
Vulnerable: capable of being hurt: susceptible to injury or disease	
Susceptible: greater likelihood of an adverse outcome given a specific exposure, in comparison with the general population. Includes both host and environmental factors (e.g., genetics, diet, physiological state, age, gender, social, economic, and geographic attributes).	American Lung Association (2001, 016626)
Vulnerable: periods during an individual's life when they are more susceptible to environmental exposures.	
Susceptible: innate (e.g., genetic or developmental) or acquired (e.g., age, disease or smoking or smoking) factors that make individuals more likely to experience effects with exposure to PM.	U.S. EPA. (2008, 157072)
Vulnerable: PM-related effects due to factors including socioeconomic status (e.g., reduced access to health care) or particularly elevated exposure levels.	
Susceptible: greater or lesser biological response to exposure.	U.S. EPA (2009, 192149)
Vulnerable: more or less exposed.	
Vulnerable: to be susceptible to harm or neglect, that is, acts of commission or omission on the part of others that can wound.	Aday, LA. (2001, 192150)
Susceptible: may be those who are significantly more liable than the general population to be affected by a stressor due to life stage (e.g., children, the elderly, or pregnant women), genetic polymorphisms (e.g., the small but significant percentage of the population who have genetic susceptibilities), prior immune reactions (e.g., individuals who have been "sensitized" to a particular chemical), disease state (e.g., asthmatics), or prior damage to cells or systems (e.g., individuals with damaged ear structures due to prior exposure to toluene, making them more sensitive to damage by high noise levels).	U.S. EPA (2003, 192145)
Vulnerable: differential exposure and differential preparedness (e.g., immunization).	
Susceptible: intrinsic (e.g., age, gender, pre-existing disease (e.g., asthma) and genetics) and extrinsic (previous exposure and nutritional status) factors.	Kleeberger and Ohtsuka (2005, 130489)
Susceptible: characteristics that contribute to increased risk of PM-related health effects (e.g., genetics, pre-existing disease, age, gender, race, socioeconomic status, healthcare availability, educational attainment, and housing characteristics).	Pope and Dockery (2006, 156881)

To examine whether air pollutants (e.g., PM) differentially affect certain populations, epidemiologic studies conduct stratified analyses to identify the presence or absence of effect modification. A thorough evaluation of potential effect modifiers may help identify populations that are more susceptible to an air pollutant (e.g., PM). Although the design of toxicological and controlled human exposure studies do not allow for an extensive examination of effect modifiers, the use of animal models of disease and the study of individuals with underlying disease or genetic polymorphisms do allow for comparisons between subgroups. Therefore, the results from these studies, combined with those results obtained through stratified analyses in epidemiologic studies, contribute to the overall weight of evidence for the increased susceptibility of specific populations to an air pollutant (e.g., PM).

This chapter discusses the epidemiologic, controlled human exposure, and toxicological studies evaluated in Chapters 6 and 7 that provide information on potentially susceptible populations. The studies highlighted include only those studies that present stratified results (e.g., males vs. females or <65 vs. ≥ 65). This approach allowed for a comparison between populations exposed to similar PM concentrations and within the same study design. In addition, numerous studies that focus on only one potentially susceptible population can provide supporting evidence on whether a population is susceptible to PM exposure and are described in Chapters 6 and 7, but these studies are not discussed in detail in this chapter. Table 8-2 provides an overview of the factors examined in the current toxicological, controlled human exposure, and epidemiologic literature and the direction of the underlying evidence in determining whether a factor increases the susceptibility of a population to PM-related health effects.

Table 8-2. Susceptibility factors evaluated.

Factor	Collective Evidence (+/-) ²
Older Adults (≥ 65)	+
Children (<18) ¹	+
Pregnancy and Developmental Effects	+*
Gender	-
Race/Ethnicity	-
Genetic factors	
- Genetic polymorphisms	+
- Epigenetics	
Cardiovascular Diseases	+
Respiratory Illnesses	+
Respiratory Contributions to Cardiovascular Effects	-*
Diabetes	+*
Obesity	+*
Socioeconomic Status (SES)	+
Educational Attainment ³	+
Residential Location ³	+
Health Status (e.g., Nutrition) ³	+*

¹ The age range that defines a child varies from study to study. In some cases it is <21 years old while in others it is <18 years old (Firestone et al., 2007, [192071](#)). For the purposes of this exercise children are defined as those individuals <18 years old because the majority of epidemiologic studies consider individuals under the age of 18 children.

² This column identifies whether the "collective" evidence from studies evaluated found that a specific factor increased (+) or did not increase (-) a population's susceptibility to PM exposure (i.e., PM exposure to all size fractions combined). In instances where only a few studies were evaluated for a specific factor it was not possible to clearly assign a (+) or (-) as a result the direction of the preliminary evidence is identified along with (*) to represent that more information is warranted.

³ These factors are surrogates of socioeconomic status and are discussed within this subsection of the chapter.

8.1. Potentially Susceptible Populations

8.1.1. Lifestage

8.1.1.1. Older Adults

Evidence for PM-related health effects in older adults spans epidemiologic, controlled human exposure, and toxicological studies. The 2004 PM AQCD found evidence for increased risk of cardiovascular effects in older adults exposed to PM (U.S. EPA, 2004, [056905](#)). Older adults represent a potentially susceptible population due to the higher prevalence of pre-existing cardiovascular and respiratory diseases found in this age range compared to younger age groups. The increased susceptibility in this population can primarily be attributed to the gradual decline in physiological processes as part of the aging process (U.S. EPA, 2006, [192082](#)). Therefore, some overlap exists between potentially susceptible older adults and the population that encompasses individuals with pre-existing diseases (Kan et al., 2008, [156621](#)). Epidemiologic studies that conduct age stratified analyses primarily focus on the association between short-term exposure to PM and cardiovascular morbidity, but additional studies have examined the association between PM and respiratory morbidity and mortality.

In recent publications, the epidemiologic evidence for cardiovascular effects in older adults in response to short-term exposure to $PM_{10-2.5}$ and $PM_{2.5}$ is limited, but taken together with evidence from studies of PM_{10} (e.g., Larriue et al., 2007, [093031](#); Le Tertre et al., 2002, [023746](#)), supports the increased risk of cardiovascular morbidity in older adults. Host et al. (2007, [155851](#)) found an increase in cardiovascular disease (CVD) hospital admissions in individuals >65 yr compared to all ages for short-term exposure to both $PM_{10-2.5}$ and $PM_{2.5}$. Barnett et al. (2006, [089770](#)) analyzed data from several cities across Australia and New Zealand and found that the excess risk of hospitalizations for cardiac diseases, congestive heart failure (CHF), ischemic heart disease (IHD), myocardial infarction (MI), and all CVD was greater among patients aged ≥ 65 yr as compared to those individuals <65 years in response to short-term exposure to $PM_{2.5}$. U.S.- and Canadian-based studies that examined the association between short-term exposure to PM and cardiovascular morbidity primarily found no evidence for increased risk among older adults. Metzger et al. (2004, [044222](#)) found no evidence of effect modification by age for cardiovascular outcomes and short-term exposure to $PM_{2.5}$ in Atlanta, Georgia, which is supported by the results from other studies that focused on short-term exposure to PM_{10} (Fung et al., 2005, [074322](#); Zanobetti and Schwartz, 2005, [088069](#)). However, Pope et al. (2008, [191969](#)) observed an increased risk of HF hospital admissions in older adults (i.e., ≥ 65 yr) in Utah, but the study used a 14-day lagged cumulative moving average of $PM_{2.5}$, which is much longer than the lags examined by the other U.S.- and Canadian-based studies. Although studies have not consistently found an association between short-term exposure to PM and respiratory-related health effects in older adults, some studies have reported an increase in respiratory hospital admissions in individuals 65 years of age and older (e.g., Fung et al., 2005, [093262](#)).

Additional evidence for an increase in cardiovascular and respiratory effects among older adults has been observed in controlled human exposure and dosimetry studies. Devlin et al. (2003, [087348](#)) found that older subjects exposed to $PM_{2.5}$ concentrated ambient particles (CAPs) experienced significant decreases in heart rate variability (HRV) (both in time and frequency) immediately following exposure, when compared to healthy young subjects. In addition, Gong et al. (2004, [055628](#)) reported that older subjects demonstrated significant decreases in HRV when exposed to $PM_{2.5}$ CAPs, but this study did not compare the response in older subjects to those elicited by young, healthy individuals. However, the study did find that healthy older adults were more susceptible to decreases in HRV compared to those with an underlying health condition (i.e., chronic obstructive pulmonary disease [COPD]) in response to PM exposure (Gong et al., 2004, [055628](#)). Dosimetry studies have shown a depression of $PM_{2.5}$ and $PM_{10-2.5}$ clearance in all regions of the respiratory tract with increasing age beyond young adulthood in humans and laboratory animals. These results suggest that older adults are also susceptible to PM-related respiratory health effects (Section 4.3.4.1).

Animal toxicological studies have attempted to characterize the relationship between age and PM-related health effects through the development of models that mimic the physiological conditions associated with older individuals. For example, Nadziejko et al. (2004, [055632](#)) observed arrhythmias in older, but not younger, rats exposed to $PM_{2.5}$ CAPs. In addition, another study (Tankersley et al., 2004, [094378](#)) that used a mouse model of terminal senescence demonstrated altered baseline autonomic tone in response to carbon black exposure, which may subsequently affect the quality and severity of cardiovascular responses (Tankersley et al., 2007, [097910](#)). Reductions in cardiac fractional shortening and significant pulmonary vascular congestion upon exposure to carbon black were also reported in older mice (Tankersley et al., 2008, [157043](#)). Overall, these studies provide biological plausibility for the increase in cardiovascular effects in older adults observed in the controlled human exposure and epidemiologic studies.

Recent epidemiologic studies have also found that individuals >65 years of age are more susceptible to all-cause (nonaccidental) mortality upon short-term exposure to both $PM_{2.5}$ (Ostro et al., 2006, [087991](#)) and PM_{10} (Samoli et al., 2008, [188455](#); Zeka et al., 2006, [088749](#)), which is consistent with the findings of the 2004 PM AQCD. Of note are the results from Ostro et al. (2006, [087991](#)) that reported a slight increase in mortality for older adults compared to all ages in single-pollutant models, but a robust effect estimate in co-pollutant models with gaseous pollutants (i.e., $PM_{2.5}+CO$ and $PM_{2.5}+NO_2$). These results differ from those in the all ages model (i.e., attenuation of the effect estimate in co-pollutant models with CO and NO_2), which suggests that older adults are more susceptible to PM exposures, even though the age-stratified effect estimates in single-pollutant models did not significantly differ. Epidemiologic studies that examined the association between mortality and long-term exposure to PM (i.e., $PM_{2.5}$) have found results

contradictory to those obtained in the short-term exposure studies. Villeneuve et al. (2002, [042576](#)), Naess et al. (2007, [090736](#)) and Zeger et al. (2008, [191951](#)) report evidence of differing PM_{2.5} relative risks by age, where risk declines with increasing age starting at age 60 until there is no evidence of an association among persons ≥ 85 yr.

The evidence from epidemiologic, controlled human exposure, and toxicological studies that focused on exposures to PM_{2.5}, PM_{10-2.5}, and PM₁₀, provide coherence and biological plausibility for the association between PM and cardiovascular morbidity in older adults. The clear pattern of positive associations only being observed in epidemiologic studies conducted in non-U.S. locations brings into question the influence of PM composition on health effects. However, the difference in effects observed between U.S. and Canadian, and international studies could also be due to possible differences in the identification of CVD-related morbidity and mortality between the studies evaluated. Although most studies examined the effect of PM on CVD outcomes in older adults, the additional evidence from epidemiologic studies that focus on respiratory morbidity and mortality in response to short-term exposure to PM also indicate that older adults represent a susceptible population. As the demographics of the U.S. population shift over the next 20 years with a larger percentage of the population (i.e., 13% of the population in 2011 and a projected 20% in 2030) encompassing individuals ≥ 65 yr (U.S. Census, 2000, [157064](#)), an increase in the number of PM-related health effects (e.g., cardiovascular and respiratory morbidity, and mortality) in individuals ≥ 65 years of age could occur.

8.1.1.2. Children

Children have generally been considered more susceptible to PM exposure due to multiple factors including more time spent outdoors, greater activity levels, exposures resulting in higher doses per body weight and lung surface area, and the potential for irreversible effects on the developing lung (U.S. EPA, 2004, [056905](#)). The 2004 PM AQCD found that studies which stratify results by age typically report associations between PM and respiratory-related health effects in children, specifically asthma (U.S. EPA, 2004, [056905](#)). Of the recent epidemiologic studies evaluated, only a few have examined the association between PM_{10-2.5} and PM_{2.5} and respiratory effects in children. Mar et al. (2004, [057309](#)) found increased respiratory effects (e.g., wheeze, cough, lower respiratory symptoms) in children 7-12 years of age compared to individuals 20-51 years of age in response to exposure to both PM_{10-2.5} and PM_{2.5} in Spokane, Washington. In addition, Host et al. (2007, [155851](#)) found an increase in respiratory-related hospital admissions with short-term exposure to PM_{10-2.5} among children ages 0-14 yr in 6 French cities. An examination of studies that also focused on PM₁₀ provide additional support for PM-induced respiratory effects in children (Mar et al., 2004, [057309](#); Peel et al., 2005, [056305](#)). A recent toxicological study provides biological plausibility for the increase in PM-related respiratory effects in children observed in the epidemiologic studies. Mauad et al. (2008, [156743](#)) using both prenatal and postnatal mice exposed to ambient PM_{2.5} in a “polluted chamber” found evidence for changes in lung function and pulmonary injury (e.g., incomplete alveolarization). Additionally, Pinkerton et al. (2004, [087465](#); 2008, [190471](#)) found evidence suggesting that the developing lung is more susceptible to PM by demonstrating that neonatal rats exposed to iron-soot PM had a reduction in cell proliferation in the lung. Overall, the evidence from epidemiologic studies that have examined the health effects associated with all size fractions of PM and toxicological studies that have examined individual PM components provide additional support to the hypothesis that children are more susceptible to respiratory effects from exposure to PM.

8.1.2. Pregnancy and Developmental Effects

While the majority of the literature focuses on epidemiologic studies that examine the potential health effects (e.g., low birth weight, growth restriction) attributed to in utero exposure to PM (see Section 7.4), it is unclear if the health effects observed are due to soluble fractions of PM that cross the placenta or physiological alterations in the pregnant woman. In the case of exposure to PM, adverse health effects in the offspring could be mediated by potentially greater susceptibility in the pregnant woman. For example, an inflammatory response leads to differential activation of multiple genes involved in immune response and regulation, cell metabolism, and proliferation all of which can lead to health effects in the developing fetus (Fedulov et al., 2008, [097482](#)). Toxicological

studies have recently examined whether exposure to air pollutants during pregnancy leads to increased allergic susceptibility in the offspring. Fedulov et al. (2008, [097482](#)) used an animal model to examine the effect of diesel exhaust particles (DEPs) along with an immunologically “inert” particle (TiO₂) on pregnant mice. The authors found that pregnant mice exhibited a local and systemic inflammatory response when exposed to either DEP or TiO₂, which was not observed in control, non-pregnant mice. In addition, the offspring of exposed pregnant mice developed AHR and allergic inflammation. This study suggests that exposure to PM_{2.5}, and even relatively inert particles, during pregnancy can potentially lead to increased allergic susceptibility in offspring and subsequently the development of asthma.

8.1.3. Gender

The 2004 PM AQCD did not find consistent evidence for a difference in health effects by gender. However, there appeared to be gender differences in the localization of particles when deposited in the respiratory tract and the deposition rate due to differences in body size, conductive airway size, and ventilatory parameters (U.S. EPA, 2004, [056905](#)). For example, females have proportionally smaller airways and slightly greater airway reactivity than males (Yunginger et al., 1992, [192074](#)).

Few recent epidemiologic studies have conducted gender-stratified analyses when examining the association between either short- or long-term exposure to PM_{10-2.5} or PM_{2.5}. Similar to the studies evaluated in the 2004 PM AQCD, the current literature has not found a consistent pattern of associations by gender for any health outcome. Pope et al. (2006, [091246](#)) observed a slightly larger, non-significant, association between short-term exposure to PM_{2.5} and daily hospital admission for acute IHD events in males. An examination of gender-specific effects by both Ostro et al. (2006, [087991](#)) and Franklin et al. (2007, [091257](#)) found conflicting associations by gender for multiple cause-specific mortality outcomes. The inconsistency in associations between males and females is further highlighted in studies that examined the health effects associated with long-term exposure to PM_{10-2.5} and PM_{2.5}. Chen et al. (2005, [087942](#)) found larger effects in females for congestive heart disease (CHD) mortality upon long-term exposure to PM_{10-2.5} in three California cities. Naess et al. (2007, [090736](#)), also observed slightly larger effect estimates in females for CVD and lung cancer mortality upon long-term exposure to PM_{2.5}, but for COPD mortality the greatest association was found in males.

The majority of the epidemiologic studies that examined the association between exposure to PM and gender focused on exposure to PM₁₀. Although most of these studies do not attribute the association to specific size fractions (i.e., PM_{10-2.5} or PM_{2.5}) or provide insight as to whether one size fraction may be driving the observed effect, the studies of PM₁₀ provide further support that gender does not appear to differentially affect PM-related health outcomes. Neither Zanobetti and Schwartz (2005, [088069](#)) nor Wellenius et al. (2006, [088748](#)) found gender to be a significant effect modifier of the risk estimates associated with short-term exposure to PM₁₀ and cardiovascular hospital admissions. These results are consistent with those found in other studies that examined the association between short-term exposure to PM₁₀ and both cardiovascular and respiratory hospital admissions (Luginaah et al., 2005, [057327](#); Middleton et al., 2008, [156760](#)). Additional studies that examined the effects of short-term and long-term exposure to PM₁₀ on respiratory morbidity and mortality (Boezen et al., 2005, [087396](#); Chen et al., 2005, [087942](#); Zanobetti and Schwartz, 2005, [088069](#); Zeka et al., 2006, [088749](#)) found results that are consistent with those reported in studies of PM_{10-2.5} and PM_{2.5} (i.e., gender is not likely to be an effect modifier).

Although human clinical studies are not typically powered to detect differences in response between males and females, one study did report significantly greater decreases in blood monocytes, basophils, and eosinophils in females compared to males following controlled exposures to UF EC (Frampton et al., 2006, [088665](#)). Overall, the evidence from primarily epidemiologic studies that examined the association between short- and long-term exposure to PM_{10-2.5} and PM_{2.5}, along with the supporting evidence from PM₁₀ studies, further confirms that although differences in dosimetry exist between males and females, neither gender consistently exhibits a higher disposition for PM-related health effects.

8.1.4. Race/Ethnicity

The 2004 PM AQCD (U.S. EPA, 2004, [056905](#)) did not evaluate the potential susceptibility of individuals of different races and ethnicities to PM exposure. The results from epidemiologic studies evaluated in this review that examined the potential effect modification of the PM-morbidity and -mortality relationships by race and ethnicity varied depending on the study location. In an analysis of the PM_{2.5}-mortality relationship, Ostro et al. (2006, [087991](#)) stratified the association by race and ethnicity, and observed a positive and marginally significant effect for whites and Hispanics, but not for blacks, in response to short-term exposure to PM_{2.5} in 9 California counties. An additional analysis performed by Ostro et al. (2008, [097971](#)) in 6 California counties using PM_{2.5} and various PM_{2.5} components, also found a significant association between mortality, specifically cardiovascular mortality, and Hispanic ethnicity (Ostro et al., 2008, [097971](#)). It should be noted that neither study, Ostro et al. (2006, [087991](#)) nor Ostro et al. (2008, [097971](#)), controlled for potential confounders (e.g., SES factors and location of residence) of the association observed between PM_{2.5} exposure and Hispanic ethnicity. As a result, Ostro et al. (2008, [097971](#)) speculated that the increased PM_{2.5}-mortality risks observed for Hispanics could be due to a variety of factors including, higher rates of: non-high school graduates, obesity, no leisure-time activity, and alcohol consumption within the Hispanic population in California. Additional evidence for the potential susceptibility of individuals by race and ethnicity were derived from studies on the health effects associated with short-term exposure to PM₁₀. Wellenius et al. (2006, [088748](#)) observed that race (i.e., white vs. other) did not significantly modify the association between short-term exposure to PM₁₀ and CHF hospital admissions. Additionally, Zeka et al. (2006, [088749](#)) did not observe any difference in mortality effect estimates when stratifying by race (i.e., black and white) upon short-term exposure to PM₁₀. To date, dosimetry studies have not extensively examined differences in particle deposition between races or ethnicities to confirm the epidemiologic findings. Although not extensively analyzed, toxicological studies have examined PM responses in different mouse and rat strains, and reported greater CV effects (Kodavanti et al., 2003, [051325](#); Tankersley et al., 2007, [097910](#)) and compromised host defense (Ohtsuka et al., 2000, [004409](#)) for some strains. These studies provide some support, in terms of biological plausibility, for differences in PM-induced health effects by race or ethnicity. However, it is unclear how the difference in the response to PM in different mouse or rat strains extrapolates to PM-induced differences between races or ethnicities. Overall, the results from the studies that examined the potential effect modification of PM associations by race and ethnicity provide some evidence for increased risk of mortality in Hispanics upon short-term exposure to PM_{2.5}. However, the evidence for this association is derived from two studies conducted in California, and it is unclear if the studies adequately controlled for potential confounders. Additional studies conducted in other locations that stratify results by ethnicity have not yet been conducted to substantiate these results.

8.1.5. Gene-Environment Interaction

A consensus now exists that gene-environment interactions merit serious consideration when examining the relationship between ambient exposures to air pollutants and the development of health effects (Gilliland et al., 1999, [155792](#); Kauffmann et al., 2004, [090968](#)). These potential interactions were not evaluated in the 2004 PM AQCD. Inter-individual variation in human responses to air pollutants suggests that some populations are at increased risk of detrimental effects due to pollutant exposure, and it has become clear that the genetic makeup of an individual can increase their susceptibility (Kleeberger and Ohtsuka, 2005, [130489](#)). Gene-environment interactions can result in health effects due to: genetic polymorphisms, which result in the lack of a protein or a change that makes a functionally important protein dysfunctional; or genetic damage in response to an exposure which potentially leads to a health response (e.g., formation of benzo [a] pyrene DNA adducts in response to PM exposure). In this review, the majority of studies examine gene-environment interactions due to genetic polymorphisms. In order to establish useful links between polymorphisms in candidate genes and adverse health effects, several criteria must be satisfied: the product of the candidate gene must be significantly involved in the pathogenesis of the adverse effect of interest; and polymorphisms in the gene must produce a functional change in either the protein product or in the level of expression of the protein (U.S. EPA, 2008, [157075](#)). Further, the issue of confounding by other environmental exposures must be carefully considered.

It has been hypothesized that the cardiovascular and respiratory health effects that occur in response to short-term PM exposure are mediated by oxidative stress (see Section 5.1.1). Research has examined this hypothesis by primarily focusing on the glutathione-S transferase (GST) genes because they have common, functionally important polymorphic alleles that significantly affect antioxidant defense function in the lung, and approximately half of the white population has a polymorphic null allele, resulting a large potential study population (Schwartz et al., 2005, [086296](#)). Exposure to free radicals and oxidants in air pollution leads to a cascade of events, which can result in a reduction in glutathione (GSH), and an increase in the transcription of GSTs. Individuals with genotypes that result in reduced or absent enzymatic activity are likely to have reduced antioxidant defenses and potentially increased susceptibility to inhaled oxidants and free radicals.

Numerous studies have examined the role of genetic polymorphisms on PM-related cardiovascular health effects using the Normative Aging Study cohort. Schwartz et al. (2005, [086296](#)) and Chahine et al. (2007, [156327](#)) found that individuals with null GSTM1 alleles had a larger decrease in HRV upon short-term exposure to PM_{2.5} compared to individuals with at least one allele. Polymorphisms in the HO-1 promoter resulted in lowered HRV upon short-term exposure to PM_{2.5} in individuals with the long repeat polymorphism compared to those individuals with the short repeat polymorphism (Chahine et al., 2007, [156327](#)). In addition, Schneider et al. (2008, [191985](#)) found that diabetic individuals with null GSTM1 alleles had larger decrements in FMD (i.e., flow-mediated dilation of the brachial artery), suggesting alterations in endothelial function. A controlled human exposure study (Gilliland et al., 2004, [156471](#)) also examined whether genetic polymorphisms increase the susceptibility of individuals to respiratory morbidity in response to PM exposure. Gilliland et al. (2004, [156471](#)) examined the effect of allergens and DEPs on individuals with either null genotypes for GSTM1 and GSTT1 or GSTP1 codon 105 variants. The authors found that individuals with the GSTM1 null or the GSTP1 I105 wildtype genotypes were more susceptible to allergic inflammation upon exposure to allergen and DEPs. Additional genes within the GST pathway have also been examined (e.g., NQO1), but the sample sizes are relatively small, which prohibits the analysis of the potential effect modification of PM-related health effects by these genes (e.g., Schneider et al., 2008, [191985](#)).

The interaction between GST genes and PM exposure has recently been extended to studies that examined the effect of PM exposure on birth outcomes. A recent study (Suh et al., 2008, [192077](#)) that examined the effect of high PM₁₀ exposures during the third trimester of pregnancy on the risk of preterm delivery, found that women with the GSTM1 null genotype were at an increased risk of preterm birth. When examining the interaction between high PM₁₀ concentrations during the third trimester of pregnancy and the presence of the GSTM1 null genotype on the risk of preterm delivery, there was evidence for a synergistic gene-environment interaction in pregnant women. This effect could occur due to oxidative stress induced by metals contained in PM₁₀, and subsequently could be modified by polymorphisms of the GSTM1 gene. This oxidative stress causes oxidative DNA damage in fetal tissues, which may lead to preterm delivery via a reduction in placental blood flow.

An examination of other genes outside the GST pathway have also been conducted to determine if specific polymorphisms increase the susceptibility of individuals to PM. Baccarelli et al. (2008, [157984](#)) in the Normative Aging Study observed that individuals with polymorphisms in MTHFR (C677T methylenetetrahydrofolate reductase), an alteration associated with reduced enzyme activity, and cSHMT (cytoplasmic serine hydroxymethyltransferase) (i.e., [CT/TT] MTHFR and [CC] cSHMT genotypes), alterations associated with higher homocysteine levels, have a reduction in SDNN, upon exposure to PM_{2.5}. Peters et al. (2009, [191992](#)) examined single nucleotide polymorphisms (SNPs) in the fibrinogen gene in myocardial infarction survivors to assess whether exposure to PM₁₀ altered steady state levels of fibrinogen, which has been implicated in promoting atherothrombosis. The authors found that individuals with single nucleotide polymorphisms (SNPs) in the fibrinogen gene have higher baseline fibrinogen levels which when combined with the inflammatory effects (i.e., increased fibrinogen levels) associated with exposure to PM could increase their risk of PM-related cardiovascular health effects. These results taken together suggest that individuals with null alleles or specific polymorphisms in genes that mediate the antioxidant response to oxidative stress, regulate enzyme activity, or regulate levels of procoagulants are more susceptible to PM. However, in some cases genetic polymorphisms may actually reduce an individual's susceptibility to PM-related health effects. For example, Park et al. (2006, [091245](#)) found that individuals with two hemochromatosis (HFE) polymorphisms (C282Y and H63D), which result in an increase in iron uptake, had smaller reductions in HRV upon exposure to PM_{2.5}. This

effect could possibly be due to the reduction in free iron that enters oxidation-reduction (redox) reactions and the subsequent reduction in reactive oxygen species (ROS).

More recently, studies have begun to focus on epigenetic effects associated with PM exposure (i.e., the effect of PM on DNA methylation) due to the fact that DNA methylation can result in gene alterations. The limited number of epidemiologic studies that examined epigenetic effects have found some evidence that long-term exposure to PM_{2.5} and PM₁₀ can influence DNA methylation (Baccarelli et al., 2009, [188183](#); Tarantini et al., 2009, [192010](#)). Additionally, a toxicological study found some evidence of hypermethylation of spermatogonial stem cells in response to the PM component of ambient urban air (Yauk et al., 2008, [157164](#)). Although epigenetic effects have been observed in response to PM exposure in some studies additional research is needed to more accurately characterize these associations.

Overall, the evidence suggests that specific genetic polymorphisms can potentially increase the susceptibility of an individual to PM exposure, but protective polymorphisms also exist, which may diminish the health effects attributed to PM exposure in some individuals. In addition, the studies that examine genetic polymorphisms or epigenetics can potentially provide additional information that can aid in identifying the specific pathways and mechanisms by which PM initiates health effects.

8.1.6. Pre-Existing Disease

In 2004, the National Research Council (NRC) published a report that emphasized the need to evaluate the effect of air pollution on susceptible populations, including those with respiratory illnesses and cardiovascular diseases (NRC, 2004, [156814](#)). The 2004 PM AQCD included epidemiologic evidence suggesting that individuals with pre-existing heart and lung diseases, as well as diabetes may be more susceptible to PM exposure. In addition, toxicological studies that used animal models of cardiopulmonary diseases and heightened allergic sensitivity found evidence of enhanced susceptibility. More recent epidemiologic and human clinical studies have directly examined the effect of PM on individuals with pre-existing diseases and toxicological studies have employed disease models to identify whether exposure to PM disproportionately affects certain populations.

8.1.6.1. Cardiovascular Diseases

The potential effect of underlying cardiovascular diseases on PM-related health responses has been examined using epidemiologic studies that stratify effect estimates by underlying conditions or secondary diagnoses, and toxicological studies that use animal models to mimic the physiological conditions associated with various cardiovascular diseases (e.g., MI, ischemia, and atherosclerosis). A limited number of controlled human exposure studies have also examined the potential relationship between CVD and exposure to PM in individuals with underlying cardiovascular conditions, but these studies have provided somewhat inconsistent evidence for these associations.

The majority of the epidemiologic literature that examined the association between short-term exposure to PM and cardiovascular outcomes focuses on cardiovascular-related hospital admissions and emergency department (ED) visits. Hypertension is the pre-existing condition that has been considered to the greatest extent when examining the association between short-term exposure to PM and cardiovascular-related HAs and ED visits. Pope et al. (2006, [091246](#)) found no evidence of effect modification of the IHD ED visit association with PM_{2.5} in individuals with secondary hypertension in Utah. This is consistent with the results of both Wellenius et al. (2006, [088748](#)) in 7 U.S. cities and Lee et al. (2008, [192076](#)) in Taipei, which found that hypertension did not modify the association between PM₁₀ and cardiovascular-related health outcomes. These results differ from those presented by Peel et al. (2007, [090442](#)), in Atlanta, which observed that exposure to PM₁₀ resulted in an increase in ED visits for arrhythmias and CHF in individuals with underlying hypertension. An additional study conducted by Park et al. (2005, [057331](#)) in Boston found that underlying hypertension increased associations between HRV, specifically a reduction in the HF parameter, and short-term exposure to PM_{2.5}.

Park et al. (2005, [057331](#)), in the analysis mentioned above, examined other underlying cardiovascular conditions and found associations between PM_{2.5} and HRV in individuals with pre-existing IHD. In a toxicological study, Wellenius et al. (2003, [055691](#)) examined the effects of

PM_{2.5} CAPs exposure on induced myocardial ischemia in dogs, which mimics the effects associated with IHD. The authors found that exposure to PM_{2.5} prior to the induced ischemia increased ST-segment elevation, indicating greater ischemia than air-exposed animals (Wellenius et al., 2003, [055691](#)). A follow-up study implicated impaired myocardial blood flow in the response (Bartoli et al., 2009, [179904](#)).

Additional studies examined the effects of PM on cardiac function in individuals with dysrhythmia. Peel et al. (2007, [090442](#)) observed some evidence for an increase in ED visits for IHD for individuals with secondary dysrhythmia and PM₁₀ exposure. However, when examining CHF hospital admissions in 7 U.S. cities, Wellenius et al. (2006, [088748](#)) found no evidence for effect modification of PM₁₀ exposure in individuals with secondary dysrhythmia.

Limited evidence is available from epidemiologic studies that examined other pre-existing cardiovascular conditions, such as CHF and MI. Pope et al. (2006, [091246](#)) observed an increase in hospital admissions for acute IHD in individuals with underlying CHF upon short-term exposure to PM_{2.5}. However, Peel et al. (2007, [090442](#)) did not find that underlying CHF contributed to an increase in the association between IHD ED visits and short-term exposure to PM₁₀. Zanobetti and Schwartz (2005, [088069](#)) also examined the potential effect modification of the association between PM₁₀ and cardiovascular-related health effects in individuals with CHF, but used MI hospital admissions as the outcome of interest. Underlying CHF was not found to increase MI hospital admissions for exposure to PM₁₀ in the cohort of more than 300,000 hospital admissions.

Wellenius et al. (2006, [088748](#)) examined the effect of previous diagnoses of acute MI on the association between CHF hospital admissions and short-term exposure to PM₁₀ in 7 U.S. cities. In this study, Wellenius et al. (2006, [088748](#)) found no evidence of effect modification of the relationship between PM₁₀ and CHF hospital admissions by previous acute MI. Toxicological studies have provided additional evidence for the cardiovascular health effects associated with exposure to PM in individuals with underlying MI. Anselme et al. (2007, [097084](#)) and Wellenius et al. (2006, [156152](#)) examined the arrhythmic effects of PM on rats that experienced an MI using two different models. Wellenius et al. (2006, [156152](#)) used a post-myocardium sensitivity model (acute MI) and observed that exposure to PM_{2.5} CAPs decreased ventricular premature beats and spontaneous supraventricular ectopic beats. In contrast, the MI model of chronic heart failure (i.e., rats that experienced an MI 3 mo prior to exposure), demonstrated a prominent increase in the incidence of premature ventricular contraction when exposed to DE (Anselme et al., 2007, [097084](#)). The discrepancy in effects observed between studies could be due to differences in the MI model or the PM exposure (i.e., CAPs vs. DE).

Additional toxicological studies examined the association between PM and pre-existing cardiovascular diseases using a murine model of atherosclerosis (ApoE^{-/-} mouse). For example, Campen et al. (2005, [083977](#); 2006, [096879](#)) examined the heart rate and ECG effects of acute exposure to PM on ApoE^{-/-} mice. With DE, dramatic bradycardia and T-wave depression were observed that were attributable to the gases (Campen et al., 2005, [083977](#)), while whole gasoline emissions induced T-wave alterations that required particles (Campen et al., 2006, [096879](#)). However, these studies along with others that used this mouse model (see Section 6.2 and 7.2) did not compare the effects observed with the ApoE^{-/-} mouse to other non-diseased mouse models, so it is unclear if the responses would differ if other strains were used in the same experimental protocol.

Controlled human exposure studies that examined the effect of pre-existing diseases on cardiovascular outcomes with exposure to PM are less consistent and difficult to interpret in the context of the results from the epidemiologic and toxicological studies. Mills et al. (2007, [091206](#); 2008, [156766](#)) investigated the effects of dilute DE, or fine and ultrafine CAPs, respectively, on subjects with coronary artery disease and prior MI. Exposure to dilute DE was found to promote exercise-induced ST-segment changes indicating myocardial ischemia, as well as inhibit endogenous fibrinolytic capacity (Mills et al., 2007, [091206](#)). The physiological responses observed in Mills et al. (2007, [091206](#)) provides a measure of coherency with the cardiovascular effects observed in epidemiologic studies, including increases in hospital admissions and ED visits for IHD and stroke associated with exposure to PM. An examination of fine and ultrafine CAPs that were low in combustion derived particles, were not found to exhibit any significant effects on vascular function (Mills et al., 2008, [156766](#)). Routledge et al. (2006, [088674](#)) reported no change in HRV in a group of adults with coronary artery disease following exposure to ultrafine carbon particles, which may be explained in part by the use of medication (beta blockers) among the majority of the subjects. Although the epidemiologic studies did not examine potential effect modification of pre-existing cardiovascular conditions on effects associated with long-term exposure to PM, a few

toxicological studies exposed animals with underlying cardiovascular conditions to PM for months. In studies that focused on the cardiovascular effects following subchronic exposure to PM in ApoE^{-/-} mice, relatively consistent physiological effects were observed across studies. Araujo et al. (2008, [156222](#)) exposed mice to ultrafine CAPs and observed enhanced size of early atherosclerotic lesions. Similarly, Chen and Nadziejko (2005, [087219](#)) and Sun et al. (2005, [087952](#); 2008, [157033](#)) exposed mice to PM_{2.5} CAPs with the same results. An additional long-term exposure study observed a decreasing trend in heart rate, physical activity, and temperature along with biphasic responses in HRV (SDNN and rMSSD) upon exposure to CAPs (Chen and Hwang, 2005, [087218](#)).

While the majority of the literature examines the potential modification of the association between PM and non-fatal cardiovascular health effects, a few new studies have also examined effect modification in mortality associations. Zeka et al. (2006, [088749](#)) found an increase in risk estimates for associations between PM₁₀ and mortality in individuals with underlying stroke, while Bateson et al. (2004, [086244](#)) found evidence for effect modification of the PM-mortality association in individuals with CHF.

Collectively, the evidence from epidemiologic and toxicological, and to a lesser extent, controlled human exposure studies indicates that individuals with underlying cardiovascular diseases are susceptible to PM exposure. Although the evidence for some outcomes was inconsistent across epidemiologic and toxicological studies, this could be due to a variety of issues including the PM size fraction used in the study along with the study location. Even with these caveats, a large proportion of the U.S. population has been diagnosed with cardiovascular diseases (i.e., approximately 51.6 million people with hypertension, 24.1 million with heart disease, and 14.1 million with coronary heart disease [see Table 8-3]), and therefore represents a large population that is potentially more susceptible to PM exposure than the general population.

Table 8-3. Percent of the U.S. population with respiratory diseases, cardiovascular diseases, and diabetes.

Chronic Condition/ Disease	Adults (18+)* Number (x 10 ⁶)	%	Age					Regional			
			18-44	45-64	65-74	75+	NE	MW	S	W	
RESPIRATORY DISEASES											
Asthma*	24.2	11.0	11.5	10.5	11.7	9.3	11.7	11.5	10.5	10.8	
Asthma (<18 yrs)	6.8*	9.3*	---	---	---	---	---	---	---	---	
COPD											
Chronic bronchitis	9.5	4.3	2.9	5.5	5.6	6.7	3.8	4.4	4.9	3.5	
Emphysema	4.1	1.8	0.3	2.4	5.0	6.4	1.4	2.3	1.9	1.6	
CARDIOVASCULAR DISEASES											
All heart disease	24.1	10.9	3.6	12.3	26.1	36.3	10.8	12.7	10.9	9.2	
Coronary heart disease	14.1	6.4	0.9	7.2	18.4	25.5	6.4	7.6	6.6	4.7	
Hypertension	51.6	23.4	7.7	32.4	52.7	53.5	22.2	23.7	25.3	20.6	
Stroke	5.6	2.6	0.5	2.4	7.6	11.2	2.1	2.8	2.9	2.2	
Diabetes	17.1	7.8	2.6	10.4	18.2	17.9	7.2	8.1	8.0	7.4	

* All data for adults except asthma prevalence data for children under 18 years of age, from CDC (2008, [156324](#); 2008, [156325](#)). For adults prevalence data based off adults responding to "ever told had asthma."

Source: Data from Pleis and Lethbridge-Çejku (2007, [156875](#)); CDC (2008, [156324](#); 2008, [156325](#)).

8.1.6.2. Respiratory Illnesses

Investigators have examined the effect of pre-existing respiratory illnesses on multiple health outcomes (e.g., mortality, asthma symptoms, CHF) in response to exposure to ambient levels of PM. Animal models have been developed and/or human clinical studies conducted to examine the possible PM effects on pre-existing respiratory conditions in a controlled setting.

Epidemiologic studies have examined the effect of short-term exposure to PM on the respiratory health of asthmatic individuals measuring a variety of respiratory outcomes. Asthmatic individuals were found to have an increase in medication use (Rabinovitch et al., 2006, [088031](#)), respiratory symptoms (i.e., asthma symptoms, cough, shortness of breath, and chest tightness) (Gent et al., 2003, [052885](#)), and asthma symptoms (Delfino et al., 2002, [093740](#); 2003, [050460](#)) with short-term exposure to PM_{2.5}; and morning symptoms (Mortimer et al., 2002, [030281](#)) and asthma attacks (Desqueyroux et al., 2002, [026052](#)) with short-term exposure to PM₁₀.

Toxicological studies that have used ovalbumin-induced allergic airway disease models provide evidence which supports the findings of the epidemiologic literature. Morishita et al. (2004, [087979](#)) used this model to assess the health effects of PM_{2.5} components. In response to short-term exposure to CAPs from Detroit, an area with pediatric asthma rates three times the national average, rats with allergic airway disease were found to preferentially retain PM derived from identified local combustion sources in association with eosinophil influx and BALF protein content after an acute exposure (Morishita et al., 2004, [087979](#)). These findings suggest that individuals with allergic airways conditions are more susceptible to allergic airways responses upon exposure to PM_{2.5}, which may be partially attributed to increased pulmonary deposition and localization of particles in the respiratory tract (Morishita et al., 2004, [087979](#)). An additional study (Heidenfelder et al., 2009, [190026](#)) examined whether genes are differentially expressed upon exposure to PM. They found that exposure to CAPs increased the expression of genes associated with inflammation and airway remodeling in rats with allergic airway disease. Although the evidence is much more limited, not all of the toxicological studies evaluated that examined the effect of underlying respiratory conditions on PM-related respiratory morbidity focused on allergic airways disease. Using an animal model of emphysema (i.e., papain-treated mice), Lopes et al. (2009, [190430](#)) found that papain-treated mice exposed to urban ambient PM demonstrated a statistically significant increase in mean linear intercept, a measure of airspace enlargement, compared to saline-treated controls exposed to filtered air. These results provide preliminary evidence, which suggests that non-allergic respiratory morbidities may also increase the susceptibility of an individual to PM-related respiratory effects.

The results from the epidemiologic and toxicological studies that focused on underlying allergic airways disease is supported by a series of controlled human exposure studies which have shown that exposure to DEPs increases the allergic inflammatory response in atopic individuals (Bastain et al., 2003, [098690](#); Diaz-Sanchez et al., 1997, [051247](#); Nordenhall et al., 2001, [025185](#)). However, not all controlled human exposure studies have found evidence for differences between the respiratory effects exhibited by healthy and asthmatic individuals. Studies by Gong et al. (2003, [042106](#); 2004, [055628](#); Gong et al., 2008, [156483](#)) reported that healthy and asthmatic subjects exposed to coarse, fine and ultrafine CAPs, exhibited similar respiratory responses. However, it should be noted that these studies excluded moderate and severe asthmatics that would be expected to show increased susceptibility to PM exposure.

In addition to examining the association between exposure to PM and respiratory effects in asthmatics, some studies examined whether individuals with COPD represent a potentially susceptible population. Desqueyroux et al. (2002, [026052](#)) did not observe an increase in the exacerbation¹ of COPD in response to short-term exposure to PM_{2.5}. However, studies that examined the effect of PM on lung function in individuals with COPD (Lagorio et al., 2006, [089800](#); Trenga et al., 2006, [155209](#)) observed declines in FEV₁, and FEV₁ and FVC, respectively in response to PM₁₀ and/or PM_{2.5}. Silkoff et al. (2005, [087471](#)) observed associations between PM₁₀ and a reduction in FEV₁ and PM_{2.5} and a reduction in PEF, in those with COPD, but only during one winter of the analysis. Only one controlled human exposure study examined the effects of PM on COPD subjects and found no significant difference in respiratory effects between healthy and individuals with COPD upon exposure to PM_{2.5} CAPs (Gong et al., 2004, [055628](#)). On the other hand the results from dosimetry studies have shown that COPD patients have increased dose rates and impaired

¹ Desqueyroux et al. (2002, [026052](#)) defined a COPD exacerbation as (a) decrease in “vesicular” breath sound, (b) bronchial obstruction, (c) tachycardia or arrhythmia, or (d) cyanosis.

mucociliary clearance relative to age matched healthy subjects, suggesting that individuals with COPD are potentially at a greater risk of PM-related health effects (Sections 4.2.4.5 and 4.3.4.3).

A few of the epidemiologic studies examined the effect of underlying respiratory illnesses on the association between short- and long-term exposure to PM and mortality. Using different pre-existing respiratory illnesses, Zeka et al. (2006, [088749](#)) and De Leon et al. (2003, [055688](#)) found that short-term exposure to PM₁₀ increased the risk of nonaccidental mortality for pneumonia and circulatory mortality for all respiratory illnesses, respectively. Additionally, Zanobetti et al. (2008, [156177](#)) observed an association between long-term exposure to PM₁₀ and mortality in individuals that had previously been hospitalized for COPD. Although these studies do not examine additional size fractions of PM, together they highlight the potential effect of underlying respiratory illnesses on the PM-mortality relationship.

Overall, the epidemiologic, controlled human exposure, and toxicological studies evaluated provide biological plausibility for the increased health effects observed in epidemiologic studies among asthmatic individuals in response to PM exposure. Although, the evidence from studies that examined associations between PM and health effects in individuals with COPD is inconsistent, taken together individuals with COPD and asthma represent a large percent of the U.S. population (~45 million people), which may be more susceptible to PM-related health effects (Table 8-3).

8.1.6.3. Respiratory Contributions to Cardiovascular Effects

Although the majority of health effects observed in individuals with pre-existing respiratory illnesses were associated with respiratory illness exacerbations, studies also examined whether underlying respiratory illnesses can lead to cardiovascular effects in response to PM exposure. Controlled human exposure and toxicological studies have also observed some cardiovascular effects in individuals with pre-existing respiratory illnesses. Gong et al. (2003, [042106](#)) observed acute responses in the cardiovascular system and systemic circulation among asthmatic individuals after exposure to PM_{2.5} CAPs. However, respiratory disease has not consistently been observed to affect cardiovascular response in controlled human exposure studies. In a toxicological study, Batalha et al. (2002, [088109](#)), using a chronic bronchitis animal model, found that the pulmonary artery lumen-to-wall ratio was decreased in rats exposed to PM_{2.5} CAPs, although the induced bronchitis didn't seem to affect the response. The majority of epidemiologic studies that examined whether underlying respiratory illnesses contributed to the manifestation of PM-related cardiovascular hospital admission or ED visits, did not report increases in effects for a variety of cardiovascular outcomes (e.g., IHD, arrhythmias, CHF, MI) for individuals with underlying respiratory infection (Wellenius et al., 2006, [088748](#)), pneumonia (Zanobetti and Schwartz, 2005, [088069](#)), or COPD (Peel et al., 2007, [090442](#); Wellenius et al., 2005, [087483](#)). However, Yeatts et al. (2007, [091266](#)), in a panel study, found evidence for cardiovascular effects, specifically reductions in HRV parameters, in asthmatic adults upon short-term exposure to PM_{10-2.5}. It must be noted that most of the aforementioned epidemiologic studies focused on exposure to PM₁₀, and, therefore, it is unclear how these results compare to those found in the controlled human exposure and toxicological studies that focused on exposure to PM_{2.5} (e.g., CAPs). Thus, it is unclear if individuals with underlying respiratory illnesses represent a population that is potentially susceptible to PM-related cardiovascular effects.

8.1.6.4. Diabetes and Obesity

It has been hypothesized that the systemic inflammatory cascade leads to an increase in cardiovascular risk (Dubowsky et al., 2006, [088750](#)). As a result, individuals with conditions linked to chronic inflammation (i.e., diabetes and obesity), have been examined to determine whether diabetes or obesity facilitate the manifestation of PM-mediated health effects, and, therefore, represent a potentially susceptible population.

Epidemiologic studies have examined whether diabetes modifies the association between cardiovascular health effects and PM exposure, but these studies have primarily focused on short-term exposure to PM₁₀. Time-series studies have provided evidence through an examination of hospital admission and ED visits and mortality, which suggests an increase in health effects in diabetic individuals in response to PM exposure. Multicity studies have found upwards of 75% greater risk of hospitalization for cardiac diseases in individuals with diabetes upon exposure to PM₁₀ (Zanobetti and Schwartz, 2002, [034821](#)). Studies conducted in Atlanta, Georgia have also

found increased risk for cardiovascular-related ED visits in diabetics, specifically for IHD, arrhythmias, and CHF (Peel et al., 2007, [090442](#)). Additional studies found some evidence that individuals with diabetes are at increased risk of mortality upon exposure to PM₁₀ (Zeka et al., 2006, [088749](#)) and PM_{2.5} (Goldberg et al., 2006, [088641](#)). However, some studies (both multicity and single-city) have not observed a modification of the risk of cardiovascular ED visits and hospital admissions in response to exposure to PM₁₀ in diabetics (Pope et al., 2006, [091246](#); Wellenius et al., 2006, [088748](#); Zanobetti and Schwartz, 2005, [088069](#)).

Panel and cohort studies have been conducted to determine the physiological changes that occur in individuals with diabetes in response to PM exposure. These studies examined both changes in inflammatory markers along with specific physiological alterations in the cardiovascular system. Schneider et al. (2008, [191985](#)) in a panel study of 22 individuals with type 2 diabetes mellitus in Chapel Hill, NC found evidence that ambient exposure to PM_{2.5} enhanced the reduction in various markers of endothelial function. Liu et al. (2007, [156705](#)) observed an increase in end-diastolic FMD and end-systolic FMD, and decreases in end-diastolic basal diameter and end-systolic basal diameter in diabetics upon exposure to PM₁₀. The authors also observed positive associations with FMD and blood pressure in diabetic individuals. A controlled human exposure study conducted by Carlsten et al. (2008, [156323](#)) found that DE did not elicit any prothrombotic effects in subjects with metabolic syndrome, which consists of physiological alterations similar to those observed in both diabetic and obese individuals. An examination of biomarkers found mixed results, with Liao et al. (2005, [088677](#)) observing an increase in vWF; Liu et al. (2007, [156705](#)) observing an increase in TBARS, but not CRP or TNF- α ; and Dubowsky et al. (2006, [088750](#)) observing an increase in CRP and WBCs. Overall, it is unclear how differences in each of the aforementioned biomarkers contribute to the potential overall cardiovascular effect observed in diabetic individuals; however, an increase in inflammation, oxidative stress, and acute phase response may contribute to cardiovascular effects. A recent toxicological study (Sun et al., 2009, [190487](#)), also demonstrated the potential for PM-related health effects in diabetics. Sun et al. (2009, [190487](#)) found that PM_{2.5} CAPs exposure for 4 mo can exaggerate insulin resistance, visceral adiposity, and inflammation in a diet-induced obesity mouse model.

Overall, epidemiologic studies have reported evidence for increased effects in diabetics in response to PM exposure, with preliminary evidence for pathophysiologic alterations from toxicological studies. This potentially susceptible population is large, with an estimated 17.1 million diabetic individuals in the U.S. (Table 8-3). However, the limited evidence from toxicological and controlled human exposure studies along with the lack of studies that examined additional PM size fractions warrants additional research to confirm the associations observed and to identify the biological pathway(s) that may result in a greater response to PM in diabetics.

In addition to diabetes, obesity has been examined as a health condition with the potential to lead to an increase in PM-related health effects. Only a few recent studies have examined the potential effect modification of PM risk estimates by obesity. Schwartz et al. (2005, [086296](#)) reported a change in HRV in obese (i.e., BMI ≥ 30 kg/m²) compared to non-obese subjects, while Dubowsky et al. (2006, [088750](#)) observed an increase in inflammatory markers (i.e., CRP, IL-6, and WBC) in response to short-term exposure to PM_{2.5} among obese individuals. Additionally, Schneider et al. (2008, [191985](#)) found some evidence for a larger reduction in FMD in individuals with a BMI >30 kg/m³ in response to PM_{2.5} exposure. These effects could be due, in part, to a higher PM dose rate in obese individuals, which has been demonstrated in children by Bennett and Zeman (2004, [155686](#)). These investigators also reported that tidal volume and resting minute ventilation increased with body mass index. Although a limited amount of research has been conducted to examine PM-related health effects in obese individuals there is an increasing trend of individuals within the U.S. that have been defined as overweight (BMI ≥ 25.0) or obese (BMI ≥ 30.0), with the prevalence of overweight individuals increasing from 20-74% from 1960 to 2004, and the prevalence of obese individuals increasing from 13.3-32.1% (NCHS, 2006, [198921](#)).

8.1.7. Socioeconomic Status

SES is a composite measure that usually consists of economic status, measured by income; social status measured by education; and work status measured by occupation (Dutton and Levine, 1989, [192052](#)). Based on data from the U.S. Census Bureau in 2006, from among commonly-used indicators of SES, about 12% of individuals and 11% of families are below the poverty line (U.S. Census, 2009, [192147](#)). Although the measure of SES is composed of a multitude of

surrogates, each of these linked factors can influence an individual's susceptibility to PM-related health effects. Additionally, low SES individuals have been found to have a higher prevalence of pre-existing diseases; inadequate medical treatment; and limited access to fresh foods leading to a reduced intake of antioxidant polyunsaturated fatty acids and vitamins, which can increase this population's susceptibility to PM (Kan et al., 2008, [156621](#)).

Surrogates of SES, such as educational attainment, have been shown in some studies to modify health outcomes of PM exposure for a population. Within the U.S. approximately 16% of the population does not have a high school degree and only 27% have a bachelor's degree or higher level of education (U.S. Census, 2009, [192148](#)). Educational attainment generally coincides with an individual's income level, which is correlated to other surrogates of SES, such as residential environment (Jerrett et al., 2004, [087379](#)). Franklin et al. (2008, [097426](#)) noted an increased risk in mortality associated with short-term exposure to PM_{2.5} and its components for individuals with low SES while additional analyses stratified by education level have also observed consistent trends of increased mortality for PM_{2.5} and PM_{2.5} species for individuals with low educational attainment (Ostro et al., 2006, [087991](#); Ostro et al., 2008, [097971](#); Zeka et al., 2006, [088749](#)). This is further supported by a reanalysis of the ACS cohort (Krewski et al., 2009, [191193](#)), which found moderate evidence for increased lung cancer mortality in individuals with a high school education or less compared to individuals with more than a high school education in response to long-term exposure to PM_{2.5}. However, when examining education level and IHD mortality due to long-term exposure to PM_{2.5} Krewski et al. (2009, [191193](#)) observed an inverse relationship.

Epidemiologic studies have also examined additional surrogates of SES, such as residential location and nutritional status to identify their influence on the susceptibility of a population. Jerrett et al. (2004, [087379](#)) examined the modification of acute mortality effects due to particulate air pollution exposure by residential location in Hamilton, Canada using educational attainment as a surrogate for SES. The authors found that the area of the city with the highest SES characteristics displayed no evidence of effect modification while the area with the lowest SES characteristics had the largest health effects. Likewise, Wilson et al. (2007, [157149](#)) examined the effect of SES on the association between mortality and short-term exposure to PM in Phoenix, but used educational attainment and income to represent SES. When stratifying Phoenix into central, middle, and outer rings of varying urban density central Phoenix, the area with the lowest SES, was found to exhibit the greatest association with PM_{2.5}. However, the association with urban density differed when examining PM_{10-2.5}, with the greatest effect being observed for the middle ring. Yanosky et al. (2008, [192081](#)) examined whether long-term exposure to traffic-related pollutants, using NO₂ as a surrogate, varied by SES at the block group level. The authors found higher levels of NO₂ associated with lower SES areas, which suggests that lower SES individuals are disproportionately exposed to traffic-related pollutants, which includes PM.

Nutritional deficiencies have been associated with increased susceptibility to a variety of infectious diseases and chronic health effects. Low SES may decrease access to fresh foods, and thus be related to nutritional deficiencies that could increase susceptibility to PM-related health effects. Baccarelli et al. (2008, [157984](#)) examined the association between exposure to PM_{2.5} and HRV in individuals with polymorphisms in MTHFR and cSHMT genes, which are associated with reduced enzyme activity and increased risk of CVD. The authors found that when individuals with these genetic polymorphisms increased their intake (above median levels) of B₆, B₁₂, or methionine no PM_{2.5} effect on HRV was observed.

8.1.8. Summary

Upon evaluating the association between short- and long-term exposure to PM and various health outcomes, studies also attempted to identify populations that are more susceptible to PM. These studies did so by: conducting stratified analyses; examining individuals with an underlying health condition; or developing animal models that mimic the physiological conditions associated with an adverse health effect. These studies identified a multitude of factors that could potentially contribute to whether an individual is susceptible to PM (Table 8-2). Although studies have primarily used exposures to PM₁₀ or PM_{2.5}, the available evidence suggests that the identified factors may also enhance susceptibility to PM_{10-2.5}.

The majority of observations made during the evaluation of the literature reviewed in this ISA are consistent with those reported in the 2004 PM AQCD. An evaluation of age-related health effects suggests that older adults have heightened responses for cardiovascular morbidity with PM exposure.

In addition, epidemiologic and toxicological studies provide evidence, which indicates that children are at an increased risk of PM-related respiratory effects. It should be noted that the health effects observed in children could be initiated by exposures to PM that occurred during key windows of development, such as in utero. Studies that focus on exposures during development have reported inconsistent findings (see Section 7.4.), but a recent toxicological study suggests that inflammatory responses in pregnant women due to exposure to PM could result in health effects in the developing fetus.

Epidemiologic studies have also examined whether additional factors, such as gender, race, or ethnicity modify the association between PM and morbidity and mortality outcomes. Consistent with the findings of the 2004 PM AQCD, gender and race do not seem to modify the association between PM and morbidity and mortality outcomes. However, some evidence, albeit from two studies conducted in California, suggest that Hispanic ethnicity may modify the association between PM and mortality.

Recent epidemiologic and toxicological studies provided evidence that individuals with null alleles or polymorphisms in genes that mediate the antioxidant response to oxidative stress (i.e., GSTM1), regulate enzyme activity (i.e., MTHFR and cSHMT), or regulate levels of procoagulants (i.e., fibrinogen) are more susceptible to PM exposure. However, some studies have shown that polymorphisms in genes (e.g., HFE) can have a protective effect upon PM exposure. Additionally, preliminary evidence suggests that PM exposure can impart epigenetic effects (i.e., DNA methylation), however, this requires further investigation.

Collectively, the evidence from epidemiologic and toxicological, and to a lesser extent, controlled human exposure studies indicate increased susceptibility of individuals with underlying cardiovascular diseases and respiratory illnesses, specifically asthma, to PM exposure. Additional controlled human exposure and toxicological studies provide some evidence for increased PM-related cardiovascular effects in individuals with underlying respiratory health conditions. However, the results are not consistent with epidemiologic studies, resulting in the need for further investigation.

Recently studies have begun to examine the influence of preexisting chronic inflammatory conditions, such as diabetes and obesity, on PM-related health effects. These studies have found some evidence for increased associations for cardiovascular outcomes along with physiological alterations in markers of inflammation, oxidative stress, and acute phase response. However more research is needed to thoroughly examine the effect of PM exposure on obese individuals and to identify the biological pathway(s) that could lead to increased susceptibility of diabetic and obese individuals to PM.

There is also evidence that SES, measured using surrogates such as educational attainment or residential location, modifies the association between PM and morbidity and mortality outcomes. In addition, nutritional status, another surrogate of SES, has been shown to have protective effects against PM exposure in individuals that have a higher intake in some vitamins and nutrients.

Overall, the epidemiologic, controlled human exposure, and toxicological studies evaluated in this review provide evidence for increased susceptibility for various populations. Although the level of evidence varies depending on the factor being evaluated collectively, it can be concluded that some populations are more susceptible to PM than the general population.

Chapter 8 References

- Aday LA (2001). At risk in America: The health and health care needs of vulnerable populations in the United States. San Francisco, CA: Jossey-Bass, Inc. [192150](#)
- American Lung Association (2001). Urban air pollution and health inequities: A workshop report. *Environ Health Perspect*, 3: 357-374. [016626](#)
- Anselme F; Lorient S; Henry J-P; Dionnet F; Napoleoni J-G; Thnillez C; Morin J-P (2007). Inhalation of diluted diesel engine emission impacts heart rate variability and arrhythmia occurrence in a rat model of chronic ischemic heart failure. *Arch Toxicol*, 81: 299-307. [097084](#)
- Araujo JA; Barajas B; Kleinman M; Wang X; Bennett BJ; Gong KW; Navab M; Harkema J; Sioutas C; Lusk AJ; Nel AE (2008). Ambient particulate pollutants in the ultrafine range promote early atherosclerosis and systemic oxidative stress. *Circ Res*, 102: 589-596. [156222](#)
- Baccarelli A; Martinelli I; Pegoraro V; Melly S; Grillo P; Zanobetti A; Hou L; Bertazzi PA; Mannucci PM; Schwartz J (2009). Living near Major Traffic Roads and Risk of Deep Vein Thrombosis. *Circulation*, 119: 3118-3124. [188183](#)
- Baccarelli A; Martinelli I; Zanobetti A; Grillo P; Hou LF; Bertazzi PA; Mannucci PM; Schwartz J (2008). Exposure to Particulate Air Pollution and Risk of Deep Vein Thrombosis. *Arch Intern Med*, 168: 920-927. [157984](#)
- Barnett AG; Williams GM; Schwartz J; Best TL; Neller AH; Petroeschevsky AL; Simpson RW (2006). The effects of air pollution on hospitalizations for cardiovascular disease in elderly people in Australian and New Zealand cities. *Environ Health Perspect*, 114: 1018-1023. [089770](#)
- Bartoli CR; Wellenius GA; Coull BA; Akiyama I; Diaz EA; Lawrence J; Okabe K; Verrier RL; Godleski JJ (2009). Concentrated ambient particles alter myocardial blood flow during acute ischemia in conscious canines. *Environ Health Perspect*, 117: 333-337. [179904](#)
- Bastain TM; Gilliland FD; Li Y-F; Saxon A; Diaz-Sanchez D (2003). Intraindividual reproducibility of nasal allergic responses to diesel exhaust particles indicates a susceptible phenotype. *Clin Immunol*, 109: 130-136. [098690](#)
- Batalha JR; Saldiva P H; Clarke RW; Coull BA; Stearns RC; Lawrence J; Murthy GG; Koutrakis P; Godleski JJ (2002). Concentrated ambient air particles induce vasoconstriction of small pulmonary arteries in rats. *Environ Health Perspect*, 110: 1191-1197. [088109](#)
- Bateson TF; Schwartz J (2004). Who is sensitive to the effects of particulate air pollution on mortality? A case-crossover analysis of effect modifiers. *Epidemiology*, 15: 143-149. [086244](#)
- Bennett WD; Zeman KL (2004). Effect of body size on breathing pattern and fine-particle deposition in children. *J Appl Physiol*, 97: 821-826. [155686](#)
- Boezen HM; Vonk JM; Van Der Zee SC; Gerritsen J; Hoek G; Brunekreef B; Schouten JP; Postma DS (2005). Susceptibility to air pollution in elderly males and females. *Eur Respir J*, 25: 1018-1024. [087396](#)
- Campen MJ; Babu NS; Helms GA; Pett S; Wernly J; Mehran R; McDonald JD (2005). Nonparticulate components of diesel exhaust promote constriction in coronary arteries from ApoE ^{-/-} mice. *Toxicol Sci*, 88: 95-102. [083977](#)
- Campen MJ; McDonald JD; Reed MD; Seagrave J (2006). Fresh gasoline emissions, not paved road dust, alter cardiac repolarization in ApoE ^{-/-} mice. *Cardiovasc Toxicol*, 6: 199-210. [096879](#)
- Carlsten C; Kaufman JD; Trenga CA; Allen J; Peretz A; Sullivan JH (2008). Thrombotic markers in metabolic syndrome subjects exposed to diesel exhaust. *Inhal Toxicol*, 20: 917-921. [156323](#)
- CDC (2008). 2006 NHIS data: table 3-1: current asthma population estimates, in thousands by age, United States: national health interview survey, 2006. Retrieved 01-DEC-09, from <http://www.cdc.gov/ASTHMA/nhis/06/table3-1.htm>. [156324](#)

Note: Hyperlinks to the reference citations throughout this document will take you to the NCEA HERO database (Health and Environmental Research Online) at <http://epa.gov/hero>. HERO is a database of scientific literature used by U.S. EPA in the process of developing science assessments such as the Integrated Science Assessments (ISA) and the Integrated Risk Information System (IRIS).

- CDC (2008). 2006 NHIS data: table 4-1: current asthma prevalence percents by age, United States: national health interview survey, 2006. Retrieved 01-DEC-09, from <http://www.cdc.gov/ASTHMA/nhis/06/table4-1.htm>. [156325](#)
- Chahine T; Baccarelli A; Litonjua A; Wright RO; Suh H; Gold DR; Sparrow D; Vokonas P; Schwartz J (2007). Particulate air pollution, oxidative stress genes, and heart rate variability in an elderly cohort. *Environ Health Perspect*, 115: 1617-1622. [156327](#)
- Chen LC; Hwang JS (2005). Effects of subchronic exposures to concentrated ambient particles (CAPs) in mice IV Characterization of acute and chronic effects of ambient air fine particulate matter exposures on heart-rate variability. *Inhal Toxicol*, 17: 209-216. [087218](#)
- Chen LC; Nadziejko C (2005). Effects of subchronic exposures to concentrated ambient particles (CAPs) in mice V CAPs exacerbate aortic plaque development in hyperlipidemic mice. *Inhal Toxicol*, 17: 217-224. [087219](#)
- Chen LH; Knutsen SF; Shavlik D; Beeson WL; Petersen F; Ghamsary M; Abbey D (2005). The association between fatal coronary heart disease and ambient particulate air pollution: Are females at greater risk? *Environ Health Perspect*, 113: 1723-1729. [087942](#)
- Delfino RJ; Gone H; Linn WS; Pellizzari ED; Hu Y (2003). Asthma symptoms in Hispanic children and daily ambient exposures to toxic and criteria air pollutants. *Environ Health Perspect*, 111: 647-656. [050460](#)
- Delfino RJ; Zeiger RS; Seltzer JM; Street DH; McLaren CE (2002). Association of asthma symptoms with peak particulate air pollution and effect modification by anti-inflammatory medication use. *Environ Health Perspect*, 110: A607-A617. [093740](#)
- Desqueyroux H; Pujet J-C; Prosper M; Squinazi F; Momas I (2002). Short-term effects of low-level air pollution on respiratory health of adults suffering from moderate to severe asthma. *Environ Res*, 89: 29-37. [026052](#)
- Devlin RB; Ghio AJ; Kehrl H; Sanders G; Cascio W (2003). Elderly humans exposed to concentrated air pollution particles have decreased heart rate variability. *Eur Respir J*, 40: 76S-80S. [087348](#)
- De Leon SF; Thurston GD; Ito K (2003). Contribution of respiratory disease to nonrespiratory mortality associations with air pollution. *Am J Respir Crit Care Med*, 167: 1117-1123. [055688](#)
- Diaz-Sanchez D; Tsien A; Fleming J; Saxon A (1997). Combined diesel exhaust particulate and ragweed allergen challenge markedly enhances human in vivo nasal ragweed-specific IgE and skews cytokine production to a T helper cell 2-type pattern. *J Immunol*, 158: 2406-2413. [051247](#)
- Dubowsky SD; Suh H; Schwartz J; Coull BA; Gold DR (2006). Diabetes, obesity, and hypertension may enhance associations between air pollution and markers of systemic inflammation. *Environ Health Perspect*, 114: 992-998. [088750](#)
- Dutton DB; Levine S (1989). Overview, methodological critique, and reformulation. In JP Bunker; DS Gomby; BH Kehrer (Ed.), *Pathways to health* (pp. 29-69). Menlo Park, CA: The Henry J. Kaiser Family Foundation. [192052](#)
- Fedulov AV; Leme A; Yang Z; Dahl M; Lim R; Mariani TJ; Kobzik L (2008). Pulmonary exposure to particles during pregnancy causes increased neonatal asthma susceptibility. *Am J Respir Cell Mol Biol*, 38: 57-67. [097482](#)
- Firestone M; Moya J; Cohen-Hubal E; Zartarian V; Xue J (2007). Identifying childhood age groups for exposure assessments and monitoring. *Risk Anal*, 27: 701-714. [192071](#)
- Frampton MW; Stewart JC; Oberdorster G; Morrow PE; Chalupa D; Pietropaoli AP; Frasier LM; Speers DM; Cox C; Huang LS; Utell MJ (2006). Inhalation of ultrafine particles alters blood leukocyte expression of adhesion molecules in humans. *Environ Health Perspect*, 114: 51-58. [088665](#)
- Franklin M; Koutrakis P; Schwartz J (2008). The role of particle composition on the association between PM_{2.5} and mortality. *Epidemiology*, 19: 680-689. [097426](#)
- Franklin M; Zeka A; Schwartz J (2007). Association between PM_{2.5} and all-cause and specific-cause mortality in 27 US communities. *J Expo Sci Environ Epidemiol*, 17: 279-287. [091257](#)
- Fung KY; Luginaah I; Gorey KM; Webster G (2005). Air pollution and daily hospital admissions for cardiovascular diseases in Windsor, Ontario. *Can J Public Health*, 96: 29-33. [074322](#)
- Fung KY; Luginaah IKMG; Webster G (2005). Air pollution and daily hospitalization rates for cardiovascular and respiratory diseases in London, Ontario. *Int J Environ Stud*, 62: 677-685. [093262](#)

- Gent JF; Triche EW; Holford TR; Belanger K; Bracken MB; Beckett WS; Leaderer BP (2003). Association of low-level ozone and fine particles with respiratory symptoms in children with asthma. *JAMA*, 290: 1859-1867. [052885](#)
- Gilliland FD; Li YF; Saxon A; Diaz-Sanchez D (2004). Effect of glutathione-S-transferase M1 and P1 genotypes on xenobiotic enhancement of allergic responses: randomised, placebo-controlled crossover study. *Lancet*, 363: 119-125. [156471](#)
- Gilliland FD; McConnell R; Peters J; Gong Jr H (1999). A Theoretical Basis for Investigating Ambient Air Pollution and Children's Respiratory Health. *Environ Health Perspect*, 107: 403-407. [155792](#)
- Goldberg MS; Burnett RT; Yale JF; Valois MF; Brook JR (2006). Associations between ambient air pollution and daily mortality among persons with diabetes and cardiovascular disease. *Environ Res*, 100: 255-267. [088641](#)
- Gong H Jr; Linn WS; Clark KW; Anderson KR; Sioutas C; Alexis NE; Cascio WE; Devlin RB (2008). Exposures of healthy and asthmatic volunteers to concentrated ambient ultrafine particles in Los Angeles. *Inhal Toxicol*, 20: 533-545. [156483](#)
- Gong H Jr; Linn WS; Sioutas C; Terrell SL; Clark KW; Anderson KR; Terrell LL (2003). Controlled exposures of healthy and asthmatic volunteers to concentrated ambient fine particles in Los Angeles. *Inhal Toxicol*, 15: 305-325. [042106](#)
- Gong H Jr; Linn WS; Terrell SL; Clark KW; Geller MD; Anderson KR; Cascio WE; Sioutas C (2004). Altered heart-rate variability in asthmatic and healthy volunteers exposed to concentrated ambient coarse particles. *Inhal Toxicol*, 16: 335-343. [055628](#)
- Heidenfelder BL; Reif DM; Harkema JR; Cohen Hubal EA; Hudgens EE; Bramble LA; Wagner JG; Morishita M; Keeler GJ; Edwards SW; Gallagher JE (2009). Comparative microarray analysis and pulmonary changes in brown Norway rats exposed to ovalbumin and concentrated air particulates. *Toxicol Sci*, 108: 207-221. [190026](#)
- Host S; Larrieu S; Pascal L; Blanchard M; Declercq C; Fabre P; Jusot JF; Chardon B; Le Tertre A; Wagner V; Prouvost H; Lefranc A (2007). Short-term Associations between Fine and Coarse Particles and Cardiorespiratory Hospitalizations in Six French Cities. *Occup Environ Med*, 18: S107-S108. [155851](#)
- Jerrett M; Burnett RT; Brook J; Kanaroglou P; Giovis C; Finkelstein N; Hutchison B (2004). Do socioeconomic characteristics modify the short term association between air pollution and mortality? Evidence from a zonal time series in Hamilton, Canada. *J Epidemiol Community Health*, 58: 31-40. [087379](#)
- Kan H; London SJ; Chen G; Zhang Y; Song G; Zhao N; Jiang L; Chen B (2008). Season, sex, age, and education as modifiers of the effects of outdoor air pollution on daily mortality in Shanghai, China: The Public Health and Air Pollution in Asia (PAPA) Study. *Environ Health Perspect*, 116: 1183-1188. [156621](#)
- Kauffmann F; Anto J; Baur MP; Bickeboller H; Clayton D; Cookson WOC; Demenais F; Helms PJ; Humphery-Smith I; Imbeaud S; Knoppers BM; Lathrop M; Little J; Pearce N; Schaid D; Silverman E; Weiss S; Wjst M (2004). Post-genome respiratory epidemiology: a multidisciplinary challenge. *Eur Respir J*, 24: 471-480. [090968](#)
- Kleeberger SR; Ohtsuka Y (2005). Gene-particulate matter-health interactions. *Toxicol Appl Pharmacol*, 207: S276-S281. [130489](#)
- Kodavanti UP; Moyer CF; Ledbetter AD; Schladweiler MC; Costa DL; Hauser R; Christiani DC; Nyska A (2003). Inhaled environmental combustion particles cause myocardial injury in the Wistar Kyoto rat. *Toxicol Sci*, 71: 237-245. [051325](#)
- Krewski D; Jerrett M; Burnett RT; Ma R; Hughes E; Shi Y; Turner MC; Pope AC III; Thurston G; Calle EE; Thun MJ (2009). Extended follow-up and spatial analysis of the American Cancer Society study linking particulate air pollution and mortality. Health Effects Institute. Cambridge, MA. Report Nr. 140. [191193](#)
- Lagorio S; Forastiere F; Pistelli R; Iavarone I; Michelozzi P; Fano V; Marconi A; Ziemacki G; Ostro BD (2006). Air pollution and lung function among susceptible adult subjects: a panel study. *Environ Health*, 5: 11. [089800](#)
- Larrieu S; Jusot J-F; Blanchard M; Prouvost H; Declercq C; Fabre P; Pascal L; Le Tertre A; Wagner V; Riviere S; Chardon B; Borelli D; Cassadou S; Eilstein D; Lefranc A (2007). Short term effects of air pollution on hospitalizations for cardiovascular diseases in eight French cities: The PSAS program. *Sci Total Environ*, 387: 105-112. [093031](#)
- Lee IM; Tsai SS; Ho CK; Chiu HF; Wu TN; Yang CY (2008). Air pollution and hospital admissions for congestive heart failure: are there potentially sensitive groups? *Environ Res*, 108: 348-353. [192076](#)

- Le Tertre A; Medina S; Samoli E; Forsberg B; Michelozzi P; Boumghar A; Vonk JM; Bellini A; Atkinson R; Ayres JG; Sunyer J; Schwartz J; Katsouyanni K (2002). Short term effects of particulate air pollution on cardiovascular diseases in eight European cities. *J Epidemiol Community Health*, 56: 773-779. [023746](#)
- Liao D; Heiss G; Chinchilli VM; Duan Y; Folsom AR; Lin HM; Salomaa V (2005). Association of criteria pollutants with plasma hemostatic/inflammatory markers: a population-based study. *J Expo Sci Environ Epidemiol*, 15: 319-328. [088677](#)
- Liu L; Ruddy TD; Dalipaj M; Szyszkowicz M; You H; Poon R; Wheeler A; Dales R (2007). Influence of personal exposure to particulate air pollution on cardiovascular physiology and biomarkers of inflammation and oxidative stress in subjects with diabetes. *J Occup Environ Med*, 49: 258-265. [156705](#)
- Lopes FD; Pinto TS; Arantes-Costa FM; Moriya HT; Biselli PJ; Ferraz LF; Lichtenfels AJ; Saldiva PH; Mauad T; Martins MA (2009). Exposure to ambient levels of particles emitted by traffic worsens emphysema in mice. *Environ Res*, 109: 544-551. [190430](#)
- Luginaah IN; Fung KY; Gorey KM; Webster G; Wills C (2005). Association of ambient air pollution with respiratory hospitalization in a government designated "area of concern": the case of Windsor, Ontario. *Environ Health Perspect*, 113: 290-296. [057327](#)
- Mar TF; Larson TV; Stier RA; Claiborn C; Koenig JQ (2004). An analysis of the association between respiratory symptoms in subjects with asthma and daily air pollution in Spokane, Washington. *Inhal Toxicol*, 16: 809-815. [057309](#)
- Mauad T; Rivero DH; de Oliveira RC; Lichtenfels AJ; Guimaraes ET; de Andre PA; Kasahara DI; Bueno HM; Saldiva PH (2008). Chronic exposure to ambient levels of urban particles affects mouse lung development. *Am J Respir Crit Care Med*, 178: 721-728. [156743](#)
- Merriam-Webster (2009). Merriam-Webster on-line. Retrieved 15-JUN-09, from <http://www.merriam-webster.com/medical/susceptible>; <http://www.merriam-webster.com/medical/vulnerable>. [192146](#)
- Metzger KB; Tolbert PE; Klein M; Peel JL; Flanders WD; Todd KH; Mulholland JA; Ryan PB; Frumkin H (2004). Ambient air pollution and cardiovascular emergency department visits. *Epidemiology*, 15: 46-56. [044222](#)
- Middleton N; Yiallourous P; Kleanthous S; Kolokotroni O; Schwartz J; Dockery DW; Demokritou P; Koutrakis P (2008). A 10-year time-series analysis of respiratory and cardiovascular morbidity in Nicosia, Cyprus: the effect of short-term changes in air pollution and dust storms. *Environ Health*, 7: 39. [156760](#)
- Mills NL; Robinson SD; Fokkens PH; Leseman DL; Miller MR; Anderson D; Freney EJ; Heal MR; Donovan RJ; Blomberg A; Sandstrom T; MacNee W; Boon NA; Donaldson K; Newby DE; Cassee FR (2008). Exposure to concentrated ambient particles does not affect vascular function in patients with coronary heart disease. *Environ Health Perspect*, 116: 709-715. [156766](#)
- Mills NL; Törnqvist H; Gonzalez MC; Vink E; Robinson SD; Soderberg S; Boon NA; Donaldson K; Sandstrom T; Blomberg A; Newby DE (2007). Ischemic and thrombotic effects of dilute diesel-exhaust inhalation in men with coronary heart disease. *N Engl J Med*, 357: 1075-1082. [091206](#)
- Morishita M; Keeler G; Wagner J; Marsik F; Timm E; Dvonch J; Harkema J (2004). Pulmonary retention of particulate matter is associated with airway inflammation in allergic rats exposed to air pollution in urban Detroit. *Inhal Toxicol*, 16: 663-674. [087979](#)
- Mortimer KM; Neas LM; Dockery DW; Redline S; Tager IB (2002). The effect of air pollution on inner-city children with asthma. *Eur Respir J*, 19: 699-705. [030281](#)
- Nadziejko C; Fang K; Narciso S; Zhong M; Su WC; Gordon T; Nadas A; Chen LC (2004). Effect of particulate and gaseous pollutants on spontaneous arrhythmias in aged rats. *Inhal Toxicol*, 16: 373-380. [055632](#)
- Naess O; Nafstad P; Aamodt G; Claussen B; Rosland P (2007). Relation between concentration of air pollution and cause-specific mortality: four-year exposures to nitrogen dioxide and particulate matter pollutants in 470 neighborhoods in Oslo, Norway. *Am J Epidemiol*, 165: 435-443. [090736](#)
- NCHS (2006). Chartbook on Trends in the Health of Americans. National Center for Health Statistics, Centers for Disease Control and Prevention. Hyattsville, MD. <http://www.cdc.gov/nchs/data/hs/hs06.pdf>. [198921](#)
- Nordenhall C; Pourazar J; Ledin M-C; Levin J-O; Sandstrom T; Adelroth E (2001). Diesel exhaust enhances airway responsiveness in asthmatic subjects. *Eur Respir J*, 17: 909-915. [025185](#)

- NRC (2004). Research priorities for airborne particulate matter: IV Continuing research progress. National Academies Press. Washington, DC. [156814](#)
- Ohtsuka Y; Brunson KJ; Jedlicka AE; Mitzner W; Clarke RW; Zhang L-Y; Eleff SM; Kleeberger SR (2000). Genetic linkage analysis of susceptibility to particle exposure in mice. *Am J Respir Cell Mol Biol*, 22: 574-581. [004409](#)
- Ostro B; Broadwin R; Green S; Feng W-Y; Lipsett M (2006). Fine particulate air pollution and mortality in nine California counties: results from CALFINE. *Environ Health Perspect*, 114: 29-33. [087991](#)
- Ostro BD; Feng WY; Broadwin R; Malig BJ; Green RS; Lipsett MJ (2008). The impact of components of fine particulate matter on cardiovascular mortality in susceptible subpopulations. *Occup Environ Med*, 65: 750-756. [097971](#)
- Park SK; O'Neill MS; Vokonas PS; Sparrow D; Schwartz J (2005). Effects of air pollution on heart rate variability: The VA normative aging study. *Environ Health Perspect*, 113: 304-309. [057331](#)
- Park SK; O'Neill MS; Wright RO; Hu H; Vokonas PS; Sparrow D; Suh H; Schwartz J (2006). HFE genotype, particulate air pollution, and heart rate variability: a gene-environmental interaction. *Circulation*, 114: 2798-2805. [091245](#)
- Peel JL; Metzger KB; Klein M; Flanders WD; Mulholland JA; Tolbert PE (2007). Ambient air pollution and cardiovascular emergency department visits in potentially sensitive groups. *Am J Epidemiol*, 165: 625-633. [090442](#)
- Peel JL; Tolbert PE; Klein M; Metzger KB; Flanders WD; Knox T; Mulholland JA; Ryan PB; Frumkin H (2005). Ambient air pollution and respiratory emergency department visits. *Epidemiology*, 16: 164-174. [056305](#)
- Peters A; Greven S; Heid I; Baldari F; Breitner S; Bellander T; Chrysohoou C; Illig T; Jacquemin B; Koenig W (2009). Fibrinogen genes modify the fibrinogen response to ambient particulate matter. *Am J Respir Crit Care Med*, 179: 484-491. [191992](#)
- Pinkerton KE; Zhou Y; Teague SV; Peake JL; Walther RC; Kennedy IM; Leppert VJ; Aust AE (2004). Reduced lung cell proliferation following short-term exposure to ultrafine soot and iron particles in neonatal rats: key to impaired lung growth? *Inhal Toxicol*, 1: 73-81. [087465](#)
- Pinkerton KE; Zhou Y; Zhong C; Smith KR; Teague SV; Kennedy IM; Ménache MG (2008). Mechanisms of particulate matter toxicity in neonatal and young adult rat lungs. Health Effects Institute. Boston, MA. 135. [190471](#)
- Pleis JR; Lethbridge-Cejku M (2007). Summary health statistics for US adults: National Health Interview Survey, 2006. National Center for Health Statistics, Centers for Disease Control and Prevention, U.S. Department of Health and Human Services. Hyattsville, Maryland. Vital Health Stat Series 10, Number 235; DHHS 2008-1563. http://www.cdc.gov/nchs/data/series/sr_10/sr10_235.pdf. [156875](#)
- Pope C; Renlund D; Kfoury A; May H; Horne B (2008). Relation of heart failure hospitalization to exposure to fine particulate air pollution. *Am J Cardiol*, 102: 1230-1234. [191969](#)
- Pope CA; Dockery DW (2006). Health effects of fine particulate air pollution: Lines that connect. *J Air Waste Manag Assoc*, 56: 709-742. [156881](#)
- Pope CA III; Muhlestein JB; May HT; Renlund DG; Anderson JL; Horne BD (2006). Ischemic heart disease events triggered by short-term exposure to fine particulate air pollution. *Circulation*, 114: 2443-2448. [091246](#)
- Rabinovitch N; Strand M; Gelfand EW (2006). Particulate levels are associated with early asthma worsening in children with persistent disease. *Am J Respir Crit Care Med*, 173: 1098-1105. [088031](#)
- Routledge HC; Manney S; Harrison RM; Ayres JG; Townend JN (2006). Effect of inhaled sulphur dioxide and carbon particles on heart rate variability and markers of inflammation and coagulation in human subjects. *Heart*, 92: 220-227. [088674](#)
- Samoli E; Peng R; Ramsay T; Pipikou M; Touloumi G; Dominici F; Burnett R; Cohen A; Krewski D; Samet J (2008). Acute effects of ambient particulate matter on mortality in Europe and North America: results from the APHENA study. *Environ Health Perspect*, 116: 1480-1486. [188455](#)
- Schneider A; Neas L; Herbst M; Case M; Williams R; Cascio W; Hinderliter A; Holguin F; Buse J; Dungan K (2008). Endothelial dysfunction: associations with exposure to ambient fine particles in diabetic individuals. *Environ Health Perspect*, 116: 1666-1674. [191985](#)
- Schwartz J; Park SK; O'Neill MS; Vokonas PS; Sparrow D; Weiss S; Kelsey K (2005). Glutathione-S-transferase M1, obesity, statins, and autonomic effects of particles: gene-by-drug-by-environment interaction. *Am J Respir Crit Care Med*, 172: 1529-1533. [086296](#)

- Silkoff PE; Zhang L; Dutton S; Langmack EL; Vedal S; Murphy J; Make B (2005). Winter air pollution and disease parameters in advanced chronic obstructive pulmonary disease panels residing in Denver, Colorado. *J Allergy Clin Immunol*, 115: 337-344. [087471](#)
- Suh YJ; Ha EH; Park H; Kim YJ; Kim H; Hong YC (2008). GSTM1 polymorphism along with PM10 exposure contributes to the risk of preterm delivery. *Mutat Res*, 656: 62-67. [192077](#)
- Sun Q; Wang A; Jin X; Natanzon A; Duquaine D; Brook RD; Aguinaldo JG; Fayad ZA; Fuster V; Lippmann M; Chen LC; Rajagopalan S (2005). Long-term air pollution exposure and acceleration of atherosclerosis and vascular inflammation in an animal model. *JAMA*, 294: 3003-3010. [087952](#)
- Sun Q; Yue P; Deiuliis JA; Lumeng CN; Kampfrath T; Mikolaj MB; Cai Y; Ostrowski MC; Lu B; Parthasarathy S; Brook RD; Moffatt-Bruce SD; Chen LC; Rajagopalan S (2009). Ambient air pollution exaggerates adipose inflammation and insulin resistance in a mouse model of diet-induced obesity. *Circulation*, 119: 538-546. [190487](#)
- Sun Q; Yue P; Kirk RI; Wang A; Moatti D; Jin X; Lu B; Schecter AD; Lippmann M; Gordon T; Chen LC; Rajagopalan S (2008). Ambient air particulate matter exposure and tissue factor expression in atherosclerosis. *Inhal Toxicol*, 20: 127-137. [157033](#)
- Tankersley CG; Bierman A; Rabold R (2007). Variation in heart rate regulation and the effects of particle exposure in inbred mice. *Inhal Toxicol*, 19: 621-629. [097910](#)
- Tankersley CG; Campen M; Bierman A; Flanders SE; Broman KW; Rabold R (2004). Particle effects on heart-rate regulation in senescent mice. *Inhal Toxicol*, 16: 381-390. [094378](#)
- Tankersley CG; Champion HC; Takimoto E; Gabrielson K; Bedja D; Misra V; El-Haddad H; Rabold R; Mitzner W (2008). Exposure to inhaled particulate matter impairs cardiac function in senescent mice. *Am J Physiol Regul Integr Comp Physiol*, 295: R252-R263. [157043](#)
- Tarantini L; Bonzini M; Apostoli P; Pegoraro V; Bollati V; Marinelli B; Cantone L; Rizzo G; Hou L; Schwartz J; Bertazzi PA; Baccarelli A (2009). Effects of particulate matter on genomic DNA methylation content and iNOS promoter methylation. *Environ Health Perspect*, 117: 217-222. [192010](#)
- Trenga CA; Sullivan JH; Schildcrout JS; Shepherd KP; Shapiro GG; Liu LJ; Kaufman JD; Koenig JQ (2006). Effect of particulate air pollution on lung function in adult and pediatric subjects in a Seattle panel study. *Chest*, 129: 1614-1622. [155209](#)
- U.S. Census (2009). Educational Attainment in the United States: 2007 (<http://www.census.gov/prod/2009pubs/p20-560.pdf>). U.S. Census Bureau, Economics and Statistics Administration, U.S. Department of Commerce. Washington, DC. P20-560. <http://www.census.gov/prod/2009pubs/p20-560.pdf>. [192148](#)
- U.S. Census (2009). U.S. census (2000): poverty. Retrieved 01-JUL-09, from <http://www.census.gov/hhes/www/poverty/hispov/hstpov2.html>. [192147](#)
- U.S. Census Bureau (2000). Census Bureau projects doubling of nation's population by 2100. Retrieved 13-MAY-01, from <http://www.census.gov/Press-Release/www/2000/cb00-05.html>. [157064](#)
- U.S. EPA (2003). Framework for cumulative risk assessment. National Center for Environmental Assessment, Office of Research and Development, U.S. Environmental Protection Agency. Washington, DC. EPA/630/P-02/001F. [192145](#)
- U.S. EPA (2004). Air quality criteria for particulate matter. U.S. Environmental Protection Agency. Research Triangle Park, NC. EPA/600/P-99/002aF-bF. [056905](#)
- U.S. EPA (2006). Aging and Toxic Response: Issues Relevant to Risk Assessment (Final). U.S. Environmental Protection Agency. Washington, DC. <http://cfpub.epa.gov/ncea/cfm/recorddisplay.cfm?deid=156648>. [192082](#)
- U.S. EPA (2008). Integrated review plan for the national ambient air quality standards for particulate matter. U.S. Environmental Protection Agency, Office of Research and Development, National Center for Environmental Assessment. Research Triangle Park, NC. [157072](#)
- U.S. EPA (2008). Integrated Science Assessment for Sulfur Oxides - Health Criteria. U.S. Environmental Protection Agency. Research Triangle Park, NC. EPA/600/R-08/047F. <http://cfpub.epa.gov/ncea/cfm/recorddisplay.cfm?deid=198843>. [157075](#)
- U.S. EPA (2009). Susceptible subpopulations. Retrieved 15-MAY-09, from <http://www.epa.gov/nerl/goals/health/populations.html>. [192149](#)

- Villeneuve PJ; Goldberg MS; Krewski D; Burnett RT; Chen Y (2002). Fine particulate air pollution and all-cause mortality within the Harvard six-cities study: variations in risk by period of exposure. *Ann Epidemiol*, 12: 568-576. [042576](#)
- Wellenius GA; Bateson TF; Mittleman MA; Schwartz J (2005). Particulate air pollution and the rate of hospitalization for congestive heart failure among medicare beneficiaries in Pittsburgh, Pennsylvania. *Am J Epidemiol*, 161: 1030-1036. [087483](#)
- Wellenius GA; Coull BA; Batalha JRF; Diaz EA; Lawrence J; Godleski JJ (2006). Effects of ambient particles and carbon monoxide on supraventricular arrhythmias in a rat model of myocardial infarction. *Inhal Toxicol*, 18: 1077-1082. [156152](#)
- Wellenius GA; Coull BA; Godleski JJ; Koutrakis P; Okabe K; Savage ST (2003). Inhalation of concentrated ambient air particles exacerbates myocardial ischemia in conscious dogs. *Environ Health Perspect*, 111: 402-408. [055691](#)
- Wellenius GA; Schwartz J; Mittleman MA (2006). Particulate air pollution and hospital admissions for congestive heart failure in seven United States cities. *Am J Cardiol*, 97: 404-408. [088748](#)
- Wilson WE; Mar TF; Koenig JQ (2007). Influence of exposure error and effect modification by socioeconomic status on the association of acute cardiovascular mortality with particulate matter in Phoenix. *J Expo Sci Environ Epidemiol*, 17: S11-S19. [157149](#)
- Yanosky JD; Schwartz J; Suh HH (2008). Associations between measures of socioeconomic position and chronic nitrogen dioxide exposure in Worcester, Massachusetts. *J Toxicol Environ Health A Curr Iss*, 71: 1593-1602. [192081](#)
- Yauk C; Polyzos A; Rowan-Carroll A; Somers CM; Godschalk RW; Van Schooten FJ; Berndt ML; Pogribny IP; Koturbash I; Williams A; Douglas GR; Kovalchuk O (2008). Germ-line mutations, DNA damage, and global hypermethylation in mice exposed to particulate air pollution in an urban/industrial location. *PNAS*, 105: 605-610. [157164](#)
- Yeatts K; Svendsen E; Creason J; Alexis N; Herbst M; Scott J; Kupper L; Williams R; Neas L; Cascio W; Devlin RB; Peden DB (2007). Coarse particulate matter (PM_{2.5-10}) affects heart rate variability, blood lipids, and circulating eosinophils in adults with asthma. *Environ Health Perspect*, 115: 709-714. [091266](#)
- Yunginger JW; Reed CE; O'Connell EJ; Melton LJ 3rd; O'Fallon WM; Silverstein MD (1992). A community-based study of the epidemiology of asthma. Incidence rates, 1964-1983. *Am Rev Respir Dis*, 146: 888-894. [192074](#)
- Zanobetti A; Bind MAC; Schwartz J (2008). Particulate air pollution and survival in a COPD cohort. *Environ Health Perspect*, 7: 48. [156177](#)
- Zanobetti A; Schwartz J (2002). Cardiovascular damage by airborne particles: are diabetics more susceptible? *Epidemiology*, 13: 588-592. [034821](#)
- Zanobetti A; Schwartz J (2005). The effect of particulate air pollution on emergency admissions for myocardial infarction: A multicity case-crossover analysis. *Environ Health Perspect*, 113: 978-982. [088069](#)
- Zeger S; Dominici F; McDermott A; Samet J (2008). Mortality in the Medicare population and chronic exposure to fine particulate air pollution in urban centers (2000-2005). *Environ Health Perspect*, 116: 1614-1619. [191951](#)
- Zeka A; Zanobetti A; Schwartz J (2006). Individual-level modifiers of the effects of particulate matter on daily mortality. *Am J Epidemiol*, 163: 849-859. [088749](#)

Chapter 9. Welfare Effects

9.1. Introduction

This chapter is a synthesis and evaluation of the most policy-relevant science used to help form the scientific foundation for review of the secondary (welfare-based) NAAQS aimed at protecting against welfare effects of ambient airborne PM. Specifically, Chapter 9 assesses the effects of atmospheric PM on the environment, including: (1) effects on visibility; (2) effects on climate; (3) ecological effects; and (4) effects on materials. These sections initially highlight the conclusions from the 2004 PM AQCD (U.S. EPA, 2004, [056905](#)), followed by an evaluation of recent publications and assessment of the expanded body of evidence. In some sections, few new publications are available, and the discussion is primarily a brief overview of the key conclusions from the previous review.

As discussed in Chapter 1, the effects of particulate NO_x and SO_x have recently been evaluated in the ISA for Oxides of Nitrogen and Sulfur – Ecological Criteria (U.S. EPA, 2008, [157074](#)). That ISA focused on the effects from deposition of gas- and particle-phase pollutants related to ambient NO_x and SO_x concentrations that can lead to acidification and nutrient enrichment, as well as on the potential for increased mercury methylation from SO₄²⁻ deposition. Thus, emphasis in this document is placed on the effects of airborne PM on visibility and climate, and on the deposition effects of PM constituents other than NO_x and SO_x, primarily metals and carbonaceous compounds.

Chapter 2 of this assessment provides an integrative overview of the major welfare effects evaluated. EPA's framework for causality, described in Chapter 1, is applied throughout the evaluation and the causal determinations are highlighted.

9.2. Effects on Visibility

9.2.1. Introduction

In recent years, most visibility research involved characterizing visibility conditions and trends over broad regional scales, improving the understanding of the atmospheric processes and pollutants responsible for the regional impacts, and attribution of visibility-impairing pollutants to emission sources, source types, and regions. The motivation for much of this work has come from the visibility protection provisions of the 1977 Clean Air Act Amendments (CAAA) that called for the development of regulations to address reduction of regional haze in 156 NPs and wilderness areas to natural conditions, and from the subsequent Regional Haze Rule (RHR) promulgated in 1999 by EPA in response to the CAA mandate. Implementation of the RHR entails planned emissions reductions to reach natural haze conditions in these protected areas by 2064 in six 10-year planning steps.

Haze conditions caused solely by PM from natural sources are generally much lower than contemporary conditions. The largest difference is between natural and current conditions for the inorganic salts ammonium sulfate and ammonium nitrate, with natural concentrations taken to be just a few tenths of a µg/m³ each (Trijonis et al., 1990, [157058](#)), while current conditions of both over large regions of the country are an order of magnitude or more larger (DeBell, 2006, [156388](#)).

Note: Hyperlinks to the reference citations throughout this document will take you to the NCEA HERO database (Health and Environmental Research Online) at <http://epa.gov/hero>. HERO is a database of scientific literature used by U.S. EPA in the process of developing science assessments such as the Integrated Science Assessments (ISA) and the Integrated Risk Information System (IRIS).

However, natural source PM can be substantial on an episodic basis for crustal mineral PM components during high windblown dust conditions and for carbonaceous PM from biomass combustion during wildfire and prescribed burning episodes. The need for information to generate RHR implementation plans has resulted in extensive use of continental-scale air quality simulation modeling and assessment of expanded ambient monitoring data sets.

Unlike the substantial remote-area visibility investigations that have been conducted in response to the RHR, relatively little work on urban visibility effects has been done in recent years. For example, there has been relatively little new research on the optical and human perceptual aspects of atmospheric visibility over the last decade or more. These topics have been the subjects of numerous earlier investigations that have been summarized in detail elsewhere (Latimer and Ireson, 1980, [035723](#); Middleton, 1952, [016324](#); Tombach and McDonald, 2004, [157054](#); Trijonis et al., 1990, [157058](#); U.S. EPA, 1979, [157065](#); Watson et al., 2002, [035623](#)), including past criteria documents on PM, SO₂ and NO_x (U.S. EPA, 1982, [017610](#); U.S. EPA, 1993, [017649](#); U.S. EPA, 2004, [056905](#)).

In spite of this fact, the understanding of urban visibility conditions has continued to improve. By applying a well established algorithm that relates PM and haze conditions to data currently collected from routine filter-based PM chemical speciation monitors located in numerous urban areas (Jayanty, 2003, [156605](#)), and to data collected from the more recently deployed high time- and size-resolved PM speciation monitors located in several cities such as those in the PM Supersites program (Solomon and Hopke, 2008, [156997](#)) urban visibility conditions can be better characterized. Comparisons between urban and remote area data in the same region afford the opportunity to differentiate between regional and local visibility impacts. The availability of better size and time resolution PM composition data, compared to that available from the routine monitoring programs, reduces the number of simplifying assumptions required to estimate visibility conditions in these areas, thereby reducing the uncertainty of the estimates. Thus, the state of the science supporting urban visibility assessments continues to improve.

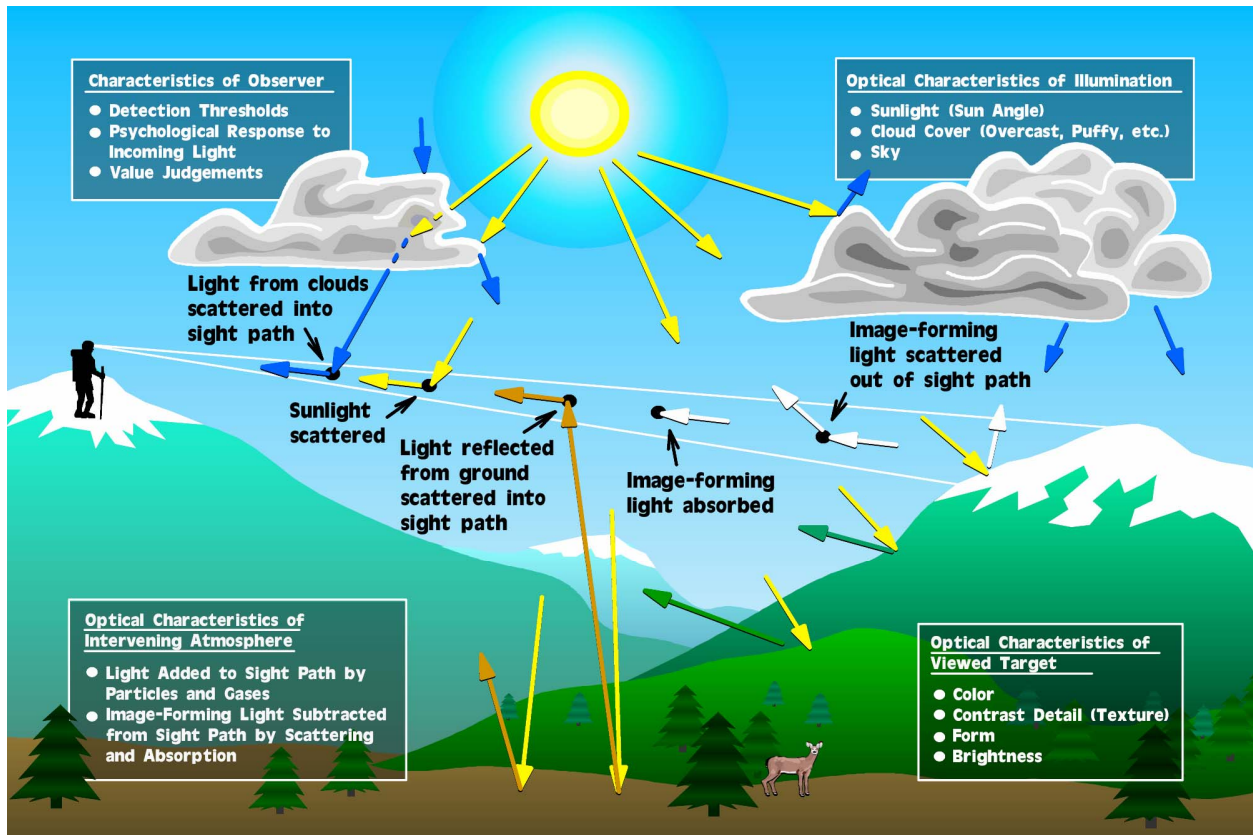
The background section below contains an overview of long-available information to help provide context to the more recently published literature summarized in subsequent sections.

9.2.2. Background

Air pollution-induced visibility impairment is caused by the loss of image-forming light (i.e., signal) and the addition of non-image forming light (i.e., noise) between an observer and the object being viewed. These changes to the light reaching the observer are a result of light being scattered and absorbed by particles and gases in the sight path (see the schematic in Figure 9-1). Electromagnetic theory developed to characterize the interaction of light with matter (Mie, 1908, [155983](#)) permits the calculation of light scattering and absorption by particles and gas molecules where the index of refraction and shape of particles by size are known (Van de Hulst, 1981, [191972](#)).

The ability of human observers to visually detect distant objects or identify changes in their appearance depends on the apparent contrast of the object against its background. The apparent contrast is affected by changes in the physicochemical characteristics of the atmosphere caused by air pollution as well as factors not related to air quality such as length of the sight path, scenic lighting and the physical characteristics of the viewed object and other elements of the scene. To rigorously determine the perceived visual effects of changes in the optical properties of the atmosphere requires the use of radiative transfer modeling to determine changes in light from the field of view experienced by the observer, followed by the use of psychophysical modeling to determine the response to the light by the eye-brain system. The complexity of such an approach discourages its common use.

Atmospheric light extinction is a fundamental atmospheric optics metric used to characterize air pollution impacts on visibility. It is the fractional loss of intensity in a light beam per unit distance due to scattering and absorption by the gases and particles in the air. Light extinction (b_{ext}) can be expressed as the sum of light scattering by particles ($b_{\text{s,p}}$), scattering by gases ($b_{\text{s,g}}$), absorption by particles ($b_{\text{a,p}}$) and absorption by gases ($b_{\text{a,g}}$). Light extinction and its components are expressed in units of inverse length, typically either inverse kilometers (km^{-1}) or, as will be the convention in this document, inverse megameters (Mm^{-1}). Traditionally, for visibility-protection applications, the most sensitive portion of the spectrum for human vision (550 nm) has been used to characterize light extinction and its components.



Source: Malm (1999, [025037](#)).

Figure 9-1. Important factors involved in seeing a scenic vista are outlined. Image-forming information from an object is reduced (scattered and absorbed) as it passes through the atmosphere to the human observer. Air light is also added to the sight path by scattering processes. Sunlight, light from clouds, and ground-reflected light all impinge on and scatter from particulates located in the sight path. Some of this scattered light remains in the sight path, and at times it can become so bright that the image essentially disappears. A final important factor in seeing and appreciating a scenic vista are the characteristics of the human observer.

A parametric analysis has shown that a constant fractional change in light extinction results in a similar perceptual change regardless of certain baseline conditions (Pitchford et al., 1990, [156871](#)). From this assessment, the deciview haze index, which is a log transformation of light extinction, similar in many ways to the decibel index for acoustic measurements, was developed (Pitchford and Malm, 1994, [044922](#)). A one deciview (1dv) change is about a 10% change in light extinction, which is a small change that is detectable for sensitive viewing situations. The haze index in deciview units is an appropriate metric for expressing the extent of haze changes where the perceptibility of the change is an issue. The RHR has adopted the deciview haze index as the metric for tracking long-term haze trends of visibility-protected federal lands (U.S. EPA, 2001, [157068](#)). Light extinction and its components are more useful metrics for characterizing the apportionment of haze to its pollutant components due to the approximately linear relationship between pollutant species concentrations and their contributions to light extinction.

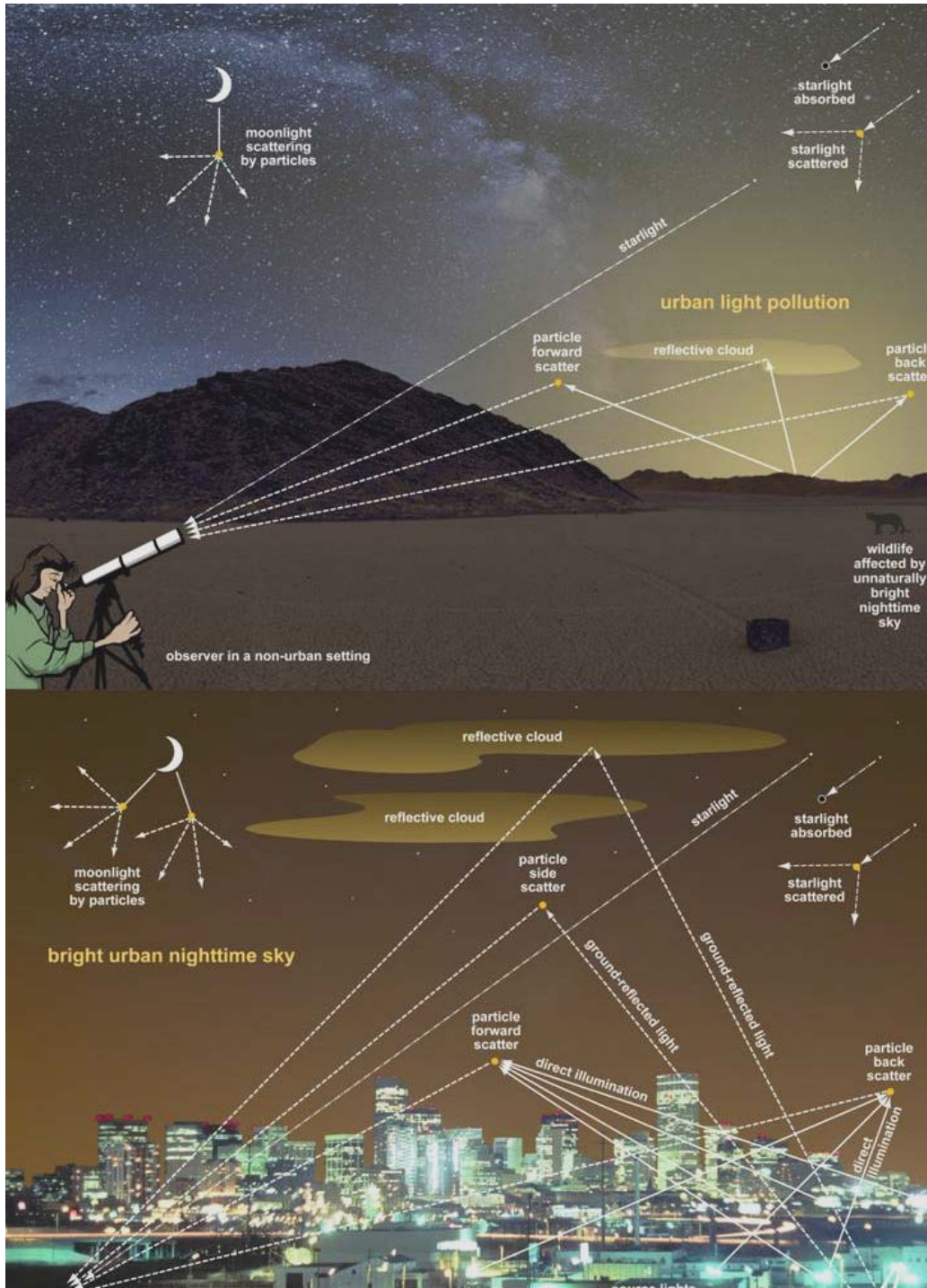


Figure 9-2. Schematic of remote-area (top) and urban (bottom) nighttime sky visibility showing the effects of PM and light pollution.

Daytime visibility has dominated the attention of those who have studied the visibility effects of air pollution, though nighttime visibility is also known to be affected by air pollution. Stargazing is a popular human activity in urban and remote settings. The reduction in visibility of the night sky is primarily dependent on the addition of light into the sight path, the brightness of the night sky, and the reduction in contrast of stars against the background (see the schematic in Figure 9-2). These are

controlled by the addition of PM, which enhances scattering, and the addition of anthropogenic sources of light. Scattering of anthropogenic light contributes to the “skyglow” within and over populated areas, adding to the total sky brightness. The visual result is a reduction of the number of visible stars and the disappearance of diffuse or subtle phenomena such as the Milky Way. The extinction of starlight is a secondary and minor effect also caused by increased scattering and absorption. Anthropogenic light sources include artificial outdoor lighting, which varies dramatically across space. Natural sources include the Moon, planets, and stars that have a predictable rhythm across time.

The nighttime visual environment has some important differences to note. Light sources and ambient conditions are typically five to seven orders of magnitude dimmer at night than in sunlight. Moonlight, like sunlight, introduces light throughout an observer’s sight path at a constant angle. On the other hand, dim starlight emanates from all over the celestial hemisphere while artificial lights are concentrated in cities and illuminate the atmosphere from below. Sight paths are often inclined upward at night as targets may be nearby terrain features or celestial phenomena. Extinction behaves the same at night as during the day, lowering the contrast of scenes through scattering and absorption; nevertheless the different light sources will yield variable changes in visibility as compared to what has been established for the daytime scenario. Little research has been conducted on nighttime visibility. Even if the air quality-visibility interactions are shown to be similar between day and night settings, the human psychophysical response at night is expected to differ. Though recent advances in the ability to instrument and quantify nighttime scenes (Duriscoe et al., 2007, [156411](#)) have been made and can be utilized to evaluate nocturnal visibility, the state of the science is not yet comparable to that associated with daytime visibility impairment. The remainder of this document focuses exclusively on daytime visibility.

9.2.2.1. Non-PM Visibility Effects

Light extinction due to the gaseous components of the atmosphere is relatively well understood and well estimated for any atmospheric conditions. Absorption of visible light by gases in the atmosphere is primarily by NO₂, and can be directly and accurately estimated from NO₂ concentrations by multiplying by the absorption efficiency. Scattering by gases is described by the Rayleigh scattering theory.

NO₂ absorbs more light in the short wavelength blue portion of the spectrum than at longer wavelengths. For this reason a plume or layer of NO₂ removes more of the blue light from the scene viewed through the layer giving a yellow or brown appearance to the layer or plume. This filtering of blue light by NO₂ can deepen the brown appearance of hazes over urban areas, although it is not the sole cause of such discoloration (U.S. EPA, 1993, [017649](#)). The photopic-weighted absorption efficiency at the 550 nm wavelength is incorporated into the revised version of the algorithm for estimating light extinction from aerosol data that is used for implementing the RHR (Pitchford et al., 2007, [098066](#)). However, NO₂ is not routinely measured at any of the monitoring sites representing visibility protected areas where its impacts are assumed to be inconsequential compared to those of PM. At background concentrations NO₂ absorption is generally less than five percent of the light scattering by clean air (Rayleigh scattering), making it imperceptible. Plume visibility models are available to assess both achromatic contrast and discoloration associated with NO₂ light absorption, for point source emissions (Latimer and Ireson, 1980, [035723](#); Seigneur et al., 1984, [156965](#)).

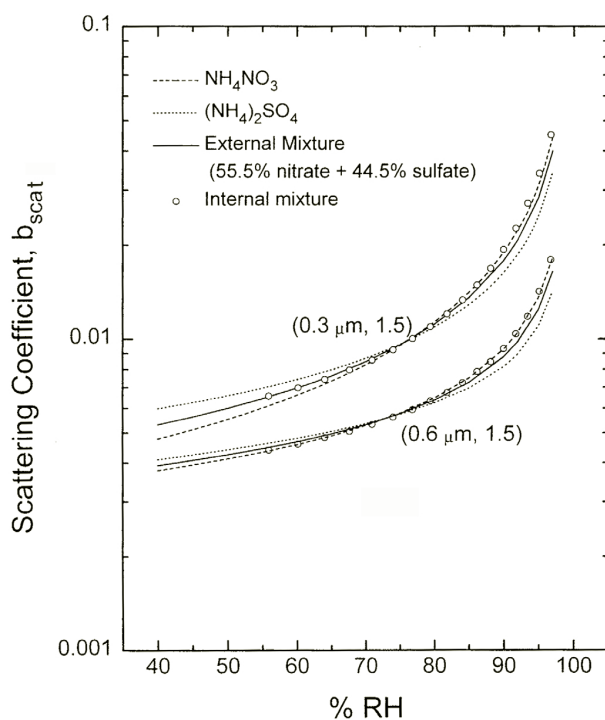
9.2.2.2. PM Visibility Effects

Particle light extinction is more complex than that caused by gaseous components. PM is responsible for most visibility impairment except under near-pristine conditions, where Rayleigh scattering is the largest contributor to light extinction or in plumes of combustion sources that are well-controlled for particulate emissions (e.g., coal-fired power plants with bag houses), where light absorption by NO₂ may dominate the light extinction.

Light-absorbing carbon (e.g., DE soot and smoke) and some crustal minerals are the only commonly occurring airborne particle components that absorb light. All particles scatter light, and generally particle light scattering is the largest of the four light extinction components. While a larger particle scatters more light than a similar shaped smaller particle of the same composition, the light scattered per unit of mass concentration (i.e., mass scattering efficiency in units of $Mm^{-1}/[\mu g/m^3]$ which reduces to m^2/g) is greatest for particles with diameters from ~ 0.3 - $1.0 \mu m$. If

the index of refraction, particle shape and concentration as a function of particle size are well characterized, Mie theory can be used to accurately calculate the light scattering and absorption by those particles. However, it is rare that these particle properties are known, so assumptions are used in place of missing information to develop a simplified calculation scheme that provides an estimate of the particle light extinction from available data sets.

Particles composed of water soluble inorganic salts (i.e., ammoniated sulfate, ammonium nitrate, sodium chloride, etc.) are hygroscopic in that they absorb water as a function of relative humidity to form a liquid solution droplet. Aside from the chemical consequences of this water growth, the droplets become larger when relative humidity increases, resulting in increased light scattering. Hence, the same PM dry concentration produces more haze. Figure 9-3 shows the effect of water growth as a function of relative humidity on light scattering for two size distributions of ammonium nitrate and ammonium sulfate particles as well as for internal and external mixtures (i.e., mixed within the same particle and in separate particles, respectively) of the two components. This figure illustrates a number of important points. The water growth effect is substantial with an increase in light scattering by about a factor of 10 between 40% and 97% relative humidity for the same dry particle concentrations. The amount of scattering is significantly dependent on the dry particle size distribution. However the growth curves for ammonium sulfate, ammonium nitrate and mixtures of the two particle components are similar at any of the dry particle size distributions. Water growth curves are also available for sodium chloride, the major component in sea salt, which is an important PM component at coastal locations.



Source: Reprinted with Permission of the American Geophysical Union from Tang (1996, [157042](#)).

Figure 9-3. Effect of relative humidity on light scattering by mixtures of ammonium nitrate and ammonium sulfate.

Using Mie theory, the scattering and absorption of any wavelength of light by a particle of known size and index of refraction (a function of the wavelength of light) can be calculated (Van de Hulst, 1981, [191972](#)). Particle density is used to convert the particle light extinction to its mass extinction efficiency (i.e., the ratio of particle light extinction to its mass). To expand the calculations from one particle at a time to the multitude of particles in ambient aerosol, information

about the aerosol size and composition distributions are needed. Aerosol mixture refers to how the major components that make up the particles are mixed. Methods have been developed to treat simple mixture models ranging from external mixtures where the various components are assumed to be in separate particles, to multi-component mixtures where individual particles contain several components (Ouimette and Flagan, 1982, [025047](#)). The latter includes internally mixed particles where two or more components are mixed within the particles, and layered aerosol with a core of one component covered by a shell of another component.

The Mie theory solution for an external mixture can be simplified to a linear relationship where the light extinction is the sum of the mass concentration of each species multiplied by its specific mass extinction efficiency (Ouimette and Flagan, 1982, [025047](#)). This formulation promotes the concept of apportioning the light extinction among the various PM species. For internally mixed aerosol, the light extinction response to adding or removing mass of any component to the aerosol is dependent on how such changes would affect the particle size, density and index of refraction distribution of the aerosol. However, a number of investigators have shown that the differences among the calculated light extinction values using external and various internal mixture assumptions are generally less than about 10% (Lowenthal et al., 1995, [045134](#); Ramsey, 1966, [013946](#); Sloane, 1983, [025039](#); Sloane, 1984, [025040](#); Sloane, 1986, [045954](#); Sloane and Wolff, 1985, [045953](#); Wolff, 1985, [044680](#)). This provides a basis to accept the apportionment of light extinction to the PM components calculated using an external mixture assumption as a meaningful surrogate for their contributions.

Ambient aerosols are usually a complex and unknown combination of both internal and external mixtures of the particle components. Despite these complexities, PM light scattering can be accurately calculated for any relative humidity if the chemical composition as a function of dry particle size is known (Hand et al., 2002, [190367](#); Malm and Pitchford, 1997, [002519](#)). However, most routinely available ambient monitoring programs do not include data with sufficient detail to make such calculations. The IMPROVE network with its greater than 150 remote area monitoring sites (DeBell, 2006, [156388](#)) and the CSN (Jayanty, 2003, [156605](#)) with its greater than 150 urban area monitoring sites collect 24-h duration fine particle samples ($PM_{2.5}$) that are analyzed for the major PM components including SO_4^{2-} , nitrate, and carbonaceous particulate. CSN also analyzes for ammonium ion, but does not monitor coarse mass ($PM_{10-2.5}$), while IMPROVE measures coarse mass but does not analyze for ammonium ion. Neither data set has sufficient size resolution to make Mie theory calculations of light extinction, nor does either program routinely monitor NO_2 concentrations, which would be required to calculate its contribution to light extinction by absorption.

A simple algorithm similar in form to the linear equation that results from Mie theory applied with an external mixture assumption is frequently used to estimate light extinction from the concentrations of the major components. The concentration of each of the major aerosol components is multiplied by a dry extinction efficiency value and for the hygroscopic components (e.g., ammoniated sulfate and ammonium nitrate) an additional multiplicative term to account for the water growth to estimate that components contribution to light extinction. Both the dry extinction efficiency and water growth terms are developed by some combination of empirical assessment and theoretical calculation using typical particle size distributions associated with each of the major aerosol components, and they are evaluated by comparing the algorithm estimates of light extinction with coincident optical measurements. Summing the contribution of each component gives the estimate of total light extinction. The most commonly used of these is referred to as the IMPROVE algorithm because it was developed specifically to use the IMPROVE aerosol monitoring data and was evaluated using IMPROVE optical measurements at the subset of sites that make those measurements (Malm et al., 1994, [044920](#)). The formula for the traditional IMPROVE algorithm is shown below.

$$\begin{aligned}
b_{\text{ext}} \approx & 3 \times f(RH) \times [\text{Sulfate}] \\
& + 3 \times f(RH) \times [\text{Nitrate}] \\
& + 4 \times [\text{Organic Mass}] \\
& + 10 \times [\text{Elemental Carbon}] \\
& + 1 \times [\text{Fine Soil}] \\
& + 0.6 \times [\text{Coarse Mass}] \\
& + 10
\end{aligned}$$

Equation 9-1

Source: DeBell (2006, [156388](#))

Light extinction (b_{ext}) is in units of Mm^{-1} , the mass concentrations of the components indicated in brackets are in $\mu\text{g}/\text{m}^3$, and $f(RH)$ is the unitless water growth term that depends on relative humidity. The dry extinction efficiency for particulate organic mass is larger than those for particulate SO_4^{2-} and nitrate principally because the density of the dry inorganic compounds is higher than that assumed for the PM organic mass components. Since IMPROVE does not include ammonium ion monitoring, the assumption is made that all SO_4^{2-} is fully neutralized ammonium sulfate and all nitrate is assumed to be ammonium nitrate. Though often reasonable, neither assumption is always true (see Section 9.2.3.1). In the eastern U.S. during the summer there is insufficient ammonia in the atmosphere to neutralize the SO_4^{2-} fully. Fine particle nitrates can include sodium or calcium nitrate, which are the fine particle fraction of generally much coarser particles due to nitric acid interactions with sea salt at near-coastal areas (sodium nitrate) or nitric acid interactions with calcium carbonate in crustal aerosol (calcium nitrate). Despite the simplicity of the algorithm, it performs reasonably well and permits the contributions to light extinction from each of the major components (including the water associated with the SO_4^{2-} and nitrate compounds) to be separately approximated.

The $f(RH)$ terms inflate the particulate SO_4^{2-} and nitrate light scattering for high relative humidity conditions. For relative humidity below 40% the $f(RH)$ value is 1, but it increases to 2 at ~66%, 3 at ~83%, 4 at ~90%, 5 at ~93% and 6 at ~95% relative humidity. The result is that both particulate SO_4^{2-} and nitrate are more efficient per unit mass than any other aerosol component for relative humidity above ~85% where its total light extinction efficiency exceeds the $10\text{m}^2/\text{g}$ associated with EC. Based on this algorithm, particulate SO_4^{2-} and nitrate are estimated to have comparable light extinction efficiencies (i.e., the same dry extinction efficiency and $f(RH)$ water growth terms), so on a per unit mass concentration basis at any specific relative humidity they are treated as equally effective contributors to visibility effects. The strong relationship demonstrated between dry light scattering and fine PM mass concentration or ambient light extinction and fine PM mass concentration under low relative humidity conditions noted by a number of investigators (Charlson et al., 1968, [095355](#); Chow et al., 2002, [037784](#); Chow et al., 2002, [036166](#); McMurry, 2000, [081517](#); Samuels et al., 1973, [070601](#); Waggoner and Weiss, 1980, [070152](#); Waggoner et al., 1981, [095453](#)) is reasonable based on this algorithm when the PM fractional composition is either relatively constant or varies most among PM components with similar dry extinction efficiency values (e.g., SO_4^{2-} , nitrate and organic mass efficiencies).

9.2.2.3. Direct Optical Measurements

Light extinction and its components (i.e., scattering and absorption by particles and gases) can be determined directly by optical measurements using commercially available instruments (Trijonis et al., 1990, [157058](#)). Though these measurements are all wavelength dependent, the convention for visibility monitoring purposes is to make measurement at or near 550 nm, which is the wavelength of maximum eye response. Direct PM light extinction, scattering and absorption measurements offer a number of advantages compared to estimates using an algorithm applied to PM speciation data. The direct optical measurements are considered more accurate because they do not depend on the assumed particle characteristics (e.g., size, shape, density, component mixture, etc.) thought to be associated with the major PM species. Also the optical measurements are made with high time resolution (e.g., minutes to hourly) compared with the filter composition based estimates that are

typically 24-h duration, allowing the former to better characterize sub-daily temporal patterns which can help in identifying influential source categories and characterize atmospheric phenomenon. The higher time resolution attainable with direct light extinction measurements are also more commensurate than the 24-h light extinction estimates from PM samples with the short exposure time associated with perceived visibility effects.

Path-averaged light extinction can be determined by long-path transmissometers that monitors the intensity of light that has traversed a known distance from a known initial intensity light source. Transmission (i.e., the ratio of the final to the initial light intensity) is the natural logarithm of the product of the path-averaged light extinction and the distance the light has traversed. Transmissometer path-length establishes the useful range of light extinction over which the measurements can be accurately measured, with path-lengths of 10 km or more required for pristine conditions and <1 km more appropriate for hazier situations or to measure the visibility impacts associated with fogs or precipitation events. The National Park Service (NPS) operated long-path transmissometers at up to 25 locations from 1986 through 2004 (DeBell, 2006, [156388](#)), but have more recently discontinued their use at all but one remote area location due to the cost of maintenance and the difficulties of performing calibration. Transmissometers are currently in routine service at five urban areas.

A number of instruments measure the light scattered by particles and gases from a source of known intensity. These include forward scattering, back scattering, polar, and integrating nephelometers. Of these the integrating nephelometers with its high sensitivity and sample control options has been more widely used for air quality-related visibility and PM monitoring purposes, while the robust design of the open air forward scattering instruments have seen extensive use by the National Weather Service (NWS) Automated Surface Observing System (ASOS) for characterizing visibility principally for transportation safety purposes (NOAA, 1998). The potential utility of the ASOS visibility network at about 900 locations for air quality monitoring has been established, but the lack of resolution in the reported data is a serious impediment to this use of the data (Richards et al., 1996, [190476](#)).

Integrating nephelometers draw air into a sample chamber, making it possible to modify the sample either by changing its humidity or controlling the particle size range that is measured. This feature makes it possible to use sample-controlled nephelometers to investigate the effects of ambient PM size and water growth characteristic on light scattering (Covert et al., 1972, [072055](#); Malm and Day, 2001, [190431](#); Rood et al., 1987, [046397](#)). For instance the coarse particle contribution to light scattering can be estimated using a nephelometer that alternately samples through a 2.5 μm size selective inlet and a 10 μm size selective inlet. This separation by size may be useful in that it would allow correction of the underestimated light scattering of larger particles due to nephelometer angular truncation errors (Anderson and Ogren, 1998, [156213](#)). For routine monitoring, integrating nephelometers are typically either used to measure the PM component of light scattering when operated at ambient relative humidity or to measure dry PM light scattering as a high-time resolution surrogate for PM mass concentration when operated with a heater or other sample air drier. Integrating nephelometers operated at ambient conditions by the IMPROVE program have replaced the long-path transmissometer as the principal optical measurement at about 30 locations (DeBell, 2006, [156388](#)).

PM light absorption can also be inferred from measured changes in the light transmitted through a filter used to sample the PM compared to an identical clean filter (Bond et al., 1999, [156281](#)). Such measurements can be made subsequent to sampling (Campbell et al., 1995, [190171](#)) or continuously during sampling by using specifically designed sampler (Hansen et al., 1982, [190368](#); Hansen et al., 1984, [002396](#)). All of the filter-based methods require adjustments to the optical measurements to account for filter and sampled particle light scattering effects associated with particles concentrated on and within the matrix of the filters (Bond et al., 1999, [156281](#)). Often PM light absorption measurements are used to infer BC concentration by assuming it is the dominant PM contributor to light absorption with a near constant absorption efficiency (Allen et al., 1999, [048923](#); Babich et al., 2000, [156239](#)). In fact commercially available aethalometers incorporate an absorption efficiency value so they can directly report BC concentrations. Like nephelometers, commercially available aethalometers can be obtained with either single or multiple-wavelength measurement capabilities, where the multi-wavelength data can be used to better characterize the PM. More recently these have been used to distinguish BC that absorbs light strongly over the full visible light spectrum (e.g., DE) from brown carbon that absorbs appreciably more at shorter wavelengths than at long wavelengths (e.g., WS) (Andreae and Gelencsér, 2006, [156215](#)).

Other approaches to measure light absorption include a photoacoustic instrument that measures the heating associated with absorbed light by suspended PM (Arnott et al., 1999, [020650](#); Moosmuller et al., 1998, [020657](#)), as well as by the difference between light extinction and light scattering measurements (Bond et al., 1999, [156281](#)).

9.2.2.4. Value of Good Visual Air Quality

The term visual air quality (VAQ) is used here to refer to the visibility effects caused solely by air quality conditions. For example, it excludes the reduced visibility caused by fog. Two broadly different approaches have traditionally been used to define and quantify the value of good VAQ. One approach assesses the monetary value associated with visibility changes; the other assesses the psychological value of visual air quality. With respect to the latter, reduced VAQ is considered an environmental stressor (Campbell, 1983, [190172](#)) that is associated with heightened amounts of anxiety, tension, anger, fatigue, depression, and feelings of helplessness (Evans et al., 1987, [190347](#); Zeidner and Shechter, 1988, [189973](#)). Though the relationship between impaired VAQ and mental health is poorly understood, there are greater emergency calls associated with psychiatric disturbances during periods with reduced VAQ (Rotton and Frey, 1982, [190477](#)). Studies have shown that reduced VAQ affects people's behavior, including reductions in outdoor activities, and increased hostility and aggressive behavior (Cunningham, 1979, [191974](#); Evans et al., 1982, [190521](#); Jones and Bogat, 1978, [190396](#); Rotton et al., 1979, [190478](#)).

The value of VAQ (both monetary and non-monetary) has been investigated in two broadly different settings, non-recreational or urban settings and recreational settings, such as the NPs and wilderness areas where visibility is protected by the RHR (Trijonis et al., 1990, [157058](#)). In urban settings, public surveys have shown that greater than 80% of the participants are aware of poor VAQ conditions (Cohen et al., 1986, [190182](#)), though attitudes towards poor VAQ have been shown to vary by socio-economic status, health, and length of residence in the urban setting (Barker, 1976, [072137](#)). The economic importance of urban visibility has been examined by a number of studies designed to quantify the benefits (or willingness to pay) associated with potential improvements in urban visibility. Urban visibility valuation research prior to 1997 was summarized in Chestnut and Dennis (1997, [014525](#)), and was also described in the 2004 PM AQCD (U.S. EPA, 2004, [056905](#)) and the 2005 PM Staff Paper (U.S. EPA, 2005, [090209](#)). These reviews summarize 34 estimates (based on different cities or model specifications) from six different studies. Since the mid 1990s, however, only one new valuation study of urban visibility has been published (Beron et al., 2001, [156270](#)) which is summarized below (Section 9.2.4.6).

In recreational settings, experience based demand models have been developed using on-site and mail-in surveys to judge the relative importance to NP visitors of various park attributes including good VAQ, to assess visitor awareness of VAQ conditions, and to explore possible relationships between VAQ and visitor satisfaction (Ross et al., 1985, [044287](#); Ross et al., 1987, [037420](#)). At the three western and two eastern NPs where this survey was conducted, visitors rated the attribute identified as "clean, clear air" among the most important features of the parks. A random sample of 1,800 visitors at one of the parks (Grand Canyon) showed that visitor awareness of VAQ impacts increased as measured visibility conditions decreased, and that overall park enjoyment and satisfaction decreased with reduced VAQ. Grand Canyon visitors when asked to indicate how they would budget their time (e.g., between visiting an archaeological site or a view lookout point) indicated that they would be willing to significantly alter their behavior to experience views under improved VAQ (Malm et al., 1984, [044292](#)).

9.2.3. Monitoring and Assessment

Monitoring and the assessment of monitoring data serve a number of goals with regard to the visibility effects of PM, including improving the understanding of the physio/chemical/optical properties of the aerosol, characterizing spatial and temporal air quality patterns, and assessing the causes (i.e., pollution sources and atmospheric processes) that are responsible for visibility impairment. Information generated by special studies employing sophisticated instrumentation are typically needed to advance the understanding of aerosol properties, while characterizing trends is the product of analyzing routine monitoring data. Whereas, assessing the causes of haze usually involves a weight-of-evidence approach applied to special study and/or routine monitoring data sets

plus the use of air quality simulation modeling. This section summarizes recently available information that is based on monitoring data.

9.2.3.1. Aerosol Properties

Particle size is the most influential physical property of aerosols with respect to their dry light extinction efficiency. Chemical composition by size is used to ascertain density (needed to convert aerodynamic to physical size and to determine particle mass as a function of size) and to identify the water growth characteristics of the aerosol (needed to calculate the particle size, density and index of refraction at ambient RH). To characterize aerosol properties of interest for visibility effects, field monitoring programs typically include particle size distribution monitoring, high size resolution particle sampling with subsequent compositional analysis, and optical monitoring. These generate data that permit optical closure assessments where the light scattering and/or light extinction estimates from the aerosol data are compared to corresponding optical data. Since component contributions to visibility are generally assessed by applying the IMPROVE or some similar algorithm to measured or modeled aerosol concentration data, this section will include recent investigations that evaluate or address various assumptions inherent in the use of these simple algorithms.

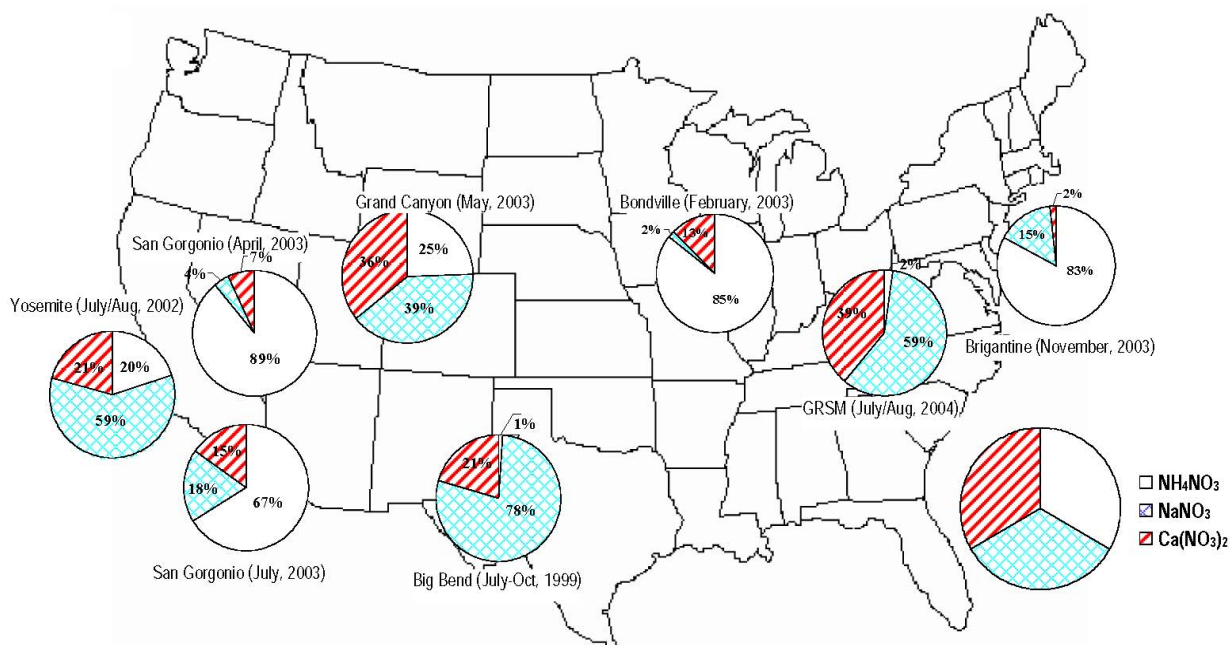
One component of the Big Bend Regional Aerosol and Visibility Observational (BRAVO) Study, conducted at Big Bend NP, TX in the summer and fall of 1999, entailed use of detailed measurements of aerosol chemical composition, size distribution, water growth, and optical properties to characterize the aerosol and assess the relationship between aerosol physical, chemical and optical properties (Malm et al., 2003, [190434](#); Schichtel et al., 2004, [179902](#)). Fine ammoniated sulfate during the BRAVO Study was about half the fine particle mass concentration and was shown to be responsible for about 35% of the light extinction. Rayleigh scattering was the second largest contributor at about 25%, followed by coarse particle (about 18%), and organic compounds (about 13%). There was little fine particle nitrate (less than 5% of the mass concentration) and most of it is apparently in the form of sodium nitrate and two thirds of it was found in the coarse mode where it comprises about 8% of the coarse particle mass concentration. Both the composition of the nitrate and the fact of much of it being in the coarse size mode ($2.5 \mu\text{m} > D > 10 \mu\text{m}$) are inconsistent with the implied assumptions of the IMPROVE algorithm.

A year-long special study of coarse particle speciation was conducted at nine IMPROVE remote area monitoring sites during 2003-2004 to provide additional information about the geographic and seasonal variations in coarse particle composition (Malm et al., 2007, [156730](#)). The same sampling and analytical methodologies procedures were used for the PM_{10} samples as are routinely used on the IMPROVE $\text{PM}_{2.5}$ samples. The IMPROVE coarse particle speciation study did not include ammonium analysis, so SO_4^{2-} and nitrate ions were assumed to be ammonium sulfate and ammonium nitrate. As expected crustal minerals were the largest contributors to coarse mass overall (about 60%), though at Mt. Rainier the fraction of coarse PM that was organic exceeded the crustal mineral by nearly two to one (i.e., 59.2% compared to 33.5%). On average across sites the organic particulate contributed significantly at about one quarter of the coarse mass, while ammonium nitrate was the third largest contributor to coarse mass (about 8%). Sea salt was negligible overall but high at the one coastal site (i.e., 12% at Brigantine, NJ). The two California sites, San Geronio and Sequoia, had the highest coarse nitrate concentrations, $0.74 \mu\text{g}/\text{m}^3$ and $0.69 \mu\text{g}/\text{m}^3$, and high fine nitrates concentrations on average, $2.66 \mu\text{g}/\text{m}^3$ and $2.14 \mu\text{g}/\text{m}^3$, respectively. Brigantine, a coastal site in New Jersey, had the highest fraction of total nitrate in the coarse size range (36%). The authors speculate that Brigantine's particulate nitrate is likely sodium nitrate, the result of nitric acid reactions with sodium chloride. The nine-site average fraction of total nitrate in the coarse size range is 26%. By contrast, coarse SO_4^{2-} concentrations are small with only about ~1% of the total SO_4^{2-} in the coarse fraction.

Routine IMPROVE monitoring data include the mass concentration, but not the composition of the coarse PM fraction, so the algorithm used to estimate light extinction does not include any provision for varied coarse PM composition as shown in this study. This study shows that about 10% of the coarse mass across the nine monitoring sites is composed of hygroscopic materials (i.e., ammonium sulfate, ammonium nitrate and sea salt), which during high humidity conditions will scatter more light than estimated by the current algorithm (e.g., ~20% bias at ~90% relative humidity). However, at coastal sites such as the Brigantine, NJ, IMPROVE site where the combined concentration of the inorganic salts (i.e., sea salt, nitrate and SO_4^{2-}) constitute a significant fraction

(~24% on average) of the coarse mass concentration, the IMPROVE algorithm underestimation of light extinction by coarse PM can be significant for high relative humidity conditions (~60% at ~90% relative humidity). The resulting underestimation of total light extinction can be much smaller since fine particle light extinction generally exceeds that contributed by coarse particles. Another issue with regard to estimating light extinction from coarse PM concentration when the composition is not crustal minerals, as has been assumed, has to do with the lower average density of the coarse mode particles that results in greater particle numbers and/or larger particles and therefore a greater light extinction efficiency (Malm and Hand, 2007, [155962](#)).

Special studies with more complete, higher time resolution and size resolved particulate inorganic ion species chemistry and precursor gases were conducted at seven of the nine sites with IMPROVE coarse particle speciation monitoring (Lee et al., 2008, [156686](#)). This work confirmed the presence of sodium and calcium nitrate (referred to as mineral nitrate) primarily in the coarse particle size range in addition to fine particle ammonium nitrate where low temperatures, high humidity and excess ammonium (beyond that required to neutralize the particulate SO_4^{2-}) favored particle phase equilibrium. Figure 9-4 is a map showing the locations and sample times and estimated composition of the total particulate nitrate for the seven locations for this special study. Sites with a high fraction of ammonium nitrate (e.g., San Gorgonio, Bondville, and Brigantine) have the highest nitrate contributions to total mass concentration and haze, whereas sites with high mineral nitrates tend to have low total nitrate contributions. This work shows that the common assumption that particulate nitrate is in the fine particle size range and consists principally of ammonium nitrate is not necessarily true.



Source: Reprinted with Permission of Atmospheric Environment from Lee et al. (2008, [156686](#))

Figure 9-4. Estimated fractions of total particulate nitrate during each field campaign comprised of ammonium nitrate, reacted sea salt nitrate (shown as NaNO_3), and reacted soil dust nitrate (shown as $\text{Ca}(\text{NO}_3)_2$).

Extinction efficiencies for individual particle species can be theoretically calculated from sized-resolved aerosol measurements and can be inferred using multiple linear regression applied to aerosol composition and light extinction measurement data. In a recent publication, Hand and Malm (2007, [155825](#)) reviewed the literature since 1990 in which aerosol mass scattering efficiency values were calculated or inferred. From these they have compiled normalized dry scattering efficiency

values for the individual species. Based on 93 separate determinations including marine, remote continental and urban areas data sets, the average dry mass scattering efficiency for ammonium sulfate is $2.5 \pm 0.6 \text{ m}^2/\text{g}$. Average values tended to be somewhat lower for the marine aerosol ($\sim 2 \text{ m}^2/\text{g}$) than for remote continental ($\sim 2.7 \text{ m}^2/\text{g}$) and urban ($2.6 \text{ m}^2/\text{g}$) areas, and values also tended to be lower for fairly clean arid locations compared with more humid polluted areas.

Based on 48 separate determinations including remote area and urban area data sets, the average dry mass scattering efficiency for ammonium nitrate is $2.7 \pm 0.5 \text{ m}^2/\text{g}$ (Hand and Malm, 2007, [155825](#)). Average values were higher in remote locations ($2.8 \pm 0.5 \text{ m}^2/\text{g}$) compared to urban locations ($2.2 \pm 0.5 \text{ m}^2/\text{g}$) though this might be accounted for by the predominate use of multiple linear regression for the remote areas, which can be biased high, compared to the use of theoretical calculations for the urban data sets.

Organic fine PM extinction efficiency of $3.9 \pm 1.5 \text{ m}^2/\text{g}$ is based on 58 separate determinations, though much higher values ($\sim 6 \text{ m}^2/\text{g}$) resulted for locations influenced by industrial and biomass combustion sources (Hand and Malm, 2007, [155825](#)). These organic fine PM extinction efficiency values were adjusted to use a consistent ratio of organic mass to OC (OC) of 1.8 for each determination of the mass concentration. This value is generally associated with aged organic PM, while for more freshly emitted PM, such as in an urban environment, a smaller ratio (e.g., 1.4) would be more appropriate. This could explain the discrepancy between two approaches used to estimate the organic PM light extinction efficiency for Phoenix (Hand and Malm, 2006, [156517](#)), which resulted in a significantly lower value where a site specific regression method was used compared to the value obtained from a method optimized for remote-area monitoring ($2.47 \text{ m}^2/\text{g}$ compared to $3.71 \text{ m}^2/\text{g}$). However in Fresno both the mass balance and light scattering balance was improved by using a ratio of 1.8 instead of 1.4 to estimate the organic compound mass (Watson and Chow, 2007, [157127](#)). Another possible or partial factor with respect to urban light extinction efficiency for organic PM may be that the size distribution of freshly emitted organic PM in urban areas extends significantly into the ultra-fine particle size range (Demerjian and Mohnen, 2008, [156392](#)) that is less efficient per mass concentration at light scattering than the generally larger-sized aged organic PM such as from a distant forest fire as was measured at the Baltimore Supersite.

Hand and Malm (2007, [155825](#)) also reviewed and made recommendations for extinction efficiencies for the other PM components including mixed coarse mode ($1.0 \pm 0.9 \text{ m}^2/\text{g}$ based on 51 determinations) and fine mode dust or soil ($3.3 \pm 0.6 \text{ m}^2/\text{g}$ based on 23 determinations), but recommending $1.0 \text{ m}^2/\text{g}$ for use with data from realistic collection efficiency samplers) and fine sea salt ($4.5 \pm 0.9 \text{ m}^2/\text{g}$ based on 25 determinations, but recommending $1.0 \text{ m}^2/\text{g}$ to $1.3 \text{ m}^2/\text{g}$ for use with data from realistic collection efficiency samplers). This work did not address light absorption efficiency of EC, CB, or crustal PM.

The Hand and Malm (2007, [155825](#)) average dry mass light scattering efficiency values are generally consistent with the values for the IMPROVE algorithm (as shown in Equation 9-1). However the adoption of the IMPROVE algorithm by EPA for calculating the haze metric used to track trends and assess the nominal pace of progress for the RHR (U.S. EPA, 2001, [157068](#)) resulted in much greater scrutiny of its performance in estimating extinction (Lowenthal and Kumar, 2003, [156712](#); Malm, 1999, [025037](#); Malm and Hand, 2007, [155962](#); Ryan et al., 2005, [156934](#)). Among the issues raised is that the algorithm tended to underestimate the light extinction for the haziest conditions and overestimate light extinction for the clearest conditions in regions such as the southeastern U.S., though it generally worked well in the arid western U.S. Furthermore, they showed the lack of mass or light scattering closure at coastal sites due to sea salt that was not accounted for by the IMPROVE algorithm. These assessments used mass concentration and light extinction closure and regression analysis methods to infer that the dry extinction efficiency for the major fine particle components would need to vary in order to avoid the biased estimates of light extinction at the extremes. Theoretical calculations of SO_4^{2-} dry extinction efficiencies for 41 days of size-resolved chemical composition data for Big Bend, TX as part of the BRAVO Study produced a range of results from $\sim 2.4 \text{ m}^2/\text{g}$ to $\sim 4.1 \text{ m}^2/\text{g}$, with the larger dry extinction efficiency values tending to be associated with higher ammonium sulfate mass concentration and narrower size distributions (Schichtel et al., 2004, [179902](#)).

In response to the technical concerns raised about the performance of the IMPROVE algorithm, a revised algorithm was developed (Pitchford et al., 2007, [098066](#)). The revised version of the algorithm differs from the original algorithm by: including a fine sea salt term related to the measured chloride ion concentration; increasing by about 30% the mass concentration of the organic aerosol component by changing the ratio of organic compound mass to OC mass from 1.4 to 1.8;

using site elevation dependent Rayleigh scattering in place of 10 Mm^{-1} that had been used at every site; adding a NO_2 light absorption term; and employing a split component model for the secondary particulate components (i.e., SO_4^{2-} , nitrate and organic species) with new water growth terms to better estimate their extinction at the high and low extremes of the range. The revised algorithm is displayed below in Equation 9-2.

$$\begin{aligned}
 b_{ext} \approx & 2.2 \times f_s(RH) \times [\textit{Small Sulfate}] + 4.8 \times f_L(RH) \times [\textit{Large Sulfate}] \\
 & + 2.4 \times f_s(RH) \times [\textit{Small Nitrate}] + 5.1 \times f_L(RH) \times [\textit{Large Nitrate}] \\
 & + 2.8 \times [\textit{Small Organic Mass}] + 6.1 \times [\textit{Large Organic Mass}] \\
 & + 10 \times [\textit{Elemental Carbon}] \\
 & + 1 \times [\textit{Fine Soil}] \\
 & + 1.7 \times f_{ss}(RH) \times [\textit{Sea Salt}] \\
 & + 0.6 \times [\textit{Coarse Mass}] \\
 & + \textit{Rayleigh Scattering (Site Specific)} \\
 & + 0.33 \times [\textit{NO}_2 \text{ (ppb)}]
 \end{aligned}$$

Equation 9-2

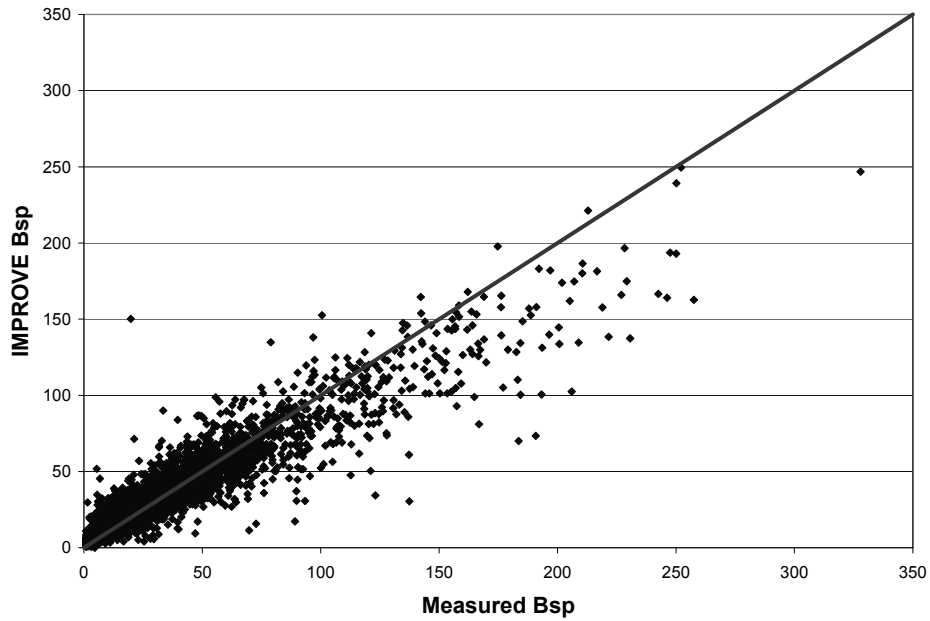
Source: Reprinted with Permission of the Air & Waste Management Association from Pitchford et al. (2007, [098066](#))

Small and large SO_4^{2-} , nitrate and organic mass are used to refer to the splitting of the concentrations of each of those three species into two size distributions. This approach accounts for increased light extinction efficiency with mass by using a simple mixing model that assume that each of these three components are comprised of an external mixture of small and large particle size modes. Conceptually, the large mode particles represent aged or cloud-processed aerosol, while the small mode particles represent relatively newly generated particles from the gas phase precursors. The former are more likely to be associated with high concentrations while the latter are likely to be at relatively low concentration.

The geometric mean diameter and standard deviations assumed for these two size modes are $0.5 \mu\text{m}$ and 1.5 for the large mode particles and $0.2 \mu\text{m}$ and 2.2 for the small mode particles. Mie theory applied to these size distributions for the three species results in dry extinction efficiencies for the small and large mode ammonium sulfate ($2.2 \text{ m}^2/\text{g}$ and $4.8 \text{ m}^2/\text{g}$), ammonium nitrate ($2.4 \text{ m}^2/\text{g}$ and $5.1 \text{ m}^2/\text{g}$) and organic mass ($2.8 \text{ m}^2/\text{g}$ and $6.1 \text{ m}^2/\text{g}$). Water growth terms specifically derived for the small and large size distribution using the upper branch of the hygroscopic growth curves for ammonium sulfate are applied to both the SO_4^{2-} and nitrate PM. No water growth is assumed for organic PM.

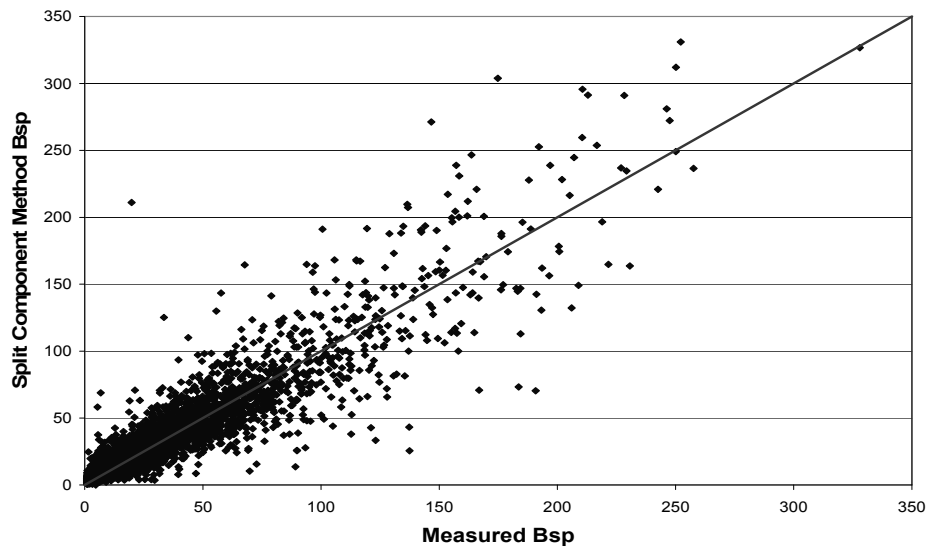
A simple empirically developed apportionment approach that was evaluated by testing the new algorithms estimated light scattering at the 21 IMPROVE sites that have nephelometer-measured light scattering data. For each sample, the fraction of the fine particle component (SO_4^{2-} , nitrate, or organic mass) that is assigned to the large mode is calculated by dividing the total concentration of the component by $20 \mu\text{g}/\text{m}^3$ (e.g., if the total fine particle nitrate concentration is $4 \mu\text{g}/\text{m}^3$, the large mode concentration is $1/5$ of $4 \mu\text{g}/\text{m}^3$ or $0.8 \mu\text{g}/\text{m}^3$, leaving $3.2 \mu\text{g}/\text{m}^3$ in the small mode). If the total concentration of a component exceeds $20 \mu\text{g}/\text{m}^3$, all of it is assumed to be in the large mode.

Figure 9-5 and Figure 9-6 are scatterplots of the estimated versus measured light scattering for the two algorithms. The revised algorithm has noticeably reduced bias at the upper and lower extremes. However, the new algorithm estimates have somewhat reduced precision (i.e., the points are more broadly scattered). States have adopted the new algorithm for the technical assessments that support their RHR State Implementation Plans, but the revised algorithm was too recently developed to be incorporated into any of the peer-reviewed technical literature reported on below. In general the differences resulting from use of the original versus the revised IMPROVE algorithm in identifying best and worst haze conditions and the apportionment of the various PM components are small with exception of coastal locations where sea salt may be a significant contributor.



Source: Reprinted with Permission of the Air & Waste Management Association from Pitchford, et al. (2007, [098066](#))

Figure 9-5. A scatter plot of the original IMPROVE algorithm estimated particle light scattering versus measured particle light scattering.



Source: Reprinted with Permission of the Air & Waste Management Association from Pitchford, et al. (2007, [098066](#))

Figure 9-6. Scatter plot of the revised algorithm estimates of light scattering versus measured light scattering.

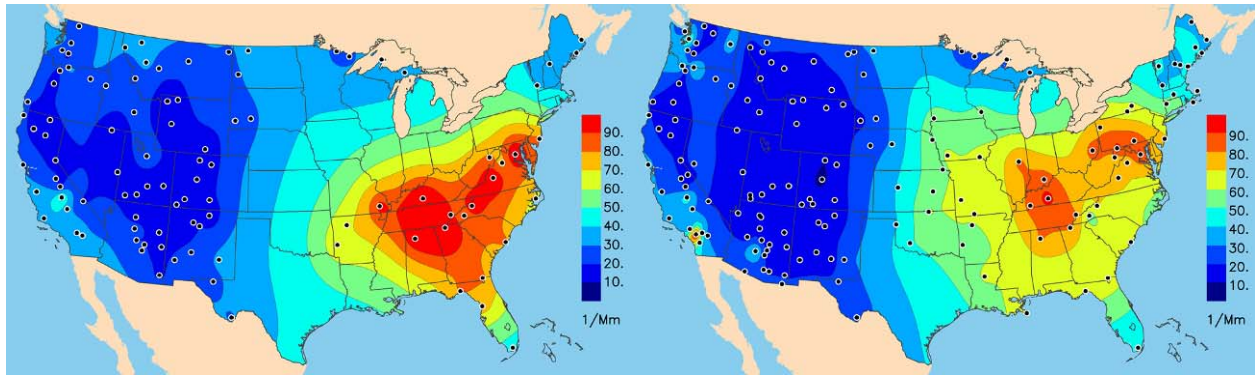
9.2.3.2. Spatial Patterns

The IMPROVE network is the basis for much of what is known about particulate species spatial and temporal patterns for remote areas of the U.S. Though IMPROVE includes some urban monitoring sites, most of what is known about urban particle speciation trends is based on the EPA Speciation Trend Network (STN) and other similarly operated state particle speciation sites jointly referred to as the Chemical Speciation Network (CSN) (Jayanty, 2003, [156605](#)). The number of IMPROVE network sites has increased considerably beginning in 2000, first to increase its ability to generate data representative of the 156 visibility-protected NPs and wilderness areas, then later as the states in the central U.S. requested additional remote-area monitoring to better understand their contributions to regional haze. The expansion of the network into the central U.S. significantly improved the understanding of spatial trends in a region of the country that had little speciation monitoring. Except as otherwise noted most of the information in this section was from the IMPROVE Report IV (DeBell, 2006, [156388](#)) and displays of data that are readily generated using the Visibility Information Exchange Web Site (VIEWS). VIEWS, the ambient monitoring data system, is one of several websites (as described in Table 9-1) sponsored by the Regional Planning Organizations (RPO) that documents substantial, though often otherwise unpublished, technical information generated to support implementation of the RHR.

Figure 9-7 shows maps of remote area light extinction estimates from PM speciation data for two years selected to demonstrate the additional information available due to the expansion of the IMPROVE network into the central U.S. The locations of monitoring sites supplying the data shown as color contours are shown as dot on the maps. Users of such contour maps are usually cautioned that the contours are only there to guide the eye to sites with similar measurements and that nothing should be implied about spatial patterns where there are no monitoring sites. Certainly these plots give proof to the wisdom of such warnings. Prior to 2001 there were no IMPROVE or any other remote-area aerosol speciation monitoring sites in the central states between northern Minnesota and Michigan to the north and Arkansas and Kentucky to the south. The lack of monitoring over such a large region in the center of the country hid the presence of high average regional haze over the midwestern U.S. Smaller scale differences are seen in the rest of the country and some of those are due to interannual variations as well as to better spatial resolution made possible by a more dense monitoring network.

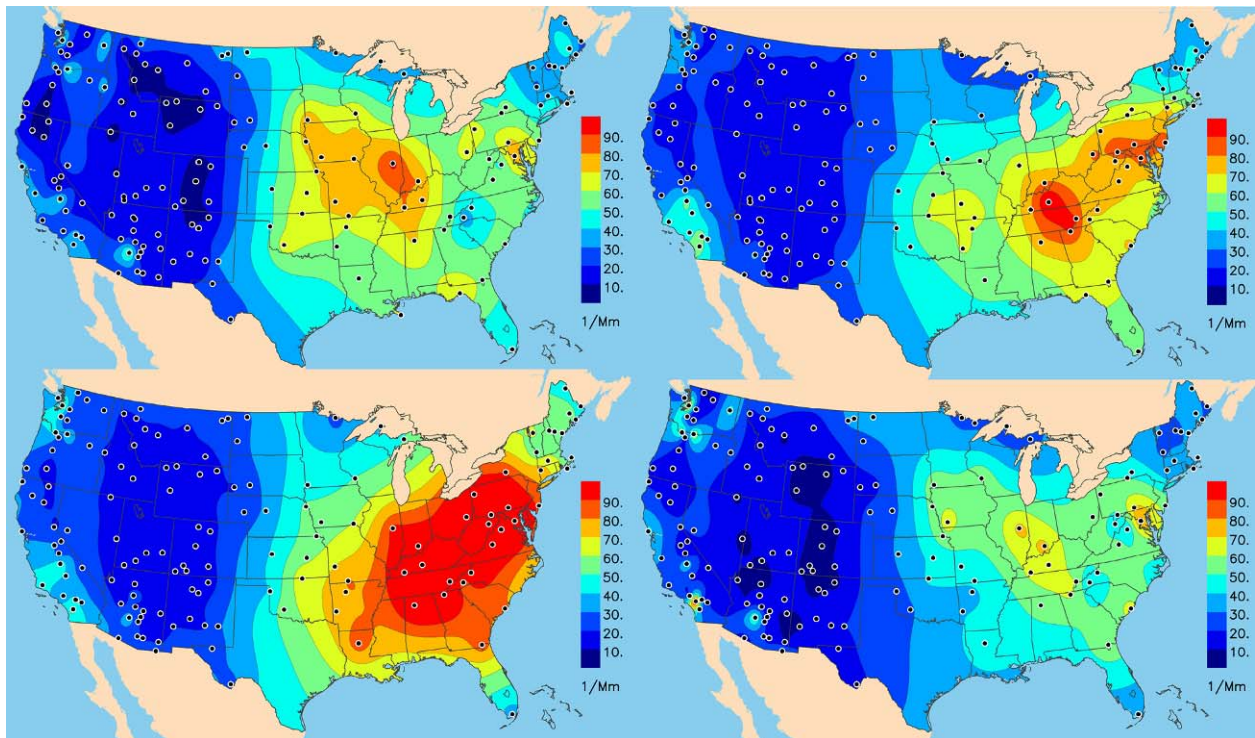
Table 9-1. Regional Planning Organization websites with visibility characterization and source attribution assessment information.

Type of Information	Name and Web Address	RPO	Information Content and Comments
RPO Home Pages	Western Regional Air Partnership http://www.wrapair.org/	WRAP	Organizational structure, plans, projects, reports and links to other sites with additional information. MANE-VU works in close cooperation with Northeast States for Coordinated Air Use Management (NESCAUM) and Mid-Atlantic Regional Air Management Association (MARAMA) to develop the technical information for RHR in the Northeast. All three web sites contain unique technical support information.
	Central Regional Air Planning Association http://www.cenrap.org/	CENRAP	
	Midwest Regional Planning Organization http://64.27.125.175/mrpo.html	MRPO	
	Visibility Improvement State and Tribal Association of the Southeast http://www.vistas-sesarm.org/	VISTAS	
	Mid-Atlantic/Northeast Visibility Union http://www.manevu.org/ http://www.nescaum.org/topics/regional-haze http://www.marama.org/visibility/	MANE-VU NESCAUM MARAMA	
Visibility - Air Quality Monitoring Data	Visibility Information Exchange Web Site http://vista.cira.colostate.edu/views/	All RPOs	All IMPROVE and most other PM speciation data, RHR compatible derived parameters, and user-friendly tools to summarize and display data.
Emission Inventory Data	Emissions Data Management System http://www.wrapedms.org/default_login.asp	WRAP	WRAP emission inventory data warehouse and tools that provides a consistent approach to regional emissions tracking
Monitoring Data Assessment	Causes of Haze Assessment http://www.coha.dri.edu/	WRAP CENRAP	Monitoring site-specific descriptive characterizations and maps, seasonal and trends analysis, air flow analysis, & receptor modeling.
Visibility Modeling	U. of California-Riverside Modeling Center http://pah.cert.ucr.edu/aqm/308/ http://pah.cert.ucr.edu/aqm/cenrap/index.shtml http://pah.cert.ucr.edu/vistas/	WRAP CENRAP VISTAS	Descriptions of input data, performance, and results of regional scale modeling (CMAQ & CAMx) & source attribution for base and future year regional haze.
Integrated Information to Support RHR SIP Preparations	Technical Support System http://vista.cira.colostate.edu/tss/	WRAP	Provides access and common formats to display and summarize emissions inventory information, monitoring data/ assessment and regional haze modeling result to aid state and tribal analyst prepare RHR implementation plans.



Source: VIEWS (<http://vista.cira.colostate.edu/views/>)

Figure 9-7. IMPROVE network PM species estimated light extinction for 2000 (left) and for 2004 (right).



Source: VIEWS (<http://vista.cira.colostate.edu/views/>)

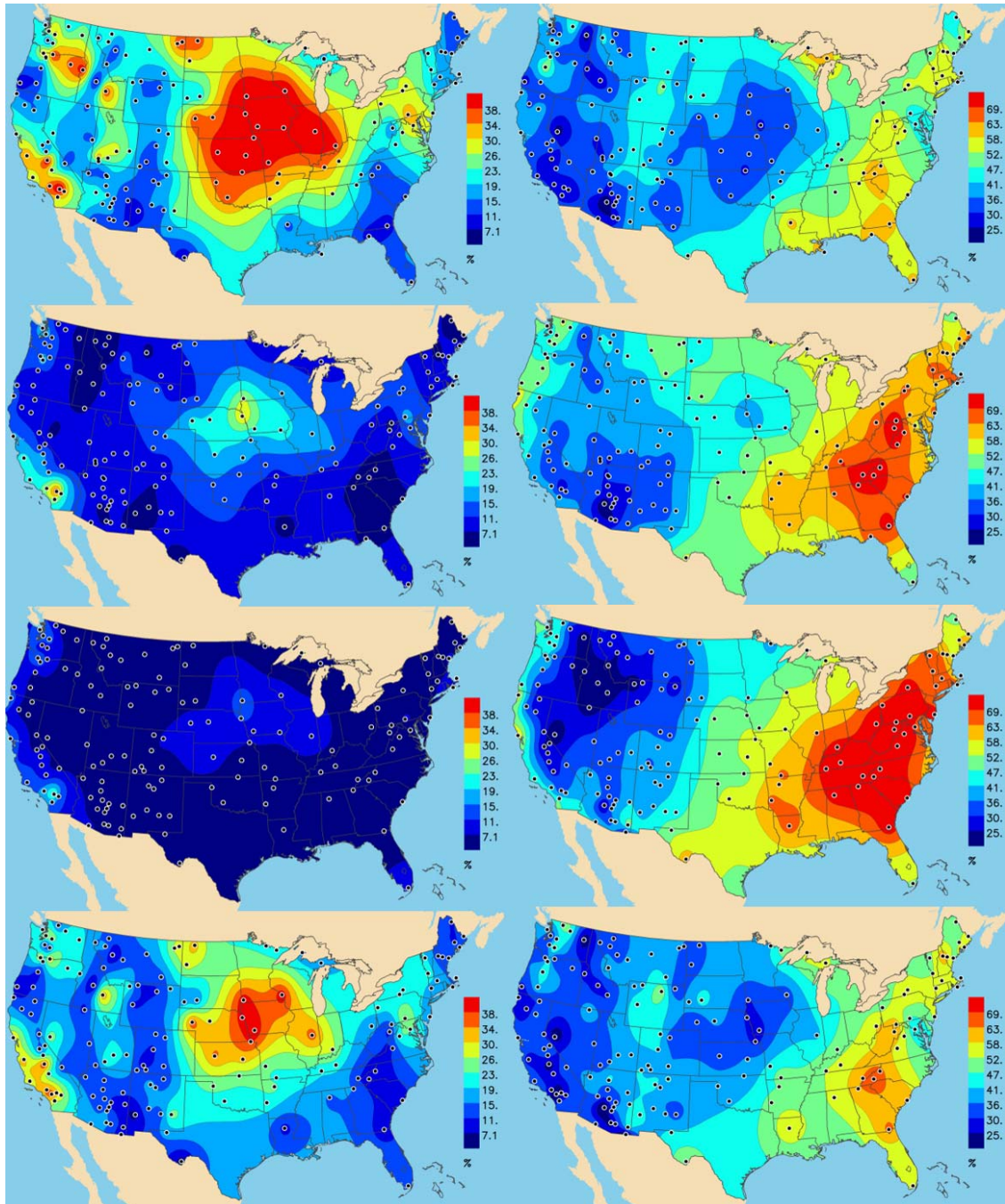
Figure 9-8. Mean estimated light extinction from PM speciation measurements for the first (top left), second (top right), third (bottom left), and fourth (bottom right) calendar quarters of 2004.

Figure 9-8 shows the seasonal pattern of PM species estimated light extinction using maps of mean values for each of the calendar quarter for 2004. The first quarter has the highest region of haze centered in the midwestern U.S.; the warmer second and third quarters have the region of highest haze over the Ohio River Valley; and the fourth quarter is a composite with high haze in both

the Midwest and Ohio River Valley. Smaller regions of haze show up in the Columbia River Valley (border between Washington and Oregon) in the colder first and fourth quarters and in Southern California in the warmer second and third quarters.

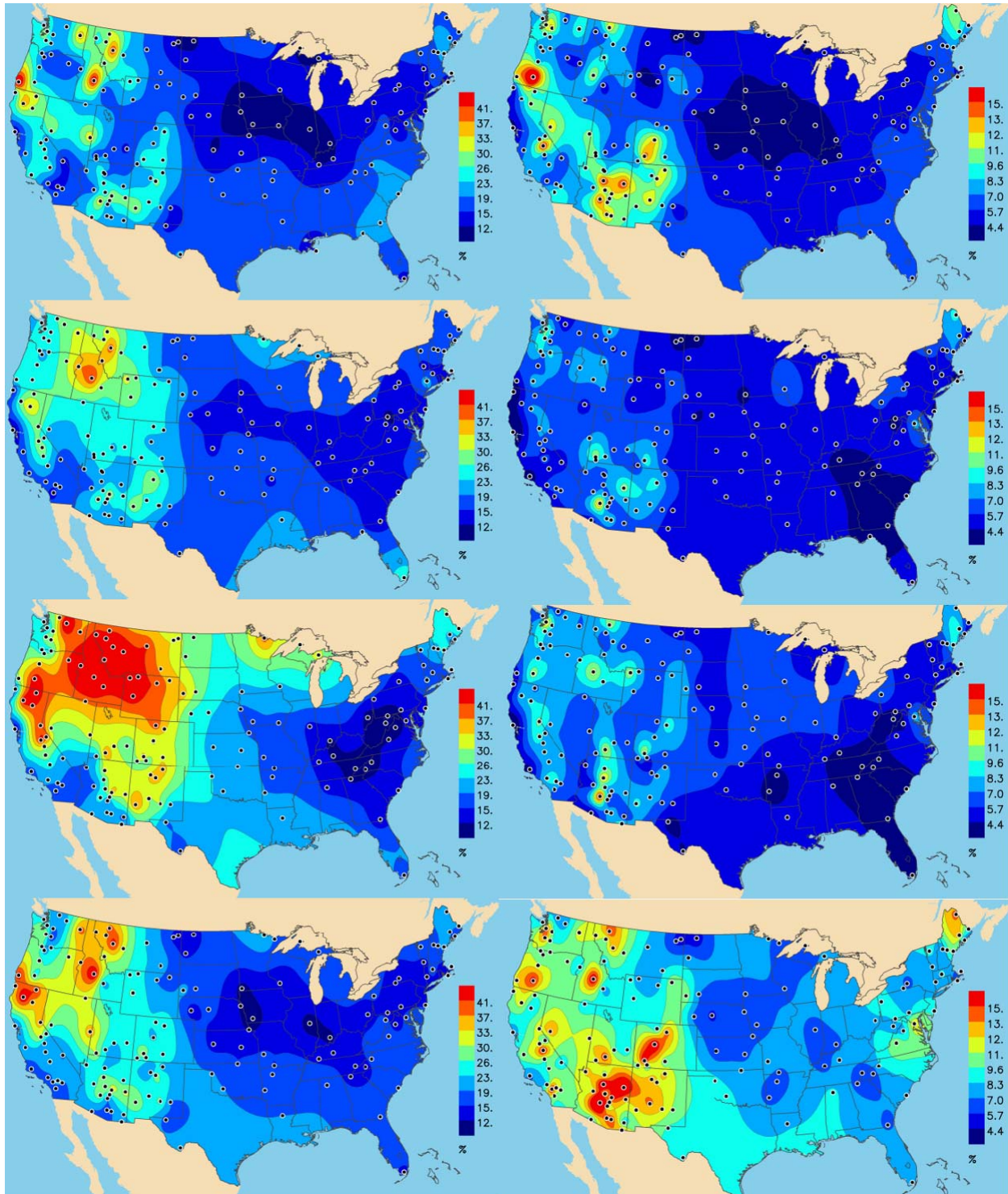
The IMPROVE algorithm permits each PM component contribution to light extinction to be separately estimated. Figure 9-9, Figure 9-10, and Figure 9-11 display the seasonal variation of the percent contribution to aerosol light extinction by the various component estimates. Figure 9-9 shows the contributions by SO_4^{2-} and nitrate particulate including the haze enhancement caused by the absorbed water in humid conditions. As shown in Figure 9-9, a large regional pattern of high contribution to haze by nitrate PM is centered in the Midwest, and during the cooler months the nitrate PM is the dominant cause of haze in the region responsible for a third to a half of the particulate light extinction. Midwestern particulate nitrate is responsible for the regional pattern of the highest haze conditions shifting from the Ohio River Valley during summer to the Midwest in the winter as shown in Figure 9-8. Particulate nitrate is also a significant contributor to particulate light extinction year-around in parts of California, where it generally contributes 20%-40%. The Pacific Northwest, parts of Idaho and Utah experience large contributions to particulate light extinction by nitrates during the colder seasons, with contributions of 20%-30%. Figure 9-9 also shows that particulate SO_4^{2-} is the predominate contributor in the eastern U.S., where it contributes 40% or more on average and during the summer months up to three quarters of the particulate light extinction over much of the East. In the western U.S. particulate SO_4^{2-} generally contribute 20-50% of the particle light extinction. Regions of the lowest fractional contributions by particulate SO_4^{2-} and nitrate for any calendar quarter are generally in the western U.S.

Figure 9-10 shows the contributions to haze by the carbonaceous PM components (i.e., organic mass and EC). They show broadly similar patterns with the greatest contributions in the western U.S. especially during the warmer months of the year. For the most part this spatial pattern results from the dominant contributions to haze by SO_4^{2-} and nitrate PM in the eastern half of the U.S., leaving relatively little for other component contributions. The fractional contribution to haze by organic PM is generally two to five times that of EC. In absolute terms, both carbonaceous components tend to have two to three times higher concentrations in the eastern U.S. than in the non-coastal western states.



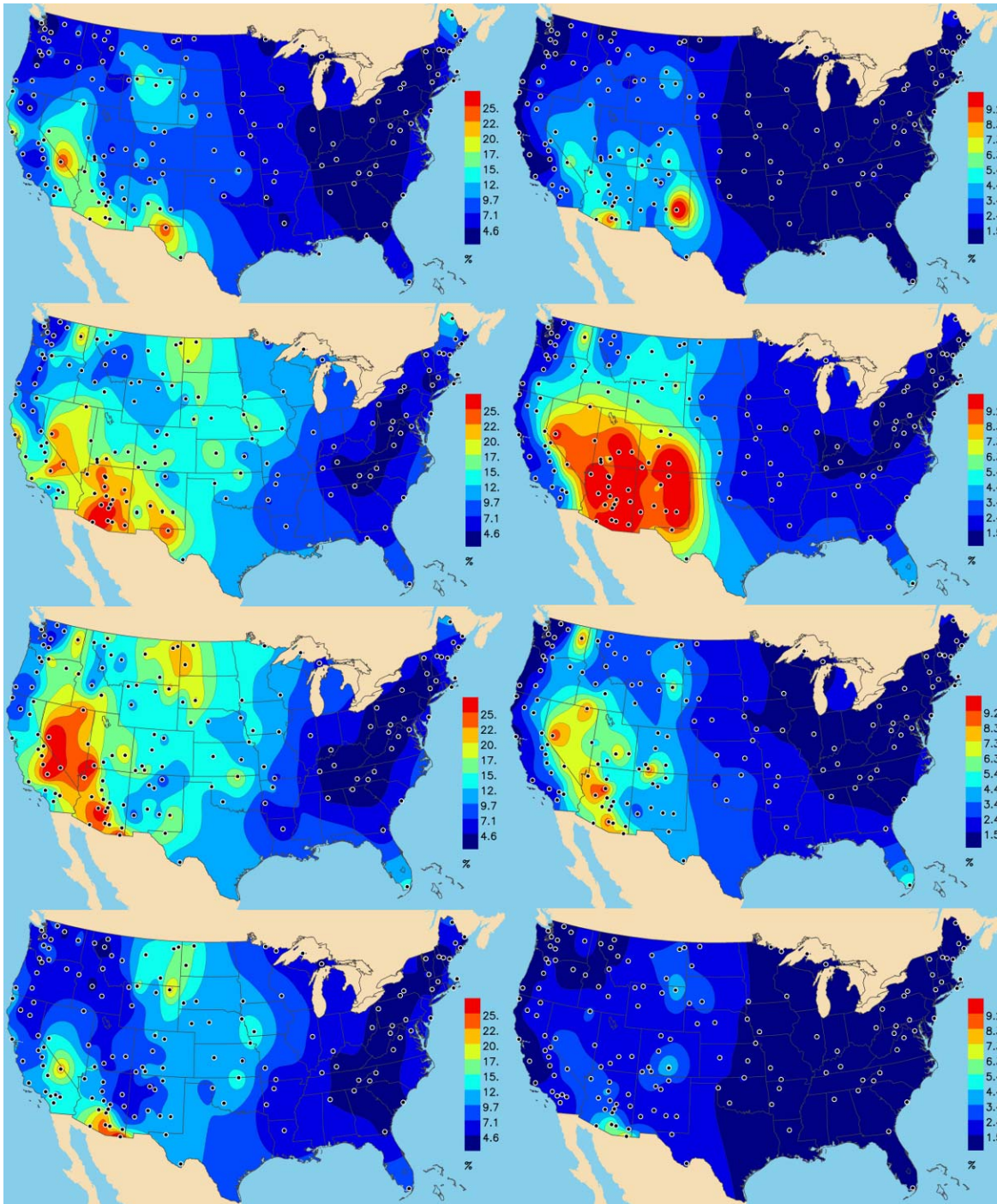
Source: VIEWS (<http://vista.cira.colostate.edu/views/>)

Figure 9-9. Percent contributions of ammonium nitrate (left column) and ammonium sulfate (right column) to particulate light extinction for each calendar quarter of 2004 (first through fourth quarter arranged from top to bottom). Note that the contour intervals are not the same for the two species contributions.



Source: VIEWS (<http://vista.cira.colostate.edu/views/>)

Figure 9-10. Percent contributions of organic mass (left column) and EC (right column) to particulate light extinction for each calendar quarter of 2004 (first through fourth quarter arranged from top to bottom). Note that the contour intervals are not the same for the two species contributions.



Source: VIEWS (<http://vista.cira.colostate.edu/views/>)

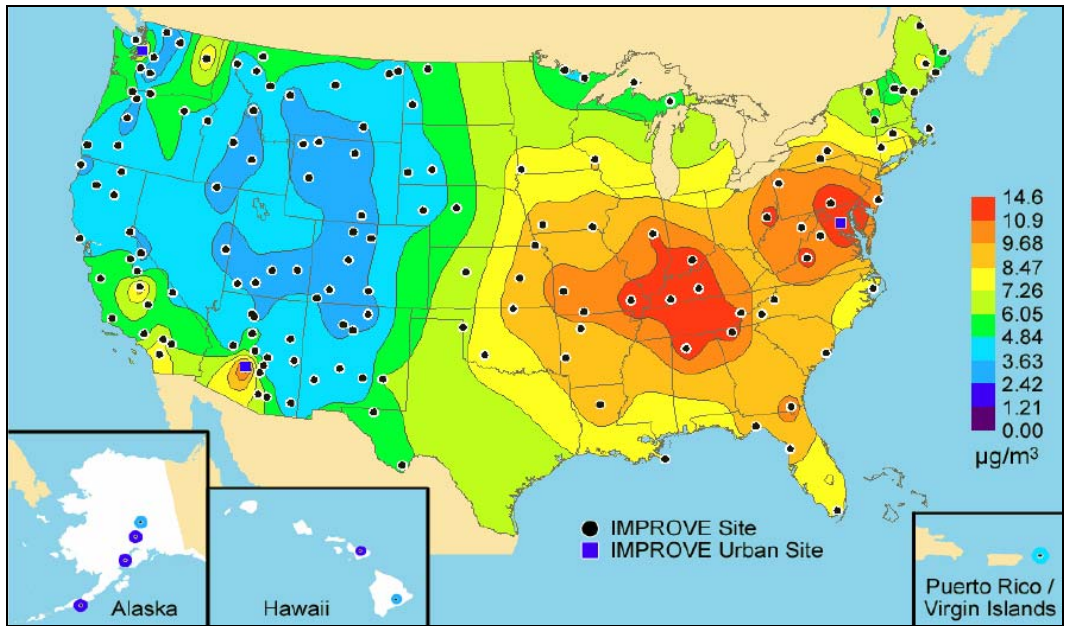
Figure 9-11. Percent contributions of coarse mass (left column) and fine soil (right column) to particulate light extinction for each calendar quarter of 2004 (first through fourth quarter arranged from top to bottom). Note that the contour intervals are not the same for the two species contributions.

Figure 9-11 shows the contributions to haze by coarse mass and fine soil components. As with the carbonaceous components, these crustal dominated components have a similar spatial pattern with regions of highest contribution to haze in the western U.S., and just as for the carbonaceous PM, the explanation for low contributions in the eastern U.S. is the dominant contributions to haze by SO_4^{2-} and nitrate PM leaving relatively little for other components. The crustal components contribute more to haze in the arid regions of the west including the southwestern deserts. In absolute terms, coarse mass concentrations are as high in the rural areas of the center of the country (including Oklahoma, Arkansas, Kansas, Missouri, and Iowa) as they are in the Desert Southwest. Typically coarse mass contributions to haze exceed those of fine mass by a factor of 2-4.

9.2.3.3. Urban and Regional Patterns

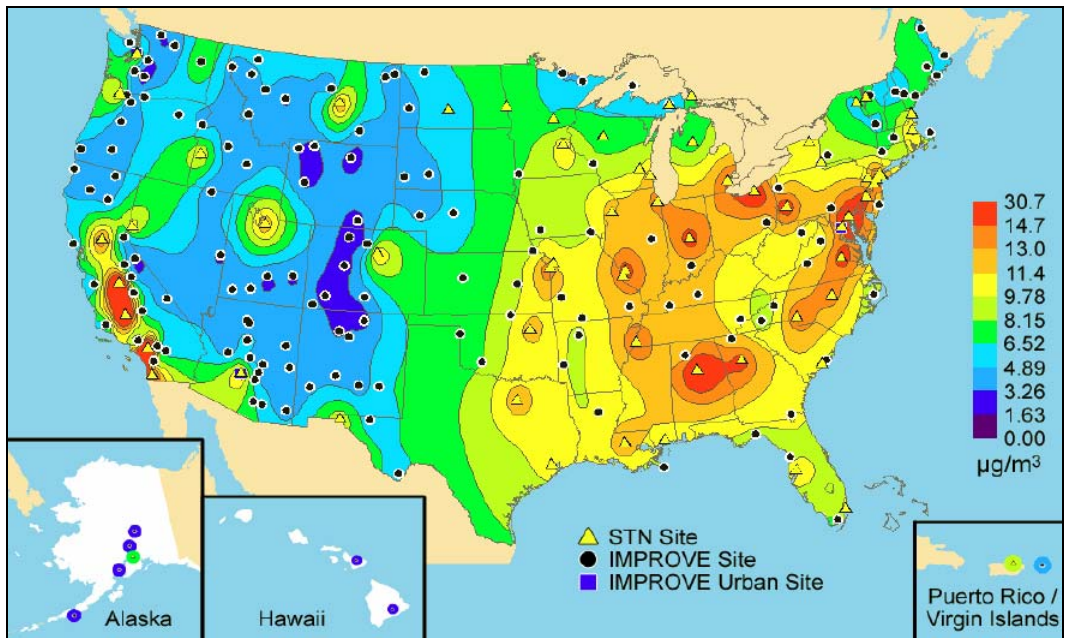
Using a combination of IMPROVE and CSN data, it is possible to compare urban $\text{PM}_{2.5}$ concentrations and composition to corresponding remote-area regional values. These are shown as paired color contours maps for IMPROVE and IMPROVE plus CSN (see Figure 9-12 through Figure 9-23). The degree of comparability of the data from these 2 networks was assessed by an analysis of two years of co-located IMPROVE and CSN data from 6 urban areas. The CSN organic mass data were adjusted for a positive sampling artifact prior to inclusion in this assessment, in a fashion similar to that used for the IMPROVE data set (pages 29-30, DeBell, 2006, [156388](#)). Note that the contour scales are different between the two maps for each component pair of maps so that each contains as much information as possible using ten concentration contours. To assess the degree to which urban areas have higher PM component concentrations compared to regional background note how many contour intervals surround the urban monitoring sites. The U.S. EPA (2004, [190219](#)) used the pairing of IMPROVE and CSN monitoring sites at 13 selected urban areas to separate local and regional contributions of three major $\text{PM}_{2.5}$ components as shown in Figure 9-24.

In Figure 9-12 and Figure 9-13, urban $\text{PM}_{2.5}$ concentrations are systematically higher than those in the surrounding non-urban regions. The urban excess is generally much higher in the western U.S. than in the East (e.g., there are five contour intervals separating Salt Lake City from its remote regional area compared to only two for Indianapolis). This implies that eastern and western urban $\text{PM}_{2.5}$ concentrations and resulting visibility are less different than the eastern and western regional concentrations and visibility.



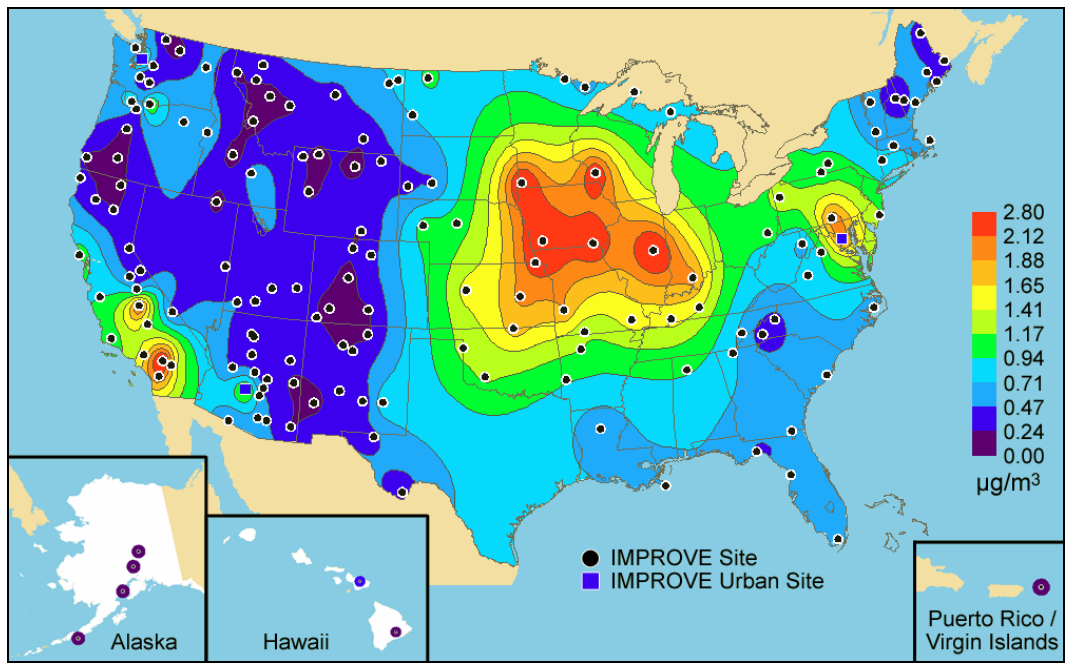
Source: Debell (2006, [156388](#)).

Figure 9-12. IMPROVE Mean PM_{2.5} mass concentration determined by summing the major components for the 2000-2004.



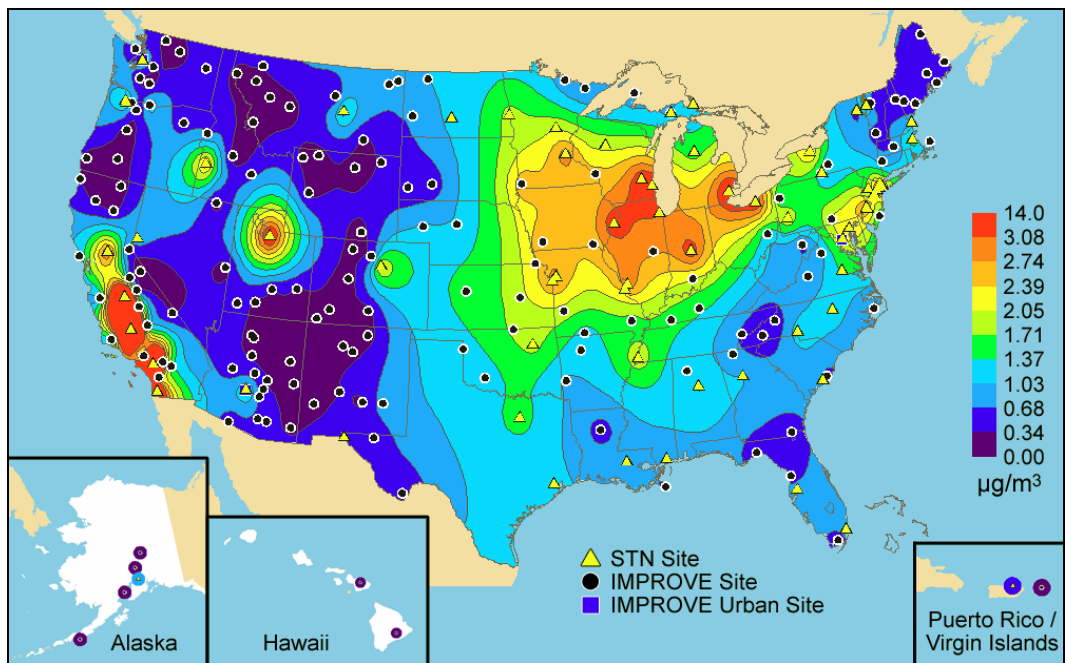
Source: Debell (2006, [156388](#)).

Figure 9-13. IMPROVE and CSN (STN) mean PM_{2.5} mass concentration determined by summing the major components for 2000-2004.



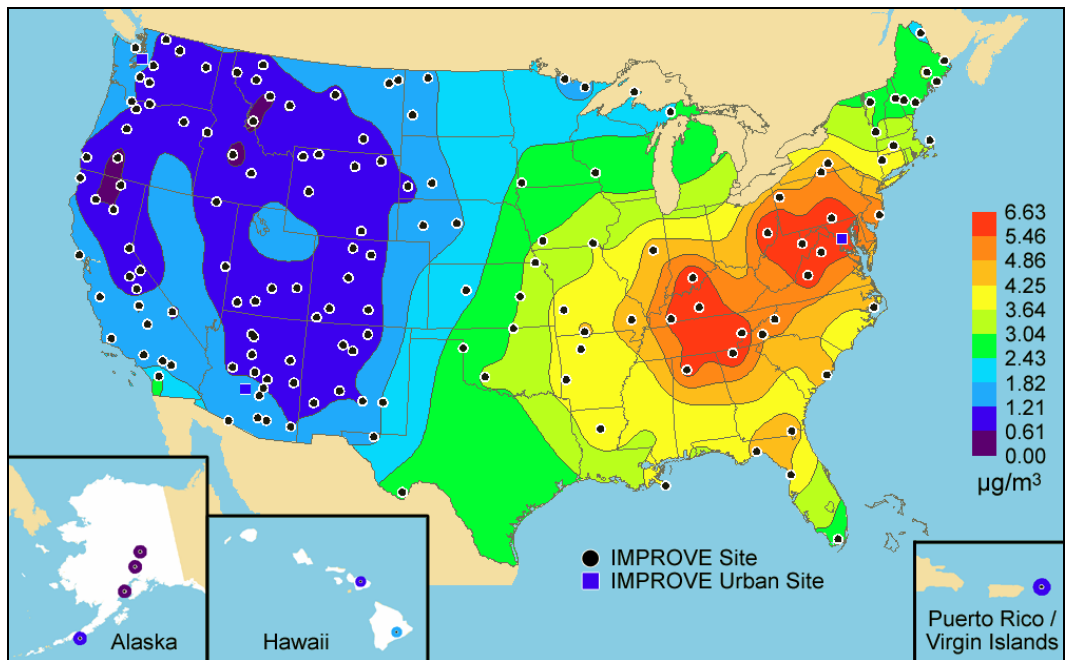
Source: Debell (2006, [156388](#)).

Figure 9-14. IMPROVE mean ammonium nitrate concentrations for 2000-2004.



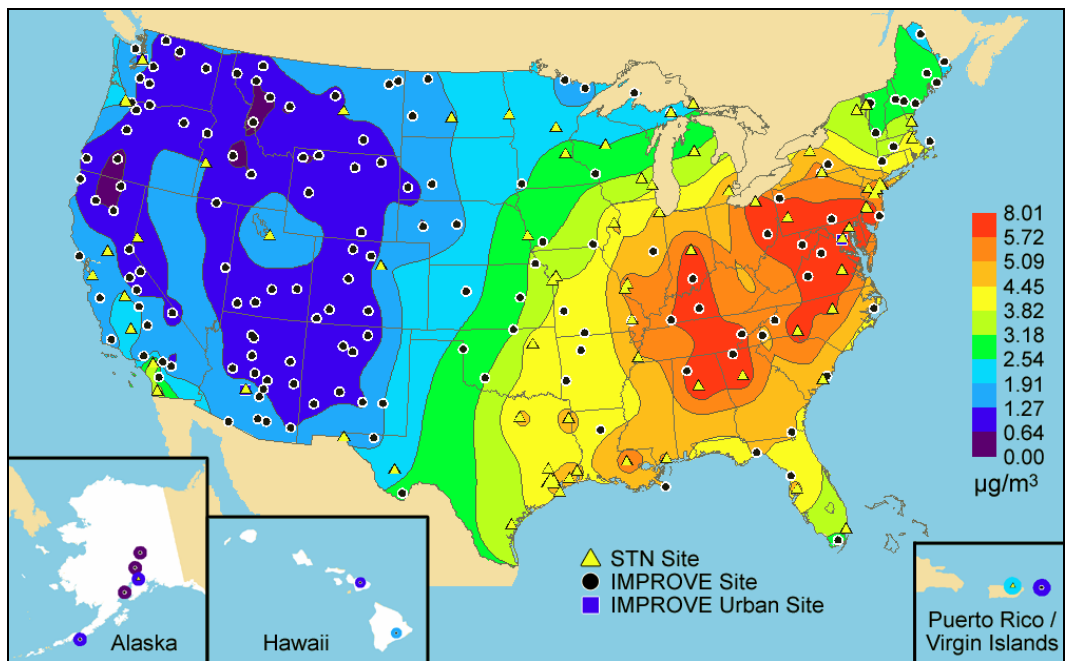
Source: Debell (2006, [156388](#)).

Figure 9-15. IMPROVE and CSN (STN) mean ammonium nitrate concentrations for 2000-2004.



Source: Debell (2006, [156388](#)).

Figure 9-16. IMPROVE mean ammonium sulfate concentrations for 2000-2004.



Source: Debell (2006, [156388](#)).

Figure 9-17. IMPROVE and CSN (STN) mean ammonium sulfate concentrations for 2000-2004.

Figure 9-14, Figure 9-15, and Figure 9-24 show the PM_{2.5} nitrate in remote and urban areas. Here the western states have urban particulate nitrate concentrations that far exceed twice the remote

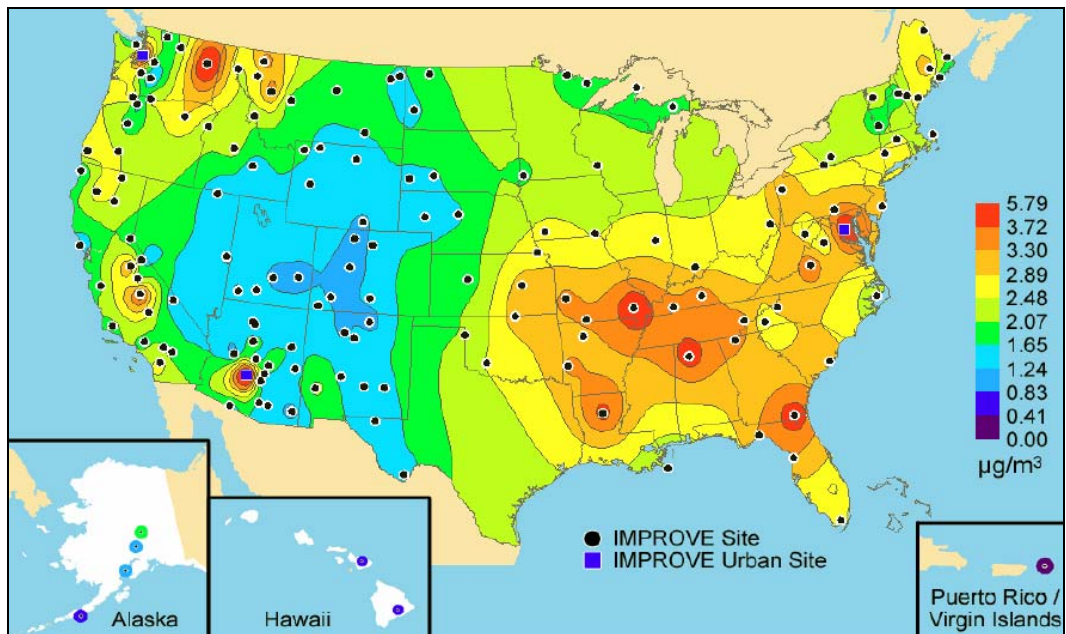
area regional concentrations. For the Central Valley of California and Los Angeles areas, the urban excess of ammonium nitrate exceeds regional concentrations by $2 \mu\text{g}/\text{m}^3$ to $12 \mu\text{g}/\text{m}^3$. In the region of the Midwest nitrate bulge, the urban concentrations were less than twice the regional concentrations for an annual urban excess of about $1 \mu\text{g}/\text{m}^3$. Northeast and southeast of the Midwest nitrate bulge, annual urban particulate nitrate concentrations are several tenths to about $1 \mu\text{g}/\text{m}^3$ above the remote area regional concentrations, with warmer southern locations tending to have the smaller concentrations of both regional and urban excess particulate nitrate.

As shown in Figure 9-16, Figure 9-17, and Figure 9-24, annual-averaged urban particulate SO_4^{2-} concentrations are generally not much higher than the regional values, with urban excess generally of less than about $0.5 \mu\text{g}/\text{m}^3$. The exceptions apparent by comparing Figure 9-16 and Figure 9-17 are in Texas and Louisiana where urban excess particulate SO_4^{2-} are $>1 \mu\text{g}/\text{m}^3$, perhaps caused by local emissions (e.g., from oil refineries). Urban contributions are a larger fraction of the total particulate SO_4^{2-} concentrations in the western U.S. because the regional concentrations are much lower than in the East. The modest additional particulate SO_4^{2-} concentrations associated with urban areas suggests that most particulate SO_4^{2-} is regionally distributed, and that IMPROVE and CSN monitoring sites can be used together to enhance the ability to delineate particulate SO_4^{2-} spatial distributions. For example, note that the additional data from urban sites shown in Figure 9-17 extends north and south of the distribution of the high particulate SO_4^{2-} loading shown in Figure 9-16 over Tennessee and Kentucky, as well as the high loadings over southern Pennsylvania, eastern West Virginia and northern Virginia. (The color-contour suggested dip in concentrations between the two eastern particulate SO_4^{2-} high concentrations regions may not exist in the atmosphere, but this cannot be verified without speciation monitoring sites in southern Ohio, the border of Kentucky and West Virginia and western Virginia.)

Urban and remote area carbonaceous $\text{PM}_{2.5}$ are displayed in Figure 9-18 and Figure 9-19 (organic mass), Figure 9-20 and Figure 9-21 (EC), and Figure 9-24 (total carbon = organic + EC concentration). Just as with particulate nitrate, both organic mass and EC concentrations are more than twice the remote-area background concentrations for western urban monitoring locations. One of the more interesting pairing of sites is for the Virgin Islands compared to the urban site at San Juan, Puerto Rico (see the map cutout Figure 9-18 through Figure 9-21). The San Juan urban excess OC is moderate, while the EC value is among the most extreme inferred in this manner. For eastern urban areas, approximately half the total carbon is local while the other half is regional. In eastern urban areas, carbonaceous and SO_4^{2-} particulate are the two major components of $\text{PM}_{2.5}$, with roughly equal contributions, and account for over 80% of the mass concentration. Edgerton et al. (2004, [156413](#)) showed that carbonaceous $\text{PM}_{2.5}$ is responsible for most of the urban excess above regional concentrations at four urban/rural paired Southeastern Aerosol Research and Characterization (SEARCH) monitoring sites in the southeastern U.S. However, the higher overall light extinction efficiency for SO_4^{2-} resulting from its hydrophilicity gives it $\sim 2:1$ dominance in responsibility for eastern urban light extinction.

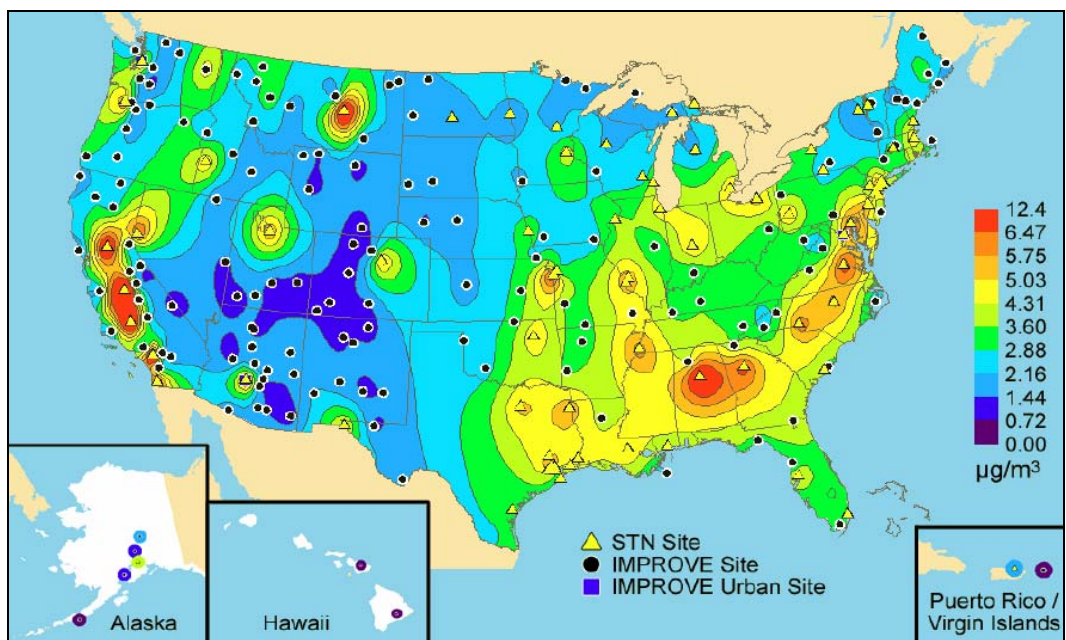
Urban and remote area soil $\text{PM}_{2.5}$ concentrations are displayed in Figure 9-22 and Figure 9-23. Urban fine soil concentrations are at most a few tenths of a $\mu\text{g}/\text{m}^3$ higher than the regional background concentrations and in some regions they are much less. Just as with carbonaceous $\text{PM}_{2.5}$, the Virgin Island, San Juan, Puerto Rico pair are interesting for fine soil. In this case, both of these island monitoring sites have high concentrations of fine soil, which is caused by the influence of the trans-Atlantic transport path of dust from Africa (Prosero, 1996, [156889](#)).

No urban-remote pair of coarse mass concentration maps is available because CSN does not monitor coarse mass. In Malm et al. (2004, [156728](#)) a map of annual mean coarse mass concentration is shown for 2003 which includes the values for IMPROVE urban sites, including two in the western U.S. with much more coarse mass than the nearby remote areas monitoring sites (i.e., $\sim 24 \mu\text{g}/\text{m}^3$ compared to $\sim 9 \mu\text{g}/\text{m}^3$ for Phoenix, AZ, and $\sim 6 \mu\text{g}/\text{m}^3$ compared to $\sim 2 \mu\text{g}/\text{m}^3$ for Puget Sound, WA) and one eastern IMPROVE site at Washington, DC with less coarse mass than the surrounding remote area values ($\sim 2 \mu\text{g}/\text{m}^3$ compared to $\sim 4 \mu\text{g}/\text{m}^3$).



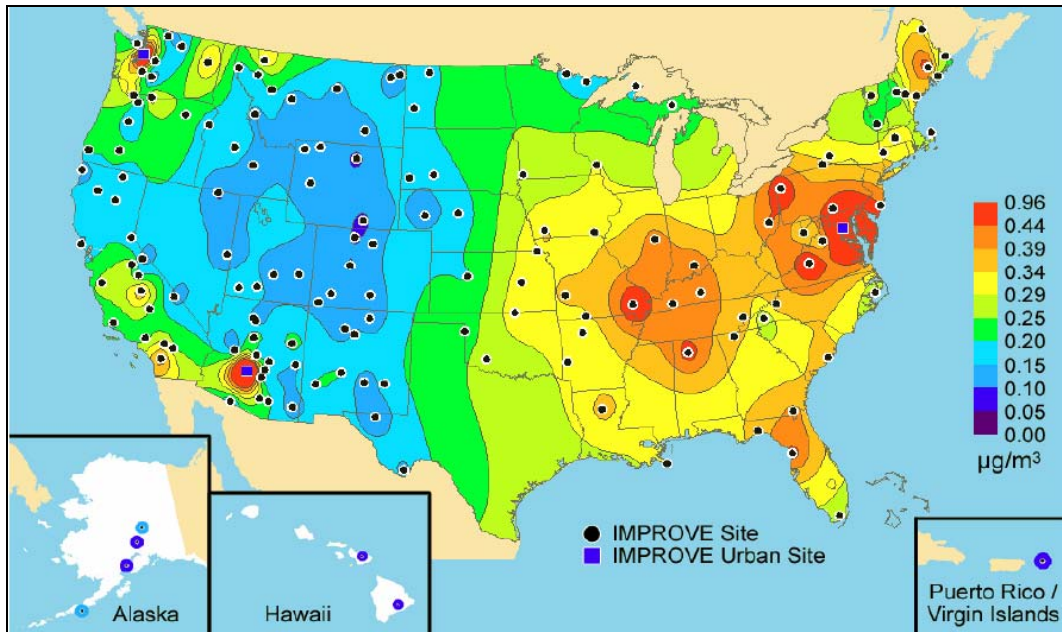
Source: Debell (2006, [156388](#)).

Figure 9-18. IMPROVE monitored mean organic mass concentrations for 2000-2004.



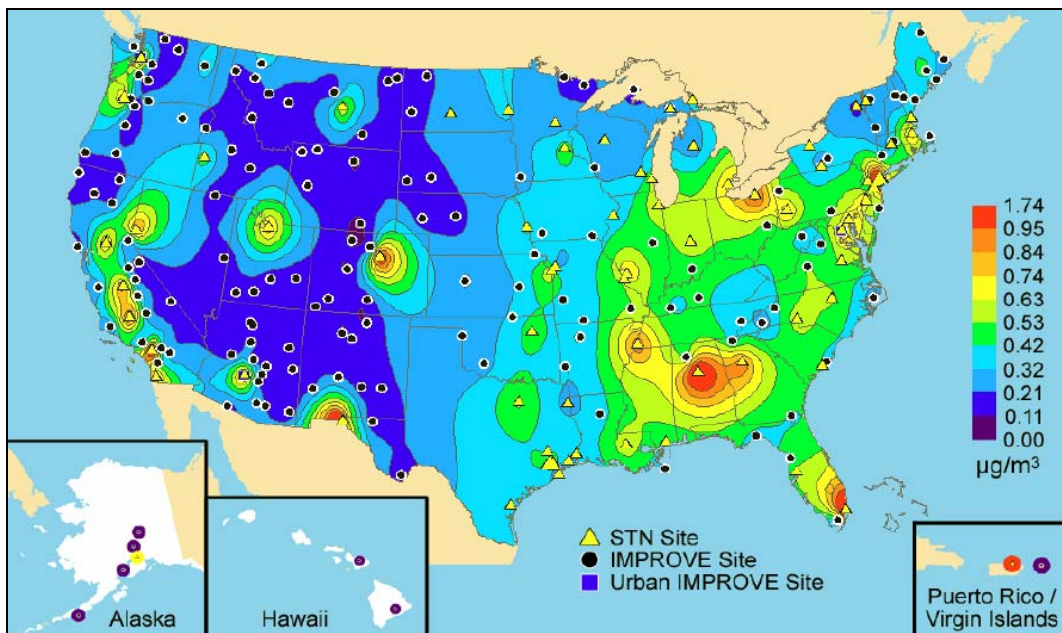
Source: Debell (2006, [156388](#)).

Figure 9-19. IMPROVE and CSN (STN) mean organic mass concentrations for 2000-2004.



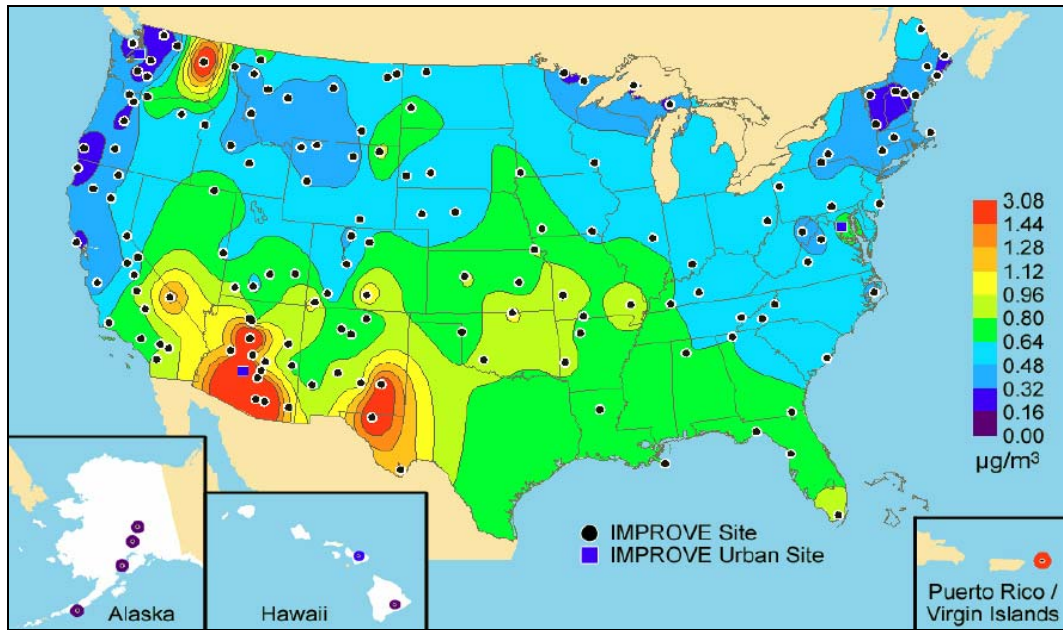
Source: Debell (2006, [156388](#)).

Figure 9-20. IMPROVE mean EC concentrations for 2000-2004.



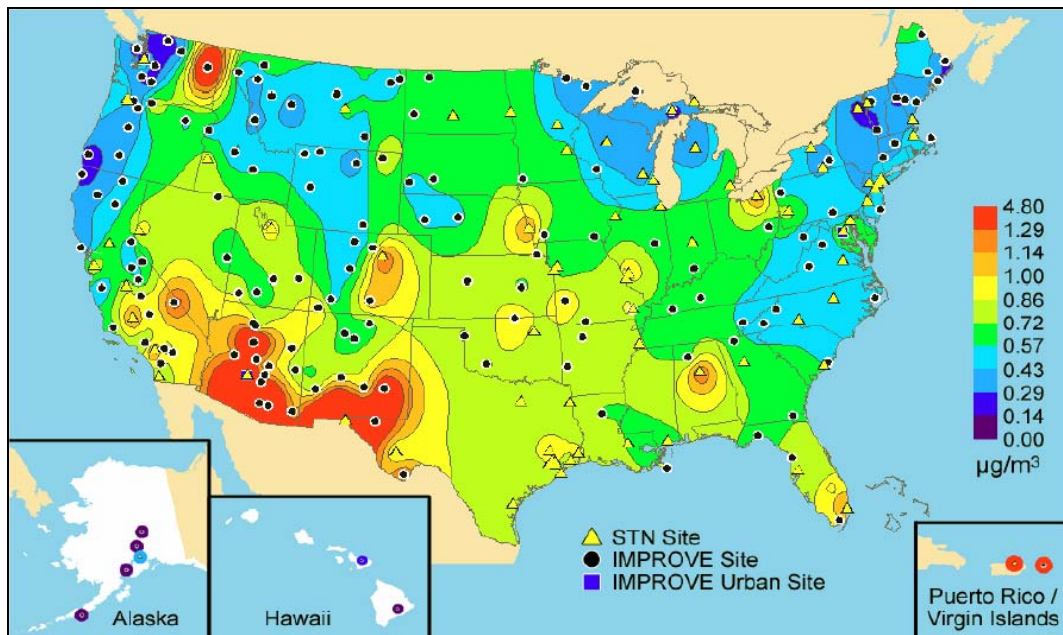
Source: Debell (2006, [156388](#)).

Figure 9-21. IMPROVE and CSN (STN) mean EC concentrations for 2000-2004.



Source: Debell (2006, [156388](#)).

Figure 9-22. IMPROVE mean fine soil concentrations for 2000-2004.



Source: Debell (2006, [156388](#)).

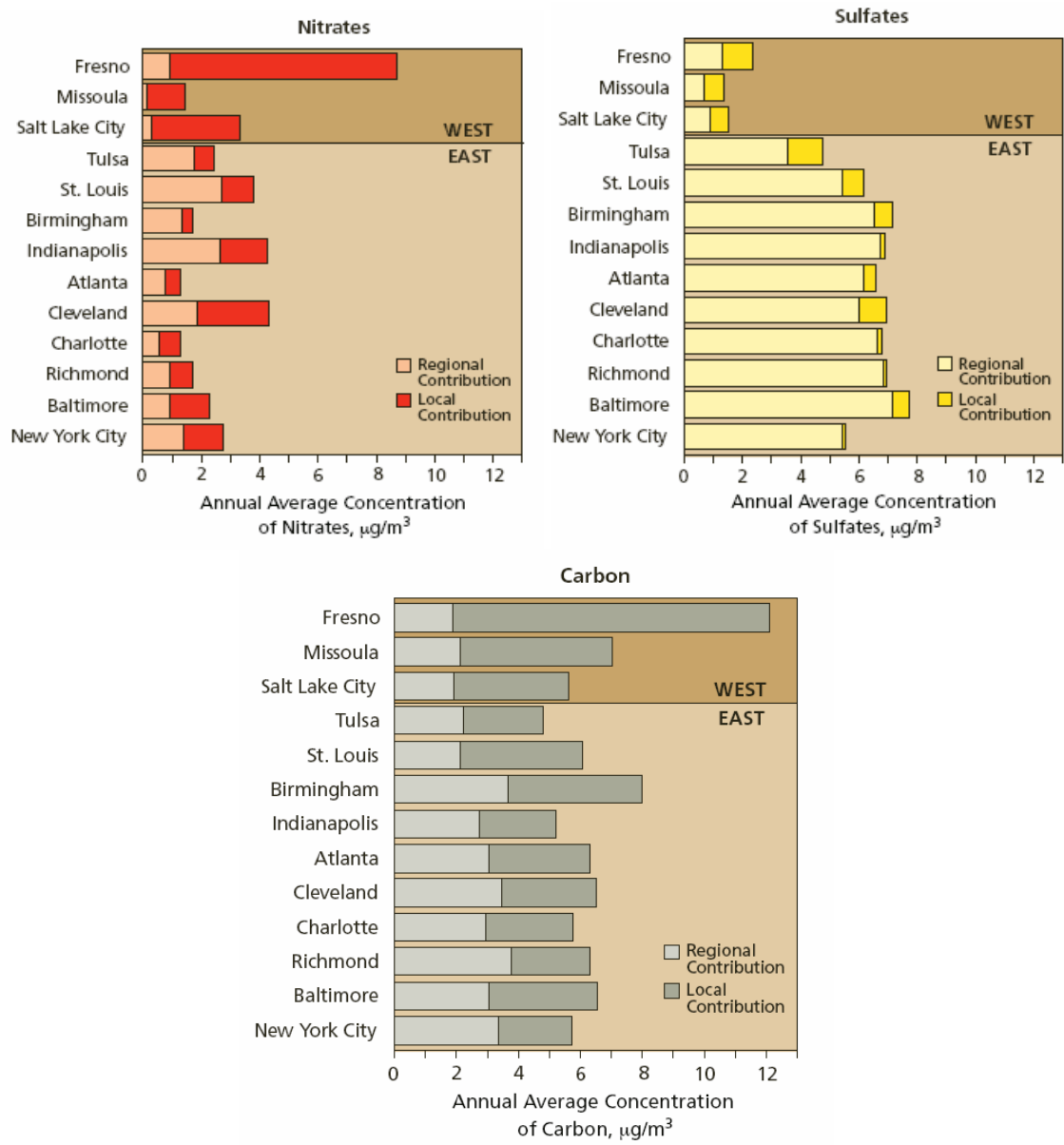
Figure 9-23. IMPROVE and CSN (STN) fine soil concentrations, 2000-2004.

Figure 9-25 shows the remote area coarse mass concentrations as measured by the IMPROVE network. The pattern of high coarse mass concentrations from Oklahoma to Iowa is comparable to the high concentrations in the desert southwest, though as shown in Figure 9-11 it contributes a

smaller relative share of the light extinction because of the higher contributions to haze by particulate nitrate and sulfate in this agricultural region of the country. Comparing Figure 9-22 and Figure 9-25 shows that the coarse mass and fine soil concentration patterns are similar for the desert southwest but there is a much lower fine soil to coarse mass concentration ratio for the agricultural center of the country, suggesting a regional difference in the size distribution of the coarse mass, perhaps due to differences in suspendable soil materials.

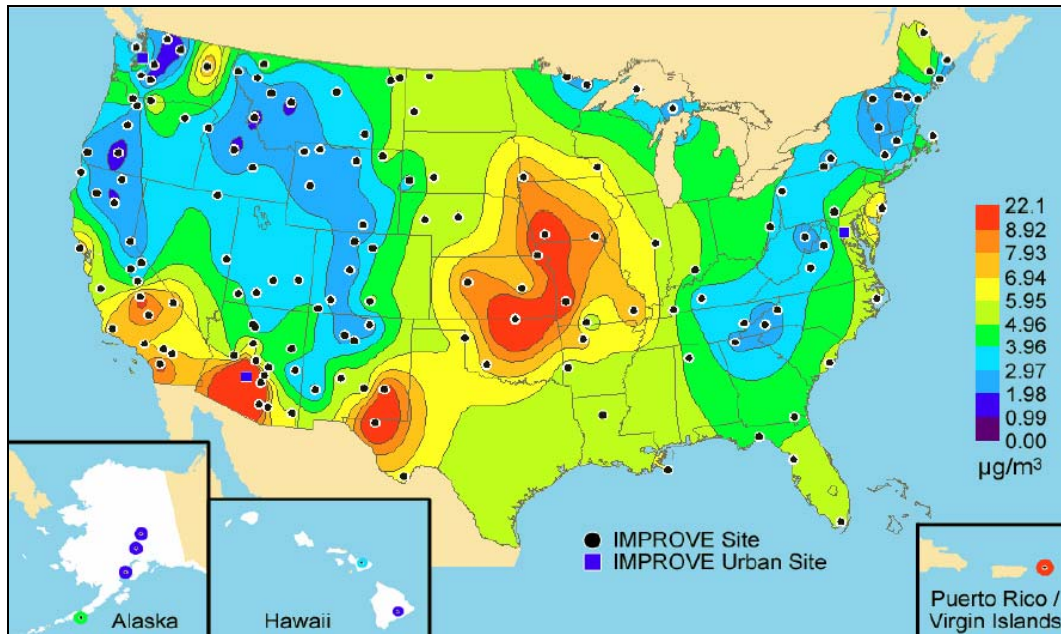
9.2.3.4. Temporal Trends

Visibility trend analysis requires relatively long data records to avoid having meteorologically driven interannual variability obscure more meaningful emissions-driven air quality trends. A requirement for long-term data limits the number of monitoring sites useful for trend analysis. Maps that show haze trends for IMPROVE sites for the 10-year period 1995-2004 for the mean of the 20% best and the 20% worst haze days where sites are required to have a minimum of 6 complete years of data during the 10-year period are shown in Figure 9-26 and Figure 9-27, respectively. The best haze days have improving haze at most sites (32 of 47), no trend at several sites (10 of 47) and degrading visibility at just one site (Great Sand Dunes, CO). The worst haze days have improving haze conditions at several sites (13 of 47), no trend at most sites (30 of 47), and degrading visibility at a few western sites (4 of 47).



Source: U.S. EPA (2004, [190219](#))

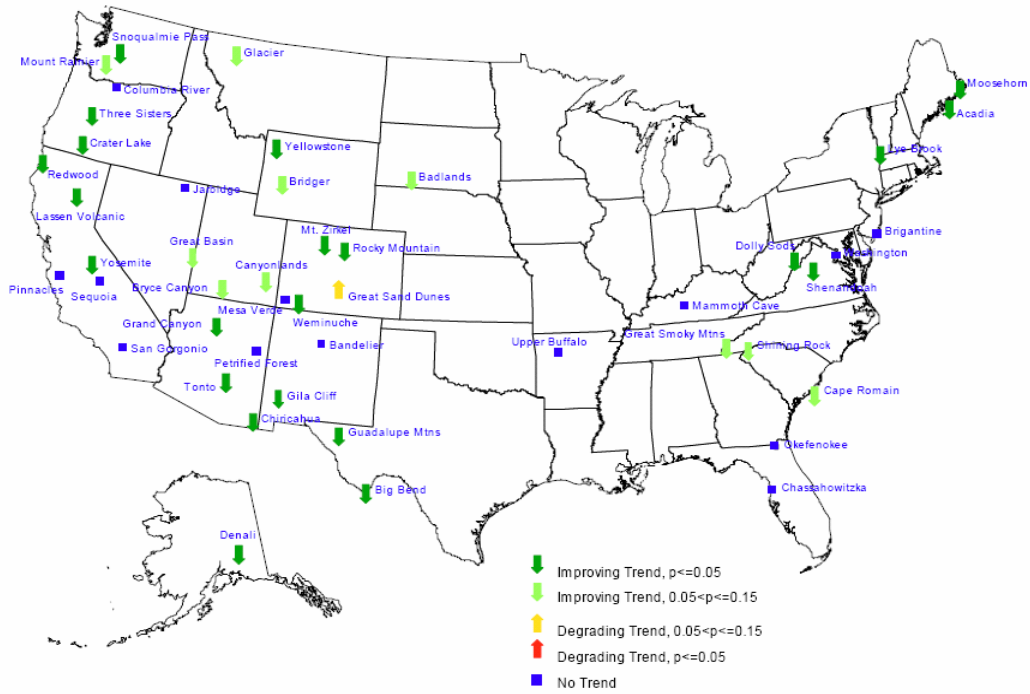
Figure 9-24. Regional and local contributions to annual average PM_{2.5} by particulate SO₄²⁻, nitrate and total carbon (i.e., organic plus EC) for select urban areas based on paired IMPROVE and CSN monitoring sites.



Source: Debell (2006, [156388](#)).

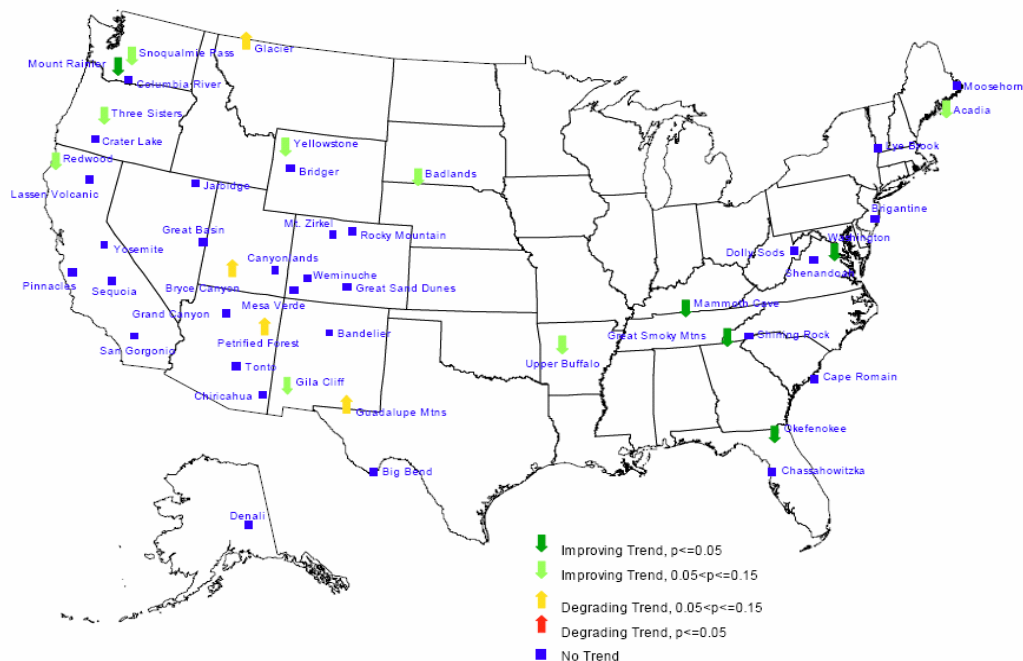
Figure 9-25. IMPROVE mean coarse mass concentrations for 2000-2004.

Eight-, ten-, and sixteen-year trends analysis conducted for the Western Regional Air Partnership (WRAP) as part of the Causes of Haze Assessment (<http://www.wrapair.or>) show that improving trends for the 20% best haze days for the sites in the western U.S. generally correspond to improving trends for all of the major components with the exception of particulate nitrate. Trends assessment for the worst haze days at western sites show consistent reductions in particulate SO_4^{2-} , but otherwise have mixed increasing and decreasing haze component trends, many of which are not statistically significant. Substantial interannual and shorter term spatial and temporal wildfire activity variations have been shown to have a significant impact on the variability of haze in the western U.S. (Park et al., 2006, [190469](#); Spracklen et al., 2007, [190485](#)). Edgerton et al. (2004, [156413](#)) showed a decreasing trend in $\text{PM}_{2.5}$ of about 18% (corresponding to 1 $\mu\text{g}/\text{m}^3$ to 2 $\mu\text{g}/\text{m}^3$) for 4 urban-rural paired SEARCH sites in the Southeastern U.S. corresponding to similar reductions in SO_4^{2-} and carbonaceous particulate.



Source: DeBell (2006, [156388](#))

Figure 9-26. Ten-year (1995-2004) haze trends for the mean of the 20% best annual haze conditions.



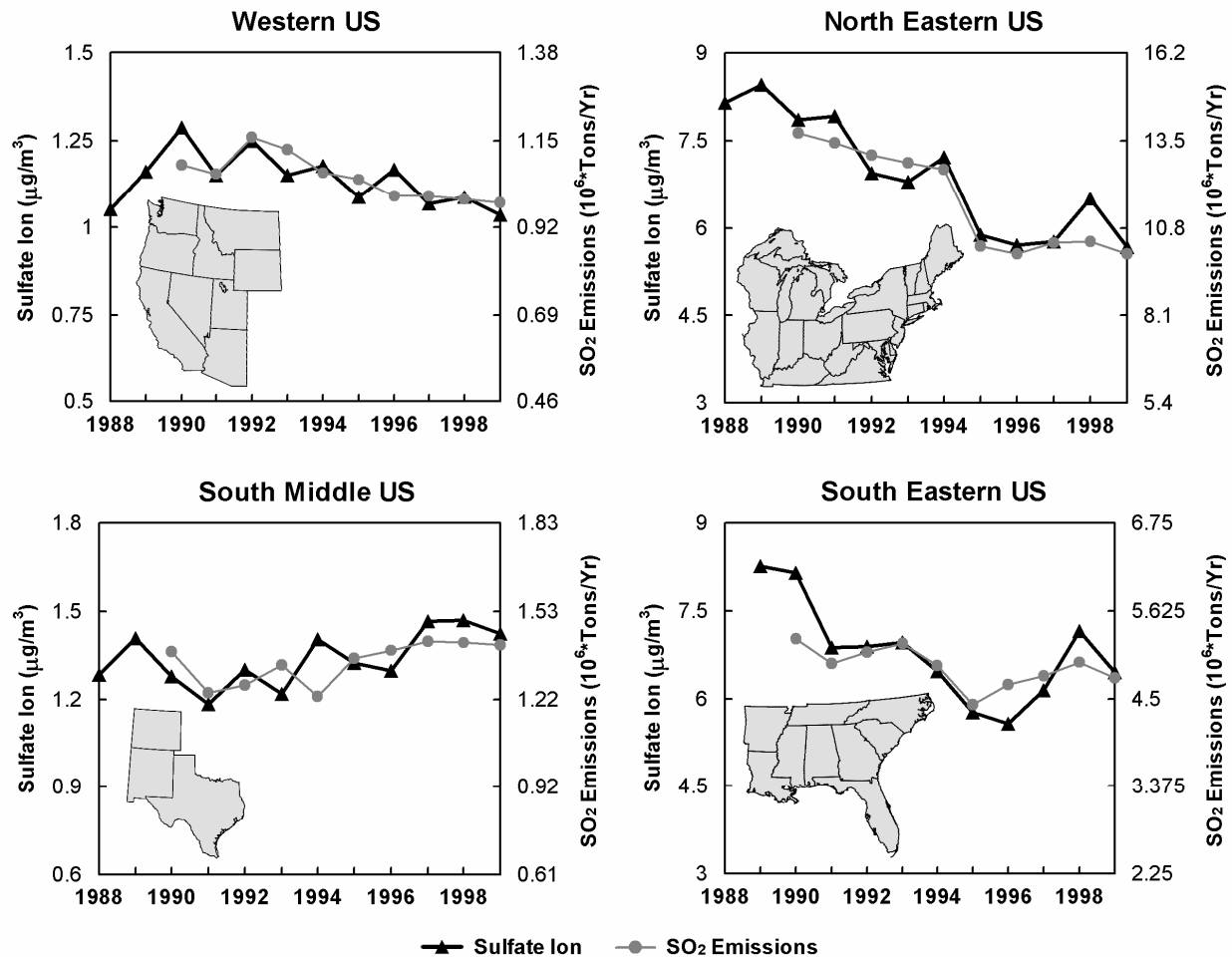
Source: Debell (2006, [156388](#))

Figure 9-27. Ten-year (1995-2004) haze trends for the mean of the 20% worst annual haze conditions.

Malm et al. (2002, [156727](#)) conducted 10-year (1988-1998) trends analyses on the combination of IMPROVE and CASTNET (Clean Air Status and Trends Network) (Baumgardner et al., 1999, [011308](#)) particulate SO_4^{2-} concentration datasets, which were shown to produce comparable SO_4^{2-} concentrations at 23 co-located monitoring sites. Figure 9-28 shows time plots of 80th percentile particulate SO_4^{2-} concentrations and annual average SO_2 emissions from the National Emissions Trends (U.S. EPA, 2000, [012211](#)) database for four regions of the U.S. Note that the concentration and emissions scales on the plots are each a factor of three, so that an equal percentage change in particulate SO_4^{2-} and SO_2 emissions slope in any plot will have the same trend line slope. Each plot shows a strong correspondence between 80th percentile particulate SO_4^{2-} and SO_2 emissions trends. The western U.S. had steadily declining trends in both, for an overall decrease of about 15%. The northeastern U.S. had a decrease of about 27% over the 10-year period with the largest 1-year decrease of about 20% between 1994 and 1995 as a result of the Phase I implementation of the Acid Rain Program. The southwestern U.S. (Texas, New Mexico and Colorado) had about a 15% increase in particulate SO_4^{2-} and SO_2 emissions over the 10-year period. The southeastern U.S. had a declining trend for the early 1990s followed by an increasing trend for the later half of the decade, with a net decrease over the decade of less than 10%. Others have shown similar decreasing particulate SO_4^{2-} concentration trends and a correspondence in trends between SO_2 emissions and particulate SO_4^{2-} concentration by region (Holland et al., 1999, [092051](#); U.S. EPA, 2004, [056905](#)).

Holland et al. (1999, [092051](#)) developed and compared NO_x emissions trends from 1989 to 1995 to corresponding trends in total nitrogen concentration (defined as particulate nitrate plus gaseous nitric acid) for the eastern U.S. (states between Louisiana to Minnesota and further east) based on data from 34 rural CASTNet dry deposition monitoring sites. They found a decrease in nitrogen median values of about 8% associated with a decrease of 5.4% in non-biogenic NO_x emissions. Trends in haze associated with particulate SO_4^{2-} and nitrate concentrations should correspond fairly well with trends in their concentration due to the simple relationship between concentration and light extinction at any relative humidity. However, nitrogen as defined in the Holland et al. (1999, [092051](#)) trend analysis includes the nitrogen from particulate nitrate and gaseous nitric acid, but nitric acid does not contribute to light extinction. For situations with limited

atmospheric ammonia or elevated temperatures, trends in nitrogen may be principally in nitric acid with no net change in nitrate light extinction. Alternately with abundant ammonia and low temperatures the trend in nitrogen may be principally in particulate nitrate and the nitrate component of haze.



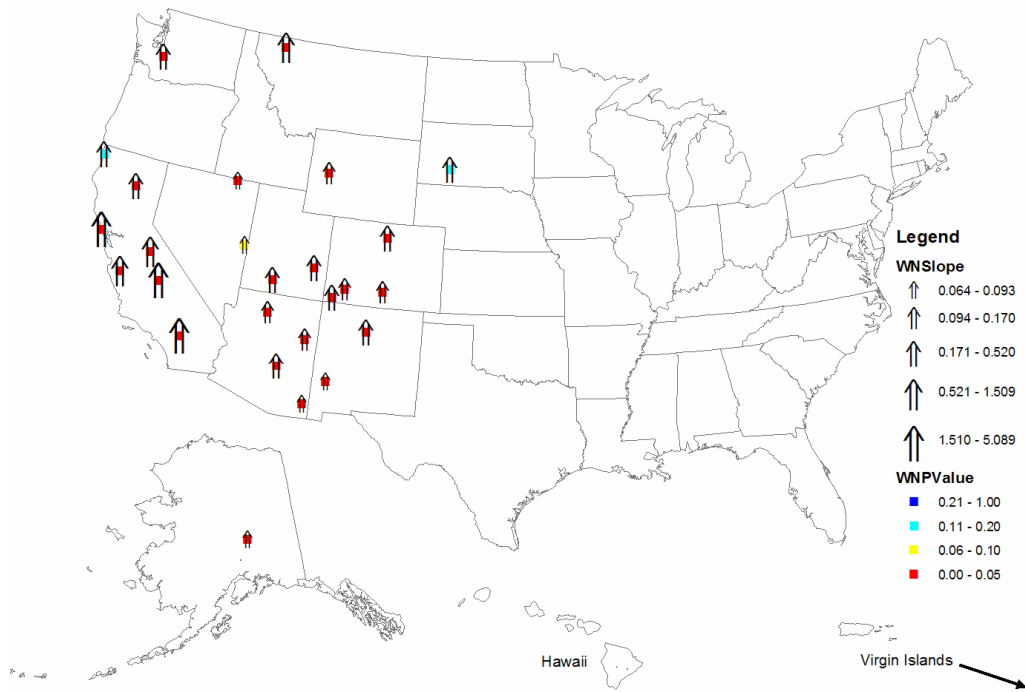
Source: Reprinted with Permission of the American Geophysical Union from Malm et al. (2002, [156727](#)).

Figure 9-28. Ten-year trends in the 80th percentile particulate SO_4^{2-} concentration based on IMPROVE and CASTNet monitoring and net SO_2 emissions from the National Emissions Trends (NET) data base by region of the U.S.

Ten-year trends (1994-2003) of particulate nitrate contribution to light extinction during the 20% worst haze conditions conducted as part of the Causes of Haze Assessment (see the link in Table 9-1) are shown in Figure 9-29. This indicates that haze from particulate nitrates is increasing across the western U.S. at a rate of several Mm^{-1} per year in parts of California and at a rate of several tenths of an Mm^{-1} across the Four-Corners states. A similar particulate nitrate trends map (not shown here) for the 20% best haze conditions that is available at the same web site shows decreasing particulate nitrate contribution to light extinction at nearly all of the western monitoring sites. While statistically significant, these trends for both the 20% worst and 20% best haze periods are influenced by an unexplained nationwide period of depressed nitrate concentrations measured by the IMPROVE network during a 4-yr period from the winter of 1996-1997 through the winter of 2000-2001. Extensive examinations of plausible monitoring methodological explanations have failed

to offer any evidence that the data are invalid (McDade, 2004, [192075](#)), but no satisfactory atmospheric or emissions-related explanation has been offered to account for this 4-yr depression of nitrate. Similar analyses of particulate nitrate haze trends are not available for the rest of the country.

Maps of remote-area 8-, 10-, and 16-yr trends for carbonaceous and crustal PM species based on IMPROVE monitoring are available for the western U.S. conducted as part of the Causes of Haze Assessment. Generally these show a broad range of results (i.e., a mixture of statistically significant upward or downward trends and insignificant trends often with neighboring sites having opposing trends) that vary considerably depending on the number of years selected (i.e., 8, 10, or 16) and whether trends are for the best, worst, or middle of the haze distribution data. The scatter in these results is undoubtedly due to the high interannual variability and varying locations of wildfire and wind-suspended dust emissions that dominate the remote-area concentrations of the carbonaceous and crustal PM species in the western U.S.



Source: <http://www.coha.dri.edu/>

Figure 9-29. Map of 10-yr trends (1994-2003) in haze by particulate nitrate contribution to haze for the worst 20% annual haze periods. The orientation, size and color of the arrows indicate the direction, magnitude and statistical level of significance of the trends. These consistent upward trends may be a misleading result due to an unexplained sampling issue (see text for additional information).

9.2.3.5. Causes of Haze

In order to attribute haze to emissions from individual sources, source types, or source regions, generally, any of a number of receptor and air quality simulation modeling approaches are applied. When using multiple approaches, the results of each are reconciled using a weight-of-evidence methodology. Commonly this methodology has been applied to the extensive datasets generated by special studies designed to estimate source-receptor relationships for a few receptor locations or for individual emission sources (Pitchford et al., 1999, [156873](#); Pitchford et al., 2005, [156874](#); Schichtel

et al., 2005, [156957](#)). More recently the Regional Planning Organizations (RPOs) have sponsored extensive regional haze source attribution assessments using weight-of-evidence methodologies to reconcile attribution results for virtually all of the remote-area IMPROVE sites to support the development of State Implementation Plans for the RHR. Additionally, a number of recent urban special studies, including those sponsored by EPA PM Supersites program (Solomon and Hopke, 2008, [156997](#)), have addressed the causes of and sources contributing to urban excess PM concentrations above region concentrations. Attribution results uncertainties are generally larger than those of the measurements upon which they are based because they also include model uncertainties and assumptions, as well as issues of representativeness (e.g., How well does the data used in the analysis represent the typical emissions, air quality and meteorological conditions of interest?). As such it is advisable to treat the attribution results reported below as semi-quantitative.

The relative importance of the PM species that contribute to haze varies by region of the U.S. and time of year as shown in Figure 9-9, Figure 9-10, and Figure 9-11, above. Generally haze in the western half of the U.S. is not dominated by any one or two PM species. In the eastern half of the U.S., SO_4^{2-} , especially during summer, and nitrate during the winter in the Midwest are the dominant haze species. As described above, urban haze can be viewed as a composite of the regional and local contributions where local contributions seem to be dominated by carbonaceous and, to a lesser extent, nitrate and crustal PM components. There have been far fewer urban investigations that explicitly consider visibility impacts, though there are numerous studies of urban PM source attribution. The order of discussion below on the cause of haze is by region beginning in the western U.S. and proceeding to the east, analogous to dominant air flow patterns across the lower 48 states and will include information from urban studies along side those of remote-area haze investigations.

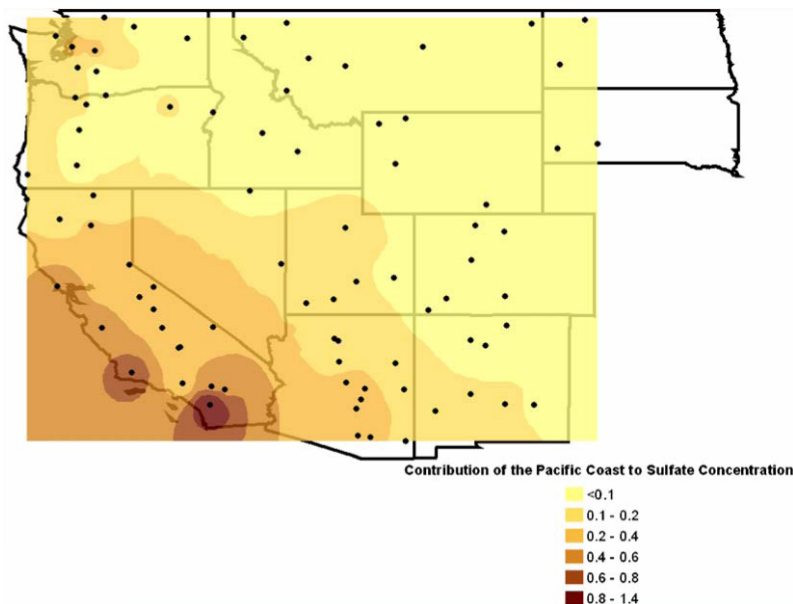
Based on modeling of an episode (September 23-25, 1996) in the California South Coast Air Basin (SCAB) and another episode (January 4-6, 1996) in the San Joaquin Valley (SVJ) by Ying and Kleeman (2006, [098359](#)), about 80% of the particulate SO_4^{2-} for both regions is from upwind sources (i.e., likely from offshore sources including marine shipping, long-range transport and natural marine sources), with most of the remaining is associated with diesel and high-sulfur fuel combustion. Kleeman et al. (1999, [011286](#)), using a combination of measurements and modeling, showed that the upwind particulate SO_4^{2-} source region for the SCAB was over the Pacific Ocean (confirmed by measurements on Santa Catalina Island) and that these particles subsequently grew with accumulation of additional secondary aerosol material, principally ammonium nitrate as they traversed the SCAB. The majority of the nitric acid that forms particulate nitrate in the SCAB is from diesel and gasoline combustion (~63%), while much of the ammonia is from agricultural sources (~40%), catalyst equipped gasoline combustion (~16%), and upwind sources (~18%). The majority of the OC found in SCAB was attributed in this study to primary emissions by transportation-related sources, including diesel (~13%) and gasoline (~44%) engines and paved road dust (~12%). At the Fullerton site in the middle of the SCAB the concentration of locally generated organics is roughly double that of the locally generated nitrates (~5.6 $\mu\text{g}/\text{m}^3$ compared to ~2.4 $\mu\text{g}/\text{m}^3$), while at Riverside on the east edge of the SCAB and near the large agricultural sources of ammonia emissions, the particulate nitrate concentrations are nearly double that of organic PM (~17 $\mu\text{g}/\text{m}^3$ compared to ~10 $\mu\text{g}/\text{m}^3$).

Ying and Kleeman (2006, [098359](#)) showed that during the winter 1996 episode in the SVJ most of the nitric acid that forms particulate nitrate is from upwind sources (~57%) with diesel and gasoline combustion contributing most of the rest (30%), while much of the ammonia is from upwind sources (~39%) and a combination of area, soil and fertilizer sources (~52%). In an assessment of PM particle size and composition in the SVJ during the winter of 2000-2001, Herner et al. (2006, [135981](#)) showed that fresh emissions of carbonaceous PM from combustion sources in urban locations (Sacramento, Modesto, and Bakersfield, CA) move quickly from ultrafine particle size (i.e., diameter ~0.1 μm) to accumulation mode by condensation with accumulation mode (i.e., diameter ~0.5 μm) particles, and that secondary nitrate particle formation occurs preferentially on the surface of hydrated ammonium sulfate particles during the afternoon when gas-phase nitric acid is at peak photo-chemical production from NO_x . Given the abundance of ammonia emissions and low ambient temperatures, particulate nitrate production in this way is only limited by the availability of nitric acid. Due to the cool winter conditions there was little SOA production during this study. Sea salt was shown to dominate the larger coarse particle mode during on-shore wind at the background coastal monitoring site at Bodega Bay, north of San Francisco, CA.

Using a regression analysis to find the dependence of particulate SO_4^{2-} concentration measured over a 3-year period (2000-2002) at 84 western IMPROVE monitoring sites on the

modeled transport trajectories to the sites for each sample period, Xu et al. (2006, [102706](#)) were able to infer the source regions that supplied particulate SO_4^{2-} in the western U.S. Among the source regions included in this analysis was the near coastal Pacific Ocean (i.e., a 300-km zone off the coast of California, Oregon, and Washington). Up to half of the particulate SO_4^{2-} measured at Southern California monitoring sites was associated with this source region. As shown in Figure 9-30 the zone of impact from this source region included large regions of California, Arizona, and Nevada. The authors made the case that high sulfur content fuel used in marine shipping and port emissions may be largely responsible. As a result, the WRAP RPO emissions inventory was modified to include marine shipping and a Pacific Offshore source region was added to source attribution by air quality simulation modeling.

The SO_4^{2-} attribution results of the WRAP air quality modeling (results available on the Technical Support System (TSS) website, see Table 9-1 for the web-link) credit the Pacific offshore source region with somewhat smaller contributions than those from the trajectory regression work by Xu et al. (2006, [102706](#)) with concentrations at the peak impact site in California that are about 45% compared to 50% by regressions and even greater differences for more distant monitoring sites. Based on the modeling attribution the Pacific offshore source region was responsible for 10-20% of the nitrate measured in Southern California.



Source: Reprinted with Permission of Atmospheric Environment from Xu et al. (2006, [102706](#)).

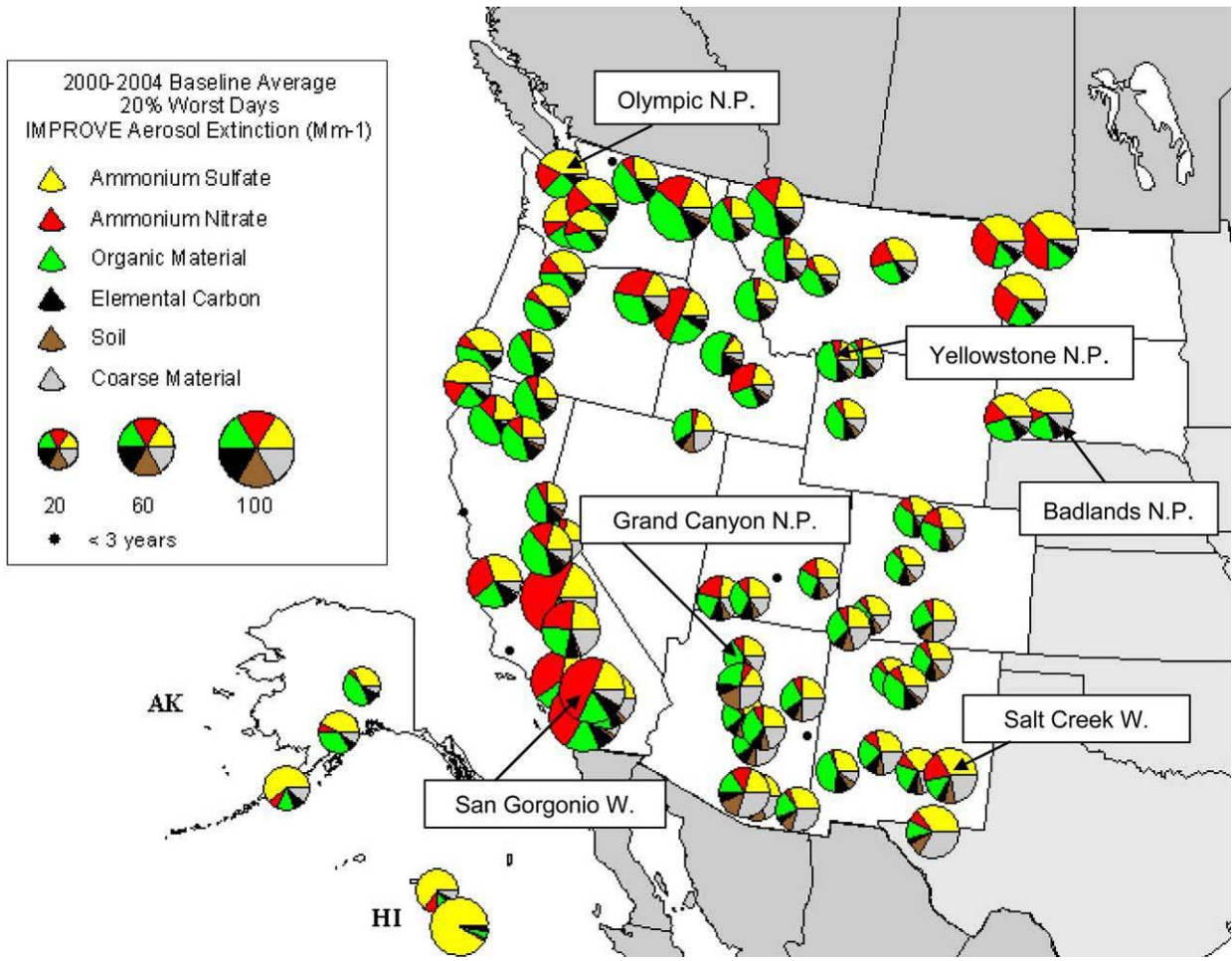
Figure 9-30. Contributions of the Pacific Coast area to the ammonium sulfate ($\mu\text{g}/\text{m}^3$) at 84 remote-area monitoring sites in western U.S. based on trajectory regression for all sample periods from 2000-2002 (dots denote locations of the IMPROVE aerosol monitoring sites).

A coordinated effort by federal, state, and county air quality organizations to determine the causes of haze in the Columbia River Gorge (a deep and narrow gap in the Cascade Mountains on the Washington/Oregon border) through extensive multiyear measurements and high spatial resolution air quality modeling of typical episodes demonstrated the multitude of emission sources that contribute to its impairment (Pitchford et al., 2007, [098066](#)). During the summer, gorge winds are generally from the west and relatively dry. More than half of the haze during a typical summer episode is from a combination of international and other distant sources (~22% at the western end of the gorge) plus regional natural sources including wildfire and secondary organic PM from biogenic emissions (~39% at the eastern end of the gorge). The Portland/Vancouver metropolitan area was responsible for a significant amount of the haze during the summer (~20% on in the western end of

the gorge), while sources within the gorge were responsible for a moderate amount of haze (~6% and ~9% at the western and eastern ends of the gorge). The wind is much more often from the east during the winter. The highest haze conditions in the gorge are during the winter and are associated with fog conditions that rapidly convert precursor gaseous emissions of NO_x and SO_2 from local and regional combustion sources and NH_4 from local and regional agricultural activities to secondary nitrate and SO_4^{2-} PM that persist as a post-fog intense haze. Contributions by these sources east of the gorge contribute ~57% of the haze on the eastern end of the gorge, with half of the nitrate and SO_4^{2-} particulate from electric utility emissions and most of the rest from transportation sources. Other sources contributing during the winter haze at the eastern end of the gorge are from sources outside the modeling domain (i.e., most of Washington and Oregon) and within the gorge (~23% and ~10%, respectively).

An assessment of concurrent measurements at the nearby Mt. Hood IMPROVE monitoring site (45 km south of the Columbia River at 1,531 m ASL) shows that Columbia River Gorge haze conditions and especially the wintertime high nitrate/ SO_4^{2-} contributions to haze are not typical of the generally higher elevation remote areas of the region (Pitchford et al., 2007, [098066](#)). However Gorge-like high wintertime nitrate and SO_4^{2-} are found at the Hells Canyon IMPROVE site, which is similarly situated in a narrow canyon of the Snake River almost 400 km east of the Gorge (from the VIEWS web site, see Table 9-1), implying that there may be a substantial vertical concentration gradient during winter in this complex terrain.

Several example monitoring locations distributed across the northern and southern portions of the western U.S. have been selected to illustrate the attribution results from the WRAP-sponsored attribution analysis tools that estimate the relative responsibility for haze of the various PM species by source region and source type. The selected sites include Olympic NP, WA; Yellowstone NP, WY; and Badlands NP, SD across the north, and San Geronio Wilderness (W), CA; Grand Canyon NP, AZ and Salt Creek W, NM across the south as shown in Figure 9-31.



Source: <http://vista.cira.colostate.edu/airdata/linkbrowser/LinkBrowserNormal.aspx>

Figure 9-31. Shows the IMPROVE monitoring sites in the WRAP region with at least three years of valid data and identifies the six sites selected to demonstrate the apportionment tools. Pie diagrams show the composition for the mean of the 20% worst haze conditions and the mean light extinction (Mm^{-1}) by the size of the circle (see figure key).

WRAP-sponsored CMAQ modeling for 2002 used virtual tracers of SO_2 and NO_x emissions that tracked the source region and category through the transport and transformation processes to particulate SO_4^{2-} and nitrate. This was used to produce pie diagrams of particulate SO_4^{2-} and nitrate attribution results by source region for each of these sites as shown in Figure 9-32 (produced using the TSS, see Table 9-1). Based on these sites, over half of the particulate SO_4^{2-} in remote areas of the Pacific coastal states is from outside of the U.S. (Pacific offshore and outside of the domain). The outside of the domain values were derived by simulating the fate of the boundary condition concentrations, which for the WRAP air quality modeling were obtained using output from the GEOS-CHEM global air quality model (Fiore et al., 2003, 047805). The SO_4^{2-} fraction from the region labeled outside of domain was approximately uniform throughout the western U.S. with site-to-site variation in the fraction caused mostly by variations in total SO_4^{2-} concentration. The more northerly sites have impacts from Canadian emissions, while the southern sites have impacts from Mexican emissions. Half of the Salt Creek, New Mexico SO_4^{2-} is from the domestic source emissions further to the east, which also contribute about 20% to Badlands particulate SO_4^{2-} concentrations. A breakout of the emission sources from within the WRAP region by source type (not shown) has most of the emissions from point sources, with the combination of motor vehicle,

area and wildfire emissions contributing from a few percent at the furthest eastern sites to about half at San Geronio.

By comparison, the particulate nitrate is much more from domestic regional emission sources, with ~60-80% being from emissions within the WRAP region. For the west coast sites about 25% of the nitrate is from a combination of Pacific offshore emissions (i.e., marine shipping) and outside domain regions. Canadian emissions are responsible for about 10-30% of the particulate nitrate for the three northern sites, but Mexican emissions do not contribute appreciably to particulate nitrate for the three southern sites. Motor vehicles are the largest contributing NO_x source category responsible for particulate nitrate for these six WRAP sites, with a combination of point, area and wildfire source categories also contributing from about 10-50% of the WRAP regional emissions.

WRAP only used the virtual tracer approach to investigate source locations and categories for SO₂ and NO_x emissions. A different type of virtual tracer modeling tool was used to track the various OC compounds and sort them into three groups for 2002. The first group labeled primary organics includes all of the organics that are emitted directly as PM from any source type and location. The second group labeled anthropogenic secondary organics is PM produced in the atmosphere by aromatic VOCs. The third category labeled biogenic secondary organics is PM produced in the atmosphere by biogenic VOCs. Organic PM in the biogenic secondary category includes those that would functionally be considered man-made emissions (e.g., those from agricultural crops and urban landscapes), though in most remote areas of the west these man-made VOC emissions are small compared to those of the natural biogenic sources. Figure 9-33, Figure 9-34, and Figure 9-35 show the monthly averaged apportionment of organic PM for the 6 selected monitoring locations.

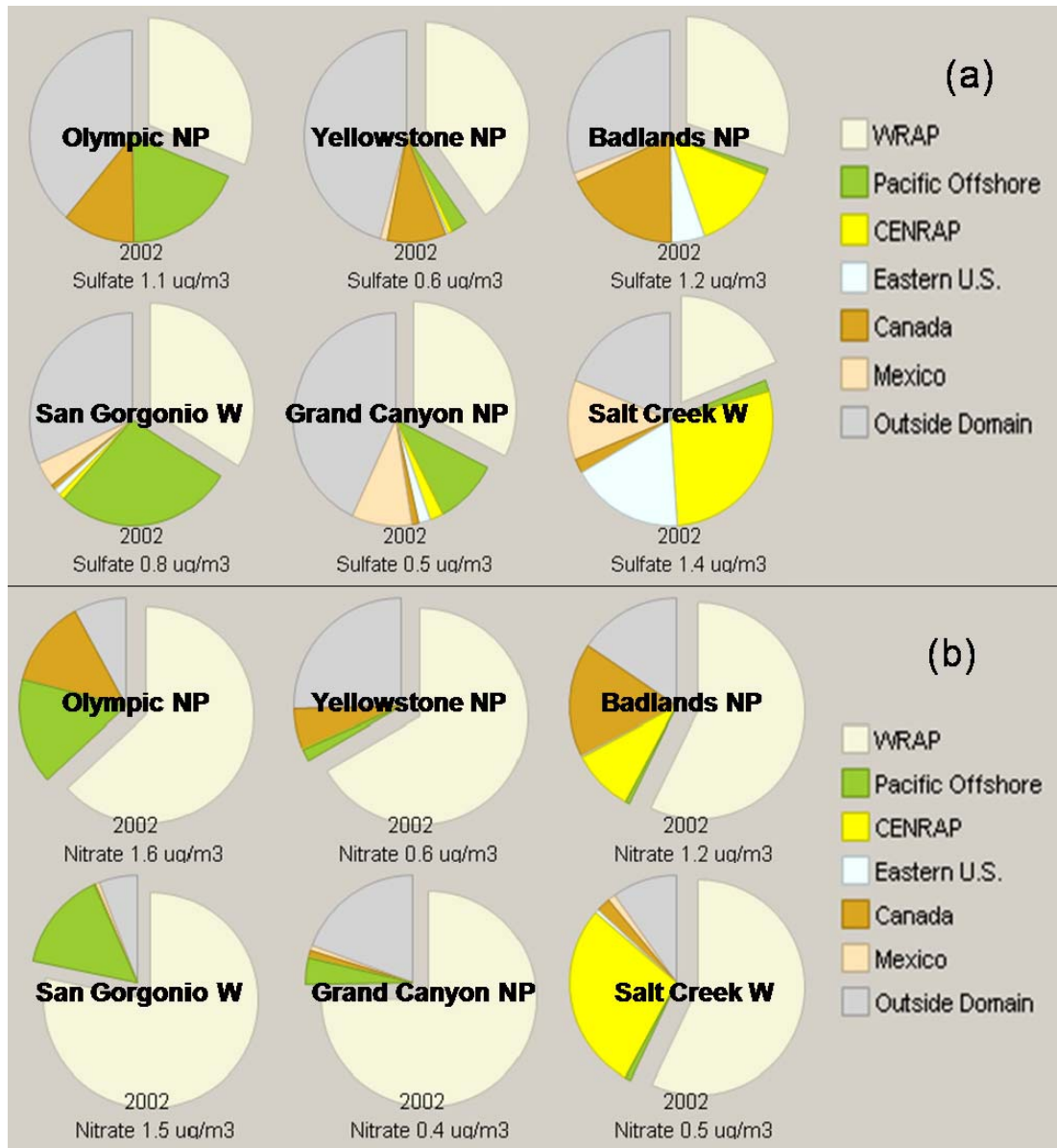
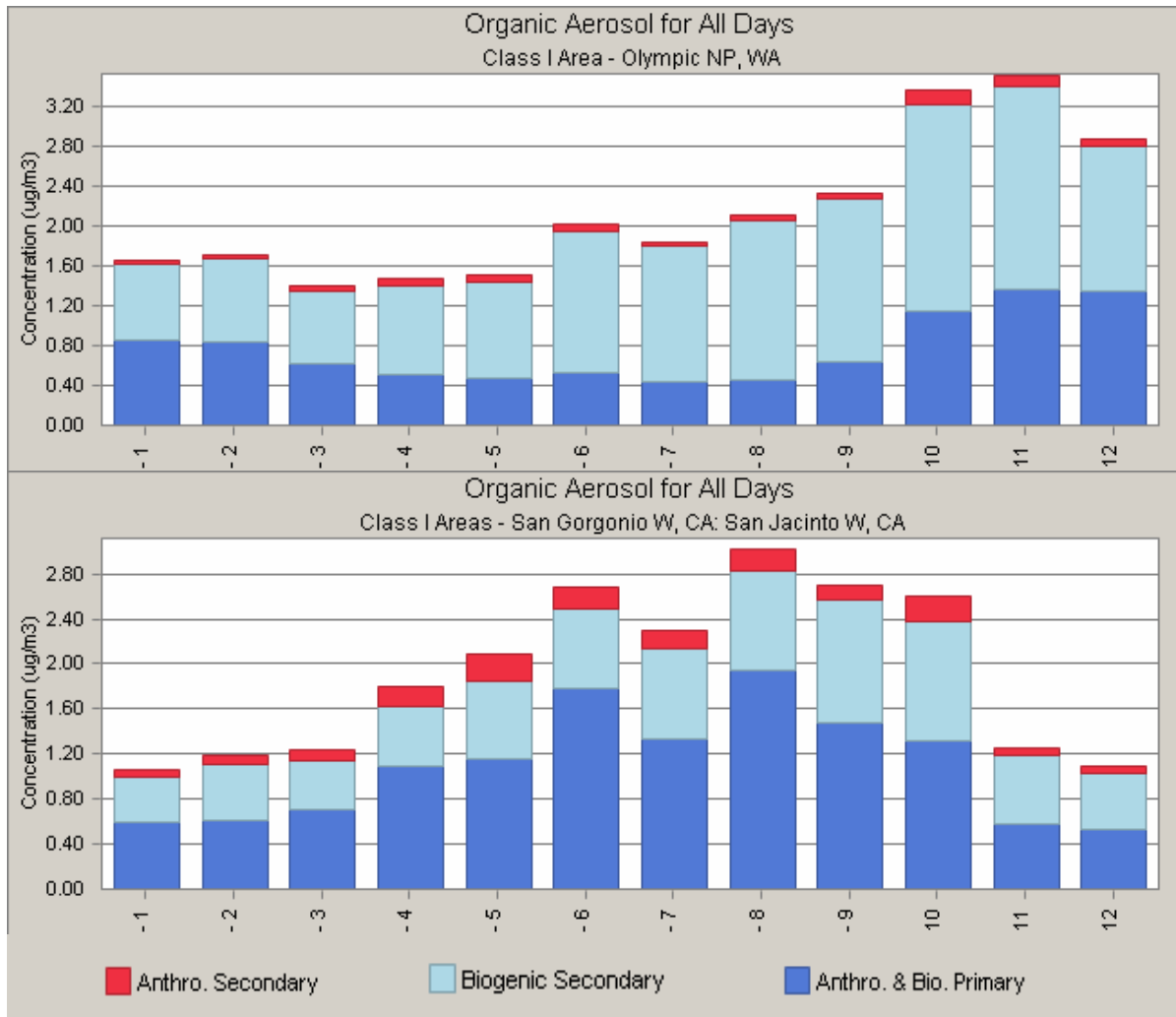


Figure 9-32. Particulate SO_4^{2-} (a) and nitrate (b) source attribution by region using CAMx modeling for six western remote area monitoring sites : top left to right Olympic NP, WA; Yellowstone NP, WY; Badlands NP, SD; bottom left to right San Gorgonio W, CA; Grand Canyon NP, AZ; and Salt Creek W, NM. WRAP includes ND, SD, WY, CO, NM and all states further west. CENRAP includes all states east of WRAP and west of the Mississippi River including MN. Eastern U.S. includes all states east of CENRAP. The Pacific Offshore extends 300km to the west of CA, OR, and WA. Outside Domain refers to the modeling domain, which extend hundreds of kilometers into the Pacific and Atlantic Oceans and from Hudson Bay Canada to just north of Mexico City. This figure was assembled from site-specific diagrams produced on the TSS web site (see Table 9-1) for 2002.

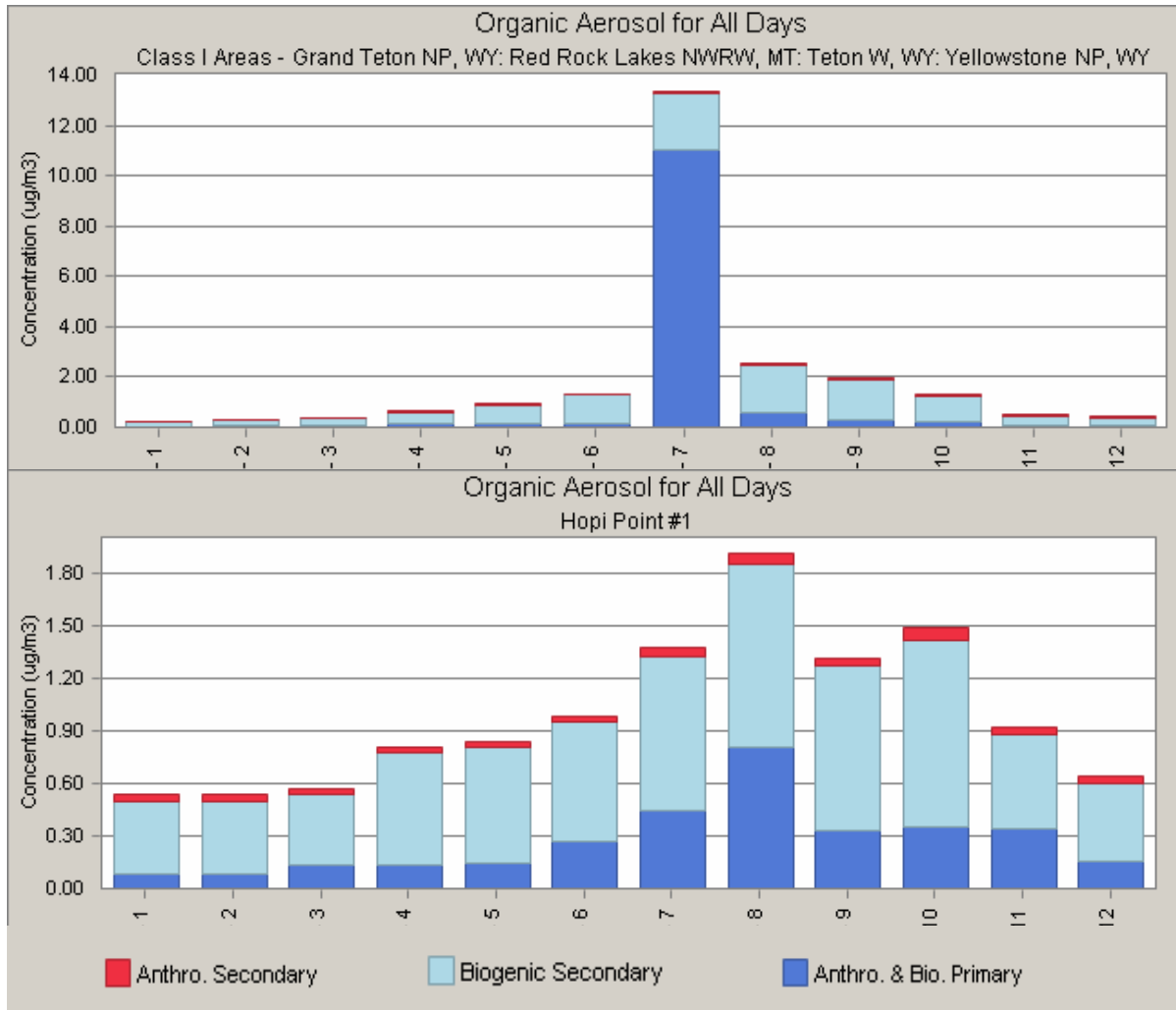


Source: From the TSS website, see Table 9-1.

Figure 9-33. Monthly averaged model predicted organic mass concentration apportioned into primary PM and anthropogenic and biogenic secondary PM categories for the Olympic NP (top) and San Geronio W (bottom) monitoring sites.

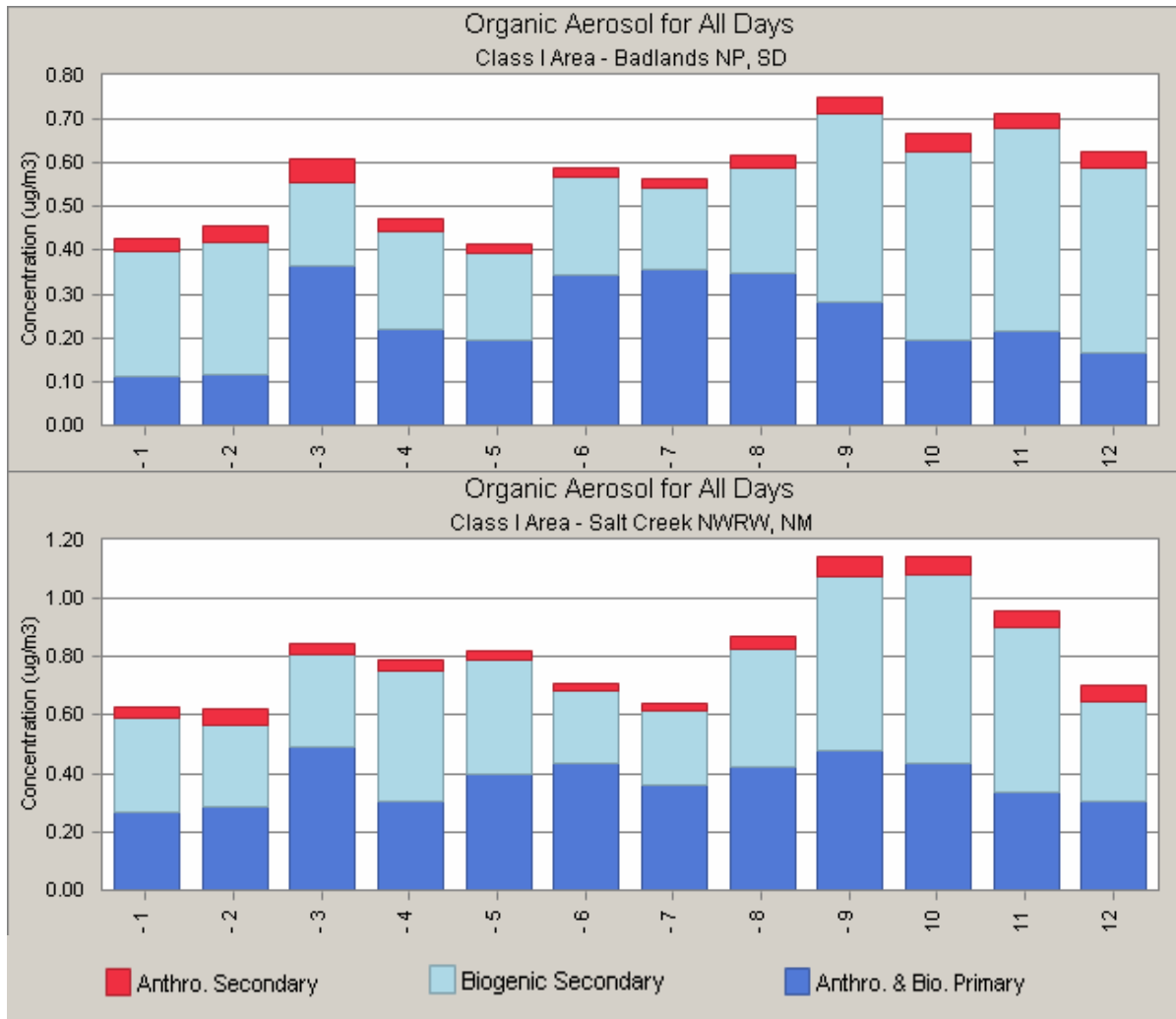
Based on the modeling results for these six sites and confirmed by measurements (see, e.g., Figure 9-10), a west-to-east decreasing gradient of organic mass exists with annual concentrations from $\sim 2 \mu\text{g}/\text{m}^3$ for the coastal state sites to $\sim 1 \mu\text{g}/\text{m}^3$ for the intermountain west sites, to $< 1 \mu\text{g}/\text{m}^3$ for the sites just east of the Rocky Mountains, discounting the large fire impacts for July at Yellowstone NP which raised its annual mean to $\sim 2 \mu\text{g}/\text{m}^3$. At all of these remote-area sites anthropogenic secondary PM is estimated to be a small fraction of the organic mass, with the largest fractional contribution at the San Geronio monitoring site immediately downwind of the major Southern California urban areas, yet having $< 10\%$ of the monthly mean organic mass from anthropogenic secondary PM. Of the six selected monitoring sites, San Geronio has the highest fraction of the organic PM from primary emissions ($\sim 57\%$), followed by Yellowstone ($\sim 55\%$), then the two eastern-most sites (Badlands $\sim 42\%$ and Salt Creek 41%), and with Grand Canyon and Olympic NPs the lowest fraction by primary emissions ($\sim 37\%$). Yellowstone NP would have had the lowest fraction of organic PM by primary emissions had it not been for the month of July (the 11-mo mean was 29%) when wild fire smoke contributed. Results from recent chamber and field studies, and modeling would seem to call into question apportionment of primary and secondary carbon done by traditional air quality model simulations of OC, as described above, due to the combined effects of

extensive evaporation of semivolatile primary emissions when diluted and to photochemical reactions of low volatility gas phase species that substantially increases the amount of secondary organic PM (Robinson et al., 2007, [156053](#)).



Source: From the TSS website, see Table 9-1.

Figure 9-34. Monthly averaged model predicted organic mass concentration apportioned into primary PM and anthropogenic and biogenic secondary PM categories for the Yellowstone NP (top) and Grand Canyon (Hopi Point) (bottom) monitoring sites.



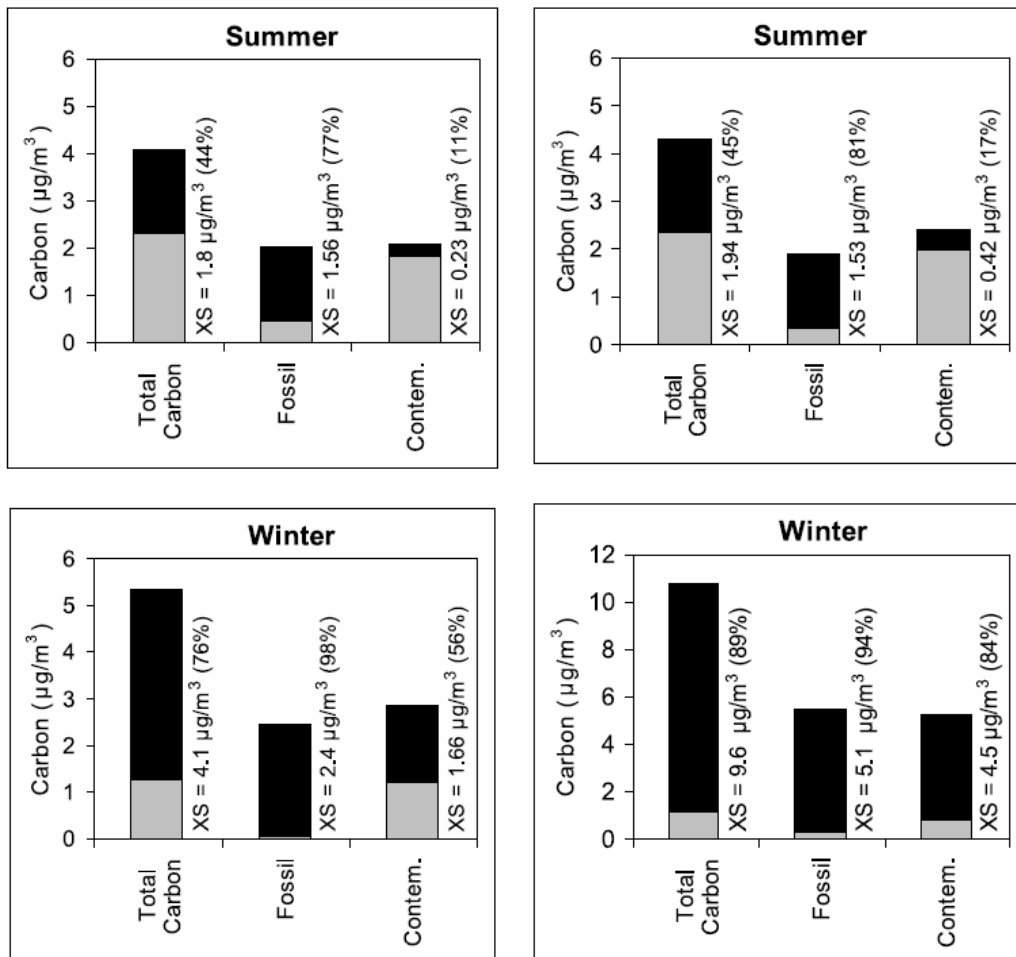
Source: From the TSS website, see Table 9-1.

Figure 9-35. Monthly averaged model predicted organic mass concentration apportioned into primary PM and anthropogenic and biogenic secondary PM categories for the Badland NP (top) and Salt Creek W (bottom) monitoring sites.

Radiocarbon (^{14}C) dating techniques were used to group ambient PM carbon into fossil and contemporary source categories at 12 IMPROVE monitoring sites across the U.S., 8 of which are in the WRAP region (Schichtel et al., 2008, [156958](#)). Results of this work showed that contemporary carbon accounts for about half the carbon in urban areas, 70-97% in near-urban areas (i.e., San Geronio) and 82-100% in remote areas. Comparing these radiocarbon dating results with the WRAP virtual tracer modeling results for organic aerosol (above), and presuming that the modeled anthropogenic secondary organic is fossil carbon and the biogenic secondary is contemporary carbon, suggests that a large fraction of the model-determined regional primary organic PM is from contemporary carbon sources (e.g., smoke from wildfires).

Schichtel et al. (2008, [156958](#)) compared radiocarbon measurements at two sets of urban/rural paired sites in the west (Mount Rainer/Seattle, and Tonto/Phoenix). Figure 9-36 shows that most of total carbon urban excess (i.e., urban site concentration minus the regional site concentration) in the summer is from fossil carbon sources (87% and 79%, respectively), while in the winter there is a surprisingly high fraction of the urban excess at both sites that is from contemporary carbon sources (41% and 47%, respectively). This implies that urban, and therefore anthropogenic, activities

generate almost as much PM_{2.5} carbon from contemporary sources (e.g., residential wood combustion) as from the fossil sources during the winter for these two western urban areas.



Source: Reprinted with Permission of the American Geophysical Union from Schichtel et al. (2008, [156958](#)).

Figure 9-36. Comparison of carbon concentrations between Seattle (Puget Sound site) and Mt. Rainer (left) and between Phoenix and Tonto (right) showing the background site concentration (gray) and the urban excess concentration (black) for total, fossil and contemporary carbon during the summer and winter studies.

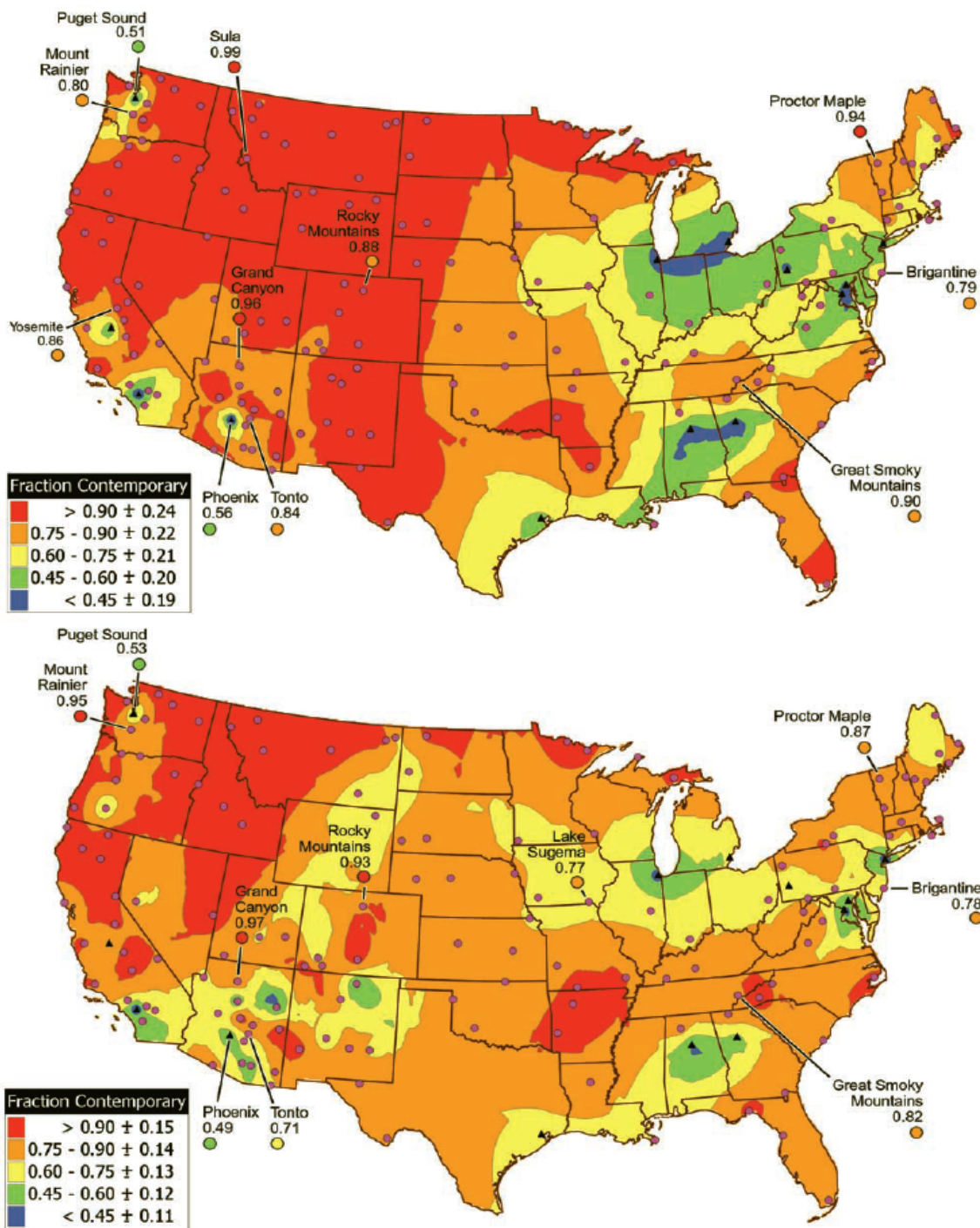
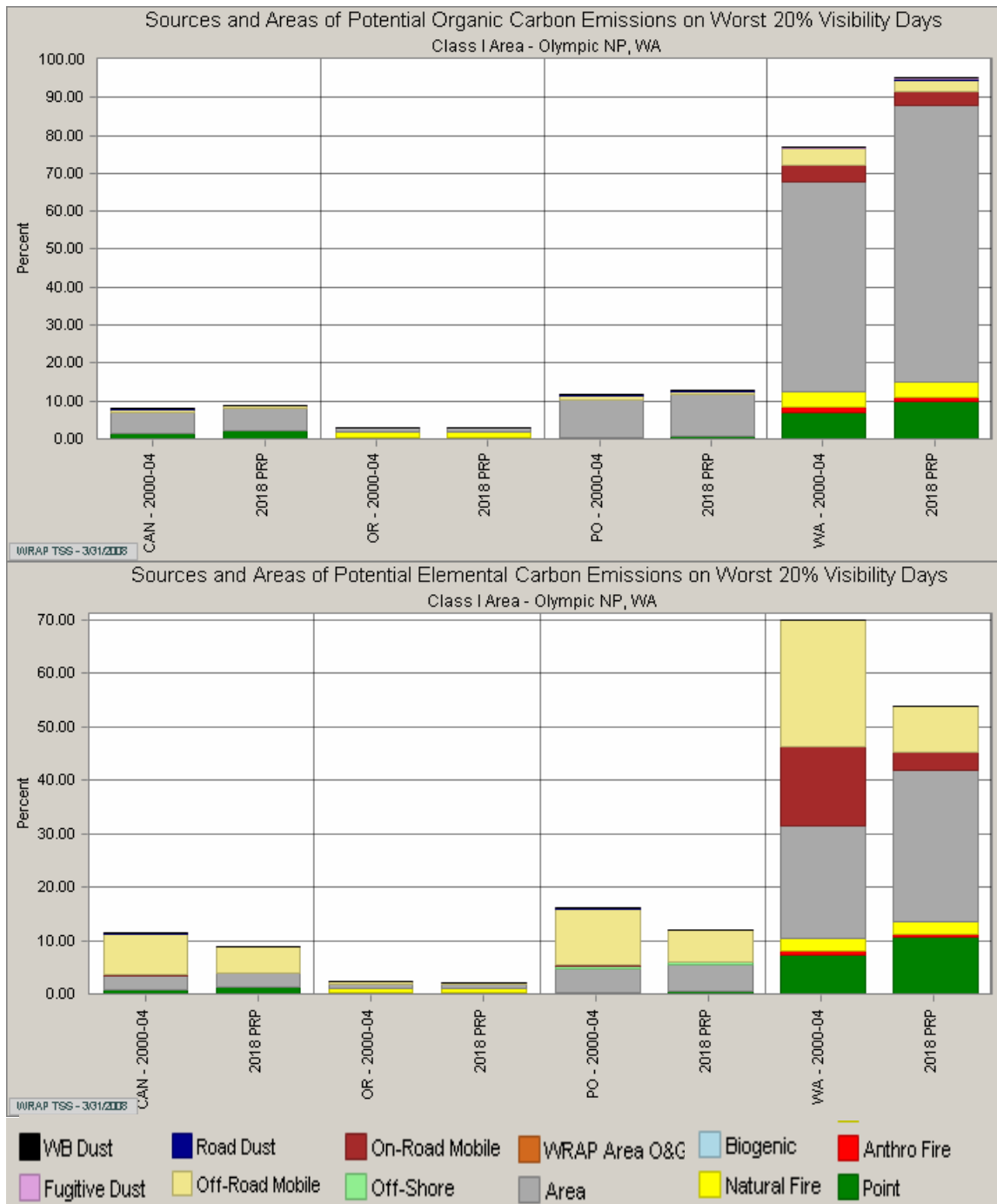


Figure 9-37. Average contemporary fraction of PM_{2.5} carbon for the summer (top) and winter (bottom), estimated from IMPROVE monitoring data (June 2004-February 2006) based on EC/TC ratios. The contemporary values from radiocarbon dating for the 12 monitoring sites are indicated in by colored circles with the site names. Color contours are shown to aid in showing sites with similar values. Site locations are indicated by circles for remote area sites and triangles for urban sites.

Contemporary carbon estimates for all of the IMPROVE network monitoring sites for data from two summer seasons (June, July and August, 2004/2005) and two winter seasons (December, 2004/2005, January and February, 2005/2006) were calculated from the measured EC to total carbon (EC/TC) ratios using the 12-site empirical relationship between radiocarbon determined contemporary carbon fraction and IMPROVE measured EC/TC ratio (Schichtel et al., 2008, [156958](#)). The results are displayed in color contour maps in Figure 9-37, which also shows the radiocarbon determined contemporary carbon for the 12 sites. The lowest contemporary carbon estimates (<60%) in both seasons are for urban areas. In the rural West, most of the sites have over 90% of their PM carbon from contemporary carbon sources during the summer and from 60% to over 90% during the winter. In the rural East, most of the sites have 45-90% of their PM carbon from contemporary carbon sources during the summer and from 60% to over 90% in the winter.

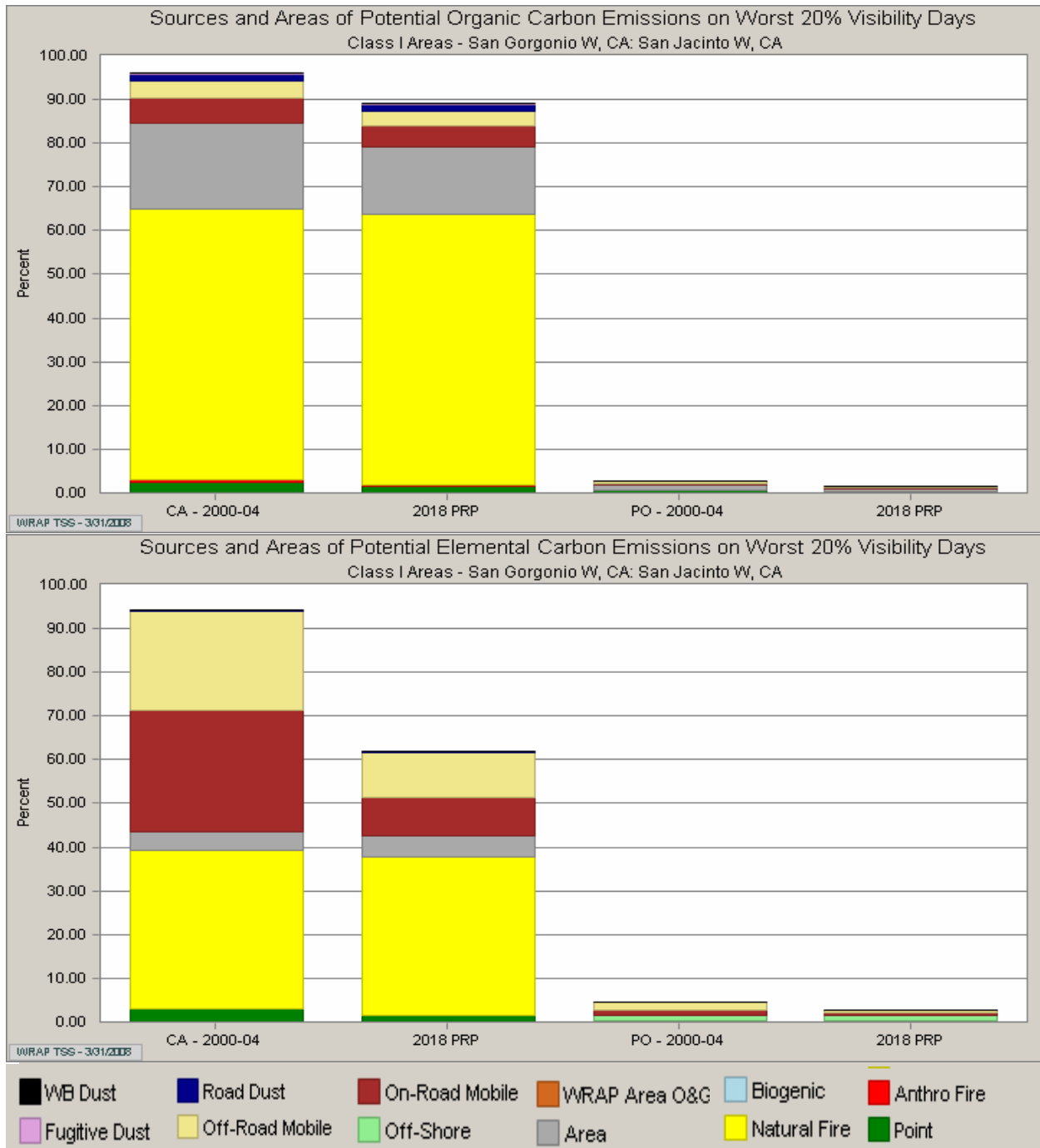
Schichtel et al. (2008, [156958](#)) showed a strong relationship between the site-averaged EC/TC ratios and the site-averaged fraction of fossil carbon separately for the summer and winter data sets (i.e., R^2 of 0.71 and 0.87, respectively). Using regression analysis they estimated that the summer and winter EC/TC ratios associated with purely fossil carbon were 0.35 ± 0.039 and 0.46 ± 0.028 , respectively, and for purely contemporary carbon the EC/TC ratios were 0.12 ± 0.011 and 0.19 ± 0.0095 . These ratios are shown to be consistent with corresponding ratios from the literature for source testing primary fossil and contemporary combustion sources respectively. They are also shown to be consistent with the 90 percentile value of the EC/TC ratio from the urban IMPROVE monitoring sites (0.41 and 0.44 for summer and winter) and the 10th percentile values of the EC/TC ratio for remote areas IMPROVE monitoring sites (0.07 and 0.16 for summer and winter), which they argue are dominated by fossil and contemporary carbon, respectively.

The largest sources of contemporary carbon are primary emissions from biomass burning and SOA from biogenic precursor gases (e.g., terpenes from conifer forests). Schichtel et al. (2008, [156958](#)) estimated the 12-site overall contribution by secondary organic PM to the summer contemporary carbon fraction as $36 \pm 6.4\%$ by assuming the EC/TC ratio for contemporary carbon during the winter represented the ratio of primary emissions only (i.e., no secondary organic PM formation in the winter) and that the EC/TC ratio for primary emissions is independent of seasons. This approach should provide a lower bound estimate of the secondary OC species. The same method applied to the fossil carbon fraction yielded an estimate of $23 \pm 10\%$ of the fossil carbon PM from secondary organic formation in the atmosphere during the summer. These estimates correspond to over 40% of the contemporary and over 35% of the fossil OC being from secondary PM formation.



Source: From the TSS website (see Table 9-1)

Figure 9-38. Results of the weighted emissions potential tool applied to primary OC emissions (top) and EC emissions (bottom) for the baseline and projected 2018 emissions inventories for Olympic NP. Only source regions (WRAP states and other regions) with the largest estimated contributions are shown (i.e., Canada, Oregon, Pacific Off-Shore, and Washington from left to right). The scale is normalized (i.e., unitless) one over distance weighted emissions multiplied by trajectory residence time.



Source: From the TSS website (see Table 9-1).

Figure 9-39. Results of the weighted emissions potential tool applied to primary OC emissions (top) and EC emissions (bottom) for the baseline and projected 2018 emissions inventories for San Geronio W. Only source regions (WRAP states and other regions) with the largest estimated contributions are shown (i.e., California and Pacific Off-Shore from left to right). The scale is normalized (i.e., unitless) one over distance weighted emissions multiplied by trajectory residence time.

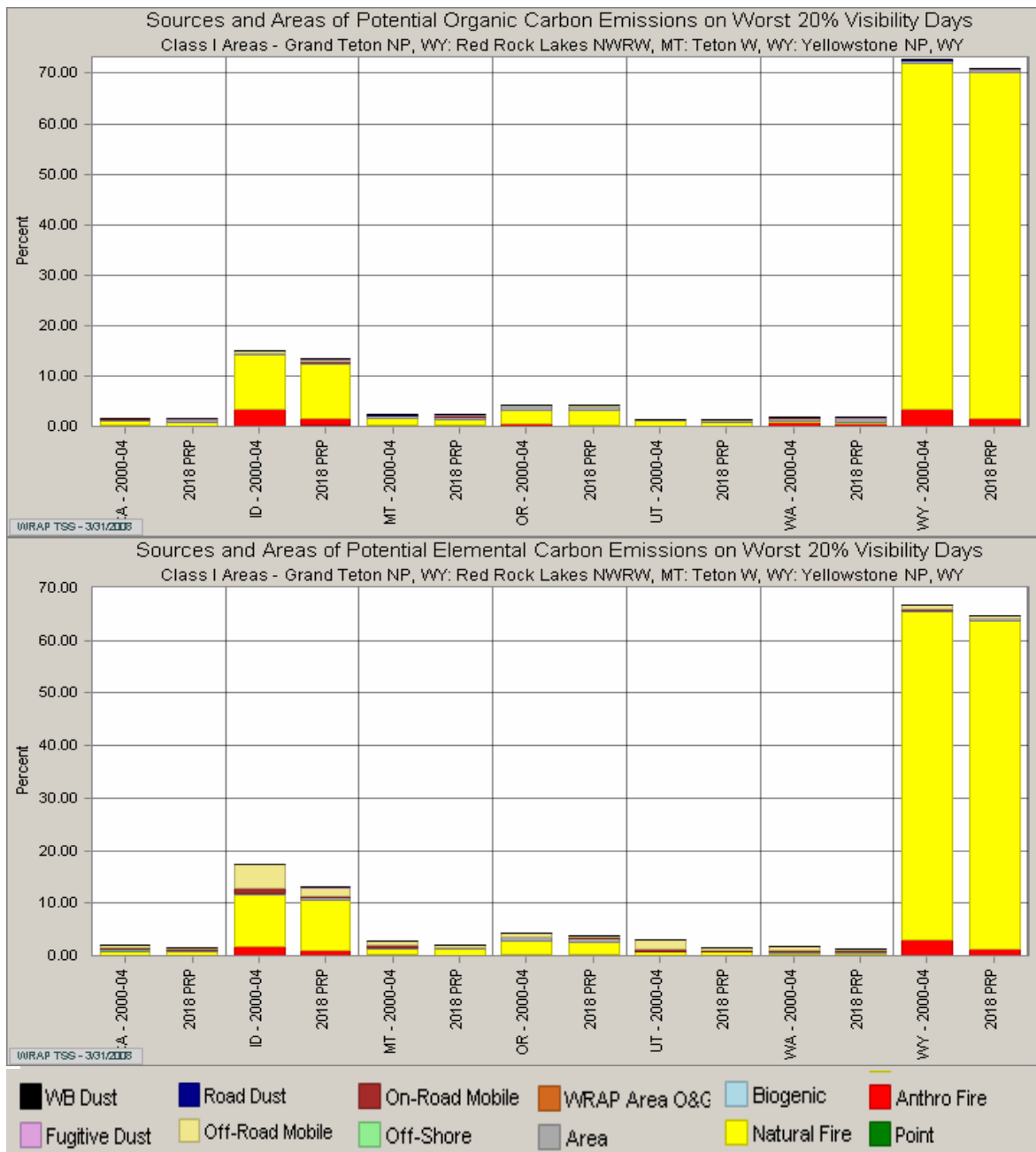
WRAP applied a weighted emissions potential analysis tool that combined gridded emissions data with back-trajectory analysis that simulated the transport pathway to the various monitoring sites to infer likely source region and emission categories for the 20% best and 20% worst haze conditions for each of the IMPROVE PM speciation monitoring locations in the West. Unlike the virtual tracer approach that uses a full regional air quality simulation model, this method does not explicitly account for chemistry or removal processes and it does not incorporate the sophisticated dispersion estimates (i.e., it uses one over distance weighting for dispersion), so it should be considered a screening tool that has been found to be helpful in identifying the likely sources contributing to haze. More information on this approach is available elsewhere (see the link to the TSS in Table 9-1). Primary OC and EC PM species results from the weighted emissions potential tool for the worst 20% haze days using the 2000-2004 base years' emissions and trajectories, and the same trajectories with 2018-projected emissions for each of the 6 selected western monitoring locations are shown in Source: From the TSS website (see Table 9-1)

Figure 9-38 through Figure 9-43.

For Olympic NP (Source: From the TSS website (see Table 9-1)

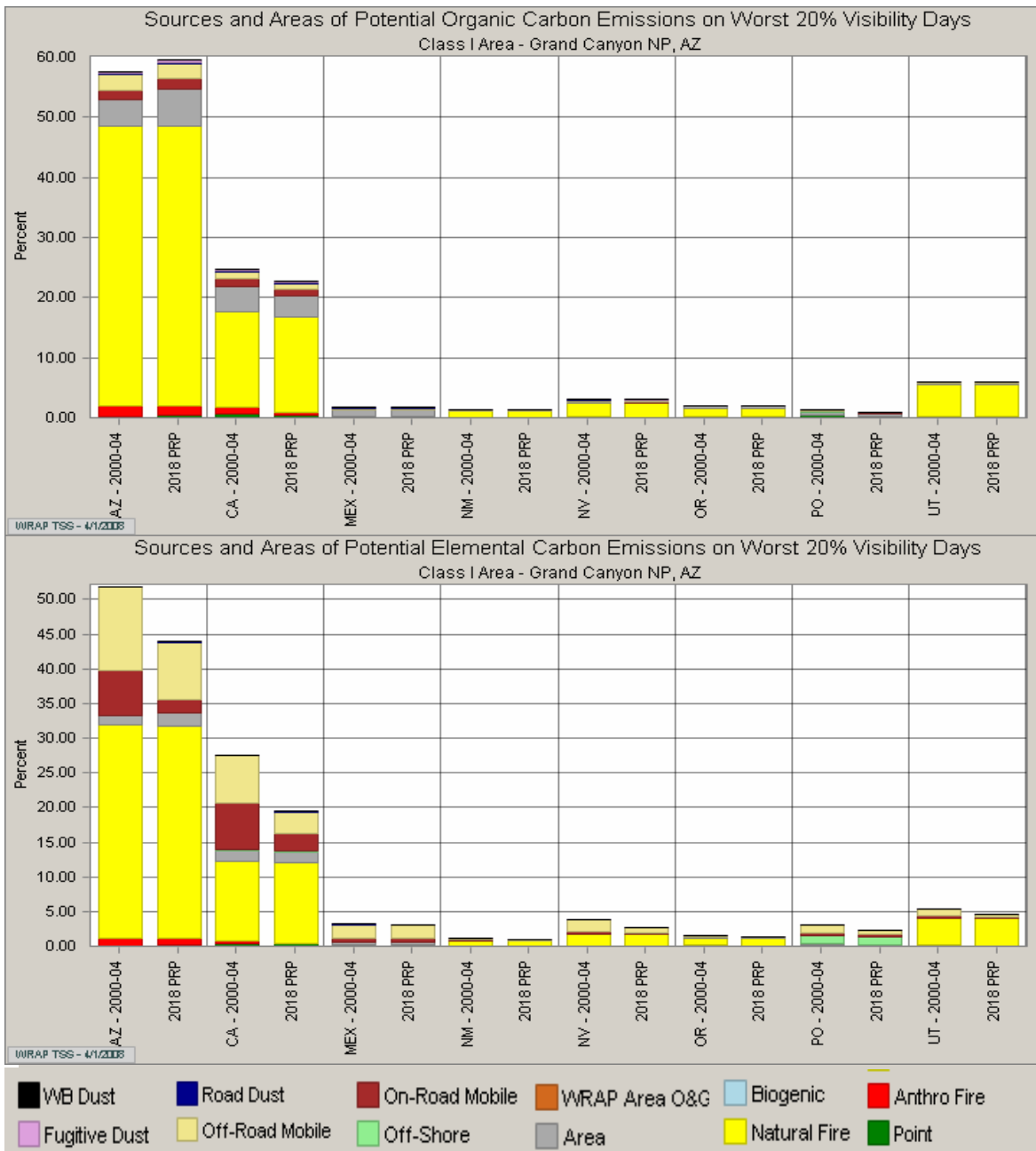
Figure 9-38), most of the primary OC as well as most of the EC PM is likely to be from the state of Washington during the worst haze days. This is because the multi-day trajectories that transport emissions on its worst days tend to be short (within 200 km based on maps available on TSS, see Table 9-1). Area sources, which include emissions from residential wood heating, watercraft, non-mobile urban and other sources too small to be labeled as point sources, are the big contributors to primary organic, while on- and off-road mobile emissions plus area sources are large contributors to the EC at Olympic NP. The 2018 projected growth in area sources and decrease in emissions of mobile source emissions is anticipated to increase the haze by primary OC while reducing the haze by EC at Olympic NP. The same analysis applied to San Geronio (Figure 9-39), is similar in that the majority of the emissions with the potential to contribute to primary OC and EC PM is from the home state, California in this case. However, the likely importance of natural fire emissions for carbonaceous PM species sites is substantially greater at San Geronio W. than it was for Olympic NP.

The weighted emissions potential results applied to Yellowstone NP and Grand Canyon NP (Figure 9-40 and Figure 9-41) show the likely dominance of natural fire emissions in the intermountain western U.S. to primary OC and EC PM during worst haze conditions for these two locations. Numerous states have emissions that have the potential to contribute noticeably to these carbonaceous species, due to relatively long multi-day trajectories (500-1,000 km) on worst haze days, though for both sites the home state has the greatest potential based on this inverse distance weighting approach. On- and off-road mobile sources in Arizona and California have significant potential to contribute to Grand Canyon carbonaceous particles, especially EC concentrations, probably due to some of the trajectories being over the populated areas of these two states to the south and southwest of Grand Canyon.



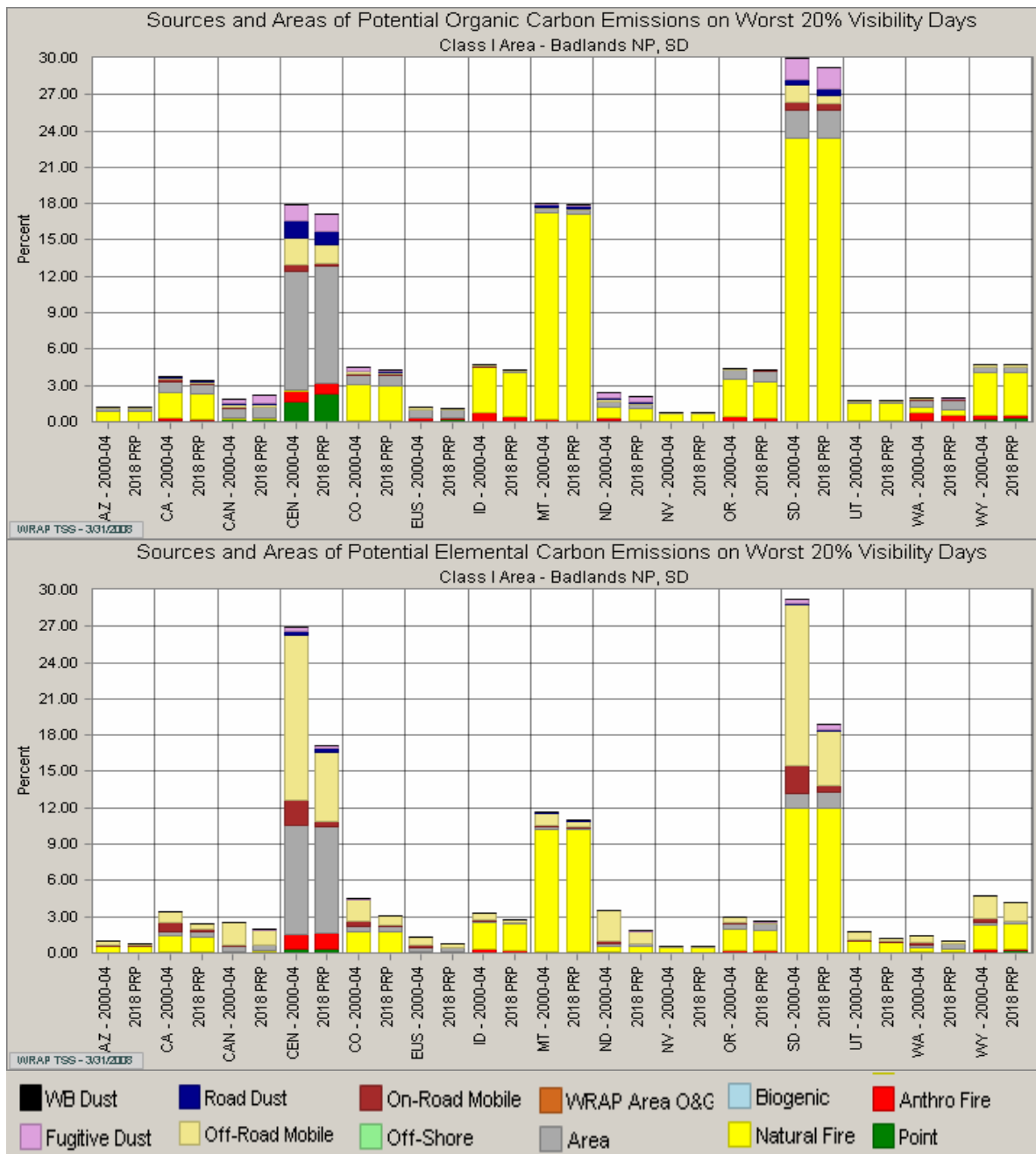
Source: From the TSS website (see Table 9-1).

Figure 9-40. Results of the weighted emissions potential tool applied to primary OC emissions (top) and EC emissions (bottom) for the baseline and projected 2018 emissions inventories for Yellowstone NP. Only source regions (WRAP states and other regions) with the largest estimated contributions are shown (i.e., California, Idaho, Montana, Oregon, Utah, Washington, and Wyoming from left to right). The scale is normalized (i.e., unitless) one over distance weighted emissions multiplied by trajectory residence time.



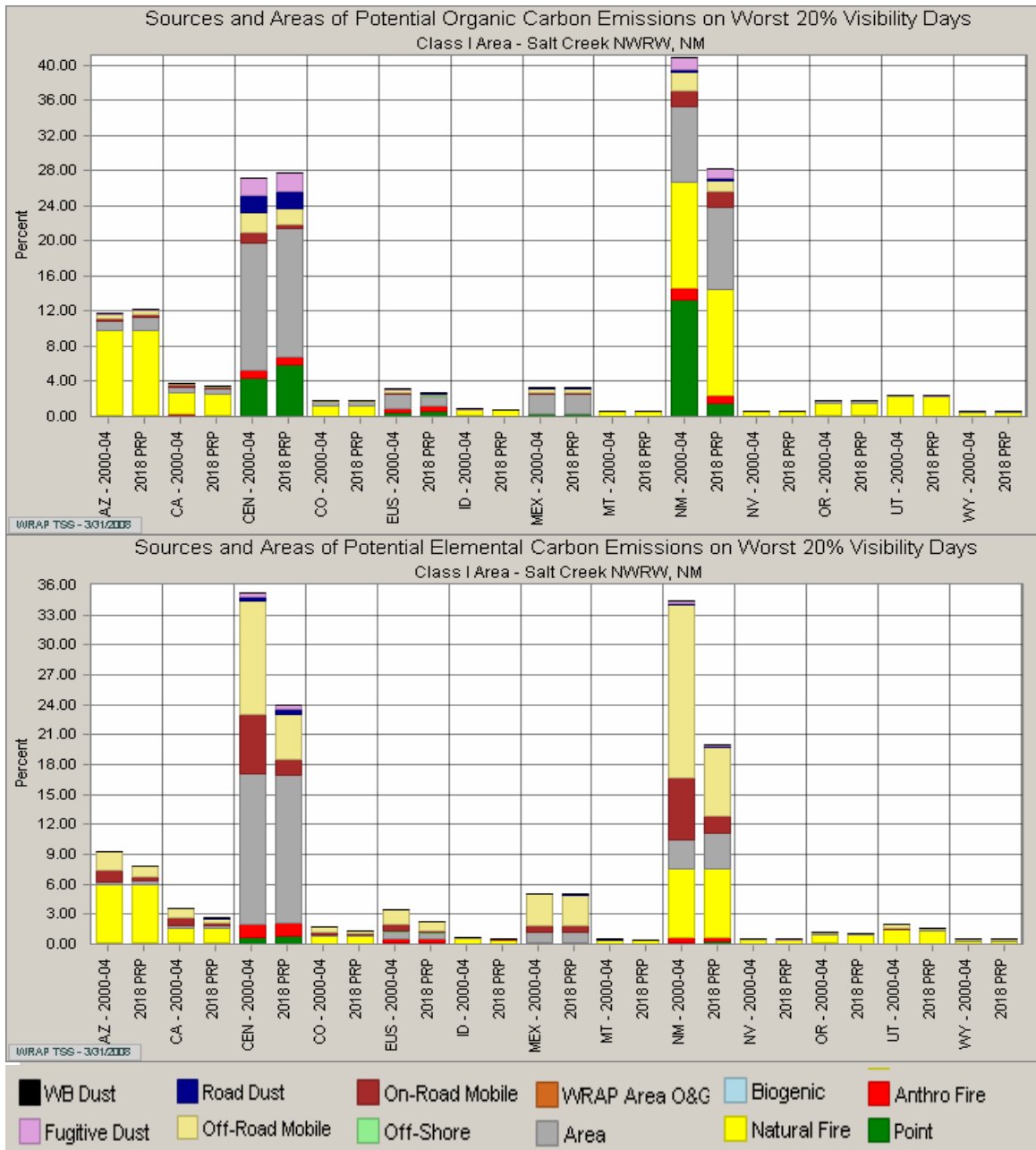
Source: From the TSS website (see Table 9-1).

Figure 9-41. Results of the weighted emissions potential tool applied to primary OC emissions (top) and EC emissions (bottom) for the baseline and projected 2018 emissions inventories for Grand Canyon NP. Only source regions (WRAP states and other regions) with the largest estimated contributions are shown (i.e., Arizona, California, Mexico, New Mexico, Nevada, Oregon, Pacific Off-shore and Utah from left to right). The scale is normalized (i.e., unitless) one over distance weighted emissions multiplied by trajectory residence time.



Source: From the TSS website (see Table 9-1).

Figure 9-42. Results of the weighted emissions potential tool applied to primary OC emissions (top) and EC emissions (bottom) for the baseline and projected 2018 emissions inventories for Badlands NP. Only source regions (WRAP states and other regions) with the largest estimated contributions are shown (i.e., Arizona, California, Canada, CenRAP, Colorado, eastern U.S., Idaho, Montana, North Dakota, Nevada, Oregon, South Dakota, Utah, Washington, and Wyoming from left to right). The scale is normalized (i.e., unitless) one over distance weighted emissions multiplied by trajectory residence time.



Source: From the TSS website (see Table 9-1).

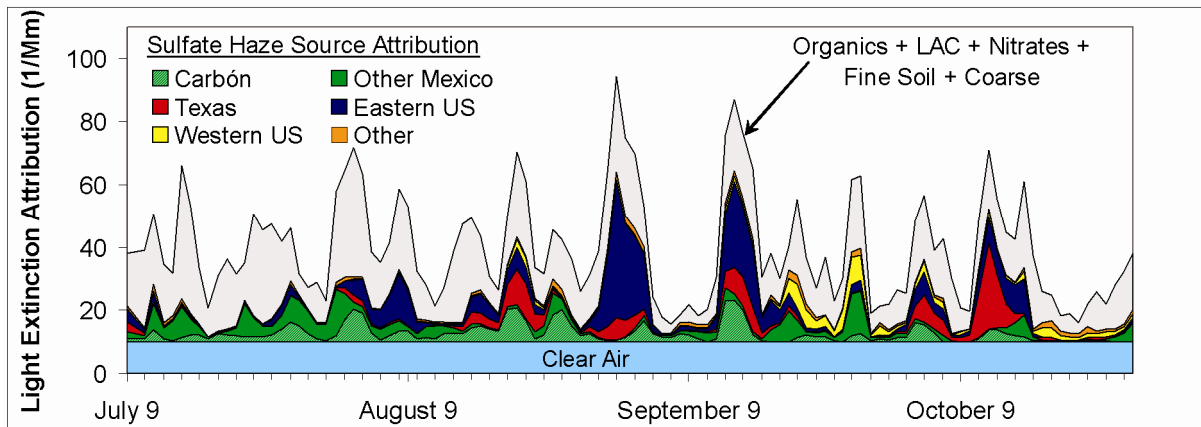
Figure 9-43. Results of the weighted emissions potential tool applied to primary OC emissions (top) and EC emissions (bottom) for the baseline and projected 2018 emissions inventories for Salt Creek W. Only source regions (WRAP states and other regions) with the largest estimated contributions are shown (i.e., Arizona, California, CenRAP, Colorado, eastern U.S., Idaho, Mexico, Montana, New Mexico, Nevada, Oregon, Utah, and Wyoming from left to right). The scale is normalized (i.e., unitless) one over distance weighted emissions multiplied by trajectory residence time.

For the most easterly of the selected WRAP sites, Badlands NP and Salt Creek, the weighted emissions potential results for primary OC and EC (Figure 9-42 and Figure 9-43) show potential contributions from a greater number of states and multi-state regions than for selected sites further to the west. This may be due in part to trajectories associated with worst haze conditions for these two sites being moderately long (~500 km) and in multiple directions. Natural fire emissions have the greatest potential to contribute to organic species PM at Badlands NP, but are less likely to be dominant at Salt Creek or at either site in its contribution to EC PM concentrations. The contributions by emissions from area and mobile sources from the home states and states to the east (Central States Regional Air Partnership states are labeled “CEN” in the figures) are potentially greater than by natural fire; this is especially true for contributions to EC PM.

WRAP applied the weighted emissions potential tool to assess likely source types and regions contributing to coarse mass concentrations. The results for the six selected monitoring sites (not shown) are as follows. Most dust at Olympic NP is likely to be from fugitive dust sources in Washington state, while at San Geronio it is likely more from road dust with smaller amounts from fugitive dust sources. The amount from wind-blown dust is small for both of these far westerly sites. Wind-blown dust is likely the largest source contributing to coarse mass at Grand Canyon NP, Badlands NP and Salt Creek W with most of it originating in the home-state for those sites. The weighted emissions potential results for coarse mass at Yellowstone are different from those of the other five selected sites in that Idaho and Montana each have a higher potential to contribute to coarse mass on the worst haze days than the home state (Wyoming), and that wind-blown and road dust both contribute substantially as does fugitive dust and natural fire.

In another WRAP-sponsored effort to better understand the causes of remote area haze in the western U.S., each of the worst haze days for all western IMPROVE monitoring sites where dust (defined as the sum of coarse mass and fine soil PM) was the largest contributor to light extinction was separately assessed to categorize the most likely dust source (Kavouras et al., 2007, [156630](#); Kavouras et al., 2009, [191976](#)) and the Causes of Haze Website – see Table 9-1). Elemental composition was used to assess the likelihood that the dust was associated with long-range transport from Asia. A regression analysis at each site between dust concentrations and coincident local wind speed was used to generate site-specific estimates of local windblown dust for each sample period. Finally, back trajectory analysis combined with maps constructed of wind erosion potential (i.e., developed by combining soil types and land cover classifications) are used in a manner similar to the weighted emissions potential analysis to identify the likelihood of regionally transported wind-blown dust as the source. These assessments were conducted on each of the 610 so-called “worst dust haze days” at 70 monitoring sites for data from 2001-2003 to classify each day by its likely contributions from Asian dust, local windblown dust, upwind transport and undetermined. The undetermined category includes those sample periods that failed to be classified into one of the other three source categories suggesting that mechanically suspended dust activities (e.g., unpaved road dust, agricultural, construction and mining activities) may be responsible.

Of the 610 “worst dust haze days” at the 70 WRAP monitoring sites, 55 sample periods are classified as Asian dust influenced, almost exclusively in the spring; 201 sample period are classified as local windblown dust, mostly in the spring but some in all seasons; 240 sample periods are classified as upwind transported dust, with a broader seasonal distribution centered on summer and few instances during winter; and 114 are in the undetermined category with most in summer and least in winter. Most dust days occurred in the deserts of Arizona, New Mexico, Colorado, western Texas and southern California, and these were dominated by local and regionally transported wind-blown dust (e.g., 84% for Salt Creek W). Asian dust caused only a few of the worst dust days during the 3-year assessment period, though it is an important source (i.e., 10-40% of the worst dust days) for sites in the more northern regions of the West with greater vegetative land-cover where local and regionally transported wind-blown dust was infrequent. The frequency of worst dust events classified as undetermined was greatest for sites in the vicinity of large urban and agricultural areas such as those in California and southern Arizona.



Source: Reprinted with Permission of the Air & Waste Management Association from Pitchford et al. (2005, [156874](#))

Figure 9-44. BRAVO study haze contributions for Big Bend NP, TX during a 4-mo period in 1999. Shown are impacts by various particulate SO_4^{2-} sources, as well as the total light extinction (black line) and Rayleigh or clear air light scattering.

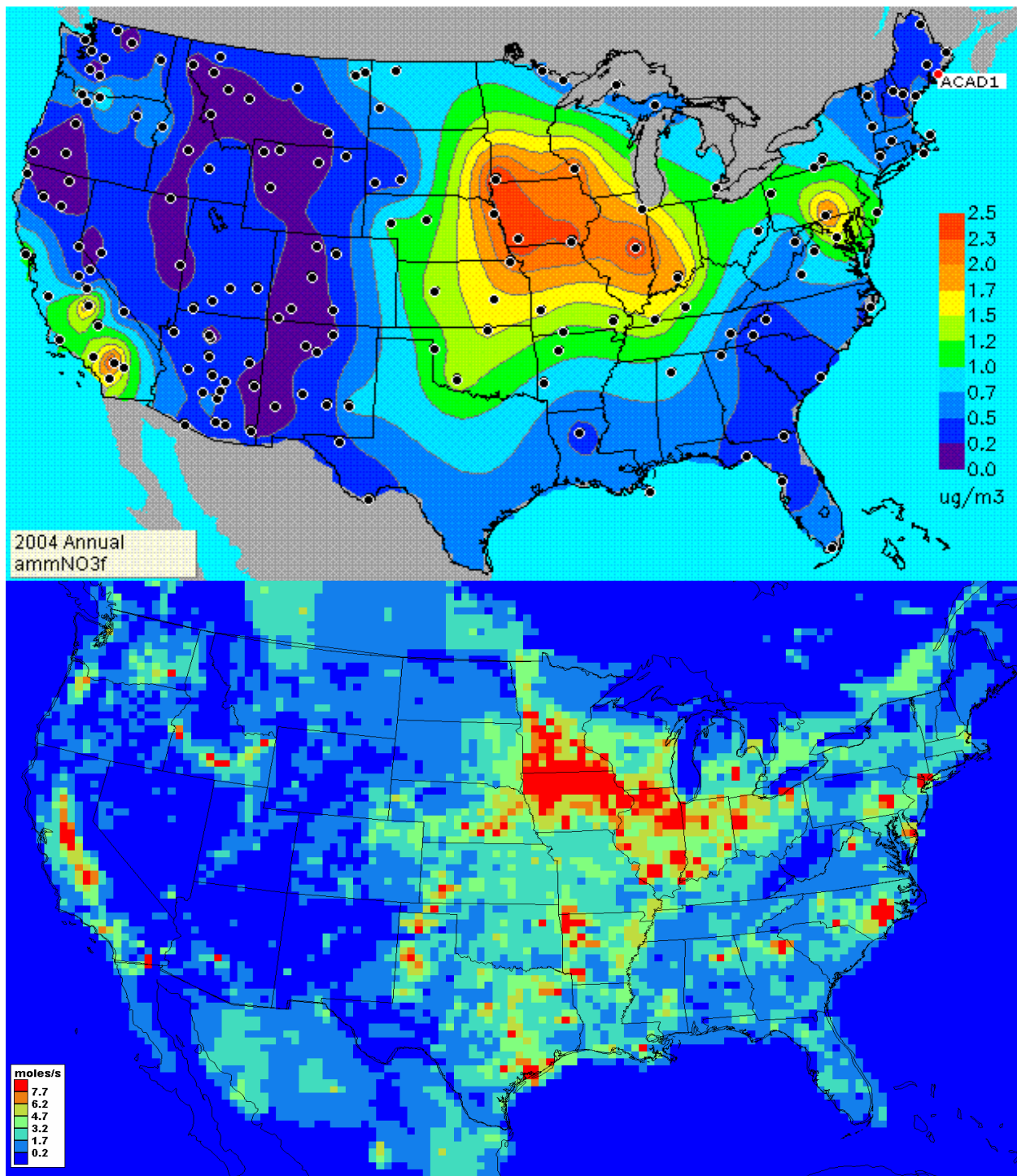


Figure 9-45. Maps of spatial patterns for average annual particulate nitrate measurements (top), and for ammonia emissions for April 2002 from the WRAP emissions inventory (bottom).

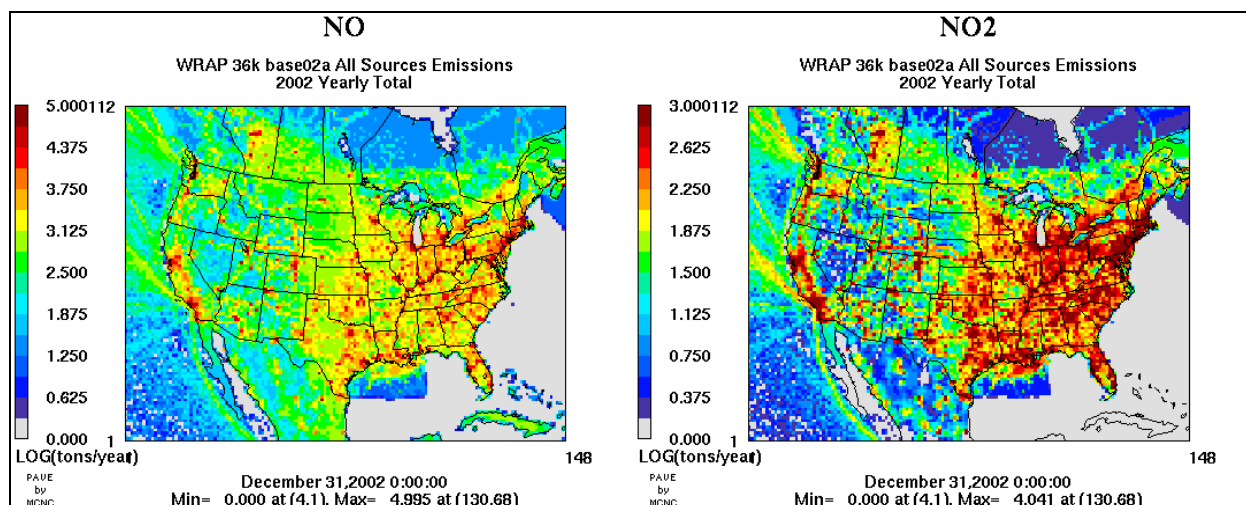


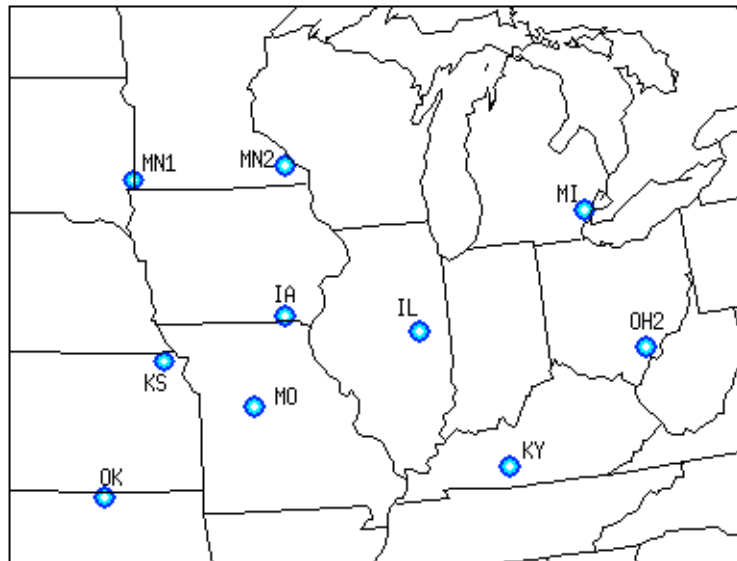
Figure 9-46. Maps of spatial patterns of annual NO (left) and NO₂ (right) emissions for 2002 from the WRAP emissions inventory.

Source attribution of the particulate SO₄²⁻ contribution to haze at Big Bend NP, TX was a primary motivation for the BRAVO study. Schichtel et al. (2005, [156957](#)) showed that during the four-month field monitoring study (July-October 1999), SO₂ emissions sources in the U.S. and Mexico were responsible for ~55% and ~38% of the particulate SO₄²⁻, respectively. Among U.S. source regions, Texas was responsible for ~16%, eastern U.S. ~30%, and the western U.S. ~9%. A large coal fired power plant, the Carbón facility in Mexico, just south of Eagle Pass, TX, was responsible for ~19%, making it the largest single contributor. Pitchford et al. (2005, [156874](#)) put these results into the context of other component contributions to regional haze, plus seasonal and longer-term variations in haze by particulate components. Figure 9-44 shows the temporal variation of the contributions by the various SO₂ emissions source regions plus the Carbón facility during the BRAVO study period. The largest particulate SO₄²⁻ peak haze periods are dominated by infrequent large contribution by emission sources in TX and the eastern U.S., while Mexican sources including the Carbón facility are more frequent contributors to haze, but at generally lower light extinction values. Particulate nitrate contributions to haze at Big Bend NP are among the lowest measured in the U.S. (~3% of light extinction on average and for worst haze episodes).

Nitrate concentrations are a significant contributor to light extinction further to the north of Texas in the center of the country. While SO₄²⁻ can be in particulate form though not fully neutralized by ammonia, nitric acid from NO_x emissions requires neutralization by ammonium to become particulate ammonium nitrate. One way to explore the causes of the Midwest nitrate bulge is to compare its spatial distribution with the spatial distributions of NO_x and ammonia emissions. Figure 9-45 shows a map of the annual average particulate nitrate concentrations (top) with a map of ammonia emissions directly below it. Animal agriculture is responsible for most of the ammonia concentration in the Midwest. The striking similarity between the ambient particulate nitrate concentration and the ammonia emissions spatial patterns with regional maximum centered on Iowa is in contrast to the NO_x (i.e., NO + NO₂) emissions spatial patterns, shown in Figure 9-46. NO_x emissions are high over a broad region of the country associated with the larger population densities and greater numbers of fossil fuel electric generation plant generally to the east of the Midwest nitrate bulge. While both ammonia and nitric acid are needed to form particulate ammonium nitrate, the maps suggest the Midwest nitrate bulge is due primarily to the abundance of free ammonia (i.e., the amount beyond what is required to neutralize the acidic particulate SO₄²⁻). By contrast, the region to the east of the Midwest nitrate bulge should have plenty of nitric acid given the higher emissions of NO_x, but apparently has a deficiency of free ammonia. The few eastern monitoring sites with locally high particulate nitrate (near southeastern PA) are located within a small region of high density animal agriculture that shows up as a high ammonia emissions region in Figure 9-45. Note that California's South Coast and Central Valley have both high ammonia and high NO_x emissions, explaining the high particulate nitrate contribution to haze there.

To better understand the role of ammonia in the formation of the Midwest nitrate bulge, the Midwest RPO and Central States Regional Air Partnership deployed a measurement program from late 2003 through early 2005 at 10 locations (9 rural and 1 urban) in the region (see Figure 9-47) to monitor particulate SO_4^{2-} , nitrate, and ammonium ions, plus the precursor gases sulfur dioxide, nitric acid, and ammonia (Kenski et al., 2004, [192078](#); Sweet et al., 2005, [180038](#)). These data have been used as input for thermodynamic equilibrium modeling to assess the changes in PM concentrations that would result from changes to precursor concentrations (Blanchard and Tanenbaum, 2006, [190005](#); Blanchard et al., 2007, [098659](#)). Blanchard and Tanenbaum (2006, [190005](#)) and Blanchard et al. (2007, [098659](#)) conclude that the current conditions at nine of the ten sites are near the point of transition between the precursor species (nitric acid and ammonia) that limits the formation of particulate nitrate. If excess ammonia increases, either by greater ammonia emissions or by anticipated decreases in SO_2 emissions, then nitric acid concentration would need to be reduced (via lower NO_x emissions) in order to reduce the particulate nitrate concentration.

Given the comparability of particulate SO_4^{2-} and nitrate with regard to their light extinction efficiencies, their visibility impacts are proportional to the sum of their mass concentrations. A reduction in SO_4^{2-} caused by SO_2 emission reductions would reduce the particulate SO_4^{2-} concentration, though according to the thermodynamic equilibrium modeling for these sites the particulate nitrate concentration will be increased somewhat. However, the total particulate SO_4^{2-} plus nitrate concentration would be reduced so visibility impacts would be decreased. At current ammonium concentrations the predicted response of changes to SO_4^{2-} and nitric acid concentrations (i.e., SO_2 and NO_x emissions changes) are similar in respect to the resulting magnitude of changes to the total particulate SO_4^{2-} plus nitrate concentrations. At all but two sites the total particulate SO_4^{2-} plus nitrate concentrations would decrease if either ammonia or nitric acid were reduced.

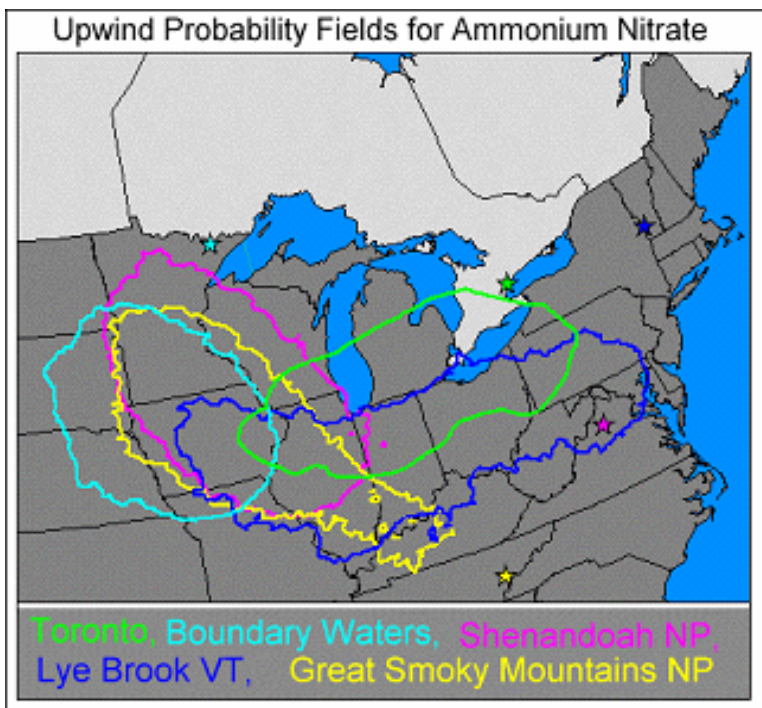


Source: Kenski et al. (2004, [192078](#))

Figure 9-47. Midwest ammonia monitoring network.

A further degree of complications in understanding the response of particulate nitrate to changes in precursor concentrations results from the temperature and humidity dependence of the partition between particulate ammonium nitrate and the disassociated gaseous nitric acid and ammonia. This dependence causes seasonal and even diurnal differences in the expected responses of particulate nitrate concentrations to changes in precursor concentrations. As expected, during the colder times of the year the total particulate concentrations are more sensitive to changes in ammonia and nitric acid concentrations than during the warmer seasons when SO_4^{2-} concentrations are greater.

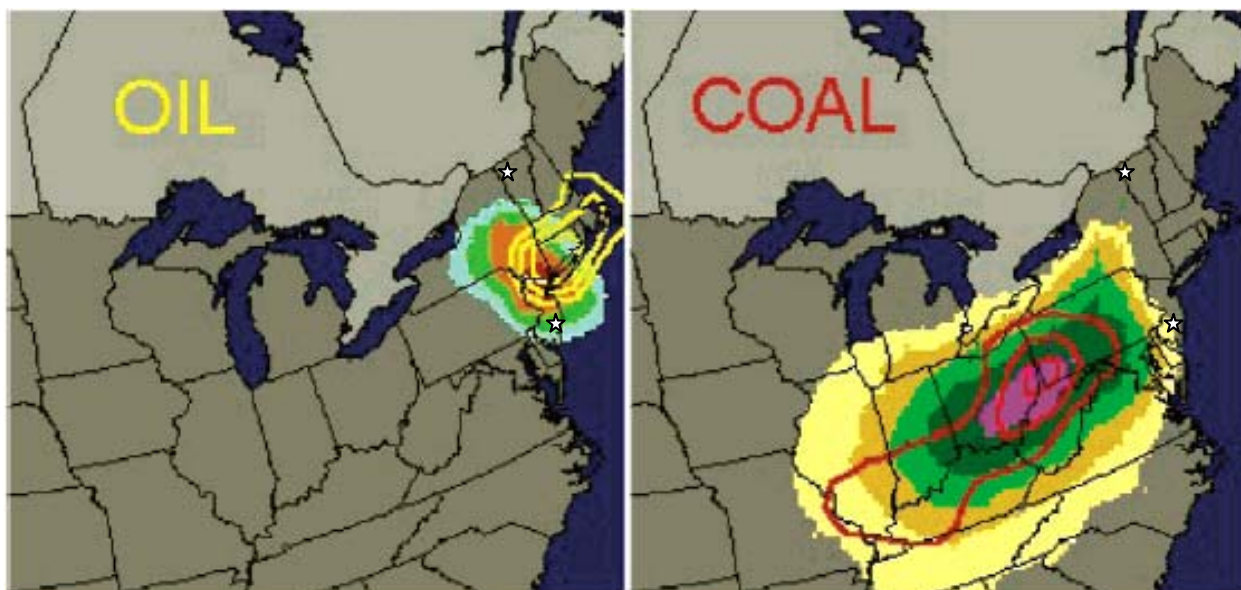
As shown in Figure 9-48, results of an air transport assessment to identify emission source areas associated with high particulate nitrate at five monitoring locations in the East (four remote-area sites and Toronto, Canada) implicate the high ammonia emissions region of the Midwest as a common source region (Canada-US Air Quality Committee, 2004, [190519](#)). This assessment does not preclude local sources of the precursor gases responsible for particulate ammonium nitrate, but does suggest that long-range transport of particulate nitrate or ammonia from the high emissions region of the Midwest is also contributing to eastern nitrate episodes.



Source: Canada-U.S. Air Committee (2004, [190519](#)).

Figure 9-48. Upwind transport probability fields associated with high particulate nitrate concentrations measured at Toronto, Canada; Boundary Water Canoe Area, MN; Shenandoah NP, VA; Lye Brook, VT; and Great Smoky Mountains NP, TN.

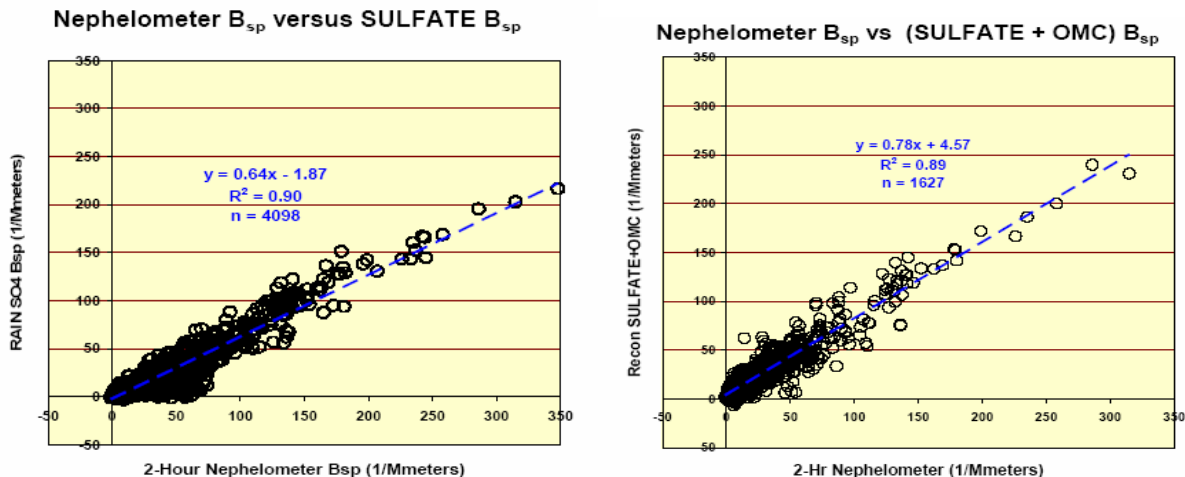
In a similar air transport assessment for measurements at Underhill, VT and at Brigantine, NJ, Hopke et al. (2005, [156567](#)) identified separate regions associated with particulate SO_4^{2-} accompanied by trace particulate components associated with coal burning (e.g., Se) and accompanied by trace particulate components associated with oil burning (e.g., V). As shown in Figure 9-49, the coal-burning related particulate SO_4^{2-} for these two monitoring sites is associated with long-range transport from the Ohio River Valley, while oil-burning related particulate SO_4^{2-} is from more nearby emissions in the high population region of coastal New York, New Jersey, Massachusetts, and Connecticut.



Source: Reprinted with Permission of Environmental Science and Technology from Hopke, et al. (2005, [156567](#)).

Figure 9-49. Trajectory probability fields for periods with high particulate SO_4^{2-} measured at Underhill, VT and Brigantine, NJ (shown as white stars) associated with oil-burning trace components (left) and with coal-burning trace components (right). Shown for comparison are the interpolated SO_2 emissions areal density contours for oil combustion sources (emissions times 10) and coal combustion sources, displayed as yellow and red contour lines, respectively.

The Regional Aerosol Intensive Network (RAIN) was established by MANE-VU to generate enhanced continuous visibility, plus fine particle mass and composition monitoring data at a string of three monitoring locations along the transport path from the Ohio River Valley to coastal Maine (NESCAUM, 2006, [156802](#)). The dominant role of particulate SO_4^{2-} in the northeast is well demonstrated by a scatter plot of RAIN data that shows the relationship between particulate SO_4^{2-} extinction, calculated using the IMPROVE algorithm plotted against directly measured particle light scattering for hourly data over a 8-mo period, beginning in July 2004 at the Acadia NP, ME monitoring site (see Figure 9-50). Particulate SO_4^{2-} explains 90% of the variance in particulate light scattering even though it is responsible for only about 64% of the total light extinction (annual averaged value from the VIEWS web site). Adding the contribution by the second-largest regional contributor to light extinction, particulate OC with about 14%, does not improve the variance explained, but does increase the slope to 0.78. The noticeable difference between these two plots is that the particulate SO_4^{2-} alone underestimates light scattering during low haze periods (points on the plot are below the regression line for light scattering $<70 \text{ Mm}^{-1}$), while the agreement is improved with the addition of particulate OC contributions to haze (regression slope is nearer to one and reduced bias for low haze periods). This implies that particulate SO_4^{2-} and any other co-varying PM species are largely responsible for the highly impacted periods, while OC and other co-varying PM species contribute more during the less extreme haze periods. Particulate nitrate contribution to light extinction at Acadia is about 10% on average.

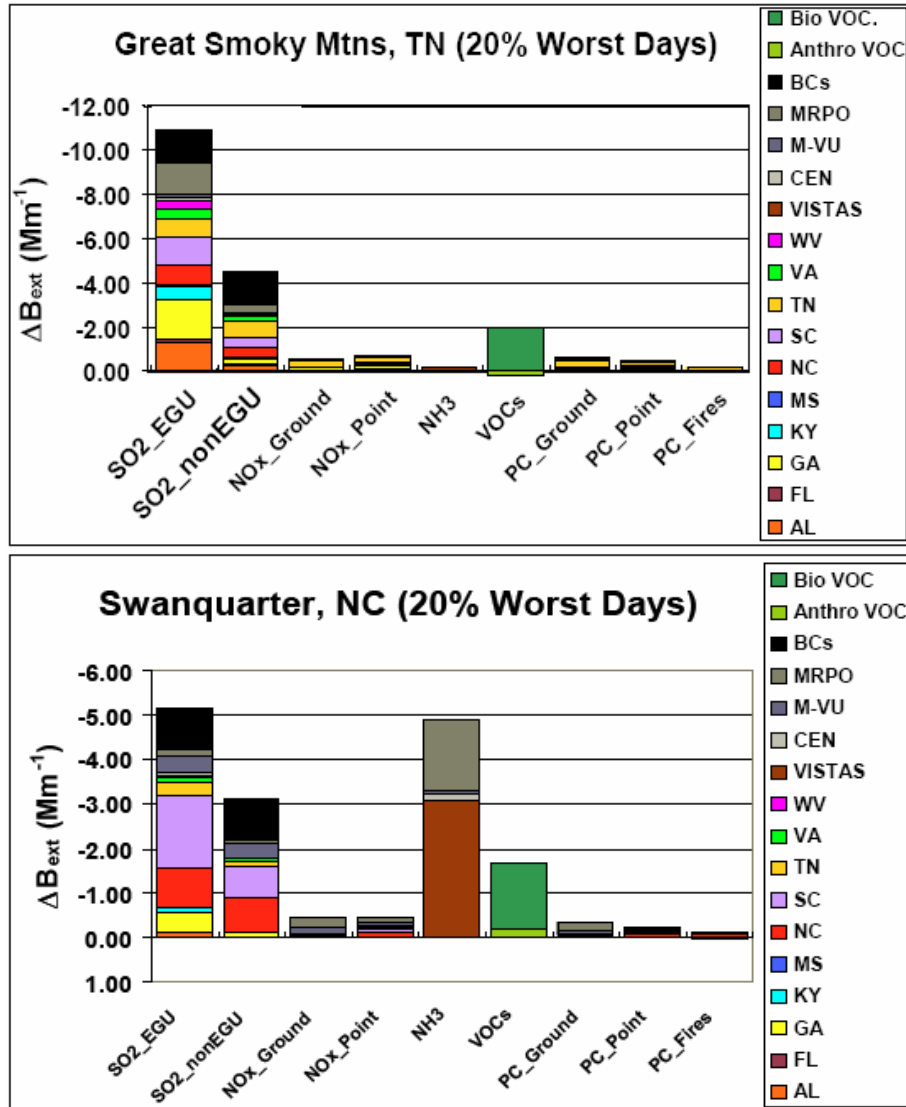


Source: RAIN Preliminary Data Analysis Report (NESCAUM, 2006, [156802](#))

Figure 9-50. Scatter plots of particulate SO_4^{2-} (left) and particulate SO_4^{2-} and organic mass (right) versus nephelometer measured particle light scattering for Acadia NP, ME.

Particulate nitrate concentrations are considerably lower in the SO_4^{2-} -dominated warmer southeastern U.S. than in the Northeast and upper Midwest. Blanchard et al. (2007, [098659](#)) conducted thermodynamic equilibrium modeling on data from the eight SEARCH monitoring sites and found that total particulate nitrate plus SO_4^{2-} is much more responsive to changes in SO_2 concentrations than to changes in nitric acid concentrations, which in turn is more responsive than changes in ammonia concentrations.

The VISTAS RPO commissioned an emissions sensitivity study using CMAQ modeling on winter and summer 2009 emissions projected from the 2002 emissions inventory (NCDENR, 2007, [156798](#)). Figure 9-51 contains bar plots for two North Carolina Class I areas that indicate projected changes in light extinction for the worst haze day due to 30% emissions reductions by particulate species, source types and location across the Southeastern states modeling domain (i.e., as far west as Texas, as far north as Pennsylvania, as far south as the Florida Keys, and as far east as ~300 km from the North Carolina coast). Great Smoky Mountains in the southern Appalachian Mountains has the greatest sensitivity to changes by SO_2 emissions from electrical generation units (EGU) and to a lesser extent other SO_2 emission sources in the region. Reductions of NO_x emissions from ground or point sources are not nearly as effective as SO_2 reductions in reducing the light extinction at Great Smoky Mountains. This is due principally to the worst days at Great Smoky Mountains occurring during the summer, when temperatures are too high to support high particulate nitrate concentrations. For the same reason, ammonia emission reductions are also ineffective. Swanquarter W, NC is a coastal location where some of the worst haze days are during the winter and include contributions from particulate ammonium nitrate. Both SO_2 and ammonia emissions reductions would be effective at reducing worst haze days at the Swanquarter W, though NO_x emissions are not as effective presumably because the atmosphere is ammonia-limited for particulate nitrate production.



Source: NCDENR (2007, [156798](#)).

Figure 9-51. CMAQ air quality modeling projections of visibility responses on the 20% worst haze days at Great Smoky Mountains NP, NC (top) and Swanquarter W, NC (bottom) to 30% reductions. This is from a projected 2009 emission inventory of visibility-reducing pollutants by source category and geographic areas.

9.2.4. Urban Visibility Valuation and Preference

The Clean Air Act §302(h) defines public welfare to include the effects of air pollution on “...visibility, ... and personal comfort and wellbeing.” Though good visibility conditions in Class I (e.g., NPs) and wilderness areas have long been recognized as important to the public welfare (see discussions in EPA (2004, [056905](#); 2005, [090209](#)) and Chestnut and Dennis (1997, [014525](#)), visibility conditions in urban areas also contribute to the public welfare. Although visibility impairment may be caused by either natural or manmade conditions (or both), it is only impairment that occurs as a result of air pollution (either alone or in combination with water vapor or other atmospheric conditions) that can be mitigated by regulations such as the RHR (40 CFR 51.300 through 309) or the Secondary NAAQS. The term visual air quality (VAQ) is used here to refer to

the visibility effects caused solely by air quality conditions, so for example it excludes the reduced visibility caused by fog. Visibly poor air quality causes people to be concerned about substantive health risks, but degraded VAQ adversely affects people in additional ways. These include the aesthetic and wellbeing benefits of better visibility, improved road and air safety, and enhanced recreation in activities like hiking and bicycling. Because the human health impacts of air pollution are assessed under the Primary NAAQS, it is necessary to separate out these non-health components associated with the visibility condition produced by a given amount of air pollution when assessing the need for additional regulation to protect the public welfare effect of visibility under the Secondary NAAQS. The degree to which previous human preference and valuation studies for VAQ have adequately made this distinction and separation is an important issue in applying results from available studies in a Secondary NAAQS (or benefits estimation for any policy affecting VAQ) context. The remainder of this discussion is focused on those aesthetic and wellbeing qualities associated with a given VAQ in urban areas.

The term “urban visibility” is used to refer to VAQ throughout a city or metropolitan area. Urban visibility includes the VAQ conditions in all locations that people experience in their daily lives, including scenes such as residential streets and neighborhood parks, commercial and industrial areas, highway and commuting corridors, central downtown areas, and views from elevated locations providing a broad overlook of the metropolitan area. Thus urban visibility includes VAQ conditions in major cities and smaller towns and encompasses all the VAQ an individual resident sees on a regular basis. Visibility conditions in urban and suburban locations are therefore distinct from visibility in rural or wilderness settings such as the Class 1 areas defined by the Clean Air Act, which include NPs and similar natural settings.

Visibility has direct significance to people’s enjoyment of daily activities and their overall wellbeing. Visibility conditions can be described both as an aesthetic quality as well as a scientifically measurable set of atmospheric conditions. Due to the subjective nature of aesthetics, people’s preferences with respect to visibility are difficult to express or quantify, but people have expressed in many different ways that they enjoy and value a clear view. A number of social science studies have been undertaken to link perceived urban visibility to an array of effects reflecting the overall desire for good VAQ, and the benefits of improving currently degraded VAQ. This wide range of diverse studies have identified types of benefits of good VAQ.

For example, psychological research has demonstrated that people are emotionally affected by low VAQ such that their overall sense of wellbeing is diminished (e.g., Bickerstaff and Walker, 2001, [156271](#)). Researchers have also shown that perception of pollution is correlated with stress, annoyance, and symptoms of depression (Evans and Jacobs, 1982, [179899](#); Jacobs et al., 1984, [156596](#); Mace et al., 2004, [180255](#)). Sociological research has demonstrated that VAQ is deeply intertwined with a “sense of place,” effecting people’s sense of the desirability of a neighborhood quite apart from the actual physical conditions of the area (e.g., ABT, 2002, [156186](#); Day, 2007, [156386](#); Elliot et al., 1999, [010716](#); Howel et al., 2002, [156571](#)). Public policy research finds that people think it is important to protect visibility, and accept the concept of setting standards to protect visibility (e.g., ABT, 2001, [156185](#); BBC Research & Consulting, 2002, [156258](#); Ely et al., 1991, [056599](#); Pryor, 1996, [056598](#)). Finally, economic valuation research has measured the amount of money that people are willing to pay to protect or improve both urban visibility (e.g., summary review in Beron et al., 2001, [156270](#); Chestnut and Dennis, 1997, [014525](#)) and natural locations such as NPs and other locations defined by the Clean Air Act as Class I visibility area (e.g., summary review in Chestnut and Dennis, 1997, [014525](#)).

Urban visibility has been examined in two types of studies directly relevant to the NAAQS review process: urban visibility preference studies and urban visibility valuation studies. The purpose of the remainder of this section is to review preference studies in four urban areas, as well as one new urban visibility valuation study not previously discussed in previous EPA Criteria Documents or OAQPS Staff Papers.

Both types of studies are designed to evaluate individuals’ desire (or demand) for good VAQ where they live, using different metrics to evaluate demand. Urban visibility preference studies examine individuals’ demand by investigating what amount of visibility degradation is unacceptable while economic studies examine demand by investigating how much one would be willing to pay to improve visibility.

9.2.4.1. Urban Visibility Preference Studies

One group of urban visibility research projects focused on identifying preferences for urban VAQ without necessarily estimating the economic value of improving visibility. This group of preference studies used a common focus group method to estimate the visibility impairment conditions that respondents described as “acceptable.” The specific definition of acceptable was largely left to each individual respondent, allowing each to identify their own preferences.

There are three completed studies that used this method, and two pilot studies that provided additional information (Table 9-2). The completed studies were conducted in Denver, Colorado (Ely et al., 1991, [056599](#)), two cities in British Columbia, Canada (Pryor, 1996, [056598](#)), and Phoenix, Arizona (BBC Research & Consulting, 2002, [156258](#)). The additional studies were conducted in Washington, DC (ABT, 2001, [156185](#); Smith and Howell, 2009, [198803](#)).

Each study collected information in a focus group setting, presenting slides depicting various visibility conditions. All four studies used photographs of a single scene from the study’s city; each photo included images of the broad downtown area and spreading out to the hills or mountains composing the scene’s backdrop. The maximum sight distance under good conditions varied by city, ranging from 8 km in Washington, DC to mountains hundreds of kilometers away in Denver. Multiple photos of the same scene were used to present approximately 20 different visibility impairment conditions. The Denver and British Columbia studies used actual photographs taken in the same location to depict various visibility conditions. The Phoenix and Washington, DC studies used photographs prepared using the WinHaze software from Air Resource Specialists (ARS). WinHaze is a computer-imaging software program that simulates visual air quality differences of various scenes, allowing the user to “degrade” an original near-pristine visibility condition photograph to create a photograph of each desired VAQ condition.

A common characteristic of the three visibility preference studies was that each was conducted in the West where distant mountains were shown in the photograph used to elicit local participant responses about visibility. Among other issues, the Washington D.C. pilot study was the first step in a process to expand the results to other regions where typical scenes may have different sensitivity to perceived visibility changes in PM air quality and where participants may have different acceptable visibility preference values.

The range of median preference values for an acceptable amount of visibility degradation from the 4 urban areas was approximately 19-33 dv. Measured in terms of visual range (VR), these median acceptable values were between approximately 59 and 20 km.

Table 9-2. Summary of urban visibility preference studies.

	Denver, CO	Phoenix, AZ	2 British Columbia cities	Washington, DC (2001)	Washington, DC (2009)
Report Date	1991	2003	1996	2001	2009
Duration of session		45 min	50 min	2 h	
Compensation	None (civic groups)	\$50	None (class room exercise)	\$50	None
# focus group sessions	17	27 total at 6 locations, Including 3 in Spanish	4	1	3 tests
# participants	214	385	180	9	64
Age range	Adults	18-65+	University students	27-58	Adults
Annual or seasonal	Wintertime	Annual	Summertime	Annual	Annual
# total scenes presented	Single scene of downtown with mountains in background	Single scene of downtown and mountains, 42 km maximum distance	Single scene from each city	Single scene of DC Mall and downtown, 8 km maximum sight	Single scene of DC Mall and downtown, 8 km maximum sight
# of total visibility conditions presented	20 conditions (+ 5 duplicates)	21 conditions (+ 4 duplicates)	20 conditions (10 each from each city)	20 conditions (+ 5 duplicates)	22 conditions

	Denver, CO	Phoenix, AZ	2 British Columbia cities	Washington, DC (2001)	Washington, DC (2009)
Source of slides	Actual photos taken between 9am and 3pm	WinHaze	Actual photos taken at 1 p.m. or 4 p.m.	WinHaze	WinHaze
Medium of presentation	Slide projection	Slide projection	Slide projection	Slide projection	Slide projection
Ranking scale used	7 point scale	7 point scale	7 point scale	7 point scale	7 point scale
Visibility range presented	11 to 40 dv	15 to 35 dv	13-25 dv (Chilliwack) 13.5-31.5 dv (Abbotsford)	9-38 dv	9-45 dv
Health issue directions	Ignore potential health impacts; visibility only	Judge solely on visibility, do not consider health	Judge solely on visibility, do not consider health	Health never mentioned, "Focus only on visibility"	Health never mentioned, "Focus only on visibility"
Key questions asked	a) Rank VAQ (1-7 scale) b) Is each slide "acceptable" c) "How much haze is too much?"	a) Rank VAQ (1-7 scale) b) Is each slide "acceptable" c) How many days a year would this picture be "acceptable"	a) Rank VAQ (1-7 scale) b) Is each slide "acceptable"	a) Rank VAQ (1-7 scale) b) Is each slide "acceptable" c) if this hazy, how many hs would it be acceptable (3 slides only) d) valuation question	a) Rank VAQ (1-7 scale) b) Is each slide "acceptable"
Mean dv found "acceptable"	20.3 dv	23-25 dv	~23 dv(Chilliwack), ~19 dv(Abbotsford)	~20 dv (range 20-25)	~30 dv

9.2.4.2. Denver, Colorado Urban Visibility Preference Study

The Denver urban visibility preference study (Ely et al., 1991, [056599](#)) was conducted on behalf of the Colorado Department of Public Health and Environment (CDPHE). The study conducted a series of focus group sessions with 17 civic and community groups in which a total of 214 individuals were asked to rate slides. The slides depicted varying values of VAQ for a well-known Denver vista, including a broad view of downtown Denver with the mountains to the west composing the scene's background. The participants were instructed to base their judgments on three factors:

1. The standard was for an urban area, not a pristine NP area where the standards might be more strict;
2. The value of an urban visibility standard violation should be set at a VAQ value considered to be unreasonable, objectionable, and unacceptable visually; and
3. Judgments of standards violations should be based on visibility only, not on health effects.

Participants were shown 25 randomly ordered slides of actual photographs. The visibility conditions presented in the slides ranged from 11-40 dv, approximating the 10th-90th percentile of wintertime visibility conditions in Denver. The participants rated the 25 slides based on a scale of 1 (poor) to 7 (excellent), with 5 duplicates included. They were then asked to judge whether the slide would violate what they would consider to be an appropriate urban visibility standard (i.e., whether the amount of impairment was "acceptable" or "unacceptable"). The individual's judgment of a slide's VAQ and whether the slide violated a visibility standard were highly correlated (Pearson correlation coefficient >80%), as were the VAQ ratings and the yes/no "acceptable" response. The participant's median response was that a visibility condition of 20.3 dv (extinction coefficient $b_{\text{ext}} = 76\text{Mm}^{-1}$, or VR ~51 km) was judged as "acceptable." The CDPHE subsequently established a Denver visibility standard at this value (defined as $b_{\text{ext}} = 76\text{Mm}^{-1}$), based on the median 50% acceptability findings from the study.

9.2.4.3. Phoenix, Arizona Urban Visibility Preference Study

The Phoenix urban visibility preference study (BBC Research & Consulting, 2002, [156258](#)) was conducted on behalf of the Arizona Department of Environmental Quality. The Phoenix study patterned its focus group survey process after the Denver study. The study included 385 participants in 27 separate focus group sessions. Participants were recruited using random digit dialing to obtain a sample group designed to be demographically representative of the larger Phoenix population. Focus group sessions were held at six neighborhood locations throughout the metropolitan area to improve the participation rate. Three sessions were held in Spanish in one region of the city with a large Hispanic population (25%), although the final overall participation of native Spanish speakers (18%) in the study was modestly below the targeted value. Participants received \$50 as an inducement to participate.

Participants were shown a series of 25 images of the same vista of downtown Phoenix, with South Mountain in the background at a distance of about 40 km. Photographic slides of the images were developed using WinHaze. The visibility impairment conditions ranged from 15-35 dv (the extinction coefficient, b_{ext} , range was approximately 45 Mm^{-1} to 330 Mm^{-1} , or a visual range of 87-12 km). Participants first individually rated the randomly shown slides on a VAQ scale of 1 (unacceptable) to 7 (excellent). Participants were instructed to rate the photographs solely on visibility, and to not base their decisions on either health concerns or what it would cost to have better visibility. Next, the participants individually rated the randomly ordered slides as “acceptable” or “unacceptable,” defined as whether the visibility in the slide is unreasonable or objectionable. Better visibility conditions (15 dv and 20 dv) were judged “acceptable” by 90% of all participants. At 24 dv nearly half of all participants thought the VAQ was “unacceptable,” with almost three-quarters judging 26 dv as unacceptable.

The Phoenix urban visibility study formed the basis of the decision of the Phoenix Visibility Index Oversight Committee for a visibility index for the Phoenix Metropolitan Area (Arizona DEQ, 2000, [019164](#)). The Phoenix Visibility Index establishes an indexed system with 5 categories of visibility conditions, ranging from “Excellent” (14 dv or less) to “Very Poor” (29 dv or greater). The “Good” range is 15-20 dv. The environmental goal of the Phoenix urban visibility program is to achieve continued progress through 2018 by moving the number of days in lower quality categories into better quality categories.

9.2.4.4. British Columbia, Canada Urban Visibility Preference Study

The British Columbia urban visibility preference study (Pryor, 1996, [056598](#)) was conducted on behalf of the Ministry of Environment. The study conducted focus group sessions that were also developed following the methods used in the Denver study. Participants were students at the University of British Columbia, who participated in one of four focus group sessions with between 7 and 95 participants. A total of 180 respondents completed surveys (29 did not complete the survey).

Participants in the study were shown slides of two suburban locations in British Columbia: Chilliwack and Abbotsford. Using the same general protocol as the Denver study, Pryor found that responses from this study found the acceptable level of visibility was 23 dv in Chilliwack and 19 dv in Abbotsford. Pryor (1996, [056598](#)) discusses some possible reasons for the variation in standard visibility judgments between the two locations. Factors discussed include the relative complexity of the scenes, potential bias of the sample population (only University students participated), and the different amounts of development at each location. Abbotsford (population 130,000) is an ethnically diverse suburb adjacent to the Vancouver Metro area, while Chilliwack (population 70,000) is an agricultural community 100 km east Vancouver in the Frazier Valley.

The British Columbia urban visibility preference study is being considered by the B.C. Ministry of the Environment as a part of establishing urban and wilderness visibility goals in British Columbia.

9.2.4.5. Washington, DC Urban Visibility Preference Studies

The Washington, DC urban visibility pilot study (ABT, 2001, [156185](#)) was conducted on behalf of the EPA, and was designed to be a pilot focus group study, an initial developmental trial run of a larger study. The intent of the pilot study was to study both focus group method design and potential survey questions. Due to funding limitations, only a single focus group session was held,

consisting of one extended session with nine participants. No further urban visibility focus group sessions were held in Washington, DC.

Due to the small number of participants, it is not possible to make statistical inferences about the opinions of the general population. The study does, however, provide additional useful information about urban visibility studies, potentially helping to both better understand previous studies as well as design future studies.

The study also adopted the general Denver study method, modifying it as appropriate to be applicable in an eastern urban setting which has substantially different visibility conditions than any of the three western locations of the other preference studies. Washington's (and the entire East) visibility is typically substantially worse than western cities, and has different characteristics. Washington's visibility impairment is primarily a uniform whitish haze dominated by sulfates, relative humidity values are higher, the low lying terrain provides substantially shorter maximum sight distances, and many residents are not well informed that anthropogenic emissions impair visibility on hazy days.

The Washington focus group session included questions on valuation, as well as on preferences. The focus group was asked to state its preferences measured in an increase in the general cost of living for certain increments of improvement in visibility on a typical summer day. A general cost of living approach is one payment vehicle approach that can be used in willingness to pay studies, especially for environmental issues arising from multiple diverse emission sources (e.g., transportation, electricity generation, industry, etc.) making a specific price increase potentially misleading.

The first part of the focus group session was designed to be an hour long, and was comparable to the focus group sessions in the Denver and Phoenix studies. A single scene was used; a panoramic shot of the Potomac River, Washington mall and downtown Washington, DC. In the first part of the session people were asked to rate the VAQ of 25 photographs (prepared using WinHaze, and projected on a large screen), judge the acceptability of visibility condition in each slide, and answer the valuation questions. The second half of the session, however, was a moderated discussion session about the format and content of the first phase of the session. In this moderated discussion, participants were asked about their understanding of each question asked in the first half of the session. Particular issues in designing a focus group session were also explored. Important participant comments included:

1. Participants had been asked how they reacted to the initial direction to base their answers only on visibility, but health was never explicitly mentioned by the focus group moderator. Participants strongly agreed with the decision to not mention that health effects are associated with visibility impairment. They understood the directions as meaning they should ignore health issues, and said their answers would have been different if they included health as well as visibility in their judgments.
2. Differentiating between haze and weather conditions was difficult. Weather was not discussed in the focus group session, and the photographs were WinHaze altered photos with identical weather conditions. Participants mentioned they were still confused about the role of weather and humidity in the different visibility conditions presented in the photos.
3. Questions about how many hours an impairment level would be acceptable were confusing. Most participants were normally indoors during most of the day, so questions about duration of outdoor conditions were difficult to answer.
4. Participants strongly agreed that not mentioning the purpose of the study, or the sponsor, until the very end (after all the questions were answered) was viewed as very important. Most felt this information would have influenced their answers.

The Smith and Howell (2009, [198803](#)) study recreated the same WinHaze images used in the 2001 Washington, DC urban visibility preference study, and followed a shortened version of the same question protocol as the 2001 study. The WinHaze images were presented to a total of 64 participants who were all employees of CRA International, Inc. (Smith and Howell also are CRA International employees).

The stated purpose of the Smith and Howell (2009, [198803](#)) study was to explore the robustness of the 2001 pilot study results. To investigate this issue, Smith and Howell (2009, [198803](#)) conducted three different tests concerning urban visibility preferences. Each participant was involved with only one test. Test 1 was designed to replicate the 2001 study. Test 2 reduced the

upper end of the range of VAQ by eliminating the 11 images used in Test 1 with a VAQ above 27.1 dv. Test 3 increased the upper end of the range of VAQ by including two new images of worse VAQ; the two new images had a VAQ of 42 dv and 45 dv. Smith and Howell (2009, [198803](#)) concluded that changing the range of VAQ presented to the participants affects the responses about whether a particular VAQ is acceptable.

9.2.4.6. Urban Visibility Valuation Studies

The one recent urban visibility benefit assessment not included in earlier reviews is “The Benefits of Visibility Improvement: New Evidence from the Los Angeles Metropolitan Area” (Beron et al., 2001, [156270](#)). Rather than a contingent valuation method (CVM) technique used in the majority of other urban visibility valuation studies, Beron et al. (2001, [156270](#)) used a housing market hedonic technique. The housing hedonic methods were used in previous urban visibility studies by Murdoch and Thayer (1988, [156788](#)) and Trijonis et al. (1985, [078468](#)). A housing market hedonic study views a housing unit as composed of a bundle of attributes, and uses housing sale price data from a large number of units in a metropolitan area to estimate the value of each component. Hedonic pricing has been used to estimate economic values for environmental effects that have a direct effect on housing market values. It relies on the measurement of differentials in property values under various environmental quality conditions including air pollution, visibility and other environmental amenities such as access to nearby beaches and parks, as well as by physical attributes of the house and attributes of the neighborhood.

Beron et al. (2001, [156270](#)) obtained data on approximately 840,000 owner-occupied, single family housing sales between 1980 and 1995 from the California South Coast Air Basin (composed of Los Angeles and Orange Counties, and the portions of Riverside and San Bernardino Counties in the greater metropolitan area). The real estate data included information on the sale price of the house, 13 housing attributes (square footage, number of bathrooms, etc.), 9 neighborhood attributes (percent poverty, school quality, FBI crime index, etc.), and three air pollution variables: ozone, particulates (measured by total suspended particulates, or TSP), and visibility. Visibility was measured as the annual average of visual range, measured in miles, and was obtained from seven airports within the study region. The visibility range was from 12.4 miles (Los Angeles International Airport, 1991) to 31.9 miles (Palm Springs Airport, 1995). Ozone data (39 monitors) and TSP data (40 monitors) were obtained from the South Coast Air Quality Management District. Annual mean values for each year were calculated for ozone and TSP.

Beron et al. (2001, [156270](#)) presented results for a hypothetical basin-wide 20% visibility improvement, or an increase from 15.3 to 18.4 miles, which is equivalent to approximately 27.6 dv to 25.8 dv. The initial results reflect the change in the purchase price of a house associated with this difference in VAQ, which can be interpreted as a present value of a stream of annual values over the lifetime of the house. The authors therefore selected a time horizon (30 yrs) and an interest rate (8%) to calculate an annual per household benefit per dv ranging from \$484 to \$1,756. The Beron results are higher than the CVM-based values summarized in Chestnut and Dennis (1997, [014525](#)), which ranged from \$12 to \$132 per dv. It should be noted that the \$132 CVM values cited by Chestnut and Dennis (1997, [014525](#)) is from a study in the Los Angeles area (Brookshire, 1979, [156298](#)). The Beron et al. (2001, [156270](#)) results are also higher than the Trijonis et al. (1990, [157058](#)) hedonic study in the Los Angeles area, which had a range of \$134 to \$360 per dv per year. All values reported here are in terms of 1994 prices.

A critical question for all urban visibility valuation studies is the extent to which the estimated values strictly reflect preferences for visibility, and do not include a component of preferences for reducing health risk from air pollution. The ability to isolate the value of visibility from within the collection of intertwined benefits from visual air quality, which is inherently multi-attributed, is a challenge for all visibility valuation studies. Each study attempts to isolate visibility from other effect categories, but different studies take different approaches.

Beron et al. (2001, [156270](#)) include two measures of air pollution directly related to health effects in their housing market hedonic study, ozone and particulates (using TSP as the metric for particulates), as well as visibility. They argue that the presence of the two health-related pollution conditions results in an estimated hedonic demand function for visibility that successfully separates the health component of demand for overall air quality from the visibility component. An alternative interpretation is that the estimated visibility function still includes a component of health risk because the housing market data does not support completely isolating the demand for visibility (due

to correlated variables, omitted variables, measurement error, model specification error, etc.) from demand for health risk reductions measured by the two health related air quality metrics.

A key issue in interpreting the Beron et al. (2001, [156270](#)) results is whether the objective measures of air quality characteristics (e.g., visibility, PM concentrations, etc.) capture people's perceptions of the different aspects of air quality in a given location. To the extent the people simultaneously use what they see regarding VAQ as an indicator of the overall air quality including potential health risks, then including all the measures in the equation is not necessarily sufficient to isolate one effect from the other.

9.2.5. Summary of Effects on Visibility

Visibility impairment is caused by light scattering and absorption by suspended particles and gases. NO₂ is the only commonly occurring atmospheric pollutant gas that absorbs visible spectrum radiation, though in most situations the amount of light absorption by NO₂ is overwhelmed by the higher amounts of particulate light extinction (i.e., the combination of scattering and absorption) usually accompanying high NO₂ concentrations. Light scattering by gases in a pollutant-free atmosphere provides a limit to visibility in pristine conditions and is the largest contributor to the total light extinction during the least visibility-impaired periods in remote regions of the western U.S. There is strong and consistent evidence that PM is the overwhelming source of visibility impairment in both urban and remote areas. EC and some crustal minerals are the only commonly occurring airborne particle components that absorb light. All particles scatter light, and generally light scattering by particles is the largest of the four light extinction components. Although a larger particle scatters more light than a similarly shaped smaller particle of the same composition, the light scattered per unit of mass is greatest for particles with diameters from approximately 0.3-1.0 μm.

For studies where detailed data on particle composition by size data are available, accurate calculations of light extinction can be made. However, routinely available PM speciation data can be used to make reasonable estimates of light extinction using relatively simple algorithms that multiply the concentrations of each of the major PM species by its dry extinction efficiency and by a water growth term that accounts for particle size change as a function of relative humidity for hygroscopic species (e.g., SO₄²⁻, nitrate, and sea salt). This permits the visibility impairment associated with each of the major PM components to be separately approximated from PM speciation monitoring data. There are six major PM components: PM_{2.5} SO₄²⁻ usually assumed to be ammonium sulfate, PM_{2.5} nitrate usually assumed to be ammonium nitrate, PM_{2.5} OC, PM_{2.5} EC, PM_{2.5} crustal material (referred to as fine soil), and PM_{10-2.5} or coarse mass.

Direct optical measurement of light extinction measured by transmissometer, or by combining the PM light scattering measured by integrating nephelometers with the PM light absorption measured by an aethalometer offer a number of advantages compared to algorithm estimates of light extinction based on PM composition and relative humidity data. The direct measurements are not subject to the uncertainties associated with assumed scattering and absorption efficiencies used in the PM algorithm approach. The direct measurements have higher time resolution (i.e., minutes to hours), which is more commensurate with the visibility effects compared with calculated light extinction using routinely available PM speciation data (i.e., 24-h duration).

Particulate SO₄²⁻ and nitrate are produced in the atmosphere from gaseous precursors, making them secondary PM species. They both have comparable light extinction efficiencies (haze impacts per unit mass concentration) at any relative humidity value, their light scattering per unit mass concentration increases with increasing relative humidity, and at sufficiently high humidity values (RH>85%) they are the most efficient particulate species contributing to haze. Particulate SO₄²⁻ is the dominant source of regional haze in the eastern U.S. (>50% of the particulate light extinction) and an important contributor to haze elsewhere in the country (>20% of particulate light extinction).

Particulate nitrate is a minor component of remote-area regional haze in the non-California western and eastern U.S., but an important contributor in much of California and in the upper Midwestern U.S. especially during winter when it is the dominant contributor to particulate light extinction. While both nitric acid (a reaction product of NO_x emissions) and ammonia are needed to form ammonium nitrate, the apparent reason for the Midwest nitrate bulge (i.e., region of high winter PM nitrate) is an abundance of atmospheric ammonia in this region principally from agricultural emissions. There is evidence that transport from the Midwest nitrate bulge region is responsible for some of the ammonium nitrate episodes experienced in downwind regions far to the east. Urban particulate nitrate concentrations are significantly elevated above surrounding remote-area

background concentrations with the largest urban contributions in the western U.S. Particulate ammonium nitrate concentrations in California and the Midwestern nitrate bulge region are an order of magnitude greater than estimated natural ammonium nitrate concentrations. Thermodynamic and air quality simulation modeling show that particulate nitrate concentrations are sensitive to changes in either NO_x emissions (from a combination of mobile and point sources) or ammonia emissions (principally from agricultural sources), with the responsiveness of particulate nitrate to emissions changes depending on the relative abundance of ammonia and nitric acid in the atmosphere.

EC and OC have the highest dry extinction efficiencies of the major PM species and are responsible for a large fraction of the haze especially in the Northwestern U.S., though absolute concentrations are as high in the eastern U.S. Both are a product of incomplete combustion of fuels, including those used in internal combustion processes (gasoline and diesel emissions) and open biomass burning (smoke from wild and prescribed fire). OC PM species are also produced by atmospheric transformation of precursor gaseous emissions. Smoke plume impacts from large wildfires dominate many of the worst haze periods in the western U.S. Carbonaceous PM is generally the largest component of urban excess $\text{PM}_{2.5}$ (i.e., the difference between urban and regional background concentration). Western urban areas have more than twice the average concentrations of carbonaceous PM than remote areas sites in the same region. In eastern urban areas, $\text{PM}_{2.5}$ is dominated by about equal concentrations of carbonaceous and SO_4^{2-} components, though the usually high relative humidity in the East causes the hydrated SO_4^{2-} particles to be responsible for about twice as much of the urban haze as that caused by the carbonaceous PM.

Radiocarbon dating of carbonaceous PM from twelve sites (eight in the West, two of which are urban) showed that about half of the urban area carbonaceous PM is from contemporary as opposed to fossil sources, while in remote areas the fraction that is contemporary ranges from 82-100%. Summer urban excess carbonaceous PM is dominated by fossil carbon for the two western urban areas (Phoenix, AZ and Seattle, WA), but nearly half of the winter urban excess for these two urban areas are from contemporary carbon sources (e.g., residential wood combustion). An empirical relationship between the radiocarbon analysis results and the more widely measured EC and OC data set was used to estimate the fraction of contemporary carbon at about 150 monitoring locations nationwide. The highest fraction of contemporary carbon is for the western remote areas sites during the summer (>90% contemporary) and the least was for eastern urban areas during the summer (<45% contemporary). Winter tended to have less extreme fractions of contemporary carbon for both remote and urban areas. A lower bound estimate of 40% of the contemporary and 35% of the fossil carbon is from secondary conversion of gaseous precursor during the summer at the twelve radiocarbon monitoring sites, suggesting that primary carbonaceous PM whether from fossil or contemporary sources represent less than two thirds of the total carbonaceous PM.

$\text{PM}_{2.5}$ crustal material (referred to as fine soil) and coarse mass (i.e., PM_{10} minus $\text{PM}_{2.5}$) are significant contributors to haze for remote areas sites in the arid Southwestern U.S. where they contribute a quarter to a third of the haze, with coarse mass usually contributing twice that of fine soil. Coarse mass concentrations are as high in the Central Great Plains as in the Southwestern deserts though there are no corresponding high concentrations of fine soil as in the Southwest. Also, the relative contribution to haze by the high coarse mass in the Great Plains is much smaller because of the generally higher haze values caused by the high concentrations of SO_4^{2-} and nitrate PM in that region.

A comprehensive assessment of the 610 worst haze sample periods over a 3-yr period in the western U.S. where dust is the major contributor categorized each site/sampler period into four causal groups: Asian dust, local windblown dust, transported regional windblown dust, and undetermined dust (i.e., not in one of the three other groups). Most dust days occurred at sites in Arizona, New Mexico, Colorado, western Texas, and southern California, and these were dominated by local and regionally transported wind-blown dust. Asian dust caused only a few of the worst dust days during the 3-year assessment period, though it is an important source of dust for the more northerly regions of the West (responsible for 10-40% of their worst dust periods) where there is rarely any windblown dust probably due to the greater ground cover. The frequency of worst dust events classified as undetermined was greatest for sites in the vicinity of large urban and agricultural areas such as those in California and Southern Arizona.

Visibility has direct significance to people's enjoyment of daily activities and their overall sense of wellbeing. For example, psychological research has demonstrated that people are emotionally affected by poor VAQ such that their overall sense of wellbeing is diminished. Urban visibility has been examined in two types of studies directly relevant to the NAAQS review process:

urban visibility preference studies and urban visibility valuation studies. Both types of studies are designed to evaluate individuals' desire for good VAQ where they live, using different metrics. Urban visibility preference studies examine individuals' preferences by investigating the amount of visibility degradation considered unacceptable, while economic studies examine the value an individual places on improving VAQ by eliciting how much the individual would be willing to pay for different amounts of VAQ improvement.

There are three urban visibility preference studies and two additional pilot studies that have been conducted to date that provide useful information on individuals' preferences for good VAQ in the urban setting. The completed studies were conducted in Denver, Colorado (Ely et al., 1991, [056599](#)), two cities in British Columbia, Canada (Pryor, 1996, [056598](#)) and Phoenix, AZ (BBC Research & Consulting, 2002, [156258](#)). The additional studies were conducted in Washington, DC (ABT, 2001, [156185](#); Smith and Howell, 2009, [198803](#)). The range of median preference values for an acceptable amount of visibility degradation from the 4 urban areas was approximately 19-33 dv. Measured in terms of visual range (VR), these median acceptable values were between approximately 59 and 20 km.

The economic importance of urban visibility has been examined by a number of studies designed to quantify the benefits (or willingness to pay) associated with potential improvements in urban visibility. Urban visibility valuation research prior to 1997 was summarized in Chestnut and Dennis (1997, [014525](#)), and was also described in the 2004 PM AQCD (U.S. EPA, 2004, [056905](#)) and the 2005 PM Staff Paper (U.S. EPA, 2005, [090209](#)). Since the mid-1990s, little new information has become available regarding urban visibility valuation.

Collectively, the evidence is sufficient to conclude **that a causal relationship exists between PM and visibility impairment.**

9.3. Effects on Climate

While most of this ISA is restricted to consideration of the emissions, transport and transformation, resulting concentrations, and effects from PM in the U.S., because the effects endpoint here is climate, a larger spatial domain is needed. However, this assessment is not intended to be comprehensive even as a survey of the enormous range and volume of science related to climate effects from PM; rather, particular attention has been paid to data relevant to the U.S.

The two principal sources for material in this section are Chapter 2, "Changes in Atmospheric Constituents and in Radiative Forcing," (Forster et al., 2007, [092936](#)) in the comprehensive Working Group I report in the Fourth Assessment Report (AR4) from the Intergovernmental Panel on Climate Change (IPCC), *Climate Change 2007: The Physical Science Basis* (IPCC, 2007, [092765](#)), hereafter IPCC AR4; and the U.S. Climate Change Science Program Synthesis and Assessment Product 2.3, "Atmospheric Aerosol Properties and Climate Impacts," by Chin et al. (2009, [192130](#)), hereafter CCSP SAP2.3. The EPA is a constituent agency member of the U.S. federated CCSP along with NOAA and NASA, which led production of CCSP SAP2.3 incorporating significant sections from EPA data and reports related particularly to U.S. emissions and measurements. Sections from each of these recent comprehensive reports are included here in their entirety or as emended as noted where they represent the most thorough summary of the climate effects of aerosols. (In the sections included from IPCC AR4 and CCSP SAP2.3, 'aerosols' is more frequently used than "PM" and that word is retained.)

9.3.1. The Climate Effects of Aerosols

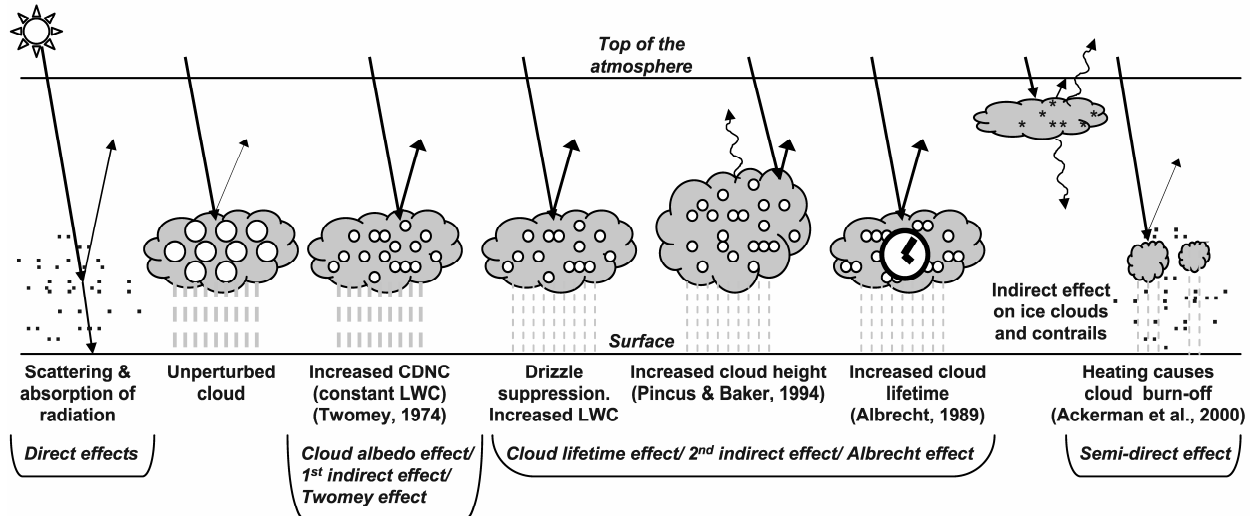
Section 9.3.1 comes directly from CCSP SAP2.3 Chapter 1 Section 1.2, with section, table, and figure numbers changed to be internally consistent with this ISA.

Aerosols exert a variety of impacts on the environment. Aerosols (sometimes referred to as particulate matter or "PM," especially in air quality applications), when concentrated near the surface, have long been recognized as affecting pulmonary function and other aspects of human health. Sulfate and nitrate aerosols play a role in acidifying the surface downwind of gaseous sulfur and odd nitrogen sources. Particles deposited far downwind might fertilize iron-poor waters in remote oceans, and Saharan dust reaching the Amazon Basin is thought to contribute nutrients to the rainforest soil.

Aerosols also interact strongly with solar and terrestrial radiation in several ways. Figure 9-52 offers a schematic overview. First, they scatter and absorb sunlight (Charlson and Pilat, 1969, [190025](#); McCormick and Ludwig, 1967, [190528](#); Mitchell, 1971, [190546](#)); these are described as “direct effects” on shortwave (solar) radiation. Second, aerosols act as sites at which water vapor can accumulate during cloud droplet formation, serving as cloud condensation nuclei or CCN. Any change in number concentration or hygroscopic properties of such particles has the potential to modify the physical and radiative properties of clouds, altering cloud brightness (Twomey, 1977, [190533](#)) and the likelihood and intensity with which a cloud will precipitate (e.g., Albrecht, 1989, [045783](#); Gunn and Phillips, 1957, [190595](#); Liou and Ou, 1989, [190407](#)).

Collectively changes in cloud processes due to anthropogenic aerosols are referred to as aerosol indirect effects. Finally, absorption of solar radiation by particles is thought to contribute to a reduction in cloudiness, a phenomenon referred to as the semi-direct effect. This occurs because absorbing aerosol warms the atmosphere, which changes the atmospheric stability, and reduces surface flux.

The primary direct effect of aerosols is a brightening of the planet when viewed from space, as much of Earth’s surface is dark ocean, and most aerosols scatter more than 90% of the visible light reaching them. The primary indirect effects of aerosols on clouds include an increase in cloud brightness, change in precipitation and possibly an increase in lifetime; thus the overall net impact of aerosols is an enhancement of Earth’s reflectance (shortwave albedo). This reduces the sunlight reaching Earth’s surface, producing a net climatic cooling, as well as a redistribution of the radiant and latent heat energy deposited in the atmosphere. These effects can alter atmospheric circulation and the water cycle, including precipitation patterns, on a variety of length and time scales (e.g., Ramanathan et al., 2001, [042681](#); Zhang et al., 2006, [190933](#)).



Source: IPCC (2007, [092765](#)) modified from Haywood and Boucher (2000, [156531](#)).

Figure 9-52. Aerosol radiative forcing. Airborne particles can affect the heat balance of the atmosphere, directly, by scattering and absorbing sunlight, and indirectly, by altering cloud brightness and possibly lifetime. Here small black dots represent aerosols, circles represent cloud droplets, and straight lines represent short-wave radiation, and wavy lines, long-wave radiation. LWC is liquid water content, and CDNC is cloud droplet number concentration. Confidence in the magnitudes of these effects varies considerably (see Chapter 3). Although the overall effect of aerosols is a net cooling at the surface, the heterogeneity of particle spatial distribution, emission history, and properties, as well as differences in surface reflectance, mean that the magnitude and even the sign of aerosol effects vary immensely with location, season and sometimes inter-annually. The human-induced component of these effects is sometimes called “climate forcing.”

Several variables are used to quantify the impact aerosols have on Earth’s energy balance; these are helpful in describing current understanding, and in assessing possible future steps.

For the purposes of this report, aerosol radiative forcing (RF) is defined as the net energy flux (downwelling minus upwelling) difference between an initial and a perturbed aerosol loading state, at a specified level in the atmosphere. (Other quantities, such as solar radiation,

are assumed to be the same for both states.) This difference is defined such that a negative aerosol forcing implies that the change in aerosols relative to the initial state exerts a cooling influence, whereas a positive forcing would mean the change in aerosols exerts a warming influence.

There are a number of subtleties associated with this definition:

(1) The initial state against which aerosol forcing is assessed must be specified. For direct aerosol radiative forcing, it is sometimes taken as the complete absence of aerosols. IPCC AR4 (2001, [156587](#)) uses as the initial state their estimate of aerosol loading in 1750. That year is taken as the approximate beginning of the era when humans exerted accelerated influence on the environment.

(2) A distinction must be made between aerosol RF and the anthropogenic contribution to aerosol RF. Much effort has been made to distinguishing these contributions by modeling and with the help of space-based, airborne, and surface-based remote sensing, as well as in situ measurements. These efforts are described in subsequent chapters (of the CCSP SAP2.3).

(3) In general, aerosol RF and anthropogenic aerosol RF include energy associated with both the shortwave (solar) and the long-wave (primarily planetary thermal infrared) components of Earth's radiation budget. However, the solar component typically dominates, so in this document, these terms are used to refer to the solar component only, unless specified otherwise. The wavelength separation between the short- and long-wave components is usually set at around three or four micrometers.

(4) The IPCC AR4 (2007, [092765](#)) defines radiative forcing as the net downward minus upward irradiance at the tropopause due to an external driver of climate change. This definition excludes stratospheric contributions to the overall forcing. Under typical conditions, most aerosols are located within the troposphere, so aerosol forcing at TOA and at the tropopause are expected to be very similar. Major volcanic eruptions or conflagrations can alter this picture regionally, and even globally.

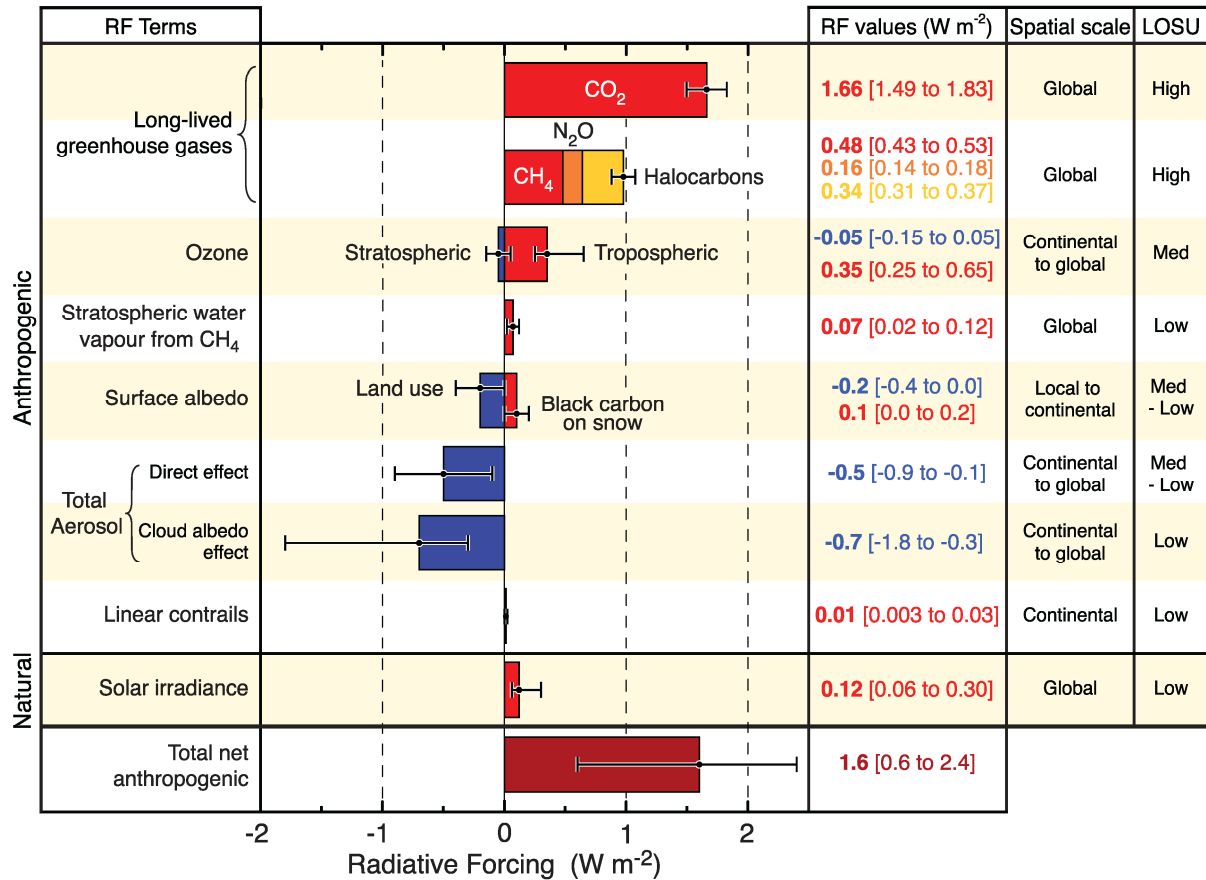
(5) Aerosol radiative forcing can be evaluated at the surface, within the atmosphere, or at top-of-atmosphere (TOA). In this document, unless specified otherwise, aerosol radiative forcing is assessed at TOA.

(6) As discussed subsequently, aerosol radiative forcing can be greater at the surface than at TOA if the aerosols absorb solar radiation. TOA forcing affects the radiation budget of the planet. Differences between TOA forcing and surface forcing represent heating within the atmosphere that can affect vertical stability, circulation on many scales, cloud formation, and precipitation, all of which are climate effects of aerosols. In this document, unless specified otherwise, these additional climate effects are not included in aerosol radiative forcing.)

(7) Aerosol direct radiative forcing can be evaluated under cloud-free conditions or under natural conditions, sometimes termed "all-sky" conditions, which include clouds. Cloud-free direct aerosol forcing is more easily and more accurately calculated; it is generally greater than all-sky forcing because clouds can mask the aerosol contribution to the scattered light. Indirect forcing, of course, must be evaluated for cloudy or all-sky conditions. In this document, unless specified otherwise, aerosol radiative forcing is assessed for all-sky conditions.

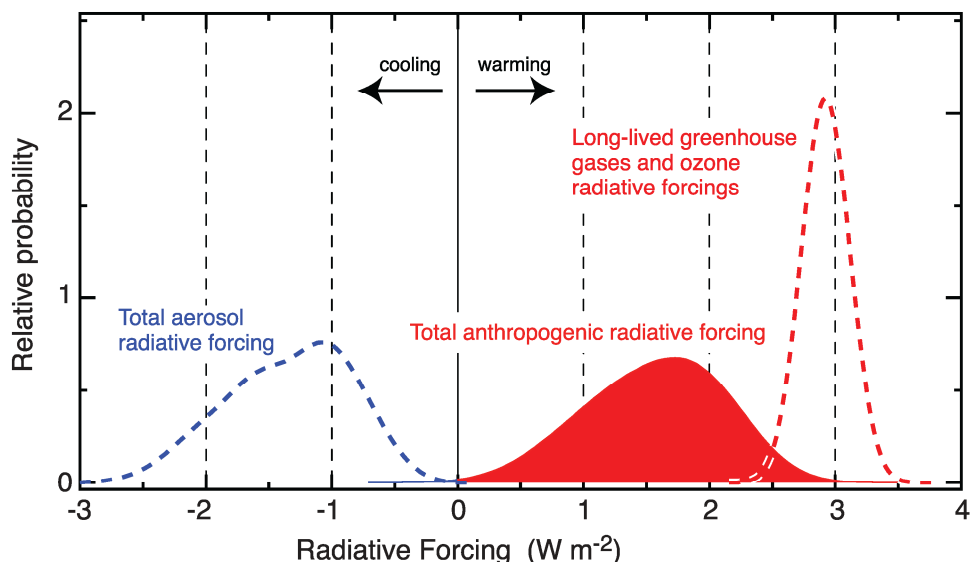
(8) Aerosol radiative forcing can be evaluated instantaneously, daily (24 h) averaged, or assessed over some other time period. Many measurements, such as those from polar-orbiting satellites, provide instantaneous values, whereas models usually consider aerosol RF as a daily average quantity. In this document, unless specified otherwise, daily averaged aerosol radiative forcing is reported.

(9) Another subtlety is the distinction between a "forcing" and a "feedback." As different parts of the climate system interact, it is often unclear which elements are "causes" of climate change (forcings among them), which are responses to these causes, and which might be some of each. So, for example, the concept of aerosol effects on clouds is complicated by the impact clouds have on aerosols; the aggregate is often called aerosol-cloud interactions. This distinction sometimes matters, as it is more natural to attribute responsibility for causes than for responses. However, practical environmental considerations usually depend on the net result of all influences. In this report, "feedbacks" are taken as the consequences of changes in surface or atmospheric temperature, with the understanding that for some applications, the accounting may be done differently.



Source: IPCC (2007, 092765).

Figure 9-53. Global average radiative forcing (RF) estimates and uncertainty ranges in 2005, relative to the pre-industrial climate. Anthropogenic CO_2 , methane (CH_4), nitrous oxide (N_2O), ozone, and aerosols as well as the natural solar irradiance variations are included. Typical geographical extent of the forcing (spatial scale) and the assessed level of scientific understanding (LOSU) are also given. Forcing is expressed in units of watts per square meter (W/m^2). The total anthropogenic radiative forcing and its associated uncertainty are also given.



Source: Adapted from IPCC (2007, [092765](#)).

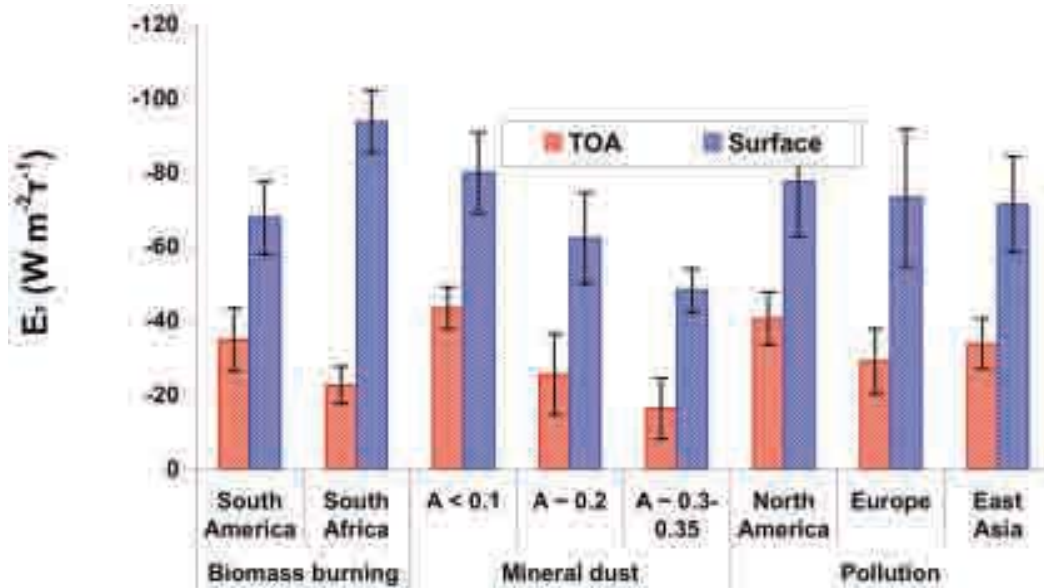
Figure 9-54. Probability distribution functions (PDFs) for anthropogenic aerosol and GHG RFs. Dashed red curve: RF of long-lived greenhouse gases plus ozone; dashed blue curve: RF of aerosols (direct and cloud albedo RF); red filled curve: combined anthropogenic RF. The RF range is at the 90% confidence interval.

In summary, aerosol radiative forcing, the fundamental quantity about which this report is written, must be qualified by specifying the initial and perturbed aerosol states for which the radiative flux difference is calculated, the altitude at which the quantity is assessed, the wavelength regime considered, the temporal averaging, the cloud conditions, and whether total or only human-induced contributions are considered. The definition given here, qualified as needed, is used throughout the report.

Although the possibility that aerosols affect climate was recognized more than 40 years ago, the measurements needed to establish the magnitude of such effects, or even whether specific aerosol types warm or cool the surface, were lacking. Satellite instruments capable of at least crudely monitoring aerosol amount globally were first deployed in the late 1970s. But scientific focus on this subject grew substantially in the 1990s (e.g., Charlson and Wigley, 1994, [189989](#); Charlson et al., 1991, [045793](#); 1992, [045794](#); Penner et al., 1992, [045825](#)), in part because it was recognized that reproducing the observed temperature trends over the industrial period with climate models requires including net global cooling by aerosols in the calculation (IPCC, 1995, [190991](#); 1996, [190990](#)), along with the warming influence of enhanced atmospheric greenhouse gas (GHG) concentrations – mainly carbon dioxide, methane, nitrous oxide, chlorofluorocarbons, and ozone.

Improved satellite instruments, ground- and ship-based surface monitoring, more sophisticated chemical transport and climate models, and field campaigns that brought all these elements together with aircraft remote sensing and in situ sampling for focused, coordinated study, began to fill in some of the knowledge gaps. By the Fourth IPCC Assessment Report, the scientific community consensus held that in global average, the sum of direct and indirect top-of-atmosphere (TOA) forcing by anthropogenic aerosols is negative (cooling) of about -1.3 W/m^2 (-2.2 to -0.5 W/m^2). This is significant compared to the positive forcing by anthropogenic GHGs (including ozone), about $2.9 \pm 0.3 \text{ W/m}^2$ (IPCC, 2007, [092765](#)). However, the spatial distribution of the gases and aerosols are very different, and they do not simply exert compensating influences on climate.

The IPCC aerosol forcing assessments are based largely on model calculations, constrained as much as possible by observations. At present, aerosol influences are not yet quantified adequately, according to Figure 9-53, as scientific understanding is designated as “Medium-Low” and “Low” for the direct and indirect climate forcing, respectively. The IPCC AR4 (2007, [092765](#)) concluded that uncertainties associated with changes in Earth’s radiation budget due to anthropogenic aerosols make the largest contribution to the overall uncertainty in radiative forcing of climate change among the factors assessed over the industrial period (Figure 9-54).



Source: Adapted with Permission of the American Geophysical Union from Zhou et al. (2005, [156183](#)).

Figure 9-55. The clear-sky forcing efficiency E_{τ} , defined as the diurnally averaged aerosol direct radiative effect (W/m^2) per unit AOD at 550 nm, calculated at both TOA and the surface, for typical aerosol types over different geographical regions. The vertical black lines represent \pm one standard deviation of E_{τ} for individual aerosol regimes and A is surface broadband albedo.

Although AOD, aerosol properties, aerosol vertical distribution, and surface reflectivity all contribute to aerosol radiative forcing, AOD usually varies on regional scales more than the other aerosol quantities involved. Forcing efficiency (E_{τ}), defined as a ratio of direct aerosol radiative forcing to AOD at 550 nm, reports the sensitivity of aerosol radiative forcing to AOD, and is useful for isolating the influences of particle properties and other factors from that of AOD. E_{τ} is expected to exhibit a range of values globally, because it is governed mainly by aerosol size distribution and chemical composition (which determine aerosol single-scattering albedo and phase function), surface reflectivity, and solar irradiance, each of which exhibits pronounced spatial and temporal variations. To assess aerosol RF, E_{τ} is multiplied by the ambient AOD.

Figure 9-55 shows a range of E_{τ} , derived from AERONET surface sun photometer network measurements of aerosol loading and particle properties, representing different aerosol and surface types, and geographic locations. It demonstrates how aerosol direct solar radiative forcing (with initial state taken as the absence of aerosol) is determined by a combination of aerosol and surface properties. For example, E_{τ} due to southern African biomass burning smoke is greater at the surface and smaller at TOA than South American smoke because the southern African smoke absorbs sunlight more strongly, and the magnitude of E_{τ} for mineral dust for several locations varies depending on the underlying surface reflectance. Figure 9-55 illustrates one further point, that the radiative forcing by aerosols on surface energy balance can be much greater than that at TOA. This is especially true when the particles have SSA substantially less than 1, which can create differences between surface and TOA forcing as large as a factor of five (e.g., Zhou et al., 2005, [156183](#)).

Table 9-3. Top-of-atmosphere, cloud-free, instantaneous direct aerosol radiative forcing dependence on aerosol and surface properties. Here TWP, SGP, and NSA are the Tropical West Pacific island, Southern Great Plains, and North Slope Alaska observation stations maintained by the DOE ARM program, respectively. Instantaneous values are given at specific solar zenith angle. Upper and middle parts are from McComiskey et al. (2008, 190523). Representative, parameter-specific measurement uncertainty upper bounds for producing 1 W/m² instantaneous TOA forcing accuracy are given in the lower part, based on sensitivities at three sites from the middle part of the table.

Parameters	TWP	SGP	NSA
AEROSOL PROPERTIES (AOD, SSA, G), SOLAR ZENITH ANGLE (SZA), SURFACE ALBEDO (A), AND AEROSOL DIRECT RF AT TOA (F)			
AOD	0.05	0.1	0.05
SSA	0.97	0.95	0.95
g	0.8	0.6	0.7
A	0.05	0.1	0.9
SZA	30	45	70
F (W/m ²)	-2.2	-6.3	2.6
SENSITIVITY OF CLOUD-FREE, INSTANTANEOUS, TOA DIRECT AEROSOL RADIATIVE FORCING TO AEROSOL AND SURFACE PROPERTIES, W/M² PER UNIT CHANGE IN PROPERTY			
dF/d(AOD)	-45	-64	51
dF/d(SSA)	-11	-50	-60
dF/dg	13	23	2
dF/dA	8	24	6
REPRESENTATIVE MEASUREMENT UNCERTAINTY UPPER BOUNDS FOR PRODUCING 1 W/M² ACCURACY OF AEROSOL RF			
AOD	0.022	0.016	0.020
SSA	0.091	0.020	0.017
g	0.077	0.043	
A	0.125	0.042	0.167

Table 9-3 presents estimates of cloud-free, instantaneous, aerosol direct RF dependence on AOD, and on aerosol and surface properties, calculated for three sites maintained by the U.S. Department of Energy's Atmospheric Radiation Measurement (ARM) program, where surface and atmospheric conditions span a significant range of natural environments (McComiskey et al., 2008, 190523). Here aerosol RF is evaluated relative to an initial state that is the complete absence of aerosols. Note that aerosol direct RF dependence on individual parameters varies considerably, depending on the values of the other parameters, and in particular, that aerosol RF dependence on AOD actually changes sign, from net cooling to net warming, when aerosols reside over an exceedingly bright surface. Sensitivity values are given for snapshots at fixed solar zenith angles, relevant to measurements made, for example, by polar-orbiting satellites.

The lower portion of Table 9-3 presents upper bounds on instantaneous measurement uncertainty, assessed individually for each of AOD, SSA, g, and A, to produce a 1 W/m² top-of-atmosphere, cloud-free aerosol RF accuracy. The values are derived from the upper portion of the table, and reflect the diversity of conditions captured by the three ARM sites. Aerosol RF sensitivity of 1 W/m² is used as an example; uncertainty upper bounds are obtained from the partial derivative for each parameter by neglecting the uncertainties for all other parameters. These estimates produce an instantaneous AOD measurement uncertainty upper bound between about 0.01 and 0.02, and SSA constrained to about 0.02 over surfaces as bright as or brighter than the ARM Southern Great Plains site, typical of mid-latitude, vegetated land. Other researchers, using independent data sets, have derived ranges of $E\tau$ and aerosol RF

sensitivity similar to those presented here, for a variety of conditions (Christopher and Jones, 2008, [189985](#); Yu et al., 2006, [156173](#); Zhou et al., 2005, [156183](#)).

These uncertainty bounds provide a baseline against which current and expected near-future instantaneous measurement capabilities are assessed in Chapter 2 (of the CCSP SAP2.3). Model sensitivity is usually evaluated for larger-scale (even global) and longer-term averages. When instantaneous measured values from a randomly sampled population are averaged, the uncertainty component associated with random error diminishes as something like the inverse square root of the number of samples. As a result, the accuracy limits used for assessing more broadly averaged model results corresponding to those used for assessing instantaneous measurements would have to be tighter, as discussed in Chapter 4 (of the CCSP SAP2.3).

In summary, much of the challenge in quantifying aerosol influences arises from large spatial and temporal heterogeneity, caused by the wide variety of aerosol sources, sizes and compositions, the spatial non-uniformity and intermittency of these sources, the short atmospheric lifetime of most aerosols, and the spatially and temporally non-uniform chemical and microphysical processing that occurs in the atmosphere. In regions having high concentrations of anthropogenic aerosol, for example, aerosol forcing is much stronger than the global average, and can exceed the magnitude of GHG warming, locally reversing the sign of the net forcing. It is also important to recognize that the global-scale aerosol TOA forcing alone is not an adequate metric for climate change (NRC, 2005, [057409](#)). Due to aerosol absorption, mainly by soot, smoke, and some desert dust particles, the aerosol direct radiative forcing at the surface can be much greater than the TOA forcing, and in addition, the radiative heating of the atmosphere by absorbing particles can change the atmospheric temperature structure, evolution, and possibly large-scale dynamical systems such as the monsoons (Kim et al., 2006, [190917](#); Lau et al., 2009, [190229](#)). By realizing aerosol's climate significance and the challenge of characterizing highly variable aerosol amount and properties, the U.S. Climate Change Research Initiative (CCRI) identified research on atmospheric concentrations and effects of aerosols specifically as a top priority (NRC, 2001, [053303](#)).

9.3.2. Overview of Aerosol Measurement Capabilities

9.3.2.1. Satellite Remote Sensing

Section 9.3.2 with the exception of the final paragraph, comes directly from CCSP SAP2.3 Chapter 2, Section 2.2 with section, table, and figure numbers changed to be internally consistent with this ISA.

A measurement-based characterization of aerosols on a global scale can be realized only through satellite remote sensing, which is the only means of characterizing the large spatial and temporal heterogeneities of aerosol distributions. Monitoring aerosols from space has been performed for over two decades and is planned for the coming decade with enhanced capabilities (Forster et al., 2007, [092936](#); King et al., 1999, [190635](#); Lee et al., 2006, [190358](#); Mishchenko et al., 2007, [190543](#)). Table 9-4 summarizes major satellite measurements currently available for the tropospheric aerosol characterization and radiative forcing research.

Early aerosol monitoring from space relied on sensors that were designed for other purposes. The Advanced Very High Resolution Radiometer (AVHRR), intended as a cloud and surface monitoring instrument, provides radiance observations in the visible and near infrared wavelengths that are sensitive to aerosol properties over the ocean (Husar et al., 1997, [045900](#); Mishchenko et al., 1999, [190541](#)). Originally intended for ozone monitoring, the ultraviolet (UV) channels used for the Total Ozone Mapping Spectrometer (TOMS) are sensitive to aerosol UV absorption with little surface interferences, even over land (Torres et al., 1998, [190503](#)). This UV-technique makes TOMS suitable for monitoring biomass burning smoke and dust, though with limited sensitivity near the surface (Herman et al., 1997, [048393](#)) and for retrieving aerosol single-scattering albedo from space (Torres et al., 2005, [190507](#)). (A new sensor, the Ozone Monitoring Instrument (OMI) aboard Aura, has improved on such UV-technique advantages, providing higher spatial resolution and more spectral channels; see (Veihelmann et al., 2007, [190627](#)). Such historical sensors have provided multi-decadal climatology of aerosol optical depth that has significantly advanced the understanding of aerosol distributions and long-term variability (e.g., Geogdzhayev et al., 2002, [190574](#); Massie et al., 2004, [190492](#); Mishchenko and Geogdzhayev, 2007, [190545](#); Mishchenko et al., 2007, [190542](#); Torres et al., 2002, [190505](#); Zhao et al., 2008, [190935](#)).

Over the past decade, satellite aerosol retrievals have become increasingly sophisticated. Now, satellites measure the angular dependence of radiance and polarization at multiple wavelengths from UV through the infrared (IR) at fine spatial resolution. From these observations, retrieved aerosol products include not only optical depth at one wavelength, but also spectral optical depth and some information about particle size over both ocean and land, as well as more direct measurements of polarization and phase function. In addition, cloud screening is much more robust than before and onboard calibration is now widely available.

Examples of such new and enhanced sensors include the MODerate resolution Imaging Spectroradiometer (MODIS, see Box 2.1 of CCSP SAP2.3), the Multi-angle Imaging SpectroRadiometer (MISR, see Box 2.2 of CCSP SAP2.3), Polarization and Directionality of the Earth's Reflectance (POLDER, see Box 2.3 of CCSP SAP2.3), and OMI, among others. The accuracy for AOD measurement from these sensors is about 0.05 or 20% of AOD (Kahn et al., 2005, [190966](#); Remer et al., 2005, [190221](#)) and somewhat better over dark water, but that for aerosol microphysical properties, which is useful for distinguishing aerosol air mass types, is generally low. The Clouds and the Earth's Radiant Energy System (CERES, see Box 2.4 of CCSP SAP2.3) measures broadband solar and terrestrial radiances. The CERES radiation measurements in combination with satellite retrievals of aerosol optical depth can be used to determine aerosol direct radiative forcing.

Table 9-4. Summary of major satellite measurements currently available for the tropospheric aerosol characterization and radiative forcing research.

Category	Properties	Sensor/platform	Parameters	Spatial coverage	Temporal coverage
Loading		AVHRR/NOAA-series	Optical depth	~daily coverage of global ocean	1981-present
		TOMS/Nimbus, ADEOSI, EP		1979-2001	
		POLDER-1,2, PARASOL		~daily coverage of global land and ocean	1997-present
		MODIS/Terra, Aqua		2000-present (Terra) 2002-present (Aqua)	
		MISR/Terra		~weekly coverage of global land and ocean, including bright desert and nadir sun-glint	2000-present
		OMI/Aura		~daily coverage of global land and ocean	2005-present
Column-integrated	Size, shape	AVHRR/NOAA-series	Ångström exponent	Global ocean	1981-present
		POLDER-1,2, PARASOL	Fine-mode fraction, Ångström exponent, non-spherical fraction	Global land and ocean	1997-present
		MODIS/Terra, Aqua	Fine-mode fraction	Global land and ocean (better quality over ocean)	2000-present (Terra) 2002-present (Aqua)
			Ångström exponent	Global ocean	
			Effective radius		
		MISR/Terra	Ångström exponent, small, medium large fractions, non-spherical fractions	Global land and ocean	2000-present
Absorption	TOMS/Nimbus, ADEOSI, EP	Absorbing aerosol index, single-scattering albedo, absorbing optical depth	Global land and ocean	1979-2001	
	OMI/Aura			2005-present	
	MISR/Terra			2000-present	
Vertical-resolved	Loading, size, and shape	GLAS/ICESat	Extinction/backscatter	Global land and ocean, 16-day repeating cycle, single-nadir measurement	2003-present (~3 mo/yr)
		CALIOP/CALIPSO	Extinction/backscatter, color ratio, depolarization ratio		2006-present

Complementary to these passive sensors, active remote sensing from space is also now possible and ongoing (see Box 2.5 of CCSP SAP2.3). Both the Geoscience Laser Altimeter System (GLAS) and the Cloud and Aerosol Lidar with Orthogonal Polarization (CALIOP) are collecting essential information about aerosol vertical distributions. Furthermore, the constellation of six afternoon-overpass spacecrafts (as illustrated in Figure 9-60), the so-called A-Train (Stephens et al., 2002, [190412](#)) makes it possible for the first time to conduct near simultaneous (within 15 minutes) measurements of aerosols, clouds, and radiative fluxes in multiple dimensions with sensors in complementary capabilities.

The improved accuracy of aerosol products (mainly AOD) from these new-generation sensors, together with improvements in characterizing the earth's surface and clouds, can help reduce the uncertainties associated with estimating the aerosol direct radiative forcing (Yu et al., 2006, [156173](#)); and references therein). The retrieved aerosol microphysical properties, such as size, absorption, and non-spherical fraction can help distinguish anthropogenic aerosols from natural aerosols and hence help assess the anthropogenic component of aerosol direct radiative forcing (Bellouin et al., 2005, [155684](#); Christopher et al., 2006, [155729](#); Kaufman et al., 2005, [155891](#); Yu et al., 2006, [156173](#)). However, to infer aerosol number concentrations and examine indirect aerosol radiative effects from space, significant efforts are needed to measure aerosol size distribution with much improved accuracy, characterize aerosol type, account for impacts of water uptake on aerosol optical depth, and determine the fraction of aerosols that is at the level of the clouds (Kapustin et al., 2006, [190961](#); Rosenfeld, 2006, [190233](#)). In addition, satellite remote sensing is not sensitive to particles much smaller than 0.1 micrometer in diameter, which comprise of a significant fraction of those that serve as cloud condensation nuclei.

Finally, algorithms are being developed to retrieve aerosol absorption or SSA from satellite observations (e.g., Kaufman et al., 2002, [190955](#); Torres et al., 2005, [190507](#)). The NASA Glory mission, scheduled to launch in 2009 and to be added to the A-Train, will deploy a multi-angle, multispectral polarimeter to determine the global distribution of aerosol and clouds. It will also be able to infer microphysical property information, from which aerosol type (e.g., marine, dust, pollution, etc.) can be inferred for improving quantification of the aerosol direct and indirect forcing on climate (Mischenko et al., 2007, [190543](#)).

In summary, major advances have been made in both passive and active aerosol remote sensing from space in the past decade, providing better coverage, spatial resolution, retrieved AOD accuracy, and particle property information. However, AOD accuracy is still much poorer than that from surface-based sun photometers (0.01-0.02), even over vegetated land and dark water where retrievals are most reliable. Although there is some hope of approaching this level of uncertainty with a new generation of satellite instruments, the satellite retrievals entail additional sensitivities to aerosol and surface scattering properties. It seems unlikely that satellite remote sensing could exceed the sun photometer accuracy without introducing some as-yet-unspecified new technology. Spacebased lidars are for the first time providing global constraints on aerosol vertical distribution, and multi-angle imaging is supplementing this with maps of plume injection height in aerosol source regions. Major advances have also been made during the past decade in distinguishing aerosol types from space, and the data are now useful for validating aerosol transport model simulations of aerosol air mass type distributions and transports, particularly over dark water. But particle size, shape, and especially SSA information has large uncertainty; improvements will be needed to better distinguish anthropogenic from natural aerosols using space-based retrievals. The particle microphysical property detail required to assess aerosol radiative forcing will come largely from targeted in situ and surface remote sensing measurements, at least for the near-future, although estimates of measurement-based aerosol RF can be made from judicious use of the satellite data with relaxed requirements for characterizing aerosol microphysical properties.

MODerate resolution Imaging Spectroradiometer

MODIS performs near global daily observations of atmospheric aerosols. Seven of 36 channels (between 0.47 and 2.13 μm) are used to retrieve aerosol properties over cloud and surface-screened areas (Li et al., 2004, [190386](#); Martins et al., 2002, [190470](#)). Over vegetated land, MODIS retrieves aerosol optical depth at three visible channels with high accuracy of $\pm 0.05 \pm 0.2\tau$ (Chu et al., 2002, [190001](#); Kaufman and Fraser, 1997, [190958](#); Levy et al., 2007, [190379](#); Remer et al., 2005, [190221](#)). Most recently a deep blue algorithm (Hsu et al., 2004, [190622](#)) has been implemented to retrieve aerosols over bright deserts on an operational basis, with an estimated accuracy of 20-30%. Because of the greater simplicity of the ocean surface, MODIS has the unique capability of retrieving not only aerosol optical depth with greater accuracy, i.e., $\pm 0.03 \pm 0.05\tau$ (Remer et al., 2002, [190218](#); 2005, [190221](#); Remer et al., 2008, [190224](#); Tanré et al., 1997, [190452](#)), but also quantitative aerosol size parameters (e.g., effective radius, fine-mode fraction of AOD) (Kaufman et al., 2002, [190956](#); Kleidman et al., 2005, [190175](#); Remer et al., 2005, [190221](#)). The fine-mode fraction has been used as a tool for separating anthropogenic aerosol from natural ones and estimating the anthropogenic aerosol direct climate forcing (Kaufman et al., 2005, [155891](#)). Figure 9-56 shows composites of MODIS AOD and fine-mode fraction that illustrate seasonal and geographical variations of aerosol types. Clearly seen from the figure is heavy pollution over East Asia in both months, biomass burning smoke over South Africa, South America, and Southeast Asia in August,

heavy dust storms over North Atlantic in both months and over Arabian Sea in August, and a mixture of dust and pollution plume swept across North Pacific in April.

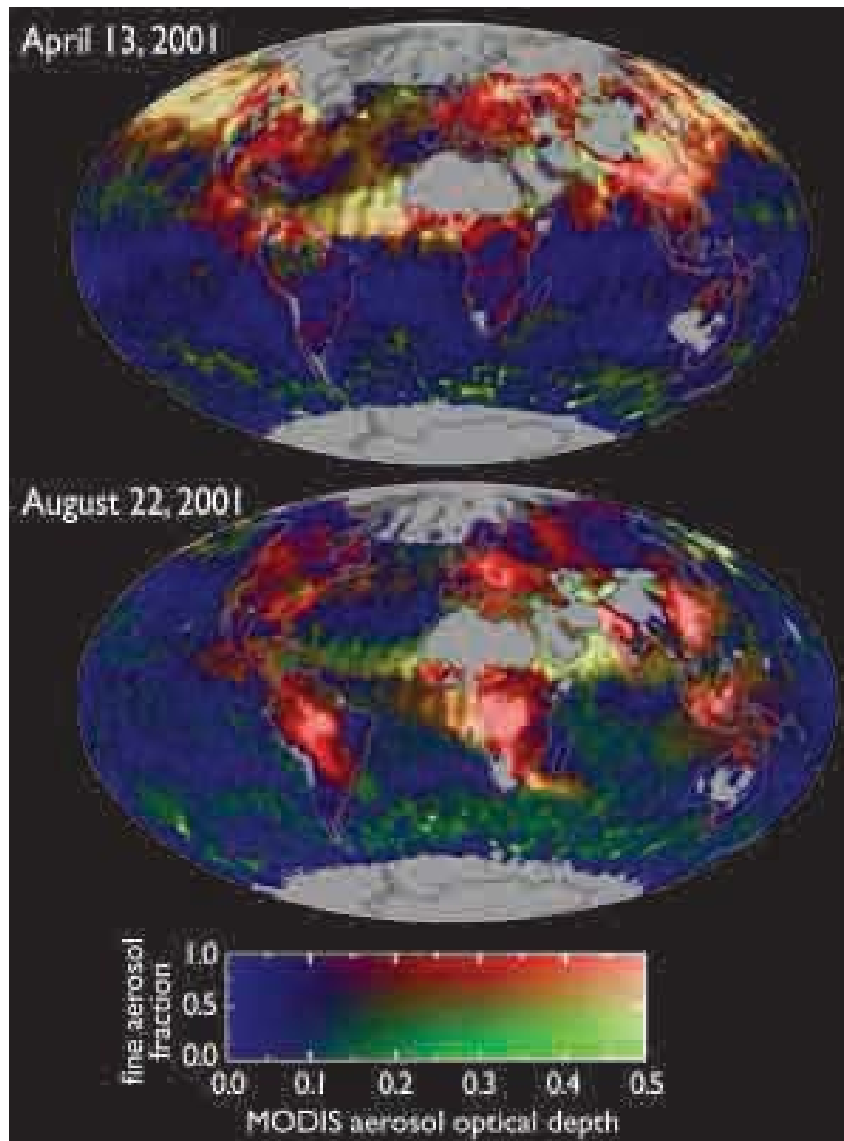
Multi-Angle Imaging SpectroRadiometer

MISR, aboard the sun-synchronous, polar orbiting satellite Terra, measures upwelling solar radiance in four visible-near-IR spectral bands and at nine view angles spread out in the forward and aft directions along the flight path (Diner et al., 2002, [189967](#)). It acquires global coverage about once per week. A wide range of along-track view angles makes it feasible to more accurately evaluate the surface contribution to the TOA radiances and hence retrieve aerosols over both ocean and land surfaces, including bright desert and sunglint regions (Diner et al., 1998, [189962](#); Kahn et al., 2005, [190966](#); Martonchik et al., 1998, [190472](#); 2002, [190490](#)). MISR AODs are within 20% or ± 0.05 of coincident AERONET measurements (Abdou et al., 2005, [190028](#); Kahn et al., 2005, [189961](#)). The MISR multi-angle data also sample scattering angles ranging from about 60° to 160° in midlatitudes, yielding information about particle size (Chen et al., 2008, [189984](#); Kahn et al., 1998, [190970](#); 2001, [190969](#); 2005, [190966](#)) and shape (Kalashnikova and Kahn, 2006, [190962](#)). The aggregate of aerosol microphysical properties can be used to assess aerosol air mass type, a more robust characterization of MISR-retrieved particle property information than individual attributes. MISR also retrieves plume height in the vicinity of wildfire, volcano, and mineral dust aerosol sources, where the plumes have discernable spatial contrast in the multi-angle imagery (Kahn et al., 2007, [190964](#)). Figure 9-57 is an example that illustrates MISR's ability to characterize the load, optical properties, and stereo height of near-source fire plumes.

POLarization and Directionality of the Earth's Reflectance

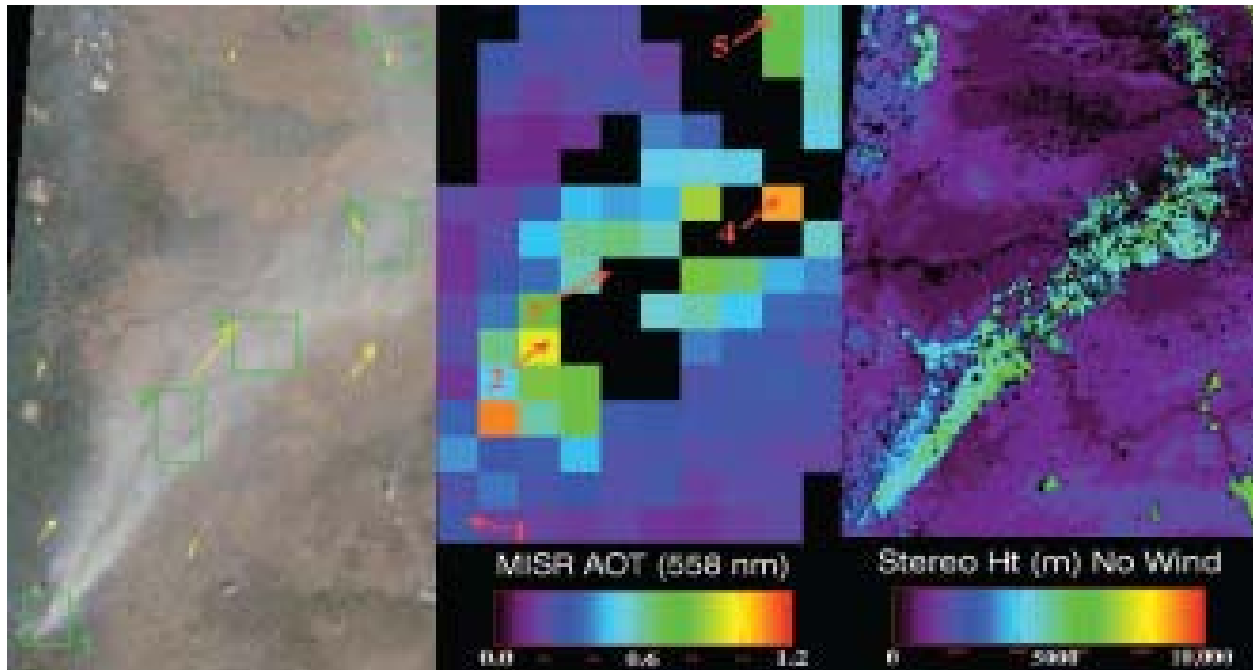
POLDER is a unique aerosol sensor that consists of wide field-of-view imaging spectro-radiometer capable of measuring multi-spectral, multi-directional, and polarized radiances (Deuzé et al., 2001, [192013](#)). The observed radiances can be exploited to better separate the atmospheric contribution from the surface contribution over both land and ocean. POLDER -1 and -2 flew onboard the ADEOS (Advanced Earth Observing Satellite) from November 1996 to June 1997 and April to October of 2003, respectively. A similar POLDER instrument flies on the PARASOL satellite that was launched in December 2004.

Figure 9-58 shows global horizontal patterns of AOD and Ångström exponent over the oceans derived from the POLDER instrument for June 1997. The oceanic AOD map (Figure 9-58a) reveals near-coastal plumes of high AOD, which decrease with distance from the coast. This pattern arises from aerosol emissions from the continents, followed by atmospheric dispersion, transformation, and removal in the downwind direction. In large-scale flow fields, such as the trade winds, these continental plumes persist over several thousand kilometers. The Ångström exponent shown in Figure 9-58 exhibits a very different pattern from that of the aerosol optical depth; specifically, it exhibits high values downwind of industrialized regions and regions of biomass burning, indicative of small particles arising from direct emissions from combustion sources and/or gas-to-particle conversion, and low values associated with large particles in plumes of soil dust from deserts and in sea salt aerosols.



Source: Adapted from (Chin et al., 2007, [190062](#)); original figure from Yoram Kaufman and Reto Stöckli.

Figure 9-56. A composite of MODIS/Terra observed aerosol optical depth (at 550 nm, green light near the peak of human vision) and fine-mode fraction that shows spatial and seasonal variations of aerosol types. Industrial pollution and biomass burning aerosols are predominately small particles (shown as red), whereas mineral dust and sea salt consist primarily of large particles (shown as green). Bright red and bright green indicate heavy pollution and dust plumes, respectively.

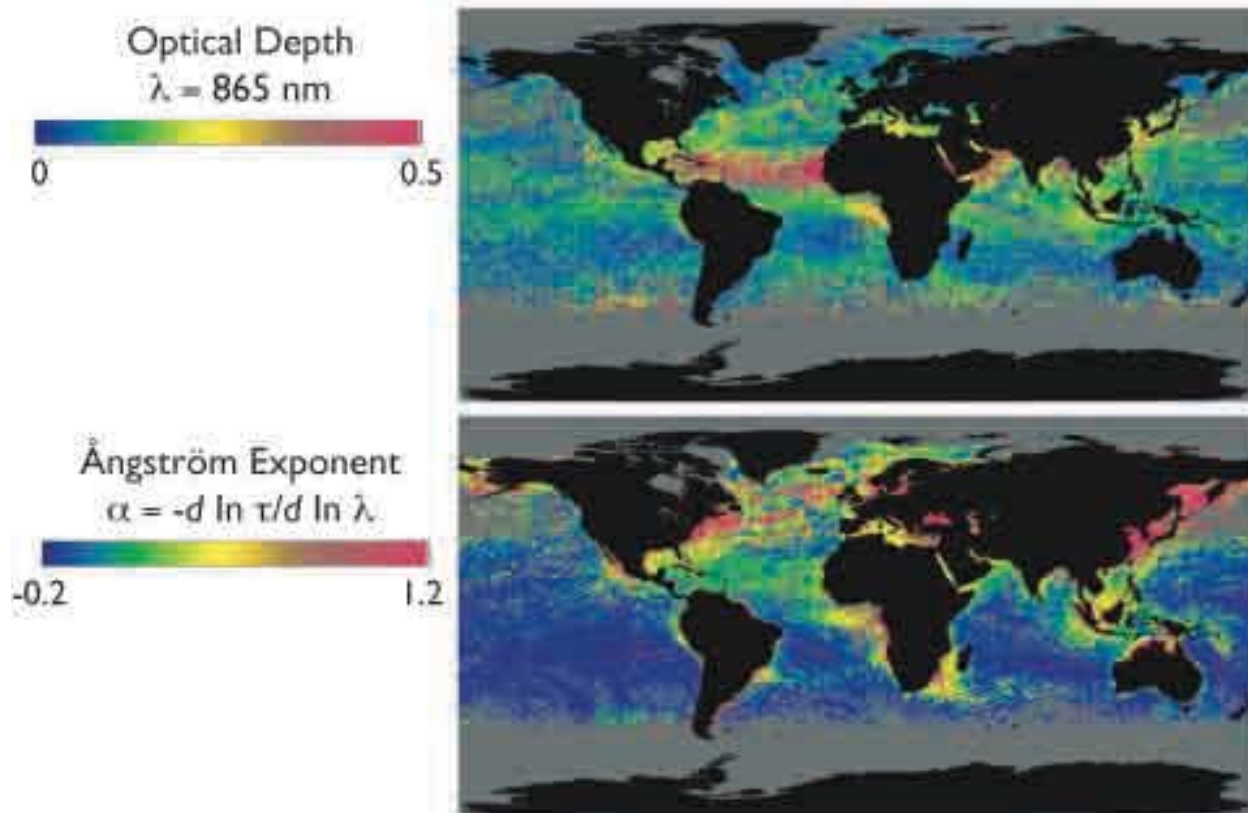


Source: Reprinted with Permission of the American Geophysical Union from Kahn et al. (2007, [190964](#)).

Figure 9-57. Oregon fire on September 4, 2003, as observed by MISR: (a) MISR nadir view of the fire plume, with five patch locations numbered and wind-vectors superposed in yellow; (b) MISR aerosol optical depth at 558 nm; and (c) MISR stereo height without wind correction for the same region.

9.3.2.2. Focused Field Campaigns

Over the past two decades, numerous focused field campaigns have examined the physical, chemical, and optical properties and radiative forcing of aerosols in a variety of aerosol regimes around the world, as listed in Table 9-5. These campaigns, which have been designed with aerosol characterization as the main goal or as one of the major themes in more interdisciplinary studies, were conducted mainly over or downwind of known continental aerosol source regions, but in some instances in low-aerosol regimes, for contrast. During each of these comprehensive campaigns, aerosols were studied in great detail, using combinations of in situ and remote sensing observations of physical and chemical properties from various platforms (e.g., aircraft, ships, satellites, and ground-based stations) and numerical modeling. In spite of their relatively short duration, these field studies have acquired comprehensive data sets of regional aerosol properties that have been used to understand the properties and evolution of aerosols within the atmosphere and to improve the climatology of aerosol microphysical properties used in satellite retrieval algorithms and CTMs.



Source : Reproduced with permission of Laboratoire d'Optique Atmosphérique (LOA), Lille, FR; Laboratoire des Sciences du Climat et de l'Environnement (LSCÉ), Gif sur Yvette, FR; Centre National d'études Spatiales (CNES), Toulouse, FR; and National Space Development Agency (NASDA), Japan.

Figure 9-58. Global maps at 18 km resolution showing monthly average (a) AOD at 865 nm and (b) Ångström exponent of AOD over water surfaces only for June, 1997, derived from radiance measurements by the POLDER.

9.3.2.3. Ground-Based In Situ Measurement Networks

Major U.S.-operated surface in situ and remote sensing networks for tropospheric aerosol characterization and climate forcing research are listed in Table 9-6. These surface in situ stations provide information about long-term changes and trends in aerosol concentrations and properties, the influence of regional sources on aerosol properties, climatologies of aerosol radiative properties, and data for testing models and satellite aerosol retrievals. The NOAA Earth System Research Laboratory (ESRL) aerosol monitoring network consists of baseline, regional, and mobile stations. These near-surface measurements include submicrometer and sub-10 micrometer scattering and absorption coefficients from which the extinction coefficient and single-scattering albedo can be derived. Additional measurements include particle concentration and, at selected sites, CCN concentration, the hygroscopic growth factor, and chemical composition.

Several of the stations, which are located across North America and world-wide, are in regions where recent focused field campaigns have been conducted. The measurement protocols at the stations are similar to those used during the field campaigns. Hence, the station data are directly comparable to the field campaign data so that they provide a longer-term measure of mean aerosol properties and their variability, as well as a context for the shorter-duration measurements of the field campaigns.

The Interagency Monitoring of Protected Visual Environment (IMPROVE), which is operated by the NP Service Air Resources Division, has stations across the U.S. located within NPs (Malm et al., 1994, [044920](#)). Although the primary focus of the network is air pollution, the measurements are also relevant to climate forcing research. Measurements include fine and coarse mode ($\text{PM}_{2.5}$ and PM_{10}) aerosol mass concentration; concentrations of elements, sulfate, nitrate, organic carbon, and elemental carbon; and scattering coefficients.

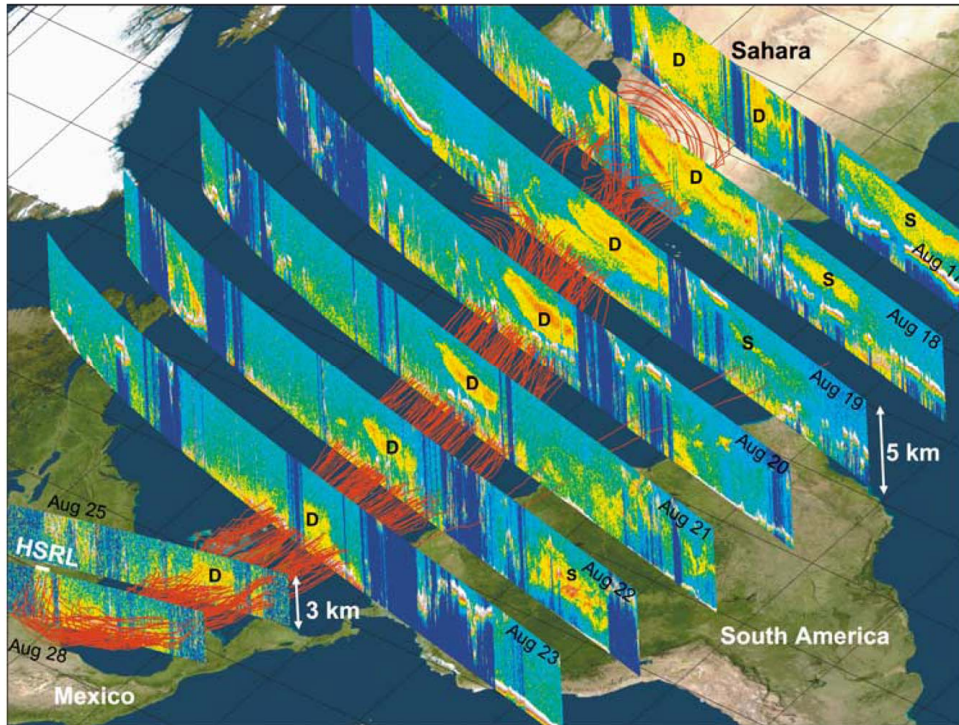
In addition, to these U.S.-operated networks, there are other national and international surface networks that provide measurements of aerosol properties including, but not limited to, the World Meteorological Organization (WMO) Global Atmospheric Watch (GAW) network (<http://www.wmo.int/pages/prog/arep/gaw/monitoring.html>), the European Monitoring and Evaluation Programme (EMEP) (<http://www.emep.int/>), the Canadian Air and Precipitation Monitoring Network (CAPMoN) (http://www.msc-smc.ec.gc.ca/capmon/index_e.cfm), and the Acid Deposition Monitoring Network in East Asia (EANET) (<http://www.eanet.cc/eanet.html>).

Clouds and the Earth's Radiant Energy System

CERES measures broadband solar and terrestrial radiances at three channels with a large footprint (e.g., 20 km for CERES/Terra) (Wielicki et al., 1996, [190637](#)). It is co-located with MODIS and MISR aboard Terra and with MODIS on Aqua. The observed radiances are converted to TOA irradiances or fluxes using the Angular Distribution Models (ADMs) that are functions of viewing angle, sun angle, and scene type (Loeb and Kato, 2002, [190432](#); Loeb et al., 2005, [190436](#); Zhang et al., 2005, [190929](#)). Such estimates of TOA solar flux in clear-sky conditions can be compared to the expected flux for an aerosol-free atmosphere, in conjunction with measurements of aerosol optical depth from other sensors (e.g., MODIS and MISR) to derive the aerosol direct radiative forcing (Christopher et al., 2006, [155729](#); Loeb and Manalo-Smith, 2005, [190433](#); Patadia et al., 2008, [190558](#); Zhang and Christopher, 2003, [190928](#); Zhang et al., 2005, [190930](#)). The derived instantaneous value is then scaled to obtain a daily average. A direct use of the coarse spatial resolution CERES measurements would exclude aerosol distributions in partly cloudy CERES scenes. Several approaches that incorporate coincident, high spatial and spectral resolution measurements (e.g., MODIS) have been employed to overcome this limitation (Loeb and Manalo-Smith, 2005, [190433](#); Zhang et al., 2005, [190930](#)).

Active Remote Sensing of Aerosols

Following the success of a demonstration of lidar system aboard the U.S. Space Shuttle mission in 1994, i.e., Lidar In-space Technology Experiment (LITE) (Winker et al., 1996, [190914](#)), the Geoscience Laser Altimeter System (GLAS) was launched in early 2003 to become the first polar orbiting satellite lidar. It provides global aerosol and cloud profiling for a one-month period out of every three-to-six months. It has been demonstrated that GLAS is capable of detecting and discriminating multiple layer clouds, atmospheric boundary layer aerosols, and elevated aerosol layers (e.g., Spinhirne et al., 2005, [190410](#)). The Cloud-Aerosol Lidar and Infrared Pathfinder Satellite Observations (CALIPSO), launched on April 28, 2006, is carrying a lidar instrument (Cloud and Aerosol Lidar with Orthogonal Polarization - CALIOP) that has been collecting profiles of the attenuated backscatter at visible and near-infrared wavelengths along with polarized backscatter in the visible channel (Winker et al., 2003, [192017](#)). CALIOP measurements have been used to derive the above-cloud fraction of aerosol extinction optical depth (Chand et al., 2008, [189974](#)), one of the important factors determining aerosol direct radiative forcing in cloudy conditions. Figure 9-59 shows an event of trans-Atlantic transport of Saharan dust captured by CALIPSO. Flying in formation with the Aqua, AURA, POLDER, and CloudSat satellites, the vertically resolved information is expected to greatly improve passive aerosol and cloud retrievals as well as allow the retrieval of vertical distributions of aerosol extinction, fine- and coarse-mode separately (Huneeus and Boucher, 2007, [190624](#); Kaufman et al., 2003, [190954](#); Léon et al., 2003, [190366](#)).



Source: Reprinted with Permission of the American Geophysical Union from Liu et al. (2008, [156709](#)).

Figure 9-59. A dust event that originated in the Sahara desert on 17 August 2007 and was transported to the Gulf of Mexico. Red lines represent back trajectories indicating the transport track of the dust event. Vertical images are 532 nm attenuated backscatter coefficients measured by CALIOP when passing over the dust transport track. The letter “D” designates the dust layer, and “S” represents smoke layers from biomass burning in Africa (17-19 August) and South America (22 August). The track of the high-spectral-resolution-lidar (HSRL) measurement is indicated by the white line superimposed on the 28 August CALIPSO image. The HSRL track is coincident with the track of the 28 August CALIPSO measurement off the coast of Texas between 28.75°N and 29.08°N.

9.3.2.4. In Situ Aerosol Profiling Programs

In addition to long-term ground based measurements, regular long-term aircraft in situ measurements recently have been implemented at several locations. These programs provide a statistically significant data set of the vertical distribution of aerosol properties to determine spatial and temporal variability through the vertical column and the influence of regional sources on that variability. In addition, the measurements provide data for satellite and model validation. As part of its long-term ground measurements, NOAA has conducted regular flights over Bondville, Illinois since 2006. Measurements include light scattering and absorption coefficients, the relative humidity dependence of light scattering, aerosol number concentration and size distribution, and chemical composition. The same measurements with the exception of number concentration, size distribution, and chemical composition were made by NOAA during regular overflights of DOE ARM’s Southern Great Plains (SGP) site from 2000-2007 (Andrews et al., 2004, [190058](#)) (<http://www.esrl.noaa.gov/gmd/aero/net/index.html>).

In summary of Sections 9.3.2.2, 9.3.2.3, and 9.3.2.4, in situ measurements of aerosol properties have greatly expanded over the past two decades as evidenced by the number of focused field campaigns in or downwind of aerosol source regions all over the globe, the continuation of existing and implementation of new sampling networks worldwide, and the implementation of regular aerosol profiling measurements from fixed locations. In addition, in situ measurement capabilities have undergone major advancements during this same time

period. These advancements include the ability to measure aerosol chemical composition as a function of size at a time resolution of seconds to minutes (e.g., Jayne et al., 2000, [190978](#)), the development of instruments able to measure aerosol absorption and extinction coefficients at high sensitivity and time resolution and as a function of relative humidity (e.g., Baynard et al., 2007, [151669](#); Lack et al., 2006, [096032](#)), and the deployment of these instruments across the globe on ships, at ground-based sites, and on aircraft. However, further advances are needed to make this newly developed instrumentation more affordable and turn-key so that it can be deployed more widely to characterize aerosol properties at a variety of sites worldwide.

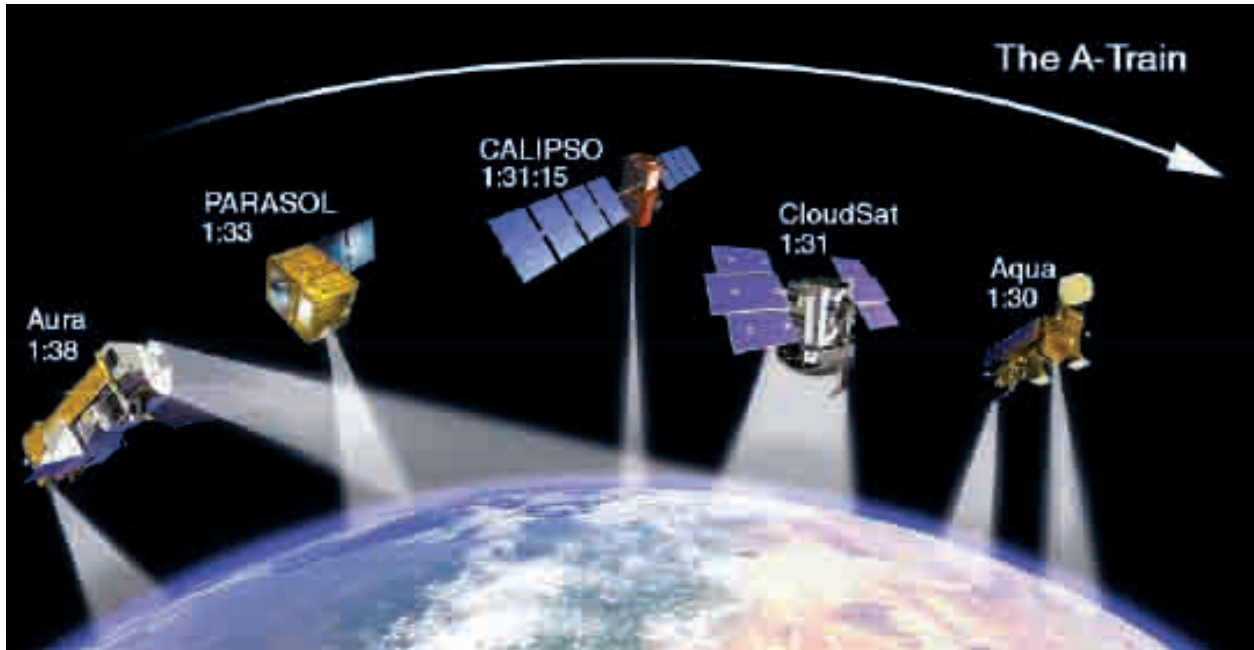


Figure 9-60. A constellation of five spacecraft that overfly the Equator at about 1:30 p.m., the so-called A-Train, carries sensors having complementary capabilities, offering unprecedented opportunities to study aerosols from space in multiple dimensions.

Table 9-5. List of major intensive field experiments that are relevant to aerosol research in a variety of aerosol regimes around the globe conducted in the past two decades.

Aerosol Regimes	Intensive Field Experiments			Major References
	Name	Location	Time Period	
Anthropogenic aerosol and boreal forest from North America and West Europe	TARFOX	North Atlantic	July 1996	Russell et al. (1999, 190363)
	NEAQS	North Atlantic	July-August 2002	Quinn and Bates (2003, 049189)
	SCAR-A	North America	1993	Remer et al. (1997, 190216)
	CLAMS	East Coast of U.S.	July-August 2001	Smith et al. (2005, 190401)
	INTEX-NA, ICARTT	North America	Summer 2004	Fehsenfeld et al. (2006, 190531)
	DOE AIOP	Northern Oklahoma	May 2003	Ferrare et al. (2006, 190561)
	MILAGRO	Mexico City, Mexico	March 2006	Molina et al. (2008, 192019)
	TexAQS/GoMACCS	Texas and Gulf of Mexico	August-September 2006	Jiang et al. (2008, 156609); Lu et al. (2008, 190455)
	ARCTS	North-central Alaska to Greenland (Arctic haze)	March-April 2008	http://www.espo.nasa.gov/arctas/
	ARCTAS	Northern Canada (smoke)	June-July 2008	
	MINOS	Mediterranean region	July-August 2001	Lelieveld et al. (2002, 190361)
	LACE98	Lindberg, Germany	July-August 1998	Ansmann et al. (2002)
	Aerosols99	Atlantic	January-February 1999	Bates et al. (2001, 043385)
Brown haze in South Asia	INDOEX	Indian subcontinent and Indian Ocean	January-April 1998 & 1999	Ramanathan et al. (2001, 190196)
	ABC	South and East Asia	Ongoing	Ramanathan and Crutzen (2003, 190198)
Anthropogenic aerosol and desert dust mixture from East Asia	EAST-AIRE	China	March-April 2005	Li et al. (2007, 190392)
	INTEX-B	Northeastern Pacific	April 2006	Singh et al. (2008, 190394)
	ACE-Asia	East Asian and Northwest Pacific	April 2001	Huebert et al. (2003, 190623); Seinfeld et al. (2004, 190388)
	TRACE-P		March-April 2001	Jacob et al. (2003, 190987)
	PEM-West A & B	Western Pacific off East Asia	September-October 1991 February-March 1994	Hoell et al. (1996, 190607 ; 1997, 057373)
Biomass burning smoke in the tropics	BASE-A	Brazil	1989	Kaufman et al. (1992, 044557)
	SCAR-B	Brazil	August-September 1995	Kaufman et al. (1998, 089989)
	LBA-SMOCC	Amazon basin	September-November 2002	Andreae et al. (2004, 155658)
	SAFARI2000	South Africa and South Atlantic	August-September 2000	King et al. (2003, 094395)
	SAFARI92		September-October 1992	Lindesay et al. (1996, 190403)
	TRACE-ADABEX	South Atlantic	September-October 1992	Fishman et al. (1996, 190566)
	DABEX	West Africa	January-February 2006	Haywood et al. (2008, 190602)
Mineral dusts from North Africa and Arabian Peninsula	SAMUM	Southern Morocco	May-June 2006	Heintzenberg et al. (2008, 190605)
	SHADE	West coast of North Africa	September 2000	Tanré et al. (2003, 190454)
	PRIDE	Puerto Rico	June-July 2000	Reid et al. (2003, 190213)
	UAE ²	Arabian Peninsula	August-September 2004	Reid et al. (2008, 190214)
Remote oceanic aerosol	ACE-1	Southern Oceans	December 1995	Bates et al. ((1998, 190063) ; Quinn and Coffman (1998, 190918))

Source: Yu (2006, [156173](#))

Table 9-6. Summary of major U.S. surface in situ and remote sensing networks for the tropospheric aerosol characterization and radiative forcing research. All the reported quantities are column-integrated or column-effective, except as indicated.

Surface Network		Measured/Derived Parameters				Spatial Coverage	Temporal Coverage
		Loading	Size, Shape	Absorption	Chemistry		
In situ	NOAA ESRL aerosol monitoring (http://www.esrl.noaa.gov/gmd/aero/)	Near-surface extinction coefficient, optical depth, CN/CNN number concentrations	Ångström exponent, hemispheric backscatter fraction, asymmetry factor, hygroscopic growth	Single-scattering albedo, absorption coefficient	Chemical composition in selected sites and periods	5 baseline stations, several regional stations, aircraft and mobile platforms	1976 onward
	NPS/EPA IMPROVE (http://vista.cira.colostate.edu/improve/)	Near-surface mass concentrations and derived extinction coefficients by species	Fine and coarse separately	Single-scattering albedo, absorption coefficient	Ions, ammonium SO ₄ ²⁻ , ammonium nitrate organics, EC, fine soil	156 NPs and wilderness areas in the U.S.	1988 onward
Remote Sensing	NASA AERONET (http://aeronet.gsfc.nasa.gov)	Optical depth	Fine-mode fraction, Ångström exponents, asymmetry factor, phase function, non-spherical fraction	Single-scattering albedo, absorption optical depth, refractive indices	N/A	~200 sites over global land and islands	1993 onward
	DOE ARM (http://www.arm.gov)					6 sites and 1 mobile facility in N. America, Europe, and Asia	1989 onward
	NOAA SURFRAD (http://www.srb.noaa.gov/surfrad/)	N/A	N/A	N/A	7 sites in the U.S.	1995 onward	
	AERONET-MAN (http://aeronet.gsfc.nasa.gov/maritime_aero_sol_network.html)				Global Ocean	2004-present periodically	
	NASA MPLNET (http://mplnet.gsfc.nasa.gov/)	Vertical profiles of backscatter/extinction coefficient	N/A	N/A	N/A	~30 sites in major continents, usually co-located with AERONET and ARM sites	2000 onward



Figure 9-61. Geographical coverage of active AERONET sites in 2006.

9.3.2.5. Ground-Based Remote Sensing Measurement Networks

The Aerosol Robotic Network (AERONET) program is a federated ground-based remote sensing network of well-calibrated sun photometers and radiometers (<http://aeronet.gsfc.nasa.gov>).

AERONET includes about 200 sites around the world, covering all major tropospheric aerosol regimes (Holben et al., 1998, [155848](#); 2001, [190618](#)), as illustrated in Figure 9-61. Spectral measurements of sun and sky radiance are calibrated and screened for cloud-free conditions (Smirnov et al., 2000, [190397](#)). AERONET stations provide direct, calibrated measurements of spectral AOD (normally at wavelengths of 440, 670, 870, and 1020 nm) with an accuracy of ± 0.015 (Eck et al., 1999, [190390](#)). In addition, inversion-based retrievals of a variety of effective, column-mean properties have been developed, including aerosol single-scattering albedo, size distributions, fine-mode fraction, degree of non-sphericity, phase function, and asymmetry factor (Dubovik and King, 2000, [190197](#); Dubovik et al., 2000, [190177](#); Dubovik et al., 2002, [190202](#); O'Neill et al., 2003, [180187](#)). The SSA can be retrieved with an accuracy of ± 0.03 , but only for AOD >0.4 (Dubovik et al., 2002, [190202](#)), which precludes much of the planet. These retrieved parameters have been validated or are undergoing validation by comparison to in situ measurements (e.g., Haywood et al., 2003, [190599](#); Leahy et al., 2007, [190232](#); Magi et al., 2005, [190468](#)).

Recent developments associated with AERONET algorithms and data products include:

- simultaneous retrieval of aerosol and surface properties using combined AERONET and satellite measurements (Sinyuk et al., 2007, [190395](#)) with surface reflectance taken into account (which significantly improves AERONET SSA retrieval accuracy) (Eck et al., 2008, [190409](#));
- the addition of ocean color and high frequency solar flux measurements; and
- the establishment of the Maritime Aerosol Network (MAN) component to monitor aerosols over the World oceans from ships of-opportunity (Smirnov et al., 2006, [190400](#)).

Because of consistent calibration, cloud-screening, and retrieval methods, uniformly acquired and processed data are available from all stations, some of which have operated for over 10 years. These data constitute a high-quality, ground-based aerosol climatology and, as such, have been widely used for aerosol process studies as well as for evaluation and validation of model simulation and satellite remote sensing applications (e.g., Chin et al., 2002, [189996](#); Kahn et al., 2005, [190966](#); Remer et al., 2005, [190221](#); Yu et al., 2003, [156171](#); 2006, [156173](#)). In addition, AERONET retrievals of aerosol size distribution and refractive indices have been used in algorithm development for satellite sensors (Levy et al., 2007, [190377](#); Remer et al., 2005, [190221](#)). A set of aerosol optical properties provided by AERONET has been used to calculate the aerosol direct radiative forcing (Procopio et al., 2004, [190571](#); Zhou et al., 2005, [156183](#)), which can be used to evaluate both satellite remote sensing measurements and model simulations.

AERONET measurements are complemented by other ground-based aerosol networks having less geographical or temporal coverage, such as the Atmospheric Radiation Measurement (ARM) network (Ackerman and Stokes, 2003, [192080](#)), NOAA's national surface radiation budget network (SURFRAD) (Augustine et al., 2008, [189913](#)) and other networks with multifilter rotating shadowband radiometer (MFRSR) (Harrison et al., 1994, [045805](#); Michalsky et al., 2001, [190537](#)), and several lidar networks including:

- NASA Micro Pulse Lidar Network (MPLNET) (Welton et al., 2001, [157133](#); Welton et al., 2002, [190631](#));
- Regional East Atmospheric Lidar Mesonet (REALM) in North America (Hoff and McCann, 2002, [190612](#); Hoff et al., 2004, [190617](#));
- European Aerosol Research Lidar Network (EARLINET) (Matthias et al., 2004, [155971](#)); and
- Asian Dust Network (AD-Net) (e.g., Murayama et al., 2001, [155992](#)).

Obtaining accurate aerosol extinction profile observations is pivotal to improving aerosol radiative forcing and atmospheric response calculations. The values derived from these lidar networks with state-of-the-art techniques (Schmid et al., 2006, [190372](#)) are helping to fill this need.

9.3.2.6. Synergy of Measurements and Model Simulations

Individual approaches discussed above have their own strengths and limitations, and are usually complementary. None of these approaches alone is adequate to characterize large spatial and temporal variations of aerosol physical and chemical properties and to address complex aerosol-climate interactions. The best strategy for characterizing aerosols and estimating their radiative forcing is to integrate measurements from different satellite sensors with complementary capabilities from in situ and surface based measurements. Similarly, while models are essential tools for estimating regional and global distributions and radiative forcing of aerosols at present as well as in the past and the future, observations are required to provide following, several synergistic approaches to studying aerosols and their radiative forcing are discussed.

Closure Experiments

During intensive field studies, multiple platforms and instruments are deployed to sample regional aerosol properties through a well-coordinated experimental design. Often, several independent methods are used to measure or derive a single aerosol property or radiative forcing. This combination of methods can be used to identify inconsistencies in the methods and to quantify uncertainties in measured, derived, and calculated aerosol properties and radiative forcings. This approach, often referred to as a closure experiment, has been widely employed on both individual measurement platforms (local closure) and in studies involving vertical measurements through the atmospheric column by one or more platforms (column closure) (Quinn et al., 1996, [192021](#); Russell et al., 1997, [190359](#)).

Past closure studies have revealed that the best agreement between methods occurs for submicrometer, spherical particles such that different measures of aerosol optical properties and optical depth agree within 10-15% and often better (e.g., Clarke et al., 1996, [190003](#); Collins et al., 2000, [190059](#); Quinn et al., 2004, [190937](#); Schmid et al., 2000, [190369](#)). Larger particle sizes (e.g., sea salt and dust) present inlet collection efficiency issues and non-spherical particles (e.g., dust) lead to differences in instrumental responses. In these cases, differences between methods for determining aerosol optical depth can be as great as 35% (Doherty et al., 2005, [190027](#); Wang et al., 2003, [157106](#)). Closure studies on aerosol clear-sky DRF reveal uncertainties of about 25% for sulfate/carbonaceous aerosol and 60% for dust-containing aerosol (Bates et al., 2006, [189912](#)). Future closure studies could integrate surface- and satellite-based radiometric measurements of AOD with in situ optical, microphysical, and aircraft radiometric measurements for a wide range of situations. There is also a need to maintain consistency in comparing results and expressing uncertainties (Bates et al., 2006, [189912](#)).

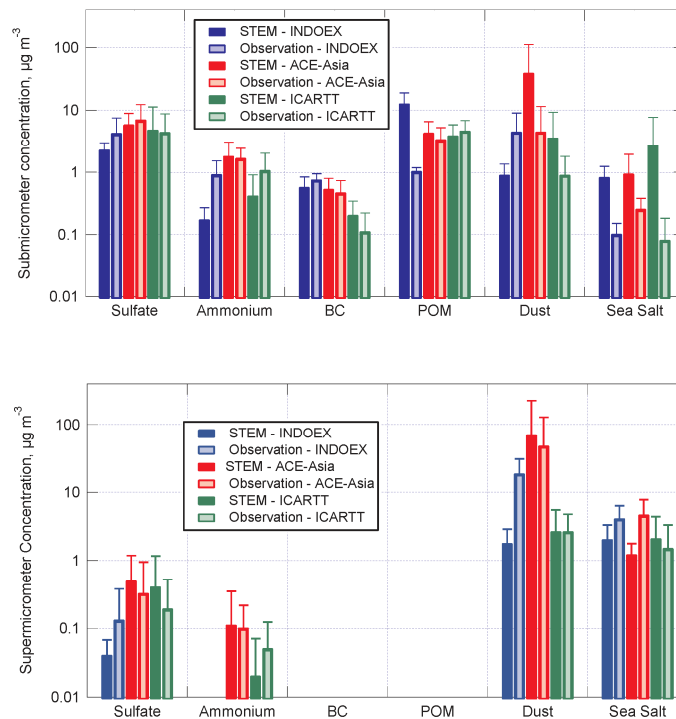
Constraining Models with In Situ Measurements

In situ measurements of aerosol chemical, microphysical, and optical properties with known accuracy, based in part on closure studies, can be used to constrain regional CTM simulations of aerosol direct forcing, as described by Bates et al. (2006, [189912](#)). A key step in the approach is assigning empirically derived optical properties to the individual chemical components generated by the CTM for use in a Radiative Transfer Model (RTM). Specifically, regional data from focused, short-duration field programs can be segregated according to aerosol type (sea salt, dust, or sulfate/carbonaceous) based on measured chemical composition and particle size. Corresponding measured optical properties can be carried along in the sorting process so that they, too, are segregated by aerosol type. The empirically derived aerosol properties for individual aerosol types, including mass scattering efficiency, single-scattering albedo, and asymmetry factor, and their dependences on relative humidity, can be used in place of assumed values in CTMs. Short-term, focused measurements of aerosol properties (e.g., aerosol concentration and AOD) also can be used to evaluate CTM parameterizations on a regional basis, to suggest improvements to such uncertain model parameters, such as emission factors and scavenging coefficients (e.g., Koch et al., 2007, [190185](#)). Improvements in these parameterizations using observations yield increasing confidence in simulations covering regions and periods where and when measurements are not available. To evaluate the aerosol

properties generated by CTMs on broader scales in space and time, satellite observations and long-term in situ measurements are required.

Improved Model Simulations with Satellite Measurements

Global measurements of aerosols from satellites (mainly AOD) with well-defined accuracies offer an opportunity to evaluate model simulations at large spatial and temporal scales. The satellite measurements can also be used to constrain aerosol model simulations and hence the assessment of aerosol DRF through data assimilation or objective analysis process (e.g., Collins et al., 2001, [189987](#); Liu et al., 2005, [190414](#); Yu et al., 2003, [156171](#); 2004, [190926](#); 2006, [156173](#); Zhang et al., 2008, [190932](#)). Both satellite retrievals and model simulations have uncertainties. The goal of data integration is to minimize the discrepancies between them, and to form an optimal estimate of aerosol distributions by combining them, typically with weights inversely proportional to the square of the errors of individual descriptions. Such integration can fill gaps in satellite retrievals and generate global distributions of aerosols that are consistent with ground-based measurements (Collins et al., 2001, [189987](#); Liu et al., 2005, [190414](#); Yu et al., 2003, [156171](#); 2006, [156173](#)). Recent efforts have also focused on retrieving global sources of aerosol from satellite observations using inverse modeling, which may be valuable for reducing large aerosol simulation uncertainties (Dubovik et al., 2007, [190211](#)). Model refinements guided by model evaluation and integration practices with satellite retrievals can then be used to improve aerosol simulations of the pre- and post-satellite eras. Current measurement-based understanding of aerosol characterization and radiative forcing is assessed in Section 9.3.3 through intercomparisons of a variety of measurement-based estimates and model simulations published in literature. This is followed by a detailed discussion of major outstanding issues in Section 9.3.4.



Source: Bates et al. (2006, [189912](#)).

Figure 9-62. Comparison of the mean concentration ($\mu\text{g}/\text{m}^3$) and standard deviation of the modeled (STEM) aerosol chemical components with shipboard measurements during INDOEX, ACE-Asia, and ICARTT.

Further complexity is added when attempting to relate surface $\text{PM}_{2.5}$ to aerosol optical depths. The main approach to derive surface $\text{PM}_{2.5}$ from satellite optical depths from MISR is based on the

use of model derived profiles to determine ratios of aerosol optical depth to surface $PM_{2.5}$ (Liu and Koutrakis, 2007, [187007](#); Liu et al., 2007, [098197](#); Van Donkelaar et al., 2006, [192108](#)).

Van Donkelaar et al. (2006, [192108](#)) derived $r = 0.69$ (MODIS) and 0.58 (MISR) with annual average ground based $PM_{2.5}$ across the U.S. and Canada. For comparison, r between AERONET total AOD and surface measurements was 0.71 . On average, MODIS tended to overestimate surface $PM_{2.5}$ by $\sim 5 \mu\text{g}/\text{m}^3$, while MISR estimates were biased high by about $3 \mu\text{g}/\text{m}^3$. Liu et al. (2007, [098197](#)) and Liu and Koutrakis (2007, [187007](#)) used MISR derived fractional AODs in their analysis and found improvement in the retrievals when fractional AODs were used instead of total AOD, allowing for better fits to the radiance data. They found that fractional AODs can explain 13-62% of the variability in $PM_{2.5}$ and its components in the eastern U.S. and 28-56% of the variability in the western U.S. The models tended to underpredict $PM_{2.5}$ by $\sim 7-8\%$ in both the East and West. The relative errors in surface $PM_{2.5}$ were estimated to be 30% in the East and 34% in the West. For AODs > 0.15 (nominal continental background values), dust particles could be distinguished from other particles with an estimated error of 4%. Performance improves substantially over polluted urban areas because they have much larger AOD. For example, Gupta et al. (2006, [137694](#)) derived a Pearson r between MODIS AOD and surface $PM_{2.5}$ of 0.96 for several urban areas around the world. The MODIS Aerosol Optical Depth (AOD)/ In-situ $PM_{2.5}$ correlation summary plot shown in Figure 9-63 below illustrates the correlation between AOD and surface $PM_{2.5}$ across the U.S. and parts of Canada. The correlation is based on coincident MODIS AOD pixels and 1-h $PM_{2.5}$ concentrations from the in-situ continuous surface monitors. The parameter plotted is the monitoring site-specific running correlation coefficient during the preceding 60 days (in color scale). The correlation coefficient has values between 1 (perfectly correlated) and -1 (perfectly anti-correlated). A value of zero indicates that the two measurements vary independently of each other.

The running time period of the correlation determination is given in the plot title, 20090704-20090901. The size of the point at each site indicates the number of coincidences between MODIS AOD pixels and the measured surface 1-h $PM_{2.5}$ concentrations for that period. Correlation significance generally increases with increasing number of coincidences. Higher correlations suggest the MODIS AOD pixel is reflective of in-situ surface $PM_{2.5}$ mass concentrations at the monitor location.

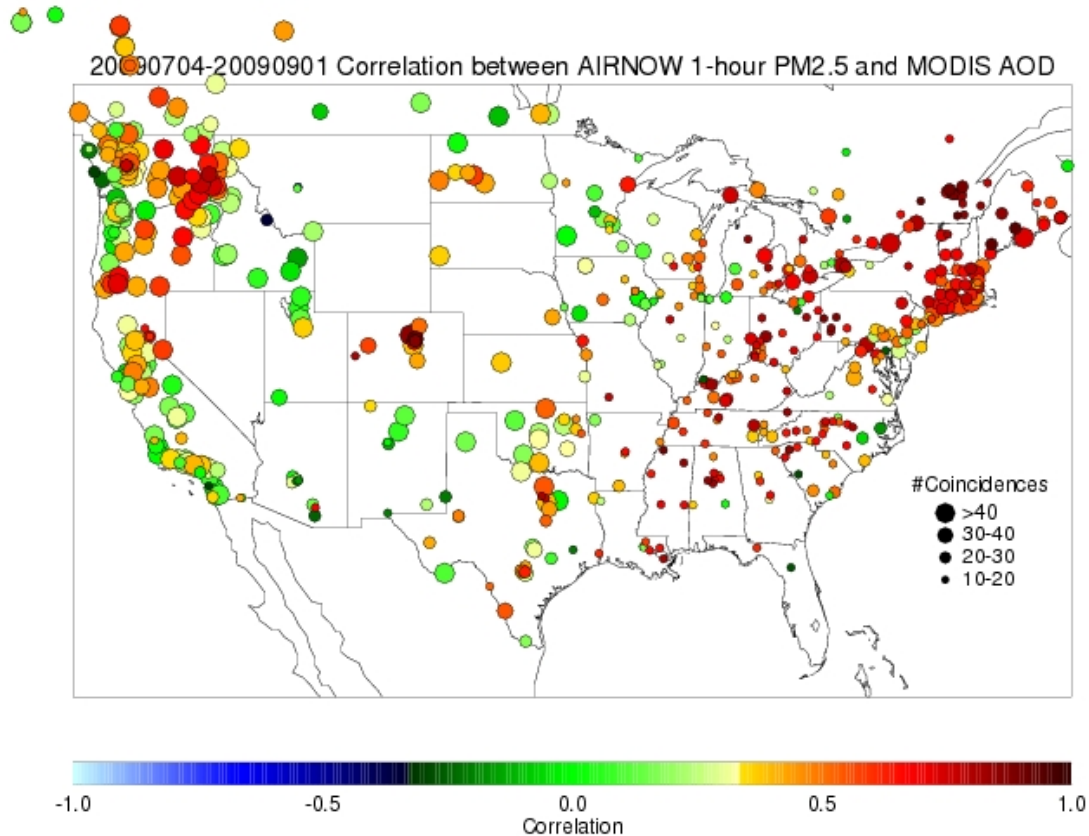


Figure 9-63. Correlations between one-hour PM_{2.5} surface measurements in the U.S. and southern Canada reported to AIRNOW and MODIS satellite AOD values for the period between 4 July and 1 September 2009. Symbol size indicates number of coincident points at that location in that period; symbol color is indexed to degree of correlation from -1 (cooler) to +1 (warmer).

The data and image of the aerosol comparison shown in Figure 9-63 were taken from the multi-agency project, Infusing satellite Data into Environmental Air Quality Applications (IDEA), a partnership of NASA, NOAA, and EPA designed to improve air quality assessment, management, and prediction by infusing NASA satellite measurements into NOAA and EPA analyses for public benefit. IDEA is funded by these three agencies and managed by the University of Maryland Baltimore County and NOAA.

9.3.3. Assessments of Aerosol Characterization and Climate Forcing

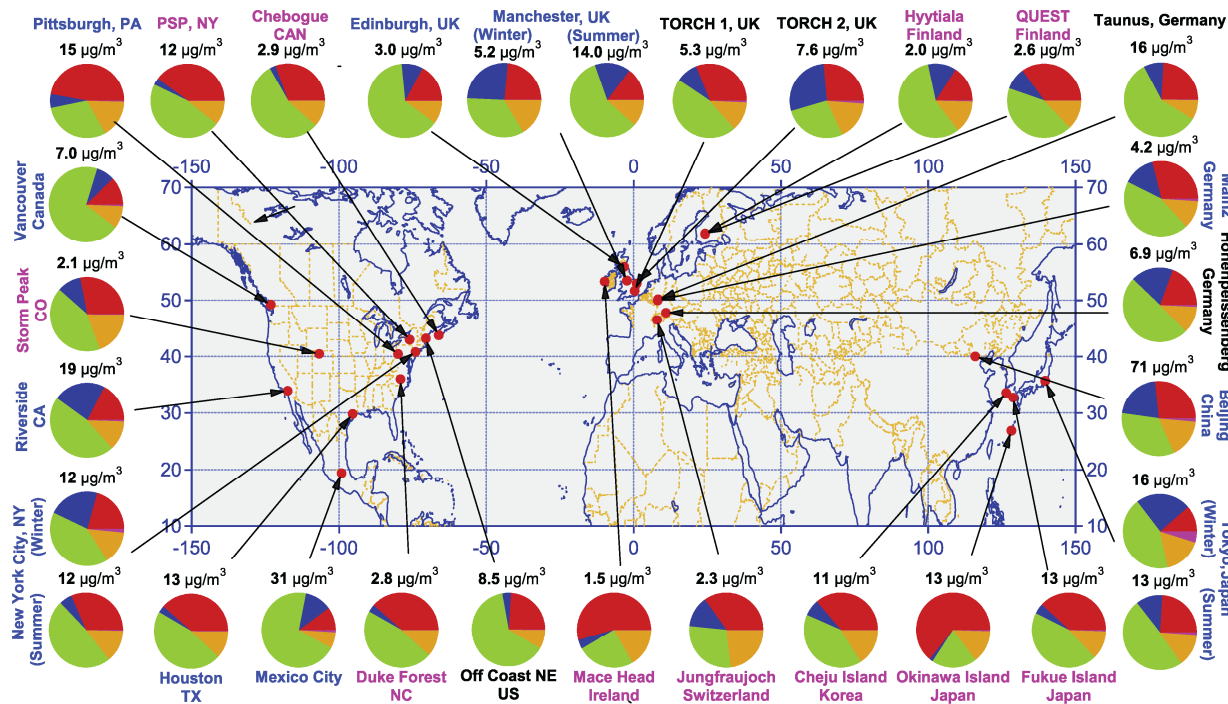
Sections 9.3.3 through 9.3.6 come directly from CCSP SAP2.3 Chapters 2, Section 2.3 through Chapter 3, Section 3.8, with section, table, and figure numbers changed to be internally consistent with this ISA.

This section focuses on the assessment of measurement-based aerosol characterization and its use in improving estimates of the direct radiative forcing on regional and global scales. In situ measurements provide highly accurate aerosol chemical, microphysical, and optical properties on a regional basis and for the particular time period of a given field campaign. Remote sensing from satellites and ground-based networks provide spatial and temporal coverage that intensive field campaigns lack. Both in situ measurements and remote sensing have been used to determine key parameters for estimating aerosol direct radiative forcing including aerosol single scattering albedo, asymmetry factor, optical depth remote sensing has also been providing simultaneous measurements of aerosol optical depth and radiative fluxes that can be combined to derive aerosol direct radiative forcing at the TOA with relaxed requirement for characterizing aerosol properties. Progress in using both satellite and surface-based measurements to study aerosol-cloud interactions and aerosol indirect forcing is also discussed.

9.3.3.1. The Use of Measured Aerosol Properties to Improve Models

The wide variety of aerosol data sets from intensive field campaigns provides a rigorous “testbed” for model simulations of aerosol properties and distributions and estimates of DRF. As described in Section 9.3.2.6, in situ measurements can be used to constrain regional CTM simulations of aerosol properties, DRF, anthropogenic component of DRF, and to evaluate CTM parameterizations. In addition, in situ measurements can be used to develop simplifying parameterizations for use by CTMs.

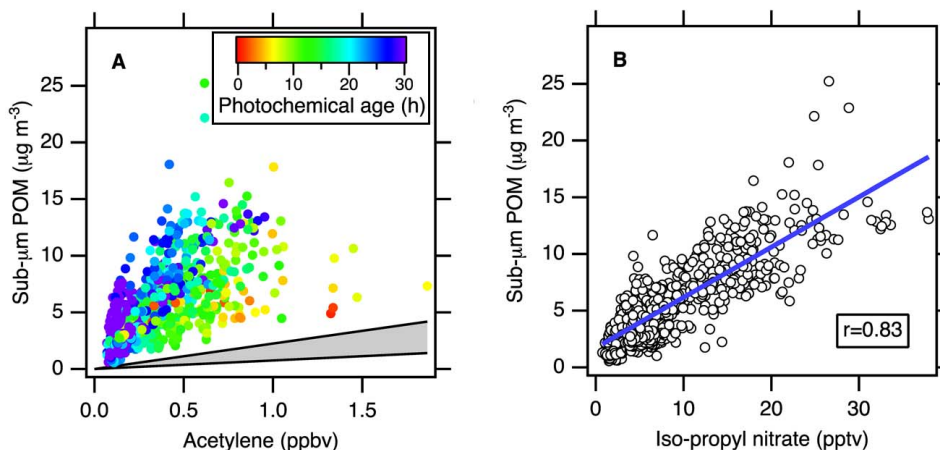
Several factors contribute to the uncertainty of CTM calculations of size-distributed aerosol composition including emissions, aerosol removal by wet deposition, processes involved in the formation of secondary aerosols and the chemical and microphysical evolution of aerosols, vertical transport, and meteorological fields including the timing and amount of precipitation, formation of clouds, and relative humidity. In situ measurements made during focused field campaigns provide a point of comparison for the CTM-generated aerosol distributions at the surface and at discrete points above the surface. Such comparisons are essential for identifying areas where the models need improvement.



Source: Data from Zhang et al. (2007, [189998](#)).

Figure 9-64. Location of aerosol chemical composition measurements with aerosol mass spectrometers. Colors for the labels indicate the type of sampling location: urban areas (blue), <100 mi downwind of major cites (black), and rural/remote areas >100 miles downwind (pink). Pie charts show the average mass concentration and chemical composition: organics (green), SO_4^{2-} (red), nitrate (blue), ammonium (orange), and chloride (purple), of non-refractory PM_{10} .

Figure 9-62 shows a comparison of submicrometer and supermicrometer aerosol chemical components measured during INDOEX, ACEAsia, and ICARTT onboard a ship and the same values calculated with the STEM Model (e.g., Bates et al., 2004, [189958](#); Carmichael et al., 2002, [148319](#); Carmichael et al., 2003, [190042](#); Streets et al., 2006, [157019](#); Tang et al., 2003, [190441](#); Tang et al., 2004, [190445](#)). To permit direct comparison of the measured and modeled values, the model was driven by analyzed meteorological data and sampled at the times and locations of the shipboard measurements every 30 min along the cruise track. The best agreement was found for submicrometer sulfate and BC. The agreement was best for sulfate; this is attributed to greater accuracy in emissions, chemical conversion, and removal for this component. Underestimation of dust and sea salt is most likely due to errors in model-calculated emissions. Large discrepancies between the modeled and measured values occurred for submicrometer particulate organic matter (POM) (INDOEX), and for particles in the supermicrometer size range such as dust (ACE-Asia), and sea salt (all regions). The model underestimated the total mass of the supermicrometer aerosol by about a factor of 3. POM makes up a large and variable fraction of aerosol mass throughout the anthropogenically influenced northern hemisphere, and yet models have severe problems in properly representing this type of aerosol. Much of this discrepancy follows from the models inability to represent the formation of secondary organic aerosols (SOA) from the precursor volatile organic compounds (VOC). Figure 9-64 shows a summary of the results from aerosol mass spectrometer measurements at 30 sites over North America, Europe, and Asia. Based on aircraft measurements of urban-influenced air over New England, de Gouw et al. (2005, [190020](#)) found that POM was highly correlated with secondary anthropogenic gas phase species suggesting that the POM was derived from secondary anthropogenic sources and that the formation took one day or more.



Source: Data from de Guow et al. (2005, [190020](#)).

Figure 9-65. Scatterplots of the submicrometer POM measured during NEAQS versus A) acetylene and B) iso-propyl nitrate. The colors of the data points in A) denote the photochemical age as determined by the ratios of compounds of known OH reactivity. The gray area in A) shows the range of ratios between submicrometer POM and acetylene observed by Kirchstetter et al. (1999, [010642](#)) in tunnel studies.

Figure 9-65 shows scatterplots of submicrometer POM versus acetylene (a gas phase primary emitted VOC species) and isopropyl nitrate (a secondary gas phase organic species formed by atmospheric reactions). The increase in submicrometer POM with increasing photochemical age could not be explained by the removal of VOC alone, which are its traditionally recognized precursors. This result suggests that other species must have contributed and/or that the mechanism for POM formation is more efficient than assumed by models. Similar results were obtained from the 2006 MILAGRO field campaign conducted in Mexico City (Kleinman et al., 2008, [190074](#)), and comparisons of GCM results with several long-term monitoring stations also showed that the model underestimated organic aerosol concentrations (Koch et al., 2007, [190185](#)). Recent laboratory work suggests that isoprene may be a major SOA source missing from previous atmospheric models (Henze and Seinfeld, 2006, [190606](#); Kröll et al., 2006, [190195](#)), but underestimating sources from certain economic sectors may also play a role (Koch et al., 2007, [190185](#)). Models also have difficulty in representing the vertical distribution of organic aerosols, underpredicting their occurrence in the free troposphere (FT) (Heald et al., 2005, [190603](#)). While organic aerosol presents models with some of their greatest challenges, even the distribution of well-characterized sulfate aerosol is not always estimated correctly in models (Shindell et al., 2008, [190391](#)).

Comparisons of DRF and its anthropogenic component calculated with assumed optical properties and values constrained by in situ measurements can help identify areas of uncertainty in model parameterizations. In a study described by Bates et al. (2006, [189912](#)), two different CTMs (MOZART and STEM) were used to calculate dry mass concentrations of the dominant aerosol species (sulfate, organic carbon, BC, sea salt, and dust).

In situ measurements were used to calculate the corresponding optical properties for each aerosol type for use in a radiative transfer model. Aerosol DRF and its anthropogenic component estimated using the empirically derived and a priori optical properties were then compared. The DRF and its anthropogenic component were calculated as the net downward solar flux difference between the model state with aerosol and of the model state with no aerosol. It was found that the constrained optical properties derived from measurements increased the calculated AOD ($34 \pm 8\%$), TOA DRF ($32 \pm 12\%$), and anthropogenic component of TOA DRF ($37 \pm 7\%$) relative to runs using the a priori values. These increases were due to larger values of the constrained mass extinction efficiencies relative to the a priori values. In addition, differences in AOD due to using the aerosol loadings from MOZART versus those from STEM were much greater than differences resulting from the a priori vs. constrained RTM runs. In situ observations also can be used to generate simplified parameterizations for CTMs and RTMs thereby lending an empirical foundation to uncertain parameters currently in use by models. CTMs generate concentration fields of individual aerosol chemical components that are then used as input to radiative transfer models (RTMs) for the calculation of DRF. Currently, these calculations are performed with a variety of simplifying assumptions concerning the RH dependence of light scattering by the aerosol.

Chemical components often are treated as externally mixed each with a unique RH dependence of light scattering. However, both model and measurement studies reveal that POM, internally mixed with water-soluble salts, can reduce the hygroscopic response of the aerosol, which decreases its water content and ability to scatter light at elevated relative humidity (e.g., Carrico et al., 2005, [190052](#); Saxena et al., 1995, [077273](#)).

The complexity of the POM composition and its impact on aerosol optical properties requires the development of simplifying parameterizations that allow for the incorporation of information derived from field measurements into calculations of DRF (Quinn et al., 2005, [156033](#)). Measurements made during INDOEX, ACE-Asia, and ICARTT revealed a substantial decrease in $f_{\text{sp}}(\text{RH})$ with increasing mass fraction of POM in the accumulation mode. Based on these data, a parameterization was developed that quantitatively describes the relationship between POM mass fraction and $f_{\text{sp}}(\text{RH})$ for accumulation mode sulfate-POM mixtures (Quinn et al., 2005, [156033](#)). This simplified parameterization may be used as input to RTMs to derive values of $f_{\text{sp}}(\text{RH})$ based on CTM estimates of the POM mass fraction. Alternatively, the relationship may be used to assess values of $f_{\text{sp}}(\text{RH})$ currently being used in RTMs.

9.3.3.2. Intercomparisons of Satellite Measurements and Model Simulation of Aerosol Optical Depth

As aerosol DRF is highly dependent on the amount of aerosol present, it is of first-order importance to improve the spatial characterization of AOD on a global scale. This requires an evaluation of the various remote sensing AOD data sets and comparison with model-based AOD estimates. The latter comparison is particularly important if models are to be used in projections of future climate states that would result from assumed future emissions. Both remote sensing and model simulation have uncertainties and satellite-model integration is needed to obtain an optimum description of aerosol distribution.

Figure 9-65 shows an intercomparison of annual average AOD at 550 nm from two recent satellite aerosol sensors (MODIS and MISR), five model simulations (GOCART, GISS, SPRINTARS, LMDZ-LOA, LMDZ-INCA) and three satellite-model integrations (MO_GO, MI_GO, MO_MI_GO). These model-satellite integrations are conducted by using an optimum interpolation approach (Yu et al., 2003, [156171](#)) to constrain GOCART simulated AOD with that from MODIS, MISR, or MODIS over ocean and MISR over land, denoted as MO_GO, MI_GO, and MO_MI_GO, respectively. MODIS values of AOD are from Terra Collection 4 retrievals and MISR AOD is based on early post launch retrievals. MODIS and MISR retrievals give a comparable average AOD on the global scale, with MISR greater than MODIS by 0.01~0.02 depending on the season. However, differences between MODIS and MISR are much larger when land and ocean are examined separately: AOD from MODIS is 0.02-0.07 higher over land but 0.03-0.04 lower over ocean than the AOD from MISR. Several major causes for the systematic MODIS-MISR differences have been identified, including instrument calibration and sampling differences, different assumptions about ocean surface boundary conditions made in the individual retrieval algorithms, missing particle property or mixture options in the look-up tables, and cloud screening (Kahn et al., 2007, [190963](#)). The MODIS-MISR AOD differences are being reduced by continuous efforts on improving satellite retrieval algorithms and radiance calibration. The new MODIS aerosol retrieval algorithms in Collection 5 have resulted in a reduction of 0.07 for global land mean AOD (Levy et al., 2007, [190379](#)), and improved radiance calibration for MISR removed ~40% of AOD bias over dark water scenes (Kahn et al., 2005, [190965](#)).

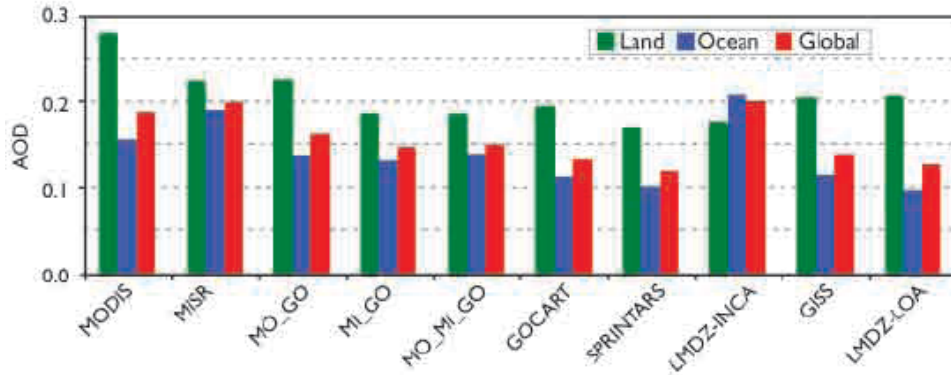
The annual and global average AOD from the five models is 0.19 ± 0.02 (mean \pm standard deviation) over land and 0.13 ± 0.05 over ocean, respectively. Clearly, the model-based mean AOD is smaller than both MODIS- and MISR-derived values (except the GISS model). A similar conclusion has been drawn from more extensive comparisons involving more models and satellites (Kinne et al., 2006, [155903](#)). On regional scales, satellite-model differences are much larger. These differences could be attributed in part to cloud contamination (Kaufman et al., 2005, [155891](#); Zhang et al., 2005, [190931](#)) and 3D cloud effects in satellite retrievals (Kaufman et al., 2005, [155891](#); Wen et al., 2006, [179964](#)) or to models missing important aerosol sources/sinks or physical processes (Koren et al., 2007, [190192](#)). Integrated satellite-model products are generally in-between the satellite retrievals and the model simulations, and agree better with AERONET measurements (e.g., Yu et al., 2003, [156171](#)). As in comparisons between models and in situ measurements (Bates et al., 2006, [189912](#)), there appears to be a relationship between uncertainties in the representation of dust in models and the uncertainty in AOD, and its global distribution.

For example, the GISS model generates more dust than the other models (Figure 9-67), resulting in a closer agreement with MODIS and MISR in the global mean (Source: Data taken from Kinne et al. (2006, [155903](#))).

Figure 9-66). However, the distribution of AOD between land and ocean is quite different from MODIS- and MISR-derived values.

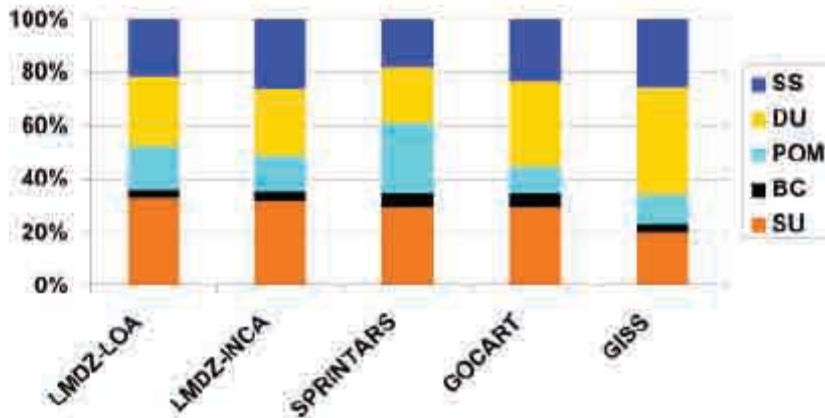
Figure 9-67 shows larger model differences in the simulated percentage contributions of individual components to the total aerosol optical depth on a global scale, and hence in the simulated aerosol single-scattering properties (e.g., single-scattering albedo, and phase function), as documented in Kinne et al. (2006, [155903](#)). This, combined with the differences

in aerosol loading (as characterized by AOD) determines the model diversity in simulated aerosol direct radiative forcing, as discussed later. However, current satellite remote sensing capability is not sufficient to constrain model simulations of aerosol components.



Source: Data taken from Kinne et al. (2006, [155903](#))

Figure 9-66. Comparison of annual mean aerosol optical depth (AOD).



Source: Data taken from Kinne et al. (2006, [155903](#))

Figure 9-67. Percentage contributions of individual aerosol components. SU – sulfate, BC – BC, POM – particulate organic matter, DU – dust, SS – sea salt; to the total aerosol optical depth (at 550 nm) on a global scale simulated by the five models.

9.3.3.3. Satellite-Based Estimates of Aerosol Direct Radiative Forcing

Table 9-7 summarizes approaches to estimating the aerosol direct radiative forcing, including a brief description of methods, identifies major sources of uncertainty, and provides references. These estimates fall into three broad categories, namely (A) satellite-based, (B) satellite-model integrated, and (C) model-based. As satellite aerosol measurements are generally limited to cloud-free conditions, the discussion here focuses on assessments of clear-sky aerosol direct radiative forcing, a net (downwelling minus upwelling) solar flux difference between with aerosol (natural + anthropogenic) and in the absence of aerosol.

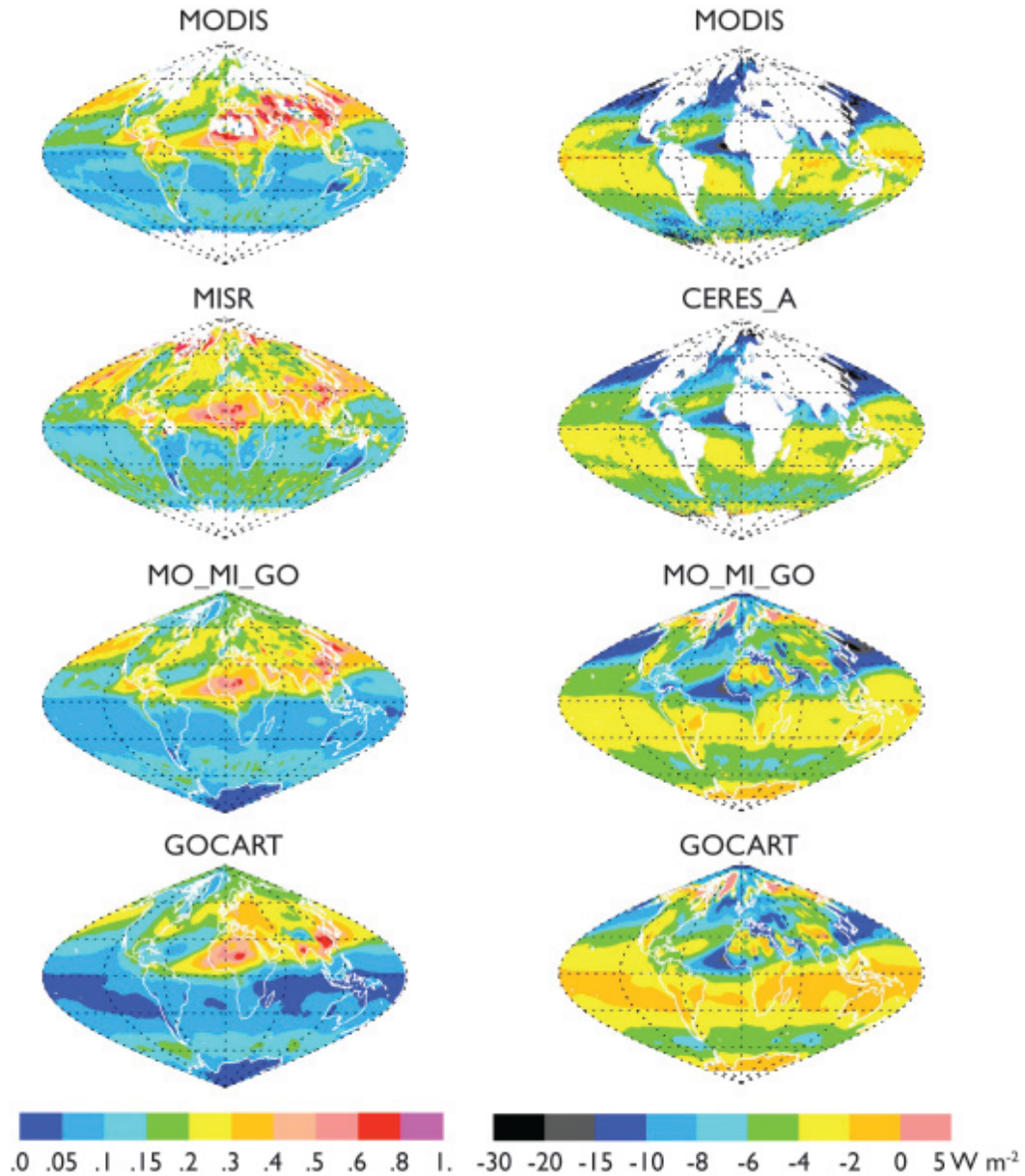
Global Distributions

Figure 9-68 shows global distributions of aerosol optical depth at 550 nm (left panel) and diurnally averaged clear-sky TOA DRF (right panel) for March-April-May (MAM) based on the different approaches. The DRF at the surface follows the same pattern as that at the TOA but is significantly larger in magnitude because of aerosol absorption. It appears that different approaches agree on large-scale patterns of aerosol optical depth and the direct radiative forcing. In this season, the aerosol impacts in the Northern Hemisphere are much larger than those in the Southern Hemisphere. Dust outbreaks and biomass burning elevate the optical depth to more than 0.3 over large parts of North Africa and the tropical Atlantic. In the tropical Atlantic, TOA cooling as large as -10 W/m^2 extends westward to Central America. In eastern China, the optical depth is as high as 0.6-0.8, resulting from the combined effects of industrial activities and biomass burning in the south, and dust outbreaks in the north. The Asian impacts also extend to the North Pacific, producing a TOA cooling of more than -10 W/m^2 . Other areas having large aerosol impacts include Western Europe, midlatitude North Atlantic, and much of South Asia and the Indian Ocean. Over the “roaring forties” in the Southern Hemisphere, high winds generate a large amount of sea salt. Elevated optical depth, along with high solar zenith angle and hence large backscattering to space, results in a band of TOA cooling of more than -4 W/m^2 . However, there is also some question as to whether thin cirrus (e.g., Zhang et al., 2005, [190931](#)) and unaccounted-for whitecaps contribute to the apparent enhancement in AOD retrieved by satellite. Some differences exist between different approaches. For example, the early post-launch MISR retrieved optical depths over the southern hemisphere oceans are higher than MODIS retrievals and GOCART simulations. Over the “roaring forties,” the MODIS derived TOA solar flux perturbations are larger than the estimates from other approaches.

Table 9-7. Summary of approaches to estimating the aerosol direct radiative forcing in three categories: (1) satellite retrievals; (2) satellite-model integrations; and (3) model simulations.

Category	Product	Brief Description	Identified Sources of Uncertainty	Major References
A Satellite retrievals	MODIS	Using MODIS retrievals of a linked set of AOD, ω_0 , and phase function consistently in conjunction with a radiative transfer model (RTM) to calculate TOA fluxes that best match the observed radiances.	Radiance calibration, cloud-aerosol discrimination, instantaneous-to-diurnal scaling, RTM parameterizations	Remer and Kaufman (2006, 190222)
	MODIS_A	Splitting MODIS AOD over ocean into mineral dust, sea salt, and biomass-burning and pollution; using AERONET measurements to derive the size distribution and single-scattering albedo for individual components.	Satellite AOD and FMF retrievals, overestimate due to summing up the compositional direct forcing, use of a single AERONET site to characterize a large region	Bellouin et al. (2005, 155684)
	CERES_A	Using CERES fluxes in combination with standard MODIS aerosol.		Loeb and Manalo-Smith (2005, 190433); Loeb and Kato (2002, 190432)
	CERES_B	Using CERES fluxes in combination with NOAA NESDIS aerosol from MODIS radiances.	Calibration of CERES radiances, large CERES footprint, satellite AOD retrieval, radiance-to-flux conversion (ADM), instantaneous-to-diurnal scaling, narrow-to-broadband conversion	Zhang et al. (2005, 086743 ; 2005, 157185); Zhang and Christopher (2003, 190928); Christopher et al. (2006, 155729); Patadia et al. (2008, 190558)
	CERES_C	Using CERES fluxes in combination with MODIS (ocean) and MISR (non-desert land) aerosol with new angular models for aerosols.		
	POLDER	Using POLDER AOD in combination with prescribed aerosol models (similar to MODIS).	Similar to MODIS	Boucher and Tanré (2000, 190041); Bellouin et al. (2003, 189911)
B. Satellite-model integrations	MODIS_G	Using GOCART simulations to fill AOD gaps in satellite retrievals.		*Aerosol single-scattering albedo and asymmetry factor are taken from GOCART simulations
	MISR_G		Propagation of uncertainties associated with both satellite retrievals and model simulations (but the model-satellite integration approach does result in improved AOD quality for MO_GO, and O_MI_GO)	
	MO_GO	Integration of MODIS and GOCART AOD.		*Yu et al. (2003, 156171 ; 2004, 190926 ; 2006, 156173)
	MO_MI_GO	Integration of GOCART AOD with retrievals from MODIS (Ocean) and MISR (Land).		
	SeaWiFS	Using SeaWiFS AOD and assumed aerosol models.	Similar to MODIS_G and MISR_G, too weak aerosol absorption	Chou et al. (2002, 190008)
C. Model simulations	GOCART	Offline RT calculations using monthly avg aerosols with a time step of 30 min (without the presence of clouds).		Chin et al. (2002, 189996); Yu et al. (2004, 190926)
	SPRINTARS	Online RT calculations every 3 hrs (cloud fraction = 0).	Emissions, parameterizations of a variety of sub-grid aerosol processes (e.g., wet and dry deposition, cloud convection, aqueous-phase oxidation), assumptions on aerosol size, absorption, mixture, and humidification of particles, Meteorology fields, not fully evaluated surface albedo schemes, RT parameterizations	Takemura et al. (2002, 190438 ; 2005, 190439)
	GISS	Online model simulations and weighted by clear-sky fraction.		Koch and Hansen (2005, 190183); Koch et al. (2006, 190184)
	LMDZ-INCA	Online RT calculations every 2 hrs (cloud fraction = 0).		Balkanski et al. (2007, 189979); Schulz et al. (2006, 190381); Kinne et al. (2006, 155903)
	LMDZ-LOA	Online RT calculations every 2 hrs (cloud fraction = 0).		Reddy et al. (2005, 190207 ; 2005, 190208)

Source: Adapted from Yu et al. (2006, [156173](#)).



Source: Yu et al. (2006, [156173](#))

Figure 9-68. Geographical patterns of seasonally (MAM) averaged aerosol optical depth at 550 nm (left panel) and the diurnally averaged clear-sky aerosol direct radiative (solar spectrum) forcing (W/m^2) at the TOA (right panel) derived from satellite (Terra) retrievals. MODIS (Remer and Kaufman, 2006, [190222](#); Remer et al., 2005, [190221](#)); MISR (Kahn et al., 2005, [190966](#)); and CERES_A (Loeb and Manalo-Smith, 2005, [190433](#)); GOCART simulations (Chin et al., 2002, [189996](#); Yu et al., 2004, [190926](#)); and GOCART-MODIS-MISR integrations (MO_MI_GO) (Yu et al., 2006, [156173](#)).

Global Mean

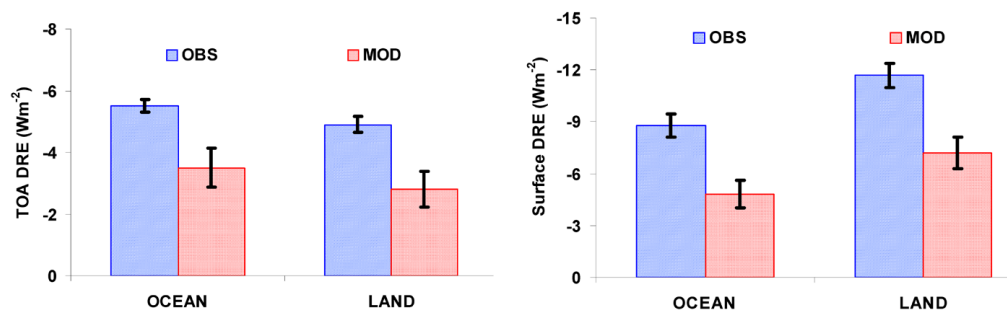
Figure 9-69 summarizes the measurement- and model-based estimates of clear-sky annual-averaged DRF at both the TOA and surface from 60°S to 60°N. Seasonal DRF values for individual estimates are summarized in Table 9-8 and Table 9-9 for ocean and land, respectively. Mean, median and standard error ϵ ($\epsilon = \sigma / (n-1)^{1/2}$), where σ is standard deviation and n is the number of methods) are calculated for measurement- and model-based estimates separately. Note that although the standard deviation or standard error reported here is not a fully rigorous measure of a true experimental uncertainty, it is indicative of the uncertainty because independent approaches with independent sources of errors are used (see Table 9-7; in the modeling community, this is called the “diversity;” see Section 9.3.6).

Ocean

For the TOA DRF, a majority of measurement-based and satellite-model integration-based estimates agree with each other within about 10%. On annual average, the measurement-based estimates give the DRF of $-5.5 \pm 0.2 \text{ W/m}^2$ (mean $\pm \epsilon$) at the TOA and $-8.7 \pm 0.7 \text{ W/m}^2$ at the surface. This suggests that the ocean surface cooling is about 60% larger than the cooling at the TOA. Model simulations give wide ranges of DRF estimates at both the TOA and surface. The ensemble of five models gives the annual average DRF (mean $\pm \epsilon$) of $-3.2 \pm 0.6 \text{ W/m}^2$ and $-4.9 \pm 0.8 \text{ W/m}^2$ at the TOA and surface, respectively. On average, the surface cooling is about 37% larger than the TOA cooling, smaller than the measurement-based estimate of surface and TOA difference of 60%. However, the ‘measurement-based’ estimate of surface DRF is actually a calculated value, using poorly constrained particle properties.

Land

It remains challenging to use satellite measurements alone for characterizing complex aerosol properties over land surfaces with high accuracy. As such, DRF estimates over land have to rely largely on model simulations and satellite-model integrations. On a global and annual average, the satellite-model integrated approaches derive a mean DRF of -4.9 W/m^2 at the TOA and -11.9 W/m^2 at the surface respectively. The surface cooling is more than a factor of 2 larger than the TOA cooling because of aerosol absorption. Note that the TOA DRF of -4.9 W/m^2 agrees quite well with the most recent satellite-based estimate of $-5.1 \pm 1.1 \text{ W/m}^2$ over non-desert land based on coincident measurements of MISR AOD and CERES solar flux (Patadia et al., 2008, [190558](#)). For comparisons, an ensemble of five model simulations derives a DRF (mean $\pm \epsilon$) over land of $-3.0 \pm 0.6 \text{ W/m}^2$ at the TOA and $-7.6 \pm 0.9 \text{ W/m}^2$ at the surface, respectively. Seasonal variations of DRF over land, as derived from both measurements and models, are larger than those over ocean.



Source: Yu et al. (2006, [156173](#))

Figure 9-69. Summary of observation- and model-based (denoted as OBS and MOD, respectively) estimates of clear-sky, annual average DRF at the TOA and at the surface. The box and vertical bar represent median and standard error, respectively.

Table 9-8. Summary of seasonal and annual average clear-sky DRF (W/m^2) at the TOA and the surface (SFC) over global OCEAN derived with different methods and data.

Products	DJF		MAM		JJA		SON		ANN	
	TOA	SFC	TOA	SFC	TOA	SFC	TOA	SFC	TOA	SFC
MODIS	-5.9		-5.8		-6.0		-5.8		-5.9	
MODIX_A*	-6.0	-8.2	-6.4	-8.9	-6.5	-9.3	-6.4	-8.9	-6.4	-8.9
CERES_A	-5.3		-6.1		-5.4		-5.1		-5.5	
CERES_B	-3.8		-4.3		-3.5		-3.6		-3.8	
CERES_C	-5.3		-5.4		-5.2				-5.3	
MODIS_G	-5.5	-9.1	-5.7	-10.4	-6.0	-10.6	-5.5	-9.8	-5.7	-10.0
MISR_G**	-6.4	-10.3	-6.5	-11.4	-7.0	-11.9	-6.3	-10.9	-6.5	-11.1
MO_GO	-4.9	-7.8	-5.1	-9.3	-5.4	-9.4	-5.0	-8.7	-5.1	-8.8
MO_MI_GO	-4.9	-7.9	-5.1	-9.2	-5.5	-9.5	-5.0	-8.6	-5.1	-8.7
POLDER	-5.7		-5.7		-5.8		-5.6		-5.7	
									-5.2***	-7.7***
SeaWiFS	-6.0	-6.6	-5.2	-5.8	-4.9	-5.6	-5.3	-5.7	-5.4	-5.9
Obs. Mean	-5.4	-8.3	-5.6	-9.2	-5.6	-9.4	-5.4	-8.8	-5.5	-8.7
Obs. Median	-5.5	-8.1	-5.7	-9.3	-5.5	-9.5	-5.4	-8.8	-5.5	-8.8
Obs. σ	0.72	1.26	0.64	1.89	0.91	2.10	0.79	1.74	0.70	1.65
Obs. ϵ	0.23	0.56	0.20	0.85	0.29	0.94	0.26	0.78	0.21	0.67
GOCART	-3.6	-5.7	-4.0	-7.2	-4.7	-8.0	-4.0	-6.8	-4.1	-6.9
SPRINTARS	-1.5	-2.5	-1.5	-2.5	-1.9	-3.3	-1.5	-2.5	-1.6	-2.7
GISS	-3.3	-4.1	-3.5	-4.6	-3.5	-4.9	-3.8	-5.4	-3.5	-4.8
LMDZ-INCA	-4.6	-5.6	-4.7	-5.9	-5.0	-6.3	-4.8	-5.5	-4.7	-5.8
LMDZ-LOA	-2.2	-4.1	-2.2	-3.7	-2.5	-4.4	-2.2	-4.1	-2.3	-4.1
Mod. Mean	-3.0	-4.4	-3.2	-4.8	-3.5	-5.4	-3.3	-4.9	-3.2	-4.9
Mod Median	-3.3	-4.1	-3.5	-4.6	-3.5	-4.9	-3.8	-5.4	-3.5	-4.8
Mod. σ	1.21	1.32	1.31	1.84	1.35	1.82	1.36	1.63	1.28	1.60
Mod. ϵ	0.61	0.66	0.66	0.92	0.67	0.91	0.68	0.81	0.64	0.80
Mod./Obs.	.60	.51	.61	.50	.64	.52	.70	.61	.64	.55

* High bias may result from adding the DRF of individual components to derive the total DRF (Bellouin et al., 2005, [155684](#)).

** High bias most likely results from an overall overestimate of 20% in early post-launch MISR optical depth retrievals (Kahn et al., 2005, [190966](#)).

*** Bellouin et al. (2003, [189911](#)) use AERONET retrieval of aerosol absorption as a constraint to the method in Boucher and Tanré (2000, [190041](#)), deriving aerosol direct radiative forcing both at the TOA and the surface.

Sources of data: MODIS (Remer & Kaufman, 2006), MODIS_A (Bellouin et al., 2005, [155684](#)), POLDER (Bellouin et al., 2003, [189911](#); Boucher and Tanré, 2000, [190041](#)), CERES_A and CERES_B (Loeb and Manalo-Smith, 2005, [190433](#)), CERES_C (Zhang et al., 2005, [190930](#)), MODIS_G, MISR_G, MO_GO, MO_MI_GO (Yu et al., 2004, [190926](#); 2006, [156173](#)), SeaWiFS (Chou et al., 2002, [190008](#)), GOCART (Chin et al., 2002, [189996](#); Yu et al., 2004, [190926](#)), SPRINTARS (Takemura et al., 2002, [190438](#)), GISS (Koch and Hansen, 2005, [190183](#); Koch et al., 2006, [190184](#)), LMDZ-INCA (Kinne et al., 2006, [155903](#); Schulz et al., 2006, [190381](#)), LMDZ-LOA (Reddy et al., 2005, [190207](#); Reddy et al., 2005, [190208](#)). Mean, median, standard deviation (σ), and standard error (ϵ) are calculated for observations (Obs) and model simulations (Mod) separately. The last row is the ratio of model median to observational median (taken from Yu et al., 2006, [156173](#)).

Table 9-9. Summary of seasonal and annual average clear-sky DRF (W/m^2) at the TOA and the surface (SFC) over global LAND derived with different methods and data.

Products	DJF		MAM		JJA		SON		ANN	
	TOA	SFC	TOA	SFC	TOA	SFC	TOA	SFC	TOA	SFC
MODIS_G	-4.1	-9.1	-5.8	-14.9	-6.6	-17.4	-5.4	-12.8	-5.5	-13.5
MISR_G	-3.9	-8.7	-5.1	-13.0	-5.8	-14.6	-4.6	-101.7	-4.9	-11.8
MO_GO	-3.5	-7.5	-5.1	-12.9	-5.8	-14.9	-4.8	-10.9	-4.8	-11.6
MO_MI_GO	-3.4	-7.4	-4.7	-11.8	-5.3	-13.5	-4.3	-9.7	-4.4	-10.6
Obs. Mean	-3.7	-8.2	-5.2	-13.2	-5.9	-15.1	-4.8	-11.0	-4.9	-11.9
Obs. Median	-3.7	-8.1	-5.1	-13.0	-5.8	-14.8	-4.7	-10.8	-4.9	-11.7
Obs. σ	0.33	0.85	0.46	1.29	0.54	1.65	0.46	1.29	0.45	1.20
Obs. ϵ	0.17	0.49	0.26	0.74	0.31	0.85	0.27	0.75	0.26	0.70
GOCART	02.9	-6.1	-4.4	-10.9	-4.8	-12.3	-4.3	-9.3	-4.1	-9.7
SPRINTARS	-1.4	-4.0	-1.5	-4.6	-2.0	-6.7	-1.7	-5.2	-1.7	-5.1
GISS	-1.6	-3.9	-3.2	-7.9	-3.6	-9.3	-2.5	-6.6	-2.8	-7.2
LMDZ-INCA	-3.0	-5.8	-4.0	-9.2	-6.0	-13.5	-4.3	-8.2	-4.3	-9.2
LMDZ-LOA	-1.3	-5.4	-1.8	-6.4	-2.7	-8.9	-2.1	-6.7	-2.0	-6.9
Mod. Mean	-2.0	-5.0	-3.0	-7.8	-3.8	-10.1	-3.0	-7.2	-3.0	-7.6
Mod Median	-1.6	-5.4	-3.2	-7.9	-3.6	-9.3	-2.5	-6.7	-2.8	-7.2
Mod. σ	0.84	1.03	1.29	2.44	1.61	2.74	1.24	1.58	1.19	1.86
Mod. ϵ	0.42	0.51	0.65	1.22	0.80	1.37	0.62	0.79	0.59	0.93
Mod./Obs.	0.43	0.67	0.63	0.61	0.62	0.62	0.53	0.62	0.58	0.62

Sources of data: MODIS_G, MISR_G, MO_GO, MO_MI_GO (Yu et al., 2004, [190926](#); 2006, [156173](#)), GOCART (Chin et al., 2002, [189996](#); Yu et al., 2004, [190926](#)), SPRINTARS (Takemura et al., 2002, [190438](#)), GISS (Koch and Hansen, 2005, [190183](#); Koch et al., 2006, [190184](#)), LMDZ-INCA (Balkanski et al., 2007, [189979](#); Kinne et al., 2006, [155903](#); Schulz et al., 2006, [190381](#)), LMDZ-LOA (Reddy et al., 2005, [190207](#); Reddy et al., 2005, [190208](#)). Mean, median, standard deviation (σ), and standard error (ϵ) are calculated for observations (Obs) and model simulations (Mod) separately. The last row is the ratio of model median to observational median. (Taken from Yu et al., 2006, [156173](#)).

The above analyses show that, on a global average, the measurement-based estimates of DRF are 55-80% greater than the model-based estimates. The differences are even larger on regional scales. Such measurement-model differences are a combination of differences in aerosol amount (optical depth), single-scattering properties, surface albedo, and radiative transfer schemes (Yu et al., 2006, [156173](#)). As discussed earlier, MODIS retrieved optical depths tend to be overestimated by about 10-15% due to the contamination of thin cirrus and clouds in general (Kaufman et al., 2005, [155891](#)). Such overestimation of optical depth would result in a comparable overestimate of the aerosol direct radiative forcing. Other satellite AOD data may have similar contamination, which however has not yet been quantified. On the other hand, the observations may be measuring enhanced AOD and DRF due to processes not well represented in the models including humidification and enhancement of aerosols in the vicinity of clouds (Koren et al., 2007, [190192](#)).

From the perspective of model simulations, uncertainties associated with parameterizations of various aerosol processes and meteorological fields, as documented under the AEROCOM and Global Modeling Initiative (GMI) frameworks (Kinne et al., 2006, [155903](#); Liu et al., 2007, [190427](#); Textor et al., 2006, [190456](#)), contribute to the large measurement-model and model-model discrepancies. Factors determining the AOD should be major reasons for the DRF discrepancy and the constraint of model AOD with well evaluated and bias reduced satellite AOD through a data assimilation approach can reduce the DRF discrepancy significantly. Other factors (such as model parameterization of surface reflectance, and model-satellite differences in single-scattering albedo and asymmetry factor due to satellite sampling bias toward cloud-free conditions) should also contribute, as evidenced by the existence of a large discrepancy in the radiative efficiency (Yu et al., 2006, [156173](#)). Significant effort will be needed in the future to conduct comprehensive assessments.

9.3.3.4. Satellite-Based Estimates of Anthropogenic Component of Aerosol Direct Radiative Forcing

Satellite instruments do not measure the aerosol chemical composition needed to discriminate anthropogenic from natural aerosol components. Because anthropogenic aerosols are predominantly sub-micron, the fine-mode fraction derived from POLDER, MODIS, or MISR might be used as a tool for deriving anthropogenic aerosol optical depth. This could provide a feasible way to conduct measurement-based estimates of anthropogenic component of aerosol direct radiative forcing (Kaufman et al., 2002, [190956](#)). Such method derives anthropogenic AOD from satellite measurements by empirically correcting contributions of natural sources (dust and maritime aerosol) to the sub-micron AOD (Kaufman et al., 2005, [155891](#)). The MODIS-based estimate of anthropogenic AOD is about 0.033 over oceans, consistent with model assessments of 0.030–0.036 even though the total AOD from MODIS is 25–40% higher than the models (Kaufman et al., 2005, [155891](#)). This accounts for $21 \pm 7\%$ of the MODIS-observed total aerosol optical depth, compared with about 33% of anthropogenic contributions estimated by the models. The anthropogenic fraction of AOD should be much larger over land (i.e., $47 \pm 9\%$ from a composite of several models) (Bellouin et al., 2005, [155684](#)), comparable to the 40% estimated by Yu et al. (2006, [156173](#)). Similarly, the non-spherical fraction from MISR or POLDER can be used to separate dust from spherical aerosol (Kahn et al., 2001, [190969](#); Kalashnikova and Kahn, 2006, [190962](#)), providing another constraint for distinguishing anthropogenic from natural aerosols.

There have been several estimates of anthropogenic component of DRF in recent years. Table 9-10 lists such estimates of anthropogenic component of TOA DRF that are from model simulations (Schulz et al., 2006, [190381](#)) and constrained to some degree by satellite observations (Bellouin et al., 2005, [155684](#); Bellouin et al., 2008, [189999](#); Christopher et al., 2006, [155729](#); Chung et al., 2005, [155733](#); Kaufman et al., 2005, [155891](#); Matsui et al., 2006, [190495](#); Quaas et al., 2008, [190916](#); Yu et al., 2006, [156173](#); Zhao et al., 2008, [190936](#)). The satellite-based clear-sky DRF by anthropogenic aerosols is estimated to be $-1.1 \pm 0.37 \text{ W/m}^2$ over ocean, about a factor of 2 stronger than model simulated -0.6 W/m^2 . Similar DRF estimates are rare over land, but a few studies do suggest that the anthropogenic DRF over land is much more negative than that over ocean (Bellouin et al., 2005, [155684](#); Bellouin et al., 2008, [189999](#); Yu et al., 2006, [156173](#)). On global average, the measurement-based estimate of anthropogenic DRF ranges from -0.9 to -1.9 W/m^2 , again stronger than the model-based estimate of -0.8 W/m^2 . Similar to DRF estimates for total aerosols, satellite-based estimates of anthropogenic component of DRF are rare over land.

On global average, anthropogenic aerosols are generally more absorptive than natural aerosols. As such the anthropogenic component of DRF is much more negative at the surface than at TOA. Several observation-constrained studies estimate that the global average, clear-sky, anthropogenic component of DRF at the surface ranges from -4.2 to -5.1 W/m^2 (Bellouin et al., 2005, [155684](#); Chung et al., 2005, [155733](#); Matsui et al., 2006, [190495](#); Yu et al., 2004, [190926](#)), which is about a factor of 2 larger in magnitude than the model estimates (e.g., Reddy et al., 2005, [190208](#)).

Uncertainties in estimates of the anthropogenic component of aerosol DRF are greater than for the total aerosol, particularly over land. An uncertainty analysis (Yu et al., 2006, [156173](#)) partitions the uncertainty for the global average anthropogenic DRF between land and ocean more or less evenly. Five parameters, namely fine-mode fraction (ff) and anthropogenic fraction of fine-mode fraction (faf) over both land and ocean, and τ over ocean, contribute nearly 80% of the overall uncertainty in the anthropogenic DRF estimate, with individual shares ranging from 13–20% (Yu et al., 2006, [156173](#)). These uncertainties presumably represent a lower bound because the sources of error are assumed to be independent. Uncertainties associated with several parameters are also not well defined. Nevertheless, such uncertainty analysis is useful for guiding future research and documenting advances in understanding.

Table 9-10. Estimates of anthropogenic components of aerosol optical depth (T_{ant}) and clear-sky DRF at the TOA from model simulations.

Data Sources	Ocean		Land		Global		Estimated uncertainty or model diversity for DRF
	T_{ant}	DRF (W/m^2)	T_{ant}	DRF (W/m^2)	T_{ant}	DRF (W/m^2)	
Kaufman et al. (2005, 155891)	0.033	-1.4					30%
Bellouin et al. (2005, 155684)	0.028	-0.8	0.13		0.062	-1.9	15%
Chung et al. (2005, 155733)						-1.1	
Yu et al. (2006, 156173)	0.031	-1.1	-0.88	-1.8	0.048	-1.3	47% (ocean), 84% (land), and 62% (global)
Christopher et al. (2006, 155729)		-1.4					65%
Matsui and Pielke (2006, 190495)		-1.6					30°S-30°N oceans
Quaas et al. (2008, 190916)		-0.7		-1.8		-0.9	45%
Bellouin et al. (2008, 189999)	0.021	-0.6	0.107	-3.3	0.043	-1.3	Update to Bellouin et al. (2005, 155684) with MODIS Collection 5 data
Zhao et al. (2008, 190936)		-1.25					35%
Schulz et al. (2006, 190381)	0.022	-0.59	0.065	-1.14	0.036	-0.77	30-40%; same emissions prescribed for all models

Sources: Schulz et al., (2006, [190381](#)) approaches constrained by satellite observations, Kaufman et al. (2005, [155891](#)); Bellouin et al. (2005, [155684](#)) 2008; Chung et al. (2005, [155733](#)); Yu et al. (2006, [156173](#)); Christopher et al. (2006, [155729](#)); Matsui and Pielke (2006, [190495](#)); Quaas et al. (2008, [190916](#)); Zhao et al. (2008, [190936](#)).

9.3.3.5. Aerosol-Cloud Interactions and Indirect Forcing

Satellite views of the Earth show a planet whose albedo is dominated by dark oceans and vegetated surfaces, white clouds, and bright deserts. The bright white clouds overlying darker oceans or vegetated surface demonstrate the significant effect that clouds have on the Earth's radiative balance. Low clouds reflect incoming sunlight back to space, acting to cool the planet, whereas high clouds can trap outgoing terrestrial radiation and act to warm the planet. In the Arctic, low clouds have also been shown to warm the surface (Garrett and Zhao, 2006, [190570](#)). Changes in cloud cover, in cloud vertical development, and cloud optical properties will have strong radiative and therefore, climatic impacts. Furthermore, factors that change cloud development will also change precipitation processes. These changes may alter amounts, locations and intensities of local and regional rain and snowfall, creating droughts, floods and severe weather.

Cloud droplets form on a subset of aerosol particles called cloud condensation nuclei (CCN). In general, an increase in aerosol leads to an increase in CCN and an increase in drop concentration. Thus, for the same amount of liquid water in a cloud, more available CCN will result in a greater number but smaller size of droplets (Twomey, 1977, [190533](#)). A cloud with smaller but more numerous droplets will be brighter and reflect more sunlight to space, thus exerting a cooling effect. This is the first aerosol indirect radiative effect, or "albedo effect." The effectiveness of a particle as a CCN depends on its size and composition so that the degree to which clouds become brighter for a given aerosol perturbation, and therefore the extent of cooling, depends on the aerosol size distribution and its size-dependent composition. In addition, aerosol perturbations to cloud microphysics may involve feedbacks; for example, smaller drops are less likely to collide and coalesce; this will inhibit growth, suppressing precipitation, and possibly increasing cloud lifetime (Albrecht, 1989, [045783](#)). In this case clouds may exert an even stronger cooling effect.

A distinctly different aerosol effect on clouds exists in thin Arctic clouds ($LWP < 25 \text{ gm}^{-2}$) having low emissivity. Aerosol has been shown to increase the longwave emissivity in these clouds, thereby warming the surface (Garrett and Zhao, 2006, [190570](#); Lubin and Vogelmann, 2006, [190466](#)).

Some aerosol particles, particularly black carbon and dust, also act as ice nuclei (IN) and in so doing, modify the microphysical properties of mixed-phase and ice-clouds. An increase in IN will generate more ice crystals, which grow at the expense of water droplets due to the

difference in vapor pressure over ice and water surfaces. The efficient growth of ice particles may increase the precipitation efficiency. In deep convective, polluted clouds there is a delay in the onset of freezing because droplets are smaller. These clouds may eventually precipitate, but only after higher altitudes are reached that result in taller cloud tops, more lightning and greater chance of severe weather (Andreae et al., 2004, [155658](#); Rosenfeld and Lansky, 1998, [190230](#)). The present state of knowledge of the nature and abundance of IN, and ice formation in clouds is extremely poor. There is some observational evidence of aerosol influences on ice processes, but a clear link between aerosol, IN concentrations, ice crystal concentrations and growth to precipitation has not been established. This report therefore only peripherally addresses ice processes. More information can be found in a review by the WMO/IUGG International Aerosol-Precipitation Scientific Assessment (Levin and Cotton, 2008, [190375](#)).

In addition to their roles as CCN and IN, aerosols also absorb and scatter light, and therefore they can change atmospheric conditions (temperature, stability, and surface fluxes) that influence cloud development and properties (Ackerman et al., 2000, [002987](#); Hansen et al., 1997, [043104](#)). Thus, aerosols affect clouds through changing cloud droplet size distributions, cloud particle phase, and by changing the atmospheric environment of the cloud.

9.3.3.6. Remote Sensing of Aerosol-Cloud Interactions and Indirect Forcing

The AVHRR satellite instruments have observed relationships between columnar aerosol loading, retrieved cloud microphysics, and cloud brightness over the Amazon Basin that are consistent with the theories explained above (Feingold et al., 2001, [190544](#); Kaufman and Fraser, 1997, [190958](#); Kaufman and Nakajima, 1993, [190959](#)), but do not necessarily prove a causal relationship. Other studies have linked cloud and aerosol microphysical parameters or cloud albedo and droplet size using satellite data applied over the entire global oceans (Han et al., 1998, [190594](#); Nakajima et al., 2001, [190552](#); Wetzel and Stowe, 1999, [190636](#)). Using these correlations with estimates of aerosol increase from the pre-industrial era, estimates of anthropogenic aerosol indirect radiative forcing fall into the range of -0.7 to -1.7 W/m² (Nakajima et al., 2001, [190552](#)).

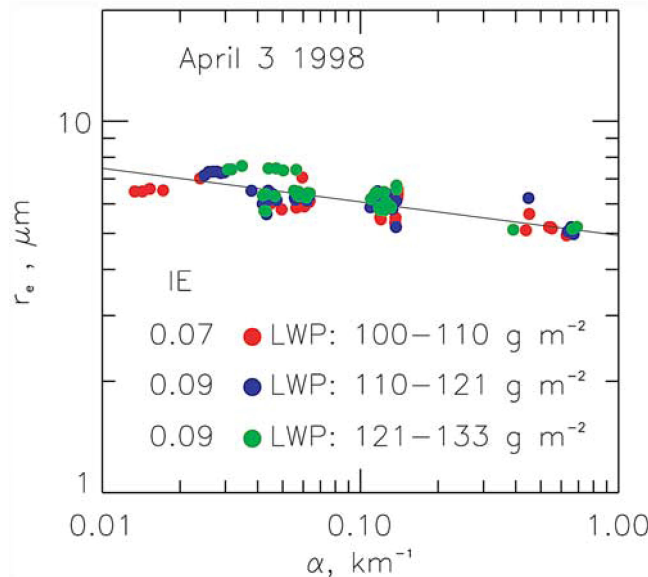
Introduction of the more modern instruments (POLDER and MODIS) has allowed more detailed observations of relationships between aerosol and cloud parameters. Cloud cover can both decrease and increase with increasing aerosol loading (Kaufman et al., 2005, [155891](#); Koren et al., 2004, [190187](#); Koren et al., 2005, [190188](#); Matheson et al., 2005, [190494](#); Sekiguchi et al., 2003, [190385](#); Yu et al., 2007, [093173](#)). The same is true of LWP (Han et al., 2002, [049181](#); Matsui et al., 2006, [190498](#)). Aerosol absorption appears to be an important factor in determining how cloud cover will respond to increased aerosol loading (Jiang and Feingold, 2006, [190976](#); Kaufman and Koren, 2006, [190951](#); Koren et al., 2008, [190193](#)). Different responses of cloud cover to increased aerosol could also be correlated with atmospheric thermodynamic and moisture structure (Yu et al., 2007, [093173](#)). Observations in the MODIS data show that aerosol loading correlates with enhanced convection and greater production of ice anvils in the summer Atlantic Ocean (Koren et al., 2005, [190188](#)), which conflicts with previous results that used AVHRR and could not isolate convective systems from shallow clouds (Sekiguchi et al., 2003, [190385](#)).

In recent years, surface-based remote sensing has also been applied to address aerosol effects on cloud microphysics. This method offers some interesting insights, and is complementary to the global satellite view. Surface remote sensing can only be applied at a limited number of locations, and therefore lacks the global satellite view. However, these surface stations yield high temporal resolution data and because they sample aerosol below, rather than adjacent to clouds they do not suffer from “cloud contamination.” With the appropriate instrumentation (lidar) they can measure the local aerosol entering the clouds, rather than a column-integrated aerosol optical depth. Under well-mixed conditions, surface in situ aerosol measurements can be used. Surface remote-sensing studies are discussed in more detail below, although the main science issues are common to satellite remote sensing.

Feingold et al. (2001, [190544](#)) used data collected at the ARM Southern Great Plains (SGP) site to allow simultaneous retrieval of aerosol and cloud properties. A combination of a Doppler cloud radar and a microwave radiometer was used to retrieve cloud drop effective radius r_e profiles in non-precipitating (radar reflectivity $Z < -17$ dBZ), ice-free clouds. Simultaneously, sub-cloud aerosol extinction profiles were measured with a lidar to quantify the response of drop sizes to changes in aerosol properties. Cloud data were binned according to liquid water path (LWP) as measured with a microwave radiometer, consistent with Twomey's (1977, [190533](#)) conceptual view of the aerosol impact on cloud microphysics. With high temporal/spatial resolution data (on the order of 20s or 100s of meters), realizations of aerosol-cloud interactions at the large eddy scale were obtained, and quantified in terms of the relative decrease in r_e in response to a relative increase in aerosol extinction ($d \ln r_e / d \ln$ extinction), as shown in Figure 9-70. Examining the dependence in this way reduces reliance on absolute measures of cloud and aerosol parameters and minimizes sensitivity to measurement error, provided errors are unbiased. This formulation permitted these responses to be related to cloud microphysical theory. Restricting the examination to updrafts only (as determined from the radar Doppler signal) permitted examination of the role of updraft in determining the response of r_e to changes in aerosol (via changes in drop number

concentration N_d). Analysis of data from 7 days showed that turbulence intensifies the aerosol impact on cloud microphysics.

In addition to radar/microwave radiometer retrievals of aerosol and cloud properties, measurements of cloud optical depth by surface based radiometers such as the MFRSR (Michalsky et al., 2001, [190537](#)) have been used in combination with measurements of cloud LWP by microwave radiometer to measure an average value of r_e during daylight when the solar elevation angle is sufficiently high (Min and Harrison, 1996, [190538](#)). Using this retrieval, Kim et al. (2003, [155899](#)) performed analyses of the r_e response to changes in aerosol at the same continental site, using a surface measurement of the aerosol light scattering coefficient instead of using extinction near cloud base as a proxy for CCN. Variance in LWP was shown to explain most of the variance in cloud optical depth, exacerbating detection of an aerosol effect. Although a decrease in r_e was observed with increasing scattering coefficient, the relation was not strong, indicative of other influences on r_e and/or decoupling between the surface and cloud layer. A similar study was conducted by Garrett et al. (2004, [190568](#)) at a location in the Arctic.



Source: Adapted with Permission of the American Geophysical Union from Feingold et al. (2003, [190551](#)).

Figure 9-70. Scatter plots showing mean cloud drop effective radius (r_e) versus aerosol extinction coefficient (unit: km^{-1}) for various liquid water path (LWP) bands on April 3, 1998 at ARM SGP site.

They suggested that summertime Arctic clouds are more sensitive to aerosol perturbations than clouds at lower latitudes. The advantage of the MFRSR/microwave radiometer combination is that it derives r_e from cloud optical depth and LWP and it is not as sensitive to large drops as the radar is. A limitation is that it can be applied only to clouds with extensive horizontal cover during daylight hours.

More recent data analyses by Feingold et al. (2003, [190551](#)), Kim et al. (2008, [130785](#)) and McComiskey et al. (2008, [190525](#)) at a variety of locations, and modeling work (Feingold, 2003, [190547](#)) have investigated (i) the use of different proxies for cloud condensation nuclei, such as the light scattering coefficient and aerosol index; (ii) sensitivity of cloud microphysical/optical properties to controlling factors such as aerosol size distribution, entrainment, LWP, and updraft velocity; (iii) the effect of optical- as opposed to radar-retrievals of drop size; and (iv) spatial heterogeneity. These studies have reinforced the importance of LWP and vertical velocity as controlling parameters. They have also begun to reconcile the reasons for the large discrepancies between various approaches, and platforms (satellite, aircraft in situ, and surface-based remote sensing). These investigations are important because satellite measurements that use a similar approach are being employed in GCMs to represent the albedo indirect effect (Quaas and Boucher, 2005, [190573](#)). In fact, the weakest albedo indirect effect in IPCC (2007, [092765](#)) derives from satellite measurements that have very weak responses of r_e to changes in aerosol. The relationship between these aerosol-cloud microphysical responses and cloud radiative forcing has been examined by

McComiskey and Feingold (2008, [190517](#)). They showed that for plane-parallel clouds, a typical uncertainty in the logarithmic gradient of a re-aerosol relationship of 0.05 results in a local forcing error of -3 to -10 W/m², depending on the aerosol perturbation. This sensitivity reinforces the importance of adequate quantification of aerosol effects on cloud microphysics to assessment of the radiative forcing, i.e., the indirect effect. Quantification of these effects from remote sensors is exacerbated by measurement errors. For example, LWP is measured to an accuracy of 25 g m⁻² at best, and since it is the thinnest clouds (i.e., low LWP) that are most susceptible (from a radiative forcing perspective) to changes in aerosol, this measurement uncertainty represents a significant uncertainty in whether the observed response is related to aerosol, or to differences in LWP. The accuracy and spatial resolution of satellite-based LWP measurements is much poorer and this represents a significant challenge. In some cases important measurements are simply absent, e.g., updraft is not measured from satellite-based remote sensors.

Finally, cloud radar data from CloudSat, along with the A-train aerosol data, is providing great opportunity for inferring aerosol effects on precipitation (e.g., Stephens and Haynes, 2007, [190413](#)). The aerosol effect on precipitation is far more complex than the albedo effect because the instantaneous view provided by satellites makes it difficult to establish causal relationships.

9.3.3.7. In Situ Studies of Aerosol-Cloud Interactions

In situ observations of aerosol effects on cloud microphysics date back to the 1950s and 1960s (Brennguier et al., 2000, [189966](#); Gunn and Phillips, 1957, [190595](#); Leaitch et al., 1992, [045270](#); Radke et al., 1989, [156034](#); Squires, 1958, [045608](#); Warner, 1968, [157114](#); Warner and Twomey, 1967, [045616](#); to name a few). These studies showed that high concentrations of CCN from anthropogenic sources, such as industrial pollution or the burning of sugarcane can increase cloud droplet number concentration Nd, thus increasing cloud microphysical stability and potentially reducing precipitation efficiency. As in the case of remote sensing studies, the causal link between aerosol perturbations and cloud microphysical responses (e.g., re or Nd) is much better established than the relationship between aerosol and changes in cloud fraction, LWC, and precipitation (see also Levin and Cotton, 2008, [190375](#)).

In situ cloud measurements are usually regarded as “ground truth” for satellite retrievals but in fact there is considerable uncertainty in measured parameters such liquid water content (LWC), and size distribution, which forms the basis of other calculations such as drop concentration, re and extinction. It is not uncommon to see discrepancies in LWC on the order of 50% between different instruments, and cloud drop size distributions are difficult to measure, particularly for droplets <10 μm where Mie scattering oscillations generate ambiguities in drop size. Measurement uncertainty in re from in situ probes is assessed, for horizontally homogeneous clouds, to be on the order of 15-20%, compared to 10% for MODIS and 15-20% for other spectral measurements (Feingold et al., 2003, [190551](#)). As with remote measurements it is prudent to consider relative (as opposed to absolute) changes in cloud microphysics related to relative changes in aerosol. An added consideration is that in situ measurements typically represent a very small sample of the atmosphere akin to a thin pencil line through a large volume. For an aircraft flying at 100 m/s and sampling at 1 Hz, the sample volume is on the order of 10 cm³. The larger spatial sampling of remote sensing has the advantage of being more representative but it removes small-scale (i.e., sub sampling volume) variability, and therefore, may obscure important cloud processes.

Measurements at a wide variety of locations around the world have shown that increases in aerosol concentration lead to increases in Nd. However the rate of this increase is highly variable and always sub-linear, as exemplified by the compilation of data in Ramanathan et al. (2001, [042681](#)). This is because, as discussed previously, Nd is a function of numerous parameters in addition to aerosol number concentration, including size distribution, updraft velocity (Leaitch et al., 1996, [190354](#)), and composition. In stratocumulus clouds, characterized by relatively low vertical velocity (and low supersaturation) only a small fraction of particles can be activated whereas in vigorous cumulus clouds that have high updraft velocities, a much larger fraction of aerosol particles is activated. Thus the ratio of Nd to aerosol particle number concentration is highly variable.

In recent years there has been a concerted effort to reconcile measured Nd concentrations with those calculated based on observed aerosol size and composition, as well as updraft velocity. These so-called “closure experiments” have demonstrated that on average, agreement in Nd between these approaches is on the order of 20% (Conant et al., 2004, [190010](#)). This provides confidence in theoretical understanding of droplet activation, however, measurement accuracy is not high enough to constrain the aerosol composition effects that have magnitudes <20%.

One exception to the rule that more aerosol particles result in larger Nd is the case of giant CCN (sizes on the order of a few microns), which, in concentrations on the order of 1 cm⁻³ (i.e., ~1% of the total concentration) can lead to significant suppression in cloud supersaturation and reductions in Nd (O'Dowd et al., 1999, [090414](#)). The measurement of these large particles is difficult and hence the importance of this effect is hard to assess. These same giant CCN, at concentrations as low as 1/liter, can significantly affect the initiation of precipitation in

moderately polluted clouds (Johnson, 1982, [190973](#)) and in so doing alter cloud albedo (Feingold et al., 1999, [190540](#)).

The most direct link between the remote sensing of aerosol-cloud interactions discussed in Section 9.3.3.6 and in situ observations is via observations of relationships between drop concentration N_d and CCN concentration. Theory shows that if re-CCN relationships are calculated at constant LWP or LWC, their logarithmic slope is $-1/3$ that of the N_d -CCN logarithmic slope (i.e., $d\ln r/d\ln \text{CCN} = -1/3 d\ln N_d/d\ln \text{CCN}$). In general, N_d -CCN slopes measured in situ tend to be stronger than equivalent slopes obtained from remote sensing – particularly in the case of satellite remote sensing (McComiskey and Feingold, 2008, [190517](#)). There are a number of reasons for this: (i) in situ measurements focus on smaller spatial scales and are more likely to observe the droplet activation process as opposed to remote sensing that incorporates larger spatial scales and includes other processes such as drop coalescence that reduce N_d , and therefore the slope of the N_d -CCN relationship (McComiskey et al., 2008, [190525](#)). (ii) Satellite remote sensing studies typically do not sort their data by LWP, and this has been shown to reduce the magnitude of the re-CCN response (Feingold, 2003, [190547](#)).

In conclusion, observational estimates of aerosol indirect radiative forcings are still in their infancy. Effects on cloud microphysics that result in cloud brightening have to be considered along with effects on cloud lifetime, cover, vertical development and ice production. For in situ measurements, aerosol effects on cloud microphysics are reasonably consistent (within $\sim 20\%$) with theory but measurement uncertainties in remote sensing of aerosol effects on clouds, as well as complexity associated with three-dimensional radiative transfer, result in considerable uncertainty in radiative forcing. The higher order indirect effects are poorly understood and even the sign of the microphysical response and forcing may not always be the same. Aerosol type and specifically the absorption properties of the aerosol may cause different cloud responses. Early estimates of observationally based aerosol indirect forcing range from -0.7 to -1.7 W/m^2 (Nakajima et al., 2001, [190552](#)) and -0.6 to -1.2 W/m^2 (Sekiguchi et al., 2003, [190385](#)), depending on the estimate for aerosol increase from pre-industrial times and whether aerosol effects on cloud fraction are also included in the estimate.

9.3.4. Outstanding Issues

Despite substantial progress, as summarized in Sections 9.3.2 and 9.3.3, most measurement-based studies so far have concentrated on influences produced by the sum of natural and anthropogenic aerosols on solar radiation under clear sky conditions. Important issues remain:

- Because accurate measurements of aerosol absorption are lacking and land surface reflection values are uncertain, DRF estimates over land and at the ocean surface are less well constrained than the estimate of TOA DRF over ocean.
- Current estimates of the anthropogenic component of aerosol direct radiative forcing have large uncertainties, especially over land.
- Because there are very few measurements of aerosol absorption vertical distribution, mainly from aircraft during field campaigns, estimates of direct radiative forcing of above-cloud aerosols and profiles of atmospheric radiative heating induced by aerosol absorption are poorly constrained.
- There is a need to quantify aerosol impacts on thermal infrared radiation, especially for dust.
- The diurnal cycle of aerosol direct radiative forcing cannot be adequately characterized with currently available, sun-synchronous, polar orbiting satellite measurements.
- Measuring aerosol, cloud, and ambient meteorology contributions to indirect radiative forcing remains a major challenge.
- Long-term aerosol trends and their relationship to observed surface solar radiation changes are not well understood.

The current status and prospects for these areas are briefly discussed below.

Measuring Aerosol Absorption and Single-Scattering Albedo

Currently, the accuracy of both in situ and remote sensing aerosol SSA measurements is generally ± 0.03 at best, which implies that the inferred accuracy of clear sky aerosol DRF would be larger than 1 W/m^2 (see Chapter 1 of the CSSP SAP2.3). Recently developed photoacoustic (Arnott et al., 1999, [020650](#)) and cavity ring down extinction cell (Strawa et al., 2002, [190421](#)) techniques for measuring aerosol absorption produce SSA with improved accuracy over previous methods. However, these methods are still experimental, and must be deployed on aircraft. Aerosol absorption retrievals from satellites using the UV-technique have large uncertainties associated with its sensitivity to the height of the aerosol layer(s) (Torres et al., 2005, [190507](#)), and it is unclear how the UV results can be extended to visible wavelengths. Views in and out of sunglint can be used to retrieve total aerosol extinction and scattering, respectively, thus constraining aerosol absorption over oceans (Kaufman et al., 2002, [190955](#)). However, this technique requires retrievals of aerosol scattering properties, including the real part of the refractive index, well beyond what has so far been demonstrated

from space. In summary, there is a need to pursue a better understanding of the uncertainty in SSA from both in situ measurements and remote sensing retrievals and, with this knowledge, to synthesize different data sets to yield a characterization of aerosol absorption with well-defined uncertainty (Leahy et al., 2007, [190232](#)). Laboratory studies of aerosol absorption of specific known composition are also needed to interpret in situ measurements and remote sensing retrievals and to provide updated database of particle absorbing properties for models.

Estimating the Aerosol Direct Radiative Forcing over Land

Land surface reflection is large, heterogeneous, and anisotropic, which complicates aerosol retrievals and DRF determination from satellites. Currently, the aerosol retrievals over land have relatively lower accuracy than those over ocean (Section 9.3.2.5) and satellite data are rarely used alone for estimating DRF over land (Section 9.3.3). Several issues need to be addressed, such as developing appropriate angular models for aerosols over land (Patadia et al., 2008, [190558](#)) and improving land surface reflectance characterization. MODIS and MISR measure land surface reflection wavelength dependence and angular distribution at high resolution (Martonchik et al., 1998, [190484](#); Martonchik et al., 2002, [190490](#); Moody et al., 2005, [190548](#)). This offers a promising opportunity for inferring the aerosol direct radiative forcing over land from satellite measurements of radiative fluxes (e.g., CERES) and from critical reflectance techniques (Fraser and Kaufman, 1985, [190567](#); Kaufman, 1987, [190960](#)). The aerosol direct radiative forcing over land depends strongly on aerosol absorption and improved measurements of aerosol absorption are required.

Distinguishing Anthropogenic from Natural Aerosols

Current estimates of anthropogenic components of AOD and direct radiative forcing have larger uncertainties than total aerosol optical depth and direct radiative forcing, particularly over land (see Section 9.3.3.4), because of relatively large uncertainties in the retrieved aerosol microphysical properties (see Section 9.3.2). Future measurements should focus on improved retrievals of such aerosol properties as size distribution, particle shape, and absorption, along with algorithm refinement for better aerosol optical depth retrievals. Coordinated in situ measurements offer a promising avenue for validating and refining satellite identification of anthropogenic aerosols (Anderson et al., 2005, [189993](#); 2005, [189991](#)). For satellite-based aerosol type characterization, it is sometimes assumed that all biomass-burning aerosol is anthropogenic and all dust aerosol is natural (Kaufman et al., 2005, [155891](#)). The better determination of anthropogenic aerosols requires a quantification of biomass burning ignited by lightning (natural origin) and mineral dust due to human induced changes of land cover/land use and climate (anthropogenic origin). Improved emissions inventories and better integration of satellite observations with models seem likely to reduce the uncertainties in aerosol source attribution.

Profiling the Vertical Distributions of Aerosols

Current aerosol profile data are far from adequate for quantifying the aerosol radiative forcing and atmospheric response to the forcing. The data have limited spatial and temporal coverage, even for current spaceborne lidar measurements. Retrieving aerosol extinction profile from lidar measured attenuated backscatter is subject to large uncertainties resulting from aerosol type characterization. Current space-borne Lidar measurements are also not sensitive to aerosol absorption. Because of lack of aerosol vertical distribution observations, the estimates of DRF in cloudy conditions and dust DRF in the thermal infrared remain highly uncertain (Lubin et al., 2002, [190463](#); Schulz et al., 2006, [190381](#); Sokolik et al., 2001, [190404](#)). It also remains challenging to constrain the aerosol-induced atmospheric heating rate increment that is essential for assessing atmospheric responses to the aerosol radiative forcing (e.g., Feingold et al., 2005, [190550](#); Lau et al., 2006, [190223](#); Yu et al., 2002, [190923](#)).

Progress in the foreseeable future is likely to come from (1) better use of existing, global, space-based backscatter lidar data to constrain model simulations, and (2) deployment of new instruments, such as high-spectral-resolution lidar (HSRL), capable of retrieving both extinction and backscatter from space. The HSRL lidar system will be deployed on the EarthCARE satellite mission tentatively scheduled for 2013 (http://asimov/esrin.esi.it/esaLP/ASESMYNW9SC_Lpearthcare_1.html).

Characterizing the Diurnal Cycle of Aerosol Direct Radiative Forcing

The diurnal variability of aerosol can be large, depending on location and aerosol type (Smirnov et al., 2002, [190398](#)), especially in wildfire situations, and in places where boundary layer aerosols hydrate or otherwise change significantly during the day. This cannot be captured by currently available, sun-synchronous, polar orbiting satellites. Geostationary satellites provide adequate time resolution (Christopher and Zhang, 2002, [190031](#); Wang et al., 2003, [157106](#)), but lack the information required to characterize aerosol types. Aerosol type information from low earth orbit satellites can help improve accuracy of geostationary satellite

aerosol retrievals (Costa et al., 2004, [190006](#); 2004, [192022](#)). For estimating the diurnal cycle of aerosol DRF, additional efforts are needed to adequately characterize the anisotropy of surface reflection (Yu et al., 2004, [190926](#)) and daytime variation of clouds.

Studying Aerosol-Cloud Interactions and Indirect Radiative Forcing

Remote sensing estimates of aerosol indirect forcing are still rare and uncertain. Improvements are needed for both aerosol characterization and measurements of cloud properties, precipitation, water vapor, and temperature profiles. Basic processes still need to be understood on regional and global scales. Remote sensing observations of aerosol-cloud interactions and aerosol indirect forcing are for the most part based on simple correlations among variables, from which cause-and-effects cannot be deduced. One difficulty in inferring aerosol effects on clouds from the observed relationships is separating aerosol from meteorological effects, as aerosol loading itself is often correlated with the meteorology. In addition, there are systematic errors and biases in satellite aerosol retrievals for partly cloud-filled scenes. Stratifying aerosol and cloud data by liquid water content, a key step in quantifying the albedo (or first) indirect effect, is usually missing. Future work will need to combine satellite observations with in situ validation and modeling interpretation. A methodology for integrating observations (in situ and remote) and models at the range of relevant temporal/spatial scales is crucial to improve understanding of aerosol indirect effects and aerosol-cloud interactions.

Quantifying Long-Term Trends of Aerosols at Regional Scales

Because secular changes are subtle and are superposed on seasonal and other natural variability, this requires the construction of consistent, multi-decadal records of climate-quality data. To be meaningful, aerosol trend analysis must be performed on a regional basis. Long-term trends of aerosol optical depth have been studied using measurements from surface remote sensing stations (e.g., Augustine et al., 2008, [189913](#); Hoyt and Frohlich, 1983, [190621](#); Luo et al., 2001, [190467](#)) and historic satellite sensors (Massie et al., 2004, [190492](#); Mishchenko and Geogdzhayev, 2007, [190545](#); Mishchenko et al., 2007, [190542](#); Zhao et al., 2008, [190935](#)). An emerging multiyear climatology of high quality AOD data from modern satellite sensors (e.g., Kahn et al., 2005, [190966](#); Remer et al., 2008, [190224](#)) has been used to examine the interannual variations of aerosol (e.g., Koren et al., 2007, [190189](#); Mishchenko and Geogdzhayev, 2007, [190545](#))

and contribute significantly to the study of aerosol trends. Current observational capability needs to be continued to avoid any data gaps. A synergy of aerosol products from historical, modern and future sensors is needed to construct as long a record as possible. Such a data synergy can build upon understanding and reconciliation of AOD differences among different sensors or platforms (Jeong et al., 2005, [190977](#)). This requires overlapping data records for multiple sensors. A close examination of relevant issues associated with individual sensors is urgently needed, including sensor calibration, algorithm assumptions, cloud screening, data sampling and aggregation, among others.

Linking Aerosol Long-Term Trends with Changes of Surface Solar Radiation

Analysis of the long-term surface solar radiation record suggests significant trends during past decades (e.g., Alpert et al., 2005, [190047](#); Pinker et al., 2005, [190569](#); Stanhill and Cohen, 2001, [042121](#); Wild et al., 2005, [156156](#)). Although a significant and widespread decline in surface total solar radiation (the sum of direct and diffuse irradiance) occurred up to 1990 (so-called solar dimming), a sustained increase has been observed during the subsequent decade. Speculation suggests that such trends result from decadal changes of aerosols and the interplay of aerosol direct and indirect radiative forcing (Norris and Wild, 2007, [190555](#); Ruckstuhl et al., 2008, [190356](#); Stanhill and Cohen, 2001, [042121](#); Streets et al., 2006, [190425](#); Wild et al., 2005, [156156](#)). However, reliable observations of aerosol trends are required to test these ideas. In addition to aerosol optical depth, changes in aerosol composition must also be quantified, to account for changing industrial practices, environmental regulations, and biomass burning emissions (Novakov et al., 2003, [048398](#); Streets and Aunan, 2005, [156106](#); Streets et al., 2004, [190423](#)). Such compositional changes will affect the aerosol SSA and size distribution, which in turn will affect the surface solar radiation (e.g., Qian et al., 2007, [190572](#)). However, such data are currently rare and subject to large uncertainties. Finally, a better understanding of aerosol-radiation-cloud interactions and trends in cloudiness, cloud albedo, and surface albedo is badly needed to attribute the observed radiation changes to aerosol changes with less ambiguity.

9.3.5. Concluding Remarks

Since the concept of aerosol-radiation-climate interactions was first proposed around 1970, substantial progress has been made in determining the mechanisms and magnitudes of

these interactions, particularly in the last 10 years. Such progress has greatly benefited from significant improvements in aerosol measurements and increasing sophistication of model simulations. As a result, knowledge of aerosol properties and their interaction with solar radiation on regional and global scales is much improved. Such progress plays a unique role in the definitive assessment of the global anthropogenic radiative forcing, as “virtually certainly positive” in IPCC AR4 (Haywood and Schulz, 2007, [190600](#)).

In Situ Measurements of Aerosols

New in situ instruments such as aerosol mass spectrometers, photoacoustic techniques, and cavity ring down cells provide high accuracy and fast time resolution measurements of aerosol chemical and optical properties. Numerous focused field campaigns and the emerging ground-based aerosol networks are improving regional aerosol chemical, microphysical, and radiative property characterization. Aerosol closure studies of different measurements indicate that measurements of submicrometer, spherical sulfate and carbonaceous particles have a much better accuracy than that for dust-dominated aerosol. The accumulated comprehensive data sets of regional aerosol properties provide a rigorous “test bed” and strong constraint for satellite retrievals and model simulations of aerosols and their direct radiative forcing.

Remote Sensing Measurements of Aerosols

Surface networks, covering various aerosol regimes around the globe, have been measuring aerosol optical depth with an accuracy of 0.01~0.02, which is adequate for achieving the accuracy of 1 W/m² for cloud-free TOA DRF. On the other hand, aerosol microphysical properties retrieved from these networks, especially SSA, have relatively large uncertainties and are only available in very limited conditions. Current satellite sensors can measure AOD with an accuracy of about 0.05 or 15-20% in most cases. The implementation of multi-wavelength, multi-angle, and polarization measuring capabilities has also made it possible to measure particle properties (size, shape, and absorption) that are essential for characterizing aerosol type and estimating anthropogenic component of aerosols. However, these microphysical measurements are more uncertain than AOD measurements.

Observational Estimates of Clear-Sky Aerosol Direct Radiative Forcing

Closure studies based on focused field experiments reveal DRF uncertainties of about 25% for sulfate/carbonaceous aerosol and 60% for dust at regional scales. The high-accuracy of MODIS, MISR and POLDER aerosol products and broadband flux measurements from CERES make it feasible to obtain observational constraints for aerosol TOA DRF at a global scale, with relaxed requirements for measuring particle microphysical properties. Major conclusions from the assessment are:

- A number of satellite-based approaches consistently estimate the clear-sky diurnally averaged TOA DRF (on solar radiation) to be about -5.5 ± 0.2 W/m² (mean \pm standard error from various methods) over global ocean. At the ocean surface, the diurnally averaged DRF is estimated to be -8.7 ± 0.7 W/m². These values are calculated for the difference between today’s measured total aerosol (natural plus anthropogenic) and the absence of all aerosol.
- Overall, in comparison to that over ocean, the DRF estimates over land are more poorly constrained by observations and have larger uncertainties. A few satellite retrieval and satellite-model integration yield the overland clear-sky diurnally averaged DRF of -4.9 ± 0.7 W/m² and -11.8 ± 1.9 W/m² at the TOA and surface, respectively. These values over land are calculated for the difference between total aerosol and the complete absence of all aerosol.
- Use of satellite measurements of aerosol microphysical properties yields that on a global ocean average, about 20% of AOD is contributed by human activities and the clear-sky TOA DRF by anthropogenic aerosols is -1.1 ± 0.4 W/m². Similar DRF estimates are rare over land, but a few measurement-model integrated studies do suggest much more negative DRF over land than over ocean.
- These satellite-based DRF estimates are much greater than the model-based estimates, with differences much larger at regional scales than at a global scale.

Measurements of Aerosol-Cloud Interactions and Indirect Radiative Forcing

In situ measurement of cloud properties and aerosol effects on cloud microphysics suggest that theoretical understanding of the activation process for water cloud is reasonably well-understood. Remote sensing of aerosol effects on droplet size associated with the albedo effect tends to underestimate the magnitude of the response compared to in situ measurements. Recent efforts trace this to a combination of lack of stratification of data by cloud water, the relatively large spatial scale over which measurements are averaged (which includes variability in cloud fields, and processes that obscure the aerosol-cloud processes), as well as measurement uncertainties (particularly in broken cloud fields). It remains a major challenge

to infer aerosol number concentrations from satellite measurements. The present state of knowledge of the nature and abundance of IN, and ice formation in clouds is extremely poor.

Despite the substantial progress in recent decades, several important issues remain, such as measurements of aerosol size distribution, particle shape, absorption, and vertical profiles, and the detection of aerosol long-term trend and establishment of its connection with the observed trends of solar radiation reaching the surface, as discussed in Section 9.3.4. Furthering the understanding of aerosol impacts on climate requires a coordinated research strategy to improve the measurement accuracy and use the measurements to validate and effectively constrain model simulations. Concepts of future research in measurements are discussed in Chapter 4 “Way Forward” (of the CCSP SAP2.3).

9.3.6. Modeling the Effect of Aerosols on Climate

9.3.6.1. Introduction

The IPCC Fourth Assessment Report (AR4) (IPCC, 2007, [092765](#)) concludes that man’s influence on the warming climate is in the category of “very likely”. This conclusion is based on, among other things, the ability of models to simulate the global and, to some extent, regional variations of temperature over the past 50-100 years. When anthropogenic effects are included, the simulations can reproduce the observed warming (primarily for the past 50 years); when they are not, the models do not get very much warming at all. In fact, all of the models runs for the IPCC AR4 assessment (more than 20) produce this distinctive result, driven by the greenhouse gas increases that have been observed to occur.

These results were produced in models whose average global warming associated with a doubled CO₂ forcing of 4 W/m² was about 3°C. This translates into a climate sensitivity (surface temperature change per forcing) of about 0.75°C/(W/m²). The determination of climate sensitivity is crucial to projecting the future impact of increased greenhouse gases, and the credibility of this projected value relies on the ability of these models to simulate the observed temperature changes over the past century. However, in producing the observed temperature trend in the past, the models made use of very uncertain aerosol forcing. The greenhouse gas change by itself produces warming in models that exceeds that observed by some 40% on average (IPCC, 2007, [092765](#)). Cooling associated with aerosols reduces this warming to the observed level. Different climate models use differing aerosol forcings, both direct (aerosol scattering and absorption of short and longwave radiation) and indirect (aerosol effect on cloud cover reflectivity and lifetime), whose magnitudes vary markedly from one model to the next. Kiehl (2007, [190949](#)) using nine of the IPCC (2007, [092765](#)) AR4 climate models found that they had a factor of three forcing differences in the aerosol contribution for the 20th century. The differing aerosol forcing is the prime reason why models whose climate sensitivity varies by almost a factor of three can produce the observed trend. It was thus concluded that the uncertainty in IPCC (2007, [092765](#)) anthropogenic climate simulations for the past century should really be much greater than stated (Kerr, 2007, [190950](#); Schwartz et al., 2007, [190384](#)), since, in general, models with low/high sensitivity to greenhouse warming used weaker/stronger aerosol cooling to obtain the same temperature response (Kiehl, 2007, [190949](#)). Had the situation been reversed and the low/high sensitivity models used strong/weak aerosol forcing, there would have been a greater divergence in model simulations of the past century.



Figure 9-71. Sampling the Arctic Haze. Pollution and smoke aerosols can travel long distances, from mid-latitudes to the Arctic, causing “Arctic Haze.” Photo taken from the NASA DC-8 aircraft during the ARCTAS field experiment over Alaska in April 2008. Credit: Mian Chin, NASA.

Therefore, the fact that a model has accurately reproduced the global temperature change in the past does not imply that its future forecast is accurate. This state of affairs will remain until a firmer estimate of radiative forcing (RF) by aerosols, in addition to that by greenhouse gases, is available.

Two different approaches are used to assess the aerosol effect on climate. “Forward modeling” studies incorporate different aerosol types and attempt to explicitly calculate the aerosol RF. From this approach, IPCC (2007, [092765](#)) concluded that the best estimate of the global aerosol direct RF (compared with preindustrial times) is -0.5 (-0.9 to -0.1) W/m^2 . The RF due to the cloud albedo or brightness effect (also referred to as first indirect or Twomey effect) is estimated to be -0.7 (-1.8 to -0.3) W/m^2 . No estimate was specified for the effect associated with cloud lifetime. The total negative RF due to aerosols according to IPCC (2007, [092765](#)) estimates is then -1.3 (-2.2 to -0.5) W/m^2 . In comparison, the positive radiative forcing (RF) from greenhouse gases (including tropospheric ozone) is estimated to be $+2.9 \pm 0.3$ W/m^2 ; hence tropospheric aerosols reduce the influence from greenhouse gases by about 45% (15-85%). This approach however inherits large uncertainties in aerosol amount, composition, and physical and optical properties in modeling of atmospheric aerosols. The consequences of these uncertainties are discussed in the next section.

The other method of calculating aerosol forcing is called the “inverse approach” – it is assumed that the observed climate change is primarily the result of the known climate forcing contributions. If one further assumes a particular climate sensitivity (or a range of sensitivities), one can determine what the total forcing had to be to produce the observed temperature change. The aerosol forcing is then deduced as a residual after subtraction of the greenhouse gas forcing along with other known forcings from the total value. Studies of this nature come up with aerosol forcing ranges of -0.6 to -1.7 W/m^2 (Knutti et al., 2002, [190178](#);

Knutti et al., 2003, [190180](#)); IPCC AR4 Chap.9); -0.4 to -1.6 W/m² (Gregory et al., 2002, [190593](#)); and -0.4 to -1.4 W/m² (Stott, 2006, [190419](#)). This approach however provides a bracket of the possible range of aerosol forcing without the assessment of current knowledge of the complexity of atmospheric aerosols.

This chapter of the CCSP SAP2.3 reviews the current state of aerosol RF in the global models and assesses the uncertainties in these calculations. First representation of aerosols in the forward global chemistry and transport models and the diversity of the model simulated aerosol fields are discussed; then calculation of the aerosol direct and indirect effects in the climate models is reviewed; finally the impacts of aerosols on climate model simulations and their implications are assessed.

9.3.6.2. Modeling of Atmospheric Aerosols

The global aerosol modeling capability has developed rapidly in the past decade. In the late 1990s, there were only a few global models that were able to simulate one or two aerosol components, but now there are a few dozen global models that simulate a comprehensive suite of aerosols in the atmosphere. As introduced in Chapter 1 (of the CCSP SAP2.3), aerosols consist of a variety of species including dust, sea salt, sulfate, nitrate, and carbonaceous aerosols (black and organic carbon) produced from natural and man-made sources with a wide range of physical and optical properties. Because of the complexity of the processes and composition, and highly inhomogeneous distribution of aerosols, accurately modeling atmospheric aerosols and their effects remains a challenge. Models have to take into account not only the aerosol and precursor emissions, but also the chemical transformation, transport, and removal processes (e.g., dry and wet depositions) to simulate the aerosol mass concentrations. Furthermore, aerosol particle size can grow in the atmosphere because the ambient water vapor can condense on the aerosol particles. This “swelling” process, called hygroscopic growth, is most commonly parameterized in the models as a function of relative humidity.

Estimates of Emissions

Aerosols have various sources from both natural and anthropogenic processes. Natural emissions include wind-blown mineral dust, aerosol and precursor gases from volcanic eruptions, natural wild fires, vegetation, and oceans. Anthropogenic sources include emissions from fossil fuel and biofuel combustion, industrial processes, agriculture practices, and human-induced biomass burning.

Following earlier attempts to quantify manmade primary emissions of aerosols (Penner et al., 1993, [045457](#); Turco et al., 1983, [190529](#)) systematic work was undertaken in the late 1990s to calculate emissions of black carbon (BC) and organic carbon (OC), using fuel-use data and measured emission factors (Cooke and Wilson, 1996, [190046](#); Cooke et al., 1999, [156365](#); Lioussé et al., 1996, [078158](#)). The work was extended in greater detail and with improved attention to source-specific emission factors in Bond et al. (2004, [056389](#)), which provides global inventories of BC and OC for the year 1996, with regional and source-category discrimination that includes contributions from industrial, transportation, residential solid-fuel combustion, vegetation and open biomass burning (forest fires, agricultural waste burning, etc.), and diesel vehicles.

Emissions from natural sources—which include wind-blown mineral dust, wildfires, sea salt, and volcanic eruptions—are less well quantified, mainly because of the difficulties of measuring emission rates in the field and the unpredictable nature of the events. Often, emissions must be inferred from ambient observations at some distance from the actual source. As an example, it was concluded (Lewis and Schwartz, 2004, [192023](#)) that available information on size-dependent sea salt production rates could only provide order-of-magnitude estimates. The natural emissions in general can vary dramatically over space and time.

Aerosols can be produced from trace gases in the atmosphere via chemical reactions, and those aerosols are called secondary aerosols, as distinct from primary aerosols that are directly emitted to the atmosphere as aerosol particles. For example, most sulfate and nitrate aerosols are secondary aerosols that are formed from their precursor gases, sulfur dioxide (SO₂) and nitrogen oxides (NO and NO₂, collectively called NO_x), respectively. Those sources have been studied for many years and are relatively well known. By contrast, the sources of secondary organic aerosols (SOA) are poorly understood, including emissions of their precursor gases (called volatile organic compounds, VOC) from both natural and anthropogenic sources and the atmospheric production processes.

Globally, sea salt and mineral dust dominate the total aerosol mass emissions because of the large source areas and/or large particle sizes. However, sea salt and dust also have shorter atmospheric lifetimes because of their large particle size, and are radiatively less active than aerosols with small particle size, such as sulfate, nitrate, BC, and particulate organic matter (POM, which includes both carbon and non-carbon mass in the organic aerosol), most of which are anthropogenic in origin.

Because the anthropogenic aerosol RF is usually evaluated (e.g., by the IPCC) as the anthropogenic perturbation since the pre-industrial period, it is necessary to estimate the

historical emission trends, especially the emissions in the pre-industrial era. Compared to estimates of present-day emissions, estimates of historical emission have much larger uncertainties. Information for past years on the source types and strengths and even locations are difficult to obtain, so historical inventories from preindustrial times to the present have to be based on limited knowledge and data. Several studies on historical emission inventories of BC and OC (e.g., Bond et al., 2007, [190050](#); Fernandes et al., 2007, [190554](#); Ito and Penne, 2005, [190626](#); Junker and Liousse, 2008, [190971](#); Novakov et al., 2003, [048398](#)), SO₂ (Stern, 2005, [190416](#)), and various species (Dentener et al., 2006, [088434](#); Van Aardenne et al., 2001, [055564](#)) are available in the literature; there are some similarities and some differences among them, but the emission estimates for early times do not have the rigor of the studies for present-day emissions. One major conclusion from all these studies is that the growth of primary aerosol emissions in the 20th century was not nearly as rapid as the growth in CO₂ emissions. This is because in the late 19th and early 20th centuries, particle emissions such as BC and POM were relatively high due to the heavy use of biofuels and the lack of particulate controls on coal-burning facilities; however, as economic development continued, traditional biofuel use remained fairly constant and particulate emissions from coal burning were reduced by the application of technological controls (Bond et al., 2007, [190050](#)). Thus, particle emissions in the 20th century did not grow as fast as CO₂ emissions, as the latter are roughly proportional to total fuel use—oil and gas included. Another challenge is estimating historical biomass burning emissions. A recent study suggested about a 40% increase in carbon emissions from biomass burning from the beginning to the end of last century (Mouillot et al., 2006, [190549](#)), but it is difficult to verify.

Table 9-11. Anthropogenic emissions of aerosols and precursors for 2000 and 1750.

Source	Species*	Emission [#] 2000 (Tg/yr)	Emission 1750 (Tg/yr)
Biomass burning	BC	3.1	1.03
	POM	34.7	12.8
	S	4.1	1.46
Biofuel	BC	9.1	0.39
	POM	9.6	1.56
	S		0.12
Fossil fuel	BC	3.0	
	POM	3.2	
	S	98.9	

Data source for 2000 emission: biomass burning – Global Fire Emission Dataset (GFED); biofuel BC and POM – Speciated Pollutant Emission Wizard (SPEW); biofuel sulfur – International Institute for Applied System Analysis (IIASA); fossil fuel BC and POM – SPEW; fossil fuel sulfur – Emission Database for Global Atmospheric Research (EDGAR) and IIASA. Fossil fuel emission of sulfur (S) is the sum of emission from industry, power plants, and transportation listed in Dentener et al. (2006, [088434](#)).

* S=sulfur, including SO₂ and particulate SO₄²⁻. Most emitted as SO₂, and 2.5% emitted as SO₄²⁻.

Source: Adapted from Dentener et al. (2006, [088434](#))

As an example, Table 9-11 shows estimated anthropogenic emissions of sulfur, BC and POM in the present day (year 2000) and pre-industrial time (1750) compiled by Dentener et al. (2006, [088434](#)). These estimates have been used in the Aerosol Comparisons between Observations and Models (AeroCom) project (Experiment B, which uses the year 2000 emission; and Experiment PRE, which uses pre-industrial emissions), for simulating atmospheric aerosols and anthropogenic aerosol RF. The AeroCom results are discussed below and in Section 9.3.6.3.

Aerosol Mass Loading and Optical Depth

In the global models, aerosols are usually simulated in the successive steps of sources (emission and chemical formation), transport (from source location to other area), and removal processes (dry deposition, in which particles fall onto the surface, and wet deposition by rain) that control the aerosol lifetime. Collectively, emission, transport, and removal determine the amount (mass) of aerosols in the atmosphere. Aerosol optical depth (AOD), which is a measure of solar or thermal radiation being attenuated by aerosol particles via scattering or absorption, can be related to the atmospheric aerosol mass loading as follows:

$$\text{AOD} = \text{MEE} \bullet \text{M}$$

Equation 9-3

where M is the aerosol mass loading per unit area (g m^{-2}), MEE is the mass extinction efficiency or specific extinction in unit of m^2/g , which is

$$\text{MEE} = \frac{3Q_{\text{ext}}}{4\pi r_{\text{eff}}^2} \bullet f$$

Equation 9-4

where Q_{ext} is the extinction coefficient (a function of particle size distribution and refractive index), r_{eff} is the aerosol particle effective radius, ρ is the aerosol particle density, and f is the ratio of ambient aerosol mass (wet) to dry aerosol mass M . Here, M is the result from model-simulated atmospheric processes and MEE embodies the aerosol physical (including microphysical) and optical properties. Since Q_{ext} varies with radiation wavelength, so do MEE and AOD. AOD is the quantity that is most commonly obtained from remote sensing measurements and is frequently used for model evaluation (see Chapter 2 of the CCSP SAP2.3). AOD is also a key parameter determining aerosol radiative effects.

Here the results from the recent multiple global-model studies by the AeroCom project are summarized, as they represent the current assessment of model-simulated atmospheric aerosol loading, optical properties, and RF for the present-day. AeroCom aims to document differences in global aerosol models and compare the model output to observations. Sixteen global models participated in the AeroCom Experiment A (AeroCom-A), for which every model used their own configuration, including their own choice of estimating emissions (Kinne et al., 2006, [155903](#); Textor et al., 2006, [190456](#)). Five major aerosol types: sulfate, BC, POM, dust, and sea salt, were included in the experiments, although some models had additional aerosol species. Of those major aerosol types, dust and sea-salt are predominantly natural in origin, whereas sulfate, BC, and POM have major anthropogenic sources.

Table 9-12 summarizes the model results from the AeroCom-A for several key parameters: Sources (emission and chemical transformation), mass loading, lifetime, removal rates, and MEE and AOD at a commonly used, mid-visible, wavelength of 550 nanometer (nm). These are the globally averaged values for the year 2000. Major features and conclusions are:

- Globally, aerosol source (in mass) is dominated by sea salt, followed by dust, sulfate, POM, and BC. Over the non-desert land area, human activity is the major source of sulfate, black carbon, and organic aerosols.
- Aerosols are removed from the atmosphere by wet and dry deposition. Although sea salt dominates the emissions, it is quickly removed from the atmosphere because of its large particle size and near-surface distributions, thus having the shortest lifetime. The median lifetime of sea salt from the AeroCom-A models is less than half a day, whereas dust and sulfate have similar lifetimes of 4 days and BC and POM 6-7 days.
- Globally, small-particle-sized sulfate, BC, and POM make up a little over 10% of total aerosol mass in the atmosphere. However, they are mainly from anthropogenic activity, so the highest concentrations are in the most populated regions, where their effects on climate and air quality are major concerns.
- Sulfate and BC have their highest MEE at mid-visible wavelengths, whereas dust is lowest among the aerosol types modeled. That means for the same amount of aerosol mass, sulfate and BC are more effective at attenuating (scattering or absorbing) solar radiation than dust. This is why the sulfate AOD is about the same as dust AOD even though the atmospheric amount of sulfate mass is 10 times less than that of the dust.
- There are large differences, or diversities, among the models for all the parameters listed in Table 9-12. The largest model diversity, shown as the % standard deviation from the all-model-mean and the range (minimum and maximum values) in Table 9-12, is in sea salt emission and removal; this is mainly associated with the differences in particle size range and source parameterizations in each model. The diversity of sea salt atmospheric loading however is much smaller than that of sources or sinks, because the largest particles have the shortest lifetimes even though they comprise the largest fraction of emitted and deposited mass.

Table 9-12. Summary of statistics of AeroCom Experiment A results from 16 global models.

Quantity	Mean	Median	Range	Stddev/mean*
SOURCES (TG/YR)				
SO ₄ ^{z-}	179	186	98-232	22%
BC	11.9	11.3	7.8-19.4	23%
Organic matter	96.6	96.0	53-138	26%
Dust	1840	1640	672-4040	49%
Sea salt	16600	6280	2180-121000	199%
REMOVAL RATE (DAY-)				
SO ₄ ^{z-}	0.25	0.24	0.19-0.39	18%
BC	0.15	0.15	0.066-0.19	21%
Organic matter	0.16	0.16	0.09-0.23	24%
Dust	0.31	0.25	0.14-0.79	62%
Sea salt	5.07	2.50	0.95-35.0	188%
LIFETIME (DAY)				
SO ₄ ^{z-}	4.12	4.13	2.6-5.4	18%
BC	7.12	6.54	5.3-15	33%
Organic matter	6.54	6.16	4.3-11	27%
Dust	4.14	4.04	1.3-7.0	43%
Sea salt	0.48	0.41	0.03-1.1	58%
MASS LOADING (TG)				
SO ₄ ^{z-}	1.99	1.98	0.92-2.70	25%
BC	0.24	0.21	0.046-0.51	42%
Organic matter	1.70	1.76	0.46-2.56	27%
Dust	19.2	20.5	4.5-29.5	40%
Sea salt	7.52	6.37	2.5-13.2	54%
MEE AT 550 NM (M2G-1)				
SO ₄ ^{z-}	11.3	9.5	4.2-28.3	56%
BC	9.4	9.2	5.3-18.9	36%
Organic matter	5.7	5.7	3.7-9.1	26%
Dust	0.99	0.95	0.46-2.05	45%
Sea salt	3.0	3.1	0.97-7.5	55%
AOD AT 550 NM				
SO ₄ ^{z-}	0.035	0.034	0.015-0.051	33%
BC	0.004	0.004	0.002-0.009	46%
Organic matter	0.018	0.019	0.006-0.030	36%
Dust	0.032	0.033	0.012-0.054	44%
Sea salt	0.033	0.030	0.02-0.067	42%
TOTAL AOT AT 550 NM	0.124	0.127	0.056-0.151	18%

Stddev/mean was used as the term "diversity" in Textor et al. (2006, [190456](#)).

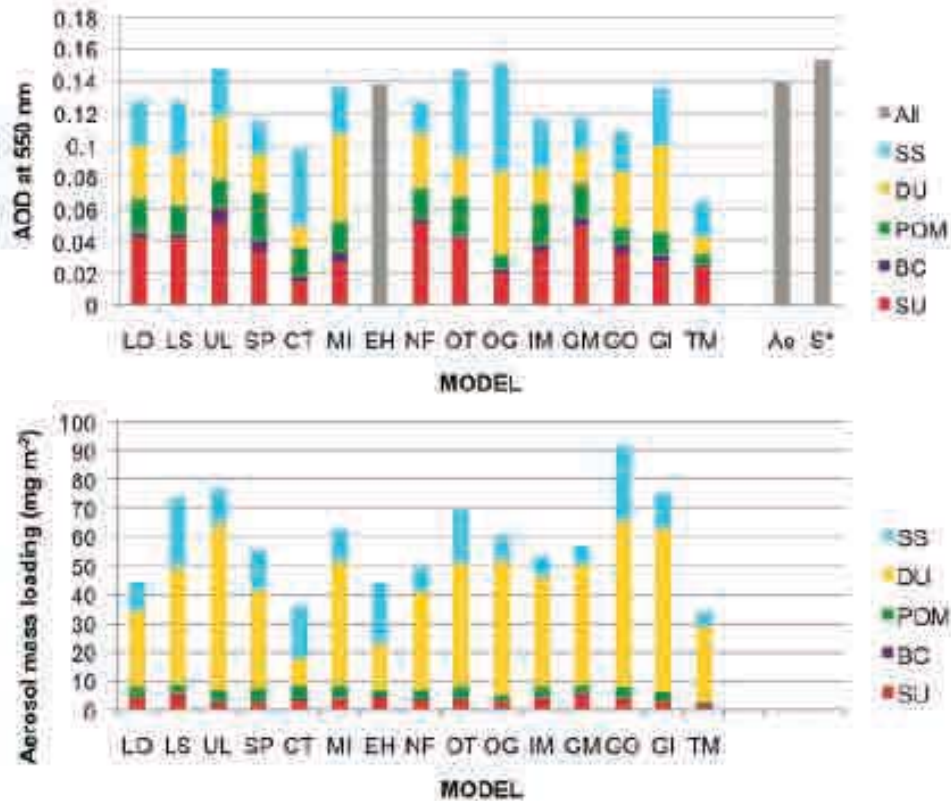
Source: Textor et al. (2006, [190456](#)) and Kinne et al. (2006, [155903](#)), and AeroCom website <http://nansen.ipsl.jussieu.fr/AEROCOM/data.html>

- Among the key parameters compared in Table 9-12, the models agree best for simulated total AOD – the % of standard deviation from the model mean is 18%, with the extreme values just a factor of 2 apart. The median value of the multi-model simulated global annual mean total AOD, 0.127, is also in agreement with the global mean values from recent satellite measurements. However, despite the general agreement in total AOD, there are significant diversities at the individual component level for aerosol optical thickness, mass loading, and mass extinction efficiency. This indicates that uncertainties in assessing aerosol climate forcing are still large, and they depend not only on total AOD but also on aerosol absorption and scattering direction (called asymmetry factor), both of which are determined by aerosol physical and optical properties. In addition, even with large differences in mass loading and MEE among different models, these terms could compensate for each other (Equation 9-3) to produce similar AOD. This is illustrated in Figure 9-72. For example, model LO and LS have quite different mass loading (44 and 74 mg m⁻², respectively), especially for dust and sea salt amount, but they produce nearly identical total AOD (0.127 and 0.128, respectively).
- Because of the large spatial and temporal variations of aerosol distributions, regional and seasonal diversities are even larger than the diversity for global annual means.

To further isolate the impact of the differences in emissions on the diversity of simulated aerosol mass loading, identical emissions for aerosols and their precursor were used in the AeroCom Experiment B exercise in which 12 of the 16 AeroCom-A models participated (Textor et al., 2007, [190458](#)). The comparison of the results and diversity between AeroCom-A and -B for the same models showed that using harmonized emissions does not significantly reduce model diversity for the simulated global mass and AOD fields, indicating that the differences in atmospheric processes, such as transport, removal, chemistry, and aerosol microphysics, play more important roles than emission in creating diversity among the models. This outcome is somewhat different from another recent study, in which the differences in calculated clear-sky aerosol RF between two models (a regional model STEM and a global model MOZART) were attributed mostly to the differences in emissions (Bates et al., 2006, [189912](#)), although the conclusion was based on only two model simulations for a few focused regions. It is highly recommended from the outcome of AeroCom-A and -B that, although more detailed evaluation for each individual process is needed, multi-model ensemble results, e.g., median values of multi-model output variables, should be used to estimate aerosol RF, due to their greater robustness, relative to individual models, when compared to observations (Schulz et al., 2006, [190381](#); Textor et al., 2006, [190456](#); Textor et al., 2007, [190458](#)).

9.3.6.3. Calculating Aerosol Direct Radiative Forcing

The three parameters that define the aerosol direct RF are the AOD, the single scattering albedo (SSA), and the asymmetry factor (g), all of which are wavelength dependent. AOD is indicative of how much aerosol exists in the column, SSA is the fraction of radiation being scattered versus the total attenuation (scattered and absorbed), and the g relates to the direction of scattering that is related to the size of the particles (see Chapter 1 of the CCSP SAP2.3). An indication of the particle size is provided by another parameter, the Ångström exponent (Å), which is a measure of differences of AOD at different wavelengths. For typical tropospheric aerosols, Å tends to be inversely dependent on particle size; larger values of Å are generally associated with smaller aerosols particles. These parameters are further related; for example, for a given composition, the ability of a particle to scatter radiation decreases more rapidly with decreasing size than does its ability to absorb, so at a given wavelength varying Å can change SSA. Note that AOD, SSA, g , Å , and all the other parameters in Equation 9-3 and Equation 9-4 vary with space and time due to variations of both aerosol composition and relative humidity, which influence these characteristics.



Source: Adapted from Kinne et al. (2006, [155903](#))

Figure 9-72. Global annual averaged AOD (upper panel) and aerosol mass loading (lower panel) with their components simulated by 15 models in AeroCom- A (excluding one model which only reported mass). SU=SO₄²⁻, BC=black carbon, POM=particulate OC, DU=dust, SS=sea salt. Model abbreviations: LO=LOA (Lille, Fra), LS=LSCE (Paris, Fra), UL=ULAQ (L'Aquila, Ita), SP=SPRINTARS (Kyushu, Jap), CT=ARQM (Toronto, Can), MI=MIRAGE (Richland, USA), EH=ECHAM5 (MPI-Hamburg, Ger), NF=CCM-Match (NCAR Boulder, USA), OT=Oslo-CTM (Oslo, Nor), OG=OLSO-GCM (Oslo, Nor) [prescribed background for DU and SS], IM=IMPACT (Michigan, USA), GM=GFDL Mozart (Princeton, NJ, USA), GO=GOCART (NASA-GSFC, Washington DC, USA), GI=GISS (NASA-GISS, New York, USA), TM=TM5 (Utrecht, Net). Also shown in the upper panel are the averaged observation data from AERONET (Ae) and the satellite composite (S*).

In the recent AeroCom project, aerosol direct RF for the solar spectral wavelengths (or shortwave) was assessed based on the 9 models that participated in both Experiment B and PRE in which identical, prescribed emissions for present (year 2000) and pre-industrial time (year 1750) listed in Table 9-11 were used across the models (Schulz et al., 2006, [190381](#)). The anthropogenic direct RF was obtained by subtracting Aero-Com-PRE from AeroCom-B simulated results. Because dust and sea salt are predominantly from natural sources, they were not included in the anthropogenic RF assessment although the land use practice can contribute to dust emissions as “anthropogenic”. Other aerosols that were not considered in the AeroCom forcing assessment were natural sulfate (e.g., from volcanoes or ocean) and POM (e.g., from biogenic hydrocarbon oxidation), as well as nitrate. The aerosol direct forcing in the AeroCom assessment thus comprises three major anthropogenic aerosol components sulfate, BC, and POM.

Table 9-13. SO₄²⁻ mass loading, MEE and AOD at 550 nm, shortwave radiative forcing at the top of the atmosphere, and normalized forcing with respect to AOD and mass. All values refer to anthropogenic perturbation.

Model	Mass load (mg m ⁻²)	MEE (m ² g ⁻¹)	AOD at 550 nm	TOA Forcing (W/m ²)	Forcing/AOD (W/m ²)	Forcing/Mass (W g ⁻¹)
PUBLISHED SINCE IPCC 2001						
A CCM3	2.23			-0.56		-251
B GEOSCHEM	1.53	11.8	0.018	-0.33	-18	-216
C GISS	3.30	6.7	0.022	-0.65	-30	-197
D GISS	3.27			-0.96		-294
E GISS*	2.12			-0.57		-269
F SPRINTARS	1.55	9.7	0.015	-0.21		-135
G LMD	2.76			-0.42		-152
H LOA	3.03	9.9	0.03	-0.41	-14	-135
I GATORG	3.06			-0.32		-105
J PNNL	5.50	7.6	0.042	-0.44	-10	-80
K UIO-CTM	1.79	10.6	0.019	-0.37	-19	-207
L UIO-GCM	2.28			-0.29		-127
AEROCOM: IDENTICAL EMISSIONS USED FOR YEAR 2000 AND 1750						
M UMI	2.64	7.6	0.02	-0.58	-29	-220
N UIO-CTM	1.70	11.2	0.019	-0.36	-19	-212
O LOA	3.64	9.6	0.035	-0.49	-14	-135
P LSCE	3.01	7.6	0.023	-0.42	-18	-140
Q ECHAMS-HAM	2.47	6.5	0.016	-0.46	-29	-186
R GISS**	1.34	4.5	0.006	-0.19	-32	-142
S UIO-GCM	1.72	7.0	0.012	-0.25	-21	-145
T SPRINTARS	1.19	10.9	0.013	-0.16	-12	-134
U ULAQ	1.62	12.3	0.02	-0.22	-11	-136
Average A-L	2.70	9.4	0.024	-0.46	-18	-181
Average M-U	2.15	8.6	0.018	-0.35	-21	-161
Minimum A-U	1.19	4.5	0.006	-0.96	-32	-294
Maximum A-U	5.50	12.3	0.042	-0.16	-10	-80
Std dev A-L	1.09	1.9	0.010	0.202	7	68
Std dev M-U	0.83	2.6	0.008	0.149	8	35
%Stddev/avg A-L	40%	20%	41%	44%	38%	385
%Stddev/avg M-U	39%	30%	45%	43%	37%	22%

Model abbreviations: CCM3=Community Climate Model; GEOSCHEM=Goddard Earth Observing System-Chemistry; GISS=Goddard Institute for Space Studies; SPRINTARS=Spectral Radiation-Transport Model for Aerosol Species; LMD=Laboratoire de Meteorologie Dynamique; LOA=Laboratoire d'Optique Atmospherique; GATORG=Gas, Aerosol Transport and General circulation model; PNNL=Pacific Northwest National Laboratory; UIO-CTM=University of Oslo CTM; UIO-GCM=University of Oslo GCM; UMI=University of Michigan; LSCE=Laboratoire des Sciences du Climat et de l'Environnement; ECHAM5-HAM=European Centre Hamburg with Hamburg Aerosol Module; ULAQ=University of IL'Aquila.

Source: Adapted from IPCC AR4 (2007, [092765](#)) and Schulz et al. (2006, [190381](#))

Table 9-14. Particulate organic matter (POM) and BC mass loading, AOD at 550 nm, shortwave radiative forcing at the top of the atmosphere, and normalized forcing with respect to AOD and mass.

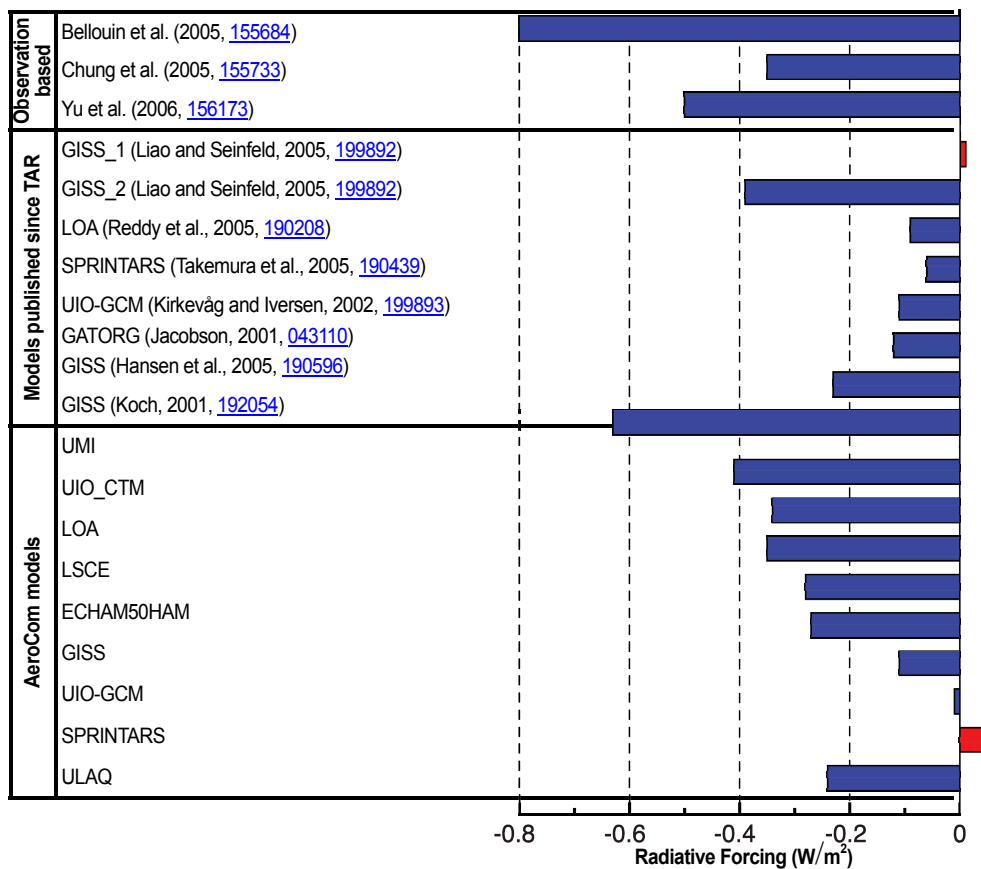
Model	Mass load (mg m ⁻²)	MEE (m ² g ⁻¹)	AOD at 550 nm	TOA Forcing (W/m ²)	Forcing/AOD (W/m ²)	Forcing/Mass (W g ⁻¹)	Mass load (mg m ⁻²)	MEE (m ² g ⁻¹)	AOD at 550 nm	TOA Forcing (W/m ²)	Forcing/AOD (W/m ²)	Forcing/Mass (W g ⁻¹)
PUBLISHED SINCE IPCC 2001												
A SPRINTARS				-0.24		-107				0.36		
B LOA	2.33	6.9	0.016	-0.25	-16	-140	0.37			0.55		
C GISS	1.86	9.1	0.017	-0.26	-15	-161	0.29			0.61		
D GISS	1.86	8.1	0.015	-0.30	-20	-75	0.29			0.35		
E GISS*	2.39			-0.18		-92	0.39			0.50		
F GISS	2.49			-0.23		-101	0.43			0.53		
G SPRINTARS	2.67	10.9	0.029	-0.27	-9	-23	0.53			0.42		
H GATORG	2.56			-0.06		-112	0.39			0.55		
I MOZGN	3.03	5.9	0.018	-0.34	-19							
J CCM							0.33			0.34		
K UIO-CTM							0.30			0.19		
AEROCOM: IDENTICAL EMISSIONS FOR YEAR 2000 & 1750												
L UMI	1.16	5.2	0.0060	-0.23	-38	-198	0.19	6.8	1.29	0.25	194	1316
M UIO-CTM	1.12	5.2	0.0058	-0.16	-28	-143	0.19	7.1	1.34	0.22	164	1158
N LOA	1.41	6.0	0.0085	-0.16	-19	-113	0.25	7.9	1.98	0.32	162	1280
OLSCE	1.50	5.3	0.0079	-0.17	-22	-113	0.25	4.4	1.11	0.30	270	1200
P ECHAMS-HAM	1.00	7.7	0.0077	-0.10	-13	-100	0.16	7.7	1.23	0.20	163	1250
Q GISS**	1.22	4.9	0.0060	-0.14	-23	-115	0.24	7.6	1.83	0.22	120	917
R UIO-GCM	0.88	5.2	0.0046	-0.06	-13	-68	0.19	10.3	1.95	0.36	185	1895
S SPRINTARS	1.84	10.9	0.0200	-0.10	-5	-54	0.37	9.5	3.50	0.32	91	865
T ULAQ	1.71	4.4	0.0075	-0.09	-12	-53	0.38	7.6	2.90	0.08	28	211
Average A-K	2.40	8.2	0.019	-0.24	-16	-102	0.37			0.44		1242
Average L-T	1.32	6.1	0.008	-0.13	-19	-106	0.25	7.7	1.90	0.25	153	1121
Minimum A-T	0.88	4.4	0.005	-0.34	-38	-198	0.16	4.4	1.11	0.08	28	211
Maximum A-T	3.03	10.9	0.029	-0.06	-5	-23	0.53	10.3	3.50	0.61	270	2103
Std dev A-K	0.39	1.7	0.006	0.09	4	41	0.08			0.06		384
Std dev L-T	0.32	2.0	0.005	0.05	10	46	0.08	1.6	0.82	0.09	68	450
%Stddev/avg A-K	16%	21%	30%	36%	26%	41%	22%			23%		31%
%Stddev/avg L-T	25%	33%	56%	39%	52%	43%	32%	21%	43%	34%	45%	40%

Source: Based on IPCC AR4 (2007, [092765](#)) and Schulz et al. (2006, [190381](#)).

The IPCC AR4 (2007, [092765](#)) assessed anthropogenic aerosol RF based on the model results published after the IPCC TAR in 2001, including those from the AeroCom study discussed above. These results (adopted from IPCC AR4) are shown in Table 9-13 for sulfate and Table 9-14 for carbonaceous aerosols (BC and POM), respectively. All values listed in Table 9-13 and Table 9-14 refer to anthropogenic perturbation, i.e., excluding the natural fraction of these aerosols. In addition to the mass burden, MEE, and AOD, Table 9-13 and Table 9-14 also list the “normalized forcing”, also known as “forcing efficiency”, one for the forcing per unit AOD, and the other the forcing per gram of aerosol mass (dry). For some models, aerosols are externally mixed, that is, each aerosol particle contains only one aerosol type such as sulfate, whereas other models allow aerosols to mix internally to different degrees, that is, each aerosol particle can have more than one component, such as black carbon coated with sulfate. For models with internal mixing of aerosols, the component values for AOD, MEE, and forcing were extracted (Schulz et al., 2006, [190381](#)).

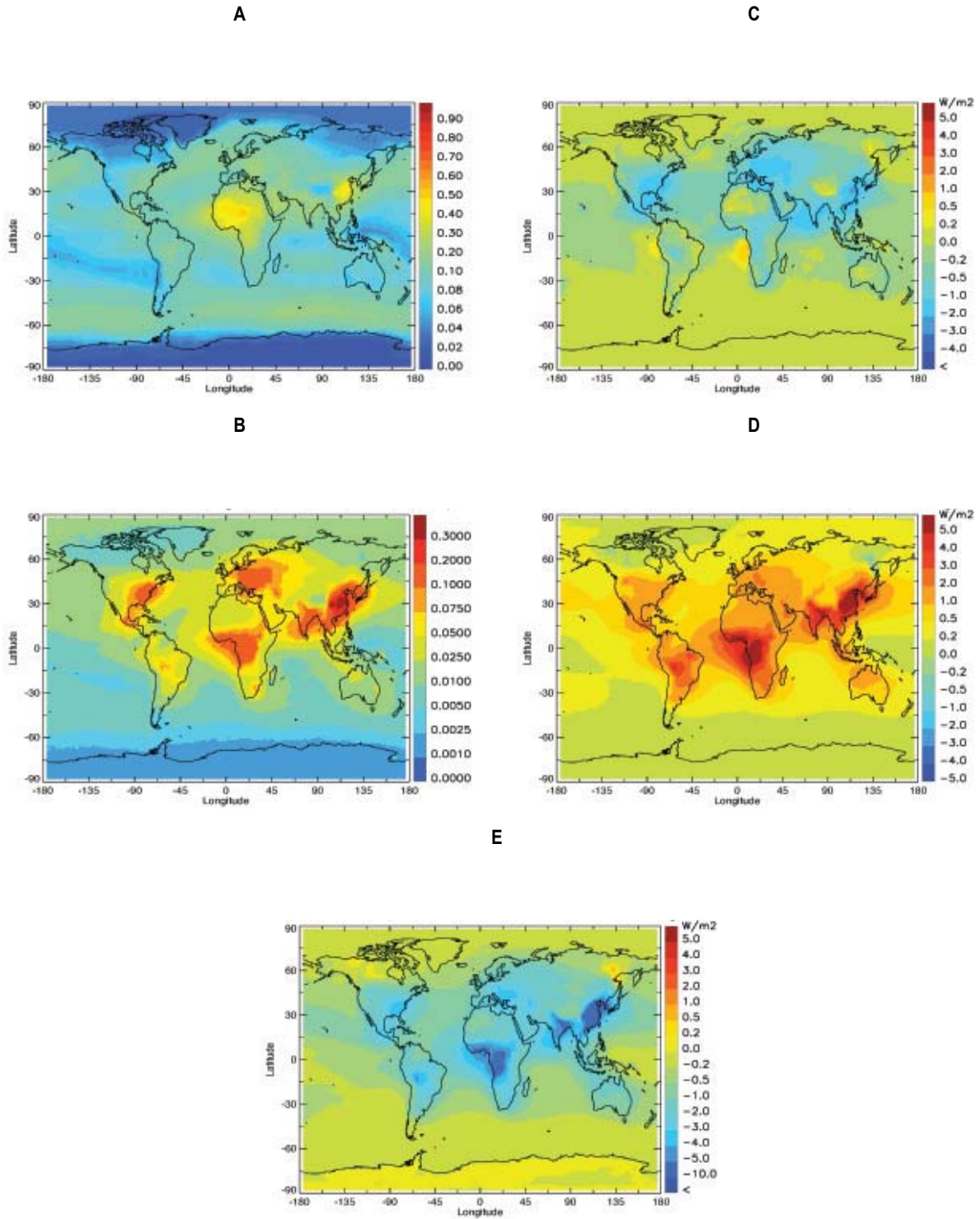
Considerable variation exists among these models for all quantities in Table 9-13 and Table 9-14. The RF for all the components varies by a factor of 6 or more: Sulfate from 0.16 to 0.96 W/m², POM from -0.06 to -0.34 W/m², and BC from +0.08 to +0.61 W/m², with the standard deviation in the range of 30 to 40% of the ensemble mean. It should be noted that although BC has the lowest mass loading and AOD, it is the only aerosol species that absorbs strongly, causing positive forcing to warm the atmosphere, in contrast to other aerosols that impose negative forcing to cool the atmosphere. As a result, the net anthropogenic aerosol forcing as a whole becomes less negative when BC is included. The global average anthropogenic aerosol direct RF at the top of the atmosphere (TOA) from the models, together with observation-based estimates (see Chapter 2 of the CCSP SAP2.3), is presented in Figure 9-73. Note the wide range for forcing in Figure 9-73. The comparison with observation-based estimates shows that the model estimated forcing is in general lower, partially because the forcing value from the model is the difference between present-day and pre-industrial time, whereas the observation-derived quantity is the difference between an atmosphere with and without anthropogenic aerosols, so the “background” value that is subtracted from the total forcing is higher in the models. The discussion so far has dealt with global average values. The geographic distributions of multi-model aerosol direct RF has been evaluated among the AeroCom models, which are shown in Figure 9-74 for total and anthropogenic AOD at 550 nm and anthropogenic aerosol RF at TOA, within the atmospheric column, and at the surface. Globally, anthropogenic AOD is about 25% of total AOD (Figure 9-74A and B) but is more concentrated over polluted regions in Asia, Europe, and North America and biomass burning regions in tropical southern Africa and South America. At TOA, anthropogenic aerosol causes negative forcing over mid-latitude continents and oceans with the most negative values (-1 to -2 W/m²) over polluted regions (Figure 9-74C). Although anthropogenic aerosol has a cooling effect at the surface with surface forcing values down to -10 W/m² over China, India, and tropical Africa (Figure 9-74E), it warms the atmospheric column with the largest effects again over the polluted and biomass burning regions. This heating effect will change the atmospheric circulation and can affect the weather and precipitation (e.g., Kim et al., 2006, [190917](#)).

Aerosol Direct Radiative Forcing



Source: IPCC (2007, [092765](#)).

Figure 9-73. Aerosol direct radiative forcing in various climate and aerosol models. Observed values are shown in the top section.



Source: Schulz et al. (2006, [190381](https://doi.org/10.1029/2006JD007593)) and AeroCom image catalog (<http://nansen.ipsl.jussieu.fr/AEROCOM/aerocomhome.html>)

Figure 9-74. Aerosol optical thickness and anthropogenic shortwave all-sky radiative forcing from the AeroCom study. Shown in the figure: total AOD (A) and anthropogenic AOD (B) at 550 nm, and radiative forcing at TOA (C), atmospheric column (D), and surface (E).

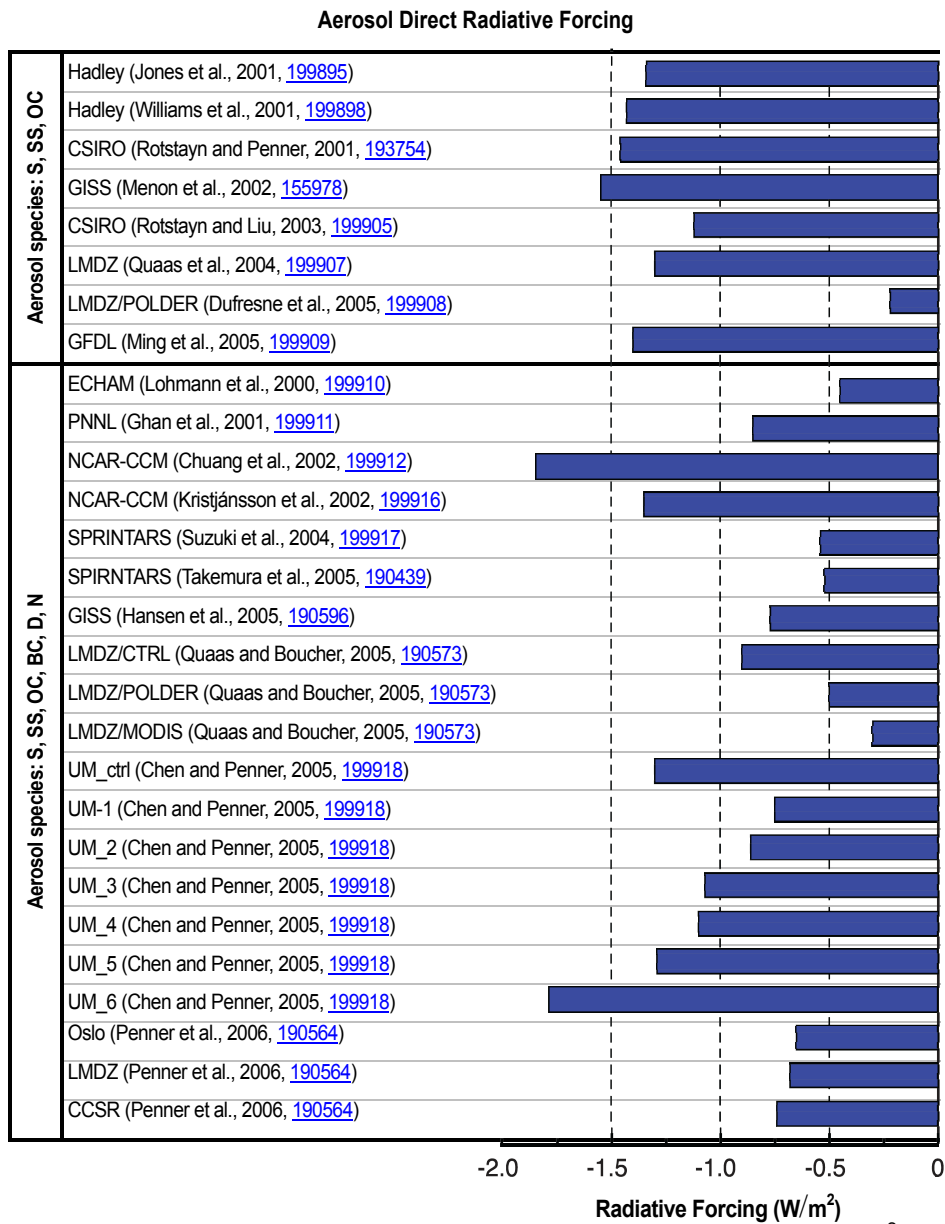


Figure 9-75. Radiative forcing from the cloud albedo effect (1st aerosol indirect effect) in the global climate models used from IPCC (2007, 092765), Chapter 2, Figure 2.14, of the IPCC AR4. Species included in the lower panel are SO₄²⁻, sea salt, organic and BC, dust and nitrates; in the top panel, only SO₄²⁻, sea salt and OC are included.

Basic conclusions from forward modeling of aerosol direct RF are:

- The most recent estimate of all-sky shortwave aerosol direct RF at TOA from anthropogenic sulfate, BC, and POM (mostly from fossil fuel/biofuel combustion and biomass burning) is $-0.22 \pm 0.18 \text{ W/m}^2$ averaged globally, exerting a net cooling effect. This value would represent the low-end of the forcing magnitude, since some potentially significant anthropogenic aerosols, such as nitrate and dust from human activities are not included because of their highly uncertain sources and processes. IPCC AR4 had adjusted the total anthropogenic aerosol direct RF to $-0.5 \pm 0.4 \text{ W/m}^2$ by adding estimated anthropogenic nitrate and dust forcing values based on limited modeling studies and by considering the observation-based estimates (see Chapter 2 of the CCSP SAP2.3).
- Both sulfate and POM cause negative forcing whereas BC causes positive forcing because of its highly absorbing nature. Although BC comprises only a small fraction of anthropogenic aerosol mass load and AOD, its forcing efficiency (with respect to either AOD or mass) is an order of magnitude stronger than sulfate and POM, so its positive shortwave forcing largely offsets the negative forcing from sulfate and POM. This points out the importance of improving the model ability to simulate each individual aerosol components more accurately, especially black carbon. Separately, it is estimated from recent model studies that anthropogenic sulfate, POM, and BC forcings at TOA are -0.4 , -0.18 , $+0.35 \text{ W/m}^2$, respectively. The anthropogenic nitrate and dust forcings are estimated at -0.1 W/m^2 for each, with uncertainties exceeds 100% (IPCC, 2007, [092765](#)).
- In contrast to long-lived greenhouse gases, anthropogenic aerosol RF exhibits significant regional and seasonal variations. The forcing magnitude is the largest over the industrial and biomass burning source regions, where the magnitude of the negative aerosol forcing can be of the same magnitude or even stronger than that of positive greenhouse gas forcing.
- There is a large spread of model-calculated aerosol RF even in the global annual averaged values. The AeroCom study shows that the model diversity at some locations (mostly East Asia and African biomass burning regions) can reach $\pm 3 \text{ W/m}^2$, which is an order of magnitude above the global averaged forcing value of -0.22 W/m^2 . The large diversity reflects the low level of current understanding of aerosol radiative forcing, which is compounded by uncertainties in emissions, transport, transformation, removal, particle size, and optical and microphysical (including hygroscopic) properties.
- In spite of the relatively small value of forcing at TOA, the magnitudes of anthropogenic forcing at the surface and within the atmospheric column are considerably larger: -1 to -2 W/m^2 at the surface and $+0.8$ to $+2 \text{ W/m}^2$ in the atmosphere. Anthropogenic aerosols thus cool the surface but heat the atmosphere, on average. Regionally, the atmospheric heating can reach annually averaged values exceeding 5 W/m^2 . Source: Schulz et al. (2006, [190381](#)) and AeroCom Image Catalog (<http://nansen.ipsl.jussieu.fr/AEROCOM/aerocomhome.html>)
- Figure 9-74D). These regional effects and the negative surface forcing are expected to exert an important effect on climate through alteration of the hydrological cycle.

9.3.6.4. Calculating Aerosol Indirect Forcing

Aerosol Effects on Clouds

A subset of the aerosol particles can act as cloud condensation nuclei (CCN) and/or ice nuclei (IN). Increases in aerosol particle concentrations, therefore, may increase the ambient concentrations of CCN and IN, affecting cloud properties. For a fixed cloud liquid water content, a CCN increase will lead to more cloud droplets so that the cloud droplet size will decrease. That effect leads to brighter clouds, the enhanced albedo then being referred to as the “cloud albedo effect” (Twomey, 1977, [190533](#)), also known as the first indirect effect. If the droplet size is smaller, it may take longer to rainout, leading to an increase in cloud lifetime, hence the “cloud lifetime” effect (Albrecht, 1989, [045783](#)), also called the second indirect effect. Approximately one-third of the models used for the IPCC 20th century climate change simulations incorporated an aerosol indirect effect, generally (though not exclusively) considered only with sulfates.

Shown in Figure 9-75 are results from published model studies indicating the different RF values from the cloud albedo effect. The cloud albedo effect ranges from -0.22 to -1.85 W/m^2 ; the lowest estimates are from simulations that constrained representation of aerosol effects on clouds with satellite measurements of drop size vs. aerosol index. In view of the difficulty of quantifying this effect remotely (discussed later), it is not clear whether this constraint provides an improved estimate. The estimate in the IPCC AR4 ranges from $+0.4$ to -1.1 W/m^2 , with a “best-guess” estimate of 0.7 W/m^2 .

The representation of cloud effects in GCMs is considered below. However, it is becoming increasingly clear from studies based on high resolution simulations of aerosol-

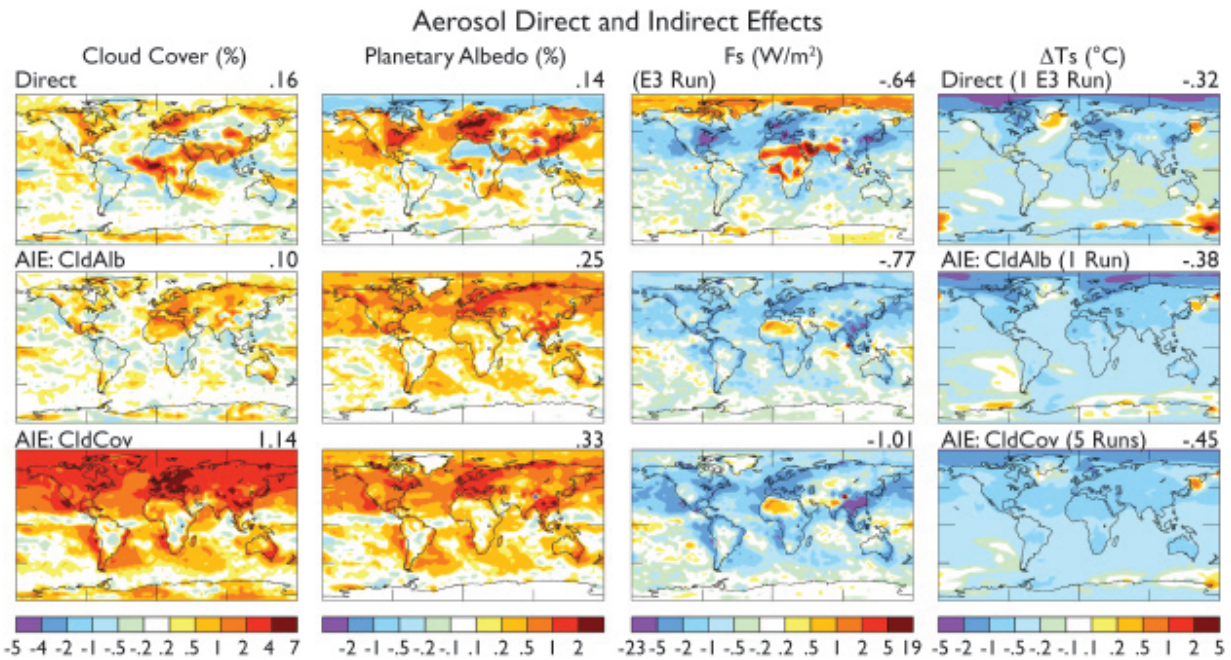
cloud interactions that there is a great deal of complexity that is unresolved in climate models. This point is examined below (High Resolution Modeling).

Most models did not incorporate the “cloud lifetime effect.” Hansen et al. (2005, [059087](#)) compared this latter influence (in the form of time-averaged cloud area or cloud cover increase) with the cloud albedo effect. In contrast to the discussion in IPCC (2007, [092765](#)), they argue that the cloud cover effect is more likely to be the dominant one, as suggested both by cloud-resolving model studies (Ackerman et al., 2004, [190056](#)) and satellite observations (Kaufman et al., 2005, [155891](#)). The cloud albedo effect may be partly offset by reduced cloud thickness accompanying aerosol pollutants, producing a meteorological (cloud) rather than aerosol effect (see the discussion in Lohman and Feichter, 2005, [155942](#)). The distinction between meteorological feedback and aerosol forcing can become quite opaque; as noted earlier, the term feedback is restricted here to those processes that are responding to a change in temperature. Nevertheless, both aerosol indirect effects were utilized in Hansen et al. (2005, [059087](#)), with the second indirect effect calculated by relating cloud cover to the aerosol number concentration, which in turn is a function of sulfate, nitrate, black carbon and organic carbon concentration. Only the low altitude cloud influence was modeled, principally because there are greater aerosol concentrations at low levels, and because low clouds currently exert greater cloud RF. The aerosol influence on high altitude clouds, associated with IN changes, is a relatively unexplored area for models and as well for process-level understanding.

Hansen et al. (2005, [059087](#)) used coefficients to normalize the cooling from aerosol indirect effects to between -0.75 and -1 W/m^2 , based on comparisons of modeled and observed changes in the diurnal temperature range as well as some satellite observations. The response of the GISS model to the direct and two indirect effects is shown in Figure 9-76. As parameterized, the cloud lifetime effect produced somewhat greater negative RF (cooling), but this was the result of the coefficients chosen. Geographically, it appears that the “cloud cover” effect produced slightly more cooling in the Southern Hemisphere than did the “cloud albedo” response, with the reverse being true in the Northern Hemisphere (differences on the order of a few tenths °C).

Model Experiments

There are many different factors that can explain the large divergence of aerosol indirect effects in models (Figure 9-75). To explore this in more depth, Penner et al. (2006, [190564](#)) used three general circulation models to analyze the differences between models for the first indirect effect, as well as a combined first plus second indirect effect. The models all had different cloud and/or convection parameterizations. In the first experiment, the monthly average aerosol mass and size distribution of, effectively, sulfate aerosol were prescribed, and all models followed the same prescription for parameterizing the cloud droplet number concentration (CDNC) as a function of aerosol concentration. In that sense, the only difference among the models was their separate cloud formation and radiation schemes. The different models all produced similar droplet effective radii, and therefore shortwave cloud forcing, and change in net outgoing whole sky radiation between pre-industrial times and the present. Hence the first indirect effect was not a strong function of the cloud or radiation scheme. The results for this and the following experiments are presented in Figure 9-77, where the experimental results are shown sequentially from left to right for the whole sky effect and in Table 9-15 for the clear-sky and cloud forcing response as well.



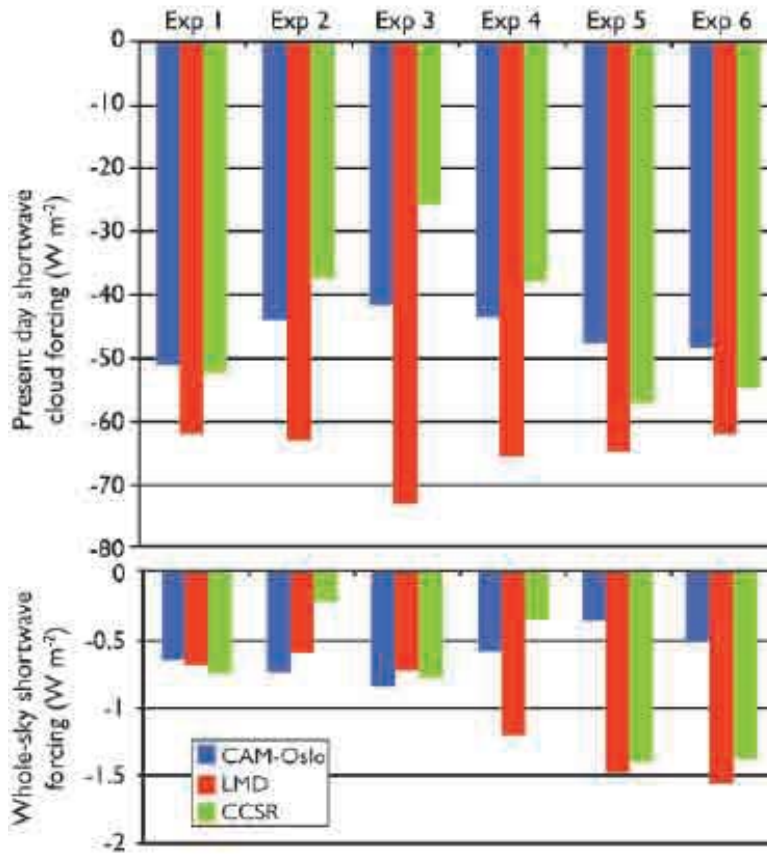
Source: Reprinted with Permission of Bioresource Technology from Hansen et al. (2005, [059087](#)).

Figure 9-76. Anthropogenic impact on cloud cover, planetary albedo, radiative flux at the surface (while holding sea surface temperatures and sea ice fixed) and surface air temperature change from the direct aerosol forcing (top row), the first indirect effect (second row) and the second indirect effect (third row). The temperature change is calculated from year 81-120 of a coupled atmosphere simulation with the GISS model.

The change in cloud forcing is the difference between whole sky and clear sky outgoing radiation in the present day minus pre-industrial simulation. The large differences seen between experiments 5 and 6 are due to the inclusion of the clear sky component of aerosol scattering and absorption (the direct effect) in experiment 6.

In the second experiment, the aerosol mass and size distribution were again prescribed, but now each model used its own formulation for relating aerosols to droplets. In this case one of the models produced larger effective radii and therefore a much smaller first indirect aerosol effect (Figure 9-77, Table 9-15). However, even in the two models where the effective radius change and net global forcing were similar, the spatial patterns of cloud forcing differ, especially over the biomass burning regions of Africa and South America.

The third experiment allowed the models to relate the change in droplet size to change in precipitation efficiency (i.e., they were now also allowing the second indirect effect – smaller droplets being less efficient rain producers – as well as the first). The models utilized the same relationship for autoconversion of cloud droplets to precipitation. Changing the precipitation efficiency results in all models producing an increase in cloud liquid water path, although the effect on cloud fraction was smaller than in the previous experiments. The net result was to increase the negative radiative forcing in all three models, albeit with different magnitudes: for two of the models the net impact on outgoing shortwave radiative increased by about 20%, whereas in the third model (which had the much smaller first indirect effect), it was magnified by a factor of three.



Source: Adapted from Penner et al. (2006, [190564](#)).

Figure 9-77. Global average present-day short wave cloud forcing at TOA (top) and change in whole sky net outgoing shortwave radiation (bottom) between the present-day and pre-industrial simulations for each model in each experiment.

Table 9-15. Differences in present day and pre-industrial outgoing solar radiation (W/m^2) in the different experiments.

Model	EXP 1	EXP 2	EXP 3	EXP 4	EXP 5	EXP 6
WHOLE-SKY						
CAM-Oslo	-0.648	-0.726	-0.833	-0.580	-0.365	-0.518
LMD-Z	-0.682	-0.597	-0.722	-1.194	-1.479	-1.553
CCSR	-0.739	-0.218	-0.733	-0.350	-1.386	-1.386
CLEAR-SKY						
CAM-Oslo	-0.063	-0.066	-0.026	0.014	-0.054	-0.575
LMD-Z	-0.054	0.019	0.030	-0.066	-0.126	-1.034
CCSR	0.018	-0.007	-0.045	-0.008	0.018	-1.160
CLOUD-FORCING						
CAM-Oslo	-0.548	-0.660	-0.807	-0.595	-0.311	0.056
LMD-Z	-0.628	-0.616	-0.752	-1.128	-1.353	-0.518
CCSR	-0.757	-0.212	-0.728	-0.345	-1.404	-0.200

EXP1: tests cloud formation and radiation schemes

EXP2: tests formulation for relating aerosols to droplets

EXP3: tests inclusion of droplet size influence on precipitation efficiency

EXP4: tests formulation of droplet size influence on precipitation efficiency

EXP5: tests model aerosol formulation from common sources

EXP6: added the direct aerosol effect

Source: Adapted from Penner et al. (2006, [190564](#)).

In the fourth experiment, the models were now each allowed to use their own formulation to relate aerosols to precipitation efficiency. This introduced some additional changes in the whole sky shortwave forcing (Figure 9-77).

In the fifth experiment, models were allowed to produce their own aerosol concentrations, but were given common sources. This produced the largest changes in the RF in several of the models. Within any one model, therefore, the change in aerosol concentration has the largest effect on droplet concentrations and effective radii. This experiment too resulted in large changes in RF.

In the last experiment, the aerosol direct effect was included, based on the full range of aerosols used in each model. While the impact on the whole-sky forcing was not large, the addition of aerosol scattering and absorption primarily affected the change in clear sky radiation (Table 9-15).

The results of this study emphasize that in addition to questions concerning cloud physics, the differences in aerosol concentrations among the models play a strong role in inducing differences in the indirect effect(s), as well as the direct one.

Observational constraints on climate model simulations of the indirect effect with satellite data (e.g., MODIS) have been performed previously in a number of studies (e.g., Lohmann et al., 2006, [190451](#); Menon et al., 2008, [190534](#); Quaas et al., 2006, [190915](#); Storlevmo et al., 2006, [190418](#)).

These have been somewhat limited since the satellite retrieved data used do not have the vertical profiles needed to resolve aerosol and cloud fields (e.g., cloud droplet number and liquid water content); the temporal resolution of simultaneous aerosol and cloud product retrievals are usually not available at a frequency of more than one a day; and higher level clouds often obscure low clouds and aerosols. Thus, the indirect effect, especially the second indirect effect, remains, to a large extent, unconstrained by satellite observations. However, improved measurements of aerosol vertical distribution from the newer generation of sensors on the A-train platform may provide a better understanding of changes to cloud properties from aerosols. Simulating the top-of-atmosphere reflectance for comparison to satellite measured values could be another way to compare model with observations, which would eliminate the inconsistent assumptions of aerosol optical properties and surface reflectance encountered when compared the model calculated and satellite retrieved AOD values.

Additional Aerosol Influences

Various observations have empirically related aerosols injected from biomass burning or industrial processes to reductions in rainfall (e.g., Andreae et al., 2004, [155658](#); Eagan et al., 1974, [190231](#); Rosenfeld, 2000, [002234](#); Warner, 1968, [157114](#)). There are several potential mechanisms associated with this response.

In addition to the two indirect aerosol effects noted above, a process denoted as the “semidirect” effect involves the absorption of solar radiation by aerosols such as black carbon and dust. The absorption increases the temperature, thus lowering the relative humidity and producing evaporation, hence a reduction in cloud liquid water. The impact of this process depends strongly on what the effective aerosol absorption actually is; the more absorbing the aerosol, the larger the potential positive forcing on climate (by reducing low level clouds and allowing more solar radiation to reach the surface). This effect is responsible for shifting the critical value of SSA (separating aerosol cooling from aerosol warming) from 0.86 with fixed clouds to 0.91 with varying clouds (Hansen et al., 1997, [043104](#)). Reduction in cloud cover and liquid water is one way aerosols could reduce rainfall.

More generally, aerosols can alter the location of solar radiation absorption within the system, and this aspect alone can alter climate and precipitation even without producing any change in net radiation at the top of the atmosphere (the usual metric for climate impact). By decreasing solar absorption at the surface, aerosols (from both the direct and indirect effects) reduce the energy available for evapotranspiration, potentially resulting in a decrease in precipitation. This effect has been suggested as the reason for the decrease in pan evaporation over the last 50 years (Roderick and Farquhar, 2002, [042788](#)). The decline in solar radiation at the surface appears to have ended in the 1990s (Wild et al., 2005, [156156](#)), perhaps because of reduced aerosol emissions in industrial areas (Kruger and Grasl, 2002, [190200](#)), although this issue is still not settled.

Energy absorption by aerosols above the boundary layer can also inhibit precipitation by warming the air at altitude relative to the surface, i.e., increasing atmospheric stability. The increased stability can then inhibit convection, affecting both rainfall and atmospheric circulation (Chung and Zhang, 2004, [190054](#); Ramanathan et al., 2001, [042681](#)). To the extent that aerosols decrease droplet size and reduce precipitation efficiency, this effect by itself could result in lowered rainfall values locally.

In their latest simulations, Hansen et al. (2007, [190597](#)) did find that the indirect aerosol effect reduced tropical precipitation; however, the effect is similar regardless of which of the two indirect effects is used, and also similar to the direct effect. So it is likely that the reduction of tropical precipitation is because of aerosol induced cooling at the surface and the consequent reduced evapotranspiration. Similar conclusions were reached by Yu et al. (2002, [190923](#)) and Feingold et al. (2005, [190550](#)). In this case, the effect is a feedback and not a forcing.

The local precipitation change, through its impacts on dynamics and soil moisture, can have large positive feedbacks. Harvey (2004, [190598](#)) concluded from assessing the response to aerosols in eight coupled models that the aerosol impact on precipitation was larger than on temperature. He also found that the precipitation impact differed substantially among the models, with little correlation among them.

Recent GCM simulations have further examined the aerosol effects on hydrological cycle. Ramanathan et al. (2005, [190199](#)) showed from fully coupled ocean-atmosphere GCM experiments that the “solar dimming” effect at the surface, i.e., the reduction of solar radiation reaching the surface, due to the inclusion of absorbing aerosol forcing causes a reduction in surface evaporation, a decrease in meridional sea surface temperature (SST) gradient and an increase in atmospheric stability, and a reduction in rainfall over South Asia. Lau and Kim (2006, [190226](#)) examined the direct effects of aerosol on the monsoon water cycle variability from GCM simulations with prescribed realistic global aerosol forcing and proposed the “elevated heat pump” effect, suggesting that atmospheric heating by absorbing aerosols (dust and black carbon), through water cycle feedback, may lead to a strengthening of the South Asia monsoon. These model results are not necessarily at odds with each other, but rather illustrate the complexity of the aerosol-monsoon interactions that are associated with different mechanisms, whose relative importance in affecting the monsoon may be strongly dependent on spatial and temporal scales and the timing of the monsoon. These results may be model dependent and should be further examined.

High Resolution Modeling

Largely by its nature, the representation of the interaction between aerosol and clouds in GCMs is poorly resolved. This stems in large part from the fact that GCMs do not resolve convection on their large grids (order of several hundred km), that their treatment of cloud microphysics is rather crude, and that as discussed previously, their representation of aerosol needs improvement. Superparametrization efforts (where standard cloud parameterizations in the GCM are replaced by resolving clouds in each grid column of the GCM via a cloud resolving model) (e.g., Grabowski, 2004, [190590](#)) could lead the way for the development of more realistic cloud fields and thus improved treatments of aerosol cloud interactions in large-scale models. However, these are just being incorporated in models that resolve both cloud and

aerosols. Detailed cloud parcel models have been developed to focus on the droplet activation problem (that asks under what conditions droplets actually start forming) and questions associated with the first indirect effect. The coupling of aerosol and cloud modules to dynamical models that resolve the large turbulent eddies associated with vertical motion and clouds [large eddy simulations (LES) models, with grid sizes of ~100 m and domains ~10 km] has proven to be a powerful tool for representing the details of aerosol-cloud interactions together with feedbacks (e.g., Ackerman et al., 2004, [190056](#); Feingold et al., 1994, [190535](#); 1999, [190540](#); Kogan et al., 1994, [190186](#); Stevens et al., 1996, [190417](#)).

This section explores some of the complexity in the aerosol indirect effects revealed by such studies to illustrate how difficult parameterizing these effects properly in GCMs could really be.

The First Indirect Effect

The relationship between aerosol and drop concentrations (or drop sizes) is a key piece of the first indirect effect puzzle. (It should not, however, be equated to the first indirect effect which concerns itself with the resultant RF). A huge body of measurement and modeling work points to the fact that drop concentrations increase with increasing aerosol. The main unresolved questions relate to the degree of this effect, and the relative importance of aerosol size distribution, composition and updraft velocity in determining drop concentrations (for a review, see McFiggans et al., 2006, [190532](#)). Studies indicate that the aerosol number concentration and size distribution are the most important aerosol factors. Updraft velocity (unresolved by GCMs) is particularly important under conditions of high aerosol particle number concentration.

Although it is likely that composition has some effect on drop number concentrations, composition is generally regarded as relatively unimportant compared to the other parameters (Dusek et al., 2006, [155756](#); Ervens et al., 2005, [190527](#); Feingold et al., 2003, [190551](#); Fitzgerald, 1975, [095417](#)). Therefore, it has been stated that the significant complexity in aerosol composition can be modeled, for the most part, using fairly simple parameterizations that reflect the soluble and insoluble fractions (e.g., Rissler et al., 2004, [190225](#)). However, composition cannot be simply dismissed. Furthermore, chemical interactions also cannot be overlooked. A large uncertainty remains concerning the impact of organic species on cloud droplet growth kinetics, thus cloud droplet formation. Cloud drop size is affected by wet scavenging, which depends on aerosol composition especially for freshly emitted aerosol. And future changes in composition will presumably arise due to biofuels/biomass burning and a reduction in sulfate emissions, which emphasizes the need to include composition changes in models when assessing the first indirect effect. The simple soluble/insoluble fraction model may become less applicable than is currently the case.

The updraft velocity, and its change as climate warms, may be the most difficult aspect to simulate in GCMs because of the small scales involved. In GCMs it is calculated in the dynamics as a grid box average, and parameterized on the small scale indirectly because it is a key part of convection and the spatial distribution of condensate, as well as droplet activation. Numerous solutions to this problem have been sought, including estimation of vertical velocity based on predicted turbulent kinetic energy from boundary layer models (Larson et al., 2001, [190212](#); Lohmann et al., 1999, [190443](#)) and PDF representations of subgrid quantities, such as vertical velocity and the vertically-integrated cloud liquid water ('liquid water path,' or LWP) (Golaz et al., 2002, [190587](#); 2002, [190589](#); Larson et al., 2005, [190220](#); Pincus and Klein, 2000, [190565](#)). Embedding cloud-resolving models within GCMs is also being actively pursued (Grabowski et al., 1999, [190592](#); Randall et al., 2003, [190201](#)). Numerous other details come into play; for example, the treatment of cloud droplet activation in GCM frameworks is often based on the assumption of adiabatic conditions, which may overestimate the sensitivity of cloud to changes in CCN (Sotiropoulou et al., 2006, [190406](#); Sotiropoulou et al., 2007, [190405](#)). This points to the need for improved theoretical understanding followed by new parameterizations.

Other Indirect Effects

The second indirect effect is often referred to as the "cloud lifetime effect", based on the premise that non-precipitating clouds will live longer. In GCMs the "lifetime effect" is equivalent to changing the representation of precipitation production and can be parameterized as an increase in cloud area or cloud cover (e.g., Hansen et al., 2005, [059087](#)). The second indirect effect hypothesis states that the more numerous and smaller drops associated with aerosol perturbations, suppress collision-induced rain, and result in a longer cloud lifetime. Observational evidence for the suppression of rain in warm clouds exists in the form of isolated studies (e.g., Warner, 1968, [157114](#)) but to date there is no statistically robust proof of surface rain suppression (Levin and Cotton, 2008, [190375](#)). Results from ship-track studies show that cloud water may increase or decrease in the tracks (Coakley and Walsh, 2002, [192025](#)) and satellite studies suggest similar results for warm boundary layer clouds (Han et al., 2002, [049181](#)). Ackerman et al. (2004, [190056](#)) used LES to show that in stratocumulus, cloud water may increase or decrease in response to increasing aerosol depending on the relative humidity of the air overlaying the cloud. Wang et al. (2003, [157106](#)) showed that all

else being equal, polluted stratocumulus clouds tend to have lower water contents than clean clouds because the small droplets associated with polluted clouds evaporate more readily and induce an evaporation-entrainment feedback that dilutes the cloud. This result was confirmed by Xue and Feingold (2006, [190920](#)) and Jiang and Feingold (2006, [190976](#)) for shallow cumulus, where pollution particles were shown to decrease cloud fraction. Furthermore, Xue et al. (2008, [190921](#)) suggested that there may exist two regimes: the first, a precipitating regime at low aerosol concentrations where an increase in aerosol will suppress precipitation and increase cloud cover (Albrecht, 1989, [045783](#)); and a second, non-precipitating regime where the enhanced evaporation associated with smaller drops will decrease cloud water and cloud fraction.

The possibility of bistable aerosol states was proposed earlier by Baker and Charlson (1990, [190016](#)) based on consideration of aerosol sources and sinks. They used a simple numerical model to suggest that the marine boundary layer prefers two aerosol states: a clean, oceanic regime characterized by a weak aerosol source and less reflective clouds; and a polluted, continental regime characterized by more reflective clouds. On the other hand, study by Ackerman et al. (1994, [189975](#)) did not support such a bistable system using a somewhat more sophisticated model. Further observations are needed to clarify the nature of cloud/aerosol interactions under a variety of conditions.

Finally, the question of possible effects of aerosol on cloud lifetime was examined by Jiang et al. (2006, [133165](#)), who tracked hundreds of cumulus clouds generated by LES from their formative stages until they dissipated. They showed that in the model there was no effect of aerosol on cloud lifetime, and that cloud lifetime was dominated by dynamical variability.

It could be argued that the representation of these complex feedbacks in GCMs is not warranted until a better understanding of the processes is at hand. Moreover, until GCMs are able to represent cloud scales, it is questionable what can be obtained by adding microphysical complexity to poorly resolved clouds. A better representation of aerosol-cloud interactions in GCMs therefore depends on the ability to improve representation of aerosols and clouds, as well as their interaction, in the hydrologic cycle. This issue is discussed further in the next chapter.

9.3.6.5. Aerosol in the Climate Models

Aerosol in the IPCC AR4 Climate Model Simulations

To assess the atmospheric and climate response to aerosol forcing, e.g., changes in surface temperature, precipitation, or atmospheric circulation, aerosols, together with greenhouse gases should be an integrated part of climate model simulation under the past, present, and future conditions. Table 9-16 lists the forcing species that were included in 25 climate modeling groups used in the IPCC AR4 (2007, [092765](#)) assessment. All the models included long-lived greenhouse gases, most models included sulfate direct forcing, but only a fraction of those climate models considered other aerosol types. In other words, aerosol RF was not adequately accounted for in the climate simulations for the IPCC AR4. Put still differently, the current aerosol modeling capability has not been fully incorporated into the climate model simulations. As pointed out in Section 9.3.6.4, fewer than one-third of the models incorporated an aerosol indirect effect, and most considered only sulfates.

The following discussion compares two of the IPCC AR4 climate models that include all major forcing agencies in their climate simulation: the model from the NASA Goddard Institute for Space Studies (GISS) and from the NOAA Geophysical Fluid Dynamics Laboratory (GFDL). The purpose in presenting these comparisons is to help elucidate how modelers go about assessing their aerosol components, and the difficulties that entail. A particular concern is how aerosol forcings were obtained in the climate model experiments for IPCC AR4. Comparisons with observations have already led to some improvements that can be implemented in climate models for subsequent climate change experiments (e.g., Koch et al., 2006, [190184](#), for GISS model). This aspect is discussed further in Chapter 4 of the CCSP SAP2.3.

Table 9-16. Forcings used in IPCC AR4 simulations of 20th century climate change. This table is adapted from SAP 1.1 Table 5.2 (compiled using information provided by the participating modeling centers, see http://www.pcmdi.llnl.gov/ipcc/model-documentation/ipcc_model_documentation.php) plus additional information from that website. Eleven different forcings are listed: well-mixed greenhouse gases (G), tropospheric and stratospheric ozone (O), SO₄²⁻ aerosol direct (SD) and indirect effects (S), black carbon (BC) and organic carbon aerosols (OC), mineral dust (MD), sea salt (SS), land use/land cover (LU), solar irradiance (SO), and volcanic aerosols (V). Check mark denotes inclusion of a specific forcing. As used here, “inclusion” means specification of a time-varying forcing, with changes on interannual and longer timescales.

	Model	Country	G	O	SD	SI	BC	OC	MD	SS	LU	SO	V
1	BCC-CMI	China	√	√	√								
2	BCCR-BCM2.0	Norway	√		√				√	√			
3	CCSM3	USA	√	√	√		√	√				√	√
4	CGCM3.1(T47)	Canada	√		√								
5	CGCM3.1(T63)	Canada	√		√								
6	CNRM-CM3	France	√	√	√		√						
7	CSIRO-Mk3.0	Australia	√		√								
8	CSIRO-Mk3.5	Australia	√		√								
9	ECHAMS/MPI-OM	Germany	√	√	√	√							
10	ECHO-G	Germany/ Korea	√	√	√	√						√	√
11	FGOALS-g1.0	China	√		√								
12	GFDL-CM2.0	USA	√	√	√		√				√	√	√
13	GFDL-CM2.1	USA	√	√	√		√				√	√	√
14	GISS-AOM	USA	√		√					√			
15	GISS-EH	USA	√	√	√	√	√	√	√	√	√	√	√
16	GISS-ER	USA	√	√	√	√	√	√	√	√	√	√	√
17	INGV-SXG	Italy	√	√	√								
18	INM-CM3.0	Russia	√		√							√	
19	IPSL-CM4	France	√		√	√							
20	MICROC3.2(hires)	Japan	√	√	√		√	√	√	√	√	√	√
21	MICROC3.2(medres)	Japan	√	√	√		√	√	√	√	√	√	√
22	MRI-CGCM2.3.2	Japan	√		√							√	√
23	PCM	USA	√	√	√							√	√
24	UKMO-HasCM3	U.K.	√	√	√	√							
25	UKMO-HadGEM1	U.K.	√	√	√	√	√	√				√	√

The GISS Model

There have been many different configurations of aerosol simulations in the GISS model over the years, with different emissions, physics packages, etc., as is apparent from the multiple GISS entries in the preceding figures and tables. There were also three different GISS GCM submissions to IPCC AR4, which varied in their model physics and ocean formulation.

(Note that the aerosols in these three GISS versions are different from those in the AeroCom simulations described in Sections 9.3.6.2 and 9.3.6.3.) The GCM results discussed

below all relate to the simulations known as GISS model ER (Schmidt et al., 2006, [190373](#)) (see Table 9-16). Although the detailed description and model evaluation have been presented in Liu et al. (2006, [190422](#)), below are the general characteristics of aerosols in the GISS ER:

Aerosol fields: The aerosol fields used in the GISS ER is a prescribed “climatology” which is obtained from chemistry transport model simulations with monthly averaged mass concentrations representing conditions up to 1990. Aerosol species included are sulfate, nitrate, BC, POM, dust, and sea salt. Dry size effective radii are specified for each of the aerosol types, and laboratory-measured phase functions are employed for all solar and thermal wavelengths. For hygroscopic aerosols (sulfate, nitrate, POM, and sea salt), formulas are used for the particle growth of each aerosol as a function of relative humidity, including the change in density and optical parameters. With these specifications, the AOD, single scattering albedo, and phase function of the various aerosols are calculated. While the aerosol distribution is prescribed as monthly mean values, the relative humidity component of the extinction is updated each hour. The global averaged AOD at 550 nm is about 0.15.

Global distribution: When comparing with AOD from observations by multiple satellite sensors of MODIS, MISR, POLDER, and AVHRR and surface based sunphotometer network AERONET (see Chapter 2 of the CCSP SAP2.3 for detailed information about data), qualitative agreement is apparent, with generally higher burdens in Northern Hemisphere summer, and seasonal variations of smoke over southern Africa and South America, as well as wind blown dust over northern African and the Persian Gulf. Aerosol optical depth in both model and observations is smaller away from land. There are, however, considerable discrepancies between the model and observations. Overall, the GISS GCM has reduced aerosol optical depths compared with the satellite data (a global, clear-sky average of about 80% compared with MODIS and MISR data), although it is in better agreement with AERONET ground-based measurements in some locations (note that the input aerosol values were calibrated with AERONET data). The model values over the Sahel in Northern Hemisphere winter and the Amazon in Southern Hemisphere winter are excessive, indicative of errors in the biomass burning distributions, at least partially associated with an older biomass burning source used (the source used here was from (Liousse et al., 1996, [078158](#))).

Seasonal variation: A comparison of the seasonal distribution of the global AOD between the GISS model and satellite data indicates that the model seasonal variation is in qualitative agreement with observations for many of the locations that represent major aerosol regimes, although there are noticeable differences. For example, in some locations the seasonal variations are different from or even opposite to the observations.

Particle size parameter: The Ångström exponent (\AA), which is determined by the contrast between the AOD at two or more different wavelengths and is related to aerosol particle size (discussed in Section 9.3.6.3). This parameter is important because the particle size distribution affects the efficiency of scattering of both short and long wave radiation, as discussed earlier. \AA from the GISS model is biased low compared with AERONET, MODIS, and POLDER data, although there are technical differences in determining the \AA . This low bias suggests that the aerosol particle size in the GISS model is probably too large. The average effective radius in the GISS model appears to be 0.3-0.4 μm , whereas the observational data indicates a value more in the range of 0.2-0.3 μm (Liu et al., 2006, [190422](#)).

Single scattering albedo: The model-calculated SSA (at 550 nm) appears to be generally higher than the AERONET data at worldwide locations (not enough absorption), but lower than AERONET data in Northern Africa, the Persian Gulf, and the Amazon (too much absorption). This discrepancy reflects the difficulties in modeling BC, which is the dominant absorbing aerosol, and aerosol sizes. Global averaged SSA at 550 nm from the GISS model is at about 0.95.

Aerosol direct RF: The GISS model calculated anthropogenic aerosol direct shortwave RF is -0.56 W/m^2 at TOA and -2.87 W/m^2 at the surface. The TOA forcing (upper left, Figure 9-78) indicates that, as expected, the model has larger negative values in polluted regions and positive forcing at the highest latitudes. At the surface (lower left, Figure 9-78) GISS model values exceed -4 W/m^2 over large regions. Note there is also a longwave RF of aerosols (right column), although they are much weaker than the shortwave RF.

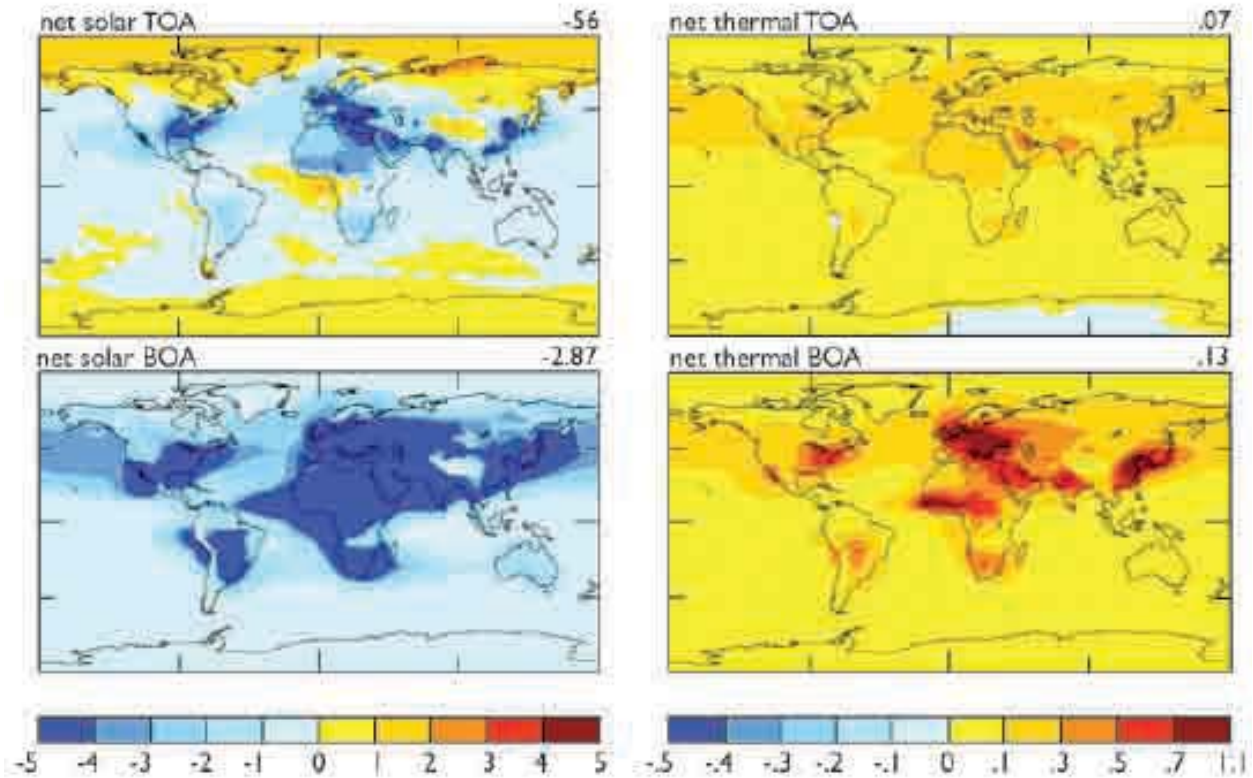
There are several concerns for climate change simulations related to the aerosol trend in the GISS model. One is that the aerosol fields in the GISS AR4 climate simulation (version ER) are kept fixed after 1990. In fact, the observed trend shows a reduction in tropospheric aerosol optical thickness from 1990 through the present, at least over the oceans (Mishchenko and Geogdzhayev, 2007, [190545](#)). Hansen et al. (2007, [190597](#)) suggested that the deficient warming in the GISS model over Eurasia post-1990 was due to the lack of this trend. Indeed, a possible conclusion from the Penner et al. (2002, [190562](#)) study was that the GISS model overestimated the AOD (presumably associated with anthropogenic aerosols) poleward of 30°N . However, when an alternate experiment reduced the aerosol optical depths, the polar warming became excessive (Hansen et al., 2007, [190597](#)). The other concern is that the GISS model may underestimate the organic and sea salt AOD, and overestimate the influence of black carbon aerosols in the biomass burning regions (Liu et al., 2006, [190422](#); deduced from Penner et al., 2002, [190562](#)). To the extent that is true, it would indicate the GISS model underestimates the aerosol direct cooling effect in a substantial portion of the tropics, outside of biomass burning areas. Clarifying those issues requires numerous modeling experiments and various types of observations.

The GFDL Model

A comprehensive description and evaluation of the GFDL aerosol simulation are given in Ginoux et al. (2006, [190582](#)). Below are the general characteristics:

Aerosol fields: The aerosols used in the GFDL climate experiments are obtained from simulations performed with the MOZART 2 model (Model for Ozone and Related chemical Tracers) (Horowitz, 2006, [190620](#); Horowitz et al., 2003, [057770](#)). The exceptions were dust, which was generated with a separate simulation of MOZART 2, using sources from Ginoux et al. (2001, [190579](#)) and wind fields from NCEP/NCAR reanalysis data; and sea salt, whose monthly mean concentrations were obtained from a previous study by Haywood et al. (1999, [040453](#)). It includes most of the same aerosol species as in the GISS model (although it does not include nitrates), and, as in the GISS model, relates the dry aerosol to wet aerosol optical depth via the model's relative humidity for sulfate (but not for organic carbon); for sea salt, a constant relative humidity of 80% was used. Although the parameterizations come from different sources, both models maintain a very large growth in sulfate particle size when the relative humidity exceeds 90%.

Global distributions: Overall, the GFDL global mean aerosol mass loading is within 30% of that of other studies (Chin et al., 2002, [189996](#); Reddy et al., 2005, [190207](#); Tie et al., 2005, [190459](#)), except for sea salt, which is 2 to 5 times smaller. However, the sulfate AOD (0.1) is 2.5 times that of other studies, whereas the organic carbon value is considerably smaller (on the order of 1/2). Both of these differences are influenced by the relationship with relative humidity. In the GFDL model, sulfate is allowed to grow up to 100% relative humidity, but organic carbon does not increase in size as relative humidity increases. Comparison of AOD with AVHRR and MODIS data for the time period 1996-2000 shows that the global mean value over the ocean (0.15) agrees with AVHRR data (0.14) but there are significant differences regionally, with the model overestimating the value in the northern mid latitude oceans and underestimating it in the southern ocean. Comparison with MODIS also shows good agreement globally (0.15), but in this case indicates large disagreements over land, with the model producing excessive AOD over industrialized countries and underestimating the effect over biomass burning regions. Overall, the global averaged AOD at 550 nm is 0.17, which is higher than the maximum values in the AeroCom-A experiments (Table 9-12) and exceeds the observed value too (A_e and S^* in Figure 9-72).



Source: Figure provided by A. Lacis, GISS.

Figure 9-78. Direct radiative forcing by anthropogenic aerosols in the GISS model (including sulfates, BC, OC and nitrates). Short wave forcing at TOA and surface are shown in the top left and bottom left panels. The corresponding thermal forcing is indicated in the right hand panels.

Composition: Comparison of GFDL modeled species with in situ data over North America, Europe, and over oceans has revealed that the sulfate is overestimated in spring and summer and underestimated in winter in many regions, including Europe and North America. Organic and black carbon aerosols are also overestimated in polluted regions by a factor of two, whereas organic carbon aerosols are elsewhere underestimated by factors of 2 to 3. Dust concentrations at the surface agree with observations to within a factor of 2 in most places where significant dust exists, although over the southwest U.S. it is a factor of 10 too large. Surface concentrations of sea salt are underestimated by more than a factor of 2. Over the oceans, the excessive sulfate AOD compensates for the low sea salt values except in the southern oceans.

Size and single-scattering albedo: No specific comparison was given for particle size or single-scattering albedo, but the excessive sulfate would likely produce too high a value of reflectivity relative to absorption except in some polluted regions where black carbon (an absorbing aerosol) is also overestimated.

As in the case of the GISS model, there are several concerns with the GFDL model. The good global-average agreement masks an excessive aerosol loading over the Northern Hemisphere (in particular, over the northeast U.S. and Europe) and an underestimate over biomass burning regions and the southern oceans. Several model improvements are needed, including better parameterization of hygroscopic growth at high relative humidity for sulfate and organic carbon; better sea salt simulations; correcting an error in extinction coefficients; and improved biomass burning emissions inventory (Ginoux et al., 2006, [190582](#)).

Comparisons between GISS and GFDL Model

Both GISS and GFDL models were used in the IPCC AR4 climate simulations for climate sensitivity that included aerosol forcing. It would be constructive, therefore, to compare the similarities and differences of aerosols in these two models and to understand what their

impacts are in climate change simulations. Figure 9-79 shows the percentage AOD from different aerosol components in the two models.

Sulfate: The sulfate AOD from the GISS model is within the range of that from all other models (Table 9-13), but that from the GFDL model exceeds the maximum value by a factor of 2.5. An assessment in SAP 3.2 (CCSP, 2008, [192028](#); Shindell et al., 2008, [190393](#)) also concludes that GFDL had excessive sulfate AOD compared with other models. The sulfate AOD from GFDL is nearly a factor of 4 large than that from GISS, although the sulfate burden differs only by about 50% between the two models. Clearly, this implies a large difference in sulfate MEE between the two models.

BC and POM: Compared to observations, the GISS model appears to overestimate the influence of BC and POM in the biomass burning regions and underestimate it elsewhere, whereas the GFDL model is somewhat the reverse: it overestimates it in polluted regions, and underestimates it in biomass burning areas. The global comparison shown in Table 9-14 indicates the GISS model has values similar to those from other models, which might be the result of such compensating errors. The GISS and GFDL models have relatively similar global-average black carbon contributions, and the same appears true for POM.

Sea salt: The GISS model has a much larger sea salt contribution than does GFDL (or indeed other models).

Global and regional distributions: Overall, the global averaged AOD is 0.15 from the GISS model and 0.17 from GFDL. However, as shown in Figure 9-79, the contribution to this AOD from different aerosol components shows greater disparity. For example, over the Southern Ocean where the primary influence is due to sea salt in the GISS model, but in the GFDL it is sulfate. The lack of satellite observations of the component contributions and the limited available in situ measurements make the model improvements at aerosol composition level difficult.

Climate simulations: With such large differences in aerosol composition and distribution between the GISS and GFDL models, one might expect that the model simulated surface temperature might be quite different. Indeed, the GFDL model was able to reproduce the observed temperature change during the 20th century without the use of an indirect aerosol effect, whereas the GISS model required a substantial indirect aerosol contribution (more than half of the total aerosol forcing) (Hansen et al., 2007, [190597](#)). It is likely that the reason for this difference was the excessive direct effect in the GFDL model caused by its overestimation of the sulfate optical depth. The GISS model direct aerosol effect (see Section 9.3.6.6) is close to that derived from observations (Chapter 2 of the CCSP SAP2.3); this suggests that for models with climate sensitivity close to $0.75^{\circ}\text{C}/(\text{W}/\text{m}^2)$ (as in the GISS and GFDL models), an indirect effect is needed.

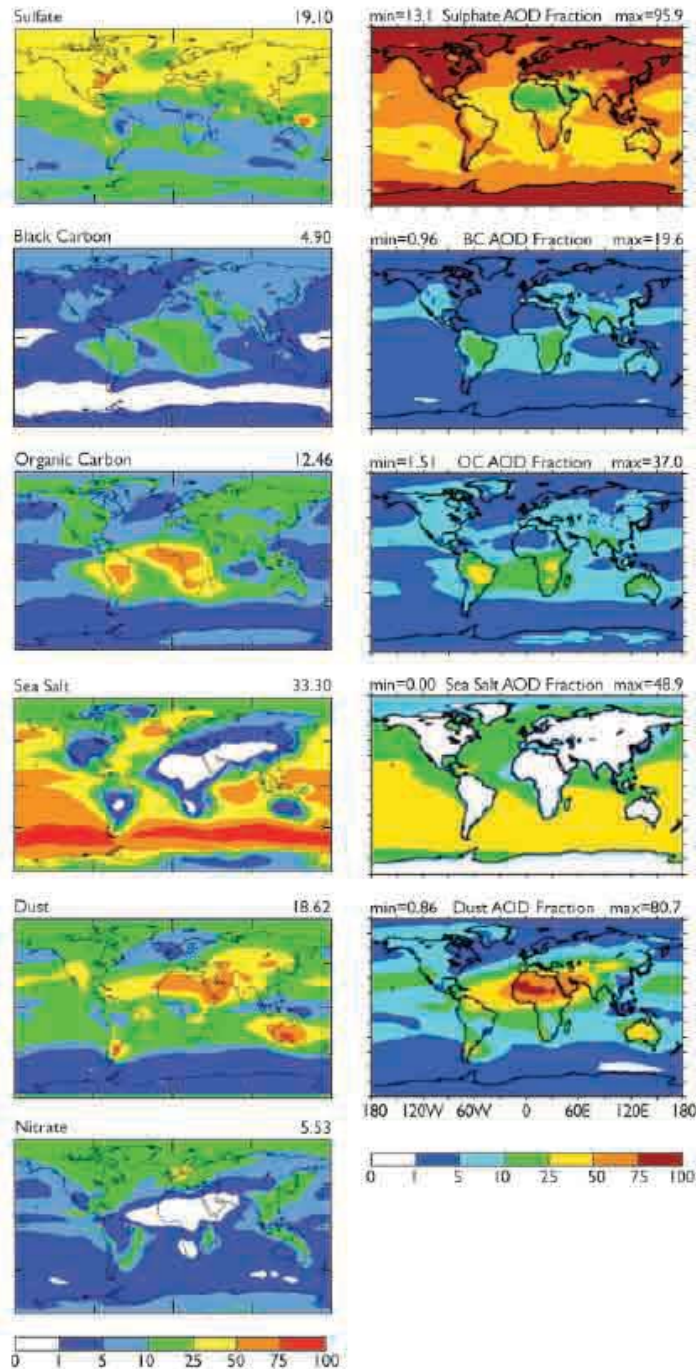


Figure 9-79. Percentage of aerosol optical depth in the GISS, left, based on Liu et al. (2006, [190422](#)), provided by A. Lacis, GISS, and GFDL, right, from Ginoux et al. (2006, [190582](#)). Models associated with the different components: SO_4^{2-} (1st row), BC (2nd row), OC (3rd row), sea-salt (4th row), dust (5th row), and nitrate (last row). Nitrate not available in GFDL model). Numbers on the GISS panels are global average, but on the GFDL panels are maximum and minimum.

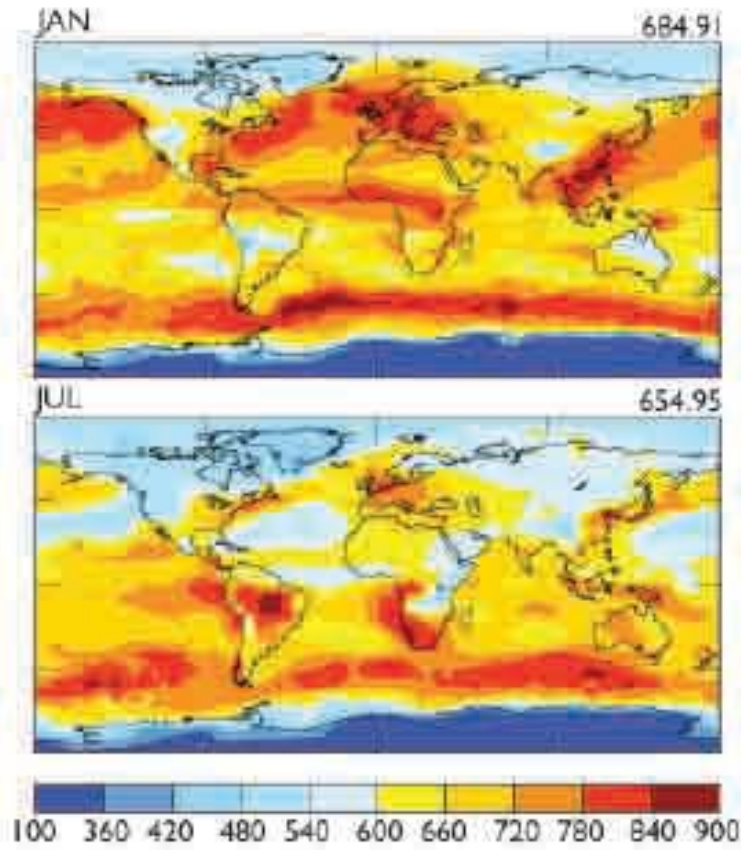
Additional Considerations

Long wave aerosol forcing: So far only the aerosol RF in the shortwave (solar) spectrum has been discussed. Figure 9-78 (right column) shows that compared to the shortwave forcing, the values of anthropogenic aerosol long wave (thermal) forcing in the GISS model are on the order of 10%. Like the shortwave forcing, these values will also be affected by the particular aerosol characteristics used in the simulation.

Aerosol vertical distribution: Vertical distribution is particularly important for absorbing aerosols, such as BC and dust in calculating the RF, particularly when longwave forcing is considered (e.g., Figure 9-78) because the energy they reradiate depends on the temperature (and hence altitude), which affects the calculated forcing values. Several model inter-comparison studies have shown that the largest difference among model simulated aerosol distributions is the vertical profile (e.g., Lohmann et al., 2001, [190448](#); Penner et al., 2002, [190562](#); Textor et al., 2006, [190456](#)), due to the significant diversities in atmospheric processes in the models (e.g., Table 9-12). In addition, the vertical distribution also varies with space and time, as illustrated in Figure 9-80 from the GISS ER simulations for January and July showing the most probable altitude of aerosol vertical locations. In general, aerosols in the northern hemisphere are located at lower altitudes in January than in July, and vice versa for the southern hemisphere.

Mixing state: Most climate model simulations incorporating different aerosol types have been made using external mixtures, i.e., the evaluation of the aerosols and their radiative properties are calculated separately for each aerosol type (assuming no mixing between different components within individual particles). Observations indicate that aerosols commonly consist of internally mixed particles, and these “internal mixtures” can have very different radiative impacts. For example, the GISS-1 (internal mixture) and GISS-2 (external mixture) model results shows very different magnitude and sign of aerosol forcing from slightly positive (implying slight warming) to strong negative (implying significant cooling) TOA forcing (Figure 9-73), due to changes in both radiative properties of the mixtures, and in aerosol amount. The more sophisticated aerosol mixtures from detailed microphysics calculations now being used/developed by different modeling groups may well end up producing very different direct (and indirect) forcing values.

Cloudy sky vs. clear sky: The satellite or AERONET observations are all for clear sky only because aerosol cannot be measured in the remote sensing technique when clouds are present. However, almost all the model results are for all-sky because of difficulty in extracting cloud-free scenes from the GCMs. So the AOD comparisons discussed earlier are not completely consistent. Because AOD can be significantly amplified when relative humidity is high, such as near or inside clouds, all-sky AOD values are expected to be higher than clear sky AOD values. On the other hand, the aerosol RF at TOA is significantly lower for all-sky than for clear sky conditions; the IPCC AR4 and AeroCom RF study (Schulz et al., 2006, [190381](#)) have shown that on average the aerosol RF value for all-sky is about 1/3 of that for clear sky although with large diversity (63%). These aspects illustrate the complexity of the system and the difficulty of representing aerosol radiative influences in climate models whose cloud and aerosol distributions are somewhat problematic. And of course aerosols in cloudy regions can affect the clouds themselves, as discussed in Section 9.3.6.5.



Source: A. Lacis, GISS.

Figure 9-80. Most probable aerosol altitude (in pressure, hPa) from the GISS model in January (top) and July (bottom).

9.3.6.6. Impacts of Aerosols on Climate Model Simulations

Surface Temperature Change

It was noted in the introduction that aerosol cooling is essential in order for models to produce the observed global temperature rise over the last century, at least models with climate sensitivities in the range of 3°C for doubled CO_2 (or $\sim 0.75^{\circ}\text{C}/(\text{W}/\text{m}^2)$). The implications of this are discussed here in somewhat more detail. Hansen et al. (2007, [190597](#)) show that in the GISS model, well-mixed greenhouse gases produce a warming of close to 1°C between 1880 and the present (Table 9-17). The direct effect of tropospheric aerosols as calculated in that model produces cooling of close to -0.3°C between those same years, while the indirect effect (represented in that study as cloud cover change) produces an additional cooling of similar magnitude (note that the general model result quoted in IPCC AR4 is that the indirect RF is twice that of the direct effect).

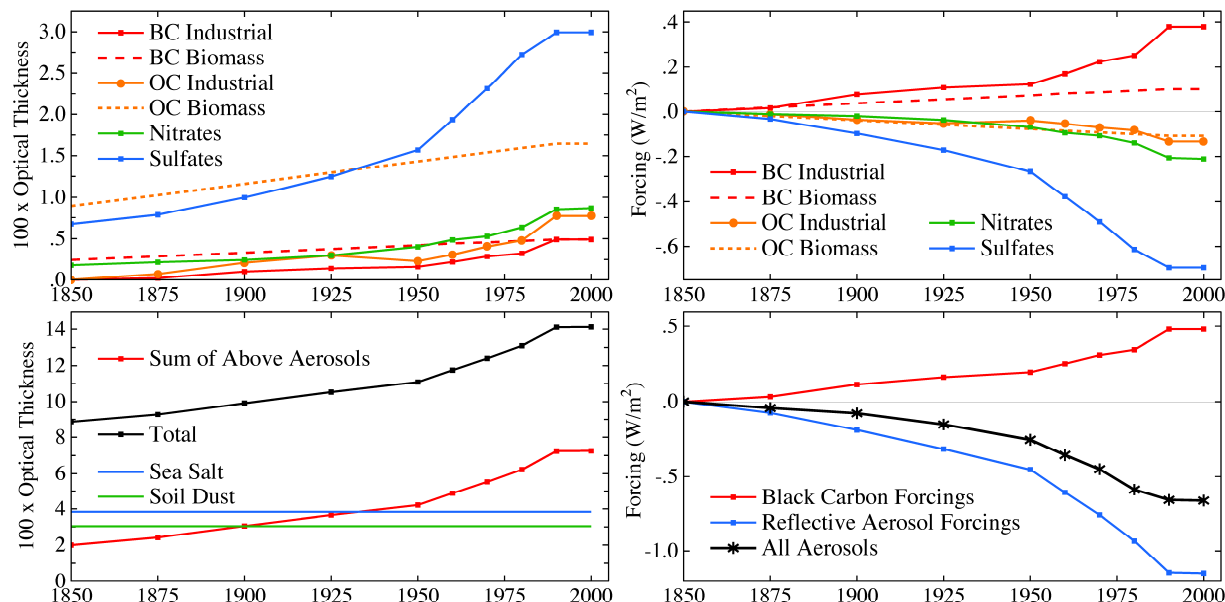
Table 9-17. Climate forcings (1880-2003) used to drive GISS climate simulations, along with the surface air temperature changes obtained for several periods.

Forcing Agent	Forcing Wm^{-2} (1880-2003)				ΔT Surface $^{\circ}C$ (year to 2003)			
	Fi	Fa	Fs	Fe	1880	1900	1950	1979
Well-mixed GHGs	2.62	2.50	2.65	2.72	0.96	0.93	0.74	0.43
Stratospheric H_2O			0.06	0.05	0.03	0.01	0.05	0.00
O_3	0.44	0.28	0.26	0.23	0.p08	0.05	0.00	-0.01
Land use			-0.09	-0.09	-0.05	-0.p07	-0.04	-0.02
Snow albedo	0.05	0.05	0.14	0.14	0.03	0.00	0.02	-0.01
Solar irradiance	0.23	0.24	0.23	0.22	0.07	0.07	0.01	0.02
Stratospheric aerosols	0.00	0.00	0.00	0.00	-0.08	-0.03	-0.06	0.04
Trop. aerosol direct forcing	-0.41	-0.38	-0.52	-0.60	-0.28	-0.23	-0.18	-0.10
Trop. aerosol indirect forcing			-0.87	-0.77	-0.27	-0.29	-0.14	-0.05
Sum of above			1.86	1.90	0.49	0.44	0.40	0.30
All forcings at once			1.77	1.75	0.53	0.61	0.44	0.29

Source: Reprinted with Permission of Springer Publishing from Hansen et al. (2007, [190597](#)). Instantaneous (Fi), adjusted (Fa), fixed SST (Fs) and effective (Fe) forcings are defined in Hansen et al. (2005, [059087](#))

The time dependence of the total aerosol forcing used as well as the individual species components is shown in Figure 9-81. The resultant warming, $0.53 (\pm 0.04) ^{\circ}C$ including these and other forcings (Table 9-17), is less than the observed value of $0.6-0.7^{\circ}C$ from 1880-2003. Hansen et al. (2007, [190597](#)) further show that a reduction in sulfate optical thickness and the direct aerosol effect by 50%, which also reduced the aerosol indirect effect by 18%, produces a negative aerosol forcing from 1880-2003 of $-0.91 W/m^2$ (down from $-1.37 W/m^2$ with this revised forcing). The model now warms $0.75^{\circ}C$ over that time. Hansen et al. (2007, [190597](#)) defend this change by noting that sulfate aerosol removal over North America and western Europe during the 1990s led to a cleaner atmosphere. Note that the comparisons shown in the previous section suggest that the GISS model already underestimates aerosol optical depths; it is thus trends that are the issue here.

The magnitude of the indirect effect used by Hansen et al. (2005, [190596](#)) is roughly calibrated to reproduce the observed change in diurnal temperature cycle and is consistent with some satellite observations. However, as Anderson et al. (2003, [054820](#)) note, the forward calculation of aerosol negative forcing covers a much larger range than is normally used in GCMs; the values chosen, as in this case, are consistent with the inverse reasoning estimates of what is needed to produce the observed warming, and hence generally consistent with current model climate sensitivities. The authors justify this approach by claiming that paleoclimate data indicate a climate sensitivity of close to $0.75 (\pm 0.25)^{\circ}C/(W/m^2)$, and therefore something close to this magnitude of negative forcing is reasonable. Even this stated range leaves significant uncertainty in climate sensitivity and the magnitude of the aerosol negative forcing. Furthermore, IPCC (2007, [092765](#)) concluded that paleoclimate data are not capable of narrowing the range of climate sensitivity, nominally $0.375-1.13 ^{\circ}C/(W/m^2)$, because of uncertainties in paleoclimate forcing and response; so from this perspective the total aerosol forcing is even less constrained than the GISS estimate. Hansen et al. (2007, [190597](#)) acknowledge that “an equally good match to observations probably could be obtained from a model with larger sensitivity and smaller net forcing, or a model with smaller sensitivity and larger forcing”.



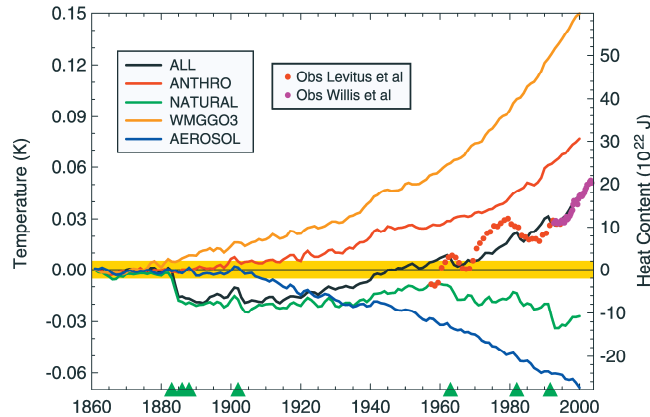
Source: Reprinted with Permission of Springer from Hansen et al. (2007, [190597](#)).

Figure 9-81. Time dependence of aerosol optical thickness (left) and climate forcing (right). Note that as specified, the aerosol trends are all “flat” from 1990-2000.

The GFDL model results for global mean ocean temperature change (down to 3 km depth) for the time period 1860-2000 is shown in Figure 9-82, along with the different contributing factors (Delworth et al., 2005, [190055](#)). This is the same GFDL model whose aerosol distribution was discussed previously. The aerosol forcing produces a cooling on the order of 50% that of greenhouse warming (generally similar to that calculated by the GISS model, Table 9-17). Note that this was achieved without any aerosol indirect effect.

The general model response noted by IPCC, as discussed in the introduction, was that the total aerosol forcing of -1.3 W/m^2 reduced the greenhouse forcing of near 3 W/m^2 by about 45%, in the neighborhood of the GFDL and GISS forcings. Since the average model sensitivity was close to $0.75 \text{ }^\circ\text{C}/(\text{W/m}^2)$, similar to the sensitivities of these models, the necessary negative forcing is therefore similar. The agreement cannot therefore be used to validate the actual aerosol effect until climate sensitivity itself is better known.

Is there some way to distinguish between greenhouse gas and aerosol forcing that would allow the observational record to indicate how much of each was really occurring? This question of attribution has been the subject of numerous papers, and the full scope of the discussion is beyond the range of this (CCSP SAP2.3) report. It might be briefly noted that Zhang et al. (2006, [157722](#)) using results from several climate models and including both spatial and temporal patterns, found that the climate responses to greenhouse gases and sulfate aerosols are correlated, and separation is possible only occasionally, especially at global scales. This conclusion appears to be both model and method-dependent: using time-space distinctions as opposed to trend detection may work differently in different models (Gillett et al., 2002, [190576](#)). Using multiple models helps primarily by providing larger-ensemble sizes for statistics (Gillett et al., 2002, [190578](#)). However, even separating between the effects of different aerosol types is difficult. Jones et al. (2005, [155885](#)) concluded that currently the pattern of temperature change due to black carbon is indistinguishable from the sulfate aerosol pattern. In contrast, Hansen et al. (2005, [059087](#)) found that absorbing aerosols produce a different global response than other forcings, and so may be distinguishable. Overall, the similarity in response to all these very different forcings is undoubtedly due to the importance of climate feedbacks in amplifying the forcing, whatever its nature.



Source: Courtesy of the American Geophysical Union from Delworth et al. (2005, [190055](#)).

Figure 9-82. Change in global mean ocean temperature (left axis) and ocean heat content (right axis) for the top 3000 m due to different forcings in the GFDL model. WMGG includes all greenhouse gases and ozone; NATURAL includes solar and volcanic aerosols (events shown as green triangles on the bottom axis). Observed ocean heat content changes are shown as well.

Distinctions in the climate response do appear to arise in the vertical, where absorbing aerosols produce warming that is exhibited throughout the troposphere and into the stratosphere, whereas reflective aerosols cool the troposphere but warm the stratosphere (Hansen et al., 2005, [059087](#); IPCC, 2007, [092765](#)). Delworth et al. (2005, [190055](#)) noted that in the ocean, the cooling effect of aerosols extended to greater depths, due to the thermal instability associated with cooling the ocean surface. Hence the temperature response at levels both above and below the surface may provide an additional constraint on the magnitudes of each of these forcings, as may the difference between Northern and Southern Hemisphere changes (IPCC, 2007, [092765](#), Chapter 9). The profile of atmospheric temperature response will be useful to the extent that the vertical profile of aerosol absorption, an important parameter to measure, is known.

Implications for Climate Model Simulations

The comparisons in Sections 9.3.6.2 and 9.3.6.3 suggest that there are large differences in model calculated aerosol distributions, mainly because of the large uncertainties in modeling the aerosol atmospheric processes in addition to the uncertainties in emissions. The fact that the total optical depth is in better agreement between models than the individual components means that even with similar optical depths, the aerosol direct forcing effect can be quite different, as shown in the AeroCom studies. Because the diversity among models and discrepancy between models and observations are much larger at the regional level than in global average, the assessment of climate response (e.g., surface temperature change) to aerosol forcing would be more accurate for global average than for regional or hemispheric differentiation. However, since aerosol forcing is much more pronounced on regional than on global scales because of the highly variable aerosol distributions, it is insufficient or even misleading to just get the global average right.

The indirect effect is strongly influenced by the aerosol concentrations, size, type, mixing state, microphysical processes, and vertical profile. As shown in previous sections, very large differences exist in those quantities even among the models having similar AOD. Moreover, modeling aerosol indirect forcing presents more challenges than direct forcing because there is so far no rigorous observational data, especially on a global scale, that one can use to test the model simulations. As seen in the comparisons of the GISS and GFDL model climate simulations for IPCC AR4, aerosol indirect forcing was so poorly constrained that it was completely ignored by one model (GFDL) but used by another (GISS) at a magnitude that is more than half of the direct forcing, in order to reproduce the observed surface temperature trends. A majority of the climate models used in IPCC AR4 do not consider indirect effects; the ones that did were mostly limited to highly simplified sulfate indirect effects (Table 9-16). Improvements must be made to at least the degree that the aerosol indirect forcing can no longer be used to mask the deficiencies in estimating the climate response to greenhouse gas and aerosol direct RF.

9.3.6.7. Outstanding Issues

Clearly there are still large gaps in assessing the aerosol impacts on climate through modeling. Major outstanding issues and prospects of improving model simulations are discussed below.

Aerosol composition

Many global models are now able to simulate major aerosol types such as sulfate, black carbon, and POM, dust, and sea salt, but only a small fraction of these models simulate nitrate aerosols or consider anthropogenic secondary organic aerosols. And it is difficult to quantify the dust emission from human activities. As a result, the IPCC AR4 estimation of the nitrate and anthropogenic dust TOA forcing was left with very large uncertainty. The next generation of global models should therefore have a more comprehensive suite of aerosol compositions with better-constrained anthropogenic sources.

Aerosol absorption

One of the most critical parameters in aerosol direct RF and aerosol impact on hydrological cycles is the aerosol absorption. Most of the absorption is from BC despite its small contribution to total aerosol short and long-wave spectral ranges, whereas POM absorbs in the near UV. The aerosol absorption or SSA, will have to be much better represented in the models through improving the estimates of carbonaceous and dust aerosol sources, their atmospheric distributions, and optical properties.

Aerosol indirect effects

The activation of aerosol particles into CCN depends not only on particle size but chemical composition, with the relative importance of size and composition unclear. In current aerosol-climate modeling, aerosol size distribution is generally prescribed and simulations of aerosol composition have large uncertainties. Therefore the model estimated “albedo effect” has large uncertainties. How aerosol would influence cloud lifetime/ cover is still in debate. The influence of aerosols on other aspects of the climate system, such as precipitation, is even more uncertain, as are the physical processes involved. Processes that determine aerosol size distributions, hygroscopic growth, mixing state, as well as CCN concentrations, however, are inadequately represented in most of the global models. It will also be difficult to improve the estimate of indirect effects until the models can produce more realistic cloud characteristics.

Aerosol impacts on surface radiation and atmospheric heating

Although these effects are well acknowledged to play roles in modulating atmospheric circulation and water cycle, few coherent or comprehensive modeling studies have focused on them, as compared to the efforts that have gone to assessing aerosol RF at TOA. They have not yet been addressed in the previous IPCC reports. Here, of particular importance is to improve the accuracy of aerosol absorption.

Long-term trends of aerosol

To assess the aerosol effects on climate change the long-term variations of aerosol amount and composition and how they are related to the emission trends in different regions have to be specified. Simulations of historical aerosol trends can be problematic since historical emissions of aerosols have shown large uncertainties – as information is difficult to obtain on past source types, strengths, and even locations. The IPCC AR4 simulations used several alternative aerosol emission histories, especially for BC and POM aerosols.

Climate modeling

Current aerosol simulation capabilities from CTMs have not been fully implemented in most models used in IPCC AR4 climate simulations. Instead, a majority employed simplified approaches to account for aerosol effects, to the extent that aerosol representations in the GCMs, and the resulting forcing estimates, are inadequate. The oversimplification occurs in part because the modeling complexity and computing resource would be significantly increased if the full suite of aerosols were fully coupled in the climate models.

Observational constraints

Model improvement has been hindered by a lack of comprehensive datasets that could provide multiple constraints for the key parameters simulated in the model. The extensive AOD coverage from satellite observations and AERONET measurements has helped a great

deal in validating model-simulated AOD over the past decade, but further progress has been slow. Large model diversities in aerosol composition, size, vertical distribution, and mixing state are difficult to constrain, because of lack of reliable measurements with adequate spatial and temporal coverage (see Chapter 2 of the CCSP SAP2.3).

Aerosol radiative forcing

Because of the large spatial and temporal differences in aerosol sources, types, emission trends, compositions, and atmospheric concentrations, anthropogenic aerosol RF has profound regional and seasonal variations. So it is an insufficient measure of aerosol RF scientific understanding, however useful, for models (or observation-derived products) to converge only on globally and annually averaged TOA RF values and accuracy. More emphasis should be placed on regional and seasonal comparisons, and on climate effects in addition to direct RF at TOA.

9.3.6.8. Conclusions

From forward modeling studies, as discussed in the IPCC (2007, [092765](#)), the direct effect of aerosols since pre-industrial times has resulted in a negative RF of about -0.5 ± 0.4 W/m^2 . The RF due to cloud albedo or brightness effect is estimated to be -0.7 (-1.8 to -0.3) W/m^2 . Forcing of similar magnitude has been used in some modeling studies for the effect associated with cloud lifetime, in lieu of the cloud brightness influence. The total negative RF due to aerosols according to IPCC (2007, [092765](#)) estimates is therefore -1.3 (-2.2 to -0.5) W/m^2 . With the inverse approach, in which aerosols provide forcing necessary to produce the observed temperature change, values range from -1.7 to -0.4 W/m^2 (IPCC, 2007, [092765](#)). These results represent a substantial advance over previous assessments (e.g., IPCC TAR), as the forward model estimated and inverse approach required aerosol TOA forcing values are converging. However, large uncertainty ranges preclude using the forcing and temperature records to more accurately determine climate sensitivity.

There are now a few dozen models that simulate a comprehensive suite of aerosols. This is done primarily in the CTMs. Model inter-comparison studies have shown that models have merged at matching the global annual averaged AOD observed by satellite instruments, but they differ greatly in the relative amount of individual components, in vertical distributions, and in optical properties. Because of the great spatial and temporal variations of aerosol distributions, regional and seasonal diversities are much larger than that of the global annual mean. Different emissions and differences in atmospheric processes, such as transport, removal, chemistry, and aerosol microphysics, are chiefly responsible for the spread among the models. The varying component contributions then lead to differences in aerosol direct RF, as aerosol scattering and absorption properties depend on aerosol size and type. They also impact the calculated indirect RF, whose variations are further amplified by the wide range of cloud and convective parameterizations in models. Currently, the largest aerosol RF uncertainties are associated with the aerosol indirect effect. Most climate models used for the IPCC AR4 simulations employed simplified approaches, with aerosols specified from stand-alone CTM simulations. Despite the uncertainties in aerosol RF and widely varying model climate sensitivity, the IPCC AR4 models were generally able to reproduce the observed temperature record for the past century. This is because models with lower/higher climate sensitivity generally used less/more negative aerosol forcing to offset the greenhouse gas warming. An equally good match to observed surface temperature change in the past could be obtained from a model with larger climate sensitivity and smaller net forcing, or a model with smaller sensitivity and larger forcing (Hansen et al., 2007, [190597](#)). Obviously, both greenhouse gases and aerosol effects have to be much better quantified in future assessments.

Progress in better quantifying aerosol impacts on climate will only be made when the capabilities of both aerosol observations and representation of aerosol processes in models are improved. The primary concerns and issues discussed in this chapter of the CCSP SAP2.3 include:

- Better representation of aerosol composition and absorption in the global models
- Improved theoretical understanding of subgrid-scale processes crucial to aerosol-cloud interactions and lifetime
- Improved aerosol microphysics and cloud parameterizations
- Better understanding of aerosol effects on surface radiation and hydrological cycles
- More focused analysis on regional and seasonal variations of aerosols
- More reliable simulations of aerosol historic long-term trends
- More sophisticated climate model simulations with coupled aerosol and cloud processes
- Enhanced satellite observations of aerosol type, SSA, vertical distributions, and aerosol radiative effect at TOA; more coordinated field experiments to provide constraints on aerosol chemical, physical, and optical properties.

9.3.7. Fire as a Special Source of PM Welfare Effects

Much interest has developed in defining more precisely the role of pyrogenic C in the boreal C cycle. This is due to: (1) the resistance of pyrogenic C to decomposition; (2) its influence on soil processes; and (3) the absorption of solar radiation by soot aerosols (Preston and Schmidt, 2006, [156030](#)).

Preston and Schmidt (2006, [156030](#)) reviewed the current state of knowledge regarding atmospheric emissions of pyrogenic C in the boreal zone. They considered chemical structures, analytical methods, formation, characteristics in soil, loss mechanisms, and longevity. Biomass is largely converted to gaseous forms during burning, but up to several percent is converted to pyrogenic C, and this includes charcoal and BC. Charcoal is defined visually; BC is defined chemically by its resistance to oxidation in the laboratory. Andreae and Gelencsér (2006, [156215](#)) reviewed a different category of light-absorbing carbon, referred to as brown carbon.

Within the boreal zone, fire is a critical driver of ecosystem process and nutrient cycling (Hicke et al., 2003, [156545](#)). For example, Bachelet et al. (2005, [156241](#)) estimated that 61% of the C gained in Alaska by primary production of boreal forests between 1922 and 1996 was lost to fire.

An updated modeling effort to evaluate the radiative effects of aerosols was presented by Stier et al. (2007, [157012](#)). Inclusion of refractive indices recommended by Bond and Bergstrom (2005, [155696](#)) significantly increased aerosol RF and resulted in better agreement with sun-photometer estimates. Although this stage of climate modeling improved the representation of aerosols, large uncertainties remain regarding the effects of aerosol mixing and aerosol-cloud interactions. Furthermore, Stier et al. (2007, [157012](#)) emphasized that these types of modeling efforts are dependent upon emission estimates that are likely to vary by a factor of 2 or more.

One important reason for the acknowledged uncertainty in estimating global emissions of carbonaceous aerosols is the influence of intermittent fires that can occur at scales large enough to affect hemispheric aerosol concentrations. To better quantify the effects of large-scale fire, Generoso et al. (2007, [155786](#)) used satellite observations of boreal fires in Russia in 2003 to evaluate the performance of a global chemistry and transport model in simulating aerosol optical thickness, transport, and deposition. Emissions estimates of BC and OC were adjusted in the model to better match satellite observations of pollutant transport over the North Pacific. This resulted in an increase in optical thickness and BC deposition by a factor of 2. The adjusted model estimated that the fires contributed 16-33% of the optical thickness and 40-56% of BC deposition north of 75° N in the spring and summer of 2003.

Large fires also occurred over the Iberian Peninsula and Mediterranean coast during 2003. A meso-scale atmospheric transport model was used with ground-based measurements and satellite optical measurements to characterize the dispersion of emitted smoke particles and quantify radiative effects across Europe (Hodzic et al., 2007, [156553](#)). The modeled wildfire emissions resulted in increases in PM_{2.5} concentrations from 20 to 200%. The increased aerosol concentration was estimated to increase radiative forcing by 10-35 W/m² during the period of strong fire influence. Absorption of radiation by BC was also estimated to decrease rates of photolysis by 30%. In this simulation, all particles were assumed to be internally mixed, and secondary aerosol formation was not considered. Meteorological conditions in Europe during the exceptionally hot summer of 2003 were linked to enhanced photochemically derived pollutants, increased wild fires, and elevated aerosol concentrations in an analysis by Vautard et al. (2007, [106012](#)).

In addition to incidental fires, routine biomass burning, usually associated with agriculture in eastern Europe, also has been shown to contribute to hemispheric concentrations of carbonaceous aerosols. In the spring of 2006, the most severe air pollution levels in the Arctic to date were recorded (Stohl et al., 2006, [156100](#)). Atmospheric transport modeling coupled with satellite fire detection data identified biomass burning for agriculture as the primary cause of the high pollution levels. Concentrations of PM_{2.5} peaked during the pollution episode at values of an order of magnitude greater than those recorded prior to the episode. The increased transport of pollution into the Arctic during 2006 was attributed to weather conditions that delayed preparations for crop planting into May. Weather patterns favorable for pollutant transport into the Arctic were related to unusually warm weather in late April and May, when the majority of agricultural biomass burning took place that year.

In the summer of 2004, 2.7 million ha were burned by wildfire in Alaska and 3.1 million ha were burned in Canada. Effects on atmospheric air quality were measured throughout the Arctic, although the concentrations of particulates varied considerably. Aerosol optical depths were also

increased at all measurement stations, which indicated that the fires were likely to have had a significant effect on the atmospheric radiation budget for the Arctic (Stohl et al., 2006, [156100](#)). At one site, a pronounced drop in albedo was observed due presumably to high deposition of light absorbing particulates on the snow surface by the North American fires in 2004.

Investigations of the effects of large fires on climate forcing have typically focused on the absorptive effects of BC. However, these fires also release large amounts of CO₂ and CH₄, as well as light scattering compounds such as OC, and can enhance cloud formation. These fires also increase radiative surface absorption through BC deposition on snow and ice, and alter surface albedo and ecosystem energy budgets within the burn perimeter. Randerson et al. (2006, [156038](#)) estimated the net climate forcing of greenhouse gases, aerosols, BC deposition on snow and ice and changes in albedo for the year subsequent to a fire and for 80 years in the future in interior Alaska. The net effect of the fire in the first year was an increase in radiative forcing, but over the 80-year recovery period, average net annual radiative forcing was decreased by the fire.

9.3.8. Radiative Effects of Volcanic Aerosols

Section 9.3.8.1. comes directly from IPCC AR4 Chapter 2, Section 2.7.2, with section, table, and figure numbers changed to be internally consistent with this ISA.

9.3.8.1. Explosive Volcanic Activity

Radiative Effects of Volcanic Aerosols

Volcanic sulfate aerosols are formed as a result of oxidation of the sulfur gases emitted by explosive volcanic eruptions into the stratosphere. The process of gas-to-particle conversion has an e-folding time of roughly 35 days (Bluth et al., 1992, [192029](#); Read et al., 1993, [192031](#)). The e-folding time (by mass) for sedimentation of sulfate aerosols is typically about 12 to 14 months (Baran and Foot, 1994, [192032](#); Barnes and Hofmann, 1997, [192044](#); Bluth et al., 1997, [192045](#); Lambert et al., 1993, [192231](#)). Also emitted directly during an eruption are volcanic ash particulates (siliceous material). These are particles usually larger than 2 μm that sediment out of the stratosphere fairly rapidly due to gravity (within three months or so), but could also play a role in the radiative perturbations in the immediate aftermath of an eruption. Stratospheric aerosol data incorporated for climate change simulations tends to be mostly that of the sulfates (Ammann et al., 2003, [192057](#); Hansen et al., 2002, [049177](#); Ramachandran et al., 2000, [192050](#); Sato et al., 1993, [192046](#); Stenchikov et al., 1998, [192049](#); Tett et al., 2002, [192053](#)). As noted in the Second Assessment Report (SAR) and the TAR, explosive volcanic events are episodic, but the stratospheric aerosols resulting from them yield substantial transitory perturbations to the radiative energy balance of the planet, with both shortwave and longwave effects sensitive to the microphysical characteristics of the aerosols (e.g., size distribution).

Long-term ground-based and balloon-borne instrumental observations have resulted in an understanding of the optical effects and microphysical evolution of volcanic aerosols (Deshler et al., 2003, [192058](#); Hofmann et al., 2003, [192062](#)). Important ground-based observations of aerosol characteristics from pre-satellite era spectral extinction measurements have been analysed by Stothers (2001, [192233](#); 2001, [192232](#)), but they do not provide global coverage. Global observations of stratospheric aerosol over the last 25 years have been possible owing to a number of satellite platforms, for example, TOMS and TOVS have been used to estimate SO₂ loadings from volcanic eruptions (Krueger et al., 2000, [192234](#); Prata et al., 2003, [192235](#)). The Stratospheric Aerosol and Gas Experiment (SAGE) and Stratospheric Aerosol Measurement (SAM) projects (e.g., McCormick and Trepte, 1987, [192328](#)) have provided vertically resolved stratospheric aerosol spectral extinction data for over 20 years, the longest such record. This data set has significant gaps in coverage at the time of the El Chichón eruption in 1982 (the second most important in the 20th century after Mt. Pinatubo in 1991) and when the aerosol cloud is dense; these gaps have been partially filled by lidar measurements and field campaigns (e.g., Antuña et al., 2003, [192251](#); Thomason and Peter, 2006, [192248](#)).

Volcanic aerosols transported in the atmosphere to polar regions are preserved in the ice sheets, thus recording the history of the Earth's volcanism for thousands of years (Kruyssen, 1971, [192236](#); Mosley-Thompson et al., 2003, [192255](#); Palmer et al., 2002, [192319](#)). However, the atmospheric loadings obtained from ice records suffer from uncertainties due to imprecise knowledge of the latitudinal distribution of the aerosols, depositional noise that can affect the signal for an individual eruption in a single ice core, and poor constraints on aerosol microphysical properties. The best-documented explosive volcanic event to date, by way of reliable and accurate observations, is the 1991 eruption of Mt. Pinatubo. The growth and decay

of aerosols resulting from this eruption have provided a basis for modeling the RF due to explosive volcanoes. There have been no explosive and climatically significant volcanic events since Mt. Pinatubo. As pointed out in Ramaswamy et al. (2001, [156899](#)), stratospheric aerosol concentrations are now at the lowest concentrations since the satellite era and global coverage began in about 1980. Altitude dependent stratospheric optical observations at a few wavelengths, together with columnar optical and physical measurements, have been used to construct the time-dependent global field of stratospheric aerosol size distribution formed in the aftermath of volcanic events. The wavelength-dependent stratospheric aerosol single-scattering characteristics calculated for the solar and longwave spectrum are deployed in climate models to account for the resulting radiative (shortwave plus longwave) perturbations.

Using available satellite- and ground-based observations, Hansen et al. (2002, [049177](#)) constructed a volcanic aerosols data set for the 1850-1999 period (Sato et al., 1993, [192046](#)). This has yielded zonal mean vertically resolved aerosol optical depths for visible wavelengths and column average effective radii. Stenchikov et al. (2006, [192260](#)) introduced a slight variation to this data set, employing UARS observations to modify the effective radii relative to Hansen et al. (2002, [049177](#)), thus accounting for variations with altitude. Ammann et al. (2003, [192057](#)) developed a data set of total aerosol optical depth for the period since 1890 that does not include the Krakatau eruption. The data set is based on empirical estimates of atmospheric loadings, which are then globally distributed using a simplified parameterization of atmospheric transport, and employs a fixed aerosol effective radius (0.42 μm) for calculating optical properties. The above data sets have essentially provided the bases for the volcanic aerosols implemented in virtually all of the models that have performed the 20th-century climate integrations (Stenchikov et al., 2006, [192260](#)). Relative to Sato et al. (1993, [192046](#)), the Ammann et al. (2003, [192057](#)) estimate yields a larger value of the optical depth, by 20 to 30% in the second part of the 20th century, and by 50% for eruptions at the end of 19th and beginning of 20th century, for example, the 1902 Santa Maria eruption (Figure 9-83).

The global mean RF calculated using the Sato et al. (1993, [192046](#)) data yields a peak in radiative perturbation of about -3 W/m^2 for the strong (rated in terms of emitted SO_2) 1860 and 1991 eruptions of Krakatau and Mt. Pinatubo, respectively. The value is reduced to about -2 W/m^2 for the relatively less intense El Chichón and Agung eruptions (Hansen et al., 2002, [049177](#)). As expected from the arguments above, Ammann's RF is roughly 20 to 30% larger than Sato's RF.

Not all features of the aerosols are well quantified, and extending and improving the data sets remains an important area of research. This includes improved estimates of the aerosol size parameters (Bingen et al., 2004, [192262](#)), a new approach for calculating aerosol optical characteristics using SAGE and UARS data (Bauman et al., 2003, [192265](#)), and intercomparison of data from different satellites and combining them to fill gaps (Randall et al., 2001, [192268](#)). While the aerosol characteristics are better constrained for the Mt. Pinatubo eruption, and to some extent for the El Chichón and Agung eruptions, the reliability degrades for aerosols from explosive volcanic events further back in time as there are few, if any, observational constraints on their optical depth and size evolution.

The radiative effects due to volcanic aerosols from major eruptions are manifest in the global mean anomaly of reflected solar radiation; this variable affords a good estimate of radiative effects that can actually be tested against observations. However, unlike RF, this variable contains effects due to feedbacks (e.g., changes in cloud distributions) so that it is actually more a signature of the climate response. In the case of the Mt. Pinatubo eruption, with a peak global visible optical depth of about 0.15, simulations yield a large negative perturbation as noted above of about -3 W/m^2 (Hansen et al., 2002, [049177](#); Ramachandran et al., 2000, [192050](#)) (see also Section 9.2 of the IPCC AR4). This modeled estimate of reflected solar radiation compares reasonably with ERBS observations (Minnis et al., 1993, [190539](#)). However, the ERBS observations were for a relatively short duration, and the model-observation comparisons are likely affected by differing cloud effects in simulations and measurements. It is interesting to note (Stenchikov et al., 2006, [192260](#)) that, in the Mt. Pinatubo case, the Goddard Institute for Space Studies (GISS) models that use the Sato et al. (1993, [192046](#)) data yield an even greater solar reflection than the National Center for Atmospheric Research (NCAR) model that uses the larger (Ammann et al., 2003, [192057](#)) optical depth estimate.

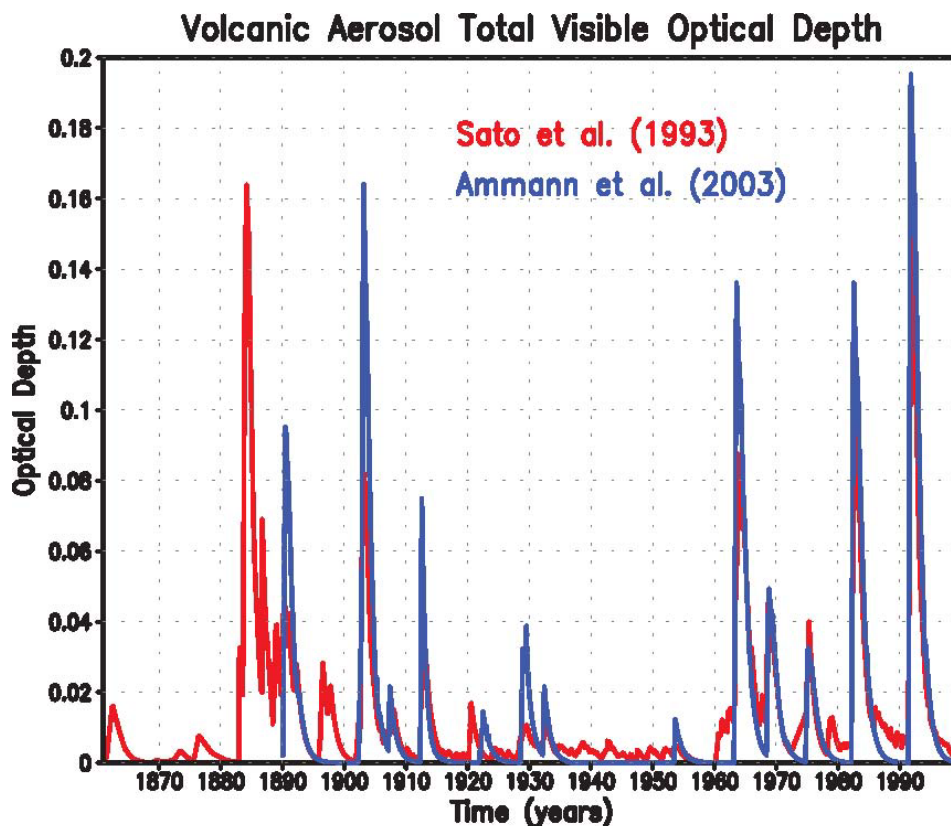


Figure 9-83. Visible (wavelength 0.55 μm) optical depth estimates of stratospheric SO_4^{2-} aerosols formed in the aftermath of explosive volcanic eruptions that occurred between 1860 and 2000. Results are shown from two different data sets that have been used in recent climate model integrations. Note that the Ammann et al. (2003, [192057](#)) data begins in 1890.

Thermal, Dynamical and Chemistry Perturbations Forced by Volcanic Aerosols

Four distinct mechanisms have been invoked with regards to the climate response to volcanic aerosol RF. First, these forcings can directly affect the Earth's radiative balance and thus alter surface temperature. Second, they introduce horizontal and vertical heating gradients; these can alter the stratospheric circulation, in turn affecting the troposphere. Third, the forcings can interact with internal climate system variability (e.g., El Niño-Southern Oscillation, North Atlantic Oscillation, Quasi-Biennial Oscillation) and dynamical noise, thereby triggering, amplifying or shifting these modes (see Section 9.2 of the IPCC AR4) (Stenchikov et al., 2004, [192274](#); Yang and Schlesinger, 2001, [192270](#)). Fourth, volcanic aerosols provide surfaces for heterogeneous chemistry affecting global stratospheric ozone distributions (Chipperfield et al., 2003, [192275](#)) and perturbing other trace gases for a considerable period following an eruption. Each of the above mechanisms has its own spatial and temporal response pattern. In addition, the mechanisms could depend on the background state of the climate system, and thus on other forcings (e.g., due to well-mixed gases) (Meehl et al., 2004, [192279](#)), or interact with each other.

The complexity of radiative-dynamical response forced by volcanic impacts suggests that it is important to calculate aerosol radiative effects interactively within the model rather than prescribe them (Andronova et al., 1999, [192286](#); Broccoli et al., 2003, [192283](#)). Despite differences in volcanic aerosol parameters employed, models computing the aerosol radiative effects interactively yield tropical and global mean lower-stratospheric warmings that are fairly consistent with each other and with observations (Hansen et al., 2002, [049177](#); Ramachandran et al., 2000, [192050](#); Ramaswamy et al., 2006, [192284](#); Stenchikov et al., 2004, [192274](#); Yang and Schlesinger, 2001, [192270](#)); however, there is a considerable range in the responses in the

polar stratosphere and troposphere. The global mean warming of the lower stratosphere is due mainly to aerosol effects in the longwave spectrum, in contrast to the flux changes at the TOA that are essentially due to aerosol effects in the solar spectrum. The net radiative effects of volcanic aerosols on the thermal and hydrologic balance (e.g., surface temperature and moisture) have been highlighted by recent studies (Free and Angell, 2002, [192281](#); Jones et al., 2003, [192278](#)) (see Chapter 6 of the IPCC AR4). See Chapter 9 (of the IPCC AR4) for significance of the simulated responses and model-observation comparisons for 20th-century eruptions. A mechanism closely linked to the optical depth perturbation and ensuing warming of the tropical lower stratosphere is the potential change in the cross-tropopause water vapour flux (Joshi and Shine, 2003, [192327](#)) (see Section 2.3.7 of the IPCC AR4).

Anomalies in the volcanic-aerosol induced global radiative heating distribution can force significant changes in atmospheric circulation, for example, perturbing the equator-to-pole heating gradient (Ramaswamy et al., 2006, [192273](#); Stenchikov et al., 2002, [192277](#)) (see Section 9.2 of the IPCC AR4) and forcing a positive phase of the Arctic Oscillation that in turn causes a counterintuitive boreal winter warming at middle and high latitudes over Eurasia and North America (Miller et al., 2005, [192258](#); Perlwitz and Graf, 2001, [192271](#); Perlwitz and Harnik, 2003, [192264](#); Rind et al., 2005, [192261](#); Shindell et al., 2003, [192069](#); Shindell et al., 2004, [192267](#); Stenchikov et al., 2002, [192277](#); Stenchikov et al., 2004, [192274](#); Stenchikov et al., 2006, [192260](#)).

Stratospheric aerosols affect the chemistry and transport processes in the stratosphere, resulting in the depletion of ozone (Brasseur and Granier, 1992, [192256](#); Chipperfield et al., 2003, [192275](#); Solomon et al., 1996, [192252](#); Tie et al., 1994, [192253](#)). Stenchikov et al. (2002, [192277](#)) demonstrated a link between ozone depletion and Arctic Oscillation response; this is essentially a secondary radiative mechanism induced by volcanic aerosols through stratospheric chemistry. Stratospheric cooling in the polar region associated with a stronger polar vortex initiated by volcanic effects can increase the probability of formation of polar stratospheric clouds and therefore enhance the rate of heterogeneous chemical destruction of stratospheric ozone, especially in the NH (Tabazadeh et al., 2002, [192250](#)). The above studies indicate effects on the stratospheric ozone layer in the wake of a volcanic eruption and under conditions of enhanced anthropogenic halogen loading. Interactive microphysics-chemistry-climate models (Dameris et al., 2005, [192055](#); Rozanov et al., 2002, [192070](#); Rozanov et al., 2004, [192072](#); Shindell et al., 2003, [192069](#); Timmreck et al., 2003, [192068](#)) indicate that aerosol-induced stratospheric heating affects the dispersion of the volcanic aerosol cloud, thus affecting the spatial RF. However the models' simplified treatment of aerosol microphysics introduces biases; further, they usually overestimate the mixing at the tropopause level and intensity of meridional transport in the stratosphere (Douglass et al., 2003, [057260](#); Schoeberl et al., 2003, [057262](#)). For present climate studies, it is practical to utilize simpler approaches that are reliably constrained by aerosol observations.

Because of its episodic and transitory nature, it is difficult to give a best estimate for the volcanic RF, unlike the other agents. Neither a best estimate nor a level of scientific understanding was given in the TAR. For the well-documented case of the explosive 1991 Mt. Pinatubo eruption, there is a good scientific understanding. However, the limited knowledge of the RF associated with prior episodic, explosive events indicates a low level of scientific understanding.

9.3.9. Other Special Sources and Effects

International shipping has been identified as an additional source of carbonaceous aerosols. Simulations with a climate model that included aerosol effects and 3 different emissions inventories showed that shipping contributed 2.3-3.6% of the total SO_4^{2-} atmospheric aerosol content and 0.4-1.4% of the total BC atmospheric aerosol content, based on global means in 2000. This modeling also showed that aerosol optical thickness over the Indian Ocean, the Gulf of Mexico, and the northeastern Pacific Ocean varied by 8 to 10%. The corresponding all-sky (that includes both cloudy and clear skies) direct radiative forcings ranged from -0.011 to -0.013 W/m^2 . The greatest effect of aerosols emitted from global shipping is likely to be an increase in cloud formation and the resulting change in reflectivity of shortwave radiation. Aerosols from shipping were estimated to contribute 17-39% of the total anthropogenic aerosol radiation forcing effect.

When BC is deposited to the surface of ice or snow, solar absorption and heating occur at the surface. This can melt additional snow or ice at the surface and the reflectivity of the surface can change. Both factors affect aspects of climate. Jacobson (2003, [155866](#); 2004, [155870](#)) and Jacobson et al. (2004, [180362](#)) estimated the warming due to fossil fuel BC and organic matter using the Gas, Aerosol, Transport, Radiation, General Circulation, Mesoscale and Ocean Model (GATOR-GCMOM). The modeling effort included consideration of the BC cycle, accounting for emissions, transport, aerosol coagulation, aerosol growth, cloud activation, aerosol-cloud coagulation, cloud-cloud coagulation, rainout, washout, dry deposition, and processes of precipitated and dry-deposited BC in snow and sea ice. Results suggested that BC absorption in snow and sea ice

increased near-surface temperatures over a 10-year simulation by about 0.06°K (Jacobson, 2003, [155868](#)).

BC soot is a potentially important agent of climate warming in the Arctic, and northern boreal wildfires may contribute substantially to this effect. Soot is approximately twice as effective as CO₂ in altering surface air temperature, and can reduce sea ice formation and snow albedo (Hansen and Nazarenko, 2004, [156521](#)).

Kim et al. (2005, [155900](#)) investigated the relationships between northern boreal wildfires and reductions in Arctic sea ice and glacial coverage. They modeled the FROSTFIRE boreal forest control burn (Hinzman et al., 2003, [155845](#)) with respect to BC aerosol transport, dispersion, and deposition. Model results suggested that boreal wildfires could be a major source of BC soot to sea ice and glaciers in Alaska. This may exacerbate summer melting of sea ice and reduce recruitment of first-year ice into multiyear ice, thereby leading to an overall reduction in sea ice. Similarly, increased BC soot on glaciers would be expected to increase summer melting and lead to an overall reduction in glacial coverage (Kim et al., 2005, [155900](#)).

Jacobson (2002, [155865](#)) proposed, based on model simulations with 12 identifiable effects of aerosol particles on climate, emission reductions of fossil fuel particulate BC and associated organic matter could potentially slow warming for a specific period more than reduction of CO₂ or CH₄ for a specific period. Jacobson's (2006, [156599](#)) calculations suggested that fossil fuel BC plus organic matter emissions reductions could eliminate 8-18% of total anthropogenic warming, and 20-45% of net warming after accounting for aerosol cooling, within a period of 3-5 years (Chock et al., 2003, [155727](#)). See also conflicting discussions (Feichter et al., 2003, [155772](#); Penner, 2003, [156851](#)); and further responses (Jacobson, 2003, [155867](#); Jacobson, 2003, [155868](#); Jacobson, 2003, [155869](#); Penner, 2003, [156851](#)).

Bond and Sun (2005, [156282](#)) reviewed published data regarding the warming potential of BC, compared with CO₂ and other GHG. Climatic effects of GHG are generally compared on the basis of top-of-the-atmosphere, globally averaged changes in radiative balance. On that basis, BC is one of the largest individual warming agents, after CO₂ and perhaps CH₄ (Bond and Sun, 2005, [156282](#); Jacobson, 2000, [056378](#); Sato et al., 2003, [156947](#)).

Reddy and Boucher (2007, [156042](#)) conducted an analysis that provided regional estimates of BC emissions from fossil fuels and biofuels. These estimates indicated that East and Southeast Asia contributed over 50% of the global BC burden and its associated direct radiative forcing. Europe was found to be the largest BC contributor in the northern latitudes. The indirect effect of BC deposition on snow was also estimated to be highest for Europe.

To improve understanding of the role of aerosols in climate forcing, Chung and Seinfeld (2002, [155732](#)) estimated the global distribution of BC, primary organic particles (those directly emitted from combustion), secondary organic particles (primary organic compounds partially oxidized in the atmosphere), and SO₄²⁻ aerosols to model the overall radiative forcing of these groups of compounds. The model was run with the assumption that the BC particles do not combine with OC or SO₄²⁻ particles (termed an external mixture), and with the assumption that the particles are represented by a core of BC surrounded by a shell of light scattering aerosols. Modeling results suggested an overall radiative cooling effect from aerosols ranging from -0.39 to -0.78 W/m².

Roberts and Jones (2004, [156052](#)) used a climate modeling approach to compare possible effects of BC on climate warming to those attributable to emissions from greenhouse gases. Results suggested that the warming effect from atmospheric BC aerosols may not be large relative to that from greenhouse gases. A different modeling approach by Roeckner et al. (2006, [156920](#)) evaluated the effects of BC and primary OC on climate under two scenarios of carbonaceous aerosol emissions. In the first scenario, BC and primary OC emissions decreased over Europe and China, but increased at lower latitudes. In the second scenario, emissions were frozen at 2000 levels. The effects of both scenarios on mean global temperature were found to be small, but higher aerosol emissions at low latitudes did result in atmospheric heating and corresponding land surface cooling that led to increased precipitation and runoff in this simulation.

Study of BC effects in tropical climates was undertaken by Wang (2007, [156147](#)). Substantial effects of direct radiative forcing by BC on the tropical Pacific were shown in model results that were similar to the El Niño Southern Oscillation activities both in the nature and scale of effects with enhancement of the Indian monsoon circulation. The model suggested that atmospheric heating by radiation absorption by BC can form temperature and pressure anomalies that favor propagation of convection from western to central and eastern Pacific. More work will be needed to distinguish between the aerosol signal and natural factors in controlling tropical precipitation in this region.

Table 9-18. Overview of the different aerosol indirect effects and their sign of the net radiative flux change at the top of the atmosphere (TOA).

Effect	Cloud Types Affected	Process	Sign of Change in TOA Radiation	Potential Magnitude	Scientific Understanding
Cloud albedo effect	All clouds	For the same cloud water or ice content more but smaller cloud particles reflect more solar radiation	Negative	Medium	Low
Cloud lifetime effect	All clouds	Smaller cloud particles decrease the precipitation efficiency thereby presumably prolonging cloud lifetime	Negative	Medium	Very low
Semi-direct effect	All clouds	Absorption of solar radiation by absorbing aerosols affects static stability and the surface energy budget, and may lead to an evaporation of cloud particles	Positive or Negative	Small	Very low
Glaciation indirect effect	Mixed-phase clouds	An increase in IN increases the precipitation efficiency	Positive	Medium	Very low
Thermodynamic effect	Mixed-phase clouds	Smaller cloud droplets delay freezing causing super-cooled clouds to extend to colder temperatures	Positive or Negative	Medium	Very low

Source: Reprinted with Permission of Cambridge University Press from Denman (2007, [156394](#))

Table 9-19. Overview of the different aerosol indirect effects and their implications for the global mean net shortwave radiation of the surface F_{sfc} (columns 2-4) and for precipitation (columns 5-7).

Effect	Sign of Change in F_{sfc}	Potential Magnitude	Scientific Understanding	Sign of Change in Precipitation	Potential Magnitude	Scientific Understanding
Cloud albedo effect	Negative	Medium	Low	n.a.	n.a.	n.a.
Cloud lifetime effect	Negative	Medium	Very low	Negative	Small	Very low
Semi-direct effect	Negative	Large	Very low	Negative	Large	Very low
Glaciation indirect effect	Positive	Medium	Very low	Positive	Medium	Very low
Thermodynamic effect	Positive or Negative	Medium	Very low	Positive or Negative	Medium	Very low

Source: Reprinted with Permission of Cambridge University Press from Denman (2007, [156394](#))

There are several other kinds of climate effects from aerosol PM. None is well understood or well quantified. The semi-direct effect, which involves absorption of solar radiation by soot particles followed by re-emission as thermal radiation, is expected to heat the air mass and increase its static stability relative to the surface. The semi-direct effect can also cause evaporation of cloud droplets, thereby partially offsetting the cloud albedo indirect effect. The glaciation effect involves an increase in IN, which is expected to cause rapid glaciation of a super-cooled liquid water cloud due to the differences in vapor pressure over ice and water. Unlike cloud droplets, these ice crystals can quickly reach precipitation size, with the potential to turn a non-precipitating cloud into a precipitating cloud. The thermodynamic effect involves a delay in freezing by the smaller cloud droplets, which can cause super cooled clouds to occur under colder temperatures. The possible consequences to radiative flux of all of the processes are outlined in Table 9-18 (top of the atmosphere effects) and Table 9-19 (surface radiative and precipitation effects) (Denman et al., 2007, [156394](#)), though significant uncertainties remain. Nevertheless, the individual processes cannot be considered in isolation because of the numerous feedbacks, and because atmospheric aerosol concentrations and climate are intimately coupled (Denman et al., 2007, [156394](#); Dentener et al., 2006, [088434](#)).

9.3.9.1. Glaciers and Snowpack

Organic compounds are incorporated into snow by wet and dry deposition processes (Lei and Wania, 2004, [127880](#); Roth et al., 2004, [056431](#)). Atmospherically deposited organics appear to be ubiquitous in snowpacks at appreciable concentrations (Grannas et al., 2007, [156492](#)). Examples include PAHs, phthalates, alkanes, phenols, low molecular weight carbonyls, POPs, and low molecular weight organic acids (Halsall, 2004, [155822](#); Nakamura et al., 2000, [156792](#); Villa et al., 2003, [156139](#)). Humic-like substances found in the snowpack may release VOCs into the atmosphere via photo-oxidation (Grannas et al., 2004, [155803](#); Grannas et al., 2007, [156492](#)). Several thousand organic species were identified by Grannas et al. (2006, [155804](#)), based on molecular weight, from a single ice core collected in Russia. Little information is available, however, regarding the chemical properties of these chemical constituents. In addition to the diversity of chemicals that are deposited into the snowpack, there are also biological organisms, including bacteria and algae. Their role in influencing snow chemistry and volatilization processes is not understood (Grannas et al., 2007, [156492](#)).

Recent research has explored connections between the atmosphere and the cryosphere (land or sea covered by snow or ice). A seasonal maximum of 40% of the Earth's land surface is covered by snow or ice, as well as several percent of the oceans. Particulate deposition to snow and ice surfaces can affect melting rates. Deposition of PM to glacial ice surfaces can affect the subsequent rate of melting. A thin cover of debris contributes to accelerated melting. A thicker cover of debris, such as that which may result from a volcanic eruption, retards melting. The difference is due to the changing balance between enhanced absorption of shortwave radiation by PM and conductive heat flow (insulation) through a buildup of material having low heat conduction (Kirkbride and Dugmore, 2003, [156645](#)). This issue is particularly important for deposition of large quantities of volcanic material. To a lesser extent, however, the same principles apply to PM deposition derived from air pollution. Under a thin layer of debris, ablation rates are higher than for clean ice. However, as the thickness of the debris layer increases, ablation rates systematically decline (Nicholson and Benn, 2006, [156806](#)). The threshold debris thickness that separates ablation increase from decrease is site specific and depends on local climate and the nature of the debris particles. Nicholson and Benn (2006, [156806](#)) presented a surface energy balance model to calculate ice melt beneath a surface debris layer, based on meteorological data and basic debris characteristics. Modeled melting rates matched observed rates, suggesting that the model produced useful results.

Long-range atmospheric transport of PM delivers a large fraction of the total input of POPs to the Arctic region (Halsall, 2004, [155822](#)). These contaminants can accumulate in Arctic food webs and have become the focus of international research and concern. Nevertheless, fate and transport of POPs within terrestrial and marine Arctic ecosystems are not well understood and are strongly affected by the presence of snow and ice. Sea ice provides a barrier to air-water exchange, and this hinders volatilization and re-emission of previously deposited contaminants (Halsall, 2004, [155822](#)). Thus, the effects of greenhouse gasses and PM on climate in the Arctic region have feedbacks to POP fate, transport, and toxicity. The transfer of POPs among the major abiotic environmental compartments in the Arctic are summarized in Figure 9-84 from Halsall (2004, [155822](#)). Recent studies detailing rate and transport of POPs are summarized in Table 9-20.

Table 9-20. Recent studies highlighting POP occurrence and fate in the major arctic compartments.

ATMOSPHERE		
1	Annual time-series of OC and PCB concentrations in the Norwegian Arctic	Oehme et al. (1996, 156001)
2	Long-term analysis of the chlordane-group and their input to the Arctic with changing sources	Bidleman et al. (2002, 155691)
3	PAH occurrence at monitoring sites across the Arctic, seasonality and gas/particle partitioning	Halsall et al. (1997, 155821)
4	PCB occurrence at monitoring sites across the Arctic, spatial differences and seasonality	Stern et al. (1997, 156096)
5	Long-term analysis of PCB and OC trends in the Canadian Arctic and seasonal patterns	Hung et al. (2001, 155856 ; 2002, 155857)
6	Trans-Pacific LRAT and impact of Asian sources on the western Canadian Arctic	Bailey et al. (2000, 155670)
FRESHWATER		
7	Annual avg water concentrations in major Russian rivers for selected OC pesticides	Alexeeva et al. (2001, 155651)
8	Long-term (decades) PCB deposition profile in Arctic lake sediments	Muir et al. (1996, 155991)
9	Mass balance of selected OCs in Canadian Arctic lake conducted with data collected over 3 yrs	Helm et al. (2002, 155835)
10	Examining the biodegradation of HCHs in Canadian Arctic watersheds	Helm et al. (2000, 155834)
MARINE		
11	Transport and entry of β -HCH into western Arctic Ocean via Pacific surface waters	Li et al. (2002, 156691)
12	Occurrence of current use pesticides in air, fog and surface seawater in the western Arctic Ocean	Chermyak et al. (1996, 155726)
13	Resolving petrogenic and anthropogenic PAH input to marine sediments in coastal Arctic seas	Yunker et al. (1996, 156175)
14	Quantifying abiotic and biotic degradation of HCHs in the Arctic Ocean water column	Harner et al. (2000, 155829)
15	PCBs and OCs in surface ocean water—Bering and Chukchi seas	Strachan et al. (2001, 156103)
16	Spatial patterns of HCHs and toxaphene in Arctic Ocean surface water	Jantunen and Bidleman (1998, 155877)
SNOW/AIR-FRESHWATER		
17	PAHs (and inorganics) in surface snow layers (snowpit) at Summit, Greenland	Masclat et al. (2000, 155966)
18	PAHs measured in snow and ice layers on Agassiz ice-cap, Ellesmere Island, Canada	Peters et al. (1995, 156856)
19	Modeling OC behaviour and fate in the surface seasonal snow pack at Amituk Lake, Canada	Wania et al. (1998, 156148)
20	OCs, PCBs and PAHs in snow and ice of the Ob-Yenisey watershed of the Russian Arctic	Melnikov et al. (2003, 156753)
OCEAN/AIR		
21	Transfer of α -HCH across the air/water interface in the western Arctic ocean	Jantunen and Bidleman (1996, 155876)
22	Calculated seasonality of OC air/water fluxes in the Canadian high Arctic	Hargrave et al. (1997, 155827)
OCEAN/ICE		
23	Transport potential of contaminants across the Arctic ocean via sea-ice drift	Pfirman et al. (1997, 156864)
24	The importance of eastern Arctic sea-ice drift as a source of contaminants to the Norwegian sea	Korsnes et al. (2002, 156657)

Source: Reprinted with Permission of Elsevier Ltd. from Halsall (2004, [155822](#))

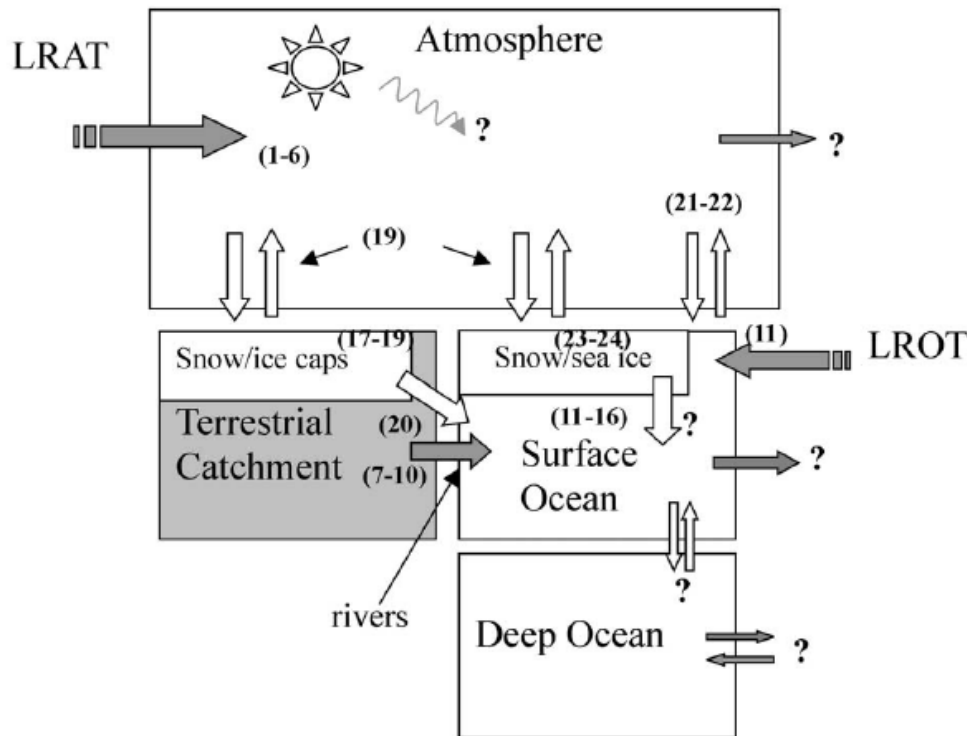


Figure 9-84. The transfer of POPs between the major abiotic compartments of the Arctic. Shaded arrows represent inputs/outputs of POPs to the Arctic. The numbers refer to selected studies detailing the occurrence and behavior of POPs, and are listed in Table 9-20. Question marks represent those areas that are least well understood. LRAT-long range atmospheric transport; LROT – long range oceanic transport.

9.3.9.2. Radiative Forcing by Anthropogenic Surface Albedo Change: BC in Snow and Ice

Section 9.3.9.2 comes directly from IPCC AR4 Chapter 2, Section 2.5.4, with section, table, and figure numbers changed to be internally consistent with this ISA.

The presence of soot particles in snow could cause a decrease in the albedo of snow and affect snowmelt. Initial estimates by Hansen et al. (2000, [042683](#)) suggested that BC could thereby exert a positive RF of $+0.2 \text{ W/m}^2$. This estimate was refined by Hansen and Nazarenko (2004, [156521](#)), who used measured BC concentrations within snow and ice at a wide range of geographic locations to deduce the perturbation to the surface and planetary albedo, deriving an RF of $+0.15 \text{ W/m}^2$. The uncertainty in this estimate is substantial due to uncertainties in whether BC and snow particles are internally or externally mixed, in BC and snow particle shapes and sizes, in voids within BC particles, and in the BC imaginary refractive index. Jacobson (2004, [155870](#)) developed a global model that allows the BC aerosol to enter snow via precipitation and dry deposition, thereby modifying the snow albedo and emissivity. They found modeled concentrations of BC within snow that were in reasonable agreement with those from many observations. The model study found that BC on snow and sea ice caused a decrease in the surface albedo of 0.4% globally and 1% in the NH, although RFs were not reported. Hansen et al. (2005, [059087](#)) allowed the albedo change to be proportional to local BC deposition according to Koch (2001, [192054](#)) and presented a further revised estimate of 0.08 W/m^2 . They also suggested that this RF mechanism produces a greater temperature response by a factor of 1.7 than an equivalent CO_2 RF, that is, the ‘efficacy’ may be higher for this RF mechanism (see Section 2.8.5.7 of the IPCC AR4). This report adopts a best estimate

for the BC on snow RF of $+0.10 \pm 0.10$ W/m², with a low level of scientific understanding (Section 2.9, Table 2.11, of the IPCC AR4).

9.3.9.3. Effects on Local and Regional Climate

Most effects of PM on climate, as assessed by IPCC (Stohl et al., 2007, [157015](#)) and summarized in this assessment, focus on global-scale processes and responses. In addition, it is also possible that PM emissions contribute to local and regional climate changes. These might include short-term cycles in rainfall or temperature and rainfall suppression, especially near cities and for orographic precipitation. Rainfall suppression, in particular, is believed to exacerbate water supply problems which are substantial in many regions, especially in the western U.S.

Aerosol particles, directly and through cloud enhancement, may reduce near-surface wind speeds locally. Slower winds, in turn, reduce evaporation. The overall impact can be a reduction in local precipitation. Jacobson and Kaufman (2006, [090942](#)) investigated the effects of PM on spatially-distributed wind speeds and resulting feedbacks to precipitation using the GATOR-GCMOM (Jacobson, 2001, [155864](#)) and supporting evidence from satellite data. The study focused on the South Coast Air Basin (SCAB) in California during February and August, 2002-2004. The modeled precipitation decrease over land in California was 2% of the baseline 1.5 mm/day due to emissions of anthropogenic aerosol particle and precursor gasses in the SCAB domain. However, the reduction over much of the Sierra Nevada, where most precipitation falls, was up to 0.5 mm/day, or 4-5% of the baseline 10-13 mm/day in that mountainous region (Jacobson, 2006, [156599](#)). The probable mechanism was described as follows. Aerosol particles and aerosol-enhanced clouds reduce wind speeds below them by stabilizing the air, reducing the vertical transport of horizontal momentum. In turn, the reduced wind speeds, and associated reduced evaporation and increased cloud lifetime, contributes to reduced local and regional precipitation (Jacobson, 2006, [156599](#)).

Effects of air pollution on regional precipitation were quantified by Givati and Rosenfeld (2004, [156475](#)). They found a 15-25% reduction in the orographic component of precipitation downwind of major coastal urban areas during the 20th century. Their study focused on orographically-forced clouds because these short-lived, shallow clouds are expected to exhibit the largest effect of air pollution on precipitation. Substantially larger precipitation suppression due to aerosol particulate pollution was found between Fresno and Sacramento in California by Givati and Rosenfeld (2004, [156475](#)). Precipitation losses over topographical barriers in the Sierra Nevada amounted to 15-25% of the annual precipitation at elevations less than 2,000 m. This precipitation suppression occurred mainly in the relatively shallow orographic clouds within the cold air mass of cyclones. The suppression that occurred on the upslope side of the mountains was coupled with similar percentage (but lower absolute volume) enhancement on the drier downslope eastern side (Givati and Rosenfeld, 2004, [156475](#)). Similar results were found in studies by Griffith et al. (2005, [156497](#)), Jirak and Cotton (2006, [156612](#)), Rosenfeld and Givati (2006, [156924](#)), and Rosenfeld et al. (2007, [156057](#)). At all of these study locations (California, Israel, Utah, Colorado, China), orographic precipitation decreased by 15-30% downwind of pollution sources, likely due to creation of more and smaller cloud droplets and resulting suppression of precipitation.

The study of Givati and Rosenfeld (2004, [156475](#)) was the first to quantify the microphysical effect of mesoscale precipitation. Following the findings of Givati and Rosenfeld (2004, [156475](#)), the effects of aerosol air pollution on precipitation at high elevation sites in the Front Range of Colorado adjacent to urban areas were investigated by Jirak and Cotton (2006, [156612](#)). Examination of precipitation trends showed that the ratio of upslope precipitation during easterly flows at high elevation west of Denver and Colorado Springs to the upwind urban sites decreased by about 30% over the past half century. These results provide further support for the hypothesis that aerosol pollution suppresses orographic precipitation downwind of pollution source areas.

Griffith et al. (2005, [156497](#)) found similar reductions in mountainous precipitation in Utah, downwind of Salt Lake City and Provo. The ratio of precipitation at mountain stations located in rural settings in Utah and Nevada remained stable, supporting the hypothesis that air pollution decreases Ro (the ratio of precipitation at the downwind site to precipitation at the upwind pollution source) over the mountains to the east of Salt Lake City.

Rosenfeld and Givati (2006, [156924](#)) extended the investigation of the suppression of precipitation by aerosol pollutants to a larger scale by examining the ratio between precipitation amounts over the hills to precipitation over upwind lowland areas throughout the western U.S. from the Pacific Coast to the Rocky Mountains. They found in these paired analyses a pattern of

decreasing precipitation by as much as 24% from the Mexican border to central California, with no decrease in northern California and Oregon and smaller decrease of 14% in Washington east of Seattle and Puget Sound. Similar decreases were found over Arizona and New Mexico (Rosenfeld, 2006, [190233](#)), Utah (Griffith et al., 2005, [156497](#)), and the east slope of the Colorado Rockies (Jirak and Cotton, 2006, [156612](#)).

Suppression of winter orographic precipitation appears to occur up to hundreds of kilometers inland of coastal urban areas (Rosenfeld, 2006, [190233](#)). Decreases in this precipitation ratio occurred during winter orographic precipitation, but not during convective summer precipitation over the same mountain ranges. This finding agrees with the expectation that aerosol-induced changes in the rate of precipitation formation would cause a decrease in precipitation from shallow and short-lived orographic clouds, but not necessarily from deeper and longer-lived thermally-driven convective clouds.

Results of these studies of aerosol effects on orographic precipitation suggest that human-caused air pollution, and fine particles in particular, have had a large effect on precipitation well beyond the local scales of the pollution sources (Rosenfeld, 2006, [190233](#)).

9.3.10. Summary of Effects on Climate

Aerosols affect climate through direct and indirect effects. The direct effect is primarily realized as planet brightening when seen from space because most aerosols scatter most of the visible spectrum light that reaches them. The IPCC AR4 reported that the radiative forcing from this direct effect was $-0.5 (\pm 0.4) \text{ W/m}^2$ and identified the level of scientific understanding of this effect as 'Medium-low'. The global mean direct radiative forcing effect from individual components of aerosols was estimated for the first time in the IPCC AR4 where they were reported to be (all in W/m^2 units): $-0.4 (\pm 0.2)$ for sulfate, $-0.05 (\pm 0.05)$ for fossil fuel-derived organic carbon, $+0.2 (\pm 0.15)$ for fossil fuel-derived black carbon, $+0.03 (\pm 0.12)$ for biomass burning, $-0.1 (\pm 0.1)$ for nitrates, and $-0.1 (\pm 0.2)$ for mineral dust. Global loadings of anthropogenic dust and nitrates remain very troublesome to estimate, making the radiative forcing estimates for these constituents particularly uncertain.

Numerical modeling of aerosol effects on climate has sustained remarkable progress since the time of the last PM AQCD, though model solutions still display large heterogeneity in their estimates of the direct radiative forcing effect from anthropogenic aerosols. The clear-sky direct radiative forcing over ocean due to anthropogenic aerosols is estimated from satellite instruments to be on the order of $-1.1 (\pm 0.37) \text{ W/m}^2$ while model estimates are -0.6 W/m^2 . The models' low bias over ocean is carried through for the global average: global average direct radiative forcing from anthropogenic aerosols is estimated from measurements to range from -0.9 to -1.9 W/m^2 , larger than the estimate of -0.8 W/m^2 from the models.

Aerosol indirect effects on climate are primarily realized as an increase in cloud brightness (termed the 'first indirect' or Twomey effect), changes in precipitation, and possible changes in cloud lifetime. The IPCC AR4 reported that the radiative forcing from the Twomey effect was -0.7 (range: -1.1 to $+4$) and identified the level of scientific understanding of this effect as 'Low' in part owing to the very large unknowns concerning aerosol size distributions and important interactions with clouds. Other indirect effects from aerosols are not considered to be radiative forcing.

Taken together, direct and indirect effects from aerosols increase Earth's shortwave albedo or reflectance thereby reducing the radiative flux reaching the surface from the Sun. This produces net climate cooling from aerosols. The current scientific consensus reported by IPCC AR4 is that the direct and indirect radiative forcing from anthropogenic aerosols computed at the top of the atmosphere, on a global average, is about -1.3 (range: -2.2 to -0.5) W/m^2 . While the overall global average effect of aerosols at the top of the atmosphere and at the surface is negative, absorption and scattering by aerosols within the atmospheric column warms the atmosphere between the Earth's surface and top of the atmosphere. In part, this is owing to differences in the distribution of aerosol type and size within the vertical atmospheric column since aerosol type and size distributions strongly affect the aerosol scattering and reradiation efficiencies at different altitudes and atmospheric temperatures. And, although the magnitude of the overall negative radiative forcing at the top of the atmosphere appears large in comparison to the analogous IPCC AR4 estimate of positive radiative forcing from anthropogenic GHG of about $+2.9$ (± 0.3) W/m^2 , the horizontal, vertical, and temporal distributions and the physical lifetimes of these two very different radiative forcing agents are not similar; therefore, the effects do not simply off-set one another.

Overall, the evidence is sufficient to conclude **that a causal relationship exists between PM and effects on climate, including both direct effects on radiative forcing and indirect effects that involve cloud feedbacks that influence precipitation formation and cloud lifetimes.**

9.4. Ecological Effects of PM

9.4.1. Introduction

PM is heterogeneous with respect to chemical composition and size; therefore, it can cause a variety of ecological effects, which have been previously described by the U.S. EPA (2004, [056905](#)) and by Grantz et al. (2003, [155805](#)). Atmospheric PM has been defined, for regulatory purposes, mainly by size fractions and less clearly so in terms of chemical nature, structure, or source. Both fine and coarse-mode particles may affect plants and other organisms; however, PM size classes do not necessarily relate to ecological effects (U.S. EPA, 1996, [079380](#)). More often the chemical constituents drive the ecosystem response to PM (Grantz et al., 2003, [155805](#)).

The previous PM assessment (U.S. EPA, 2004, [056905](#)) included the acidifying effects of particulate N and S. The 2008 NO_xSO_x ISA (U.S. EPA, 2008, [157074](#)) assessed the effects of particle- and gas-phase N and S pollution on acidification, N enrichment, and Hg methylation. Acidification of ecosystems is driven primarily by deposition resulting from SO_x , NO_x , and NH_x pollution. Acidification from the deposition resulting from current emission levels causes a cascade of effects that harm susceptible aquatic and terrestrial ecosystems, including slower growth and injury to forests and localized extinction of fishes and other aquatic species. In addition to acidification, atmospheric deposition of reactive N resulting from current NO_x and NH_x emissions along with other non-atmospheric sources (e.g., fertilizers and wastewater), causes a suite of ecological changes within sensitive ecosystems. These include increased primary productivity in most N-limited ecosystems, biodiversity losses, changes in C cycling, and eutrophication and harmful algal blooms in freshwater, estuarine, and ocean ecosystems. In some watersheds, additional SO_4^{2-} from atmospheric deposition increases Hg methylation rates by increasing both the number and activity of S-reducing bacteria. Methylmercury is a powerful toxin that can bioaccumulate to toxic amounts in food webs at higher trophic levels.

This assessment of PM effects on ecosystems considers both direct and indirect exposure pathways. Atmospheric PM may affect ecological receptors directly following deposition on surfaces or indirectly by changing the soil chemistry or by changing the amount of radiation reaching the Earth's surface. Indirect effects acting through the soil are often thought to be most significant because they can alter nutrient cycling and inhibit nutrient uptake (U.S. EPA, 2004, [056905](#); U.S. EPA, 2008, [157074](#)). The U.S. EPA (2004, [056905](#)) reported that the effects of PM can be both chemical and physical. Physical effects of particle deposition on vegetation may include abrasion and radiative heating. However, chemical effects may be more significant (U.S. EPA, 2008, [157074](#)).

In general, anthropogenic stressors can result in damaged ecosystems that do not recover readily (Odum, 1993, [076742](#); Rapport and Whitford, 1999, [004595](#)). Ecosystems sometimes lack the capacity to adapt to an anthropogenic stress and are unable to maintain their normal structure and functions unless the stressor is removed (Rapport and Whitford, 1999, [004595](#)). These stresses result in a process of ecosystem degradation marked by a decrease in biodiversity, reduced primary and secondary production, and a lower capacity to recover and return to the original ecosystem state. In addition, there can be an increased prevalence of disease, reduced nutrient cycling, increased dominance of exotic species, and increased dominance by smaller, short-lived opportunistic species (Odum, 1985, [039482](#); Rapport and Whitford, 1999, [004595](#)).

Ecosystems are often subjected to multiple stressors, of which atmospheric PM deposition is only one. Additional stressors are also important, including O₃ exposure, climatic variation, natural and human disturbance, the occurrence of invasive non-native plants, native and non-native insect pests, disease, acidification, and eutrophication among others. PM deposition interacts with these other stressors to affect ecosystem patterns and processes.

The possible effects of particulate (and other) air pollutants on ecosystems have been categorized by Guderian (1977, [004150](#)) as follows:

- accumulation of pollutants in plants and other ecosystem components (such as soil and surface- and groundwater),
- damage to consumers as a result of pollutant accumulation,
- changes in species diversity because of shifts in competition,
- disruption of biogeochemical cycles,
- disruption of stability and reduction in the ability to self-regulate,
- breakdown of stands and associations, and
- expansion of denuded zones.

The general conclusion of the last PM assessment (U.S. EPA, 2004, [056905](#)) was that ecosystem response to PM can be difficult to determine because the changes are often subtle. For example, changes in the soil may not be observed until pollutant deposition has occurred for many decades, except in the most severely polluted areas around heavily industrialized point sources. The presence of co-occurring pollutants generally makes it difficult to attribute ecological effects to PM alone or to one constituent in the deposited PM. In other words, the potential for alteration of ecosystem function and structure exists but can be difficult to quantify except in cases of extreme amounts of deposition, especially when there are other pollutants present in the ambient air that may produce additive or synergistic responses.

New information on the ecological effects of coarse and fine particle PM is presented in the following discussion in the context of effects that were known from the last PM AQCD (U.S. EPA, 2004, [056905](#)). The general effects of the chemical constituents of PM are discussed; however, a rigorous assessment of each chemical constituent (e.g., Hg, Cd, Pb, etc.) is not given. Both direct and indirect effects will be discussed and the strength of the scientific evidence will be evaluated using the causality framework.

9.4.1.1. Ecosystem Scale, Function, and Structure

Information presented in this section was collected at multiple scales, ranging from the physiology of a given species to population, community, and ecosystem-level investigations. For this assessment, “ecosystem” is defined as a functional entity consisting of interacting groups of living organisms and their abiotic (chemical and physical) environment. Ecosystems cover a hierarchy of spatial scales and can comprise the entire globe, biomes at the continental scale, or small, well-circumscribed systems such as a small pond.

Ecosystems have both structure and function. Structure may refer to a variety of measurements including the species richness, abundance, community composition and biodiversity as well as

landscape attributes. Competition among and within species and their tolerance to environmental stresses are key elements of survivorship. When environmental conditions are shifted, for example, by the presence of anthropogenic air pollution, these competitive relationships may change and tolerance to stress may be exceeded. “Function” refers to the suite of processes and interactions among the ecosystem components and their environment that involve nutrient and energy flow as well as other attributes including water dynamics and the flux of trace gases. Plant processes including photosynthesis, nutrient uptake, respiration, and C allocation, are directly related to functions of energy flow and nutrient cycling. The energy accumulated and stored by vegetation (via photosynthetic C capture) is available to other organisms. Energy moves from one organism to another through food webs, until it is ultimately released as heat. Nutrients and water can be recycled. Air pollution alters the function of ecosystems when elemental cycles or the energy flow are altered. This alteration can also be manifested in changes in the biotic composition of ecosystems.

There are at least three levels of ecosystem response to pollutant deposition: (1) the individual organism and its environment; (2) the population and its environment; and (3) the biological community composed of many species and their environment (Billings, 1978, [034165](#)). Individual organisms within a population vary in their ability to withstand the stress of environmental change. The response of individual organisms within a population is based on their genetic constitution, stage of growth at time of exposure to stress, and the microhabitat in which they are growing (Levine and Pinto, 1998, [029599](#)). The range within which organisms can exist and function determines the ability of the population to survive. Those able to cope with the stresses survive and reproduce. Competition among different species results in succession (community change over time) and, ultimately, produces ecosystems composed of populations of species that have the capability to tolerate the stresses (Guderian, 1985, [019325](#); Rapport and Whitford, 1999, [004595](#)). Available information on individual, population and community response to PM will be discussed.

9.4.1.2. Ecosystem Services

Ecosystem structure and function may be translated into ecosystem services. Ecosystem services identify the varied and numerous ways that ecosystems are important to human welfare. Ecosystems provide many goods and services that are of vital importance for the functioning of the biosphere and provide the basis for the delivery of tangible benefits to human society. Hassan et al. (2005, [092759](#)) define these to include supporting, provisioning, regulating, and cultural services:

- Supporting services are necessary for the production of all other ecosystem services. Some examples include biomass production, production of atmospheric O₂, soil formation and retention, nutrient cycling, water cycling, and provisioning of habitat. Biodiversity is a supporting service that is increasingly recognized to sustain many of the goods and services that humans enjoy from ecosystems. These provide a basis for three higher-level categories of services.
- Provisioning services, such as products (Gitay et al., 2001, [092761](#)), i.e., food (including game, roots, seeds, nuts and other fruit, spices, fodder), fiber (including wood, textiles), and medicinal and cosmetic products (including aromatic plants, pigments).
- Regulating services that are of paramount importance for human society such as (a) C sequestration, (b) climate and water regulation, (c) protection from natural hazards such as floods, avalanches, or rock-fall, (d) water and air purification, and (e) disease and pest regulation.
- Cultural services that satisfy human spiritual and aesthetic appreciation of ecosystems and their components.

9.4.2. Deposition of PM

Deposition of PM is discussed in Chapter 3.3.4. Additional material specifically related to ecosystems is discussed in this section.

9.4.2.1. Forms of Deposition

Research summarized by the previous NAAQS PM assessment illustrated the complexity of deposition processes. Airborne particles, their gas-phase precursors, and their transformation products are removed from the atmosphere by wet and dry deposition processes. These deposition processes transfer PM pollutants to other environmental media where they can alter the structure, function, diversity, and sustainability of complex ecosystems. Dry deposition of PM is most effective for coarse particles. These include primary geologic materials and elements such as iron and manganese. By contrast, wet deposition is more effective for fine particles of secondary atmospheric origin and elements such as cadmium, chromium, lead, nickel, and vanadium (Reisinger, 1990, [046737](#); Smith, 1990, [084015](#); U.S. EPA, 2004, [056905](#)). The relative magnitudes of the different deposition modes vary with ecosystem type, location, elevation, and chemical burden of the atmosphere (U.S. EPA, 2004, [056905](#)). There are differences in the deposition behavior of fine and coarse particles. Coarse particles generally settle nearer their site of formation than do fine particles. In addition, the chemical constitution of individual particles is correlated with size. For example, much of the base cation and heavy metal burden is present on coarse particles.

Fine PM is often a secondary pollutant that forms within the atmosphere, rather than being directly emitted from a pollution source. It derives from atmospheric gas-to-particle conversion reactions involving nucleation, condensation, and coagulation, and from evaporation of water from contaminated fog and cloud droplets. Fine PM may also contain condensates of VOCs, volatilized metals, and products of incomplete combustion, including polycyclic aromatic hydrocarbons (PAH) and BC (soot) (U.S. EPA, 2004, [056905](#)).

Fine PM may act as a carrier for materials such as herbicides that are phytotoxic. Fine PM provides much of the surface area of particles suspended in the atmosphere, whereas coarse PM provides much of the mass of airborne particles. Surface area can influence ecological effects associated with the oxidizing capacity of fine particles, their interactions with other pollutants, and their adsorption of organic compounds. Fine and coarse particles also respond to changes in atmospheric humidity, precipitation, and wind, and these can alter their deposition characteristics.

Coarse PM is mainly a primary pollutant, having been emitted from pollution sources as fully formed particles derived from abrasion and crushing processes, soil disturbances, desiccation of marine aerosol emitted from bursting bubbles, hygroscopic fine PM expanding with humidity to coarse mode, and/or gas condensation directly onto preexisting coarse particles. Suspended primary coarse PM may contain iron, silica, aluminum, and base cations from soil, plant and insect fragments, pollen, fungal spores, bacteria, and viruses, as well as fly ash, brake lining particles, and automobile tire fragments. Coarse mode particles can be altered by chemical reactions and/or physical interactions with gaseous or liquid contaminants.

Exposure to a given mass concentration of PM may lead to widely differing phytotoxic and other environmental outcomes depending upon the particular mix of PM constituents involved. Especially important in this regard are S and N components of PM, which are addressed in the 2008 NO_xSO_x ISA, and effects of particulate heavy metals and organic contaminants. This variability has not been characterized adequately. Though effects of specific chemical fractions of PM have been described to some extent, there has been relatively little research aimed at defining the effects of unspiciated PM on plants or ecosystems.

9.4.2.2. Components of PM Deposition

Trace Metals

Atmospheric deposition can be the primary source of some metals to some watersheds. Metal inputs can include the primary crustal elements (Al, Ca, K, Fe, Mg, Si, Ti) and the primary anthropogenic elements (Cu, Zn, Cd, Cr, Mn, Pb, V, Hg). The crustal elements are derived largely from weathering and erosion, whereas the anthropogenic elements are derived from combustion, industrial sources, and other man-made sources (Goforth and Christoforou, 2006, [088353](#)).

Heavy metal deposition to ecosystems depends on their location as well as upwind emissions source strength. The deposition velocity tends to be dependent on particle size and chemical species. Larger particles deposit more efficiently than smaller particles. Heavy metals preferentially associate

with fine particles. Fine particles also have the longest atmospheric residence times. Depending on climate and topography, fine particles may remain airborne for days to months and may be transported thousands of kilometers from their source.

Ecosystems immediately downwind of major heavy metal emissions sources may receive locally heavy dry deposition. Trace element investigations conducted in roadside, industrial, and urban environments have also shown that substantial amounts of particulate heavy metals can accumulate on surfaces.

A significant trace metal component of PM is mercury (Hg). Hg is toxic and can move readily through environmental compartments. Atmospheric and depositional inputs of Hg include both natural and anthropogenic sources. Natural geologic contributions to Hg in the environment include geothermal and volcanic activity, geologic metal deposits, and organic-rich sedimentary rocks. These natural emissions combine with anthropogenic emissions from such sources as power plants, landfills, sewage sludge, mine waste, and incineration (Gustin, 2003, [155816](#); Schroeder and Munthe, 1998, [014559](#)). Emissions from natural sources are controlled by geologic features, including substrate Hg content, rock type, the degree of hydrothermal activity, and the presence of heat sources (Gustin, 2003, [155816](#)). The significance of natural Hg sources relative to anthropogenic sources varies geographically. For example, Nevada occurs within a global mercuriferous belt, with area emissions about three times higher than the value assumed for global modeling (Gustin, 2003, [155816](#)). In Nevada, natural and anthropogenic Hg emissions are approximately equal (Gustin, 2003, [155816](#)).

The U.S. EPA (1997, [157066](#)) compiled an assessment of the sources and environmental effects of Hg in the U.S. A variety of factors were found to influence Hg deposition, fate and transport (Table 9-21). Such factors relate in particular to speciation of the Hg that is emitted, the forms in which it is deposited from the atmosphere, and transformations that occur within the atmosphere and within the aquatic, transitional, and terrestrial compartments of the receiving watershed. There have been studies that have reconstructed, from lake sediment records, the atmospheric depositional history of trace metals and PAHs in lakes adjacent to coal-fired power plants. For example, Donahue et al. (2006, [155751](#)) analyzed sediment from Wababun Lake, which is located in Alberta, Canada in proximity (within 35 km) to 4 power plants built since 1950. Trace metal concentrations of Hg, Cu, Pb, As, and Se in lake sediment increased by 1.2- to 4-fold. The total PAH flux to surface sediments was 730-1,100 $\mu\text{g}/\text{m}^2/\text{yr}$, which was two to five times higher than in 2 lakes situated 20 km to the north and 70 km to the south. Further discussion of Hg effects on ecosystems can be found in Section 9.4.5.

Table 9-21. Factors potentially important in estimating Hg exposure.

Factor	Importance and Possible Effect on Mercury Exposure
Type of anthropogenic source of mercury	Different combustion and industrial process sources are anticipated to have different local scale impacts due to physical source characteristics (e.g., stack height), the method of waste generation (e.g., incineration or mass burn) or mercury control devices and their effectiveness.
Mercury emission rates from stack	Increased emissions will result in a greater chance of adverse impacts on environment.
Mercury species emitted from stack	More soluble species will tend to deposit closer to the source.
Form of mercury emitted from stack	Transport properties can be highly dependent on form.
Deposition differences between vapor and particulate-bound mercury	Vapor-phase forms may deposit significantly faster than particulate-bound forms.
Transformations of mercury after emission from source	Relatively nontoxic forms emitted from source may be transformed into more toxic compounds.
Transformation of mercury in watershed soil	Reduction and revolatilization of mercury in soil limits the buildup of concentration.
Transport of mercury from watershed soils to water body	Mercury in watershed soils can be a significant source to water bodies and subsequently to fish.
Transformation of mercury in water body	Reduction, methylation, and demethylation of mercury in water bodies affect the overall concentration and the MHg fraction, which is bioaccumulated in fish.
Facility locations	Effects of meteorology and terrain may be significant.
Location relative to local mercury source	Receptors located downwind are more likely to have higher exposures. Influence of distance depends on source type.
Contribution from non-local sources of mercury	Important to keep predicted impacts of local sources in perspective.
Uncertainty	Reduces confidence in ability to estimate exposure accurately.

Source: Modified from U.S. EPA (1997, [157066](#))

Organics

Organic compounds that may be associated with deposited PM include persistent organic pollutants (POPs), pesticides, SOCs, polyaromatic hydrocarbons (PAHs) and flame retardants among others. Organic compounds partition between gas and particle phases, and organic particulate deposition depends largely on the particle sizes available for adsorption (U.S. EPA, 2004, [056905](#)). Dry deposition of organic materials is often dominated by the coarse fraction. Gas-particle phase interconversions are important in determining the amount of dry deposition.

Most persistent organic pollutants (POPs) enter the biosphere via human activities, including synthetic pesticide application, output of polychlorinated dibenzo dioxins (PCDD) from incinerators, and accidental release of PCBs from transformers (Lee, 2006, [088968](#)). Once they are introduced into the environment, their accumulation and magnification in biological systems are determined by physiochemical properties and environmental conditions (Section 9.4.6). Uptake by plants can occur at the soil/plant interface and at the air/plant interface (Krupa et al., 2008, [198696](#)). For lipophilic POPs, such as PCDDs and PCBs, the air/plant response route generally dominates (Lee, 2006, [088968](#); Thomas et al., 1998, [156118](#)), but uptake through above-ground plant tissue also occurs. In a study of zucchini (*Cucurbita pepo*), Lee et al. (2006, [088968](#)) found chlordanes pesticide components in all vegetation tissues examined: root, stem, leaves, fruits.

Many pesticides and SOCs are carcinogenic or estrogenic and pose potential threats to aquatic and terrestrial biota. Although deposition of SOCs was previously reported for the Sierra Nevada Mountains in California and the Rocky Mountains in Colorado, little was previously known about the occurrence, distribution, or sources of SOCs in alpine, sub-Arctic, and Arctic ecosystems in the western U.S. The snowpack is efficient at scavenging of both particulate and gas phase pesticides from the atmosphere (Halsall, 2004, [155822](#); Lei and Wania, 2004, [127880](#)). Analysis of pesticides in snowpack samples from seven NPs in the western U.S. by Hageman et al. (2006, [156509](#)) illustrated the deposition and fate of 47 pesticides and their degradation products. Correlation analysis with latitude, temperature, elevation, PM, and two indicators of regional pesticide use suggested that regional patterns in historic and current agricultural practices are largely responsible

for the distribution of pesticides in the NPs. Pesticide deposition to parks in Alaska was attributed to long-range atmospheric transport.

PAHs include hundreds of different compounds that are characterized by possessing two or more fused benzene rings. They are widespread contaminants in the environment, and are formed by incomplete combustion of fossil fuels and other organic materials. Eight PAHs are considered carcinogenic and 16 are classified by EPA as priority pollutants. They are common air pollutants in metropolitan areas, derived from vehicular traffic and other urban sources. Especially high concentrations have been found near Söderberg aluminum production industries and areas where heating during winter via wood burning is common. Other sources, in addition to gasoline and diesel engines, include forest fires and various forms of fossil fuel combustion (Sanderson and Farant, 2004, [156942](#)).

The behavior of PAHs is strongly determined by their chemical characteristics, especially their nonpolarity and hydrophobicity. They readily adsorb to particulates in the air and to sediments in water. Srogi (2007, [180049](#)) provided a thorough review of PAH concentrations in various environmental compartments and their use for assessing environmental risks and possible effects on ecosystems and human health.

Deposition and fate of PAH has been an important area of research. Because they are carcinogenic, PAHs are important environmental contaminants. Root-soil behavior of PAHs is an area of active study. Soil-bound PAHs are associated with soil organic matter and are therefore generally not easily available for root uptake. PAHs are readily adsorbed to root surfaces but there seems to be little movement to the interior of the root or movement up to the shoots (Gao and Zhu, 2004, [155782](#)). Paddy rice is the main food crop planted in China. As an aquatic plant having aerial roots, the movement of PAHs into rice roots may be different than their movement into more widely studied land-grown food crops. PAH concentrations in the rice roots were more correlated with the water and air compartments than with the soil (Jiao et al., 2007, [155879](#)).

The total PAH concentration in grasses adjacent to a highway have been measured to be about eight times higher than in grasses from reference sites not close to a highway (Crépineau et al., 2003, [155741](#)). Howe et al. (2004, [155854](#)) found that concentrations of PAHs and hexachlorobenzene (HCB) in spruce (*Picea* spp.) needles at 36 sites in eastern Alaska varied by an order of magnitude. Samples collected near the city of Fairbanks generally had higher concentrations than samples collected from rural areas. The relative importance of combustion sources versus petrogenic sources was highest in the near-coastal areas, as reflected in variation in the concentration of ratios of isomeric PAHs.

Use of flame retardants has increased in recent years in response to fire product safety regulations. However, some flame retardant chemicals are toxic and are readily transported atmospherically. Use of some has been banned in Europe and some of the United States because of their persistence and tendency to bioaccumulate (Hoh et al., 2006, [190378](#)).

Base Cations

With respect to ecosystem effects from PM deposition, the inclusion of base cations (especially Ca, Mg, and K) in atmospheric deposition is generally considered to be a positive effect. Base cations are important plant nutrients that are in some locations present in short supply and that are further depleted by the acidic components of deposition. Increased base cation deposition can help to ameliorate adverse effects of acidification of soils and surface waters and reduce the toxicity of inorganic Al to plant roots and aquatic biota. These topics are covered in detail in the recent 2008 NO_xSO_x ISA (U.S. EPA, 2008, [157074](#)).

Although the effects of base cation deposition inputs to terrestrial ecosystems are most commonly considered to be positive, under very high base cation deposition, plant health can be adversely affected. Dust that is high in base cations can settle on leaves and other plant structures and remain for extended periods of time. This is especially likely in arid environments because rainfall can serve to wash dry deposited materials off the foliage. Extended dust coverage can result in a variety of adverse impacts on plant physiology (Grantz et al., 2003, [155805](#)). For example, van Heerden et al. (2007, [156131](#)) documented decreased chlorophyll content, inhibition of CO₂ assimilation, and uncoupling of the oxygen-evolving complex in desert shrubs exposed to high limestone dust deposition near a limestone quarry in Namibia.

Based on the Integrated Forest Study (IFS) data, the U.S. EPA (2004, [056905](#)) concluded that particulate deposition has a greater effect on base cation inputs to soils than on base cation losses associated with the inputs of sulfur, nitrogen, and H⁺. These atmospheric inputs of base cations have considerable significance, not only to the base cation status of these ecosystems, but also to the potential of incoming precipitation to acidify or alkalize the soils in these ecosystems. This topic is discussed in detail in the recent NO_xSO_x ISA (U.S. EPA, 2008, [157074](#)).

9.4.2.3. Magnitude of Dry Deposition

Using Vegetation for Estimating Atmospheric Deposition

Whereas direct real-time measurement of deposition or air concentrations of atmospheric contaminants is desirable, it is not always practical (Howe et al., 2004, [155854](#)). Instead, passive time-integrative methods are frequently used. These can involve analysis of vegetative tissues as a record of pollutant exposure, or analysis of lake sediment cores or ice cores to determine changes in pollutant input over time. There is a general assumption that the concentration of an analyte in vegetation reflects the time-integrated concentration of that analyte in the air. The development of deposition layers in sediment or ice cores allows the possibility of determining the effects of changes in the atmospheric concentration over periods of years, decades, or longer.

Biomonitoring methods are important in air pollution assessment and provide a complement for more typical instrumental analyses. It is well known that mosses can accumulate large amounts of heavy metals in response to atmospheric deposition. Mosses accumulate dissolved materials and PM deposited from the atmosphere and have been used extensively in Europe as surrogate collectors for estimating bulk (wet plus dry) deposition of metals. The ease and low cost of this method has enabled regional assessments to be conducted throughout Europe.

Despite its wide use, however, several papers have pointed out complications in the use of mosses to quantify metal deposition rates. Zechmeister (1998, [156178](#)) found that the uptake efficiency for 12 heavy metals in three species of moss was similar, but that uptake efficiency in a fourth species was uncorrelated with the other species for about half the metals considered. Zechmeister (1998, [156178](#)) also showed that productivity of an individual species can vary greatly among sites. To calculate atmospheric deposition of metals from accumulation in mosses, both the metal concentration and the rate of biomass production is needed. Further complication was shown in the study of Shakya et al. (2008, [156081](#)), which revealed that accumulation of Cu, Zn and Pb decreased chlorophyll content. Sites with greater deposition amounts may therefore have lower rates of productivity than cleaner sites.

Differences in uptake efficiencies among species and productivity among sites has led to the use of a single moss species placed in mesh bags that can be distributed to areas where that species of moss does not grow naturally. Studies to standardize this passive deposition monitoring approach have been limited. Adamo et al. (2007, [155644](#)) evaluated the effects of washing with water, oven drying, and acid washing as pretreatments and found little difference in uptake efficiencies, although the ratio of the collecting surface area to mass was found to be a key factor in uptake efficiency.

Couto et al. (2004, [155739](#)) investigated dry versus bulk deposition of metals using transplanted moss bags. This study showed that at some sites dry deposition exceeded bulk deposition, a likely outcome of wash-off of dry deposited particles. This study also documented intercationic displacement and leaching as a result of acidic precipitation. The authors concluded that the accumulated metal concentration represented an unstable equilibrium between inputs and outputs of elements that were a function of the local environment and weather during the exposure period. They also concluded that it was not possible to extrapolate calibrations between metal accumulation in moss and atmospheric deposition of metals to areas with different weather conditions, precipitation pH, and air contaminant concentrations. Zechmeister et al. (2003, [157175](#)) also presented results demonstrating the problems with dry deposited particles that can be washed off by rain. These studies indicate that moss is not a completely effective collector of total particle deposition. Deposition estimates from moss accumulation probably represent values that fall between wet deposition and total deposition.

A European moss biomonitoring network has been in place since 1990 (Harmens et al., 2007, [155828](#)). Sampling surveys are repeated every five years. The survey conducted in 2005/2006

occurred in 32 countries at over 7,000 sites. The network reports metal concentrations associated with live moss tissue. Trends analysis of these data showed statistically significant decreases over time in moss concentrations for As, Cu, V, and Zn. Trends were not observed for Cr, Fe, or Ni. Results for individual countries participating in the survey have also been published. In Hungary, major pollution sources were readily detected by moss sampling (Otvos et al., 2003, [156831](#)). Somewhat higher metal concentrations in mosses in 1997 than in other European countries were attributed to the use of a different moss species in the Hungarian survey (Otvos et al., 2003, [156831](#)). Similar sampling in Romania showed regions with contamination that were among the highest in Europe. These results were consistent with known air quality problems in Romania (Lucaciu et al., 2004, [155947](#)). Because particulate deposition is not well characterized using this method, spatial patterns and temporal trends for particulate metal deposition in Europe only provide crude estimates of relative deposition patterns.

The use of moss to assess heavy metal deposition has received much less attention in the U.S. than in Europe. A study conducted in the Blue Ridge Mountains, VA, found that metal concentrations in moss were related to elevation and canopy species at some sites (Schilling and Lehman, 2002, [113075](#)). However, metal concentrations in moss were not related to concentrations in the O horizon of the soil. Other measurement methods for trace metal deposition were not available to compare with moss concentrations.

Epiphytic lichens have also been used to evaluate heavy metal accumulation. Helena et al. (2004, [155833](#)) found substantially increased concentrations of metals in lichens transplanted from a relatively clean region to an area in proximity to a metal smelter. The presence of specific species of bryophyte or lichen can serve as an effective bioindicator of metal contamination (Cuny et al., 2004, [155742](#)). In some studies, tree bark has been used as a biomonitor for atmospheric deposition of heavy metals (Baptista et al., 2008, [155673](#); Pacheco and Freitas, 2004, [156011](#); Rusu et al., 2006, [156062](#)).

Biomonitoring using mosses, lichens, or other types of vegetation has been established as a means of identifying spatial patterns in atmospheric deposition of heavy metals in relation to power plants, industry, and other point and regional emissions sources. More recently, a number of studies (López et al., 2002, [155943](#); 2003, [155944](#); 2003, [155945](#)) have used cattle that have been reared predominantly on local forage as a means of monitoring atmospheric inputs of Cu, Ar, Zn, and Hg. For example, Hg emissions from coal fired power plants in Spain had a substantial effect on Hg accumulation by calves (López et al., 2003, [155944](#)). Accumulation of Hg by cattle extended to ~140-200 km downwind from the source.

Yang and Zhu (2007, [156168](#)) investigated the effectiveness of pine needles as passive air samplers for SOCs, such as PAHs, that are partially or completely particle-associated in the atmosphere. PAH distribution patterns are complicated by their properties, which span a broad range of octanol-air partition coefficients. This allows them to be present in both vapor and particle phases. In addition, the air-plant partitioning of PAHs is affected by air temperature and atmospheric stability (Krupa et al., 2008, [198696](#); Yang and Chen, 2007, [092847](#)). DeNicola et al. (2005, [155747](#)) documented the suitability of a Mediterranean evergreen oak (*Quercus ilex*) to serve as a passive biomonitor for atmospheric contamination with PAH in Italy.

Deposition to Canopies

Tree canopies have been shown to increase dry deposition from the atmosphere, including deposition of PM. Dry deposition rates in the canopy are commonly estimated by the difference between throughfall deposition and deposition measured by an open collector, although the use of this approach to specifically quantify particulate deposition is complicated by gaseous deposition to leaf surfaces and, for some elements, leaching and uptake. Avila and Rodrigo (2004, [155664](#)) found that trace metal deposition in throughfall in a Spanish oak forest were higher than bulk deposition for Cu, Pb, Mn, V, and Ni, but not for Cd and Zn. This study also found that dry deposition of Cu, Pb, Zn, Cd and V occurred, but that canopy uptake of Zn and Cd also occurred. Leaching of Mn and Ni from the foliage was observed as well. Leaching of Ni, Cu, Mn, Rb, and Sr from a red spruce-balsam fir canopy by acidic cloud water was also measured in a study by Lawson et al. (2003, [089371](#)). These studies suggest that leaching of trace metals from forest canopies varies with tree species and the acidity of precipitation. Throughfall therefore cannot be assumed to represent total deposition of heavy metals without evaluating uptake and leaching at the specific study site. Physical models have

provided an alternative to estimating dry deposition to canopies with throughfall measurements. Recently, Pryor and Binkowski (2004, [116805](#)) identified an additional complication in that models typically hold particle size constant. Nevertheless, there may be significant modification of particle size distributions during the deposition process.

The use of pine and oak canopies as bioindicators of atmospheric trace metal pollution was investigated by Aboal et al. (2004, [155642](#)). As an ecosystem pool, metals in leaves were likely to be much more important than those in mosses. The authors concluded, however, that these tree species were not effective bioindicators of atmospheric deposition of heavy metals. Metal concentrations in leaves were found to be one to three orders of magnitude lower than in mosses collected in this study.

The effectiveness of tree canopies in capturing particulates was investigated as a method for improving air quality by Freer-Smith et al. (2004, [156451](#)). This study showed that with consideration of planting design, location of pollution source, and tree species, planting of trees can be effective at reducing particulate air pollution. However, this approach does not address the possible effects of the captured pollution on trees, soils and surface waters.

High-elevation forests generally receive larger particulate deposition loadings than equivalent low elevation sites. Higher wind speeds at high elevation enhance the rate of aerosol impaction. Orographic effects enhance rainfall intensity and composition and increase the duration of occult deposition. High-elevation forests are often dominated by coniferous species with needle-shaped leaves that enhance impaction and retention of PM delivered by all three deposition modes.

Deposition to Soil

As with mosses, accumulation of heavy metals in surface soils provides a general reflection of the spatial distribution of industrial pollution. The distribution of toxic elements in urban soils has been an important area of study (Madrid et al., 2002, [155956](#); Markiewicz et al., 2005, [155963](#)). Generally, Cu, Pb, Zn, and Ni have accumulated in urban soils compared with their rural counterparts (Yuangen et al., 2006, [156174](#)). In the study of Romić and Romić (2003, [156055](#)), relationships were found between urban activities and concentrations of metals in soils in developed areas surrounding Zagreb, Croatia. Goodarzi et al. (2002, [155801](#)) compared deposition estimated by moss bags to concentrations of metals in A-horizon soils in the vicinity of a large smelter. Statistically significant correlations were observed between the moss bag deposition estimates and the soil metal concentrations for Cd, Pb, Zn, and in some cases also Cu. These correlations suggested that atmospheric deposition of metals caused elevated metal concentrations in the upper mineral horizon of these soils. No correlations were found for Hg or As in this study.

Studies have also been conducted to assess metal accumulation in peat because of the tendency of most metals to be immobilized through binding with organic matter. Steinnes et al. (2005, [156095](#)) presented geographical patterns of metal concentrations in surface peat throughout Norway that corresponded to pollution sources, although the peat samples were collected in 1979. Zaccone et al. (2007, [179930](#)) found that variations of metal concentrations with depth in a single Swiss peat core corresponded with the depositional history that would be expected from the industrial revolution, although Cs¹³⁷ activity exhibited a distribution in the profile that was not fully consistent with the Chernobyl nuclear reactor accident. A detailed study of Finnish peat showed that relationships between depth profiles of metal concentrations and deposition history can match well for some metals at some sites, but not well for the same metals at other sites (Roberts et al., 2003, [156051](#)). They also found that Zn and Cd accumulation rates were independent of deposition history at each of three study sites.

Metal deposition to soil is also a significant concern adjacent to roadways. Urban stormwater can be rich in heavy metals and other contaminants derived from atmospheric deposition, and can be a major source of pollutant inputs to water bodies in urban settings. Urban stormwater runoff can also be toxic to aquatic biota, partly due to trace metal concentrations (Greenstein et al., 2004, [155808](#); Sabin et al., 2005, [088300](#); Schiff et al., 2002, [156959](#)). These processes are largely a function of the impervious nature of much of the ground surface in urban areas (i.e., buildings, roads, sidewalks, parking lots, construction sites). Dry-deposited pollutants can build up, especially in arid and semi-arid environments, and then be washed into surface waters with the first precipitation event. The concentrations of Cd, Ca, Cu, Pb, and Zn in road runoff were found to be significantly higher during winter in Sweden. This seasonal pattern was attributed to the intense wearing of the

pavement that occurred during winter due to the use of studded tires in combination with chemical effects of deicing salts (Bäckström et al., 2003, [156242](#)).

9.4.3. Direct Effects of PM on Vegetation

Exposure to airborne PM can lead to a range of phytotoxic responses, depending on the particular mix of deposited particles. This was well known at the time of the previous PM criteria assessment, as summarized below. Most direct phytotoxic effects occur in severely polluted areas surrounding industrial point sources, such as limestone quarries and other mining activities, cement kilns, and metal smelting facilities (U.S. EPA, 2004, [056905](#)). Experimental application of PM constituents to foliage typically elicits little response at the more common ambient concentrations. The diverse chemistry and size characteristics of ambient PM and the lack of clear distinction between effects attributed to phytotoxic particles and to other air pollutants further confound the understanding of the direct effects on foliar surfaces.

Deposition of PM can cause the accumulation of heavy metals on vegetative surfaces. Low solubility limits foliar uptake and direct heavy metal toxicity because trace metals must be brought into solution before they can enter into the leaves or bark of vascular plants. In those instances when trace metals are absorbed, they are frequently bound in leaf tissue and are lost when the leaf drops off (Hughes, 1981, [053595](#)).

Depending on the size of the particles, the PM deposited on the leaf surface can affect the plant's metabolism and photosynthesis by blocking light, obstructing stomatal apertures, increasing leaf temperature and altering pigment and mineral content (Naidoo and Chirkoot, 2004, [190449](#)) (Section 9.4.3.1.). Fine PM has been shown to enter the leaf through the stomata and penetrate into the mesophyll layers where it alters leaf chemistry (Da et al., 2006, [190190](#)). Kuki et al. (2008, [155346](#)) also showed increased leaf permeability and increased activity of enzymes in response to fine PM lead (Section 9.4.5.).

Studies of the direct toxic effects of particles on vegetation have not yet advanced to the stage of reproducible exposure experiments. In general, phytotoxic gases are deposited more readily, assimilated more rapidly, and lead to greater direct injury of vegetation as compared with most common particulate materials. The dose-response functions obtained in early experiments following the exposure of plants to phytotoxic gases generally have not been observed following the application of particles (U.S. EPA, 2004, [056905](#)).

9.4.3.1. Effects of Coarse-mode Particles

The current state of scientific knowledge regarding the direct effects of coarse PM on plants has not changed since publication of the previous PM criteria assessment (U.S. EPA, 2004, [056905](#)). The summary provided here is taken from that report. In many rural areas and some urban areas, the majority of the mass in the coarse particle mode derives from the elements Si, Al, Ca, and Fe, suggesting a crustal origin as fugitive dust from disturbed land, roadways, agriculture tillage, or construction activities. Large particles tend to deposit near their source (Grantz et al., 2003, [155805](#)) and rapid sedimentation of coarse particles tends to restrict their direct effects on vegetation largely to roadsides and forest edges, which often receive the greatest deposition (U.S. EPA, 2004, [056905](#)).

Dust

Dust can cause both physical and chemical effects. Consequences are often mediated via impacts on leaf cuticles and waxes. Deposition of inert PM on above-ground plant organs sufficient to coat them with a layer of dust may result in changes in radiation received, a rise in leaf temperature, and the blockage of stomata. Crust formation can reduce photosynthesis and the formation of carbohydrates needed for normal growth, induce premature leaf-fall, damage leaf tissues, inhibit growth of new tissue, and reduce starch storage. Dust may decrease photosynthesis, respiration, and transpiration; and it may result in the condensation and reactivity of gaseous pollutants with PM, thereby causing visible injury symptoms and decreased productivity (U.S. EPA, 2004, [056905](#)). Leaves with trichomes may be more prone to the accumulation of dust on leaf surfaces (Kuki et al., 2008, [155346](#)).

The chemical composition of PM is usually the key phytotoxic factor leading to plant injury. For example, cement-kiln dust liberates calcium hydroxide on hydration. It can then penetrate the epidermis and enter the mesophyll, causing an increase in leaf surface pH. In turn, surface pH can be important for surface microbial colonization and wax formation and degradation.

Salt

Sea-salt particles can serve as nuclei for the absorption and subsequent reaction of other gaseous and particulate air pollutants. Direct effects on vegetation reflect these inputs and salt injury caused by the sodium and chloride that constitute the bulk of these particles. The source of most salt spray near the coast is aerosolized ocean water. Sea salt can cause damage to plants; however, it is not covered in this assessment because it is not of anthropogenic origin. However particulate salt may be input to an ecosystem from deicing salt.

Injury to vegetation from the application of deicing salt is caused by salt spray blown or drifting from the highways (Viskari and Karenlampi, 2000, [019101](#)). The most severe injury is often observed nearest the highway. Conifers planted near roadway margins in the eastern U.S. often exhibit foliar injury due to toxic amounts of saline aerosols deposited from deicing solutions (U.S. EPA, 2004, [056905](#)).

9.4.4. PM and Altered Radiative Flux

The effects of PM on radiative flux and the subsequent effects on vegetation have been described in Section 4.2.3.2 of the previous PM assessment (U.S. EPA, 2004, [056905](#)); a brief overview is presented below. Atmospheric PM can affect ambient radiation, which can be considered in both its direct and diffuse components. Foliar interception by canopy elements occurs for both up- and down-welling radiation. Therefore, the effect of atmospheric PM on atmospheric turbidity influences canopy processes both by radiation attenuation and by changing the efficiency of radiation interception in the canopy through conversion of direct to diffuse radiation (Hoyt, 1978, [046638](#)). Diffuse radiation is more uniformly distributed throughout the canopy and increases canopy photosynthetic productivity by distributing radiation to lower leaves. The enrichment in photosynthetically active radiation (PAR) present in diffuse radiation may offset a portion of the effect of an increased atmospheric albedo due to atmospheric particles. Mercado et al. (2009, [190444](#)) estimated the effects of variations in diffuse light on the terrestrial carbon sink during the last century using a global model. The results indicated that the terrestrial carbon sink increased by approximately 25% during the “global dimming” period (1950-1980), likely driven by increased diffuse light despite decreased PAR. However, under a future scenario in which SO_4^{2-} and BC aerosols decline, the diffuse-radiation and the associated terrestrial C sink also decline (Mercado et al., 2009, [190444](#)).

The effects of regional haze on the yield of crops because of reduction in solar radiation were examined by Chameides et al. (1999, [011184](#)) in China, where regional haze is especially severe. Based on model results, it was estimated that approximately 70% of crops were being depressed by at least 5-30% by regional scale air pollution and its associated haze (Chameides et al., 1999, [011184](#); U.S. EPA, 2004, [056905](#)).

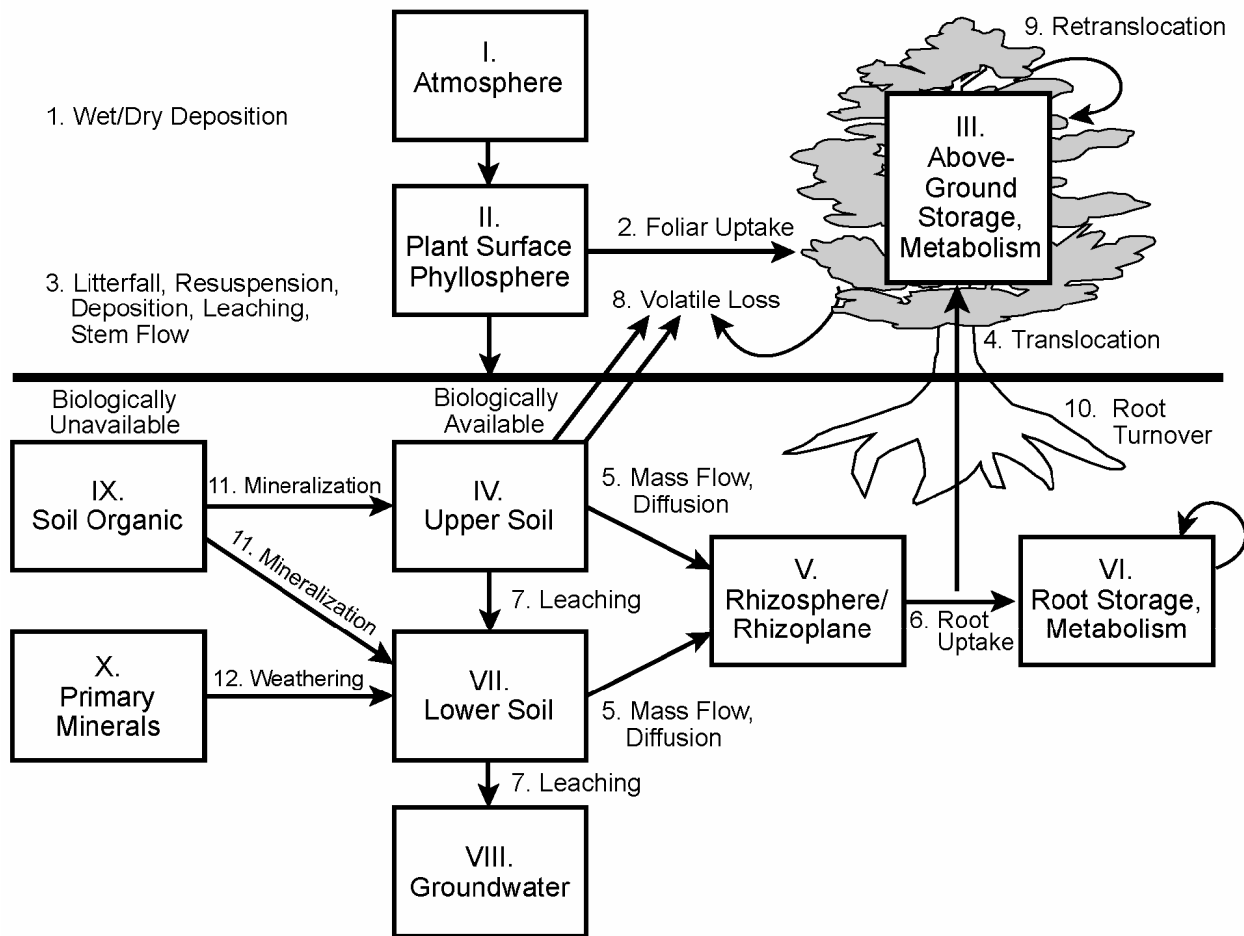
9.4.5. Effects of Trace Metals on Ecosystems

Trace metals may enter the ecosystems as both fine and coarse particles. All but 10 of the 90 elements that comprise the inorganic fraction of the soil occur at concentrations of <0.1% (1,000 $\mu\text{g/g}$) and are termed “trace” elements or trace metals. Trace metals with a density greater than 6 g/cm^3 , referred to as “heavy metals” (e.g., Cd, Cu, Pb, Cr, Hg, Ni, Zn), are of particular interest because of their potential toxicity to plants and animals. Although some trace metals are essential for vegetative growth or animal health, they are all toxic in large quantities. Most trace elements exist in the atmosphere in particulate form as metal oxides (Ormrod, 1984, [046892](#)). Aerosols containing trace elements derive predominantly from industrial activities. Generally, only the heavy metals Cd, Cr, Ni, and Hg are released from stacks in the vapor phase (McGowan et al., 1993, [046731](#)). Atmospherically deposited PM can interact with a variety of biogeochemical

processes. The potential pathways of accumulation of trace metals in terrestrial ecosystems, as well as the possible consequences of trace metal deposition on ecosystem functions, are summarized in Figure 9-85 (U.S. EPA, 2004, [056905](#)). A number of mass balance approaches (Macleod et al., 2005, [155954](#); Toose and Mackay, 2004, [156123](#)), and metal speciation and transport models (Bhavsar et al., 2004, [155689](#); Bhavsar et al., 2004, [155690](#); Gandhi et al., 2007, [155781](#)) have been developed in recent years.

Atmospheric Pb is a component of PM in some regions. The effects of Pb on ecosystems were discussed in the 2006 Pb AQCD (U.S. EPA, 2006, [090110](#)), which concluded that, due to the deposition of Pb from past human practices (e.g., leaded gasoline, ore smelting) and the long residence time of Pb in many aquatic and terrestrial ecosystems, a legacy of environmental Pb burden exists, over which is superimposed much lower contemporary atmospheric Pb loadings. The potential for ecological effects of the combined legacy and contemporary Pb burden to occur is a function of the bioavailability or bioaccessibility of the Pb. This, in turn, is highly dependent upon numerous site factors (e.g., soil OC content, pH, water hardness). Although the more localized ecosystem impacts observed around smelters are often striking, effects generally cannot be attributed solely to Pb, because of the presence of many other stressors (e.g., other heavy metals, oxides of sulfur and nitrogen) that can also act singly or in concert with Pb to cause readily observable environmental effects (U.S. EPA, 2004, [056905](#); U.S. EPA, 2008, [157074](#)).

Effects of fine particle trace elements were described by the U.S. EPA (2004, [056905](#)), and some additional more recent research has also been conducted, especially on the topic of vegetative uptake of trace elements from the soil. The state of scientific understanding as presented by the U.S. EPA (2004, [056905](#)) as well as a discussion of more recent research findings are presented below.



Source: U.S. EPA (2004, [056905](#))

Figure 9-85. Relationship of plant nutrients and trace metals with vegetation. Compartments (roman numerals) represent potential storage sites; whereas arrows (Arabic numerals) represent potential transfer routes.

9.4.5.1. Effects on Soil Chemistry

Trace metals are naturally found in small amounts in soils, ground water, and vegetation. Many are essential micronutrients required for growth by plants and animals. Naturally occurring mineralization can produce metal concentrations in soils and vegetation that are high compared to atmospheric sources. Many metals are bound by chemical processes in the soil, reducing their availability to biota. However, epiphytic or parasitic root colonizing microorganisms can solubilize and transport metals for root uptake (Lingua et al., 2008, [155935](#)). It can be difficult to assess the extent to which observed heavy metal concentrations in soil are of anthropogenic origin. This is because soil parent material, pedogenesis, and anthropogenic inputs all influence the amounts and distribution of trace elements in soil. Trace element concentrations in some natural soils that are remote from air pollution can be higher than soils derived from other parent materials that receive anthropogenic inputs (Burt et al., 2003, [155709](#)). The general effects of metals from atmospheric deposition are presented in the following discussion.

There is not a standard method available for quantifying the bioavailability of heavy metals in soil. A variety of models, isotopic studies, and sequential extraction methods have been used (Collins et al., 2003, [155737](#); Feng et al., 2005, [155774](#); Shan et al., 2003, [156972](#)). Total metal concentration in soil does not give a good indication of potential biological effects because soils vary in their

ability to bind metals in forms that are not bioavailable. There are various methods available for assessing bioavailability of metals, but soils are heterogeneous and there is no ideal method for evaluating what conditions the soil biota experience. Almås et al. (2004, [155654](#)) argued that the actual measurement of biological effects is the best criterion for determining bioavailability. In particular, the replacement of metal-sensitive microorganisms by metal-tolerant organisms within each functional group may be one of the most sensitive indicators of metal exposure. An increase in microbial trace metal tolerance *per se* would not be problematic if it was not for the fact that this increase in tolerance is generally accompanied by a decrease in microbial diversity (Almas et al., 2004, [155654](#); Lakzian et al., 2002, [156671](#)).

Heavy metals deposited from the atmosphere to forests accumulate either in the organic forest floor or in the upper mineral soil layers and metal concentration tends to decrease with soil depth. The accumulation of heavy metals in soil is influenced by a variety of soil characteristics, including pH, Fe and Al oxide content, amount of clay and organic material, and cation exchange capacity (CEC) (Hernandez et al., 2003, [155841](#)). Thus, the pattern of distribution of heavy metals in soils depends on both the soil characteristics and the metal characteristics.

Burt et al. (2003, [155709](#)) investigated the concentrations and chemical forms of trace metals in smelter-contaminated soils collected in the Anaconda and Deer Lodge Valley area of Montana, one of the major mining districts of the world for over a century (1864-1983). The relative distributions of trace metals within the more soluble soil extraction forms were similar to their respective total concentrations. This suggested a relationship between the concentrations of total trace elements and concentrations of soluble mobile fractions. Sequential extractions do not provide direct characterization of trace metal speciation, but rather an indication of chemical reactivity (Burt et al., 2003, [155709](#); Ramos et al., 1994, [046736](#)). Soluble and exchangeable forms are considered readily mobile and bioavailable. Those bound to clay minerals or organic matter are considered generally unavailable.

There is concern that Pb contamination of forest soil could move into groundwater. This would be important in view of the large quantity of Pb deposited from the atmosphere in the 1960s and 1970s in response to combustion of leaded gasoline. This issue was investigated by Watmough et al. (2004, [077809](#)) who applied a stable isotope (^{207}Pb) to the forest floors of white pine (*Pinus strobus*) and sugar maple (*Acer saccharum*) stands. Added Pb was rapidly lost from the forest floor, likely due to high litter turnover in these forest types. However, Pb concentrations in the upper 30 cm of mineral soil were strongly correlated with soil OM, suggesting that Pb does not readily move down the soil profile to the ground water, but rather is associated with the organic content of the upper soil layers (Watmough et al., 2004, [077809](#)).

The upper soil layers are typically an active site of litter decomposition and plant root uptake, both processes may be affected by metal components of PM. Surface litter decomposition is reduced in soils having high metal concentrations. This is likely due to the sensitivity to metals of microbial decomposers and reduced palatability of plant litter having high metal concentration (Johnson and Hale, 2008, [155881](#)). Root decomposition is a key component of nutrient cycling. Johnson and Hale (2008, [155881](#)) measured in situ fine root decomposition at Sudbury, Ontario and Rouyn-Noranda, Quebec. Elevated soil metal concentrations (Cu, Ni, Pb, Zn) did not necessarily reduce fine root decomposition. Only at sites having high concentrations of metals did decomposing roots show increased metal concentrations over time.

9.4.5.2. Effects on Soil Microbes and Plant Uptake via Soil

Upon entering the soil environment, PM pollutants can alter ecological processes of energy flow and nutrient cycling, inhibit nutrient uptake, change ecosystem structure, and affect ecosystem biodiversity. Many of the most important effects occur in the soil. The soil environment is one of the most dynamic sites of biological interaction in nature. It is inhabited by microbial communities of bacteria, fungi, and actinomycetes. These organisms are essential participants in the nutrient cycles that make elements available for plant uptake. Changes in the soil environment that influence the role of the bacteria and fungi in nutrient cycling determine plant and ultimately ecosystem response.

Many of the major indirect plant responses to PM deposition are chiefly soil-mediated and depend on the chemical composition of the individual components of deposited PM. Effects may result in changes in biota and in soil conditions that affect ecological processes, such as nutrient cycling and uptake by plants.

The soil environment is rich in biota. Bacteria and fungi are usually most abundant in the rhizosphere, the soil around plant roots that all mineral nutrients must pass through. Bacteria and fungi benefit from the nutrients that are present in root exudates and make mineral nutrients available for plant uptake. The soil-mediated ecosystem impacts of PM are largely determined by effects on the growth of bacteria and mycorrhizal fungi that are involved in nutrient cycling and plant nutrient uptake.

Soil Nutrient Cycling

Accumulation of heavy metals in litter can interfere with nutrient cycling. Microorganisms are responsible for decomposition of organic matter, which contributes to soil fertility. Toxic effects on the microflora can be caused by Zn, Cd, and Cu. The U.S. EPA (2004, [056905](#)) judged that addition of only a few mg of Zn per kg of soil can inhibit sensitive microbial processes. Enzymes involved in the cycling of N, P, and S (especially arylsulfatase and phosphatase) seem to be most affected (Kandeler et al., 1996, [094392](#)).

Soil organic matter cycling is known to be sensitive to disturbance due to heavy metal pollution. This can cause increased litter accumulation at sites close to metal emissions point sources. The relative importance of the various processes that might be responsible for this observation is poorly known. Boucher et al. (2005, [155699](#)) conducted CO₂ evolution studies in microcosms having metal-rich and metal-poor plant materials. Their results suggested that there was a pool of less readily decomposable C that appeared to be preferentially preserved in the presence of high metal (Zn, Pb, Cd) concentrations in the leaves of the metallophyte *Arabidopsis halleri*. An additional possibility is that increased lignification of the cell walls increased the amount of insoluble C (Mayo et al., 1992, [155974](#)).

Yuangen et al. (2006, [156174](#)) found that urban soil basal respiration rates were positively correlated with soil acetic acid-extractable Cd, Cu, Ni, and Zn. The soil microbial biomass was negatively correlated with the concentrations of Pb fractions, but not with other metals. Overall microbial biomass was lower for urban soils as compared with rural soils (Yuangen et al., 2006, [156174](#)).

Metal Toxicity to Microbial Communities

It is believed that increased accumulation of litter in metal-contaminated areas is due to the effects of metal toxicity on microorganisms. Smith (1991, [042566](#)) reported the effects of Cd, Cu, Ni, and Zn on the symbiotic activity of fungi, bacteria, and actinomycetes. In particular, the formation of mycorrhizae has been shown to be reduced when Zn, Cu, Ni, and Cd were added to the soil.

Most studies of the effects of heavy metals on soils have been conducted under laboratory conditions. However, Oliveira and Pampulha (2006, [156827](#)) performed a field study to evaluate long-term changes in soil microbiological characteristics in response to heavy metal contamination. Dehydrogenase activity, soil ATP content, and enumeration of major soil microbial groups illustrated the effects of contamination. There was a marked decrease in total numbers of the different microbial groups. In particular, asymbiotic nitrogen-fixers and heterotrophic bacteria were found to be sensitive. Dehydrogenase activity was confirmed to be a good assay for determining the effect of heavy metals on physiologically active soil microbial biomass.

The toxic effects of heavy metals on soil microorganisms are well known. However, less is known about the relative sensitivity of different types of soil microorganisms (Rajapaksha et al., 2004, [156035](#)). Vaisvalavicius et al. (2006, [157080](#)) assessed the toxicity of high concentrations of Pb (839 mg/kg), Zn (844 mg/kg), and Cu (773 mg/kg) in the upper 0-0.1 m soil layer. Microbial abundance of all groups was reduced and enzymatic activity was lower than for uncontaminated soil. In particular, actinomycetes, oligonitrophobic and mineral N assimilating bacteria were most affected.

Effects of heavy metals in soil on microbes depends on soil pH, organic content, and the type of heavy metal exposure (Kucharski and Wyszowska, 2004, [156662](#)). Some studies have shown that heavy metals inhibit microbial activity in soil (Smejkalova et al., 2003, [156987](#); Vasundhara et al., 2004, [156133](#)). However, Wyszowska et al. (2007, [179948](#)) showed that heavy metals can either

inhibit or stimulate the growth of soil microbes. Populations of *Azotobacter* spp. decreased, but populations of oligotrophic and copiotrophic bacteria, actinomyces, and fungi increased in response to heavy metal exposure. Acute metal stress causes a decrease in microbial biomass as metal-sensitive microbes are inhibited (Joynt et al., 2006, [155887](#)).

Studies of the impacts of metal stress on the microbial community composition in soil have generally been based on microbial culturing techniques that can select only a subset of the natural soil population of microbes. More recent culture-independent studies have been conducted using phospholipids or nucleic acid biomarkers to reveal information regarding changes in microbial community structure (Joynt et al., 2006, [155887](#)). Using this approach, Joynt et al. (2006, [155887](#)) demonstrated that soils contaminated with both metals (Pb, Cr) and organic solvent compounds over a period of several decades had undergone changes in community composition, but still contained a phylogenetically diverse group of bacteria. This may reflect adaptation to the potentially toxic conditions through such processes as natural selection, gene exchange, and immigration. Comparison between a severely contaminated soil with a similar soil that had much lower amounts of contamination showed considerably lower microbial diversity in the contaminated soil, particularly for asymbiotic nitrogen fixers and heterotrophic bacteria (Oliveira and Pampulha, 2006, [156827](#)).

As pollution increases, it is expected that the more sensitive species will be lost and the more tolerant species remain. This gives rise to the concept of pollution-induced community tolerance (PICT), which has been demonstrated for populations of bacteria and fungi (Davis et al., 2004, [155744](#)). These researchers assessed the effects of long-term Zn exposure on the metabolic diversity and tolerance to Zn of a soil microbial community across a gradient of Zn pollution. PICT was found to correlate better with total soil Zn than with the concentration of Zn in soil pore water.

Soil Microbe Interactions with Plant Uptake of Metals

Atmospherically-deposited metals accumulate in upper soil horizons where fine roots are most developed. The availability for plant uptake of metals in soil depends on metal speciation and soil pH. In addition, metal binding to dissolved organic matter (DOM) reduces bioavailability (Sauvé, 2001, [156948](#)). Because organic matter typically decreases with soil depth, the affinity of metals for organic matter can influence metal bioavailability at different soil depths. Fine roots (<2 mm diameter) provide the major site of uptake and transport to the above-ground plant and generally contain a large proportion of the total metals found in plants (Gordon and Jackson, 2000, [155802](#)).

Fine roots are often colonized by mycorrhiza and interact with other soil microbes. Recent published evidence supports that mycorrhiza and bacteria influence plant uptake and tolerance of metals. Mycorrhiza are fungi that colonize plant roots to form a symbiosis. Mycorrhiza take up nutrients from the soil and transfer them to the plant in exchange for carbon from the plant. Like plants, some species and strains of mycorrhiza are more tolerant of metals in the soil (Ray et al., 2005, [190473](#)), so that unpolluted and polluted sites may host different species and strains of mycorrhiza (Vogel-Mikus et al., 2005, [190501](#)).

Mycorrhiza have been observed to cause a range of effects on plants. In some cases, plants colonized with mycorrhiza showed improved nutrient uptake and decreased metal uptake (Berthelsen et al., 1995, [078058](#); Nogueira et al., 2004, [190460](#); Vogel-Mikus et al., 2006, [190502](#)). Mycorrhiza have been shown to accumulate metals and act as a sink (Berthelsen et al., 1995, [078058](#); Carvalho et al., 2006, [155715](#)) often preventing the metals in the roots from allocation to shoots (Kaldorf et al., 1999, [190399](#); Soares and Siqueira, 2008, [190482](#); Zhang et al., 2005, [192083](#)). For example, estuarine salt marshes are often located close to urban and industrial areas and receive elevated amounts of trace metal contaminants from point and non-point (including atmospheric deposition) sources. Vegetation is important in the retention and accumulation of heavy metals in salt marshes. Carvalho et al. (2006, [155715](#)) conducted experiments on the effects of arbuscular mycorrhizal fungi (AMF) on the uptake of Cd and Cu by *Aster tripolium*, a common plant species in polluted salt marshes and a host of AMF. Carvalho et al. (2006, [155715](#)) found that AMF colonization increased metal accumulation in the root system of *Aster tripolium* without enhancing translocation to the shoot. By trapping toxic metals in the roots, this plant species may reduce the extent of vegetative stress caused by metal exposure and act as an effective sink for these metals. In a review paper Christie et al. (2004, [190174](#)) concluded that mycorrhiza may directly improve plant tolerance to

metals by binding and immobilizing metals and indirectly improve plant tolerance by improving uptake of nutrients that increase plant growth.

There is recent evidence that bacteria and mycorrhiza act together to improve plant tolerance to metals. Like mycorrhiza some bacteria are more tolerant to metals than others (Vivas et al., 2003, [190499](#)). Combined inoculation of *Trifolium sp.* by the arbuscular mycorrhiza, *Glomus mosseae*, and the bacterium, *Brevivacillus sp.*, conferred tolerance to Cd by increasing nutrient status and rooting development and by decreasing Cd uptake by the plant (Vivas et al., 2003, [190499](#)). A similar result was observed for Zn uptake (Vivas et al., 2006, [190500](#)).

In some cases, mycorrhizae will not prevent metal uptake (Weissenhorn et al., 1995, [073826](#)). In fact, mycorrhiza may facilitate the accumulation of metals in plants and enhance the translocation of metals from the root to the shoot (Citterio et al., 2005, [190176](#); Vogel-Mikus et al., 2005, [190501](#); Zimmer et al., 2009, [192085](#)). There is evidence of variable responses depending on the combination of mycorrhiza and bacteria species. Zimmer et al. (2009, [192085](#)) recently showed that the willow tree (*Salix sp.*) colonized with the ectomycorrhizal fungus, *Hebeloma crustuliniforme*, and the bacteria, *Micrococcus luters*, increased total Cd and Zn accumulation due to enhanced mycorrhizal formation. In these cases where soil microbes cause increased metal accumulation, there is a potential to use the system for phytoremediation.

Plants also vary in the extent to which they take up heavy metals from the soil. Variability has been shown to occur in response to different plant species and different metals. For example, Szabó and Fodor (2006, [156109](#)) exposed winter wheat (*Triticum aestivum*), maize (*Zea mays*) and sunflower (*Helianthus annuus*) to a variety of micro-pollutants. Cadmium accumulation was significant in both vegetative and reproductive plant parts. Vegetative winter wheat accumulated substantial amounts of Hg, but the other species did not. Lead, Cu, and Zn showed only moderate enrichment in crops (Szabó and Fodor, 2006, [156109](#)).

There is some evidence to support that shallow-rooted plant species are most likely to take up metals from the soil (Martin and Coughtrey, 1981, [047727](#)). However, there is little evidence confirming this observation. It may be more likely that shallow roots of species are likely to take up metals because the metal often accumulates in shallow soil layers. Even though atmospheric PM will usually deposit on soils before being taken up by plants, it could also be deposited to aquatic systems with subsequent transfer to terrestrial plants. Contamination of stream sediments by heavy metals can impact adjacent terrestrial ecosystems when high flows cause resuspension and subsequent streamside deposition of sediment particles. For example, Ozdilek et al. (2007, [156010](#)) showed that metal concentrations in vegetation along the Blackstone River in Massachusetts and Rhode Island were generally inversely related to the distance from the riverbank, with higher metal concentrations in plant tissues located near the river. The ability of plants to take up metals from soil is an important part of metal cycling in the environment. This uptake process allows the metals to enter the food web, where they might exert mutagenic, carcinogenic, and teratogenic effects (Hunaiti et al., 2007, [156579](#)).

9.4.5.3. Plant Response to Metals

Some metals, including Cu, Co, Ni, and Zn, are essential micronutrients needed for plant growth. Others, including Hg, Cd, and Pb are not essential for plants. Though all heavy metals can be directly toxic at sufficiently high concentrations, only Cu, Ni, and Zn have been documented as being frequently toxic to plants (U.S. EPA, 2004, [056905](#)), while toxicity due to Cd, Co, and Pb has been observed less frequently (Smith, 1990, [046896](#)). Toxic doses depend on the type of ion, ion concentration, plant species and the stage of plant growth (Memon and Schroder, 2009, [190442](#)). Toxicity response is also dependent on the nutritional status of the plant and the development of mycorrhizae (Strandberg et al., 2006, [156105](#)). Plants respond to high concentrations of metals in soil through a variety of mechanisms and there are substantial differences among plant species in their response to heavy metal exposure. Mechanisms of metal tolerance included exclusion or excretion rates, genetics (Patra et al., 2004, [081976](#); Yang et al., 2005, [192104](#)), mycorrhizal interactions (Gohre and Paszkowski, 2006, [190355](#)), storage capability and accumulation (Clemens, 2006, [190179](#)), and various cellular detoxification mechanisms (Gratao et al., 2005, [190364](#); Hall, 2002, [190365](#)).

One of the most important mechanisms that increases plant tolerance to metals is chelation with phytochelatin, such as metallothioneins and peptide ligands that are synthesized within the plant from glutathione (Memon and Schroder, 2009, [190442](#)). Phytochelatin are intracellular

metal-binding peptides that act as specific indicators of metal stress. Because they are produced by plants as a response to sublethal concentrations of heavy metals, they can indicate that heavy metals play a role in forest decline (Gawel et al., 1996, [012278](#)). Phytochelatin concentrations have previously been measured in coniferous trees in the northeastern U.S. The U.S. EPA (2004, [056905](#)) and Grantz et al. (2003, [155805](#)) summarized studies indicating that both the number of dead red spruce trees and phytochelatin concentrations increased sharply with elevation in the northeastern U.S. Red spruce stands showing varying degrees of decline indicated a systematic and significant increase in phytochelatin concentrations associated with the extent of tree injury. These data suggest that metal stress might contribute to tree injury and forest decline in the northeastern U.S. The extent to which low to moderate amounts of heavy metal deposition, which might occur at locations that are not in close proximity to a large point source, contribute to adverse impacts on forest vegetation is not known. Although the phytochelatin data suggest a linkage, more direct experimental data would be needed to confirm such a finding.

In general, plant growth is negatively correlated with trace metal and heavy metal concentration in soils and plant tissue (Audet and Charest, 2007, [190169](#)). Trace metals, particularly heavy metals, can influence forest growth. Growth suppression of foliar microflora has been shown to result from Fe, Al, and Zn. These three metals can also inhibit fungal spore formation, as can Cd, Cr, Mg, and Ni (see Smith, 1990, [046896](#)). Metals cause stress and decreased photosynthesis (Kucera et al., 2008, [190408](#)) and disrupt numerous enzymes and metabolic pathways (Strydom et al., 2006, [190486](#)). Excessive concentrations of metals result in phytotoxicity through: (i) changes in the permeability of the cell membrane; (ii) reactions of sulfhydryl (-SH) groups with cations; (iii) affinity for reacting with phosphate groups and active groups of ADP or ATP; and (iv) replacement of essential ions (Patra et al., 2004, [081976](#)).

In addition to disrupting photosynthesis and other metabolic pathways, metals have been shown to alter frost hardiness and impair nutrition. A recent review by Taulavuori (2005, [190489](#)) suggests that metal-induced stress reduces frost hardiness of plants, a particular concern at high elevation sites. Kim et al. (2003, [155899](#)) found decreased concentration of K in needles and Ca in stems of *Pinus sylvestris* seedlings exposed to Cd addition. This response suggests a disturbance of nutrition in response to Cd. Pollutant-caused needle loss can reduce the interception of pollutants from the atmosphere, and therefore reduce their concentrations in stemflow. This may be responsible for the observation that species diversity of lichens is sometimes higher on trees affected by die-back (Hauck, 2003, [155830](#)).

Da Silva et al. (2006, [190190](#)) have shown that PM had anatomical and physiological effects on plants growing near an iron pelletization factory in Brazil. The effects of PM occurred due to foliar uptake. Structural characteristics such as peltate trichomes may have formed a barrier lessening the penetration of metallic iron into the mesophyll in some species. Iron was shown to penetrate the trichomes, epidermic cells (adaxial and abaxial surfaces), stomata, xylem cells, collenchyma, endodermis and mesophyll tissues. Once entering the stomata, the PM penetrates within the mesophyll, it may modify the chemical balance of the mesophyll (Da et al., 2006, [190190](#)).

A greenhouse study evaluated the combined effects of iron dust on restinga vegetation (coastal vegetation of Brazil) that commonly grows near iron ore industries. Kuki et al. (2008, [155346](#)) found that iron dust had differing effects on gas exchange, chlorophyll content, iron content and antioxidant enzyme activity on two plant species common to the restinga, *Schinus terebinthifolius* (an invasive exotic in the U.S.) was not affected by the iron dust. However, *Sophora tomentosa* showed increased iron content and membrane permeability to the leaves, increasing activity of antioxidant enzymes. These results showed that the plants used different strategies to cope with PM pollution. *S. terebinthifolius* avoided stress, while *S. tomentosa* used antioxidant enzyme systems to partially neutralize oxidative stress.

Plant foliage can accumulate elemental Hg over time in response to air exposure and concentrations in soil (Erickson et al., 2003, [155769](#); Frescholtz et al., 2003, [190352](#)). A mesocosm experiment was conducted by Erickson et al. (2003, [155769](#)) where aspen trees were grown in gas-exchange chambers in Hg-enriched soil ($12.3 \pm 1.3 \mu\text{g/g}$) and the Hg content in the foliage was analyzed. Foliar Hg increased with leaf age for 2-3 mo and then stabilized at leaf concentrations near 150 ng/g. About 80% of the Hg found in above-ground biomass was present in the leaves. The concentration of Hg in trees grown in the same mesocosms in containers of low Hg soil ($0.03 \pm 0.01 \mu\text{g/g}$) exhibited foliar Hg concentrations that were similar to those of trees grown in Hg-enriched soil. Almost all of the foliar Hg originated from the atmosphere. Clearly, plant foliage

can be a major sink for airborne Hg, which can subsequently enter the soil after litterfall (Erickson et al., 2003, [155769](#)). However, this study did not determine the extent to which atmospheric Hg was dry-deposited on the foliage, as opposed to gaseous uptake through the stomata. Foliar/air Hg exchange has been shown to be dynamic and bi-directional (Millhollen et al., 2006, [190447](#)). These investigators compared foliar Hg accumulation over time in three tree species with fluxes measured using a plant gas-exchange system subsequent to soil amendment with HgCl₂. Root tissue Hg concentrations were strongly correlated with soil Hg concentrations, suggesting that below-ground accumulation of Hg by roots may be an important process in the biogeochemical cycling of Hg in soil systems. Nevertheless, measured foliar Hg fluxes indicated that deposition of atmospheric Hg constituted the dominant flux of Hg to the leaf surface (Millhollen et al., 2006, [190447](#)). Grigal (2003, [155811](#)) also found that Hg in vegetation is derived almost exclusively from the atmosphere. Mercury uptake from soil is limited, partly because roots adsorb Hg but transport it to foliage very poorly (Grigal, 2002, [156498](#)). Grigal (2003, [155811](#)) provided a thorough review of the sequestration of Hg in forest and peatland ecosystems. A fundamental aspect of Hg cycling is its strong relationship to organic matter. For that reason, peatlands sequester much larger quantities of Hg than would be expected on the basis of their land area. Thus, if global climate change affects C storage, it may indirectly affect Hg storage because of the strong relationship between Hg and organic matter (Grigal, 2003, [155811](#)).

Arbuscular mycorrhizal (AM) fungi can play important roles in mitigating toxicity of heavy metals in plants. For example, AM symbiosis is known to be involved in plant adaptation to As-contaminated soils. Higher plants that are adapted to As contaminated soils are generally associated with mycorrhizal fungi (Gonzalez-Chavez et al., 2002, [155800](#)). It has also been shown that AM symbioses can influence plant coexistence and community diversity (O'Connor, 2002). Some plants associated with AM fungi can successfully colonize sites that are heavily contaminated by heavy metals (Pennisi, 2004, [156018](#)).

Dong et al. (2008, [192106](#)) cultivated white clover (*Trifolium repens*) and ryegrass (*Lolium perenne*) in As-contaminated soil (water extractable As 82.7 mg/kg). The growth and P nutrition of both species largely depended on AM symbiosis. The AM-inoculated plants showed selective uptake and transfer of P over As.

PM pollution has the potential to alter species composition over long time scales. Kuki et al. (2009, [190411](#)) showed that early establishment stages of *Sophora tomentosa* species were negatively affected by the combination of iron ore and acidifying particles. The deleterious effects of the PM included deficient germination and toxic concentrations in roots. In contrast, *S. terebinthifolius* was not affected by the PM revealing species resistance to the pollution. The difference among species response suggests that over a long time period the imbalance will likely change the species composition (Kuki et al., 2009, [190411](#)).

The process of removing toxins from soil or water using photoautotrophs is referred to as phytoremediation. Some plant species have good ability to extract heavy metals from soil, thereby offering potential for phytoremediation (Clemens, 2006, [190179](#); Hooda, 2007, [190382](#); Padmavathamma and Li, 2007, [190465](#)). For example, several species of willow (*Salix* spp.) accumulate high concentrations of Zn and Cd in aboveground biomass (Lunácková et al., 2003, [155948](#); Meers et al., 2007, [155977](#); Rosselli et al., 2003, [156058](#)). A first estimation of the order of magnitude of potential metal removal by willow was 2 to 27 kg/ha/yr of Zn and 0.25 to 0.65 kg/ha/yr for Cd (Meers et al., 2007, [155977](#)). Build-up of high concentrations of trace metals in soil is difficult to remediate because of the long residence times of metals in the environment. Plants that survive on heavy metal-contaminated soils have been studied to elucidate the mechanisms that allow them to tolerate such conditions and interactions between soil contamination and vegetation composition (Becker and Brändel, 2007, [156260](#); Hall, 2002, [190365](#)). There are numerous other plants that have been investigated for application to phytoremediation. Plants that hyperaccumulate metals have special potential for remediation of metal-contaminated sites. About 400 species have been reported. Brassicaceae has the largest numbers of taxa, with 11 genera and 87 species known to hyperaccumulate one or more metal contaminants (Prasad and DeOliveira, 2003, [156885](#)).

Plant uptake is often the first step for a metal to enter higher levels of the food web. Consumers of vegetation may often receive heavy loading of metals from their diets. Metals may also bioaccumulate in some species and tissue concentrations are magnified at the higher trophic levels, so-called biomagnifications (see Section 9.4.5.7. on Biomagnification).

9.4.5.4. Effects on Aquatic Ecosystems

The atmospheric deposition of PM into the ocean has important implications for primary productivity and carbon sequestration. In part, metals in PM deposition may limit phytoplankton growth in parts of the ocean (Crawford et al., 2003, [156370](#)). In particular, Fe and Zn can influence the productivity of algae that are involved in CaCO₃ production. The production of both particulate organic C and CaCO₃ drive the ocean's biological carbon pump (Shulz et al., 2004, [156087](#)). Thus, in oceanic areas of trace metal limitation, changes in trace metal atmospheric deposition can affect biogenic calcification, with potential consequences for CO₂ partitioning between the ocean and atmosphere.

A study by Sheesley et al. (2004, [156084](#)) illustrated the value of bioassay procedures to provide an initial screening of ambient PM toxicity. They used two species of green algae and two extraction methods to compare the toxicities of atmospheric PM collected at two urban/industrial sites and one rural site near the southern shore of Lake Michigan. Toxicities varied by site, by extraction solvent, and by bioassay. Results suggested that toxicity was not related to the total mass of PM in the extract, but to the chemical components of the PM. It is noteworthy that the concentrations of contaminants in PM in this type of short-term and acute toxicity testing are much higher than would be found in the natural environment. Thus, the purpose of this type of testing is to provide an initial screening-level comparison of relative toxicities of atmospheric PM from different source areas. It does not provide the data that would be needed to assess risk (Sheesley et al., 2004, [156084](#)).

9.4.5.5. Effects on Animals

There has been little work focusing on animal indicators of PM effects in the field. However, there have been several recent studies on snails, amphibians, earthworms, and bivalves that are discussed below.

Bioindicator organisms can be especially useful for monitoring PM effects over geographical and temporal scales. Terrestrial invertebrates have been used to monitor contaminants in both air and soil. Snails (*Helix* sp.) accumulate trace metals and agrochemicals, and can be used as effective biomonitors for urban air pollution (Beeby and Richmond, 2002, [155680](#); Regoli et al., 2006, [156046](#); Viard et al., 2004, [055675](#)). Demonstrated biological effects include growth inhibition, impairment of reproduction, and induction of metallothioneins that are involved in metal detoxification (Gomot-de and Kerhoas, 2000, [155798](#); Regoli et al., 2006, [156046](#)). The use of sentinel species to detect the effects of complex mixtures of air pollutants is of particular value because the chemical constituents are difficult to characterize, exhibit varying bioavailability, and are subject to various synergistic effects.

Regoli et al. (2006, [156046](#)) caged land snails (*Helix aspersa*) at five locations in the urban areas of Ancona, Italy. After four weeks of exposure to ambient air pollution, the snails were analyzed for trace metals and PAHs. Biomarkers were measured that correlated with contaminant accumulation, including concentrations of metallothioneins, activity of biotransformation enzymes, and peroxisomal proliferation. In addition, indicators of oxidative stress were measured, such as oxyradical scavenging capacity, onset of cellular damage, and loss of DNA integrity. Results documented substantial accumulation of metals and PAHs in snail digestive tissues in urban areas having high traffic congestion. Cellular reactivity was also found, suggesting that this species is an effective bioindicator for multipollutant air quality and PM monitoring.

Some amphibian ecotoxicological research has focused on heavy metal exposure. Contaminant uptake can occur by oral, pulmonary, and dermal exposure (James et al., 2004, [155874](#); Johnson et al., 1999, [155880](#); Lambert, 1997, [155916](#)). This is potentially important because of documented declines in amphibian populations in the U.S. and elsewhere in recent decades (Houlahan et al., 2000, [155853](#)). Toads were shown to be fairly tolerant of Cd exposure (James et al., 2004, [155874](#)). It is not clear whether current amounts of terrestrial metal contamination pose an increased risk to amphibians in general.

Estuarine and marine bivalves provide potential bioindicators for Hg bioaccumulation. For example, Coelho et al. (2006, [190181](#)) investigated Hg concentrations in *Scrobicularia plana*, a long-lived, deposit-feeding bivalve in southern Europe. Annual bioaccumulation rates were shown to be strongly correlated with Hg concentrations in suspended particulate matter (SPM), a response to

their deposit-feeding tactics (Verdelhos et al., 2005, [190497](#)). The ability to predict annual accumulation rates for indicator species, such as this bivalve, may facilitate management actions to avoid deleterious effects on humans through consumption of bivalves above a certain age/size class.

Earthworms often constitute a large percentage of soil animal biomass and they are considered to be relatively sensitive indicators of soil metal contamination. They are continuously exposed to the soil via dermal contact in the soil solution or ingestion of large quantities of soil pore water, polluted food and/or soil particles (Lanno et al., 2004, [190415](#)). Hobbelen et al. (2006, [190371](#)) determined the important metal pools for bioaccumulation by earthworms *Lumbricus rubellus*, which live in the upper 5cm of soil and *Aporrectodea caliginosa*, which live in the upper 25 cm of soil. Soil concentration explained much of earthworm concentrations, however Cd concentration in *A. caliginosa* was best explained by pore water concentrations and no variable tested explained Zn tissue concentrations. Massicotte et al. (2003, [155968](#)) compared the cell viability and phagocytic potential of three earthworm species (*Lumbricus terrestris*, *Eisenia andrei*, and *Aporrectodea tuberculata*) in response to atmospheric emissions of metals from a cement factory in Quebec, Canada. Cell viability actually increased in proximity (0.5 km) to the cement factory for *A. tuberculata*, and this might have been due to beneficial effects of increased Ca deposition. There were no significant differences observed for the other two species (Massicotte et al., 2003, [155968](#)).

Biogeochemical cycling of Hg in the Arctic has been investigated, in part because observed Hg concentrations in marine animals may pose health risks for local human populations. The lifetime of gaseous elemental Hg (GEM) in the atmosphere, which constitutes about 95% of atmospheric Hg, is generally about one year (Lin and Pehkonen, 1999, [190426](#)). However, during spring (typically March through June), the lifetime of GEM in the Arctic is much shorter, and atmospheric GEM can be depleted in less than one day during atmospheric Hg depletion episodes (AMDE) (Lindberg et al., 2002, [190429](#); Skov et al., 2004, [190481](#)). During the AMDE, GEM is rapidly oxidized to reactive gaseous Hg that can be deposited to the ground surface (Skov et al., 2004, [190481](#)). Because of the increased solar flux to the Arctic during spring and seasonal melting of sea ice, there may be an increased efficiency of Hg bioaccumulation in Arctic food webs than would be expected based on data collected at mid-latitudes. Skov et al. (2004, [190481](#)) developed a simple parameterization for AMDE and included it in the Danish Eulerian Hemispheric Model (DEHM). The model was shown to reproduce the general structure of AMDE, suggesting that the limiting factor for AMDE may be the surface temperature of sea ice.

9.4.5.6. Biomagnification across Trophic Levels

Biomagnification is the progressive accumulation of chemicals with increasing trophic level (LeBlanc, 1995, [155921](#)). Organic Hg is the most likely metal to biomagnify, in part because organisms can efficiently assimilate methylmercury and it is slowly eliminated (Croteau et al., 2005, [156373](#); Reinfelder et al., 1998, [156047](#)). Of the trace metals, there is also evidence that Cd, Pb, Zn, Cu and Se biomagnify.

The study of trophic transfer and biomagnification is limited by the difficulty in discriminating food webs and the uncertainty associated with assignment of trophic position to individual species (Croteau et al., 2005, [156373](#)). Use of stable isotopes can help to establish linkages. However, it is difficult to determine the extent to which biomagnification occurs in a given ecosystem without thoroughly investigating physiological biodynamics, habitat, food web structure, and trophic position of relevant species. Thus, development of an understanding of ecosystem complexity is necessary to determine what species might be at greatest risk from toxic metal exposure (Croteau et al., 2005, [156373](#)).

Terrestrial

Bioaccumulation of heavy metals can occur through the plant-herbivore and litter-detritivore food webs. The U.S. EPA (2004, [056905](#)) concluded that Cd and Zn can bioaccumulate in earthworms. Other invertebrates inhabiting soil litter may also accumulate metals. Although food web accumulation of a metal may not result in mortality, it might reduce breeding potential or result in other non-lethal effects that adversely affect organism responses to environmental cues.

Metal accumulation in litter can be found mainly around brass works, cement factories, and Pb and Zn smelters. Organisms that feed on earthworms living in soils with elevated metal

concentrations may also accumulate Pb and Zn. Increased concentrations of heavy metals have been found in a variety of mammals living in areas with elevated heavy metal concentrations in the soils.

The transfer of metals from plants to terrestrial snails is an interesting system for biomagnifications because snails accumulate metals in their soft tissue and can contribute significantly to the transfer of pollutants to primary consumers and terrestrial predators (Dallinger et al., 2001, [192109](#)). Notten et al. (2005, [190461](#)) studied the transfer of Cu, Zn, Cd and Pb in terrestrial soil-plant-snail food chains in metal-polluted soils of the Netherlands. The food chain included perennial plant species *Urtica dioica* and the herbivorous snail *Cepaea nemoralis*. The transfer of metal from the soil to the plant compartment was low (coefficient of determination $R^2 = 0.20$). Total concentration of metals in soils was a poor predictor of leaf concentration. Low metal concentration in the leaves was thought to be due to low pore water metal concentrations and was also thought to be partly caused by low translocation from roots within the plant. The Cu, Zn and Cd concentrations in the snails were always higher than concentrations in the leaves indicating bioaccumulation. The metal transfer from the leaf to snail was highest among all routes tested, suggesting that transfer from diet is important. Similar results were found by Beeby and Richmond (2002, [155680](#)) with the snail, *Helix aspersa*, and the plant, *Taraxacum sp.*, for Zn, Pb, Cd, but not for Cu.

Many types of predators including shrews, thrushes and beetle larvae include snails as part of their diet (Gomot-De and Pihan, 2002, [190357](#); Seifert et al., 1999, [190480](#)). Seifert et al. (1999, [190480](#)) found the shrews eating snails with elevated Cd had critical levels of Cd in their kidneys. Scheifler et al. (2007, [190379](#)) found that Cd in snails lead to toxic levels in beetle larvae that caused increased amounts of mortality.

Aquatic

In general, it has been assumed that metal biomagnification in aquatic ecosystems is an exception rather than the rule (Gray, 2002, [155806](#)). More recent research has demonstrated aquatic biomagnification of certain metals. For example, Stewart et al. (2004, [156097](#)) used stable isotopes of C and N to show biomagnification of Se in San Francisco Bay food webs. Croteau et al. (2005, [156373](#)) identified trophic position of estuarine organisms and food web structure in the delta of San Francisco Bay to document Cd biomagnification in invertebrates that live on macrophytes and also in fish. Concentrations of Cd were biomagnified 15 times within two trophic links in each food web. In contrast, no tendency towards biomagnification was observed for Cu.

In aquatic ecosystems, biomagnification of trace metals does not necessarily occur. Nguyen et al. (2005, [155997](#)) found biodiminution for most metals in Lake Balaton, Hungary, with the exception of slight enrichment of Zn from PM to zooplankton and of Cd from sediment to mussels.

Once transported to aquatic ecosystems, trace metals often preferentially bind to sediment particles. Some of these sediment-bound metals may be unavailable to biota; in contrast, metals bound to sediment organic matter may exhibit varying degrees of bioavailability (Di Toro et al., 2005, [155750](#)). Piol et al. (2006, [156028](#)) studied the bioavailability of sediment-bound Cd to the freshwater oligochaete *Lumbriculus variegatus*. They found that Cd uptake depended on the amount of free dissolved Cd(II), and the Cd contribution from sedimentary particles to biological uptake was negligible.

Marine bivalve mollusks bioaccumulate trace metals and other contaminants (LaBrecque et al., 2004, [155913](#)) and therefore may be used as bioindicators of contamination. In addition, they constitute an important link to human health by virtue of their importance as a food source (Cheggour et al., 2005, [155723](#); Li et al., 2002, [156691](#)).

9.4.5.7. Effects near Smelters and Roadsides

The high PM concentrations in proximity to mining, smelting, roadsides and other industrial sources result in heavy metal loadings that may be particularly damaging to nearby ecosystems.

Smelters

The Harjavalta region is one of the most intensively studied heavy metal polluted areas in the world. Kiikkilä et al. (2003, [156637](#)) reviewed available data on heavy metal deposition and environmental effects in this area. Emissions from the smelter were as high as 1,100 t/yr of dust, 140 t/yr Cu, 96 t/yr Ni, 162 t/yr Zn, and 94 t/yr Pb in 1987. Deposition amounts decreased substantially after 1990, to only a few percent of the amounts that occurred during the 1980s.

Kiikkilä (2003, [156637](#)) investigated the effects of heavy metal pollution in proximity to a Cu-Ni smelter at Harjavalta, Finland. The deposition of heavy metals increased within 30 km of the smelter. Only slight changes in the understory vegetation were observed at distances greater than 8 km from the smelter. At 4 km distance, species composition of vegetation, insects, birds, and soil microbiota changed and tree growth was reduced. Within about 1 km, only the most resistant organisms were surviving.

The number of soil organisms clearly decreased and their community structure was altered close to the Harjavalta smelter (Kiikkilä, 2003, [156637](#)). However, this effect was only pronounced within about 2 km of the smelter. This suggests that the soil microfauna are relatively resistant to metal pollution effects.

Soil microbial activity decreased close to the Harjavalta smelter (Kiikkilä, 2003, [156637](#)), as reflected by microbial respiration, distribution of species within physiological groups, and microbial and fungal biomass. The fungi appeared to be more sensitive to metal contamination than the bacteria (Pennanen et al., 1996, [156016](#)). The rate of litter decomposition decreased, causing an accumulation of needle litter on top of the forest floor near the smelter (Fritze et al., 1989, [079635](#)).

Inhibition of nutrient cycling and displacement by Cu and Ni of base cations from cation exchange sites on the soil resulted in a decrease in base cation concentrations in the organic soil layer (Derome and Lindroos, 1998, [155749](#); Kiikkilä, 2003, [156637](#)) close to the Harjavalta smelter. In addition, Mg, Ca, and Mn concentrations in Scots pine (*Pinus sylvestris*) needles were low, and this was attributed by Kiikkilä (2003, [156637](#)) to the toxic effects of Cu and Ni to plant fine roots and also to ectomycorrhizal root tips (Helmisaari et al., 1999, [155836](#)). Nutrient translocation during fall was also affected close to the smelter; as a consequence needle concentrations of K were relatively high (Nieminen et al., 1999, [155998](#)).

Tree growth (Scots pine) has been poor (Malkönen et al., 1999, [155961](#)) and most vegetation was absent within 0.5 km of the smelter. Effects on plant species occurrence close to the smelter were almost entirely negative. In contrast, some animal species responded positively, including a leaf miner, three species of aphid, and some ants, beetles, and spiders.

Salemaa et al. (2004, [156069](#)) investigated heavy metal concentrations in understory plant species growing at varying distances from the Harjavalta Cu-Ni smelter. Heavy metal concentrations (except Mn) were highest in bryophytes, followed by lichens, and were lowest in vascular plants. Vascular plants are generally able to restrict the uptake of toxic elements, and therefore were able to grow closer to the smelter than lichens. A pioneer moss (*Pohlia nutans*) was unusual in that it survived close to the smelter despite its accumulation of high amounts of Cu and Ni.

Changes in breeding success of cavity-nesting passerine birds close to the Harjavalta smelter were attributed to habitat changes in response to metal toxicity (Eeva et al., 2000, [155761](#); Kiikkilä, 2003, [156637](#)). Calcium supply is also well known to be important for breeding success in passerine bird species. Eggshell thickness, egg size, clutch size, and hatchability of pied flycatcher (*Ficedula hypoleuca*) were found to be depressed near the Cu smelter at Harjavalta, SW Finland (Eeva and Lehikoinen, 2004, [155762](#)). Availability of Ca-rich food to the birds was estimated by counting snail shells in the nests postfledging. The number of snail shells correlated positively with the Ca concentration of nestling feces and adult breeding success. In addition, the negative impact of Cu on the number of fledglings was stronger at locations where Ca concentration was low (Eeva and Lehikoinen, 2004, [155762](#)).

Documentation of effects on individual species, such as was reported above, does not reveal what the impacts might be on ecosystem function. Nevertheless, the mere fact that multiple species, operating at different trophic levels, have been shown to be affected by the ambient deposition in proximity to the smelter suggests that effects on ecosystem function may indeed have occurred. More research is needed, however, to fully evaluate effects on function as opposed to abundance of individual species.

Roadsides

Heavy metal particles are important constituents of road dust. These particles accumulate on the road surface from brake linings, road paint, tire debris, diesel exhaust, road construction materials, and catalyst materials. Road dust can be suspended in the atmosphere and contribute metals to soil, air, and urban runoff (Adachi and Tainosho, 2004, [081380](#); Davis et al., 2001, [024933](#); Smolders and Degryse, 2002, [156091](#)). In particular, Zn oxide comprises 0.4-4.3% of tire tread (Smolders and Degryse, 2002, [156091](#)) and tire wear is a substantial source of environmental Zn pollution. Adachi and Tainosho (2004, [081380](#)) used a field emission screening electron microscope equipped with an energy dispersive x-ray spectrometer to characterize heavy metal particles embedded in tire dust. Samples were classified into four likely source categories, based on cluster analysis. Based on morphology and chemical composition, the samples were identified as having derived from yellow paint (CrPbO₄ particles), brake dust (particulate Ti, Fe, Cu, Sb, Zr, Ba and heavy minerals [Y, Zr, La, Ce]), and tire tread (Zn oxide).

Since publication of EPA's 2004 PM criteria assessment, some additional research has been conducted on the effects of windblown PM. Effects on physical, chemical, and biological attributes of both plants and animals have been documented (Englert, 2004, [087939](#); Gleason et al., 2007, [155794](#); Kappos et al., 2004, [087922](#)). Experiments by Gleason et al. (2007, [155794](#)) suggest that most direct effects on plants of windblown PM originating from on-road surfaces occur within 40 m of the source. Windblown PM from roads or agriculture can cover plant photosynthetic structures (Sharifi et al., 1999, [156082](#)), cause impact damage (Armbrust and Retta, 2002, [156225](#)), or interfere with physiological mechanisms (Burkhardt et al., 2002, [155708](#)). As previously discussed in Section 9.4.5.5, land snails in urban areas have been shown to be a good indicator of traffic pollution.

9.4.5.8. Toxicity to Mosses and Lichens

At the time of the most recent air quality criteria report for PM (U.S. EPA, 2004, [056905](#)), trace metal toxicity to lichens had been demonstrated in relatively few cases. Nash (1975, [016763](#)) documented Zn toxicity in the vicinity of a Zn smelter near Palmerton, PA. Experimental data had suggested that lichen tolerance to Zn and Cd generally ranges between 200 and 600 ppm (Nash, 1975, [016763](#)).

The effects of deposited metals on the mosses have not been well studied. Tremper et al. (2004, [156126](#)) exposed mosses of two species to roadside conditions and sampled them over a period of 3 mo. Under field conditions, chlorophyll concentrations in moss tissue were not affected by metal contamination and accumulation.

Mosses and lichens readily take up metals from atmospheric deposition. Otnyukova (2007, [156009](#)) demonstrated vertical gradients within a coniferous forest canopy in the fruticose lichen genus *Usnea* with respect to lichen thallus morphology and heavy metal concentration. Abnormal thalli at the tree-top level contained higher concentrations of Al, Fe, Zn, F, Sr, and Pb. This vertical pattern within the tree canopy is in general accordance with known deposition of PM to plants (Otnyukova, 2007, [156009](#)).

There is an extensive literature on the use of mosses and lichens for estimating deposition (biomonitors) and indicating metal exposure in ecosystems (bioindicators) (see Section 9.4.2.3.).

9.4.6. Organic Compounds

VOCs in the atmosphere are partitioned between the gas and particle phases. As described by the U.S. EPA (2004, [056905](#)), the partitioning depends on vapor pressure, temperature, surface area of the particles, and the nature of the particles and of the chemical being adsorbed. A wide variety of organic contaminants are deposited from the atmosphere. These include chemicals such as DDT, PCBs, and PAHs.

Important organic atmospheric contaminants are generally those that are transported long distances in the atmosphere, subsequently deposited into remote locations, and bioaccumulated to sufficient concentrations that they can affect humans, wildlife, or other biota (Swackhamer et al., 2004, [190488](#)). Certain physical and chemical properties facilitate the movement of these contaminants from land and water surfaces into the atmosphere, provide stability, and enhance accumulation in lipids. Some, including the relatively small (up to 4 rings) PAHs degrade relatively

rapidly in the atmosphere or at the surface subsequent to atmospheric deposition. Below is a summary of the findings of the U.S. EPA (2004, [056905](#)), followed by discussion of more recent research findings.

Plants may be used as passive monitors to compare the deposition of organic compounds between sites. Vegetation can be used semi-quantitatively to indicate organic pollutant amounts if the mechanism of accumulation is considered. Organic compounds can enter the plant via the roots or be deposited as particles on the leaves and be taken up through the cuticle or stomata. The pathways depend on the chemical and its physical properties. These include, for example, lipophilicity, water solubility, vapor pressure, and Henry's law constant. Environmental conditions can also be important, including temperature and organic content of soil, plant species, and the foliar surface area and lipid content.

Organic particulates in the atmosphere are diverse in their makeup and sources. Vegetation itself is an important source of hydrocarbon aerosols. Terpenes, particularly α -pinene, β -pinene, and limonene, released from tree foliage may react in the atmosphere to form submicron particles. These naturally generated organic particles contribute significantly to the blue-haze aerosols formed naturally over forested areas (Geron et al., 2000, [019095](#); U.S. EPA, 2004, [056905](#)).

The low water solubility and high lipo-affinity of many organic xenobiotics control their interaction with the vegetative components of natural ecosystems. Foliar surfaces are covered with a waxy cuticle layer that helps reduce moisture loss and short-wave radiation stress. This epicuticular wax consists largely of long-chain esters, polyesters, and paraffins, which accumulate lipophilic compounds. Organic air contaminants in the particulate or vapor phase can be adsorbed to, and accumulate in, the epicuticular wax of leaf surfaces. Direct uptake of organic contaminants through the cuticle and vapor-phase uptake through the stomata are not well characterized for most trace organics.

Soil acts as an important storage compartment for POPs, including PCBs and PAHs. There is a continuous process of partitioning between the soil pool and the atmosphere, and this controls the regional and global transport of these compounds (Backe et al., 2004, [155668](#); Wania and Mackay, 1993, [157110](#)). Over time, POPs move towards equilibrium between the environmental compartments, and this process can be described using the fugacity concept (Backe et al., 2004, [155668](#); Mackay, 1991, [042941](#)). Fugacity reflects the tendency of a chemical constituent to escape one environmental compartment and move to another. When an equilibrium distribution is achieved, the fugacity quotient values in each compartment will be equal. Soil/air partitioning is controlled by a variety of factors. These include soil properties, such as organic matter content, moisture, porosity, texture, and structure, as well as the physiochemical properties of the pollutant, including vapor pressure and water solubility.

The accumulation of PAHs in vegetation, due to their lipophilic nature, could contribute to human and other animal exposure via food consumption. As a result, plant uptake of PAHs has been an important area of research (Gao and Zhu, 2004, [155782](#)). Most bioaccumulation of PAHs by plants occurs by leaf uptake (Tao et al., 2006, [156112](#)). Root uptake also occurs. It appears that roots preferentially accumulate the lower molecular weight PAHs due to their greater water solubility (Wild and Jones, 1992, [156155](#)).

Various models have been developed to simulate plant uptake of organic contaminants. The simple partition-limited model of Chiou et al. (2001, [156342](#)) has been further expanded to increase complexity and to include root uptake pathways (e.g., Fryer and Collins, 2003, [156454](#); Yang et al., 2005, [192104](#); Zhu et al., 2004, [156184](#)).

In evaluating receptor choice for studies of contaminant exposure to plants, and also remediation potential, it is important to consider differences among species. For example, Parrish et al. (2006, [156014](#)) assessed the bioavailability of PAHs in soil. During the first growing season, zucchini (*Cucurbita pepo* ssp. *pepo*) accumulated significantly more PAHs than did other related plant species, including up to three orders of magnitude greater concentrations of the six-ring PAHs. Parrish et al. (2006, [156014](#)) also noted differences in PAH uptake by two different species of earthworm.

The leaves of *Quercus ilex* have been shown to readily accumulate PAHs *in situ*. Young leaves accumulated PAHs within three weeks of bud break. Mature leaves showed seasonality, with higher PAH concentrations during winter (Alfani et al., 2005, [154319](#)).

It is difficult to discriminate between PAHs that are adsorbed to plant root surfaces as opposed to those that are actually taken up by the roots. In general, soil bound PAHs are associated with soil organic matter and are therefore not readily available for root uptake (Fismes et al., 2002, [141156](#);

Jiao et al., 2007, [155879](#)). Wild et al. (2005, [156156](#)) used two-photon excitation microscopy to visualize the uptake and transport of two PAHs (anthracene and phenanthrene) from a contaminated soil into living wheat and maize roots. Jiao et al. (2007, [155879](#)) developed a sequential extraction method to discriminate between PAH adsorption in rice roots.

Maize roots and tops of plants have been shown to directly accumulate PAHs from aqueous solution and from air in proportion to exposure amounts. Root concentration factors are log-linear functions of log-based octanol-water partition coefficients ($\log K_{ow}$); similarly, leaf concentration factors are log-linear functions of log-based octanol-air partition coefficients ($\log K_{oa}$) (Lin et al., 2007, [155933](#)). Although the bulk concentrations of PAHs in various plant tissues can differ greatly, the observed differences disappear after they are normalized to lipid content (Lin et al., 2007, [155933](#)). This suggests that the lipid content of different plant tissues may influence PAH distribution within the plant.

Previously, there was relatively little information available regarding incorporation of atmospherically deposited PAHs into aquatic food webs. It is known that PAHs can be transferred to higher trophic levels, including fish, and that this transfer can be mediated by aquatic invertebrates, which generally comprise an important part of fish diets. High mountain lakes offer an effective receptor for quantification of biomagnification in aquatic ecosystems from atmospheric PM deposition. There are typically no sources of organic contaminants in their watersheds, and atmospheric inputs dominate as sources of contamination. In addition, such lakes tend to have relatively simple food webs. Vives et al. (2005, [157099](#)) investigated PAH content of brown trout (*Salmo trutta*) and their food items. Total PAH concentrations tended to be highest in organisms that occupy littoral habitats, and lowest in pelagic organisms. This may reflect more efficient transfer of PAHs to underlying sediments in shallower water and associated degradation within the water column.

Some atmospheric organic contaminants have been shown to accumulate in biota at remote locations. For example, polybrominated diphenyl ethers (PBDEs), which are man-made chemicals used as flame retardants in materials manufacturing, have been found to accumulate in lichens and mosses collected at King George Island, maritime Antarctica (Yogui and Sericano, 2008, [189971](#)). Because contaminant concentrations were not statistically different at sites close to and distant from human facilities in Antarctica, the authors concluded that long-range atmospheric transport was the likely primary source of PBDEs to King George Island. Law et al. (2003, [190420](#)) reviewed available data for accumulation of PBDEs and other brominated flame retardants in wildlife. These compounds have become widely distributed in the environment, including in the deep-water, oceanic food webs.

Ohyama et al. (2004, [190462](#)) chose salmonid fish, mainly rainbow trout (*Oncorhynchus mykiss*), as an indicator species to evaluate the transport and bioaccumulation of organochloride compounds in the northern and central Sierra Nevada. They found that elevation was an important factor affecting residual concentrations of polychlorinated biphenyls (PCBs) in fish muscle tissue. On this basis, Ohyama et al. (2004, [190462](#)) concluded that PCB residue in rainbow trout, a widely distributed salmonid species, provided a good monitoring tool for studying the effects of mountainous topography on the long-range transport and distribution of persistent organic pollutants.

Semivolatile compounds can undergo repeated volatilization on surfaces, such as plant foliage, in response to diel changes in temperature. As a consequence, such compounds can be deposited, re-emitted, and re-deposited multiple times. This behavior can cause these compounds to move large distances in a leap-frog fashion (Krupa et al., 2008, [198696](#)). It is believed that POPs can be atmospherically transported throughout the world because of their volatility and response to changes in temperature. This "global distillation theory" (Holmqvist et al., 2006, [190380](#); Wania and Mackay, 1993, [157110](#)) predicts that POPs in the northern hemisphere are generally transported towards the Arctic, and in the southern hemisphere they are transported toward the Antarctic. In general, POP concentrations measured in the Arctic are higher than in the Antarctic. They have been detected in all levels of the Arctic food web (Oehme et al., 1995, [011267](#)). Bioconcentration of organochlorines has been shown in the Arctic food web, including fish, seals, and polar bears (Oehme et al., 1995, [011267](#)). Concentrations measured in Arctic polar bears are especially high (AMAP, 2004, [190168](#)).

Holmqvist et al. (2006, [190380](#)) measured levels of PCBs in longfin eels (*Anguilla dieffenbachii*) in 17 streams on the west coast of South Island, New Zealand. The PCBs were at low levels, and were believed to originate from atmospheric transport from industrial areas in Asia. Characteristics of the longfin eel that make it susceptible to bioaccumulation of lipophilic persistent

pollutants include high lipid content (up to 40%), long lifespan (up to 90 yrs), and position near the top of the food chain (Holmqvist et al., 2006, [190380](#)).

Long-range transport of atmospherically deposited contaminants can be augmented by biotransport. A good example of this phenomenon was documented by Ewald et al. (1998, [190348](#)), who showed that biotransport by migrating sockeye salmon (*Oncorhynchus nerka*) in the Copper River watershed, Alaska, had a greater influence than atmospheric transport on bioaccumulation of PCBs and DDT in lake food webs. Organic pollutants accumulated by salmon during their ocean residence were effectively transferred 410 km inland to their spawning lake. Arctic grayling (*Thymallus arcticus*) in the salmon spawning lake were found to contain organic pollutants more than twice as high as arctic grayling in a near-by salmon-free lake. The pollutant composition of the grayling in the salmon spawning lake was similar to that of the migrating salmon (Ewald et al., 1998, [190348](#)), suggesting that salmon migration contributed to bioaccumulation of organic contaminants in the lake used for spawning by the salmon.

An assessment of the ecological effects of airborne metals and SOCs was conducted for eight NPs by the Western Airborne Contaminants Assessment Project (WACAP) (Landers et al., 2008, [191181](#)). From 2002-2007, WACAP researchers conducted analysis of the biological effects of airborne contaminants in seven ecosystem compartments: air, snow, water, sediments, lichens, conifer needles and fish. The goals were to identify where the pollutants were accumulating, identify ecological indicators for those pollutants causing ecological harm, and to determine the source of the air masses most likely to have transported the contaminants to the parks.

The results from WACAP were summarized by Landers et al. (2008, [191181](#)), which concluded that bioaccumulation of SOCs were observed throughout park ecosystems. Vegetation tended to accumulate PAHs, CUPs, and HCHs. Conifer needles were a good indicator of pesticides, however the ecological consequences of this accumulation are unexamined. SOCs in vegetation and air showed different patterns, possibly because each medium absorbs different types of SOCs with varying efficiencies. Mean ammonium nitrate concentration in ambient fine particulates <2.5 µm diameter was a good predictor of dacthal, endosulfan, chloradane, trifluralin, DDT and PAH concentrations in vegetation.

Concentrations of SOCs were five to seven orders of magnitude higher in fish tissue than in sediments. Fish accumulated more PCBs, chlordanes, DDT and dieldrin than vegetation. Fish lipid and age were the most reliable predictors of SOC concentrations. Most fish appeared normal during field necropsies; however, individuals with both male and female reproductive organs were collected at two sites. The incidence of this condition has increased since the pre-organic pollutant era. Additionally, elevated concentrations of vitellogenin, a female protein involved in egg production, were found in male fish from three sites, and directly related to the concentration of several organochlorines at one site.

The lake sediment records showed steadily increasing mercury deposition over time at lakes in two parks, Mt. Ranier NP and Rocky Mountain NP. Apportionment of the mercury to its atmospheric sources is not quantified at this time; however, the pattern in the sediment suggests a local source rather than a global source. Mercury concentrations in fish exceeded contaminant health thresholds for some piscivorous fish, mammals and birds in most parks. The average mercury concentration in fish from one site and individual fish from three additional sites exceeded the U.S. EPA contaminant health thresholds for humans.

Although this assessment focuses on chemical species that are components of PM, it does not specifically assess the effects of particulate versus gas-phase forms; therefore, in most cases it is difficult to apply the results to this assessment based on particulate concentration and size fraction.

9.4.7. Summary of Ecological Effects of PM

Ecological effects of PM include direct effects to metabolic processes of plant foliage; contribution to total metal loading resulting in alteration of soil biogeochemistry and microbiology, plant and animal growth and reproduction; and contribution to total organics loading resulting in bioaccumulation and biomagnification across trophic levels. These effects were well-characterized in the 2004 PM AQCD (U.S. EPA, 2004, [056905](#)). Thus, the summary below builds upon the conclusions provided in that review.

PM deposition comprises a heterogeneous mixture of particles differing in origin, size, and chemical composition. Exposure to a given concentration of PM may, depending on the mix of deposited particles, lead to a variety of phytotoxic responses and ecosystem effects. Moreover, many

of the ecological effects of PM are due to the chemical constituents (e.g., metals, organics, and ions) and their contribution to total loading within an ecosystem.

Investigations of the direct effects of PM deposition on foliage have suggested little or no effects on foliar processes, unless deposition levels were higher than is typically found in the ambient environment. However, consistent and coherent evidence of direct effects of PM has been found in heavily polluted areas adjacent to industrial point sources such as limestone quarries, cement kilns, and metal smelters (Sections 9.4.3 and 9.4.5.7). Where toxic responses have been documented, they generally have been associated with the acidity, trace metal content, surfactant properties, or salinity of the deposited materials.

An important characteristic of fine particles is their ability to affect the flux of solar radiation passing through the atmosphere, which can be considered in both its direct and diffuse components. Foliar interception by canopy elements occurs for both up- and down-welling radiation. Therefore, the effect of atmospheric PM on atmospheric turbidity influences canopy processes both by radiation attenuation and by changing the efficiency of radiation interception in the canopy through conversion of direct to diffuse radiation. Crop yields can be sensitive to the amount of radiation received, and crop losses have been attributed to increased regional haze in some areas of the world such as China. On the other hand, diffuse radiation is more uniformly distributed throughout the canopy and may increase canopy photosynthetic productivity by distributing radiation to lower leaves. The enrichment in photosynthetically active radiation (PAR) present in diffuse radiation may offset a portion of the effect of an increased atmospheric albedo due to atmospheric particles. Further research is needed to determine the effects of PM alteration of radiative flux on the growth of vegetation in the U.S.

The deposition of PM onto vegetation and soil, depending on its chemical composition, can produce responses within an ecosystem. The ecosystem response to pollutant deposition is a direct function of the level of sensitivity of the ecosystem and its ability to ameliorate resulting change. Many of the most important ecosystem effects of PM deposition occur in the soil. Upon entering the soil environment, PM pollutants can alter ecological processes of energy flow and nutrient cycling, inhibit nutrient uptake, change ecosystem structure, and affect ecosystem biodiversity. The soil environment is one of the most dynamic sites of biological interaction in nature. It is inhabited by microbial communities of bacteria, fungi, and actinomycetes, in addition to plant roots and soil macro-fauna. These organisms are essential participants in the nutrient cycles that make elements available for plant uptake. Changes in the soil environment can be important in determining plant and ultimately ecosystem response to PM inputs.

There is strong and consistent evidence from field and laboratory experiments that metal components of PM alter numerous aspects of ecosystem structure and function. Changes in the soil chemistry, microbial communities and nutrient cycling, can result from the deposition of trace metals. Exposures to trace metals are highly variable, depending on whether deposition is by wet or dry processes. Although metals can cause phytotoxicity at high concentrations, few heavy metals (e.g., Cu, Ni, Zn) have been documented to cause direct phytotoxicity under field conditions. Exposure to coarse particles and elements such as Fe and Mg are more likely to occur via dry deposition, while fine particles, which are more often deposited by wet deposition, are more likely to contain elements such as Ca, Cr, Pb, Ni, and V. Ecosystems immediately downwind of major emissions sources can receive locally heavy deposition inputs. Phytochelatins produced by plants as a response to sublethal concentrations of heavy metals are indicators of metal stress to plants. Increased concentrations of phytochelatins across regions and at greater elevation have been associated with increased amounts of forest injury in the northeastern U.S.

Overall, the ecological evidence is sufficient to conclude **that a causal relationship is likely to exist between deposition of PM and a variety of effects on individual organisms and ecosystems, based on information from the previous review and limited new findings in this review.** However, in many cases, it is difficult to characterize the nature and magnitude of effects and to quantify relationships between ambient concentrations of PM and ecosystem response due to significant data gaps and uncertainties as well as considerable variability that exists in the components of PM and their various ecological effects.

9.5. Effects on Materials

Effects of air pollution on materials are related to both aesthetic appeal and physical damage. Deposited particles, primarily carbonaceous compounds, cause soiling of building materials and culturally important items, such as statues and works of art. Physical damage from dry deposition of PM also can accelerate natural weathering processes. The major deterioration phenomenon affecting building materials in response to atmospheric deposition is most likely sulfation, leading to secondary salt crystallization which forms gypsum (Marinoni et al., 2003, [092520](#)).

This section (a) summarizes information on exposure-related effects on materials associated with particulate pollutants as addressed in the 2004 PM AQCD (U.S. EPA, 2004, [056905](#)); and (b) presents relevant information derived from very limited research conducted and published since completion of that document. Most recent work on this topic has been conducted outside the U.S.

There is a variety of factors that contribute to the deterioration of monuments and buildings of cultural significance. They include: (1) biodeterioration processes; (2) weathering of materials exposed to the air; and (3) air pollution from both anthropogenic and natural sources (Herrera and Videla, 2004, [155843](#)). Because of the diversity in climate, proximity to marine aerosol sources, and pollution of various types, the magnitude and relative importance of these causal agents vary by location.

Much existing literature on damage to structural materials of cultural heritage has not seriously considered the importance of biodeterioration processes and the relationship that often exists between environmental characteristics and the microbial communities that colonize monuments and buildings. In general, high humidity, high temperature, and air pollution often enhance the biodeterioration hazard. Herrera and Videla (2004, [155843](#)) concluded that heterotrophic bacteria, fungi, and cyanobacteria were the main microbial colonizers of buildings that they investigated in Latin America. Their analyses suggested that the major deterioration mechanism of limestone at the Mayan site of Uxmal in a non-polluted rural environment was biosolubilization induced by metabolic acids produced by bacteria and fungi. The rock decay at Tulum, near the seashore, was mainly attributed to the marine influence. At Medellin, it appeared that biodeterioration effects from microbes synergistically enhanced the effects of atmospheric factors on material decay. Deterioration of structural material in the Cathedral of La Plata, located in a mixed urban/industrial environment, was attributed mainly to atmospheric pollutants (Herrera and Videla, 2004, [155843](#)).

Ambient particles can cause soiling of man-made surfaces. Soiling generally is considered an optical effect. Soiling changes the reflectance from opaque materials and reduces the transmission of light through transparent materials. Soiling can represent a significant detrimental effect, requiring increased frequency of cleaning of glass windows and concrete structures, washing and repainting of structures, and, in some cases, reduces the useful life of the object. Particles, especially carbon, may also help catalyze chemical reactions that result in the deterioration of materials (U.S. EPA, 2004, [056905](#)).

Soiling is dependent on atmospheric particle concentration, particle size distribution, deposition rate, and the horizontal or vertical orientation and texture of the exposed surface (Haynie, 1986, [157198](#)). The chemical composition and morphology of the particles and the optical properties of the surface being soiled will determine the time at which soiling is perceived by human observers (Nazaroff and Cass, 1991, [044577](#)).

Ferm et al. (2006, [155135](#)) reported development of a simple passive particle collector for estimating dry deposition to objects of cultural heritage. The observed mass of deposited particles mainly belonged to the coarse particulate mode. The sampler collects particles from all directions. It replicates at least some of the complexity of particle deposition to actual objects, and is easier to analyze than a precious object (Ferm et al., 2006, [155135](#)).

Soiling of urban buildings constitutes a visual nuisance that leads to the loss of architectural value. Soiling can include reversible darkening of the building surfaces and also irreversible damage. Water runoff patterns on the building surfaces are influenced by the type of surface material, architectural elements, and climate. Therefore, soiling does not occur uniformly across the building. Public perception of soiling entails complex interactions between the extent of soiling, architecture, and aesthetics (Grossi and Brimblecombe, 2004, [155813](#)).

One of the most significant air pollution damage features affecting urban buildings and monuments is the formation of black crusts. Quantification of different forms of carbon in black crusts is difficult. There is often a carbonate component which is derived from the building material, plus OC and EC, derived from air pollution. EC is considered to be a tracer for combustion sources,

whereas OC may derive from multiple sources, including atmospheric deposition of primary and secondary pollutants, and the decay of protective organic treatments (Bonazza et al., 2005, [155695](#)). Bonazza et al. (2005, [155695](#)) quantified OC and EC in damage layers on European cultural heritage structures. OC predominated over EC at almost all locations investigated. Traffic appeared to be the major source of fine carbonaceous particles, with organic matter as the main component (Putaud et al., 2004, [055545](#)). Viles and Gorbushina (2003, [156138](#)) found that soiling in Oxford, U.K. showed a relationship with traffic and NO₂ concentrations.

In addition to the soiling effects of EC, much soiling appears to be largely of microbiological origin (Viles and Gorbushina, 2003, [156138](#)). Microbial biofilms, composed mainly of fungi, can stain exposed rock surfaces with yellow, orange, brown, gray, or black colors. Microorganisms may be able to trap PM more efficiently than the stone surface itself. In addition, microbial growth may be stimulated by organic or nutrient constituents in PM deposition.

Viles et al. (2002, [156137](#)) investigated the nature of soiling on limestone tablets in relation to ambient air pollution and climate at three contrasting sites in Great Britain over periods of one to eight years. Spectrophotometer and microscope observations suggested that there were not consistent trends in soiling over time at the study sites. Each site behaved differently in terms of the temporal development of soiling and the differences between sheltered and exposed limestone tablets. In addition, organisms played important roles in the soiling response, even at the highly polluted site.

Some work has been conducted on public perception regarding the lightness of historic buildings and the aesthetic need for cleaning subsequent to soiling by air pollution. Brimblecombe and Grossi (2005, [155703](#)) found a strong relationship between the perceived lightness of a building and the opinion that it was dirty. This relationship was used to establish levels of blackening that might be publicly acceptable.

Recently, the importance of organic contaminant deposition to the overall air pollution damage to building materials has been recognized. Low molecular weight organic anions such as formate, acetate, and oxalate are ubiquitous in black crusts in damage layers on stones and mortars sampled from monuments and buildings throughout Europe (Sabbioni et al., 2003, [049282](#)). This has been observed at urban, suburban, and rural sites.

9.5.1. Effects on Paint

Studies have evaluated the soiling effects of particles on painted surfaces (U.S. EPA, 2004, [056905](#)). Particles composed of EC, acids, and various other constituents are responsible for the soiling of structural painted surfaces. Coarse-mode particles (>2.5 μm) initially contribute more soiling of horizontal and vertical painted surfaces than do fine-mode particles (<2.5 μm), but are more easily removed by rain (Haynie and Lemmons, 1990, [044579](#)). Rain interacts with coarse particles, dissolving the particle and leaving stains on the painted surface (Creighton et al., 1990, [044578](#); Haynie and Lemmons, 1990, [044579](#)). Particle deposition contributes to increased frequency of cleaning of painted surfaces and physical damage to the painted surface. Air pollution affects the durability of paint finishes by promoting discoloration, chalking, loss of gloss, erosion, blistering, and peeling (U.S. EPA, 2004, [056905](#)). There have been no new developments in this field subsequent to the review of the U.S. EPA (2004, [056905](#)).

9.5.2. Effects on Metal Surfaces

Metals undergo natural weathering processes. The effects of air pollutants on natural weathering processes depend on the nature of the pollutant(s), the deposition rate, and the presence of moisture (U.S. EPA, 2004, [056905](#)). Pollutant effects on metal surfaces are governed by such factors as the presence of protective corrosion films and surface electrolytes, the orientation of the metal surface, and surface moisture. Surface moisture facilitates particulate deposition and promotes corrosive reactions. Formation of hygroscopic salts increases the duration of surface wetness and enhances corrosion.

A corrosion film, such as for example the rust layer on the surface of some metals, may provide some protection against further corrosion. Its effectiveness in retarding the corrosion process is affected by the solubility of the corrosion layer and the pollutant exposure. Other than the effects of acidifying compounds, there has not been additional research conducted in recent years on the effects of PM deposition on metal corrosion.

9.5.3. Effects on Stone

Air pollutants can enhance the natural weathering processes on building stone. The development of crusts on stone monuments has been attributed to the interaction of the stone's surface with pollutants, wet or dry deposition of atmospheric particles, and dry deposition of gypsum particles. Because of a greater porosity and specific surface, mortars have a high potential for reacting with environmental pollutants (Zappia et al., 1998, [012037](#)).

Most research evaluating the effects of air pollutants on stone structures has concentrated on gaseous pollutants (U.S. EPA, 2004, [056905](#)). The dark color of gypsum is attributed to soiling by carbonaceous particles. A lighter gray colored crust is attributed to soil dust and metal deposits (Ausset et al., 1998, [040480](#); Camuffo, 1995, [076278](#); Lorusso et al., 1997, [084534](#); Moropoulou et al., 1998, [040485](#)). Lorusso et al. (1997, [084534](#)) attributed the need for frequent cleaning and restoration of historic monuments in Rome to exposure to total suspended particulates.

Grossi et al. (2003, [155812](#)) investigated the black soiling rates of building granite, marble, and limestone in two urban environments with different climates. Horizontal specimens were exposed, both sheltered and unsheltered from rainfall. Limestone showed soiling proportional to the square root of the time of exposure, but granite and marble did not.

Black soiling is caused mainly by particulate EC (PEC). For that reason, it is most prevalent in urban environments due to the formation of carbonaceous fine particles from the incomplete combustion of fossil fuels. Traffic emissions, especially from diesel engines, and wood burning are important sources of PEC (Grossi et al., 2003, [155812](#)).

Kamh (2005, [155888](#)) studied the effects of weathering on Conway Castle, an historical structure in Great Britain built about 1289 AC. The weathering was identified as honeycomb, blackcrust, exfoliation, and discoloration, with white salt efflorescence at some parts. These features are diagnostic for salt weathering (Goudie et al., 2002, [156486](#)), and this was confirmed by laboratory analyses, including scanning electron microscopy and x-ray diffraction. The authors concluded that the salt was derived from three sources: sea spray, chemical alteration of the carbonate in mortar into SO_4^{2-} salts by acidic deposition, and wet deposition of air pollutants on the stone surface. The salt content on the rock surface fills the rock pores and then exerts high pressure on the rock texture due to hydration of the salt in the cold humid environment. In particular, CaSO_4 and Na_2SO_4 exert enough pressure on hydration as to deteriorate construction rock at both the micro- and macroscale (Moses and Smith, 1994, [156785](#)).

9.5.4. Summary of Effects on Materials

Building materials (metals, stones, cements, and paints) undergo natural weathering processes from exposure to environmental elements (wind, moisture, temperature fluctuations, sunlight, etc.). Metals form a protective film of oxidized metal (e.g., rust) that slows environmentally induced corrosion. However, the natural process of metal corrosion is enhanced by exposure to anthropogenic pollutants. For example, formation of hygroscopic salts increases the duration of surface wetness and enhances corrosion.

A significant detrimental effect of particle pollution is the soiling of painted surfaces and other building materials. Soiling changes the reflectance of opaque materials and reduces the transmission of light through transparent materials. Soiling is a degradation process that requires remediation by cleaning or washing, and, depending on the soiled surface, repainting. Particulate deposition can result in increased cleaning frequency of the exposed surface and may reduce the usefulness of the soiled material. Attempts have been made to quantify the pollutant exposure at which materials damage and soiling have been perceived. However, to date, insufficient data are available to advance the knowledge regarding perception thresholds with respect to pollutant concentration, particle size, and chemical composition. Nevertheless, the evidence is sufficient to conclude that **a causal relationship exists between PM and effects on materials.**

Chapter 9 References

- Abdou W; Diner D; Martonchik J; Bruegge C; Kahn R; Gaitley B; Crean K; Remer L; Holben B (2005). Comparison of coincident Multiangle Imaging Spectroradiometer and Moderate Resolution Imaging Spectroradiometer aerosol optical depths over land and ocean scenes containing Aerosol Robotic Network sites. *J Geophys Res*, 110: D10S07. [190028](#)
- Aboal JR; Fernández JA; Carballeira A (2004). Oak leaves and pine needles as biomonitors of airborne trace elements pollution. *Environ Exp Bot*, 51: 215-225. [155642](#)
- ABT (2001). Assessing Public Opinions on Visibility Impairment Due to Air Pollution: Summary Report. [156185](#)
- ABT (2002). Sense of Place and Stewardship: Final Focus Group Report. [156186](#)
- Ackerman A; Kirkpatrick M; Stevens D; Toon O (2004). The impact of humidity above stratiform clouds on indirect aerosol climate forcing. *Nature*, 432: 1014-1017. [190056](#)
- Ackerman AS; Toon OB; Hobbs PV (1994). Reassessing the dependence of cloud condensation nucleus concentration on formation rate. *Nature*, 367: 445-447. [189975](#)
- Ackerman AS; Toon OB; Stevens DE; Heymsfield AJ; Ramanathan V; Welton EJ (2000). Reduction of tropical cloudiness by soot. *Sci New York*, 288: 1042-1047. [002987](#)
- Ackerman T; Stokes G (2003). The atmospheric radiation measurement program. *Phys Today*, 56: 38-44. [192080](#)
- Adachi K; Tainosho Y (2004). Characterization of heavy metal particles embedded in tire dust. *Environ Int*, 30: 1009-1017. [081380](#)
- Adamo P; Crisafulli P; Giordano S; Minganti V; Modenesi P; Monaci F; Pittao E; Tretiach M; Bargagli R (2007). Lichen and moss bags as monitoring devices in urban areas. Part II: Trace element content in living and dead biomonitors and comparison with synthetic materials. *Environ Pollut*, 146: 392-399. [155644](#)
- Albrecht B (1989). Aerosols, cloud microphysics, and fractional cloudiness. *Science*, 245: 1227-1230. [045783](#)
- Alexeeva LB; Strachan WMJ; Shlychkova VV; Nazarova AA; Nikanorov AM; Korotova LG (2001). Organochlorine pesticides and trace metal monitoring of Russian rivers flowing to the Arctic Ocean. *Mar Pollut Bull*, 43: 71-85. [155651](#)
- Alfani A; De Nicola F; Maisto G; Prati MV (2005). Long-term PAH accumulation after bud break in *Quercus ilex* L leaves in a polluted environment. *Atmos Environ*, 39: 307-314. [154319](#)
- Allen GA; Lawrence J; Koutrakis P (1999). Field validation of a semi-continuous method for aerosol black carbon (aethalometer) and temporal patterns of summertime hourly black carbon measurements in southwestern PA. *Atmos Environ*, 33: 817-823. [048923](#)
- Almas AR; Bakken LR; Mulder J (2004). Changes in tolerance of soil microbial communities in Zn and Cd contaminated soils. *Soil Biol Biochem*, 36: 805-813. [155654](#)
- Alpert P; Kishcha P; Kaufman Y; Schwarzbard R (2005). Global dimming or local dimming?: Effect of urbanization on sunlight availability. *Geophys Res Lett*, 32: 17. [190047](#)
- AMAP (2004). AMAP Assessment 2002: Persistent Organic Pollutants in the Arctic. Arctic Monitoring and Assessment Programme. Oslo, Norway. [190168](#)
- Ammann CM; Meehl GA; Washington WM; Zender CS (2003). A monthly and latitudinally varying volcanic forcing dataset in simulations of 20th century climate. *Geophys Res Lett*, 30: 1657. [192057](#)
- Anderson HR; Atkinson RW; Bremner SA; Marston L (2003). Particulate air pollution and hospital admissions for cardiorespiratory diseases: are the elderly at greater risk? *Eur Respir J*, 40: 39s-46s. [054820](#)

Note: Hyperlinks to the reference citations throughout this document will take you to the NCEA HERO database (Health and Environmental Research Online) at <http://epa.gov/hero>. HERO is a database of scientific literature used by U.S. EPA in the process of developing science assessments such as the Integrated Science Assessments (ISA) and the Integrated Risk Information System (IRIS).

- Anderson T; Charlson R; Bellouin N; Boucher O; Chin M; Christopher S; Haywood J; Kaufman Y; Kinne S; Ogren J (2005). An "A-Train" strategy for quantifying direct climate forcing by anthropogenic aerosols. *Bull Am Meteorol Soc*, 86: 1795-1809. [189993](#)
- Anderson T; Wu Y; Chu D; Schmid B; Redemann J; Dubovik O (2005). Testing the MODIS satellite retrieval of aerosol fine-mode fraction. *J Geophys Res*, 110: D18204. [189991](#)
- Anderson TL; Ogren JA (1998). Determining aerosol radiative properties using the TSI 3563 integrating nephelometer. *Aerosol Sci Technol*, 29: 57-69. [156213](#)
- Andreae MO; Gelencsér A (2006). Black carbon or brown carbon? The nature of light-absorbing carbonaceous aerosols. *Atmos Chem Phys*, 6: 3131-3148. [156215](#)
- Andreae MO; Rosenfeld D; Artaxo P; Costa AA; Frank GP; Longo KM; Silva-Dias MAF (2004). Atmospheric science: smoking rain clouds over the Amazon. *Sci New York*, 303: 1337-1341. [155658](#)
- Andrews E; Sheridan PJ; Ogren JA; Ferrare R (2004). In situ aerosol profiles over the Southern Great Plains cloud and radiation test bed site: 1. Aerosol optical properties. *J Geophys Res*, 109: D06208. [190058](#)
- Andronova NG; Rozanov EV; Yang F; Schlesinger ME; Stenchikov GL (1999). Radiative forcing by volcanic aerosols from 1850 to 1994. *J Geophys Res*, 104: 16807-16826. [192286](#)
- Antuña JC; Robock A; Stenchikov G; Zhou J; David C; Barnes J; Thomason L (2003). Spatial and temporal variability of the stratospheric aerosol cloud produced by the 1991 Mount Pinatubo eruption. *J Geophys Res*, 108: 4624. [192251](#)
- Arizona DEQ (2000). Phoenix metropolitan area visibility briefing paper. Arizona Department of Environmental Quality. Phoenix, AZ. [019164](#)
- Armbrust DV; Retta A (2002). Wind and sandblast damage to growing vegetation. *Ann Arid Zone*, 39: 273-284. [156225](#)
- Arnott WP; Moosmuller H; Rogers CF; Jin T; Bruch R (1999). Photoacoustic spectrometer for measuring light absorption by aerosol; instrument description. *Atmos Environ*, 33: 2845-2852. [020650](#)
- Audet P; Charest C (2007). Heavy metal phytoremediation from a meta-analytical perspective. *Environ Pollut*, 147: 231-237. [190169](#)
- Augustine J; Hodges G; Dutton E; Michalsky J; Cornwall C (2008). An aerosol optical depth climatology for NOAA's national surface radiation budget network (SURFRAD). *J Geophys Res*, 113: D11204. [189913](#)
- Ausset P; Bannery F; Del Monte M; Lefevre RA (1998). Recording of pre-industrial atmospheric environment by ancient crusts on stone monuments. *Atmos Environ*, 32: 2859-2863. [040480](#)
- Avila A; Rodrigo A (2004). Trace metal fluxes in bulk deposition, throughfall and stemflow at two evergreen oakstands in NE Spain subject to different exposure to the industrial environment. *Atmos Environ*, 38: 171-180. [155664](#)
- Babich P; Wang PY; Allen G; Sioutas C; Koutrakis P (2000). Development and Evaluation of a Continuous Ambient PM_{2.5} Mass Monitor. *Aerosol Sci Technol*, 32: 309-324. [156239](#)
- Bachelet D; Lenihan J; Neilson R; Drapek R; Kittel T (2005). Simulating the response of natural ecosystems and their fire regimes to climatic variability in Alaska. *Can J For Res*, 35: 2244-2257. [156241](#)
- Backe C; Cousins IT; Larsson P (2004). PCB in soils and estimated soil-air exchange fluxes of selected PCB congeners in the south of Sweden. *Environ Pollut*, 128: 59-72. [155668](#)
- Bäckström M; Nilsson U; Håkansson K; Allard B; Karlsson S (2003). Speciation of heavy metals in road runoff and roadside total deposition. *Water Air Soil Pollut*, 147: 343-366. [156242](#)
- Bailey R; Barrie LA; Halsall CJ; Fellin P; Muir DCG (2000). Atmospheric organochlorine pesticides in the western Canadian Arctic: evidence of trans-Pacific transport. *J Geophys Res*, 105: 11805-11811. [155670](#)
- Baker M; Charlson R (1990). Bistability of CCN concentrations and thermodynamics in the cloud-topped boundary layer. *Nature*, 345: 142-145. [190016](#)
- Balkanski Y; Schulz M; Claquin T; Guibert S (2007). Reevaluation of mineral aerosol radiative forcings suggests a better agreement with satellite and AERONET data. *Atmos Chem Phys*, 7: 81-95. [189979](#)
- Baptista MS; Vasconcelos MTSD; Cabral JP; Freitas MC; Pacheco AMG (2008). Copper, nickel and lead in lichen and tree bark transplants over different periods of time. *Environ Pollut*, 151: 408-413. [155673](#)

- Baran AJ; Foot JS (1994). New application of the operational sounder HIRS in determining a climatology of sulphuric acid aerosol from the Pinatubo eruption. *J Geophys Res*, 99: 25673-25679. [192032](#)
- Barker ML (1976). Planning for environmental indices: observer appraisals of air quality. In K Craig; E Zube (Ed.), *Perceiving Environmental Quality* (pp. 175-203). New York: Plenum Press. [072137](#)
- Barnes JE; Hofmann DJ (1997). Lidar measurements of stratospheric aerosol over Mauna Loa Observatory. *Geophys Res Lett*, 24: 1923-1926. [192044](#)
- Bates T; Anderson T; Baynard T; Bond T; Boucher O; Carmichael G; Clarke A; Erlick C; Guo H; Horowitz L (2006). Aerosol direct radiative effects over the northwest Atlantic, northwest Pacific, and North Indian Oceans: estimates based on in-situ chemical and optical measurements and chemical transport modeling. *Atmos Chem Phys Discuss*, 6: 175-362. [189912](#)
- Bates T; Huebert B; Gras J; Griffiths B; Durkee P (1998). The International Global Atmospheric Chemistry (IGAC) Project's First Aerosol Characterization Experiment (ACE 1)-Overview. *J Geophys Res*, 103: 16297-16318. [190063](#)
- Bates T; Quinn P; Coffman D; Covert D; Miller T; Johnson J; Carmichael G; Uno I; Guazzotti S; Sodeman D (2004). Marine boundary layer dust and pollutant transport associated with the passage of a frontal system over eastern Asia. *J Geophys Res*, 109: D19S19. [189958](#)
- Bates TS; Quinn PK; Coffman DJ; Johnson JE; Miller TL; Covert DS; Wiedensohler A; Leinert S; Nowak A; Neususs C (2001). Regional physical and chemical properties of the marine boundary layer aerosol across the Atlantic during Aerosols99: an overview. *J Geophys Res*, 106: 20,767-20,782. [043385](#)
- Bauman JJ; Russell PB; Geller MA; Hamill P (2003). A stratospheric aerosol climatology from SAGE II and CLAES measurements: 2. Results and comparisons. *J Geophys Res*, 108: 4383. [192265](#)
- Baumgardner RE Jr; Isil SS; Bowser JJ; Fitzgerald KM (1999). Measurements of rural sulfur dioxide and particle sulfate: analysis of CASTNet data, 1987 through 1996. *J Air Waste Manag Assoc*, 49: 1266-1279. [011308](#)
- Baynard T; Lovejoy ER; Pettersson A; Brown SS; Lack D; Osthoff H; Massoli P; Ciciora S; Dube WP; Ravishankara AR (2007). Design and application of a pulsed cavity ring-down aerosol extinction spectrometer for field measurements. *Aerosol Sci Technol*, 41: 447-462. [151669](#)
- BBC Research & Consulting (2002). Phoenix Area Visibility Survey. Draft Report. Available at http://www.azdeq.gov/environ/air/download/vis_021903f.pdf. [156258](#)
- Becker T; Brändel M (2007). Vegetation-environment relationships in a heavy metal-dry grassland complex. *Folia Geobot*, 42: 11-28. [156260](#)
- Beeby A; Richmond L (2002). Evaluating *Helix aspersa* as a sentinel for mapping metal pollution. *Ecol Indic*, 1: 261-270. [155680](#)
- Bellouin N; Boucher O; Haywood J; Reddy MS (2005). Global emissions of aerosol direct radiative forcing from satellite measurements. *Nature*, 438: 1138-1141. [155684](#)
- Bellouin N; Boucher O; Tanré D; Dubovik O (2003). Aerosol absorption over the clear-sky oceans deduced from POLDER-1 and AERONET observations. *Geophys Res Lett*, 30: 1748. [189911](#)
- Bellouin N; Jones A; Haywood J; Christopher S (2008). Updated estimate of aerosol direct radiative forcing from satellite observations and comparison against the Hadley Centre climate model. *J Geophys Res*, 113: D10205. [189999](#)
- Beron K; Murdoch J; Thayer M (2001). The Benefits of Visibility Improvement: New Evidence from the Los Angeles Metropolitan Area. *J R Estate Finance Econ*, 22: 319-337. [156270](#)
- Berthelsen BO; Olsen RA; Steinnes E (1995). Ectomycorrhizal heavy metal accumulation as a contributing factor to heavy metal levels in organic surface soils. *Sci Total Environ*, 170: 141-149. [078058](#)
- Bhavsar SP; Diamond ML; Evans LJ; Gandhi N; Nilsen J; Antunes P (2004). Development of a coupled metal speciation-fate model for surface aquatic systems. *Environ Toxicol Chem*, 23: 1376-1385. [155689](#)
- Bhavsar SP; Diamond ML; Gandhi N; Nilsen J (2004). Dynamic coupled metal transport-speciation model: application to assess a zinc-contaminated lake. *Environ Toxicol Chem*, 23: 2410-2420. [155690](#)
- Bickerstaff K; Walker G (2001). Public understandings of air pollution: the 'localisation' of environmental risk. *Global Environ Change*, 11: 133-145. [156271](#)

- Bidleman TF; Jantunen LMM; Helm PA; Bronstrom-Lunden E; Juntto S (2002). Chlordane isomers and enantiomers suggest changing sources in Arctic air. *Environ Sci Technol*, 36: 539-544. [155691](#)
- Billings WD (1978). *Plants and the ecosystem*. Belmont, CA: Wadsworth Publishing Company, Inc. [034165](#)
- Bingen C; Fussen D; Vanhellefont F (2004). A global climatology of stratospheric aerosol size distribution parameters derived from SAGE II data over the period 1984-2000: 2. Reference data. *J Geophys Res*, 102: D06202. [192262](#)
- Blanchard C; Tanenbaum S (2006). Weekday/weekend differences in ambient air pollutant concentrations in Atlanta and the southeastern United States. *J Air Waste Manag Assoc*, 56: 271-284. [190005](#)
- Blanchard CL; Tanenbaum S; Hidy GM (2007). Effects of sulfur dioxide and oxides of nitrogen emission reductions on fine particulate matter mass concentrations: regional comparisons. *J Air Waste Manag Assoc*, 57: 1337-50. [098659](#)
- Bluth GJS; Doiron SD; Schnetzler CC; Krueger AJ; Walter LS (1992). Global tracking of the SO₂ clouds from the June, 1991 Mount Pinatubo eruptions. *Geophys Res Lett*, 19: 151-154. [192029](#)
- Bluth GJS; Rose WI; Sprod IE (1997). Stratospheric loading of sulfur from explosive volcanic eruptions. *J Geol*, 105: 671-683. [192045](#)
- Bonazza A; Sabbioni C; Ghedini N (2005). Quantitative data on carbon fractions in interpretation of black crusts and soiling on European built heritage. *Atmos Environ*, 39: 2607-2618. [155695](#)
- Bond T; Bhardwaj E; Dong R; Jogani R; Jung S; Roden C; Streets D; Trautmann N (2007). Historical emissions of black and organic carbon aerosol from energy-related combustion, 1850-2000. *Global Biogeochem Cycles*, 21: GB2018. [190050](#)
- Bond TC; Anderson TL; Campbell D (1999). Calibration and Intercomparison of Filter-Based Measurements of Visible Light Absorption by Aerosols. *Aerosol Sci Technol*, 30: 582-600. [156281](#)
- Bond TC; Bergstrom RW (2005). Light absorption by carbonaceous particles: an investigative review. *Aerosol Sci Technol*, 39: 1-41. [155696](#)
- Bond TC; Streets DG; Yarber KF; Nelson SM; Woo J-H; Klimont Z (2004). A technology-based global inventory of black and organic carbon emissions from combustion. *J Geophys Res*, 109: D14203. [056389](#)
- Bond TC; Sun H (2005). Can reducing black carbon emissions counteract global warming? *Environ Sci Technol*, 39: 5921-5926. [156282](#)
- Boucher O; Tanré D (2000). Estimation of the aerosol perturbation to the Earth's radiative budget over oceans using POLDER satellite aerosol retrievals. *Geophys Res Lett*, 27: 1103-1106. [190041](#)
- Boucher U; Balabane M; Lamy I; Cambier P (2005). Decomposition in soil microcosms of leaves of the metallophyte *Arabidopsis halleri*: Effect of leaf-associated heavy metals on biodegradation. *Environ Pollut*, 135: 187-194. [155699](#)
- Brasseur G; Granier C (1992). Mount Pinatubo aerosols, chlorofluorocarbons, and ozone depletion. *Science*, 257: 1239-1242. [192256](#)
- Brenguier J; Chuang P; Fouquart Y; Johnson D; Parol F; Pawlowska H; Pelon J; Schuller L; Schroder F; Snider J (2000). An overview of the ACE-2 CLOUDYCOLUMN closure experiment. *Tellus B Chem Phys Meteorol*, 52: 815-827. [189966](#)
- Brimblecombe P; Grossi CM (2005). Aesthetic thresholds and blackening of stone buildings. *Sci Total Environ*, 349: 175-189. [155703](#)
- Broccoli AJ; Dixon KW; Delworth TL; Knutson TR; Stouffer RJ; Zeng F (2003). Twentieth-century temperature and precipitation trends in ensemble climate simulations including natural and anthropogenic forcing. *J Geophys Res*, 108: 4798. [192283](#)
- Brookshire D (1979). *Methods Development for Assessing Air Pollution Control Benefits. Volume 2: Experiments in Valuing Nonmarket Goods. A Case Study of Alternative Benefit Measures of Air Pollution in the South Coast Air Basin of Southern California*. EPA. Washington, DC. [156298](#)
- Burkhardt J; Kaiser H; Kappen L; Goldbach HE (2002). The possible role of aerosols on stomatal conductivity for water vapour. *Basic Appl Ecol*, 2: 351-364. [155708](#)

- Burt R; Wilson MA; Mays MD; Lee CW (2003). Major and trace elements of selected pedons in the USA. *J Environ Qual*, 32: 2109-2121. [155709](#)
- Campbell D; Copeland S; Cahill T (1995). Measurement of Aerosol Absorption Coefficient from Teflon Filters using Integrating Plate and Integrating Sphere Techniques. *Aerosol Sci Technol*, 22: 287-292. [190171](#)
- Campbell FW (1983). Ambient Stressors. *Environ Behav*, 15: 355-380. [190172](#)
- Camuffo D (1995). Physical weathering of stones. Presented at In: Saiz-Jimenez, C., ed. The deterioration of monuments: proceedings of the 2nd international symposium on biodeterioration and biodegradation; January 1994; Sevilla, Spain. *Sci. Total Environ*. 167: 1-14. [076278](#)
- Canada-US Air Quality Committee (2004). Canada-United States transboundary particulate matter science assessment. Meteorological Service of Canada. Toronto, Ontario, Canada. En56-203/2004E. http://www.msc-smc.ec.gc.ca/saib/smog/transboundary/toc_e.html. [190519](#)
- Carmichael G; Tang Y; Kurata G; Uno I; Streets D; Thongboonchoo N; Woo J; Guttikunda S; White A; Wang T (2003). Evaluating regional emission estimates using the TRACE-P observations. *J Geophys Res*, 108: 8810. [190042](#)
- Carmichael GR; Calori G; Hayami H; Uno I; Cho SY; Engardt M; Kim SB; Ichikawa Y; Ikeda Y; Woo JH; Ueda H; Amann M (2002). The MICS-Asia study: model intercomparison of long-range transport and sulfur deposition in East Asia. *Atmos Environ*, 36: 175-199. [148319](#)
- Carrico C; Kreidenweis S; Malm W; Day D; Lee T; Carrillo J; McMeeking G; Collett J (2005). Hygroscopic growth behavior of a carbon-dominated aerosol in Yosemite National Park. *Atmos Environ*, 39: 1393-1404. [190052](#)
- Carvalho LM; Caçador I; Martins-Loução MA (2006). Arbuscular mycorrhizal fungi enhance root cadmium and copper accumulation in the roots of the salt marsh plant *Aster tripolium* L. *Plant Soil*, 285: 161-169. [155715](#)
- CCSP (2008). Climate Projections Based on Emissions Scenarios for Long-lived and Short-lived Radiatively Active Gases and Aerosols. A Report by the U.S. Climate Change Science, Program and the Subcommittee on Global Change Research. Department of Commerce. Washington, DC. [192028](#)
- Chameides WL; Yu H; Liu SC; Bergin M; Zhou X; Mearns L; Wang G; Kiang CS; Saylor RD; Luo C; Huang Y; Steiner A; Giorgi F (1999). Case study of the effects of atmospheric aerosols and regional haze on agriculture: an opportunity to enhance crop yields in China through emission controls? *PNAS*, 96: 13626-13633. [011184](#)
- Chand D; Anderson T; Wood R; Charlson R; Hu Y; Liu Z; Vaughan M (2008). Quantifying above-cloud aerosol using spaceborne lidar for improved understanding of cloudy-sky direct climate forcing. *J Geophys Res*, 113: D13206. [189974](#)
- Charlson R; Pilat M (1969). Climate: the influence of aerosols. *J Appl Meteorol*, 8: 1001-1002. [190025](#)
- Charlson R; Wigley T (1994). Sulfate aerosol and climate change. *Sci Am*, 270: 28-35. [189989](#)
- Charlson RJ; Ahlquist NC; Horvath H (1968). On the generality of correlation of atmospheric aerosol mass concentration and light scatter. *Atmos Environ*, 2: 455-464. [095355](#)
- Charlson RJ; Langner J; Rodhe H; Leovy CB; Warren SG (1991). Perturbation of the northern hemisphere radiative balance by backscattering from anthropogenic sulfate aerosols. *Tellus Dyn Meteorol Oceanogr*, 43AB: 152-163. [045793](#)
- Charlson RJ; Schwartz SE; Hales JM; Cess RD; Coakley JA Jr; Hansen JE; Hofmann DJ (1992). Climate forcing by anthropogenic aerosols. *Science*, 255: 423-430. [045794](#)
- Cheggour M; Chafik A; Fisher NS; Benbrahim S (2005). Metal concentrations in sediments and clams in four Moroccan estuaries. *Mar Environ Res*, 59: 119-137. [155723](#)
- Chen W; Kahn R; Nelson D; Yau K; Seinfeld J (2008). Sensitivity of multiangle imaging to the optical and microphysical properties of biomass burning aerosols. *J Geophys Res*, 113: D10203. [189984](#)
- Chen Y; Penner JE (2005). Uncertainty analysis of the first indirect aerosol effect. *Atmos Chem Phys Discuss*, 5: 4507-4543. [199918](#)
- Chernyak SM; Rice CP; McConnell LL (1996). Evidence of currently used pesticides in air, ice, fog, seawater and surface microlayer in the Bering and Chukchi Seas. *Mar Pollut Bull*, 32: 410-419. [155726](#)

- Chestnut LG; Dennis RL (1997). Economic benefits of improvements in visibility: acid rain Provisions of the 1990 Clean Air Act Amendments. *J Air Waste Manag Assoc*, 47: 395-402. [014525](#)
- Chin M; Diehl T; Ginoux P; Malm W (2007). Intercontinental transport of pollution and dust aerosols: implications for regional air quality. *Atmos Chem Phys*, 7: 5501-5517. [190062](#)
- Chin M; Ginoux P; Kinne S; Torres O; Holben B; Duncan B; Martin R; Logan J; Higurashi A; Nakajima T (2002). Tropospheric aerosol optical thickness from the GOCART model and comparisons with satellite and Sun photometer measurements. *J Atmos Sci*, 59: 461-483. [189996](#)
- Chin M; Kahn RA; Remer LA; Yu H; Rind D; Feingold G; Quinn PK; Schwartz SE; Streets DG; DeCola P; Halthorne R (2009). Atmospheric aerosol properties and climate impacts. Synthesis and assessment product 2.3. A report by the U.S. Climate Change Science Program and the Subcommittee on Global Change Research. National Aeronautics and Space Administration. Washington, DC. [192130](#)
- Chiou CT; Sheng G; Manes M (2001). A partition-limited model for the plant uptake of organic contaminants from soil and water. *Environ Sci Technol*, 35: 1437-1444. [156342](#)
- Chipperfield MP; Randel WJ; Bodeker GE; Johnston P (2003). Global ozone: past and future. In *Scientific Assessment of Ozone Depletion: 2002* (pp. 4.1-4.90). Geneva: World Meteorological Organization. [192275](#)
- Chock DP; Song Q; Hass H; Schell B; Ackermann I (2003). Comment on "Control of fossil-fuel particulate black carbon and organic matter, possibly the most effective method of slowing global warming" by Jacobson, M. Z. *J Geophys Res*, 108: ACH12.1-ACH13.4. [155727](#)
- Chou M; Chan P; Wang M (2002). Aerosol radiative forcing derived from SeaWiFS-retrieved aerosol optical properties. *J Atmos Sci*, 59: 748-757. [190008](#)
- Chow JC; Watson JG; Edgerton SA; Vega E (2002). Chemical composition of PM10 and PM25 in Mexico City during winter 1997. *Sci Total Environ*, 287: 177-201. [036166](#)
- Chow JC; Watson JG; Lowenthal DH; Richards LW (2002). Comparability between PM25 and particle light scattering measurements. *Environ Monit Assess*, 79: 29-45. [037784](#)
- Christie P; Li XL; Chen BD (2004). Arbuscular mycorrhiza can depress translocation of zinc to shoots of host plants in soils moderately polluted with zinc. *Plant Soil*, 261: 209-217. [190174](#)
- Christopher S; Jones T (2008). Short-wave aerosol radiative efficiency over the global oceans derived from satellite data. *Tellus B Chem Phys Meteorol*, 60: 636-640. [189985](#)
- Christopher SA; Zhang J (2002). Daytime variation of shortwave direct radiative forcing of biomass burning aerosols from GOES-8 imager. *J Atmos Sci*, 59: 681-691. [190031](#)
- Christopher SA; Zhang J; Kaufman YJ; Remer L (2006). Satellite-based assessment of the top of the atmosphere anthropogenic aerosol radiative forcing over cloud-free oceans. *Geophys Res Lett*, 111: L15816. [155729](#)
- Chu D; Kaufman Y; Ichoku C; Remer L; Tanré D; Holben B (2002). Validation of MODIS aerosol optical depth retrieval over land. *Geophys Res Lett*, 29: 8007. [190001](#)
- Chuang CC; Penner JE; Prospero JM; Grant KE; Rau GH; Kawamoto K (2002). Cloud susceptibility and the first aerosol indirect forcing: Sensitivity to black carbon and aerosol concentrations. *J Geophys Res*, 107: 4564. [199912](#)
- Chung C; Zhang G (2004). Impact of absorbing aerosol on precipitation: Dynamic aspects in association with convective available potential energy and convective parameterization closure and dependence on aerosol heating profile. *J Geophys Res*, 109: D22103. [190054](#)
- Chung CE; Ramanathan V; Kim D; Podgorny IA (2005). Global anthropogenic aerosol direct forcing derived from satellite and ground-based observations. *J Geophys Res*, 110: D24207. [155733](#)
- Chung SH; Seinfeld JH (2002). Global distribution and climate forcing of carbonaceous aerosols. *J Geophys Res*, 107: 4407. [155732](#)
- Citterio S; Prato N; Fumagalli P; Aina R; Massa N; Santagostino A; Sgorbati S; Berta G (2005). The arbuscular mycorrhizal fungus *Glomus mosseae* induces growth and metal accumulation changes in *Cannabis sativa* L. *Chemosphere*, 59: 21-29. [190176](#)

- Clarke A; Porter J; Valero F; Pilewskie P (1996). Vertical profiles, aerosol microphysics, and optical closure during the Atlantic Stratocumulus Transition Experiment: Measured and modeled column optical properties. *J Geophys Res*, 101: 4443-4453. [190003](#)
- Clemens S (2006). Toxic metal accumulation, responses to exposure and mechanisms of tolerance in plants. *Biochimie*, 88: 1707-1719. [190179](#)
- Coakley JA; Walsh CD (2002). Limits to the aerosol indirect radiative effect derived from observations of ship tracks. *J Atmos Sci*, 59: 668-680. [192025](#)
- Coelho JP; Rosa M; Pereira E; Duarte A; Pardal MA (2006). Pattern and annual rates of *Scrobicularia plana* mercury bioaccumulation in a human induced mercury gradient (Ria de Aveiro, Portugal). *Estuar Coast Mar Sci*, 69: 629-635. [190181](#)
- Cohen S; Evans GW; Stokols D; Krantz DS (1986). *Behavior, Health, and Environmental Stress*. New York: Plenum Press. [190182](#)
- Collins D; Johnsson H; Seinfeld J; Flagan R; Gasso S; Hegg D; Russell P; Schmid B; Livingston J; Ostrom E (2000). In situ aerosol-size distributions and clear-column radiative closure during ACE-2. *Tellus B Chem Phys Meteorol*, 52: 498-525. [190059](#)
- Collins RN; Merrington G; McLaughlin MJ; Morel JL (2003). Organic ligand and pH effects on isotopically exchangeable cadmium in polluted soils. *Soil Sci Soc Am J*, 67: 112-121. [155737](#)
- Collins W; Rasch P; Eaton B; Khattatov B; Lamarque J; Zender C (2001). Simulating aerosols using a chemical transport model with assimilation of satellite aerosol retrievals: Methodology for INDOEX. *J Geophys Res*, 106: 7313-7336. [189987](#)
- Conant W; VanReken T; Rissman T; Varutbangkul V; Jonsson H; Nenes A; Jimenez J; Delia A; Bahreini R; Roberts G (2004). Aerosol-cloud drop concentration closure in warm cumulus. *J Geophys Res*, 109: D13204. [190010](#)
- Cooke W; Wilson J (1996). A global black carbon aerosol model. *J Geophys Res*, 101: 19,395-19,409. [190046](#)
- Cooke WF; Lioussé C; Cachier H; Feichter J (1999). Construction of a $1^\circ \times 1^\circ$ fossil fuel emission data set for carbonaceous aerosol and implementation and radiative impact in the ECHAM 4 model. *J Geophys Res*, 104: 22137-22162. [156365](#)
- Costa M; Silva A; Levizzani V (2004). Aerosol characterization and direct radiative forcing assessment over the ocean. Part I: Methodology and sensitivity analysis. *J Appl Meteorol*, 43: 1799-1817. [190006](#)
- Costa MJ; Levizzani V; Silva AM (2004). Aerosol characterization and direct radiative forcing assessment over the ocean. Part II: Application to test cases and validation. *J Appl Meteorol*, 43: 1818-1833. [192022](#)
- Couto JA; Fernández JA; Aboal JR; Carballeira A (2004). Active biomonitoring of element uptake with terrestrial mosses: a comparison of bulk and dry deposition. *Sci Total Environ*, 324: 211-222. [155739](#)
- Covert DS; Charlson RJ; Ahlquist NC (1972). A study of the relationship of chemical composition and humidity to light scattering by aerosols. *J Appl Meteorol*, 11: 968-976. [072055](#)
- Crawford DW; Lipsen MS; Purdie DA; Lohan MC; Statham PJ; Whitney FA; Putland JN; Johnson WK; Sutherland N; Peterson TD; Harrison PJ; Wong CS (2003). Influence of zinc and iron enrichments on phytoplankton growth in the northeastern subarctic Pacific. *Limnol Oceanogr*, 48: 1583-1600. [156370](#)
- Creighton PJ; Liou PJ; Haynie FH; Lemmons TJ; Miller JL; Gerhart J (1990). Soiling by atmospheric aerosols in an urban industrial area. *J Air Waste Manag Assoc*, 40: 1285-1289. [044578](#)
- Crépineau C; Rychen G; Feidt C; Le Roux Y; Lichtfouse E; Laurent F (2003). Contamination of pastures by polycyclic aromatic hydrocarbons (PAHs) in the vicinity of a highway. *J Agric Food Chem*, 51: 4841-4845. [155741](#)
- Croteau MN; Luoma SN; Stewart AR (2005). Trophic transfer of metals along freshwater food webs: Evidence of cadmium biomagnification in nature. *Limnol Oceanogr*, 50: 1511-1519. [156373](#)
- Cunningham M (1979). Weather, mood, and helping behavior: Quasi experiments with the sunshine Samaritan. *J Pers Soc Psychol*, 37: 1947-1956. [191974](#)
- Cuny D; Denayer FO; De Foucault B; Schumacker R; Colein P; Van Haluwyn C (2004). Patterns of metal soil contamination and changes in terrestrial cryptogamic communities. *Environ Pollut*, 129: 289-297. [155742](#)

- Da Silva LC; Oliva MA; Azevedo AA; De Araujo JM (2006). Responses of restinga plant species to pollution from an iron pelletization factory. *Water Air Soil Pollut*, 175: 241-256. [190190](#)
- Dallinger R; Wang Y; Berger B; Mackay EA; Kägi JH (2001). Spectroscopic characterization of metallothionein from the terrestrial snail, *Helix pomatia*. *Eur J Med Chem*, 268: 4126-4133. [192109](#)
- Dameris M; Grewe V; Ponater M; Deckert R; Eyring V; Mager F; Matthes S; Schnadt C; Stenke A; Steil B; Brühl C; Giorgetta MA (2005). Long-term changes and variability in a transient simulation with a chemistry-climate model employing realistic forcing. *Atmos Chem Phys Discuss*, 5: 2121-2145. [192055](#)
- Davis AP; Shokouhian M; Ni S (2001). Loading estimates of lead, copper, cadmium, and zinc in urban runoff from specific sources. *Chemosphere*, 44: 997-1009. [024933](#)
- Davis MRH; Zhao FJ; McGrath SP (2004). Pollution-induced community tolerance of soil microbes in response to a zinc gradient. *Environ Toxicol Chem*, 23: 2665-2672. [155744](#)
- Day R (2007). Place and the experience of air quality. *Health Place*, 13: 249-260. [156386](#)
- DeBell L (2006). Spatial and seasonal patterns and temporal variability of haze and its constituents in the United States: Report IV. ICooperative Institute for Research in the Atmosphere. Colorado State University Fort Collins, CO. [156388](#)
- Delworth T; Ramaswamy V; Stenchikov G (2005). The impact of aerosols on simulated ocean temperature and heat content in the 20th century. *Geophys Res Lett*, 32: N/A. [190055](#)
- Demerjian KL; Mohnen VA (2008). Synopsis of the temporal variation of particulate matter composition and size. *J Air Waste Manag Assoc*, 58: 216-233. [156392](#)
- Denman KL; Brasseur G; Chidthaisong A; Ciais P; Cox PM; Dickinson RE; Hauglustaine D; Heinze C; Holland E; Jacob D; Lohmann U; Ramachandran S; da Silva Dias PL; Wofsy SC; Zhang X (2007). Couplings Between Changes in the Climate System and Biogeochemistry. In *Climate Change 2007: The Physical Science Basis. Contribution of Working Group I to the Fourth Assessment Report of the Intergovernmental Panel on Climate Change* (pp. 499-587). Cambridge and New York: Cambridge University Press. [156394](#)
- Dentener F; Stevenson D; Ellingsen K; Van Noije T; Schultz M; Amann M; Atherton C; Bell N; Bergmann D; Bey I; Bouwman L; Butler T; Cofala J; Collins B; Drevet J; Doherty R; Eickhout B; Eskes H; Fiore A; Gauss M; Hauglustaine D; Horowitz L; Isaksen ISA; Josse B; Lawrence M; Krol M; Lamarque JF; Montanaro V; Müller JF; Peuch VH; Pitari G; Pyle J; Rast S; Rodriguez J; Sanderson M; Savage NH; Shindell D; Strahan S; Szopa S; Sudo K; Van Dingenen R; Wild O; Zeng G (2006). The global atmospheric environment for the next generation. *Environ Sci Technol*, 40: 3586-3594. [088434](#)
- Derome J; Lindroos A-J (1998). Effects of heavy metal contamination on macronutrient availability and acidification parameters in forest soil in the vicinity of the Harjavalta Cu-Ni smelter, SW Finland. *Environ Pollut*, 99: 225-232. [155749](#)
- Deshler T; Hervig ME; Hofmann DJ; Rosen JM; Liley JB (2003). Thirty years of in situ stratospheric aerosol size distribution measurements from Laramie, Wyoming (41°N), using balloon-borne instruments. *J Geophys Res*, 108: 4167. [192058](#)
- Deuzé J; Bréon F; Devaux C; Goloub P; Herman M; Lafrance B; Maignan F; Marchand A; Nadal F; Perry G (2001). Remote sensing of aerosols over land surfaces from POLDER-ADEOS-1 polarized measurements. *J Geophys Res*, 106: 4913-4926. [192013](#)
- De Gouw J; Middlebrook A; Warneke C; Goldan P; Kuster W; Roberts J; Fehsenfeld F; Worsnop D; Canagaratna M; Pszenny A (2005). Budget of organic carbon in a polluted atmosphere: Results from the New England Air Quality Study in 2002. *J Geophys Res*, 110: D16305. [190020](#)
- De Nicola F; Maisto G; Prati MV; Alfani A (2005). Temporal variations in PAH concentrations in *Quercus ilex* L. (holm oak) leaves in an urban area. *Chemosphere*, 61: 432-440. [155747](#)
- Diner D; Beckert J; Bothwell G; Rodriguez J (2002). Performance of the MISR instrument during its first 20 months in Earth orbit. *IEEE Trans Geosci Remote Sens*, 40: 1449-1466. [189967](#)
- Diner D; Beckert J; Reilly T; Bruegge C; Conel J; Kahn R; Martonchik J; Ackerman T; Davies R; Gerstl S (1998). Multi-angle Imaging SpectroRadiometer (MISR) instrument description and experiment overview. *IEEE Trans Geosci Remote Sens*, 36: 1072-1087. [189962](#)

- Di Toro DM; McGrath JH; Berry WJ; Paquin PR; Mathew R; Wu KB; Santore RC (2005). Predicting sediment metal toxicity using a sediment biotic ligand model: Methodology and initial application. *Environ Toxicol Chem*, 24: 2410-2427. [155750](#)
- Doherty S; Quinn P; Jefferson A; Carrico C; Anderson T; Hegg D (2005). A comparison and summary of aerosol optical properties as observed in situ from aircraft, ship, and land during ACE-Asia. *J Geophys Res*, 110: D04201. [190027](#)
- Donahue WF; Allen EW; Schindler DW (2006). Impacts of coal-fired power plants on trace metals and polycyclic aromatic hydrocarbons (PAHs) in lake sediments in central Alberta, Canada. *J Paleolimnol*, 35: 111-128. [155751](#)
- Dong Y; Zhu YG; Smith FA; Wang Y; Chen B (2008). Arbuscular mycorrhiza enhanced arsenic resistance of both white clover (*Trifolium repens* Linn.) and ryegrass (*Lolium perenne* L.) plants in an arsenic-contaminated soil. *Environ Pollut*, 155: 174-181. [192106](#)
- Douglass AR; Schoeberl MR; Rood RB; Pawson S (2003). Evaluation of transport in the lower tropical stratosphere in a global chemistry and transport model. *J Geophys Res*, 108: 4259. [057260](#)
- Dubovik O; Holben B; Eck TF; Smirnov A; Kaufman YJ; King MD; Tanre D; Slutsker I (2002). Variability of absorption and optical properties of key aerosol types observed in worldwide locations. *J Atmos Sci*, 59: 590-608. [190202](#)
- Dubovik O; King MD (2000). A flexible inversion algorithm for retrieval of aerosol optical properties from sun and sky radiance measurements. *J Geophys Res*, 105: 20673-20696. [190197](#)
- Dubovik O; Lapyonok T; Kaufman Y; Chin M; Ginoux P; Sinyuk A (2007). Retrieving global sources of aerosols from MODIS observations by inverting GOCART model. *Atmos Chem Phys Discuss*, 7: 3629-3718. [190211](#)
- Dubovik O; Smirnov A; Holben BN; King MD; Kaufman YJ; Eck TF; Slutsker I (2000). Accuracy assessments of aerosol optical properties retrieved from AERONET sun and sky radiance measurements. *J Geophys Res*, 105: 9791-9806. [190177](#)
- Dufresne L-L; Quaas J; Boucher O; Denvil S; Fairhead L (2005). Contrasts in the effects on climate of anthropogenic sulfate aerosols between the 20th and the 21st century. *Geophys Res Lett*, 32: L21703. [199908](#)
- Duriscoe DM; Luginbuhl CB; Moore CA (2007). Measuring Night-Sky Brightness with a Wide-Field CCD Camera. *Publ. Astron. Soc. Pac.*, 119: 192-213. [156411](#)
- Dusek R; Frank GP; Hildebrandt L; Curtius J; Schneider J; Walter S; Chand D; Drewnick F; Hings S; Jung D; Borrmann S; Andreae MO (2006). Size matters more than chemistry for cloud-nucleating ability of aerosol particles. *Science*, 312: 1375-1378. [155756](#)
- Eagan RC; Hobbs PV; Radke LF (1974). Measurements of cloud condensation nuclei and cloud droplet size distributions in the vicinity of forest fires. *J Appl Meteorol*, 13: 553-557. [190231](#)
- Eck TF; Holben BN; Reid JS; Dubovik O; Smirnov A; O'Neill NT; Slutsker I; Kinne S (1999). Wavelength dependence of the optical depth of biomass burning, urban, and desert dust aerosols. *J Geophys Res*, 104: 31333-31350. [190390](#)
- Eck TF; Holben BN; Reid JS; Sinyuk A; Dubovik O; Smirnov A; Giles D; O'Neill NT; Tsay SC; Ji Q; Mandoos AAI; Khan MR; Reid EA; Schafer JS; Sorokine M; Newcomb W; Slutsker I (2008). Spatial and temporal variability of column-integrated aerosol optical properties in the southern Arabian Gulf and United Arab Emirates in summer. *J Geophys Res*, 113: in press. [190409](#)
- Edgerton ES; Hartsell BE; Jansen JJ; Hansen DA; Waid CJ; Kandasamy K (2004). 5-Year Trend Analysis of PM_{2.5} Data from the SEARCH Network. Presented at Regional and Global Perspectives on Haze: Causes, Consequences and Controversies, Visibility, Asheville, NC. [156413](#)
- Eeva T; Lehikoinen E (2004). Rich calcium availability diminishes heavy metal toxicity in Pied Flycatcher. *Funct Ecol*, 18: 548-553. [155762](#)
- Eeva T; Tanhuanpää S; Råbergh C; Airaksinen S; Nikinmaa M; Lehikoinen E (2000). Biomarkers and fluctuating asymmetry as indicators of pollution-induced stress in two hole-nesting passerines. *Funct Ecol*, 14: 235-243. [155761](#)
- Elliot SJ; Cole DC; Krueger P; Voorberg N; Wakefield S (1999). The power of perception: health risk attributed to air pollution in an urban industrial neighborhood. *Risk Anal*, 19: 621-634. [010716](#)

- Ely DW; Leary JT; Stewart TR; Ross DM (1991). The establishment of the Denver Visibility Standard. Presented at Presented at: 84th annual meeting & exhibition of the Air & Waste Management Association; June; Vancouver, British Columbia. Pittsburgh, PA: Air & Waste Management Association; paper no. 91-48.4. [056599](#)
- Englert N (2004). Fine particles and human health - a review of epidemiological studies. *Toxicol Lett*, 149: 235-242. [087939](#)
- Ericksen JA; Gustin MS; Schorran DE; Johnson DW; Lindberg SE; Coleman JS (2003). Accumulation of atmospheric mercury in forest foliage. *Atmos Environ*, 37: 1613-1622. [155769](#)
- Ervens B; Feingold G; and SMKreidenweis SM (2005). The influence of water-soluble organic carbon on cloud drop number concentration. *J Geophys Res*, 110: D18211.1-D18211.14. [190527](#)
- Evans GW; Jacobs SV (1982). Air Pollution and Human Behavior. In Evans, GW (Ed.), *Environmental Stress* (pp. 105-132). New York, NY: Cambridge University Press. [179899](#)
- Evans GW; Jacobs SV; Dooley D; Catalano R (1987). The Interaction of Stressful Life Events and Chronic Strains on Community Mental Health. *Am J Community Psychol*, 15: 23-24. [190347](#)
- Evans GW; Jacobs SV; Frager NB (1982). Behavioral responses to air pollution. In A Baum; J Singer (Ed.), *Advances in Environmental Psychology* (pp. 237-269). Hillsdale, NJ: Erlbaum. [190521](#)
- Ewald G; Larsson P; Linge H; Okla L; Szarzi M (1998). Biotransport of organic pollutants to an inland Alaska lake by migrating sockeye salmon (*Oncorhynchus nerka*). *Arctic*, 51: 40-47. [190348](#)
- Fehsenfeld FC; Ancellet G; Bates TS; Goldstein AH; Hardesty RM; Honrath R; Law KS; Lewis AC; Leaitch R; McKeen S; Meagher J; Parrish DD; Pszenny AAP; Russell PB; Schlager H; Seinfeld J; Talbot R; Zbinden R (2006). International consortium for atmospheric research on transport and transformation (ICARTT): North America to Europe -overview of the 2004 summer field study . *J Geophys Res*, 111: D23S01.1-D23S01.36. [190531](#)
- Feichter J; Sausen R; Graßl H; Fiebig M (2003). Comment on "Control of fossil-fuel particulate black carbon and organic matter, possibly the most effective method of slowing global warming" by M. Z. Jacobson. *J Geophys Res*, 108: 4767. [155772](#)
- Feingold G (2003). Modeling of the first indirect effect: Analysis of measurement requirements. *Geophys Res Lett*, 30: ASC7.1-ASC7.4. [190547](#)
- Feingold G; Furrer R; Pilewskie P; Remer LA; Min Q; Jonsson; Hafliði (2003). Aerosol indirect effect studies at southern great plains during the May 2003 intensive operations period . *J Geophys Res*, 111: D5. [190551](#)
- Feingold G; Jiang H; Harrington J (2005). On smoke suppression of clouds in Amazonia. *Geophys Res Lett*, 32: L02804.1-L02804.4. [190550](#)
- Feingold G; Remer LA; Ramaprasad J; Kaufman YJ (2001). Analysis of smoke impact on clouds in Brazilian biomass burning regions: An extension of Twomey's approach. *J Geophys Res*, 106: 22907-22922. [190544](#)
- Feingold G; Stevens B; Cotton WR; Walko RL (1994). An explicit microphysics/LES model designed to simulate the Twomey Effect. *Atmos Res*, 33: 207-233. [190535](#)
- Feingold GW; Cotton WR; Kreidenweis SM; Davis JT (1999). The impact of giant cloud condensation nuclei on drizzle formation in stratocumulus: Implications for cloud radiative properties. *J Atmos Sci*, 56: 4100-4117. [190540](#)
- Feng MH; Shan XQ; Zhang SZ; Wen B (2005). Comparison of a rhizosphere-based method with other one-step extraction methods for assessing the bioavailability of soil metals to wheat. *Chemosphere*, 59: 939-949. [155774](#)
- Ferm M; Watt J; O'Hanlon S; De Santis F; Varotsos C (2006). Deposition measurement of particulate matter in connection with corrosion studies. *Anal Bioanal Chem*, 384: 1320-30. [155135](#)
- Fernandes SD; Trautmann NM; Streets DG; Roden CA; Bond TC (2007). Global biofuel use, 1850-2000. *Global Biogeochem Cycles*, 21: GB2019.1-GB2019.15. [190554](#)
- Ferrare R; Feingold G; Ghan S; Ogren J Schmid B; Schwartz SE; Sheridan P (2006). Preface to special section: Atmospheric radiation measurement program May 2003 intensive operations period examining aerosol properties and radiative influences . *J Geophys Res*, 111: D05S01. [190561](#)
- Fiore AM; Jacob DJ; Mathur R; Martin RV (2003). Application of empirical orthogonal functions to evaluate ozone simulations with regional and global models. *J Geophys Res*, 108: 4431. [047805](#)

- Fishman J; Hoell JM; Bendura RD; McNeal RJ; Kirchhoff V (1996). NASA GTE TRACE A experiment (September-October 2002): Overview. *J Geophys Res*, 101: 23865-23880. [190566](#)
- Fismes J; Perrin-Ganier C; Empereur-Bissonnet P; Morel JL (2002). Soil-to-root transfer and translocation of polycyclic aromatic hydrocarbons by vegetables grown on industrial contaminated soils. *J Environ Qual*, 31: 1649-1656. [141156](#)
- Fitzgerald JW (1975). Approximation formulas for the equilibrium size of an aerosol particle as a function of its dry size and composition and the ambient relative humidity. *J Appl Meteor Climatol*, 14: 1044-1049. [095417](#)
- Forster P; Ramaswamy V; Artaxo P; Berntsen T; Betts R; Fahey DW; Haywood J; Lean J; Lowe DC; Myhre G; Nganga J; Prinn R; Raga G; Schultz M; Van Dorland R (2007). Changes in atmospheric constituents and in radiative forcing, Chapter 2. In Solomon S, Qin D; Manning M; Chen Z; Marquis M; Averyt KB; Tignor M; Miller HL (Ed.), IPCC Fourth Assessment Report (AR4): Climate Change 2007: Working Group I Report: The Physical Science Basis. (pp. 129-234). Cambridge, U.K. and New York, NY: Intergovernmental Panel on Climate Change; Cambridge University Press. [092936](#)
- Fraser R; Kaufman Y (1985). The relative importance of aerosol scattering and absorption in remote sensing. *IEEE Trans Geosci Remote Sens*, GE-23: 625-633. [190567](#)
- Free M; Angell JK (2002). Effect of volcanoes on the vertical temperature profile in radiosonde data. *J Geophys Res*, 107: 4101. [192281](#)
- Freer-Smith PH; El-khatib A; Taylor G (2004). Capture of particulate pollution by trees: a comparison of species typical of semi-arid areas (*Ficus nitida* and *Eucalyptus globulus*) with European and North American species. *Water Air Soil Pollut*, 155: 173-187. [156451](#)
- Frescholtz TF; Gustin MS; Schorran DE; Fernandez GCJ (2003). Assessing the source of mercury in the foliar tissue of quaking aspen. *Environ Toxicol Chem*, 22: 2114-2119. [190352](#)
- Fritze H; Niini S; Mikkola K; Makinen A (1989). Soil microbial effects of a Cu-Ni smelter in southwestern Finland. *Biol Fertil Soils*, 8: 87-94. [079635](#)
- Fryer ME; Collins CD (2003). Model intercomparison for the uptake of organic chemicals by plants. *Environ Sci Technol*, 37: 1617-1624. [156454](#)
- Gandhi N; Bhavsar SP; Diamond ML; Kuwabara JS; Marvin-DiPasquale M; Krabbenhoft DP (2007). Development of a mercury speciation, fate, and biotic uptake (BIOTRANSPEC) model: Application to Lahontan Reservoir (Nevada, USA). *Environ Toxicol Chem*, 26: 2260-2273. [155781](#)
- Gao YZ; Zhu LZ (2004). Plant uptake, accumulation and translocation of phenanthrene and pyrene in soils. *Chemosphere*, 55: 1169-1178. [155782](#)
- Garrett T; Zhao C; Dong X; Mace G; Hobbs P (2004). Effects of varying aerosol regimes on low-level Arctic stratus. *Geophys Res Lett*, 31: L17105.1-L17105.4. [190568](#)
- Garrett TJ; Zhao C (2006). Increased Arctic cloud longwave emissivity associated with pollution from mid-latitudes. *Nature*, 440: 787-789. [190570](#)
- Gawel JE; Ahner BA; Friedland AJ; Morel FMM (1996). Role for heavy metals in forest decline indicated by phytochelatin measurements. *Nature*, 381: 64-65. [012278](#)
- Generoso S; Bey I; Attié J-L; Bréon F-M (2007). A satellite- and model-based assessment of the 2003 Russian fires: impact on the arctic region. *J Geophys Res*, 112: 5302. [155786](#)
- Geogdzhayev I; Mishchenko M; Rossow W; Cairns B; Lacis AA (2002). Global two-channel AVHRR retrievals of aerosol properties over the ocean for the period of NOAA-9 observations and preliminary retrievals using NOAA-7 and NOAA-11 data. *J Atmos Sci*, 59: 262-278. [190574](#)
- Geron C; Rasmussen R; Arnts RR; Guenther A (2000). A review and synthesis of monoterpene speciation from forests in the United States. *Atmos Environ*, 34: 1761-1781. [019095](#)
- Ghan S; Laulainen N; Easter R; Wagener R; Nemesure S; Chapman E; Zhang Y; Leung R (2001). Evaluation of aerosol direct radiative forcing in MIRAGE. *J Geophys Res*, 106: 5295-5316. [199911](#)
- Gillett NP; Hegerl GC; Allen MR; Stott PA; Schnur R (2002). Reconciling two approaches to the detection of anthropogenic influence on climate. *J Clim*, 15: 326-329. [190576](#)

- Gillett NP; Zwiers FW; Weaver AJ; Hegerl GC; Allen MR; Stott PA (2002). Detecting anthropogenic influence with a multi-model ensemble. *J Geophys Res*, 29: 31.1-31.4. [190578](#)
- Ginoux P; Chin M; Holben B; Lin SJ; Tegen I; Prospero JM; Dubovik O (2001). Sources and distributions of dust aerosols simulated with the GOCART model. *J Geophys Res*, 20: 20255-20273. [190579](#)
- Ginoux P; Horowitz LW; Ramaswamy V; Geogdzhayev IV; Holben BN; Stenchikov G; Tie X (2006). Evaluation of aerosol distribution and optical depth in the geophysical fluid dynamics laboratory coupled model CM2.1 for present climate. *J Geophys Res*, 111: D22210. [190582](#)
- Gitay H; Brown S; Easterling W; Jallow B (2001). Ecosystems and their goods and services. In *Climate change 2001: impacts, adaptation and vulnerability. Contribution of working group II to the third assessment report of the Intergovernmental Panel on Climate Change* (pp. 237-342). Cambridge, United Kingdom: Cambridge University Press. [092761](#)
- Givati A; Rosenfeld D (2004). Quantifying precipitation suppression due to air pollution. *J Appl Meteorol*, 43: 1038-1056. [156475](#)
- Gleason SM; Faucette DT; Toyofuku MM; Torres CA; Bagley CF (2007). Assessing and mitigating the effects of windblown soil on rare and common vegetation. *Environ Manage*, 40: 1016-1024. [155794](#)
- Goforth MR; Christoforou CS (2006). Particle size distribution and atmospheric metals measurements in a rural area in the South Eastern USA. *Sci Total Environ*, 356: 217-227. [088353](#)
- Gohre V; Paszkowski U (2006). Contribution of the arbuscular mycorrhizal symbiosis to heavy metal phytoremediation. *Planta*, 223: 1115-1122. [190355](#)
- Golaz JC; Larson VE; Cotton WR (2002). A PDF based model for boundary layer clouds. Part I: Method and model description. *J Atmos Sci*, 59: 3540-3551. [190587](#)
- Golaz JC; Larson VE; Cotton WR (2002). A PDF-Based Model for Boundary Layer Clouds. Part II: Model Results. *J Atmos Sci*, 59: 3552-3571. [190589](#)
- Gomot-de Vaufléury A; Kerhoas I (2000). Effects of cadmium on the reproductive system of the land snail *Helix aspersa*. *Bull Environ Contam Toxicol*, 64: 434-442. [155798](#)
- Gomot-De Vaufléury A; Pihan F (2002). Methods for toxicity assessment of contaminated soil by oral or dermal uptake in land snails: Metal bioavailability and bioaccumulation. *Environ Toxicol Chem*, 21: 820-827. [190357](#)
- Gonzalez-Chavez C; Harris PJ; Dodd J; Meharg AA (2002). Arbuscular mycorrhizal fungi confer enhanced arsenate resistance on *Holcus lanatus*. *New Phytol*, 155: 163-171. [155800](#)
- Goodarzi F; Sanei H; Garrett RG; Duncan WF (2002). Accumulation of trace elements on the surface soil around the Trail smelter, British Columbia, Canada. *Environ Geol*, 43: 29-38. [155801](#)
- Gordon W; Jackson R (2000). Nutrient concentrations in fine roots. *Ecology*, 81: 275-280. [155802](#)
- Goudie AS; Elaine W; Viles HA (2002). The roles of salt and fog in weathering: a laboratory simulation of conditions the northern Atacama Desert, Chile. *Catena*, 48: 255-266. [156486](#)
- Grabowski WW (2004). An improved framework for superparameterization. [embedding of cloud-resolving model in each column of large-scale model for small-scale and mesoscale processes representation]. *J Atmos Sci*, 61: 1940-1952. [190590](#)
- Grabowski WW; Wu X; Moncrieff MW (1999). Cloud resolving modeling of tropical cloud systems during phase III of GATE. Part III: Effects of cloud microphysics. *J Atmos Sci*, 56: 2384-2402. [190592](#)
- Grannas AM; Hockaday WC; Hatcher PG; Thompson LG; Mosley-Thompson E (2006). New revelations on the nature of organic matter in ice cores. *J Geophys Res*, 111: D04304. [155804](#)
- Grannas AM; Jones AE; Dibb J; Ammann M; Anastasio C; Beine HJ; Bergin M; Bottenheim J; Boxe CS; Carver G; Chen G; Crawford JH; Dominé F; Frey MM; Guzmán MI; Heard DE; Helmig D; Hoffmann MR; Honrath RE; Huey LG; Hutterli M; Jacobi HW; Klán P; Lefer B; McCo (2007). An overview of snow photochemistry: evidence, mechanisms and impacts. *Atmos Chem Phys*, 7: 4329-4373. [156492](#)
- Grannas AM; Shepson PB; Filley TR (2004). Photochemistry and nature of organic matter in Arctic and Antarctic snow. *Global Biogeochem Cycles*, 18: GB1006. [155803](#)

- Grantz DA; Garner JHB; Johnson DW (2003). Ecological effects of particulate matter. *Environ Int*, 29: 213-239. [155805](#)
- Gratao PL; Polle A; Lea PJ; Azevedo RA (2005). Making the life of heavy metal-stressed plants a little easier. *Funct Plant Biol*, 32: 481-494. [190364](#)
- Gray JS (2002). Biomagnification in marine systems: The perspective of an ecologist. *Mar Pollut Bull*, 45: 46-52. [155806](#)
- Greenstein D; Tiefenthaler L; Bay S (2004). Toxicity of parking lot runoff after application of simulated rainfall. *Arch Environ Contam Toxicol*, 47: 199-206. [155808](#)
- Gregory JM; Stouffer RJ; Raper SCB; Stott PA; Rayner NA (2002). An observationally based estimate of the climate sensitivity. *J Clim*, 15: 3117-3121. [190593](#)
- Griffith DA; Solak ME; Yorty DP (2005). Is air pollution impacting winter orographic precipitation in Utah? Weather modification association. *J Weather Modif*, 37: 14-20. [156497](#)
- Grigal DF (2002). Inputs and outputs of mercury from terrestrial watersheds: a review. *Environ Rev*, 10: 1-39. [156498](#)
- Grigal DF (2003). Mercury sequestration in forests and peatlands: A review. *J Environ Qual*, 32: 393-405. [155811](#)
- Grossi CM; Brimblecombe P (2004). Aesthetics of simulated soiling patterns on architecture. *Environ Sci Technol*, 38: 3971-3976. [155813](#)
- Grossi CM; Esbert RM; Diaz-Pache F; Alonso FJ (2003). Soiling of building stones in urban environments. *Build Environ*, 38: 147-159. [155812](#)
- Guderian R (1977). Accumulation of pollutants in plant organs. In *Air pollution: phytotoxicity of acidic gases and its significance in air pollution control* (pp. 66-74). Berlin, Germany: Springer-Verlag. [004150](#)
- Guderian R (1985). *Air pollution by photochemical oxidants: formation, transport, control, and effects on plants*. New York: Springer-Verlag. [019325](#)
- Gunn R; Phillips BB (1957). An experimental investigation of the effect of air pollution on the initiation of rain. *J Atmos Sci*, 14: 272-280. [190595](#)
- Gupta P; Christopher SA; Wang J; Gehrig R; Lee Y; Kumar N (2006). Satellite remote sensing of particulate matter and air quality assessment over global cities. *Atmos Environ*, 40: 5880-5892. [137694](#)
- Gustin MS (2003). Are mercury emissions from geologic sources significant? A status report. *Sci Total Environ*, 304: 153-167. [155816](#)
- Hageman KJ; Simonich SL; Campbell DH; Wilson GR; Landers DH (2006). Atmospheric deposition of current-use and historic-use pesticides in snow at national parks in the western United States. *Environ Sci Technol*, 40: 3174-3180. [156509](#)
- Hall JL (2002). Cellular mechanisms for heavy metal detoxification and tolerance. *J Exp Bot*, 53: 1-11. [190365](#)
- Halsall CJ (2004). Investigating the occurrence of persistent organic pollutants (POPs) in the Arctic: their atmospheric behaviour and interaction with the seasonal snow pack. *Environ Pollut*, 128: 163-175. [155822](#)
- Halsall CJ; Barrie LA; Fellin P; Muir DCG; Rovinski FY; Kononov EY (1997). Spatial and temporal variation of polycyclic aromatic hydrocarbons in the arctic atmosphere. *Environ Sci Technol*, 31: 3593-3599. [155821](#)
- Han Q; Rossow WB; Chou J; Welch RM (1998). Global survey of the relationship of cloud albedo and liquid water path with droplet size using ISCCP. *J Clim*, 11: 1516-1528. [190594](#)
- Han Q; Rossow WB; Zeng J (2002). Three different behaviors on liquid water path of clouds in aerosol-cloud interactions. *J Atmos Sci*, 59: 726-735. [049181](#)
- Hand JL; Kreidenweis SM; Sherman DE; Collett JL Jr; Hering SV; Day DE; Malm WC (2002). Aerosol size distributions and visibility estimates during the big bend regional aerosol visibility and observational study (BRAVO). *Atmos Environ*, 36: 5043-5055. [190367](#)
- Hand JL; Malm WC (2006). Review of the IMPROVE Equation for Estimating Ambient Light Extinction Coefficients-Final Report. [156517](#)
- Hand JL; Malm WC (2007). Review of aerosol mass scattering efficiencies from ground-based measurements since 1990. *J Geophys Res*, 112: D16203. [155825](#)
- Hansen AC; Zhang Q; Lyne PWL (2005). Ethanol-diesel fuel blends--a review. *Bioresour Technol*, 96: 277-285. [059087](#)

- Hansen AD; Rosen AH; Novakov T (1982). Real-Time Measurement of the Absorption Coefficient of Aerosol Particles. *Appl Opt*, 21: 3060-3062. [190368](#)
- Hansen ADA; Rosen H; Novakov T (1984). The aethalometer - an instrument for the real-time measurement of optical absorption by aerosol particles. *Sci Total Environ*, 36: 191-196. [002396](#)
- Hansen J; Nazarenko L (2004). Soot climate forcing via snow and ice albedos. *PNAS*, 101: 423-428. [156521](#)
- Hansen J; Sato M; Mazarenko L; Ruedy R; Lacis A; Koch D; Tegen I; Hall T; Shindell D; Santer B; Stone P; Novakov T; Thomason L; Wang R; Wang Y; Jacob D; Hollandsworth S; Bishop L; Logan J; Thompson A; Stolarski R; Lean J; Willson R; Levitus S; Antonov J; Rayner N; Parker D; Christy J (2002). Climate forcings in Goddard Institute for Space Studies S12000 simulations. *J Geophys Res*, 107: 4347. [049177](#)
- Hansen J; Sato M; Ruedy R; Kharecha P; Lacis A; Miller R; Nazarenko L; Lo K; Schmidt GA; Russell G; Aleinov I; Bauer S; Baum E; Cairns B; Canuto V; Chandler M; Cheng Y; Cohen A; Del Genio A; Faluvegi G; Fleming E; Friend A; Hall T; Jackman C; Jonas J; Kelley M; Kiang NY; Koch D; Labow G; Lerner J; Menon S; Novakov T; Oinas V; Perlwitz JA; Perlwitz Ju; Rind D; Romanou A; Schmunk R; Shindell D; Stone P; Sun S; Streets D; Tausnev N; Thresher D; Unger N; Yao M; Zhang S (2007). Climate simulations for 1880-2003 with GISS modelE. *Clim Dynam*, 29: 661-696. [190597](#)
- Hansen J; Sato M; Ruedy R; Lacis A; Oinas V (2000). Global warming in the twenty-first century: an alternative scenario. *PNAS*, 97: 9875-9880. [042683](#)
- Hansen J; Sato M; Ruedy R; Nazarenko L; Lacis A; Schmidt GA; Russell G; Aleinov I; Bauer M; Bauer S; Bell N; Cairns B; Canuto V; Chandler M; Cheng Y; Del Genio A; Faluvegi G; Fleming E; Friend A; Hall T; Jackman C; Kelley M; Kiang N; Koch D; Lean J; Lerner J; Lo K; Menon S; Miller R; Minnis P; Novakov T; Oinas V; Perlwitz JA; Perlwitz Ju; Rind D; Romanou A; Shindell D; Stone P; Sun S; Tausnev N; Thresher D; Wielicki B; Wong T; Yao M; Zhang S (2005). Efficacy of climate forcings. *J Geophys Res*, 110: D18104. [190596](#)
- Hansen JE; Sato M; Ruedy R (1997). Radiative forcing and climate response. *J Geophys Res*, 102: 6831-6864. [043104](#)
- Hargrave BT; Barrie LA; Bidleman TF; Welch HE (1997). Seasonality in exchange of organochlorines between arctic air and seawater. *Environ Sci Technol*, 31: 3258-3266. [155827](#)
- Harmens H; Norris DA; Koerber GR; Buse A; Steinnes E; Rühling A (2007). Temporal trends in the concentration of arsenic, chromium, copper, iron, nickel, vanadium and zinc in mosses across Europe between 1990 and 2000. *Atmos Environ*, 41: 6673-6687. [155828](#)
- Harner T; Jantunen LMM; Bidleman TF; Barrie LA; Kylin H; Strachan WMJ; Macdonald RW (2000). Microbial degradation is a key elimination pathway of hexachlorocyclohexanes from the Arctic Ocean. *Geophys Res Lett*, 27: 1155-1158. [155829](#)
- Harrison L; Michalsky J; Berndt J (1994). Automated multifilter rotating shadow-band radiometer: an instrument for optical depth and radiation measurements. *Appl Opt*, 33: 5118-5125. [045805](#)
- Harvey LDD (2004). Characterizing the annual-mean climatic effect of anthropogenic CO₂ and aerosol emissions in eight coupled atmosphere-ocean GCMs. *Clim Dynam*, 23: 569-599. [190598](#)
- Hassan R; Scholes R; Ash N (2005). *Ecosystems and human well-being: current state and trends, volume 1*. United Kingdom: Shearwater Books. [092759](#)
- Hauck M (2003). Epiphytic lichen diversity and forest dieback: The role of chemical site factors. *Bryologist*, 106: 257-269. [155830](#)
- Haynie FH (1986). Environmental factors affecting corrosion of weathering steel. Presented at Materials degradation caused by acid rain: developed from the 20th state-of-the-art symposium of the American Chemical Society; June 1985; Arlington, VA., Washington, DC. [157198](#)
- Haynie FH; Lemmons TJ (1990). Particulate matter soiling of exterior paints at a rural site. *Aerosol Sci Technol*, 13: 356-367. [044579](#)
- Haywood J; Boucher O (2000). Estimates of the direct and indirect radiative forcing due to tropospheric aerosols: A review. *Rev Geophys*, 38: 513-543. [156531](#)
- Haywood J; Francis P; Osborne S; Glew M; Loeb N; Highwood E; Tanré D; Myhre G; Formenti P; Hirst E (2003). Radiative properties and direct radiative effect of Saharan dust measured by the C-130 aircraft during SHADE: 1. Solar spectrum : The Saharan Dust Experiment (SHADE). *J Geophys Res*, 108: SAH 4-1. [190599](#)

- Haywood J; Schulz M (2007). Causes of the reduction in uncertainty in the anthropogenic radiative forcing of climate between IPCC (2001) and IPCC (2007). *Geophys Res Lett*, 34: L20701. [190600](#)
- Haywood JM; Pelon J; Formenti P; Bharmal N; Brooks M; Capes G; Chazette P; Chou C; Christopher S; Coe H; Cuesta J; Derimian Y; Desboeufs K; Greed G; Harrison M; Heese B; Highwood EJ; Johnson B; Mallet M; Marticorena B; Marsham J; Milton S; Myhre G; Osborne SR; Parker DJ; Rajot JL; Schulz M; Slingo A; Tanré D; Tulet P (2008). Overview of the dust and biomass burning experiment and African monsoon multidisciplinary analysis special observing Period-0. *J Geophys Res*, 113: D00C17. [190602](#)
- Haywood JM; Ramaswamy V; Soden BJ (1999). Tropospheric aerosol climate forcing in clear-sky satellite observations over the oceans. *Science*, 283: 1299-1303. [040453](#)
- Heald CL; Jacob DJ; Park RJ; Russell LM; Huebert BJ; Seinfeld JH; Liao H; Weber RJ (2005). A large organic aerosol source in the free troposphere missing from current models. *Geophys Res Lett*, 32: L18809.1-L18809.4. [190603](#)
- Heintzenberg J (2008). The SAMUM-1 experiment over Southern Morocco: overview and introduction. *Tellus B Chem Phys Meteorol*, 61: 2-11. [190605](#)
- Helena P; Franc B; Cvetka RL (2004). Monitoring of short-term heavy metal deposition by accumulation in epiphytic lichens (*Hypogymnia Physodes* (L.) Nyl.). *J Atmos Chem*, 49: 223-230. [155833](#)
- Helm PA; Diamond ML; Semkin R; Bidleman TF (2000). Degradation as a loss mechanism in the fate of α -hexachlorocyclohexane in Arctic watersheds. *Environ Sci Technol*, 34: 812-818. [155834](#)
- Helm PA; Diamond ML; Semkin R; Strachan WMJ; Teixeira C; Gregor D (2002). A mass balance model describing multi-year fate of organochlorine compounds in a high arctic lake. *Environ Sci Technol*, 36: 996-1003. [155835](#)
- Helmisaari H-S; Makkonen K; Olsson M; Viksna A; Mälkönen E (1999). Fine-root growth, mortality and heavy metal concentrations in limed and fertilized *Pinus silvestris* (L.) stands in the vicinity of a Cu-Ni smelter in SW Finland. *Plant Soil*, 209: 193-200. [155836](#)
- Henze DK; Seinfeld JH (2006). Global secondary organic aerosol from isoprene oxidation. *Geophys Res Lett*, 33: L09812.1-L09812.4. [190606](#)
- Herman JR; Bhartia PK; Torres O; Hsu C; Seftor C; Celarier E (1997). Global distribution of UV-absorbing aerosols from Nimbus 7/TOMS data. *J Geophys Res*, 102: 16911-16922. [048393](#)
- Hernandez L; Probst A; Probst JL; Ulrich E (2003). Heavy metal distribution in some French forest soils: Evidence for atmospheric contamination. *Sci Total Environ*, 312: 195-219. [155841](#)
- Herner JD; Ying Q; Aw J; Gao O; Chang DPY; Kleeman MJ (2006). Dominant Mechanisms that Shape the Airborne Particle Size and Composition Distribution in Central California. *Aerosol Sci Technol*, 40: 827-844. [135981](#)
- Herrera LK; Videla HA (2004). The importance of atmospheric effects on biodeterioration of cultural heritage constructional materials. *Int Biodeterior Biodegradation*, 54: 125-134. [155843](#)
- Hicke JA; Asner GP; Kasischke ES; French NHF; Randerson JT; Collatz GJ; Stocks BJ; Tucker CJ; Los SO; Field CB (2003). Postfire response of North American boreal forest net primary productivity analysed with satellite observations. *Global Change Biol*, 9: 1145-1157. [156545](#)
- Hinzman LD; Fukuda M; Sandberg DV; Chapin III FS; Dash D (2003). FROSTFIRE: an experimental approach to predicting the climate feedbacks from the changing boreal fire regime. *J Geophys Res*, 108: 8153. [155845](#)
- Hobbelen PHF; Koolhaas JE; van Gestel CAM (2006). Bioaccumulation of heavy metals in the earthworms *Lumbricus rubellus* and *Aporrectodea caliginosa* in relation to total and available metal concentrations in field soils. *Environ Pollut*, 144: 639-646. [190371](#)
- Hodzic A; Madronich S; Bohn B; Massie S; Menut L; Wiedinmyer C (2007). Wildfire particulate matter in Europe during summer 2003: meso-scale modeling of smoke emissions, transport and radiative effects. *Atmos Chem Phys*, 7: 4043-4064. [156553](#)
- Hoell JM; Davis DD; Liu SC; Newell R; Shipham M; Akimoto H; McNeal RJ; Bemdura RJ; Drewry JW (1996). Pacific exploratory mission-west A (PEM-WEST A): September- October, 1991. *J Geophys Res*, 101: 1641-1653. [190607](#)
- Hoell JM; Davis DD; Liu SC; Newell RE; Akimoto H; McNeal RJ; Bendura RJ (1997). The Pacific exploratory mission-west phase B: February-March, 1994. *J Geophys Res*, 102: 28223-28239. [057373](#)

- Hoff R; Engel-Cox J; Krotkov N; Palm S; Rogers R; McCann K; Sparling L; Jordan N; Torres O; Spinhirne J (2004). Long-range transport observations of two large forest fire plumes to the northeastern U.S. In Proceedings of the 22nd International Laser Radar Conference (pp. 683-686.). Paris: European Space Agency. [190617](#)
- Hoff RM; McCann KJ (2002). Regional East Atmospheric Lidar Mesonet: REALM. In L. Bissonette; G Roy; G Vallée (Ed.), Lidar Remote Sensing in Atmospheric and Earth Sciences (pp. 281-284). Val-Bélair, Quebec: Def. R&D Can. Valcartier. [190612](#)
- Hofmann D; Barnes J; Dutton E; Deshler T; Jäger H; Keen R; Osborn M (2003). Surface-based observations of volcanic emissions to stratosphere. In Volcanism and the Earth's Atmosphere (pp. 57-73). Washington, DC: American Geophysical Union. [192062](#)
- Hoh E; Zhu L; Hites RA (2006). Dechlorane plus, a chlorinated flame retardant, in the Great Lakes. Environ Sci Technol, 40: 1184-1189. [190378](#)
- Holben BN; Eck TF; Slutsker I; Tanré D; Buis JP; Setzer A; Vermote E; Reagan JA; Kaufman YJ; Nakajima T; Lavenu F; Jankowiak I; Smirnov A (1998). AERONET: A federated instrument network and data archive for aerosol characterization. Rem Sens Environ, 66: 1-16. [155848](#)
- Holben BN; Smirnov A; Eck TF; Slutsker I; Abuhassan N; Newcomb WW; Schafer JS; Tanre D; Chatenet B; Lavenu F (2001). An emerging groundbased aerosol climatology: aerosol optical depth from AERONET. J Geophys Res, 106: 12067-12098. [190618](#)
- Holland EA; Dentener FJ; Braswell BH; Sulzman JM (1999). Contemporary and pre-industrial global reactive nitrogen budgets. Biogeochemistry, 46: 7-43. [092051](#)
- Holmqvist M; Stenroth P; Berglund O; Nystrom P; Olsson K; Jellyman D; McIntosh AR; Larsson P (2006). Low levels of persistent organic pollutants (POPs) in New Zealand eels reflect isolation from atmospheric sources. Environ Pollut, 141: 532-538. [190380](#)
- Hooda V (2007). Phytoremediation of toxic metals from soil and waste water. J Environ Biol, 28: 367-376. [190382](#)
- Hopke PK; Zhou L; Poirot RL (2005). Reconciling Trajectory Ensemble Receptor Model Results with Emissions. Environ Sci Technol, 39: 7980-7983. [156567](#)
- Horowitz L (2006). Past, present, and future concentrations of tropospheric ozone and aerosols: Methodology, ozone evaluation, and sensitivity to aerosol wet removal. J Geophys Res, 111: D22211.1-D22211.16. [190620](#)
- Horowitz LW; Walters S; Mauzerall DL; Emmons LK; Rasch PJ; Granier C; Tie X; Lamarque J-F; Schultz MG; Tyndall GS; Orlando JJ; Brasseur GP (2003). A global simulation of tropospheric ozone and related tracers: Description and evaluation of MOZART, version 2. J Geophys Res, 108: D24. [057770](#)
- Houlahan JE; Findlay CS; Schmidt BR; Meyer AH; Kuzmin SL (2000). Quantitative evidence for global amphibian population declines. Nature, 404: 752-755. [155853](#)
- Howe TS; Billings S; Stolzberg RJ (2004). Sources of polycyclic aromatic hydrocarbons and hexachlorobenzene in spruce needles of eastern Alaska. Environ Sci Technol, 38: 3294-3298. [155854](#)
- Howel D; Moffatt S; Prince H; Bush J; Dunn CE (2002). Urban Air Quality in North-East England: Exploring the Influences on Local Views and Perceptions. Risk Anal, 22: 121-130. [156571](#)
- Hoyt D; Frohlich C (1983). Atmospheric transmission at Davos, Switzerland 1909-1979. Clim Change, 5: 61-71. [190621](#)
- Hoyt DV (1978). A model for the calculation of solar global insolation. Solar Energy, 21: 27-35. [046638](#)
- Hsu NC; Tsay SC; King MD; Herman JR (2004). Aerosol properties over bright-reflecting source regions. IEEE Trans Geosci Remote Sens, 42: 557-569. [190622](#)
- Huebert BJ; Bates T; Russell PB; Shi G; Kim YJ; Kawamura K; Carmichael G; Nakajima T (2003). An overview of ACE-Asia: Strategies for quantifying the relationships between Asian aerosols and their climatic impacts. J Geophys Res, 108: 8633. [190623](#)
- Hughes MK (1981). Cycling of trace metals in ecosystems. In NW Lepp (Ed.), Effect of heavy metal pollution on plants. Volume 2: metals in the environment (pp. 95-118). London, United Kingdom: Applied Science Publishers. [053595](#)
- Hunaiti AA; Al-Oqlah A; Shannag NM; Abukhalaf IK; Silvestrov NA; Von Deutsch DA; Bayorh MA (2007). Toward understanding the influence of soil metals and sulfate content on plant thiols. J Toxicol Environ Health A Curr Iss, 70: 559-567. [156579](#)

- Huneeus N; Boucher O (2007). One-dimensional variational retrieval of aerosol extinction coefficient from synthetic LIDAR and radiometric measurements. *J Geophys Res*, 112: D14303.1-D14303.14. [190624](#)
- Hung HH; Halsall CJ; Blanchard P (2001). Are PCBs in the Canadian Arctic atmosphere declining? Evidence from 5 years of monitoring. *Environ Sci Technol*, 35: 1303-1311. [155856](#)
- Hung HH; Halsall CJ; Blanchard P; Li HH; Fellin P; Stern G; Rosenberg B (2002). Temporal trends of organochlorine pesticides in the Canadian Arctic atmosphere. *Environ Sci Technol*, 36: 862-868. [155857](#)
- Husar RB; Prospero JM; Stowe LL (1997). Characterization of tropospheric aerosols over the oceans with the NOAA advanced very high resolution radiometer optical thickness operational product. *J Geophys Res*, 102: 16,889-16,909. [045900](#)
- IPCC (1995). Radiative forcing of climate change and an evaluation of the IPCC IS92 emission scenarios. In *Climate Change 1994* (pp. 193-204). New York: Cambridge University Press. [190991](#)
- IPCC (1996). Radiative forcing of climate change. In *Climate Change 1995* (pp. 65-131). New York: Intergovernmental Panel on Climate Change. [190990](#)
- IPCC (2001). *Climate Change 2001: The Scientific Basis*. Contribution of Working Group I to the Third Assessment Report (TAR) of the Intergovernmental Panel on Climate Change [Houghton, J.T., Y. Ding, D.J. Griggs, M. Noguer, P.J. van der Linden, X. Dai, K. Maskell, and C.A. Johnson (eds.)]. Cambridge, UK and New York, NY, USA: Intergovernmental Panel on Climate Change, Cambridge University Press. [156587](#)
- IPCC (2007). *Climate Change 2007: The Physical Science Basis*. Contribution of Working Group I to the Fourth Assessment Report (AR4) of the Intergovernmental Panel on Climate Change. Cambridge, UK and New York, NY: Intergovernmental Panel on Climate Change, Cambridge University Press. [092765](#)
- Ito A; Penne JE (2005). Historical emissions of carbonaceous aerosols from biomass and fossil fuel burning for the period 1870-2000. *Global Biogeochem Cycles*, 19: GB2028.1-GB2028.14. [190626](#)
- Jacob DJ; Crawford JH; Kleb MM; Connors VS; Bendura RJ; Raper JL; Sachse GW; Gille JC; Emmons L; Heald CL (2003). The Transport and Chemical Evolution over the Pacific (TRACE-P) aircraft mission: design, execution, and first results. *J Geophys Res*, 108: 9000. [190987](#)
- Jacobs SV; Evans GW; Catalano R; Dooley D (1984). Air pollution and depressive symptomatology: Exploratory analyses of intervening psychosocial factors. *Popul Environ*, 7: 260-272. [156596](#)
- Jacobson MZ (2000). A physically-based treatment of elemental carbon optics: implications for global direct forcing of aerosols. *Geophys Res Lett*, 27: 217-220. [056378](#)
- Jacobson MZ (2001). GATOR-GCMM: a global through urban scale air pollution and weather forecast model: 1. Model design and treatment of subgrid soil, vegetation, roads, rooftops, water, sea ice, and snow. *J Geophys Res*, 106: 5385-5402. [155864](#)
- Jacobson MZ (2001). Global direct radiative forcing due to multicomponent anthropogenic and natural aerosols. *J Geophys Res*, 106: 1551-1568. [043110](#)
- Jacobson MZ (2002). Control of fossil-fuel particulate black carbon and organic matter, possibly the most effective method of slowing global warming. *J Geophys Res*, 107: 4410. [155865](#)
- Jacobson MZ (2003). Development of mixed-phase clouds from multiple aerosol size distributions and the effect of the clouds on aerosol removal. *J Geophys Res*, 108: 4245. [155866](#)
- Jacobson MZ (2003). Reply to comment by D. P. Chock et al. on "Control of fossil-fuel particulate black carbon and organic matter, possibly the most effective method of slowing global warming". *J Geophys Res*, 108: 4770. [155867](#)
- Jacobson MZ (2003). Reply to comment by J. E. Penner on "Control of fossil-fuel particulate black carbon and organic matter, possibly the most effective method of slowing global warming". *J Geophys Res*, 108: 4772. [155868](#)
- Jacobson MZ (2003). Reply to comment by J. Feichter et al. on "Control of fossil-fuel particulate black carbon and organic matter, possibly the most effective method of slowing global warming". *J Geophys Res*, 108: 4768. [155869](#)
- Jacobson MZ (2004). Climate response of fossil fuel and biofuel soot, accounting for soot's feedback to snow and sea ice albedo and emissivity. *J Geophys Res*, 109, : D21201. [155870](#)
- Jacobson MZ (2006). Effects of externally-through-internally-mixed soot inclusions within clouds and precipitation on global climate. *J Phys Chem B*, 110: 6860-6873. [156599](#)

- Jacobson MZ; Kaufman YJ (2006). Wind reduction by aerosol particles. *Geophys Res Lett*, 33: L24814. [090942](#)
- Jacobson MZ; Seinfeld JH; Carmichael GR; Streets DG (2004). The effect on photochemical smog of converting the U.S. fleet of gasoline vehicles to modern diesel vehicles. *Geophys Res Lett*, 31: L02116. [180362](#)
- James SM; Little EE; Semlitsch RD (2004). Effects of multiple routes of cadmium exposure on the hibernation success of the American toad (*Bufo americanus*). *Arch Environ Contam Toxicol*, 46: 518-527. [155874](#)
- Jantunen LMM; Bidleman TF (1996). Air-water gas exchange of hexachlorocyclohexanes (HCHs) and the enantiomers of α -HCH in Arctic regions. *J Geophys Res*, 101: 28837-28846. [155876](#)
- Jantunen LMM; Bidleman TF (1998). Organochlorine pesticides and enantiomers of chiral pesticides in Arctic Ocean water. *Arch Environ Contam Toxicol*, 35: 218-228. [155877](#)
- Jayanty R (2003). Overview of PM_{2.5} Chemical Speciation Nationwide Network Program. Presented at Specialty Conference of the American Association for Aerosol Research, Pittsburgh, PA, April, 2003, Research Triangle Park, NC. [156605](#)
- Jayne JT; Leard DC; Zhang X; Davidovits P; Smith KA; Kolb CE; Worsnop DR (2000). Development of an aerosol mass spectrometer for size and composition analysis of submicron particles. *Aerosol Sci Technol*, 33: 49-70. [190978](#)
- Jeong MJ; Li Z; Chu DA; Tsay SC (2005). Quality and Compatibility Analyses of Global Aerosol Products Derived from the Advanced Very High Resolution Radiometer and Moderate Resolution Imaging Spectroradiometer. *J Geophys Res*, 110: D10S09. [190977](#)
- Jiang H; Feingold G (2006). Effect of aerosol on warm convective clouds: Aerosol-cloud-surface flux feedbacks in a new coupled large eddy model. *J Geophys Res*, 111: D01202. [190976](#)
- Jiang J; Oberdrster G; Elder A; Gelein R; Mercer P; Biswas P (2008). Does nanoparticle activity depend upon size and crystal phase? *Nanotoxicology*, 2: 33-42. [156609](#)
- Jiang W; Smyth S; Giroux E; Roth H; Yin D (2006). Differences between CMAQ fine mode particle and PM_{2.5} concentrations and their impact on model performance evaluation in the lower Fraser valley. *Atmos Environ*, 40: 4973-4985. [133165](#)
- Jiao XC; Xu FL; Dawson R; Chen SH; Tao S (2007). Adsorption and absorption of polycyclic aromatic hydrocarbons to rice roots. *Environ Pollut*, 148: 230-235. [155879](#)
- Jirak IL; Cotton WR (2006). Effect of air pollution on precipitation along the Front Range of the Rocky Mountains. *J Appl Meteorol*, 45: 236-245. [156612](#)
- Johnson D; Hale B (2008). Fine root decomposition and cycling of Cu, Ni, Pb, and Zn at forest sites near smelters in Sudbury, ON, and Rouyn-Noranda, QU, Canada. *Hum Ecol Risk Assess*, 14: 41-53. [155881](#)
- Johnson DB (1982). The role of giant and ultragiant aerosol particles in warm rain initiation. *J Atmos Sci*, 39: 448-460. [190973](#)
- Johnson MS; Franke LS; Lee RB; Holladay SD (1999). Bioaccumulation of 2,4,6-trinitrotoluene and polychlorinated biphenyls through two routes of exposure in a terrestrial amphibian: Is the dermal route significant? *Environ Toxicol Chem*, 18: 873-878. [155880](#)
- Jones A; Roberts DL; Woodage MJ (2001). Indirect sulphate aerosol forcing in a climate model with an interactive sulphur cycle. *J Geophys Res*, 106: 20293-20301. [199895](#)
- Jones GS; Jones A; Roberts DL; Stott PA; Williams KD (2005). Sensitivity of global-scale climate change attribution results to inclusion of fossil fuel black carbon aerosol. *Geophys Res Lett*, 32: L14701. [155885](#)
- Jones JW; Bogat GA (1978). Air pollution and human aggression. *Psychol Rep*, 43: 721-722. [190396](#)
- Jones PD; Moberg A; Osborn TJ; Briffa KR (2003). Surface climate responses to explosive volcanic eruptions seen in long European temperature records and mid-to-high latitude tree-ring density around the Northern Hemisphere. In Robock A; Oppenheimer C (Ed.), *Volcanism and the earth's atmosphere* (pp. 239-254). Washington, DC: American Geophysical Union. [192278](#)
- Joshi M; Shine K (2003). A GCM study of volcanic eruptions as a cause of increased stratospheric water vapor. *J Clim*, 16: 3525-3534. [192327](#)

- Joynt J; Bischoff M; Turco R; Konopka A; Nakatsu CH (2006). Microbial community analysis of soils contaminated with lead, chromium and petroleum hydrocarbons. *Microb Ecol*, 51: 209-219. [155887](#)
- Junker C; Liousse C (2008). A global emission inventory of carbonaceous aerosol from historic records of fossil fuel and biofuel consumption for the period 1860-1997. *Atmos Chem Phys*, 8: 1195-1207. [190971](#)
- Kahn R; Banerjee P; McDonald D (2001). The sensitivity of multiangle imaging to natural mixtures of aerosols over ocean. *J Geophys Res*, 106: 18219-18238. [190969](#)
- Kahn R; Banerjee P; McDonald D; Diner D (1998). Sensitivity of multiangle imaging to aerosol optical depth, and to pure-particle size distribution and composition over ocean. *J Geophys Res*, 103: 32195-32213. [190970](#)
- Kahn R; Gaitley B; Martonchik J; Diner D; Crean K; Holben B (2005). Multiangle Imaging Spectroradiometer (MISR) global aerosol optical depth validation based on 2 years of coincident Aerosol Robotic Network (AERONET) observations. *J Geophys Res*, 110: D10S04. [189961](#)
- Kahn R; Li W; Martonchik J; Bruegge C; Diner D; Gaitley B; Abdou W; Dubovik O; Holben B; Smirnov A; Jin Z; Clark D (2005). MISR low-light-level calibration, and implications for aerosol retrieval over dark water. *Science*, 62: 1032-1052. [190965](#)
- Kahn R; Li W; Moroney C; Diner D; Martonchik J; Fishbein E (2007). Aerosol source plume physical characteristics from space-based multiangle imaging. *J Geophys Res*, 112: D11205. [190964](#)
- Kahn RA; Gaitley BJ; Martonchik JV; Diner DJ; Crean KA; Holben B (2005). MISR global aerosol optical depth validation based on two years of coincident AERONET observations. *J Geophys Res*, 110: D10S04. [190966](#)
- Kahn RA; Garay MJ; Nelson DL; Yau KK; Bull MA; Gaitley BJ; Martonchik JV; Levy R (2007). Satellite-derived aerosol optical depth over dark water from MISR and MODIS: comparisons with AERONET and implications for climatological studies. *J Geophys Res*, 112: D18205. [190963](#)
- Kalashnikova O; Kahn R (2006). Ability of multiangle remote sensing observations to identify and distinguish mineral dust types: Part 2 Sensitivity over dark water. *J Geophys Res*, 111: D11207. [190962](#)
- Kaldorf M; Kuhn AJ; Schroder WH; Hildebrandt U; Bothe H (1999). Selective element deposits in maize colonized by a heavy metal tolerance conferring arbuscular mycorrhizal fungus. *J Plant Physiol*, 154: 718-728. [190399](#)
- Kamh GME (2005). The impact of landslides and salt weathering on Roman structures at high latitudes - Conway Castle, Great Britain: A case study. *Environ Geol*, 48: 238-254. [155888](#)
- Kandeler E; Kampichler C; Horak O (1996). Influence of heavy metals on the functional diversity of soil microbial communities. *Biol Fertil Soils*, 23: 299-306. [094392](#)
- Kappos AD; Bruckmann P; Eikmann T; Englert N; Heinrich U; Hoppe P; Koch E; Krause GH; Kreyling WG; Rauchfuss K; Rombout P; Schulz-Klemp V; Thiel WR; Wichmann HE (2004). Health effects of particles in ambient air. *Int J Hyg Environ Health*, 207: 399-407. [087922](#)
- Kapustin VN; Clarke AD; Shinozuka Y; Howell S; V Brekhovskikh V; Nakajima T; Higurashi A (2006). On the determination of a cloud condensation nuclei from satellite: Challenges and possibilities. *J Geophys Res*, 111: D04202. [190961](#)
- Kaufman Y (1987). Satellite sensing of aerosol absorption. *J Geophys Res*, 92: 4307-4317. [190960](#)
- Kaufman Y; Boucher O; Tanré D; Chin M; Remer L; Takemura T (2005). Aerosol anthropogenic component estimated from satellite data. *Geophys Res Lett*, 32: L17804. [155891](#)
- Kaufman Y; Fraser R (1997). The effect of smoke particles on clouds and climate forcing. *Science*, 277: 1636-1639. [190958](#)
- Kaufman Y; Haywood J; Hobbs P; Hart W; Kleidman R; Schmid B (2003). Remote sensing of vertical distributions of smoke aerosol off the coast of Africa. *Geophys Res Lett*, 30: 1831. [190954](#)
- Kaufman YD; Tanré D; Boucher O (2002). A satellite view of aerosols in the climate system. *Nature*, 419: 215-223. [190956](#)
- Kaufman YJ; Hobbs PV; Kirchoff VWJH; Artaxo P; Remer LA; Holben BN; King MD; Ward DE; Prins EM; Longo KM; Mattos LF; Nobre CA; Spinhirne JD; Ji Q; Thompson AM; Gleason JF; Christopher SA; Tsay S-C (1998). Smoke, clouds, and radiation--Brazil (SCAR-B) experiment. *J Geophys Res*, 103: 31783-31808. [089989](#)
- Kaufman YJ; Koren I (2006). Smoke and pollution aerosol effect on cloud cover. *Science*, 313: 655-658. [190951](#)

- Kaufman YJ; Martins JV; Remer LA; Schoeberl MR; Yamasoe MA (2002). Satellite retrieval of aerosol absorption over the oceans using sunglint. *Geophys Res Lett*, 29: 34.1-34.4. [190955](#)
- Kaufman YJ; Nakajima T (1993). Effect of Amazon smoke on cloud microphysics and albedo—Analysis from satellite imagery. *J Appl Meteorol*, 32: 729-744. [190959](#)
- Kaufman YJ; Setzer A; Ward D; Tanre D; Holben BN; Menzel P; Pereira MC; Rasmussen R (1992). Biomass Burning Airborne and Spaceborne Experiment in the Amazonas (BASE-A). *J Geophys Res*, 97: 14581-14599. [044557](#)
- Kavouras IG; Etyemezian V; DuBois DW; Xu J; Pitchford M (2009). Source reconciliation of atmospheric dust causing visibility impairment in Class I areas of the western United States. *J Geophys Res*, 114: D02308. [191976](#)
- Kavouras IG; Etyemezian V; Xu J; DuBois DW; Green M; Pitchford M (2007). Assessment of the local windblown component of dust in the western United States. *J Geophys Res*, 112: D08211. [156630](#)
- Kenski DM; Gay D; Fitzsimmons S (2004). Ammonia and its role in midwestern haze. Presented at Regional and Global Perspectives on Haze: Causes, Consequences and Controversies Visibility Specialty Conference, Asheville, NC. [192078](#)
- Kerr R (2007). Another global warming icon comes under attack. *Science*, 317: 28-29. [190950](#)
- Kiehl JT (2007). Twentieth century climate model response and climate sensitivity. *Geophys Res Lett*, 34: 1-4. [190949](#)
- Kiikkilä O (2003). Heavy-metal pollution and remediation of forest soil around the Harjavalta Cu-Ni smelter, in SW Finland. *Silva Fennica*, 37: 399-415. [156637](#)
- Kim CG; Bell JNB; Power SA (2003). Effects of soil cadmium on *Pinus sylvestris* L. seedlings. *Plant Soil*, 257: 443-449. [155899](#)
- Kim MK; Lau KM; Chin M; Kim KM; Sud Y; Walker GK (2006). Atmospheric teleconnection over Eurasia induced by aerosol radiative forcing during boreal spring. *PNAS*, 19: 4700-4718. [190917](#)
- Kim SW; Yoon SC; Kim J (2008). Columnar Asian dust particle properties observed by sun/sky radiometers from 2000 to 2006 in Korea. *Atmos Environ*, 42: 492-504. [130785](#)
- Kim Y; Hatsushika H; Muskett RR; Yamazaki K (2005). Possible effect of boreal wildfire soot on Arctic sea ice and Alaska glaciers. *Atmos Environ*, 39: 3513-3520. [155900](#)
- King M; Kaufman Y; Tanré D; Nakajima T (1999). Remote sensing of tropospheric aerosols from space: Past, present, and future. *Bull Am Meteorol Soc*, 80: 2229-2259. [190635](#)
- King MD; Platnick S; Moeller CC; Revercomb HE; Chu DA (2003). Remote sensing of smoke, land, and clouds from the NASA ER-2 during SAFARI 2000. *J Geophys Res*, 108: SAF38.1-SAF38.12. [094395](#)
- Kinne S; Schulz M; Textor C; Guibert S; Balkanski Y; Bauer SE; Bernsten T; Berglen TF; Boucher O; Chin M; Collins W; Dentener F; Diehl T; Easter R; Feichter J; Fillmore D; Ghan S; Ginoux P; Gong S; Grini A; Hendricks J; Herzog M; Horowitz L; Isaksen I; Iversen T; Kirkevåg A; Kloster S; Koch D; Kristjansson JE; Krol M; Lauer A; Lamarque JF; Lesins G; Liu X; Lohmann U; Montanaro V; Myhre G; Penner J; Pitari G; Reddy S; Seland O; Stier P; Takemura T; Tie X (2006). An AeroCom initial assessment—optical properties in aerosol component modules of global models. *Atmos Chem Phys*, 6: 1815-1834. [155903](#)
- Kirchstetter TW; Harley RA; Kreisberg NM; Stolzenberg MR; Hering SV (1999). On-road measurement of fine particle and nitrogen oxide emissions from light- and heavy-duty motor vehicles. *Atmos Environ*, 33: 2955-2968. [010642](#)
- Kirkbride MP; Dugmore JA (2003). Glaciological response to distal tephra fallout from the 1947 eruption of Hekla, south Iceland. *J Glaciol*, 49: 420-428. [156645](#)
- Kirkevåg A; Iversen T (2002). Global direct radiative forcing by process-parametrized aerosol optical properties. *J Geophys Res*, 107: 4433. [199893](#)
- Kleeman MJ; Hughes LS; Allen JO; Cass GR (1999). Source contributions to the size and composition distribution of atmospheric particles: southern California in September 1996. *Environ Sci Technol*, 33: 4331-4341. [011286](#)
- Kleidman R; O'Neill N; Remer L; Kaufman Y; Eck T; Tanré D; Dubovik O; Holben B (2005). Comparison of Moderate Resolution Imaging Spectroradiometer (MODIS) and Aerosol Robotic Network (AERONET) remote-sensing retrievals of aerosol fine mode fraction over ocean. *J Geophys Res*, 110: 1-16. [190175](#)

- Kleinman MT; Araujo JA; Nel A; Sioutas C; Campbell A; Cong PQ; Li H; Bondy SC (2008). Inhaled ultrafine particulate matter affects CNS inflammatory processes and may act via MAP kinase signaling pathways. *Toxicol Lett*, 178: 127-130. [190074](#)
- Knutti R; Stocker TF; Joos F; Plattner GK (2002). Constraints on radiative forcing and future climate change from observations and climate model ensembles. *Nature*, 416: 719-723. [190178](#)
- Knutti R; Stocker TF; Joos F; Plattner GK (2003). Probabilistic climate change projections using neural networks. *Clim Dynam*, 21: 257-272. [190180](#)
- Koch D (2001). Transport and direct radiative forcing of carbonaceous and sulfate aerosols in the GISS GCM. *J Geophys Res*, 106: 20311-20332. [192054](#)
- Koch D; Bond TC; Streets D; Unger N; van der Werf GR (2007). Global impact of aerosols from particular source regions and sectors. *J Geophys Res*, 112: D02205. [190185](#)
- Koch D; Hansen J (2005). Distant origins of Arctic black carbon: A Goddard Institute for Space Studies ModelE experiment. *J Geophys Res*, 110: D04204. [190183](#)
- Koch D; Schmidt G; Field C (2006). Sulfur, sea salt, and radionuclide aerosols in GISS ModelE. *J Geophys Res*, 111: D06206. [190184](#)
- Kogan YL; Lilly DK; Kogan ZN; Filyushkin V (1994). The effect of CCN regeneration on the evolution of stratocumulus cloud layers. *Atmos Res*, 33: 137-150. [190186](#)
- Koren I; Kaufman YJ; Remer LA; Martins JV (2004). Measurement of the effect of Amazon smoke on inhibition of cloud formation. *Science*, 303: 1342-1345. [190187](#)
- Koren I; Kaufman YJ; Rosenfeld D; Remer LA; Rudich Y (2005). Aerosol invigoration and restructuring of Atlantic convective clouds. *Geophys Res Lett*, 32: L14828. [190188](#)
- Koren I; Martins JV; Remer LA; Afargan H (2008). Smoke invigoration versus inhibition of clouds over the Amazon. *Science*, 321: 946-949. [190193](#)
- Koren I; Remer KA; Kaufman YJ; Rudich Y; Martins JV (2007). On the twilight zone between clouds and aerosols. *Geophys Res Lett*, 34: L08805. [190192](#)
- Koren I; Remer LA; Longo K (2007). Reversal of trend of biomass burning in the Amazon. *Geophys Res Lett*, 34: L20404. [190189](#)
- Korsnes R; Pavlova O; Godtlielsen F (2002). Assessment of potential transport of pollutants into the Barents Sea via sea ice--an observational approach. *Mar Pollut Bull*, 44: 861-869. [156657](#)
- Kristjánsson JE; Staple A; Kristiansen J; Kaas E (2002). A new look at possible connections between solar activity, clouds and climate. *Geophys Res Lett*, 29: 2107. [199916](#)
- Kroll JH; Ng NL; Murphy SM; Flagan RC; Seinfeld JH (2006). Secondary organic aerosol formation from isoprene photooxidation. *Environ Sci Technol*, 40: 1869-1877. [190195](#)
- Krueger AJ; Schaefer SJ; Krotkov N; Bluth G; Barker S (2000). Ultraviolet remote sensing of volcanic emissions. In *Remote Sensing of Active Volcanism* (pp. 25-43). Washington, DC: American Geophysical Union. [192234](#)
- Kruger O; Grasl H (2002). The indirect aerosol effect over Europe. *Geophys Res Lett*, 29: 1925. [190200](#)
- Krupa S; Booker F; Bowersox V; Lehmann CT; Grantz D (2008). Uncertainties in the current knowledge of some atmospheric trace gases associated with U.S. agriculture: A review. *J Air Waste Manag Assoc*, 58: 986-993. [198696](#)
- Kruysse A (1971). Acute inhalation toxicity of acrolein in hamsters. Central Institute for Nutrition and Food Research. The Netherlands. R 3516. [192236](#)
- Kucera T; Horakova H; Sonska A (2008). Toxic metal ions in photoautotrophic organisms. *Photosynthetica*, 46: 481-489. [190408](#)
- Kucharski J; Wyszowska J (2004). Inter-relationship between number of microorganisms and spring barley yield and degree of soil contamination with copper. *Plant Soil Environ*, 50: 243-249. [156662](#)
- Kuki KN; Oliva MA; Costa AC (2009). The simulated effects of iron dust and acidity during the early stages of establishment of two coastal plant species. *Water Air Soil Pollut*, 196: 287-295. [190411](#)

- Kuki KN; Oliva MA; Pereira EG; Costa AC; Cambraia J (2008). Effects of simulated deposition of acid mist and iron ore particulate matter on photosynthesis and the generation of oxidative stress in *Schinus terebinthifolius* Radii and *Sophora tomentosa* L. *Sci Total Environ*, 403: 207-214. [155346](#)
- LaBrecque JJ; Benzo Z; Alfonso JA; Cordoves Manuelita Quintal PR; Gomez CV; Marciano E (2004). The concentrations of selected trace elements in clams, *Trivela mactroidea* along the Venezuelan coast in the state of Miranda. *Mar Pollut Bull*, 49: 659-667. [155913](#)
- Lack DA; Lovejoy ER; Baynard T; Pettersson A; Ravishankara AR (2006). Aerosol Absorption Measurement using Photoacoustic Spectroscopy: Sensitivity, Calibration, and Uncertainty Developments. *Aerosol Sci Technol*, 40: 697 - 708. [096032](#)
- Lakzian A; Murphy P; Turner A; Beynon JL; Giller KE (2002). *Rhizobium leguminosarum* bv. *viciae* populations in soils with increasing heavy metal contamination: abundance, plasmid profiles, diversity and metal tolerance. *Soil Biol Biochem*, 34: 519-529. [156671](#)
- Lambert A; Grainger RG; Remedios JJ; Rodgers CD; Corney M; Taylor FW (1993). Measurements of the evolution of the Mt. Pinatubo aerosol cloud by ISAMS. *Geophys Res Lett*, 20: 1287–1290. [192231](#)
- Lambert MRK (1997). Environmental effects of heavy spillage from a destroyed pesticide store near Hargeisa (Somaliland) assessed during the dry season, using reptiles and amphibians as bioindicators. *Arch Environ Contam Toxicol*, 32: 80–93. [155916](#)
- Landers DH; Simonich SL; Jaffe DA; Geiser LH; Campbell DH; Schwindt AR; Schreck CB; Kent ML; Hafner WD; Taylor HE; Hageman KJ; Usenko S; Ackerman LK; Schrlau JE; Rose NL; Blett TF; Erway MM (2008). The fate, transport, and ecological impacts of airborne contaminants in western national parks (USA). U.S. Environmental Protection Agency, Office of Research and Development, NHEERL, Western Ecology Division. Corvallis, Oregon. EPA/600/R-07/138. http://www.nature.nps.gov/air/studies/air_toxics/WACAPreport.cfm. [191181](#)
- Lanno R; Wells J; Conder J; Bradham K; Basta N (2004). The bioavailability of chemicals in soil for earthworms. *Ecotoxicol Environ Saf*, 57: 39-47. [190415](#)
- Larson VE; Golaz J-C; Jiang H; Cotton WR (2005). Supplying local microphysics parameterizations with information about subgrid variability: Latin hypercube sampling. *J Atmos Sci*, 62: 4010-4026. [190220](#)
- Larson VE; Wood R; Field PR; Golaz J-C (2001). Small-scale and mesoscale variability of scalars in cloudy boundary layers: One-dimensional probability density functions. *J Atmos Sci*, 58: 1978-1996. [190212](#)
- Latimer DA; Ireson RG (1980). Workbook for estimating visibility impairment. U.S. Environmental Protection Agency. Research Triangle Park, NC. EPA-450/4-80-031. [035723](#)
- Lau K-M; Kim K-M (2006). Observational relationships between aerosol and Asian monsoon rainfall, and circulation. *Geophys Res Lett*, 33: L21810. [190226](#)
- Lau K; Kim M; Kim K (2006). Asian summer monsoon anomalies induced by aerosol direct forcing—the role of the Tibetan Plateau. *Clim Dynam*, 36: 855-864. [190223](#)
- Lau KM; Kim KM; Sud YC; Walker GK (2009). A GCM study of the response of the atmospheric water cycle of West Africa and the Atlantic to Saharan dust radiative forcing. *Ann Geophys*, 27: 4023-4037. [190229](#)
- Law RJ; Alaee M; Allchin CR; Boon JP; Lebeuf M; Lepom P; Ster GA (2003). Levels and trends of polybrominated diphenylethers and other brominated flame retardants in wildlife. *Environ Int*, 29: 757-770. [190420](#)
- Lawson ST; Scherbatskoy TD; Malcolm EG; Keeler GJ (2003). Cloud water and throughfall deposition of mercury and trace elements in a high elevation spruce-fir forest at Mt Mansfield, Vermont. *J Environ Monit*, 5: 578-583. [089371](#)
- Leahy L; Anderson T; Eck T; Bergstrom R (2007). A synthesis of single scattering albedo of biomass burning aerosol over southern Africa during SAFARI 2000. *Geophys Res Lett*, 34: L12814. [190232](#)
- Leaith WR; Banic CM; Isaac GA; Couture MD; Liu PSK; Gultepe I; Li S-M; Kleinman L; Daum PH; MacPherson JI (1996). Physical and chemical observations in marine stratus during the 1993 North Atlantic Regional Experiment: Factors controlling cloud droplet number concentrations. *J Geophys Res*, 101: 29123-29135. [190354](#)
- Leaith WR; Isaac GA; Strapp JW; Banic CM; Wiebe HA (1992). The relationship between cloud droplet number concentrations and anthropogenic pollution: observations and climatic implications. *J Geophys Res*, 97: 2463-2474. [045270](#)

- LeBlanc GA (1995). Trophic-level differences in the bioconcentration of chemicals: Implications in assessing environmental biomagnification. *Environ Sci Technol*, 29: 154-160. [155921](#)
- Lee JK (2006). Toxicity and tissue distribution of magnetic nanoparticles in mice [erratum]. *Toxicol Sci*, 90: 267. [088968](#)
- Lee T; Yu XY; Ayres B; Kreidenweis SM; Malm WC; Collett JL (2008). Observations of fine and coarse particle nitrate at several rural locations in the United States. *Atmos Environ*, 42: 2720-2732. [156686](#)
- Lee TE; Miller SD; Turk FJ; Schueler C; Julian R; Deyo S; Dills P; Wang S (2006). The NPOESS VIIRS day/night visible sensor. *Bull Am Meteorol Soc*, 87: 191-199. [190358](#)
- Lei YD; Wania F (2004). Is rain or snow a more efficient scavenger of organic chemicals? *Atmos Environ*, 38: 3557-3571. [127880](#)
- Lelieveld J; Berresheim H; Borrmann S; Crutzen PJ; Dentener FJ; Fischer H; Feichter J; Flatau PJ; Heland J; Holzinger R; Korrmann R; Lawrence MG; Levin Z; Markowicz KM; Mihalopoulos N; Minikin A; Ramanathan V; De Reus M; Roelofs GJ; Scheeren HA; Sciare J; Schlager H; Schultz M; Siegmund P; Steil B; Stephanou EG; Stier P; Traub M; Warneke C; Williams J; Ziereis H (2002). Global air pollution crossroads over the Mediterranean. *Science*, 298: 794-799. [190361](#)
- Léon J; Tanré D; Pelon J; Kaufman Y; Haywood J; Chatenet B (2003). Profiling of a Saharan dust outbreak based on a synergy between active and passive remote sensing. *J Geophys Res*, 108: 8575. [190366](#)
- Levin Z; Cotton WR (2008). Report from the WMO/ IUGG International Aerosol Precipitation Science, Assessment Group (IAPSAG). In *Aerosol pollution impact on precipitation: A scientific review* (pp. 482). Geneva, Switzerland: World Meteorological Organization. [190375](#)
- Levine JS; Pinto JP (1998). The production of CO by biomass burning. Presented at Proceedings of the International Conference on Atmospheric Carbon Monoxide and Its Environmental Effects, Washington, DC. [029599](#)
- Levy R; Remer L; Dubovik O (2007). Global aerosol optical properties and application to MODIS aerosol retrieval over land. *J Geophys Res*, 112: D13210. [190377](#)
- Levy R; Remer L; Mattoo S; Vermote E; Kaufman Y (2007). Second-generation algorithm for retrieving aerosol properties over land from MODIS spectral reflectance. *J Geophys Res*, 112: D13211. [190379](#)
- Lewis ER; Schwartz SE (2004). Sea salt aerosol production: Mechanisms, methods, measurements and models: A critical review. Washington, DC: American Geophysical Union. [192023](#)
- Li R-R; Kaufman YJ; Hao WM; Salmon JM; Gao B-C (2004). A technique for detecting burn scars using MODIS data. *IEEE Trans Geosci Remote Sens*, 42: 1300-1308. [190386](#)
- Li Y-F; MacDonald RW; Jantunen LMM; Harner T; Bidleman TF; Stachen WMJ (2002). The transport of β -hexachlorocyclohexane to the western Arctic Ocean: a contrast to α HCH. *Sci Total Environ*, 291: 229-246. [156691](#)
- Li Z; Chen H; Cribb M; Dickerson R; Holben B; Li C; Lu D; Luo Y; Maring H; Shi G; Tsay S-C; Wang P; Wang Y; Xia X; Zheng Y; Yuan T; Zhao F (2007). Preface to special section on East Asian studies of tropospheric aerosols: An international regional experiment (EAST-AIRE). *J Geophys Res*, 112: D22S00. [190392](#)
- Liao H; Seinfeld JH (2005). Global impacts of gas-phase chemistry/aerosol interactions on direct radiative forcing by anthropogenic aerosols and ozone. *J Geophys Res*, 110: D18208. [199892](#)
- Lin CJ; Pehkonen SO (1999). The chemistry of atmospheric mercury: a review. *Atmos Environ*, 33: 2067-2070. [190426](#)
- Lin H; Tao S; Zuo Q; Coveney RM (2007). Uptake of polycyclic aromatic hydrocarbons by maize plants. *Environ Pollut*, 148: 614-619. [155933](#)
- Lindberg SE; Brooks S; Linn CJ; Scott KJ; Landis MS; Stevens RK; Goodsite M; Richter A (2002). Dynamic oxidation of gaseous mercury in the Arctic troposphere at polar sunrise. *Environ Sci Technol*, 36: 1245-1256. [190429](#)
- Lindesay JA; Andreae MO; Goldammer JG; Harris G; Annegarn HJ; Garstang M; Scholes RJ; van Wilgen BW (1996). International Geosphere Biosphere Programme/International Global Atmospheric Chemistry SAFARI-92 field experiment: Background and overview. *J Geophys Res*, 23521-23530: 101. [190403](#)
- Lingua G; Franchin C; Todeschini V; Castiglione S; SBiondi; Burlando B; Parravicini V; PTorrigiani; GBerta (2008). Arbuscular mycorrhizal fungi differentially affect the response to high zinc concentrations of two registered poplar clones. *Environ Pollut*, 153: 137-147. [155935](#)

- Liou KN; Ou S-C (1989). The role of cloud microphysical processes in climate: an assessment from a one-dimensional perspective. *J Geophys Res*, 94: 8599-8607. [190407](#)
- Liousse C; Penner JE; Chuang C; Walton JJ; Eddleman H; Cachier H (1996). A global three-dimensional model study of carbonaceous aerosols. *J Geophys Res*, 101: 19,411-19,432. [078158](#)
- Liu H; Pinker R; Holben B (2005). A global view of aerosols from merged transport models, satellite, and ground observations. *J Geophys Res*, 110: D10S15. [190414](#)
- Liu J; Ballaney M; Al-Alem U; Quan C; Jin X; Perera F; Chen LC; Miller RL (2008). Combined Inhaled Diesel Exhaust Particles and Allergen Exposure Alter Methylation of T Helper Genes and IgE Production In Vivo. *Toxicol Sci*, 102: 76-81. [156709](#)
- Liu L; Lacis AA; Carlson BE; Mishchenko MI; Cairns B (2006). Assessing Goddard Institute for Space Studies ModelE aerosol climatology using satellite and ground-based measurements. *J Geophys Res*, 111: D20212. [190422](#)
- Liu X; Penner J; Das B; Bergmann D; Rodriguez J; Strahan S; Wang M; Feng Y (2007). Uncertainties in global aerosol simulations: Assessment using three meteorological data sets. *J Geophys Res*, 112: D11212. [190427](#)
- Liu Y; Koutrakis P (2007). Estimating Fine Particulate Matter Component Concentrations and Size Distributions Using Satellite- Retrieved Fractional Aerosol Optical Depth: Part I—Method Development. *J Air Waste Manag Assoc*, 57: 1351-1359. [187007](#)
- Liu Y; Koutrakis P; Kahn R; Turquety S; Yantosca RM (2007). Estimating fine particulate matter component concentrations and size distributions using satellite-retrieved fractional aerosol optical depth: part 2--a case study. *J Air Waste Manag Assoc*, 57: 1360-9. [098197](#)
- Loeb N; Kato S (2002). Top-of-atmosphere direct radiative effect of aerosols over the tropical oceans from the Clouds and the Earth's Radiant Energy System (CERES) satellite instrument. *PNAS*, 15: 1474-1484. [190432](#)
- Loeb N; Manalo-Smith N (2005). Top-of-Atmosphere direct radiative effect of aerosols over global oceans from merged CERES and MODIS observations. *J Clim*, 18: 3506-3526. [190433](#)
- Loeb NG; Kato S; Loukachine K; Smith NM (2005). Angular distribution models for top-of-atmosphere radiative flux estimation from the Clouds and the Earth's Radiant Energy System instrument on the Terra Satellite. part I: Methodology. *J Atmos Ocean Tech*, 22: 338-351. [190436](#)
- Lohman U; Feichter J (2005). Global indirect aerosol effects: a review. *Atmos Chem Phys*, 5: 715-737. [155942](#)
- Lohmann U; Feichter J; Chuang CC; Penner JE (1999). Prediction of the number of cloud droplets in the ECHAM GCM. *J Geophys Res*, 104: 9169-9198. [190443](#)
- Lohmann U; Feichter J; Penner JE; Leaitch WR (2000). Indirect effect of sulfate and carbonaceous aerosols: A mechanistic treatment. *J Geophys Res*, 105: 12193-12206. [199910](#)
- Lohmann U; Koren I; Kaufman YJ (2006). Disentangling the role of microphysical and dynamical effects in determining cloud properties over the Atlantic. *Geophys Res Lett*, 33: L09802. [190451](#)
- Lohmann U; Leaitch WR; Barrie L; Law K; Yi Y; Bergmann D; Bridgeman C; Chin M; Christensen J; Easter R; Feichter J; Jeuken A; Kjellstrom E; Koch D; Land C; Rasch P; Roelofs GJ (2001). Vertical distributions of sulfur species simulated by large scale atmospheric models in COSAM: comparison with observations. *Tellus B Chem Phys Meteorol*, 53: 646 - 672. [190448](#)
- López Alonso M; Benedito JL; Miranda M; Castillo C; Hernández J; Shore RF (2002). Cattle as biomonitors of environmental semi-metal and trace metal concentrations in Galicia (NW Spain). *Arch Environ Contam Toxicol*, 43: 103-108. [155943](#)
- López Alonso M; Benedito JL; Miranda M; Castillo C; Hernández J; Shore RF (2003). Mercury concentrations in cattle from NW Spain. *Sci Total Environ*, 302: 93-100. [155945](#)
- López Alonso M; Benedito JL; Miranda M; Fernández JA; Castillo C; Hernández J; Shore RF (2003). Large-scale spatial variation in mercury concentrations in cattle in NW Spain. *Environ Pollut*, 125: 173-181. [155944](#)
- Lorusso S; Marabelli M; Troili M (1997). Air pollution and the deterioration of historic monuments. *J Environ Pathol Toxicol Oncol*, 16: 171-173. [084534](#)
- Lowenthal DH; Kumar N (2003). PM2.5 mass and light extinction reconstruction in IMPROVE. *J Air Waste Manag Assoc*, 53: 1109-1120. [156712](#)

- Lowenthal DH; Rogers CF; Saxena P; Watson JG; Chow JC (1995). Sensitivity of estimated light extinction coefficients to model assumptions and measurement errors. *Atmos Environ*, 29: 751-766. [045134](#)
- Lu M-L; Feingold G; Jonsson H; Chuang P; Gates H; Flagan RC; Seinfeld JH (2008). Aerosol-cloud relationships in continental shallow cumulus. *J Geophys Res*, 113: D15201. [190455](#)
- Lubin D; Vogelmann AM (2006). A climatologically significant aerosol longwave indirect effect in the Arctic. *Nature*, 439: 453-456. [190466](#)
- Lubin DS; Satheesh S; McFarquar G; Heymsfield A (2002). Longwave radiative forcing of Indian Ocean tropospheric aerosol. *J Geophys Res*, 107: 8004. [190463](#)
- Lucaciu A; Timofte L; Culicov O; Frontasyeva MV; Oprea C; Cucu-Man S; Mocanu R; Steinnes E (2004). Atmospheric deposition of trace elements in Romania studied by the moss biomonitoring technique. *J Atmos Chem*, 49: 533-548. [155947](#)
- Lunácková L; Masarovicová E; Kráová K; Stresko V (2003). Response of fast growing woody plants from family Salicaceae to cadmium treatment. *Bull Environ Contam Toxicol*, 70: 576-585. [155948](#)
- Luo Y; Lu D; Zhou X; Li W; He Q (2001). Characteristics of the spatial distribution and yearly variation of aerosol optical depth over China in last 30 years. *J Geophys Res*, 106: 14501. [190467](#)
- Mace BL; Bell PA; Loomis RJ (2004). Visibility and Natural Quiet in National Parks and Wilderness Areas: Psychological Considerations. *Environ Behav*, 36: 5-31. [180255](#)
- Mackay D (1991). Multimedia environmental models: the fugacity approach. Chelsea, MI: Lewis Publishers. [042941](#)
- Macleod M; McKone TE; Mackay D (2005). Mass balance for mercury in the San Francisco Bay area. *Environ Sci Technol*, 39: 6721-6729. [155954](#)
- Madrid L; Diaz-Barrientos E; Madrid F (2002). Distribution of heavy metal contents of urban soils in parks of Seville. *Chemosphere*, 49: 1301-1309. [155956](#)
- Magi B; Hobbs P; Kirchstetter T; Novakov T; Hegg D; Gao S; Redemann J; Schmid B (2005). Aerosol properties and chemical apportionment of aerosol optical depth at locations off the United States East Coast in July and August 2001. *J Atmos Sci*, 62: 919-933. [190468](#)
- Malkönen E; Derome J; Fritze H; Helmissaari H-S; Kukkola M; Kytö M; Saarsalmi A; Salemaa M (1999). Compensatory fertilization of Scots pine stands polluted by heavy metals. *Nutr Cycling Agroecosyst*, 55: 239-268. [155961](#)
- Malm W; Bell P; McGlothin GE (1984). Field testing a methodology for assessing the importance of good visual air quality. Presented at Air Pollution Control Association, June, 1984, San Francisco, CA. [044292](#)
- Malm WC (1999). Introduction to visibility. Cooperative Institute for Research in the Atmosphere. Fort Collins, CO. [025037](#)
- Malm WC; Day DE (2001). Estimates of aerosol species scattering characteristics as a function of relative humidity. *Atmos Environ*, 35: 2845-2860. [190431](#)
- Malm WC; Day DE; Kreidenweis SM; Collett JL; Lee T (2003). Humidity dependent optical properties of fine particle during the Big Bend Regional Aerosol and Visibility Observational Study (BRAVO). *J Geophys Res*, 108: 4279. [190434](#)
- Malm WC; Hand JL (2007). An examination of the physical and optical properties of aerosols collected in the IMPROVE program. *Atmos Environ*, 41: 3407-3427. [155962](#)
- Malm WC; Pitchford ML (1997). Comparison of calculated sulfate scattering efficiencies as estimated from size-resolved particle measurements at three national locations. *Atmos Environ*, 31: 1315-1325. [002519](#)
- Malm WC; Pitchford ML; McDade C; Ashbaugh LL (2007). Coarse particle speciation at selected locations in the rural continental United States. *Atmos Environ*, 41: 2225-2239. [156730](#)
- Malm WC; Schichtel BA; Ames RB; Gebhart KA (2002). A ten-year spatial and temporal trend of sulfate across the United States. *J Geophys Res*, 107: 4627. [156727](#)
- Malm WC; Schichtel BA; Pitchford ML; Ashbaugh LL; Eldred RA (2004). Spatial and monthly trends in speciated fine particle concentration in the United States. *J Geophys Res*, 109: 3306. [156728](#)

- Malm WC; Trijonis J; Sisler J; Pitchford M; Dennis RL (1994). Assessing the effect of SO₂ emission changes on visibility. *Atmos Environ*, 28: 1023-1034. [044920](#)
- Marinoni N; Birelli MP; Rostagno C; Pavese A (2003). The effects of atmospheric multipollutants on modern concrete. *Atmos Environ*, 37: 4701-4712. [092520](#)
- Markiewicz Patkowska J; Hursthouse A; Przybyla-Kij H (2005). The interaction of heavy metals with urban soils: sorption behaviour of Cd, Cu, Cr, Pb and Zn with a typical mixed brownfield deposit. *Environ Int*, 31: 513–521. [155963](#)
- Martin MH; Coughtrey PJ (1981). Impact of metals on ecosystem function and productivity. In Lepp, N. W. (Ed.), *Effect of heavy metal pollution on plants: volume 2, metals in the environment* (pp. 119-158). Barking, United Kingdom: Applied Science Publishers. [047727](#)
- Martins J; Tanré D; Remer L; Kaufman Y; Mattoo S; Levy R (2002). MODIS cloud screening for remote sensing of aerosol over oceans using spatial variability. *Geophys Res Lett*, 29: MOD4. [190470](#)
- Martonchik J; Diner D; Crean K; Bull M (2002). Regional aerosol retrieval results from MISR. *IEEE Trans Geosci Remote Sens*, 40: 1520-1531. [190490](#)
- Martonchik J; Diner D; Pinty B; Verstraete M; Myneni R; Knjazikhin Y; Gordon H (1998). Determination of land and ocean reflective, radiative, and biophysical properties using multiangle imaging. *IEEE Trans Geosci Remote Sens*, 36: 1266-1281. [190484](#)
- Martonchik JD; Diner D; Kahn R; Verstraete M; Pinty B; Gordon H; Ackerman T (1998). Techniques for the Retrieval of aerosol properties over land and ocean using multiangle data. *IEEE Trans Geosci Remote Sens*, 36: 1212-1227. [190472](#)
- Masclet PP; Hoyau V; Jaffrezo JL; Cachier H (2000). Polycyclic aromatic hydrocarbons deposition on the ice sheet of Greenland. Part I. Superficial snow. *Atmos Environ*, 34: 3195-3207. [155966](#)
- Massicotte R; Robidoux PY; Sauve S; Flipo D; Fournier M; Trottier B (2003). Immune response of earthworms (*Lumbricus terrestris*, *Eisenia andrei* and *Aporrectodea tuberculata*) following in situ soil exposure to atmospheric deposition from a cement factory. *J Environ Monit*, 5: 774-779. [155968](#)
- Massie S; Torres O; Smith S (2004). Total ozone mapping spectrometer (TOMS) observations of increases in Asian aerosol in winter from 1979 to 2000. *J Geophys Res*, 109: D18211. [190492](#)
- Matheson MA; Coakley JA; Tahnk WR (2005). Aerosol and cloud property relationships for summertime stratiform clouds in the northeastern Atlantic from Advanced Very High Resolution Radiometer observations. *J Geophys Res*, 110: D24204. [190494](#)
- Matsui T; Masunaga H; Kreidenweis SM; Pielke RA; Tao W-K; Chin M; Kaufman YJ (2006). Satellite-based assessment of marine low cloud variability associated with aerosol, atmospheric stability, and the diurnal cycle. *J Geophys Res*, 111: D17204. [190498](#)
- Matsui T; Pielke R; (2006). Measurement-based estimation of the spatial gradient of aerosol radiative forcing. *Geophys Res Lett*, 33: L11813. [190495](#)
- Matthias I; Ansmann A; Müller D; Wandinger U; Althausen D (2004). Multiyear aerosol observations with dual wavelength Raman lidar in the framework of EARLINET. *J Geophys Res*, 109: 1-15. [155971](#)
- Mayo JM; Legge AH; Yeung EC; Krupa SV; Bogner JC (1992). The effects of sulphur gas and elemental sulphur dust deposition on *Pinus contorta* x *Pinus banksiana*: Cell walls and water relations. *Environ Pollut*, 76: 43-50. [155974](#)
- McComiskey A; Feingold G (2008). Quantifying error in the radiative forcing of the first aerosol indirect effect. *Geophys Res Lett*, 35: L20810. [190517](#)
- McComiskey A; Feingold G; Frisch AS; Turner D; Miller M; Chiu JC; Min Q; Ogren JA (2008). An assessment of aerosol-cloud interactions in marine stratus clouds based on surface remote sensing. *J Geophys Res*, 114: D09203. [190525](#)
- McComiskey A; Schwartz SE; Schmid B; Guan H; Lewis ER; Ricchiuzzi P; Ogren JA (2008). Direct aerosol forcing: Calculation from observables and sensitivity to inputs. *J Geophys Res*, 113: D09202. [190523](#)
- McCormick M; Trepte C (1987). Polar stratospheric optical depth observed between 1978 and 1985. *J Geophys Res*, 92: 4297-4306. [192328](#)
- McCormick R; Ludwig J (1967). Climate modification by atmospheric aerosols. *Science*, 9: 1358 - 1359. [190528](#)

- McDade C (2004). Summary of IMPROVE nitrate measurements. Retrieved 29-JUL-09, from http://vista.cira.colostate.edu/improve/publications/GrayLit/gray_literature.htm. [192075](#)
- McFiggans G; Artaxo P; Baltensperger U; Coe H; Facchini MC; Feingold G; Fuzzi S; Gysel M; Laaksonen A; Lohmann U; Mentel TF; Murphy DM; O'Dowd CD; Snider JR; Weingartner E (2006). The effect of physical and chemical aerosol properties on warm cloud droplet activation. *Atmos Chem Phys*, 6: 2593-2649. [190532](#)
- McGowan TF; Lipinski GE; Santoleri JJ (1993). New rules affect the handling of waste fuels. *Chem Eng*, 100: 122-128. [046731](#)
- McMurry PH (2000). A review of atmospheric aerosol measurements. *Atmos Environ*, 34: 1959-1999. [081517](#)
- Meehl GA; Washington WM; Ammann CM; Arblaster JM; Wigley TML; Tebaldi C (2004). Combinations of natural and anthropogenic forcings in twentieth-century climate. *J Clim*, 17: 3721-3727. [192279](#)
- Meers E; Vangronsveld J; Tack FMG; Vandecasteele B; Ruttens A (2007). Potential of five willow species (*Salix* spp.) for phytoextraction of heavy metals. *Environ Exp Bot*, 60: 57-68. [155977](#)
- Melnikov S; Carroll J; Gorshkov A; Vlasov S; Dahle S (2003). Snow and ice concentrations of selected persistent organic pollutants in the Ob-Yenisey River watershed. *Sci Total Environ*, 306: 27-37. [156753](#)
- Memon AR; Schroder P (2009). Implications of metal accumulation mechanisms to phytoremediation. *Environ Sci Pollut Res Int*, 16: 162-175. [190442](#)
- Menon S; Del Genio AD; Kaufman Y; Bennartz R; Koch D; Loeb N; Orlikowski D (2008). Analyzing signatures of aerosol cloud interactions from satellite retrievals and the GISS GCM to constrain the aerosol indirect effect. *J Geophys Res*, 113: D14S22. [190534](#)
- Menon S; Hansen J; Nazarenko L; Luo Y (2002). Climate effects of black carbon aerosols in China and India. *Science*, 297: 2250-2253. [155978](#)
- Mercado LM; Bellouin N; Sitch S; Boucher O; Huntingford C; Wild M; Cox PM (2009). Impact of changes in diffuse radiation on the global land carbon sink. *Nature*, 458: 1014-U1087. [190444](#)
- Michalsky J; Schlemmer J; Berkheiser W; (2001). Multiyear measurements of aerosol optical depth in the Atmospheric Radiation Measurement and Quantitative Links program. *J Geophys Res*, 106: 12099-12108. [190537](#)
- Middleton WEK (1952). *Vision through the atmosphere*. Toronto, ON, Canada: University of Toronto Press. [016324](#)
- Mie G (1908). Beiträge zur Optik trüber Medien, speziell kolloidaler Metallösungen. *Ann Phys*, 330: 377-445. [155983](#)
- Miller RL; Schmidt GA; Shindell DT (2005). Forced annular variations in the 20th century Intergovernmental Panel on Climate Change Fourth Assessment Report models. *J Geophys Res*, 111: D18101. [192258](#)
- Millhollen AG; Gustin MS; Obrist D (2006). Foliar mercury accumulation and exchange for three tree species. *Environ Sci Technol*, 40: 6001-6006. [190447](#)
- Min Q; Harrison LC (1996). Cloud properties derived from surface MFRSR measurements and comparison with GEOS results at the ARM SGP site. *Geophys Res Lett*, 23: 1641- 1644. [190538](#)
- Ming Y; Ramaswamy V; Ginoux PA; Horowitz LW; Russell LM (2005). Geophysical Fluid Dynamics Laboratory general circulation model investigation of the indirect radiative effects of anthropogenic sulfate aerosol. *J Geophys Res*, 110: D22206. [199909](#)
- Minnis P; Harrison EF; Stowe LL; Gibson GG; Denn FM; Doelling DR; Smith WL Jr (1993). Radiative Climate Forcing by the Mount Pinatubo Eruption. *Science*, 259: 1411-1415. [190539](#)
- Mischenko M; Cairns B; Kopp G; Schueler CF; Fafaul BA; Hansen JE; Hooker RJ; Itchkawich T; Maring HB; Travis LD (2007). Accurate monitoring of terrestrial aerosols and total solar irradiance. *Bull Am Meteorol Soc*, 88: 677-691. [190543](#)
- Mishchenko MI; Geogdzhayev IV (2007). Satellite remote sensing reveals regional tropospheric aerosol trends. *Optics Express*, 15: 7423-7438. [190545](#)
- Mishchenko MI; Geogdzhayev IV; Cairns B; Rossow WB; Lacis AA (1999). Aerosol retrievals over the ocean by use of channels 1 and 2 AVHRR data: sensitivity analysis and preliminary results. *Appl Opt*, 38: 7325-7341. [190541](#)
- Mishchenko MI; Geogdzhayev IV; Rossow WB; Cairns B; Carlson BE; Lacis AA; Liu L; Travis LD (2007). Long-term satellite record reveals likely recent aerosol trend. *Science*, 315: 1543. [190542](#)

- Mitchell JM Jr (1971). The effect of atmospheric aerosols on climate with special reference to temperature near the Earth's surface. *J Appl Meteorol*, 10: 703-714. [190546](#)
- Molina LT; Madronich S; Gaffney JS; Singh HB (2008). Overview of MILAGRO/INTEX-B Campaign. International Global Atmospheric Chemistry (Newsletter). Seattle, WA. http://www.igac.noaa.gov/newsletter/igac38/Apr_2008_IGAC_38.pdf. [192019](#)
- Moody E; King M; Platnick S; Schaaf C; Gao F (2005). Spatially complete global spectral surface albedos: value-added datasets derived from Terra MODIS land products. *IEEE Trans Geosci Remote Sens*, 43: 144-158. [190548](#)
- Moosmuller H; Arnott WP; Rogers CF (1998). Photoacoustic and filter measurements related to aerosol light absorption during the Northern Front Range Air Quality Study (Colorado 1996/1997). *J Geophys Res*, 103: 28,149-28,157. [020657](#)
- Moropoulou A; Bisbikou K; Torfs K; Van Grieken R; Zezza F; Macri F (1998). Origin and growth of weathering crusts on ancient marbles in industrial atmosphere. *Atmos Environ*, 32: 967-982. [040485](#)
- Moses CA; Smith BJ (1994). Limestone weathering in the supratidal zone: an example from Mallorca. In DA Robinson; RBG Williams (Ed.), *Rock weathering and landform evolution* (pp. 432-451). Chichester, West Sussex, United Kingdom: John Wiley & Sons. [156785](#)
- Mosley-Thompson E; Mashiotta TA; Thompson LG (2003). High resolution ice core records of Late Holocene volcanism: Current and future contributions from the Greenland PARCA cores. In *Volcanism and the Earth's Atmosphere* (pp. 153-164). Washington, DC: American Geophysical Union. [192255](#)
- Mouillot F; Narasimha A; Balkanski Y; Lamarque J-F (2006). Global carbon emissions from biomass burning in the 20th century. *Geophys Res Lett*, 33: L01801. [190549](#)
- Muir DCG; Omelchenko A; Grift NP; Savoie DA; Lockhart WL; Wilkinson P; Brunskill GJ (1996). Spatial trends and historical deposition of polychlorinated biphenyls in Canadian midlatitude and arctic lake sediments. *Environ Sci Technol*, 30: 3609-3617. [155991](#)
- Murayama T; Sugimoto N; Uno I; Kinoshita K; Aoki K; Hagiwara N; Liu Z; Matsui I; Sakai T; Shibata T; Arai K; Sohn B-J; Won J-G; Yoon S-C; Li T; Zhou J; Hu H; Abo M; Iokibe K; Koga R; Iwasaka Y (2001). Ground-based network observation of Asian dust events of April 1998 in East Asia. *J Geophys Res*, 106: 18345-18360. [155992](#)
- Murdoch JC; Thayer MA (1988). Hedonic price estimation of variable urban air quality. *J Environ Econ Manage*, 15: 143-146. [156788](#)
- Naidoo G; Chirkoot D (2004). The effects of coal dust on photosynthetic performance of the mangrove, *Avicennia marina* in Richards Bay, South Africa. *Environ Pollut*, 127: 359-366. [190449](#)
- Nakajima T; Higurashi A; Kawamoto K; Penner JE (2001). A possible correlation between satellite-derived cloud and aerosol microphysical parameters. *Geophys Res Lett*, 28: 1171-1174. [190552](#)
- Nakamura K; Nakawo M; Ageta Y; Goto-Azuma K; Kamiyam K (2000). Post-depositional loss of nitrate in surface snow layers of the Antarctic ice sheet. *Bull. Glaciol. Res.*, 17: 11-16. [156792](#)
- Nash TH (1975). Influence of effluents from a zinc factory on lichens. *Ecol Monogr*, 45: 183-198. [016763](#)
- Nazaroff WW; Cass GR (1991). Protecting museum collections from soiling due to the deposition of airborne particles. *Atmos Environ*, 25: 841-852. [044577](#)
- NCDENR (2007). Technical Analyses Supporting Regional Haze State Implementation Plan. , North Carolina Department of Environment and Natural Resources. NC. [156798](#)
- NESCAUM (2006). Regional Aerosol Intensive Network (RAIN) Preliminary Data Analysis. Northeast States for Coordinated Air Use Management. Boston, MA. <http://www.nescaum.org/documents/2006-05-memo8-rain.pdf>. [156802](#)
- Nguyen HL; Leermakers M; Elskens M; De Ridder F; Doan TH; Baeyens W (2005). Correlations, partitioning and bioaccumulation of heavy metals between different compartments of Lake Balaton. *Sci Total Environ*, 341: 211-226. [155997](#)
- Nicholson L; Benn DI (2006). Calculating ice melt beneath a debris layer using meteorological data. *J Glaciol*, 52: 463-470. [156806](#)

- Nieminen T; Derome J; Helmisaari H-S (1999). Interactions between precipitation and Scots pine canopies along a heavy-metal pollution gradient. *Environ Pollut*, 106: 129–137. [155998](#)
- Nogueira MA; Magalhaes GC; Cardoso EJBN (2004). Manganese toxicity in mycorrhizal and phosphorus-fertilized soybean plants. *J Plant Nutr*, 27: 141-156. [190460](#)
- Norris J; Wild M (2007). Trends in aerosol radiative effects over Europe inferred from observed cloud cover, solar “dimming”, and solar “brightening”. *J Geophys Res*, 112: D08214. [190555](#)
- Notten MJM; Oosthoek AJP; Rozema J; Aerts R (2005). Heavy metal concentrations in a soil-plant-snail food chain along a terrestrial soil pollution gradient. *Environ Pollut*, 138: 178-190. [190461](#)
- Novakov T; Ramanathan V; Hansen JE; Kirchstetter TW; Sato M; Sinton JE; Sathaye JA (2003). Large historical changes of fossil-fuel black carbon aerosols. *Geophys Res Lett*, 30: 1-4. [048398](#)
- NRC (2001). *Climate change science: an analysis of some key questions*. National Research Council. National Academy Press. Washington, DC. [053303](#)
- NRC (2005). *Radiative forcing of climate change: expanding the concept and addressing uncertainties*. Washington DC: National Research Council; The National Academies Press. [057409](#)
- O'Dowd C; McFiggans G; Creasey DJ; Pirjola L; Hoell C; Smith MH; Allan BJ; Plane JMC; Heard DE; Lee JD; Pilling MJ; Kulmala M (1999). On the photochemical production of new particles in the coastal boundary layer. *Geophys Res Lett*, 26: 1707-1710. [090414](#)
- O'Neill NT; Eck TF; Smirnov A; Holben BN; Thulasiraman S (2003). Spectral discrimination of coarse and fine mode optical depth. *J Geophys Res*, 108: 4559. [180187](#)
- Odum EP (1985). Trends expected in stressed ecosystems. *Bioscience*, 35: 419-422. [039482](#)
- Odum EP (1993). Major ecosystem types of the world. In Odum, E. P. (Ed.), *Ecology and our endangered life-support systems*. Sunderland, MA: Sinauer Associates, Inc. [076742](#)
- Oehme M; Biseth A; Schlabach M; Wiig O (1995). Concentrations of polychlorinated dibenzo-p-dioxins, dibenzofurans and non-ortho substituted biphenyls in polar bear milk from Svalbard (Norway). *Environ Pollut*, 90: 401-407. [011267](#)
- Oehme M; Haugen J-E; Schlabach M (1996). Seasonal changes and relation between levels of organochlorines in Arctic ambient air: First results from an all-round-year monitoring program at Ny-Ålesund, Norway. *Environ Sci Technol*, 30: 2294-2304. [156001](#)
- Ohyama K; Angermann J; Dunlap DY; Matsumura F (2004). Distribution of polychlorinated biphenyls and chlorinated pesticide residues in trout in the Sierra Nevada. *J Environ Qual*, 33: 1752-1764. [190462](#)
- Oliveira A; Pampulha ME (2006). Effects of long-term heavy metal contamination on soil microbial characteristics. *J Biosci Bioeng*, 102: 157-161. [156827](#)
- Ormrod DP (1984). Impact of trace element pollution on plants. In Treshow, M. (Ed.), *Air pollution and plant life* (pp. 291-314). Chichester, United Kingdom: John Wiley & Sons Ltd. [046892](#)
- Otnyukova T (2007). Epiphytic lichen growth abnormalities and element concentrations as early indicators of forest decline. *Environ Pollut*, 146: 359-365. [156009](#)
- Otvos E; Pazmandi T; Tuba Z (2003). First national survey of atmospheric heavy metal deposition in Hungary by the analysis of mosses. *Sci Total Environ*, 309: 151-160. [156831](#)
- Ouimette JR; Flagan RC (1982). The extinction coefficient of multicomponent aerosols. *Atmos Environ*, 16: 2405-2420. [025047](#)
- Ozdilek HG; Mathisen PP; Pellegrino D (2007). Distribution of heavy metals in vegetation surrounding the Blackstone River, USA: Considerations regarding sediment contamination and long term metals transport in freshwater riverine ecosystems. *J Environ Biol*, 28: 493-502. [156010](#)
- Pacheco AMG; Freitas MC (2004). Are lower epiphytes really that better than higher plants for indicating airborne contaminants? An insight into the elemental contents of lichen thalli and tree bark by INAA. *Journal of Radioanal Chem*, 259: 27-33. [156011](#)

- Padmavathiamma PK; Li LY (2007). Phytoremediation technology: Hyper-accumulation metals in plants. *Water Air Soil Pollut*, 184: 105-126. [190465](#)
- Palmer AS; Morgan VI; Curran MAJ; van Ommen TD; Mayewski PA (2002). Antarctic volcanic flux ratios from Law Dome ice cores. *Ann Glaciol*, 35: 329-332. [192319](#)
- Park RJ; Jacob DJ; Kumar N; Yantosca RM (2006). Regional visibility statistics in the United States: Natural and transboundary pollution influences, and implications for the regional haze rule. *Atmos Environ*, 40: 5405-5423. [190469](#)
- Parrish ZD; White JC; Isleyen M; Gent MPN; Iannucci-Berger W; Eitzer BD; Kelsey JW; Mattina MI (2006). Accumulation of weathered polycyclic aromatic hydrocarbons (PAHs) by plant and earthworm species. *Chemosphere*, 64: 609-618. [156014](#)
- Patadia F; Gupta P; Christopher SA (2008). First observational estimates of global clear-sky shortwave aerosol direct radiative effect over land. *J Geophys Res*, 35: L04810. [190558](#)
- Patra M; Bhowmik N; Bandopadhyay B; Sharma A (2004). Comparison of mercury, lead and arsenic with respect to genotoxic effects on plant systems and the development of genetic tolerance. *Environ Exp Bot*, 52: 199-223. [081976](#)
- Pennanen T; Frostegård Å; Fritze H; Bååth E (1996). Phospholipid fatty acid composition and heavy metal tolerance of soil microbial communities along two heavy metal-polluted gradients in coniferous forests. *Appl Environ Microbiol*, 62: 420-428. [156016](#)
- Penner J; Quaas J; Storelvmo T; Takemura T; Boucher O; Guo H; Kirkevåg A; Kristjansson JE; Seland O (2006). Model intercomparison of indirect aerosol effects. *Atmos Chem Phys*, 6: 3391-3405. [190564](#)
- Penner JE (2003). Comment on "Control of fossil-fuel particulate black carbon and organic matter, possibly the most effective method of slowing global warming. *J Geophys Res*, 108: 4771. [156851](#)
- Penner JE; Dickinson RE; O'Neill CA (1992). Effects of aerosol from biomass burning on the global radiation budget. *Science*, 256: 1432-1433. [045825](#)
- Penner JE; Eddleman H; Novakov T (1993). Towards the development of a global inventory for black carbon emissions. *Atmos Environ*, 27: 1277-1295. [045457](#)
- Penner JE; Zhang SY; Chin M; Chuang CC; Feichter J; Feng Y; Geogdzhayev IV; Ginoux P; Herzog M; Higurashi A; Koch D; Land C; Lohmann U; Mishchenko M; Nakajima T; Pitari G; Soden B; Tegen I; Stowe L (2002). A comparison of model- and satellite derived aerosol optical depth and reflectivity. *J Atmos Sci*, 59: 441-460. [190562](#)
- Pennisi E (2004). The secret life of fungi. *Science*, 304: 1620-1622. [156018](#)
- Perlwitz J; Graf HF (2001). Troposphere-stratosphere dynamic coupling under strong and weak polar vortex conditions. *J Geophys Res Lett*, 28: 271-274. [192271](#)
- Perlwitz J; Harnik N (2003). Observational evidence of a stratospheric influence on the troposphere by planetary wave reflection. *J Clim*, 16: 3011-3026. [192264](#)
- Peters AJ; Gregor DJ; Teixeira CF; Jones NP; Spencer C (1995). The recent depositional trend of polycyclic aromatic hydrocarbons and elemental carbon to the Agassiz Ice cap, Ellesmere Island, Canada. *Sci Total Environ*, 160/161: 167-179. [156856](#)
- Pfirman SL; Kögeler JW; Rigor I (1997). Potential for rapid transport of contaminants from the Kara Sea. *Sci Total Environ*, 202: 111-122. [156864](#)
- Pincus R; Klein SA (2000). Unresolved spatial variability and microphysical process rates in large-scale models. *J Geophys Res*, 105: 27059-27065. [190565](#)
- Pinker R; Zhang B; Dutton E (2005). Do satellites detect trends in surface solar radiation? *Science*, 308: 850-854. [190569](#)
- Piol MN; López AG; Miño LA; Dos Santos Afonso M; Verrengia Guerrero NR (2006). The impact of particle-bound cadmium on bioavailability and bioaccumulation: A pragmatic approach. *Environ Sci Technol*, 40: 6341-6347. [156028](#)
- Pitchford M; Green M; Kuhns H; Tombach I; Malm W; Scruggs M; Farber R; Mirabella V; White WH; McDade C (1999). Project MOHAVE Final Report. [156873](#)

- Pitchford M; Maim W; Schichtel B; Kumar N; Lowenthal D; Hand J (2007). Revised algorithm for estimating light extinction from IMPROVE particle speciation data. *J Air Waste Manag Assoc*, 57: 1326-36. [098066](#)
- Pitchford ML; Malm WC (1994). Development and applications of a standard visual index. *Atmos Environ*, 28: 1049-1054. [044922](#)
- Pitchford ML; Polkowsky BV; McGown MR; Malm WC; Molenaar JV; Mauch L (1990). Percent change in extinction coefficient: a proposed approach for federal visibility protection strategy. In CV Mathai (Ed.), *Transactions: Visibility and Fine Particles* (pp. 37-49). Pittsburgh, PA: Air and Waste Management Association. [156871](#)
- Pitchford ML; Schichtel BA; Gebhart KA; Barna MG; Malm WC; Tombach IH; Knipping EM (2005). Reconciliation and Interpretation of the Big Bend National Park Light Extinction Source Apportionment: Results from the Big Bend Regional Aerosol and Visibility Observational Study- Part II. *J Air Waste Manag Assoc*, 55: 1726-1732. [156874](#)
- Prasad MNV; DeOliveira FHM (2003). Metal hyperaccumulation in plants: Biodiversity prospecting for phytoremediation technology. *Electron J Biotechnol*, 6: 110-146. [156885](#)
- Prata A; Rose W; Self S; O'Brien D (2003). Global, long-term sulphur dioxide measurements from TOVS data: a new tool for studying explosive volcanism and climate. In *Volcanism and the Earth's Atmosphere* (pp. 75-92). Washington, DC: American Geophysical Union. [192235](#)
- Preston CM; Schmidt MWI (2006). Black (pyrogenic) carbon: a synthesis of current knowledge and uncertainties with special consideration of boreal regions. *Biogeosciences*, 3: 397-420. [156030](#)
- Procopio AS; Artaxo P; Kaufman YJ; Remer LA; Schafer JA; Holben BN (2004). Multiyear analysis of Amazonian biomass burning smoke radiative forcing of climate. *J Geophys Res*, 31: L03108. [190571](#)
- Prospero JM (1996). Saharan dust transport over the North Atlantic Ocean and Mediterranean: an overview. In Guerzoni S; Chester R (Ed.), *The Impact of Desert Dust Across the Mediterranean* (pp. 133-152). The Netherlands: Kluwer Academic Publishers. [156889](#)
- Pryor SC (1996). Assessing public perception of visibility for standard setting exercises. *Atmos Environ*, 30: 2705-2716. [056598](#)
- Pryor SC; Binkowski FS (2004). An analysis of the time scales associated with aerosol processes during dry deposition. *Aerosol Sci Technol*, 38: 1091-1098. [116805](#)
- Putaud J-P; Raes F; Van Dingenen R; Brüggemann E; Facchini M-C; Decesari S; Fuzzi S; Gehrig R; Hüglin C; Laj P; Lorbeer G; Maenhaut W; Mihalopoulos N; Müller K; Querol X; Rodriguez S; Schneider J; Spindler G; ten Brink H; Törseth K; Wiedensohler A (2004). A European aerosol phenomenology--2: chemical characteristics of particulate matter at kerbside, urban, rural and background sites in Europe. *Atmos Environ*, 38: 2579-2595. [055545](#)
- Qian Y; Wang W; Leung L; Kaiser D (2007). Variability of solar radiation under cloud-free skies in China: The role of aerosols. *Geophys Res Lett*, 34: L12804. [190572](#)
- Quaas J; Boucher O (2005). Constraining the first aerosol indirect radiative forcing in the LMDZ GCM using POLDER and MODIS satellite data. *Geophys Res Lett*, 32: L17814. [190573](#)
- Quaas J; Boucher O; Bellouin N; Kinne S (2008). Satellite-based estimate of the direct and indirect aerosol climate forcing. *J Geophys Res*, 113: D05204. [190916](#)
- Quaas J; Boucher O; Breon F-M (2004). Aerosol indirect effects in POLDER satellite data and the Laboratoire de Météorologie Dynamique-Zoom (LMDZ) general circulation model. *J Geophys Res*, 109: D08205. [199907](#)
- Quaas J; Boucher O; Lohmann U (2006). Constraining the total aerosol indirect effect in the LMDZ GCM and ECHAM4 GCMs using MODIS satellite data. *Atmos Chem Phys Discuss*, 5: 9669-9690. [190915](#)
- Quinn PK; Anderson T; Bates T; Dlugi R; Heintzenberg J; Von Hoyningen-Huene W; Kumula M; Russel P; Swietlicki E (1996). Closure in tropospheric aerosol-climate research: A review and future needs for addressing aerosol direct shortwave radiative forcing. *Contrib Atmos Phys*, 69: 547-577. [192021](#)
- Quinn PK; Bates TS (2003). North American, Asian, and Indian haze: Similar regional impacts on climate? *Geophys Res Lett*, 30: 1555. [049189](#)
- Quinn PK; Bates TS; Baynard T; Clarke AD; Onasch TB; Wang W; Rood MJ; Andrews E; Allan J; Carrico CM; Coffman D; Worsnop D (2005). Impact of particulate organic matter on the relative humidity dependence of light scattering: A simplified parameterization. *Geophys Res Lett*, 32: 1-4. [156033](#)

- Quinn PK; Coffman D; Kapustin V; Bates TS; Covert DS (1998). Aerosol optical properties in the marine boundary layer during ACE 1 and the underlying chemical and physical aerosol properties. *J Geophys Res*, 103: 16547-16563. [190918](#)
- Quinn PK; Coffman DJ; Bates TS; Welton EJ; Covert DS; Miller TL; Johnson JE; Maria S; Russell L; Arimoto R; Carrico CM; Rood MJ; Anderson J (2004). Aerosol optical properties measured aboard the Ronald H. Brown during ACE-Asia as a function of aerosol chemical composition and source region. *J Geophys Res*, 109: 109. [190937](#)
- Radke LF; Coakley JA; King MD (1989). Direct and remote sensing observations of the effects of ships on clouds. *Science*, 246: 1146-1149. [156034](#)
- Rajapaksha R; MT-K; Bååth E (2004). Metal toxicity affects fungal and bacterial activities in soil differently. *Appl Environ Microbiol*, 5: 2966 – 2973. [156035](#)
- Ramachandran S; Ramaswamy V; Stenchikov GL; Robock A (2000). Radiative impact of the Mount Pinatubo volcanic eruption: Lower stratospheric response. *J Geophys Res*, 105: 24409-24429. [192050](#)
- Ramanathan V; Chung C; Kim D; Bettge T; Buja L; Kiehl JT; Washington WM; Fu Q; Sikka DR; Wild M (2005). Atmospheric brown clouds: Impact on South Asian climate and hydrologic cycle. *PNAS*, 102: 5326-5333. [190199](#)
- Ramanathan V; Crutzen P (2003). Atmospheric Brown “Clouds”. *Atmos Environ*, 37: 4033-4035. [190198](#)
- Ramanathan V; Crutzen PJ; Kiehl JT; Rosenfeld D (2001). Aerosols, climate and the hydrological cycle. *Science*, 294: 2119-2124. [042681](#)
- Ramanathan V; Crutzen PJ; Lelieveld J; Mitra AP; Althausen D; Anderson J; Andreae MO; Cantrell W; Cass GR; Chung CE; Clarke AD; Coakley JA; Collins WD; Conant WC; Dulac F; Heintzenberg J; Heymsfield AJ; Holben B; Howell S; Hudson J; Jayaraman A; Kiehl JT; Krishnamurti TN; Lubin D; McFarquhar G; Novakov T; Ogren JA; Podgorny IA; Prather K; Priestley K; Prospero JM; Quinn PK; Rajeev K; Rasch P; Rupert S; Sadourny R; Satheesh SK; Shaw GE; Sheridan P; Valero FPJ (2001). Indian Ocean Experiment: An integrated analysis of the climate forcing and effects of the great Indo-Asian haze. *J Geophys Res*, 106: 28371-38398. [190196](#)
- Ramaswamy V; Boucher O; Haigh J; Hauglustaine D; Haywood J; Myhre G; Nakajima T; Shi G; Solomon S (2001). Radiative forcing of climate change, Chapter 6. In Houghton JT; Ding Y; Griggs DJ; Noguer M; van der Linden PJ; Da X; Maskell K; Johnson CA (Ed.), IPCC Third Assessment Report (TAR): Climate Change 2001: Working Group I: The Scientific Basis (pp. 349-416). Cambridge, U.K. and New York, NY: Intergovernmental Panel on Climate Change; Cambridge University Press. [156899](#)
- Ramaswamy V; Ramachandran S; Stenchikov G; Robock A (2006). A model study of the effect of Pinatubo volcanic aerosols on the stratospheric temperatures+. In Kiehl JT; Ramanathan V (Ed.), *Frontiers of climate modeling* (pp. 152–178). Cambridge, UK: Cambridge University Press. [192273](#)
- Ramaswamy V; Schwarzkopf MD; Randel WJ; Santer BD; Soden BJ; Stenchikov GL (2006). Anthropogenic and natural influences in the evolution of lower stratospheric cooling. *Science*, 311: 1138-1141. [192284](#)
- Ramos L; Hernandez LM; Gonzalez MJ (1994). Sequential fractionation of copper, lead, cadmium and zinc in soils from or near Donana National Park. *J Environ Qual*, 23: 50-57. [046736](#)
- Ramsey JM (1966). Concentrations of carbon monoxide at traffic intersections in Dayton, Ohio. *Arch Environ Occup Health*, 13: 44-46. [013946](#)
- Randall CE; Bevilacqua RM; Lumpe JD; Hoppel KW (2001). Validation of POAM III aerosols: Comparison to SAGE II and HALOE. *J Geophys Res*, 106: 27525–27536. [192268](#)
- Randall D; Khairoutdinov M; Arakawa A; Grabowski W (2003). Breaking the cloud parameterization deadlock. *Bull Am Meteorol Soc*, 84: 1547-1564. [190201](#)
- Randerson JT; Liu H; Flanner MG; Chambers SD; Jin Y; Hess PG; Pfister G; Mack MC; Treseder KK; Welp LR; Chapin FS; Harden JW; Goulden ML; Lyons E; Neff JC; Schuur EAG; Zender CS (2006). The impact of boreal forest fire on climate warming. *Science*, 314: 1130-1132. [156038](#)
- Rapport DJ; Whitford WG (1999). How ecosystems respond to stress: Common properties of arid and aquatic systems. *Bioscience*, 49: 193-203. [004595](#)
- Ray P; Reddy UG; Lapeyrie F; Adholeya A (2005). Effect of coal ash on growth and metal uptake by some selected ectomycorrhizal fungi in vitro. *Int J Phytoremediation*, 7: 199-216. [190473](#)

- Read WG; Froidevaux L; Waters JW (1993). Microwave limb sounder measurement of stratospheric SO₂ from the Mt. Pinatubo Volcano. *Geophys Res Lett*, 20: 1299–1302. [192031](#)
- Reddy M; Boucher O; Balkanski Y; Schulz M (2005). Aerosol optical depths and direct radiative perturbations by species and source type. *Geophys Res Lett*, 32: L12803. [190208](#)
- Reddy M; Boucher O; Bellouin N; Schulz M; Balkanski Y; Dufresne J; Pham M (2005). Estimates of multi-component aerosol optical depth and direct radiative perturbation in the LMDZT general circulation model. *J Geophys Res*, 110: D10S16. [190207](#)
- Reddy MS; Boucher O (2007). Climate impact of black carbon emitted from energy consumption in the world's regions. *Geophys Res Lett*, 34: 1802. [156042](#)
- Regoli F; Gorbi S; Fattorini D; Tedesco S; Notti A; Machella N; Bocchetti R; Benedetti M; Piva F (2006). Use of the land snail *Helix aspersa* sentinel organism for monitoring ecotoxicologic effects of urban pollution: An integrated approach. *Environ Health Perspect*, 114: 63-69. [156046](#)
- Reid J (2008). An overview of UAE2 flight operations: Observations of summertime atmospheric thermodynamic and aerosol profiles of the southern Arabian Gulf. *J Geophys Res*, 113: D14213. [190214](#)
- Reid JS; Kinney JE; Westphal DL; Holben BN; Welton EJ; Tsay S-C; Eleuterio DP; Campbell JR; Christopher SA; Colarco PR; Jonsson HH; Livingston JM; Maring HB; Meier ML; Pilewskie P; Prospero JM; Reid EA; Remer LA; Russell PB; Savoie DL; Smirnov A; Tanré D (2003). Analysis of measurements of Saharan dust by airborne and ground-based remote sensing methods during the Puerto Rico Dust Experiment (PRIDE). *J Geophys Res*, 108: 8586. [190213](#)
- Reinfelder JR; Fisher NS; Luoma SN; Nichols JW; Wang W-X (1998). Trace element trophic transfer in aquatic organisms: A critique of the kinetic model approach. *Sci Total Environ*, 219: 117-135. [156047](#)
- Reisinger LM (1990). Analysis of airborne particles sampled in the southern Appalachian Mountains. *Water Air Soil Pollut*, 50: 149-162. [046737](#)
- Remer L; Gassó; Hegg D; Kaufman Y; Holben B (1997). Urban/industrial aerosol: ground based sun/sky radiometer and airborne in situ measurements. *J Geophys Res*, 102: 16849-16859. [190216](#)
- Remer L; Kaufman Y (2006). Aerosol direct radiative effect at the top of the atmosphere over cloud free ocean derived from four years of MODIS data. *Atmos Chem Phys*, 6: 237-253. [190222](#)
- Remer L; Kaufman Y; Tanré D; Mattoo S; Chu D; Martins J; Li R; Ichoku C; Levy R; Kleidman R; Eck T; Vermote E; Holben B (2005). The MODIS aerosol algorithm, products and validation. *J Atmos Sci*, 62: 947-973. [190221](#)
- Remer L; Kleidman RG; Levy RC; Kaufman YJ; Tanre D; Mattoo S; Vanderlei Martins J; Ichoku C; Koren I; Yu H; Holben BN (2008). An emerging aerosol climatology from the MODIS satellite sensors. *J Geophys Res*, 113: D14S01. [190224](#)
- Remer L; Tanré D; Kaufman Y; Ichoku C; Mattoo S; Levy R; Chu D; Holben B; Dubovik O; Smirnov A; Martins J; Li R; Ahman Z (2002). Validation of MODIS aerosol retrieval over ocean. *Geophys Res Lett*, 29: 8008. [190218](#)
- Richards LW; Dye TS; Arthur M; Byars MS (1996). Analysis of ASOS Data for Visibility Purposes, Final Report . Systems Applications International, Inc.. San Rafael, CA. STI-996231-1610-FR. [190476](#)
- Rind D; Perlwitz J; Lonergan P (2005). AO/NAO response to climate change: 1. Respective influences of stratospheric and tropospheric climate changes. *J Geophys Res*, 110: D12107. [192261](#)
- Rissler J; Swietlicki E; Zhou J; Roberts G; Andreae MO; Gatti LV; Artaxo P (2004). Physical properties of the sub-micrometer aerosol over the Amazon rain forest during the wet-todry season transition—comparison of modeled and measured CCN concentrations. *Atmos Chem Phys*, 4: 2119-2143. [190225](#)
- Roberts DL; Jones A (2004). Climate sensitivity to black carbon aerosol from fossil fuel combustion. *J Geophys Res*, 109: 6202. [156052](#)
- Roberts ES; Richards JH; Jaskot R; Dreher KL (2003). Oxidative stress mediates air pollution particle-induced acute lung injury and molecular pathology. *Inhal Toxicol*, 15: 1327-1346. [156051](#)
- Robinson AL; Donahue NM; Shrivastava MK; Weitkamp EA; Sage AM; Grieshop AP; Lane TE; Pierce JR; Pandis SN (2007). Rethinking organic aerosols: Semivolatile emissions and photochemical aging. *Science*, 315: 1259-1262. [156053](#)

- Roderick ML; Farquhar GD (2002). The cause of decreased pan evaporation over the past 50 years. *Science*, 298: 1410-1411. [042788](#)
- Roeckner E; Stier P; Feichter J; Kloster S; Esch M; Fischer-Bruns L (2006). Impact of carbonaceous aerosol emissions on regional climate change. *Clim Dynam*, 27: 553-571. [156920](#)
- Romic M; Romic D (2003). Heavy metals distribution in agricultural topsoils in urban area. *Environ Geol*, 43: 795-805. [156055](#)
- Rood MJ; Covert DS; Larson TV (1987). Hygroscopic properties of atmospheric aerosol in Riverside, California. *Tellus B Chem Phys Meteorol*, 39B: 383-397. [046397](#)
- Rosenfeld D (2000). Suppression of rain and snow by urban and industrial air pollution. *Science*, 287: 1793-1796. [002234](#)
- Rosenfeld D (2006). Aerosols, clouds, and climate. *Science*, 312: 1. [190233](#)
- Rosenfeld D; Dai J; Yu X; Yao Z; Xu X; Yang X; Du C (2007). Inverse relations between amounts of air pollution and orographic precipitation. *Science*, 315: 1396-1398. [156057](#)
- Rosenfeld D; Givati A (2006). Evidence of orographic precipitation suppression by air pollution-induced aerosols in the western United States. *J Appl Meteor Climatol*, 45: 893-911. [156924](#)
- Rosenfeld D; Lansky I (1998). Satellite-based insights into precipitation formation processes in continental and maritime convective clouds. *Bull Am Meteorol Soc*, 79: 2457-2476. [190230](#)
- Ross DM; Malm WC; Loomis RJ (1985). The psychological valuation of good visual air quality by national park visitors. Presented at 78th annual meeting of the Air Pollution Control Association, June, 1985, Detroit, MI. [044287](#)
- Ross DM; Malm WC; Loomis RJ (1987). An examination of the relative importance of park attributes at several national parks. In Bhardwaja, P. S. (Ed.), *Visibility protection: research and policy aspects, an APCA international specialty conference Grand Teton National Park, WY; Pittsburgh, PA: Air Pollution Control Association*. [037420](#)
- Rosselli W; Keller C; Boschi K (2003). Phytoextraction capacity of trees growing on a metal contaminated soil. *Plant Soil*, 256: 265-272. [156058](#)
- Roth CM; Goss K-U; Schwarzenbach RP (2004). Sorption of diverse organic vapors to snow. *Environ Sci Technol*, 38: 4078-4084. [056431](#)
- Rotstain LD; Liu Y (2003). Sensitivity of the first indirect aerosol effect to an increase of the cloud droplet spectral dispersion with droplet number concentration. *J Clim*, 16: 3476-3481. [199905](#)
- Rotstain LD; Penner JE (2001). Indirect aerosol forcing, quasi-forcing, and climate response. *J Clim*, 14: 2960-2975. [193754](#)
- Rotton J; Barry T; Milligan M; Fitzpatrick M (1979). The air pollution experience and interpersonal aggression. *Appl Psychol*, 9: 397-412. [190478](#)
- Rotton J; Frey J (1982). Atmospheric conditions, seasonal trends, and psychiatric emergencies. In *Replications and Extensions* (pp. Unknown). Washington, DC: American Psychological Association. [190477](#)
- Rozanov EV; Schlesinger ME; Andronova NG; Yang F; Malyshev SL; Zubov VA; Egorova TA; Li B (2002). Climate/chemistry effects of the Pinatubo volcanic eruption simulated by the UIUC stratosphere/troposphere GCM with interactive photochemistry. *J Geophys Res*, 107: ACL 12-1. [192070](#)
- Rozanov EV; Schlesinger ME; Egorova TA; Li B; Andronova N; Zubov VA (2004). Atmospheric response to the observed increase of solar UV radiation from solar minimum to solar maximum simulated by the University of Illinois at Urbana-Champaign climate-chemistry model. *J Geophys Res*, 109: D01110.1-D01110.16. [192072](#)
- Ruckstuhl C; Philipona R; Behrens K; Coen MC; Dürr B; Heimo A; Mätzler C; Nyeki S; Ohmura A; Vuilleumier L; Weller M; Wehrli C; Zelenka A (2008). Aerosol and cloud effects on solar brightening and recent rapid warming. *Geophys Res Lett*, 35: L12708. [190356](#)
- Russell P; Kinne S; Bergstrom R (1997). Aerosol climate effects: local radiative forcing and column closure experiments. *J Geophys Res*, 102: 9397-9407. [190359](#)
- Russell P; Livingston J; Hignett P; Kinne S; Wong J; Chien A; Bergstrom R; Durkee P; Hobbs P (1999). Aerosol-induced radiative flux changes off the United States mid-Atlantic coast: comparison of values calculated from sun photometer and in situ data with those measured by airborne pyranometer. *J Geophys Res*, 104: 2289-2307. [190363](#)

- Rusu A-M; Jones GC; Chimonides PDJ; Purvis OW (2006). Biomonitoring using the lichen *Hypogymnia physodes* and bark samples near Zlatna, Romania immediately following closure of a copper ore-processing plant. *Environ Pollut*, 143: 81-88. [156062](#)
- Ryan PA; Lowenthal D; Kumar N (2005). Improved light extinction reconstruction in interagency monitoring of protected visual environments. *J Air Waste Manag Assoc*, 55: 1751-1759. [156934](#)
- Sabbioni C; Ghedini N; Bonazza A (2003). Organic anions in damage layers on monuments and buildings. *Atmos Environ*, 37: 1261-1269. [049282](#)
- Sabin LD; Lim JH; Stolzenbach KD; Schiff KC (2005). Contribution of trace metals from atmospheric deposition to stormwater runoff in a small impervious urban catchment. *Water Res*, 39: 3929-3937. [088300](#)
- Salemaa M; Derome J; Helmisaari HS; Nieminen T; Vanha-Majamaa I (2004). Element accumulation in boreal bryophytes, lichens and vascular plants exposed to heavy metal and sulfur deposition in Finland. *Sci Total Environ*, 324: 141-160. [156069](#)
- Samuels HJ; Twiss S; Wong EW (1973). Visibility, light scattering and mass concentration of particulate matter: report of the California Tri-City Aerosol Sampling Project. Air Resources Board. CA. [070601](#)
- Sanderson EG; Farant JP (2004). Indoor and outdoor polycyclic aromatic hydrocarbons in residences surrounding a Soderberg aluminum smelter in Canada. *Environ Sci Technol*, 38: 5350-5356. [156942](#)
- Sato M; Hansen J; Koch D; Lucis A; Ruedy R; Dubovik O; Holben B; Chin M; Novakov T (2003). Global atmospheric black carbon inferred from AAEONET. Presented at Proceedings of the National Academy of Science. [156947](#)
- Sato M; Hansen JE; McCormick MP; Pollack JB (1993). Stratospheric aerosol optical depths, 1850-1990. *J Geophys Res*, 98: 22987-22994. [192046](#)
- Sauvé S (2001). Speciation of metals in soils. Presented at , Pensacola, FL. [156948](#)
- Saxena P; Hildemann LM; McMurry PH; Seinfeld JH (1995). Organics alter hygroscopic behavior of atmospheric particles. *J Geophys Res*, 100: 18,755-18,770. [077273](#)
- Schichtel BA; Gebhart K; Barna MG; Malm WC; Green MC (2004). Big Bend Regional Aerosol and Visibility Observational (BRAVO) Study Results: Air Quality Data and Source Attribution Analyses Results from the National Park Service. Colorado State University CIRA. Ft. Collins, CO
.http://vista.cira.colostate.edu/improve/Studies/BRAVO/Studybravo.htm. [179902](#)
- Schichtel BA; Gebhart KA; Malm WC; Barna MG; Pitchford ML; Knipping EM; Tombach IH (2005). Reconciliation and interpretation of big bend national park particulate sulfur source apportionment: Results from the big bend regional aerosol and visibility observational study-part I. *J Air Waste Manag Assoc*, 55: 1709-1725. [156957](#)
- Schichtel BA; Malm WC; Bench G; Fallon S; McDade CE; Chow JC; Watson JG (2008). Fossil and contemporary fine particulate carbon fractions at 12 rural and urban sites in the United States. *J Geophys Res*, 113: D02311. [156958](#)
- Schiff K; Bay S; Stransky C (2002). Characterization of stormwater toxicants from an urban watershed to freshwater and marine organisms. *Urban Water*, 4: 215-227. [156959](#)
- Schilling JS; Lehman ME (2002). Bioindication of atmospheric heavy metal deposition in the Southeastern US using the moss *Thuidium delicatulum*. *Atmos Environ*, 36: 1611-1618. [113075](#)
- Schmid B; Ferrare R; Flynn C; Elleman R; Covert D; Strawa A; Welton E; Turner D; Jonsson H; Redemann J; Eilers J; Ricci K; Hallar AG; Clayton M; Michalsky J; Smirnov A; Holben B; Barnard J (2006). How well do state-of-the-art techniques measuring the vertical profile of tropospheric aerosol extinction compare? *J Geophys Res*, 111: 1-25. [190372](#)
- Schmid B; Livingston JM; Russell PB; Durkee PA; Jonsson HH; Collins DR; Flagan RC; Seinfeld JH; Gassó S; Hegg DA; Öström E; Noone KJ; Welton EJ; Voss KJ; Gordon HR; Formenti, P.(9) Andreae, M.O (2000). Clear sky closure studies of lower tropospheric aerosol and water vapor during ACE-2 using airborne sunphotometer, airborne in situ, space-borne, and ground-based measurements. *Tellus B Chem Phys Meteorol*, 52: 568-593. [190369](#)
- Schmidt GA; Ruedy R; Hansen JE; Aleinov I; Bell N; Bauer M; Bauer S; Cairns B; Canuto V; Cheng Y; del Genio A; Faluvegi G; Friend AD; Hall TM; Hu Y; Kelley M; Kiang NY; Koch D; Lacis AA; Lerner J; Lo KK; Miller RL; Nazarenko L; Oinas V; Perlwitz J; Perlwitz J; Rind D; Romanou A; Russell GL; Sato MKI; Shindell DT; Stone PH; Sun S; Tausnev N; Thresher D; Yao MS (2006). Present-day atmospheric simulations using GISS Model E: Comparison to in situ, satellite and reanalysis data. *J Clim*, 19: 153-192. [190373](#)

- Schoeberl MR; Douglass AR; Zhu Z; Pawson S (2003). A comparison of the lower stratospheric age spectra derived from a general circulation model and two data assimilation systems. *J Geophys Res*, 108: 4113. [057262](#)
- Schroeder WH; Munthe J (1998). Atmospheric mercury -- an overview. *Atmos Environ*, 32: 809-822. [014559](#)
- Schulz M; Textor C; Kinne S; Balkanski Y; Bauer S; Bernsten T; Berglen T; Boucher O; Dentener F; Guibert S; Isaksen ISA; Iversen T; Koch D; Kirkevåg A; Liu X; Montanaro V; Myhre G; Penner JE; Pitari G; Reddy S; Seland O; Stier P; Takemura T (2006). Radiative forcing by aerosols as derived from the AeroCom present-day and preindustrial simulations. *Atmos Chem Phys*, 6: 5225-5246. [190381](#)
- Schwartz SE; Charlson RJ; Rodhe H (2007). Quantifying climate change- Too rosy a picture? *Nature*, 2: 23-24. [190384](#)
- Seifert M; Anke S; Holzinger S; Jaritz M; Arnhold W; Anke M (1999). Cadmium and strontium content of mice, shrews, and some invertebrates. *J. Trace Microprobe Tech.*, 17: 357-365. [190480](#)
- Seigneur C; Johnson CD; Latimer DA; Bergstrom RW; Hogo H (1984). Users manual for the Plume Visibility Model (PLUVUE II). Final report 23 Feb-29 Aug 83. Systems Applications, Inc. San Rafael, CA . PB-84-158302. [156965](#)
- Seinfeld JH; Carmichael GR; Arimoto R; Conant WC; Brechtel FJ; Bates TS; Cahill TA; Clarke AD; Doherty SJ; Flatau PJ; Huebert BJ; Kim J; Markowicz KM; Quinn PK; Russell LM; Russell PB; Shimizu A; Shinozuka Y; Song CH; Tang Y; Uno I; Vogelmann AM; Weber RJ; Woo J-H; Zhang XY (2004). ACEAsia: Regional climatic and atmospheric chemical effects of Asian dust and pollution. *Bull Am Meteorol Soc*, 85: 367-380. [190388](#)
- Sekiguchi M; Nakajima T; Suzuki K; Kawamoto K; Higurashi A; Rosenfeld D; Sano I; Mukai S (2003). A study of the direct and indirect effects of aerosols using global satellite data sets of aerosol and cloud parameters. *J Geophys Res*, 108 D22: 4699. [190385](#)
- Shakya K; Chettri MK; Sawidis T (2008). Impact of heavy metals (copper, zinc, and lead) on the chlorophyll content of some mosses. *Arch Environ Contam Toxicol*, 54: 412-421. [156081](#)
- Shan XQ; Wang ZW; Wang WS; Zhang SZ; Wen B (2003). Labile rhizosphere soil solution fraction for prediction of bioavailability of heavy metals and rare earth elements to plants. *Anal Bioanal Chem*, 375: 400-407. [156972](#)
- Sharifi MR; Gibson AC; Rundel PW (1999). Phenological and physiological responses of heavily dusted creosote bush (*Larrea tridentata*) to summer irrigation in the Mojave Desert. *Flora*, 14: 369-378. [156082](#)
- Sheesley RJ; Schauer JJ; Hemming JD; Barman MA; Geis SW; Tortorelli JJ (2004). Toxicity of ambient atmospheric particulate matter from the Lake Michigan (USA) airshed to aquatic organisms. *Environ Toxicol Chem*, 23: 133-140. [156084](#)
- Shindell DT; Levy H; Schwarzkopf II MD; Horowitz LW; Lamarque JF; Faluvegi G (2008). Multimodel projections of climate change from short-lived emissions due to human activities. *J Geophys Res*, 113: D11109. [190393](#)
- Shindell DT; Schmidt GA; Mann ME; Faluvegi G (2004). Dynamic winter climate response to large tropical volcanic eruptions since 1600. *J Geophys Res*, 109: D05104. [192267](#)
- Shindell DT; Schmidt GA; Miller RL; Mann M (2003). Volcanic and solar forcing of climate change during the preindustrial era. *J Clim*, 16: 4094-4107. [192069](#)
- Shindell DT; Teich H; Chin M; Dentener F; Doherty RM; Faluvegi G; Fiore AM; Hess P; MacKenzie IA; Sanderson MG; Schultz MG; Schulz M; Stevenson DS; Textor C; Wild O; Bergmann DJ; Bian H; Cuvelier C; Duncan BN; Folberth G; Horowitz LW; Jonson J; Kaminski JW; Marmer E; Park R; Pringle KJ; Schroeder S; Szopa S; Takemura T; Zeng G; Keating TJ; Zuber A (2008). A multi-model assessment of pollution transport to the Arctic. *Atmos Chem Phys*, 8: 5353-5372. [190391](#)
- Shulz KG; Zondervan I; Gerringa LJA; Timmermans KR; Veldhuls MJW; Riebesell U (2004). Effect of trace metal availability on coccolithophorid calcification. *Nature*, 430: 673-676. [156087](#)
- Singh HB; Brune WH; Crawford JH; Flocke F; Jacob DJ (2008). Chemistry and transport of pollution over the Gulf of Mexico and the Pacific: spring 2006 INTEX-B campaign overview and first results. *Atmos Chem Phys Discuss*, 9: 2301-2318. [190394](#)
- Sinyuk A; Dubovik O; Holben B; Eck TF; Breon FM; Martonchik J; Kahn R; Diner DJ; Vermote EF; Roger JC; Lapyonok T; Slutsker I (2007). Simultaneous retrieval of aerosol and surface properties from a combination of AERONET and satellite data. *Rem Sens Environ*, 107: 90-108. [190395](#)

- Skov H; Christensen JH; Goodsite ME; Heidam NZ; Jensen B; Wahlin P; Geernaert G (2004). Fate of elemental mercury in the Arctic during atmospheric mercury depletion episodes and the load of atmospheric mercury to the Arctic. *Environ Sci Technol*, 38: 2373-2382. [190481](#)
- Sloane CS (1983). Optical properties of aerosols--comparison of measurements with model calculations. *Atmos Environ*, 17: 409-416. [025039](#)
- Sloane CS (1984). Optical properties of aerosols of mixed composition. *Atmos Environ*, 18: 871-878. [025040](#)
- Sloane CS (1986). Effect of composition on aerosol light scattering efficiencies. *Atmos Environ*, 20: 1025-1037. [045954](#)
- Sloane CS; Wolff GT (1985). Prediction of ambient light scattering using a physical model responsive to relative humidity: validation with measurements from Detroit. *Atmos Environ*, 19: 669-680. [045953](#)
- Smejkalova M; Mikanova O; Boruvka L (2003). Effects of heavy metal concentrations on biological activity of soil microorganisms. *Plant Soil Environ*, 49: 321-326. [156987](#)
- Smirnov A; Holben B; Eck T; Dubovik O; Slutsker I (2000). Cloud screening and quality control algorithms for the AERONET database. *Rem Sens Environ*, 73: 337-349. [190397](#)
- Smirnov A; Holben B; Eck T; Slutsker I; Chatenet B; Pinker R (2002). Diurnal variability of aerosol optical depth observed at AERONET (Aerosol Robotic Network) sites. *Geophys Res Lett*, 29: 2115. [190398](#)
- Smirnov A; Holben B; Sakerin S; Kabanov DM; Slutsker I; Chin M; Diehl TL; Remer LA; Kahn R; Ignatov A; Liu L; Mishchenko M; Eck TF; Kucsera TL; Giles D; Kopelevich OV (2006). Shipbased aerosol optical depth measurements in the Atlantic Ocean, comparison with satellite retrievals and GOCART model. *Geophys Res Lett*, 33: L14817. [190400](#)
- Smith AE; Howell S (2009). An assessment of the robustness of visual air quality preference study results. CRA International. Washington, DC. [http://yosemite.epa.gov/sab/sabproduct.nsf/B55911DF9796E5E385257592006FB737/\\$File/CRA+VAQ+Pref+Robustness+Study+3+30+09+final.pdf](http://yosemite.epa.gov/sab/sabproduct.nsf/B55911DF9796E5E385257592006FB737/$File/CRA+VAQ+Pref+Robustness+Study+3+30+09+final.pdf). [198803](#)
- Smith WH (1990). Forest nutrient cycling: toxic ions. In *Air pollution and forests: interactions between air contaminants and forest ecosystems* New York, NY: Springer-Verlag. [046896](#)
- Smith WH (1990). Forests as sinks for air contaminants: vegetative compartment. In *Air pollution and forests: interactions between air contaminants and forest ecosystems* (pp. 147-180). New York, NY: Springer-Verlag. [084015](#)
- Smith WH (1991). Air pollution and forest damage. *Chem Eng News*, 6945: 30-43. [042566](#)
- Smith WL Jr; Charlock TP; Kahn R; Martins JV; Remer LA; Hobbs PV; Redemann J; Rutledge CK (2005). EOS Terra aerosol and radiative flux validation: An overview of the Chesapeake Lighthouse and aircraft measurements from satellites (CLAMS) experiment. *J Atmos Sci*, 62: 903-918. [190401](#)
- Smolders E; Degryse F (2002). Fate and effect of zinc from tire debris in soil. *Environ Sci Technol*, 36: 3706-3710. [156091](#)
- Soares CRFS; Siqueira JO (2008). Mycorrhiza and phosphate protection of tropical grass species against heavy metal toxicity in multi-contaminated soil. *Biol Fertil Soils*, 44: 833-841. [190482](#)
- Sokolik I; Winker D; Bergametti G; Gillette DA; Carmichael G; Kaufman YJ; Gomes L; Schuetz L; Penner JE (2001). Introduction to special section: outstanding problems in quantifying the radiative impacts of mineral dust. *J Geophys Res*, 106: 18015-18027. [190404](#)
- Solomon PA; Hopke PK (2008). A Special Issue of JA&WMA Supporting Key Scientific and Policy-and Health-Relevant Findings from EPA's Particulate Matter Supersites Program and Related Studies: An Integration and Synthesis of Results. *J Air Waste Manag Assoc*, 58: 137. [156997](#)
- Solomon S; Portmann RW; Garcia RR; Thomason LW; Poole LR; McCormick MP (1996). The role of aerosol variations in anthropogenic ozone depletion at northern midlatitudes. *J Geophys Res*, 101: 6713-6727. [192252](#)
- Sotiropoulou REP; Medina J; Nenes A (2006). CCN predictions: is theory sufficient for assessments of the indirect effect? *Geophys Res Lett*, 33: L05816. [190406](#)
- Sotiropoulou REP; Nenes A; Adams PJ; Seinfeld JH (2007). Cloud condensation nuclei prediction error from application of Kohler theory: Importance for the aerosol indirect effect. *J Geophys Res*, 112: D12202. [190405](#)

- Spinhirne J; Palm S; Hart W; Hlavka D; Welton E (2005). Cloud and Aerosol Measurements from the GLAS Space Borne Lidar: initial results. *Geophys Res Lett*, 32: L22S03. [190410](#)
- Spracklen DV; Logan JA; Mickley LJ; Park RJ; Yevich R; Westerling AL; Jaffe DA (2007). Wildfires drive interannual variability of organic carbon aerosol in the western U.S. in summer. *Geophys Res Lett*, 34: L16816. [190485](#)
- Squires P (1958). The microstructure and colloidal stability of warm clouds: Part I - the relation between structure and stability. *Tellus Dyn Meteorol Oceanogr*, 10: 256-261. [045608](#)
- Srogi (2007). Monitoring of environmental exposure to polycyclic aromatic hydrocarbons: a review. *Environ Chem Lett*, 5: 169-195. [180049](#)
- Stanhill G; Cohen S (2001). Global dimming: a review of the evidence for a widespread and significant reduction in global radiation with discussion of its probable causes and possible agricultural consequences. *Agr Forest Meteorol*, 107: 255-278. [042121](#)
- Steinnes E; Hvatum OØ; Bølviken B; Varskog P (2005). Atmospheric supply of trace elements studied by peat samples from ombrotrophic bogs. *J Environ Qual*, 34: 192-197. [156095](#)
- Stenchikov G; Hamilton K; Robock A; Ramaswamy V; Schwarzkopf MD (2004). Arctic Oscillation response to the 1991 Pinatubo eruption in the SKYHI GCM with a realistic quasi-biennial oscillation. *J Geophys Res*, 109: D03112. [192274](#)
- Stenchikov G; Hamilton K; Stouffer RJ; Robock A; Ramaswamy V; Santer B; Graf H-F (2006). Arctic Oscillation response to volcanic eruptions in the IPCC AR4 climate models. *J Geophys Res*, 111: D07107. [192260](#)
- Stenchikov G; Robock A; Ramaswamy V; Schwarzkopf MD; Hamilton K; Ramachandran S (2002). Arctic Oscillation response to the 1991 Mount Pinatubo eruption: Effects of volcanic aerosols and ozone depletion. *J Geophys Res*, 107: D24. [192277](#)
- Stenchikov GL; Kirchner I; Robock A; Graf H-F; Antuña JC; Grainger RG; Lambert A; Thomason L (1998). Radiative forcing from the 1991 Mount Pinatubo volcanic eruption. *J Geophys Res*, 103: 13837-13857. [192049](#)
- Stephens G; Vane DG; Boain RJ; Mace GG; Sassen K; Wang Z; Illingworth AJ; O'Connor EJ; Rossow WB; Durden SL; Miller SD; Austin RT; Benedetti A; Mitrescu C; The CloudSat Science Team (2002). The CloudSat mission and the A-Train. *Bull Am Meteorol Soc*, 83: 1771-1790. [190412](#)
- Stephens GL; Haynes JM (2007). Near global observations of the warm rain coalescence process. *Geophys Res Lett*, 34: L20805. [190413](#)
- Stern DI (2005). Global sulfur emissions from 1850 to 2000. *Chemosphere*, 58: 163-175. [190416](#)
- Stern GA; Halsall CJ; Barrie LA; Muir DCG; Fellin P; Rosenberg B (1997). Polychlorinated biphenyls in arctic air. 1. Temporal and spatial trends: 1992-1994. *Environ Sci Technol*, 31: 3619-3628. [156096](#)
- Stevens B; Feingold G; Walko RL; Cotton WR (1996). On elements of the microphysical structure of numerically simulated non-precipitating stratocumulus. *J Atmos Sci*, 53: 980-1006. [190417](#)
- Stewart AR; Luoma SN; Schlekert CE; Doblin MA; Hieb KA (2004). Food web pathway determines how selenium affects aquatic ecosystems. *Environ Sci Technol*, 38: 4519-4526. [156097](#)
- Stier P; Seinfeld JH; Kinne S; Boucher O (2007). Aerosol absorption and radiative forcing. *Atmos Chem Phys*, 7: 5237-5261. [157012](#)
- Stohl A; Andrews E; Burkhardt JF; Forster C; Herber A; Hoch SW; Kowal D; Lunder C; Mefford T; Ogren JA; Sharma S; Spichtinger N; Stebel K; Stone R; Ström J; Tørseth K; Wehrli C; Yttri KE (2006). Pan-Arctic enhancements of light absorbing aerosol concentrations due to North American boreal forest fires during summer 2004. *J Geophys Res*, 111: D22214. [156100](#)
- Stohl A; Berg T; Burkhardt JF; Fjæraa AM; Forster C; Herber A; Hov Ø; Lunder C; McMillan WW; Oltmans S; Shiobara M; Dimpson D; Solberg S; Stebel K; Ström J; Tørseth K; Treffeisen R; Virkkunen K; Yttri KE (2007). Arctic smoke - record high air pollution levels in the European Arctic due to agricultural fires in Eastern Europe in spring 2006. *Atmos Chem Phys*, 7: 511-534. [157015](#)
- Storlevmo T; Kristjansson JE; Myhre G; Johnsd M; Stordal F (2006). Combined observational and modeling based study of the aerosol indirect effect. *Atmos Chem Phys*, 6: 3583-3601. [190418](#)

- Stothers RB (2001). A chronology of annual mean effective radii of stratospheric aerosols from volcanic eruptions during the twentieth century as derived from ground-based spectral extinction measurements. *J Geophys Res*, 106: 32043–32049. [192233](#)
- Stothers RB (2001). Major optical depth perturbations to the stratosphere from volcanic eruptions: Stellar extinction period, 1961–1978. *J Geophys Res*, 106: 2993–3003. [192232](#)
- Stott PA (2006). Observational constraints on past attributable warming and predictions of future global warming. *J Clim*, 19: 3055-3069. [190419](#)
- Strachan WMJ; Burniston DA; Williamson M; Bohdanowicz H (2001). Spatial difference in persistent organochlorine pollutant concentrations between the Bering and Chukchi Seas. *Mar Pollut Bull*, 43: 132-142. [156103](#)
- Strandberg B; Axelsen JA; Pedersen MB; Jensen J; Attrill MJ (2006). Effect of a copper gradient on plant community structure. *Environ Toxicol Chem*, 25: 743-753. [156105](#)
- Strawa A; Castaneda R; Owano T; Baer P; Paldus B (2002). The measurement of aerosol optical properties using continuous wave cavity ring-down techniques. *J Atmos Ocean Tech*, 20: 454-465. [190421](#)
- Streets D; Bond T; Lee T; Jang C (2004). On the future of carbonaceous aerosol emissions. *J Geophys Res*, 109: D24212. [190423](#)
- Streets D; Wu Y; Chin M (2006). Two-decadal aerosol trends as a likely explanation of the global dimming/brightening transition. *Geophys Res Lett*, 33: L15806. [190425](#)
- Streets DG; Aunan K (2005). The importance of China's household sector for black carbon emissions. *Geophys Res Lett*, 32: L12708. [156106](#)
- Streets DG; Zhang Q; Wang L; He K; Hao J; Wu Y; Tang Y; Carmichael GR (2006). Revisiting China's CO emissions after the Transport and Chemical Evolution over the Pacific (TRACE-P) mission: Synthesis of inventories, atmospheric modeling, and observations. *J Geophys Res*, 111: D14306. [157019](#)
- Strydom C; Robinson C; Pretorius E; Whitcutt JM; Marx J; Bornman MS (2006). The effect of selected metals on the central metabolic pathways in biology: A review. *WaterSA*, 32: 543-554. [190486](#)
- Suzuki K; Nakajima T; Numaguti A; Takemura T; Kawamoto K; Higurashi A (2004). A study of the aerosol effect on a cloud field with simultaneous use of GCM modeling and satellite observation. *J Atmos Sci*, 61: 179-194. [199917](#)
- Swackhamer DL; Paerl HW; Eisenreich SJ; Hurley J; Hornbuckle KC; McLachlan M; Mount D; Muir D; Schindler D (2004). Impacts of atmospheric pollutants on aquatic ecosystems. *Issues in Ecology*, 12: 1-24. [190488](#)
- Sweet C; Caughey M; Gay D (2005). Midwest Ammonia Monitoring Project: Summary for October 2003 through November 2004. Illinois State Water Survey. IL.http://www.ladco.org/reports/rpo/monitoring/ammonia_study_monitoring_report.pdf. [180038](#)
- Szabó L; Fodor L (2006). Uptake of microelements by crops grown on heavy metal-amended soil. *Commun Soil Sci Plant Anal*, 37: 2679-2689. [156109](#)
- Tabazadeh A; Drdla K; Schoeberl MR; Hamill P; Toon OB (2002). Arctic "ozone hole" in a cold volcanic stratosphere. *PNAS*, 99: 2609-2612. [192250](#)
- Takemura T; Nakajima T; Dubovik O; Holben B; Kinne S (2002). Single-scattering albedo and radiative forcing of various aerosol species with a global three-dimensional model. *PNAS*, 15: 333-352. [190438](#)
- Takemura T; Nozawa T; Emori S; Nakajima T; Nakajima T (2005). Simulation of climate response to aerosol direct and indirect effects with aerosol transport-radiation model. *J Geophys Res*, 110: D02202. [190439](#)
- Tang IN (1996). Chemical and size effects of hygroscopic aerosols on light scattering coefficients. *J Geophys Res*, 101: 245?219. [157042](#)
- Tang Y; Carmichael GR; Seinfeld JH; Dabdub D; Weber RJ; Huebert B; Clarke AD; Guazzotti SA; Sodeman DA; Prather KA; Uno I; Woo JH; Yienger JJ; Streets DG; Quinn PK; Johnson JE; Song CH; Grassian VH; Sandu A; Talbot RW; Dibb JE (2004). Three-dimensional simulations of inorganic aerosol distributions in East Asia during spring 2001. *J Geophys Res*, 109: D19S23. [190445](#)

- Tang Y; Carmichael GR; Woo JH; Thongboonchoo N; Kurata G; Uno I; Streets DG; Blake DR; Weber RJ; Talbot RW; Kondo Y; Singh HB; Wang T (2003). Influences of biomass burning during the Transport and Chemical Evolution Over the Pacific (TRACE-P) experiment identified by the regional chemical transport model. *J Geophys Res*, 108: 8824. [190441](#)
- Tanré D; Haywood J; Pelon J; Léon JF; Chatenet B; Formenti P; Francis P; Goloub P; Highwood EJ; Myhre G (2003). Measurement and modeling of the Saharan dust radiative impact: Overview of the Saharan Dust Experiment (SHADE). *J Geophys Res*, 108: 8574. [190454](#)
- Tanré D; Kaufman Y; Herman M; Mattoo S (1997). Remote sensing of aerosol properties over oceans using the MODIS/ EOS spectral radiances. *J Geophys Res*, 102: 16971-16988. [190452](#)
- Tao S; Jiao X; Chen S; Xu F; Li Y; Liu F (2006). Uptake of vapor and particulate polycyclic aromatic hydrocarbons by cabbage. *Environ Pollut*, 140: 13–15. [156112](#)
- Taulavuori K; Prasad MNV; Taulavuori E; Laine K (2005). Metal stress consequences on frost hardness of plants at northern high latitudes: a review and hypothesis. *Environ Pollut*, 135: 209-220. [190489](#)
- Tett SFB; Jones GS; Stott PA; Hill DC; Mitchell JFB; Allen MR; Ingram WJ; Johns TC; Johnson CE; Jones A; Roberts DL; Sexton DMH; Woodage MJ (2002). Estimation of natural and anthropogenic contributions to twentieth century temperature change. *J Geophys Res*, 107: 4306. [192053](#)
- Textor C; Schulz M; Guibert S; Kinne S; Balkanski Y; Bauer S; Berntsen T; Berglen T; Boucher O; Chin M; Dentener F; Diehl T; Easter R; Feichter H; Fillmore D; Ghan S; Ginoux P; Gong S; Grini A; Hendricks J; Horowitz L; Huang P; Isaksen I; Iversen T; Kloster S; Koch D; Kirkevåg A; Kristjansson JE; Krol M; Lauer A; Lamarque JF; Liu X; Montanaro V; Myhre G; Penner J; Pitari G; Reddy S; Sel Ø; Stier P; Takemura T; Tie X (2006). Analysis and quantification of the diversities of aerosol life cycles within AEROCOM. *Atmos Chem Phys*, 6: 1777-1813. [190456](#)
- Textor C; Schulz M; Guibert S; Kinne S; Balkanski Y; Bauer S; Berntsen T; Berglen T; Boucher O; Chin M; Dentener F; Diehl T; Feichter J; Fillmore D; Ginoux P; Gong S; Grini A; Hendricks J; Horowitz L; Huang P; Isaksen ISA; Iversen T; Kloster S; Koch D; Kirkevåg A; Kristjansson JE; Krol M; Lauer A; Lamarque JF; Liu X; Montanaro V; Myhre G; Penner JE; Pitari G; Reddy MS; Seland O; Stier P; Takemura T; Tie X (2007). The effect of harmonized emissions on aerosol properties in global models?an AeroCom experiment. *Atmos Chem Phys*, 7: 4489-4501. [190458](#)
- Thomas GO; Smith KEC; Sweetman AJ; Jones KC (1998). Further studies of the air-pasture transfer of polychlorinated biphenyls. *Environ Pollut*, 102: 119–128. [156118](#)
- Thomason LW; Peter T (2006). Assessment of Stratospheric Aerosol Properties (ASAP): Report on the Assessment Kick-Off Workshop, Paris, France, 4-6 November 2001 . Presented at Assessment of Stratospheric Aerosol Properties , Paris, France. [192248](#)
- Tie X; Madronich S; Walters S; Edwards DP; Ginoux P; Mahowald N; Zhang R; Lou C; Brasseur C (2005). Assessment of the global impact of aerosols on tropospheric oxidants. *J Geophys Res*, 110: 1-32. [190459](#)
- Tie XX; Brasseur GP; Briegleb B; Granier C (1994). Two-dimensional simulation of Pinatubo aerosol and its effect on stratospheric ozone. *J Geophys Res*, 99: 20545-20562. [192253](#)
- Timmreck C; Graf H-F; Steil B (2003). Aerosol chemistry interactions after the Mt. Pinatubo Eruption . In A Robock and C Oppenheimer (Ed.), *Volcanism and the Earth's Atmosphere* (pp. 213-226). Washington, DC: American Geophysical Union. [192068](#)
- Tombach I; McDonald K (2004). Visibility and Radiative Balance Effects. In P.H. McMurry MFS, and J.S. Vickery (Ed.), *Particulate Matter Science for Policy Makers: A NARSTO Assessment* (pp. 325-354). Cambridge, MA: Cambridge University Press. [157054](#)
- Toose LK; Mackay D (2004). Adaptation of fugacity models to treat speciating chemicals with constant species concentration ratios. *Environ Sci Technol*, 38: 4619–4626. [156123](#)
- Torres O; Bhartia P; Herman J; Ahmad Z; Gleason J (1998). Derivation of aerosol properties from satellite measurements of backscattered ultraviolet radiation: Theoretical bases. *J Geophys Res*, 103: 17009-17110. [190503](#)
- Torres O; Bhartia P; Herman J; Sinyuk A; Ginoux P; Holben B (2002). A long-term record of aerosol optical depth from TOMS observations and comparison to AERONET measurements. *J Atmos Sci*, 59: 398-413. [190505](#)

- Torres O; Bhartia P; Sinyuk A; Welton E; Holben B (2005). Total Ozone Mapping Spectrometer measurements of aerosol absorption from space: Comparison to SAFARI 2000 groundbased observations. *J Geophys Res*, 110: D10S18. [190507](#)
- Tremper AH; Agneta M; Burton S; Higgs DEB (2004). Field and laboratory exposures of two moss species to low level metal pollution. *J Atmos Chem*, 49: 111-120. [156126](#)
- Trijonis J; Thayer M; Murdoch J; Hagemen R (1985). Air quality benefit analysis for Los Angeles and San Francisco based on housing values and visibility. California Air Resources Board. Sacramento, CA. [078468](#)
- Trijonis JC; Malm WC; Pitchford M; White WH; Charlson R (1990). Acidic deposition: State of science and technology. Report 24. Visibility: Existing and historical conditions-causes and effects. Final report. [157058](#)
- Turco RP; Toon OB; Whitten RC; Pollack JB; Hamill P (1983). The global cycle of particulate elemental carbon: a theoretical assessment. In Pruppacher HR (Ed.), *Precipitation Scavenging, Dry Deposition, and Resuspension* (pp. 1337- 1351). New York: Elsevier Science. [190529](#)
- Twomey S (1977). The influence of pollution on the shortwave albedo of clouds. *J Atmos Sci*, 34: 1149-1152. [190533](#)
- U.S. EPA (1979). *Protecting Visibility*, an EPA Report to Congress. U.S. Environmental Protection Agency. Washington, DC. [157065](#)
- U.S. EPA (1982). Air quality criteria for particulate matter and sulfur oxides, Vol 1, 2, 3. U.S. Environmental Protection Agency, Environmental Criteria and Assessment Office. Washington, D.C.. EPA 600/8-82-029a; EPA 600/8-82-029b; EPA 600/8-82-029c. <http://nepis.epa.gov/Exe/ZyPURL.cgi?Dockey=3000188Z.txt>; <http://nepis.epa.gov/Exe/ZyPURL.cgi?Dockey=300018EV.txt>; <http://nepis.epa.gov/Exe/ZyPURL.cgi?Dockey=300053KV.txt>. [017610](#)
- U.S. EPA (1993). Air quality criteria for oxides of nitrogen, 3 Volumes. Environmental Criteria and Assessment Office, Office of Health and Environmental Assessment, U.S. Environmental Protection Agency. Research Triangle Park, NC. EPA/600/8-91/049. <http://cfpub.epa.gov/ncea/cfm/recordisplay.cfm?deid=40179>. [017649](#)
- U.S. EPA (1996). Air quality criteria for particulate matter. U.S. Environmental Protection Agency. Research Triangle Park, NC. EPA/600/P-95/001aF-cF. [079380](#)
- U.S. EPA (1997). Mercury Study Report to Congress. U.S. Environmental Protection Agency. Washington, DC. [157066](#)
- U.S. EPA (2000). National air pollutant emission trends, 1900-1998. U.S. Environmental Protection Agency. Washington, DC. [012211](#)
- U.S. EPA (2001). Draft Guidance for tracking progress under the regional haze rule. U.S. Environmental Protection Agency. Washington, DC. [157068](#)
- U.S. EPA (2004). Air quality criteria for particulate matter. U.S. Environmental Protection Agency. Research Triangle Park, NC. EPA/600/P-99/002aF-bF. [056905](#)
- U.S. EPA (2004). The Particle Pollution Report: Current Understanding of Air Quality and Emissions through 2003. U.S. Environmental Protection Agency. Research Triangle Park, NC. EPA 454-R-04-002. [190219](#)
- U.S. EPA (2005). Review of the national ambient air quality standards for particulate matter: Policy assessment of scientific and technical information OAQPS staff paper. U.S. Environmental Protection Agency. Washington, DC. EPA/452/R-05-005a. http://www.epa.gov/ttn/naaqs/standards/pm/data/pmstaffpaper_20051221.pdf. [090209](#)
- U.S. EPA (2006). Air quality criteria for lead, in 2 Volumes. Office of Health and Environmental Assessment, Environmental Criteria and Assessment Office, Office of Research and Development, U.S. Environmental Protection Agency. Research Triangle Park, NC. EPA-600/R-5/144aF-bF. [090110](#)
- U.S. EPA (2008). Integrated science assessment for oxides of nitrogen and sulfur: Ecological criteria. U.S. Environmental Protection Agency. Research Triangle Park, NC. EPA/600/R-08/082F. [157074](#)
- Vaisvalavicius R; Motuzas A; Prosycevas I; Levinskaite L; Zakarauskaite D; Grigaliuniene K; Butkus V (2006). Effect of heavy metals on microbial communities and enzymatic activity in soil column experiment. *Arch Agron Soil Sci*, 52: 161-169. [157080](#)
- Van Aardenne JA; Dentener FJ; Olivier JGJ; Klein Goldewijk CGM; Lelieveld J (2001). A 1"degree" x 1"degree" resolution data set of historical anthropogenic trace gas emissions for the period 1980-1990. *Global Biogeochem Cycles*, 15: 909-928. [055564](#)

- Van de Hulst H (1981). Light scattering by small particles. New York: Dover. [191972](#)
- Van Donkelaar A; Martin RV; Park RJ (2006). Estimating ground-level PM_{2.5} using aerosol optical depth determined from satellite remote sensing. *J Geophys Res*, 111: D21. [192108](#)
- van Heerden PDR; Krüger GHJ; Kilbourn Louw M (2007). Dynamic responses of photosystem II in the Namib Desert shrub, *Zygophyllum prismatocarpum*, during and after foliar deposition of limestone dust. *Environ Pollut*, 146: 34-45. [156131](#)
- Vasundhara G; Jayashree G; Muraleedhara-Kurup G (2004). Sequestration of nickel and copper by *Azotobacter chroococcum* SB1. *Bull Environ Contam Toxicol*, 72: 1122-1127. [156133](#)
- Vautard R; Maldi M; Menut L; Beekmann M; Colette A (2007). Boundary layer photochemistry simulated with a two-stream convection scheme. *Atmos Environ*, 41: 8275-8287. [106012](#)
- Veihelmann B; Levelt PF; Stammes P; Veefkind JP (2007). Simulation study of the aerosol information content in OMI spectral reflectance measurements. *Atmos Chem Phys*, 7: 3115-3127. [190627](#)
- Verdelhos T; Neto JM; Marques JC; Pardal MA (2005). The effect of eutrophication abatement on the bivalve *Scrobicularia plana*. *Estuar Coast Shelf Sci*, 63: 261-268. [190497](#)
- Viard B; Pihan F; Promeyrat S; Pihan J-C (2004). Integrated assessment of heavy metal (Pb, Zn, Cd) highway pollution: bioaccumulation in soil, graminaceae and land snails. *Chemosphere*, 55: 1349-1314. [055675](#)
- Viles HA; Gorbushina AA (2003). Soiling and microbial colonisation on urban roadside limestone: A three year study in Oxford, England. *Build Environ*, 38: 1217-1224. [156138](#)
- Viles HA; Taylor MP; Yates TJS; Massey SW (2002). Soiling and decay of N.M.E.P. limestone tablets. *Sci Total Environ*, 292: 215-229. [156137](#)
- Villa S; Vighi M; Maggi V; Finizio A; Bolzacchini E (2003). Historical trends of organochlorine pesticides in an Alpine glacier. *J Atmos Chem*, 46: 295-311. [156139](#)
- Viskari E-L; Karenlampi L (2000). Roadside Scots pine as an indicator of deicing salt use - a comparative study from two consecutive winters. *Water Air Soil Pollut*, 122: 405-419. [019101](#)
- Vivas A; Barea JM; Biro B; Azcon R (2006). Effectiveness of autochthonous bacterium and mycorrhizal fungus on *Trifolium* growth, symbiotic development and soil enzymatic activities in Zn contaminated soil. *J Appl Microbiol*, 100: 587-598. [190500](#)
- Vivas A; Voros A; Biro B; Barea JM; Ruiz-Lozano JM; Azcon R (2003). Beneficial effects of indigenous Cd-tolerant and Cd-sensitive *Glomus mosseae* associated with a Cd-adapted strain of *Brevibacillus* sp in improving plant tolerance to Cd contamination. *Appl Soil Ecol*, 24: 177-186. [190499](#)
- Vives I; Grimalt JO; Ventura M; Catalan J (2005). Distribution of polycyclic aromatic hydrocarbons in the food web of a high mountain lake, Pyrenees, Catalonia, Spain. *Environ Toxicol Chem*, 24: 1344-1352. [157099](#)
- Vogel-Mikus K; Drobne D; Regvar M (2005). Zn, Cd and Pb accumulation and arbuscular mycorrhizal colonisation of pennycress *Thlaspi praecox* Wulf. (Brassicaceae) from the vicinity of a lead mine and smelter in Slovenia. *Environ Pollut*, 133: 233-242. [190501](#)
- Vogel-Mikus K; Pongrac P; Kump P; Necemer M; Regvar M (2006). Colonisation of a Zn, Cd and Pb hyperaccumulator *Thlaspi praecox* Wulfen with indigenous arbuscular mycorrhizal fungal mixture induces changes in heavy metal and nutrient uptake. *Environ Pollut*, 139: 362-371. [190502](#)
- Waggoner AP; Weiss RE (1980). Comparison of fine particle mass concentration and light scattering extinction in ambient aerosol. *Atmos Environ*, 14: 623-626. [070152](#)
- Waggoner AP; Weiss RE; Ahlquist NC; Covert DS; Will S; Charlson RJ (1981). Optical characteristics of atmospheric aerosols. *Atmos Environ*, 15: 1891-1909. [095453](#)
- Wang C (2007). Impact of direct radiative forcing of black carbon aerosols on tropical convective precipitation. *Geophys Res Lett*, 34: 5709. [156147](#)
- Wang Y-Z; Ingram JL; Walters DM; Rice AB; Santos JH; Van Houten B; Bonner JC (2003). Vanadium-induced STAT-1 activation in lung myofibroblasts requires H₂O₂ and P38 MAP kinase. *Free Radic Biol Med*, 35: 845-855. [157106](#)

- Wania F; Hoff JT; Jia CQ; Mackay D (1998). The effects of snow and ice on the environmental behaviour of hydrophobic organic chemicals. *Environ Pollut*, 102: 43-51. [156148](#)
- Wania F; Mackay D (1993). Global fractionation and cold condensation of low volatility organochlorine compounds in polar regions. *Ambio*, 22: 10-18. [157110](#)
- Warner J (1968). A reduction in rainfall associated with smoke from sugar-cane fires—an inadvertent weather modification? *J Appl Meteorol*, 7: 247-251. [157114](#)
- Warner J; Twomey S (1967). The production of cloud nuclei by cane fires and the effect on cloud droplet concentration. *J Atmos Sci*, 24: 704-706. [045616](#)
- Watmough SA; Hutchinson TC; Dillon PJ (2004). Lead dynamics in the forest floor and mineral soil in south-central Ontario. *Biogeochemistry*, 71: 43-68. [077809](#)
- Watson JG; Chow JC (2007). Receptor models for source apportionment of suspended particles. In *Introduction to Environmental Forensics* (pp. 273-298). San Diego, CA: Academic Press. [157127](#)
- Watson JG; Zhu T; Chow JC; Engelbrecht J; Fujita EM; Wilson WE (2002). Receptor modeling application framework for particle source apportionment. *Chemosphere*, 49: 1093-1136. [035623](#)
- Weissenhorn I; Leyval C; Berthelin J (1995). Bioavailability of heavy metals and abundance of arbuscular mycorrhiza in a soil polluted by atmospheric deposition from a smelter. *Biol Fertil Soils*, 19: 22-28. [073826](#)
- Welton E; Voss K; Quinn P; Flatau P; Markowicz K; Campbell J; Spinhirne J; Gordon H; Johnson J (2002). Measurements of aerosol vertical profiles and optical properties during INDOEX 1999 using micro-pulse lidars. *J Geophys Res*, 107: 8019. [190631](#)
- Welton EJ; Campbell JR; Spinhirne JD; Scott VS (2001). Global monitoring of clouds and aerosols using a network of micro-pulse lidar systems. In Singh, U.N. T. Itabe N. Sugimoto (Ed.), *Lidar remote sensing for industry and environment monitoring* (pp. 151-158). Bellingham, WA: Society of Photo-Optical Instrumentation Engineers. [157133](#)
- Wen T; Wang Y; Chang SY; Liu G (2006). On-line measurement of water-soluble ions in ambient particles. *Adv Atmos Sci*, 23: 586-592. [179964](#)
- Wetzel MA; Stowe LL (1999). Satellite-observed patterns in stratus microphysics, aerosol optical thickness, and shortwave radiative forcing. *J Geophys Res*, 104: 31287-31299. [190636](#)
- Wielicki B; Barkstrom B; Harrison E; Lee R; Smith G; Cooper J (1996). Clouds and the Earth's radiant energy system (CERES): An Earth observing system experiment. *Bull Am Meteorol Soc*, 77: 853-868. [190637](#)
- Wild E; Dent J; Thomas GO; Jones KC (2005). Direct observation of organic contaminant uptake, storage, and metabolism within plant roots. *Environ Sci Technol*, 39: 3695-3702. [156156](#)
- Wild SR; Jones KC (1992). Polynuclear aromatic hydrocarbons uptake by carrots grown in sludge amended soil. *J Environ Qual*, 21: 217- 225. [156155](#)
- Williams KD; Jones A; Roberts DL; Senior CA; Woodage MJ (2001). The response of the climate system to the indirect effects of anthropogenic sulfate aerosols. *Clim Dynam*, 17: 846-856. [199898](#)
- Winker D; Couch R; McCormick M (1996). An overview of LITE: NASA's Lidar In-Space Technology Experiment. *IEEE Micro*, 84: 164-180. [190914](#)
- Winker DM; Pelon J; McCormick MP (2003). The CALIPSO mission: spaceborne lidar for observation of aerosols and clouds. *PNAS*, 4893: 1-11. [192017](#)
- Wolff GT (1985). Characteristics and consequences of soot in the atmosphere. *Environ Int*, 11: 259-269. [044680](#)
- Wyszkowska J; Boros E; Kucharski J (2007). Effect of interactions between nickel and other heavy metals on the soil microbiological properties. *Plant Soil Environ*, 53: 544-552. [179948](#)
- Xu J; DuBois D; Pitchford M; Green M; Etyemezian V (2006). Attribution of sulfate aerosols in Federal Class I areas of the western United States based on trajectory regression analysis. *Atmos Environ*, 40: 3433-3447. [102706](#)
- Xue H; Feingold G (2006). Large eddy simulations of tradewind cumuli: Investigation of aerosol indirect effects. *J Atmos Sci*, 63: 1605-1622. [190920](#)

- Xue H; Feingold G; Stevens B (2008). Aerosol effects on clouds, precipitation, and the organization of shallow cumulus convection. *J Atmos Sci*, 65: 392-406. [190921](#)
- Yang CY; Chen CJ (2007). Air pollution and hospital admissions for chronic obstructive pulmonary disease in a subtropical city: Taipei, Taiwan. *J Toxicol Environ Health A Curr Iss*, 70: 1214-1219. [092847](#)
- Yang F; Schlesinger M (2001). Identification and separation of Mount Pinatubo and El Niño-Southern Oscillation land surface temperature anomalies. *J Geophys Res*, 106: 14757-14770. [192270](#)
- Yang XE; Jin XF; Feng Y; Islam E (2005). Molecular mechanisms and genetic basis of heavy metal tolerance/hyperaccumulation in plants. *J Integr Plant Biol*, 47: 1025-1035. [192104](#)
- Yang Z; Zhu L (2007). Performance of the partition-limited model on predicting ryegrass uptake of polycyclic aromatic hydrocarbons. *Chemosphere*, 67: 402-409. [156168](#)
- Ying Q; Kleeman MJ (2006). Source contributions to the regional distribution of secondary particulate matter in California. *Atmos Environ*, 40: 736-752. [098359](#)
- Yogui G; Sericano J (2008). Polybrominated diphenyl ether flame retardants in lichens and mosses from King George Island, maritime Antarctica. *Chemosphere*, 73: 1589-1593. [189971](#)
- Yu H; Dickinson R; Chin M; Kaufman Y; Zhou M; Zhou L; Tian Y; Dubovik O; Holben B (2004). The direct radiative effect of aerosols as determined from a combination of MODIS retrievals and GOCART simulations. *J Geophys Res*, 109: D03206. [190926](#)
- Yu H; Kaufman YJ; Chin M; Feingold G; Remer LA; Anderson TL; Balkanski Y; Bellouin N; Boucher O; Christopher S; Decola P; Kahn R; Koch D; Loeb N; Reddy MS; Schulz M; Takemura T; Zhou M (2006). A review of measurement-based assessments of the aerosol direct radiative effect and forcing. *Atmos Chem Phys*, 6: 613-666. [156173](#)
- Yu H; Liu S; Dickinson R (2002). Radiative effects of aerosols on the evolution of the atmospheric boundary layer. *J Geophys Res*, 107: 4142. [190923](#)
- Yu IJ; Park JD; Park ES; Song KS; Han KT; Han JH; Chung YH; Choi BS; Chung KH; Cho MH (2003). Manganese distribution in brains of Sprague-Dawley rats after 60 days of stainless steel welding-fume exposure. *Neurotoxicology*, 24: 777-785. [156171](#)
- Yu LE; Yung LL; Ong C; Tan Y; Balasubramaniam KS; Hartono D; Shui G; Wenk MR; Ong W (2007). Translocation and effects of gold nanoparticles after inhalation exposure in rats. *Nanotoxicology*, 1: 235-242. [093173](#)
- Yuangeng Y; Campbell CD; Clark L; Camerson CM; Paterson E (2006). Microbial indicators of heavy metal contamination in urban and rural soils. *Chemosphere*, 63: 1942-1952. [156174](#)
- Yunker MB; Snowdon LR; MacDonald RW; Smith JN; Fowler MG; Skibo DN (1996). Polycyclic aromatic hydrocarbon composition and potential sources for sediment samples from the Beaufort and Barents Seas. *Environ Sci Technol*, 30: 1310-1320. [156175](#)
- Zaccone C; Coccoza C; Cheburkin AK; Shotykh W; Miano TM (2007). Highly Organic Soils as “Witnesses” of Anthropogenic Pb, Cu, Zn, and ¹³⁷Cs Inputs During Centuries. *Water Air Soil Pollut*, 186: 263-271. [179930](#)
- Zappia G; Sabbioni C; Riontino C; Gobbi G; Favoni O (1998). Exposure tests of building materials in urban atmosphere. *Sci Total Environ*, 224: 235-244. [012037](#)
- Zechmeister HG (1998). Annual growth of four pleurocarpous moss species and their applicability for biomonitoring heavy metals. *Environ Monit Assess*, 52: 441-451. [156178](#)
- Zechmeister HG; Hohenwallner D; Riss A; Hanus-Illy A (2003). Variation in heavy metal concentrations in the moss species *Abietinella abietina* (Hedw.) Fleisch. according to sampling time, within site variability and increase in biomass. *Sci Total Environ*, 301: 55-65. [157175](#)
- Zeidner M; Shechter M (1988). Psychological responses to air pollution: some personality and demographic correlates. *J Environ Psychol*, 8: 191-208. [189973](#)
- Zhang J; Christopher S (2003). Longwave radiative forcing of Saharan dust aerosols estimated from MODIS, MISR, and CERES observations on Terra. *Geophys Res Lett*, 30: 2188. [190928](#)
- Zhang J; Christopher S; Remer L; Kaufman Y (2005). Shortwave aerosol radiative forcing over cloud-free oceans from Terra. I: Angular models for aerosols. *J Geophys Res*, 110: D10S23. [190929](#)

- Zhang J; Christopher S; Remer L; Kaufman Y (2005). Shortwave aerosol radiative forcing over cloud-free oceans from Terra. II: Seasonal and global distributions. *J Geophys Res*, 110: D10S24. [190930](#)
- Zhang J; Reid JS; Holben BN (2005). An analysis of potential cloud artifacts in MODIS over ocean aerosol optical thickness products. *Geophys Res Lett*, 32: L15803. [190931](#)
- Zhang J; Reid JS; Westphal DL; Baker NL; Hyer EJ (2008). A system for operational aerosol optical depth data assimilation over global oceans. *J Geophys Res*, 113: D10208. [190932](#)
- Zhang KM; Wexler AS; Niemeier DA; Zhu YF; Sioutas W; Sioutas C (2005). Evolution of particle number distribution near roadways Part III: traffic on-road size resolved particulate emission factors. *Atmos Environ*, 39: 4155-4166. [086743](#)
- Zhang Q; Jimenez JL; Canagaratna MR; Allan JD; Coe HL Ulbrich I; Alfarra MR; Takami A; Middlebrook AM; Sun YL; Dzepina K; Dunlea E; Docherty K; DeCarlo PF; Salcedo D; Onasch T; Jayne JR; Miyoshi T; Shimo A; Hatakeyama S; Takegawa N; Kondo Y; Schneider J; Drewnick F; Borrmann S; Weimer S; Demerjian K; Williams P; Bower K; Bahreini R; Cottrell L; Griffin RJ; Rautiainen J; Sun JR; Zhang YM; Worsnop DR (2007). Ubiquity and dominance of oxygenated species in organic aerosols in anthropogenically-influenced Northern Hemisphere midlatitudes. *Geophys Res Lett*, 34: L13801. [189998](#)
- Zhang Q; Jimenez JL; Canagaratna MR; Jayne JT; Worsnop DR (2005). Time- and size-resolved chemical composition of submicron particles in Pittsburgh: Implications for aerosol sources and processes. *J Geophys Res*, 110: 1-19. [157185](#)
- Zhang X; Zwiers FW; Stott PA (2006). Multi-model multisignal climate change detection at regional scale. *J Clim*, 19: 4294-4307. [190933](#)
- Zhang XH; Zhu YG; Chen BD; Lin AJ; Smith SE; Smith FA (2005). Arbuscular mycorrhizal fungi contribute to resistance of upland rice to combined metal contamination of soil. *J Plant Nutr*, 28: 2065-2077. [192083](#)
- Zhang XZ; Sun HW; Zhang ZY (2006). [Bioaccumulation of titanium dioxide nanoparticles in carp]. *Huanjing Kexue*, 27: 1631-5. [157722](#)
- Zhao TXP; Laszlo I; Guo W; Heidinger A; Cao C; Jelenak A; Tarpley D; Sullivan J (2008). Study of long-term trend in aerosol optical thickness observed from operational AVHRR satellite instrument. *J Geophys Res*, 113: D07201. [190935](#)
- Zhao TXP; Yu H; Laszlo I; Chin M; Conant WC (2008). Derivation of component aerosol direct radiative forcing at the top of atmosphere for clear-sky oceans. *J Quant Spectrosc Radiat Transf*, 109: 1162-1186. [190936](#)
- Zhou M; Yu H; Dickinson RE; Dubovik O; Holben BN (2005). A normalized description of the direct effect of key aerosol types on solar radiation as estimated from aerosol robotic network aerosols and moderate resolution imaging spectroradiometer albedos. *J Geophys Res*, 110: D19202. [156183](#)
- Zhu Y; Hinds WC; Shen S; Sioutas C (2004). Seasonal trends of concentration and size distribution of ultrafine particles near major highways in Los Angeles. *Aerosol Sci Technol*, 38: 5-13. [156184](#)
- Zimmer D; Baum C; Leinweber P; Hryniewicz K; Meissner R (2009). Associated bacteria increase the phytoextraction of cadmium and zinc from a metal-contaminated soil by mycorrhizal willows. *Int J Phytoremediation*, 11: 200-213. [192085](#)